



## **PROCEEDINGS OF THE INTERNATIONAL SOLVENT EXTRACTION CONFERENCE**

Edited by

**Kathryn C. Sole**  
Anglo American Research Laboratories

**Peter M. Cole**  
Hydrometallurgy Consultant

**John S. Preston**  
Mintek

**David J. Robinson**  
Anglo American Platinum Corporation

International conference held in Cape Town, South Africa, from 17 to 21 March 2002.  
Organised by the ISEC 2002 South African Organising Committee, and supported by  
the South African Chemical Institute, the South African Institution of Chemical Engineers,  
and the South African Institute of Mining and Metallurgy.

Copyright Reserved

The South African Institute of Mining and Metallurgy  
P O Box 61127, Marshalltown 2107, South Africa  
[www.saimm.co.za](http://www.saimm.co.za)

All rights reserved.

No part of this publication may be reproduced, stored in a retrieval system,  
or transmitted in any form or by any means, electronic, mechanical photocopying,  
recording or otherwise without the written permission of the copyright owner.

Although the greatest care has been taken in the compilation of the entire contents,  
the editors and publishers do not accept responsibility for errors or omissions.

First Edition Copyright March 2002  
ISBN 1-919783-24-5 (set of 2 volumes)

Produced by Documentation Transformation Technologies, Irene  
Reprographics by Disc Express, Sandton  
Printed and bound by NBD / Paarl Print, Cape Town

Published by Chris van Rensburg Publications (Pty) Ltd  
P O Box 29159, Melville 2109, South Africa

The Organising Committee of ISEC 2002 is not responsible for statements or opinions  
and is absolved of liability due to misuse of information contained in this publication.

## TABLE OF CONTENTS

Foreword	xix
Preface	xxi
Acknowledgements	xxiii

### VOLUME 1

#### **Plenary Addresses**

Solvent extraction as an enabling technology in the nickel industry <i>Bacon G, Mihaylov I</i>	1
Developments in platinum group metals refining and the utilisation of solvent extraction technology <i>Charlesworth P</i>	14
Tailored solvents and colloids for green processing of chemicals and biochemicals <i>Hatton TA</i>	15
Achieving high performance low cost processes for the manufacture of organic chemicals using phase transfer catalysis <i>Halpern M</i>	24
Supercritical fluids: Clean solvents for extraction, reaction and crystallisation <i>O'Neil AS, Hamley PA, Poliakoff M</i>	34
Room temperature ionic liquids as alternatives to traditional organic solvents in solvent extraction <i>Visser AE, Holbrey JD, Rogers RD</i>	474

#### **Fundamentals: Coalescence and Interfacial Phenomena** 44

Electric fields in solvent extraction <i>Bart H-J</i>	45
Behaviour of interfacial tension at an oil-water interface in the presence of an applied electric field <i>Kuipa PK, Hughes MA</i>	53
Interfacial orientation of porphyrin at the liquid-liquid interface using UV-vis external reflection spectroscopy <i>Ogawa N, Moriya Y, Nakata S</i>	58
Mass spectrometry and laser microspectrometry for the study of interfacial reaction in solvent extraction systems <i>Watari H</i>	64
The drainage and rupture of the film between colliding drops in the presence of surfactant <i>Yeo LY, Matar OK, Perez de Ortiz ES, Hewitt GF</i>	70
Estimation of coalescence parameters for population balance models <i>Simon M, Bart H-J</i>	77
Flotation-assisted electrostatic coalescence <i>Bailes PJ, Edalat A</i>	83
Drop coalescence behaviour for extraction systems containing industrial extractants <i>Ban T, Kawaizumi F, Nii S, Takahashi K</i>	89
Non-invasive experimental study and modelling of toluene-in-water turbulently agitated liquid-liquid dispersions <i>Ribeiro MM, Baptista M, Texeira P, Soeiro JM, Ribeiro LM, Guimarães MML, Cruz-Pinto JJC</i>	95
AC fields in solvent extraction – influence on droplet formation and mass transfer <i>Gneist G, Bart H-J</i>	101

<b>Fundamentals: Advances in Solvent Extraction Theory</b>	<b>107</b>
Application of preferential solvation concept for interpretation of the mechanisms of solvent extraction: Part I: Acid solvent extraction by amines. Part II: Metal solvent extraction by acidic extractants <i>Kislik V</i>	108
Microemulsions and third phase formation <i>Osseo-Asare K</i>	118
Prediction of diffusivities in liquid associating systems <i>Bosse D, Bart H-J</i>	125
Study of the interaction of tributylphosphate, non-ionic surfactant and water by Fourier Transform infrared spectroscopy <i>Chang Z-D, Wei X-F, Wang J, Liu H-Z, Chen J-Y</i>	131
Analysis of amine-based extraction systems containing more than one organic phase: invariance and implications for extraction efficiency and selectivity <i>Eyal AM, Hazan B, Canari R, Vitner A, Reuveny T</i>	137
Computational time saving in the Monte Carlo simulation of liquid-liquid dispersions <i>El-Hassan Z, Perez de Ortiz ES</i>	143
An expression of equilibrium constants in synergistic extraction <i>Hasegawa Y, Matsubayashi I, Inagaki A</i>	149
Some fundamental aspects of the cloud point phenomenon and application to the extraction of phenol from aqueous streams <i>Materna K, Cote G, Szymanowski J</i>	155
Equilibria based on $g^E$ -models in a Co / Ni / phosphinic acid system <i>Manski R, Bart H-J, Görge A, Traving M, Strube J, Bäcker W</i>	161
Estimation of activities in the extraction of iron(III) with tri-n-butylphosphate and of cobalt(II) with Aliquat 336 from magnesium chloride media <i>Azimi A, Rice NM</i>	167
Aqueous two-phase equilibrium data for polyethylene glycol, potassium phosphate and bromelain <i>Moreira AS, Silva DN, Chiavone-Filho O</i>	174
Selectivity of metal extraction at the micellar mechanism <i>Sinegribova OA, Muravirova OV</i>	180
Micellar mechanism peculiarities of metal extraction by organophosphorus extractants in the presence of surfactants <i>Sinegribova OA, Muravirova OV</i>	186
Structure-reactivity studies of solvent extractants in metal extraction <i>Yuan C, Li S</i>	192
Colloid structures formed in extraction systems with organophosphorus extractants <i>Yurtov EV, Murashova NM</i>	197
A structure parameter characterising steric effect of organophosphorus acid extractants <i>Zhu T</i>	203
<b>Fundamentals: Kinetics and Mass Transfer</b>	<b>208</b>
Mass transfer coefficients of single liquid drops in extraction columns <i>Hashem MA, Saien J</i>	209
The development of mathematical correlations for mass transfer of film contacting of two aqueous phases <i>Jahim J, Slater MJ</i>	215

The effect of ionic surfactants on the mass transfer at the liquid-liquid interface for a toluene/water/ acetone system <i>Mendes-Tatsis MA, Pursell M, Tang S, San Miguel G</i>	221
Numerical approach to the motion and external mass transfer of a drop swarm by the cell model <i>Mao Z-S, Chen JY</i>	227
Mass transfer and microdrops at interfaces investigated on molecular level <i>Merzliak T, Schmäh M, Schott R, Pfennig A</i>	233
Study of salt effects on the kinetics of solute transfer and extraction at a free liquid-liquid interface <i>Simonin J-P, Hendrawan H</i>	238
Computer simulation of the mass transfer process between a single drop and an unbounded continuous phase <i>Uribe AR, Santamaría MP, Korchinsky WJ</i>	245
Influencing the rate of mass transfer in reactive extraction using high voltage <i>Wildberger A, Bart H-J</i>	251
A study on multi-component mass transfer coefficients of drop swarm <i>Wei H, Fei W</i>	257
Kinetic study of nickel(II) extraction from chloride solutions <i>Buch A, Pareau D, Stambouli M, Durand G</i>	262
Kinetics of rare earth extraction with sec-octylphenoxy acetic acid <i>Yue ST, Liao WP, Li DQ, Su Q</i>	268
Kinetics and mechanism of metal extraction onto a microcapsule containing organo-phosphorus extractant <i>Kamio E, Matsumoto M, Kondo K</i>	274
<b>Extractants</b>	<b>279</b>
New types of extractant to transport metal sulphates in base metal recovery processes <i>Gunn DM, Miller HA, Swart RM, Seward GW, Tasker PA, West LC, White DJ</i>	280
Physico-chemical properties of Cyanex® 301 <i>Cote G, Martin J-V, Bauer D, Mottot Y</i>	291
Towards recognition of the anion in the extraction of alkali metal salts by crown ethers and calixarenes <i>Moyer BA, Bonnesen PV, Delmau LH, Havelock TJ, Kavallieratos K, Levitskaia TG</i>	299
Extraction of gold from hydrochloric acid solutions by calixarenes <i>Belhamel K, Dzung NTK, Benamor M, Ludwig R</i>	307
Separation and concentration of Pd(II) with immobilised maleonitrile-dithiocrown ethers <i>Mickler W, Bukowsky H, Holdt H-J</i>	313
Separation of palladium from platinum <i>du Preez JGH, Hosten EC, Knoetze SE</i>	319
On the liquid-liquid extraction of Pt(IV/II) from hydrochloric acid by N-acyl(aryloyl)-N',N'dialkyl-thioureas: A multinuclear ( <sup>1</sup> H, <sup>13</sup> C, <sup>195</sup> Pt) NMR speciation study of the extracted complexes <i>Koch KR, Westra A</i>	327
Extraction of silver from concentrated chloride solutions: use of tri-n-butyl- and tri-n-octyl-phosphine sulphides <i>Capela RS, Paiva AP</i>	335
Extraction of base metals with binary extractants <i>Belova VV, Voshkin AA, Kholkin AI, Fleitlikh I Yu, Pashkov GL</i>	341

Diazopyrazolones as solvent extractants for copper from ammonia leach solutions <i>Campbell J, Cupertino D, Emeleus LC, Harris SG, Owens S, Parsons S, Swart RM, Tasker PA, Tinkler OS, White DJ</i>	347
Synergistic solvent extraction of Cu(II), Zn(II) and Ni(II) based on supramolecular assemblies <i>Gasperov V, Gloe K, Leong AJ, Lindoy LF, Mahinay MS, Stephan H, Tasker PA, Wichmann K</i>	353
Beta-diketone copper extractants: structure and stability <i>Kordosky G, Virnig M, Mattison P</i>	360
Solvent extraction of iron(III) from hydrochloric acid solutions by dihexyl sulphoxide <i>Sato T, Ishikawa I, Sato K, Noguchi Y</i>	366
Solvent extraction of iron(II) from hydrochloric acid solutions using N,N'-dimethyl-N,N'-diphenylmalonamide <i>Costa MC, Paiva AP</i>	371
Study of Sc and Zr extraction reactions by reactive materials containing acidic organo-phosphorus extractants <i>Cortina JL, Korovin V, Shestak Y</i>	377
Solvent extraction of tetravalent titanium, zirconium and tin from hydrochloric acid solutions by an $\alpha$ -hydroxyoxime <i>Sato T, Suzuki K, Sato K, Takahashi T</i>	384
Aggregation and metal ion extraction properties of novel, silicon-substituted alkylene-diphosphonic acids <i>McAlister DA, Dietz ML, Chiarizia R, Herlinger AW</i>	390
Separation of NaOH from salts by weak hydroxyl acids <i>Havelock TJ, Bonnesen PV, Brown GM, Chambliss CK, Levitskaia TG, Moyer BA</i>	396
Extraction of selected metal cations with the alkylaryl-phosphinic acid: 2,4,4-trimethylpentyl-phenylphosphinic acid <i>Nucciarone D, Jakovljevic B, Fir B, Hillhouse J, Depalo M</i>	402
Thermodynamics of the extraction of selected metal ions by di(2-ethylhexyl)alkylene-diphosphonic acids <i>Otu EO, Chiarizia R</i>	408
Comparison of solvent extraction method and ion-exchange method for the separation among alkaline earth metal ions in the presence of cryptands as the masking reagents <i>Tsurubou S, Umetani S, Komatsu Y</i>	414
Solvent extraction of metal ions with novel 4-acyl-5-pyrazolones having crown ether moiety as intramolecular synergist <i>Umetani S, Yamazaki S, Ogura K</i>	420
A novel synergism found in the extraction of In(III) ion with TTA and TOPO in carbon tetrachloride <i>Hokura A, Noro J, Kusakabe S, Sekine T</i>	425
Solvent extraction of indium(III) and iron(III) from sulphuric acid media by mixtures of D <sub>2</sub> EHPA and Cyanex 923 <i>Wang C, Liu D, Zhang J</i>	430
Extraction of rare earth ions by sec-nonaphenoxyacetic acid <i>Wang YG, Meng SL, Li DQ, Jin MJ, Li CZ</i>	436
Chemistry of solvent extraction of scandium(III) from sulfate solutions quaternary ammonia sulfates <i>Stepanov SI, Kharchev AE, Chekmarev AM</i>	441
Extraction of uranium(VI) from phosphate media in poly(ethyleneglycol) solutions <i>Safiulina AM, Sinegribova OA, Shkinev VM</i>	447

Development of environmentally benign new solvent extraction reagents from chitosan, a natural polysaccharide <i>Inoue K, Yoshizuka K, Ohto K</i>	453
<b>Novel Developments and Applications</b>	<b>458</b>
Novel electrochemical processing using conventional organic solvents <i>O'Keefe T, O'Keefe M, Fang R, Sun J, Dahlgren E</i>	459
Advanced liquid-liquid extraction system using photochemical reduction for metals <i>Nishihama S, Hirai T, Komasawa I</i>	467
Room temperature ionic liquids as alternatives to traditional organic solvents in solvent extraction <i>Visser AE, Holbrey JD, Rogers RD</i>	474
Toward "in silico" design of new potential extractants using chemical informatics methods <i>Varnek A, Wipff G, Solov'ev V</i>	481
Electrical tomography and other measurements in liquid-liquid systems <i>Korchinsky WJ, Bolton GT</i>	487
Solvent impregnated resins: Performance and environmental applications in metal extraction <i>Warshawsky A, Cortina JL</i>	493
Study of the sorption of Zn(II) with XAD-7 resin impregnated with Ionquest 801 <i>Benamor M, Draa MT</i>	500
Evaluation of alkylguanidine based solvent impregnated resins for gold cyanide extraction <i>Kautzmann RM, Sampaio CH, Korovin V, Shestak Y, Aguilar M, Cortina JL</i>	506
Sol-gel synthesized adsorbents for noble metal separations <i>Lee JS, Tavlarides LL</i>	512
Hydrophobic gel separation agents (X). Solvent extraction separation of copper(II) and lanthanide(III) in the presence or absence of hydrophobic silica gels <i>Komatsu Y, Kokusen H, Tsurubou S</i>	518
Coalescence extraction – from molecular dynamics to chemical engineering application <i>Schaadt A, Bart H-J</i>	524
Liquid-liquid extraction in aqueous biphasic systems: Partitioning behavior of silica and hematite in the dextran/triton X-100/water system <i>Zeng X, Osseo-Asare K</i>	530
The partitioning of some dyes and the effect of KSCN in polyethylene glycol/salts aqueous two-phase systems <i>Xu Y, Lu J, Li DQ</i>	537
Application of solvent extraction to the production of multicomponent composite powders <i>Shibata S, Yamamoto H</i>	543
<b>Analytical Applications</b>	
Determination of protonation constants of 2,2':6',2"-terpyridine by liquid-liquid distribution data <i>Andersson S, Ekberg C, Liljenzin J-O, Skarnemark G</i>	549
Separation of precious metals with crown ethers as their ion-pair complexes by means of solvent extraction <i>Honjo T, Hossain KZ, Camagong CT</i>	555
The binding constants of metal fulvate and humate complexes <i>Helal AA, Mourad Gh A, Khalifa SM</i>	558

Ion-pair extraction and one-drop flame atomic absorptiometric determination of silver with benzo-monothiacrown and bromothymol blue <i>Kojima I, Katsuzaki M, Yamada M, Yamaguchi M, Sakamoto H</i>	565
Extraction and spectrophotometric determination of copper(II) with isonitroso-5-methyl-2-hexanone and 5-methyl-2,3-hexanedione dioxime <i>Tandel SP, Jadhav SB, Malve SP</i>	570
Extraction behavior of soft metal ions with polythioether derivatives containing O or N donor atoms <i>Chayama K, Adachi K, Mori T, Tsuji H</i>	576
Application of Courier 30SX analyser to nickel laterite solvent extraction <i>Hughes DV, Kongas M, Saloheimo K</i>	581
<b>Biotechnology, Pharmaceutical and Nutriceutrical Applications</b>	<b>588</b>
Opportunities for extraction technology in chiral separations <i>De Haan AB, Kuipers NJM, Steensma M</i>	589
Mass transfer performance of two-phase electrophoresis with an emulsion solution as organic phase <i>Liu JG, Luo GS, Pan S, Zhai SL, Wang JD</i>	597
Study on the three-phase extraction of penicillin G with a single step method <i>Chen J, Liu H-Z, Wang B, An ZT, Liu QF</i>	602
Extraction of drug traces with liquid membrane systems <i>Grote M, Haciosmanoglu B, Nolte J</i>	607
Selectivity in the extraction of carboxylic acids by amine-based extractants <i>Eyal AM, Hazan B, Canari R, Vitner A, Reuveny T</i>	614
Optimisation of process conditions for industrial separation of amino acid enantiomers by fractional reactive extraction <i>Steensma M, Kuipers NJM, De Haan AB, Kwant G</i>	620
Extraction of borage seed oil by compressed carbon dioxide: Effect of process parameters <i>Gaspar F, Lu T, Santos R, Al-Duri B</i>	626
Liquid-liquid equilibrium data for the corn oil / oleic acid / aqueous ethanol system <i>Gonçalves CB, Meirelles AJ</i>	632
Liquid-liquid extraction for deacidification of vegetable oils <i>Batista E, Antoniassi R, Wolf Maciel MR, Meirelles AJA</i>	638
Influence of operating factors on the rhubarb extraction process <i>Lu YC, Luo GS, Dai YY</i>	644
Extraction of lysozyme with reverse micelles using a contactor agitated by automatic suction of liquid type stirrer <i>Zhang W, Liu H, Chen J</i>	650
Extraction of lysozyme by reversed micellar solution in a sieve-tray column <i>Nishii Y, Hara C, Kinugasa T, Nii S, Takahashi K</i>	656
Modeling of solubilities of essential oils in liquid carbon dioxide present in three odoriferous plants <i>Sousa EMBD, Silva DN, Chiavone-Filho O, Meireles MAA</i>	662
Evaluation of improved solvents for caprolactam extraction <i>Van Delden ML, Kuipers NJM, de Haan AB, Lerner O</i>	668
Extraction and enrichment of physiologically active lipids and nutrients from plant materials using supercritical fluid extraction <i>Westerman D, Al-Duri B, Santos R, Bosley J</i>	674

Forward and backward extraction of BSA using mixed reversed micellar system of CTAB and 4-methyl-2-pentanone <i>Zhang W, Lui H, Chen J</i>	680
<b>Membranes</b>	<b>686</b>
Optical sensor for chromium(VI) monitoring: optimisation of chromium(VI) transport through liquid membranes <i>Castillo E, Granados M, Cortina JL</i>	687
Application of novel extractants for actinide(III) / lanthanide(III) separation in hollow fibre modules <i>Geist A, Weigl M, Müllrich U, Gompper K</i>	693
Hollow fibre membrane-based non-dispersive extraction Ag(I) from alkaline cyanide media using LIX 79 <i>Kumar Pabby A, Melgosa A, Haddad R, Sastre AM</i>	699
Selective extraction of lithium ion with novel lipophilic phthalocyanine derivatives and its permeation through supported liquid membrane <i>Kondo K, Matsumoto M, Yoshida T, Kamio E</i>	706
Extraction of cadmium from phosphoric acid with an emulsion liquid membrane: water transport and membrane rupture <i>Gallego Lizon T, Perez de Ortiz ES</i>	712
Transfer properties of cadmium(II) and zinc(II) from hydrochloric acid with HEH/EHP using microporous hollow fibre membrane <i>Luo F, Jia Q, Li DQ, Wu YL</i>	718
A kinetic study of the extraction of zinc from hydrochloric acid solutions by a surfactant liquid membrane containing trioctylamine <i>Pérocheau S, Stambouli M, Pareau D, Durand G</i>	724
Extraction and separation of nickel and cobalt by electrostatic pseudo liquid membrane <i>Heckley PS, Ibana DC, McRae C</i>	730
Membrane selection in membrane-assisted metal extraction and stripping processes <i>Soldenhoff KH, McCulloch J</i>	736
Axial dispersion characteristics in hollow fibre modules for membrane extractions <i>Yujun W, Guangsheng L, Yan W, Youyuan D</i>	742
Swelling and stability of emulsions in liquid membrane extraction <i>Koroleva M Yu, Yurtov EV</i>	748
<b>Environmental Applications</b>	<b>754</b>
Commercial-scale recovery of hexavalent chromium for recycle water by anion liquid-liquid extraction <i>Monzyk B, Conkle HN, Rose JK, Chauhan SP</i>	755
Operation of a NDSX pilot plant for recovery of Cr(VI) from ground waters <i>Ortiz I, Galán B, Castenáda D, Irabien A</i>	762
Screening of reagents for recovery of zinc(II) from hydrochloric spent pickling solutions <i>Regel-Rosocka M, Miesi I, Sastre AM, Szymanowski J</i>	768
A continuous solvent extraction process for refining of pickling baths <i>Caron L, Pareau D, Stambouli M, Durand G</i>	774

Copper recovery from spent ammoniacal etching solutions <i>Ismael MRC, Carvalho JMR</i>	781
Recovery of nickel from spent electroless nickel plating baths by solvent extraction <i>Tanaka M, Kobayashi, M, Seki T</i>	787
Recovery of cobalt and nickel from spent catalysts using Cyanex 923 <i>Gupta B, Tandon SN, Deep A</i>	793
Cyanide recovery by solvent extraction <i>Dreisinger DB, Wassink B, Ship K, King JA, Hames M, Hackl RP</i>	798
Mercury recovery from dental amalgams using solvent extraction <i>Silva de Lima LA, Pereira de Souza C, Pereira Leite JY, Curbelo Garnica AI</i>	804
Supercritical fluid extraction-oxidation technology to remediate PCB contaminated soils / sediments <i>Zhou W, Anitescu G, Tavlarides LL</i>	809
Supercritical CO <sub>2</sub> extraction of halogenated flame retardants from polymer materials using different modifiers <i>Gamse T, Marr R</i>	816
Metal ion and dye extraction from textile wastewater by microemulsions <i>Cordeiro Beltrame LT, Barros Neto EL, Dantas Neto AA, Castro Dantas TN</i>	822
Recovery of polyphenols from olive mill waste-waters by precipitation and liquid-liquid extraction <i>Carvalho JMR, Santos C, Ismael R, Ferreira L</i>	828
Methyl tert-butyl ether – a new solvent for phenol and acetic acid extraction from waste water <i>Strătulă C, Oprea F, Panaiteescu C, Petre M, Boțoc, G</i>	834
Point source recovery of hydrocarbons from wastewaters by solvent extraction <i>Halevy M, Jones P</i>	840
Catalyst recovery from the wet peroxide oxidation process by means of non-dispersive solvent extraction <i>Urtiaga AM, Muela C, Ortiz I</i>	846
<b>Hydrometallurgical Applications</b>	<b>852</b>
Copper recovery using leach / solvent extraction / electrowinning technology: Forty years of innovation, 2.2 million tonnes of copper annually <i>Kordosky GA</i>	853
Solvent extraction in the primary and secondary processing of zinc <i>Cole PM, Sole KC</i>	863
Some design and operating problems encountered in solvent extraction plants <i>Ritcey GM</i>	871
The extraction of copper, zinc, cadmium and lead from waste streams in the lead-zinc industry <i>Cox M, Flett DS, Gotfryd L</i>	879
The extraction of arsenic(V) and sulphuric acid from acidic sulphate media by tri-n-butyl phosphate in Shellsol A or T: I - An equilibrium study <i>Demirkiran A, Rice NM, Wright AR</i>	884
The extraction of arsenic(V) and sulphuric acid from acidic sulphate media by tri-n-butyl phosphate in Shellsol A or T: II – Flowsheet development <i>Demirkiran A, Rice NM</i>	890

The solvent extraction properties of di-n-hexyl sulphoxide in relation to the refining of platinum-group metals <i>Du Preez AC, Preston JS</i>	896
Recovery of Ag and Au from aqueous thiourea solutions by liquid-liquid extraction <i>Dzul Erosa MS, Navarro Mendoza R, Saucedo Medina TI, Lapidus Lavine G, Avila-Rodriguez M</i>	902
Opportunities and challenges in developing a solvent extraction process for rhodium based on the use of stannous chloride <i>Demopoulos GP, Shang Y, Benguerel E, Riddle M</i>	908
Extraction of chlorocomplexes of platinum and palladium by diamines and their salts with organic acids <i>Belova VV, Jidkova TI, Kholkin AI, Brenno Yu Yu, Jidkov LL</i>	916
Commissioning of the new Harmony Gold Refinery <i>Feather A, Bouwer W, O'Connell R, Roux J</i>	922
Behaviour of Os(IV) aquachloro and aquochlorohydroxo complexes in solvent extraction from sulphuric acid media <i>Mayboroda A, Lang H, Troshkina ID, Chekmarev AM</i>	928
Solvent extraction and hydrochemical preparation of gold powders with dithiozone derivatives <i>Sánchez-Loredo MG, Grote M</i>	934
The application of solvent extraction to the refining of gold <i>Grant RA, Drake VA</i>	940
Pilot-plant solvent extraction of cobalt and nickel for Avmin's Nkomati project <i>Feather A, Bouwer W, Swarts A, Nagel V</i>	946
Separation of cobalt and nickel by solvent extraction from sulphate liquors obtained by the acid leaching of a product from the Caron process <i>García Liranza E, Moreno Daudinot A, Viera Martínez R, Rosales Bárzaga B</i>	952
Modelling methodology for the simulation of extraction processes – cobalt/nickel <i>Leistner J, Görge A, Bäcker W, Górká A, Strube J</i>	958
Cobalt-nickel separation by solvent extraction in Cuba <i>Moreno Daudinot AM, García Liranza E</i>	964
Bateman pulsed column pilot-plant campaign to extract cobalt from the nickel electrolyte stream at Anglo Platinum's Base Metal Refinery <i>Nagel V, Gilmore M, Scott S</i>	970
Extraction equilibria of Ni(II) and Zn(II) with LIX 984 <i>Draa MT, Benamor M</i>	976
The effect of organophosphoric extractant concentration and initial phase volume ratio on cobalt(II) and nickel(II) extraction <i>Maljković D, Lenhard Z</i>	982
Options of copper(II) and zinc(II) extraction from chloride media with bifunctional extractants <i>Borowiak-Resterna A, Kyuchoukov G, Szymanowski J</i>	988
Impurity removal from copper tankhouse liquors by solvent extraction <i>Cox M, Flett DS, Velea T, Vasiliu C</i>	995
Studies of copper extraction using the system saponified coconut oil / isoamyl alcohol / kerosene / copper sulphate solution <i>De Barros Neto EL, Dantas Neto AA, Castro Dantas TN, Duarte LJN, de Araújo ACM</i>	1001
Copper hydrometallurgy process evolution: Changing operating parameters and philosophies throughout the life of Giralambone Copper Company solvent extraction circuit <i>Dudley KA, Readett DJ, Crane PA, MacKenzie JMW</i>	1007

Application of two types of commercial extractants for copper in China <i>Jiaoyong Y</i>	1014
Pilot copper solvent-extraction testing using the Bateman Pulsed Column <i>Buchalter EM, Kleinberger R, Grinbaum B, Nielson C</i>	1021
Ammonia leach - solvent extraction – electrowinning process for treatment of high alkaline gangue-containing copper ores <i>Liu D, Jiang K, Wang C, Zhang P</i>	1027
Solvent extraction of copper from high concentration pressure acid leach liquors <i>Sole KC</i>	1033
Purification of copper electrolyte with Cyanex 923 <i>Wang C, Jiang K, Liu D, Wang H</i>	1039
Extending zinc production possibilities through solvent extraction <i>Martín D, Díaz G, García MA, Sánchez F</i>	1045
Effect of TBP as a modifier for extraction of zinc and cadmium with a mixture of DEHPA and MEHPA <i>Keshavarz Alamdari E, Darvishi D, Sadrnezhaad SK, Mos'hefi Shabestari Z, O'hadizadeh A, Akbari M</i>	1052
Zinc extraction and stripping with D2EHPA: Further consideration as a test system <i>Antonelli D, Vegliò F, Mansur MB, Biscaia Jnr. EC, Slater MJ</i>	1058
The integrated recovery of rare earths from apatite raw material in the Odda process of fertilizer production by solvent extraction. A plant experience <i>Al-Shawi AW, Engdal SE, Jenssen OB, Jørgensen TR, Røsæg M</i>	1064
Extraction of lanthanides and yttrium with PC-88A from aqueous phosphate media <i>Abdeltawab AA, Nii S, Kawaizumi F, Takahashi K</i>	1070
Extractive leaching in the technology of rare metal raw materials: Problems and perspectives <i>Chizhevskaya SV, Chekmarev AM, Cox M</i>	1076
Development of a solvent extraction process for the production of pure neodymium oxide from synthetic Mt Weld process liquor <i>Cheng CY, Soldenhoff K, Vaisey M</i>	1082
Separations and recoveries of uranium, thorium and lanthanides using CYANEX 923 <i>Gupta B, Malik P, Deep A</i>	1089
Solvent extraction pilot plant results for recovery of copper and nickel from an ammoniacal leach of deep-sea manganese nodules <i>Hubred GL</i>	1095
Possible application of offshore oil and gas phase separation technology to hydro-metallurgical solvent extraction <i>Stanbridge D, Sullivan J</i>	1102
<b>Nuclear Applications</b>	<b>1109</b>
Virtues and vices of reagents for actinide partitioning in the 21 <sup>st</sup> century <i>Nash KL</i>	1110
Update on the science and technology of tributyl phosphate <i>Navratil JD</i>	1118
Compounds of hexavalent uranium and dibutyl phosphate in nitric acid <i>Powell BA, Navratil JD, Thompson C</i>	1124
Effect of U(VI) concentration on equilibrium and kinetics in flow-extraction of U(VI) in HNO <sub>3</sub> /supercritical CO <sub>2</sub> and TBP system <i>Meguro Y, Iso S, Yoshida Z</i>	1131

New insights in third phase formation in the U(VI)HNO <sub>3</sub> -TBP-alkane system <i>Jensen MP, Chiarizia R, Ferraro JR, Borkowski M, Nash KL, Thiagarajan P, Littrell KC</i>	1137
Supercritical CO <sub>2</sub> fluid leaching (SFL) of uranium from solid wastes using HNO <sub>3</sub> -TBP complex as a reactant <i>Tomioka O, Meguro Y, Iso S, Yoshida Z, Enokida Y, Yamamoto I</i>	1143
Structural studies by NMR and molecular dynamic calculations of lanthanide complexes with ethoxy malonamides in solution <i>Berthon C, Guibard P, Bousquet M, Giminez C</i>	1148
Extraction of Ln(III) and Am(III) from nitrate media by malonamides and polydentate N-bearing ligands <i>Charbonnel MC, Flandin JL, Giroux S, Presson MT, Morel JP</i>	1154
Aggregation of complexes formed in the liquid-liquid extraction of nitric acid and/or metallic cations by malonamides <i>Martinet L, Berthon L, Peineau N, Madic C, Zemb T</i>	1161
Extraction of trivalent actinides and long-lived fission products by different classes of functionalized calixarenes <i>Dozol JF, Garcia-Carrera A, Lamare V, Rouquette H</i>	1168
Modelling of nitric acid and actinide / lanthanide extraction by CMPO-like calixarenes <i>Garcia-Carrera A, Dozol JF, Dannus P, Böhmer V, Sastre-Requena AM</i>	1174
Extraction of actinides and lanthanides with diphenyl[dibutylcarbamoylmethyl]phosphine oxide in the absence of a solvent <i>Myasoedov BF, Kulyako Yu M, Malikov DA, Trofimov TI, Chmutova MK</i>	1180
Dissolution of actinide oxides in supercritical fluid carbon dioxide modified with various organic ligands <i>Samsonov MD, Trofimov TI, Vinokurov SE, Lee SC, Myasoedov BF, Wai CM</i>	1187
Modelling the influence of organic phase composition on the extraction of trivalent actinides <i>Nilsson M, Liljenzin J-O, Ekberg C</i>	1193
Application of SISAK for fast continuous solvent extraction processes to study exotic nuclides <i>Skarnemark G, Alstad J, Eberhardt K, Gregorich KE, Hoffman DC, Johansson M, Kirbach U, Langrock G, Mendel M, Ninov V, Nitsche H, Nähler A, Omtvedt JP, Omtvedt LA, Stavsetra L, Sudowe R, Trautmann N, Wiehl N</i>	1199
SANEX-BTP process development studies <i>Hill C, Guillaneux D, Berthon L</i>	1205
Automatically controlled solvent extraction cycle for advanced co-decontamination process <i>Andaur C, Falcón M, Gauna A, Granatelli F, Russo A, Vaccaro J, Balmaceda V</i>	1210
Development and characterisation of a universal solvent mixture for the separation of cesium, strontium, actinides and rare earth elements from acidic radioactive waste <i>Todd TA, Law JD, Herbst RS, Romanovskiy VN, Smirnov IV, Babain VA, Esimantovski VM, Zaitsev BN, Nazin EG, Egorov GF</i>	1216
Development and pilot scale testing of solvent extraction flowsheets for the separation of radionuclides from acidic radioactive waste <i>Law JD, Todd TA, Herbst RS</i>	1222
Extended flowsheet testing of the universal extraction (UNEX) process for the simultaneous separation of Cs, Sr and actinides from acidic waste <i>Law JD, Herbst RS, Todd TA, Romanovskiy VN, Esimantovkiy VM, Smirnov IV, Babain VA, Zaitsev BN</i>	1229
Comparison of solvent extraction processes and ion exchange resins for reprocessing actinide effluents <i>Pescayre L, Douche C, Thiébaut C</i>	1235

Preparation of N,N'-diacylpiperazines and their extraction properties for U(VI) <i>Xing-Cun Y, Bo-Rong B, Wei-Guo C</i>	1241
<b>Petrochemical Applications</b>	<b>1245</b>
Designer solvents for liquid-liquid extraction <i>Van Dyk B, Nieuwoudt I</i>	1246
Revamp of an aromatics extraction complex using high performance mass transfer internals <i>Bravo J, Bergerman S</i>	1253
A new approach to improve the sulfolane aromatic extraction column <i>Fei W, Wen X</i>	1260
Non-equilibrium stage modelling of lube extraction processes <i>Jain A, Sen PK, Chopra SJ</i>	1265
Selective recovery of aldehydes and ketones from hydrocarbon mixtures by reactive extraction with aqueous salt solutions <i>Kuzmanović B, Jallo R, Kuipers NJM, De Haan AB, Kwant G</i>	1271
Extraction of sulphonated triphenylphosphines from oleum and separation of reagents from hydroformylation of hexene carried out in microemulsion <i>Miesiac I, Tic W, Sobczynska A, Szymanowski J</i>	1277
Development of a novel process for the purification of a phenolic derivative <i>Mikus O, Hutton BM</i>	1283
The separation of phenolic compounds from neutral oils and nitrogen bases <i>Venter DL, Nieuwoudt I</i>	1289
Wax fractionation with supercritical fluid extraction <i>Nieuwoudt I, Crause JC, du Rand M, Schwarz CE</i>	1296
Novel application perspectives for metal extractants : olefin separations <i>Wentink BAE, Krooshof PWT, Kuipers NJM, de Haan AB, Mulder H</i>	1301
<b>Process Engineering and Design</b>	<b>1307</b>
Hydrodynamic behaviour in packed countercurrent columns for supercritical fluid extraction <i>Brunner G, Stockfleth R</i>	1308
A case study of an industrial packed column design using single drop mass transfer data <i>Barnard P, Slater MJ, Wu X-P</i>	1316
Industrial applications of CENTREK centrifugal extractors <i>Kuznetsov GI, Pushkov AA, Kosogorov AV</i>	1322
Sieve tray extractors: A closer look at capacity limitations <i>Seibert F, Fair JR, Bravo JL</i>	1328
Hydrodynamics and mass transfer of a rotating disk column <i>Yamaguchi M, Yamashita H, Noda H</i>	1334
Experiments with a short Kühni column used in batch mode <i>Antonelli D, Vegliò F, Mansur MB, Biscaia Jnr. EC, Slater MJ</i>	1339
The importance of hold-up in piloting of kinetically controlled SX processes in columns <i>Grinbaum B</i>	1345
Axial mixing in a reciprocating plate column <i>Garnica AIC, Duarte MML, de Souza CP</i>	1352
Design of pulsed extraction columns based on laboratory-scale experiments <i>Groß-Hardt E, Henschke M, Klinger S, Pfennig A</i>	1358

A distributor for liquid-liquid extraction columns <i>Vogelpohl A, Koch J</i>	1364
Application of drift flux theory to packed extraction columns <i>Hutahaean LS, van Brunt V, Kanel JS</i>	1370
A backflow model to determine backmixing in a vibrating plate extraction column for a dissociation extraction <i>Hutton B, Heyberger A, Myburgh P, Godwin I</i>	1376
Liquid-liquid miniplant extractor – a novel tool for process design <i>Kolb P, Bart H-J</i>	1382
Advanced methods for designing today's optimum solvent extraction mixer settler unit <i>Gigas B, Giralico MA</i>	1388
Testing novel features in mixer-settler prototypes <i>Gauna A, Andaur C, Granatelli F</i>	1396
The influence of experimental drop size errors on liquid-liquid extraction modelling evaluation <i>Gomes MLACN, Guimarães MML, Cardia Lopez JMM, Madureira CMN, Stichlmair J, Cruz-Pinto JCC</i>	1402
Verification of a process in a demonstration plant: How long does it take to find all the problems? <i>Grinbaum B, Kogan L</i>	1408
Performance characteristics for a Karr reciprocating plate extraction column <i>Stella A, Pratt HRC, Stevens GW</i>	1414
Getting the balance right – Some practical design considerations for solvent extraction circuits <i>Laing G</i>	1421
Organic removal using CoMatrix filtration <i>Greene WA</i>	1428
<b>Author Index</b>	<b>1435</b>

## FOREWORD

We all have defining moments in life. Today one is defined for most of us by the question "What were you doing when you heard about the World Trade Center?"

One of my defining moments was travelling to Gatlinburg for the first real gathering of solvent extraction experts. About half an hour before we were due to land, we suddenly fell out of the sky. A few moments and several thousand metres later we were cruising down one of those Tennessee Valleys, banking on every bend, and breathing almost normally. The Captain said "On the next turn, look up, everyone. That's the US Air Force coming past!"

We did, and the sky was black with aeroplanes. The Bay of Pigs had just broken, and everything that could fly was heading south-east. The threat of a nuclear holocaust was very real. It was with a certain amount of unease and camaraderie that we gathered, uncomfortably near to Oak Ridge, a centre for nuclear development which would almost certainly be targeted if the holocaust burst forth.

Forty years on, we gather in Cape Town. The threats to our gathering are not as immediate as they were when we first met. The Organising Committee had some nervous moments when we wondered whether the Conference might go ahead, but in the end sense prevailed, and we are gathering to review the progress of our branch of science and technology.

Any reasonable review of papers from Gatlinburg and those presented here show that we have made immense progress on many fronts. Our speciality has developed in an orderly, almost stately way. It has become a mature technology, and has yielded solutions to difficult problems which have generally been as economically sound as they have been environmentally safe.

But I remain concerned that we lack a fundamental understanding of the liquid state. If you tell me the chemical composition of a gas mixture, I can do an excellent job of predicting its properties over a wide range of temperatures and pressures. I can even predict how and under what conditions its components are likely to react, and what the outcome of the reaction is likely to be, and my predictions will be within a few percent of what can be measured. But let the components condense, and I am lost.

If you tell me the composition and crystal structure of a solid, I can also predict its properties accurately. I may need to know something about its history, and I probably cannot predict its reactivity with any accuracy, but I can tell you when it should melt to a high degree of accuracy. Once it melts, however, I am again lost.

I cannot even predict from first principles the properties of a solution of a grain of common salt in a glass of water. Even empirical models break down if I add another salt to the solution. To be sure, we are making progress on these problems, but it is slow and we seek some insights to guide us to new directions.

If a single solution is intractable, how much more so is the world of solvent extraction. Take two separate solutions, carefully chosen to be essentially immiscible. Mix them to encourage them to react, and hope they have reached equilibrium. Separate them and see the results.

The description of this process is what concerns the majority of papers at this Conference. There is more on the theory of the mixing process than there is on the theory of species in solution. The body of empirical knowledge continues to grow, and in the midst of it we see some glimmers of patterns emerging, but they are glimmers, destroyed by slight changes in experimental conditions. I am always amused by the fact that we deal with subtle equilibria, and everyone knows that equilibria are affected by temperature, yet few bother to examine temperature as a controlled variable in their solvent extraction studies.

Difficult separations have been achieved because the experimenter saw fit to raise or lower the temperature at which he or she did the extractions, yet their findings have not found widespread application in solvent extraction technology. Similarly pressure is a controllable variable which few other than the supercritical extraction people worry about. Yet one subtle separation has been achieved because the developers realised that a solvent that had been abandoned because of its low boiling point could be used successfully under modest pressure.

This Conference provides an opportunity to exchange such ideas. Sadly, the exchanges cannot be captured in the Proceedings. The papers collected here represent the findings of, largely, individual workers from small groups. The collective wisdom of the workers is what is sustained by these Conferences, and it is for this reason that it is a privilege to host them.

Many people have been responsible for making this Conference possible. The Organising Committee has worked hard and well. The Mintek Secretariat has provided an underpinning of confidence and efficiency. The International Committee and the local professional institutions have been most supportive. The many Sponsors of the Conference are an indication of the value placed on the efforts of the researchers, and the hope that still more economically attractive processes will evolve from gatherings such as ours.

We are grateful to all who have submitted the papers collected here. Many of you will be present at the Conference, and I hope that you will not only have an intellectually stimulating meeting, but also will be able to find time to enjoy the natural wonders that make Cape Town one of the more beautiful cities in the world.

Philip Lloyd  
Chair: Organising Committee

## PREFACE

The ISEC 2002 gathering in Cape Town, South Africa, marks some important milestones in the field of solvent extraction. Although it is now the second time that this meeting has been held in the southern hemisphere (following ISEC '96 held in Melbourne, Australia), ISEC comes to the mineral-rich continent of Africa for the first time. Representing a maturing technology, these proceedings bear testimony to the many advances made in the understanding and application of solvent extraction during recent times.

At this first ISEC meeting of the new century, it is appropriate to reflect on our industry's achievements, as well as taking a look into the future. Solvent extraction (SX) started life as an analytical technique, developed in an era before sophisticated spectrometric instruments were able to detect trace quantities of elements in myriad hostile matrices. The purification of radioactive isotopes during the Manhattan project was the first application of SX for small-scale production. Two decades later, SX entered the hydrometallurgical arena, with the commissioning of the first copper SX plant in Arizona. Today, SX still has a strong and critical presence in both the hydrometallurgical and nuclear industries. As a glance at the contents pages of these volumes will show however, its applications now extend to industries as diverse as biotechnology, food technology, pharmaceuticals and petrochemicals. While many of these industries have traditionally been perceived to be associated with causes of pollution, it is encouraging to note the increasing use of SX dedicated to solving or remediating environmental problems.

Although the "solvent" part of solvent extraction raises concerns in many circles today over the safety, toxicity and environmental friendliness of this technology, the alternative description, "liquid-liquid extraction", has been side-lined for many years, despite being the nomenclature recommended by the International Union of Pure and Applied Chemistry (IUPAC). However, the time may have now come when the latter terminology more accurately represents many of the new advances in our field. Interesting developments are occurring with two-phase aqueous extraction systems, ionic liquids, magnetic fluid extraction and supercritical fluid extraction, amongst others. None of these techniques make use of traditional organic solvents. It may be that the first ISEC of the 21<sup>st</sup> century may also be the last! Should we be looking forward to ILLEC in Beijing in 2005?

While globalisation in many of our industries is now a reality, the need was never greater for technical innovation, for movement down the cost curve, and for more efficient recovery and use of our natural resources. However, in South Africa, as in many other parts of the western world, we see a declining interest in technical subjects at tertiary educational institutions. It is hoped that this conference will, in some way, help revitalise educational and research efforts.

The proceedings of ISEC 2002 comprise some 200 technical papers, representing contributions from 34 countries and almost 600 authors. For the first time, the ISEC proceedings are presented in CD-ROM format. This necessitated completely electronic organisation of the conference, with all papers being submitted, refereed, revised and edited via a series of e-mail iterations. This process was not without teething problems, but we hope that the final result will be both user-friendly and useful. Progress in this regard will, no doubt, proceed in leaps and bounds in years to come.

The editors gratefully acknowledge those efforts made by the many people involved in the compilation of these proceedings and those who have contributed to the success of the conference. The authors of the papers, many of whom are not English speaking, are thanked for their contributions. The critical inputs of some 100 referees from the global solvent-extraction community has ensured that a high technical standard has prevailed. Appreciation is also extended to the plenary speakers for their insightful and stimulating presentations, and to the session chairs and members of the International Committee for their contributions. Our corporate colleagues all provided generous sponsorship, and we urge delegates, in turn, to support these companies into the future.

Finally, we thank Yvonne Clayden and Jean Martins of the Mintek Conference Secretariat for their invaluable contributions (and their limitless patience with tiresome scientists!); Trevor Burt who assisted with the publication; Pam Oberholzer, Ken Brown and Steve Oberholzer of African Conferences and Incentives (our conference travel agents); Moonshine Advertising for all our graphics design and maintaining our website; Nigel Walker of Document Transformation Technologies for production of the CD-ROM; and our long-suffering publisher, Chris van Rensburg. The editors also extend personal thanks to our employers for their indulgence and support of the many hundreds of hours involved in the preparation of these proceedings, while we were getting paid to do "real" jobs!

It is our hope that you will enjoy both the technical and social aspects of the conference, and will find the ISEC 2002 proceedings a stimulating and valuable reference source for many years to come.

Kathy Sole  
Peter Cole  
John Preston  
Dave Robinson

December 2001

## PREFACE

The ISEC 2002 gathering in Cape Town, South Africa, marks some important milestones in the field of solvent extraction. Although it is now the second time that this meeting has been held in the southern hemisphere (following ISEC '96 held in Melbourne, Australia), ISEC comes to the mineral-rich continent of Africa for the first time. Representing a maturing technology, these proceedings bear testimony to the many advances made in the understanding and application of solvent extraction during recent times.

At this first ISEC meeting of the new century, it is appropriate to reflect on our industry's achievements, as well as taking a look into the future. Solvent extraction (SX) started life as an analytical technique, developed in an era before sophisticated spectrometric instruments were able to detect trace quantities of elements in myriad hostile matrices. The purification of radioactive isotopes during the Manhattan project was the first application of SX for small-scale production. Two decades later, SX entered the hydrometallurgical arena, with the commissioning of the first copper SX plant in Arizona. Today, SX still has a strong and critical presence in both the hydrometallurgical and nuclear industries. As a glance at the contents pages of these volumes will show however, its applications now extend to industries as diverse as biotechnology, food technology, pharmaceuticals and petrochemicals. While many of these industries have traditionally been perceived to be associated with causes of pollution, it is encouraging to note the increasing use of SX dedicated to solving or remediating environmental problems.

Although the "solvent" part of solvent extraction raises concerns in many circles today over the safety, toxicity and environmental friendliness of this technology, the alternative description, "liquid-liquid extraction", has been side-lined for many years, despite being the nomenclature recommended by the International Union of Pure and Applied Chemistry (IUPAC). However, the time may have now come when the latter terminology more accurately represents many of the new advances in our field. Interesting developments are occurring with two-phase aqueous extraction systems, ionic liquids, magnetic fluid extraction and supercritical fluid extraction, amongst others. None of these techniques make use of traditional organic solvents. It may be that the first ISEC of the 21<sup>st</sup> century may also be the last! Should we be looking forward to ILLEC in Beijing in 2005?

While globalisation in many of our industries is now a reality, the need was never greater for technical innovation, for movement down the cost curve, and for more efficient recovery and use of our natural resources. However, in South Africa, as in many other parts of the western world, we see a declining interest in technical subjects at tertiary educational institutions. It is hoped that this conference will, in some way, help revitalise educational and research efforts.

The proceedings of ISEC 2002 comprise some 200 technical papers, representing contributions from 34 countries and almost 600 authors. For the first time, the ISEC proceedings are presented in CD-ROM format. This necessitated completely electronic organisation of the conference, with all papers being submitted, refereed, revised and edited via a series of e-mail iterations. This process was not without teething problems, but we hope that the final result will be both user-friendly and useful. Progress in this regard will, no doubt, proceed in leaps and bounds in years to come.

The editors gratefully acknowledge those efforts made by the many people involved in the compilation of these proceedings and those who have contributed to the success of the conference. The authors of the papers, many of whom are not English speaking, are thanked for their contributions. The critical inputs of some 100 referees from the global solvent-extraction community has ensured that a high technical standard has prevailed. Appreciation is also extended to the plenary speakers for their insightful and stimulating presentations, and to the session chairs and members of the International Committee for their contributions. Our corporate colleagues all provided generous sponsorship, and we urge delegates, in turn, to support these companies into the future.

Finally, we thank Yvonne Clayden and Jean Martins of the Mintek Conference Secretariat for their invaluable contributions (and their limitless patience with tiresome scientists!); Trevor Burt who assisted with the publication; Pam Oberholzer, Ken Brown and Steve Oberholzer of African Conferences and Incentives (our conference travel agents); Moonshine Advertising for all our graphics design and maintaining our website; Nigel Walker of Document Transformation Technologies for production of the CD-ROM; and our long-suffering publisher, Chris van Rensburg. The editors also extend personal thanks to our employers for their indulgence and support of the many hundreds of hours involved in the preparation of these proceedings, while we were getting paid to do "real" jobs!

It is our hope that you will enjoy both the technical and social aspects of the conference, and will find the ISEC 2002 proceedings a stimulating and valuable reference source for many years to come.

Kathy Sole  
Peter Cole  
John Preston  
Dave Robinson

December 2001

## **ISEC 2002 ORGANISING COMMITTEE**

Chair: Organising Committee : Prof Philip Lloyd, University of Cape Town  
Chair: Technical Programme : Dr Kathy Sole, Anglo American Research Laboratories (Pty) Ltd  
Treasurer : John Riordan, Bateman Engineering  
Technical Programme : Peter Cole, Hydrometallurgy Consultant  
: Angus Feather, Mintek  
: Dr Leon Krüger, De Beers  
: Dr John Preston, Mintek  
Technical Tours : Dr Dave Robinson, Anglo American Platinum Corporation  
Exhibition : Andrew Nisbett, Cognis Corporation  
Conference Secretariat : Yvonne Clayden, Mintek  
: Jean Martins, Mintek  
Conference Travel Agent : Ken Brown, African Conferences and Incentives  
: Pam Oberholzer, African Conferences and Incentives  
Sponsoring Institute : Dr Michael Booth, South African Chemical Institute  
Representatives : Wim Mandersloot, South African Institution of Chemical Engineers  
: Cathy McInnes, South African Institute of Mining and Metallurgy

## **ISEC 2002 SPONSORS**

Anglo American Platinum Corporation  
Anglo American Research Laboratories  
Cytec Industries, Inc.

Avecia	ExxonMobil
Bateman Advance Technologies	Impala Platinum
Bateman Engineering	Mintek
Bayer	Rhodia
Cognis	Sasol
CSIR BioChemtek	Schümann Sasol
Engen Chemicals	Shell Chemicals

## **INTERNATIONAL COMMITTEE ON SOLVENT EXTRACTION**

Prof Geoff W. Stevens, University of Melbourne, Australia (Secretary General)  
Prof Michael Cox, University of Hertfordshire, United Kingdom (Secretary)  
Dr Douglas S. Flett, St Barbara Consultancy, United Kingdom (Treasurer)  
Prof Hans-Jörg Bart, University of Kaiserslautern, Germany  
Prof Weiyang Fei, Tsinghua University, PR China  
Prof Stan Hartland, ETH-Zurich, Switzerland  
Dr Gary A. Kordosky, Cognis Corporation, USA  
Prof Philip J. Lloyd, University of Cape Town, South Africa  
Prof Yitzhak Marcus, The Hebrew University of Jerusalem, Israel  
Dr Hans Reinhardt, MEAB Metallextraktion AB, Sweden  
Dr Gordon M. Ritcey, Gordon Ritcey and Associates, Canada  
Prof Taichi Sato, Shizuoka University, Japan  
Prof Larry L. Tavlarides, Syracuse University, USA  
Prof Hitoshi Watarai, University of Osaka, Japan  
Prof Eugeny V. Yurtov, Mendeleev University of Chemical Technology, Russia  
Prof Yuri A. Zolotov, Lomonosov Moscow University, Russia

## **ISEC 2002 TECHNICAL REVIEW PANEL**

Dr Abdullah Al-Shawi, Norsk Hydro, Norway  
Prof Philip Bailes, University of Bradford, United Kingdom  
Prof Hans-Jörg Bart, University of Kaiserslautern, Germany  
Dr Andrew Bond, PG Research Foundation, Inc., USA  
Dr Joe Boyle, ExxonMobil Process Research Laboratories, USA  
Prof Gerd Brunner, Technische Universität Hamburg-Harburg, Germany  
Prof Paul Calvert, University of Arizona, USA  
Prof A. Chekmarev, Mendeleev University of Chemical Technology of Russia, Russia  
Dr Chu Yong Cheng, CSIRO, Australia  
Dr Svetlana Chizhevskaya, Mendeleev University of Chemical Technology of Russia, Russia  
Mr Peter Cole, Hydrometallurgy Consultant, South Africa  
Dr José Luis Cortina Pallas, Universitat Politècnica de Catalunya, Spain  
Prof Gérard Cote, Ecole Nationale Supérieure de Chimie de Paris, France  
Prof Michael Cox, University of Hertfordshire, United Kingdom  
Prof Andre de Haan, University of Twente, The Netherlands  
Dr Mark Dietz, Argonne National Laboratory, USA  
Mr Jean François Dozol, CEA Cadarache, France  
Prof Josef Draxler, Montanuniversität Leoben, Germany

Dr David Dreisinger, University of British Columbia, Canada  
Prof Jan du Preez, University of Port Elizabeth, South Africa  
Ms Rene du Preez, Mintek, South Africa  
Asst Prof Christian Ekberg, Chalmers University of Technology, Sweden  
Prof Aharon Eyal, Hebrew University of Jerusalem, Israel  
Mr Angus Feather, Mintek, South Africa  
Dr Douglas Flett, St Barbara Consultancy, United Kingdom  
Dr Filipe Gaspar, University of Birmingham, United Kingdom  
Dr Andreas Geist, Forschungszentrum Karlsruhe, Germany  
Prof Karsten Gloe, Technical University of Dresden, Germany  
Dr Brian Green, Mintek, South Africa  
Dr Baruch Grinbaum, TAMI-IMI, Israel  
Dr Martin Henschke, RWTH Aachen, Germany  
Dr Don Ibana, Curtin University of Technology, Australia  
Mr Adish Jain, Engineers India Limited, India  
Dr Jeff Kanel, Dow Chemical Co, USA  
Prof Judson King, University of California Office of the President, USA  
Dr Dave Kinneberg, Metalor USA Refining, USA  
Prof Klaus Koch, Universiteit van Stellenbosch, South Africa  
Prof Walter Korchinsky, UMIST, United Kingdom  
Dr Gary Kordosky, Cognis Corporation, USA  
Dr Marina Koroleva, Mendeleev University of Chemical Technology, Russia  
Mr Jack Law, Idaho National Engineering and Environmental Laboratory, USA  
Prof Philip Lloyd, University of Cape Town, South Africa  
Dr Rainer Ludwig, Freie Universität Berlin, Germany  
Prof Yitzhak Marcus, Hebrew University of Jerusalem, Israel  
Prof Fabri Marsicano, University of the Witwatersrand, South Africa  
Dr Ron Molnar, Lakefield Research, Canada  
Dr Bruce Monzyk, Battelle Memorial Research Institute, USA  
Dr Michael Mooiman, Metalor USA Refining, USA  
Dr Bruce Moyer, Oak Ridge National Laboratory, USA  
Dr David Muir, CSIRO Minerals, Australia  
Mr Victor Nagel, Bateman Engineering, South Africa  
Dr Kenneth Nash, Argonne National Laboratory, USA  
Dr N. Naumenko, A. A. Bochvar All-Russian Research Institute of Inorganic Materials, Russia  
Prof James Navratil, Clemson University, USA  
Dr Donato Nucciarone, Cytec Inc., Canada  
Prof Michael Nicol, Murdoch University, Australia  
Prof Izak Nieuwoudt, The University of Stellenbosch, South Africa  
Prof Nobuaki Ogawa, Akita University, Japan

Prof Tom O'Keefe, University of Missouri-Rolla, USA  
Dr Immaculada Ortiz, University of Cantabria, Spain  
Prof Susanna Ortiz, Imperial College of Science, Technology and Medicine, United Kingdom  
Prof Kwadwo Osseo-Asare, Pennsylvania State University, USA  
Dr Emmanuel Otu, Indiana University Southeast, USA  
Prof Erkki Paatero, Lappeenranta University of Technology, Finland  
Dr Jilska Perera, University of Melbourne, Australia  
Prof Andreas Pfennig, RWTH Aachen, Germany  
Dr John Preston, Mintek, South Africa  
Prof N Räbiger, University of Bremen, Germany  
Dr Nevill Rice, University of Leeds, United Kingdom  
Mr John Riordan, Bateman Engineering, South Africa  
Dr Gordon Ritcey, Gordon Ritcey and Associates, Canada  
Dr David Robinson, Anglo American Platinum Corporation, South Africa  
Prof Ana Maria Sastre, Universitat Politècnica de Catalunya, Spain  
Dr Jos Schaekers, BHP Billiton, South Africa  
Dr Frank Seibert, The University of Texas at Austin, USA  
Prof Jean-Pierre Simonin, Université P. M. Curie, France  
Prof Oksana Sinegribova, Mendeleev University of Chemical Technology, Russia  
Prof Gunner Skarnemark, Chalmers University of Technology, Sweden  
Dr Michael Slater, University of Bradford, United Kingdom  
Dr Karin Soldenhoff, Australian Nuclear Science and Technology Organisation, Australia  
Dr Kathryn Sole, Anglo American Research Laboratories, South Africa  
Prof R. Steiner, University of Erlangen, Germany  
Prof Geoff Stevens, University of Melbourne, Australia  
Prof Johann Stichlmair, Lehrstuhl für Fluidverfahrenstechnik, Germany  
Dr Natalia Streletsova, WMC Resources Limited, Australia  
Prof Jan Szymanowski, Poznan University of Technology, Poland  
Prof Larry Tavlarides, Syracuse University, USA  
Mr Owen Tinkler, Avecia, USA  
Mr Terry Todd, Idaho National Engineering and Environmental Laboratory, USA  
Dr Agustin Uribe Ramirez, Universidad de Guanajuato, Mexico  
Dr Michael Virnig, Cognis Corporation, USA  
Prof Alfons Vogelpohl, Technical University of Clausthal, Germany  
Prof Hitoshi Watarai, Osaka University, Japan  
Dr Michael Weigl, Forschungszentrum Karlsruhe GmbH, Germany  
Prof Jochen Winkelmann, University of Halle, Germany  
Prof Bernhard Wolf, Johannes Gutenberg-Universität, Mainz  
Prof Manabu Yamaguchi, Himeji Institute of Technology, Japan  
Prof Eugene Yurtov, Mendeleev University of Chemical Technology, Russia

## **ISEC 2002 SESSION CHAIRS**

Prof Hans-Jörg Bart, University of Kaiserslautern, Germany  
Mr Peter Cole, Hydrometallurgy Consultant, South Africa  
Dr José Luis Cortina Pallas, Universitat Politècnica de Catalunya, Spain  
Prof Andre de Haan, University of Twente, The Netherlands  
Dr David Dreisinger, University of British Columbia, Canada  
Asst Prof Christian Ekberg, Chalmers University of Technology, Sweden  
Prof Weiyang Fei, Tsinghua University, PR China  
Mr Richard Grant, Johnson Matthey, United Kingdom  
Dr Jeff Kanel, Dow Chemical Co, USA  
Dr Dave Kinneberg, Metalor USA Refining, USA  
Prof Klaus Koch, Universiteit van Stellenbosch, South Africa  
Dr Gary Kordosky, Cognis Corporation, USA  
Dr Norbert Kuipers, University of Twente, The Netherlands  
Mr Geoff Laing, Bateman Engineering, Australia  
Prof Philip Lloyd, University of Cape Town, South Africa  
Dr Rainer Ludwig, Freie Universität Berlin, Germany  
Mr Jeremy Mann, Anglo American Research Laboratories, South Africa  
Dr Indje Mihaylov, INCO Technical Services, Canada  
Dr Bruce Monzyk, Battelle Memorial Research Institute, USA  
Dr Bruce Moyer, Oak Ridge National Laboratory, USA  
Prof James Navratil, Clemson University, USA  
Prof Izak Nieuwoudt, The University of Stellenbosch, South Africa  
Dr Donato Nucciarone, Cytec Inc., Canada  
Prof Susanna Ortiz, Imperial College of Science, Technology and Medicine, United Kingdom  
Dr Emmanuel Otu, Indiana University Southeast, USA  
Prof Andreas Pfennig, RWTH Aachen, Germany  
Prof Ana Maria Sastre, Universitat Politècnica de Catalunya, Spain  
Dr Karin Soldenhoff, Australian Nuclear Science and Technology Organisation, Australia  
Prof Geoff Stevens, University of Melbourne, Australia  
Prof Peter Tasker, University of Edinburgh, Scotland  
Prof Larry Tavlarides, Syracuse University, USA  
Dr Vincent van Brunt, University of South Carolina, USA  
Prof Alfons Vogelpohl, Technical University of Clausthal, Germany



## SOLVENT EXTRACTION AS AN ENABLING TECHNOLOGY IN THE NICKEL INDUSTRY

Gord Bacon and Indje Mihaylov

Inco Technical Services Limited, Mississauga, Canada

The last decade had witnessed unprecedented growth in the development and implementation of solvent extraction technology in the extractive metallurgy of nickel and cobalt. Solvent extraction is proving to be a powerful tool, opening new opportunities for simpler, more cost efficient and environmentally sound metal refining processes. These advances, however, could not have been possible without the cooperative efforts between the nickel industry and the people and organizations involved with reagents, materials and equipment development and supply as well as solvent extraction research, aided by the accumulated knowledge and practical experience from the copper and uranium solvent extraction operations. This paper provides an overview of these developments and some of the challenges ahead.

### INTRODUCTION

Historically, the main source for primary nickel production has been the nickel-iron-copper sulphide ores (typically 1-3% Ni). The ability to upgrade these ores to a sulphide concentrate is essential as it ensures that the subsequent processing involves low volume high-grade nickel material. However, with a few notable exceptions, the known sulphide ore resources are located deep underground and their mining costs are high. As the more economical of these resources are gradually exhausted, the complexity of mining and processing inevitably increases.

The sulphide ores represent only about 30% of the world's land-based nickel resources. The remaining ~70% are represented by the nickeliferous lateritic ores (typically 1-2% Ni), which are also a major source for cobalt. The laterites are located close to surface and can be mined at significantly lower costs. Unfortunately, they are not readily amenable to upgrading thus resulting in higher processing costs than for the sulphides. For this reason, the use of these resources has been largely limited to the high-Ni saprolitic fraction leaving as generally uneconomical the much more abundant limonitic fraction.

Two hydrometallurgical technologies had played a key role in the development of commercially viable nickel recovery processes for these resources. One has been the pressure acid leaching of laterites using horizontal agitated autoclaves. Substantial advances in autoclave design and engineering were made over the last 10–12 years as part of the successful introduction of pressure leaching technology for treating refractory gold ores as well as zinc and nickel sulphide concentrates. Although the autoclaves used in these processes typically operate below 220°C, the accumulation of engineering know-how and operating experience spurred renewed interest in applying the technology to laterites.

The other hydrometallurgical technology has been the solvent extraction (SX) of base metals. Its acceptance by the nickel industry has been primarily influenced by the following factors:

- development and commercial availability of new solvent extraction reagents,
- demonstrated success in copper refining over a wide range of throughputs, and
- developments in solvent extraction equipment design and engineering.

Other factors, common to all base metals producers, such as declining ore grades and increasing ore complexity, decreasing (in real terms) prices and pressure to meet increasingly stringent environmental regulations, require continuous improvement, development and implementation of innovative techniques to address these issues.

Solvent extraction has a significant potential as a metal refining hydrometallurgical process—its operation is continuous, easily automated and requires little supervision. Unlike alternative separation/concentration techniques, no solids handling is routinely required (except for occasional crud and in some rare cases scale handling). These features contribute to low operating costs and high on-line availability of the typical solvent extraction circuit.

The first relatively large-scale SX application in hydrometallurgy—for uranium refining—dates back to the years around World War II. Solvent extraction is also well established in the refining of precious metals and rare earths. However, because in this case the amount of material to be processed is relatively small, the refining circuits are generally smaller in size, requiring less capital to build and to modify as needed in the future.

On the other hand, the business of base metals mining and refining is very capital intensive. For example, the capital cost of a nickel laterite plant is generally in the range of US\$8–12 per pound of Ni annual production. With few exceptions, the plants producing base metals as their primary product are by necessity large to maximize the economy-of-scale benefits and be economically viable. Hence, the acceptance of solvent extraction as a new technology in base metals refining is a fairly complex task. It requires not only a credible demonstration of the particular process at all levels of testing/piloting and in good integration with the upstream and downstream operations, but also a careful evaluation of the available engineering designs to support the technology and all potential risks associated with its implementation. It is thus not surprising that it usually takes years before the industry would embrace an otherwise technically and economically viable SX process. At the same time, the continuing pressure to develop more efficient and environmentally sensitive refining technologies inevitably dictates that the whole range of available process tools, and combinations thereof, are carefully evaluated in the quest to determine the optimum one for the specific feed material and the specific circumstances of the base metal producer.

One relevant example has been the development of the technology for the copper H<sub>2</sub>SO<sub>4</sub> leach-solvent extraction-electrowinning (L/SX/EW) operations. This particular experience had a substantial effect on the large scale solvent extraction application in the nickel industry and it is from that point of view that some of the major advances are reviewed below.

## COMING OF AGE IN COPPER SOLVENT EXTRACTION

The classical route for Cu recovery from sulphide ores involves concentration, smelting and electrorefining. It is well suited when the ore also contains appreciable amounts of precious metals. The route becomes uneconomical for low grade sulphides (and with minimal precious metals content) and for oxide ores. The preferred way to extract Cu from these types of ores is by mild H<sub>2</sub>SO<sub>4</sub> leach producing a dilute (~0.5–4.0 g/L Cu) CuSO<sub>4</sub> solution with a pH of ~1.4–2.0. The solution would then be treated to precipitate and concentrate the copper in one form or another—for example, by cementation using metallic iron or by precipitation using H<sub>2</sub>S. The concentrate would then be processed through smelting and electrorefining.

Solvent extraction provided a winning alternative to these routes. Building upon the class of known Cu-selective hydroxyoxime reagents used in analytical chemistry methods, the first commercial Cu extractants were developed in the mid-1960's. These extractants (LIX® 63, and particularly LIX® 64 and LIX® 65N) were able to selectively transfer copper from the dilute acidic leach solution with minimal Fe co-extraction (the main impurity) into a concentrated CuSO<sub>4</sub> solution (typically ~50 g/L Cu and 150–180 g/L H<sub>2</sub>SO<sub>4</sub>) from which copper could be electrowon. The acidic raffinate after extraction is used for leaching while the highly acidic lean copper electrolyte electrowinning is used for copper stripping from the loaded organic. In this elegant refining scheme, by separation and concentration, the SX process provides the link between leaching and electrowinning to produce high purity electrolytic copper.

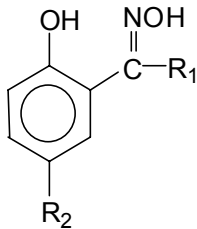
The use of solvent extraction resulted in significantly reduced operating costs (by some estimates, about 50% lower than for the cementation with Fe route). One of the newest Cu L/SX/EW plants, Codelco's Radomiro Tomic, is said to have cash production costs of about US\$ 0.38/lb of Cu. This lowering of costs allowed to include as copper resources feed materials previously considered uneconomical. Today, there are roughly about 50 such plants with a total production capacity of close to 2 million tonnes of Cu per year. The individual SX circuit capacity of these plants ranges from ~200 to ~3,000 m<sup>3</sup>/h of pregnant leach solution (PLS), proving that the technology can deliver a reliable and consistent performance over a wide range of throughputs. It is also quite telling that about 50% of these plants were commissioned during the last 10 years and another ~27% during the 1980s. This pattern of exponential growth is a testament to the success of the SX technology for this copper recovery route.

Perhaps the most important factor for the success of the solvent extraction in this case has been the development of solvent extractants and fine-tuning of their performance to meet the range of optimal process conditions both for the leaching and electrowinning side, as dictated by the individual plant's copper sources conditions. That meant having a copper-selective extractant, with fast extraction and stripping kinetics, able to maintain high Cu extractions over the pH range of the PLS and the product raffinate (*i.e.*, to pHs of as low as 1.2–1.4) while allowing at the same time to be readily stripped using lean copper electrolyte (typically ~30–35 g/L Cu and ~200 g/L H<sub>2</sub>SO<sub>4</sub>) to produce feed to electrowinning. One particular advantage of this Cu SX system is that no base addition is necessary during the extraction, resulting in base reagent cost saving and a simplified circuit operation since no pH control is necessary.

The constituents of the proprietary extractants, available from Avecia (formerly Zeneca) and Cognis (formerly Henkel), are nonyl (C9) and dodecyl (C12) hydroxyphenyl ketoximes and aldoximes (Table 1). The ketoximes are weaker extractants than the aldoximes but are more readily stripped at lower free H<sub>2</sub>SO<sub>4</sub> levels. Thus, the majority of the copper SX plants use specific formulations to balance the extraction and stripping properties required. These formulations include ketoxime/aldoxime mixtures (such as LIX® 984 and LIX® 973 from Cognis) or an aldoxime with the addition of various modifiers, such as nonylphenol (*e.g.*, Acorga® P5100 from Avecia), tridecanol (*e.g.*, LIX® 622), or proprietary esters (*e.g.*, Acorga® M5640). The last few years had also seen a gradual trend of phasing out the C12 in favour of the C9 aldoximes.

The Cu/Fe selectivity, phase-separation and crud formation, and to a certain degree the extractant stability, also affect the choice for a particular formulation of the SX plant organic. Crud formation has been and continues to be one of the biggest problems in the operation of these circuits; detailed studies on crud formation have identified a number of contributing factors (*e.g.*, colloidal silica, surfactants, solids, certain organic additives, *etc.*).

*Table 1. Chelating hydroxyoxime extractants for copper.*

	Type	R1	R2	Trade name
Ketoxime	C <sub>6</sub> H <sub>5</sub>	C <sub>12</sub> H <sub>25</sub>	LIX® 64	
Ketoxime	C <sub>6</sub> H <sub>5</sub>	C <sub>9</sub> H <sub>19</sub>	LIX® 65N	
Ketoxime	CH <sub>3</sub>	C <sub>9</sub> H <sub>19</sub>	LIX® 84	
Aldoxime	H	C <sub>9</sub> H <sub>19</sub>	Acorga® P50	
Aldoxime	H	C <sub>12</sub> H <sub>25</sub>	LIX® 860	

Improvements in mixer-settler design have also helped to minimize crud formation and phase entrainment (organic loss to raffinate and to copper electrolyte and transfer of leach solution with the loaded organic to copper stripping) and to maximize settler throughputs. Entrainment of leach solution with the loaded organic is particularly critical in those cases when the leach solution has high levels of Fe, Mn and Cl; in such circumstances, installation of a dedicated wash stage for the loaded organic is often required.

In addition to the standard box-type agitated mixer with gravity settler design, proprietary mixer-settlers are also in use. Krebs mixer-settlers were introduced in late 1980s at Phelps Dodge's Morenci and at WMC's Olympic Dam. By employing a conical pumper and superimposed launder for early phase-separation in the settler, the settler specific throughput is significantly (up to ~2x) increased, resulting in reduced capital costs and organic inventory needs. Their performance, however, has reportedly had a mixed success. Another proprietary mixer-settler introduced for Cu SX in the late 1990s is Outokumpu's Vertical Smooth Flow (VSF) unit. Examples of this technology in the Cu industry include two Chilean plants (at Zaldivar and Radomiro Tomic) and the latest SX plant at Phelps Dodge's Morenci operation. Key features of the VSF technology are the separation of the pumping and mixing functions allowing for a controlled and gentle mixing achieved with a helical Spirok impeller. This results in minimized overmixing and air entrapment leading to lower phase entrainment and crud formation.

Other developments include the implementation of methods for organic removal from raffinate and strip solution (e.g., coalescers, multimedia filters, Jameson cell) and for the clay treatment of the organic to remove organic-soluble contaminants (e.g., surfactants) which negatively effects plant performance (e.g., worsened phase separation, poorer extraction kinetics, etc.).

All SX plants represent a fire-hazard risk. This fact alone has historically been a major stumbling block for the adoption of otherwise technically and economically sound SX processes. The development and introduction of higher flash point diluents helped in reducing the fire hazards. The demonstrated effectiveness of fire prevention and fire fighting measures over time have increased the confidence in the ability of the technology to mitigate this risk. However, recent incidents (December 1999 and October 2001) at WMC Olympic Dam's Cu SX plant have shown that a lot more is needed in the areas of equipment design, layout and plant operating practices. Notwithstanding the success of the L/SX/EW process, it should be noted that the development of a similar chloride route has not been successful. Suitable copper extractants were developed (e.g., Acorga® CLX-50 for the Cuprex process), but difficulties in electrowinning high purity copper from chloride solutions are a major impediment. This example shows that as with any other tool, solvent extraction is not, and cannot be, a fit-for-all hydrometallurgical process.

The Cu L/SX/EW plant operations clearly showed that the solvent extraction technology does work over a wide range of scales. This engineering and operating experience, together with the already accumulated knowledge from existing nickel-cobalt solvent extraction operations, was particularly important for the acceptance of the technology for the large scale commercial hydrometallurgical processes for laterites, in development over the last several years.

## SOLVENT EXTRACTION IN NICKEL/COBALT REFINING

From solvent extraction's perspective, there are three principal types of solutions important in commercial Ni/Co refining, reflecting the range of lixivants used to solubilise Ni/Co values:

- chloride solutions—resulting from Cl<sub>2</sub> and/or HCl leaching of nickel matte, intermediates or secondary nickel sources (e.g., at Falconbridge's Kristiansand, SLN's Le Havre, SMM's Niihama, and Metallurgie Hoboken refineries);
- ammoniacal (ammonia–ammonium carbonate) solutions—resulting from leaching of reduction roasted laterites as part of the Caron process (e.g., QNI's Yabulu refinery, Tocantins in Brazil and Punta Gorda in Cuba) and of nickel-cobalt hydroxide precipitate (as practised by Cawse); and
- sulphate solutions—resulting from O<sub>2</sub> pressure leaching and/or H<sub>2</sub>SO<sub>4</sub> leaching of sulphide concentrates and precipitates, matte and lateritic ores.

### Chloride Solutions

In strong chloride solutions, the separation task is helped by the fact that cobalt forms anionic chloro-complexes (e.g., CoCl<sub>3</sub><sup>-</sup> and CoCl<sub>4</sub><sup>2-</sup>) while Ni does not. Hence, an anion-exchange extractant such as a tertiary alkyl amine in its salt form (R<sub>3</sub>NH<sup>+</sup>Cl<sup>-</sup>) is able to selectively extract Co away from the Ni-containing concentrated chloride (typically ≥ 5 N Cl) solution. Other metals, often present as impurities, such as Fe, Cu and Zn, also form strong chloro-complexes and can be selectively removed from the nickel solution as well. Impurities, such as Pb and Mn can also be extracted from the nickel solution, if required. Nickel is electrowon from the purified NiCl<sub>2</sub> solution and the generated Cl<sub>2</sub> is used in the upstream leaching operation. The cobalt is readily stripped from the loaded amine organic with any low in chlorides solution (such as water) producing a CoCl<sub>2</sub> solution with ≥60 g/L Co. This solution is typically low in acid and after additional purification, if required, becomes the starting point for producing a variety of Co products, such as Co metal (electrowinning), metal powders, salts, etc.

Not surprisingly, the first commercial SX applications in the Ni industry were based on this chemistry. Major developments in this area from late 1960s to mid-1970s resulted in the adoption of the selective Co extraction with tertiary amines such as tri-iso-octyl amine (TiOA) or tri-n-octyl amine (TnOA) from concentrated Ni/Co chloride solutions at several refineries at about the same time in early to mid-1970s, with most of the operations continuing to this day.

Because Ni is not chemically co-extracted, the Co/Ni ratios in the Co product can be very high, from at least ~3,000 to as high as 8,000–10,000. The main problem in reaching and maintaining these ratios has been the transfer of entrained Ni solution with the Co-loaded organic to stripping. For example, the Ni/Co feed to Co SX at Kristiansand contains about 220 g/L Ni (and ~11 g/L Co) and it would not take much physical entrainment of that solution into the loaded organic to substantially raise the nickel level in the cobalt strip product.

Various measures are in place to reduce the aqueous entrainment with the loaded organic. They include the use of one or more scrub stages in which the cobalt-loaded organic is contacted with an aqueous solution to remove entrained nickel; in most cases, this solution is a small portion of the cobalt strip product solution (subsequently reverted to extraction) in order to chemically displace less extractable metals, such as Mn, from the organic. Other measures include special design mixer-settlers to minimise entrainment or additional mechanically forced phase-separators (e.g., centrifugal separators).

Despite the very convenient Ni/Co separation chemistry, there are two particular process and engineering challenges. The first one is having to operate with highly corrosive Cl<sup>-</sup> solutions. Since the start-up of these refineries about a quarter century ago, the development of various acid-resistant composite materials and the accumulation of considerable expertise in materials selection have made the task of designing and building SX circuits for this type of solutions somewhat easier, yet it is still a challenge. The second one is the necessity to use all-aromatic diluents for the amine organic. There are several reasons for that, the primary one being the

need to keep the viscosity of the Co-loaded organic low and thus minimise the entrainment of Ni solution. The problem with these diluents is that they have lower flash points than the aliphatic diluents with low (e.g., ~20 vol%) or no aromatic content, are more volatile and more corrosive.

One such diluent initially used by some of these refineries was xylene, which has a flash point of only ~26°C and thus represents a major fire hazard. While it is not clear whether the choice of diluent was a factor in the May 1972 major fire at the new Ni/Co refinery at Kristiansand, this event did raise serious and long-lasting concerns about SX as a reliable hydrometallurgical process in the minds of many. On the positive side, there were subsequently significant developments in the areas of SX plant layout, piping design and construction, materials and instrumentation selection as well as fire fighting measures at Kristiansand and elsewhere to minimize the risk of this happening again.

Today's aromatic diluent formulations used by some of these refineries, such as Exxon's Aromatic® 100 and Shell's ShellSol® A100 have higher flash points of ~42–47°C and are thus safer alternatives. Using diluents with even higher flash-points, such as Exxon's Aromatic® 150 and Shell's ShellSol® A150 (flash points of ~63–64°C), would be preferable whenever possible.

### **Ammoniacal Solutions**

In early 1970s, a small Cu and Ni SX plant was commissioned and operated for some time by the SEC Corporation in El Paso, Texas. The plant treated a 70–90 g/L Cu, 30–40 g/L Ni liquor after the crystallization of CuSO<sub>4</sub> from Cu electrolytes of a close-by Phelps Dodge refinery. Following Cu extraction with LIX® 64N (LIX® 65N containing ~1 vol% LIX® 63; see Table 1), Ni was then extracted at pH 9–10, with LIX® 64N and using ammonia for pH control. The Ni-loaded organic was washed (pH~3–5) to remove entrained ammonia and then stripped with dilute H<sub>2</sub>SO<sub>4</sub> at pH~2 producing NiSO<sub>4</sub> electrolyte for Ni electrowinning. Although a very small scale (about 2 t of Cu and 0.5 t of Ni per day), this plant operation was significant in that it focussed the attention of a major extractant supplier on opportunities to use Cu extractants in Ni refining.

In 1975 Nippon Mining's Hitachi refinery began using LIX® 64N for Ni extraction in about the same way. Following sequential Zn and Co removal in separate SX steps, Ni was extracted from a sulphate solution (~30 g/L Ni) at pH~9–10 using ammonia for pH control; Ni was recovered to final product by electrowinning and spent electrolyte was used to strip the Ni from the organic. This operation (producing about 3,300 t of Ni and 1,300 t of Co per year in early 1980s) provided invaluable information and a working resolution for the problem of hydroxyoxime degradation. Further to the known almost irreversible Co extraction as Co(II) and accumulation in the hydroxyoxime organic as Co(III), it was discovered that LIX® 64N was losing its oxime group (C=NOH) by conversion to ketone (C=O) through Co-catalysed oxidation, hence losing its extractive capacity. Fortunately, it was found that the ketone could be re-oximated with high yields to the original oxime through contact with hydroxylamine salts in alkaline solutions. This regeneration process was further developed into a workable technology with the involvement of the extractants manufacturer. Without the re-oximation process, the commercial application of the ammoniacal SX process for Ni would not have been possible.

The QNI's Yabulu refinery uses the high cost and energy intensive Caron process, developed in the 1920s; at Yabulu, it involved ore drying and grinding, followed by reduction roast and ammonia-ammonium carbonate leaching of the reduced ore, Co removal by precipitation with H<sub>2</sub>S as mixed Ni/Co sulphide (Ni:Co~2) and shipment for refining elsewhere, Ni recovery by precipitation as NiCO<sub>3</sub> with subsequent calcination to NiO and partial reduction to 85–90% Ni in the final NiO product. By mid-1980s, the local (Greenvale) laterite feed was being exhausted and the plant had to switch to processing New Caledonian and Indonesian laterites with higher Co content. The change to imported laterite feed meant increased transportation costs; the higher Co content would have required a substantial expansion of the existing Ni/Co sulphide plant with increased costs for drying the sulphide and shipping it for refining overseas while reducing the proportion of the nickel available for on site NiO production. The net result would have been substantially higher operating costs, undermining the viability of the entire operation.

In the modified Yabulu refinery operation, the  $\text{NH}_3$  /  $(\text{NH}_4)_2\text{CO}_3$  leach liquor, containing ~10 g/L Ni, ~0.5 g/L Co, 80–90 g/L  $\text{NH}_3$  and ~60 g/L  $\text{CO}_2$ , is first pre-boiled to reduce the free ammonia from ~80 g/L to ~40 g/L (Ni extraction decreases with increasing ammonia concentration) and then the liquor is aerated to oxidize Co(II) to Co(III) to prevent co-extraction in the subsequent Ni ammoniacal SX (ASX) process. Nickel is extracted with LIX® 87QN, an extractant formulation prepared by Cognis for QNI containing LIX® 84 and undisclosed modifiers. The Ni extraction most likely proceeds through a cation-exchange reaction with  $\text{Ni}^{2+}$  replacing loaded  $\text{NH}_4^+$  from the extractant. Nickel stripping from the extractant requires contact with high-strength ammonia–ammonium carbonate solution (~280 g/L  $\text{NH}_3$  and ~230 g/L  $\text{CO}_2$ ) and produces strip liquor with ~80 g/L Ni. From this liquor, Ni is recovered to basic nickel carbonate and nickel oxide as before. The cobalt from the raffinate is removed by  $\text{H}_2\text{S}$  as sulphide, but the produced quantity is ~3 times less due to substantially lower nickel content (28% Ni and 14% Co before ASX, 2% Ni and 42% Co thereafter).

The development and implementation in late 1980s of the ASX process at Yabulu, in cooperation with the extractant supplier (Cognis), was crucial to the refinery's continuing operation. It also provided the additional confidence in the SX technology to proceed with the introduction in the late 1990s of a Co refining process, involving several SX steps, for on-site production of cobalt oxide hydroxide which also had the benefit of keeping all of the primary nickel for refining on site. The ASX process also enabled the refinery to expand the range of laterite feed materials it can process. At the present time, feasibility studies are in progress to expand the refinery (from the ASX process onwards) to almost double capacity to treat the mixed Ni/Co hydroxide from the Ravensthorpe pressure acid leach laterite project.

The ASX process does suffer from several disadvantages, although none are too critical: slow extraction and even slower (>5 min per stage required) stripping, a need to reductively strip accumulating cobalt from the organic and to operate the re-oximation process, relatively slow phase-separation. In addition, the small amounts of copper in the feed to extraction would accumulate in the organic due to high pH conditions in both extraction and stripping; copper removal would require separate  $\text{H}_2\text{SO}_4$  stripping. The transfer of ammonium with the organic between Ni extraction and stripping at Yabulu is inconsequential, as the solutions at both ends of the SX process are ammoniacal, but it is an issue in other refining schemes.

A similar SX process was adopted for the Cawse project. In this most technically successful operation (start-up early 1999) of all three Western Australian pressure acid leach laterite projects to date, an intermediate Ni/Co hydroxide precipitate is re-leached in  $\text{NH}_3$  /  $(\text{NH}_4)_2\text{CO}_3$  solution and then nickel is selectively extracted with LIX® 84 from the resulting solution (~12–15 g/L Ni and ~2–3 g/L Co). Unlike at Yabulu, the nickel-loaded organic is first scrubbed/washed to remove loaded ammonium, producing  $(\text{NH}_4)_2\text{SO}_4$  solution. This scrub/wash operation is also essential in minimizing the co-extraction of zinc, present in small quantities in the feed to extraction. The scrubbed/washed nickel-loaded organic is then stripped with  $\text{H}_2\text{SO}_4$  from the spent nickel electrolyte from electrowinning. Copper and cobalt removal from the organic as well as re-oximation is required.

With a nameplate capacity of only 9,000 t of Ni and 1,600 t of Co (in cobalt sulphide) per year Cawse is a relatively small operation but serves as a proving case for the technologies involved, including the solvent extraction.

### Sulphate Solutions

As a common solution matrix in Ni/Co hydrometallurgy, the Ni/Co SX from sulphate solutions had received considerable attention in the areas of extractants and applications development. The Ni/Co commercial SX processes to date involve the use of five extractants (Table 2).

Table 2. Development/commercial application of cobalt-nickel extractants for sulphate solutions.

Extractant	1960's	1970's	1980's	1990's	2000's
D2EHPA 					
Versatic® 10 					
PC-88A / Ionquest® 801 					
Cyanex® 272 					
Cyanex® 301 					

Three of these extractants are used for selective Co extraction from Ni/Co solutions. In chronological order of development to market, they are the di-2-ethylhexyl phosphoric acid, known as D2EHPA, the 2-ethylhexyl phosphonic acid mono 2-ethylhexyl ester, available as PC-88A (Daihachi Chemical Industries) and Ionquest® 801 (Albright&Wilson), and the bis (2,4,4-trimethylpentyl) phosphinic acid, available from Cytec Canada Inc. as Cyanex® 272.

The first SX process for Co separation from Ni was developed using D2EHPA in mid-1960s. The process developed for Eldorado Nuclear refinery in Canada was actually for ammoniacal leach solutions and prior to extraction the leach solution was aerated to oxidize Co(II) to Co(III). D2EHPA extracted Co as Co(III) pentamine in some preference to Ni; in the hydroxyoxime processes (QNI, Cawse), Co(II) is oxidized to Co(III) prior to SX so that it will *not* be extracted. Due to D2EHPA's relatively low Co/Ni selectivity, many extraction stages are required. This was perhaps a reason to choose sieve-plate pulsed column in the piloting. The loaded organic was scrubbed with high-cobalt amine solution. The D2EHPA process was further developed in the early 1970s at CANMET in Ottawa for sulphate leach solutions. The organic was pre-loaded with ammonia or sodium to avoid adding base for pH control (pH 5–6) during Co(II) extraction. The cobalt was stripped with H<sub>2</sub>SO<sub>4</sub> to produce electrolyte suitable for electrowinning.

At about the same time, a similar D2EHPA process was developed in the UK (Warren Springs laboratory) and later adopted at the Rustenburg base metals refinery, still in operation today. Cobalt is separated from the primary Ni feed to EW by precipitation of Co(OH)<sub>3</sub> with electrolytically produced Ni(OH)<sub>3</sub>. A reductive re-leach of the solids produces a Ni/Co sulphate solution, which is fed, after removal of impurities such as Fe, Cu, and Pb, to the Co D2EHPA SX circuit. The organic is pre-loaded with Na prior to extraction. A large number of extraction and scrubbing stages is needed to achieve the required Co/Ni ratio in the Co strip solution.

The development of the D2EHPA process was a major advance in Ni/Co refining from sulphate solutions which also focussed the attention of extractant developers on the organophosphine chemistry. Some of the disadvantages of using D2EHPA are the very strong Fe extraction, requiring a reductive or HCl stripping, low degree of Co/Ni selectivity, and preferential Ca, Mg and Mn extraction ahead of cobalt and nickel. In the Rustenburg operation, NaOH is used for iron removal thus the feed to Co SX contains only traces of Ca and Mg—both are co-extracted and occasional gypsum removal from the Co strip stages is necessary.

The D2EHPA separation process was introduced at Nippon Mining's Hitachi refinery in 1975. Several years later Daihachi introduced the organophosphonic acid extractant PC-88A. In many respects it was similar to D2EHPA. However, it was a poorer Ni extractant (same Ni extraction required a higher pH) and was thus more selective for cobalt over nickel. The testwork at Nippon Mining confirmed at least an order of magnitude better Co/Ni separation with PC-88A. On that basis, the new extractant was adopted at the refinery, despite being more expensive than D2EHPA. The rest of the SX operation remained essentially the same. The use of the PC-88A for cobalt continues to this day at least one major Ni/Co refinery.

In 1980 Cyanamid (now Cytec) Canada Inc. developed at their Welland, Ontario, plant a new extractant, Cyanex® CNX, which showed a significant promise as a selective reagent for Co over Ni. Inco's research laboratory in Mississauga, Ontario, was apparently the first facility outside Cyanamid to test the new reagent. It was not "perfect" (for example, it was in solid rather than in liquid form) but the internal Inco results were very encouraging and had a positive effect on the continuing efforts at Cyanamid. In early 1982, an improved version, Cyanex® 272, became available ("27" signified Co, "2"—the "second generation" reagent).

Keeping with the trend from D2EHPA and PC-88A/Ionquest® 801, Cyanex® 272 is an even poorer Ni extractant, while still extracting Co at about the same pH (i.e., pH 5–6), resulting in a substantially higher Co/Ni separation factor. With Cyanex® 272 it is much easier (less extraction and scrub stages) to achieve the required high Co/Ni ratios in the cobalt strip product, on par with what is achieved in the chloride system.

Due to its superior Co/Ni selectivity, Cyanex® 272 was relatively quickly adopted in Ni/Co refineries: the first plant to use this reagent was started in 1985 and by 1990 there were three more plants, including two major Co refineries in Europe. By 1995, the number of plants had doubled, with the latest addition being the newly upgraded and expanded Outokumpu's Harjavalta Ni/Co refinery, now part of the OM Group, Inc.

At Harjavalta, the Co SX process with Cyanex® 272 replaced Outokumpu's older process of Co removal from the  $\text{NiSO}_4$  electrolyte by precipitation as  $\text{Co(OH)}_3$  with  $\text{Ni(OH)}_3$ . Hence, the Ni:Co ratio in the feed to Co SX is >100 (typical feed (g/L): 130 Ni, 0.8–1.0 Co). Selective Co extraction from a solution with such a high Ni:Co ratio would not have been feasible with D2EHPA or PC-88A/Ionquest® 801. The Rustenburg base metals refinery uses that same Outokumpu process and its Co D2EHPA circuit is on the redissolved  $\text{Co(OH)}_3$  stream (Ni:Co ratio of only ~0.3); the Nippon Mining Co PC-88A circuit used to process Ni/Co feed with Ni:Co ratio of ~2–3 only.

The development of Cyanex® 272 in Canada expanded the range of possible SX applications in Co/Ni refining and enabled the replacement of more costly and/or environmentally and operator unfriendly technologies. According to Cytec's estimates, by the end of 1995, about 50% of the world Co production involved a Cyanex® 272 Co refining step. At the present time the total number of refineries (including Murrin-Murrin and Bulong) using the reagent has grown to about 10–12. Perhaps, the biggest disadvantage of Cyanex® 272 is its relatively high cost, hence its users are careful to limit entrainment and soluble losses to outgoing aqueous streams.

The fourth extractant used for Ni/Co refining in sulphate solutions is the Versatic® 10 carboxylic acid. Similarly to D2EHPA, it has been around for a long time, it is not particularly selective and its price is one of its most attractive features. Unlike D2EHPA, Versatic® 10 is selective for Ni and Co over Ca and Mg. Unlike all three organophosphorus reagents, Versatic® 10 is selective for Ni over Co; the selectivity is minimal, however, and cannot be used in reality. There have been considerable efforts to increase the extractant's affinity for Ni by introduction of various modifiers and improve its selectivity for Ni over Co. Although not particularly successful to date, the approach is worth pursuing, given the low cost of the extractant. Versatic® 10 is also a weaker extractant, requiring pH of ~7 for efficient Ni extraction, which exacerbates its biggest problem, namely, the high aqueous solubility (3–5 g/L) and relatively poor phase separation.

For ~20 years SMM' Niijhama refinery used Versatic® 10 to transfer Ni and Co from sulphate into a concentrated chloride solution. Similarly to the Rustenburg refinery operation, the feed to Versatic® 10 SX was the Ni/Co product solution from the reductive re-leach of  $\text{Co}(\text{OH})_3$  precipitate after the removal of impurities such as Fe, Mn and Cu. Ammonia was used for pH control and the raffinate was contacted with  $\text{H}_2\text{SO}_4$  to recover some of the solubilised organic. Nickel and Co were stripped with HCl, producing ~200 g/L Ni+Co strip solution. Cobalt was then selectively extracted with a tertiary amine; both Co and Ni were recovered by electrowinning.

Recent interest in Versatic® 10 results largely from its application at the Bulong laterite plant for Ni SX. This plant (design capacity of ~9,000 t of Ni and ~1,000 t of Co per year) is the only one of the three new Western Australian laterite projects to use SX directly on the partially neutralized Ni/Co leach solution. At Bulong, there are two SX circuits on the entire volume of the dilute Ni/Co leach solution after partial neutralization with limestone ((g/L): 3.5 Ni, 0.3 Co, 1.0 Mn, 15 Mg, 0.5 Ca). Cyanex® 272 is first used for Co and ammonia is added for pH control. Cyanex® 272 extracts Mn preferentially to Co while the selectivity for Co over Mg is relatively small at the unfavourable Co:Mg ratio in the feed. Hence, the loaded organic is largely carrying Mn and Mg, with Co representing at most ~10% of the total metal load. Because the feed to extraction is also Ca-saturated some Ca would be extracted in one extraction stage and displaced in another, resulting in likely gypsum formation; aqueous phase dilution in extraction due to the water from the ammonia for pH control will help to minimise the formation of gypsum.

The raffinate from the Cyanex® 272 circuit is processed through the Versatic® 10 circuit. Here Ni is separated from the Ca and Mg; any Co not extracted in the Cyanex® 272 circuit will follow the Ni and report into the electrowon Ni metal; ammonia is used for pH control and Ni electrolyte bleed is needed to balance the transfer of co-extracted ammonia to nickel stripping. One main problem at the circuit has been the cross-contamination with Cyanex® 272, resulting in higher Ca extraction and displacement within the extraction stages, leading to gypsum precipitation.

The fifth, and the newest, reagent used for Ni/Co refining in sulphate solutions is Cyanex® 301, developed by Cytec in late 1980s as a selective extractant for Zn over Ca and Mg. Although similar in many respects to Cyanex® 272 (both extractants also are manufactured at the same Welland plant), the replacement of both oxygens with sulphur (Table 2) results in a reagent with a very different extractive strength and selectivity for base metals.

The Ni/Co extraction with Cyanex® 301 is a key feature of the Inco-Goro hydrometallurgical process for laterites (Figure 1). The Goro Nickel plant, presently at detailed engineering stage, is expected to have an annual capacity of 54,000 tonnes of Ni and 5,400 tonnes of Co.

The use of Cyanex® 301 allows Ni and Co to be removed quickly (fast extraction kinetics) and efficiently (>99.9% extraction) from the large flow of relatively dilute partially neutralised leach solution (~4.5 g/L Ni) without the co-extraction of any of the major impurities (Mn, Ca, Mg), without the need for pH control and having to add expensive base reagents. Any traces of Cu in solution after partial neutralization are removed by ion-exchange ahead of SX, to prevent practically irreversible Cu extraction. Due to strong Ni and Co extraction, the strip kinetics is relatively slow and contact with strong acid is required. The use of HCl produces a concentrated Ni/Co strip solution (~80–100 g/L Ni) with about 20 times reduction in volume, significantly reducing the size of the downstream refining circuits. Zinc is completely co-extracted with Ni and Co but is selectively removed by ion-exchange from the chloride solution. Cobalt separation from Ni is done using a tertiary amine extractant. Nickel is recovered by pyrohydrolysis as the desired NiO product, while the HCl is regenerated and recycled back to Cyanex® 301 stripping.

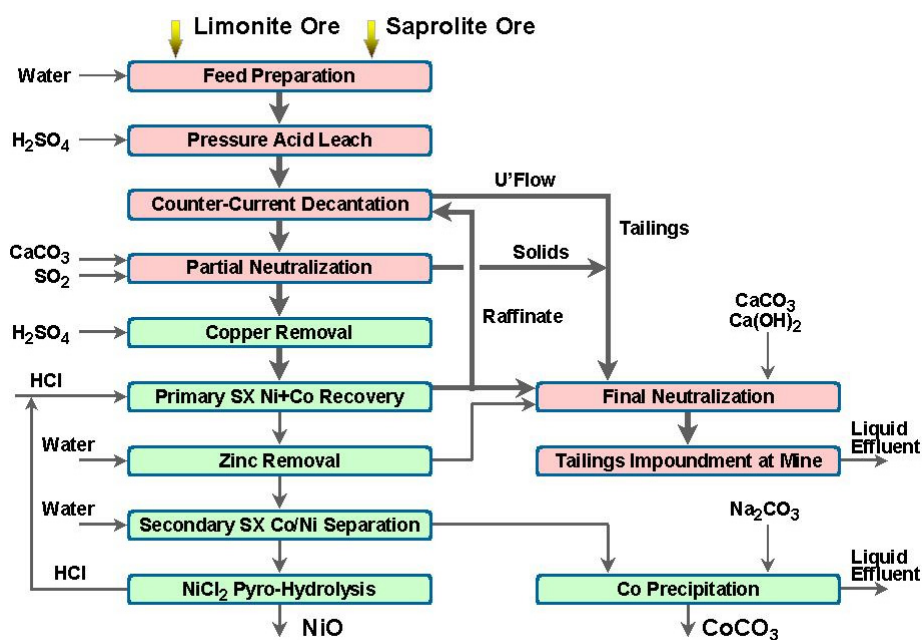


*Figure 1. The Goro process.*

Compared with the other four extractants, Cyanex® 301 has the lowest aqueous solubility which is even lower under the acidic conditions of the raffinate ( $pH \leq 1.5$ ). The phase separation in both extraction and stripping is fast, thus contributing to very low soluble and entrainment losses.

Extensive testing of the Cyanex® 301 process was required as there were no commercial operations using this new reagent. It was carried out at the Inco's laboratory, mini-plant and pilot plant scale operations in Canada and at the fully integrated pilot plant operation at Goro. In close collaboration with Cytec's Phosphine Technical Centre, the stability of the extractant was thoroughly investigated. The product of Cyanex® 301 ( $R_2P(S)SH$ ) degradation was identified (a disulphide,  $R_2P(S)S-S(S)PR_2$ ) and several processes to convert it back into  $R_2P(S)SH$  were developed. The Cyanex® 301 degradation was caused by metal-catalysed (e.g., Fe) oxidation by air. By operating under an  $O_2$ -excluded atmosphere, the degradation rate was demonstrated to be essentially nil. In the Goro pilot plant operations (processing 12 t (dry basis) of ore per day) to date, the Cyanex® 301 circuit have performed very much as expected, and in fact with much less troubles than anticipated.

In many respects, Cyanex® 301 may be regarded as a sulphide, performing a similar function to  $H_2S$  in selectively recovering Ni and Co from the laterite acid leach solution as practised at Moa Bay and more recently at Murrin-Murrin. One major difference, and advantage of using Cyanex® 301, is that this selective Ni/Co recovery is achieved without the safety concerns associated with the use of  $H_2S$  and without the need for solids handlings and subsequent re-dissolution of the sulphide precipitate. The Cyanex® 301 development by Cytec and the development of the technology for Ni/Co refining by Inco is yet another demonstration of the potential of SX to streamline and improve refining operations in the nickel industry.

### Equipment and Materials

At the present time, all SX operations in Ni/Co refining use mixer-settlers contacting equipment. Proprietary technologies, such as the Krebs mixer-settler and Outokumpu's Vertical Smooth Flow (VSF) mixer-settler were first developed in mid-1970s to early 1980s and introduced at Ni refineries in France and Finland, respectively. Both technologies are used to this day and are continuously evolving.

In the last ~5 years, there has been a renewed interest in using columns in Ni/Co SX circuits. This has been due in part to the considerable efforts of Bateman Projects Engineering in Israel of promoting their pulsed column technology for Ni/Co refining. However, it also reflects nickel industry's increased confidence in SX technology and the ever present need for further operational and capital cost savings. Columns have been used for decades as contacting equipment for many processes in the chemical industry, including liquid extraction, but except for a few cases of uranium refining (e.g., in France), there have been no hydrometallurgical applications.

This all changed with the successful introduction of the Bateman disc and doughnut pulsed columns in late 1990s for uranium extraction at WMC's Olympic Dam operation, which served as a powerful stimulus for a number of metal refineries to consider possible adoption in their operations. Pilot tests were carried out in the last 2–3 years at many Ni/Co refineries; examples include Impala's base metals refinery and QNI's Yabulu refinery.

The use of columns instead of mixer-settlers is advantageous in processes where many extraction or stripping stages are required, where extractants are costly, flammable, volatile, where processes require special atmosphere and/or well sealed environment, and where processes are particularly sensitive to moving parts and materials of construction. Columns are often easier to operate than mixer-settlers. Columns with axial energy input provide much more uniform size distribution of droplets, thus leading to reduced organic entrainment in outgoing aqueous streams.

With significantly reduced organic vapours, acid and other emissions, due to their fully sealed environment, and with their more uniform mixing thus leading to lower organic entrainment in the outgoing aqueous streams, the pulsed columns are a particularly attractive option for minimizing the impact of the solvent extraction operations on the environment.

As part of the testwork and piloting of the Inco-Goro process for laterites, the Bateman pulsed columns technology was also evaluated. The use of pulsed columns for both SX circuits is attractive for a number of reasons, including the ability to seal the equipment, to maintain the required atmosphere and to limit fugitive organic and acid emissions, lack of internal moving parts, reduced fire risks, simpler operation and minimum organic entrainment losses.

The increased interest in columns application in Ni/Co refining had also attracted the attention of other developers/suppliers of columns equipment. One example is Koch-Otto York who have many years of experience in various types of columns technology for the chemical industry.

These increased activities in the area of contacting equipment are expected to result not only in improvements in known technologies but also in novel, more efficient and safer ways of carrying the process of solvent extraction in the hydrometallurgical refineries.

As the scope of solvent extraction systems and range of applications increases, so does the challenge of finding and proving the right materials for the equipment. Despite significant advances in that area, there are still concerns particularly when the materials have to withstand *combinations* of various corrosive reagents, such as organic extractants, diluents and modifiers, in contact with corrosive acids, gases, etc., sometimes at elevated temperatures. These concerns, of course, are not limited to solvent extraction processes only. In addition, the science of detection and removal of any products of such interactions needs further development to better address this types of issues in refining operations.

## **CONCLUSIONS**

The use of solvent extraction for nickel/cobalt refining in the nickel industry have substantially progressed since its earliest applications in the 1970s. The successful development of new extractants and the advances in contacting equipment technology (mixer-settlers and columns) have significantly expanded the scope of technologically and economically sound nickel-cobalt refining options. All these are very much needed as the industry is faced with having to process feed materials of increasing complexity and often decreasing grades while meeting at the same time the challenges of stricter limits on the environment impact of its operations.



## DEVELOPMENTS IN PLATINUM-GROUP METALS REFINING AND THE UTILIZATION OF SOLVENT EXTRACTION TECHNOLOGIES

Peter Charlesworth

Anglo American Platinum Corporation Limited, Anglo Platinum Research Centre,  
Johannesburg, South Africa

The discovery of the platinum-bearing ore bodies of the Bushveld Igneous Complex (primarily in the Merensky and UG2 reefs) in South Africa in 1923 sparked the growth of a significant industry which today contributes some 4 % of the South African GDP. The production of platinum-group metals has developed steadily from exploration through mining and overseas toll treatment to the current situation whereby South Africa leads the world in the production of high-purity platinum-group metals for a variety of demands and applications. Over the last few years, South Africa has been responsible for the production of 70 to 80 % of the world's platinum, with Anglo Platinum being responsible for approximately one half of this production. The variety of demands for platinum, from jewellery through to industrial and automotive catalysts and the future fuel cells, has established platinum as the true "metal of the millennium". Ongoing forecasts for significant growth in demand place South Africa and this industry in a good position.

The early refining routes used in South Africa were largely based upon the classical gravimetric analytical methods by which the metals had been separated on a small scale over many decades. While these were reliable, they were expensive to operate, often required skilled operators, were time-consuming, and were often both capital- and inventory-intensive. The development of ion exchange and, more recently, solvent extraction separation technologies for a range of metals from the base metals through to the lanthanides and actinides presented an opportunity for improved processing routes which were eagerly engaged by Anglo Platinum. The current Anglo Platinum Precious Metals Refinery is the most modern, efficient and productive platinum-producing refinery in the world. The core separation processes are based largely on the selective solvent extraction (using some commercially available reagents and other proprietary reagents) of either individual elements or groups of elements producing individual platinum-group metal feed streams for final purification.



## TAILORED SOLVENTS AND COLLOIDS FOR GREEN PROCESSING OF CHEMICALS AND BIOCHEMICALS

T. Alan Hatton

Massachusetts Institute of Technology, Cambridge, USA

Alternative solvents and extraction concepts can be developed to minimise the deleterious effect of solvent losses to the environment. Two new concepts are discussed here. First, the tailoring of solvents can minimise the extent to which they may be lost to the environment, and can minimise the number of unit operations required in a chemical process; this approach is demonstrated to be effective in a sequence of reactions required in the synthesis of an HIV protease inhibitor. Secondly, the use of bulk solvents can be avoided by covalently attaching solvent-like polymers to the surfaces of colloidally dispersed magnetic nanoparticles, that can be recovered directly using high gradient magnetic separations.

### INTRODUCTION

Solvents are used ubiquitously in chemical synthesis and separation operations. Solvent extraction, in particular, has evolved to be the workhorse of many processes as it provides a versatile and selective class of unit operations for the recovery or removal of a wide range of materials from both aqueous and organic solutions. A continuing challenge facing the chemical and biochemical industries is how to enhance the selectivity and capacity of these processes, and how to adapt them for new separations problems, such as in the biotechnology arena, where the interest has progressed from proteins through to larger materials such as nucleic acids and viral particles, and even cells. In recent years, there has also been a growing interest in micro-scale separations for the purification of products from micro-reactors used in, e.g., combinatorial chemistry, and for the pre-treatment of compounds to be analysed in micro-scale total analysis systems. At the same time, increasing attention has had to be paid to alleviating potential impacts of solvent usage on the environment caused by solvent losses through entrainment or dissolution in aqueous discharge streams, and through air emissions.

In this paper we discuss recent developments in our laboratory to develop alternative solvents and extraction concepts for the separation and production of chemicals and biochemicals. We show that in some cases conventional solvents can be tailored to modify their physical properties while retaining their chemical functionalities, and that this can lead to dramatic advances in pollution reduction through elimination of many energy-intensive unit operations required in some pharmaceutical processing. We also show that some advantages can accrue by avoiding the use of bulk organic solvents altogether by relying on the use of non-volatile colloidal aggregates and coated nanoparticles dispersed within aqueous feed phases that are able to capture targeted solutes rapidly and efficiently, and that can be recovered by means other than settling or centrifugation.

## TAILORED SOLVENTS

The implementation of various pollution prevention regulations has resulted in an increased awareness of organic solvent use in chemical processing, and has reinforced the need to develop new technologies for the minimisation or elimination of solvent wastes. In many instances, the attributes that make a solvent ideal for a particular application, such as in chemical synthesis operations, can hamper subsequent processing steps in which the products or byproducts must be recovered in a second phase in which the solvent is significantly soluble in its own right, tetrahydrofuran (THF) in water being one such example. For these synthetic applications, significant processing advantages may be gained by using alternative solvents for existing processes or by developing new chemical routes to desired products that can exploit more benign solvent systems. Rational design and implementation of these solvents can lead to significant decreases in the environmental burden associated with solvent losses and in energy usage through the simplification of process flowsheets.

As one example of a "green" replacement for traditional solvents used in fine chemical processing, we have modified the solvent tetrahydrofuran (THF) to reduce its volatility and water solubility significantly while retaining its chemical characteristics. The structures of THF and nOTE (*n*-octyl tetrahydrofurfuryl ether), and some of their physical properties are shown in Figure 1. The addition of the alkyl tail to the THF ring through the ether linkage essentially eliminates solvent losses through vapor emissions and aqueous discharge streams, and allows for simplified processing options in reaction sequences.

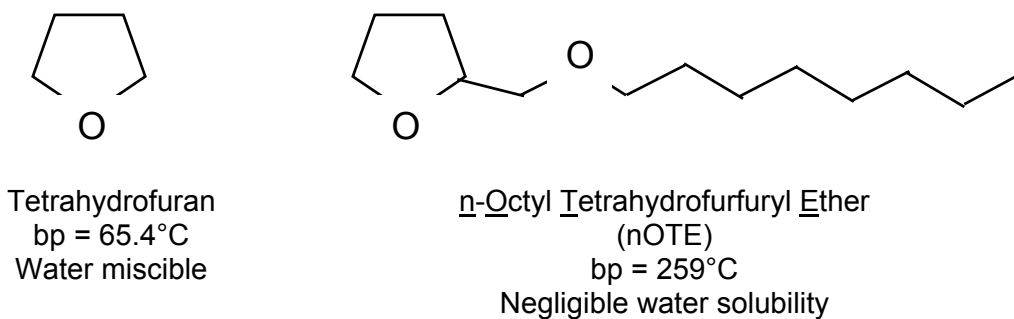
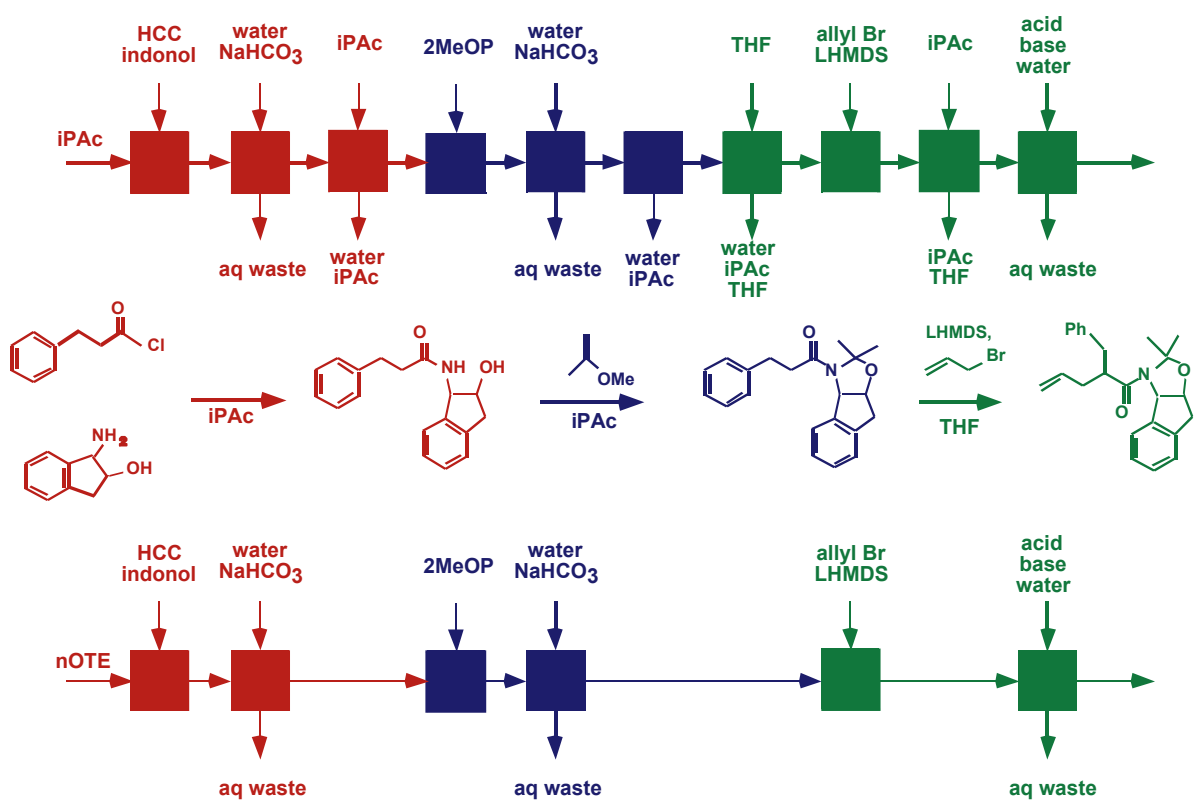


Figure 1. Tetrahydrofuran and its tailored analog, nOTE.

Figure 2 shows the energy-intensive separations and solvent exchanges that can be avoided using this new class of solvents (most notably or nOTE) in a series of reactions in the synthesis of the Merck HIV protease inhibitor, Crixivan. The traditional process uses iPAC in some of the reactions, but in others it is necessary to switch over to THF. This poses a problem as the reaction cannot be quenched with water and washed when it is carried out in THF because THF and water are completely miscible. It is therefore necessary to conduct another solvent switch, this time back to iPAC. In all cases, the aqueous waste streams leaving the different units must be treated offline, usually requiring either energy-intensive distillation or incineration. The new solvent, nOTE, can be used during the entire reaction sequence, so the solvent switches can be avoided, along with their attendant waste generation and need for offline separations, and the loss of the solvent to the aqueous wash streams is negligible owing to nOTE's very low solubility in water. Moreover, as the water uptake by nOTE is low, the need for drying is also obviated, or drastically reduced relative to that with iPAC, which has a fairly high capacity for water. Thus, it is clear that the solvent replacement strategy in this case can lead to rather significant reductions in the number of unit operations required, as well as in the off-line separations needed to regenerate the solvents, or to prepare the streams for discharge.



*Figure 2. Comparison of the published process for a series of reactions in the synthesis of intermediates for the HIV protease inhibitor Crixivan with the proposed process.*

## COLLOIDAL STRUCTURES IN TWO-PHASE SYSTEMS

Often co-solvents or solubilising agents are added to solvents to enhance their selectivity and/or capacity for targeted solutes, and sometimes these form micelles to provide a more positive interaction with the solute than that afforded by the pure solvent on its own. The separation of proteins using reversed micellar phases provides one example, in which the proteins are encapsulated within the cores of surfactant-stabilized water-in-oil microemulsion drops in equilibrium with a bulk aqueous phase. The selectivity of such operations can be enhanced dramatically by the addition of cosurfactants with specificity for the targeted protein. In the hydrometallurgical field, micelles have also been implicated in the selective extraction of metals from aqueous liquors. A drawback of these systems is that organic solvents are still used, which may have undesirable environmental consequences. Thus, there is interest in avoiding the use of bulk organic solvents altogether, one means being the use of biphasic aqueous systems, in which colloidal interactions can lead to the formation of two immiscible phases, each of which is composed primarily of water. For instance, the two polymers poly(ethylene glycol) and dextran, each of which is very soluble in water, are nonetheless themselves incompatible when mixed together in an aqueous solution, and cause a phase separation, such that one phase is rich in the PEG and the other in dextran. It has been shown that proteins, viruses, nucleic acids and even cells can partition between the two phases. It has also been shown that certain metal ions in solution can partition favourably to one phase over the other, pointing the way to an organic-solvent-free extraction operation, which could have many environmental benefits.

Biphasic aqueous systems can also be generated using micellar solutions that tend to phase separate as the temperature is increased, owing to increased micelle-micelle interactions, leading to a micelle-rich and a micelle-poor phase. Proteins and viruses can be separated through volume exclusion effects, and organics through solubilisation in the micelle-rich phase. Again, the avoidance of a bulk organic phase could provide a route to greener processing of process streams.

## COLLOIDAL EXTRACTANTS

In the examples cited above, the colloidal material is an integral part of the phase itself, and it is the bulk partitioning of materials between the two macroscopic phases, as mediated by the presence of the colloid, that is exploited in the separation process. Traditionally, interfacial transport between the two immiscible macroscopic liquids is enhanced by distributing one of these phases as a coarse dispersion in the other to provide the surface areas required for effective mass transfer operations. These operations can be beset by difficulties associated with poor contacting between the phases through flow maldistributions, while entrainment in the disengagement zones poses environmental discharge concerns. It is possible to avoid the use of macroscopically biphase systems by exploiting the solubilising powers of the colloids directly as colloidally dispersed extractants distributed spontaneously within the feed phase. We describe here two different systems, one based on the self-assembly of surfactant molecules to form micelles, and the other on the use of tailored nanoparticles coated with polymers or surfactants to provide the solvation of the targeted solutes.

### Micellar Systems

Surfactant molecules self-assemble to form micelles with oily interiors that can solubilise hydrophobic compounds, surrounded by hydrophilic coronae that stabilise the colloidal dispersion against macroscopic phase separation. Surfactant micelles formed within the feed stream effectively remove organic solutes from the surrounding aqueous phase, and hence can be treated as solvents in their own right. The process is single-phased, with intimate contact between the feed and the colloidal extractant, which disperses spontaneously and does not require strong agitation to maintain the dispersion. Difficulties associated with flow maldistributions and channeling are by-passed, but the traditional use of countercurrent-type operations is no longer possible because of the thermodynamic stability of the dispersion, and the difficulty in getting the micelles to move independently of the surrounding fluid. Also, phase disengagement cannot be accomplished through normal gravitational or centrifugal settling operations, unless a phase separation can be induced through changes in the environmental conditions, such as temperature, pressure or ionic strength to form two immiscible phases, one rich in the loaded micellar solutions (the coacervate) and the other consisting primarily of the treated water phase. The loaded micelles can be separated from the feed mixture by ultrafiltration, however, where the membrane retains the loaded surfactant micelles and the solvent phase (usually water) is recovered as a clear permeate; this process is known as micellar-enhanced ultrafiltration (MEUF).

The effective loading of the micelles in MEUF is limited by the single-stage nature of the system, although in principle the membrane modules can be staged. An alternative approach which utilises the full capacity of the micellar systems in a true countercurrent process in a mechanically-simple process is to pass the micellar solution through the lumens of a hollow fibre bundle, with the feed phase introduced to the shell side of the membrane module. The micellar suspension can be treated as an aqueous-based solvent phase immiscible with the aqueous feed because of the intervening membrane since although water can pass through the membrane, the micelles cannot. The solute itself diffuses across the membrane and is picked up by the micelles. The large capacity of the micelles for the solute provides a strong

driving force for this trans-membrane diffusion, while the large membrane area available in hollow fibre membrane modules offsets the diffusional resistances offered by the membrane such that this process has potentially a greater volumetric efficiency than conventional two-phase solvent extraction processes. The recovery of the solute from the loaded micelles and regeneration of the micellar solution after the contacting step must be accomplished efficiently if this process is to find technological acceptance. Steam stripping, carbon adsorption, and solvent extraction are among the approaches that have been used successfully to perform the task. The efficiency of these approaches can be enhanced if the micelles are disrupted prior to the recovery stage so that they release their loads; in some cases the released solutes reporting to the aqueous phase may be at concentrations well above their aqueous solubilities and they form a separate phase, either solid or liquid, which can be removed by filtration, centrifugation or decantation. Temperature is one method that can be used to alter the micellar structures.

Figure 3 illustrates these concepts with a thermally-reversible block co-polymer micellar solubilisation process. The solubilisation of naphthalene in solutions of triblock Pluronic® poly(ethylene oxide)-poly(propylene oxide)-poly(ethylene oxide) (PEO-PPO-PEO) copolymers is seen to be a strong function of temperature; at low temperatures the polymers are readily soluble in water and do not form hydrophobic domains for the solubilization of the solute. As the temperature is increased, the PPO block is dehydrated and the micelles begin to form, providing the hydrophobic environment required for solubilisation. Thus, the capacity of the aqueous phase is greatly enhanced by the presence of the micelles. These observations can be exploited in the development of strategies for the removal of trace contaminants from aqueous streams as shown in Figure 4. In the micellar phase, the aqueous phase concentration (or activity) is low, even for high overall concentrations in the micellar solution, and the driving force for extraction or absorption of the solute in a countercurrent membrane process (the concentration difference across the membrane between the water phases) is kept high during the process. Upon cooling, the micelles fall apart and release the solubilised solute to the water phase. The dramatically increased aqueous phase concentration (or activity) provides a large driving force for either phase separation of the solute as a solid (e.g., naphthalene) or liquid (e.g., toluene), or, as shown here, for a stripping operation. The stripped polymer solution is then heated to form micelles again, and the solution is recirculated to the beginning of the process. Only small temperature changes would be required to change the capacity of the micellar solutions dramatically.

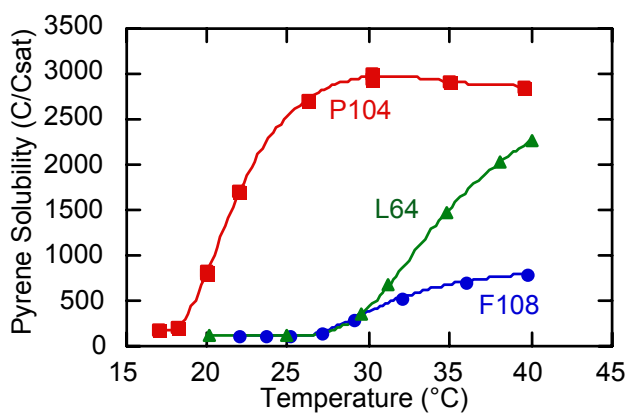


*Figure 3. The solubility enhancement of pyrene in Pluronic® PEO-PPO-PEO block copolymer solutions relative to the saturation solubility in water depends on the polymer molecular weight and composition. Significant solubilization occurs only at temperatures above which micelles begin to form.*

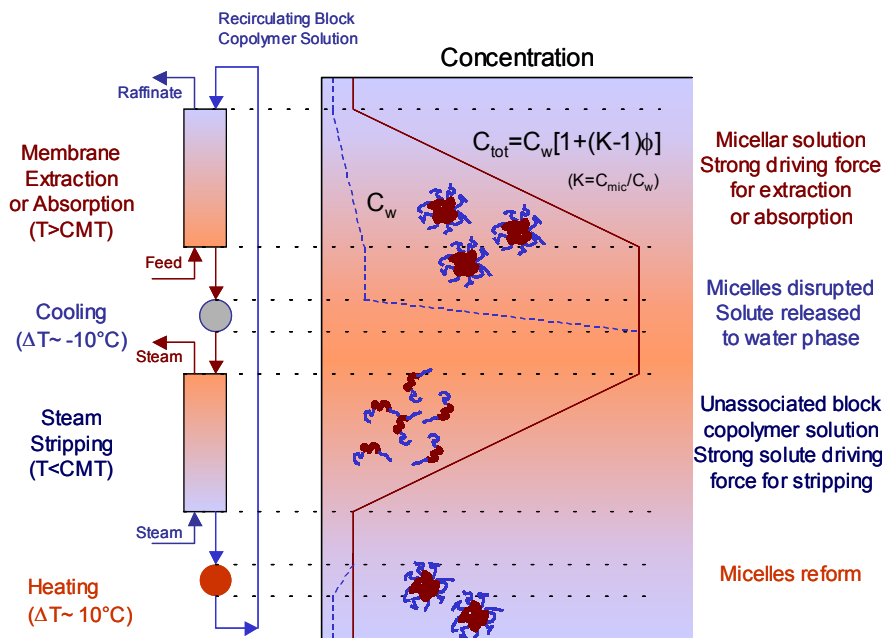


*Figure 4. Implementation of the block copolymer micelle solubilization scheme for removal of trace organics from contaminated waste streams showing the importance of small temperature swings for micelle regeneration.*

Rosslee and Abbott have recently reported another example in which the reversible assembly and issolution of micelles can be used to good advantage in separations. Redox-active surfactants such as (11-ferrocenylundecyl)trimethylammonium bromide form micelles which can solubilize hydrophobic compounds selectively when in the reduced state. On oxidation of the ferrocenyl moiety, however, these micelles break up into the monomers, releasing the solubilized materials. When a mixture of two hydrophobic compounds deposited on a substrate surface is challenged with the micellar solution, they are solubilized within the micellar cores, potentially with some selectivity for one component over the other such that the micelles are enriched in that component relative to the feed mixture. The solubilizate-laden micelles can now be transported to the cathode where the surfactants are oxidised, the micelles fall apart, and the released solutes deposit on the cathode surface. The surfactant monomers are returned to the anode, reduced to amphiphilic form and self-assemble to form new micelles ready to solubilize the solutes. While the selectivity in any given step is small, the separation effectiveness can be enhanced dramatically by redissolving the deposited material now enriched slightly in one of the compounds, and going through the micelle dissolution process once again to deposit an even richer mixture on the electrode surface. In one set of experiments in which this cycle was repeated five times an initial equimolar mixture of the two compounds was resolved to 97% purity.

The two examples given here rely on changes in the temperature and the oxidation state of the surfactant, respectively, for the disruption of the micelles and release of the solubilizates. Other stimuli can also be used for this purpose, as there are many other physical driving forces that can be used to alter the state of the surfactant, including pH, ionic strength, pressure and, in the case of photoresponsive surfactants, light. The challenge in some cases would be to scale these processes up from small-scale operations ideally suited for microchemical and low volume/high value-added operations to large-scale production

operations. Nonetheless, they offer intriguing opportunities for the green processing of chemicals and biochemicals by colloidal solvent extraction in which the use of bulk organic solvents can be bypassed in favour of the higher molecular weight and non-volatile surfactant and polymer self-assembled colloidal extractants.

### Coated Nanoparticles as Extractants

Possible disadvantages of self-assembled surfactant micellar systems include the necessary presence of monomeric surfactants at the critical micelle concentration, which cannot be ultrafiltered and can end up either in the recovered product phase or as counter-contaminants of the feed stream being treated. This problem can be overcome to a large extent using specially prepared nanoparticles coated with various self-assembled layers of surfactants and polymers to provide an environment for effective recovery and/or separation of materials from dilute solutions. With coatings covalently attached to the particle surface, these particles behave as micellar systems but without some of the disadvantages of monomer loss and micelle dissolution upon dilution or change in solution conditions. The particles must be captured and regenerated for subsequent reuse, and the solute must be recovered. This capture can be done through ultrafiltration, or the particles can be induced to agglomerate to form large flocs that can be microfiltered. Alternatively, deep-bed filtration of the particles can be attempted. These techniques can be confounded if there are other nano- or microscopic materials present, such as particulates or cell debris, and it would be advantageous to use another handle to latch onto the particles. One approach is to use magnetic nanoparticles, which can then be recovered by high gradient magnetic field separation techniques.

One class of particles that we have synthesized is shown on Figure 5, where the stabilizing comb-like polymer is amphiphilic in character; along the polyacrylic acid backbone are attached both PEO and PPO polymers, the PEO providing the stabilization of the particles in suspension, and the PPO collapsing to provide a strongly hydrophobic shell surrounding the particle. The solutes of interest can be either solubilized directly within the layer, or can adsorb through specific interactions with the external moieties on the coating surface. These particles have high surface areas per unit volume, and minimal transport resistances owing to the small diffusional distances between particles. They can also be used in systems with high solids content, such as cell suspensions or in the extraction of natural products.

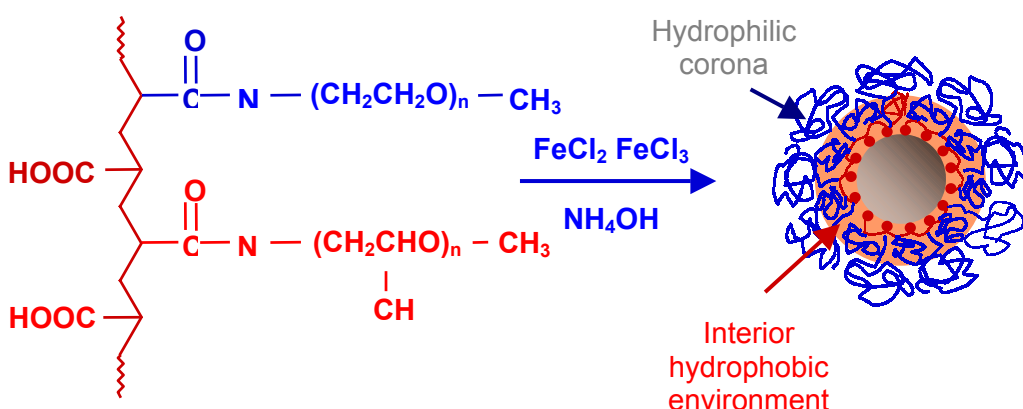


*Figure 5. Synthesis and structure of an amphiphilic magnetic nanoparticle. The PPO domains can solubilise organic solutes, while the PEO chains stabilise the particle dispersion in water.*

We compare the partitioning of a range of solutes between water and the PPO shell with the results reported by a number of workers on Pluronic® copolymer micelles. Clearly, the good agreement between the two sets of data shown in Figure 6 indicates that the environment afforded by the chemisorbed polymers on the particle surfaces is similar to that in the Pluronic® micelle cores, and that high solute loadings (~0.1-0.5 g/g PPO) can be attained. The particles themselves can be filtered from the aqueous solution using high gradient magnetic separation, in which the particle-laden stream is passed through a bed of stainless steel mesh inserted between the poles of an electromagnet that can generate fields of up to 2 Tesla; the wires in the mesh dehomogenise the magnetic field, creating very high gradients near the wire surfaces that are sufficient to hold even the small (10 nm) particles at the wire surface, effectively removing them from the suspension. The particles are collected by turning the magnets off and flushing the mesh with a clean aqueous stream. They can be regenerated either by steam-stripping of the particles while trapped in the bed, or the solute can be removed by extraction with a small amount of solvent and recovered by distillation. The partitioning of weak acids or bases to the coated nanoparticles can be controlled by pH, which can be selected relative to the  $pK_a$  of the material to either drive the solubilisation of the stripping operation.

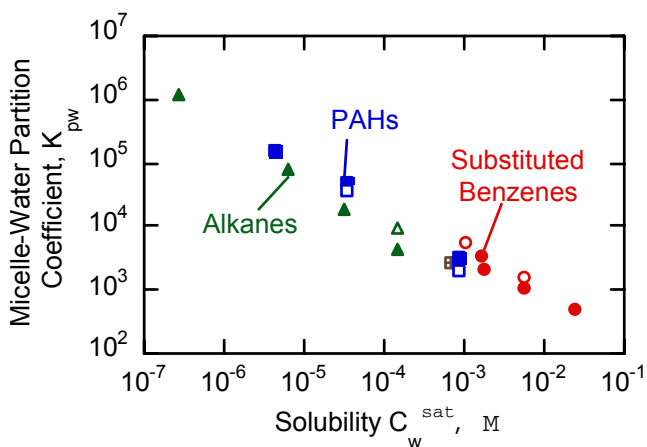


Figure 6 . Partitioning of organic solutes to PPO domains in Pluronic(r) micelles (solid symbols) and magnetic nanoparticle shells (open symbols).

In these systems the solvent phase is tethered to the nanoparticles, which themselves can be readily recovered through the application of an external magnetic field, and this can provide some unique benefits from the standpoint of green processing applications.

## CONCLUSIONS

The need for alternative approaches for using solvents in chemical and biochemical separation processes is dictated by the increasing awareness that their impact on the environment must be minimised. We have shown that by simple modification of a conventional solvent (THF) through the attachment of an alkyl tail, we can change its physical properties significantly to minimize both its water solubility and its potential to be lost to the environment through vapour emissions, and yet can retain its chemical functionality. The utility of such a solvent was demonstrated in the industrially-relevant process for the synthesis of an HIV protease inhibitor, where it was noted that we can eliminate many of the unit operations used in the published process

We have also discussed a few methods for the avoidance of a bulk organic solvent altogether through the use of colloidal extractants dispersed within the aqueous feed phase, either in the form of micelles, or as amphiphilic polymers attached to magnetic nanoparticles. Advantages associated with these systems include the wide range of polymeric species that can be envisaged, and that can be tailored to the specific needs in any particular chemical separations process. This is a rich area that has significant potential in a range of process industries, and provides many challenging and rewarding avenues for research and development.

#### **ACKNOWLEDGEMENTS**

I wish to acknowledge the contributions of the current and former students to the research results reported here. Linda Molnar, Bain Chin, Laura Cermenati and Professor Steve Buchwald participated in the tailored solvents work, supported by the DOE, EPA and NSF. Patricia Hurter and Paschalis Alexadridis conducted the thermodynamics and solubilisation studies on Pluronic® copolymer systems. Geoff Moeser, undergraduate student Kaitie Roach and Professors Paul E. Laibinis and William H. Green were responsible for the work on the polymer-stabilised magnetic fluids, which was supported by the NSF. Geoff Moeser has also received support in the form of a Fellowship from Kodak.



# ACHIEVING HIGH-PERFORMANCE LOW-COST PROCESSES FOR THE MANUFACTURE OF ORGANIC CHEMICALS USING PHASE TRANSFER CATALYSIS<sup>[1]</sup>

Marc Halpern

PTC Organics, Inc., Mt. Laurel, New Jersey, USA

Phase Transfer Catalysis, PTC, is widely used in the commercial manufacture of specialty and commodity organic chemicals. PTC can be described as catalytic one-step extraction and reaction of anions. PTC can also be used to simultaneously extract and react anions (or easily ionized organic compounds) from waste streams and convert them into value added products. Such waste streams can include cyanide from mining, mercaptans from petrochemicals and phenol from chemical processes. PTC processes provide many cost and performance benefits, including high yield, short cycle time, flexible choice of solvent, reduced solvent usage, lower excess of reactants, use of alternate less expensive raw materials and a variety of safety and environmental benefits.

## INTRODUCTION

Phase transfer catalysis (PTC) is used in hundreds of commercial processes to manufacture organic chemicals including agricultural chemicals, monomers, polymers, pharmaceuticals, additives, dyes and colors, photographic chemicals, flavors and fragrances, explosives, rubber chemicals and a wide variety of specialty and fine organic chemicals [2, 3]. PTC can also be used to remove certain anions from waste streams and convert them into value added products. This paper will describe the mechanism of PTC, selected applications of PTC, the benefits of PTC and how PTC may be used to convert byproduct streams (such as cyanide from mining operations, mercaptans from petrochemicals and phenol from chemical processes) into value added products.

## MECHANISM

Since this paper is being presented at a Solvent Extraction conference, phase transfer catalysis may be described as a catalytic one-step process for EXTRACTION and REACTION of anions. The goal of most PTC systems is to convert anions into value added products. Figure 1 illustrates the mechanism of PTC [4] by example, for the extraction and reaction of cyanide to produce the agricultural chemical and pharmaceutical intermediate benzyl cyanide. The catalyst is a quaternary ammonium cation, Aliquat® 336 (trademark of Cognis Corporation; methyltricaprylyl ammonium), represented by Q<sup>+</sup>. Starting at the left side of Figure 1, the ion pair Q<sup>+</sup>CN<sup>-</sup> distributes between the aqueous phase and the organic phase. For the case of the highly lipophilic Aliquat 336 shown here, this distribution happens to be > 99% in the organic phase. Once the cyanide has been transferred to the organic phase, it can react with benzyl chloride to produce the benzyl cyanide product and liberate

chloride as the leaving group byproduct. When the irreversible organic phase reaction liberates the chloride leaving group, it pairs with  $\text{Q}^+$  to form  $\text{Q}^+\text{Cl}^-$  which also equilibrates between the two phases. The  $\text{Q}^+$  cation can then pick up another cyanide anion from the aqueous phase and the cycle restarts. The cyanide anion reacts with greatly enhanced reactivity due to three reasons: (1) the cyanide anion is actually solubilized in the organic phase by  $\text{Q}^+$  and therefore the reaction with the benzyl chloride is homogeneous (not interfacial), (2) the cyanide anion is stripped of most of its hydration shell once transferred into the non-polar organic phase and is thereby greatly activated and (3) the bulky  $\text{Q}^+$  cation forms a loose ion pair with the cyanide anion, rendering the cyanide ion much more reactive than if it were associated with a small  $\text{Na}^+$ , for example. In all, the mechanism includes two “extraction” steps, one ion exchange step and one actual chemical reaction in which bonds are formed or broken. Only the chemical reaction is irreversible (the other three steps are equilibrium steps) and that is what drives the catalytic system forward to completion. On balance, the phase transfer catalyst  $\text{Q}^+$ , transfers cyanide to the organic reaction phase and transfers the chloride leaving group to the aqueous phase while benzyl chloride is converted into benzyl cyanide.

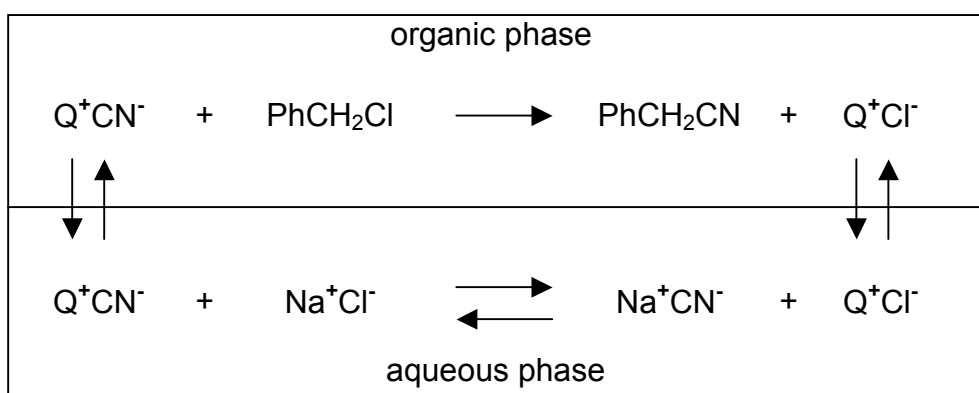


*Figure 1. Phase transfer catalysis mechanism (illustrated by CN/Cl reaction example).*

### SCOPE OF APPLICATION

There are literally hundreds of anions which can be successfully transferred and reacted under PTC conditions. As a result there are 10,000 publications and 2,000 patents which describe applications in 40 broad reaction categories. Table 1 shows examples (partial list) of anions which have been reacted under PTC conditions. Note that the list includes neutral molecules such as phenol, mercaptans and carboxylic acids which can easily be ionized to anions at high pH. Table 2 shows the reaction categories in which PTC excels.

*Table 1. Examples of anions successfully reacted under PTC conditions.*

Bases	hydroxide, carbonate
Inorganic Nucleophiles	cyanide, azide, fluoride, bromide, iodide, thiocyanate, cyanate
Organic Nucleophiles	phenol, alcohols, carboxylic acids, mercaptans, heterocycles, Most organic compounds containing an O-H, C-H, N-H or S-H group with a pKa of under 23
Oxidizing Agents	permanganate, hypochlorite (bleach), dichromate, peroxide
Reducing agents	bороhydride, formate, dithionite, nitrite

*Table 2. Selected reaction categories in which PTC excels.*

Etherification (O-Alkylation)
Esterification (carboxylic acids with alkyl halides)
Transesterification
N-Alkylation
Thioetherification (S-Alkylation)
C-Alkylation (nucleophilic)
Cyanation
Fluorination
Iodination
Azidation
Hydrolysis (Saponification)
A variety of nucleophilic aliphatic substitutions
A variety of nucleophilic aromatic substitutions
Reactions of N-H, O-H, and S-H groups with highly water-sensitive compounds including acyl halides, sulfonyl halides, phosphorous halides, esters, phosgene, others
Dehydrohalogenation
Carbene Reactions
Oxidation
Epoxidation
Reduction
Hydrogenation
Carbonylation
Michael Addition
Aldol Condensation
Darzens Condensation
Wittig
Condensation Polymerization
Radical Polymerization
Transition Metal Co-Catalyzed Reactions
HCl/HBr Reactions
Any reaction above for polymer modification

As will be shown in the next section, there are many benefits in using PTC in industrial applications, most of which focus on cost savings and/or pollution prevention. Following are some examples of industrial applications and highlights of their key benefits:

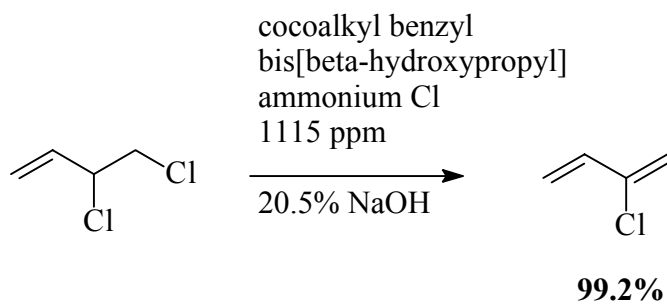


*Figure 2. Continuous dehydrohalogenation to produce a large scale monomer [5].*

Achieved:  
Productivity: 16 tons/hr, 99.2% yield and NaOH usage of only 0.8 mole % excess!

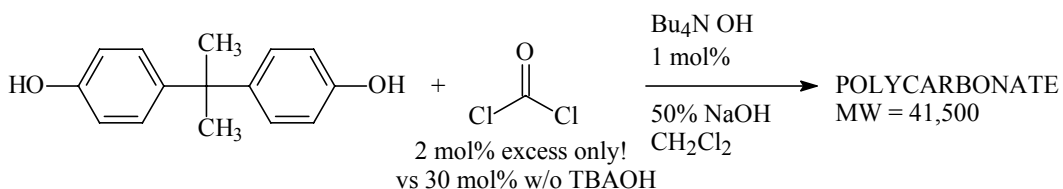


*Figure 3. Outstanding reduction of excess hazardous high volume raw material [6].*

Achieved:

Great improvement in safety and environmental by reducing phosgene excess by 94%!  
PTC provides 200X less hydrolysis of phosgene/chloroformate according to GE patent.

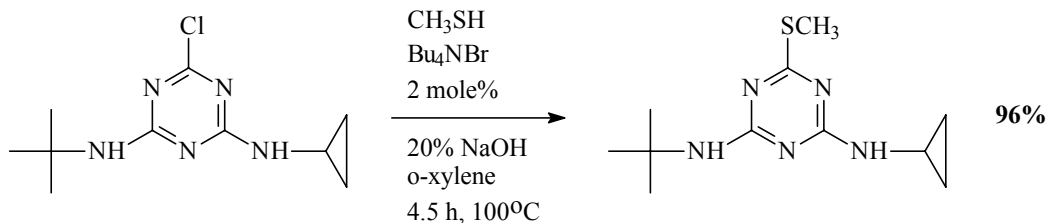


*Figure 4. Thiolation [7] (using methyl mercaptan).*

Achieved:

High yield for > 40 triazines, reduced cycle time by eliminating unit operations;  
no isolation of intermediates; achieved single solvent for 3 steps with low emissions.

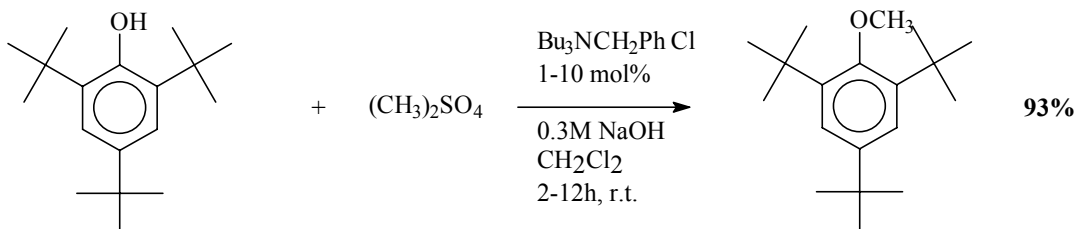


*Figure 5. Etherification [8] (O-alkylation).*

- PTC usually best Williamson ether synthesis
- high yield etherification
- no need for excess pre-formed alkoxide
- usually short cycle time and easy workup
- non-dry mild reaction conditions
- aliphatic and phenolic O-alkylation many commercial bis-phenol A processes

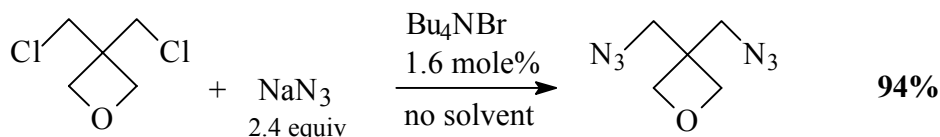


*Figure 6. High yield solvent-free hazardous nucleophilic displacement [9].*

Achieved:

High yield, with no solvent; reduced excess of explosive reactant; scaled up to 200 L.

### Sulfur Removal from Diesel Fuel [10]

Legislation in the US and Europe reduced the permitted sulfur levels in diesel fuels by 84% during the past few years. PTC/H<sub>2</sub>O<sub>2</sub> was used as part of a process to achieve excellent desulfurization of diesel oil. A key sulfur component of diesel oil is dibenzothiophene and was quantitatively oxidized using 0.5 wt% Aliquat 336, 0.3 wt% phosphotungstic acid and 11% aq. H<sub>2</sub>O<sub>2</sub> (6.4 wt% on a 100% basis) at 60°C. Since H<sub>2</sub>O<sub>2</sub> is expensive, the PTC oxidative desulfurization (ODS) is preceded by hydrodesulfurization (HDS). HDS of gas oils to < 0.5 wt% sulfur is difficult. Thus, sequential HDS followed by PTC ODS was used to achieve 0.005 wt% sulfur, which is an order of magnitude lower than US and European requirements.

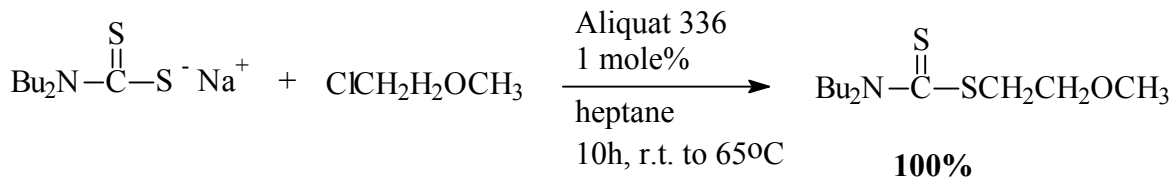


*Figure 7. Thioesterification for lubricant [11].*

### Carbonylation

Phase-transfer catalysis offers a variety of conceptual and practical advantages when performing carbonylations as described in [2] (Chapter 13). Among the advantages unique to PTC is the ability to transfer the anionic forms of metal carbonyls to the organic phase, in which CO is about 10 times more soluble than in water, which further leads to less hydrolysis of CO to formate and esters to acids. For example, malonic esters can be made by PTC carbonylation of ethyl chloroacetate at 1 atm CO at 25°C in the presence of cobalt carbonyl [12]. Ni(CN)<sub>2</sub> was used for the PTC double carbonylation of alkynols, using PEG-400 as the phase-transfer catalyst, LaCl<sub>3</sub> as an additional co-catalyst, toluene as the solvent, and 5.0 N NaOH as the optimum base concentration [13]. Yields of ene-dicarboxylic acids were up to 97%. PTC carbonylation has also been used to convert alkyl halides to acids and esters, and aryl halides to aryl carboxylic acids.

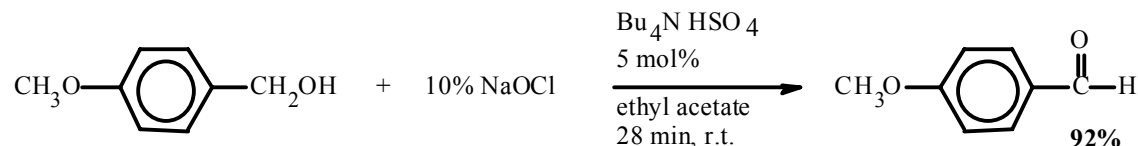


*Figure 8. Oxidation [14] (hypochlorite).*

Achieved:

High yield in short reaction time at room temperature;  
inexpensive oxidizing agent/no transition metal with high selectivity (vs. over-oxidation).

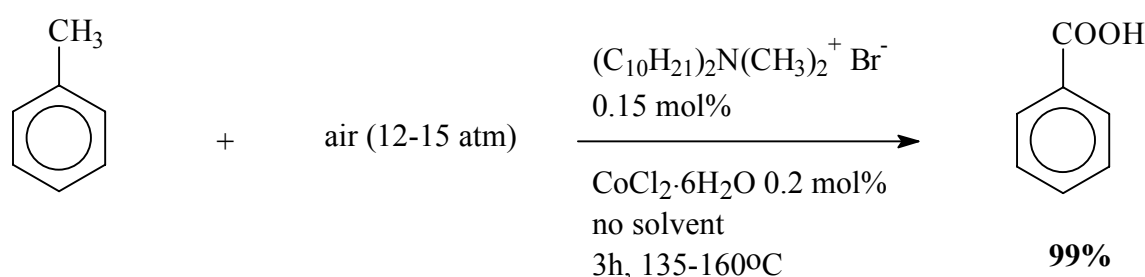


Figure 9. Oxidation [15] (air).

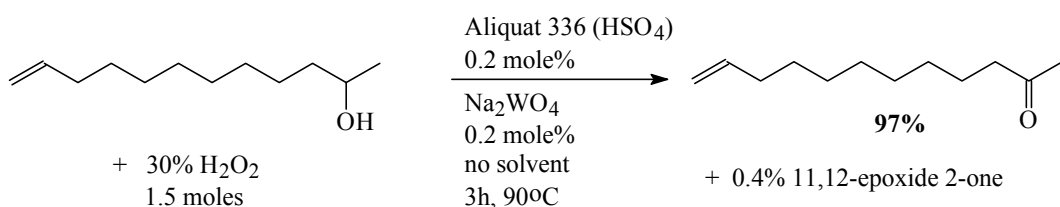


Figure 10. Oxidation [16] (hydrogen peroxide).

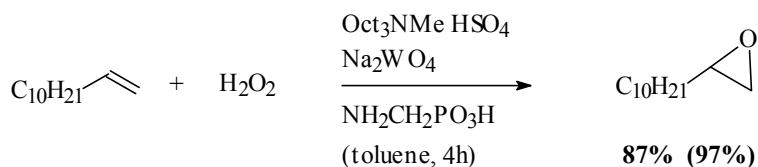


Figure 11. Epoxidation [17].

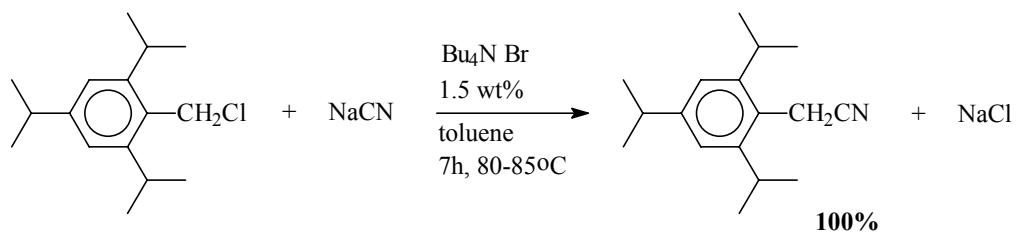


Figure 12. Cyanation [18].

Achieved:

Yield increase of 19% vs previous DMSO process. 100% recycle of toluene solvent vs no recycle of DMSO with 40% less solvent taking up reactor space. 95% (!) less cyanide excess, 85% (!) less aqueous waste, 3 less workup unit operations and better controlled exotherm through agitation vs. stepwise cyanide addition.

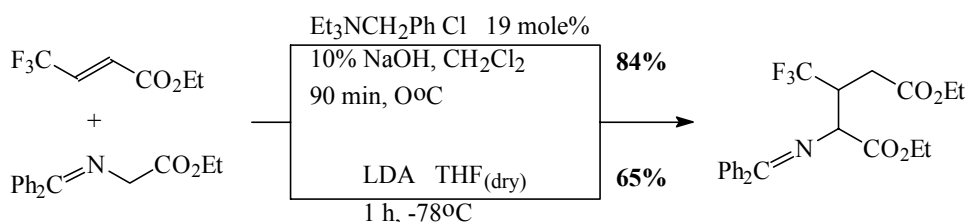


Figure 13. Michael Addition [19].

Achieved:

Eliminated very expensive hazardous organic strong base (LDA) at very expensive very low temperature with 19% yield increase!  
Multiple Michael addition to acrylates used for lubricants also reported [20].

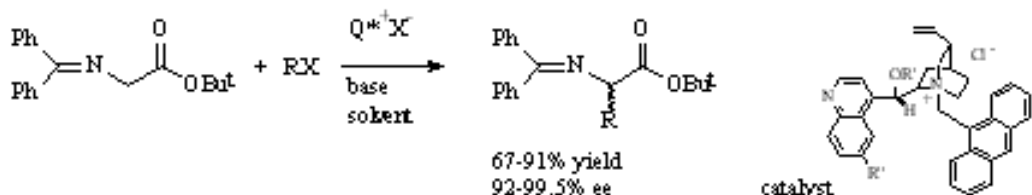


Figure 14. Chiral alkylation [21].

## BENEFITS OF PHASE TRANSFER CATALYSIS

Table 3 shows the primary benefits provided by PTC systems. There are several fundamental underlying reasons for the ability of PTC to provide these benefits and they are mostly related to the two phase nature of PTC systems and the ability to carefully regulate the transfer of species between the phases. As noted in the Mechanism section above, high reaction rates are achieved due to the co-location of the reactants in a single phase, the reduced hydration of the anion and the looseness of the ion pair. This results in advantageously reduced cycle time. The lower energy of activation achieved in PTC systems can also be exploited to perform the reaction at lower temperatures. Reduced temperature may sometimes be important not only to reduce energy costs but also to reduce the heat history of the reactants and products, thereby increasing the purity or assay of the product which in turn may lead to lower separation costs. PTC systems often achieve higher yield than non-PTC systems, because byproducts can be minimized and equilibrium reactions can be replaced by irreversible reactions (e.g., performing esterification by the reaction of an alkyl halide with a carboxylic acid salt instead of an alcohol with a carboxylic acid). One surprising advantage of PTC systems is the ability to work with highly water sensitive compounds such as acyl halides, phosgene, sulfonyl halides, phosphoryl halides, esters and anhydrides. This ability is due to the ability to “protect” the water sensitive compound from hydrolysis by either working under anhydrous solid-liquid PTC conditions, or if a water phase is used, by using the catalyst to transfer the anion to the organic phase with very low agitation thereby minimizing interfacial hydrolysis. When hydrolysis is minimized, yield increases. The ability to minimize hydrolysis also results in significant cost savings by reducing the amount of excess reactant used to several mole%. As shown in the applications section above, this has been achieved to reduce excess phosgene from 30 mole% to 2 mole%, excess cyanide from 70 mole% to 5 mole% and excess expensive borohydride from 30 mole % to 4 mole%.

Another great advantage of PTC is the flexibility in choosing solvent. The proper choice of phase transfer catalyst can allow almost any anion to be transferred into almost organic liquid. Therefore, any reactant or product which is a liquid can be used as the solvent and so-called "solvent-free PTC" is achieved. If a solvent is absolutely necessary, it can be chosen based on cost, recovery, toxicity, environmental considerations, recrystallization procedures in later or earlier steps or almost any other reason. The choice of solvent in PTC is rarely dependent on the ability of that solvent to dissolve salts. Therefore, one can very often replace DMSO, DMF, NMP, DMA and other polar aprotic solvents with solvents which are easy to recover such as toluene and MIBK.

One of the greatest cost advantages in using PTC is the ability to substitute expensive hazardous strong bases with inexpensive inorganic bases. Often, the combination of PTC with sodium hydroxide can replace sodium methoxide, ethoxide, t-butoxide, sodium amide, sodium hydride, sodium metal and sometimes even LDA. Savings achieved are usually in the range of \$1,250 to \$18,000 per ton of strong base purchased [22].

### **PTC APPLICATION TO BYPRODUCTS FROM MINES AND CHEMICAL PROCESSING**

This ISEC 2002 conference is attended by a significant number of professionals from the mining and heavy chemicals industries who may not be likely to be interested in the manufacture of fine organic chemicals. However, we may be able to offer those individuals the opportunity to substitute some of their waste treatment costs with profit!

For example, mining and electroplating companies generate large aqueous waste streams containing cyanide. PTC can be used to catalytically extract cyanide from an aqueous phase and react it with an alkylating agent, such as benzyl chloride (list price ~ \$1.5/kg) to produce a value added product such as benzyl cyanide (list price ~ \$5/kg). This represents a significant opportunity for cyanide stream generators since it currently costs money to treat cyanide streams and with PTC it may be possible to generate profit from these streams. The economic feasibility would have to be evaluated on a stream-by-stream basis and depends on many factors, including the concentration of the cyanide in the stream. This reaction is illustrated in the Mechanism section above.

Organic compounds which are easily ionizable to anions at pH of 12 and under can also be catalytically extracted and reacted in one step from aqueous streams to produce value added products. An excellent example includes extracting phenol (or phenol derivatives such as bisphenol A, resorcinol and others) from a dilute aqueous stream at pH 11 and react it with any of a variety of alkylating agents to form phenyl ethers. In one report, 99.9% removal of phenol from a 5000 ppm aqueous stream was achieved using PTC and benzoyl chloride to produce an ester in 15 minutes at room temperature in either a batch or continuous process [23].

Mercaptans can likewise be catalytically extracted and reacted in one step from aqueous, gaseous or organic streams to produce thioethers (organic sulfides). It is noteworthy that mercaptans can be converted into thioethers without the need to pre-form the sodium mercaptide salt. The mercaptide salt can be formed *in situ* by passing the mercaptan over the base (e.g., NaOH) in the presence of the phase transfer catalyst and alkylating agent to efficiently produce the thioether.

## SUMMARY

Phase transfer catalysis provides great economic benefit and high performance in the manufacture of a very wide range of organic chemicals. Although significant expertise is required to develop and commercialize PTC opportunities, companies could improve profit and process performance by partnering with a process development company with dedicated and highly specialized expertise in industrial PTC (such as PTC Organics, www.ptcorganics.com) to identify, develop and commercialize opportunities. In addition, companies which generate waste streams with certain anions (such as cyanide from mining) may be able to convert their waste treatment cost centers to profit generators by applying the fundamentals and practical aspects of phase transfer catalysis.

*Table 3. Benefits of phase transfer catalysis.*

- **Increase Productivity**
  - ⇒ increase yield
  - ⇒ reduce cycle time
  - ⇒ increase reactor volume efficiency
- **Improve Environmental Performance**
  - ⇒ eliminate, reduce or replace solvent for lower emissions and/or easier workup
- **Increase Quality**
  - ⇒ improve selectivity
  - ⇒ reduce variability
- **Enhance Safety**
  - ⇒ control exotherms
  - ⇒ use less hazardous raw materials
- **Reduce Other Manufacturing Costs**
  - ⇒ eliminate workup unit operations
  - ⇒ use alternate less expensive or easier to handle raw materials such as replacing NaOMe/OEt, t-butoxide, NaH, NaNH<sub>2</sub>, Na metal or LDA
  - ⇒ reduce excess reactants
  - ⇒ reduce temperature

## REFERENCES

1. This article is reprinted with permission from PTC Communications, Inc. and is taken from the course manual “Practical Phase Transfer Catalysis” 2000 (course information can be found at [www.phasetransfer.com](http://www.phasetransfer.com) and [www.ptcorganics.com](http://www.ptcorganics.com)), and articles from the journal “Phase Transfer Catalysis Communications”, primarily Volume 3 Issue 2, pages 17-27, 1997 and the webpage [www.phasetransfer.com/overview.htm](http://www.phasetransfer.com/overview.htm).
2. M. Halpern (1991), Ullmann’s Encyclopedia of Industrial Chemistry, Vol. A19, VCH, Weinheim, p. 293.
3. C. Starks, C. Liotta and M. Halpern (1994), Phase Transfer Catalysis: Fundamentals, Applications and Industrial Perspectives, Chapman and Hall, New York.
4. C. Starks (1971), *J. Amer. Chem. Soc.*, **93**, 195; C. Starks and R. Owens (1973), *J. Amer. Chem. Soc.*, **95**, 3613.
5. L. Maurin (1983), *US Pat.*, No. 4,418,232 .
6. E. Boden, P. Phelps, D. Ramsey, P. Sybert, L. Flowers and R. Odle (1995), *US Pat.*, No. 5,391,692.
7. H. Grace and M. Wood (1994), *Eur. Pat.*, No. 0 648 755 A1.
8. A. McKillop, J. Fiaud and R. Hug (1974), *Tetrahedron*, **30**, 1379.
9. A. Malik, G. Manser, R. Carson and G. Archibald (1996), *US Pat.*, No. 5,523,424.
10. F. Collins, A. Lucy and C. Sharp (1997), *J. Mol. Catal. A*, **117**, 397.
11. L. Farny, A. Horodysky and R. Nipe (1996), *US Pat.*, No. 5,514,189.
12. M. Kantam, N. Reddy and B. Choudary (1990), *Synth. Comm.*, **20**, 2631.
13. Z. Zhou and H. Alper (1996), *Organometallics*, **15**, 3282.
14. G. Lee and H. Freedman (1978), *US Pat.*, No. 4,079,075.
15. J. Dakka, A. Zoran and Y. Sasson, *Eur. Pat. Appl.*, No. EP 0 300 921.
16. K. Sato, M. Aoki, J. Takagi and R. Noyori (1997), *J. Amer. Chem. Soc.*, **119**, 12386.
17. K. Sato, M. Aoki, M. Ogawa, T. Hashimoto and R. Noyori (1996), *J. Org. Chem.*, **61**, 8310.
18. G. Dozeman, P. Fiore, T. Puls and J. Walker (1997), *Org. Proc. Res. Dev.*, **1**, 137.
19. D. Gestmann, A. Laurent and E. Laurent (1996), *J. Fluorine Chem.*, **80**, 27.
20. M. Sabahi and R. Irwin (1994), *US Pat.*, No. 5,347,043.
21. E. Corey, F. Xu and M. Noe (1997), *J. Amer. Chem. Soc.*, **119**, 12414; B. Lygo and P. Wainwright (1997), *Tetrahedron Lett.*, 8595.
22. M. Halpern (2001), *Phase Transfer Catalysis Comm.*, **14**, 1.
23. V. Krishnakumar and M. Sharma (1984), *Ind. Eng. Chem. Proc. Des. Dev.*, **23**, 410.



## SUPERCRITICAL FLUIDS: CLEAN SOLVENTS FOR EXTRACTION, REACTION AND CRYSTALLISATION

Adam S. O'Neil, Paul A. Hamley and Martyn Poliakoff

School of Chemistry, University of Nottingham, Nottingham, England

Supercritical fluids are becoming increasingly attractive as an environmentally acceptable replacement for organic solvents in chemical reactions and material processing. This paper highlights the properties of supercritical fluids, especially supercritical CO<sub>2</sub>, which offer particular advantages for extraction. The paper includes references to a number of reviews, which together provide a brief introduction to the State of the Art.

### INTRODUCTION

Supercritical fluids have excited the interest of physical chemists for the past 150 years. Indeed, a gas which displays some of the properties of a liquid remains fascinating even today [1]. However it is only recently that the fluids have aroused substantial technological interest. The primary reason for this is their solvent power which can often approach, and occasionally exceed, those of organic solvents but without the environmental complications associated with the use of those solvents.

In the early 1980s, there was significant research into possible applications of supercritical fluids but, sadly, the proponents of these fluids oversold their wares. The result was considerable disillusionment about the real value of supercritical solvents. Now, with the Montreal Protocol and a generally heightened environmental awareness, supercritical fluids are beginning to show their true value. However, it is not just the spectre of environmental regulation which is driving this comeback. The renewed interest is based on a broad foundation of recent academic research which has shown that supercritical fluids can provide an additional degree of control and performance in reaction chemistry and materials processing, which would be difficult to achieve with conventional solvents.

Supercritical fluids are gases compressed until their densities approach those of liquids. Such compression can only occur above the so-called 'critical temperature' of the fluid; at lower temperatures, the fluid will simply liquefy on compression. Several materials have critical temperatures close to room temperature (Figure 1). Of these CO<sub>2</sub> is currently the most commonly used due to its easy availability and relative cheapness.

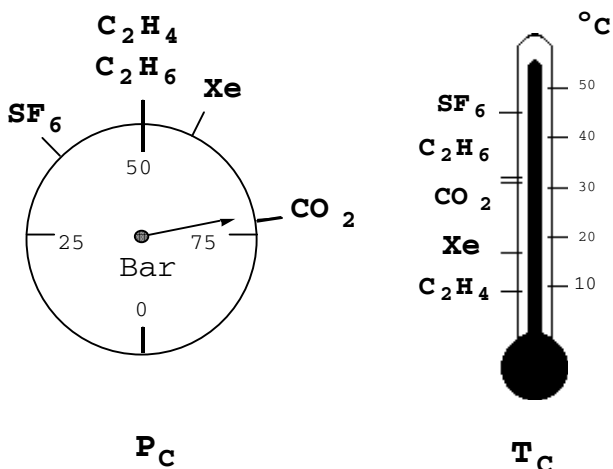


*Figure 1. Schematic representation of the critical temperatures ( $T_c$ ) and critical pressure ( $P_c$ ) of selected pure materials with critical points near room temperature.*

This paper draws attention to some recent developments and concentrates on the particular properties of supercritical fluids which differentiate them from more conventional solvents. Apart from the excellent books by McHugh and Krukonis [2] and Jessop and Leitner [3], there have been recent reviews in the area of extraction and reaction chemistry [4], extraction, materials processing [5, 6], and new industrial applications [7].

## SUPERCritical SOLVENTS

The solvent properties of supercritical fluids have been known since the 19th century. Broadly, the solubility of non-polar materials in sc $CO_2$  is similar to that in light hydrocarbons, such as hexane. However, unlike solubility in hexane, the solubility in sc $CO_2$  can be “tuned”; the higher the applied pressure and hence the higher density of the fluid, the greater the solubility in the fluid. Furthermore, heating sc $CO_2$  under constant pressure causes a reduction in density which, in turn, can lead to a drop in solubility. Thus, one has the interesting possibility of depositing dissolved material onto a *heated surface* directly from the supercritical solution. Such deposition would be extremely difficult in an ordinary solvent. The solvent power of  $CO_2$  can be enhanced by adding so-called “modifiers”. The most common modifier is MeOH but it has a tendency to self-associate, thus limiting its effect at high concentrations. Work in our laboratory suggested that HCFC compounds, e.g.,  $CH_2FCF_3$  (R134a), etc., might be quite effective modifiers for sc $CO_2$  [8] and this has now been confirmed by Abbott and coworkers [9]. The critical points of mixtures are more complicated than for pure substances and the relevant phase behaviour is described in References [2, 3]. Although phase behaviour can appear discouragingly complex to those starting in the field, it cannot be ignored. Fortunately, once the basics have been mastered, the behaviour of a particular system is often quite easy to understand.

In the context of this Conference, it is important to stress that sc $CO_2$  differs from conventional hydrocarbon solvents in its affinity for fluorinated compounds, many of which are more soluble in sc $CO_2$  than they are in alkane solvents under similar conditions. The origins of this increased affinity are beyond the scope of this paper but, somewhat simplistically, it can be considered to be the result of the inherent volatility of the fluorinated compounds and also to thermodynamically favorable interactions between the fluorinated materials and  $CO_2$ . Whatever the origins of the effect, it has generated interest in the use of

fluorinated materials to aid the extraction of metal [10, 11] and in the use of fluorinated surfactants to create aqueous inverse micelles [12-16] and to emulsify polymers [10]. Indeed, DeSimone has coined the phrase “CO<sub>2</sub>-philic” to describe the behaviour of these fluorinated materials.

### RAPID EXPANSION

The dependence of solubility on fluid density has led to the development of a whole technology of powder and particle formation, based on the Rapid Expansion of Supercritical Solution (RESS) [17]. The technique is almost self-explanatory. It involves pumping a supercritical solution through an expansion nozzle or valve, see Figure 2(a).

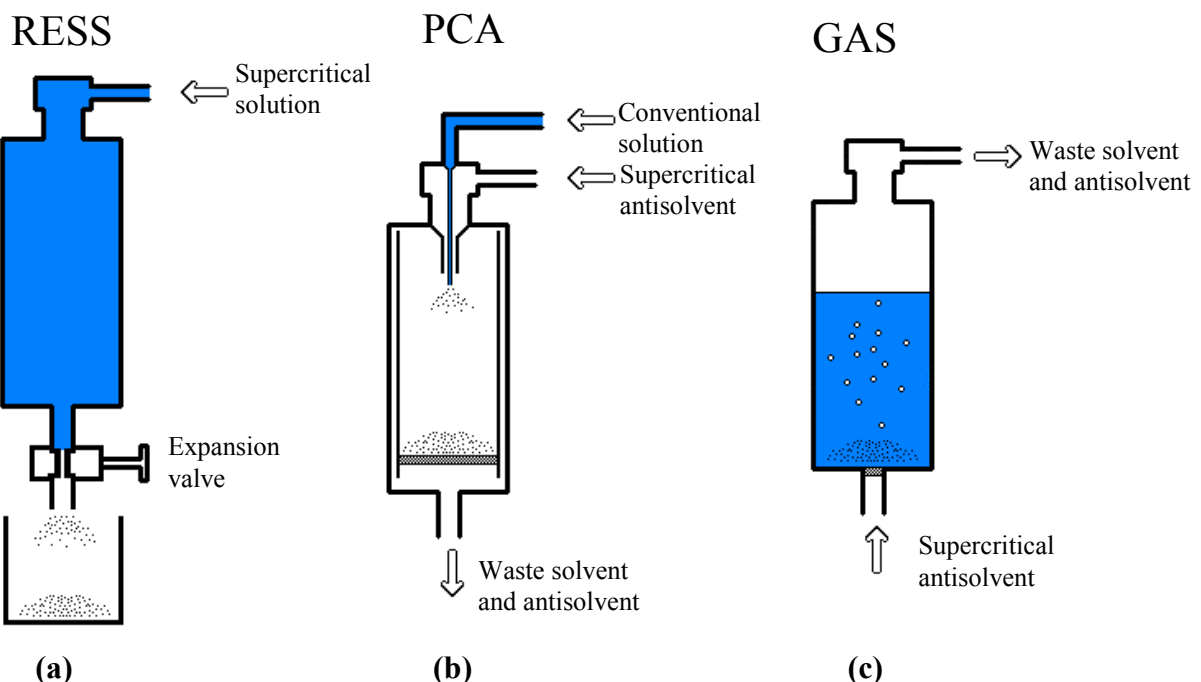


Figure 2. Principles of (a) the RESS, (b) PCA and (c) GAS processes for precipitating powdered materials using supercritical fluids. For further details, see references [17-33].

The solute is precipitated as a very uniform powder. The particle size and other properties of the powder can be controlled by varying the expansion conditions and by the careful design of the nozzle. Originally developed by Smith and coworkers [17], the technique has been heavily investigated by Debenedetti and coworkers [18, 19]. RESS has the disadvantage that it requires a relatively large amount of supercritical solvent, but this should be less of a hindrance in the deposition of coatings than it would be in the preparation of bulk materials.

RESS expansion is used for the recovery of extracts in the majority of analytical scale supercritical extractions. Although analytical techniques are largely outside the scope of this lecture, it should be noted that supercritical fluid extraction has widespread applications for detection of residual monomers or oligomers in polymeric materials, and more generally for the characterisation of thermally labile high molecular weight compounds such as polymer additives and stabilisers [34].

## SUPERCritical ANTISOLVENTS

A more recent development has been the use of supercritical fluids to precipitate materials which are insoluble in the supercritical solvents. The technique is similar to that used by synthetic chemists when they add one solvent to another to induce precipitation. There have been a number of different variations of the supercritical technique, the most important of which are the GAS (Gas Anti-Solvent, Figure 2(c)) and the PCA (Precipitation by Compressed Antisolvent, Figure 2(b)) [21-25] approaches. In the GAS process scCO<sub>2</sub> is pumped into a solution of a material dissolved in an organic solvent [2, 20, 33]; GAS precipitation has been used for materials as diverse as hormones and explosives. During PCA a solution is injected into a flow of antisolvent, for example a polymer in tetrahydrofuran (thf) is pumped into a vessel containing scCO<sub>2</sub>, the thf is stripped off, and the polymer is precipitated.

The advantage of both the GAS and PCA techniques is that the particle size of precipitated material can be controlled very precisely to generate a highly uniform product. Variations have already attracted interest in the pharmaceutical industry [35-39] where the morphology of a material can have a profound effect on its therapeutic value. The technique can also be combined with coating technology so that the material can be both precipitated and coated with a surfactant material in a single process.

Precipitation can also provide a method of synthesis. C<sub>60</sub>(gas) inclusion compounds have previously only been produced by using very high temperatures and pressures to force gas into the solid lattice [40]. Supercritical fluid antisolvent has been shown to provide a much simpler route to these compounds [26]. With CO<sub>2</sub> as an antisolvent, C<sub>60</sub> was precipitated as a solid around the CO<sub>2</sub> molecules, creating C<sub>60</sub>(CO<sub>2</sub>). We have extended this work to preparation [41] of hydrocarbon intercalates which cannot be prepared by the traditional forcing methods. These intercalates include C<sub>60</sub>(C<sub>2</sub>H<sub>4</sub>), C<sub>60</sub>(C<sub>2</sub>H<sub>6</sub>), C<sub>60</sub>(C<sub>3</sub>H<sub>6</sub>) and C<sub>60</sub>(C<sub>3</sub>H<sub>8</sub>). Our specific antisolvent techniques used included a new method, strongly analogous to conventional antisolvent precipitation. This method involves simple layering of a pressurised gas (ca. 10 MPa) over a C<sub>60</sub> solution. Slow diffusion of this gas into the solution creates a gradual reduction in solvating power and hence reduction in its ability to hold the C<sub>60</sub> in solution. This process was observed to progress over 2-3 days and to produce crystals of material that were measurable on a mm scale. Some of the crystals were of sufficient quality to allow characterisation by single crystal X-ray diffraction. This has proved successful for compounds which previously have been found to be extremely difficult to crystallise, virtually all other work in this area relies on powders as the only means of diffraction analysis [40].

## SUPERCRITICAL EXTRACTION

The use of SCFs for extraction is well established technique [2]. In the words [42] of Chien Wai, supercritical extraction is “over the hump”. For the extraction of metals, much of the current research is focused on finding the optimal ligands for sequestering and solubilizing the target ions [43]. This search is now beginning to lead to an understanding of the factors affecting solubility of such complexes [11]. When fully developed, this understanding will have a significant influence on the design of ligands for selective SCF extraction and for reaction chemistry [4]. There are several attractive aspects of scCO<sub>2</sub> for extraction. Firstly, it can eliminate the need for using volatile organic compounds. Secondly, the extractant can be recovered totally free of solvent merely by reduction in pressure. Thirdly, and most significantly, pressure can be used to tune the solvent power of scCO<sub>2</sub> and hence to alter the selectivity of the extraction. One of the interesting recent developments is the use of scCO<sub>2</sub> for reactive extraction. Recently, Wai and coworkers reported a striking example [44] of this, the reactive extraction of uranium oxide, UO<sub>2</sub>, into scCO<sub>2</sub> using the CO<sub>2</sub>-soluble complex TBP-HNO<sub>3</sub> (TBP = tri-*n*-butyl-phosphate) to convert the oxide to the nitrate, which had previously been shown to be soluble in scCO<sub>2</sub> modified with TBP [43].

## IMPREGNATION OF POLYMERS

As explained above, supercritical CO<sub>2</sub> is widely used for extraction on an industrial scale [2]. The appeal of scCO<sub>2</sub> is the absence of toxic residues and a relatively low temperature needed for the extraction process. Precisely the same properties make scCO<sub>2</sub> a useful solvent for the *impregnation* of materials into polymers and porous solids. Our research group at Nottingham has used this approach for a number of chemical reactions [45, 46], and the technique is being used for impregnating dyes into polymeric materials [47-49].

Dyeing is traditionally carried out in water, which generates very substantial clean-up problems before the wastewater can be discharged from the dye works [50-53]. The problem is exacerbated by the intense colour of the dyestuffs. Supercritical dyeing totally eliminates the need for water but there are still problems in achieving the uniformity of dyeing needed for the clothing industry. The technique has the interesting ability to dye several types of synthetic material simultaneously, for example, both the teeth and the backing material of zip fasteners.

At Nottingham, we have developed spectroscopic techniques for monitoring the impregnation of metal complexes into polymers [54]. We have found that impregnation is relatively uniform over small distances (centimetres) [55]. Once impregnated into the polymers, the metal compounds can be induced to react with the polymers photochemically [56] or even to modify the polymer either by isomerization of olefinic bonds or hydrogenation [46].

## REACTIONS IN SUPERCRITICAL FLUIDS

A number of chemical processes are traditionally run under conditions which are supercritical. Probably the best known example is the high-pressure polymerisation of ethylene which has been carried out for nearly 50 years [2]. Supercritical fluids (SCFs) offer a wide range of opportunities as solvents for chemical reactions and supercritical CO<sub>2</sub> is becoming increasingly important as a benign replacement for more toxic media [4, 57-60]. High pressure reactions, however, are more capital intensive than conventional low pressure processes. Therefore, supercritical fluids will only gain widespread acceptance in those areas where the fluids give real chemical advantages as well as environmental benefits.

Our research group initially became involved with SCFs via inorganic and organometallic chemistry, a field which we comprehensively reviewed recently [4]. We were among the first to recognise that the miscibility of H<sub>2</sub> with SCFs could be exploited for new chemistry and we generated a number of previously unknown organometallic dihydrogen complexes [61]. More recently we developed the use of miniature flow reactors to isolate new, highly labile alkene and dihydrogen complexes from SCF solution [62, 63]. At the same time, other groups were working on enhanced homogeneously catalysed reduction of CO<sub>2</sub> [59, 64, 65] and increasing the efficiency of catalytic hydrogenation of fats [66], our work on H<sub>2</sub>-complexes and flow reactors lead us to the supercritical hydrogenation of organic compounds. This initiated a fruitful collaboration between the University of Nottingham and Thomas Swan & Co. Ltd. The attraction of scCO<sub>2</sub> is that it offers new possibilities in chemical processing as well as being cleaner. Many of the limitations in current catalytic hydrogenation stem from the inherently low solubility of H<sub>2</sub> in conventional solvents. Above the critical temperature of CO<sub>2</sub>, 31.6 °C, H<sub>2</sub> is completely miscible with CO<sub>2</sub>. It also offers the possibility of converting from batch to continuous processes, with the advantages of smaller reactors, lower inventories of chemicals and increased safety. Several groups have reported the use of continuous reactors for hydrogenation[66-74]. Our own work has focused on the hydrogenation of compounds of interest to the fine chemicals industry. We have shown that scCO<sub>2</sub> and supercritical propane can be used as solvents for the continuous supercritical hydrogenation of a wide range of organic functionalities [68, 69].

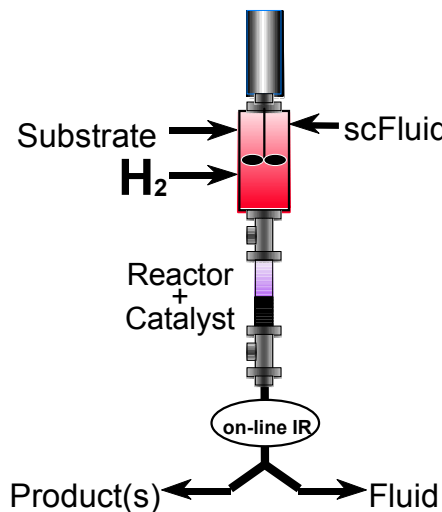


Figure 3. Schematic diagram of a supercritical flow reactor.

The organic substrate, H<sub>2</sub> and scCO<sub>2</sub> are mixed by the stirrer, and are then passed over a heterogeneous catalyst bed, such as Pd/Deloxan (a polyamino-siloxane support from Degussa), Figure 3. Depressurization of the system downstream gives phase separation of the CO<sub>2</sub> and organic products. Conditions can be optimised to give very high selectivity and efficiency in such a reactor. We have shown how this concept can be extended to other organic reactions, for example Friedel Crafts alkylation [75], etherification [76] using a solid acid catalyst and hydroformylation [77]. In each reaction, scCO<sub>2</sub> appears to offer significant advantages, as well as process intensification. Thus, supercritical hydrogenation of isophorone gives 99.6% selectivity for dihydro-isophorone [69], better than is achieved in most commercial hydrogenation processes for this compound. In the Friedel-Crafts reaction, there is high selectivity for mono-alkylation and long catalyst lifetime [75]. In hydroformylation, there is a very good selectivity and catalyst lifetime [77]. In all of the reactions, the products are recovered free from any liquid solvent, which greatly simplifies the subsequent work-up.

Near critical (ncH<sub>2</sub>O) and supercritical water (scH<sub>2</sub>O) have attracted much attention in the synthesis of metal oxides [4, 78, 79]. Most of the published work has been done in batch reactors, with limited control of the process. In contrast, flow reactors allow a better control of the experimental conditions. We have previously reported the synthesis of a large range of different nano-particulate single metal oxides in a flow reactor [80]. The materials, as fresh prepared, are crystalline, have very small particle sizes and a narrow size distribution. Flow reactors seem especially suitable for the synthesis of heterometallic compounds [78]. A solution containing a mixture of the metal salts at room temperature was mixed with a stream of water heated up to 400 °C by a pre-heater. After the mixing point, the mixture was cooled down immediately by a water cooler. Reaction temperatures at the mixing point were between 260 and 370 °C depending on the experiments. The pressure was kept constant and equal to 25 MPa by a back-pressure regulator (BPR). The high self-dissociation constant of water at near critical conditions allowed hydrolysis of the metal salts without addition of any base. The lower dielectric constant induced super-saturation and precipitation of small hydroxides, which underwent fast dehydration. The products were passed through a filter (to remove large aggregates) upstream of the BPR and were collected as suspensions. The solids were decanted and dried at 100°C. Examples include Ce<sub>1-x</sub>Zr<sub>x</sub>O<sub>2</sub> [80] and La<sub>2</sub>CuO<sub>4</sub> [81].

## EXPERIMENTAL TECHNIQUES

The prospects of carrying out experiments at high-pressure are often very discouraging to new workers in the field. Our group at Nottingham has developed a range of techniques to enable supercritical fluid experiments to be carried out on a small scale so that new ideas can be tested effectively, rapidly and, above all, safely. We have developed a range of miniature cells and components which together form a modular system. Even quite complicated apparatus can be assembled very easily from the basic modules [4, 82]. The high compressibility of supercritical fluids adds a whole new dimension to chemistry by allowing the solvent to be tuned. Unfortunately, it also adds an extra parameter which has to be optimised. The key to our work has been the use of spectroscopy, particularly infrared and Raman, to monitor processes in supercritical fluids [83, 84]. Reaction conditions can then be monitored in real time and conditions can be optimised much more effectively. In this way, quite wide areas of chemistry can be explored rapidly and the most useful applications of supercritical fluids can be identified.

## CONCLUSIONS

Working at high-pressure always introduces additional complications to any procedure. Therefore, the use of supercritical fluids in a particular process must be based on sound scientific reasons to justify the extra complexity. Fortunately, supercritical fluids offer a whole range of new opportunities to chemists. These opportunities are far more profound than merely complying with environmental legislation. The value of supercritical fluids lies in control. They allow materials and reactions to be manipulated more precisely, more effectively, and more efficiently than in conventional solutions. Supercritical science is inherently interdisciplinary. Scientists who are interested in applying supercritical fluids to their particular problem will find that workers in the field are willing to collaborate and are especially receptive to new ideas.

## ACKNOWLEDGEMENTS

We are grateful for the support of EPSRC Clean Technology Unit, the Royal Society, ICI, and the Royal Academy of Engineering for supporting work at Nottingham. We thank our colleagues, collaborators and coworkers for their help and advice and Mr. M. Guyler and Mr. K. Stanley for their technical assistance.

## REFERENCES

1. M. Poliakoff, P. J. King (2001), *Nature*, **412**, 125.
2. M. A. McHugh, V. J. Krukonis (1994), *Supercritical Fluid Extraction*, 2nd edn., Butterworth-Heinemann, Boston, MA.
3. P. G. Jessop, W. Leitner (1999), *Chemical Synthesis Using Supercritical Fluids*, Wiley-VCH, Weinheim.
4. J. A. Darr, M. Poliakoff (1999), *Chem. Rev.*, **99**, 495.
5. A. Cooper, S. Howdle (2000), *Materials World*, **8**, 10.
6. A. I. Cooper (2000), *J. Mater. Chem.*, **10**, 207.
7. D. Adams (2000), *Nature*, **407**, 938.
8. A. Kordikowski, D. G. Robertson, A. I. Aguiar-Ricardo, V. K. Popov, S. M. Howdle, M. Poliakoff (1996), *J. Phys. Chem.*, **100**, 9522.
9. A. Abbott, C. Eardley, J. Scheirer (1999), *J. Phys. Chem. B*, **103**, 8790.
10. J. L. Kendall, D. A. Canelas, J. L. Young, J. M. DeSimone (1999), *Chem. Rev.*, **99**, 543.
11. N. G. Smart, T. Carleson, T. Kast, A. A. Clifford, M. D. Burford, C. M. Wai (1997), *Talanta*, **44**, 137.
12. E. L. V. Goetheer, M. A. G. Vorstman, J. T. F. Keurentjes (1999), *Chem. Eng. Sci.*, **54**, 1589.
13. M. J. Clarke, K. L. Harrison, K. P. Johnston, S. M. Howdle (1997), *J. Am. Chem. Soc.*, **119**, 6399.
14. Y. Ikushima (1997), *Adv. Colloid Interface Sci.*, **71-2**, 259.
15. K. P. Johnston, K. L. Harrison, M. J. Clarke, S. M. Howdle, M. P. Heitz, F. V. Bright, C. Carlier, T. W. Randolph (1996), *Science*, **271**, 624.
16. E. D. Niemeyer, F. V. Bright (1998), *J. Phys. Chem. B*, **102**, 1474.
17. R. D. Smith (1988), *U.S. Patent*, No. 734,451.
18. C. A. Eckert, B. L. Knutson, P. G. Debenedetti (1996), *Nature*, **383**, 313.
19. J. W. Tom, P. G. Debenedetti (1991), *J. Aerosol Sci.*, **22**, 555.
20. P. M. Gallagher, V. J. Krukonis, L. J. VandeKieft (1991), *Proc. Second Intl. Symp. on Supercritical Fluids*, Johns Hopkins University, Boston, p. 45.

21. E. Reverchon (1998), *Proc. 5th Meeting on Supercritical Fluids*, Vol. T1, Nice, France, p. 221.
22. E. Reverchon, G. Della Porta, D. Sannino, L. Lisi, P. Ciambelli (1998), *Stud. Surf. Sci. Catal.*, **118**, 349.
23. S. D. Yeo, P. G. Debendetti, M. Radosz, R. Giesa, H.-W. Schmidt (1995), *Macromolecules*, **28**, 1316.
24. D. J. Dixon, K. P. Johnston (1993), *J. Appl. Poly. Sci.*, **50**, 1929.
25. T. W. Randolph, A. D. Randolph, M. Mebes, S. Yeung (1993), *Biotech. Prog.*, **9**, 429.
26. C. N. Field, P. A. Hamley, J. M. Webster, D. H. Gregory, J. J. Titman, M. M. Poliakoff (2000), *J. Am. Chem. Soc.*, **122**, 2480.
27. E. Reverchon, G. Della Porta (1999), *Powder Techn.*, **106**, 23.
28. E. Reverchon, G. Della Porta, D. Sannino, P. Ciambelli (1999), *Powder Techn.*, **102**, 127.
29. E. Reverchon (1999), *J. Supercrit. Fluids*, **15**, 1.
30. E. Reverchon, G. Della Porta, I. De Rosa, P. Subra, D. Letourneur (2000), *J. Supercrit. Fluids*, **18**, 239.
31. E. Reverchon, G. Della Porta, M. G. Falivene (2000), *J. Supercrit. Fluids*, **17**, 239.
32. E. Reverchon, G. Della Porta, P. Pallado (2001), *Powder Techn.*, **114**, 17.
33. J. G. Cai, Z. Y. Zhou, X. Deng (2001), *Chin. J. Chem. Eng.*, **9**, 258.
34. T. L. Chester, J. D. Pinkston, D. E. Raynie (1996), *Anal. Chem.*, **68**, 487R.
35. J. Jung, M. Perrut (2001), *J. Supercrit. Fluids*, **20**, 179.
36. A. Kordikowski, T. Shekunov, P. York (2001), *Pharm. Res.*, **18**, 682.
37. H. H. Y. Tong, B. Y. Shekunov, P. York, A. H. L. Chow (2001), *Pharm. Res.*, **18**, 852.
38. B. Y. Shekunov, J. Baldyga, P. York (2001), *Chem. Eng. Sci.*, **56**, 2421.
39. S. Beach, D. Latham, C. Sidgwick, M. Hanna, P. York (1999), *Org. Proc. Res. Dev.*, **3**, 370.
40. G. E. Gadd, P. J. Evans, S. Kennedy, M. James, M. Elcombe, D. Cassidy, S. Moricca, J. Holmes, N. Webb, A. Dixon, P. Prasad (1999), *Fullerene Sci. Technol.*, **7**, 1043.
41. A. S. O'Neil, J. M. Webster, C. Wilson, A. J. Blake, M. Poliakoff (2001), *Proc. 8th Meeting Supercritical Fluids*, M. Bernard, F. Cansell (eds.), ISASF, Bordeaux, in press.
42. C. L. Phelps, N. G. Smart, C. M. Wai (1996), *J. Chem. Ed.*, 1163.
43. M. J. Carrott, B. E. Waller, N. G. Smart, C. M. Wai (1998), *Chem. Commun.*, 373.
44. M. D. Samsonov, C. M. Wai, S.-C. Lee, Y. Kulyako, N. G. Smart (2001), *Chem. Commun.*, 1868.
45. S. M. Howdle, J. M. Ramsay, A. I. Cooper (1994), *J. Poly. Sci., Part B: Poly. Phys.*, **32**, 541.
46. M. J. Clarke, A. I. Cooper, S. M. Howdle, M. Poliakoff (2000), *J. Am. Chem. Soc.*, **122**, 2523.
47. S. G. Kazarian, B. L. West, M. F. Vincent, C. A. Eckert (1997), *Am. Lab.*, **29**, B18.
48. N. H. Brantley, S. G. Kazarian, C. A. Eckert (2000), *J. Appl. Polymer Sci.*, **77**, 764.
49. N. H. Brantley, D. Bush, S. G. Kazarian, C. A. Eckert, (1999), *J. Phys Chem. B*, **103**, 10007.
50. E. Bach, E. Cleve, J. Schuttken, E. Schollmeyer, A. W. Rucker (2001), *Col. Techn.*, **117**, 13.
51. E. Bach, E. Cleve, E. Schollmeyer (1998), *J. Textile Inst.*, **89**, 647.
52. E. Bach, E. Cleve, E. Schollmeyer (1998), *J. Textile Inst.*, **89**, 657.
53. E. Cleve, E. Bach, E. Schollmeyer (1998), *Angew. Makromolek. Chem.*, **256**, 39.
54. M. Poliakoff, S. M. Howdle, S. G. Kazarian (1995), *Angew. Chem. Intl. Ed. Engl.*, **34**, 1275.
55. A. I. Cooper, S. M. Howdle, C. Hughes, M. Jobling, S. G. Kazarian, M. Poliakoff, L. A. Shepherd, K. P. Johnston (1993), *Analyst*, **118**, 1111.

56. M. J. Clarke, M. Jobling, S. M. Howdle, M. Poliakoff (1994), *J. Am. Chem. Soc.*, **116**, 8621.
57. P. T. Anastas, T. C. Williamson (1998), *Green Chemistry*, Oxford University Press.
58. R. Noyori (1999), *Chem. Rev.*, **99**, 353.
59. P. G. Jessop, T. Ikariya, R. Noyori (1999), *Chem. Rev.*, **99**, 475.
60. R. S. Oakes, A. A. Clifford, C. M. Rayner (2001), *J. Chem. Soc. Perkin Trans. 1*, 917.
61. S. M. Howdle, M. A. Healy, M. Poliakoff (1990), *J. Am. Chem. Soc.*, **112**, 4804.
62. J. A. Banister, P. D. Lee, M. Poliakoff (1995), *Organometallics*, **14**, 3876.
63. P. D. Lee, J. L. King, S. Seebald, M. Poliakoff (1998), *Organometallics*, **20**, 524.
64. P. G. Jessop, Y. Hsiao, T. Ikariya, R. Noyori (1994), *J. Am. Chem. Soc.*, **116**, 8851.
65. P. G. Jessop, T. Ikariya, R. Noyori (1994), *Nature*, **368**, 231.
66. T. Tacke, S. Wieland, P. Panster (1996), *High Pressure Chemical Engineering*, P. Rudolph von Rohr, C. Trepp (eds.), Elsevier, Netherlands, p. 12.
67. K.-H. Pickel, K. Steiner (1994), *Proc. 3rd Int. Symp. Supercritical Fluids*, Strasbourg, France, p. 25.
68. M. G. Hitzler, M. Poliakoff (1997), *Chem. Commun.*, 1667.
69. M. G. Hitzler, F. R. Smail, S. K. Ross, M. Poliakoff (1998), *Org. Proc. Res. Dev.*, **2**, 137.
70. A. Bertucco, P. Canu, L. Devetta, A. G. Zwahlen (1997), *Ind. Eng. Chem. Res.*, **36**, 2627.
71. L. Devetta, P. Canu, A. Bertucco, K. Steiner (1997), *Chem. Eng. Sci.*, **52**, 4163.
72. J. W. King, R. L. Holliday, G. R. List, J. M. Snyder (2001), *J. Am. Oil Chem. Soc.*, **78**, 107.
73. M. B. O. Andersson, J. W. King, L. G. Blomberg (2000), *Green Chem.*, **2**, 230.
74. V. Arunajatesan, B. Subramaniam, K. W. Hutchenson, F. E. Herkes (2001), *Chem. Eng. Sci.*, **56**, 1363.
75. M. G. Hitzler, F. R. Smail, S. K. Ross, M. Poliakoff (1998), *Chem. Commun.*, 359.
76. F. R. Smail, W. K. Gray, M. G. Hitzler, S. K. Ross, M. Poliakoff (1999), *J. Am. Chem. Soc.*, **121**, 10711.
77. N. J. Meehan, A. J. Sandee, J. N. H. Reek, P. J. C. Kamer, P. W. M. N. van Leeuwen, M. Poliakoff (2000), *Chem. Commun.*, 1497.
78. T. Adschiri, K. Kanazawa, K. Arai (1992), *J. Am. Ceram. Soc.*, **75**, 1019.
79. Y. Hakuta, H. Terayama, S. Onai, T. Adschiri, K. Arai (1997), *Proc. 4th Int. Symp. Supercritical Fluids*, Sendai, Japan, p. 255.
80. A. Cabanas, J. A. Darr, E. Lester, M. Poliakoff (2000), *Chem. Commun.*, 901.
81. A. A. Galkin, B. G. Kostyuk, V. V. Lunin, M. Poliakoff (2000), *Angew. Chem.*, **39**, 2738.
82. S. M. Howdle, M. Poliakoff (1994), *NATO Advanced Study Institute Supercritical Fluids - Fundamentals for Application*, E. Kiran (ed.), Kluwer Academic Publishers, Dordrecht, pp. 527.
83. S. M. Howdle, M. W. George, M. Poliakoff (1999), *Chemical Synthesis Using Supercritical Fluids*, W. Leitner, P. G. Jessop (eds.), VCH, pp. 147.
84. S. J. Barlow, M. W. George, M. Poliakoff (2001), *Handbook of Vibrational Spectroscopy*, J. Chalmers, P. Griffiths (eds.), J. Wiley, Chichester.



## ELECTRIC FIELDS IN SOLVENT EXTRACTION

Hans-Jörg Bart

Institute of Thermal Process Engineering, University of Kaiserslautern,  
Kaiserslautern, Germany

Electric fields influence mass transfer and hydrodynamics in solvent extraction. The transfer of ionic species may be affected by external electrical fields or an ionic Helmholtz double layer near the interface. The latter one is induced by adsorbed ionic surfactants and its influence can be quantified and related to  $\xi$  potential measurements. This will be shown in detail with the extraction of organic acids, where negative layers repulse and positive ones attract the solute anion and thus change the mass transfer velocity. The aspects of electric migration due to external fields on basis of the Nernst-Planck equation will be discussed too. Hydrodynamic effects like formation, coalescence and break-up of the droplets are also affected by electrical fields, which are again related to a change in mass transfer behaviour as is expressed with several examples.

### INTRODUCTION

The driving forces in separation processes are usually based on chemical potentials. Additional forces like centrifugal, gravity, pressure forces and electrical gradients can promote and intensify a certain task. The latter ones are important for mass transport and diffusion of electrolytes and also influence coalescence and formation of droplets [1-6]. In contrast to this, in wide industrial use are only electrostatic coalescers in the oil industry to separate fine dispersed aqueous droplets from crude oil [7].

In the following, aspects of droplet hydrodynamics and mass transfer in an electrical field will be discussed in detail. A special focus is on ionic surfactants which adsorb at the liquid-liquid interface. Their influence on mass transfer may then be via a different mechanism. A blocking effect of adsorption layers in a diffusional transport regime is well known and results in a reduction of mass transfer [8-11] and even Marangoni instabilities [12,13] are found. However, in the kinetic mass transfer regime, both an enhancement and retardation of mass transfer [13] is with Gibbs surfactant layers. When extracting ionic species, ionic surfactants will induce an electrostatic double layer, which can be related to the  $\xi$ -potential. As a result, in addition to the chemical potentials, an electrostatic potential difference exists. In order to quantify these effects, a combination of electrostatic and chemical potential differences as driving force has to be considered [14]. In an alternative manner, electrostatic fields can be used to induce migration of ions to the interface, even in the kinetically controlled transfer regime [15]. Furthermore, electrohydrodynamics with single droplets or droplet swarms will predominately change the mean Sauter diameters compared to the interfacial area and thus the mass transfer characteristics [16].

## REACTIVE MASS TRANSFER WITH ELECTRIC FIELDS

### Equilibria

As a prerequisite to understand chemical kinetics, one should know beforehand the reactive phase equilibria. The dissociation and complexation behaviour of the aqueous and organic species have to be taken into account for a proper hydrodynamic description. Recent  $g^E$ -models [17, 18] based on the Pitzer model [19] are capable of describing the non-ideal behaviour of strong and weak electrolyte mixtures. As an example, the extraction of acetic acid (HAc) with tri-octylamine (TOA) in toluene compared to isododecane in the presence of sodium chloride will be discussed. In this system the following reactions will occur:



The following extractive reaction stoichiometry will be seen, where a and b are derived from independent spectrometric data [20] (bar indicates organic species) :



$$K_{ab} = \frac{\overline{\text{TOA}_b \cdot \text{HX}_a}}{(\text{HX})^a \cdot (\text{TOA})^b} \times \frac{\gamma_{\overline{\text{TOA}_b \cdot \text{HX}_a}}}{\gamma_{\text{HX}}^a \cdot \gamma_{\text{TOA}}^b} \quad (5)$$

The Hildebrand-Scott-parameters which account for the non-idealities of the organic complexes and the physically extracted compounds HAc,  $(\text{HAc})_2$  are shown in Table 1 and the Pitzer parameters can be found elsewhere [21]. On the basis of binary data, it is possible to predict the behaviour of the quaternary systems  $\text{H}^+$ ,  $\text{Na}^+$ ,  $\text{Ac}^-$ , TOA resp.  $\text{H}^+$ ,  $\text{Na}^+$ ,  $\text{Cl}^-$ , TOA. For the quaternary system  $\text{H}^+$ ,  $\text{Na}^+$ ,  $\text{Ac}^-$ ,  $\text{Cl}^-$ , TOA, a new compound  $\text{TOA}\cdot\text{HCl}\cdot(\text{HAc})_2$  has to be introduced to correlate the experimental data. Figure 1 depicts the distribution coefficient of the anions ( $P_{\text{anion}}$ ) as a function of the aqueous acetic acid molality. As could be shown experimentally, in accordance with theory that there is no influence of electric fields on the phase equilibria of ionic solutes in aqueous/organic systems [15, 22].

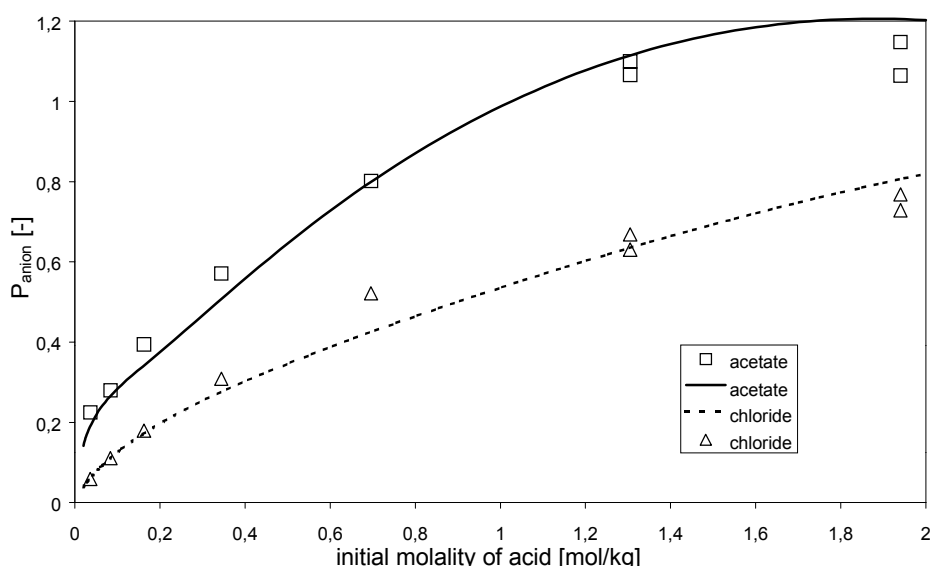


Figure 1. Distribution coefficient  $P$  of different anions as a function of the acetic acid concentration.

Table 1. Equilibrium constants and Hildebrand-Scott solubility parameters  $\delta$ .

System a:b	Toluene		Isododecane	
	$\ln K_{a:b}$ [-]	$\delta$ [cal $^{1/2}$ cm $^{-3/2}$ ]	$\ln K_{a:b}$ [-]	$\delta$ [cal $^{1/2}$ cm $^{-3/2}$ ]
toluene	-	8.9	-	-
isododecane	-	-	-	7.0
TOA	-	8.5	-	8.5
HA	2.726	10.1	1.883	10.1
(HA) $_2$	7.469	10.1	6.633	10.1
TOA·HA	4.778	9.567	3.768	9.567
TOA·(HA) $_2$	-	-	7.845	9.593
TOA·(HA) $_3$	14.953	9.610	-	-
TOA·(HA) $_4$	-	-	16.750	9.881

### Mass Transfer

In systems with liquid ion exchangers, the following transfer regimes may exist:

- chemical reaction regime,
- diffusion controlled regime and
- mixed regime, with both diffusional and kinetic resistances.

A discrimination can be made in a Lewis-cell type cell with a constant interfacial area. As is known, with increasing power input, diffusional resistances diminish as the diffusional boundary layer is reduced. The chemical reaction regime occurs when a plateau is reached when plotting initial mass transfer rates versus power input (rpm or vibrational rate), as is discussed in detail in literature [23, 24].

In order to model the chemical rate determined regime, the equilibrium equation with the 1:1 complex in a dilute system



can be split into the following molecular steps according to Danesi [25]:



The subscript "ad" represents those species which are adsorbed at the interface. Therefore, the first reaction step depicts protonation at the interface of an adsorbed TOA molecule. The first step is in quasi stationary equilibrium, which is in contrast to the two following rate determining steps:



This reaction represents the formation of an ion-pair molecule which is adsorbed at the interface. This molecule is then replaced by a fresh TOA molecule from the organic bulk phase in the third and last reaction step:



The interfacially adsorbed anion exchanger species are balanced according to Gibbs' law:

$$[\text{TOA}_{\text{ad}}] + [\text{TOAH}^+_{\text{ad}}] + [\text{TOAHA}_{\text{ad}}] = \frac{\alpha_m \cdot [\text{TOA}]}{\gamma_m + [\text{TOA}]} \quad (10)$$

$\alpha_m$  and  $\gamma_m$  are the adsorption constants which have been determined by interfacial tension measurements to be  $1.489 \times 10^{-3}$  for  $\alpha_m$  and  $8.156 \times 10^{-2}$  mol/kg for  $\gamma_m$  in isododecane [22]. To guarantee that the model is able to describe the equilibrium state ( $t = \infty$ ), the activities of the species are used instead of their concentrations. Combining the rate determining steps (Eqns. 7-9) and Eqn. (10) yields the kinetic rate equation,  $R'$ :

$$R' = \frac{(a_{\text{H}^+} \cdot a_{\text{A}^-} \cdot a_{\text{TOA}} - 1/K_{\text{EX}} \cdot a_{\text{TOAHA}}) \cdot (\alpha_m \cdot a_{\text{TOA}} / (\gamma_m + a_{\text{TOA}}))}{C_1 + C_2 \cdot a_{\text{H}^+} + C_3 \cdot a_{\text{H}^+} \cdot a_{\text{A}^-} + C_4 \cdot a_{\text{H}^+} \cdot a_{\text{TOA}} + C_5 \cdot a_{\text{TOA}} + C_6 \cdot a_{\text{TOAHA}}} \quad (11)$$

The constants  $C_1$  to  $C_6$  are functions of the kinetic parameters, where  $k_{-3}$  is calculated from  $K_{\text{EX}}$  ( $K_1 = 3.015$  [kg/mol],  $k_{-2} = 0.0108$  [ $\text{s}^{-1}$ ],  $k_2 = 83.07$ ,  $k_3 = 1814$ ,  $k_{-3} = 7192$  all in [kg/(mol s)]):

$$C_1 = \frac{k_{-2}}{k_2 \cdot k_3 \cdot K_1}, C_2 = \frac{k_{-2}}{k_2 \cdot k_3}, C_3 = \frac{1}{k_3}, C_4 = \frac{1}{k_2}, C_5 = \frac{1}{k_2 \cdot K_1}, C_6 = \frac{1}{k_{-2} \cdot K_{\text{EX}}} \quad (12)$$

At an equal interfacial covering of surfactants, the mass transfer of acetate is enhanced by cationic surfactants (DTACl, dodecyl trimethylammonium chloride), unaffected by nonionic surfactants (TX100 octylpolyethylene glycolether)<sub>10</sub>), and slowed down by anionic surfactants (NaLS, sodium lauryl sulfate; NaDdS, sodium dodecyl sulfate). This can be quantified when calculating the true interfacial concentrations,  $m_{\text{PG},i}$ , in the electrochemical double layer with the Boltzmann equation:

$$m_{\text{PG},i} = m_{\text{B},i} \cdot \exp \left( -\frac{z \cdot e \cdot \Psi_0}{k \cdot T} \right) \quad (13)$$

where  $m_{\text{B},i}$  is the bulk concentration,  $z$  is the valence,  $e$  is the elemental charge,  $k$  is the Boltzmann-constant and  $T$  represents the absolute temperature. The interfacial potential  $\Psi_0$  is calculated in accordance with the electric double layer theory after Stern [27], with the approximation of  $\Psi$  is about the zeta potential,  $\xi$  [28]:

$$\tanh \left( \frac{z \cdot e \cdot \Psi}{4 \cdot k \cdot T} \right) = \tanh \left( \frac{z \cdot e \cdot \Psi_0}{4 \cdot k \cdot T} \right) \cdot \exp (-\kappa \cdot x) \quad (14)$$

Here  $\kappa$  is the Debye-Hückel constant and  $x$  the distance to the interface which is estimated to be 3 nm [26] in the discussed system. There is a difference between bulk and interfacial concentrations in magnitudes, e.g., bulk pH = 3 and the interfacial pH = 1.0 after 60 min. at 298 K with  $7.5 \times 10^{-7}$  mol/m<sup>2</sup> NaDdS (or pH = 6.7 with DTACl) in a system of 1 % acetic acid, 10 % tri-n-octylamine in isododecane. This is similar for all ionic species involved according to the attraction/repulsion forces.

The model simulations in the kinetic regime are given in Figure 2. The nonionic surfactant TX100 has no influence; the cationic surfactant (DTACl) shows enhanced kinetics and the anionic surfactants (NaDdS, NaLS) a slowed down kinetics in a model derived in a surfactant-free environment. However, this interfacial polarization effect will dampen with higher ionic strengths and under system conditions where molecular or eddy diffusion dominate the mass transfer process in relation to the interfacial chemical reaction rate resistance.

The influence of the interfacial charge of the anionic surfactant NaDdS and the cationic surfactant DTACl on the transfer rate is shown in Figure 3. The upper limit in these experiments is given by the critical micelle concentration (cmc) of the components. In the range of lower interfacial charge, the systems behave as in Figure 2, an increase of the surfactant concentrations leads in the same way to a decrease of the initial flux for NaDdS as to an increase for DTACl. But at higher concentrations the mass transfer for the cationic surfactant increases non-proportionally with the interfacial charge and in a similar manner is even an increase instead of a stronger decrease in the anionic case. This can be explained by the constitution of the surfactant film at the interface, because an increase of the surfactant concentration leads to a transformation of the gas-analogous film into a condensed and strictly ordered surfactant film, which makes penetration and mass transfer easier. This is in accordance as with the other systems, e.g., water/acetone/toluene in the presence of NaDdS [29].

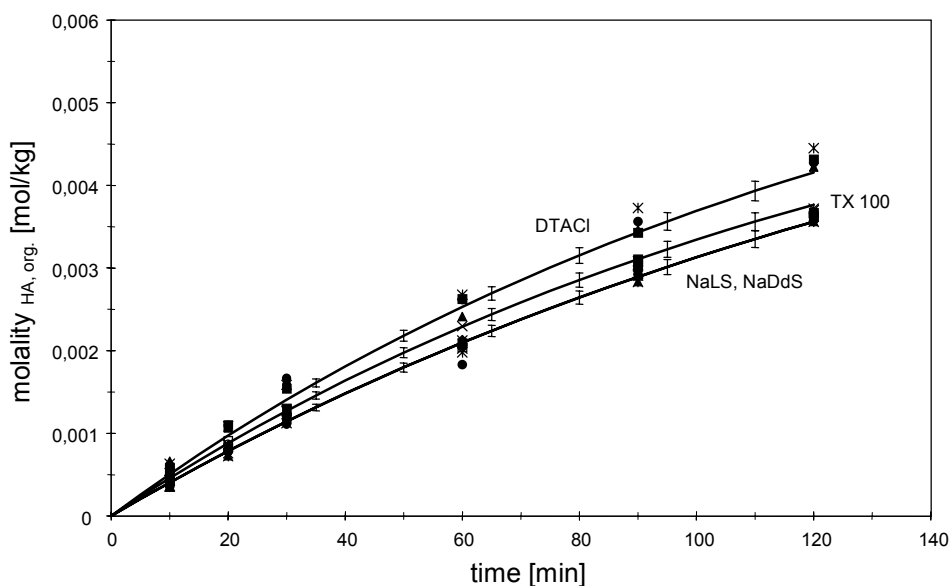


Figure 2. Model comparison at an equal amphiphile interfacial covering of  $7.5 \times 10^{-7} \text{ mol/m}^2$  (1 % acetic acid, 10 % tri-n-octylamine in isododecane, 298 K).

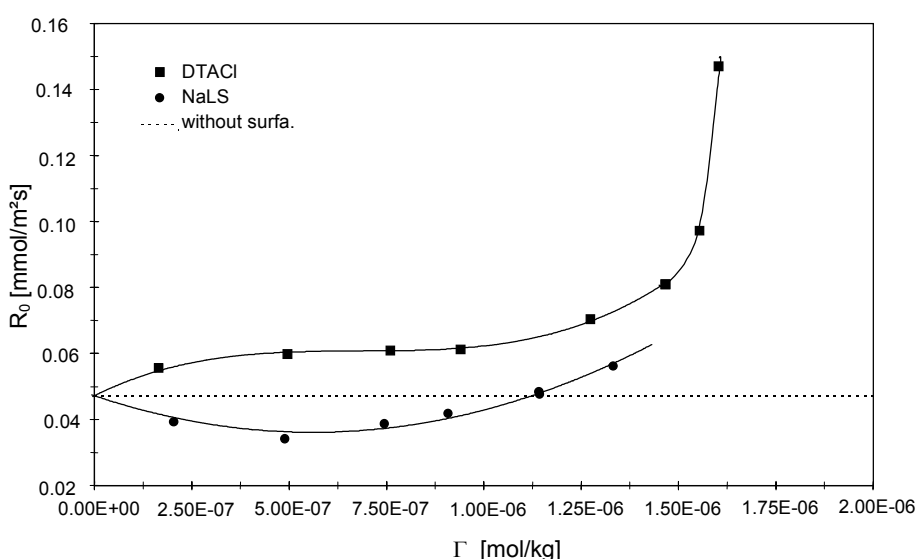


Figure 3. Influence of surfactants on the reaction limited regime, variation of  $\Gamma$  (1 % acetic acid, 10 % tri-n-octylamine in isododecane, 298 K,  $n_{or} = 180 \text{ rpm}$ ).

At surfactant concentrations near the cmc, an enhanced blocking of the surface and change of interfacial rheology and thus reduction of mass transfer may occur [30]. However, even low surfactant concentrations with species of high adsorption affinity may show a similar effect. As to this, it is essential to know the adsorption behaviour of single or mixed adsorption layers to properly predict their impact on interfacial transfer kinetics.

Similar results to those with surfactants can be obtained when applying DC fields. The mass transfer of ionic species in an electric field, when there is no current applied, is according to the Nernst-Planck equation [13]:

$$N_i = -D_i \cdot \nabla c_i - D_i \cdot c_i \cdot \nabla \ln \gamma_i + \frac{t_i}{Z_i} \cdot \sum_{j=1}^{n-1} Z_j \cdot (D_j - D_n) \cdot \nabla c_j \\ + \frac{t_i}{Z_i} \cdot \sum_{j=1}^n Z_j \cdot c_j \cdot D_j \cdot \nabla \ln \gamma_j \quad (15)$$

where  $z$  is the valence and the transference number of species  $j$  is:

$$t_j = \frac{\kappa_j}{\kappa} \quad (16)$$

composed from the equivalent conductivity  $\kappa_j$  of species  $i$  and of the mixture  $\kappa$ . In a reaction controlled regime the first two diffusion related terms are zero and only the migration term and its thermodynamic correction term remains. A comparison of the model calculations with a field-free system is in Figure 4 [15].

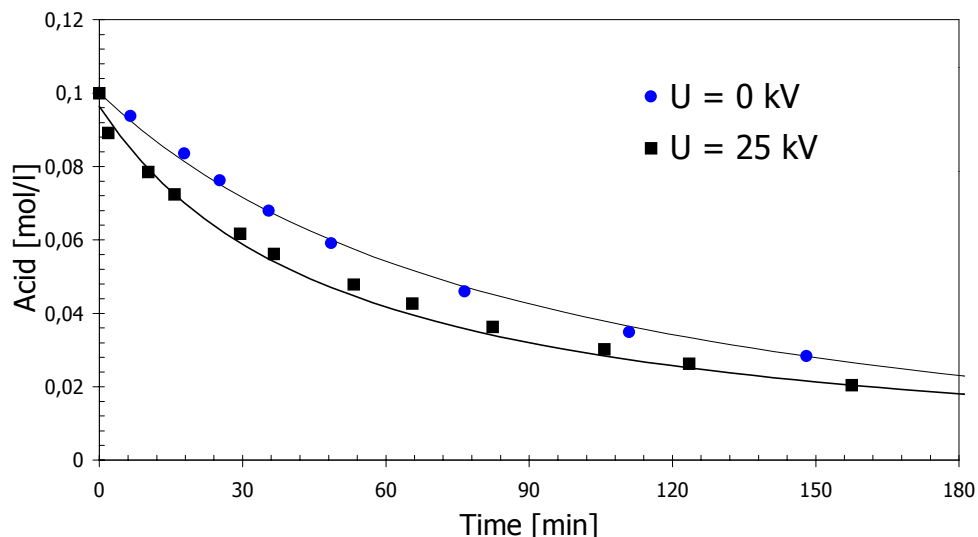


Figure 4. Mass transfer enhancement of acid extraction by a DC field (0.1 mol/l acid, 5 % tri-n-octylamine in toluene, 298 K).

The influence of electrical fields on hydrodynamics and thus on mass transfer has been discussed in an excellent review by Yamaguchi [3, 4]. It is thus possible to produce monodispersed droplet swarms up to extreme viscosities in the nano-scale (see Figure 5 [15]). Here the force balance on a nozzle leads to a disruption of drops. Under similar conditions breakage of an emulsion will occur, when due to polarization droplets form chains and will coalesce to bigger droplets [31]. Thus coalescence and droplet formation in the electric field is sensitive to minor changes in geometry or system parameters involved. This may be the one of the reasons that despite the attractiveness of the use of electrical fields there is no major application seen in conventional solvent extraction.

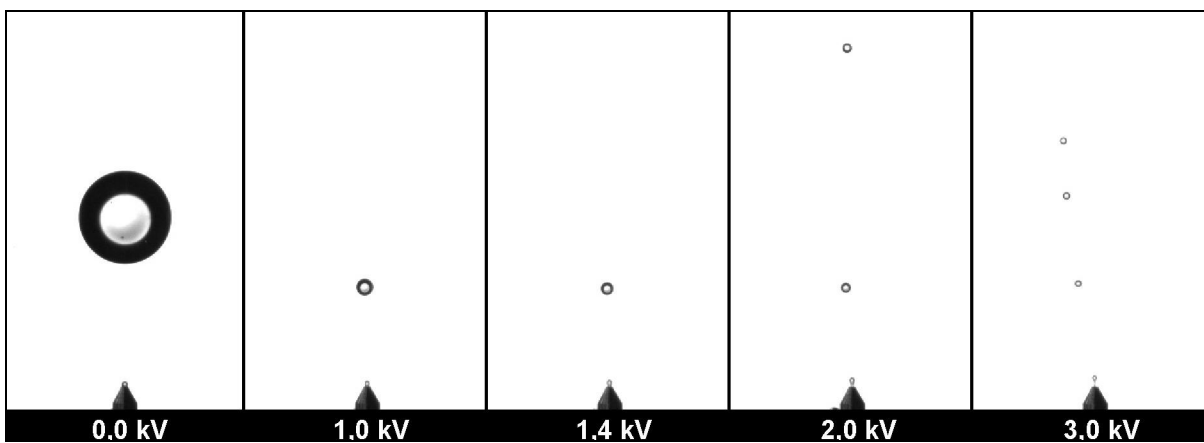


Figure 5. Drop formation in an AC field with silicone oil (298 K,  $\eta = 1000 \text{ mPas}$ ) in water.

## CONCLUSIONS

Solvent extraction is a mature unit operation and non-conventional applications like membrane extractors, aqueous-two-phase systems etc. are in the focus of research and development. As to that, electric fields as additional driving force for ionic species affect mass transfer rates. This can be due to ionic migration and polarization layers at the interface with a change of interfacial concentrations and thus reaction kinetic rates. Even Marangoni instabilities at charged interfaces have been reported. Moreover, electric fields have impact on droplet formation and coalescence and thus droplet diameter and mass transfer. As has been shown, even nanoscale particles can be produced with minor efforts and high reproducibility for special applications. As to that, there are several niches concerning electrical fields in solvent extraction, which are of industrial relevance and of interest for further exploitation.

## REFERENCES

1. C. H. Byers and K. R. Anarnath (1995), *Chem. Eng. Progr.*, 63-69.
2. A. D. Moore (1973), *Electrostatics and its Applications*, John Wiley, New York.
3. M. Yamaguchi (1994), *Liquid-Liquid Extraction Equipment*, J. G. Godfrey and M. J. Slater (eds.), Wiley, New York, pp. 585-624.
4. M. Yamaguchi (1994), *Electric Fields Applications*, T. Tsuda (ed.), Wiley-VCH, Weinheim, pp. 185-204.
5. J. D. Thornton (1968), *Rev. Pure Appl. Chem.*, **18**, 197.
6. T. C. Scott (1989), *Sep. Purif. Methods*, **18**, 65.
7. L. C. Waterman (1965), *Chem. Eng. Progr.*, **61** (10), 51-57.
8. V. G. Levich (1962), *Physicochemical Hydrodynamics*, Prentice Hall, New York.
9. J. T. Davies (1972), *Turbulence Phenomena*, Academic Press, New York.
10. W. Nitsch and G. Weber (1976), *Chem. Ing. Techn.*, **48**, 715.
11. K. L. Lin and K. Osseo-Asare (1986), *Recent Developments in Separation Science*, N. N. Li and J. M. Carlo (eds.), CRC Press, Cleveland, pp. 55-74.
12. D. Agbe and M.A. Mendes-Tatsis (2000), *Int. J. Heat Mass Transfer*, **43**, 1025-1034.
13. V. Mohan, K. Padnanabhan and K. Chandrasekharan (1993), *Adv. Space Res.*, **3** (5), 188-180.

14. H.-J. Bart (2001), Heat and Mass Transfer, D. Mewes and F. Mayinger (eds.), Springer, Heidelberg.
15. A. Wildberger and H.-J. Bart (2002), *Proc. International Solvent Extraction Conference ISEC 2002*, K. C. Sole, P. M. Cole, J. S. Preston, and D. J. Robinson (eds.), South African Institute of Mining and Metallurgy, Johannesburg, pp. 251 - 256.
16. G. Gneist and, H.-J. Bart (2002), *Proc. International Solvent Extraction Conference ISEC 2002*, K. C. Sole, P. M. Cole, J. S. Preston, and D. J. Robinson (eds.), South African Institute of Mining and Metallurgy, Johannesburg, pp 101 - 106.
17. T. J. Edwards, G. Maurer, J. Newman and J. M. Prausnitz (1978), *AIChE J.*, **24**, 966-976.
18. B. Mock, L. B. Evans and C. C. Chen (1986), *AIChE J.*, **32**, 1655-1664.
19. K. S. Pitzer (1973), *J. Phys. Chem.*, **77**, 268.
20. H. Ziegenfuß and G. Maurer (1994), *Fluid Phase Equilibria*, **102**, 211-255.
21. M. Roos and H.-J. Bart (2001), *J. Chem. Eng. Data*, in press.
22. C. Czapla (2000), Zum Einfluss von Grenzflächenladungen auf den Reaktionsmechanismus organischer Säuren bei der Reaktivextraktion, Shaker, Aachen.
23. W. Nitsch (1989), DECHHEMA-Monography, Vol. 114, VCH, Weinheim, 285-302.
24. V. Hancil, M. J. Slater and W. Yu (1990), *Hydrometallurgy*, **25**, 375-386.
25. P. R. Danesi, R. Chiarizia and M. Muhammed (1978), *J. Inorg. Nucl. Chem.*, **40**, 1581-1589.
26. C. Czapla and H.-J. Bart (2001), *Ind. Engng. Chem. Res.*, in press.
27. R. J. Hunter (1981), Zeta Potential in Colloid Science, Oxford University Press, New York.
28. J. Lyklema, J. de Coninck and S. Rovillard (1998), *Langmuir*, **14**, 5659-5663.
29. K. J. Hüttlinger and J. R. Schegk (1984), *Chem. Ing. Techn.*, **56** (7), 544-555.
30. S. Raatz and G. Härtel (2000), DECHHEMA-Monography, Vol. 136, Wiley-VCH, Weinheim, pp. 317-339.
31. R. Marr and J. Draxler (1992), Membrane Handbook, W. S. W. Ho and K. K. Sirkar (eds.), Van Nostrand Reinhold, New York, pp. 701-717.



## BEHAVIOR OF INTERFACIAL TENSION AT AN OIL-WATER INTERFACE IN THE PRESENCE OF AN APPLIED ELECTRICAL FIELD

Pardon K. Kuipa and Michael A. Hughes\*

Department of Chemical Engineering, National University of Science and Technology,  
Bulawayo, Zimbabwe

\*Department of Chemical Engineering, University of Bradford, Bradford, UK

The effect of an applied electrical field on the interfacial tension at an oil/water interface has been explored. Water droplets were formed at a charged nozzle immersed in a low dielectric constant liquid. The diameters of detaching water droplets were measured by recording the volume of a given number of detaching droplets and interfacial tension was calculated from the drop diameter using the Harkins-Brown formula. The oil phase in our studies was heptane with and without a metal extractant. The metal extractant studied was P50 (5-nonylsalicylaldoxime). In another range of experiments the oil phase was a mixture of heptane and octanol in different proportions. A decrease in drop diameter (corresponding to a decrease in the interfacial tension) with increased applied voltage was observed in all instances. The decrease in interfacial tension, which denotes the accumulation of charge carriers (ions) at the interface, depends upon the transport numbers and concentrations of the ions in the two phases and also upon the current. The behavior of interfacial tension in the presence of an applied electrical field is the same for systems with and without extractant in the organic phase. The purpose of the study was to gain an insight into the phenomenon of mass transfer intensification of a solute across an interface of two immiscible liquids by an electric field applied normal to the interface.

### INTRODUCTION

Several workers have studied a variation in the interfacial tension due to an applied potential difference between two immiscible liquids in contact. The observed interfacial tension changes were termed "electrocapillarity" by Lippman [1], who studied the mercury-aqueous phase interface. This phenomenon when observed at the interface of two immiscible nonmetallic liquid phases, such that one of the phases is electrically conducting whilst the other one is not, e.g. water-organic phase system, was termed "electroadsorption" by Guastalla [2]. The mercury-water interface behaves quite differently from the water-organic interface since the former is entirely polarizable, whilst the latter is hardly polarizable. At the mercury water interface, interfacial polarization takes place by the excess or deficit of electrons at the metal surface, which accompanies an unsymmetrical distribution of ions on the solution side of the interface. Charge transfer across the interface is negligible in such a system. Since we cannot expect the presence of free electronic charge at an oil-water interface, the polarization and thus formation of double layers in such a system is due only to unsymmetrical distribution of cationic and anionic species at the interface. The observed phenomenon is similar to concentration polarization as is clear from the passage of a small current in our systems.

When an electric field is applied across an ionic solution there are changes in concentration in the vicinity of the electrodes but not in the region between the electrodes. In a solvent extraction system there can be concentration changes at the liquid-liquid interface as well as at the electrodes, since an ion generally has different transport numbers in the two solvents. The change in charge carrier concentration at the liquid-liquid interface depends on the rate of flow of ions through the interface and the rate of diffusion to and from the interface. Accumulation of charges at the interface results in local variations in interfacial tension that may lead to instabilities of the Marangoni type to set in [3]. When both phases are perfectly insulating there is no free charge at the interface.

## EXPERIMENTAL PROCEDURE

### Reagents

The diluents (heptane and octanol) used for this work were of Analar grade. P50 (5-nonylsalicylaldoxime) was 98% pure. Water for interfacial tension measurements was double distilled.

### Interfacial Tension Measurements

The effective interfacial tension between the organic and aqueous phases in the presence of applied electric fields was measured by a modified drop volume method, equipped with a high voltage unit. Figure 1 is a schematic diagram of the experimental device used. The volume of liquid corresponding to a number of drops was read off from a 10 ml x 0.02 ml burette. All measurements were performed at room temperature,  $25 \pm 1^\circ\text{C}$ .

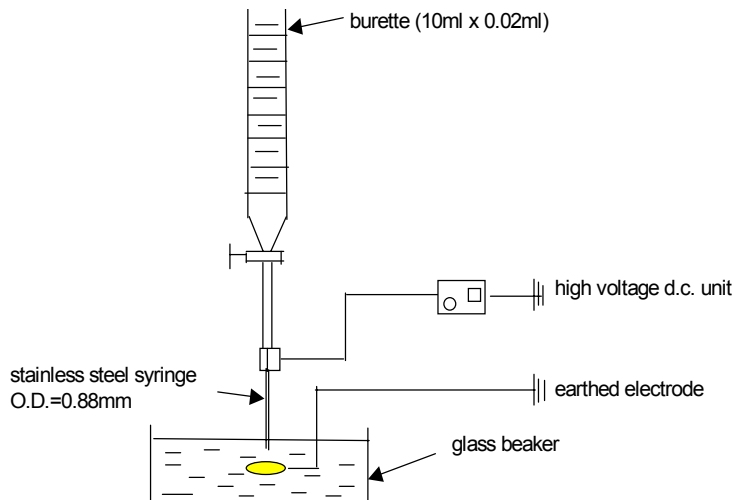


*Figure 1. Schematic of the apparatus used for interfacial tension measurements.*

The drop volume method was chosen because it could easily be adapted to work involving charged droplets. A variable voltage of up to 2000 V was applied to the base of the stainless steel syringe. The outside diameter of the tip of the stainless steel syringe was measured with a traveling microscope and found to be 0.88 mm; this is where the drops were formed. The disc electrode in the organic phase was earthed and its diameter was 25 mm. If the average drop volume at a particular electric field strength is known, the effective interfacial tension can be roughly estimated by the Harkins-Brown formula [4],

$$\gamma_e = V_E (\rho_1 - \rho_2) g F / r \quad (1)$$

where,  $\rho_1$  and  $\rho_2$  are the densities of the aqueous and organic phases respectively,  $r$  is the outer radius of the tip of the stainless steel syringe,  $g$  is the acceleration due to gravity,  $V_E$  is the average drop volume of the aqueous phase at a particular field strength and  $F$  is the Harkins-Brown correction term for the small amount of liquid that is left behind when the drop falls off the nozzle and is a function of  $V_E/r^3$ , the value of the latter ( $V_E/r^3$ ) ranging from 1.0 to 270 in this work. The range of values for  $V_E/r^3$  from 1.0 to 270 corresponds to drop volumes of  $0.68 \text{ mm}^3$  and  $184 \text{ mm}^3$  and  $F$  values of 0.2603 and 0.1979, respectively. Values of  $F$  were obtained through the extrapolation of tabulated values of  $F$  against  $v/r^3$ ,  $v$  being the drop volume [5]. In general,  $F$  values range from 0.159 to 0.2559 for corresponding  $v/r^3$  values of  $\infty$  and 0.403, respectively.

In this work, the use of the Harkins-Brown formula to estimate the effective interfacial tension in the presence of an applied electrical field assumes that the correction factor,  $F$ , is the same for a drop which is detaching from both an uncharged and a charged nozzle. In reality, the drop will be subjected not only to an acceleration force due to gravity but also to an acceleration force ( $QE_0$ ) due to the electric field, where  $Q$  is the droplet charge and  $E_0$  is the actual field strength acting on the drop. However, the use of the Harkins-Brown formula for the calculation of the effective interfacial tension of a system under electrical stress, *i.e.*, electrical field, will give a good approximation of the real values.

## RESULTS

The effect of the applied voltage on the effective interfacial tension of the liquid-liquid systems investigated in this work is summarized in Figures 2 and 3 for the water/0.05M P50/octanol-heptane diluent mixture and the water /octanol-heptane diluent mixture systems, respectively.

The effect of applied voltages on observed current passing between 0.05 M P50 octanol-heptane solvent mixtures and water with the high voltage electrode situated in the organic phase and the earthed electrode in the aqueous phase, is summarized in Figure 4.

## DISCUSSION

If thermodynamic equilibrium is assumed at the interface, the Gibbs adsorption isotherm extended to include the electrostatic term may be written as:

$$-d\gamma = \sum_i \Gamma_i RT d \ln C_i + q dV^a \quad (2)$$

where,  $\Gamma_i$  is the surface excess of the component  $i$ ,  $C_i$  its bulk concentration,  $q$  the surface charge density and  $V^a$  is the interfacial potential difference.  $R$  is the gas constant and  $T$  is the absolute temperature. For systems whose electrical conductance is high,  $V^a$  is approximately the same as the applied voltage  $V$ , whilst for the systems in our study the actual potential difference is different from the applied voltage so that

$$V^a = kV, \quad 0 < k < 1 \quad (3)$$

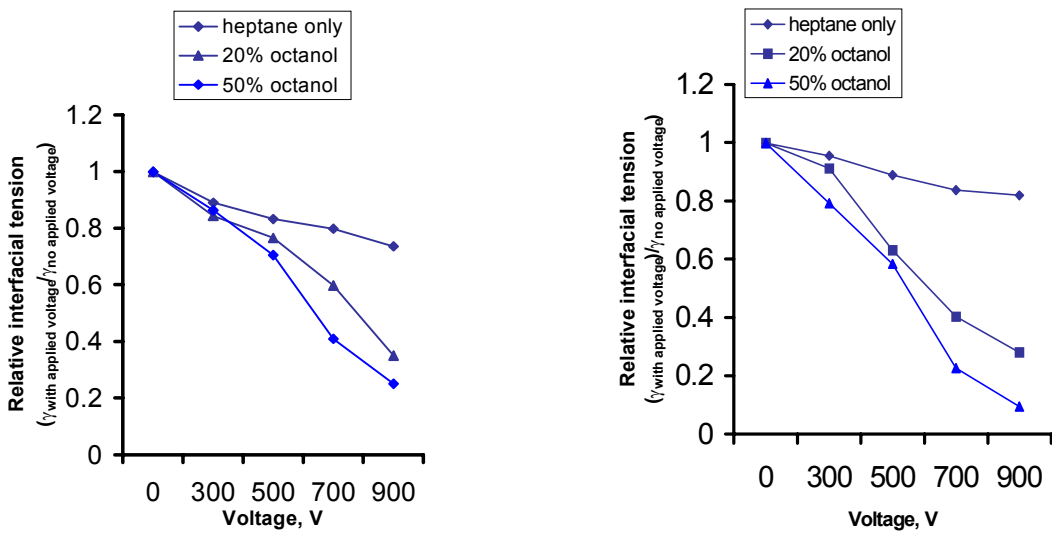


Figure 2. Voltage-interfacial tension relationship for the water/P50/(heptane-octanol mixture) system.

Figure 3. Voltage-interfacial tension relationship for the water/(heptane-octanol mixture) system.

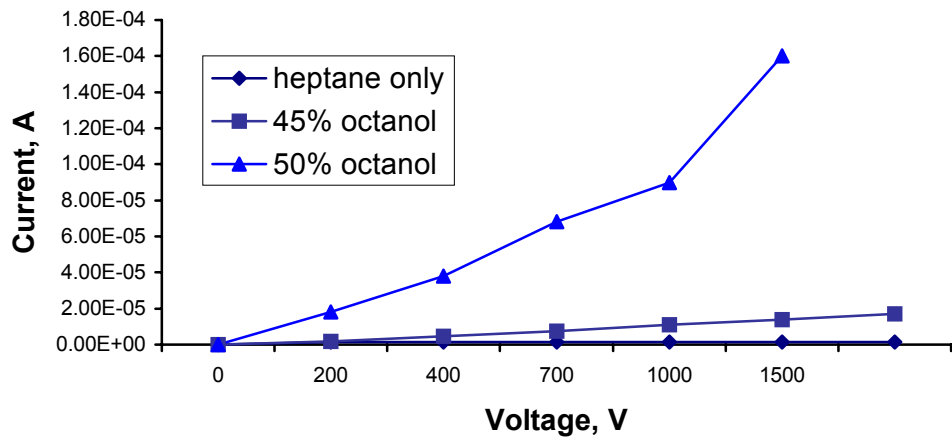


Figure 4. Effect of applied voltage on the observed current for the water/0.05M P50/(heptane-octanol mixture) system.

For a constant composition of the system  $d \ln C_i = 0$ , so that

$$-\left(\frac{d\gamma}{dV^a}\right)_{C_i} = q \quad (4)$$

where,  $q$  is the surface charge density. According to our results, for the systems studied, the interfacial tension decreases with increasing applied voltage ( $\gamma_{\text{with applied voltage}} < \gamma_{\text{without applied voltage}}$ ) so that the term in brackets in equation (4) is negative and thus  $q$  is positive. Then we have a picture of the interfacial double layer consisting of an array of cations on the aqueous side and that of surface-active agent anions on the oil side of the interface. These conclusions are based upon the Helmholtz double layer model. It is envisaged that the

systems studied will in real terms consist of the Gouy-Chapman diffuse double layers on both sides of the interface with the possibility of the Stern adsorption layer being formed if surface active components are present.

We have previously reported [6] that a change in the sign of the applied voltage does not result in a suppression or enhancement of the observed extraction rate across the liquid-liquid interface. This seems to imply that the surface-active anions accumulating on the organic side of the interface are not necessarily those of the extractant but rather those of the charge carriers, which are present within the bulk of the organic phase. The surface charge densities for our systems were not calculated, since the value of the constant,  $k$  in equation (3), is unknown.

For octanol-heptane diluent mixtures, we have reported previously [6] that extraction rates are enhanced with increasing applied voltages when the amount of *n*-octanol in the organic phase exceeds 45%. Octanol is readily adsorbed and desorbed at the oil/water interface [7] so that the cohesion and packing of the extractant are lowered. The fast renewals of extractant at the liquid-liquid interface resulting from the circulation produced by octanol desorption and adsorption is responsible for the extraction rate enhancement. Alternatively, the enhancement could be associated with the number of charge carriers associated with the octanol. Accumulation of charge carriers at the interface makes it unstable, resulting in fast renewal of extractant, since interfacial turbulence is created as a result of the instability.

## CONCLUSIONS

The behavior of interfacial tension in the presence of an applied electrical field is the same for systems with and without extractant in the organic phase. This could imply that the observed decrease in interfacial tension of a liquid-liquid system under the influence of an applied electrical field is due to the accumulation of charge carriers at the interface (owing to the difference in transport numbers of the charge carriers in each phase) rather than the accumulation of extractant at the liquid-liquid interface. Accumulation of charges at the interface makes the interface unstable, resulting in local variations in interfacial tension which may cause instabilities of the Marangoni type and consequently interfacial turbulence to set in. In solvent extraction systems the interfacial turbulence should result in better renewal of the interface between the aqueous and organic phases, thereby increasing the rates of mass transfer, as has been observed by several researchers.

## REFERENCES

1. G. Lippmann (1873), *Ann. Physik*, **149**, 546. Cited in M. Dupeyrat and J. Michel (1969), *J. Colloid Interf. Sci.*, **29** (4), 605-612.
2. J. Guastalla (1957), *Proc. 2nd Int. Congr. Surface Activity (London)*, **3**, 112. Cited in M. Blank (1966), *J. Colloid Interf. Sci.*, **22**, 51-57.
3. V. Mohan, K. Padmanabhan and K. Chandrasekharan (1983), *Adv. Space Research*, **3** (5), 177-180.
4. Findlay and J. A. Kitchener (1960), *Practical Physical Chemistry*, Longmans, London.
5. International Critical Tables (1928), Vol. 4, McGraw-Hill Book Co., Inc.
6. P. K. Kuipa and M. A. Hughes (1999), *Sep. Sci. Techn.*, **34** (13), 2679-2684.
7. J. T. Davies and E. K. Rideal (1963), *Interfacial Phenomena*, Academic Press, 2nd edn., London, pp. 334 and 337.



# INTERFACIAL ORIENTATION OF PORPHYRIN AT THE LIQUID-LIQUID INTERFACE USING UV-VIS EXTERNAL REFLECTION SPECTROSCOPY

Nobuaki Ogawa, Yoshio Moriya and Shinichi Nakata

Faculty of Engineering and Resource Science, Akita University, Akita City, Japan

The adsorption state of diprotonated tetraphenylporphyrin at the toluene-aqueous acid interface was investigated by the UV-vis external reflection (ER) spectroscopy. The degree of aggregation and the orientation angle were estimated to be 4 and 19°, respectively. The tilting orientation was supported by *p*-polarized spectrum where the 473 and 720 nm bands were observed positively and the 412 nm band negatively at a higher angle of incidence than Brewster's angle, which was explained by the assignments of bands and the interfacial selection rule. The ER method can yield not only a spectrum of the interfacial species itself, but also information on its interfacial orientation.

## INTRODUCTION

The *in situ* measurements of adsorbed species at the liquid-liquid interface may give us significant information relating to the states of aggregation and orientation, which may not occur in homogeneous bulk phase. In recent years, various spectroscopic methods for the measurements of interfacial adsorbed species have been facilitated remarkably. Two typical methods are attenuated total internal reflection (ATR) [1,2] and double phase transmission spectroscopy, represented by a centrifugal liquid membrane method [3] within the visible wavelength region.

The organic phase encountered in solvent extraction systems usually contains strongly light-absorbing solute, and hence the spectrum of interfacial species may be considerably affected by the absorption bands of organic bulk species. Our previous work [4], therefore, proposed the external reflection (ER) method, by which we could observe an ER spectrum with some negative absorption bands relating only to the interfacial adsorbed species, as for the diprotonated porphyrin in a *J*-aggregate at the toluene-4 M sulfuric acid interface.

In this report, we studied in detail the aggregation and orientation states of tetraphenylporphyrin (TPP) in diprotonated form adsorbed at the same liquid-liquid interface, based on the decreased absorbance in the organic phase with the interfacial adsorption. Furthermore, we obtained a characteristic spectrum of the interfacial adsorbed species in polarization ER spectroscopy and qualitatively discussed the interfacial orientation.

## EXPERIMENTAL

A simple device, which we call the Prism-Cell method, is schematically illustrated in Figure 1, and was used for the quantitative analysis of the interfacial adsorption. After pouring the same volume ( $3 \text{ cm}^3$ ) of 4 M sulfuric acid and toluene into the Prism-Cell, a small portion of the solution of TPP ( $20 \mu\text{M}$ ) was added stepwise and homogenized within the upper toluene phase. The absorption spectrum of organic phase ( $A_{\text{org}}$ ) (as well as that of aqueous phase ( $A_{\text{aq}}$ )) and the spectrum of ER (as well as ATR) were measured by a vertical shift of the prism-cell as described previously [4]. The fixed angle of incidence ( $\theta$ ) for ER and ATR measurements on our system were calculated to be  $\theta_E = 73.0^\circ$  and  $\theta_A = 74.4^\circ$ , respectively. A double beam spectrometer (Perkin Elmer, Lambda 40) was used for this work. For the measurement of polarized ER spectrum, a pair of dichroic sheet polarizer was inserted across the incident beam in front of the detector. The measurements were carried out at the temperature 298 K.

A new apparatus for the measurements of liquid-liquid interfacial species at the variable angle of incidence was devised as shown in Figure 2, which we call the Optical Fiber method. It was assembled from focus lens (L), optical fiber (F) of  $600 \text{ mm}\phi$  (purchased from Perkin Elmer), a Gran-Thompson polarizing prism (P) attached on the mobile arms around the center of a goniometer where a cylindrical cell of  $2 \text{ cm}$  diameter (C) was positioned by xyz-stage. The monochromatic light directly conducted into the fiber was reflected at the liquid-liquid interface, polarized by P, depolarized by a depolarizer (D) and then derived into detector. A single beam spectrometer (Hitachi 239) was used for this work. The measurements were carried out at room temperature,  $298 \pm 2 \text{ K}$ .

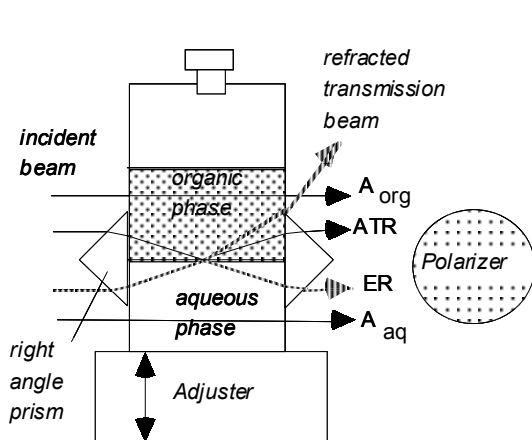


Figure 1. The Prism-Cell method.

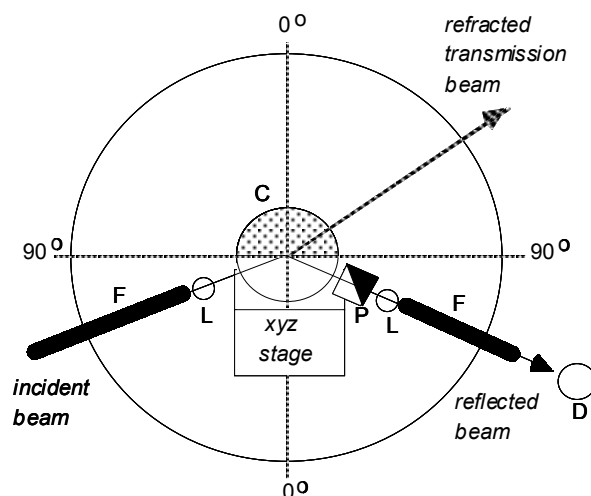


Figure 2. The Optical Fiber method.

## RESULTS AND DISCUSSION

### Interfacial Species and the ER spectrum

The tetraphenylporphyrin (TPP) is diprotonated and adsorbed at the toluene-4 M sulfuric acid interface as  $(\text{H}_2\text{TPP}^{2+})_n$  in a J-aggregate [5] under the equilibration represented as



where the subscript o and i refer to the bulk organic phase and the interface, respectively. The diprotonation and aggregation attained quasi-equilibrium after  $\sim 1 \text{ h}$ , and the ER spectrum measured by the Prism-Cell method with no polarizer was observed in the same manner as described previously [4]. That is, the negative absorption bands at 720, 473 and 412 nm were observed without the interference of strong Soret band in the organic bulk phase as shown in Figure 3.

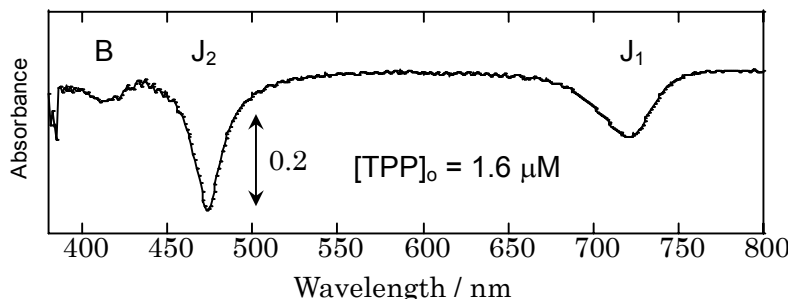


*Figure 3. External reflection spectrum of J-aggregate.*

For understanding the origin of spectral bands, we can refer to the discussion on the J-aggregate of water-soluble tetra(4-sulfophenyl) porphyrin ( $\text{TPPS}^{4-}$ ) in acidic aqueous media [6]. According to the work, two absorption bands at 707 nm (J<sub>1</sub> band) and 492 nm (J<sub>2</sub> band) were assigned to the characteristic transition of linear oscillator polarized in the long axis of rod-like aggregate ( $(\text{H}_2\text{TPPS}^{2+})_n$ ,  $n=11$ ) in a slipped face-to-face stacking structure where the participation of inter-porphyrin charge resonance excited states should be taken into account. Another diffuse absorption band around at 420 nm (B band) was assigned to the transition inner pyrrole ring plane (in the short axis), where the counterpart of the 491 nm band of porphyrin Soret origin was appeared. In our spectra, the former two should correspond to the bands at 720 nm (J<sub>1</sub> band) and 473 nm (J<sub>2</sub> band), and the later to the band at 412 nm (B band).

#### **Estimation of Orientation Angle and the Degree of Aggregation**

The spectra of ER and  $A_{\text{org}}$  were measured under the varied conditions of the initial concentrations of TPP,  $[\text{TPP}]_0$ , as well as that of initial solution  $A_{\text{soln}}$ , in order to analyze the saturated interfacial concentration of the  $\text{H}_2\text{TPP}^{2+}$  and the degree of aggregation ( $n$ ) for the  $(\text{H}_2\text{TPP}^{2+})_n$  in our experimental system. Absorption intensity at the minimum absorption wavelength ( $\lambda_{\text{min}}/\text{nm}$ ) was represented by  $\Delta A_E^{\lambda}$  hereafter, which was estimated by the difference between the absorbance at the  $\lambda_{\text{min}}$  and that at 530 nm where no band was observed. The ratio of the  $\Delta A_E^{\lambda}$  among the three bands was constant in the concentration region of  $0.2 < [\text{TPP}]_0/\mu\text{M} < 2.5$ . It means all of the three bands belong to only one species and also suggests that the interfacial orientation is consistent in the concentration region.

The interfacial concentration ( $\text{mol cm}^{-2}$ ) of the  $\text{H}_2\text{TPP}^{2+}$  could be estimated from the reduced absorbance in the organic phase by neglecting a trace amount of aqueous species, and by taking into account the organic bulk volume  $V_o$  ( $\text{dm}^3$ ) and the interfacial area  $S_i$  ( $\text{cm}^2$ ). The relation between the  $\Delta A_E^{473}$  and the interfacial concentration of the  $\text{H}_2\text{TPP}^{2+}$  was shown in Figure 4, where a linear relation was observed in the lower concentration region. On the assumption of a monolayer adsorption state, the saturated interfacial concentration was estimated to be  $2.67 \times 10^{10} \text{ mol cm}^{-2}$ . The value means the occupied area per molecule to be  $0.63 \text{ nm}^2$  at the interfacial saturation. When a roughly estimated value of  $3 \text{ nm}^2$  was used as a molecular area ( $a$ ) occupied by  $\text{H}_2\text{TPP}^{2+}$  from the value  $3.2 \text{ nm}^2$  as that for tetrakis(*N*-methyl-4-pyridyl)porphine [7], the orientation angle of the pyrrole ring plane against the surface normal to be  $12^\circ$  [8], though a different value  $19.4^\circ$  was obtained by a value of  $a=1.9 \text{ nm}^2$  from the molecular mechanics (MM2) calculation [3]. In any event, the pyrrole ring plane must be appreciably tilting at the interface.

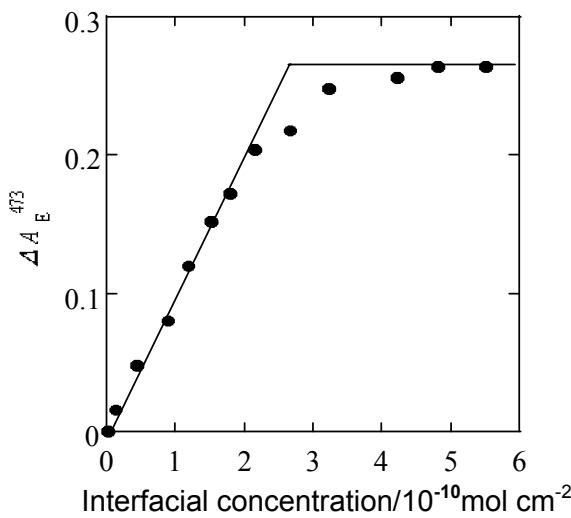


Figure 4. Intensity of ER absorption at 473 nm vs. interfacial concentration

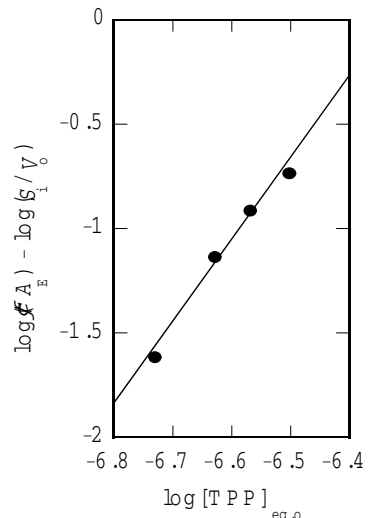


Figure 5. Determination of the degree of aggregation.

The degree of aggregation ( $n$ ) was estimated using data within the low concentration region. The quasi-equilibration constant  $K$  for Eq. (1) would be represented as

$$K = [(\text{H}_2\text{TPP}^{2+})_n]_i [\text{TPP}]_{e,o}^{-n} [\text{H}^{+}]^{-2n}, \quad (2)$$

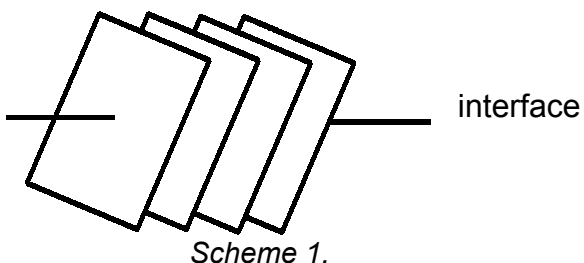
using the equilibrated concentrations of TPP in the organic phase ( $[\text{TPP}]_{e,o}$ ). The value of  $\Delta A_E^\lambda$  could be expressed by

$$\Delta A_E^\lambda = \rho n [(\text{H}_2\text{TPP}^{2+})_n]_i (S_i/V_o) \quad (3)$$

where the  $\rho$  refer to a coefficient ( $M^{-1}$ ) at  $\lambda$ . Then we could obtain the following equation:

$$\log(\Delta A_E^\lambda) - \log(S_i/V_o) = n \log[\text{TPP}]_{e,o} + \log(\rho n K) + 2n \log[\text{H}^+] \quad (4)$$

where the last two terms could be constant under our experimental conditions. The plot of  $\log(\Delta A_E^{473}) - \log(S_i/V_o)$  vs.  $\log[\text{TPP}]_{e,o}$  within the range  $0.18 < [\text{TPP}]_{e,o}/\mu\text{M} < 0.32$  was shown in Figure 5. The plot gave a slope 3.9, hence the J-aggregate could be represented as  $(\text{H}_2\text{TPP}^{2+})_4$  [8]. Therefore, we can imagine the interfacial adsorption state of the J-aggregate as drawn in Scheme 1.



### Measurements of Polarized Spectra

The polarized ER spectra were measured by the Prism-Cell method with polarizer. Figure 6 shows the s- and p-polarized ER spectra (where a signal around 550 nm is not a spectral band) at the fixed angle ( $73^\circ$ ) of incidence by the Prism-Cell method under the condition of initial concentration  $[\text{TPP}]_0 = 1.6 \mu\text{M}$ . In the s-polarized spectrum denoted by s in Figure 6, the absolute intensities of  $J_1$  and  $J_2$  bands were strengthened while that of B band was reduced as compared with the spectrum depicted in Figure 3. In the p-polarized spectrum denoted by p in Figure 6, on the other hand, the two bands of  $J_1$  and  $J_2$  appeared with positive absorbance while the B-band was negatively strengthened [8]. This positive/negative band observation may be the first example observed in the liquid-liquid boundary system, as far as we know.

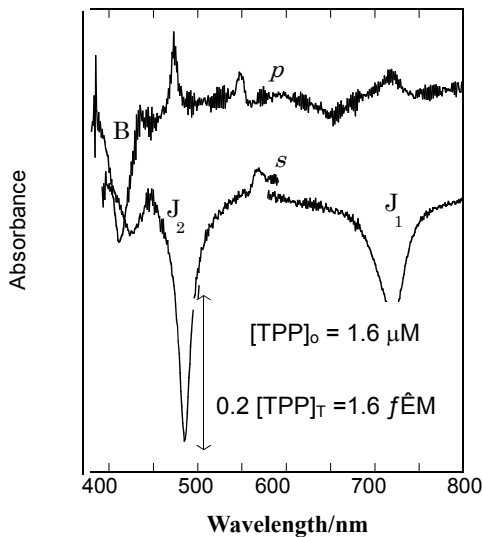


*Figure 6. The s- and p-polarized ER Spectra of interfacial species (by the Prism-Cell method).*

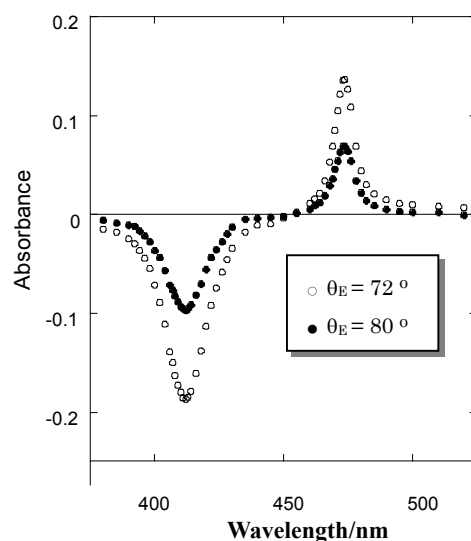


*Figure 7. The p-polarized ER spectra at the angle of incidence 72° and 80° (by the Optical Fiber method).*

The ER spectroscopic measurements, in general, suffer from the defect that the reflection factor at the interface may be low and produce a low ratio of signal/noise (S/N). It was amplified especially in the *p*-polarized spectrum measured by the Prism-Cell method using double beam spectrometer as depicted in Figure 6. Therefore, some measurements for *p*-polarized spectra were carried out also by the Optical Fiber method (see Figure 2) using a single beam spectrometer. The reflection intensities of blank ( $I_0$ ) and of sample ( $I$ ) were measured, respectively, within 380-520 nm at  $\theta_E = 72^\circ$  and  $80^\circ$ , and then the absorbance value as  $\log(I_0/I)$  was plotted against the wavelength. Figure 7 represents the *p*-polarization spectra measured after the contact of the same volume ( $4 \text{ cm}^3$ ) of 4 M sulfuric acid and  $1 \mu\text{M}$  TPP solution within a cylindrical cell. In the figure, a positive absorption band ( $J_2$ ) and a negative one (B) were clearly shown, where the intensity of both  $J_2$  and B at  $\theta_E = 72^\circ$  was higher than that at  $80^\circ$ .

#### Qualitative Orientation using the Interface Selection Rule

The observation of positive/negative absorption bands for surface-boundary substances can be an intrinsic phenomenon, which appears only within the *p*-polarized ER method. The feasibility of the positive/negative appearance was shown by Hansen's approximate formulae for the three phase system in the literature [9]. Using the IR-ER method for the LB film of cadmium stearate on GaAs substrate, Hasegawa [10] showed that the characteristic IR bands of functional groups appeared with positive/negative absorbance according to the interface selection rule [9] where absorption bands could intensified when the  $\theta_E$  approached the Brewster's angel ( $\theta_B$ ), and also that the orientation angle against the surface normal could be determined by the use of anisotropic principle [10]. Taking into account the difficulties of IR-ER measurements for the oil-water system, it will be very useful for us to get spectral information on the interfacial molecular orientation by a polarized vis-ER measurement. Therefore, our new observation of *p*-polarized ER spectrum with positive/negative bands will be significant for the qualitative orientation analysis of interfacial species, from where the sense of electronic transition moment for each of chromophores will be obtained.

According to the interface selection rule for ER method, the positive absorption band of  $J_2$  as well as  $J_1$  could be assigned to the chromophores having a parallel electron-transition moment to the interface while another band B to that having a perpendicular moment under our experimental condition of  $\theta_E > \theta_B$  ( $47.4^\circ$  for our interfacial system). The decrease tendency of absorbance at the higher angle of incidence ( $80^\circ$ ) in Figure 7 was consistent with the interface selection rule already mentioned. Then, it would be concluded that the pyrrole ring plane of  $\text{H}_2\text{TPP}^{2+}$  in *J*-aggregate must be oriented vertically or obliquely against the interface, since the

B-band has already assigned as the electron transition inner pyrrole ring plane. Therefore, the tilting orientation model depicted in Scheme 1 was supported by the observation of *p*-polarization ER spectroscopy, though a quantitative analysis on the orientation by ER spectroscopy would have to be carried out by a method as shown in the literature [11]. We also did the preliminary experiment for a porphyrin in dodecane-aqueous acid system. In detail, we will discuss the data in near future.

## CONCLUSIONS

The application of ER method to *in situ* measurements of a liquid-liquid interface enables us not only to obtain a spectrum of an interfacial species itself, without any interference of organic bulk phase, but also to have much information about the interfacial molecular orientation. Thus, the degree of aggregation and orientation angle of diprotonated tetraphenylporphyrin adsorbed at the liquid-liquid interface were estimated. Furthermore, a tilting orientation model was supported by the *p*-polarized ER spectrum.

## REFERENCES

1. J. M. Perera, J. K. McCulloch, B. S. Murray, F. Grieser, and G. W. Stevens (1992), *Langmuir*, **8**, 366-368.
2. R. Okumura, T. Hinoue, and H. Watarai (1996), *Anal. Sci.*, **12**, 393-397.
3. H. Nagatani and H. Watarai (1998), *Anal. Chem.*, **70**, 2860-2865.
4. Y. Moriya, N. Ogawa, T. Kumabe, and H. Watarai (1998), *Chem. Lett.*, 221-222.
5. Y. Chida and H. Watarai (1994), *Bull. Chem. Soc. Jpn.*, **69**, 341-347, and references therein.
6. O. Ohno, Y. Kaizu, and H. Kobayashi (1993), *J. Chem. Phys.*, **99**, 4128-4139.
7. M. T. Martin, I. Prieto, L. Camacho, and D. Mobius (1996), *Langmuir*, **12**, 6554-6560.
8. Y. Moriya, R. Amano, T. Sato, S. Nakata, and N. Ogawa (2000), *Chem. Lett.*, 556-557.
9. W. N. Hansen (1970), *Symp. Faraday Soc.*, **4**, 27-35.
10. T. Hasegawa, S. Takeda, A. Kawaguchi, and J. Umemura (1995), *Langmuir*, **11**, 1236-1243, and references therein.
11. E. Okamura, T. Hasegawa, and J. Umemura (1995), *Biophys. J.*, **69**, 1142-1147.



## MASS SPECTROMETRY AND LASER-MICROSCOPY FOR THE STUDY OF INTERFACIAL REACTION IN SOLVENT EXTRACTION SYSTEMS

Hitoshi Watarai

University of Osaka, Toyonaka, Japan

For the study of formation reactions of metal-complexes at the liquid-liquid interfaces of solvent extraction systems, new experimental approaches using mass spectrometry and laser-induced fluorometry of micro-flow two-phase systems were developed. Mass spectrometry of the directly introduced two-phase micro-flow system can measure the compositions or structures of complex species formed in the interface as well as in the bulk phases. In the extraction of Cu(II) with a pyridylazo extractant (L), the formations of  $\text{CuL}^+$  and  $\text{CuL}_2$  were detected simultaneously. A remarkable solvent effect was found in the distribution among the species measured by this method. On the other hand, laser-induced fluorometry of a two-phase sheath flow system succeeded in measuring fast interfacial reactions. In the extraction of Zn(II) with *n*-alkyl substituted oxine, the interfacial complexation within 5 ms could be measured.

### INTRODUCTION

Interfacial reaction has been recognised as an important reaction step which determines kinetic extraction mechanisms of metal ions [1]. Some specific reactions were found at liquid-liquid interfaces, for example, the formation of the binuclear complex of europium(III) [2] and the formation of the aggregate of Pd(II)-binding porphyrins [3]. For the development of interfacial chemistry of liquid-liquid interfaces, it is necessary to invent new measurement methods for interfacial reactions. So far, we have developed various measurement methods including a high-speed stirring method [4] and a centrifugal liquid membrane method [5].

In the present report, we describe two novel methods developed for the measurement of interfacial reactions: two-phase micro-flow electrospray ionization/ mass spectrometry and two-phase sheath flow/laser-induced fluorometry. These two methods can afford new information which has never been obtained by the other techniques.

Electrospray ionization (ESI) is a versatile and effective ionization technique for liquid samples for various mass spectrometric (MS) measurements. Advantages of ESI/MS in solution chemistry research are well recognised because of its high potential in structural identification or chemical speciation of the compounds in a dilute solution. In some cases, chemical equilibria and kinetics of complexation in solution could be discussed by ESI/MS. However, the solvents used in ESI/MS are usually limited to polar or protic solvents such as methanol, acetonitrile, dimethylsulfoxide and water. Non-polar organic solvents such as heptane and toluene, which are used very often in solvent extraction of metal ions, cannot be introduced directly to the ESI, because of their very low conductivities [6]. If these kinds of inert solvents could be used in ESI/MS, the realm of MS measurement will be significantly extended. In the present study, a novel method was invented which introduced an inert organic solvent phase into ESI/MS by producing organic droplets in a flowing aqueous phase at the position just prior to the ionization.

Various kinetic measurement methods have been developed for the study of extraction rates and complexation at the liquid/liquid interface. For example, the two-phase stopped flow method has succeeded in measuring the interfacial reaction in a time range of 0.1 s to a few seconds [7]. The centrifugal liquid membrane method and the high-speed stirring method proved to be useful for measurements of processes longer than several seconds. However, for fast reactions that finish within several ms, the previous methods cannot be applied. In the present study, laser-induced fluorometry of a two-phase sheath flow system was invented for the measurement of the interfacial complexation rates within 5 ms.

## EXPERIMENTAL

### Two-Phase Micro-Flow Electrospray Ionisation/Mass Spectrometry

The device for the two-phase micro-flow electrospray ionization was made by using a stainless steel outer capillary (0.4 mm o.d., 0.2 mm i.d.) and an inner silica capillary (0.158 mm o.d., 0.050 mm i.d.). A schematic drawing of the device is shown in Figure 1. The tip of the silica capillary was made as fine as 13 µm o.d. and 7 µm i.d. by pulling it under heating with a CO<sub>2</sub> laser (SYNRAD, 10.5 µm, 12.0 W). The silica capillary tip was positioned about 1 mm inside of the tip of the stainless capillary. Water-saturated toluene phase containing 1.0 x 10<sup>-3</sup> M 2-(5-bromo-2-pyridylazo)-5-diethylaminophenol (5-Br-PADAP) was pumped into the inner silica capillary with a flow rate of 0.001- 0.02 ml/h. Into the stainless steel capillary, 5.0 x 10<sup>-6</sup> M Cu(II) in aqueous 0.0010 M acetic acid was introduced from the tee connector with the flow rate of 0.1 ml/h as an outer phase. For the pumping of both phases, syringe pumps (Harvard 11) were used. A high voltage of 4.4 kV was applied to the stainless steel for the generation of electrospray. The ESI interface was positioned about 2 cm apart from the inlet hole in the interface (controlled at 600 V) of the TOF/MS (Jaguar, Sensar, Utah). Nitrogen curtain gas was flowed at the rate of 1000 ml/min between the interface and a nozzle positioned inside the interface. The nozzle voltage was changed in the range of 100 – 500 V and the voltage in the skimmer was set at 70 V.

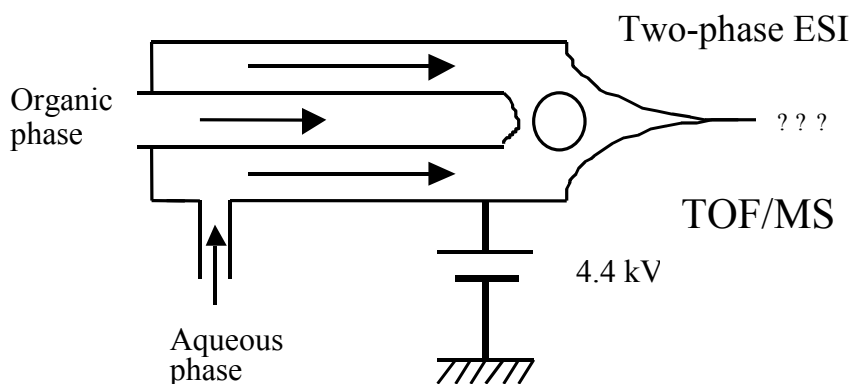


*Figure 1. Schematic drawing of the electrospray ionization interface of the two-phase micro-flow oil/water system.*

### Two-Phase Sheath Flow/Laser-Induced Fluorometry [8]

Figure 2 is the schematic representation of the fluorescence measurement cell of the two-phase sheath flow system. The inner phase is the organic solution flow and the outer phase is the aqueous solution flow. When the linear velocities of two solutions are matched, a stable and turbulence-free two-phase flow was formed. When these conditions were satisfied, the interface was regarded as a steady interface except moving from left to right in Figure 2. In this configuration, the distance along the flows from the capillary outlet can be

converted to the reaction time at a constant linear velocity. This unique feature of the sheath flow system allows us to integrate fluorescence at a certain distance for a long time. The inside cross section of the quartz cell was  $250\text{ }\mu\text{m} \times 250\text{ }\mu\text{m}$  square, and one side of the cell wall was scraped for the observation with a high NA objective. The organic solution was introduced into the cell through a fused silica capillary, whose inner and outer diameters were  $50\text{ }\mu\text{m}$  and  $150\text{ }\mu\text{m}$ , respectively, and whose outlet was narrowed to  $30\text{ }\mu\text{m}$  by pulling under irradiation with a CO<sub>2</sub> laser. The cell was placed on the stage of an inverted microscope (TE300, Nikon).

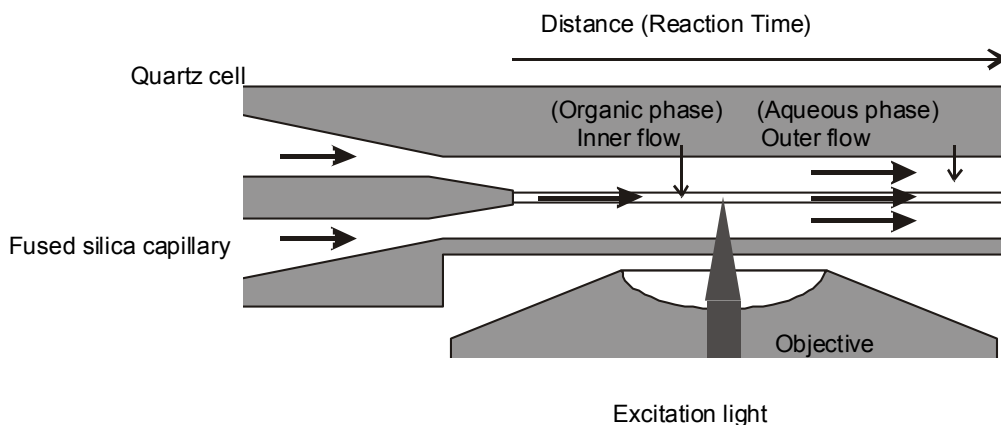


*Figure 2. Schematic representation of the laser-induced fluorometric measurement cell of the two-phase sheath flow extraction system [8].*

In the present study, the 1-butanol/water system was employed as an extraction solvent due to its low interfacial tension ( $1.8\text{ mN m}^{-1}$ ). When the inner organic phase is a solvent with higher interfacial tension such as toluene ( $36.2\text{ mN m}^{-1}$ ), the organic phase tended to become droplets at a low flow rate. The extraction system of Zn<sup>2+</sup> with 5-octyloxymethyl-8-quinolinol (Hocqn) was chosen as a test sample, because the complex formed was highly fluorescent [9]. To detect quite small amounts of the complex, laser-induced fluorescence microscopy was employed.

The organic solution was  $1.3 \times 10^{-3}\text{ mol dm}^{-3}$  Hocqn in 1-butanol, and the aqueous solution containing  $1.1 \times 10^{-2}\text{ mol dm}^{-3}$  ZnCl<sub>2</sub> and  $1.0 \times 10^{-3}\text{ mol dm}^{-3}$  2-morpholinoethanesulfonic acid (MES) as a buffer. The pH of the aqueous solution was kept within 6.0 – 6.4. Prior to two-phase sheath flow experiments, the aqueous solution was stirred with pure 1-butanol for saturation.

For excitation of the complex in the sheath flow system, the second harmonic light (pulse width, 150 fs; 400 nm; 70 mW; 82 MHz) of a Ti:sapphire laser (Tsunami, Spectra-Physics) was used. The excitation light was reflected by a dichroic mirror (DM455, Nikon) toward the cell and focused on the pillar-shaped organic phase flow by a 20× objective (SuperFluor, Nikon). An intensified cooled CCD camera (PentaMax, Princeton Instruments) detected the fluorescence emitted from the complex formed in the organic phase flow. To measure its fluorescence spectra, a streak scope (C4334, Hamamatsu Photonics) was used. Undesirable light caused by the scattering of excitation light and the Raman scattering of the solvent was removed by the dichroic mirror and a barrier filter (535AF45, Omega Optical; passing 550 – 580 nm) placed in front of the CCD camera. By travelling the microscope stage, the excitation point at the interface was shifted along the flow and the fluorescence intensities of the points were measured as a function of time.

## RESULTS AND DISCUSSION

### Mass Spectra of Cu(II) Extraction System by the Two-Phase Flow ESI/MS

Under the conditions of 0.02 ml/h flow rate of the organic phase and 400 V in the nozzle voltage, a good ESI/MS spectrum was obtained as shown in Figure 3. The 1:1 complex ( $m/z = 410$ ) and 1:2 complex ( $m/z = 760$ ) of Cu(II) with 5-Br-PADAP as well as the free extractant ( $m/z = 349$ ) were detected clearly. These peaks were measured only when aqueous Cu(II) solution and organic 5-Br-PADAP solution were flowed. From this result, it was shown that the two-phase flow ESI/MS could detect the complexes formed in the two-phase system and that a highly hydrophobic solute like a 5-Br-PADAP was detected by ESI/MS for the first time in the present method.

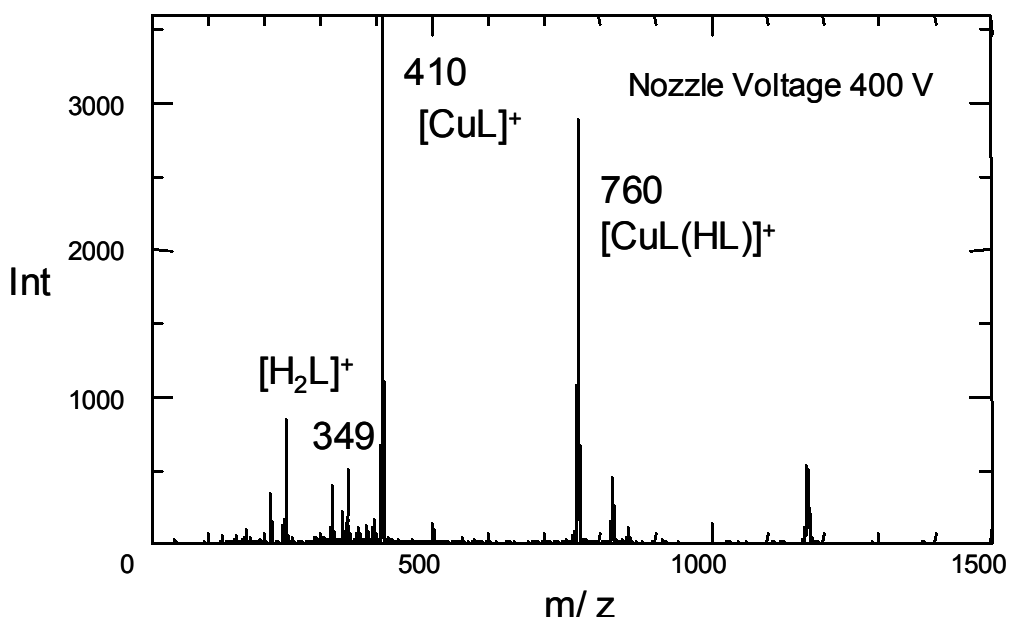


Figure 3. Mass spectra of the copper(II)-5-Br-PADAP complexes in micro-flow toluene-water system including  $1.0 \times 10^{-3}$  M 5-Br-PADAP in the organic phase with a flow rate of 0.02 ml/h and  $5.0 \times 10^{-6}$  M Cu(II) in the aqueous 0.0010 M acetic acid with a flow rate of 0.1 ml/h.

The nozzle voltage was one of the critical conditions to detect the complexes. When the nozzle voltage was less than 300 V, solvent cluster peaks became larger and the signal of the complex was not observed. At 500 V, both complex peaks and solvent cluster peaks were decreased. In 400 V, the complex signals were highest and the solvent cluster peaks were lowest. These effects were explained in terms of the collision activated dissociation (CAD). The CAD was increased in the higher nozzle voltage, so that the higher voltage reduced effectively the back-ground signals of solvent clusters and enhanced the complex signals.

The flow rate of the organic phase was another critical condition to be optimised. Accompanied by the increase of the flow rate of the organic phase from 0.001 ml/h to 0.02 ml/h, the signals of the complex were increased. The reaction probability between Cu(II) ion and 5-Br-PADAP was thought to be increased at the higher flow rate. Under the three different flow rates, the time-resolved MS was measured for the signal of 1:1 complex. The time-resolved MS revealed that the organic phase was flowed as droplets giving 500 counts in an average per 10 second per single droplet. This result allowed us to calculate the volume of the single organic droplet as 18 nl in an average.

### **Measurement of Fast Interfacial Reaction of Zn(II)**

The linear velocities of the both phases were matched at  $0.2 \text{ m s}^{-1}$  by controlling the flow rate. The diameter of the inner flow was  $30 \mu\text{m}$  and the specific interfacial area, defined as the interfacial area per unit volume of the organic phase, was calculated as  $1.3 \times 10^3 \text{ cm}^{-1}$ . Figure 4 shows the results of the kinetic measurement. The fluorescence intensity was converted to the complex concentration by the use of the fluorescence intensities of  $\text{Zn}(\text{ocqn})_2$  in 1-butanol of the concentration of  $1.1 \times 10^{-5} \text{ mol dm}^{-3}$  used as an inner phase. The distance from the capillary outlet to the observing spot was converted to the reaction time. The spectra of fluorescence emitted from the observing spots measured by the streak scope were in agreement with that of  $\text{Zn}(\text{ocqn})_2$  extracted into 1-butanol phase, proving that the detected fluorescence was generated only from the complex. In the system shown in Figure 4, the observed fluorescence intensity was increased with the reaction time, and the slope of  $5.4 \times 10^{-4} \text{ mol dm}^{-3} \text{ s}^{-1}$  was thought to be the complexation rate of  $\text{Zn}^{2+}$  with Hocqn.

In a short contact time less than 5 ms as in the present case, the distribution of Hocqn between the bulk phases is not completed. Simple calculation by assuming  $5 \times 10^{-5} \text{ cm}^2 \text{ s}^{-1}$  as a diffusion coefficient of Hocqn in water estimated about  $2 \mu\text{m}$  as its diffusion depth in aqueous phase after 5 ms. Therefore, the complexation was postulated to take place only in the interfacial reaction zone, which might be depending on the diffusion coefficient and the concentration of the reactant. The rate-determining step of this complexation reaction can be assumed to be the formation of a 1:1 complex of  $\text{Zn}^{2+}$  and Hocqn. When Hocqn is distributed in the aqueous interfacial reaction zone according to the local distribution equilibrium and reacts with  $\text{Zn}^{2+}$  in the interfacial region, the extraction rate of  $\text{Zn}(\text{ocqn})_2$  in the organic interfacial region might be given by:

$$\frac{d[\text{Zn}(\text{ocqn})_2]_{\text{oi}}}{dt} = k[\text{Zn}^{2+}]_{\text{ai}}[\text{Hocqn}]_{\text{ai}} \quad (1)$$

where  $[\text{Zn}(\text{ocqn})_2]$ ,  $[\text{Zn}^{2+}]$ , and  $[\text{Hocqn}]$  represent the concentrations of the  $\text{Zn}(\text{ocqn})_2$ ,  $\text{Zn}^{2+}$ , and Hocqn, respectively. The subscripts oi and ai refer to the organic interfacial region and aqueous interfacial region, respectively. The distribution constant of Hocqn in the interfacial region of 1-butanol/water system was estimated to be about  $10^{4.5}$ . Hence, the rate constant  $k$  was calculated as  $1 \times 10^6 \text{ mol}^{-1} \text{ dm}^3 \text{ s}^{-1}$ . The magnitude of this value is thought to be close to the values reported in the Eigen mechanism.

### **CONCLUSIONS**

Two-phase micro-flow electrospray ionization/mass spectrometry was invented and proved as a promising technique in the study of complexation in the solvent extraction systems. It was suggested that not only the bulk phase species but also the interfacial species could be detected by this method.

The measurement of the fast (within 5 ms) extraction process of  $\text{Zn}^{2+}$  with Hocqn was demonstrated by the two-phase sheath flow method with laser-induced fluorometry. The interface in the flow system was stable, and the specific interfacial area was  $1.3 \times 10^3 \text{ cm}^{-1}$ .

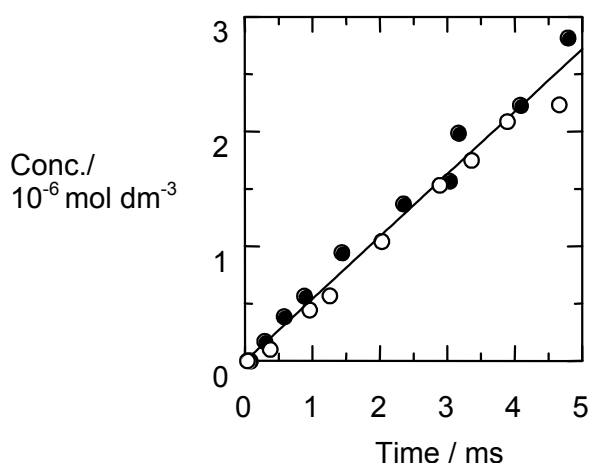


Figure 4. Formation rate of the fluorescent Zn-ocqn complex in the 1-butanol/water interfacial region. The linear flow velocities are  $0.26 \text{ m s}^{-1}$  (●), and  $0.20 \text{ m s}^{-1}$  (○). Organic phase was  $1.3 \times 10^{-3} \text{ mol dm}^{-3}$  Hocqn in 1-butanol. Aqueous phase included  $1.1 \times 10^{-2} \text{ mol dm}^{-3}$   $\text{Zn}^{2+}$  and  $1.0 \times 10^{-3} \text{ mol dm}^{-3}$  MES, and pH was 6.3.

Since the contribution of interfacial reaction is extremely multiplied under the condition of the high specific interfacial area, the two-phase micro-flow method proposed in the present study is strongly promising for the study of liquid/liquid interfacial reactions in various extraction systems.

#### ACKNOWLEDGEMENTS

The author thanks Dr. T. Fukumoto, Dr. S. Tsukahara, Mr. A. Matsumoto and Mr. T. Tokimoto for their assistance. This work was supported by a Grant-in-Aid for Scientific Research (No. 12304045) from the Ministry of Education, Science and Culture.

#### REFERENCES

1. H. Watarai (2000), Liquid Interfaces in Chemical, Biological, and Pharmaceutical Applications, A. G. Volkov (ed.), Marcel Dekker, Inc., New York, pp. 355-372.
2. M. Fujiwara, S. Tsukahara and H. Watarai (1999), *Phys. Chem. Chem. Phys.*, **1**, 2949-2951.
3. N. Fujiwara, S. Tsukahara and H. Watarai (2001), *Langmuir*, in press.
4. H. Watarai (1993), *Trends Anal. Chem.*, **12**, 313-318.
5. Y. Yulizar, A. Ohashi, H. Nagatani and H. Watarai (2000), *Anal. Chim Acta.*, **419**, 107-114.
6. R. J. Pfeifer and C. D. Hendricks (1968), *AIAA J.*, **6**, 496.
7. H. Nagatani and H. Watarai (1996), *Anal. Chem.*, **68**, 1250-1253.
8. T. Tokimoto, S. Tsukahara and H. Watarai, *Chem. Lett.*, **2001**, 204-205
9. H. Kokusen, K. Suzuki, K. Ohashi and K. Yamamoto (1988), *Anal. Sci.*, **4**, 617.



## THE DRAINAGE AND RUPTURE OF THE FILM BETWEEN COLLIDING DROPS IN THE PRESENCE OF SURFACTANT

Leslie Y. Yeo, Omar K. Matar, E. Susana Perez de Ortiz and Geoffrey F. Hewitt

Department of Chemical Engineering & Chemical Technology  
Imperial College of Science, Technology & Medicine, London, U.K.

The understanding of the coalescence process between two drops is essential in determining the stability of liquid-liquid systems. By solving the equation governing the evolution of the continuous phase film trapped between two drops colliding at constant velocity coupled with that describing the surfactant interfacial concentration in the lubrication approximation, we show that the interface is rendered immobile due to the presence of a small amount of surfactant. Film rupture is therefore delayed due to the Marangoni effect retarding the drainage of the film. In this study, the effects of the viscosity ratio, surface diffusivity, approach velocity and the van der Waals interaction force are reported.

### INTRODUCTION

During the approach of two drops in a dispersion of two immiscible liquids, a thin film of the continuous phase is trapped between the interface of the drops. This film then proceeds to drain as the interfaces deform under the influence of the interaction forces acting on the drops. If the film succeeds in draining to a thickness at which van der Waals forces become significant in the time at which the drops are in contact with each other, the film ruptures resulting in the coalescence of the drops. The study of the film drainage and rupture process is therefore vital in the determination of the stability of liquid-liquid systems.

In practical systems of interest, surface active agents are often present. Due to spontaneous deformations at the drop interface, concentration gradients arise resulting in the Marangoni effect. The influence of surfactant on the drainage and rupture of the film between two drops colliding at a constant approach force has been investigated by Chesters and Bazhlekov [1]. In this paper, we consider the constant approach velocity case which is more appropriate for inertial collisions, which is often more relevant in practical liquid-liquid systems.

### PROBLEM FORMULATION

The approach of two drops with radii,  $R_i^*$  ( $i = 1, 2$ ), at a velocity,  $V^*$  (\* indicating a dimensional quantity), is considered (Figure 1). The following simplifying approximations have been adopted:

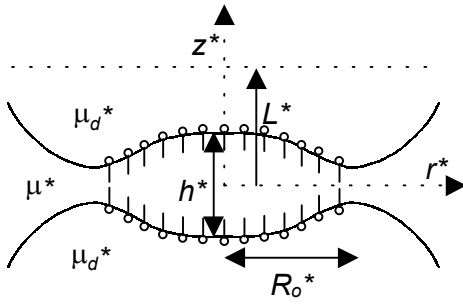


Figure 1. Schematic diagram of the film drainage region.

- The film is sufficiently thin compared to the radial extent ( $\epsilon = h_o^*/R_o^* \ll 1$ , where  $h_o^*$  is the initial film thickness and  $R_o^*$  is the initial rim radius of the film) such that the lubrication approximation applies. Symmetry relative to the plane  $z^* = 0$  can also be assumed since the effect of drop size on the film curvature is negligible as a result. An equivalent radius,  $R^*$ , can then be defined as follows:

$$\frac{1}{R^*} = \frac{1}{2} \left( \frac{1}{R_1^*} + \frac{1}{R_2^*} \right). \quad (1)$$

As a consequence of symmetry, it can also be assumed that the interfacial properties are the same at both interfaces and hence the interfacial concentration of surfactant,  $\Gamma^*$ , and the interfacial tension,  $\gamma^*$ , are equal at both the drop interfaces [2].

- In the drop, there is a characteristic penetration length,  $L^*$ , of magnitude  $\epsilon R^*$  from the interface at which the velocity and the velocity gradient approach zero [2,3].
- A dilute and uniformly distributed amount of surfactant is present at the interface initially. The surfactant is assumed to be insoluble in both the dispersed and continuous phases. A linear surfactant equation of state, justifiable for dilute concentrations, is adopted:

$$\gamma^* = \gamma_o^* - \left( \frac{\partial \gamma^*}{\partial \Gamma^*} \right) \Gamma^*, \quad (2)$$

where  $\gamma_o^*$  is the interfacial tension when the interface is free of surfactant.

The following transformations are applied to render the variables dimensionless:

$$\begin{aligned} r &\equiv \frac{r^*}{R_o^*}; & R_i &\equiv \frac{R_i^*}{R_o^*}; & z &\equiv \frac{z^*}{h_o^*}; & h &\equiv \frac{h^*}{h_o^*}; & t &\equiv \frac{\epsilon S^* t^*}{\mu^* R_o^*}; & p &\equiv \frac{h_o^* p^*}{S^*}; \\ \lambda &\equiv \frac{\mu^*}{\mu_d^*}; & \Gamma &\equiv \frac{\Gamma^*}{\Gamma_m^*}; & \gamma &\equiv \frac{(\gamma^* - \gamma_m^*)}{S^*}; & B &\equiv \frac{B^*}{S^* h_o^{m-1}}; & S^* &\equiv \gamma_o^* - \gamma_m^*, \end{aligned} \quad (3)$$

where  $h$  is the film thickness,  $t$  is the time,  $S^*$  the spreading pressure and  $p$  the film pressure;  $\mu^*$  and  $\mu_d^*$  are the continuous and the dispersed phase viscosities, respectively;  $\gamma_m^*$  is the interfacial tension when the interfacial surfactant concentration is at its saturation,  $\Gamma_m^*$ .  $B$  is the dimensionless Hamaker constant and  $m$  is a parameter for which value of 3 is assumed [4].

The lubrication equations can then be written both for the film and in the drops:

$$\frac{\partial p}{\partial r} = \frac{\partial^2 v}{\partial z^2}; \quad \frac{\partial p_i}{\partial r} = \lambda \frac{\partial^2 v_i}{\partial z^2}, \quad (4)$$

where  $v$  is the radial velocity in the film, and,  $p_i$  and  $v_i$  are the pressure and radial velocity in drop  $i$ , respectively. Taking into account the tangential shear stress balance at the interfaces,

$$\frac{\partial v}{\partial z} - \lambda \frac{\partial v_1}{\partial z} = \frac{\partial \gamma}{\partial r}, \quad (5)$$

$$\lambda \frac{\partial v_2}{\partial z} - \frac{\partial v}{\partial z} = \frac{\partial \gamma}{\partial r}, \quad (6)$$

where equation (5) applies to the interface above  $z = 0$  and equation (6) applying to the bottom interface, it can then be shown [2,5] by integration of the lubrication equations (the boundary conditions being the velocity and velocity gradient in the drop diminishing at the characteristic penetration length, symmetry at  $z = 0$  and continuity of velocities at the interface) that:

$$\frac{\partial h}{\partial t} = \frac{1}{12r} \frac{\partial}{\partial r} \left( rh^3 \frac{\partial p}{\partial r} \right) - \frac{1}{r} \frac{\partial}{\partial r} (rhv_{int}). \quad (7)$$

Here,  $v_{int}$  is the interfacial velocity which is given by:

$$v_{int} = \frac{R}{2\lambda} \frac{\partial \gamma}{\partial r} - \frac{hR}{4\lambda} \frac{\partial p}{\partial r}. \quad (8)$$

The dimensionless film pressure can be written as:

$$p = \frac{2 \epsilon \gamma_m^*}{RS^*} - \frac{1}{2} \frac{\epsilon^2 \gamma_m^*}{S^*} \left[ \frac{1}{r} \frac{\partial}{\partial r} \left( r \frac{\partial h}{\partial r} \right) \right] + \frac{B}{h^m}, \quad (9)$$

and the equation describing the evolution of surfactant interfacial concentration reads:

$$\frac{\partial \Gamma}{\partial t} = \frac{1}{Pe_s} \left[ \frac{1}{r} \frac{\partial}{\partial r} \left( r \frac{\partial \Gamma}{\partial r} \right) \right] - \frac{1}{r} \frac{\partial}{\partial r} (rv_{int} \Gamma), \quad (10)$$

where  $Pe_s$  is the surface Péclet number ( $Pe_s = S^* h_o^* / \mu^* D_s$  where  $D_s$  is the surface diffusivity).

Given an initially undeformed spherical drop with uniform concentration,  $\Gamma_o$ ,

$$h = h_{oo} + \frac{r^2}{\epsilon R} \quad \text{and} \quad \Gamma = \Gamma_o \quad \text{at } t = 0, \quad (11)$$

where  $h_{oo}$  is the initial film thickness at  $t = 0$ . The following boundary conditions apply:

$$\begin{aligned} \frac{\partial h}{\partial r} &= 0; \quad \frac{\partial^3 h}{\partial r^3} = 0; \quad \frac{\partial \Gamma}{\partial r} = 0 \quad \text{at } r = 0, \\ \frac{\partial h}{\partial t} &= -V; \quad p = 0; \quad \frac{\partial \Gamma}{\partial r} = 0 \quad \text{at } r = \infty, \end{aligned} \quad (12)$$

where  $V = V^* \mu^* / \epsilon^2 S^*$ .

The two coupled fourth-order nonlinear parabolic partial differential equations describing the evolution of the film and the interfacial concentration of surfactant as given by equations (7) and (10) were solved starting from the initial conditions, equation (11), subject to the boundary conditions, equation (12), using the numerical Method of Lines [6]. Spatial derivatives were discretised using fourth-order centred differences and Gear's method was used to advance the solution in time. A uniform grid of up to 1000 points was used, the grid being refined to achieve convergence. In the case of film rupture, the computations were halted at a film thickness of approximately 0.1 as the increasingly singular spatial derivatives near the rupture region posed a difficulty for it to be resolved. In the simulations, we assume  $R = 4$  [3] and  $\gamma_m^* = S^* = 40$  dynes/cm;  $h_{\infty}$  was taken to be 1 unless otherwise stated.

## RESULTS

### Interface Immobilisation

The effect of surfactant on film drainage can be seen in Figure 2. It is seen that the drainage of the film is retarded even at the addition of a small amount of surfactant. As the initial concentration of surfactant is increased, the drainage profile tends to that of a surfactant-free system with immobile interfaces (*i.e.*,  $v_{int} = 0$ ) for which the flow is only driven by the radial pressure gradient. These results are in agreement with previous theoretical and experimental findings [7-9] which report interfacial immobilisation in the presence of a small quantity of surfactant. A typical surfactant interfacial concentration evolution profile is illustrated in Figure 3(a) indicating that the initial deformation of the interface due to the approach of the drops results in depletion of surfactant at the centre. This gives rise to the Marangoni effect where interfacial tension gradients arise to oppose the flow of liquid out from the drainage region. Consequently, the surfactant gets replenished in the deformation region. The corresponding film thickness evolution profile is shown in Figure 3(b) showing the formation of a dimple. Surfactant is observed to deplete at the dimple rim as fluid is expelled away from this region.

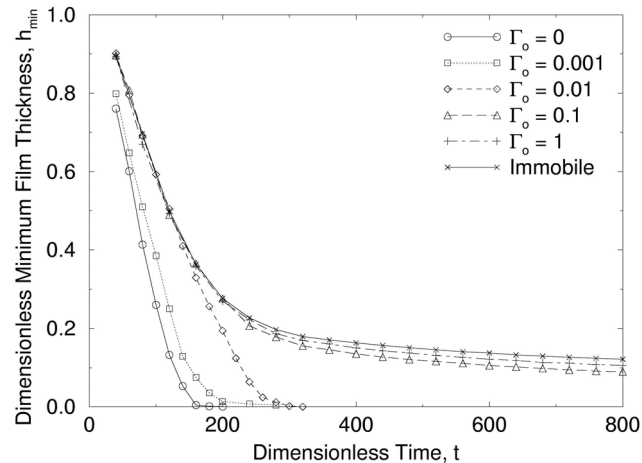


Figure 2. Minimum film thickness as a function of time for various surfactant loadings. The rest of the parameters are  $\lambda = 1$ ,  $Pe_s = 1000$  (where applicable),  $B = 0$  &  $V = 0.01$ . Also shown is the solution for the surfactant-free immobile interface.

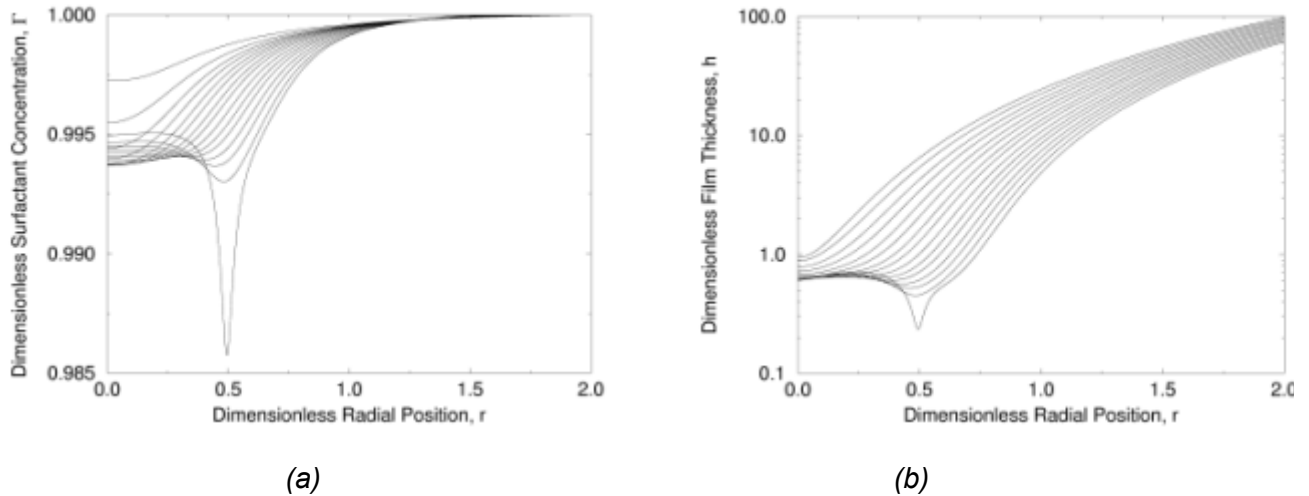


Figure 3. Surfactant concentration (a) & film thickness (b) evolution profiles for 15 equal time steps up to  $t = 117.1$ . Other parameters are  $\lambda = 1$ ,  $Pe_s = 1000$ ,  $\Gamma_o = 1$ ,  $B = 10^{-3}$  &  $V = 0.5$ .

### Viscosity Ratio

The effect of the viscosity ratio on the drainage process is illustrated in Figure 4. It can be seen that the viscosity ratio has little effect on film drainage. This is consistent with the experimental observations in [9]. The viscosity ratio is not expected to significantly influence the drainage of the film because of the resulting immobility of the interface due to the presence of surfactant, as discussed previously [1,9]. Since the flow in the dispersed phase is insignificant for immobile interfaces, the drop phase viscosity therefore no longer influences the interface.

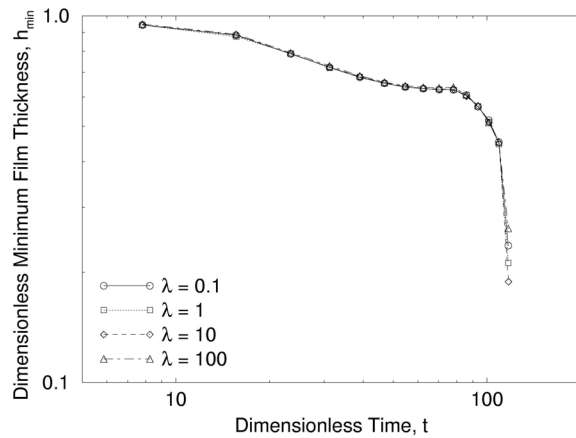


Figure 4. Effect of viscosity ratio,  $\lambda$ , on the minimum film thickness. The rest of the parameter values are  $Pe_s = 1000$ ,  $\Gamma_o = 1$ ,  $V = 0.5$  &  $B = 10^{-3}$ .

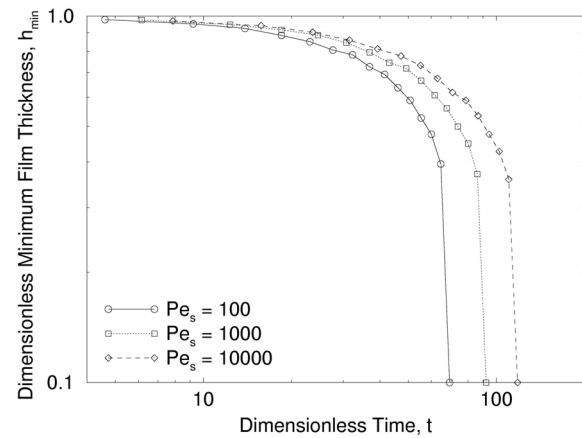


Figure 5. Minimum film thickness as a function of the surface Péclet number  $Pe_s$ . Other parameter values are  $\lambda = 1$ ,  $\Gamma_o = 0.0025$ ,  $V = 0.01$  &  $B = 10^{-4}$ .

### Surface Péclet Number

The surface Péclet number,  $Pe_s$ , represents the significance of surfactant transport by Marangoni convection relative to that by surface diffusion. Low  $Pe_s$  values indicate the dominance of surface diffusion whereas high  $Pe_s$  values indicate that the spreading of surfactant due to Marangoni stresses is the dominant mechanism. Figure 5 depicts the effect of  $Pe_s$  on the dynamics of the film drainage process. As Marangoni convection becomes increasingly significant with increasing

$\text{Pe}_s$ , it can be seen that the latter stages of film drainage is affected, the film taking longer to drain. It should be noted that there is little difference in the early stages of the film drainage because the surfactant concentration gradient at the interface is small. However, as the drops approach each other, interfacial deformation takes place leading to a large negative concentration gradient being present in the drainage region. For systems with high  $\text{Pe}_s$ , the Marangoni stresses that arise as a consequence of these concentration gradients act to retard the interfacial velocity and thus the drainage of the film. For systems with low  $\text{Pe}_s$  on the other hand, there is little effect of the surfactant on the interfacial dynamics since diffusion serves to distribute the surfactant quickly with little disturbance caused to the interface.

### Approach Velocity

The role of the approach velocity on the dynamics of film thinning is described in Figure 6. As the drops collide with increasing velocities, dimpling begins to occur as seen by the rim position for larger velocities in the figure. For low velocities, dimpling does not occur since there are insufficient hydrodynamic forces to cause deformation to the film. As such, the film drains quickly and proceeds towards rupture, as shown by the minimum film thickness curves in Figure 6.

### van der Waals Interaction Forces

As the film thins to thicknesses of the order 1000 Angstroms, intermolecular interactions such as the van der Waals attraction become significant. As a result, there is a negative contribution to the disjoining pressure leading towards the rupture of the film as observed in Figure 3(b). The liquid in the film is expelled together with surfactant away from the rupture region thereby causing a sharp depletion of surfactant as shown in Figure 3(a). Figure 7 shows the rate of film thinning as a function of the dimensionless Hamaker constant,  $B$ . Clearly, as the magnitude of  $B$  increases, the film tends to rupture quickly at a large critical rupture thickness since the van der Waals attraction is strong. In Figure 7, it can be seen that for  $B = 10^{-6}$ , the effect of the van der Waals force, which is extremely weak in this case, is not significant even at a film thickness of 0.1 dimensionless units and hence rupture does not occur even at this stage.

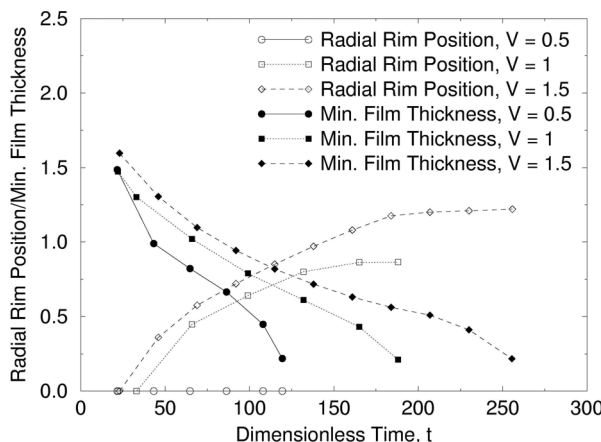


Figure 6. Radial rim position & minimum film thickness as a function of the approach velocity  $V$ . The rest of the parameters are  $\lambda = 1$ ,  $\text{Pe}_s = 1000$ ,  $\Gamma_o = 1$ ,  $B = 10^{-3}$  &  $h_{oo} = 2.63$ .

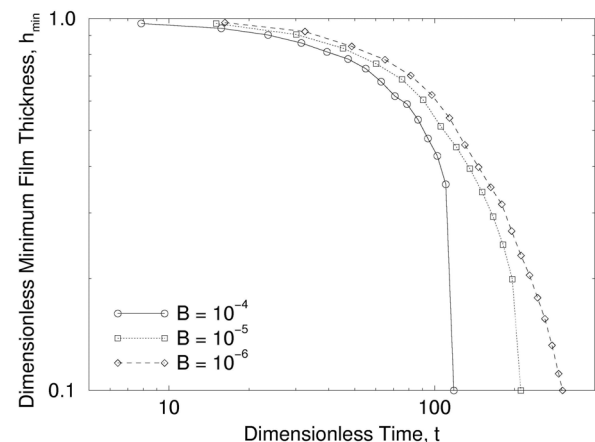


Figure 7. Variation of the minimum film thickness with the dimensionless Hamaker constant  $B$ . The other parameters are  $\lambda = 1$ ,  $\text{Pe}_s = 10000$ ,  $\Gamma_o = 0.0025$  &  $V = 0.01$ .

## CONCLUSIONS

The drainage of the film trapped between two drops colliding at constant approach velocity in the presence of insoluble surfactant has been studied. The interface is rendered immobile even when small amounts of surfactant are present, thereby retarding the drainage of the film and hence film rupture. This is a consequence of concentration gradients that arise out of deformations caused to the film during the approach of the drops. These concentration gradients seek to replenish the surfactant locally depleted in the film deformation region therefore retarding interfacial mobility by opposing the flow of the liquid outwards.

The role of the viscosity ratio, surface Péclet number, approach velocity and van der Waals force have been investigated. Viscosity ratio is not found to have any influence on film drainage since the interface is immobilised and thus there is no flow in the dispersed phase. As the surface Péclet number is increased, Marangoni forces become increasingly dominant thereby retarding the drainage of the film. When the drops collide at higher approach velocities, dimpling of the film is observed and hence the film takes longer to drain as compared to low velocity collisions. Finally, the effect of van der Waals forces on film drainage and rupture was examined.

## REFERENCES

1. A. K. Chesters and I. B. Bazhlekov (2000), *J. Colloid Interf. Sci.*, **230**, 229-243.
2. L. Y. Yeo, O. K. Matar, E. S. Perez de Ortiz and G. F. Hewitt (2001), *J. Colloid Interf. Sci.*, **241**, 233-247.
3. D. Li and S. Liu (1996), *Langmuir*, **12**, 5216-5220.
4. J. D. Chen and J. C. Slattery (1982), *AIChE J.*, **28** (6), 955-963.
5. L. Y. Yeo, O. K. Matar, E. S. Perez de Ortiz and G. F. Hewitt, in preparation.
6. W. E. Schiesser (1991), *The Numerical Method of Lines*, Academic Press, San Diego.
7. R. S. Allan, G. E. Charles and S. G. Mason (1961), *J. Colloid Sci.*, **16**, 150-165.
8. C. Y. Lin and J. C. Slattery (1982), *AIChE J.*, **28** (1), 147-156.
9. E. Klaseboer, J. Ph. Chevaillier, C. Gourdon and O. Masbernat (2000), *J. Colloid Interf. Sci.*, **229**, 274-285.



## ESTIMATION OF COALESCENCE PARAMETERS FOR POPULATION BALANCE MODELS

Martin Simon and Hans-Jörg Bart

Institute of Thermal Process Engineering, University of Kaiserslautern,  
Kaiserslautern, Germany

The description of the hydrodynamics of extraction columns is increasingly done with population balance models. The droplet population balance model describes the axial change of local column hold-up and local droplet size distributions due to the basic phenomena like droplet rising, axial dispersion, droplet breakage, and coalescence. The experimental set-up on the basis of a simple apparatus with low experimental effort will be shown for the investigation of the coalescence parameters depending on inlet droplet diameter and hold - up. The experimental results and an correlation describing the coalescence phenomena for the system n-butylacetate / water will be presented.

### INTRODUCTION

Up to now the design of an extraction column is not feasible without widespread experiments. The usually applied back-mixing model cannot describe the real hydrodynamic behaviour because of its simplicity. The dispersed phase hold - up and the droplet size distribution change with time and column height due to the dynamic processes droplet rising  $v_d$ , axial dispersion  $D_{ax}$ , droplet breakage  $S_B$  and random inter-droplet coalescence  $S_C$ . The droplet population balance model developed since the Eighties [1] takes these kinetic processes into account and gives a more realistic picture of the local hydrodynamics:

$$\frac{\partial P(t, z, d)}{\partial t} = v_d \frac{\partial P(t, z, d)}{\partial z} + D_{ax} \frac{\partial^2 P(t, z, d)}{\partial z^2} + S_B + S_C \quad (1)$$

Let  $P(t, z, d) \Delta d$  be the volume fraction of drops of diameter between  $d \pm \Delta d/2$  at column height  $z$  at time  $t$ .  $P(t, z, d)$  may also be interpreted as the probability density to find a droplet of diameter  $d \pm \Delta d/2$  located at time  $t$  at column level  $z$ . The first term on the right hand side of equation (1) represents the transport of droplets due to droplet diameter depended rising velocity  $v_d$ , the second part describes the axial dispersion of droplets. The source terms  $S_B$  and  $S_C$  take the death and birth of droplets with size  $d \pm \Delta d/2$  due to the breakage and the coalescence of droplets into account. The basis for each simulation is the estimation of the above mentioned model parameters. The model parameters droplet rising velocity  $v_d$ , the axial dispersion coefficient  $D_{ax}$  and the breakage term  $S_B$  are already topics of investigations in a RDC geometry [2]. But due to a lack of data, special attention has to be paid to determine the parameters incorporated in the coalescence term  $S_C$ .

The number of coalescence events of droplets of diameter between  $d_1 \pm \Delta d_1/2$  with droplets of diameter between  $d_2 \pm \Delta d_2/2$  per unit volume and per unit time is given by  $\omega(d_1, d_2)N(d_1)\Delta d_1 N(d_2)\Delta d_2$ , where  $N(d)\Delta d$  denotes the number of droplets per unit volume and  $\omega(d_1, d_2)$  is the so called coalescence frequency. The loss of droplets due to coalescence with other drops is:

$$S_c^-(t, z, d, P)\Delta d = P(t, z, d)\Delta d \int_0^{\sqrt[3]{d_{\max}^3 - d^3}} \omega(d_1, d_2) \frac{P(t, z, d_1)}{V(d_1)} dd_1 \quad (2)$$

The gain of droplets of diameter between  $d \pm \Delta d/2$  is given by the integration over all possible pairs of droplets ( $d_1 \pm \Delta d_1/2, d_2 \pm \Delta d_2/2$ ) with the droplet volume  $V(d_1) + V(d_2) = V(d)$ :

$$S_c^+(t, z, d, P)\Delta d = \frac{1}{2} V(d)\Delta d \int_0^d \omega(d_1, d_2) \frac{P(t, z, d_1)}{V(d_1)} \frac{P(t, z, d_2)}{V(d_2)} \left( \frac{d}{d_2} \right)^2 dd_1 \quad (3)$$

Since the integral counts every event twice, the factor  $\frac{1}{2}$  has to be inserted. To determine the coalescence term  $S_c$  the model parameter  $\omega(d_1, d_2)$  must be known. The coalescence frequency  $\omega(d_1, d_2)$  can be calculated from the coalescence probability  $p$ , the residence time  $t_r$  of the droplets in a volume  $V$  and the volume  $V$  itself where coalescence occurs.

## EXPERIMENTAL

To determine the coalescence frequency it must be guaranteed that only coalescence occurs during an experiment. Otherwise, it is not possible to determine correctly the coalescence frequency. In Figure 1 the experimental set-up ( $D = 80$  mm) is shown which fulfills the requirements.

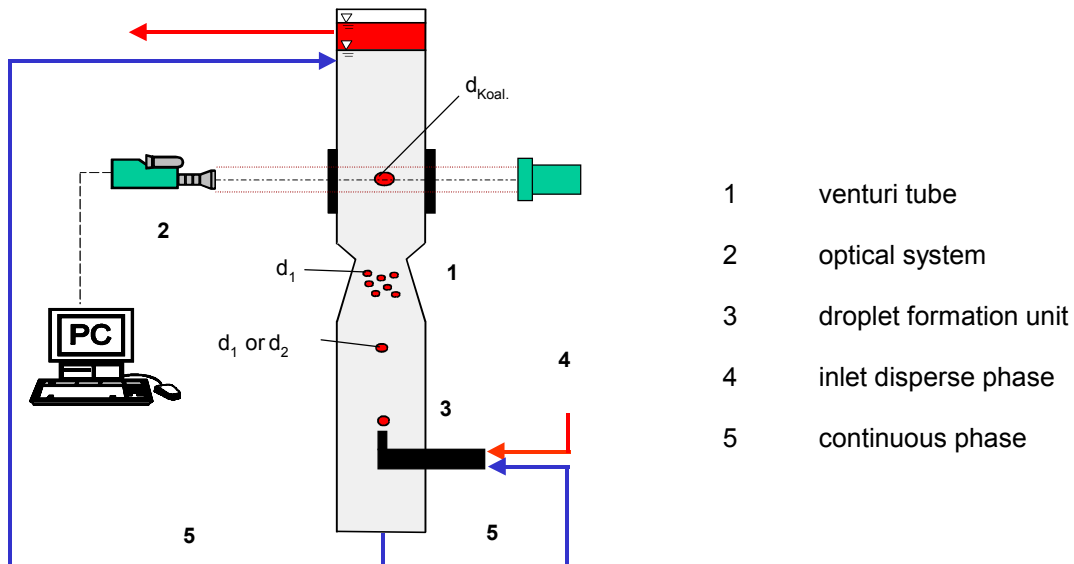


Figure 1. Experimental set – up for coalescence experiments.

The core of the apparatus is a venturi tube with a length of  $L = 250$  mm and a diameter ratio of  $D_s / D = 0.45$  (the smallest diameter of the venturi tube to the apparatus diameter). The continuous phase flows from the top to the bottom of the apparatus and the dispersed phase vice versa.

The droplet formation unit generates monodispersed droplets which is important for the analysis later. Due to the smaller cross section of the venturi tube the velocity of the continuous phase is higher than in the other cross section areas. In this way it is possible to capture the droplets of different diameters depending on the continuous throughput flow in the venturi tube. In this volume the droplets can only interact in such a way that they coalesce.

For a typical experiment swarm droplets of diameter  $d_1$  will be generated. The throughput of the continuous phase is set in that way that the droplets  $d_1$  can not pass the smallest cross section of the venturi tube. When a minimum hold-up is realized coalescence will occur in the venturi tube. After the formation of the swarm droplet class  $d_1$ , droplets of diameter  $d_2 < d_1$  are formed. As a result of the turbulence and the droplet swarm influence, both droplet classes are mixed within the venturi tube. Coalescence events between equal or different sized swarm droplets may occur. Instead of a second droplet swarm  $d_2$  it is possible to form single droplets of diameter  $d_3 > d_1 > d_2$  which pass the venturi tube due to the higher buoyancy force.

The droplet diameters of all droplets which pass the venturi tube can be detected with the optical system above the venturi tube. Following the detection the digital image processing calculate the position, the rising velocity and the size of the droplets. In this way, it is possible to investigate the coalescence probability between swarm droplets  $d_1$  and single droplets  $d_3$  or between equal and different sized swarm droplets of diameter  $d_1$  and  $d_2$  depending on the hold-up,  $\Phi$ , of the dispersed phase. Furthermore, with this procedure it can be determined whether the different rising velocities of two droplets ( $v_3 > v_1$ ) or the residence time,  $t_r$ , and the random movement of droplets in a certain volume,  $V$ , have more influence on the coalescence frequency.

The coalescence experiments are realized with the salt conditioned ( $I = 10^{-4}$  mol/l NaCl) EFCE standard test system n-butylacetate / water. To avoid mass transfer the phases are saturated. The droplet diameter was varied in the range of  $1.5\text{ mm} < d_i < 3.0\text{ mm}$  for the swarm droplets and  $2.5\text{ mm} < d_3 < 3.5\text{ mm}$  in the case of single droplets. Additionally, the hold-up was varied between 0.5% and 5%.

## RESULTS

The coalescence probability of droplets strongly depends on the droplet size and the hold-up. In Figure 2 it can be seen that the coalescence probability generally increases with the hold-up. In contrast to this, the dependency of the coalescence probability on the droplet diameter is different. Up to a swarm droplet diameter of  $d_1 = 2.0\text{ mm}$  the coalescence probability increases as the droplet diameter increases. Although the number of droplets of  $d_1 = 1.5\text{ mm}$  realizing a definite hold-up is greater than realizing the same hold-up with a droplet diameter of  $d_1 = 2.0\text{ mm}$ , its coalescence probability is less. It seems that only the volume of dispersed phase (hold-up) in combination with the droplet diameter is important. The number of droplets seems to have not such a great influence on the coalescence probability.

But beyond droplet diameters of  $d_1 = 2.0\text{ mm}$  the coalescence probability shows another dependency on the droplet diameter. Realizing comparable hold-up values the coalescence probability decreases with larger droplet diameters (dotted line in Figure 2). This can be explained by the rigid sphere of the smaller droplets. Using the information of the droplet detection system (Figure 1) droplets up to  $d_1 = 2.0\text{ mm}$  have the shape of a sphere. But above this diameter the droplet shape becomes more and more deformable. This leads to an enlargement of the film drainage time between two droplets during the coalescence process so that the residence time of two droplets staying side by side is not sufficient to cause coalescence [3].

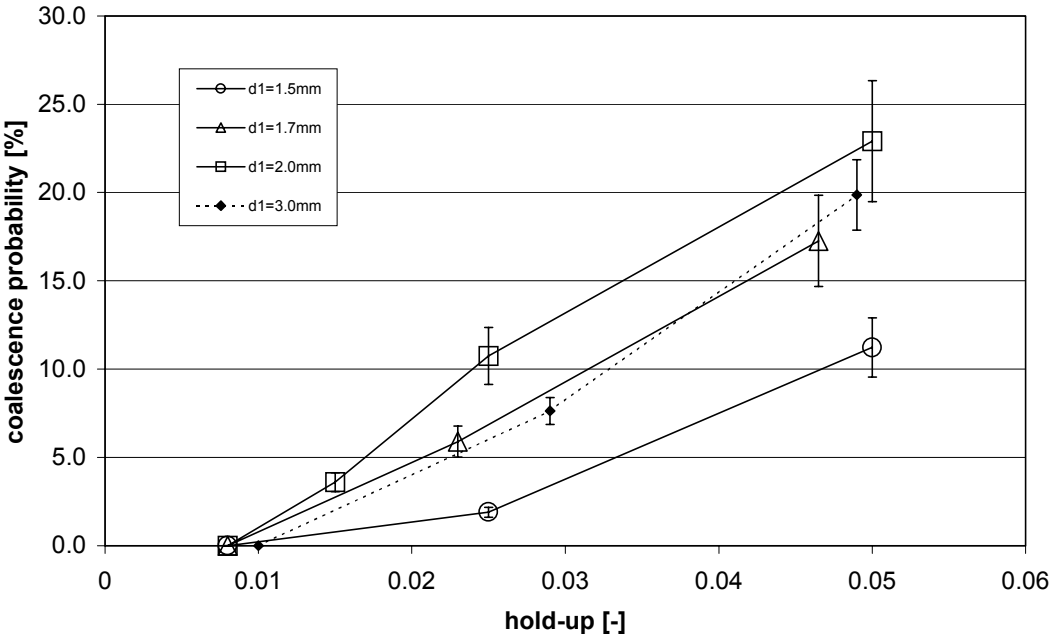


Figure 2. Coalescence probability vs. hold-up for equal sized droplets.

Furthermore, it could be observed that the effect of coalescence between a swarm droplet  $d_1$  and a single droplet  $d_3$  as a result of different rising velocities can be neglected as found elsewhere [4]. Therefore, the idea that the coalescence phenomenon is a random process which mainly depends on the residence time of droplets in a certain volume becomes more important. Coalescence will especially occur in regions where the residence time of droplets is high and the energy input is not in the breakage range. This is, for example, under the stators of agitated columns.

## MODELLING

The modelling and simulation of the inter-droplet coalescence process is done since the Sixties. The investigations start with the works in stirred vessels by Howarth [5] and Coualaloglou and Tavlarides [6]. Coualaloglou and Tavlarides developed a phenomenological model which based on the drainage film theory. Based on this work Sovova [7] and Ramkrishna *et al.* [3] enhanced the model to improve the prediction of the droplet size distribution and the hold-up in liquid – liquid dispersion. They proposed models that take factors like droplet size, system properties and turbulence intensity into account. But in respect of their complexity empirical models were developed [8] which are simpler than those mentioned above.

As a result of the experiments presented above it can be pointed out that the coalescence frequency depends on the droplet diameter, the hold-up and the residence time if the system properties do not change with time. The system properties of the system used are too complex as they could be completely taken into account in the model.

Therefore a simple model is used to describe the coalescence behaviour in liquid – liquid dispersion:

$$\omega(V_1, V_2) = k_1 (V_1 + V_2)^{k_2} \left(\frac{N}{t_r}\right)^{k_3} \phi^{k_4} \quad (4)$$

It takes the swarm droplet volumes,  $V_1$ , and,  $V_2$ , the number of coalesced droplets,  $N$ , the hold-up,  $\Phi$ , and the mean residence time,  $t_r$ , into account. The number of coalescence events per unit time is relating to the minimum residence time in a column compartment to observe coalescence. The constants  $k_i$  represent the fitting parameters.

As it can be seen in Figure 3, the coalescence frequency of equal sized droplets increases with hold-up and droplet diameter up to  $d_1 = 2.0\text{mm}$ . The model shows a good comparison to the experimental data within an accuracy of 10%.

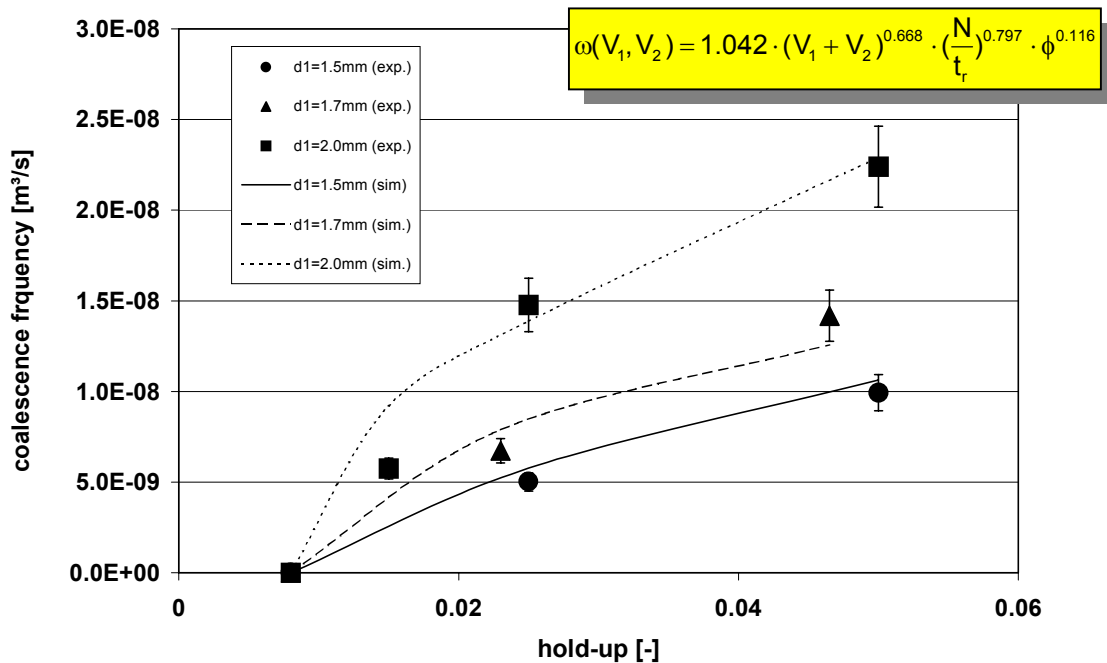


*Figure 3. Theoretical and experimental coalescence frequency vs. hold-up for equal sized droplets.*

But the coalescence frequency of larger and different sized droplets can not be calculated with this model. The deformable shape of the larger droplets totally changes the coalescence procedure.

## CONCLUSIONS

As has been shown, the determination of coalescence frequencies is possible with the presented experimental set-up. Coalescence increases with the increase of the droplet volumes up to a diameter of  $d_1 = 2.0\text{ mm}$ , the hold-up and the residence time. To guarantee the reproducibility of the experimental data it is essential to condition the system. Concerning the modelling of the experimental data it must be said that further experiments are necessary to describe the coalescence phenomena of larger sized droplets. To validate the experimental data of the venturi tube, coalescence experiments should be done in a real RDC compartment. Furthermore it is necessary to investigate other standard test systems with and without mass transfer.

## ACKNOWLEDGEMENTS

The authors wish to thank the DFG for financial support and Mrs. T. Schiek and Mr. T. Dreher for their help with the experiments.

## SYMBOLS

D	venturi tube diameter	[m]
$D_s$	smallest diameter of the venturi tube	[m]
$D_{ax}$	axial dispersion coefficient	[m/s]
$d_i$	droplet diameter of class i	[m]
$k_1$	constants in eq. (4)	$[m^{0.996} s^{-0.203}]$
$k_2, k_3, k_4$	constants in eq. (4)	[ $-$ ]
I	ionic strength	[mol/l]
L	venturi tube length	[m]
N	number of coalesced droplets	[ $-$ ]
$P(t,z,d)$	probability density for droplet with diameter d at height z at time t	[ $m^{-1}$ ]
p	coalescence probability	[ $\%$ ]
$S_B^+$	source term for the gain of droplets due to breakage	[ $m^{-1} s^{-1}$ ]
$S_B^-$	source term for the lost of droplets due to breakage	[ $m^{-1} s^{-1}$ ]
$S_C^+$	source term for the gain of droplets due to coalescence	[ $m^{-1} s^{-1}$ ]
$S_C^-$	source term for the lost of droplets due to coalescence	[ $m^{-1} s^{-1}$ ]
t	time	[s]
$t_r$	residence time	[s]
V	volume of an compartment	[ $m^3$ ]
$V_i$	volume of a droplet with size d of class i	[ $m^3$ ]
$v_i$	droplet rising velocity of class i	[m/s]
$v_r$	relative velocity between continuous and dispersed phase	[m/s]
$v_r^*$	terminal characteristic velocity of a single droplet	[m/s]
z	column height	[m]

### *Greek symbols*

$\phi(t,z)$	dispersed phase hold-up	[ $-$ ]
$\omega(V_1, V_2)$	coalescence frequency for droplets of volume $V_1$ and $V_2$	[ $m^3 s^{-1}$ ]

### *subscripts*

ax	axial
c	continuous phase
d	dispersed phase
i	droplet class i
1	swarm droplets of diameter $d_1$
2	swarm droplets of diameter $d_2$
3	single droplets of diameter $d_3$

## REFERENCES

1. C. Gourdon, G. Casamatta, G. Muratet (1994), Liquid – Liquid Extraction Equipment, J.C. Godfrey and M.J. Slater (eds.), John Wiley & Sons, pp. 141-226.
2. G. Modes, H.-J. Bart (1999), *Chem. Eng. Tech.*, **22**, 231-236.
3. T. Tobin, D. Ramkrishna (1999), *Canad. J. Chem. Eng.*, **77**, 1090-1104.
4. S. Mohanty, A. Vogelpohl (1997), *Chem. Eng. Proces.*, **36**, 385-395.
5. D. Howarth (1964), *Chem. Eng. Sci.*, **36**, 1567-1573.
6. C. A. Coulaloglou, L.L. Tavlarides (1977), *Chem. Eng. Sci.*, **34**, 1141-1149.
7. H. Sovova (1981), *Chem. Eng. Sci.*, **36**, 1567-1573.
8. G. Casamatta, A. Vogelpohl (1985), *Ger. Chem. Eng. Tech.*, **8**, 96-103.



## FLOTATION-ASSISTED ELECTROSTATIC COALESCENCE

Philip J. Bailes and Arian Edalat

University of Bradford, Bradford, United Kingdom

A novel electrostatic coalescer is described in which the resolution of a stable water-in-oil emulsion is augmented by sparging air into the system. Batch experiments have been carried out using two types of high voltage alternating waveform to energise the electrodes in a study which covers a range of applied voltages and frequencies. The extent of coalescence in the emulsion is measured by the intensity of light transmitted through the separator and is reported in terms of the mean greyness of digital video images of the emulsion. The results confirm the efficacy of flotation-assisted electrostatic coalescence for stable, high water content emulsion and demonstrate the influence of applied voltage waveform.

### INTRODUCTION

There are several areas of process engineering where considerable benefits accrue from being able to enhance the rate at which droplets of one liquid can be removed from another liquid in which they are substantially immiscible. Amongst the physical methods available for achieving such enhancement, electrostatic coalescence offers cost effective separation and minimal environmental impact for systems where the continuous phase is electrically insulating. Such circumstances arise in solvent extraction operations, emulsion liquid membrane processes, and in the desalting and dehydration of crude oil emulsions. Of particular interest in all these applications is the possibility of using electric fields to treat systems in which the volume fraction of the electrically conducting dispersed phase is high and perhaps stabilised by the presence of surface active agents.

The electric field augments phase separation by promoting coalescence between the droplets. Increased rates of separation have been observed using AC, DC and pulsed electric fields applied between electrodes which may be bare metal, insulation coated, or of composite construction [1]. The mechanisms whereby electrostatic coalescence occurs all involve the attraction of opposite charges on the surface of proximate droplets, the net effect of which is to increase the incidence of collision followed by coalescence. The overall increase in droplet size which results from this process improves the general rate of sedimentation and therefore increases the rate of phase separation. Although the benefits of using electric fields to create larger droplets from many smaller droplets are self-evident, there are still significant practical limitations on what can be accomplished with existing technology. For example, a major obstacle is the inhibiting effect that surface active agents, either naturally present or deliberately introduced, can have on the electrically augmented coalescence process. Another barrier may arise from the need to successfully treat such stable emulsions when the concentration of the conducting dispersed phase is relatively high, say 60% or thereabouts, since this increases the likelihood of a conduction path forming between the electrodes; the attendant current leakage and loss of electric field can have a very deleterious effect on separator efficiency.

Research with liquid systems of this type has recently shown [2,3] that electrically augmented coalescence occurs more rapidly when the stable emulsion to be treated is subject to simultaneous gas flotation. At this stage the explanation for the observed process improvement is not known but it is likely that the gas bubbles serve to remove excess surfactant from the coalescing system. The gas-liquid interface provides accommodation for the surface active molecules that are released back into the organic phase when many small liquid droplets coalesce to form fewer larger droplets and these droplets coalesce with the bulk interface. The use of gas sparging as an adjunct to electrical resolution is attractive from a practical point of view since it preserves the mechanical simplicity and low maintenance costs that are generally associated with electric treaters. Moreover, the technique offers scope for innovative separator design and it is in this context that a novel flotation-assisted electrostatic coalescer has been developed. The work reported here relates to batch tests that have been conducted with this prototype.

## EXPERIMENTAL

The test separator (depicted in Figure 1) was designed so that the upper high voltage electrode plate (30 mm × 180 mm) was horizontal and separated from the emulsion to be treated by a 5 mm air gap; whereas the lower earthed electrode plate was inclined to the horizontal plane and positioned beneath the emulsion. The lower electrode was wave-shaped and incorporated four separate copper tubes (3.2 mm o.d.) that followed the same profile for the purpose of sparging air into the water-in-oil emulsion. This electrode had slots cut through it at the bottom of the troughs in its profile to allow liquid to pass through the plate. The body of the vessel underneath the lower electrode was divided into three sections by two weirs which ensured that in operation the bulk water interface formed three steps each level with the bottom of the troughs in the wave-shaped electrode. The upper electrode and lower electrode plates were made from aluminium and brass, respectively; the walls and base of the separator were fabricated from Perspex™.

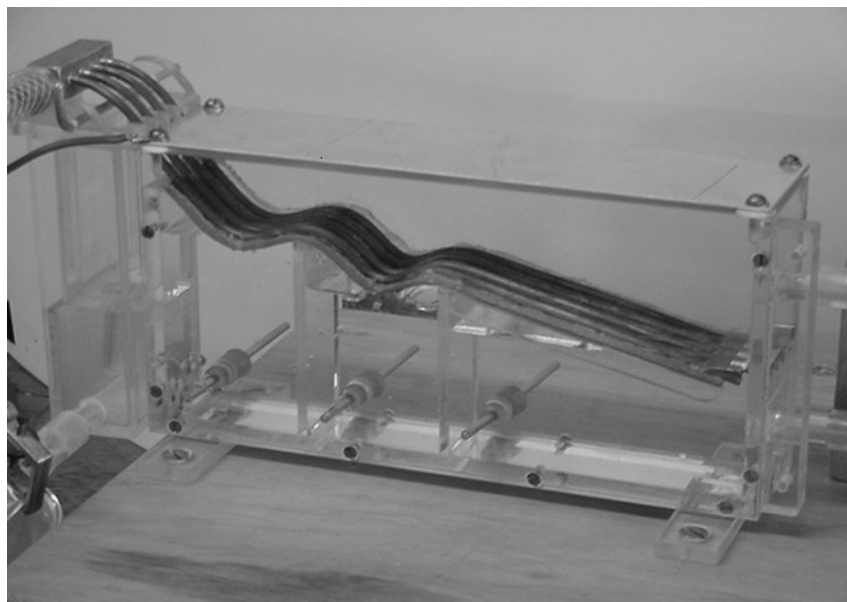


Figure 1. The experimental coalescer.

High voltage was supplied to the apparatus from a Trek 20/20C high voltage amplifier which was used in conjunction with a low voltage function generator. The high voltage waveform was monitored by employing 1/2000 voltage divider coupled to an oscilloscope.

The test emulsions were prepared under ambient conditions by mixing distilled water (40 vol %) into the organic phase (mineral oil - heavy white/odourless kerosene in the ratio 4 : 1, 58 vol %) in the presence of anhydrous lanolin (2 vol %) in the proportions shown. This formulation for the water-in-oil emulsion was developed after extensive trial and error investigations in a previous study [4]. Mixing was accomplished using a Silverson L4RT homogeniser with the impeller speed gradually increased to  $10200\text{ s}^{-1}$  while the aqueous phase was slowly added to the agitated organic phase. The mixing time for a 500 ml batch was 10 minutes and the resultant emulsion was stable for at least 2.5 h.

Phase separation performance was quantified by a light transmission method. For this purpose the separator was illuminated from behind the section where the emulsion depth was greatest and digital video images were recorded through the front face of the separator. The lighting and the size and location of the area being recorded were maintained constant throughout the study. For the work reported here, the video camera was used with a 16 mm focal length lens. The camera was connected to a Kodak Motion Corder Analyzer (Model 1000 B) which has a 1086 frame memory, a resolution of 640 by 480 pixels and a trigger facility. The sequence of images stored on the Motion Corder was transferred to OPTIMAS, an image analysis package which can be used to analyse images based on the different shades of grey of each pixel. The frame storage capability of the Motion Corder meant that it was not possible to record images continuously for the whole of a batch experiment. Instead the progress of each batch was observed at intervals using a sequence of 10 short video samples each made up of 10 frames which were then analysed for their mean greyness. For each sample this information, together with the time of its recording (including the initial pre-treatment zero time value), was exported to an Excel sheet for further analysis.

The procedure for each experiment was that a 196 ml batch of freshly made emulsion was placed in the separator which already contained distilled water up to the maximum level in each section. Once digital images of the untreated emulsion had been recorded, an air flow of  $133\text{ ml s}^{-1}$  was introduced to the emulsion and at the same time the designated electric field was applied. Images of the emulsion were then recorded and saved as the demulsification process proceeded. Each batch was evaluated for 665 s divided for image sampling purposes into the following intervals 15 s, 90 s, 200 s, 320 s, 382 s, 443 s, 507 s, 600 s and 665 s. The field and the flotation were switched off at the end of 600s recording. The state of the emulsion after treatment was recorded at the 665 s image sample. If required a physical sample of the emulsion was removed at this time for observation under a microscope. The applied electrostatic fields were of two alternating types as shown in Figure 2, with most of the experiments being conducted with the type B field.

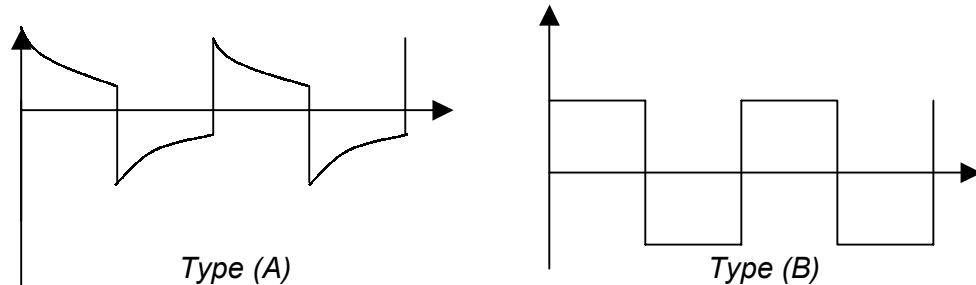
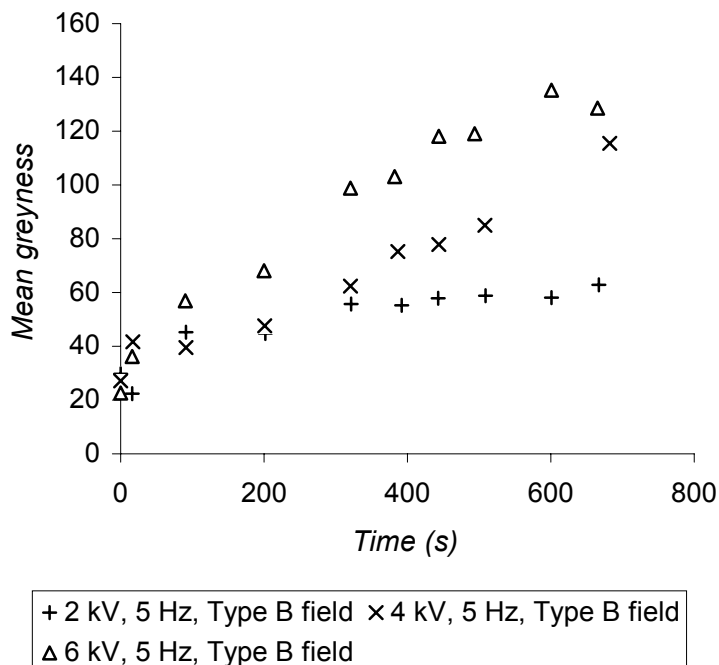


Figure 2. Electrostatic field types.

## RESULTS AND DISCUSSION

It is apparent from the data shown in Figure 3 that as the time of treatment proceeds mean greyness values increase, establishing a similar trend for each of the applied voltages. The mean greyness value indicates the extent of coalescence and therefore phase separation in the emulsion. Confirmation of this may be seen from the photomicrographs given in Figure 4 which depict the state of the system moments after the treatment end point. Also, it should be noted that in the absence of dispersed phase the light transmitted through the separator registered a mean greyness value of 176.5.



*Figure 3. Rate of change of mean greyness value as a function of applied voltage magnitude.*

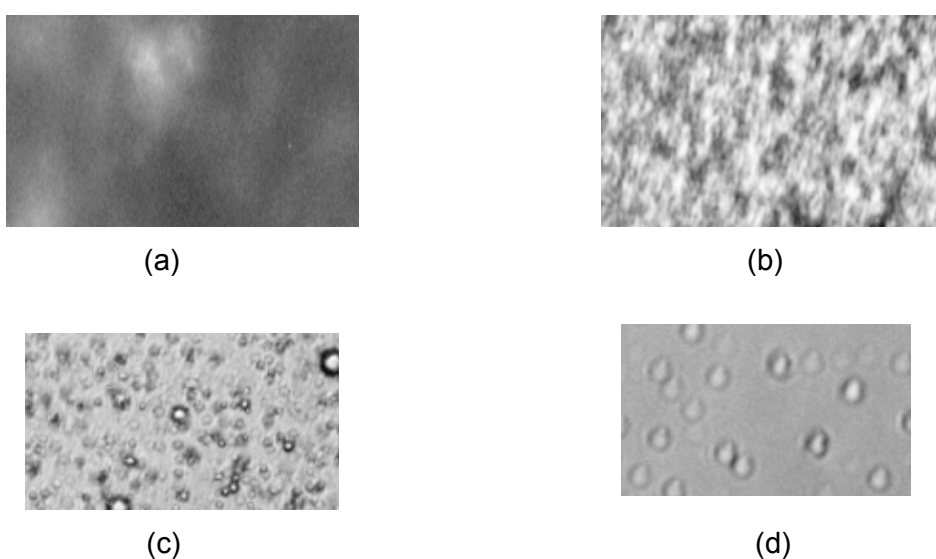


*Figure 4. Micrographic images of (a) untreated emulsion; (b) 2 kV, 5 Hz, Type B field; (c) 4 kV, 5 Hz, Type B field; (d) 6 kV, 5 Hz, Type B field.*

Further evidence of the beneficial effect on coalescence of increasing the applied voltage magnitude is given in Figure 5 which shows the mean greyness values obtained at 665 s for three different frequencies. For a given frequency, voltage comparisons are valid since each batch has received energisation by the same number of cycles. It is clear that for the range of frequencies used the best phase separation occurs at 50Hz except at the highest applied voltage. Here it is possible that the sudden fall in performance may be explained by the combined effects of voltage magnitude and rate of change being such as to cause Rayleigh instability and hence droplet break-up. As far as the general trend with frequency is concerned, it is known from the electrical analysis of a broadly equivalent circuit [5] that the dynamic response of the circuit influences the magnitudes of the electric field appearing in the emulsion. In particular, because the equivalent resistance of the emulsion is negligible compared to that of the air gap, the voltage drop across the emulsion is relatively small compared to the applied voltage source for an appreciable time in each cycle. At low frequencies, resistive currents dominate for most of the cycle except immediately after a change in direction of the applied voltage at which time the displacement currents are important. At moderate and higher frequencies the displacement current components remain important throughout the cycle and therefore the magnitude of the voltage applied between the electrodes and across the emulsion itself are comparable.

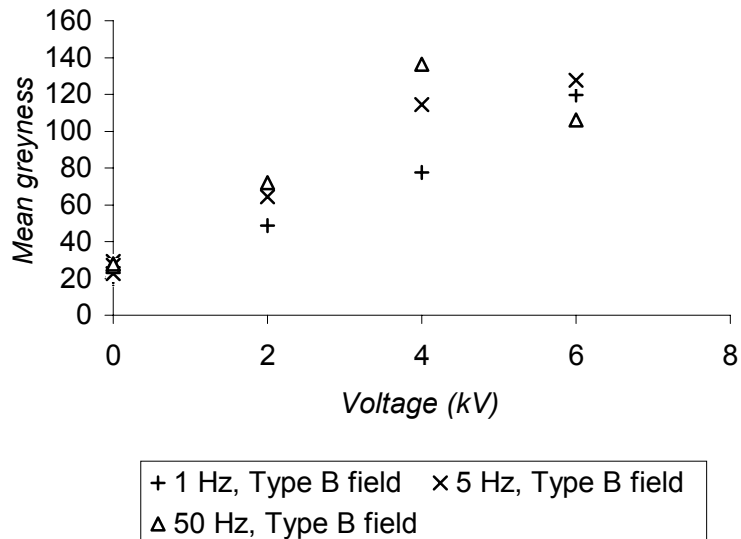


*Figure 5. Mean greyness at 665 s after the application of different voltages as a function of frequency.*

In the context of the present work where the same potential difference is applied across the electrodes for frequencies of 1 Hz, 5 Hz and 50 Hz it is therefore to be expected that the field in the emulsion would increase accordingly. The higher field strength then experienced by the droplets being the reason for the observed improvement in phase separation with increasing frequency.

Further evidence of the importance to be attached to the dynamic response of the coalescer may be seen in Figure 6 where the performance of the flotation-assisted electrostatic coalescer is improved by changing the waveform of the source voltage. Somewhat surprisingly, the type A waveform outperforms the type B waveform perhaps indicating that the temporal field profile experienced by the droplets in the emulsion is also a factor in achieving good coalescence.

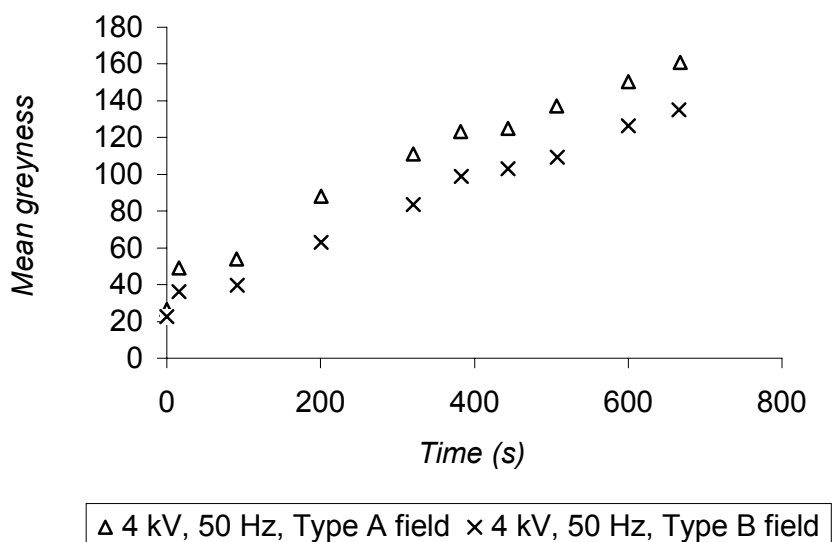


Figure 6. Mean greyness as a function of the shape of the applied waveform.

## CONCLUSIONS

A novel flotation-assisted electrostatic coalescer has been demonstrated to give efficient resolution of a stable water-in-oil emulsion. Phase separation, monitored by a non-invasive method employing digital video image analysis, is shown to be a function of source voltage waveform, magnitude, and frequency.

## REFERENCES

1. J. S. Eow, M. Ghadiri, A. O. Sharif and T. J. Williams (2001), *Chem. Eng. J.*, **3808**, 1-20.
2. P. J. Bailes (1996), *Eur. Pat. No. 0632 739B1* (June).
3. P. J. Bailes and P. K. Kuipa (1997), *Proc. First European Congress on Chem. Eng.*, Florence, (4), 2861-2864.
4. A. Edalat (2000), *MSc Dissertation*, University of Bradford, UK,
5. F. M. Joos and R. W. L. Snaddon (1985), *Chem. Eng. Res. Des.*, **63** (5), 305-310.



## DROP COALESCENCE BEHAVIOR FOR EXTRACTION SYSTEMS CONTAINING INDUSTRIAL EXTRACTANTS

Takahiko Ban, Fumio Kawaizumi, Susumu Nii and Katsuroku Takahashi

Department of Chemical Engineering, Nagoya University, Nagoya, Japan

A prediction of drop coalescence behavior based on HLB values of extractants has been examined for industrial liquid-liquid extractant systems. Similar experiment was conducted with surfactants, SPAN systems, for which HLB values are known. The dependence of drop coalescence behavior on HLB of extractant systems is similar to that of the surfactant systems. HLB of the extractants works as one controlling factor for drop coalescence. Additionally, drop size of dispersed phase has been measured in a single stage mixer-settler column for three extractant systems, TOPO, TOA and PC88A. The change of drop size with extractant concentration can be explained qualitatively from drop coalescence behavior.

### INTRODUCTION

Liquid-liquid dispersions play an essential role in separation processes and reaction systems. This is because large interfacial area due to dispersion promotes mass transfer and reaction rates. Estimation of the drop size controlling the interfacial area in liquid-liquid extraction columns is important for both extraction efficiency and operation of the apparatus. Thus a number of relationships have been proposed to describe the effect of column geometry, agitation conditions, physical properties of the liquid-liquid system, and direction of mass transfer on the drop size [1, 2]. It should be noted, however, that the observed holdup effects of dispersed phase on the drop size are different, depending on the authors. This fact suggests that the drop coalescence behavior depends on the liquid-liquid systems investigated. The drop size is affected greatly by the coalescence of dispersed drops. Thus a number of theoretical and experimental researches have been reported of drop coalescence [3-9]. The predictions of drop coalescence behavior treated in these papers are based on the film drainage theory in which only the physical properties of fluids (interfacial tension, density and viscosity) are taken into consideration. Experimental data reported are those obtained in limited situations. Equations for prediction of coalescence are complicated and contain parameters which are practically unavailable. For this reason predicting the coalescence behavior in some of actual cases is extremely difficult.

In this work, among the physicochemical parameters of systems we paid special attention to HLB (hydrophile-lipophile balance) to apply it as an index to predict drop coalescence behavior in practical cases. Drop coalescence behavior in liquid-liquid system has been monitored for ten systems containing industrial extractants, e.g., PC88A (2-ethylhexyl-phosphonic acid mono-2-ethylhexyl ester), D2EHPA (di(2-ethylhexyl)phosphoric acid), TBP (tri-*n*-butyl phosphate), MIBK (methylisobutyl ketone), LIX 84I (2-hydroxy-5-nonylacetophenone oxime), LIX 860IC (5-dodecylsalicylaldoxime), TOA (triocetylamine), Et2CO (diethylketone), BA (benzoylacetone) and TOPO (tri-*n*-octylphosphine oxide). Factors investigated are concentration and HLB of the extractants. Similar experiment was conducted with surfactants, SPAN systems, for which HLB values are known. Average coalescence times for the extractants are compared with those for the surfactants.

Additionally, drop size of dispersed phase has been measured in a single stage mixer-settler column for three systems containing industrial extractants, e.g., TOPO, TOA and PC88A.

## EXPERIMENTAL

### Measurement of Coalescence Time

Coalescence times of two droplets growing at the adjacent glass nozzles standing in parallel were measured. Details of coalescence cell are shown in Figure 1. This apparatus is wholly made of glass and PTFE. Two nozzles **B** with an inner diameter 1.9 mm are introduced in the coalescence cell **A** with an inner diameter 22 mm. The whole apparatus was set in a thermostat air bath to have a good temperature control.

Dispersed phase was fed to both nozzles **B** using a micro-feeder which pushes two syringes simultaneously at the rate 0.5 mm/s. Continuous phase is fed downward into the coalescence cell at flow rate 1.5 mm/s. The drop diameter is 3-5 mm. A video camera was used to monitor the time course of coalescence for the droplets formed at the top of adjacent nozzles in water.

Coalescence time is here defined as the period from the contact time to coalescence time. About 10 runs of measurements of time for coalescence were carried out for each condition. If no drop coalescence occurred in five minute, the measurement was stopped.

### Measurement of Drop Size

The mixer settler column is 100 mm in diameter and 100 mm in height. Single stage of the column (see Figure 2) consists of a lower mixer part and an upper settler part, and a drop coalescer is set between them. The coalescer is a three-dimensional lattice made of glass fiber mesh coated with PTFE. A 6-blade lifter turbine is installed in the mixer.

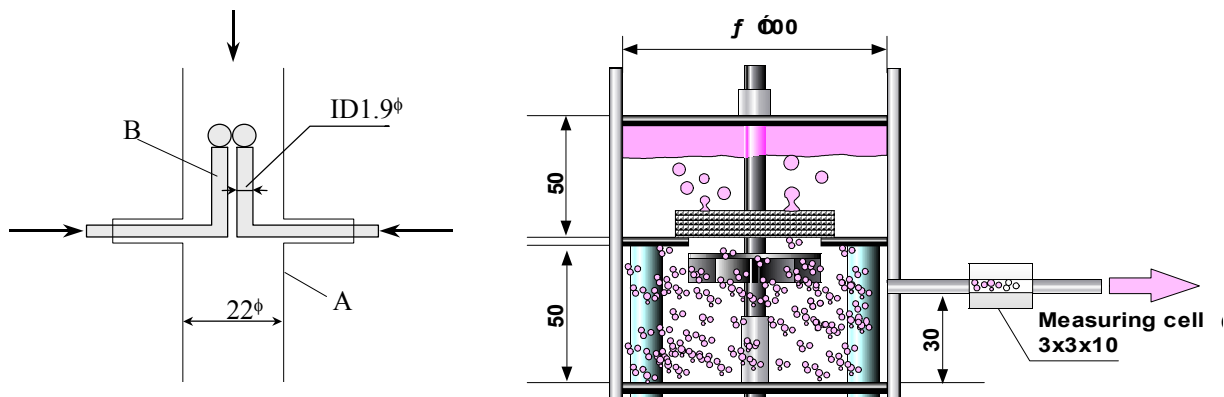


Figure 1. Details of coalescence cell.

Figure 2. Single stage of mixer-settler extraction column.

Aqueous phase (continuous phase) is led to the bottom of mixer through two pipes (not shown in Figure 2) and is discharged from the bottom of the settler through two down spouts. Organic phase (dispersed phase) is also introduced from bottom of the mixer and is drawn from the top of the settler. Liquid samples in the mixer are drawn out from the pipe passing through the rectangular measuring cell. The volume of dispersed phase as well as the total amount of the liquid sample were measured to determine holdup of dispersed phase. Drop size was determined from photograph of the rectangular measuring cell.

## RESULTS AND DISCUSSION

### Relation between coalescence time and HLB

Experimental system is heptane-extractants-water. Figure 3 refers to average coalescence time plotted against extractants concentration (wt%) for various extractants. Average coalescence times,  $t_c$ , for PC88A are very smaller even at their low concentrations. TOPO showed no drop coalescence in the concentration range measured. The values of  $t_c$  for TOA decrease with the increase in the concentration. In general the presence of surface-active substance retards droplets from coalescing. This is because the interfacial tension gradient arising from the concentration difference in the film by natural drainage opposes the film drainage. However, the drop coalescence times decrease with increasing the extractants concentration except for TOPO. The similar result was obtained when a solute is transferred from dispersed phase to continuous phase [11]. As a result of slight solubility of these extractants in water, the effect of mass transfer of these extractants may promote drop coalescence. TOPO having strong hydrophobicity show no effect on the drop coalescence. In heptane-water system, i.e., without extractants, drop coalescence never occurred in the present experimental condition.

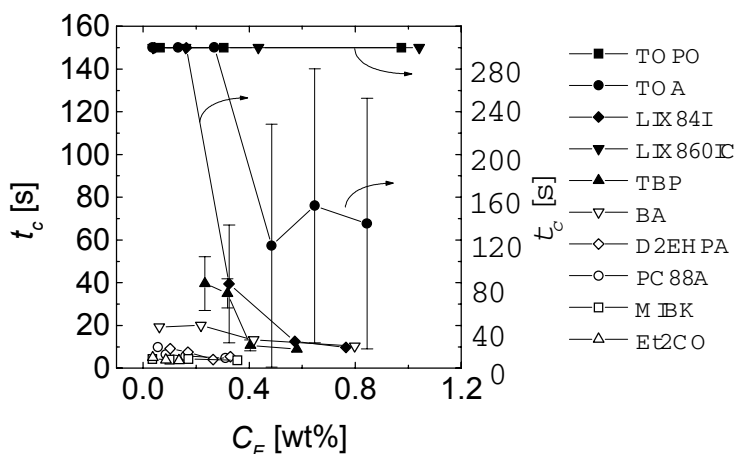
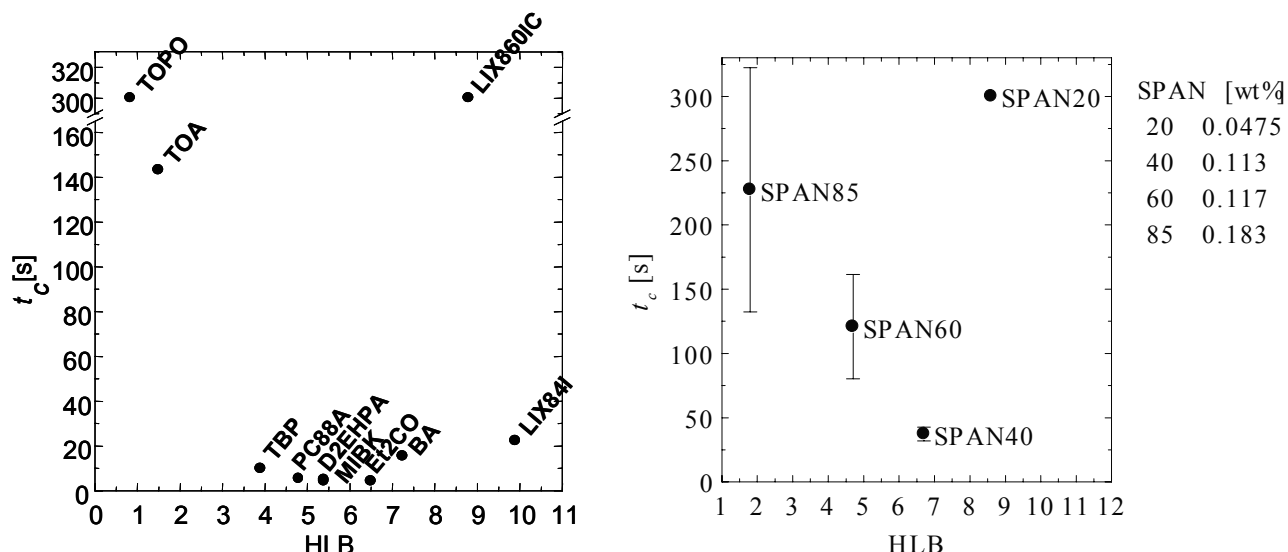


Figure 3. Effect of concentration on coalescence time.

HLB values of extractants were calculated by Oda method [11]. The relation between coalescence time and HLB in the extractant systems is shown in Figure 4(a). Coalescence time in Figure 3 refers to coalescence time averaged for the concentration range where the change in coalescence times with the concentration is small. When no coalescence occurs, coalescence time is taken as 300 s. Average coalescence time decreases with increase in HLB for HLB values lower than about 8. BA having HLB value 7.3 and LIX84I having HLB value 9.9 retard droplets coalescing. LIX860IC having HLB value 8.8 shows no drop coalescence. Coalescence times for TOPO and TOA having strong hydrophobicity are very long. Substances with HLB value above 8 are appropriate for use as o/w emulsifier with the results that the oil droplets are prevented from coalescing. The results for surfactants for which HLB values are available are shown in Figure 4(b). Since the surfactants are insoluble in heptane, the measurement of coalescence time was done in toluene-surfactants-water system.

The most remarkable finding is the strong resemblance between the result for the extractants and that for the surfactants system. SPAN85 having HLB value 1.8 significantly retards droplets coalescing. The higher the HLB values become, the shorter the coalescence times become for HLB values lower than 8. No drop coalescence was observed for SPAN 20 having HLB value 8.6. Our results indicate that irrespective of the kind of surface-active substance coalescence time decreases with the increase in HLB for HLB values lower than about 8, while

coalescence time increases at HLB values higher than 8. This implies that hydrophilicity or highly lipophilicity of extractants prevents the droplets from coalescing. Thus, HLB works as a clue to predict drop coalescence behavior for industrial extractants for which reliable data of physical and chemical properties are unavailable.

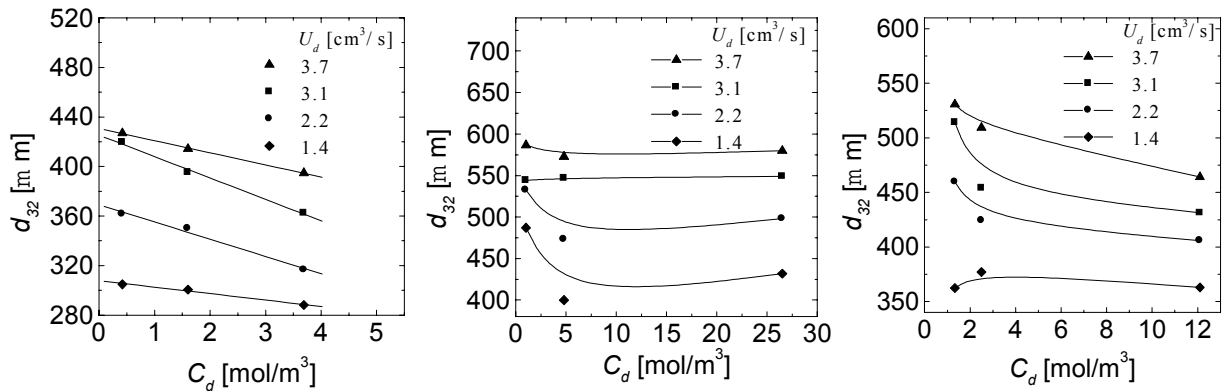


*Figure 4. Relation between coalescence time and HLB in extractant (a) and surfactant (b) systems.*

#### Relation between Drop Size and Holdup

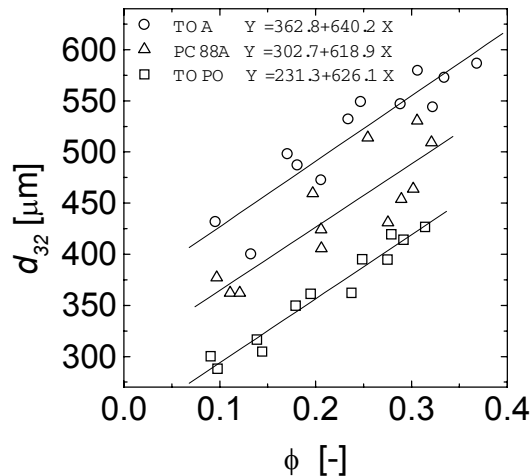
Drop size and holdup of dispersed phase were measured in TOPO, TOA and PC88A systems. As shown Figure 4(a), coalescence time for TOPO is the longest and that for PC88a is the shortest in these systems. The Sauter mean diameters,  $d_{32}$ , of dispersed phase are plotted against hold up in Figure 5. Sauter mean diameter for both TOPO and PC88A decreases with the concentration, while one for TOA remains constant with the concentration. Although PC88A shows very short coalescence time, the Sauter mean diameter decreases with the concentration, i.e. the coalescence effect is minor. As shown in Figure 3, coalescence behavior for both TOPO and PC88A is independent of the concentration. Thus the factor controlling drop size in these systems is breakage effect by their surface activity rather than coalescence effect. On the other hand coalescence time for TOA decreases with concentration. The enhancement of coalescence frequency by increasing the concentration maintains drop size at constant value.

Figure 6 represents the relation between Sauter mean diameter and holdup. The Sauter mean diameter increases linearly with holdup for all systems. In contrast to our expectation that PC88A will show the highest slope as a reflection of its shortest coalescence time among the three, the slopes of these lines in three systems are similar. Estimation of drop size needs consideration of the competition between coalescence and breakage effects.



*Figure 5. Effect of extractant concentration on Sauter mean diameter.*

(a) TOPO (b) TOA (c) PC88A.



*Figure 6. Relation between Sauter mean diameter and holdup.*

## CONCLUSION

The relation between coalescence times and HLB in both the extractants and surfactants systems was investigated in the present work. The results for the extractants show that coalescence time decreases with the increase in HLB for HLB values lower than about 8, while it increases with HLB value higher than 8. The similar result was obtained for industrial surfactants SPAN. HLB of the extractants works as a reference for prediction of coalescence.

Drop size of dispersed phase was measured in the single stage mixer-settler column. The results show that the change of drop size with extractant concentration can be explained qualitatively from drop coalescence behavior. However, the assumption that drop size is predictable from drop coalescence behavior was unsuccessful for the system investigated.

## REFERENCES

1. P. H. Calderbank (1958), *Trans. Inst. Chem. Eng.*, **36**, 443-463.
2. A. Kumar and S. Hartland (1994), *Trans. Inst. Chem. Eng.*, **72**, 89-104.
3. G. E. Charles and S. G. Mason (1960), *J. Colloid Sci.*, **15**, 236-267.
4. S. Liu and D. Li (1999), *Chem. Eng. Sci.*, **54**, 5667-5675.
5. G. V. Jeffreys and J. L. Hawksley (1965) *AIChE J.*, **11**, 413-417.
6. G. V. Jeffreys and J. L. Hawksley (1965), *AIChE J.*, **11**, 418-424.
7. J. C. Lee and T. D. Hodgson (1968), *Chem. Eng. Sci.*, **23**, 1375-1397.
8. I. Komasawa and J. Ingham (1978), *Chem. Eng. Sci.*, **33**, 479-485.
9. W. Meon, W. Rommel and E. Blass (1993), *Chem. Eng. Sci.*, **48**, 159-168
10. T. Ban, F. Kawaizumi, S. Nii and K. Takahashi (2000), *Chem. Eng. Sci.*, **55**, 5385-5391.
11. R. Oda (1957), *Kaimenkasseizai no Gosei to sono oyou*, Maki Shoten, Japan, pp. 501-502.



## NON-INVASIVE EXPERIMENTAL STUDY AND PHENOMENOLOGICAL MODELLING OF TOLUENE-IN-WATER TURBULENTLY AGITATED LIQUID-LIQUID DISPERSIONS

M. M. Ribeiro, M. Baptista, P. Teixeira\*, J. M. Soeiro\*, L. M. Ribeiro\*,  
M. M. L. Guimarães and J. J. C. Cruz-Pinto\*\*

Dep. Engenharia Química, Instituto Superior de Engenharia do Porto, Porto, Portugal

\* Faculdade de Engenharia, Universidade do Porto, Porto, Portugal

\*\* Dep. Química, Universidade de Aveiro, Aveiro, Portugal

Liquid-liquid dispersions usually show highly dynamic behaviour, marked by simultaneous drop size- and operating conditions-dependent breakage and coalescence. This complex behaviour is difficult to realistically model and accurately probe by non-invasive experimental means. In this work, an experimental batch/continuous agitated vessel with attendant dispersed phase imaging system was set-up, and is described here (together with drop size data treatment procedures), in order to non-invasively study toluene-in-water turbulently agitated liquid-liquid dispersions. The data is physically interpreted and compared with the results of numerical simulations using a specifically developed, population balance numerical algorithm, combined with a detailed description of the hydrodynamics according to three different drop interaction models, as developed by different authors (Coulaloglou and Tavlarides, Sovová, and Tsouris).

### INTRODUCTION

In process vessels, agitation-induced turbulence, which is required to create and maintain a dispersed phase with the specific interfacial area adequate for mass transfer, directly controls drop breakage and coalescence frequencies (and thus drop size and interfacial area distributions) as well as the instantaneous kinetics of the (transfer or reaction) process through the individual drop surfaces. Mass transfer efficiency of liquid-liquid mixers thus becomes highly dependent on these hydrodynamic phenomena. In multi-component systems, this behaviour is also of paramount importance to the overall rate and selectivity of the process.

Present knowledge of these processes is still embarrassingly scarce, in particular when contrasted with the present availability of physically realistic, fast and efficient algorithms with effective predictive power and suitable for real plant control applications [1, 2].

During the last decades several drop-size measurement techniques have been developed or adapted from solid particle size measurement. Bae and Tavlarides [3] discussed the operating range of several available techniques. Most of these were employed for measuring the drop size distribution (or average drop size) in lean dispersions under steady state conditions. However, techniques that involve sampling of the drops are not adequate for unsteady-state experiments. Even under steady state conditions, capillary techniques are very tedious and time consuming when very lean dispersions are involved. Recent experiments made in a Kühni column at the Technical University of Munich [4] highlighted and supported this assertion.

Recently, drop size studies have been made easier by developments in video and image processing technology [5], but still suffer from flaws originated from intrusion or wall effects, mainly at high volume fractions.

These experimental studies provide the factual basis for modelling procedures to describe drop size distribution by means of population balance techniques, and indicate that there are a number of different possible coalescence mechanisms [6]; however, there have been difficulties in identifying mechanisms that correlate well to the data collected.

Early computer simulations of agitated liquid-liquid systems were based on *ad hoc* heuristics to describe peculiarly idealised interactions within the dispersed phase. Most of the present day approaches, however, employ highly sophisticated models based on sound kinetic-statistical principles (Brownian collision and homogeneous turbulence, for instance) and describe the relevant material and equipment properties by means of phenomenologically significant parameters. Such approaches are usually based on population balance techniques and explicitly include detailed descriptions of environmental conditions on breakage and coalescence events. Among such models, Coulaloglou and Tavlarides' model [7], for the locally isotropic regime, enjoys well-deserved prominence, despite some acknowledged deficiencies. This model has been described as adequately accurate, both when mass transfer is present and absent, and has been extensively put to use for both stirred vessels and extraction columns. However, Sovová [8] and Tsouris [9] have cast doubts about its description of the coalescence event. We shall compare these three models with our experimental data.

All the above authors use the same expression for the breakage frequency,

$$g(d) = C_1 \cdot \frac{\varepsilon^{1/3} \cdot d^{-2/3}}{1+\phi} \exp\left(-\frac{C_2 \sigma \cdot (1+\phi)^2}{\rho_D \varepsilon^{2/3} \cdot d^{5/3}}\right) \quad (1)$$

and, for the collision frequency,

$$h(d, d') = C_3 \cdot \frac{\varepsilon^{1/3}}{(1+\phi)} \cdot (d^2 + d'^2) \cdot (d^{2/3} + d'^{2/3})^{1/2} \quad (2)$$

where  $C_1$ ,  $C_2$  and  $C_3$  are constants,  $d$  and  $d'$  are the diameters of the colliding drops,  $\phi$  is the dispersed phase holdup,  $\varepsilon$  is the energy dissipation per unit mass,  $\sigma$  is the interfacial tension and  $\rho_D$  is the dispersed phase density.

Coalescence frequency is modelled as a product of two factors, the collision frequency and the coalescence efficiency. To describe the coalescence efficiency, Coulalouglo and Tavlarides [7] have used a probabilistic model, based on the argument that coalescence occurs when the contact time between the two colliding drops exceeds the time necessary to drain the liquid film between them to rupture thickness. The expression obtained for the coalescence efficiency, considering drop size above the turbulence micro-scale, is

$$\lambda(d, d') = \exp\left[-C_4 \cdot \frac{\mu_c \cdot \rho_c \cdot \varepsilon}{\sigma^2 \cdot (1+\phi)^3} \left(\frac{d \cdot d'}{d + d'}\right)^4\right] \quad (3)$$

where  $C_4$  is a constant and  $\rho_c$  and  $\mu_c$  are, respectively, the density and viscosity of the continuous phase.

Based on the assumption that coalescence is controlled by the ratio between the interfacial energy and the energy of collision, Sovová [8] suggested the following equation for the coalescence efficiency:

$$\lambda(d, d') = \exp\left[-C_5 \frac{\sigma \cdot (d^2 + d'^2) \cdot (d^3 + d'^3) \cdot (1+\phi)^2}{\rho_D \cdot \varepsilon^{2/3} \cdot d^3 \cdot d'^3 \cdot (d^{2/3} + d'^{2/3})}\right] \quad (4)$$

where  $C_5$  is another constant.

Tsouris [9] argued that Sovová's equation (4) excessively inflates the coalescence frequency of the larger drop sizes, while Coulalouglou's expression (3) overestimates smaller drop coalescence. Therefore, he used another form of the coalescence efficiency function

$$\lambda(d, d') = \exp \left[ -c_6 \cdot \frac{\mu_C \cdot (1 + \phi)}{\rho_C \cdot \varepsilon^{1/3} \cdot (d + d')^{4/3}} \right] \quad (5)$$

where  $C_6$  is a constant.

## EXPERIMENTAL SETUP AND MEASUREMENT TECHNIQUE

The liquid-liquid system used for the experiments consists of toluene as the dispersed phase and distilled water as the continuous phase. The apparatus used is shown in Figure 1. A glass vessel with flat bottom and four baffles was used. A standard Rushton turbine of 0.1 m diameter (1/2 of vessel diameter) provided the agitation.

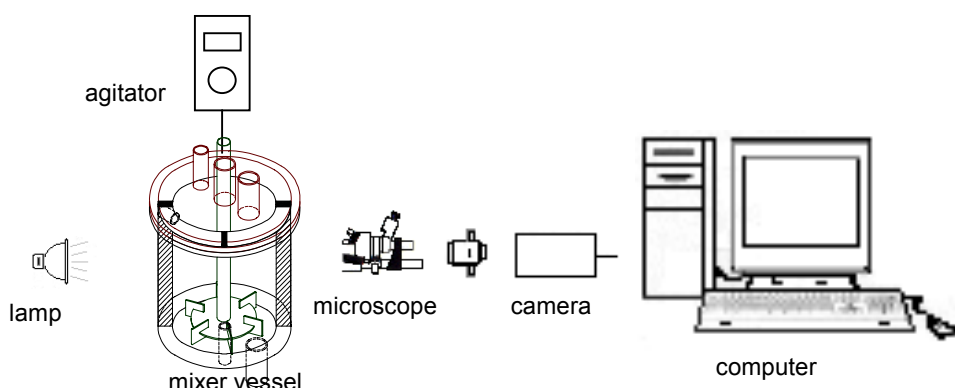


Figure 1. Schematic drawing of the mixer and data acquisition equipment.

In order to measure the drop size distribution, new techniques have been developed, based on image acquisition by means of a video camera and microscope. As mentioned above, Pacek [5] used such a technique but illuminated invasively, thus disturbing the local hydrodynamics. We aimed at a feasible non-invasive technique, even if limited to lower hold-ups. After exhaustively testing a large variety of video cameras available in the market, one of them was selected for its speed and sensitivity: the *Sensicam Long Exposure*. This camera was mounted behind a low magnification *Nikon SMZ-2T* microscope, supported by a purpose-built structure, enabling focusing and targeting. For the present work, the magnification was 25 times the actual size, and the focus was located approximately 15 mm behind the vessel wall.

Opposite, the lighting system was mounted. Several types of lighting systems were tried, from fluorescent tubes, to point sources, electronic flat lamps and halogen lamps. Only the latter exhibited consistently good results using four 12 Volt-lamps (focused beam, rear heat dissipation support, *Phillips ref. Masterline Plus*).

From the video pictures acquired, drop sizes were measured by means a routine developed in *Scion Image* software. In this specific routine, a mouse is used to place three points on the perimeter of each drop. The software then inserts a circle showing the size and the location of the drop, and these data are stored in an ASCII (.txt) file. If the operator misplaces one of the points, which would lead to a wrong size determination, he can visually detect it and repeat the three-point selection. After all drops have been measured for each experiment, the .txt file is exported to *Microsoft Excel* and the drop size in pixels recalculated to centimetres. The drop volumes were classified into 50 different logarithmic size fractions, from  $10^{-7} \text{ cm}^3$  to  $10^{-2} \text{ cm}^3$ .

## PROCEDURE AND RESULTS

Experimental drop size distributions were compared with the results predicted by numerically solving three different coalescence models (Sovová, Tsouris and Coulalougou and Tavlarides).

Experimental batch runs under different sets of operating conditions (hold-up and agitation rates) were planned (agitation rates 99/111 rpm; hold-ups 1.85/2.17 %) and performed, taking into consideration the conflicting requirements for image quality (moderate hold-ups and not too small drops) and homogeneous dispersion in the vessel.

Common ( $C_1$ ,  $C_2$  and  $C_3$ ) and specific ( $C_4$ ,  $C_5$  and  $C_6$ ) model parameters were adjusted to the pooled data from four batch experiments, using a standard Levenberg-Marquardt routine and the visual and numerical (sum-of-squares of deviations) quality of the adjustments were noted and compared (see Table 1 and Figures 2, 3 and 4 for some examples).

*Table 1. Optimised breakage and coalescence parameters for the three different models.*

Coalescence Model	Ssq Deviation	Breakage $C_1$	Breakage $C_2$	Coalescence $C_3$	Coalescence
Coulalougou/ Tavlarides	1.32864e-5	2.37516e-3	3.16059e-2	1e-3	$C_4 = 1.8443e+1$
Sovová	1.32834e-5	2.37445e-3	3.16619e-2	1e-3	$C_5 = 1.50335e-5$
Tsouris	1.32863e-5	2.37505e-3	3.16068e-2	1e-3	$C_6 = 3.01719e-3$

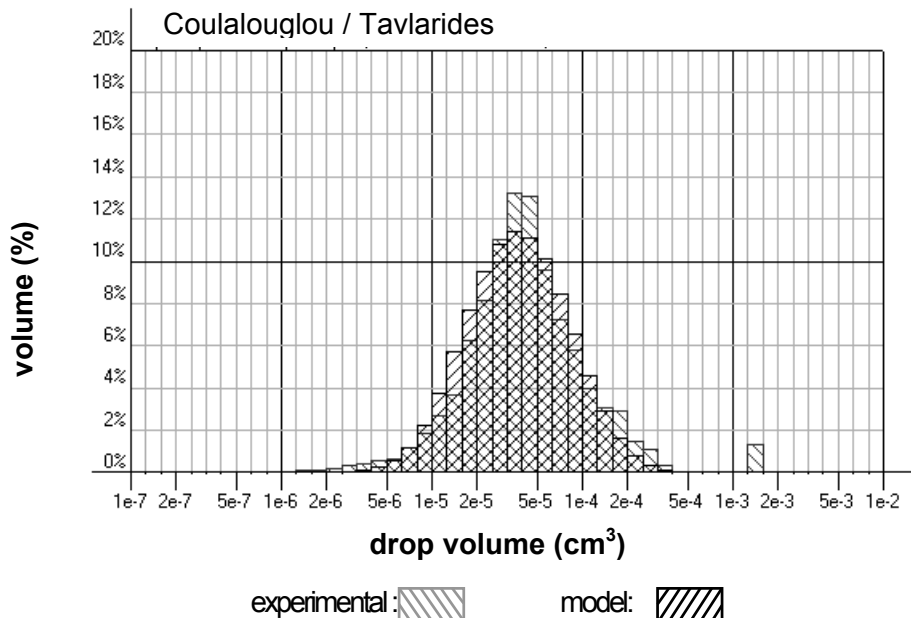


*Figure 2. Experimental and simulated (according to Coulalougou and Tavlarides' model) histograms of size distributions, in a batch vessel, for 100 rpm and 1.85 % hold-up.*

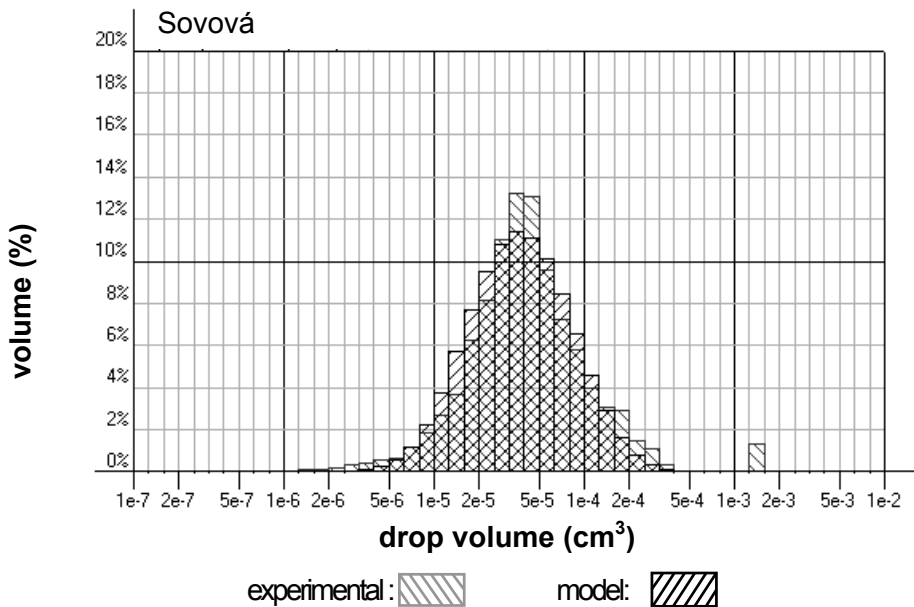


*Figure 3. Experimental and simulated (according to Sovová's model) histograms of size distributions, in a batch vessel, for 100 rpm and 1.85 % hold-up.*

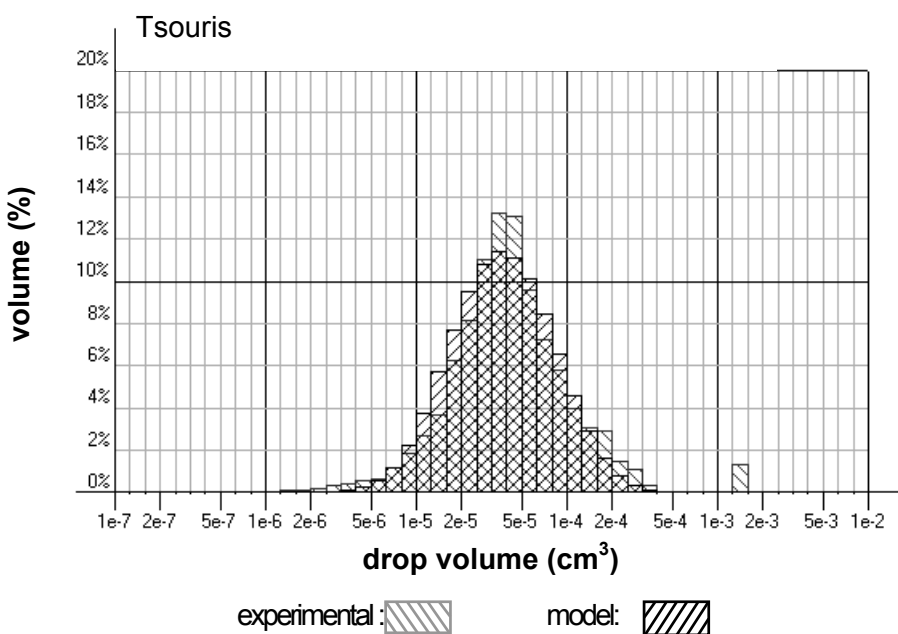


*Figure 4. Experimental and simulated (according to Tsouris' model) histograms of size distributions, in a batch vessel, for 100 rpm and 1.85 % hold-up.*

In order to test the predictive performance of the three models, 13 continuous runs (agitation rate 113 rpm, hold-up 1.85%, and residence time 167 s) were performed under the same operating conditions. Using the kinetic parameters from the batch runs, the averaged data were used to optimise the (unknown) drop feed distribution parameters ( $V_{\text{aver.feed}}$  and  $\sigma_{\text{feed}}/V_{\text{aver.feed}}$ ) and weighed sum-of-squares of the deviations (see Table 2).

*Table 2. Optimised feed drop distribution parameters for the three different models under continuous operating conditions.*

Model	Ssq of deviations	$V_{\text{aver.feed}}$	$\sigma_{\text{feed}}/V_{\text{aver.feed}}$
Coulalouglou/Tavlarides	2.26441e-5	9.33067e-4	2.99811e-1
Sovová	2.24796e-5	9.30824e-4	3.00424e-1
Tsouris	2.26381e-5	9.32955e-4	2.99840e-1

## DISCUSSION AND CONCLUSIONS

The quality of the adjustment of hydrodynamic parameters from the batch runs is excellent ( $\sim 10^{-5}$ ) for all three models as well as the agreement between the common parameters. Using the continuous runs as independent benchmarks, the predictive power of all three models is also remarkable, both as measured by the quality of the adjustment ( $\sim 2 \cdot 10^{-5}$ ) and by the agreement between the feed parameters' estimations.

Quite astonishing is the fact that such different models seem to have the same descriptive and predictive power. This may be ascribed to the narrow range of operating conditions used (and indeed required so far) by the size measurement set-up used.

## REFERENCES

1. L. M. Ribeiro, P. F. R. Regueiras, M. M. L. Guimarães, C. M. N. Madureira, J. J. C. Cruz-Pinto (1995), *Computers Chem. Engng.*, **19** (3), 333-343.
2. L. M. Ribeiro, P. F. R. Regueiras, M. M. L. Guimarães, C. M. N. Madureira, J. J. C. Cruz-Pinto (1997), *Computers Chem. Engng.*, **21** (5), 543-558.
3. J. H. Bae and L. L. Tavlarides (1989), *AIChE J.*, **35** (7), 1073-1084.
4. M. L. N. Gomes (1999) 'Comportamento Hidrodinâmico de Colunas Agitadas de Extracção Líquido-Líquido' Ph.D. Thesis, University of Minho, Braga, Portugal.
5. A. W. Pacek, I. P. T. Moore and A. W. Nienow (1994), *AIChE J.*, **40**, 1940-1949.
6. A.W. Pacek, C. C. Mann and A. W. Nienow (1997) *Progrès Récents en Génie des Procédeés*, **52**, 263.
7. C. A. Coulaloglou and L. L. Tavlarides (1977), *Chem. Eng. Sci.*, **32**, 1289.
8. H. Sovová (1981), *Chem. Eng. Sci.*, **36**, 1567.
9. C. Tsouris (1992), Modelling and Control of Extraction Columns, Ph.D. Thesis, University of Syracuse, USA.



## AC FIELDS IN SOLVENT EXTRACTION – INFLUENCE ON DROPLET FORMATION AND MASS TRANSFER

Guido Gneist and Hans-Jörg Bart

Institute of Thermal Process Engineering, University of Kaiserslautern, Germany

The influence of a high frequency electric field on droplet formation and mass transfer was investigated. Different parameters, such as capillary geometry and conductivity of the continuous water phase, were varied to study the influence on droplet size. As a result, the conical capillary leads to smaller Sauter-diameters in comparison to the flat one. In the same way, the lower conductivity of continuous phase resulted in smaller droplet sizes, as desired. Further, the dispersion of highly viscous liquids in water was demonstrated. Finally, mass transfer enhancement was visualized with an optical double flash system.

### INTRODUCTION

The application of different electric fields (DC, pulsed DC and AC) in solvent extraction is widely recorded in literature [1-6]. Herein an improvement of interfacial mass transfer is described by reducing the effective interfacial tension, increasing interfacial area for mass transfer and enhancing interfacial disturbance and drop circulation.

Concerning the increase of interfacial mass transfer area, mono-dispersed droplets of isododecane and toluene, down to 90 µm, were produced in distilled water using high frequency electric fields, with voltages up to 20 kV [7, 8]. Here for low dispersed phase flow rates (0.05 and 0.1 ml/min) a significant reduction of droplet diameter with increasing voltage was shown between 0 and 4 kV. In exceeding this limit, only a slight decrease was detected. A frequency change from 45 to 30 kHz was necessary to reach higher voltages above 4 kV and did not affect the droplet size. The two different flow rates did also not change the droplet size. In contrast, the different geometry of the capillaries used (glass capillary with axial electrode and stainless steel capillary) had a strong influence on droplet size. If the reverse dispersion type (water in organic) was investigated, the conductivity of the disperse water phase was an important factor in the spraying process.

In this paper the influence of capillary geometry and conductivity of the continuous water phase on droplet size, using in a high frequent AC field, were investigated. The conductivity was adjusted by adding NaCl to the continuous distilled water phase. Besides, the possibility of dispersing highly viscous liquids, such as Silicone Oil, in water was also studied. Additionally, the visualization of mass transfer enhancement under field conditions is given in the physical toluene/acetone/water system.

## EXPERIMENTAL PROCEDURE

The experimental set-up (see Figure 1) for droplet formation (1) is a double casing glass tube which is sealed with two Teflon plugs with boreholes for the nozzles. Herewith it is possible to disperse the heavy phase top down, as well as the light phase bottom-up to observe both dispersion types. The apparatus is placed inside a rectangular Plexiglas tank (2), thermostated with water at 298 K. The dispersed phase is fed into the nozzle by a dosing pump (5) with constant flow rate of 0.05 ml/min.

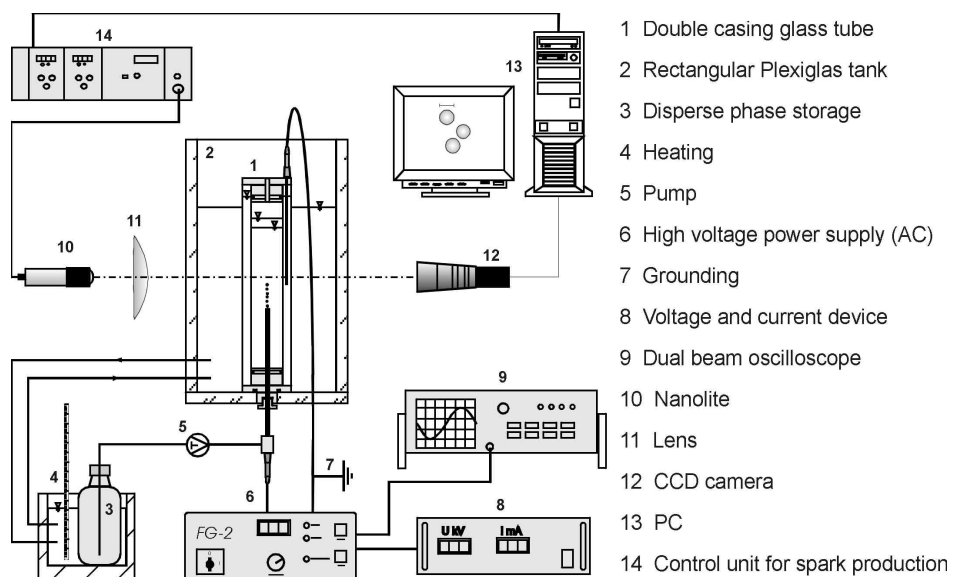


Figure 1. Experimental set-up.

For the experiments different types of isolated stainless steel capillaries are used (flat capillary (ID = 0.13 and 0.25 mm), cone shaped capillary (ID = 0.25 mm)). The high voltage power supply (6) is connected to the capillary and the ground electrode, where the double casing filled with an electrolyte (solution of 0.5 mol/l NaCl/H<sub>2</sub>O) acts as a grounded electrode (7). The applied voltage, the current and the AC frequency are then measured (8, 9). An optical double flash system is used for the analysis of droplet diameter. It comprises a nanolite (10) connected to a control unit (14), a planoconvex lens (11) and a CCD camera (12). Droplet images are taken under various experimental conditions and afterwards analysed with the use of digital image processing software (13). The measured droplet sizes are used to calculate droplet size distributions and Sauter-diameters. The physical properties of the liquids used are listed in Table 1.

Table 1. Physical properties of the liquids.

Liquid	Interfacial tension $\gamma$ [mN/m]**	Viscosity $\eta$ [mPa s]	Density $\rho$ [kg/m <sup>3</sup> ]
Isododecane	44.8	1.49	751
Isotridecanol	14.0	41.9	848
Silicone Oil 550	37.8	220.5	1060
Silicone Oil DC200	37.8	1000	970
Toluene	35.0	0.59	867
Acetone		0.316	791
Water		0.95	998

\*\* together with water

## CAPILLARY GEOMETRY

The results of droplet formation for isododecane in distilled water, using two different stainless steel capillaries, are shown in Figure 2. Both capillaries had the same inner diameter of 0.25 mm, but a different shape of the tips (flat and conical). For 0 kV the results strongly depend on the wetting of the material, which is influenced by the mechanical treatment of the tip and the cleaning procedure. Both capillaries were cut and machine polished and one of them afterwards received the conical shape by turning. The different finish of the tip could be an explanation for the deviation at 0 kV. If no wetting is expected, the droplets should have the same size. Between 0 and 1 kV, no stable voltage was available with the high voltage source. With increasing voltage the droplet size decreases and the wetting effect vanishes. A distinct influence of capillary geometry on droplet size is visible. Together with the conical capillary smaller droplets are formed. The relation between exposed cross-sectional area of liquid and cross-sectional area of capillary has to be considered in a correlation for droplet size.

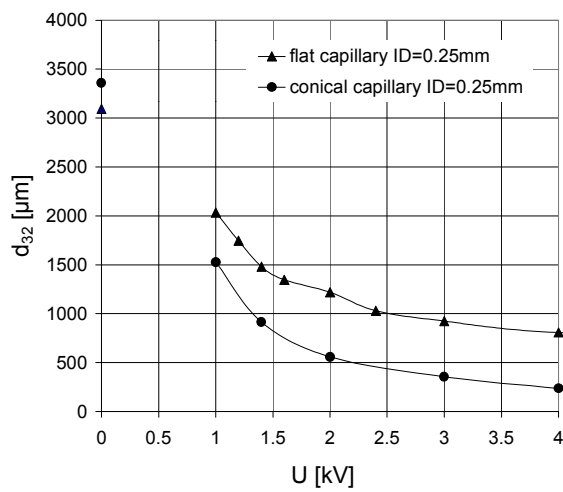


Figure 2. Sauter-diameter vs. applied voltage for different capillaries for isododecane droplets in distilled water.

## CONDUCTIVITY OF CONTINUOUS WATER PHASE

For all experiments the flow of current was measured as a function of applied voltage. In Figure 3 the typical current-voltage-plots are shown for varying conductivity of the continuous water phase at a constant frequency of 45 kHz.

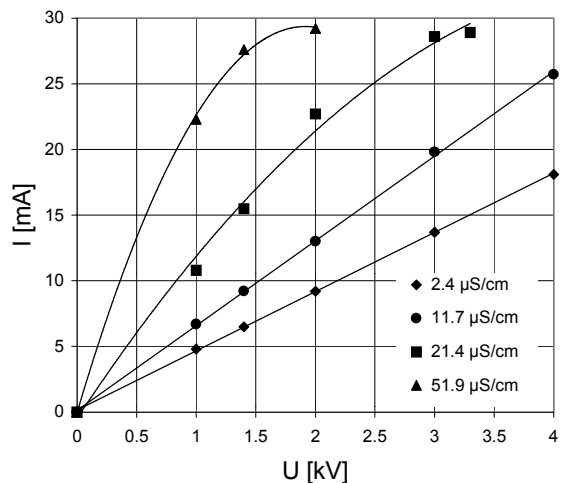


Figure 3. Flow of current vs. applied voltage for varying conductivity of continuous water phase.

Below 12  $\mu\text{S}/\text{cm}$  a linear relationship between current and voltage is visible, which loses its linearity with increasing conductivity. For 21.4  $\mu\text{S}/\text{cm}$  it was not possible to obtain higher voltages than 3.3 kV and for 51.9  $\mu\text{S}/\text{cm}$  not higher than 2.0 kV. Besides, increasing conductivity and current flow resulted in the production of heat in the apparatus.

The reducing effect of applied voltage on droplet size is neutralised with increasing conductivity of continuous water phase (Figure 4 (a)). The curves shift again to larger Sauter-diameters. Above 11.4  $\mu\text{S}/\text{cm}$  this effect is not negligible. With increasing conductivity the duration of charges at the droplet surface is minute, so that the resulting electric force, acting on the droplet, is reduced. The smallest droplets are produced together with the lowest conductivity. Additionally, with growing conductivity and flow of current, the power input is enhanced, which is directly visible in Figure 4 (b). At higher conductivity, the power input has to be raised to form the same droplet size.

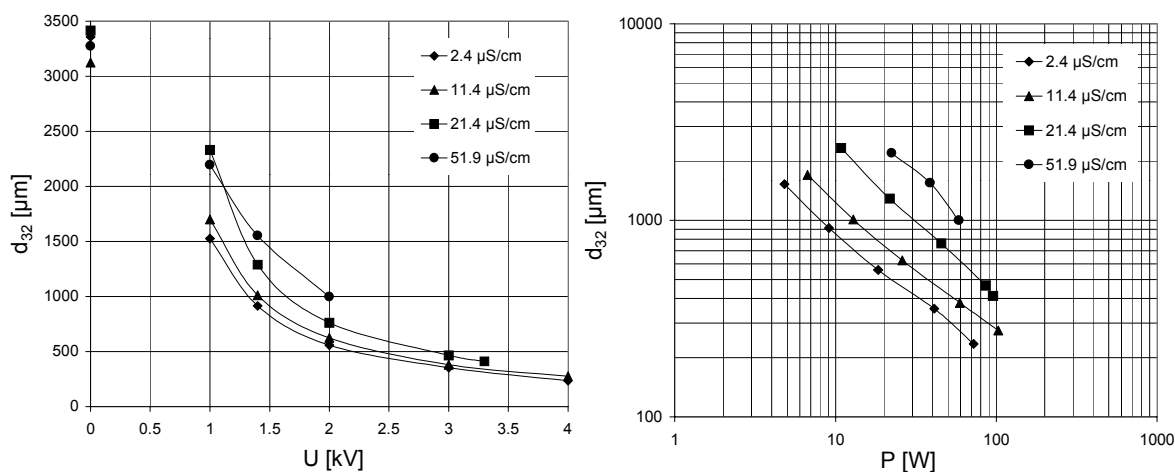


Figure 4. Sauter-diameter with respect to the applied voltage (a) and power input (b) for varying conductivity of continuous water phase (isododecane/water, cone shaped capillary ID=0.25mm).

## HIGHLY VISCOUS LIQUIDS

If dispersion of a highly viscous liquid into a medium of low viscosity, such as water, is achieved, some problems appear, because of low shear stress. Together with the presented method, it is possible to break the liquid-liquid surface and to form mono-sized droplets without any problem, as demonstrated in Figure 5.

The results of different organic solvents with a distinct variation of viscosity, shown in Figure 6, yield no clear dependence between viscosity and droplet size. For example, it is possible to calculate the different droplet sizes at 0 kV, without taking viscosity effects into account. The force balance between interfacial tension force and the force due to gravity are alone responsible for the resulting droplet size at 0 kV. With exceeding 0 kV, the electric field force prevails the force balance. The curves approach each other with increasing voltage.

## MASS TRANSFER

The electric field acts directly at the liquid-liquid interface. By changing the size and the shape of the interface, it is possible to influence the transfer of species between the liquids. Together with the optical system used, a relatively high concentration of acetone in water (3.7 mol/l) was chosen to visualize mass transfer inside a continuous toluene phase (Figure 7). With increasing voltage the droplet elongates, because of the electric stress, and the optical inhomogeneities

(schlieren) are greatly enhanced. These inhomogeneities are a result of density differences and therefore are an index for mass transfer. To get more insight into these interfacial phenomena under field conditions, a schlieren arrangement is being implemented at the moment and will be used for further investigations.

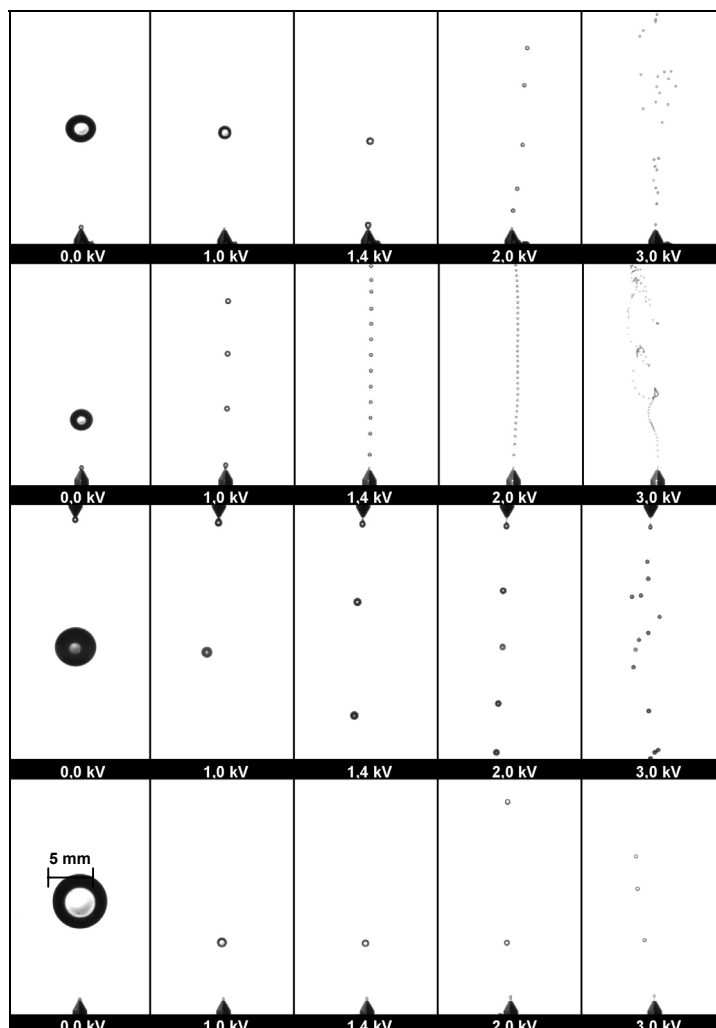


*Figure 5. Dispersion patterns with increasing voltage for different organic solvents in distilled water (images from top down: isododecane, isotridecanol, Silicone Oil 550, Silicone Oil DC200).*

## CONCLUSIONS

The influence of capillary geometry on droplet diameter was investigated in the isododecane/water system by applying a high frequency (45 kHz) electric field to the capillary. Using the conical capillary instead of the flat one, smaller droplets were formed, which indicates a relation between exposed cross-sectional area of the liquid and cross-sectional area of the capillary. The influence of continuous water phase conductivity on droplet size was also studied in the isododecane/water system. Here the lowest conductivity resulted in droplets with the smallest size. In this context, the conductivity of the water phase should not exceed 10  $\mu\text{S}/\text{cm}$ , to avoid a high flow of current and power input. Moreover, the presented technique, using high frequency AC fields, is successful, if highly viscous liquids have to be dispersed in low viscosity media, such as water. Concerning mass transfer enhancement, an observation of interfacial phenomena under field conditions was demonstrated with an optical double flash system and will be adjusted by a newly implemented schlieren arrangement.

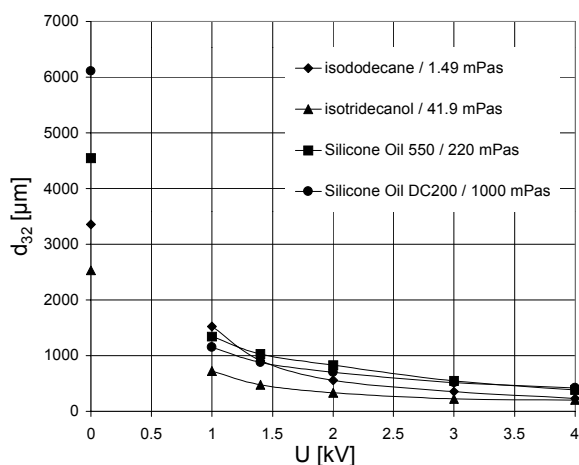


Figure 6. Sauter-diameter with respect to the applied voltage for different organic solvents with varying viscosity in distilled water.

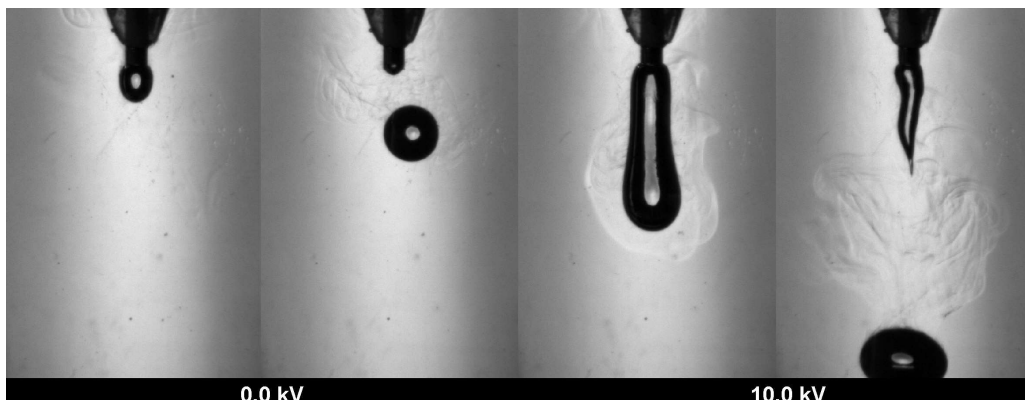


Figure 7. Mass transfer of acetone (3.7 mol/l) from a water droplet into a continuous toluene phase for 0 and 10 kV.

## ACKNOWLEDGEMENTS

The authors wish to thank the DFG for financial support and Mrs. K. Hauling and Mrs. A. Owzar for their help with the experiments.

## REFERENCES

1. G. Stewart and J.D. Thornton (1967), *I. Chem. E. Symposium Series* No. 26, pp. 29.
2. A.G. Bailey (1986), *Atom. Spray Techn.*, **2**, 95-134.
3. C.H. Byers and J.J. Perona (1988), *AIChE J.*, **34** (9), 1577-1580.
4. W. He, J.S. Chang and M.H.I. Baird (1997), *J. Electrostatics*, **40&41**, 259-264.
5. T.C. Scott (1987), *AIChE J.*, **33** (9), 1557-1559.
6. M. Sato (1984), *J. Electrostatics*, **15**, 237-247.
7. G. Gneist and H.-J. Bart (2000), *J. Electrostatics*, submitted.
8. G. Gneist and H.-J. Bart (2001), *Chem. Ing. Techn.*, in press.



# APPLICATION OF PREFERENTIAL SOLVATION CONCEPT FOR INTERPRETATION OF THE MECHANISMS OF SOLVENT EXTRACTION. I. ACID SOLVENT EXTRACTION BY AMINES. II. METAL SOLVENT EXTRACTION BY ACIDIC EXTRACTANTS

Vladimir Kislik

Casali Institute of Applied Chemistry, School of Applied Science and Technology,  
The Hebrew University of Jerusalem, Jerusalem, Israel

A novel competitive complexation/solvation modeling approach is introduced to explain the mechanisms of solvent extraction. The theory is based on the modified competitive preferential solvation theory, the concept of amphoteric properties of extractants and the concept of different aggregation structures' formation at increasing extractant loading. Four possible stages of extraction behavior, interacting mechanisms and aggregate structures formation, depending on solute-solvent affinity constant ratios and solvent concentrations, are discussed. Extractants are considered amphoteric and may perform as acids (electron acceptors) or bases (electron donors). A mathematical description for quantification of the results is also introduced. Based on the presented theory, analysis of different acid-amine and metal ion-organic acid extraction systems are presented. It gives a key for preliminary quantitative prediction of suitable extraction systems.

## INTRODUCTION

Solvent extraction is an efficient industrial scale technology for the separation and concentration of solutes from leachates, fermentation broths or industrial waste solutions. Complex chemistry of extraction processes is still not completely understood [1,2]. In some cases the complicated behavior of extraction systems conflicts with the stoichiometric ion-exchange models [3,4]. The difference in the extraction trends must be attributed to solvation (coordination) effects. In order to analyze solvation effects, identification, and most importantly, quantification of solvent-solute interactions must be accomplished. Coordination models, explaining qualitatively some mechanisms of metal solvent extraction, meet difficulties when modeling anion exchangers, acid solvent extraction and, especially, at the attempts of quantification of the models.

The Competitive complexation/solvation theory is based on the modified competitive preferential solvation (COPS) theory [5], the Lewis acid-base concept [1-4], the concept of amphoteric properties of extractants and the concept of different aggregation structures' formation at increasing extractant loading [3,4]. In this paper extraction of acids by amines and metal ions by acidic extractants is interpreted on the base of the new theory. The data, available from the literature [1,2] and our experiments [6,7], are used for interpretation.

## BASIC STATEMENTS OF THE THEORY

### I. As loading of organic phase by extracted solute increases, interacting mechanisms and compounds formed are changing

The most general extraction isotherm consists of four stages at loading of organic phase by extracted solute (see Figure 1):

Region 1: Comparatively low extraction at low solute concentration in the aqueous phase.

Region 2: Drastic rise of distribution curve where the small increase of solute concentration in the aqueous phase has a strong effect on its organic phase concentration.

Region 3: The distribution curve approaches saturation and levels-off to nearly a plateau.

Region 4: Above-stoichiometric extraction is pronounced at high solute concentrations with massive formation of the third phase. The distribution curve rises once more.

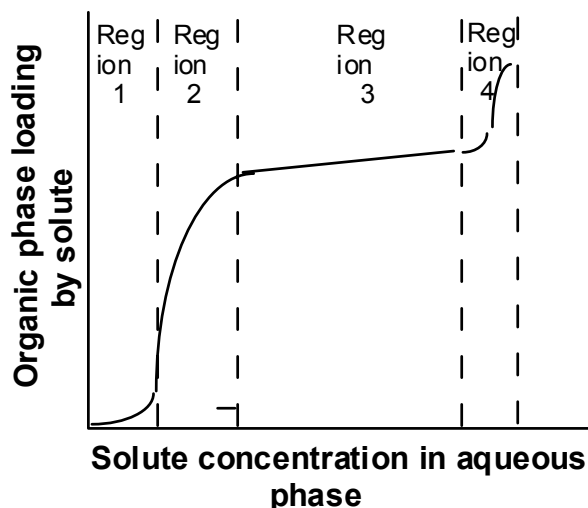


Figure 1. General scheme of organic phase loading as a function of solute concentration in the aqueous phase.

The division of the distribution curve between the regions depends on many factors, such as properties and concentrations of solute extracted, the properties of the extractants and solvents (modifiers, synergistic agents) used, temperature, acidity of the treated (feed) aqueous solutions and the structure of initial compounds, the structure of the organic compounds formed, aggregation, etc.

### II. Both strong (ion-exchange, "chemical", electrostatic) and weak (solvating, "physical", "intermolecular", hydrogen, coordinate) interactions have to be taken into consideration in all regions of the general extraction isotherm (Figure 1)

In the following, postulates of the COPS theory [3-5] are modified for extraction systems. Solute in the phases is surrounded by a solvation shell. This means that it interacts with all the constituents of the environment and, therefore, "free" solute, free extractant, or free solute-extractant complex do not exist. Components of the solvation shell compete to form a complex according to their electronic-geometric affinity  $k_i$  (interaction strength), which is constant at a given temperature and pressure. Coefficient,  $k_i$ , represents the total, complexing and solvating affinity constant.

Competition between the constituents of the solvation shell takes place according to their affinity constants  $k_i$  and the number of potentially available molecules of every component, i.e., on its actual concentration. The solute is partitioned among all constituents of the solvation shell medium. A set of equations [3,4] are developed for calculation of the solute

partitioning factors,  $P_{Si}$ , and its concentrations (molar fractions,  $C_{Si}$ ) in the mixed solvation shell (extractant, E, water (in organic), W, active adduct, A, and diluent, D) at equilibrium.

The value of the physicochemical property X (for example, chemical shift  $\delta$  in NMR, molar extinction coefficient  $\varepsilon$  in UV-VIS, changes in free energy  $\Delta G$ , etc.), measured in mixed solvents, is considered to be the weighed sum of this same property measured in pure solvent constituents. The contribution of each solvent on the shift of this property, X, is additive. Considering three component solute-extractant-water system we obtain, after some algebra, the linear equation for the measured property X [3-5]:

$$\frac{X_{SW} - X}{C_E} = \frac{k_{SE}}{k_{SW}} v_W (X_{SW} - X_{SE}) - [\frac{k_{SE}}{k_{SW}} v_W - v_E] (X_{SW} - X) \quad (1)$$

and the saturation factor Z at  $C_E > C_S^0$ :

$$Z = \frac{C_{Sorg}}{C_S^0 - C_{Sorg}} = \frac{X_{SW} - X}{X_{SW} - X_{SE}} = \frac{k_{SE} v_W C_E}{k_{SW} + (k_{SE} v_W - k_{SW} v_E) C_E} \quad (2)$$

where  $k_{SE}/k_{SW}$  is the affinity constant ratio;  $C_S^0$  is the initial (or total) concentration of the solute;  $C_{Saq}$ ,  $C_{Sorg}$ ,  $C_{SE}$ ,  $C_{SW}$  are the solute concentrations (molar fractions) in the aqueous phase, in the organic phase, in the mixed solvation shell of the organic phase (extractant, water, active adduct and diluent), respectively, at equilibrium;  $v_E$  and  $v_W$  are partial molar volumes of extractant and water.

### **III. Extractants are considered amphoteric and may perform as acids (electron acceptors) or bases (electron donors), depending on the structure of their functional groups and composition of the organic phase, and on the structure of the solutes and composition of the aqueous phase**

According to the Lewis and Pearson classification, many substances can be both bases and acids. Any specie with a  $pK_a$  value higher than the given one, may be conjugate base to it. An empirical quantum chemical method's approach is applied, which employs the concepts of donor-acceptor interactions. For example, at extraction with acidic organic extractants, titanium(IV) hydroxo-ion [4], hydrated (coordinated) by water molecules at the aqueous phase  $pH \geq 2$ , is considered as a conjugate base (electron donor) to extractant. In this case, the extractant in an inert organic diluent behaves as an electron acceptor (acid). At  $pH \leq -0.9$  ( $\geq 8$  mol/kg HCl) of the aqueous solutions, titanium ion, coordinated (solvated) by HCl molecules, behaves as a conjugate acid (electron acceptor) to the same acidic organic extractant. In this case, the extractant behaves as an electron donor (base).

### **IV. Aggregation, as a process that affects extraction, should be considered in all regions of the general extraction isotherm (Figure 1)**

At low solute concentrations in the organic phase, solute-extractant complex, surrounded by its solvation shell, forms a geometric structure which is denoted as a nucleus aggregate. According to the COPS theory the solute is partitioned between different solvents to form some kind of a virtual physical unity, called solvation shell. It is a statistical thermodynamics' denomination that is convenient for mathematical description. The nucleus aggregate describes the same but real physical unity with stereospecific bonds and orientation in the bulk organic solution. The nucleus aggregate is open to the bulk phase and is characterized by the fast exchange with the bulk solvents.

Region 1 is characterized by solute-extractant equivalent concentration ratios,  $C_{S\text{org}}/C_{SE} < 1$  (more than one equivalent of extractant to one equivalent of solute) and  $P_{SE\text{s}} \geq P_{SE\text{c}}$ , where  $P_{SE\text{c}}$  and  $P_{SE\text{s}}$  represent partitioning factors of the solute in the complexed and solvated forms, respectively [3]. The structures of the nuclei aggregates in this region are formed mainly through the weak interactions. pH dependence in this region is not pronounced, but stability pH limitations of the formed complexes are observed.

Region 2 is characterized by solute-extractant equivalent concentration ratios,  $C_{S\text{org}}/C_{SE} \approx 1$  and  $P_{SE\text{s}} \leq P_{SE\text{c}}$ . Formation of nuclei aggregates in this region is driven mainly by strong interactions. The interactions in this region are strongly dependent on pH or anion concentration in the aqueous phase. Divergence of the distribution curve slope from the 1/1 equivalents of the S-E complex is explained by weak interactions.

According to the presented theory, the difference between regions 1 and 2 is mainly in the magnitude of the affinity constant ratios:

$$\frac{k_{SE\text{c}}}{k_{SW}} / \frac{k_{SE\text{s}}}{k_{SW}} = \frac{k_{SE\text{c}}}{k_{SE\text{s}}} \quad (3)$$

at the same concentrations of extractant, water in organic phase and affinity coefficient of solute in pure water.  $k_{SE\text{c}}$  and  $k_{SE\text{s}}$  are affinity constants of the solute toward extractant in the complexed and in the solvating forms, respectively. So, all coordination structure schemes of the nuclei aggregates in Region 1 may belong to Region 2, but at  $k_{SE\text{c}} > k_{SE\text{s}}$ . It follows that the slopes of the distribution curve in Fig. 1 for Regions 1 and 2 may have all magnitudes between two extreme structures: at  $k_{SE\text{c}} \rightarrow 0$  and at  $k_{SE\text{s}} \rightarrow 0$ .

With increasing concentration of solute the nuclei aggregates interact, grow in size via a step-wise aggregation and form linear or ringed (cyclic) aggregates. This is Region 3, in which the equivalent of solute to the equivalent of extractant ratio is:  $C_{S\text{org}}/C_{SE} \geq 1$ . Region 3 is characterized mainly by bridging of the nuclei aggregates through the solute, extractant, or active adduct (including water) molecules. Competition between these components influences the slope value of the curve. All components of the linear aggregates are also open to the bulk phase, and exchange between the aggregate and the bulk solvents continues to be fast.

At high solute concentrations upon reaching a critical size, the structural reorganization of the linear (or cyclic) aggregates takes place, and supramolecular structures - reversed micelle-like, or crosslinked cluster-like, are formed. This is Region 4, characterized by  $P_{SE\text{s}} < P_{SE\text{c}}$  and  $C_{S\text{org}}/C_{SE} \gg 1$ . Above-stoichiometric loading and massive third phase formation are typical for this region. The exchange rate between the components of the solvation shell and the bulk phase depends on the orientation of the polar groups relative to the bulk phase, and, as a rule, is controlled by diffusion kinetics. Host-guest interaction models can be used for analysis of these systems. Region 4 is beyond the practical interest of technologists and will not be discussed in this paper.

### **Summarizing Remarks for the Presented Theory**

Affinity constant ratio  $k_{SE}/k_{SW}$  can be obtained from the slope of the equation (1) plots:  $(X_{SW} - X)/C_E$  vs  $(X_{SW} - X)$ . The intercept gives the hypothetical differences between the property, measured in pure extractant and in pure water. Thus, the agreement between the direct experimental determination of the measured property in pure solvents and their graphically obtained values of  $X_{SW}-X_{SE}$  may be examined. Only relative values (affinity constant ratios) can be measured in solution because of the ubiquitous nature of molecular interactions. Affinity constant ratio's value of unity suggests the same values of solvation effects of the

solute with extractant in the organic phase and with water in the aqueous phase; a large value of  $k_{SE}/k_{SW}$  means strong or very strong complexation-solvation effects with extractant. A positive sign of a slope means that the solvation of the reactant molecules is stronger than the product molecules. The negative slope shows that the solvation of product molecule is stronger than the reactant's.

The presented model overcomes some limitations of "chemical modeling approach" [1,2]. The last is a useful tool to describe the data quantitatively, if complexation is strong (as in the region 2). In the presented theory the separate mathematical descriptions are developed for different regions of the extraction system. Interchanges in the linearity of equation (1), or the different slopes in the loading curve over the solute concentration range, mean that the affinity constant ratios and/or concentrations of the components in the aggregate are different. It means, also, that the different charge-transfer complexation mechanisms, and consequently the different values of  $k_{SEc}$ , or the different solvation mechanisms, and consequently different values of  $k_{SEs}$ , take place at different solute concentrations. So, we have to use one more experimentally measured property, such as UV-VIS or quantitative IR measurements, to determine  $k_{SEc}/ k_{SEs}$ . Regions 1-4 in the distribution curve (Figure 1) with different values of the slopes testify different compositions of the aggregates formed.

## ACID SOLVENT EXTRACTION BY AMINES

### **Acid-Amine (in inert diluent)-Water (S-E-W) System**

Let us consider a relatively simple system: monobasic acid, S - monobasic amine, E - water, W - inert organic diluent, D (kerosene). Some preliminary assumptions: 1. All components of the system are monomers in a pure, initial state; 2. Volume change on mixing of the solvents is neglected; 3. Diluent D is inert enough and does not participate in solvation; 4. Solubility of water in the bulk organic solvents' mixture is excluded: water, after equilibration, separation and centrifugation is present only in the solvation shell.

A set of equations, derived from equation (1), were developed for different measured properties X [3,4]. For example, at measured chemical shift,  $X=\delta$  (NMR), the equation is:

$$\frac{\delta_{SW} - \delta}{C_E} = \frac{k_{SE} V_{Worg}}{k_{SW}} (\delta_{SW} - \delta_{SE}) - \left[ \frac{k_{SE}}{k_{SW}} V_{Worg} - V_E \right] (\delta_{SW} - \delta) \quad (4)$$

Experimentally obtained [2] data of lactic acid extraction by Alamine-336, and data, calculated according the presented theory [3], is compared in Figure 2. It shows that the presented theoretical approach satisfactorily quantitatively describes the studied extraction system.

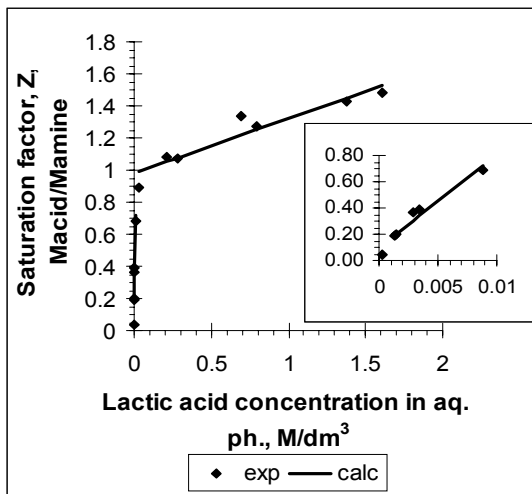


Figure 2. Comparison of experimental data [2] and calculated data [3] in regards to lactic acid extraction by Alamine 336.

### System with Mixture of Two Acids - Selectivity

If both monobasic acids,  $S_1$  and  $S_2$ , are miscible in the organic and aqueous phases and differ mainly in their acidity, expected interactions and associations, formed at extraction, are obeyed expression:

$$\frac{k_{S_1E} C_{S_1org}}{k_{S_1W} C_{S_1aq}} > \frac{k_{S_2E} C_{S_2org}}{k_{S_2W} C_{S_2aq}} \quad (5)$$

Two cases may be considered. At relatively low initial concentrations of both acids, expected interactions correspond to Regions 1 and 2 of the general extraction isotherm (Fig. 1) with nuclei aggregates forming. According to Statements II, III and IV of the presented theory, electrostatic, ion-pair interaction mechanisms (Region 2) will dominate with the stronger acid,  $S_1$ , and H-bonding (Region 1) will dominate with the weaker acid,  $S_2$ . The weaker acid plays here a synergistic, enhancing role for the distribution of a stronger acid into organic phase.  $\frac{k_{S_1E}}{k_{S_1W}}$  and  $\frac{k_{S_2E}}{k_{S_2W}}$  constant values are the same inside every region, therefore, the difference between magnitudes of concentration ratios (and selectivity) at equilibrium will increase with increasing initial concentrations of both acids.

At relatively high initial concentrations of both acids (prevailing stoichiometry 1-1 for stronger acid), expected interactions will correspond to Region 3 with linear (or cyclic) aggregates, formed preferentially through the H-bond bridging by the weaker acid. With the increase of initial concentrations the difference between magnitudes of concentration ratios (selectivity) at equilibrium will pass through a maximum because of the competition between the weaker  $S_2$  and the stronger  $S_1$  acids for the H-bonding. According to the presented theory (statements II and III), the maximal selectivity will be at different amine - stronger acid compositions for the same amine and every two acids used. Preliminary data for these compositions may be calculated, using relations derived from equations (1) and (2):

$$\frac{(X_{SW} - X)_{max}}{C_E} = \frac{k_{SE}}{k_{SW}} v_W (X_{SW} - X_{SE}) - [\frac{k_{SE}}{k_{SW}} v_W - v_E] (X_{SW} - X)_{max} \quad (6)$$

$$\frac{1}{Z_{max}} = 1 + \frac{k_{SW}}{k_{SE}} \times \frac{[C_{Worg}]_{max}}{C_E} \quad (7)$$

Determining experimentally  $[C_{Worg}]_{max}$  for both,  $S_1$  and  $S_2$  acids at already obtained affinity coefficient ratios, we can determine water concentration limits for selective separation of two acids. It is especially important when using amine - acid mixtures as extractants for the weak acids. The theory predicts and permits the preliminary evaluation of Water-swing separation.

### **System with Two Acids when One of them, $S_1$ , is Water Immiscible (Acid-Base-Coupled (ABC) extractants [3])**

Concentration of the water immiscible acid in the aqueous phase is  $C_{S1aq} \rightarrow 0$ . Therefore,

relationship  $\frac{C_{S1org}}{C_{S1aq}} \gg \frac{C_{S2org}}{C_{S2aq}}$  will be correct for almost all range of acid  $S_2$  concentration. This

means that the concentration of acid  $S_2$  in the solvation shell will be very small. Only at very high  $S_2$  concentrations in the aqueous phase the extraction of this acid will be detectable. The interactions and the aggregates forming are typical for Regions 3 and 4. The presented theory shows (without any experiments) that ABC may be useful extractants only for strong mineral or carboxylic acids.

### **System with a Mixture of Two Amines**

In the mixture of two monobasic amines, at  $\frac{k_{SE1}}{k_{SW}} \times \frac{C_{Sorg}}{C_{Saq}} > \frac{k_{SE2}}{k_{SW}} \times \frac{C_{Sorg}}{C_{Saq}}$  and  $\frac{k_{SE2}}{k_{SW}} < \frac{k_{SE1}}{k_{SW}}$  the

weaker amine  $E_2$  will perform as a weak acid (Statement III), and all considerations, presented in the section for two acids, are valid here. So, the weaker amine plays here a synergistic, enhancing effect on the distribution of the acid into the organic phase. It is evident from the theory that the initial concentration of the weak amine,  $E_2$ , has to be lower than amine  $E_1$  and acid  $S$ . If the amine  $E_2$  is immiscible in the aqueous phase, the above considerations for the two acids, where one is immiscible, are valid in this case as well. Preliminary data for these compositions may be calculated using independent experiments.

### **System with Active Solvent as an Adduct**

The solute-solvent interactions in the S-E-W-A system are different for every adduct and result in different affinity constant ratios:  $k_{SE}/k_{SW}$ ,  $k_{SE}/k_{SA}$ ,  $k_{SA}/k_{SW}$  and concentration ratios:  $C_{SE}/C_{SW}$ ,  $C_{SA}/C_{SW}$ ,  $C_{SE}/C_{SA}$  in the solvation shell. An active adduct may be water-immiscible, partly or completely soluble in both, organic and aqueous phases. In this case, the concentrations of  $C_{Worg}$ ,  $C_{Aorg}$ ,  $C_{Aaq}$  in the bulk organic and aqueous phases have to be measured at the absence of acid,  $S$ .

Using the equations of statement II, preliminary data may be calculated using independent experimental data, obtained for the simple three-component S-E-A, S-A-W and E-A-W systems, in analogy to the S-E-W system. According to the amphotropy of extractants (Statement III) an active solvent (adduct) at  $\frac{k_{AE}}{k_{AW}} > \frac{k_{SE}}{k_{SW}}$  performs as a weak acid and all

considerations, presented above for the two acids, are valid here. In this case, an active adduct,  $A$ , has a synergistic, enhancing effect on the distribution of the acid into the organic phase. This is explained by replacing a hydrogen bonded amine molecule by an active

adduct molecule in the solvation shell (nucleus aggregate). Therefore, apparent concentration of amine increases for acid-amine interactions. Headley and coworkers [8] denominate this phenomenon as a "relative increase of amine basicity". Evidently, the concentration of the adduct in the organic phase,  $C_{Aorg}$ , has to be lower than amine  $C_E$  and acid  $C_{Sorg}$ . Comparing values of the relations:  $\frac{k_{SE}}{k_{SW}} \times \frac{C_{Sorg}}{C_{Saq}}$ ,  $\frac{k_{SE}}{k_{SA}} \times \frac{C_E}{C_A}$  and  $\frac{k_{AE}}{k_{AW}} \times \frac{C_{Aorg}}{C_{Aaq}}$ , one can calculate  $[C_{Aorg}]_{max}$  and  $[C_{Aaq}]^0$  compositions for optimal extraction of the acid of interest at its different concentrations. The presented theory predicts the solvent-swing regeneration and permits its preliminary quantification.

It should be stressed that the presented theory predicts the synergistic, enhancing effect of weak amines or weak acids or neutral protic, polar/polarizable solvents as adducts to the basic amine extractant on extraction of acids. Classical theories do not indicate any direct knowledge regarding this effect.

## METAL SOLVENT EXTRACTION BY ACIDIC EXTRACTANTS

### Metal-Extractant-Water (M-E-W) System

Let us consider an M-E-W extraction system in which metal ion,  $M^{z+}$ , a molecules, monobasic acidic organic extractant,  $E=HL$ , b-molecules, water (W), c molecules participate in a single reaction act. Here, z is the oxidation state of metal ion. All assumptions presented in the previous section, are valid here as well. Using different measured properties, X, we obtain relations, derived from equation (1). For UV-VIS,  $X = \varepsilon$  is a molar extinction coefficient:

$$\frac{\varepsilon_{MW} - \varepsilon}{C_E} = \frac{k_{ME} v_W}{k_{MW}} (\varepsilon_{MW} - \varepsilon_{ME}) - \left[ \frac{k_{ME}}{k_{MW}} v_W - v_E \right] (\varepsilon_{MW} - \varepsilon) \quad (9)$$

where

$\frac{A}{C_{Morg}} = \varepsilon$ ,  $\frac{A_{ME}}{C_{Morg}} = \varepsilon_{ME}$ ,  $\frac{A_{MW}}{C_{Morg}} = \varepsilon_{MW}$  and A is a measured absorbency. At  $a=1$ , partitioning factors are  $P_{ME} = b/(n+1)$  and  $P_{MW} = (n-b)/(n+1)$ . The metal central ion is coordinated by z charged ligands  $L^-$ , by  $b-z$  neutral HL molecules and by c water molecules, filling metal ion coordination sites, n, up to saturation.

As an example, the re-investigated data of titanium(IV) extraction by DEHPA [6,7] are presented in Figure 3. The values of affinity constant ratios, average equilibrium constants and intercepts were calculated, using the presented theory equations, for different regions of the extraction isotherm. Figure 3 shows a good agreement between experimentally obtained (points) and calculated (lines) data.

The M-E-W is the simplest extraction system. Real systems are those with two or more metal ions ( $M_1$ ,  $M_2$ ,  $M_3$ ) have to be selectively separated, and/or with a mixture of extractants ( $E_1$ ,  $E_2$ ) and/or with different active solvents as adducts ( $A_1$ ,  $A_2$ ), used, for synergistic effect. These systems are analyzed in a way, described in the previous section. Analysis and predictions are based on the experimentally determined affinity constant ratios and coordination structures (numbers) of the aggregates, formed at different concentrations of the metals, extractants, adducts. For example, the contribution of every component in the complicated M-E-A-W system, where A is an active adduct, may be evaluated at the determined affinity constant ratios  $k_{ME}/k_{MW}$ ,  $k_{ME}/k_{MA}$ ,  $k_{MA}/k_{MW}$ . These data may be realized through a series of conventional equilibrium extraction experiments with simple three component systems M-E-W, M-E-A, M-A-W, and E-A-W.

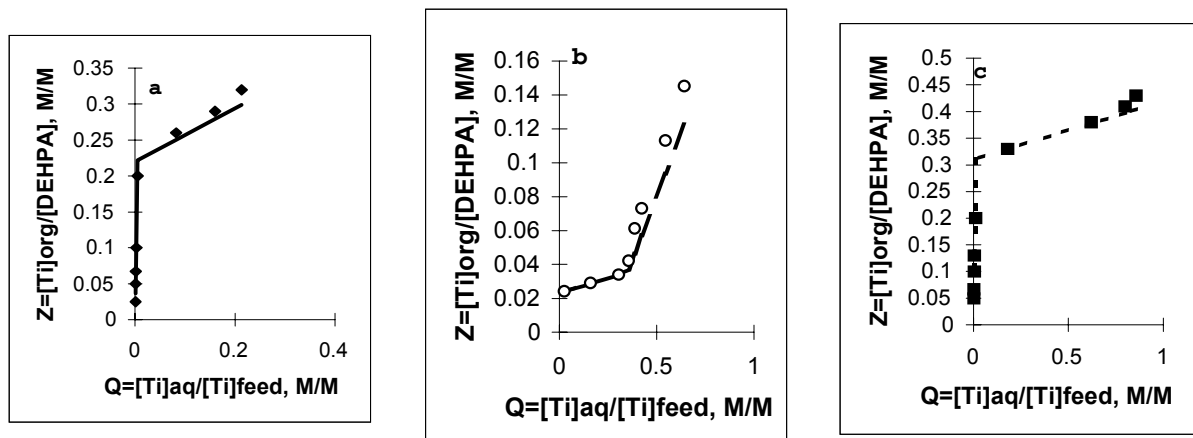


Figure 3. Comparison of experimentally obtained (points) and theoretically calculated (lines) data of extraction of titanium(IV) chlorides by DEHPA in benzene from the aqueous solutions at initial acidities (HCl): a) 0.1 mol/kg, b) 2.0 mol/kg and c) 7.6 mol/kg.

### ADVANTAGES OF THE PRESENTED THEORY

The presented theory constitutes a general framework for interpretation of ion-molecular interaction data in the solvent extraction systems. More parameters such as water and active adduct are introduced to the quantitative consideration of the extraction systems. A mathematical description for the process simulation is proposed.

Affinity constant ratios are easily acceptable through the independent measurements conducted with simple three-component-systems. Experimental determination of the affinity constant ratios and solvation shell compositions, quantitative, or even semi-quantitative spectrometric determination of solute in the complexed and solvated forms permits to set up an exact form of the aggregates formed. Composition and behavior predictions of the extraction system of interest may be analyzed. Relation

$$K_{SE} = \frac{k_{SE}}{k_{SW}} v_W - v_E \quad (10)$$

between equilibrium constant  $K_{Si}$  of the classical theories and affinity constant ratio,  $k_{Si}/k_{Sj}$ , obtained by the measurements of the same property, permits to use available equilibrium constant data for calculations in the presented theory.

The theory of partitioning in the homogenous media implies that the components act independently in their interaction with a given solute. In other words, the values of  $k_{SE}$  are independent of the values of  $k_{SW}$  or  $k_{SA}$ , and are transferable from one system to the other. Influence of different solvent adducts to extractant on the effectiveness and selectivity of the extraction process, is predictable once some solvent parameters are ascertained. Transferability can be proved by different independent experiments with three component systems through relations:

$$\frac{k_{SE}}{k_{S_2E}} = \frac{k_{(S_1E)_1}}{k_{(S_1W)_1}} \times \frac{k_{(S_2W)_2}}{k_{(S_2E)_2}} = \frac{k_{(S_1E)_1}}{k_{(S_1A)_1}} \times \frac{k_{(S_2A)_2}}{k_{(S_2E)_2}} \quad (11)$$

$$\frac{k_{SE_1}}{k_{SE_2}} = \frac{k_{(SE_1)_1}}{k_{(SW)_1}} \times \frac{k_{(SW)_2}}{k_{(SE_2)_2}} = \frac{k_{(SE_1)_1}}{k_{(SA)_1}} \times \frac{k_{(SA)_2}}{k_{(SE_2)_2}} \quad (12)$$

$$\frac{k_{SA_1}}{k_{SA_2}} = \frac{k_{(SA_1)_1}}{k_{(SW)_1}} \times \frac{k_{(SW)_2}}{k_{(SA_2)_2}} = \frac{k_{(SA_1)_1}}{k_{(SE)_1}} \times \frac{k_{(SE)_2}}{k_{(SA_2)_2}} \quad (13)$$

where the systems (all in the same inert diluent), experimentally verified, are: S<sub>1</sub>-E-W, S<sub>1</sub>-E-A and S<sub>2</sub>-E-W, S<sub>2</sub>-E-A, respectively, for equation (11); S-E<sub>1</sub>-W, S-E<sub>1</sub>-A and S-E<sub>2</sub>-W, S-E<sub>2</sub>-A, respectively, for equation (12); S-A<sub>1</sub>-E, S-A<sub>1</sub>-W, and S-A<sub>2</sub>-E, S-A<sub>2</sub>-W, respectively, for equation (13).

Co-solvent independence, established experimentally, allows us to compare directly the solvating-complexing power (competition order) of various extractants, adducts, diluents at a fixed other components of the system. Once determined and tabulated, the data may be used in any system, containing these components. Independence and transferability of affinity constants have been proved for many organic systems [5], using chromatographic techniques, NMR, UV-VIS, potentiometric titrations, kinetic measurement techniques. Nevertheless, it still remains to be proved for different extraction systems of interest.

The presented theory predicts the synergistic, enhancing effect of weak amines, weak acids and active solvents as adducts to the basic amine extractant on extraction effect of acids. Classical theories do not indicate any direct knowledge about this effect.

The presented competitive complexation/solvation modeling approach is an attempt to describe the mechanisms of solvent extraction with quantitative evaluation of different compounds, formed in the organic phase at different concentrations of the solute in the aqueous phase. Of course, the theory has many simplifications and limitations but it may be a starting point for the quantification of solvent extraction processes in aim to predict suitable extraction systems for different solutes separation.

## REFERENCES

1. A. M. Eyal and R. Canari (1995), *Ind. Eng. Chem. Res.*, **34** (5), 1789-1798.
2. J. Tamada and C. King (1989), Extraction of Carboxylic Acids by Amine Extractants, Ph.D. Thesis, Lawrence Berkeley Laboratory, University of California.
3. V. Kislik (2001), *Sep. Sci. Technol.*, **36** (13), 2899-2926.
4. V. Kislik (2001), Submitted to *Sep. Sci. Technol.*
5. O. B. Nagy, H. Muanda ad J. B. Nagy (1978), *J. Chem. Soc., Faraday Trans.*, **1** (74), 2210-2229.
6. V. Kislik and A. Eyal (1993), *Proc. ISEC '93*, Society of Chemical Industry, London, Vol. 2, pp.1353-1360.
7. V. Kislik and A. Eyal (1993), *Solvent Extr. Ion Exch.*, **11** (2), 285-310.
8. A. D. Headley (1991), *J. Org. Chem.*, **56**, 3688-3691.



## MICROEMULSIONS AND THIRD PHASE FORMATION

K. Osseo-Asare

Department of Materials Science and Engineering, Penn State University,  
University Park, PA, USA

The formation of a third phase, a process in which the organic phase splits into two immiscible liquids, has a detrimental effect on solvent extraction operations. The phase splitting is generally attributed to the limited solubility of the extracted complexes in hydrocarbon diluents, with the solubility decreasing in the order: aromatic diluent > cyclic diluent > aliphatic diluent. Third phase research has, therefore, been preoccupied with efforts to establish the stoichiometry of the species responsible for the limited solubility. In contrast, relatively little effort has been devoted to investigations focusing on the phase behavior of the relevant systems and on the molecular structure of the heavy organic extract. This paper departs from the previous approaches by promoting the view that the solvent extraction third phase corresponds to the middle phase in a microemulsion fluid system. Using tri-n-butylphosphate (TBP) as a model extractant, phase evolution and aggregation concepts from microemulsion science are used to develop a general framework for interpreting and predicting the patterns of phase behavior in solvent extraction third-phase-forming systems.

### INTRODUCTION

In an excellent review of third phase formation published in 1967, Kertes [1] described the literature as consisting of “fairly abundant but essentially fragmentary data”. In the intervening thirty-five years more papers on third phase formation have appeared [1-6]. However, the data remain fragmentary and a comprehensive theory of third phase formation is yet to be developed. The purpose of this paper is to offer some ideas [5, 6] that can help fill this gap in our knowledge.

Third phase formation, the separation of the organic phase into two liquids, has a detrimental effect on solvent extraction separations. Fluid mixing is complicated by the presence of two organic liquids. Also, the fact that phase splitting tends to be associated with relatively concentrated organic extracts puts severe restrictions on the highest metal loadings that can be tolerated.

The available reports on third phase formation typically involve basic reagents, such as organophosphorus esters, ethers, and amines [1, 2]. Extraction systems based on tri-n-butyl phosphate (TBP;  $(C_4H_9O)_3P=O$ ) are among those most vulnerable towards organic phase splitting [1, 2]. Recognition that phase separation is related to the limited solubility of the extracted complexes in hydrocarbon diluents has led to research programs that emphasize a search for the stoichiometry of the poorly soluble species. In contrast, investigations that focus on phase behavior have received little attention.

The experimental evidence indicating the presence of molecular aggregates in TBP extracts was critically reviewed in a previous publication from this laboratory [6]. For highly acidic aqueous solutions and highly concentrated metal salt solutions, the extracted species tend to be in the form of ion-pairs. These species are expected to exhibit surfactant-like behavior since they possess both hydrophobic (*i.e.*, the trialkyl radicals) and hydrophilic (*i.e.*,  $P=O(H_2O)_xM^{z+}$ ,  $P=O(H_2O)_yH^+$ ) groups. Thus, as with classical surfactants [7-10], extracted TBP complexes can self-organize into reverse micelles in nonpolar organic solvents. The polar regions of reverse micelles can solubilize water molecules to form water-in-oil (w/o) microemulsions. The earlier paper [6] emphasized the role of aggregation in the extraction of acids and metal ions by TBP. However, the relationship between aggregation and third phase formation was briefly examined and it was postulated that "The solvent extraction third phase corresponds to the middle phase in a microemulsion fluid system". Using TBP as a model extractant, the present paper further examines this claim and elaborates on how microemulsion science provides the missing framework needed to develop a thoroughgoing understanding of third phase formation in solvent extraction systems.

### MICROEMULSION PHASE BEHAVIOR

A microemulsion contains three essential ingredients: water, oil, and surfactant [7-10]. In many practical systems one or more electrolytes (*e.g.*, metal salts and/or mineral acids) and a cosurfactant (*e.g.*, a medium-chain alcohol) may also be present. Kahlweit and coworkers [11-13] have shown that the patterns of phase behavior in microemulsion systems can be effectively visualized and systematized with the aid of phase diagrams. Following their approach [11], Figure 1 presents a schematic ternary phase diagram for a hypothetical water (A)-oil (B)-surfactant (C) system. The area delineated by a, b, and c represents a three-phase triangle; mixtures with compositions within this region will split into three phases, *i.e.*, (a), (b), and (c). On the other hand, regions  $\alpha$ ,  $\beta$ , and  $\gamma$  represent two-phase domains. In region  $\alpha$  phase (b) is in equilibrium with (c), in region  $\beta$  phases (a) and (c) are in mutual equilibrium, while in region  $\gamma$  phase (a) is in equilibrium with phase (b).

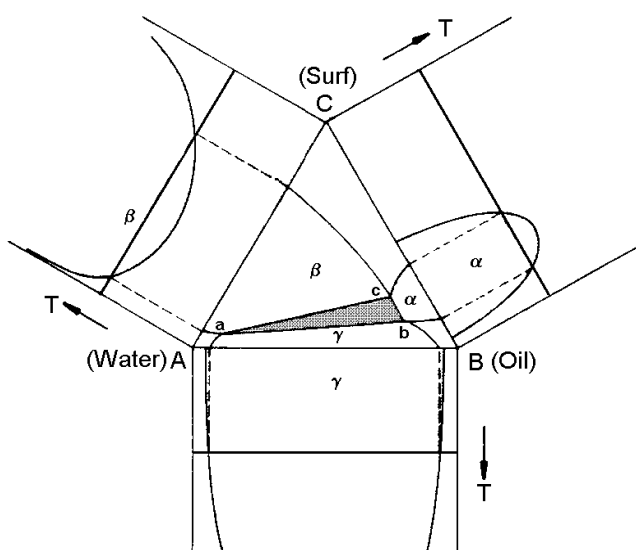


*Figure 1. A schematic ternary phase diagram for a hypothetical water (A)-oil (B)-surfactant (C) system (after Kahlweit et al. [11]).*

As temperature, surfactant, or oil is altered, the shape and size of the three-phase region also varies. This change will reflect changes in the corresponding binary phase equilibria. Thus, Figure 1 is only valid for a particular temperature ( $T_1$ ), and as the temperature is raised, the miscibility gap ( $\beta$ ) in the A-C diagram grows while the corresponding gap ( $\alpha$ ) for the B-C diagram becomes smaller. These effects translate into elongation of side ac of the three-phase triangle and shrinking of side bc. Accordingly, as illustrated in Figure 2, as the temperature is raised, point c moves clockwise relative to a mixture composition at point P. The corresponding test-tube profiles are shown in Figure 3.

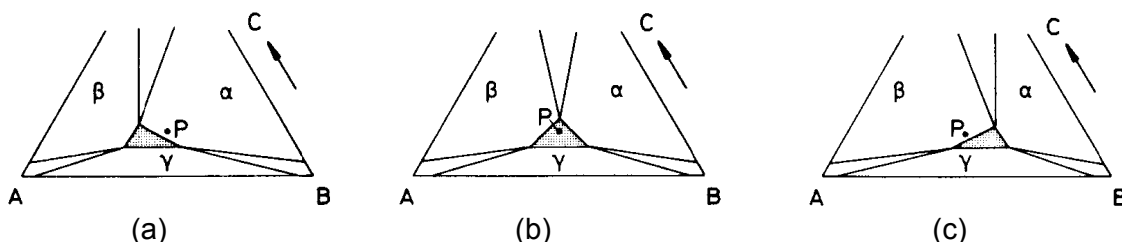


*Figure 2. Schematic illustration of the effect of temperature on the three-phase triangle (after Kahlweit et al. [11]). Temperature increases in the direction (a) → (b) → (c).*

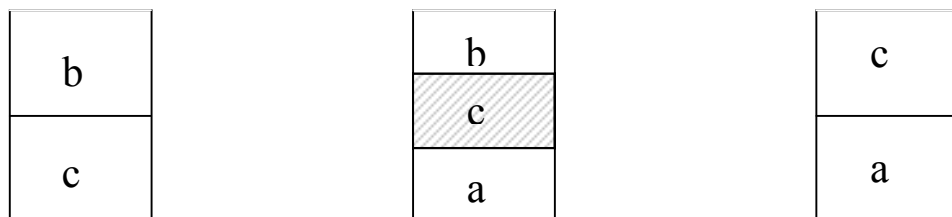


*Figure 3. Test-tube profiles corresponding to the temperature changes in Figure 2.*

The effects of surfactant, oil, and electrolyte on microemulsion phase behavior can also be visualized by considering the corresponding effects on the binary phase diagrams. Consider oils  $B_1$ ,  $B_2$ ,  $B_3$ , and  $B_4$ , where the hydrophobicity decreases in the order  $B_1 > B_2 > B_3 > B_4$ . Furthermore, let the surfactant be completely miscible with the least hydrophobic oil,  $B_4$ . Then, as the oil is changed from  $B_4$  to  $B_1$ , the oil-surfactant (B-C) miscibility gap is expected to decrease in the order  $(B_1-C) > (B_2-C) > (B_3-C) > (B_4-C)$ . Thus, the miscibility gap should be highest for the most hydrophobic oil, i.e.,  $B_1$ . Accordingly, as the hydrophobicity of the oil increases (e.g., by going from an aromatic to an aliphatic hydrocarbon), the three phase interval should become enlarged.

## PHASE DIAGRAMS FOR TBP SYSTEMS

In general solvent extraction diluents and the related aqueous solutions have very little mutual solubility and, therefore, the corresponding water-diluent binary phase diagram should exhibit a very wide miscibility gap, as depicted for the binary A-B diagram in Figure 1. It is apparent, therefore, that if one could justify making the following correspondence: aqueous solution:water (A), diluent:oil (B), and TBP:surfactant (C), then Figure 1 can be taken to represent a pseudoternary phase diagram for a hypothetical TBP-diluent-water-electrolyte system. Access to such diagrams for a specific TBP-diluent-water-acid-metal salt system would permit one to readily assess how process variables, such as TBP, diluent,  $H_2O$ , acid, and metal content, as well as temperature influence third phase formation.

Unfortunately such ternary phase diagrams are not available for most of the relevant solvent extraction systems. In the case of TBP, a few binary phase diagrams are available and some of these are used below to illustrate the utility and power of the microemulsion model of third phase formation.

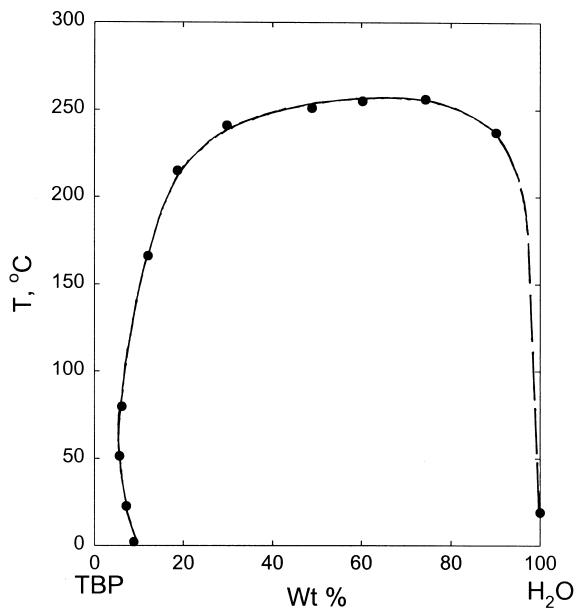


*Figure 4. Binary phase diagram for the TBP-H<sub>2</sub>O system (after Rozen et al. [14].)*

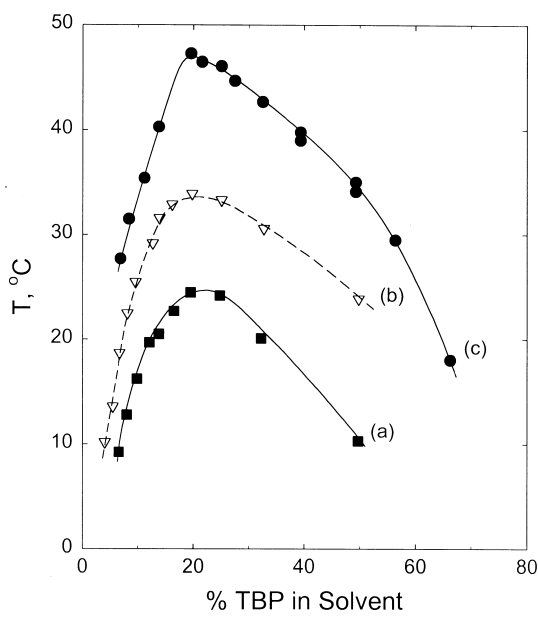


*Figure 5. Pseudobinary phase diagram for the system TBP-kerosene-H<sub>2</sub>O-HNO<sub>3</sub>-Th(NO<sub>3</sub>)<sub>4</sub> (after Healy and McKay [15]). Concentrations in the initial aqueous solutions: (a) 0.69 M Th(NO<sub>3</sub>)<sub>4</sub>, (b) 0.69 M Th(NO<sub>3</sub>)<sub>4</sub> + 0.96 M HNO<sub>3</sub>, (c) 0.86 M Th(NO<sub>3</sub>)<sub>4</sub>.*

Figure 4 presents the binary phase diagram for the TBP-H<sub>2</sub>O system [14]. It can be seen that there is a large miscibility gap up to approximately 225 °C. An upper critical temperature is observed at about 250 °C, above which water and TBP become mutually soluble. If TBP is taken to represent a surfactant (C), then it can be seen that the miscibility gap in Figure 4 matches the trend shown in Figure 1 for the binary A-C diagram of an arbitrary water-surfactant system. A pseudobinary phase diagram for the system TBP-kerosene-H<sub>2</sub>O-HNO<sub>3</sub>-Th(NO<sub>3</sub>)<sub>4</sub> [15] is shown in Figure 5. Below each curve is a two-phase region where a diluent-rich solution (left-hand side) is in equilibrium with a TBP-rich phase (right-hand side). It can also be seen that mutual solubility is enhanced by increase in temperature and that there is an upper critical temperature above which the TBP-rich and the diluent-rich phases become mutually soluble. If the diluent represents oil (B), then referring again to Figure 1, it can be seen that Figure 5 follows the trend depicted in the binary B-C phase diagram.

Figure 5 further shows that in the absence of HNO<sub>3</sub> the miscibility gap increases with Th(NO<sub>3</sub>)<sub>4</sub> concentration (curves a and c). Also, for a given metal concentration, increasing the nitric acid concentration extends the miscibility gap (curves a and b). An expansion of the miscibility gap in the binary B-C phase diagram signals enhanced third phase formation. This effect is illustrated in Figure 6 for the TBP-kerosene-H<sub>2</sub>O-HNO<sub>3</sub>-UO<sub>2</sub>(NO<sub>3</sub>)<sub>2</sub> system [16]. It can be seen that raising the acid concentration increases the volume of the third phase.

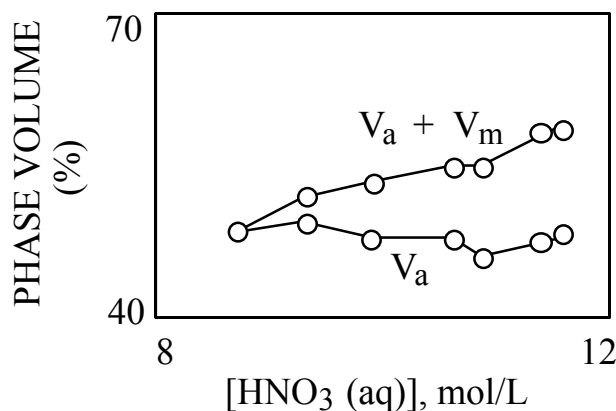


*Figure 6. Effect of HNO<sub>3</sub> concentration on third phase formation in the system TBP-kerosene-water-UO<sub>2</sub>(NO<sub>3</sub>)<sub>2</sub>-HNO<sub>3</sub> (data from Solovkin et al. [16]). Volumes after third phase formation: V<sub>a</sub> = volume of the aqueous phase, V<sub>m</sub> = volume of the middle (third) phase.*

Third phase formation is also affected by the nature of the aliphatic diluent. Figure 7 shows a comparison of the HCl extraction isotherms for 50% TBP solutions in n-hexane, n-octane, and n-dodecane [17]. It can be seen that the aqueous acidity marking the onset of third phase formation follows the order: hexane > octane > dodecane. It can also be seen that the concentration of HCl in the lower organic phase increases from n-hexane to n-dodecane; the opposite trend is observed for the upper organic phase. These effects are consistent with the above discussion on microemulsion phase behavior. The longer chain hydrocarbons are more hydrophobic and are, therefore, expected to be more sensitive to third phase formation.

## AGGREGATION AND THIRD PHASE FORMATION

It is well established that ion-pairs of the type  $(TBP)_x(H_2O)_yH^+ \cdot A^-$ ,  $(TBP)_x(H_2O)_yH^+ \cdot MA_n^-$ , and  $(TBP)_x(H_2O)_yM^{z+} \cdot zA^-$  form in TBP extraction systems [1, 6]. It has been suggested that anhydrous ion-pairs, e.g.,  $TBPH^+ \cdot ClO_4^-$ , also occur in some systems [18]. This latter complex is reminiscent of alkylammonium salts which are recognized surfactants capable of forming reverse micelles. Evidence for the presence of reverse micelles and microemulsions in TBP solvent extraction systems include the observed abrupt increases in viscosity with increase in acid and metal uptake, dramatic electrical conductivity changes, and the co-extraction of water molecules (as reflected, for example, in volumetric changes of the organic phase) [6].

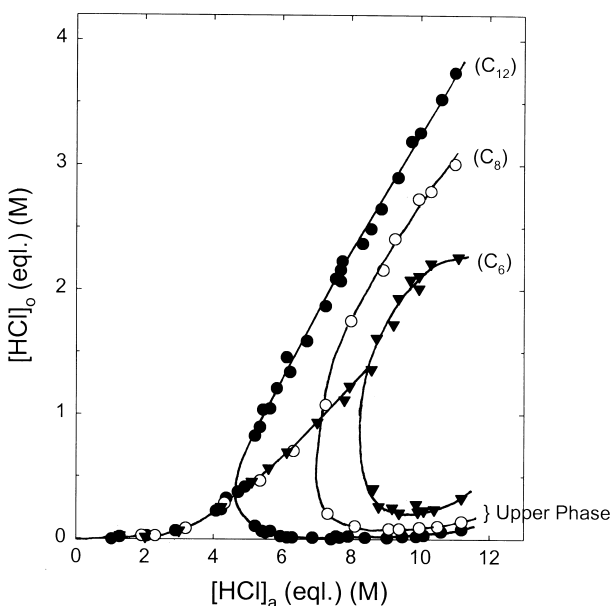


*Figure 7. HCl extraction isotherms for 50% TBP solutions in n-hexane ( $C_6$ ), n-octane ( $C_8$ ), and n-dodecane ( $C_{12}$ ) (after Kopacz and Jezowska-Trzebiatowska [17]).*

Reverse micelles present in an oil interact with each other through a variety of forces, including van der Waals interactions between the solubilized water droplets, and steric interactions between the hydrophobic surfactant chains [3, 4, 19, 20]. If these interactions are sufficiently attractive, the reverse micelles begin to aggregate, squeezing out the oil molecules. Eventually phase separation (a kind of precipitation or flocculation) occurs, resulting in a heavier micelle-rich phase below a lighter micelle-depleted phase. If in fact reverse micelles occur in TBP solvent extraction systems, then it is reasonable to suppose that a similar micellar interaction is responsible for third phase formation. Indeed recent work by Erlinger *et al.* [3, 4], based on investigations of aggregation phenomena in a quaternary malonoamide extractant system, strongly support the original proposal [6] forwarded in 1991 that: "The solvent extraction third phase corresponds to the middle phase in a microemulsion fluid system".

## REFERENCES

1. A. S. Kertes (1967), Solvent Extraction Chemistry of Metals, H. A. C. McKay, T. V. Healy, I. L. Jenkins, and A. Naylor (eds.), CRC Press, Cleveland, OH, pp. 377-400.
2. P. R. Vasudeva Rao and Z. Kolarik (1996), *Solv. Extr. Ion Exch.*, **14**, 955-993.
3. C. Erlinger, D. Gazeau, T. Zemb, C. Madic, L. LeFrancois, M. Hebrant, and C. Tondre (1998), *Solv. Extr. Ion Exch.*, **16**, 707-738.
4. C. Erlinger, L. Belloni, T. Zemb, and C. Madic (1999), *Langmuir*, **15**, 2290-2300.
5. K. Osseo-Asare (1999), Metal Separation Technologies Beyond 2000: Integrating Novel Chemistry with Processing, K. C. Liddell and D. J. Chaiko (eds.), TMS, Warrendale, PA, pp. 339-346.
6. K. Osseo-Asare (1991), *Adv. Colloid Interface Sci.*, **37**, 123-173.
7. I. D. Robb (ed.) (1982), Microemulsions, Plenum, New York.
8. S. E. Friberg, and P. Bothorel (eds.) (1987), Microemulsions: Structure and Dynamics, CRC Press, Boca Raton, FL.
9. R. Zana (ed.) (1987), Surfactant Solutions, New Methods of Investigation, Marcel Dekker, New York.
10. P. Kumar and K. L. Mittal (eds.) (1999), Handbook of Microemulsion Science and Technology, Marcel Dekker, New York, NY.
11. C.-U. Herrmann, G. Klar, and M. Kahlweit (1981), *J. Colloid Interface Sci.*, **82**, 6-13.
12. M. Kahlweit, E. Lessner, and R. Strey (1984), *J. Phys. Chem.*, **88**, 1937-1944.
13. M. Kahlweit, R. Strey, P. Firman, D. Haase, J. Jen, and R. Schomäcker (1988), *Langmuir*, **4**, 499-511.
14. A. M. Rozen, L. P. Khorkhorina, G. D. Agashkina, E. G. Tetrin, A. N. Mal'tseva, and E. V. Voronetskaya (1970), *Sov. Radiochem.*, **12**, 312-321.
15. T. V. Healy and H. A. C. McKay (1956), *Trans. Farad. Soc.*, **52**, 633-642.
16. A. S. Solovkin, N. S. Povitskii, and K. P. Lunichkina (1960), *Russ. J. Inorg. Chem.*, **5**, 1026-1028.
17. S. Kopacz and B. Jezowska-Trzebiatowska (1970), *Russ. J. Inorg. Chem.*, **15**, 539-547.
18. D. G. Whitney and R. M. Diamond (1963), *J. Phys. Chem.*, **67**, 209-216.
19. C. Regnaut and J. C. Ravey (1989), *J. Chem. Phys.*, **91**, 1211-1221.
20. F. Pitre, C. Regnaut, and M. P. Pilani (1993), *Langmuir*, **9**, 2855-2860.



## PREDICTION OF DIFFUSIVITIES IN LIQUID ASSOCIATING SYSTEMS

D. Bosse and H.-J. Bart

Institute of Thermal Process Engineering, University of Kaiserslautern,  
Kaiserslautern, Germany

A model for the prediction of Fick diffusion coefficients in binary associating systems has been developed. Due to association reactions between solute molecules such systems can be regarded as multicomponent systems. Therefore, the proposed model is based on a multicomponent approach for the Maxwell-Stefan diffusivities combined with an extension of the commonly used UNIFAC model which takes association reactions explicitly into account.

### INTRODUCTION

Diffusion plays an important role in all kinds of separation processes, e.g., distillation, extraction, membrane processes, etc. Since the increasing use of nonequilibrium stage modelling [1] a deeper insight into mass transfer has become more important in order to allow accurate and reliable predictions in any kind of equipment. Due to their slowness, diffusional processes are often the rate determining step in reactive liquid systems [2], e.g., extraction with a solvent of much higher viscosity than the solute. A further complexity is that the liquid state cannot be as properly described as the gas phase. Thermodynamic non-idealities - caused by different sizes, shapes, and interaction energies as well as association and solvation of molecules – strongly influence the diffusional behaviour of the different species. These effects usually result in large deviations between experimental data and predicted values.

Diffusion problems are tackled with Fick's law or the Maxwell-Stefan (MS) equation. The relation between the two has been given by Taylor and Krishna [3]. For a binary mixture this yields:

$$D = \Gamma D \quad (1)$$

As can be seen from this equation the Fick diffusivities,  $D$ , equals the MS diffusion coefficients,  $D$ , times the thermodynamic correction factor,  $\Gamma$ . The main difference between both descriptions is that the MS-approach separates diffusional processes from thermodynamic non-idealities while the Fick diffusion coefficients must also account for the non-idealities in the mixture, therefore, the MS-description is preferred throughout this work.

This work deals with diffusional mass transfer in binary associating systems. On first sight, only two constituents are present in such mixtures, namely the monomer molecules of a solute, e.g., alcohol, aldehyde, etc., and a solvent. In reality we are dealing with a multicomponent mixture due to association effects between solute molecules which lead to cluster formation. Hence, the binary diffusivity measured in such systems equals an effective diffusivity that accounts for these effects. Modelling systems with associating constituents as binary mixtures is not straightforward, since reality is not properly reflected. Therefore, the

main goal of this work is to present a new approach for the prediction of diffusivities in liquid associating systems. For this purpose a diffusivity model derived on the basis of the MS-equation has been applied in conjunction with an extension of the well-known UNIFAC model. The solute associates formed in the mixture are treated as separate constituents. A transformation from the multicomponent mixture to the 'pseudo-binary' mixture is also presented. Hence, it is possible to compute binary diffusivities of solute – solvent mixtures on a multicomponent basis.

## THEORY

### Mixture Composition and Formation of Associates

In binary systems with a solute (A) and an inert solvent (B) self-association reactions between solute molecules can occur according to the reaction:



In the following the species in the mixture are indicated by the subscripts '1' for A, '2' for  $A_2$ , ..., ' $n-1$ ' for  $A_{n-1}$ , and 'n' for B. The equilibrium constant of the  $i$ th reaction is defined by:

$$K_i = \frac{(\gamma_i x_i)}{(\gamma_1 x_1)^i} \quad (3)$$

Here  $\gamma_i$  refers to the activity coefficient and  $x_i$  to the mole fraction of the species considered. The relation between the overall binary mole fractions of A and B, indicated by  $\tilde{x}_1$  and  $\tilde{x}_n$ , and the multicomponent mole fractions is given by:

$$\tilde{x}_1 = \frac{\sum_{i=1}^{n-1} i x_i}{\sum_{i=1}^{n-1} i x_i + x_n} \quad (4)$$

$$\tilde{x}_n = \frac{x_n}{\sum_{i=1}^{n-1} i x_i + x_n} \quad (5)$$

For given equilibrium constants these equations yield the real mixture composition. How these constants are determined is shown below.

### Maxwell-Stefan Diffusivities

On the basis of the Maxwell-Stefan equation Rutten [4] has derived an expression that allows computation of the MS-diffusivities of a pseudo-binary mixture with polymerization, i.e., association, on the basis of a multicomponent approach.

$$\tilde{D} = \frac{1}{x_{sum}} \sum_{i=1}^{n-1} \sum_{j=1}^{n-1} \left[ \frac{i x_n + x_{sum}}{x_n + x_{sum}} \right] j A_{ij} x_j \quad (6)$$

In this equation  $x_{sum}$  is defined as

$$x_{sum} = \sum_{i=1}^{n-1} i x_i \quad (7)$$

and  $A_{ij}$  is an element of the inverse matrix of  $[B]$  with dimension  $(n-1)$  whose elements are given by:

$$B_{ii} = \frac{x_i}{D_{in}} + \sum_{k=1, k \neq i}^n \frac{x_k}{D_{ik}} \quad (8)$$

$$B_{ij} = -x_i \left( \frac{1}{D_{ij}} - \frac{1}{D_{in}} \right) \quad (9)$$

The diffusivities given in equations (8-9) are the MS-diffusivities of the multicomponent mixture. At infinite dilution equation (6) reduces to the following expressions in which the left hand sides can be determined from experimental diffusivity data at infinite dilution or from an appropriate model, e.g., Wilke-Chang [5]:

$$X_1 \rightarrow 0 \quad \tilde{D} = D_{1n} = D_{AB} \quad (10)$$

$$X_n \rightarrow 0 \quad \tilde{D} = \left[ \sum \frac{x_i}{D_{in}} \right]^{-1} \quad (11)$$

In order to estimate values for the multicomponent diffusivities, these diffusivities have been related to the monomer pair diffusivity using van der Waals radii,  $R_{vdW}$ .

$$D_{in} = \frac{R_{vdW,1}}{R_{vdW,i}} D_{1n} \approx i^{-1/3} D_{1n} \quad (12)$$

$$D_{ij} = \frac{R_{vdW,1} R_{vdW,n}}{R_{vdW,i} R_{vdW,j}} D_{1n} \approx i^{-1/3} j^{-1/3} \frac{R_{vdW,n}}{R_{vdW,1}} D_{1n} \quad (13)$$

The van der Waals radius in turn is defined by

$$R_{vdW} = \left( \frac{3V_{vdW}}{4\pi N_A} \right)^{1/3} \quad (14)$$

whereas the van der Waals volumes,  $V_{vdW}$ , of the associates are taken as multiples of the volume of the monomer solute. Values for the van der Waals volumes have been listed by Edward [6] and Bondi [7].

The monomer pair diffusivity may now be computed as follows. Equation (10) yields the diffusivity at infinite dilution in pure solvent which is equal to the binary experimental value. In order to obtain the infinite dilution diffusivity in pure solute the equations (11-13) must be combined, which yields a value depending on the mixture composition, i.e. equilibrium constants. At intermediate composition the multicomponent diffusion coefficient of the monomer pair is computed from the infinite dilution diffusivities using a mixing rule, e.g., Vignes [8]. Once these diffusivities have been calculated, the computation of the binary diffusivity given in equation (6) is straightforward.

### Calculation of Equilibrium Constants with the UNIFAC Association Model

In 1999 Asprion extended the commonly used UNIFAC model to account also for association effects [9]. In his work, binary and ternary mixtures of alcohols in both inert and solvating solvents were investigated by spectroscopic analysis in respect to the structure of the associates and solvates formed. Associates can be regarded as molecular clusters of a single species, while solvates are molecular clusters of different components. In addition to the structure analysis, phase equilibrium measurements were conducted in order to obtain new sets of interaction parameters for the UNIFAC model. The resulting UNIFAC association model has been shown to be superior to the commonly used versions of UNIQUAC and UNIFAC. In the following the derivation of this model with respect to systems in which only association reactions occur, i.e., an alcohol as solute in an inert solvent, will be presented.

In this model, associates are regarded as separate chemical species with reaction equilibria defined by equations (2-3). The required equilibrium constants were determined from independent FT-IR measurements. For correlation purposes the number of associates considered in the model was reduced by assuming that, besides dimer association, only one higher associated species had been formed. This higher oligomer can be seen as a representative for all higher associates occurring in the mixture. For the calculation of the equilibrium constant the following relation is favoured

$$\ln K_k = -\frac{\Delta_R h_k^{\text{Ref.}}}{RT} + \frac{\Delta_R s_k^{\text{Ref.}}}{R} \quad k = Di, Po \quad (15)$$

whereas the reaction enthalpy and reaction entropy for the dimer reaction are given by:

$$\Delta_R h_{Di}^{\text{Ref.}} = \frac{\Delta_R h_{Po}^{\text{Ref.}}}{n-1} - \Delta h_{Di} \quad (16)$$

$$\Delta_R s_{Di}^{\text{Ref.}} = \frac{\Delta_R s_{Po}^{\text{Ref.}}}{n-1} - \Delta s_{Di} \quad (17)$$

$n$  refers to the number of solute molecules in an associate. The values for the dimer reaction enthalpy and entropy for the alcohol-inert solvent systems investigated are as follows:

$$\Delta h_{Di} = -12.023 \text{ kJ/mol} \quad (18)$$

$$\Delta s_{Di} = -30.031 \text{ J/(mol K)} \quad (19)$$

Example values for the reaction enthalpy and reaction entropy, which are assumed to be independent of temperature and pressure, of higher oligomers can be found in Table 1.

*Table 1. Reaction enthalpies and entropies for solvents n-hexane and cyclohexane.*

Component	$n$	$-\frac{\Delta_R h_{Po}^{\text{Ref.}}}{n-1}$	$-\frac{\Delta_R s_{Po}^{\text{Ref.}}}{n-1}$
		[kJ/mol]	[J/(mol K)]
Methanol	5	27.524	51.174
Ethanol	5	27.524	54.162
1-Propanol	5	27.524	56.690

Since association has been considered in terms of chemical reactions the UNIFAC parameters for the OH-group have been adapted accordingly. The resulting parameters are given in Tables 2-3, values of the other groups have been adopted from [10].

*Table 2. Parameters  $R_k$  and  $Q_k$  for OH-group.*

Group	Main group	$R_k$	$Q_k$
OH	OH	0.530	0.584

*Table 3. Interaction parameters for the OH-main group with the CH<sub>3</sub>-main group.*

$a_{mn}$	CH <sub>3</sub>	OH
CH <sub>3</sub>	0	578.9
OH	107.5	0

On the basis of this information it is possible to compute multicomponent activity coefficients and together with the information given in [3] the multicomponent thermodynamic correction factor are also accessible.

### Thermodynamic Correction Factor

As can be seen from the definition of the thermodynamic correction factor (here given only for the binary case) the second derivative of a  $g^E$ -model is required.

$$\Gamma = 1 + x_1 \left. \frac{\partial \ln \gamma_1}{\partial x_1} \right|_{T, P, \Sigma} \quad (20)$$

The symbol  $\Sigma$  indicates that the differentiation is to be carried out using the restriction that  $\tilde{x}_1 + \tilde{x}_2 = 1$ . The solution of equation (20) for the UNIQUAC model which has been used to compute  $\Gamma$  has been presented in [3].

## RESULTS

For the binary system ethanol-cyclohexane MS-diffusivities and Fick diffusivities have been calculated with the approach proposed here (model 1) and with a combination of the Vignes equation and the UNIQUAC model (model 2). In order to minimise prediction errors the diffusivity at infinite dilution,  $D^0$ , for cyclohexane in ethanol has been adopted from the experimental data, while the Wilke-Chang equation has been applied to compute  $D^0$  for ethanol in cyclohexane. In Figure 1 the results of these calculations are presented together with data acquired from diaphragm cell experiments [11]. These data have also been transformed to MS-diffusivities by means of the UNIQUAC model (calc.).

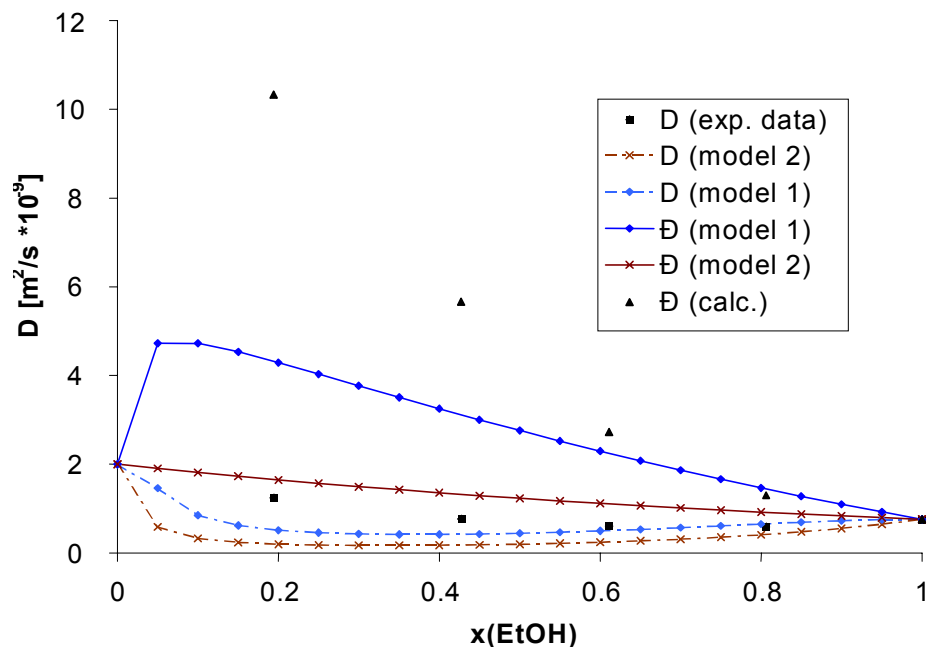


Figure 1. Comparison of experimental data and simulation for system ethanol-cyclohexane.

At lower alcohol concentrations the MS data points show a strong increase in value. The model 1 proposed here qualitatively follows this trend, while the Vignes equation used in model 2 can only predict ideal behaviour. The larger deviations between the data points and the association model can be explained with difficulties in describing the thermodynamic correction factor properly. At lower concentrations of alcohol, i.e., up to  $\tilde{x}(\text{EtOH}) \approx 0.3 - 0.4$ ,  $\Gamma$

falls rapidly from  $\Gamma=1$  in pure benzene to values around 0-0.2. Rutten assumed an inaccuracy in the MS-diffusivities in this region of 50% [4]. Consideration of these deviations would lead to a good agreement between model 1 and the experimental MS-diffusivities. The success of the model proposed here can also be seen in a comparison of the Fick diffusivities. The association model is superior to model 2. Nevertheless, deviations between the experimental data and model 1 can be seen at lower alcohol concentrations. An explanation for these differences is that the commonly used UNIQUAC equation has also been used in the association model to compute  $\Gamma$ .

## CONCLUSIONS

In this work a new model for the prediction of diffusivities in binary associating systems has been presented. Binary Fick diffusivities are computed on the basis of a multicomponent approach for the MS-diffusivities combined with an extension of the commonly used UNIFAC equation. Within this model the associates formed are regarded as separate species.

A first assessment of the association model has been carried out in a comparison of this model with a combination of the Vignes equation and the UNIQUAC model. The results show that the approach proposed here is superior to the other model in describing experimental Fick diffusivities. MS-diffusivities calculated from the literature data can only be qualitatively recalculated because of inaccuracies in  $\Gamma$  at lower alcohol concentrations.

In order to improve the prediction quality of the association model proposed here the thermodynamic correction factor will be calculated using the extended version of the UNIFAC model which has been shown to predict activity coefficients of associating mixtures with high accuracy [9]. Additionally, more experimental data of associating solutes in an inert solvent need to be measured for further model verification.

## ACKNOWLEDGEMENT

The authors are grateful to the Deutsche Forschungsgemeinschaft for financial support of this work.

## REFERENCES

1. R. Krishnamurthy and R. Taylor (1985), *AIChE*, **31**, 449-456.
2. H. J. Bart (2001), *Reactive Extraction*, Springer, Berlin.
3. R. Taylor and R. Krishna (1993), *Multicomponent Mass Transfer*, John Wiley & Sons, New York.
4. P. W. M. Rutten (1992), *Diffusion in Liquids*, Delft University Press, Delft.
5. C. R. Wilke and P. Chang (1955), *AIChE*, **1**(2), 264-270.
6. J. T. Edward (1970), *J. Chem. Educ.*, **47**, 261-270.
7. A. Bondi (1964), *J. Phys. Chem.*, **68**, 441-451.
8. A. Vignes (1966), *Ind. Eng. Chem. Fundam.*, **5**, 189-199.
9. N. Asprion (1996), *Anwendung der Spektroskopie in thermodynamischen Untersuchungen assoziierender Lösungen*, Dissertations Druck Darmstadt GmbH, Darmstadt.
10. A. Fredenslund, R. L. Jones and J. M. Prausnitz (1975), *AIChE*, **21**, 1086-1099.
11. C. Ramakanth, A. K. Mukherjee, K. Ashok and T. R. Das (1991), *J. Chem. Eng. Data*, **36**(4), 384-387.



## STUDY OF THE INTERACTION OF TRIBUTYLPHOSPHATE, NON-IONIC SURFACTANT AND WATER BY FOURIER-TRANSFORM INFRARED SPECTROSCOPY

Zhi-Dong Chang, Xiao-Fang Wei, Jing Wang, Hui-Zhou Liu and Jia-Yong Chen

Young Scientist Laboratory of Separation Science & Engineering,  
State Key Laboratory of Biochemical Engineering, Institute of Chemical Metallurgy,  
Chinese Academy of Sciences, Beijing, China

The interaction of tributylphosphate, the non-ionic surfactant, Tween80, and water has been investigated using Fourier Transform infrared spectroscopy. Results show that if water molecules are present, molecules of tributylphosphate can form a reversed micelle structure. Molecules of tributylphosphate and Tween80 can coalesce through a water bridge. The interaction points between  $\text{H}_2\text{O}$  and tributylphosphate can be  $\text{P}=\text{O}$  or  $\text{P}-\text{O}-\text{C}$ .

### INTRODUCTION

Tributylphosphate (TBP) has been used in recent research as a co-extractant to extract proteins in reversed micelles extraction systems and predispersed extraction systems [1]. The interaction of TBP, surfactant and water is a very important factor in the extraction. Although the interaction of TBP with the water molecule has been reported [2], few papers have been published on the interaction of TBP, water and surfactant molecules. The work reported in this paper focuses on the interaction of TBP, water and non-ionic surfactant, Tween80, molecules.

### EXPERIMENTAL

TBP of analytical grade and Tween80 of chemical grade were obtained from Beijing Chemical Reagent Company. Distilled water was used in all experiments.

TBP, Tween80 and water were mixed together in various proportions using a WH-90A mini-mixer made by Yarong Biochemical Instruments (Shanghai, China). The mixture was analyzed using a Vector22 Fourier Transform Infrared (FTIR) spectrometer made by Bruker Optik (Germany). The FTIR scan time used was 32 and the resolution,  $2 \text{ cm}^{-1}$ .

### RESULTS AND DISCUSSION

An infrared spectrum for TBP is shown in Figure 1. The typical absorption bands for TBP are due to the presence of C-H,  $\text{P}=\text{O}$  and  $\text{P}-\text{O}-\text{C}$  groups. Bands at  $2800\text{--}3000 \text{ cm}^{-1}$  are due to symmetry and asymmetry stretching of methyl and methylene C-H absorption [3]. Absorption bands at  $1200\text{--}1500 \text{ cm}^{-1}$  are due to bending, twisting, wagging and scissoring of methyl and methylene C-H [2]. Bands at  $1280 \text{ cm}^{-1}$  and  $950\text{--}1100 \text{ cm}^{-1}$  bands are due to  $\text{P}=\text{O}$  stretching and  $\text{P}-\text{O}-\text{C}$  stretching respectively [4]. The spectrum for Tween80 is shown in Figure 2.

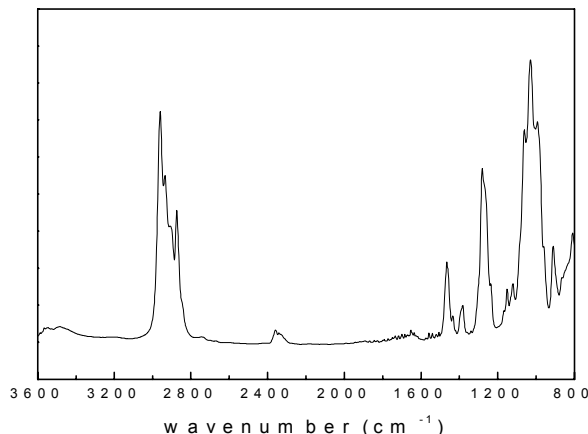


*Figure 1. The infrared spectrum for TBP.*

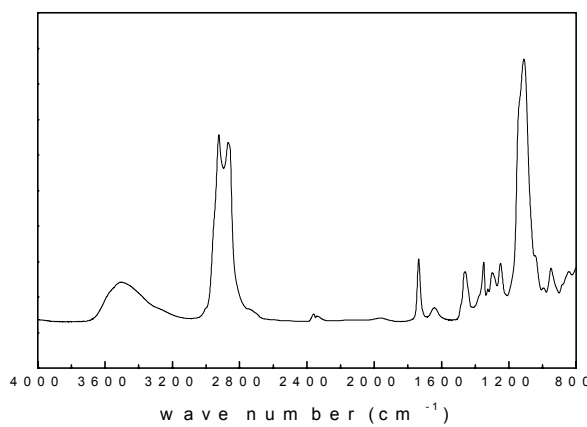


*Figure 2. The infrared spectrum for Tween80.*

When the TBP/Tween80 mixture ratio was 1:4.1, it was observed that the 2800~3000 cm<sup>-1</sup> CH stretching band changed with an increase of water content. The four absorption peaks in this region are due to C-H asymmetric stretching of CH<sub>3</sub> (2958 cm<sup>-1</sup>), C-H asymmetric stretching of -CH<sub>2</sub>- (2924 cm<sup>-1</sup>), C-H symmetric stretching of CH<sub>3</sub> (2872 cm<sup>-1</sup>) and C-H symmetric stretching of -CH<sub>2</sub>- (2853 cm<sup>-1</sup>). Using Gauss functions to fit the curves, it was found that the area of each peak and the peak positions changed with the water content. The area percentage of each peak after normalization and the peak positions are shown in Figures 3 to 6. The results show that when the mole percentage of water in solution exceeded 75%, the peak position and peak area percentage changed sharply. The position of C-H asymmetric stretching of methyl at 2962 cm<sup>-1</sup> shifted to 2945 cm<sup>-1</sup> and the area percentage rose from 1.6% to 41%. The position of C-H asymmetric stretching of methylene nearby 2921 cm<sup>-1</sup> shifted to 2926 cm<sup>-1</sup>, and the area percentage decreased from 40% to 13%. The position of C-H symmetric stretching of methyl at 2864 cm<sup>-1</sup> first shifted to 2898 cm<sup>-1</sup> then to 2880 cm<sup>-1</sup>. The area percentage rose from 25% to 60% and then fell to 40%. The position of C-H symmetric stretching of methylene at 2942 cm<sup>-1</sup> shifted to 2865 cm<sup>-1</sup> with the increase in water content. When the water content exceeded 75%, the peak position shifted to 2853 cm<sup>-1</sup> and the area percentage dropped from 25% to 2%. An explanation for these phenomena follows. In pure solutions, the wave number of C-H symmetric and asymmetric stretching of methyl for TBP is higher than that for Tween80. When blended together, the peak positions shift but no other absorption peaks appear. This result suggests that when Tween80 mixes with TBP, the environment in the solution is suitable to both of them. Their hydrocarbon chains can stretch

out easily and coalesce together. When water is added, hydrogen bonds are formed between water molecules and oxygen molecules of the polyethylene oxide chain of Tween80, causing polyethylene oxide chain bending and overlapping. Thus the C-H stretching of methylene is restrained and the absorption position shifts to a higher wave number. The area percentage of methylene decreases since bending and overlapping of polyethylene oxide chains affect the absorption. Since the supposed molecule structure arrangement is that the hydrophilic portion points inwards with the hydrophobic portion pointing outwards, the hydrophobic chain can stretch out completely and thus enhance the absorption of infrared light.

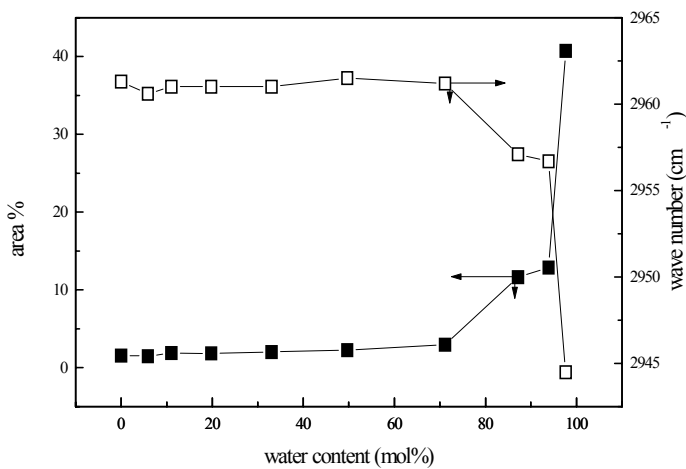


Figure 3. Relation of peak position and area ratio with water content at  $2960\text{ cm}^{-1}$ .

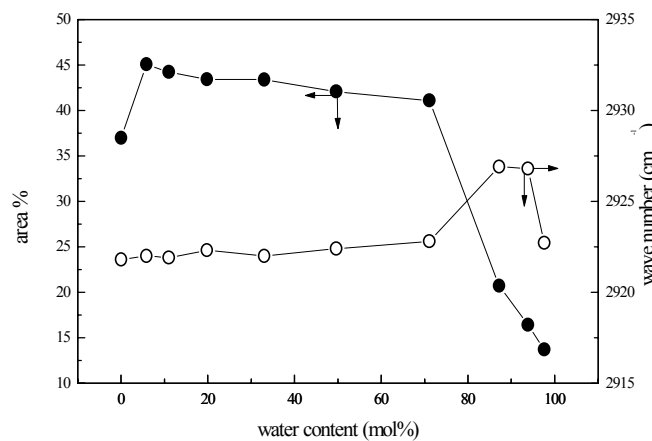


Figure 4. Relation of peak position and area ratio with water content at  $2934\text{ cm}^{-1}$ .

Peaks at  $1487$ ,  $1468$ ,  $1458$  and  $1451\text{ cm}^{-1}$  represent bending of  $-\text{CH}_2-$ , scissoring of  $-\text{CH}_2-$ , asymmetric bending of  $-\text{CH}_3$  and deforming of C-H respectively [5]. The effect of water content on the area percentage of each peak is shown in Figure 7. Although no obvious shift in the positions of the four peaks occurred the absorption intensities of these peaks were observed to change. The area percentages at  $1487$  and  $1468\text{ cm}^{-1}$ , which are associated with the vibration of methylene, decreased. These results reflect that the peaks may be due to the vibration of the methylene of polyethylene oxide. On the other hand, the polyethelene oxide chain coalesces tightly, affecting the absorption of infrared light. The increase of area percentages at  $1458$  and  $1450\text{ cm}^{-1}$  from  $8.2\%$  and  $61\%$  to  $15\%$  and  $68.5\%$ , respectively, demonstrated that the methyl group was exposed on the outside of the molecular aggregation. In addition it was

inferred that the absorption peak at  $1450\text{ cm}^{-1}$  was due to the vibration of methyl. The peak at  $1324\text{ cm}^{-1}$  is assigned twisting of  $-\text{CH}_2-$ . Figure 8 shows that an increase in the water content caused a gradual shift of the peak position to  $1328\text{ cm}^{-1}$ .

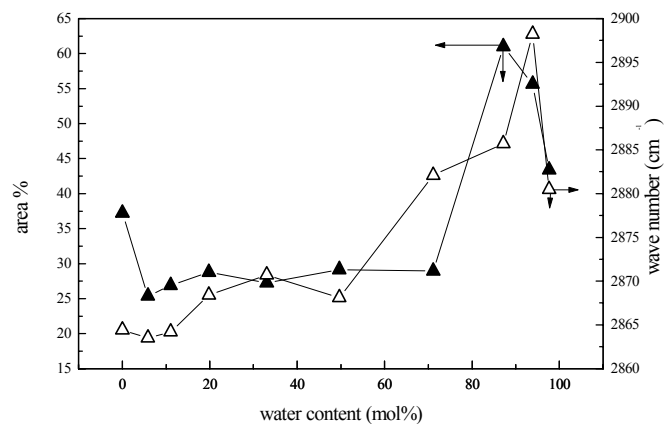


Figure 5. Relation of peak position and area ratio with water content at  $2874\text{ cm}^{-1}$ .

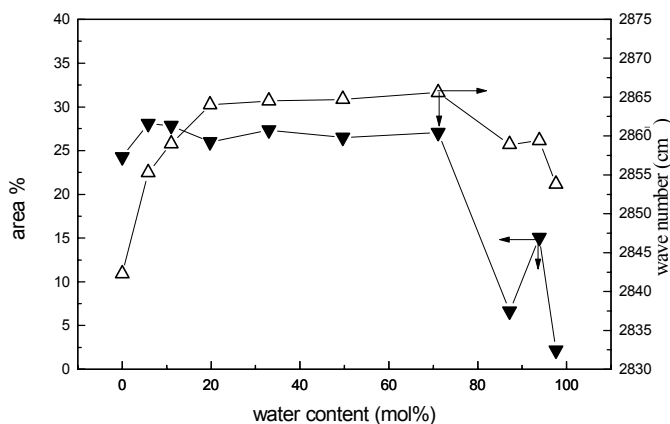


Figure 6. Relation of peak position and area ratio with water content at  $2853\text{ cm}^{-1}$ .

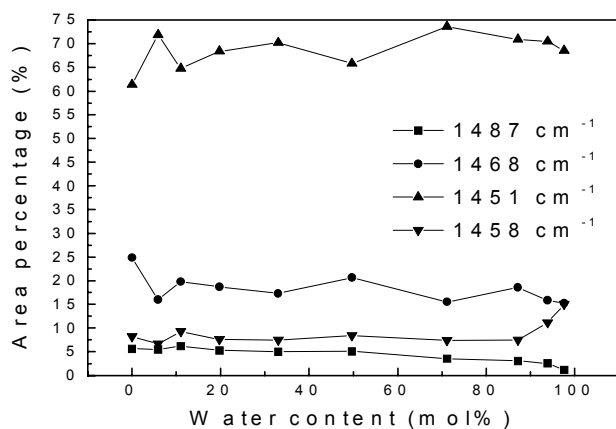


Figure 7. Relation of peak position with water content.

This indicates that the large space obstruction caused by the bulky chain of polyethylene oxide, results in higher energy requirements for the bending of methylene. Peaks at 1146, 1120 and 1100  $\text{cm}^{-1}$  are assigned stretching of C-O of Tween80. Peak positions and area percentages changing with water contents are shown from Figures 9 to 11. The observed decrease in peak positions at 3~6  $\text{cm}^{-1}$  indicates that a hydrogen bond was formed between a water molecule and the O of C-O-C group. This would reduce the interaction of C-O.

## CONCLUSIONS

It was deduced from the results of a FTIR spectroscopic analysis that a reversed micelle structure was formed when water was added to the TBP and Tween80 mixed system. The interaction points between  $\text{H}_2\text{O}$  and TBP can be P=O or P-O-C. Water and TBP can form hydrogen bond at P=O and C-O-P. Molecules of TBP and Tween80 can coalesce through a water bridge.

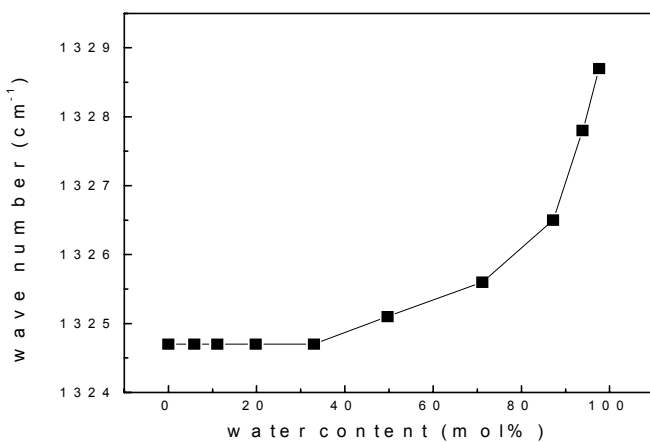


Figure 8. Relation of peak position with water content at  $1324 \text{ cm}^{-1}$ .

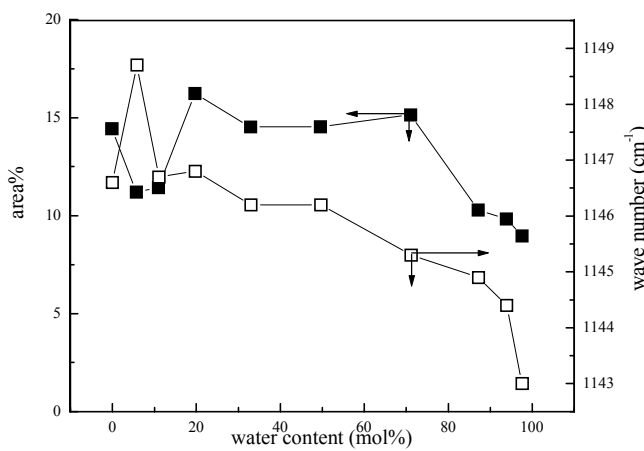
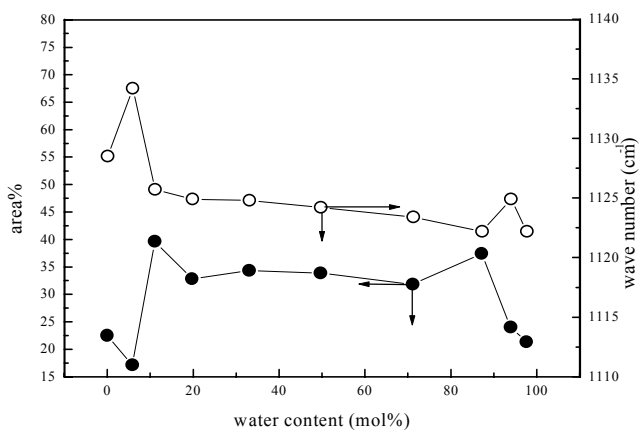
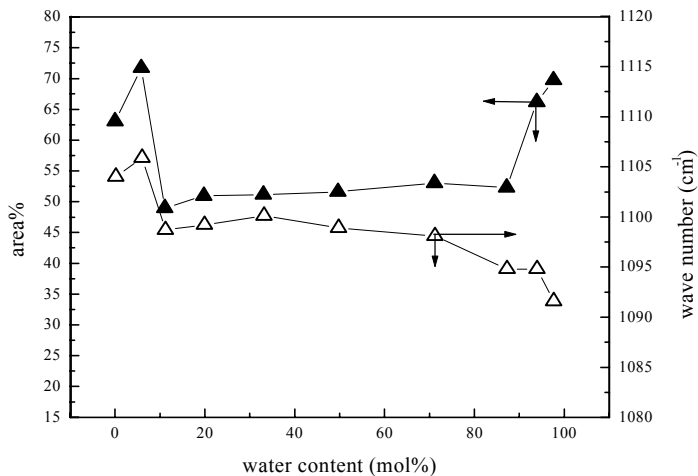


Figure 9. Relation of peak position and area ratio with water content at  $1146 \text{ cm}^{-1}$ .



*Figure 10. Relation of peak position and area ratio with water content at 1120 cm<sup>-1</sup>.*



*Figure 11. Relation of peak position and area ratio with water content at 1100 cm<sup>-1</sup>.*

## ACKNOWLEDGEMENT

This work was supported by the National Nature Science Foundation of China (Grant No. 29836130).

## REFERENCES

1. F. Sebba (1985), *Sep. Sci. Tech.*, **20** (5&6), 331-334.
2. Y. Zhang (1999), Dissertation for Master Degree, Institute of Chemical Metallurgy, Chinese Academy of Sciences.
3. H. A. Scymanski (1964), *Interpreted Infrared Spectra*, Vol. 1, Plenum Press, New York.
4. V. P. Tomaselli, H. Zarrabi and K. D. Moller (1980), *Applied Spectroscopy*, **34** (4), 415-417.
5. L. L. Burger (1984), *Science and Technology of Tributyl Phosphate*, Vol. 1, W. W. Schultz, J. D. Navratil and A. S. Kertes (eds.), CRC Press, Boca Raton, FL, pp. 25-67.



# ANALYSIS OF AMINE-BASED EXTRACTION SYSTEMS CONTAINING MORE THAN ONE ORGANIC PHASE: INVARIANCE AND IMPLICATIONS FOR EXTRACTION EFFICIENCY AND SELECTIVITY

Aharon M. Eyal, Betty Hazan, Riki Canari, Asher Vitner, and Tali Reuveny

Casali Institute of Applied Chemistry, The Hebrew University of Jerusalem, Jerusalem, Israel

Single organic-phase extraction systems were formed while extracting acrylic acid by tricaprylylamine (TCA) (no diluent), TCA in kerosene, or TCA in kerosene with 2% octanol. In contrast, two organic phases were formed on extracting maleic acid, and on extracting maleic and acrylic acid from their mixed solution using TCA in kerosene. The preference of maleic acid for the heavy phase over the light one is 80- to 1.6-fold larger than that of acrylic acid (it increases with the increase of the maleic-to-amine molar ratio). These results are explained by extraction mechanisms and the phase rule. Formation of two organic phases can be used successfully for selective separation between a product acid and other acids that preferably distribute into the second organic phase.

## INTRODUCTION

In some cases of using amine-based extractants for extracting mineral acids [1], carboxylic acids [2,3], or metals (like uranium [4]), the organic phase splits into two phases - heavy and light. This phenomenon is undesired in many cases, but could be beneficial in others, e.g., enhancing enrichment in extraction [2,3]. A second organic phase can be of particular interest for selective extraction in a number of industrial systems, e.g., extraction from an aqueous solution containing a mixture of two carboxylic acids.

The present paper analyses the third phase formation based on the Gibbs phase rule determining the general relationship between the degrees of freedom of the system, the number of phases, and the number of components. The effect of diluent properties is discussed and, for the case of extraction from solutions containing maleic and acrylic acids, distribution between the two organic phases and selectivity are analyzed, based on the extraction mechanism.

## THEORY

### Gibbs Phase Rule

The extraction in a three-phase system can be analyzed based on the Gibbs phase rule. This rule determines the general relationship between the degrees of freedom of the system, the number of phases, and the number of components [5,6].

Consider a system containing C number of distinct chemical species (components a, b, c, etc.) and P phases ( $\alpha$ ,  $\beta$ ,  $\gamma$ ), where all the species distribute between the phases and none enters into reaction. The state of each phase is defined by the temperature, T, the pressure, p, and the activity of each of the species in that phase. In other words, the number of the variables for each phase is:

2 (temperature and pressure) + C – 1 (the concentration of one of the component is determined by the sum of the others) = C + 1

Thus, the total number of the variables in all the phases is:

$$P(C+1) = \text{the total number of variables in all the phases} \quad (1)$$

(It should be noted that these variables specify the state of the phases, but not their size). Phases which are in equilibrium must have the same temperature, pressure, and chemical potential,  $\mu$ , for each of the species. Thus, assuming three phases ( $\alpha$ ,  $\beta$ ,  $\gamma$ ) and two species (a, b), there are the following equations between the variables:

$$T_\alpha = T_\beta \quad (2a) \qquad T_\beta = T_\gamma \quad (2b)$$

$$p_\alpha = p_\beta \quad (2c) \qquad p_\beta = p_\gamma \quad (2d)$$

$$\mu_{\alpha,a} = \mu_{\beta,a} \quad (2e) \qquad \mu_{\beta,a} = \mu_{\gamma,a} \quad (2f)$$

$$\mu_{\alpha,b} = \mu_{\beta,b} \quad (2g) \qquad \mu_{\beta,b} = \mu_{\gamma,b} \quad (2h)$$

The total number of equations is: (P-1) temperature equations + (P-1) pressure equations + (P-1) equations of  $\mu$  for species a + (P-1) equations of  $\mu$  for species b, or:

$$(P-1)^* (C+2) = \text{the total number of equations} \quad (3)$$

The number of variables of which their values may be freely chosen by the experimentalist is defined as the degrees of freedom of the system F. According to the Gibbs phase rule, the degrees of freedom can be calculated by subtracting the total number of equations (Equation (3)) from the total number of the variables in all the phases (Equation (1)), hence:

$$F = P(C+1) - (P-1)^* (C+2) \quad (4a)$$

$$\text{or} \quad F = C + 2 - P \quad (4b)$$

Equation (4b) defines the Gibbs phase rule.

## MATERIALS AND METHODS

### Materials

The amine used was tricaprylyl amine (TCA), supplied as Alamine 336 (A-336) by Cognis (MW~391, 95%). The diluents were a low-aromatic kerosene, Isopar K (Exxon), and 1-octanol (Merck, 99%). The acids were maleic acid (MW = 116, BDH, 99%-100.5%) and acrylic acid (MW = 72, Aldrich, 99%).

### Methods

In the single-acid extraction systems, 4 g aliquots of the organic phase were mixed at 25°C for 30 min with 1g aliquots of aqueous phases containing various concentrations of maleic acid. In two-acid extraction systems, 3 g aliquots of the organic phase loaded with the two acids were mixed at 25°C for 30 min with 1 g aliquots of aqueous phases. In some of the

experiments, the various phases (two or three) were separated by centrifugation. The organic phases were washed with 1 N NaOH solution. The wash solutions were analyzed by high performance liquid chromatography (HPLC) (where the temperature was 42°C, the column was Polyspher<sup>R</sup> OA KC (Merck), the mobile phase was 0.01 N H<sub>2</sub>SO<sub>4</sub>, and the flow rate was 0.4 ml/min).

## RESULTS

### Single-acid Extraction System

Table 1 shows that three-phase extraction systems were formed while extracting maleic acid by A-336 (no diluent), A-336 in kerosene, or A-336 in kerosene + 2% octanol (where the initial amine:acid molar ratios were in the range between 1 and 4.5). In contrast, two-phase extraction systems were formed while extracting acrylic acid by A-336 (no diluent), A-336 in kerosene, A-336 in kerosene + 2% octanol, or A-336 in kerosene + 10% octanol. Two-phase extraction systems were also formed while extracting maleic acid by A-336 in kerosene + 10% octanol.

*Table 1. Number of phases formed in extraction systems containing a single acid.*

Extractant	Maleic 0.1-0.45 mol/kg	Acrylic 0.1-0.45 mol/kg
A-336 (no diluent)	+++	---
0.45 mol/kg A-336 in kerosene	+++	---
0.45 mol/kg A-336+ 2% octanol in kerosene	+++	---
0.45 mol/kg A-336+10% octanol in kerosene	---	---

+++ Three-phase extraction system; --- Two-phase extraction system.

Table 2 presents the extraction of maleic acid by A-336 with no diluent. The final maleic acid concentration for all these experiments was 0.014 mol/kg in the aqueous phase, and 0.012 and 1.71 mol/kg in the light and the heavy organic phases, respectively.

*Table 2. Maleic acid extraction systems containing three components and three phases.*

Initial composition (g)			Final composition (g)		
Water	Maleic	A-336	Light organic phase	Heavy organic phase	Aqueous phase
1.54	0.47	2.01	0.33	2.30	1.49
1.70	0.35	2.01	0.8	1.75	1.5
2.04	0.24	2.00	1.3	1.2	1.76
1.93	0.11	2.02	1.76	0.5	1.81

Figure 1 presents results for the extraction of maleic acid by 0.45 mol/kg A-336 in kerosene. The concentration of the acid in the light and the heavy organic phases, and the volume ratio between the organic phases are presented as a function of the acid concentration in the aqueous phase. Figure 1 shows that the acid concentrations in the heavy and the light phase are almost independent of the acid concentration in the aqueous phase. Those concentrations are about 1.5 and 0.01 mol/kg for the heavy and the light phase, respectively. In addition, the ratio between the heavy organic and the light organic phases increases linearly with increasing acid concentration in the aqueous phase.

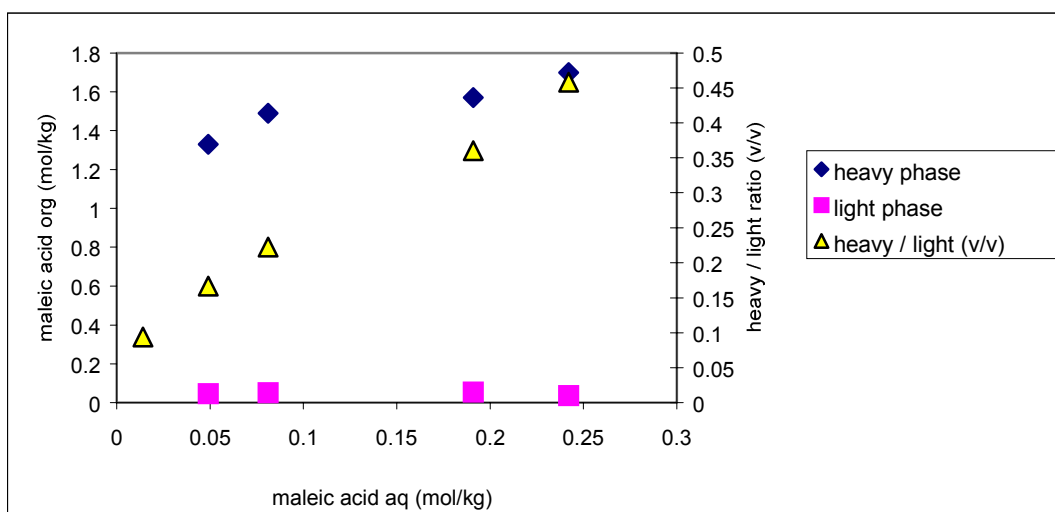


Figure 1. Extraction of maleic acid by 0.45 mol/kg Alamine 336 in kerosene.

### Two-acid Extraction System

Table 3 describes the extraction of maleic and acrylic acid from an aqueous solution by 0.45 mol/kg A-336 in kerosene. It shows the volume ratio between the organic phases (heavy/light), the acid concentrations in the two organic phases, the calculated molar ratio between the acids in each organic phase (e.g.,  $\text{light}_{\text{maleic}/\text{acrylic}}$ ), the preference of each acid for the heavy phase over the light phase (e.g.,  $P_{(\text{H/L})\text{maleic}}$ ), and the ratio between the organic phase preference for the maleic acid and that for acrylic acid ( $R = P_{(\text{H/L})\text{maleic}} / P_{(\text{H/L})\text{acrylic}}$ ).

Table 3. Extraction from solutions containing both maleic and acrylic acid by 0.45 mol/kg A- 336 in kerosene.

Amine/Maleic/ Acrylic	Heavy/ Light	Maleic		Acrylic		Acrylic/Maleic		P (Heavy/Light)		R Maleic/Acrylic
Initial molar ratio	(v/v)	Heavy mol/kg	Light mol/kg	Heavy mol/kg	Light mol/kg	Light	Heavy	Maleic	Acrylic	P/P
0.45:0.1:0.1	0.08	0.142	0.0012	0.088	0.058	49.5	0.62	121	1.5	79.7
0.45:0.1:0.2	0.08	0.144	0.0021	0.197	0.15	7.1	1.4	67	1.3	52.1
0.45:0.1:0.6	0.23	0.305	0.028	1.360	0.28	10.0	4.5	11	4.9	2.2
0.45:0.2:0.1	0.22	0.353	0.013	0.293	0.048	3.7	0.83	28	6.1	4.5
0.45:0.2:0.2	0.22	0.642	0.014	0.592	0.072	5.3	0.92	47	8.2	5.8
0.45:0.2:0.4	0.23		0.019		0.148	7.9				
0.45:0.2:0.5	0.29	0.652	0.023	0.954	0.21	9.2	1.5	28	4.5	6.3
0.45:0.3:0.1	0.24	0.35	0.0075	0.214	0.020	2.7	0.62	46	10.6	4.3
0.45:0.3:0.2	0.29		0.013	0.509	0.050	3.8			10.2	
0.45:0.3:0.3	0.33	0.82	0.016	0.751	0.074	4.7	0.92	52	10.1	5.1
0.45:0.45:0.1	0.40	0.704	0.014	0.250	0.015	1.1	0.35	51	16.7	3.0
0.45:0.45:0.2	0.47	0.409	0.012	0.406	0.032	2.8	0.99	35	12.5	2.8
0.45:0.7:0.1	0.56	0.841	0.0033	0.127	too low			255		
0.45:0.7:0.2	0.56	0.519	0.0066	0.329	0.0067	1.0	0.64	78	49.4	1.6

Table 3 shows that:

1. Although one organic phase was observed in the extraction of acrylic acid by 0.45 mol/kg A-336 in kerosene (Table 1), two organic phases were formed in all the systems containing both maleic and acrylic acid.
2. The ratio between the heavy-to-light organic phase decreases from 0.56 to 0.08 on decreasing the molar ratio between the total acids (maleic + acrylic) to amine in the system from 0.9/0.45 to 0.2/0.45.
3. The preference values of acrylic acid for the heavy phase over the light ( $P_{(H/L)\text{acrylic}}$ ) are higher than unity, but lower than those for maleic acid. The value of the acrylic preference  $P_{(H/L)\text{acrylic}}$  increases on increasing maleic acid concentrations in the system.
4. The ratio between the organic phase preference for the maleic acid and that for acrylic acid ( $R = P_{(H/L)\text{maleic}} / P_{(H/L)\text{acrylic}}$ ) is very sensitive to the maleic acid concentration. It decreases from about 80 to 1.6 on increasing the maleic acid to amine molar ratio in the system from 0.1/0.45 to 0.7/0.45.

## DISCUSSION

### Gibbs Phase Rule

Let us analyze the number of the degrees of freedom in the systems described above based on Gibbs phase rule. In all of the systems, the temperature (T) and pressure (P) are determined (25°C and atmospheric, respectively).

### Acid - amine - water system

In the system containing acrylic acid, amine and water (Table 1), the number of components, C, is 3 and the number of phases is 2. There are three degrees of freedom ( $F = C + 2 - P = 3$ ), but since T and P are determined, there is only one degree of freedom left. One may control the concentration of the acid in the aqueous phase, which determines that in the organic phase. In contrast, in a system containing maleic acid, amine and water (Table 2), the number of components is also 3, but the number of phases is 3. In such a case there are 2 degrees of freedom, but since T and P are determined, no degree of freedom is left and the system becomes invariant (as long as there are 3 phases). At the given T and P, the concentrations of the maleic acid in the light and the heavy organic phases and that in the aqueous phase were fixed: 0.012, 1.71, and 0.014 mol/kg, respectively.

### Acid - amine - diluent - water system

Figure 1 shows that in a system containing maleic acid, amine, kerosene, and water, three phases were formed as in the previous case. However, unlike in that case, there are 4 components, which increases the number of degrees of freedom from zero to 1. Hence, here, as in the case of amine-water-acrylic acid with two phases, one may control the concentration of the acid in one of the phases (which is the degree of freedom) which determines the concentration in the other.

### Two acids - amine - diluent - water system

In the case of extraction systems containing both acrylic and maleic acid (Table 3), two organic phases were also formed. With five components, 3 phases and fixed P and T, the numbers of degrees of freedom in this system is two. Indeed, controlling the concentration of the two acids in the aqueous phase determines their concentration in each of the organic phases).

## **Formation of Three Phases, Extraction Mechanisms, and Practical Aspects**

### **Single-acid extraction system**

In the system containing maleic acid, amine, and water (no diluent), the polarity of the ion pairs  $R_3NH^+ - OOC-C=C-COOH$  is high. Therefore, the mutual solubility between the free amine ( $R_3N$ ) molecules and those of the ion pairs is low. As a result, two organic phases were formed in this case. The solubility of the non-polar diluent (kerosene) in the maleic ion-pairs medium is very low too. Thus, two organic phases were also observed in the system containing maleic acid, amine, kerosene, and water. Being a more polar diluent, octanol acts as a co-solvent and increases the mutual solubility of free amine and amine-maleic acid ion pairs. Hence, the organic phase does not split into two in the case of the extraction system with high octanol content.

Acrylic acid ( $pK_{a,Acrylic} = 4.24$ ) extraction is different from that of the maleic acid ( $pK_{a,1, Maleic} = 1.83$ ). The ion pairs of the weaker acid (acrylic acid) are less polar than those of the maleic and the mutual solubility between the free amine molecules and the ion pairs is higher. As a result, a single organic phase was formed in all the acrylic acid extraction systems.

Hartl and Marr [2,3] suggest improving separation and enrichment in extraction of certain carboxylic acids by choosing conditions where three phases (an aqueous and two organics) are formed.

### **Extraction system containing two acids**

In the extraction of both acrylic and maleic acid from their mixture solutions, the solubility of the maleic acid ion pairs in the light organic phase is low. That is still true when that light phase contains acrylic acid ion pairs. As a result, the organic phase splits in two. Once a heavy, more polar phase forms, the acrylic acid ion pairs prefer it over the light phase, which is less polar ( $P_{(H/L)Acrylic}$  are higher than unity). The polarity of the heavy phase increases with increasing concentration of maleic acid ion pairs. Therefore,  $P_{(H/L)Acrylic}$  increases with increasing maleic acid concentration in the system. Since ion pairs of both acids prefer the heavy phase, the volume of this phase increases with increasing the total concentration of ion pairs (acrylic or/and maleic acid) in the system.

The high affinity of the organic base (the amine) for the acids enables selectivity for extracting the acid over the nonacidic components in the mixture [7]. But the most difficult impurities from which to separate the carboxylic acid in a fermentation broth, are other carboxylic acids. Thus, the selectivity in extraction of carboxylic acids from aqueous solutions containing their mixtures is an important issue. The three-phase systems can be used successfully for selective separation between a product acid and other carboxylic acids that preferably distribute into the second organic phase, in addition to the selective separation of carboxylic acids from non-acidic compounds (like sugars) that preferably distribute into the aqueous phase.

## **REFERENCES**

1. M. Robaglia and T. Kikindai (1971), *C. R. Acad. Sci., Ser. C*, **273** (25), 1685-8.
2. J. Hartl and R. Marr (1993), *Chem. Ing. Tech.*, **65** (7), 810-18.
3. J. Hartl and R. Marr (1993), *Proceedings ISEC '93*, Society of Chemical Industry, London, pp. 1683-88.
4. J. M. P. J. Verstegen (1965), *J. Inorg. Nucl. Chem.*, **27**, 201-207.
5. K. Denbigh (1984), *The Principles of Chemical Equilibrium*, 4th edition, Cambridge University Press, Cambridge, pp. 182-194.
6. V. Fried, H. F. Hameka and U. Blukis (1977), *Physical Chemistry*, Macmillan Publication Co., U.S.A., pp. 188-9.
7. S. T. Yang, S. A. White and S. T. Hsu (1991), *Ind. Eng. Res.*, **30**, 1335-1342.



## COMPUTATIONAL TIME SAVING IN THE MONTE CARLO SIMULATION OF LIQUID-LIQUID DISPERSIONS

Zaki El Hassan and E. Susana Perez de Ortiz\*

Department of Chemistry & Chemical Engineering, University of Paisley, Paisley, UK

\*Department of Chemical Engineering, Imperial College, London, UK

This work examines the Monte Carlo models for the simulation of liquid-liquid dispersions proposed in the literature and discusses the implications of their simplifying assumptions on the dynamics of the simulated dispersion and the transfer processes that may take place in it. Following an analysis of the computational load caused by the calculation of the different events taking place in the dispersion, a time saving approximation is proposed for the overall coalescence frequency that preserves the accuracy of the simulation while achieving significant reductions in the computational time. The proposed algorithm allows the implementation of sophisticated interaction models for drops breakage and coalescence as well as other deterministic processes.

### INTRODUCTION

Design of liquid-liquid extractors or mixing equipments relies heavily on laboratory or pilot-plant scale tests. Most of the design depends on experience and trial and error rather than a well-established theoretical basis. This may be attributed to the complexity of the mixing systems' hydrodynamics. The interactions between mass transfer, heat transfer, reaction kinetics and flow structure make it a difficult task to model and design extraction contactors from fundamentals. The existence of regions of substantially different turbulence structure inside the tank requires a rigorous description of the local turbulence features and of the boundary conditions where the regions meet. Two main approaches are found in the literature for modelling such systems. One is to use non-interacting models that ignore the micromixing effects and use averages for the system properties such as the surface area. They include the effective interfacial area models and drop size and residence time distribution models.

The second approach is based on the use of the interaction models that incorporate both microscale and macroscale processes. They provide a vehicle for treating drop breakage and coalescence and account for their effect on the overall process. The importance of micromixing has been illustrated by Curl [1] who showed that for chemically reacting systems, any reaction of order other than one is sensitive to micromixing. Stochastic systems that involve random motions of particles or lumps of fluid that require an statistical treatment are best treated by using the population balance equations (PBE), stochastic simulation methods or Monte Carlo simulation techniques.

The PBEs originated in the treatment of microbial growth. The first time the framework of PBEs appeared in the chemical engineering literature was by Hulbert and Katz [2]. Randolph and Larson [3] discussed the application of PBEs in crystallization. Ramkrishna and coworkers [4-6] studied PBEs in connection with small populations in which random fluctuations would be important. They also discussed the general features of population balances with regard to their applicability in chemical engineering problems [4,6-8]. Valentas and coworkers [9,10], Jeon and Lee [11], Sovova [12], and Shah *et al.* [13] used PBEs to simulate liquid-liquid dispersions but at the expense of accuracy as simplifications were introduced. Normally, when the different rate expressions are incorporated in PBEs, mixed integro-differential equations result that render PBEs of limited use except for simplified cases.

The difficulties associated with PBEs when rate processes were included in the models led to the search for other methods that could be used to analyse realistic situations. The development of digital computers made it possible to overcome most of the PBE's limitations encountered when dealing with complicated equations by using Monte Carlo simulations. Monte Carlo methods may prove more convenient for the following reasons:

1. Techniques are flexible, powerful, and free of convergence problems.
2. They eliminate the need for solving complicated integro-differential equations that result when transfer processes modelling is added to the simulation.
3. The simulation gives information about fluctuations of mean population characteristics as well as their individual entities around the average values, a feature not always possible with PBEs.
4. They allow for easy implementation of the basic expressions for mass and heat transfer rates without unnecessary simplification that may cause significant differences between experimental and simulation results.

The use of Monte Carlo techniques in particulate systems description was pioneered by Spielman and Levenspiel [14] then followed by Zeitlin and Tavlarides [15], Shah *et al.* [16], Bapat *et al.* [17], Hsia and Tavlarides [18], and Okufi [19], among others. This research refers to liquid-liquid and solid-liquid dispersions. Ramkrishna [6] established the connection between PBEs and Monte Carlo simulation techniques by using the method of the interval of quiescence (IQ).

## MODELS AND ASSUMPTIONS

Application of the Monte Carlo simulation techniques requires *a priori* knowledge of the processes at the microscale level which, in case of dispersion splitting and coagulation, are the mechanisms of breakage and coalescence. The development of an adequate algorithm can make it possible to handle mass transfer, heat transfer, as well as complex chemical reactions taking place in the dispersion.

The accuracy of the simulation of liquid-liquid dispersions depends on both the drop interaction models used and the robustness of the simulation algorithm. The approximations made vary from the assumption of interactions between identical drops to more sophisticated ones that use the dispersion characteristics to effect reasonable approximations. They are normally dictated by the computational resources available.

Most Monte Carlo models start by creating a digitised drop size sample according to a predetermined distribution, depending on the nature of the process and the underlying assumptions. In cases where a solute and mass transfer are involved, a trivariate distribution is normally created. In general, the initial time is considered to be zero and the solute is uniformly distributed. In cases where stages are involved, then each drop may have an initial age and a concentration different from the others. Using appropriate phenomenological

models, breakage and coalescence frequencies are assigned. A suitable technique for time management is then selected and the simulation started. The system properties are examined during the assigned time interval then the type(s) of stochastic event(s) taking place are determined and executed. Methods used to execute deterministic events vary according to the models chosen and level of accuracy required. The simulation is continued until a predetermined criterion is achieved. This may be steady state in population size distribution, a predetermined number of events, or a specific population size.

The most fundamental work done in the simulation of liquid-liquid dispersion was carried out by Bapat *et al.* [17] where a fully fledged Monte Carlo model was implemented using the phenomenological models developed earlier by Coualaglou and Tavlarides [20]. The interactions between drops were simulated without introducing any simplifying assumptions that can reduce accuracy or render the results of limited value. No restrictions were made on the sizes of drops coalescing or the daughter droplets resulting from breakage. Their model allowed the implementation of other processes such as mass transfer with relative ease. The penalty for such rigorous approach was a fast increase in computational resources as the sample size was increased and following drops splitting. El Hassan [21] analysed this increase and found it to be proportional to the square of population size.

Several researchers used different approaches to deal with the simulation time problems in their quest to reduce the computational resources required. Laso *et al.* [22, 23] developed a model that significantly reduced computational load with the following assumptions:

1. Drops are assigned to classes with representative sizes.
2. Only breakage into equally sized drops was allowed.
3. Only coalescence between two equally sized drops was allowed.

Das [24] studied only breakage but used similar restrictions regarding daughter droplets sizes. Skelland and Kanel [25] considered mass transfer in agitated systems using similar assumptions for coalescence and breakage as those used by Laso *et al.* [22, 23] but added the effect of drops circulation and rebounding to their model. Balmelli and Steiner [26] used an approach similar to Bapat *et al.* [17] but used representative drop sizes to describe the properties of drops within a certain category. A similar approach was used by Mousa and de Ven [27]. Ribeiro *et al.* [28-30] produced an efficient algorithm that does not restrict interactions to similar drops categories but used representative drop sizes increased algorithmically.

## NEW MODEL

In this paper we present the first step in a new approach [21] to dispersion simulation intended to reduce the computational load while preserving accuracy. This is achieved by minimising the number of assumptions made and by restricting the simplifications.

An examination of the computational load due to the different events was made using a Monte Carlo simulation of a dispersion of 2000 drops in the size range 0.0-0.5 mm and performed using the phenomenological models of Coualaglou and Tavlarides [20] and a full spectrum of drop sizes.

The breakage frequency  $g(a)$  of a drop of diameter  $a$  is given by:

$$g(a) = k_1 \frac{\overline{u^2(a)}^{1/2}}{a} \exp \left[ -k_2 \frac{\sigma}{\rho_d a \overline{u^2(a)}} \right]$$

and the corresponding equation for coalescence frequency  $f(a,a')$  between two drops of diameters  $a$  and  $a'$  is:

$$f(a, a') = k_3 (a + a')^2 \left( \overline{u^2(a)} + \overline{u^2(a')} \right)^{1/2} \exp \left[ k_4 \frac{\mu_c \rho_d}{\sigma^2} \frac{\left( \overline{u^2(a+a')} \right)^{3/2}}{a + a'} \left( \frac{aa'}{a + a'} \right)^4 \right]$$

where  $k_1, k_2, k_3, k_4$  are constants,  $\sigma$  is the interfacial tension,  $\rho$  the density,  $\mu$  is the viscosity,  $u$  the fluctuation velocity across drop diameter, and the subscripts  $c$  and  $d$  refer to the continuous and dispersed phases, respectively.

The algorithm is similar to that developed by Bapat *et al.* [17]. An analysis of the time taken to update the state of the dispersion after each of the different events showed that the main computational load was due to the calculation of the population coalescence frequencies. The model uses a full spectrum of drop sizes, thus avoiding the use of representative drop sizes to simulate the population, where the only approximation made is that of the population coalescence frequencies. This was therefore identified as the section of the simulation with potential for computational time saving. An analysis of the variation with drop size of the overall coalescence frequency of that drop with the rest of the drop population revealed that that the sensitivity is low and smooth, unlike the abrupt changes observed in the breakage frequencies after events are executed. Thus if the drop population is divided into categories of small diameter increments, and the mean size within each category is used in the calculations instead of the spectrum of sizes, the error introduced is small provided that the actual number of drops in the dispersion is used. This is shown in Table 1 for different numbers of categories.

*Table 1. Percentage error in population coalescence frequency.*

Number of Categories	Coalescence Frequency % error
50	0.036
120	0.0059
180	0.0018

Therefore the proposed model uses representative drop sizes only to update coalescence frequencies while keeping the actual drop sizes, ages, and other properties unchanged. Although two drops in one category may have the same coalescence frequencies, their breakage, coalescence, circulation, and rebound probabilities remain distinct. Therefore this approach introduces a minimum of simplifications and does not affect population behaviour in any significant manner.

The model also shifts the emphasis from repetitive CPU operations to the proper utilisation of the storage capacity of the random access memory.

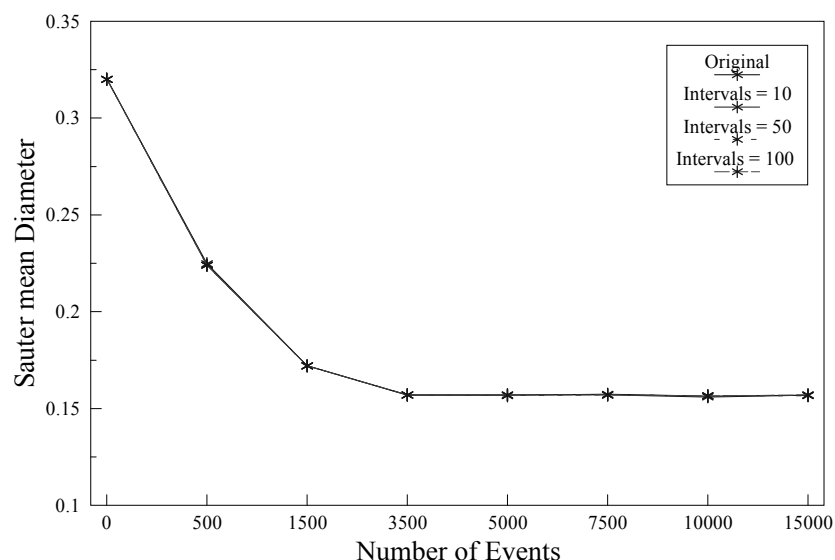
The resulting computational time savings in comparison with a non-simplified algorithm exceeds 97% for any significant number of events as shown in Table 2.

As can be seen, this approach resulted in a very significant reduction in computing load. As the only approximation was in the method by which the coalescence frequency was calculated, it is necessary to show that there was no degradation in the quality of properties used in the simulation and this is shown in Table 2 for a population sample of 2000 drops. All the percentages used in comparison are calculated using a rigorous algorithm similar to that developed by Bapat *et al.* [17].

*Table 2. The new algorithm - computer time saving.*

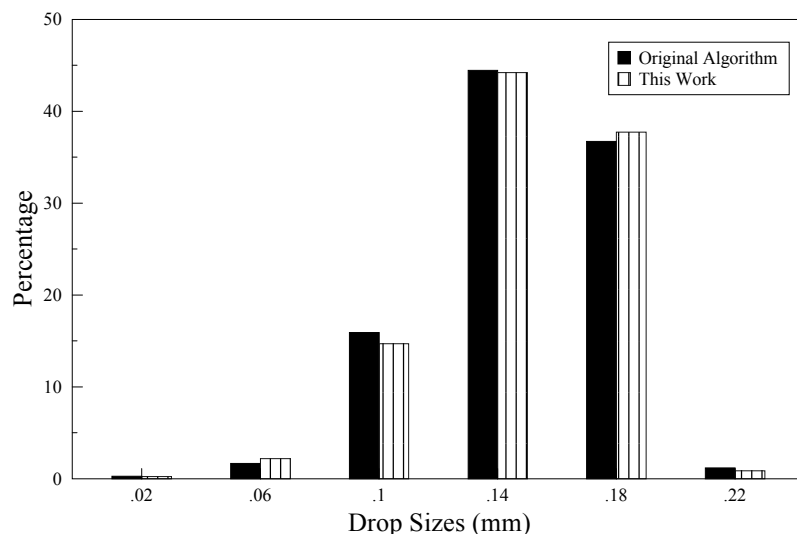
Events	Computer Time Saving (%)		
	10 Intervals	50 Intervals	100 Intervals
500	88.7	88.1	87.1
1500	96.4	96.1	95.8
3500	97.4	97.3	97.1
5000	97.3	97.2	97.1
7500	97.2	96.8	97.1
10000	97.2	97.1	97.1
15000	97.1	97.1	97.0

Figure 1 shows that the evolution of the population Sauter mean diameter obtained with the new model is similar to that resulting from the use of the more rigorous simulation algorithm.



*Figure 1. Evolution of Sauter mean diameter.*

A comparison of the drop size distributions calculated with the two algorithms after 5000 events is shown in Figure 2. It can be seen that the results are quite similar.



*Figure 2. Comparison of drop size distributions.*

## CONCLUSIONS

A computer time-saving Monte Carlo algorithm for the simulation of liquid-liquid dispersions in stirred tanks is presented. The only simplification with respect to more rigorous algorithms is in the calculation of overall coalescence frequency for which the drop size spectrum in each category has been substituted by a mean drop size while retaining the total number of drops in the dispersion. Dispersion updating after all other events is calculated using the entire drop spectrum and unsimplified phenomenological equations. The reductions achieved in the computational load are above 85%.

## REFERENCES

1. R. L. Curl (1963), *Am. Inst. Chem. Eng. J.*, **9** (2), 175.
2. H. H. Hulbert and S. L. Katz (1964), *Chem. Eng. Sci.*, **19**, 555.
3. A. D. Randolph and M. A. Larson (1971), Theory of Particulate Processes Analysis and Techniques of Continuous Crystallization, Academic Press, New York.
4. D. Ramkrishna and J. D. Borwanker (1976), *Chem. Eng. Sci.*, **31**, 435.
5. R. K. Bajpai, D. Ramkrishna and A. Prokop (1977), *Biotech. Bioengng.*, **19**, 1761.
6. D. Ramkrishna (1981), *Chem. Eng. Sci.*, **36**, 1203.
7. D. Ramkrishna and J. D. Borwanker (1973), *Chem. Eng. Sci.*, **28**, 1423.
8. D. Ramkrishna and J. D. Borwanker (1974), *Chem. Eng. Sci.*, **29**, 1711.
9. K. L. Valentas, O. Bilous and N. R. Amundson (1966), *Ind. Eng. Chem. Fundam.*, **5** (2), 271.
10. K. L. Valentas and N. R. Amundson (1966), *Ind. Eng. Chem. Fundam.*, **5** (4), 533.
11. Y. M. Jeon and W. K. Lee (1986), *Ind. Eng. Chem. Fundam.*, **25**, 293.
12. H. Sovova (1981), *Chem. Eng. Sci.*, **36**, 1567.
13. B. H. Shah and J. D. Borwanker (1976), *Math. Biosci.*, **31**, 1.
14. L. A. Spielman and O. Levenspiel (1965), *Chem. Eng. Sci.*, **20**, 247.
15. M. A. Zeitlin and L. L. Tavlarides (1972), *Can. J. Chem. Eng.*, **50**, 207.
16. B. H. Shah, J. D. Borwanker and D. Ramkrishna (1977), *Am. Inst. Chem. Eng. J.*, **23**, 897.
17. P. M. Bapat, L. L. Tavlarides and G. W. Smith (1983), *Chem. Eng. Sci.*, **38**, 2003.
18. M. A. Hsia and L. L. Tavlarides (1983), *Chem. Eng. J.*, **26**, 189.
19. S. Okufi (1984), PhD Thesis, University of London.
20. C. A. Coulaloglou. and L. L. Tavlarides (1976), *Am. Inst. Chem. Eng. J.*, **22**, 289.
21. Z. M. O. El Hassan (1990), PhD Thesis, University of London.
22. M. Laso, L. Steiner and S. Hartland (1987), *Chem. Eng. Sci.*, **42** (10), 2429.
23. M. Laso, L. Steiner and S. Hartland (1987), *Chem. Eng. Sci.*, **42** (10), 2437.
24. P. K. Das (1996), *Computers Chem. Eng.*, **20** (3), 307.
25. A. H. P. Skelland and J. S. Kanel (1992), *Ind. Eng. Chem. Res.*, **31**, 908.
26. M. Balmelli and L. Steiner (2000), *Chem. Eng. Proc.*, **39**, 201.
27. T. Mousa and T. G. M. van de Ven (1995), *Colloid Surf.*, 221.
28. L. M. Ribeiro, P. F R. Regueiras, M. M. L. Guimaraes and J. J. C. Cruz-Pinto (2000), *Adv. Eng. Software*, **31**, 985.
29. L. M. Ribeiro, P. F R. Regueiras, M. M. L. Guimaraes, C. M. N. Madureira, and J. J. C. Cruz-Pinto (1995), *Computers Chem. Eng.*, **19** (3), 333.
30. L. M. Ribeiro, P. F R. Regueiras, M. M. L. Guimaraes, C. M. N. Madureira, and J. J. C. Cruz-Pinto (1997), *Computers Chem. Eng.*, **21** (5), 543.



## AN EXPRESSION OF EQUILIBRIUM CONSTANTS IN SYNERGISTIC EXTRACTION

Yuko Hasegawa, Izuru Matsubayashi, and Akiko Inagaki

Department of Chemistry, Faculty of Science, Science University of Tokyo, Tokyo, Japan

To examine the effect of water molecules dissolved in the organic phase on the magnitude of synergistic extraction, the water solubility, the residual hydration number of the central metal in the chelates and the adducts, the extraction constants of the chelates, and the formation constants of the phen adducts to the chelate have been determined. Using the data obtained from the extraction of europium(III) and zinc(II) with pivaloyltrifluoroacetone (PTA) and/or 1,10-phenanthroline into chloroform, benzene, carbon tetrachloride, and hexane, the adduct formation constants introduced the term of water concentration in the organic phase were calculated. The difference of the constants among the solvents is much smaller than that defined conventionally. It has been concluded that the water content in organic phases, and the hydration and dehydration of the relevant species are the important factors controlling the magnitude of synergistic effects, because water molecules in the organic phases compete with a Lewis base in adduct formation.

### INTRODUCTION

The magnitude of the synergistic extraction of metal ions with a  $\beta$ -diketone and a Lewis base, depends on the nature of the solvents [1]. The solvent effects have been discussed on the basis of the dielectric constants [2] and solubility parameter of organic solvents [3-5]. However, less attention has been paid to the effect of the water in organic phases on the synergistic effects, although the organic phase is always saturated with water in solvent extraction system, and the content in the organic phase is largely different among organic solvents.

The present study has been aimed to examine the effect of water molecules dissolved in the organic phase on the magnitude of synergistic extraction. Since europium(III) is a typical hard acid and zinc(II) is in a middle of hard and soft acids, and their surface charge density should be similar to each other, they have been chosen to compare the involvement of water in organic phase to the adduct formation.

## EXPERIMENTAL

Most experiments were performed in a thermostated room at 298 K.

### Stability Constants of Metal Complexes with Phen in 0.1 M Ionic Medium

Chloroform solution containing various amounts of phen ( $(0.5\text{--}1.0)\times10^{-4}\text{ M}$ : 1 M = 1 mol·dm<sup>-3</sup>) was shaken with zinc(II) ( $1.5\times10^{-2}\text{ M}$  at maximum) aqueous solution at  $\text{pC}_\text{H}$  2 – 3 ( $\text{pC}_\text{H} = -\log[\text{H}^+]$ ) for an hour, where phen is 1,10-phenanthroline and was purchased as monohydrate. Similarly  $\text{CCl}_4$  containing phen was shaken with europium(III) (0.03 M at maximum) perchlorate aqueous solutions at  $\text{pC}_\text{H}$  3.5 - 5.5. The concentration of phen in the organic phases was determined from the absorbance at 265.8 nm.

### Adduct Formation Constants of PTA-Chelates with Phen in Organic Solvents

The procedure was performed in a similar way to that described elsewhere [6]. The aqueous solution containing europium(III) ( $(0.2\text{--}1.2)\times10^{-3}\text{ M}$ ) or zinc(II) ( $1.1\times10^{-4}\text{ M}$ ) adjusted the total ion concentration to 0.1 M with sodium perchlorate, 8.0 mL, was shaken with the identical volume of an organic solution containing PTA (0.05 - 0.2 M) and/or phen ( $< 5.0\times10^{-3}\text{ M}$ ). The hydrogen ion concentration was measured potentiometrically using  $1.00\times10^{-2}\text{ M}$  perchloric acid at 0.1 M ( $\text{H, NaClO}_4$ ) as a standard of  $\text{pC}_\text{H}$  2.00. The europium(III) concentration in the organic phase was determined by ICP-AES (inductively coupled plasma atomic emission spectrometry; HITACHI P-4000) after back extraction into 0.1 M perchloric acid. The concentration of europium(III) in aqueous phases was calculated by subtracting the concentration of europium(III) transferred into the organic phase from the initial concentration in the vial. The zinc(II) concentration in the organic phase was measured after the back extraction by atomic absorption spectrophotometer (HITACHI Z-6000). The zinc(II) concentration in the aqueous phase was also measured.

### Hydration Number of the PTA-Chelates and their Adducts with Phen

The PTA-chelate solutions were prepared by shaking europium(III) or zinc(II) perchlorate solution at  $\text{pC}_\text{H}$  5 - 6 with an organic solution of PTA at a given concentration. The adduct of europium(III) chelate with phen was prepared by extracting europium(III) with PTA and phen into an organic solvent. A portion of the organic phase was transferred into another tube and the water concentration was measured by coulometric Karl-Fischer titration (Hiranuma Sangyo Model AQ-7, Ibaraki, Japan), using HYDRANAL Coulomat AK as the anolyte, serving as a generator of  $\text{I}_2$ , and HYDRANAL Coulomat CG-K as catholyte were obtained from Riedel-de Haën (Seelze, Germany).

## RESULTS AND DISCUSSION

### Stability Constants of Metal Complexes with Phen in 0.1 M Ionic Medium

Since neither  $\text{Zn}^{II}$  nor  $\text{Eu}^{III}$  was extracted, the distribution ratio of phen accompanied with the formation of aqueous complexes with metal ion ( $\text{M}^{m+}$ ) can be represented as follows,

$$D_\text{B} = \frac{[\text{B}]_\text{o}}{[\text{B}] + [\text{HB}^+] + [\text{MB}^{m+}] + \Lambda} = \frac{K_{d,\text{B}}}{(1 + [\text{H}^+]/K_{a,\text{B}}) + \sum n \beta_n [\text{M}^{m+}] [\text{B}]^{n-1}} \quad (1)$$

where,  $\beta_n = [\text{MB}_n^{m+}] [\text{M}^{m+}]^{-1} [\text{B}]^{-n}$ . Assuming the formation of only the first complex, Eq. (1) can be represented as,

$$\log D_\text{B} + \log \left( 1 + \frac{[\text{H}^+]}{K_{a,\text{B}}} \right) = \log K_{d,\text{B}} - \log \left( 1 + \frac{\beta_1 [\text{M}^{m+}]}{1 + [\text{H}^+]/K_{a,\text{B}}} \right) \quad (2)$$

Figure 1 shows the relation of Eq. (2) when phen distributes between a given organic solvent and 0.1 M NaClO<sub>4</sub> in the presence of zinc(II) and europium(III). The values on Y-axis in the flat lines to X-axis agreed with  $\log K_{d,B}$ , i.e., 2.72 (CHCl<sub>3</sub>) and 0.11 (CCl<sub>4</sub>). When the data in Figure 1 were analyzed using  $pK_{a,B}$  4.77,  $5.98 \pm 0.07$  for Zn<sup>II</sup> complex was obtained as  $\log \bar{\beta}_1$ , while it was less than 1.8 for Eu<sup>III</sup> complex. The different stability of the complex for Eu<sup>III</sup> from that for Zn<sup>II</sup> may reflect the different affinity of these metal ions to oxygen atom in H<sub>2</sub>O and nitrogen atom in phen.

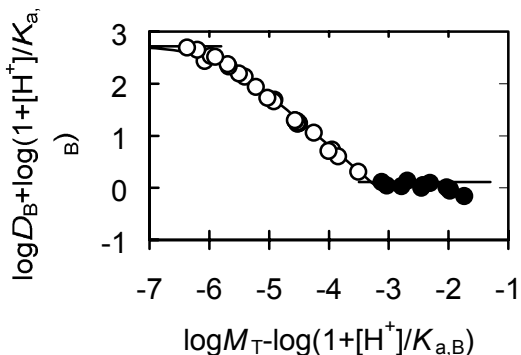


Figure 1. Correlation between  $\log D_B + \log(1+[H^+]/K_{a,B})$  and  $\log M_T - \log(1+[H^+]/K_{a,B})$ .  
aq : 0.1 M NaClO<sub>4</sub>, ○ Zn<sup>II</sup> org : CHCl<sub>3</sub>, ● Eu<sup>III</sup> org : CCl<sub>4</sub>.

### Synergistic Extraction of Europium(III) and Zinc(II) with PTA and Phen

When the distribution ratio ( $D$ ) of europium(III) or zinc(II) between 0.1 M NaClO<sub>4</sub> and an organic solution at a given concentration of PTA,  $\log D$ , was plotted as a function of pC<sub>H</sub> (Eu<sup>III</sup>: 3.1 - 4.3, Zn<sup>II</sup>: 3.5 - 5.8), straight lines having slope of +m were obtained. Accordingly, under the present experimental condition, the formation of the ionic chelates such as EuA<sup>2+</sup> and ZnA<sup>+</sup> can be ignored. When Eu<sup>III</sup> was extracted with PTA of several concentration (0.05 - 0.2 M) at a given pC<sub>H</sub>, the plot of  $\log D$  vs.  $\log [HA]_o$  also gave a straight line having a slope of +3. Using  $pK_a$  (7.01) and the distribution constant of PTA ( $\log K_d$  : 2.51 (CHCl<sub>3</sub>), 2.15 (C<sub>6</sub>H<sub>6</sub>), 2.15 (CCl<sub>4</sub>), 1.87 (C<sub>6</sub>H<sub>14</sub>)) [7], the extraction constants denoted as  $K_{exm0} = [MA_m]_o[M^{m+}]^{-1}[A^-]^{-m}$  were calculated. The values of  $K_{exm0}$  obtained are summarized in Table 1.

Table 1. The extraction constants of PTA-chelate, the adduct formation constants with phen, and the saturated solubility of water in pure organic solvents at 298 K.

	Eu <sup>III</sup>		Zn <sup>II</sup>		Water solubility in organic solvents /M
	$\log K_{ex30}$	$\log \bar{\beta}_1$	$\log K_{ex20}$	$\log \bar{\beta}_1$	
CHCl <sub>3</sub>	$18.1_3 \pm 0.0_5$	$7.6_1 \pm 0.0_6$	$9.6_5 \pm 0.0_5$	$8.5_6 \pm 0.0_6$	$(7.2 \pm 0.2) \times 10^{-2}$
C <sub>6</sub> H <sub>6</sub>	$18.2_9 \pm 0.0_7$	$9.4_0 \pm 0.0_9$	$9.3_0 \pm 0.0_5$	$10.7_7 \pm 0.0_8$	$(3.8 \pm 0.1) \times 10^{-2}$
CCl <sub>4</sub>	$17.5_8 \pm 0.1_2$	$10.1_4 \pm 0.1_5$	$8.9_7 \pm 0.0_4$	$10.3_9 \pm 0.0_4$	$(8.5 \pm 0.3) \times 10^{-3}$
C <sub>6</sub> H <sub>14</sub>	$16.7_4 \pm 0.1_4$	$11.1_2 \pm 0.2_0$	$8.2_7 \pm 0.0_4$	$11.0_1 \pm 0.0_3$	$(3.5 \pm 0.4) \times 10^{-3}$

Figure 2 shows the enhancement of the distribution ratio of europium(III) (a) and zinc(II) (b) in the presence of phen. Since the plot gives a straight line with a slope of 1, the stoichiometry between  $\beta$ -diketonato chelate and phen can be regarded as 1:1, and the total metal concentration in the organic phase,  $M_{o,T}$ , can be regarded as  $[MA_m]_o[B]_o$ . Accordingly the total concentration of phen in the vial,  $B_T$ , can be represented by Eq. (3).

$$B_T = [B] + [BH^+] + [MB^{m+}] + [B]_o + M_{o,T} \\ = [B]_o \{1 + (1 + [H^+]/K_{a,B} + \beta_1[M^{m+}])/K_{d,B}\} + M_{o,T}. \quad (3)$$

where  $\log K_{d,B}$  is 0.76 for  $C_6H_6$  and -1.24 for  $C_6H_{14}$ .

When metal ion is extracted with  $\beta$ -diketone and phen, the distribution ratio of the metal ion can be generally represented as

$$D = \frac{[MA_m]_o + [MA_m \cdot B]_o + \Lambda}{[M^{m+}] + [MA^{m-}] + \Lambda + [MB^{m+}] + [MB_2^{m+}] + \Lambda} \quad (4)$$

Then the net enhancement of the distribution ratio of the metal (II or III) in the presence of phen can be represented as

$$\log(D[A]^{-m} K_{exm0}^{-1}) + \log(1 + \beta_1[B]) = \log \bar{\beta}_1 + \log[B]_o \quad (5)$$

where  $\bar{\beta}_1 = [MA_m \cdot B]_o / [MA_m]_o [B]_o^{-1}$  (6)

and  $[A^-]$  is calculated from the following equation;

$$A_T = [HA] + [A^-] + [HA]_o + m[MA_m \cdot B]_o \\ = [A^-] \{1 + [H^+](1 + K_d)/K_a\} + m M_{o,T} \quad (7)$$

The values of  $\bar{\beta}_1$  were determined using the data in Fig. 2. The adduct formation constants obtained are also listed in Table 1. As seen from Table 1, the adduct formation constants are similar between zinc(II) and europium(III). Although the reason can not be explained easily, plausibly it may reflect the different hydration tendency and the different coordination numbers.

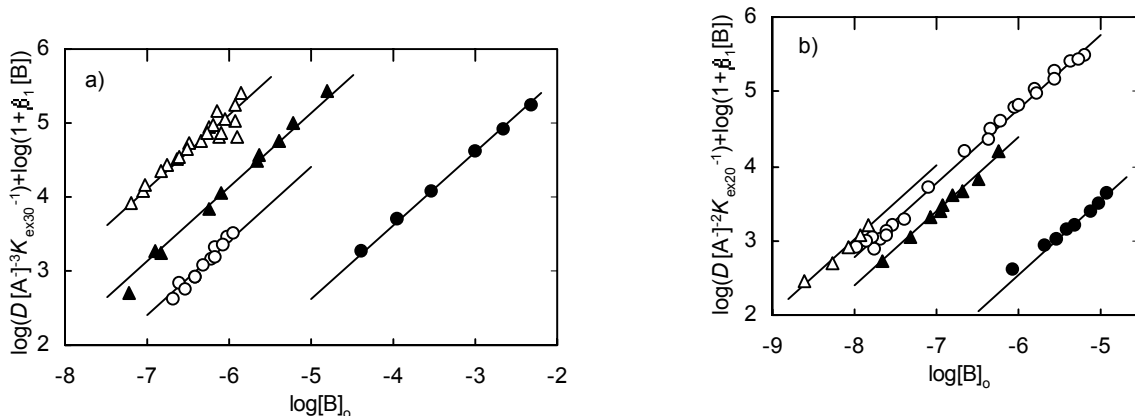


Figure 2. The change in the distribution ratio ( $D$ ) of a) europium(III) or b) zinc(II) containing PTA as a function of phen concentration at equilibrium

●:  $CHCl_3$ , ○:  $C_6H_6$ , ▲:  $CCl_4$ , Δ:  $C_6H_{14}$ .

### Hydration Number of the PTA-Chelates and their Adducts with Phen

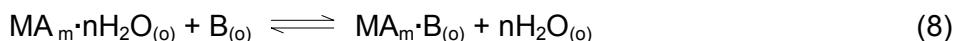
When the water concentration in the benzene, carbon tetrachloride and hexane was measured in the extraction of  $Eu^{III}$  with PTA, the concentration of water in the organic solvents increased linearly with increasing the concentration of the  $Eu^{III}$  extracted, as similarly as reported in chloroform [8]. The value at the intercept agreed with water solubility in the pure organic solvents. Then the residual hydration numbers ( $n_0$ ) of  $Eu^{III}$  are obtained from dividing the increment of water content,  $[H_2O]_{o,T} - [H_2O]_{solv}$ , by the concentration of  $[Eu(pta)_3]$  in the organic phase;  $2.4 \pm 0.0$  in  $CHCl_3$ ,  $2.5 \pm 0.1$  in  $C_6H_6$ ,  $2.2 \pm 0.0$  in  $CCl_4$ , and  $2.1 \pm 0.1$  in  $C_6H_{14}$ . The order

of the residual hydration numbers of central metal in the PTA chelates among organic solvents is similar to that of the water solubility. The residual hydration numbers of  $[Zn(pta)_2]$  and  $[Eu(pta)_3 \cdot phen]$  ( $n_1$ ) were determined in a similar way. In the all organic solutions studied, the hydration numbers of  $[Eu(pta)_3 \cdot phen]$  were almost zero. This may suggest that almost all hydrated molecules would be released from europium(III) on the formation of the adducts. The number in the PTA chelate of zinc(II) was  $1.1 \pm 0.1$  in  $CHCl_3$ ,  $1.4 \pm 0.2$  in  $C_6H_6$ ,  $0.8 \pm 0.1$  in  $CCl_4$ , and  $0.8 \pm 0.1$  in  $C_6H_{14}$ , although it was expected to be 2.0 assigning 6 to the coordination number of zinc(II). The reason for the much smaller values than expected can be not explained at present. The coordination number of zinc(II) in the PTA chelate extracted may be a mixture between 4 and 6. In the worst case it may suggest that water content can not be determined exactly in the presence of zinc(II) by Karl-Fischer titration. The detailed discussion must wait until more data are accumulated.

### A Novel Definition for the Equilibrium Constants in Organic Solvents Saturated with Water.

In general, the term of water is excluded from the equilibrium constant in complexation in organic solutions as represented by Eq. (6), because the involvement of water molecules in organic solvents has not been treated in the complexation in the organic phases.

However, the formation constants of the adducts can be represented as,



Then the adduct formation constant should be written as

$$K_1 = [MA_m \cdot B]_o [H_2O]_o^n [MA_m \cdot nH_2O]_o^{-1} [B]_o^{-1} \quad (9)$$

The equilibrium constant,  $K_1$ , may be related to the adduct formation constant,  $\bar{\beta}_1$ :

$$K_1 = \bar{\beta}_1 [H_2O]_o^n \quad (10)$$

where we can use the saturated water solubility in the organic solvent as the concentration of water. The values of  $K_1$  are calculated from the adduct formation constant according to the conventional definition, the hydration number, and the water solubility. As listed in Table 2, the numbers are similar among the solvents studied, although in  $CHCl_3$  the value is a little smaller than others. Accordingly, the difference of the magnitude of the synergistic extraction among organic solvents can be explained by the difference of water concentration in the organic phases as seen from Eq. (10).

*Table 2. Formation constants of phen adduct to  $\beta$ -diketonato chelate according to proposed definition ( $\log K_1$ ).*

	$CHCl_3$	$C_6H_6$	$CCl_4$	$C_6H_{14}$
$Eu^{III}$	$4.9 \pm 0.1$	$5.9 \pm 0.1$	$5.6 \pm 0.2$	$6.1 \pm 0.2$
$Zn^{II}$	$7.4 \pm 0.1$	$8.8 \pm 0.2$	$8.7 \pm 0.1$	$9.1 \pm 0.1$

From the present study it has been concluded that the involvement of water in organic solvents should be treated, whenever the extraction is compared among organic solvents. As the expression of the magnitude of the synergistic extraction of metal ions with  $\beta$ -diketone and a Lewis base, in other words, as the expression of the adduct formation equilibrium, we would like to offer Eq. (8), and as the equilibrium constant, Eq. (9) instead of Eq. (6).

## ACKNOWLEDGEMENTS

The authors are grateful to Messrs. K. Nakaya and T. Saito, Science University of Tokyo, for their experimental aid. This research was partially supported by a Grant-in-Aid for Scientific Research (C), No. 11640614 for the Ministry of Education, Science and Culture, Japan.

## REFERENCES

1. T. V. Healy (1963), *Nucl. Sci. Eng.*, **16**, 413.
2. S. A. Pai, J. N. Mathur, P. K. Khopkar, and M. S. Subramanian (1977), *J. Inorg. Nucl. Chem.*, **39**, 1209.
3. K. Akiba, M. Wada, and T. Kanno (1981), *J. Inorg. Nucl. Chem.*, **43**, 1031.
4. A. T. Kandil and K. Farah (1981), *Radiochim. Acta*, **28**, 165.
5. S. Nakamura, H. Imura, and N. Suzuki (1985), *Inorg. Chim. Acta*, **109**, 157.
6. S. Yajima and Y. Hasegawa (1998), *Bull. Chem. Soc. Jpn.*, **71**, 7825.
7. T. Sekine, Y. Hasegawa, and N. Ihara (1973), *J. Inorg. Nucl. Chem.*, **35**, 3968.
8. Y. Hasegawa, M. Miratsu, T. Kondo (2000), *Inorg. Chim. Acta*, **303**, 291.



## SOME FUNDAMENTAL ASPECTS OF THE CLOUD POINT PHENOMENON AND APPLICATION TO THE EXTRACTION OF PHENOL FROM AQUEOUS STREAMS

Katarzyna Materna, Gerard Cote\* and Jan Szymanowski

Poznan University of Technology, ICTE, Poznan, Poland

\*Ecole Nationale Supérieure de Chimie de Paris, Paris, France

This paper shows the influence of various parameters on the cloud point of a series of new oxyethylated methyl dodecanoates and an oxyethylated alcohol. In particular, the salting-out effect (decrease of the cloud point) arising from the presence of NaCl or NaHCO<sub>3</sub> is explained by the existence of a hydration shell with enhanced water structure as well as a zone with decreased salt concentration (*i.e.*, with excess water molecules) around the -(OCH<sub>2</sub>CH<sub>2</sub>)<sub>n</sub>- chain, as compared with the bulk. On the opposite, the salting-in effect (increase of the cloud point) is explained by depletion of water around the -(OCH<sub>2</sub>CH<sub>2</sub>)<sub>n</sub>- chain. Extraction data are also reported for phenol chosen as a model pollutant.

### INTRODUCTION

The concern to protect the environment becomes everyday stronger and despite major progresses achieved over the last three decades in the field of separation techniques, the removal of pollutants from aqueous industrial streams and wastewaters remains an important challenge. Indeed, well-established techniques such as liquid-liquid extraction exhibit important restrictions and drawbacks. For instance, the diluents and extractants constituting the organic solvents are partly lost in the aqueous phases by solubility and mechanical dispersion as fine droplets and, therefore may be the source of an induced pollution. Furthermore, the use of large volumes of hydrocarbons as diluents may be hazardous. As a result, new separation methods based on innovative concepts are currently being investigated. Thus, the cloud-point extraction technique, which does not use any organic diluent, attracts an increasing attention [1-5].

Cloud-point separations use aqueous micellar solutions of nonionic surfactants that undergo a phase separation (cloud-point phenomenon) upon appropriate temperature increase. From a physical point of view, the increase of temperature provokes the dehydration of the hydrophilic groups of the surfactant molecules, an increase of the aggregation number and the swelling of the micelles until the micellar solution becomes turbid and the separation of a surfactant-rich phase takes place. Such a phase separation leads to a surfactant-rich phase (the extract) in which the solutes are transferred and an almost micelle-free dilute solution of the nonionic surfactants (the raffinate). The phase separation is reversible, and on cooling the mixture to a temperature below the cloud point, the two phases merge to form once again a clear solution.

In its principle, the cloud point extraction technique is highly attractive, but despite many fundamental studies few data are available in the literature for evaluating its applicability in environmental cleanup engineering, as for instance the decontamination of industrial aqueous streams or polluted soils.

Earlier works were based on the use of oxyethylated alkylphenols as non-ionic surfactants, but it is obvious that such compounds are not acceptable in the aimed application because they are toxic and resistant to biodegradation. On the other hand, nonionics such as the new narrow-range oxyethylated methyl dodecanoates [ $C_{11}H_{23}CO(OCH_2CH_2)_nOCH_3$ ] recently synthesized from inexpensive materials avoid such a difficulty, as they hydrolyse easily and give non-toxic and non-surface active moieties [5-7].

Another concern is the consumption of energy to heat the aqueous solutions above their cloud points (*i.e.*, the temperature denoted hereafter CP at which a given micellar solution splits into two liquid phases). Indeed, a simple calculation shows that about 1.2 kWh is needed to increase the temperature of 1 m<sup>3</sup> of water by 1 °C. As a result, the consumption of energy to cause the splitting of the micellar phase is rather high, especially because an overheating ( $\Delta T = T_{set.} - CP$ , where  $T_{set.}$  denotes the settling temperature) of at least 10°C is essential to obtain less hydrophilic surfactant-rich phases and higher distribution coefficients for pollutants such as phenols [5]. However, the overheating  $\Delta T$  should not be too high as the distribution coefficients and yields of extraction of solutes (*e.g.*, phenol) first increase with overheating, then reach a maximum and finally decrease at high values of  $\Delta T$  and/or  $T_{set.}$ . Thus, it is of high importance to control the cloud point to optimise both the efficiency of extraction and consumption of energy.

In the present paper, the influence of various parameters on the cloud point of aqueous solutions of nonionics, including various oxyethylated methyl dodecanoates and an oxyethylated alcohol, is reported and discussed. Extraction data for phenol, a model pollutant, are also presented.

## EXPERIMENTAL

The various oxyethylated methyl dodecanoates [ $C_{11}H_{23}CO(OCH_2CH_2)_nOCH_3$ ] used were kindly provided by the Institute of Heavy Organic Synthesis, Kedzierzyn-Kozle (Poland) and are denoted hereafter as OMD-n, where n refers to the average degree of oxyethylation. The surfactants effectively tested exhibited average degrees of oxyethylation equal to 6, 8, 10 and 12 and their compositions determined by GC and HPLC were reported in previous papers [5-7]. Simulsol OX 1006L [ $C_{10}H_{21}(OCH_2CH_2)_6OH$ ] from Seppic (France) was also used in some experiments. Sodium chloride [NaCl], sodium hydrogenocarbonate [NaHCO<sub>3</sub>], potassium thiocyanate [KSCN] and phenol of reagent grade were from PROLABO (France) and used as delivered. Finally, deionised water was used for the preparation of all the aqueous solutions.

The cloud points were determined in a classical way by heating the micellar solutions above their CP and then by leaving their temperature to slowly decrease under intensive mixing, until the instant of complete disappearance of the turbidity (the temperatures at which the solutions became transparent were assumed to be the cloud points). The determination was repeated at least three times for each solution and the error on the average values of CP did not exceed 1°C.

The concentration of phenol in aqueous solutions was determined spectrophotometrically at 270 nm by using a SECOMAM S.750 spectrophotometer (France).

## RESULTS AND DISCUSSION

### Effects of Various Parameters on the Cloud Point of Non-Ionic Surfactant Solutions

#### **Surfactant concentration**

The cloud point of nonionics is influenced by the concentration of the latter and exhibits a minimum [3,8]. However, in a limited range of concentration, the cloud point is rather insensitive to the concentration of the nonionic surfactant used. Thus, the cloud points of aqueous solutions of oxyethylated methyl dodecanoates are fairly constant between 10 and 50 g.L<sup>-1</sup> [5]. As all our experiments were performed within this range, the effect of surfactant concentration is no longer considered below.

#### **Surfactant hydrophile-lipophile balance**

The appearance of cloudiness is greatly dependent on the structure of the non-ionic surfactant used. Such a dependence can be understood by considering the packing ratio  $P = \upsilon/a_0 l_c$  where  $a_0$  is the cross-sectional area of the hydrophilic group of the surfactant, and  $\upsilon$  and  $l_c$  are the volume and effective length of the hydrophobic tail, respectively [9,10].  $P$  provides a measure of the hydrophile-lipophile balance (HLB). Schott sought a universal relationship between the HLB value and the cloud point of nonionic surfactants [11]. In fact, examination of the cloud points of 165 nonionic surfactants showed that there is no universal relationship between calculated HLB and experimental CP (a graph plotting CP vs HLB consists not of a line but of a band), but that within a homologous series of surfactants having the same hydrophobic moiety and varying degrees of oxyethylation, Eq. (1) applies rather well [11]:

$$CP (\text{ }^{\circ}\text{C}) = a + b \text{ HLB} + c (\text{HLB})^2 \quad (1)$$

In many cases, the term in  $(\text{HLB})^2$  can be ignored and a linear relationship gives the best fit. For instance, in the absence of electrolyte, the following equation was found for the cloud point of the series of oxyethylated methyl dodecanoates of interest here [ $C_{11}\text{H}_{23}\text{CO(OCH}_2\text{CH}_2)_n\text{OCH}_3$ , with  $n = 5$  to 14] [5] :

$$CP (\text{ }^{\circ}\text{C}) = -245.8 + 20.27 \times (\text{HLB})^G \quad (2)$$

where  $(\text{HLB})^G$  represents the hydrophile-lipophile balance in Griffin's scale (*i.e.*,  $(\text{HLB})^G = 20M_H/M_S$  where  $M_H$  and  $M_S$  denote the molecular weight of the hydrophilic groups and the molecular weight of the surfactant, respectively; [for OMD-n,  $M_H = 44(n+1)$ ]).

#### **Electrolyte concentration**

The cloud point of a solution of nonionic surfactant can be deeply altered by the presence of various materials including electrolytes, cosurfactants and organic solutes [1,12]. The influence of electrolytes is usually explained in terms of salting-out and salting-in effects, but the formation of complexes between the polyoxyethylene groups of the nonionic surfactants and the metal cations of the electrolyte, including alkali-metal cations (*e.g.*,  $K^+$ ), may also contribute to alter the cloud point [9,13].

The influence of various electrolytes on the cloud point of different narrow-range oxyethylated methyl dodecanoates (OMD-n) is considered in Figure 1. Examination of this figure shows that the cloud point corresponding to a given oxyethylated methyl dodecanoate decreases with the concentration of  $\text{NaCl}$  and that of  $\text{NaHCO}_3$ , but increases with the concentration of  $\text{KSCN}$ . This exemplifies the salting-out and salting-in effects, respectively, and can be interpreted in terms of water structure. Indeed, generally, ions that are water structure formers (*e.g.*,  $\text{Cl}^-$ ) lower the cloud points, whereas ions that are water structure breakers (*e.g.*,  $\text{SCN}^-$  and  $\text{I}^-$ ) increase the cloud points [8,13].

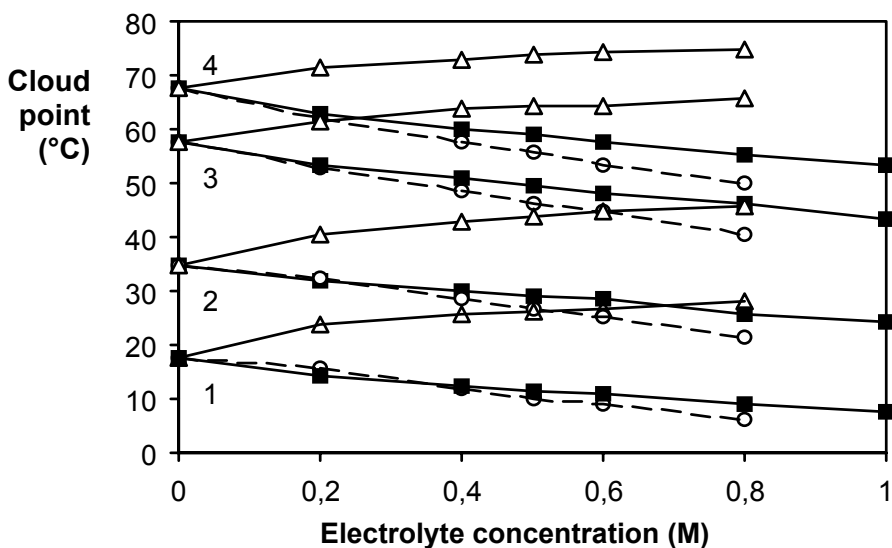


*Figure 1.: Effect of the concentration of different electrolytes on the cloud point of aqueous solutions containing 10 g.L<sup>-1</sup> of various oxyethylated methyl dodecanoates (OMD-n) :*  
 (1) OMD-6, (2) OMD-8, (3) OMD-10 and (4) OMD-12; black squares : NaCl [5];  
 open circles : NaHCO<sub>3</sub> [this work]; open triangles : KSCN [this work].

Florin *et al.* have developed a model for the cloud point of high-molecular-weight poly(ethylene oxide), PEO, in aqueous salt solution [14,15]. The basic feature of this model is the existence of a hydration shell with enhanced water structure as well as a zone with decreased salt concentration (*i.e.*, with excess water molecules) around the PEO chain, as compared with the bulk. When the temperature is increased, water molecules are forced back into the bulk solution from the salt-deficient regions, which allows the overlap of the latter and finally the splitting of the solution.

Florin *et al.* have established that the observed change in the cloud points due the presence of an electrolyte arises from the difference  $w - w_o$  given by Eq. (3) :

$$w - w_o = b (\mu_1 - \mu_1^\circ) + \lambda \quad (3)$$

where  $w$  and  $w_o$  are the molar-free-energy contributions from PEO chain - PEO chain interactions and overlaps of hydration shells and salt-deficient zones (if any), in the presence and absence of salt, respectively,  $b$  is the sum of transferred water molecules per  $-\text{O}-\text{CH}_2-\text{CH}_2-$  monomer unit,  $\mu_1$  and  $\mu_1^\circ$  refer to the chemical potential of water in the bulk and in the standard state, respectively, and  $\lambda$  includes all the remaining salt effects. Florin *et al.* found that  $b$  greatly varies from one salt to another. For instance, for PEO solutions at 90°C,  $b$  is close to 3 for NaCl, but only to 0.3 for KI. A negative value of  $b$  is even obtained at 96°C, which indicates depletion of water near the PEO chains, instead of excess as described above.

The difference  $w - w_o$  varies almost linearly with absolute temperature in the case of PEO solutions :

$$w - w_o = \alpha - \beta \quad (\alpha = 15.47 \text{ J.K}^{-1}.\text{mol}^{-1}; \beta = 5682 \text{ J.mol}^{-1}; R^2 = 0.9994) \quad (4)$$

If Eq. (3) and Eq. (4) are identified,  $(\mu_1 - \mu_1^\circ)$  is replaced by  $RT\ln a_w$  and T is identified to the cloud point, one obtains:

$$1/CP = (\alpha / [\beta + \lambda]) - (bR / [\beta + \lambda]) \ln a_w \quad (5)$$

where R and  $a_w$  denote the gas constant and the water activity (at CP), respectively. If Eq. (5) is assumed to be applicable to the aqueous solutions of oxyethylated methyl dodecanoates considered in the present work and if CP° refers to the cloud point in the absence of electrolyte, Eq. (5) can be rewritten as:

$$CP^\circ/CP = 1 - (bR/\alpha) \ln a_w \quad (6)$$

By using the water activity data available in the literature [16], the experimental results given in Figure 1 have been replotted under the form of a CP°/CP vs.  $\ln a_w$  graph, which leads to a series of straight lines as expected from Eq. (6) [for instance, for OMD-10 in the presence of NaHCO<sub>3</sub> : CP°/CP = 0,9999 - 2,1091  $\ln a_w$  with  $R^2 = 0,9993$ ]. From the slopes of these straight lines the following values of b were derived : 1.8 ± 0.2, 3.6 ± 0.5 and - 1.9 ± 0.3 for NaCl, NaHCO<sub>3</sub> and KSCN, respectively. The value of 1.8 ± 0.2 found for NaCl with OMD-n is slightly lower than that previously reported with PEO ( $b \approx 3$ ) [15], but nevertheless clearly illustrates the process of dehydration. On the other hand, the negative value obtained for KSCN suggests that this salt creates a depletion of water around the -(OCH<sub>2</sub>CH<sub>2</sub>)<sub>n</sub>- chain (*i.e.*, a zone with increased concentration of salt), as compared with the bulk, as already observed with KI. However, the extent of the phenomenon is surprisingly large here.

### **Phenol concentration**

The presence of organic solutes is known to have a great effect on the cloud points via the phenomenon of micellar extraction. In general, long-chain nonpolar solutes, such as saturated aliphatic hydrocarbons, which are solubilized in the inner core of the micelles, appear to cause an increase in the cloud point of the solutions, whereas polar and polarizable compounds, such as fatty acids and alcohols of moderate chain length, phenol, benzene, etc., which are solubilized in the outer regions of the micelles, depress it [1,12].

It was observed here that the presence of phenol decreases the cloud point of aqueous solutions of Simulsol OX 1006L in 1 M NaCl according to Eq. (7) (Table 1):

$$CP(^{\circ}C) = -622.5[\text{Phenol}] + 34.95 \quad ([\text{Phenol}] \text{ in M}; R^2 = 0.9979) \quad (7)$$

which shows that the phenol depresses the cloud point much more effectively ( $\Delta CP/\Delta[\text{Phenol}] \approx -622 \text{ } ^{\circ}\text{C.M}^{-1}$ ) than electrolytes such as NaCl ( $\Delta CP/\Delta[\text{NaCl}] \approx -9 \text{ } ^{\circ}\text{C.M}^{-1}$ ). However, if the cloud point extraction method is applied for the removal of low concentrations of phenol [or other organic pollutant] (*e.g.*, < 10<sup>-3</sup> M), the cloud point should be rather constant along the process line.

### **Characteristics of the Surfactant-rich Phase and Extraction Data for Phenol**

In our previous work performed with oxyethylated methyl dodecanoates [5], it was shown that the volume of the surfactant-rich phase and, as a result, the volume phase ratio ( $V_s/V_w$ ) sharply decreases with increasing overheating ( $\Delta T = T_{\text{set.}} - CP$ ) and/or settling temperature  $T_{\text{set.}}$  [ $\Delta T$  and  $T_{\text{set.}}$  were varied simultaneously]. The results obtained in the present study with Simulsol OX 1006L at constant settling temperature (*i.e.*,  $T_{\text{set.}} = 50^{\circ}\text{C}$ ) and reported in Table 1 show that an increase of  $\Delta T$  caused by an increase of the initial concentration of phenol, at constant  $T_{\text{set.}}$ , effectively decreases the ratio  $V_s/V_w$ . As expected, it is also observed that the distribution coefficient of phenol,  $D_{\text{Phenol}}$  increases as the surfactant-rich phase becomes less hydrophilic (*i.e.*, as  $V_s/V_w$  decreases). However, due to the combination of the increase of  $D_{\text{Phenol}}$  and the decrease of  $V_s/V_w$ , the yield of phenol extraction remains remarkably constant. Finally, it should be noticed that with  $[\text{Phenol}]_{\text{initial}} = 49.4 \text{ mM}$ , the system is already turbid at room temperature, but that the efficiency of phenol extraction is as good as in the other experiments. This suggests that it could be more efficient to perform all the extraction procedure above CP (*i.e.*, as in classical liquid-liquid extraction, but without organic diluent), which is possible as the dispersion of the surfactant is easy here. Indeed, this would avoid consumption of much energy to make the solution turbid, without loss of extraction performance.

**Table 1.** Extraction data for phenol and physical characteristics of the extraction system.  
 [Simulsol OX 1006L] = 40 g.L<sup>-1</sup>; phenol variable in 1 M NaCl (pH ≈ 3); T<sub>set.</sub> = 50°C.

[Phenol] <sub>initial</sub> (mM)	CP (°C)	Overheating (°C)	V <sub>S</sub> /V <sub>W</sub> (*)	D <sub>Phenol</sub>	Phenol extracted (%)
0	34.5	15.5	-	-	-
0.97	34.2	15.8	0.095	28.5	72.9
1.9	34.0	16.0	0.080	31.9	71.8
4.8	31.7	18.3	0.079	34.9	73.2
9.9	29.0	21.0	0.079	33.3	72.3
19.9	22.5	27.5	0.074	35.8	72.6
49.4 (**)	< 20	> 30	0.052	49.9	72.2

(\*) V<sub>S</sub> = volume of the surfactant-rich phase; V<sub>W</sub> = volume of the separated aqueous phase

(\*\*) The system is already turbid at room temperature

## REFERENCES

1. W.L. Hinze and E.Pramauro (1993), *Crit. Rev. Anal. Chem.*, **24**, 133-177 and references therein.
2. S. Akita, M. Rovira, A.M. Sastre and H. Takeuchi (1998), *Sep. Sci. Technol.*, **33**, 2159-2177 and references therein.
3. E. Lins de Barros Neto (1999), Doctorate Thesis, Institut National Polytechnique de Toulouse, France.
4. J. Szymanowski and W. Apostoluk (2000), *J. Colloid Interface Sci.*, **228**, 178-181 and references therein.
5. K. Materna, I. Milosz, I. Miesiac, G. Cote and J. Szymanowski (2001), *Environ. Sci. Technol.*, **35**, 2341-2346 and references therein.
6. J. Szymanowski, D. Makowska and W. Hreczuch (1999), *Proc. 4<sup>th</sup> Word Conf. Deterg.: Strategies for the 21<sup>st</sup> Century*, AOCS Press, Champaign, USA, pp. 255-260.
7. Z. Siwek, W. Hreczuch, J. Szymanowski and G. Bekierz (1999), *Proc. 4<sup>th</sup> Word Conf. Deterg. : Strategies for the 21<sup>st</sup> Century*, AOCS Press, Champaign, USA, pp. 273-279.
8. T. Okada (1992), *Anal. Chem.*, **64**, 2138-2142 and references therein.
9. D.J. Mitchell and B.W. Ninham (1981), *J. Chem. Soc., Faraday Trans. 2*, **77**, 601-629.
10. D. Myers (1999), Surfaces, Interfaces, and Colloids: Principles and Applications, 2nd edn., Wiley-VCH, New York, p. 373.
11. H. Schott (1969), *J. Pharm. Sci.*, **58**, 1443-1449.
12. M.J. Rosen (1989), Surfactants and Interfacial Phenomena, 2nd edn., Wiley Interscience, New York, p. 191.
13. F. Tokiwa, T. Matsumoto (1975), *Bull. Chem. Soc. Jpn.*, **48**, 1645-1646.
14. R. Kjellander and E. Florin (1981), *J. Chem. Soc., Faraday Trans. 1*, **77**, 2053-2077.
15. E. Florin, R. Kjellander and J.C. Eriksson (1984), *J. Chem. Soc., Faraday Trans. 1*, **80**, 2889-2910.
16. G.G. Aseyev (1999), Electrolytes: Equilibria in Solutions and Phase Equilibria. Calculation of Multicomponent Systems and Experimental Data on the Activities of Water, Vapor Pressures, and Osmotic Coefficients, Begell House Inc. Publishers, New York.



## EQUILIBRIA BASED ON G<sup>E</sup>-MODELS IN A Co/Ni/ PHOSPHINIC ACID SYSTEM

Ralf Manski, Hans-Jörg Bart, Astrid Görge\*\*, Michael Traving\*, Jochen Strube\*  
and Werner Bäcker\*

Institute of Thermal Process Engineering, University of Kaiserslautern, Germany

\*Fluid Process Technology, Bayer AG, Leverkusen, Germany

\*\*H.C. Starck GmbH & Co. KG, Goslar, Germany

Solvent extraction studies of cobalt and nickel have been carried out using a phosphinic acid. The percentage extraction of metal ions increased with increasing equilibrium pH. Cobalt was preferentially extracted over nickel. The equilibria data were correlated with a stoichiometry of 1:4 for cobalt and 1:6 for nickel using activity coefficient corrections. The complex stoichiometry of the system has been confirmed using FT-IR spectroscopy. The models used for calculating activity coefficients were the Pitzer model for the aqueous phase and the regular solution theory of Hildebrand and Scott for the organic phase.

### INTRODUCTION

The separation of cobalt and nickel solutions into pure components is difficult, because of their similar physico-chemical properties. Solvent extraction has proven to be an efficient tool [1, 2]. To provide a model for equilibria and kinetics which is consistent for a broad concentration range non-idealities of both phases have to be taken into account [3]. This can be done using activity coefficients which are partial molar quantities of the Gibbs excess enthalpy. The Gibbs excess enthalpy can be calculated using suitable models such as the Pitzer model for electrolyte solutions [4] and the regular solution theory of Hildebrand and Scott [5] for organic species. The Pitzer model contains several parameters which can be regressed from the experimental data. To be exact in the models, the stoichiometry of the metal complex has to be known. Complex stoichiometry which can be found in the literature are mostly derived from slope analysis at low concentrations. For consistent modeling, it is desirable to know if there is a concentration dependency of the organic metal complex structure. FT-IR analysis is a useful tool in this respect [6].

### EXPERIMENTAL

The phosphinic acid was diluted with solvent. Three different stock solutions were prepared by dissolving cobalt salt in water. Solution I contains 34 g/l cobalt and 2.6 g/l nickel. Solution III contains 10 % of the concentration from solution I, solution II 50 % of the concentration of solution I. The two phases were contacted in a shaker machine for 20 h to reach thermodynamic equilibrium. The equilibrium data are shown in Figure 1. Cobalt is preferably extracted over nickel at low pH-values. At high pH values it was possible to extract the total amount of cobalt and nickel from the aqueous phase.

Atomic absorption spectrophotometry, AAS, (Hitachi Z 8100) was used for the analysis of metal concentration in both phases. Direct organic phase analysis was found to be less accurate than re-extracting the organic phase with acid. The error in the metal mass balance was up to 10 % for direct organic AAS analysis and less than 5 % for the stripped organic solution.

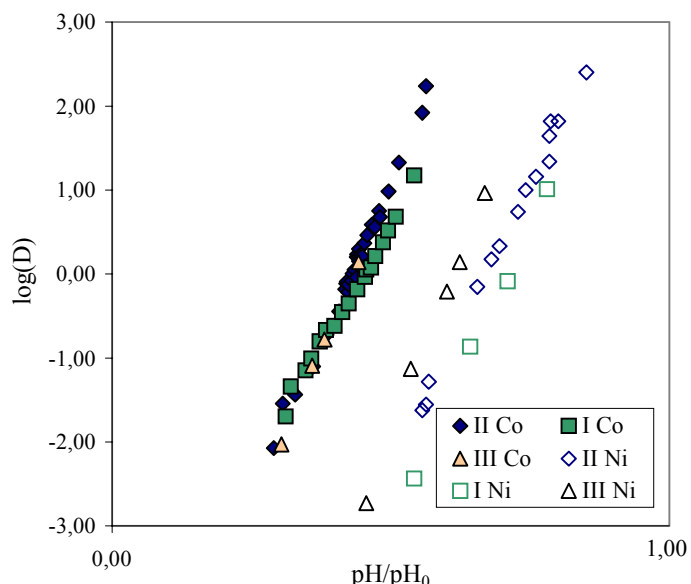


Figure 1. Equilibrium data of Co/Ni/phosphinic acid.

### ORGANIC-PHASE FT-IR SPECTROSCOPY

The predominant metal complex for phosphinic acid in the organic phase according to literature is 1:4 for cobalt ( $\text{CoR}_2(\text{RH})_2$ ) and 1:6 for nickel ( $\text{NiR}_2(\text{RH})_4$ ) [7-11]. The authors did not mention, however, the concentration range valid for those complexes. Most of the information was derived from slope analysis, which is only valid for low concentrations. FT-IR measurements were carried out to investigate directly the structure in the organic phase. Resonances of IR-active groups can be identified in an IR-spectrum. The valence oscillation of the P=O double binding is identified in the range of  $1240\text{-}1180\text{ cm}^{-1}$  [12]. Phosphinic and phosphoric acids can be identified by characteristic vibrational bands in that area. Sainz-Diaz *et al.* [6] investigated the Zn-D2EHPA system by FT-IR measurements. Two distinct bands were identified at  $1234\text{ cm}^{-1}$  and  $1206\text{ cm}^{-1}$  for the phosphoric acid. The band at  $1234\text{ cm}^{-1}$  decreases for increasing metal loading on the ion exchanger, whereas the other band increased. Thus a correlation to the unloaded ion exchanger molecule and one for the metal loaded dimer is possible. The same behavior was observed for Ni-D2EHPA.

FT-IR spectrophotometric analysis were carried out with a Nicolet FT-IR Avatar 320 using KBr-windows. The reproducibility of FT-IR measurements was determined to be within 8 %. Figure 2 shows the FT-IR spectrum for the phosphinic acid dissolved in solvent. With increasing cobalt loading, two diminishing bands can be identified and one increasing band can be identified, respectively.

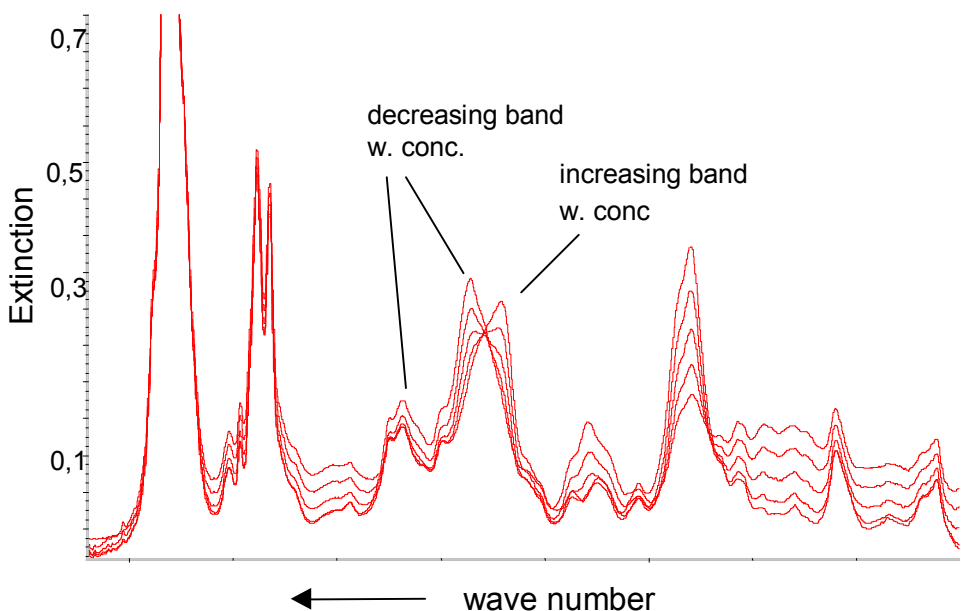


Figure 2. FT-IR-spectrum of Co loaded phosphinic acid.

In Figure 3, FT-IR measurements of the phosphinic acid with different cobalt loadings are plotted over the diminishing band height. Here a linear relationship between metal loading and band height is observed. This strongly indicates that the complex in the organic phase does not vary with concentration. The same observations were made for nickel. A calibration curve was determined by measuring the unloaded ion exchanger at different dilutions in an aliphatic solvent. Figure 4 shows a linear relationship between ion exchanger concentration and band height. Now it is possible to actually assign a concentration of free ion exchanger in loaded organic phases. To determine the actual cobalt complex one has to determine the actual sodium concentration which remained in the organic phase resulting from pre-neutralization. A similar procedure for nickel yields the Ni-complex behavior in the organic phase.

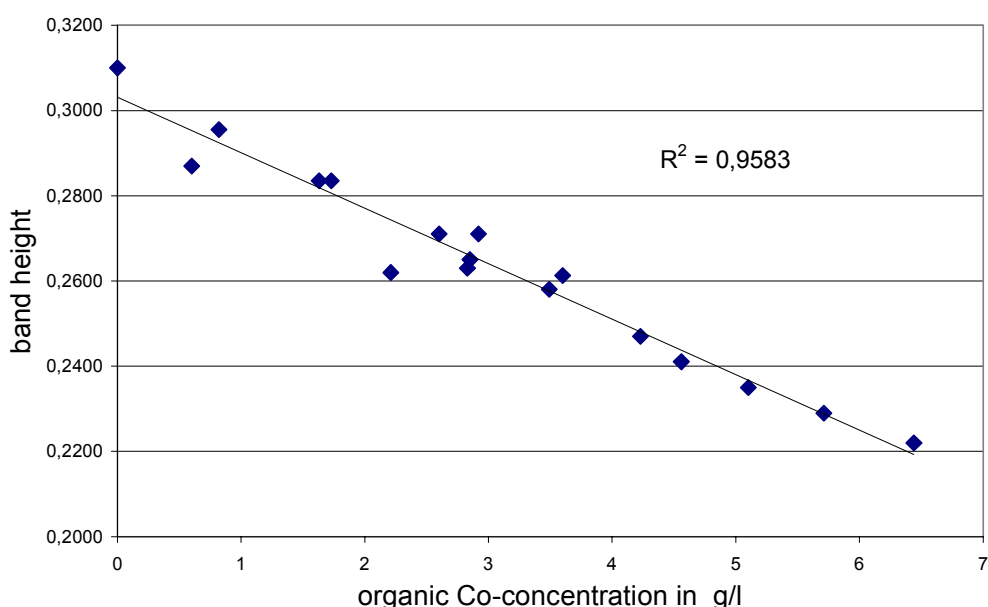


Figure 3. Reducing band for cobalt loaded phosphinic acid.

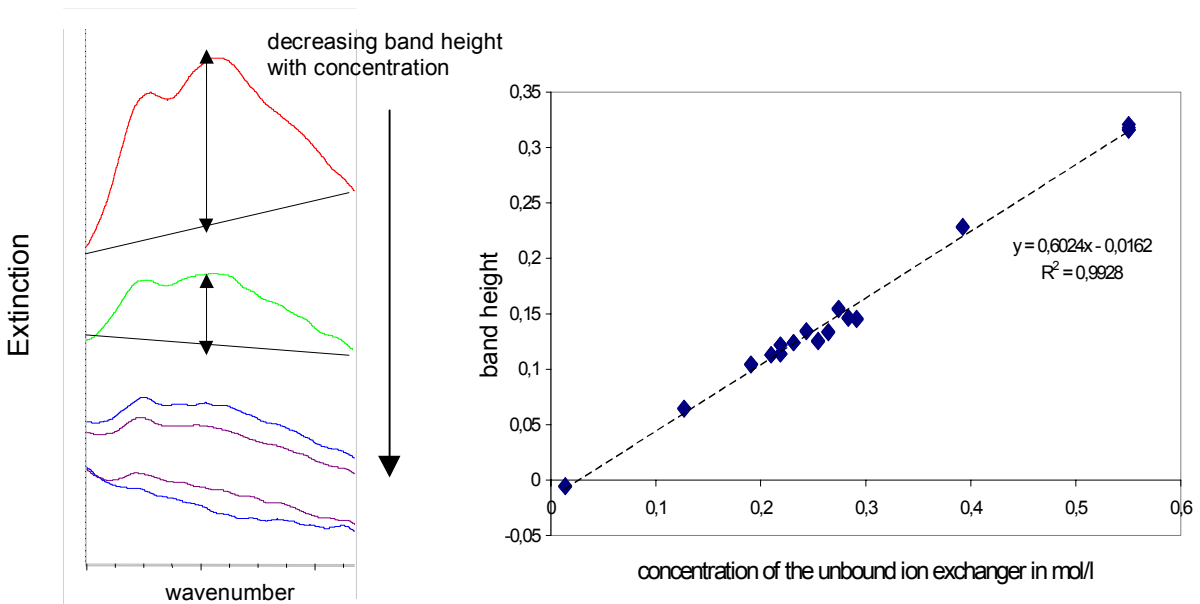


Figure 4. Calibration curve with different phosphinic acid concentration.

The present evaluation of the FT-IR measurements could not confirm the complexes proposed in the literature. The evaluation rather indicates a 1:2 complex for cobalt ( $\text{CoR}_2$ ) and nickel ( $\text{NiR}_2$ ). Further experiments are crucial to show whether this observation holds for lower metal loadings, which would be more compatible to the literature cited. However, no dependency or a change of the stoichiometry of the metal complex with concentration, in the concentration range studied, was found for the cobalt and nickel complexes.

### EQUILIBRIA MODELLING WITH $\text{g}^\text{E}$ -MODELS

Phosphorus-based ion exchangers exist as dimers in kerosene like diluents [13, 14]. With the stoichiometry given in the literature the equilibrium reaction can therefore be written as:



The mass action law then reads as:

$$K_{\text{Co}} = \frac{\overline{\text{CoR}_2(\text{RH})_2} \cdot [\text{H}^+]^2}{\overline{(\text{RH})_2}^2 \cdot [\text{Co}^{2+}]} \cdot \frac{\gamma_{\text{CoR}_2(\text{RH})_2} \cdot \gamma_{\text{H}^+}^2}{\gamma_{(\text{RH})_2}^2 \cdot \gamma_{\text{Co}^{2+}}} \quad (3)$$

$$K_{\text{Ni}} = \frac{\overline{\text{NiR}_2(\text{RH})_4} \cdot [\text{H}^+]^2}{\overline{(\text{RH})_2}^3 \cdot [\text{Ni}^{2+}]} \cdot \frac{\gamma_{\text{NiR}_2(\text{RH})_4} \cdot \gamma_{\text{H}^+}^2}{\gamma_{(\text{RH})_2}^3 \cdot \gamma_{\text{Ni}^{2+}}} \quad (4)$$

To calculate the activity coefficients,  $\gamma_i$ , the Pitzer model[4] is used for the aqueous phase and the Hildebrand-Scott [5] solubility parameter is used for the organic species. Pitzer parameters, Masson parameters and solubility parameters were taken from the literature [15]-[17]. The freely available computer program SXLSQI of Baes *et al.* [18] is used to correlate the experimental data by regressing free parameters of the  $\text{g}^\text{E}$ -models. Figure 5 shows good correspondence of the model with correlated parameters and the experimental equilibrium data.

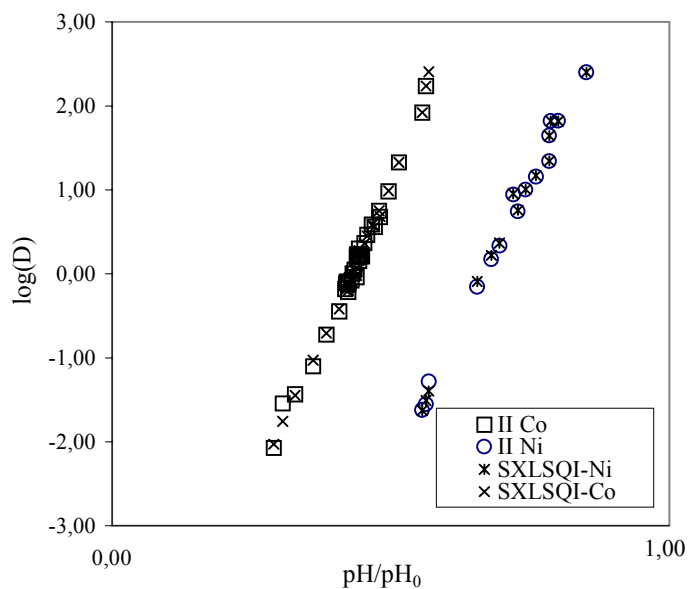


*Figure 5. Correlated equilibria data using activity coefficients.*

## CONCLUSIONS

The extraction equilibria for reactive extraction of divalent cobalt and nickel from acid solutions using a commercial phosphinic acid as extractant were studied. The percentage extraction of metal ions increased with increasing equilibrium pH. Cobalt was preferentially extracted over nickel. The correlated data using activity coefficients leads to higher model depth. Predictions over the concentration range measured are thus possible. The  $\log D$  over  $pH$  plot yields linear relationships. In order to model the equilibrium data and reaction kinetics, the predominant metal complex in the organic phase has to be known. The stoichiometry of the slope analysis is only valid for low concentrations, therefore the organic phase was investigated by FT-IR spectroscopy analysis over a wide concentration range. Characteristic bands were attributed to the loaded and unloaded ion exchanger. Linear relationships of the characteristic bands with concentration show that the stoichiometry of the metal complex is no function of concentration. With this, FT-IR analysis has proven to be a suitable tool to determine the organic metal complex under extreme conditions.

## ACKNOWLEDGEMENTS

The authors wish to thank Bayer AG and H.C. Starck for their support of this work. Melanie Schmidt is thanked for conducting the FT-IR experiments.

## REFERENCES

1. G. W. Ritcey and A. W. Ashbrook (1984), Solvent Extraction: Principles and Applications to Process Metallurgy, Part I, Elsevier Scientific Publishing Company, Amsterdam.
2. M. Cox (1992), Solvent Extraction in Hydrometallurgy, Marcel Dekker, Inc., New York.
3. H. J. Bart (2001), Reactive Extraction, Springer, Berlin.
4. K. S. Pitzer (1973), *J. Phys. Chem.*, **77** (2), 268-277.
5. J. M. Hildebrand and R. L. Scott (1950), The Solubility of Nonelectrolytes, Reinhold, New York.
6. C. I. Sainz-Diaz, H. Klocker, R. Marr and H. J. Bart (1996), *Hydrometallurgy*, **42**, 1-11.
7. B. K. Tait (1993), *Hydrometallurgy*, **32**, 365-372.
8. K. Yoshizuka, Y. Sakumoto, Y. Baba and K. Inoue (1990), *Hydrometallurgy*, **23**, 309-318.
9. K. C. Sole and J. B. Hiskey (1992), *Hydrometallurgy*, **30**, 345-365.
10. N. B. Devi, K. C. Nathsarma and V. Chakravortty (1994), *Hydrometallurgy*, **34**, 331-342.
11. Z. Hubicki and H. Hubicka (1996), *Hydrometallurgy*, **40**, 65-76.
12. H. W. Williams and I. Fleming (1991), Strukturaufklärung in der organischen Chemie: Eine Einführung in die spektroskopischen Methoden, Thieme, Stuttgart.
13. Z. Kolarik and R. Grimm (1976), *J. Inorg. Nucl. Chem.*, **38**, 1721-1727.
14. M. Kunzmann and Z. Kolarik (1992), Proc ISEC '90, Kyoto, Japan, pp. 207-211.
15. K. S. Pitzer (1991), Activity Coefficients in Electrolyte Solutions: Ion Interaction Approach: Theory and Data correlation, K.S. Pitzer (ed.), CRC Press, Boca Raton.
16. F. J. Millero (1972), Water and Aqueous Solutions: Structure, Thermodynamics, and Transport Processes: The Partial Molar Volumes of Electrolytes in Aqueous Solutions, R.A. Horne (ed.), Wiley-Interscience, New York.
17. A. F. M. Barton (1991), Handbook of Solubility Parameters and Other Cohesion Parameters, CRC Press, Boca Raton.
18. C. F. Baes, B. A. Moyer, G. N. Case and I. Faith (1990), *Sep. Sci. Technol.*, **25** (13-15), 1675-1688.



# ESTIMATION OF ACTIVITIES IN THE EXTRACTION OF IRON(III) WITH TRI-N-BUTYL PHOSPHATE AND OF COBALT(II) WITH ALIQUAT 336 FROM MAGNESIUM CHLORIDE MEDIA

Ali Azimi and Nevill M. Rice\*

National Iranian Copper Industries Co. (NICICO), Tehran, Iran

\*Department of Mining and Mineral Engineering, School of Process, Environmental and Materials Engineering, University of Leeds, Leeds, U.K.

Activities in both phases in the extraction of iron(III) from chloride media, containing  $\text{FeCl}_3$ ,  $\text{MgCl}_2$  and HCl by tri-*n*-butyl phosphate (TBP) were estimated. The activity of water in the  $\text{H}_2\text{O}-\text{FeCl}_3$  system was calculated from freezing point data in the literature for  $\text{FeCl}_3$  concentrations up to 1.3 molal and the corresponding  $\text{FeCl}_3$  activity estimated using the Gibbs-Duhem equation. The activity of TBP in the  $\text{FeCl}_3-\text{H}_2\text{O}-\text{TBP}$  system was estimated by application of a multi-component Gibbs-Duhem equation to the distribution and water content data for the extraction of iron by TBP at 25°C but the technique could not be applied to extraction from  $\text{FeCl}_3 - \text{MgCl}_2$  mixtures due to lack of activity coefficient data in mixed electrolytes. The composition of the extracted complex was confirmed as  $\text{FeCl}_3 \cdot 3\text{TBP}$  by slope analysis. An attempt to obtain thermodynamic data for modelling of the extraction of cobalt(II) chloro-complexes from  $\text{MgCl}_2$  media by Aliquat 336 in xylene using vapour pressure osmometry was unsuccessful because the system failed to come to equilibrium due to slow aggregation and the presence of impurities and other components.

## INTRODUCTION

The extraction of iron with several different reagents was studied as part of the development of methods for separation and recovery of metals leached from lateritic nickel ores by HCl [1-10]. Iron(III) can be extracted from chloride media, including HCl,  $\text{MgCl}_2$  and HCl -  $\text{MgCl}_2$  mixtures, by several solvating, cation or anion exchange type extractants [6,8,10,11]. Tri-*n*-butyl phosphate (TBP) has been used in a pilot plant for removing Fe(III) from  $\text{NiCl}_2$  leach liquors in the Falconbridge Matte Leach Process [12,13] when only three loading stages were required as a result of the high  $\text{NiCl}_2$  tenor. An attempt to replicate this at low  $\text{NiCl}_2$  concentration in 6 M HCl with ~5 g/L  $\text{Ni}^{2+}$  required many more stages [14]. Hayman [6] confirmed the improvement in Fe(III) extraction at high concentrations of  $\text{NiCl}_2$  or  $\text{MgCl}_2$  due to the increased aqueous ionic activity of  $\text{FeCl}_3$  at high ionic strength. The extraction of Fe(III) by neutral extractants is well-documented [15-19]. High  $\text{Cl}^-$  concentration is important for stabilising  $\text{FeCl}_3$  complexes though protonated  $\text{HFeCl}_4$  may also be extracted at high acidity. After removing iron from the liquor, Co may be recovered by extracting anionic Co(II) chloro-complexes with alkyl-amines including Aliquat 336 [8,20].

## MODEL FOR THE EXTRACTION OF IRON WITH TBP

For the extraction of the  $\text{FeCl}_3$  complex, the extraction equilibrium can be written as:



from which the thermodynamic extraction equilibrium constant,  $K_{(\text{ex})}$ , may be defined:

$$K_{(\text{ex})} = a_{\text{FeCl}_3 \cdot 3\text{TBP}} / a_{\text{FeCl}_3} a^3_{\text{TBP}} \quad (2)$$

$$\text{whence: } \log D_{\text{Fe}} = \log K' + \log \alpha_3 + 3 \log m_{\text{TBP}} + 3 \log a_{\text{Cl}^-} \quad (3)$$

$D_{\text{Fe}}$  is the distribution ratio of iron(III),  $\alpha_3$  the fraction of aqueous iron as the  $\text{FeCl}_3$  complex,  $m_{\text{TBP}}$  the molality of free TBP,  $a_{\text{Cl}^-}$  the chloride ion activity and  $K'$  a composite term given by

$$K' = K_{(\text{ex})} \beta_3 (\gamma_{\pm} \gamma_{\text{TBP}} / \gamma_0) \quad (4)$$

$\beta_3$  is the overall stability constant of  $\text{FeCl}_3$  complexes;  $\gamma_{\pm}$ , the mean aqueous ionic activity coefficient of  $\text{FeCl}_3$ ,  $\gamma_{\text{TBP}}$  and  $\gamma_0$  are the activity coefficients of the organic TBP and iron species.  $\gamma_{\pm}$  should be constant at constant ionic strength and  $\gamma_0$  is assumed to be constant for constant TBP concentration. To apply this model the parameters in equations (3) and (4) should be known. Data for stability constants are available in the literature [21,22] to enable calculation of  $\alpha_3$  but the organic phase activity coefficients need to be determined from data for the activity of water in the relevant electrolyte solutions. Activities of TBP during solvent extraction have been reported in connection with nuclear fuel processing [23-25] and for the extraction of  $\text{ZnCl}_2$  [26] using the Gibbs-Duhem equation [27] to determine  $\text{H}_2\text{O}$  activity in the organic phase. The formation of  $\text{TBP} \cdot \text{H}_2\text{O}$  in the organic phase is generally agreed [23-25]. Mean ionic activity coefficients for several aqueous metal chloride solutions have been reported [28-34] but only freezing point data were available for  $\text{FeCl}_3$  (for concentrations up to 1.3 molal [35]).

### Gibbs-Duhem Equation

For a two-component system at constant temperature and pressure where  $N$  represents the number of moles of each component, A and B, and  $a$  the corresponding activity the Gibbs-Duhem equation is:

$$N_A d \ln a_A + N_B d \ln a_B = 0 \quad (5)$$

Integration and rearrangement leads to:

$$-\ln a_A = \int_1^{AB} (N_B / N_A) d \ln a_B \quad (6)$$

Therefore if  $N_A$ ,  $N_B$  (or their respective mole fraction,  $X$ , or molality,  $m$ ) and  $a_B$  are known,  $a_A$  may be evaluated by graphical or numerical integration of a plot of  $N_B / N_A$  against  $\ln a_B$  between the appropriate limits. For evaluation of the activity coefficient of  $\text{FeCl}_3$  from freezing point data [9] the equation can be transformed to:

$$-\ln \gamma_{\pm} = j + \int_0^m j d \ln m_{\text{Fe}} - \frac{\Delta \theta}{\lambda} \int_0^{\Delta \theta} (1-j) d \Delta \theta \quad (7)$$

$$\text{for } j = 1 - (\Delta \theta / v m \lambda) \quad (8)$$

where  $\Delta \theta$  is the depression of the freezing point,  $\lambda$  the freezing point depression constant of  $\text{H}_2\text{O}$  (= 1.860 at  $0^\circ\text{C}$ ),  $\$$  for  $\text{H}_2\text{O} = 5.4 \times 10^{-4}$  and  $v$ , the number of ions = 4 for  $\text{FeCl}_3$ . The activity of water,  $a_w$ , may be calculated [31,32] from the osmotic coefficient,  $\Phi$ , in electrolytes of molality,  $m$ , using:

$$-\ln a_w = v m \lambda \Phi / 1000 \quad (9)$$

The activity of TBP was estimated by application of a multi-component Gibbs-Duhem equation

$$\int d \ln a_A = - \int (N_B / N_A a_B) da_B - \int (N_C / N_A a_C) da_C \quad (10)$$

to the distribution data and water content data for the extraction of iron from  $\text{FeCl}_3$  solutions with TBP at  $25^\circ\text{C}$  [8]. (Note that  $a_w$  is equal in each phase at equilibrium).

## EXPERIMENTAL METHOD

The distribution of Mg and Fe(III) between water and TBP (BDH, A.R grade) or TBP in Shellsol A (Shell Chemicals Ltd) was measured by contacting equal volumes of each phase in sealed containers for two hours at 298 K in a shaking thermostat bath. The phases were separated after standing in the bath for several hours. Organic phases were stripped with water and the metal content of both phases determined by atomic absorption spectrophotometry using a Varian Techtron AA-775 double beam instrument and standard addition method (to compensate for matrix effects). Co(II) extraction with Aliquat 336 (tri-n-octylmethylammonium chloride, Henkel) in xylene or Shellsol A was measured similarly. H<sub>2</sub>O in the organic phase was measured by Karl Fischer titration using a conductimetric end point and calibrated against weighed samples of water. The effect of Fe(III), which lowered the apparent concentration of water, was compensated by titration against the H<sub>2</sub>O content of methanol solutions of FeCl<sub>3</sub>.9.3H<sub>2</sub>O (BDH) (1 mg Fe(III) ≡ 0.9 mg H<sub>2</sub>O). Densities were measured using a density bottle calibrated with distilled water [35].

## RESULTS AND DISCUSSION

### TBP- MgCl<sub>2</sub>-H<sub>2</sub>O System

For concentrations up to 3 mol/L Mg the value of D<sub>Mg</sub> is <10<sup>-3</sup>[8] so that Mg extraction may be ignored. The aqueous activity of water in MgCl<sub>2</sub> was calculated from the osmotic coefficient [28,29] using (9), and the activities of H<sub>2</sub>O and TBP in the organic phase were estimated using (6). Figure 1 shows the Gibbs-Duhem plot and Figure 2 the organic activities of water, a<sub>w</sub> and TBP, a<sub>TBP</sub>, as a function of their respective mole fractions, X. Henry's law a = k<sub>H</sub>X, was obeyed by both TBP and water with a<sub>TBP</sub> = 0.7 X<sub>TBP</sub> and a<sub>w</sub> = 1.5 X<sub>w</sub>, using slopes from the "trend lines".

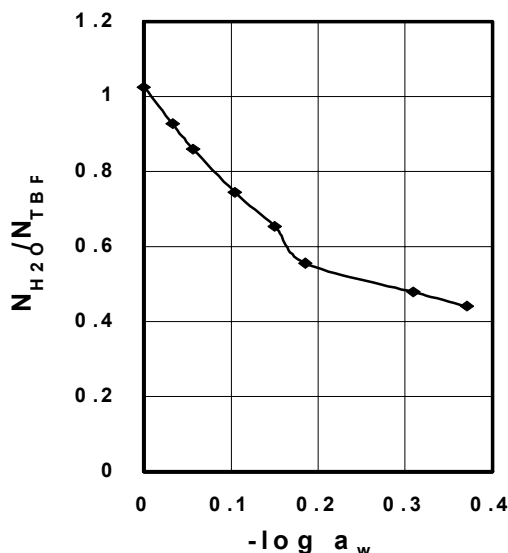


Figure 1. Gibbs-Duhem plot for the TBP-MgCl<sub>2</sub>-H<sub>2</sub>O system.

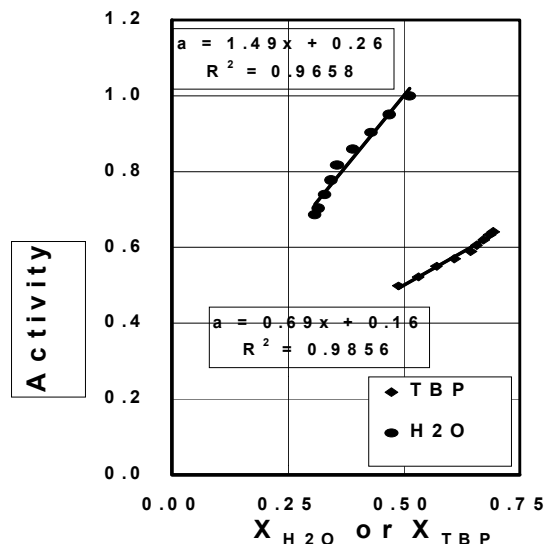


Figure 2. Organic phase activities of TBP and H<sub>2</sub>O in the TBP- MgCl<sub>2</sub>-H<sub>2</sub>O system.

### FeCl<sub>3</sub> - H<sub>2</sub>O System

Table 1 shows  $\gamma_{\pm}$  for FeCl<sub>3</sub>, and also values of a<sub>FeCl<sub>3</sub></sub>, calculated from freezing point data [35] by equation (7) with the integration limits set as described in [8]. (Note: a<sub>FeCl<sub>3</sub></sub> = 27m<sup>4</sup> $\gamma_{\pm}^4$ ).

*Table 1. Activity coefficients of aqueous  $\text{FeCl}_3$  from freezing point data [35].*

Molarity $M_{\text{FeCl}_3}$ (mol dm $^{-3}$ )	Molality $m_{\text{FeCl}_3}$ (mol kg $^{-1}$ )	Solution density (kg dm $^{-3}$ )	Freezing point depression (K)	Water activity	Activity coefficient of $\text{FeCl}_3 \gamma_{\pm}$	Activity of $\text{FeCl}_3$ by Eqn. (11)
0.0086	0.0086				0.548*	$1.4 \times 10^{-8}$
0.031	0.031	1.0043	0.206	0.998	0.558	$2.4 \times 10^{-6}$
0.062	0.062	1.0086	0.385	0.996	0.585	$4.7 \times 10^{-5}$
0.125	0.125	1.0171	0.753	0.992	0.648	$1.16 \times 10^{-3}$
0.189	0.190	1.0256	1.14	0.988	0.700	$8.45 \times 10^{-3}$
0.255	0.256	1.0341	1.56	0.985	0.754	0.0375
0.321	0.324	1.0426	2.00	0.980	0.790	0.116
0.388	0.392	1.0512	2.47	0.977	0.828	0.300
0.457	0.463	1.0590	3.00	0.970	0.857	0.670
0.526	0.534	1.0680	3.56	0.965	0.910	1.50
0.597	0.608	1.0779	4.18	0.960	0.943	2.92
0.669	0.683	1.0870	4.35	0.954	0.976	5.33
0.917	0.840	1.1060	6.38	0.940	1.031	15.18
0.970	1.000	1.1248	8.22	0.923	1.146	46.6
1.120	1.171	1.1440	10.45	0.903	1.231	116.5
1.290	1.350	1.1636	13.08	0.880	1.422	366.7

\* Debye-Hückel value

### $\text{FeCl}_3 - \text{H}_2\text{O} - \text{TBP}$ System

The activity of TBP was evaluated using equation (10) with A  $\equiv$  TBP, B  $\equiv$   $\text{FeCl}_3$  and C  $\equiv$   $\text{H}_2\text{O}$  by separate plotting and integration of  $N_B / N_A a_B$  vs.  $a_B$  and  $N_C / N_A a_C$  vs.  $a_C$ .  $a_{\text{FeCl}_3}$  was obtained by interpolation of the data from Table 1. The first integral was evaluated graphically and the second numerically by curve fitting. The integration limits were taken to be the activity values for water saturated TBP (0.498) and very dilute  $\text{FeCl}_3$  solution with  $a_{\text{FeCl}_3} = 3 \times 10^{-5}$  and  $a_w = 0.998$ . Mole fractions of total and free TBP,  $X_{\text{TBP}}$ , were estimated ( $m_{\text{TBP free}} = m_{\text{TBP tot}} - 3m_{\text{Fe org}}$ ). Results shown in Table 2 display no simple relationship between  $a_{\text{TBP}}$  and  $X_{\text{TBP}}$  and behaviour is far from ideal.

*Table 2. Calculated activity of TBP in the  $\text{FeCl}_3 - \text{H}_2\text{O} - \text{TBP}$  system (TBP = 3.754 mol kg $^{-1}$ ).*

Aq. $m_{\text{FeCl}_3}$ (mol kg $^{-1}$ )	Org $m_{\text{FeCl}_3}$ (mol kg $^{-1}$ )	Water activity	Activity of $\text{FeCl}_3$	Activity of TBP	$X_{\text{TBP}}$ Total	$X_{\text{TBP}}$ Free
0.0572	0.0027	0.996	$3.3 \times 10^{-5}$	0.495	0.493	0.492
0.0813	0.0037	0.994	$1.57 \times 10^{-4}$	0.493	0.495	0.493
0.165	0.0127	0.989	$4.25 \times 10^{-3}$	0.483	0.511	0.506
0.324	0.0237	0.981	0.116	0.457	0.528	0.518
0.549	0.137	0.966	1.732	0.424	0.528	0.470
1.13	0.732	0.906	109.5	0.118	0.507	0.210
1.21	0.819	0.898	160.3	0.109	0.514	0.177
1.4	0.985	0.878	458.0	0.0802	0.508	0.108

### $\text{FeCl}_3 - \text{MgCl}_2 - \text{H}_2\text{O} - \text{TBP}$ System

The Gibbs-Duhem method could not be extended to this system due to lack of activity coefficient data for mixed aqueous solutions of  $\text{FeCl}_3$  and  $\text{MgCl}_2$ . Although expressions exist to calculate mean ionic coefficients of 1:1/1:1 and 1: 1/1:2 mixtures [29] nothing exists for 1:2/1:3 mixtures so it is necessary to rely on empirical data and empirical or semi-empirical models for such systems.

### Extraction of Fe(III) from MgCl<sub>2</sub> solutions with TBP

Jansz [30] has reported the activities of Cl<sup>-</sup> ions in MgCl<sub>2</sub>/HCl mixtures. His data for a<sub>Cl<sup>-</sup></sub> were used to plot the variation of Fe extraction with a<sub>Cl<sup>-</sup></sub> with undiluted TBP from 0.0196 M (1.1 g/L) Fe(III) in 0.1 M HCl with varying MgCl<sub>2</sub> concentration (Figure 3). The effect of varying TBP concentrations (in Shellsol A) on the extraction of Fe from 1.1 g/L Fe(III) in 4.0 M MgCl<sub>2</sub>/0.1 M HCl is presented in Figure 4. The slopes of both graphs are close to 3, indicating that the model equation (3) is valid and that the extraction proceeds according to reaction (1).

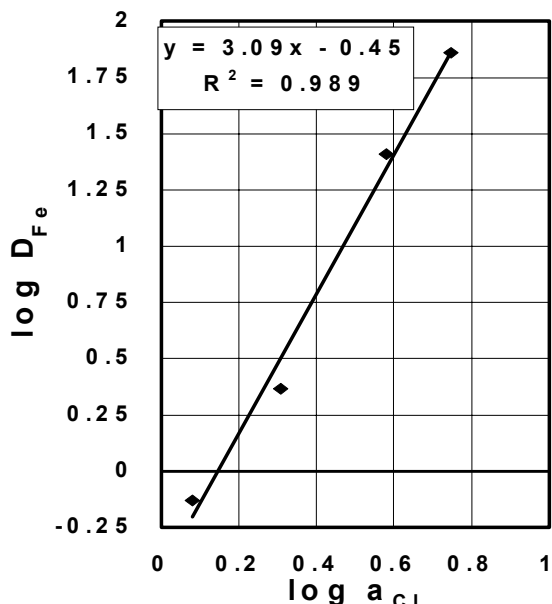


Figure 3. Extraction of Fe(III) from MgCl<sub>2</sub> media with 100 % TB.P

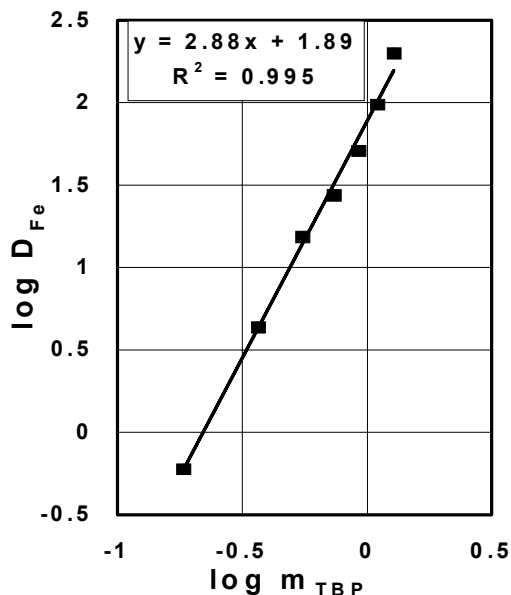


Figure 4. Extraction of Fe(III) from 4.0 M MgCl<sub>2</sub> at varying TBP concentrations in Shellsol A.

### Extraction Of Cobalt(II) With Aliquat 336

Ignoring possible aggregation of the extractant, the extraction of chloro-complexes of Co(II) with Aliquat 336 may be represented by the reaction:



from which:  $\log D_{Co} = \log K' + \log a_n + m \log [R_4NCl]_{(org)} + (2-n) \log a_{Cl^-}$  (13)

From (13) the slope of a plot of log D<sub>Co</sub> vs. log [R<sub>4</sub>NCl]<sub>(org)</sub> = m (14)

and [36] the slope of a plot of log D<sub>Co</sub> vs. log a<sub>Cl<sup>-</sup></sub> should = i<sub>org</sub> - i<sub>aq</sub> = m + 2 - n (15)

Figures 5 and 6 show variation of the extraction of Co(II) by Aliquat 336 from MgCl<sub>2</sub> solutions containing, initially, 1 g/L Co(II) and also 0.05 M HCl with log[R<sub>4</sub>NCl]<sub>(org)</sub> and log a<sub>Cl<sup>-</sup></sub> respectively in order to evaluate m and n from (14) and (15). Figure 5 shows that the value of m increases with increasing aqueous chloride concentration to a maximum of 2 in 6 M Cl<sup>-</sup>, i.e., the organic co-ordination number, i<sub>org</sub> = 4, as expected for tetrahedrally co-ordinated CoCl<sub>4</sub><sup>2-</sup>. However, although the slope in Figure 6 = 3.3 on average, it is closer to 2 at low a<sub>Cl<sup>-</sup></sub> and increasing whereas according to (15) it should fall as a<sub>Cl<sup>-</sup></sub> and hence n increases. This is clearly not true, probably due to aggregation of Aliquat so that the model (13) is inadequate.

### Vapour Pressure Osmometry of Aliquat 336 Solutions in Xylene

In order to allow for aggregation and replace [R<sub>4</sub>NCl]<sub>(org)</sub> by a<sub>R<sub>4</sub>NCl</sub> in the model equation (13) an attempt was made to obtain association data for Aliquat 336 in xylene using vapour pressure osmometry (VPO). Owing to experimental difficulties, i.e., the system failed to reach a constant temperature within a finite time, no useful data could be obtained. The failure of the system to achieve equilibrium can be explained in terms of slow formation of aggregates of Aliquat in the

xylene [37]. A study of tri-*n*-dodecylammonium chloride and nitrate in toluene by VPO has recently reported the formation of dimers of the chloride [38]. It is also probable that the purity of the extractant sample used was insufficient for VPO [37].

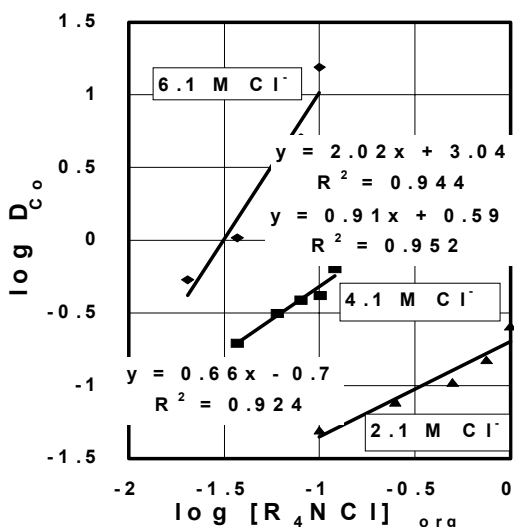


Figure 5. Variation of cobalt(II) extraction by Aliquat 336 concentration from  $MgCl_2$  solutions.

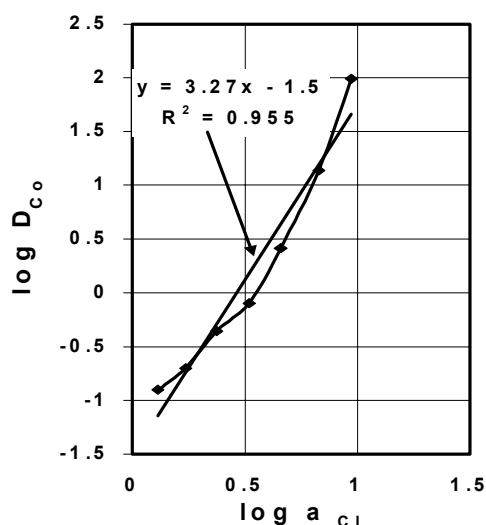


Figure 6. Variation of cobalt(II) extraction by Aliquat 336 (0.625 M) with chloride activity.

## CONCLUSIONS

An attempt to derive a thermodynamic model for the extraction of Fe(II) from  $MgCl_2$  solutions by TBP was partially successful but lack of activity data for mixed ionic media prevented application to the  $FeCl_3 - MgCl_2 - H_2O - TBP$  system and demonstrated the need for empirical data. No useful data could be obtained by VPO for modelling of the extraction of Co(II) with Aliquat 336.

## ACKNOWLEDGEMENTS

The authors wish to thank the U.K. SERC (now EPSRC) for provision of a scholarship for AA.

## REFERENCES

1. N.M. Rice and R.W. Gibson (1997), *Proc. 27th CIM Ann. Hydromet. Meeting*, Sudbury, Ont., I. Mihaylov (ed.), CIM, Montreal, pp. 247-262.
2. N.M. Rice (1990), *Leeds University Mining Association (LUMA) Journal*, Leeds University, pp. 59-89.
3. N.M. Rice and L.W. Strong (1975), *Proc. Symp. Hydrometallurgy '75*, Manchester, *I. Chem. Eng. Symp. Series*, No.42, pp. 6.1-6.13.
4. L.W. Strong (1978), Leaching of Lateritic Nickel Ores, PhD Thesis, University of Leeds.
5. C.E. Jimenez-Novoa (1980), The Effect of Metal Chloride Additions upon the Extraction of Nickel from Laterite Ores by Hydrochloric Acid, PhD Thesis, University of Leeds.
6. J.A. Hayman (1984), Recovery of Metals from Nickel Laterite Chloride Leach Liquors, PhD Thesis, University of Leeds.
7. N.M. Rice and D.C. Smith (1986), *Proc. Int. Solv. Extr. Conf. ISEC '86*, Munich, Germany, pp. 633-637.
8. A. Azimi (1987), Separation and Recovery of Cobalt and Iron from Laterite Chloride Leach Liquors by Solvent Extraction, PhD Thesis, University of Leeds.

9. R.W. Gibson (1995), The Hydrometallurgical Recovery of Nickel from Laterite Ores by a Chloride Route with Proprietary Extractants Cyanex 301 and 302, PhD Thesis, University of Leeds.
10. N.M. Rice and R.W. Gibson (1996), *Proc. Int. Solv. Extr. Conf. ISEC '99*, Melbourne, Australia, pp. 715-720.
11. N.M. Rice (1978), *Hydrometallurgy*, **3**, 111-133.
12. P.G. Thornhill, E. Wigstøl and G. van Weert (1971), *J. Metals*, **23** (7), 13-18.
13. E. Wigstøl and K.F. Frøyland (1972), *Proc. Int. Symp. Solvent Extraction in Metallurgical Processes*, Antwerp, Belgium, Benelux Metallurgie, pp. 62-72.
14. J. Lupton and G.L. Perry (1972), Recovery of Cu and Ni from an Egyptian Oxidised Ore, 3<sup>rd</sup> Year BSc Dissertations, University of Leeds.
15. I. Eger (1974), *Proc. Int. Solv. Extr. Conf. ISEC '74*, Lyon, France, pp. 1729-1736.
16. J.S. Preston and A.C. du Preez (1985), *Mintek Report*, No. M228, Randburg, 37pp.
17. J. Aggett and T.E. Clark (1970), *J. Inorg. Nucl. Chem.*, **32**, 2037-2043.
18. G. Weidmann (1960), *Canad. J. Chem.*, **38**, 459-464.
19. R. Sibut-Pinote, M. Prevost and M. Menier (1977), *Proc. Int. Symp. Chloride Hydromet.*, Benelux Metallurgie, Brussels, Belgium, pp. 368-384.
20. A.J. Monhemius (1972), The Solvent Extraction of Cobalt with Tertiary Amines, PhD Thesis, Imperial College, University of London.
21. L.G. Sillen and A.R. Martell (1964 and 1971), Stability Constants of Metal Ion Complexes, Spec. Publ. Nos 17 and 25, RCS, London.
22. R.M. Smith and A.R. Martell (1981) Critical Stability Constants, IUPAC Chem. Data Series No. 21, Pergamon, Oxford.
23. C.J. Hardy, D.C. Fairhurst, H.A.C. McKay, A.M. Wilson (1964), *Trans. Faraday Soc.*, **60**, 1626-1636.
24. H.A.C. McKay (1952), *Nature*, **169**, 464.
25. J.W. Roddy and J. Mrochek (1966), *J. Inorg. Nucl. Chem.*, **28**, 3019-3026.
26. N.M. Rice and M.R. Smith (1973), *Proc Conf. Physical Chemistry of Process Metallurgy*, The Richardson Conference, Institute of Mining and Metallurgy, London, pp. 55-64.
27. L.S. Darken (1950), *J. Amer. Chem. Soc.*, **72**, 2909-2914.
28. R.A. Robinson and R.H. Stokes (1959), Electrolyte Solutions, 2nd edn., Butterworths, London.
29. H.S. Harned and B.B. Owen (1958), The Physical Chemistry of Electrolyte Solutions, 3rd edn., ACS Monograph No.137, Reinhold, New York.
30. J.J.C.J Jansz (1983), *Hydrometallurgy*, **11**, 13-32.
31. R.G. Bates, B.R. Staples and R.A. Robinson (1970), *Anal. Chem.*, **42**, 867-871.
32. G. Senanayake (1986), Ionic Activities in Strong Salt Solutions and Mixed Solvents of Hydrometallurgical Importance, PhD Thesis, Murdoch University.
33. T. Sekine and Y. Hasegawa (1977), Solvent Extraction Chemistry – Fundamentals and Applications, Marcel Dekker, New York.
34. Y. Marcus and A.S. Kertes (1969), Ion Exchange and Solvent Extraction of Metal Complexes, Wiley–Interscience, New York.
35. R.C. Weast and M.J. Astle (eds.) (1982), CRC Handbook of Chemistry and Physics, 62nd edn., CRC Press, Boca Raton, FL, pp. D-208 and F-5.
36. N.M. Rice and M.R. Smith (1975), *J. Appl. Chem. Biotechnol.*, **25**, 379-402.
37. A.S. Kertes and H. Gutmann (1972), Surfactants in Organic Solvents: The Physical Chemistry of Aggregation and Micellization, Institute of Chemistry, Hebrew University, Jerusalem, Israel, 131 pp.
38. Y. Belaustegi, N. Etxebarria, M.A. Olazabal *et al.* (1996), *J. Solution Chem.*, **25**, 1113-1124.



## AQUEOUS TWO-PHASE EQUILIBRIUM DATA FOR POLYETHYLENE GLYCOL, POTASSIUM PHOSPHATE AND BROMELAIN

Albina S. Moreira, Douglas N. Silva, Osvaldo Chiavone-Filho

UFRN, Dept. de Engenharia Química, Natal, Brasil

Liquid-liquid equilibrium data for the aqueous two-phase system with polyethylene glycol (PEG), potassium phosphate and the enzyme bromelain are presented. The project of an analytical cell is described, together with the developed experimental procedure. The concentration of the salt was directly determined for the potassium by atomic absorption spectrophotometry. PEG was quantified with the help of a calibration curve and measures of refractive index. For the determination of the bromelain concentrations in the partition experiments, direct measurements of absorption in the UV range was applied. The method of Lowry was used as reference for the determination of protein content. The dependence of the pH on the partition coefficients was evaluated at a determined tie-line length. The viability of this system for the bromelain extraction was demonstrated.

### INTRODUCTION

The extraction of natural products is gaining importance due to the increasing demands of the pharmaceutical and food industries. Bromelain is an enzyme extracted from the pineapple and presents a series of applications, *i.e.*, meat tenderizer, enrichment of flours, dehydrated eggs, soy milk, brewery, digestion of worms, treatment of wounds and burns, improvement of the efficiency of X-raying the uterus, minimization of menstrual pains, anti-inflammatory agent, and as an inhibitor of cancerous cells [1].

Liquid-liquid extraction using aqueous systems with polymers and salts has shown to be a feasible technique for the partition and concentration of enzymes [2]. The knowledge of liquid-liquid equilibrium data is fundamental for the design and operation of such unities of extraction.

In this work, liquid-liquid equilibrium data for the system  $\text{H}_2\text{O} + \text{PEG-3350} + \text{KH}_2\text{PO}_4/\text{K}_2\text{HPO}_4$  at 298.15 and 313.15 K are presented. Furthermore, experimental results of the partition coefficient of the bromelain in the aqueous mixtures with PEG3350 and potassium phosphate are also given in a range of pH.

## EXPERIMENTAL SET-UP AND PROCEDURE

The designed analytical cell is described in Figure 1.

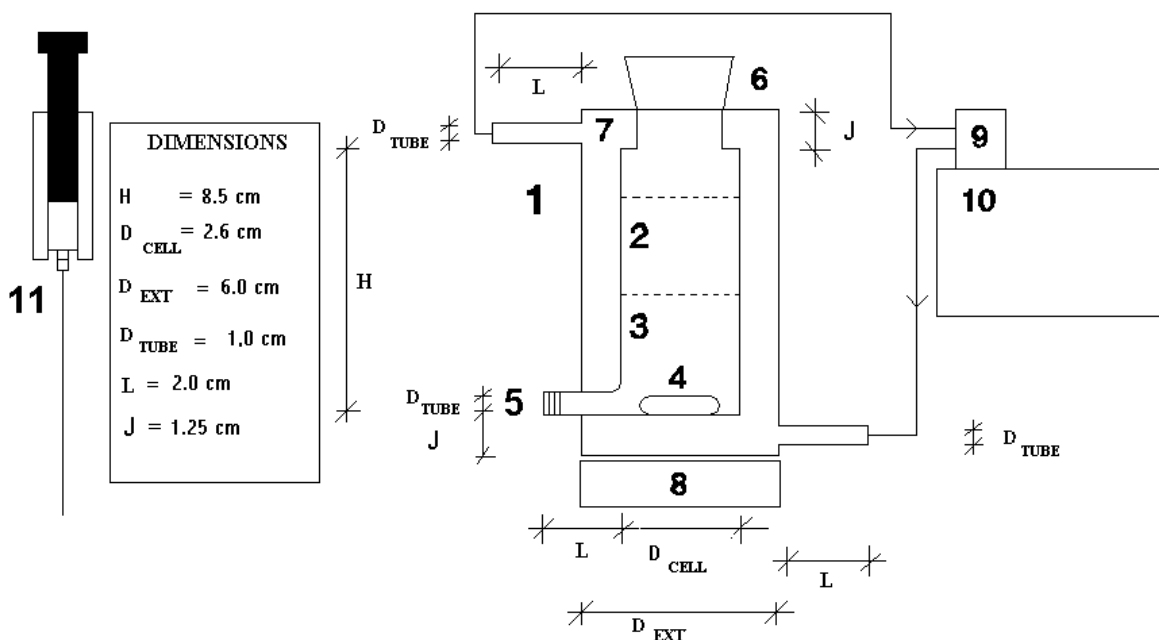


*Figure 1. Liquid-liquid equilibrium device: (1) analytical cell with jacket; (2) upper liquid phase; (3) lower liquid phase; (4) magnetic bar; (5) connector and septum for cleaning and sampling of the lower liquid phase; (6) conical join for cleaning, sampling of the upper liquid phase and measurement of the temperature; (7) jacket; (8) magnetic stirrer; (9) temperature controller and pump for circulating thermostatized water; (10) thermostatic bath; (11) syringe.*

Based on the literature data [2], due to the similarity of the system, and also by trial-and-error, the initial global concentrations to form two liquid phases could be found, in order to start the determination of the phase diagram.

For each tie-line, a mixture of known and appropriate composition inside the two-phase region is poured into the cell. The system is then subjected to mixing for about four hours at constant temperature. The mixture is then left resting for at least twelve hours, usually overnight, for complete separation of the phases in equilibrium. Finally, samples of the top and bottom phases are withdrawn for analysis, in a careful way to avoid disturbance of the system.

### METHODS OF ANALYSIS

The concentration of salt was directly determined for the potassium by atomic absorption spectrophotometry. PEG was quantified with the help of a calibration curve and measures of refractive index of various synthetic solutions of concentrations determined gravimetrically (see Figure 2). The water content was obtained by difference. It may be observed that the solutions with higher salt content (10 and 12 wt%) presented stable behavior (one liquid phase) up to a limited concentration of PEG.

The method of Lowry [3] was firstly applied, as reference, to determine the protein content present in the bromelain, which was provided by SIGMA. Then a calibration curve was prepared with known enzyme concentrations using direct measurements of absorbance at the recommended wavelength of 280 nm (see calibration curve in Figure 3).

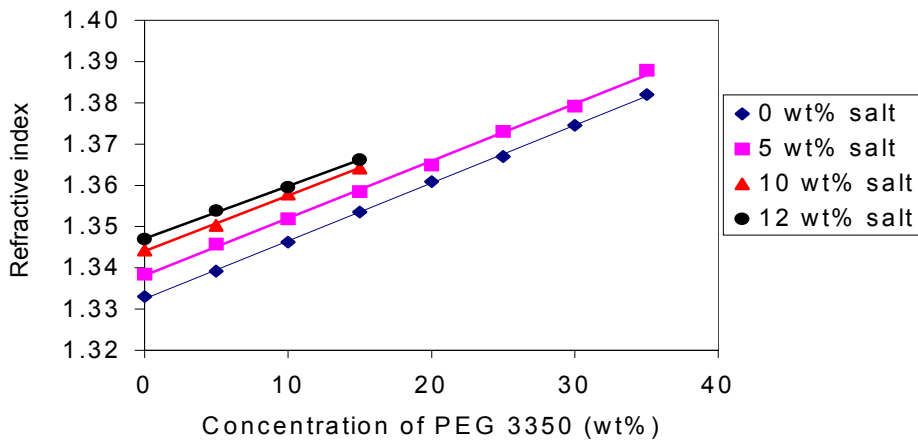


*Figure 2. Calibration curves for the determination of PEG concentration at 298.15 K as a function of the potassium phosphate concentration and refractive index.*

This direct method presented satisfactory reproducibility with the advantage that it is not destructive, requiring no reagent and few dilutions for both phases in the partition experiments. It is noteworthy that partition experiments without enzyme were also carried out in parallel in order to determine the absorption of the other species presented, *i.e.*, PEG and potassium phosphate, and proceed the proper discount [4]. The variation of the pH of the solutions was provided by the combination of the salts mono and di-potassium phosphate mass ratios ( $\text{KH}_2\text{PO}_4/\text{K}_2\text{HPO}_4$ ).

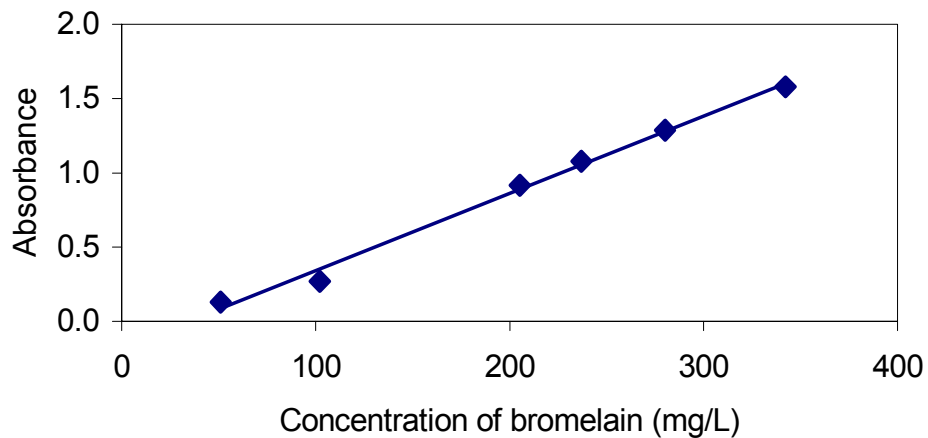


*Figure 3. Calibration curve of absorbance of bromelain in water by the direct method at 280 nm [ $\text{Abs} = 0.0052 (\text{C in mg/L}) - 0.1807$ ].*

## RESULTS AND DISCUSSION

In order to verify the efficiency of the projected equilibrium cell and also the experimental procedure, liquid-liquid equilibrium data for the aqueous system with PEG3350 and potassium phosphate (KPH) were determined at 298.15 and 313.15 K (see Tables 1 and 2).

Based on the data obtained (Figures 4 and 5), the partition experiments for the bromelain were defined in terms of initial concentration, since it is recommended to work with significant tie-line lengths, that produce adequate differences of volume, density and viscosity between the two liquid phases. It is noteworthy that there are two differences between the diagrams presented in Figures 4 and 5, i.e., temperature and pH, resulting a somewhat distinct behavior.

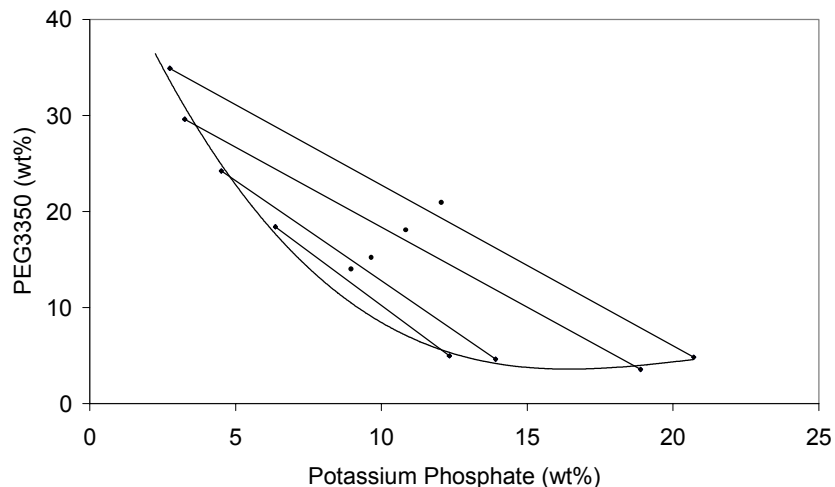


Figure 4. Phase diagram for the aqueous system PEG3350/potassium phosphate at 298.15 K and pH = 7.0.

Table 1. Liquid-liquid equilibrium data for the aqueous\* system PEG3350/potassium phosphate at 298.15 K and pH = 7.0.

Feed		Bottom phase		Top phase	
KHP (wt%)	PEG3350 (wt%)	KHP (wt%)	PEG3350 (wt%)	KHP (wt%)	PEG3350 (wt%)
8.96	14.00	12.33	4.97	6.36	18.40
9.66	15.23	13.92	4.63	4.51	24.21
10.83	18.07	18.89	3.56	3.25	29.61
12.05	20.93	20.71	4.84	2.75	34.92

\*Water content is obtained by difference.

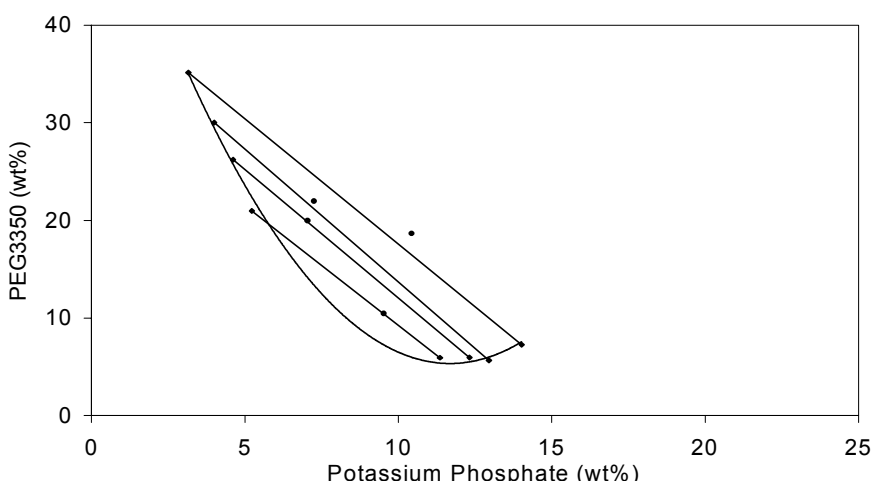


Figure 5. Phase diagram for the aqueous system PEG3350/potassium phosphate at 313.15 K and pH = 4.5.

*Table 2. Liquid-liquid equilibrium data for the aqueous\* system PEG3350/potassium phosphate at 313.15 K and pH = 4.5.*

Feed		Bottom phase		Top phase	
KHP (wt%)	PEG 3350 (wt%)	KHP (wt%)	PEG 3350 (wt%)	KHP (wt%)	PEG 3350 (wt%)
9.53	10.45	11.36	5.93	5.22	20.96
7.05	19.94	12.32	5.94	3.99	30.00
7.25	21.96	12.95	5.65	4.00	30.01
10.43	18.64	14.02	7.25	3.16	35.13

\*Water content is obtained by difference.

Figure 6 shows the partition coefficient of the bromelain as a function of the pH for the aqueous two-phase system with PEG3350 + KH<sub>2</sub>PO<sub>4</sub>/K<sub>2</sub>HPO<sub>4</sub>. It can be observed that the values of the partition coefficient (K) are larger than 1, meaning that the salting-out effect is occurring. Experiments with the same system including dextran and using the salt just as buffer for a range of pH values, revealed the opposite behavior (K < 1) in terms of partition coefficient, i.e., the bromelain was concentrated to the dextran-rich phase, which may be explained by the affinity effect, since dextran and bromelain are macromolecules. However, the results obtained with the PEG/salt system indicate the viability of bromelain separation and it is also more economic than the using dextran.

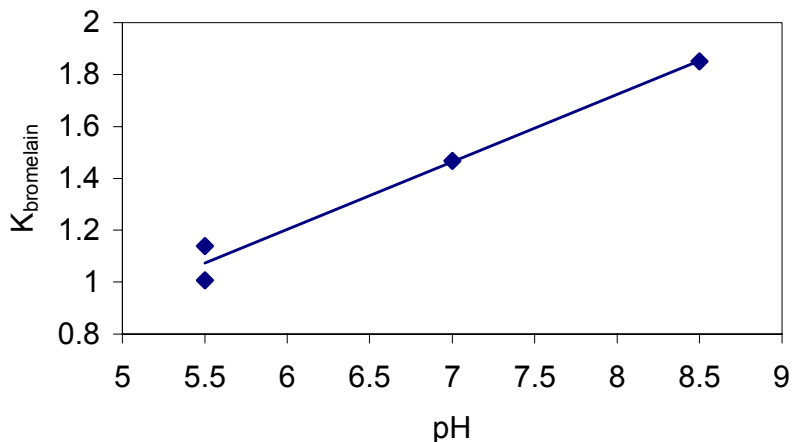


*Figure 6. Partition coefficient of the bromelain in aqueous PEG3350 + KH<sub>2</sub>PO<sub>4</sub>/K<sub>2</sub>HPO<sub>4</sub> as a function of the pH at 298.15 K and with tie-line length of 30.4 wt%.*

## CONCLUSIONS

The analytical methodology employed for determination of liquid-liquid equilibrium data was demonstrated to be adequate and simple. The results presented satisfactory reproducibility.

One drawback was the determination of the first feed composition adequate for the liquid-liquid experiments. These difficulties were due to the fact that the system is multicomponent and the solubility dependences in terms of temperature and pH were not completely known.

The partition coefficient values obtained for the bromelain in the aqueous system with PEG3350 + potassium phosphate indicated the viability of the concentration and storage of this enzyme with the studied system of separation.

## **ACKNOWLEDGEMENTS**

We would like to acknowledge the financial support granted by the Brazilian agency CNPq (Conselho Nacional de Desenvolvimento Científico e Tecnológico).

## **REFERENCES**

1. L. O. Freiman and A. U. O. Sabaa-Srur (1996), *Ciência e Tecnologia de Alimentos*, **16** (3), 246-249.
2. P. A. Albertsson (1971), Partition of Cell Particles and Macromolecules, 2nd edn., John Wiley and Sons, New York.
3. R. L. Scopes (1993), Protein Purification: Principles and Practice, 3rd edn., Springer, New York.
4. Q. Peng, Z. Li and Y. Li (1995), *Fluid Phase Equilib.*, **107**, 303-315.



## SELECTIVITY OF METAL EXTRACTION AT THE MICELLAR MECHANISM

Oxana A. Sinegribova and Ol'ga V. Muraviova

D. Mendeleyev University of Chemical Technology of Russia, Moscow, Russia

The present work is devoted to the study of the influence of colloidal particle formation on the selectivity for rare and non-ferrous metal extraction using organophosphorus extractants. The extraction systems containing salts of different metals, neutral and acid organophosphorus extractants (TBP, HDEHP) and various surfactants were the objects of the investigation. It was shown that the selectivity of extraction could be changed due to the surfactant addition. The selectivity of metal extraction depends on the aqueous phase composition, pH, nature and content of added surfactant. The study of the kinetics of extraction indicated that in the presence of surfactant the mass transfer of individual metals took place with the different rates, hence the dynamic separation of metals could be possible.

### INTRODUCTION

Due to the amphiphilic nature of common commercially available metal extractants, they have a tendency to aggregate into micelles, microemulsions and lyotropic liquid crystals under certain conditions. This phenomenon may affect the extraction performance: namely the kinetic and thermodynamic features of metal extraction may be changed due to the formation of colloidal particles depending on their composition and type [1,2].

It was shown earlier that the selective separation of two similar metal ions is performed less efficiently in the micellar system [3]. The addition of TBP and isodecanol to the systems containing acid extractants leads to a dramatic decrease of Co/Ni separation factor [4]. Stoyanov found that the cause of this phenomenon is the formation of micelles. He showed that the presence of modifiers (alcohol, TBP, etc.) increased water content in the organic phase and therefore favoured the formation of mixed micelles [5].

But the extractability and selectivity can be controlled by proper manipulation of the micellar structure [6]. Sometimes the formation of colloidal structures can promote the selectivity of extraction. The structural-mechanical barrier consisting of the aggregated droplets of aqueous phase is a possible reason for the increase of the Pt/Pd separation coefficients in the emulsion extraction systems with tetraoctylammonium di-(2-ethyl)phosphate [7].

Only a few studies have been applied to the problem of selectivity of extraction by the micellar mechanism. The present work is devoted to the study of the influence of colloidal particle formation on the selectivity for rare and non-ferrous metal extraction using organophosphorus extractants. The extraction systems containing salts of different metals, acid or neutral organophosphorus extractants and surfactants were the objects of the investigation. Surfactants with low surfactive properties, which can really increase the metal distribution coefficients [8], were used.

## EXPERIMENTAL

In the present work the following substances have been used: HDEHP(di(2-ethylhexyl) phosphoric acid), TBP (tributylphosphate), TOPO (trioctylphosphinoxide), toluene, aliphatic alcohols (from butanol to decanol); nitrates, sulphates and chlorides of yttrium, lanthanum, zirconium, hafnium with the content of main material not less than 98 %. The concentration of metals was determined by complexometric titration with EDTA.

For the study of the effect of colloidal formation on the dynamic selectivity, the kinetic curves of metal extraction were obtained. The mass transfer was carried out across the flat interface in a horizontal rotating cell (HRC). HRC is a device with a flat interface submitted to weak mechanical action directed into the interfacial field. When the cylindrical cell is placed in horizontal position the interface becomes parallel to the axis of symmetry of the cylinder. At the cylinder wall aqueous, organic phases and wall are brought in contact. During the cell rotating the perimeter of the phase contact slips over the cylinder surface. As a result of the slipping, interfacial perturbations arise providing effective interfacial renewal [9].

## RESULTS AND DISCUSSION

The effect of nature and concentration of added surfactant on the extractability of lanthanide extraction by the solutions of HDEHP in toluene was studied. The values of the ratio of the distribution coefficients for La and Y at the addition of different SAS are presented in Table 1. The concentration of added surfactant corresponds to the maximum of the metal distribution coefficients [10].

The data of Table 1 show that the increase of ratio  $D_Y/D_{La}$  depends on the composition of aqueous phase considerably. The ratio  $D_Y/D_{La}$  increases with decrease of the hydrocarbon length. The higher increase of ratio is observed in the presence of  $\text{CH}_3\text{COOH}$ . TBP and TOPO improve the ratio of the distribution coefficients for La and Y to the same extent.

The dependence of the ratio of the distribution coefficients for La and Y on the concentration of added surfactant is presented in the Table 2.

The ratio of the distribution coefficients  $D_Y/D_{La}$  increases with the increase of the SAS content in the extraction system as compared with the systems without surfactant. The dependence of values of the ratio  $D_Y/D_{La}$  on the concentration of added SAS has a maximum. The ratio depends on the composition of aqueous phase and higher for the extraction from hydrochloric medium.

It was found that the location of yttrium in the lanthanide extractability row by HDEHP (La, Ce, Pr, Nd, Eu, Dy, Er, Yb were used) depends on the process conditions, namely on the composition of the aqueous phase, on the molar ratio between the concentrations of the extractant, metal and the added surfactant. At the certain conditions, for example, at the extraction from hydrochloric medium ( $U = [\text{octanol}]/[\text{HDEHP}] = 0.1$ ), yttrium is outstanding from these lanthanide extractability row:  $\text{La} < \text{Ce} < \text{Pr} < \text{Nd} < \text{Eu} < \text{Dy} < \text{Er} < \text{Yb} < \text{Y}$ .

*Table 1. Comparison of extractability of La and Y in the presence of surfactant.*

Surfactant	[surfactant], mol/L	D <sub>Y/D<sub>La</sub></sub>		
		Extraction from hydrochloric medium	Extraction from nitric medium	Extraction from sulphuric medium
-	0	2.0	2.6	2.4
butanol	0.04	6.4	4.5	6.0
isopentanol	0.04	5.7	4.0	4.7
hexanol	0.04	4.3	3.4	3.6
octanol	0.02	3.4	3.4	3.1
decanol	0.02	3.2	3.2	2.3
CH <sub>3</sub> COOH	0.08	6.6	5.7	6.0
TBP	0.02	2.5	3.3	2.9
TOPO	0.02	2.6	3.4	2.9

Aqueous phase: [Me<sup>3+</sup>] = 0.1 mol/L, pH 2.0. Organic phase: [HDEHP] = 0.2 mol/L in toluene.

*Table 2. Effect of surfactant content on extractability of La and Y.*

[surfactant], mol/L	D <sub>Y/D<sub>La</sub></sub>					
	butanol		octanol		TOPO	
	Extraction from hydrochlor. medium	Extraction from nitric medium	Extraction from hydrochlor. medium	Extraction from nitric medium	Extraction from hydrochlor. medium	Extraction from nitric medium
0.0	2.0	2.6	2.0	2.6	2.0	2.6
0.01	3.6	3.0	2.9	2.9	1.9	2.7
0.02	5.5	4.3	3.4	3.4	2.6	3.3
0.04	6.4	4.5	2.9	3.4	2.1	2.5
0.08	5.9	4.0	2.6	3.6	1.3	1.4

Aqueous phase: [Me<sup>3+</sup>] = 0.1 mol/L, pH 2.0. Organic phase: [HDEHP] = 0.2 mol/L in toluene.

The possibility of the dynamic separation of lanthanides was verified in HRC using octanol as the added surfactant. The extraction of lanthanides (Y, La, Pr, Dy, Er) proceeds with identical rates in the absence of SAS, the kinetic curves coincide practically, and kinetic separation is not possible (Figure 1). But for the addition of octanol to the extraction system, when the micellar mechanism of extraction occurs, the process proceeds with different rate, and the micellar mechanism of extraction occurs, the process proceeds with different rate, and dynamic separation can take place. It should be noted that the presence of octanol causes an increase in the mass transfer rate. For the extracted metals the separation of REE on the yttrium, light and heavy groups can take place.

The influence of surfactant present in the extraction system on the extraction of Zr and Hf by the solutions of HDEHP in toluene from different medium was studied. It was established that the composition of aqueous phase affects the ratio D<sub>Zr</sub>/D<sub>Hf</sub>. For the extraction from nitric and hydrochloric medium, the addition of octanol practically does not affect the separation factor, and the difference between the distribution coefficients for Zr and Hf is low or is absent. For the extraction from sulphuric medium, the ratio D<sub>Zr</sub>/D<sub>Hf</sub> is more considerable. Data of the extractability of zirconium and hafnium in the presence of butanol and octanol

show dependence on the concentration of added alcohol for the extraction from sulphuric medium (Table 4).

The rise of the selectivity of zirconium and hafnium extraction by HDEHP can be obtained at a certain concentration of added alcohol. But at these conditions, a decrease of the distribution coefficients is observed [10].

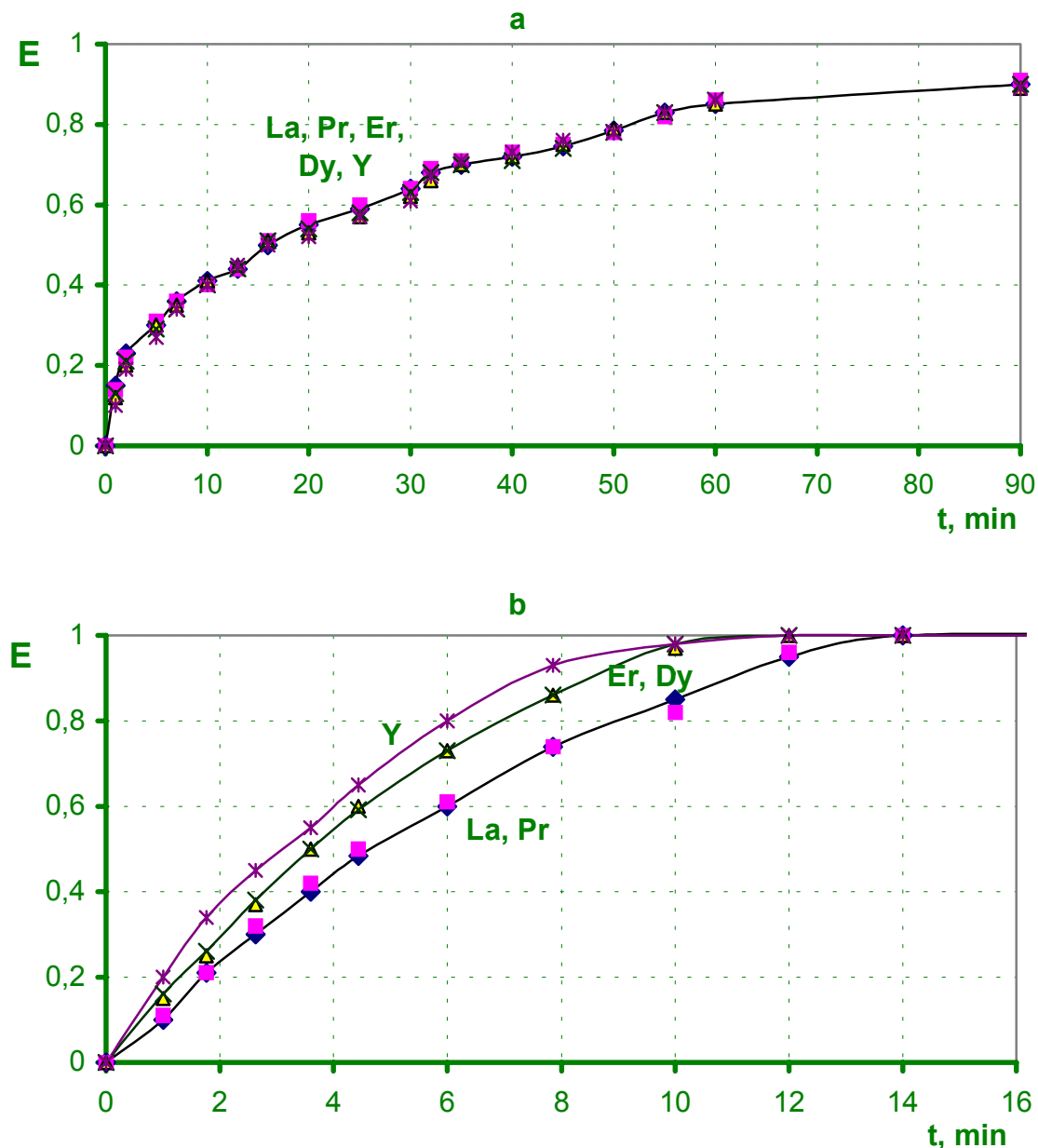


Figure 1. Effect of octanol on kinetics of lanthanides extraction by HDEHP from hydrochloric medium in octanol presence. a - without octanol; b - in the presence of octanol,  $[LnCl_3]=0.1$  mol/L, pH 2;  $[HDEHP]=0.2$  mol/L in toluene.

It should be noted that for the HDEHP extraction of Zr and Hf from different medium, in contrast to lanthanide extraction, the selectivity decrease was not observed, so the surfactant presence can lead to an increase the distribution coefficients of Zr and Hf without the selectivity decreasing.

The relation between the distribution coefficients of zirconium and hafnium in the presence of different SAS (at concentration of added surfactant corresponding to maximum of the metal distribution coefficients) for different media is presented in Table 5.

*Table 4. Effect of alcohol content on the extractability at extraction of Zr and Hf by HDEHP from sulphuric medium*

[surfactant], mol/L	butanol			octanol		
	D <sub>Zr</sub>	D <sub>Hf</sub>	D <sub>Zr</sub> /D <sub>Hf</sub>	D <sub>Zr</sub>	D <sub>Hf</sub>	D <sub>Zr</sub> /D <sub>Hf</sub>
0	0.62	0.48	1.29	0.62	0.48	1.29
0.01	1.02	0.63	1.62	1.66	1.29	1.29
0.02	1.31	0.69	1.90	1.31	0.99	1.32
0.04	1.60	0.82	1.95	1.30	0.96	1.35
0.08	1.95	1.78	1.10	1.04	0.72	1.44
0.16	1.65	1.17	1.41	0.62	0.37	1.68
0.24	1.03	0.84	1.23	0.49	0.32	1.53

Aqueous phase: [Me] = 0.075 mol/L; pH 0.3. Organic phase: [HDEHP] = 0.4 mol/L in toluene.

*Table 5. Effect of surfactant addition on the extractability of Zr and Hf by HDEHP from different media.*

surfactant	[surfactant], mol/L	D <sub>Zr</sub> /D <sub>Hf</sub>		
		Extraction from hydrochloric medium	Extraction from nitric medium	Extraction from sulphuric medium
-	0	1.04	1.06	1.29
CH <sub>3</sub> COOH	0.08	1.20	1.11	1.52
butanol	0.08	1.13	1.20	1.40
isopentanol	0.08	1.20	1.14	1.87
hexanol	0.08	1.16	1.12	1.68
octanol	0.10	1.13	1.10	1.68
decanol	0.10	1.14	1.11	1.61

Aqueous phase: [Me] = 0.075 mol/L; pH 0.3. Organic phase: [HDEHP] = 0.4 mol/L in toluene.

The ratio D<sub>Zr</sub>/D<sub>Hf</sub> depends on the composition of the aqueous phase and is higher for extraction from sulphuric medium. This phenomenon is probably explained by the processes of complexing, which are more intensive in sulphuric system as compared with the hydrochloric and nitric systems. The dependence of the ratio between the distribution coefficients of zirconium and hafnium from the hydrocarbon length of aliphatic alcohol has a maximum at the extraction from sulphuric medium.

The influence of SAS addition on the extraction of Zr and Hf by solutions of TBP in toluene from different media has also been investigated. Two systems were considered: the system in which zirconium is preferably extracted (extraction from nitric solutions) and the system in which hafnium is preferably extracted (extraction in the presence of NCS<sup>-</sup> anion). The enhancement of extractability in the presence of alcohol is greater for Hf. In the extraction system when zirconium and hafnium are extracted from nitric medium by TBP, the increase of metal distribution coefficients is more obvious for Hf, the selectivity of metal extraction in the presence of alcohol decreases as compared with the systems without surfactant. But the

selectivity of the process can be considerably increased by surfactant addition to the system with the  $\text{NCS}^-$  anion, where Hf is preferably extracted (Table 3).

Analysis of the data of Table 3 shows that the increase of ratio  $D_{\text{Hf}} / D_{\text{Zr}}$  depends on the hydrocarbon length of the added alcohol and on the composition of aqueous phase.

*Table 3. Effect of surfactant additions on the extractability of Zr and Hf by TBP in the presence of  $\text{CNS}^-$  - anions.*

surfactant	Extraction from hydrochloric medium				Extraction from sulphuric medium			
	[surfactant], mol/L	$D_{\text{Hf}}$	$D_{\text{Zr}}$	$D_{\text{Hf}} / D_{\text{Zr}}$	[surfactant], mol/L	$D_{\text{Hfr}}$	$D_{\text{Zr}}$	$D_{\text{Hf}} / D_{\text{Zr}}$
-	-	4.00	2.83	1.41	-	1.00	0.053	18.87
butanol	0.073	9.06	5.63	1.61	0.0365	1.45	0.13	11.15
isopentanol	0.0365	7.31	4.51	1.62	0.0365	2.72	0.12	22.64
hexanol	0.0365	7.89	3.72	2.12	0.0365	2.93	0.10	29.25
octanol	0.073	8.98	3.21	2.81	0.0365	3.00	0.08	37.50
decanol	0.0365	5.61	2.43	2.31	0.0365	1.84	0.05	36.80

Aqueous phase:  $[\text{Me}] = 0.075 \text{ mol/L}$ ;  $[\text{HCl}] / [\text{MeO}_2] ([\text{H}_2\text{SO}_4] / [\text{MeO}_2]) = 2.0$ ;  $[\text{NH}_4\text{CNS}] = 100 \text{ g/L}$ .

Organic phase: [TBP] = 1.46 mol/L in toluene.

## CONCLUSIONS

The increase in the selectivity of metal extraction in the presence of SAS can be obtained under the definite conditions. The selectivity of metal extraction depends on the aqueous phase composition, pH, nature and content of added surfactant, and on the nature of extracted metals. The study of the kinetics of metal extraction indicated that the mass transfer of individual metals took place at different rates when the micellar mechanism of extraction occurred. So, at these conditions the dynamic separation of metals could be possible.

## REFERENCES

1. A.M. Chekmarev, O.A. Sinegribova, V. Kim (1997), *J. Colloid. Chem. (Russ.)*, **7**, 399-405.
2. W. Nitsch, P. Plucinski (1994), *J. Phys. Chem.*, **6**, 8983-8999.
3. Y. Miyake, Y. Nakata et al. (1990), *Proc. ISEC '90*, Kyoto, Japan, pp. 823-829.
4. F. Xun, J.A. Golding (1987), *Solv. Extr. Ion Exch.*, **2**, 205-211.
5. E.S. Stoyanov (1993), *Proc. ISEC '93*, York, UK, pp. 793-729.
6. R.D. Neuman, Z.-J. Yu, T. Ibrahim (1996), *Proc. ISEC '96*, Melbourne, Australia, pp.135-141.
7. E.V. Yurtov, O.V. Gafanova, T.P. Sidorova et al. (1998), *Proc. XI Russ. Conf. Extr.*, Moscow, Russia, p.198.
8. O.A. Sinegribova, O.V. Muraviova (2001), *Proc. 3rd European Cong. Chem. Eng.*, Nuremberg, Germany, paper № P 15-11.
9. V. V. Tarasov, O. A. Sinegribova, O. V. Sviridenkova. (1999), *Proc. ISEC '99*, Barcelona, Spain, pp. 825-828.
10. N.V. Bukar, V.Kim, O.A. Sinegribova (1999), *J. Inorg. Chem. (Russ.)*, **7**, 1124-1129.



# MICELLAR MECHANISM PECULIARITIES OF METAL EXTRACTION BY ORGANOPHOSPHORUS EXTRACTANTS IN THE PRESENCE OF SURFACTANT

Oxana A. Sinegribova and Ol'ga V. Muraviova

D. Mendeleyev University of Chemical Technology of Russia, Moscow, Russia

The main focus of the present work is the study of surfactant's influence on the metal loading of the extractant for extraction of different metals by organophosphorus extractants. It was found that the addition of co-surfactant to the extraction system could change the metal loading of the extractant. The isotherms of extraction of calcium, yttrium and zirconium from different medium were obtained using n-butanol or n-octanol as the example of the added surfactant. It was shown that in the presence of surfactant in the extraction system, the metal loading of HDEHP and TBP increased significantly as compared with the extraction process without surfactant. The metal loading of extractant depends on the surfactant amount and on the conditions of the extraction.

## INTRODUCTION

The conception of micellar mechanism, which is due to addition of co-surfactant into the extraction system, is one of intensively developing conceptions of the solvent extraction theory. But in general the investigations in this field were carried out with the aim of increasing the distribution coefficients and mass transfer coefficients of metals.

Most extractants are surfactants, which are able to form different types of colloid structures at certain conditions. Such structures can consist of thermodynamically stable aggregates, like micelles, microemulsions, lyotropic liquid crystals, and thermodynamically unstable particles [1]. The structurisation in extraction systems can take place in the bulk and at the interface. The structures formed in extraction systems can influence the parameters of the extraction process: distribution coefficient, separation coefficient, extraction rate, and phase separation rate. The colloidal structures of different types may take a part in the formation of the viscous interfacial films [2].

The parameters of the extraction process can be improved due to micellar mechanisms of metal extraction. But the main attention has been paid to the enhancement of metal distribution coefficients. Due to the addition of surfactant in the extraction system the distribution coefficients of iron [3,4], aluminium [4], cobalt and nickel [5,6] etc. can increase considerably. It was shown that the colloidal formation by Ca, La, and Zr in the presence of aliphatic alcohol changes the distribution coefficients of these metals [7]. The dependence of distribution coefficient on  $\mathbf{U}$ , the molar ratio between the concentrations of n-octanol and HDEHP (di (2-ethylhexyl) phosphoric acid) ( $\mathbf{U}=[\text{n-octanol}]/[\text{HDEHP}]$ ), has a maximum. The value  $\mathbf{U}_{\text{opt}}$  corresponding to the maximum value of the distribution coefficient depends on the nature of extracted metal, nature and concentration of added alcohol and pH.

The change of extraction parameters due to micellar mechanisms has not been studied systematically. In the present work a lot of attention has been paid to the study of surfactant's influence on the metal loading of the extractant for the extraction of different metals by organophosphorus extractants such as HDEHP and tributylphosphate (TBP). The extraction was carried out from sulphuric, nitric and hydrochloric medium. The micellar mechanism of extraction was realised due to the addition of the co-surfactant with low surfactive activity into the extraction system. Ca, Y, Zr were used as extractable metals.

## EXPERIMENTAL

The following substances have been used: HDEHP, TBP, toluene, aliphatic alcohols (from butanol to decanol); nitrates, sulphates and chlorides of Ca, Y and Zr with the content of main material not less than 98 %. The concentration of metals was determined by complexometric titration with EDTA. The content of water in organic phase was determined by Karl Fisher method.

In order to determine the hydrodynamic radius of colloidal aggregates in the organic phase the methods of photon-correlation spectrometry were used. Photon-correlation spectrometer included He-Ne laser with the operation wavelength of the light 632.8 nm, photometer F-221 and correlator "Unicor SP" with 128 high-speed signal processors. Computing program allowed in the real-time mode to calculate the correlation function, using cumulant method [8].

## RESULTS AND DISCUSSION

Figure 1 presents the isotherms of yttrium extraction from hydrochloric medium into toluene solutions of HDEHP at different content of butanol (different values of  $U$ ). The loading capacity of extractant depends on the amount of added alcohol. The maximum loading capacity is achieved at the concentration of alcohol corresponding to the maximum of distribution coefficients  $U = U_{opt}$  ( $U_{opt} = 0.2$ ). In this case the course of isotherm is steep and the loading capacity of extractant increases significantly as compared with the data obtained in the extraction system without butanol. At following increase of the molar ratio butanol/HDEHP the loading capacity decreases.

The loading capacity of extractant in the presence of 1-octanol (at  $U_{opt}$ ) depends on the composition of aqueous phase (Figure 2). The most loading capacity of extractant was observed for the extraction from hydrochloric medium.

It follows from extraction isotherms presented above that by the realization of micellar mechanism the metal capacity of extractant can be increased. The metal loading capacity of HDEHP depends on the nature of added alcohol (Figures 3 and 4). The enhancement of the loading capacity for calcium extraction is higher than for yttrium.

The addition of butanol or octanol in the extraction system containing TBP,  $HNO_3$  and Zr can influence on the metal loading capacity too (Figure 5).

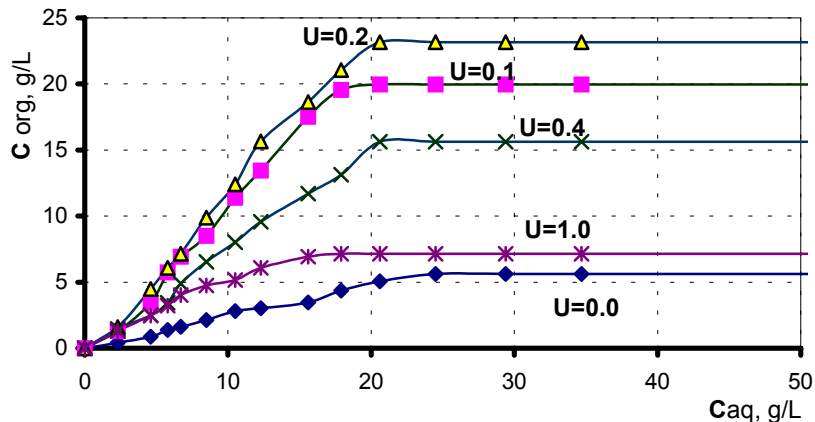


Figure 1. Isotherms of yttrium extraction by HDEHP from hydrochloric medium at the presence of n-butanol. [HDEHP] = 0.2 mol/L in toluene, pH 2.

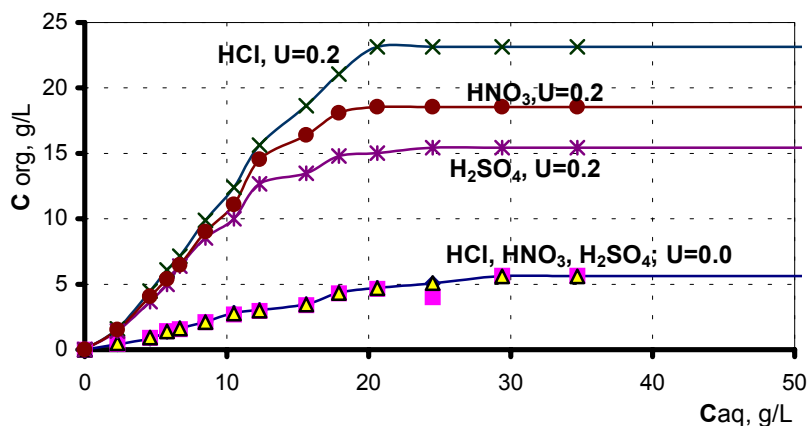


Figure 2. Isotherms of yttrium extraction by HDEHP from different medium at the presence of n-butanol. [HDEHP] = 0.2 mol/L in toluene, pH 2.

The hydrodynamic radius of particles in organic phase was determined for the estimation of the colloidal aggregate size in extraction system  $\text{MeCl}_n/\text{HCl}/\text{HDEHP}/\text{toluene}/\text{n-octanol}$  at the loading of extractant. It was established that in the presence of alcohol the hydrodynamic radius of particles increases considerably as compared with radius of particles without octanol. For example, the value of the hydrodynamic radius for calcium is equal 18.4 nm in the system without alcohol and 159 nm at the concentration of added octanol corresponding to maximum of distribution coefficient of Ca ( $\mathbf{U} = \mathbf{U}_{\text{opt}} = 0.2$ ). The lanthanum radius is equal 23.7 nm without octanol and 223 nm at the concentration of added SAS corresponding to the maximum of distribution coefficient of La ( $\mathbf{U} = \mathbf{U}_{\text{opt}} = 0.1$ ). The measurement of the colloidal particle size in the organic phase indicated that in dependence of added alcohol content the reversed micelles or microemulsion were formed in the organic phase. The obtained data confirmed the supposition about the structural transition in the extraction system containing metal di-2-ethylhexylphosphate and n-octanol [6].

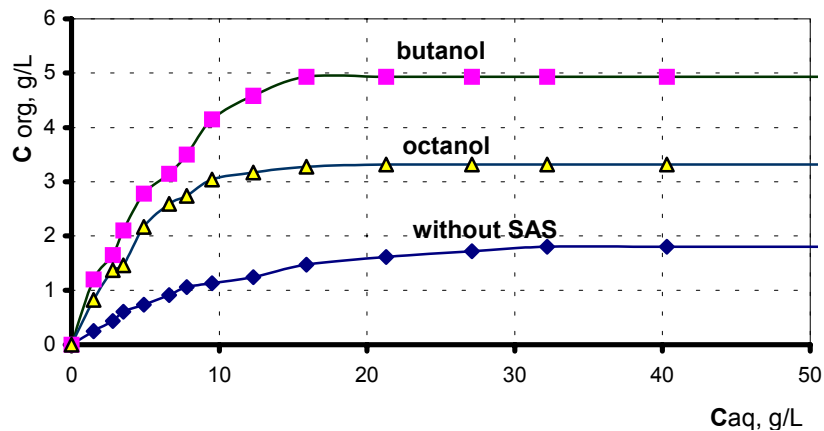


Figure 3. Isotherms of extraction of calcium from hydrochloric medium in the presence of *n*-butanol and *n*-octanol. [HDEHP] = 0.2 mol/L in toluene,  $U = U_{opt}$  (butanol:  $U = 0.3$ ; octanol:  $U = 0.2$ ), pH 2.

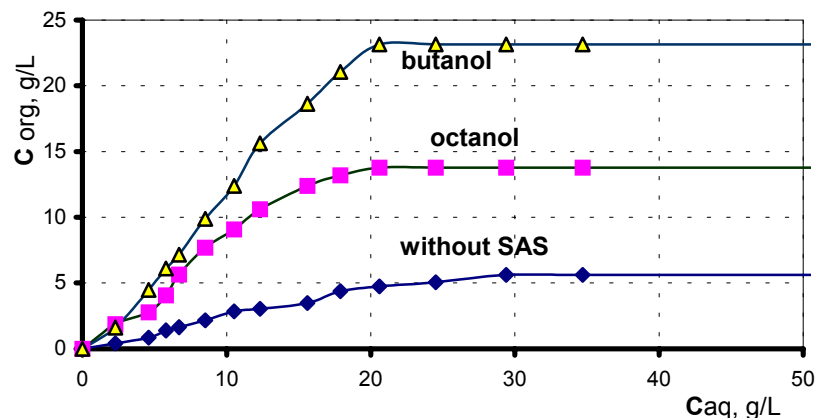


Figure 4. Isotherms of extraction of yttrium from hydrochloric medium in the presence of *n*-butanol and *n*-octanol. [HDEHP] = 0.2 mol/L in toluene,  $U = U_{opt}$  (butanol:  $U = 0.2$ ; octanol:  $U = 0.1$ ), pH 2.

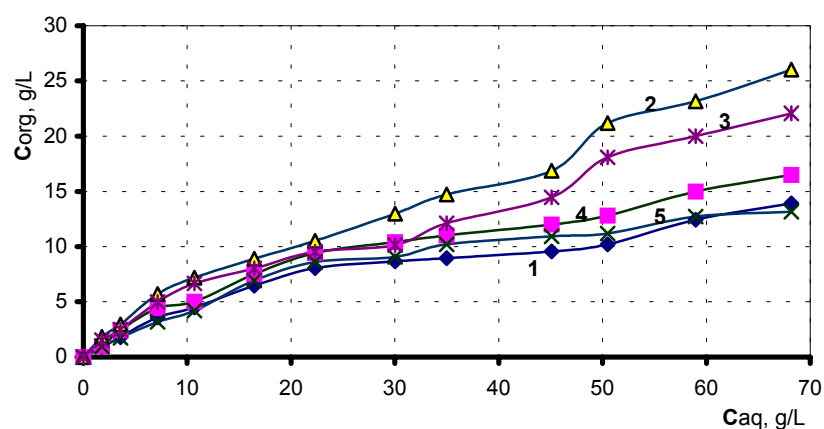


Figure 5. Isotherms of zirconium extraction by TBP from nitric medium in the presence of *n*-butanol and *n*-octanol. [TBP] = 1.46 mol/L in toluene,  $[HNO_3]_{aq} = 4$  mol/L. 1-without alcohol, 2-butanol,  $U = 0.025$ ; 3- butanol,  $U = 0.1$ ; 4- octanol,  $U = 0.025$ ; 5- octanol  $U = 0.1$ .

Table 1 presents the values of water content in the organic phase received at the extraction of yttrium in the presence of different aliphatic alcohols. The concentration of added surfactant corresponds to the maximum of the metal distribution coefficient.

*Table 1. Composition of organic phase at the extraction of yttrium by HDEHP from hydrochloric medium.*

Alcohol	U	D	[Me] <sub>org</sub> , mol/L	[H <sub>2</sub> O] <sub>org</sub> , mol/L	[H <sub>2</sub> O]/[Me]
-	0	0.42	0.0295	0.044	1.48
butanol	0.2	0.55	0.0355	0.212	5.98
isopentanol	0.2	0.53	0.0342	0.157	4.60
hexanol	0.2	0.52	0.0340	0.116	3.42
octanol	0.1	0.50	0.0335	0.062	1.86
decanol	0.1	0.46	0.0315	0.053	1.68

Aqueous phase: [LnCl<sub>3</sub>] = 0.1 mol/L, pH 2.0. Organic phase: [HDEHP] = 0.2 mol/L in toluene

The data of Table 1 indicate that water content is higher in the alcohol presence as compared with system without alcohol. Water content in the organic phase decreases with the rise of the hydrocarbon length of aliphatic alcohol. The water content depends on the composition of initial aqueous phase. At the extraction of lanthanides from hydrochloric medium the water content in the organic phase is higher as compared with the value received at the extraction from nitric medium, presented in Table 2. The water content in the organic phase increases with increase of concentration of added alcohol.

*Table 2. Effect of alcohol concentration on composition of organic phase at the extraction of lanthanum by HDEHP from nitric medium.*

Alcohol	U	D	[Me] <sub>org</sub> , mole/L	[H <sub>2</sub> O] <sub>org</sub> , mole/L	[H <sub>2</sub> O]/[Me]
-	0	0.38	0.0273	0.027	1.34
butanol	0.05	0.41	0.0290	0.078	2.70
	0.1	0.44	0.0305	0.089	2.92
	0.2	0.51	0.0336	0.154	4.61
	0.4	0.43	0.0300	0.164	5.48
	0.6	0.37	0.0270	0.214	7.92
	1.0	0.32	0.0240	0.252	10.51
octanol	0.05	0.40	0.0286	0.049	1.72
	0.1	0.43	0.0300	0.051	1.71
	0.2	0.37	0.0271	0.051	1.88
	0.4	0.31	0.0237	0.052	2.19
	0.6	0.28	0.0221	0.057	2.58
	1.0	0.23	0.0186	0.058	3.12

Aqueous phase: [Ln(NO<sub>3</sub>)<sub>3</sub>] = 0.1 mol/L, pH 2.0. Organic phase: [HDEHP] = 0.2 mol/L in toluene

The water content also depends on the nature of extractable metal. Table 3 presents the data of the water content at the extraction of Ca, La and Zr by HDEHP from hydrochloric medium at the presence of n-octanol, where the concentration of added alcohol corresponds to the maximum of the metal distribution coefficients.

*Table 3. Composition of organic phase at the extraction of same metals by HDEHP from hydrochloric medium in the presence of n-octanol.*

Metal	D	U	[Me] <sub>org</sub> , mol/L	[H <sub>2</sub> O] <sub>org</sub> , mol/L	[H <sub>2</sub> O]/[Me]
Ca	1.01	0.2	0.0502	0.380	7.56
La	0.50	0.1	0.0335	0.062	1.86
Zr	1.84	0.025	0.0486	0.075	1.54

Ca: [Me]=0.1 mol/L, pH 2.0; [HDEHP]=0.2 mol/L in toluene

La: [Me]=0.1 mol/L, pH 2.0; [HDEHP]=0.2 mol/L in toluene

Zr: [Me]= 0.075 mol/L, [HCl]= 2.0 mol/L; [HDEHP]=0.4 mol/L in toluene

The analysis of the data of Table 3 shows that the most water content is observed in the system containing calcium di-2-ethylhexylphosphates.

## CONCLUSIONS

It was found that the addition of co-surfactant to the extraction system could change the metal loading of the extractant. In the presence of surfactant in the extraction system, the metal loading of HDEHP and TBP increased as compared with the extraction process without surfactant. The metal loading of extractant depends on the added surfactant amount and on the conditions of the extraction process realisation.

## REFERENCES

1. E. Paatero and J. Sjoblom (1990), *Hydrometallurgy*, **1**, 231-250.
2. V. Tarasov and G. Yagodin (1988), *Solvent Extr. Ion Exch.*, **10**, 141-153.
3. L. Huiznou, Y. Shuqiu and C.Jiayong (1990), *Proc. ISEC '90*, Kyoto, Japan, pp. 793-799.
4. M. de L. Dias Lay, E.S. Perez de Ortiz *et al.* (1996), *Proc. ISEC '96*, University of Melbourne Press, Melbourne, pp. 409-415.
5. N.-F. Zhou, J. Wu, P.K. Sarathy, F. Lui and R.D. Neuman (1990), *Proc. ISEC '90*, Kyoto, Japan, pp. 165-171.
6. R.D. Neuman, S.J.Park, N.F. Zhou and P.Shah (1993), *Proc. ISEC '93*, Society of Chemical Industry, London, pp. 1689-1895.
7. N.V. Bukar, V.Kim and O.A. Sinegribova (1999), *J. Inorg. Chem. (Russ.)*, **7**, 1124-1129.
8. G. Fourche, M. Bellocq and S. Brunetti (1982), *J. Colloid Interface Sci.*, **2**, 302-310.



## STRUCTURE-REACTIVITY STUDIES OF SOLVENT EXTRACTANTS IN METAL EXTRACTION

Chengye Yuan and Shusen Li

Shanghai Institute of Organic Chemistry, Chinese Academy of Sciences, Shanghai, China

The structure-reactivity relationship of solvent extractants in metal separation was studied both qualitatively and quantitatively. Pearson's HSAB principle is successfully applied to the qualitative prediction and molecular modification of solvent extractants. Molecular orbital calculations are a useful tool to estimate the charge density of the coordination atom or group. Molecular mechanics calculations are good for the evaluation of the steric contribution of the molecules. Based on experimental data a series of multiple regression analyses involving extraction constants and polar and steric parameters were established. Such treatments are helpful for the prediction and design of extractant molecules with high selectivity in cobalt and nickel separation in particular, since the formation of different configurations of coordination compounds plays an important role during the extraction process.

### INTRODUCTION

The technological and economical behavior of extraction systems are dependent on the performance of extractants that are closely related to the chemical structure of the latter. Consequently, structure reactivity studies of solvent extractants can, in very practical terms, contribute both to the discovery of new selective extractants and to the progress of extraction chemistry in general. Both qualitative and quantitative examinations of structure-reactivity relationship of extractants are helpful for the design and selection of extractants.

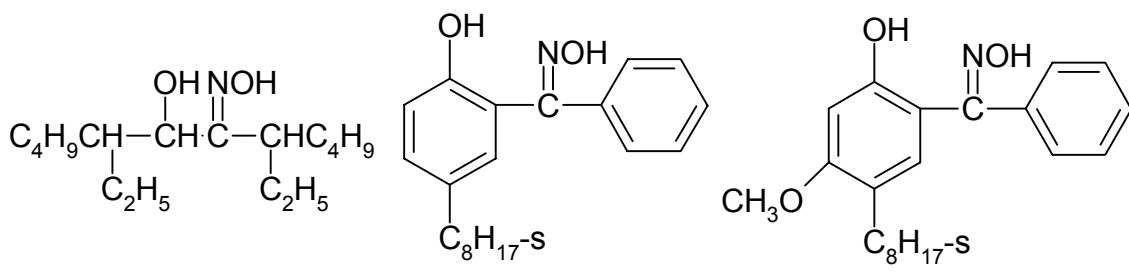
### QUALITATIVE STRUCTURE-REACTIVITY STUDIES

Metal extraction may be considered simply as the replacement reaction of water molecule in the hydration shells of metallic ions in aqueous solution by an organic ligand (extractant):



Both metal ions (acceptor) and coordinating atoms (donor) are classified as either hard, soft or borderline acids and bases according to Pearson's scale.

Oxygen-containing ligands, including ether, alcohol, carboxylate, phosphate and phosphonates are referred to hard bases, which prefer to coordinate with hard acids, such as lanthanides, actinides, niobium, tantalum, zirconium or hafnium. As soft bases, sulfur-containing ligand (thioether, thiourea, thiocarboxylate, or dithiophosphate) prefer to combine with soft acids such as copper. It is therefore not difficult to rationalize the fact that LIX 63 was replaced by LIX 64 for copper extraction in acidic medium.



LIX 63 (N-509)

LIX 64 (N-510)

N-530

Since in the molecule LIX 63, both OH and N–OH are coordination groups in which O is a hard base, while Cu<sup>++</sup> is a soft acid. Consequently as an aliphatic hydroxyoxime, LIX 63 is poor in copper extraction. However, the hardness of the donor atoms can be modified by the inductive or conjugative effect of the neighboring atom and group. LIX 64 being an aromatic hydroxyoxime, the conjugation effect of benzene ring decreases the hardness of the base and the extraction ability of copper will be enhanced accordingly. Moreover, introduction of additional electron-withdrawing groups (NO<sub>2</sub>, Cl) makes the molecule more powerful in copper extraction. Unfortunately, in such case, the resulting loaded organic phase turns out to have poor stripping ability towarding the back extraction process. It is very interesting to note that the compound N–530, chemically known as *p*–octyl–*m*–methoxyl benzophenone oxime, is an excellent copper extractant. Structurally it is understandable, located on the *meta*-position, the methoxyl group possesses electron-withdrawing ability that makes the phenolic OH more acidic. On the other hand, the methoxyl group is a well-known electron-donating group toward the *para*–substituent, that results the higher electron density on the oximido nitrogen atom. Consequently, N–530 exhibits high extraction ability and loading capacity in copper extraction. Beside these, the copper extraction kinetics of this reagent are quite good. As an empirical principle, HSAB is therefore not only useful for the prediction but also helpful for the design of extractants.

Molecular orbital calculations were applied by us to estimating the charge density and bond order of hydroxyoxime-type extractants (Table 1). The calculation results are fully consistent with the experimental data [1,2] and theoretical predictions. Unfortunately, such treatment is not in a position to evaluate the contribution of steric effect of substituents that are very important in solvent extraction.

Concerning the quantitative structure activity relationship (QSAR) studies, we have demonstrated that the reactivity of solvent extractants is dependent on the polar and steric effect of the substituent as well as solubility contributions as represented by the equation:

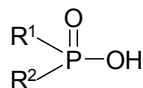
$$\log K_{\text{ex}} = \log K_{\text{ex}_0} + \rho \sum \sigma + \delta \sum E_s + k \sum C$$

Nevertheless, our equation consisted of three most important structural effects of substituents, since solvent extraction is a multiple component equilibrium process between two heterogeneous phases. Moreover, the contribution of the configuration of extracted species, dimer constant of extractants and influence of diluents are not included in such treatment. Consequently this equation can only be regarded as an approximate approach.

Table 1. Molecular orbital calculation of hydroxyoxime extractants.

En.	Compd.	Charge density (q)			Bond order (p)			Remarks
		-OH (HOMO)	>N=	>N-OH	C-N	N-O	C-OH	
1		0.1330	0.9101	1.8981	0.8092	0.3169	0.1711	N-509
2		0.0481	1.2501	1.9470	0.7958	0.6992	0.2616	N-510
3		0.0489	1.2596	1.9470	0.7960	0.1968	0.2588	LIX 70
4		0.0393	1.2494	1.9474	0.7956	0.1974	0.3844	NO2-N-510
5		0.0400	1.2669	1.9489	0.7910	0.1914	0.2723	N-530
6		0.0811	1.2797	1.9539	0.8429	0.1806	0.2630	SME 529
7		0.0928	1.2290	1.9494	0.8648	0.1960	0.2632	Acorga P50

A series of mono-basic phosphorus-based compounds was studied for cobalt and nickel separation [4].



R<sup>1</sup>=R<sup>2</sup>=n-C<sub>8</sub>H<sub>17</sub>O (**1**), i-C<sub>8</sub>H<sub>17</sub>O (**2**), s-C<sub>8</sub>H<sub>17</sub>O (**3**)

R<sup>1</sup>=n-C<sub>8</sub>H<sub>17</sub>, R<sup>2</sup>=n-C<sub>8</sub>H<sub>17</sub>O (**4**), i-C<sub>8</sub>H<sub>17</sub>O (**5**), s-C<sub>8</sub>H<sub>17</sub>O (**6**)

R<sup>1</sup>=i-C<sub>8</sub>H<sub>17</sub>, R<sup>2</sup>=n-C<sub>8</sub>H<sub>17</sub>O (**7**), i-C<sub>8</sub>H<sub>17</sub>O (**8**), s-C<sub>8</sub>H<sub>17</sub>O (**9**)

R<sup>1</sup>=s-C<sub>8</sub>H<sub>17</sub>, R<sup>2</sup>=n-C<sub>8</sub>H<sub>17</sub>O (**10**), i-C<sub>8</sub>H<sub>17</sub>O (**11**), s-C<sub>8</sub>H<sub>17</sub>O (**12**)

R<sup>1</sup>=cyc-C<sub>6</sub>H<sub>11</sub>, R<sup>2</sup>=n-C<sub>8</sub>H<sub>7</sub>O (**13**), i-C<sub>8</sub>H<sub>17</sub>O (**14**), s-C<sub>8</sub>H<sub>17</sub>O (**15**)

R<sup>1</sup>=i-C<sub>3</sub>H<sub>7</sub>, R<sup>2</sup>=n-C<sub>12</sub>H<sub>25</sub>O (**16**), i-C<sub>14</sub>H<sub>29</sub> (**17**)

R<sup>1</sup>=CH<sub>3</sub>, R<sup>2</sup>=i-C<sub>14</sub>H<sub>29</sub>O (**18**)

R<sup>1</sup>=R<sup>2</sup>=n-C<sub>8</sub>H<sub>17</sub> (**19**), i-C<sub>8</sub>H<sub>17</sub> (**20**), s-C<sub>8</sub>H<sub>17</sub> (**21**)

where i-C<sub>8</sub>H<sub>17</sub> and s-C<sub>8</sub>H<sub>7</sub> represent

C<sub>4</sub>H<sub>9</sub>CH(C<sub>2</sub>H<sub>5</sub>)CH<sub>2</sub>- and C<sub>6</sub>H<sub>13</sub>CH(CH<sub>3</sub>)- respectively

i-C<sub>14</sub>H<sub>29</sub> denotes C<sub>7</sub>H<sub>15</sub>CH(C<sub>5</sub>H<sub>11</sub>)CH<sub>2</sub>-

As shown by us, in structure-reactivity studies of organophosphorus compounds, the classic Taft constants could be used as a substituent polar parameter. It is not necessary to have another set of polar parameters specific for organophosphorus compounds [5]. There are no suitable parameters for long-chain alkyl or alkoxy groups that are critical for the extractant molecule. Based on the measurement of pKa values of mono-basic phosphorus acids, we estimated a series of alkyl and alkoxy groups directed linked to phosphorus atom and showed that these parameters are related to "Group Connectivity" [6] and chemical properties including IR,  $^{31}\text{P}$  NMR as well as hydrolytic constant in alkaline hydrolysis [7]. In this study, it is important to establish steric parameters for substituents, of extractants. We used Charton's v parameters, that are based on the Van der Waals radius between atoms, as the measure for the steric effect. During the nickel and cobalt extraction, formation of extraction species with different configurations takes place. Cobalt forms complexes with tetrahedral configuration, while nickel gives a complex with square planar configuration. The influence of the steric effect on these two configurations is significant remarkable. Therefore we introduce  $\Sigma E_{\text{ex}}^{\text{Co}}$  and  $\Sigma E_{\text{PA}}^{\text{Ni}}$  parameters for cobalt and nickel extraction correspondingly.

$$\log K_{\text{ex}}^{\text{Co}} = 0.86 \sum \sigma^p + 1.00 \sum E_{\text{PA}}^{\text{Co}} - 3.17$$

$$\log K_{\text{ex}}^{\text{Ni}} = 3.03 \sum \sigma^p + 1.00 \sum E_{\text{PA}}^{\text{Ni}} + 5.86$$

In the above formulae,  $\Sigma E_{\text{PA}}^{\text{Co}}$  and  $\Sigma E_{\text{PA}}^{\text{Ni}}$  could be used, as we expected, as the steric parameter for metal extraction with related configurations (Table 2).

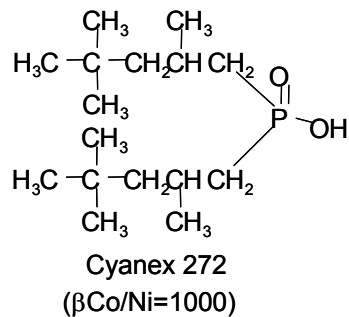
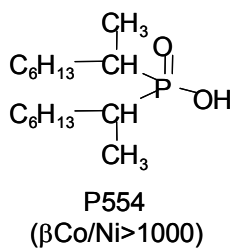
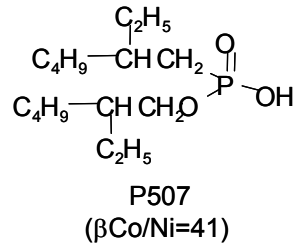
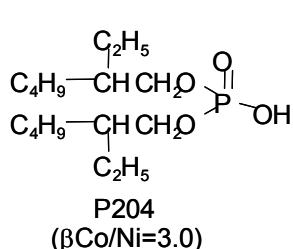
*Table 2. Extraction of Co and Ni by mono-basic phosphorus-based extractants.*

No.	R <sub>1</sub>	R <sub>2</sub>	-Σσ	ΣE <sub>ex</sub>	log P	-log K <sub>Co</sub>	-log K <sub>Ni</sub>	Log β <sub>Co/Ni</sub>
1	n-C <sub>8</sub> H <sub>17</sub> O	n-C <sub>8</sub> H <sub>17</sub> O	0.98	0.025	3.28	4.33	4.57	0.24
2	i-C <sub>8</sub> H <sub>17</sub> O	i-C <sub>8</sub> H <sub>17</sub> O	1.10	0.046	3.51	5.42	6.13	0.71
3	s-C <sub>8</sub> H <sub>17</sub> O	s-C <sub>8</sub> H <sub>17</sub> O	1.36	0.338	3.51	5.82	----	----
4	n-C <sub>8</sub> H <sub>17</sub>	n-C <sub>8</sub> H <sub>17</sub> O	1.60	0.023	3.36	5.55	6.35	0.80
5	n-C <sub>8</sub> H <sub>17</sub>	i-C <sub>8</sub> H <sub>17</sub> O	1.66	0.034	3.48	5.66	7.13	1.47
6	n-C <sub>8</sub> H <sub>17</sub>	s-C <sub>8</sub> H <sub>17</sub> O	1.79	0.180	3.48	5.85	7.63	1.78
7	i-C <sub>8</sub> H <sub>17</sub>	n-C <sub>8</sub> H <sub>17</sub> O	1.70	0.098	3.48	5.62	6.98	1.36
8	i-C <sub>8</sub> H <sub>17</sub>	i-C <sub>8</sub> H <sub>17</sub> O	1.76	0.109	3.59	5.87	8.16	2.29
9	i-C <sub>8</sub> H <sub>17</sub>	s-C <sub>8</sub> H <sub>17</sub> O	1.89	0.255	3.59	6.27	8.91	2.63
10	s-C <sub>8</sub> H <sub>17</sub>	n-C <sub>8</sub> H <sub>17</sub> O	1.77	0.289	3.48	5.77	7.34	1.57
11	s-C <sub>8</sub> H <sub>17</sub>	i-C <sub>8</sub> H <sub>17</sub> O	1.83	0.300	3.59	6.15	8.61	2.46
12	s-C <sub>8</sub> H <sub>17</sub>	s-C <sub>8</sub> H <sub>17</sub> O	1.96	0.495	3.59	6.28	8.62	2.34
13	Cycl-C <sub>6</sub> H <sub>11</sub>	n-C <sub>8</sub> H <sub>17</sub> O	1.74	0.230	2.08	5.66	7.20	1.54
14	Cycl-C <sub>6</sub> H <sub>11</sub>	i-C <sub>8</sub> H <sub>17</sub> O	1.80	0.241	2.19	5.64	7.93	2.29
15	Cycl-C <sub>6</sub> H <sub>11</sub>	s-C <sub>8</sub> H <sub>17</sub> O	1.93	0.436	2.19	5.81	8.06	2.25
16	i-C <sub>3</sub> H <sub>7</sub>	n-C <sub>12</sub> H <sub>25</sub> O	1.63	0.229	1.65	5.62	6.91	1.29
17	i-C <sub>3</sub> H <sub>7</sub>	i-C <sub>14</sub> H <sub>29</sub> O	1.74	0.240	2.50	5.72	6.73	1.01
18	CH <sub>3</sub>	i-C <sub>14</sub> H <sub>29</sub> O	1.40	0.014	0.98	5.19	5.75	0.56
19	n-C <sub>8</sub> H <sub>17</sub>	n-C <sub>8</sub> H <sub>17</sub>	2.22	0.022	3.44	5.80	----	----
20	i-C <sub>8</sub> H <sub>17</sub>	i-C <sub>8</sub> H <sub>17</sub>	2.42	0.172	3.67	6.00	8.08	2.08
21	s-C <sub>8</sub> H <sub>17</sub>	s-C <sub>8</sub> H <sub>17</sub>	2.56	0.554	3.67	5.92	9.95	4.03

Molecular mechanics calculations were introduced to evaluate the steric contribution of the substituent in solvent extraction [8] (Table 3). The theoretical prediction was supported by experimental data.

Table 3. Substituent steric parameters.

Group	$E_s^P(R)$	$E_s^P(RO)$	$E_{s,ex}(R)$	$E_{s,ex}(RO)$	$\nu$	$E_s$
Me	0.50	0.38	-0.037	0.0	0.52	-1.24
Et	0.75	0.62	0.0	0.003	0.56	-1.31
n-Pr	0.85	0.72	0.007	0.003	0.68	-1.60
i-Pr	1.12	0.98	0.216	0.021	0.76	-1.71
n-Bu	0.91	0.77	0.010	0.003	0.68	---
i-Bu	1.05	0.91	0.053	0.015	0.98	---
s-Bu	1.17	1.02	0.246	0.102	1.02	-2.37
t-Bu	1.36	1.21	0.545	---	1.24	-2.78
n-Am	0.91	0.77	0.010	0.010	0.68	---
i-Am	0.92	0.78	---	---	0.68	---
cyc-Hex	1.07	0.93	0.218	---	6.87	-1.01
n-Oct	0.90	0.76	0.011	0.012	0.68	---
i-Oct	1.10	0.96	0.068	0.023	1.01	---
s-Oct	1.25	1.05	0.277	0.169	1.05	---



## ACKNOWLEDGEMENTS

The project was supported by the National Natural Science Foundation of China.

## REFERENCES

1. S. Chen, Y. D. Jiang and K. C. Chen (1981), *Acta Chim. Sin.*, **39**, 749–760.
2. C. Y. Yuan, C. M. Zhou and K. C. Chen (1981), *Acta Chim. Sin.*, **39**, 699–710.
3. C. Y. Yuan (1980). *Proc. ISEC '80*, Liege, Belgium, Paper No. 80–81.
4. C. Y. Yuan, Q. R. Xu and S. G. Yuan (1988), *Solvent Extr. Ion Exch.*, **6**, 393–416.
5. C. Y. Yuan and S. S. Hu (1986), *Acta Chim. Sin.*, **44**, 590–601.
6. P. J. Hanson (1984), *J. Chem. Soc., Perkin Trans. I*, 101–103.
7. C. Y. Yuan, S. G. Yuan and S. S. Hu (1988), *Acta Chim. Sin.*, **46**, 159–164.
8. S. S. Li and C. Y. Yuan (1989), *Acta Phys. Chim. Sin.*, **5**, 56–61.



## COLLOID STRUCTURES FORMED IN EXTRACTION SYSTEMS WITH ORGANOPHOSPHORUS EXTRACTANTS

E.V. Yurtov and N.M. Murashova

Mendeleyev University of Chemical Technology of Russia, Moscow, Russia

Colloid structures, such as organogels, microemulsions, liquid crystals and amorphous sediments, found in extraction systems with organophosphorus extractants are discussed. Micellar organogels, microemulsions and liquid crystals are shown in the system sodium di(2-ethylhexyl)phosphate/decane/water. The formation of crystalline organogels and amorphous sediments was studied in the systems di(2-ethylhexyl)phosphoric acid/copper hydroxide/ hydrocarbon/water and di(2-ethylhexyl)phosphoric acid/neodymium hydroxide/ decane/water. Concentration regions and rheological properties of the structures were investigated. Properties of emulsions, stabilized by disperse structures of copper and neodymium di(2-ethylhexyl)phosphates were studied. Some ways of prevention of disperse structures formation in systems with organophosphorus extractants are discussed.

### INTRODUCTION

Colloid structure formation in extraction systems, near the interface and in the bulk, leads to interfacial films and crud formation. It can be an undesirable phenomenon because it can result in extraction rate reduction and phase separation difficulty, which impedes performance of the extraction equipment. On the other hand, the processes of structure transformation can increase the interfacial mass-transfer. The structures may arise from the formation of surface-active or low-soluble compounds during the extraction process. Such colloid structures, as reverse micelles and microemulsions, are known in extraction systems with organophosphorus extractants [1-5]. Formation and properties of different colloid structures in the extraction systems with di-(2-ethylhexyl)phosphoric acid (DEHPA) and alkali, non-ferrous and rare-earth metals were investigated in this contribution.

The formation of crud, a highly viscous and stable disperse structure, which looks like a deposit, paste, emulsion or gel at the interface between two partially settled phases, is known for a number of extraction systems, containing, for example, the organophosphorus compounds TBP and dibutylphosphoric acid. Investigation of colloid structure formation in the extraction systems gives the possibility of clarifying the behavior and properties of extraction systems and to predict the formation of interfacial films and crud in technology processes.

## EXPERIMENTAL

The following extractants were used in this work: di(2-ethylhexyl)phosphoric acid (DEHPA) from Merck (Germany) with the main substance content more than 98 % and DEHPA of technical grade from OAO Himprom (Russia), which contained 66.0 % di(2-ethylhexyl)-phosphoric and 19.5 % mono-(2-ethylhexyl)phosphoric acid. Copper and rare-earth elements' hydroxides were obtained by the reaction of NaOH with copper sulfate or rare-earth metal nitrate solution.

The samples were prepared by mixing DEHPA organic solution with the required quantity of water and the hydroxide. Emulsions were obtained by means of water phase (water + hydroxide precipitate) and organic phase (DEHPA solution) mixing for 2 min with stirrer (rotation rate  $3000\text{ min}^{-1}$ ). The ratio of water and organic phase volume was 3:2). Emulsion stability was determined by the method of phase separation in centrifuge (at acceleration 90 g). A rotation viscometer, Rhoetest 2, was used for viscosity measurement.

## RESULTS AND DISCUSSION

### Micellar Organogels, Microemulsions and Liquid Crystals

A number of extractants and extracted compounds including DEHPA and its salts can form disperse structures, typical for surfactants are normal and reverse micelles, micellar organogels, microemulsions, vesicles, liquid crystals. Di(2-ethylhexyl)phosphates are able to form reverse micelles (spherical in the systems DEHPNa/benzene/water [1] and DEHPNa/toluene/water [5], and giant cylindrical in the systems cobalt di(2-ethylhexyl)phosphate/heptane/water [2] and DEHPNa solution in dry heptane [4]). When the concentration of the surfactant exceeds a critical value, long and flexible cylindrical micelles can entangle, forming the micellar organogel structure. The gelation is accompanied by viscosity growth. Viscous and thixotropic (*i.e.*, able to restore the structure after mechanical destruction) micellar organogels of DEHPNa arise in the system DEHPA/NaOH/decane/water both with pure and technical DEHPA. The organogels in the system with technical DEHPA form only at the excess of NaOH ( $[\text{NaOH}]/[\text{DEHPA}] = 1.4 - 1.8$ ) [6].

Salts of di(2-ethylhexyl)phosphoric acid are able to form bilayer structures: vesicles and lamellar liquid crystals. For example, addition of small amount of  $\text{CCl}_4$  to crystalline di(2-ethylhexyl) phosphates of rare-earth metals leads to the formation of anisotropic and viscous liquid crystals [7]. Liquid crystals are formed in the system DEHPNa/decane/water in the region of high concentrations (90% mass and more) of DEHPNa. The picture of DEHPNa liquid crystal under a polarizing microscope is shown in Figure 1.

Microemulsion formation is possible in DEHPA salts systems, both containing aliphatic alcohols and without cosurfactants. The formation of microemulsion of W/O (water-in-oil) type was described in the extraction system: water solution of NaOH or  $\text{NH}_4\text{OH}$ /DEHPA and sec- octyl alcohol solution in kerosene [3]. Bicontinuous and O/W (oil-in-water) microemulsions are found to exist in the ternary system DEHPNa/hexane/water [4].

The peculiarity of the DEHPA/NaOH/decane/water system is the possibility of the formation of several colloid structures, such as reverse micelles, micellar organogels, microemulsions and liquid crystals. These structures can coexist with each other and with DEHPNa solution in water and in decane. The regions of different phase equilibria in the system DEHPA (technical)/NaOH/decane/water are shown in Figure 2. Similar regions of phase equilibria were obtained in the system with pure DEHPA.

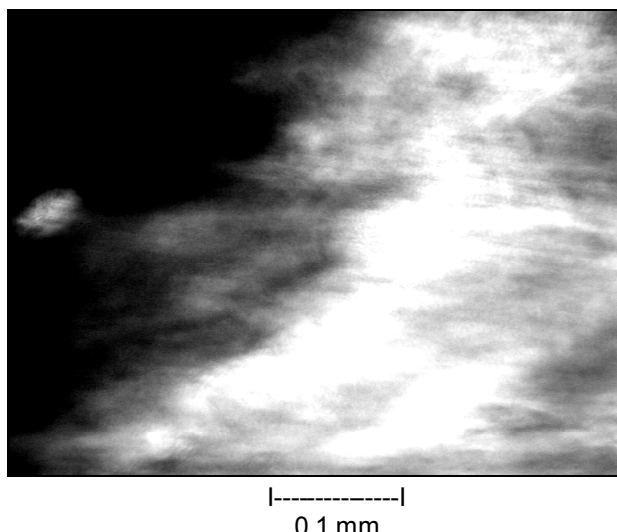


Figure 1. The picture under a polarizing microscope of the liquid crystal in the system DEHPNa/decane/water.  $[DEHPNa] = 2.7 \text{ mol/l}$ ,  $W = [H_2O]/[DEHPNa] = 16.0$ .

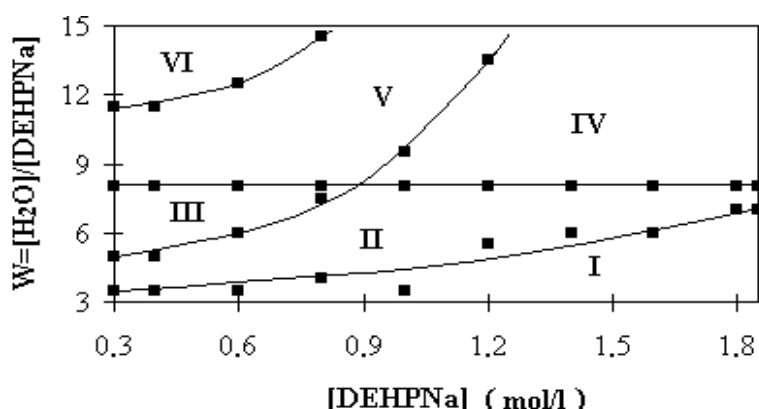


Figure 2. Phase equilibria in the system DEHPA (technical)/NaOH/decane/water at 20 °C.  $[NaOH]/[DEHPA] = 1.5$ . I - spherical DEHPNa micelles solution; II - micellar organogel; III - DEHPNa organic solution/microemulsion; IV - microemulsion/liquid crystal; V - DEHPNa organic solution/microemulsion/liquid crystal; VI - DEHPNa organic solution/liquid crystal.

The considered disperse structures of DEHPNa possess different values of viscosity. At low shear rate ( $1\text{-}10 \text{ s}^{-1}$ ) and 20 °C viscosity of liquid crystals is in the range  $10^1$  to  $10^3 \text{ Pa.s}$  (their viscosity strongly depends upon water concentration), viscosity of micellar organogels is  $10^0$  to  $10^{-1} \text{ Pa.s}$ , microemulsions are  $10^{-1}$  to  $10^{-2} \text{ Pa.s}$ , while the viscosity of spherical micelle solutions is close to the viscosity of the solvent. Viscous disperse structures such as liquid crystals and, possibly, micellar organogels can take part in crud formation.

### Crystalline Organogels and Amorphous Sediments

Beside the disperse structures arising due to the association of organic-soluble extractants and extracted compounds, formation of colloid structures of low-soluble compounds is possible. For example, the formation of water gels in extraction systems containing organophosphorus extractants (TBP and dibutylphosphoric acids) and such elements as Si and Zr is known [8-10].

It was found that basic copper di(2-ethylhexyl)phosphate ( $\text{Cu(OH)DEHP}$ ) formed a gel in organic phase (organogel). Because little crystals build the structure of this gel, it can be called crystalline organogel. A picture of the crystalline organogel in the system DEHPA (technical)/ $\text{Cu(OH)}_2$ /decane/water obtained under an optical microscope is shown in Figure 3. The organogels of  $\text{Cu(OH)DEHP}$  are blue, transparent or slightly cloud, they are irreversibly destroyed by mechanical stress.

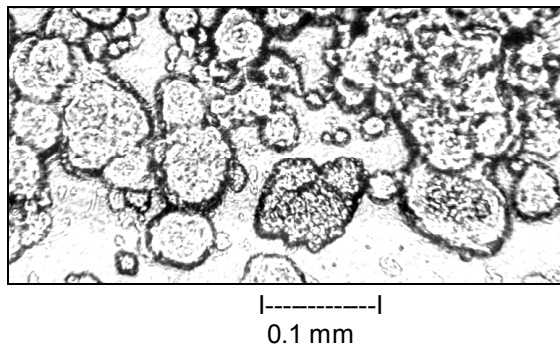


*Figure 3. Picture under an optical microscope of the organogel in the system DEHPA (technical)/ $\text{Cu(OH)}_2$ /decane/water. [DEHPA] = 0.05 mol/l; [DEHPA]/[Cu] = 1.4.*

The region of gelation in the system DEHPA (technical)/ $\text{Cu(OH)}_2$ /decane/water is shown in Figure 4. Water, present in the system and arising from the hydroxide neutralization, separates from the organic phase (organogel), so the water phase is not considered in the diagram. The gelation takes place in narrow diapason of the acid and the base concentration ratio. If the ratio of the acid and the base concentrations exceeds the region of the gelation (at the acid excess), organic solution is formed. At the base excess crystalline sediment arises. The limits of the gelation of basic copper di(2-ethylhexyl)phosphate slightly alter in different hydrocarbon solvents. The values of the gelation limits in decane, hexane and toluene are presented in Table 1. Gelation is also possible in other organic solvents, for example, in decanol.

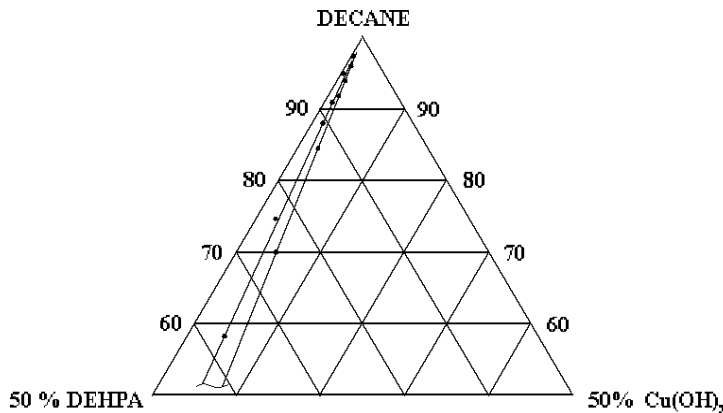


*Figure 4. The region of the crystalline organogel existence at 20 °C. DEHPA technical.*

*Table 1. The gelation limits in the systems DEHPA (technical)/ $\text{Cu(OH)}_2$ /organic solvent/ water at 20 °C.*

Solvent	Minimum concentration of DEHPA, necessary for the gelation, mol/l	Ratio of molar concentrations of the acid and the base ([DEHPA] : [ $\text{Cu(OH)}_2$ ])	
		Lower limit of gelation	Upper limit of gelation
decane	0.025	1.0 : 1.0	1.6 : 1.0
hexane	0.010	1.2 : 1.0	1.8 : 1.0
toluene	0.050	1.2 : 1.0	2.2 : 1.0

Amorphous sediments, consisting of basic di(2-ethylhexyl)phosphate and organic solvent, arise in the systems DEHPA (technical)/lanthanide hydroxides/decane/water in the determined region of the ratio of the acid and the base concentrations. In the system with  $\text{Nd}(\text{OH})_3$  the formation of bulk amorphous sediment is found in the region  $[\text{DEHPA}]/[\text{Nd}(\text{OH})_3] \leq 1.5$  (concentration of technical DEHPA: 0.3 mol/l). This region corresponds to the existence of mono-substituted basic salt  $\text{Nd}(\text{OH})_2\text{DEHP}$ . Compact crystalline sediments and organic solutions are observed at higher  $[\text{DEHPA}]/[\text{Nd}(\text{OH})_3]$  values. Colloid structure formation in the systems with other lanthanides (Ho, Yb, Dy, Sm) is found to be similar.

### Emulsion Stabilization

In the region of the amorphous sediments existence in the system DEHPA (technical)/ $\text{Nd}(\text{OH})_3$ /decane/water stable emulsions can be obtained. The emulsions can stay at ambient conditions more than six months without visible change. Their separation in a centrifugal field was studied. Curves of the organic phase separation for the emulsions with different  $[\text{DEHPA}]/[\text{Nd}(\text{OH})_3]$  values are shown in Figure 5. Unlike stable emulsions (curve 1), arising in the region of the amorphous sediment existence, emulsions obtained in the region of the crystalline sediment existence, are unstable (curve 3).

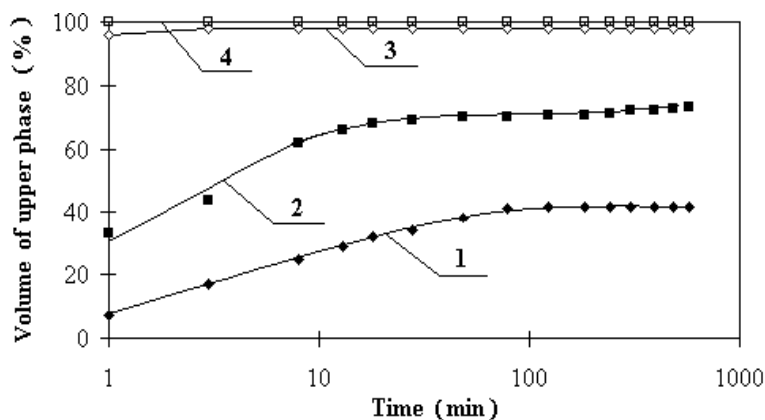


Figure 5. Separation of the emulsions stabilized by copper and neodymium di(2-ethylhexyl)-phosphates in a centrifugal field 90 g.  $[\text{DEHPA}] = 0.3 \text{ mol/l}$ ; DEHPA - technical  
**1** -  $[\text{DEHPA}]/[\text{Nd}(\text{OH})_3] = 1.2$ ; **2** -  $[\text{DEHPA}]/[\text{Cu}(\text{OH})_2] = 1.2$ ; **3** -  $[\text{DEHPA}]/[\text{Nd}(\text{OH})_3] = 2.0$ ;  
**4** -  $[\text{DEHPA}]/[\text{Nd}(\text{OH})_3] = 2.0$ .

Stability of emulsions in the system DEHPA (technical)/ $\text{Cu}(\text{OH})_2$ /decane/water changes with increase of the ratio of the acid and the base concentrations in the same manner. Stable emulsions can be prepared in the system at  $1.0 < [\text{DEHPA}]/[\text{Cu}(\text{OH})_2] < 1.6$ , i.e., in the region of  $\text{Cu}(\text{OH})_2$  and DEHPA concentration ratio, corresponding to the crystalline organogel formation. The curves of the organic phase separation for the emulsions in the system DEHPA (technical)/ $\text{Cu}(\text{OH})_2$ /decane/water within the gelation region (curve 2) and outside it (curve 4) are presented in Figure 5. In the systems, containing micellar organogel, microemulsion or liquid crystal of DEHPNa the formation of stable emulsions was not found.

Knowledge of the regions of existence and properties of disperse structures which can take part in crud formation permits recommending methods of prevention of undesirable structurization in extraction systems.

### Prevention of Crud Formation

Methods which prevents formation of a colloid structure of one certain type can not prevent a structure of another type arising. For example, octanol addition (1 mol of the alcohol per 1 mol of DEHPA salt) prevents the formation of DEHPNa micellar organogel, but this method is not effective in the case of crystalline organogel of  $\text{Cu}(\text{OH})\text{DEHP}$ .

The common recommendation for reduction of crud formation is to carry out the extraction process far from the region of the corresponding structure formation. For example, the probability of formation of micellar organogels, crystalline organogels and amorphous sediments will decrease at low concentrations of extracted compound, at great excess of the extractant and at low pH values in water phase.

Purification of the extractant can prevent crud formation. For example, purification of TBP from radiolysis products decreases crud formation [10]. The removal of mono(2-ethylhexyl)phosphoric acid from technical DEHPA by alkaline washing results in the narrowing of the gelation region in the system DEHPA/Cu(OH)<sub>2</sub>/decane/water from [DEHPA]/[Cu(OH)<sub>2</sub>] = 1.0 - 1.6 (without purification) to [DEHPA]/[Cu(OH)<sub>2</sub>] = 1.6 - 1.8 (after washing).

## CONCLUSIONS

Various colloid structures can take part in crud formation in different extraction systems:

- water gels (arising, for example, in the systems with organophosphorus compounds and such elements, as Si and Zr [8-10] ;
- micellar organogels (formed, for example, by sodium di(2-ethylhexyl)phosphate);
- crystalline organogels (as in the case of basic di(2-ethylhexyl)phosphate of copper);
- bulk amorphous sediments (as basic di-(2-ethylhexyl)phosphates of lanthanides);
- emulsions, stabilized by water gels or crystalline organogels or amorphous sediments.

The regions of existence and properties of these disperse structures are different, so various methods are necessary to prevent their formation.

## ACKNOWLEDGEMENTS

This work was partly supported by Russian Federal Program "Integration" (grant A0078/3,5)

## REFERENCES

1. A. Faure, T. Ahlnas, A.M. Tistchenco, C. Chachaty (1987), *J. Phys. Chem.*, **91**, 1827-1834.
2. Z.-J. Yu, R.D. Neuman (1996), *Proc. ISEC '96*, Melbourne, Australia, pp. 135-140.
3. C.-K. Wu, H.-C. Kao, S.-C. Li, T.-C. King, K.-H. Hsu (1980), *Proc. ISEC '80*, Liege, Belgium, abstract N 80-23.
4. Z.-J. Yu, R.D. Neuman (1995), *Langmuir*, **11**, 1081-1086.
5. A.M. Chekmarev, N.V. Bukar, V. Kim, O.A. Sinegribova, E.I. Chibrikina (1996), *Proc. ISEC '96*, Melbourne, Australia, pp. 389-393.
6. E.V. Yurtov, N.M. Murashova (1999), *Proc. ISEC '99*, Barcelona, Spain, pp. 579-584.
7. Yu. I.Trifonov, E.K. Legin, D.N Suglobov (1990), *Proc. ISEC '90*, Kyoto, Japan, pp. 279-284.
8. S.V. Chizhevskaya, O.A. Sinegribova, A.M. Chekmarev, M. Cox (1996), *Proc. ISEC '96*, Melbourne, Australia, pp. 683-688.
9. G.M. Ritcey, E.W. Wong (1988), *Proc. ISEC '88*, Moscow, Russia, pp. 116-119.
10. G.S. Markov, M.M. Moshkov, V.A. Shcherbakov (1993), *Proc. ISEC '93*, York, UK, pp. 1531-1537.



# A STRUCTURE PARAMETER CHARACTERIZING THE STERIC EFFECT OF ORGANOPHOSPHOROUS ACID EXTRACTANTS

Tun Zhu

Institute of Chemical Metallurgy, Chinese Academy of Sciences, Beijing, P.R. China

It is suggested in the present paper to take the angle between the two substituting groups and the phosphorus atom,  $\Delta RPR'$  as the steric parameter of the extractants. For extracted coordination compounds with an octahedral configuration, the substituting groups from two coordinated organophosphorous acids are approximately in the same plane, thus the larger the angle  $\Delta RPR'$ , the larger the interaction between them, resulting in a greater steric effect. In a tetrahedral configuration, the substituting groups are located in two perpendicular planes, and the interaction is much weaker.

## INTRODUCTION

Steric effects have great influence on the selectivity of organophosphorous acid (OPA) extractants. Extractants with stronger steric effects usually have better separation abilities for metal ions with similar properties. Steric hindrance has been adopted by many authors as a means of interpreting the extraction ability of organophosphorous acids, but there is a lack of a clear description of the steric hindrance of these compounds from structural point of view. Usually it is believed that for extractants with the same structure, the steric effect is decided by the bulk and the degree of branching of the substituting groups in the compounds.

Systematic studies on alkylphosphorous acids (AOPA) have been done by Yuan and coworkers [1]. An empirical equation relating the extraction equilibrium constants and the polarity and the steric hindrance of the substituents in the AOPA has been established, based on the regression of the solvent extraction constants of cobalt and nickel extracted by more than twenty AOPA. For one AOPA there are two different steric parameters for cobalt and nickel, respectively. These parameters are not factors characterizing the structure of the extractant molecule itself, but rather coefficients denoting the selectivity of this reagent for a specific metal, although it may relate to the steric effect of the substituting group in the compound.

## EXPERIMENTAL

### Calculation Molecular Parameters

Molecular parameters of some AOPA were calculated by use the Sybyl programm of the molecular mechanics(force field) program, produced by Tripol Company and the Gasteiger-Marsili-Hückel method.

## RESULTS AND DISCUSSION

### Stability Energies of $\text{Co}^{2+}$ and $\text{Ni}^{2+}$

Of the seven d electrons in the weak octahedral ligand field of cobaltous ions, five electrons are in the lower energy  $t_{2g}$  orbital, four of which are paired, and the other two are in the higher energy  $e_g$  orbital and unpaired. In a tetrahedral field, on the other hand, four are paired in the lower energy  $e_g$  orbital and the remaining three unpaired in  $t_{2g}$ . Strong interactions between the ligands, such as steric or electronic effects, will weaken the formation of the higher coordination number octahedral coordination compound and favor the tetrahedral complex. Cobalt(II) forms a large number of tetrahedral coordination compounds compared to the other first row transition metal ions. This is in accordance with the fact that for  $d^7 \text{ Co}^{2+}$  the ligand field stabilization energies have the least adverse effect on the tetrahedral field relative to the octahedral field as compared to any other d-transition element ions with one to nine d electrons.

For the  $d^8 \text{ Ni}^{2+}$  ion in an octahedral coordination environment, six electrons are paired in the lower energy  $t_{2g}$  orbital and two unpaired in the  $e_g$  orbital, whereas in tetrahedral coordination compounds, four electrons remain paired in the lower energy  $e_g$  orbital with the other four in  $t_{2g}$ , of which two are paired. It will be noted that compared with Co(II), Ni(II) has one more electron in the low energy orbital (although it is paired) in a weak octahedral coordination environment, and in the tetrahedral symmetry one more electron (paired) in the higher energy orbital. The difference in the electronic configuration offers much more stabilization energy for Ni(II) in octahedral coordination compounds than the tetrahedral ones. This explains the existence of a much larger number of Ni(II) octahedral coordination compounds than those having other configurations. The different behaviour of Co(II) and Ni(II) in forming coordination compounds provides a chemical basis for the separation of the two metals.

The sulphate system occupies the most important place in the hydrometallurgy of cobalt and nickel. In sulphate solution cobalt and nickel exist as divalent hydrated ions, with solvent extraction of cobalt and nickel usually taking place through cation exchange, and consequently, acidic extractants, particularly AOPA are mostly widely used. These AOPA are di(2-ethylhexyl)phosphoric acid (DEHPA), 2-ethylhexyl-phosphonic acid mono-2-ethylhexyl ester (EH(EH)PA) and di(2,4,4-trimethylpentyl)phosphinic acid (DTMPPA, Cyanex 272). The separation ability of the above reagents for cobalt over nickel increases along the sequence, it is believed, because of increasing the steric hindrance.

### The Distance between Substituting Groups and The Phosphorus Atom

For the same kind of alkylphosphorous acids, it is obvious that the larger the bulk of the component groups the higher is the steric hindrance. In addition, Danesi and coworkers believed that as an oxyalkyl group is substituted by an alkyl one, the distance between the group and the phosphorus atom was shortened due to the elimination of the oxygen atom, and thus the steric hindrance was increased [2].

Some data quoted in that work [2] are not in harmony with this statement. One such example is the extraction ability of di(1,3,3-trimethylbutyl)phosphoric acid (denoted as I) and di(2,4,4-trimethyl pentyl)phosphinic acid (as II see Figure 1) for cobalt and nickel.

The extraction equilibrium constants,  $K_{\text{ex}}$  of Co(II) and Ni(II) as extracted with I were,  $5.6 \times 10^{-6}$  and  $1.5 \times 10^{-6}$ , and with II were  $6.0 \times 10^{-8}$  and  $1.6 \times 10^{-10}$ , respectively for formation of  $\text{CoA}_2\text{.H}_2\text{A}_2$ , and  $\text{NiA}_2\text{.2H}_2\text{A}_2$ . The ratio  $K_{\text{ex(Co)}}/K_{\text{ex(Ni)}}$  is 3.7 and  $3.8 \times 10^2$ , for I and II, respectively, and thus the separation factor of II over I is greater than  $10^2$ . If one takes account of the steric hindrance only in terms of bulk of the substituting groups and their distance from the central ion in the AOPA, these two acids should have similar steric effects.

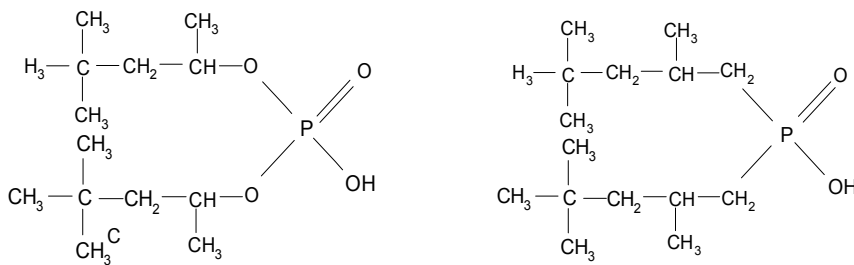
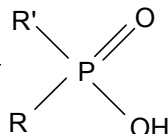


*Figure 1. Di(1,3,3-trimethylbutyl)phosphoric acid (I) and di(2,4,4-trimethyl pentyl) phosphinic acid (II).*

The covalent radii of O and C are 74pm and 77.2pm, respectively. The bond length of P-O on average is 162 pm and that of P-C is 185 pm, respectively, therefore, the distance of the bulk of the substituents from the central ion in complexes is only marginally different, and the bulk of the two substituents are also similar. The other factors determining the value of  $K_{ex}$ , such as partition coefficients of the extractants and the extracted species are also not expected to be so different. The large difference in separation factor of cobalt over nickel, or the ease of conversion of the octahedral to the tetrahedral cobalt complex in case II should not be attributed to the distance between the central ion and the substituting groups. In order to obtain a sound explanation for this large difference in the extraction abilities of I and II, a close look at the structure of the compounds is necessary.

### The Bond Angle and The Steric Hindrance

OPA's coordinate either their two oxygen atoms to the central ion or one to the central ion, with the second forming a hydrogen bond with another OPA molecule. However, the ligand cannot



rotate around the ligand-central ion  $\sigma$  bond freely. The bulk of the substituents and the angle  $\Delta RPR'$ , where R and R' represent the alkyl substituents, are the main factors governing the steric hindrance of the acid molecules. The angle  $\Delta RPR'$ , the dihedral angle between the R-P-R' plane and the O-P-O' plane of the acid, the electrostatic point charge of the P and the two O atoms of the aforementioned three commercial AOPA have been calculated by use of the Sybyl program. Some of the results obtained are shown in Table 1.

*Table 1.  $\Delta RPR'$ , dihedral angles and charges of atoms in alkylphosphorous acids,  $R(R')P(O')OH$ .*

Extractants	Groups*		$\Delta RPR'$ degree	Dihedral angle degree	charge		
	R	R'			P	O	O'
DEHPA	OEH	OEH	104.68	90.18	0.161	-0.345	-0.772
EH(EH)PA	OEH	EH	115.65	91.19	0.028	-0.367	-0.794
DTMPAA	TMP	TMP	120.09	89.48	0.092	-0.393	-0.814

\*OEH = oxy-2-ethylhexyl, EH = 2-ethylhexyl, TMP=2,4,4-trimethylpentyl.

It can be seen from the calculation results that the direct bonding of an alkyl group to P, increases the angle  $\Delta RPR'$  and the charges on the two O atoms, but hardly affects the value of the dihedral angles, which are all nearly  $90^\circ$ .

When an OPA molecule coordinates to a metal ion, these parameters calculated in the free state will certainly undergo change, but some inferences may be deduced from the calculated results.

- (1) When two such acid molecules coordinate to the central ion in a square planar configuration (*i.e.*, in an octahedral configuration), all the four substituting groups extend into a space nearly vertical to the oxygen coordination plane (*i.e.*, X-Y plane). The hindrance along z and -z direction is expected to rise with an increase of the  $\Delta RPR'$  angle as well as the bulk of R and R'.
- (2) When two such acid molecules coordinate with tetrahedral symmetry, the substituting groups extend into two different spaces, the central planes of which are almost perpendicular, then the interaction between the substituted groups should be very weak, no matter what the  $\Delta RPR'$  is.

### **Configuration Change of Extract and Steric Hindrance**

In the literature [1,2] the extraction constant  $K_{ex}$  is taken as a measure of steric hindrance, but  $K_{ex}$  does not only reflect steric hindrance, it is also dependent on the acidity of the OPA, the partition coefficient of the reagent itself and the extracted metal complexes, and even on some other factors. For the extraction of cobalt and nickel the steric effect of the OPA mainly causes a change in the configuration of the cobalt extract. Therefore, the equilibrium between the tetrahedral and octahedral configuration complexes could much more directly reflect the steric effect of the extractants. Data in Table 2, which were determined earlier in this laboratory [3,4], show that the trend of  $\Delta RPR'$  is in good accord with the thermodynamic parameters of the configuration equilibrium of the cobalt tetrahedral and octahedral extracts. In a neutral octahedral configuration, four oxygen atoms from two coordinated AOPA are in the same plane (*i.e.*, X-Y plane), the other two neutral ligands, which usually are water molecules, are aligned alone the Z axis. The IR spectra of nickel extracts demonstrate a strong water absorption peak, which reveals a high water content in the extract [3,4].

As aforementioned, for the  $d^7$   $Co^{2+}$  the ligand field stabilization energies have the least adverse effect on the tetrahedral field relative to octahedral field. The value of  $\Delta G^\circ$  for the equilibrium between the octahedral and tetrahedral configuration decreases with increasing  $\Delta RPR'$  value, while the value of  $\Delta S^\circ$  increased significantly, and so the latter may reflect more directly the effect of the steric hindrance.

*Table 2.  $\Delta RPR'$  and the thermodynamic parameters of tetrahedral and octahedral equilibrium of extracted cobalt complexes.*

Extractant	$\Delta RPR'$ degree	$\Delta G^\circ$ kJ/mol	$\Delta H^\circ$ kJ/mol	$\Delta S^\circ$ J/mol · K
DEHPA	104.68	0.638	66.1	221
EH(EH)PA	115.65	-10.1	63.2	245
DTMPPA	120.09	-15.6	124	459

### **The Effect of Electron Density of Donor Atoms**

The steric effect of OPAs is not the only factor determining the configuration of the cobalt extracts. The electron density of the donor oxygen atom in the OPA is, in some cases, an even more important factor. The calculated charge on the oxygen atoms in Table 1 increases along the series of phosphoric acid, phosphonic acid, and phosphinic acid. The charge on the oxygen atom in the P-OH group will be significantly increased with increasing dissociation of the  $H^+$ . It is obvious that the higher the oxygen negative charge on the POH group, the weaker is the acidity.

The negatively charged donor atoms around the central ion repel one another. This, just as for steric hindrance, will destabilize complexes of high coordination number. The fact is that weak ligands with high negatively charged donor atom, even in the presence of only a small steric effect likely to form tetrahedral coordination compounds with Co(II) rather than octahedral ones. Further evidence supporting this statement is the fact that anionic ligands, such as  $\text{Cl}^-$ ,  $\text{SCN}^-$ ,  $\text{Br}^-$ ,  $\text{I}^-$ , form tetrahedral coordination compounds with cobalt, but no stable octahedral coordination compounds have been detected.

The electron density of the oxygen atoms in organophosphorous acids is determined by the electron withdrawing ability of the substituting groups. The replacement of oxyalkyl groups with weaker electron withdrawing alkyl groups results in an increase in the electron density on the oxygen atoms of the  $\text{P=O}$  and  $\text{POH}$  groups. When a metal coordination compound is formed with these ligands, there is an energy balance between the enhancement of donor strength of the ligand and the strengthening repulsive interaction between the donor atoms.

This energy balance favours the extracted tetrahedral coordination compounds of cobalt(II) over the octahedral ones, because of the inherent low degree of stability of the octahedral coordination configuration. The higher oxygen electron density in an OPA results in a higher ratio of the tetrahedral to octahedral configuration in the extracted compounds. There is another reason for the increase of the ratio along the sequence of dialkylphosphoric acid, alkyl-phosphonic acid mono-alkyl ester and dialkyl phosphinic acid. The cobalt tetrahedral complexes contain no water (as demonstrated by the IR spectra [3,4]) and are more lipophilic than the octahedral extracts, and, therefore, have higher partition coefficients between the organic and aqueous phases. The increase in the proportion of the cobalt tetrahedral complexes increases the extractability, and partly compensates for the decrease of extraction caused by the reduction in the acidity of the AOPA along the above sequence. Therefore, the cobalt extraction equilibrium constants are only slightly decreased, as shown in Table 3. This different behaviour of the two metals results in an increase of the separation factor of cobalt over nickel along the same sequence.

*Table 3. Extraction constants of cobalt and nickel with alkylphosphorous acid<sup>#</sup>*

Extractants	$pK_a^*$	$K_{\text{ex(Co)}}$	$K_{\text{ex(Ni)}}$	$K_{\text{ex(Co)}} / K_{\text{ex(Ni)}}$
DEHPA	3.57	$5.50 \times 10^{-6}$ ( $4.3 \times 10^{-6}$ )	$1.10 \times 10^{-6}$ ( $2.2 \times 10^{-6}$ )	5(2.2)
EH(EH)PA	4.10	$1.07 \times 10^{-6}$ ( $3.6 \times 10^{-7}$ )	$1.51 \times 10^{-8}$ ( $1.7 \times 10^{-8}$ )	71(21)
DTMPPA	5.05	$1.66 \times 10^{-7}$ ( $6.0 \times 10^{-8}$ )	$2.00 \times 10^{-10}$ ( $1.6 \times 10^{-10}$ )	830 (380)

# Data in the brackets are from [2], others were determined in this laboratory.

\* In 75% ethanol [5].

## ACKNOWLEDGEMENTS

The author deeply thanks Associate Professor Xie Guirong in the Division of Computer Application of the Institute of Chemical Metallurgy, for the helping in operation of the Sybyl program. This work was supported by National Nature Science Foundation of China (No. 50074028; 29836130).

## REFERENCES

- Y. Chenye, X. Qingren, Y. Shengang, L. Haiyan, F. Hanzhen, W. Fubing and C. Wuhua (1988), *Solvent Extr. Ion Exch.*, **6** (3), 363 - 416.
- P.R. Danesi, L. Reichley-Yinger, M.L. Kaplan, E.P. Horwitz, and H. Diamond (1985), *Solvent Extr. Ion Exch.*, **3** (4), 435 - 452.
- L. Jinshan, Z. Tun, and C. Jiayong (1987), *Wuji Huaxue*, **3** (5), 7-15.
- L. Jinshan (1984), Master Degree Dissertation, Institute of Chemical Metallurgy, Chinese Academy of Sciences, Beijing.
- M. Cox, *Proc. Int. Solvent Extr. Conf. ISEC '83*, Denver, CO, pp. 268 - 269.



## MASS TRANSFER COEFFICIENTS OF SINGLE LIQUID DROPS IN EXTRACTION COLUMNS

Mohsen A. Hashem and J. Saien\*

Dept. of Chem. Eng., Faculty of Eng., El-Minia University, El-Minia, Egypt

\*Dept. of Applied Chem., University of Bu-Ali Sina, Hamadan, Iran

Hydrodynamic behaviour and mass transfer coefficients of single liquid drops have been measured in a 150 mm diameter column. The column was operated in two different modes as a spray tower and perforated plate tower. The systems employed were toluene/water for the hydrodynamic study and toluene/benzoic acid/water for the mass transfer study. Experiments were performed using different needle sizes to obtain drops of different diameter. The relationship between the drop velocity and the down flow of the continuous phase was examined experimentally. Mass transfer coefficients (MTCs) have been measured for single liquid drops rising through nonflowing and flowing water and have been compared with the coefficients measured for free rise conditions in an empty column. The MTCs were determined as a function of drop size, mass transfer direction, compartment height and down flow of the continuous phase.

From the data obtained, it is concluded that the drop size is a key variable affecting hydrodynamics and mass transfer processes. The drop velocities were found to decrease as down flow rate of continuous phase increased. The effect of continuous phase velocity on the MTC is significant with a slight increase in drop size occurring with increasing flow rate. The degree of enhancement of the dispersed phase film coefficient due to the presence of plates has been ascertained. Finally the coefficients for mass transfer direction from the dispersed phase into the continuous phase ( $d \rightarrow c$ ) are slightly higher than that for the opposite direction, ( $c \rightarrow d$ ).

### INTRODUCTION

In the field of solvent extraction processes various types of equipment have been developed during the last few decades. Therefore, the user is faced with a critical choice between contactors and most of the time has to decide according to subjective criteria. Nowadays, various extractors that are operated with and without a supply of mechanical energy are available in industry. Spray and perforated-plate (sieve plate) columns are commonly used in commercial liquid-liquid extraction systems. In these towers many drops are formed simultaneously and rise (or fall) in a swarm.

One of the ways to increase the mass transfer rates between the dispersed and the continuous phase is to provide for frequent coalescence and redispersion of the drops especially for the systems which show high internal circulation in the drop during formation at orifice or nozzles [1]. Perforated plate extraction towers are unique in that they provide repeated coalescence and redispersion for the drops and offer the advantage of cross flow of the continuous phase in addition to yielding high extraction coefficients with practically no axial mixing. The perforated plate columns may be considered as a series of short spray columns arranged one above the other. In practice, however, there are numerous applications of liquid-liquid extraction where perforated columns are preferred [2].

The present work aims at the prediction of mass transfer rates from single liquid drop to a continuous phase and investigates the effect of drop size, mass transfer direction, height of compartment and continuous phase velocity on the mass transfer coefficients of single liquid drop in a perforated plate (sieve-plate) and spray columns. Since knowledge of particle velocity is of fundamental importance for the description of mass transfer process, it is necessary to consider some aspects of the fluid mechanics of a single particle in free motion through a continuous fluid phase. Hence, the relevant hydrodynamics to mass transfer consideration are first reviewed briefly, with respect to drop size and terminal velocity because the primary focus of this paper is on mass transfer of a single liquid drop.

## EXPERIMENTAL

### Systems Tested

The systems investigated in this work were, toluene / water for the hydrodynamic studies and toluene / benzoic acid / water for the mass transfer studies. Solute concentration was determined by using a spectrophotometer (UV-1601 Shimadzu). The organic liquid were special-grade chemicals and were used without further purification. The physical properties of the system used (toluene / water) are as following:  $\rho_c = 998 \times 10^3 \text{ g/m}^3$ ,  $\rho_d = 862 \times 10^3 \text{ g/m}^3$ ,  $\mu_c = 0.00098 \text{ g/ms}$ ,  $\mu_d = 0.00059 \text{ g/ms}$ ,  $\gamma = 34 \text{ mN/m}$ , where  $\gamma$  interfacial tension,  $\rho_c$ ,  $\rho_d$  density of the continuous and dispersed phase and  $\mu$  its viscosity, respectively.

### Single Drop Apparatus

The experimental apparatus were essentially the same as described in a previous paper [3]. A summary of column details is given in Table 1. Main parts of the apparatus consisted of Perspex extraction column 0.150 m diameter, a glass funnel for sample collection and one of several sizes of glass capillary for drop formation. The rising time of the drops through given distance was measured with a stopwatch and the equivalent spherical drop diameter,  $d$ , was calculated knowing the flow rate and counting the number of drops formed in unit time.

*Table 1. Perforated column details.*

Column diameter, mm	150
Plate hole diameter, mm	5
Number of holes	37
Plate thickness, mm	3
Variable plate spacing, mm	20, 40, 60
Area of perforations, %	47

## Experimental Procedure

Prior to the commencement of measurements the apparatus was thoroughly cleaned and the system run to achieve saturation of the phases. The column was filled with the aqueous phase (distilled water) before the solvent (dispersed phase) is fed. Rotameters on the lines to and from the column enabled accurate flow settings and adjustment to be made thus ensuring that balanced flows were rapidly achieved and then maintained. A positive displacement pump was used to introduce the organic phase into the bottom of the column. Experiments were performed using different glass needles to obtain drops of different size. At least 300 drops were timed for each run. This was considered long enough for steady state conditions to be achieved [4]. Drops were spaced more than 30 mm apart typically, sufficient to avoid interactions according to Skelland [5]. In the perforated plate column, the droplets leaving the plates were allowed to rise a measured distance through the aqueous phase before being collected by suction through a small inverted funnel. The interfacial area in the funnel was kept small by occasionally pulling the drops into a pipette. After each experiment the column was thoroughly cleaned with decontaminating agent (Decon 90) to prevent the problem of contamination.

## Interpretation of Data

The overall mass transfer coefficients for drops of known size may be measured by passing solvent drops of known composition through an aqueous phase of known composition and collecting drops in an inverted glass funnel at the top of the column [6]. Analysis of solvent drops after passage through the column in a known time allows an overall time-averaged mass transfer coefficient, ( $K_{od}$ ), to be calculated from the following equations:

$$(C_o - C_i) / (C^* - C_i) = (1 - \exp(-6 K_{od} t / d)) \quad (1)$$

$$K_{od} = -(d / 6 t) \ln(1 - E) \quad (2)$$

where  $E = (C_i - C_o) / (C_i - C^*)$  and  $C_i$  is the inlet and  $C_o$  outlet solvent concentration, and since there was no solute initially in the water, the drop concentration in equilibrium with the aqueous phase,  $C^* = 0$ .

## RESULTS AND DISCUSSION

### Hydrodynamics

#### *Terminal velocities of single drops*

The experimental terminal velocities for toluene/water system are plotted versus drop diameter in Figure 1. Also shown are the terminal velocities for the drops raising singly as predicted by the correlations of Grace [7] for comparison with measured values. The terminal velocity is observed to increase with increasing droplet diameter. The reasonable agreement indicates that all drops in this work experienced some internal circulation.

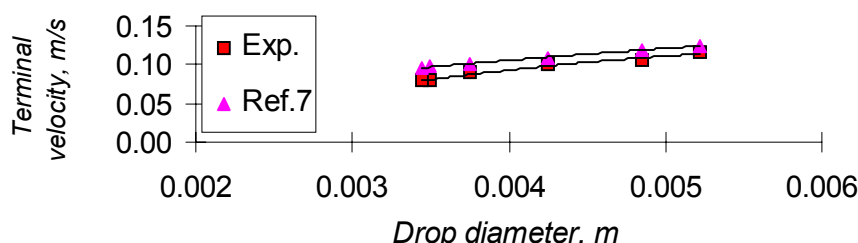


Figure 1: Terminal velocity versus drop diameter.

### **Effect of continuous phase velocity**

Figure 2 shows the profile of down flow of the continuous phase against the velocity under various flow rates conditions. The drop velocity decreases as the down flow rate increases as expected.

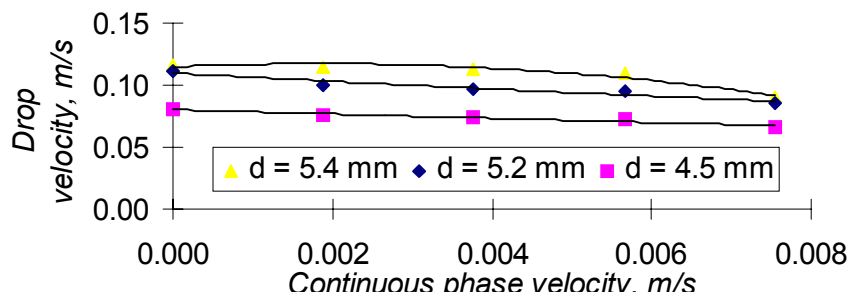


Figure 2: Effect of continuous phase velocity on drop velocity.

### **Mass Transfer**

#### **Spray and perforated columns**

Figure 3 shows the mass transfer coefficient for spray and perforated columns. The mass transfer coefficient in the presence of a sieve plate is higher than that without plates. This is due to the fact that during the operation of a spray column the use of continuous phase cause convection currents through the column leading to axial mixing in that phase. This reduces the extraction rate because of the deviation from true counter current behaviour. In a sieve plate contactor the distortion of the drop by direct contact with the edge of the plate holes during the passage disturbs the concentration profile inside the droplet and increases the mass transfer coefficient. The enhancement of up to about 80 % presumed due to the influence of plates is far greater than the value of 30 % obtained in the absence of plates. The results obtained are in qualitative agreement with observations of other investigators [8].

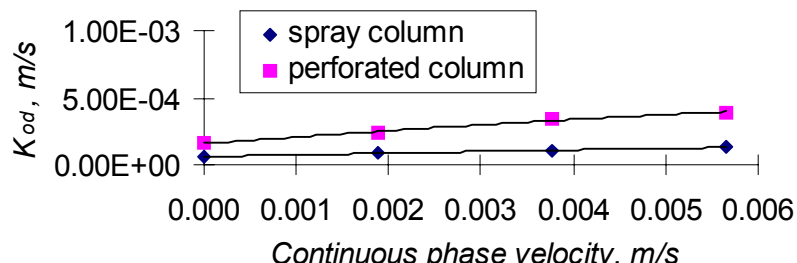


Figure 3: Mass transfer coefficient in spray and perforated plate column.

### **Effect of drop size and direction of solute transfer**

Figure 4 shows the dependence of the average mass transfer coefficient on drop size and direction of the mass transfer. The coefficients of mass transfer from the continuous to the dispersed ( $c \rightarrow d$ ) appear to be smaller than those obtained for the opposite direction of transfer ( $d \rightarrow c$ ). The difference in the coefficient is, however, small with slight increase in drop size from  $d \rightarrow c$ . Direct comparison of the results is difficult owing to the variation of drop size with direction of solute transfer. With solute transfer from  $d \rightarrow c$ , the drop size increased probably due to changes in interfacial tension. In addition the mechanism of mass transfer is known to be dependent on drop size, with the mass transfer mechanism varying from molecular diffusion for very small drops, which behave as a rigid spheres, to the development of internal droplet circulation, oscillation and turbulent eddy transfer mechanisms as the drop size is increased.

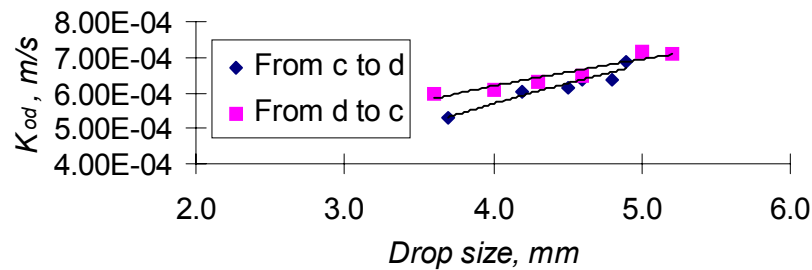


Figure 4 : Dependency of the MTC on drop size and direction of solute transfer.

### Effect of continuous phase velocity

The effect of the continuous phase velocity on the mass transfer coefficient was found to be significant [9] with only a slight increase in the drop size occurring with increasing the continuous phase velocity. The enhancement factor ( $E$ ), defined as the ratio of mass transfer coefficient at a given value of down flow to that at zero down flow,  $K_{od}/K_{odo}$ , as a function of continuous phase velocity (Figure 5) shows how increase of the continuous phase velocity increases the ratio. The study of the continuous phase velocity was also useful in that it enable a comparison between the unsteady state and the stationary phase methods for single liquid drops. The obtained results were in good agreement with those of other workers [10-11]. The effect of down flow on the dispersed phase mass transfer coefficient is associated directly with movement of drops through holes. Other important effects are obtained by reducing drop relative velocities [12] and increasing in contact time leading to reduction in  $k_d$  and a change in the product  $K_d t / d$  which affects the fraction extraction. The main benefit is the enhancement of mass transfer through the droplet/continuous phase interface as demonstrated by other investigators [13-15].

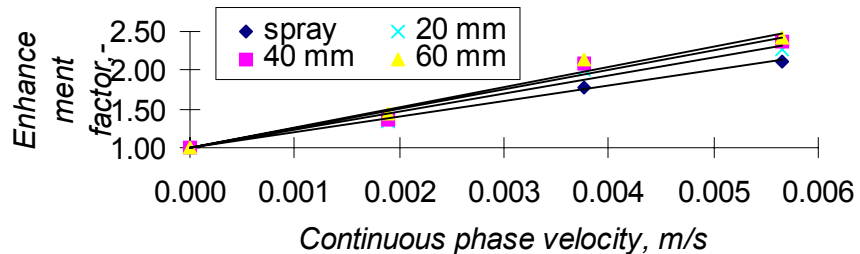


Figure 5: Enhancement factor vs. continuous phase velocity in perforated plate column.

### Effect of compartment height

The mass transfer coefficients slightly increase by increasing the height through which drops rise after leaving the plate (Figure 6). This may be due to the period of time needed to reach maximum velocity after leaving a plate. For liquid-liquid extraction, it can be concluded that efficiencies in the order of 70 % to 80 % are normally obtained for a perforated plate. The degree of enhancement of the dispersed phase film coefficient due to the presence of plates has been ascertained. The experiments using variable rise heights indicate that most of the mass transfer during rise is important and the mass transfer during formation is not dominant. A common plate design with a free area of 42 % was used throughout the experiments.

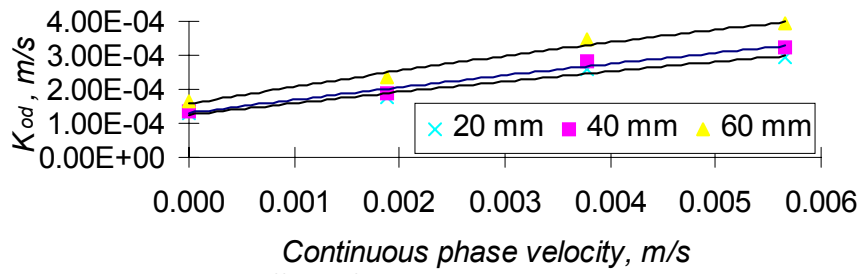


Figure 6 :Effect of compartment height on mass transfer coefficients.

## CONCLUSIONS

The drop size is a key variable affecting hydrodynamics and mass transfer processes. The drop velocity was found to decrease as down flow rate of continuous phase increased. The mass transfer coefficient in the presence of plates is higher than that without plates. The coefficients for mass transfer from the dispersed phase into the continuous phase direction ( $d \rightarrow c$ ) are slightly higher than that for the opposite direction of transfer ( $c \rightarrow d$ ). The effect of continuous phase velocity on the mass transfer coefficient is significant with a slight increase in the drop size occurring with increasing flow rate. The mass-transfer coefficients slightly increased by increasing the height through which drops rise after leaving the plate.

## REFERENCES

1. G. S. Laddha and T. E. Degaleesanb (1976), Transport Phenomena in Liquid Extraction, Chap. 9 and 11, Tata McGraw-Hill Publishing Co. Ltd.
2. J. D. Thornton (1992), The Science and Practice of Liquid-Liquid Extraction, Oxford University Press, Oxford.
3. M. A. Hashem and A. A. El-bassuoni (2001), *Proc. First Int. Conf. Computational Methods in Multiphase Flow*, University of Central Florida, USA.
4. J. C. Godfrey and M. J. Slater (1991), *Trans. IChemE.*, **69** (A) (3), 130 -141.
5. A. H. P. Skelland and N. C. Vasti (1985), *Can J. Chem. Eng.*, **63** (6), 390 - 398.
6. M. J. Slater, M. H. I. Baird and T. B. Liang (1988), *Chem. Eng. Sci.*, **43** (2), 233-245.
7. J. R. Grace, T. H. Wairegi and T. H. Nguyen (1976), *Trans. IChemE.*, **54** (3), 167-173.
8. B. Hoting, M.Qi and A. Vogelpohl (1993), *Proc. ISEC'93*, Society of Chemical Industry, London.
9. H. Haverland and M.J. Slater (1994), Liquid Extraction Equipment, M. J. Slater and J. C. Godfrey (eds.), J. Wiley and Sons, Chapter 10.
10. M. A. Hashem (2000), *Proc. 3<sup>rd</sup> Int. Conf. RETBE'2000*, Faculty of Eng., Alexandria University, Egypt.
11. Ingham, M. J. Slater and J. Retamales (1995), *Trans. IChemE.*, **73**(A) (7),492-496.
12. J. C. Godfrey, D. A. Houlton, S. T. Marley, A. Marrocchelli and M. J. Slater (1985), *Chem. Eng. Res. Des.*, **66** (5), 445-454.
13. M. A. Hashem and M. J. Slater (1996), *Proc. Fluid Mixing 5 Conference*, IChemE., University of Bradford, UK.
14. W. Kowalski and Z. Ziolkowski (1981), *Int. Chem. Eng.*, **21**, 323-327.
15. G. H. Sedahmed, A. M. El-Kayar, H. A. Farag and S. A. Noseir (1996), *Chem. Eng. J.*, **62**, 61-65.



# THE DEVELOPMENT OF MATHEMATICAL CORRELATIONS FOR MASS TRANSFER OF FILM CONTACTING OF TWO AQUEOUS PHASES

Jamaliah Jahim and M. J. Slater\*

Department of Chemical & Process Engineering, Universiti Kebangsaan Malaysia,  
Bangi, Malaysia

\*Department of Chemical Engineering, University of Bradford, West Yorkshire, UK

The use of a thin film-type contactor appeared sensible and might be applicable to aqueous two-phase systems (ATPS), as well as many other liquid-liquid systems when the phase ratio is extreme. In drop contactors at high phase ratio (continuous/dispersed) there are operating difficulties with low hold up and entrainment of many small drops. A study of a thin flowing film of one phase exposed to the other was made and the kinetics of mass transfer using such film contact were investigated. The experiments reported here concern PEG 3350 (light phase)/Na<sub>2</sub>SO<sub>4</sub> (heavy phase) with bovine serum albumin (BSA) plus  $\alpha$ -amylase dissolved in the heavy phase. The heavy phase was allowed to flow down a sloping metal channel in a bath of light phase. Mass transfer occurred from the heavy phase; samples of heavy phase were collected at the end of the channel for different flow rates and slope angles. Data of mass transfer coefficients have been interpreted using various empirical equations for mass transfer across a horizontal, vertical and sloping system. A correction factor to describe the enhancement of both film mass transfer coefficients caused by rippling or/and internal circulation in the film has been used.

The best fit correlation for BSA that is for single resistance in the top phase was found to be an equation derived by Baird, whilst for two-phase resistance with  $\alpha$ -amylase for mass transfer in the top phase and bottom phase, the combination of Baird [1] and Higbie [2] equations was found to give good agreement. Correlations for predicting overall effective diffusivity, D<sub>oe</sub> for both systems have also been made but do not give satisfactory results since the range of D<sub>oe</sub>/D<sub>m</sub> values is very large.

## INTRODUCTION

Aqueous two-phase systems (ATPS) have a great potential in future industries when the formation of two liquid phases that occurs can give the basis for analogies with liquid-liquid (organic-aqueous) extraction processes, which are quite common in chemical industries. These aqueous two-phase systems could become a suitable alternative for large scale processing of microbial products especially for the extractions concerning complex, polar and water-soluble products (antibiotics, sugars, glycolipeptides, etc.). Details of the use of such systems in downstream processing on a large scale have been published elsewhere [3-5].

Although the systems are capable of processing streams with small particulate material, it can be difficult to carry out solid-liquid separation on a large scale like centrifugation in the early stage of a protein recovery process [6]. Therefore, the removal of solids using ATPS can be integrated into a liquid-liquid separation step and the clarification steps can be combined with an initial purification. At present, ATPS are only successful on the laboratory scale, and are not widely used in large-scale industrial operations. The potential of commercial mixer-settler systems and centrifugal separators of various design for processing of large flow rates have been investigated by several authors in ATPS [4,5,7].

The separation on a pilot scale (1-20 kg ATPS) in the presence of microbial cells has been successfully demonstrated by continuous phase separation in a disk stack centrifuge and in a nozzle discharge disk stack centrifuge when they are compared with the settling under gravity [8]. Continuous countercurrent column extractions with ATPS have also recently been investigated. Sawant *et al.* and Pawar *et al.* studied a spray column (in which the PEG phase is dispersed into fine droplets) [9-11]. Bhawsar *et al.* have investigated the mass transfer and hydrodynamics in a pulse sieve plate column [12]. Studies on York-Scheibel columns with alternating zones of mixing and coalescence have been reported by Pawar *et al.*[11]. This simple, effective pilot-plant scale equipment is of great interest for industrial extraction.

In this work, the use of ATPS for the recovery and separation of proteins such as  $\alpha$ -amylase and bovine serum albumin (BSA) was investigated. The work covers the experiments to prepare the equilibrium diagram for the proteins since no information on this has been published. The equilibrium diagram is used to determine the partition coefficients in the studied systems. A novel preliminary study is focused on the kinetics of the mass transfer behaviour in an inclined film flow channel using ATPS. The mass transfer experiments that involve the estimation of film thickness and contact time and determination of degree of extraction to be able to calculate the experimental mass transfer coefficients of the system.

## MATERIAL AND METHODS

### Chemicals

PEG with an average molecular weight of 3350 was purchased from Sigma Ltd. Co., England while  $\text{Na}_2\text{SO}_4$  was purchased from BDH Chemicals Ltd, Poole UK. Both chemicals were analytical grade. BSA and  $\alpha$ -amylase produced by bacteria, *B. subtilis* were industrially prepared and supplied by Sigma Ltd. All stock of the solutes was stored at temperature below 4°C. Enzyme  $\alpha$ -amylase was supplied freeze-dried in a mixture of starch powder while BSA was supplied in a solution with 8.5% of sodium chloride.

### Preparation of Phase Systems

The pre-mixed immiscible PEG-rich phase and salt-rich phase solutions were prepared to be used in all kinetic experiments. These phases were made by adding weighed amounts of PEG 3350 and  $\text{Na}_2\text{SO}_4$  to the amount of water that gave the required total system of 7.6% mass PEG 3350/ 9.7% mass  $\text{Na}_2\text{SO}_4$ /82.8% mass water. The phase diagram of the PEG3350/ $\text{Na}_2\text{SO}_4$ /water system has been prepared by Snyder and co-workers [12]. The mixture was stirred by means of a stainless steel disk turbine attached to a stirrer RZR-200 (Heidolph, Germany), for about 2-3 hours to equilibrate. The mixture was left overnight in the separating funnel to allow settling at room temperature. The two phases were then separated and they were filtered to obtain clear phases free from any particles.

### System Compositions and Physical Properties.

The phase composition and the physical properties of viscosities and densities based on the data prepared by Snyder are shown in Table 1. They used the analysis technique using high-performance liquid chromatography (HPLC)-gel chromatography to determine compositions of the ATPS. The determination of density was repeated and the results obtained were little

different from Snyder's data [12]. Density measurements were carried out using a vibrating U-tube densitometer DMA 35 (Anton Paar, Austria) at  $25 \pm 0.5^\circ\text{C}$ . The reproducibilities of the densities of the bottom phase and top phase were estimated to be  $1125 \pm 5 \text{ kg m}^{-3}$  and  $1071 \pm 5 \text{ kg m}^{-3}$ , respectively.

*Table 1. Composition, density and viscosity of the phases at  $20^\circ\text{C}$  on PEG3350/ $\text{Na}_2\text{SO}_4$  tie line [12].*

Tie line	Top phase			Bottom phase		
	PEG/Salt/Water (%w/w)	Viscosity $\mu/(\text{Pa.s})$	Density, $\rho/(\text{kg/m}^3)$	PEG/Salt/Water (%w/w)	Viscosity $\mu/(\text{Pa.s})$	Density, $\rho/(\text{kg/m}^3)$
F	23.6/4.9/71.5	0.0134	1076.6	1.3/12.1/86.7	0.0015	1106.6

### Enzyme and Protein Assay

The determination of  $\alpha$ -amylase using  $\alpha$ -Amylase Diagnostic® kit is based on hydrolytic activity or catalytic activity of  $\alpha$ -amylase in the sample. One unit of  $\alpha$ -amylase is defined as the millimolar absorptivity of para-nitrophenol (PNP) at 405 nm degraded from hydrolysis of substrates (ET-G<sub>7</sub>PNP) per minute at  $37^\circ\text{C}$ . The procedure to measure protein using Protein Assay Kits supplied by Sigma Ltd. Co. is based on Peterson's modification of the micro-Lowry method. Absorbance is read at suitable wavelength between 500 nm to 800 nm and protein concentration is determined from a calibration curve using BSA as standard.

### Mass Transfer Experiments Using a Sloping Channel.

The experiments were performed in a square glass tank with capacity of 50 L of top phase as shown in Figure 1. The mass transfer coefficients were measured for the flow of thin film on the sloping channel (length between 0.25-0.4 m) at room temperature of  $25 \pm 1^\circ\text{C}$ . The lower end of the channel was held with a wire mounted to a metal strip which was placed across the tank, while the other end was plugged into a slot on a supporting stand for particular required angles. Five different flow rates controlled by means of a syringe pump were used; 16, 20, 26, 28 and 36  $\text{mm}^3/\text{s}$ . The initial concentration of both solutes were 6024.0 U/L (slope  $14.5^\circ$ ) and 6576.2 U/L (slopes  $23.7^\circ$  and  $45^\circ$ ) for  $\alpha$ -amylase and 3790.64 mg/L for BSA.

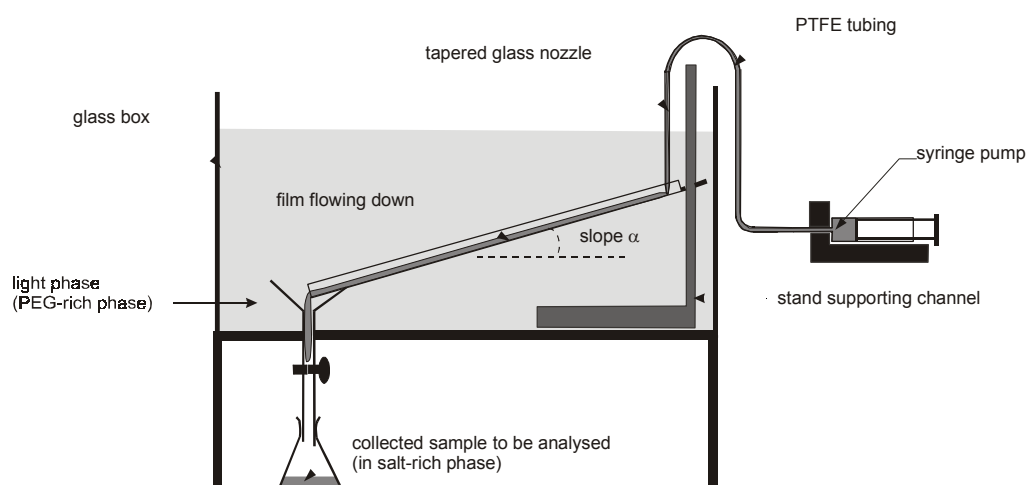


*Figure 1. Experimental set-up of flowing film on a sloping channel.*

The thickness of the film was calculated from the hold-up of the film. This was done by allowing the film to flow into a beaker that was placed next to the funnel collector for two minutes to obtain a steady flow. The channel was then moved quickly sideways using the holding wire, draining the flow into the funnel collector and at the exact moment the pump was turned off. When the film had drained off, the bottom phase plus some top phase was collected. The bottom phase was separated and weighed to obtain the volume by dividing the weight with the known bottom phase density. Knowing the wetted area of the channel, the mean film thickness can be determined. The width of the film was taken to be 4.5 mm, the width of the channel. The contents of protein and  $\alpha$ -amylase left in the bottom phase were analysed. This was done by letting the film flow to run for 2-3 minutes to reach steady state before the sample was taken. Samples collected were diluted before further analysis.

### **Calculations**

The degree of extraction, E was calculated using the equation defined as

$$E = 1 - (c_{\text{out}}/c_{\text{in}}) \quad (1)$$

where  $c_{\text{in}}$  is the concentration of the heavy phase at inlet flow and  $c_{\text{out}}$  is the concentration at the outlet flow. The overall mass transfer coefficient from the experiment can be calculated from

$$K_{\text{od}} = -h/t * \ln(1-E) \quad (2)$$

where h is the measured film thickness and t is the contact time of the film travelling from the inlet to the outlet of the flow.

The film thickness, h can be calculated from the mean of film thickness for laminar film flow given by Nusselt, for two-film liquid flow,

$$h = [3\mu Q/wg(\rho - \rho_c)\sin \theta]^{1/3} \quad (3)$$

where w is the width of the liquid film, Q is the liquid volumetric flowrate per unit width,  $(\rho - \rho_c)$  is the density difference for adjoining phases and  $\theta$  is inclination of the channel to the horizontal.

## **RESULTS**

The overall mass transfer coefficient,  $K_{\text{od}}$  is given as

$$1/K_{\text{od}} = 1/k_b + 1/mk_t \quad (4)$$

where  $k_b$  and  $k_t$  are film mass transfer coefficient for dispersed and continuous phases respectively.

The mass transfer coefficient for both films, dispersed in film form (bottom phase) and continuous (top phase) can be calculated using existing correlations that are for films flowing or rising on sloping, horizontal or vertical surfaces. For both films, a time-dependent process is assumed and diffusion coefficients are needed. The values of  $K_{\text{od}}$  found from these correlations were lower than those from the experiment if molecular diffusivity is used. Therefore the second term of effective diffusivity proposed by Handlos and Baron (1957), originally proposed for drops, here multiplied by a correction factor  $k_H$  was used to estimate the diffusivity due to the mixing in the film caused by rippling or wave motion at interface [14,15]. The effective diffusivity is defined as

$$D_e = k_H h u / 2048 [1 + (\mu_d / \mu_c)] \quad (5)$$

where  $u$  is velocity of the film and  $k_H$  is a correction factor which is adjusted so that overall mass transfer coefficients agree with results from experiment. The overall diffusivity,  $D_{oe}$  is given as

$$D_{oe} = D_M + D_e \quad (6)$$

Molecular diffusivity,  $D_M$  for  $\alpha$ -amylase and BSA is calculated using the correlation of Young-Carrodd-Bell [13] which was adapted from the Stokes-Einstein equation. The best correlation to be considered here is the correlation that has lowest value of  $k_H$  since high values may be unrealistic. In the comparison for the two-film system for  $\alpha$ -amylase, it was found that the combination model of Baird [1] for continuous phase and Higbie [2] for film or dispersed phase gave the lowest correction factor  $k_H=1$  at the lowest slope of the channel and lowest  $k_H$  at highest slope. For the results of the BSA system, where the resistance is in the continuous phase, the best equation fitted with the experiments found was by using the Baird equation [1]. The data are shown in Figure 2.

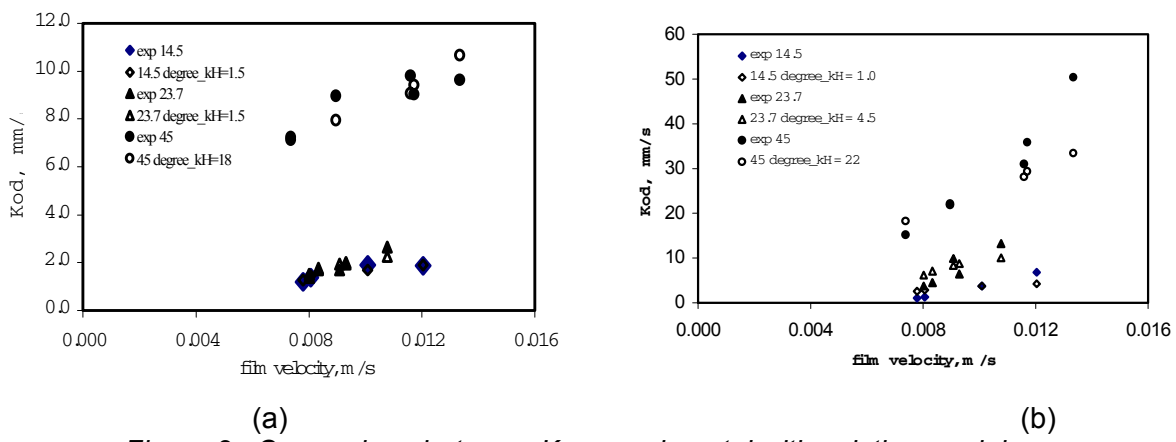


Figure 2. Comparison between  $K_{oe}$  experimental with existing model:  
 (a) for BSA (b) for  $\alpha$ -amylase.

The results also show that mass transfer coefficients of  $\alpha$ -amylase are higher compared to those found for BSA. There are marked increases for both  $\alpha$ -amylase and BSA at angle  $45^\circ$  with increasing velocity compare to those at lower angle at  $14.5^\circ$  and  $23.7^\circ$ . As the velocity of the film increases, the film thickness also increases, and perhaps more mixing within the film or at the interface.

### Empirical Correlation of Mass Transfer Coefficient

In an attempt to find empirical correlations for mass transfer in films, the forces that might affect the mass transfer process are gravity forces, interfacial shear stress, viscous forces, interfacial tension force and inertia forces. Large number of correlations have been tried using dimensionless numbers with regards to the mentioned forces with data from various organic-aqueous system, and the best correlations found were in the form of

$$D_{oe}/D_M = 1 + b \cdot Re^m [1 + a Eot^n] \quad (7)$$

where for  $D_{oe}/D_M \rightarrow 1$ ,  $a$   $Re \rightarrow 0$  and  $Eot \rightarrow 0$  for conditions with no rippling. The curve fitting between the experimental data and the empirical model was carried out using Microcal Origin® to obtain best fit constants of  $a, b, m$  and  $n$ .  $D_{oe}$  can then be calculated and used in calculating  $K_{oe}$  values. It was found that the exponents are unrealistically high, so the method of correlation is not satisfactory from a physical point of view.

## CONCLUSIONS

The application of ATPS in particular appears promising for biochemical separations, although few investigations of chemical engineering aspects have been made. Much work has been done on theoretical prediction of film thickness on sloping plates for laminar flow. There are only a few equations for turbulent flow. Some work has been done to model rippling on film surfaces (mainly gas/liquid) but the subject is complex and most correlations are empirical, and there is little agreement between them. Measurements of film thickness have been made in this work in a simple way and reasonable agreement with theory for laminar flow was found. According to Baird et al. [1], rippling occurs in laminar flow at Reynolds numbers between 6 to 500. No obvious agreement with correlations was found, therefore more work is required to determine the validity of the correlations. More accurate methods of film thickness measurement are desirable for liquid-liquid systems. Only when this work is done can mass transfer coefficients be better correlated.

## ACKNOWLEDGEMENTS

The author wishes to acknowledge the National University of Malaysia for the financial support during the study at the University of Bradford, United Kingdom.

## REFERENCES

1. M. H. I. Baird, A. Rohatgi and W. He (1988), *Chem. Eng. Res. Des.*, **66**, 122.
2. R. Higbie (1935), *Trans. Amer. Inst. Chem. Engr.* **31**, 365.
3. H. Hustedt, K. H. Kroner and N. Papamichael (1988), *Proc. Biochem.*, **23** (5), 129.
4. M.-R. Kula (1979), Applied Biochemistry and Bioengineering, L. Wingard and L. Goldstein (eds), Academic Press, New York, p. 71.
5. M.-R. Kula (1985), Comprehensive Biotechnology, A. Humphrey and C. L. Cooney (eds.), Vol. 2, Pergamon Press, p. 451.
6. J. G. Huddleston, S. O'Brien, H. Picard and A. Lyddiatt (1993), Solvent Extraction in Process Industries, D. Logsdail and M. J. Slater (eds.), Vol. 2, SCI, London, p. 1048.
7. K. Kroner, H. Hustedt, S. Granda and M.-R. Kula (1978), *Biotechnol. Bioeng.*, **20**, 1966.
8. T. Minuth, H. Gieren, U. Pape, H. C. Rath, J. Thommes and M.-R. Kula (1997), *Biotechnol. Bioeng.*, **55** (2), 339.
9. S. B. Sawant, J. B. Joshi and S. K. Sikdar (1990), *Biotechnol. Bioeng.*, **36**, 106.
10. P. A. Pawar, K. R. Jafarabad, S. B. Sawant and J. B. Joshi (1993), *Eng. Commun.*, **122**, 151.
11. P. A. Pawar, U. Parasu Veera, S. B. Sawant and J. B. Joshi (1997), *Can. J. Chem. Eng.* **75**, 751.
12. S. M. Snyder, K. D. Cole and D. C. Szlag (1992), *J. Chem. Eng. Data*, **37** (2), 268.
13. M. E. Young, P. A. Carroad and R. L. Bell (1980), *Biotechnol. Bioeng.*, **22**, 947.
14. R. E. Emmert and R. L. Pigford (1954), *Chem. Engng. Prog.*, **50**, 87.
15. S. Kamei and J. Oishi (1955), *Mem. Fac. Engng., Kyoto Univ.*, **17**, 277.



# THE EFFECT OF IONIC SURFACTANTS ON THE MASS TRANSFER AT THE LIQUID-LIQUID INTERFACE FOR A TOLUENE/WATER/ACETONE SYSTEM

**M. A. Mendes-Tatsis, M. Pursell, S. Tang and G. San Miguel**

Department of Chemical Engineering and Chemical Technology,  
Imperial College of Science, Technology and Medicine, London, United Kingdom

The study of the transfer of a solute across an interface between two immiscible liquid phases is fundamental in liquid-liquid extraction. When that transfer causes spontaneous interfacial convection (Marangoni convection) and/or when the system is "contaminated" by surfactants, theoretical predictions for the rate of solute transfer may become invalid.

In this work the transfer of acetone from toluene into water has been studied using a Schlieren optical system for the visualisation of the interface and a Mach-Zehnder interferometer to obtain measurements of concentrations close to the interface. The effect of the presence of soluble ionic surfactants in the system was found to decrease the total moles transferred per unit area when compared to the case of the "clean" system.

## INTRODUCTION

Mass transfer in liquid-liquid systems has been studied for many years and the knowledge acquired has been applied to the design of mass transfer contacting equipment such as liquid/liquid extractors [1]. This type of contactor is used successfully in various production processes such as in the extraction of metals from aqueous solutions, in the field of biotechnology and in the chemical and pharmaceutical industries and also in the treatment of effluents from the same plants.

Usually, industrial effluent streams are "soups" containing different chemicals and chemicals with surfactant properties. However, this is normally not taken into consideration in the design of contacting equipment where the system is considered "clean"; it is often assumed that the material to be extracted is the only one present in the "soup" and the only one being transferred.

Another commonly applied simplifying assumption is the exclusion of the role of the interface in the mass transfer process. Interfacial area and ways of maximising it are always given consideration but interfacial phenomena, which may be present, such as Marangoni phenomena, are usually ignored. However, for a fixed interfacial area, mass transfer rates may be increased if interfacial phenomena are taken into account, as has been well documented (e.g., [2-5]). It is, therefore, very important to get an accurate picture of the role played by the interfacial region in realistic systems. The interface acts not only as the boundary across which mass transfer happens but also where adsorption/desorption effects, from small concentrations of "minor" components in the "soup", occur which may cause or inhibit interfacial convection and therefore affect the mass transfer process.

Traditional mass transfer theories describe processes where ternary systems are involved but many times they fail when applied to industrial cases. In the case of liquid-liquid extraction, the European Federation of Chemical Engineers (EFCE) has proposed several ternary test systems so that an experimental database could be created against which theories could be tested. Although useful as a start, the test systems proposed are not fully representative of real industrial systems where, in most cases, more than one species undergoes mass transfer, most certainly in the presence of surface active impurities. The presence of surfactants in the systems is usually accepted as being detrimental to the mass transfer process (e.g., [1,6,7]), as their adsorption at the interface may create a barrier to the transfer of other species or dampen any interfacial movements. On the other hand, reports, which conclude that the adsorption/desorption of surfactants at an interface may produce Marangoni convection, which enhances mass transfer, have also been published [5,8].

The objective of this work is to study the interphase transfer of acetone from toluene into water for the cases when the interface is "clean" and when it is "contaminated" with soluble ionic surfactants, when the system is quiescent. Comparisons are made between the two systems using visual observations made with a Schlieren optical system and using quantitative results obtained with a Mach-Zehnder interferometer.

## EXPERIMENTAL SYSTEMS AND METHODS

The system toluene/acetone/water was chosen for this investigation for several reasons: (i) it has been selected by EFCE as a model ternary system and physical properties are easily available [9]; (ii) it has been part of previous investigations (e.g., [10-12]) and was found to be Marangoni unstable, contrary to predictions by Sternling and Scriven's stability criteria [13]; and (iii) its optical properties make it a good choice to be used with the apparatus employed in this study.

Two easily available ionic surfactants have been selected: sodium dodecyl sulphate (SDS), which is anionic, and dodecyl trimethyl ammonium bromide (DTAB), which is cationic.

The apparatus used for the experiments has been described in detail elsewhere [5]. It consists of a Schlieren system to obtain images which indicate the stability of the interfaces under study and a Mach-Zehnder interferometer to obtain interferograms. These interferograms have been obtained for planar interfaces for the toluene+acetone/water system and have been analysed to enable the calculation of the values of concentrations at different locations from the interface and at different times, from which concentration profiles were plotted.

Theoretical mass transfer predictions have been made for the ternary system, based on Fickian diffusion of the solute into water. The theoretical concentration profiles may be obtained from the solution of Fick's 2<sup>nd</sup> law [14]:

$$C_S = C_{Si} \operatorname{erfc} \left( \frac{x}{2\sqrt{D_S t}} \right) \quad (1)$$

where  $C_S$  is the concentration of solute at any distance  $x$  from the interface at time  $t$ .  $C_{Si}$  is the interfacial concentration, which in the case of a ternary system may be estimated through the solute partition coefficient.

Instead of discussing plots of concentration profiles for the different conditions, it may be preferable to show the integral mass transfer results, i.e., results in terms of the summation of the molar mass transferred at all the planes of reference in the phase, as opposed to transfer at a single plane of reference. The reason for this is that if the mass transfer rate closer to the interface is higher than that further away from the interface, then a comparison between the experimental concentrations measured at near the interface and their theoretical predictions may give a distorted result.

Therefore, the mass transfer results are presented in terms of the total moles of acetone transferred per unit area,  $M_S$ , which is given by the area under the corresponding curve of concentration,  $C_S$ , plotted against distance from the interface.

## EXPERIMENTAL RESULTS

### Toluene+Acetone/Water

Figure 1 shows the Schlieren image sequence for the transfer of acetone (0.8 M) from toluene (in the drop) into the continuous “clean” water phase. These images clearly show that interfacial convection started immediately after formation of the drop and lasted for several minutes, which is in agreement with similar results obtained in the literature (e.g., [10-12]).

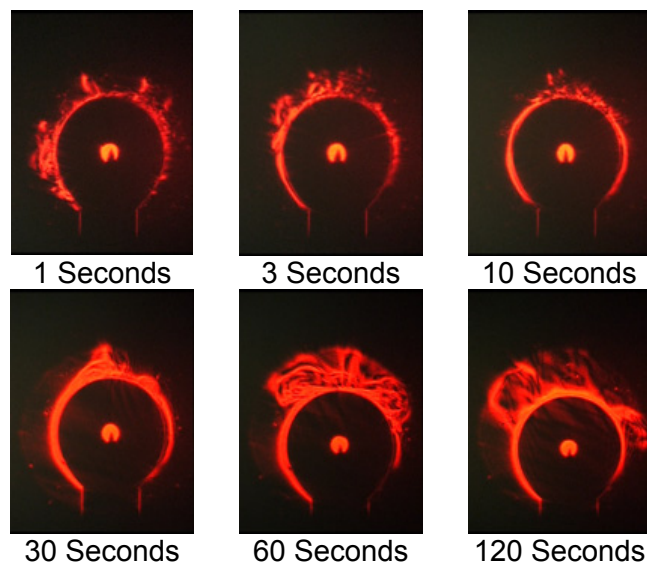


*Figure 1. Schlieren image sequence for the transfer of acetone (0.8 M) from the toluene drop into “clean” water.*

In Figure 2, the theoretical and the experimental results for the total moles transferred up to a distance of 6 mm from the interface are presented. A comparison of the two curves shows that the experimental results are in close agreement with those theoretically predicted by Fick’s 2<sup>nd</sup> Law. This is really unexpected from the Schlieren images presented in Figure 1, which show intense interfacial convection, usually indicating a higher mass transfer rate than theoretically predicted. Further work is necessary to investigate this result.

### Toluene+Acetone/Water +SDS

Experiments have been carried out to investigate the effect the addition of an anionic surfactant, SDS, to the water has on the interfacial stability and on the integral mass transfer of acetone into water.

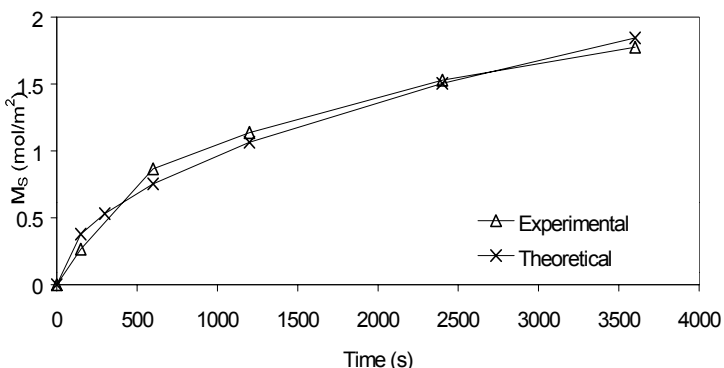


Figure 2. Comparison between experimental and theoretical values of the total moles of acetone transferred per unit area from toluene into “clean” water vs. time.

A Schlieren image sequence for the transfer of acetone (0.8 M) from toluene into water with SDS (0.05 g per 100 ml) is presented in Figure 3. It shows that the addition of SDS to the aqueous phase dampens interfacial convection that was present in the “clean” system shown in Figure 1.

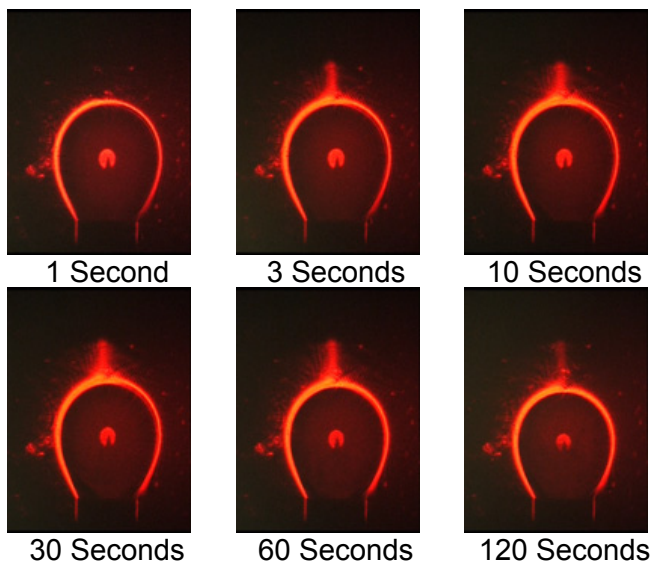


Figure 3. Schlieren image sequence for the transfer of acetone (0.8 M) from the toluene drop into water containing SDS (0.05 g/100 ml).

The plot of the total moles transferred per unit area vs. time for this case of transfer of acetone into water with the added surfactant SDS is shown in Figure 4. The addition of SDS to the aqueous phase decreases the integral mass transferred per unit area in comparison to the “clean” system, which is consistent with the observed damped interfacial convection in the Schlieren images. This is in agreement with the accepted idea that the presence of surfactants in a system decrease mass transfer rates.

#### Toluene+Acetone/Water +DTAB

Experiments have also been carried out to investigate the effect of DTAB, a cationic surfactant on the interfacial stability of the toluene+acetone/water system. Just like for the previous experiments the surfactant was added to the aqueous phase.

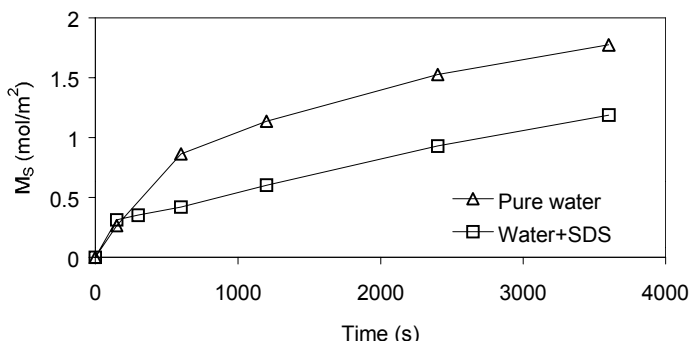


Figure 4. Total moles of acetone transferred per unit area from toluene into “clean” water and into water containing SDS (0.05 g/100 ml).

Figure 5 shows the corresponding Schlieren image sequence for the transfer of acetone from toluene in the drop into water with DTAB (0.05 g/100 ml). The effect of this cationic surfactant on the interfacial stability is found to be similar to that of the anionic surfactant, SDS, described above, *i.e.*, the interfacial convection is dampedened.

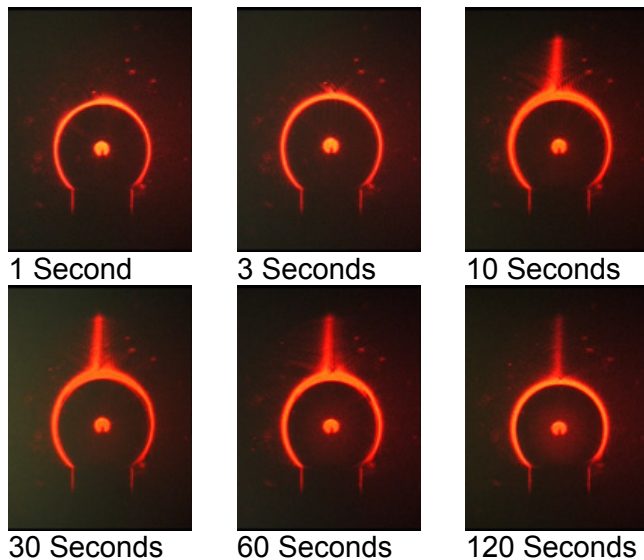


Figure 5. Schlieren image sequence for the transfer of acetone from the toluene drop into water containing DTAB (0.05 g/100 ml).

Figure 6 shows the change with time of the total moles of acetone transferred per unit area from the toluene to the water with the added surfactant DTAB as well as the curve for the transfer of acetone into a “clean” water phase. As for the case of the addition of SDS there is a decrease on the total moles transferred when DTAB is added to the water in comparison with the “clean” system. This is also consistent with the dampedened interfacial convection observed in Figure 5.

## CONCLUSIONS

Schlieren images and interferometric results have been presented for the transfer of acetone from toluene into “clean” water and into water “contaminated” with two different ionic surfactants. In the “clean” system mass transfer is accompanied by interfacial convection, which is not predicted by stability criteria but is in agreement with previous experimental work published. However, the interfacial convection observed does not have much effect on the

integral mass transferred in comparison with the theoretical prediction. This is unexpected and further work is under way to investigate this finding.

The effect of the addition of the ionic surfactants investigated is similar for both cases and it indicates a decrease in the total moles transferred per unit area when compared to the case of the “clean” system.

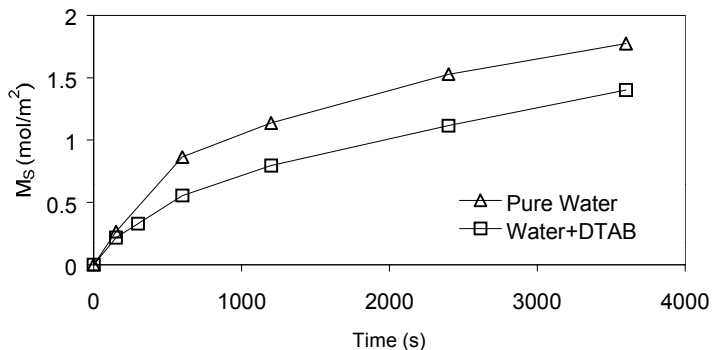


Figure 6. Total moles of acetone transferred per unit area from toluene into “clean” water and into water containing DTAB (0.05 g/100 ml).

#### ACKNOWLEDGEMENT

The authors gratefully acknowledge the financial support provided by EPSRC, under Grant No GR/M42848.

#### REFERENCES

1. J. C. Godfrey and M. J. Slater (1994), Liquid-Liquid Extraction Equipment, John Wiley & Sons.
2. H. Sawistowski (1971), Recent Advances in Liquid-Liquid Extraction, C. Hanson (ed.), Pergamon Press, pp. 293-365.
3. J. C. Berg (1972), Recent Developments in Separation Science, Vol. 2, CRC Press, Boca Raton, FL, pp. 1-29.
4. E. S. Perez de Ortiz (1991), Science and Practice of Liquid-Liquid Extraction, J. D. Thornton (ed.), Clarendon Press.
5. D. Agble and M. A. Mendes-Tatsis (2000), *Int. J. Heat Mass Transfer*, **43** (6), 1025-1034.
6. P. C. Blokker (1957), *Proc. 2nd Int. Congr. Surface Activity*, Vol. 1, pp. 503-510.
7. I. Komasawa, T. Saito and T. Otake (1972), *Inst. Chem. Eng.*, **12** (2), 345-351.
8. E. Nakache, M. Dupeyrat and M. Vignes-Adler (1983), *J. Colloid Int. Sci.*, **94**, 187-192.
9. T. Misek, R. Berger and J. Schröter (1984), Standard Test Systems for Liquid Extraction, European Federation of Chemical Engineering, 2nd edn., Institution of Chemical Engineers, Rugby.
10. K. H. Javed, J. D. Thornton and T. J. Anderson (1989), *AIChE J.*, **35** (7), 1125-1136.
11. M. Pertler, M. Haberl, W. Rommel and E. Blass (1995), *Chem. Eng. Proc.*, **34**, 269-277.
12. C. von Reden, M. J. Slater and A. Gorak (1996), *Proc. ISEC '96*, Melbourne, pp. 99-104.
13. C. V. Sternling and L. E. Scriven (1959), *AIChE J.*, **5/4**, 514-523.
14. J. Crank (1975), The Mathematics of Diffusion, Oxford University Press, London.



## NUMERICAL APPROACH TO THE MOTION AND EXTERNAL MASS TRANSFER OF A DROP SWARM BY THE CELL MODEL

Zai-Sha Mao and Jiayong Chen

Institute of Process Engineering, Chinese Academy of Sciences, Beijing, China

The cell model developed for solid particles sedimentation and viscous flow through porous media was extended to simulate the drop behavior in a dense swarm. Zero shear stress or zero vorticity condition was designated at the external cell boundary. Numerical simulation in terms of stream function and vorticity was carried out to shed light on the interaction between drops and bulk liquid phase. The drag coefficient and external mass transfer rate from the simulation was also compared with correlations reported in literature. It is found that the cell model with the zero shear at the external cell boundary was satisfactory on the overall performance of prediction, but more modeling efforts are necessary to get closer agreement with experimental data.

### INTRODUCTION

Understanding of drop behavior in swarms is the prerequisite for establishing the mathematical model of a multiphase system for scientific scale-up of related process equipment. To approach this goal, numerous experimental data have been accumulated, but it is quite difficult to retrieve universal correlations for the purpose of prediction and process design. As for theoretical analysis, significant progress has been achieved in interpretation of the behavior of single drops and bubbles by theoretical and numerical approaches. For examples, Leal and coworkers solved numerically the buoyancy-driven motion of single deformable bubbles and drops in a curvilinear orthogonal coordinate system [1,2]. The authors also used the similar numerical scheme for interpretation of the motion and mass transfer of single drops in extraction systems [3-5]. However, theoretical approach to a drop swarm remains a great challenge.

In view of the successful application of the cell model to solid particle assemblages [6,7], efforts are taken to extend its use to fill the gap in the knowledge between single drop and drop swarm. As for the fluid particles, only one report is available on studying the motion and transfer of a bubble swarm [8].

To meet the pressing need for understanding the motion and transport behavior of drops in a swarm, the cell model is tentatively used for numerical simulation of spherical drops in a swarm. The prediction of drag coefficient and external mass transfer rate by the cell models is compared with several correlations. It is found that the Happel cell model gives more reasonable prediction of drop swarm behavior in the dispersion at low Reynolds numbers, and the Kawabara cell model tends to overestimate the friction to drops.

## FORMULATION OF CELL MODELS

A spherical cell is depicted in Figure 1. To resolve the fluid flow and mass transfer to the drop, the Navier-Stokes and convective diffusion equations are solved in an axisymmetrical coordinate system. For this purpose, we adopted the numerical scheme used previously for buoyancy-driven motion of single particles and deformable drops in an infinite medium [1-5,9].

For mathematical formulation of the viscous flow in such an assemblage, it is usual to adopt the following assumptions. (1) the liquid is incompressible, viscous and Newtonian; (2) the flow is laminar and axisymmetric; (3) the drop remains spherical; (4) the flow and mass transfer are steady-state; (5) the physical properties are not altered by mass transfer, so the mass transfer and liquid flow problems are not coupled. Thus, the liquid flow in a cell is described by the Navier-Stokes equations and the external mass transfer by a convective diffusion equation.

The axisymmetrical flow in the cell may be described by a set of partial differential equations in terms of stream function  $\psi$  and vorticity  $\omega$  in a sectional plane ( $x,y$ ) passing through the axis of symmetry as indicated in Figure 2. The non-dimensional governing equations are expanded in the computational plane ( $\xi,\eta$ ) which is the orthogonal mapping of the physical domain in the plane ( $x,y$ ) as follows [1,4]:

$$L_1^2(y_1\omega_1) - \frac{Re_1}{2} \frac{1}{h_{\xi_1} h_{\eta_1}} \left[ \frac{\partial \psi_1}{\partial \xi_1} \frac{\partial}{\partial \eta_1} \left( \frac{\omega_1}{y_1} \right) - \frac{\partial \psi_1}{\partial \eta_1} \frac{\partial}{\partial \xi_1} \left( \frac{\omega_1}{y_1} \right) \right] = 0 \quad (1)$$

$$L_2^2 \psi_1 + \omega_1 = 0 \quad (2)$$

$$L_2^2(y_2\omega_2) + \frac{Re_2}{2} \frac{1}{h_{\xi_2} h_{\eta_2}} \left[ \frac{\partial \psi_2}{\partial \xi_2} \frac{\partial}{\partial \eta_2} \left( \frac{\omega_2}{y_2} \right) - \frac{\partial \psi_2}{\partial \eta_2} \frac{\partial}{\partial \xi_2} \left( \frac{\omega_2}{y_2} \right) \right] = 0 \quad (3)$$

$$L_2^2 \psi_2 + \omega_2 = 0 \quad (4)$$

$$\frac{u_\xi}{h_\xi} \frac{\partial c}{\partial \xi} + \frac{u_\eta}{h_\eta} \frac{\partial c}{\partial \eta} = \frac{1}{Pe h_\xi h_\eta y} \left[ \frac{\partial}{\partial \xi} \left( \frac{h_\eta y}{h_\xi} \frac{\partial c}{\partial \xi} \right) + \frac{\partial}{\partial \eta} \left( \frac{h_\xi y}{h_\eta} \frac{\partial c}{\partial \eta} \right) \right] \quad (5)$$

where the differential operator is

$$L^2 = \frac{1}{h_\xi h_\eta} \left[ \frac{\partial}{\partial \xi} \left( \frac{f}{y} \frac{\partial}{\partial \xi} \right) + \frac{\partial}{\partial \eta} \left( \frac{1}{fy} \frac{\partial}{\partial \eta} \right) \right] \quad (6)$$

As depicted in Figure 2, the external domain is affixed with a left-handed reference frame ( $\xi_1, \eta_1$ ) and the drop domain is in a right-handed reference frame ( $\xi_2, \eta_2$ ). The typical grid on which partial differential equations are discretized and solved may be specified analytically for the domain between two concentric spheres [9].

Most of the boundary conditions for the cell model are routinely used: no slip and  $\psi=0$  at the drop surface,  $\psi=0$  and  $\omega=0$  at the axis of symmetry. Uniform flow is *a priori* assumed at the outer cell boundary. For the second boundary condition at the outer cell boundary, Happel proposed the shear-free boundary condition [6], and Kuwabara adopted the zero vorticity

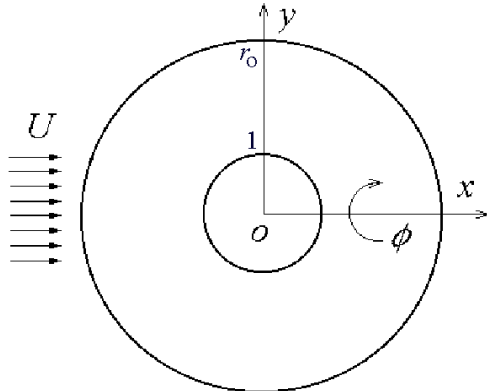


Figure 1. Schematic of the unit cell with the axisymmetrical reference coordinate system fixed on the spherical drop.

boundary condition [10] as listed in Table 1. The aim of these two conditions is to isolate a cell from the neighboring cells, but it seems that the zero vorticity boundary condition forces a more stringent constraint on the inter-cell interaction. Mass transfer controlled by external resistance occurs rarely in practical solvent extraction. This case is simulated in this work as a first effort. For external mass transfer,  $c=0$  at the interface is assumed since no mass transfer resistance exists in the drop phase,  $c=1$  is designated to the upstream half of the outer cell boundary and at the downstream half the zero gradient of  $c$  along the flow direction is adopted.

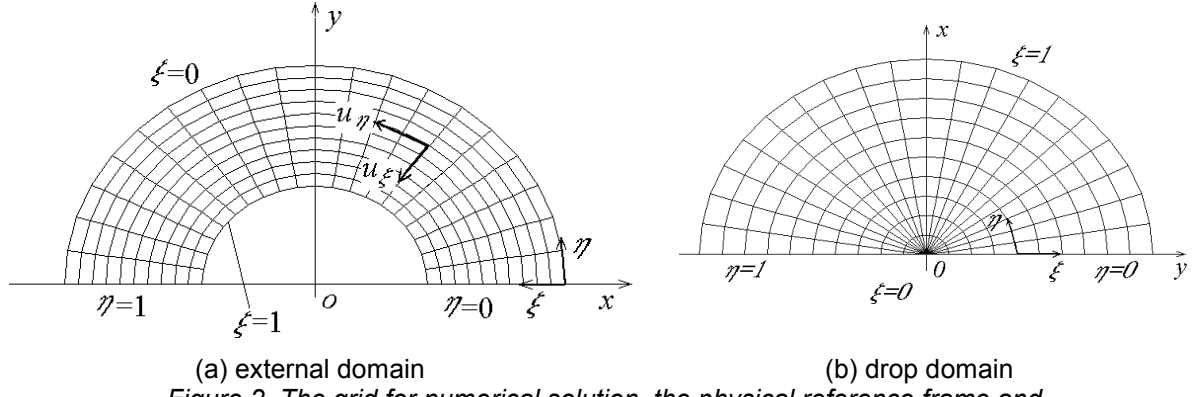


Figure 2. The grid for numerical solution, the physical reference frame and the computational coordinate system.

Table 1. Outer cell boundary conditions for the cell models.

Model H (Hapell) [6]	
$\psi = \frac{1}{2}y^2$	(uniform flow)
$\tau_{\xi\eta} = 0$	(free shear boundary)
Model K (Kuwabara) [10]	
$\psi = \frac{1}{2}y^2$	(uniform flow)
$\omega = 0$	(zero vorticity boundary)

The drag coefficient may be evaluated by the following line integral along the drop surface:

$$C_D = 2 \oint \left( \tau_{\xi\eta} \frac{\partial y_2}{\partial \eta_2} - \tau_{\xi\xi} \frac{\partial x_2}{\partial \eta_2} \right) y_2 d\eta_2 \quad (10)$$

and evaluation of terms in equation (15) is referred to [2,5]. The Sherwood number based on  $k_{od}$  is

$$Sh_c = \frac{2Rk_{od}}{D_1} = - \frac{2 \int_0^1 f_1 y_1 \left. \frac{\partial c}{\partial \xi_1} \right|_{\xi_1=1} d\eta_1}{\int_0^1 y_1 h_{\eta_1} d\eta_1} \quad (11)$$

## NUMERICAL SIMULATION

First the grid-independence of numerical simulation was tested. For a drop moving at  $Re=100$  with  $\lambda=1.33$  and  $\zeta=0.91$  in a swarm with the voidage  $\varepsilon=0.9$ , numerical simulation was repeated with Model H on successively denser meshes of  $41\times 21$ ,  $41\times 41$ ,  $81\times 41$ ,  $81\times 81$ ,  $121\times 81$  and  $121\times 121$ . It is found that the simulations on grids finer than  $41(\text{in } \xi)\times 81(\text{in } \eta)$  grid give similar numerical value of  $C_D$  within 0.7%. Sherwood numbers predicted by  $81\times 81$  and  $161\times 161$  grids differ at a level of 3%. Therefore, all the subsequent simulation were done on the uniform  $81\times 81$  grid.

For a spherical drop at  $Re=100$  with the voidage  $\varepsilon=0.7$  and  $0.9$ , the streamline contours are presented in Figure 3, showing the wake region is much smaller than that of a single buoyant drop in an unbounded medium. Since Model K imposes most stringent constraint on liquid flow by uniform liquid flow and zero vorticity at the outer boundary, it predicts greater drag coefficient than Model H as shown in Figure 4.

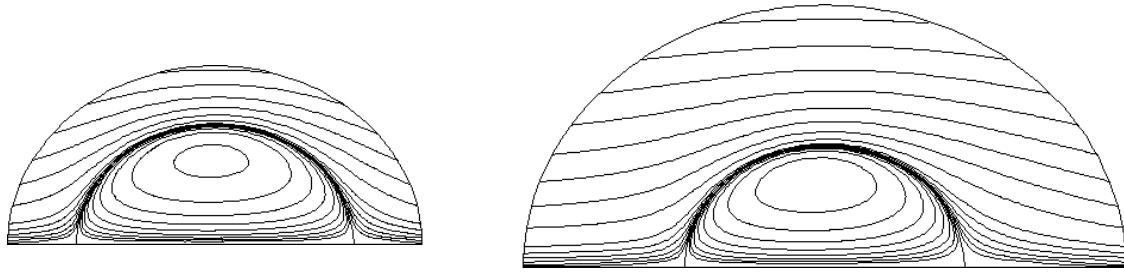


Figure 3. The streamline maps for a spherical drop with  $Re=100$ ,  $\lambda=1.33$ ,  $\zeta=0.91$ .

## COMPARISON OF MODELS WITH LITERATURE CORRELATIONS

### Drag Coefficient

To date many works have been published on the drag coefficients of drop swarms and many correlations were proposed. Among them, the correlation by Kumar and Hartland [11] is thought more reliable. The explicit expression for the drag coefficient is

$$C_D = \left( 0.53 + \frac{24}{Re} \right) \frac{1 + 4.56(1-\varepsilon)^{0.73}}{\varepsilon} \quad (12)$$

Comparison between the correlation and the prediction is shown in Figure 4, suggesting that Model H is in close agreement with the correlation when  $Re \leq 20$  and  $\varepsilon \geq 0.7$ , but Model K gives overestimated drag coefficients.

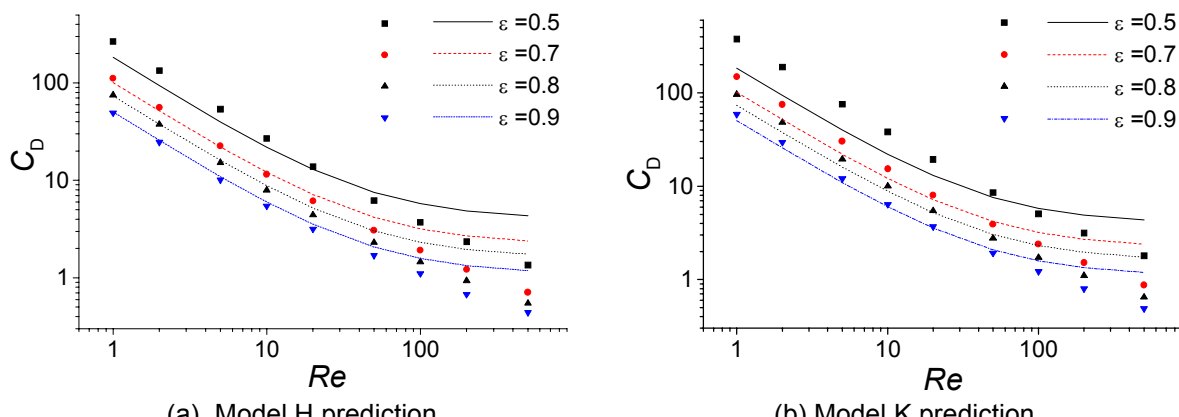


Figure 4. Comparison of the Kumar-Hartland correlation with the predicted drag coefficients for two cell models. Symbols stands for model prediction, lines are the correlation values.

## Mass Transfer Coefficient

Figure 5 shows the contour lines of solute in the continuous around a drop. It suggests that the most effective region for external mass transfer is the drop front where the solute concentration gradient is large, and that the recirculation in the drop wake distorts the concentration contour lines. The rate of external mass transfer to single drops has been studied by many authors, and Steiner [12] presented a new correlation for external mass transfer of single rigid drops ( $Re$  between 10 and 1000):

$$\frac{Sh_c - Sh_{cr}}{Sh_{ca} - Sh_{cr}} = 1 - \exp(-4.18 \times 10^{-3} Pe^{0.42}) \quad (13)$$

$$Sh_{cr} = 2.43 + 0.775 Re^{1/2} Sc_c^{1/3} + 0.0103 Re Sc_c^{1/3} \quad (14)$$

$$Sh_{ca} = (2/\sqrt{\pi}) Re^{1/2} Sc_c^{1/2} \quad (15)$$

However, the report on external mass transfer of drop swarms is rare and inconvenient. Tentative comparison between the Steiner's correlation and the prediction of  $Sh_c$  is shown in Figure 6, suggesting only partial agreement in the middle and low range of Peclet numbers. The prediction indicates obvious dependence of Sherwood number on the voidage, but the Steiner correlation ignored such a relation. It is believed that the cell model needs to be improved by taking the factors such as drop deformation, turbulence or drop oscillation into account. Besides, more proper and physical outer cell boundary conditions are desired.

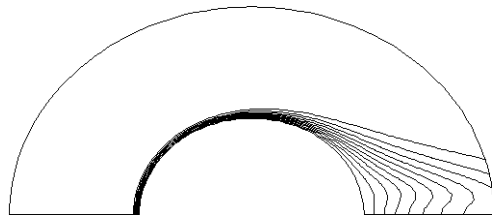


Figure 5. Concentration contour lines around a spherical drop with  $Re=100$  and  $Pe=1000$  ( $\lambda=1.33$ ,  $\zeta=0.91$ ).

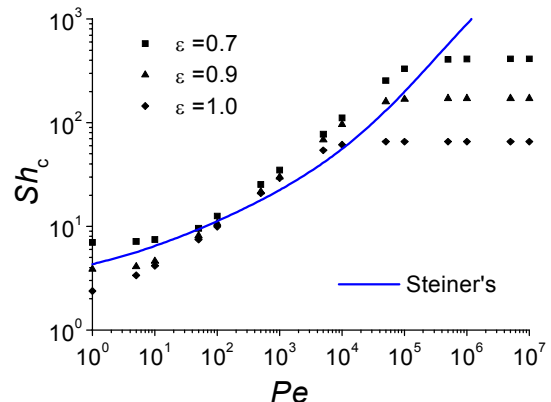


Figure 6. Comparison of the Steiner correlation with the predicted mass transfer coefficients for two cell models ( $Re=100$ ,  $\lambda=1.33$ ,  $\zeta=0.91$ ). Solid line for Steiner's correlation and symbols for cell model H prediction.

## CONCLUSIONS

Comparison of free surface cell model and free vorticity cell model with the correlations of drag coefficient of drops in spray towers indicates that Model H (free shear at the outer cell boundary) presents smaller deviation from the correlations in the range of  $Re$  below 20 and  $\epsilon$  greater than 0.7. Model K seems to overestimate the drag coefficient. Model H gives reasonable value of  $Sh$  with the same order of magnitude as the empirical correlation and presents the qualitatively correct trend. However, the cell model needs further development if its applicability is to be extended to higher Reynolds number and dense drop swarms.

## NOMENCLATURE

$C_D$	drag coefficient in a swarm, $8Rg\Delta\rho/3\rho_c U^2$
$c$	solute concentration
$D$	molecular diffusivity of solute, $\text{m}^2\cdot\text{s}^{-1}$
$f(\xi, \eta)$	distortion function, $f = h_\eta/h_\xi$
$h_\xi, h_\eta$	scaling factor
$k_{od}$	mass transfer coefficient, $\text{m}\cdot\text{s}^{-1}$
$Pe$	Peclet number for mass transfer, $2RU/D$
$R$	volume-equivalent drop radius, m
$Re$	Reynolds number, $2RU\rho_c/\mu_c$
$r_o$	cell radius
$Sc$	Schmidt number, $\mu/D$
$Sh$	Sherwood number, $2Rk_{od}/D$
$U$	superficial fluid velocity or terminal velocity, m/s
$x, y$	coordinate in physical plane

*Greek symbols:*

$\varepsilon$	voidage of multi-particle system
$\lambda$	relative viscosity, $\mu_2/\mu_1$
$\mu$	viscosity, $\text{Pa}\cdot\text{s}$
$\xi, \eta$	coordinate in computational plane, $0 \leq \xi, \eta \leq 1$
$\rho$	density, $\text{kg}/\text{m}^3$
$\tau$	stress tensor component
$\psi$	stream function
$\zeta$	relative density, $\rho_2/\rho_1$
$\omega$	vorticity

Subscripts

$c, 1$	continuous phase
$d, 2$	drop

## ACKNOWLEDGEMENTS

The authors are grateful to National Natural Science Foundation of China (No. 29836130) for financial support.

## REFERENCES

1. G. Ryskin and L.G. Leal (1984), *J. Fluid Mech.*, **148**, 1-17.
2. D.S. Dandy and L.G. Leal (1989), *J. Fluid Mech.*, **208**, 161-192.
3. T.W. Li, C.G. Sun, Z.-S. Mao and J.Y. Chen (1999), *Huagong Yejin*, **20** (1), 29-37.
4. Z.-S. Mao, T.W. Li and J.Y. Chen (2001), *Int. J. Heat Mass Transfer*, **44** (6), 1235-1247.
5. T.W. Li, Z.-S. Mao, J.Y. Chen and W.Y. Fei (2001), *Chinese J. Chem. Eng.* (in press).
6. J. Happel (1958), *AIChE J.*, **4** (2), 197-201.
7. B.P. LeClair and A.E. Hamielec (1968), *Ind. Eng. Chem. Fundam.*, **7** (4), 542-549.
8. B.P. LeClair and A.E. Hamielec (1971), *Can. J. Eng. Chem.*, **49** (6), 713-720.
9. Z.-S. Mao and J.Y. Chen (1997), *Chinese J. Chem. Eng.*, **5** (2), 105-116 (1997).
10. S. Kuwabara, (1959), *J. Phys. Soc. Japan*, **14** (4), 527-532.
11. A. Kumar and S. Hartland (1985), *Can. J. Chem. Eng.*, **63** (3), 368-376.
12. L. Steiner (1986), *Chem. Eng. Sci.*, **41** (8), 1978-1986.



## MASS TRANSFER AND MICRODROPS AT INTERFACES INVESTIGATED ON MOLECULAR LEVEL

Tatiana Merzliak, Marita Schmäh, Robin Schott and Andreas Pfennig

Lehrstuhl für Thermische Verfahrenstechnik, RWTH Aachen, Germany

To investigate the origin of the various instabilities when mass transfer takes place across an interface molecular simulations have been performed on different levels of detail. Very detailed molecular-dynamics simulations give insight into the mobility of the molecules at an interface. To investigate the behaviour of a larger number of molecules for a larger time span, Monte-Carlo simulations for a lattice system have been performed. In these simulations the occurrence of nano droplets of some 1000 molecules has been observed. Based on diffusional and thermodynamic properties of the system a first stability criterion for the occurrence of the nano droplets has been derived.

### INTENTION OF THE PROJECTS

Interfaces and especially the mass transfer at interfaces as well as in the interfacial region are of great importance in many fields of chemical engineering. However, there are no models available so far which could describe mass transfer correctly in detail. Even some phenomena such as Marangoni instabilities can not be fully explained to satisfaction although it is known that these instabilities have a great influence, e.g., on liquid-liquid extraction (see e.g. [1]). The following projects were initiated aiming at examining liquid-liquid interfaces using different space and time scales. Basis for all models is the microscopic understanding of the phenomena at interfaces which is achieved by simulations on a molecular level.

### SIMULATION TECHNIQUES

For the simulation of interfaces and the interfacial region as well as in the bulk phases molecular-dynamics (MD) simulations are performed. In MD the trajectories of up to some 1000 molecules are determined by solving the equations of motion of all particles acting in the force field of all neighbours. The systems are only some nm in size and simulation times are some ns on a high-performance computer. The results correspond very well to macroscopic data regarding, e.g., equilibrium information and diffusion coefficients. Since diffusion is a relatively slow process MD is not a very efficient technique to simulate diffusion for larger systems.

Thus we have chosen to augment these simulations with a technique which does not take the detailed movements of all molecules into account but is able to model diffusive phenomena on a larger scale correctly. With lattice Monte-Carlo (MC) simulations some million particles can be simulated for a simulation time of some  $\mu$ s. Instead of solving the differential equations of motion exchange energies and probabilities of exchange between neighbouring molecules which are located on fixed lattice sites are considered. Comparison of the results obtained with both techniques show very good agreement. Thus a combination of MD and lattice-MC techniques can bridge the gap in space and time scales usually encountered.

## MD RESULTS

With MD simulations a system with a stable liquid-liquid interface was simulated consisting of Lennard-Jones particles with appropriate interaction energies. Self-diffusion coefficients are calculated based on the mean square displacement using different time steps. For an adequate time step the coefficients are examined as function of distance from the interface for the three spatial directions. The result is shown in Figure 1.

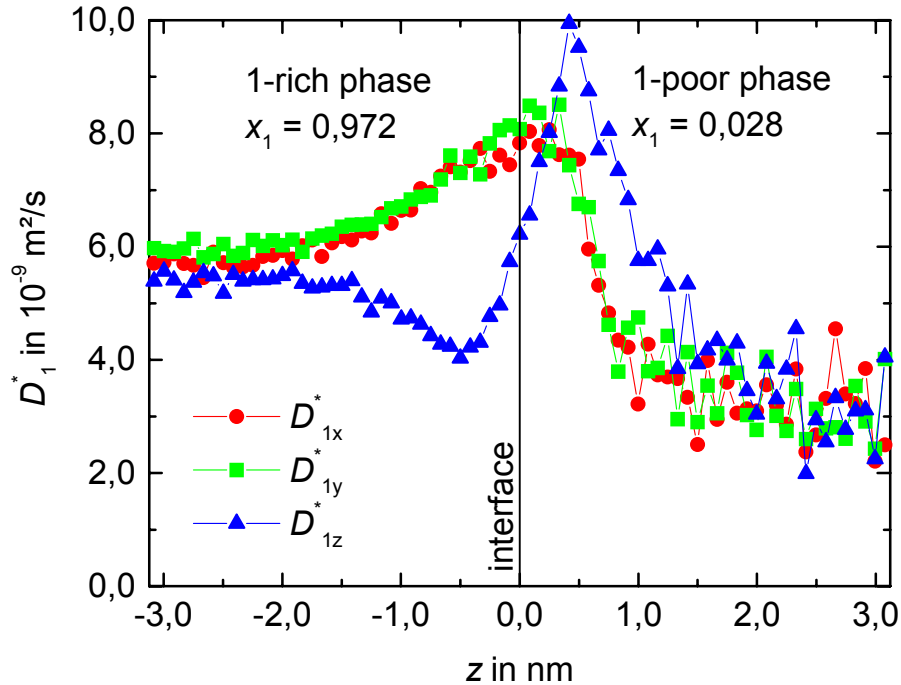


Figure 1. Diffusion coefficients as function of the distance to the interface.

In Figure 1 the self-diffusion coefficients of component 1 are shown. Since all properties of the two components present in the system are symmetrical with respect to component index, the properties of component 2 correspond to the mirror image of this plot with respect to the interface. The mutual solubility of the two components which are modelled with argon parameters is 2.8 %. The miscibility gap is induced by a less attractive cross-interaction energy between the components. Since at the interface the two phases have to interact due to geometrical reasons while they would rather prefer to separate the overall density at the interface is reduced and the mobility of the molecules described with the self-diffusion coefficient is thus increased. In the spatial directions parallel to the interface, x and y, the mobility of the molecules is identical as expected.

The deviation of the diffusion coefficient in z-direction (perpendicular to the interface) from that parallel to the interface can be explained by recalling that the partition coefficient deviates from unity. Thus the molecules of one component crossing the interface in one direction have a reduced tendency to return while this tendency is much higher when the interface is crossed in the opposite direction. Thus in this case particles of component one crossing the interface from the left to the right will return with a higher probability than if the interface would not be present. Thus the apparent mobility is reduced which leads to a smaller self-diffusion coefficient in z direction directly to the left of the interface. The opposite argument holds directly to the right of the interface leading to a self-diffusion coefficient somewhat higher than that parallel to the interface.

## LATTICE-MC RESULTS

Results of various MC simulations show that under certain conditions mass transfer across interfaces induces the formation of nano droplets in the close vicinity of the interface. It should be noted that for the occurrence of this effect roughly a million particles have to be simulated for some  $\mu\text{s}$ . The simulations are performed for a diffusion tube where the compositions of the phases brought into contact are shown in Figure 2. One of the phases is a binary equilibrium phase while to the other binary equilibrium phase 20% of the transfer component 3 are added.

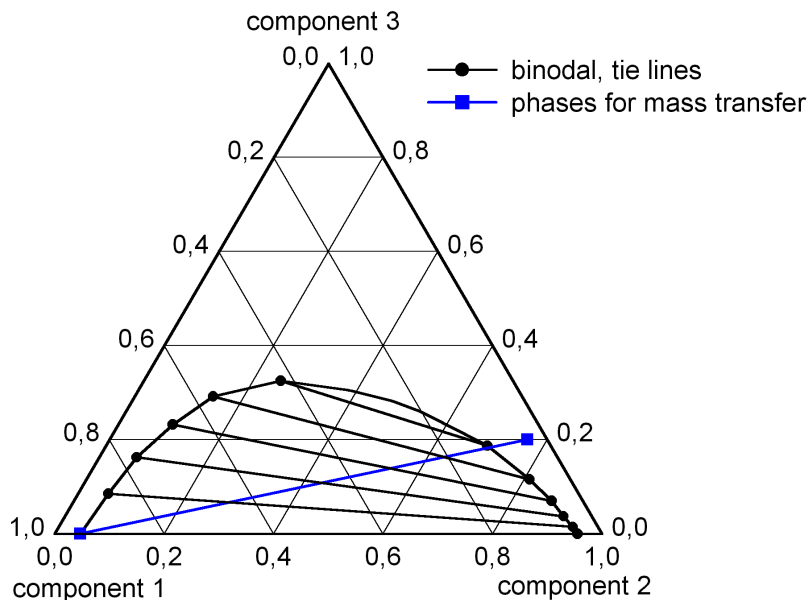


*Figure 2. Phases brought into contact which lead to the formation of nano droplets.*

In Figure 3 the resulting concentration profiles in the diffusion tube are shown as function of the contact time. The grey scale shows the concentration of component 2 which is the solvent in the upper phase. To this phase the transfer component has been added which then starts to be transferred into the lower 1-rich phase. After roughly  $2 \mu\text{s}$  the occurrence of a nano droplet can be seen, where a stable region of 1-rich phase is formed within the 2-rich phase. Because of the sharp change in grey value between the nano droplet and the surrounding phase it can be concluded that this droplet has a distinct interface [2]. Some nano droplets directly above the interface are shown in Figure 4. Here only molecules of component 1 are shown which are directly connected via next-neighbour contacts to more than 100 molecules of component 1. Thus only clusters of molecules of component 1 are visualized. The rough nature of the major interface is nicely seen. Also several nano droplets of some 1000 molecules have formed at a distance of approximately 20 nm from the interface

These nano droplets can now interact among each other and with the major interface via attractive or repulsive long-range forces. The long-range forces may be assumed as resulting from attractive van-der-Waals forces between nano droplets accounted for, e.g., by the Hamaker constant and from electrostatic forces due to orientation of polar molecules at the interface and the formation of diffusive double layers at the interface if ionic species are present [3]. The different combination of the nano-droplet behaviour due to attractive or repulsive forces together with the characteristics of coalescence may then lead to different macroscopic interfacial instabilities like, e.g., spontaneous emulsification or large eruptions.

To investigate the origin of the nano droplets further and to derive a quantitative stability criterion the diffusive properties of the chosen lattice system are evaluated according to Fick and Maxwell-Stefan theory where thermodynamic behaviour is well described by the GEQUAC model [4].

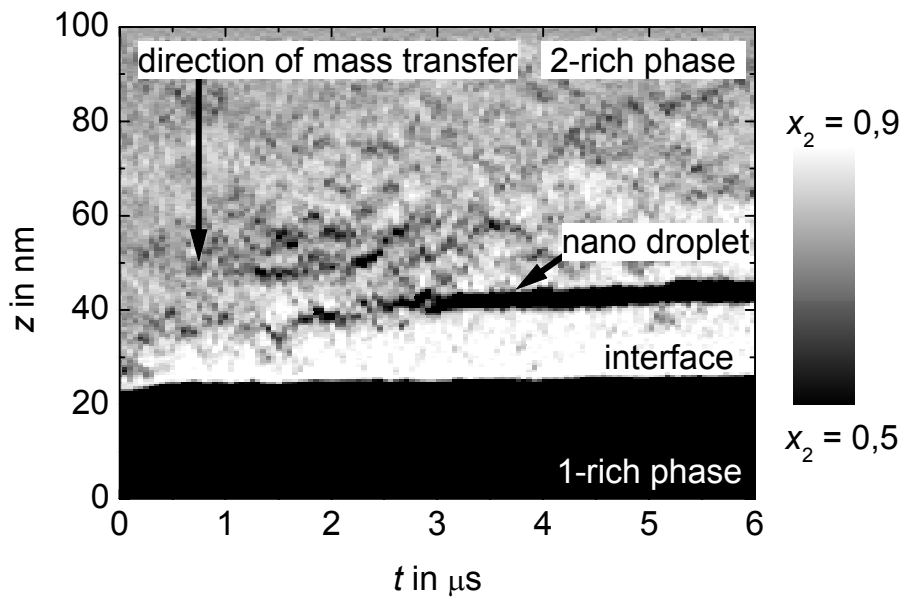


Figure 3. Formation of nano droplet induced by mass transfer.

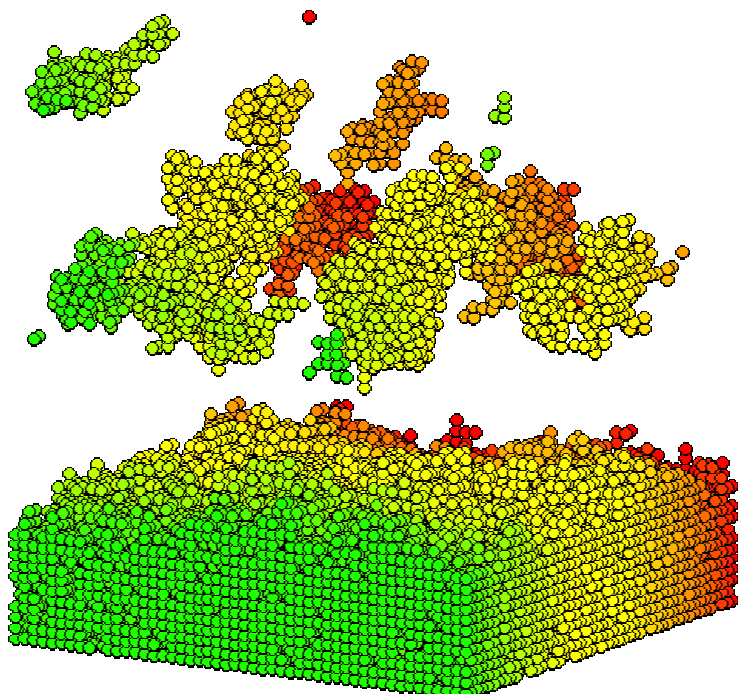
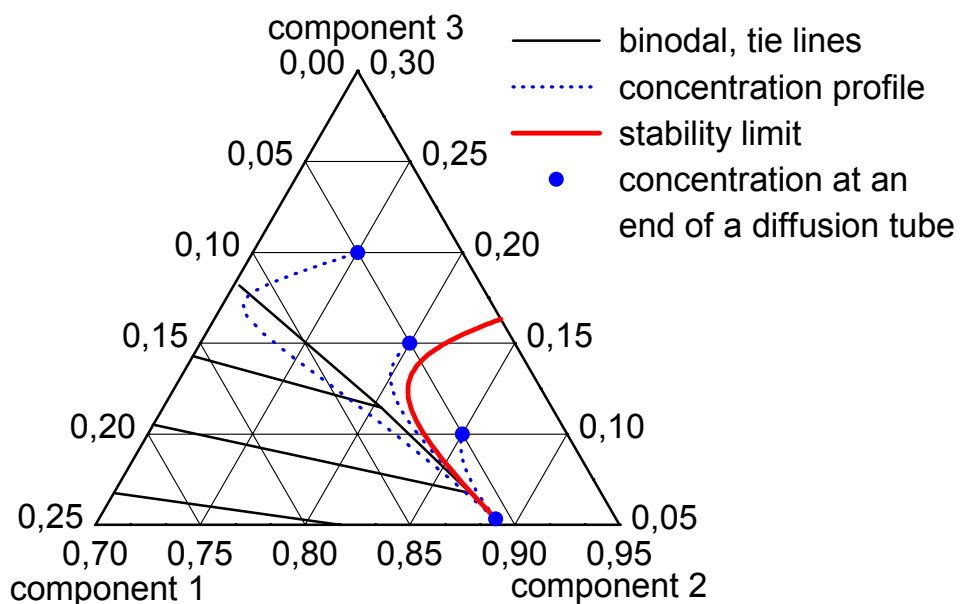


Figure 4. Some nano drops directly above the interface.

## DISCUSSION OF RESULTS

Based on the diffusive and thermodynamic properties a first stability criterion for nano-droplet formation was developed. Calculations show that the concentration profile in a diffusion tube may cross the binodal even if the connecting line between the concentrations corresponding to the ends of a diffusion tube runs outside the miscibility gap (Figure 5). The stability criterion in Figure 5 does not yet take interfacial tension into account. The consideration of the interfacial tension causes shifting of the stability limit towards the spinodal.



*Figure 5. Stability criterion.*

Future work will be directed at the development of a quantitative understanding of the discussed effects and an improvement of the stability criterion.

#### ACKNOWLEDGEMENTS

Funding of the ongoing work by the German Science Foundation in the framework of the SFB 540 projects and the SPP programme 1105 is gratefully acknowledged.

#### REFERENCES

1. M. Henschke, A. Pfennig (1998), *AIChE J.*, **45** (10), 2079-2086.
2. A. Pfennig (2000), *Chem. Eng. Sci.*, **55** (22), 5333-5339.
3. A. Pfennig, A. Schwerin (1998), *Ind. Eng. Chem. Res.*, **37**, 3180-3188.
4. K. Egner, J. Gaube, A. Pfennig (1999), *Fluid Phase Equilib.*, **158**, 381-389.



# STUDY OF SALT EFFECTS ON THE KINETICS OF SOLUTE TRANSFER AND EXTRACTION AT A FREE LIQUID/LIQUID INTERFACE

Jean-Pierre Simonin and Hendrawan Hendrawan

Laboratoire Liquides Ioniques et Interfaces Chargées, Université P.M. Curie, Paris, France

The effect of a salt on the kinetics of (*i*) transfer of acetic acid and (*ii*) extraction of metal cations, Co<sup>2+</sup> and Zn<sup>2+</sup>, by di(2-ethylhexyl) phosphoric acid (D2EHPA), was studied using the rotating membrane cell technique. In case (*i*), the kinetic rate of transfer could not be correlated with the value of the activity coefficient of solute in the aqueous phase. In case (*ii*), it was found that the reaction is unlikely to be purely interfacial. The effect of salt on the kinetics was interpreted in terms of metal-(salt anion) association, transfer of extractant into the aqueous phase and primary electrolyte effect on the extractant-metal reaction in the aqueous phase.

## INTRODUCTION

The use of a salt, added to the aqueous phase, to modify the partitioning or the extraction velocity of a solute is well known. In contrast with the former issue, references that have addressed the latter issue are rather scarce: one of the first papers mentioning this effect was written by McClellan *et al.* in 1971 [1] in which acceleration of the kinetics of extraction of Fe(III) was observed by addition of NaClO<sub>4</sub>. The papers published subsequently have generally considered the effect of simple inorganic salts such as LiCl, NaCl, NaClO<sub>4</sub> on the extraction kinetics of metal cations, including Fe(III) [2,3], Cu(II) [4] or Zn(II) [5], by an extractant in a diluent. Another paper considered the extraction of HCl by trilaurylamine in toluene [6]. In these references, salt effects were regarded either from a chemical viewpoint when the major factor was expected to be the formation of a complex between the solute and an ion of the salt, or from a physical viewpoint, with a dominant effect of departures from ideality. In the latter case, quantitative descriptions rested on the assumption (e.g., [4-7]) that any kinetic parameter *k* appearing in the kinetic equations should be replaced by *kγ*, where *γ* denoted an activity coefficient. This procedure sometimes [4] involved an estimation of the individual activity coefficient of an ion, with well-known problems associated with assessing this quantity [8]. In other papers [6,7], the mean salt activity coefficient was taken instead of the individual activity coefficient. So, influence of the salt on the solute in the bulk alone was taken into account, although the reaction was believed to occur at the interface. Besides, if the main reaction pathway is not interfacial and involves transport of the extractant into the aqueous phase, then addition of salt may change the solubility of the extractant and this could contribute to modify the kinetics. This is what may happen for an acidic extractant such as di(2-ethylhexyl) phosphoric acid (D2EHPA) [2,5] for which complexation has been reported to occur in a region near the interface [9,10].

In this paper, a study of salt effects on solute transfer [11] kinetics, which topic has not been investigated before, is presented first. Next, the case of the extraction kinetics of metal cations by D2EHPA is considered; this first approach is aimed at an elucidation of the mechanisms of extraction, which are still unclear, and electrolyte effects on this type of system. The use of a technique that controls the hydrodynamics is of primordial importance for that purpose. Here, the rotating membrane cell technique is employed. Its principle is described in the following section.

## DESCRIPTION OF THE TECHNIQUE

The characteristics of the rotating membrane cell (RMC) technique [12] are described below. A sketch of the set-up is shown in Figure 1. The cell consists of a thin Millipore™ membrane (hydrophilic PVDF, HVLP type), ca. 120 µm thick and 0.8 cm in diameter, that is glued on the base of a cylinder made of Perspex with the use of a polyurethane mastic (Scotch-Seal 5300). This mastic was chosen for its excellent chemical resistance to organic solvents.

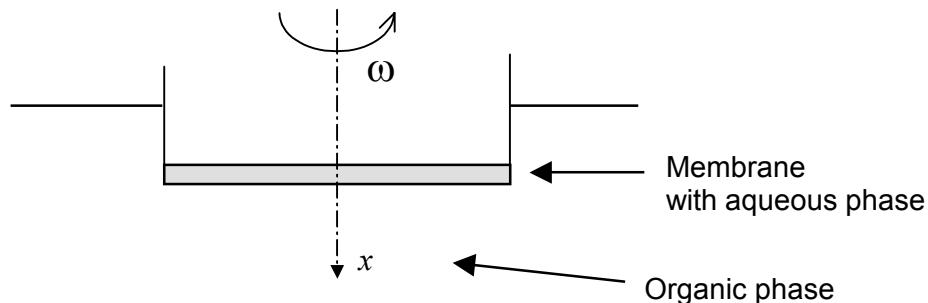


*Figure 1. Sketch of the RMC. Membrane: thickness = 120 µm, diameter = 8 mm.*

The membrane contained the aqueous phase. It was set into rotation at a known speed and, at  $t=0$ , it was immersed into the organic phase. Analysis of the extracted matter was performed by using radio-labelled species. The membrane was chosen for its good chemical compatibility with acid solutions and aliphatic solvents. Its average pore size was 0.45 micron (manufacturer's value). The experimental value found for the void porosity was  $\sigma = 0.685 \pm 0.015$ , compared to the manufacturer's value of 0.70.

The main feature of the RMC is that diffusive transport is controlled in both phases. Moreover, the diffusion coefficients of solute may be measured experimentally with a suitable technique. Then, the contributions from Fickian diffusion in the membrane and convective transport in the outer phase may be subtracted from the overall process, so yielding the contribution from interfacial transfer alone. Previous work [13] has shown that good control of the hydrodynamics is achieved with this technique. Thus the RMC technique does not require prior calibration.

In contrast with the rotating diffusion cell of Albery, the RMC method operates in a transient regime. For a purely interfacial reaction, the proportion of matter transferred from the aqueous phase (denoted by A) to the organic phase (B) may be expressed as [12]

$$P(t) \approx 1 - \exp(-t/\tau) \quad (1)$$

in which  $\tau$  is the mean time for the transfer of solute from A to B. It is given by

$$\tau = \tau_f + \tau_A + \tau_B \quad (2)$$

with

$$\tau_f = L / k_f \quad ; \quad \tau_A = L^2 / (3 D_A) \quad ; \quad \tau_B = L \sigma \delta / (K D_B) \quad (3)$$

Here  $L$  is the membrane thickness,  $D_X$  is the diffusion coefficient in phase X,  $k_f$  is the A-to-B ("forward") rate constant,  $\tau_f$  is the characteristic time for the interfacial forward reaction,  $\tau_A$  represents the mean diffusion time in the membrane and  $\tau_B$  is the mean residence time of the species in the diffusion layer. The parameter  $\delta$  represents the diffusion layer thickness, given by

$$\delta = 1.612 (\nu/\omega)^{1/2} / Sc^{1/3} \quad (4)$$

in which  $Sc = \nu/D_B$  is the Schmidt number,  $\nu$  is the kinematic viscosity of B and  $K$  is the partition coefficient ( $K = k_f/k_r$ , with  $k_r$  the reverse rate constant). In the case where the interfacial kinetics are very fast ( $k_f$  and  $k_r$  infinite, but still  $k_f/k_r = K$ )  $\tau$  becomes

$$\tau_\infty = \tau_A + \tau_B \quad (5)$$

which gives the diffusive limit (DL) for the extracted rate of matter :  $P_\infty(t) = 1 - \exp(-t/\tau_\infty)$ .

## STUDY OF SOLUTE TRANSFER KINETICS

The solutions were composed of  $0.01 \text{ mol L}^{-1}$  HCl,  $10^{-3} \text{ mol L}^{-1}$  acetic acid (to avoid adsorption), salt and were spiked with tracer amounts of radio-labelled acetic acid. The organic phase was isopropyltetradecanate (isopropylmyristate). The diffusion coefficients of acetic acid (AA) in the aqueous phases (containing salt),  $D_{\text{sol}}$ , were determined using the open-ended capillary technique. Then the apparent diffusion coefficient in the membrane,  $D_A$ , was obtained from the values of  $D_{\text{sol}}$  and the measurement of the membrane tortuosity factor, performed using impedance spectroscopy [12], yielding:  $D_A = D_{\text{sol}}/1.88$ . The activity coefficient of acetic acid in the aqueous phase was determined experimentally by classic solvent partitioning. All experiments were conducted at room temperature  $22 \pm 1^\circ\text{C}$ . In absence of salt, we obtained a value for the rate constant,  $k_f^{(0)} = (2.4 \pm 0.1) \times 10^{-6} \text{ m s}^{-1}$ . This value compares well with a previous value of  $2 \times 10^{-6} \text{ m s}^{-1}$  obtained with a similar cell [14], in which a gel was used instead of membrane.

In Figure 2, the experimental values for  $k_f$  vs. LiCl concentration are compared [13] with the quantity  $\gamma k_f^{(0)}$ ,  $\gamma$  being the activity coefficient of AA in the solution containing salt.

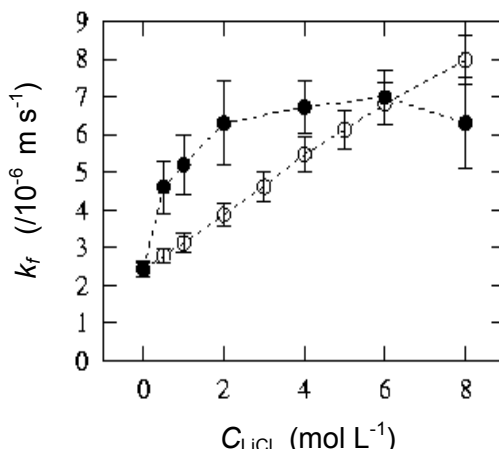


Figure 2. Kinetic rate  $k_f$  variation vs. LiCl concentration. Experimental result (●) compared with  $\gamma k_f^{(0)}$  (○). Vertical bars indicate experimental uncertainty.

It is seen that, for finite salt concentrations, the two plots do not coincide, except at high concentration around  $6 \text{ mol L}^{-1}$ . The same qualitative behaviour was observed in the case of NaCl and KCl. Therefore, the common assumption that activity should replace concentration is not verified in the present case. This observation may be attributed to the fact that, as mentioned in the Introduction section, the effect of the salt on the solute at the interface has not been taken into account. However a conclusive interpretation of this phenomenon seems difficult to give at present. A priori this effect may result from interplay between several effects such as ion-solute interactions, change of solute hydration, as well as dynamical effects, all occurring in the interfacial region. Nonetheless, the model assuming that  $k_f$  should coincide with the quantity  $\gamma k_f^{(0)}$  may be supplemented by the introduction of the activity coefficient of an “intermediate”, or “activated” species, as in Brönsted's postulate [15]. This gives

$$k_f = \gamma k_f^{(0)} / \gamma_X \quad (6)$$

where X denotes the “activated” AA. This relation may be justified by using a barrier-crossing model, as utilised in earlier work [14]. In this framework, X is located at the barrier top and is expected to correspond to an intermediary state of incomplete solvation. Then, equation 6 may be derived [13] by noting that the activation energy is decreased by a quantity of  $k_B T \ln(\gamma/\gamma_X)$  ( $k_B$  is the Boltzmann constant and  $T$  the temperature) corresponding to the change in the difference between the chemical potential of the solute in the aqueous bulk and at transition state. The results of Figure 2 show that  $\gamma_X \leq 1$  between 0 and  $6 \text{ mol L}^{-1}$ ; this suggests that the free energy of the solute at the interface be decreased by addition of salt; at higher concentration  $\gamma_X > 1$ . The

decrease of  $\gamma_X$  at low and moderate salt concentration may be interpreted in terms of direct ion-solute (e.g. ion-dipole), or indirect water-mediated attractive interactions and excluded volume effects that are less important at the interface than in the bulk because of the depletion in the interfacial ionic population. However, one must keep in mind that dynamical effects, that are not included in the above barrier model, may play an important role [16] because the time scale for solvation exchange dynamics is likely to be comparable with the time scale of the interfacial transfer process. So, ions may modify the water re-organisation dynamics around the acetic acid molecules in the interfacial region and this could facilitate the transfer of acetic acid.

## STUDY OF EXTRACTION KINETICS

The effect of a salt, added to the aqueous phase, on the kinetics of extraction of Co(II) and Zn(II) by 0.02-0.5 mol L<sup>-1</sup> D2EHPA in dodecane were studied for various salts, at pH's between 3 and 5. The concentration of radioactive Zn(II) in the aqueous phases was on the order of 10<sup>-4</sup> mol L<sup>-1</sup>; for Co(II) it was 2×10<sup>-8</sup> mol L<sup>-1</sup>. No inactive solute was added (it was verified that addition of 10<sup>-3</sup> mol L<sup>-1</sup> metal ion did not change the result). The possibility of using tracer amounts of Co(II) was an interesting feature (see below). An advantage of Zn(II) was that it led to high values of the partition coefficient  $K$ . Thus, the processes on the organic side of the interface (re-extraction and transport) should not influence the kinetics of this solute [17]; instead, the kinetics may be expected to be controlled by diffusion in the membrane and processes in the interfacial aqueous region. In this study, the extractant D2EHPA was purified using the method of Partridge and Jensen. The diluent (dodecane) was purified using silica powder. In the case of metal cations extracted by D2EHPA, the extraction mechanism is not firmly established yet, some authors proposing an interfacial process while others suggest transport of the extractant into the aqueous phase accompanied by reaction in a thin zone near the interface [18]. Thus, the aqueous/organic partitioning of D2EHPA was studied experimentally, using standard phosphate titration.

Firstly, the influence of the identity of the anion was investigated. So, solutions of HCl, HNO<sub>3</sub>, HClO<sub>4</sub> and a 0.1 mol L<sup>-1</sup> acetate buffer, at pH=3, were prepared, together with a HNO<sub>3</sub> solution (pH 3) that was equilibrated with a 0.2 mol L<sup>-1</sup> D2EHPA. For these solutions the concentration of the anion of the salt is on the order of 10<sup>-3</sup> mol L<sup>-1</sup>. Then these solutions were used to study the extraction kinetics of Co(II) by a 0.2 mol L<sup>-1</sup> D2EHPA solution. The rotation speed of the cell was 800 rpm. The result of these experiments is depicted in Figure 3(a), in which -ln(1-P) is plotted against  $t$  (see equation 1). It is seen that the kinetics for the acetate buffer and the equilibrated HNO<sub>3</sub> are significantly above those for the other solutions. Moreover, for the latter, the extraction velocity is found to be independent of the nature of the anion.

The fact that the rates for equilibrated nitric acid (ENA) and acetate buffer coincide is striking. Moreover, they are close to the prediction for the diffusive limit (DL) for cobalt in ENA (the region between the two dashed lines in Figures 3(a) and (b)), which was computed as follows: the diffusion coefficients of Co(II) in ENA was measured (by spiking ENA solution with radio-labelled cobalt ion), yielding  $D_{CoENA} \pm SD$  within the membrane; then the values  $D_{CoENA} + SD$  and  $D_{CoENA} - SD$  were plugged into equations 1 and 5. Let us denote by CIDL the corresponding confidence interval for the DL. The difference observed between equilibrated and non-equilibrated HNO<sub>3</sub> solutions suggests that the presence of D2EHPA in the aqueous phase (concentration of D2EHPA measured in ENA pH3 = 1.1×10<sup>-4</sup> mol L<sup>-1</sup>) accelerates significantly the kinetics, which becomes diffusion-controlled. In this case, we may suppose that a complex is formed between Co(II) and the extractant in the aqueous phase; according to this picture,  $D_{CoENA}$  is the diffusion coefficient of the complex in the aqueous phase. Figure 3(a) shows that the rate of extraction from ENA seems to be mainly controlled by diffusion; the transfer of cobalt from ENA is fast. Results at pH 5 for a 0.1 mol L<sup>-1</sup> acetate buffer are shown in Figure 3(b). For this system, the experimental points are located above the diffusive limit for the cobalt ion in the buffer (lower dotted line); however, they lie within the CIDL (dashed lines) at 600 and 800 rpm. In the case of

Zn(II), the kinetics were found to be fast with all anions; moreover, they were faster than the DL for all aqueous solutions.

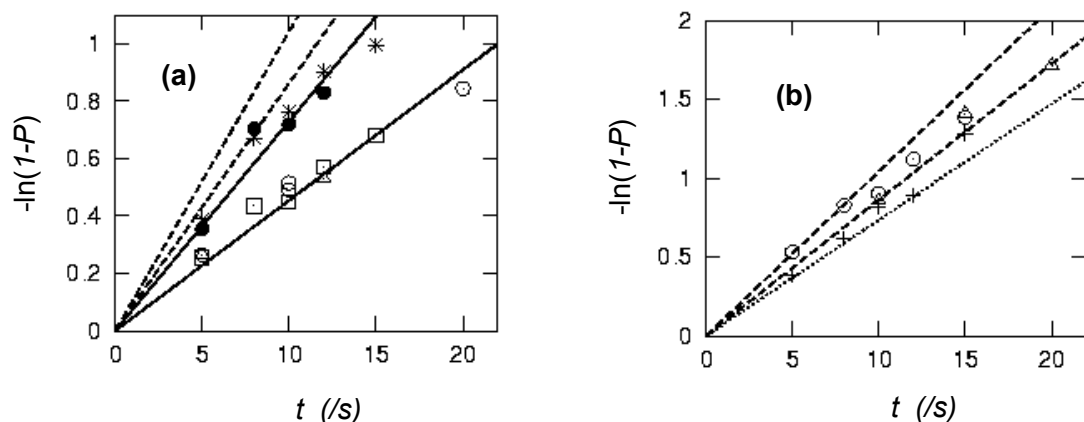


*Figure 3 (a) and (b). Influence of the nature of the anion on the kinetics. Plot of  $-\ln(1-P)$  vs. time. (a) Experimental results: equilibrated  $\text{HNO}_3$  (●), acetate buffer (\*)  $\text{HNO}_3$  (○),  $\text{HClO}_4$  (□),  $\text{HCl}$  (Δ). Solid lines: adjustments using equation 1; dashed lines: CIDL for cobalt in ENA. (b) Kinetics with acetate buffer at pH 5: rotation speed = 400 rpm (+), 600 rpm (Δ), 800 rpm (○). Dotted line: DL for cobalt ion in the buffer; dashed lines: CIDL for cobalt in ENA.*

The fact that the experimental rate can exceed the DL in some cases (in Figure 3(b) and for Zn(II)) is *a priori* an anomalous result. However, it may be interpreted according to a mass transfer with chemical reaction (MTWCR) process [9,10,18] in which the metal cation reacts with (the ionised form of) D2EHPA in the aqueous phase and is then transferred to the organic phase. Such a mechanism is suggested by the experiments using ENA. Besides, in Figure 3(b), the anomaly is removed if  $D_{\text{CoENA}}$  is taken to compute the DL because, actually, the value measured for  $D_{\text{CoENA}}$  was indeed found to be greater than that of cobalt in the pH5 buffer; then, the kinetics correspond to a diffusion-controlled process. Within this framework, the reaction of D2EHPA with Zn(II) is fast for all anions; it is fast with Co(II) for the acetate ion and slower for the other anions. We notice that fast kinetics have previously been found for Zn(II) in HClO<sub>4</sub> [9], and that the acceleration produced by the acetate ion has been observed in earlier work [19] for cobalt. The latter effect was explained by a complexation of cobalt by acetate, accompanied by a removal of co-ordinated water molecules; since the release of water was believed to be the limiting step, it was proposed that the acetate complex was a more reactive species. When the kinetics are slow, the present results do not help to discriminate between an interfacial and a MTWCR process; both processes may occur. For fast reactions, it must be underlined that the above scenario supposes that the extractant be transferred rapidly enough to the aqueous phase. However, to our knowledge, the transport process of D2EHPA into an aqueous phase is not well known. Besides, the kinetics were found to be independent of the D2EHPA concentration, in the range 0.1-0.5 mol L<sup>-1</sup>, for HNO<sub>3</sub> pH3 (results not shown); this fact seems difficult to reconcile with the MTWCR picture. Therefore, the elucidation of the extraction mechanism will require further investigation.

Lastly, the effect of salt concentration was studied at constant pH, pH=3. Figure 4 presents the variation of the quantity  $\tau - \tau_B$  vs. the concentration of the anion for zinc and cobalt extraction. Here,  $\tau$  was determined by fitting eq 1 to the experimental data;  $\tau_B$  was computed from eq 3. The value of  $\tau_A$  is ca. 10.6 s for Co(II) complexed by D2EHPA in ENA. Figure 4 shows that the kinetics of zinc extraction are not modified greatly by the addition of nitrate ion, the kinetics remaining apparently fast. In the case of cobalt, nitrate and perchlorate slow down the kinetics similarly (great values of  $\tau$  correspond to slow kinetics). In the latter case, if we assume that it is the reaction of D2EHPA (solubilised in the aqueous phase) with cobalt that controls the kinetics,

then it is easy to show that  $\tau_f$  should be replaced by  $k^{-1}$  in equation 3. With  $k$  the apparent rate constant for the reaction in the aqueous phase; then, taking  $\tau_A=10.6$  s, we find that  $k$  would be roughly decreased by a factor of 3 or 4 when the anion concentration is varied from  $10^{-3}$  to 1 mol L<sup>-1</sup>. It is interesting to notice that this variation of  $k$  may be interpreted by a primary kinetic salt effect on the homogeneous reaction between cobalt and D2EHPA: a plot of  $\log_{10}(k/k_0)$  against  $I^{1/2}$ , with  $I$  the ionic strength, can be represented using the extended Debye-Hückel version of Brönsted formula [20,21] with a closest approach distance of ca.  $8\times 10^{-10}$  m, which is a realistic value. It is clear however that, although appealing, such an interpretation will require prior confirmation of the extraction mechanism.

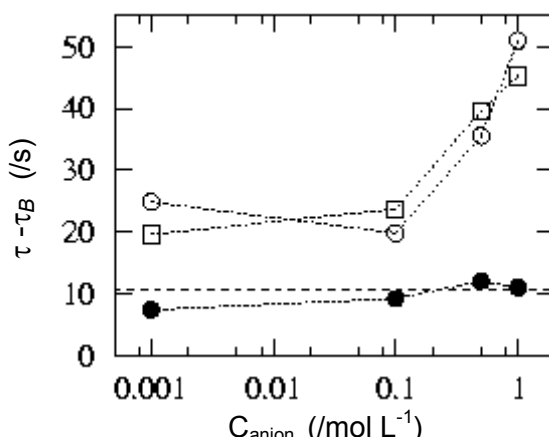


Figure 4. Influence of anion concentration on the kinetics. Plot of  $\tau - \tau_B$ . Kinetics for Co(II) in  $\text{HNO}_3$  ( $\circ$ ), in  $\text{HClO}_4$  ( $\square$ ), and Zn(II) in  $\text{HNO}_3$  ( $\bullet$ ). Horizontal dashed line:  $\tau_A$  for Co(II) in ENA.

#### ACKNOWLEDGEMENTS

Useful references were found in the Ph.D. thesis of C. Bouvier (supervisor: G. Cote). The technical help of N. Prulière, F. Dardoize and G. Clodic is acknowledged.

#### REFERENCES

1. B.E. McClellan and O. Menis (1971), *Anal. Chem.*, **43**, 436.
2. J.W. Roddy, C.F. Coleman and S. Arai (1971), *J. Inorg. Nucl. Chem.*, **33**, 1099.
3. T. Sato, T. Nakamura and M. Ikeno (1985), *Hydrometallurgy*, **15**, 209.
4. L. Zhou, W. Fürst and H. Renon (1988), *Hydrometallurgy*, **21**, 213.
5. L.A. Ajawin, E.S. Perez de Ortiz and H. Sawitowski (1983), *Chem. Eng. Res. Des.*, **61**, 62.
6. J. Aparicio, M. Valiente and M. Muhammed (1985), *Solvent Extr. Ion Exch.*, **3**, 485.
7. P.R. Danesi and R. Chiarizia (1977), *Proc. Int. Solvent Extr. Conf. ISEC '77*, **21**, 219; and discussion following this paper, p. 226-227.
8. H.S. Frank (1977), *J. Phys. Chem.*, **67**, 4413.
9. D.B. Dreisinger and W.C. Cooper (1989), *Solvent Extr. Ion Exch.*, **7**, 335.
10. M.A. Hughes and P.K. Kuipa (1996), *Ind. Eng. Chem. Res.*, **35**, 1976.
11. G.J. Hanna and R.D. Noble (1985), *Chem. Rev.*, **85**, 583.
12. J.P. Simonin and J. Weill (1998), *Solvent Extr. Ion Exch.*, **16**, 1493.
13. J.P. Simonin and H. Hendrawan (2000), *J. Phys. Chem. B*, **104**, 7163.
14. J.P. Simonin (1995), *Solvent Extr. Ion Exch.*, **13**, 941.
15. R. Livingston (1930), *J. Chem. Educ.*, **7**, 2887.
16. I. Benjamin (1992), *J. Chem. Phys.*, **96**, 577.

17. P.R. Danesi (1992), Principles and Practices of Solvent Extraction, J. Rydberg, C. Musikas, G.R. Choppin (eds.), M. Dekker, New York, pp. 157-207.
18. S. Durand-Vidal, J.P. Simonin and P. Turq (2000), Electrolytes at Interfaces, Kluwer, Dordrecht, pp. 251-261.
19. D.T. Wasan, Z.M. Gu and N.N. Li (1984), *Faraday Discuss. Chem. Soc.*, **77**, 67.
20. G. Scatchard (1930), *J. Am. Chem. Soc.*, **52**, 52.
21. J.P. Simonin and H. Hendrawan (2001), *PCCP*, in press.



# COMPUTER SIMULATION OF THE MASS TRANSFER PROCESS BETWEEN A SINGLE DROP AND AN UNBOUNDED CONTINUOUS PHASE

Agustín R. Uribe, Mariana P. Santamaría and W. J. Korchinsky\*

Universidad de Guanajuato, Guanajuato, México

\*University of Manchester Institute of Science and Technology, Manchester, England

A computer simulation of the mass transfer process of a single solute between two immiscible liquid phases is carried out by solving the dimensionless conservation equations for momentum and mass transport simultaneously using Computational Fluid Dynamics techniques. The simulation involves Reynolds numbers up to 450 and Peclet numbers of 100, 1000 and 10,000. In this work, the single drops are considered spherical in shape with no surface-active contaminants and no turbulence. Some concentration profiles and theoretical results are presented.

## INTRODUCTION

The study of fluid flow and mass transfer from drops to an immiscible continuous phase is of fundamental importance in many industrial processes such as liquid-liquid extraction. With the results from these studies it is possible to estimate the rate of extraction and, therefore, the efficiency of the extraction column. Although much experimental work has been carried out over the years, it is until recently that, with the use of powerful computers and sophisticated numerical methods, it has been possible to study this process from a more fundamental point of view. The Computational Fluid Dynamics (CFD) techniques developed and improved since the 1980s have helped increase the accuracy and speed of the solution to the conservation equations using more advanced and powerful hardware and software.

In general, multiphase flow is not solvable by CFD [1], but there are some cases where reasonable solutions are possible, such as when the second phase appears as a discrete particle of known size and shape whose motion may be approximately computed with drag coefficient formulations or rigorously computed with refined meshes applying boundary conditions at the particle surface. Attempts to predict the shape and movement of drops travelling through a continuous phase have been proposed by several authors [2].

Frequently, the study of mass transfer to or from liquid drops is carried out experimentally, but a numerical solution to the conservation equations is presented here. The results obtained from these studies are of importance in equipment design, since they allow the prediction of the mass transfer rate in multi-drop systems. In this work it is assumed that the drops are spherical and axisymmetric travelling at intermediate Reynolds numbers [3] and Peclet numbers ranging from 100 to 10,000. It is also assumed that there is only mass transfer of one solute between the phases.

## THEORETICAL TREATMENT

The conservation equations of motion and diffusion used in the present study are as follows:

$$\frac{\partial \mathbf{v}}{\partial \Theta} = \frac{1}{Re^C} \nabla^2 \mathbf{v} - \mathbf{v} \cdot \nabla \mathbf{v} - \nabla P \quad (1)$$

$$\frac{\partial \mathbf{v}}{\partial \Theta} = \frac{1}{Re^D} \nabla^2 \mathbf{v} - \mathbf{v} \cdot \nabla \mathbf{v} - \nabla P \quad (2)$$

$$\frac{\partial x_i}{\partial \Theta} = \frac{1}{Pe^C} \nabla^2 x_i - \mathbf{v} \cdot \nabla x_i \quad (3)$$

$$\frac{\partial y_i}{\partial \Theta} = \frac{1}{Pe^D} \nabla^2 y_i - \mathbf{v} \cdot \nabla y_i \quad (4)$$

where the superscript  $D$  represents the dispersed phase and  $C$  represents the continuous phase,  $x_i$  is the mass fraction of the solute in the continuous phase and  $y_i$  is the mass fraction in the dispersed phase. The following dimensionless variables are used

$$\mathbf{v}^* = \frac{\mathbf{v}}{U_\infty}, \quad \nabla^* = d \nabla, \quad P = \frac{P^*}{\rho U_\infty}, \quad y_i = \frac{y_i^* - y_i^0}{m x_i^\infty - y_i^0}, \quad m x_i = \frac{m x_i^* - y_i^0}{m x_i^\infty - y_i^0}, \quad r = \frac{r^*}{d}$$

where the superscript \* represents the untransformed variables and  $m$  is the mass distribution coefficient. The following dimensionless groups result from the conservation equations.

$$Re^P = \frac{\rho^P d U_\infty}{\mu^P} = \frac{\text{Convective transport of momentum}}{\text{Molecular transport of momentum}} \quad (5)$$

$$Pe^P = \frac{U_\infty d}{D^P} = \frac{\text{Convective transport of mass}}{\text{Diffusive transport of mass}} \quad (6)$$

$$\Theta = \frac{t U_\infty}{d} = \frac{\text{Drop rising time}}{\text{Time to travel a distance equivalent to a drop diameter}} \quad (7)$$

In these equations,  $U_\infty$  is the drop rising velocity,  $d$  is the drop diameter,  $y_i^0$  is the initial mass fraction in the dispersed phase,  $x_i^\infty$  is the solute mass fraction far from the drop interface into the continuous phase,  $\rho^P$  and  $\mu^P$  are the density and viscosity of the  $P$ -phase, respectively. The physical limiting conditions imposed on the problem are

$$x_i = 1, \quad y_i = 0, \quad \mathbf{v} = \delta_x \quad \text{at} \quad t = 0 \quad (8)$$

$$x_i = 1, \quad \mathbf{v} = \delta_x \quad \text{at} \quad r \rightarrow \infty \quad (9)$$

$$\frac{\partial y_i}{\partial r} = 0, \quad \frac{\partial \mathbf{v}}{\partial r} = 0 \quad \text{at} \quad r \rightarrow 0 \quad (10)$$

$$y_i = m x_i, \quad \mathbf{v}^x = \mathbf{v}^y \quad \text{at} \quad r = 1/2 \quad (11)$$

$$\mathbf{j}_r^x = \mathbf{j}_r^y, \quad \boldsymbol{\tau}_{r\theta}^x = \boldsymbol{\tau}_{r\theta}^y \quad \text{at} \quad r = 1/2 \quad (12)$$

Where  $r = 1/2$  at the drop surface and  $\delta_x$  is the unit vector in the  $x$ -direction. The initial solute mass fraction in the continuous and the dispersed phases, as well as the initial fluid velocity, are given in Equation (8); the solute mass fraction and the fluid velocity far from the drop surface into the continuous phase are given in Equation (9); the conditions of symmetry at the centre of the drop (zero flux) are given in Equation (10); the mechanical and the phase equilibrium at the drop surface are given in Equation (11) and, finally, the continuity of the mass and the momentum flux at the drop surface are given in Equation (12). The equations (1)-(4) are solved in their dimensionless form in order to simplify the representation and interpretation of the results and the possibility to use them for any liquid-liquid system. These equations are nonlinear due to the inertial terms, therefore the solution is complicated to

achieve. The ratio of the convective terms to the diffusive terms is given by the Reynolds number ( $Re$ ) for the momentum transport and by the Peclet number ( $Pe$ ) for the mass transport equation. At larger  $Re$  and  $Pe$ , the solution is quite difficult to achieve due to instability problems, leading to the use of a mesh with a very large number of nodes with the corresponding increase in the computational time. The larger  $Re$  used was 450 based on the properties of the continuous phase and the larger  $Pe$  was 10,000. Although these do not represent the real systems, the solution obtained is suitable for comparison purposes. The dimensionless hydrodynamic time,  $\Theta$ , represents the ratio between the rising time and the time taken by the drop to travel its own diameter.

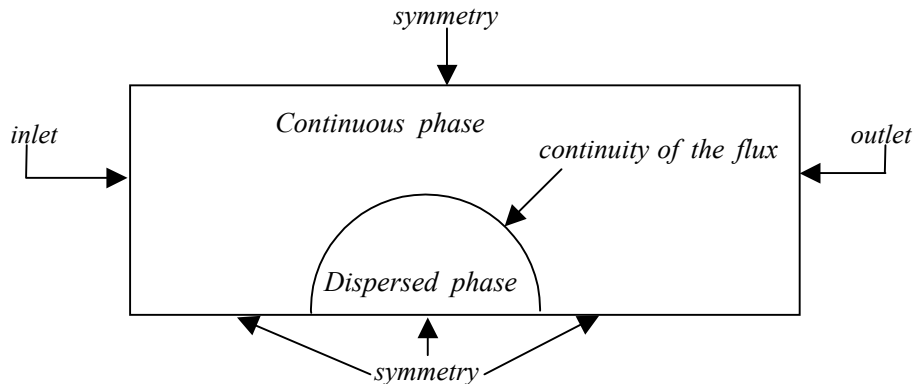


Figure 1. Schematic representation of the computational domain

The computational boundary conditions used here are different from those on the physical system, because they are adjusted to the computational domain, as shown in Figure 1.

## NUMERICAL RESULTS

The system of equations (1)-(4) was solved using the finite element method [4] in a Silicon Graphics Workstation model sgi 1400 with two Pentium-III Xeon processors. The Finite Element computer code FEMLAB [5], based on MATLAB for solving partial differential equations, was used. The momentum and mass transport equations were solved in unsteady state.

Two important assumptions were considered in the solution of the system of equations: a) the drops are completely spherical and b) the problem is axisymmetric. In this work it is considered that there is only one component transferring between the phases, although the presence of more than one component is common and it would lead to a more complicated solution.

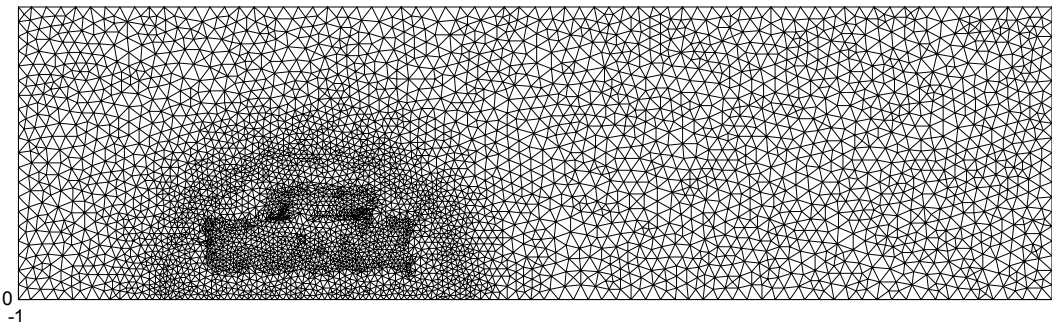
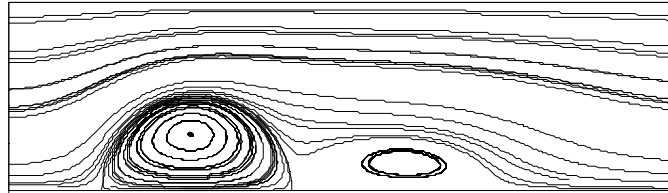
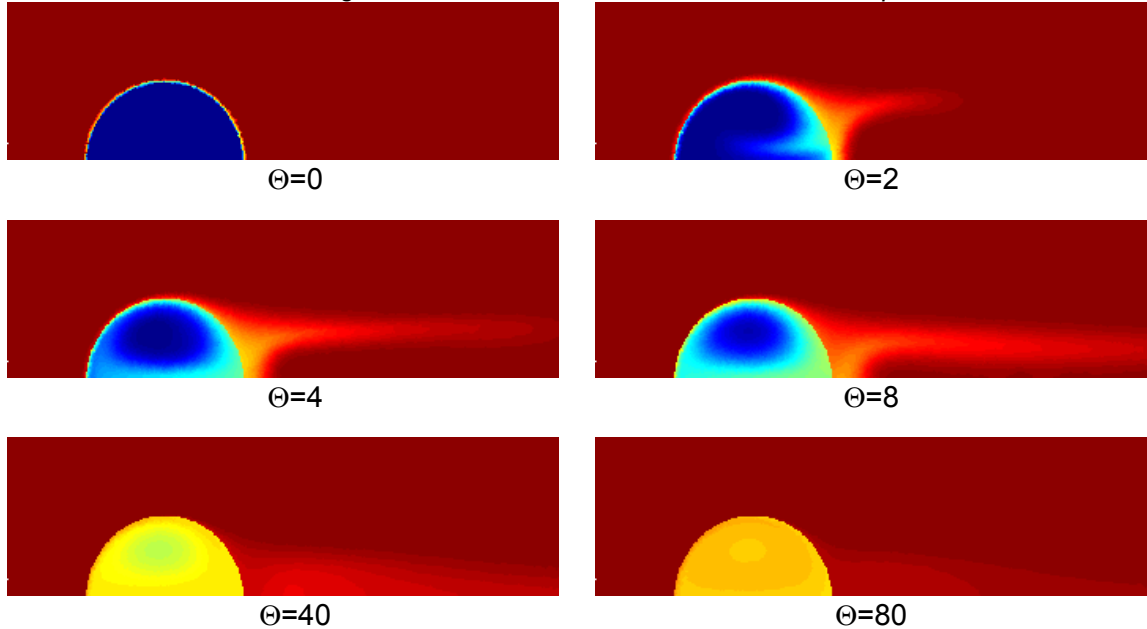


Figure 2. Typical computational mesh (nodes: 4563, triangles: 8906).

A typical mesh, which consists of 4563 nodes and 8906 triangles, is shown in Figure 2. The streamlines around the drop at the beginning of the mass transfer process are shown in Figure 3 which represent the velocity field. In this figure it can be observed that a wake is formed behind the drop, detached from the drop interface, which affects the drop movement and the mass transfer rate.



*Figure 3. Streamlines inside and around the drop.*



*Figure 4. Concentration profiles for  $Re^C = 26$ ,  $Re^D = 66$ ,  $Pe^P = 1000$ , at different values of  $\Theta$ .*

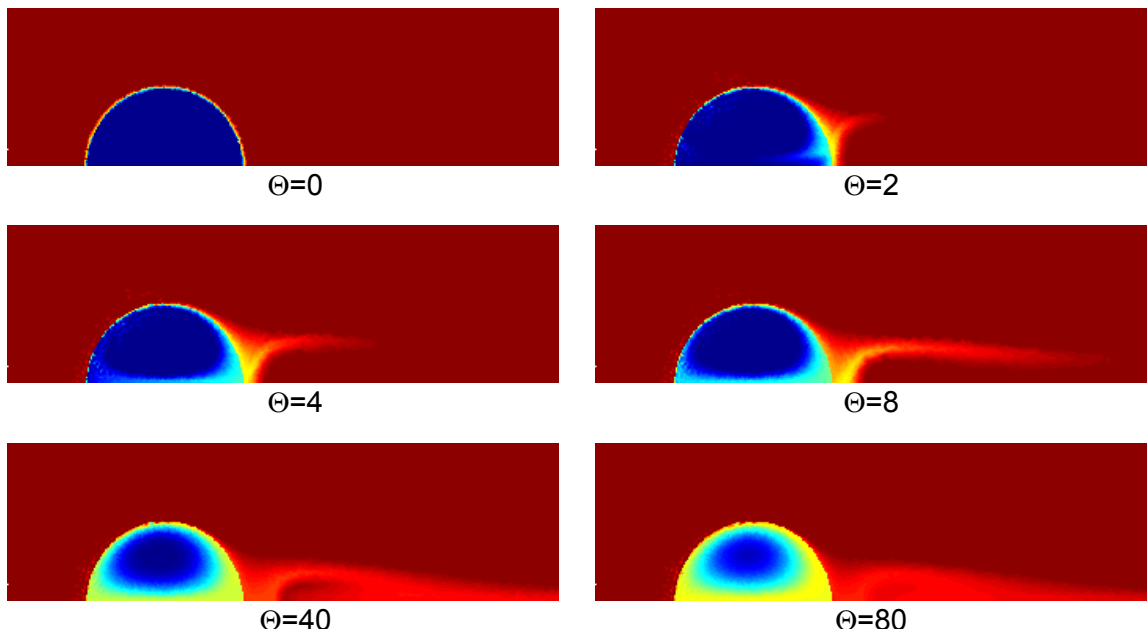


*Figure 5. Concentration profiles for  $Re^C = 26$ ,  $Re^D = 66$ ,  $Pe^P = 10,000$ , at different values of  $\Theta$ .*

Two sequences of graphics representing the development of the concentration distribution of the solute between the drop and the continuous phase are shown in Figures 4 and 5. The value of the distribution coefficient ( $m$ ) used in these simulations is 0.7. It is worth noting that steady state is reached at approximately  $\Theta = 40$  for  $Pe^P = 1000$ ,  $Re^D = 26$  and  $Re^C = 66$ , whereas for  $Pe^P = 10,000$  at the same values of the Reynolds numbers, the steady-state is not yet reached at  $\Theta = 80$ .

It is observed that for larger Peclet numbers at the same Reynolds number, the time taken by the drop to reach the steady state is longer because the inertial terms remain the same, but the diffusive terms are smaller, therefore affecting the mass transfer rate. At larger Reynolds numbers, the nonlinear inertial terms become more important leading to a solution more difficult to achieve due to the presence of oscillation. In these figures, it can be observed that, in the absence of turbulence or oscillations, the solute travels around the drop in a circular motion passing from the front to the rear stagnation point along the surface and comes back to the front through the axis of symmetry. The solute is transported from the drop surface to the stagnation ring by diffusion. Since the diffusion is a slow process, the time taken by the solute to go from the drop surface to the stagnation ring is much longer than the time taken to travel around the drop surface. If the convective transport rate of mass is kept constant, as the Peclet increases the diffusive term decreases and therefore the solute takes longer to travel from the surface to the bulk of the drop.

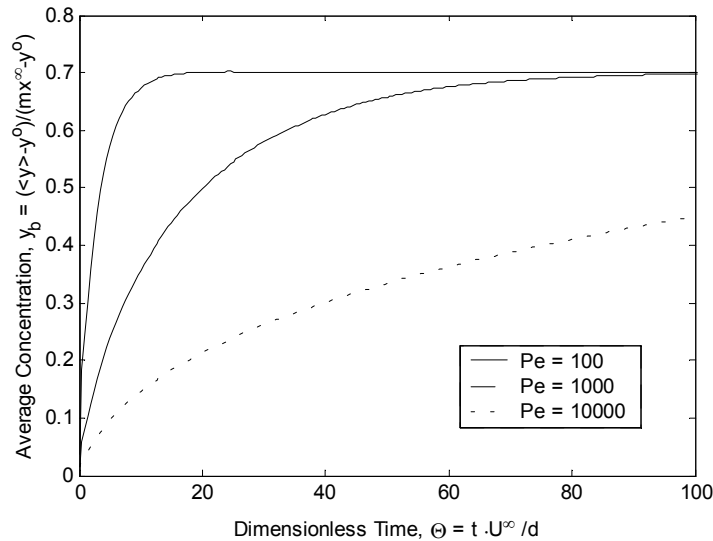


*Figure 6. Plot of dispersed phase average concentration vs dimensionless time for  $Re^C = 26$  and  $Re^D = 66$  at different Peclet numbers.*

Three plots of the average concentration of the solute inside the drop for three different values of the Peclet number at the same Reynolds number against the dimensionless time are shown in Figure 6. Since the Reynolds is kept constant, the convective transport rate of mass is also kept constant. Therefore, it can be observed that for larger Peclet numbers, the time taken by the solute to reach the steady (equilibrium) state increases. Three plots of the bulk average concentration in the dispersed phase against the dimensionless time are shown in Figure 7 for three different values of the Reynolds number ( $Re^C = 66, 200, 450$ ) and  $Pe^P = 100$ . There is not an appreciable difference between the three plots. This can be explained by observing that, since the Peclet number is quite small, the diffusive mass transfer rate is more important than the convective transport rate and therefore the total mass transfer rate is almost constant with varying Reynolds numbers. It is expected that for larger Peclet numbers, the effect of the Reynolds number will also be large.

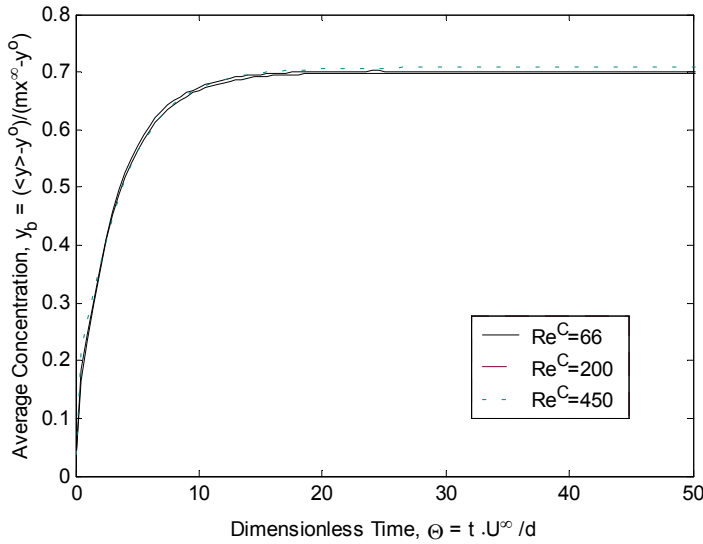


*Figure 7. Plot of dispersed phase average concentration vs. dimensionless time for  $Pe^P = 100$  at different Reynolds numbers*

## CONCLUSIONS

A numerical study of the mass transfer process between a single, spherical drop traveling through an unbounded, still continuous phase is presented. The studies were carried out assuming that no turbulence is present and, therefore, the flow is laminar and the mass transfer is carried out by convection around the drop and by diffusion towards the stagnation ring. It is observed that the most important dimensionless groups that represent this phenomenon are the Reynolds number, the Peclet number and the hydrodynamic time. For a constant Reynolds number, the mass transfer rate decreases as the Peclet number increases due to a constant convective term but a lower diffusive term.

The results presented in this work agree with qualitative observations in real systems [3]. This is an important step in the solution of the mass transfer process in drops in more complex situations where other influences are present such as bulk turbulence, interfacial turbulence (Marangoni effect), surface active contaminants, moving and varying drop shapes, multicomponent mass transport, etc. The study of the mass transfer process in single drops will allow us to extrapolate the results to mass transport in bubbles and in multidrop columns for design and process scale up.

## REFERENCES

1. R. H. Perry, D. W. Green and J. O. Maloney (1999), Perry's Chemical Engineers' Handbook, 7th edn., McGraw Hill Company, Inc., pp. 6.47-6.48.
2. D. S. Dandy and L. G. Leal (1989), *J. Fluid Mech.*, **208**, 161-192.
3. A. R. Uribe-Ramírez and W. J. Korchinsky (2000), *Chem. Eng. Sci.*, **55** (16), 3305-3318.
4. Y. W. Kwon and H. Bang (1997), The Finite Element Method Using MATLAB, CRC Press LLC, FL.
5. Comsol, Inc (2000), FEMLAB Reference Manual.
6. W. A. Sirignano (1999), Fluid Dynamics and Transport of Droplets and Sprays, Cambridge University Press, UK.



## INFLUENCING THE RATE OF MASS TRANSFER IN REACTIVE EXTRACTION USING HIGH VOLTAGE

Andreas Wildberger and Hans-Jörg Bart

Institute of Thermal Process Engineering, University of Kaiserslautern,  
Kaiserslautern, Germany

Mass transfer of p-toluenesulfonic acid, PTA, dissolved in water extracted with tri-n-octylamine, TOA, dissolved in toluene was investigated in a planar mass transfer cell with a constant interfacial area when high electrostatic fields (DC) were applied. Mass transfer was found to be markedly accelerated, and this can be explained by the field induced potential gradient which is the driving force. An electrostatically extended kinetic model based on the Nernst-Planck equation was developed to quantify the enhancement of mass transfer. The theory was also proved with a cation exchange system as is zinc chloride/di-2-ethylhexylphosphoric acid ester (D2EHPA) in toluene.

### INTRODUCTION

Several studies have been conducted on the effect of applied electrical fields on liquid-liquid mass transfer rates between a drop (the dispersed conducting phase) and a nonconducting continuous phase [1-4]. The applied field was found to alter the shape of the droplet and charge the droplet, which influences drop rise velocity, phase separation, coalescence and mass transfer. Little has been reported on the effect of applied electrical fields on liquid-liquid mass transfer when such fields are applied across a plane interface [5]. Generally, interfacial turbulence, and increased mass transfer rates have been observed [6-9]. Kuipa and Hughes expected the enhanced mass transfer to be depended on the organic diluent and of local variations in surface tension and surface boundary layer created by the electrical field [5].

However, no attempt was made to study the influence of electric fields in a reaction controlled regime. This work focuses on the development of an electrostatically extended kinetic model which describes the mass transfer enhancement in reactive extraction.

### EXPERIMENTAL

Mass transfer was investigated in a stirring cell having a constant interfacial area [10], while high electric fields (DC) up to 25 000 volts were applied. The cell was modified with two teflon-coated ring-electrodes (Figure 1). The upper one (in organic phase) was positively charged, while the other one (in aqueous phase) was grounded. The distance of each from the interface was 1 cm. The external field applied between those electrodes was then perpendicular to the liquid-liquid interface.

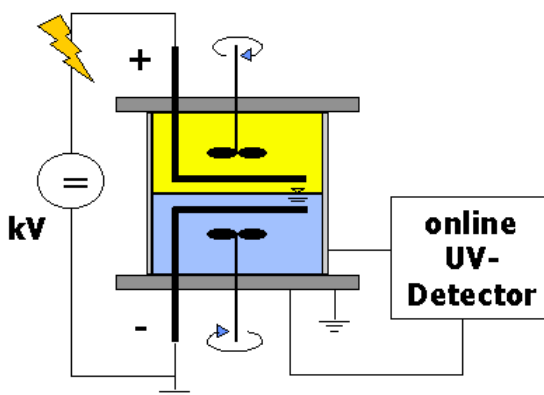


Figure 1. Mass transfer cell.

The reactive extraction system investigated was p-toluenesulfonic acid (PTA) dissolved in water, tri-n-octylamine (TOA) dissolved in toluene. The PTA concentration was determined by an online UV-detector (Fig. 1). All experiments were carried out at 298 K. All chemicals used were of analaR grade.

## EQUILIBRIA

PTA (HA) was found to chemically react with the amino-function of the liquid ion exchanger (TOA) at the interface to form a 1:1 complex.

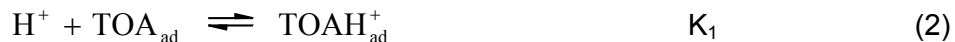


Despite being under the influence of strong electric fields (up to 25 000 volts), no equilibrium shift was found. Thus the external field does not affect the extraction equilibria or induce further chemical reactions under these electrostatic conditions [11].

## MASS TRANSFER

### Kinetics

The following model can be applied to simulate mass transfer when mass transfer is kinetically controlled (plateau area) [12-16]. In order to model the reactive mass transfer of PTA, the equilibrium equation (1) is split into the following three partial reaction steps:



The index "ad" represents these species which are adsorbed at the interface. The first reaction step depicts the protonation of an at the interface adsorbed TOA molecule.



This reaction represents the formation of an ion-pair molecule which is adsorbed at the interface. This molecule is then replaced by a fresh TOA-molecule from the organic bulk phase in the third and last reaction step:



The interfacially adsorbed anion exchanger species are balanced according to the Gibbs' law:

$$[\text{TOA}_{\text{ad}}] + [\text{TOAH}^+_{\text{ad}}] + [\text{TOAHA}_{\text{ad}}] = \frac{\alpha_m \cdot \overline{[\text{TOA}]}}{\gamma_m + \overline{[\text{TOA}]}} \quad (5)$$

$\alpha_m$  and  $\gamma_m$  are the adsorption constants which have been determined by interfacial tension measurements to be  $8.49 \times 10^{-4}$  for  $\alpha_m$  and  $2.98 \times 10^{-2}$  mol/kg for  $\gamma_m$  in toluene [15]. The rate determining steps (Eq. (2)-(4) and Eq. (5)) are combined to obtain the kinetic rate equation,  $R'$ :

$$R' = \frac{(a_{H^+} \cdot a_{A^-} \cdot a_{\text{TOA}} - 1/K_{\text{EX}} \cdot a_{\text{TOAHA}}) \cdot (\alpha_m \cdot a_{\text{TOA}} / (\gamma_m + a_{\text{TOA}}))}{C_1 + C_2 \cdot a_{H^+} + C_3 \cdot a_{H^+} \cdot a_{A^-} + C_4 \cdot a_{H^+} \cdot a_{\text{TOA}} + C_5 \cdot a_{\text{TOA}} + C_6 \cdot a_{\text{TOAHA}}} \quad (6)$$

The constants  $C_1$  -  $C_6$  are functions of the kinetic parameters, where  $k_3$  is calculated from  $K_{\text{EX}}$  ( $K_1 = 503.908$  [kg/mol],  $k_2 = 93.016$ ,  $k_{-2} = 0.019$  [ $s^{-1}$ ],  $k_3 = 58.450$ ,  $k_{-3} = 12.934$  all in [kg/mol s]):

$$C_1 = \frac{k_{-2}}{k_2 \cdot k_3 \cdot K_1}, C_2 = \frac{k_{-2}}{k_2 \cdot k_3}, C_3 = \frac{1}{k_3}, C_4 = \frac{1}{k_2}, C_5 = \frac{1}{k_2 \cdot K_1}, C_6 = \frac{1}{k_{-2} \cdot K_{\text{EX}}} \quad (7)$$

The model was found to correlate the experimental data within a very good agreement over a wide concentration range (see Figure 2).

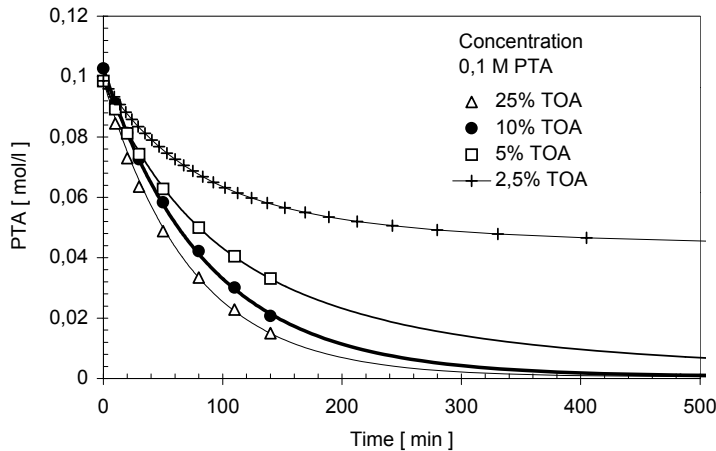


Figure 2. Simulation of the mass transfer kinetics of PTA with the kinetic model.

### Influence of Electric Fields

The Nernst-Planck equation (8) describes the movement of ions caused by diffusion and migration driving forces under isotherm conditions. Convection effects are neglected [13,17]:

$$\dot{N} = \dot{N}_{\text{diffusion}} + \dot{N}_{\text{migration}} \quad (8)$$

The molar Flux  $\dot{N}_{\text{diffusion}}$  [mol/s] becomes negligible because the system is kinetically controlled (plateau area) and only the migration term (Eq. (9)) becomes important as driving force for the movement of the ions inside the applied electric field:

$$\dot{N} = \dot{N}_{\text{migration}} = -A \frac{D_i c_i z_i e}{kT} \nabla \psi \quad (9)$$

(with:  $c_i$  concentration of the ionic species  $i$  [mol/l],  $A$  the mass transfer area [ $m^2$ ],  $D_i$  the diffusion coefficient of the ionic species  $i$  [ $m^2/s$ ],  $z_i$  charge number of the ionic species  $i$  [-],  $e$  elementary charge [C],  $\psi$  electrical potential [V],  $k$  Boltzmann constant [J/K],  $T$  temperature [K]).

For  $\Delta\psi = \psi_2 - \psi_1$ , with 2: interface and 1: bulk, as the driving force for the ion movement from bulk to interface equation 10 is obtained, which calculates the interfacial concentration of the ionic solute [17].

$$c_2 = -\frac{z_i e(\psi_2 - \psi_1)c_1}{kT} + c_1 \quad (10)$$

Equation 10 was integrated in the above used kinetic model. Thus an electrostatic expanded kinetic model was developed, which considers the field influence in the interfacial concentration of the ionic mass transfer components. The  $\text{A}^-$  concentration is increased at the interface by the applied field, while the interfacial concentration of the  $\text{H}^+$  ions is decreased. When no external field is applied and the interfacial potential becomes zero, the interfacial concentrations in the kinetic regime are the same as in the bulk.

### Computer Aided Determination of the Interface Potential

The potential drop which is generated by the applied electric field was determined considering the special geometry involved with the software program called EMAS (Ansoft Corporation Europe, UK). EMAS numerically evaluates potential fields by the finite element method based on the field theory of Maxwell [18]. EMAS considers the exact geometry of the electrostatic condenser (which is the geometry of cell and the used electrodes), the temperature, the electrical properties of the liquids used (like the dielectric constants or conductivity data) as well as the vectorial character of the field.

The potential was found to linearly drop from the interface to the grounded electrode inside the aqueous phase. The interface potential  $\psi_2$  was obtained to be 578 V, when a voltage of 20 kV was applied. The potential decreases from 20 kV at the upper electrode in organic phase till a value of 0 V at the other electrode in aqueous phase. Thus the bulk potential on aqueous side  $\psi_1$  is zero. It was also found, that the interface potential linearly increases with increasing the applied external voltage.

### Comparison of Theory and Experiment

Under the influence of a high electric field (DC) the mass transfer of PTA was found to be accelerated while the same equilibrium composition in the kinetically controlled regime is obtained (see Figure 3).

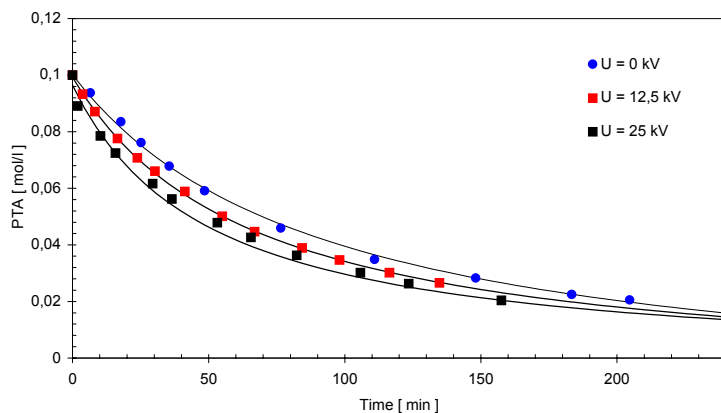


Figure 3. Mass transfer enhancement of PTA by a strong external field (DC) (PTA: 0,1 mol/l; TOA: 5%).

The acid anions are attracted by the positive charge of the upper electrode and move favourably to the interface. Thus the concentration of the acid anions is enhanced at the interface by the positive charge. The higher the voltage applied, the higher will be the interfacial concentration of the anions. The enhancement of mass transfer was found to be linear with increasing the voltage [11].

In light of proving the model it was also important to investigate mass transfer kinetics when using positively charged solutes (cationic ion exchange system) under the same conditions. In this case a diminution of mass transfer is expected. Zinc chloride was extracted with di(2-ethylhexyl)phosphoric acid ester (D2EHPA) dissolved in isododecane [15,19] under the same conditions as in Figure 3. The  $H^+$  concentration was measured online and zinc was analysed by atomic absorption spectroscopy.

As shown in Figure 4, the mass transfer kinetics of zinc ions are retarded under the same electric fields. This elucidates the correctness of the model assumption and is in accordance with the obtained concentration profiles in case of surfactant induced charging of the liquid-liquid interface [20]. The simulated mass transfer enhancement is given in Figure 5. A good representation of the experimental values is obtained.

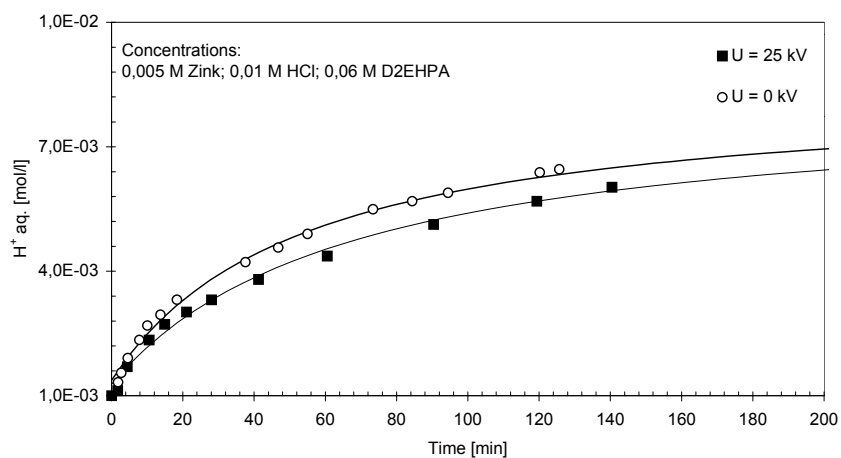


Figure 4. Mass transfer diminution of zinc ions by a strong external field (DC).

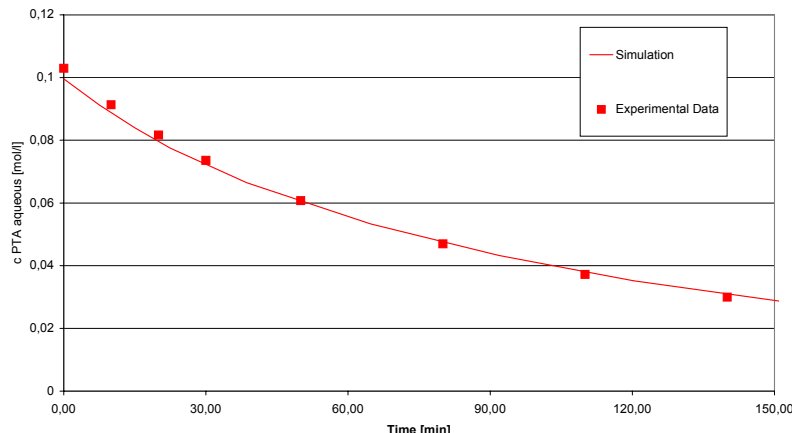


Figure 5. Simulation of mass transfer kinetics of PTA by a strong external field ( $U: 20\text{ kV}$ , PTS:  $0,1\text{ mol/l}$ ; TOA: 5%).

## CONCLUSIONS

Mass transfer was found to be accelerated (respectively reduced) in an electric high voltage field (DC). This is depending on either the field polarity or the charge of the solutes. Thus the application of high voltage in reactive extraction provides a potential to easily influence the selectivity of extraction. Because solutes are differently attracted by the field induced potential drop depending on the charge of the ionic solute. It is also possible to oppress a current flow by isolating the electrodes, which enables a low costing process and provides high safety aspects. This and the acceleration of mass transfer are interesting aspects in light of industrial application

of high voltage assisted extraction. In order to describe the process, a kinetic model was developed which satisfactorily correlates the experimental data.

### ACKNOWLEDGEMENTS

The support of the Deutsche Forschungsgemeinschaft (DFG) is gratefully acknowledged.

### REFERENCES

1. T. C. Scott (1989), *Sep. Purif. Methods*, **18** (1), 65-109.
2. N.-V. T. E. Carleson (1986), *AIChE*, **32** (10), 1739-1742.
3. P. J. Bailes (1981), *Ind. Eng. Chem. Process Des. Dev.*, **20**, 564-570.
4. M. Yamaguchi (1995), Electric Field Applications: Application of Electric Fields to Solvent Extraction, T. Tsuda (ed.), VCH, Weinheim, pp. 185-203.
5. P. K. Kuipa and M. A. Hughes (1999), *Sep. Sci. Technol.*, **34** (13), 2643-2661.
6. V. Mohan, P. Jayasankar and K. Padmanabhan (1986), *Proc. Int. Solv. Extr. Conf.*, Munich, Germany, Vol. 1, pp. 507-510.
7. L. J. Austin, L. Banczyk and H. Sawistowski (1971), *Chem. Eng. Sci.*, **26**, 2120-2121.
8. V. Mohan, K. Padmanabhan and K. Chandrasekharan (1983), *Adv. Space Res.*, **3** (5), 177-180.
9. M. Hund and F. Lancelot (1986), *Proc. Int. Solv. Extr. Conf.*, Munich, Germany, Vol. 1, pp. 511-517.
10. W. Nitsch (1989), Transportprozesse und chemische Reaktionen an fluiden Phasengrenzflächen, DECHEMA-Monographie, 144, VCH, Weinheim.
11. A. Wildberger, S. Schmidt and H.-J. Bart (2001), Mass Transfer Enhancement in Reactive Extraction by an Electric Field, Proc. ECCE 3, Nuremberg, Germany, in press.
12. M. Roos (2000), Zum Einfluß von Salzen auf die Reaktivextraktion organischer Säuren, Shaker, Aachen.
13. H.-J. Bart (2001), Reactive Extraction, Springer, Berlin.
14. C. Czapla (2000), Zum Einfluß von Grenzflächenladungen auf den Reaktionsmechanismus organischer Säuren bei der Reaktivextraktion, Shaker, Aachen.
15. S. Schmidt (2000), Diploma thesis, Universität Kaiserslautern, Germany.
16. H.-J. Bart (2002), *Proc. Int. Solv. Extr. Conf.*, Cape Town, South Africa, pp. 45-52.
17. J. A. Wesselingh and R. Krishna (2000), Mass Transfer in Multicomponent Mixtures, Delft University Press, Delft, The Netherlands.
18. I. Wolff (1997), Maxwellsche Theorie, Springer, Berlin.
19. M. Mörters (2001), Zum Stoffübergang in Tropfen bei der Reaktivextraktion, Shaker, Aachen.
20. C. Czapla and H.-J. Bart (2000), *Chem. Eng. Technol.*, **23**, 1058-62.



## A STUDY ON MULTI-COMPONENT MASS TRANSFER COEFFICIENTS OF DROP SWARM

Haiguo Wei and Weiyang Fei

Department of Chemical Engineering, Tsinghua University, Beijing, P.R. China

The multi-component mass transfer coefficients of drop swarm of aromatic extraction by sulpholane were measured in a 100mm internal diameter glass column and compared with those of single drops. It is shown from the experiments that the mass transfer coefficients of benzene are larger than those of toluene and much larger than those of xylene.

Several kinds of equations for single drop mass transfer coefficients were used to estimate the multi-component ones and compare with those of experimental, but none of them could fit the results well. The situation becomes more complex since the Marangoni phenomenon exists for the aromatic extraction by sulpholane system. Therefore, further study is necessary for the estimation of multi-component mass transfer coefficients of drop swarm for this important commercial system.

### INTRODUCTION

Solvent extraction has been widely used in petrochemical, pharmaceutical, hydrometallurgical and environmental industries. However, the design of commercial extraction columns is still difficult. Scale-up of extractors is often dependent on pilot plant experiments, which are expensive and time-consuming. The uncertainty of estimation of mass transfer coefficients is one of the main problems faced by the design engineers.

Measuring mass transfer coefficient with single drop experiments seems a promising method to solve the problem. Many researchers [1-4] completed extensive studies on this field and proposed many equations to evaluate mass transfer coefficient. However, most of the equations are restricted to their experimental conditions. The interactions among drops in commercial extraction columns have significant impact on mass transfer but can't be considered in single drop mass transfer models. Therefore, it is essential to measure mass transfer coefficient of drop swarms directly.

The estimation of multi-component mass transfer coefficients of drop swarm is essential when the non-equilibrium stage model is used for the simulation of a commercial extraction column [5]. However, the literature on measurement and prediction of multi-component mass transfer coefficients are still scarce.

Therefore, the multi-component mass transfer coefficients of drop swarm for aromatic extraction by sulfolane system were measured and compared with those of single components in this paper. The complexity of calculating multi-component mass transfer coefficients of drop swarm was also discussed.

## EXPERIMENTAL

### Apparatus

Figure 1 shows a diagram of the experimental apparatus. The flanged glass column has a 100 mm internal diameter and 600 mm working height. Both ends of the column were sealed by plexiglass using flanges. The bottom plexiglass has ten 3 mm pores. One is in the center, and the others are evenly distributed on a 50 mm circle concentric with the center pore. Stainless steel needles with blunt tips were inserted into the column through the pores. Two funnels were arranged 100 mm and 500 mm away from the bottom to collect samples.

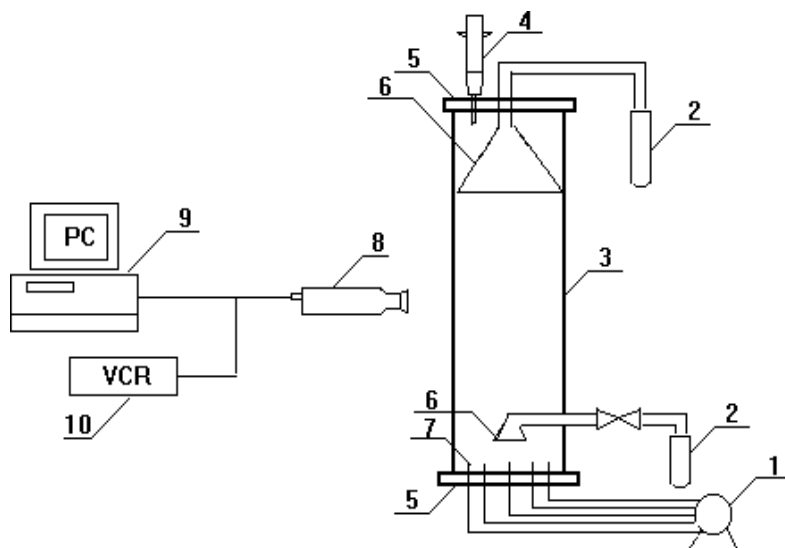


Figure 1. Diagram of experimental apparatus.

- 1.multichannel syringe pump 2.sampling tube 3.extraction column 4.syringe  
5.flange 6.funnel 7.needle 8.video camera 9. PC computer 10.video tape recorder.

The drop swarm was produced by a multi-channel syringe pump (Cole-Parmer Ins. Co., model 74900-10), which guarantee that each syringe pump has the same flow rate. Seven different gauges of medical needles were used in the experiments to produce different size drops. Teflon pipe was used as connector between needles and syringes. A computerized video imaging system, consisting of a PC computer with a capture card, a video camera and a video tape recorder, was installed to record the movements of drops.

### Test System

The continuous phase is pure sulfolane. The dispersed phases are either multi-component mixture of benzene, toluene, xylene and n-heptane or binary mixtures benzene/n-heptane, toluene/n-heptane and xylene/n-heptane. The concentrations of each component in mixtures are always 10% (wt%). The physical properties of the components are shown in Table 1.

### Method of Analysis

The concentrations of samples are measured by gas chromatography. The instruments are HP5890 Series II GC connecting with HP3365 workstation, HP-1 quartz glass capillary (25 m × 0.2 mm × 0.33 μm), GCD-300 flame ionic detector(FID) and automatic hydrogen generator. The method of area normalization with calibration factor was applied in the calculation.

*Table 1. Physical properties of experimental systems.*

Component	$\rho$ (Kg · m <sup>-3</sup> )	$\mu$ (mPa · S)
benzene	872.5	0.596
toluene	862.3	0.547
p-xylene	859.9	0.605
n-heptane	680.5	0.396
sulfolane	1263.2	11.4

### Procedure

The column was filled with sulfolane. The whole column is airtight and does not have elastic parts, so an equal volume organic phase will leave from the top funnel when drop swarms enter the column. The interface of the two phases at the top funnel was controlled through injecting or sucking continuous phase by the syringe at the upper Plexiglass. The formation time of each drop was about 2 to 3 seconds. Drop size was calculated according to the flow rate of the pump and the time used to produce a certain number of drops. Assuming the overall mass transfer coefficient  $K_{od}$  of drop swarms doesn't change with time, it can be calculated by the following equations:

$$K_{od} = -\frac{d_p}{6t} \ln(1 - E) \quad (1)$$

$$E = (y_2 - y_1) / (y^* - y_1) \quad (2)$$

where  $y_1$ ,  $y_2$  are the samples concentration at 100 mm and 500 mm above the column bottom respectively, and  $y^*$  is the equilibrium concentration of continuous phase.

## EXPERIMENTAL RESULTS

### Multi-Component Mass Transfer Coefficients of Drop Swarm

The multi-component drop swarm mass transfer coefficients of benzene, toluene and xylene are shown in Figure 2. It is clear from the figure that the mass transfer coefficients of benzene are larger than those of toluene and much larger than those of xylene. The differences of mass transfer coefficients among benzene, toluene and xylene are significant. Therefore, it will cause huge error if the same mass transfer coefficients or tray efficiencies are used in design procedure according to the equilibrium stage model. On the other hand, the larger the drop diameter, the larger the mass transfer coefficients for all the components.

### Mass Transfer Coefficients of Drop Swarm in Binary Mixture

The drop swarm mass transfer coefficients of benzene, toluene and xylene in binary mixtures are shown in Figure 3. The effects of component and drop size on the mass transfer coefficients are similar with those of multi-component system. The mass transfer coefficients of benzene are about three times larger than those of xylene, and are about 50% larger than those of toluene.

### Comparison of Mass Transfer Coefficients between Multi-Component and Binary System

The comparison of toluene mass transfer coefficients between multi-component and binary system is shown in Figure 4. The mass transfer coefficients of toluene in multi-component system is slightly larger than those of in binary system and increased more quickly with the drop size.

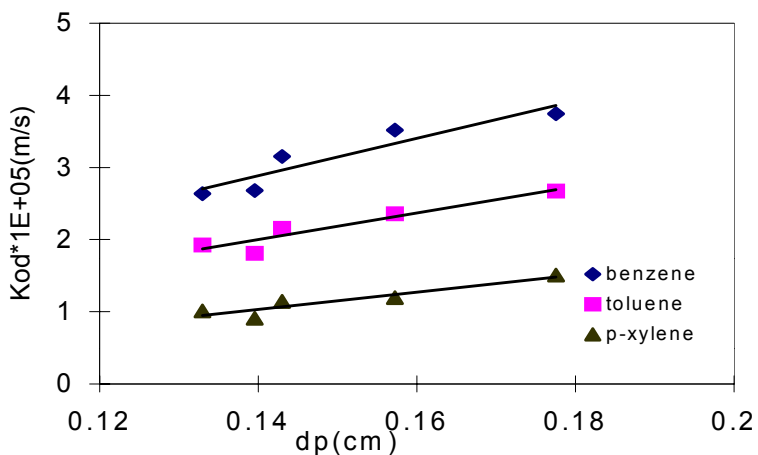


Figure 2. Mass transfer coefficients of drop swarms in multi-component mixture.

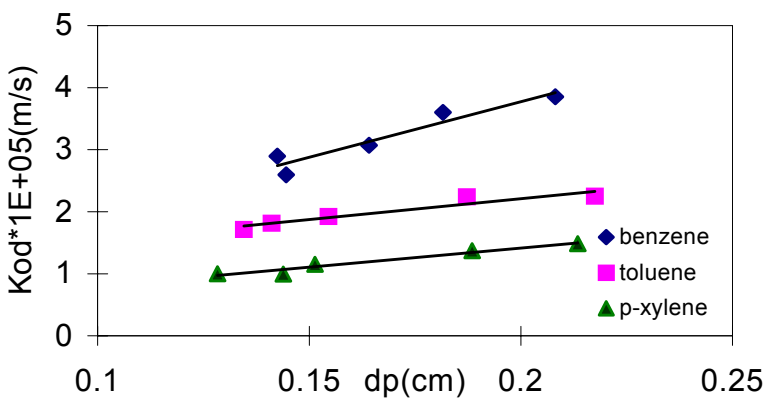


Figure 3. Mass transfer coefficients of drop swarms in binary mixture.

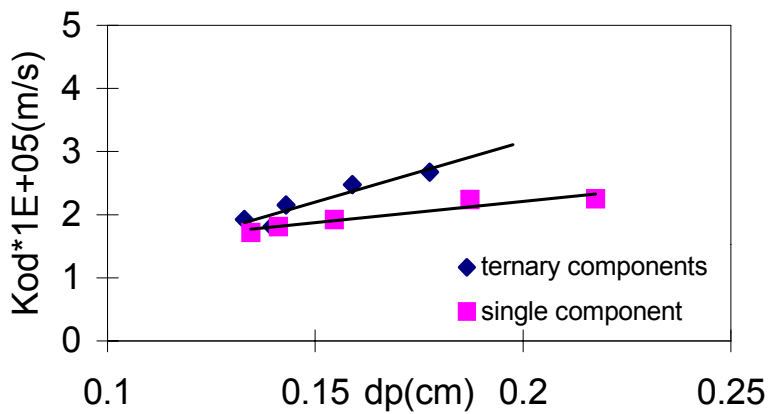


Figure 4. Mass transfer coefficients of toluene's drop swarms.

## DISCUSSION

There are many equations used to calculate the inside and outside drop mass transfer coefficients. These models can be classified into three categories, which are suitable for stagnant, circulating and oscillating drops respectively. Slater [3] and Kumar *et al.* [4] reviewed these models and proposed empirical correlations for the prediction of single drop mass transfer coefficient. However, most of them could not fit experimental data of this paper very well after extensive calculation and comparison [6]. It seems that the main reasons of this discrepancy are the difference between the mass transfer of single drop and drop swarm and the serious Marangoni effect during the mass transfer of test systems.

## CONCLUSIONS

1. It is shown from the multi-component mass transfer experiments of drop swarm that the mass transfer coefficients of benzene are about 50% larger than those of toluene and 200% larger than those of xylene.
2. According to the comparison between multi-component and binary system experiments the mass transfer coefficients of toluene in multi-component systems are slightly larger than those in binary systems.
3. The existing models could not fit experimental data of multi-component mass transfer experiments of drop swarm very well. Therefore, further study is necessary in this area.

## ACKNOWLEDGEMENTS

The authors wish to express their appreciation to the Solvent Extraction Laboratory, State Key Laboratory of Chemical Engineering, China, for its support.

## SYMBOLS

$d_p$	[m]	drop diameter
$E$	[‐]	fraction degree of extraction
$K_{od}$	[m s <sup>‐1</sup> ]	overall dispersed phase mass transfer coefficient
$t$	[s]	time
$y_1$	[mol l <sup>‐1</sup> ]	dispersed phase concentration at 100mm above the bottom
$y_2$	[mol l <sup>‐1</sup> ]	dispersed phase concentration at 500mm above the bottom
$y$	[mol l <sup>‐1</sup> ]	dispersed phase concentration

### Greek letters

$\mu$	[Pa S]	viscosity
$\rho$	[kg m <sup>‐3</sup> ]	density

## REFERENCES

1. G. S. Laddha and J. M. Smith (1976), *Transport Phenomena in Liquid Extraction*, Tata McGraw-Hill, New Delhi.
2. E. Blass, G. Goldmann, K. Hirschmann, *et.al.* (1986), *Ger. Chem. Eng.*, **9**, 222-238.
3. M. J. Slater (1994), *Liquid-Liquid Extraction Equipment*, J.C. Godfrey, M. J. Slater, (eds.), John Wiley & Sons, Chichester, pp. 45-94.
4. A. Kumar and S. Hartland (1999), *Trans. IChemE*, **77**, 372-384.
5. W. Y. Fei, X. M. Wen and R. X. Xie (1996), *Tsinghua Sci. Tech.*, **1** (4), 332.
6. W. Y. Fei and H. G. Wei, *Chinese J. Chem. Eng.*, in press.



## KINETIC STUDY OF NICKEL(II) EXTRACTION FROM CHLORIDE SOLUTIONS

A. Buch, D. Pareau , M. Stambouli and G. Durand

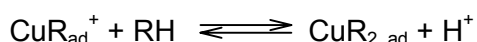
Laboratoire de Chimie et Génie des Procédés, Ecole Centrale Paris, Paris, France

The rate of nickel(II) extraction from aqueous chloride solutions by 2-ethylhexanal oxime (EHO) in dodecane has been studied as a function of the concentrations of extractant, metal and salt and of the equilibrium pH.

The extraction kinetics have been carefully studied and a mechanism in agreement with the experimental results has been proposed for pH > 4. The limiting step is an interfacial reaction between a neutral nickel adsorbed species and a molecule of EHO.

### INTRODUCTION

The extraction of nickel(II) by oximes is relatively slow [1-3]. For example, more than 1 hour is necessary for reaching equilibrium of nickel(II) extraction by 2-ethylhexanal oxime (EHO). Only a few authors have studied the kinetics of nickel(II) extraction by oximes, but a great number of them have investigated copper or nickel extraction by hydroxyoximes. All these systems involve an interfacial mechanism [4-6]. The limiting step of copper extraction by an hydroxyoxime (2-hydroxy-5-alkylbenzaldehyde oxime) is indeed often the complexation of an adsorbed species (containing one molecule of extractant and one atom of metal) with a second molecule of extractant as shown[4, 5]:



where the subscript, ad, denotes an interfacial adsorbed species and RH represents the acidic hydroxyoxime.

Another kind of limiting step has been determined for copper extraction by LIX 65N [6]:



In this case CuR<sup>+</sup> in the aqueous phase reacts with an adsorbed molecule of the extractant.

Chen [7] has however shown that in the case of nickel(II) extraction by dodecylsalicylaldoxime (HL), the rate-limiting step involves two reactions, one at the interface ( $\text{Ni}^{2+} + \text{HL} \rightarrow \text{NiL}^+ + \text{H}^+$ ) and one in the bulk aqueous phase ( $\text{Ni}^{2+} + \text{L}^- \rightarrow \text{NiL}^+$ ).

It can be seen that the kinetic interpretations of these systems are not simple. Our contribution is the determination of the limiting step of nickel(II) extraction by EHO, because of the interesting properties of this extractant in acid solutions.

EHO can adopt two configurations, known as (Z) and (E) [2,8,9]. As proposed by Kopczynski [8], the organic phase containing EHO was pre-equilibrated with the aqueous phase containing no metal, to ensure a pre-equilibrium condition with the (Z) and (E) configurations. Furthermore, the authors have reported the aggregation of this oxime previously [3]. EHO was found to form dimers and trimers. These results are used in this work to calculate the EHO monomer concentrations.

## EXPERIMENTAL

The principal reagent (EHO) was prepared by reaction of 2-ethylhexanal with hydroxyl ammonium chloride [3, 10]. The measured EHO purity was 98.5%. The diluent used was dodecane (Aldrich, 99%+). The aqueous solutions were prepared by dissolving nickel chloride salts (Fluka 99%) in water.

150 mL of aqueous nickel phase were contacted at 24°C in a homothetic cell with 150 mL of organic phase containing EHO. The pH was controlled using a specific calomel electrode.

Ni concentrations in the aqueous phase were measured by atomic absorption spectrometry (AA300 Varian). The metal contained in the organic phase was stripped with HNO<sub>3</sub> and its concentration in the aqueous stripping phase was measured by the same method.

The interfacial tension was measured by the drop volume method at 293 K.

## KINETIC STUDY OF NICKEL EXTRACTION BY EHO

This study was performed using a vigorously stirred cell. A homothetic cell (Rushton type) was designed in order to ensure a good reproducibility of the experimental results. In the previous thermo dynamical study [3], two different ranges of pH were considered. For pH > 4, the only range of pH considered in this study, the extracted complex was shown to be NiCl(Ox)(HOx)<sub>4</sub>.

By considering the global rate of extraction  $r = k_g (x - x_{eq})$  ( per surface unit), a kinetic model can be written as:

$$x(t) = x_{eq} + (x_0 - x_{eq}) \cdot \exp(-\alpha \cdot t) \quad (1)$$

where  $\alpha = \frac{ak_g V_t}{A}$ , A is the aqueous volume, V<sub>t</sub> the total volume of both phases, a the specific interfacial area (per total unit volume) (unknown but reproducible), and k<sub>g</sub> the kinetic constant. x<sub>0</sub>, x<sub>eq</sub>, x are respectively the concentrations of aqueous nickel at the initial time, at equilibrium and at time t. Experimental results (x, t) were fitted by the exponential expression of x (t) using the Microcal origin® program. The values for a.k<sub>g</sub> could then be determined.

### Influence of Hydrodynamic Parameters

The extraction rate of nickel(II) by EHO in a chloride solution is relatively low. If stirring is not sufficient, diffusion can be the rate limiting step. Experiments were performed with various stirring speeds and the experimental data was manipulated as described above. The calculated values of a.k<sub>g</sub> were found to be constant for a stirring speed greater than 650 rpm: diffusion was therefore not limiting in these conditions. In all further experiments a stirring speed of 700 rpm was used.

### Influence of Temperature

By varying temperature from 4 to 40°C, the different values of  $a.k_g$  were plotted versus  $1/T$ . A straight line was obtained for pH = 6.2 and the activation energy was calculated from the slope to be  $52.3 \pm 6.7$  kJ/mol. This value was greater than 40 kJ/mol, the range that represents the chemical nature of the kinetic regime.

### Influence of Chemical Parameters

Nickel concentration was varied between 2.5 to 9 mmol/L.  $a.k_g$  was found to be independent of Ni concentration and had the value  $(4.7 \pm 0.5).10^{-4}$  s<sup>-1</sup>. The reaction rate was therefore first order with respect to nickel. Other chemical parameters such as pH, EHO and NaCl concentrations were studied.

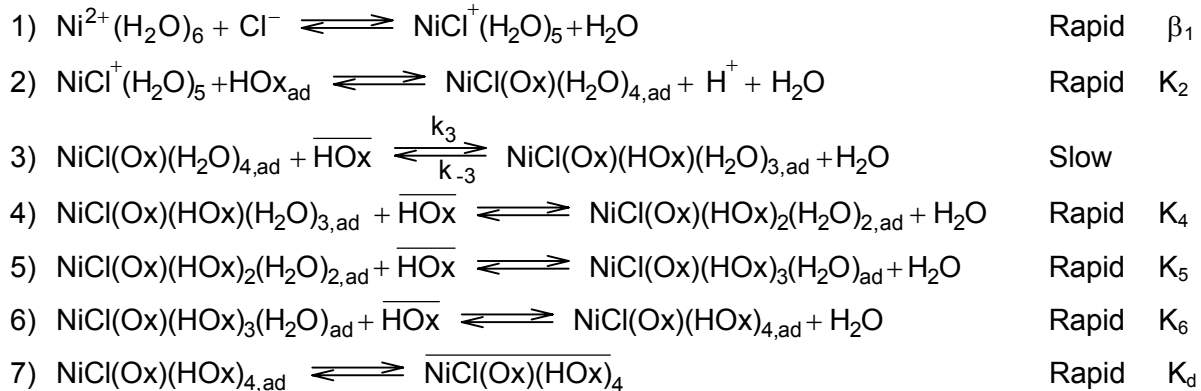
## EXTRACTION MECHANISM

Different experiments were performed to study the influence of EHO and NaCl concentrations and of pH under the following conditions:

- EHO concentration varying from 0.1 to 0.55 mol/L for pH 6.2 and NaCl 0.5 mol/L
- pH varying from 6 to 7 for NaCl 0.5 and 1 mol/L and EHO 0.295 mol/L
- NaCl concentration varying between 0.3 to 1 mol/L for pH 6.2 and EHO 0.295 mol/L.

The experimental data was manipulated using the model presented below.

The following mechanism was proposed and its accordance with the experimental results was tested.



where the overbar represents a species in the organic phase.

Activities were defined on the molarity scale, with reference to  $C_o=1$  mol/L. In the organic phase, the ionic strength was very low, so the activity coefficients could be considered to be constant. Furthermore,  $[\text{Ni}] = [\text{Ni}^{2+}] \cdot \alpha_{\text{Ni}}$ , with  $\alpha_{\text{Ni}} = 1 + \sum_{j=1}^m \beta_j \cdot a_{\text{Cl}^-}^j$ . where  $\beta_j$  is the associated complexation constant [11]. Only  $\beta_1$  is considered here. The activity coefficient of Ni was considered to be constant because nickel was present in trace amounts.

The apparent equilibrium constants can be written as :

$$\beta_1 = \frac{a_{\text{NiCl}^+(\text{H}_2\text{O})_5}}{a_{\text{Ni}^{2+}} a_{\text{Cl}^-}} = \frac{[\text{NiCl}^+(\text{H}_2\text{O})_5] \cdot \alpha_{\text{Ni}}}{[\text{Ni}] \cdot a_{\text{Cl}^-}} \quad (2)$$

$$K_2 = \frac{[NiCl(Ox)(H_2O)_4]_{ad} \cdot a_{H^+}}{[NiCl(H_2O)_5] \cdot [HOx]_{ad}} \quad (3)$$

$$K_4 K_5 K_6 K_d = \frac{[NiCl(Ox)(HOx)_4]}{[NiCl(Ox)(HOx)(H_2O)_3]_{ad} \cdot [HOx]^3} \quad (4)$$

The rate of the limiting step (reaction 3 in the mechanism proposed) is defined as:

$$r_3 = k_3 \cdot [NiCl(Ox)(H_2O)_4]_{ad} \cdot \overline{[HOx]} - k_{-3} \cdot [NiCl(Ox)(HOx)(H_2O)_3]_{ad} \quad (5)$$

or by replacing  $[NiCl(Ox)(H_2O)_4]_{ad}$  and  $[NiCl(Ox)(HOx)(H_2O)_3]_{ad}$  by their expressions:

$$r_3 = K_2 \cdot k_3 \cdot [HOx]_{ad} \cdot \frac{\overline{[HOx]}}{a_{H^+}} \cdot \frac{\beta_1 \cdot a_{Cl^-}}{\alpha_{Ni}} \cdot x - \frac{k_{-3}}{K_4 K_5 K_6 K_d \cdot \overline{[HOx]}^3} \cdot y \quad (6)$$

with  $y = \overline{[NiCl(Ox)(HOx)_4]}$

Introducing  $r_{3,eq} = 0$ :

$$r_3 - r_{3,eq} = K_2 \cdot k_3 \cdot [HOx]_{ad} \cdot \frac{\overline{[HOx]}}{a_{H^+}} \cdot \frac{\beta_1 a_{Cl^-}}{\alpha_{Ni}} (x - x_{eq}) - \frac{k_{-3}}{K_4 K_5 K_6 K_d \cdot \overline{[HOx]}^3} (y - y_{eq}) \quad (7)$$

This expression is correct only if  $\overline{[HOx]} = \overline{[HOx]}_{eq}$ ,  $a_{H^+} = a_{H^+,eq}$  and  $a_{Cl^-} = a_{Cl^-,eq}$ .

These hypotheses were justified because, for each experiment, only nickel concentrations varied. pH was kept constant and  $Cl^-$  and EHO were present in large excess.

The mass balance of nickel gives for equal volumes of both phases:  $(y - y_{eq}) = - (x - x_{eq})$

The kinetic constant  $a \cdot k_g$  is finally expressed as:

$$a \cdot k_g = K_2 \cdot k_3 \cdot [HOx]_{ad} \frac{\overline{[HOx]}}{a_{H^+}} \frac{\beta_1 a_{Cl^-}}{\alpha_{Ni}} + \frac{k_{-3}}{K_4 K_5 K_6 K_d \cdot \overline{[HOx]}^3} \quad (8)$$

The concentration of the adsorbed monomer (the only adsorbed EHO species) may be considered as constant when the total EHO concentration varies because of its excellent surfactant properties. The plot of the interfacial tension  $\chi$  versus  $\log[HOx]$  was indeed a straight line with  $\chi$  (N/m) =  $-7.9 \log [HOx] + 23.1$  ( $r^2 = 0.995$ )), showing that the interface was saturated with EHO monomers. This result is in a good agreement with previous findings that oximes are more interfacially active in aliphatic than in aromatic diluents [6].

From equation (8), the expressions of  $a \cdot k_g = f\left(\frac{\beta_1 a_{Cl^-}}{\alpha_{Ni}}\right)$ ,  $a k_g = f\left(\frac{1}{a_{H^+}}\right)$  and of  $a \cdot k_g \cdot [HOx]^3 = f\left(\overline{[HOx]}^4\right)$  were plotted and showed linear relationships (Figures 1, 2 and 3).

The model is therefore shown to be in good agreement with the experimental results.

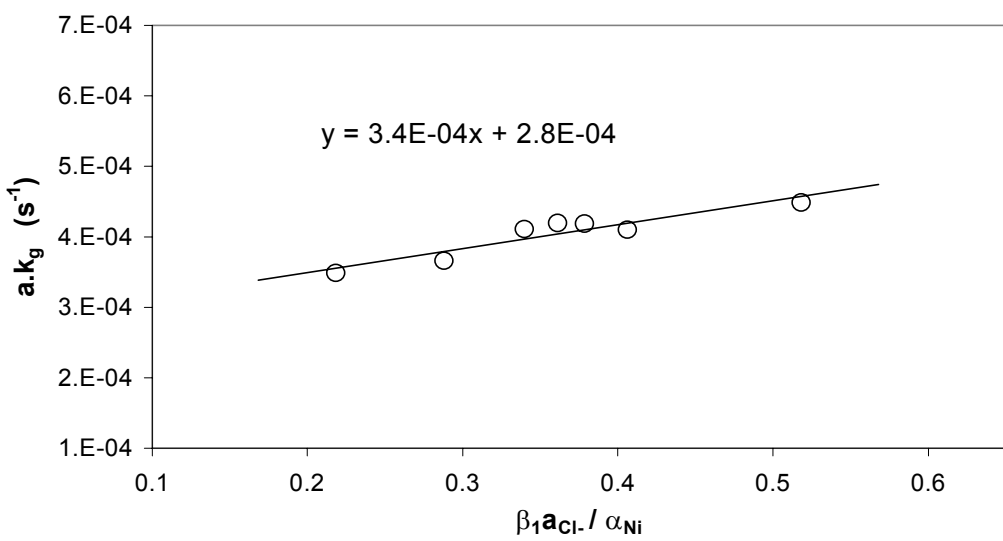


Figure 1. Plot of  $a.k_g$  versus NaCl activity,  $pH=6.2$ ,  $[EHO]_{\text{total}}=0.295 \text{ mol/L}$ .

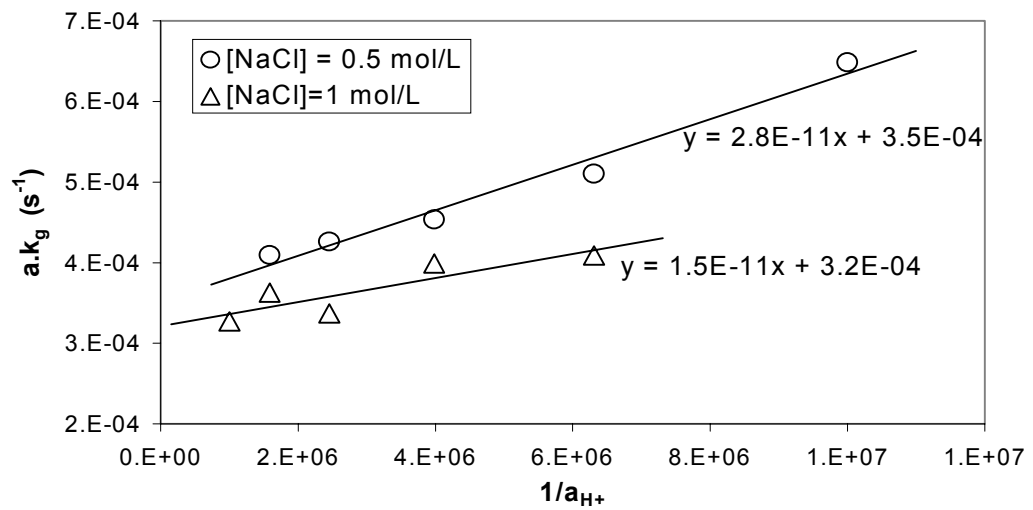


Figure 2. Plot of  $a.k_g$  versus  $a_{\text{H}^+}$ ,  $[EHO]_{\text{total}}=0.295 \text{ mol/L}$ .

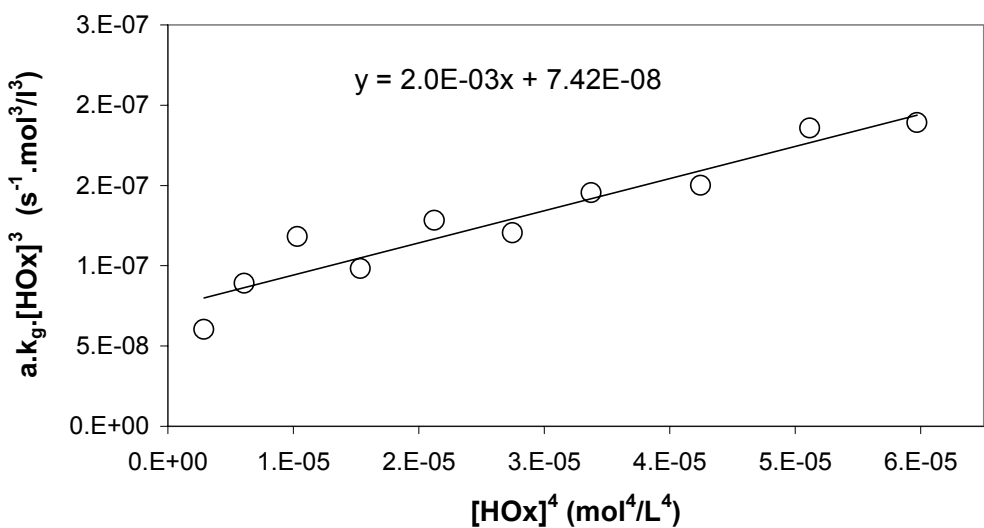


Figure 3. Validation of the model for EHO variations,  $pH=6.2$ ,  $[\text{NaCl}]=0.5 \text{ mol/L}$

The values of  $K_2 \cdot k_3 \cdot [HOx]_{ad}$  and  $\frac{k_{-3}}{K_4 K_5 K_6 K_d}$  were estimated from these three series of experiments. The values obtained were essentially constant, thus confirming the validity of the proposed mechanism:

$$K_2 \cdot k_3 \cdot [HOx]_{ad} = (2.4 \pm 0.3) \cdot 10^{-9} \quad \frac{k_{-3}}{K_4 K_5 K_6 K_d} = (9.0 \pm 0.7) \cdot 10^{-8}$$

## CONCLUSION

A kinetic mechanism proposed for the extraction of nickel by EHO was found to be consistent with experimental results. The limiting step was the first reaction of the solvation of the adsorbed neutral nickel species  $NiCl(Ox)(H_2O)_4$  by EHO. The slow reaction rate can be attributed to the solvation shell of this complex being very strong thus causing the substitution of a supplementary water molecule to be difficult. The further substitution reactions are then facilitated by the presence, in the solvation shell, of several EHO molecules.

The proposed kinetic mechanism is valid for pH greater than 4. When pH is lower, the nickel extraction reaction is not reversible and the kinetic mechanism is supposed to be fundamentally different, needing then another complete kinetic study.

## ACKNOWLEDGMENT

We gratefully acknowledge the support provided by Dr J.S. Preston for the synthesis of EHO.

## REFERENCES

1. L.D. Redden and R.D. Groves (1993), *Sep. Sci. Technol.*, **28**, 201-225.
2. G.L. Pashkov, N.P. Bezrukova, V.N. Volk, I. Yu. Fletlich, N.I. Pavlenko, G.E. Selutin, and E.D. Korniyets (1991), *Solv. Extr. Ion Exch.*, **9**, 549-567
3. A. Buch, D. Pareau, M. Stambouli and G. Durand (2001), *Solv. Extr. Ion Exch.*, **19**, 277-299.
4. D. Stepiak-Biniakiewicz, J. Szymanowski, K. Alejski and K. Prochaska (1994), *Solv. Extr. Ion Exch.*, **8(3)**, 425-444.
5. J. Szymanowski and R. Cierpiszewski (1992), *Solv. Extr. Ion Exch.*, **12(4)**, 663-683.
6. R. Belcher, F. Ingman, A.S. Kertes, H.W. Nurnberg, P. Papoff, E. Pungor, W.F. Pickering, S. Siggia and Y.A. Zolotov (1980), Critical Reviews in Analytical Chemistry, B. Campbell (ed.), CRC Press.
7. F. Chen, H. Ma, H. Freiser and S. Muralidharan (1995), *Langmuir*, **11**, 3235-3242.
8. T. Kopczynski, M. Lozynski, K. Prochaska, A. Burdzy, R. Cierpiezewski and J. Szymanowski (1994), *Solv. Extr. Ion Exch.*, **12(4)**, 701-725.
9. N.P. Bezrukova and V.E. Kolesnichenko (1996), *Solv. Extr. Ion Exch.*, **14(6)**, 1017.
10. V.M. Peshkova, V.M. Savostina and E.K. Ivanova (1977), Oximes, Nauka, Moscow.
11. S. Kotryl and L. Sucha (1985), Handbook of Chemical Equilibria in Analytical Chemistry, Ellis Horwood Limited.



## KINETICS OF RARE EARTH EXTRACTION WITH SEC-OCTYLPHENOXY ACETIC ACID

S. T. Yue\*, W. P. Liao, D. Q. Li and Q. Su

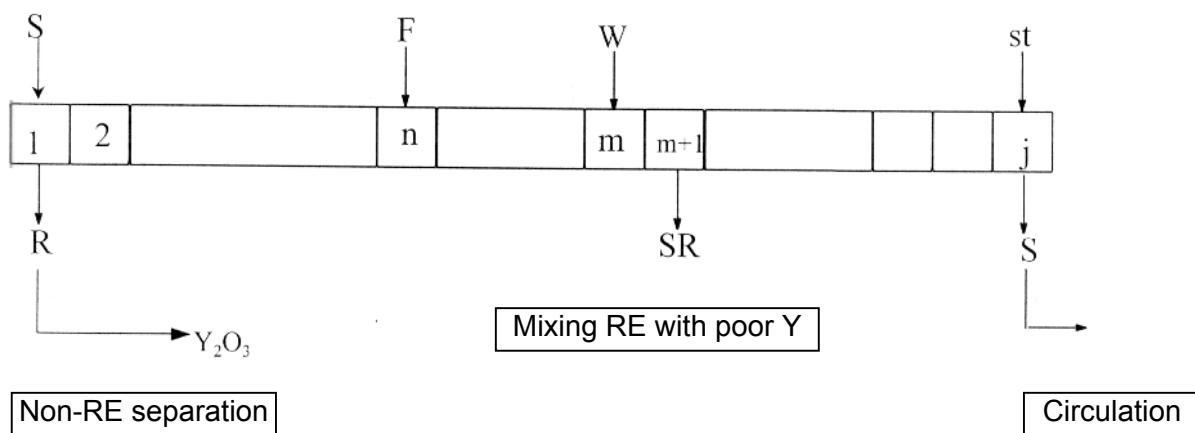
Laboratory of Rare Earth Chemistry and Physics, Changchun Institute of Applied Chemistry, Chinese Academy of Sciences, Changchun, P. R. China

\* Department of Chemistry, South of China Normal University, Guangzhou, P. R. China

The extraction kinetics of La(III), Gd(III), Er(III), Yb(III), and Y(III) with sec-octylphenoxy acetic acid in heptane have been investigated by using a constant interfacial area cell with laminar flow at 30°C. The results obtained have indicated that extraction rate is affected by the nature of the extracted species. For the extraction of Er(III), Yb(III) and Y(III), extraction rate is controlled by the reaction rate of M(III) and extractant molecules at the two-phase interface. For the extraction of Gd(III), extraction rate is decided by a mixed chemical reaction-diffusion. But, for the extraction of La(III), extraction rate is limited by diffusion. An interfacial extraction reaction model has also been derived.

### INTRODUCTION

It is well known that yttrium can be used in many fields, such as metallurgy, ceramics, lasers, and electronics, especially in fluorescent materials whose need for high purity yttrium oxide is always increasing. In China the resource of yttrium is very rich, and high purity yttrium has mainly been obtained by the process of naphthenic acid extraction [1-3]. However, there are some problems in the naphthenic acid extracting process. It is a very interesting project to develop a new process for extracting high purity yttrium, which is superior to the naphthenic acid.



S: HAB, F: feed, W: washings, st: stripping solution,  
S': HAB regeneration, R: raffinate, SR: stripped RE solution

Figure 1. Process scheme of separating yttrium by HAB extraction.

Ye *et al.* synthesized a carboxylic acid type of extractant, sec-octylphenoxy acetic acid (HA), whose composition is very simple. Under the same conditions, the natures of HA extraction are better than those of the naphthenic acid [4]. Li *et al.* [5,6] studied the mechanism of extracting rare earth(III) with HA and put forward HAB two solvent extraction system [two kinds of extractant system, HAB stands for HA+HB (another acidic extractant)]. Figure1 shows the process scheme of separating yttrium with HAB extraction system. But, the reports about the kinetics of rare earth extraction with HA have not been seen. It is very necessary to understand kinetics of the system. In this work, the extraction kinetics of Y(III), La(III), Gd(III), Er(III), Yb(III) with HA was examined following a thermodynamic study [5].

## EXPERIMENTAL SECTION

Interfacial tension measurements were performed as described in [7]. Apparatus and procedure employed in the study of extraction kinetics were described previously [8]. Both aqueous and organic phase volume were  $9.25 \times 10^{-5} \text{ m}^3$  ( $92.5 \text{ cm}^3$ ). Two phase interfacial area was  $2.1 \times 10^{-3} \text{ m}^2$  ( $21 \text{ cm}^2$ ). The pH in aqueous phase was adjusted by a NaAc-HAc buffer solution and the total concentration of NaAc and HAc was 0.2 mol/l. A Model 720 pH meter (Orion Co., America) was used to measure pH values in aqueous solutions.

Sec-octylphenoxy acetic acid (HA) was provided by Shanghai Institute of Organic Chemistry, Chinese Academy of Sciences. Its purity was more than 93%. After dissolving in heptane, HA was washed in turn by sodium carbonate, hydrochloric acid, distilled water, and was then saponified with ammonia water. The extent of ammonia saponification was 57.3%. The stock solutions of rare earths were prepared by dissolving their oxides (which had purity of greater than 99.99%) in concentrated hydrochloric acid and evaporating the excess HCl.

## RESULTS

### Data Treatment

Experimental data were treated following Danesi [9]. Assuming that the mass transfer process could be formally treated as a pseudo-first-order reversible reaction with respect to the metal cation:



The rate equation can be written as:

$$-\frac{d[M]_{(o)}}{dt} = (Q/V) (k_{oa}[M]_{(o)} - k_{ao}[M]_{(a)}) \quad (2)$$

Integrating gives:

$$\ln (1 - [M]_{(o)} / [M]_{(o)}^e) = - (Q/V)(k_{oa} + k_{ao})t \quad (3)$$

At constant stirring speed, the pseudo-first-order rate constants,  $k_{oa}$  and  $k_{ao}$ , are function of the concentration of HA in the organic phase and the concentration of the hydrogen ion in the aqueous phase:

$$k_{ao} = f_1([HA]_{(o)}, [H^+]_{(a)}) \quad (4)$$

$$k_{oa} = f_2([HA]_{(o)}, [H^+]_{(o)}) \quad (5)$$

At equilibrium, equation (2) is equal to zero, then

$$Kd = [M]_{(o)}^e / [M]_{(a)}^e = k_{ao} / k_{oa} \quad (6)$$

Equation (6) is substituted into (3), i.e.

$$\ln (1 - [M]_{(o)} / [M]_{(o)}^e) = - (Q/V)(1 + Kd) k_{oa} t \quad (7)$$

The function  $\ln(1 - [M]_{(o)} / [M]^e_{(o)})$  vs. time was plotted for each experiment. The slopes of the plots were used to evaluate  $k_{oa}$  and  $k_{ao}$ . All plots were straight lines, indicating that the mass transfer process could be treated as a pseudo-first-order reversible reaction with respect to the metal cation.

### Interfacial Tension Measurements of HA

The interfacial excess of HA at the n-heptane-water interface was determined from the plot of the interfacial tension ( $\gamma$ , mN/m) vs  $\log c$ ,  $c$  being the concentration of HA. The plot is shown in Figure 2 and the interfacial excess  $\Gamma$  derived from the linear part of the plot according to the Gibbs equation (eq. (8)) is  $3.54 \times 10^{-6} \text{ mol} \cdot \text{l}^{-2}$ .

$$\Gamma = -\frac{1}{2.303RT} \left( \frac{\partial \gamma}{\partial \log c} \right)_T \quad (8)$$

Here,  $\gamma$  is interfacial tension (in mN/m),  $c$  is the bulk concentration (in mol/l),  $R = 8.314 \text{ J} \cdot \text{K}^{-1} \cdot \text{mol}^{-1}$ , and  $T$  is the absolute temperature. It is evident that HA possesses high interfacial activity.

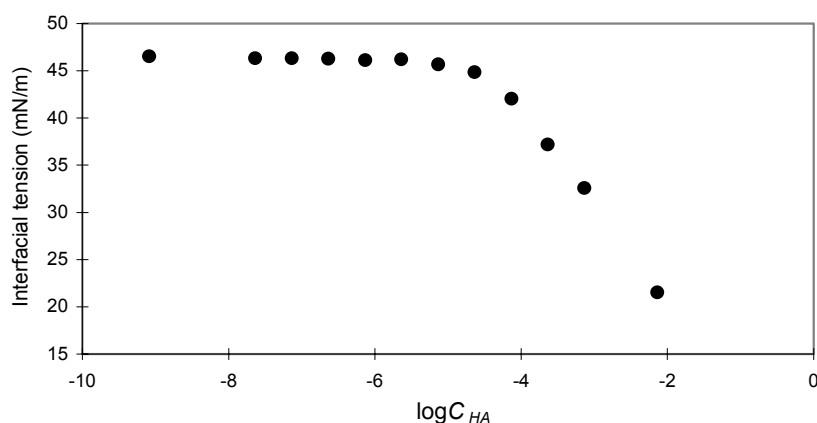


Figure 2. Interfacial tension of HA vs.  $\log c$ .

### Dependence of $\log k_{ao}$ on Stirring Speed

The apparatus used for the kinetic experiments is a constant interfacial area cell with laminar flow [8]. In a constant interfacial area cell, the thickness of the stationary interfacial film is thicker at a lower stirring speed and the diffusion limits the rate because of a relatively fast chemical reaction. With the increase of the stirring speed, the stationary diffusion film becomes thinner and the diffusion resistance smaller. At some value of the stirring speed, the extraction rate may be limited by the chemical reaction only, or the extraction rate is independent on the stirring rate and it is called "kinetics plateau". Hence, this kind of stirring cell allows an easy discrimination between limitation by diffusion or chemical reaction [10].

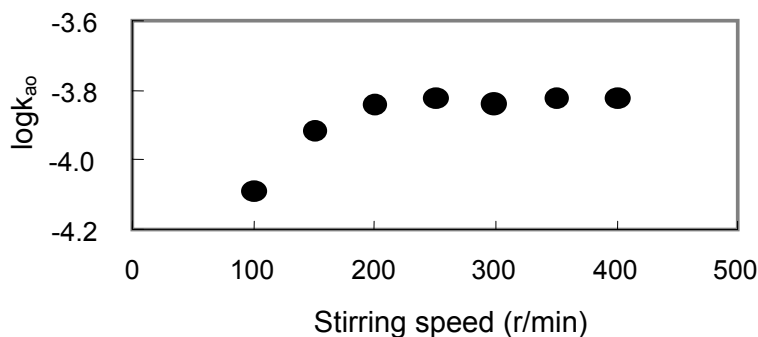


Figure 3. Dependence of  $\log k_{ao}$  vs. stirring speed.

Figure 3 shows the influence of the stirring speed on the extraction rate of yttrium(III) with sec-octylphenoxy acetic acid dissolved in heptane. When the stirring speed attained 200 r/min, the extraction rate was independent on the stirring speed. All other kinetic experiments were measured at 250 r/min in order to maintain same hydrodynamic conditions.

### Dependence of $\log k_{ao}$ on pH

In the pH range from 3.5 to 4.5, the effect of pH on extraction rate was studied. The orders of  $[H^+]$  for La(III), Gd(III), Er(III), Yb(III), Y(III) are  $-0.32$ ,  $-0.46$ ,  $-1.1$ ,  $-0.73$ ,  $-0.79$ , respectively. Because  $k_{ao}$  is function of the concentration of HA and  $H^+$ , for the extraction of La and Gd it is possible that the effect of the concentration of HA on the extraction rate is larger than that of  $[H^+]$ , which the order of  $[H^+]$  for the extraction of La and Gd is lower.

### Dependence of $\log k_{ao}$ on the Concentration of Extractant

The influence of extractant concentration on the extraction rate shows that with the increase of atomic weight from La to Yb the extraction rate decreases. The orders of extractant for La(III), Gd(III), Er(III), Yb(III), and Y(III) extraction with HA are  $1.2$ ,  $1.0$ ,  $1.2$ ,  $1.2$  and  $1.2$ , respectively.

### Dependence of $\log k_{ao}$ on Temperature

It was found that the extraction rate increased with temperature and the experimental data obeyed Arrhenius equation. The apparent activation energies for La(III), Gd(III), Er(III), Yb(III) and Y(III) extraction were calculated from the slope of  $\log k_{ao}$  versus  $1/T$  shown in Figure 4 and were  $18.4$  kJ/mol,  $30.0$  kJ/mol,  $46.2$  kJ/mol,  $55.2$  kJ/mol and  $49.9$  kJ/mol, respectively. Generally speaking [12], when an extraction activation energy ( $E_a$ ) is more than  $42$  kJ/mol, the extraction process is controlled by chemical reaction. When  $E_a$  is lower than  $20$  kJ/mol, species diffusion is rate-determining step. When  $E_a$  is in the range from  $20$  to  $42$  kJ/mol, the extraction rate is controlled by a mixed chemical reaction-diffusion. Thus, the extraction rate for Er(III), Yb(III) and Y(III) with HA is controlled by chemical reaction, Gd(III) is controlled by a mixed chemical reaction-diffusion, and La(III) is controlled by a diffusion.

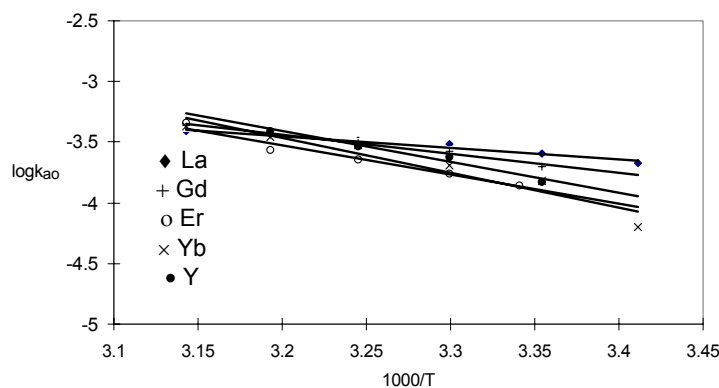


Figure 4. Dependence of  $\log k_{ao}$  vs.  $1/T$ .

## DISCUSSION

According to experimental results, the following rate equations are obtained:

$$-\frac{d[La^{3+}]_{(a)}}{dt} = k[La^{3+}]_{(a)}[H_2A_2]_{(o)}^{1.2}[H^+]_{(a)}^{-0.32} \quad (9)$$

$$-\frac{d[Gd^{3+}]_{(a)}}{dt} = k[Gd^{3+}]_{(a)}[H_2A_2]_{(o)}^{1.0}[H^+]_{(a)}^{-0.45} \quad (10)$$

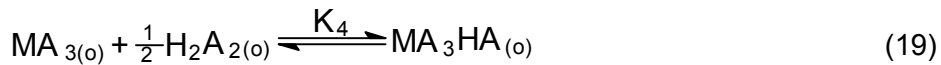
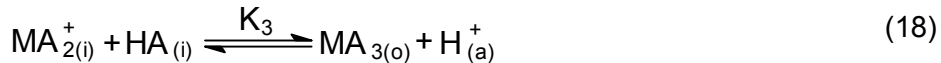
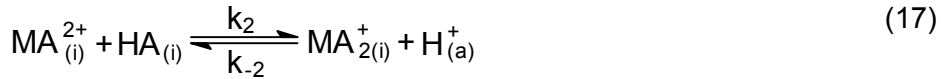
$$-\frac{d[Er^{3+}]_{(a)}}{dt} = k[Er^{3+}]_{(a)}[H_2A_2]_{(o)}^{1.2}[H^+]_{(a)}^{-1.1} \quad (11)$$

$$-\frac{d[Yb^{3+}]_{(a)}}{dt} = k[Yb^{3+}]_{(a)}[H_2A_2]_{(o)}^{1.2}[H^+]_{(a)}^{-0.73} \quad (12)$$

$$-\frac{d[Y^{3+}]_{(a)}}{dt} = k[Y^{3+}]_{(a)}[H_2A_2]_{(o)}^{1.2}[H^+]_{(a)}^{-0.79} \quad (13)$$

The molecules of HA can adsorb on the interface easily because of their surface activity and create a surface excess. Part of the molecules dissociates and diffuses, and interface double layer can result. Rare earth ions in aqueous solution can not easily enter the organic phase directly. Thus, it is more likely that the chemical reaction of extraction for rare earth ions with HA occurs at the two-phase interface. The previous thermodynamic study of rare earth extraction with HA [3] showed that the complex extracted into the organic phase for La(III), Gd(III), Er(III), Yb(III) was  $MA_3 \cdot HA$  and for Y was  $YA_3$ .

Based on the results of above kinetics and thermodynamics, the following extraction reaction mechanism for Er(III), Yb(III) and Y is put forward (there is no equation (19) for the extraction of Y(III)) :



From equations (14) and (15), one can obtain:

$$[HA]_{(i)} = K_1^{1/2} K_2 [H_2A_2]_{(o)}^{1/2} \quad (20)$$

If one assumes an instantaneous state and ignores the  $k_{-2}$  rate constant, the concentration of  $[MA^{2+}]_{(i)}$  can be easily calculated.

$$[MA^{2+}]_{(i)} = k_1 [M^{3+}]_{(a)} [HA]_{(i)} / (k_{-1} [H^+]_{(a)} + k_2 [HA]_{(i)}) \quad (21)$$

Assuming that equation (17) is the controlling-rate-step, one can write the following rate law:

$$R_f = k_2 [MA^{2+}]_{(i)} [HA]_{(i)} \quad (22)$$

Both equation (20) and (21) are substituted into equation (22), then:

$$R_f = k_1 k_2 K_1 K_2^2 [M^{3+}]_{(a)} [H_2A_2]_{(o)} / (k_{-1} [H^+]_{(a)} + k_2 K_2 K_1^{1/2} [H_2A_2]_{(o)}^{1/2}) \quad (23)$$

When  $k_{-1} [H^+]_{(a)} \gg k_2 K_2 K_1^{1/2} [H_2A_2]_{(o)}^{1/2}$ , equation (23) can be simplified as:

$$R_f = k [M^{3+}]_{(a)} [H_2A_2]_{(o)} [H^+]_{(a)}^{-1} \quad (24)$$

where  $k = k_1 k_2 k_{-1}^{-1} K_1 K_2^2$ .

The above mechanism is consistent with the experimental results.

## NOMENCLATURE

a	aqueous phase
o	organic phase
V	volume of either the aqueous or organic phase, cm <sup>3</sup>
k <sub>oa</sub>	backward pseudo-first-order rate constant, cm·s <sup>-1</sup>
k <sub>ao</sub>	forward pseudo-first-order rate constant, cm·s <sup>-1</sup>
Q	interfacial area, cm <sup>2</sup>
e	equilibrium
H <sub>2</sub> A <sub>2</sub>	dimer of extractant in organic phase
K <sub>d</sub>	distribution ratio of M
i	interface
K <sub>1</sub> ,K <sub>2</sub> ,K <sub>3</sub> ,K <sub>4</sub>	equilibrium constant
k <sub>1</sub> ,k <sub>2</sub>	forward reaction rate constant
k <sub>-1</sub> ,k <sub>-2</sub>	backward reaction rate constant

## ACKNOWLEDGEMENTS

Sec-octylphenoxy acetic acid was kindly supplied by Shanghai Institute of Organic Chemistry, Chinese Academy of Sciences. The project was supported by the National Program (G1998061301) and National Natural Science Foundation of China (29771028, 29801004).

## REFERENCES

1. A. Peng, Z.R. Dai, C.X. Wang (1982), Rare Earth Chemistry Symposium, Science Press, Beijing, pp. 39-49.
2. Z.R. Dai, C.X. Wang, Z.Y. Wang (1985), *Chinese Patent*, CN85102220B.
3. Department of Chemistry, Beijing University (1978), Rare Metals, Vol. 5, pp. 8-17.
4. W.Z. Ye, J.Y. Yan, Q.Y. Xu (1995), *Chinese Patent*, Open No. CN1108309A.
5. X.Y. Zhang, Q.B. Bo, D.Q. Li (2000), *Chinese J. Appl. Chem.*, **17** (2), 198-200.
6. D.Q. Li, Z.H. Wang, S.L. Meng (1996), *Chinese Rare Earths*, **17** (6), 41-43.
7. S.Y. Zhu, G.X. Zhao (1981), *Chemistry*, **6**, 21-26.
8. Z. Zheng, J. Lu, D.Q. Li, G.X. Ma (1998), *Chem. Eng. Sci.*, **53** (13), 2327-2333.
9. P.R. Danesi, G.F. Vandegreft (1981), *J. Phys. Chem.*, **85**, 3646-3651.
10. C.Q. Chen, T. Zhu (1994), *Solvent Extr. Ion Exch.*, **12** (5), 1013-1032.
11. J.Z. Ni, G.Y. Hong (1998), Progress in New Rare Earth Materials and Separation Processes: The Synthesis and Nature of New Extractants of Rare Earths, Science Press, Beijing, pp. 3-10.
12. J.F. Yu, C. Ji (1992), *Chem. J. Chinese Univ.*, **13** (2), 224-226.



# KINETICS AND MECHANISM OF METAL EXTRACTION ONTO A MICROCAPSULE CONTAINING ORGANOPHOSPHORUS EXTRACTANT

Eiji Kamio, Michiaki Matsumoto and Kazuo Kondo

Doshisha University, Kyotanabe, Japan

In this study, the adsorption behavior of gallium and indium onto a microcapsule containing 2-ethylhexylphosphonic acid mono 2-ethylhexyl ester is investigated by the shallow bed method. Firstly, the adsorption capacities were determined according to the Langmuir adsorption isotherm model. Subsequently, the adsorption rates of gallium and indium were measured and evaluated by homogeneous particle diffusion model. Furthermore, the initial extraction rates of the metals were evaluated for different metal concentrations. The resulted initial extraction rates were compared with those for the solvent extraction system measured using a stirred transfer cell, from which the adsorption behavior could be predicted.

## INTRODUCTION

In recent years, the need of more specific systems for metal recovery from both ecological and economic aspects has led to the development of new adsorbents such as solvent impregnated resins, polymer gels swollen with solvent, microcapsules containing extractant, and so on [1]. Among these new techniques, we have investigated the use of microcapsules as an effective method for recovery and separation of metals. In the previous study [2], we made the extraction equilibria clear and proposed a metal separation system using a column packed with microcapsules containing 2-ethylhexylphosphonic acid mono-2-ethylhexyl ester (abbreviated as EHPNA, trade name PC-88A). From the results, it was found that the microcapsules have a place in extraction chromatography at analytical application scale and are of potential application at an industrial scale. When we apply these microcapsules to industrial application, a fundamental study of transport phenomena of metal ions in a microcapsule is required for evaluating the extraction behavior. However, there are only few reports to evaluate the transport phenomena of metal ions into such adsorbents [3].

In our study, to make the extraction behavior clear, the kinetic experiments of gallium and indium for the microcapsule and solvent extraction systems are carried out.

## EXPERIMENTAL

### Reagents

The microcapsules containing EHPNA were prepared as was described previously [2]. The aqueous phase was prepared by dissolving gallium chloride ( $\text{GaCl}_3 \cdot 6\text{H}_2\text{O}$ ) or indium sulfate ( $\text{In}_2(\text{SO}_4)_3 \cdot 7\text{H}_2\text{O}$ ) in  $0.1\text{mol}/\text{dm}^3$  ( $\text{H, Na}_2\text{SO}_4$ ) solution. The pH of the solution was adjusted with a pH meter. The metal concentrations in the aqueous solutions were measured with an inductively coupled plasma spectrometer (ICPS).

### Adsorption Isotherm

The equilibrium adsorption isotherm of gallium or indium was measured under batch conditions. The aqueous solutions of pH 2.2 containing the metal ions at several concentrations and 0.1g of the microcapsules were contacted for over 1 day to attain equilibrium. Then the metal concentration in the aqueous solutions was measured. The amount of metal adsorbed into the microcapsule was determined by mass balance before and after equilibrium. All experiments were carried out at room temperature.

### Kinetic Study for Microcapsule System with Shallow Bed

Figure 1 shows the shallow bed used in this study. 0.05g of the microcapsules were packed into the bed. The bed was conditioned by feeding aqueous solution at pH 2.2 for 30 min. After 30 min, the aqueous solution containing 0.1 mol/m<sup>3</sup> of gallium or indium ion was introduced for appropriate periods. As soon as this time passed, a scrubbing solution of pH 3.0 was introduced into the bed at a fast flow rate to remove the feed solution remaining in the bed. Two minutes is enough to remove completely the metal ion remaining in the bed. Then the resulting microcapsules were collected and contacted with the stripping solution for 1 day.

### Experimental conditions

Flow rate : 70 cm<sup>3</sup>/min

Reynolds number of feed solution : 2.5

Microcapsules packed: 0.05g

pH of the feed : 2.20

pH of the scrubbing solution : 3.00

Stripping solution :

2.0 mol/dm<sup>3</sup> H<sub>2</sub>SO<sub>4</sub> for gallium

5.0 mol/dm<sup>3</sup> H<sub>2</sub>SO<sub>4</sub> for indium

Temperature : 313K

$$Re = d_p u \rho / \mu$$

$$d_p : \text{particle diameter} \\ = 1.5 \times 10^{-4} \text{ m}$$

$$u : \text{relative rate between fluid and particle} \\ = 10.1 \times 10^{-3} \text{ m/s}$$

$$\rho : \text{fluid density} \\ = 1.03 \times 10^6 \text{ g/m}^3$$

$$\mu : \text{fluid viscosity} \\ = 0.65 \text{ g/(m·s)}$$

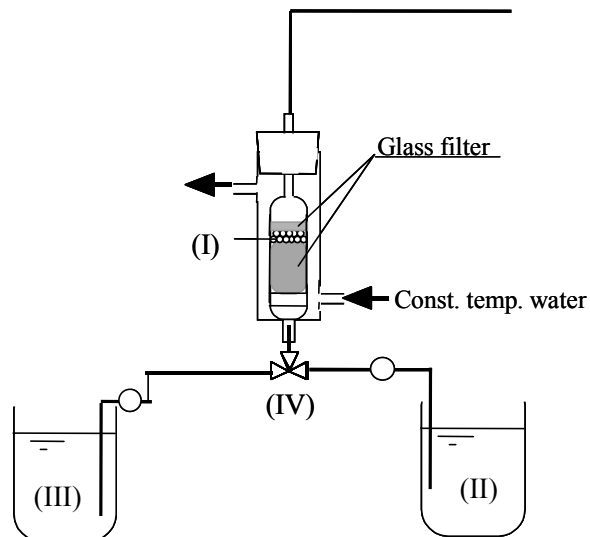


Figure 1. Experimental apparatus of shallow bed method; (I) shallow bed, (II) feed solution (pH = 2.20), (III) scrubbing solution (pH = 3.00), (IV) three-way cock.

### Kinetic Experiment for Solvent Extraction System

A stirred transfer cell was used to measure the rates of gallium and indium extraction by EHPNA at 313K. In this study, undiluted EHPNA was used as the organic phase. The solutions in the cell were stirred at 140 rpm. The aqueous solution containing no metal ion was contacted with the organic phase to attain equilibrium. Then the stock solution containing the metal ion was introduced into the lower compartment of the cell. Small samples were taken at intervals from both phases. The organic samples were treated with the stripping solution. The metal concentration was measured by ICPS.

## RESULTS

### Adsorption Isotherms

The experimental isotherm results for both metals correlated well with the calculated results based on Langmuir isotherm model. By the least-squares method, saturation capacities,  $q_\infty$ , and equilibrium constants,  $K$ , were determined.

### Kinetic Study for Microcapsule System with Shallow Bed

Figures 2 and 3 show the uptakes for gallium and indium adsorption, respectively. As shown in Figure 2, the adsorption rates of gallium increase with increasing the gallium concentration in the bulk. The extraction behavior was evaluated by a homogeneous particle diffusion model based on Fick's law. As a result, it was suggested that the extraction rate would be controlled by intraparticle diffusion of the metal-extractant complex. On the other hand, it is clear from Figure 3 that the adsorption rates of indium decrease with increasing the bulk concentrations. This is opposite tendency for general ion-exchanger or solvent extraction systems. However, at the early periods of the adsorption, the initial adsorption rates increase with increasing the bulk concentration as shown in Figure 4.

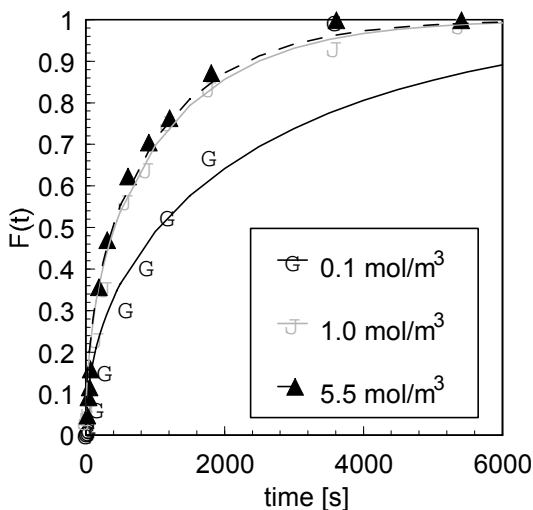


*Figure 2. Uptake for gallium adsorption. Solid and broken lines are theoretical result based on homogeneous particle diffusion model.*

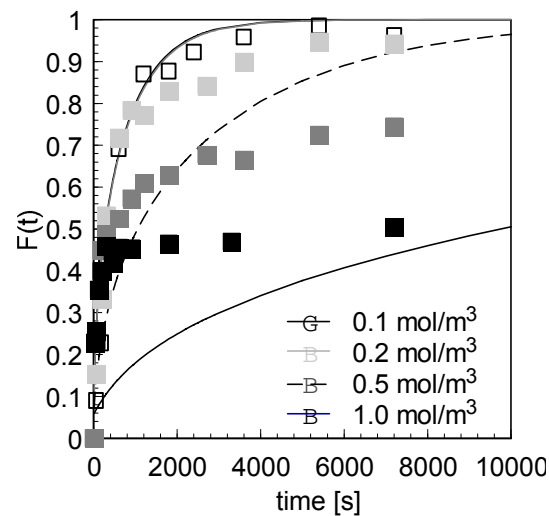


*Figure 3. Uptake for indium adsorption. Solid and broken lines are theoretical result based on homogeneous particle diffusion model.*

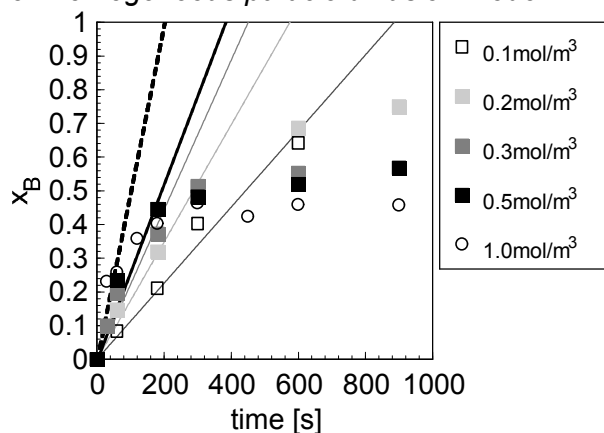


*Figure 4. Uptakes for indium adsorption in early periods of adsorption.*

### Kinetic Experiment for Solvent Extraction System

Figures 5 and 6 show the relationship between initial extraction rate and metal concentration for gallium and indium, respectively. In these figures, the results for microcapsule systems were also shown. From the figures, it is clear that the calculated initial extraction rates for both systems are almost the same.

In the case of indium extraction, an interesting phenomenon was observed. As soon as the adsorption started, it was found that a white precipitation was formed in the aqueous phase at high metal concentration. This was collected and separated from the aqueous phase by centrifugation. Then, the precipitate was washed with 0.1 mol/m<sup>3</sup> (H, Na)<sub>2</sub>SO<sub>4</sub> solution of pH=2.2. Some was dissolved in 5 mol/m<sup>3</sup> H<sub>2</sub>SO<sub>4</sub> solution and the concentrations of indium and phosphorus were measured with ICPS. They were dried and its P=O bond was identified with FT-IR. From the result of measurement with ICPS, it was found that the molar ratio of In/P in the precipitate was 1.0. From the FT-IR spectrum, the characteristic peaks of EHPNA were observed at 1350 cm<sup>-1</sup> for P=O, 2925 cm<sup>-1</sup> for alkyl chain.

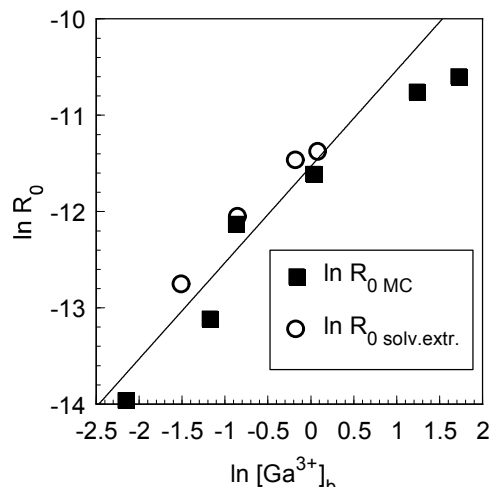


Figure 5. Effect of gallium concentration on initial extraction rate.

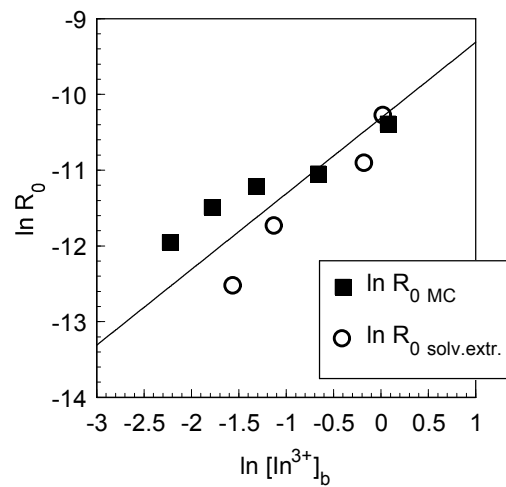


Figure 6. Effect of indium concentration on initial extraction rate.

### DISCUSSION

From the experimental results, it is suggested that the precipitate could be an aggregated indium-EHPNA complex. From this result, it is suggested that the pore in the microcapsule is closed with the indium-extractant precipitations.

We propose that the adsorption behavior occurring at the interface is as follows. At high metal concentration, one or two of the extractant molecule react with the metal ion and the metal-extractant complex ions ( $MR^{2+}$ ,  $MR_2^{+}$ ) are adsorbed at the interface. Only the metal-extractant complex ( $MR_3$ ) can diffuse toward the center of the microcapsules. If there are many metal ions in the liquid film, the metal-extractant complex ions would be mainly formed. Therefore, at early stage of the adsorption, the adsorption rate is fast because of the adsorption of metal ions onto the surface of the microcapsules. However, if the extractant has a high affinity with the metal ion, the aggregated precipitate would be formed at the interface and the exchange reaction of extractants between the complexes does not occur because the metal-extractant precipitate exists stably. As a result, the adsorption rate is considered to become low. On the other hand, if there is only a little metal ion in the bulk, a small amount of the metal-extractant complex ions are formed and no precipitate would be formed at the surface of the microcapsules. Therefore, the metal-extractant complex ions can be reacted with the active non-reacted extractant molecules, and the metal-extractant complex ( $MR_3$ ) will be easily formed. So the adsorption rate under low concentration condition will become faster than that under high concentration condition.

The calculated initial rates for both microcapsule and solvent extraction systems were almost the same. Therefore, it is suggested that chemical reaction controls the adsorption rate at the early periods.

## CONCLUSIONS

The kinetics of adsorption of gallium and indium were investigated in the microcapsule system and solvent extraction system in order to elucidate the adsorption mechanism. It was found that the adsorption of gallium into the microcapsule would be mainly controlled by intraparticle diffusion of metal complex. For indium adsorption, it was suggested that metal-EHPNA complex precipitation was formed at the surface of the microcapsules and it would prevent the diffusion of metal complex into the microcapsules. From the comparison of the results for both microcapsule and solvent extraction system, chemical reaction would control the adsorption at the early periods.

## NOMENCLATURE

$F(t)$	=	fractional attainment of equilibrium	[ $\text{-}$ ]
$R_0$	=	Initial extraction rate	$[\text{mol}\cdot\text{m}^{-2}\cdot\text{s}^{-1}]$

## REFERENCES

1. N. Kabay, M. Demircioglu, H. Ekinci, M. Yuksel, M. Saglam, and M. Streat (1998), *Reactive Funct. Polym.*, **38**, 219-226.
2. E. Kamio, M. Matsumoto and K. Kondo (1999), *Proc. Regional Symp. Chem. Eng.*, Songkhla, Thailand, pp. B59-1 – B59-6.
3. J. L. Cortina, R. Arad-Yellin, N. Miralles, A. M. Sastre, and A. Warshawsky (1998), *Reactive Funct. Polym.*, **38**, 269-278.



## NEW TYPES OF EXTRACTANT TO TRANSPORT METAL SULFATES IN BASE METAL RECOVERY PROCESSES

Donald M. Gunn, Hamish A. Miller, Ronald M. Swart\*, Peter A. Tasker,  
Lee C. West and David J. White

Department of Chemistry, The University of Edinburgh, Edinburgh, UK  
\*AVECIA Ltd., Manchester, UK

Extractants to transport metal salts have been developed using components that are structurally related to the commercial phenolic oximes. The structures have been engineered to generate sulfate-binding sites so that both the metal cation and the sulfate counterion of divalent metal sulfates can be extracted without changing the pH or transferring any ions to an aqueous feed. Such extractants should be useful in opening up new flowsheets to recover base metals from sulfate streams when it is desirable to avoid any interstage pH-adjustment in solvent extraction or any neutralisation of effluent streams. Proof-of-concept has been established for systems to transport copper(II) sulfate or nickel(II) sulfate. Stripping the metal sulfate and recycling the extractants can be accomplished using pH-swing mechanisms, exploiting a key design feature of the extractants, that the metal sulfate is bound in a zwitterionic form.

### INTRODUCTION

This paper describes the design of novel reagents that are capable of transporting metals *salt*s in metal-recovery circuits (see Figure 1). A programme to develop ligands that bind both a metal cation and its attendant anion or anions was initiated in 1999 with “blue skies” funding from the UK’s Engineering and Physical Sciences Research Council. This was considered timely because developments in the area of supramolecular chemistry [1] have greatly improved our understanding of how to design organic complexing agents for anions [2] using a combination of electrostatic and secondary bonding forces. The programme aimed to exploit this new area of science to achieve high strength and selectivity of extraction of salts of base metals using “ditopic ligands” which have separated, tailor-made, binding sites for the cation and anion(s).

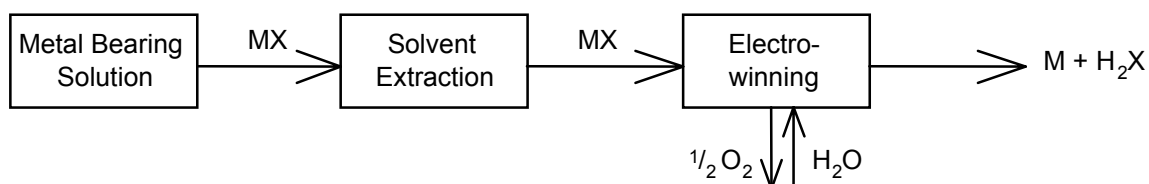
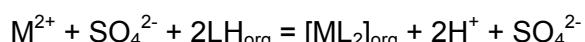


Figure 1. Transport of a metal cation and its attendant anion in a hydrometallurgical circuit.

The concept of transporting a metal salt across a hydrometallurgical circuit is well known for processes involving nitrate and chloride media. Copper recovery from chloride leaching of sulfidic ores has been proposed [3] by using extraction equilibria,



which are dependent on chloride ion concentrations and temperature. In such processes the transfer of the anion(s) to the organic phase is dependent on them being part of the coordination sphere of the metal cation to generate a neutral, organic-soluble, complex. Because the sulfate anion is a relatively poor ligand for base metal cations it is not easy to use this mechanism to transport metal sulfates and, partly as a consequence of this, ion-exchange reagents are generally used for the recovery of base metals from sulfate media. Most commonly in solvent extraction such ion-exchange reagents operate on a pH-swing mechanism,



releasing acid in the front end of a circuit. This is beneficial in primary metal recovery if the leaching step consumes acid and it leads to an almost ideal materials balance in the well established [4] processes to recover copper from oxidic ores *via* a heap leach/solvent extraction/electrowinning circuit as shown in Figure 2.

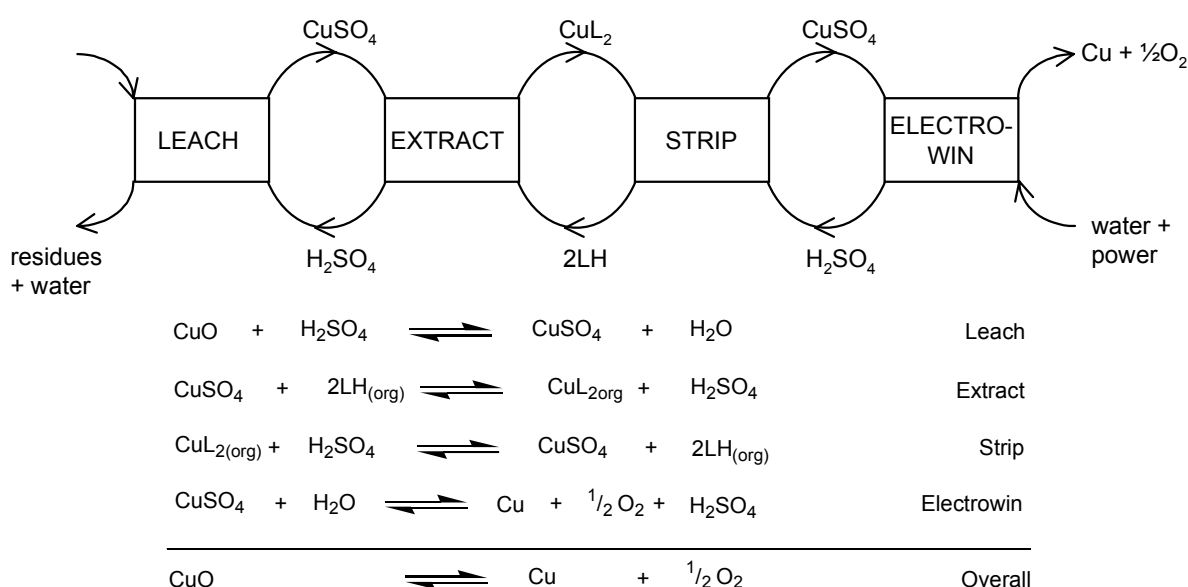


Figure 2. A simplified flowsheet and materials balance for the recovery of copper from oxidic and transition ores by heap leaching, solvent extraction and electrowinning.

Acidic cation-exchange extractants of this type are not so well suited to recovery from pregnant leach solutions where the leach process does not consume acid, or for recovery from secondary sources such as acidic tailings or acid main drainage streams because neutralisation of the acid released in raffinate will be required. For such situations a “subtractive” rather than exchange process is preferred in which the metal sulfate is removed from the aqueous feed.



In designing ligands to operate in this way it is important from the outset to address the following issues:

- (i) An effective mechanism to control loading and stripping must be defined which will allow us to generate an advance with high concentration of metal sulfate and to recycle the reagent efficiently. Whilst it is now possible in theory to design good binding sites for the metal cation and its attendant sulfate anion using relatively well established principles of co-ordination chemistry and supramolecular chemistry [5], it is not obvious how to reverse the complexation reactions. It was decided at the outset to tackle this problem by developing extractants which will bind the metal sulfate in a zwitterionic form of the ligand where the transfer of protons from one site to another creates two charged compartments, one to accommodate the metal cation and the other the sulfate dianion (see Figure 3). It is then possible to use “pH-swing” processes to remove the cation and sulfate anion from the ligand (see below).
- (ii) The metal-binding site, e.g., the dianionic compartment in the schematic ligand in Figure 3, will need to show high selectivity for the desired metal in the sulfate feed solution. It was proposed to tackle this design feature by incorporating other metal-ligating atoms into this compartment to generate a multidentate ligand with donor atoms types and dispositions to meet the preferences of the desired metal ion.
- (iii) For use in base-metal recovery the new extractants based on ditopic ligands must be relatively simple to manufacture and give good mass transfer efficiencies. This presents major challenges. Most of the complexing agents that have been developed recently for binding anions have high molecular weights and rigid, often macrocyclic, structures to pre-organise the functionalities which bind to the anion.

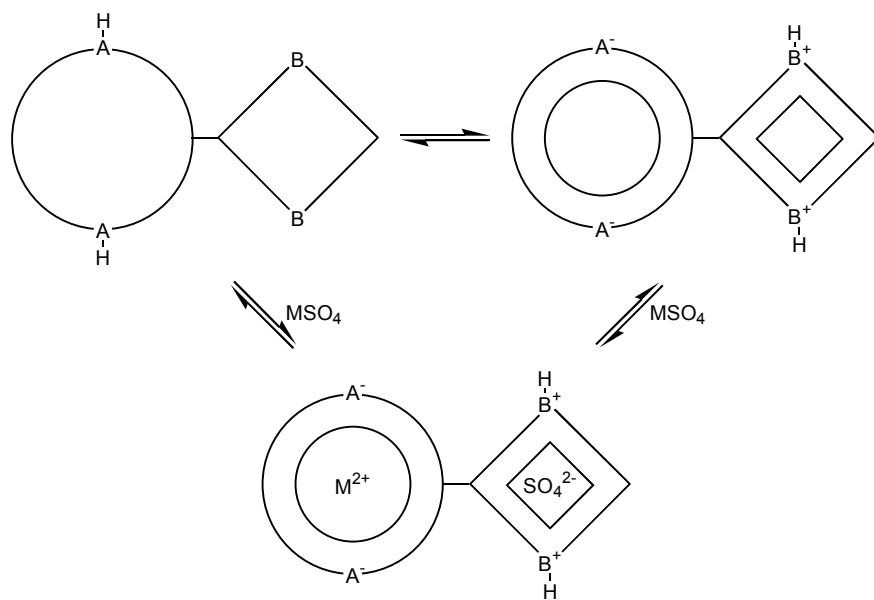


*Figure 3. Schematic representation of a ditopic ligand in which a divalent metal sulfate is bound in the charged “compartments” of a zwitterionic form of a diacidic/dibasic system.*

This paper describes the proof-of-concept of developing relatively simple ditopic ligands of the type shown in Figure 3 to bind metal sulfates and of exploiting the zwitterionic nature of these to establish convenient load/strip protocols to generate a concentrated advance electrolyte and to recycle the ligand. Details of the development and testing reagents to meet the requirements of specific nickel-recovery flowsheets will be presented orally at the meeting.

## PROTOTYPE DITOPIC LIGANDS

One of the simplest ways of incorporating the design features outlined in Figure 3 into a ligand superstructure is to use a linear molecule in which the central portion supplies the metal-binding site and the terminal groups the anion-binding site. Complexation of the metal cation can then be used to assist the preorganisation of the functionalities which are needed to bind the anion (see Figure 4).

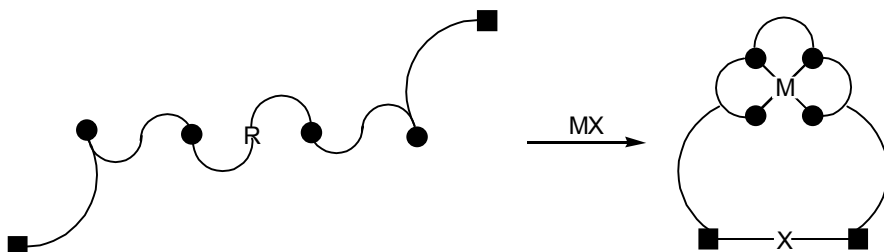


*Figure 4. Metal-ion templating of the anion binding site in a linear multidentate ligand.*

A donor set array as in Figure 4 can be constructed easily from phenolic aldehydes or ketones which are already in commercial production as precursors for the phenolic oxime extractants **I** used in copper recovery.

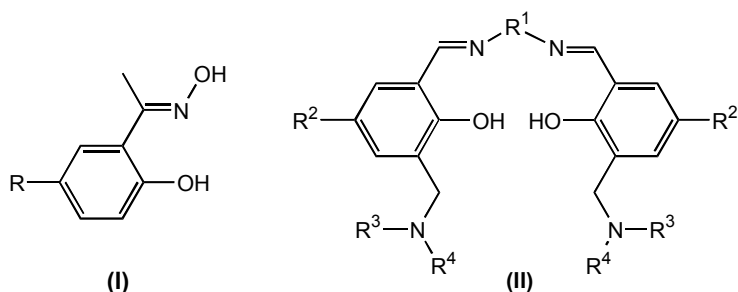


*Figure 5. The commercial oxime extractants **I** for copper and the prototype metal-salt extractants **II** described in this paper.*

The prototype ligands were prepared [6] from the parent phenolic aldehydes **III** in a two stage synthesis in yields approaching 95%, using the scheme outlined in Figure 6. Compounds with a solubilizing  $C_9H_{19}$  substituent  $R^2$  have been used in solvent extraction experiments and with  $CH_3$ - and  $^{13}C_4H_9$ -groups for characterisation and structure determination. Bis-imine ligands derived from salicylaldehyde, "salen-type" systems, have been much studied previously and the nature of the bridge  $R^1$  between the two imine nitrogen atoms has been extensively varied to "tune" metal binding. Appending amido groups in the sites *ortho* to the phenolic oxygen atoms has been used previously to provide hydrogen-bonding functionality [7].

The distinctive feature of the prototype ligands (Figure 6) is that their pendant tertiary amine groups allow formation of complexes of metal salts by incorporating the metal cation and its attendant anion into a zwitterionic form of the ligand which is created by transfer of the phenolic protons to the pendant amine groups. This process, and the templating of the sulfate-binding site are illustrated in Figure 7 for the system **IV** with a flexible  $-(CH_2)_2-$  bridge, and morphilino pendant arms.

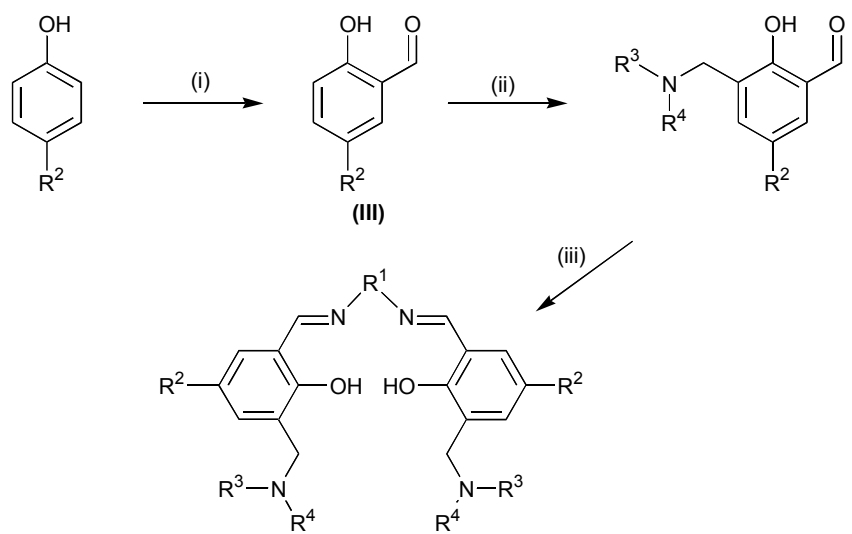


**Figure 6.** The synthesis of the “salen”-type prototype metal-salt ligands: (ia) MgOMe, MeOH-toluene, reflux 3 h; (ib) paraformaldehyde, distillation; (ii) secondary amino-ethoxymethane, MeCN, N<sub>2</sub>, reflux 66 h; (iii) diamine, Et<sub>2</sub>O-EtOH (1:1), r.t. 24 h.

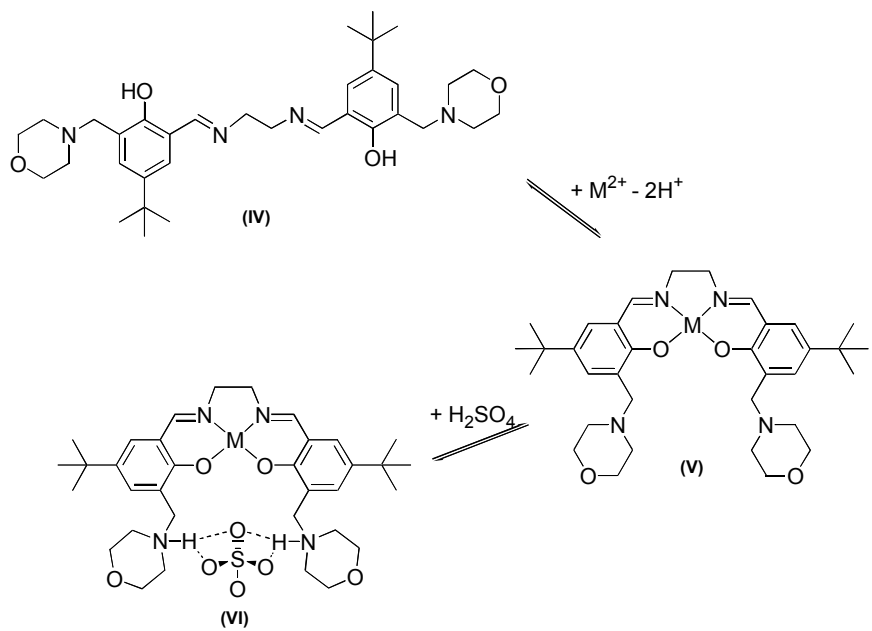


**Figure 7.** The templating of the sulfate binding site in the prototype ligands showing formation of the “nickel-only” complex **V** and the nickel sulfate complex **VI**.

## CHARACTERISATION OF METAL-SALT COMPLEXES

An X-ray structure (Figure 8) determination of the nickel(II) sulfate complex **VI** of the *t*-butyl-substituted ligand indicates clearly that in the solid state the sulfate dianion is located between the protonated morpholinium units forming strong bifurcated hydrogen bonds.

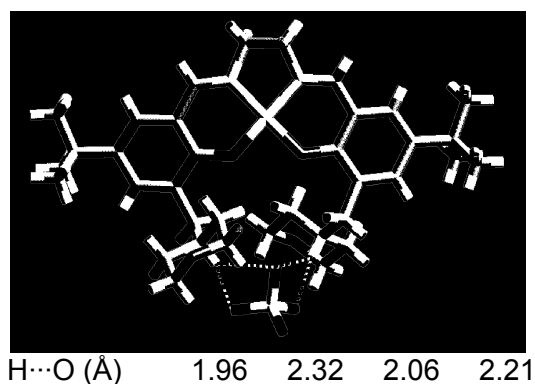


*Figure 8. The solid-state structure of the nickel sulfate complex VI, with the morpholinium-NH to sulfate hydrogen-bonding dimensions.*

The importance of the “metal-templating” of the pendant tertiary amine groups is illustrated by comparing the distances [8,9] between the morpholino nitrogen atoms in the free ligand with those in the “nickel-only” complex (**V** in Figure 8). The “metal-only” complexes can be formed by carrying out the complex formation at relatively high pH (see below). The morpholino nitrogen atoms are separated [8] by 16.2 Å in the free ligand **IV** compared with 5.17 Å in the “nickel-only” complex **V**. This distance is very similar to that (5.16 Å) in the nickel sulfate complex **VI**.

A wide range of solid-state metal salt complexes of the “salen” prototype ligands has been characterised in our laboratories using X-ray crystallography and other methods. An interesting feature of this chemistry is that “metal only” complexes analogous to **V** in Figure 7 can be treated with diacids to generate polymeric structures with unusual dianion-bridged three-dimensional arrays of complex units [8].

In addition to establishing the viability of metal complex formation using the ligand zwitterions, the solid state structures provide some insight into the design features that are likely to prove important in the development of reagents to be used in liquid phase transport processes. In particular, the geometry of the sulfate-binding site will be dependent on both the “templating” properties of the metal cation and the nature of the bridging unit R<sup>1</sup> in the ligand structure. These will greatly influence the “strength” and selectivity of reagents. Also the solubility of the ligand:metal salt assembly will be very dependent on using functionalities in the pendant tertiary amines which envelop the sulfate group, restricting the formation of intermolecular H-bonded assemblies which will lead to polymeric (insoluble) materials.

#### **EXTRACTION STUDIES – PROOF OF CONCEPT WITH TRANSPORT OF COPPER(II) SULFATE**

Initially proof-of-concept was established by contacting a 0.01 M solution of the o-phenylene-bridged ligand (**VII** in Figure 9) with an excess of copper(II) sulfate at room temperature. At equilibrium (with no pH-adjustment) a 95-100% loading of copper and sulfate was confirmed by ICP OES analysis. It proved impossible to strip copper from ligand **VII** without using acids of such a concentration that significant decomposition of the ligand resulted.

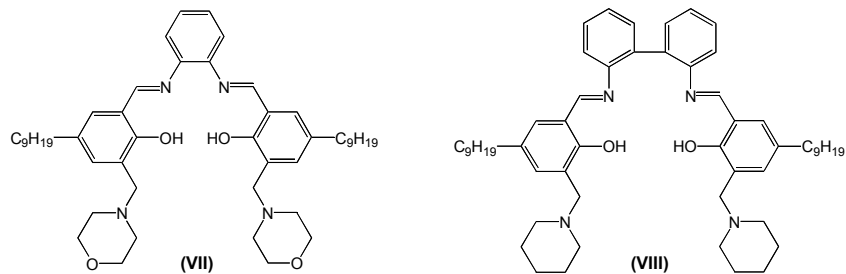


*Figure 9. "Salen-type" ligands used in extraction experiments.*

One of the strategies envisaged to recover metal salts from these new types of extractants exploits their zwitterionic nature and is illustrated in Figure 10. Because the charges on the binding sites result from protonation/deprotonation reactions we can envisage controlling loading and stripping using “pH-swing” processes. Ideally the system needs to show a pH-profile which has a high stability of the metal-sulfate complex (top right, Figure 10) at a pH close to that of the aqueous feed. The  $\text{pH}_{1/2}$  for reprotoonation of the metal-cation binding site needs to be accessible for stripping with 1-5 M  $\text{H}_2\text{SO}_4$  to yield the sulfate salt of the ligand (bottom, Figure 10). The  $\text{pK}_{\text{a}}$ s of the pendant groups binding the sulfate need to be such that the free ligand (top left, Figure 10) can be easily regenerated with base (ammonia is shown in Figure 10).

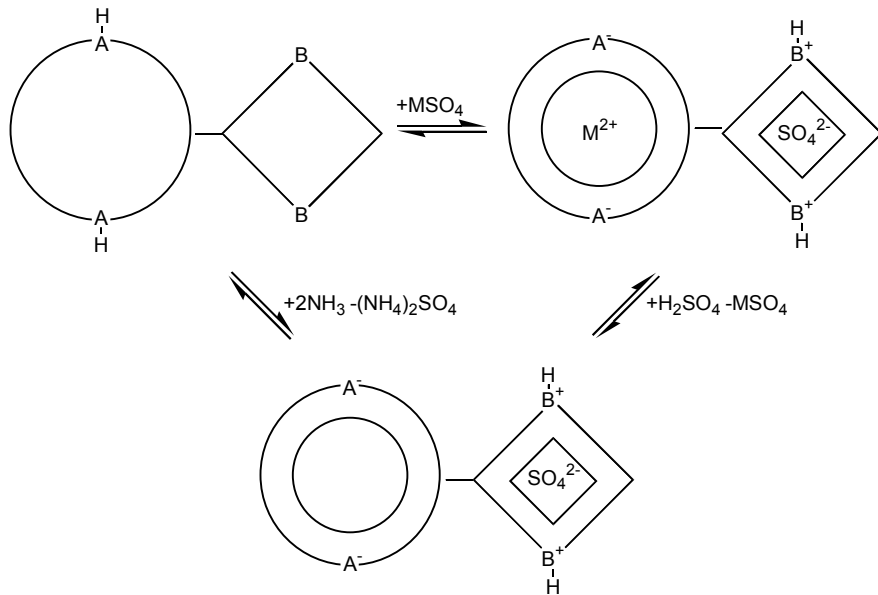


*Figure 10. Exploiting the zwitterionic binding sites in the prototype ligands to recycle the extractant and recover metal and sulfate.*

In order to establish the viability of this load(strip protocol for copper sulfate it was clear that the "strength" of the binding site for Cu(II) needs to be "de-tuned" from that in the *o*-phenylene-bridged ligand **VII**. This was approached by incorporating a bridging unit R<sup>1</sup> which will distort the N<sub>2</sub>O<sub>2</sub><sup>2-</sup> donor set of the "salen-unit" away from the planar arrangements preferred by copper(II). Several approaches to this were tried, but the most successful appeared to be the incorporation of a 2,2'-biphenyl-linkage (**VIII** in Figure 9). The solubility of this extractant and its metal complexes was also enhanced by replacing the morpholino units in the pendant arms by piperidino groups. This extractant again showed 95-100% loading of copper from copper(II) sulfate without pH adjustment, but could be stripped to  $\leq 5\%$  copper loading with sulfuric acid pH 1.0 (see Figure 11). The results presented in Figure 11 were obtained [10] by contacting preloaded 0.01M solutions of **VIII** in chloroform with aqueous H<sub>2</sub>SO<sub>4</sub>/Na<sub>2</sub>SO<sub>4</sub>.

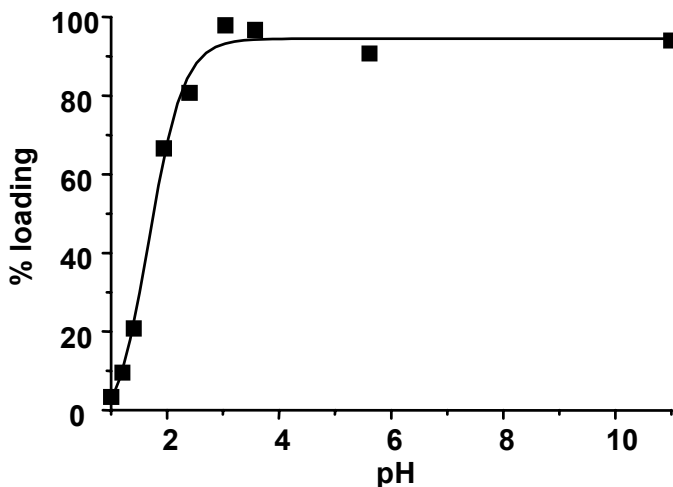


Figure 11. Copper loading of ligand **VIII** as a function of pH.

Ammonia solutions can be used very effectively to strip sulfate from the morpholinium binding site of **VIII**. After contracting either a fully CuSO<sub>4</sub>-loaded, or the copper-stripped solution of **VIII** in chloroform referred to above, with aqueous ammonia (pH  $\geq$  11.0) the sulfate loading, as judged by ICP OES, falls to <1%. The reagent **VIII** is robust, and when taken through a cycle of loading with CuSO<sub>4</sub>, copper-stripping with 2 M H<sub>2</sub>SO<sub>4</sub> and sulfate-stripping with ammonia it can be reloaded with CuSO<sub>4</sub> to the same level (>95% of theory) which was observed initially. If the sequence of operations outlined above were to be coupled with conventional electrowinning of copper from sulfate the materials balance would be given by

CuSO <sub>4</sub> + L <sub>org</sub> = [CuLSO <sub>4</sub> ] <sub>org</sub>	Extract
CuLSO <sub>4</sub> + H <sub>2</sub> SO <sub>4</sub> = CuSO <sub>4</sub> + [LH <sub>2</sub> SO <sub>4</sub> ] <sub>org</sub>	Strip 1
[LH <sub>2</sub> SO <sub>4</sub> ] <sub>org</sub> + 2NH <sub>3</sub> = L <sub>org</sub> + [NH <sub>4</sub> ] <sub>2</sub> SO <sub>4</sub>	Strip 2
CuSO <sub>4</sub> + H <sub>2</sub> O = Cu + ½ O <sub>2</sub> + H <sub>2</sub> SO <sub>4</sub>	Electrowin
<hr/>	
CuSO <sub>4</sub> + H <sub>2</sub> O + 2NH <sub>3</sub> = Cu + ½ O <sub>2</sub> + [NH <sub>4</sub> ] <sub>2</sub> SO <sub>4</sub>	Overall

These “shake-out” experiments establish the proof-of-concept of transporting a metal sulfate across a hydrometallurgical circuit and illustrate that the prototype “salen” extractants can be tailored to show strength, pH-profiles for loading and stripping, and solubility characteristics which would allow them to be applied in a wide range of operations. The practicalities of their use in primary copper recovery from sulfate media using a flowsheet involving the material balance outlined above would give some cause for concern in terms of the consumption of ammonia and generation of ammonium sulfate as a by product. It is timely to review with potential end-users how and where the new reagents could be most effectively used in developing flowsheets for base metal recovery. In order to facilitate such discussions, we have focused recently on identifying reagents for the recovery of nickel-from-sulfate media. Results are given below and will be presented in more detail in the context of circuit design at the forthcoming meeting.

## RECOVERY OF NICKEL FROM SULFATE FEED SOLUTIONS

The development [11] of a number of new leaching processes for the recovery of nickel potentially provides opportunities for reagents to transport nickel(II) sulfate. Preliminary work using the “salen-type” extractants (Figure 9) showed that while these readily form  $\text{NiSO}_4^-$ -complexes, the kinetics of loading and stripping are very poor (>24 hours is often needed to approach equilibrium) and the “strength” of the  $\text{N}_2\text{O}_2^{2-}$  binding site is often not sufficient to give high loadings. Consequently we considered extending the design concept to ligands related to this prototype but with the metal cation binding site having six donor atoms to favour the formation of octahedral complexes. The systems which will be described here have trifurcated structures (Figure 12) and provide trianionic and tricationic sites to bind the metal salts. An important feature of such systems is that when binding divalent metal sulfates the overall charge on the metal sulfate complex is zero and good solubility in low polarity organic solvents is possible. Also on the grounds of electrostatic contributions to bonding the “strength” of these trifurcated reagents is expected to be greater than the analogous bifurcated systems. Both of these features have been realised for  $\text{NiSO}_4$ -complex formation with the reagents outlined in Figure 12. Other types of metal salt-ligands containing *pseudo*-octahedral binding sites will be described [12] elsewhere.

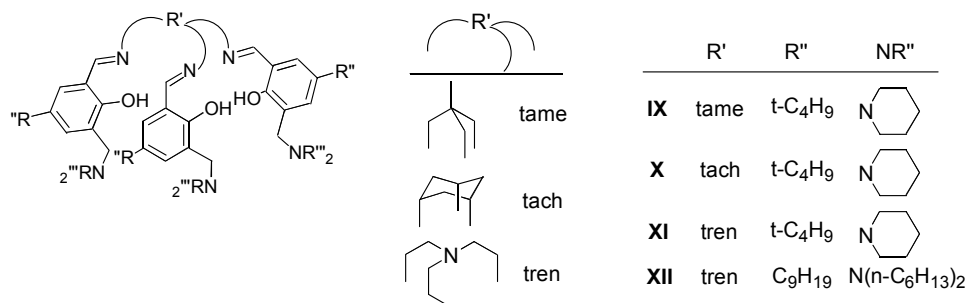


*Figure 12. Trifurcated ligands providing tricationic sulfate-binding and trianionic six co-ordinate metal-binding sites.*

These trifurcated reagents can be prepared in high yields by adaptations of the route outlined in Figure 6. The reagents shown in Figure 12 all form nickel complexes readily under conditions analogous to those used for the “salen-type” ligands and spectroscopic and magnetic data support the formulation of these as *pseudo*-octahedral high spin systems. The six co-ordinate geometry of  $\text{Ni}^{2+}$  in these systems has been confirmed by X-ray crystallography for the  $\text{NiSO}_4$  complex of **IX**.

For the development of nickel-recovery processes based on sulfate transport, the reagents will be required to have a high solubility in commercial hydrocarbon solvents, good kinetics of extraction and convenient stripping protocols to allow the SX-based recovery to be interfaced with conventional nickel reduction processes. In the context of the latter it was found that  $\text{NiSO}_4$ -loaded forms of all the ligands **IX-XII** (Figure 12) can be directly stripped by aqueous ammonia to generate nickel ammonium sulfate. This can be used as a feedstock for the conventional Sherrit-reduction process from which the ammonia can be recycled as in the flowsheet based on:

$\text{NiSO}_4 + \text{L}_{\text{org}} = [\text{NiLSO}_4]_{\text{org}}$	Extract
$[\text{NiLSO}_4]_{\text{org}} + 6\text{NH}_3 = \text{L}_{\text{org}} + [\text{Ni}(\text{NH}_3)_6]\text{SO}_4$	Strip
$[\text{Ni}(\text{NH}_3)_6]\text{SO}_4 + \text{H}_2 = \text{Ni} + [\text{NH}_4]_2\text{SO}_4 + 4\text{NH}_3$	Sherrit reduction
$[\text{NH}_4]_2\text{SO}_4 + \text{Ca}(\text{OH})_2 = 2\text{NH}_3 + \text{CaSO}_4 + 2\text{H}_2\text{O}$	Ammonia regeneration
$\text{NiSO}_4 + \text{H}_2 + \text{Ca}(\text{OH})_2 = \text{Ni} + \text{CaSO}_4 + 2\text{H}_2\text{O}$	Overall

Good solubility in hydrocarbons and phase disengagement are shown by the bis-hexylamine-functionalised reagent **XII**. Shake-out work defining loading/stripping isotherms, kinetics measurements and the results of minirig trials will be reported at the forthcoming meeting.

## CONCLUSIONS

An understanding of the principles of “supramolecular chemistry” allows us to design receptors for anions by incorporating functionalities which use secondary bonding to generate stable complexes. One of the potential advantages of incorporating anion-binding sites into metal extractants is that the processes can function without changing the pH or transferring any ions to an aqueous feed.

Having established that it is possible to synthesise such reagents easily from commercially available components, and that they can be tailored to transport metal sulfates in solvent extraction-based circuits, it is timely to review the best areas for their exploitation. It is envisaged that these would involve processes to recover base metals from sulfate streams when it is desirable to avoid any interstage pH-adjustment in solvent extraction or any neutralisation of effluent streams, but other possibilities should be explored. Developing extractants to meet the needs of a particular flowsheet would be best undertaken in collaboration with potential end-users, suppliers of the engineering and a reagent manufacturer.

## ACKNOWLEDGEMENTS

This work has been supported by the Engineering and Physical Sciences Research Council under a ROPA grant and by the Scottish Higher Education Funding Council under a POC award. Bryn Harris, Hatch International (B.Harris@hatch.ca), and Geoff Seward, Hydromet Services International (gseward@25kingfisher.fsnet.co.uk), are thanked for their contributions to defining areas of application of the new reagents which will be described more fully at the meeting. We are also grateful to Avecia for providing access to equipment, expertise and materials for the project and to Edinburgh Research and Innovation, in particular Tom Higgison, for support.

## REFERENCES

1. I. M. Atkinson and L. F. Lindoy (2000), *Self-Assembly in Supramolecular Systems*, The Royal Society of Chemistry, London.
2. A. Bianchi, K. Bowman-James and E. Garcia-España (eds.) (1997), *Supramolecular Chemistry of Anions*, Wiley-VCH, New York; F. P. Schmidtchen and M. Berger (1997), *Chem Rev.*, **97**, 1609; P. A. Gale (2000), *Coord. Chem. Rev.*, **199**, 181; P. D. Beer and P. A. Gale (2001), *Angew. Chem. Int. Ed.*, **40**, 486.
3. R. G. Reddy and R. N. Weizenbach (eds.) (1993), *Proc. The Paul Quenaeu International Symposium on Extractive Hydrometallurgy of Copper, Nickel and Cobalt*, Vol 1: Fundamental Aspects, The Minerals, Metals and Materials Society, Warrendale, PA, pp. 881-910; R.F. Dalton, A. Burgess and P. H. Quan (1993), *Hydrometallurgy*, **30**, 385.
4. J. Szymanowski (1993), *Hydroxyoximes and Copper Hydrometallurgy*, CRC Press, Boca Raton.

5. For metal salt binding ditopic receptors: S. S. Flack, J-L. Chaumette, J. D. Kilburn, G. J. Langley and M. Webster (1993), *J. Chem. Soc., Chem. Commun.*, 399; P. B. Savage, S. K. Holmgren and S. H. Gellman (1994), *J. Am. Chem. Soc.*, **116**, 4069; M. T. Reetz (1996), Comprehensive Supramolecular Chemistry, J. L. Atwood, J. E. D. Davies, D. D. MacNicol and F. Vogle (eds.), Elsvier Science Ltd, Oxford, pp. 553-563; N. Pelizzi, A. Casnati, A. Friggeri and R. Ungaro (1998), *J. Chem. Soc., Perkin Trans. 2*, 1307; P. D. Beer and J. B. Cooper (1998), *J. Chem. Soc., Chem. Commun.*, 129.
6. D. J. White, N. Laing, H. A. Miller, S. Parsons, S. Coles and P. A. Tasker (1999), *J. Chem. Soc., Chem. Commun.*, 2077; P. A. Tasker and D. J. White (1999), *Br. Pat.*, 9907485.8.
7. D. M. Rudkevich, Z. Brzozka, M. Palys, H. C. Visser, W. Verboom and D. N. Reinhoudt (1994), *Angew. Chem. Int. Ed. Engl.*, **33**, 467.
8. H. A. Miller, N. Laing, S. Parsons, A. Parkin, P. A. Tasker and D. J. White (2000), *J. Chem. Soc., Dalton Trans.*, 3773.
9. S. Shanmuga, S. Raj, R. Thirumurugan, G. Shanmugam, H-K. Fun, J. Manonmani and M. Kandaswamy (1999), *Acta Cryst.*, **C55**, 94.
10. In contact with aqueous sulfate solutions at low pHs sulfur to ligand and sulfur to metal ratios of >1 are observed implying that  $\text{HSO}_4^-$  is loaded.
11. V. H. Ness and N. L. Hayward (2000), *Proc. SME Annual Meeting*, Littleton, CO.
12. K. Smith, H. A. Miller and P. A. Tasker, unpublished work; K. Smith (2000), Final year report, Department of Chemistry, University of Edinburgh.



## PHYSICO-CHEMICAL PROPERTIES OF CYANEX® 301

Gerard Cote, Jean-Valéry Martin\*, Denise Bauer\*\* and Yves Mottot\*

Ecole Nationale Supérieure de Chimie de Paris, Paris, France

\* Rhodia Recherches, Aubervilliers, France

\*\* Ecole Supérieure de Physique et de Chimie Industrielles de Paris, Paris, France

This paper gives a rapid overview of the physical and chemical properties of Cyanex® 301. In particular, it is shown that purified bis(2,4,4-trimethylpentyl)dithiophosphinic acid, the active substance of Cyanex® 301, has a weak tendency to dimerize in non-polar organic diluents. The dimerization constant  $K_2$  is close to 5 ( $M^{-1}$ ) in *n*-heptane equilibrated with an aqueous phase of ionic strength of 0.02 M. The aqueous pKa and the logarithm of the partition ratio ( $K_D = [HL] / [HL]$ ) of the monomeric form of bis(2,4,4-trimethylpentyl)dithio-phosphinic acid were estimated to be close to 1.7 and 4.8 (at low ionic strength), respectively. Other properties of Cyanex® 301 such its chemical stability and resistance to  $\gamma$ -irradiation, as well as the nature of the metal species extracted into the organic phases are discussed.

### INTRODUCTION

The organothiophosphorus compounds have attracted a great attention in solvent extraction over the last three decades and their properties have been extensively investigated [1]. Cyanex® 301 is an organothiophosphorus extractant which is commercially available from Cytec and contains about 80% (in weight) of bis(2,4,4-trimethylpentyl)dithiophosphinic acid [denoted hereafter either HL or R<sub>2</sub>PSSH] as the active substance. Originally, Cyanex® 301 was developed for the selective extraction of zinc from effluent streams containing calcium, such as those generated in the manufacture of rayon by the viscose process, but it was found that this reagent is also capable to extract a great number of metal and metalloid species in a large range of acidity [2]. Some possible fields of applications of Cyanex® 301 reported in the recent literature include the treatment of spent catalysts and electroplating baths (removal of Ni) [3], the purification of wet-phosphoric acid (removal of Cd by Solvent Impregnated Resin technology) [4], the treatment of phosphoric acid process liquors [5], the management of tannery waste [6] and the production of separated rare earths [7]. It was also recently discovered that Cyanex® 301 and its analogues are capable of separating actinides(III) from lanthanides(III) in nitric acid media, which is of high strategic importance for the development of advanced nuclear waste reprocessing schemes [8-15]. It has been demonstrated that the high actinides(III)/lanthanides(III) separation factors obtained with such extractants are due to a covalent effect in the M(III)-S bond, which is greater for actinides(III) (e.g., Am<sup>3+</sup>) than for lanthanides(III) (e.g., Eu<sup>3+</sup>). However, despite numerous studies dedicated to Cyanex® 301, and more generally to the organodithiophosphinic acids, some physical and chemical properties of such compounds are not yet very well known or even remain controversial.

The purpose of the present paper is to give a rapid overview of the properties of purified and non-purified Cyanex 301®. Properties such as self-association in the organic phases, acidic dissociation ( $pK_a$ ), distribution between aqueous and organic phases, adsorption at the liquid-liquid interfaces, chemical and radiolytic stabilities are considered. Some crystallographic data of crystallized bis(2,4,4-trimethylpentyl)dithiophosphinic acid are also given. Finally, the nature of the extracted species is discussed.

## PHYSICO-CHEMICAL PROPERTIES

### Chemical Composition

In earlier works, Cyanex® 301 was used as delivered by Cytec (or previously by Cyanamid). Recently, Zhu *et al.* have proposed a method based on the formation, isolation and recrystallization of ammonium bis(2,4,4-trimethylpentyl)dithiophosphinate and regeneration of the acidic form with 4 M HCl, for purifying Cyanex® 301 [16]. Alternatively, El Aouni has proposed a derived method based on the formation of sodium bis(2,4,4-trimethylpentyl)dithiophosphinate [17]. The composition of purified and non-purified Cyanex® 301 has been investigated by various authors with different techniques. The results are summarized in Table 1.

*Table 1. Composition of purified and non-purified Cyanex® 301 (HL).*

Samples	Species and concentrations (R = 2,4,4-trimethylpentyl)	Analytical methods	Ref.
Non-purified Cyanex® 301	R <sub>2</sub> PS <sub>2</sub> H 75 - 83 %      R <sub>3</sub> PS 5 - 8 % R <sub>2</sub> PSOH 3 - 6 %      unknown ≈ 2 %	GC-MS <sup>31</sup> P-NMR	[18]
Non-purified Cyanex® 301	R <sub>2</sub> PS <sub>2</sub> H 78 %      R <sub>3</sub> PS 14 % R <sub>2</sub> PSOH 0.8 %      R <sub>2</sub> PO <sub>2</sub> H 3.5 % unknown ≈ 3.6 %	GC	[19]
Purified Cyanex® 301	R <sub>2</sub> PS <sub>2</sub> H > 99% (up to 99.8 %)	Potentiometric titration <sup>31</sup> P-NMR	[16] [8]
Purified Cyanex® 301	R <sub>2</sub> PS <sub>2</sub> H ≈ 98 %	GC Metal loading at saturation	[17]

Examination of Table 1 mainly shows that the composition of Cyanex® 301 varies from one sample to another, and that the purification method proposed by Zhu *et al.* is efficient.

### Some Physical and Spectrometric Characteristics of Purified Cyanex® 301

At room temperature, purified Cyanex® 301 is a greenish liquid. Some of its physical and spectrometric characteristics are given in Table 2. When purified Cyanex® 301 is left at 0°C, white needle shaped crystals (typically 5-15 μm width x 100 - 200 μm length) of pure bis(2,4,4-trimethylpentyl)dithiophosphinic acid slowly form. These crystals were found to belong to the monoclinic system with  $a = 1.784 \pm 0.003$  nm,  $b = 0.4849 \pm 0.0006$  nm,  $c = 1.127 \pm 0.005$  nm and  $\alpha = \beta = 90^\circ$ ,  $\gamma = 125.1 \pm 0.2^\circ$ . Examination of Table 2 shows that pure bis(2,4,4-trimethylpentyl)dithiophosphinic acid exhibits only a low interfacial activity at the 0.1 M H<sub>2</sub>SO<sub>4</sub> / *n*-decane interface as its Critical Adsorption Concentration is close to 0.03 M.

Table 2. Some properties of purified Cyanex® 301.

Properties	Data		Ref.
Density at 24°C (kg dm <sup>-3</sup> ) Viscosity at 24°C (mPa s)	0.946 18.1		[20]
Interfacial tension at the 0.1 M H <sub>2</sub> SO <sub>4</sub> / <i>n</i> -decane interface, at 25°C (mN m <sup>-1</sup> )	43.7 (C = 0.0001 M) 43.7 (C = 0.001 M) 41.0 (C = 0.01M)	39.3 (C = 0.1 M) 30.1 (C = 1 M)	This work
Proton decoupled <sup>31</sup> P-NMR spectrum (in CDCl <sub>3</sub> )	Only 2 peaks at 67.0 and 67.1 ppm (85% H <sub>3</sub> PO <sub>4</sub> as external standard)	The presence of two peaks in the spectrum is due to the existence of diastereoisomers as each of the two 2,4,4-trimethylpentyl chains contains one stereogen center	This work [2]
Some characteristic absorption bands in the IR spectrum (cm <sup>-1</sup> )	S-H stretching : 2580 P-CH <sub>2</sub> bending : 820	C-P-C bending : 805 P=S stretching : 611	This work

### Self-Association in the Organic Diluents, Distribution between Aqueous and Organic Phases and Aqueous Acidic Dissociation Constant

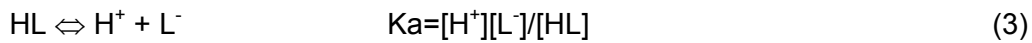
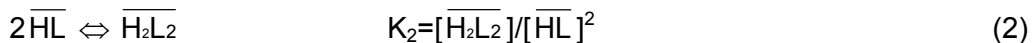
Although the self-association of purified and non-purified Cyanex® 301 in the organic diluents has been investigated by various authors and various techniques, the subject is still a matter of controversy (Table 3). Indeed, on the one hand, three independent studies based on vapour pressure osmometry and a very recent work based on SANS (small angle neutron scattering) unambiguously indicate that Cyanex® 301 exists as a monomer in toluene (or deuterated toluene), benzene and heptane, at least up to about 0.1 - 0.2 M (0.4 M in toluene), regardless it is purified or not [21-23]. On the second hand, distribution ratio measurements between aqueous and organic phases at pH 3.66 suggest that purified bis(2,4,4-trimethylpentyl)dithiophosphinic acid is dimeric in *n*-heptane, when its total concentration ranges between 0.2 and 1.0 M [20]. These two diametrically opposed conclusions have their unconditional followers and some extraction mechanisms proposed in the literature from metal distribution measurements may be not operative since they have been established considering that bis(2,4,4-trimethylpentyl)dithiophosphinic acid is either monomeric or dimeric, without any further evidence. Thus, the question is of importance.

In inert diluents, the self-association of the dialkyldithiophosphinic acids is possible only through the formation of S – H … S hydrogen bonds. Allen *et al.* have investigated this phenomenon by infrared spectroscopy and found that diethyldithiophosphinic acid and diphenyldithiophosphinic acid in carbon tetrachloride, chloroform and cyclohexane exhibit a very sharp νSH band at 2550 – 2560 cm<sup>-1</sup> (due to the monomeric form of the studied acids) and a broad νSH band at about 2400 cm<sup>-1</sup> (due the dimeric form), whose relative intensities and areas greatly vary with the dithiophosphinic acid concentration: at 0.1 M the IR spectra show mainly the sharp νSH band at 2550 – 2560 cm<sup>-1</sup>, whereas above 2 M the broad νSH band at about 2400 cm<sup>-1</sup> is dominant [25]. Such observations suggest that the two studied dithiophosphinic acids are mainly monomeric in dilute solutions (*i.e.*, up to about 0.1 M), but dimeric in concentrated solutions, which is in a rather good qualitative agreement with the results reported in Table 3 for bis(2,4,4-trimethylpentyl)dithiophosphinic acid.

If equilibria (1-3) are considered, the distribution coefficient D<sub>Cyanex® 301</sub> of bis(2,4,4-trimethylpentyl)dithiophosphinic acid is given by Eq. (4) and Eq. (5) :

Table 3. Aggregation of Cyanex® 301 in organic diluents.

Techniques	Experimental conditions	Aggregation number found ( <i>n</i> )	Ref
Vapour pressure osmometry	0.2 M and 0.4 M non-purified Cyanex® 301 in toluene	<i>n</i> = 1.05 (0.2 M) <i>n</i> = 1.04 (0.4 M)	[21]
Vapour pressure osmometry	About 0.1 M non-purified Cyanex® 301 in benzene at room temperature	<i>n</i> = 0.90 (i.e., <i>n</i> ≈ 1)	[22]
Vapour pressure osmometry	0.016 to 0.16 M non-purified Cyanex® 301 in heptane at 28°C	<i>n</i> = 1 (no detectable deviation from the standard)	[23]
SANS (small angle neutron scattering)	0.1 M purified Cyanex® 301 (99%) in deuterated toluene	<i>n</i> = 1.07	[24]
Distribution ratio measurements between aqueous and organic phases	0.2 M to 1.0 M purified Cyanex® 301 in <i>n</i> -heptane at 25°C (pH = 3.66)	<i>n</i> ≈ 2	[20]



$$D_{Cyanex\text{®}301} = 2K_2 \left( \frac{K_D}{(1+K_a/[H^+])} \right)^2 [Cyanex\text{®}301] + \frac{K_D}{(1+K_a/[H^+])} \quad (4)$$

$$\log D_{Cyanex\text{®}301} = \log K_D - \log 2 + \log \left\{ 1 + (1 + 8K_2 C_{Total})^{0.5} \right\} - \log (1 + K_a / [H^+]) \quad (5)$$

where overbars refer to the species in organic phases,  $[Cyanex\text{®}301] = [HL] + [L^-]$  (i.e., total aqueous concentration) and  $C_{Total} \approx \overline{HL} + 2\overline{H_2L_2}$ .

Examination of Chen's data in *n*-heptane [20] obtained at an ionic strength of 0.02 M shows both a linear dependence of  $D_{Cyanex\text{®}301}$  vs  $[Cyanex\text{®}301]$  and a linear dependence of  $\log D_{Cyanex\text{®}301}$  vs pH :

$$D_{Cyanex\text{®}301} = 5.44 \times 10^6 [Cyanex\text{®}301] + 7.17 \times 10^2 \quad \text{at pH} = 3.66 \quad (R^2 = 0.983) \quad (6)$$

$$\log D_{Cyanex\text{®}301} = 6.98 - 0.997 \text{pH} \quad (R^2 = 0.996) \quad (7)$$

By identifying Eq. (4) and Eq. (6), one obtains  $K_D/(1+Ka/[H^+]) = 7.17 \times 10^2$  and  $2K_2(K_D/(1+Ka/[H^+]))^2 = 5.44 \times 10^6$  (at 25°C, pH = 3.66 and I = 0.02 M), and as a result  $K_2 \approx 5$  ( $M^{-1}$ ) in *n*-heptane. Furthermore, comparison of Eq. (5) and Eq. (7) indicates that  $Ka/[H^+] \gg 1$  in the range of pH investigated (i.e., 2.4 – 4.0) and thus that  $pKa < 2.4$ . Then, at pH = 3.66 and I = 0.02 M,  $K_D [H^+]/Ka \approx K_D/(1+Ka/[H^+]) = 7.17 \times 10^2$ , which leads to  $\log(K_D/Ka) \approx 6.5$ . Finally, by identifying Eq. (5) and Eq. (7), it comes also  $\log(K_D/Ka) - \log 2 + \log(1+(1+8K_2C_{\text{Total}})^{0.5}) = 6.98$ , which gives  $\log(K_D/Ka) \approx 6.6$ , as  $C_{\text{Total}} = 0.4$  M, and thus corroborates the previous determination.

The value of about 5 estimated above for the dimerization constant of bis(2,4,4-trimethylpentyl)dithiophosphinic acid in *n*-heptane, at 25°C, is in a good agreement with the established order of aggregation [23] : alkylphosphinic ( $\log K_2 = 3$  in kerosene [26] and 2.3 in CHCl<sub>3</sub> [27], for Cyanex® 272) > alkylthiophosphinic ( $\log K_2 = 1.3$  in heptane for Cyanex® 302 [H]) > alkylidithiophosphinic acid ( $\log K_2 = 0.7$  in *n*-heptane for Cyanex® 301 [this work]).

The pKa values of organophosphorus acid can be predicted from appropriate statistical relationships [28]. For the XYPSSH dithiophosphinic acids in water containing 7% ethanol, Eq. (8) was established [28,29]:

$$pKa = 1.74 + 0.01\sigma^\phi \quad (8)$$

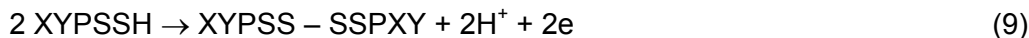
where  $\sigma^\phi = -1.21, -1.44, -1.21$  and  $-1.11$  for X (or Y) =  $-(CH_2)_4CH_3, -CH_2-C(CH_3)_3, -(CH_2)_5CH_3$  and  $-(CH_2)_7CH_3$ , respectively. The coefficient 0.01 in Eq. (8) suggests that the nature of the substituent X and Y in XYPSSH has only a little influence on the pKa values. Thus, the pKa of bis(2,4,4-trimethylpentyl)dithiophosphinic acid can be estimated to be close to 1.7 in aqueous 7% ethanol, but also in water as the presence of a moderate concentration of ethanol has only a little effect on the pKa values [29,30]. Such a value is indeed lower than 2.4, as stated above. If the value of 1.7 is retained for aqueous pKa at low ionic strength, thus  $\log K_D$  can be estimated to be close to 4.8, which is credible. In summary, the following values can be proposed for bis(2,4,4-trimethylpentyl)dithiophosphinic acid in the system water / *n*-heptane, at low ionic strength :  $pKa \approx 1.7$ ,  $\log K_D \approx 4.8$  and  $\log K_2 \approx 0.7$ . Obviously, such estimates are rough.

However, a value of 5 for the dimerization constant  $K_2$  means that about 40 % of bis(2,4,4-trimethylpentyl)dithiophosphinic acid is already under its dimeric form at  $C_{\text{Total}} = 0.1$  M and it is surprising that the presence of this form was not detected by vapour pressure osmometry, especially in heptane (Table 3). The presence of impurities when non-purified Cyanex® 301 was used, as well as the possible use of dry diluents in which the tendency for aggregation could be weaker than in organic phases equilibrated with water may explain such a discrepancy [31]. Nevertheless further investigations based on the coupled use of various techniques (e.g., VPO, SANS, distribution ratio measurements, etc.) are necessary to elucidate all the involved phenomena.

Finally, it is of interest that in oxygenated diluents such as diethylether or in inert diluents modified by long chain alcohols, the S – H … O hydrogen bonding becomes predominant and the dimerization of the dithiophosphinic acids, including Cyanex® 301, can be ignored, even at high concentration [25,31,32], as assumed in our previous works [33-35].

## **Chemical Stability and Resistance towards Radiolysis**

The dithiophosphorus acids can be easily oxidized into disulphides according to Eq. (9) :



For similar alkyl chains, it was found that the dialkyldithiophosphinic acids are slightly more easily oxidable than their dithiophosphoric analogues (e.g.,  $E^\circ = 0.13$  V for  $X = Y = i\text{-C}_4\text{H}_9$ , whereas  $E^\circ = 0.23$  V for  $X = Y = i\text{-C}_4\text{H}_9\text{O}$ ) [36]. The strong reductive properties of phosphorus dithioic acids determine the instability of their complexes with some metals. In particular, it is known that copper(II) dithiophosphate complexes are converted in polar media into polynuclear copper(I) compounds having a 1:1 metal : ligand stoichiometry [36]. More recently, Sole *et al.* have confirmed the 1:1 stoichiometric ratio between copper and Cyanex® 301 and postulated a structure for the oligomeric complex [22]. It is of interest that the reduction of copper(II) into copper(I) may be intermolecular rather than intramolecular in nature (*i.e.*, the molecules of Cyanex® 301 which act as reducing-agent against copper(II) are not those engaged in the copper(II) complex, but the free Cyanex® 301 molecules in excess) [17]. Evidence of such a behaviour is that the organic solutions of purified Cyanex® 301 loaded with copper(II) at saturation do not undergo transformation, whereas the reduction takes place in the presence of free Cyanex® 301.

Logically, Sole *et al.* found that contact with nitric acid solutions which are oxidizing causes rapid destruction of Cyanex® 301, even at low acid strength and for short periods of time [19]. Even under milder conditions, the dithiophosphorus acids are prone to oxidation with the formation of disulphides in the organic solvent phases. However, they can be regenerated by reduction with metal powders (e.g., Ni, Co, Zn, etc.) [37,38].

Another commonly cited problem with earlier generation of dithiophosphoric acid extractants was their poor hydrolytic and thermal stabilities [39]. Such difficulties are largely overcome with Cyanex® 301 as the latter exhibits no significant degradation when subjected to prolonged periods of exposure to sulphuric acid solutions, even under severe conditions (e.g., 3 M  $\text{H}_2\text{SO}_4$ , 60°C, 3000 hours) [19].

Finally, due to the interest of dithiophosphinic acids for separating actinides(III) from lanthanides(III), the radiolytic stability of non-purified and purified Cyanex® 301 was investigated by Chen *et al.* [40]. It was found that Cyanex® 301 is severely damaged by  $\gamma$ -irradiation, but that purified Cyanex® 301 is more resistant than the non-purified reagent. For instance, the damage percentage of  $\text{R}_2\text{PSSH}$  in purified and non-purified Cyanex® 301 in xylene amounts to 54% and 94%, after a dose of  $10^5$  Gy, respectively. Dialkylmonothiophosphinic acid, dialkylphosphinic acid and various other phosphorus compounds form under  $\gamma$ -irradiation.  $\text{H}_2\text{SO}_4$  also forms after a dose of  $10^6$  Gy.

## **Extracted Species**

From the analysis of metal distribution data by the slope analysis method, various types of extracted complexes have been identified :  $\text{ML}_2$ ,  $\text{ML}_2\text{HL}$ ,  $\text{ML}_2(\text{HL})_2$ ,  $\text{M}(\text{HL}_2)_2\text{.}(\text{HL})_2$ ,  $\text{ML}_3$ ,  $\text{ML}_3\text{.HL}$ ,  $\text{ML}_3\text{.}3\text{HL}$ , etc. Generally, the dithiophosphinates behave as chelating or bridging (in polynuclear complexes) ligands, whereas the non-dissociated dithiophosphinic acid molecules can contribute to the formation of auto-adducts. However, in some cases the formulas proposed for the species extracted in the organic phases may be erroneous as they have been established by assuming that Cyanex® 301 is either totally monomeric or totally dimeric in the organic phases, regardless the actual situation. Thus, considering that purified Cyanex® 301 is totally dimeric in kerosene, Zhu *et al.* found that the plot  $\log D_{\text{Am}}$  vs.  $[\text{H}_2\text{L}_2]_{\text{free}}$  is linear with a slope of 2 (curve 1 in Figure 1) and concluded that  $\text{Am}^{3+}$  is extracted by Cyanex® 301 by formation of  $\text{ML}_3\text{.HL}$  according to Eq. (10) [16] :



However, if one considers that Cyanex® 301 is not totally dimerized in kerosene in the range of concentration investigated (i.e., 0,2 – 1,0 M) and that its dimerization constant is equal to 4 (which is close to 5 as estimated in the preceding paragraph for *n*-heptane), one obtains a plot  $\log D_{Am}$  vs.  $\overline{HL}_{free}$  which is also linear, but whose slope is equal to 3 (curve 2 in Figure 1), which leads to the conclusion that  $Am^{3+}$  is extracted merely as  $AmL_3$  according to Eq. (11) :

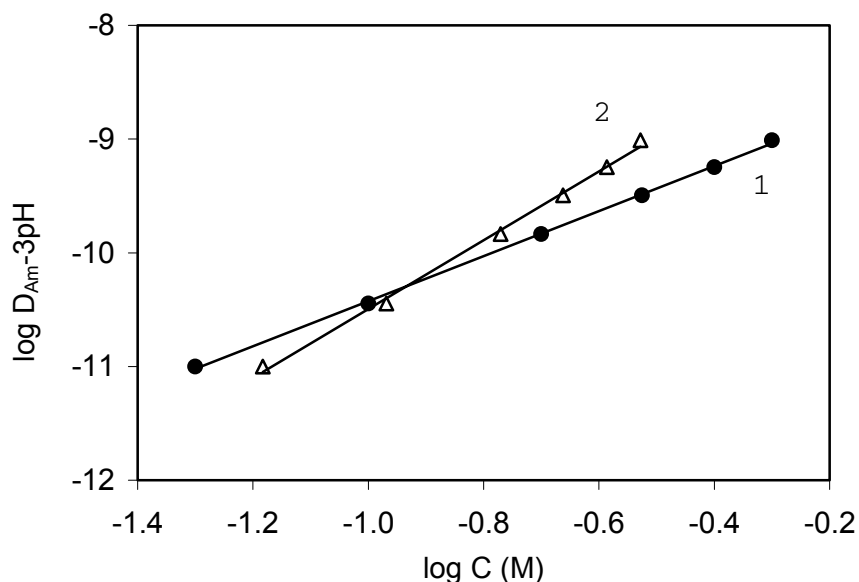


Figure 1. Plot  $\log D_{Am} - 3pH$  vs  $\log C$ . (1) Cyanex® 301 is assumed to be totally dimerized and  $C = [H_2L_2]$ ; slope = 1.98 ( $R^2 = 0.999$ ) [16]; (2) Cyanex® 301 is assumed to be partly dimerized with  $\log K_2 = 0.6$  and  $C = [HL]$ ; slope = 3.02 ( $R^2 = 0.997$ ).

Thus, most equations proposed in the literature for the extraction of metals under experimental conditions where Cyanex® 301 can distribute more or less equally between its monomeric and dimeric forms should be considered critically.

Another interesting phenomenon related to the extracted complexes is the formation of mixed ligand complexes for producing synergistic effects [7,14,15]. We point out that in the presence of O-bearing co-extractant, the formation of S – H  $\cdots$  O hydrogen bonds should be favoured and that the tendency of Cyanex® 301 to dimerize should be depressed.

## REFERENCES

1. G. Cote and D. Bauer (1989), *Rev. Inorg. Chem.*, **10**, 121-144.
2. S. Facon, M.A. Rodriguez, G. Cote and D. Bauer (1993), Solvent Extraction in the Process Industries (*Proc. ISEC '93*), Vol. 1, D.H. Logsdail and M.J. Slater (eds.), Society of Chemical Industry, Elsevier Applied Science, London, pp. 557-564.
3. R. Singh, A.R. Khwaja, B. Gupta and S.N. Tandon (1999), *Solv. Extr. Ion Exch.*, **17**, 367-390.

4. L.H. Reyes, I.S. Medina, R.N. Mendoza, J.R. Vazquez, M.A. Rodriguez and E. Guibal (2001), *Ind. Eng. Chem. Res.*, **40**, 1422-1433.
5. C. Koopman, G.J. Witkamp and G.M. Van Rosmalen (1999), *Sep. Sci. Technol.*, **34**, 2997-3008.
6. A.R. Khwaja, R. Singh and S.N. Tandon (2000), *J. Environ. Eng.*, **126**, 307-312.
7. M.L.P. Reddy, J.R. Bosco Bharathi, Smitha Peter and T.R. Ramamohan (1999), *Talanta*, **50**, 79-85.
8. C. Hill, C. Madic, P. Baron, M. Ozawa and Y. Tanaka (1998), *J. Alloys Compounds*, **271-273**, 159-162.
9. J. Chen, R.Z. Jiao and Y.J. Zhu (1999), *Radiochim. Acta*, **86**, 151-154.
10. H. Hoshi, A. Tsuyoshi and K. Akiba (1999), *Solv. Extr. Res. Dev. (Japan)*, **6**, 113-121 and (2001), *Solv. Extr. Res. Dev. (Japan)*, **8**, 159-164.
11. H. Hoshi, A. Tsuyoshi and K. Akiba (2000), *J. Radioanal. Nucl. Chem.*, **243**, 621-624.
12. Y. Wei, M. Kumagai, Y. Takashima, G. Modolo and R. Odoj (2000), *Nucl. Technol.*, **132**, 413-423.
13. H. Mimura, H. Hoshi, K. Akiba and Y. Onodera (2001), *J. Radioanal. Nucl. Chem.*, **247**, 375-379.
14. G. Ionova, S. Ionov, C. Rabbe, C. Hill, C. Madic, R. Guillaumont and J.C. Krupa (2001), *Solv. Extr. Ion Exch.*, **19**, 391-414.
15. G. Ionova, S. Ionov, C. Rabbe, C. Hill, C. Madic, R. Guillaumont, G. Modolo and J.C. Krupa (2001), *New. J. Chem.*, **25**, 491-501.
16. Y. Zhu, J. Chen and R. Jiao (1996), *Solv. Extr. Ion Exch.*, **14**, 61-68.
17. M. El Aouni (1998), Doctorate Thesis, Ecole Centrale de Paris, France.
18. K.C. Sole and J.B. Hiskey (1992), *Hydrometallurgy*, **30**, 345-365.
19. K.C. Sole, J.B. Hiskey and T.L. Ferguson (1993), *Solv. Extr. Ion Exch.*, **11**, 783-796.
20. J. Chen, R. Jiao and Y. Zhu (1996), *Chin. J. Appl. Chem.*, **13**, 45-48.
21. B.K. Tait (1993), *Hydrometallurgy*, **32**, 365-372.
22. K.C. Sole and J.B. Hiskey (1995), *Hydrometallurgy*, **37**, 129-147.
23. A. Almela and M.P. Elizalde (1995), *Anal. Proc. Incl. Anal. Com.*, **32**, 145-147.
24. M.P. Jensen, R. Chiarizia and V. Urban (2001), *Solv. Extr. Ion Exch.*, **19**, 865-884.
25. G. Allen and R.O. Colclough (1957), *J. Chem. Soc.*, 3912-3915.
26. C. Sella and D. Bauer (1988), *Solv. Extr. Ion Exch.*, **6**, 819-833.
27. L. Ke-an, S. Muralidharan and H. Freiser (1985), *Solv. Extr. Ion Exch.*, **3**, 895-908.
28. D.D. Perrin, B. Dempsey and E.P. Serjeant (1981), pKa Prediction for Organic Acids and Bases, Chapman and Hall, London, pp. 91-95.
29. T.A. Mastryukova and M.I. Kabachnik (1969), *Russ. Chem. Rev.*, **38**, 795-811.
30. M. Rovira, J.L. Cortina and A.M. Sastre (1999), *Solv. Extr. Ion Exch.*, **17**, 333-349.
31. J.R. Ferraro, G.W. Mason and D.F. Peppard (1961), *J. Inorg. Nucl. Chem.*, **22**, 285-291.
32. G.W. Mason, S. Lewey and D.F. Peppard (1964), *J. Inorg. Nucl. Chem.*, **26**, 2271-2284.
33. S. Facon, G. Cote and D. Bauer (1991), *Solv. Extr. Ion Exch.*, **9**, 717-734.
34. M. Avila Rodriguez, G. Cote and D. Bauer (1992), *Solv. Extr. Ion Exch.*, **10**, 811-827.
35. M. Avila Rodriguez, G. Cote, R. Navarro Mendoza, T.I. Saucedo Medina and D. Bauer (1998), *Solv. Extr. Ion Exch.*, **16**, 471-485.
36. V.V. Ovchinnikov, V.F. Toropova, A.R. Garifzyanov, R.A. Cherkasov and A.N. Pudovik (1985), *Phosphorus Sulfur*, **22**, 199-210.
37. J.J.R. Perraud, D.F. Colton, J.P. Duterque and Y. Okita (2000), *U.S. Pat.*, No 6.022,991 A (Feb. 8).
38. W.A. Rickelton, I.O. Mihaylov, E. Krause, B.J. Love and P.K. Louie (1997), *French Pat. Appl.*, No 2,749,192 A1 (Dec. 5).
39. G. Cote and D. Bauer (1984), *Anal. Chem.*, **56**, 2153-2157.
40. J. Chen, R. Jiao and Y. Zhu (1996), *Solv. Extr. Ion Exch.*, **14**, 555-565.



## TOWARD RECOGNITION OF THE ANION IN THE EXTRACTION OF ALKALI METAL SALTS BY CROWN ETHERS AND CALIXARENES

Bruce A. Moyer, Peter V. Bonnesen, Lætitia H. Delmau,  
Tamara J. Haverlock, Konstantinos Kavallieratos and Tatiana G. Levitskaia

Chemical and Analytical Sciences Division, Oak Ridge National Laboratory, TN, USA

Recent results are reviewed concerning major factors that govern selectivity for monovalent anions when host-guest chemistry is employed in the extraction of salts from aqueous solution. Such factors include solvation, ion-pairing, and anion binding by anion receptors. From these considerations, we may begin to anticipate the ability to control the selectivity for the anion as well as the cation in salt extraction by designed receptors.

### INTRODUCTION

Despite the attractive selectivity that crown ethers, calixarenes, and other host molecules offer toward *cations*, the role of the anion has not been fully understood nor controlled by design. In recent years, research in this laboratory has focused on ion-pair extraction employing cation and anion receptors for alkali metal salts. Interest in such systems stems in part from the desire to strip extracted salts with water, resulting in processes that yield a pure salt product stream with little secondary waste. Examples include processes for nuclear-waste treatment that produce aqueous streams of cesium nitrate [1] or sodium pertechnetate [2] suitable for vitrification and disposal. These processes respectively employ calixcrown and crown ether extractants to bind the cation, leaving the co-extracted anion to be solvated by diluent, modifier, and water molecules. Solvation principles [3] may thus be used to gain a modest degree of control over the selectivity toward the anion. For univalent anions, extractability tends to increase with increasing anion thermochemical radius. This monotonic selectivity trend has been referred to as "bias," the steepness of which may be manipulated by judicious selection of diluent and any modifier [4]. Exploiting such considerations, the extractability of trace pertechnetate anion from a sodium nitrate waste matrix by a crown ether is possible because pertechnetate is the largest anion in the system. On the other hand, the extractability of trace cesium from a nitrate matrix is more challenging, owing to the difficulty associated with extraction of a small, hydrated anion. Extraction in this case is possible because nitrate has a high concentration and is overwhelmingly the most abundant anion in many nuclear wastes.

In the context of ion-pair extraction by neutral cation receptors like crown ethers, the question naturally arises as to how one can gain better control of the anion co-extraction and escape from reliance upon ion-solvation effects. In this paper, the major effects governing anion selectivity in ion-pair extraction are examined from the point of view of systems studied in this laboratory. Results reflect both solvation and ion-pairing effects in simple systems involving crown ethers. Novel approaches involve the use of separate anion hosts in synergistic combination with cation hosts. Ultimately, such research is aimed at improving processes for the extraction of certain cations such as cesium or sodium by increasing the strength of the extraction and by minimizing matrix effects. A practical benefit would be increased net

strength of extraction of salts from aqueous matrices that contain high concentrations of chloride, nitrate, or other hydrated anions common in hydrometallurgy. Second, one may possibly disrupt the bias-type of selectivity favoring large anions to gain true anion recognition. Third, given the availability of extractants that are each specific to a given salt, one may then possibly combine such extractants without mutual interference. Thus, processes may be envisioned in which one or more targeted salts may be extracted by design from a complex salt mixture.

### SYSTEMS EMPLOYING ONLY A CATION RECEPTOR

In a low-polarity diluent system, the simplest mechanism for the extraction of an alkali metal salt with a univalent anion may be written as:



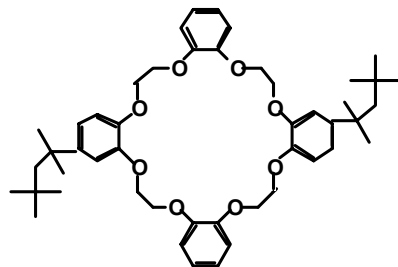
where Crown is any lipophilic neutral metal ion receptor. Many extraction reactions involving crown ethers or calixarenes in fact follow such a stoichiometry [5]. To evaluate how the net driving force depends on anion interactions, it is instructive to examine this reaction in terms of its component thermochemical steps. A particularly useful thermochemical scheme comprises Gibbs energy changes associated with a) partitioning of the individual metal ion  $M^+$  from water to the solvent phase [ $\Delta G_p^\circ(M^+)$ ], b) partitioning of the individual anion  $X^-$  from water to the solvent phase [ $\Delta G_p^\circ(X^-)$ ], c) complexation of the metal ion by the cation receptor CE in the solvent phase [ $\Delta G_{\text{cpx}}^\circ(CEM^+)$ ], and d) ion pairing in the solvent phase [ $\Delta G_{\text{ip}}^\circ(CEM^+X^-)$ ]. The standard Gibbs energy change  $\Delta G_{\text{ex}}^\circ$  associated with the net extraction may be expressed as sum of the four component steps:

$$\Delta G_{\text{ex}}^\circ = \Delta G_p^\circ(M^+) + \Delta G_p^\circ(X^-) + \Delta G_{\text{cpx}}^\circ(CEM^+) + \Delta G_{\text{ip}}^\circ(CEM^+X^-) \quad (2)$$

Generally, the tetraphenylarsonium tetraphenylborate (TATB) extrathermodynamic assumption is employed for evaluating the ion-partitioning terms [3]. Under this reasonable assumption, the values of  $\Delta G_p^\circ$  are set equal for tetraphenylarsonium and tetraphenylborate, thus allowing the evaluation of  $\Delta G_p^\circ$  values for individual ions.

In cases where ion-pairing is weak or effectively does not occur, anion selectivity can be understood entirely on the basis of the behavior of the anion-partitioning term  $\Delta G_p^\circ(X^-)$  [4]. Many such values have been reported in the form of standard Gibbs energies of transfer  $\Delta G_{\text{tr}}^\circ(X^-)$ , which for simplicity are not distinguished here from  $\Delta G_p^\circ(X^-)$  [6]. Unfortunately, quantitative tools for predicting ion partitioning are rather imprecise. Electrostatic theory agrees qualitatively with the general observation that the extractability of anions of a given charge type increases with increasing anionic thermochemical radius ( $r_-$ ). One may say that extraction is "biased" toward larger anions, as distinct from peak selectivity or recognition. Often electrostatic relationships are expressed in terms of  $1/r_-$ , and certain thermodynamic quantities such as standard Gibbs energies of ion hydration or transfer often plot nearly linearly with this variable. From tabulated  $\Delta G_{\text{tr}}^\circ(X^-)$  values [6], it may be seen that values of  $\Delta G_{\text{tr}}^\circ(X^-)$  for a range of anions with a given diluent indeed correlate with  $1/r_-$ , and the slope of the fitted line depends upon the diluent. Toward understanding this effect, electrostatic theory distinguishes among diluents mainly in terms of the dielectric constant, which has unfortunately turned out to be a poor parameter for correlating diluent effects in ion partitioning. Rather, statistical analysis has shown that the most important diluent property governing partitioning of anions is the diluent's ability to donate a hydrogen bond relative to that of water [7]. It follows from this statistical analysis that the slope of plots of  $\Delta G_{\text{tr}}^\circ(X^-)$  vs.  $1/r_-$  correlates with the diluent hydrogen-bond-donor (HBD) strength. By way of a simple conclusion, the closer the diluent is to water in donating hydrogen bonds, the less anion discrimination or bias is possible. To maximize anion discrimination, the diluent should therefore be chosen to have no HBD ability.

A practical example is the extraction of trace pertechnetate ( $\text{TcO}_4^-$ ) as a sodium salt by a crown ether from a concentrated sodium nitrate matrix [2]. In this case, one requires the maximum discrimination or bias in favor of the larger pertechnetate ( $r_- = 0.252 \text{ nm}$  [4]) vs. nitrate ( $r_- = 0.196 \text{ nm}$  [4]). It follows that one should choose a diluent system with low HBD strength, as a hydrogen-bond donor would bind more strongly to the smaller nitrate ion and thereby lower selectivity for pertechnetate. Accordingly, 1-octanol in comparison with non-HBD solvents such as 2-octanone gave poor extraction of pertechnetate [8].



4,5"-bis(*tert*-octylbenzo)dibenzo-24-crown-8

To quantify the thermochemical terms in eq. 2 by way of a specific example, Figure 1 shows the stepwise extraction of cesium nitrate and perchlorate salts by a representative cesium-selective crown ether, 4,5"-bis(*tert*-octylbenzo)dibenzo-24-crown-8 (see structure at right) [9]. Through equilibrium analysis of liquid-liquid distribution data, it has been possible to evaluate these component steps in terms of their standard Gibbs energies with use of 1,2-dichloroethane as a model (as opposed to a process-suitable) diluent. The use of this diluent was helpful in this regard, as a) values of  $\Delta G_p^\circ$  are available [6], b) extraction behavior is simple, and c) the intermediate dielectric constant (10.4) permits examination of the ion-pairing step. It may be seen in Figure 1 that partitioning of the individual ions into the solvent is highly unfavorable, but the favorable complexation of the cation by the crown ether more than compensates, drawing the cesium ion into the solvent phase. Ion pairing provides additional stabilization. The overall process, corresponding to eq. 1, is favorable for each salt, whence  $\Delta G_{\text{ex}}^\circ = -1.7 \text{ kJ mol}^{-1}$  for  $\text{CsNO}_3$  extraction and  $-18.0 \text{ kJ mol}^{-1}$  for  $\text{CsClO}_4$  extraction.

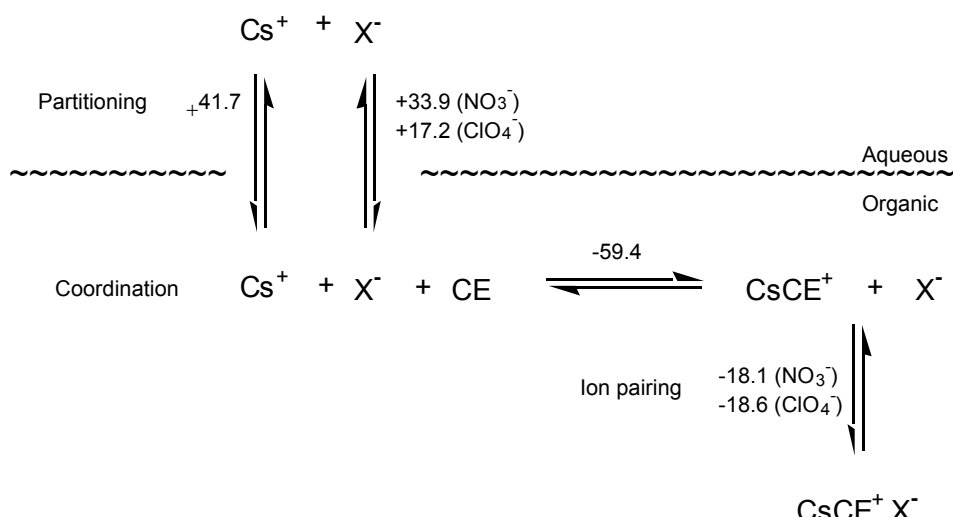


Figure 1. Thermochemical scheme for the extraction of cesium salts by 4,5"-bis(*tert*-octylbenzo)dibenzo-24-crown-8 (CE) in 1,2-dichloroethane at 25 °C. The numbers associated with the equilibria are standard Gibbs energies in  $\text{kJ mol}^{-1}$ .

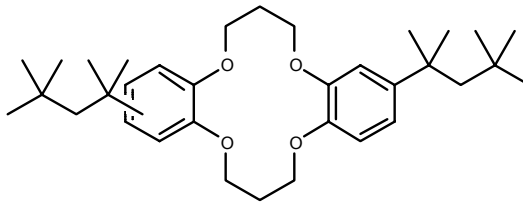
By reference to Figure 1, it may be appreciated that two processes govern anion selectivity: anion partitioning and ion-pairing. In the example shown, the overall extraction of the perchlorate salt of cesium is favored over nitrate by 16.3 kJ mol<sup>-1</sup>, consistent with the thermochemical radii (0.196 nm and 0.250 nm for nitrate [4] and perchlorate [6], respectively). Moreover, it is clear that almost all of the selectivity comes from the anion-partitioning process and is thus governed essentially by solvation. Ion pairing in this case has almost no effect on anion preference, attributable to the fact that the ion-pair is ligand-separated as a consequence of the efficient encapsulation of the Cs<sup>+</sup> ion by the crown ether [9]. Maximal anion discrimination is thus achieved, as ion-pairing is minimized.

Thermochemical measurements corresponding to the system shown in Figure 1 have been made for a large series of anions under the same conditions. The standard Gibbs energy change for the process in which the ions are completely dissociated in the solvent phase may be defined:

$$\Delta G_{\text{ex}\pm}^\circ = \Delta G_p^\circ(M^+) + \Delta G_p^\circ(X^-) + \Delta G_{\text{cpx}}^\circ(\text{CEM}^+) \quad (3)$$

As expected, linear plots of the corresponding constant  $\log K_{\text{ex}\pm}$  vs.  $\Delta G_p^\circ(X^-)/(2.303RT)$  were obtained. This has allowed the determination of values of  $\Delta G_p^\circ(X^-)$  for anions not yet reported in the literature(kJ mol<sup>-1</sup>): picrate (3.4), MnO<sub>4</sub><sup>-</sup> (12.4), CF<sub>3</sub>SO<sub>3</sub><sup>-</sup> (20.5), CF<sub>3</sub>COO<sup>-</sup> (34.9), CH<sub>3</sub>SO<sub>3</sub><sup>-</sup> (48.1), and CH<sub>3</sub>COO<sup>-</sup> (56.5).

By contrast, Figure 2 illustrates a case where ion-pairing does have a significant impact on anion selectivity. The system shown involves the extraction of sodium salts by bis(*tert*-octylbenzo)-14-crown-4 (structure at right) in 1,2-dichloroethane at 25 °C [10]. This crown ether was shown to bind Na<sup>+</sup> ion as a 1:1 metal:ligand open-face sandwich and a 1:2 metal:ligand sandwich complex in the same system. In the formation of the open-face sandwich complex NaCE<sup>+</sup>X<sup>-</sup>, the ion-pairing step favors nitrate by 13.6 kJ mol<sup>-1</sup>, owing to the ability of the anion to engage in contact ion-pairing with the Na<sup>+</sup> cation. As a result, the ion-pairing interaction nearly cancels the perchlorate selectivity of the ion-partitioning step, and the net reaction favors perchlorate by just 3.1 kJ mol<sup>-1</sup>. On the other hand, sandwich formation prevents contact ion-pairing, and the result is reminiscent of the case in Figure 1. Namely, the ion-pairing step discriminates weakly between the anions, because the charge-separation is large in the ligand-separated ion-pair. Consequently, the ion-partitioning step controls the selectivity, and perchlorate is favored in the net reaction by 15.6 kJ mol<sup>-1</sup>, in fairly good agreement with the results obtained in Figure 1 with an entirely different system.



Another way to modulate anion selectivity through the ion-pairing interaction entails modifying the cation-receptor molecule by adding HBD groups. Figure 3 illustrates such an example, in which the *syn*-bis(methoxy) and *syn*-dihydroxy derivatives of bis(*tert*-octylbenzo)-14-crown-4 are compared [11]. In the experiment, each crown ether was used to extract aqueous solutions containing single sodium salts, and <sup>22</sup>Na tracer techniques were employed to determine the distribution ratio of each salt. From largest to smallest, the anions tested include ReO<sub>4</sub><sup>-</sup>, ClO<sub>4</sub><sup>-</sup>, SCN<sup>-</sup>, I<sup>-</sup>, NO<sub>3</sub><sup>-</sup>, Br<sup>-</sup>, and Cl<sup>-</sup>. Sodium chloride extraction was too feeble for reliable measurement in the case of the *syn*-bis(methoxy) derivative and could not be determined. A correction for loading was applied to the distribution data, and the corrected distribution ratio  $D_0$  is shown plotted vs. the reciprocal of the anionic thermochemical radius augmented by a small correction term ( $\Delta r_- = 0.017$  nm). The size correction  $\Delta r_-$  is that which linearizes plots of Gibbs energies of anion hydration vs.  $1/(r_- + \Delta r_-)$

[12]. As shown in Figure 3, both crown ether systems exhibit a strong bias toward large anions, as indicated by the arbitrary lines drawn with negative slope. If one refers to the slope ( $m$ ) as a measure of bias, then it may be concluded that the effect of the hydroxy groups is to attenuate this bias. The hydrogen-bond donation provided by the hydroxy groups would be expected to boost extraction of all anions. However, the hydrogen-bonding interaction would be strongest with the smallest anions and would thereby enhance their extraction to a greater degree than that of the larger anions. The net effect is to make the negative slope of the line less steep. It may be noted that some recognition may be exhibited in the case of the  $\text{SCN}^-$  ion, which lies somewhat above the line in the case of the *syn*-dihydroxy crown.

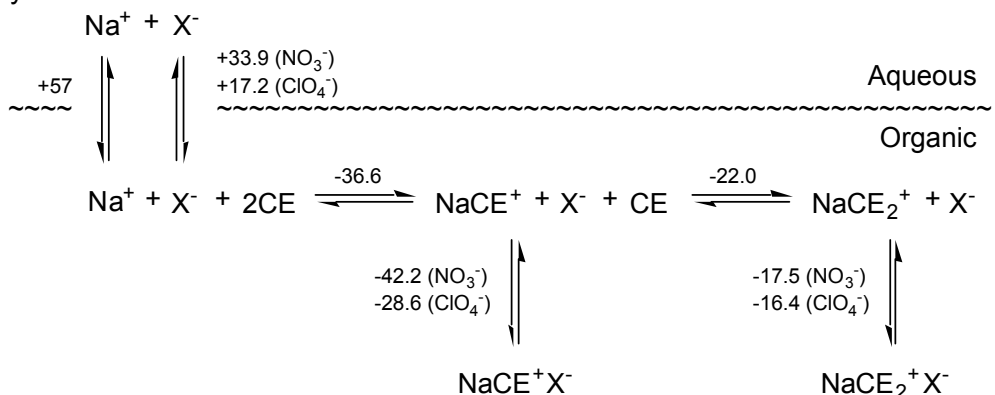


*Figure 2. Thermochemical scheme for the extraction of sodium salts by bis(tert-octylbenzo)-14-crown-4 in 1,2-dichloroethane at 25 °C. The numbers associated with the equilibria are standard Gibbs energies in kJ mol<sup>-1</sup>.*

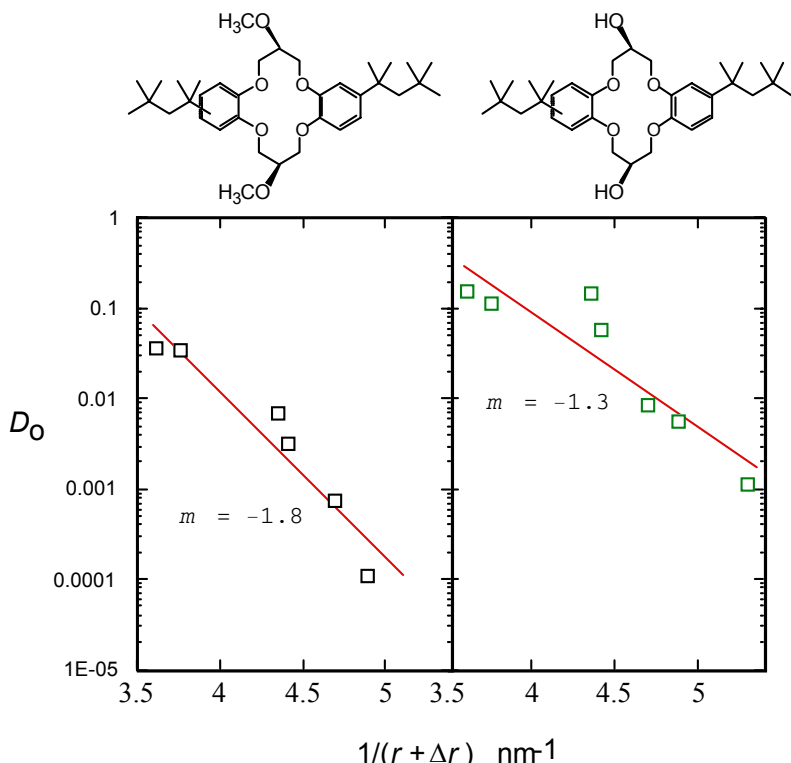
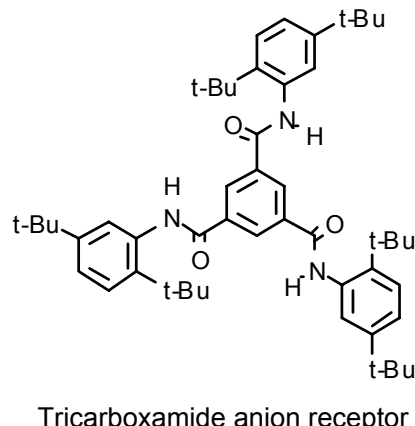


*Figure 3. Extraction of individual sodium salts at 0.5 M by two derivatives of bis(tert-octylbenzo)-14-crown-4 at 50 mM in 1,2-dichloroethane at 25 °C. From left to right, points in the plots each correspond to the anions  $\text{ReO}_4^-$ ,  $\text{ClO}_4^-$ ,  $\text{SCN}^-$ ,  $\text{I}^-$ ,  $\text{NO}_3^-$ ,  $\text{Br}^-$ ,  $\text{Cl}^-$ ; chloride was not determined in the left plot and was omitted.*

## DUAL-HOST SYSTEMS

As illustrated in Figure 4, it is possible to fundamentally alter the extractability of the anion in ion-pair extraction of alkali metals by the addition of an anion receptor [13]. By combination of a tripodal tricarboxamide-type anion receptor with 4,5"-bis(*tert*-octylbenzo)dibenzo-24-crown-8 in 1,2-dichloroethane, the extraction of cesium nitrate at 25 °C is synergistically enhanced. According to the equilibrium constant for nitrate binding measured independently by  $^1\text{H}$  NMR, the enhancement in driving force is potentially as much as -13.7 kJ mol<sup>-1</sup> in this case. Electro-spray mass-spectrometry results confirmed the 1:1 binding of the nitrate anion by the receptor. Comparable results were obtained with tripodal triamide receptors based on tris(2-aminoethyl)amine (tren) [14]. Synergistic enhancements in the distribution experiments were comparable to, though somewhat less than, the values expected from the NMR binding constants. Detailed equilibrium analyses remain to be performed, including determination of the ion-pairing constants and intermolecular association between the two receptors. Ion-pairing may be weak, as conditions were chosen to favor dissociation, and the complexation of the anion is likely to decrease the stability of the ion pair by increasing charge separation. Likewise, intermolecular association as judged from vapor-phase-osmometry data is weak in these systems, though not absent.



Tricarboxamide anion receptor

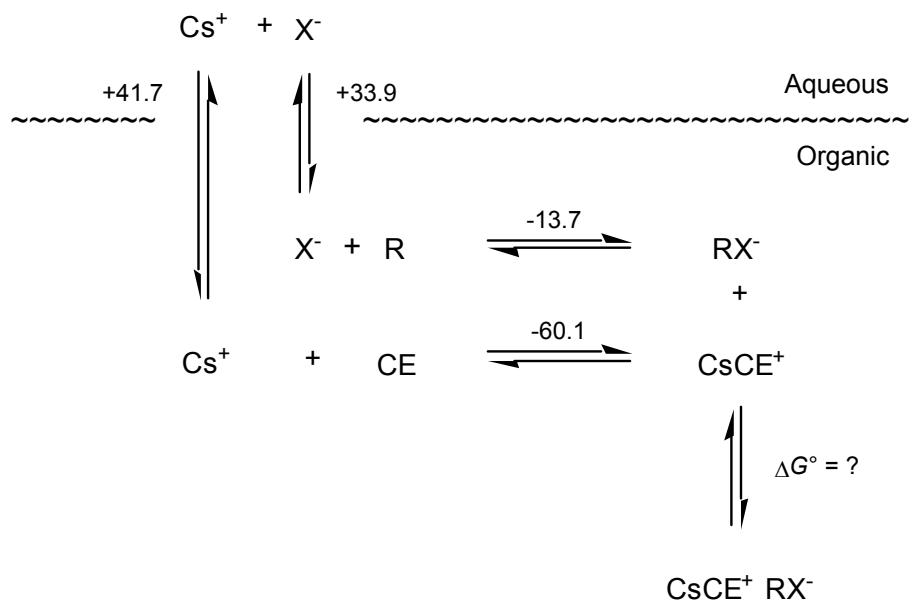


*Figure 4. Scheme showing stepwise extraction of cesium nitrate into an organic solvent containing 4,5"-bis(*tert*-octylbenzo)dibenzo-24-crown-8 and a tripodal tricarboxamide-type anion receptor in 1,2-dichloroethane at 25 °C.*

In experiments using more powerful disulfonamide anion receptors combined with a calixcrown  $\text{Cs}^+$  ion receptor, the synergistic enhancement in the extraction of cesium salts was found to increase with decreasing anion size [15].  $^{137}\text{Cesium}$  tracer distribution experiments shown in Figure 5 were performed using aqueous phases containing 0.10 M  $\text{NaX}$  (inextractable) and  $5 \times 10^{-6}$  M  $\text{CsX}$  [in order of increasing  $\Delta G_p^\circ(\text{X}^-)$ ,  $\text{X}^- = \text{ClO}_4^-$ ,  $\text{I}^-$ ,  $\text{NO}_3^-$ ,  $\text{Br}^-$ ,  $\text{Cl}^-$ ]. Organic phases contained 0.010 M of calix[4]arene-bis(benzo-18-crown-6) **1** either alone or with 0.035 M of sulfonamides **2**, **3**, or **4** in 1,2-dichloroethane at 25 °C. Based on previous results [16], these experimental conditions are expected to minimize ion-pairing and

its role in anion selectivity. Control experiments performed with organic phases containing sulfonamides alone gave negligible extraction relative to the calixarene used alone. The results in Figure 5 show that receptors **2** and **3** dramatically enhance Cs<sup>+</sup> ion extraction by the calixcrown for small anions. In general, the degree of enhancement agreed with that expected from independently measured anion-binding constants measured by NMR titrations. As follows from eq. 3, the cesium distribution ratio using the calixcrown alone varies linearly with  $\Delta G_p^\circ(X^-)$ . Remarkably, the combined systems also give linear plots, indicating that there is no special recognition for any of these anions. The effect of the anion receptors is apparently to attenuate the bias for the large anions. As discussed above, such behavior resembles that expected for hydrogen-bond donor diluents.

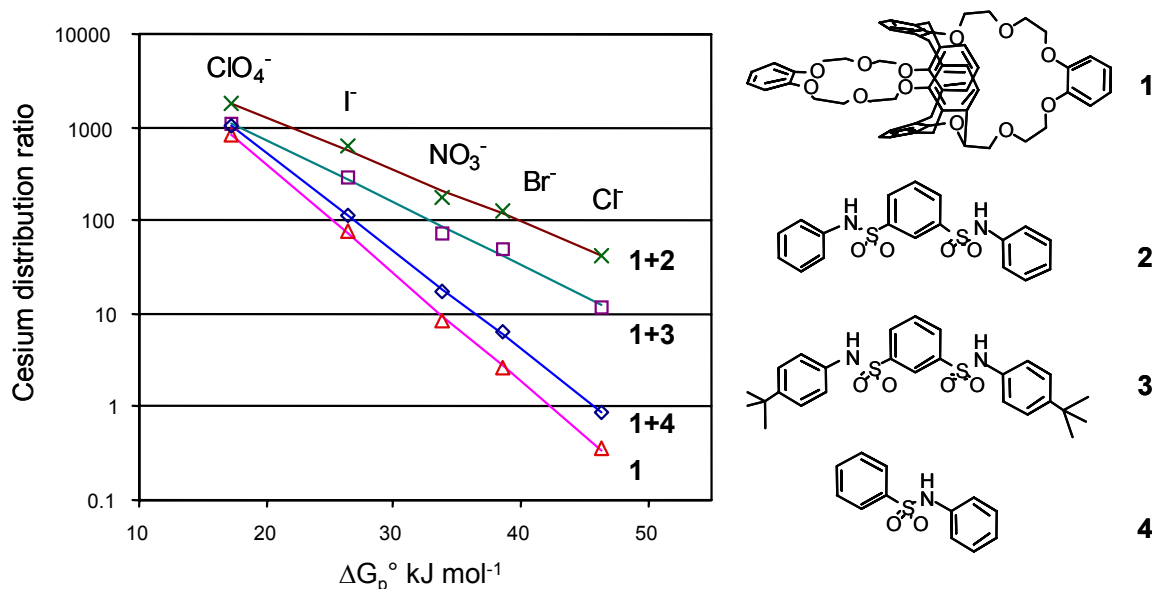


Figure 5. Plot showing the synergistic effect involving combinations of calixcrown **1** with sulfonamide anion receptors **2** - **4** in 1,2-dichloroethane in the extraction of trace Cs<sup>+</sup> ion from 0.1 M sodium salt solutions at 25 °C.

## CONCLUSIONS

Recent results show how one may manipulate interactions involving the co-extracted monovalent anion in ion-pair extraction systems involving neutral cation and anion receptors. In the absence of other specific interactions, solvation effects govern anion selectivity in systems involving only the cation host. A persistent dependence on the reciprocal anion thermochemical radius has been linked to the often-observed bias-type selectivity favoring large anions. Diluent effects are pronounced, though limited mainly to influencing the steepness of this bias effect. Ion-pairing interactions attenuate this bias, but if the cation is fully encapsulated so as to prevent contact ion-pairing, minimal attenuation occurs. Contact ion-pairing is a strong effect and was observed to nearly cancel the bias due to solvation alone. Hydrogen-bonding groups on the cation receptor may also interact with the anion to attenuate bias.

A promising novel approach entails the combination of cation and anion receptors. Significant synergistic effects are observed that can be definitely attributed to anion binding. However, systems so far investigated exhibit only attenuated bias with little or no evidence for true anion recognition. Future efforts are focusing on use of anion receptors possessing multiple hydrogen-bond donor groups and sufficient constraints so as to foster anion

recognition. Detailed equilibrium models are needed to understand the net process in terms of discrete thermochemical steps. One interaction not yet well characterized entails interaction between the two hosts. This potentially antagonistic effect has not proved strong in the case of the tricarboxamide hosts but remains an open question with sulfonamide and pyrrole-type receptors under current investigation.

Ditopic hosts combining cation and anion receptors into a single molecule offer incentives for future study but represent a particular challenge. Such ion-pair receptors must discourage intra- and inter-molecular interactions between hydrogen-bond donor and acceptor groups while maintaining maximal preorganization for the incoming ion-pair. Given that such systems may be found, a key advantage may lie in efficient encapsulation of the ion-pair as a unit, minimizing the role of the diluent and perhaps permitting use of aliphatic diluents with little or no modifier. It therefore seems possible that practical processes may be devised for selective salt extraction from a complex aqueous mixture. Additionally, for particular purposes in which it would be advantageous to target multiple salts simultaneously, well-designed ditopic hosts could be combined without antagonistic interaction.

### ACKNOWLEDGMENTS

This research was sponsored by the Division of Chemical Sciences, Geosciences, and Biosciences, Office of Basic Energy Sciences, U.S. Department of Energy, under contract DE-AC05-00OR22725 with Oak Ridge National Laboratory, managed and operated by UT-Battelle, LLC. The participation of T.G.L. and K.K. was made possible by an appointment to the ORNL Postgraduate Program administered by the Oak Ridge Associated Universities.

### REFERENCES

1. P. V. Bonnesen, L. H. Delmau, B. A. Moyer, and R. A. Leonard (2000), *Solvent Extr. Ion Exch.*, **18**, 1079-1108.
2. R. A. Leonard, C. Conner, M. W. Liberatore, P. V. Bonnesen, D. J. Presley, B. A. Moyer, and G. J. Lumetta (1999), *Sep. Sci. Technol.*, **34**, 1043-1068.
3. Y. Marcus (1985), *Ion Solvation*, Wiley, Chichester.
4. B. A. Moyer and P. V. Bonnesen (1997), *Supramolecular Chemistry of Anions*, A. Bianchi, K. Bowman-James, and E. Garcia-Espana (eds.), Wiley-VCH, New York, pp. 1-44.
5. Y. Takeda (1984), *Top. Curr. Chem.*, **12**, 1-38.
6. Y. Marcus (1997), *Ion Properties*, Marcel Dekker, New York.
7. Y. Marcus, M. J. Kamlet, and R. W. Taft (1988), *J. Phys. Chem.*, **92**, 3613-3622.
8. P. V. Bonnesen, B. A. Moyer, D. J. Presley, V. S. Armstrong, T. J. Haverlock, R. M. Counce, and R. A. Sachleben (1996), Report ORNL/TM-13241, Oak Ridge National Laboratory, Oak Ridge, TN, U.S.A..
9. T. G. Levitskaia, J. C. Bryan, R. A. Sachleben, J. D. Lamb, and B. A. Moyer (2000), *J. Am. Chem. Soc.*, **122**, 554-562.
10. B. A. Moyer, T. J. Haverlock, and R. A. Sachleben (1999), *Proc. Internat. Solvent Extraction Conference (ISEC '99)*, Barcelona, Spain, pp. 660-674.
11. R. A. Sachleben, J. H. Burns, J. C. Bryan, P. V. Bonnesen, T. J. Haverlock, and B. A. Moyer, unpublished results.
12. D. A. Johnson (1982), *Some Thermodynamic Aspects of Inorganic Chemistry*, 2nd edn., Cambridge University Press, London.
13. K. Kavallieratos, R. A. Sachleben, G. J. Van Berkel, and B. A. Moyer (2000), *Chem. Commun.*, 187-188.
14. K. Kavallieratos, A. M. Danby, G. J. Van Berkel, M. A. Kelly, R. A. Sachleben, B. A. Moyer, and K. Bowman-James (2000), *Anal. Chem.*, **72**, 5258-5264.
15. K. Kavallieratos and B. A. Moyer (2001), *Chem. Commun.*, 1620-1621.
16. T. J. Haverlock, P. V. Bonnesen, R. A. Sachleben and B. A. Moyer (2000), *J. Inclusion Phenom. Macrocyclic Chem.*, **36**, 21-37.



## EXTRACTION OF GOLD FROM HYDROCHLORIC ACID SOLUTIONS BY CALIXARENES

Kamel Belhamel<sup>a,c</sup>, Nguyen T. K. Dzung<sup>b,c</sup>, Mohamed Benamor<sup>a</sup> and Rainer Ludwig<sup>c</sup>

<sup>a</sup> Département de Genié des Procédés, Université de Bejaia, Algeria

<sup>b</sup> Institute for Technology on Rare Elements, Atomic Energy Commission, Hanoi, Vietnam

<sup>c</sup> Freie Universität Berlin, Berlin, Germany

The design of extractants for noble metal ions, especially Au(III), which are based on the concept of ion recognition is reported. The structure of extractants that recognize  $[\text{AuCl}_4]^-$  was optimized with respect to extraction efficiency, high selectivity, complete back extraction and fast kinetics. For that purpose, functional groups were attached to a macrocyclic backbone which places them in suitable positions to match the metal coordination sphere. The most useful of these calixarenes are nitrogen- and sulfur-containing ones having a cavity which is large enough to wrap around the desired metal ion. The study also includes the comparison with extractants of similar structure but different donor atoms, e.g., amides instead of thioamides. The synthesis of such new ligands is straightforward and proceeds in good yields. The extraction equilibria were characterized in terms of concentration and pH-dependency. Quantitative extraction from hydrochloric acid solutions ( $> 0.01 \text{ M}$ ) is achieved with ligands **1** and **3**. Ligands **2** and **4** extract  $> 99\%$  Au(III) at  $\text{HCl} \geq 1 \text{ M}$ , where they exist in their protonated forms. A 99.9% recovery in one step is possible by stripping with diluted thiourea/HCl (ligands **1**, **3**) or thiourea/H<sub>2</sub>O (ligands **2**, **4**). In the latter cases, stripping is also possible by deprotonating the ligand. The equilibria were reached in less than 5 minutes of overhead shaking. The selectivity over the metals accompanying gold in ores, especially iron at excess concentrations, is promising.

### INTRODUCTION

A type of macrocyclic ligand with the name calix[n]arene enjoys a remarkable interest in various fields of chemistry in recent years, which is highlighted by several books [e.g., 1-3]. Over 50 reviews concerning their synthesis, properties and applications were published, including their use in solvent extraction studies [4-8].

The interest in this class of compounds, which consists of a large number of derivatives results mainly from the possibility of designing 3-dimensional ligand structures in order to match the coordination sphere of the ion or molecule to be extracted. Based on the previous studies, it is now possible to derive some design principles concerning, for example, the size of the cavity, the molecular flexibility, and the arrangement of ionophilic functional groups. Other important factors for the application in extraction are (i) the inexpensive starting materials, (ii) the chemical stability, and (iii) the insolubility in water thanks to branched alkyl chains. The extractant can be imagined as a macrocyclic skeleton onto which various functional groups are attached and the hydrophobic and ionophilic properties are kept in balance.

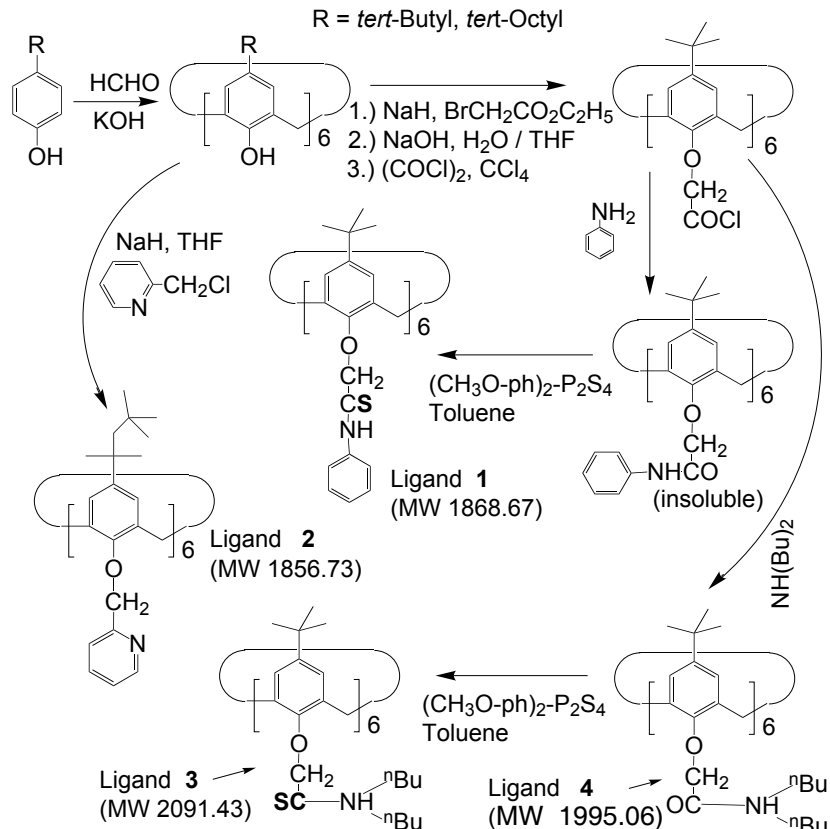
In this work we report on the design, synthesis and extraction properties of calixarenes with the aim of examining their usefulness for the extraction of gold from HCl leaching of Algerian ores. Previously, we investigated the noble metal extraction by calix[4]arenes bearing amide groups [9] and the current work was undertaken to improve the extraction behaviour.

## LIGAND DESIGN AND EXPERIMENTAL

In order to discriminate between the anionic  $[\text{AuCl}_4]^-$  and other metal ions, which exist predominantly as cations in 1 M HCl, we considered various structural features, especially:

- The ligand should have a cavity large enough to include the gold complex. Calix[6]arenes with a flexible, ca.  $0.3 \times 0.76$  nm cavity appear suitable.
- The ligand must be able to participate in coordination and should therefore contain donor atoms such as sulphur and/or nitrogen.
- These donor atoms should be allowed to arrange themselves into the optimum position around the metal, thus a certain degree of molecular flexibility is to be balanced with the degree of molecular pre-organization.
- The desired high extraction yield must be balanced with stability of the extracted complex in order to allow easy backextraction. One approach to this goal are the protonation / deprotonation equilibria of ligands **2** and **4**.

The synthesis of the ligands is outlined in Scheme 1. Each step proceeds in reasonably high chemical yield. The products were identified on the bases of their NMR- and mass-spectra, by elemental analysis and chromatographically. Details of the synthesis will be reported in a subsequent paper.



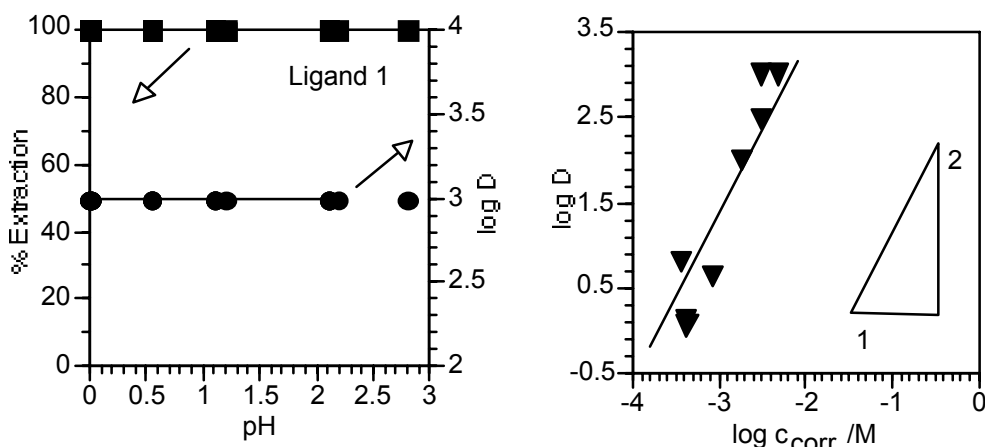
Scheme 1. Extractants used for this work, and their synthesis.

Metal extraction was carried out batchwise with equal volumes at 298K.  $\text{CHCl}_3$  saturated with water served as solvent. Metal contents before and after extraction were analyzed by means of atomic absorption spectrophotometry after dilution with 1 M HCl. Quantitative stripping was done with 10 mM thiourea dissolved in water (ligands **2**, **4**) or 1 M HCl (ligands **1**, **3**) and a 100% mass balance was obtained. Using thiourea in water or diluted HCl, partial stripping is possible in one step as tested for ligands **1** and **2**, respectively. The agitation speed was 54 rpm in an overhead shaker. Solutions were prepared by handling  $\text{AuCl}_3$  under  $\text{N}_2$  in a glove bag and dissolving in HCl. For the pH-dependent extraction, the pH was adjusted by adding ammonia or HCl to 0.1 M HCl solutions. Equilibrium pH values were measured with a combination glass electrode. The concentration of uncomplexed ligand (corrected) was calculated by taking into account the complexation. Selectivity studies were done as competitive extraction. The chemical stability was tested by repeated extraction and stripping cycles, in the course of which no degradation was observed.

## RESULTS AND DISCUSSION

### Extraction Equilibria

Figure 1 shows the results for the extraction of Au(III) by ligand **1**. The term '% Extraction' is defined as the percentage of extracted metal into the organic phase with respect to the overall metal concentration. The extraction is quantitative above 3 mM ligand concentration within the investigated pH range. From the  $pK_a$  of the parent [aniline $\cdot\text{H}^+$ ] (4.5), it is concluded that ligand **1** can exist in a mono-protonated form under these conditions. Due to the high  $D$ -values, a variation with the pH cannot be measured, while higher pH-values were not applied in order to avoid metal hydrolysis. The extracted species is assumed to be  $[(\text{AuCl}_3)\cdot\text{LH}^+\cdot\text{L}]$ .

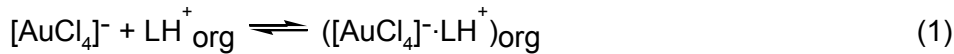


Figures 1a and 1b. Effect of pH (left) and of concentration (right) on the extraction of gold by ligand **1**. Aq. phase: 14 mg/l Au(III) (0.07 mM) in HCl, pH 2.8 (right figure), Org. phase:  $\text{CHCl}_3$  containing ligand **1** (3.3 mM in left figure).

Figure 2 shows the extraction data obtained with the pyridine derivative **2**. Quantitative extraction from 1 M HCl is achieved with 5 mM ligand solution. In contrast to ligand **1**, the stoichiometry of metal:ligand in the extracted complex is 1:1. The pH-dependency is attributed to the protonation of the ligand. Due to electrostatic interactions within one ligand molecule, we assume mono-protonation under the conditions applied. The following equations were applied to calculate the extraction constant  $K_{\text{ex}}$  according to the equilibrium (1), the acid constant  $K_a$  of ligand **2**, and the line in the plot of  $\log D$  vs. pH:

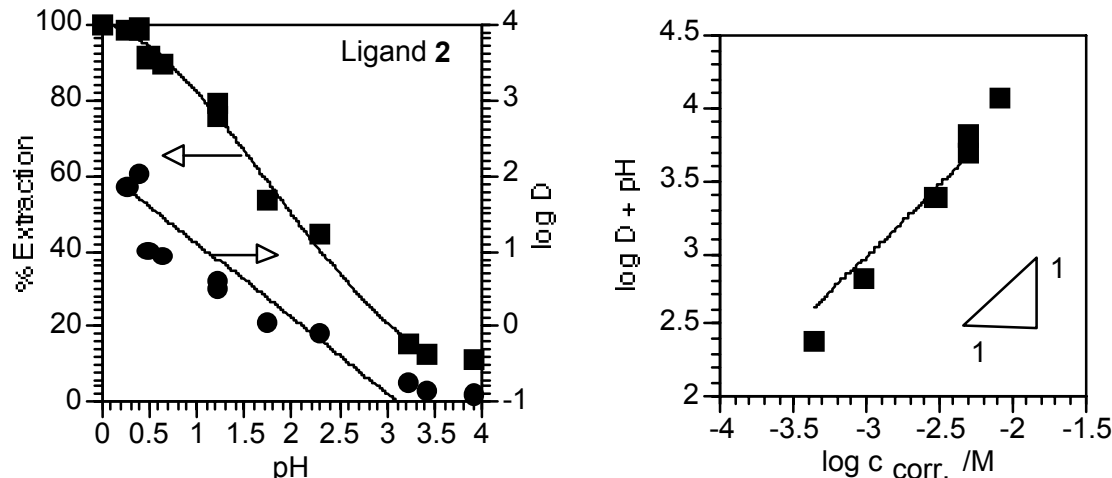
$$K_{\text{ex}} = \frac{D}{[\text{LH}^+]_{\text{org}}} = \frac{D}{\left( \frac{[\text{H}^+] \cdot c^0}{[\text{H}^+] + K_a} \right)}$$

with  $K_a = \frac{[\text{L}] \cdot [\text{H}^+]}{[\text{LH}^+]}$

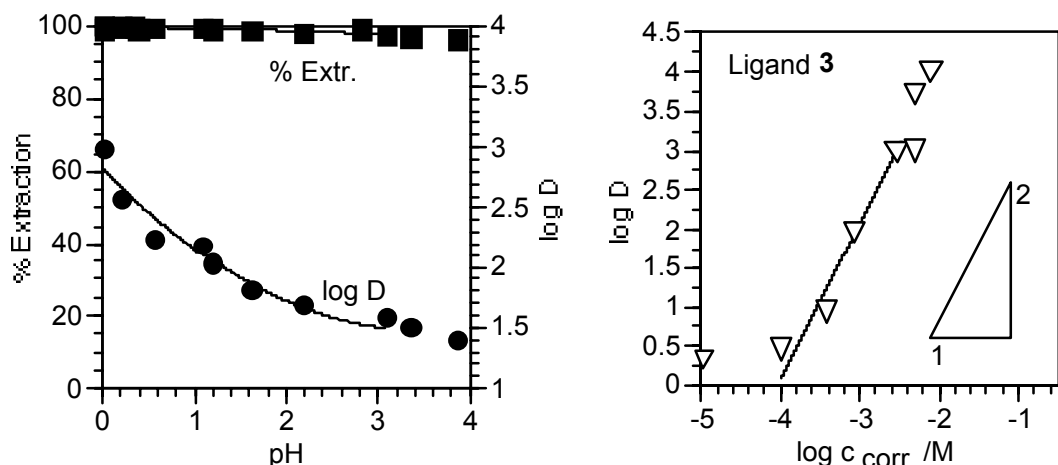


$$\log D = \log K_{\text{ex}} - \text{pH} + \log \left( \frac{c^0}{(\text{H}^+ + K_a)} \right) \quad \text{with } c^0 \text{ as the initial concentration}$$

$$\log K_{\text{ex}} = 6.064, \text{p}K_a = -1.65$$



Figures 2a and 2b. Extraction of Au(III) by pyridine derivative 2. Aq. phase: 14 mg/l Au(III) in HCl,  $c_{\text{HCl}} = 1 \text{ M}$  (right figure), Org. phase:  $\text{CHCl}_3$  containing ligand 2 (5 mM in left figure).



Figures 3a and 3b. Extraction data for thioamide derivative 3.  
The experimental conditions are the same as in Figure 2.

The thioamide derivative 3 is characterized by very high extraction of Au(III) as seen in Figure 3. The high extractability and the stoichiometry are comparable with the behaviour of ligand 1. The extraction depends on the pH, but not on the chloride concentration (*vide infra*). The mechanism is interpreted as protonation of the ligand and extraction of  $([\text{AuCl}_4]^- \cdot \text{LH}^+ \cdot \text{L})$ . However, the slope of  $\log D$  vs. pH is less than  $| -1 |$ , therefore only an apparent extraction constant was estimated for pH = 0 according to equation (2):  $\log K_{\text{ex}} = 8.08$ .



$$\log D = \log K_{\text{ex}} + 2 \log [\text{L}] \quad \text{at pH} = 0$$

Finally, ligand **4** has a structure resembling that of **3**, but carbonyl oxygen atoms replace the thiocarbonyl sulphur atoms. The distribution ratios are lower compared with **3**, which proves the important role of the sulphur atoms in the complexation. Upon protonation of one nitrogen atom, ligand **4** nearly quantitatively extracts Au(III). The occupation of the ligand cavity by the chloro complex of Au(III) probably contributes to the good extraction.

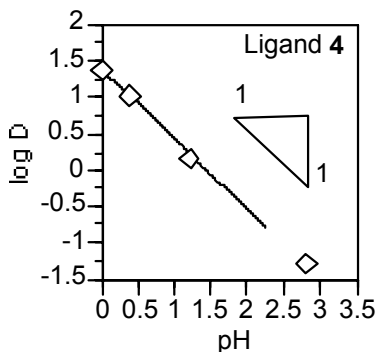
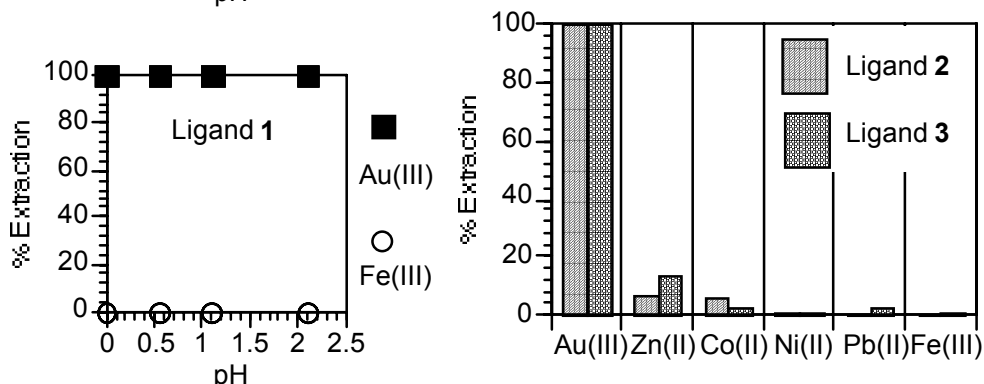


*Figure 4 (on the left):*  
pH-Dependent extraction of Au(III) by amide **4**.  
Aq. phase: 14 mg/l Au(III) in HCl,  
Org. phase: CHCl<sub>3</sub> contg. 5 mM ligand.



*Figures 5a and b: Selectivity data for ligands **1**, **2** and **3** in competitive extraction.*  
Aq. phase: 14 mg/l Au(III) in 1 M HCl, 2 mM Fe(III) (Fig. 5a, left) or 0.1 mM each of Zn<sup>2+</sup>, Co<sup>2+</sup>, Ni<sup>2+</sup>, Pb<sup>2+</sup>, Fe<sup>3+</sup> (Fig. 5b, right side), Org. phase: CHCl<sub>3</sub> containing 5 mM ligand.

### Selectivity

The selectivity of ligands **1** to **3** for gold over metals which are present in excess in Algerian ore was examined by competitive extraction. Figure 5a shows that (i) the quantitative extraction of gold by ligand **1** is maintained in the presence of excess Fe(III), and (ii) iron is not extracted from the aqueous solutions of various acidity.

The selectivity data for ligands **2** and **3** are shown in Figure 5b. The quantitative extraction of gold from 1 M HCl is not affected by the presence of other metals at comparable concentrations. Among these metals, zinc is extracted to the highest extent with 7% and 13%, respectively. We interpret the good selectivity as the result of the ligand design: The metal cations, even if they have an affinity towards nitrogen or sulphur atoms in the ligands, are much smaller than the cavity of calix[6]arenes and are therefore unable to interact with all donor atoms in order to match their coordination sphere.

## Extraction Kinetics

The time necessary to reach distribution equilibrium was examined in batch experiments. The results in Table 1 show that the equilibria are reached very fast for all extractants. We attribute this to the remaining molecular flexibility of the ligand. Thus steric crowding as well as slow conformational equilibria, which can occur in the smaller calix[4]arenes or in tautomeric equilibria for example, are avoided. The stripping equilibria were established fast as well, which is attributed to fast decomplexation and deprotonation equilibria.

Table 1. Kinetics of Au(III) extraction (0.1 mM in 1 M HCl) into CHCl<sub>3</sub> containing 5 mM ligand at 54 rpm overhead shaking at 298 K

%Ex / t, min	1	3	5	10	20	30	70	100
Ligand 1	99.61	>99.99	>99.99	>99.99	>99.99	>99.99	>99.99	>99.99
Ligand 2	98.36	98.86	99.24	99.92	>99.99	>99.99	>99.99	>99.99
Ligand 3	98.25	98.46	98.53	98.91	99.86	99.97	99.98	>99.99
Ligand 4	98.78	98.61	99.28	99.28	99.44	99.44	99.78	>99.99

## Influence of Chloride Salt Concentration

Increasing the concentration of chloride ions by adding up to 5 M NaCl to 0.1 M HCl solutions results in slightly higher distribution ratios with ligand **2**, while the near quantitative extraction by ligand **3** remained unaffected. The small increase of log  $D_{\text{Au}}$  in case of ligand **2** is interpreted as change in activity coefficients (salting out), because the [AuCl<sub>4</sub>]<sup>-</sup>-complex predominates already at low concentrations of Cl<sup>-</sup>.

## CONCLUSIONS

High distribution ratios of Au(III) are observed when the ligand contains both sulphur and nitrogen as donor atoms, resulting in quantitative extraction from HCl solution. Ligands containing only nitrogen as donor atoms extract Au(III) quantitatively when they are protonated. The oxygen atoms of the ligands are considered to play only a minor role in gold complexation. The results on selectivity and kinetics are further proof that this type of macrocyclic ligands have the potential for application in recovery of valuable metals from dilute solutions.

## ACKNOWLEDGEMENTS

We appreciate the funding of this work by Deutscher Akademischer Austauschdienst (DAAD) and the Stiftung Industrieforschung.

## REFERENCES

1. Z. Asfari, V. Böhmer, J. Harrowfield and J. Vicens (eds.) (2001), Calix 2001, Kluwer Academic Publishers, Dordrecht, and references cited therein.
2. C. D. Gutsche (1998), Calixarenes Revisited, Royal Society of Chemistry, Cambridge.
3. G. J. Lumetta and R. D. Rogers (eds.) (1999), Calixarene Molecules for Separations, American Chemical Society, Washington DC.
4. R. Ludwig (1995), JAERI Review 95-022, JAERI, Tokai-mura, Japan.
5. M. A. McKervey, M. J. Schwing-Weill and F. Arnaud-Neu (1996), Comprehensive Supramolecular Chemistry: Molecular Recognition. Receptors for Cationic Guests, Vol. 1, G. W. Gokel (ed.), Pergamon, New York, pp. 537-603.
6. A. T. Yordanov and D. M. Roundhill (1998), *Coord. Chem. Rev.*, **170**, 93-124.
7. D. M. Roundhill (1995), Progress in Inorganic Chemistry, Vol. 43, K. D. Karlin (ed.), Wiley, New York, pp. 533-591.
8. R. Ludwig (2000), *Fres. J. Analyt. Chem.*, **367**, 103-128.
9. R. Ludwig and S. Tachimori (1996), *Solv. Extr. Res. Dev., Jpn.*, **3**, 244-254.



## SEPARATION OF PALLADIUM(II) WITH IMMOBILIZED MALEONITRILE-DITHIOCROWN ETHERS

W. Mickler, H. Bukowsky and H-J. Holdt

Universität Potsdam, Institut für Anorganische Chemie und Didaktik der Chemie,  
Potsdam, Germany

As extractants for the selective separation and recovery of palladium (II) from industrially spent liquors crowned dithiomaleonitriles are proposed. These macrocyclic chelate ligands extract palladium (II) at sufficient rate in very good yields. The synthesis of the immobilized ligands proceeds from the 2-allyloxy-1, 2-propanediol. The silylated macrocycle is immobilized by a spacer onto activated silica gel. By modification of the cavity of the macrocycle the extraction rate can be optimised. The best results were observed with the maleonitrile-dithio-12-crown-4. The composition of the extracted compounds has to be found as 1:1. The separation is unsatisfactory in the case of Ag(I), Hg(II), Tl(I) and of the most 3d-elements.

### INTRODUCTION

Especially in the last few years the recovery and separation of palladium(II) from spent autocatalysts or industrial wastes has become increasingly important [1]. For the technical realisation of such processes commercial extractants as di(n-alkyl)sulfide ((Hex)<sub>2</sub>S) [2, 3, 4] were widely used. Recently an extraction process on the basis of substituted amines in presence of LIX 63 as accelerator[5] has been described. More classical separation technologies for the platinum group metals have been reported [6]. Moreover substituted acylpyrazolones [7], calix[4]arenes [8], hydroxyquinolines [9] or phenyloximes [10] are proposed for the separation of palladium.

Generally, ligands containing sulphur as donor atoms are particularly well suited for the separation of thiophilic palladium (II) by liquid-liquid-extraction [11]. This quality we advantageously used in the case of crowned dithiomaleonitrile [12]. For the accumulation and separation of small concentrated cations from diluted solutions the utilization of ion exchangers is helpful. In this case the selectivity of the anchor groups of the resin and the advantage of a continuous operation are usefully associated.

As supporting material for immobilizing ligands especially silica gel is used frequently because both the hydrosilylation of the extractant and the reaction following with the matrix are performed easily. Additionally, the mechanical stability of the ion exchanger and its hydrophilic surface, cause rapid kinetic of the exchange process and have advantages over the commercial liquid ion exchangers.

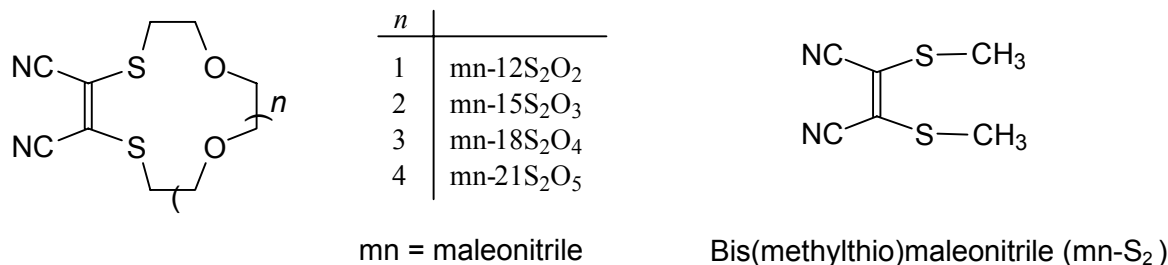
## EXPERIMENTAL

To allow a comparison with the commercial extractant di-n-hexylsulphide the extraction behaviour of the selected macrocyclic compounds was studied with the free ligand dissolved in chloroform. The liquid-liquid-extractions were performed as single experiments in separation funnels at room temperature. The metal concentration was generally in the range of  $10^{-4}$  mol•L<sup>-1</sup>, in nitric acid 0.01 mol•L<sup>-1</sup>. All chemicals were of analytical grade. The metal stock solutions were prepared by dilution of a Merck-standard solution with bidistilled water. Generally, the concentration of the ligands was adjusted to  $10^{-2}$  mol•L<sup>-1</sup> in a phase ratio to the model solution of 1+1 (1 mL).

A mechanical shaker performed each extraction cycle within 120 minutes. After re-extraction of the organic phase with an aqueous thiourea solution (2 mol•L<sup>-1</sup>) the metal concentration was determined by AAS (AAS 1100 B, Perkin Elmer). The distribution coefficient:  $D = \frac{C_{M^{n+}}^{(org)}}{C_{M^{n+}}^{(aq)}}$  was calculated from the metal concentration in the aqueous phase before extraction and from the organic phase after re-extraction. The slope  $n$  of the function  $\log D = f(c_L)$  corresponds to the number of coordinated ligands.

### Extractants

As extractants were used a series of maleonitrile-dithiocrown ethers with different lengths of the oligo(oxyethylene)unit [13,14,15]. For comparison the acyclic compound bis(methylthio)maleonitrile ( $mn\text{-S}_2$ ) and the commercial extractant di(n-hexyl)sulfide [ $(\text{Hex})_2\text{S}$ ] were used.



The scheme of the syntheses of the allylsubstituted maleonitrile-dithio-12-crown-4 ( $mn\text{-}12\text{S}_2\text{O}_2\text{-allyl}$ ) is given in Figure 1.

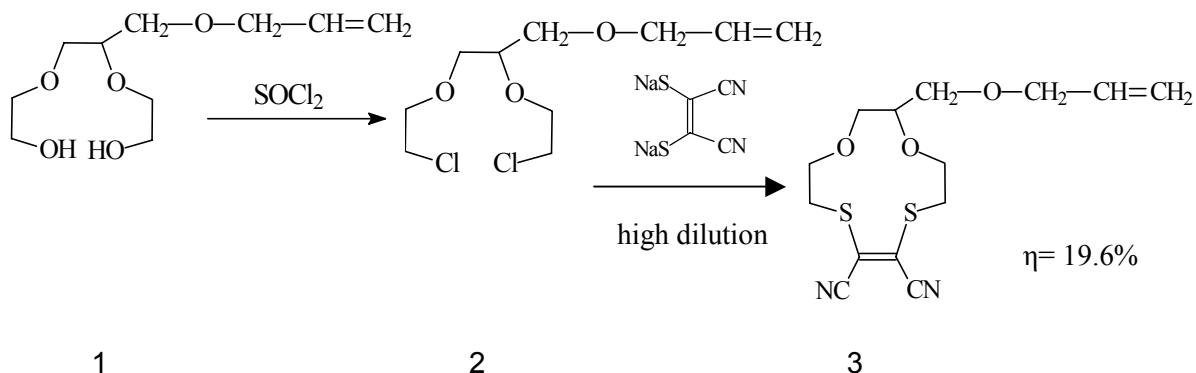


Figure 1. Synthesis of the allylsubstituted maleonitrile-dithio-12-crown-4.

By the reaction of 2-allyloxy-1,2-propanediol with potassium t-butoxide and chloracetic acid the dicarbon acid was formed and subsequently changed by a reduction to the diole (1). With the help of thionylchloride the dichloro compound (2) was synthesized which, together with a dithiolate ((Z)-disodium-1,2-dicyanethene-1,2-dithiolate), under high dilution conditions formed the macrocycle (3). Then the allylsubstituted maleonitrile-dithio-12-crown-4 can be silylated and the resulting alkoxy silane is immobilized onto activated silica gel. The substituent forms in the same time a spacer and should be modified in the future. All compounds were purified by distillation *in high vacuo*. The macrocycle (3) was isolated in a good overall yield (19.6 %).

## RESULTS AND DISCUSSION

In Figure 2 the results of the extraction of palladium (II) with the examined extractants are shown. The function  $\log D = f(c_{\text{ligand}})$  illustrates the influence of different structural parameters on the extraction behaviour. The time needed to reach the extraction equilibrium was determined in preceding experiments to 120 minutes. From the slope of the curves the expected composition of the extracted species as (PdL) has to be found.

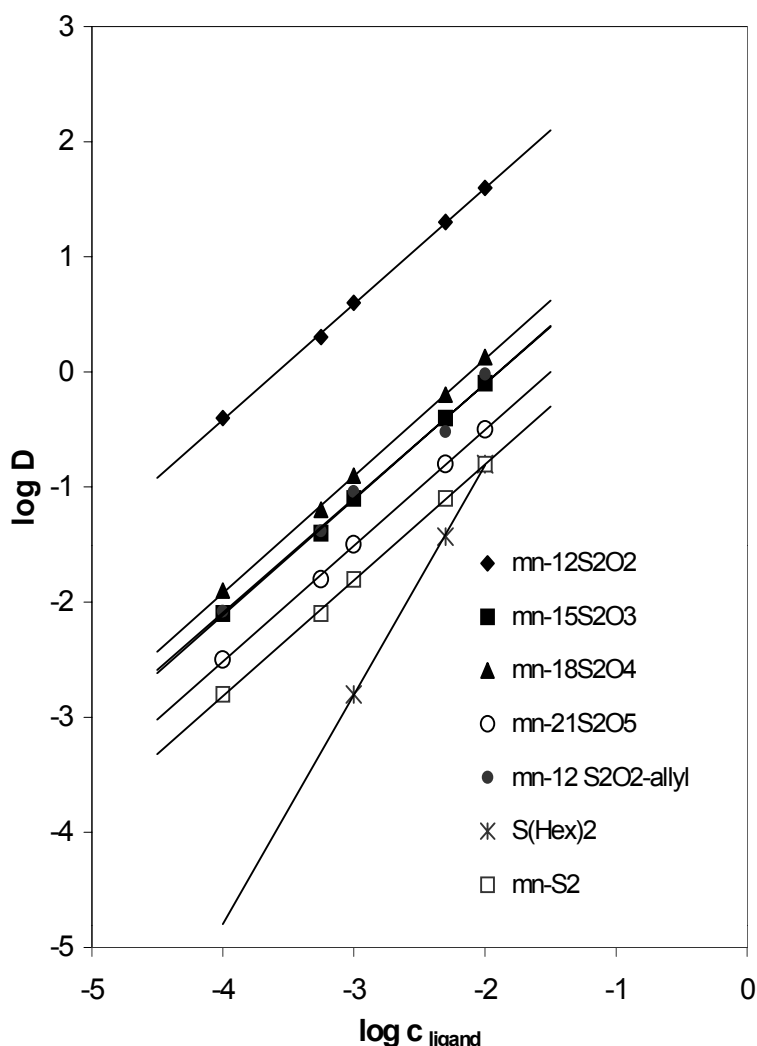


Figure 2. Extraction of Pd(II) with maleonitrile-dithiocrown ethers and di(*n*-hexyl)sulfide.

In the case of the commercial extractant di(n-hexyl)sulfide the expected slope of the function has to be found and leads to the composition of the extracted chelate as 1:2. Generally, it can be seen that all the tested maleonitrile-dithiocrown ethers show better distribution coefficients than the frequently used commercial extractant di(n-hexyl)sulfide and the acyclic compound mn-S<sub>2</sub>. The reason for the low palladium (II) extractability of mn-S<sub>2</sub> is the free rotatability of the methyl groups hindering the chelation of the palladium (II) with the sulphur atoms.

Furthermore, the extraction behaviour can be discussed by the fact that 1,2-dithioethenes are weak chelate-forming ligands [16] and in the case of bis(methylthio)maleonitrile [17] the donor power of both of the sulphur atoms is further decreased by the electron withdrawing effect of the cyano groups. This quality is advantageously used in the case of crowned dithiomaleonitrile. By macrocyclic fixing the dithio unit is available for the complex formation without any hindrance and so the transfer of palladium (II) into the organic extraction phase is possible, as is illustrated by the increasing distribution coefficients. The best results for the extraction of palladium (II) were observed in the case of maleonitrile-dithio-12-crown-4 (mn-12S<sub>2</sub>O<sub>2</sub>). In comparison to this, the increasing length of the oligo(oxyethylene) unit from mn-12S<sub>2</sub>O<sub>2</sub>, mn-15S<sub>2</sub>O<sub>3</sub>, mn-18S<sub>2</sub>O<sub>4</sub> to mn-21S<sub>2</sub>O<sub>5</sub> cause a decreasing separation coefficient. One reason for this unsatisfying result is the reduced availability of the sulphur atoms for the complex formation by the increased flexibility of the macrocycle. The differences between mn-12S<sub>2</sub>O<sub>2</sub> and its allylsubstituted derivative (mn-12S<sub>2</sub>O<sub>2</sub>-allyl) are caused by the steric hindrance of the allyl-chain of the chelate formation. The separation of palladium (II) is disturbed because the free rotatable substituent covers the donor atoms of the macrocycle. The chelate formation and also the stability of the palladium complex would be improved by fixing the maleonitrile-dithiocrown ether with its substituent on a matrix.

*Table 1. Formation constants of PdCl<sub>2</sub>-chelates in methanolic solutions.*

Complex	log K <sub>a</sub>
[PdCl <sub>2</sub> (mn-12S <sub>2</sub> O <sub>2</sub> )]	6.20 ± 0.30
[PdCl <sub>2</sub> (mn-18S <sub>2</sub> O <sub>4</sub> )]	4.70 ± 0.10
[PdCl <sub>2</sub> (mn-21S <sub>2</sub> O <sub>5</sub> )]	4.67 ± 0.02
[PdCl <sub>2</sub> (mn-15S <sub>2</sub> O <sub>3</sub> )]	3.90 ± 0.01
[PdCl <sub>2</sub> (mn-S <sub>2</sub> )]	3.60 ± 0.50

In Table 1 the formation constants of the complexes determined by UV spectroscopy in methanol are given. The order of log K<sub>a</sub> is in good agreement with the results found by liquid-liquid-extraction so that the relatively high complex stability of the palladium complex of mn-12S<sub>2</sub>O<sub>2</sub> may be regarded as an important reason for its good extractability.

The extraction behaviour of the tested dithiocrown ethers towards palladium (II) and some competition elements is summarized in Figure 3. As it can be seen from Table 2, especially palladium is extracted selectively with a good yield. The separation coefficient towards nickel was about 1.4·10<sup>3</sup>.

*Table 2. Extraction rate (E %) and selectivity (S) of the extraction of palladium, lead and different 3d-elements with mn-12S<sub>2</sub>O<sub>2</sub>.*

element	chromium	iron	nickel	copper	cadmium	zinc	lead	palladium
E %	0.00	0.56	2.75	1.60	1.78	2.45	1.03	97.3
S (towards Pd)	--	1.3·10 <sup>4</sup>	1.4·10 <sup>3</sup>	2.4·10 <sup>3</sup>	2.2·10 <sup>3</sup>	1.6·10 <sup>3</sup>	3.9·10 <sup>3</sup>	--

One of the reasons for this behaviour may be the coordination structure of the formed complexes. In opposite to most of the 3d-elements palladium (II) favours a square-planer coordination geometry. For that reason the relatively inflexible structure of the macrocycles supports especially those elements which prefer a planar structure.

This fact could be also verified by its extraction behaviour with 4-acylpyrazolones. These ligands prefer spatial geometries. In the case of the 3d-elements almost stable octahedral complex structures are formed so that a high extraction rate could be found [18]. The extraction of palladium (II) with 1-phenyl-3-methyl-4(2-ethylhexanoyl)-5-pyrazolone at pH 2.3 shows only a rate of 34 %. This could mainly be due to the unfavourable geometrical structure of the extracted chelate.

Especially a good selectivity of the palladium (II) extraction with maleonitrile-dithiocrown ethers was also observed towards silver and mercury, so that interesting applications to the separation of noble metals should be possible. A comparison of the extraction behaviour of the various elements showed slightly better results for the soft and thiophilic elements such as nickel or lead, against chromium and iron.

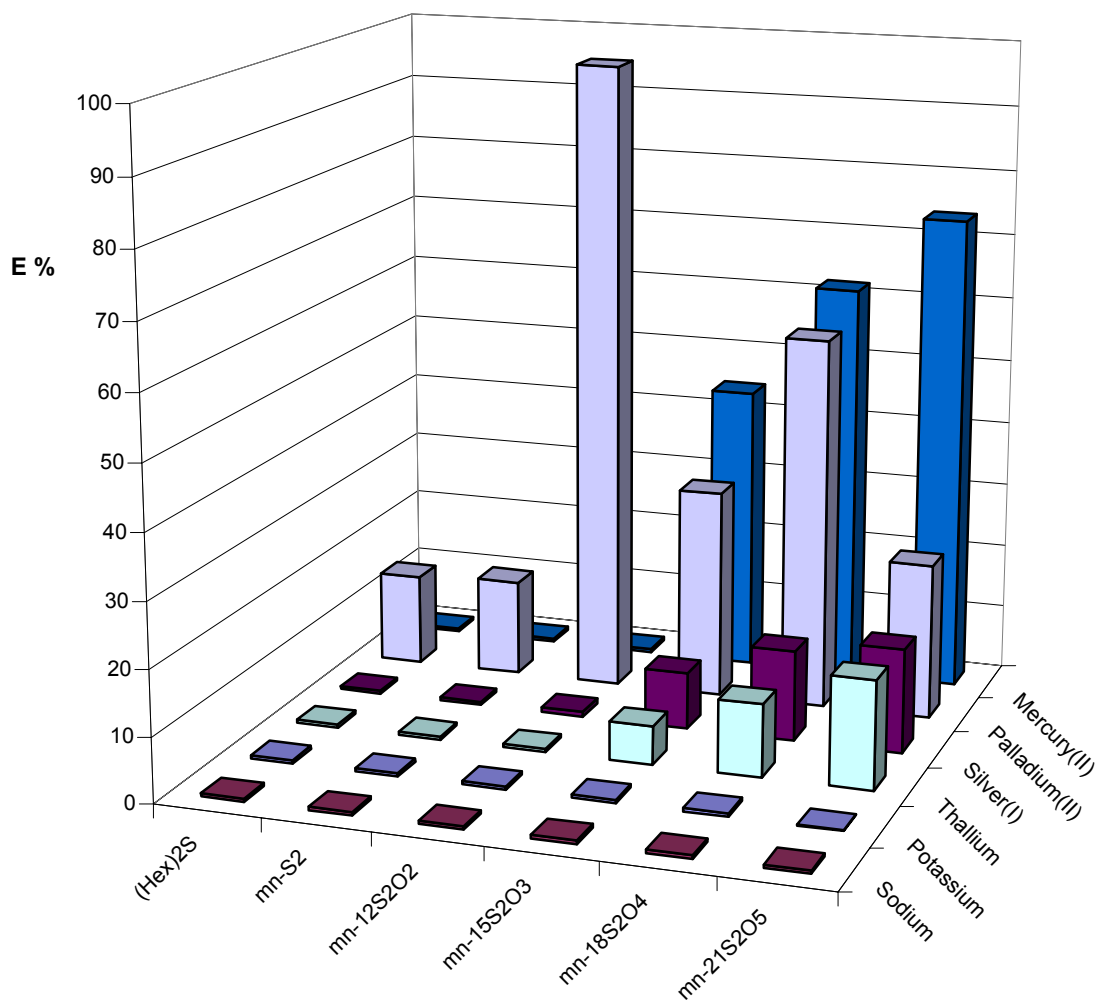


Figure 3. Extraction of different metals with maleonitrile-dithiocrown ethers and  $(\text{Hex})_2\text{S}$ .

## REFERENCES

1. C. Nowotny, W. Halwachs and K. Schugerl (1997), *Sep. Purif. Technol.*, **12**, 135.
2. R. K. Lea, J. D. Edwards, F. D. Colton (1983), *US Pat.*, No. US 4390366 (June 28).
3. N. Katsutoshi (1998), *JP Pat.*, No. JP 10130744 (May 19).
4. S. Yasukatsu and O., Tomonaga (2001), *JP Pat.* No. JP 2001107156 (April 17).
5. C. Foulon, D. Pareau, M. Stambouli and G. Durand (1999), *Hydrometallurgy*, **54**, 49.
6. W. Hasenpusch (1987), *Chem. Labor Betr.*, **38**, 454.
7. A. Zhang (2000), *Solvent Extr. Ion Exch.*, **18**, 1189.
8. A. T. Yordanov, O. M. Falana, H. Koch and D. M. Roundhill (1997), *Inorg. Chem.*, **36**, 6468.
9. G. B. Harris, S. Monette and D. Vleeschhouwer (1993), *Proc. 4th Int. Symp. Hydrometallurgy*, CIM, Montreal, pp. 777.
10. M. v. d. Puy, D. S. Sorlano and D. J. Howard (1986), *Europ. Pat.*, No. EP 0166151(January 02).
11. M. Cox (1992), Liquid-liquid Extraction in Hydrometallurgy: Sciences and Practice of Liquid-liquid Extraction, Vol. 2, J. D. Thornton (ed.), Clarendon Press, Oxford, pp. 63.
12. H.-J. Holdt (1993), *Pure Appl. Chem.*, **65**, 477.
13. H.-J. Holdt and J. Teller (1988), *Z. Chem.*, **28**, 249.
14. H.-J. Drexler, H. Reinke and H.-J. Holdt (1998), *Z. Anorg. Allg. Chem.*, **624**, 1376.
15. H.-J. Holdt, K. Gloe, H. Stephan, H. Bukowsky, W. Mickler, H.-J. Drexler and C. Grütter (2001), *Chem. Eur. J.*, submitted for publication.
16. G. N. Schrauzer and H. N. Rabinowitz (1968), *J. Am. Chem. Soc.*, **90**, 4297.
17. G. Bähr and G. Schleitzer (1957), *Chem. Ber.*, **90**, 438.
18. W. Mickler, A. Reich and E. Uhlemann (1999), *Proc. ISEC '99*, Barcelona, pp. 356.



## SEPARATION OF PALLADIUM FROM PLATINUM

Jan G. H. du Preez, Eric C. Hosten and Shimoné E. Knoetze

Research Unit for Metal Ion Separation, University of Port Elizabeth,  
Port Elizabeth, South Africa

In this paper it is shown how the basic coordination chemistry of Pd, Pt and contaminants can be applied to suggest possibilities for the development of separating agents which can preferentially extract Pd(II). The method is applied and illustrated by the synthesis of pyrazole derivatives in both the form of extractants and a resin. It is shown how Pd(II) can be selectively extracted from Pt(IV) from dilute HCl solutions contaminated with base metals. The durability of the agents is also illustrated.

### INTRODUCTION

The platinum group metals are found in a very complex ore body. They appear together with gold, silver and some base metals like iron, cobalt, nickel and copper. They are mainly found in the same matrix in the form of their sulfides, arsenides, selenides and tellurides. The separation and isolation of the metals are thus formidable tasks since the process is further complicated by the kinetic stability of the various complex species. A number of separating schemes are employed industrially, however, systems which utilise HCl media seem to be most important, especially as far as separation of palladium from platinum is concerned.

In our laboratory we have for many years directed efforts to develop improved or novel separating agents for metal ions. The method followed was always to first study those aspects of the coordination chemistry of the relevant metal ions in order to determine their preferences and those of possible contaminants. Information thus obtained is then applied to investigate possible avenues for improved separation.

When this approach was applied to the above problem two types of methods emerged:

Type I: Separation of chloro-anionic complexes present in the HCl feed solutions, namely  $\text{PtCl}_6^{2-}$ ,  $\text{PdCl}_4^{2-}$  and also  $\text{Pd}_2\text{Cl}_6^{2-}$ . Differences in ion pairing and/or phase transferability are exploited by using suitable cationic species. The lower charge density of the  $\text{PtCl}_6^{2-}$  complex results in the preference of the latter over  $\text{PdCl}_4^{2-}$  for most cations, especially those which also have low charge densities like quaternary ammonium cations. Conditions which favour formation of  $\text{Pd}_2\text{Cl}_6^{2-}$ , however, should be avoided. This separation can be achieved by employing the cationic site in the form of a precipitant, an extractant or an active site on a resin. Since the basis of this separation is ion pairing, the kinetics of the reaction are relatively fast.

These reactions can be represented by equations 1(a) and 1(b).



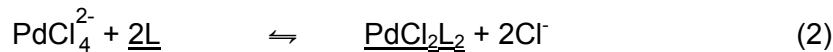
Apart from the above reactions, it must be borne in mind that the HCl effect of the above species is not the same; normally it is smaller for  $\text{PtCl}_6^{2-}$  than for  $\text{PdCl}_4^{2-}$  when quaternary ammonium cations are used. Further interference via the reaction of  $\text{Pd}_2\text{Cl}_6^{2-}$  species is only experienced when very bulky low charge density cations and low  $\text{Cl}^-$  concentrations are used.

A very large variety of cations has been applied by researchers in this area. These can be divided into two main categories (i) low charge density cations, e.g., quaternary ammonium [1], phosphonium [2] and arsonium species [3,4], and (ii) "protonic" cations obtained by protonation of neutral donor species. These can be described as relatively high charge density cations. This group can be subdivided into two categories: firstly those containing neutral donor atoms like oxygen for which these metals have very low affinities. A large variety of such oxygen donor extractants has been applied for the extraction of the above chloro complexes, e.g., C-O compounds like alcohols [5,6], ketones [7,8], ethers [6], esters [6] and P-O compounds [9-11]. In all of the above cases, the extraction occurs via the formation of an oxonium counter cation.

Secondly, "protonic" cations formed by protonation of neutral donor atoms having the potential to coordinate to these metals as such, e.g., amines, i.e., primary, secondary and tertiary amines. Such amines include aliphatic amines, e.g., tri-n-octylamine [12] and triisobutylamine [13].

Type II: Separation by using the differences in the kinetic stability of  $\text{PtCl}_6^{2-}$  and  $\text{PdCl}_4^{2-}$  through the application of a suitable soft donor ligand/extractant, which will replace the  $\text{Cl}^-$  from  $\text{PdCl}_4^{2-}$ , but not from  $\text{PtCl}_6^{2-}$ . These ligands are ones with good covalent capability for which the palladium has a high affinity. This type are, almost without exception, also reducing agents which have low protonation constants.

The reactions are represented in equation (2).



With reference to type II, the most important compounds are sulfur donor atom ligands, in particular thioethers. Di-n-octylsulfide is a typical example [14]. This extractant reacts by replacing the  $\text{Cl}^-$  in  $\text{PdCl}_4^{2-}$  through the formation of  $\text{PdCl}_2\text{L}_2$  where L = extractant. In contrast to the extraction of type I, this process is kinetically controlled and equilibrations occur normally slowly. Back extraction can only be achieved by another ligand exchange process.

Thioethers are reducing agents. At the redox potential required to obtain Pt as Pt(IV), some oxidation of the thioether to sulfoxides occurs leading to the destruction of the separating agent thus shortening its lifetime. A great advantage of the thioethers however, is their very low protonation constants which is required to avoid cation formation leading to extraction of  $\text{PtCl}_6^{2-}$ .

## SELECTION OF ACTIVE CENTRE FOR SEPARATING AGENT

In our previous studies with amines as potential separating agents for base metals, we recognised promise for the application of some of these for Pd/Pt separation. At the basis of the potential application of these as separating agents lies their affinity for the specific metal ion ( $\text{Pd}^{(\text{II})}$ ) relative to the affinity for protons as well as the affinity for contaminants (e.g., base metals).

As a first-order approximation for the potential application of amines in terms of the above arguments, species distribution curves using published [15] formation constants of their complexes with  $\text{Ni}^{2+}$  (a  $3d$  transition metal ion) as formed in aqueous solution were compiled (see Figure 1). The dotted curves are the species formed with  $\text{H}^+$ . These curves clearly suggest that amine complexes of aliphatic amines with  $\text{Ni}^{2+}$  will not be formed in acidic media, although the difference in stability between the  $\text{H}^+$  and  $\text{Ni}^{2+}$  gets smaller upon chelation (compare results of  $\text{NH}_3$  with ethylene diammine (en) for  $\text{Ni}^{2+}$  (Figure 1 (top))).

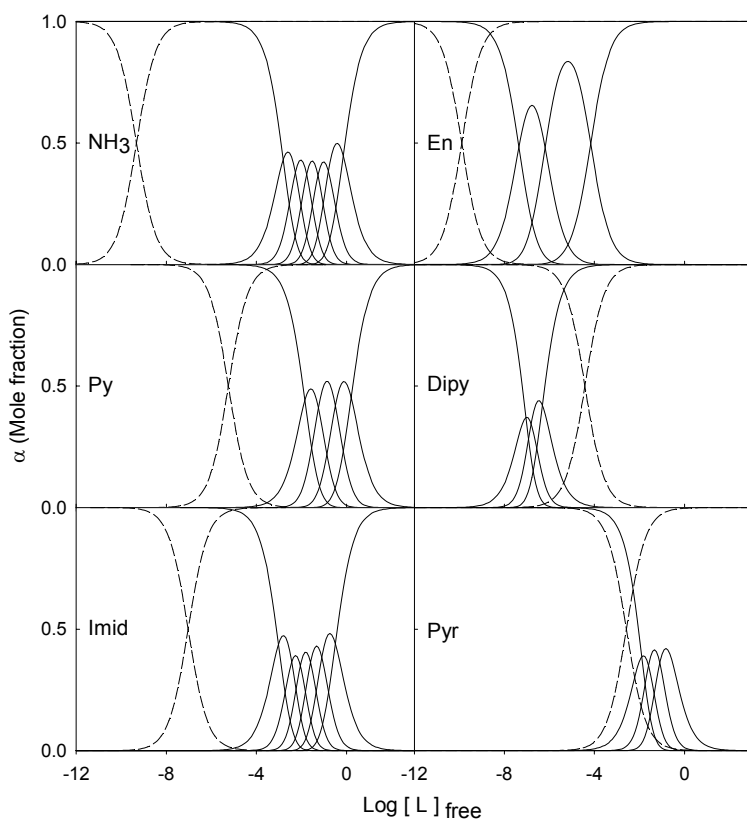


*Figure 1. Species distribution curves for  $\text{Ni}^{(\text{II})}$  complexes with some amines.*

In the case of the corresponding aromatic N donor ligands (compare results of py and dipy with  $\text{Ni}^{2+}$  - Figure 1 (middle)), it is clear that the difference in complexing capability becomes even smaller (py) and is reversed with the bidentate aromatic ligand (dipy). In the latter case it will be very difficult to "strip"  $\text{Ni}^{2+}$  from such an extracted phase by pH control if such a ligand is used as extractant.

In the case of the diazines imidazole and pyrazole (Figure 1 (bottom)) it is indicated that imidazole has an intermediate behaviour when compared to ammonia and pyridine. Pyrazole, on the other hand, poorly coordinates to both  $\text{Ni}^{2+}$  and  $\text{H}^+$ .

In considering the above data to determine the separation potential of these amines it must be borne in mind that the curves represent formation of complexes in a single phase (aqueous). For effective separation, two-phase systems will be required. Phase transfer of the H<sup>+</sup> with its counter anion will provide a barrier towards protonation in a nonpolar organic phase. It has been indicated that derivatives of imidazole and pyridine can extract base metal ions from slightly acidic aqueous solutions via coordination (pH values > ~2) [16,17].

The great difference in behaviour between the 3d and 4d transition metals should also be considered if these data are to be applied to palladium(II). The amine complexes of Pd(II) are much more stable than those of Ni<sup>2+</sup> (its 3d analogue – dotted lines) (see the species distribution curves for the NH<sub>3</sub> complexes of Pd(II) in Figure 2). Palladium(II) is already completely in the form of Pd(NH<sub>3</sub>)<sub>4</sub><sup>2+</sup> at a free NH<sub>3</sub> concentration of 1x10<sup>-5</sup> M whereas the first NH<sub>3</sub> complex, of Ni<sup>2+</sup>, i.e., Ni(NH<sub>3</sub>)<sup>2+</sup> is not yet present in significant concentrations (Figure 1(b)) at the same free NH<sub>3</sub> concentration.

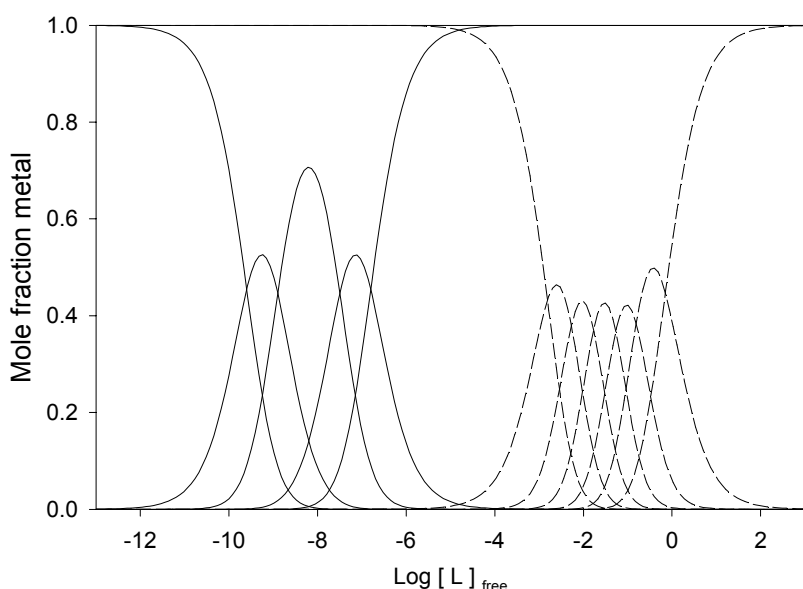


Figure 2. Comparison of the stabilities of Pd(II) and Ni(II) ammine complexes.

When the above information is now applied to select a possible neutral N-donor separating agent which will operate exclusively by the Type II method, pyrazole derivatives were chosen. Its low protonation constant will limit/exclude cation formation, its small formation constants with base metals should seriously limit base metal interferences, but it can be expected to complex strongly with Pd(II).

## EXPERIMENTAL

The preparation of N-decylpyrazole and the procedure followed for the extraction studies were described previously[18]. The same method was followed to functionalise the chlorinated resin.

Batch studies: An amount of dried resin was weighed off and allowed to equilibrate overnight with a HCl solution of the required concentration. The HCl was filtered off and the resin was agitated with a certain volume of 0.1 M Pd(II) (large excess) in the same concentration of HCl at  $\approx$ 180 rev/min for approximately 2 hours. The palladium solution was filtered through a sintered glass quickfit funnel (pyrex G<sub>2</sub>) and the brownish coloured resin was washed with 5

x 25 ml fractions of the required concentration HCl solution. The resin was then "stripped" using 0.75 M NH<sub>4</sub>HSO<sub>3</sub> at pH 6.8.

Column studies were performed using a 300 mm long column with 10 mm internal diameter. Stripping was done by the same reagents as for the batch studies.

## RESULTS AND DISCUSSION

### Pyrazole Derivatives as Separating Agents

These were studied as extractants as well as resins.

#### Extractants

A variety of N-substituted pyrazole compounds was prepared having bulky substituents containing aliphatic, aromatic and mixed groups, in order to study the effect of different parameters like stereochemistry and base strength. The results obtained from N-decylpyrazole (dpyraz) will be discussed in this paper.

The extraction studies were started by equilibrating 0.02 M solutions of each of Pd(II) and Pt(IV) 3.5 M in HCl with 0.18 M chloroform solutions of dpyraz. Analysis of aqueous phases was performed at 30 min intervals. The Pt(IV) extraction occurred almost instantaneously and stayed at ~23% from 30 minutes to 180 minutes. Pd(II) extraction gradually increased from 69% after 30 minutes to 91% after 180 minutes. The fast extraction of Pt(IV) renders the suspicion that cationic species are formed in the organic phase whereas the Pd(II) extraction appeared to be via ligand exchange as anticipated.

HCl phase transfer studies therefore followed, in which equal volumes of 0.18 M solutions of a number of extractants in CHCl<sub>3</sub> were each equilibrated with aqueous HCl solutions varying from 1 M to 5 M. (See Table 1 for the data for dpyraz and 3-methyl-decylpyrazole (mdpyraz)).

*Table 1. Results of HCl loading for pyrazole derivatives in CHCl<sub>3</sub> solutions.*

MHCl	dpyraz	mdpyraz
1	1.51	13.9
2	3.55	-
3	12.72	81.2
4	39.4	89.1
5	70.9	91.8

The fractional HCl loading of dpyraz at 3-4 M HCl readily explains why PtCl<sub>6</sub><sup>2-</sup> is extracted from 3.5 M HCl solutions. Studies were subsequently performed at lower HCl concentrations since % HCl loading of only 0.11%, 0.13% and 0.15% were found for 0.1, 0.2 and 0.5 M HCl solutions, respectively. The results of mdpyraz show how HCl loading is affected by only a small increase in basicity of the extractant.

*Table 2. Approximate calculation of separation factors for palladium and platinum as a function of HCl concentration.*

HCl Concentration (M)	% Pd(II) Extraction after 4 hours	% Pt(IV) Extraction after 4 hours	Separation Factor
0.2	97.41	0.01	14000
0.5	82.62	0.97	85
1	69.28	1.36	50

Extraction curves of Pd(II) obtained from a mixture of 0.02 M Pd(II) and 0.02 M Pd(II) in various HCl solutions using 0.18 M dpyraz in  $\text{CHCl}_3$  solution are represented in Figure 3. The corresponding extraction of Pt(IV) from the same solutions are given in Table 2.

These results indicate how Pt(IV) extraction can be correlated with HCl loading and thus cation formation in the organic phase. At the same time Pd(II) extraction is lowered with increase in HCl loading in the region of 0.2 to 1 M aqueous HCl solutions. Electronic spectral analysis of the organic phases indicated the presence of  $\text{PdCl}_2 \cdot 2\text{dpyraz}$  ( $\lambda_{\text{max}} \sim 404$  nm) (those for  $\text{PdCl}_4^{2-}$  (476 nm) and  $\text{Pd}_2\text{Cl}_6^{2-}$  at 440 nm are found at higher wavelengths) [18].

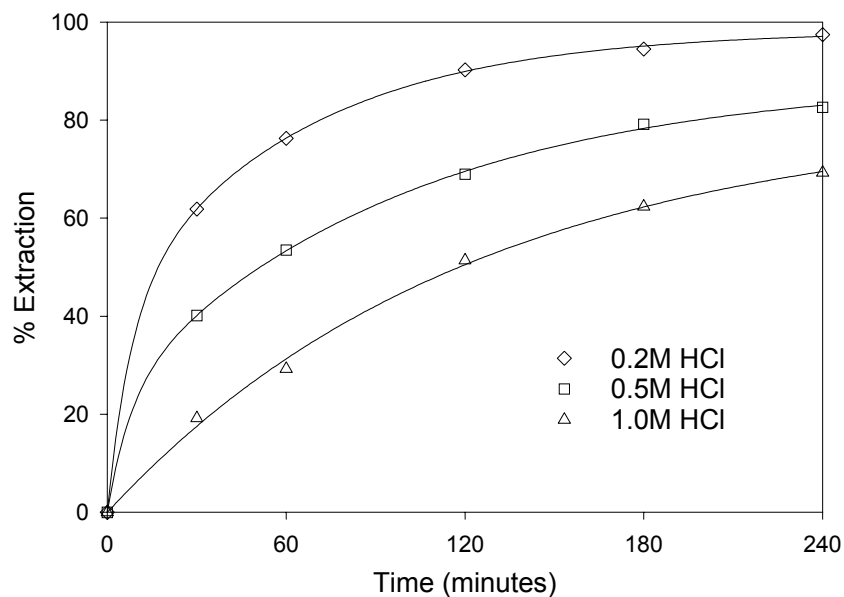


*Figure 3. Extraction curves of Pd(II) from dilute HCl solutions by 0.18 M dpyraz solutions in  $\text{CHCl}_3$ .*

When the above extraction values are used to calculate approximate separation factors, a large value is obtained for 0.2 M HCl solutions though rapidly decreasing with increase in HCl concentration (See Table 2).

Extraction studies performed on base-metals showed that only Fe(III) is extracted from 3 M HCl solutions.

#### **Resin studies**

In view of the positive results obtained from the solvent extraction system, especially in the 0.2-1 M HCl region, studies were undertaken with a pyrazole functionalised XAD-16 resin. Batch studies, palladium capacity studies and selectivity studies were performed.

The capacity loading of Pd (g/l) as a function of aqueous HCl concentration is given in Table 3. The decrease of loading of Pd with increase of HCl concentration is again emphasised by these data. The relatively low capacity could possibly be related to the fact that only 50% of the Cl in the chlorinated resin could be replaced by pyrazole in the functionalisation reaction.

*Table 3. The capacity loading of palladium as a function of aqueous HCl concentration.*

Aqueous HCl concentration (M)	Palladium capacity (g/l)
0.1	17.8
0.2	17.7
0.5	7.9
1.0	7.9
3.5	7.2

The curves generated for the loading and stripping of palladium and platinum from a mixture of palladium and platinum in 0.2 M HCl are depicted in Figure 4. The selectivity values (obtained by the ratio of the areas of Pd(II) divided by that of Pt(IV) in the stripping phase as a function of aqueous HCl concentrations from different column studies are given in Table 4.

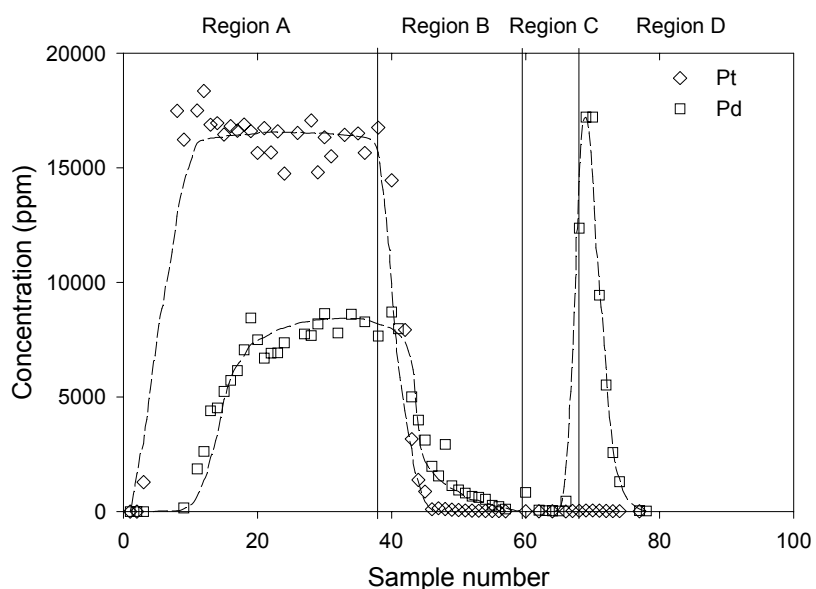


*Figure 4. Curves generated for the loading (Region A), washing (Region B) and Stripping (Region C) of palladium (0.1 M), and platinum (0.1 M) from their mixture in 0.2 M HCl.*

*Table 4. Selectivity/separation factor as a function of aqueous HCl concentration (M).*

Aqueous HCl Concentration (M)	Selectivity/Separation Factor
0.1	146
0.2	130
0.5	66
1.0	46
3.5	5

Although the selectivity of the resin was much less than that of the solvent extraction system, the kinetics was fast.

In order to determine the durability of the resin, a comparison of capacity loading and selectivity values for the new and 8-month old resin was made (See Table 5).

*Table 5. A comparison of capacity loading and selectivity values for the new and 8-month old resin.*

Aqueous HCl concentration (M)	New Resin		8-month old resin	
	Capacity Loading (g/l)	Selectivity	Capacity Loading (g/l)	Selectivity
0.1	17.7	146	10.0	40.7
0.2	17.7	146	9.6	33.0

In conclusion, the results obtained in this study indicate that reasonably stable and efficient separating agents can be prepared for the isolation of Pd(II) from Pt(IV) using pyrazole derivatives.

#### ACKNOWLEDGEMENTS

We thank the University of Port Elizabeth, National Research Foundation, Thrip and Impala Platinum for financial assistance.

#### REFERENCES

1. P. Senise and L.M. Pitombo (1971), *Talanta*, **11**, 1185.
2. P. Senise and F. Levi (1964), *Anal. Chim. Acta*, **30**, 422 and **30**, 509.
3. F. Jasim, R.J. Magee and C.L. Wilson (1960), *Rec. Trav. Chim.*, **79**, 541.
4. F. Jasim, R.J. Magee and C.L. Wilson (1962), *Microchim. Acta*, 160.
5. A.M. Golub and T.V. Pomeranets (1965), *Ukr. Khim. Zh.*, **31**, 104.
6. T.S. Katykhin, M.K. Nikitin, V.P. Sergeev and S.K. Kalinini (1967), *Primenvnie Ekstraktsii i Ionnogo Obmena v Analize Blagorodnykh Metallov*, Izd. Tsctmetinformatsiya, Moskva, p. 39.
7. J. Forsythe, R. Magee and C. Wilson (1950), *Talanta*, **3**, 324.
8. J. Forsythe, R. Magee and C. Wilson (1950), *Talanta*, **3**, 330.
9. E. Berg and W. Senn (1958), *Anal. Chim. Acta*, **19**, 12.
10. E. Berg and W. Senn (1958), *Anal. Chim. Acta*, **19**, 109.
11. A.T. Casey, E. Davies, T.L. Meek and S.E. Wagner (1967), *Solvent Extraction Chemistry*, North-Holland, Amsterdam, p. 327.
12. J. Timitaro, K. Kon, F. Takeo and M. Hiroko (1962), *J. Atom. Energy Soc. Jap.*, **4**, 117.
13. V.F. Borbat, P.I. Bobikov and E.F. Kouba (1965), *Zh. Anal. Chim.*, **20**, 192.
14. R.I. Edwards (1977), *Chem. Abstr.*, **87**, 12108.
15. A.E. Martell and R.M. Smith (1982), *Critical Stability Constants*, Vol. 2 and Vol. 4, Plenum Press, New York.
16. J.G.H. du Preez, C. Mattheus, N. Sumter, W. Edge, C. Potgieter and B.J.A.M. van Brecht (1998), *Solv. Extr. Ion Exch.*, **16**, 1033-1046.
17. J.G.H. du Preez, C. Mattheus, N. Sumter, S. Ravindran, C. Potgieter and B.J.A.M. van Brecht (1998), *Solv. Extr. Ion Exch.*, **16**, 565-586.
18. J.G.H. du Preez, S.E. Knoetze and S. Ravindran (1999), *Solv. Extr. Ion Exch.*, **17**, 317-332.



# ON THE LIQUID-LIQUID EXTRACTION OF Pt(IV/II) FROM HYDROCHLORIC ACID BY *N*-ACYL(AROYL)-*N'*,*N'*-DIALKYLTHIOUREAS: A MULTINUCLEAR ( $^1\text{H}$ , $^{13}\text{C}$ AND $^{195}\text{Pt}$ ) NMR SPECIATION STUDY OF THE EXTRACTED COMPLEXES

Klaus R. Koch\*, Jörn Miller and Arjan N. Westra

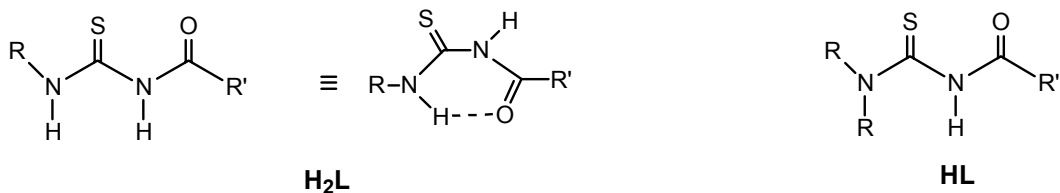
Department of Chemistry, University of Stellenbosch, Stellenbosch, South Africa

An investigation into the nature of the complex species which are formed by the extraction of Pt(IV/II) from hydrochloric acid using *N*-benzoyl-*N'*,*N'*-diethylthiourea and *N*-benzoyl-*N'*,*N'*-di(*n*-butyl)thiourea in chloroform and toluene has been carried out. The study reveals that for Pt<sup>IV</sup> extraction a remarkably complicated distribution of complex species is obtained, arising from *inter alia* possible redox reactions between Pt<sup>IV</sup> and the ligands. In the case of Pt<sup>II</sup> extraction with *N*-acyl(aroyl)-*N'*,*N'*-dialkylthioureas, which is relatively simpler, several protonated species containing coordinated chloride ions ([Pt(L-S,O)(HL-S)Cl], *cis*-[Pt(HL-S)<sub>2</sub>Cl<sub>2</sub>] and *trans*-[Pt(HL-S)<sub>2</sub>Cl<sub>2</sub>]), as well as the well-known *cis*-[Pt(L-S,O)<sub>2</sub>] complex (depending on the extraction conditions), are found in the organic phase.

## INTRODUCTION

Although the discovery of platinum in the sixteenth century did not lead to an immediate realisation of any usefulness for it, it has become one of the most sought-after metals today. With applications for this transition metal as diverse as the manufacture of autocatalysts, to the development of new anti-cancer drugs based on *cis*-platin and its derivatives, to the making of jewellery and ornaments, it is not surprising that research into improved separation of this precious metal, and the other platinum group metals (PGMs), is ongoing. While previous processes for the separation of the platinum group metals (Pt, Pd, Ru, Rh, Os and Ir) were based on the selective precipitation of the metals from a solution mixture, solvent extraction has proven to be more advantageous in many respects, *viz.* efficiency, yield and operating time [1], and investigations into the selective solvent extraction of the platinum group metals are therefore of continued interest.

The ligands *N*-acyl(aroyl)-*N'*-alkylthiourea ( $\text{H}_2\text{L}$ ) and *N*-acyl(aroyl)-*N'*,*N'*-dialkylthiourea (HL) have been shown to form very stable neutral complexes with many metal ions, particularly so with the platinum group metals [2,3]. In fact, these ligands have been found to selectively coordinate the PGMs making them ideal candidates for use in the liquid-liquid extraction [4,5], as well as preconcentration and separation [6,7], of the PGMs.



$\text{R}' = \text{phenyl or alkyl group}$

In a study by König *et al.* [4] the efficacy of several *N*-benzoyl-*N'*,*N'*-dialkylthioureas as extraction reagents was illustrated (dialkyl = dimethyl, diethyl, di-*n*-propyl, di-*n*-butyl, di-*n*-hexyl). The authors found that by controlling the pH of the aqueous phase, the PGMs ( $\text{Pt}^{II}$ ,  $\text{Pd}^{II}$ ,  $\text{Ru}^{III}$ ,  $\text{Rh}^{III}$ ,  $\text{Os}^{III}$ ,  $\text{Ir}^{III}$ ) can be separated from several important metals such as iron, cobalt, nickel, copper and zinc. Furthermore, by controlling the pH and the temperature, it is, to some degree, also possible to separate the platinum group metals from each other. Ligands with longer alkyl moieties produce larger distribution coefficients, better phase separation and thus improved extraction. The differences in the extractive abilities of the ligands was ascribed to varying solubilities of the ligands and complexes in the solvents used, as well as to the large variation in complex stabilities; the longer alkyl groups lead, due to larger +I-effects, to increased electron density at the coordinative centers of the ligands (the O- and S-atoms) and thus to more stable complexes. A subsequent investigation by Vest *et al.* [5] showed that the dialkyl-substituted benzoylthioureas,  $\text{HL}$ , are far more efficient in the liquid-liquid extraction of the PGMs than the monoalkyl-substituted analogues,  $\text{H}_2\text{L}$ .

In both the afore-mentioned investigations, however, no description of the coordination chemistry of  $\text{Pt}^{II}$  (or the other PGMs) with the *N*-acyl(aroyl)-*N'*,*N'*-alkylthioureas,  $\text{H}_2\text{L}$ , and *N*-acyl(aroyl)-*N'*,*N'*-dialkylthioureas,  $\text{HL}$ , was given, but in recent years several papers have appeared in this regard. Investigations have shown that the potentially bidentate  $\text{H}_2\text{L}$  ligands co-ordinate to the  $\text{Pt}^{II}$  through the S-atom only, similar to simple unsubstituted thioureas, and not via the O-atom also [8-10]. Crystallographic evidence reveals the monoalkyl-substituted ligands to be locked into a planar six-membered O-C-N-C-N-H ring by means of an intramolecular N-H...O hydrogen bond, thus disallowing coordination via the carbonyl oxygen (Figure 1 (a)). The  $\text{HL}$  ligands, however, coordinate to the  $\text{Pt}^{II}$  via both the S- and the O-atom forming essentially square-planar bis-complexes with loss of the thioamidic proton (Figure 1 (b)). Coordination to  $\text{Pt}^{II}$  by the monoalkyl- and dialkyl-substituted ligands differs in another respect in that the *N*-acyl(aroyl)-*N'*,*N'*-alkylthioureas react with  $\text{PtCl}_4^{2-}$  in neutral aqueous solution to yield mixtures of *cis*- and *trans*- $[\text{Pt}(\text{H}_2\text{L}-\text{S})_2\text{Cl}_2]$  complexes whilst complexation with *N*-acyl(aroyl)-*N'*,*N'*-dialkylthioureas in most cases yields only *cis*- $[\text{Pt}(\text{L}-\text{S},\text{O})_2]$  complexes. *N*-naphthoyl-*N'*,*N'*-dibutylthiourea is the only dialkyl-substituted ligand of this type to have been reported to yield *trans*- as well as *cis*- isomers [11].

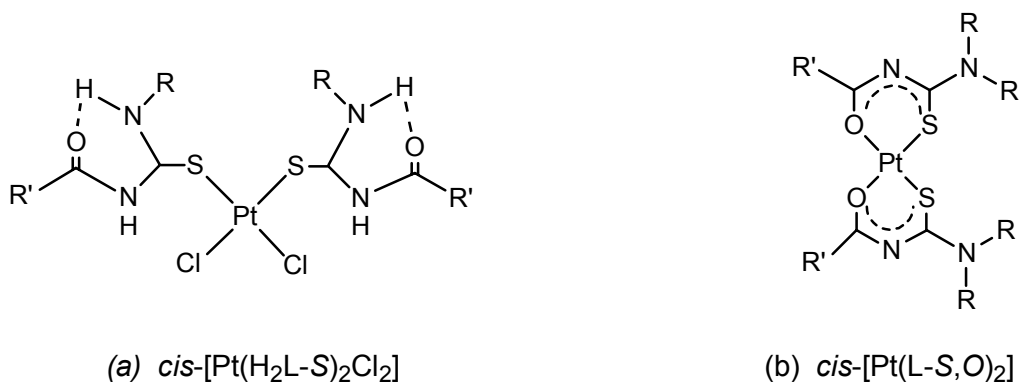


*Figure 1. Complexation of  $\text{Pt}^{II}$  with *N*-acyl(aroyl)-*N'*,*N'*-alkylthioureas leads to mixtures of *cis*-, (a), and *trans*- isomers whilst complexation with *N*-acyl(aroyl)-*N'*,*N'*-dialkylthioureas leads predominantly to *cis*-, (b), isomers.*

Whereas the investigations [8-11] into the fundamental coordination chemistry of the  $\text{H}_2\text{L}$  and  $\text{HL}$  type ligands of the PGMs have been performed in essentially neutral solutions, the solvent extraction studies by Vest *et al.* [5] revealed that optimum extraction of the PGMs by the ligands of interest occurred in 2 M hydrochloric acid media, conditions under which  $\text{Pt}^{II}$  species other than those already identified [8-11] might also exist. An investigation of the acid-base chemistry of various *cis*- $[\text{Pt}(\text{L}-\text{S},\text{O})_2]$  complexes [12] elucidated this point ( $\text{HL} = \text{N}$ -benzoyl- $\text{N}'$ , $\text{N}'$ -di(*n*-butyl)thiourea,  $\text{N}$ -(4Br-phenyl)- $\text{N}'$ , $\text{N}'$ -di(*n*-butyl)thiourea,  $\text{N}$ -(4NO<sub>2</sub>-phenyl)-

*N,N'*-di(n-butyl)thiourea). It was shown that treatment of a solution of the uncharged complex *cis*-[Pt(L-S,O)<sub>2</sub>] in chloroform with hydrochloric acid solution results in the formation of three protonated complexes: a partially ring-opened [Pt(L-S,O)(HL-S)Cl] complex which, in the presence of excess conc. HCl, disappeared, presumably becoming further protonated in the acid medium to yield a *cis*-[Pt(HL-S)<sub>2</sub>Cl<sub>2</sub>] complex which in turn isomerizes slowly to the *trans*-[Pt(HL-S)<sub>2</sub>Cl<sub>2</sub>] complex.

The results of investigations by Koch and co-workers give an indication of the types of Pt<sup>II</sup> species that possibly exist in the extraction processes described by Vest *et al.* Since much of the platinum in the extractive industrial process streams occurs in the oxidation state +4 however (as the species PtCl<sub>6</sub><sup>2-</sup>), investigations into the extraction of Pt<sup>IV</sup> and the resultant Pt<sup>IV</sup> species are therefore also of importance. The Pt<sup>IV</sup> chloro-complex (PtCl<sub>6</sub><sup>2-</sup>) is however kinetically less labile than the Pt<sup>II</sup> chloro-complex (PtCl<sub>4</sub><sup>2-</sup>) and this results in slower formation of the extractable Pt<sup>IV</sup> species; the system is thus more difficult to investigate. Moreover, the possibility of a redox reaction between Pt<sup>IV</sup> and the thiourea ligands cannot be excluded. Vest *et al.* improved the rate of extraction of Pt<sup>IV</sup> by addition of tin(II) chloride [13], a reagent which, apart from stabilizing Pt—Cl bonds, also reduces the Pt<sup>IV</sup> to Pt<sup>II</sup> [14].

This paper reports on our preliminary attempts at Pt<sup>IV</sup> speciation in the extraction of this ion with *N*-benzoyl-*N,N'*-diethylthiourea, HL<sup>1</sup>, and *N*-benzoyl-*N,N'*-di(n-butyl)thiourea, HL<sup>2</sup>, as well as Pt<sup>II</sup> speciation in the coordination of this ion with *N*-propanoyl-*N*-morpholinothiourea, HL<sup>3</sup>.

## EXPERIMENTAL

### Preparation of ligands and *cis*-[Pt(L<sup>3</sup>-S,O)<sub>2</sub>] complex

All ligands, HL<sup>1</sup> – HL<sup>3</sup>, were prepared as previously described [9] and were characterised by means of <sup>1</sup>H and <sup>13</sup>C NMR spectroscopy. The neutral complex *cis*-[Pt(L<sup>3</sup>-S,O)<sub>2</sub>] was also prepared and characterized as previously reported [9].

### Solvent extraction procedure

Phase intermixtures in the extractions was achieved either by the use of a shaking apparatus or by means of magnetic stirring. In the first case 1.0 mL of an acidified (2 M HCl) aqueous H<sub>2</sub>PtCl<sub>6</sub>·H<sub>2</sub>O solution (initial concentration of platinum was 23.1 g/L) and 1.0 mL of a CDCl<sub>3</sub> solution of HL<sup>1</sup> (metal/ligand ratio 1:4) were thoroughly mixed at room temperature in a tightly stoppered test-tube on a shaking apparatus for 24 hours. The organic layer was filtered through Extrelut® (to remove traces of water) directly into an NMR tube and spectra acquired. In the second instance extractions were performed by magnetically stirring the two phases in a water-jacketted reaction vessel; the latter allowed temperature control. 10.0 mL of an acidified (2 M HCl) aqueous H<sub>2</sub>PtCl<sub>6</sub>·H<sub>2</sub>O solution (initial concentration of platinum was 22.1 g/L) was vigorously stirred with 10.0 mL of a toluene solution of HL<sup>2</sup> (metal/ligand ratio 1:8) at 80°C. After 3 hours of stirring a sample of the organic phase was filtered through Extrelut® directly into an NMR tube and spectra acquired.

### Protonation experiments

An aliquot of 0.15 mL 6 M aqueous HCl was added directly to an NMR tube containing 0.6 mL of *cis*-[Pt(L<sup>3</sup>-S,O)<sub>2</sub>] complex in CDCl<sub>3</sub>. After vigorously shaking the tube to ensure thorough intermixing of the two phases, the acidified organic layer was allowed to separate and NMR spectra were recorded ca. 7 minutes after acid addition. After spectral acquisition the mineral acid was removed, the organic layer washed with water and then treated with 5 M ammonia solution, and NMR spectra were re-acquired.

## NMR spectroscopy

$^1\text{H}$  and  $^{195}\text{Pt}$  NMR spectra were recorded in 5 mm tubes in chloroform-d ( $^1\text{H}$  and  $^{195}\text{Pt}$ ) or toluene-d<sub>8</sub> ( $^{195}\text{Pt}$ ) solution, using a Varian INOVA 600 MHz spectrometer operating at 600 and 128 MHz respectively ( $^1\text{H}$  at 25°C and  $^{195}\text{Pt}$  at 30°C).  $^1\text{H}$  chemical shifts are quoted relative to the residual  $\text{CDCl}_3$  solvent resonance at 7.26 ppm. The  $^{195}\text{Pt}$  NMR spectra were recorded using spectral widths typically 130 kHz with 15  $\mu\text{s}$  pulses (~90°) and 1.0 s pulse delay. All  $^{195}\text{Pt}$  chemical shifts are quoted relative to external  $\text{H}_2\text{PtCl}_6$  (500mg ml<sup>-1</sup> in 30% v/v  $\text{D}_2\text{O}/1\text{ M HCl}$ ) and are estimated to be accurate to  $\pm 4$  ppm.

## RESULTS AND DISCUSSION

### Pt<sup>IV</sup> speciation

In the first attempt at characterising the Pt<sup>IV</sup> species that occur in the extraction of  $[\text{PtCl}_6]^{2-}$  with an *N*-acyl(aryl)-*N',N'*-dialkylthiourea, an acidified aqueous solution of Pt<sup>IV</sup> was vigorously mixed with a  $\text{CDCl}_3$  solution containing *N*-benzoyl-*N',N'*-diethylthiourea, HL<sup>1</sup>, on a shaking apparatus for 24 hours as described in the experimental section. The organic layer coloured dark yellow indicating the formation of platinum complexes and NMR spectra of this solution were acquired.  $^{195}\text{Pt}$  spectra in the region between 220 and –3700 ppm, relative to the external standard, were recorded; uncertainty as to the species that had formed necessitated this large spectral region but the limits were based on the premise that both Pt<sup>IV</sup> and Pt<sup>II</sup> species would be found in this range. The only indication of platinum in the organic layer however was a very broad (334 Hz) and undefinable peak at –3646 ppm which, despite a long acquisition time (9 h), was of extremely low intensity. The appearance of this peak, as well as a very complex  $^1\text{H}$  spectrum different from that of the ligand, is proof that extraction of the metal had taken place but the very low intensity of the  $^{195}\text{Pt}$  peak suggested that several species were extracted and that the extent of metal separation had been very poor.

To improve the extent of metal separation, a second extraction was performed at higher temperature with a toluene solution containing *N*-benzoyl-*N',N'*-di(n-butyl)thiourea, HL<sup>2</sup>, as described in the experimental section. König *et al.* [4] had concluded that ligands with longer alkyl moieties lead to improved platinum extraction, as does a higher operating temperature; the latter change necessitated the use of an organic solvent with a higher boiling point. After 3 hours of phase contact at 80°C the toluene solution had an extremely dark brown/red appearance indicating significant metal extraction; this was confirmed by the  $^1\text{H}$  spectrum which revealed a plethora of peaks the complexity of which prevented interpretation. To ensure that all possible species would be registered, the platinum spectral region from 3500 to –6000 ppm (relative to the external standard) was scanned, but  $^{195}\text{Pt}$  peaks were only observed between –3100 and –3700 ppm. In this range several peaks appeared (at least 7) with varying line-widths (64 – 208 Hz) but again with surprisingly low intensity despite an acquisition time of 13½ hours. After several days a white/yellow precipitate had formed in the toluene solution. The precipitate was separated, rinsed and re-dissolved in  $\text{CDCl}_3$  and NMR spectra acquired. The  $^1\text{H}$  NMR spectrum is consistent with a species that contains the *N*-benzoyl-*N',N'*-di(n-butyl)thiourea ligand. Moreover, the presence of a  $^1\text{H}$  peak at 11.16 ppm, characteristic of an N-H resonance, confirms that the thioamidic N-atom of the ligand is protonated. The corresponding  $^{195}\text{Pt}$  spectrum of this solution consists of a single, relatively sharp (180 Hz), resonance at -3205 ppm. In the investigation of the acid-base chemistry of various *cis*-[Pt<sup>II</sup>(L-S,O)<sub>2</sub>] complexes by Koch *et al.* [12], the complex *cis*-bis(*N*-benzoyl-*N',N'*-di(n-butyl)thiourea)platinum(II) was prepared and the  $^1\text{H}$  and  $^{195}\text{Pt}$  NMR spectra of this complex and its protonated forms acquired. The authors concluded that one of the doubly protonated forms of *cis*-bis(*N*-benzoyl-*N',N'*-di(n-butyl)thiourea)platinum(II) was a complex denoted as *cis*-[Pt<sup>II</sup>(HL<sup>2</sup>-S)<sub>2</sub>Cl<sub>2</sub>] in which the carbonyl O-donor of the ligand had been displaced from the metal centre by a coordinating chloride ion upon protonation of the thioamidic nitrogen. The resultant N-H resonance was found to appear at 11.14 ppm and the

platinum resonance for this protonated complex was reported at -3218 ppm. Comparison of these  $^1\text{H}$  and  $^{195}\text{Pt}$  chemical shifts (11.14 ppm and -3218 ppm respectively) with those obtained for the re-dissolved precipitate in the present investigation (11.16 ppm and -3205 ppm respectively) suggests that *cis*-[Pt<sup>II</sup>(HL<sup>2</sup>-S)<sub>2</sub>Cl<sub>2</sub>] is one of the species formed in the extraction of Pt<sup>IV</sup> with *N*-benzoyl-*N'*,*N*-di(*n*-butyl)thiourea and thus that some Pt<sup>IV</sup> is reduced to Pt<sup>II</sup> in the process of extraction. The reduction of Pt<sup>IV</sup> by the ligands was not unexpected since several investigations into anti-cancer drugs have revealed that many sulfur-containing biomolecules act as reducing agents, reducing antitumour-active platinum(IV) drugs to their platinum(II) analogues [15].

Although the serendipitous crystallization of one of extracted platinum species has allowed its characterisation, the complexity of the extracted mixture, as revealed by the  $^1\text{H}$  and  $^{195}\text{Pt}$  NMR spectra, indicates that the speciation in the liquid-liquid extraction of Pt<sup>IV</sup> with the ligands of interest must be approached in a piecemeal fashion. This would entail the preparation of possible complex species under experimental conditions relevant to the extraction process, characterisation of these species by means of multinuclear ( $^1\text{H}$ ,  $^{13}\text{C}$  and  $^{195}\text{Pt}$ ) NMR spectroscopy and subsequent correlation of these species-characterisation results with the results obtained from extraction experiments. Since the preparation and characterisation of Pt<sup>II</sup> species will elucidate not only speciation in the solvent extraction of Pt<sup>II</sup> but also that of Pt<sup>IV</sup>, attention was first focused on Pt<sup>II</sup> speciation; a description of the complexes of Pt<sup>II</sup> with *N*-propanoyl-*N'*-morpholinothiourea, HL<sup>3</sup>, follows.

### Pt<sup>II</sup> speciation

Reaction of *N*-propanoyl-*N'*-morpholinothiourea with PtCl<sub>4</sub><sup>2-</sup> (see the Experimental section) yields a product the  $^{195}\text{Pt}$  NMR spectrum of which shows only a single resonance at  $\delta(^{195}\text{Pt}) = -2743$  ppm (Figure 2(a)).

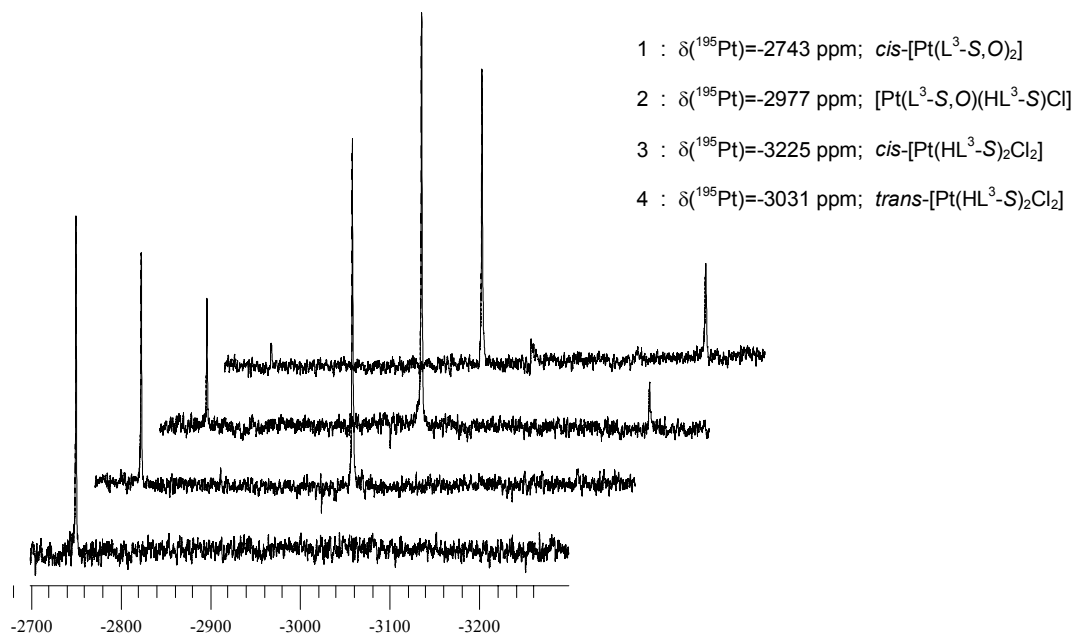


Figure 2. (a)  $^{195}\text{Pt}$  NMR spectrum of *cis*-[Pt(L<sup>3</sup>-S,O)<sub>2</sub>] in  $\text{CDCl}_3$  before acid addition.  
 (b)-(d) Spectra of solution (a) to which 6 M HCl has been added, acquired at the time intervals as indicated.

Although *trans* configurations of Pt<sup>II</sup> complexes with *N*-acyl(aroyl)-*N,N*'-dialkylthioureas are known [11], formation of exclusively the *cis* isomer predominates [12] and since the <sup>195</sup>Pt chemical shift obtained for the product (-2743 ppm) is consistent with <sup>195</sup>Pt shift trends reported by Koch *et al.* for several *cis*-[Pt(L-S,O)<sub>2</sub>] complexes [10, 12, 16], it is concluded that the product obtained is *cis*-bis(*N*-propanoyl-*N*'-morpholinothiourea)platinum(II) (*cis*-[Pt(L<sup>3</sup>-S,O)<sub>2</sub>]; Figure 4). The corresponding <sup>1</sup>H NMR spectrum is consistent with only a single unprotonated complex species, as confirmed by the absence of the characteristic amido N-H resonance in the 10-12 ppm range (detailed <sup>1</sup>H assignments are trivial and will not be given here).

Addition of 0.15 mL 6 M HCl directly to the NMR tube containing *cis*-[Pt(L<sup>3</sup>-S,O)<sub>2</sub>] in CDCl<sub>3</sub> as described in the experimental section, yields a <sup>1</sup>H spectrum (acquired ca. 7 min after addition of the HCl) showing the presence of at least two additional species in solution, characterised by N-H resonances at 10.70 and 10.57 ppm (Figure 3(i)). The appearance of the two N-H resonances reveals that the additional species occur as a result of the protonation of the coordinated ligands by some HCl partitioned into the CDCl<sub>3</sub> phase. After 1 hour 23 min a third protonated species becomes evident, as indicated by an N-H resonance at 10.29 ppm (Figure 3(ii)); the corresponding <sup>195</sup>Pt spectrum at this time (Figure 2(b)) consists of only two resonances at  $\delta = -2743$  and -2977 ppm. With time the concentrations of two of the protonated species increase, as indicated by the increasing intensities of the peaks at 10.57 and 10.29 ppm (Figure 3(iii)-3(viii)) and eventually exist at concentrations which enable them to be detected in the <sup>195</sup>Pt spectra,  $\delta(^{195}\text{Pt}) = -3225$  and -3031 ppm (Figure 2(c) and 2(d)). The protonated species giving rise to the <sup>1</sup>H peak at 10.70 ppm and the <sup>195</sup>Pt peak at -2977 ppm slowly increases and then decreases in concentration whilst the original unprotonated complex,  $\delta(^{195}\text{Pt}) = -2743$  ppm, decreases markedly with time.

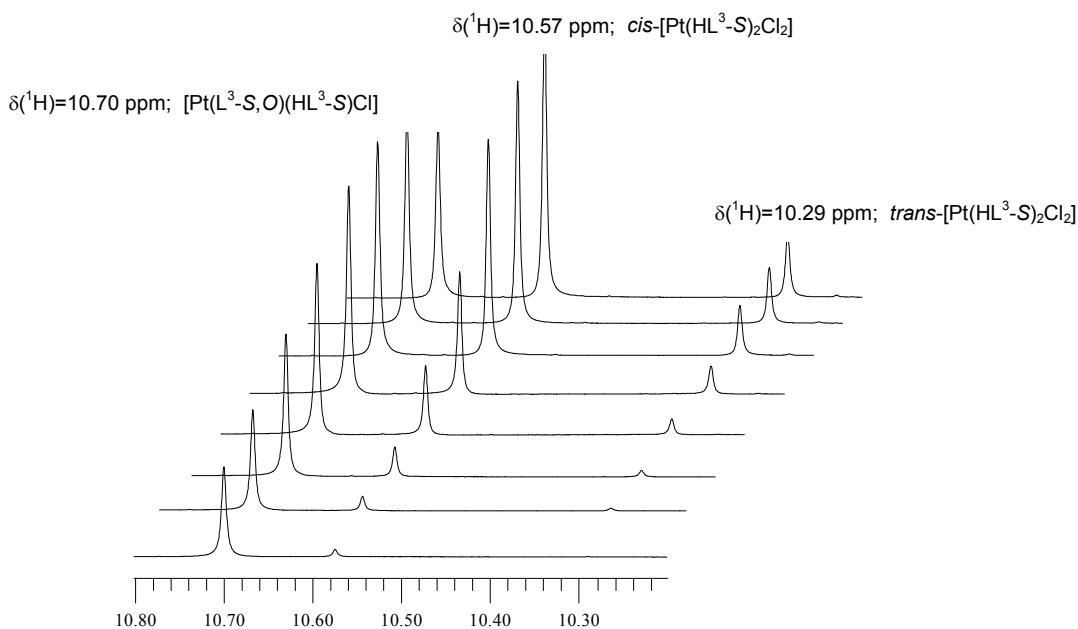


Figure 3. Partial <sup>1</sup>H NMR spectra of *cis*-[Pt(L<sup>3</sup>-S,O)<sub>2</sub>] in CDCl<sub>3</sub> acquired as a function of time after addition of 6 M HCl.

Treatment of the CDCl<sub>3</sub> phase with a small volume of 5 M ammonia as described in the experimental section, results in <sup>1</sup>H and <sup>195</sup>Pt spectra which are identical to those of the initial *cis*-[Pt(L<sup>3</sup>-S,O)<sub>2</sub>] complex with no evidence of any other complex species in solution. Whereas the protonation steps had taken several hours to occur, the solution treated with base had reverted to the original *cis*-[Pt(L<sup>3</sup>-S,O)<sub>2</sub>] complex within minutes (ca. 10 min) indicating that the deprotonation reactions take place much more rapidly across the phase boundary.

In a previous investigation by Koch *et al.* [8], the  $^{195}\text{Pt}$  spectrum of a mixture of *cis*- and *trans*-bis(*N*-benzoyl-*N'*-propylthiourea)dichloroplatinum(II) in  $\text{CDCl}_3$  showed two resonances at -3219 and -3040 ppm. The resonance at -3219 ppm has been assigned to the *cis*-bis(*N*-benzoyl-*N'*-propylthiourea)dichloroplatinum(II) complex (which has also been characterised by means of x-ray crystallography) and the one at -3040 ppm to the *trans*- isomer. Based on these assignments the  $^{195}\text{Pt}$  peak at -3225 ppm in the present investigation is assigned to the doubly protonated species *cis*-[Pt(HL<sup>3</sup>-S)<sub>2</sub>Cl<sub>2</sub>] (Figure 4); a species formed when, upon protonation of the thioamidic N-atoms of *cis*-[Pt(L<sup>3</sup>-S,O)<sub>2</sub>], the carbonyl O-donor atoms are displaced from the metal centre by coordinating chloride ions leaving the ligands monodentately coordinated through the S-atoms only. The smaller  $^{195}\text{Pt}$  peak which develops over time at -3031 ppm is assigned to the *trans*-[Pt(HL<sup>3</sup>-S)<sub>2</sub>Cl<sub>2</sub>] isomer (Figure 4), resulting from the isomerization of the *cis* complex. These assignments are consistent with the generally observed trend that the *cis* isomers for complexes of the type [PtA<sub>2</sub>X<sub>2</sub>] usually appear 200-500 ppm upfield of the *trans* isomers, depending on the nature of the donor atom of ligand A (X = Cl<sup>-</sup>) [17]. The  $^{195}\text{Pt}$  peak at -2977 ppm is assigned to a singly protonated species [Pt(L<sup>3</sup>-S,O)(HL<sup>3</sup>-S)Cl] (Figure 4), a species in which only one of the ligands has been protonated to become monodentately (S-) coordinated to the platinum centre whilst the second ligand remains bidentately (S,O-) bound.  $^{195}\text{Pt}$  chemical shifts are extremely sensitive to changes in the coordination sphere of the metal [17] and an upfield shift change of 234 ppm {-2743 ppm – (-2977 ppm)} as compared to an upfield shift change of 482 ppm {-2743 ppm – (-3225 ppm)}, known to result from a change in coordination sphere from two O-atoms to two chloride ions, would indicate a species in which only one O-atom has been replaced by only a single chloride ion.

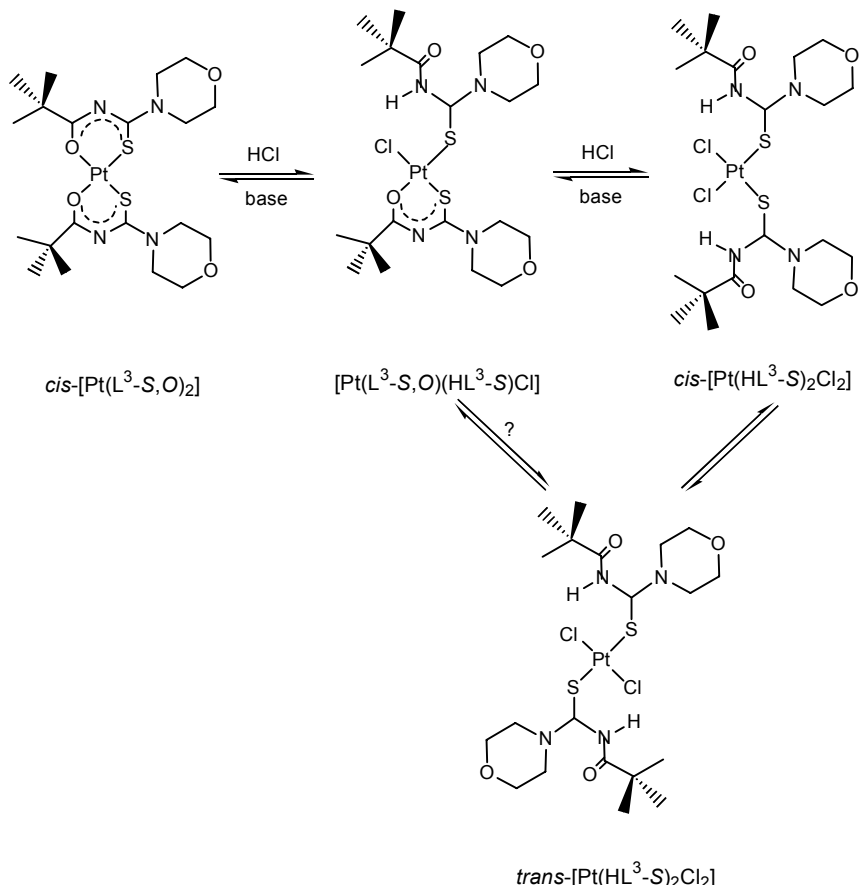


Figure 4. Schematic representation of the formation of various Pt<sup>II</sup> species on addition of HCl to a  $\text{CDCl}_3$  solution of *cis*-[Pt(L<sup>3</sup>-S,O)<sub>2</sub>].

## CONCLUSION

The results of our investigation confirm that Pt<sup>IV</sup> complex species are indeed extracted by *N*-acyl(aryl)-*N,N*'-dialkylthioureas yielding remarkably complex <sup>1</sup>H and <sup>195</sup>Pt NMR spectra of the extracts which are difficult to interpret directly. The possibility of redox reactions between Pt<sup>IV</sup> and the ligands cannot be excluded at present, warranting further study (currently in progress). Nevertheless <sup>1</sup>H and <sup>195</sup>Pt NMR studies of the simpler Pt<sup>II</sup> system shows that under acidic extractive conditions a variety of protonated complexes such as [Pt(L<sup>3</sup>-S,O)(HL<sup>3</sup>-S)Cl], *cis*-[Pt(HL<sup>3</sup>-S)<sub>2</sub>Cl<sub>2</sub>] and *trans*-[Pt(HL<sup>3</sup>-S)<sub>2</sub>Cl<sub>2</sub>], may exist in equilibrium in the organic phase. Treatment of the acidified solution with dilute alkali results in reversion to the *cis*-[Pt(L<sup>3</sup>-S,O)<sub>2</sub>] complex.

## ACKNOWLEDGEMENTS

We thank the University of Stellenbosch, the National Research Foundation (NRF) and Anglo Platinum for financial assistance.

## REFERENCES

1. F. Hartley (1991), Chemistry of the Platinum Group Metals: Recent Developments, Elsevier, Amsterdam, pp.9-31.
2. L. Beyer, E. Hoyer, J. Liebscher and H. Hartmann (1981), *Z. Chem.*, **21**, 81-91.
3. P. Muhl, K. Gloe, F. Dietze, E. Hoyer and L. Beyer (1986), *Z. Chem.*, **26**, 81-94.
4. K.-H. König, M. Schuster, B. Steinbrech, G. Schneeweis and R. Schlodder (1985), *Fres. Z. Anal. Chem.*, **321**, 457-460.
5. P. Vest, M. Schuster and K.-H. König (1989), *Fres. Z. Anal. Chem.*, **335**, 759-763.
6. M. Schuster (1992), *Fres. Z. Anal. Chem.*, **342**, 791-794.
7. K. R. Koch (2001), *Coord. Chem. Rev.*, **216-217**, 473-488.
8. S. Bourne and K. R. Koch (1993), *J. Chem. Soc., Dalton Trans.*, 2071-2072.
9. K. R. Koch, C. Sacht and S. Bourne (1995), *Inorg. Chim. Acta*, **232**, 109-115.
10. K. R. Koch, C. Sacht, T. Grimbacher and S Bourne (1995), *S. Afr. J. Chem.*, **48**, 71-77.
11. K. R. Koch, J. du Toit, M. Caira and C. Sacht (1994), *J. Chem. Soc., Dalton Trans.*, 785-786.
12. K. R. Koch, T. Grimbacher and C. Sacht (1998), *Polyhedron*, **17**, 267-274.
13. P. Vest, M. Schuster and K.-H. König (1991), *Fres. J. Anal. Chem.*, **339**, 142-144.
14. K. R. Koch and J. Yates (1983), *Anal. Chim. Acta*, **147**, 235-245.
15. T. Shi, J. Berglund and L. Elding (1997), *J. Chem. Soc., Dalton Trans.*, 2073-2077.
16. A. Irving, K. R. Koch and M. Matoetoe (1993), *Inorg. Chim. Acta*, **206**, 193-199.
17. P. Pregosin (1982), *Coord. Chem. Rev.*, **44**, 247-291.



# EXTRACTION OF SILVER FROM CONCENTRATED CHLORIDE SOLUTIONS: USE OF TRI-*n*-BUTYL- AND TRI-*n*-OCTYLPHOSPHINE SULPHIDES

Rita S. Capela and Ana P. Paiva

Departamento de Química e Bioquímica, C.E.C.U.L.,  
Faculdade de Ciências da Universidade de Lisboa, Lisboa, Portugal

Tri-*n*-butyl- and tri-*n*-octylphosphine sulphides have been synthesised by reaction of the respective phosphines with sulphur, the results collected for their characterisation and purity being in accordance with expected data. Both alkylphosphine sulphides were then evaluated for silver extraction from concentrated chloride media, a stabilised sodium thiosulphate aqueous solution being utilised for the stripping of the metal ion. The selectivity of both extractants towards the precious metal, when 10- to 60-fold molar contents of Cu(II), Fe(III) and Pb(II) are present in the feed aqueous medium, was also investigated. The information obtained from the study of the dependency of silver ion distribution data on acid and chloride contents, as well as on extractant concentration, allows the proposal of the most probable silver extraction pathways. The overall results achieved are systematically compared with those previously obtained for triisobutylphosphine sulphide, commercially available from Cytec under the trade name of Cyanex 471X.

## INTRODUCTION

Chloride hydrometallurgy has been frequently considered for the treatment of complex sulphide ores and concentrates [1], and it is known that the resulting leaching solutions usually may contain traces of silver in their composition.

Precipitation in silver chloride form and cementation [2] are widely used methods to separate the precious metal from complex chloride aqueous phases. However, in addition to those, solvent extraction can be an interesting approach to efficiently and selectively recover silver remaining dissolved in highly concentrated chloride leaches [1], as the anionic chlorocomplexes of the type  $\text{AgCl}_2^-$ ,  $\text{AgCl}_3^{2-}$  and  $\text{AgCl}_4^{3-}$  are known to be responsible for the increasing solubility of silver chloride when high chloride concentrations coexist in the aqueous solution [3].

Several organic extractants have been investigated for silver recovery from concentrated chloride media [4]; amongst the most efficient, a monomeric amide derivative of a calix[4]arene [5], diphenyl- and di-*n*-butylthioureas [6] and triisobutylphosphine sulphide (TIBPS, active ingredient of Cyanex 471X, commercially available from Cytec) [7] deserve a special mention.

In fact, all extractants proved to be very efficient for silver extraction, the thiourea derivatives and TIBPS acting through a sort of “solvation” reaction pathway [4, 6], whereas silver cation suffered extraction by the calix[4]arene compound through an anionic exchange equilibrium [5].

When selectivity of extraction is considered, base metals such as Fe(III), Cu(II) and Pb(II) seriously affect the performance of thiourea derivatives towards Ag(I), as they also are extensively co-extracted [6]. TIBPS is much more selective for silver under similar experimental conditions, with separation factor values of 9, 23 and 111 achieved for Ag(I) / Cu(II), Ag(I) / Fe(III) and Ag(I) / Pb(II), respectively, when the three metal ions co-existed with Ag(I) in 10- to 60-fold molar excesses in the initial aqueous solution [7].

With the exception of triphenylphosphine sulphide (TPPS) [8], no other phosphine sulphide than TIBPS has been tested for silver recovery from chloride solutions. The presence of the aromatic rings in the TPPS structure markedly decreased the extraction affinity of the organic compound for Ag(I) contained in concentrated chloride solutions, which is a quite surprising result [8] if the similarities of TIBPS and TPPS are taken into account. However, this poor extraction behaviour would not be expected if new phosphine sulphides with different aliphatic alkyl groups other than isobutyl were used instead.

In order to check the influence of the nature of the alkyl groups of phosphine sulphides for Ag(I) extraction from concentrated chloride solutions, tri-*n*-butyl- and tri-*n*-octylphosphine sulphides (TBPS and TOPS, respectively) were synthesised and tested for silver recovery. In fact, it seems interesting to evaluate if an isomeric branched or linear alkyl group in the extractants (isobutyl in TIBPS and *n*-butyl in TBPS) differentiates their affinity towards Ag(I), both in terms of efficiency and selectivity. In addition, the size of the alkyl group in the organic molecule may also play an important role in the metal ion extraction, therefore the performance of TOPS was simultaneously investigated.

## EXPERIMENTAL

Tri-*n*-butyl- and tri-*n*-octylphosphine sulphides were synthesised by reaction of the respective phosphines with excess sulphur ( $S_8$ ) under a nitrogen atmosphere, using toluene as solvent [9]. The extent of both reactions was controlled by T.L.C. After completeness, the solvent was evaporated on the rotary evaporator. The yields obtained were quantitative. The purity of both liquids was checked by GC, revealing values of about 95% for TBPS and 90% for TOPS. Characterisation was accomplished by IR, MS and  $^1H$ ,  $^{13}C$  and  $^{31}P$  NMR, the results obtained being in accordance with expected data.

Aqueous solutions for the extraction experiments were prepared using hydrochloric acid and sodium chloride, generally containing 2 M HCl + 3 M NaCl; however, for the study of the chemical reactions involved or the influence of acidity, different proportions of both reagents, or HCl alone, were also used. Ag(I) feed solutions, with concentrations of about  $1.4 \times 10^{-3}$  M, were made by dissolution of the required amount of  $AgNO_3$  (Merck, 99.5% purity) in the base-electrolytes. In addition to Ag(I), solutions containing  $3 \times 10^{-2}$  M Cu(II),  $9 \times 10^{-2}$  M Fe(III) and  $1 \times 10^{-2}$  M Pb(II) were prepared from the respective chloride salts in the 2 M HCl + 3 M NaCl aqueous phase. All chemicals were pro-analysis. For the stripping experiments, a stabilised sodium thiosulphate solution whose composition is referred to by Rickelton and Robertson [10] was employed. Organic phases were obtained by dissolution of TBPS or TOPS in 1,2-dichloroethane (1,2-DCE, Riedel-de-Haen, 99.8%).

Extraction and stripping experiments were carried out by mixing equal volumes of aqueous and organic phases (A/O=1) for 30 minutes, at room temperature and at a constant stirring speed of 1000 rpm, which was enough to guarantee a good emulsion. A similar procedure was also adopted for the evaluation of the selectivity of both extractants towards Ag(I). For the investigation of the extraction reactions and influence of acidity, a double-wall cell with circulation of water from a thermostat, in order to control the temperature (25°C), was used instead.

Analysis of the metal contents in the aqueous phases, before and after extraction, was carried out by Flame Atomic Absorption Spectrophotometry using a Unicam 929 model. For each sample, three aliquots were analysed and the values obtained were critically treated and only accepted if a reasonable relative standard deviation was obtained. Metal ion concentrations in organic phases were calculated by mass balance. For the majority of the cases, at least two sets of experiments were accomplished in order to confirm all data obtained.

## RESULTS AND DISCUSSION

### Extraction and Stripping

In order to check whether TBPS and TOPS are suitable extractants for silver ion from concentrated chloride base-electrolytes, 0.1 M solutions of both organic compounds in 1,2-DCE were used to extract  $1.4 \times 10^{-3}$  M of Ag(I) contained in a 2 M HCl + 3 M NaCl aqueous phase. The results obtained are presented in Table 1, the values displayed being the average of at least four experiments for each ligand.

*Table 1. Percentages of Ag(I) extraction by TBPS and TOPS.*

Extractant	% of Ag(I) extraction
TBPS	85 ± 3
TOPS	76 ± 4

Both TBPS and TOPS are good extractants for Ag(I) recovery from typical concentrated chloride aqueous phases, TBPS being the most efficient of the two. For an identical set of experimental conditions, TIBPS exhibits Ag(I) extraction values of about 77% [7], therefore TBPS seems to be slightly more efficient than TIBPS. This latter ligand is comparable to TOPS as far as its extraction performance towards the precious metal is concerned.

Stripping of the Ag(I) loaded organic solutions was accomplished by use of a stabilised 1 M sodium thiosulphate solution [10]. The performance of this aqueous phase for recovery of the Ag(I) contained in the loaded TBPS or TOPS solvents is presented in Table 2.

*Table 2. Percentages of Ag(I) stripping from TBPS and TOPS.*

Extractant	% of Ag(I) stripping
TBPS	76
TOPS	96

Table 2 shows that the stabilised sodium thiosulphate aqueous solution is an efficient Ag(I) stripping agent. Ag(I) from TOPS is easier to strip than from TBPS, this order being the inverse of the one found for extraction. For similar experimental conditions, stripping of Ag(I) from TIBPS is more difficult to achieve, as values of only 57% were reported [7].

Concerning total Ag(I) recovery, the use of TBPS allowed a 65% silver recovery, whereas TOPS achieved an overall performance of about 73%. Both extractants compare well with the solvent extraction behaviour of TIBPS for Ag(I) recovery from concentrated chloride phases [7]. In addition, it can be concluded that changing the *n*-butyl groups in TBPS to their branched isomers in TIBPS decreases the extraction efficiency towards Ag(I), as well as the stripping of the precious metal from the organic solvent. TOPS can also be considered a promising extractant.

### Selectivity of Ag(I) Extraction

The behaviour of TBPS and TOPS towards Ag(I) when the precious metal co-exists with larger concentrations of base metals such as Cu(II), Fe(III) and Pb(II) is quite interesting to evaluate, as it is a situation which can occur if a chloride leaching of a complex sulphide ore or concentrate is considered. Therefore, a synthetic feed solution containing  $1.4 \times 10^{-3}$  M Ag(I), in addition to  $3 \times 10^{-2}$  M Cu(II),  $9 \times 10^{-2}$  M Fe(III) and  $1 \times 10^{-2}$  M Pb(II) in a 2 M HCl + 3 M NaCl base-electrolyte, was put in contact with either a 0.1 M 1,2-DCE solution of TBPS or TOPS, following the general experimental conditions reported earlier. Data related to TIBPS are also included [7]. The results obtained are listed in Table 3.

Table 3. Selectivity of TBPS, TOPS and TIBPS for Ag(I) extraction.

Extractant	Separation Factor Ag(I) / Cu(II)	Separation Factor Ag(I) / Fe(III)	Separation Factor Ag(I) / Pb(II)
TBPS	4	5	20
TOPS	5	8	99
TIBPS [7]	9	23	111

A general insight through the contents of Table 3 reveals that TBPS and TOPS exhibit a quite good selectivity for Ag(I). In fact, it must not be forgotten that all the basic metals are much more abundant in the feed aqueous solution than the precious metal itself. TOPS shows a better selectivity for Ag(I) than TBPS.

This feature can be considered an interesting result if data related to TBPS are compared with those of TIBPS. It can be concluded that changing the isobutyl groups in TIBPS to their linear isomers in TBPS affects negatively the selectivity of TBPS for Ag(I), which is precisely the inverse situation found for the extraction / stripping of Ag(I) in the absence of other metal ions.

The stabilised sodium thiosulphate solution was also applied on the metal ion stripping of the loaded organic phases resulting from the selectivity experiments. It has been found that the stripping agent is not selective for Ag(I), as Cu(II) and Fe(III) were also extensively stripped. In addition to the poor extraction performance exhibited by both ligands towards Pb(II), the stripping of this metal ion by the thiosulphate aqueous solution has not been successful.

### Extraction Pathways involving TBPS and TOPS

In order to establish the probable Ag(I) extraction pathways by TBPS and TOPS, several series of extraction experiments were carried out in order to evaluate the dependence of Ag(I) distribution coefficient on extractant and chloride concentrations. The extraction of  $1.4 \times 10^{-3}$  M of Ag(I) contained in a 2 M HCl + 3 M NaCl medium was accomplished using different concentrations of TBPS and TOPS, whereas a 0.06 M solution of TBPS or TOPS was used to extract  $1.4 \times 10^{-3}$  M of Ag(I) from solutions with different chloride concentrations, although containing a fixed 2 M HCl portion. The temperature of extraction was controlled at 25°C. The overall results obtained are plotted in Figures 1 and 2.

The experimental extractant / Ag(I) ratio, given by the slope of the straight lines which best fit the distribution data, have the values of 1.8 for TBPS ( $R^2 = 0.990$ ) and 2.3 for TOPS ( $R^2 = 0.991$ ). Regarding the chloride / Ag(I) ratio, using a similar approach, the analysis of the slopes give -4.0 for TBPS ( $R^2 = 0.995$ ) and -4.1 for TOPS ( $R^2 = 0.998$ ). Therefore, a preliminary conclusion is that both extractants follow identical Ag(I) extraction pathways, as the data collected are similar.

The influence of the aqueous medium acidity on the overall extraction process was also investigated for both extractants. Sets of extraction experiments involving 0.1 M concentrations of TBPS or TOPS in 1,2-DCE were carried out, using aqueous solutions with  $1.4 \times 10^{-3}$  M of Ag(I) contained in a 5 M total chloride concentration, for which the HCl content varied between 1 and

5 M. Therefore, whenever necessary, addition of NaCl was made. The results obtained put in evidence that increasing concentrations of HCl slightly enhance Ag(I) extraction, e.g., from 1 M to 5 M HCl, extraction of Ag(I) by TBPS passed from 75% to 82%, whereas for TOPS it increased from 66% to 82%.

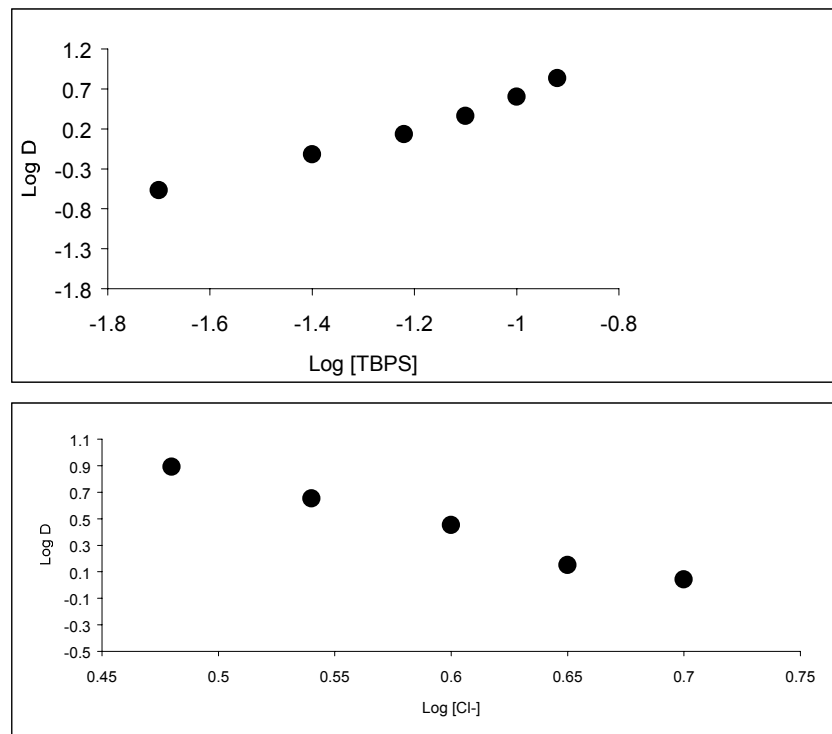


Figure 1. Dependence of Ag(I) distribution coefficient on TBPS and chloride concentration.

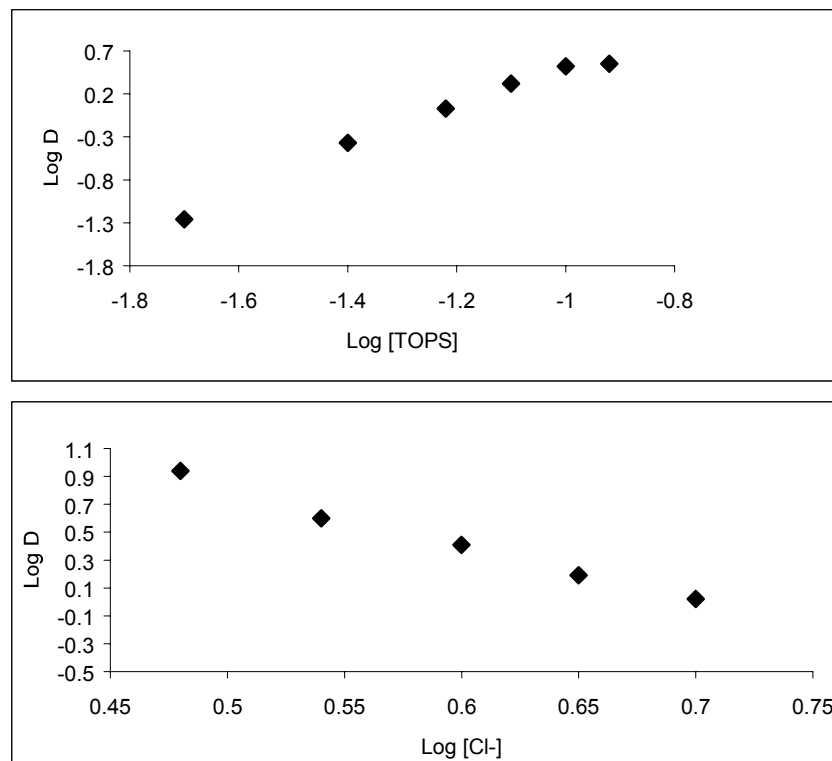
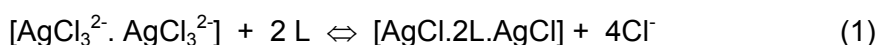


Figure 2. Dependence of Ag(I) distribution coefficient on TOPS and chloride concentration.

A possible interpretation of these acidity data is that a direct chemical exchange of H<sup>+</sup> on the extraction reaction is not likely to occur, however H<sup>+</sup> or Na<sup>+</sup> must appear as counter cations of the Ag(I) anionic chlorocomplexes. It is reasonable to suppose that, in the absence of Na<sup>+</sup>, the viscosity and density of the aqueous solutions should decrease, and the mentioned effect of those parameters certainly facilitates the physical phenomena associated with the extraction process, therefore enhancing the Ag(I) extraction efficiency.

Based on the experimental extractant / Ag(I) ratio, two molecules of TBPS or TOPS must be involved with each Ag(I) species. However, the values of -4 collected for the slopes of the chloride / Ag(I) ratios are more difficult to explain. According to literature, for chloride solutions between 1 and 5 M NaCl, the predominant Ag(I) chlorocomplex is always AgCl<sub>3</sub><sup>2-</sup> [3]. A possible explanation is that TBPS or TOPS may have the particularity to act over a sort of AgCl<sub>3</sub><sup>2-</sup> dimer, namely AgCl<sub>3</sub><sup>2-</sup>.AgCl<sub>3</sub><sup>2-</sup>, giving rise to something such as AgCl.2L.AgCl (L = TBPS or TOPS) in the organic phase and releasing 4 Cl<sup>-</sup> for each Ag(I) species, Equation (1).



This interpretation is based on the assumption that D, for these systems, may be defined as presented in Equation (2).

$$D = [\text{AgCl} \cdot 2\text{L} \cdot \text{AgCl}] / [\text{AgCl}_3^{2-} \cdot \text{AgCl}_3^{2-}]_{\text{eq}} \quad (2)$$

The influence of chloride ion on Ag(I) extraction by TBPS and TOPS seems to be different from that suffered by TIBPS under similar experimental conditions, as the slope of log D vs. log [Cl<sup>-</sup>] for Ag(I) extraction by this latter extractant was found to be -2.4 [7].

However, Abe and Flett also studied Ag(I) extraction from chloride media by TIBPS [11], stating the formation of L<sub>2</sub>AgCl species, although mentioning a slope of -3.6 for the log D vs. log [Cl<sup>-</sup>]. This latter result was attributed to the presence of inextractable anionic Ag(I) complexes in the aqueous phase [11]. Hence, the interpretation of this particular feature deserves further research.

## REFERENCES

1. N. M. Rice, R. W. Gibson (1996), *Proc. ISEC 1996*, University of Melbourne Press, Melbourne, pp. 715-720.
2. M. Cox (1992), Principles and Practices of Solvent Extraction, J. Rydberg, C. Musikas and G. R. Choppin (eds.), Marcel Dekker, New York, pp. 381-393.
3. J. J. Fritz (1985), *J. Soln. Chem.*, **14** (12), 865-879.
4. A. P. Paiva (2000), *Solv. Ext. Ion Exch.*, **18** (2), 223-271.
5. K. Ohto, H. Yamaga, E. Murakami and K. Inoue (1997), *Talanta*, **44** (6), 1123-1130.
6. A. P. Paiva (1999), *Proc. ISEC 1999*, Society of Chemical Industry, London, pp. 399 - 404.
7. A. P. Paiva and L. M. Abrantes (1994), *Proc. EPD Congress 1994*, The Minerals, Metals and Materials Society, Warrendale, PA, pp. 243-255.
8. L. M. Abrantes, A. P. Paiva and G. Cote (1996), *Proc. ISEC 1996*, University of Melbourne Press, Melbourne, pp. 129-134.
9. P. D. Bartlett and G. Meguerian (1956), *J. Am. Chem. Soc.*, **78**, 3710-3715.
10. W. A. Rickelton and A. J. Robertson (1987), *Min. Metall. Processing*, **Feb**, 7-10.
11. Y. Abe and D. S. Flett (1990), *Proc. ISEC 1990, Part B*, Japan, pp. 1127-1132.



## EXTRACTION OF BASE METALS WITH BINARY EXTRACTANTS

V.V. Belova, A.A. Voshkin, A.I. Kholkin, I.Yu. Fleitlikh\* and G.L. Pashkov\*

Kurnakov Institute of General and Inorganic Chemistry of RAS, Moscow, Russia

\*Institute of Chemistry and Chemical Technology of SB RAS, Krasnoyarsk, Russia

Study on the extraction of Fe, Cu, Ni and Co from chloride and sulphate solutions with different binary extractants varying aqueous acidity has been carried out. In binary extractant systems iron(III) is extracted from chloride solutions with high distribution coefficients for a wide range of aqueous acidities. Compositions of extracted species are different depending on acidity. Usually both iron and copper are poorly extracted from sulphate solutions with anion-exchange and neutral extractants. Nevertheless, Fe(III) as well Cu(II) are effectively extracted from cobalt and nickel sulphate electrolytes with binary extractants due to the high concentration of the sulphate in the aqueous phase. Using the mixtures of binary extractants and aldoximes the separation of Ni and Co can be achieved. The highest separation coefficients are however realized in the extraction from nitrate solutions.

### INTRODUCTION

Establishment of basic principles of binary extraction of acids and metal salts and advantages of binary extraction in comparison with extraction using initial ion-exchange and neutral extractants has lead to further developments of the extraction method. To date a series of fundamental and applied research initiatives into mineral acid and metal salt extraction with binary extractants have been performed [1-5]. However, there are a great number of extraction systems, which are in need of a study to solve some problems in extraction and separation of the substances. In this work the the solvent extraction behaviour of Fe(III) and non-ferrous metals with binary extractants in chloride and sulphate solutions is examined in order to indicate conditions for the recovery and separation of these metals.

### EXPERIMENTAL

#### Extraction of Fe(III) from Chloride and Sulphate Solutions

For the extraction of iron with binary extractants of different compositions, chloride and sulphate solutions with a wide range of aqueous acidities were used. Salts of trioctylmethylammonium, such as 4-tert-butylphenolate, caprylate and di(2-ethylhexyl)-phosphate, were employed as extractants. The binary extractants ( $R_4NA$ ) were prepared by mixing equimolar amounts of  $R_4NCl$  and organic acid (HA) in toluene and with subsequent washing of organic solutions with 1 M NaOH or water.

### Extraction of Fe(III) and Cu(II) from Sulphate Electrolytes

For refining sulphate nickel and cobalt electrolytes binary extractants of different composition based on quaternary ammonium bases (QAB) were examined. Ni and Co electrolytes were prepared as saturated solutions of sulphates of these metals with concentrations of Ni ~120 g/l and Co ~118 g/l. Sulphates of copper or iron were added into the electrolytes prepared adjusting  $C_{Fe(Cu)} = 1$  g/l. Solutions of salts of trioctylmethylammonium with different organic acids (di(2-ethylhexyl)phosphoric, caprylic, 2-ethylheptylcarboxylic acids) were used as extractants.

### Extraction of Ni and Co from Sulphate and Nitrate Solutions

Aldoximes of simple structure have been shown to extract nickel selectivity from cobalt in aqueous solutions [10-12]. However, owing to the thermodynamic stability of the extracted species in aldoxime systems, stripping of Ni is difficult. To study improved stripping extraction of Ni and Co from sulphate and nitrate solutions by mixtures of binary extractants and heptanealdehyde (Ox) of linear structure were examined. Salts of trialkylbenzylammonium, trialkylmethylammonium and tetraoctylammonium with anions of organic acids (caprylic,  $\alpha,\alpha$ -monocarboxylic) were used as binary extractants.

## RESULTS AND DISCUSSION

### Extraction of Fe(III) from Chloride and Sulphate Solutions

In previous studies of the extraction of Fe(III) from chloride solutions with binary extractants we found that the complex acid, HFeCl<sub>4</sub>, is extracted from acidic solutions [2]. The extraction power of binary extractants based on tetraalkylammonium and trialkylammonium decreases in the series: 2,6-tert-butylphenolate > 2-kumylphenolate > 4-tert-butylphenolate >  $\alpha$ -monocarboxylate > *n*-caprylate. The use of binary extractants instead of alkylammonium chloride leads to decreasing distribution coefficients of iron,  $D_{Fe}$ . As a result, the concentration of iron in raffinates increases in the stripping by water in comparison with the R<sub>4</sub>NCl system according to principles of binary extraction.

Using 4-tert-butylphenol and caprylic acid, the C<sub>R4NCl</sub>: C<sub>HA</sub> ratios were 1:3 and 1:2 respectively. The experimental data (Figure 1, curves 1-3) show that iron(III) is extracted by the binary extractants from chloride solutions for a wide range of aqueous acidities. Dependencies of distribution coefficients exhibit a minimum, obviously, due to different extraction mechanisms.

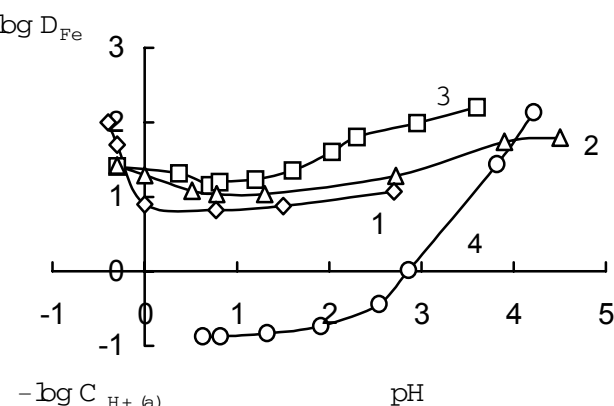


Figure 1. Extraction of Fe(III) from chloride (1-3) and sulphate (4) solutions by 0.01 M solutions of alkylphenolate (1), caprylate (2, 4) and dialkylphosphate (3) of trioctylmethylammonium in toluene depending on aqueous acidity.

$$C_{Cl(a)} = 2.5 \text{ M} \quad (1-3); \quad C_{SO_4(a)} = 2.5 \text{ M} \quad (4).$$

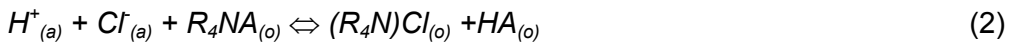
The extraction of iron from sulphate solutions occurs to an appreciable extent only from weak acidic media (Figure 1, curve 4). The enhancement of distribution coefficients of iron with increasing pH of the aqueous phase more than 2 is observed for all dependencies.

As indicated previously [7], iron from chloride acidic solutions is mainly extracted by anion-exchange extractants as ion associates involving the  $\text{FeCl}_4^-$  anion. The absorption spectra of the organic phases after iron extraction by binary extractants from acidic chloride solutions exhibit absorption bands at  $\lambda_{\text{max}}$  equal to 318 and 365 nm in the visible range, characterized for the spectrum of  $\text{FeCl}_4^-$  complex anion [7]. This indicates that iron is recovered from chloride solutions in the region of 2 M HCl to pH values  $\sim 2$  in the form of  $\text{FeCl}_4^-$  complex anion. Studying the distribution of chloride between toluene solutions of alkylphenolate, caprylate, dialkylphosphate of QAB and acidic chloride solutions the binary extractants were found to transfer to the chloride form in a range of 1-3 M HCl [4]. The distribution of iron under these conditions proceeds through anion-exchange mechanism:

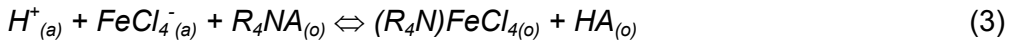


Subscripts (a) and (o) denote species in the aqueous and organic phases respectively.

With a decrease in aqueous acidity, an equilibrium:



is shifted to the formation of the binary extractant for the systems involving dialkylphosphate and caprylate of QAB, and distribution of iron can occur through binary mechanism:



It seems reasonable that the decrease in distribution coefficients of iron in the range 2 M HCl to pH  $\sim 1$  is accounted for by decreasing portion of the extracted species  $\text{FeCl}_4^-$ . In QAB caprylate system a formation of iron caprylate in the organic phase is also possible. It is known that in the Fe(III) extraction by caprylic acid a three-nuclear complex,  $\text{Fe}_3\text{A}_9$ , is recovered into the organic phase [8]. Thus, when both anionic and cationic forms are distributed into the organic phase, extraction of iron by caprylate of trioctylmethylammonium can be described as a summary equation:

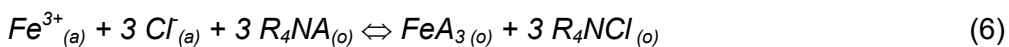


The observed increase of  $D_{\text{Fe}}$  values at pH  $> 3$  (Figure 1) is obviously related to this phenomenon.

Trioctylmethylammonium dialkylphosphate involves a strong organic acid ( $\text{pK}_a \sim 2$ ), and extraction of iron as a dialkylphosphate should occur at lower pH values. The spectra of extracts were observed to indeed change at pH  $\sim 0.8$ . The absorption maxima at 318 and 365 nm gradually disappeared, and a new band with  $\lambda_{\text{max}} = 285$  nm appeared. The extraction of iron also improves with increasing pH  $> 1$  (Figure 1, curve 3). According to published data on Fe extraction by di(2-ethylhexyl)phosphoric acid as the complex  $\text{FeA}_3$  [9] and data on the state of binary extractant [4], iron distribution by trioctylmethylammonium dialkylphosphate in an intermediate range can be represented as a summary equation:



and in a range of pH  $> 3$  as follows:



The extraction of iron from sulphate solutions is more pronounced at lower acidity in QAB caprylate system (Figure 1, curve 4) due to the high energy of hydration of sulphate. With increasing pH, the Fe extraction improves due to forming caprylate of iron,  $\text{Fe}_3\text{A}_9$ , in the organic phase.

### Extraction of Fe(III) and Cu(II) from Sulphate Electrolytes

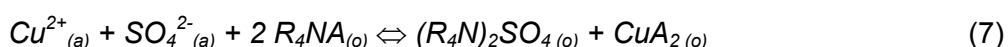
A choice of binary extractants for extraction and (or) separation of Fe(III) and Cu(II) is defined by objects and solvable problems. For selective recovery of copper from Fe-containing solutions, for example, solutions after leaching of oxidized ores dialkyldithiophosphate of tetraalkylammonium can be employed as an extractant [2]. This system is characterized by high separation coefficients,  $\beta_{\text{Cu}/\text{Fe}}$ , up to  $1 \cdot 10^4$ , a high extractant capacity and fast extraction and stripping kinetics. Copper can be stripped using ammonia solutions.

*Table 1. Extraction and stripping of Cu and Fe in systems Ni electrolyte – QAB salts.  
Stripping solution – 0.05 M  $\text{H}_2\text{SO}_4$*

Extractant	$C_{\text{ex}}, M$	$D_M$		Stripping efficiency, %	
		Cu	Fe	Cu	Fe
Caprylate	0.53	3.94	-	71.1	-
	0.45	1.63	74	90.7	1.0
	0.25	-	33	-	36.4
	0.15	0.002	1.64	-	75.5
Alkylcarboxylate	0.53	5.23	-	82.8	-
	0.45	1.38	60	95.0	12.3
	0.38	0.212	48	97.3	27.5
	0.25	-	16	-	41.2
Alkylphosphate	0.45	0.009	74	94.4	5.4
	0.25	-	5.90	-	28.2
	0.15	0.001	1.22	-	53.9

$C_{\text{ex}}$  - concentration of extractant

The data shows that the most effective extraction of copper occurs from Ni sulphate solutions by carboxylate and caprylate of QAB (Table 1). Iron can be recovered by different QAB salts from Ni sulphate solutions. In contrast to the copper extraction, the highest distribution coefficients for iron are observed in QAB alkylphosphate system. Extraction of sulphates of Cu and Fe by salts of QAB with organic acids can be described in general form as follows (using copper example):



Extraction of Cu and Fe proceeds due to the high concentration of the sulphate in the aqueous phase. Copper and iron can be stripped by water or weak acidic solutions owing to a decrease in sulphate concentration in the aqueous phase. Indeed, Cu and Fe are effectively stripped from the organic phase by a 0.05 M solution of  $\text{H}_2\text{SO}_4$  in systems involving alkylcarboxylate and caprylate of QAB using one step of stripping. At the same time, the values of  $D_{\text{Cu}}$  and  $D_{\text{Fe}}$  remain high in the extraction by these extractants (Table 1). Extraction of Cu and Fe from Co sulphate solutions was found to be effective also in systems involving QAB salts. Then these metals can be stripped from the organic phase with a 0.05M solution of  $\text{H}_2\text{SO}_4$  (Table 2).

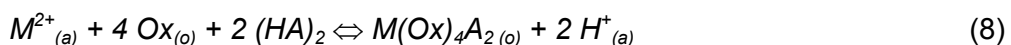
*Table 2. Extraction and stripping of Cu and Fe in Co electrolyte – QAB salts systems.  
Stripping solution – 0.05 M H<sub>2</sub>SO<sub>4</sub>*

Extractant	C <sub>ex</sub> , M	D <sub>M</sub>		Stripping efficiency, %	
		Cu	Fe	Cu	Fe
Caprylate	0.60	2.29	46	77.1	10.5
	0.50	-	8.5	-	25.8
	0.45	0.32	2.28	96.0	48.4
Alkylcarboxylate	0.60	2.13	17	92.8	17.6
	0.50	-	4.73	-	32.0
	0.45	0.134	1.55	97.6	52.0

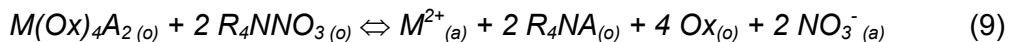
### Extraction of Ni and Co from Sulphate and Nitrate Solutions

Systems involving mixtures of binary and neutral extractants are of a special interest. When a neutral extractant forms more stable complexes with coordination to the atom of one of the metals, an increase of separation coefficients would be expected. In the extraction of Ni and Co with mixtures of binary extractants and heptanealdoxime it was shown that extraction characteristics obtained for simpler binary extractant systems remained the same for these systems. In particular, the extraction of metals doesn't depend on pH values, and the extraction of salts decreases in the series: Ni(NO<sub>3</sub>)<sub>2</sub> > NiCl<sub>2</sub> > NiSO<sub>4</sub>. With increasing concentration of an anion of mineral salt in the aqueous phase, distribution coefficients of metals enhance. An increase in a concentration of organic acid in the organic phase results in decreasing distribution coefficients due to interactions of monocarboxylic acid with aldoxime and R<sub>4</sub>NA forming compounds such as HA<sup>n</sup>Ox and R<sub>4</sub>NA<sup>m</sup>HA. In some extraction systems Co(II) in the organic phase oxidizes partially by oxygen of air. Conditions preventing cobalt oxidation in the organic phase were found.

Data obtained are given in Table 3 from which it follows that the highest separation coefficients of Ni and Co ( $\beta_{Ni/Co}$ ) are realized in the extraction from nitrate solutions using the mixtures of QAB alkylcarboxylates with aldoxime. Besides, the distribution coefficients of nickel from sulphate solutions are less than 0.2 complicating the use of these extractants in the technological processes. In a range of high pH values metals are extracted by mixtures of binary extractants and Ox through cation-exchange mechanism:



Intermediate complexes such as M(Ox)<sub>4</sub>AB (B<sup>-</sup> - nitrate, for example) can be also formed in the organic phase. Nickel and cobalt can be stripped from the organic phase by water through binary mechanism in consequence of forming a stable salt, R<sub>4</sub>NA:



Thus, the use of mixtures of binary extractants with aldoxime results in increasing distribution coefficients,  $\beta_{Ni/Co}$ , in comparison with binary extractants owing to the primary coordination of molecules of aldoxime to the atom of nickel [12]. On the other hand, metals can be stripped from the organic phase more easily compared to the system involving only aldoxime. To obtain more concentrated raffinate of nickel mixtures of ammonium bicarbonate and ammonia should be used for stripping.

*Table 3. Extraction of Ni and Co from sulphate and nitrate solutions by mixtures of R<sub>4</sub>NA and aldoxime in toluene*

Extractant	Solution	C <sub>M</sub> (init.), g/l		pH <sub>eq.</sub>	D <sub>Ni</sub>	D <sub>Co</sub>	$\beta_{Ni/Co}$
		Ni	Co				
I	sulphate	5	75	5.1	0.075	0.014	5.36
				5.2	0.094	0.027	3.48
	nitrate	5	86	5.0	1.65	0.116	14.2
				5.2	1.75	0.081	21.6
II	sulphate	5	75	5.7	0.211	0.028	7.54
				5.7	0.250	0.035	7.14
	nitrate	5	86	5.3	3.04	0.081	37.5
				5.4	3.45	0.048	71.9

I – 0.5 M trialkylbenzylammonium dialkylphosphate + 1 M Ox

II – 0.5 M trialkylbenzylammonium caprylate + 1 M Ox

#### ACKNOWLEDGEMENTS

Financial support of Russian Foundation for Basic Research (grant N 00-03-32036) is gratefully acknowledged.

#### REFERENCES

1. A. I. Kholkin and V. I. Kuzmin (1982), *Zh. Neorg. Khim.*, **27**, 2070-2074.
2. A. I. Kholkin, G. L. Pashkov, I. Yu. Fleitlikh, V. V. Belova, K. S. Luboshnikova, V. V. Sergeev, A. M. Kopanov and G. K. Kulmuhamedov (1994), *Hydrometallurgy*, **36**, 109-125.
3. A. I. Kholkin, V. V. Belova, G. L. Pashkov, I. Yu. Fleitlikh and V. V. Sergeev (1999), *J. Molec. Liquids*, **82**, 131-146.
4. V. V. Belova and A. I. Kholkin (1998), *Solv. Extr. Ion Exch.*, **16**, 1233-1255.
5. A. I. Kholkin, G. L. Pashkov and V. V. Belova (2000), *Min. Pro. Extr. Met. Rev.*, **21**, 217-248.
6. I. Yu. Fleitlikh, A. I. Kholkin, G. L. Pashkov, K. S. Luboshnikova, V. V. Sergeev, G. K. Kulmuhamedov and T. V. Galantseva (1995), *Tsvetnii Metallii*, 22-26.
7. Yu. A. Zolotov, I. V. Seryakova, I. I. Antipova-Karataeva, Yu. I. Kutsenko and A. V. Karyakin (1962), *Zh. Neorg. Khim.*, **7**, 1197-1204.
8. A. I. Kholkin, L. M. Gindin, K. S. Luboshnikova, P. Muhl and K. Gloe (1976), *J. Radioanal. Chem.*, **30**, 383-395.
9. E. S. Berketov and A. A. Zaytsev (1975), *Radiokhim.*, **17**, 371-372.
10. J. S. Preston (1983), *Hydrometallurgy*, **25**, 107-124.
11. G. L. Pashkov, N. P. Bezrukova, V. N. Volk, I. Yu. Fleitlikh, N. I. Pavlenko, G. E. Selutin and E. D. Korniets (1991), *Solv. Extr. Ion Exch.*, **9**, 549-567.
12. I. Yu. Fleitlikh, A. I. Kholkin, V. V. Sergeev, K. S. Luboshnikova, G. L. Pashkov, I. V. Makarov and L. V. Zelentsova (1997), *Tsvetnii Metallii*, **3**, 31-35.



# DIAZOPYRAZOLONES AS SOLVENT EXTRACTANTS FOR COPPER FROM AMMONIA LEACH SOLUTIONS

**John Campbell\*, Domenico C. Cupertino\*, Lucy C. Emeleus, Steven G. Harris, Susan Owens\*, Simon Parsons, Ronald M. Swart\*, Peter A. Tasker, Owen S. Tinkler\*\* and David J. White**

Department of Chemistry, The University of Edinburgh, Edinburgh, UK

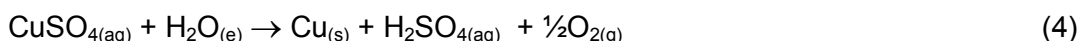
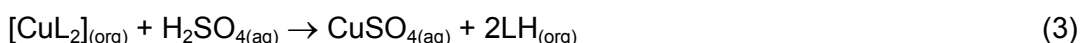
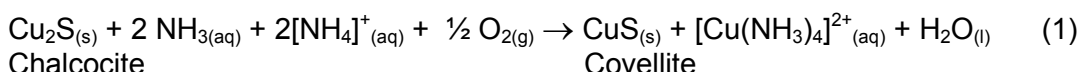
\*AVECIA, Manchester, UK

**\*\*AVECIA, Phoenix, AZ, USA**

4-Diazopyrazol-5-one ligands carrying a range of substituents can be readily prepared by coupling aryl diazonium salts on to the appropriate pyrazolones. Hydrocarbon-soluble versions have been shown to be selective and robust extractants for copper from ammoniacal sulfidic ore leach solutions. Cobalt(III), copper(II), nickel(II) and zinc(II) complexes with 4-(4-*tert*-butylphenyldiazo)-3-methyl-1-phenyl-5-pyrazolone (LH) have been characterised by X-ray crystallography. Solvent extraction studies with analogous compounds have shown that pH<sub>1/2</sub> values for copper(II) vary depending on the substitution on the pyrazolone ring. Using two stages of extraction and two stages of stripping, the N-*tert*-butyl analogue gave stage efficiencies of 90% in extract and 95% in strip. Using an advance electrolyte of 45g/l copper(II), recovery of greater than 93% was achieved. Whilst diazopyrazolone extractants are strong enough for use with ammoniacal feeds and show good loading and stripping characteristics, the compounds are highly coloured and this may limit their use as commercial extractants.

## INTRODUCTION

Over 2.3 million tonnes of copper, equivalent to one fifth of total world production, are currently recovered each year by hydrometallurgical processes involving solvent extraction from acidic sulfate leach solutions. The economic and environmental benefits of such processes make them attractive alternatives to smelting. A considerable amount of research and development [1,2] has been directed at recovery of copper from chloride and ammoniacal leach solutions as these will extend the range of ores which can be efficiently processed hydrometallurgically. More recently, a process has been developed based on ammoniacal leaching of chalcocite-based ores under mild conditions [3]. This generates two copper streams - an enriched ore, covellite, which can be treated in a conventional smelter, and a concentrated aqueous solution (ca. 5 M, pH 8.5 - 10) containing ammine complexes (Equation 1).



Solvent extraction with a weakly acidic reagent, as in Equation 2, regenerates the leachant, which is recycled. Stripping the copper from the loaded organic solution with acid (Equation 3), followed by electrowinning the copper (Equation 4), regenerates the extractant without overall consumption of acid. The recycling of reagents between the unit operations leads to a remarkable materials balance with the overall process being represented by Equation 5. Overall, more than 97 % of the total copper present in the ore can be recovered by the combination of hydrometallurgical and smelting processes with less than 3 % being lost to tailings [1].

The pH of the lixiviant and the leach conditions employed are such that very little of the iron present in the ores and, only small quantities of other transition metals, are transferred to the pregnant leach solution (PLS). Typically the PLS has a composition of ca. 280 g l<sup>-1</sup> Cu, 440 ppm Zn, <1 ppm Fe, 1 ppm Mn and <<1 ppm Ni [4]. As a consequence, and in marked contrast to the acid leach process, the solvent extractant used to recover the copper is not required to show very high selectivity for copper over iron or high "strength" because the extraction equilibrium (Equation 2) is effectively buffered by [NH<sub>4</sub>]<sup>+</sup>/NH<sub>3</sub>. A "weak" extractant also has the advantage that stripping the copper with spent electrolyte is facile and a good copper transfer efficiency is obtained in the circuit. A reagent such as, 1-phenyl-3-heptyl-1,3-propane dione (mixed isomer heptyl substituent, Figure 1) provides "strength" and selectivity well suited to ammoniacal recovery processes. However, a potential problem with organic reagents which contain reactive carbonyl groups is their ability to form the corresponding imines in the presence of high levels of NH<sub>3</sub> and at the temperature typically used in the leaching process, 45°C. Apart from the potential loss of the active reagent from the system, these imines may also build up in the organic phase leading to poor stripping and may contribute to poor phase disengagement which will consequently lead to high entrainment of the aqueous phase in the loaded organic. For these reasons other systems are now being considered [5].

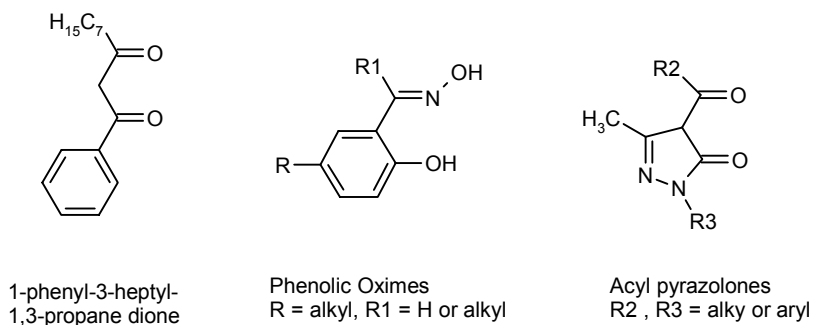


*Figure 1. Structures of commercial metal extractants and acylpyrazolones.*

Acylpyrazolones (Figure 1) also form neutral  $\beta$ -diketonate-type complexes suitable for extraction of a range of metals into organic solvents[ 6-9] and have been considered [10] as alternatives for use in ammoniacal leach circuits. However, the low solubility of their metal complexes limits [10] their usefulness. The structurally related diazopyrazolones (Figure 2) have not been previously investigated as copper extractants, but possess very well defined synthetic chemistry [11] due to their extensive use in the dyestuffs industry [12]. They have been shown [13] to form neutral 2:1 complexes with copper with an N<sub>2</sub>O<sub>2</sub><sup>2-</sup> donor set analogous to that in the very successful phenolic oxime extractants (Figure 1) used to recover copper from acidic leach solutions. In this paper we report the extraction properties of a series of diazopyrazolones with a range of first row transition metals. The crystallography of the complexes has been reported previously [14].

## RESULTS AND DISCUSSION

### Preparation of the Ligands

The free ligands (Figure 2) **1-7** were readily prepared by coupling the appropriate pyrazolone and diazonium salt derived from the required *para*-substituted aniline. All are highly coloured (yellow/orange), and diazopyrazolones have been used extensively for over a century in the dyestuffs industry [12]. Ligands **1-4** with N-phenyl, N-methyl and unsubstituted pyrazolone units are solids which are easily recrystallised and characterised, their solubilities and those of their copper(II) complexes in hydrocarbon solvents were poor. Incorporation of a *t*-butyl group on the pyrazolone and a branched alkyl group in the *para*-position of the phenylazo group gave ligands **5-7**, with much higher solubility in hydrocarbons and could only be isolated as viscous oils.

### Metal Complexes

All the complexes are very highly coloured. The colour changes associated with complex formation can be used to monitor the displacement of metals from the ligand in solvent extraction experiments. Whilst the solubilities of the metal complexes in hydrocarbons were generally low, ligands **5-7** and their copper complexes were judged to be sufficiently soluble to allow solvent extraction experiments to be performed.

Ligand No.	R1	R2	
<b>1</b>	t-Bu	Ph	
<b>2</b>	H	Ph	
<b>3</b>	t-Bu	H	
<b>4</b>	t-Bu	Me	
<b>5</b>	t-Bu	t-Bu	
<b>6</b>	s-Bu	t-Bu	
<b>7</b>	branched-nonyl	t-Bu	

Figure 2. Structures of diazopyrazolones.

### Solvent Extraction

It is convenient to assess the strength of extractants that operate on a “pH-swing” controlled process of the type shown in Equation 2, by determining their pH<sub>½</sub> values (the pH values associated with 50 % theoretical loading of a particular metal). The pH<sub>½</sub> values for 0.1 M toluene solutions of **5-7** obtained with acidic solutions of copper(II) sulfate were ca. 3.7, much higher than those for the “strong” phenolic oxime extractants (Figure 1), which are used commercially for the recovery of copper from acid sulfate leach solutions and have pH<sub>½</sub> values of < 2.0. The diazopyrazolone pH<sub>½</sub> value of ca. 4 is almost ideal for an ammoniacal leach circuit. Good loading is likely with the [NH<sub>4</sub><sup>+</sup>]/NH<sub>3</sub> buffered feed solution, whilst almost quantitative stripping is expected when using spent tankhouse electrolyte (pH 0 - 0.5).

S-curves can also be used to assess the selectivity of metal extraction. A toluene solution of **1** was contacted with aqueous solutions of cobalt(II), nickel(II), copper(II) and zinc(II) sulfates at various pH values (Figure 3). The pH<sub>½</sub> values obtained (Cu; 4.7, Zn; 5.8 and Ni; >7.0) are consistent with selectivities which follow the Irving-Williams order of complex stabilities, but with the nickel(II) complex formation being more disfavoured than normal relative to zinc. Reproducibility of extraction of cobalt was poor and the results were consistent with extraction of cobalt(II) and subsequent oxidation to cobalt(III). Such oxidation is likely to make stripping difficult on both thermodynamic and kinetic grounds. If cobalt is present this will be converted by the leachant to kinetically inert and thermodynamically stable cobalt(III) ammine complexes in the ammoniacal pregnant leach solution.

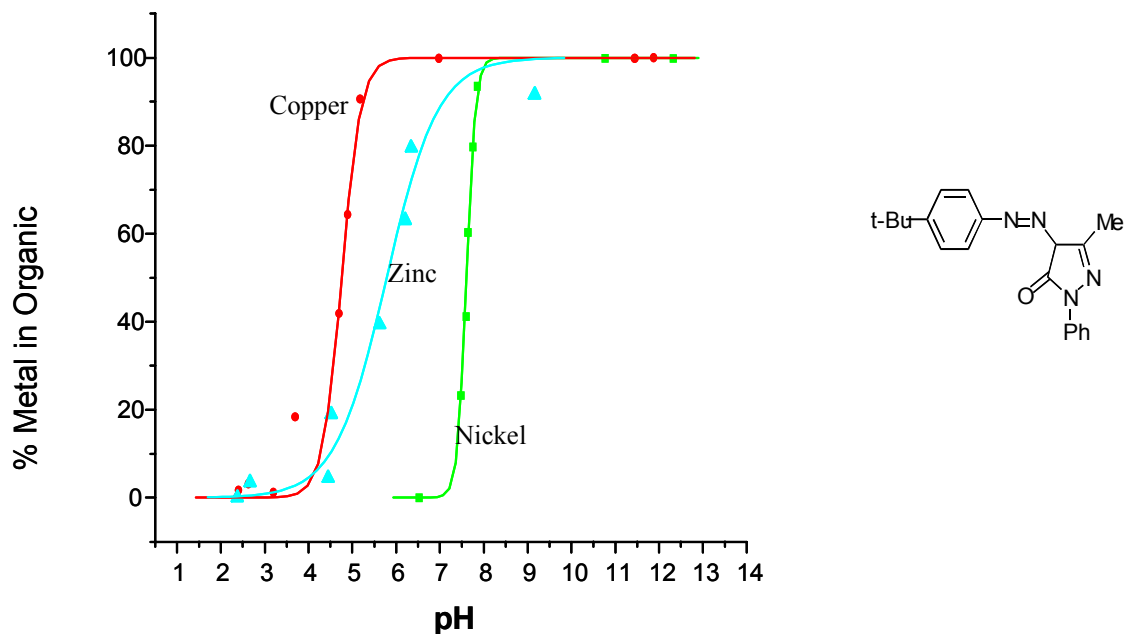


Figure 3. Extraction of copper, zinc and nickel by ligand 1 as a function of pH.

The position of the isotherm confirms that the azopyrazolones are weak extractants for copper when compared with conventional low pH phenolic oxime extractants because of their much higher pH<sub>½</sub> for extraction (ca. 3.7 vs. 0.3).

The extraction isotherms for analogues with R1 as tert-butyl and R2 as tert-butyl, s-butyl or nonyl are all very similar and weak. Figure 4 shows that extraction isotherms where R2 is tert-butyl but R1 varies from tert-butyl through methyl to phenyl become weaker though sharper.

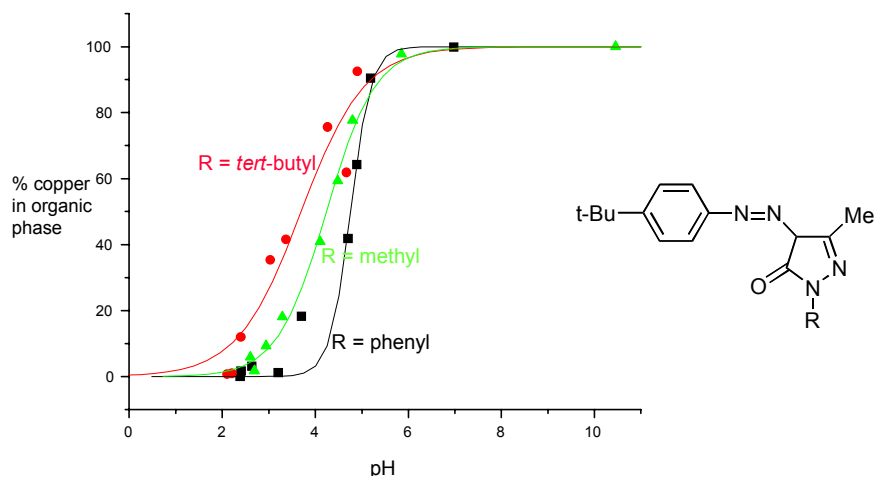
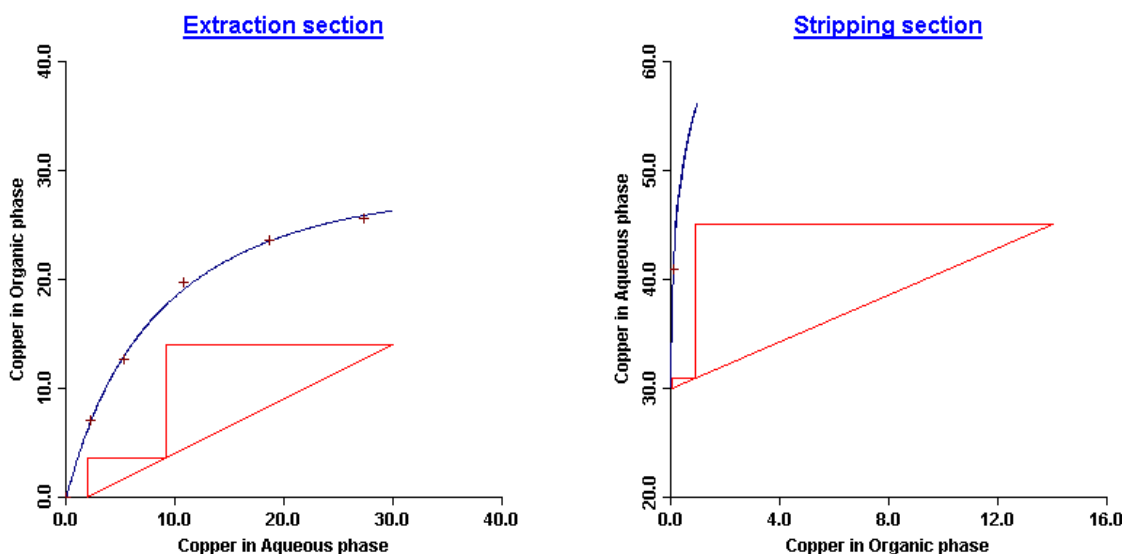


Figure 4. Extraction of copper by ligands 1,4 and 5 as a function of pH.

Figure 5 shows equilibrium isotherms for **7** with McCabe-Thiele constructions for the recovery of copper from a Cu 30 g l<sup>-1</sup>, SO<sub>4</sub><sup>2-</sup> 75 g l<sup>-1</sup>, NH<sub>3</sub> 45 g l<sup>-1</sup> feed and stripping with 30 g l<sup>-1</sup> copper and 180 g l<sup>-1</sup> sulfuric acid. The McCabe-Thiele data were modelled using the programme MINCHEM [15] for a process based on 2 stages of extraction and 2 stages of stripping and assuming 90 and 95 % stage efficiencies in extract and stripping respectively. The computed model indicates that copper recoveries in excess of 93 % may be expected, while producing a regenerated electrolyte containing 45 g l<sup>-1</sup> copper from which the copper metal value may then be recovered in a conventional electrowinning process.



*Figure 5. McCabe-Thiele constructions for the recovery of copper with Ligand 7 1.0 M in kerosene (20 % aromatic/80 % aliphatic content). All scales g l<sup>-1</sup>.*

The stability of the solvent extractant to the basic conditions of an ammoniacal leach process is of paramount importance. A preliminary assessment of the robustness of the diazopyrazolone **5** was performed by contacting separate samples of a 0.056 M solution of **5** in toluene with equal volumes of 34 g l<sup>-1</sup> (19 × excess of copper) and 3.4 g l<sup>-1</sup> (1 × excess of copper) ammoniacal copper feeds at room temperature over a period of 552 h (23 days). Analysis of both the aqueous and organic phases using ICP-AES showed that, within experimental error, the amount of copper extracted did not decrease over this time period demonstrating that the ligand does not undergo chemical degradation and is stable to prolonged contact with ammoniacal feeds. An important feature of the diazopyrazolone ligands which underpins their potential for use in a copper/ammoniacal circuit is that they are significantly weaker complexing agents for copper than the structurally related phenolic oximes. A series of X-ray structure determinations has been reported previously [15] in an attempt to define the origin of this difference.

## CONCLUSIONS

Diazopyrazolone ligands of the types described above are good candidates for extractants to recover copper from ammoniacal pregnant leach solutions. Good copper transfer efficiency can be obtained; they are relatively weak extractants and are very efficiently stripped by acidic spent tankhouse electrolyte. Whilst the buffering effect of the ammoniacal feed solution ensures good loading of copper into the organic phase in the extract stages and they appear to show good resistance to chemical degradation, their intense colour may restrict their use as commercial metal extractants.

## ACKNOWLEDGEMENTS

We thank AVECIA for a postgraduate studentship (LCE) and postdoctoral fellowship (DJW) and AVECIA and the EPSRC for funding for the ICP-AES equipment. Figures 1 and 5 and some associated text are reproduced by permission of the Royal Society of Chemistry.

## REFERENCES

1. W. P. C. Duyvesteyn and B.J. Sabacky (1993), Extractive Metallurgy of Copper, Nickel and Cobalt, Vol. 1: Fundamental Aspects, R.G. Reddy and R.N. Weizenbach (eds.), The Minerals, Metals and Materials Society, Warrendale, PA, pp. 881-910.
2. C. Bouvier, G. Cote, R. Cierpiszewski and J. Szymanowski, (1998) *Solvent Extr. Ion Exch.*, **16** (6), 1465.
3. W.P.C. Duyvesteyn (1993), *U.S. Patent*, No. 5176802.  
K.D. MacKay (1979), *U.S. Patent*, No. 4175012.  
J.M. Sierakoski (1993), *WO Patent*, No. 93/04208.
4. W.P.C. Duvesteyn (1995), Australasian Institute of Mining and Metallurgy Publication Series, Vol. 95, Ch. 13 (3), pp. 29-42.
5. M.J. Virnig, *WO Patent*, 97/29215, 1997.  
M.J. Virnig, *WO Patent*, 97/09453, 1997.
6. Y.A. Zolotov and N.M. Kuzmin (1977), Extraction of Metals with Acylpyrazolones, Nauka, Moscow. *Chem. Abs.* 89 : B81023X.
7. S. Miyazaki, H. Mukai, S. Umetani, S. Kihara and M. Matsui (1989), *Inorg. Chem.*, **28**, 3014.
8. S.A. Pai, K.V. Lohithakshan, P.D. Mithapar, S.K. Aggarwal and H.C. Jain (1996), *Radiochim. Acta*, **73** (2), 83.
9. P. Thakur, K.C. Dash, M.P.L. Reddy, R. Luxmi Varma, T.R. Ramamohan and A.D. Damodaran (1996), *Radiochim. Acta*, **75** (1), 11.
10. W. Mickler and E. Uhlemann (1993), *Sep. Sci. Technol.*, **28**(10), 1913.
11. J. March (1985), Advanced Organic Chemistry, 3rd edn., Wiley, New York, pp. 804-805.
12. W.M. Tuddenham and P.A. Dougall (1978), Kirk-Othmer Encyclopædia of Chemical Technology, 3rd edn., Vol. 6, M. Grayson and D. Eckroth (eds.), Wiley, New York, pp. 819-868.
13. F.A. Snavely, B.D. Krecker and C.G. Clark (1959), *J. Am. Chem. Soc.*, **81**, 2337.
14. L.C. Emeleus, D.C. Cupertino, S.G. Harris, S. Owens, S. Parsons, R.M. Swart, P.A. Tasker and D.J. White (2001), *J. Chem. Soc., Dalton Trans.*, 1239-1245.
15. J. Morrison and B. Townson (1989), *Proc. Extraction Metallurgy*, The Institute of Mining and Metallurgy, London, pp. 397-407.



## SYNERGISTIC SOLVENT EXTRACTION OF Co(II), Ni(II), Cu(II) AND Zn(II) BASED ON SUPRAMOLECULAR ASSEMBLIES

V. Gasperov, K. Gloe\*, A. J. Leong\*\*, L. F. Lindoy, M. S. Mahinay\*\*, H. Stephan\*, P. A. Tasker\*\*\* and K. Wichmann\*

Centre for Heavy Metal Research, School of Chemistry, University of Sydney, Australia

\*Institute of Inorganic Chemistry, TU Dresden, Dresden, Germany

\*\*James Cook University, Townsville, Australia

\*\*\*Department of Chemistry, University of Edinburgh, Edinburgh, UK

The aim of the studies now reported was to investigate synergistic extraction of Co(II), Ni(II), Cu(II) and Zn(II) with a mixed ligand system consisting of a macrocyclic amine and an organic acid. A key design feature of such mixed extractant systems is their ability to form supramolecular assemblies which are preorganized for metal complexation and which are able to reversibly transfer metal cations from an aqueous feed solution. Experiments were performed to elucidate the inter-dependence of the extraction behaviour on the metal ion type, the nature of the diluent as well as the concentration ratio of both extractants, and the pH of the aqueous solution. Furthermore, an NMR titration study of assembly formation in solution and an X-ray structure of a relevant crystallized ligand adduct have been obtained in order to aid understanding of the observed solvent extraction results.

### INTRODUCTION

There is a current need in solvent extraction processes for a rational approach towards the development of selective reagents for toxic and/or valuable metal-ion mixtures even if they are only present at low concentrations. Synergistic effects can contribute to both enhanced selectivity as well as to more efficient metal extraction behaviour [1-3]. The use of supramolecular ligand systems as extractants may help control separation processes [4-6] and also aid the discovery of novel synergistic principles [7]. A key system type showing high synergistic behaviour towards metal extraction involves the combination of a crown ether and a cation-exchanging extractant of, for example, a chelating or organic acid type. In such cases the generally accepted explanation for observed synergism is related to complex formation of the metal ion with both components giving rise to a saturated coordination sphere of the metal ion that in turn yields increased lipophilicity of the extracted complex [7].

The supramolecular self-assembly process offers a new approach to the design of synergistic systems. Based on weak hydrogen bonding, two or more potential ligand molecules can form an organized assembly that, taken together, may be considered to approximate an assembled coordination sphere of the metal ion. Such ligand assemblies have been investigated between cyclam and 4-*tert*-butylbenzoic acid [8], 2-benzylphenol and 2-benzylphenolate [9] as well as between guanosine and isoguanosine nucleosides [10, 11]. Recently we have discussed some general aspects of tailoring molecular assemblies for metal ion binding using host-guest systems formed between carboxylic acids and macrocyclic amine-containing ligands [12]. Overall, the aims of the presented study were two-fold: (i) to investigate the formation of selected molecular assemblies incorporating *tert*-butylbenzoic acid **HR** and the azamacrocyclic **L** (Figure 1) and (ii) to use these molecular assemblies in selected solvent extraction experiments.

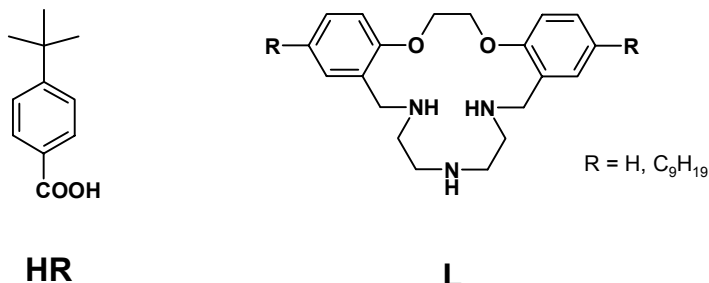


*Figure 1.* Compounds investigated.

## EXPERIMENTAL

Where available, all chemicals were A.R. grade. Macrocycle **L** ( $R = H$ ) was prepared as described elsewhere [13]; an analogous procedure starting from 4-nonylsalicylaldehyde [14] was employed for **L** ( $R = C_9H_{19}$ ). Slow crystallization of an acetonitrile solution containing **L** ( $R = H$ ) and **HR** in a ratio of 1:2 yielded crystals of the corresponding 2:1 adduct which were suitable for X-ray structure determination [15]. The nmr titration experiments were performed on a AM 300 Bruker spectrometer at 25 °C. Weighted amounts (3-5 mg) of **HR** were added incrementally to a solution (0.075 M) of **L** ( $R = C_9H_{19}$ ) in  $CDCl_3$  contained in the nmr tube while the corresponding induced  $^{13}C$  and  $^1H$  chemical shifts were monitored.

Extraction studies were performed at  $25 \pm 1^\circ C$  in 2 cm<sup>3</sup> microcentrifuge tubes by mechanical shaking. The phase ratio  $V_{(org)}:V_{(w)}$  was 1:1 (0.5 cm<sup>3</sup> each); the shaking period was 30 min for Co(II), Cu(II), Zn(II) and 24 h for Ni(II). All samples were centrifuged after extraction. The metal concentration in both phases was determined radiometrically using  $\beta$ -emission ( $^{63}Ni$ ; liquid scintillation counter Tricarb 2500/Canberra Packard), and  $\gamma$ -radiation ( $^{60}Co$ ,  $^{64}Cu$ ,  $^{65}Zn$ ; NaI(Tl) scintillation counter Cobra II/Canberra Packard). The pH of aqueous solution was adjusted using 0.05 M 2-[N-morpholino]ethanesulfonic acid (MES)/ NaOH (pH = 5.5).

## RESULTS AND DISCUSSION

The general reaction scheme for the solvent extraction of a metal ion by a mixed extraction system consisting of a macrocyclic amine and an organic acid is given in Figure 2.

For a synergistic effect by the present mechanism to operate, the formation of an assembled extractant package with defined stoichiometry should be favourable and this species will be responsible for the metal ion transfer from the aqueous into the organic phase. The benefits of such assembly formation could be manifested as improvements in both technical (extractability, selectivity) and economic (solvent losses, easier synthesis of a preorganized extractant) parameters.

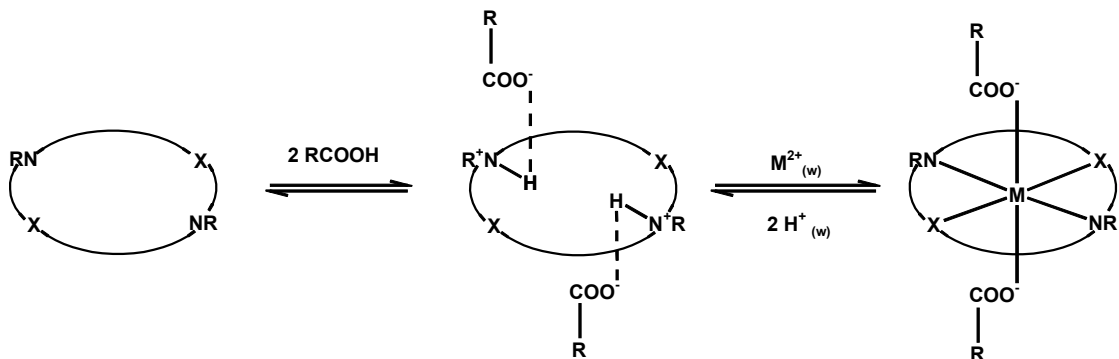


*Figure 2. General scheme for metal extraction on the bases of a 2:1 assembly between an organic acid and a macrocyclic amine.*

### Formation of Supramolecular Assemblies

$^{13}\text{C}$  and  $^1\text{H}$  NMR titration studies in  $\text{CDCl}_3$  were performed in order to probe the formation of defined assemblies between 4-*tert*-butylbenzoic acid (**HR**) and the macrocyclic amine (**L**) ( $R = \text{C}_9\text{H}_{19}$ ). The results of the investigation are illustrated in Figure 3 and provide clear evidence for the existence of 1:1 and 2:1 adduct species (**HR** : **L**) in solution. A similar result was obtained from parallel titrations involving **HR** and **L** ( $R = \text{H}$ ).

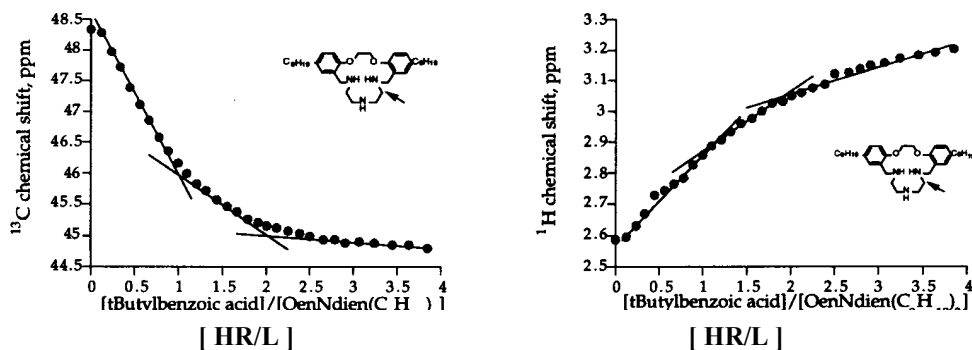


*Figure 3. Plots of the chemical shifts of the  $^{13}\text{C}$  and  $^1\text{H}$  resonance vs. the ratio  $\text{HR}/\text{L}$ .*

Such a stoichiometry is also confirmed in the solid state by an X-ray structure analysis of a crystalline 2:1 assembly between **HR** and **L** ( $R = \text{H}$ ); details are shown in Figure 4. The carboxylic groups interact directly via hydrogen bonds with two amine nitrogens of the macrocycle and one included water molecule [15].

### Solvent Extraction Studies

Preliminary extraction experiments have been performed for  $\text{Co}(\text{II})$ ,  $\text{Ni}(\text{II})$ ,  $\text{Cu}(\text{II})$  and  $\text{Zn}(\text{II})$  in the system  $\text{M}(\text{NO}_3)_2\text{-NaNO}_3\text{-MES/NaOH buffer/L-}\text{HR-CHCl}_3$  in order to investigate the prospect of enhanced affinity of the extractant assembly for suitable metal ions. The results shown in Figure 5 provide clear evidence for the existence of a strong synergistic effect in all cases. The order of increasing extractability by the extractant assembly is  $\text{Ni}(\text{II}) > \text{Cu}(\text{II}) > \text{Co}(\text{II}) \sim \text{Zn}(\text{II})$ .

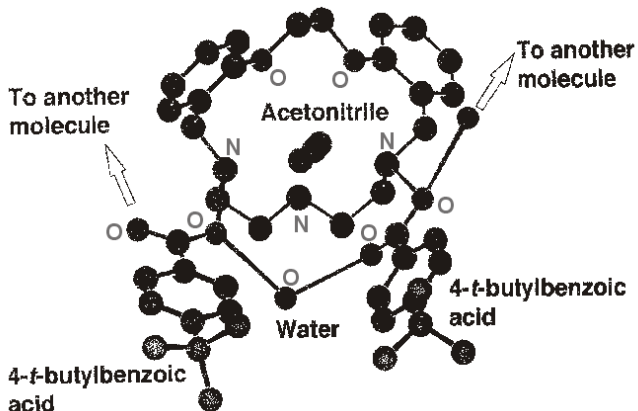


Figure 4. X-ray crystal structure of the supramolecular 2:1 assembly between **HR** and **L** ( $R = H$ ).

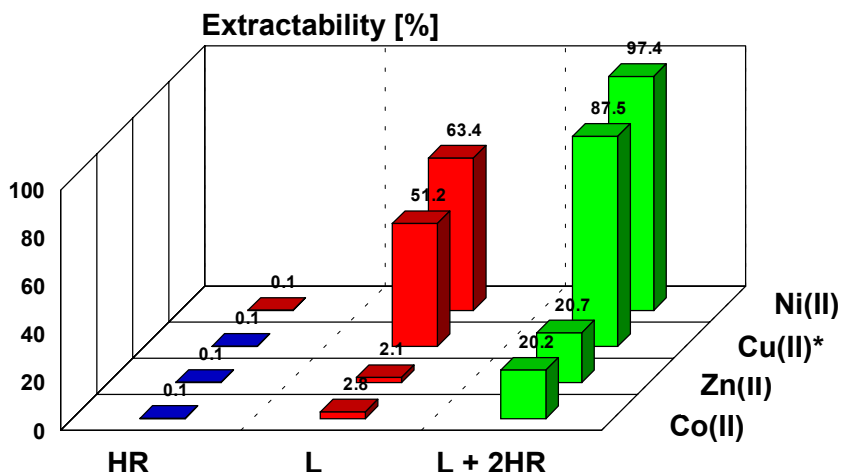
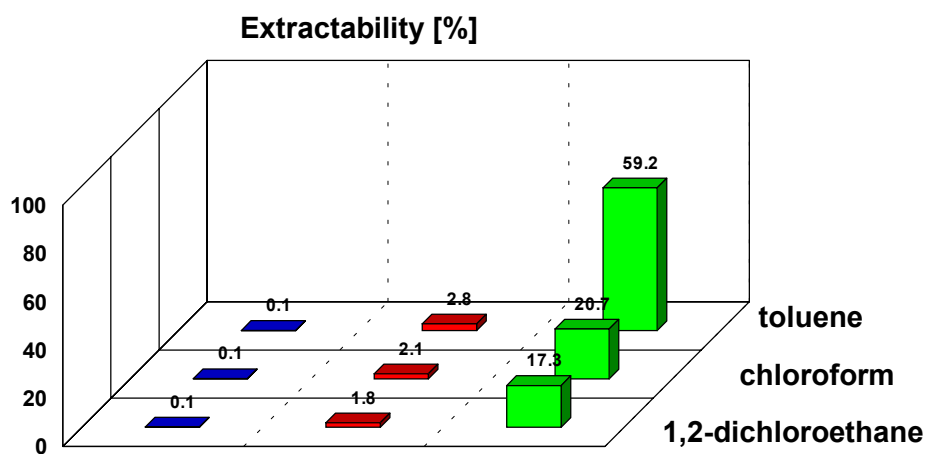


Figure 5. Influence of assembly effect on metal ion extraction by **HR/L** ( $R = C_9H_{19}$ ).  
 $[M(NO_3)_2] = 1 \cdot 10^{-4} M$ ; pH = 5.5 (MES/NaOH buffer);  $[NaNO_3] = 1 M$ ;  $[HR] = 2 \cdot 10^{-3} M$  and  
 $[L] = 1 \cdot 10^{-3} M$  in chloroform (\* without  $NaNO_3$ ).

The graduation observed for Ni(II), Co(II) and Zn(II) is in a good agreement with the order of the stability constants obtained in methanol [16]. It is interesting to note that in competition extraction experiments a pronounced preference for Zn(II) over Co(II) has been observed although the single metal extraction data are comparable. Of the metal ions studied, the Ni(II) system was observed to be very slow to reach equilibrium; hence a shaking time for the Ni(II) case of 24 h was employed while for the other metal ion cases it was 30 min.

The influence of the diluent on the extractability of Zn(II) serves to illustrate the importance of weak interactions between the components in the extraction system. Employment of toluene yielded a significant improvement in extraction efficiency in contrast to the use of more polar chlorinated hydrocarbons (cf. Figure 6). Most likely the competitive formation of hydrogen bonding between the extractants and diluents is responsible for the decreased extraction efficiency in the latter cases.

As expected, the extraction equilibrium strongly depends on the pH of the aqueous phase. As shown in Figure 7, the synergistic effect of the extractant assembly is significantly enhanced at pH values higher than 5. The increasing slope of the curve in the Log  $D_{Zn}$  – pH diagram is obviously connected with the complicated pH-dependent behaviour of the species present in solution.



*Figure 6. Influence of diluents on the assembly effect for Zn(II) extraction.*  
 $[Zn(NO_3)_2] = 1 \cdot 10^{-4} M$ ;  $pH = 5.5$  (MES/NaOH buffer);  $[NaNO_3] = 1 M$ ;  $[HR] = 2 \cdot 10^{-3} M$  and  
 $[L] (R = C_9H_{19}) = 1 \cdot 10^{-3} M$  in different diluents.

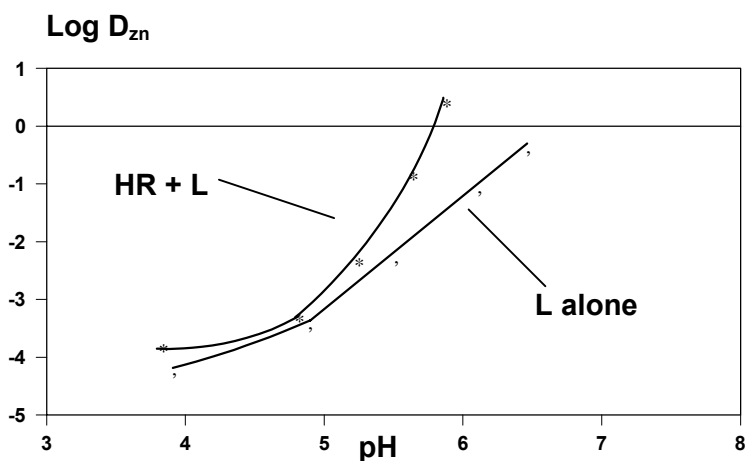


*Figure 7. Influence of pH on assembly effect for Zn(II) extraction.*  
 $[Zn(NO_3)_2] = 1 \cdot 10^{-4} M$ ;  $[NaNO_3] = 1 M$ ; pH variation with  $HNO_3$ ;  $[L] = 1 \cdot 10^{-3} M$  and  
 $[L](R = C_9H_{19}) = [HR] = 1 \cdot 10^{-3} M$  in chloroform.

In order to gain information about speciation, a series of experiments was performed involving Zn(II) extraction with the individual extractants alone and with them present in varying ratios. The extraction dependence on extractant concentrations is shown in Figure 8.

The results indicate apparent stoichiometries for the Zn(II) complexes extracted by **L** ( $R = C_9H_{19}$ ) alone of 1:1 and 2:1 ( $L:M$ ) [similar behaviour was also observed for Ni(II)]. The addition of **HR** to the organic phase results in an improvement in extraction efficiency and a change of speciation of the complexes formed. It is clear from Figure 8 that, for an extractant ratio **HR : L** of 1:1, extraction is very significantly increased. Further addition of **HR** to yield a **HR : L** ratio of 2:1 gives an additional slight rise, whereas for the 3:1 or 4:1 mixtures the extraction remains almost the same. The observance of an optimum synergistic effect for the 2:1 assembly is in clear agreement with the general ligand assembly effect postulate illustrated in Figure 2. Perhaps surprisingly, the slopes of the curves in the  $\log D_{zn}$ - $\log c_L$  diagram at constant **HR : L** ratios are in all cases about 2 and are significantly higher than for the macrocycle alone (slope about 1.5). A series of structural studies in both solution and the solid state on different metal complexes of azamacrocycles of the present type have shown a

considerable variation of coordination patterns occurs, the latter depending on a range of experimental factors [13, 16, 17]. As a consequence, in the absence of further data it appears inappropriate to speculate here about the architectures adopted by the metal complex species in the present systems. This aspect will be the subject of a future study.

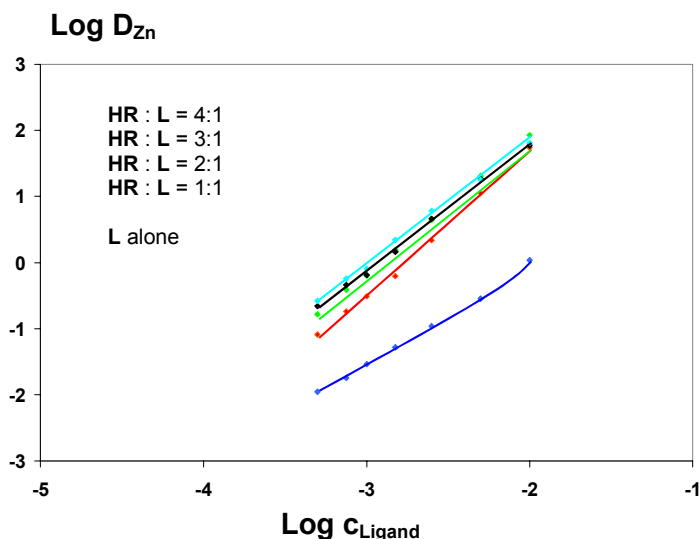


**Figure 8.** Variation of  $\log D_{Zn}$  with ligand concentration at different  $HR : L$  ( $R = C_9H_{19}$ ) ratios for Zn(II) extraction.  $[Zn(NO_3)_2] = 1 \cdot 10^{-4} M$ ;  $[NaNO_3] = 1 M$ ;  $pH=5.5$  (MES/NaOH buffer);  $[L] = 5 \cdot 10^{-4} \dots 1 \cdot 10^{-2} M$  in chloroform.

#### ACKNOWLEDGEMENT

We thank the Australian Research Council, DFG and DAAD for support.

#### REFERENCES

1. Y. Marcus and A. S. Kertes (1968), Ion Exchange and Solvent Extraction of Metal Complexes, Wiley-Interscience, London.
2. T. Sekine and Y. Hasegawa (1977), Solvent Extraction Chemistry, Marcel Dekker, New York.
3. J. Rydberg, C. Musikas and G. R. Choppin (eds.) (1992), Principles and Practices of Solvent Extraction, Marcel Dekker, New York.
4. B. A. Moyer (1996), Comprehensive Supramolecular Chemistry, J.-M. Lehn, J. L. Atwood, J. E. O. Davies, D. D. McNicol and F. Vögtle (eds.), Vol. 1, Pergamon Press, Oxford, pp. 377-416.
5. J. S. Bradshaw and R. M. Izatt (1977), *Acc. Chem. Res.*, **30**, 338-345.
6. C. Chartroux, K. Wichmann, G. Goretzki, T. Rambusch, K. Gloe, U. Müller, W. Müller and F. Vögtle (2000), *Ind. Eng. Chem. Res.*, **39**, 3616-3624.
7. A. H. Bond, M. L. Dietz and R. Chiarizia (2000), *Ind. Eng. Chem. Res.*, **39**, 3442-3464.
8. K. R. Adam, M. Antolovich, I. M. Atkinson, A. J. Leong, L. F. Lindoy, B. J. McCool, R. L. Davis, C. H. L. Kennard, P. A. Tasker (1994), *Chem. Comm.*, 1539-1540.

9. J. C. Bryan, L. H. Delmau, B. P. Hay, J. B. Nicholas, L. M. Rogers, R. D. Rogers, B. A. Moyer (1999), *Struct. Chem.*, **10**, 187-203.
10. J. T. Davis, M. Cai, J. Fettinger, V. Sidorov (2000), *Proc. 219<sup>th</sup> ACS National Meeting*, San Francisco, paper IEC 152.
11. J. D. Lamb, S. C. Lee, J. T. Davies, M. Cai (2000), *Proc. 219<sup>th</sup> ACS National Meeting*, San Francisco, paper IEC 153.
12. K. R. Adam, I. M. Atkinson, S. Farquhar, A. J. Leong, L. F. Lindoy, M. S. Mahinay, P. A. Tasker, D. Thorp (1998), *Pure Appl. Chem.*, **70**, 2345-2350.
13. K. R. Adam, L. F. Lindoy, H. C. Lip, J. H. Rea, B. W. Skelton and A. H. White (1981), *J. Chem. Soc., Dalton Trans.*, 74-79.
14. R. Aldred, R. Johnston, D. Levin and J. Neilan (1994), *J. Chem. Soc., Perkin Trans. I*, 1823-1831.
15. C. H. L. Kennard, University of Queensland, unpublished work.
16. I. M. Atkinson, K. A. Byriel, P. S. K. Chia, C. H. L. Kennard, A. J. Leong, L. F. Lindoy, M. P. Lowe, S. Mahendran, G. Smith, G. Wei (1998), *Austral. J. Chem.*, **51**, 985-991 and references therein.
17. K. R. Adam, A. J. Leong, L. F. Lindoy, B. J. McCool, A. Ekstrom, I. Liepa, P. A. Harding, K. Henrick, M. McPartlin, P. A. Tasker (1987), *J. Chem. Soc., Dalton Trans.*, 2537-2542.



## BETA-DIKETONE COPPER EXTRACTANTS: STRUCTURE AND STABILITY

Gary A. Kordosky, Michael J. Virnig and Phillip Mattison\*

Cognis Corporation, Tucson, United States of America

\*Cognis Corporation, Cincinnati, United States of America

The beta-diketone based reagent, LIX 54, has many outstanding properties for the extraction of copper from ammonia leach solutions. However, it has recently been found that the beta-diketone in LIX 54 reacts slowly with free ammonia in the presence of copper to form a ketimine product. The ketimine product results in a reduced rate of copper stripping, higher entrainment of aqueous in the loaded and stripped organic, and higher entrainment of organic in the pregnant strip electrolyte. Several new beta-diketone molecules were synthesized and their copper extraction properties as well as their resistance to ketimine formation were determined. These new beta-diketone molecules retain many of the outstanding properties of LIX 54 while the formation of ketimine is significantly reduced as the structure of the beta-diketone is altered in a systematic way.

### INTRODUCTION

The beta-diketone reagent, LIX 54, was introduced in 1975 as a reagent designed specifically for the extraction of metals from ammonia solutions [1]. The outstanding properties of this reagent when compared to the oxime copper extraction reagents include:

- High fluidity which allows the use of high reagent concentrations such that the organic phase in a continuous solvent extraction circuit can transfer up to ~ 32 g/l Cu.
- Low chemical loading of ammonia.
- Ease of stripping copper from the loaded copper organic phase, allowing the plant operator to tailor the acid and copper concentrations in the pregnant strip solution.

Over the years LIX 54 has been used in a number of small copper solvent extraction (SX) plants to extract copper from ammonia leach solutions, including spent etchant solutions from the circuit board industry [2] and ammonia leach solutions resulting from the leaching of lead dross [3]. For the most part, these plants are conservatively designed and the free ammonia in the leach solution is relatively low. Some plants have been in operation for over 15 years and feedback from the plant operators suggested that these plants were running relatively well.

During the development of the ammonia leaching process for Escondida copper concentrates, LIX 54 was run in the pilot-plant campaign and, from available reports, the small continuous solvent-extraction plant appeared to run well [4]. The Escondida commercial copper leach / SX / electrowinning plant at Coloso, Chile, was designed to produce a leach solution having about 32 to 35 g/l Cu, 40 g/l total ammonia at a pH of 9.5.

The commercial solvent extraction plant had a 2 extraction, 1 wash, 1 strip stage configuration with a three minute mixer retention in extraction and in strip. The organic phase was made up to a concentration that loaded about 32 g/l Cu.

## THE PROBLEM

When the Escondida plant at Coloso started up, the solvent extraction circuit operated very well for some period of time; entrainment was low and the stripping of the organic was efficient. Because the Coloso plant was on and off line as startup problems were encountered and solved, the behavior of the organic in the solvent extraction plant was not well documented during this time. After about 4 to 6 months of operation, it was noted that the stripping efficiency of the organic had decreased and entrainment had increased considerably, particularly entrainment of aqueous in the loaded and stripped organic, along with entrainment of organic in the pregnant strip solution. This, in turn, resulted in poor copper transfer efficiency, high ammonia consumption across the solvent extraction circuit and organic carryover to the tankhouse.

Both Cognis and Escondida made an effort to solve the problem by finding a simple method to regenerate clean circuit organic. Clay treatment, which is used successfully to treat many contaminated circuit organic solutions in typical acid leach copper solvent extraction circuits [5], was only partially effective in treating the Coloso circuit organic. Escondida developed an effective organic regeneration process consisting of contacting the circuit organic with a 600 to 900 g/l sulfuric acid solution followed by clay treatment of the acid-treated organic. Acid treatment caused formation of a viscous tarry third phase that entrained circuit organic and acid, creating a disposal problem. Cleaned organic performed well for only a short period of time before becoming contaminated again, meaning that any cleaning process had to be run continuously.

## IDENTIFICATION OF THE OFFENDING SPECIES

Infrared analysis showed that the circuit organic from the Coloso plant contained a small amount of ketimine functionality (Figure 1). Further work showed that ketimine was formed by the reaction of the beta-diketone extractant in LIX 54 with ammonia and, to add an ironic twist, the formation of ketimine takes place faster in the presence of copper than in the absence of copper.

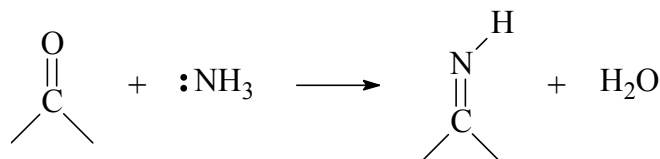


Figure 1. Ketimine formation.

High purity ketimine was produced by the reaction of the beta-diketone in LIX 54 with a concentrated solution of ammonia. This high purity ketimine was used to spike fresh LIX 54 solutions in diluent so that the properties of the LIX 54 solutions spiked with ketimine could be compared to the properties of fresh LIX 54 solutions having no ketimine and with the properties of the organic phase from the Coloso plant. A ketimine-spiked solution of LIX 54 showed the same problems as the organic phase from the solvent extraction plant at Coloso, but not to the same extent as seen in the plant. Thus it appeared that the ketimine was indeed part of the problem, but perhaps not the only problem.

A series of simple spiking tests showed that many of the reagents used in the upstream processing of the ore or in other parts of the plant interacted with ketimine-spiked LIX 54 to give much slower copper stripping kinetics and much higher entrainment than ketimine by itself. Additionally it was shown conclusively that the presence of ketimine in the circuit organic caused the clay treatment process to be less effective than it normally is.

At this time the decision was made to develop an alternative to the beta-diketone extractant in LIX 54 with the goal being the development of an extractant that would retain all the good properties of LIX 54, but, would not form ketimine under the existing circuit conditions.

### ALTERNATIVE MOLECULES

Because the active extractant in LIX 54 (Figure 2) has two carbon-oxygen double bonds that could react with ammonia to form ketimine, it was reasoned that the first step of the process to develop an alternative to the beta-diketone in LIX 54 was to determine the structure of any and all ketamines in the circuit organic. Somewhat to Cognis' surprise, the ketamine shown in Figure 3 was the only ketamine found in the circuit organic.

Organic chemistry tells us that the most likely direction from which ammonia attacks a

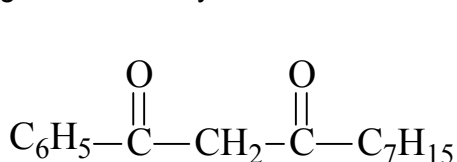


*Figure 2. Active extractant in LIX 54.*

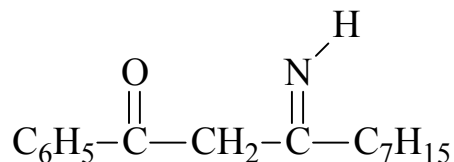


*Figure 3. Only ketimine formed by LIX 54.*

carbon-oxygen double bond is at the carbonyl carbon. A careful look at the structure of the beta-diketone in LIX 54 (Figure 4) shows that the carbonyl carbon which forms the ketimine is not particularly sterically hindered since there are two small hydrogen atoms bonded to  $\text{C}^*$  in addition to one larger C atom.

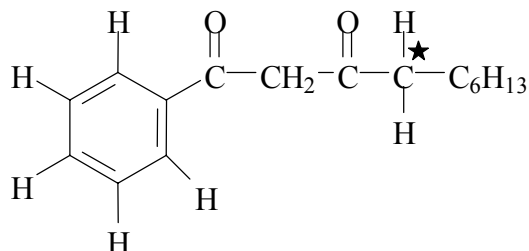


*Figure 4. Active extractant in LIX 54.*

It was then reasoned that one way to decrease or even prevent formation of the offending ketimine was to synthesize beta-diketones that had greater steric hindrance around the reactive carbonyl carbon. It is known from organic chemistry that one way to increase steric hindrance around a carbonyl carbon is to increase the bulk around the carbon (shown as  $\text{C}^*$ ) next to the reactive carbonyl carbon. One way to increase the bulk around  $\text{C}^*$  is to increase the number of carbons and decrease the number of hydrogens bonded to  $\text{C}^*$ .

To test the reasoning, three alternative beta-diketone molecules were synthesized: XI-55, XI-N54 and XI-57 shown in Figures 5, 6 and 7, respectively.

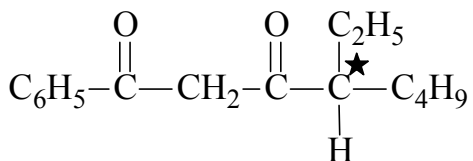


Figure 5. Active extractant in XI-55.

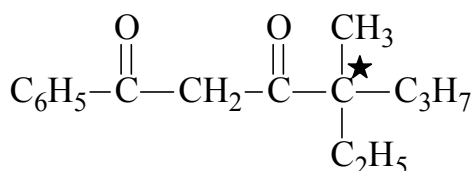


Figure 6. Active extractant in XI-N54.

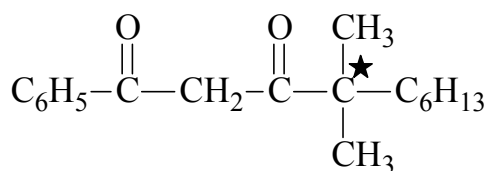


Figure 7. Active extractant in XI-57.

Note that while the basic molecular structure of the beta-diketone in LIX 54 has been retained in each of the new betadiketones, there is a systematic change in the structure of the new beta-diketones at C<sup>\*</sup> when compared to the beta-diketone in LIX 54. The betadiketone in LIX 54 has two hydrogens and one carbon bonded to C<sup>\*</sup>, in XI-55 there is one hydrogen and two carbons bonded to C<sup>\*</sup> and in both XI-N54 and XI-57 there are three carbons bonded to C<sup>\*</sup>.

## TESTING OF NEW MOLECULES

### Extraction

The three new molecules were synthesized and purified to give low viscosity light yellow liquids. The three new molecules were formulated in Conoco 170E at a level sufficient to load about 30 g/l Cu and then run through performance tests along with LIX 54-100. In the first test, 25 ml of the respective organic phase was vigorously contacted for two minutes with 25 ml of a standard synthetic leach solution containing 30 g/l Cu, 30 g/l NH<sub>3</sub> and 30 g/l ammonium sulfate. After the phases separated, the organic phase was filtered and analyzed for copper by atomic absorption spectrophotometry (AA) and for ammonia content using a Cognis method [6]. A portion of the organic phase was contacted vigorously two more times with fresh synthetic leach solution twice for two minutes each contact, then filtered and analyzed to give a copper maximum load.

A second sample of XI-57 was vigorously contacted with a synthetic stability leach solution containing 30 g/l Cu, 44 g/l NH<sub>3</sub> and 20 g/l ammonium sulfate in a round bottom flask fitted with a stirring rod and paddle for one week at 45 °C. This sample of "aged XI-57" was stripped with sulfuric acid until no copper was present on the organic phase and then taken through the same set of experiments as described directly above. The results of this series of copper and ammonia loading tests are shown in Table 1.

Table 1. Copper and ammonia loading for various beta-diketones.

	LIX 54	XI-55	Neo-54	XI-57	XI-57 Aged
Max load (g/l Cu)	30.0	27.8	27.3	30.2	26.8
One contact (g/l Cu)	23.5	22.4	20.8	21.3	19.7
Max load (%)	78	81	76	71	74
NH <sub>3</sub> loading (g/l)	0.32	0.28	0.13	0.094	0.10

The new beta-diketones retain the very good fluidity of LIX 54. Both XI-55 and neo-54 have about the same extractive strength as LIX 54 as shown by the % copper max loading after one contact with a synthetic standard leach solution, while XI-57 appears to be a slightly weaker extractant than LIX 54. Ammonia loading on the new beta-diketones is less than the ammonia loading on LIX 54, in the case of Neo-54 and XI-57 less than 1/2. These new beta-diketones appear to retain the very good properties of LIX 54.

### Ketimine Formation

The various beta-diketones were then tested for ketimine formation using an accelerated ketimine formation test. A 0.95 molar solution of the respective beta-diketone in the diluent Conoco 170E was vigorously contacted for six days at 45 °C with the synthetic stability leach solution containing 30 g/l Cu, 44 g/l NH<sub>3</sub> and 20 g/l ammonium sulfate. After the test was completed, the organic phase was stripped of the loaded copper by vigorous contact with an aqueous solution of 150 g/l sulfuric acid until the respective organic phase was light yellow in color indicating that all the copper had been stripped. The organic phase was then washed twice with water and filtered. The ketimine content of the organic phase was determined by gas chromatography with a detection limit of 0.01%. The results are given in Table 2.

*Table 2. Ketimine formation of various beta-diketones.*

Beta-diketone	Ketimine content by weight
LIX 54	0.98%
XI-55	None detected
XI-N54	None detected

Neither XI-55 nor XI-N54 form ketimine under conditions where LIX 54 shows significant ketimine formation.

### Stripping Kinetics

Stripping kinetics were determined for fresh and aged samples of the respective beta-diketones. A sample of the respective organic phase was vigorously contacted one time at an O/A = 1 with the standard synthetic leach solution for two minutes. Within a few minutes after the phases had separated, 100 ml of the copper loaded organic phase was added to a 2.25 inch square box and stirred at 1750 rpm with a slotted impeller 1.25 inches in diameter. Then 100 ml of an aqueous solution containing 35 g/l Cu and 150 g/l sulfuric acid was added over 5 seconds. Samples of the dispersion were removed at specified times, the organic phase for each sample analyzed for copper and stripping kinetics calculated. Under these conditions, all fresh beta-diketones strip almost completely in 30 seconds. Stripping kinetics for aged and aged then clay treated beta-diketones are given in Table 3.

*Table 3. Percent copper stripping for various aged beta-diketones.*

Time (s)	LIX 54-100		XI-55		XI-N54	XI-57
	Aged	Clay treated*	Aged	Clay treated**	Aged	Aged
30	41%	95%	70%	98%	100%	92%
60		100%		100%		100%
120			96%			
180	98%					

\* Clay treatment is with 3 g clay / 100 ml of aged organic phase.

\*\* Clay treatment is with 1 g clay / 100 ml of aged organic phase.

LIX 54 stripping kinetics are unique. A LIX 54 solution loaded with copper from an ammonia solution will show slower strip kinetics the longer the solution stands before being stripped. If LIX 54 after being stripped is reloaded with copper from ammonia and then stripped immediately, the strip kinetics are very rapid. Interestingly, if the loaded LIX 54 is washed with phthalate buffer solution to remove ammonia, the strip kinetics do not slow with time.

When the new more hindered beta-diketones are loaded with copper and allowed to stand for a long period of time, the stripping kinetics are rapid even when ammonia is not scrubbed from the loaded organic. The authors have no explanation why the strip kinetics of LIX 54 slow with time when a small amount of co-loaded ammonia remains on the organic phase.

It is known that stripping kinetics are slowed by the presence of ketimine. Aged LIX 54 shows a dramatic slowing of copper strip kinetics that can be reversed with a heavy clay treatment. Aged XI-55 shows some slowing of stripping kinetics that can be reversed with a light clay treatment, while aged XI-N54 and XI-57 both show rapid strip kinetics. This suggests that XI-55 may form a very small amount of ketimine or some other species that retards copper stripping, but that XI-N54 and XI-57 do not.

### **Long-Term Continuous Circuit Testing**

A sample of XI-57 was compared to LIX 54-100 in a small continuous SX mini-plant treating a leach solution from the Coloso ammonia leach plant under conditions similar to those in the Coloso SX plant. Within several weeks after start up, the LIX 54 in the mini-plant began to show slower stripping kinetics and increased transfer of ammonia to the wash stage. After three months in the mini-plant, the XI-57 retained fast copper stripping kinetics and ammonia transfer to the wash stage was less than 25% of the ammonia transfer shown by LIX 54. Infrared analysis of the XI-57 that had been in the mini-plant for three months did not detect the presence of ketimine. The results of the long-term continuous circuit testing were consistent with the previous tests. XI-57 did not appear to form ketimine under conditions where LIX 54 forms ketimine, ammonia transfer was much less than with LIX 54, copper stripping kinetics remain rapid and XI-57 was shown to be a slightly weaker copper extractant than LIX 54.

## **CONCLUSION**

The goal of synthesizing beta-diketones that resist ketimine formation while still retaining the very good properties of LIX 54 was achieved by applying well-known organic chemistry principals relating chemical structure to reactivity. The new more hindered beta-diketones do not form ketimine under conditions where the less hindered beta-diketone in LIX 54 readily forms ketimine. A reagent based on the structure of either XI-N54 or XI-57 should be an excellent extractant for copper from ammonia.

## **REFERENCES**

1. Preliminary Report (1975): LIX 54 - A New Reagent for Metal Extractions from Ammoniacal Solutions, Cognis Corporation.
2. Closed Loop Recycling of Alkaline Etchants, Technical Bulletin, Sigma Innovation AB, Sweden.
3. W. Hopkins, W. H. Hunter, K. Nakade, A. Asano and S. Kobayashi (1983), Hydrometallurgy: Research, Development and Plant Practice, K. Osseo-Asare and J. D. Miller (eds.), The Minerals, Metals and Materials Society, Warrendale, PA, pp. 985–999.
4. W. P. C. Duyvesteyn and B. J. Sabacky (1993), Extractive Metallurgy of Copper, Nickel and Cobalt, Vol. I: Fundamental Aspects, R. G. Reddy and R. N. Weizenbach (eds.), The Minerals, Metals and Materials Society, Warrendale, PA, pp. 881–910.
5. G. A. Kordosky, W. H. Champion and P. L. Mattison (1983), Hydrometallurgy: Research, Development and Plant Practice, K. Osseo-Asare and J. D. Miller (eds.), The Minerals, Metals and Materials Society, Warrendale, PA, pp. 617–628.
6. Blue Line Technical Bulletin, Determination of NH<sub>3</sub> in Solutions of LIX Reagents, Cognis Corporation, Tucson, USA.



## SOLVENT EXTRACTION OF IRON(III) FROM HYDROCHLORIC ACID SOLUTIONS BY DIHEXYL SULPHOXIDE

Taichi Sato\*, Izumi Ishikawa, Keiichi Sato and Yoshitomo Noguchi

Faculty of Engineering, Shizuoka University, Hamamatsu, Japan

\* Also at Queen's University, Metallurgical Engineering Department, Kingston, Ontario, Canada

The extraction of iron(III) from aqueous solutions containing hydrochloric acid and/or lithium chloride has been carried out using dihexyl sulphoxide (DHSO, R<sub>2</sub>SO) in benzene. The organic extracts were examined by infrared and ultraviolet spectroscopies. As a result, it was found that the distribution coefficient rises with increasing chloride ion concentration in the aqueous solution, and that the extraction equilibrium of iron(III) from hydrochloric acid solutions by DHSO can be expressed as:



### INTRODUCTION

As the presence of a sulphur atom facilitates the combination of extractants with class b metal ions, sulphur-containing compounds have been used as solvent extractants for various valuable metals. In particular, it has been found that dialkyl-sulphides and -sulphoxides are effective extractants for silver and mercury [1-4]. The present authors have therefore examined the extraction of silver(I) and mercury(II) by dihexyl sulphide (DHS, R<sub>2</sub>S) [5,6], and the extraction of mercury(II) by dihexyl sulphoxide (DHSO, R<sub>2</sub>SO) [6]. However, since DHSO contains an oxygen atom in addition to a sulphur one, it is expected that the extractability of metals by DHSO should be generally more effective than that by DHS. Accordingly, when DHSO is used as an extractant for a metal such as mercury, it is an important problem to separate the valuable metal from iron(III). Thus this study extends the work to obtain further information on the extraction of iron(III) from hydrochloric acid solutions by DHSO in order to compare with the results for the extraction of mercury [6].

### EXPERIMENTAL

The DHSO was synthesized by means of oxidation from DHS (Daihachi Chem. Ind. Co., Ltd.) [7]: 35 cm<sup>3</sup> each of acetic acid and acetic anhydride and 20 cm<sup>3</sup> of a 30% aqueous solution of hydrogen peroxide were added to 50 cm<sup>3</sup> of DHS drop-wise during 1 h; the mixture was cooled with ice and then stirred for 3 h at 273 K. After the completion of the reaction was confirmed by TLC, the DHSO was extracted into chloroform and washed first with water, then with 10 % sodium carbonate, and finally with water again. The white crystals obtained after the removal of chloroform by evaporation were purified by recrystallization.

Aqueous solutions of iron were prepared by dissolving ferric chloride (FeCl<sub>3</sub>.6H<sub>2</sub>O) in hydrochloric acid of selected concentration. In general, the concentration of the metal salt was 1 g dm<sup>-3</sup> except for the loading tests. All chemicals were of analytical reagent grade.

Equal volumes (15 cm<sup>3</sup> each) of organic and aqueous phases were placed in a 50 cm<sup>3</sup> stoppered conical flask and shaken for a selected time in the thermostatic water bath at 293 K, except for the experiment on temperature effect. Preliminary experiments showed that equilibrium was complete in 10 min. The mixture was quickly separated by centrifugation, and then both phases were assayed to determine the distribution coefficient ( $E_a^{\circ}$ , the ratio of the equilibrium concentration of metal in the organic phase to that in the aqueous phase). Iron in the organic phase was stripped with 1 mol dm<sup>-3</sup> hydrochloric acid. The concentration of iron in aqueous solution was determined by EDTA titration using xylenol orange (XO) as the indicator. The chloride concentration and the water content in the organic phase were determined by the use of Volhardt's method and Karl Fischer titration, respectively.

The infrared (IR) spectra of the organic extracts were determined on JASCO models IRA-1 (4000-650 cm<sup>-1</sup>) and IR-F (700-200 cm<sup>-1</sup>) using a capillary film between thallium halides or polyethylene films. The ultraviolet (UV) absorption spectra were recorded on a Hitachi model 340 spectrophotometer using 1.0 x 1.0 cm fused silica cells.

## RESULTS AND DISCUSSION

### Extraction Isotherms

The extraction of iron(III) from hydrochloric acid solutions by DHSO was carried out by varying the aqueous acidity. The distribution coefficient rose sharply with increasing initial concentration of hydrochloric acid as shown in Figure 1. When hydrochloric acid in the aqueous phase was replaced by lithium chloride, the extraction behaviour of iron(III) resembled that from hydrochloric acid solutions alone.

The log-log plots of  $E_a^{\circ}$  vs.  $[R_2SO]_{eq} = [R_2SO]_{init} - 2[Fe]_{org}$  at a constant hydrochloric acid concentration gave straight lines with the following slopes: 2.08, 1.80 and 1.75 at 4, 5 and 6 mol dm<sup>-3</sup> HCl, respectively, and 1.94, 1.82, 1.75 and 1.76 at 0.1 mol dm<sup>-3</sup> HCl + LiCl (of 5, 6, 7 and 8 mol dm<sup>-3</sup>), respectively. These results show that the dependence of distribution coefficient on the DHSO concentration is second-power at constant aqueous acidity.

In the extraction of iron(III) from hydrochloric acid solutions by DHSO, the continuous variation of  $[Fe]_{org}$  plotted as a function of mole fraction  $[Fe]_{init\ aq}/([Fe]_{init\ aq} + [R_2SO]_{init})$  at a fixed total concentration of  $[Fe]_{init\ aq} + [R_2SO]_{init} = 0.04$  mol dm<sup>-3</sup>, at 6 mol dm<sup>-3</sup> HCl and at 0.2 mol dm<sup>-3</sup> HCl + 5.8 mol dm<sup>-3</sup> LiCl gave a maximum of 0.33. This shows that the combination of DHSO with iron is in the molar ratio of 2:1 depending on aqueous acidity. However, since the distribution coefficient from acid alone is higher than that from a mixture of hydrochloric acid and lithium chloride, the effect of proton concentration on the distribution coefficient has been examined [6]. When the initial hydrochloric acid concentration was varied at a constant chloride concentration in the aqueous phase ( $[Cl]_{init\ aq} = [HCl]_{init\ aq} + [LiCl]_{init\ aq}$ ), the distribution coefficient increased linearly with increasing the proton concentration in aqueous phase as indicated in Figure 2. The slopes ( $\partial \log E_a^{\circ} / \partial \log [H]_{init\ aq}$ ) were 0.80, 0.78, 0.64 and 0.66 at the total  $[Cl]_{init\ aq}$  of 5, 6, 7 and 8 mol dm<sup>-3</sup>, respectively, with 0.02 mol dm<sup>-3</sup> DHSO. It is thus presumed that the dependence of distribution coefficient on the proton concentration in aqueous phase is the first-power. Besides, the loading test of iron in the organic phase indicated the stoichiometry of the extracted species. With increasing the initial aqueous iron concentration at 6 mol dm<sup>-3</sup> HCl, the molar ratio  $[Fe] / [Cl] / [R_2SO] / [H_2O]$  in the organic phase approaches 1:4:2:0, exhibiting the composition  $FeCl_3 \cdot HCl \cdot 2R_2SO$  (as  $HFeCl_4 \cdot 2R_2SO$ ).

Hence the following equilibrium equation is inferred for the extraction of iron(III) from hydrochloric acid solutions by DHSO:

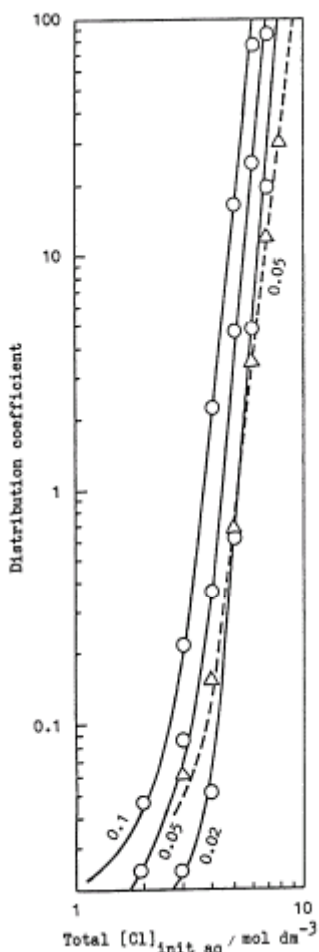
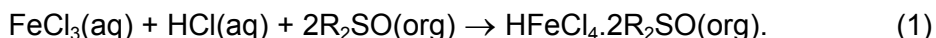


*Figure 1. Extraction of iron(III) from HCl solutions by DHSO in benzene. The numerals on the curves are DHSO concentrations in  $\text{mol dm}^{-3}$ . Solid and broken lines represent the extraction from HCl solutions and mixed  $0.1 \text{ mol dm}^{-3}$  HCl / LiCl solutions, respectively.*

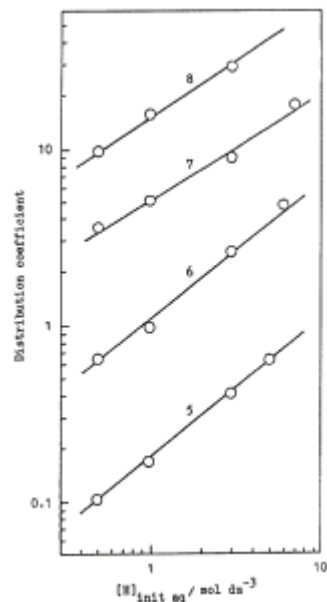


*Figure 2. Dependence of distribution coefficient on aqueous proton concentration for the extraction of iron(III) from mixed solutions of HCl and LiCl with  $0.02 \text{ mol dm}^{-3}$  DHSO in benzene (numerals on the lines are total  $[\text{Cl}]_{\text{init aq}}$  ( $= [\text{HCl}]_{\text{init aq}} + \text{LiCl}_{\text{init aq}}$ ) /  $\text{mol dm}^{-3}$ ).*

### IR and UV Spectra

The organic extracts with  $0.2 \text{ mol dm}^{-3}$  DHSO in benzene, from aqueous solutions containing ferric chloride of  $2$ ,  $5$  and  $20 \text{ g dm}^{-3}$  at  $0.2 \text{ mol dm}^{-3}$   $\text{HCl} + 5.8 \text{ mol dm}^{-3}$   $\text{LiCl}$ , were examined by IR spectroscopy. The IR spectra of the organic extracts exhibit the absorption due to the  $\text{S=O}$  stretching vibration at  $990 \text{ cm}^{-1}$ , shifted from the band which appears at  $1050 \text{ cm}^{-1}$  in a free DHSO [6]. With increasing metal concentration, its absorption band increases in intensity, and in addition the  $\text{Fe-Cl}$  stretching frequency appears at  $378 \text{ cm}^{-1}$ .

The UV spectra of the organic extracts were examined in the extraction with  $0.1 \text{ mol dm}^{-3}$  DHSO in cyclohexane from aqueous solutions containing ferric chloride of  $0.02 \text{ g dm}^{-3}$  in hydrochloric acid. In the spectra of aqueous ferric chloride solutions in hydrochloric acid, the

absorption at 335 nm appears in 2-4 mol dm<sup>-3</sup> HCl, and then the absorption bands at 245, 316 and 364 nm appear gradually with increasing the acid concentration in 5-9 mol dm<sup>-3</sup> HCl. According to Metzler *et al.* [8], the absorptions at 245, 316 and 365 nm are due to FeCl<sub>4</sub><sup>-</sup>. This is supported by the reports that the dominant species of ferric chloride is FeCl<sub>4</sub><sup>-</sup> [9,10]. In contrast, as shown in Figure 3, the spectra of the organic extracts show the absorption bands at 316 and 364 nm similar to the pattern of the aqueous ferric chloride solutions in 5-9 mol dm<sup>-3</sup> HCl. We have also observed that the absorptions at 245, 314 and, 364 nm due to the species FeCl<sub>4</sub><sup>-</sup> for the organic extracts from hydrochloric acid solutions at higher acidities by an  $\alpha$ -hydroxyoxime [11]. Accordingly, it is inferred that the organic extracts from aqueous solutions containing ferric chloride in hydrochloric acid exist as the stoichiometric composition of HFeCl<sub>4</sub>.2R<sub>2</sub>SO.

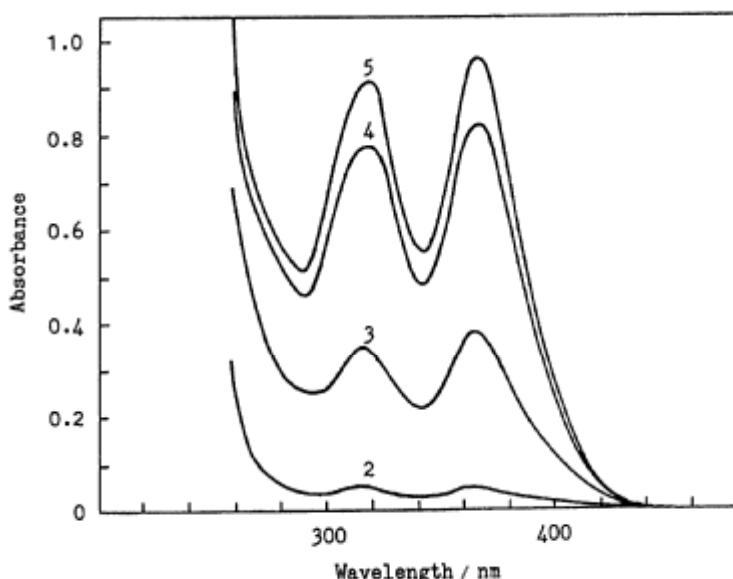


Figure 3. Absorption spectra of the organic extracts with 0.1 mol dm<sup>-3</sup> DHSO in cyclohexane from aqueous solutions containing ferric chloride 0.02 g dm<sup>-3</sup> in hydrochloric acid (numerals on curves are initial HCl concentrations / mol dm<sup>-3</sup>).

Table 1. Temperature-dependence of distribution coefficient for the extraction of iron(III) from 4 and 6 mol dm<sup>-3</sup> hydrochloric acid solutions with DHSO in benzene.

[HCl] init ag /mol dm <sup>-3</sup>	[DHSO] /mol dm <sup>-3</sup>	E <sub>a</sub> <sup>o</sup>				
		283K	293K	303 K	313 K	323K
4	0.05	0.422	0.360	0.345	0.321	0.287
6	0.02	5.02	4.55	4.36	4.16	3.40

### Temperature Effect

The extraction of iron(III) from 4 and 6 mol dm<sup>-3</sup> hydrochloric acid solutions with 0.05 and 0.02 mol dm<sup>-3</sup> DHSO in benzene, respectively, was carried out at temperatures between 283 and 323 K. The results showed that the distribution coefficient decreases with rising temperature. From this, the values of heat of reaction (change of enthalpy,  $-\Delta H$ ) in Eq. (1) were estimated as 9.19 and 14.7 kJ mol<sup>-1</sup>, respectively. When the heat of reaction for DHSO (hard base) with iron (hard acid) is compared to that for DHSO (hard base) with mercury (soft acid), estimated as 35.2 kJ mol<sup>-1</sup> [6], the former value is expected to be smaller than the latter one.

## CONCLUSION

The extraction of iron(III) from hydrochloric acid solutions by DHSO has been examined under different conditions. As a result, it is seen that the extraction of iron(III) involves the solvating reaction according to:



In comparison with the results for the extraction of mercury(II) [6], since the extraction from hydrochloric acid solutions by DHSO for mercury (II) is effective at low aqueous acidity more than that for iron(III), the separation of mercury(II) from iron(III) is preferably carried out at below  $2 \text{ mol dm}^{-3}$  HCl .

## REFERENCES

1. V. A. Mikhailov, T. G. Torgov, E. N. Gil'bert, L. N. Mazalov and A. V. Nikolaev (1971), *Proc. Int. Solvent Extr. Conf., ISEC '71*, Vol. II, Society of Chemical Industry, London, pp. 112-119.
2. V. A. Mikhailov, N. A. Korol and D. D. Bogdanova (1974), *Proc. Int. Solvent Extr. Conf., ISEC '74*, Vol. 3, Society of Chemical Industry, London, pp. 2745-2764.
3. V. A. Mikhailov, A. S. Shatskaya, D. D. Bogdanova and V. G. Torgova (1976), *Izv. Sib. Otd. Akad. Nauk SSSR. Ser. Khim. Nauk.*, **3** (7), 33-44.
4. V. A. Mikhailov, (1979), *Proc. Int. Solvent Extr. Conf., ISEC '77*, Vol. 1, Can. Inst. Min. Met., Montreal, pp. 52-60.
5. T. Sato, I. Ishikawa and T. Nakamura (1983), *Solvent Extr. Ion Exch.*, **1**, 541 -552.
6. T. Sato I. Ishikawa and K. Sato (1998), *J. Min. Mater. Process. Inst. Jpn.*, **114**, 33-39.
7. K. Ogura and G. Tsuchihashi (1983), *Bull. Chem. Soc. Jpn.*, **45**, 2203-2204.
8. D. E. Metzler and R. J. Myers (1950), *J. Am. Chem. Soc.*, **72**, 3376-3378.
9. S. Lindenbaum and G. E. Boyd (1963), *J. Phys. Chem.*, **67**, 1238-1241.
10. P. M. Cusher and S. M. S. Kennard (1959), *J. Am. Chem. Soc.*, **81**, 2976-2982.



## SOLVENT EXTRACTION OF IRON(III) FROM HYDROCHLORIC ACID SOLUTIONS USING N,N'-DIMETHYL-N,N'-DIPHENYLMALONAMIDE

M. C. Costa and A. P. Paiva\*

C.E.C.U.L. / F.E.R.N, Universidade do Algarve, Campus de Gambelas, Faro, Portugal

\*Departamento de Química e Bioquímica, C.E.C.U.L., Faculdade de Ciências da Universidade de Lisboa, Lisboa, Portugal

This work is focused on the ability of N,N'-dimethyl-N,N'-diphenylmalonamide to extract iron(III). The results have shown that iron(III) can be efficiently and selectively extracted from hydrochloric acid solutions. The effect of variables including acidity and chloride concentration of the aqueous phases, as well as the influence of the diluent, is researched and discussed. The analysis of the aqueous solutions after contact with the organic phase showed that iron(III) was quantitatively extracted from HCl solutions between 0 to 12 M, maintaining the total chloride concentration with LiCl at 12 M. Regarding selectivity studies, the extraction of other metals such as Cu(II), Zn(II) and In(III), usually present in typical pregnant leaching solutions, was also investigated. Significant selectivity over these metals can be achieved, since no extraction other than iron(III) was detected. Preliminary assays of the stripping of iron(III) from the organic phase to a purified aqueous medium showed that iron(III) can be partially recovered. The overall results obtained for this malonamide derivative are generally compared, in terms of extraction and stripping properties, with the behaviour of N,N'-dimethyl-N,N'-diphenyltetradecylmalonamide, the subject of previous studies.

### INTRODUCTION

The extractive properties of diamides were clearly demonstrated by Musikas and co-workers [1,2], who developed studies concerning their utilisation in the nuclear processing industry as solvent extraction agents. Therefore, N,N'-tetraalkylmalonamides were considered important alternatives to the organophosphorus compounds - e.g., tributylphosphate (TBP) - because they efficiently extract trivalent, tetravalent and hexavalent actinides and lanthanides from nitric acid medium [3,4] and because of their environmental advantages [5]. The ability of malonamides to extract polyvalent metals can be explained by the weak basic nature of the amide carbonyl group [4,6]. In the last decade considerable effort on the development of different molecular structures has been made with the aim of optimising the extractive performances of malonamides for the nuclear industry metals. Thus, the synthesis of different structures is being stimulated since the nature of the N-substituents in diamides greatly affects the distribution ratios of several actinides and lanthanides [7,8]. In fact, the selection of the substituents on the nitrogen atoms (R and R') is very important to facilitate metal-ion co-ordination and to allow the solubility of the diamide and its adducts in the organic phase. In order to attain both objectives, R and R' should have different sizes. If R is a small group (typically methyl) and R' a bigger one, both criteria are satisfied: the stereochemical hindrance around the carbonyl oxygen atoms is kept to a minimum and both oxygen atoms can co-ordinate to a metal ion [8] and the lipophilic character of the ligands is attained by the presence of a higher chain - alkyl or aryl groups - at R'. In order to increase the solubility of the diamide in the organic solvent (and thus of the metallic complexes) one of the methylenic hydrogen atoms can be substituted by an alkyl group [9].

N,N'-dimethyl-N,N'-diphenylmalonamide (DMDPHMA), whose structure is presented in Figure 1, was chosen for this research. In this molecule the aforementioned criteria for the selection of R and R' are satisfied.

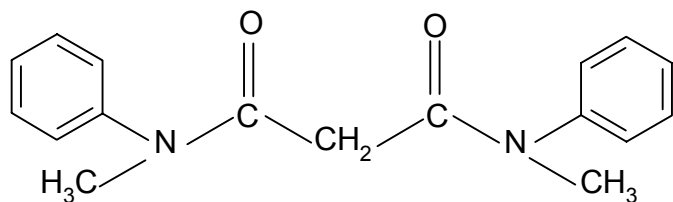


*Figure 1. General structure of DMDPHMA.*

The phenyl groups, bonded to the nitrogen atoms, act as electron acceptors, thus giving the molecular structure a less basic character. These phenyl rings affect the extractive properties of DMDPHMA for the extraction of metallic nitrates from highly concentrated nitric media [10], as the competition between metallic complexes and the acid for the diamide is reduced.

Previous studies using substituted diamides have shown that these compounds can also be successfully used for the extraction of Fe(III) from hydrochloric acid medium [11,12]. The selectivity exhibited over some basic metals is a very promising result that led to this research.

## EXPERIMENTAL

### Synthesis of DMDPHMA

N,N'-dimethyl-N,N'-diphenylmalonamide was synthesised by reaction of methylaniline and dimethylmalonate: methylaniline (222 g, 2.051 mol) was mixed with dimethyl malonate (137 g, 0.99 mol) and then heated at 180 °C for 3 h. After distillation the mixture still reacted for 1 h. A white solid formed on cooling. The product was washed with diethyl ether and recrystallised from ethyl acetate to give pure DMDPHMA. The synthesised compound (26% overall yield) was characterised by melting point and elemental analysis (CE Instruments EA 1110 CHNS-O) (Table 1), and by spectroscopic techniques such as mass spectroscopy and <sup>1</sup>H NMR. For mass spectroscopy Trio 1000 equipment was used. The <sup>1</sup>H (300 MHz) NMR spectrum was obtained with a Bruker AMX-300 spectrometer using CDCl<sub>3</sub> as solvent and TMS as the standard. Mass spectroscopy and <sup>1</sup>H NMR data are presented in Tables 2 and 3, respectively.

*Table 1. Melting point and elemental analysis for DMDPHMA.*

Melting point Literature [8] This work	(°C)		
	105-106	107-108	
Elemental analysis Theoretical Experimental	C (%)	H (%)	N (%)
	72.3	6.4	9.9
	72.3	6.6	9.4

*Table 2. Proton NMR assignments for DMDPHMA.*

Molecular structure	$^1\text{H}$ NMR
	$^1\text{H}$ NMR assignments: 3.0 (2 H, s, a) 3.2 (6 H, s,b) 7.0-7.1 (4 H, d, c) 7.3-7.4 (6 H, t, d)

s – singlet, d – doublet, t – triplet

$^1\text{H}$  NMR data are in agreement with previous reported results [8].

*Table 3. Mass spectroscopy data for DMDPHMA.*

Molecular peak: $\text{C}_{17}\text{H}_{18}\text{N}_2\text{O}_2 \cdot \ddagger = 282$ (48%)
$\text{C}_{10}\text{H}_{10}\text{NO}_2 \cdot \ddagger = 176$ (23%)
$\text{C}_9\text{H}_{10}\text{NO} \cdot \ddagger = 148$ (37%)
$\text{C}_8\text{H}_8\text{NO} \cdot \ddagger = 134$ (83%)
$\text{C}_7\text{H}_8\text{N} \cdot \ddagger = 106$ (100%)
$\text{C}_6\text{H}_5 \cdot \ddagger = 77$ (91%)

The obtained spectrum is in accordance with the expected fragmentation of the molecule.

### Solvent Extraction Experiments

Extraction experiments were performed by shaking the aqueous and the organic phases for 15 minutes at a constant speed (1000 rpm), at a temperature of 25 °C, with a ratio of 1 between the two phases. DMDPHMA solutions (~0.1 M and ~0.01 M) in toluene,  $\text{CCl}_4$  or 1,2-dichloroethane were used as the organic phases. Hydrochloric acid solutions (1, 3, 4, 5, 6, 7, 8, 10 and 12 M) and metal feed solutions with ~0.01 M iron(III) in HCl (prepared by dissolving iron(III) chloride hexahydrate) were used as aqueous phases. Solutions containing ~0.01 M of other metals (copper(II) and indium(III)) as chloride salts were also used. In some metal solutions the total chloride concentration was maintained at 12 M by adding LiCl. The metal content in the aqueous phases was analysed before and after extraction by flame atomic absorption spectroscopy (Shimatzu AA 680), using three aliquots of each sample. The values obtained were treated and only accepted if a reasonable standard deviation were obtained. In all cases three sets of experiments were performed in order to confirm the data obtained. The aqueous and the loaded organic phases were analysed by UV-visible spectroscopy (Shimatzu UV 160).

Stripping experiments were conducted by contact with the loaded organic phase with distilled water or diluted HCl solution (~0.4 M) using the same conditions as for extraction.

All chemicals and reagents used were of analytical reagent grade.

## RESULTS AND DISCUSSION

### Extraction of Iron(III)

The ability of DMDPHMA to extract iron(III) from hydrochloric acid solutions was studied. The results obtained are presented in Figure 2. Iron(III) extraction increases as the hydrochloric acid concentration increases. For  $C_{\text{HCl}} \geq 7 \text{ M}$  metal extraction is higher than 90%, while only 25% was achieved from  $C_{\text{HCl}} = 5 \text{ M}$ . For  $C_{\text{HCl}} \leq 3 \text{ M}$  metal extraction is lower than 2%. Thus, it is possible to conclude that the extraction of iron(III) depends on the hydrochloric acid concentration.

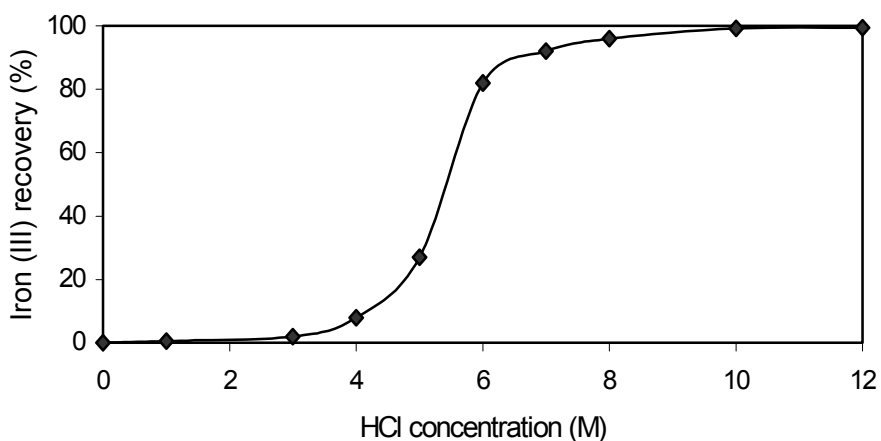


Figure 2. Iron(III) extraction with DMDPHMA from HCl solutions.

The use of different diluents such as  $\text{CCl}_4$  and 1,2-dichloroethane does not significantly affect the extraction of iron(III): 5-6% was achieved for  $C_{\text{HCl}} \leq 3 \text{ M}$ , when each of the alternative diluents were used.

Similar extraction behaviour was obtained for analogous experimental conditions with the corresponding alkylated malonamide ( $\text{N,N}'\text{-dimethyl-N,N}'\text{-diphenyltetradecylmalonamide}$ , DMDPHTDMA) [13].

The results of iron(III) extraction with DMDPHMA (~0.1 M) from HCl solutions from 0 to 12 M, with 12 M of total chloride concentration achieved by adding LiCl, show a quite different extraction profile: in these cases iron(III) is totally removed, regardless of the acid concentration. Even in solutions containing only LiCl (12 M), the metal is also completely extracted. When the concentration of the extractant is decreased (~0.01 M), the extraction of iron is almost unaffected, and therefore, the metal is still removed with an efficiency higher than 90%.

Studies with the alkylated malonamide (DMDPHTDMA) showed different extraction behaviour: no extraction was detected for  $C_{\text{HCl}} < 4 \text{ M}$ , while for higher acid concentrations the metal was completely removed [11,12]. This suggests that alkylated and the non-alkylated malonamides extract iron(III) by different extraction mechanisms.

Solvent extraction essays from hydrochloric acid solutions containing metals other than iron(III) – Cu(II), Zn(II) and In(III) - were carried out. No extraction was detected in the presence or in the absence of iron(III). The selectivity of Fe(III) over the metals under study is a very important result, mainly considering that in particular conditions zinc is frequently co-extracted together with iron by extractants commonly used (e.g., TBP, Alamine 336, D2EHPA) [14,15]. The co-extraction of iron(III) and copper from chloride media is also reported [15] (e.g., Alamine 336). The selectivity towards a large number of other base metal cations, usually present in pregnant mineral leaching solutions, such as Fe(II), Pb and Ni, is being researched.

In this project a preliminary attempt to find out which iron(III) species is preferably extracted by DMDPHMA from chloride media is made based on the extraction data obtained and on evidence given by spectroscopic techniques. The results presented above and the ultra-violet spectra of the charged organic phases (Figure 3) suggest that iron is extracted in the form of anionic chlorocomplex tetrachloroferrate  $\text{FeCl}_4^-$ .

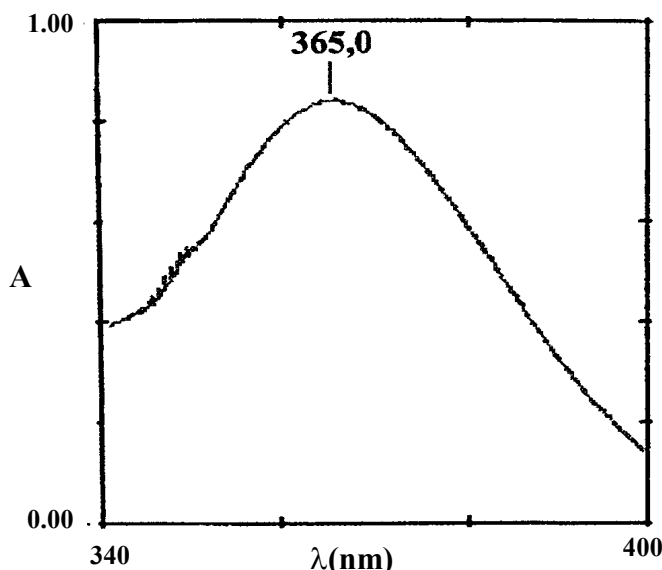


*Figure 3. Region of the UV-spectrum of loaded DMDPHMA.*

In fact the peak observed at 365 nm can probably be assigned to the anionic chlorocomplex, since the literature refers to the existence of an intense charge-transfer band at 364 nm for this complex [16]. This peak was clearly identified in the aqueous phases containing a hydrochloric acid concentration higher than 4 M, proving that the increase in chloride concentration favours the formation of  $\text{FeCl}_4^-$  and therefore iron(III) extraction.  $\text{FeCl}_4^-$  is referred to in the literature as predominant at high  $\text{Cl}^-$  concentrations [17]. For lower chloride concentrations chloro, aqua, and hydroxy species are mentioned [17] and, therefore, different spectra for the aqueous solutions were obtained (a peak near 340 nm appeared in that region of the UV spectrum), indicating that the anionic chlorocomplex species is not predominant. The new band is probably due to the presence of iron complexes containing chloride ions and water in their co-ordination sphere [18], which are not extracted by DMDPHMA.

Further studies to clarify the mechanism of extraction are being carried out.

The extraction data of malonamides for iron(III) from a hydrochloric acid medium show a different behaviour from those presented by the same compounds in the extraction of actinides and lanthanides from nitric acid solutions. A reason for this difference is obviously related with the utilisation of different media, where logically different equilibria are involved, leading possibly to different mechanisms of extraction.

### Stripping Experiments

Stripping experiments of iron(III) from the loaded organic phase to a purified aqueous phase were carried out using water and diluted HCl solutions (~0.4 M). In both cases iron(III) was only partially re-extracted after 15 minutes of contact between the two phases. Results from 23% to 38% were obtained with diluted acid solutions, while 28% was achieved using water.

Assays performed with the loaded alkylated malonamide, DMDPHTDMA, showed that iron(III) was quantitatively re-extracted by water or diluted HCl solutions [11], which proves the importance of the malonamide structure for efficient metal stripping.

## REFERENCES

1. C. Musikas and H. Hubert (1987), *Solvent Extr. Ion. Exch.*, **5** (5), 877-893.
2. C. Musikas (1988), *Sep. Sci. Technol.*, **23**, 1211-1218.
3. L. Nigond, C. Musikas and C. Cuillerdier (1994), *Solvent Extr. Ion. Exch.*, **12** (2), 297-229.
4. Q. Tian and A. Hughes (1994), *Hydrometallurgy*, **36**, 79-94.
5. M. Weigl, A. Geist, K. Gompper and J. Kim (2001), *Solvent Extr. Ion. Exch.*, **19** (2), 215-323.
6. L. Spjuth, J. O. Liljenzin, M. J. Hudson, M. G. B. Drew, P. B. Iveson and C. Madic (2000), *Solvent Extr. Ion. Exch.*, **18** (1), 1-23.
7. C. Cuillerdier, C. Musikas, P. Hoel, L. Nigond and X. Vitart (1991), *Sep. Sci. Technol.*, **26**, 1229-1236.
8. G. Y. S. Chan, M. G. B. Drew, M. J. Hudson, P. B. Iveson, J. O. Liljenzin, M. Skalberg, L. Spjuth and C. Madic (1997), *J. Chem. Soc., Dalton Trans.*, 649-660.
9. L. Spjuth, J. O. Liljenzin, M. Skalberg, M. J. Hudson, G. Y. S. Chan, M. G. B. Drew, M. Feaviour, P. B. Iveson and C. Madic (1997), *Radiochim. Acta*, **78**, 39-46.
10. L. Spjuth, J. O. Liljenzin, M. Skalberg, M. J. Hudson, G. Y. S. Chan, M. G. B. Drew, M. Feaviour, P. B. Iveson and C. Madic (1996), *Proc. Int. Solv. Ext. Conf.*, Melbourne, Australia, pp. 1309-1314.
11. M. C. Costa, C. E. Fernandes, M. J. Hudson and P. B. Iveson (1999), *Proc. Int. Solv. Ext. Conf.*, Barcelona, Spain, pp. 271-275.
12. C. E. Fernandes (1998), *Final Report for the Chemistry Degree*, University of Madeira, Portugal, 87 pp.
13. M. C. Costa, A. P. Paiva, *in preparation*.
14. M. C. Costa (1996), Processamento hidrometalurgico para recuperacao de metais basicos e preciosos, PhD Thesis, Faculty of Sciences of Lisbon University, Portugal.
15. J. Monhemius (1981), *Chem. Ind.*, **20**, 410-416.
16. A. B. P. Lever (1968), *Inorganic Electronic Spectroscopy*, Elsevier, Amsterdam, 295 pp.
17. F. A. Cotton and G. Wilkinson (1988), *Advanced Inorganic Chemistry*, John Wiley & Sons, New York, 717 pp.
18. N. Greenwood and A. Earnshaw (1984), *Chemistry of the Elements*, Pergamon Press, Oxford, 1264 pp.



## STUDY OF Sc AND Zr EXTRACTION REACTIONS BY REACTIVE MATERIALS CONTAINING ACIDIC ORGANOPHOSPHOROUS EXTRACTANTS

Jose-Luis Cortina, Vadim Korovin\* and Yuriy Shestak\*

Department of Chemical Engineering, Polytechnical University of Catalonia,  
Barcelona, Spain

\*Pridneprovski Scientific Centre, Ukrainian Academy of Sciences,  
Dnieprodzerzhinsk, Ukraine

Extraction properties of polymer reactive materials prepared by impregnation of macroporous polymers with DEHPA have been evaluated. NMR spectroscopy was used to determine the extraction mechanism of Sc and Zr with DEHPA (HA) in both carbon tetrachloride and when impregnated onto solid adsorbents. Extraction of Sc and Zr from acidic solutions showed changes in the composition of the extracted complexes when compared with liquid /liquid extraction. While in liquid/liquid extraction systems mixed complexes of Zr and Sc with anions of the aqueous phase ( $\text{NO}_3^-$  and  $\text{Cl}^-$ ) and the anionic form of DEHPA ( $\text{A}^-$ ) are extracted, in solid supports simples complexes of Zr and Sc with the anionic form of DEHPA ( $\text{A}^-$ ) were found. The ability to interact with extracted cations by both ion-exchange mechanism and formation of co-ordination bond with P=O group of DEHPA=HA molecules was corroborated. The availability of two active centers on HA ligands allows the formation of polynuclear complexes with metal ions.

### INTRODUCTION

Selective adsorption systems based on extractant supported in carriers are seen as an important emerging alternative approach to well established technologies such as solvent extraction (SX) and ion exchange (IX). These materials, in which the active phase is impregnated or physically immobilised into a porous carrier may be used widely for metal extraction, separation and preconcentration schemes in, for example, reversed-phase extraction chromatography, membrane extraction, and hydrometallurgy of rare-earth, non-ferrous and noble metals. These supported extractant materials are produced either by direct impregnation of a porous carrier by the liquid extractant (SIR), or by introduction of the extractant during synthesis of the porous matrix (solid extractants (TVEX)).

They have a number of processing advantages over techniques like resin ion exchange and liquid-liquid extraction. Thus when compared to conventional ion exchange resins they provide increased selectivity for a metal without the reduction in kinetics and capacity experienced by chelating ion exchange resins. Also when compared with liquid-liquid extraction, these systems provide a more efficient extractant use with minimal use of organic solvents, leading to a reduction in waste and hence a more environmentally desirable process. Authors of early papers did not notice any differences between the capacity of the extractant when present in the porous matrix and when used in liquid-liquid extraction.

However, recently it has been shown in a number of cases that the polymer matrix influences not only the extraction kinetics, but also the formation of metal complexes with the extractant in the organic phase [1-3].

These peculiarities on the metal extracted complexes and the influence of the solid carrier have been studied and described by partners of the present paper. Earlier work [3-6] comparing the extraction of a number of metals by extractants in the liquid phase and present in a polymer matrix by means of IR, NMR spectroscopy and mercury porosimetry has shown that: the porous matrix did not only change the composition and structure of extracted complexes, but also, in a number of cases, led to an increase in extractant capacity. This is the case for neutral extractants where the influence of the matrix on metal extraction was largely dependent on the extraction mechanism; for solvation extraction mechanism of a single metal the polymer matrix showed very little influence either on extractant capacity or the composition of extracted compounds; for systems forming metal complexes with labile co-ordination spheres the presence of the polymer matrix changes the composition and correlation of extracted compounds, simultaneously increasing the extractant capacity near extractant saturation.

The present paper describes the extraction of rare-earth (Zr(IV), Sc(III)) metals with impregnated reactive polymers containing DEHPA. These reactive materials were prepared by polymerisation of the polymer monomers in the presence of DEHPA. The extraction patterns in terms of metal extraction reactions and identification of extracted complexes in both organic solvents and solid supports were studied by using NMR spectroscopy.

## EXPERIMENTAL

### Preparation of DEHPA Solid Adsorbents

Synthesis of solid extractant (TVEX) containing DEHPA was carried out in a glass reactor fitted with a mixer, thermometer and back-flow condenser. Starch solution (0.4%), used as emulsion stabiliser, was first added to the reactor [7]. Then reaction mixture containing styrene, divinylbenzene, DEHPA and benzoyl peroxide as initiator of radical copolymerisation were fed into the reactor at 323 K with agitation. Polymerisation was carried out for 8 h. The TVEX granules were washed with water and dried with nitrogen. DEHPA loading was evaluated by washing a known amount of resin with ethanol, which elutes DEHPA for subsequent determination by potentiometric titrations.

### Rare Earth Extraction Evaluation

#### *Liquid-liquid and solid-liquid experiments*

Liquid-liquid extraction experiments were performed using 0.05 mol/L solutions of Sc(III) and 0.5 mol/L solutions of Zr(IV) and variable concentrations of HCl (from 0.2 to 7.9 mol/L) and HNO<sub>3</sub> (from 2.2 to 8.1 mol/L), respectively. DEHPA solutions in CCl<sub>4</sub> were 0.3 mol/L for Sc(III) experiments and 0.5 and 1.8 mol/L for Zr(IV) experiments. Equal volumes of aqueous and organic phases were used. Agitation times of 30 minutes were enough to reach equilibrium. For solid extraction systems a volumetric phase ratio of 4 (resin/aqueous) was used while equilibration times of 1440 minutes were used. Detailed description of the different runs is collected in tables 1 and 2. Sc and Zr concentration in aqueous phase was measured using photometric titration by EDTA.

#### *NMR spectroscopy measurements*

<sup>31</sup>P (81.04 MHz) and <sup>45</sup>Sc (48.62 MHz) NMR high resolution spectra were recorded using impulse spectrometer Bruker CXP-200. Positive chemical shifts correspond to decrease of magnetic field. Chemical shifts were referenced to a 85 % phosphoric acid solution for <sup>31</sup>P and a 0.1 mol/L acidified Sc(ClO<sub>4</sub>)<sub>3</sub> solution <sup>45</sup>Sc. Relative intensities of badly resolved

spectra were defined by searching system parameters (position, width, height) minimising root-mean-square deviation of calculated and experimental spectra [7].

## SCANDIUM EXTRACTION

$^{45}\text{Sc}$  NMR spectra of liquid and solid Sc-containing extracts comprise broad singlet signals with chemical shifts -9.6 ppm (535-560 Hz) for  $\text{CCl}_4$  extracts and -10.4 ppm (2420-2480 Hz) for solid ones. Measured values of chemical shift indicated the absence of  $\text{Cl}^-$  ions in scandium co-ordination sphere. Former studies revealed [8] that inclusion of every  $\text{Cl}^-$  ion to Sc co-ordination sphere resulted in signal shift approximately 45 ppm to low field up to +249 ppm for  $[\text{ScCl}_6]^{3+}$  complex.

$^{31}\text{P}$  NMR spectra of extracts and TVEX in Figure 1 showed up to a maximum of three peaks (A, B and C). Signal A (1.2-1.7 ppm) in spectra of initial DEHPA in  $\text{CCl}_4$  and TVEX-DHEPA corresponds to non-coordinated DEHPA molecules while signal B (-4.5-4.7 ppm) in all Sc-containing samples corresponds to DEHPA molecules bound with scandium. Besides, a third signal C in the spectra of some specimen with chemical shift twice as much as the chemical shift for signal B (Figure 1, spectra 2, 4, 5) was associated to DEHPA molecules bound with 2 Sc ions (*i.e.*, “bridge” extractant molecules).

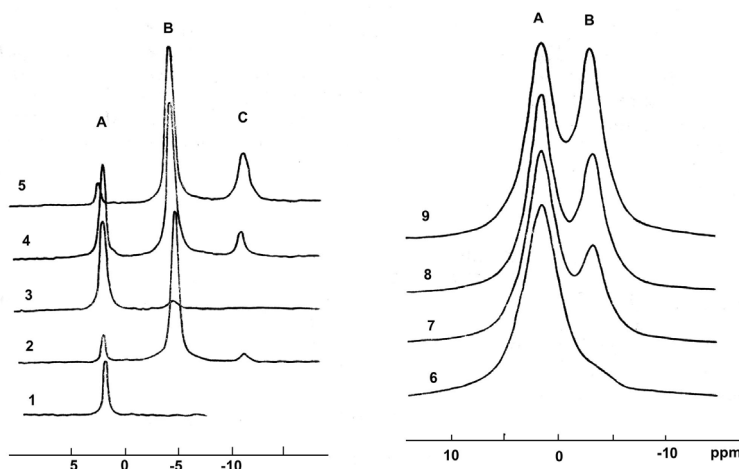


Figure 1.  $^{31}\text{P}$  NMR spectra of initial 0.3 mol/L DEHPA in  $\text{CCl}_4$  (1); Sc-containing extracts (2-5) and TVEX-DEHPA samples (6-9).

Average solvate number (ASN) (Table 1), which defines the number of extractant molecules bonded with metal ion, was calculated on the basis of DEHPA/Sc mol ratio (R) and relative intensity (I) of B and C signals (signals from bonded extractant molecules) using the following equation  $\text{ASN} = R^* (I_B + I_C) / 100$ .

ASN values of 6 for  $\text{CCl}_4$  suggested that the extraction of scandium proceeds with the formation of the complex  $\text{Sc}(\text{A}_2\text{H})_3$ . ASN values less than 6 together with absence of  $\text{Cl}^-$  ions in Sc first co-ordination sphere may be explained by either inclusion of water molecules or formation of scandium polymer bonds with HA. Since the amount of extractant “bridge” molecules is negligible (according to NMR data), decrease of ASN value may be explained by inclusion of water molecules to Sc first co-ordination sphere.

Table 1. Scandium average solvate number in extracts and TVEX-DEHPA.

Run #	Sample	[HCl], mol/L	R $C_{HA}/C_{Sc}$	Relative Signal Intensity, % (I)			ASN
				I <sub>A</sub>	I <sub>B</sub>	I <sub>C</sub>	
<b>Solvent Extraction</b>							
1	0.3 mol/L HA in CCl <sub>4</sub>	0.2	5.6	4.6	91.0	4.4	5.3
2		1.1	5.8	5.2	90.7	4.1	5.5
3		2.3	19.5	72.5	27.5	0	5.3
4		4.0	28.6	86.1	13.9	0	5.0
5		5.7	22.9	74.7	25.3	0	5.8
6		8.0	6.1	12.9	76.8	10.3	5.3
7		1.1	3.6	4.6	58.4	37.0	3.5
8		7.4	6.0	12.3	78.2	9.5	5.3
9	Extract # 2	Water	5.8	4.7	91.9	3.4	5.5
10	Extract # 4	Water	28.6	79.4	20.6	0	5.9
11	Extract # 6	Water	6.1	8.3	88.0	3.7	5.6
<b>TVEX-DEHPA</b>							
12	TVEX-DEHPA	0.2	5.6	97.2	2.8	0	0.2
13		1.1	5.6	92.4	7.6	0	0.4
14		2.4	5.6	72.7	27.3	0	1.5
15		4.2	5.6	70.4	29.6	0	1.7
16		6.3	5.6	61.5	38.5	0	2.2
17		7.60	5.62	59.8	40.2	0	2.3

For conditions with minimum ASN values of 4 (run # 7) extraction will take place with scandium ions bound to 4 DEHPA molecules and 2 water molecules as could be seen in the following two possible structures:

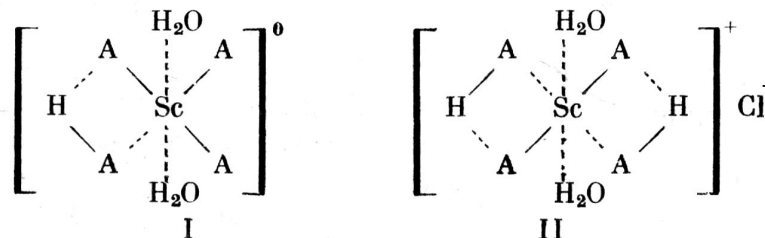
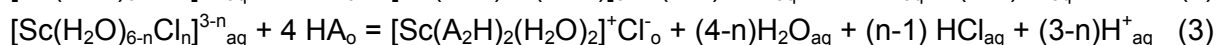
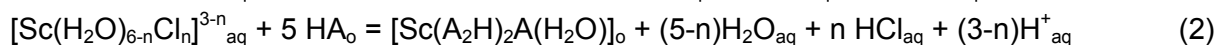
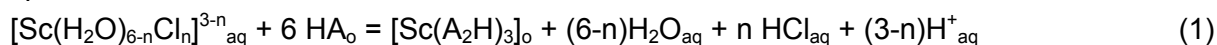


Figure 2. Proposed Sc-DEHPA structures.

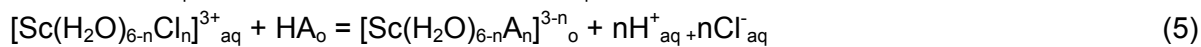
Rinsing of CCl<sub>4</sub> phases with water (runs 9-11) resulted in an increase of content of HA molecules co-ordinated to scandium, a decrease of concentration of non-coordinated extractant, decrease of "bridge" molecule amount and an ASN increase. Besides, analysis of rinsing water revealed the presence of HCl and absence of scandium ions. These facts confirm the entry of Cl<sup>-</sup> ions to scandium extracted complexes.

Thus, present results allow concluding that Cl<sup>-</sup> ions are not found in the first co-ordination sphere and, the extraction mechanism could be described as:



where n = 0 – 3 depending upon acidity of aqueous phase.

For TVEX-DEHPA scandium is extracted as complexes with common formula  $[\text{Sc}(\text{H}_2\text{O})_6\text{A}_n]_{3-n}$ , where n equals 0 - 3 according to ASN values. Thus, Sc extraction by TVEX-DEHPA is accompanied by substitution of  $\text{Cl}^-$  ions in Sc first coordination sphere by  $\text{A}^-$  ions; and extraction mechanism may be presented by the following equations:



## ZIRCONIUM EXTRACTION

$^{31}\text{P}$  NMR spectra of DHEPA solution in  $\text{CCl}_4$  and TVEX-DHEPA consist of three singlet signals A, B and C (Figure 3). Signal A (+1.6 to -1.8 ppm) corresponds to non-bonded extractant molecules while signal B (-5.9 to -5.3 ppm) was associated to monodentate extractant ligands ( $\text{A}^-$ ) in Zr co-ordination sphere. Signal C (-15.1 to -15.2 ppm) was associated to bridge ligands that simultaneously interact with two zirconium ions forming polynuclear complexes Zr-A-Zr. It should be pointed out that the amount of "bridge" DHEPA molecules is small in all the organic phases with a maximum of 7 %.

Based on DHEPA/Zr mole ratio (R) and relative intensity (I) of B and C signals in the NMR spectra, the average solvate number of DEHPA molecules for Zr cations was calculated for the studied system. The data obtained are given in Table 2.

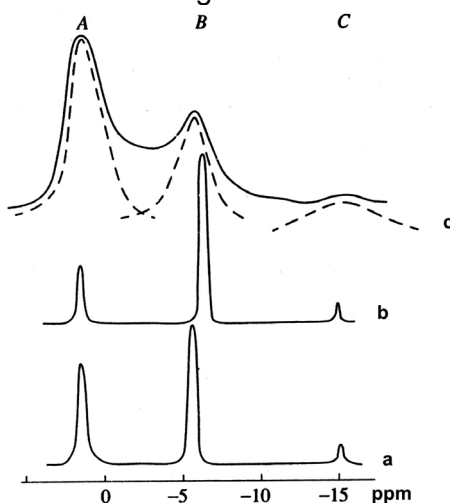


Figure 3.  $^{31}\text{P}$  NMR spectra of zirconium extracts: (a) 0.3 mol/L DEHPA; (b) 0.3 mol/L DEHPA after water rinsing, (c) TVEX-DEHPA.

ASN value for zirconium extraction by 0.3 mol/L (runs 1-5) and 1.9 mol/L (runs 8-12) DEHPA in  $\text{CCl}_4$  is less than 4, i.e., amount of  $\text{A}^-$  ions in co-ordination sphere of  $\text{Zr}^{4+}$  ion is not sufficient to compensate its charge. Consequently, for the studied conditions extraction takes place with formation of compound mixed complexes with  $\text{A}^-$  and  $\text{NO}_3^-$  anions; and extraction mechanism may be described by the following equation:

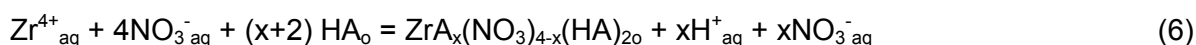


Table 2. Zirconium extraction by DEHPA and TVEX-DHEPA runs.

Run	Organic Phase	[HNO <sub>3</sub> ], mol/L	Loading, mol Zr/L	HA/ Zr Ratio	Intensity, %			ASN
					I <sub>A</sub>	I <sub>B</sub>	I <sub>C</sub>	
1 2 3 4 5	0.300 mol/L DEHPA in CCl <sub>4</sub>	2.2	0.07	8.7	63.4	36.6	0	3.2
		4.2	0.10	6.0	47.7	48.6	3.7	3.2
		5.1	0.10	6.0	48.0	48.0	4.0	3.1
		6.0	0.09	6.2	44.3	51.4	4.3	3.4
		8.1	0.10	5.9	52.9	42.4	4.7	2.8
6	Extract, run 1	water	0.070	8.72	33.9	63.9	2.2	5.8
7	Extract, run 5	water	0.103	5.88	28.9	65.6	5.5	4.2
8 9 10 11 12	1.875 mol/L DEHPA in CCl <sub>4</sub>	2.2	0.62	6.1	43.9	49.8	6.3	3.4
		3.8	0.45	8.5	58.1	38.9	3.0	3.6
		5.0	0.68	6.0	45.0	48.6	6.4	3.3
		6.1	0.62	6.2	42.9	49.7	7.3	3.5
		8.1	0.65	5.9	48.3	44.8	6.9	3.0
13 14 15 16 17	TVEX – 35.6 wt. % DEHPA	2.2	0.37	6.0	73.2	21.3	5.5	1.6
		4.0	0.38	5.9	75.0	23.0	2.0	1.5
		5.1	0.38	5.9	78.1	19.7	2.2	1.3
		5.7	0.36	6.2	78.9	18.7	2.4	1.3
		7.9	0.38	5.9	80.8	16.7	2.5	1.1

On the basis of ASN value, the following complexes are extracted within the studied aqueous phase acidity (2.2 - 8.1 mole/L): Zr(NO<sub>3</sub>)<sub>4</sub>(HA)<sub>2</sub> (I), ZrA(NO<sub>3</sub>)<sub>3</sub>(HA)<sub>2</sub> (II), ZrA<sub>2</sub>(NO<sub>3</sub>)<sub>2</sub>(HA)<sub>2</sub> (III). Their structure may be presented by the following formulas:

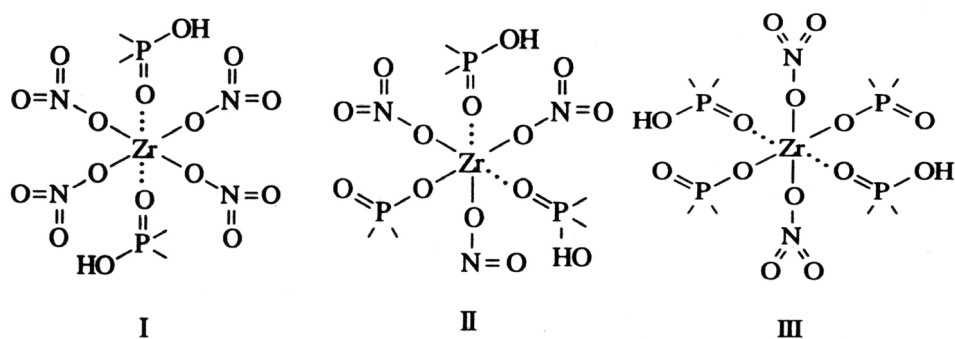
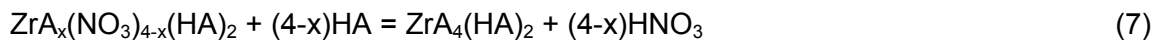


Figure 4. Proposed Zr-DEHPA structures.

ASN value decreases with acidity increase that may be caused by decrease of compound III content and increase of content of forms I and II at increase of NO<sub>3</sub><sup>-</sup> content in organic phase. CCl<sub>4</sub> extracts from experiments 1 and 5 were rinsed with water. Zirconium was not found in rinsing water however acidity of aqueous phase increased. The amount of non-bonded DEHPA molecules essentially decreased (see Figure 3 curve b); the amount of bonded extractant molecules increased with an ASN increase from 3.2 to 5.8 (runs # 1 and 6) and from 2.8 to 4.2 (runs # 5 and 7). The water rinsing resulted in removal of NO<sub>3</sub><sup>-</sup> ions from organic phase and substitution of these positions by A<sup>-</sup> anions which gives the following Zr extraction reaction:



For Zr extraction by TVEX-DEHPA the ASN value is half as much for solvent extraction and decreases from 1.6 to 1.1 with an increase of the aqueous phase acidity. This indicates that one zirconium cation interacts with one or two HA molecules in solid extractant forming mainly complexes I and II in organic phase.

## CONCLUSIONS

Differences in metal extraction by DEHPA and TVEX-DEHPA is caused by the extractant state in the porous carrier. Small signal broadening in TVEX spectra as compared with DHEPA solution in  $\text{CCl}_4$  indicates the liquid state of the extractant in matrix. Part of the extractant is held due to physical adsorption and "meshing" of big and branched alkyl radicals in the polymer structure. This limits the mobility of extractant molecules and decreases their competitiveness with nitric ions during filling of Zr co-ordination sphere. This mechanism is similar to sorption of metal cations by ion-exchange resins where functional groups are fixed in a polymer frame.

## REFERENCES

1. V. Korovin (1991), *Khim. Technol.*, **5**, 3-13.
2. V. Korovin, Y.G. Shestak and Y. Pogorelov (1996), *Proc. 12th Int. Congr. Chem. Proc. Eng.*, Praha, Sec. 3, p.127.
3. J. L. Cortina and A. Warshawsky (1996), Ion Exchange and Solvent Extraction, Vol. 13, J. Marinsky and Y. Marcus (eds.), Marcel Dekker, New York, pp. 204-299.
4. J. L. Cortina, N. Miralles, M. Aguilar and A. Sastre (1995), *Hydrometallurgy*, **37**, 301-302.
5. V. Korovin, S. B. Randarevich, Y. N. Pogorelov and S. V. Bodaratsky (1996), *Russ. J. Coordin. Chem.*, **22** (8), 633-640.
6. V. Korovin and S. Randarevich (1988), *Proc. ISEC '88*, Vol. 3, Moscow, pp. 159-162.
7. B. Bandi (1988), Methods of Optimization, Moscow.
8. Y. Buslaev (1982), *Doklady AN, SSSR*, **8**, 261-264.



# SOLVENT EXTRACTION OF TETRAVALENT TITANIUM, ZIRCONIUM AND TIN FROM HYDROCHLORIC ACID SOLUTIONS BY AN $\alpha$ -HYDROXYOXIME

Taichi Sato\*\*\*, Kiyohito Suzuki\*, Keiichi Sato\* and Toshio Takahashi\*\*\*

\* Faculty of Engineering, Shizuoka University, Hamamatsu, Japan

\*\* Queen's University, Metallurgical Engineering Department, Kingston, Ontario, Canada

\*\*\* Lion Corporation, Materials Science Research Center, Tokyo, Japan

The extraction of tetravalent titanium, zirconium and tin from hydrochloric acid solutions by LIX 63 (5,8-diethyl-7-hydroxy-6-dodecanone oxime, HR) in kerosene was investigated. The organic extracts were examined by infrared and nuclear magnetic resonance spectroscopy. In the range of 0.1-10 mol dm<sup>-3</sup> HCl, the extraction efficiency of LIX 63 is in the order Sn > Ti > Zr at [HCl] < 1 mol dm<sup>-3</sup>, Ti > Zr > Sn at [HCl] = 1-3 mol dm<sup>-3</sup> and Ti > Sn > Zr at [HCl] > 3 mol dm<sup>-3</sup>. As a result, the equilibrium equations are proposed as follows: for Ti(IV),  $\text{Ti}(\text{OH})_2^{2+}(\text{aq}) + 2\text{HR}(\text{org}) \leftrightarrow \text{Ti}(\text{OH})_2\text{R}_2(\text{org}) + 2\text{H}^+(\text{aq})$  and  $\text{Ti}(\text{OH})_2\text{Cl}_2(\text{aq}) + 2\text{HR}(\text{org}) \leftrightarrow \text{Ti}(\text{OH})_2\text{Cl}_2 \cdot 2\text{HR}(\text{org})$ ; for Zr(IV),  $\text{ZrCl}_4(\text{aq}) + \text{HR}(\text{org}) \leftrightarrow \text{ZrCl}_4 \cdot \text{HR}(\text{org})$ ; for Sn(IV),  $\text{SnCl}_2^{2+}(\text{aq}) + 2\text{HR}(\text{org}) \leftrightarrow \text{SnCl}_2\text{R}_2(\text{org}) + 2\text{H}^+(\text{aq})$  and  $\text{SnCl}_4(\text{aq}) + \text{HR}(\text{org}) \leftrightarrow \text{SnCl}_4 \cdot \text{HR}(\text{org})$ .

## INTRODUCTION

The extraction of divalent metals such as copper, nickel and cobalt by  $\alpha$ -hydroxyoximes has been reported extensively [1], but little attention has been paid to the extraction of tri- and tetravalent metals. From the viewpoint of hydrometallurgical processing, however, solvent extraction of tri- and tetravalent elements is of significance because of an increase in industrial demand. Accordingly, our studies have been conducted on the complexes formed in the extraction of copper from hydrochloric acid solutions by an  $\alpha$ -hydroxyoxime (such as 5,8-diethyl-7-hydroxy-6-dodecanone oxime, HR, the active component of LIX 63), and in addition the extraction of divalent cobalt, nickel and copper and trivalent gallium, indium, thallium and iron [2-5]. The present paper extends the work to the extraction of tetravalent titanium, zirconium and tin from hydrochloric acid solutions by an  $\alpha$ -hydroxyoxime.

## EXPERIMENTAL

LIX 63 (Henkel Corp., now Cognis) used as the  $\alpha$ -hydroxyoxime was purified by the method according to an earlier paper [6], and diluted with purified kerosene. Stock solutions of metal chlorides were prepared as follows: titanium chloride solution is obtained by dissolving titanium hydroxide, precipitated by addition of ammonium hydroxide to titanium tetrachloride, in hydrochloric acid. Aqueous solutions of zirconium and tin were obtained by dissolving their chlorides ( $\text{ZrCl}_4$  and  $\text{SnCl}_4 \cdot x\text{H}_2\text{O}$ ) in hydrochloric acid of the selected concentration. The concentrations of titanium, zirconium and tin were generally 1 g dm<sup>-3</sup> as the respective chlorides, except for loading tests. All chemicals used were of an analytical reagent grade.

Equal volumes (15 cm<sup>3</sup> each) of the aqueous and organic phases placed in 50 cm<sup>3</sup> stoppered conical flask were shaken for a certain period by a mechanical shaker at 298 K, except the experiments on temperature effect. Preliminary experiments showed that the equilibria for titanium, zirconium and tin were attained in 8, 2 and 3 h, respectively. After separation of both phases by centrifugation, the aliquots of the both phases were pipetted for analysis. Metals in the organic phase were stripped with 1 mol dm<sup>-3</sup> sodium hydroxide solution and concentrated hydrochloric acid for titanium, 6 mol dm<sup>-3</sup> nitric acid and 2-ethylhexyl alcohol for zirconium and 2 mol dm<sup>-3</sup> hydrochloric acid and 2-ethylhexyl alcohol for tin, respectively. The addition of the alcohol plays the role of promoting the dehydration of the extracted species. The extraction coefficient, E<sub>a</sub><sup>°</sup>, was determined as the ratio of the equilibrium concentration of metal in the organic phase to that in the aqueous phase.

The concentration of titanium in aqueous solution was obtained by adding excess of EDTA and back-titration with zinc sulphate solution at pH 7 using Eriochrome Black T. The concentrations of zirconium and tin were assayed by EDTA titration using xylene orange as the indicator. The infrared (IR) spectra were recorded on JASCO models IRA-1 (4000-650 cm<sup>-1</sup>) and IR-F (700-200 cm<sup>-1</sup>) using a capillary film between thallium halide plates or polyethylene films. The nuclear magnetic resonance (NMR) spectra were obtained for the organic extracts dissolved in carbon tetrachloride using a Hitachi model R-24 with the use of tetramethylsilane as the internal reference.

## RESULTS AND DISCUSSION

### Extraction Isotherms

The extraction of tetravalent titanium, zirconium and tin from hydrochloric acid solutions by different concentrations of LIX 63 in kerosene gives the results shown in Figures 1 to 3. Figure 1 shows that with increasing in the aqueous acidity, the distribution coefficient for titanium(IV) decreases gently up to 1 mol dm<sup>-3</sup> and rises to a maximum at 2 mol dm<sup>-3</sup> and then falls. In Figure 2, with increasing in the aqueous acidity, the distribution coefficient for zirconium rises to a maximum at 2 mol dm<sup>-3</sup> and then falls up to 7 mol dm<sup>-3</sup> and rises again. The distribution behaviour of tin(IV) resembles that of titanium(IV) as seen in Figure 3: with increasing in the aqueous acidity, the distribution coefficient decreases to a minimum at 2 mol dm<sup>-3</sup> and rises to a maximum at 3 mol dm<sup>-3</sup> and then falls. When the extraction efficiency of LIX 63 for titanium(IV), zirconium(IV) and tin(IV) is compared at the aqueous acidity in the range of 0.1-10 mol dm<sup>-3</sup> HCl, it is in the order Sn > Ti > Zr at [HCl] < 1 mol dm<sup>-3</sup>, Ti > Zr > Sn at [HCl] = 1-3 mol dm<sup>-3</sup> and Ti > Sn > Zr at [HCl] > 3 mol dm<sup>-3</sup>, respectively. In the extraction of titanium(IV) at 1 mol dm<sup>-3</sup> =< [HCl], when hydrochloric acid in aqueous solution is partly replaced by lithium chloride, the distribution coefficient rises with the total chloride ion concentration.

This suggests that the total chloride concentration is the controlling factor (Figure 1). From this, it is deduced that there are two different regions in which the extraction occurs involving different mechanism. The variation of the distribution coefficient is attributed to the chelation mechanism similar to a cation exchange reaction in the weak acid region, and arises from a solvating reaction at higher acidities. But there is no simple aquated Ti<sup>4+</sup> ion because of the extremely high charge-to-radius ratio, and in aqueous solutions hydrolyzed species occur and basic oxo salts or hydrated oxides may precipitate. Besides, as the titanyl ion, TiO<sup>2+</sup>, seems to exist neither in solutions nor in crystalline salts, the species [Ti(OH)<sub>2</sub>(H<sub>2</sub>O)<sub>4</sub>]<sup>2+</sup> is in general considered to be the prevailing species in dilute aqueous solutions of titanium salts. However, since the extraction of zirconium(IV) at [HCl] =< 1 mol dm<sup>-3</sup> reveals the rising in the distribution coefficient with increasing in the total chloride ion concentration for the aqueous solutions of 0.7 mol dm<sup>-3</sup> HCl + LiCl, the results shown in Figure 2 arise from a solvating reaction. In addition, the extraction of zirconium(IV) from aqueous solutions at pH 2 by LIX

63 forms a third phase. In contrast, the extraction of tin(IV) is analogous to that of titanium(IV): the distribution coefficient is not much affected with increasing in the total chloride ion concentration for the aqueous solutions of  $0.4 \text{ mol dm}^{-3}$  HCl + LiCl.

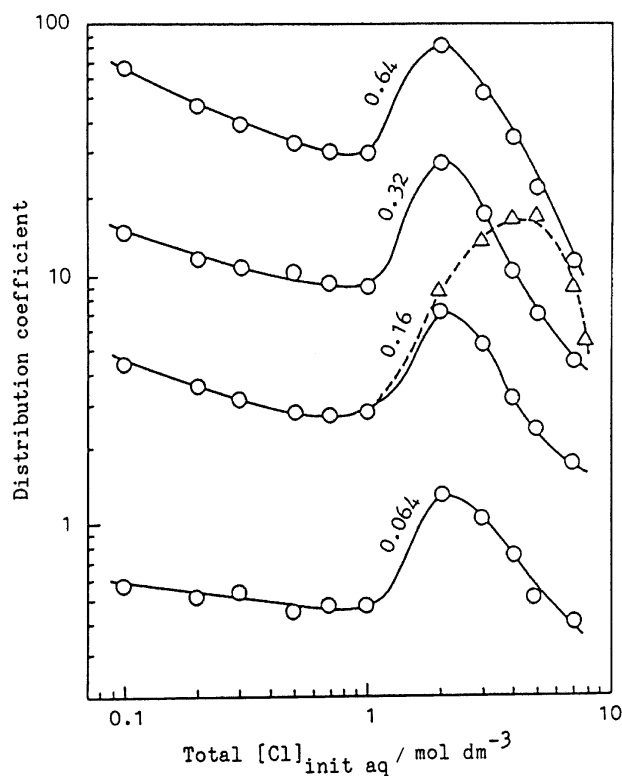


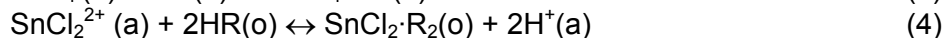
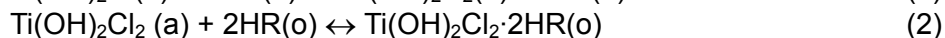
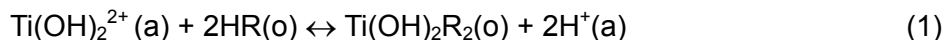
Figure 1. Extraction of titanium(IV) from HCl solutions by LIX 63 in kerosene. Numerals upon the curves are LIX 63 concentrations /  $\text{mol dm}^{-3}$ ; continuous and broken lines represent the extraction from HCl solutions and mixed  $1 \text{ mol dm}^{-3}$  HCl / LiCl solutions, respectively.

Table 1. Slope of log-log plots of  $E_a^\circ$  vs.  $[\text{HR}]_{\text{eq}}$  for the extraction of titanium(IV), zirconium(IV) and tin(IV) from hydrochloric acid solutions with LIX 63 in kerosene.

$[\text{HCl}]_{\text{init aq}}$ $\text{mol dm}^{-3}$	Slope		
	Ti	Zr	Sn
0.1	1.8	-	2.0
0.3	1.7	1.1	1.9
0.5	1.8	0.8	1.8
1	1.8	1.1	1.4
2	1.9	1.2	1.2
3	1.9	1.1	1.2
5	1.8	1.1	1.0
10	1.8	1.0	1.0

Log-log plots of  $E_a^\circ$  vs.  $[\text{HR}]_{\text{eq}} = [[\text{HR}]_{\text{init}} - n[\text{M}]_{\text{org}}]$  where  $\text{M} = \text{Ti}, \text{Zr}$  or  $\text{Sn}$  and  $n$  denotes the solvation number, at constant hydrochloric acid concentration give the straight lines with slopes of 1-2 as illustrated in Table 1. It is thus seen that their distribution coefficients have first- and second-power dependences on LIX 63 concentration, indicating the formation of mono- and di-solvates.

This is also supported by the loading test of the metals in the organic phase. When the metals are extracted with  $0.064 \text{ mol dm}^{-3}$  LIX 63, the molar ratio of the extract  $[\text{Ti}] / [\text{Cl}] / [\text{HR}] / [\text{H}_2\text{O}]$ , seems to approach to 1:2:2:1 at 2 mol  $\text{dm}^{-3}$  HCl,  $[\text{Zr}] / [\text{Cl}] / [\text{HR}] / [\text{H}_2\text{O}]$  to 1:4:1:4 at 2 mol  $\text{dm}^{-3}$  HCl and  $[\text{Sn}] / [\text{Cl}] / [\text{HR}] / [\text{H}_2\text{O}]$  to 1:2:2:1 and 1:4:1:1 at 0.4 and 5 mol  $\text{dm}^{-3}$  HCl. These results suggest the formation of  $\text{TiCl}_2 \cdot 2\text{HR} \cdot \text{H}_2\text{O}$ ,  $\text{ZrCl}_4 \cdot \text{HR} \cdot 4\text{H}_2\text{O}$ ,  $\text{SnCl}_2 \cdot \text{R}_2 \cdot \text{H}_2\text{O}$  and  $\text{SnCl}_4 \cdot \text{HR} \cdot \text{H}_2\text{O}$ , respectively. Hence the following equilibrium equations are proposed:



Here, (a) and (o) represents the species in the aqueous and organic phase, respectively.

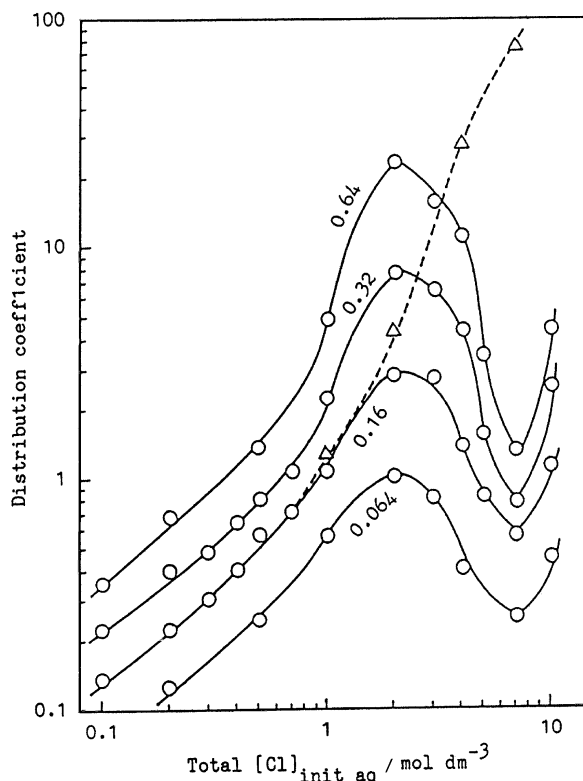
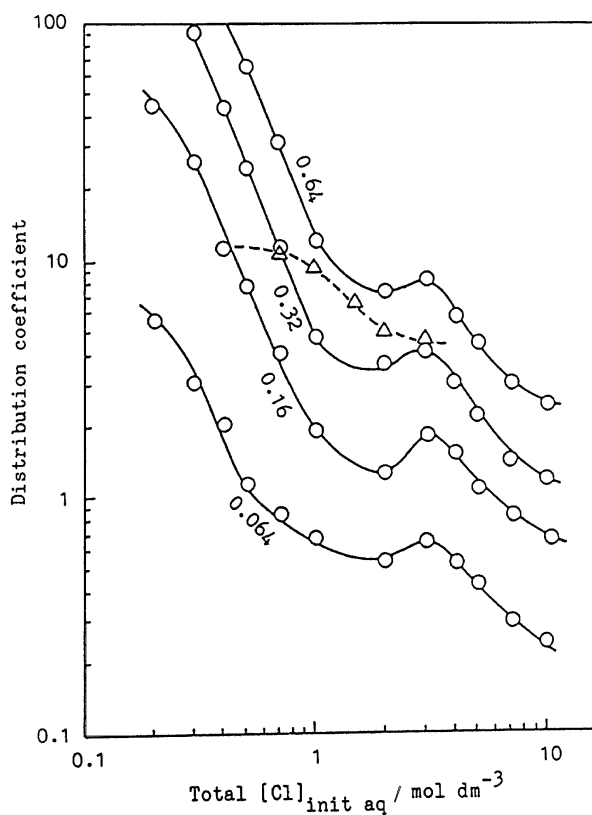


Figure 2. Extraction of zirconium(IV) from HCl solutions by LIX 63 in kerosene. Numerals upon the curves are LIX 63 concentrations /  $\text{mol dm}^{-3}$ ; continuous and broken lines represent the extraction from HCl solutions and mixed  $0.7 \text{ mol dm}^{-3}$  HCl / LiCl solutions, respectively.

### IR and NMR Spectra

The organic phases of  $0.01 \text{ mol dm}^{-3}$  LIX 63 in *n*-hexane equilibrated with 2 mol  $\text{dm}^{-3}$  hydrochloric acid solutions containing each metal salts of 1, 10 and  $25 \text{ g dm}^{-3}$  were examined by IR spectroscopy. As for all organic extracts, the C-O stretching vibration which appears at  $1030 \text{ cm}^{-1}$  for free extractant shifts to higher frequency at  $1035\text{-}1040 \text{ cm}^{-1}$ , whereas the C=N stretching vibration at  $1650 \text{ cm}^{-1}$  shifts to lower frequency at  $1610\text{-}1620 \text{ cm}^{-1}$ . From this it is deduced that the species formed in the organic phase possesses the structure in which oxime group coordinates to the metal through oxygen and nitrogen atoms. Additionally the stretching modes of Ti-Cl, Ti-O, Zr-Cl, Zr-O, Sn-Cl and Sn-O appear at 280, 515, 328, 495, 335 and  $490 \text{ cm}^{-1}$ , respectively, due to the formation of the species in Eqs. (2), (3) and (5).



*Figure 3. Extraction of tin(IV) from HCl solutions by LIX 63 in kerosene. Numerals upon the curves are LIX 63 concentration / mol dm<sup>-3</sup>; continuous and broken lines represent the extraction from HCl solutions and mixed 0.4 mol dm<sup>-3</sup> HCl / LiCl solutions, respectively.*

The organic extracts from aqueous solutions containing tin chloride in 0.4 and 5 mol dm<sup>-3</sup> HCl with 0.1 mol dm<sup>-3</sup> LIX 63 in carbon tetrachloride were examined by NMR spectroscopy. At 0.4 mol dm<sup>-3</sup> HCl, the OH resonance due to oxime at  $\tau$  5.9 exhibits the shift to higher field and the decrease in the intensity with increasing in the metal concentration in the organic phase, arising from the substitution of hydrogen ion of LIX 63 by the metal ion. At 5 mol dm<sup>-3</sup> HCl, LIX 63 shows the peak at  $\tau$  1.6, due to the compound HCl-HR [3] formed in the extraction of hydrochloric acid, shifts to higher field. Similar NMR spectra are also observed for the extracts of other metals.

#### Temperature Effect

The results for the extraction of each metals at temperature between 283-313 K are indicated in Table 2. It is seen that the distribution coefficients increase with rising temperature. Thus the value of the heat of reaction ( $-\Delta H$ , change in enthalpy) are estimated: 15.4 (Ti), 16.6 (Zr), 4.36 (Sn) and 7.93 (Sn) kJ mol<sup>-1</sup> at 2, 2, 0.5 and 5 mol dm<sup>-3</sup> HCl, respectively.

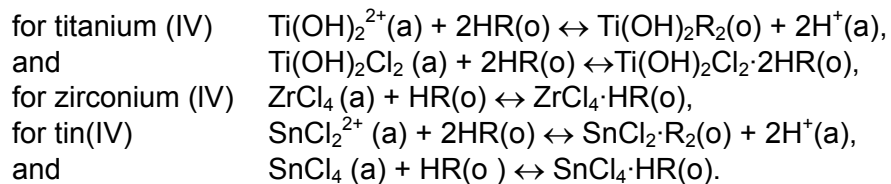
*Table 2. Temperature-dependence of the distribution coefficient for the extraction of titanium(IV), zirconium(IV) and tin(IV) from hydrochloric acid solutions with LIX 63 in kerosene.*

Metal	[HCl] <sub>init aq</sub> mol dm <sup>-3</sup>	[HR] mol dm <sup>-3</sup>	E <sub>a</sub> <sup>o</sup>			
			283 K	293 K	303 K	313 K
Ti	2	0.064	4.61	6.21	8.26	10.4
Zr	2	0.064	0.561	0.832	1.21	1.69
Sn	0.5	0.16	6.31	8.11	10.1	12.8
Sn	5	0.16	0.971	1.18	1.49	1.86

## CONCLUSION

The extraction of tetravalent titanium, zirconium and tin from hydrochloric acid solutions by LIX 63 in kerosene has been investigated over the concentration range of 0.1 to 10 mol dm<sup>-3</sup> hydrochloric acid. With increasing in the aqueous acidity, the distribution coefficient for titanium(IV) decreases gently up to 1 mol dm<sup>-3</sup> and then rises to a maximum at 2 mol dm<sup>-3</sup> and falls again; for zirconium(IV), the distribution coefficient rises to a maximum at 2 mol dm<sup>-3</sup> and then falls up to 7 mol dm<sup>-3</sup> and rises again; for tin-(IV), the distribution behaviour is analogous to that of titanium(IV) but the distribution coefficient decreases to a minimum at 2 mol dm<sup>-3</sup> and then rises to a maximum at 3 mol dm<sup>-3</sup> and falls again. When the extraction efficiency of LIX 63 is compared with each metal, its order is observed as Sn > Ti > Zr at [HCl] = < 1 mol dm<sup>-3</sup>, Ti > Zr > Sn at [HCl] = 1-3 mol dm<sup>-3</sup> and Ti > Sn > Zr at [HCl] >= 3 mol dm<sup>-3</sup>.

As a result, the extraction of tetravalent titanium, zirconium and tin from hydrochloric acid solutions by LIX 63 proceeds according to the following equations:



## REFERENCES

1. D. S. Flett, J. Melling and M. Cox (1983), *Handbook of Solvent Extraction*, T. C. Lo, M. H. I. Baird and C. Hanson (eds.), Wiley, New York, pp. 629-647.
2. T. Sato, M. Ito, T. Sakamoto and R. Otsuka (1987), *Hydrometallurgy*, **18**, 105-115.
3. T. Sato, M. Ito and K. Sato (1996), *Proc. Int. Solvent Extr. Conf.*, Vol. 1, University of Melbourne Press, Melbourne, pp. 665-670.
4. T. Sato, K. Suzuki and K. Sato (1989), *Proc. 2nd Int. Conf. on Separations and Technology*, Vol. 2, Canadian Society of Chemical Engineers, Ottawa, pp. 539-547.
5. T. Sato, K. Sato and Y. Noguchi (2001), *J. Min. Mater. Proces. Inst. Jpn.*, **117**, 226-229.
6. T. A. B. Al-DiWan, M. A. Hughes and R. J. Whewell (1977), *J. Inorg. Nucl. Chem.*, **39**, 1419-1424.



## AGGREGATION AND METAL ION EXTRACTION PROPERTIES OF NOVEL, SILICON-SUBSTITUTED ALKYLENEDIPHOSPHONIC ACIDS

Daniel R. McAlister, Mark L. Dietz\*, Renato Chiarizia\* and Albert W. Herlinger

Department of Chemistry, Loyola University Chicago, Chicago, IL, USA

\*Chemistry Division, Argonne National Laboratory, Argonne, IL, USA

In conjunction with efforts to develop novel actinide extractants exhibiting solubility in supercritical carbon dioxide, the effect of adding silicon-based functionalities to diphosphonic acids has been investigated. Specifically, a series of silyl-substituted diphosphonic acids has been prepared and characterized, and their aggregation and metal ion extraction properties compared with alkyl-substituted diphosphonic acids, reagents previously demonstrated to be effective extractants of actinides from acidic aqueous media into various organic solvents. In addition, the influence of the number of methylene groups bridging the phosphorus atoms of the diphosphonic acids on their extraction behavior has been investigated. Variations in the extraction behavior of the compounds arising from differences in the number of bridging methylene groups have been shown to be attributable to a combination of factors, in particular, the aggregation state of the ligand, the size of the chelate rings formed upon complexation, the basicity of the phosphoryl group and the relative acidities of the ligands.

### INTRODUCTION

Partial esters of diphosphonic acids in organic solvents have been shown to be efficient metal ion extractants, exhibiting a particular affinity for tri-, tetra- and hexavalent actinides and Fe(III) [1]. In previous work, which grew out of an effort to synthesize supercritical CO<sub>2</sub>-soluble diphosphonic acid ligands, a series of silyl-substituted diphosphonic acids was investigated to determine the effect of incorporating a silicon functionality into a diphosphonic acid. While the incorporation of the silyl functionality was shown to have a relatively minor effect on the aggregation and metal ion extraction properties of the ligands, a more profound effect on these properties was observed as the length of the alkyl chain bridging the phosphorus atoms was varied. This work represents the first step toward understanding this effect, as part of a broader effort to determine the relationship between structure and function in diphosphonic acids.

### EXPERIMENTAL

All materials, instrumentation and experimental conditions used in this study were as previously described [2, 3]. The aggregation states of the ligands in toluene at 25°C were determined by vapor pressure osmometry using a Jupiter Model 833 vapor pressure osmometer. Infrared spectra were obtained by taking 64 scans at 2 cm<sup>-1</sup> resolution on a Mattson Genesis Series FTIR spectrometer. <sup>31</sup>P NMR spectra were collected on a Varian 400 MHz spectrometer, with chemical shifts reported relative to an external 85% H<sub>3</sub>PO<sub>4</sub>.

reference. Duplicate measurements showed that the reproducibility of the distribution ratio measurements was generally within five percent, although the uncertainty interval was higher for the highest and lowest D values ( $D > 10^3$ , or  $D < 10^{-3}$ ).

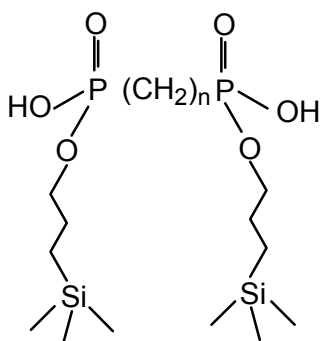


*Figure 1. General structure of silyl-substituted diphosphonic acids.*

## RESULTS AND DISCUSSION

### Aggregation

The aggregation state of the silyl-substituted diphosphonic acids (Figure 1) was found to vary dramatically as a function of the number of methylene groups bridging the phosphorus atoms. As can be seen in Table 1, the ligands with an odd number of bridging methylene groups exist as dimers, while those with an even number tend to form more highly aggregated species. While the origin of this even/odd effect is not fully understood in these systems, it appears to be due to the “zig-zag” pattern adopted by the alkyl chain separating the phosphorus atoms. This affects the orientation of the P=O and P-OH groups of the ligands and changes the geometry of the hydrogen bonded aggregates which can be formed between the ligand molecules. As is observed with normal “straight chain” alkanes, this even/odd effect also manifests itself in the melting points of the ligands, with the ligands containing an even number of bridging methylene groups exhibiting higher than expected melting points (Table 1). Molecular mechanics calculations are currently being performed to determine the most energetically stable conformations of these ligand aggregates.

*Table 1. Properties of silyl-substituted diphosphonic Acids.*

compound	n <sup>1</sup>	aggregation	$\delta$ <sup>31</sup> P NMR	P=O str. (cm <sup>-1</sup> )	m.p. (°C)
H <sub>2</sub> DTMSP[MDP]	1	dimeric	20.0	1230	32-34
H <sub>2</sub> DTMSP[EDP]	2	hexameric	31.4	1212	90-92
H <sub>2</sub> DTMSP[PrDP]	3	dimeric	33.5	1197	46-47
H <sub>2</sub> DTMSP[BuDP]	4	trimeric/hexameric	34.4	1194	75-78
H <sub>2</sub> DTMSP[PDP]	5	dimeric	34.7	1192	N/A
H <sub>2</sub> DTMSP[HDP]	6	hexameric	34.4	1192	N/A

<sup>1</sup>number of bridging methylene groups

### <sup>31</sup>P NMR and Infrared Spectroscopy

Due to the electron withdrawing effect of one phosphoryl group of the diphosphonic acid on the other, the P=O basicity and P-OH acidity of these ligands are expected to vary with the number of bridging methylene groups separating the phosphorus atoms. This is illustrated

clearly in the  $^{31}\text{P}$  NMR and infrared spectroscopy of these ligands. The  $^{31}\text{P}$  chemical shifts observed for these ligands are essentially the same as those observed for the corresponding monophosphonates in which the second phosphorus atom has been replaced by an electronegative substituent, such as chlorine [4]. As this electronegative group is separated from the phosphorus atom by an increasing number of methylene groups, the electron withdrawing effect diminishes and the P=O basicity increases, while the P-OH acidity decreases. The magnitude of this difference is expected to be the greatest between the ligands with one and two bridging methylene groups, for which the difference in  $^{31}\text{P}$  chemical shift is the greatest. When more than three methylene groups bridge the two phosphorus atoms, the  $^{31}\text{P}$  chemical shift observed is essentially the same as that for a monophosphonate, where the second phosphorus atom has been replaced by an alkyl substituent. Beyond this point, the P=O basicity and P-OH acidity are expected to remain constant with the incorporation of more bridging methylene groups, as evidenced by the constant  $^{31}\text{P}$  chemical shift observed for the ligands with four or more bridging methylene groups. Attempts are currently underway to determine the  $\text{pK}_\text{a}$ s of a series of analogous water-soluble, substituted diphosphonic acids to provide a more quantitative description of this effect.

A similar trend is observed in the infrared spectra of this series of ligands. As more methylene groups are incorporated between the phosphorus atoms of these ligands, the P=O stretching vibration is shifted to lower energy (Table 1). As in the  $^{31}\text{P}$  NMR spectra, the largest difference in energy is observed between the phosphoryl stretching bands of the ligands with one and two bridging methylene groups. The position of the stretching bands for the ligands with more than three bridging methylene groups are essentially identical. It should be noted that the position of the phosphoryl stretching band is very sensitive to hydrogen bonding. However, the same trend is also observed for the analogous series of tetraethyl diphosphonates, which do not form hydrogen-bonded aggregates, suggesting that this trend is primarily due to the electronic effect of phosphoryl groups on each other.

### Solvent Extraction

Figure 2a shows the nitric acid dependent extraction of Am(III) by 0.01 M solutions of the extractants in *o*-xylene. (For brevity, in this section, the ligands are denoted by their number of bridging methylene groups in parentheses.) Because a detailed investigation of the solvent extraction properties of this series of ligands has been described previously [2,3], for the purposes of the present discussion, it is sufficient to note that the extraction of Am(III) clearly exhibits the general trends expected as the number of methylene groups separating the phosphorus atoms is varied. A slope of negative three is exhibited by the acid dependencies of all of the extractants over at least part of the acid concentration range studied. This indicates that three protons are displaced from the extractant aggregates upon metal ion complexation, consistent with the plus three charge of the Am(III) cations. At higher acid concentrations, the extractants with more than three bridging methylene groups tend to exhibit acid dependency plots with a less negative or even positive slope. This suggests an increased importance of extraction by the neutral (fully protonated) extractant and provides evidence to support the reduced acidity of these ligands suggested by the  $^{31}\text{P}$  NMR and infrared spectroscopy experiments (*vide supra*).

Figures 2b and 2c show the extractant dependencies for Am(III) extraction by the series of silyl-substituted diphosphonic acid ligands. The plots for the ligands with an odd number of bridging methylene groups exhibit extractant dependency slopes of two, suggesting that two dimeric ligand units participate in the extraction of each Am(III) cation. The efficiency of Am(III) extraction decreases as the number of bridging methylene groups incorporated into the ligand increases from 1 to 3 to 5, even though the basicity of the phosphoryl oxygen increases over the same series. This suggests that the chelate effect is the dominant factor in determining the differences in the efficiency of metal ion extraction observed for this series

of ligands. The six-membered rings formed upon complexation of metal ions by (1) is favored over the larger rings possible upon complexation by (3) or (5). Even though a true chelate effect is not expected to be present when considering the larger ring sizes possible upon complexation of metal ions by (3) and (5), the higher efficiency of metal extraction by (3) may be due to a small entropic advantage due to the closer proximity of two phosphoryl groups.

The ligands with an even number of bridging methylene groups exhibit Am(III) extraction dependency plots with slopes less than two, suggesting the importance of extraction by a single, highly aggregated species. Ligand (2) exhibits an extractant dependency slope of one, except at the lowest extractant concentrations, suggesting that Am(III) is primarily extracted by a single hexameric aggregate of (2). Ligands (4) and (6) exhibit extractant dependency slopes that are close to two at lower concentrations and decrease slightly as the extractant concentration increases. This agrees with the vapor pressure osmometry data, which suggests that these ligands exist as an equilibrium mixture of trimeric and hexameric species and monomeric and hexameric species in toluene, respectively. Thus, at lower extractant concentrations, Am(III) is extracted by two trimeric aggregates of (4), while at higher extractant concentrations, extraction by a single hexameric aggregate becomes important. The extraction of Am(III) by (6) involves monomeric and hexameric species. VPO data indicate that (6) is slightly less aggregated at a given extractant concentration than (2). This suggests that the ligand (6) monomer plays a more important role in metal ion extraction than the ligand (2) monomer, at a given extractant concentration, and may explain why an extractant dependency of slope one is not observed for (6). Additionally, since fitting of the vapor pressure osmometry data suggests that (6) tends to be more highly aggregated than (4) at a given extractant concentration, the slightly more efficient extraction of Am(III) observed for (6) versus (4) suggests that extraction by this single hexameric aggregate is more efficient than extraction by two trimeric species. Furthermore, extraction of Am(III) by (4) and (6) is more efficient than extraction by the dimeric ligands (3) or (5) under analogous conditions, suggesting that extraction by the single hexameric species is more efficient than extraction by two dimeric extractant units, except in the case of (1), where the chelate effect is the dominant factor in determining extraction efficiency.

#### **Comparison of Silyl-Substituted and 2-Ethylhexyl-Substituted Diphosphonic Acids**

Vapor pressure osmometry, solvent extraction and  $^{31}\text{P}$  NMR and infrared spectroscopy experiments show that incorporation of a silyl functionality into a diphosphonic acid does not adversely affect its metal ion extraction properties relative to analogous alkyl-substituted diphosphonic acids. Silyl-substituted diphosphonic acids exhibit the same aggregation behavior as and typically extract metal ions 2-3 times more efficiently than their 2-ethylhexyl-substituted analogues [2,3].  $^{31}\text{P}$  NMR and infrared spectroscopy experiments suggest that this increased extraction efficiency may be due to a slightly higher P=O basicity in the silyl-substituted diphosphonic acids [3].

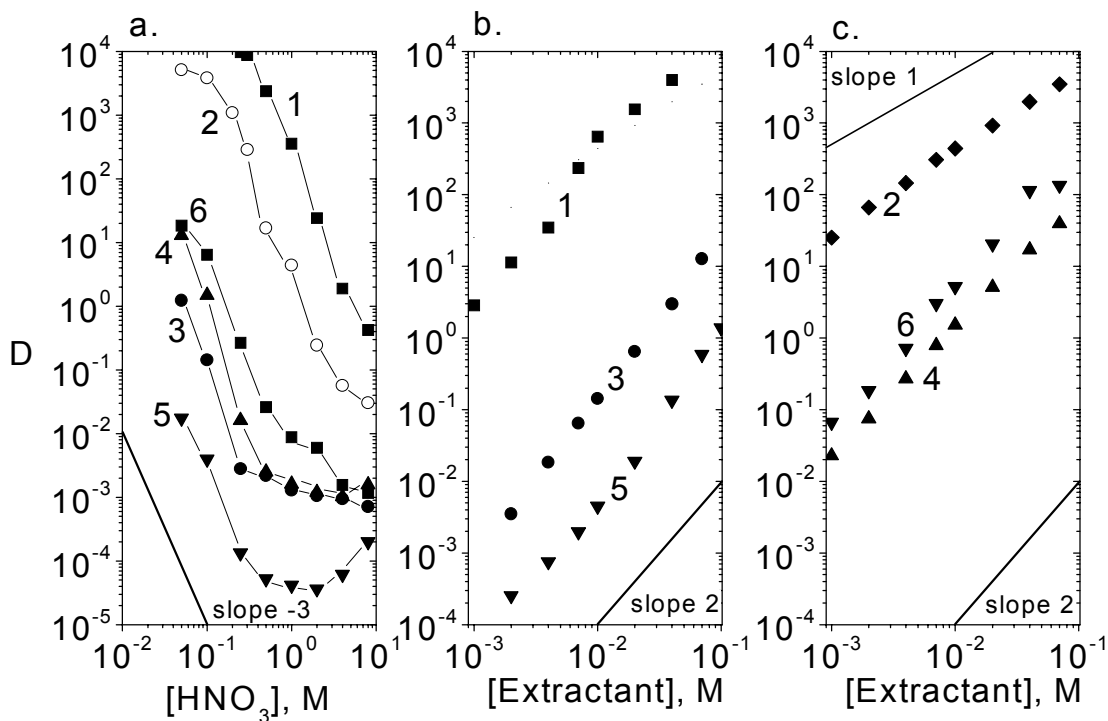


*Figure 2. Solvent extraction of Am(III) from aqueous nitric acid by silyl-substituted diphosphonic acids in o-xylene. a. Acid dependencies for the extraction of Am(III) by 0.01 M extractant in o-xylene. b. Extractant dependencies for Am(III) extraction from 1.0 M (1) or 0.1 M HNO<sub>3</sub> (3 and 5) by silyl-substituted diphosphonic acids with odd numbers of bridging methylene groups. c. Extractant dependencies for Am(III) extraction from 0.1 M HNO<sub>3</sub> by silyl-substituted diphosphonic acids with even numbers of bridging methylene groups. (Numbers on plots refer to the number of bridging methylene groups).*

## CONCLUSIONS

The extraction of metal cations by a series of silyl-substituted diphosphonic acids has been shown to be affected by a number of factors, including the aggregation state of the ligand, the size of the chelate rings formed upon complexation, the basicity of the phosphoryl group and the relative acidities of the ligands. Metal ion extraction is most efficient when one methylene group bridges the two phosphorus atoms of the partially esterified diphosphonic acid extractant, due to the stability of the six-membered chelate rings formed upon metal ion complexation. As more bridging methylene groups are added, metal ion extraction tends to become less efficient and the aggregation state of the ligand becomes a more important factor in determining this efficiency. The incorporation of a silyl functionality into diphosphonic acids does not adversely affect the solvent extraction properties relative to analogous alkyl-substituted diphosphonic acids, with the silyl-substituted ligands typically extracting metal ions 2-3 times more efficiently, presumably due to the slightly higher basicity of their P=O groups.

## **ACKNOWLEDGEMENTS**

Work performed under the auspices of the Environmental Management Sciences Program of the Offices of Science and Environmental Management, US Department of Energy, under grant number DE-FG07-98ER14928 (LUC) and contract number W-31-109-ENG-38 (ANL). The submitted manuscript has been created by the University of Chicago as Operator of Argonne National Laboratory ("Argonne") under contract No. W-31-109-ENG-38 with the U.S. Department of Energy. The U.S. Government retains for itself, and others acting on its Behalf, a paid-up, nonexclusive, irrevocable worldwide License in said article to reproduce, prepare derivative works, distribute copies to the public, and perform Publicly and display publicly, by or on behalf of the Government.

## **REFERENCES**

1. R. Chiarizia, E. P. Horwitz, P. G. Rickert and A. W. Herlinger (1996), *Solv. Extr. Ion Exch.*, **14**, 773-792.
2. D. R. McAlister, M. L. Dietz, R. Chiarizia and A. W. Herlinger (2001), *Sep. Sci. Technol.*, in press.
3. D. R. McAlister, M. L. Dietz, R. Chiarizia and A. W. Herlinger (2002), in press.
4. K. Moedritzer and R. R. Irani (1961), *J. Inorg. Nucl. Chem.*, **22**, 297-304.



## SEPARATION OF NaOH FROM SALTS BY WEAK HYDROXY ACIDS

**Tamara J. Haverlock, Peter V. Bonnesen, Gilbert M. Brown, C. Kevin Chambliss,  
Tatiana G. Levitskaia, and Bruce A. Moyer**

Chemical and Analytical Sciences Division, Oak Ridge National Laboratory, Oak Ridge, USA

Promising liquid-liquid extraction chemistry has been identified for the separation of sodium hydroxide from alkaline salt solutions. Recent data show that a putative cation-exchange process using weakly acidic, lipophilic phenols or fluorinated alcohols appears especially attractive for practical use. Specific application of this concept is envisioned for treatment of nuclear waste stored at various United States Department of Energy (US DOE) sites.

### INTRODUCTION

The separation of sodium hydroxide from alkaline nuclear wastes represents significant potential value in terms of recycle to waste retrieval and sludge washing, whereupon additions of fresh sodium hydroxide to the waste can be avoided [1]. Potential savings are large because of the huge costs associated with waste disposal and the construction of new waste tanks, both of which are directly related to the net volume of the waste.

Eight fundamental approaches that could be undertaken for liquid-liquid extraction of sodium hydroxide have been conceptualized [2]. The eight approaches may be divided into two categories according to whether the underlying mechanism is ion-pair extraction or cation exchange. Ion-pair extraction involves transfer of sodium and hydroxide ions to the organic solvent and was found to be weak in the systems examined, as the selectivity of such processes tends to disfavor small, highly hydrated anions. The cation-exchange approach employs weak hydroxy acids such as phenols or fluorinated alcohols as sodium ion extractants. At the elevated pH values characteristic of alkaline tank waste, the hydroxy acids give up their protons in exchange for sodium ions. Contact of the resulting sodium phenoxide- or alkoxide-containing solvent with water results in hydrolysis, in which the protons given up by the water exchange with the organic-phase sodium ions to yield an aqueous sodium hydroxide solution and simultaneous regeneration of the neutral phenol or alcohol in the organic phase. Hence, there is no net consumption of reagent chemicals. Since only hydroxide *equivalents* and not actual hydroxide ions are extracted, the process has been termed “pseudo hydroxide extraction.” A series of experiments have demonstrated this concept with both selected phenols and novel fluorinated alcohols [2-4]. It was shown that the separation of sodium hydroxide is efficient and selective in competition with other salts present in alkaline tank waste. This paper summarizes the key findings and reports additional results toward a conceptual process.

## PROCESS REQUIREMENTS

Figure 1 depicts an idealized extraction cycle for a conceptual process. Waste containing NaOH, together with other salts and radionuclides, is passed through a multi-stage, counter-current contacting device (e.g., mixer-settlers, centrifugal contactors, or hollow-fiber dispersionless contactors) wherein NaOH is transferred to the solvent. The loaded solvent enters a multi-stage stripping section in which the NaOH is transferred to water, allowing the solvent to be recycled. The treated aqueous waste (still alkaline, but with a significantly reduced NaOH concentration) is then committed to further processing, ultimately to include a waste-immobilization process such as vitrification. The separated NaOH can then be used for further waste processing. Ideally, the entire process would require no adjustment of the waste stream, consume no chemicals, and add nothing to either the exiting partially NaOH-depleted waste or NaOH product streams. Use of water for stripping is highly compatible with such a process, necessitating extractants that release the NaOH upon contact with water. Except for perhaps simple evaporation, no further separation steps would then be needed to put the obtained NaOH product to direct use. Hence, extractant systems that are particularly attractive have adequate selectivity for NaOH, good loading directly from the waste, and good stripping into water. However, it should be kept in mind that practical extraction systems must ultimately possess other characteristics. Such characteristics include having accessible and economical extractants, good phase disengagement, good kinetics, minimal loss of the extractant to the aqueous phase, resistance to formation of third phases, and adequate chemical and radiolytic stability.

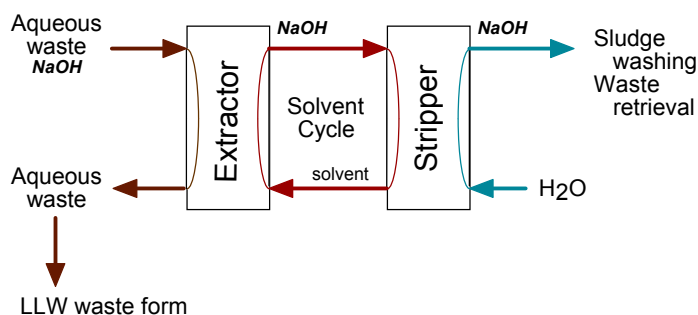


Figure 1. "Ideal" extraction cycle depicting the removal of NaOH from alkaline tank waste.

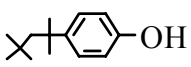
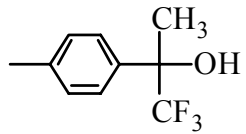
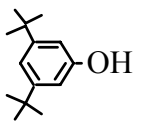
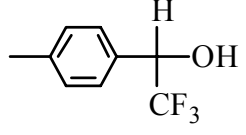
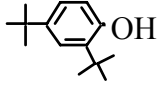
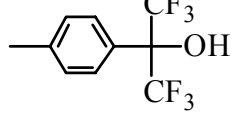
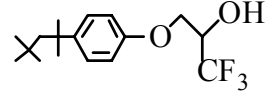
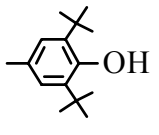
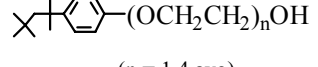
## SODIUM HYDROXIDE EXTRACTION

Isotherm behavior demonstrated the efficiency of sodium extraction from hydroxide solutions for the more acidic hydroxy acids tested. Table 1 lists the alkylated phenols and fluorinated alcohols used as extractants in the study. In the first set of experiments, equal volumes of an organic phase consisting of 0.2 M extractant dissolved in 1-octanol and an aqueous phase containing varying concentrations of sodium nitrate or sodium hydroxide with a spike of  $^{22}\text{Na}$  radio-tracer were gently equilibrated in vials on a rotating device at 25 °C [3]. A well-studied water-immiscible alcohol, 1-octanol, was chosen as the diluent to provide a suitable solvation environment for organic-phase sodium salts, as few alternative non-alcohol diluents compare in ability to solvate both cations and anions [5]. Plots of the equilibrium concentrations of sodium in the organic phase vs. the equilibrium concentrations of NaOH in the aqueous phase are shown in Figure 2. Most of the tested hydroxy acids significantly enhanced the extraction of sodium from aqueous NaOH over that which is extracted by 1-octanol alone. In contrast, little or no enhancement of sodium extraction from aqueous NaNO<sub>3</sub> solution by the same compounds was seen (plots not shown), an encouraging demonstration of the specificity of the tested hydroxy compounds toward hydroxide, albeit under non-competitive conditions.

Sodium hydroxide may be efficiently recovered from the solvent by stripping with water. Comparative data for the efficacy of the various hydroxy acids in extraction of NaOH together with data demonstrating the recovery of NaOH are given in Table 2. In the experiments, equal

with data demonstrating the recovery of NaOH are given in Table 2. In the experiments, equal volumes of an organic solution containing 0.20 M hydroxy acid in 1-octanol and an aqueous solution containing 7.0 M NaOH and a spike of  $^{22}\text{Na}$  radio-tracer were equilibrated at 25 °C [3]. Following extraction, the loaded solvents were stripped with an equal volume of pure water. Parallel experiments were performed with 7.0 M NaOH that did not contain the  $^{22}\text{Na}$  radio-tracer, and the total concentration of base in the aqueous strip solution was determined by titration. The data collectively demonstrate near-quantitative recovery of sodium hydroxide into water for all solvents tested, as evidenced by the near-unity values of the ratio  $[\text{base}]/[\text{Na}^+]_{\text{strip}}$ .

*Table 1. Compound key for hydroxy-acid extractants.*

<b>1a</b>	$\text{HF}_2\text{C}(\text{CF}_2)_7\text{CH}_2\text{OH}$	<b>3a</b>		<b>4a</b>	
<b>1b</b>	$\text{F}_3\text{C}(\text{CF}_2)_7\text{CH}_2\text{OH}$	<b>3b</b>		<b>4b</b>	
<b>1c</b>	$\text{F}_3\text{C}(\text{CF}_2)_5(\text{CH}_2)_3\text{OH}$	<b>3c</b>		<b>4c</b>	
<b>2a</b>		<b>3d</b>			
<b>2b</b>					
					(n = 1.4 avg)

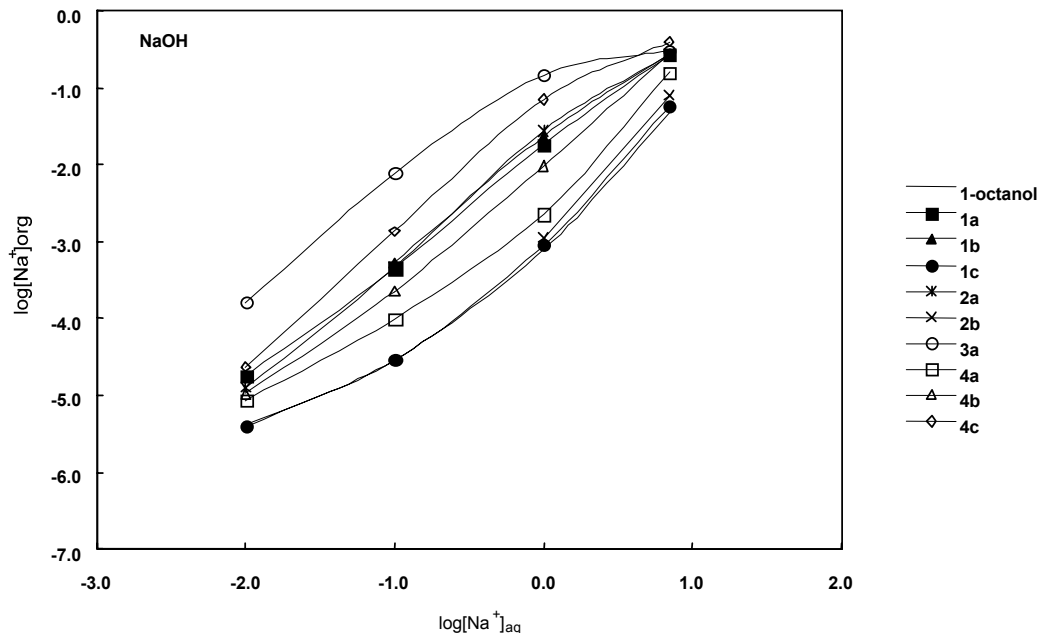


*Figure 2. Equilibrium isotherms for the extraction of sodium hydroxide by hydroxy acids at 0.20 M and 25 °C.*

*Table 2. Extraction and stripping results for recovery of hydroxide ion from aqueous 7.0 M NaOH.*

Compound	[Na] <sub>extr</sub> <sup>a</sup> (M)	[Na] <sub>strip</sub> <sup>b</sup> (M)	% strip	[base] <sub>strip</sub> <sup>c</sup> (M)
<b>1a</b>	0.29	0.29	100%	0.30
<b>1b</b>	0.29	0.28	97%	0.30
<b>1c</b>	0.058	0.058	100%	0.056
<b>2a</b>	0.28	0.28	100%	0.30
<b>2b</b>	0.087	0.087	100%	0.087
<b>3a</b>	0.31	0.26	82%	0.26
<b>3b</b>	0.29	0.26	91%	ND
<b>3c</b>	0.22	0.22	100%	ND
<b>3d</b>	0.049	0.048	98%	0.056
<b>4a</b>	0.18	0.18	100%	0.19
<b>4b</b>	0.29	0.29	100%	0.28
<b>4c</b>	0.40	0.39	96%	0.36
<b>1-octanol</b>	0.050	0.050	100%	0.056

<sup>a</sup>The equilibrium concentration of sodium in the organic phase following extraction. The concentration of fluorinated alcohol or alkylated phenol in 1-octanol was 0.2 M. <sup>b</sup>The equilibrium concentration of sodium in the aqueous strip phase. <sup>c</sup>The equilibrium concentration of titratable base in the aqueous strip phase. ND = Not determined.

Consistent with previous results on phenols [6-8], Figure 2 and Table 2 show that the strength of sodium extraction from NaOH solutions correlates directly with acidity or hydrogen-bond donor strength of the tested hydroxy acids, as perturbed by steric effects. By reference to Figure 2, relative differences in extraction efficiency for these compounds appear to become more pronounced at hydroxide concentrations less than 1 M, owing to the saturation seen for some compounds and steepened extraction by 1-octanol alone at higher hydroxide concentrations. Appreciable extraction of sodium from 7.0 M NaOH is observed for solvents containing compounds **1a**, **1b**, **2a**, **3a-c**, and **4a-c**, whereas extraction for solvents containing **1c**, **2b**, and **3d** is on the order of that observed for 1-octanol alone. The extraction of sodium from 7.0 M NaOH reveals the expected trend following the direction of decreasing extraction strength with increasing  $pK_a$  values [8]. Weak extraction by **1c** and **2b** is a reflection of this trend. Comparison of the data for compounds **4a-c** illustrates “fine tuning” of acidity within a single class of hydroxy acids by variation of a substituent -X (-X = -CH<sub>3</sub>, -H, or -CF<sub>3</sub>) in the core molecule *para*-CH<sub>3</sub>-C<sub>6</sub>H<sub>4</sub>-C(CF<sub>3</sub>)(X)-OH. The electron-withdrawing effect increases in the order -CH<sub>3</sub> < -H < -CF<sub>3</sub>, and accordingly, the resultant acidity of the alcohol as reflected by the amount of sodium extracted into the solvent phase ([Na]<sub>org</sub>, Table 2) also increases in that order. Not surprisingly, the stripping efficiency for these compounds (and also phenols **3a-d**) follows the opposite trend of the extraction efficiency. While solvents containing **3a** were impressive with respect to sodium extraction, only 82% of the extracted sodium ions were recovered as the hydroxide salt in a single contact. It may therefore be concluded that **3a** is approaching an upper limit of acidity in terms of efficient recovery of sodium hydroxide.

In order to evaluate extraction selectivity for hydroxide under competitive conditions, the extractants **1a**, **2a** and **3a** at 0.2 M in 1-octanol were equilibrated with aqueous solutions containing high concentrations of competing anions. Experiments employed solutions containing 1.75 M NaOH (typical of alkaline tank waste) plus either 3.5 M NaCl or 3.5 M NaNO<sub>3</sub>. A third aqueous solution was a complex simulant of an actual tank waste (Hanford tank AW-101 Double-Shell Slurry Feed, designated DSSF-7) that is high in hydroxide, nitrate, and aluminate ions, any of which may be co-extracted with sodium ion [3]. Extraction of OH<sup>-</sup> equivalents from the waste simulant gave very high selectivities over Al(OH)<sub>4</sub><sup>-</sup> ion with selectivity factors ranging from 280 (**1a**) to 650 (**2a**). Selectivity factors exceeded 20 for the key anion NO<sub>3</sub><sup>-</sup>. Since nitrate extraction is largely due to the background salt extraction by 1-octanol, it may be expected that selectivity will improve with use of higher, more practical concentrations of extractant.

For a process to be economical, the solvent must also prove to be recyclable as well as selective. Experiments were performed using solvent systems **1a** and **3a** at 0.2 M in 1-octanol and equilibrated with the waste simulant containing  $^{22}\text{Na}$  tracer at 25 °C to demonstrate recyclability of the extractants [3]. Both solvent systems performed consistently through four cycles with both extraction and stripping results at each cycle remaining constant, implying complete regeneration of the solvent in the stripping steps as well as negligible loss of extractant to the aqueous phases. However, recovery of the hydroxide from the phenol (**3a**) required a second strip that was not needed with **1a**. Preliminary results have shown that in the same tests, **4c** was not completely recyclable, which may be related to insufficient lipophilicity. Further work on the lipophilicity issue is in progress.

Toward maximizing solvent capacity, experiments have shown that extractant concentrations up to 1 M may be employed. In initial tests at 25 °C, it was found that when **1a** and **3b** are used at 1 M, the solvent becomes loaded with sodium exceeding 1 M. However, the viscosity increased significantly at high sodium loading, and gel formation was observed. This problem is readily alleviated at elevated temperatures, and isotherms at 60 °C are shown in Figure 3 for 1 M solutions of selected hydroxy acids [**1a**, **2a**, **3a**, **3b**] in 1-octanol. Sodium hydroxide was released from these loaded solvents on contact with water at 60 °C. To test a more complex case, 1 M **3a** was used as the extractant for hydroxide removal from a simple simulant containing 1.9 M free hydroxide, 0.70 M  $\text{NaAl(OH)}_4$ , and 3.5 M  $\text{NaNO}_3$ . The simulant was contacted successively three times at 60 °C with fresh solvent. After each contact, the simulant was analyzed for aluminum and sodium by ICAP (Thermo Jarrel Ash), while hydroxide was determined by titration. Essentially all free hydroxide was recovered, along with 24% of the sodium. Aluminum was not extracted. Subsequently, as shown by powder X-ray diffraction, Bayerite (a form of aluminum trihydroxide) precipitated in the simulant, releasing one additional recoverable mole of free hydroxide for each Al(III) precipitated.

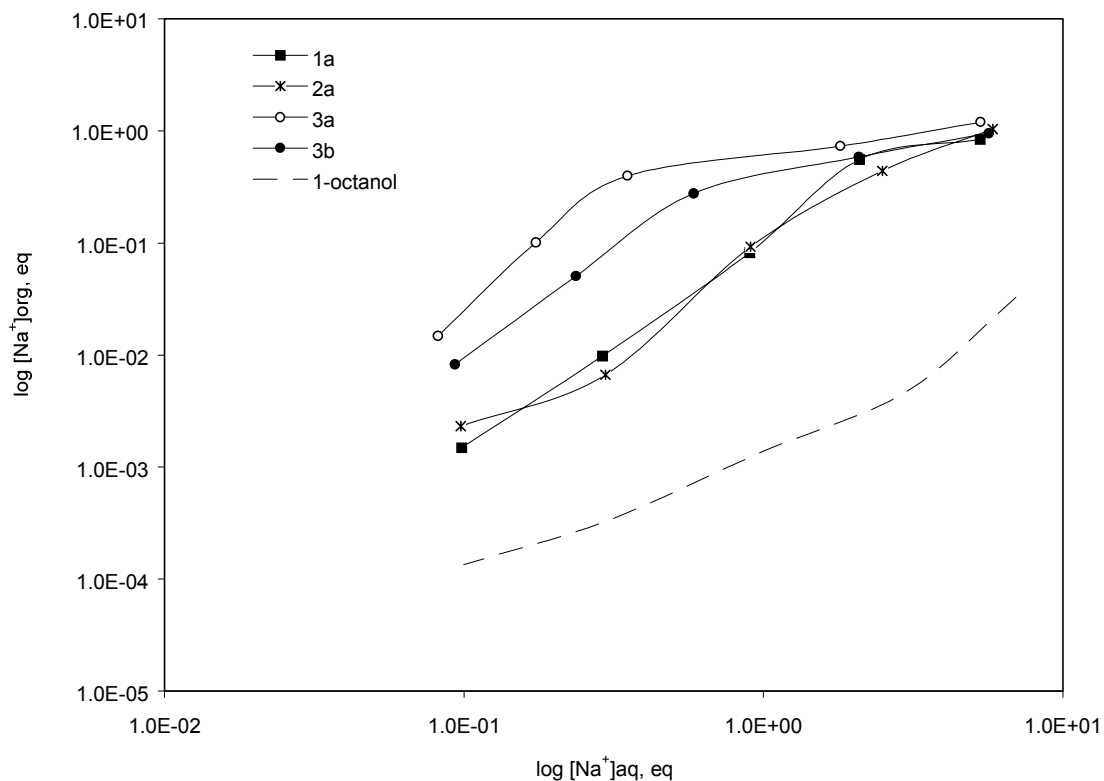


Figure 3. Equilibrium isotherms for the extraction of sodium hydroxide by selected hydroxy acids at 60 °C.

## CONCLUSIONS

Sodium hydroxide recovery adds value to the problem of tank waste remediation by enabling NaOH recycle for sludge-washing processes, thereby reducing the volume of waste that must undergo expensive vitrification. Extraction systems utilizing the concept of "pseudo hydroxide extraction" have been identified that have adequate selectivity for NaOH, good loading directly from the waste, and feasible stripping into water. A series of experiments demonstrated this concept with both selected phenols and novel fluorinated alcohols as cation exchangers for sodium ion. The majority of the hydroxy acids tested significantly enhanced the extraction of sodium from aqueous NaOH over that which is extracted by 1-octanol alone, but effected little or no enhancement of sodium extraction from aqueous NaNO<sub>3</sub> solution. These results from non-competitive extraction, as well as results from competitive extraction from a tank waste simulant are an encouraging demonstration of the specificity of the tested hydroxy compounds toward hydroxide. Furthermore, correlation between the strength of sodium extraction from NaOH solutions and the acidity or hydrogen-bond donor strengths of the tested hydroxy acids and phenols was demonstrated, as perturbed by steric effects. Not surprisingly, stripping efficiency for these compounds follows the opposite trend of the extraction efficiency, with those having the greatest extraction strength unable to release the hydroxide completely to water. Finally, in a test with an actual tank waste simulant, it was shown that over 90% of the total free hydroxide present can be extracted by a solvent containing the economical 4-*tert*-octylphenol (**3a**) at 1M, with the hydroxide subsequently recovered by stripping into water. Future research efforts are directed at testing this system with real waste at the USDOE's Hanford site.

## ACKNOWLEDGMENTS

This research was sponsored by the Environmental Management Science Program, Offices of Science and Environmental Management, U. S. Department of Energy, under contract DE-AC05-00OR22725 with Oak Ridge National Laboratory, managed and operated by UT-Battelle, LLC. The participation of C.K.C. and T.G.L. was made possible by appointments to the Oak Ridge National Laboratory Postgraduate Program administered by the Oak Ridge Associated Universities. The authors also wish to thank J.C. Bryan for assistance with X-ray powder diffractometry.

## REFERENCES

1. D. E. Kurath, K. P. Brooks, G. W. Hollenberg, D. P. Sutija, T. Landro, and S. Balagopal (1997), *Sep. Purif. Technol.*, **11**, 185-198.
2. B. A. Moyer, P. V. Bonnesen, C. K. Chambliss, T. J. Haverlock, A. P. Marchand, H.-S. Chong, A. S. McKim, K. Krishnudu, K. S. Ravikumar, V. S. Kumar, and M. Takhi (2001), Nuclear Site Remediation: First Accomplishments of the Environmental Science Program, P. G. Eller and W. R. Heineman (eds.), ACS Symposium Series, Vol. 778, American Chemical Society, Washington, DC, pp. 114-132.
3. C. K. Chambliss, T. J. Haverlock, P. V. Bonnesen, N. L. Engle, and B. A. Moyer, *Environ. Sci. Technol.*, submitted.
4. B. A. Moyer, C. K. Chambliss, P. V. Bonnesen, and T. J. Keever (1999), U.S. Patent Application Ser. No. 09/404, 104, Sept. 23.
5. B. A. Moyer and Y. Sun (1997), Ion Exchange and Solvent Extraction, Vol. 13, Y. Marcus and J. A. Marinsky (eds.), Marcel Dekker, New York, pp. 295-391.
6. R. R. Grinstead (1971), U.S. Patent 3,598,547, Aug. 10.
7. R. R. Grinstead (1971), U.S. Patent 3,598,548, Aug. 10.
8. (a) P. D. Bolton, C. H. Rochester, and B. Rossall (1970), *Trans. Faraday Soc.*, **66**, 1348-1350. (b) C. H. Rochester and B. Rossall (1967), *J. Chem. Soc. B*, 743-748.



## EXTRACTION OF SELECTED METAL CATIONS WITH THE ALKYLARYLPHOSPHINIC ACID: 2,4,4-TRIMETHYLPENTYLPHENYLPHOSPHINIC ACID

D. Nucciarone, B. Jakovljevic, B. A. Fir Medeiros, J. Hillhouse and M. DePalo

Cytec Canada, Inc., Niagara Falls, Ontario, Canada

The synthesis and physical properties of 2,4,4-trimethylpentylphenylphosphinic acid (TMPPPA) is described. Extraction of several metals, mostly from the first row transition elements, was examined and compared to that of other phosphinic acids. As a function of increasing pH the metals studied were found to extract in the order:



The metals Mn(II), Ca(II), and Cu(II) were observed to have very similar pH extraction profiles. Compared to bis(2,4,4-trimethylpentyl)phosphinic acid - the main component of CYANEX® 272 - the extraction order was similar, with the exception of Ca(II), which was observed to extract in preference to Co(II) and Mg(II). For all the metals studied extraction was observed at lower pH for TMPPPA by 1.1 to 1.6 pH units compared to CYANEX 272.

### INTRODUCTION

Organophosphorus acids of the type  $\text{R}_2\text{P}(\text{O})\text{OH}$  where R = alkyl, alkoxy, aryl or aryloxy have been extensively studied, particularly the alkyl and alkoxy derivatives. These latter two have found numerous commercial applications. To a lesser degree, diaryl and, more specifically, mixed alkyl/aryl derivatives have not been as thoroughly studied. While references to diaryl and mixed alkyl/aryl phosphoric acids and phosphonic acid esters can be found, there is little information available on the metal extraction behaviour of mixed alkyl/aryl phosphinic acids. With the advent of new synthetic methods allowing more facile preparation of this class of compounds, a more thorough investigation of these compounds was begun.

Replacement of an alkyl moiety with an aryl moiety on phosphorus would be expected to allow the introduction of unique electronic and steric effects. Compared to a saturated aliphatic substituent, an aryl group will act as an electron-withdrawing group and result in a stronger acid. The magnitude of this effect can be controlled by appropriate substitution on the phenyl ring. In addition to electronic effects the presence of a phenyl ring also permits tailoring of steric interactions between the co-ordinating ligand and the metal centre.

In an example where a mixed alkyl/aryl phosphinic acid showed improved characteristics over the dialkyl analogue, Mason *et al.*, examined octylphenylphosphinic acid and cyclooctylphenylphosphinic acid as extractants for M(III) and M(VI) cations (including selected actinides and lanthanides) [1]. They observed that the alkylphenyl derivatives were more effective extractants for M(III) cations than the dialkyl counterparts.

In this study we undertook to prepare and characterize 2,4,4-trimethylpentylphenylphosphinic acid and examine the extraction behaviour of various metal cations selected from the first row transition metals and alkali earths.

## EXPERIMENTAL

### Synthesis of TMPPPA

The general reaction of phosphine with 2,4,4-trimethylpent-1-ene under free radical initiated conditions was used to produce a blend of primary, secondary, and tertiary phosphines [2]. Isolation of the primary phosphine by distillation and subsequent reaction with bromobenzene using Pd catalysis produced a mixture containing (2,4,4-trimethylpentyl)phenylphosphine, with smaller quantities of the alkyldiphenylphosphine and unreacted primary alkylphosphine [3]. The crude mixture was washed with water to remove aqueous soluble salts. Excess bulk solvent (*o*-xylene) and unreacted primary alkylphosphine were removed to give a concentrate containing the alkylarylpophosphine as the principle component. Oxidation with 2 equivalents of hydrogen peroxide (as a 25% solution) gave, upon separation of the aqueous and organic phases, a mixture containing 88% TMPPPA, 7% (2,4,4-trimethylpentyl)diphenylphosphine oxide and 2% 2,4,4-trimethylpentylphosphonic acid.

Phosphonic acid impurities were reduced by dissolving the crude material (176 g) in methylene chloride (260 mL) and washing 3 times with 100 mL portions of 0.2 M NaOH.

Phosphine oxide levels were reduced by neutralizing the bulk organic phase with NaOH to form a micellar phase. This micellar phase was isolated, washed twice with hexanes, then converted back to the free acid by contacting with aqueous sulfuric acid.

This general procedure resulted in a purified white solid with a melting point of 66-69°C. Analysis by gas chromatography indicated a product purity of 98%. Nuclear magnetic resonance spectroscopy showed a signal for the phosphinic acid at 46.3 ppm (singlet) relative to 85% phosphoric acid as external standard.

### Metal Distribution Experiments

Single metal extraction studies were conducted as follows: A 200 mL solution containing  $1 \times 10^{-3}$  M metal sulfate and 0.5 M sodium sulfate was mixed with 200 mL of 0.1 M TMPPPA in EXXSOL D80® at room temperature (23-24°C). The pH was adjusted by dropwise addition of 50 g/L NaOH (accurately measured). At each pH value selected the mixture was allowed to agitate for 10 minutes then an equal volume of the organic and aqueous phase sampled. The aqueous phase was analyzed for metal content by atomic absorption spectrophotometry and the concentration of the metal in the organic phase determined by difference. Each experiment was done in duplicate.

### pKa Measurements

Solutions containing an accurately weighed amount of the purified phosphinic acid (0.2 g) in 75% isopropanol were titrated with standardized 0.1 N NaOH in water. The average of triplicate analyses gave a pKa of  $5.35 \pm 0.03$  at 23°C.

## RESULTS AND DISCUSSION

### General

The physical behaviour of the mixed organic and aqueous phases showed good phase separation behaviour at lower pH (< 5) with both phases separating cleanly after one minute but becoming worse at higher pH (> 5) with times increasing to up to 3.5 minutes.

Throughout these studies the aqueous phase remained clear but the organic phase was cloudy (due to the dispersion of fine droplets of the aqueous phase), the latter being easily clarified by centrifuging.

Figure 1 shows plots of % extraction versus pH for nine metal cations. The order of extraction as a function of increasing pH was seen to be:



The following general observations are noted. Fe(III) extracts at low pH and is well separated from its next nearest neighbor, Zn(II). Mn(II), Ca(II), and Cu(II) displayed overlapping extraction curves. Mg(II) and Ni(II) displayed extraction maximum near pH 4.9-5.0 with subsequent decline at higher pH. Extraction data for Mg(II) and Ni(II) above ca. pH 5.0 is not presented. At and above this pH, solids began forming which dispersed in the organic phase. This behaviour was reversible such that lowering the pH restored homogeneous liquid phases, but was otherwise not investigated further. This suggests a solubility issue of the Mg and Ni complexes which may be addressed by changing the nature of the diluent or addition of modifiers.

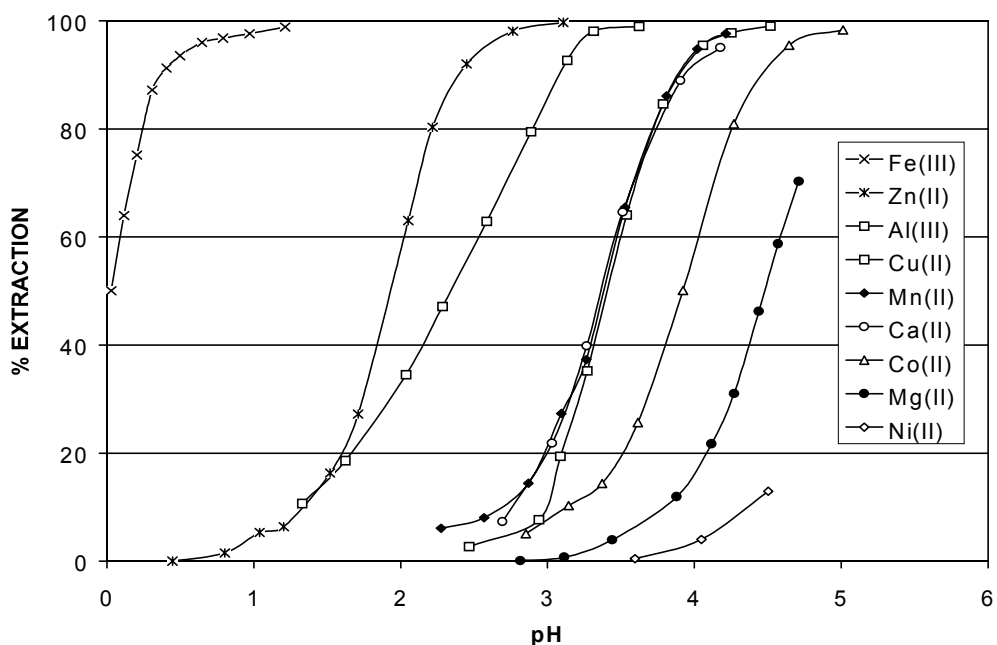


Figure 1. Extraction of metal ions by TMPPPA from sulfate solutions.

In comparison, the ordering for CYANEX 272 is:



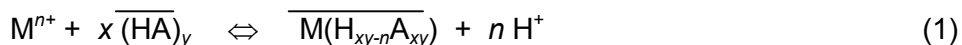
Comparison of the order of extraction of the metals with CYANEX 272 shows a similar ordering except for Ca(II). Whereas Ca(II) extracts at higher pH than Co(II) with CYANEX 272, this element is extracted at lower pH than Co(II) for TMPPPA. The practical implication is the possibility of gypsum precipitation in SX processes having sulfate feed liquors containing Ca(II) [4].

Table 1 shows pH values at 50% extraction for the extractants TMPPPA and CYANEX 272 [5,6]. The data presented was obtained under the same conditions and allows direct comparison. Comparison with CYANEX 272 shows the extraction pH for all metals is lower by 1.1 to 1.6 pH units for TMPPPA (where data are available).

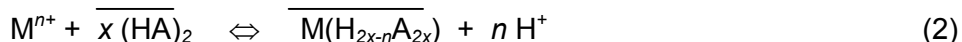
*Table 1. Comparison of  $pH_{50}$  for TMPPA and CYANEX 272.*

Metal Cation	$pH_{50}$		$\Delta pH_{50}$ (TMPPA-CYANEX 272)
	TMPPA	CYANEX 272 [5,6]	
Fe(III)	0.03	1.6	-1.6
Zn(II)	1.9	3.0	-1.1
Al(III)	2.4	3.4	-1.0
Mn(II)	3.4	4.9	-1.5
Ca(II)	3.4	-	-
Cu(II)	3.4	4.6	-1.2
Co(II)	3.9	5.2	-1.3
Mg(II)	-	5.95	-
Ni(II)	-	7.05	-

Extraction of cationic metal species by organophosphorus acids can be described by the general equation:



where  $n$  is the charge on the metal cation and  $y$  is the degree of association of the organophosphorus acid. Under the conditions studied, a value of  $y = 2$  has been observed [1], therefore Equation (1) becomes:



An equilibrium constant,  $K$ , can be defined from (2) as:

$$K = \frac{[\overline{M(H_{2x-n}A_{2x})}][H^+]^n}{[M^{n+}][\overline{(HA)_2}]^x} \quad (3)$$

Defining the distribution coefficient,  $D$ , as the ratio of the total metal concentration in the organic phase to that in the aqueous phase gives:

$$K = D[H^+]^n / [\overline{(HA)_2}]^x \quad (4)$$

and

$$\log D = n[\text{pH}] + \log K + x \log [\overline{(HA)_2}] \quad (5)$$

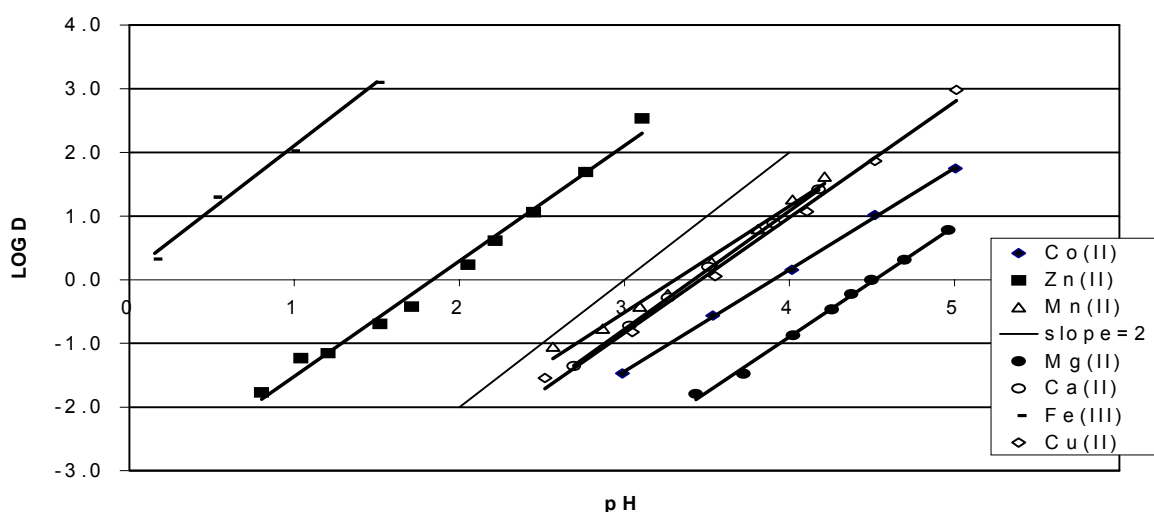
Under conditions where  $(HA)_2$  is constant, a plot of  $\log D$  versus pH should yield a straight line with slope  $n$ . Under these experimental conditions, the extractant concentration is much greater than the metal concentration, thus  $(HA)_2$  can be considered constant.

Values of  $n$  obtained from the plots of  $\log D$  versus pH are listed in Table 2. A plot of  $\log D$  versus pH for the various metals is shown in Figure 2.

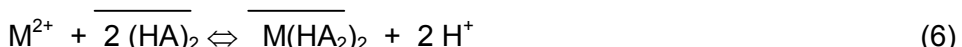
Table 2. Values of  $n$  from plots of  $\log D$  versus  $pH$ .

Metal Cation	$n$	
	This work	CYANEX 272 [5,6]
Fe(III)	2.0	1.7
Zn(II)	1.8	1.8
Mn(II)	1.7	1.6
Ca(II)	1.9	-
Cu(II)	1.8	1.7
Co(II)	1.7	1.8
Mg(II)	1.7	-
Ni(II)	-	1.8

Figure 2. Plot of  $\log D$  versus  $pH$ .



Values obtained are all slightly less than two for the dipositive cations, as would be described by the stoichiometry:



Similar results were obtained for the case of CYANEX 272 [5,6]. The extraction behaviour observed for Ni(II) did not permit this type of analysis. Data for Al(III) did not show a straight line relationship for  $\log D$  versus  $pH$ . The value  $n = 2$  for Fe(III) is significantly lower than the expected value of 3 (*vide infra*).

### Iron Behaviour

A survey of the literature shows that the nature of the Fe(III) species extracted by CYANEX 272 varies markedly depending on the extraction conditions. For Fe(III) extracted with CYANEX 272 under the same conditions as reported in this study, a similar value of  $n = 2$  was observed [5,6]. With sulfate anion present in significant quantities (at 0.5 M), iron sulfate species predominate in the aqueous phase under acidic conditions [7,8]. Under these conditions, an equilibrium between ferrous and ferric has also been suggested [6]. Assuming a ferric species, then a 2:1 phosphinate:iron ratio for the extracted complex suggests that the iron species in the solvent phase may be a mixed ligand species containing both an inorganic and organic component. The nature of the extracted specie(s) in sulfate systems requires further investigation.

In a second study of Fe(III) extraction with CYANEX 272, curve-fitting models suggest that, in a nitrate medium, three species predominate having the stoichiometries  $\text{FeA}_3$ ,  $\text{FeA}_3(\text{HA})_3$ , and  $\text{Fe}(\text{NO}_3)_3(\text{HA})_3$ , where A is the phosphinate anion [9]. In the same study these authors rejected the presence of polynuclear complexes. The presence of  $\text{FeOH}^{2+}$  at  $\text{pH} < 2$  was seen as being of little significance. The extraction efficiency was found to be dependent on the nature of the anion such that extraction efficiency followed the order nitrate > chloride > sulfate at any given pH.

In a third study, where Fe(III) extraction by DEHPA, PC-88A, and CYANEX 272 was examined, results showed a phosphinate:iron ratio of 1:1 when Fe(III) was extracted by CYANEX 272 from a chloride media at 0.05 N acid strength [10]. Interestingly, a 2.8:1 stoichiometry was observed for both DEHPA and PC-88A under stronger acid conditions of 0.35 N. The phosphinate complex was postulated to be a dihydroxyphosphinatoiron(III) species,  $\text{FeA(OH)}_2$ .

## CONCLUSIONS

The extraction of several metals by the mixed alkyl/aryl phosphinic acid, TMPPPA, has shown a shift to lower pH compared to its dialkyl counterpart. Fe(III) is shifted to a low  $\text{pH}_{50}$  value of 0.03, separating it cleanly from its next neighbour Zn(II) having  $\text{pH}_{50}$  of 1.93. This may make it attractive for Fe(III) impurity removal from acidic sulfate solutions. Extraction of Ca preferable to Co makes it less attractive in Co extraction applications from sulfate media. Manganese, similar to CYANEX 272, is also extracted at lower pH than Co.

## REFERENCES

1. G. W. Mason, N. L. Schofer, and D. F. Peppard (1970), *J. Inorg. Nucl. Chem.*, **32**, 3375-3386.
2. W. A. Rickelton (1996), Kirk Othmer Encyclopedia of Chemical Technology, 4th edn., Vol. 18, John Wiley & Sons, Inc., pp. 656-668.
3. J. Hillhouse (1997), *U.S. Pat.*, No. 5,550,295, (Aug. 27).
4. J. Babjak (1986), *U.S. Pat.*, No. 4,610,861, (Sep. 9).
5. K. C. Sole (1993), Solvent Extraction of First Row Transition Metals by Thiosubstituted Organophosphinic Acids, PhD Thesis, University of Arizona, United States of America.
6. K. C. Sole and J. B. Hiskey (1992), *Hydrometallurgy*, **30**, 345-365.
7. R. B. Bhappu (1986), Iron Control in Hydrometallurgy, J.E. Dutrizac and A.J. Monhemius (eds.), Ellis Horwood Limited, Chichester, pp. 183-201.
8. T. Nishimura, Q. Wang, and Y. Umetsu (1996), Iron Control and Disposal, J.E. Dutrizac and G.B. Harris (eds.), The Canadian Institute of Mining, Metallurgy and Petroleum, Montreal, pp. 535-548.
9. N. Miralles, A. M. Sastre, E. Figuerola, and M. Martinez (1992), *Hydrometallurgy*, **31**, 1-12.
10. A. Sandhibigraha, P. V. R. Bhaskara Sarma, and V. Chakravortty (1996), *Scand. J. Metall.*, **25**, 135-140.



# THERMODYNAMICS OF THE EXTRACTION OF SELECTED METAL IONS BY DI(2-ETHYLHEXYL) ALKYLENEDIPHOSPHONIC ACIDS

Emmanuel O. Otu and Renato Chiarizia\*

Department of Chemistry, Indiana University Southeast, New Albany, IN, USA

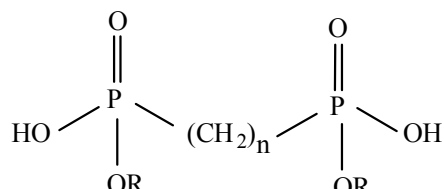
\*Chemistry Division, Argonne National Laboratory, Argonne, IL, USA

The thermodynamics of extraction of Am(III), Sr(II) and U(VI) from aqueous HNO<sub>3</sub> solutions by o-xylene solutions of P,P'-di(2-ethylhexyl) methylene- (H<sub>2</sub>DEH[MDP]), ethylene- (H<sub>2</sub>DEH[EDP]), and butylene- (H<sub>2</sub>DEH[BuDP]) diphosphonic acids has been studied by the temperature coefficient method in the 25.0 to 60.0 °C range. Both extractant aggregation and extraction stoichiometries did not change with temperature. The extraction of Am(III) by H<sub>2</sub>DEH[MDP], and that of U(VI) by all three extractants are strongly driven by both enthalpy and entropy variations. The extraction of Sr(II) by H<sub>2</sub>DEH[MDP] is enthalpy driven. The extraction of Am(III) by H<sub>2</sub>DEH[EDP] and H<sub>2</sub>DEH[BuDP] is mainly driven by entropy changes. The extraction of Sr(II) by H<sub>2</sub>DEH[EDP] and H<sub>2</sub>DEH[BuDP] is characterized by an unfavorable entropy change and is not indicative of a micellar-type extraction mechanism.

## INTRODUCTION

P,P'-di(2-ethylhexyl) alkylidendiphosphonic acids have been proposed for actinide separation and pre-concentration procedures [1]. In Structure I, n is one, two or four, for P,P'-di(2-ethylhexyl) methylene- (H<sub>2</sub>DEH[MDP]), ethylene- (H<sub>2</sub>DEH[EDP]), and butylene- (H<sub>2</sub>DEH[BuDP]) diphosphonic acid, respectively. Solvent extraction reagents containing the diphosphonic acid group, the solvent extraction equivalent of the Diphenix® resin [2], exhibit extraordinary affinity for tri-, tetra- and hexavalent actinides [3-5].

In toluene solutions H<sub>2</sub>DEH[MDP] exists as dimers [6], H<sub>2</sub>DEH[EDP] as hexamers [7], while H<sub>2</sub>DEH[BuDP] exists mainly as trimeric aggregates [5]. The effect of these aggregation states on metal extraction has been reported in previous works [3-5]. Extractant dependencies higher than one were measured for the extraction of Am(III), Sr(II) and U(VI) by either H<sub>2</sub>DEH[MDP] or H<sub>2</sub>DEH[BuDP]. However, with H<sub>2</sub>DEH[EDP], extractant dependencies equal to unity were reported for these ions indicating that, with H<sub>2</sub>DEH[EDP], extraction probably takes place through a micellar-type mechanism similar to other highly aggregated extraction systems [8-10].



The objective of this work was to gain information on the thermodynamics of metal solvent extraction by the di(2-ethylhexyl) alkylenediphosphonic acids, by using the method of the temperature coefficient of the metal distribution ratio. Given the pronounced differences in extraction processes and type of metal species formed in the organic phase, it was reasonable to expect that the extraction of metal ions by H<sub>2</sub>DEH[MDP], H<sub>2</sub>DEH[EDP] and H<sub>2</sub>DEH[BuDP] should be accompanied by different enthalpic and entropic contributions to the overall stability of the species formed.

## EXPERIMENTAL

<sup>241</sup>Am and <sup>233</sup>U were obtained from ANL stocks. <sup>85</sup>Sr was obtained from Isotope Products Laboratories (Burbank, CA). The extractants were prepared and purified as described in previous works [3-5]. All other reagents were of analytical grade.

The aggregation of the extractants in toluene at various temperatures was measured by vapor pressure osmometry (VPO) using a Jupiter Model 833 vapor pressure osmometer as described previously [5-7,11]. The extractant solutions used for the VPO measurements were first equilibrated with appropriate nitric acid solutions in order to run the VPO measurements under conditions similar to those used for distribution ratio measurements. The distribution ratios, D, defined as the ratio of metal concentrations in the organic and aqueous phase, were measured following the procedure reported earlier [11]. The measured molar D values were converted to molal values by multiplying them by the appropriate aqueous to organic phase density ratio.

## RESULTS AND DISCUSSIONS

### Aggregation

The aggregation state of the extractants redetermined at temperatures up to 60°C confirmed the results of previous studies at 25°C for concentrations up to about 0.1 M, i.e., H<sub>2</sub>DEH[MDP] is dimeric, H<sub>2</sub>DEH[EDP] is hexameric, and H<sub>2</sub>DEH[BuDP] is predominantly trimeric in toluene [5-7]. The details of the VPO results and data treatment are reported elsewhere [11].

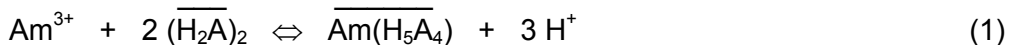
### Extraction Equilibria

The extraction stoichiometries of the target ions by the extractants at ambient temperature have previously been determined [3-5]. Although the extractant aggregation did not change in the 25 to 60°C temperature range, it was necessary to redetermine the extraction stoichiometries at various temperatures. The temperature coefficient method for the determination of thermodynamic parameters is based on the assumption that the same equilibria are operative in the temperature range of interest. If the extraction equilibria were different at different temperatures, the temperature coefficient method would not be applicable and calorimetric measurements would be required. The acid dependencies for the three reagents were always equal to the formal charges of the metal cation being extracted. The extractant dependencies were essentially the same as those previously reported at room temperature [3-5] and are summarized in Table 1.

*Table 1. Extractant dependencies in the 25 to 60 °C temperature range.*

Ion	H <sub>2</sub> DEH[MDP]	H <sub>2</sub> DEH[EDP]	H <sub>2</sub> DEH[BuDP] trimer
Am(III)	2.0	1.0	1.5
Sr(II)	2.0	1.0	2.0
U(VI)	1.0	1.0	1.0

The extraction equilibrium of americium by the dimeric H<sub>2</sub>DEH[MDP] can be written as:



where H<sub>2</sub>A stands for the diphosphonic acid and the bar indicates organic phase species. Similar equations can be written for the other extractants and metal ions using the values of the extractant (Table 1) and acid dependencies determined experimentally. By neglecting aqueous phase nitrate ion complexation [12], the thermodynamic equilibrium constant for the exemplificative case of the Am(III)-H<sub>2</sub>DEH[MDP] system can be written as:

$$K_{\text{Am},\text{MDP}} = 4D \frac{[\text{H}^+]^3}{C_{\text{H}_2\text{A}}^2} \frac{\gamma_{\pm,\text{HN}}^6}{\gamma_{\pm,\text{AmN}}^4} \quad (2)$$

where D is the molal distribution ratio,  $\gamma_{\pm,\text{HN}}$  and  $\gamma_{\pm,\text{AmN}}$  are the mean ionic molal activity coefficients of HNO<sub>3</sub> and Am(NO<sub>3</sub>)<sub>3</sub>, respectively, and C<sub>H<sub>2</sub>A</sub> is the molal analytical concentration of the extractant. Corresponding extraction equilibria and equilibrium constant expressions can also be written for the hexameric H<sub>2</sub>DEH[EDP] and the trimeric H<sub>2</sub>DEH[BuDP], as well as for Sr(II) and U(VI) extraction by the three extractants. The mean molal activity coefficients of americium (europium was used as a stand-in), strontium and uranyl nitrates at tracer concentration level in solutions of HNO<sub>3</sub> at the relevant ionic strengths were calculated according to the method of Kusik and Meissner [13]. Other details of the equilibrium constants calculations can be found elsewhere [14]. The values of the thermodynamic equilibrium constant calculated at different temperatures are given in Table 2.

*Table 2. Equilibrium constants for the extraction of Am(III), Sr(II) and U(VI) by H<sub>2</sub>DEH[MDP], H<sub>2</sub>DEH[EDP] and H<sub>2</sub>DEH[BuDP] in o-xylene.*

T °C	logK Am(III)			logK Sr(II)			logK U(VI)		
	MDP	EDP	BuDP	MDP	EDP	BuDP	MDP	EDP	BuDP
25	8.82	4.67	1.49	1.80	-1.17	-2.21	5.63	7.31	5.06
30	8.78	4.66	1.50	1.78	-1.22	-2.16	5.54	7.23	5.01
35	8.75	4.68	1.54	-	-	-	5.54	7.14	4.96
40	8.71	4.66	1.54	1.70	-1.32	-2.17	5.38	7.07	4.92
45	8.68	4.66	1.58	1.67	-1.38	-2.19	5.32	7.00	4.88
50	8.65	4.66	1.59	1.64	-1.42	-2.16	5.22	6.93	4.83
60	8.59	4.64	1.67	1.58	-1.50	-2.15	5.10	6.78	4.76

The uncertainties in these equilibrium constant values (in log units), estimated from the statistical analysis of the logK data, are 0.05 for americium, 0.03 for strontium, and 0.08 for uranium, respectively. The logK values clearly reflect the fact that H<sub>2</sub>DEH[MDP] has the highest extraction efficiency for the three metal ions (except for U(VI)) and H<sub>2</sub>DEH[BuDP] the least [3-5].

### Free Energy, Enthalpy and Entropy Variations

The enthalpy and entropy changes of the extraction processes were calculated from the slopes (= -ΔH°/2.303R) and intercepts (= ΔS°/2.303R), respectively, of the plots of logK vs. 1/T, with R = 8.314 JK<sup>-1</sup>mol<sup>-1</sup>. Previously discussed conditions regarding the constancy of ΔH° and aqueous phase activity coefficients over the temperature range investigated apply here as well [15-17]. Plots of logK for each metal ion vs. 1/T are shown in Figure 1.

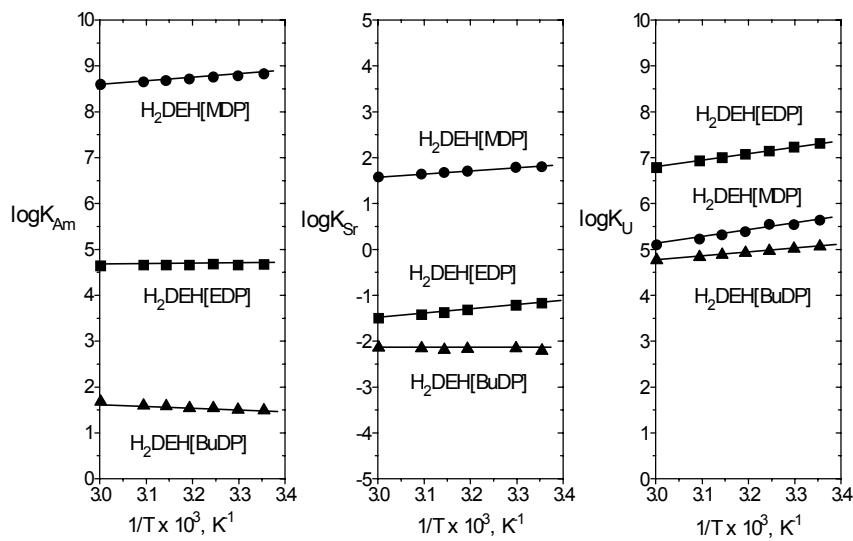


**Figure 1.** Effect of temperature on the extraction of Am(III), Sr(II) and U(VI) from aqueous  $\text{HNO}_3$  by  $\text{H}_2\text{DEH}[\text{MDP}]$ ,  $\text{H}_2\text{DEH}[\text{EDP}]$  and  $\text{H}_2\text{DEH}[\text{BuDP}]$  in *o*-xylene.

The  $\Delta H^0$  and  $\Delta S^0$  values calculated from the plots, along with the  $\Delta G^0$  values calculated from  $\Delta G^0 = -2.303RT \log K$  are given in Table 3. The uncertainties reported for  $\Delta H^0$  and  $\Delta S^0$  are the standard errors of the slopes and intercepts, respectively. Those for  $\Delta G^0$  were obtained from the standard error of  $\log K$ .

In the extraction of a metal cation by a liquid cation exchanger, the net enthalpy and entropy variations of the extraction reaction are the result of several different processes. The dehydration of the metal cation generally involves a positive enthalpy variation ( $\Delta H > 0$ ) as a result of the breakage of ion-water bonds, and a positive entropy variation ( $\Delta S > 0$ ) due to an increase of disorder in the system. The opposite will occur for the hydration of the proton. On the other hand, metal coordination by the organic ligand will result in a negative enthalpy variation ( $\Delta H < 0$ ), as a consequence of replacing relatively weak hydrogen bonds with stronger metal coordination bonds, and in a negative entropy variation ( $\Delta S < 0$ ) due to the increase of order caused by the new bonds. The deprotonation of the extractant will produce opposite effects.

Among the ions investigated, Am(III) behaves in a way which is easier to rationalize based on the arguments outlined above. The  $\Delta H^0$  values for Am(III) extraction exhibit a trend along the  $\text{H}_2\text{DEH}[\text{MDP}]$ ,  $\text{H}_2\text{DEH}[\text{EDP}]$ ,  $\text{H}_2\text{DEH}[\text{BuDP}]$  series, with the reaction being exothermic for the first, thermoneutral for the second, and endothermic for the third extractant, respectively. The trend in  $\Delta H^0$  can be interpreted as arising from the formation of progressively less stable chelate rings along the diphosphonic acids series, as the length of the alkyl chain separating the two phosphorus atoms of the molecule increases. A favorable enthalpic term is observed only for Am(III) extraction by  $\text{H}_2\text{DEH}[\text{MDP}]$ , a ligand with which the metal can form several highly stable six-membered chelate rings. In all cases, the extraction is facilitated by a favorable entropic term, as typically observed for the formation of chelate complexes [18]. The almost zero or positive enthalpy variation with a concomitant favorable entropy variation confirm for  $\text{H}_2\text{DEH}[\text{EDP}]$  and for  $\text{H}_2\text{DEH}[\text{BuDP}]$  a micellar-like type of extraction process [15,19]. The diphosphonic acids form organic phase aggregates characterized by highly ordered structures. When the metal ion is transferred to the organic phase, it becomes part of these structures adding little order to the system. Consequently, the entropy variation is mainly determined by the disorder generated by the metal ion dehydration.

*Table 3: Thermodynamic parameters for the extraction of Am(III), Sr(II) and U(VI) by H<sub>2</sub>DEH[MDP], H<sub>2</sub>DEH[EDP] and H<sub>2</sub>DEH[BuDP] in o-xylene.*

Ion	Extractant	ΔG° at 25 °C kJ/mol	ΔH° kJ/mol	ΔS° at 25 °C J/mol/K
Am(III)	H <sub>2</sub> DEH[MDP]	-50.3 ± 0.1	-12.5 ± 0.2	127 ± 1
	H <sub>2</sub> DEH[EDP]	-26.7 ± 0.5	-1.4 ± 0.5	85 ± 2
	H <sub>2</sub> DEH[BuDP]	-8.5 ± 0.7	9.5 ± 0.9	60 ± 4
Sr(II)	H <sub>2</sub> DEH[MDP]	-10.3 ± 0.1	-12.3 ± 0.4	-7 ± 1
	H <sub>2</sub> DEH[EDP]	6.7 ± 0.3	-18.2 ± 0.4	-84 ± 2
	H <sub>2</sub> DEH[BuDP]	12.6 ± 0.2	2.1 ± 1.2	-35 ± 4
U(VI)	H <sub>2</sub> DEH[MDP]	-32.2 ± 0.5	-29.9 ± 2.1	8 ± 2
	H <sub>2</sub> DEH[EDP]	-41.7 ± 0.6	-28.5 ± 0.7	44 ± 3
	H <sub>2</sub> DEH[BuDP]	-28.9 ± 0.3	-16.3 ± 0.3	42 ± 2

The extraction of Sr(II) by H<sub>2</sub>DEH[MDP] is enthalpy driven. With H<sub>2</sub>DEH[EDP] and H<sub>2</sub>DEH[BuDP], Sr(II) extraction is very inefficient, as indicated by the positive values of ΔG°, as a result of strongly unfavorable entropic terms. The H<sub>2</sub>DEH[EDP] results are indicative of strong metal-ligand coordination and attendant increased ordering. The negative entropic terms for all three extractants also suggest that the hydration of the exchanged protons predominates over the dehydration of the metal ion. Overall, in the extraction of Sr(II) by the three diphosphonic acids, the enthalpy and entropy changes do not lend themselves to indicate a micellar-type extraction mechanism.

The extraction of U(VI) by all three extractants is strongly driven by both enthalpy and entropy variations, which testifies to the extremely high affinity exhibited especially by H<sub>2</sub>DEH[MDP] and H<sub>2</sub>DEH[EDP] for U(VI). The negative enthalpy change associated with metal coordination predominates over the other opposing enthalpic factors. The increasing ΔS° values observed for U(VI) extraction in moving from H<sub>2</sub>DEH[MDP] to the other extractants may be due, at least in part, to the overlapping of a solvation mechanism with the ion exchange mechanism. Extraction of uranyl nitrate by alkylphosphoric acids as solvated complexes at relatively high aqueous acidities is well-known [20], and has been reported for alkylenediphosphonic acids as well [3-5]. In a solvation mechanism, the neutral salt is transferred into the organic phase without simultaneous transfer of protons in the other direction. Consequently, the positive entropy variation associated with the dehydration of the extracted cation and anions dominates the net entropy variation. A solvation mechanism is more likely for extractants having a more basic P=O group as observed along the H<sub>2</sub>DEH[MDP], H<sub>2</sub>DEH[EDP], H<sub>2</sub>DEH[BuDP] series (21), and would therefore explain the ΔS° trend reported for U(VI) in Table 3.

#### ACKNOWLEDGMENTS

This work was funded by the Office of Basic Energy Sciences, Division of Chemical Sciences, U.S. Department of Energy under contract number W-31-109-ENG-38. The submitted manuscript has been created by The University of Chicago as Operator of Argonne National Laboratory ("Argonne") under Contract No W-31-109-ENG-3B with The US Department of Energy. The US Government retains for itself, and others acting on its behalf, a paid-up, nonexclusive, irrevocable worldwide license in said article to reproduce, prepare derivative works, distribute copies to the public, and perform publicly and display publicly, by or on behalf of the Government.

## REFERENCES

1. E.P. Horwitz, R. Chiarizia and M.L. Dietz (1997), *US Pat.*, No. 5,651,883 (July 29).
2. R. Chiarizia, E. P. Horwitz, S. D. Alexandratos, and M. J. Gula (1997), *Sep. Sci. Technol.*, **32**, 1-35.
3. R. Chiarizia, E. P. Horwitz, P. G. Rickert and A. W. Herlinger (1996), *Solv. Extr. Ion Exch.*, **14**, 773-792.
4. R. Chiarizia, A. W. Herlinger and E. P. Horwitz (1997), *Solv. Extr. Ion Exch.*, **15**, 417-432.
5. R. Chiarizia, A. W. Herlinger, Y. D. Cheng, J. R. Ferraro, P. G. Rickert and E. P. Horwitz (1998), *Solv. Extr. Ion Exch.*, **16**, 505-526.
6. A. W. Herlinger, J. R. Ferraro, R. Chiarizia and E. P. Horwitz (1997), *Polyhedron*, **16**, 1843-1854.
7. A. W. Herlinger, R. Chiarizia, J. R. Ferraro, P. G. Rickert and E. P. Horwitz (1997), *Solv. Extr. Ion Exch.*, **15**, 401-416
8. B. A. Moyer, C. F. Baes, Jr., G. N. Case, G. J Lumetta and N. M. Wilson (1993), *Sep. Sci. Technol.*, **28**, 81-113.
9. G. S. Rao, G. W. Mason and D. F. Peppard (1966), *J. Inorg. Nucl. Chem.*, **28**, 887-897.
10. R. Chiarizia, R. C. Gatrone and E. P. Horwitz (1995), *Solv. Extr. Ion Exch.*, **13**, 615-645.
11. E. O. Otu and R. Chiarizia (2001), *Solv. Extr. Ion Exch.*, **19**, in press.
12. S. Kotrly and L. Sucha (1985), Handbook of Chemical Equilibria in Analytical Chemistry, J. Wiley & Sons, New York, pp. 116-117.
13. C. L. Kusik and H. P. Meissner (1978), Fundamental aspects of Hydrometallurgical Processes, *AICHE Symposium Series*, **173**, pp. 14-20.
14. E. O. Otu and R. Chiarizia (2001), *Solv. Extr. Ion Exch.*, submitted.
15. E. O. Otu and A. D. Westland (1990), *Solv. Extr. Ion Exch.*, **8**, 827-842.
16. E. O. Otu (1998), *Solv. Extr. Ion Exch.*, **16**, 1161-1176.
17. E. O. Otu (1999), *Thermochimica Acta*, **329**, 117-121.
18. G. R. Choppin and A. Morgenstern (2000), *Solv. Extr. Ion Exch.*, **18**, 1029-1049.
19. P.R. Danesi, R. Chiarizia, M.A. Raieh and G. Scibona (1975), *J. Inorg. Nucl. Chem.*, **37**, 1489-1493.
20. Y. Marcus and S. Kertes (1969), Extraction by Compound Formation, in Ion Exchange and Solvent Extraction of Metal Complexes, J. Wiley & Sons, New York, p. 545.
21. D. R. McAlister, M. L. Dietz, R. Chiarizia, P. R. Zalupski and A. W. Herlinger (2001), *Sep. Sci. Technol.*, in press.



# COMPARISON OF SOLVENT EXTRACTION METHOD WITH ION-EXCHANGE METHOD FOR THE SEPARATION AMONG ALKALINE EARTH METAL IONS IN THE PRESENCE OF CRYPTANDS AS THE MASKING REAGENTS

Shigekazu Tsurubou, Shigeo Umetani\* and Yu Komatsu\*\*

Asahi University, Gifu, Japan

\* Kyoto University, Kyoto, Japan

\*\* Kanazawa Institute of Technology, Ishikawa, Japan

Synergetic solvent extraction and ion-exchange methods have been examined and compared for the selectivity among alkaline earth metal ions in the presence of cryptands as ion-size selective masking reagents. Cryptand [2.2.2] and [2.2.1] were applied as the ion-size selective masking reagents for both the synergetic solvent extraction of alkaline earth metal ions with benzoyltrifluoroaceton (BFA) and tri-n-butylphosphate (TBP) into cyclohexane, and ion exchange with the strongly acidic cation exchange resin (Amberlite 200CT). Quantitative separation between Mg and Ca was achieved in the presence of cryptand [2.2.1] by the synergetic solvent extraction method. Also, Mg and Ca were quantitatively separated from Sr in the presence of cryptand [2.2.2] by both separation methods examined here.

## INTRODUCTION

It is well known that the selectivity of metal ions in the solvent extraction and ion-exchange methods are largely governed by their ion size. Generally, the extractability of metal ions having smaller ionic radii is higher with open chain chelating reagents such as  $\beta$ -diketones. The selectivity series for divalent metal ions given by ion exchange reaction, are reverse relationship compared to that of solvent extraction. On the other hand, the stability of the complex formation between the macrocyclic ionophores such as cryptands and the metal ions especially alkali and alkaline earth metal ions exhibits a quite different tendency. Thus, combining the chelating reagents (or ion-exchange resins) and macrocyclic ionophores could possibly result in more selective or quantitative separation systems.

The stability constants of inclusion complexes between several kinds of cryptands and alkali, alkaline earth metal cations have been reported by Lehn *et al.* in 1975 [1]. Some stability constants of alkali and alkaline earths with cryptand [2.2.1] and [2.2.2] are shown in Table 1. These stability constants show the considerable differences between neighboring two metals, for example, between Mg and Ca with cryptand [2.2.1] and between Ca and Sr with cryptand [2.2.2]. In this study, the comparison of the effect of cryptands on the synergetic solvent extraction and the ion-exchange methods has been examined.

*Table 1. Formation constants ( $\log \beta$ )<sup>\*</sup> [ $M^{2+} + CR \rightarrow M(CR)^{2+}$ ].*

Cryptand	Mg	Ca	Sr
[2.2.1]	< 2	6.95	7.35
[2.2.2]	< 2	4.4	8.0

\* taken from [10].

## EXPERIMENTAL

### Materials

Cryptand [2.2.1] and cryptand [2.2.2] were purchased commercially from Merck, BFA and TBP from Dojindo and Nacalai Tesque, respectively, and they were used without further purification. Ion-exchange resin (Amberlite 200CT) was purchased from ORGANO, and was conditioned with dilute hydrochloric acid solution and sodium chloride solution in order to convert the resin to the sodium form. Other chemicals were reagent-grade materials. Distilled, and de-ionized water was used throughout.

### Apparatus

The metal ion concentrations in the aqueous phase were determined by an atomic absorption spectrophotometer (Shimadzu, Model AA-660). pH measurements were made with a Horiba (Model F-22) pH meter. A Taitec (Model BR-30LF) bioshaker was used to equilibrate the aqueous and organic (or the ion-exchange resin) phases at a controlled temperature ( $25\pm1^\circ\text{C}$ ).

### Procedure

#### *Solvent extraction method*

A 10 ml portion of an aqueous phase containing the required amount of metal ion (less than  $2\times10^{-4}\text{M}$ ), cryptand (0.01M) and 0.02M Good's buffer such as tris(hydroxymethyl)-aminomethane was adjusted to the desired pH with hydrochloric acid and tetramethyl ammonium hydroxide. The aqueous phase was shaken for 2-20 h until the reaction reached equilibrium with an equal volume of an organic phase (cyclohexane) containing the required amount of BFA and TBP or TOPO at  $25\pm1^\circ\text{C}$ . After centrifugation of the mixture, the pH in the aqueous phase was measured. The metal concentration in the aqueous phase was determined by atomic absorption spectrophotometry and in the organic phase was similarly measured after back-extraction with a hydrochloric acid solution.

#### *Ion exchange method*

A 5 ml portion of an aqueous phase containing the required amount of metal ion (less than  $2\times10^{-4}\text{ M}$ ), cryptand (0.02 M) and 0.02 M Good's buffer such as tris- (hydroxymethyl)-aminomethane was adjusted to the desired pH with hydrochloric acid and tetramethyl ammonium hydroxide. The aqueous phase was shaken for 3-5 h until the reaction reached to the equilibrium with required amount of ion-exchange resin (0.02-0.1g) at  $25\pm1^\circ\text{C}$ . After centrifugation of the mixture, the pH in the aqueous phase was measured. The metal concentration in the aqueous phase was determined by atomic absorption spectrophotometry and the amount of metal ions adsorbed onto ion-exchange resin were calculated from the concentrations of aqueous phase before and after the reaction.

## RESULTS AND DISCUSSION

### Synergetic Extraction of Alkaline Earth Metal Ions with BFA and TBP in the Presence of Cryptand [2.2.1] or [2.2.2] [2],[3]

The results for the extraction of magnesium, calcium and strontium with  $2.5 \times 10^{-3}$  M BFA and TBP into cyclohexane are shown in Figure 1. Logarithm of the distribution ratio of metal ions between the cyclohexane and the aqueous phase,  $\log D$ , is plotted against the pH. Alkaline earths were extracted in the order  $Mg > Ca > Sr$ , which is the same order in which their ionic radii decrease. The slopes of the straight portion of the plots are two, indicating that two protons are released through the extraction reaction.

Figure 2 shows the results for the extraction of Mg and Ca into cyclohexane with  $2.5 \times 10^{-3}$  M BFA and TBP in the presence of 0.01 M cryptand [2.2.1]. The distribution ratio of Ca decreases rapidly over pH 7.5, while that of Mg are quite similar to those in the absence of cryptand [2.2.1] as shown in Figure 1. Mg can be separated from Ca quantitatively at the pH range 8.5 - 9.5 where more than 98% of Mg ( $\log D^* > 1.80$ ) is extracted into cyclohexane with slope of +2, while more than 99% of Ca ( $\log D^* < -2$ ) remains in the aqueous phase at the same time. On the other hand, the distribution of Sr was very low ( $\log D^* < -3$ ) in the pH range 7.0 - 9.5. The application of cryptand [2.2.2] to the synergistic extraction of alkaline earths with BFA and TBP has been also examined. Figure 3 shows the results for the extraction of Mg, Ca and Sr into cyclohexane with 0.015 M BFA and TBP in the absence (blank symbols) and presence (solid symbols) of 0.01 M cryptand [2.2.2]. Very low and constant (about  $\log D^* \sim -2.0$ ) extraction of Sr was observed over pH 5.2, while that of Mg and Ca are quite similar to those in the absence of cryptand [2.2.2]. By controlling the concentration of BFA and TBP, Sr can be separated quantitatively from Mg and Ca in the pH range 6.7-8.0, where more than 99% ( $\log D^* > 2$ ) of Ca and Mg are extracted into cyclohexane with slopes of +2, while more than 99% ( $\log D^* < -2$ ) of Sr remains in the aqueous phase at the same time.

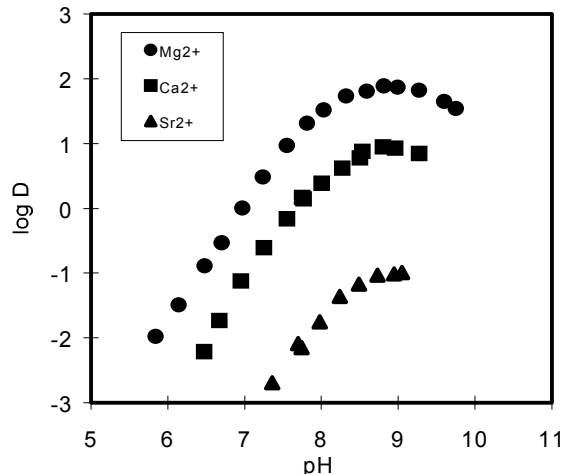


Figure 1. Extraction of alkaline earths into cyclohexane with BFA and TBP.  
 $[Mg^{2+}] = 3 \times 10^{-5}$  M,  $[Ca^{2+}] = 2 \times 10^{-4}$  M,  $[Sr^{2+}] = 10^{-4}$  M  
 $[BFA]_0 = [TBP]_0 = 2.5 \times 10^{-3}$  M.

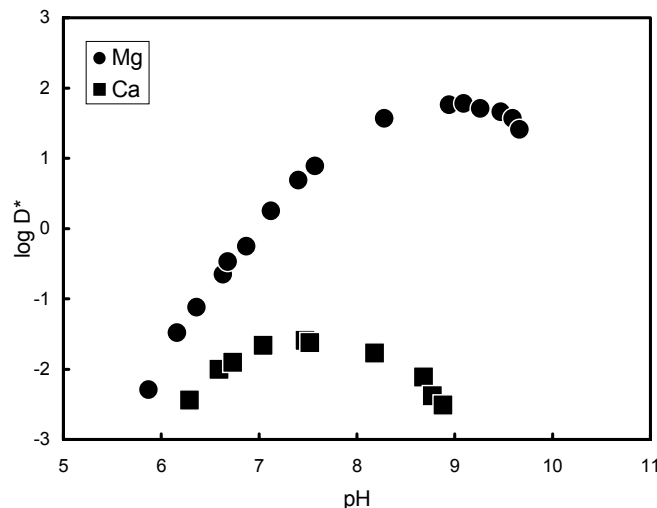
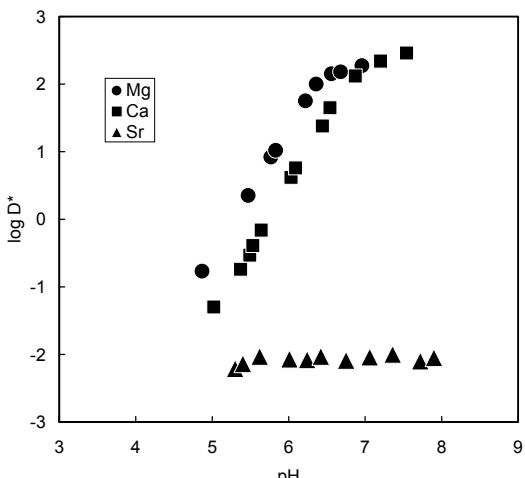


Figure 2. Extraction of Mg and Ca into cyclohexane with BFA and TBP in the presence of cryptand[2.2.1].  
 $[BFA]_0 = [TBP]_0 = 2.5 \times 10^{-3}$  M,  $[L] = 0.01$  M.



**Figure 3.** Extraction of Mg, Ca and Sr into cyclohexane with BFA and TBP in the presence of cryptand[2.2.2].  
[BFA]<sub>0</sub>=[TBP]<sub>0</sub>=0.015 M, [L]=0.01 M.

In the synergetic extraction of alkaline earths ( $M^{2+}$ ) with BFA (HA) and TBP, the extraction constant,  $K_{ex,s}$ , can be written as follows:

$$\log K_{ex,s} = \log D + 2 \text{ pH} + 2 \log [HA]_0 + 2 \log [TBP]_0 \quad (1)$$

where subscript o denotes the organic phase and D,  $[MA_2(TBP)_2]_0/[M^{2+}]$ , is the distribution ratio of alkaline earth metal ions. The distribution ratio of alkaline earth metal ions in the presence of cryptand [2.2.1] or [2.2.2] (L),  $D^*$ , can be expressed as follows:

$$D^* = K_{ex,s} [HA]_0^2 [TBP]_0^2 / [H^+]^2 \{ 1 + \beta[L] \} \quad (2)$$

where  $\beta$  is the complex formation constant of cryptand [2.2.1] or [2.2.2] with alkaline earth metal ions in the aqueous phase, defined as  $[ML^{2+}]_0/[M^{2+}][L]$ . Dividing D by  $D^*$  gives

$$D/D^* = 1 + \beta[L] \quad (3)$$

The values of  $\log K_{ex,s}$  and  $\log \beta$  for alkaline earth metal ions calculated from Eqs. (1), (2) and (3) are summarized in Table 2. These  $\log \beta$  values are in good agreement with those in Table 1.

From these results, combining the chelating reagents and the macrocyclic ionophores, such as cryptand [2.2.1] and cryptand [2.2.2], having an opposite complexation tendency has been proved to be a powerful means to separate alkaline earth metal ions each other.

**Table 2.** Extraction parameters for alkali and alkaline earth metals.

	$\log K_{ex,s}$	$\log \beta$	$\log \beta^*$
(A)	Mg	-3.50	---
	Ca	-4.60	6.85
(B)	Ca	-4.24	---
	Sr	-5.78	7.93

\* taken from [1].

### **Ion-Exchange Separation of Alkaline Earth Metal Ions with Strongly Acidic cation Exchange Resin (Amberlite 200CT)**

Conventional strongly acidic cation exchange resins, such as the commercially available Amberlite 200CT and Dowex 50W, can generally adsorb alkaline earth metal ions exclusively. In the ion-exchange reaction, metal ions having smaller ionic radii exhibit lower distribution ratio. However, the separation among alkaline earth metal ions is difficult to obtain with strongly acidic cation exchange resins. Figure 4 shows the results for the adsorption of alkaline earth metal ions onto Amberlite 200CT as a function of pH in the presence of cryptand [2.2.1].

The percent adsorption of Ca and Sr decreases rapidly above pH 6, while that of Mg is almost similar to these in the absence of cryptand [2.2.1]. Mg can be separated from most of the Ca and Sr in the pH range 6–8 where almost 100% of Mg is adsorbed by the resin, while more than 75–80% of Ca and Sr remain in the aqueous phase. By adding 2-propanol to the aqueous phase, the masking effect of cryptand is enhanced, resulting in a decrease of percent adsorption of Ca and Sr. This can be explained by the fact that the lower dielectric solvents are less capable of solvating cations, thus favoring their complex formation with cryptands in the aqueous phase [4].

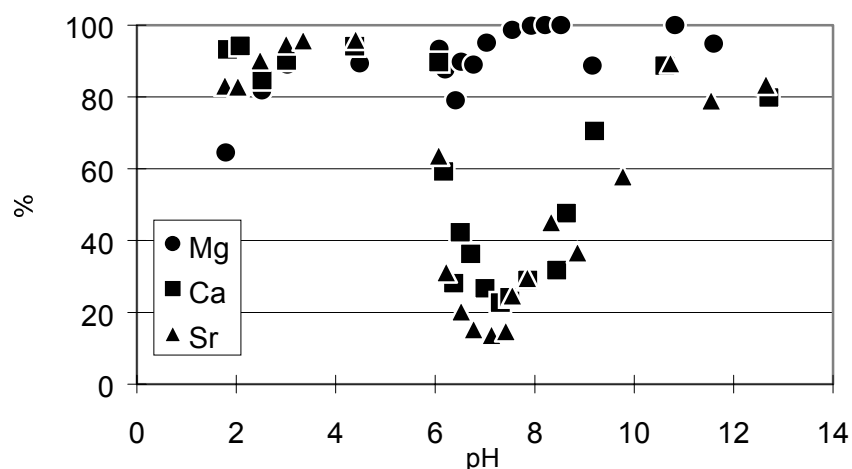


**Figure 4.** Adsorption of alkaline earth metal ions.  
Amberlite200CT(Na)=0.02g, [2.2.1]=0.02M, 30%-2prop.

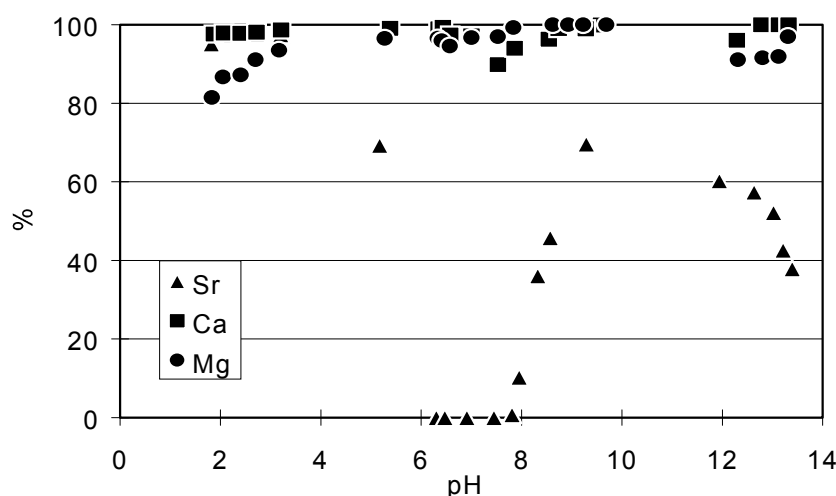


**Figure 5.** Adsorption of alkaline earth metal ions,  
Amberlite200CT(Na)=0.02g, [2.2.2]=0.02M, 30%-2prop.

Figure 5 also shows the results for the percent adsorption of alkaline earth metal ions onto Amberlite 200CT as a function of pH in the presence of cryptand [2.2.2]. Sr can be separated from Mg and Ca quantitatively in the pH range 6–8 where more than 90% of Mg and Ca are adsorbed onto resin, while 100% of Sr remains in the aqueous phase. Effective complex formation of metal ions with cryptands can be achieved at pH 6-7 according to the stability constants, respectively. However, discussions about the increasing adsorption of metal ions in higher pH region have not been extended at this time.

## CONCLUSIONS

Highly selective separation systems for alkaline earth metal ions have been successfully developed via synergistic extraction with benzoyltrifluoroacetone (BFA) and tri-n-butylphosphate (TBP), and by ion exchange with Amberlite 200CT in the presence of cryptands [2.2.1] and [2.2.2] as the ion-size selective masking reagents. On comparison of the above two methods, under these experimental conditions, quantitative separation among alkaline earth metal ions was not obtained by ion exchange, while the synergistic solvent extraction method could achieve quantitative separation of Mg from Ca and Sr in the presence of cryptand [2.2.1] and of Mg and Ca from Sr in the presence of cryptand [2.2.2]. However, combining the chelating reagent or ion-exchange resin and cryptands has been proven to be a powerful means to separate alkaline earth metal ions. This concept is universal and is of particular interest because it generates many opportunities for analytical and separation chemistry.

## REFERENCES

1. J. M. Lehn, J. Sauvage (1975), *J. Am. Chem. Soc.*, **97**, 6700-6707.
2. S Tsurubou, T. Sasaki, S. Umetani and M. Matsui (1997), *Anal. Sci.*, **13**, 127-130.
3. S. Tsurubou, S. Umetani and Y. Komatsu (1999), *Anal. Chim. Acta*, **394**, 317-324.
4. M. L. Dietz, R. Chiarizia, E. P. Horwitz, R. A. Bartsch and V. Talanov (1997), *Anal. Chem.*, **69**, 3028-3037.



## SOLVENT EXTRACTION OF METAL IONS WITH NOVEL 4-ACYL-5-PYRAZOLONES HAVING CROWN ETHER MOIETY AS INTRAMOLECULAR SYNERGIST

Shigeo Umetani, Shoko Yamazaki\* and Kaoru Ogura\*\*

Kyoto University, Uji, Japan

\* Nara University of Education, Nara, Japan

\*\*Ube National College of Technology, Ube, Japan

Novel 4-acyl-5-pyrazolones having the crown ether moiety as the intramolecular synergist have been synthesized and the solvent extraction of various metal ions are examined. It is expected that the crown ether moiety could behave as the intramolecular synergist and that the selectivity could be governed by the acylpyrazolone and the crown ether parts. These ligands are powerful and selective extracting reagents for alkali, alkaline earth and divalent transition metal ions, and the selectivity is quite unique depending on the intramolecular synergist.

Alkali metal ions are readily extracted into chloroform. The selectivity is governed primarily by the crown ether moiety depending on the cavity size. Alkaline earth metal ions are also readily extracted into chloroform, however in this case, the selectivity is governed by both the acylpyrazolone and the crown ether parts. Among the divalent transition metal ions, the extraordinarily high extractability is observed for  $Mn^{2+}$ ,  $Cd^{2+}$  and  $Pb^{2+}$ . Such anomalous extraction is also given in the synergistic extraction of  $Mn^{2+}$ ,  $Cd^{2+}$  and  $Pb^{2+}$  with acylpyrazolone and benzo-crown ethers used separately.

### INTRODUCTION

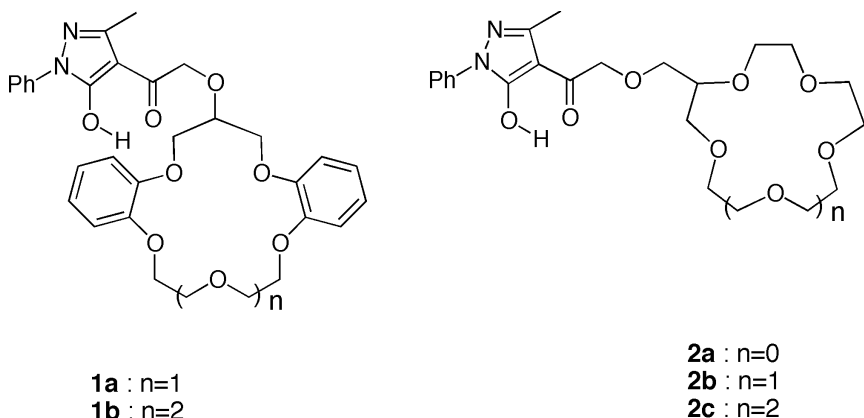
Macrocyclic ligands such as crown ethers and cryptands have been utilized in the metal ion separations [1]. Many novel macrocyclic ligands have been prepared as ion pair extraction reagents exhibiting excellent separation ability [2]. It was shown that water soluble macrocyclic ligands could enhance the separability when they were added in the aqueous phase as ion size selective masking reagents in the extraction of alkali, alkaline earth and lanthanide metal ions with the chelate extraction reagents [3, 4]. On the contrary, it is known that neutral macrocyclic ligands can work as synergists when they were added in the organic phase. In both cases, unique separability would be expected since the selectivity of the macrocyclic ligands and the chelating reagents is quite different.

In this work, 4-acyl-5-pyrazolone-substituted dibenzo-16-crown-5, dibenzo-19-crown-6 (**1a-b**), 12-crown-4, 15-crown-5 and 18-crown-6 (**2a-c**) were designed and synthesized by facile coupling reactions between  $\alpha$ -chloro 4-acyl-5-pyrazolone and the corresponding hydroxy crown ethers. It is expected that the crown ether moiety could work as the intramolecular synergist and the selectivity would be governed by the acylpyrazolone and the crown ether parts.

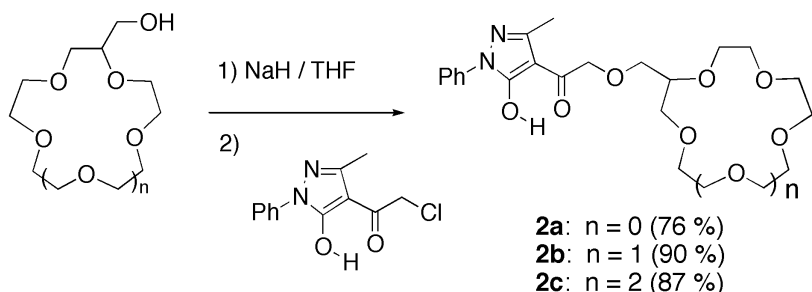
## EXPERIMENTAL

### Materials

4-Acyl-5-pyrazolone-substituted dibenzo-16-crown-5 and dibenzo-19-crown-6 (**1a-b**) were synthesized from 1-phenyl-3-methyl-4-chloroacetyl-5-pyrazolone and readily accessible hydroxy crown ethers. Hydroxy crown ethers were treated with NaH in THF at room temperature. The addition of 1-phenyl-3-methyl-4-chloroacetyl-5-pyrazolone to the mixture and stirring overnight produced **1a-b** in 48% and 95% yields, respectively. The detailed procedures, elemental analysis and spectroscopic data are available in the literature [5].



4-Acyl-5-pyrazolone-substituted 12-crown-4, 15-crown-5 and 18-crown-6 (**2a-c**) were also prepared from 1-phenyl-3-methyl-4-chloroacetyl-5-pyrazolone and commercially available hydroxy crown ethers in a similar manner. The details will be published elsewhere.



Other chemicals were of reagent-grade materials. Distilled, and de-ionized water was used throughout.

### Extraction Procedure

A  $10 \text{ cm}^3$  aliquot of an aqueous phase containing  $1 \times 10^{-4} \text{ M}$  of metal ion, 0.1 M tetramethylammonium chloride to keep the ionic strength at 0.1 and 0.01 M 2-morpholinoethanesulfonic acid as buffering component was adjusted to the desired pH with hydrochloric acid or tetramethylammonium hydroxide solution. The aqueous phase was shaken with an equal volume of chloroform containing the required amount of ligand at  $25^\circ\text{C}$  for one hour. A shaking time of 1 h was found to be long enough to reach equilibrium. After centrifugation, the pH of the aqueous phase was measured and taken as the equilibrium value. The metal concentration in the aqueous phase was determined by atomic absorption spectrometry. That in the organic phase was measured in the same way after back-extraction by stripping with hydrochloric acid solution. The sum of the metal concentrations in the two phases agreed well with the initial concentration.

## RESULTS AND DISCUSSION

### Extraction of Alkali and Alkaline Earth Metal Ions

The extraction of alkali metal ions into chloroform with 0.01 M **2a** is shown in Figure 1. 0.1 M tetramethylammonium chloride was added to the aqueous phase to keep the ionic strength at 0.1. Alkali metal ions were extracted in the order  $\text{Li}^+ > \text{Na}^+ > \text{K}^+ > \text{Rb}^+ > \text{Cs}^+$  with **2a**,  $\text{Na}^+ > \text{K}^+ > \text{Rb}^+ > \text{Cs}^+ > \text{Li}^+$  with **2b** and  $\text{K}^+ > \text{Na}^+ > \text{Rb}^+ > \text{Cs}^+ > \text{Li}^+$  with **2c**. Alkali and alkaline earth metal ions are not extractable with acylpyrazolone alone because of water molecules attached to the metal chelate that reduce the hydrophobicity remarkably. As seen in the figure, the separability and the extractability with these ligands are notable. It is clear that the crown ether moiety works as an intramolecular synergist. The extraction reaction was found to follow Eqn. (1) according to the slope analysis.



where M and HA stand for the metal ion and the extraction reagent, and the subscript o denotes the species in the organic phase. The extraction constant ( $K_{\text{ex}}$ ) can be written as follows

$$K_{\text{ex}} = [\text{MA}_n]_o [\text{H}^+]^n / [\text{M}^{n+}] [\text{HA}]^n_o = D [\text{H}^+]^n / [\text{HA}]^n_o \quad (2)$$

where D is the distribution ratio defined as  $[\text{MA}]_o / [\text{M}^+]$ . It was found that **2b** and **2c** are more powerful than the combination of 1-phenyl-3-methyl-4-benzoyl-5-pyrazolone and benzo-15-crown-5 or benzo-18-crown-6.

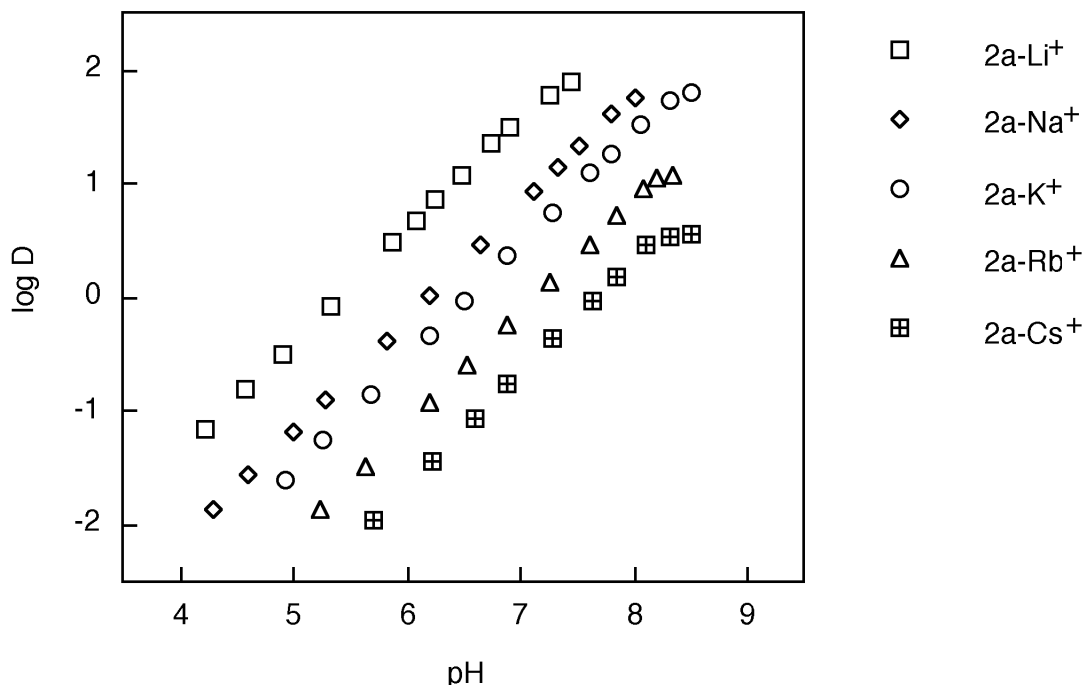


Figure 1. Extraction of alkali metal ions with **2a**.

The  $\log K_{\text{ex}}$  values for the extraction of alkali metal ions with **2a-c** are plotted in Figure 2 (a) against the  $\log K$  values which are the formation constant with 12-crown-4, 15-crown-5 and 18-crown-6 in methanol measured by conductometric titration. Fairly good linear relationship can be seen between  $\log K_{\text{ex}}$  and  $\log K$  indicating that the extraction selectivity with **2a-c** for the extraction of alkali metal ions is governed primarily by the crown ether moiety depending on the cavity size.

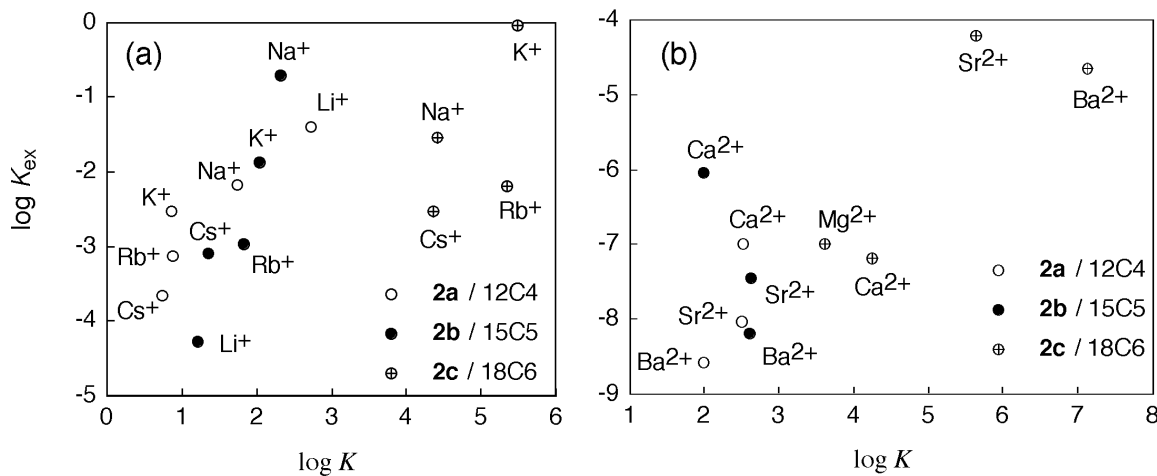


Figure 2. Relationship between the extraction constants ( $\log K_{\text{ex}}$ ) with **2a-c** and the formation constants ( $\log K$ ).

Alkaline earth metal ions were extracted in the order  $\text{Mg}^{2+} > \text{Ca}^{2+} > \text{Sr}^{2+} > \text{Ba}^{2+}$  with **2a**,  $\text{Ca}^{2+} > \text{Mg}^{2+} > \text{Sr}^{2+} > \text{Ba}^{2+}$  with **2b** and  $\text{Sr}^{2+} > \text{Ba}^{2+} > \text{Ca}^{2+} > \text{Mg}^{2+}$  with **2c**. The  $\log K_{\text{ex}}$  values for the extraction of alkaline earth metal ions with **2a-c** are plotted in Figure 2 (b) against the formation constants, the  $\log K$ , with 12-crown-4, 15-crown-5 and 18-crown-6 in methanol measured by conductometric titration. However, no good linear relationship could be seen in the figure, unlike the case for alkali metal ions, indicating that the selectivity is governed by both the acylpyrazolone and the crown ether parts.

#### Extraction of Divalent Transition Metal Ions

The extractions of divalent transition metal ions were made with 0.01 M **2c** into chloroform and are shown in Figure 3.

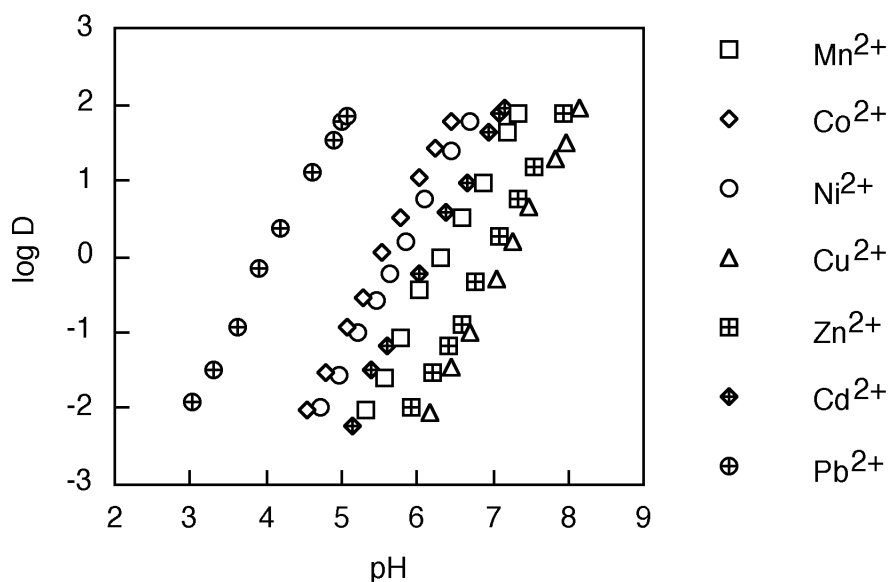


Figure 3. Extraction of divalent transition metal ions with **2c**.

Divalent transition metal ions were extracted in the order,  $\text{Pb}^{2+} > \text{Mn}^{2+} > \text{Cd}^{2+} > \text{Cu}^{2+} > \text{Zn}^{2+} > \text{Co}^{2+} > \text{Ni}^{2+}$  with **1a** and  $\text{Pb}^{2+} > \text{Cu}^{2+} > \text{Mn}^{2+} > \text{Zn}^{2+} > \text{Co}^{2+} > \text{Cd}^{2+} > \text{Ni}^{2+}$  with **1b**. With **2a-c** the orders are  $\text{Cu}^{2+} > \text{Zn}^{2+} > \text{Co}^{2+} > \text{Pb}^{2+} > \text{Ni}^{2+} > \text{Mn}^{2+} > \text{Cd}^{2+}$  with **2a**,  $\text{Pb}^{2+} > \text{Cu}^{2+} > \text{Zn}^{2+} > \text{Co}^{2+} > \text{Ni}^{2+} > \text{Cd}^{2+} > \text{Mn}^{2+}$  with **2b** and  $\text{Pb}^{2+} > \text{Co}^{2+} > \text{Ni}^{2+} > \text{Cd}^{2+} > \text{Mn}^{2+} > \text{Zn}^{2+} > \text{Cu}^{2+}$  with **2c**. The extraction orders with the present ligands are unique. Among the divalent transition metal ions, the extraordinarily high extractability was seen for  $\text{Mn}^{2+}$ ,  $\text{Cd}^{2+}$  and  $\text{Pb}^{2+}$ . It is well known that the extractability for these metal ions is much lower than the other divalent transition metal ions such as  $\text{Cu}^{2+}$ ,  $\text{Co}^{2+}$ ,  $\text{Ni}^{2+}$  and  $\text{Zn}^{2+}$  with the conventional chelating extractants. It was reported that the formation constants ( $K$ ) of divalent transition metal ions with 15-crown-5 or 18-crown-5 are low except for that of  $\text{Pb}^{2+}$  with 18-crown-6 [2]. No linear relationship can not be seen between  $\log K_{\text{ex}}$  and  $\log K$ . Such anomalous extraction was also given in the synergistic extraction with 1-phenyl-3-methyl-4-benzoyl-5-pyrazolone and benzo-15-crown-5 or benzo-18-crown-6. The adduct formation constants ( $\beta$ ) defined as Eqn. (3) were obtained examining the effect of the benzo-crown ether ( $L$ ) concentration in the organic phase.



The  $\log \beta$  values for  $\text{Mn}^{2+}$ ,  $\text{Cd}^{2+}$  and  $\text{Pb}^{2+}$  with both benzo-15-crown-5 and benzo-18-crown-6 are considerably larger than those for the other divalent transition metal ions, which can not be rationalized considering the formation constants ( $K$ ) as described above. The extraordinarily high extractability for  $\text{Mn}^{2+}$ ,  $\text{Cd}^{2+}$  and  $\text{Pb}^{2+}$  would be attributable to the specific adduct formation reaction presumably based on the complex structure.

## REFERENCES

1. Y. A. Zolotov (1997), *Macrocyclic Compounds in Analytical Chemistry*, John Wiley & Sons, New York.
2. R. M. Izatt, K. Pawlak, J. S. Bradshaw and R. L. Bruening (1991), *Chem. Rev.*, **91**, 1721.
3. S. Tsurubou, M. Mizutani, Y. Kadota, T. Yamamoto, S. Umetani, T. Sasaki, Q. T. H. Le and M. Matsui (1995), *Anal. Chem.*, **67**, 1465-1469.
4. S. Tsurubou, S. Umetani and Y. Komatsu (1999), *Anal. Chim. Acta*, **394**, 317-324.
5. S. Yamazaki, M. Hanada, Y. Yanase, C. Fukumori, K. Ogura, T. Saeki and S. Umetani (1999), *J. Chem. Soc., Perkin Trans. 1*, 693-696.



## A NOVEL SYNERGISM FOUND IN THE EXTRACTION OF In(III) ION WITH TTA AND TOPO IN CARBON TETRACHLORIDE

Akiko Hokura, Junji Noro\*, Satoshi Kusakabe and the late Tatsuya Sekine

Science University of Tokyo, Tokyo, Japan

\*Nissan Arc Co., Ltd., Yokosuka, Japan

Solvent extraction of indium(III) with 2-thenoyltrifluoroacetone (Htta) in carbon tetrachloride from aqueous 0.1 mol dm<sup>-3</sup> sodium nitrate solution at pH 2 was measured in the absence and presence of trioctylphosphine oxide (TOPO). Addition of TOPO enhanced the extraction, although the solvation of In(tta)<sub>3</sub> by TOPO was not found. The complexes extracted by the cooperation with Htta and TOPO was presumed to be In(tta)<sub>a</sub>(OH)<sub>3-a</sub>(TOPO)<sub>b</sub> where *a* and *b* are 2 and/or 1. The possibility of the extraction of hydroxide has been discussed.

### INTRODUCTION

Indium(III) in aqueous solutions is effectively extracted with several chelating extractants [1] such as 2-thenoyltrifluoroacetone (Htta) [2]. It is also known that In<sup>3+</sup> ion is extracted with a solvating type extractant such as trioctylphosphine oxide (TOPO) as an ion pair with a bulky anion [3]. When both a chelating and a solvating type extractant are used together, the extraction is often better than the net extraction by both extractants. This is known as synergism. Although the synergistic extraction is marked among trivalent lanthanoids as was demonstrated with 2-thenoyltrifluoroacetone (Htta) and with tributylphosphate (TBP) [2], the extraction of indium(III) with Htta was not enhanced by an addition of TBP. This observation can be explained in terms that the six coordination sites on In<sup>3+</sup> ion are fully occupied by the three molecules of bi-dentate chelate ion, and there should be no room for TBP to form the adduct compound. However, an addition of TOPO enhanced the extraction of In(III) in aqueous perchlorate solutions with Htta in carbon tetrachloride [4]. Moreover, the extracted complex seemed to contain less than three molecules of tta<sup>-</sup>. The role of anions in this extraction equilibrium was examined in the present study.

### EXPERIMENTAL

All the solvent extraction experiments were carried out in a room thermostated at 298 K. The Htta and TOPO, both supplied by Dojindo Laboratories, were crystallized from toluene and hexane, respectively. A weighed amount of Htta or TOPO was dissolved in carbon tetrachloride for each stock solution. The Htta solution was left standing overnight before use. The indium(III) nitrate was dissolved in aqueous 9.00x10<sup>-2</sup> mol dm<sup>-3</sup> sodium nitrate solution containing 1.00x10<sup>-2</sup> mol dm<sup>-3</sup> nitric acid, or otherwise an indium standard solution (contains In<sup>3+</sup> by 1000 ppm in 1 mol dm<sup>-3</sup> HNO<sub>3</sub>) for the atomic absorption spectrometry was diluted with a sodium nitrate solution. A portion of the aqueous solution and the same volume of carbon tetrachloride solution containing each or both of Htta and TOPO were placed in a stoppered glass tube of 20 cm<sup>3</sup>. The two phases were agitated by a mechanical shaker for 2 h and centrifuged off. The indium ion extracted into the organic phase was stripped by 1 mol dm<sup>-3</sup> nitric acid. The amount of indium in the stripped solution and that in the aqueous phase were determined by atomic absorption spectrometry using a Hitachi Z-6100 atomic absorption spectrometer. The pH of the aqueous phase was measured by a potentiometer using the solution containing 0.01 mol dm<sup>-3</sup> HClO<sub>4</sub> and 0.09 mol dm<sup>-3</sup> NaClO<sub>4</sub> as the standard for pH 2.

## RESULTS AND DISCUSSION

The distribution ratio of In(III) between aqueous 0.1 mol dm<sup>-3</sup> nitrate solution of pH 2 and carbon tetrachloride containing certain amounts of TOPO and Htta is shown in Figure 1. When TOPO was absent, the plot of logarithm of the distribution ratio vs. logarithm of Htta at initial concentration gave a straight line of slope +3. Thus this extraction equilibrium can be expressed by equation (1) and the formation of chelate complexes in the aqueous phase should be negligible.



$$K_{\text{ex}30} = \frac{[\text{In}(\text{tta})_3]_{\text{org}}[\text{H}^+]^3}{[\text{In}^{3+}][\text{Htta}]_{\text{org}}^3} \quad (2)$$

The value of this constant is obtained from the data in Figure 1(A) was 10-2.53. This value is reported in the previous paper [4] as 10-2.55 by separate data. When TOPO was added, the distribution ratio was enhanced, though the slope became smaller than +3. When In<sup>3+</sup> was extracted from 1 mol dm<sup>-3</sup> aqueous NaClO<sub>4</sub> solution with TOPO only, the extracted species was found to be In(ClO<sub>4</sub>)<sub>3</sub>(TOPO)<sub>4</sub> [3]. However, Figure 1(B) shows that the slope of log-log plot for the extraction with TOPO only is approximately +2.5. Then, the chemical form of In(III) extracted with TOPO from the nitrate medium is thus expected to be In(NO<sub>3</sub>)<sub>3</sub>(TOPO)<sub>2</sub> and In(NO<sub>3</sub>)<sub>3</sub>(TOPO)<sub>3</sub>. Since the extracted amount is small compared to that with the cooperation of Htta and TOPO, this extraction is neglected in the following discussions. As is seen in Figure 1(B), the addition of Htta enhanced the extraction of In(III) but reduced the slope of the extraction curves.

The smaller slope than +3 in Figure 1(A) indicates that the extracted species contain less than three tta<sup>-</sup> ions, namely, other anion(s) should be included in them. Reduction of In(III) to In(II) or In(I) will scarcely occur, because the extraction of In(tta)<sub>3</sub> has been established and TOPO is not a reducing reagent. In order to identify the cooperating anion with tta<sup>-</sup>, indium ion was extracted from aqueous sodium nitrate or sodium perchlorate solutions of different ionic concentration. The hydrogen-ion concentration was kept at 0.01 mol dm<sup>-3</sup>. Figure 2 gives the results. The distribution ratio seems to be independent of the concentration of both anions at least below 0.1 mol dm<sup>-3</sup>. This fact excludes these anions from the counter anion.

Since highly charged cations are susceptible to hydrolysis in aqueous solutions, the effect of hydroxyl ion was examined. Figure 3 gives the extraction curves of In(III) from the aqueous solutions of various pH. Although the slopes were not always +3 exactly, the present authors assume that the extracted species may contain tta<sup>-</sup> and hydroxyl ion. Supposing that the extracted species are In(tta)<sub>3</sub>, In(tta)<sub>2</sub>OH, and In(tta)(OH)<sub>2</sub>, the number of TOPO molecules adducting to these species is assumed to be 1 or 2 from the slope of plots in Fig. 1(B). Thus the chemical form of the extracted species can be written as In(tta)<sub>a</sub>(OH)<sub>3-a</sub>(TOPO)<sub>b</sub>. The extraction constants are defined by equation (3) and the distribution ratio of indium(III) can be written as equation (4).

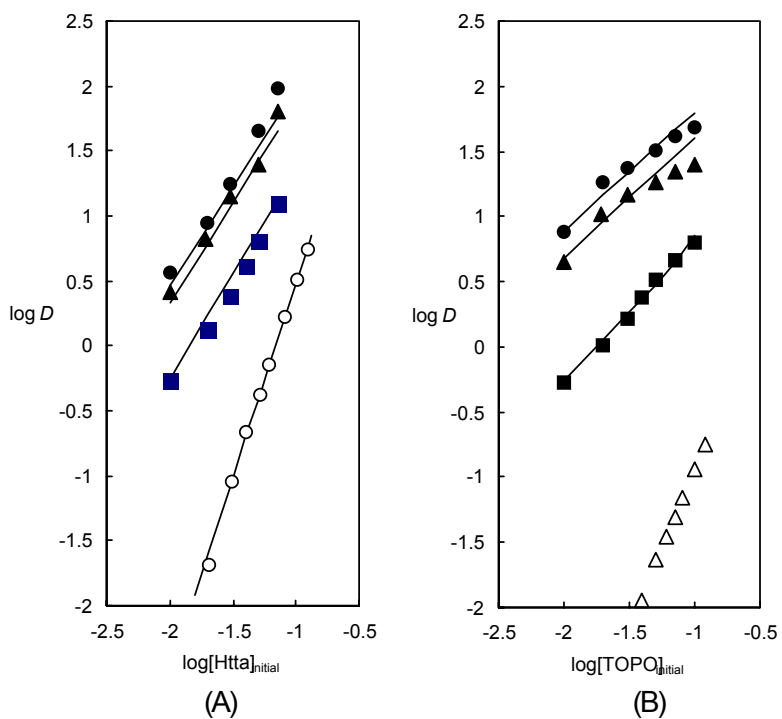


*Figure 1. Distribution ratio of indium(III). Aqueous phase: 0.01 mol dm<sup>-3</sup> HNO<sub>3</sub> and 0.09 mol dm<sup>-3</sup> NaNO<sub>3</sub> initially containing 1×10<sup>4</sup> mol dm<sup>-3</sup> In<sup>3+</sup>. Organic phase: CCl<sub>4</sub> containing (A) various amounts of Htta with; 0, 0.01, 0.0375, and 0.05 mol dm<sup>-3</sup> TOPO from bottom to top and (B) various amounts of TOPO with 0, 0.01, 0.0375, and 0.05 mol dm<sup>-3</sup> Htta from bottom to top, respectively. Solid lines are calculated by using the constants in the text on the basis of equation (4).*

$$K_{\text{exab}} = \frac{[\ln(\text{tta})_a(\text{OH})_{3-a}(\text{TOPO})_b]_{\text{org}} [\text{H}^+]^3}{[\ln^{3+}] [\text{Htta}]_{\text{org}}^a [\text{TOPO}]_{\text{org}}^b} \quad (3)$$

$$D = \frac{[\ln(\text{tta})_3]_{\text{org}} + [\ln(\text{tta})_2(\text{OH})(\text{TOPO})_b]_{\text{org}} + [\ln(\text{tta})(\text{OH})_2(\text{TOPO})_{b'}]_{\text{org}}}{[\ln^{3+}]} \quad (4)$$

$$= \frac{K_{\text{ex30}} [\text{Htta}]_{\text{org}}^3 + K_{\text{ex2b}} [\text{Htta}]_{\text{org}}^2 [\text{TOPO}]_{\text{org}}^b + K_{\text{ex1b}} [\text{Htta}] [\text{TOPO}]_{\text{org}}^{b'}}{[\text{H}^+]^3}$$

The Htta and TOPO associate in carbon tetrachloride. The association constant has been reported as  $K_{as} = [(\text{Htta})(\text{TOPO})]_{\text{org}} / [\text{Htta}]_{\text{org}}[\text{TOPO}]_{\text{org}} = 101$  [5]. The decrease in the concentrations of both reagents by this association equilibrium was taken into account. Curve fitting calculation based on a non-linear least squares approximation gave the constants as follows, although the accuracy is not always satisfactory;  $\log K_{ex22} = 0.97$ ,  $\log K_{ex21} = -0.30$ ,  $\log K_{ex12} = -1.09$ , and  $\log K_{ex11} = -2.93$ .

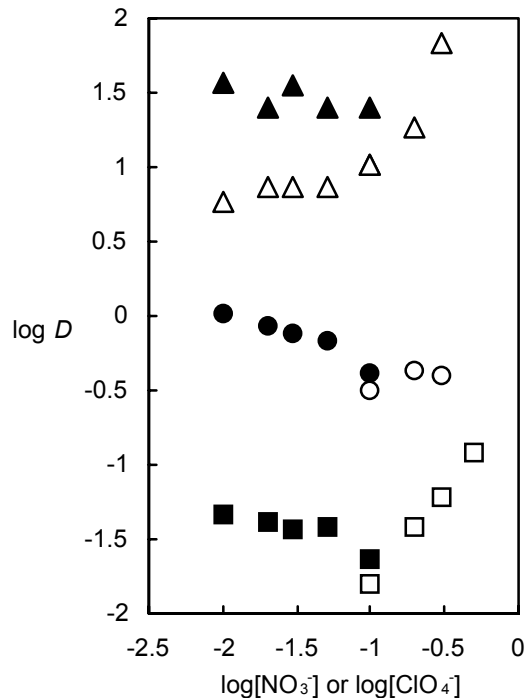


*Figure 2. The extraction of indium(III) as a function of anion concentration in an aqueous phase initially containing  $[H^+] = 0.01 \text{ mol dm}^{-3}$ . Open and filled symbols are for perchlorate and nitrate media, respectively. The organic phase is; squares = TOPO only ( $0.05 \text{ mol dm}^{-3}$  for nitrate medium and  $0.03 \text{ mol dm}^{-3}$  for perchlorate medium), circles = Htta only ( $0.05 \text{ mol dm}^{-3}$  for both media), and triangles = mixture containing the same concentration of Htta and TOPO ( $0.05 \text{ mol dm}^{-3}$  for nitrate medium and  $0.02 \text{ mol dm}^{-3}$  for perchlorate medium).*

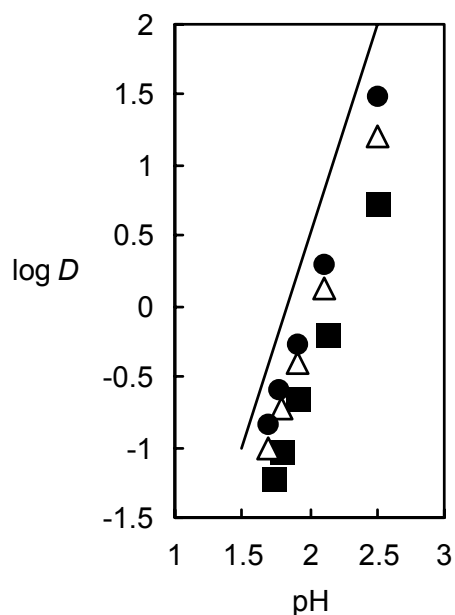


*Figure 3. Extraction of indium(III) as a function of pH in the aqueous phase at equilibrium. The initial concentration of  $In^{3+}$  was  $8.76 \times 10^{-5} \text{ mol dm}^{-3}$  in  $0.1 \text{ mol dm}^{-3} NaNO_3$ . The organic phases initially contain;*

- (a)  $0.03 \text{ mol dm}^{-3}$  Htta and  $0.01 \text{ mol dm}^{-3}$  TOPO,
- (b)  $0.02 \text{ mol dm}^{-3}$  Htta and  $0.02 \text{ mol dm}^{-3}$  TOPO, and
- (c)  $0.01 \text{ mol dm}^{-3}$  Htta and  $0.05 \text{ mol dm}^{-3}$  TOPO

*from top to bottom. The solid line shows the slope +3.*

The hydroxyl ion is regarded as an anion of very poor extractability in the ion-pair extraction systems. Moreover, the molar ratio of these hydroxides to the  $\text{In}^{3+}$  ion in the aqueous phase of pH=2 is estimated as  $10^{-2.43}$  (3.7%) for  $\text{In}(\text{OH})^{2+}$  and  $10^{-5.35}$  (0.0005%) for  $\text{In}(\text{OH})_2^+$ , respectively, from the hydrolysis constant  $K_{11} = 10^{-4.31}$  and  $K_{12} = 10^{-9.35}$  (in 0.5 mol dm<sup>-3</sup> NaNO<sub>3</sub> medium [6], the hydrolysis constants being defined by  $K_{xy} = [\text{In}_x(\text{OH})_y]^{3x+y}[\text{H}^{+}]^y/[\text{In}^{3+}]^x$ ). Therefore, the hydroxides of In(III) ion should be negligible in both phases of the present extraction system. Although  $\text{In}(\text{OH})_3$  is scarcely extractable,  $\text{In}(\text{OH})^{2+}$  and  $\text{In}(\text{OH})_2^+$  might be stabilized in the organic phase by the aid of lipophilic ligands. As a similar case to the hydroxide, extraction of In(III) chloride complexes is reported by Brunette *et al.* [7].

Brunette *et al.* extracted indium(III) in aqueous chloride-perchlorate solutions with acylpyrazolones (HL) and TOPO in toluene [7]. The chemical form of the extracted complexes was reported as  $\text{InL}_3(\text{TOPO})_2$ ,  $\text{InClL}_2(\text{TOPO})_2$ , and  $\text{InCl}_2\text{L}(\text{TOPO})_2$ . The  $\text{InL}_3(\text{TOPO})_2$  type of complex was not found in the present study. This may be attributed to the different ability of ligand molecule to form hydrogen bonds with TOPO. Acylpyrazolone has a nitrogen atom that can form hydrogen bond with water and TOPO can also form hydrogen bond with this water molecule. Even though the Htta molecule has a sulfur atom, it may have much weaker interactions with TOPO. From [7], the extraction constant of  $\text{InL}_3$  defined by the same form with equation (2) is  $10^{1.50}$  when In(III) is extracted with 1-phenyl-3-methyl-4-benzoylpyrazol-5-one from perchlorate medium to toluene. Since this value for  $\text{In}(\text{tta})_3$  in the present study is  $10^{-2.6}$ , Htta is a poorer extractant for In(III) than HL; otherwise the extraction of hydroxides will be not recognized, hidden under a good extraction by other superior extractants.

The extraction of hydroxide is assumed to explain the unusual extraction behavior of In(III) complex in the present system and it should be proved by further studies. However, if the hydroxide is actually extracted, the present extraction system may be regarded as a new type of synergism in which three different types of extractant cooperate. Formation of poly-nuclear hydroxide in the aqueous solutions is also reported;  $K_{34} = 10^{9.29}$  (in 3 mol dm<sup>-3</sup> NaClO<sub>4</sub>) [8]. This may impair the extraction of In(III) in its higher concentrations.

## ACKNOWLEDGEMENTS

The authors thank Miss Yuko Ueno and Mr. Yohei Unno for their experimental work.

## REFERENCES

1. (a) J. Stary (1964), *The Solvent Extraction of Metal Chelates*, Pergamon Press. (b) A. K. De, S. M. Khodkar and R. A. Chalmers van Nostrand (1970), *Solvent Extraction of Metals*, Reinhold, London. (c) T. Sekine and Y. Hasegawa (1977), *Solvent Extraction Chemistry, Fundamentals and Applications*, Marcel Dekker, New York.
2. T. Sekine and D. Dyrssen (1967), *J. Inorg. Nucl. Chem.*, **29**, 1481.
3. M. Yamada, S. Kusakabe, J. Prekopova and T. Sekine (1996), *Anal. Sci.*, **12**, 405.
4. J. Noro, A. Hokura, I. Tanaka, M. Yamada and T. Sekine (1999), *Proc. ISEC '99*, Society of Chemical Industry, London, pp. 561-566.
5. T. Sekine, T. Saitou and H. Iga (1983), *Bull. Chem. Soc. Jpn.*, **56**, 700.
6. P. L. Brown, J. Ellis and R. N. Sylva (1982), *J. Chem. Soc. Dalton Trans.*, 1911.
7. J. P. Brunette, M. Taheri, G. Goetz-Grandmont and M. J. F. Leroy (1985), *Solv. Extr. Ion Exch.*, **3**, 309.
8. C. F. Baes, Jr. and R. E. Mesmer (1976), *The Hydrolysis of Cations*, John Wiley, New York.



## SOLVENT EXTRACTION OF INDIUM(III) AND IRON(III) FROM SULPHURIC ACID MEDIA BY MIXTURES OF D<sub>2</sub>EHPA AND CYANEX 923

Chun Wang\*, Daxing Liu and Jin Zhang

Beijing General Research Institute of Mining and Metallurgy, Beijing, P. R. China

The extraction equilibria of In(III) and Fe(III) by di(2-ethylhexyl) phosphoric acid (D<sub>2</sub>EHPA), 2-ethylhexyl phosphonic acid 2-ethylhexyl ester (EHEHPA), Cyanex 923 and binary mixtures of D<sub>2</sub>EHPA-Cyanex 923, D<sub>2</sub>EHPA-TRPO and D<sub>2</sub>EHPA-TBP were studied. The stripping of In(III) and Fe(III) from the loaded organic phase was conducted using H<sub>2</sub>SO<sub>4</sub>. It was found that it is easier to strip In(III) and Fe(III) from D<sub>2</sub>EHPA-Cyanex 923 and D<sub>2</sub>EHPA-TRPO than from D<sub>2</sub>EHPA. 90% In(III) can be stripped from D<sub>2</sub>EHPA-Cyanex 923 by using 250 g/L H<sub>2</sub>SO<sub>4</sub> in a single stage. The In(III) loading capacity with D<sub>2</sub>EHPA-Cyanex 923 was determined. The effects of equilibrium time, phase ratio, temperature, extractant concentration were observed. The kinetics of In(III) and Fe(III) extraction and stripping were also studied to achieve a better separation of In(III) and Fe(III). Compared with D<sub>2</sub>EHPA, the mixture of D<sub>2</sub>EHPA and Cyanex 923 has the following advantages: 1) lower stripping acidity and higher stripping yield of indium(III); 2) is easier to strip Fe(III) from the loaded organic phase; 3) its loading capacity is comparable to that with D<sub>2</sub>EHPA at real leach liquor acidity.

### INTRODUCTION

Indium is one of the most important rare metals used in electronic devices and alloys. Indium consumption has been increasing significantly in recent years because of its applications in high-tech products such as InP semiconductors, and indium tin oxide (ITO) used in the LCDs of portable electronics.

Indium is recovered usually as a by-product from zinc or lead residues, or slags derived from zinc or lead smelting and refining processes. One of the important processes is to recover indium(III) from sulphuric acid leach liquors of zinc residues by solvent extraction using organophosphorus compounds. Di(2-ethylhexyl) phosphoric acid (D<sub>2</sub>EHPA, marketed as P204 in China) is used as an extractant at Laibing Smelter, Huaxi Group Co., China [1]. Toho Zinc Co., Ltd. employs a mixture of D<sub>2</sub>EHPA and tributylphosphate (TBP) [2].

Fundamental studies on the extraction of indium(III) with organophosphorus compounds have been conducted by several researchers. Sato studied In(III) extraction with D<sub>2</sub>EHPA and 2-ethylhexyl phosphoric acid 2-ethylhexyl ester (EHEHPA, marketed as PC-88A in Japan and P507 in China) from H<sub>2</sub>SO<sub>4</sub>, HNO<sub>3</sub> and HCl media [3]. Inoue compared In(III) extraction from HNO<sub>3</sub> media with D<sub>2</sub>EHPA, PC-88A and Cyanex 272. The extraction with these reagents

decreases in the order: D<sub>2</sub>EHPA > PC-88A > Cyanex 272 [4]. Bauer studied In(III) recovery from mixed hydrochloric acid-sulphuric acid media with bis(2,4,4-trimethylpentyl)-dithiophosphinic acid (marketed as Cyanex 301). In(III) is co-extracted with As(III), Cd(II), Cu(II) and Fe(III), so this reagent shows no improved selectivity for In(III) over other impurities. A high concentration of HCl, *i.e.*, 7 mol/L, is used to strip In(III) [5].

D<sub>2</sub>EHPA is still one of the most important extractants applied on an industrial scale. However, the strong extraction of In(III) and Fe(III) make the stripping of these elements very difficult, high concentrations of HCl, *i.e.*, 6-8 Mol/L, are used to conduct stripping [6]. Fe(III) will be accumulated gradually in the organic phase of the SX circuit, and this will eventually result in extractant poisoning.

Rickelton studied In(III) recovery by D<sub>2</sub>EHPA modified with Cyanex 923 (a mixture of straight-chained phosphine oxides) or Cyanex 925 (a branched chain phosphine oxide) [7]. Better stripping of In(III) and Fe(III) from the loaded organic phase can be accomplished with 2 mol/L H<sub>2</sub>SO<sub>4</sub> when D<sub>2</sub>EHPA is modified with Cyanex 923 or Cyanex 925.

In this paper, the extraction equilibria of In(III) and Fe(III) by di(2-ethylhexyl) phosphoric acid (D<sub>2</sub>EHPA), 2-ethylhexyl phosphonic acid 2-ethylhexyl ester (EHEHPA), Cyanex 923 and binary mixtures of D<sub>2</sub>EHPA-Cyanex 923, D<sub>2</sub>EHPA-TRPO and D<sub>2</sub>EHPA-TBP were studied. The effects on extraction and stripping of In(III) and Fe(III) were studied. Synthetic as well as actual leach liquors were used [8]. The purpose of this study was to evaluate the potential of D<sub>2</sub>EHPA-Cyanex 923 mixtures for indium recovery on a commercial scale.

## EXPERIMENTAL

### Reagents

Indium and ferric sulphate solutions were prepared by dissolving the analytical grade reagents in deionized water. The synthetic leach solution was prepared by mixing In(III) sulphate, Fe(III) sulphate, and sulphuric acid solutions. The actual liquor solution was supplied by a domestic zinc refinery in China, and its chemical composition is shown in Table 1.

*Table 1. Chemical composition of the real leach liquor.*

Element	In	Fe	Zn	Cd	Mn	Cu	Ca	Mg	H <sub>2</sub> SO <sub>4</sub>
Content(g/L)	0.39	49.58	11.18	0.22	2.81	0.27	0.50	0.73	19.28

Cyanex 923 was kindly supplied by Cytec Industries Inc. D<sub>2</sub>EHPA, EHEHPA, TBP and Trialkyl phosphine oxide (TRPO) were supplied by China's Chemical Plants. All extractants were used without further purification. Kerosene was used as a diluent. All other reagents were of chemical grade.

### Extraction, Stripping and Analytical Procedures

All batch experiments, including extraction and stripping, were conducted by equilibrating measured volumes of aqueous and organic phases in separating funnels and shaking for 1-10 min at room temperature.

Aqueous feed and raffinate solutions were analyzed by atomic absorption spectrophotometry (AAS) using a Perkin-Elmer model TC5100 instrument or inductively coupled plasma atomic emission spectrometry (ICP-AES) using a Perkin-Elmer model Optima 3000 instrument. The metal contents in the loaded organics were determined by mass balance. The simulated continuous counter-current tests were also conducted in a series of separating funnels.

## RESULTS AND DISCUSSION

### In(III) Extraction

In(III) extraction was conducted with 5% v/v D<sub>2</sub>EHPA, 5% v/v EHEHPA, 5% v/v Cyanex 923 and binary mixtures of 5% D<sub>2</sub>EHPA-5% Cyanex 923, 5% D<sub>2</sub>EHPA-5% TRPO and 5% D<sub>2</sub>EHPA-5% TBP under different sulphuric acid concentrations (Figure 1).

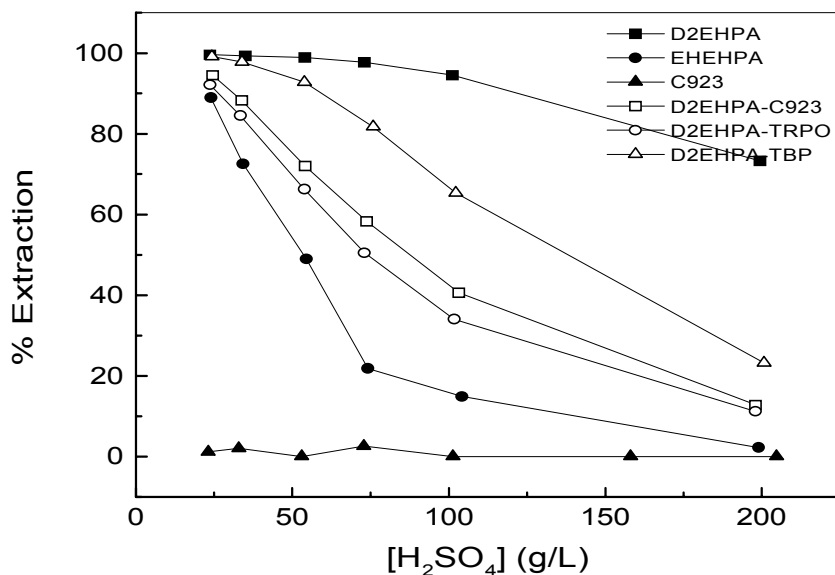


*Figure 1. Effect of aqueous acidity on the In(III) extraction. Organic Phase: 5% v/v D<sub>2</sub>EHPA, 5% v/v EHEHPA, 5% v/v Cyanex 923, 5% D<sub>2</sub>EHPA-5% Cyanex 923, 5% D<sub>2</sub>EHPA-5% TRPO or 5% D<sub>2</sub>EHPA-5% TBP; Aqueous phase: 1 g/L In(III); Phase ratio(O/A): 1.*

In the ranges of 25 g/L to 250 g/L sulphuric acid, In(III) is not extracted by Cyanex 923. The In(III) extractions with the other five solvents decrease with increasing aqueous acidity in the order: D<sub>2</sub>EHPA > D<sub>2</sub>EHPA-TBP > D<sub>2</sub>EHPA-Cyanex 923 > D<sub>2</sub>EHPA-TRPO > EHEHPA. At the real leach liquor acidity, *i.e.*, 20 g/L H<sub>2</sub>SO<sub>4</sub>, the In(III) extraction with mixtures of D<sub>2</sub>EHPA and Cyanex 923, TRPO or TBP is close to that with D<sub>2</sub>EHPA. Up to 92% In(III) can be extracted in a single stage. However, the extraction with these mixtures decrease more significantly with increasing aqueous acidity than D<sub>2</sub>EHPA does. This means the In(III) stripping from these loaded organic phases will be accomplished more easily with sulphuric acid, *e.g.*, 200 g/L H<sub>2</sub>SO<sub>4</sub>.

### Fe(III) Extraction

The Fe(III) extraction with with 5% v/v D<sub>2</sub>EHPA, 5% D<sub>2</sub>EHPA-5%TRPO, 5% D<sub>2</sub>EHPA-5% TBP or 5% D<sub>2</sub>EHPA-5% Cyanex 923 under different sulphuric acid concentrations was studied.

The Fe(III) extraction decreases with increasing aqueous acidity in the order: D<sub>2</sub>EHPA > D<sub>2</sub>EHPA-TRPO ~ D<sub>2</sub>EHPA-TBP ~ D<sub>2</sub>EHPA-Cyanex 923. At aqueous acidity of 20 g/L H<sub>2</sub>SO<sub>4</sub>, 25.9%, 14.6%, 10.1% and 8.9% Fe(III) are extracted, respectively. The modification of D<sub>2</sub>EHPA with alkyl phosphine oxides, therefore, can reduce Fe(III) extraction.

### In(III) Stripping

The stripping of In(III) from the loaded D<sub>2</sub>EHPA, D<sub>2</sub>EHPA-TRPO, D<sub>2</sub>EHPA-TBP or D<sub>2</sub>EHPA-Cyanex 923 was conducted using sulphuric acid of different concentrations (Figure 2).

The In(III) stripping increases with increasing sulphuric acid concentration in the order: D<sub>2</sub>EHPA < D<sub>2</sub>EHPA-TBP < D<sub>2</sub>EHPA-TRPO ~ D<sub>2</sub>EHPA-Cyanex 923. In a single stage, 44.1%, 64.8%, 89.4%, and 92.2% of In(III) can be stripped, respectively, from the loaded organic phase with 250 g/L H<sub>2</sub>SO<sub>4</sub>. This result indicates that In(III) stripping can be achieved more easily with mixtures of D<sub>2</sub>EHPA and Cyanex 923 than with D<sub>2</sub>EHPA only.

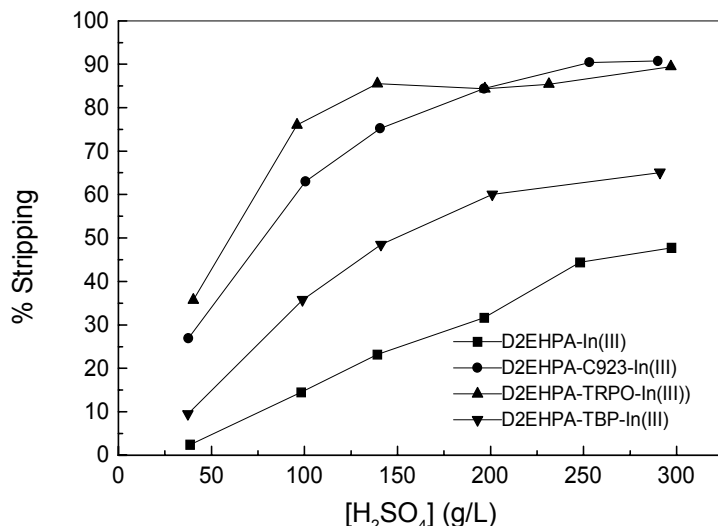


*Figure 2. In(III) stripping with sulphuric acid of different concentrations. Organic Phase: 5% v/v D<sub>2</sub>EHPA, 5%D<sub>2</sub>EHPA-5%Cyanex 923, 5%D<sub>2</sub>EHPA-5%TRPO or 5%D<sub>2</sub>EHPA-5%TBP loaded with 1.9~2.0 g/L In(III); Aqueous phase: sulphuric acid solutions; Phase ratio(O/A): 1.*

### Fe(III) Stripping

Fe(III) stripping with sulphuric acid of different concentrations was also studied and shown in Figure 3. The Fe(III) stripping increases with increasing sulphuric acid concentration in the order: D<sub>2</sub>EHPA < D<sub>2</sub>EHPA-TBP < D<sub>2</sub>EHPA-Cyanex 923 < D<sub>2</sub>EHPA-TRPO. In a single stage, 12.2%, 25.6%, 47.7% and 57.4% of Fe(III) can be stripped from the loaded organic phases with 220 g/L H<sub>2</sub>SO<sub>4</sub>.

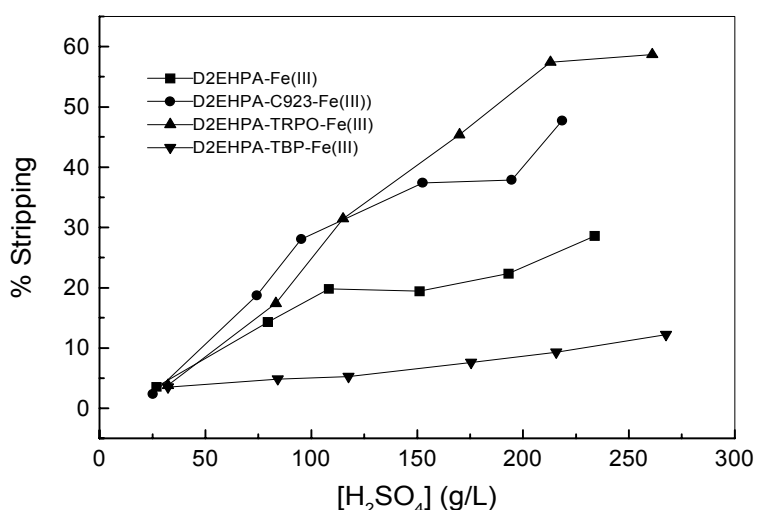


*Figure 3. Fe(III) stripping with sulphuric acid of different concentrations. Organic Phase: 5% v/v D<sub>2</sub>EHPA, 5%D<sub>2</sub>EHPA-5%Cyanex 923, 5%D<sub>2</sub>EHPA-5%TRPO or 5%D<sub>2</sub>EHPA-5%TBP loaded with 1.2~1.4 g/L In(III); Aqueous phase: sulphuric acid solutions; Phase ratio(O/A): 1.*

### In(III) Loading Capacity

5% D<sub>2</sub>EHPA, 5% D<sub>2</sub>EHPA-5% Cyanex 923 and 5% D<sub>2</sub>EHPA-5% TRPO were contacted with equal volume of a liquor containing 2 g/l In(III) and 20 g/L H<sub>2</sub>SO<sub>4</sub> in a separating funnel. After equilibrium, the raffinate was measured to determine the In(III) content, then the loaded organic phase was re-contacted with a fresh In(III) liquor. The extraction was run 3 times. The In(III) loadings are shown in Table 2. The result indicates that at the real leach liquor acidity, D<sub>2</sub>EHPA modified with Cyanex 923 or TRPO, is comparable in the In(III) loading capacity to D<sub>2</sub>EHPA.

Table 2. In(III) loading capacity

Solvents	D <sub>2</sub> EHPA	D <sub>2</sub> EHPA-Cyanex 923	D <sub>2</sub> EHPA-5%TRPO
In(III) content in organain phase(g/l)	4.71	4.43	4.26

### Effect of Contact Time on In(III) and Fe(III) Extraction and Stripping

To achieve better separation of In(III) and Fe(III) in the extraction and stripping, the effect of contact time was studied and shown in Figure 4 and 5, respectively.

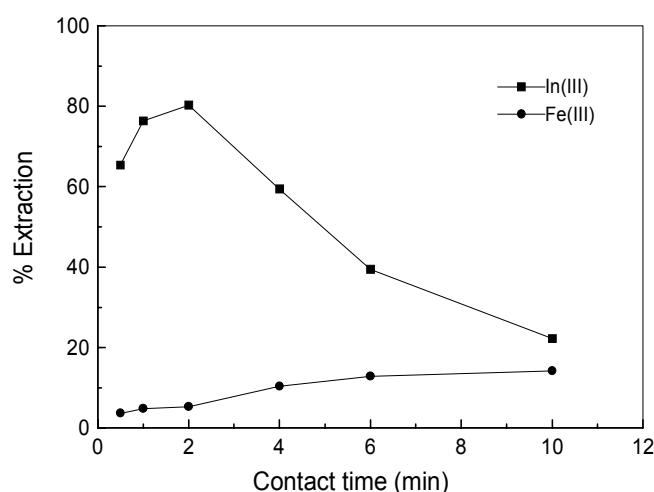
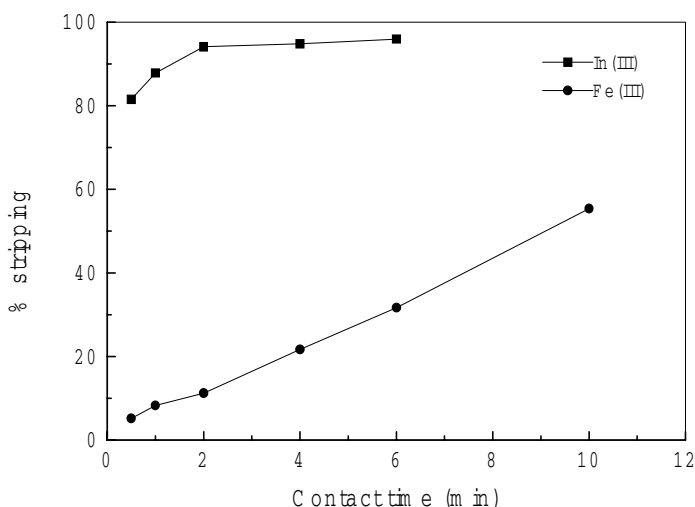


Figure 4. Effect of contact time on In(III) and Fe(III) extraction. Organic phase: 10% D<sub>2</sub>EHPA-10% Cyanex 923; Aqueous phase: real leach liquor containing 0.39 g/L In(III), 49.85 g/L Fe(III) and 19.28 g/L H<sub>2</sub>SO<sub>4</sub>; Phase ratio(O/A): 1.

The extraction of In(III) increases with increasing contact time, and up to the 80.3% In(III) is loaded at 2 min, then decreases sharply. Also, Fe(III) extraction increases with increasing contact time. 5.3% Fe is extracted at 2 min. The decrease in In(III) extraction, thus, can be ascribed to the competitive extraction of Fe(III). The contact time for extraction should be controlled at 1-2 min.

Both In(III) and Fe(III) stripping increase with increasing contact time. 94.1% In(III) can be stripped at 2 min and only up to 95.5% at 6 min. While 1.2% and 31.7% Fe(III) is stripped at 2 min and 6 min, respectively. The contact time for In(III) stripping should be 2 min.



*Figure 5. Effect of contact time on In(III) and Fe(III) stripping. Organic phase: 10% D<sub>2</sub>EHPA-10% Cyanex 923 loaded with 0.33 g/L In(III) and 0.8 g/L Fe(III); Aqueous phase: 250 g/L H<sub>2</sub>SO<sub>4</sub>; Phase ratio(O/A): 1.*

## CONCLUSIONS

In contrast with D<sub>2</sub>EHPA employed in indium recovery, the mixture of D<sub>2</sub>EHPA and Cyanex 923 has lower stripping acidity and higher stripping yield of indium(III), and same In(III) loading capacity at the real leach liquor acidity. The kinetics difference in In(III) and Fe(III) extraction and stripping should be used to achieve better separation.

It can be argued that the D<sub>2</sub>EHPA-Cyanex 923 mixture has certain potential for recovering indium from acidic leach liquors derived from zinc process residues.

## ACKNOWLEDGEMENTS

The late Dr. W. A. Rickelton, Cytec Canada Inc, is greatly appreciated for his valuable advice. This paper is published with the permission of BGRIMM.

## REFERENCES

1. Z. Chen (1996), Zinc and Indium Metallurgy Practice, Central South University of Technology Publisher, Changsha, pp. 35.
2. K. Yamaguchi, and K. Tomii (1980), *J. Min. Metall. Inst. Jpn.*, **96**, 257-258I.
3. T. Sato and K. Sato (1992), *Hydrometallurgy*, **30**, 367-383.
4. K. Inoue, Y. Baba and K. Yoshizuka (1988), *Hydrometallurgy*, **19**, 393-399.
5. M. A. Rodriguez, G. Cote and D. Bauer (1992), *Solvent Extr. Ion Exch.*, **5**, 811-827.
6. S. Facon, M. A. Rodriguez, G. Cote and D. Bauer (1993), *Proc. Int. Solvent Extraction Conf.*, Vol. 1, Society of Chemical Industry, London, pp. 557-564.
7. W. A. Rickelton (1993), *Proc. Int. Solvent Extraction Conf.*, Vol. 1, Society of Chemical Industry, London, pp. 533-540.
8. C. Wang and D. Liu (1998), *BGRIMM Research Report*, No. KY 081-1, Beijing, pp. 27-40.



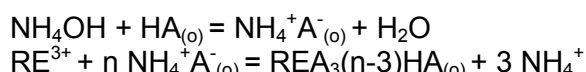
## EXTRACTION OF RARE EARTH IONS BY SEC-NONAPHENOXYACETIC ACID

Y. G. Wang, S. L. Meng, D. Q. Li, M. J. Jin\* and C. Z. Li\*

Laboratory of Rare Earth Chemistry and Physics, Changchun Institute of Applied Chemistry,  
Chinese Academy of Sciences, P.R. China

\*Shanghai Institute of Organic Chemistry, Chinese Academy of Sciences, P.R. China

The extraction of rare earths with CA-100 as a function of hydrogen ion concentration has been studied under constant ionic strength of aqueous phase. The extraction order of rare earth ions is:  $\text{Sc}^{3+} >> \text{Eu}^{3+} > \text{Sm}^{3+}(\text{Nd}^{3+}) > \text{Pr}^{3+} > \text{Ce}^{3+} > \text{La}^{3+} > \text{Gd}^{3+}(\text{Tb}^{3+}) > \text{Dy}^{3+} > \text{Tm}^{3+} > \text{Ho}^{3+} > \text{Er}^{3+} > \text{Yb}^{3+} > \text{Lu}^{3+} > \text{Y}^{3+}$ , which suggests that light lanthanides are more strongly extracted by CA-100.  $\text{Sc}^{3+}$  and  $\text{Y}^{3+}$  have the highest and lowest extractability among rare earth ions, respectively. According to the separation factors,  $\text{Sc}^{3+}$  can be separated from  $\text{RE}^{3+}$  easily;  $\text{Y}^{3+}$  can be separated from  $\text{RE}^{3+}$ , especially from light and middle lanthanides. The organic phase loaded with  $\text{Y}^{3+}$  stripped with HCl has been studied and it is obvious that the stripping acidity is low. The extraction mechanism can be written as follows on the basis of slope analysis of  $\log D$  vs. pH and  $\log D - 3\text{pH}$  vs.  $\log (\text{CA-100})_{[\text{O}]}$ :



### INTRODUCTION

The rare earth separation process using P507 and naphthenic acid solvent extraction combined with P507 extraction resin chromatography and redox, etc. has been applied widely in China [1]. This process provides industrial production of all the individual RE (except Pm) up to 99.99% or higher purity. However, the industrial practice indicates that there are some problems with the P507 and naphthenic acid extraction process. To explore some new extractants or extraction systems superior to P507 or naphthenic acid has consequently been an interesting subject for many researchers.

From a practical point of view, reagents of the carboxylic acid type are relatively inexpensive and readily available. Some application in commercial processes for the separation of rare earth metals with carboxylic acids have been found [2]. However, the extraction of the rare earth metals by carboxylic acids has not been studied in detail [3]. Alkylphenoxyacetic acid is an extractant developed by Shanghai Institute of Organic Chemistry, Chinese Academy of Science. Studies indicate that these extractants have several advantages including low solubility and stronger acidity in aqueous phase and larger distribution constant in organic solvent- water. Hence, they may be prospective extractants superior to naphthenic acid [4]. The extraction of some rare earth elements with CA-12 (sec-octylphenoxyacetic acid) from chloride medium has been studied. Li *et al.* [5] proposed HAB two solvent-extraction system on the basis of CA-12, which greatly improved the separation factors of  $\text{Y}^{3+}$  with heavy  $\text{RE}^{3+}$  elements. CA-100 (sec-nonylphenoxyacetic acid), with a larger alkyl group, has a similar structure to that of CA-12 and its molecular structure can be expressed as follows:



To date, extraction behavior of rare earth elements with CA-100 has not been reported.

There is a sharp rise in demand of lanthanides (Ln), yttrium (Y) and scandium (Sc) due to the quick growth of advanced industries such as electronics, new ceramics, metallurgy, and laser. Scandium and yttrium often co-exist with lanthanide due to the similarity in their chemical properties and the separation by solvent extraction is of practical significance [6,7]. The purpose of this paper is to explore the extraction behavior of rare earth elements in hydrochloric acid media by CA-100 and facilitate the RE hydrometallurgy process.

## EXPERIMENTAL

### Reagents and Apparatus

Before used as an extractant, CA-100 was purified by washing with  $\text{Na}_2\text{CO}_3$  and HCl twice, finally by washing with distilled water to neutrality. Stock solutions containing rare earths were prepared by dissolving the RE oxide (>99.9%) in hydrochloric acid and standardized by EDTA titration using xylenol orange as an indicator. A Shimadzu Model UV-365 spectrophotometer was used to analysis the concentration of metal ions in aqueous phase. A model pHs-3c pH meter was employed to measure pH value in aqueous phase. All other reagents were of analytical grade.

### Procedure

Equal volumes (5 ml) of organic and aqueous solutions were placed in equilibrium tubes and shaken for 20 minutes at 303K. The system was at equilibrium within this shaking time. The ionic strength ( $\mu$ ) in the aqueous phase was kept at 1 M with  $\text{NH}_4\text{Cl}$  solution. Phase were separated by centrifuging. Concentration of extractants was determined by titration with standard sodium hydroxide in an ethanol-water mixture using phenolphthalein as an indicator. The concentration of RE(III) in the aqueous phase was determined spectrophotometrically by the Arsenazo III method at 650-670 nm. The organic phase concentration of rare earth elements was determined by difference. The distribution ratio (D) of RE was defined as  $D = C_{(o)} / C_{(a)}$ .

## RESULTS AND DISCUSSION

### Effect of Equilibrium Aqueous pH

The effects of equilibrium aqueous pH on extraction equilibrium were studied under constant ionic strength of aqueous phase. The results shown in Table 1 indicate that the distribution ratios of RE increase with increasing pH with constant concentration of extractant and metal ion. The extraction order of rare earth ions is:  $\text{Sc}^{3+} >> \text{Eu}^{3+} > \text{Sm}^{3+}(\text{Nd}^{3+}) > \text{Pr}^{3+} > \text{Ce}^{3+} > \text{La}^{3+} > \text{Gd}^{3+}(\text{Tb}^{3+}) > \text{Dy}^{3+} > \text{Tm}^{3+} > \text{Ho}^{3+} > \text{Er}^{3+} > \text{Yb}^{3+} > \text{Lu}^{3+} > \text{Y}^{3+}$ , which suggests that light lanthanides are more strongly extracted by CA-100.  $\text{Sc}^{3+}$  and  $\text{Y}^{3+}$  have the highest and lowest extractability among rare earth ions, respectively. Similar results were obtained in the literature [4]. The slopes of the  $\log D$  vs. pH of rare earth elements are near three.

Table 1.  $pH_{1/2}$  value in rare earth elements extraction by CA-100.

parameter	Sc	Y	La	Ce	Pr	Nd	Sm	Eu
$pH_{1/2}$	2.14	3.01	2.78	2.76	2.75	2.73	2.73	2.71
parameter	Gd	Tb	Dy	Ho	Er	Tm	Yb	Lu
$pH_{1/2}$	2.79	2.79	2.82	2.89	2.93	2.86	2.93	2.95

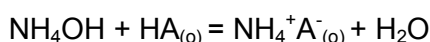
From the list of separation factors of rare earths with respect to  $Sc^{3+}$  and  $Y^{3+}$  shown in Table 2, it can be seen that  $Sc^{3+}$  can be separated from  $RE^{3+}$  easily;  $Y^{3+}$  can be separated from  $RE^{3+}$ , especially from light and middle lanthanides. Compared with the data reported in literature [4], the selectivity towards  $RE^{3+}$  with CA-100 is better than that with CA-12, which may be partly due to the high steric hindrance of the former. It is suggested that CA-100 may be a useful reagent for the separation of  $Sc^{3+}$  and  $Y^{3+}$  from  $RE^{3+}$ .

Table 2. Separation factors( $\beta$ ) of  $RE^{3+}$  with respect to  $Sc^{3+}(Y^{3+})$ .

$RE^{3+}$	$Sc^{3+}$		$Y^{3+}$	
	$\bullet pH_{1/2}$	$\beta_{RE^{3+}/Sc^{3+}}$	$\bullet pH_{1/2}$	$\beta_{Y^{3+}/RE^{3+}}$
$Sc^{3+}$			0.87	407.38
$Y^{3+}$	0.87	407.38		
$La^{3+}$	0.64	83.18	0.23	4.90
$Ce^{3+}$	0.62	72.44	0.25	5.62
$Pr^{3+}$	0.61	67.61	0.26	6.03
$Nd^{3+}$	0.59	58.88	0.28	6.92
$Sm^{3+}$	0.59	58.88	0.28	6.92
$Eu^{3+}$	0.57	51.29	0.3	7.94
$Gd^{3+}$	0.65	89.12	0.22	4.57
$Tb^{3+}$	0.65	89.12	0.22	4.57
$Dy^{3+}$	0.68	109.65	0.19	3.72
$Ho^{3+}$	0.75	177.82	0.12	2.29
$Er^{3+}$	0.79	234.42	0.08	1.74
$Tm^{3+}$	0.72	144.54	0.15	2.82
$Yb^{3+}$	0.79	234.42	0.08	1.74
$Lu^{3+}$	0.81	269.15	0.06	1.51

### Effect of Extractant Concentration on the RE(III) Extraction

Figure 1 illustrates the effect of extractant concentration on the extraction of  $RE^{3+}$  in hydrochloric acid solution. Here, Nd represents light rare earth elements and Yb represents heavy rare earth elements. The distribution ratio increases with the increase of extractant concentration. The plots of  $\log D-3$  pH vs.  $\log [HA]_{(o)}$  of Nd and Yb give straight lines with slopes almost four, whereas the slope of Sc near three. It can be inferred from the results shown in Table 1 that three or four moles of hydrogen ions are released per mole of extracted metal ion. CA-100 must be ammoniated before extracting reaction to form ammoniate ( $NH_4^+A^-$ ) in order to exchange cation ions with RE(III) smoothly. Therefore it can be assumed that the RE(III) extraction with CA-100 can be expressed as follows:



where HA represent CA-100, n equal to four or three.

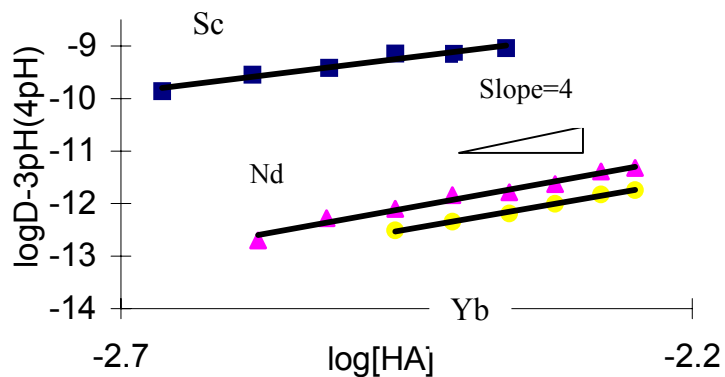


*Figure 1. Effect of extractant concentration on extraction of some rare earth elements.*

### Stripping

The organic phase loaded  $\text{Y}^{3+}$  was stripped with HCl. The aqueous phase concentration of Y was determined and the plot of the stripping efficiency versus different concentration of HCl is shown in Figure 2. When the concentration of HCl is large than 0.01 M, 90%  $\text{Y}^{3+}$  is stripped. The low stripping acidity is obvious.

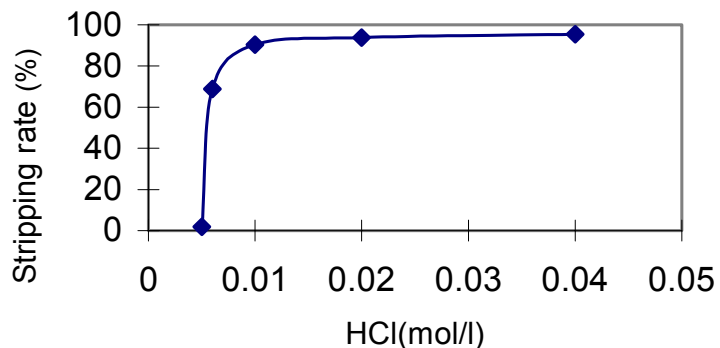
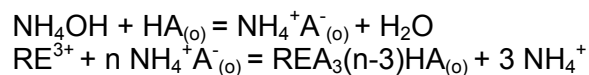


*Figure 2. Effect of acidities on stripping of yttrium.*

### CONCLUSION

The effects of hydrogen ion concentration and extractant concentration on extraction of scandium, yttrium and lanthanides with CA-100 have been studied and the extraction mechanism can be written as follows:



According to the separation factors,  $\text{Sc}^{3+}$  can be separated from  $\text{RE}^{3+}$  easily;  $\text{Y}^{3+}$  can be separated from  $\text{RE}^{3+}$ , especially from light and middle lanthanides. Due to the higher steric hindrance, the selectivity towards  $\text{RE}^{3+}$  with CA-100 is better than that with CA-12. Hence, CA-100 may be a prospecting extractant for extraction and separation of rare earth elements.

## ACKNOWLEDGEMENTS

The authors wish to thank Shanghai Institute of Organic Chemistry, Chinese Academy of Sciences for supplying the CA-100. Project supported by State Key Project of Fundamental Research (G19980661301) and the National Natural Science Foundation of China (29771028,29801004).

## REFERENCES

1. D. Q. Li, Z. H. Wang, S. L. Meng *et al.* (1994), *Hydrometallurgy '94*, Chapman and Hall, London, pp. 627-634.
2. L. Sherrington (1983), *Handbook of Solvent Extraction*, T. C. Lo, M. H. I. Baird and C. Handson (eds.), Wiley-Interscience, New York, NY, pp. 717.
3. A. C. Du. Preez and J. S. Preston (1992), *Solvent Extr. Ion Exch.*, **10**, 207-230.
4. W. Z. Ye (1998), *Development in New Rare Earth Materials and Separation Processes*, J. Z. Ni and G. Y. Hong (eds.), Science Press, Beijing, pp. 3-10.
5. D. Q. Li, Z. H. Wang and S. L. Meng (1996), *Chinese Rare Earths*, **17** (6), 41-43.
6. L. Z. Xue, D. Q. Li (1992), *Chin. J. Appl. Chem.*, **9** (4), 21-25.
7. J. M. Liu, R. D. Yang and Y. S. Ma (1991), *Chin. Rare Earths*, **12** (1), 15-19.



# CHEMISTRY OF SOLVENT EXTRACTION OF SCANDIUM(III) FROM SULFATE SOLUTIONS BY QUATERNARY AMMONIUM SULFATES

S. I. Stepanov, A. E. Kharchev and A. M. Chekmarev

D.Mendeleev University of Chemical Technology of Russia, Moscow, Russia.

Scandium(III) extraction from sulfate solutions by methyltrialkylammonium sulfate and methylcyclohexyldioctylammonium sulfate in toluene was investigated, using the methods of distribution, slope analyses and mathematical modeling of extraction isotherms. The formation of complexes, which partially dissociate in organic phase,  $(R_4N)_3[Sc(SO_4)_3]$  with methyltrialkylammonium sulfate and  $(R_4N)_2SO_4\cdot Sc_2(SO_4)_3$  with methylcyclohexyldioctylammonium sulfate, was established. The thermodynamic constants of extraction equilibrium were calculated.

## INTRODUCTION

Scandium exists in water sulfate solutions in form of the complexes  $Sc(SO_4)_n^{3-2n}$ , where  $n = 1-3$  [1]. In a small excess of sulfate ligands, the cationic complexes  $ScSO_4^+$  are formed. When the concentration of  $SO_4^{2-}$  groups is increased, the anionic complexes  $Sc(SO_4)_2^-$  preferably with  $Li_2SO_4$  and  $Sc(SO_4)_3^{3-}$  with  $Na_2SO_4$  are formed. With sulphates of  $NH_4^+$ ,  $K^+$ ,  $Rb^+$  and  $Cs^+$  both type of complexes are observed. When the pH of the sulfate solutions is increased, hydrolysed complexes of scandium are formed, due to replacement of sulfate ligands by hydroxyl groups. Complexes of the composition  $Sc(OH)SO_4$ ,  $Sc_3O_2(OH)_3SO_4$ , and  $Sc_4(OH)_{10}SO_4$  are formed at the same time. At  $pH \geq 4.9$ , insoluble scandium hydroxysulfates are precipitated [2].  $SO_4^{2-}$  groups can be co-ordinated as monodentate or bidentate ligands in scandium anionic complexes. In this case the symmetry of  $SO_4^{2-}$  ion is decreased from  $T_d$  to  $C_{2v}$ . The highest possible number of sulfate ligands that can be included into the inner sphere of scandium anionic complexes is 3, forming the  $Sc(SO_4)_3^{3-}$  anion.

Numerous double sulfates of scandium with alkaline metals and ammonium such as  $MeSc(SO_4)_2$  and  $Me_3Sc(SO_4)_3$  were prepared. These salts can be isolated from solutions in solid phase as different hydrates [1]. So in sulfate solutions in presence of access of  $SO_4^{2-}$  groups, two anionic complexes of scandium exist preferably: less stable  $Sc(SO_4)_3^-$  and more stable  $Sc(SO_4)_3^{3-}$ . They can be extracted by quaternary ammonium salts (QAS). This work reports the solvent extraction of scandium from sulfate solutions by QAS.

## EXPERIMENTAL

For the extraction experiments  $Sc_2(SO_4)_3$ ,  $Na_2SO_4$  and  $H_2SO_4$  of analytical grade were used. As extractants, 0.1 M solutions of methyltrialkylammonium sulfate (TAMAS) and methylcyclohexyldioctylammonium sulfate (MChDOAS) in toluene were used. TAMAS and MChDOAS were prepared from methylsulfate forms of QAS by consecutive contact of the organic salts with water solutions of 50%  $H_2SO_4$ , 10% NaOH and 10%  $Na_2SO_4$ . In the case of MChDOAS, sodium sulfate, which was extracted by MChDOAS, was isolated as solid salts by

precipitation in acetone. The acetone was evaporated in a vacuum. The extraction was carried out in thermostatic separate funnels at temperature  $T = 25 \pm 0.1^\circ\text{C}$ , with initial ratio of organic and water phase volumes O:W = 1:1 and contacting time 15 min. Organic and water phases were separated and metal contents in water solutions were determined by complexonometric [3] or spectrophotometric methods with xylanol orange as indicator [4].

## RESULTS AND DISCUSSION

In Figure 1 the extraction isotherms of Sc from sulfate solutions by 0.1 M TAMAS and 0.1 M MChDOAS in toluene are presented. As one can see that the loading of the organic phase depends on extractant's structure and composition of water solution. The differences are due to the formation of various extractable complexes. The decrease of loading for Sc extraction from sulfate acidic solutions is explained by competitive distribution of sulfuric acid. At the same time,  $\text{H}_2\text{SO}_4$  addition into the initial solutions of Sc was necessary to prevent metal hydrolysis.

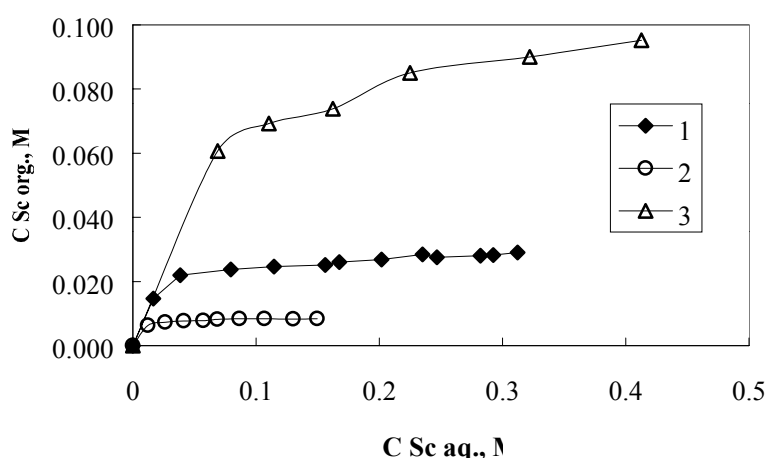


Figure 1. Scandium extraction isotherms from sulfate solutions by QAS.

- 1- $\text{H}_2\text{O} - \text{Sc}_2(\text{SO}_4)_3 - 0.1 \text{ M TAMAS} - \text{toluene};$
- 2- $\text{H}_2\text{O} - \text{Sc}_2(\text{SO}_4)_3 - 0.5 \text{ M Na}_2\text{SO}_4 - 0.2 \text{ M H}_2\text{SO}_4 - 0.1 \text{ M TAMAS} - \text{toluene};$
- 3- $\text{H}_2\text{O} - \text{Sc}_2(\text{SO}_4)_3 - 0.1 \text{ M TAMAS} - \text{toluene}.$

### Theoretical

In the present work the mathematical modelling of the extraction isotherms were carried out using software «EXTREQ». The basis for this computing program is a method that takes into account the hydration of organic components for calculation of non-ideality of organic phase, suggested by Sergievsky [5]. The following equations were used for description of scandium sulfate extraction in all cases.

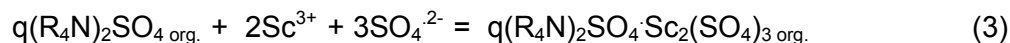
Model of physical partition: chemical reaction



and constant of distribution

$$\ln K_{101}^T = \ln \frac{C_{\text{Sc.org}}}{a_{\text{Sc}}} + H_{101}(1 - a_w) \quad (2)$$

## Model of solvates formation: chemical reaction



and constant of extraction

$$\ln K_{pqv}^T = \ln \frac{C_{Sc.org}^q}{a_{Sc} C_{ext}^q} + H_{pqv}(1 - a_w) \quad (4)$$

where  $K_{pqv}^T$  is the thermodynamic constant of distribution or extraction;  $C_{Sc.org}$ , metal concentration in organic phase;  $a_{Sc}$ , metal activity in water phase;  $C_{ext}^q$ , equilibrium free extractant concentration;  $H_{pqv}$ , hydration parameter;  $p$ , number of  $Sc_2(SO_4)_3$  molecule in extractable compound;  $q$ , number of extractant molecule in extractable compound,  $v$ , stage of dissociation ( $v = 1$ , no dissociation;  $v = 2$ , first stage dissociation, etc.) In both equations (2) and (4), the hydration parameter includes non-ideality of organic phase, mainly interactions of water – organic components.

Equation (4) with  $q = 1$  will describe monosolvate extraction; equation (4) with  $q = 3$  will describe three chargeable complex extraction. The extractable compound can dissociate in the organic phase. Generally the equation for the extraction constant can be written as:

$$\ln K_{pqv}^T = \ln \frac{C_{Sc.org}^{qv}}{a_{Sc} C_{ext}^q} + H_{pqv}(1 - a_w) \quad (5)$$

In the case of extraction of two or more compounds, the equations are combined to determine all the extraction constants. The software «EXTREQ» gives the possibility of calculating extraction constants and hydration parameters for four simultaneously extractable compounds by one extractant using experimental distribution data. Relative errors between experimental and calculated isotherms and standard deviation of experimental points were used as criteria of the accuracy.

## Extraction of Scandium by MChDOAS

A molar ratio  $(R_4N)_2SO_4:Sc_2(SO_4)_3 = 1:1$  in case of MChDOAS (Figure 1) is evidence of monosolvate formation  $(R_4N)_2SO_4 \cdot Sc_2(SO_4)_3$ . Recently monosolvate formation for the extraction of Li, Na, Zn(II), Cu(II), Co(II) and Ni(II) sulfates by MChDOAS was established [6]. The mechanism of anion intercalation for explaining of this kind extraction was presented. The experimental results obtained allowed consideration of the distribution of scandium from sulfate solutions to toluene solutions of MChDOAS by anion intercalation extraction.

For confirmation of monosolvate formation of scandium sulfate with MChDOAS, mathematical modeling of extraction isotherm was carried out. In the literature, experimental thermodynamic data for binary water solutions of scandium sulfate are not found. Therefore, we calculated activity coefficients and water activity in such solutions using comparative methods and experimental data for different trivalent metals sulfates, nitrates and chlorides and scandium chloride and nitrate. Values obtained were used for simulation of all extraction isotherms.

In Table 1 the results of mathematical modeling of scandium sulfate extraction by 0.1 M MChDOAS in toluene under the assumption of physical distribution and formation of different solvates with or without dissociation into organic phase are presented. As should be seen from analysis of error values, the extractable monosolvate is partially dissociated in the organic phase. So results of mathematical modeling verify the formation of monosolvate of scandium sulfate with MChDOAS, which is partially dissociated under high values of water activity.

*Table 1. Results of mathematical modeling of Sc isotherm by 0,1 M MChDOAS in toluene.*

pqv	101	101	102	111	112	121	122	131	132
$\ln K'_{\text{pqv}}$	3.716	0.003	4.840	6.461	9.077	0.856	24.08	1.621	29.91
$H_{\text{pqv}}$	99.8	-31.71	168.1	-71.04	222.2	-5.588	136.2	-41.80	244.0
% error	68.9		8.42		3.66		6.45		51.17

So, the chemistry of scandium extraction from sulfate solutions can be presented by two equations:



It is necessary to note, that another equation for first dissociation stage of monosolvate can be written:



Thermodynamic parameters of extraction equilibrium with MChDOAS are presented in Table 3.

### Extraction of Scandium by TAMAS

In contrast to MChDOAS, the partitioning of scandium from binary water solutions and from sulfuric solutions contained salting-out agent into toluene solutions of TAMAS is accompanied by the formation of a most stable three chargeable complex  $(\text{R}_4\text{N})_3[\text{Sc}(\text{SO}_4)_3]$ . In this case, the molar ratio  $(\text{R}_4\text{N})_2\text{SO}_4:\text{Sc}_2(\text{SO}_4)_3$  is 3:1. The distribution of this complex is confirmed by results of slope analyses (Figure 2).

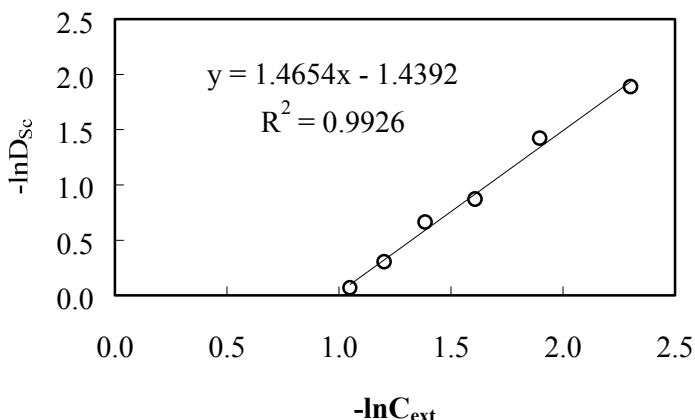


*Figure 2. The dependence of  $\ln D_{\text{Sc}}$  vs.  $\ln C_{\text{ext}}$  for Sc extraction from sulfate solutions, containing 0.001 M  $\text{Sc}_2(\text{SO}_4)_3$ , 0.5 M  $\text{Na}_2\text{SO}_4$  and 0.2 M  $\text{H}_2\text{SO}_4$  by TAMAS in toluene.*

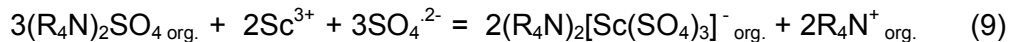
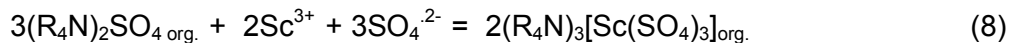
The dependence of  $\ln D_{\text{Sc}}$  vs.  $\ln C_{\text{ext}}$  is a straight line with tangent of angle equal 1.465, that corresponds to  $q = 3$  in equation (3). Mathematical modeling, which was carried out for both isotherms with TAMAS, showed adequate description only for model of three chargeable anionic complex extraction with its partial dissociation under high values of water activity. In Table 2, the results of the mathematical calculations of the extractable complexes concentrations in frame of selected model for  $\text{Sc}_2(\text{SO}_4)_3$  extraction by TAMAS are presented.

*Table 2. Results of mathematical modeling of Sc extraction isotherm from 0.5 M Na<sub>2</sub>SO<sub>4</sub> and 0.2 M H<sub>2</sub>SO<sub>4</sub>, water solutions by 0.1 M TAMAS in toluene.*

No n/n	C <sub>Sc</sub> M	a <sub>w</sub>	C <sub>Sc.org</sub> M	C <sub>Sc.org.calc.</sub> M	% error	C <sub>131, org</sub> M	C <sub>132,org</sub> M
1	0.0123	0.9755	6.26E-03	5.99E-03	-4.3	4.69E-04	5.52E-03
2	0.0262	0.9728	7.28E-03	7.35E-03	1.0	1.53E-03	5.82E-03
3	0.0414	0.9699	7.70E-03	7.67E-03	-0.3	3.05E-03	4.63E-03
4	0.0572	0.9669	7.79E-03	7.86E-03	1.0	4.70E-03	3.16E-03
5	0.0687	0.9648	8.16E-03	8.10E-03	-0.8	5.79E-03	2.31E-03
6	0.0864	0.9610	8.34E-03	8.26E-03	-1.0	7.06E-03	1.20E-03
7	0.1068	0.9563	8.37E-03	8.37E-03	0.0	7.87E-03	4.98E-04
8	0.1302	0.9510	8.31E-03	8.49E-03	2.1	8.31E-03	1.78E-04
9	0.1495	0.9462	8.34E-03	8.34E-03	0.0	8.27E-03	6.86E-05

\* C<sub>131, org</sub> - concentrations of extractable complex and \*\* C<sub>132, org</sub> – dissociated complex in organic phase.

The chemistry of Scandium extraction from sulfate solutions by TAMAS can be described the following equations:



In Table 3 thermodynamic data for extraction equilibrium of scandium sulfate with MChDOAS and TAMAS are presented.

*Table 3. Thermodynamic parameter of Sc extraction from sulfate solutions by QAS.*

Composition of water phase	Composition of extractable compounds	Num. of points	ln K <sup>T</sup> <sub>pqv</sub>	H <sub>pqv</sub>	% error
0.1 M MChDOAS in toluene					
Sc <sub>2</sub> (SO <sub>4</sub> ) <sub>3</sub> , H <sub>2</sub> O	(R <sub>4</sub> N) <sub>2</sub> SO <sub>4</sub> ·Sc <sub>2</sub> (SO <sub>4</sub> ) <sub>3</sub> . R <sub>4</sub> NSO <sub>4</sub> ·Sc <sub>2</sub> (SO <sub>4</sub> ) <sub>3</sub> + R <sub>4</sub> N <sup>+</sup>	6	6.461 9.077	-71.04 222.2	3.66
0.1 M TAMAS in toluene					
Sc <sub>2</sub> (SO <sub>4</sub> ) <sub>3</sub> , H <sub>2</sub> O	(R <sub>4</sub> N) <sub>3</sub> [Sc(SO <sub>4</sub> ) <sub>3</sub> ] (R <sub>4</sub> N) <sub>2</sub> [Sc(SO <sub>4</sub> ) <sub>3</sub> ] + R <sub>4</sub> N <sup>+</sup>	12	15.237 16.865	110.4 327.7	2.25
Sc <sub>2</sub> (SO <sub>4</sub> ) <sub>3</sub> , 0.5 M Na <sub>2</sub> SO <sub>4</sub> , 0.05 M H <sub>2</sub> SO <sub>4</sub> ,	(R <sub>4</sub> N) <sub>3</sub> [Sc(SO <sub>4</sub> ) <sub>3</sub> ] (R <sub>4</sub> N) <sub>2</sub> [Sc(SO <sub>4</sub> ) <sub>3</sub> ] + R <sub>4</sub> N <sup>+</sup>	9	29.079 36.083	102.5 250.0	1.16
Sc <sub>2</sub> (SO <sub>4</sub> ) <sub>3</sub> , 0.5 M Na <sub>2</sub> SO <sub>4</sub> , 0.05 M H <sub>2</sub> SO <sub>4</sub> , a <sub>w</sub> = 0.9755	(R <sub>4</sub> N) <sub>3</sub> [Sc(SO <sub>4</sub> ) <sub>3</sub> ] (R <sub>4</sub> N) <sub>2</sub> [Sc(SO <sub>4</sub> ) <sub>3</sub> ] + R <sub>4</sub> N <sup>+</sup>	9	26.567 29.958	102.5 250.0	1.16

The scandium extraction from binary solutions is accompanied by formation of three chargeable complex in organic phase too. But under these conditions, when the salting-out agent is absent in water solutions, the distributed species can be the neutral molecule Sc<sub>2</sub>(SO<sub>4</sub>)<sub>3</sub> only. So, in this case formation of anionic complex is the result of complexing reaction or replacement of water molecule on sulfate groups in organic phase. These reactions embodied high values of the hydration parameters. The negative value of H<sub>111</sub> for scandium extraction by MChDOAS corresponds to more hydration number of extractant in comparison with extractable monosolvate.

For the isotherm obtained in the presence of  $\text{Na}_2\text{SO}_4$ , the extrapolation of the function  $\ln K_{\text{pqv}}^T$  vs.  $(1-a_w)$  at  $a_w = 0.9755$  was made. This water activity corresponds to the standard condition of "indefinitely dilute solution" of scandium sulfate in 0.5 M  $\text{Na}_2\text{SO}_4 + 0.05$  M  $\text{H}_2\text{SO}_4$  water solution. The calculated value of  $\ln K_{\text{pqv}}^T$  shows that the addition of the salting-out agent increases the extraction constant of non-dissociated sulfate complex of scandium up to 4 orders of magnitude and the dissociated complex up to 5 orders. The extraction constant of scandium from nitrate solutions by TAMAN is up to 12 orders less than from sulfate media [7]. So, sulfate media are preferable for recovery scandium by QAS.

## CONCLUSIONS

Scandium(III) can be extracted from water sulfate solutions as the neutral salt or anionic complexes by quaternary ammonium sulfates. Extraction of  $\text{Sc}_2(\text{SO}_4)_3$  by MChDOAS is accompanied by the formation of the monosolvate  $(\text{R}_4\text{N})_2\text{SO}_4 \cdot \text{Sc}_2(\text{SO}_4)_3$ , presumably by the mechanism of anionic intercalation. Extraction of  $\text{Sc}_2(\text{SO}_4)_3$  by TAMAS is accompanied by the formation of three chargeable anionic complex  $(\text{R}_4\text{N})_3[\text{Sc}(\text{SO}_4)_3]$ . This process is due to a complexing reaction or replacement of water molecule on sulfate groups in the organic phase. From sulphate solutions with excess salting-out agent, the more stable anionic complex  $(\text{R}_4\text{N})_3[\text{Sc}(\text{SO}_4)_3]$  is extracted by an anion-exchange mechanism. The above compounds can be partially dissociated in the organic phase under conditions of high water activity.

## REFERENCES

1. L.N.Komissarova (ed.) (1986), Compounds of Rare Earth Elements: Sulfates, Selenites, Tellurates, Chromates, Nauka, Moscow, pp. 3-247.
2. B.G. Korshunov, A.M. Reznik, S.A. Semenov (1987), Scandium, Metallurgy, Moscow, pp. 40-59.
3. G. Schwarzenbach, H. Flashka (1970), Complexonometric Titration, Nauka, Moscow, pp. 157-163.
4. M.K. Achmedly, D.G. Gambarov (1963), *J. Analyt. Chem. (Russ.)*, **22**, 1183-1187.
5. V.V. Sergievsky (1976), Review of Science and Technique. Inorganic Chemistry, Vol. 5, VINITI, Moscow, pp. 5-82.
6. S.I. Stepanov, A.M. Chekmarev (1996), Value Adding through Solvent Extraction, Vol. 1, *Proc. ISEC '96*, D.C. Shallcross, R. Paimin, L.M. Prvcic (eds.), The University of Melbourne Press, Melbourne, pp. 659-664.
7. S.I. Stepanov, N.G. Kijatkina, O.N. Fedotov (1987), *J. Inorg. Chem. (Russ.)*, **32**, 2517-2521.



## EXTRACTION OF URANIUM(VI) FROM PHOSPHATE MEDIA IN POLY(ETHYLENE GLYCOL) SOLUTIONS

Alfia M. Safiulina, Oxana A. Sinegribova and Valerii M. Shkinev\*

D. Mendeleev University of Chemical Technology of Russia, Moscow, Russia

\*Vernadsky Institute of Geochemistry and Analytical Chemistry,  
Russian Academy of Sciences, Moscow, Russia

Extraction of uranium(VI) from concentrated phosphate media using aqueous poly(ethylene glycol) (PEG) solutions with different molecular masses (1500, 4000, 6000, 20 000) was studied. The phase diagram for the PEG/phosphate salts/water system has been examined and the causes of phase formation from the position of the theory of regular solutions was explained after a theoretical analysis of the PEG/water and phosphate salt/water systems. A study of the distribution coefficients of uranium(VI) between the phases as a function of pH indicated that uranium extraction increased with the pH of the salt phase. Extraction of uranium at pH 13.6 and 20°C was studied as a function of its concentration in the salt phase. The separation coefficients of uranium from Ca, Cr, Cu, Mg, B, Zn, Co, and Ni were greater than 100.

### INTRODUCTION

Liquid-liquid extraction systems based on water-soluble polymers are used for the separation of biomolecules in biotechnology [1]. The studies, first initiated at the Vernadsky Institute in Moscow in 1983, have shown that not only biomolecules but common metal ions as well are unevenly distributed between the two phases in Aqueous Biphasic Systems (ABS), one of which is the salt-rich phase and the other is the PEG-rich phase [2-5]. Pioneering research has been done on the application of ABS to the separation of actinides [2-5]. The experiments indicated that such systems are suitable for the extraction of various metals, including actinides [2-7]. This system usually contains two aqueous phases: either two solutions of two-water soluble polymers, or one solution of water-soluble polymer and a solution of an inorganic salt. The components of the systems are distributed between these two aqueous phases. Poly(ethylene)glycol (PEG) is popular polymer for such systems. The advantages of polymer systems, as compared with traditional extraction systems, are the following: PEG systems are cheap; the components are readily available; they are non-toxic in nature, inflammable, and contain no organic diluent.

The aim of our work is to study the extraction of uranium(IV) from higher pH solutions and provide a thermodynamic description of the phase formation in ABS from a study of the PEG/water and salt/water systems.

## EXPERIMENTAL

### Reagents and Methods

The inorganic salts were of chemical purity grade. PEG from Loba Chemie with different molecular masses from 1500 to 20 000 was used in the extraction experiments. 2 ml of 40 mass % solution of potassium phosphate, uranium solution aliquot and 2 ml of 40 mass % PEG solution were diluted with water to a volume of 6 ml. The mixture was shaken for 7 min. After phase separation, aliquots of each phase were withdrawn and analysed by x-ray fluorescence analysis. Measurements of solution pH were made on a LPU-01 pH meter after phase separation.

The distribution coefficients were calculated as the ratio of the uranium concentration in the PEG-enriched phase (PEG-phase) to that in the phosphate salt-enriched phase (salt phase).

## RESULTS AND DISCUSSION

### Phase Diagrams

Some phase diagrams of phosphate salt/PEG systems are given in Figure 1.

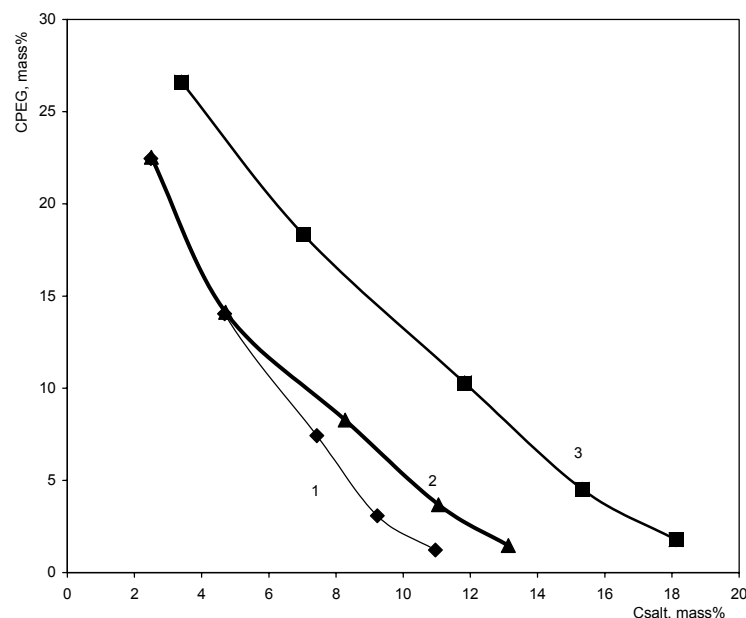


Figure 1. Phase diagrams: (1)  $\text{PEG1500} / \text{K}_3\text{PO}_4 / \text{H}_2\text{O}$ ; (2)  $\text{PEG1500} / (\text{NH}_4)_2\text{SO}_4 / \text{H}_2\text{O}$ ; (3)  $\text{PEG1500} / \text{K}_2\text{HPO}_4 / \text{H}_2\text{O}$ .

The heterogeneity areas are situated above the corresponding lines in the diagrams. The system chosen for the investigation of uranium extraction contained 12 mass % PEG 1500 and 12 mass % phosphate salts. Comparison of the phosphate and sulfate systems indicated that order of affinity of the salt for phase formation is  $\text{K}_3\text{PO}_4 = (\text{NH}_4)_2\text{SO}_4 > \text{K}_2\text{HPO}_4$ . The molecular mass of PEG influences the viscosity and phase separation rate of the systems. It is practically convenient to work with PEG of a molecular mass between 1500 and 4000, at a polymer concentration lower than 40 %.

The phase separation rate of such systems was faster than 5 min. The pH of the salt systems influences the phase separation rate. For concentrated solutions, the phase separation is better.

### Thermodynamic Description

To studying the three component system (water/soluble polymer/inorganic salts), two bi-component systems (water/inorganic salt and water/water-soluble polymer) were considered. The bi-component system water/inorganic salt was analyzed from the point of view of the theory of electrolyte solutions. It was found that salts containing anions ( $\text{PO}_4^{3-}$ ,  $\text{CO}_3^{2-}$ ,  $\text{HPO}_4^{2-}$ ,  $\text{SO}_4^{2-}$ ,  $\text{SCN}^-$ ), capable of creating two-phase equilibria in the three-component system, are characterized by weak interactions with water (negative hydration energy  $\Delta G > 0$  in Table 1) and by positive deviation from Raoult's law ( $\gamma_w > 1.0$ ) (Figure 2) in the water/inorganic salt binary system.

*Table 1. Hydration energies of salts.*

Salt	$\Delta G_{\text{hydr}}$ (kcal/mol)	Salt	$\Delta G_{\text{hydr}}$ (kcal/mol)
$\text{Na}_3\text{PO}_4$	7,85	$\text{Cu}(\text{NO}_3)_2$	-3.09
$\text{Na}_2\text{HPO}_4$	4,04	$\text{Zn}(\text{NO}_3)_2$	-3.7
$\text{NaH}_2\text{PO}_4$	-0,74	$\text{NH}_4\text{NO}_3$	-1.46
$\text{Na}_2\text{SO}_4$	3,22	$\text{NaF}$	0,67
$\text{NaHSO}_4$	2,06	$\text{KF}$	-3,46
$(\text{NH}_4)_2\text{SO}_4$	1,27	$\text{LiBr}$	-7,24
$\text{Na}_2\text{CO}_3$	1,96	$\text{LiI}$	-6,27
$\text{K}_2\text{SO}_4$	4,22	$\text{CsF}$	-8,65
$\text{KHSO}_4$	1,99	$\text{Ca}(\text{NO}_3)_2$	-1,82
$\text{KH}_2\text{PO}_4$	0,76	$\text{Li}_2\text{SO}_4$	0,11
$\text{K}_2\text{CO}_3$	-4,2		

The negative derivation from Raoult's law ( $\gamma_w < 1.0$ ), exhibited by the interaction of salts with water, characterize the salts of metals with anions, in the presence of which two phases are not formed (for example,  $\text{LiCl}$ ,  $\text{NaCl}$ ,  $\text{NaNO}_3$ ). The ability of salts to achieve phase formation is connected, as a rule, with the negative hydration energy, and hence with more intensive interaction of cations and anions between themselves than with water.

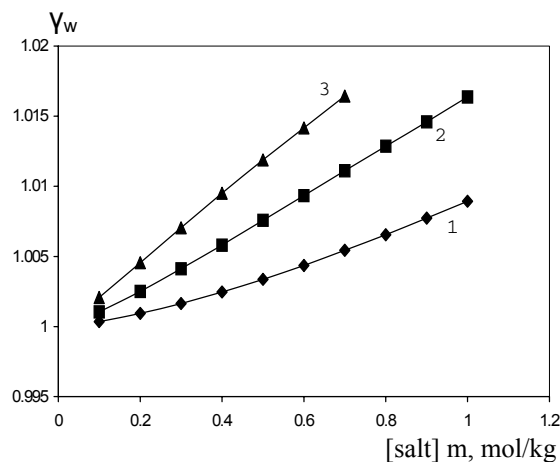


*Figure 2. Activity coefficients of water in the system potassium phosphate salts/ $\text{H}_2\text{O}$ . (1)  $\text{KH}_2\text{PO}_4$ , (2)  $\text{K}_2\text{HPO}_4$ , (3)  $\text{K}_3\text{PO}_4$ .*

In the present work, the experimental data concerning the dependency of water activity on the concentration and molecular masses of PEG for the temperatures 298, 313, 323, and 333 K [8] were treated and discussed from the point of view of the theory of polymer solutions (Figure 3).

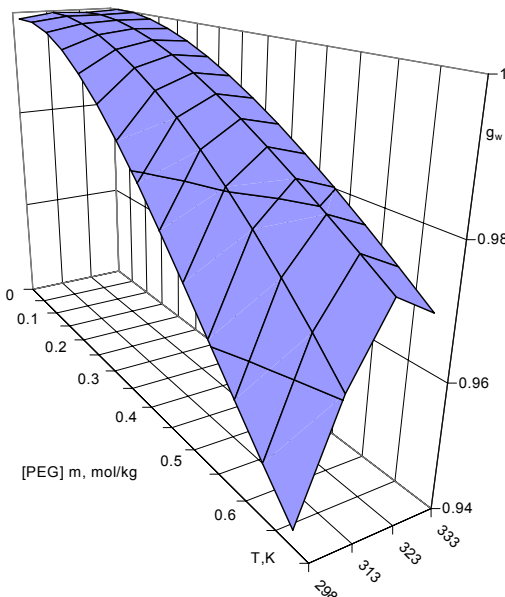


Figure 3. Activity coefficients of water in the system PEG1500 /  $H_2O$ .

It was shown that these dependencies can be explained by a thermal effect, namely by an entropy increase on mixing of molecules with different sizes (Flory-Huggins theory). Quantitative description is possible if one takes into account the value of the coordination number. The Van-der-Waals force effect was described and  $\gamma_{vw}$  was estimated in the approximation to the theory of regular solutions:  $\gamma_{vw} = \exp(2T_c/T)$ . The value of  $\gamma_{hydr}$  was determined from  $\gamma_{hydr} = 1/\gamma_{vw}$ . If the pure substance was considered as the standard condition,  $\gamma_{hydr} = \exp(-2T_c/T)$ . The hydration number ( $h$ ) was found, which was equal to 2 at the cloud-point temperature for the binary solution; at lower temperatures, it is equal to 4 according to the equation  $1/\gamma_{hydr} = \exp(h)$ , where  $h = 2T_c/T$ . So the influence of Van-der-Waals forces on phase separation is important.

It was shown earlier [9] that some phase diagrams for polymer systems contain two cloud points. The upper part of diagram, corresponding to upper cloud point, is a result of the influence of Van-der-Waals forces. The appearance of the lower critical point may be caused by the formation of crystallohydrates in these systems. It corresponds with the temperature effect on the phase separation process: for such systems, when temperature rises the expansion of the two-phase field is typical. So it can be concluded from the investigation of PEG/water systems that the properties of solutions are determined by the entropy factor.

### Extraction of Uranium

For practical purposes, it is important to study the distribution of species in multi-component systems. The distribution of uranium(VI) in the phosphate salts/PEG system was studied (Figure 4). There are conditions for the selective recovery of uranium.

The distribution of uranium has been examined at different pH values of the equilibrium salt-phase. Earlier, the distribution coefficients of some common and actinide metals were examined for PEG/ammonium sulphate systems [2-5] and for the phosphate system at pH values lower than 11 [2].

Optimal conditions for uranium extraction from phosphate solutions are pH 11 to 14. Distribution coefficients are near 2.0 for molecular masses of PEG from 1500 to 4000. For higher molecular masses of PEG (6000, 20 000), the distribution coefficients increased (Figure 5).

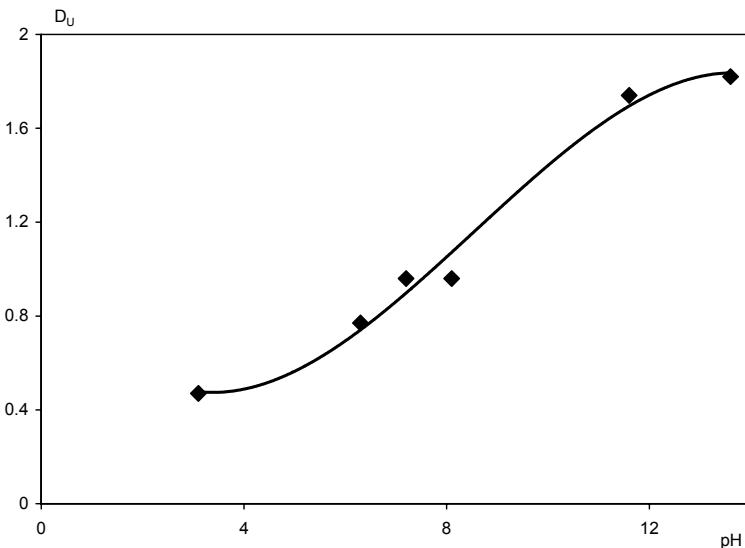


Figure 4. Influence of pH the on distribution coefficient of U(VI) in the system PEG1500 (12 mass %) / potassium phosphate salts (12 mass %) /  $H_2O$ .

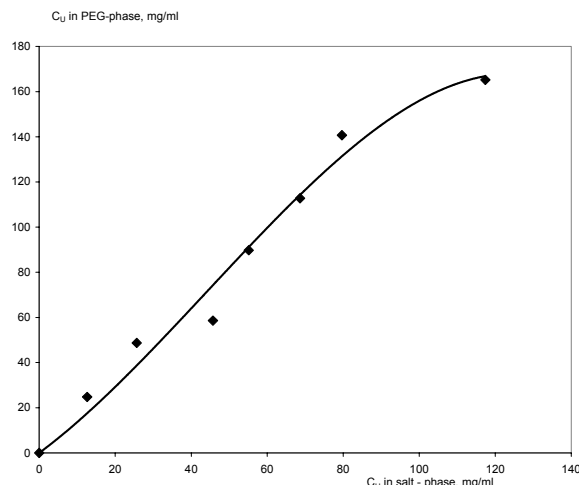
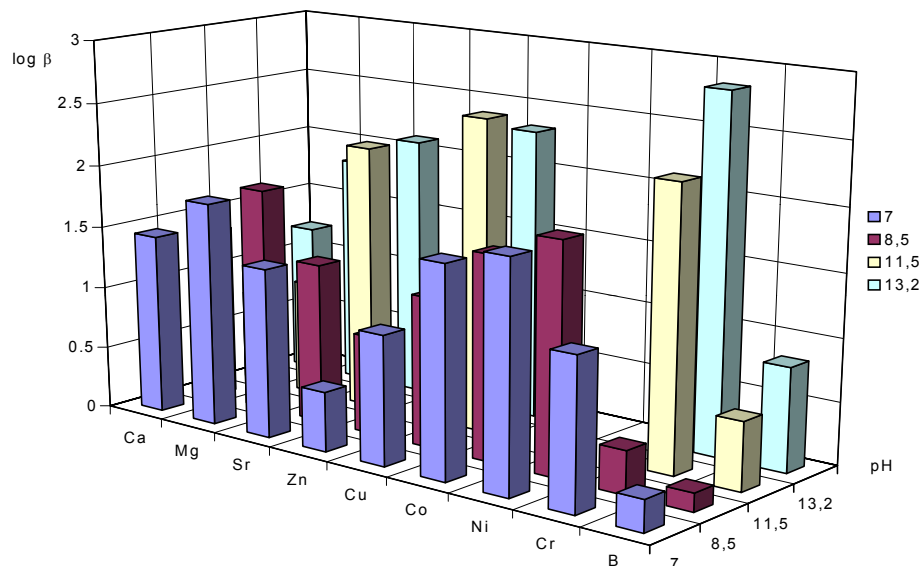


Figure 5. Distribution of uranium (VI) in the system PEG1500 (12 mass %) / potassium phosphate (12 mass %) /  $H_2O$ . pH = 13.6 and  $20^{\circ}C$ .

The extraction of uranium at these conditions is very selective. The separation coefficients of uranium from Zn, Cu, Cr, Ni and other elements are higher than 100 and it is possible to separate uranium from common metals (Figure 6).

## CONCLUSIONS

Conditions for optimal extraction of uranium from concentrated phosphate solutions were selected. A theoretical description of the PEG/water and phosphate salt/water systems was carried out. Selective extraction of uranium was shown.



*Figure 6. Separation coefficients ( $\beta = \log D_U/D_{me}$ ) for the system PEG1500 (12 mass %) / potassium phosphate salts (12 mass %) /  $H_2O$ .*

## REFERENCES

1. P.-A. Albertsson (1971), Partition of Cell Particles and Macromolecules, Almquist and Wiksell, Stockholm.
2. N. P. Molochnikova, V. M. Shkinev and B. F. Myasoedov (1992), *Solvent Extr. Ion Exch.*, **10** (4), 697-712 .
3. T. I. Zvarova, V. M. Shkinev, G. A. Vorob'eva, B. Ya. Spivakov and Yu. A. Zolotov (1984), *Mikrochim. Acta*, 449-458.
4. V. M. Shkinev, N. P. Molochnikova, T. I. Zvarova, B. Ya. Spivakov, B. F. Myasoedov and Yu. A. Zolotov (1985), *J. Radioanalyst. Nucl. Chem.*, **88** (1), 115-120.
5. B. Ya. Spivakov, T. I. Nifant'eva and V. M. Shkinev (1995), Aqueous Biphasic Separations: Biomolecules to Metal Ions, R. D. Rogers and M. A. Eiteman (eds.), Plenum, New York, pp. 83-90.
6. R. D. Rogers, A. H. Bond and C. B. Bauer (1993), *Sep. Sci. Technol.*, **28**, 1091.
7. R. D. Rogers, A. H. Bond, C. B. Bauer, J. Zhang, S. D. Rein, R. R. Chomko and D. M. Roden (1995), *Solvent Extr. Ion Exch.*, **13** (4), 689-713.
8. Z. N. Gao, X. L. Wen and H. L. Li (1998), *Polish J. Chem.*, **72**, 2346.
9. E. A. Bekturov and Z. Ch. Bakauova (1981), *Alma-ata, Kazach SSR*, p. 149.



## DEVELOPMENT OF ENVIRONMENTALLY BENIGN NEW SOLVENT EXTRACTION REAGENTS FROM CHITOSAN, A NATURAL POLYSACCHARIDE

Katsutoshi Inoue, Kazuharu Yoshizuka, and Keisuke Ohto

Department of Applied Chemistry, Faculty of Science and Engineering,  
Saga University, Japan

Two types of lipophilic chitosan, O,O'-decanoyl chitosan (1) and O,O'-decanoyl N,N-didecanoyl chitosan (2) as well as that chemically modified with functional groups of dithiocarbamate (3) were synthesized as solvent extraction reagents for metal ions from chitosan, which is a natural polysaccharide produced from shells of crabs, shrimps, prawns and so on, a biomass waste discharged from marine food industries. Although the reagent (1) was soluble in toluene, the reagents (2) and (3) were soluble not only in toluene but also in kerosene and hexane. In the solvent extraction with the reagent (1), Cu(II) was selectively extracted while only negligible amount of Fe(III) was extracted though it was selectively extracted over Cu(II) in the extraction with the reagent (2). On the other hand, in the extraction with the reagent (3), Cu(II) and Ni(II) were selectively extracted over Fe(III).

### INTRODUCTION

Chitosan is a basic polysaccharide containing primary amino groups. It is produced from shells of some Crustacean such as crabs, shrimps, prawns etc. as discharged from marine food industries in large amount as biomass wastes. It is currently being used for various purposes such as coagulating reagent in waste water treatments or as raw materials for cosmetics, reagents for improving soils for agriculture and so on. Although chitosan itself is hydrophilic solid powder, it is possible to make it lipophilic and soluble in some organic diluents by means of some chemical modifications of hydroxyl groups, for example, by acylating them by using chloride of some carboxylic acids with long-chain alkyl radicals [1]. In addition, the primary amino groups of chitosan are reactive and suitable for various chemical modifications. Thus it is possible to immobilize a variety of functional groups with high affinity to specified metal ions, suggesting the possibility of the development of very new solvent extraction reagents from chitosan, environmentally benign natural polysaccharide.

From the viewpoints as such, we prepared O,O'-decanoyl chitosan which has the free primary amino groups and O,O'-decanoyl N,N-didecanoyl chitosan in which the primary amino group is also acylated with two decanoyl groups as well as O,O'-decanoyl dithiocarbamate chitosan the primary amino groups of which are chemically modified with dithiocarbamate to test their solvent extraction behaviors for some metal ions (see Figure 1).

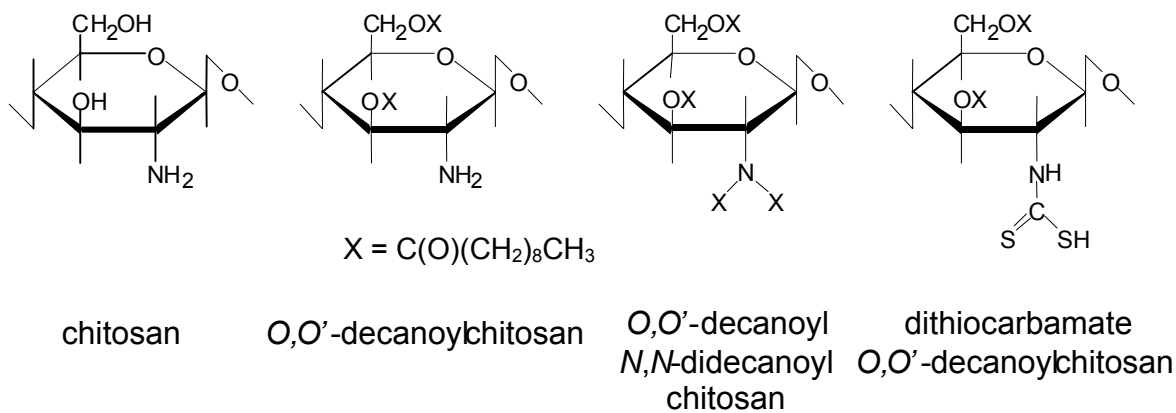


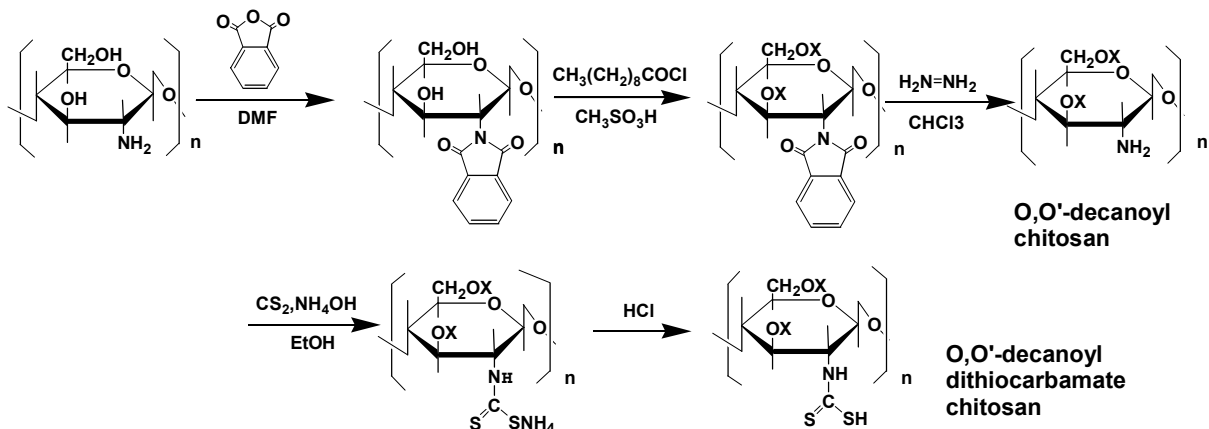
*Figure 1. Chemical structures of chitosan and some lipophilic chitosan employed in the present work.*

## EXPERIMENTAL

$O,O'$ -decanoyl chitosan was synthesized according to the method proposed by Nishimura *et al.* [1] as shown in Scheme 1. Here, prior to the acylation of hydroxyl groups of chitosan with decanoyl chloride, primary amino groups were protected against the attack by the decanoyl chloride by interacting phthalic acid anhydride which was deprotected by using hydrazine after the acylation. The product was soluble in chloroform and toluene, but insoluble in kerosene.  $O,O'$ -decanoyl  $N,N$ -didecanoyl chitosan was prepared by directly interacting decanoyl chloride with chitosan according to the method of Fujii *et al.* [2]. The product was soluble not only in chloroform and toluene but also in hexane and kerosene.

$O,O'$ -decanoyl dithiocarbamate chitosan was synthesized by interacting  $O,O'$ -decanoyl chitosan with carbon disulfide. The sulfur content was measured by using a Mitsubishi Chemicals model TOX-10 total halogen analyzer, from which the extent of the immobilization of the functional groups of dithiocarbamate onto glucosamine unit of  $O,O'$ -decanoyl chitosan was evaluated as high as 96 % [3] while it was only 25 % in the case of immobilization onto chitosan, the solid feed material [4]. It was soluble not only in chloroform and toluene but also in hexane and kerosene.

### Preparation of the Reagents



*Scheme 1. Synthetic route of  $O,O'$ -decanoyl chitosan and  $O,O'$ -decanoyl dithiocarbamate chitosan.*

## Procedure

All experiments of solvent extraction and adsorption were carried out batch wise at 30 °C. Aqueous metal solutions for solvent extraction or adsorption tests were prepared by dissolving metal sulfate or nitrate in 0.1 M aqueous HEPES (2-[4-(2-hydroxyethyl)-1-piperazinyl]ethanesulfonic acid) buffer solution the pH of which was adjusted by adding small amount of nitric acid or sulfuric acid. Initial metal concentration was 0.1 or 0.2 mM for all metal ions in the cases of solvent extraction tests and adsorption tests, respectively. In the solvent extraction tests with O,O'-decanoyl chitosan, chloroform and toluene was used as diluents while, in those with O,O'-decanoyl N,N-didecanoyl chitosan and O,O'-decanoyl dithiocarbamate chitosan, kerosene was used.

Equal volumes (5 ml) of organic and aqueous phases were contacted for 12 h to attain equilibrium in the solvent extraction tests while 30 mg chitosan powder was shaken in 10 ml aqueous metal solution for 24 h in the adsorption tests. Metal concentration in the aqueous phase was measured by using Seiko model SAS 7500 or Shimadzu model AA-6650F atomic absorption spectrophotometer. Metal concentration in the organic phase and amount of metal adsorption on chitosan was calculated by mass balance.

## RESULTS AND DISCUSSION

### O,O'-Decanoyl Chitosan

Figure 2 shows the plot of % extraction against equilibrium pH in the extraction of some metal ions with O,O'-decanoyl chitosan in chloroform. As seen from this figure, iron(III) is not practically extracted with this solvent while copper(II) is highly selectively extracted over all of other metal ions. Similarly, also in the case of toluene as the diluent, only copper(II) was extracted with this reagent while other metals including iron(III) were not practically extracted.

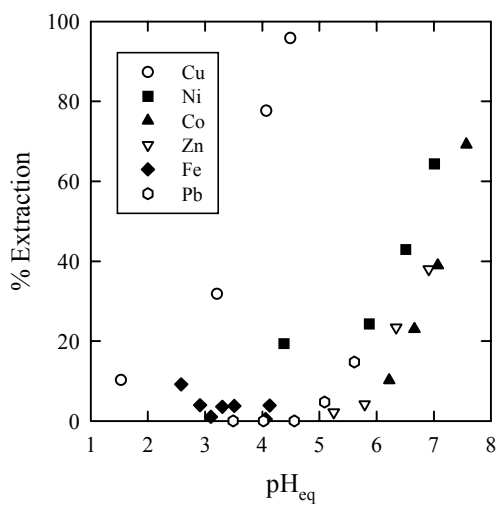


Figure 2. Percentage extraction of some metal ions with O,O'-decanoyl chitosan in chloroform.

Figure 3 shows the plot of % adsorption against equilibrium pH in the adsorption of the same metal ions on chitosan itself. Very different from the result shown in Figure 2, iron(III) is selectively adsorbed over other metals including copper(II). In addition, the extraction with O,O'-decanoyl chitosan takes place at pH greater than 2, which is lower than that at which adsorption on chitosan takes place by 1 pH unit; that is, copper(II) is more strongly extracted with O,O'-decanoyl chitosan than chitosan itself by making chitosan lipophilic. It may be inferred that only the nitrogen atom of primary amino group takes part in the coordination with metal ions in the extraction with O,O'-decanoyl chitosan while oxygen atom of the hydroxyl

group adjacent to the primary amino group also take part in the coordination in the adsorption on chitosan itself as was suggested in the previous paper [5]. In these respects, further works should be necessary in future to elucidate the exact and detailed mechanisms of solvent extraction and adsorption reactions.

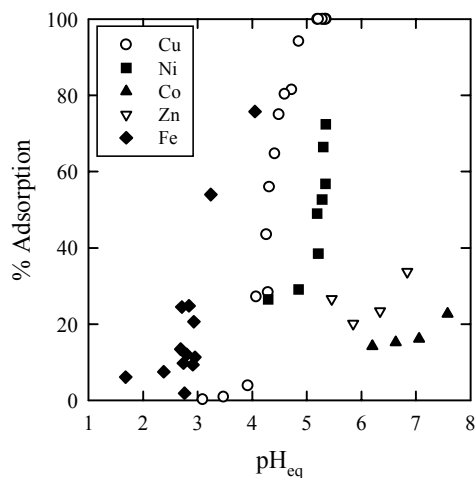


Figure 3. Percentage adsorption of some metal ions on chitosan.

#### O,O'-Decanoyl N,N-Didecanoyl Chitosan

Figure 4 shows the plots of % extraction of metal ions with O,O'-decanoyl N,N-didecanoyl chitosan in kerosene. In this case, iron(III) is selectively extracted over copper(II), which is much more selectively extracted over other divalent metal ions. In the solvent extraction with lipophilic N,N-diacyl chitosan which have two carbonyl groups at the  $\alpha$ -position adjacent to nitrogen atom, it is very natural to consider that oxygen atoms of the two carbonyl groups take part in the coordination, which may be responsible to the high selectivity to iron(III) over copper(II) different from the extraction with O,O'-decanoyl chitosan. Remarkable differences between chloroform and kerosene were not observed in this case.

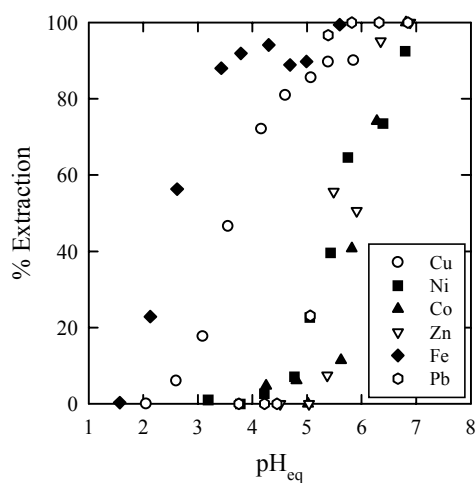


Figure 4. Percentage extraction of some metal ions with O,O'-decanoyl N,N-didecanoyl chitosan in kerosene.

#### O,O'-Decanoyl Dithiocarbamate Chitosan

Figure 5 shows the plot of % extraction against equilibrium pH in the extraction of some metal ions with 2.3 kg/m<sup>3</sup> O,O'-decanoyl dithiocarbamate chitosan in kerosene. As seen from this figure, copper(II) is nearly quantitatively extracted over the whole pH greater than 1, very selectively over other metal ions tested. Although nickel(II) is extracted at pH higher than that

at which the extraction of copper(II) takes place, it is much more selectively extracted over other metal ions including iron(III), which is selectively extracted over cobalt(II) and zinc(II). The sequence of the selectivity among metal ions in this extraction system is also different from that in the adsorption on chitosan chemically modified with dithiocarbamate groups the extent of immobilization of which was about 25 % on glucosamine unit of chitosan. That is, the order of the selectivity among metal ions in the adsorption on the dithiocarbamate chitosan was as follows: Cu(II) > Fe(III) > Ni(II) ~ Co(II) [4].

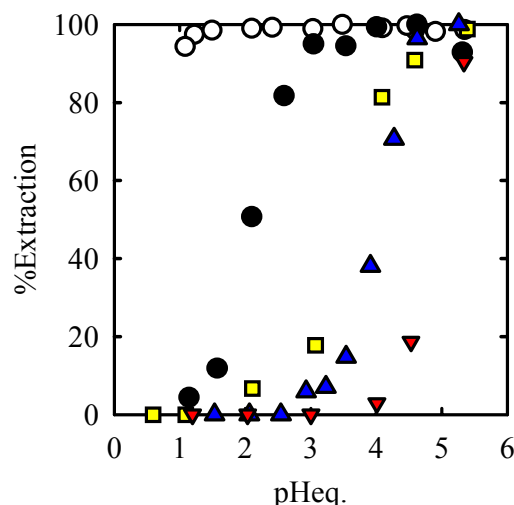


Figure 5. Percentage extraction of some metal ions with O,O'-decanoyl dithiocarbamate chitosan in kerosene. ○: Cu(II), ●: Ni(II), □: Fe(III), ▲: Co(II), ▼: Zn(II).

It should be considered that the extent of the immobilization of the functional groups and its characteristics as a soft base are much enhanced by making polymer matrices of chitosan lipophilic.

## ACKNOWLEDGEMENT

This work was financially supported in part by grant in aid for scientific research on priority areas by The Ministry of Education, Science, Sports and Culture of Japanese Government (No. 12015234) and by Kyushu Industrial Technology Centre (KITEC) under the R&D work “99:A-1) Development of the technology for recovering valuable metals and removing toxic metals by the effective use of biomass wastes”.

## REFERENCES

1. S. Nishimura, O. Kohgo, K. Kurita, C. Vittavatvong, and H. Kuzuhara (1990), *Chem. Lett.*, 243.
2. S. Fujii, H. Kumagai, and M. Honda (1980), *Carbohydr. Res.*, **83**, 389.
3. K. Inoue, K. Yoshizuka, K. Ohto, and H. Nakagawa (2001), *Chem. Lett.*, 698.
4. T. Asakawa, K. Inoue, and T. Tanaka (2000), *Kagaku Kogaku Ronbunshu* (in Japanese), **26**, 321.
5. K. Inoue, Y. Baba, and K. Yoshizuka (1993), *Bull. Chem. Soc. Jpn.*, **66**, 2915.



## NOVEL ELECTROCHEMICAL PROCESSING USING CONVENTIONAL ORGANIC SOLVENTS

T. O'Keefe, M. O'Keefe, R. Fang, J. Sun and E. Dahlgren

Department of Metallurgical Engineering and Graduate Center for Materials Research,  
University of Missouri-Rolla, Rolla, MO, USA

Recent research studies have demonstrated the feasibility of conducting spontaneous electrochemical displacement or redox reactions in conventional solvent extraction organic solutions. Even though the solvents are poor electrolytic conductors, local oxidation/reduction reactions are possible. The patented process was initially designed to use solid metals to remove ferric or ceric ions or metal cation impurities such as copper, lead, cadmium and silver directly from the organic phase. Examples of organic solvents that were successfully used includes D2EHPA, TBP, LIX, Dipex and Alamine. One promising application identified during these studies was Fe<sup>3+</sup> removal from a zinc electrowinning circuit utilizing zinc or iron metal powder in D2EHPA. This process is being evaluated in laboratory pilot tests, with emphasis on producing a usable iron product.

Based on similar chemistry, a unique new process has been developed for the metallization of surfaces in the fabrication of integrated circuits on silicon wafers. After the initial chip surface is coated with Al or a similar barrier metal, an adherent seed layer of Cu, Pd or Au is selectively deposited onto the substrate metal from a suitable organic solution. Once in place, the deposited layer provides an anchoring intermediate film for subsequent build-up of other metals using standard commercial electroless or electrodeposition processes to complete the circuitry. The organic solution process is currently under evaluation for a number of potential commercial semiconductor manufacturing applications. Initial feasibility tests have shown that deposition from the organics has certain advantages over similar aqueous based cementation metallization systems currently used in the electronics industry, but the systems must be optimized.

The basic process and nature of the reactions involved, as well as possible commercial applications of spontaneous electrochemical reactions in organics, will be discussed. The influence of various operating parameters on the reaction rates and efficiencies of these processes, as well as a possible electrochemical model of the process, are presented. Overall, the potential for incorporating electrochemical concepts into the development of new processes or enhancing existing solvent extraction systems seems promising.

### INTRODUCTION

The purification and concentration of leach solutions is a necessary step in most hydro-metallurgical processes because of the adverse effects of trace metal impurities on product quality, recovery and efficiency. Some of the more common treatment options include precipitation, crystallization, electrolysis, cementation, ion exchange and solvent extraction.

Each of these unit operations has certain unique characteristics and advantages, but the ability to provide a favorable distribution of the chemical components between the reacting phases with good, selective separation is essential. From this perspective, solvent extraction is particularly attractive in providing a wide range of options for use in metal production from either primary or waste sources.

The solvent extraction process is based on the ability to control the chemical equilibria operative in an organic/aqueous system. The vast majority of the reactions do not involve electron transfer, but in recent years the use of gaseous reducing agents such as hydrogen as well as photochemical reduction have been proposed, in selected cases, as alternatives to conventional chemical stripping. The concept of incorporating oxidation/reduction reactions to supplement the bulk chemical stripping reactions has been expanded to include the use of solid metals as the reducing agents [1]. Even though the electrical resistances of the organic solutions used were extremely high, it was demonstrated that spontaneous, short range, heterogeneous electrochemical reactions directly in the organic media were possible. Thus, cementation type reactions, similar to those carried out in aqueous solutions, were shown to also be feasible in organic solvents.

A brief overview of direct electrochemical reactions in organic media, termed galvanic stripping, will be presented. Two examples of the use of galvanic stripping will be described. One involves the removal of  $\text{Fe}^{3+}$  from acid zinc sulfate process streams. In a second application area, a completely new form of solid metal deposition that could be used in the electronics industry is presented. The nature of the reactions occurring and the general role that electrochemical reactions may have in organic solvent systems is discussed. A possible model for the mechanism of the reactions is also presented.

### GALVANIC STRIPPING - PROCESS DESCRIPTION

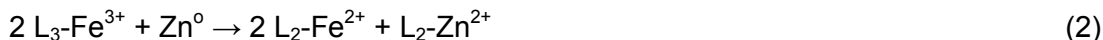
Aqueous solution purification and concentration that involve electrochemical reactions are utilized in a variety of hydrometallurgical operations. While the representation of these displacement or cementation reactions is relatively simple, the specific mechanisms involved may be considerably more complex [2]. The basis for the cementation reaction is the ability of a less noble metal ( $M_2$ ) to serve as the reducing agent for a more noble cation ( $M_1^+$ ) present in an aqueous electrolyte as depicted in Eq. (1).



The equilibrium potentials for  $M_1^+/M_1$  and  $M_2^+/M_2$  reflect the relative driving force for oxidation and reduction and each can be written as a separate, half cell reaction, a condition which is unique to electrochemical reactions. While the thermodynamics of the cementation reactions can be used to theoretically predict reaction tendencies, in actual practice the reactions are often strongly influenced by the system kinetics. As a result, the degree and types of polarization inherent to the systems often dictate the extent and efficiency of the reactions. One outcome of this behavior is that a wide range of chemical and operating modifications may be employed to control the cementation reactions and provide a broader range of separation options.

In principle, the galvanic stripping process to be described in this paper is a cementation reaction. The major difference is the nature of the liquid media in which the reactions occur. In this particular variation of the reaction, organic solvents are used instead of aqueous electrolytes. While some organics are good conductors and capable of sustaining electrochemical reactions, the particular organics employed in galvanic stripping are poor electrolytic conductors. This condition imparts a high degree of polarization to the system and forces the spontaneous reactions to occur over a relatively short range because of the high solution resistivities.

The galvanic stripping reactions might be written using the chemical format given previously for aqueous cementation. Though not indicated in Eq. (1), the metal cations are complexed with water in a hydration sheath. In galvanic stripping the chelation or primary solution structure is an organic entity, probably similar to that encountered in standard solvent extraction. Examples of reactions involving either complete or partial reduction of an  $M_1$  cation by the less noble metal  $M_2$  using a suitable organic ligand L are:



Two process variations can be used to carry out the galvanic stripping reactions and are referred to as simultaneous or separate stripping as illustrated in Figure 1. In simultaneous galvanic stripping the loaded organic, the solid metal reductant and the aqueous stripping phase are allowed to react before settling and separating. This arrangement seems more efficient for partial reduction separations, for example reducing  $Fe^{3+}$  to  $Fe^{2+}$  or  $Ce^{4+}$  to  $Ce^{3+}$  that then easily transfer into the aqueous stripping phase. In separate stripping the reduction reaction and stripping reactions are conducted in two steps. For low concentration cation impurity removal, metal deposition or seed crystal nucleation for microelectronic applications, the separate stripping process has been more effective. An example of the latter is the cementation of Cu on Al, Pd on Al, or Au on Cu.

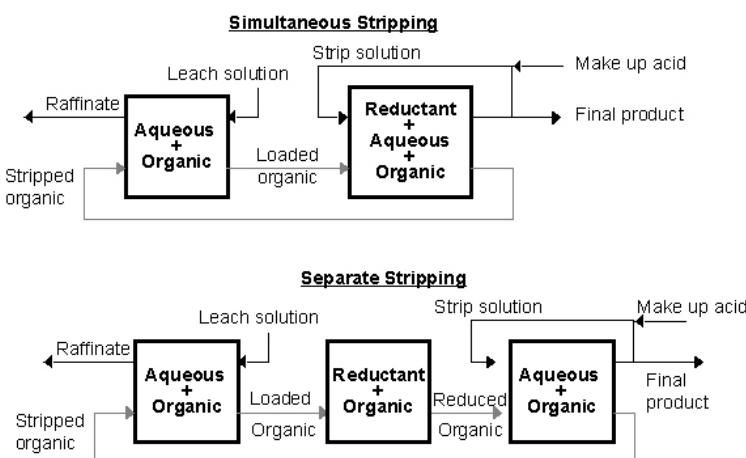


*Figure 1. Process flow sheet for simultaneous and separate galvanic stripping.*

## GALVANIC STRIPPING APPLICATIONS

### Feasibility Studies

The first successful demonstration of galvanic stripping was the deposition of copper onto zinc powder from a LIX reagent. Next a broader range of combinations of organic solvents and metal/metal ion systems was investigated to determine if the reactions occurred only in isolated instances or were more generic in nature [3]. Somewhat surprisingly, reactions were observed to occur in a variety of organic solvents such as D2EHPA, TBP, Acorga, Cyanex, Alamine and Dipex. In total,  $Ag^+$ ,  $Cd^{2+}$ ,  $Cu^{2+}$ ,  $Co^{2+}$ ,  $Pb^{2+}$ ,  $Au^{3+}$ ,  $Fe^{3+}$ ,  $Ce^{4+}$ ,  $Pd^{2+}$  and  $Ni^{2+}$  were reduced using Al, Fe, Zn, Cd, Cu and Mn as the solid metal reductants. Of course, the correct combination of organic/ion/metal is necessary and the selection criteria are based on solubility and reactivity in the organic and the thermodynamic driving force generated by the two metal/ion half cells.

Attempts to measure the potentials of the metal/ion half-cells had limited success because of the lack of a stable reference electrode in the low conductivity organic solutions. Another observation regarding the possibility of obtaining a redox reaction in the organic phase was the dependence on the metal ion used for loading. For example, in some cases where copper sulfate was used, no reaction occurred, but deposition was possible with copper chloride. Obviously, the operating conditions as well as the thermodynamic stability and reducibility of the components themselves must be considered, as is often the case for aqueous cementation reactions.

### FERRIC ION REMOVAL - ZINC ELECTROLYTES

The application of galvanic stripping that involves the selective removal of  $\text{Fe}^{3+}$  from zinc sulfate electrolytes appears to offer some attractive advantages [4]. Di(2-ethylhexyl) phosphoric acid (D2EHPA) was the organic solvent of choice and either metallic zinc or iron was used to reduce  $\text{Fe}^{3+}$  to  $\text{Fe}^{2+}$ , the latter then being easily removed into an aqueous stripping phase. Extensive fundamental and applied studies have been made on both systems. The critical operating parameters were identified and correlated with the efficiency, recovery and kinetics of the anodic and cathodic reactions of interest. A recent article surveyed the removal and recovery of  $\text{Fe}^{3+}$  from sulfuric acid processing solutions using solvent extraction and ion exchange [5]. Though promising, the conclusion was that no commercially proven system is available, considering both the extraction and stripping aspects to produce a "useful" iron product. When galvanic stripping was used it was possible to recover the iron in various forms that could have commercial value.

Initially, batch screening tests were made on  $\text{Fe}^{3+}$  separation using either simultaneous or separate galvanic stripping at a beaker scale. Once the feasibility of using galvanic stripping in this application was demonstrated, a small, continuous pilot apparatus was designed and operated. The schematic flow sheet for the continuous galvanic stripping of  $\text{Fe}^{3+}$  is shown in Figure 2. The results from the small continuous pilot run were reasonably successful and in good agreement with the previous batch tests. Some of the pertinent operating parameters and results are given in Table 1.

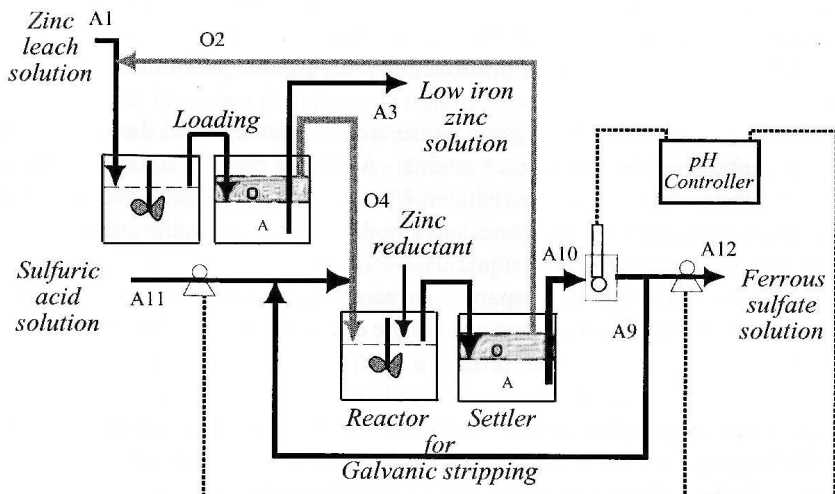


Figure 2. Flow sheet for continuous galvanic stripping of  $\text{Fe}^{3+}$  from a Zn leach solution.

*Table 1. Simultaneous galvanic stripping for Fe<sup>3+</sup> removal.*

Conditions	Results
30 vol% D2EHPA SX-12 Diluent (A/O) 1.0 Loading (A/O) 2.0 Striping Strip pH 1.5 – 2.1 Zn Powder Reductant Fe <sup>3+</sup> 5 – 11 g/L	Fe <sup>3+</sup> removal 50% (one stage) Rate 75 µg/cm <sup>2</sup> /min @40°C Stoichiometry 1.3 – 4 Fe <sup>2+</sup> Strip 90 – 110 g/L Electrolytic Fe Product Crystallized FeSO <sub>4</sub> Product

A complete impurity distribution chemical analysis between the initial zinc sulfate electrolyte and processed organic was made. A number of undesirable impurities such as Ni, Co, Ge and Ti did not extensively load into the organic, but small concentrations of Sn, In, Cu, Cd and Pb did load into the organic. The two major impurities that reported to the final aqueous iron product stream were Zn and As. The Zn can be controlled by using a proper strip solution pH and As may be eliminated by a pre-treatment of the organic prior to reduction. The most promising aspects of the continuous runs were the reasonably efficient elimination of Fe<sup>3+</sup> and a the production of a concentrated Fe<sup>2+</sup> solution as a final iron product. The Fe<sup>2+</sup> concentration in the final aqueous strip solution was in the range of 100 g/L. Assuming the As levels could be decreased, this solution might be used in water treatment applications. In other tests it was demonstrated that electrolytic iron could be won from the solution. In a separate study, a very pure ferrous sulfate product was crystallized that resulted in a final solid salt with a very low impurity content [4].

In summary, galvanic stripping offers some potentially attractive alternatives for removing Fe<sup>3+</sup> from process streams while simultaneously producing a useful final iron product. Other options have also been evaluated, such as using scrap steel as the reductant and operating in a separate rather than a simultaneous mode. Each has advantages and disadvantages that must be considered for the intended application.

## ELECTROCHEMICAL MODEL

Even though it was clear that spontaneous electrochemical reactions could be conducted directly in high resistance organic media, the actual mechanistic path for galvanic stripping was less evident. With simultaneous stripping and an abundance of water as a second phase it is arguable that the electron transfer steps might occur in the aqueous phase. This mechanism appeared less likely for metal deposition from organics using the separate stripping mode because the amount of water was very limited, often in a range of 1% or less. The availability of some water definitely enhanced the reaction rates. One assumption is that water is acting as an intermediate component in the metal/ion electrochemical step at the interface between the solid metal and the organic phase.

In order to gain more insight into the fundamental aspects of the reactions, Electrochemical Impedance Spectroscopy (EIS) measurements were made using zinc electrodes in dehydrated D2EHPA. The Nyquist plot generated is shown in Figure 3a. A simple two-element model was derived from the two capacitive semi-circles present in the plot. The water content was increased to saturation and the EIS curves that resulted are shown in Figure 3b. The first large semi-circle decreased significantly and the second small semi-circle was no longer evident as water was added. Each semi-circle was assumed to represent a reaction layer. The large capacitive loop with 74 MΩ resistance and 7 pF capacitance being the bulk or solution layer. The second small capacitive loop with 1.6 MΩ

resistance and  $10^4$ F capacitance was thought to represent the interface or charge transfer layer. From a high value of  $1.6\text{ M}\Omega$  the second loop is seen to decrease to a value too low to measure, an indication that the reaction resistance decreased with increased water content. The water does increase the bulk conductivity, which may assist the reaction, but the critical function is to decrease the charge transfer resistance at the electrode interface. Therefore, the presence of water would be expected to improve zinc dissolution in D2EHPA, a condition that was observed in the galvanic stripping experiments. Though these results are very preliminary in nature, the tests show that there is a definite opportunity to conduct fundamental studies on organic solvents using electrochemical techniques.

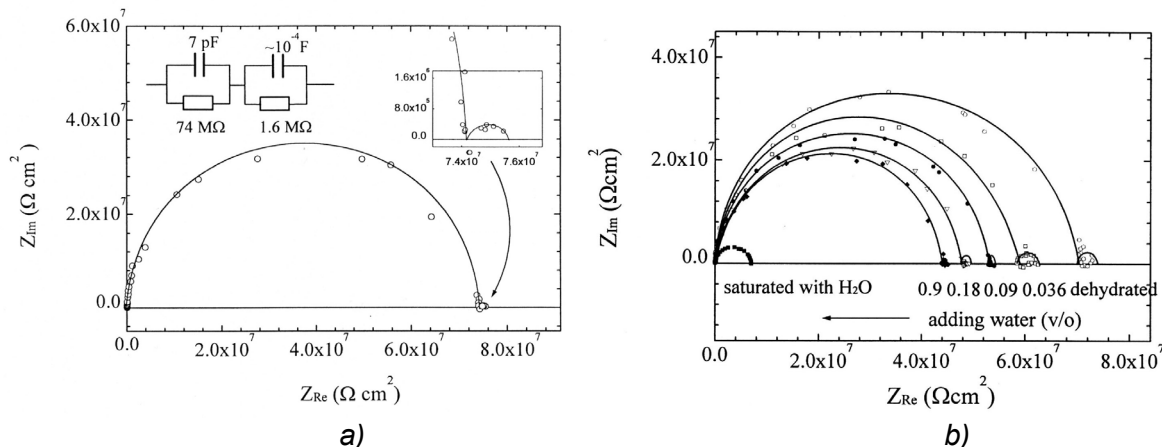


Figure 3. a) Nyquist plot of Zn-Zn cell in dehydrated D2EHPA with simulation of a two layer mechanism. b) Effect of water on zinc dissolution in D2EHPA at 25°C measured by the Zn-Zn cell at open circuit potential in the frequency range of  $10^6$  to  $10^{-2}$  Hz.

## METAL DEPOSITION FOR MICROELECTRONIC APPLICATIONS

The separate galvanic stripping process depicted in Figure 1 can be utilized for metal deposition from organics if the more noble ions loaded into the organic phase are brought into contact with a less noble metallic substrate. As shown in Figure 4a, deposition of more noble ions (e.g., Cu<sup>2+</sup>) on the surface of the less noble substrate (e.g., Al) occurs by a process similar to immersion plating in aqueous solutions. Dissolution of the active substrate into the organic phase is accompanied by an electrochemical reduction of the ions that leads to the formation of metallic seed crystals or nuclei on the surface of the substrate. An inherent part of the process is that deposition occurs only on electrochemically active surfaces and not on electrically non-conducting materials or more noble metals.

There are number of microelectronic applications that might benefit from the organic solution selective area deposition process. Many microelectronic manufacture processes require a sequence of deposition, patterning and etching to fabricate multilayer structures with the required electrical functionality. Integrated circuits on silicon wafers, printed circuit boards made of copper on an insulating dielectric, and microelectromechanical systems (MEMS) all require deposition, print and etch processing steps. Typically, metals and insulating films are deposited over the entire surface and the film is then patterned and etched to remove unwanted material.

Since the deposition of metals from organic solutions is a selective process the seed layers (Figure 4b) will plate only in the patterned areas that are metallic. Subsequent build up of metal thickness to complete the circuits can then be accomplished using conventional aqueous electroless and electrolytic plating processes.

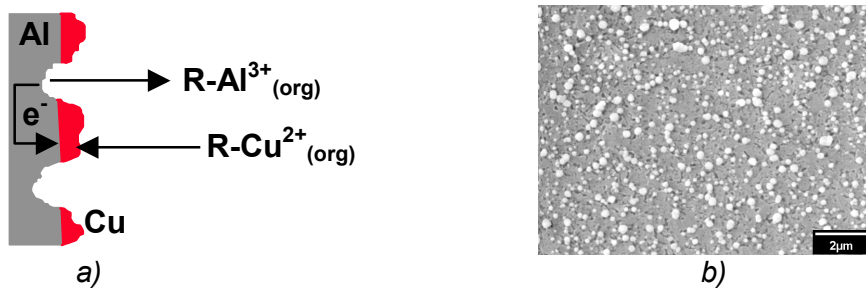


Figure 4. a) Schematic drawing of deposition of Cu onto Al from organic solutions.  
b) Scanning electron micrograph of Cu seed crystals (white) on an Al substrate.

Previous work on the deposition of metals from organic solutions focused on the deposition of metals onto the Al bond pads of silicon integrated circuits (ICs) [6-8]. In some cases, it is desirable to deposit copper or nickel onto the bond pads to facilitate solder attachment of the IC during packaging. Selected area deposition of Cu or Pd from organic solutions acts as a seed layer for the subsequent deposition of electroless copper or nickel from aqueous solutions eliminates the need for subsequent patterning steps. In addition, the process can be scaled to accommodate individual die (on the order of a few mm on a side) or entire wafers (up to 200mm in diameter). The studies found that metal loaded organic solutions could be used to deposit adherent Cu and Pd nuclei that were able to act as seed layers for subsequent metallic copper build-up directly onto Al bond pads. Attempts to deposit copper directly from aqueous plating baths onto the aluminum bond pads were not successful as either no deposition occurred or the film that was deposited did not adhere to the bond pad.

Deposition onto thin (500Å) metal films such as Ta, TaN, Ti, and TiN used as diffusion barriers between copper and low-k dielectric insulators on advanced integrated circuits [9] and the deposition of Au onto Cu for MEMS applications has also been investigated (Figure 5). The feasibility of depositing Cu and Pd seed layers from organic solutions on barrier metals has demonstrated that organic solution processing offers many advantages over aqueous processing. Due to the tenacity of the native oxides on tantalum and titanium based alloys, aqueous electrochemical processes for depositing seed layers onto these materials has proven to be very difficult, if not impossible. Utilizing the unique properties of conventional organic solvents in conjunction with electrochemically driven deposition has the capability to extend the technology to these and other applications as well.

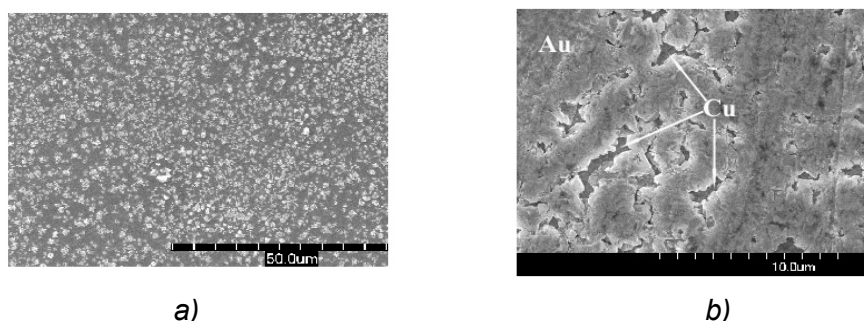


Figure 5. a) Au seed crystals on a Cu substrate. b) Semi-continuous Au film on a Cu substrate.

## CONCLUSIONS

Localized electrochemical reactivity in poorly conducting organic solvents has been demonstrated. The unique aspect of the galvanic stripping and deposition from organics described is the use of solid metals as the reducing agents. Displacement, or redox, reactions were possible in a substantial number of organic/ion/metal systems. Several promising commercial applications have been identified and development efforts continue in these areas. From a more fundamental standpoint, these complex heterogeneous reactions offer some interesting possibilities for extending the utilization of electrochemical principles to advance solvent extraction and organic solution processing.

## ACKNOWLEDGEMENTS

This work has been partially supported over the years through the HSRC Project/Kansas State University, Brewer Science/U.S. Air Force Research Laboratory, the U. S. Department of Education GAANN Fellowship Program, the University of Missouri-Rolla Graduate Center for Materials Research, and the U.S. Defense Advanced Research Projects Agency.

## REFERENCES

1. T. J. O'Keefe (1993), *U. S. Pat.*, No. 5,228,903.
2. J. D. Miller (1981), Metallurgical Treatises, TMS-AIME, pp. 95-117.
3. L. M. Chia, M. P. Nevia, C. Flores and T. J. O'Keefe (1994), Extraction and Processing for the Treatment and Minimization of Wastes, TMS, Warrendale, PA, pp. 279-292.
4. J. Barrera, J. Sun, T. J. O'Keefe and S. E. James (2000), Lead-Zinc 2000, TMS, Warrendale, PA, pp. 763-778.
5. P. A. Riveros, J. E. Dutrizac, E. Bengueral and G. Haulachi (1998), *Min. Proc. Ext. Met. Rev.*, **18**, 105-145.
6. R. Fang, H. Gu, M. J. O'Keefe, T. J. O'Keefe, W.-S. Shih, K. D. Leedy and R. Cortez (2001), *J. Electr. Mater.*, **30** (4), 349 - 354.
7. M. J. O'Keefe, K. D. Leedy, J. T. Grant, M. Fang, H. Gu and T. O'Keefe (1999), *J. Vac. Sci. Tech. B*, **17** (5), 2366-2372.
8. H. Gu, T. J. O'Keefe, M. J. O'Keefe, K. D. Leedy, R. Cortez, R. E. Strawser and W-S Shih (2000), *Electrochem. Soc. Proc.*, **99-33**, 242-248.
9. H. Gu, R. Fang, T. J. O'Keefe, M. J. O'Keefe, W.-S. Shih, J. A. M. Snook, K. D. Leedy and R. Cortez (2001), *Mat. Res. Soc. Proc.*, **612**, D9.19.



## ADVANCED LIQUID-LIQUID EXTRACTION SYSTEM USING PHOTOCHEMICAL REDUCTION FOR METALS

Syouhei Nishihama, Takayuki Hirai, and Isao Komasawa

Department of Chemical Science and Engineering, Graduate School of Engineering Science,  
Osaka University, Toyonaka, Japan

An advanced liquid-liquid extraction system using photochemical reduction for metal ions has been investigated. The distribution of the target metals between the aqueous and organic phases in the extraction system can be controlled by the reduction of the metals, and selective extraction or stripping processes. Kinetic studies for such extraction systems revealed that the photochemical reduction of the metals is the rate-determining step. The photochemical reduction of the metals mainly progressed at the interface and in the organic phase, following photoabsorption at the absorption band for the metal extracted. The technique can be applied to the cobalt-poisoning problem in the hydroxyoxime-type extractant systems.

### INTRODUCTION

Liquid-liquid extraction is a major method employed for separation of metals on an industrial scale. Such extractive separation processes are generally based on differences in the complex formation abilities between metals and their extractants. Separation of some metals is, therefore, difficult when using a conventional extraction system. For the development of more effective separation processes, introduction of functional chemical reactions to the system has been investigated [1]. Redox reactions for the target metal has also been investigated as the reaction to the extraction system. This system is based on the principle that ions with different valencies behave differently with respect to their extractability [2]. There are three possible ways for producing the redox reaction: (1) chemical reaction, (2) electrochemical reaction, and (3) photochemical reaction. In these reactions, the photochemical reaction has the advantages of little discharge of waste and good integration with the extraction system. The photochemical redox reaction can be introduced to both the metal ion in the aqueous phase [3,4] and to the extracted species in the organic phase [5-8], and high selective separation can be carried out. There are, however, relatively few reports concerning the mechanism for such extraction systems.

In the present work, the mechanism of advanced liquid-liquid extraction systems combined with the photochemical reduction of target metals has been investigated. The photoreductive stripping of Fe(III) [9] and photoreductive extraction of V(V) [10] were investigated as case studies. The photochemical reduction of Fe(III) and V(V) in separate aqueous or organic phases was first investigated. The photochemical reduction was then applied to the extraction (stripping) system, and the mechanism of extraction was investigated based on kinetic studies. The advanced extraction system was then applied to the cobalt-poisoning problem in hydroxyoxime extractant systems [11].

## EXPERIMENTAL

The commercial extractants 2-ethylhexyl phosphonic acid mono-2-ethylhexyl ester (EHPNA), bis(2-ethylhexyl)phosphoric acid (D2EHPA), 2-hydroxy-5-nonylacetophenone oxime (LIX-84I), and 2-hydroxy-5-nonylbenzophenone oxime (LIX-65N) were used as extractants, without further purification. In the cases of the Fe and Co systems, aqueous feed solutions were prepared by dissolving each metal chloride in dilute HCl solutions. In the case of the V system, the aqueous feed solution was prepared by dissolving either NaVO<sub>3</sub> or VOSO<sub>n</sub>H<sub>2</sub>O into dilute H<sub>2</sub>SO<sub>4</sub>. The organic solutions were prepared by diluting each extractant with *n*-dodecane.

The extraction equilibrium data were obtained by conventional procedures, at an organic/aqueous (O/A) volume ratio of 1, at 298 K. The photochemical reaction of metals in both single aqueous and organic solutions and photoreductive stripping or extraction were carried out using a beaker-type glass bottle (32 mm in diameter). A 500 W xenon lamp with an irradiation intensity of 580 kW/m<sup>2</sup> was used as the light source for the Fe and V systems, and a 500 W halogen lamp with an irradiation intensity of 706 kW/m<sup>2</sup> was used for the Co system. The wavelength of irradiated light was adjusted by the Pyrex glass material of the reaction bottle (greater than 300 nm) or by using appropriate cut-off filters. The concentrations of metals in the aqueous solutions were analyzed using an inductively coupled argon plasma atomic emission spectrophotometer.

## RESULTS AND DISCUSSION

### Extraction Equilibrium Formulations

Figure 1 shows the effect of the equilibrium pH value on the distribution ratios in Fe/EHPNA and V/D2EHPA systems. Generally, the distribution ratios for the metals having larger valencies are larger than those for metals having smaller valencies. For the Fe system, the distribution ratio for Fe(II) is much lower than that for Fe(III) over the pH range investigated, thus indicating that selective stripping of Fe may be expected to progress by reduction during the stripping process. The slope analysis method revealed that the extraction equilibria for these metals could be expressed as in Eqs. (1) and (2).



For the V system, however, the distribution ratio for V(V) is smaller than that for V(IV), which is contrary to the valences, since, in an acidic solution with a pH value of 0-2, V(V) and V(IV) exist as VO<sub>2</sub><sup>+</sup> and VO<sup>2+</sup>, respectively. Selective extraction of V is thus expected by reduction, especially at high pH. The slope analysis method revealed that the extraction equilibria for these metals could be expressed as in Eqs. (3) and (4).



### Photochemistry of the Metals in Aqueous and Organic Solutions

In the case of Fe(III), no photochemical reduction occurs without a radical scavenger in both aqueous and organic solutions. In aqueous solution, however, the reaction progresses in the presence of a radical scavenger, such as formic acid. This is because the photochemical reduction of Fe(III) in aqueous solution occurs by electron donation from water, and the OH radical produced, which promotes the reverse reaction, is scavenged by formic acid. In the case of V(V), photochemical reduction occurs in both aqueous and organic solutions without

a radical scavenger. The rate of photochemical reduction was investigated following Ar bubbling in order to purge dissolved oxygen. A pseudo-first order kinetic plot for the variation in the concentration of V(V) revealed that the rate of photochemical reduction of V(V), in both aqueous and organic solutions, is first order with respect to V(V) concentration and is independent of pH, sulfuric ion concentration, and extractant concentration.

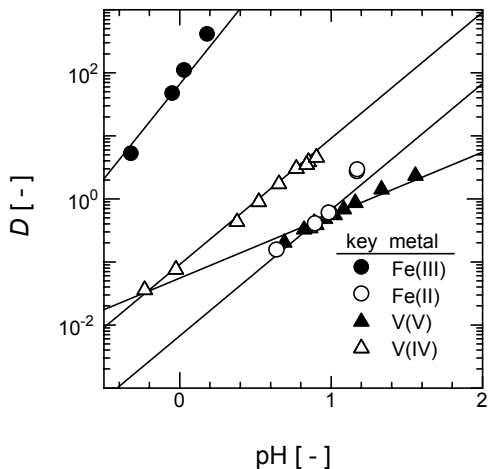


Figure 1. Effect of the aqueous pH on the distribution ratio for Fe with EHPNA and V with D2EHPA.  $[(RH)_2]_{feed} = 0.5 \text{ mol/l}$  and  $[M]_{feed} = 0.01 \text{ mol/l}$ .

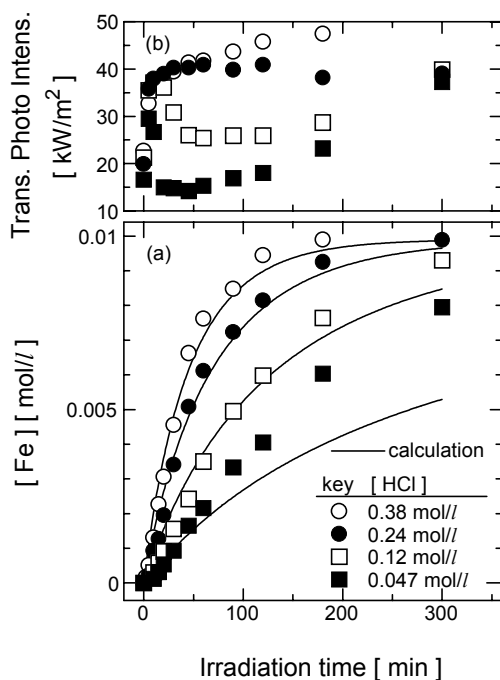


Figure 2. Effect of irradiation time on (a)  $[\text{Fe(III)}]$  and (b) the transmitted photointensity. Comparison of observed data with prediction shown by solid lines.  $[(RH)_2]_{feed} = 0.1 \text{ mol/l}$  and  $[\text{Fe(III)}]_{feed} = 0.01 \text{ mol/l}$ .

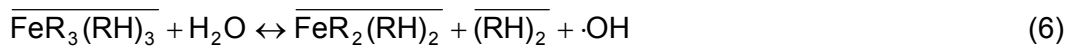
### Photoreductive Stripping of Fe(III)

The organic solution following extraction of Fe(III) was contacted with a dilute HCl solution at O/A = 1, which was not expected to strip Fe(III), and then photoirradiated with the Xe lamp with vigorous agitation by a magnetic stirrer. The photoreductive stripping of Fe(III) progresses by photoirradiation following an initial induction period caused by dissolved oxygen in the extraction system. In addition, the photoreductive stripping of Fe(III) progressed when only organic phase was irradiated. Because photochemical reduction is found not to occur in the organic solution, Fe(III) is likely to be photoexcited in the organic phase and to be reduced at the interface by electron donation from water. A kinetic study revealed that the rate of photoreductive stripping is expressed by Eq. (5):

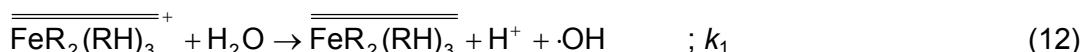
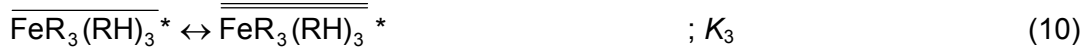
$$r_{\text{Fe}} = -\frac{d[\overline{\text{Fe}}]}{dt} = k_{\text{Fe}} \frac{[\overline{\text{Fe}}][\text{H}^+]}{[(RH)_2]^{0.5}} \quad (5)$$

where  $k_{\text{Fe}} = 0.0275 \text{ l}^{0.5} \text{ mol}^{-0.5} \text{ min}^{-1}$ . Figure 2(a) shows the effect of photoirradiation time on the concentration of Fe in the aqueous phase, as compared with the calculated value based on Eq. (5). The experimental values agree well with the calculated values during the initial part of the run, but with increasing irradiation time the deviations become notable in the run with the solution of lower HCl concentration. Figure 2(b) shows the variation with time on the photointensity of transmitted light. In the case of HCl concentration of 0.047 mol/l, the transmitted light intensity increased as the photoreductive stripping of Fe(III) progressed, and the photoreaction progressed more effectively than that predicted based on the initial photoreductive stripping rate.

The overall reaction mechanism for the photoreductive stripping of Fe(III) can be divided into two reaction stages, the photochemical reduction of extracted species of Fe(III) to Fe(II) at the interface, followed by the stripping of Fe(II) into the aqueous phase, as follows:



This reaction scheme is deduced on the assumptions that the rate-determining step is the photochemical reduction of Fe(III), as shown by Eq. (6), and that the rate of distribution of the reduced Fe(II) is fast. The Fe(III)-extractant complex is found to be excited in the organic phase and to be donated an electron from the water at the aqueous/organic interface. Assuming the extractant to exist as a monomeric species at the interface, the elementary reaction of Eq. (6) can be expressed in more detail as in Eqs. (8)-(13):



If the rate-determining step is the photochemical reduction of Fe(III) as shown by Eq. (12), the overall reaction rate equation can be expressed by Eq. (14).

$$r = -\frac{d[\overline{\text{Fe}}]}{dt} = k_1 [\overline{\text{FeR}_2(\text{RH})_3}^+] = \frac{k_1 K_2 K_3 K_4}{K_1^{0.5}} \frac{[\overline{\text{FeR}_3(\text{RH})_3}][\text{H}^+]}{[(\overline{\text{RH}})_2]^{0.5}} \quad (14)$$

This agrees with the result from the experimental kinetic study, as shown by Eq. (5), indicating that the mechanism of photoreductive stripping of Fe(III) is expressed by the proposed scheme.

### Photoreductive Extraction of V(V)

The extractant D2EHPA in *n*-dodecane was contacted with the aqueous solution, containing NaVO<sub>3</sub>, at O/A = 1, under the photoirradiation following Ar bubbling with agitation by a magnetic stirrer. Figure 3 shows the effect of photoirradiation time on the distribution ratio for V. The variation with time of the distribution ratio can be predicted by assuming that the rate of the reaction is dominated by the photochemical reduction of V in the aqueous and organic phases, which were obtained otherwise. Such predictions, which are shown by dotted lines in Figure 3, however, lead to much lower values for the distribution ratio than the experimental results. This difference may be caused by photochemical reduction of V at the interface between the aqueous and organic phases, as was also found in the case for the photoreductive stripping of Fe(III). The prediction lines, considering the photochemical reduction of V(V) at the interface, can express the experimental data, thus indicating that the photochemical reduction of V progresses in the aqueous phase, in the organic phase, and at the interface. However, the reduction in the aqueous phase hardly contributes to the overall photoreductive extraction.

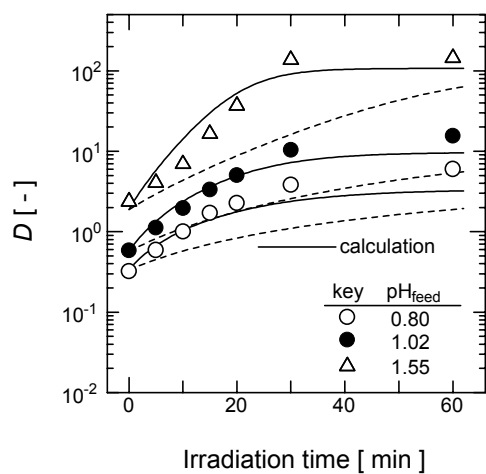


Figure 3. Effect of the irradiation time on the distribution ratio for V. Solid lines: photochemical reduction at the interface only, dotted lines: photochemical reduction only in the aqueous and organic phases.  $[(RH)_2]_{feed} = 0.5 \text{ mol/l}$  and  $[NaVO_3]_{feed} = 0.01 \text{ mol/l}$ .

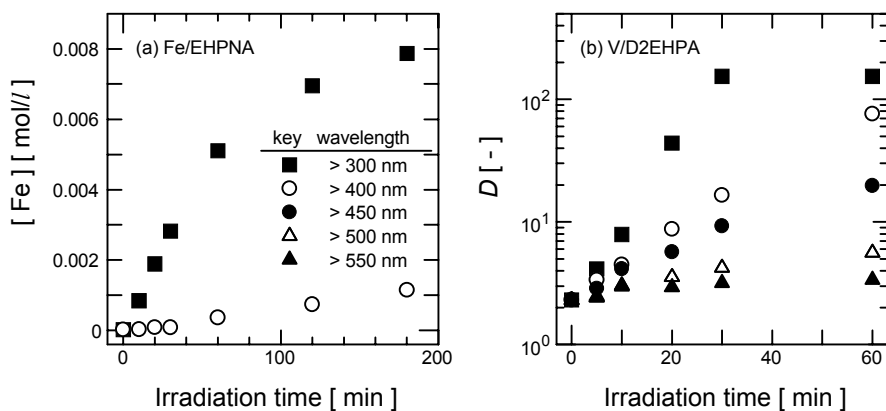


Figure 4. Effect of the wavelength of the light source on the rate of (a) photoreductive stripping of Fe(III) and (b) photoreductive extraction of V(V). (a) Fe/EHPNA system,  $[(RH)_2]_{feed} = 0.1 \text{ mol/l}$ ,  $[\overline{Fe}]_{feed} = 0.0088 \text{ mol/l}$ , and  $[HCl]_{feed} = 0.24 \text{ mol/l}$ , and (b) V/D2EHPA system,  $[(RH)_2]_{feed} = 0.5 \text{ mol/l}$ ,  $[NaVO_3]_{feed} = 0.01 \text{ mol/l}$ , and  $pH_{feed} = 1.52$ .

### Effect of the Wavelength of the Irradiated Light

Figure 4 shows the effect of the wavelength of the irradiated light, when varied by the use of appropriate cut-off filters, on the variation with time in the photoreductive stripping of Fe(III) and photoreductive extraction of V(V). The reaction hardly occurs when irradiated light of less than 400 nm is cut off in the Fe system, and hardly occurs when irradiated light of less than 500 nm is cut off in the V system. This may be caused by the ability for photoabsorption of the extracted species. In the case of Fe(III), the absorption band, caused by Fe(III) extracted species, appears at 200-350 nm. In the case of V(V), the absorption band, caused by V(V), appears at 300-500 nm. These results thus indicate the photochemical reduction of the metals in the organic phase and at the interface progresses following photoabsorption at the absorption band for the metal extracted.

### Reusability of the Organic Phase

The reuse of an organic solution following photoirradiation was also investigated. In the case of Fe, the aqueous feed solution and organic solution were contacted at O/A = 1. The Fe loaded organic solution was then contacted with 0.36 mol/l HCl solution at O/A = 1 and the phases photoirradiated for 300 min. In the case of V, the aqueous and organic solutions were contacted at O/A = 1 and were photoirradiated for 60 min. The resultant organic solution was then stripped using 6 mol/l HCl at O/A = 0.5. These resultant organic solutions were then used for repeated processing after washing with 3 mol/l HCl and then water. Figure 5 shows the concentration of Fe or V in the organic phase during the repeated extraction-stripping processing. The results thus show that the organic phase possesses sufficient loading and stripping capacity for use in repeated processing and confirm the possible reuse of the organic phase following photoirradiation.

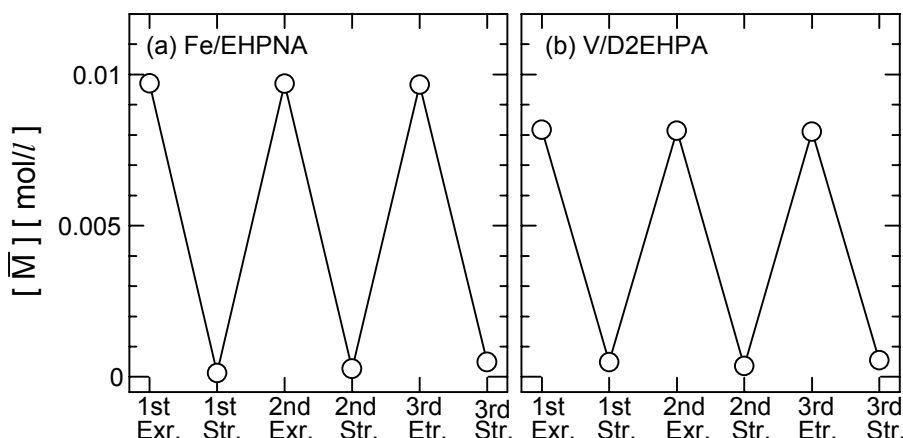


Figure 5. The concentration of (a) Fe and (b) V in the organic phase following the repeated extraction-stripping processing.  $[(RH)_2]_{\text{feed}} = (a) 0.1 \text{ mol/l}$  and  $(b) 0.5 \text{ mol/l}$ ,  $[M]_{\text{feed}} = 0.01 \text{ mol/l}$ , and  $pH_{\text{feed}} = (a) 1.47$  and  $(b) 0.86$ .

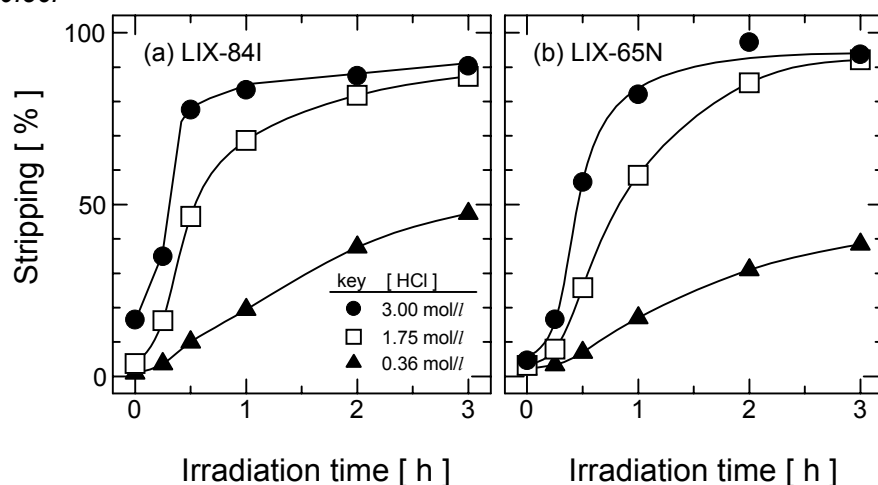


Figure 6. Effect of the HCl concentration on rate of photoreductive stripping in (a) LIX-84I and (b) LIX-65N systems.  $[RH]_{\text{feed}} = 10 \text{ vol\%}$ , and  $[Co]_{\text{feed}} = (a) 6.53 \text{ mmol/l}$  and  $(b) 9.37 \text{ mmol/l}$ .

### **Application for the Cobalt-Poisoning Problem**

It is well known that Co(II) when extracted via commercial chelating extractants, such as hydroxyoxime type extractants, is difficult to recover by conventional stripping procedures, owing to cobalt poisoning. This poisoning is because Co is oxidized to the trivalent state by oxygen in the extraction system, and is then stabilized in the organic phase, which suppresses quantitative stripping. Effective stripping is therefore expected to be carried out, if the oxidized Co(III) complex can be photoreduced within the organic phase. The photoreductive stripping of Co was then carried out by a similar procedure to the photoreductive stripping of Fe using a halogen lamp. Only visible light with a wavelength greater than 550 nm was irradiated, since Co-LIX 84I has a large absorption band at 400-800 nm. Figure 6 shows the effect of HCl concentration on the photoreductive stripping of Co in LIX-84I and LIX-65N systems. Successive stripping can be carried out in both systems using the photoreductive stripping technique. The photoreductive stripping of cobalt is improved by increasing the concentration of HCl in both systems, and a stripping efficiency of about 90 % can be achieved with 3 mol/l HCl following photoirradiation for 3 h. The organic phase in this process also possesses sufficient loading and stripping capacity for use in repeated processing, as for the Fe and V systems.

### **CONCLUSION**

Advanced liquid-liquid extraction systems using photochemical reduction for metal ions have been investigated, with the following results: (1) The distribution ratio of metals can be controlled by photochemical reduction of the metals. The mechanisms of the extraction system combined with photochemical reduction were elucidated based on kinetic studies, in which the photochemical reduction of the metals is the rate-determining step. (2) The photochemical reduction of the metals in the organic phase and at the interface takes place following photoabsorption at the absorption band for the extracted metal. The organic solution following photoirradiation is reusable for repeated extraction-stripping processing. (3) The photoreductive stripping technique can solve the cobalt-poisoning problem in hydroxyoxime extractant systems.

### **NOMENCLATURE**

- = organic phase species
- = = interface species

### **REFERENCES**

1. S. Nishihama, T. Hirai, and I. Komasawa (2001), *Ind. Eng. Chem. Res.*, **40**, in press.
2. M., Benedict, T. Pigford, and H. Levi (1981), Nuclear Chemical Engineering, McGraw-Hill Book Company, New York.
3. T. Hirai, N. Onoe, and I. Komasawa (1993), *J. Chem. Eng. Japan*, **26**, 64.
4. T. Hirai and I. Komasawa (1996), *J. Chem. Eng. Japan*, **29**, 731.
5. T. Hirai and I. Komasawa (1995), *Ind. Eng. Chem. Res.*, **34**, 237.
6. T. Hirai, N. Onoe, and I. Komasawa (1993), *J. Chem. Eng. Japan*, **26**, 416.
7. T. Hirai, T. Manabe, and I. Komasawa (1995), *J. Chem. Eng. Japan*, **28**, 486.
8. T. Hirai, T. Manabe, and I. Komasawa (1997), *J. Chem. Eng. Japan*, **30**, 268.
9. S. Nishihama, T. Hirai, and I. Komasawa (1999), *Ind. Eng. Chem. Res.*, **38**, 4850.
10. S. Nishihama, T. Hirai, and I. Komasawa (2000), *Ind. Eng. Chem. Res.*, **39**, 3018.
11. S. Nishihama, N. Sakaguchi, T. Hirai, and I. Komasawa (2000), *Ind. Eng. Chem. Res.*, **39**, 4986.



## ROOM TEMPERATURE IONIC LIQUIDS AS ALTERNATIVES TO TRADITIONAL ORGANIC SOLVENTS IN SOLVENT EXTRACTION

Ann E. Visser, John D. Holbrey, and Robin D. Rogers

The Department of Chemistry and Center for Green Manufacturing,  
The University of Alabama, Tuscaloosa, AL, USA

We describe a new class of solvents comprised of low melting salts known as room temperature ionic liquids. Recent interest has focused on their unique properties as alternative solvents in synthesis and separations. The properties of both hydrophobic and hydrophilic ionic liquids reveal how water content, density, viscosity, surface tension, melting point, and thermal stability are affected by changes in the nature of both cation and anion. Applications for ionic liquids, with particular attention to their solvating ability and utilization as replacements for organic solvents in liquid/liquid separations, are described.

### INTRODUCTION

Much of the interest surrounding Ionic Liquids (IL) has centered on their unusual properties for catalysis [1] and, recently, as solvent alternatives for synthesis [2] and liquid/liquid separations [3-6]. Performing ordinary chemical processes using alternative reaction media demonstrates the basis for a shift in manufacturing paradigm towards “green chemistry,” and an aim to reduce or eliminate hazards and risks involved with current processes that rely heavily on volatile organic compounds (VOCs) as the solvent medium. Incorporating green chemistry to provide benign conditions or processes will promote the research, development, and implementation of innovative chemical technologies to achieve pollution prevention [7].

#### Ionic Liquids

In the current understanding, IL are composed of large, organic cations (Figure 1) which, when appended with alkyl groups and combined with various anions, result in low melting salts [8].

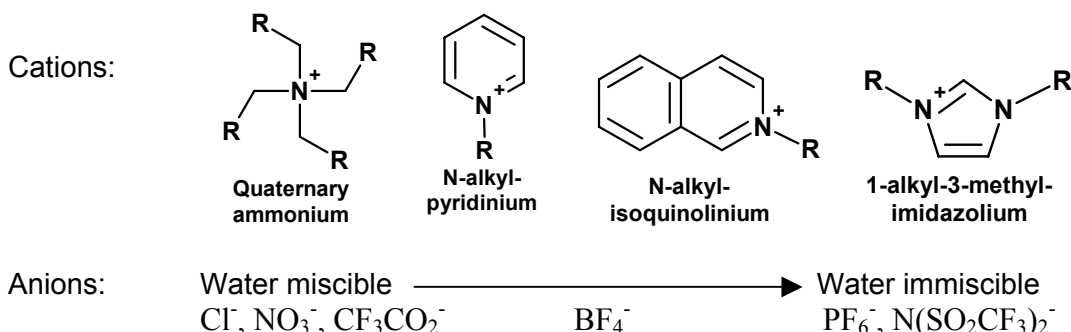


Figure 1. Representative IL compositions.

These novel compounds are, thus, ionic and melt at or below 150 °C (an accepted upper temperature limit). In contrast to molten ionic melts (*i.e.*, NaCl at 800 °C), the asymmetric organic cations in IL interrupt the crystal packing and can substantially lower the melting points. Room Temperature Ionic Liquids (RTIL) are a subdivision of IL that are liquid at room temperature and, thus, facilitate their use at ambient temperatures.

## SUMMARY

Depending on composition, IL can be hydrophobic or hydrophilic [8,9]. An inherent property of many IL is their minuscule volatility and easily manipulated properties, characteristics of a unique class of solvents. IL principally have an organic cation, usually among ammonium [10-12], phosphonium, pyridinium [13,14], pyrrolidinium [15], or imidazolium [8,9], each with the possibility for attaching various alkyl groups to the ring or quaternary onium cation. Depending on the type of cation investigated and the length of the alkyl chain, the resulting IL may have a melting point above room temperature and several crystal structures have been reported [16].

We have initially focused on IL incorporating the 1-alkyl-3-methylimidazolium ( $[C_n\text{mim}]^+$ ) cation [3,4], where the alkyl group is usually an *n*-alkane and increasing the length of the alkane chain affects the resulting properties (*e.g.*, viscosity, hydrophobicity, and melting point) [8,9]. For example,  $[C_8\text{mim}][\text{PF}_6^-]$  is a liquid at room temperature with a glass transition temperature at -75 °C [9] and  $[C_{10}\text{mim}][\text{PF}_6^-]$  melts at 38 °C [3]. IL composed of several different cations or anions (*i.e.*, multi-component mixtures) can also be envisaged to further expand the family of ionic liquids.

Choice of cations and anions can be used to control the IL water miscibility with the nature of the anion having the greatest effect on hydrophobicity. The anions may also impart unique chemistry to the systems, rendering the IL capable of digesting materials such as nuclear fuel components [17] and kerogens [18]. For liquid/liquid separations,  $\text{PF}_6^-$  and  $\text{N}(\text{SO}_2\text{CF}_3)_2^-$  produce water immiscible IL useful for partitioning both organic and inorganic solutes [3-6]. Our previous results [9] indicate water content has a profound effect on physical properties and, in liquid/liquid separation systems, IL analyses after equilibration with water provide the most accurate analysis of the IL properties under those conditions. Table 1 presents some physical properties of water-equilibrated  $[C_n\text{mim}][\text{PF}_6^-]$  IL which illustrate the cation effect.

*Table 1. Physical properties of water-equilibrated IL [9].*

Parameter	$[C_4\text{mim}][\text{PF}_6^-]$	$[C_6\text{mim}][\text{PF}_6^-]$	$[C_8\text{mim}][\text{PF}_6^-]$
Water content (ppm)	11700	8837	6666
Viscosity (cP)	397	452	506
Density (g/mL)	1.35	1.24	1.16
Melting point (°C)	4		
Glass transition (°C)	-83	-75	-75
Thermal decomposition (°C)	360	390	374
Surface tension (dyn/cm)	49.8	36.8	34.2

Even ‘hydrophobic’ RTIL incorporating the  $\text{PF}_6^-$  anion contain significant amounts of water. Previous partitioning results show that an increase in the alkyl chain length produces higher distribution ratios [3,9] for more hydrophobic solutes which is consistent with the decreasing water content. The rheological properties hinge largely on water content.

For comparison, Table 2 lists some physical properties for IL composed of the  $[C_4mim]^+$  cation and various anions. Since both hydrophobic and hydrophilic IL are represented, the properties listed here are those for IL that have been ‘dried’ on a vacuum line for 4 hours while heating to 70 °C.

*Table 2. Physical properties of related dried IL [9].*

Parameter	$[C_4mim]-[Cl]$	$[C_4mim]-[BF_4]$	$[C_4mim]-[PF_6]$	$[C_4mim]-[N(SO_2CF_3)_2]$
Water content (ppm)	2200	4530	590	474
Viscosity (cP)	na	219	450	69
Density (g/mL)	1.08	1.12	1.36	1.43
Melting point (°C)	41	na	10	na
Glass transition (°C)	na	-97	-80	-104
Thermal decomposition (°C)	254	403	349	439
Surface tension (dyn/cm)	na	46.6	48.8	37.5

### Solvent Properties

IL are generally considered to be highly polar, yet non-coordinating solvents. Solvatochromatic studies have shown that IL have polarities similar to those of short-chain alcohols and other polar, aprotic solvents (e.g., DMSO, DMF, etc.) [8,19-21]. Some IL are immiscible with several organic solvents (e.g., alkanes). Primary solvent features of IL are the ability for H-bond donation from the cation to polar or dipolar solutes. H-bond accepting functionality in the anion can vary from  $Cl^-$ , which is a good H-bond acceptor, to  $PF_6^-$ , which is poor. In addition, cations containing  $\pi-\pi$  or  $CH-\pi$  interactions may serve to enhance aromatic solubility.

From empirical observation, most IL tend to be immiscible with non-polar solvents. Thus, IL can be washed or contacted with either diethylether or hexane to extract non-polar reaction products. On increasing solvent polarity, esters (e.g., ethylacetate) exhibit variable solubility with IL depending on the nature of the IL. Polar or dipolar solvents (chloroform, acetonitrile and methanol) appear to be totally miscible with all IL (excepting tetrachloroaluminate IL and the like, which are reactive).

We have recently shown that hydrophobic  $PF_6^-$  IL can, in fact, be made totally miscible with water by the addition of alcohols [22]. Ethanol forms biphasic mixtures with  $[C_4mim][PF_6]$ ,  $[C_6mim][PF_6]$ , and  $[C_8mim][PF_6]$ , depending on temperature, although mixtures containing ethanol, water, and IL may be totally miscible at specific compositions as shown in Figure 2. Successful solubilization of IL has many potential uses for washing and removal of ionic liquids from products and reactors or catalysis supports, and has important implications in designing IL/aqueous extraction systems.

### Liquid/Liquid Separations

Water immiscible RTIL (e.g.,  $PF_6^-$  salts) have been pursued as a class of alternative solvent media to illustrate how their unique properties encourage their use in place of traditional organic solvents in liquid/liquid separations [3,9,23]. Some of our recent results are summarized below.

### Organic solutes

Our initial results [23] for aromatic solute partitioning between water and  $[C_4mim][PF_6]$  indicated that neutral, hydrophobic, aromatic solutes have an affinity for the ionic liquid phase and that traditional hydrophobicity parameters (*i.e.*, 1-octanol/water log P) can be a guide to predicting IL affinity. With charged or ionizable solutes, a change in the aqueous phase pH results in certain ionizable solutes exhibiting pH-dependent partitioning such that their affinity for the RTIL decreases upon ionization [23] (*e.g.*, the pH dependent partitioning of thymol blue, Figure 3 [3]).

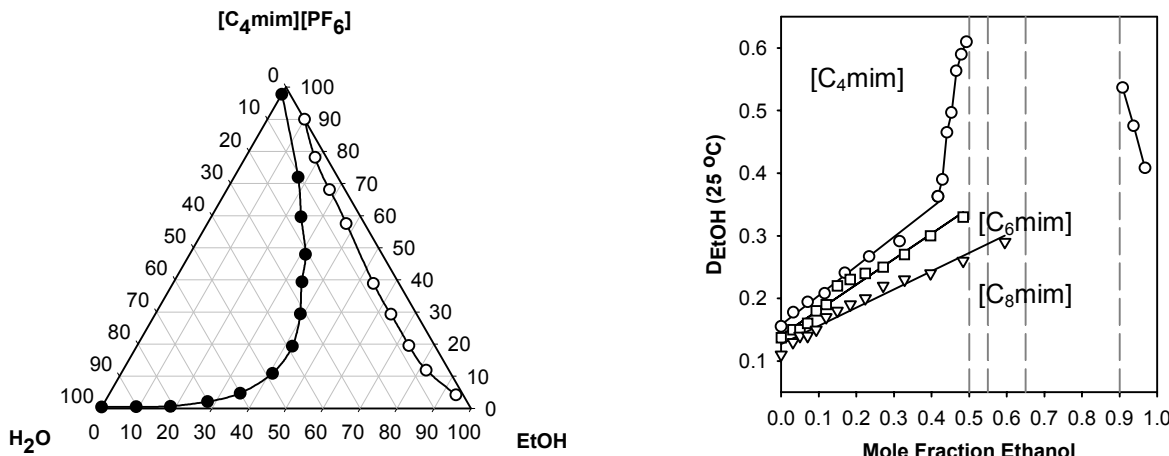


Figure 2. Ethanol/water/[ $\text{C}_4\text{mim}][\text{PF}_6]$  ternary phase diagram and solute distribution in IL.

Extraction efficiency and selectivity can be controlled by changing IL components: for example, IL/aqueous systems containing alkyl-isoquinolinium cations show increased distribution ratios [24] for organic solutes in comparison to imidazolium-based IL, as shown in Figure 4.

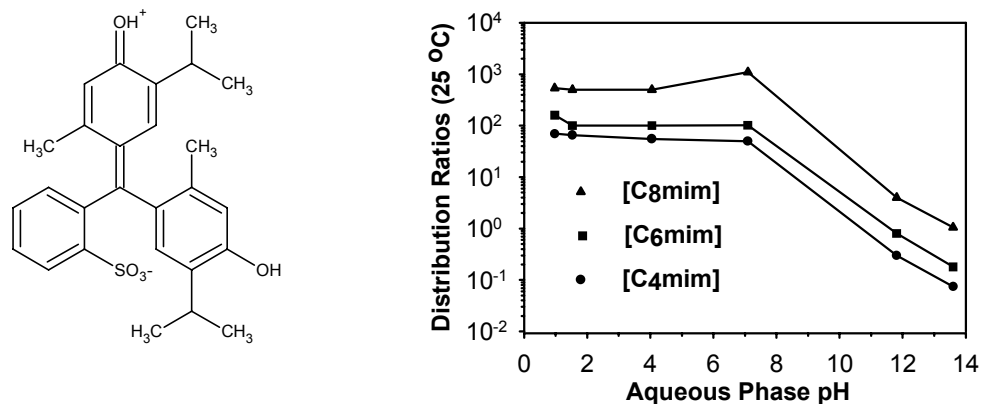


Figure 3. pH switchable partitioning of thymol blue in  $[\text{C}_n\text{mim}][\text{PF}_6]$ /aqueous biphasic systems.

### Metal ions

There is considerable interest in replacing organic extracting phases with IL for recovery of metals from waste water, mining, nuclear fuel, and waste reprocessing, and immobilizing transition metal catalysts. The hydrated nature of most metal ions lowers their affinity for the IL phase, thus, in the typical  $[\text{C}_n\text{mim}][\text{PF}_6]$ /water system, hydrated metal ions do not partition to IL from water. Enhancing the affinity of metal ions for the less polar phase can be achieved by changing the hydration environment of the metal ion using either organic ligands [4,5] which provide a more hydrophobic region around the metal, or with inorganic anions [5] that form softer more extractable anionic complexes with the metal. The challenges in adapting IL to traditional separations include finding extractants which quantitatively partition to the solvent phase and can still readily complex target metal ions, or finding conditions under which specific metal ion species can be selectively extracted from aqueous streams containing inorganic complexing ions.

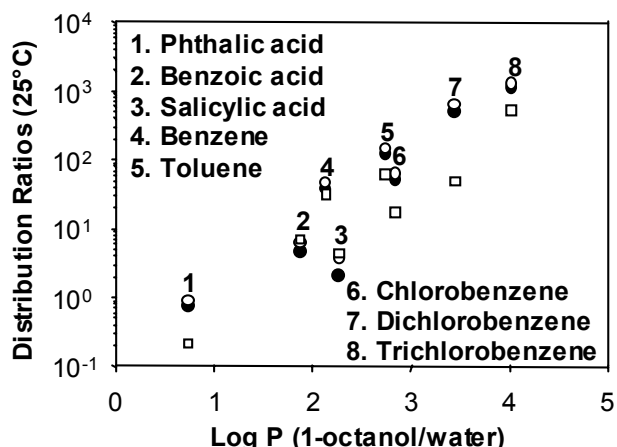


Figure 4. Organic solute distribution ratios in  $[C_{14}isoq][BETI]$  ( $\circ$ ),  $[C_8isoq][BETI]$  ( $\bullet$ ), and  $[C_4mim][PF_6]$  ( $\square$ ).

### Anionic extractants

The distribution ratios from aqueous to IL phases of some metal ions may be enhanced in the presence of coordinating anions such as halides or pseudohalides. Metal ions such as  $Hg^{2+}$  have large formation constants with halides, and their effect has been observed on the partitioning of  $Hg^{2+}$  in other systems [25]. Halides, cyanate, cyanide, and thiocyanate have been studied [5] as anionic extractants in  $[C_4mim][PF_6]$ /aqueous systems. The results appear to indicate that the metal ion transfer to the IL phase depends on the relative hydrophobicity of the metal complex;  $Hg-I$  complexes having the highest formation constants and highest distribution ratios [5].

### Organic extractants

Macrocyclic ligands such as crown ethers have been widely used for metal ion extraction. A series of 18-crown-6 ligands were investigated as extractants for  $Sr^{2+}$  and  $Cs^+$  in  $[C_nmim][PF_6]/HNO_3$  [4] with unexpected results which highlight the complexity of IL-based liquid/liquid systems and other system factors which have a dramatic effect on metal ion extraction and the stability of the IL.

Ionizable extractants can also be used to complex metal ions and increase lipophilicity. The azo dyes 1-(2-pyridylazo)-naphthol (PAN) and 1-(2-thiazolyl)-2-naphthol (TAN) are conventional metal extractants which quantitatively remain in  $[C_6mim][PF_6]$  when contacted with an aqueous phase between pH 1 – 13. Distribution ratios for  $Fe^{3+}$ ,  $Co^{2+}$ , and  $Cd^{2+}$  show that the metal ions can be extracted from the aqueous phase at basic pH and stripped from the IL under acidic conditions [5].

### Task Specific Ionic Liquids

Task Specific Ionic Liquid (TSIL) can be designed to incorporate a complexing functionality as an integral part of an IL [6]. These TSIL can be used as the extracting phase, or may be mixed with a second, more conventional IL to modify rheological properties. Figure 5 demonstrates the utility of one such TSIL prepared by tethering a ligating moiety to an imidazolium cation [6].

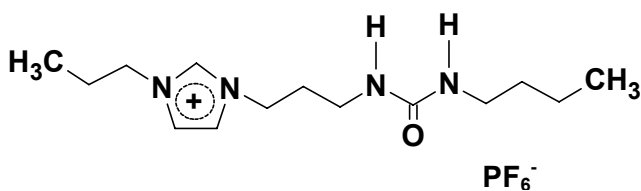
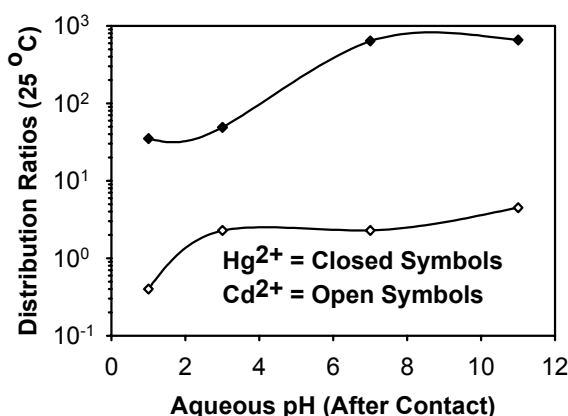


Figure 5.  $\text{Hg}^{2+}$  and  $\text{Cd}^{2+}$  distribution ratios with 1:1 TSIL: $[\text{C}_4\text{mim}][\text{PF}_6]$  as the extracting phase.

## CONCLUSIONS

At an early stage in a rapidly developing field of separation science, RTIL have clearly demonstrated versatility and promise for design of facilitated separation schemes. From the “green chemistry” standpoint, the chemical and physical properties of RTIL warrant their further study and exploration. The potential for RTIL is great, but these results must be considered with a certain degree of caution; there is a necessary, yet missing, fundamental understanding of these systems and cation-anion-solute interactions. There is, however, every reason for optimism; the number of new and exciting examples of RTIL separations schemes is limited only by time and imagination.

## ACKNOWLEDGEMENTS

This work is supported by U.S. Environmental Protection Agency through grant number R-82825701-0 and by the PG Research Foundation.

## REFERENCES

1. R. Sheldon (2001), *Chem. Commun.*, Advance article.
2. T. Welton (1999), *Chem. Rev.*, **99**, 2071-2083.
3. A. E. Visser, R. P. Swatloski, and R. D. Rogers (2000), *Green Chem.*, **2**, 1-4.
4. A. E. Visser, R. P. Swatloski, W. M. Reichert, S. T. Griffin, and R. D. Rogers (2000), *Ind. Eng. Chem. Res.*, **39**, 3596-3604.
5. A. E. Visser, R. P. Swatloski, S. T. Griffin, D. H. Hartman, and R. D. Rogers (2001), *Sep. Sci. Technol.*, **36**, 785-804.
6. A. E. Visser, R. P. Swatloski, W. M. Reichert, R. D. Rogers, R. Mayton, S. Sheff, A. Wierzbicki, and J. H. Jr. Davis (2001), *Chem. Commun.*, 135-136.
7. P. T. Anastas and J. C. Warner (1998), *Green Chemistry: Theory and Practice*, Oxford University Press, New York.
8. P. Bonhôte, A.-P. Dias, N. Papageorgiou, K. Kalyanasundaram, and M. Grätzel (1996), *Inorg. Chem.*, **35**, 1168-1178.
9. J. G. Huddleston, A. E. Visser, W. M. Reichert, H. D. Willauer, G. A. Broker, and R. D. Rogers (2001), *Green Chem.*, **3**, 156-164.

10. K. G. Furton and R. Morales (1991), *Anal. Chim. Acta*, **246**, 171-179.
11. S. K. Poole, P. H. Shetty, and C. F. Poole (1989), *Anal. Chim. Acta*, **218**, 241-264.
12. J. Sun, M. Forsyth, and D. R. MacFarlane (1998), *J. Phys. Chem. B*, **102**, 8858-8864.
13. J. Robinson and R. A. Osteryoung (1979), *J. Amer. Chem. Soc.*, **101**, 323-327.
14. C. M. Gordon, J. D. Holbrey, A. R. Kennedy, and K. R. Seddon (1998), *J. Mater. Chem.*, **8**, 2627-2636.
15. D. R. McFarlane, J. Sun, J. Golding, P. Meakin, and M. Forsyth (2000), *Electrochim. Acta*, **45**, 1271-1278.
16. J. D. Holbrey and K. R. Seddon (1998), *J. Chem. Soc., Dalton Trans.*, 2133-2140.
17. W. R. Pitner, D. W. Rooney, K. R. Seddon, and R. C. Thied (2000), *World Pat.*, No. 9941752.
18. L. M. Dutta (1994), M. Phil. Thesis, University of Sussex.
19. S. N. V. K. Aki, J. F. Brennecke, and A. Samanta (2001), *Chem. Commun.*, 413-414.
20. A. J. Carmichael and K. R. Seddon (2000), *J. Phys. Org. Chem.*, **13**, 591-595.
21. M. J. Muldoon, C. M. Gordon, and I. R. Dunkin (2001), *J. Chem. Soc. Perkin Trans. 2*, 433-435.
22. R. P. Swatloski, A. E. Visser, W. M. Reichert, G. A. Broker, L. M. Farina, J. D. Holbrey, and R. D. Rogers (2001), *Chem. Commun.*, 2070-2071.
23. J. G. Huddleston, H. D. Willauer, R. P. Swatloski, A. E. Visser, and R. D. Rogers (1998), *Chem. Commun.*, 1765-1766.
24. A. E. Visser, J. D. Holbrey, and R. D. Rogers (2001), *Chem. Commun.*, in press.
25. R. D. Rogers and S. T. Griffin (1998), *J. Chromatogr. B*, **711**, 277-283.



## TOWARDS "*IN SILICO*" DESIGN OF NEW POTENTIAL EXTRACTANTS USING CHEMICAL INFORMATICS METHODS

Alexandre Varnek, Georges Wipff and Vitaly P. Solov'ev\*

Université Louis Pasteur, Strasbourg, France

\* Institute of Physiologically Active Compounds, Chernogolovka, Russia

This article concerns the design of a prototype of information system for solvent extraction of metals including a comprehensive factual database, an expert system to analyse experimental extraction data and a generator of virtual libraries of extractants. A prototype of the solvent extraction database is developed. Each database record corresponds to one extraction reaction and contains three information parts (bibliographic, extraction system description and extraction properties) including chemical structural 2D and 3D information for extractants, as well as thermodynamic and kinetic data in textual, numerical and graphical forms. As expert system we use the Substructural Molecular Fragments method which models structure-property relationships using information retrieved from the database. Its performance is assessed on the distribution coefficients of Hg, In and Pt extracted by 26 phosphoryl-containing monopodands, and of uranium extracted by 32 mono- and tripodands or by 22 monoamides. The generation of virtual combinatorial libraries of potential metal binders using substructural molecular fragments is discussed.

### INTRODUCTION

A theoretical design of an extraction process with desired characteristics requires development of an information platform involving collection and generalization of available experimental data on extraction kinetics and thermodynamics (database), coupled with the chemical informatics methods that establish quantitative structure-extraction property relationships and generate potential metal binders. So far, such an ensemble of computational tools has not been developed.

This article concerns the development of an informational system for complexation/extraction of metals which involves three main elements: (i) a database, (ii) an expert system, and (iii) a combinatorial module. Figure 1 illustrates links between these modules. On the learning stage, a data set selected from the database is used by the expert system in order to establish relationships between structure of the molecules and their complexation/extraction properties. Then, the combinatorial module generates libraries of virtual compounds, from which the expert system selects "the best" potential metal binders using knowledge obtained on the learning stage. Tri-dimensional structures of selected candidates and explicit characteristics of host-guest interactions in solution could then be obtained using molecular modelling methods. New processes proposed on the basis of theoretical calculations can be experimentally tested, in turn providing the database with new information.

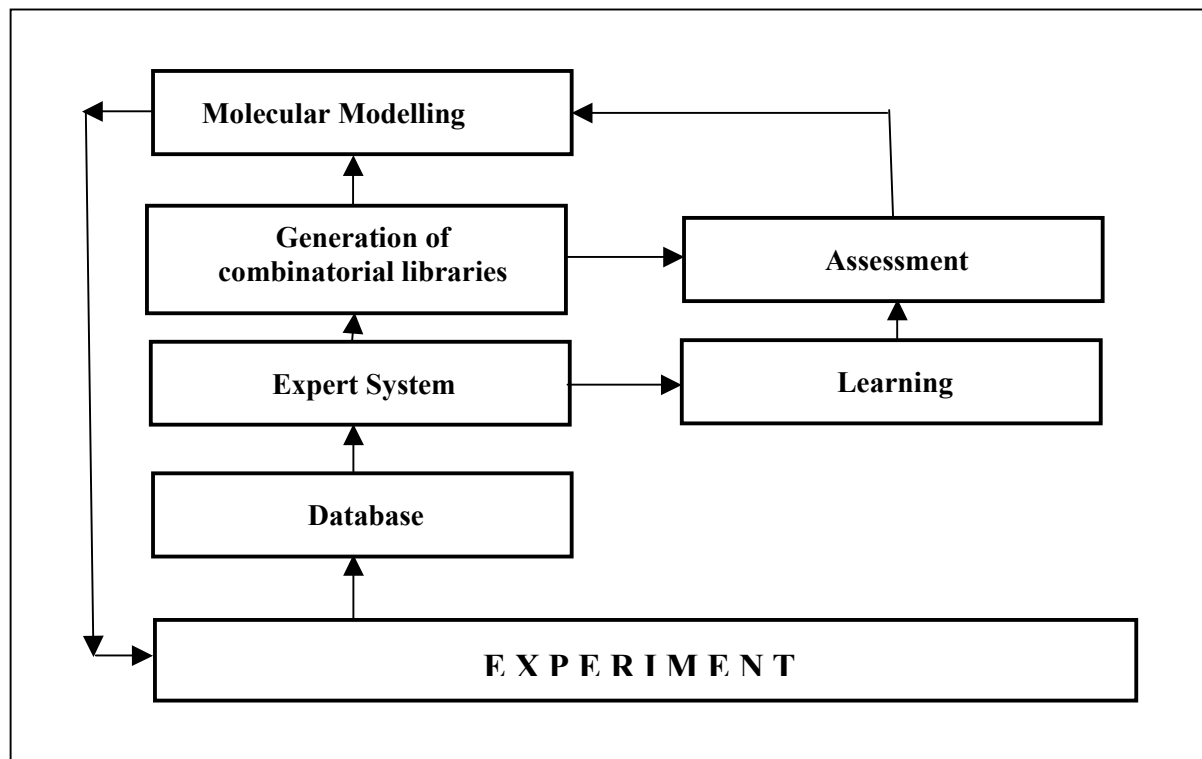


*Figure 1. Informational system on solvent extraction.*

## SOLVENT EXTRACTION DATABASE AND RELATED COMPUTATIONAL TOOLS

### Sources of Extraction Data in the Literature

A bibliographic search performed from 1970-1999 on solvent extraction with PASCAL, Science Citation Index and Chemical Abstracts databases resulted in (together with SEPSYS database [1, 2]) about 12,000 references, some of them concerning several individual extraction systems. This information could probably be enriched by numerous publications in the Russian and Chinese scientific literature which are not covered by "western" bibliographic databases (see [3-5]). According to our estimates, about 20,000 papers on extraction chemistry (including Russian and Chinese bibliographic sources, industrial reports, etc.) reviewing 50,000 – 70,000 extraction systems have been published since 1970.

### Solvent Extraction Database: Graphical Interface and Related Programs

A graphical user-friendly interface for a Solvent eXtraction Database (**SXD**) [6] has been designed using DELPHI programming platform for WINDOWS 98/2000/NT. It allows the user to load, to store in the SDF format [7] and to retrieve bibliographic and structural 2D and 3D information as well as experimental data presented in numerical and graphical forms, and to compare data from different records. **SXD** uses its own editor of 2D structures whereas the WebLabViewer Lite program [8], freely available from the INTERNET, is used for visualization and manipulation of 3D structures.

### Record and Queries Fields

Each **SXD** record describes one extraction system and contains three main parts: 1) bibliographic part including title, source (journal, book, proceedings), date of publication, authors and their addresses, keywords, abstract; 2) description of extraction system, *i.e.*, extractant(s): compound name, CAS number, empirical formula, molecular weight, 2D and 3D structures, concentrations (Figure 2); extracted species: cation, anion and their concentrations in aqueous phase; aqueous phase: background compound(s), their

concentrations, pH, ionic strength; organic phase: diluent(s) and their concentrations, background compounds and their concentrations; experimental conditions: temperature, pressure, experimental and equilibration technique; 3) extraction properties, *i.e.*, extraction equilibrium: reaction, thermodynamic data (extraction constant, free energy, enthalpy and entropy of extraction), partition coefficient and separation coefficient; extraction kinetics: extraction process, kinetic data (rate constant, activation free energy, enthalpy and entropy); other parameters represented as tables or graphs. The graphical interface of **SXD** allows experimental data to be stored in 85 fields grouped in 6 sections, and permits data-treatment to be carried out.

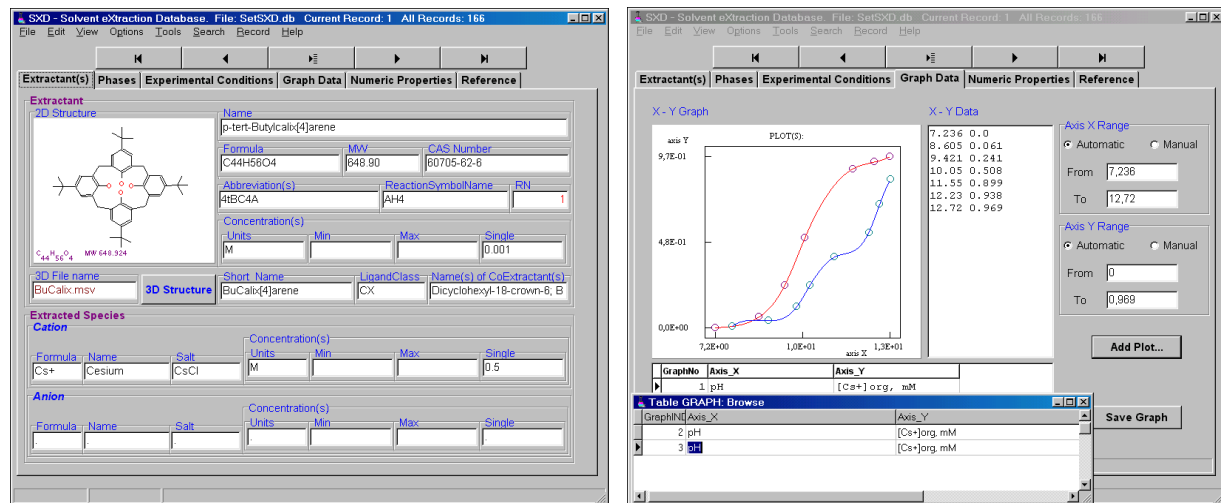


Figure 2. Two of six informational pages of Solvent Extraction Database.

### Retrieval of Data and Their Analysis

A search of information can be performed by any individual textual, numerical and 2D structure field or by their combinations using AND, OR and NOR Boolean operators. The search engine of **SXD** is based on the Borland Database Engine (BDE) for textual and numerical information, and tools developed here for 2D structural information. A CURVE option in the graphical interface of **SXD** performs a comparison of graphs from different records. It verifies if selected graphs have the same notation for "X" and "Y" axes, and superposes curves in a separate window using user-defined scale. If necessary, the program extrapolates or interpolates original curves. The program can also create the input files for commercial program packages for additional treatment of the curves. Data retrieved from the database can be used as an input for the TRAIL expert system discussed below.

## EXPERT SYSTEM

### Substructural Molecular Fragments Method and Related Computer Tools

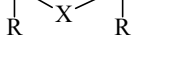
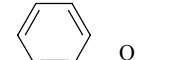
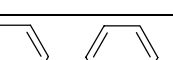
An expert systems on solvent extraction has to be able (i) to classify and generalize the data from SXD, (ii) to establish relationships between the composition of extraction systems and their properties, and, (iii) to propose new extraction systems possessing desirable properties. Development of such an expert system represents a difficult task due to the large number of variables affecting the thermodynamic and kinetic parameters of solvent extraction. In this paper, we present its first version based on recently developed Substructural Molecular Fragments (SMF) method [6-9] which allows one to model structure-property relationships for the series of different molecules participating in similar processes. Currently, this method uses only one variable-molecular structure of extractant, assuming that other components of extraction systems (nature of cation, anions, pH, diluent(s), background compounds, etc.)

and experimental conditions are the same for a given series of processes. The SMF method is based on the representation of molecular graph by fragments (atom-bond “sequences” or “augmented atoms”) and on the calculation of their contributions to a given property.

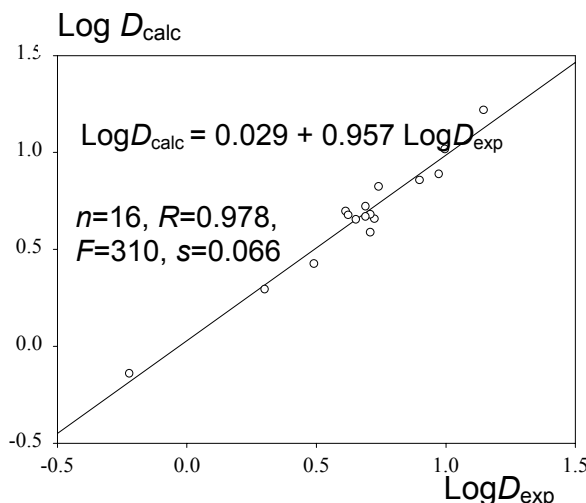
The TRAIL program [9] has been developed to calculate structure-property correlations based on the SMF partitioning. TRAIL generates all possible types of fragments coupled with one of three linear or non-linear fitting equations, which correspond to 147 fitting models involving 49 typical sets of fragments. Selection of the best models is based on statistical parameters such as correlation coefficient ( $R$ ), standard deviation ( $s$ ), Fischer's criterion ( $F$ ),  $R_H$ -factor of Hamilton, the fitness criterion of Kubinyi ( $F/T$ ) [10].

Earlier, we have shown that the SMF method represents an efficient tool to model the octanol/water partition coefficient, stability constants of host-guest complexes in water and in non-aqueous solution [6, 9].

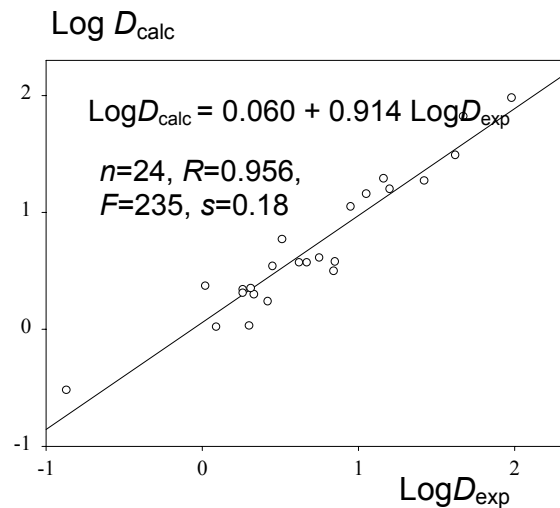
**Table 1.** Phosphoryl-containing podands and amides extraction properties of which were calculated by the SMF method.

Podands	R	X	n	Y	m
	a: b: c: d: e: f:	Ph Ph Tol Ph Ph Ph	CH <sub>2</sub> (CH <sub>2</sub> ) <sub>n</sub> -O-(CH <sub>2</sub> ) <sub>m</sub> (CH <sub>2</sub> ) <sub>n</sub> -O-(CH <sub>2</sub> ) <sub>m</sub> (CH <sub>2</sub> ) <sub>n</sub> -O-(CH <sub>2</sub> ) <sub>m</sub> (CH <sub>2</sub> -O-CH <sub>2</sub> ) <sub>3</sub> CH <sub>2</sub> (CH <sub>2</sub> -O-CH <sub>2</sub> ) <sub>3</sub> CH <sub>2</sub>	- 1 2 2 - -	- - - - - -
	a: b: c: d:	Ph Bu, Ph, Tol Ph Ph	(CH <sub>2</sub> ) <sub>n</sub> (CH <sub>2</sub> ) <sub>n</sub> (CH <sub>2</sub> ) <sub>n</sub> (CH <sub>2</sub> ) <sub>n</sub>	0 1 3, 5 1, 3-5	(CH <sub>2</sub> ) <sub>m</sub> (CH <sub>2</sub> ) <sub>m</sub> (CH <sub>2</sub> ) <sub>m</sub> (CH <sub>2</sub> ) <sub>m</sub>
	a: b: c: d: e:	Bu, Ph, Tol Bu, Ph Ph OEt, Ph, Tol Ph	(CH <sub>2</sub> ) <sub>n</sub> (CH <sub>2</sub> ) <sub>n</sub> (CH <sub>2</sub> ) <sub>n</sub> (CH <sub>2</sub> ) <sub>n</sub> (CH <sub>2</sub> ) <sub>n</sub>	0 1 2 0 1	O(CH <sub>2</sub> ) <sub>2</sub> O(CH <sub>2</sub> ) <sub>2</sub> O O(CH <sub>2</sub> ) <sub>2</sub> O(CH <sub>2</sub> ) <sub>2</sub> O O(CH <sub>2</sub> ) <sub>2</sub> O(CH <sub>2</sub> ) <sub>2</sub> O OCH <sub>2</sub> P(O)MeCH <sub>2</sub> O OCH <sub>2</sub> P(O)MeCH <sub>2</sub> O
			(CH <sub>2</sub> ) <sub>n</sub>	0, 1	

## Amides



## Podands



compound	exp	calc
	0.380	0.269
	0.602	0.625
	0.708	0.663
$R$	0.973	
$s$	0.071	

compound	exp	calc
	1.20	0.78
	-0.20	-0.38
	1.72	1.40
$R$	0.996	
$s$	0.11	

*Figure 3. Extraction of uranyl nitrate by amides in toluene (left) and by phosphoryl-containing podands in dichloroethane (right). Experimental data are taken from [11] (for amides) and [12] (for podands). The graphs show the correlation between experimental and calculated distribution coefficients ( $\log D$ ) on the learning stage, tables report the experimental (exp) and "predicted" (calc)  $\log D$  values for the molecules from the validation set.  $R$  and  $s$  are correlation coefficient and standard deviation for the correlation between experimental and predicted  $\log D$  values.*

### Assessment of Thermodynamics Parameters for Solvent Extraction

The SMF method was used to assess the extraction constants for the complexes of uranyl cation by phosphine oxides, and on distribution coefficients of Hg, In and Pt extracted by phosphoryl-containing monopodands, and those of uranium extracted by podands or by amides [6, 9]. Figure 3 illustrates the performance of this method to model distribution coefficients ( $\log D$ ) for  $\text{UO}_2^{2+}$  extraction. On the learning stage TRAIL selects the best (of

147) computational models to establish structure-property relationships for the molecules from the learning set (Table 1), which then are used for prediction calculations for the compounds from the validation set. One may see, that "predicted" log D values are very close to the experimental ones. Thus, the SMF method is a reliable tool for structure - extraction property modelling.

## GENERATION OF COMBINATORIAL VIRTUAL LIBRARIES

To generate virtual combinatorial libraries of potential extractants we used an algorithm based on the *Markush* structures [13]. It allows the user to attach a certain number of fragments to a molecular "core". A set of the extractants cores has been prepared analyzing all ligands from SXD database by the SMF partitioning. The generation module allows the user to select interactively molecular "bricks" and to launch computer "synthesis" of their possible combinations. The generated set of virtual compounds is saved in the SDF format to be used as an input by TRAIL for selection the best potential extractants.

## CONCLUSION

Three main elements of Informational system for solvent extraction (a prototype of a comprehensive database, an expert system, and a combinatorial module) have been developed and tested. This opens a perspective for computational design of new efficient extractant molecules.

## REFERENCES

1. W. J. McDowell, D. C. Michelson, B. A. Moyer and C. F. Coleman (1983), *Proc. Int. Solvent Extr. Conf. ISEC '83*, Amer. Inst. Chem. Eng., New York, pp. 257-258.
2. W. J. McDowell, D. C. Michelson, B. A. Moyer and C. F. Coleman (1983), *Solvent Extr. Ion Exch.*, 1-4.
3. Handbook on Solvent Extraction (Russ.) (1976), Vol. 1-3, ATOMIZDAT, Moscow.
4. E. A. Mejov (1999), Handbook on Extraction by Amines and Quaternary Ammonium Bases (Russ.), ENERGOATOMIZDAT, Moscow.
5. Z. I. Nikolotova (1999), Extraction of Lanthanides and Actinides by Neutral Extractants (Russ.), ENERGOATOMIZDAT, Moscow.
6. A. Varnek, G. Wipff and V. P. Solov'ev (2001), *Solvent Extr. Ion Exch.*, submitted.
7. A. Dalby, J. G. Nourse, W. D. Hounshell, A. K. I. Gushurst, D. L. Grier, B. A. Leland and J. Laufer (1992), *J. Chem. Inf. Comput. Sci.*, **32**, 244-255.
8. Molecular Simulations, Inc. (2000), <http://www.msi.com> (accessed June 2000).
9. V. P. Solov'ev, A. Varnek and G. Wipff (2000), *J. Chem. Inf. Comput. Sci.*, **40**, 847-858.
10. H. Kubinyi (1994), *Quant. Struct.-Act. Relat.*, **13**, 285-294.
11. C. Rabbe, C. Sella, C. Madic and A. Godard, (1999), *Solvent Extr. Ion Exch.*, **17**, 87-112.
12. A. N. Turanov, V. K. Karandashev and V. E. Baulin (1998), *Radiokhim.*, **40**, 36-43.
13. W. War (1997), *J. Chem. Inf. Comput. Sci.*, **37**, 134-140.



## ELECTRICAL TOMOGRAPHY AND OTHER MEASUREMENTS IN LIQUID-LIQUID SYSTEMS

W. J. Korchinsky and G. Bolton\*

Department of Chemical Engineering, UMIST, Manchester, UK

\*Industrial Tomography Systems, Manchester, UK

Successful application of electrical capacitance tomography (ECT) to a stirred tank and to a countercurrent flow column has demonstrated the usefulness of such a technique to monitoring performance of liquid-liquid contacting equipment. In addition, electrical resistance tomography (ERT) has been widely used for investigating the behaviour of stirred tanks. These techniques have the potential, matched by no other existing technique, to monitor dispersed phase distribution in a liquid-liquid contactor. The results to date obtained with an ECT system are summarised. The potential for this method and other tomographic measurements are discussed.

Beyond the tomographic measurements, there is a need for other measurements to provide the values for the many additional parameters that are required to make possible accurate predictions of liquid-liquid extraction equipment performance. Models are available to explain dispersion hydrodynamics, including breakup and coalescence, and mass transfer rates, for single component and multicomponent transfer. The number of parameters which must be available to use these models is daunting. Can sufficient measurements ever be made to provide accurate predictions of all parameter values?

### INTRODUCTION

The literature, and that includes the various Proceedings of ISECs over the years, contains numerous models of the liquid-liquid extraction process. Now successful modelling of a process implies that a check of the accuracy of the model can be made. Every model is represented by equations with defined variables and perhaps model parameters, which it is hoped can be measured and used in the checks of the model's accuracy. For instance, dispersed phase holdup may be predicted either directly, by correlations such as that of Kumar and Hartland [1], or through some model of dispersed phase behaviour such as the population balance equations [2] provide. In the former case one needs only to measure the holdup, and all the variables in the prediction equation, such as physical properties, operating conditions, etc. In the latter case one is presented with variables such as drop size distribution functions, breakage and coalescence frequencies, daughter drop size distributions and – how many more? Has the accuracy of the approach been adequately tested? How sensitive is performance to the change in value of each of the defined parameters – rarely mentioned! How many measurements would be required just to obtain a set of drop population balance equations which were accurate and reliable in predicting column hydrodynamic behaviour? On-line measurement of required variables may in some cases be attainable, but at what cost would attainment of all the desired measurements be achieved? Few have tackled the problem of prediction of performance for multicomponent systems.

Are pilot plants here to stay?

## HYDRODYNAMICS

On-line, non-invasive, measurement by Electrical Capacitance Tomography of dispersed phase hold-up fraction in a mixer and column extractor has been demonstrated successfully at UMIST [3]. Earlier attempts using other methods, such as the work on ultrasound techniques by Tavlarides and coworkers [4] looked promising, but the technique has not been applied widely. The use of electrical capacitance (ECT) and resistance (ERT) tomography techniques in process monitoring and control is a rapidly developing field, as expertly summarised by Williams and Beck in 1995 [5]. The techniques promise to give very useful on-line measurement of various processes in industrial plants. Most developed are ECT measurements in solid-gas systems, and ERT measurements in liquid-gas and miscible and immiscible liquid-liquid systems. The instantaneous, non-invasive, measurement of dispersed phase hold-up, this important parameter of extraction operation, would be of considerable interest to researchers and process operators.

At the last ISEC, the preliminary results of the application of ECT to liquid-liquid systems were announced [6]. Since, there has been further publication of results, which are now summarised. The typical capacitance sensor system employed is illustrated, for a mixer, in Figure 1. Eight to twelve capacitance electrodes, in this case of 50 mm height, are attached to the wall (in this case the outside of a Perspex wall). Except for a gap between electrodes, the electrodes cover the circumference of the vessel. To obtain accurate capacitance measurements between electrodes, grounded 'driven guards' are placed above and below the electrodes, and a screen to protect from outside interference is placed around the entire electrode system.

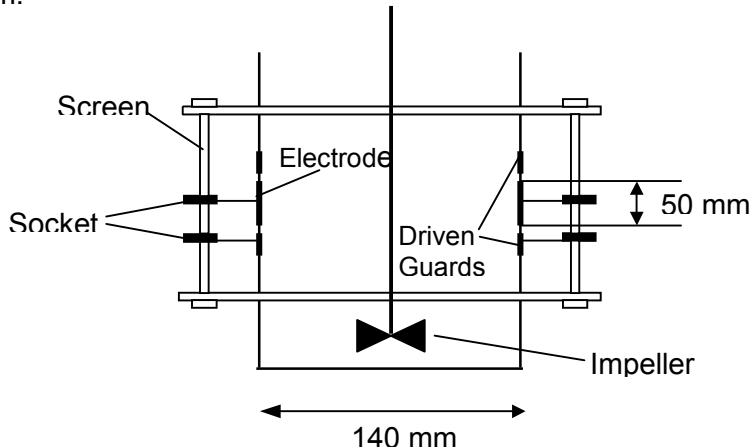


Figure 1. Detailed diagram of the stirred tank capacitance sensor.

The electrical signals from the capacitance sensors are transferred to a data acquisition system and then to a computer, where software is used to reconstruct images of electrical permittivity distribution which are translated into liquid phase distributions. Stirred tank dispersed phase content in a stirred tank can be averaged and illustrated on-line by colour projections of the capacitance data – see Figure 2. Accuracy of determination of the holdup is within 5%rel.

On-line visualisation of the unsteady state approach to steady state in a mixing tank has been demonstrated – over a 100 scans per second can be generated. Clear indications of phase mal-distribution in a counter-current flow column have been demonstrated. There was some difficulty applying the same system to a much larger (1 m) diameter vessel, but some progress was made. Multiple sets of sensors could be applied to give instant on-line-measurements of the change of hold-up with height. Multiple sets of sensors have been applied with an ERT system [7] to track variation with height. Images of vortex formation and

geometry, gas-liquid mixing, and brine tracer distribution were generated. Identification of non-standard conditions inside mixing vessels is a particularly important application of these measurement systems, aside from their potential use in providing quantitative information for model prediction methods. Other work at UMIST on tomographic techniques is in the area of two-phase and three-phase flows, fluidised beds, foams and froths.

- *Available* – On-line - dispersed phase hold-up measurement.

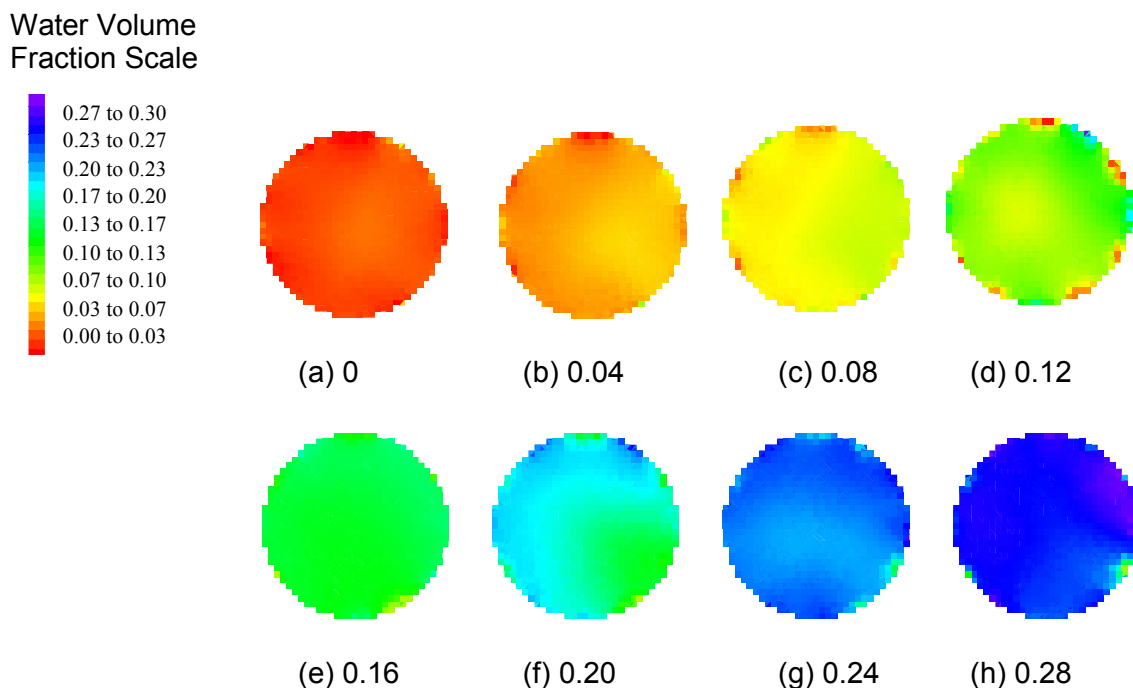


Figure 2. Colour-scale tomographic images of homogenous mixtures of water dispersed in kerosene for several water volume fractions.

### Drop Size and Population Balances

Measurement of drop sizes has largely been by photography, from outside the column, necessarily focussing on the drops near the column wall. Are they representative of all the drops in the column? There has been recent work reported on on-line drop size measurements by Ritter and Kraume [8], 2000 and by Wille *et al.* [9], 2001. The Kumar and Hartland [1] prediction equations, developed for the RDC, show the dependency on operating conditions and system physical properties, and a constant C, which depends on mass transfer direction.

But the Sauter-mean diameter does not in most cases accurately represent the performance of the entire dispersed phase, so one needs to develop prediction methods for the measured drop size distribution. The Mugele-Evans [10] distribution function has largely been employed. When drop size control at the inlet is maintained [11], values of the function parameters may be determined which give good predictions of drop size distribution and column performance. But the distribution function parameters have not been widely determined.

- *Available* - Sauter mean drop size, column averages
- *Required* - Drop size distribution function parameters

But the drop size distribution changes, in most cases, with column position – in particular with column vertical position. How do we model this change? Drop population balances have been developed by many researchers– see Kumar and Hartland [12], Ribeiro *et al.* [13], Hoting and Vogelpohl [14], Shen and Tavlarides [15] and Zamponi *et al.* [16]. The developed equations model the change in size distribution, and dispersed phase holdup, but require the values of a number of additional parameters. From a given drop size distribution, the birth and death rates of each size of drops determine the distribution changes with height. An example of the equations developed [13] is given below - the original may be consulted for an explanation of all the variables used. It is given here only to illustrate the complexity of the calculations required.

$$\begin{aligned} \frac{\partial}{\partial t} f(v, c, \tau, t) + \frac{\partial}{\partial c} [f(v, c, \tau, t) \dot{c}] + \frac{\partial}{\partial \tau} f(v, c, \tau, t) = \\ 2 \int_{v' > v} \int_{c'} \int_{\tau'} f(v', c', \tau', t) g(v') \beta(v|v') \delta(\tau) \delta(c' - c) dv' dc' d\tau' + \\ 2 \int_{v' > v} \int_{c'} \int_{\tau'} \int_{\tau''} f(v', c', \tau', t) f\left(v - v', \frac{vc - v'c'}{v - v'}, \tau'', t\right) h(v', v - v') \lambda(v', v - v') \delta(\tau) dv' dc' d\tau' d\tau'' + \\ \frac{1}{\theta} f_{\text{feed}}(v, t) \delta(\tau) \delta(c - c_{\text{feed}}) - f(v, c, \tau, t) \left[ g(v) + \int_{v'} \int_{c'} \int_{\tau'} f(v', c', \tau', t) h(v, v') \lambda(v, v') dv' dc' d\tau' + \frac{1}{\theta} \right] \end{aligned} \quad (1)$$

#### *Required*

- Drop breakage rate
- Number of daughter drops produced by breakup of a drop of given volume
- Drop probability density
- Drop collision frequency
- Coalescence frequency

Have they all been measured? Certainly not! These are still mostly empirically set and the theory tested by how well the measured change in drop size distribution is predicted with a particular set of these parameters. But widespread applicability is some way off. To quote Gourdon *et al.* [17], “If ...one considers the gap between the demand of the scientists and the impact on the economy of the sort of the results that could be obtained, it is questionable whether the endeavour is worth the trouble”!

## MASS TRANSFER

To develop models which predict accurate mass transfer rates, the hydrodynamic models need to be integrated into an appropriate mass transfer model. The model must then accurately predict mass transfer driving forces and rates. To determine driving forces, equilibrium concentrations and therefore chemical potentials in highly non-ideal liquid-liquid systems must first be determined.

### **Equilibrium Prediction**

To be able to design from first principles, it must be possible to predict driving forces, or departure from equilibrium conditions. Although measurements of equilibrium concentrations can be made for specific systems, a model of liquid phase behaviour which will accurately predict these is still not available. Additional data which can be used to develop a suitable model are needed.

*Required*

- “Chemical potential ” or activity coefficients for highly non-ideal liquid systems

### Mass Transfer Rate Prediction

#### Single-component mass transfer

A relatively simple model of mass transfer in a continuous contactor has been developed by Chartres and Korchinsky [18]. Differential equations representing solute balances in the dispersed phase droplets, and the continuous phase, were written. With measured drop size distributions, dispersed phase holdup, and concentration profiles, these equations, with appropriate boundary conditions, may be solved to generate values of the continuous phase axial dispersion coefficient, and drop size-dependent mass transfer coefficients [19]. These equations assume no change with height, no coalescence and break-up, and no interaction between species transferring in a multicomponent system.

*Required:*

- Drop size dependent mass transfer coefficients
- Continuous phase axial dispersion coefficients

#### Multicomponent mass transfer

To model multicomponent mass transfer the Maxwell-Stefan equations are recommended. The Maxwell-Stefan equations have been developed by Krishna *et al.* and are well explained in books written in 1993 [20] and 2000 [21]. The basic equation for diffusion in multicomponent systems is

$$F_i = - \frac{d\mu_i}{dz} = - RT \frac{d \ln a_i}{dz} = - RT \frac{d \ln \gamma_i x_i}{dz} = \sum_{j \neq i} \zeta_{i,j} x_j (u_i - u_j) \quad (2)$$

This can be rearranged to a form which can be used more readily,

$$f_i = F_i c x_i = - c R T x_i \frac{d \ln \gamma_i x_i}{dz} = R T \sum_{j \neq i} \frac{x_j N_i - x_i N_j}{\mathfrak{D}_{i,j}} \quad (3)$$

where the friction coefficient,  $\zeta$ , has been replaced by the Maxwell Stefan diffusion coefficient,  $\mathfrak{D}_{i,j}$ , ie  $\mathfrak{D}_{i,j} = RT / \zeta_{ij}$ . The net component fluxes,  $N_i$ , have replaced the products,  $c x_i u_i$ . It is not possible to measure the Maxwell-Stefan diffusivities directly, but for binary systems they can be calculated from measured Fick Diffusivities,  $D_{i,j}$  as follows

$$\Gamma = 1 + x_i \frac{d(\ln \gamma_i)}{dx_j} = \frac{D_{i,j}}{\mathfrak{D}_{i,j}} \quad (4)$$

where  $\Gamma$  is the “thermodynamic correction factor”. A matrix of mass transfer coefficients may also be defined in terms of the Stefan-Maxwell diffusivities.

*Required:*

- Multicomponent Maxwell-Stefan diffusivities (or the equivalent mass transfer coefficients)
- Activity coefficients and Fick diffusivities

Applications of the Maxwell-Stefan approach to multicomponent liquid-liquid systems have been reported, by Negri and Korchinsky [22], Taylor and Krishna [20], Brodkorb and Slater [23], Wesselingh and Krishna [21], and Uribe-Ramirez and Korchinsky [24], but this work has only scratched the surface. As stated by Wesselingh and Krishna [21], the prediction of rates in multicomponent systems is unreliable because there is a “lack of good data on multicomponent diffusivities” (or mass transfer coefficients).

## CONCLUDING REMARKS

There are a large number of variables which must be predicted to apply developed models successfully. There is still little confidence in applying these models widely. Furthermore, there are variables which may affect performance considerably and are not "modelled". To mention only a few - concentration of cruds, slimes, fines, surfactants, and colouring (black!) agents in the mixture, and the accumulated effect of equipment wall ageing, distributor clogging, etc! More models and measurements? Or pilot plant performance studies?

## ACKNOWLEDGEMENTS

The authors are grateful to the EPSRC and Separation Processes Service, AEA Technology for their financial support of the electrical capacitance studies.

## REFERENCES

1. A. Kumar and S. Hartland (1994), Liquid-Liquid Extraction Equipment, J. C. Godfrey and M. J. Slater (eds.), John Wiley & Sons, pp. 625-735.
2. K. J. Valentas and N. R. Amundson (1966), *Ind. Eng. Chem. Fund.*, **5** (4), 533-542.
3. G. T. Bolton, W. J. Korchinsky, and R. C. Waterfall (1999), *Trans. IChemE.*, **77A**, 699-708.
4. J. C. Bonnet and L. L. Tavlarides (1987), *Ind. Eng. Chem. Res.*, **26**, 811-815.
5. R. W. Williams and M. S. Beck (1995), Process Tomography Principles, Techniques and Applications, Butterworth-Heinemann, Oxford.
6. G. T. Bolton, W. J. Korchinsky, R. C. Waterfall and P. D. Martin (1999), *Proc. Int. Solvent Extraction Conf.*, Barcelona.
7. P. J. Holden, M. Wang, R. Mann, F. J. Dickin and R. B. Edwards (1999), *Trans. IChemE.*, **77**, 709-712.
8. J. Ritter and M. Kraume (2000), *Chem. Eng. Technol.*, **23**, 579-581.
9. M. Wille, G. Langer and U. Werner (2001), *Chem. Eng. Technol.*, **24**, 475-479.
10. R. A. Mugele and H. D. Evans (1951), *Ind. Eng. Chem.*, **43**, 1317-1324.
11. W. J. Korchinsky (1994), Chapter 9, Liquid-Liquid Extraction Equipment, J. C. Godfrey and M. J. Slater (eds.), John Wiley & Sons, pp. 247-275.
12. A. Kumar and S. Hartland (1999), *Ind. Eng. Chem. Res.*, **38**, 1040-1056.
13. L. M. Ribeiro, P. F. R. Regueiras, M. M. L. Guimarães and J. J. C. Cruz-Pinto (2000), *Advances in Engineering Software*, **31**, 985-990
14. B. Hoting and A. Vogelpohl (1996), *Proc. Int. Solvent Extraction Conf.*, Melbourne, pp. 231-236.
15. W-P Shen and L. L. Tavlarides (1996), *Proc. Int. Solvent Extraction Conf.*, Melbourne, pp. 813-818.
16. G. Zamponi, J. Stichlmair, A. Gerstlauer and E. D. Gilles (1996), *Proc. Int. Solvent Extraction Conf.*, Melbourne, pp. 1049-1054.
17. C. Gourdon, G. Casamatta and G. Muratet (1994), Chapter 7, Liquid-Liquid Extraction Equipment, Ed: J. C. Godfrey and M. J. Slater, John Wiley & Sons, pp.137-226.
18. R. Chartres and W. J. Korchinsky (1975), *Trans. Inst. Chem. Eng.*, **53**, 237-254.
19. C. H. Young and W.J. Korchinsky (1985), *J. Chem. Tech. Biotech.*, **35a**, 347-357.
20. R. Taylor and R. Krishna (1993), Multicomponent Mass Transfer, John Wiley and Sons, NY.
21. J. A. Wesselingh and R. Krishna (2000), Mass Transfer in Multicomponent Mixtures, Delft University Press, Amsterdam.
22. D. Negri and W. J. Korchinsky (1986), *Chem. Eng. Sci.* **41**, 2401- 2406.
23. M. J. Brodkorb and M. J. Slater (1999), *Proc. Int. Solvent Extraction Conf.*, Barcelona.
24. A. Uribe-Ramirez and W. J. Korchinsky (2000), *Chem. Eng. Sci.*, **55**, 3319-3328.



## SOLVENT IMPREGNATED RESINS: PERFORMANCE AND ENVIRONMENTAL APPLICATIONS IN METAL EXTRACTION

The late Abraham Warshawsky and Jose L. Cortina\*

Department of Organic Chemistry, Weizmann Institute of Science, Rehovot, Israel

\*Universitat Politecnica de Catalunya, Barcelona, Spain

In this paper the extraction performance of solvent impregnated resins in heavy metal removal and separation in environmental applications is presented. Solvent impregnated resins were prepared by both direct adsorption of the active component onto macroporous polymeric supports and by co-polymerization of styrene and divinylbenzene in the presence of the active component. Resins based on two types of extractant functionalities (phosphoric and phosphinic acids) were evaluated. Separation of Zn, Cu and Cd was achieved using pH changes as parametric pumping and by modifying ligand metal extraction properties using mixtures of organophosphorous extractants.

### INTRODUCTION

Novel metal decontamination and water treatment technologies are required for a range of purposes in the European Union and with special needs in the metallurgical and mining sectors [1]. Both types of industries are characterised by using huge volumes of water streams with high contents of strong acids and bases, high content of electrolytes and moderate to low levels of metal ions. Many of the separation, transformation and destruction processes required already exist, such as ion exchange (IX), solvent extraction (SX) and membrane filtration processes. However, improvements are needed, notably in economic efficiency of the treatment and minimisation (volume reduction)/neutralisation/further processing and treatment of by products. This is reflected in the large number of scientific contributions during the last decades and the impetus is in the development of new separation chemistry techniques, particularly for treatment of liquid wastes and effluents [2-3]. These advances result from recent progress in the field of fundamental chemistry involving the synthesis of new classes of extractants, exchangers and absorbents capable of significantly improving the selectivity and the efficiency of a number of separation techniques (SX, supported liquid membranes, etc.). Despite the high selectivity of the chelating and IX resins, the application of these resins in separation processes on a technological scale seems to be limited by the complexity of their synthesis, the very often difficult and time-consuming procedures needed for covalently linking the functional group to the backbone of the resin, and their high cost.

Taking into account these limitations in the preparation of chelating and IX resins and the recent advances in the synthesis of new organic reagents for SX, which are bound to significantly improve both separation efficiency and selectivity for a wide range of chemical species, the development of solvent impregnated resins (SIR) as a link between SX and IX processes has become an important field of development in separation science. The place and limits of these materials in the domain of metal recovery methods covering the IX and SX sectors are shown in Figure 1 [4]. As can be seen the role of SIR materials will be closely related to that played by IX covering the low level range (below 1 g/l).

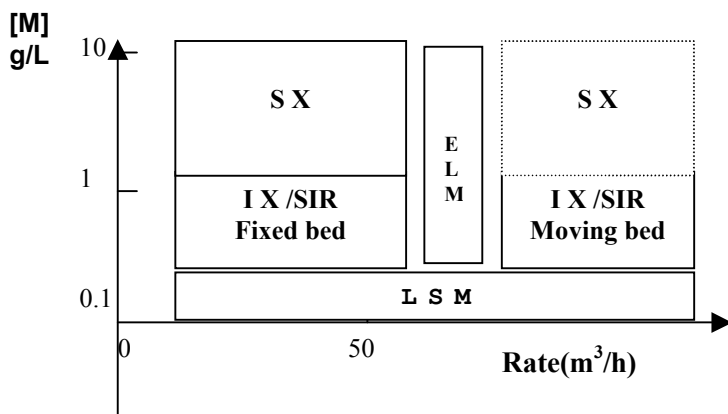


*Figure 1. Semiquantitative application limits for selected metal separation processes. (Ion Exchange(IX), Solvent Extraction (SX), Solvent Impregnated Resins (SIR), Supported Liquid Membranes (SLM) and Emulsified Liquid Membranes (ELM)).*

Since SIRs are posed in competition to IX materials and liquid-liquid metal extractants dissolved in organic diluents, SIR development efforts have been directed mainly to evaluation and performance studies. Preparative procedures remained simple and are mainly directed towards improvement in metal binding efficiencies and separation factors and are published elsewhere [5-6]. Reactive polymer (anion exchangers) supports have become important since they were shown to improve resin process kinetics and efficiency in removing metal ions from ppm or ppb range concentrations. Some of this work now in press [7-8] concerns mainly the newly discovered phenomena of extractant migration within SIR containing DEHPA, DEHTPA and DEHDTPA and comparison between SIR and their chemically-bound analogues. While important progress has been achieved in applications of SIR in analytical chemistry [6] maturation of such resins for hydrometallurgical applications are still to be achieved. More recently, new solutions to improve the separation of mixtures of dissolved heavy metals by means of parametric pumping with variation of pH have been presented for IX resins [12]. The most important property of this method is the fact that it is a regenerant-free separation or ion exchange process. Separation is possible if a parameter of substantial influence on the sorption equilibrium is varied.

In the present paper the application of SIRs in the removal and separation of toxic and heavy metal ions (Zn, Cu, Cd) present in many industrial streams at low levels is presented. Acidic organophosphorous derivatives (DEHPA, Cyanex 272) have been used as active component due to their high affinity and complexing properties with heavy and toxic metal ions and also for their suitable properties in the stripping step. The possibility of using parametric pumping with variation pH is presented.

## NON-FERROUS METAL REMOVAL FROM INDUSTRIAL LIQUORS

Many non-ferrous metal industries are generating basically two types of metal containing effluents: highly concentrated liquors from spent baths of electroplating or tanning operations and diluted streams typically generated by rinsing operations. While the first type are directed to recovery operations such as chemical precipitation, electrowinning or cementation, the second type of liquor needs a pre-concentration step in order to reduce volume and to achieve suitable concentrations to be treated like the spent baths. Additionally, as those diluted streams could contain mixtures of metal ions, a separation step is required to achieve suitable conditions for subsequent recovery. Metal ion mixtures are also found in acidic waters generated by dedusting off gases of many domestic and industrial waste incineration plants, thermal power stations and metallurgical plants. These solutions contain a wide range of non-ferrous metals such as Zn, Cd, Pb, Cu in the order of 0.5 to 0.01 g/L and non-metals such as As, Sb and Bi, typically of the order 0.01 to 0.001 g/L. The main components of such a stream are summarised in Table 1.

*Table 1. Typical composition of acidic metallurgical waste effluent.*

Metals (M): 0.1-0.5 g/l	Non metals (NM): < 0.01g/l	Common anions (A <sup>a-</sup> ) (150 to 0.1 g/l)	Common cations (C <sup>c+</sup> )(100 to 0.1 g/l)
Zn	As	Cl <sup>-</sup>	Ca <sup>+2</sup>
Cu	Sb	SO <sub>4</sub> <sup>-2</sup>	Na <sup>+</sup>
Cd	Bi	NO <sub>3</sub> <sup>-</sup>	Mg <sup>+2</sup>
Pb	Se		H <sup>+</sup> (pH (1-6))

\*Variation ranges are indication of typical values

Although traditionally these solutions are treated by the physico-chemical process of precipitation with lime, current efforts are directed to the selective recovery and separation of the metals Zn, Cd and Pb for subsequent treatment by electrolysis (for Zn, Pb, Cu) or cementation by powder metallic zinc (for Cd). Those effluents with relatively low levels of metal ions cannot be treated efficiently by SX but can be treated by transforming the SX system into the corresponding SIR system.

### Separation and Preconcentration of Heavy Metals

A great effort has been directed to the separation of Zn from Cu and Cd, and problems were encountered when applying strong cation exchange (bearing sulphonate acid groups) or chelating (bearing carboxylic, diiminoacetic or aminophosphinic groups) resins. Benefiting from the extensive extraction studies of Zn, Cu and Cd using organophosphorus extractants in SX applications [13] significant pioneering work was initiated on the homologues SIR systems [5-8]. Impregnated resins containing acidic organophosphorous derivatives (Cyanex 272 and DEHPA) impregnated onto Amberlite XAD2 or Levextrel type resins (Lewatit 1026 OC, Lewatit TP807) were made and tested. The behaviour of such materials (in terms of selectivity) was controlled modulating polymer properties or by modifying extraction properties or by using mixtures of extractants [6].

The extraction dependence of divalent metals on SIR containing acidic organophosphorous extractants on the acidity of the aqueous solutions is described by the following general reaction:



The pH<sub>50</sub> (pH for which a 50% extraction efficiency is achieved) has been used to measure the separation factors. A practical ΔpH<sub>50</sub> (M<sub>1</sub>/M<sub>2</sub>)≥1 allows an effective separation efficiency of M<sub>1</sub> (>95%) over M<sub>2</sub> (<5%). The pH<sub>50</sub> and ΔpH<sub>50</sub> values for the set of selected metals for SX, IX and SIR systems (Table 2) shows that sulphonate, phosphoric and carboxylic groups do not allow efficient separation factors, yet phosphinic acid extractants such as Cyanex 272 could offer an appropriate answer to solve this separation problem.

The pH dependence functions for the selected group of metals (Table 1) were determined by batch experiments. Results for Cyanex 272 impregnated resins with the highest separation factors are shown in Figure 2. The extraction function of Zn(II) in relation to Cu(II) and especially to Cd(II) makes this resin suitable for use in the separation of this metal couple.

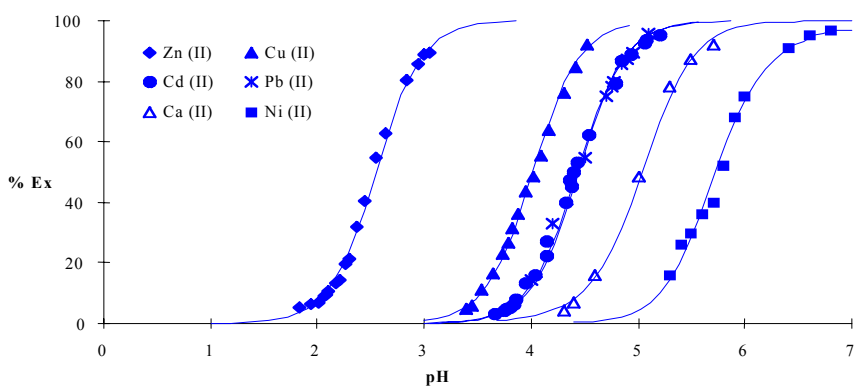


*Figure 2. Extraction of Zn (II), Cu (II), Cd(II), Pb(II), Ca(II) and Ni(II) as a function of pH for Cyanex 272 impregnated resin.*

*Table 2. ΔpH<sub>50</sub> of Zn(II), Cu(II) and Cd(II) with solvent impregnated and Levextrel resins.*

Resin	Zn/Cd	ΔpH <sub>50</sub> Zn/Cu	Cd/Cu	%M <sub>1</sub> /M <sub>2</sub> Zn/Cd	(pH <sub>opt</sub> ) Zn/Cu
<b>Impregnated Resins</b>					
DEHPA / XAD2	0.8	0.5	0.3	85/5 (2)	85/20 (2)
Lewatit 1026 (DHEPA)	1	0.6	0.4	85/10 (2)	85/10 (2)
Cyanex 272 / XAD2	2.0	1.3	0.6	99/1 (3.5)	99/5 (3)
Lewatit TP807 (Cyanex 272)	2.0	1.5	0.5	99/1 (3.5)	99/5 (3)
<b>Ion Exchange Resins</b>					
Lewatit TP207*	1.2	0.8	0.4	NA**	NA**

\* Lewatit 207, chelating resin containing aminophosphinic groups.

NA\*\* no available data.

The extraction efficiency of SIR resins prepared by direct adsorption of Cyanex 272 onto a macroporous polymeric support of styrene-divinylbenzene (Amberlite XAD2) and those prepared by polymerisation of styrene-divinylbenzene in the presence of Cyanex 272 (Levextrel type) were evaluated in column operations. The breakthrough curves obtained for solutions containing Zn(II), Cu (II) and Cd(II) in the low concentration range 10-50 ppm are shown in Figure 3.

In column runs known amounts of swollen resins (10 g) were slurry-packed in an Omnifit borosilicate glass column fitted with porous 25-micron polyethylene frits and Teflon end pieces. A peristaltic pump at the column entrance delivered solution at constant flow rate of 0.5 to 1 mL/min. Metal ions were determined by following the change in concentration with throughput of the samples collected to follow the extraction histories. After each metal extraction experiment, the flow of the metal solution was stopped and the resin washed successively with water, stripping solution at flow rate of 1 mL/min through the resin bed in the column. Metal ion concentration was determined in all the samples.

As can be seen metal capacity of the SIR resins is highly dependent on operating pH and Cd(II) extracted at the higher pH values show lower resin loadings. Metal solutions were in sulphate media (1000 ppm) and pH was adjusted to 5.5 by adding sodium hydroxide. As the metal extraction process progresses the metal/proton exchange reaction takes places, the increased proton concentration causes decreased pH of the feed solution which in turns results in favoured extraction of Zn(II) and Cu(II) at lower pH values. Consequently, relative high metal loadings between 20 and 30 g metal/kg resin were obtained.

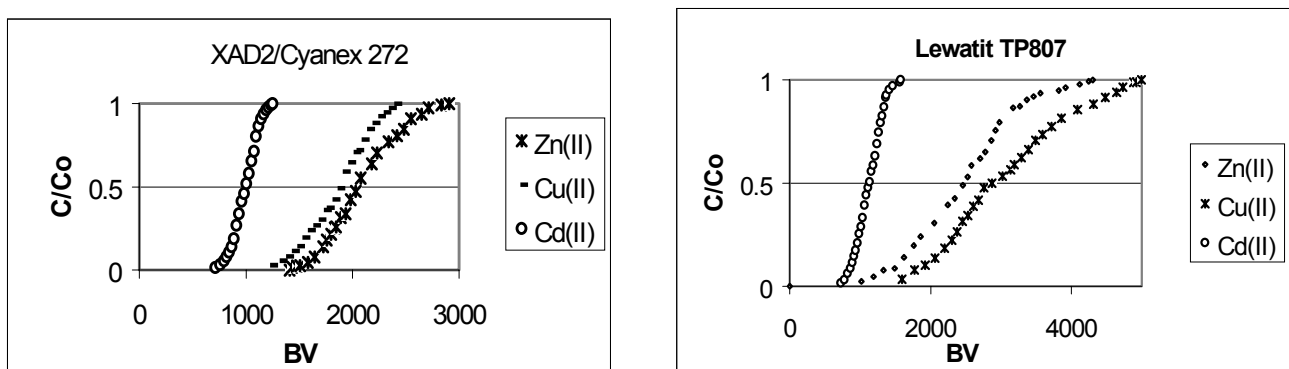


Figure 3. Breakthrough curves of XAD2/Cyanex 272 and Levextrel TP807'84 resins.

Elution runs for single systems were performed using 1 mol/L HCl solutions and results are shown in Figure 4. Concentrated solutions containing 4 g/L metals can be obtained.

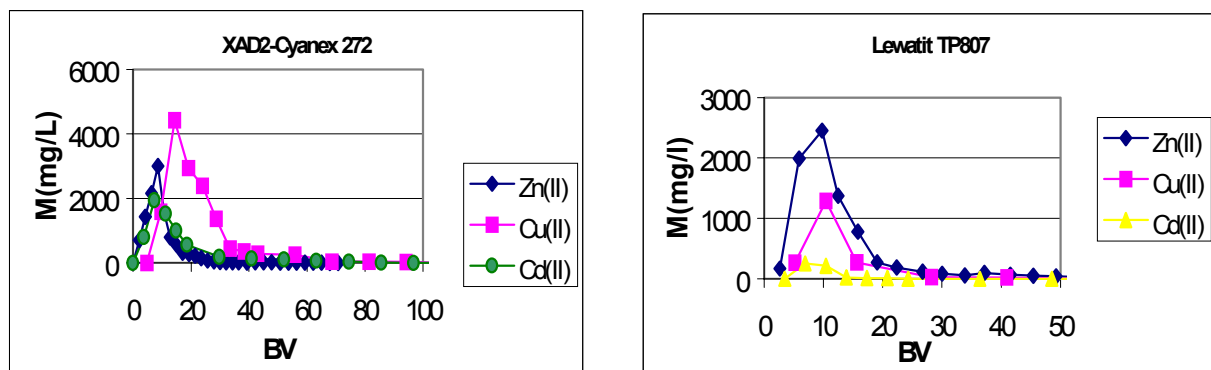


Figure 4. Breakthrough and elution curves of XAD2/Cyanex 272 and Levextrel TP807'84 resins.

Preconcentration factors (PF) achieved are shown in Table 3. Higher preconcentration factors obtained operating with lower flow rates allow the achievement of concentrated solutions (up to 10-20 g/L) suitable for subsequent cementation or electrowining steps.

Table 3. Preconcentration factors (PF) of Zn(II), Cu and Cd(II) with SIR.

Resin	PF (Zn(II))	PF(Cu(II))	PF(Cd(II))
Reagent: DEHPA: XAD2/DEHPA	40	45	45
Lewatit 1026 OC	60	70	60
Reagent: Cyanex 272: XAD2/Cyanex	65	70	50
Lewatit TP807	60	55	80

The strong acid dependency observed during the column operation was evaluated as a possible separation method to be efficiently applied using parametric pumping. Only few publications in the literature describe the variation of weak parameters (e.g., variation of ionic strength and the change of molecular sizes) as a factor in parametric pumping that will allow separation of heavy metals. The main current activity in this direction was only the use of pH as a controlling factor in parametric pumping. In this study parametric pumping assays were performed by dividing an original solution into two half volumes. Both half volumes were by turns contacted with a Cyanex 272 resins and an exchange reaction occurs during each contact. As favourable parameter values were adjusted, Cu and Cd were transported from one solution to the other whereas Zn was transported in the opposite direction.

Direct parametric pumping assays were performed by simply varying the pH of the solutions. Using more strongly acidic impregnated resins containing DEHPA, a significant effect was found when the hydrogen ion concentration of low pH solution exceeded the concentration of the heavy metals by some magnitude. On the other hand, the pH of the higher-pH solution is limited by the precipitation of heavy metal hydroxides, and additionally increases the DEHPA molecules distribution to the aqueous phases. Direct efficient mode separations were not possible using resins containing phosphoric groups (e.g., DEHPA) and effort was directed to resins containing a weaker acidic organophosphorous function such as phosphinic groups (Cyanex 272). Parametric pumping experiments were carried out at laboratory scale using 1-litre volume containers. The pH was controlled and automatically adjusted by means of a pH-controlling unit with two dosage pumps for adding acid or base if required. In each half-cycle, the stirrer with the resin material rotated for 120 minutes due to the kinetic behaviour of those resins, in each solution. Between the contacts with the two solutions, the liquid in the resin packing was centrifuged off.

Separation experiments of the couples Zn/Cu and Zn/Cd with Lewatit TP807 using the direct mode were carried out and results are shown in Figures 5 and 6.

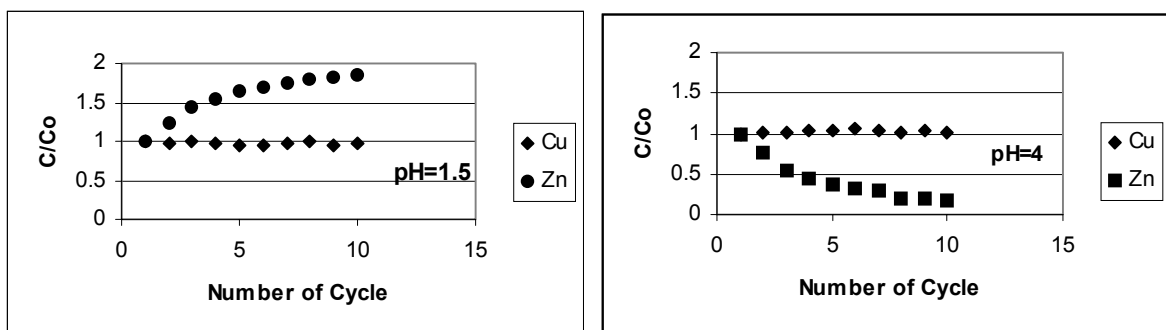


Figure 5. Parametric pumping assays for the system Zn/Cu Lewatit TP807 in the two half volumes system.  $C_o$  (Zn(II)) =  $C_o$  (Cu(II)) = 2 mmol/L.

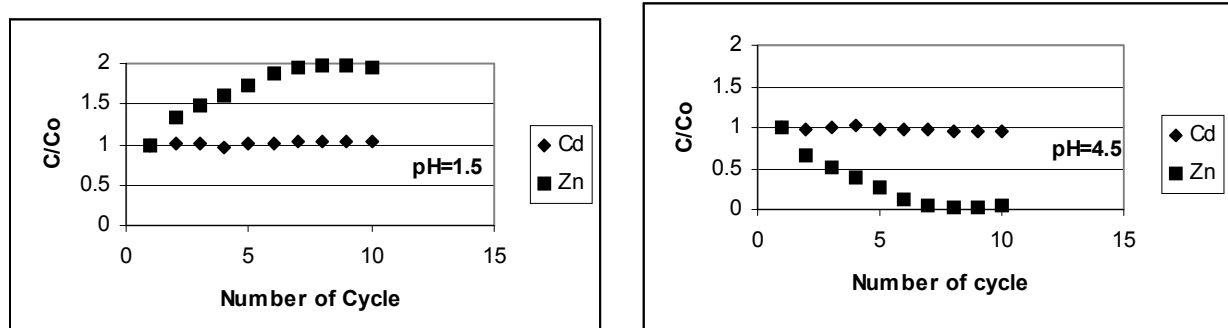


Figure 6. Parametric pumping assays for the system Zn /Cd and Lewatit TP807 in the two half volumes system.  $C_o$  (Zn(II)) =  $C_o$  (Cd(II)) = 2 mmol/L.

Separations in the direct mode were achieved. The pH values were adjusted according to the pH-dependency functions of Cyanex 272 resins given in Figure 2. Figure 5 shows the separation of Zn from Cu. Zn is extracted at pH 3 whereas the extraction of Cu commenced only after reaching pH 4 or higher. Zinc therefore was transported into the pH 1.5 vessel. After ten cycles, the pH 4 vessel contained a Cu(II) solution with 2% Zn(II). Similarly, Figure 6 shows the separation of Zn from Cd, using in this case, a vessel of pH 4.5 where Zn was transported into the pH 1.5 vessel. After ten cycles, the pH 4.5 vessel contained a Cd(II) solution with 1% Zn(II).

## CONCLUSIONS

Solvent impregnated resins and Levextrel-type resins containing phosphoric and phosphinic derivatives can be used to efficiently concentrate diluted solutions of Zn, Cu and Cd and when using phosphinic containing resins efficient separation factors of Cd over Zn could be achieved if acidity of the solution could be controlled. Parametric pumping experiments to achieve these objectives were assayed and preliminary results obtained open new ways to successfully achieve the needed pH control.

## ACKNOWLEDGEMENTS

We wish to acknowledge to Bayer AG, Rohm & Haas for resin supply and to Cytec for extractants supply. This work was supported by CICYT Project QUI99-1025-C03-02 (MEC, Spain) and by MOSA in Israel and MAE in Spain for grants allowing an exchange research collaboration program. A. Warshawsky was the holder of the Rebbecca and Israel Sieff professorial chair in organic chemistry. His colleagues and friends were saddened to learn of his death during publication of this manuscript.

## REFERENCES

1. Environmental Signals 2000 (2000), Environmental Assessment Report No 6, European Environment Agency, Copenhagen.
2. G. Tiravanti, D. Petruzzelli and R. Passino (1996), *Waste Manag.*, **16**, 597-605.
3. H. J. Bart and A. Schoneberger (2000), *Chem. Eng. Technol.*, **23**, 653-660.
4. A. Warshawsky (1981), Ion Exchange and Solvent Extraction, Vol. 8, J. A. Marinsky and Y. Marcus (eds.), Marcel Dekker, New York, p. 229.
5. J. L. Cortina and A. Warshawsky (1996), Ion Exchange and Solvent Extraction, Vol. 13, J. A. Marinsky and Y. Marcus (eds.), Marcel Dekker, New York, p. 209.
6. A. Warshawsky, A. G. Strikovsky, J. Jerabek and J. L. Cortina (1997), *Solvent Extr. Ion Exch.*, **15** (2), 259-283.
7. J. Jerabek, L. Hankova, A. G. Strikovsky and A. Warshawsky (1996), *React. Polym.*, **28**, 149.
8. A. Strikovsky, K. Jerabek, J. L. Cortina, A. M. Sastre and A. Warshawsky, *React. Funct. Polym.*, **28**, 149-158.
9. A. G. Strikovsky, A. Warshawsky, L. Hankova and K. Jerabek (1998), *Acta Polym.*, **49**, 600-605.
10. A. Warshawsky, A. G. Strikovsky and M. Vilensky (2001), *Sep. Sci. Techn.*, in press.
11. A. Warshawsky and M. Vilensky (2001), *Sep. Sci. Techn.*, in press.
12. W. H. Holl, C. Stohr, R. Kiefer and C. Bratosch (2000), Ion Exchange at the Millenium, J.A. Greig (ed.), Imperial College Press, p. 377.
13. G. M. Ritcey and A. M. Ashbrook (1984), Solvent Extraction. Principles and Applications to Process Metallurgy, Part 1, Elsevier, Amsterdam.
14. E. Castillo, M. Granados, M. D. Prat and J. L. Cortina (2000), *Solvent Extr. Ion Exch.*, **143**, 243-245.
15. Z. M. Ahmed (1980), *React. Polym., Ion Exch. Sorbents*, **5**, 227-235.
16. J. E. Sabadell and N. H. Sweed (1970), *Sep. Sci.*, **5**, 171-181.



## STUDY OF THE SORPTION OF Zn(II) WITH XAD-7 RESIN IMPREGNATED WITH IONQUEST 801

M. Benamor and M. T. Draa

Department of Chemical Engineering, University of Bejaia, Bejaia, Algeria

Studies have been conducted on the sorption characteristics of Zn(II) from nitrate media with XAD-7 macroporous resin containing Ionquest 801 (2-ethylhexylphosphonic acid mono-2-ethylhexyl ester, HEHEHP, HL). The evaluation of the impregnation procedure shows that the extractant retention on the polymer is better in the case of an excess of water in ethanol-water mixture. It reaches a plateau value of 2.85 mol HL/kg dry resin for an impregnation solution of 0.33 mol HL/L, and an ethanol-water ratio of 1:2.

The impregnated resin shows good affinity towards the extraction of Zn(II). The sorption of the metal increases with aqueous pH solution and extractant retention in the resin phase.

Experimental data were numerically analyzed, and the results show that sorption equilibrium on the impregnated resin can be satisfactorily explained by taking into account the formation of  $ZnL_2$  complexes in the resin phase and  $ZnL^+$  in the aqueous phase.

### INTRODUCTION

The recovery of metal ions from dilute solutions using solvent impregnated resins (SIR) has been proposed as a technological alternative to solvent extraction technique [1]. It has been shown that macromolecular resins containing an extractant within their lattice provide the best use of the advantages of both solvent extraction and ion exchange. A significant number of works dealing with sorption and separation of metal with SIR has been carried out [1, 2]. Numerous metal extractants were used in these studies. They include acidic organophosphorus extractant like DEHPA [3, 4], CYANEX 272 [5], PC-88A [6], neutral extractants like TBP [7] and also basic extractants like tri-*n*-octylamine (TOA) [8]. These extractants were impregnated on different supports [1, 2]. The stability of impregnated resins depends principally on the type of support used and the nature of the organic reagent retained. Generally these support are hydrophobic macroporous organic polymers with a high surface area and good mechanical stability. The amberlite resins XAD are among the most suitable [1, 2].

The objectives of these studies were mainly devoted to explaining the impregnation processes, to elucidate the equilibrium reactions involved as well as kinetics. The approaches used in studying chemical equilibrium are based on those developed for liquid-liquid extraction [4]. But, in spite of these efforts, discrepancies result still exist. In this paper, a sensitive method for sorption of Zn(II) with Ionquest 801 impregnated in polymeric support, amberlite XAD-7 resin, has been developed and the operating parameters have been evaluated.

## EXPERIMENTAL

### Apparatus and Reagents

The pH of the aqueous phase was measured with a 3420 electrochemistry analyzer (Jenway) with a combined glass-saturated calomel electrode. The concentration of metal ions was analyzed with a Shimadzu atomic absorption spectrophotometer (model AA 6501f.) with an air-acetylene flame.

Ionquest 801 (2-ethylhexylphosphonic acid mono-2-ethylhexyl ester, HEHEHP), denoted hereafter by HL, was supplied by Albright and Wilson and used as received. Zinc nitrate, and other inorganic chemicals were of analytical reagent grade and were used without purification.

Stock solutions of Zn(II) ( $1\text{g}/\text{dm}^3$ ) were prepared by dissolving the corresponding salts in a solution of nitric acid ( $10^{-2}\text{ M}$ ). The aqueous solution consisted of  $0.1\text{ M}(\text{Na}^+, \text{H}^+, \text{Zn}^{2+})\text{NO}_3^-$ . The total nitrate concentration was kept constant at  $0.1\text{ M}$ . The aqueous pH was adjusted by changing different fractions of  $\text{HNO}_3$  and  $\text{NaNO}_3$ .

Amberlite XAD-7 resin (Rohm and Hass, size 0.3-0.9 mm) was used as support. The resin was washed in 50% methanol-water solution containing  $4\text{ M HCl}$  in order to remove inorganic impurities.

### Impregnation Procedure

The impregnated resins were prepared according to a slightly modified version of the dry method [1]. Amounts of 5 g of fresh resin XAD-7 were placed for 12 h in an ethanol-water mixture containing Ionquest 801 at different concentrations. After filtration, the Ionquest 801 content of the impregnated resin was determined after washing a given amount of the resin with ethanol, and titration with NaOH.

### Zinc Extraction with XAD7-Ionquest 801

The extraction of Zn(II) was carried out with batch experiments at room temperature. Samples of 0.2 g of resin containing Ionquest 801 were put in contact with 50 ml of an aqueous solution and were magnetically mixed. Preliminary work showed that a 2 h mixing time is sufficient to reach equilibrium.

## RESULTS AND DISCUSSION

### Evaluation of the Impregnation Method

The impregnation procedure was evaluated as a function of both solvent and extractant concentration. The evaluation of the impregnation procedure shows that the extractant retention on the polymer is better in the case of an excess of water in ethanol-water mixture. This is probably the result of different solubility of the extractant in these solutions. The same result was observed by Cortina *et al.* [9] in the case of DEHPA-XAD-2.

Figure 1 shows the relation between the quantity of adsorbed extractant  $q_{\text{HL}}$  (mol HL/kg Res) and the extractant concentration in the impregnation solution  $C_{\text{HL}}$  (mol HL/L). It is evident that  $q_{\text{HL}}$  increases with increasing  $C_{\text{HL}}$  until it reaches a plateau value of approximately 2.85 mol HL/kg resin for an impregnation solution of 0.3 mol HL/L, and an ethanol-water ratio of 1:2.

The model of Langmuir was used to characterize the sorption isotherms by the following expression:

$$\frac{q}{q_m} = \frac{bC}{1+bC} \quad (1)$$

where:

$q$  = moles of the adsorbed solute per mass unit of adsorbent (mol/kg)

$q_m$  = maximum concentration of the adsorbed solute per mass unit of the adsorbent (mol/kg)

$C$  = concentration of the solute at equilibrium in the impregnation solution (mol/L).

The parameters of the model were obtained from experimental data by the non-linear least square method. The values of these parameter obtained are:  $q_m = 2.89$  mol/kg,  $b = 27.29$  (L/mol). The curve obtained is depicted in Figure 1 (solid line). Good agreement exists between experimental and calculated values.

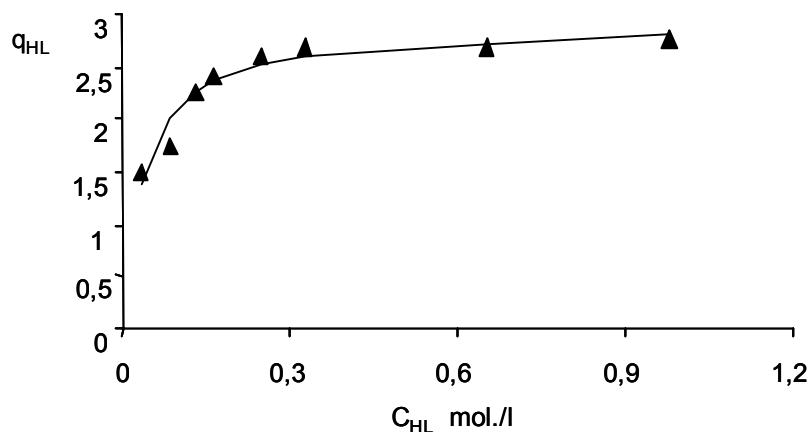


Figure 1. Influence of the extractant Concentration on the resin.  
Loading impregnation solution ethanol-water Mixture 1:2.  $q_{HL}$  : mol.HL / kg resin.

### Effect of pH and Extractant Concentration on Metal Sorption

The distribution of metal ions between the aqueous phase and the resin phase containing Ionquest 801 can be directly obtained as:

$$D = [M]_{R,T} / [M^{m+}]_T \quad (2)$$

where  $[M]_{R,T}$  is the total concentration of metals in the resin phase in mol/kg dry impregnated resin and  $[M^{m+}]_T$  represents the concentration of the different species in the aqueous phase. The total concentration of metals in the resin phase can be expressed as:

$$[M]_{R,T} = \{ [M^{m+}]_0 - [M^{m+}]_T \} \times (V/m_R) \quad (3)$$

where  $[M^{m+}]_0$  is the initial total concentration of the metal in the aqueous phase,  $V$  denotes the volume of the aqueous phase, and  $m_R$  is the mass of dry impregnated resin.

Figure 2 depicts the influence of the equilibrium pH on the distribution coefficient  $D$  at different resin loading  $[HL]_{R,T}$ . It is found that the distribution coefficient increases with aqueous pH; the slope of  $\log D$  versus  $pH_{eq}$  varying between 1.5 and 2 suggests that one or two protons are exchanged during the extraction sorption.

In order to investigate the influence of the extractant concentration, this latter was varied between 0.03 and 0.97 mol/L (Figure 3). The results obtained illustrate that for a constant pH,  $\log D$  increases with the free extractant concentration of the resin and the slope of  $\log D$  versus  $\log [HL]_R$  is close to 2 indicating that two molecules are associated with the extracted metal complex.

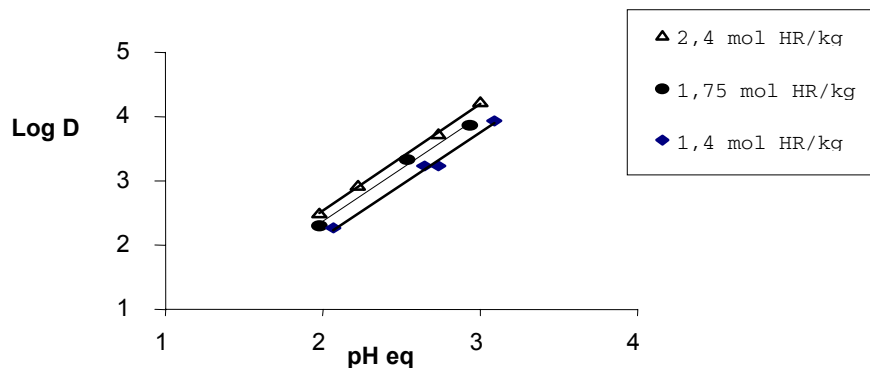


*Figure 2. Influence of the equilibrium pH on the sorption of Zn(II) in the XAD-7 impregnated resin with Ionquest 801 for three different resin loading 0.1M NaNO<sub>3</sub>.*

The influence of the metal concentration shows also that there is no polynuclear complex species formed during the sorption of the metal between the extractant and the metal in the resin phase.

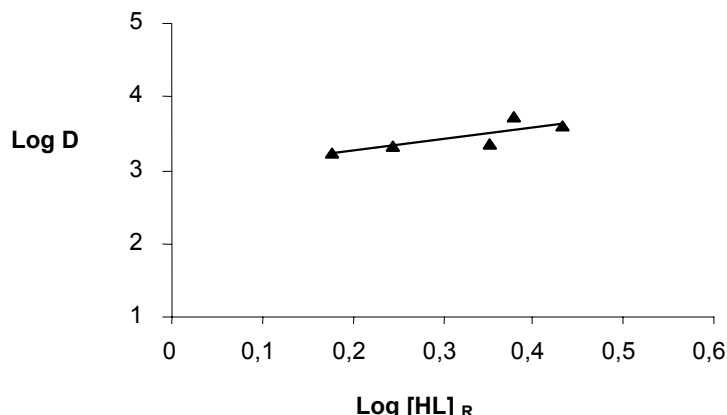
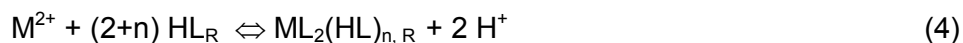


*Figure 3. Influence of the extractant concentration of the resin on the distribution coefficient of Zn(II), pH<sub>eq.</sub> = 2.75.*

### Sorption Equilibrium

Divalent metal ion extraction using impregnated resins with organophosphorus extractants can be described by the general reaction [1, 2]:



where the subscript R designs the resin phase.

$$K_{mn} = \frac{[ML_2(HL)_n]_R [H^+]^2}{[M^{2+}] [HL]_R^{2+n}} \quad (5)$$

The corresponding equilibrium constant  $K_{mn}$  based on concentration is defined by taking into account that the extractant adsorbed in the resin phase is involved also in other equilibrium like distribution between the resin and aqueous phase, dissociation in the aqueous phase, and dimerization in the resin phase. We can derive the following mass balance for  $[HL]$  in the case of low metal concentration [2]:

$$[HL]_{o,R} = \{1 + (1/K_D) + (K_a/K_D[H^+])\}[HL]_R + 2K_2 [HL]_R^2 \quad (6)$$

where  $[HL]_{o,R}$ ,  $[HL]_R$  and  $[HL]$  are the initial, free and aqueous phase concentrations of extractant, respectively.

In order to model these extraction equilibrium, the equilibrium constant of the extractant ( $pK_A$ ,  $K_D$ ,  $K_2$ ) must be known. In the case of Ionquest 801, the value of  $pK_a$  of HL was taken from reference [11] and is equal to 3.

The best formulation of the complexes formed in the resin phase is obtained by minimization of the error squares sum defined by:

$$U = \sum (\log D_{exp} - \log D_{calc})^2 \quad (7)$$

where  $D_{exp}$  is the experimental distribution coefficient and  $D_{calc}$  is the one calculated assuming the formation of one set of species and the above mass balance equations. This is achieved by searching the best values of the equilibrium constants  $K_{mn}$  as well as the distribution and the dimerization constant  $K_D$ ,  $K_2$  for extractant, which minimize the error squares sum  $U$ . The Microsoft Excel 97 program was used for this purpose. The standard deviation  $\sigma(\log D)$  is calculated by:

$$\sigma(\log D) = (U/N_p)^{1/2} \quad (8)$$

where  $N_p$  is the difference between the total number of data points and the total number of equilibrium constants calculated.

In the first attempt, and following the slope analysis results, the value of  $n$  was varied between 0-2. Table 1 shows the best formulation for the metal-HL complexes, together with the calculated equilibrium constants obtained. This results show that only a single Zn(II)-HL complex is formed on the macroporous resin and the simultaneous formation of binary complex is rejected.

*Table 1. Results of the numerical calculation obtained in the Zn(II)/XAD-7 system for various model species: case where only free cationic metal in the aqueous phase.*

Specie	U	$\sigma(\log D)$	$\log K_{mn}$
ZnL <sub>2</sub>	0.277	0.13	-1.57

Another scheme consistent with the results of slope analysis was also considered. This latter takes into consideration the reaction between the metal and the ionized extractant in the aqueous phase [10] following the mechanism:



This second model gave a better value of  $U$  (0.19) than the first case. Table 2 depicts the principal result obtained together with the corresponding equilibrium constants.

*Table 2. Results of the numerical calculation obtained in the Zn(II)/XAD-7 system:  
case where the aqueous phase contains ionized complexes species.*

Specie	U	$\sigma(\log D)$	pK <sub>A</sub>	$\log K_D$	$\log K_2$	$\log K_{ex1}$	$\log K_{ex2}$
ZnL <sub>2</sub>	0.19	0.10	3	2.15	3.04	2.73	5

## CONCLUSION

The extraction of Zn(II) from nitrate solutions by impregnated resins containing Ionquest 801 on the amberlite XAD-7 polymeric support in a batch system has been investigated. The evaluation of the impregnation procedure shows that that the extractant retention on the polymer is favoured in the case of an excess of water in ethanol-water mixture. This retention reaches a constant value of 2.85 mol HL/kg dry resin for an impregnation solution of 0.33 mol HL/L, and an ethanol-water ratio of 1:2.

The impregnated resin shows good affinity towards the extraction of Zn(II). The sorption of the metal increases with aqueous pH solution and extractant retention in the resin phase. The data were analyzed numerically and the results show that by taking into account the formation of ZnL<sub>2</sub> in the resin phase, and ZnL<sup>+</sup> complexes between metal and ionized extractant in the aqueous phase, the experimental result could be satisfactorily explained.

## ACKNOWLEDGEMENT

We are grateful to Albright and Wilson (USA) for kindly donating Ionquest 801.

## REFERENCES

1. J. L. Cortina and A. Warshawsky (1997), *Ion Exchange and Solvent Extraction*, Vol.13, J. A. Marinsky and Y. Marcus (eds.), Marcel-Dekker, New York, pp. 195-293.
2. R. S. Juang (1999), *Proc. Nat. Sci. Counc. ROC(A)*, **23** (3), 353-364.
3. J. L. Cortina, N. Miralles, A. Aguilar and A. M. Sastre (1994), *Solvent Extr. Ion Exch.*, **12**, 371- 391.
4. R. S. Juang and M. L. Chen (1997), *Sep. Sci. Technol.*, **32** (5), 1017.
5. J. L. Cortina, N. Miralles, A. M. Sastre, A. Aguilar, A. Profumo, and M. Pesavento (1993), *React. Polym.*, **21**, 103-116.
6. S. Akita and H. Takeuchi (1990), *J. Chem. Eng. Jpn.*, **23**, 439.
7. I. Villaescusa, V. Salvado, J.de Pablo, M. Valiente and J. Aguilar (1992), *React. Polym.*, **17**, 69-73.
8. S. Akita, K. Hirano, Y. Ohashi and H. Takeuchi (1993), *Solvent Extr. Ion Exch.*, **11** (5), 797.
9. J. L. Cortina, N. Miralles, A. Aguilar and A. M. Sastre (1994), *Solvent Extr. Ion Exch.*, **12**, 349-369.
10. R. N. Mendoza, T. I. Saucedo Medina, A. Vera, M. Avila Rodriguez and E. Guibal (2000), *Solvent Extr. Ion Exch.*, **18** (2), 319.
11. J. L. Perera, J. K. McCulloch, B. S. Murray, F. Geiser and G. W. Stevens (1992), *Langmuir*, **8**, 2.



## EVALUATION OF ALKYLGUANIDINE BASED SOLVENT IMPREGNATED RESINS FOR GOLD CYANIDE EXTRACTION

Rubens M. Kautzmann, Carlos H. Sampaio, Vadim Korovin\*, Yuriy Shestak\*,  
Manuel Aguilar\*\* and Jose L. Cortina\*\*

Universidad Federal de Rio Grande do Sul, Porto Alegre, Brazil

\*Pridneprovsky Scientific Center of Ukrainian NAS, Dnieprodzerzhinsk, Ukraine

\*\*Universitat Politecnica de Catalunya, Barcelona, Spain

In this work a new family of solvent-impregnated resins based on alkylguanidine functionality (LIX 79) has been synthesised and chemically and physically characterised. Solvent-impregnated resins are prepared by both direct adsorption of the active component onto macroporous polymeric supports and by co-polymerisation of styrene and divinylbenzene in the presence of the active component. The extraction performance of these new materials on metalcyanides from mineral leaching solutions has been evaluated and separation factors and extraction efficiency for the materials are determined. It is shown that gold(I) is extracted into the organic phase by formation of the species  $\text{RH}^+\text{Au}(\text{CN})_2^-$ . Stripping of gold from loaded resin phases is carried out using NaOH, NaCN and NaOH/NaCN mixture solutions. Finally the application of those impregnated resins to extract gold from cyanide solutions is evaluated on different mineral leaching solutions derived from two auriferous Brazilian minerals.

### INTRODUCTION

The application of hydrometallurgy to the recovery of precious metals from dilute ore sources is increasing in use [1]. For example, dump, heap and vat leaching in cyanide media of selected ores are employed commercially in the gold mining industry. In the case of gold the circuit consisting of leaching, carbon adsorption and electrowinning is the most economical way to produce gold.

Although, in this process gold extraction is achieved using activated carbon, in recent years, research efforts have attempted its substitution by ion exchange (IX) or solvent extraction (SX) reagents. The main objective of the application of IX and SX is to solve existing problems associated with the use of activated carbon and thereby improve the selective recovery of goldcyanide, increase loading and stripping efficiencies, and develop an integrated process of leaching and extraction such as resin/solvent-in-leach (RIL/SIL) and resin/solvent-in-pulp (RIP/SIP).

Commercially available resins and extractants are unable to compete with activated carbon due to poor selectivity and the requirement for complex elution and regeneration processes. Since typical leach solutions contain gold as  $\text{Au}(\text{CN})_2^-$  at pH about 10, it was reasoned that these shortcomings might be overcome if an extractant or a resin containing a functional group (L), which would operate on the hydrogen ion cycle shown in the following reaction were used:



where the equilibrium lies far to the right at pH < 10 and far to the left at pH > 12.5. Gold cyanide extraction will be accomplished by the following reaction:



A new reagent that can accomplish the required type of pH cycle, has recently been commercialised by Cognis Co [2]. The reagent, known as LIX 79 contains a guanidine ion-pairing functionality. In previous studies [3,4] the extraction of gold(I) from aurocyanide aqueous solutions using LIX 79 was evaluated and showed that the aurocyanide complex is extracted preferentially over other metal cyano complexes at alkaline pH. This study has been extended to the evaluation of this extractant when immobilised onto polymeric macroporous supports.

Solid adsorbents prepared by immobilisation of liquid extractant onto polymeric materials has been proposed in the last decades as an alternative to solvent extraction by combining the mass transfer properties of solvent-extraction systems with the simplicity provided by polymeric adsorbents on plant design and operation. The impregnated adsorbents can be prepared by simple immobilisation of the extractant onto macroporous supports or by polymer synthesis in the presence of the extractant as has been used by Bayer [5] and Sorbent Center [6].

This paper deals with recent investigations in the application of impregnated resin adsorbents (TVEX-LIX 79) in the extraction, separation and recovery of gold cyanide from leaching solutions. The impregnated resins prepared were obtained by polymerisation of styrene and divinylbenzene in the presence of LIX 79. Solid-liquid studies of gold cyanide extraction using batch and column experiments were performed. The influence of both reagent and polymer functional structure on the extraction ability and the influence of the aqueous composition were studied.

## EXPERIMENTAL PROCEDURE

### Materials Preparation

The extractant LIX 79 was used as supplied by the manufacturer (Cognis Corp.); the active substance of the extractant is based on the guanidine functional group, the structure of which is shown in Figure 1.

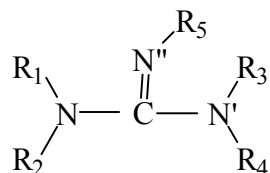


Figure 1. Basic structure of the guanidine functional group ( $R_1$  to  $R_4$  represent alkyl groups).

### Preparation of impregnated adsorbents

Synthesis of solid extractant (TVEX) containing 40–50 % LIX79 was carried out in a glass reactor fitted with a mixer, thermometer and backflow condenser [7]. Starch solution (1%), used as emulsion stabiliser, was first added to the reactor. Then reaction mixture containing styrene, divinylbenzene, LIX79 and benzoyl peroxide as initiator of radical co-polymerisation was fed into the reactor at 55 °C with agitation. Polymerisation was carried out for 5 h at 85–90 °C. The TVEX granules were washed with water and dried with nitrogen.

XAD2-LIX 79 resins were prepared according to a modified version of the wet impregnation method described previously [8]. The amount of LIX 79 impregnated in both types of resins was evaluated by washing a known amount of resin with ethanol, which completely elutes these extractants for subsequent determination by potentiometric titrations. Impregnates prepared achieved loadings of 0.33 g LIX 79/g resin for XAD2 impregnates and 0.20, 0.35 g LIX 79/g resin for TVEX impregnates.

### Aqueous solutions

Stock solutions of  $\text{Au}(\text{CN})_2^-$ ,  $\text{Zn}(\text{CN})_4^{2-}$ ,  $\text{Ag}(\text{CN})_2^-$ ,  $\text{Fe}(\text{CN})_6^{4-}$  and  $\text{Cu}(\text{CN})_3^{2-}$  ( $1\text{g} \cdot \text{dm}^{-3}$ ) were prepared by dissolving the corresponding salts (Johnson Mathey, A.R. grade) in sodium cyanide solution. Real cyanide leach liquors were obtained by leaching of a gold mineral ore from Brazil. The compositions of the solutions are shown in Table 1.

Table 1. Composition of the Metal Cyanide Solutions (mg/L.)

Metal	Leach Liquor 1	Leach Liquor 2	Synthetic Liquor
Gold	11.6	9.6	10.0
Silver	0.7	5.7	5.0
Copper	12.4	20.4	30.0
Iron	10.7	25.7	30.0
Zinc	3.1	6.1	4.0

### Experimental Procedures

Samples between 0.1-0.2 g of impregnates, were mixed mechanically in glass tubes with an aqueous solution (20 ml) until equilibrium was achieved. The composition of the aqueous solutions varied depending on the nature of the experiment. After phase separation the equilibrium pH was measured using a combined electrode. Metal content in both phases were determined using atomic absorption spectrophotometry or inductively coupled plasma spectrophotometry, depending on solution composition. Experiments were repeated on average three times and the accuracy of the estimation of the metal concentration in the loaded resin phase by mass balance was checked by experiments in which complete stripping of the loaded resin phase was carried out and the stripped solution was analysed. An average accuracy of 97%, between calculated and analytical results, was regularly obtained.

## RESULTS AND DISCUSSION

### Influence of the Extractant Concentration

Figure 2 shows the variation in gold extraction against pH for experiments carried out with aqueous phases of 10 mg/l gold(I) and resin impregnated phases which contained different LIX 79 loadings.

As expected, as the extractant concentration increased the corresponding gold extraction curve shifted to more alkaline pH values. The figure also compares the performance of prepared TVEX and XAD2 impregnated resins against a liquid LIX 79/Kerosene mixture. Gold loadings of 20 g/kg achieved with TVEX (0.35 g/g) in solutions at pH 10 are comparable with those published elsewhere with the resin analogue of LIX 79 extractant (AURIX) [9].

### Gold Extraction Mechanism

The expected general equilibrium from which the aurocyanide complex is extracted by LIX 79 can be represented by the reaction:



where R denotes the extractant molecule and the subscript res, a species in the resin phase.

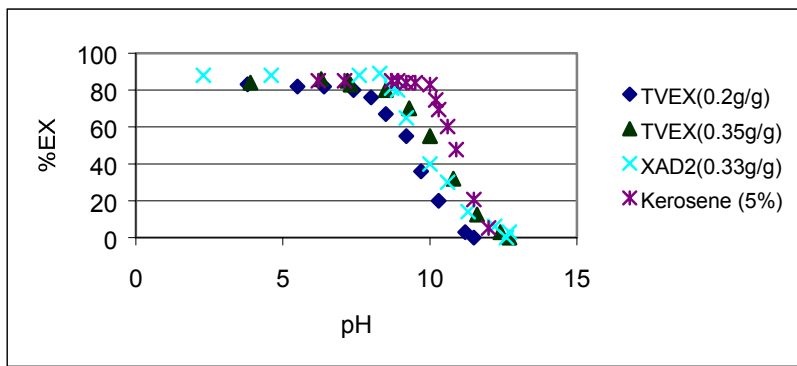


Figure 2. The influence of the LIX79 loadings of the impregnates on gold(I) extraction.

Assuming ideal behaviour for the reaction in eqn (3) in resin and aqueous phases, the stoichiometric equilibrium constant ( $K_{ex}$ ) can be written as:

$$K_{ex} = \frac{[RH^+Au(CN)_2^-]_{res}}{[R]_{res}[H^+][Au(CN)_2^-]} \quad (4)$$

and taking into account the distribution coefficient  $D_{Au}$

$$D_{Au} = \frac{[Au(I)]_{res, tot}}{[Au(I)]_{aq, tot}} \quad (5)$$

dependence of the distribution coefficient and operation parameters can be described by the following equation:

$$\log D_{Au} = \log K_{ex} - pH + \log[R]_{res} \quad (6)$$

The  $pH_{50}$ , pH where a 50% of extraction ( $D_{Au}=1$ ) is obtained, is defined by the following equation:

$$pH_{50} = \log K_{ex} + \log[R]_{res} \quad (7)$$

Figure 3 shows that the variation of  $pH_{50}$  as a function of LIX 79 loadings has a linear relation with a slope of 0.99 and an intercept of 12.9 as the  $\log K_{ex}$  value. This shows that gold cyanide extraction on LIX 79 impregnates occurs via formation of a  $RH^+Au(CN)_2^-$  complex onto the resin phase. This is similar to the described behaviour for this reagent when used in liquid-liquid extraction systems.

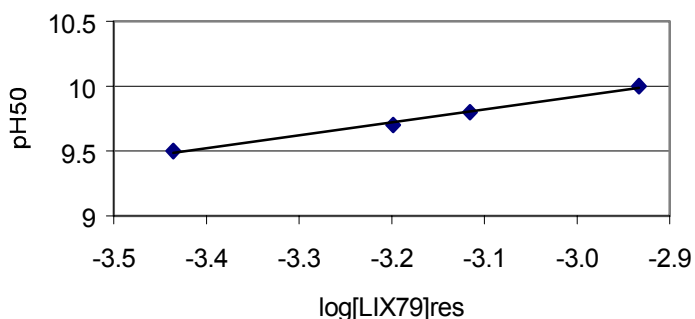


Figure 3. Dependence of  $pH_{50}$  on LIX79 loading on the resin impregnates.

### Selectivity of the TVEX/LIX79-Au(CN)<sub>2</sub>-Extraction System

The selectivity of TVEX/LIX 79 resin for various metal cyano complexes is illustrated in Figure 4, which represents the percentage of metal extraction against equilibrium pH. The aurocyanide complex is extracted at the most alkaline pH value and, consequently, gold loading can be increased relative to the other metal-cyano complexes present in the aqueous phase in this pH range.

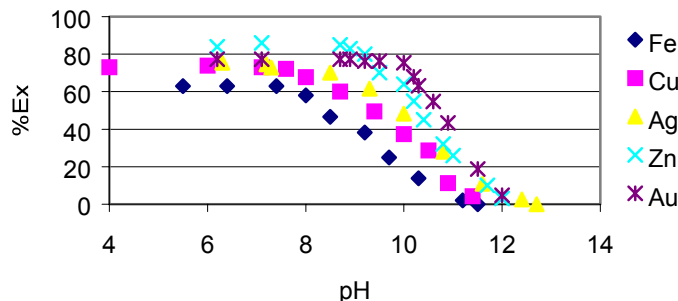


Figure 4. Extraction-pH dependence of  $\text{Au}(\text{CN})_2^-$ ,  $\text{Zn}(\text{CN})_4^{2-}$ ,  $\text{Ag}(\text{CN})_2^-$ ,  $\text{Fe}(\text{CN})_6^{4-}$  and  $\text{Cu}(\text{CN})_3^{2-}$  with TVEX/LIX79 (0.35 g/g) impregnates.

The following extraction sequence can be tentatively established for these metal-cyano complexes:  $\text{M}(\text{CN})_2 > \text{M}(\text{CN})_4^{n-} \sim \text{M}(\text{CN})_6^{n-}$ ; thus the extraction of these complexes depends on the metal co-ordination number. In general, the complexes with lower co-ordination numbers were extracted preferentially to those with higher numbers and the lower charge complexes were extracted preferentially to higher charge complexes.

Extraction experiments were performed with the real leach liquors (Table 1) and the results expressed in terms of the separation factors ( $K_{\text{Au/metal}}$ ), are compared with those for synthetic liquor in Table 2.

Table 2. Separation factors for synthetic and mineral leaching solutions.

Solution	pH <sub>eq</sub>	K <sub>Au/Ag</sub>	K <sub>Au/Zn</sub>	K <sub>Au/Fe</sub>	K <sub>Au/Cu</sub>
Synthetic	10,2	3	6	40	20
Synthetic	10,4	4	8	45	23
Leach 1	10,4	2	4	20	15
Leach 2	10,6	2	5	30	15

The results show that independent of the aqueous solution, the apparent order follows the series:

$$K_{\text{Au/Ag}} > K_{\text{Au/Zn}} > K_{\text{Au/Cu}} > K_{\text{Au/Fe}}$$

This selectivity is in agreement with the fact that the hydrophilicity of the polymer matrix and the ionic density (number of ionic groups per unit volume) play important roles in determining the selectivity characteristics of a resin. Ion-water interactions are stronger in the aqueous phase than in the resin phase, for the simple reason that more free water is available for solvation in the aqueous phase. Thus on this basis alone, the ions with the greatest ionic charge tend to have a lower extraction onto the resin phase. In the resin phase a low degree of hydrophilicity and a low ionic density increases the selectivity for gold and silver and favors those metals over the base metals, iron and copper.

### Stripping

The stripping of gold from loaded TVEX resins (0.2 g/g and 0.35 g/g) was studied using various stripping reagents. Table 3 shows the effect of both the stripping reagent and its concentration on stripping. Stripping efficiency follows the order NaOH > NaCN and tends to increase with increasing reagent concentration, although good gold recoveries were obtained using low NaOH or NaCN concentrations. When the stripping process is completed, the active component [R] of the extractant is deprotonated (eqn (3) shifts to the left), and no metal ions are present in the polymer phase.

Table 3. Stripping of  $\text{Au}(\text{CN})_2^-$  from TVEX/LIX 79 impregnated resins.

Eluant	Stripping %	
	LIX79 (0.2 g/g)	LIX79 (0.35 g/g)
NaOH 0.2 M	94±3	93±1
NaOH 0.5 M	95±2	96±2
NaOH 1.0 M	98±1	96±2
NaCN 0.1 M	90±2	92±3
NaCN 0.2 M	97±2	96±2

### CONCLUSIONS

The use of LIX 79 extractant supported onto polymeric substrate of styrene divinylbenzene allowed gold extraction from alkaline cyanide media. Gold extraction seems to be independent on the initial metal concentration, slightly dependent of the organic diluent and more dependent on the extractant concentration and aqueous pH values. The aurocyanide complex is extracted preferentially over other metal cyano complexes at alkaline pH values. Stripping is accomplished using NaOH or NaCN solutions, the efficiency of stripping slightly increases with the increase in the reagent concentration.

### ACKNOWLEDGEMENTS

This work has been supported by CICYT (QUI99-1025-C03-02) and CIRIT (SGR96-101) Cognis is thanked for providing LIX 79 used in this work.

### REFERENCES

1. M.B. Moiman, J.D. Miller, J.B. Hiskey, A.R. Hendrickson (1984), Comparative of Process Alternatives for Gold Recovery from Cyanide Leach Solutions, J.B. Hiskey (ed.), AIME, **93**, 108.
2. G.A. Kordosky GA, J.M. Sierakowski, M.J. Virnig, P.L. Mattison (1992), *Hydrometallurgy*, **30**, 291-305.
3. M. Virnig, G.A. Wolfe (1996), *Proc. Int. Solvent Extraction Conf. ISEC '96*, University of Melbourne Press, Melbourne, pp. 311-316.
4. A. Sastre, A. Madi, J.L. Cortina, F.J. Alguacil (1999), *J. Chem. Tech. Biochem.*, **74**, 310-314.
5. V. Korovin, S. Randarevich (1988), *Proc. Int. Solvent Extraction Conf. ISEC '88*, Vol. 3, Moscow, pp. 159-162.
6. R. Kroebel, A. Meyer (1976), *Proc. Int. Solvent Extraction Conf. ISEC '74*, Vol. 3, Lyon France, pp. 2095-2107.
7. V. Korovin (1991), *Khim. Technol.*, **5**, 3-13.
8. J.L. Cortina, E. Meinhardt, O. Roijals, V. Martí (1998), *React. Funct. Polym.*, **36**, 149-165.
9. J.M.W. Mackenzie (1993), *Proc. Randol Gold Forum*, Beaver Creek, CO, pp. 287-292.



## SOL-GEL SYNTHESIZED ADSORBENTS FOR NOBLE METAL SEPARATIONS

J. S. Lee and L. L. Tavlarides

Department of Chemical Engineering and Materials Science, Syracuse University, NY, USA

Sol-gel adsorbent materials are synthesized with imidazole and pyrazole chelation ligands which have advantages over conventional solvent extraction systems for selective separation of platinum, palladium, and gold in the presence of copper and iron from leach solutions. These adsorbents are effective for the hydrochloric acid concentration range of 0.1 M to 5.0 M. The sol-gel synthesis starting with precursor silanes and siloxanes results in gel particles of desired pore characteristics and high capacity and stability. Characterization studies, such as adsorption isotherms, breakthrough curves for fixed bed operation, and material stability show promising results for applications to noble metal extraction.

### INTRODUCTION

The technology of noble metal extraction from ores has been developed for a long period of time, but it is still an important research topic because the demand for noble metals continues to increase in various applications such as catalysts, electronics, and corrosion-resistant materials. In addition, the recovery of precious metals from industrial wastes, such as from spent electronic components and catalysts, receives great attention because significant amounts of noble metal-containing wastes are being generated from such industries [1].

Refining processes employing solvent extraction techniques for precious metal mining can achieve highly selective separations and effective enrichments [2], and many organic chelants have been developed to improve the efficiency of currently available extraction processes [3]. These organic chelants are used as solvent extractants or immobilized sorbents on solid supports such as polymer resins [4] and ceramics [5]. The use of immobilized chelating agents on solid supports is a favorable alternative for the recovery of noble metals from dilute leaching solutions.

Recently, our research group reported a sol-gel processing technique synthesizing organo-ceramic adsorbents for the extraction of heavy metal ions [6]. The developed adsorbent, SOL-AD-IV, has significantly improved metal uptake capacities for mercury and cadmium ions compared to those developed by covalent attachment or solvent impregnation on silica matrices. Similarly, two organo-ceramic adsorbents functionalized with imidazole (SOL-IPS) and pyrazole (SOL-PzPs) are developed for the extraction of palladium, platinum, and gold chlorides from hydrochloric acid solutions (0.1 M – 5.0 M).

In this paper, synthesis of adsorbents by sol-gel processing and adsorptive characteristics for the separation of palladium, platinum, and gold chlorides in HCl solutions are discussed.

## EXPERIMENTS

### Materials and Reagents

SOL-IPS and SOL-PzPs adsorbents are synthesized by the sol-gel processing technique as reported in our patent application [7]. N-(3-triethoxysilylpropyl)-4,5-dihydroimidazole (Gelest, Inc.) and N-(trimethoxysilylpropyl)-pyrazole are used as functional precursors for SOL-IPS and SOL-PzPs, respectively, and tetraethoxysilane is used as the cross-linking silane for both adsorbents. Results of pore characterization, elemental analysis, and maximum uptake capacity of palladium(II) chlorides are summarized in Table 1.

*Table 1. Ligand density, metal uptake capacity and pore characteristics of SOL-IPS and SOL-PzPs adsorbents.*

Adsorbent	Ligand density <sup>a</sup> , mmol/g	Metal uptake capacity <sup>b</sup> , mmol/g			Pore characteristics	
		Pd(II)	Pt(IV)	Au(III)	D, Å	SA, m <sup>2</sup> /g
SOL-IPS	2.98	1.54	1.41	2.43	ND <sup>c</sup>	ND <sup>c</sup>
SOL-PzPs	3.16	1.41	0.56	1.48	37	437

a: results of elemental analysis for carbon and nitrogen

b: SOL-IPS at [HCl] = 0.1 M and SOL-PzPs at [HCl] = 2.0 M

c: Not detectable in mesoporous range

Palladium, platinum, and gold chloride solutions are formulated by dissolving potassium tetrachloropalladate(II) (Alfa Aesar Co.), potassium hexachloroplatinate(IV) (Aldrich Chemical Co.), and potassium tetrachloroaurate(III) (Aldrich Chemical Co.) in hydrochloric acid solutions at appropriate concentrations. All other chemicals used in this study are reagent grade.

### Characterization

The metal concentrations are measured with an atomic absorption spectrophotometer (Perkin-Elmer Model 2380) and an ICP-OES (Perkin-Elmer OPTIMA 3300DV). Average pore sizes and surface areas of the adsorbents are measured by nitrogen adsorption at 77 K with Micromeritics ASAP 2000. Carbon and nitrogen contents of synthesized adsorbents are measured by the elemental analysis (Oneida Research Services Inc., Whitesboro, NY).

Maximum uptake capacities for Pd(II), Pt(IV), and Au(III) chlorides at various HCl concentrations are measured by equilibrating desired amounts of adsorbents (0.1 – 0.25 g) with 7–10 mmol/L of the metal chloride solutions at 25°C. For equilibrium adsorption isotherms, desired amounts of adsorbents are equilibrated with the metal chloride solutions at desired HCl concentrations (0.1 mol/L for SOL-IPS and 2.0 mol/L for SOL-PzPs). Multi-metal breakthrough experiments are performed for SOL-IPS and SOL-PzPs adsorbents by using 2.0 g-packed 0.8 cm ID columns and feed solutions containing 0.1 mmol/L each of Pd(II), Pt(IV), and Au(III) chlorides, and 2.5 mmol/L each of copper and iron at desired HCl concentrations (0.1 mol/L for SOL-IPS and 2.0 mol/L for SOL-PzPs). The feed solutions are passed through the columns at approximately 1.0 ml/min flow rate. The stability of SOL-IPS and SOL-PzPs are tested in each 0.5 g of adsorbent packed column (0.8 cm ID). The metal loading solutions are 200 ml of 4.75 mmol/L palladium chloride at 0.1 mol/L (SOL-IPS) and 2.0 mol/L (SOL-PzPs) HCl concentrations that are circulated through the columns for 24 hours at 1.0 ml/min flow rate. After the palladium loading, the columns are washed with 10 ml of water and then stripped with 50 – 75 ml of 0.5 mol/L thiourea in 0.1 mol/L HCl solution. The stripped columns are washed with 0.5 mol/L HCl solution before the next palladium loading. These loading, washing, stripping, and washing cycles are repeated until the desired criteria are satisfied.

## RESULTS AND DISCUSSION

### Maximum Uptake Capacity

Maximum uptake capacities of SOL-IPS and SOL-PzPs for Pd(II), Pt(IV), and Au(III) chlorides are determined at various HCl concentrations to determine appropriate operational conditions. As shown in Figure 1, the uptake capacity of SOL-IPS for Pd(II) is approximately 0.5 mmol/g larger than that for Pt(IV) within the studied HCl concentration range. The uptake capacity for Au(III) rapidly decreases as HCl concentration increases 0.1 M to 1.0 M, and it is even smaller than that for Pd(II) or Pt(IV) at 1.0 M HCl concentration. Hence, the capacity difference for these metal chlorides is insignificant when HCl concentration is higher than 1.0 M. On the other hand, the metal uptake capacities of SOL-PzPs are significantly different with those of SOL-IPS. Uptake capacities of SOL-PzPs for Pd(II) and Au(III) are much higher than that for Pt(IV) within the studied HCl concentration range (< 5.0 M). Hence, this adsorbent can be employed to extract Pd(II) and Au(III) from solutions at HCl concentration range of 0.1 M - 5.0 M.

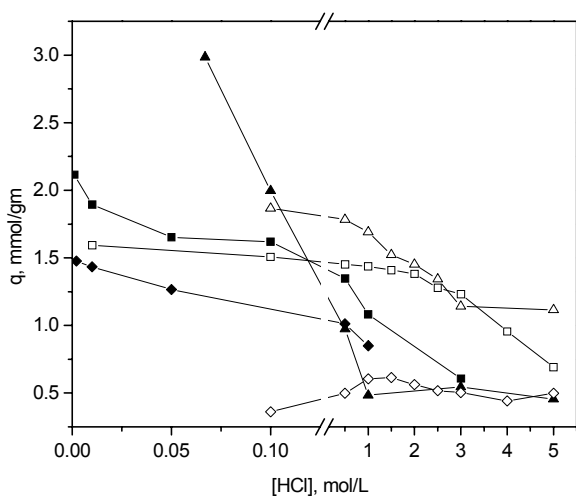
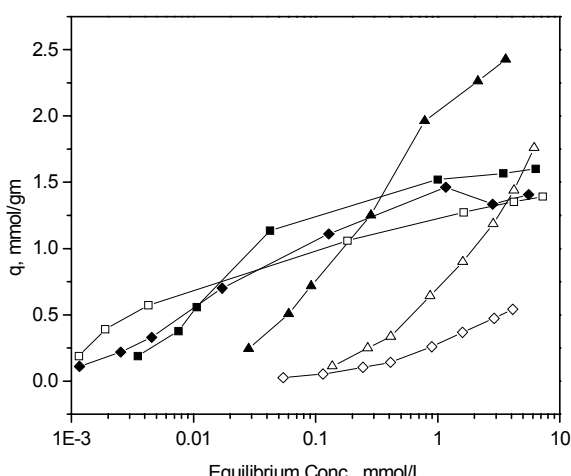


Figure 1. Maximum metal uptake capacities of SOL-IPS (solid symbols) and SOL-PzPs (open symbols) for palladium (■, □), platinum (◊, △), and gold (▲, Δ) chlorides at various HCl concentrations.

### Equilibrium Loading Capacity

The experimental results of equilibrium loading capacity at 0.1 mol/L HCl concentration show that SOL-IPS has a higher uptake capacity for palladium chloride over platinum and gold chlorides when the metal concentrations in the solutions are smaller than 0.2 mmol/L (Figure 2). On the other hand, the uptake capacity for gold chloride is higher than that for palladium and platinum chlorides when the metal concentrations are higher than 0.2 mmol/L. For SOL-PzPs, palladium uptake rapidly increases at low concentration while the uptake capacities for platinum and gold chlorides increase steadily as the solution concentrations increase. This implies that the adsorbent has stronger affinity for palladium chloride than for platinum and gold chlorides, thus an almost complete separation of palladium over platinum and gold is expected at low metal concentrations (< 0.2 mmol/L).



*Figure 2. Equilibrium adsorption isotherms of SOL-IPS at  $[HCl] = 0.1 \text{ mol/L}$  (solid symbols) and SOL-PzPs at  $[HCl] = 2.0 \text{ mol/L}$  (open symbols) for palladium ( $\blacksquare$ ,  $\square$ ), platinum ( $\diamond$ ,  $\square$ ), and gold ( $\blacktriangle$ ,  $\Delta$ ) chlorides.*

### Multi-metal Breakthrough Curves

For both adsorbent systems, multi-metal breakthrough experiments are performed to demonstrate the capability to extract noble metals from highly concentrated transition metal solutions (Figure 3). The breakthroughs of iron and copper from both adsorbent columns occur immediately after starting the experiments. From both columns, the breakthroughs of gold and platinum chlorides occur together, and these metals are exchanged by palladium chloride. The displacements of gold and platinum chlorides by palladium chlorides are approximately 55% and 33% from the maximum loadings (at  $C/C_0 = 1$ ), respectively, for SOL-IPS (within 2,800 and 6,500 bed volumes) and 44% and 100% for SOL-PzPs (within 300 and 6,000 bed volumes), respectively. The displacements of gold and platinum chlorides indicate that SOL-IPS and SOL-PzPs have higher affinity for palladium chloride than for gold and platinum chloride. However, no difference in affinity is observed between gold and platinum chlorides in both adsorbent systems. These experiments show that both adsorbent systems can be used to selectively extract noble metals from concentrated transition metal solutions. In addition, SOL-PzPs shows high possibility to separate palladium from mixture solutions with platinum and gold chlorides at relatively high HCl concentrations (~2.0 M). After complete loading, the loaded palladium, platinum, and gold are recovered with 92 - 100% efficiency by using only ten bed volumes of 0.5 M thiourea in 0.1 M HCl solution. In addition, only trace amounts of platinum is detected in the eluted solution from loaded SOL-PzPs column.

### Material Stability

Experimental results of operational stability of SOL-IPS and SOL-PzPs in packed columns show that the palladium uptake capacities of SOL-IPS and SOL-PzPs are maintained at approximately 100% of the original capacity for six cycles, and decreases to 85% after 17 cycles (Figure 4). The column fails after that due to increase in pressure drop in both columns. The decreasing trends of palladium uptake capacity of these two adsorbents virtually overlap even though the two adsorbents have different functional groups and are operated at different HCl concentrations. Hence, the major reason for pressure drop and the degradation of performance seems to be due to deposition of thiourea on adsorbents leading to column plugging. To avoid degradation of adsorbents and to minimize pressure buildup in packed columns, other stripping agents are recommended even though thiourea is the most powerful stripping agent for noble metals reported in the literature.

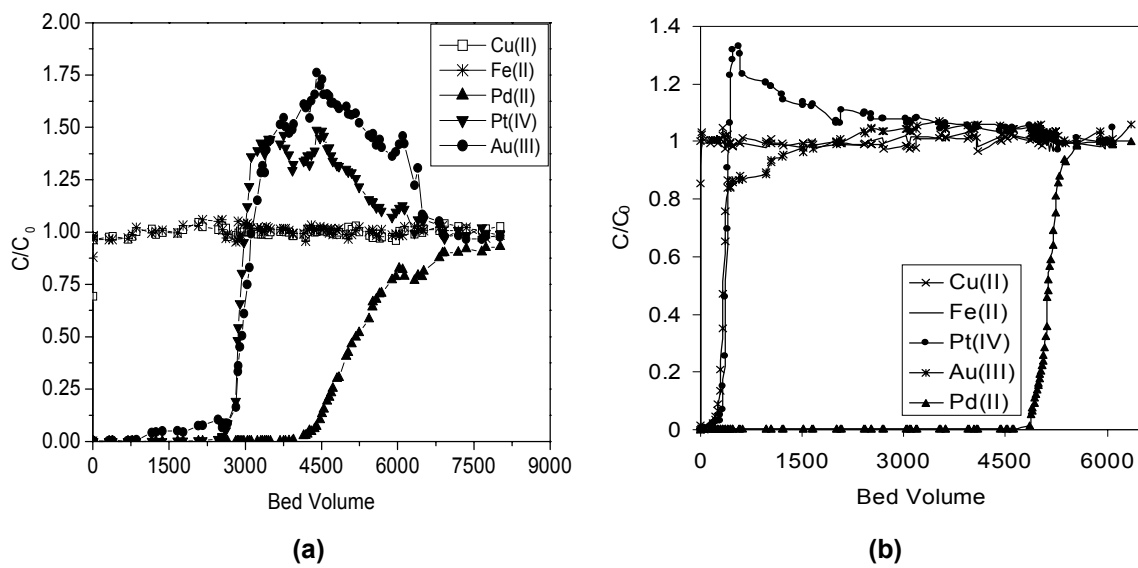


Figure 3. Multi-metal breakthrough curves in columns of SOL-IPS (bed volume = 3.36 ml) at  $[HCl] = 0.1\text{ M}$ , (a) and SOL-PzPs (bed volume = 2.98 ml) at  $[HCl] = 2.0\text{ M}$ , (b): flow rate = 1.0–1.1 ml/min; maximum loading of SOL-IPS = 0.88 mmol Pd/g, 0.50 mmol Pt/g, and 0.47 mmol Au/g; maximum loading of SOL-PzPs = 0.77 mmol Pd/g, 0.0 mmol Pt/g, and 0.03 mmol Au/g.

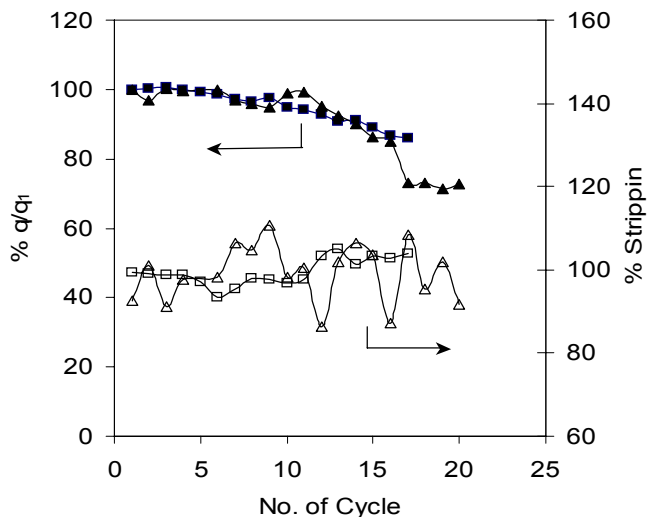


Figure 4. Results of stability tests of SOL-IPS ( $\blacktriangle$  and  $\square$ ) and SOL-PzPs ( $\blacksquare$  and  $\square$ ) by repeated Pd(II) loading and stripping cycles:  $q_i$  is palladium uptake capacity at  $i^{\text{th}}$  cycle;  $q_1$  is palladium uptake capacity at 1<sup>st</sup> cycle (1.42 mmol/g for SOL-IPS and 1.37 mmol/g for SOL-PzPs).

## COMPARISON OF ADSORBENTS FOR NOBLE METAL EXTRACTION

Most adsorbents for extracting noble metals reported in the literature are polymer resins developed through solvent impregnation, ligand coupling (covalent bonding), and copolymerization techniques. Of these approaches, the copolymerization technique generally produces higher ligand density than other techniques. However, the actual metal uptake capacities of these copolymers are usually lower than the predicted capacities obtained from metal-ligand stoichiometry due to the presence of ligands inaccessible to metal ions. The organo-ceramic adsorbents synthesized in this study, however, show high metal uptake capacities as well as high ligand densities. These imply that most of the ligands incorporated

into these silica structures can be accessed by metal ions. Also, these organo-ceramic adsorbents normally have faster equilibration time than chelating resins. In addition to these desirable properties, SOL-PzPs, in particular, has stronger selectivity for Pd(II) than polymer resins functionalized with similar functional groups (3(5)-methylpyrazole and 3,5-dimethylpyrazole) [8, 9]. Hence, this adsorbent is an attractive alternative for selective extraction of Pd(II) as compared to polymer resins at high HCl concentrations.

## CONCLUSIONS

Organic-ceramic adsorbents functionalized with imidazole (SOL-IPS) and pyrazole (SOL-PzPs) are synthesized by sol-gel processing technology for the separation of noble metals at low and high HCl concentrations, respectively. From multi-metal breakthrough experiments, both adsorbents show no adsorption of copper and iron, which exist in excessive quantities in noble metal leaching solutions. More importantly, the pyrazole functionalized adsorbent shows strong selectivity for palladium chloride over platinum and gold chlorides. Hence, this adsorbent has a high potential for application in the separation and recovery of noble metals from leaching solutions of ores, spent catalysts, and disposed microelectronic components. Further investigation is on going to selectively recover platinum and gold in copper and iron enriched HCl solutions. Accordingly, complete extraction and separation of palladium, platinum, and gold can be achieved with sequential fixed beds using these adsorbents.

## ACKNOWLEDGEMENT

The financial support from National Science Foundation through grant No. CTS-9805118 is gratefully acknowledged.

## REFERENCES

1. C-H. Kim, S.I. Woo, and S. H. Jeon (2000), *Ind. Eng. Chem. Res.*, **39**, 1185-1192.
2. D. O'Sullivan (1992), *Chem. Eng. News*, (Oct. 26), 20.
3. B. Cote, E. Benguerel, and G.P. Demopoulos (1993) *Precious Met.*, **17**, 593-617.
4. K. Sanjiv, V. Rakesh, B. Venkataramani, V.S. Raju, and S. Gangadharan (1995), *Solv. Extr. Ion Exch.*, **13**, 1097-1112.
5. N.A. D'yachenko, A.K. Trofimchuk, and V.V. Sukhan (1999), *Zh. Anal. Khim.*, **54**, 151-161.
6. J.S. Lee, S. Gomez-Salazar, and L.L. Tavlarides (2001), *React. Funct. Polym*, in press.
7. L.L. Tavlarides, N.V. Deorkar, J.S. Lee, US Pat. Appl.No. 09/573,304. Filed 5/18/2000.
8. G.V. Myasoedova, N.I. Shcherbinina, E.A. Zakhartchenko, S.S. Kolobov, L.V. Lileeva, P.N. Komozin, I.N. Marov, and V.K. Belyaeva (1997), *Solv. Extr. Ion Exch.*, **15**, 1107-1118.
9. I.I. Antokol'skaya, G.V. Myasoedova, L.I. Bol'shakova, M.G. Ezernitskaya, M.P. Volynets, A.V. Karyakin, and S.B. Savvin (1976), *Zh. Anal. Khim.*, **31**, 742-745.



# HYDROPHOBIC GEL SEPARATION AGENTS (X). SOLVENT EXTRACTION SEPARATION OF COPPER(II) AND LANTHANIDE(III) IN THE PRESENCE OR ABSENCE OF HYDROPHOBIC SILICA GELS

Yu Komatsu, Hisao Kokusen and Shigekazu Tsurubou\*

Faculty of Engineering, Kanazawa Institute of Technology, Ishikawa, Japan

\*Department of Chemistry, School of Dentistry, Asahi University, Gifu, Japan

In an ongoing research program dedicated to the improvement of solvent extraction methodology for the separation of metal ions, we have developed a new extraction system called Triple Phase Extraction Systems that can significantly improve both the extractability and selectivity of such separations. Triple phase extraction is a method involving the introduction of a hydrophobic silica gel separation agent, having an alkyl chain, into a solvent extraction system, thereby improving extractability and selectivity. This is a phenomenon unique to triple phase extraction systems and is not achieved in a synergic extraction systems. We describe extraction of copper(II) ions with TTA and extraction of rare earth with H<sub>2</sub>Clbbpen. We think that the triple phase extraction method is adaptable to macro-scale separations.

## INTRODUCTION

Solvent extraction is a useful method for the separation and reservation of precious metals. The improvement of selectivity and extractability has been extensively examined [1,2]. Many synergic extraction systems, which use a synergic effect to improve the extractability, have been investigated [3]. In many synergistic extraction systems, selectivity decreases. A further disadvantage arises from the use of halogenated hydrocarbons as carrier solvents (or diluents) because of the adverse environmental effects of their use. We found that, by modifying the characteristic behavior of a typical solvent extraction system by the addition of a hydrophobic silica gel, we could achieve the desired increase in selectivity. For obvious reasons, we call this new technique Triple Phase Extraction System (TPES) [4-6]. It is a method of adding the hydrophobic silica gel separation agent, which has an alkyl chain, into a general solvent extraction system. In this method, metal complexes are extracted into organic solvent. After that, metal complex distributed to silica gel separation materials. Therefore, high extraction ability is shown. In this case, the selectivity improves because the distribution constant is different according to metal complex. The extraction of a transition metal ion and lanthanide ion is described in this paper.

## EXPERIMENTAL

### Reagents and Apparatus

The synthesis of hydrophobic silica gels were performed according to previously described methods [7]. Hydrophobic silica gel materials in which octadecyl group, dodecyl group and phenyl group are introduced are abbreviated as C18g, C12g and C6g, respectively. Carbon content of synthesized C18g was 22%. The synthesis of H<sub>2</sub>Clbbpen in Figure 1 was performed according to the method of Neves *et al.* [8]. TTA (4,4,4-trifluoro-1-(2-thienyl)-1,3-butanedione) was made by Dojindo Laboratories. All other chemicals were reagent-grade materials and deionized water was used throughout. The pH and the metal concentration in the aqueous phase were determined with a Hitachi-Horiba F-13 pH meter equipped with glass electrode and a Seiko SPS-1200R inductively coupled argon plasma spectrometer was used to determine metal concentrations. For metal concentrations in the organic phase the solution was first back extracted into 1 M sulfuric acid and then analysed by ICP. Gel separation agent were separated using centrifugation or filtration.

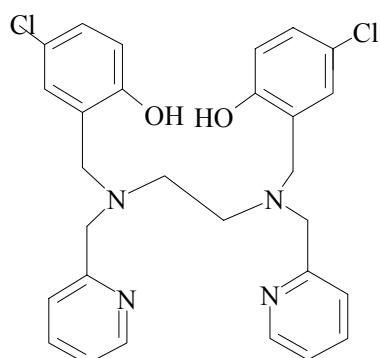


Figure 1. *N,N'-bis(5-chloro-2-hydroxybenzyl)-N,N'-bis(2-methylpyridyl)ethanediamine (H<sub>2</sub>Clbbpen).*

### Extraction of Metal Ion

#### Extraction of copper(II) ion with TTA

In a 30 cm<sup>3</sup> centrifuge tube, an aliquot of toluene (10 cm<sup>3</sup>) containing 0.01 M TTA was equilibrated with an equal volume of an aqueous phase containing 0.1 M sodium nitrate and 0.02 M buffer (chloroacetic acid and acetic acid) containing 1.0 × 10<sup>-4</sup> M Cu<sup>2+</sup>. After the two phases were separated by centrifugation, the pH and Cu(II) concentration of the aqueous phase were measured. In the TPES experiment, 5 g of the gel per 100 cm<sup>3</sup> solvent was added.

#### Extraction of lanthanide ions with H<sub>2</sub>Clbbpen and picrate ion

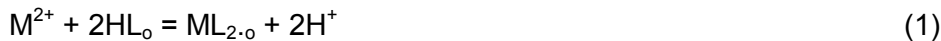
Lanthanide ions were extracted in a manner similar to that of copper(II) extraction. In a 30 cm<sup>3</sup> centrifuge tube, an aliquot of toluene (10 cm<sup>3</sup>) containing 0.02 M H<sub>2</sub>Clbbpen and an equal volume of an aqueous phase containing 1.0 × 10<sup>-4</sup> M Ln<sup>3+</sup>, 0.01 M sodium picrate and the 0.02 M buffer (acetic acid, 2-(N-morpholino)ethanesulfonic acid (MES), 3-(N-morpholino)-propanesulfonic acid (MOPS) and N-tris(hydroxymethyl)methyl-3-aminopropanesulfonic acid). After aqueous and other phase were separates by centrifugation, the pH and lanthanide concentration of aqueous phase were determined.

## RESULTS AND DISCUSSION

#### Extraction Mechanism and Equilibrium Analysis

Figure 2 shows the extraction scheme of triple phase extraction system in the case of extraction of transition metal ions. First, metal ion was complexed with extractant in aqueous phase. The metal complex is distributed to an organic phase. Second, extracted metal

complexes in the organic phase are distributed to the gel phase. Each distribution constant is assumed to be P and P'. The extraction constant and extraction equilibrium of a general solvent extraction system can be shown as follows.



$$K_{ex} = [ML_2]_o [H^+]^2 / [M^{2+}] [HL]_o^2 \quad (2)$$

$$D = [ML_2]_o / [M^{2+}] \quad (3)$$

where subscript o denote the species in the organic phase.

First, in the absence of hydrophobic silica gel,  $[ML_2]_{(o+s)}$  equals  $[ML]_o$ . Therefore, the extraction constant reduces to that of the general extraction.

In the presence of the gel, we have the following formulation.

$$[ML_2]_o + [ML_2]_g = C - [M] \quad (4)$$

where subscript s denote the species in the solid phase (gel phase) and C represents the initial concentration of metal ions. Therefore, the metal concentration except for aqueous phase  $[ML_2]_{(o+s)}$  can be calculated in equation (5) and there are following relation on  $[ML_2]_o$  and  $[ML_2]_g$ .

$$[ML_2]_{(o+s)} = [ML_2]_o + [ML_2]_g \quad (5)$$

$$P' = [ML_2]_g / [ML_2]_o \quad (6)$$

By using these equations, the metal concentration except for aqueous phase  $[ML_2]_{(o+s)}$  can be described as follows.

$$[ML_2]_{(o+s)} = \{1 + P'\}[ML_2]_o \quad (7)$$

This equation was substituted for expression (2), the extraction constant of triple phase extraction system( $K_{ex}'$ ) was described as follows.

$$\begin{aligned} K_{ex}' &= [ML_2]_o \{1 + P'\} [H^+]^2 / [M^{2+}] [HL]_o^2 \\ &= \{1 + P'\} K_{ex} \end{aligned} \quad (8)$$

The effect of addition of hydrophobic silica gel can be quantitatively discussed by using partition constant (P'). The extraction curve was analyzed based on such a formulation.

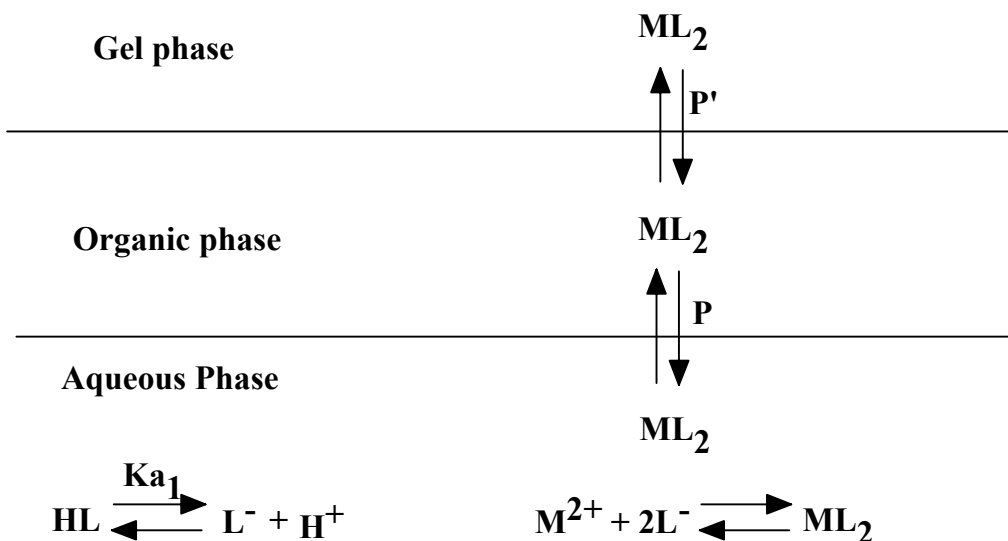


*Figure 2. Extraction mechanism of triple phase separation system.*

HL : Extractant; P: Distribution constant of metal complexes between organic and aqueous phase;  
P': Distribution constant of metal complexes between organic and gel phase;  
 $K_{a1}$  and  $K_{a2}$  : dissociation constants of ligand.

### Extraction of Transition Metal Ion using TTA

Log D vs. pH plot when the copper ion is extracted by using various separation materials and TTA is shown in Figure 3, and a half extraction pH is shown in Table 1. The overall extraction equilibrium, constant ( $K_{ex}$ ) and extraction constant of triple phase extraction system ( $K_{ex}'$ ) of copper(II) ion can be described as:



$$K_{ex} = [CuL_2]_o [H^+]^2 / [Cu^{2+}] [HL]_o^2 \quad (10)$$

$$\begin{aligned} K_{ex}' &= [CuL_2]_o \{1 + P'\} [H^+]^2 / [Cu^{2+}] [HL]_o^2 \\ &= \{1 + P'\} K_{ex} \end{aligned} \quad (11)$$

As can be seen from Figure 3, the results conform to a linear relationship between the log Cu extracted and the pH as predicted from Eqn. (11) both in the presence and absence of the gel. The added distribution occurring with the gel increases the extractability at each pH, as seen in the lower values of  $pH_{1/2}$  corresponding to a higher value of the distribution constant. Table 2 shows the relation of extraction solvent and distribution constant ( $P'$ ) when the copper ion is extracted by using TTA with C18g. When using a small organic solvent of the permittivity and the dipole moment is used the magnitude of the distribution constant is large. It is thought that the ratio which extracted complex distributes into the gel phase is large because the solubility of complex is small. Extractability increases when the introduced alkyl chain becomes long. Moreover, when the solvent with small solubility of complex is used, the distribution constant is large and an increase in the extractability is large.

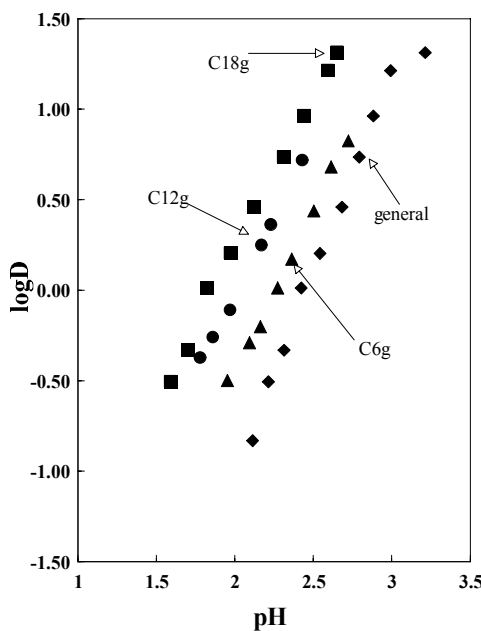


Figure 3.  $\log D$  vs.  $pH$  of TTA- $Cu^{2+}$  extraction system.

$Cu^{2+} : 1.0 \times 10^{-4} M$ ; TTA :  $0.01 M$ ; Buffer :  $0.02 M$ ; Sodium Nitrate :  $0.01 M$ ; Organic solvent : Toluene; Hydrophobic gel separation agent  $5 g/100 cm^3$  solvent.

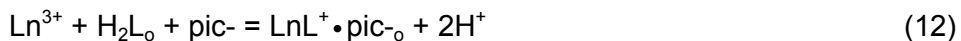
Table 1.  $pH_{1/2}$  of triple phase extraction systems.

Extraction system	C18g	C12g	C6g	general
$pH_{1/2}$	1.82	2.08	2.24	2.38

$Cu^{2+} : 1.0 \times 10^{-4} M$ ; TTA :  $0.01 M$ ; Buffer :  $0.02 M$ ; Sodium nitrate :  $0.1 M$ .  
Organic solvent : Toluene ; Hydrophobic gel separation agent  $5 g/100 cm^3$  solvent.

### **Ion Pair Extraction of Rare Earth Metal Ion using H<sub>2</sub>Clbbpen**

Lanthanide ions can be extracted with H<sub>2</sub>Clbbpen and picrate ion into toluene and dichloroethane as an ion pair species. Extractability of system decreases when the toluene was used. The solubility of the extracted ion pair species was small because the permittivity of the toluene is smaller than that of dichloroethane, and the extractability is also small. The overall ion pair extraction equilibrium, extraction constant ( $K_{ex}$ ) and extraction constant of triple phase extraction system ( $K_{ex}'$ ) of lanthanide ion can be described as:



$$K_{ex} = [LnL^+ \cdot pic^-_o][H^+]^2 / [Ln^{3+}][H_2L_o][pic^-] \quad (13)$$

$$\begin{aligned} K_{ex}' &= [LnL^+ \cdot pic^-_o]\{1 + P'\}[H^+]^2 / [Ln^{3+}][H_2L_o][pic^-] \\ &= \{1 + P'\}K_{ex} \end{aligned} \quad (14)$$

From Figure 4 may be seen that the log D vs. pH plot is in accord with the scheme developed in Eqns. (12)-(14). In each of the systems the data exhibit a linear relationship of slope 2, with the pH<sub>1/2</sub> moving to lower values as the length of the alkyl chain is increased. It is also seen that differences in pH<sub>1/2</sub> from neighboring Ln ions also increases, signifying an increase of selectivity (see Table 2).

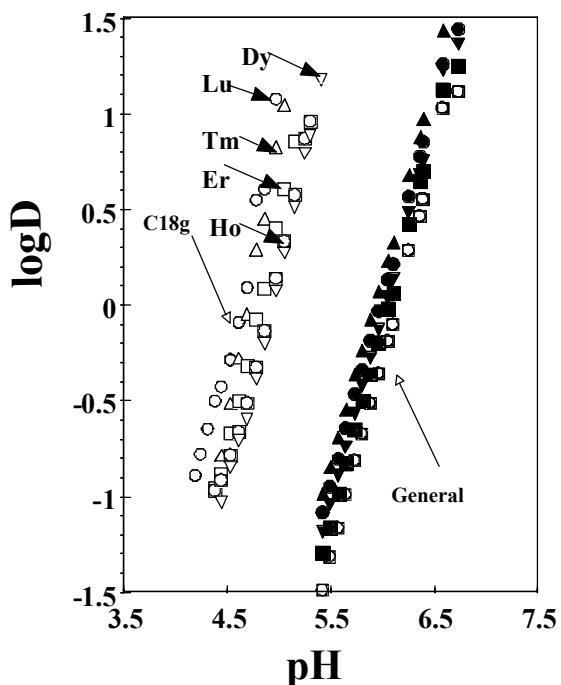


*Figure 4. log D vs. pH of ion pair extraction of lanthanide metal.*  
 Ln<sup>3+</sup> : 1.0 × 10<sup>-4</sup> M ; H<sub>2</sub>Clbbpen:0.01 M ; Buffer : 0.02M ; Sodium picrate : 0.01 M ;  
 Organic solvent : Toluene; Hydrophobic gel separation agent 5 g/100 cm<sup>3</sup> solvent.

When the extraction constants of the same metal are compared, it is seen that the extraction constant of triple phase extraction system is large. Separation factors of triple phase extraction systems are larger than that of a general extraction system. Therefore, it is understood that extractability and selectivity improved by adding the hydrophobic gel separation agent. The selectivity of lanthanide metal ion improves for the difference of the distribution constant. The distribution constant was increasing with decreasing ionic radii of lanthanide metal ions. The selection improves because the distribution constant of heavy lanthanide metal ion with a high extraction constant is large. This phenomenon is unique to triplephase extraction system and is not seen in a synergic extraction system. This method should be broadly applicable to many metal ion separation processes.

*Table 2. Extraction constants and distribution constants of general and triple phase extraction systems.*

	$\log K_{ex}$	$\log K'_{ex}$	P'
La <sup>3+</sup>	-10.42	-9.27	13.1
Pr <sup>3+</sup>	-9.42	-8.42	9.0
Nd <sup>3+</sup>	-9.53	-8.30	16.0
Sm <sup>3+</sup>	-9.16	-7.62	33.5
Eu <sup>3+</sup>	-8.98	-7.48	27.1
Gd <sup>3+</sup>	-9.28	-7.64	42.5
Tb <sup>3+</sup>	-8.48	-6.95	32.7
Dy <sup>3+</sup>	-8.01	-6.62	23.4
Ho <sup>3+</sup>	-8.21	-6.55	44.5
Er <sup>3+</sup>	-8.10	-6.40	48.9
Tm <sup>3+</sup>	-7.81	-6.18	41.5
Yb <sup>3+</sup>	-7.46	-5.58	74.5
Lu <sup>3+</sup>	-7.93	-5.99	85.3

$\log K_{ex}$  : Extraction constant of normal extraction.

$\log K'_{ex}$  : Extraction constant of three phase extraction.

P': Distribution constant.

## REFERENCES

1. T. Sekine, I. Kobelova, J. Noro and N. Thi Kim Dung (1994), *Anal. Sci.*, **10**, 743-748.
2. T. Sekine, A. Abdurahman, and N. Thi Kim Dung (1994), *Anal. Sci.*, **10**, 955-958.
3. H. Kokusen, Y. Sohrin, H. Hasegawa, Y. Hata, S. Kihara and M. Matsui (1996), *J. Chem. Soc., Dalton Trans.*, **1996**, 195-201.
4. Y. Komatsu, S. Umetani, S. Tsurubou, Y. Michiue and T. Sasaki (1998), *Chem. Lett.*, **1998**, 1167-1170.
5. Y. Kuo, (1984), *Chem. Eng. Progr.*, **1984**, 37-42.
6. C. Rostaing, G. Cote and D. Bauer, (1987), *Proc. Summer School on Extraction, PROGEC*, Toulouse, France, C.I-1-C.I-10.
7. K. K. Unger (1974), *Porous Silica*, Elsevier Scientific, Amsterdam.
8. A. Neves, S. M. D. Erthal, I. Vencato and A. S. Ceccato (1992), *Inorg. Chem.*, **31**, 4749-4755.



## COALESCENCE EXTRACTION - FROM MOLECULAR DYNAMICS TO CHEMICAL ENGINEERING APPLICATION

Achim Schaad and Hans-Jörg Bart

Institute of Thermal Process Engineering  
University of Kaiserslautern, Kaiserslautern, Germany

Coalescence Extraction is an effective solvent extraction method which uses single phase extraction followed by spinodal phase decomposition. After a rapid temperature or composition quench the phases separate within seconds even in the presence of emulsifying agents. Phase separation kinetics are studied using crystal violet as surfactant. The formation of phase boundary during coalescence extraction is analysed by a microscopy set-up. Furthermore, coalescence extraction is carried out using a reactive solvent extraction mixture. Iodine, which is used as transfer component, is quantitatively transferred into the organic phase. In order to investigate the structure and dynamics from the very beginning of phase separation, molecular dynamics techniques are applied. The resulting diffusion coefficients are in good accordance with the literature.

### INTRODUCTION

An efficient solvent extraction method has been investigated which is called either 'Coalescence Extraction' [1] or 'Phase Transition Extraction' [2]. It is based on the use of a primary solvent which, in combination with the feed, forms a homogeneous solution. This homogeneous phase has enormous extraction potential for the treatment of cell fragments and other highly viscous materials. In the next step, a secondary solvent (Composition-Induced Phase Separation, CIPS) or a significant temperature change (Temperature-Induced Phase Separation, TIPS) is used to enter the spinodal two-phase region in which an extract and a raffinate are formed. The phases separate within seconds, even in the presence of emulsifying agents [3]. Furthermore, the interfacial surface area, which is one of the most relevant determinants of extraction rates, reaches its theoretical limit.

Stable emulsions may frequently develop in solvent extraction (e.g., with fermentation broths) which make the separation of the desired product difficult. Furthermore, the shear stress induced by vigorous stirring can in many cases damage high molecular weight compounds [4]. In addition, the product yield may be reduced through partially adsorbed solute molecules adhering to solid surfaces due to wetting and leaching problems of an organic solvent. This paper describes a strategy to solve these problems.

Although many experimental and theoretical studies have been carried out, which were summarised by [5], a fundamental understanding of the phase separation process does not yet exist.

## EXPERIMENTAL

The non-reactive system investigated contains a solvent mixture of 4-methyl-2-pentanone (MIBK), acetonitrile and an aqueous solution of crystal violet dye [6]. Crystal violet acts both as a surfactant and as a transfer component. Several functional groups cause its intensive colour. The surface-active properties of crystal violet are verified by measuring the interfacial tension. The second solvent system used is a binary mixture of 2,6-dimethylpyridine and water. Iodine is used as a model transfer component. A reaction takes place between 2,6-dimethylpyridine and iodine, forming charge-transfer complexes and ionic species [7]. Both selected solution systems have very low critical solution temperatures (CST).

An experimental set-up has been designed to study the dynamic behaviour of the phase separation process (Figure 1). It consists of a temperature-controlled cell (volume: 0.7 ml) and a CCD-camera which is mounted on an optical microscope. This allows an on-line observation of the phase separation process. Structures are resolved up to a size of 2  $\mu\text{m}$ . Two temperature baths are used for rapid temperature quenching. The solution is stirred in order to achieve fast heat transfer. The resulting frames are grabbed by a computer and analysed with commercially available software.

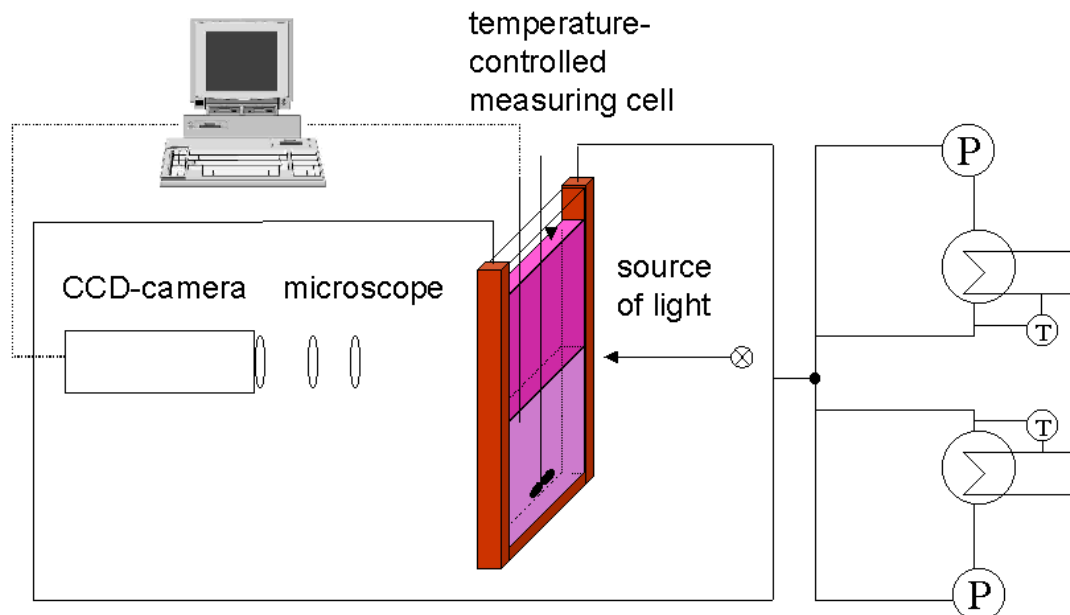
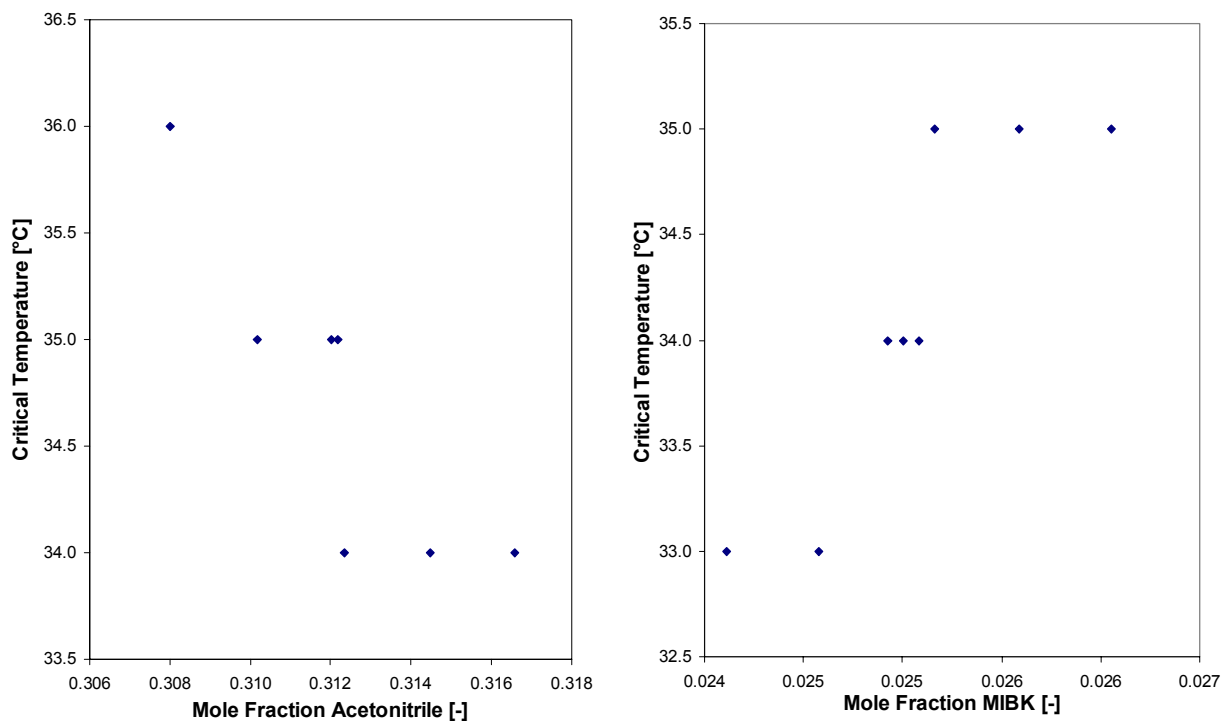


Figure 1. Experimental set-up.

## RESULTS AND DISCUSSION

### Non-Reactive Coalescence Extraction

The non-reactive solvent mixture is investigated with regard to critical temperature, equilibria, kinetics of phase separation and microscopic structure of the phase boundary during phase disengagement. The correlation of critical temperature and composition of the solvent mixture is investigated using a crystal violet concentration of 5 mg/l in the aqueous phase (Figure 2). The upper critical solution temperature (UCST) of the mixture increases with increasing amount of MIBK. The opposite effect is observed when the mole fraction of acetonitrile increases, as it is known from the literature [8]. Even very small changes in composition cause significant changes in critical temperature. This is useful with respect to a technical application.



*Figure 2. Critical solution temperature.*

The equilibrium concentrations of crystal violet are measured by UV-spectroscopy. When only MIBK is used as organic solvent in a conventional extraction process, the efficiency of extraction is very poor compared with a mixture of acetonitrile/MIBK or with coalescence extraction, that is CIPS (Figure 3).

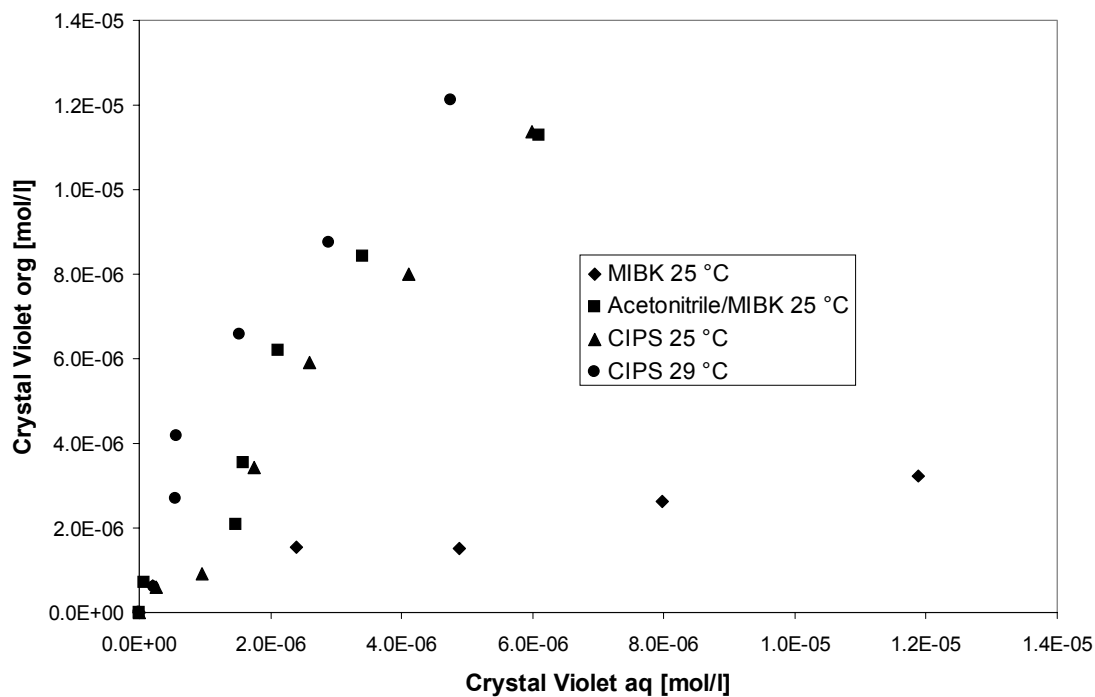


*Figure 3. Equilibria.*

Furthermore, Figure 3 shows that equilibria of conventional extraction and coalescence extraction are identical within tolerance as expected. In addition, equilibria are investigated at different temperatures. Significantly higher distributions of dye in the organic phase are observed at higher temperatures.

The phase separation kinetics are measured by several visualisation techniques. A series of macroscopic photos are taken by a stirring cell during the phase separation process using a digital camera. These images show that the solvent extraction method used influences the separation kinetics heavily. When the same amount of surfactant is dissolved both in conventional extraction and coalescence extraction, the kinetics of phase separation are found to be faster in orders of magnitude in the latter. In conventional extraction, intensive mixing of the phases yields a stable (30 minutes) emulsion zone. Since a single extraction phase is obtained in the case of coalescence extraction, moderate stirring is sufficient here. Moreover, the phases separate within seconds even in the presence of emulsifying agents. Since the coalescence process is very fast there are no well-defined phase boundaries to which surface-active compounds can adsorb [5].

Microscopic photos are taken during the phase separation process. A typical morphology of a emulsion-zone formed in conventional extraction processes consists of polydisperse droplets in the order of magnitude of 90  $\mu\text{m}$  (Figure 4 A). This almost rigid emulsion zone between the organic and the aqueous phase decreases during the phase separation process until a sharp phase boundary is obtained. The duration of this process ( $> 30 \text{ min}$ ) depends on the energy input which is brought into the system.

During the coalescence process, the situation is completely different, not only with respect to the dynamics, but also to the structure of the phase boundary. At the beginning of phase separation a interface between the phases appears which is initially very diffuse. At the same time dynamic domains on both sides of the phase boundary start to grow during the phase separation process. These domains spread out from the phase boundary. Figure 4 B shows the interconnectivity of phases which is characteristic of spinodal decomposition [5].

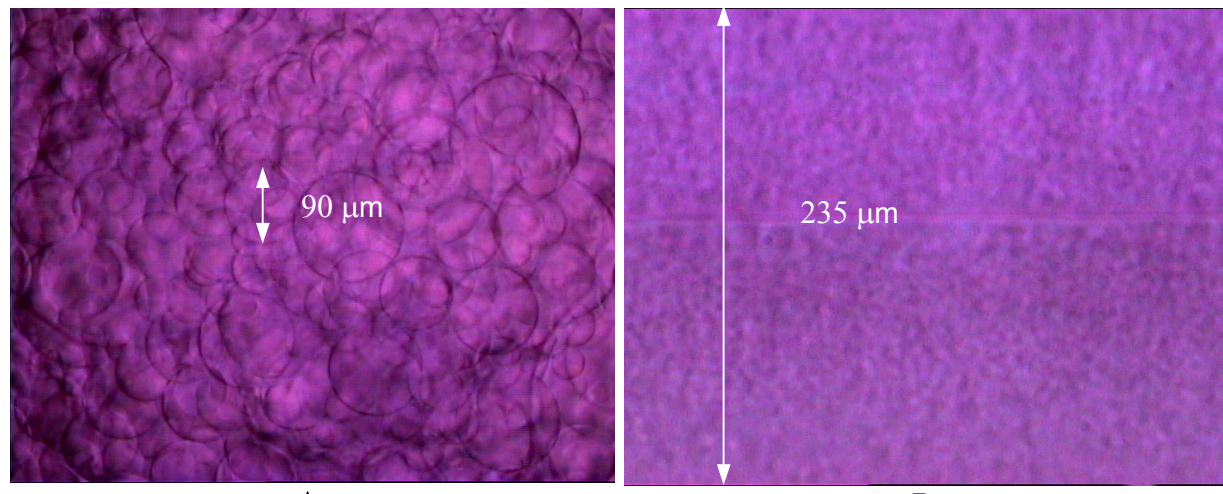


Figure 4. Microscope photos (A: Conventional Extraction, B: CIPS),

### Reactive Coalescence Extraction

The binary mixture of 2,6-dimethylpyridine and water has a lower consolute point at a temperature of 33.9 °C and a 2,6-dimethylpyridine concentration of 2.78 M [10]. Iodine, which is used as model transfer component, is bound through 2,6-dimethylpyridine by complexation. Equilibria measurements of different iodine concentrations (up to 100 mg/l) show a quantitative mass transfer in the organic phase. Using a 2.2 M 2,6-dimethylpyridine solution (critical

temperature: 34.3 °C [10]) the interfacial tension is measured at different temperatures as close as possible to the consolute point, resulting in a linear correlation. The interfacial tension decreases with decreasing temperature. If the regression curve is extrapolated to a interfacial tension of zero a critical temperature of 35.7 °C is obtained which is very close to published data.

### Molecular Dynamics Simulations

Since the phase separation kinetics in coalescence extraction are very fast, experiments will fail to study the first stages of this process. In order to investigate the structure and dynamics from the very beginning of phase separation, molecular dynamics techniques are applied. Molecular dynamics simulations involve numerical solution to Newton's equations of motion for a set of molecules [9]. Commercially available software is used to determine the diffusion coefficient of a 5 mole % solution of 2,6-dimethylpyridine in water. A periodic three-dimensional box (box-length: 16.8 Å) is built consisting of 5 molecules of 2,6-dimethylpyridine and 95 molecules of water (Figure 5). Afterwards, a minimisation is performed to optimise the conformation of the model so that such conformation corresponds to one at 0 K. Finally, a molecular dynamics simulation is carried out at a temperature of 298 K. From the resulting trajectories a mean-square displacement (MSD) is calculated as a function of the position of each diffusing molecule. As a result, the interdiffusion constant D is obtained using the Einstein relation (1) where N is the number of the atoms, r the position of the particle and t corresponds to the simulation-time in fs.

$$D = \frac{1}{6Nt} \langle |r(t) - r|^2 \rangle \quad (1)$$

D is obtained by calculating the slope of MSD vs. time. The result of this non-ideal solvent system,  $0.99 \cdot 10^{-10} \text{ m}^2 \text{ s}^{-1}$ , is in accordance with the literature value of  $1.03 \cdot 10^{-10} \text{ m}^2 \text{ s}^{-1}$  [10].

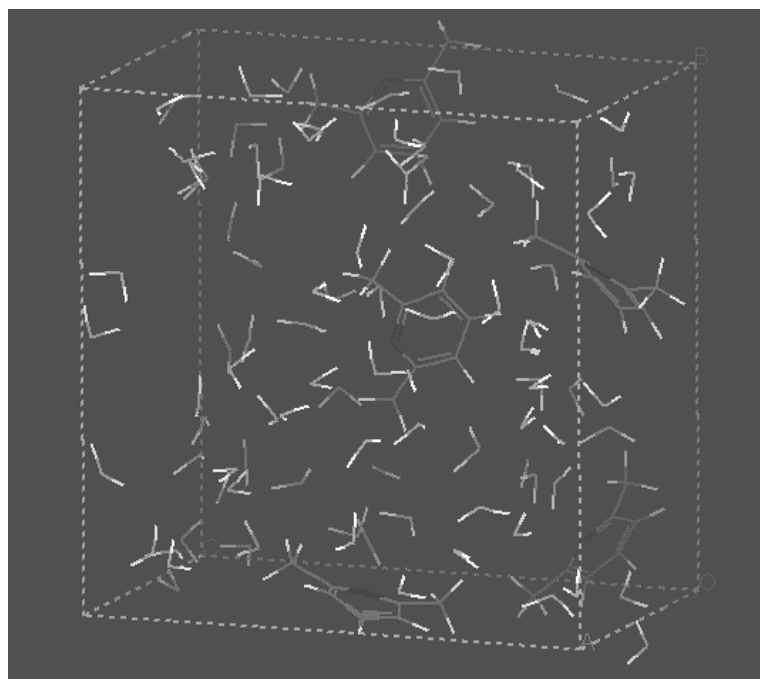


*Figure 5. Periodic three-dimensional 2,6-dimethylpyridine/water-box.*

## CONCLUSIONS

This work investigated coalescence extraction which is a benign extraction tool using partially immiscible solvents. When significant concentrations of surfactant are present, phase separation is found to be much faster than in conventional solvent extraction. The phase separation process is studied using microscopic measurements, yielding detailed information on the dynamics of phase separation. Molecular dynamics simulations are applied to investigate this process from the very beginning. The resulting diffusion coefficients are in accordance with the literature. Further work will deal with a detailed study of the binary system discussed last. The aim of such work is to investigate the structure and dynamics of the phase separation process. Conventional molecular dynamics simulations are useful to obtain diffusion coefficients and to analyse the structure of the phase boundary. Since the simulation time of conventional molecular dynamics is limited to a few nanoseconds, molecular dynamics can analyse only one part of the separation process. The molecular model used has to be simplified in order to obtain a complete theoretical description by using Dissipative Particle Dynamics (DPD) simulations. On the one hand, microscopic processes are investigated; on the other hand, molecular dynamics simulations are used. DPD will bridge the gap between the different time- and length-scales.

## ACKNOWLEDGEMENTS

We would like to thank Deutsche Forschungsgemeinschaft (DFG) for supporting this work.

## REFERENCES

- 1 J. D. Lamb and R. T. Peterson (1995), *Sep. Sci. Techn.*, **30** (17), 3237-3244.
- 2 A. Ullmann, Z. Ludmer, R. Shinnar (1995), *AIChE J.*, **41** (3), 488-500.
- 3 R. Gupta, R. Mauri, R. Shinnar (1999), *Ind. Eng. Chem. Res.*, **38**, 2418-2424.
- 4 H. Hsien-Wen (1980), Techniques of Chemistry, Chap. VI., A. Weissberger (ed.), Wiley-Interscience, New York.
- 5 J. D. Gunton, M. San Miguel, P. S. Sahni (1983), Phase Transitions and Critical Phenomena, Vol. 8, C. Domb and J. L. Lebowitz (eds.), Academic Press, London, pp. 269-466.
- 6 R. Gupta, R. Mauri, R. Shinnar (1996), *Ind. Eng. Chem. Res.*, **35**, 2360-2368.
- 7 I. I. Schuster and J. D. Roberts (1979), *J. Org. Chem.*, **44** (15), 2658-2662.
- 8 B. J. Hales, G. L. Bertrand, L. G. Hepler (1966), *J. Phys. Chem.*, **70** (12), 3970-3975.
- 9 J. P. O'Connel and M. Neurock (2000), *AIChE Symp. Ser.*, **96** (323), 5-22.
- 10 J. C. Clunie and J. K. Baird (1999), *Phys. Chem. Liq.*, **37**, 357-371.



## LIQUID-LIQUID EXTRACTION IN AQUEOUS BIPHASE SYSTEMS: PARTITIONING BEHAVIOR OF SILICA AND HEMATITE IN THE DEXTRAN/TRITON X-100/WATER SYSTEM

**Xi Zeng and Kwadwo Osseo-Asare**

Department of Materials Science & Engineering, Pennsylvania State University,  
University Park, PA, USA

A two-phase system may be produced when a water-soluble polymer is added to another water-soluble polymer, an inorganic salt, or a surfactant in aqueous solution. Compared to conventional solvent extraction media, aqueous biphasic systems are potentially more environmental friendly since they can be formulated with non-toxic and degradable polymers. The feasibility of employing aqueous biphasic systems for fine particle separations was investigated by using dextran/Triton X-100/water mixtures as separation media, with hematite and silica as model materials. For the entire pH range investigated (pH 2-12), hematite preferred the bottom dextran-rich phase. In contrast silica exhibited a pH-dependent partitioning behavior. It was found that the partitioning behavior of both silica and hematite could be modified significantly in the presence of ionic surfactants. The physicochemical origins of these effects are discussed.

### INTRODUCTION

A two-phase system often forms when two different water-soluble polymers are mixed in water. This kind of aqueous biphasic system has been used as an extraction medium for bioseparations after the pioneering work of Albersson in the mid-1950s. Other aqueous biphasic systems of biotechnological interest are also known, such as those composed of a polymer and a surfactant or a polymer and an inorganic salt [1-3]. Recently, the application of aqueous biphasic extraction has broadened to include processing of ultrafine particles [4-6] and separation of metal ions [7].

In our laboratory, work is in progress to apply aqueous biphasic systems as the extraction media for ultrafine particle processing [8-10]. The partitioning behavior of several inorganic particles, e.g., pyrite, hematite, silica, alumina, and titania, has been studied in polyethylene glycol (PEG)/Na<sub>2</sub>SO<sub>4</sub> systems. As in conventional liquid-liquid extraction [11], the partitioning behavior relies on the surface properties of the solids and the interfacial interactions between the particles and the surrounding liquid solution. The distribution of particles is dependent upon many factors, such as the surface hydrophilic/hydrophobic balance, solution pH, the nature and concentration of collectors (surfactants), and specific interaction between the polymer and the oxides.

Previous work in the literature has mainly focused on the partition of solids in polymer/salt aqueous biphasic systems; little work has been reported for other systems. The only available result of solid partition in polymer/polymer biphasic systems concerns the work of Baxter *et al.* [6] who studied the partition of dispersed TiO<sub>2</sub> pigment and latex particles in the PEG/poly(N-vinylpyrrolidone) (PVP) system. In the available published literature, no research has been reported yet about the partition of inorganic particles in the polymer/surfactant system, although this system has been used in bioseparation [12-14]. This paper presents the results of an investigation into the partitioning behavior of particles (hematite and silica) in polymer/surfactant systems (dextran (Dex)/Triton X-100 (TX100)). First, the partitioning behavior at different pH values is presented; then, the feasibility of applying electrostatic force to modify particle partition is exploited. In polymer/nonionic surfactant systems, electrostatic interaction can have a significant effect on the distribution of biological materials [12-14]. In these systems, a weakly charged environment develops if an ionic surfactant is added, which is concentrated in the top surfactant-rich phase. Thus, Coulombic attraction or repulsion is produced between the surfactant-rich phase and charged proteins; therefore, the partitioning of proteins is affected by this electrostatic interaction [12-14].

## EXPERIMENTAL

Dextran (average molecular weight 24,500), Triton X-100, ferric oxide (< 5 μm size), were purchased from Sigma-Aldrich Co. Dodecyltrimethylammonium bromide (DTAB), sodium dodecyl sulfate (SDS), sodium hydroxide, and nitric acid were all of reagent grade (Aldrich). Distilled water was used in all experiments. The composition of the Dex/TX100 system was 9.0 wt% polymer, 11.0 wt% surfactant, and 80.0 wt% water. In this system, the bottom phase was enriched in dextran, the other component was concentrated in the top phase [12-14]. The experimental procedures used in this study were as previously described [8-10].

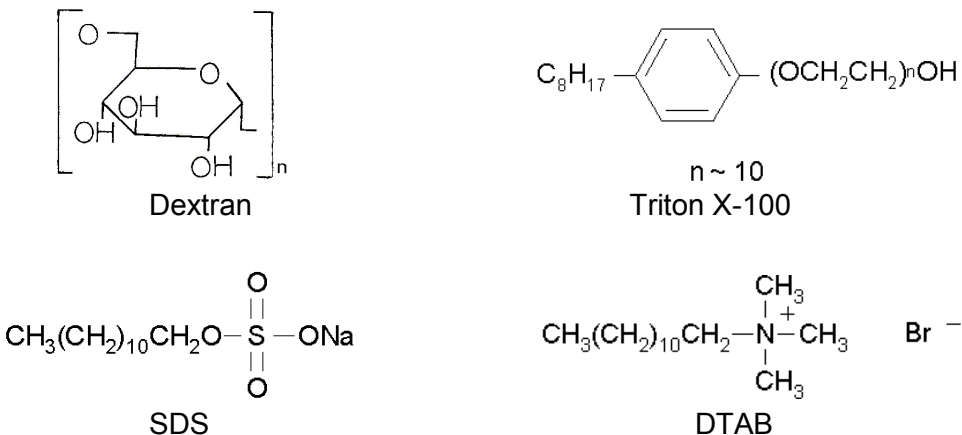


Figure 1. Chemical structures of polymer and surfactants.

## RESULTS AND DISCUSSION

### Partitioning Behavior of Silica in the Dextran/Triton X-100 System

#### *Effect of pH on the silica partition*

Figure 2 shows the partitioning behavior of silica in the Dex/TX100/H<sub>2</sub>O system. Below pH 3.5, almost all the silica particles go into the top surfactant-rich phase. When the pH increases from 4.0 to 8.0, the particles begin to concentrate at the interface, and the yields in the top phase decrease with increase in pH. Between pH 9.0 and 11.3, the solids prefer the bottom polymer-rich phase. At pH 11.5 and 11.7, the oxide particles mainly stay at the

interface. With further increase in pH from 11.8 to 12.5, the solids transfer to the top phase again. For the cases when the solids accumulated at the interface, for purposes of mass balance, the particles were combined with the silica in the bottom polymer-rich phase.

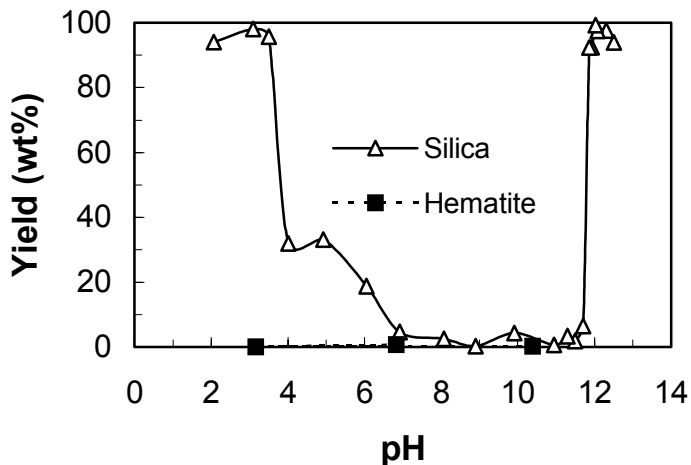


Figure 2. Effect of pH on the partitioning behavior of silica and hematite in the top phase of Dex/TX100 system. (Dex: 9 wt%, TX100, 11 wt%, solid: 2 g/L).

It is known that nonionic surfactants, such as Triton X-100, can adsorb on silica surface in aqueous solution [15-17]. The adsorption happens through the hydrogen bonding between the oxyethylene groups of TX100 molecules and the neutral silanol groups on solid surfaces [15-17]. On the other hand, dextran can also adsorb on silica, a result of hydrogen bonding between the surface silanol groups, and the glycosidic and hydroxylic acceptor sites in the repeating glucose units of the polysaccharide [18, 19]. However, this polymer only shows poor affinity to the solid surface [19].

According to the results available in the literature, in aqueous solution both dextran and Triton X-100 can adsorb on silica through hydrogen bonding [15-19]. Therefore, when silica particles are dispersed in the Dex/TX100 system, a competitive adsorption process occurs at the solid/liquid interface between the polymer and surfactant molecules. Therefore, the partition behavior of silicon dioxide is determined by the relative strength of the Dex/SiO<sub>2</sub> and TX100/SiO<sub>2</sub> interactions. At acidic pH values (< 3.5), most of silanol groups on the surface remain neutral since the pH<sub>PZC</sub> of silica is around pH 2 [20]. The interaction of TX100/SiO<sub>2</sub> may be stronger than Dex/SiO<sub>2</sub>, because dextran only shows poor affinity to the solid surface [19]. Therefore, the particles prefer to stay in the top surfactant-rich phase. With increase of pH, the surface acquires negative charges through deprotonation of silanol groups. Since the oxygen atom in the oxyethylene unit of Triton X-100 is partially negatively charged, which introduces certain level of electrostatic repulsion between the surfactant and the oxide. This repulsion force is demonstrated by the adsorption experiments in the literature which show that the uptake of TX100 by silica decreases with increase in pH [15, 16]. Thus, it follows that like increase in pH, the TX100/SiO<sub>2</sub> interaction becomes weak, even maybe less than that the Dex/SiO<sub>2</sub> interaction. The particles then begin to transfer from the surfactant-rich phase to the interface, then to the polymer-rich phase. This may explain the experimental trend in the pH range of 3.5 to 11.3.

The result at pH above 11.5 is very interesting; the particles preferred the top phase again. This behavior is difficult to explain from current literature about adsorption of dextran and TX100 on silica. From this experimental result, it can be deduced that the interaction of dextran/silica is less than that between TX100 and silica. Since the adsorption amount of TX100 on silica decrease with increase of pH [15, 16], it looks like that the adsorption of dextran on silica is suppressed by high pH environment. However, this needs to be demonstrated with other experiments at high pH, like adsorption study.

### Effects of surfactants on the silica partition

Figure 3 show the partition of silica in the dextran/Triton X-100 system in the presence of SDS and DTAB. With  $1.4 \times 10^{-3} M$  SDS, silica particles stay in the top phase at pH 2; at the interface from pH 3 to 5, and at pH 12; and in the bottom phase at pH 7 and 10. At higher SDS concentration ( $3.5 \times 10^{-3} M$ ), silica particles stay in the bottom dextran-rich phase from pH 8 to 12. However, below pH 7, this amount of SDS causes the whole system to form only one phase. From Figure e, it can be seen that with addition of  $1.3 \times 10^{-3} M$  DTAB, silica always stays in the top phase from pH 4 to 11.

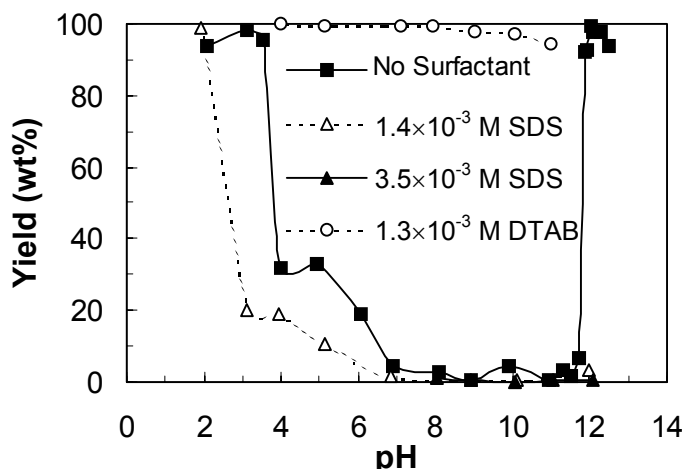


Figure 3. Effect of pH on the partitioning behavior of silica in the top phase of Dex/TX100 system in the presence of SDS and DTAB.  
(Dex: 9 wt%, TX100, 11 wt%, silica: 2 g/L; SDS & DTAB: as indicated in the figure).

In the polymer/nonionic surfactant aqueous biphasic system, ionic surfactants mainly concentrate in the top surfactant-rich phase. They form mixed micelles with the nonionic surfactant. Therefore, a weak charged environment is introduced into this kind of aqueous biphasic system [12-14]. In the Dex/TX100 system, the partition of silica in the top phase at certain pH values is due to hydrogen bonding between the oxyethylene groups of the nonionic surfactant and silanol groups on the solid surface. Addition of SDS makes the micelles in the top phase negatively charged [12-14]. Since silica is negatively charged above its pH<sub>PZC</sub> (about pH 2), it is expected that there is electrostatic repulsion between the mixed micelles and solid particles. Adsorption experiments show that TX100 adsorption on silica is suppressed from the mixed solution of TX100 and SDS [21]. Therefore, the particles are expected to move out from the top phase to the interface or bottom phase. The results show this really happens.

In this system, as with SDS, DTAB prefers the top surfactant-rich phase and forms mixed micelles with TX100 [12-14]. Thus, a weakly positively charged environment is formed in the top phase. Electrostatic attraction is then developed between the micelles in the top phase and silica surface. Therefore, silica particles are expected to prefer the top phase in the presence of DTAB. The experimental results demonstrate this expectation. From pH 4 to 11, silica particles stay in the top surfactant-rich phase with  $3.5 \times 10^{-3} M$  DTAB, irrespective of whether they are at the interface or in the bottom phase before addition of cationic surfactant.

## Partitioning Behavior of Hematite in the Dextran/Triton X-100 System

### Effects of pH on hematite partition

Figure 2 shows the partitioning behavior of hematite in the Dex/TX100 system at pH 3, 7, and 11. Under all the pH conditions, hematite stayed in the bottom polymer-rich phase. Like other metal oxides, hematite surface is covered by metal hydroxyl groups (Fe-OH), which make the surface hydrophilic. According to Albertsson's relative hydrophilic/hydrophobic scale, PEG is more hydrophobic than dextran [1]. Triton X-100 is a surfactant composed of a hydrocarbon chain and a chain of about 10 oxyethylene units which is the repeating unit of PEG, as shown in Figure 1. Therefore, it is reasonable to deduce that the solution of Triton X-100 is more hydrophobic than that of PEG. Hence, in the Dex/TX100 system, the bottom dextran-rich phase is more hydrophilic than the top surfactant-rich layer. Therefore, if one only considers the hydrophilic/hydrophobic properties, then hematite particles prefer the more hydrophilic bottom phase, not the more hydrophobic top one.

It is known that dextran interacts strongly with ferric oxide in aqueous solution and can even solubilize the oxide to form iron-dextran complexes [22, 23]. At the same time, the adsorption of nonionic surfactants on metal oxides is believed to be a physical process through hydrogen bonding and van der Waals attraction [15]. Thus, it is reasonable to conclude that dextran has stronger interaction with hematite than TX100; hence, the particles prefer to stay in the bottom dextran-rich phase. From the above discussion, it can be seen that both hydrophilic/hydrophobic properties and specific polymer-solid interaction favor the distribution of hematite into the dextran-rich phase.

### Effects of surfactants on hematite partition

Figure 4 shows the partitioning behavior of ferric oxide from pH 2 to 12 in the presence of DTAB and SDS. At all the pH values,  $3.5 \times 10^{-3}$  M SDS has no effect on the hematite partition. Addition of  $3.2 \times 10^{-3}$  M DTAB could modify the distribution of hematite particles. At high pH (pH 5, 8-11), the solids mainly stay in the top TX100-rich phase, although there are some particles at the interface. At pH 4, most of the oxide particles concentrate at the interface. In acidic solution (pH 2 and 3), the particles reside in the bottom phase, similar to the DTAB-free system. It needs to be noticed that at pH 6, 7, and 12, the system forms only one phase, not two phases. At these three pH values, no partition results are available.

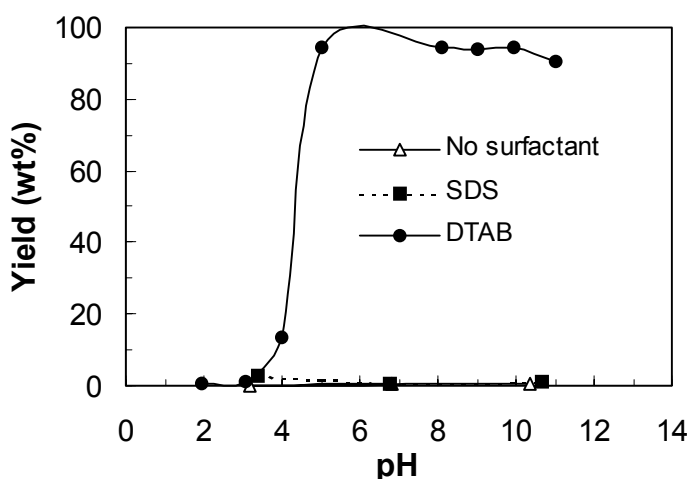


Figure 4. Effect of pH on the partitioning behavior of hematite in the top phase of Dex/TX100 system in the presence of DTAB and SDS.

(Dex: 9.0 wt%, TX100, 11.0 wt%, silica: 2.0 g/L, SDS:  $3.5 \times 10^{-3}$  M, DTAB:  $3.2 \times 10^{-3}$  M).

The pH<sub>PZC</sub> of ferric oxides is known to occur in the pH range from 5 to 8.6 [20]. Below this pH, the hematite surface is positively charged; the surface acquires negative charges above this pH. It is known that cationic surfactants can adsorb on the oxide surfaces above the pzc through electrostatic attraction [24]. Since in this system, DTAB concentrates in the top phase and forms mixed micelles with TX100 [12-14]. Therefore, at high pH values, DTAB adsorbs on hematite surface through electrostatic attraction and transfers the particles from the bottom to the top phase. In acidic solution, DTAB cannot adsorb on the surface of ferric oxide due to Coulombic repulsion, because both surfactant and solid surface are positively charged. Thus, the oxide surface is still covered with dextran layer. Hence, the oxide remains in the bottom phase. Although SDS can modify the surface chemistry of ferric oxide at certain pH values in conventional aqueous solution, it has no effect on the partitioning behavior of hematite in this system. Since dextran strongly interacts with ferric oxide in solution [22, 23], it appears that SDS is not able to replace the strongly adsorbed dextran layer on the hematite surface so that the particles continue to stay in the bottom phase.

## CONCLUSIONS

The principle behind the partition of inorganic particles in aqueous biphasic systems is the physicochemical interaction between the solid surface and the surrounding liquid solution. This study demonstrates that many factors, such as hydrophilic/hydrophobic properties, polymer-solid specific interaction, adsorption of surfactant on the solid surface, may influence the partition of metal oxides in aqueous biphasic systems. The experimental results show that in the dextran/Triton X-100 system, hematite stays in the bottom dextran-rich phase at all the pH values, while the partitioning behavior of silica is pH-dependent. Presence of ionic surfactants may modify the solid partition in this system. For silica particles, addition of SDS moves the solid from top phase to the interface or bottom phase; DTAB attracts the particles to the top phase from the interface or the bottom phase in the pH range of 4 to 11. However, only DTAB can transfer the hematite particles from bottom phase to the top phase or interface at high pH values; SDS has no effect on the partition.

## ACKNOWLEDGEMENT

This research was supported by the Department of Energy, Grant No. DE-FG22-96 PC96211.

## REFERENCES

1. P. A. Albertsson (1986), Partition of Cell Particles and Macromolecules, 3rd edn., Wiley-Interscience, New York.
2. B. Y. Zaslavsky (1995), Aqueous Two-Phase Partitioning, Marcel Dekker Inc., New York.
3. H.-K. Rajni Eds. (2000), Aqueous Two-Phase Systems, Humana Press, New Jersey.
4. K. P. Ananthapadmanabhan and E. D. Goddard (1988), *U. S. Pat.*, No. 4,725,358 (Feb. 16).
5. D. J. Chaiko, R. Mensah-Biney, C. J. Mertz and A. Rollins (1993), *Sep. Sci. Tech.*, **28**, 765-780.
6. S. M. Baxter, P. R. Sperry and Z. Fu (1997), *Langmuir*, **13**, 3948-3952.
7. R. D. Rogers, A. H. Bord and C. B. Bauer (1993), *Sep. Sci. Technol.*, **28**, 1091-1126.
8. K. Osseo-Asare and X. Zeng (2000), *Int. J. Miner. Proc.*, **58**, 319-330.

9. K. Osseo-Asare and X. Zeng (1999), Metal Separation Technology Beyond 2000, K. C. Liddell and D. J. Chaiko (eds.), The Minerals, Metals, and Materials Society, Warrendale, PA, pp. 347-356.
10. X. Zeng and K. Osseo-Asare (2001), *Coll. Surf. A*, **177**, 247-254.
11. E. Kusaka, Y. Kamata, Y. Fukunaka and Y. Nakahiro (1998), *Coll. Surf. A*, **139**, 155-162.
12. U. Sivars, K. Bergfeldt, L. Piculell and F. Tjerneld (1996), *J. Chrom. B*, **680**, 43-53.
13. U. Sivars and F. Tjerneld (2000), *Biochim. Biophys. Acta*, **1474**, 133-146.
14. U. Sivars, J. Abramson, S. Iwata and F. Tjerneld (2000), *J. Chrom. B*, **743**, 307-316.
15. W. Kwok, H. A. Nasr-El-Din, R. E. Hayes and D. Sethi (1993), *Coll. Surf. A*, **78**, 193-209.
16. R. Denoyel and J. Rouquerol (1991), *J. Coll. Interf. Sci.*, **143**, 555-572.
17. T. Gu and B.-Y. Zhu (1990), *Coll. Surf.*, **44**, 81-87.
18. I. Baudin, A. Richard and R. Audebert (1990), *J. Coll. Interf. Sci.*, **138**, 324-331.
19. B. A. Jucker, H. Harms, S. J. Hug and A. J. B. Zehnder (1997), *Coll. Surf. B*, **9**, 331-343.
20. G. A. Parks (1965), *Chem. Rev.*, **65**, 177-198.
21. Y. Gao, C. Yue, S. Lu, W. Gu and T. Gu (1984), *J. Coll. Interf. Sci.*, **100**, 581-583.
22. S. H. Kilcoyne and B. Webster (2000), *Magn. Reson. Chem.*, **38**, S20-S26.
23. B. Knight, L. H. Bowen, R. D. Bereman, S. Huang and E. D. Grave (1999), *J. Inorg. Biochem.*, **73**, 227-233.
24. R. Sivamohan (1990), *Int. J. Miner. Proc.*, **28**, 247-288.



## THE PARTITIONING OF SOME DYES AND THE EFFECT OF KSCN IN POLYETHYLENE GLYCOL/SALTS AQUEOUS TWO-PHASE SYSTEMS

Y. Xu, J. Lu \* and D.Q. Li \*

Department of Chemical Engineering, Hebei Institute of Technology, Tangshan, P.R. China

\*Laboratory of Rare Earth Chemistry and Physics, Changchun Institute of Applied Chemistry, Chinese Academy of Sciences, Changchun, P.R. China

The partitioning behaviors of three dyes in three oil/water biphasic systems were compared with that in three polyethylene glycol (PEG)/salt aqueous two-phase systems. It was found that the partitioning behaviors in PEG2000/salt aqueous two-phase systems are strongly correlated with that in the ethyl ether/water biphasic system. Potassium thiocyanate could alter the pH difference between the two phases, and thus affect the distribution ratios of the charged dye molecules. And the pH difference between two phases can be employed as the measurement of electrostatic driving force for the partitioning of small charged dye molecules in the PEG 2000/salt aqueous two-phase system.

### INTRODUCTION

Aqueous two-phase systems (ATPSs) have been studied extensively as gentle, non-denaturing systems for the separation of proteins, cell matter, and other biomolecules [1,2]. Although a considerable amount of research has gone into studying partitioning in ATPS, many of the phenomena concerning these complex systems are not yet completely understood. It had been observed that some salts can alter the partition coefficients of charged proteins in aqueous two-phase systems [3,4]. A combination of the proper salt and the proper pH, which affect the net charge of the protein, can steer the preferential partitioning to either phase. Previous studies of the salt effect have focused on the changes in potential difference between the two phases, and the investigations were mostly confined to the biomaterials in polymer/polymer ATPS [5,6].

Dyes have been used as affinity ligands in the partitioning of biomolecules. The dyes have either been bound directly to PEG [7,8] or simply allowed to selectively partition to one phase, thus influencing the direction of biomolecule partitioning [9,10]. Some dyes have also been used to extract metal ions from the salt-rich to PEG-rich phase [11,12]. Although there have been some studies on the nature of the dye characteristics responsible for the partitioning behavior in polymer/salt ATPS [13,14], more investigations are still needed. Most of the dyes are small charged molecules, the salt effect on their partitioning behavior in ATPS is not understood, and their electrochemical partitioning in ATPS has not been extensively investigated.

In this paper, the partitioning of Arsenazo III (AZ), Xylenol Orange (XO) and Cresol Red (CR) in three different organic solvent/water biphasic systems and three polyethylene glycol 2000 (PEG2000)/salt ATPSs was studied. The relationship between the distribution ratio in the oil/water biphasic systems ( $\text{InD}_o$ ) and that in PEG2000/salt ATPSs ( $\text{InD}$ ) was discussed. Then the effect of potassium thiocyanate on the partitioning of the dyes in the three PEG2000/salts (ammonium sulfate, dipotassium hydrogen phosphate and trisodium citrate) aqueous two-phase systems was investigated.

## EXPERIMENTAL

### Materials

PEG2000 was of reagent grade and all the chemicals were of analytical grade. The stock solutions of PEG2000 (32% w/v), ammonium sulfate (35% w/v), trisodium citrate (36% w/v), dipotassium hydrogen phosphate, (35% w/v) and potassium thiocyanate (6.0 mol/L) were prepared with distilled water. 0.01 mol/L arsenazolIII, xylenol orange water solution, and cresol red alcohol solution was used.

### Methods

For the measurements of distribution ratio for the dyes, 3 ml PEG2000 and 2 ml relevant salt stock solutions were mixed in graduated tubes, then 0.1 ml of dye solution and different amounts of potassium thiocyanate solution were added to the final volume of 5.5 ml. The systems were vortex mixed for 3 min (established by primary experiments), then disengaged by centrifugation. After determining the phase ratio, a 0.5 ml aliquot of each phase was taken for analysis. The concentrations of dyes were determined with spectrophotometry. pH values of the two phases were determined with a Model pHs-3C pH meter (Shanghai China). The  $\Delta\text{pH}$  is the pH of the top phase ( $\text{pH}_t$ ) minus that of bottom phase ( $\text{pH}_b$ ). All measurements were made in duplicate at room temperature. The method to estimate the partitioning behavior of the dyes in the three oil/water biphasic systems was same as described above.

## RESULTS AND DISCUSSION

The work from Rogers' group had indicated a preference for molecules with sulfonated aromatic rings to partition to the PEG-rich phase in PEG/salt ATPS [12,13]. For the substituted benzenes, partitioning behavior in PEG-salt ATPS was found to be strongly correlated with their partitioning in 1-octanol/water biphasic systems [15,16]. Here, the partitioning behavior of three dyes that contain the sulfonated aromatic rings in the molecules in three different oil (1-octanol, ethyl ether and hexane)/water biphasic systems was investigated (Figure 1). In the non-polar hexane system, the distribution ratios of all three dyes are low. In the 1-octanol system, the distribution ratio of CR alone reached very high, and that of AZ and XO increased slightly. We compared the distribution ratios of the dyes in the three oil/water biphasic systems with that in the three PEG2000/salt ATPSs and good linear relationships (the correlation coefficient  $R^2 = 0.9754$ ) were observed for the ethyl ether system (Figure 2 for ATPS with trisodium citrate). It is shown that the partitioning behavior of the dyes with sulfonated aromatic rings in PEG2000/salt ATPSs is strongly correlated with their partitioning in ethyl ether/water biphasic system. So, it is believed that the partition data in ethyl ether/water biphasic system can be used to estimate the partitioning behavior in the PEG/salt ATPSs for the small charged dye molecules with sulfonated aromatic rings.

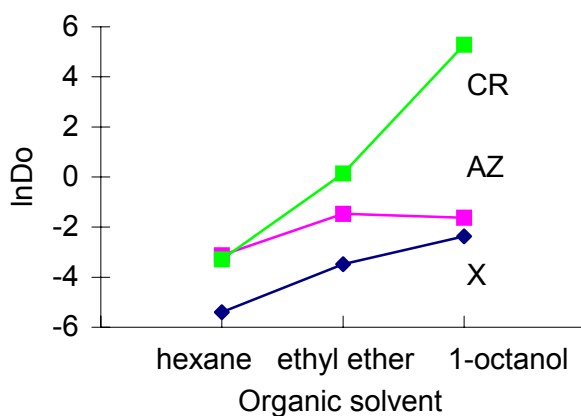


Figure 1. Distribution of dyes in oil/water biphasic systems.

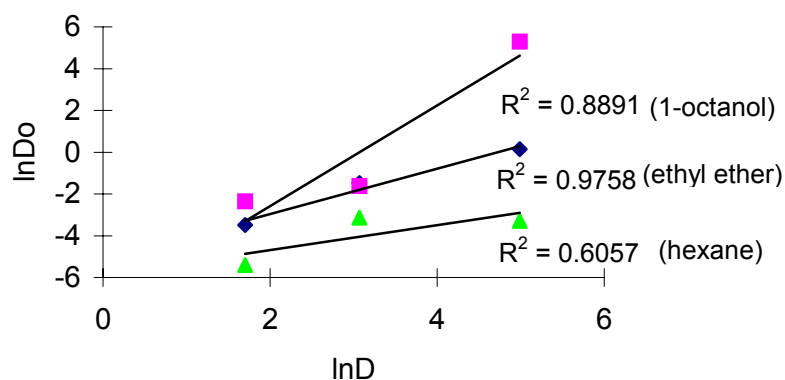


Figure 2. Relationship between the distribution ratio of dyes in oil/water systems and PEG2000 (18% w/v)/trisodium citrate (13% w/v) ATPS.

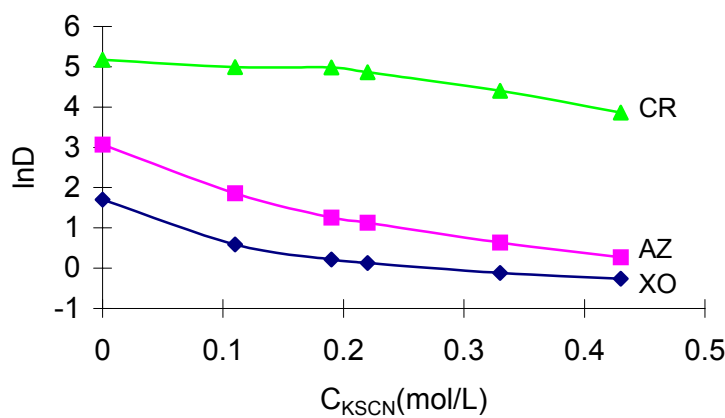
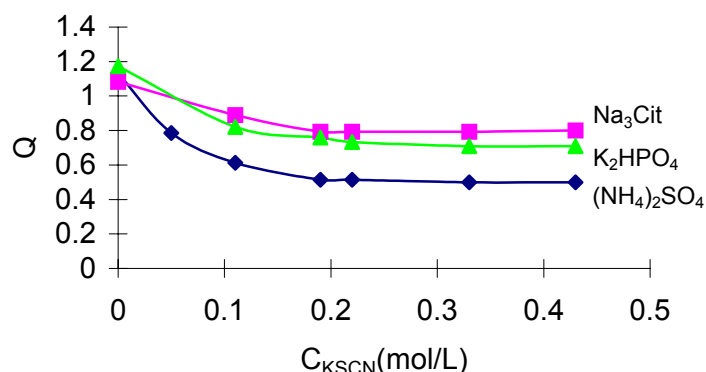


Figure 3. Effect of potassium thiocyanate on the distribution ratio of the dyes in PEG2000 (18% w/v)/trisodium citrate (13% w/v) ATPS, pH, 8.0.

In the presence of thiocyanate, the partition coefficients of positively charged proteins increase and those of negatively charged decrease in the PEG/dextran ATPS [4]. The effect of potassium thiocyanate was also observed in the PEG/ammonium sulfate ATPS for the charged proteins [17]. The effect of potassium thiocyanate on the distribution ratio of these

three small charged dyes in the three PEG2000/salt ATPSs has been examined. For these three negatively charged dye molecules, the distribution ratios decrease with the increase of potassium thiocyanate concentration in the all three PEG2000/salt ATPSs (shown in Figure 3 for ATPS with trisodium citrate), that is similar to the partitioning behavior of charged proteins in the ATPS. The more the dye molecules negatively charged, the greater the distribution ratio decreased.

In the PEG/dextran ATPS, the thiocyanates favor the PEG-rich (top) phase while the sulfates and phosphates favor the dextran-rich (bottom) phase [18]. Here, the effect of potassium thiocyanate on the phase ratio ( $Q$ ), which is defined as the ratio of the volume of PEG-rich phase to that of salt-rich phase, of the three PEG2000/salt ATPSs is studied (Figure 4). The adding of potassium thiocyanate causes the PEG-rich phase shrinking and the salt-rich phase expending. It had been pointed out that the thiocyanates have no ability to form two-phase systems in aqueous mixtures with PEG [19,20]. In the presence of phase-forming salt trisodium citrate, dipotassium hydrogen phosphate or ammonium sulfate, the thiocyanate also shows ability to salt out PEG, and so it is believed that the new polymer/mixed salts ATPSs are formed.



*Figure 4. Effect of KSCN on the phase ratio of the PEG2000 (18% w/v)/salt (13% w/v) ATPSs.*

Previous studies of salt effects on protein partitioning have focused on changes in the potential difference measured by two Ag/AgCl electrodes [5,6]. In our experiments, it is found that the addition of potassium thiocyanate can alter the pH difference between the top and bottom phase in the three PEG2000/salt ATPSs. The pH difference between two phases is believed to represent the distribution of proton in the aqueous two-phase system. The pH can be determined by glass electrode, and the electrode potential is expressed as ( $\varphi_g$ ):

$$\varphi_g = A - (2.303 RT/F)pH$$

$$\Delta pH = pH_t - pH_b$$

$$\Delta\varphi_g = \varphi_{gt} - \varphi_{gb}$$

$$\text{Then } \Delta\varphi_g = -(2.303 RT/F)\Delta pH \quad (1)$$

$A$  is a constant.  $\varphi_{gt}$  and  $\varphi_{gb}$  denote the glass electrode potential of top and bottom phases, respectively.  $\Delta\varphi_g$  can be thought to be the measurement of the driving force of proton distribution and employed to represent the electrostatic driving force for partitioning of the charged molecules.

$$\text{Suppose } \Delta\varphi = B\Delta\varphi_g \quad (2)$$

where B is a constant related to the systems. For the small charged dye molecules, the partitioning coefficient in the classical equation presented by Albertsson [1] should be substituted by the distribution ratio:

$$\ln D = \ln D_i + (z_p F/RT) \Delta\varphi \quad (3)$$

$D_i$  includes all the other factors affecting the dye partitioning,  $z_p$  denotes the average charge number of the dye molecules. Combining Eq. (3) with Eq. (2):

$$\ln D = \ln D_i - 2.303 B z_p \Delta pH \quad (4)$$

We correlated the natural logarithm of distribution ratio ( $\ln D$ ) of the dyes with the  $\Delta pH$ s in the three PEG2000/salt ATPS, the linear relationships were obtained and the parameters are listed in Table 1. The pH difference between the two phases of the PEG2000/salt ATPS can be taken as the measurement of electrostatic driving force for partitioning of the small charged dye molecules.

*Table 1. The regression parameters of  $\ln D$  to  $\Delta pH$  for the dyes in PEG2000/salt ATPS.*

PEG2000/trisodium citrate			PEG2000/ dipotassium hydrogen phosphate			PEG2000/ammonium sulfate		
slope	intercept	R <sup>2</sup>	slope	intercept	R <sup>2</sup>	slope	intercept	R <sup>2</sup>
4.64	1.69	0.9949	6.51	0.61	0.9798	7.68	1.33	0.9727
3.29	0.60	0.9788	4.01	0.58	0.9873	3.78	0.33	0.9750
1.62	4.82	0.5021	2.12	3.79	0.9966	0.038	5.38	0.3084

## CONCLUSIONS

For small charged dye molecules that contain the sulfonated aromatic rings, their partitioning behavior in the PEG2000/salt ATPSs is strongly correlated with that in the ethyl ether/water biphasic system. The partition data in the ethyl ether/water biphasic system can be used to predict the partitioning behavior in the PEG/salt ATPSs for the small charged dye molecules. In the three PEG2000/salt ATPSs, the distribution ratios of Arsenazo III, Xylenol Orange and Cresol Red are all affected by the potassium thiocyanate. As potassium thiocyanate is added to the three PEG2000/salt ATPSs, the respective PEG2000/mixed salts ATPSs are believed to be formed. It is through its effect on the pH difference between the two phases, that the potassium thiocyanate can alter the distribution ratio of the charged dyes in the PEG2000/salt ATPSs. There is a linear relationship between the  $\ln D$  and  $\Delta pH$ , and the  $\Delta pH$  can be employed as the measurement of the electrostatic driving force for the partitioning of small charged molecules in PEG2000/salt ATPS.

## ACKNOWLEDGMENTS

This work is supported by the State Key Project of Fundamental Research of China (G1998061301) and the National Natural Science Foundation of China (29771028, 29801004).

## REFERENCES

1. P.A.Albertsson (1986), Partition of Cell Particles and Macromolecules, 3rd edn., Wiley, New York.
2. H. Walter, G. Johansson (1994), Methods in Enzymology, Aqueous Two-Phase System, Vol. 228, Academic Press, San Diego, CA.
3. J.E. Ramirez-Vick, A.A. Garcia (1996-97), *Sep. Purif. Meth.*, **25**, 8-129.
4. G. Johansson (1974), *Acta Chem. Scand. B*, **28**, 873-882.
5. A. Pfennig, A. Schwerin, J. Gaube (1998), *J. Chromatogr. B*, **711**, 45-52.
6. R.S. King, H.W. Blanch, J.M. Prausnitz (1988), *AIChE J.*, **34**, 1585-1594.
7. A. Cordes, M.R. Kula (1986), *J. Chromatogr.*, **376**, 375-384.
8. G. Johansson, M. Joelsson (1987), *J. Chromatogr.*, **411**, 161-166.
9. K.A. Giuliano (1991), *Anal. Biochem.*, **197**, 333-339.
10. D.Q. Lin, Z.Q. Zhu, L.H. Mei (1996), *Biotechnol. Techn.*, **10**, 41-46.
11. T.I. Zvarova, V.M. Shkinev, G.A. Vorob'eva et al. (1984), *Mikrochim. Acta*, III, 449458.
12. R.D. Rogers, A.H. Bond, C.B. Bauer (1993), *Sep. Sci. Technol.*, **28**, 139-153.
13. R.D. Rogers, A.H. Bond, C.B. Bauer et al. (1996), Value Adding Through Solvent Extraction, *Proc. ISEC '96*, Vol. 2, The University of Melbourne Press, Melbourne, pp. 1537-1542.
14. J.G. Huddleston, H.D. Willauer, K.R. Boaz et al. (1998), *J. Chromatogr. B*, **711**, 237-244.
15. R.D. Rogers, H.D. Willauer, S.T. Griffin et al. (1998), *J. Chromatogr. B*, **711**, 255-263.
16. H.D. Willauer, J.G. Huddleston, S.T. Griffin et al. (1999), *Sep. Sci. Technol.*, **34**, 1069-1090.
17. Y. Xu, J. Lu and D.Q. Li (2000), *Chinese Chem. Lett.*, **11**, 453-454.
18. B.Yu. Zaslavsky, L.M. Miheeva and Yu.P. Aleschko-Ozhevskii (1988), *J. Chromatogr.*, **39**, 267-281.
19. K. P. Ananthapadmanabhan, E.D. Goddard (1986), *J. Colloid Interf. Sci.*, **113**, 294-296.
20. K. P. Ananthapadmanabhan, E.D. Goddard (1987), *Langmuir*, **3**, 25-31.



## APPLICATION OF SOLVENT EXTRACTION TO PRODUCTION OF MULTICOMPONENT COMPOSITE POWDERS

Junji Shibata and Hideki Yamamoto

Department of Chemical Engineering, Kansai University, Osaka, Japan

Fundamental studies were carried out using liquid-liquid extraction to produce composite powders comprising two or three metal oxalates and to develop control of the particle size. The combination of samarium and cobalt was selected as the two-component composite powders. Stripping and crystallization occurred at the same time by contacting diluted Versatic Acid 10 loaded with the two metals and the aqueous solution containing oxalic acid. The effect of aqueous pH, oxalic acid concentration and agitation speed on the physical and the chemical properties such as crystallization percent, particle size and shape of each metal oxalate powder obtained in this process was examined. Analysis by using EDX showed that the two metal oxalates were distributed uniformly in the composite powders.

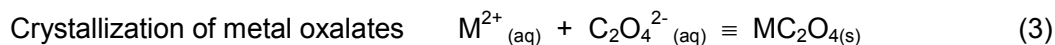
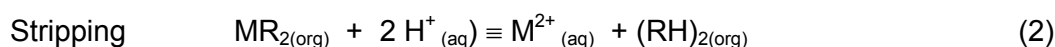
### INTRODUCTION

Composite metal and metal oxide powders of high purity are indispensable as industrial materials in the fields of electrical engineering, electronics and metallurgy. It is difficult to mechanically mix metal or metal oxide powders uniformly for the production of alloy or composite oxide powders. If insoluble metal salts are allowed to collect as crystallization products in a crystallization-stripping process, the conventional melting and crushing process can be avoided [1-4].

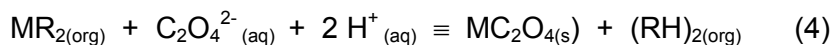
After mixing the organic phase containing metals at the fixed composition, fine metal oxalate powders are produced using a crystallization-stripping method [5-7]. The composite metal oxalates are converted to composite metal or metal oxide powders by roasting in H<sub>2</sub> or air. Versatic Acid 10 and D2EHPA, both acidic extractants, were chosen in the experiments, and the metal oxalate powders were produced using oxalic acid as a crystallization reagent. The mixed metal oxalates containing samarium and cobalt were precipitated from the organic phase containing these metals. The physical properties of the powders, such as particle size, shape and thermal decomposition, were measured in order to evaluate them for industrial purposes.

### SOLVENT EXTRACTION-CRYSTALLIZATION STRIPPING PROCESS

Solvent extraction usually comprises three processes, namely extraction, scrubbing and stripping. Extraction is the operation in which an objective component is separated from the aqueous phase into the organic phase using an extraction reagent; scrubbing is the operation in which undesirable components in the organic phase are removed to the aqueous phase; stripping is the operation where the objective component is returned from the organic phase to the aqueous phase again. Our process is a modification of conventional solvent extraction by adding a crystallization operation, in which the metal salts of low solubility are precipitated in the aqueous phase. The crystallization operation means the collection of stripped metal ions as insoluble salts in the aqueous phase. The reaction mechanism of this process is shown by the following equations.



The overall crystallization-stripping reaction is shown as:



where subscripts, aq, org, and s mean aqueous, organic and solid phases, respectively.

## EXPERIMENTAL METHOD

Versatic acid 10 and D2EHPA diluted in kerosene were used in the concentration range of 0.5 ~ 1.0 mol/dm<sup>3</sup>. Aqueous solutions containing Sm(III) and Co(II) were prepared at a fixed concentration as an aqueous feed. Crystallization-stripping experiments were carried out as follows. Fifty cm<sup>3</sup> of the organic phase containing metals and the same volume of oxalic acid solution were placed in a 4-necked flask and agitated with an impeller. One hundred cm<sup>3</sup> of the solvent mixture was separated in the separation funnel into organic-aqueous-solid phases. Metals in the organic phase were stripped using 2 mol/dm<sup>3</sup> HCl. Metal concentrations were determined by using an atomic absorption spectrometer (Z-6000 Hitachi Ltd.). The crystallization products were washed several times with acetone, and the composition was identified by X-ray diffraction analysis (JDX-3530 JOEL Ltd.). The size and shape of crystallization products were observed by SEM (JSM-5410 JOEL Ltd.). Thermal decomposition analysis of the crystallization products was carried out in order to confirm the temperatures at which metal oxalates were converted to oxides.

## RESULTS AND DISCUSSION

The aim of this study is to clarify the phenomena and mechanisms of the crystallization-stripping of metals from the organic phase containing Sm(III) and Co(II). Extraction curves of Sm(III) and Co(II) with Versatic Acid 10 and D2EHPA are shown in Figure 1. The figure shows that the metal ions can be extracted at different pH values with Versatic Acid 10 and D2EHPA. Sm(III) is extracted in the lowest pH range (pH 0-1) with D2EHPA, while Co(II) is extracted at pH 2-3.5 with D2EHPA. It is found that the separation of Sm(III) from Co(II) is carried out easily by the extraction with D2EHPA. On the other hand, Sm(III) and Co(II) are extracted at a higher pH with Versatic Acid 10 than they are extracted with D2EHPA. The difference in extraction behavior is based on the value of dissociation constants of the two extractants.

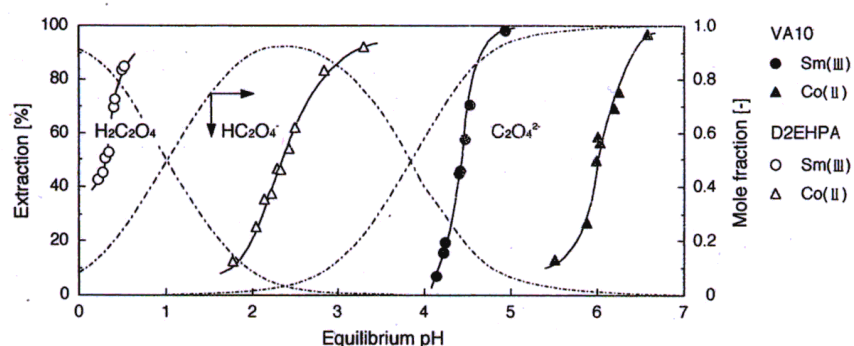


Figure 1: Mole fraction of oxalic acid in aqueous solution and extraction curves with various extractants

Figure 1 also shows a distribution diagram for oxalic acid in an aqueous solution. Oxalate ion ( $C_2O_4^{2-}$ ), which contributes to the formation of insoluble metal oxalates, exists in the condition of  $pH > 4.0$ . As the extraction is a reversible reaction, an aqueous solution of a lower pH than equilibrium pH of the extraction is required in order to strip the metals from Versatic acid 10. The extraction curves of Sm and Co with Versatic acid 10 locate in the pH region, 4-5 and 5.5-6.5, respectively, while the extractions of Sm and Co with D2EHPA take place in the pH region, 0-1 and 1.5-3, respectively. It is considered that the Versatic acid 10 is favorable for crystallization- stripping from the viewpoint of the distribution of oxalate ion ( $C_2O_4^{2-}$ ) and the position of the extraction curve.

The crystallization-stripping was carried out in a concentration of  $0.1\text{mol}/\text{dm}^3$  oxalic acid. The  $0.1\text{ mol}/\text{dm}^3$  Versatic Acid 10 containing  $0.01\text{mol}/\text{dm}^3$  Sm(III) or  $0.085\text{mol}/\text{dm}^3$  Co(II) was stripped by oxalic acid solution. Stripping and crystallization approach almost 100% within 300 s for Sm(III) and 1200s for Co(II). Figure 2 shows the relationship between pH and stripping, and pH and crystallization. The crystallization of Sm(III) takes place in aqueous solution prior to Co(II) crystallization because of the low solubility of Sm(III) oxalate. The crystallization of Sm(III) oxalate takes place in the wide pH range of 0.5 to 6, while Co(II) oxalate is quantitatively crystallized in the pH range of 2 to 6. The decrease in crystallization of Sm(III) in the higher pH is explained by the fact that the stripping does not proceed in the pH region, whereas the decrease in Co(II) crystallization in the lower pH is due to the high solubility of Co(II) oxalate in the pH region. The crystallization product was separated by filtration and washed with acetone several times. Then, undesirable components were removed from the surface of the crystallization products. The products were dried in a vacuum dryer at room temperature.

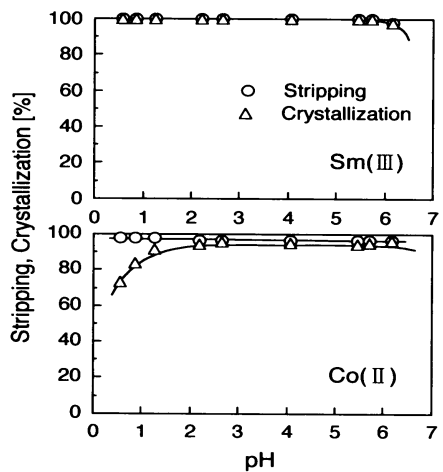
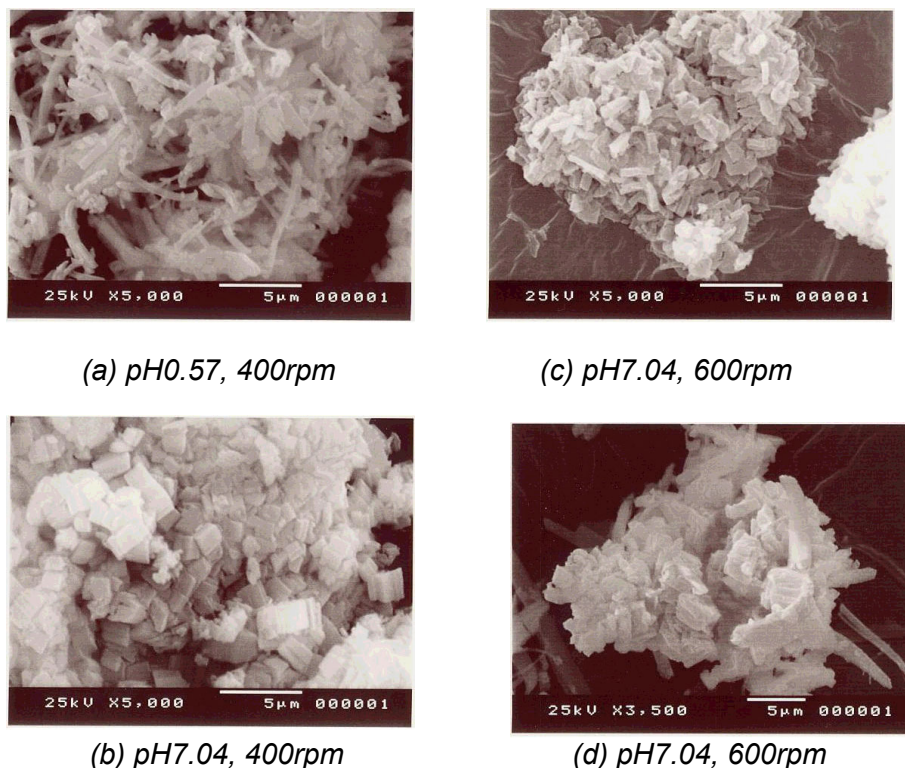


Figure 2 : Stripping, and crystallization of Sm(III) and Co(II) as a function of pH

Photos 1(a)-(d) show the complex oxalates of Sm(III) and Co(II). The size and shape of crystallization products for Sm(III) and Co(II) depend on the conditions, such as pH and mixing speed where the crystallization are carried out. The mixed organic phase was prepared by mixing each organic phase containing Sm(III) and Co(II) for the production of composite metal oxalates with the interest composition. The composition ratio of Sm(III):Co(II) =2:17 is required in the magnet industry field. Though the size and shape of the crystallization products depend on the conditions such as pH and mixing speed, Sm(III) and Co(II) oxalates in the crystallization product are both angular crystal as small as  $1\text{ }\mu\text{m}$  in the condition of pH 7 and 600 rpm. It is found from the EDX analysis that Sm(III) and Co(II) are uniformly distributed in the product crystallized in the above condition. For the condition of pH 0.6 and 400 rpm, Sm(III) and Co(II) oxalates in the crystallization products are the angular crystal of  $1\text{ }\mu\text{m}$  and the needle-like crystal of  $1\times 7\text{ }\mu\text{m}$ , respectively.

X-ray analysis showed the crystallization products to be  $\text{Sm}_2(\text{C}_2\text{O}_4)_3 \cdot 10\text{H}_2\text{O}$  and  $\text{CoC}_2\text{O}_4 \cdot 2\text{H}_2\text{O}$ . The temperature at which metal oxalates are converted to metal oxides should be lower for a practical use. The results of thermal decomposition analysis for each metal oxalate are shown in Figure 3. Sm(III) oxalate is decomposed to become the oxide in air at temperature of 913K, while the decomposition of Co(II) oxalate to the oxide takes place in air at temperature of 553K.



*Photo 1. SEM analysis of Sm(III)-Co(II) oxalate powders prepared under different conditions.*

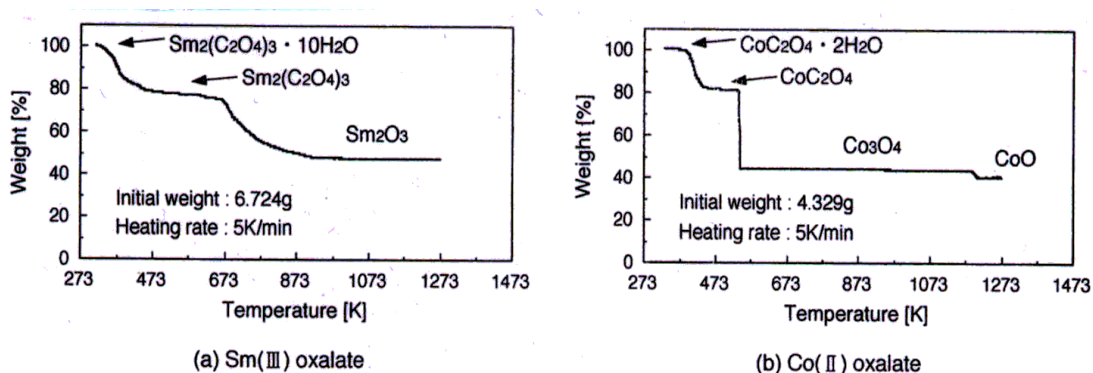


*Figure 3: Thermogravimetric analysis of metal oxalates*

## CONCLUSIONS

The studies of a production process for metal oxide and metal powders were carried out using a solvent extraction method. Crystallization-stripping is a suitable method to produce composite powders comprising two or three metal salts. Though the size and shape of crystallization products depend on the conditions such as pH and mixing speed, Sm(III) and Co(II) oxalates in the crystallization product are both angular particle as small as 1  $\mu\text{m}$  at conditions of pH 7 and 600 rpm. Sm(III) and Co(II) are uniformly distributed in the products crystallized in the above condition.

## REFERENCES

1. A. Okuda, J. Shibata, M. Sano and S. Nishimura (1986), *J. Min. Material Inst. Japan*, **102**, 869-874.
2. J. Shibata, A. Okuda, M. Sano and S. Nishimura (1988), *J. Min. Material Inst. Japan*, **104**, 97-102.
3. M. Sano, J. Shibata, S. Mutagami and S. Nishimura (1988), *J. Min. Material Inst. Japan*, **104**, 173-176.
4. J. C. Lee, K. I. Rhee and H.-S. Yu (1990), *Hydrometallurgy*, **51**, 831-843.
5. J. Shibata, S. Matsumoto and H. Yamamoto (2000), *Proc. Second Int. Conf. Processing Materials for Properties*, San Francisco, pp. 435-438.
6. K. Sasabe, J. Shibata and H. Yamamoto (2001), *J. Min. Material Inst. Japan*, **117**, 288-292.
7. J. Shibata and H. Yamamoto (2001), *Proc. TMS Annual Meeting*, Warrendale, PA, pp. 657-661.



## DETERMINATION OF PROTONATION CONSTANTS OF 2,2':6',2"-TERPYRIDINE FROM LIQUID-LIQUID DISTRIBUTION DATA

S. Andersson, C. Ekberg, J-O. Liljenzin and G. Skarnemark

Department of Nuclear Chemistry, Chalmers University of Technology, Gothenburg, Sweden

Spent nuclear fuel is a problem that has to be dealt with in the future. Transmutation of the most dangerous long-lived radionuclides into other less harmful ones can be considered a complement to direct disposal in a repository. Separation of the interesting nuclides is an important issue and liquid-liquid extraction is a suitable technique to achieve the necessary separation yields.

One group of extractants that can be used is oligopyridines and in this work basic research to determine the protonation constants of 2,2':6',2"-terpyridine has been performed. Results show that complexes with up to three hydrogen atoms, bound to the terpyridine molecule, exist. Terpyridine forms a strong complex with Cu(II)-ions, which facilitate spectrophotometric determination of the distribution of terpyridine between the two phases. This distribution, measured at different pH-values in the aqueous phase, makes it possible to determine the protonation constants.

### INTRODUCTION

Transmutation of the long-lived radionuclides in the nuclear waste into short-lived or stable nuclides can be considered a complement to disposal in a deep geological repository. The process requires a partitioning step where the material that has been converted is separated from the rest, which must be recirculated back for further neutron irradiation in the transmuter unit. The recirculated material consists mainly of actinides that have been selectively separated from the fuel fission products.

It is difficult to separate, for example, Am and Cm from trivalent lanthanides because of their similar chemical properties in aqueous solutions. The use of extractants containing soft donor ligands (e.g., N or S) facilitates the separation, probably because they form complexes with actinides that have more covalency in the bonds than lanthanides [1]. They also make it possible to get a sufficient yield of separation, both quantitatively and qualitatively. Knowledge of basic thermodynamic properties is important to be able to understand the separation process in more complex systems.

In this work a method to determine the protonation constants of 2,2':6',2"-terpyridine has been developed. The concentration of terpyridine in both phases are evaluated spectrophotometrically, facilitated by the fact that Cu(II)-ions form strong complexes with terpyridine. If the distribution of terpyridine is known at different pH-values, the protonation constants can be derived through modelling. This method to derive protonation constants, through a combination of solvent extraction and spectrophotometry, has not been used in this system before.

## THEORY

### Background

To understand the extraction behaviour of different extractants, it is important to be familiar with their basic thermodynamic properties, among them the protonation constants (often called the basicity of the reagent). The most common way to examine these parameters is to perform a potentiometric titration [2], but the method used in this work has, in comparison, some major advantages. With potentiometric titrations it is difficult to derive all three protonation constants, both from experimental difficulties, e.g., precipitation, and the fact that the solubility of terpyridine in water is very low.

### Simulations

A computer program, Spartan [3, 4], has been used to calculate the spatial positions and electrostatic charges of the different elements of the molecules, the density of the electrostatic and polarisation potential, the molecular orbitals, the dipole momentum, the heat of formation among other parameters. By addition of hydrogen atoms it is possible to predict where the first hydrogen ion will attach to the molecule through studying the heat of formation of the different possible complexes. It is also possible to see the difference in spatial constellation of the molecules, when protonation has occurred. When the stability constants have been determined, it is possible to compare them with the heat of formation of the complexes.

### Calculations

The reactions between terpyridine (Tp) and hydrogen ions can be expressed as



The number of hydrogen ions attached to the terpyridine molecule depends on the concentration of hydrogen ions in the aqueous phase. By varying this concentration it is possible to obtain the protonation constants.

The concentrations of the protonated complexes can be expressed with the protonation constants  $\beta_1$ - $\beta_3$  as

$$\{TpH^+\} = \beta_1 \{Tp\} \{H^+\} \quad (4)$$

$$\{TpH_2^{2+}\} = \beta_2 \{Tp\} \{H^+\}^2 \quad (5)$$

$$\{TpH_3^{3+}\} = \beta_3 \{Tp\} \{H^+\}^3 \quad (6)$$

At this stage the assumption that the activity coefficient of each species is constant is reasonable, since constant ion strength in the aqueous phase has been used throughout the experiments and the concentration of terpyridine always has been kept low in comparison with the total ionic strength. The activity coefficients are from this point included in the protonation constants themselves [5].

The distribution coefficient, *i.e.*, the ratio between the total concentration of terpyridine in the organic and aqueous phases can be written as (equal volumes of the two phases assumed)

$$D = \frac{\lambda}{1 + \beta_1[H^+] + \beta_2[H^+]^2 + \beta_3[H^+]^3} \quad (7)$$

where

$$\lambda = \frac{\text{Total concentration of } Tp \text{ in organic phase}}{\text{Total concentration of } Tp \text{ in aqueous phase}} \quad (8)$$

The value of  $H^+$  that should be used is the free hydrogen concentration in the aqueous phase. A total mass balance over the system concerning hydrogen makes it possible to express this concentration as

$$[H^+] = \frac{[H_{tot}]}{1 + \beta_1[Tp] + 2\beta_2[Tp][H^+] + 3\beta_3[Tp][H^+]^2} \quad (9)$$

Everything but the free terpyridine concentration in the aqueous phase is known in this expression. A balance over the system dealing with terpyridine makes it possible to calculate this concentration as

$$[Tp] = \frac{[Tptot]}{\lambda + 1 + \beta_1[H^+] + \beta_2[H^+]^2 + \beta_3[H^+]^3} \quad (10)$$

Guessing the free hydrogen ion concentration in equation (10) gives a value of the terpyridine concentration. These together are used in equation (9) to calculate a new hydrogen ion concentration. The procedure is repeated until the guessed and calculated values agree. This iterative calculation method makes it possible to get a theoretical value of the distribution of terpyridine between the two phases. By varying the values of  $\beta_1$  to  $\beta_3$  and comparing the theoretical distribution coefficient with the experimental one, it is possible to determine the protonation constants. The experimental distribution coefficient is given from the concentration of terpy in the two phases, spectrophotometrically determined. These are according to earlier assumptions, specific for 1 M ionic strength.

## EXPERIMENTAL

### Materials

2,2':6',2''-terpyridine (98% purity) as well as the organic solvent, *tert*-butylbenzene (99% purity), were obtained from Aldrich. Concentrated nitric acid (min. 65%) to produce the aqueous phases with different hydrogen ion concentrations came from Riedel-de Haën, as did the NaOH (0.1 M and 0.01 M) used for the titrations. The copper(II)-sulphate-5-hydrate (min 99%) and the sodium nitrate (>99%) used for keeping the ion strength constant in the aqueous phases was obtained from Merck. Ethanol used, both in the ordinary method (95% purity) and in the spectrophotometric measurements (min 99.5%), came from Kemetyl.

### Procedure and Apparatus

Liquid-liquid extraction experiments were performed to determine the distribution of terpyridine in a system with *tert*-butylbenzene as the organic phase and with varying hydrogen ion concentrations in the aqueous phase. 1 ml of each phase were added to a glass test tube and after 5 minutes of vigorous shaking the phases were allowed to settle. The temperature was held at 298 K to avoid temperature dependent changes in the protonation constants [6, 7]. The aqueous phases were prepared in advance and titrated with

sodium hydroxide to determine the true hydrogen ion concentrations. The hydrogen concentration was varied between 0.0001 M and 0.4 M, and the ionic strength was kept constant at 1 M with sodium nitrate. Experiments have also been performed at higher pH values. The composition of the organic phase before contact with the aqueous phase consisted of 0.01 M or 0.1 M terpyridine in *tert*-butylbenzene (the higher concentration at higher pH values).

The same method to obtain the concentration of terpyridine in both phases was used. 0.4 ml 0.08 M Cu<sup>2+</sup> solution (a mixture of 20% ethanol and 80% distilled water, which enables the same method to be used for concentration evaluation in both organic and aqueous phase) was added to a 10 ml volumetric flask. 1 ml 2 M hydrochloric acid was added to assure that the hydrogen ion concentration, in the method for concentration evaluation, was held constant. Some 95% ethanol was added and followed by 10 to 1000 µl of the sample from one of the phases in the shaking tube. Triple samples from each phase were always taken to minimise the statistical fluctuations and facilitate the spectrum evaluation. Ethanol was then added to a total volume of 10 ml and the solution was analysed in a spectrophotometer Perkin Elmer Lambda 19 UV/VIS/NIR. The wavelengths used were in the interval 320-345 nm, where *tert*-butylbenzene itself has no absorption peaks. Through shaking a test tube with only *tert*-butylbenzene and an aqueous phase of known hydrogen ion concentration it was seen that the hydrogen ion concentration in the aqueous phase did not change. All titrations were performed with an ABU91 autoburette from Radiometer Copenhagen.

Other metal ions than copper have also been tested. Preparatory experiments to determine the, in this case, most suitable metal ion that forms a complex with terpyridine have been performed. Iron, nickel, cobalt, iron and magnesium were all tested, but copper was selected because of the shape of its spectrum with terpyridine. Some other metal ions also forms complexes with terpyridine [6, 8-11].

A calibration to determine the concentration of terpyridine in a sample has been performed. A linear relation between absorption and concentration (regardless of which phase the sample were taken from) was found to exist. In most cases the spectra of the organic and aqueous phases have been superimposed and the factor that has to be multiplied to one of the curves to fit the other gives the distribution coefficient of terpyridine. In some cases, though, the shape of the spectrum and the detection limit of the spectrophotometer prevent this method and the calibration line has to be used instead. Good agreement between both methods has been found.

## RESULT AND DISCUSSION

Spartan simulation of where the hydrogen ions will attach to the terpyridine molecule makes it possible to predict what the complexes will look like. The first hydrogen is attached to the central nitrogen atom, but is transferred to one of the outer nitrogen atoms as a second hydrogen is added. Previous work on stability constants has not proven that a third complex exists, but according to the results given in this paper the terpyridine molecule is able to add a third hydrogen, *i.e.*, all of the nitrogen may have hydrogen ions attached to themselves. Figure 1 shows the spatial constellation of the protonated complexes. The results are consistent with earlier published in this area [12], although only the energy aspect has been included in this paper.

The calculations have been performed in a semi-empirical manner and no surrounding media has been regarded. The heat of formation of the complexes can be found in Table 1.

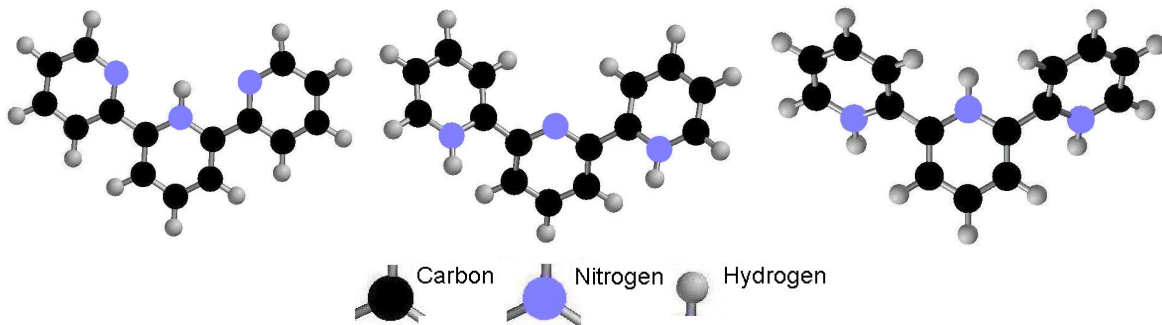


*Figure 1. Terpyridine with the hydrogen ions attached at the energetically most favourable sites.*

*Table 1. Heat of formation of protonated terpyridine.*

Tp, no H	398.1 kJ/mol
Tp, H on the central nitrogen	894.1 kJ/mol
Tp, H on the outer nitrogen	944.6 kJ/mol
Tp, 2H on the outer nitrogen atoms	1798.6 kJ/mol
Tp, 2H on the central and outer nitrogen atoms	1860 kJ/mol
Tp, 3H on all three nitrogen atoms	3068.9 kJ/mol

In Figure 2 the result of the experiments are shown. Both the experimental and calculated values of the distribution ratio are included, and good agreement between the two series can be found. It is not possible to explain the shape of the curve without taking the third protonated complex into account.

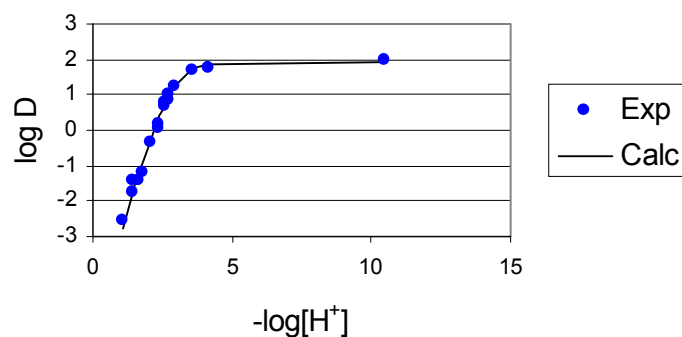


*Figure 2. Calculated and experimental distribution coefficients (298K, 1M NaNO<sub>3</sub>).*

A slope analysis in the lower pH region has been performed. In this part the existence of the three-protonated complex should dominate and taking the logarithm of equation (7) and neglecting the concentration of the first two complexes, a theoretical slope of 3 is found. The slope of the calculated curve in Figure 2 is ~2.8, which shows that a third complex really exists.

The stability constants can be found in Table 2. The statistical uncertainties in the stability constants have been estimated by the chi-square method [13] and are found in Table 2. It is difficult to compare the values of the stability constant with others earlier presented [6, 7, 14-18] because of a wide variety in temperature, ion strength and evaluation method, together with the fact that a third complex has been used to explain the shape of the extraction curve in this paper.

*Table 2. The acidity stability constants of terpyridine, 298K, 1M NaNO<sub>3</sub>.*

$\log \beta_1$	$3.21 \pm 0.2$
$\log \beta_2$	$2.84 \pm 0.2$
$\log \beta_3$	$1.81 \pm 0.5$

One conclusion that can be made from this work is that it is possible to determine the protonation constants of terpy with the above-described method. The complex of terpyridine with three hydrogen ions bound to it has been found to exist.

### ACKNOWLEDGEMENTS

The authors wish to thank the Swedish Nuclear Fuel and Waste Management Co., SKB, and the European Union (PARTNEW FIKW-CT2000-00087) for the financial support.

### REFERENCES

1. C. Musikas, X. Vitart, J. Y. Pasquiou and P. Hoël (1986), C. . King and J. D. Navratil (eds.), Litarvan Literature, pp. 359.
2. I. Hagström, L. Spjuth, Å. Enarsson, J. O. Liljenzin, M. Skålberg, M. J. Hudson, P. B. Iveson, C. Madic, P. Y. Cordier, C. Hill and N. Francois(1999), *Solvent Extr. Ion Exch.*, **17**(2), 221-242.
3. H. Ottosson, An Introduction to Computational Chemistry Spartan. Chalmers University of Technology, Gothenburg [*Internet*]. Available from: <<http://www.oc.chalmers.se/spartanc/Spartantutorial.html>> [Accessed 17 July 2001].
4. Queensland Parallel Supercomputing Foundation (1997), Spartan 4.1 [*Internet*]. Available from: <<http://www.qpsf.edu.au/software/spartan.html>> [Accessed 17 July 2001].
5. C. Ekberg (1999), Uncertainties in Actinide Solubility Calculations Illustrated Using the Th-OH-PO<sub>4</sub> System, PhD Thesis, Chalmers University of Technology, Sweden.
6. J. I. Bullock and P. W. G. Simpson (1981), *J. Chem. Soc., Faraday Trans. 1*, **77**, 1991-1997.
7. P. O'D. Offenhartz, P. George and G. P. Haight Jr, *J. Phys. Chem.*, **67**, 116-118.
8. H. Alemu, B. Hundhammer and T. Solomon (1990), *J. Electroanal. Chem.*, **294**, 165-177.
9. C. Piguet, B. Bocquet, E. Müller and A. F. Williams (1989), *Helvet. Chim. Acta*, **72**, 323-337.
10. S. Rüttimann, C. M. Moreau and A. F. Williams (1992), *Polyhedron*, **11**(2), 635-646.
11. R. M. Awadallah, M. K. Sherif and T. I. El Desouky (1984), *J. Indian Chem. Soc.*, **61**, 403-405.
12. M. G. B. Drew, M. J. Hudson, P. B. Iveson, M. L. Russel, J. O. Liljenzin, M. Skålberg, L. Spjuth and C. Madic (1998). *Chem. Soc., Dalton Trans.*, 2973-2980.
13. G. Meinrath, C. Ekberg, A. Landgren and J-O. Liljenzin (2000), *Talanta*, **51**(2), 231-246.
14. P. Y. Cordier, C. Rabbe, N. Francois, C. Madic and Z. Kolarik, Jaeri-Conf 99-004, 278-284.
15. A. A. Schildt and S-Y. Wong (1984), *J. Coord. Chem.*, **13**, 331-339.
16. R. B. Martin and J. A. Lissfelt (1956), *J. Am. Chem. Soc.*, **78**, 938.
17. B. R. James and R. J. P. Williams (1961), *J. Chem. Soc.*, 2007.
18. K. Y. Kim and G. H. Nancollas (1977), *J. Phys. Chem.*, **81**, 948.



# SEPARATION OF PRECIOUS METALS WITH CROWN ETHERS AS THEIR ION-PAIR COMPLEXES BY MEANS OF SOLVENT EXTRACTION

T. Honjo, K. Z. Hossain and C. T. Camagong

Department of Chemistry, Faculty of Science, Kanazawa University, Kanazawa, Japan

This article is a summary of the new data revealed by the present authors on extraction and back-extraction of precious metals (Pt, Pd, Rh, Ir, Au and Ag, etc.) as their ion-pair complexes with or without crown ethers in organic solvents, along with the papers reported previously.

## INTRODUCTION

The growing demands of precious metals attract great attention to their separation and purification, however, it is always a difficult task to achieve their mutual separation. The behaviour of precious metals (platinum, palladium, rhodium, iridium, gold and silver, etc.) traces in solvent extraction has been examined in detail with or without crown ethers in organic solvents. The effect of various factors on the extraction and back-extraction of precious metals at ppm to ppb levels has been investigated. On the basis of these results, several new analytical methods have been developed by combining with atomic absorption spectrometry (AAS) and inductively coupled plasma atomic emission spectrometry (ICP-AES).

## EXPERIMENTAL

The experimental procedures were almost the same as have been described in the previous papers [1-5]. Crown ethers and organic solvents used were 12-crown-4(12C4), 15-crown-5(15C5), 18-crown-6(18C6), dibenzo-18-crown-6(DB18C6), dicyclohexyl-18-crown-6(DC18C6) and dibenzo-24-crown-8(DB24C8) in organic solvents such as benzene, toluene, nitrobenzene, o-dichlorobenzene, cyclohexane, dichloromethane, chloroform, 1,2-dichloroethane and 1-octanol. The effect of various factors (acid concentration, pH, solvent, crown ether, potassium thiocyanate, hydrochloric acid, reagent concentration, shaking time, phase volume ratio, composition of the extracted species, separation and foreign ions, etc.) on the extraction and back-extraction of precious metals at ppm to ppb levels has been investigated in detail.

## RESULTS AND DISCUSSION

### Extraction Behaviour of Platinum(IV) in Chloroform with Crown Ether from Acidic Media [1]

A new method for the extraction of platinum(IV) from hydrochloric acid media has been established based on the formation of ion-pair complex of platinum hexachloro anion,  $\text{PtCl}_6^{2-}$ , with DC18C6 oxonium cation,  $(\text{H}_3\text{ODC18C6})_2^{2+}$ , in chloroform by means of extraction and back-extraction combined with ICP-AES.

Platinum(IV) in the presence of palladium(II) and rhodium(III) can be extracted quantitatively with 0.05 mol/L DC18C6 in chloroform at 8 mol/L hydrochloric acid within 5 min, where palladium(II) and rhodium(III) can not be extracted at all. Stripping of the extracted platinum(IV) was achieved with 0.1 mol/L hydrochloric acid within 5 min. The content of platinum in palladium chloride and rhodium chloride of guaranteed reagent grade was determined after its separation by DC18C6 extraction at 8 mol/L hydrochloric acid, and it was found to be 16.39 g/g and 8.94g/g, respectively.

#### **Separation of Trace Amounts of Palladium(II) with Crown Ether from Hydrochloric acid and Potassium Thiocyanate Media [2]**

A new method for the separation of trace amounts of palladium(II) from hydrochloric acid and potassium thiocyanate media has been established based on the formation of an ion-pair complex of palladium thiocyanate anion,  $\text{Pd}(\text{SCN})_4^{2-}$ , and the cationic potassium complex of DC18C6,  $(\text{KDC18C6})_2^{2+}$ , in chloroform.

Palladium(II) in the presence of rhodium(III) can be extracted completely with 0.05 mol/L DC18C6 in chloroform at 1 mol/L hydrochloric acid in the presence of 0.05 mol/L potassium thiocyanate within 4 min where rhodium(III) can not be extracted at all. Stripping of the extracted palladium was achieved with 0.1 mol/L ammonia buffer within 4 min.

The method can be combined with subsequent FAAS determination of palladium. The procedure was applied to determine palladium traces in chloroplatinic acid and rhodium chloride. The content of palladium traces in chloroplatinic acid and rhodium chloride of guaranteed reagent grade was found to be 31.66 g/g and 11.98 g/g, respectively.

#### **Separation of Trace Amounts of Rhodium(III) with Tri-*n*-butylphosphate from Nitric Acid and Sodium Trichloroacetate media [3]**

A new method for the quantitative extraction and separation of trace amounts of rhodium(III)from nitric acid and sodium trichloroacetate media has been established based on the formation of an ion-pair complex of hexahydrated rhodium cation,  $\text{Rh}(\text{H}_2\text{O})_6^{3+}$ , and the trichloroacetate (TCA) anion in tri-*n*-butyl phosphate (TBP). The effect of various factors (solvent, pH, sodium trichloroacetate, shaking time, phase volume ratio, composition of the extracted species, foreign ions, transformation of rhodium chlorocomplexes into hexahydrated cation, etc.) on the extraction and back-extraction of rhodium has been investigated.

The matrix of platinum(IV) and palladium(II) in rhodium(III) is previously removed by extraction with DC18C6 in chloroform, and then rhodium(III) can be extracted completely with TBP from nitric acid and sodium trichloroacetate media at pH 3 within 5 min. Stripping of the extracted rhodium was achieved with 8 mol/L perchloric acid within 20 min.

The method can be combined with subsequent FAAS determination of rhodium. The procedure was applied to determine rhodium traces in chloroplatinic acid and palladium chloride. The content of rhodium traces in chloroplatinic acid and palladium chloride of guaranteed reagent grade was found to be 24.09 g/g and 18.07 g/g, respectively.

#### **Extraction of Iridium(IV) from Hydrochloric Acid Media with Crown Ether in Chloroform and its Determination by ICP-AES [4]**

A new method for the quantitative extraction and determination of trace amounts of iridium(IV) from hydrochloric acid media has been established based on the formation of an ion-association complex of iridium hexachloro anion,  $\text{IrCl}_6^{2-}$ , with DC18C6 oxonium cation,  $(\text{H}_3\text{ODC18C6})_2^{2+}$ , in chloroform, then determination by ICP-AES.

Iridium(IV) can be extracted completely with 0.05 mol/L DC18C6 in chloroform at 8 mol/L hydrochloric acid within 5 min along with Pt(IV). Stripping of the extracted iridium(IV) was achieved with 1 mol/L hydrochloric acid within 5 min. The separation of platinum(IV) and iridium(IV) was conducted with 0.1 mol/L tri-*n*-octylamine (TOA) in benzene at 5 mol/L hydrochloric acid within 5 min, where platinum(IV) can be extracted completely, while iridium(IV) can not be extracted at all.

The procedure was used to determine traces of iridium in palladium chloride and rhodium chloride. The iridium content of palladium and rhodium chloride of guaranteed reagent grade was found to be 15.73 g/mL and 13.24 g /mL, respectively.

#### **Separation of Gold(III)with 18-Crown-6 from Hydrochloric Acid Media by means of Solvent Extraction [5]**

A new method for the separation of gold(III) at trace amounts from hydrochloric acid media was developed based on the formation of an ion-pair complex of gold tetrachloro anion,  $\text{AuCl}_4^-$ , with 18C6 oxonium cation,  $(\text{H}_3\text{O}18\text{C}6)^+$ , in 1,2-dichloroethane.

Gold(III) in the presence of silver(I) can be quantitatively extracted with 0.05 mol/L 18C6 in 1,2-dichloroethane from 4 mol/L hydrochloric acid within 5 min. A back-washing step was necessary for the complete separation of gold(III) and silver(I), otherwise, 2 to 6% of silver can be found in the gold extract. Stripping of the extracted gold(III) was achieved with 0.2 mol/L ammonia in the presence of 0.1 mol/L  $\text{Na}_2\text{S}_2\text{O}_3$  media within 5 min.

The method can be combined with subsequent FAAS determination of gold(III). The procedure was applied to determine gold(III) traces in first-class silver reagents such as silver nitrate and silver sulfate, where their content was under 0.25 ng/g (detection limit) after 20 times preconcentration.

#### **Separation of Silver(I) with dicyclohexyl-18-CROWN-6 from Hydrochloric Acid Media by means of Solvent Extraction**

A new method for the separation of silver(I) at trace amounts from hydrochloric acid media was developed based on the formation of an ion-pair complex of silver thiocyanate anion,  $\text{Ag}(\text{SCN})_4^{3-}$ , with cationic potassium complex of DC18C6,  $(\text{KDC}18\text{C}6)_3^{3+}$ , in 1,2-dichloroethane.

Silver(I) can be quantitatively extracted with 0.05 mol/L DC18C6 in 1, 2-dichloroethane from 1.0 mol/L hydrochloric acid in the presence of 0.05 mol/L potassium thiocyanate within 5 min. Stripping of the extracted silver was achieved with 3.0 mol/L potassium thiocyanate within 5 min.

#### **REFERENCES**

1. K. Z. Hossain and T. Honjo (1999), *Proc. Int. Conf. Solvent Extr., ISEC '99*, Society of Chemical Industry, London, pp. 585-590.
2. K. Z. Hossain and T. Honjo (2000), *Fresenius J. Anal. Chem.*, **367**, 141-145.
3. K. Z. Hossain and T. Honjo (2000), *Fresenius J. Anal. Chem.*, **368**, 480-483.
4. K. Z. Hossain, C.T. Camagong and T. Honjo (2001), *Fresenius J. Anal. Chem.*, **369**, 543-545.



## THE BINDING CONSTANTS OF METAL FULVATE AND HUMATE COMPLEXES

A.A. Helal, Gh. A. Mourad and S.M. Khalifa

Hot Labs. Center, Atomic Energy Authority, Cairo, Egypt

The solvent-extraction technique was used to measure the binding constants for Eu and Th fulvate complexes. For comparison, the binding constant for the Eu humate complex was also measured. The investigations were carried out radiometrically using  $(^{152,154})\text{Eu}$  and  $^{234}\text{Th}$ . The results indicated that in case of fulvic acid, one parameter,  $\beta_1$ , was required to fit the binding as a function of carboxylate concentration. In case of humic acid, two parameters,  $\beta_1$  and  $\beta_2$ , were required where  $\text{Eu}^{3+}$  bound forming 1:1 and 1:2 complexes. In both cases, the strength of binding increased with  $\text{pK}_a$  and degree of ionization of the ligands and with valency of the metal ions.

### INTRODUCTION

Naturally occurring fulvic acid (FA) and humic acid (HA) are known to be strong complexing agents to metal ions in the environment. As natural polyelectrolytes, humic compounds are heterogeneous mixtures possessing many types of acidic functional groups that can bind with cations in aqueous media. There are two types of metal fulvate and humate complexations: electrostatic binding due to the polyelectrolyte effect and inner sphere complexation including chelation. As pointed out by Rashid [1], FAs are low molecular weight humic compounds. They are weakly aromatized, poorly condensed compounds with a preponderance of aliphatic side chains. As compared with HAs, FAs are less polymerized. They are generally enriched in oxygen-containing functional groups. Therefore, they are soluble both in acids and bases. FAs are believed to form more readily than the corresponding HAs [2]. Once formed, FAs probably undergo condensation reactions to form more complex HAs.

An important characteristic of a metal fulvate or humate complex is its binding constant (BC), the value of which provides an index of the affinity of the cation for the ligand. Numerical values of BCs for metal fulvate and humate complexes would be of considerable value in predicting the behavior of radionuclides, trace elements, and toxic heavy metals in soils and sediments. As reviewed by Monsallier *et al.* [3], many experimental procedures have been used for the measurements of BCs such as solvent extraction (SX) [4], gel permeation chromatography [5], UV spectroscopy [6], ion exchange [7], laser-induced photoacoustic spectroscopy [8], time-resolved laser fluorescence spectroscopy [9], ultrafiltration [8,10] and dialysis [7,11]. Depending on the method, the results vary considerably.

According to Takamatsu and Yoshida [12], there are two difficulties in determining the BCs of metal fulvate and humate complexes, one related to determining concentrations of humic compound as complexant, and the other related to procedures for measuring the actual BCs. The average molecular weight, the maximum complexing ability and the number of titratable functional groups have been used to represent the concentration of humic compound as complexant. Because of variations in the physico-chemical characteristics of the humic compounds and the different methods used to measure the BC, the reported constants have no consistency [1]. SX is a suitable method for radionuclide investigation since it allows measurements at tracer level concentrations. Although extensive use has been made of the SX (and other methods) for determining BCs of metal humate complexes, little application has been made in studies of metal complexes of FAs. In particular, data on lanthanides and actinides are limited. In this work, the BCs of  $^{(152,154)}\text{Eu}$  and  $^{234}\text{Th}$  with FA, and the BC of  $^{(152,154)}\text{Eu}$  with peat HA were determined using the SX technique.

## EXPERIMENTAL

### Chemicals and Materials

The chemicals used were of analytical purity. Di(2-ethylhexyl)phosphoric acid, HDEHP, was obtained from Union Carbide, and purified according to Peppard *et al.* [13]. FA was isolated from the agricultural soil of Orman garden, an old garden located at the West Bank of Nile river in Cairo, Egypt. The HA is isolated from a sample of peat. The method of separation and purification of FA and HA is the conventional method [14].

### Tracers

The radiotracer  $^{(152,154)}\text{Eu}$  was prepared locally by neutron activation of  $\text{Eu}_2\text{O}_3$  in the Egyptian reactor (ARE-RR-1).  $^{234}\text{Th}$  was separated from natural uranium by SX using 30% TBP diluted in benzene [15]. The radiochemical purity of  $^{234}\text{Th}$  and  $^{(152,154)}\text{Eu}$  was checked by measuring the respective  $\gamma$ -spectrum with Ge(Li) detector using a multichannel analyzer. The  $\gamma$ -emissions of both tracers was counted with a NaI(Tl) well counter of ORTEC type.

### Procedures

The FA and HA samples were characterized by elemental analysis, potentiometric titration, and visible spectroscopy. The acid-base behavior of FA and HA was determined at an ionic strength ( $\mu$ ) of 0.1 M by direct titration [16]. The absorption in the visible region was measured using a Shimadzu recording spectrometer 160A.

For the SX experiments, the organic phases consisted of toluene containing HDEHP. Because of the precipitation problems encountered when contacting HA solutions with organic phase [15], the latter was pre-equilibrated several times against equal volumes of the corresponding buffer solutions before use. This pre-equilibration was continued until no pH change was observed in the fresh aqueous phase. The aqueous phases were prepared by using the suitable buffer solutions for the desired pH values. These buffer solutions also contained the necessary quantity of  $\text{NaClO}_4$  to make the total ( $\mu$ ) 0.1 M.

Primary distribution experiments were performed to evaluate the time needed for equilibration for each of the ligands. For both  $\text{Eu}^{3+}$  and  $\text{Th}^{4+}$ , the obtained results showed that the equilibrium is reached within 2.5 h in case of FA and 1.5 h in case of HA. A working solution of FA or HA was prepared by dissolving ca. 0.1 g in 10 ml of 0.1 M NaOH with overnight stirring under nitrogen gas. The solution was titrated to the desired pH with 0.1 M  $\text{HClO}_4$ , and diluted to 100 ml with the suitable buffer solution [4] of the same pH. Aliquots of this working solution were diluted with the buffer to obtain solutions of varying HA concentrations. The free humate concentration (in eq/l) was determined by multiplying the concentration (g/l) by the total capacity (eq/g) and by the degree of ionization corresponding to the pH of the investigation.

Five ml of each phase and 10  $\mu$ l of tracer were added to 20 ml glass scintillation vials (coated with silicon compounds [17] to minimize the adsorption of activity by the wall of the vial). Five ml of the buffer solution, without FA or HA, was used as a blank for each experiment. The vials were vigorously shook in a thermostated shaker at room temperature ( $25 \pm 1^\circ\text{C}$ ) for the suitable time, then they were centrifuged and the phases separated and centrifuged before removing aliquots for counting. The remainder of the aqueous phases was used to measure the final pH and the final HA concentrations in the HA experiments.

## RESULTS AND DISCUSSION

The elemental analysis of FA and HA samples indicated that the ratios of C, O, H, N and S are 51.0, 38.2, 4.4, 2.8 and 3.6% for FA and 48.5, 41.7, 5.4, 1.2 and 3.2% for HA. The higher atomic ratios O/C and H/C of HA than FA may reflect higher amounts of COOH and show that aliphatic C may be more abundant in FA.

Figures 1 and 2 give the potentiometric titration curves and the first derivatives of FA and HA samples. The curves have double inflections and, in general, they are similar to those obtained for weak acids. The first derivatives indicate that each sample has two maxima, which implies two kinds of ionizing functional groups. This phenomenon has been explained [4] by the presence of two carboxylate groups; the stronger acid group is located ortho to phenolic groups on aromatic rings, while all the other carboxylates fall in the second, weaker group. The first maxima occurs at 2.5 and 4.0 meq/g for FA and HA, respectively. The total carboxylate capacities are calculated from the second maxima and found to be 4.0 and 6.0 meq/g for FA and HA, respectively. The first maxima occur at pH 5.89 and 6.83, while the second maxima occur at pHs 8.37 and 9.16 for FA and HA, respectively.

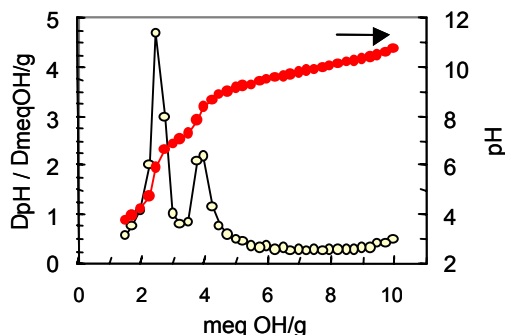


Figure 1. The titration and derivative curves of FA.

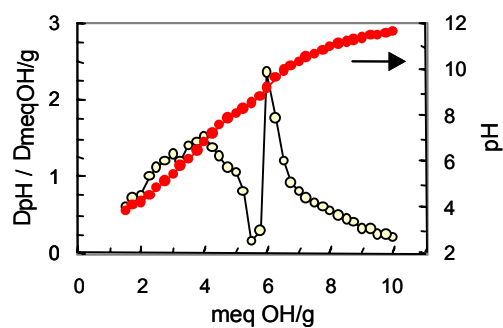


Figure 2. The titration and derivative curves of HA.

The dissociation of an acidic functional group (HA) from the humic or fulvic molecule proceeds as:



For which the ionization constant ( $K$ ) is:

$$K = [\text{A}^-][\text{H}^+]/[\text{HA}] \quad (2)$$

The titration data provide estimates for ( $\text{A}^-$ ) and ( $\text{HA}$ ) at any given pH, from which the ionization constant can be determined. Since  $K$  is normally of a very small value, the negative logarithm ( $pK$ ) is often recorded:

$$pK = -\log [\text{A}^-][\text{H}^+]/[\text{HA}] \quad (3)$$

$$= \text{pH} - \log [\text{A}^-]/[\text{HA}] \quad (4)$$

At half-neutralization,  $pK = pH$  and this is commonly referred to as  $pK_a$  of the acidic group. A variety of equilibrium functions have been developed to characterize the acid-base behavior of polyelectrolytes; the most common one is the Henderson-Hasselbalch equation [18] which was applied to evaluate the  $pK_a$  of FA and HA samples:

$$pH = pK_a + n \log [\alpha / (1-\alpha)] \quad (5)$$

where  $pK_a$  and  $n$  are constants depend on concentration as well as ionic strength, and  $\alpha$  is the degree of ionization. The  $pK_a$  values at 50% ionization ( $\alpha = 0.5$ ) was found to be 3.86 and 5.4 for FA and HA, respectively (at  $\mu = 0.1 M$  in sodium perchlorate medium).

The ratio of absorbances of dilute aqueous sample solutions at 465 and 665 nm, defined as  $E_4/E_6$  ratio, is widely used for characterization purposes. This ratio is independent of the concentration of the humic compound, but varies for different humic substances. As pointed out by Chen *et al.* [19], the magnitude of  $E_4/E_6$  ratio is inversely proportional to the degree of condensation or the molecular weight, i.e., the high  $E_4/E_6$  ratio indicates a smaller molecule which contains less carbon, but more oxygen and -COOH groups. The  $E_4/E_6$  ratios are found 4.14 and 5.93 for FA and HA, respectively. Comparing the deduced results of  $E_4/E_6$  ratio with that of elemental composition and potentiometric titration indicate that they are in good agreement with each other.

### Determination of the Binding Constants

The following equation is used to measure the binding constants for FA and HA [15]:

$$(D_o/[L])(1/D_2 - 1/D_1) = \beta_1 + \beta_2[L]$$

where  $D_o$  is the distribution ratio of the investigated cation,  $D_1$  and  $D_2$  are the distribution in presence of the buffer anion and the ligand (FA or HA), respectively, L is the ligand (FA or HA) and  $\beta_1$  and  $\beta_2$  are the binding constants. Therefore, a plot of  $(D_o/[FA \text{ or } HA])(1/D_2 - 1/D_1)$  vs.  $[FA \text{ or } HA]$  gives a straight line of intercept  $\beta_1$  and a slope of zero (or negative) if only a 1:1 complex is formed, or a straight line of intercept  $\beta_1$  and a slope of  $\beta_2$  if a 1:2 complex is formed.

### Binding of Eu<sup>3+</sup> and Th<sup>4+</sup> with FA

The plots of  $(D_o/[FA])(1/D_2 - 1/D_1)$  vs.  $[FA]$  showed linear curves with negative slopes in case of both Eu<sup>3+</sup> and Th<sup>4+</sup> (Figure 3 is an example). Thus, the binding function required analysis with one constant  $\beta_1$ , which implies the formation of 1:1 complex only. This result agrees with the potentiometric titration of FA, where the first maximum, occurring at pH 5.89, is stronger than the second one indicating that the sample has mainly one kind of ionizing functional groups.

The obtained binding constants for Eu<sup>3+</sup> and Th<sup>4+</sup> are plotted against the degree of ionization ( $\alpha$ ) of the fulvate polyelectrolyte, Figure 4. The strength of binding of both Eu<sup>3+</sup> and Th<sup>4+</sup> to FA increases with the degree of ionization, which is a function of pH. FA acts as weak-acid polyelectrolytes in which ionization of COOH groups is controlled by pH. Increasing pH of the solution results in additional ionization of the acidic functional groups of FA, and causes the increase in the binding constant.

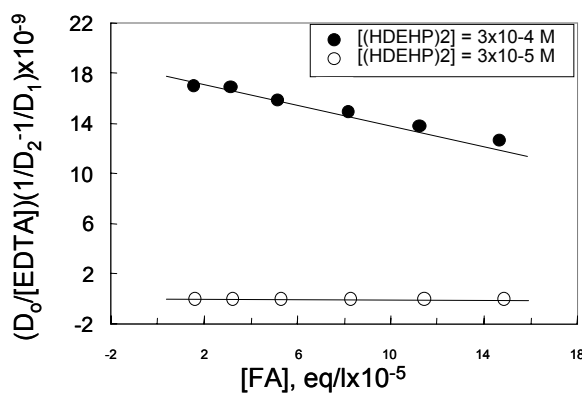


Fig. (3): Effect of [FA] on the extraction of Eu by HDEHP

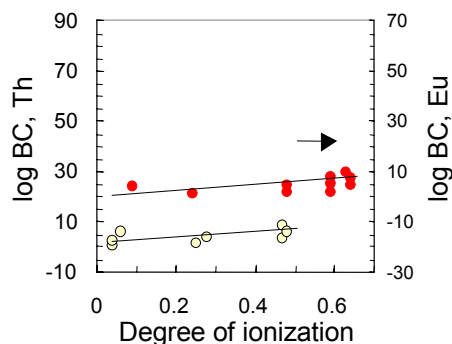


Fig. (4): Variation of log BC for Eu(III) and Th(IV) with the degree of ionization of FA

From the straight lines in Figure 4, the following equations could be derived for the value of the binding constant as a function of the degree of ionization of FA:

$$\text{For Eu}^{3+}: \text{Log } \beta_1 = 1.07 + 7.807 \alpha$$

$$\text{For Th}^{4+}: \text{Log } \beta_1 = 2.23 + 7.28 \alpha$$

Thus, the values of the binding constant at 50% ionization ( $\alpha = 0.5$ ) are 4.974 and 5.87 for  $\text{Eu}^{3+}$  and  $\text{Th}^{4+}$ , respectively. As expected, the binding constant of  $\text{Th}^{4+}$  is higher than that of  $\text{Eu}^{3+}$  since tetravalent cations are bound in greater amounts than trivalent ones, for any given pH and ( $\mu$ ). These values are in good agreement with those reported. By comparing the values of  $\text{log } \beta_1$  and  $\text{pK}_a$  of fulvic acid obtained in this work and in previous works, it is noted that the binding constants of  $\text{Eu}^{3+}$  and  $\text{Th}^{4+}$  increase with increasing  $\text{pK}_a$ .

### Binding of $\text{Eu}^{3+}$ and $\text{Th}^{4+}$ with EDTA

For confirmation, both  $\text{Eu}^{3+}$  and  $\text{Th}^{4+}$  were extracted by HDEHP from an aqueous phase containing EDTA, as a ligand form 1:1 complex, at the same conditions. The plots of the factor  $\{\text{D}_o/[\text{EDTA}]\}\{(1/\text{D}_2-1/\text{D}_1)\}$  against [EDTA] is illustrated in Figure 5. As the figure shows, the curves are linear with negative slopes, the same behavior like fulvic acid. This result confirms the formation of 1:1 complex for the binding of both  $\text{Eu}^{3+}$  and  $\text{Th}^{4+}$  with fulvic acid.

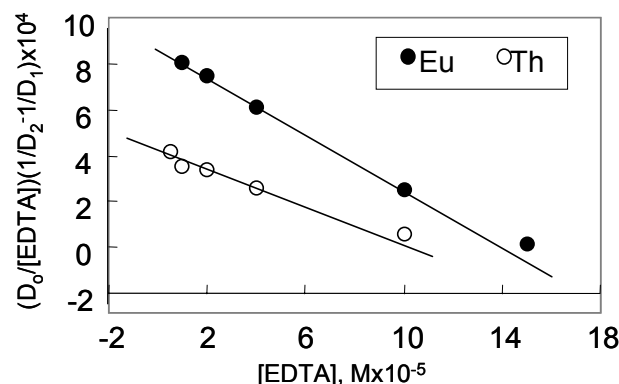


Fig. (5): Effect of [EDTA] on the extraction of Eu and Th by HDEHP

### Binding of Eu<sup>3+</sup> with HA

The BCs for Eu<sup>3+</sup> with HA are elucidated at the same conditions for comparison with FA. The maximum binding capacity of humic materials for any given metal ion is approximately equal to the content of acidic functional groups, primarily COOH. The first derivative of the potentiometric titration curve of HA, Figure 2, indicates the presence of two kinds of functional groups. The second maximum occurs at pH 9.16, which is a suitable value for the ionization of phenolic groups.

The plots of  $\{D_0/[HA]\}\{(1/D_2 - 1/D_1)\}$  versus [HA], (Figure 6 is an example), were linear with positive slopes. In these curves, the intercepts represent the values of  $\beta_1$  and the slopes represent the values of  $\beta_2$ . This result implies the formation of 1:1 and 1:2 complexes. The variation of the BC's of Eu<sup>3+</sup> with the degree of ionization of HA is illustrated in Figure 7. As previously indicated in case of FA, the BC increases with increasing the degree of ionization, which is a function of pH of the solution. From Figure 7, the following equations are derived as a relation between the BC's and the degrees of ionization:

$$\log \beta_1 = 3.402 + 13.045 \alpha$$

$$\log \beta_2 = 7.696 + 12.225 \alpha$$

Thus, the values of the BC's (at  $\alpha = 0.5$ ) are:  $\log \beta_1 = 9.925$  and  $\log \beta_2 = 13.809$ . The same behavior is observed where the BC of HA (which has higher  $pK_a$ ) is higher than that of FA (of lower  $pK_a$ ).

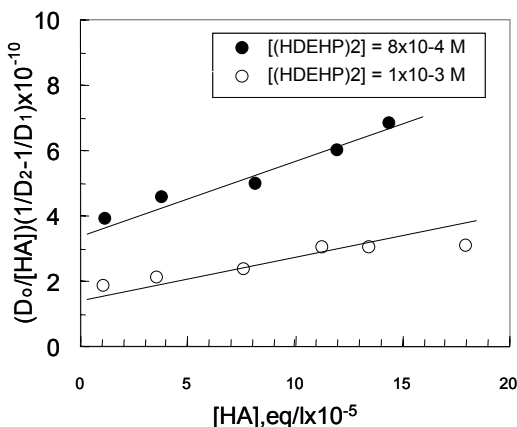


Fig. (6): Effect of [HA] on the extraction of Eu by HDEHP

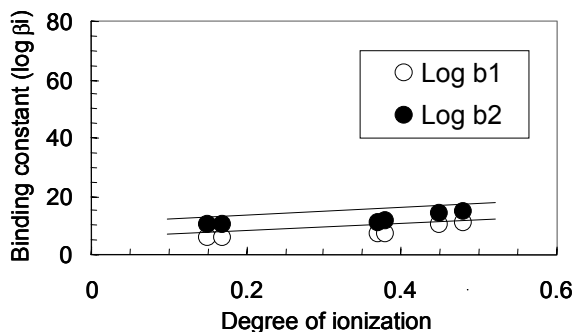


Fig. (7): Variation of log BC for Eu<sup>3+</sup> with the degree of ionization of HA

### CONCLUSIONS

In light of the preceding results, the following conclusions could be obtained:

1. Solvent extraction was found a suitable technique for measuring the binding constants of radionuclides used in tracer level.
2. FA and HA act as weak acid polyelectrolytes in which ionization of COOH groups is controlled by pH, thereby affecting their ability to bind metal ions.
3. Both Eu<sup>3+</sup> and Th<sup>4+</sup> bound to the carboxylate site in FA forming 1:1 complex only, while Eu<sup>3+</sup> bound to HA forming 1:1 and 1:2 complexes.
4. The binding constants were found to increase with  $pK_a$  of the ligand and valency of the metal ion.

## REFERENCES

1. M.A. Rashid (1985), Geochemistry of Marine Humic Compounds, Springer-Verlag, Berlin, p. 58.
2. L.A. Grishina and K.O. Korotkov (1978), *Soviet Soil Science*, **10**, 23.
3. J.N. Monsallier, F.J. Scherbaum, G. Buckau, J.I. Kim, M.U. Kumke, C.H. Specht and F.H. Frimmel (2001), *J. Photochem. Photobiol. A: Chemistry*, **138**, 55.
4. R. Torres and G.R. Choppin (1984), *J. Radiochim. Acta*, **35**, 143.
5. V. L. Moulin (1985), Les acides humiques et leurs interactions avec les éléments métalliques Cu(II), Eu(III), Th(IV), U(VI), Dissertation, Université Claude Bernard, Lyon.
6. J.I. Kim and C.M. Marquardt (1999), *J. Radiochim. Acta*, **87**, 105.
7. A. Diercks, A. Vancluysen and A. Maes (1992), Report RCM 00392, TU, München, Germany.
8. J.I. Kim, G. Buckau, E. Bryant and R. Klenze (1989), *J. Radiochim. Acta*, **48**, 135.
9. J.I. Kim, H. Vimmer and R. Klenze (1991), *J. Radiochim. Acta*, **54**, 35.
10. M. Caceci (1994), *J. Radiochim. Acta*, **39**, 51.
11. L. Carlsen (1985), Report: CEC, EUR 9780/I, EN, Brussels.
12. T. Takamatsu and T. Yoshida (1978), *J. Soil Science*, **125** (6), 377.
13. D.F. Peppard, G. W. Mason, J. L. Maier and W. J. Driscoll (1957), *J. Inorg. Nucl. Chem.*, **4**, 334.
14. G.A. Mourad (1999), M.Sc. Thesis, Zagazig University, Egypt.
15. A.A. Helal (1999), Proc. Int. Solvent Extr. Conf. ISEC '99, Society of Chemical Industry, London, pp. 213-218.
16. A.A. Helal, D. M. Imam and H. F. Aly (1996), *Egypt. J. Anal. Chem.*, **5**, 79.
17. M.S. Caceci and G. R. Choppin (1983), *J. Radiochim. Acta*, **33**, 113.
18. A. Katchalsky and O. Spitnik (1947), *J. Polymer Sci.*, **2**, 432.
19. Y. Chen, N. Senesi and Schnitzer N. (1977), *Soil Sci. Soc. Am. J.*, **41**, 352.



## ION-PAIR EXTRACTION AND ONE-DROP FLAME ATOMIC ABSORPTIOMETRIC DETERMINATION OF SILVER WITH BENZO-MONOTHIACROWN AND BROMOTHYMPOL BLUE

Isao Kojima, Miwa Katsuzaki, Miho Yamada, Makoto Yamaguchi  
and Hidefumi Sakamoto\*

Department of Applied Chemistry, Nagoya Institute of Technology, Nagoya, Japan

\* Department of Applied Chemistry, Faculty of Systems Engineering,  
Wakayama University, Wakayama, Japan

Ion-pair extraction of silver ion into chloroform has been studied with benzo-monothia-15-crown-5 (5,6-benzo-1,4,7,10-tetraoxa-13-thiacyclopentadeca-5-ene, B-15TC) in the presence of a counter anion. B-15TC was synthesized from catechol via 1,2-bis(2'-hydroxyethoxy)-benzene and 1,2-bis(p-toluenesulfonyl-oxyethoxy)-benzene in three steps. Counter anions studied were perchlorate and picrate ions, bromothymol blue (BTB), bromocresol green (BCG), ethyl orange (EO), cobalt(III)-dihydroxyazobenzene complex (Co-DHAB). The order of percent extraction was BTB > Co-DHAB > BCG > picrate ion > EO > perchlorate ion at pH less than 4 and BTB > Co-DHAB > BCG > EO > picrate ion > perchlorate ion at pH larger than 4. Silver ion was quantitatively extracted into chloroform at pH of 4.5-5.2 in the presence of BTB. The compositions of the extracted species are  $\text{Ag}^+ : \text{B-15TC} : \text{BTB}^- = 1:1:1$  and 1:2:1. With the combined use of the extraction concentration and one-drop flame atomic absorption spectrometry using 50 $\mu\text{l}$  volume of the chloroform extract, silver in a standard botanical sample of National Institute of Environmental Studies, NIES-CRM No. 9 Sargasso, was determined.

### INTRODUCTION

Thiacrown ethers obtained by replacing oxygen atoms in crown ethers with sulfur atoms have a great affinity for softer metal ions such as silver, copper(I) and mercury and extract these metal ions as ion-pair complexes in the presence of a bulky and univalent organic or inorganic anion [1-4]. In addition, 1,2-bis(alkylthia)ethanes were also used as a good extractant for these metal ions in the presence of a counter anion [3,5]. Of these reagents, a commercially available 3, 6-dithiaoctane (8-2S) was well applied to the selective extraction of silver and copper(I) in some standard reference materials and to the determination of silver [6-8] and copper [9] by one-drop flame atomic absorption spectrometry with a direct nebulization of 50  $\mu\text{l}$  volume of the chloroform extract. On the other hand, owing to the unpleasant odor specific to the sulfur compound, the use of 8-2S is disliked for chemist.

The present paper describes the selective extraction of silver ion with a non-odor 5,6-benzo-1,4,7,10-tetraoxa-13-thiacyclopentadeca-5-ene (B-15TC) in the presence of BTB and the determination of silver in a certified reference material (NIES-CRM No. 9, Sargasso) by one-drop flame AAS with the direct nebulization of 50  $\mu\text{l}$  of the chloroform extract without the deuterium background correction.

## EXPERIMENTAL

### Preparation of B-15TC

B-15TC was synthesized in a similar way described previously [10,11] in three steps, as is shown in Figure 1. Only the final synthetic step, *i.e.*, cyclization reaction, is described here. Bis(2-hydroxyethyl)sulfide (1.10 g, 0.01 mol) was dissolved in 400 ml of dry dioxane. To this solution, NaH (69% in oil, 600 mg, 0.025 mol) was added and then the resulted solution was refluxed. To this refluxing solution, 1,2-bis(p-toluenesulfonyloxyethoxy)benzene (5.1 g, 0.01 mol) dissolved in 50 ml of dry dioxane was dropwise added for 8 h and the mixture was refluxed for 2 d under a nitrogen atmosphere. The solvent was evaporated off under a reduced pressure. After the residue was dissolved in water (50 ml), the extraction with chloroform (25 ml) was done five times. The chloroform extract was dried over MgSO<sub>4</sub>. A crude white crystal obtained after the evaporation of solvent was dissolved in benzene and was recrystallized. The yield was 22%. M.p.131-132°C; <sup>1</sup>H-NMR(CDCl<sub>3</sub>) δ=6.88(s, 4H), 3.78-4.12(m, 12H), 2.82(t, J=6.8 Hz, 4H).

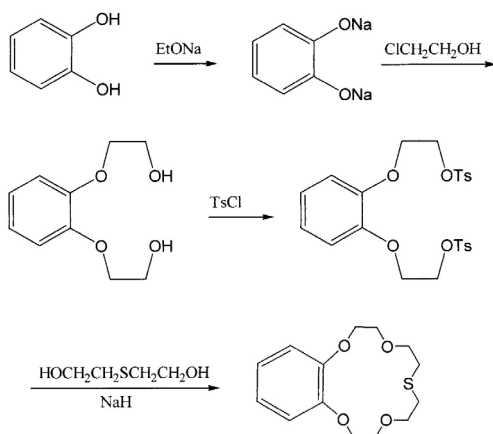


Figure 1. Synthetic route of B-15TC.

### Apparatus

An atomic absorption spectrometer equipped with 100 mm burner head (Seiko Model SAS-727, Chiba, Japan) was used with a discrete nebulization technique using a fuel-lean air-acetylene flame at 328.1 nm under the same operating conditions previously reported [8]. The signal intensity was recorded on a strip-chart recorder (National, VP-6612a, Osaka, Japan). Sample was decomposed in a closed double PTFE digestion bomb with a polypropylene jacket (San-ai Kagaku, Nagoya, Japan) by microwave-assisted heating (Hitachi MRH-4 microwave oven for kitchen use). The pH of the solutions was measured with a Radiometer (Copenhagen, Denmark) Type PHM-22 pH meter with a combined electrode.

### Reagents

A silver standard solution (2 mg/g in 0.5 M HNO<sub>3</sub>) was prepared by dissolving a silver metal of 99.99% purity (Nacalai Tesque, Kyoto) in HNO<sub>3</sub> directly in a PTFE bottle of 120 ml capacity, followed by diluting by mass with water. Working aqueous silver solutions were prepared by diluting the stock solution to the appropriate concentrations by mass with 0.05 M H<sub>2</sub>SO<sub>4</sub>. B-15TC was directly dissolved in chloroform (0.01 M). Chloroform of analytical-reagent grade (Wako Pure Chemicals, Osaka, Japan) was used without further purification. Anion solutions of bromocresol green (BCG, 10<sup>-3</sup> M), bromothymol blue (BTB, 3 × 10<sup>-3</sup> M), picric acid (Pic, 10<sup>-2</sup> M) and ethyl orange (EO, 10<sup>-2</sup> M) from Wako were prepared by dissolving in water or in an alkaline solution. The solution of cobalt-dihydroxyazobenzene complex (Co-DHAB, 3.3 × 10<sup>-3</sup> M) was prepared, as was described in [8]. To control the extraction pH, an ammonium acetate of analytical-reagent grade (2.0 M) was used. The acids used for sample

digestion and dilution were of analytical-reagent grade (Wako). Water purified by a Milli-Q system (Millipore, USA) was used throughout.

### Sample Decomposition

A dry sample of 300 mg was decomposed with an acid mixture by microwave-assisted heating, as was done in a previous study [8]. After the complete evaporation of the digest to dryness, the dry residue was dissolved in 3 ml of a 0.05 M H<sub>2</sub>SO<sub>4</sub> solution in the same vial and the total mass was weighed.

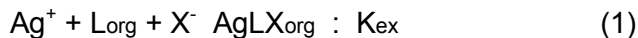
### Extraction Procedure

Into a 10 ml stoppered glass test-tube, 1 ml of the sample solution (weighed), 0.5 ml of the anion solution, 1 ml of an ammonium acetate solution, 2.5 ml of water and 0.3 ml (weighed) of the chloroform solution of B-15TC were placed. Silver ion was extracted by shaking for 15 min by a Ayela cute mixer (CM-1000, Tokyo Kikai, Tokyo). For a complete phase separation, the centrifugation at 3000 rpm was used. A 50 µl of chloroform extract was used for a FAAS measurement, as was described in a previous paper [8].

## RESULTS AND DISCUSSION

### Equilibrium Treatment

Suppose that the extracted species of silver ion with B-15TC (L) in the presence of BTB (X<sup>-</sup>) is the same as that obtained in the extraction with 1,2-bis(alkylthio)-ethane [3,5,12] or thiacrown ether [13,14] in the presence of perchlorate or picrate ion, i.e., two monomeric 1:1:1 and 1:2:1 complexes for Ag<sup>+</sup>:B-15TC:X<sup>-</sup>, then the extraction equilibria can be written as:



where the overall extraction constant, K<sub>ex</sub>, and the formation constant, K<sub>1</sub>, are given by

$$\text{K}_{\text{ex}} = [\text{AgLX}]_{\text{org}} / [\text{Ag}^+] [\text{L}]_{\text{org}} [\text{X}] \quad (3)$$

$$\text{K}_1 = [\text{AgL}_2\text{X}]_{\text{org}} / [\text{AgLX}]_{\text{org}} [\text{L}]_{\text{org}} \quad (4)$$

The subscript, <sub>org</sub>, refers to the organic phase. The distribution ratio of silver, D, is given by

$$\begin{aligned} \text{D} &= \text{E V}_{\text{aq}} / \{(100 - \text{E})\text{V}_{\text{org}}\} \\ &= \text{K}_{\text{ex}} [\text{L}]_{\text{org}} [\text{X}] \{1 + \text{K}_1 [\text{L}]_{\text{org}}\} \end{aligned} \quad (5)$$

where V<sub>org</sub> and V<sub>aq</sub> refer to the organic and aqueous volumes used for extraction equilibrium study, respectively, and E refers to the percent extraction of silver ion into chloroform. Then the plot of log D against log [X] at a constant concentration of B-15TC in chloroform should yield a straight line with a slope of unity and the plot of log D against log [L]<sub>org</sub> should yield a curve varying from slope of 1 to 2.

### Extraction Behavior

The extraction behavior of silver ion from the aqueous solution of a constant anion concentration was examined in a pH range less than 5.5. The results obtained with different anions are shown in Figure 2. The order of percent extraction of silver ion was BTB > Co-DHAB > BCG > picrate ion > EO > perchlorate ion at pH less than 4 and BTB > Co-DHAB > BCG > EO > picrate ion > perchlorate ion at pH larger than 4. Only BTB gave a quantitative extraction of silver ion at pH range larger than 4.5. Taking into account of these results, the effect of BTB concentration was tested. The quantitative extraction of silver ion (>99%) was observed at the BTB concentration larger than 3 × 10<sup>-4</sup> M. In addition, the effects of perchlorate and sulfate ion concentrations were also tested. Even with perchlorate ion, the percent extraction was low (5% at 0.1 M and 17% at 1.0 M), while silver ion was not extracted with hydrogensulfate ion.

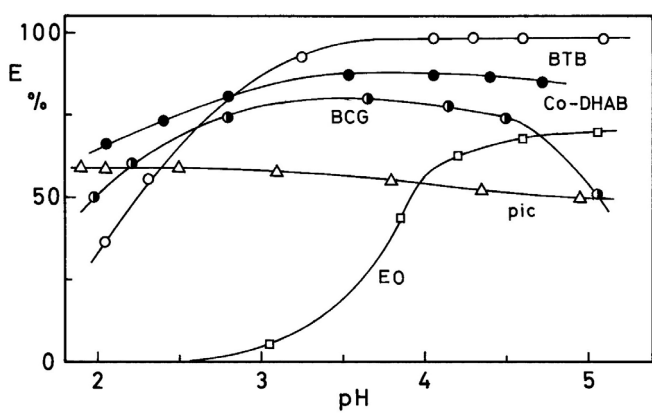


*Figure 2. Extraction of silver ion in the presence of anions.*  
 BTB :  $2 \times 10^{-4} M$ ; BCG :  $10^{-4} M$ ; Co-DHAB :  $3.3 \times 10^{-4} M$ ; Pic :  $10^{-2} M$ ; EO :  $10^{-3} M$ ; Vorg : Vaq = 0.5 ml : 5.0 ml; CAg,aq :  $1.0 \times 10^{-6} M$ .

### Composition of Extracted Species

At a constant B-15TC concentration of 0.01 M and at a pH of 4.5, a plot of log D against log [X] is shown in Figure 3.

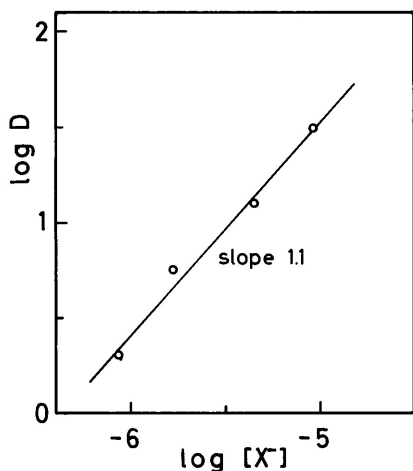


*Figure 3. A plot of log D against log [X] at [B-15TC]org = 0.01 M.*  
 Vorg : Vaq = 0.5 ml : 5.0 ml ; n = 1.

Similarly, a plot of log D against log [L]org at a constant BTB concentration of  $2 \times 10^{-4} M$  and at a pH of 4.5 is given in Figure 4. A straight line with a slope of 1.1 in Figure 3 and a curve in Figure 4 were obtained. With the same data in Figure 4, a plot of  $(\log D - \log [X]) - \log [L]_{org}$  against  $\log [L]_{org}$  is shown in Figure 5. As is evident from Figure 5, this plot gave a curve. Comparing this plot with a normalized curve obtained with  $Y = \log(1 + x)$  and  $X = \log x$ , a reasonable fit with  $\log K_{ex} = 8.06$  and with  $X = 0$  at  $\log K_1[X]_{org} = -1.90$  was obtained. These results show that the extracted species are 1:1:1 and 1:2:1 and the values of  $\log K_{ex}$  and  $\log K_1$  are 8.06 and 1.90, respectively.

### Determination of Silver in Sargasso

On the basis of the previous facts [6,7], the proposed method was applied to the determination of silver in a certified reference botanical material (NIES-CRM No. 9, Sargasso) from National Institute of Environmental Studies (Japan). The analytical results obtained are  $0.305 \pm 0.005 \mu\text{g/g}$  ( $n=6$ , Vorg : Vaq = 0.3 ml : 5.0 ml). The results agreed well with the certified value ( $0.31 \pm 0.02 \mu\text{g/g}$ ) and also were very reproducible.

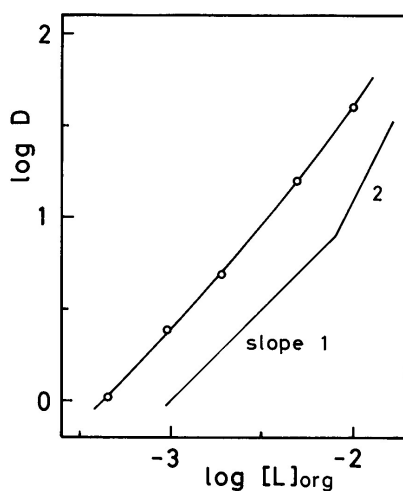


Figure 4. A plot of  $\log D$  against  $\log [L]_{\text{org}}$  at  $[BTB] = 2 \times 10^{-4} \text{ M}$ .  
 $V_{\text{org}} : V_{\text{aq}} = 0.5 \text{ ml} : 5.0 \text{ ml} ; n = 1$ .

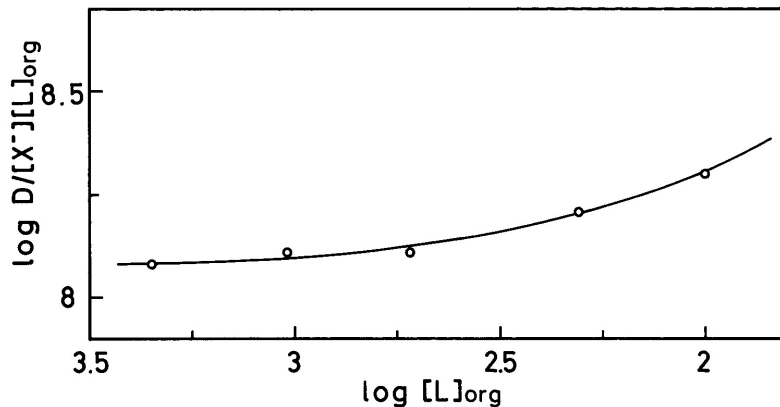


Figure 5. A plot of  $(\log D - \log [X] - \log [L]_{\text{org}})$  against  $\log [L]_{\text{org}}$ .  
 $V_{\text{org}} : V_{\text{aq}} = 0.5 \text{ ml} : 5.0 \text{ ml}$ .

## REFERENCES

1. D. Sevdic, L. Fekete, H. Meider (1980), *J. Inorg. Nucl. Chem.*, **42**, 885-889.
2. K. Saito, Y. Masuda, E. Sekido(1983), *Anal. Chim. Acta*, **151**, 447-455.
3. A. Ohki, M. Takagi, K. Ueno (1984), *Anal. Chim. Acta*, **159**, 245-253.
4. M. Oue, K. Kimura, T. Shono (1987), *Anal. Chim. Acta*, **194**, 293-298.
5. F. Dietze, K. Gloe, R. Jacobi, P. Muehl, J. Beger, M. Petrich, L. Beyer, E. Hoyer (1989), *Solv. Extr. Ion Exch.*, **7**, 223-247.
6. I. Kojima, A. Takayanagi (1996), *J. Anal. At. Spectrom.*, **11**, 607-610.
7. I. Kojima, M. Kataoka, M. Yamada, M. Yamaguchi (2000), *Anal. Sci.*, **16**, 1045-1048.
8. I. Kojima, M. Katsuzaki (1997), *Anal. Sci.*, **13**, 1021-1023.
9. I. Kojima, M. Ito, T. Mizuno, A. Matsumori, A. Asai (2000), *Anal. Sci.*, **16**, 1175-1178.
10. H. Sakamoto, K. Kimura, Y. Koseki, M. Matsuo, T. Shono (1986), *J. Org. Chem.*, **51**, 4974-4979.
11. M. Oue, K. Akama, K. Kimura, M. Tanaka, T. Shono (1989), *Anal. Sci.*, **5**, 165-169.
12. K. Chayama, N. Koyama, H. Tsuji, E. Sekido (1998), *Bunseki Kagaku*, **47**, 993- 998.
13. D. Sevdic, H. Meider (1977), *J. Inorg. Nucl. Chem.*, **39**, 1403-1407.
14. E. Sekido, K. Chayama (1986), *Nippon Kagaku Kaishi*, **1986**, 907-914.



## EXTRACTION AND SPECTROPHOTOMETRIC DETERMINATION OF COPPER(II) WITH 3-ISONITROSO-5-METHYL-2-HEXANONE AND 5-METHYL-2,3-HEXANEDIONE DIOXIME

S.P. Tandel, S.B. Jadhav and S. P. Malve

Institute of Science 15, Mumbai, India

Simple and selective methods are proposed for the extraction of copper(II) and its spectrophotometric determination using 3-isonitroso-5-methyl-2-hexanone (HIMH) and 5-methyl-2,3-hexanedione dioxime ( $H_2MHDDO$ ). Copper(II) forms greenish-yellow coloured complexes with both reagents, which can be extracted into isoamyl alcohol at pH 6.5-8.5 (HIMH) and into chloroform at pH 7.0-8.5 ( $H_2MHDDO$ ). The extracted species show absorption maxima at 390 (HIMH) and 370 nm ( $H_2MHDDO$ ), and the calibration curves are linear in the concentration ranges 0.1-7.0 and 0.1-10.0  $\mu\text{g ml}^{-1}$  of copper(II), respectively. The molar absorptivities of the complexes are  $1.001 \times 10^4$  (HIMH) and  $6.61 \times 10^3 \text{ l mol}^{-1} \text{ cm}^{-1}$  ( $H_2MHDDO$ ), and the Sandell's sensitivities of the proposed methods are 6.1 and 9.2 ng  $\text{cm}^{-2}$  respectively. These methods are applied for the determination of copper in synthetic mixtures, pharmaceuticals, dyes and alloy samples.

### INTRODUCTION

The significance of copper as a transition metal lies in its wide spectrum of applications, covering many frontier areas of studies, such as medicine, industry, food and beverages. It is also present in all body tissues, but liver, brain and kidney contain the highest amounts. Both deficiency and excess concentration of copper can cause adverse effects on the human body. Hence owing to the significance of copper, it was considered worthwhile to explore the possibilities of developing a simpler, sensitive, selective and rapid method for the determination of traces of copper in various synthetic mixtures, dyes, alloy and pharmaceutical samples.

Various substituted and unsubstituted ketoximes have been surveyed in the literature for spectrophotometric determination forming coloured chelates, especially with transition metal ions, and which were easily extractable in most common organic solvents [1-3]. The literature survey reveals that a wide variety of reagents have been employed for its spectrophotometric determination but most of them suffer from limitations such as heating time, long time of colour development, long time of equilibration, critical pH, and interference from many ions.

Owing to the increasing commercial importance, in the present communication, 3-isonitroso-5-methyl-2-hexanone (HIMH) and 5-methyl-2,3-hexanedione dioxime ( $H_2MHDDO$ ) have been proposed as new analytical reagents for the extractive spectrophotometric determination of copper. These methods are simple, selective, rapid and accurate.

## EXPERIMENTAL

### Apparatus

A Shimadzu model UV/VIS 1601A spectrophotometer and a digital ELICO (model LI-120 type) pH meter with combined glass electrodes were used.

### Reagents

All chemicals used were of analytical grade unless otherwise stated. Double distilled water was used throughout.

### Copper(II) Solution

A stock solution of copper ( $10\ 000\ \mu\text{g ml}^{-1}$ ) was prepared by dissolving an accurately weighed amount of Merck copper sulphate (9.8228 g) in 250 ml double-distilled water with a few drops of concentrated sulphuric acid and standardized by a known method [4].

### Synthesis of Ligands

#### *3-Isonitroso-5-methyl-2-hexanone (HIMH)*

The ligand was synthesized by the procedure reported in the literature by reaction of n-amyl nitrite with 5-Methyl-2-hexanone (Merck) [5].

#### *5-Methyl-2,3-hexanedione dioxime (H<sub>2</sub>MHDDO)*

The ligand was synthesized by the procedure reported in the literature by reaction of HIMH with hydroxylamine hydrochloride under alkaline conditions [6].

A 0.5% reagent solution of HIMH or H<sub>2</sub>MHDDO was prepared in absolute ethanol for all extraction studies.

### General Extraction Procedures

#### *3-Isonitroso-5-methyl-2-hexanone (HIMH)*

To an aliquot of solution containing 1- 100 µg copper in a 50 ml separating funnel, a solution of 0.3 ml of 0.5% alcoholic HIMH and 1 ml of buffer solution was added and the volume was made to 10 ml with double distilled water. The aqueous medium was equilibrated with 10 ml isoamyl alcohol for 20 s. The two layers were allowed to separate. The absorbance of the organic extract was measured at 390 nm against a reagent blank.

#### *5-Methyl-2,3-hexanedione dioxime (H<sub>2</sub>MHDDO)*

To an aliquot of solution containing 1- 100 µg copper in a 50 ml separating funnel, a solution of 0.4 ml of 0.5% alcoholic H<sub>2</sub>MHDDO and 0.6 ml of buffer solution was added and the volume was made to 10 ml with double distilled water. The aqueous medium was equilibrated with 10 ml chloroform for 25 s. The two layers were allowed to separate. The absorbance of the organic extract was measured at 370 nm against a reagent blank.

## RESULTS AND DISCUSSION

### Absorption Spectra

The absorption spectra of copper(II) complexes with HIMH and H<sub>2</sub>MHDDO are shown in Figure 1. The copper(II) complexes with HIMH and H<sub>2</sub>MHDDO show maxima at 390 nm and 370 nm, respectively.

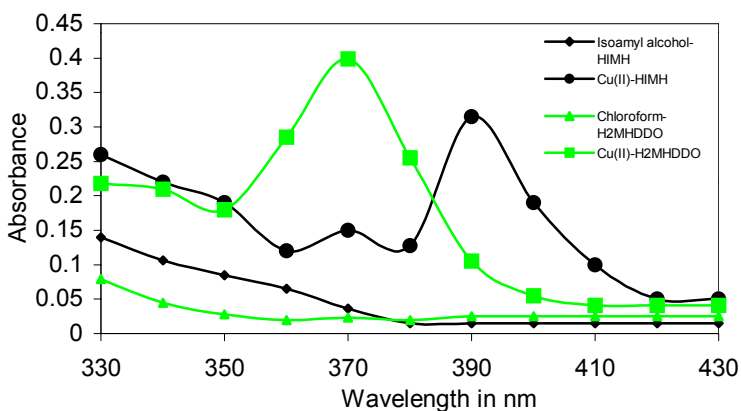


*Figure 1. Absorption spectra of copper complexes.*

### Extraction Conditions

A preliminary study showed that the formation of extractable copper-HIMH/H<sub>2</sub>MHDDO complexes is affected by the hydrogen ion concentration. The optimum pH range for the absorbance was studied by means of the standard procedure. The results are shown in Figure 2. A maximum and constant absorbance was observed over the pH range 6.5-8.5 for the Cu(II)-HIMH complex and 7.0-8.5 for the Cu(II)-H<sub>2</sub>MHDDO complex.

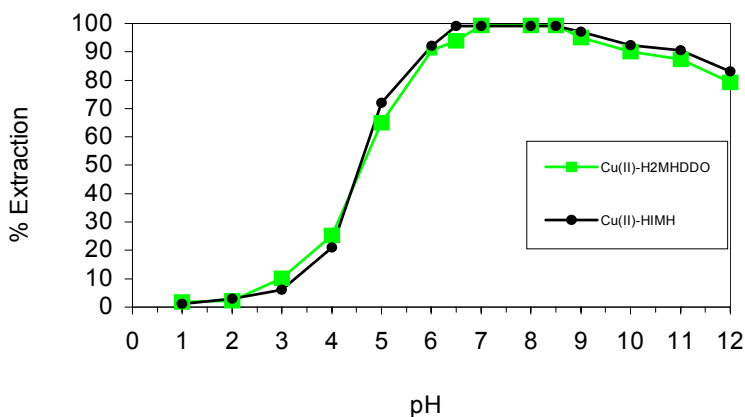


*Figure 2. Effect of pH on extraction of copper.*

### Effect of Ligand Concentration

The influence of ligand concentration on the absorbance of the extracted complexes was studied, with the variation of HIMH (H<sub>2</sub>MHDDO) concentration (0.005%-0.05%) the extraction of 20 µg (40µg) copper(II) showed increasing absorbance up to 0.015 (0.020%). Further increase in ligand concentration has no effect on the extraction.

### Choice of Extracting Solvent

Copper(II) was extracted with HIMH and H<sub>2</sub>MHDDO into various solvents. The results are given in Table 1. The extraction of the copper(II) complexes was quantitative only in isoamyl alcohol and chloroform, respectively.

### Shaking Period and Stability

Copper(II)-HIMH (H<sub>2</sub>MHDDO) complexes were extracted with varying periods of shaking in the range of 5-40 s. The optimum period of shaking required for the complete transfer of complex into organic phase was found to be 20 s (25 s). The extracted complexes are stable for 7h (10 h).

*Table 1. Extraction of copper(II) complexes with various solvents.*

Solvent	Extraction with H <sub>2</sub> MHDDO (%)	Extraction with HIMH (%)
Chloroform	99.3	80.1
Toluene	94.2	96.0
Benzene	90.1	94.0
Carbon tetrachloride	79.0	75.4
Iso-amyl alcohol	76.4	99.1
Dichloromethane	55.6	40.1
1-Octanol	44.7	35.0
Monochlorobenzene	42.1	25.0
Xylene	24.3	22.6
Cyclohexane	10.1	7.8

### Nature of the Extracted Species

To ascertain the nature of the extracted species, a fixed amount of copper(II) was extracted with varying ligand concentration. The distribution coefficient (D) of copper(II) was calculated at different molar concentrations of ligands. The logarithmic plots of D against [Ligand]<sub>M</sub> gave a straight line with a slope close to 2 indicating the composition of the extracted species as 1:2, i.e., Cu(HIMH)<sub>2</sub> and Cu(H<sub>2</sub>MHDDO)<sub>2</sub> are shown in Figure 3.

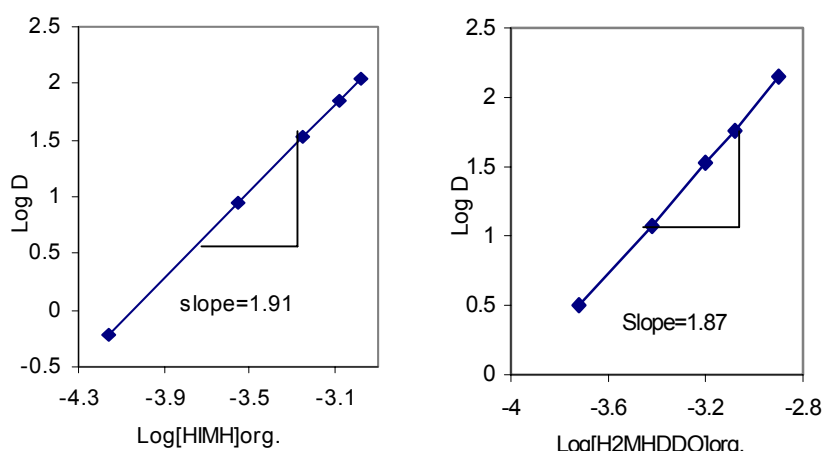


*Figure 3. Logarithmic plots of D against ligand concentration.*

### Beer's Range and Sensitivity

A calibration graph for the copper(II)-HIMH complex was prepared for the determination of copper(II) under optimum experimental conditions, i.e., 1ml of buffer solution of pH 8.0, 0.015% HIMH, shaking time 20 s and isoamyl alcohol as solvent. Beer's law was obeyed in the concentration range of 0.1-7.0  $\mu\text{g ml}^{-1}$  of copper(II). The molar absorptivity and Sandell's sensitivity were calculated to be  $1.001 \times 10^4 \text{ l mol}^{-1} \text{ cm}^{-1}$  and 6.1 ng  $\text{cm}^2$ , respectively.

A calibration graph for copper(II)-H<sub>2</sub>MHDDO complex was prepared for the determination of copper(II) under optimum experimental conditions, i.e., 0.6 ml of buffer solution of pH 8.0, 0.020% H<sub>2</sub>MHDDO, shaking time 25 s. and chloroform as solvent. Beer's law was obeyed in the concentration range of 0.1-10.0  $\mu\text{g ml}^{-1}$  of copper(II). The molar absorptivity and Sandell's sensitivity were calculated to be  $6.61 \times 10^3 \text{ l mol}^{-1} \text{ cm}^{-1}$  and 9.2 ng  $\text{cm}^2$ , respectively.

### Precision and Accuracy of the Method

These methods were applied for 10 replicate determinations of 20  $\mu\text{g}$  or 40  $\mu\text{g}$  copper(II). The relative standard deviation for HIMH was 0.89% and for H<sub>2</sub>MHDDO 0.95%.

### Effect of Foreign Ions

Copper(II) was extracted in the presence of large number of foreign ions. The tolerance amount of an ion was taken as the amount which causes an error of not more than  $\pm 2\%$  in the recovery of Cu(II). The results are given in Table 2.

*Table 2. Effect of foreign ions on the extraction of 20  $\mu\text{g}$  / 40  $\mu\text{g}$  copper with HIMH and  $\text{H}_2\text{MHDDO}$ , respectively.*

Ion added	Tolerance limit ( $\mu\text{g}$ )		Ion added	Tolerance limit ( $\mu\text{g}$ )		Ion added	Tolerance limit ( $\mu\text{g}$ )	
	HIMH	$\text{H}_2\text{MHDDO}$		HIMH	$\text{H}_2\text{MHDDO}$		HIMH	$\text{H}_2\text{MHDDO}$
Li +	10000	10000	Sn 2+	4000	6000	Bromide	20000	10000
Na +	10000	10000	Te 4+	3000	5000	Iodide	20000	10000
K +	10000	10000	Hg 2+	3000	5000	Nitrate	20000	10000
Ca 2+	10000	10000	Cr 3+	2000	4000	Acetate	20000	20000
Mg 2+	10000	10000	Fe 2+	2000	1000	Tartrate	20000	20000
Mn 2+	10000	4000	Cd 2+	2000	3000	Citrate	20000	20000
Al 3+	10000	5000	Se 4+	1000	2000	Sulphate	20000	20000
Ti 3+	10000	5000	Pt 4+	1000	1000	Urae	15000	10000
W 6+	10000	10000	Ag +	1000	1000	Sulphite	15000	10000
Zn 2+	9000	2000	Pb 2+	**	**	Thiosulphate	15000	10000
Ru 3+	8000	4000	Co 2+	**	**	Nitrite	10000	5000
Mo 6+	8000	5000	Ni 2+	**	**	Thiocyanate	10000	20000
Bi 3+	8000	5000	Pd 2+	**	**	EDTA	***	***
Rh 3+	8000	6000	Fluoride	20000	10000	Cyanide	***	***
U 6+	7000	4000	Chloride	20000	20000			

$\text{Ni}^{2+}, \text{Co}^{2+}, \text{Pb}^{2+}$  ----- Masked by Citrate  
 $\text{Pd}^{2+}$  ----- Masked by Thiocyanate  
\*\* ----- Interfering  
\*\*\* ----- Seriously Interfering

### Determination of Copper in Synthetic Mixtures

The developed method has been applied for the extraction and determination of copper 20  $\mu\text{g}$  / 40  $\mu\text{g}$  from various synthetic mixtures which contain copper, selenium, manganese, sodium, rhodium, zinc and magnesium. The results are shown in Table 3.

*Table 3. Determination of copper in synthetic mixtures.*

Sample	HIMH		$\text{H}_2\text{MHDDO}$		RSD %	
	Pre.Meth	NaDDTC*	Pre.Meth	NaDDTC*	HIMH	$\text{H}_2\text{MHDDO}$
Cu(20/40), Se(50), Mn(50)	19.95	19.92	39.95	39.90	0.81	0.55
Cu(20/40), Na(50), Rh(50)	19.96	19.94	39.96	39.92	0.68	0.72
Cu(20/40), Zn(50), Mg(50)	19.97	19.95	39.94	39.93	0.51	0.46

\*----- Sodium salt of diethyl dithiocarbamate [7]

### Analysis of Pharmaceutical Samples

To a Supradyn / Fersolate CM / Theragran-M tablet add, 10 ml aqua-regia and heat nearly to dryness followed by 2 ml of  $\text{HClO}_4$  to decompose organic matter. Finally the residue was treated with dilute HCl and the solution was evaporated nearly to dryness. The residue was dissolved in 10 ml double-distilled water and a suitable aliquot of this solution was used for copper analysis by the developed method. The results are shown in Table 4.

### **Estimation of Copper from Dye Sample**

To about 0.1 g of the dye sample, 10 ml of liquid formulation of concentrated sulfuric and nitric acids was added and evaporated nearly to dryness. It was treated with hydrogen peroxide (5ml, 30 V) every time, until the solution became colourless. Finally, it was treated with dilute HCl and the solution was evaporated nearly to dryness. The residue was extracted in distilled water and a suitable aliquot of this solution was used for copper analysis by the developed method. The results are shown in Table 4.

### **Estimation of Copper from Brass Sample**

About 0.2 g of an oven dried ( $110^{\circ}\text{C}$ ) brass sample was dissolved in 10 ml of aqua-regia and heated to nearly dryness. The residue was treated with 5 ml concentrated HCl. The residue was extracted in distilled water and a suitable aliquot of this solution was used for copper analysis by the developed method. The results are shown in Table 4.

*Table 4. Determination of copper in real samples.*

Samples	Reported values	Amount found <sup>b</sup>	S.D.	R.S.D. (%)
<i>Pharmaceutical Samples<sup>a</sup></i>				
Supradyn (Nicolas Piramal Ind. Ltd.)	0.862	0.856	0.0072	0.84
Fersolate CM (Wellcome India Ltd.)	0.661	0.654	0.0063	0.96
Theragram-M (Sarabhai Chemicals)	2.036	2.028	0.02	0.99
<i>Dye Sample<sup>c</sup></i>				
Phthalocyanine blue (Fluka Chemicals)	9.70	9.61	0.14	1.46
<i>Alloy Samples<sup>c</sup></i>				
Brass (Ita Lab. Mumbai)	59.46	59.31	0.741	1.25

a---- Certified values in milligrams.

b---- Average of five determinations.

c---- Values are in percentage.

### **CONCLUSIONS**

The proposed methods are highly sensitive and selective for the spectrophotometric determination of microgram amounts of copper. They offer advantages like reliability and reproducibility in addition to their simplicity and instant colour development, and suffer from less interference. They have been successfully applied for the determination of palladium/copper at trace level in synthetic mixtures, pharmaceutical samples, dyes and alloy samples. An R.S.D. less than 1.50% for sample analysis underlines the versatility of the developed method.

### **REFERENCES**

1. J. R. Pemberton and H. Diehl (1969), *Talanta*, **16** (4), 542.
2. T. S. Reddy and S. B. Rao (1979), *Curr. Sci.*, **48** (10), 439.
3. A. K. Shetty and A. P. Argekar (1996), *Anal. Sci.*, **12** (2), 255.
4. A. I. Vogel (1961), Textbook of Qualitative Inorganic Analysis, Longmans, Green & Co Ltd., London.
5. S. Diel and H. Dost(1902), *Ber.*, **35**, 3290.
6. G. Ponsai and M. Toress (1929), *Gazz. Chim. Ital.*, **59**, 461.
7. E.B. Sandell (1959), Colorimetric Determination of Traces of Metals, Interscience, New York, pp. 444-448.



## EXTRACTION BEHAVIOR OF SOFT METAL IONS WITH POLYTHIOETHER DERIVATIVES CONTAINING O OR N DONOR ATOMS

Kenji Chayama, Kenta Adachi, Tomoaki Mori and Haruo Tsuji

Department of Chemistry, Faculty of Science and Engineering,  
Konan University, Kobe, Japan

Three new polythioether derivatives containing an oxygen or a nitrogen atom in the molecules were synthesized. The liquid-liquid extraction of several metal ions with 1,9-diphenyl-2,5,8-trithianonane (9-2Ph-SSS), 1,9-diphenyl-5-oxa-2,8-dithianonane (9-2Ph-SOS) and 1,9-diphenyl-5-aza-2,8-dithianonane (9-2Ph-SNS) were examined. The aqueous solution containing the metal ion and counter anion such as picrate ion were shaken with a 1,2-dichloroethane solution of the reagent. Soft metal ions such as silver(I), copper(I), palladium(II), mercury(II) and gold(III) were extracted well with these three reagents. On the other hand, the hard and the intermediate metal ions were not extracted at all with these reagents. The extraction efficiency of copper(I) and palladium(II) were relatively low in the case of 9-2Ph-SOS. The extraction behaviors of soft metal ions with these reagents were characterised by the kind of donor atom in the center position of the molecules.

### INTRODUCTION

Organic analytical reagents used for the solvent extraction of metal ions have several types of donor atoms, such as oxygen, nitrogen and sulfur. The selectivities of reagents are mainly dependent on the kind of donor atoms in the reagents. The reagents that have sulfur atoms are selective for soft metal ions such as gold, silver, copper, palladium and mercury. These metals are important for the industries of electronic devices, catalysts or as jewels and coins. However, reagents containing sulfur atoms as mercapto groups are not stable because of the oxidation of the mercapto groups to form disulfide groups. Therefore sulfur-containing reagents are limited to use in reducing conditions. Reagents containing sulfur as thioether groups are much more stable than the reagents with mercapto groups, because the oxidation rate of sulfide to sulfoxide is slower than that of the mercapto group to sulfide.

We have synthesized reagents containing the thioether group [1-6]. Some of them are cyclic compounds called thiacrown ethers which have a cavity that loads a metal ion of appropriate size [1,2,7]. In order to separate a specific metal ion from others, it may be effective to create a reagent which has a host site to incorporate the guest ions. However it is difficult to synthesize the rigid cavity in the molecules. Thiacrown ether has a flexible structure so that it apparently does not work as a specific reagent for a soft metal ion. On the other hand, acyclic polythioether is also selective for the soft metal ions as well as cyclic ones, because the thioether groups acts as a softer Lewis base than the mercapto group [5-10]. It is clarified that the selectivity of the polythioethers depend on the character of the donor atoms,

nevertheless of the structures. There is another way to separate the soft metal ions from each other, by synthesizing polythioethers that have a donor atom other than sulfur. The combination of donor atoms such as oxygen, nitrogen and sulfur may enable the separation of soft metal ions from each other. Inserting the hetero atoms into the thioethers might change the selectivity of the reagent or weaken the binding ability of the reagent for the metal ion in some cases. In this study, we synthesize three reagents, 1,9-diphenyl-2,5,8-trithianonane (9-2Ph-SSS), 1,9-diphenyl-5-oxa-2,8-dithianonane (9-2Ph-SOS) and 1,9-diphenyl-5-aza-2,8-dithianonane (9-2Ph-SNS), as solvent extraction reagents. The extraction behaviors of metal ions with these reagents were examined.

## EXPERIMENTAL

### Synthesis of the Reagents

The reagent 1,9-diphenyl-2,5,8-trithianonane (9-2Ph-SSS) was synthesized as described previously [8]. The reagent containing an oxygen atom in the molecule 1,9-diphenyl-5-oxa-2,8-dithianonane (9-2Ph-SOS) was synthesized by the reaction of di-(2-mercaptoethyl)ether with benzyl bromide. The reaction gave a crude product which was then purified by column chromatography. The reagent containing a nitrogen was synthesized by the reaction of bis(2-chloroethyl)amine hydrochloride with benzyl mercaptane. The product was crystallized as the salt with HCl. These synthetic routes are shown in Figure 1.

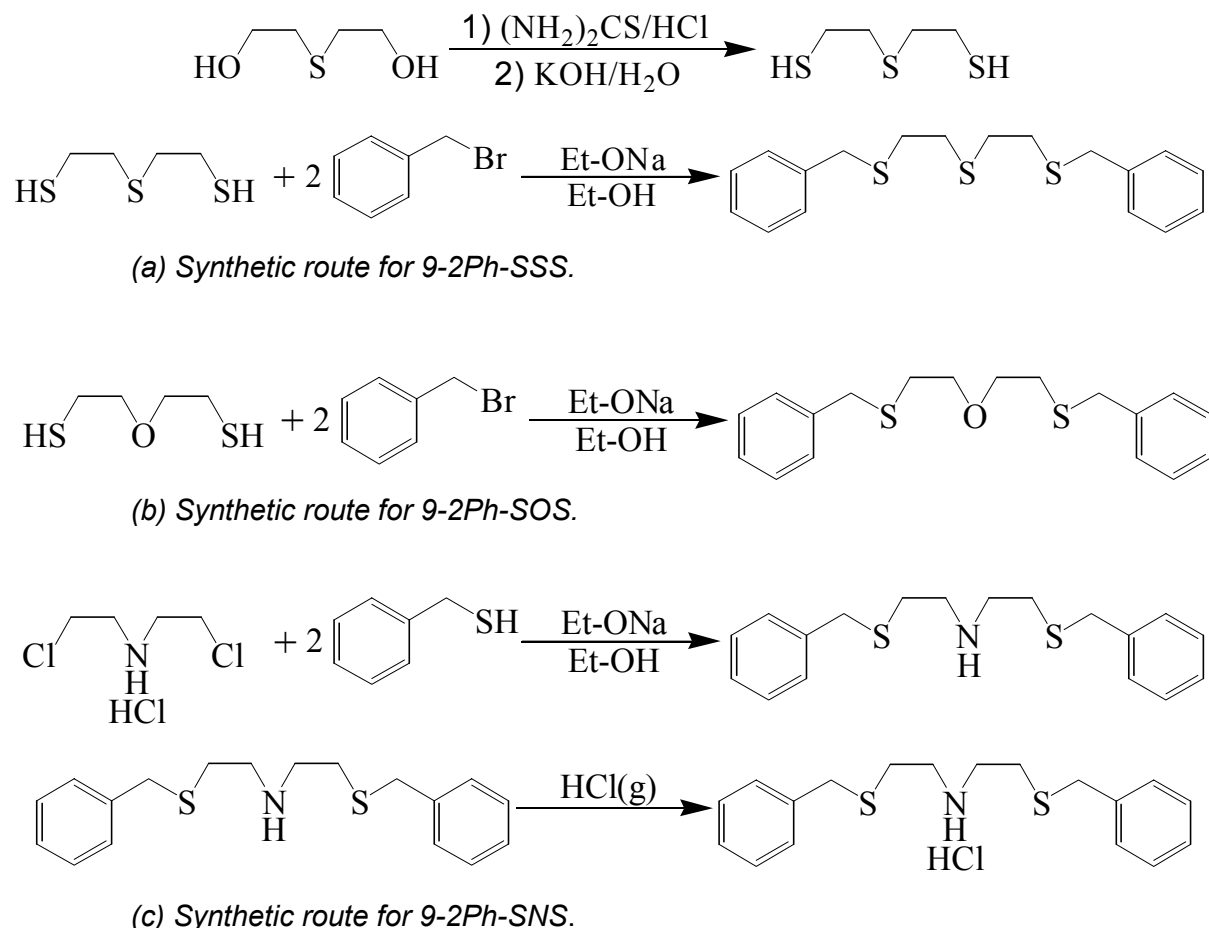


Figure 1. Synthetic routes for 9-2Ph-SSS, 9-2Ph-SOS and 9-2Ph-SNS.

## Other Reagents and Apparatus

The reagents used for liquid-liquid extraction were of reagent grade except 1,2-dichloroethane. The extraction solvent 1,2-dichloroethane, was shaken three times with 2 M (mol/dm<sup>3</sup>) potassium hydroxide solution followed by shaking three times with water, dried over calcium chloride, and distilled. Extraction was carried out in a Taiyo M incubator. A Hitachi Z-8000 atomic absorption spectrophotometer was used to determine the concentration of metal ions in the aqueous solutions. The pH of the aqueous solutions was measured with a Hitachi-Horiba M-7 pH meter.

## Liquid-Liquid Extraction of the Metal Ions

An aliquot (10 ml) of aqueous solution containing the metal ion ( $5 \times 10^{-5}$  M), picrate ion ( $1 \times 10^{-3}$  M) and acetate buffer ( $1 \times 10^{-2}$  M) was adjusted to an ionic strength of 0.1 M with sodium sulfate. This solution and 10 ml of the reagent solution in 1,2-dichloroethane in a stoppered cylindrical tube were shaken (180 strokes min<sup>-1</sup>) for 30 min at  $25 \pm 0.1^\circ\text{C}$ . The mixture was then centrifuged for 5 min at 2000 rpm. After the two phases were separated, the pH of the aqueous phase was measured and the concentrations of the metal ion in the aqueous and organic phases determined by atomic absorption spectrophotometry.

## RESULTS AND DISCUSSION

### Liquid-Liquid Distribution of 9-2Ph-SNS

The cyclic and acyclic polythioethers are insoluble in water. However the monoazapoly-thioethers are soluble in acidic aqueous solution. The distribution behavior of 9-2Ph-SNS between 1,2-dichloroethane and water was different from that of polythioethers which do not contain any nitrogen atoms. Protonated 9-2Ph-SNS distributed to the aqueous phase from 1,2-dichloroethane phase at pH less than 1. As the pH in aqueous phase increased, 9-2Ph-SNS was transferred to the organic phase. More than 99% reagent distributed to an organic phase at pH over 6.0. In this study, picrate ion was used as the counter anion to form the ion pair with the metal complex cation. However the protonated reagent 9-2Ph-SNS forms an ion pair with picrate ion, even in the case of the absence of the metal ion. This causes the reduction of picrate ion concentration in the aqueous phase, and results in a decrease of the extraction efficiency of metal ions. Then, the extraction behavior of picrate ion with 9-2Ph-SNS was examined. It is clarified that picrate ion formed an ion pair with 9-2Ph-SNS and distributed to the organic phase below pH 1.0.

### Liquid-Liquid Extraction of Metals

Liquid-liquid extraction of the metals Mg(II), Ca(II), Mn(II), Zn(II), Co(II), Ni(II), Cu(II), Fe(II), Cd(II), Ag(I), Cu(I), Pd(II), Hg(II) and Au(III) was performed. As shown in Figure 2, soft metal ions such as Ag(I), Cu(I), Hg(II) and Au(III) ions which are classified [11] as class *b* metal ions were selectively extracted with these reagents. On the other hand, hard (class *a*) and intermediate (class *ab*) metal ions such as Mg(II), Ca(II), Mn(II), Zn(II), Co(II) and Ni(II) were not extracted at all. Although Cu(II) ion belonging to class *ab* was slightly extracted, Cd(II) ion belonging to class *b* was not extracted at all. Copper(II) was extracted slightly with 9-2Ph-SNS. However, 9-2Ph-SOS or 9-2Ph-SSS did not extract Cu(II) at all.

### Liquid-Liquid Extraction of Silver(I)

Liquid-liquid extraction of silver(I) was examined. Figure 3 shows the plots of percent extraction of silver(I) versus pH in the aqueous phase. Silver(I) ion was extracted more than 99% with each reagent above pH 4.0. In the case of 9-2-Ph-SNS, the percent extraction decreases with the increase of the acid concentration. It is thought that the distribution of the reagent containing a nitrogen atom might be shifted to the aqueous phase, and the protonated species forms an ion pair with picrate ion which causes a decrease of the picrate ion as a counter anion for the metal complex cation.

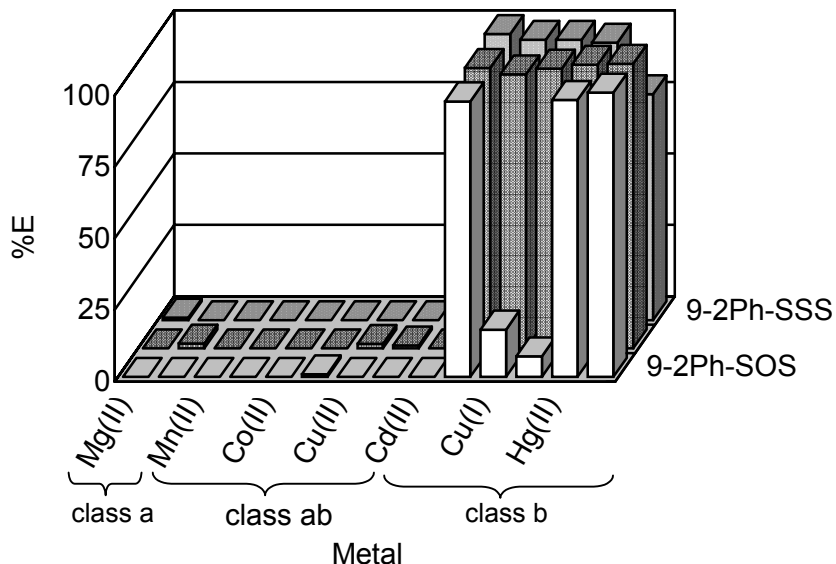


**Figure 2.** Extraction of metal ions with three polythioether derivatives.  
Initial concentration: Metal ion;  $5 \times 10^{-5}$  M, Picrate ion;  $1 \times 10^{-3}$  M,  
Reagent;  $5 \times 10^{-4}$  M. pH 5.0. Extraction time: 30 min.

The molar ratio methods was performed to clarify the composition of the extracted species. The results indicate that the molar ratio of the silver(I) ion to 9-2Ph-SOS, 9-2Ph-SNS and 9-2Ph-SSS is 1:2 for all three reagents. For each reagent, the molar ratio of the silver(I) to picrate ion were examined, and found to be 1:1 for each reagent. Therefore the molar ratio of the extracted species for each reagent silver(I):reagent:picrate ion was 1:2:1. It is thought that the extracted complex might be formed as a 1:2 complex of silver to ligand in which the silver ion takes an octahedral configuration.

#### Liquid-Liquid Extraction of Copper(I)

Liquid-liquid extraction of copper(I) ion was examined with 9-2Ph-SSS and 9-2Ph-SNS. Figure 4 shows the plots of percent extraction of copper(I) ion versus pH in the aqueous phase. As copper(II) in the aqueous solution was transformed to copper(I) by a reducing agent such as hydroxyl amine, the decrease of percent extraction of copper below pH 4.5 may depend upon the decrease of reducting power of hydroxyl amine in acidic media. The composition of extracted species were examined by means of the molar ratio method and slope analysis. The relationship between the extraction constant  $K_{ex}$  and the distribution ratio  $D_{Cu(I)}$  is expressed as follows:



$$\log D_{Cu(I)} = \log K_{ex} + m \log [L] + n \log [\text{Pic}] \quad (2)$$

When the reagent 9-2Ph-SNS was used, the plots of  $\log D_{Cu(I)}$  vs.  $\log [\text{Pic}]$  gave a straight line with slope 1, suggested "n" in Eqn. (1) and (2) is taken as  $n = 1$ . These results suggest that the composition of the extracted species with 9-2Ph-SNS were  $Cu(I) : \text{Pic}^- = 1:1$ . The plots of  $\log D_{Cu(I)}$  vs.  $\log [L]$  gave a straight line with slope 2, suggested "m" in Eqn. (1) and (2) is taken as  $m = 2$ . Therefore the composition of extracted species might be  $Cu(I):L:\text{Pic}^- = 1:2:1$ . However, the extracted species of copper(I) with 9-2Ph-SSS was  $Cu(I):L:\text{Pic}^- = 1:1:1$ . As shown in Figure 2, the extraction efficiency of copper(I) with 9-2Ph-SOS was about 15% at pH 4.5, much less than that for 9-2Ph-SSS (98.0% at pH 4.9) and 9-2Ph-SNS(95.0 at pH 4.9). It shows that the replacement of the central donor atom from sulfur to oxygen decreases the extraction efficiency. It is thought that the copper(I) ion usually takes the tetrahedral configuration in the complex. The results suggest that the 9-2Ph-SNS reagent acts as a bidentate ligand; on the other hand, the 9-2Ph-SSS reagent acts as a tridentate ligand in the copper(I) complex.

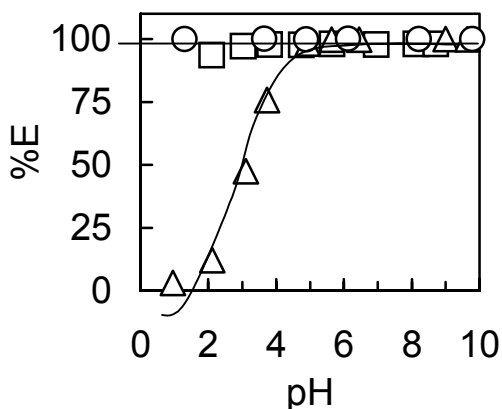


Figure 3. Plots of %E vs. pH for the extraction of silver(I) with 9-2Ph-SXS. □: 9-2Ph-SOS, Δ: 9-2Ph-SNS, ○: 9-2Ph-SSS.

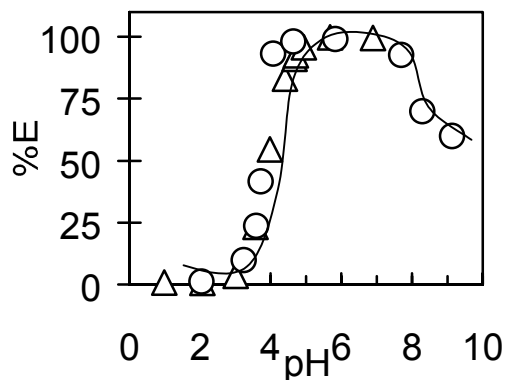


Figure 4. Plots of %E vs. pH for the extraction of copper (I) with 9-2Ph-SXS. Δ: 9-2Ph-SNS, ○: 9-2Ph-SSS.

## CONCLUSION

The liquid-liquid extraction of several metal ions with 9-2Ph-SSS, 9-2Ph-SOS and 9-2Ph-SNS was examined. Soft metal ions such as silver(I), copper(I), palladium(II), mercury(II) and gold (III) were extracted well with these three reagents. On the other hand, the hard and the intermediate metal ions were not extracted at all with these reagents. The result shows the selectivity of these reagents for the soft metal ions did not change even when the central sulfur atom was replaced with oxygen atom or the nitrogen atom. The extraction efficiency of copper(I) and palladium(II) was relatively low in the case of 9-2Ph-SOS. These results suggest that the replacement of the sulfur donor atoms by an oxygen or nitrogen may change the extraction tendency of soft metal ions. There may be a possibility to separate soft metal ions from each other with the use of such polythioether derivatives containing other kinds of donor atoms.

## REFERENCES

1. E. Sekido, K. Chayama and M. Muroi, *Talanta* (1985), **32**, 797.
2. E. Sekido, K. Chayama and H. Iwamoto (1988), *Anal. Sci.*, **4**, 511.
3. K. Chayama and E. Sekido (1986), *Anal. Sci.*, **3**, 535.
4. K. Chayama and E. Sekido (1990), *Bull. Chem. Soc. Jpn.*, **63**, 2420.
5. K. Chayama and E. Sekido (1990), *Anal. Sci.*, **6**, 883.
6. K. Chayama and E. Sekido (1991), *Anal. Chim. Acta*, **248**, 511
7. K. Chayama, K. Hara, Y. Tamari, H. Tsuji, Y. Kusaka, E. Sekido and Y. Mori (1993), *Proc. Intl. Solvent Extraction Conf., ISEC '93*, York, pp. 585.
8. K. Chayama, N. Koyama, Y. Tamari, H. Tsuji and E. Sekido (1996), *Proc. Intl. Solvent Extraction Conf., ISEC '96*, Melbourne, pp. 461.
9. K. Chayama, N. Awano, Y. Tamari, H. Tsuji and E. Sekido (1993), *Bunseki Kagaku* (in Japanese), **42**, 687.
10. K. Chayama, C. Kurihara, H. Tsuji and E. Sekido (1998), *Bunseki Kagaku*, **47**, 1077.
11. S. Ahrlund, J. Chatt and N.R. Davis (1958), *Quart. Rev., London*, **12**, 265.



## APPLICATION OF COURIER 30SX ANALYSER TO NICKEL LATERITE SOLVENT EXTRACTION

**David Hughes, Matti Kongas and Kari Saloheimo**

Outokumpu Mintec, Espoo, Finland

The paper covers the application of an on-line process analyser to solvent extraction in a laterite nickel ore treatment process in Australia. It covers the considerations in design of a sample multiplexing system specifically engineered for this process type.

The paper shows the considerations in the choice of sample handling in the solvent extraction stages of iron, zinc, and copper removal from nickel-cobalt solution and subsequently in the preparation of purified nickel and cobalt solutions for metal reduction. The wavelength-dispersive X-ray analyser equipment is described. The considerations in installation of the analyser and its sample handling in the industrial area of the plant are also described.

The project was among the first in which this analyser was installed and started up with this sample system. During the implementation of the project, the design of the sample handling and its operating program were firmed up based on deepening understanding of the design parameters of the process. Both the process solution characteristics, solution pumping parameters and the climate of the semi-arid environment affected the final design choices. The lessons learned in this project are reviewed. They can be applied to similar projects both in nickel laterite processes, and in copper oxide heap-leach, solvent extraction, electrowinning (SXEW) plants.

### CONSIDERATIONS IN DESIGN OF THE SAMPLE HANDLING SYSTEM

Outokumpu Mintec and its predecessors in the Outokumpu concern have manufactured on-line X-ray fluorescence analysers since 1969. The majority of these have been delivered to froth flotation plants, for which a gravity flow sample presentation system was developed, since keeping solids in suspension was an important part of the implementation of on-line analysis. For nickel and zinc refineries in which a number of analyser systems have been installed, the critical function of sample presentation was the extraction of solids from the sample to enable analysis of the trace elements remaining in solution. This need led to the development of a batch sampling and filtration system that is still in use. This system has been perceived to be too complicated and slow for solvent extraction plants. When the boom in copper heap-leaching, solvent extraction and electrowinning came in Chile in the early 1990s, it became necessary to rethink the approach to analysis needs and sample handling for plants of this kind. [1]

The project to design an X-ray analyser system aimed specifically at solvent extraction plants was originally specified with the Chilean copper plants in mind. Typical copper heap-leach, solvent extraction plants under construction in the Chilean copper field cover a much larger area than flotation plants for similar copper production. Sixteen to twenty sample points are scattered over an area as large as 250 m by 150 m. Usually most of these can however be located at the edge of the tank farm area. The floor of the tank farm on larger sites is 10 to 15 m lower than the level of the mixer settlers. Sample transport must be designed to operate over the long distances and with the small head or hydraulic gradient available.

The process streams to be sampled must all be solids free, unless crud formation is a big problem, but the danger exists of blockage due to crystallization, especially at high altitudes where winter temperatures can be below zero. System design must counteract the tendency of solution flowing in small pipes to cool and crystallise.

The need has also been seen to limit to a minimum the quantity of valuable solution, electrolyte that has to be discarded or recycled by pumping.

A fourth goal is to provide prompt and frequent analyses. To give sufficiently frequent data for effective control of the process, whether automatic or manual, repeating analyses every ½ hour is perceived to be necessary. Since the equipment is designed for 16 sample streams, this implies making a new measurement every two minutes. With a measurement time of 1 minute, that leaves 1 minute for rinsing the parts of the system intimately connected to the measurement cell or cuvette.

Chemically the solutions are aggressively corrosive. The acid content of electrolytes can be as high as 200 g/l H<sub>2</sub>SO<sub>4</sub>, and the REDOX potential may be 400 to 550 mV relative to the standard hydrogen electrode. The PLS and raffinates contain much less acid, but in Chile they are marked by high contents of chloride since chloride salts have not been naturally leached out of the ore bodies in the extremely arid climate.

In the design process this all led to the idea that the samples could be taken from gravity fed fast loops terminating in the tank farm area, or from process pipes in which the solution was being pumped to the mixer settlers. The flow of samples would be driven by the hydraulic gradient of 5% to 10%, or by process pump pressure, and the maximum pressure at the analyser site would be between 1 and 2 bar. This was determined by the topography of the mixer-settler pad and the tank farm.

The need to minimise the amount of sample taken into the sample multiplexer of the system, and the desire to keep sample handling time to a minimum has led to a much simplified sample multiplexing system based on using small bore piping with a minimal dead volume. The total sample take-off from a fast loop or a process pipe is envisaged to be no more than 1 ½ litre for short final pipes. The design of the sampling system, now designated COURIER 30SX, also includes stringent rinsing to forestall the possibility of crystallisation. A carefully planned rinsing sequence has been designed to meet the criterion that for a system with an X-ray analyser alone the time between successive analyses in the sample sequence should be no more than 2 minutes. Further, to reduce the cooling of the samples as they enter the multiplexer the rinsing water is hot, or at least warm. Since the water consumption is small and water in a fixed pipe cools as it stands in the pipe, a local water heater has been chosen to supply hot water on demand.

The design launched in 1997 is very compact compared with earlier COURIER 30-series analyser implementations. It includes the basic analyser with a measurement cuvette that was adapted for corrosive solution samples, a simple sample presentation connection (PSM – Probe Sample Multiplexer) consisting basically of two valves and a surface level sensor to

detect the presence of sample in the cuvette, and a multiplexer for sixteen incoming sample streams. This is a block of PVDF (polyvinylidifluoride) in which the bodies of the sample valves, rinsing and draining valves are machined and all the channels are drilled. Valve actuators from a major valve supplier are used. The multiplexer, affectionately known as the "cheese", permits grouping incoming samples in four manifolds or groups that can be disposed of to the drain separately, and are well isolated from each other. Thus samples containing only traces of an element whose analysis is important are not contaminated by samples in which this element is present in large quantities. These are connected to a main channel from which the COURIER analyser is fed. The main channel also communicates with an optional header tank and valves for feeding two small titrators that are tightly integrated in the system. This tank can also be used for de-aerating frothy samples before feeding them to the COURIER analyser to maintain adequate analytical accuracy. See Figure 1.



*Figure 1. The sample multiplexer SXM, water heater and COURIER analyser, Area 37, Murrin Murrin.*

The design of the system and its software included pressure tests of the valve block and valves, which demonstrated that it would stand up to the demands of the copper SX-EW plant installation for which it was designed. In other tests the feasibility of measuring loaded organic and aqueous solutions in the same measuring cuvette was established. The system program was thus designed to allow measuring organic (up to 4 streams) and aqueous solutions in the same installation. With this design marketing of the new system began in 1997.

## FIRMING THE SPECIFICATIONS FOR THE MURRIN MURRIN PROJECT

Although the main target of the development project had been copper solvent extraction plants, at least half of the first enquiries were from Australian laterite nickel acid-leach SX plants, of which Anaconda's Murrin Murrin project showed firm interest.

Discussions with Fluor, Anaconda's engineers, and with Anaconda staff brought a rude awakening to the fact that the process conditions in the laterite nickel plant to be built on the flat plain of the Australian outback are quite different from those in a copper SXEW plant built in the Andes. The crystallization temperature of the process solutions is tens of degrees higher, due to the different chemical composition of the solutions. The pressure in transport lines is not maximum 1 ½ bar but maximum 6 bars, because gravity cannot be used for transport in the same way as in mountainous territory. The cooling of the X-ray tube and electronics in the analyser cannot be left to circulating plant water, since that might be hotter than the upper limit for proper working of the analyser. And it might rain!

Over a period of a few months a range of typical process sample connections was developed that answered most conceivable needs in both copper SXEW plants and the nickel laterite plants. At the same time the changes made in the sample connection specifications were implemented in revisions of the design of the installation during successive rounds of correspondence with Fluor and Anaconda. Existing types of heavy-duty sample valves have been applied in these connection schemes. To comply with the concept of a system that could be started up quickly and would not need on-site programming of sample handling, the use of these was specified and built into the standard sample handling software and configuration tools. This meant a second round of programming as the specifications were firmed up, and by the time the system was started up the software was ready.

Chilean users welcomed a system pre-installed in an analyser shelter, and delivered as one package. For Australian customers specifications were drawn up by the engineering companies, and locally built shelters were fitted out by the Outokumpu subsidiaries that sold the systems. Lessons learnt from experience of these have been written into revised specification sheets. Common needs are to protect the equipment, which is comparable to laboratory equipment, from cold, direct solar radiation variations in temperature in general, and from dust and rain. The special nature of the industrial environment means that both the outer cladding and the inner floors and walls of the shelter must resist the acid in electrolytes if spills occur. This means being resistant to up to 200 g/l acid.

Forced cooling of circulating water has been applied previously in Australian installations of Outokumpu analysers to ensure reliable temperature control of the analyser. The temperature control of the analyser is important to ensure repeatable measurements, since thermal expansion or contraction changes the measurement geometry. It was decided at the start of the Murrin Murrin project that the circulating cooling water should be cooled in an auxiliary circuit through a commercially available chiller, rather than be running plant water through the heat exchanger.

## APPLICATION OF COURIER TECHNOLOGY TO THE NI-CO PROCESS

Outokumpu has used wavelength-dispersive X-ray fluorescence technology since the first COURIER 300 analyser was installed in the Pyhäsalmi flotation plant in 1969. Although we have manufactured energy-dispersive analysers over the years and do so at this moment, the wavelength-dispersive technology offers significant advantages in on-line analysis for metallurgical processes. The most important is the ability to distinguish the fluorescent radiation of trace elements in concentrated metal salt solutions, for instance in solutions of nickel sulphate containing 100 g/l Ni the detection limits of iron, cobalt, copper and zinc are between 1 and 2.5 mg/l. The X-ray tube used as a source of primary radiation excites so

high an intensity of fluorescent radiation that actual measuring times can be 60 seconds, or even less for measuring higher contents. Another advantage is that the structure of the Johansson-type curved fixed-crystal spectrometers is so robust that after 13 years of use spectrometers from an analyser being replaced have been transferred to the new analyser.

Every technology has its limits, and in the case of wavelength dispersive X-ray fluorescence the major limitations are the long air-path in the spectrometer that limits the usefulness of the analyser to elements heavier than titanium, and the fact that elements whose fluorescent X-rays have an energy 50% or more of the tube voltage, such as cadmium, have higher detection limits because of the scattered primary radiation background visible in their spectrometers.

In 1997 a number of on-line analysers using the sampling technology current at the time were installed in the new solvent extraction process at the Harjavalta nickel plant of Outokumpu Oy (this plant is now OMG Harjavalta Nickel Oy). [2] The requirements for control as expressed in the Harjavalta plant are shown in Table 1. The analysers installed at Harjavalta met these requirements to the satisfaction of the plant.

*Table 1. Requirements for control of nickel cobalt solvent extraction.*

Process stage	Purpose of control
Atmospheric and autoclave leach	Minimising trace contents of Fe, Cu, As in range 1 – 10 mg/l
Solvent extraction	Monitoring separation of cations Fe, Cu, Zn from Ni and Co in ranges 1 – 10 mg/l
	Monitoring separation of cations Co from Ni so that trace content of either in the other's solution is 1 – 10 mg/l
Reduction	Control of metal ion / ammonia ratio so that molar ratio is 1.00 ±1%

The enquiry from Murrin Murrin covered solvent extraction, in two stages: separation of magnesium, iron copper and zinc from nickel and cobalt in the first, and of cobalt from nickel in the second. The two analyser systems were installed in 1999, and commissioning and precalibration was performed in March 2000. The levels of accuracy achieved during precalibration are shown in Table 2.

*Table 2. Results of precalibration at Murrin Murrin.*

Sample type / Element	Minimum (g/l)	Maximum (g/l)	Error (1 SD) (g/l)	Error relative to average content (%)
Area 39 / High Ni				
Fe	1.0	2.0	0.0304	1.89
Co	1.0	2.0	0.0488	3.05
Ni	80.0	100.0	0.699	0.777
Area 39 / Low Ni				
Co	10.0	30.0	0.354	1.55
Ni	5.0	10.0	0.166	2.18
Area 37 / High Ni				
Co	0.10	0.20	0.0034	2.64
Ni	70	90	1.18	1.46
Area 38 High Co				
Co	70	90	0.423	0.529
Ni	0.00	0.20	0.013	10.9

Of the other chemical quantities of interest, an integrated titrator was supplied to measure ammonia (*i.e.*, dissolved ammonia gas present as ammonium hydroxide) by titration with acid. Compared with setting up the X-ray fluorescence analyser, tuning the titrator requires more work to define titration algorithm parameters, such as dose increment in ml, time between doses in seconds, maximum drift between successive pH readings before making a new dose increment, etc. Titration of ammonia showed itself repeatable over the whole range of ammonia content to an acceptable degree of accuracy. The results of some test titrations were compared with the given laboratory contents of the test solutions are shown in Figure 2.

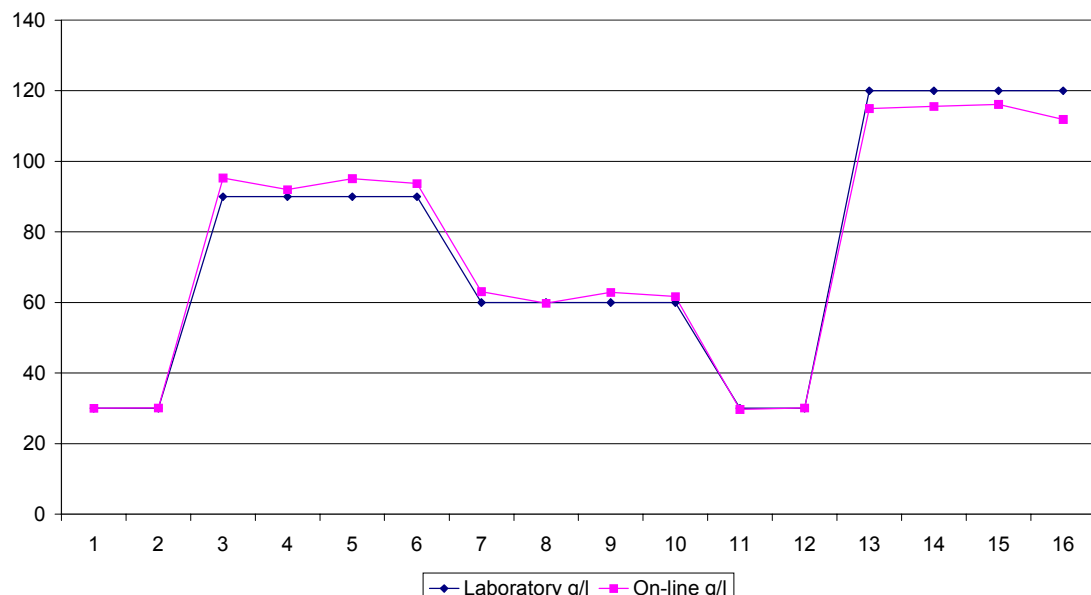


Figure 2. Titration of ammonia during precalibration at Murrin Murrin.

The precalibration described above was made with artificial samples provided for the plant laboratory for the purpose. At the time of the commissioning process material was not available and comparison with the plant laboratory could not be made. Later, information on the current performance of the on-line analysers relative to the corresponding laboratory analyses of the samples has become available. This is presented in the conclusion of the paper.

## CONCLUSION

Cooperation between equipment supplier, end-user and the engineering office has proved valuable to all parties and enabled supply of a system which takes the demands of industrial analyser applications into account.

Comparisons made of the analyses from the COURIER analysers and the plant laboratory following the precalibration and plant start-up show good correspondence between the two. The following examples are from the nickel sulphate stream, showing equally good performance at approximately 100 g/l Ni in Figure 3, and at less than 1 g/l Co in Figure 4. For the purpose of monitoring the trace elements in strong salt solutions, the performance of the on-line analysers is satisfactory.

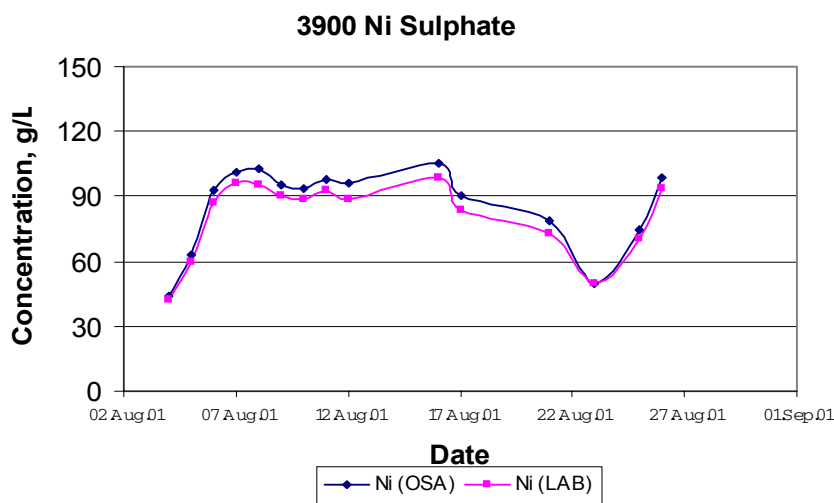


Figure 3. Correspondence of COURIER and laboratory for nickel in nickel sulphate stream.

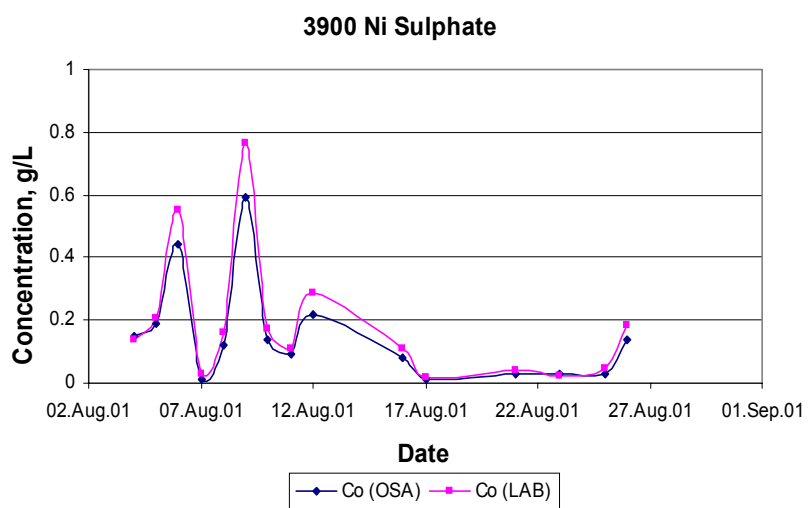


Figure 4. Correspondence of COURIER and laboratory for cobalt in nickel sulphate stream.

## ACKNOWLEDGEMENTS

Outokumpu Mintec Oy gratefully acknowledges the permission of Anaconda's Murrin Murrin Operations to publish precalibration and performance comparison data.

## REFERENCES

1. J.J Whittaker, W. Robledo, D. V. Hughes, M. Kongas (1999), *Proc. SME Annual Meeting*, Littleton, CO.
2. K. Knuutila, S-E Hultholm, B. Saxén, L. Rosenback (1997), *Proc. ALTA Ni/Co Pressure Leach and Hydrometallurgy Forum*, Melbourne.



## OPPORTUNITIES FOR EXTRACTION TECHNOLOGY IN CHIRAL SEPARATIONS

André B. de Haan, Norbert J.M. Kuipers, Maartje Steensma

University of Twente, Enschede, The Netherlands

The availability of optically pure enantiomers is a key issue for the life-science industry. In this field extractive resolutions may become a competing technology for the separation and purification of optical isomers provided that the reported technical limitations are resolved. Most of the studied systems suffer from low productivities due to the applied low enantiomer and chiral selector concentrations. Transformation into a feasible process requires significantly increased productivities by using high feed and selector concentrations applied in a fractional extraction concept to obtain complete separation combined with maximum process flexibility. One of the key issues will be the development of industrial scale contacting equipment that can provide up to 100 equilibrium stages to cope with the inherent low selectivities (1.5-4) encountered in extractive resolutions while keeping the inventory of the expensive chiral selector to a minimum.

### INTRODUCTION

Chirality is a key issue for products within the life-science industry [1-5]. Very often the two mirror images (enantiomers) of a molecule will show different interactions with a biological receptor or enzyme, and only one single enantiomer is responsible for the desired biological activity of a compound while the other enantiomer represents a 50% impurity that often leads to unwanted (harmful) side effects. However, because suitable single-isomer manufacturing technology was not available in the past, most of the drugs, agrochemicals, flavors and fragrances used nowadays are marketed as racemic mixtures. Increased pressure on companies to develop and produce enantiomerically pure products has made the efficient and economical production of enantiomerically pure chiral products one of the major challenges facing the modern life-science industry (fine-chemicals, pharmaceuticals, agrochemicals, nutraceuticals, flavors, fragrances).

There are two main routes to the production of optically pure enantiomers: resolutions and stereoselective syntheses [1-5]. In principle asymmetric synthesis is the most cost-effective method for producing single-enantiomer products, because the entire precursor is converted to the desired enantiomer. Despite this obvious advantage, stereoselective synthesis can be particularly difficult because the stringent requirements for enantiomeric purity require exceptional enantioselectivity (>100) from the catalyst system and a final purification step is usually required to remove residual undesired enantiomer from the final product. Due to this inherent limitation of asymmetric synthesis, most processes use resolution methods for the production of synthetic single enantiomer products. A resolution process uses the competitive advantage that it is relatively straightforward to synthesize a racemic mixture that can always be resolved into a product with the desired enantiomeric purity. The industrially applied resolution methods can be divided into selective crystallization, selective conversion and preparative chromatography [1-5]. Although most widely applied for its high selectivity, diastereomeric salt crystallization is relatively inflexible and requires considerable efforts in development. Selective conversion suffers from the same limitations as asymmetric synthesis. Finally industrial scale preparative chromatography for chiral separations still suffers from low productivity and high capital costs.

These limitations of the currently available resolution technologies have initiated many attempts to develop new competing chiral separation technologies. Within this field of chiral separations, extraction technology may become an industrially attractive option. This is mainly because, although the selectivity of a single extraction is usually small, staging of multiple extractions is easily achieved and well established. In this paper we explore recent developments in various extraction technologies for the separation of chiral components.

## PRINCIPLES OF ENANTIOSELECTIVE EXTRACTION

Chiral discrimination requires at least three points of interaction between the selector and one of the guest enantiomers [6,7]. This so-called “three-point model” is schematically illustrated in Figure 1. In this model, the three interaction points of one enantiomer G(+) cannot be situated in the same locations as the corresponding three points of the other enantiomer G(-) and can therefore not be recognized in the same way. Although chiral solvents are the simplest way to achieve enantioselective recognition, most methods make use of a chiral additive (chiral selector, carrier, reagent) that is added to an achiral solvent. An obvious advantage of these systems is the possibility of tailoring the selector molecules to the applications. Chiral separation is achieved by the formation of diastereomeric complexes (host-guest, HG) between the chiral selector (host, H) and racemic solute (guest, G):



Enantioselectivity,  $\beta$ , arises from the difference in the equilibrium constants  $K^+$  and  $K^-$  of both diastereomeric complexation reactions and is expressed as:

$$\ln \beta = \ln \frac{K^+}{K^-} = -\frac{\Delta \Delta G}{RT}$$
(3)

where  $\Delta \Delta G$  is the difference in the Gibbs energy of complexation for both diasteromeric complexation reactions. The simplest way to classify chiral selectors is to distinguish them by their size and the shape of their binding sites. The first class consists of molecules that complex with specific groups on the guest surface. Most of such selectors are based on derivatives from naturally occurring optical active compounds such as tartaric acid alkyl esters (**1**) and various amino acids such as L-proline and L-hydroxyproline (**2**). To improve enantioselectivity the selectors are often employed as transition metal complexes with Cu(II), Co(II), Ni(II) or various lanthanides. The main function of the metal ion is to enhance the enantioselectivity of the starting compound by creating a three-dimensional optically active complex that can be used for enantioselective extraction by ligand-exchange.

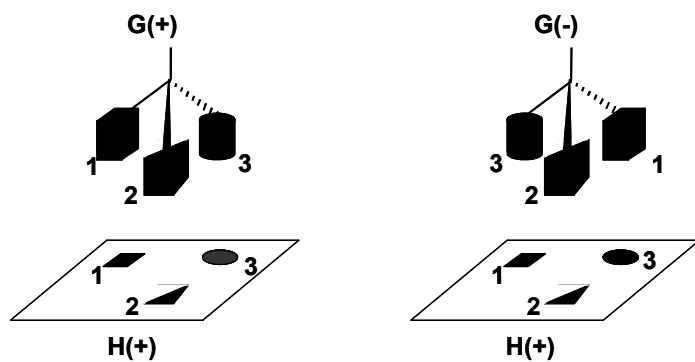
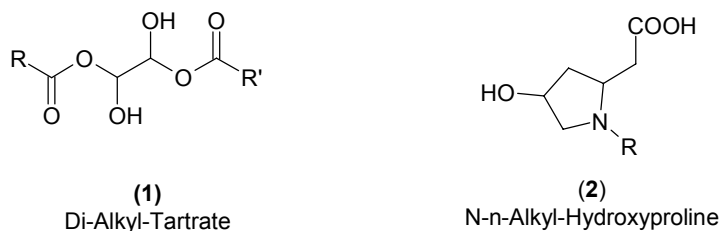


*Figure 1. Schematic representation of the Three-Point interaction model.*

The second class of chiral selectors consists of molecules that form an inclusion complex with the guest by interacting at many different points over the guest surface. Important examples are  $\alpha$ -,  $\beta$ -, or  $\gamma$ -cyclodextrins that are composed of six, seven or eight optically active glucopyranose units [8]. Besides cyclodextrins, linear polysaccharides such as maltodextrins and maltooligosaccharides might also be effective to incorporate the required enantioselectivity into one of the two phases. A group of synthetic chiral resolution agents that exhibit stereoselective inclusion complexation are chiral crown ethers [9]. Chirality is introduced by attaching two halves of the macrocyclic ether ring to chiral side groups, such as tartaric acid derivatives, dinaphthyl compounds etc. Analogous to cyclodextrins aqueous micellar aggregates are also able to provide a pseudophase with a hydrophobic interior. Micellar chiral recognition has been shown possible by either using chiral surfactants or by comicellar systems in which chiral selectors are solubilized in the hydrophobic interior [10].



## EXTRACTIVE RESOLUTON TECHNIQUES

### Liquid-Liquid Extraction

In liquid-liquid extraction optical isomers are separated by enantioselective partitioning between two liquids. In most other studies reported until now, the enantioselectivity is obtained by dissolving a suitable chiral selector in an organic solvent with minimal physical solubility of the enantiomers. The main classes that have been studied are amino acids, amino alcohols and organic acids because two simultaneous hydrogen bond interactions can provide relatively high enantioselectivity. Of these three groups most of the reported work is related to the extractive resolution of amino acids with selectors such as N-n-alkyl-L-proline copper(II) complexes [11,12]. The use of copper (II) is essential to create a selector that is capable of an enantioselective ligand exchange reaction with amino acids (AA):



According to this mechanism the overall distribution ratio is then determined by the combined solubility of the physically dissolved and complexed amino acid:

$$D = \frac{[\overline{AA}] + [\overline{AA - Cu - L}]}{[AA]} \quad (6)$$

In most studies concerning the separation of amino alcohols and organic acids dialkyl-tartrate esters have been used as chiral selectors [13,14].

### Liquid Membranes

In liquid-membrane separations enantioselective transport through the membrane is possible if chiral carriers are used that preferentially transport one of the two enantiomers. Pickering [15] studied emulsion liquid membranes for the separation of racemic phenylalanine with copper(II) N-decyl-L-hydroxyproline as the carrier dissolved in a decane/hexanol mixture as the membrane phase. Unfortunately, the enantioselectivity reduces during the course of extraction due to loss of the desired D-isomer from the source phase. This observation clearly indicates that the emulsion liquid membrane process is not sufficiently selective to achieve full separation in one stage due

to the inherent strong depletion of the enantiomer in the feed. Staging however is expensive and complicated by the required emulsification and de-emulsification steps. Related selectors have also been employed in supported and contained liquid membranes. As expected, the stability of the supported liquid membrane appeared the main issue. Long-term stability is achieved in a contained liquid membrane system. Pirkle [16] used selectors based on N-(1-naphthyl)leucine to separate the enantiomers of amino acid derivatives. As with the emulsion liquid membranes, the initially high enantioselectivity dropped quickly because the feed phase was depleted in the desired enantiomer.

### Supercritical Fluid Extraction

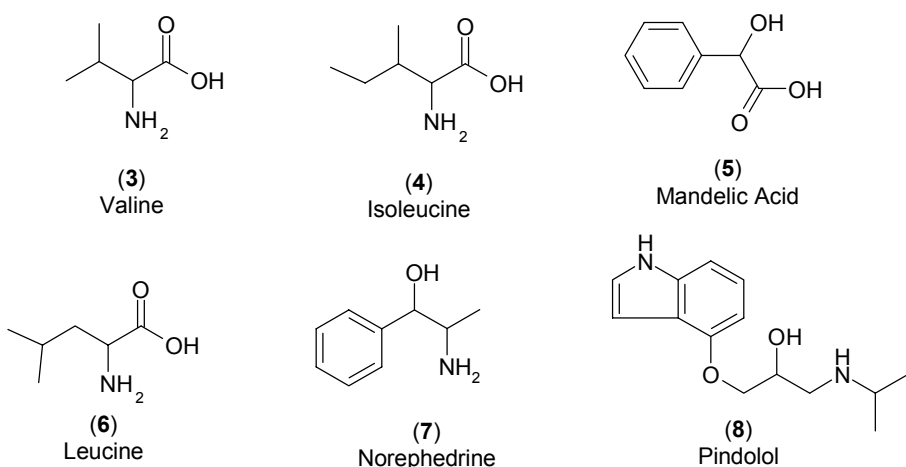
Enantioselective extraction by supercritical fluids (SFE) is possible by adding less than one equivalent of a resolving agent to establish a complex equilibrium of both free enantiomers and their diastereomeric salts [17]. The enantioselectivity of extraction arises from the preferred complexation of the resolving agent with one of the enantiomers combined with poor solubility of the diastereomeric complex in supercritical CO<sub>2</sub> that permits the selective extraction of the free optically active enantiomer. Published results indicate that SFE might be more selective for the separation of enantiomeric mixtures than conventional extraction because differences in solubility, dissociation constants and stability are larger in supercritical carbon dioxide than traditional solvents.

### Aqueous Two-Phase Extraction

Introduction of chiral differentiation in aqueous two-phase systems requires the incorporation of enantioselective interactions. This can be accomplished by the introduction of a selector that partitions preferentially into one phase or by the attachment of a chiral ligand to one of the polymers. In a dextran-PEG system 95% of the bovine serum albumin selector (BSA) dissolved in the dextran-rich phase and provides an enantioselective environment for the resolution of racemic tryptophan [18]. Besides BSA other chiral selectors such as monosaccharides, disaccharides, peptides, proteins, antibodies and optically active amino acids may be used as was disclosed by Hsu [19].

### Membrane Filtration Assisted Extraction

An alternative to separate the selector molecules the raffinate may be the use of membrane filtration. To be effective the membrane pores should retain the selector molecules and selector-enantiomer complex while the free enantiomer molecules can freely exchange phases. Complete retention is possible with sufficiently large selector molecules or aggregates such as enantioselective micelles [20], dendrimers, proteins or cyclodextrins [21]. Again the obtained selectivities (1.5-4) for the separation of amino acids with nonionic micelles containing a Cu(II)-amino acid derivative selector [20,22] are not sufficient to obtain >99% pure enantiomers with a single-stage separation process.



## FRACTIONAL EXTRACTION

The characteristic feature of enantiomer resolution is that the mixture has to be separated into two fractions consisting of the individual nearly pure enantiomers. Because of the low selectivities, mostly 1.2 up to 4, a series of extraction stages are required to obtain high optical purities. As shown in Figure 2, classical countercurrent extraction suffers from the disadvantage that only one of the two enantiomers can be obtained with sufficient purity by removing the other more or less selectively from the raffinate. For most chiral separations the recovery will be low because the extract composition is limited by the equilibrium between the racemate feed and the chiral selector containing solvent. In order to combine complete separation and high recovery of the enantiomers in two optically pure fractions, fractional extraction is the most promising liquid-liquid separation technique. Figure 2 illustrates that two solutes can be separated nearly completely by isolating one solute in the extraction solvent and the other solute in the raffinate by applying a wash solvent. Takeuchi [23] used a N-n-dodecyl-L-hydroxyproline copper(II) complex dissolved in n-butanol to resolve racemic valine (**3**) in rotating segmented glass columns. Yokouchi [24] demonstrated that the same selector could also be used for the full separation of racemic isoleucine (**4**) in a setup based on a cascade of 21 small mixer-settler units. An analytical vertical rotating column setup was used by Nishizawa [25] to achieve full (>99.9%) separation of ( $\pm$ )-mandelic acid (**5**) with N-n-dodecyl-L-proline copper(II) complex in butanol. In all three examples water was used as the wash fluid. N-n-dodecyl-L-hydroxyproline was used in octanol by Ding [26] to separate DL-leucine (**6**) into its pure enantiomers with microporous hollow fibre modules in which the polypropylene pores were filled with a cross-linked polyvinylalcohol gel. Complete separation could be obtained, provided that the velocity of the water and solvent flow are low enough to provide sufficient contacting stages. All four examples demonstrate that full separation and recovery of pure enantiomers from racemic mixtures can be achieved when fractional extraction is used.

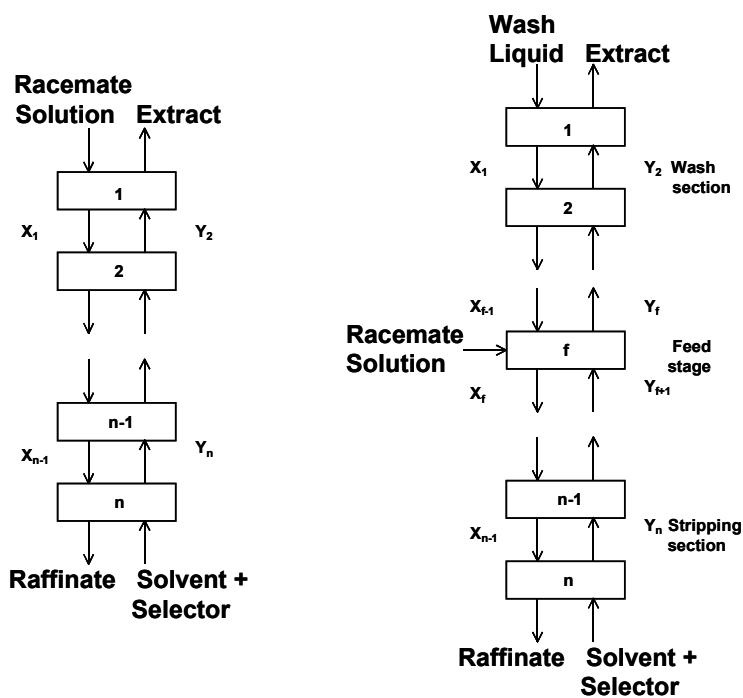


Figure 2. Countercurrent and fractional extraction.

## FUTURE OUTLOOK

The presented overview illustrates that extraction based technologies are in principle able to achieve full separation of enantiomer mixtures when the concept of fractional extraction is applied. Absolutely essential in the design of such extractive resolution installations is their application within a flexible multi-purpose environment used for the production of the majority of enantiopure products. Being unable to develop new selector systems with high selectivity for each new product within the common time-frame available for process development, the extractive resolution installation should be able to separate whole classes of products (amino acids, organic acids, amines, alcohols etc.) with a single selector system in one extraction unit. As illustrated in Table 1 for the separation of various amino acid enantiomers [23] this requires design and operation at limited selectivities, typically in the range of 1.2-4.

*Table 1. Effect of amino acid on minimum number of stages required for separation with copper(II) N-n-dodecyl-L-hydroxyproline at 25 °C.*

Amino acid	Selectivity [23]	N <sub>min</sub> (-)
Alanine	1.41	20
Valine	2.86	7
Norvaline	2.40	8
Leucine	2.04	10
Norleucine	2.50	8
Isoleucine	3.54	6
Methionine	1.62	14
Tyrosine	1.25	30
Phenylalanine	1.83	11

This challenge, encountered in virtually all chiral separation processes, strongly limits the application of the various technologies to those that can be staged relatively easily. The development of suitable contactors that provide competitive and reliable staging concepts will be one of the main challenges to initiate the application of extraction technology for the industrial separation of optical isomers. An idea about the minimum number of stages such contactors should provide can be obtained from the Underwood-Fenske relation. From Table 1 it can be seen that for the reported selectivities a minimum of 30 theoretical stages is required to separate all amino acid enantiomers into a 99% pure extract and raffinate containing the other enantiomer in 90% purity. This means that under practical operating conditions one can expect to need around 60 stages. Furthermore Table 1 illustrates that especially at low selectivities, a small increase in selectivity results in a significant decrease in the number of stages required. Such desired increases in selectivity are easily obtained by reducing the extraction temperature as illustrated by Figure 3a. However, as illustrated in Figure 3b, care has to be taken not to enter into a kinetically determined region where the reduction in number of stages by increased selectivity is outweighed by a larger increase in the size of each stage to allow sufficient time for mass transfer.

*Table 2. Process conditions for several fractional extraction resolution studies*

Selector conc. in solvent (mM)	Enantiomer feed conc. (mM)	Racemate	Solvent/Feed (w/w)	Wash/Feed (w/w)	Selector excess	Selectivity β (-)	Ref
Fractional Extraction							
5 <sup>(1)</sup>	2.4	Valine	10	10	20	1.55	23
10 <sup>(1)</sup>	13	Mandelic acid	15	27	11	n.a.	24
5 <sup>(2)</sup>	10	Isoleucine	8	14	4	1.95	25
9 <sup>(1)</sup>	4.9	Leucine	40	10	70	2.86	26
SLM fractional extraction							
200 <sup>(3)</sup>	26	Norephedrine	-	-	8	1.2	27

<sup>(1)</sup> Copper(II) N-n-dodecyl-L-hydroxyproline, <sup>(2)</sup> Copper(II) N-n-dodecyl-L-proline,

<sup>(3)</sup> SS-dihexyltartrate and RR-dehexyltartrate

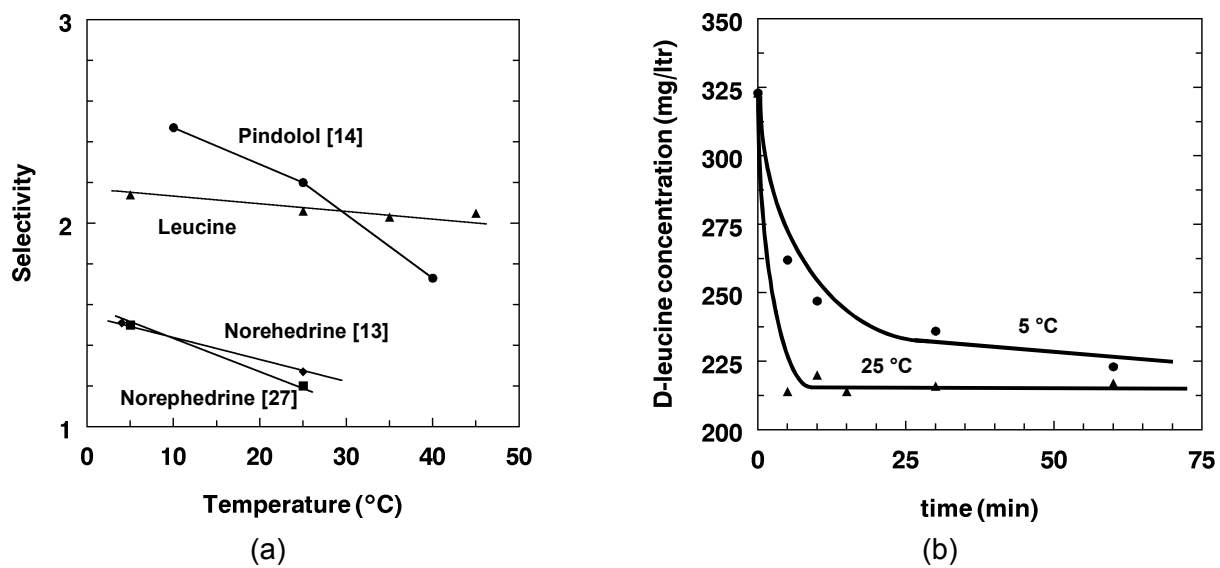


*Figure 3. Effect of temperature on (a) the selectivity of norephedrine (7), pindolol (8) and leucine (6) resolution with various selector systems and (b) the extraction kinetics of D-leucine with Cu(II) N-n-dodecyl-L-hydroxyproline.*

Looking at the operating conditions of various fractional extraction studies reported so far (Table 2) one easily sees that only very low racemate and selector concentrations have been applied. It is therefore not surprising that extractive resolutions have so far been discarded as uneconomical due to the reported very low overall productivities. However, besides selector and racemate solubility there is no particular reason to operate the process at such low concentrations. Even for the reported studies the racemate as well as the selector solubility easily allow operation at more than 10 times higher concentration levels. However, to be economically attractive, even higher concentration levels comparable to conditions applied in reactive extraction processes for metals recovery and purification need to be achieved. Operating the extractive resolution process at selector concentrations in the 20-30 wt% range would correspond to 0.3-0.5 M and results in approximately 100 times higher productivities. As illustrated by Figure 4, the use of higher selector concentrations has the additional advantage of increased operational selectivities because the contribution of the non-selective physical distribution of the enantiomers is reduced.

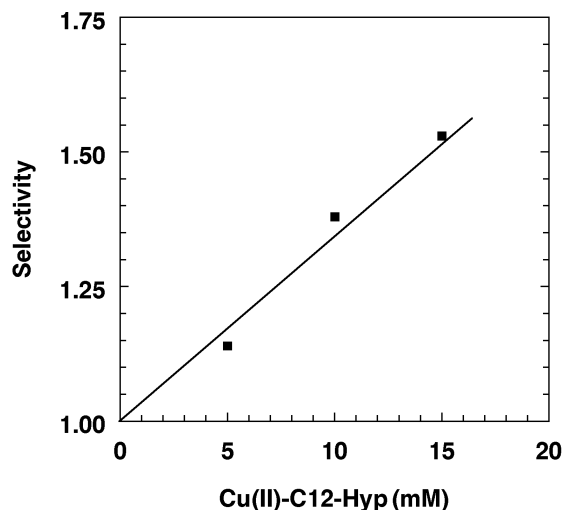


*Figure 4. Effect of selector concentration on the apparent selectivity for the resolution of DL-leucine (10 mM) with Cu(II) N-n-dodecyl-L-hydroxyproline at 25 °C.*

## CONCLUSIONS

Separation of enantiomers by extractive resolution has been proven technically feasible for the resolution of amino acids, amino alcohols and organic acids. However, a large amount of work still needs to be done to transform the reported analytical concepts into an industrially applicable multi-purpose technology. The encountered intrinsically low selectivities limit the possible technologies to those that are easily staged in a fractional extraction concept with up to 100 stages. For economical operations of such extractive resolution processes it is essential to increase the enantiomer and selector concentrations to levels common in the reactive extraction of metal ions. Under these conditions productivity increases up to 100 times come within reach. Finally it is of great essence to extend the application of extractive resolution towards other classes of enantiomers such as amines, alcohols, esters and ethers to be able to deal with the broad variety of products originating from the life-science industry.

## REFERENCES

1. R. A. Sheldon (1993), *Chirotechnology, Industrial Synthesis of Optically Active Compounds*, Marcel Dekker Inc., New York.
2. A. N. Collins, G. N. Sheldrake and J. Crosby (1992), *Chirality in Industry, The Commercial Manufacture and Applications of Optically Active Compounds*, John Wiley, Chichester.
3. A. N. Collins, G. N. Sheldrake and J. Crosby (1997), *Chirality in Industry II, The Commercial Manufacture and Applications of Optically Active Compounds*, John Wiley, Chichester.
4. S. Ahuja (1997), *Chiral Separations*, American Chemical Society, Washington DC.
5. A. B. de Haan and B. Simandi (2001), *Ion Exchange and Solvent Extraction*, Vol. 15, J.A. Marinsky, Y. Marcus (eds.), Marcel Dekker, New York, pp. 255-294.
6. T. H. Webb and C. S. Wilcox (1993), *Chem. Soc. Rev.*, **22**, 383-395.
7. S. Topiol and M. Sabio (1996), *Enantiomer*, **1**, 251-265.
8. D. W. Armstrong and H. L. Jin (1987), *Anal. Chem.*, **59**, 2237-2241.
9. D. J. Cram (1988), *Angew. Chem. Int. Ed. Engl.*, **7**, 1009-1020.
10. A. Dobashi and M. Hamada (1997), *J. Chromatogr. A*, **780**, 179-189.
11. T. Takeuchi, R. Horikawa and T. Tanimura (1982), *Anal. Chem.*, **56**, 11523-1155.
12. P. J. Pickering and J. B. Chaudhuri (1999), *Chirality*, **11**, 241-248.
13. V. Prelog, Z. Stojanac and K. Kovacevic (1982), *Helv. Chim. Acta*, **65**, 377-384.
14. Y. Abe, T. Shoji, M. Kobayashi, W. Qing, N. Asai and H. Nishizawa (1995), *Chem. Pharm. Bull.*, **43**, 262-265.
15. P. J. Pickering and J. B. Chaudhuri (1997), *Chirality*, **9**, 261-167.
16. W. H. Pirkle and W. E. Bowen (1994), *Tetrahedron Asymmetry*, **5**, 773-776.
17. B. Simandi, S. Keszei, E. Fogassy, S. Kemeny and J. Sawinsky (1998), *J. Supercrit. Fluids*, **13**, 331-336.
18. B. Ekberg, B. Sellergren and P-A. Albertsson (1998), *J. Chromatogr.*, **333**, 211-214.
19. J. T. Hsu (1990), *US Patent*, No. 4,980,065.
20. A. L. Creagh, B. B. E. Hasenack, A. van der Padt, E. J. R. Sudholter and K. van't Riet (1994), *Biotechn. Bioeng.*, **44**, 690-698.
21. T. Kokugan, Kaseno, T. Takada and M. Shimizu (1995), *J. Chem. Eng. Jpn.*, **28**, 267-273.
22. P. E. M. Overdevest and A. van der Padt (1999), *CHEMTECH*, **29**, 12, 17-22.
23. T. Takeuchi, R. Horikawa and T. Tanimura (1990), *Sep. Sci. Technol.*, **25**, 941-951.
24. Y. Yokouchi, Y. Ohno, K. Nakagomi, T. Tanimura and Y. Kabasawa (1998), *Chromatography*, **19**, 374-375.
25. H. Nishizawa, K. Tahara, A. Hayashida and Y. Abe (1993), *Anal. Sci.*, **9**, 611-615.
26. H. B. Ding, P. W. Carr and E. L. Cussler (1992), *AIChE J.*, **38**, 1493-1498.
27. J. T. F. Keurentjes, L. J. W. M. Nabuurs and E. A. Vegter (1996), *J. Membr. Sci.*, **113**, 351-360.



## MASS TRANSFER PERFORMANCE OF TWO-PHASE ELECTROPHORESIS WITH AN EMULSION SOLUTION AS ORGANIC PHASE

J. G. Liu, G. S. Luo, S. Pan, S. L. Zhai and J. D. Wang

Department of Chemical Engineering, Tsinghua University, Beijing, China

A two-phase electrophoresis process has been applied to the treatment of dilute organic acid solution. An electric field can both affect the primary distribution equilibrium state and enhance the mass transfer performance of a system. However, due to the low electric conductivity of the organic phase, the electrical efficiency can be low. In order to achieve higher efficiencies, a new system has been proposed. In this system the organic phase has been replaced with an emulsion solution of 49.9 wt% kerosene / 49.9 wt% water / 0.2 wt% Tween. Results show that the electrical resistance is significantly reduced. In addition electro osmosis is shown to be much lower than for an electrodialysis process, and the concentration of acid is increased severalfold. The effects of initial concentration and current density on current efficiency and on the recovery of organic acid are discussed.

### INTRODUCTION

The recovery of organic acids from dilute solutions is important, because of the negative environmental impact posed by their disposal. Nonetheless there are at present few efficient ways to treat these dilute solutions.

Solvent extraction is a technique commonly used in the recovery of organic acids due to high selectivities exhibited by solvents. Organic solvent requirement can however be high, and high recoveries are difficult to achieve. Electrodialysis is another technique that can be used. It can be operated in a continuous way, and does not need any regeneration steps. However, the electro osmosis in this process is a serious problem [1]. Two-phase electrophoresis is a novel separation technique, which combines the advantages of traditional extraction and electrophoresis [2-5]. It can effectively control water osmosis. In this process the heat generated by the electrode reactions can be removed utilizing the two-phase flow. Also applying an electrical field into a separation system can enhance separation efficiency. Electricity can serve as a driving force to enhance mass transfer. However the relatively low electrical conductivity of organic solvents results in a high voltage requirement for a given current density.

This work focused on the two-phase electrophoresis process where the organic phase was replaced with an emulsion solution to improve the conductivity of the whole system. The effects of initial concentration of organic acid and current density on current efficiency and on recovery of organic acid were explored. In addition electro osmosis in the two-phase electrophoresis process was investigated and compared to the case for electrodialysis.

## EXPERIMENTAL

### Reagents

All reagents were purchased from Beijing Chemical Products Company and used without any further purification. Acetic acid was of AR grade.

### Anion Exchange Membranes

AM-203 anion-exchange membrane was obtained from Shanghai Shengle Chemical Plant. The exchange capacity was 1.9 meq/g, the membrane resistance was about  $10\Omega/cm^2$ ; and the selectivity was 96%. In order to keep the size of membrane the same during the experiments, the anion-exchange membrane was immersed in the acid solution for more than 12 hours.

### Experimental Setup and Procedures

Figure 1 shows a schematic diagram of the experimental setup used. For the two-phase electrophoresis experiments, one phase was the water solution, and the other was an emulsion solution consisting of 49.9 wt% kerosene / 49.9 wt% water / 0.2 wt% Tween. To improve the electrical conductivity of the emulsion solution, a quantity of organic acid was introduced into it prior to use. The cathode was located in the water phase and the anode in the emulsion phase. Peristaltic pumps were used for circulating water and emulsion solutions. The constant current required in the operation was achieved using a DYY-III DC power supply. During the two-phase electrophoresis experiments, samples of the water phase were removed at specific intervals and analyzed by titration. A stirrer was used on the emulsion solution side to prevent phase separation of the emulsion solution.

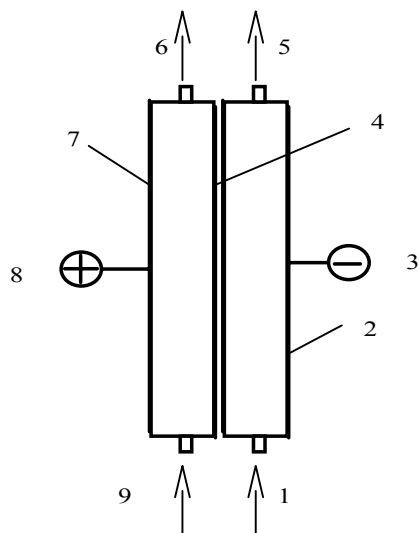


Figure 1. Schematic diagram of experimental set-up.

(1) inlet of water phase; (2) water phase chamber; (3) cathode; (4) anion-exchange membrane; (5) outlet of water phase; (6) outlet of emulsion phase; (7) emulsion phase chamber; (8) anode; (9) inlet of emulsion phase.

The current efficiency ( $\eta$ ) and recovery (R) were the two parameters used to evaluate the performance of the two-phase electrophoresis process. They were defined as follows:

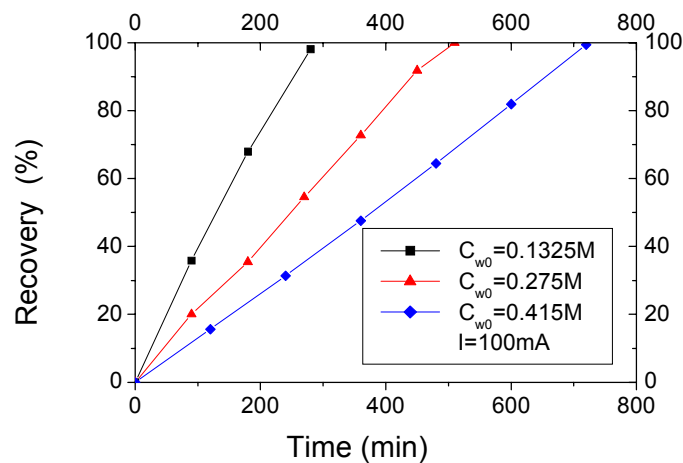
$$\eta = \frac{(C_0 V_0 - C_1 V_1)F}{It} \times 100\% \quad R = \left(1 - \frac{C_1}{C_i}\right) \times 100\%$$

where F is Faraday's constant, I the applied current, and t the time.  $V_0$  and  $V_1$  are the volumes of water phase at different times.  $C_0$  and  $C_1$  are the organic acid concentrations associated with the volumes of water phase.  $C_i$  is the initial concentration of organic acid in the water phase.

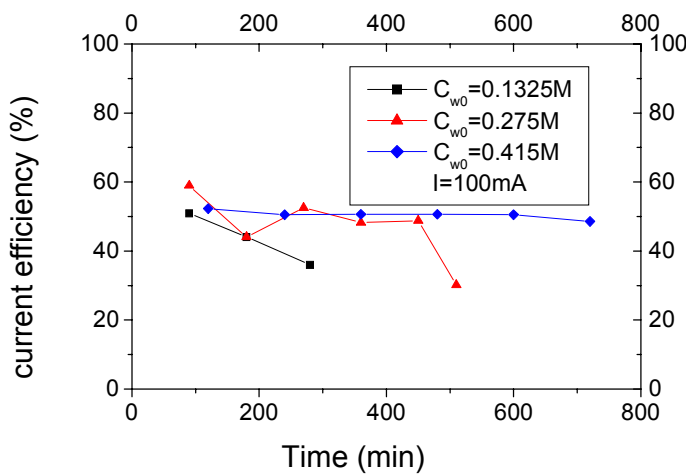
## RESULTS AND DISCUSSIONS

### **Effect of Initial Concentration on Current Efficiency and Recovery**

The effects of initial organic acid concentration on recovery and current efficiency are shown in Figures 2 and 3. In the process of two-phase electrophoresis, acid ions and hydrogen ions play an important role in current conducting. Current density plays an important role on the mass transfer rate of organic acid. To keep the same current density and change the initial concentration in water solution, the time for achieving the same recovery is increased with an increase of initial concentration. The reason is that the total amount of acid in the water phase increases but the solute transfer rate does not increase in proportion.



*Figure 2. Influence of initial concentration on recovery.*



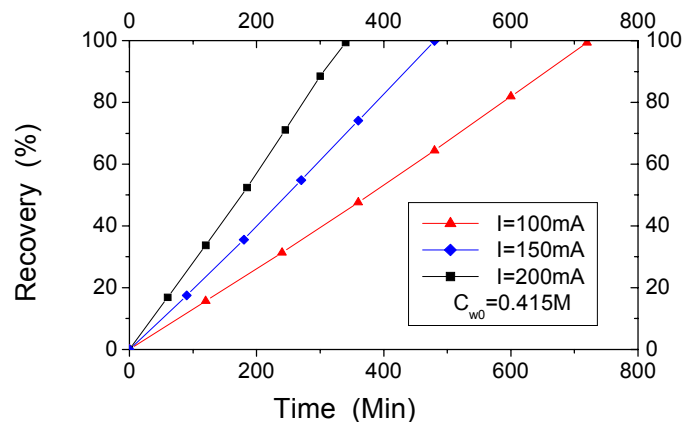
*Figure 3. Influence of initial concentration on current .*

Figure 3 shows that the overall current efficiency increases slightly with the increase of initial organic acid concentration in the water phase, which may be due to the higher electrical conductivity at the high initial acid concentration.

In the process, acid ions move into the emulsion phase continuously under the action of the electric field. The solute concentration of the water phase decreases during the course of the experiment. The electrical conductivity of the emulsion increases while the conductivity of the water phase decreases. When nearly all the solute in the water phase has passed into the emulsion solution, the ions that then play the greatest role in conducting current come from the electrolysis of water. As shown in Figure 3, at this time, the conductivity of the whole system decreased along with the current efficiency.

### **Effect of Current Density on Current Efficiency and Recovery**

The effects of current density on the recovery and on the current efficiency are shown in Figure 4 and Figure 5. The experimental results showed that for the same concentration, the rate of change of recovery increased with the increase in current density. To achieve a given recovery of organic acid, a shorter time is required due to the high solute transfer rate passing through the anion-exchange membrane under high current density.



*Figure 4. Influence of current density on recovery.*

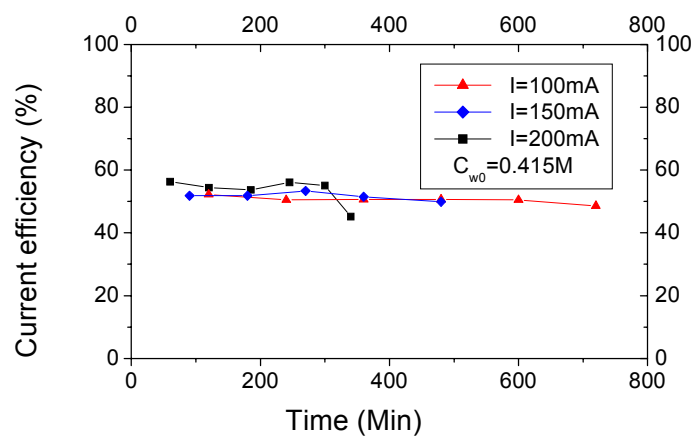


*Figure 5. Influence of current density on current efficiency.*

Figures 4 and 5 showed that the effects of current density on current efficiency were relatively minor. For the same initial organic acid of water solution, the current efficiency was nearly stable during the operation for each current density.

### **Effect of Current Density on Water Electro-osmosis**

The volumes of electro-osmosis water for electrodialysis and two-phase electrophoresis are compared in Table 1. The electro-osmosis water for electrodialysis is serious. It increased with the increase of current density. In electrodialysis, electro-osmosis effects limited the concentration of organic acid on the anode side. In the process of two-phase electrophoresis, the electro osmosis is negligible and poses no limitation on acid concentration.

*Table 1. Effect of current density on water electro-osmosis.*

	Electrodialysis (0.55 M)			Two-phase electrophoresis (0.415 M)		
	50	100	150	100	150	200
Current density (mA)	50	100	150	100	150	200
Initial volume of cathode side (ml)	60	80	80	60	60	60
Initial volume of anode side (ml)	40	40	40	60	60	60
Operation time (min)	540	520	120	720	480	340
Vol. of electro-osmosis water (ml)	15	31	45	~0	~0	~0

### **CONCLUSIONS**

This study showed that when the organic phase is replaced with an emulsion solution in two-phase electrophoresis the electrical conductivity increases. When compared with electro dialysis, the electro osmosis in two-phase electrophoresis was very low. The current efficiency was about 50% in the cases of different initial acid concentrations. From the experimental results it may be concluded that the recovery of organic acid was high. Nearly complete removal of the organic acid from water phase can be achieved if the operating time is long enough. The two-phase electrophoresis process can be applied to treat dilute acid solutions with high recoveries and current efficiencies.

### **REFERENCES**

1. G. S. Luo and F. Y. Wu (2000), *Sep. Sci. Technol.*, **35**( 15), 2485-2496.
2. J. Stichlmair (1987), *German Pat.*, DBP3742292 (Dec.14).
3. J. Stichlmair, J. Schmidt and R. Proplesch (1992), *Chem. Eng. Sci.*, **47** (12), 3015-3022.
4. C. W. Theos and W. M. Clark (1995), *Appl. Biochem. Biotech.*, **154**, 143-157.
5. J. G. Liu, G. S. Luo, S. L. Zhai (1999), *Mod. Chem. Ind. (China)*, **19** (8), 8-11.



## STUDY ON THE THREE-PHASE EXTRACTION OF PENICILLIN G WITH A SINGLE-STEP METHOD

J. Chen, H. Z. Liu, B. Wang, Z. T. An and Q. F. Liu

Young Scientist Laboratory of Separation Science and Engineering,  
State Key Laboratory of Biochemical Engineering, Institute of Chemical Metallurgy,  
Chinese Academy of Sciences, Beijing, China

A novel three-phase extraction with a single-step method is developed for the extraction of penicillin G from the whole fermentation broth and filtered supernatant. The three phases are composed of organic solvent and two aqueous phases, which were traditionally composed of polymer and corresponding polymer or salts. The organic solvent must have low solubility compared to the polymers. In the extraction process, the extraction and purification was finished with a single step in the three phases. The color grade, water content and contamination index of butyl acetate in the first circle are used for estimating the extraction ratio and purification degree. For average results for the filtrate of fermentation broth, the color grade is 2, the water content is less than 1.03 and the contamination index is less than 0.3. For whole-broth processing, the color grade is 5, the water content is less than 1.2 and the contamination index is less than 0.28. The extraction processes, such as flocculation, demulsion, decoloration and freezing dehydration, are integrated into the three-phase extraction. The novel three-phase extraction can be recognized as an advanced method for complex systems, such as the purification of bioproducts from fermentation broths.

### INTRODUCTION

An important step in the production of antibiotics is the recovery and concentration of product from the fermentation broth in which it is produced. The physicochemical properties that distinguish the desired solute from other fermentation products must be exploited in the selection of an appropriate separation technique for this step. Physical sorption, ion-exchange (IX) and solvent extraction (SX) have all been employed successfully in isolation of different antibiotics. For the extraction of penicillin G, the simple adsorption operation has the characteristics of low selectivity, high labor need and low reversibility. Although IX has higher selectivity and yield, it is not suitable for the low stability of the penicillin due to the long cycle. SX is an important method with relatively high selectivity and yield.

Impetus for the large-scale use of SX for antibiotics recovery was provided by the critical need for increased supplies of penicillin during the Second World War. Since that time, refinements in extractor design and improvements in fermentation technology have yielded considerable increases both in equipment throughput capacities and in overall product yields, although the basic technology itself has changed little over the years[1]. But SX requires some complex processes, such as flocculation, demulsion, decoloration and freezing dehydration, for the further purification of antibiotics, and it is still necessary to operate the costly podbielniad, Alfa-Laval and other centrifugal contractors in the plant.

During the past decades, the main progresses of antibiotics industry have been focused on solvent selection. Treybal [2] and King [3] have documented several criteria that should be considered in the selection of solvents for extraction processes in general. Yang [4] has reported that a new mixed solvent can be used to increase the yield by improving the pH values to 2.5 - 5 to minimize the solute degradation by acid hydrolysis. Yang [5] has also patented a new extractant used in the extraction process without demulsifier. Qi [6] has studied the extraction by alcohol, which was superior to the BA solvent in some aspects. With the development of antibiotics, there are urgent needs for the new extraction methods such as UF membrane separation showing high extraction ratios and low demulsion to the penicillin extraction. But these are only used to clarify fermentation broths instead of rotary pricoat filters, and do not give any downstream benefits [7]. Pan *et al.* [8] reviewed the progress of aqueous two-phase extraction in antibiotic separations, but low extraction ratio and high cost limited its application.

In this paper, a new method of three-phase extraction with a single step is presented to overcome the defects of present techniques for both filtered broth and whole fermentation broth. The extraction and purification of penicillin G in the three-phase system will be finished with single step, and the target product and by-products will be separated into different layers together. The product quality was improved and the technique was greatly simplified.

## EXPERIMENTAL

80 g clean, filtered supernatant or whole fermentation broth, 12.5 g polyethylene glycol and 15 g ammonia sulphate were placed together in a stoppered tubes. These were shaken for half an hour, then the aqueous two phases were formed. 50 ml BA was added into the mixture solution, and 10% sulfuric acid was added to adjust the pH to 1.8~2.2. The centrifugation was needed after drastic agitation. There were four layers for the filtered supernatant: clear organic phase at topside, a very thin layer of emulsion at second layer, a deep color aqueous phase at the third layer, and a clear aqueous phase at the bottom phase. The clear organic phase was taken out to check its penicillin concentration, color grade, water content and contamination index. For the whole fermentation broth, three layers can be seen clearly: clear organic phase at topside, the liquid and solid mixture of mycelium and dark color matter at middle phase, and a clear aqueous phase at the bottom phase.

Penicillin concentration was measured by polarimeter for its polarizability, which was in proportion to its concentration. Micro-water content was measured by Karl-Fischer titration. Color degree was determined through the method of comparing the standard color degrade. Contamination index was the ratio of foreign acid to penicillin acid, and the foreign acid was the difference between the total acid and penicillin acid in the loaded organic phase. The present techniques standard of first cycle BA check was provided by North China Pharmaceutics Company.

## RESULTS AND DISCUSSION

As shown in Tables 1 and 2, the results of the organic solvent in three-phase extraction with the single step was all better than the present standard at different batch filtered supernatant and different molecular weights of PEG. The quality of the organic phase after first circle was improved and the process was simplified. The emulsion during the extraction process was still lowered deeply. The quality of the product by the three-phase extraction is shown in Table 3.

*Table 1. Extraction results of the filtered supernatant with three-phase extraction (O/A=1/2, T=18°C).*

Molecular weight of PEG	Organic phase	Biological activity (u/ml)	pH	Extraction (%)	First circle butyl acetate measurement		
					Color degree	Water (%)	Contamination index
6000	BA	35181	2	97.1	Pure Penicillin G solution		
1000	BA	31486	2	95.1	2 <sup>-</sup>	1.01	0.29
2000	BA	31486	2	97.7	2 <sup>+</sup>	0.99	0.27
4000	BA	32800	2	91.1	2	1.02	0.21
6000	BA	28896	2	90.0	2	0.93	0.26
6000	BA + 2.5% butyl alcohol	33800	4	84.3	2	1.32	0.34
4000	BA+T <sub>2</sub> Demulsifier	32800	2	88.5	3	1.24	0.30
Mixing 1000, 2000, 4000 and 6000	BA	32425	2.5	83.0	1 <sup>+</sup>	1.00	0.26

*Table 2. Comparison between three-phase extraction with present standard techniques.*

	Color degree	Water (%)	Contamination index	Emulsion status	Extraction (%)
Present techniques	4~5	1~ 1.3	0.3 ~ 0.4	Demulsifier and centrifugation was needed to demulsify	> 95% in 3-step extraction
Three-phase extraction with single step	2	< 1.03	< 0.3	Without demulsifier, centrifugation was enough	see Table 1

*Table 3. The crystallization of potassium salt of penicillin G.*

Biological activity (u/mg)	Appearance	pH	Density (g/cm <sup>-3</sup> )	Melting point (°C)	264 nm	280 nm	325 nm	400 nm
1598 (1597)	White crystal powder	6.0 (6.0)	4.28 (4.26)	215 (215)	0.870 (0.890)	0.071 (0.067)	0.116 (0.176)	0.894 (0.922)

The data in brackets show typical values for the product using the current extraction method.

The extraction and purification were finished in the single step since the steps of demulsion, freezing dehydration and decoloration in present techniques were omitted. Because the aqueous two phases were formed by adding high polymer PEG and ammonia sulphate, the effect of adsorption of color matter, sedimentation of protein and flocculation of protein was enhanced. The aqueous two phases were used as the liquid filtration membrane, which hold back the color matter, protein and other organic acid, while the penicillin acid can pass through it smoothly.

Compared with the aqueous two phase extraction, penicillin asymmetrically partitioned in the system of 11.6% PEG 6000, 13.9% ammonia sulphate aqueous two phases. The partition coefficient was 18.7, and the volume ratio of top phase to bottom phase was 0.34. The extraction of the top phase was 42.7%. The complex back treatment and longer phase separation time were still limitations to its application [9], although low emulsion and denature in aqueous two phases were prominent characteristics for penicillin extraction. In the three-phase system of the same weight of PEG and ammonia sulphate, the percentage of extraction was 90.0%, water content 0.93, contamination index 0.26, color degree 2 (Table 1). In the three-phase system, the viscosity of aqueous two phases was lowered, and the extraction speed was enhanced.

It is shown in Table 4 that the quality of the first stage BA was also better than the present techniques for the whole fermentation broth, and nearly equal to the standard for the filtered broth. Three-phase extraction with single step will still improve the penicillin quality of extraction from the whole fermentation broth.

*Table 4. The extraction result of the fermentation broth with three-phase extraction  
(O/A=1/2, T=18°C.)*

Molecular weight of PEG	Organic phase	Biological activity (u/ml)	pH	Extraction (%)	First stage butyl acetate check		
					Color degree	Water (%)	Contamination index
6000	BA	52000	2	80.1	4 <sup>+</sup>	1.10	0.25
6000	BA	50960	2	83.2	5 <sup>-</sup>	1.10	0.22
1000	BA	52100	2	76.1	5 <sup>-</sup>	1.06	0.24
2000	BA	52100	2	73.0	5 <sup>-</sup>	1.06	0.27
4000	BA	52100	2	78.0	5 <sup>-</sup>	1.23	0.28

Filtration was omitted during its extraction for the whole fermentation broth, during which the biological activity loss will be 10~20% at this step. So, extraction directly from the whole fermentation broth was a tendency for its advanced development. The costly advanced Decantor extractors are widely used in the world, and it was necessary to select suitable demulsifier and control the solution viscosity to improve the extraction of Penicillin G. The three-phase extraction with single step method will omit the procedures of filtration, flocculation, demulsion and decoloration, and produce a higher quality product. The detailed comparison between the three-phase extraction with single step with present techniques is shown in Table 5.

There are complex phenomena for the aqueous two-phase extraction from the whole fermentation broth. Four layers appeared after the extraction: top phase, interface phase, bottom phase and solid phase. The multiple phases and low extraction coefficient will limit its application. With the three-phase system, the percentage of extraction was 77.0 %, water content 1.1, contamination index 0.25 and color degree 4<sup>+</sup>. Another advantage was that it is easier to deal with different phases respectively and recycle in the middle phase.

*Table 5. Comparison between three-phase extraction with present techniques for the whole fermentation broth.*

	Equipment	Pretreatment	After treatment	First stage BA check	Extraction ratio
Present standard technique	Decantor extractor	suitable demulsifer, and certain viscosity	Bulky solid and liquid volume	Color degree < 5 Water < 1.3 % Contamination index < 0.3	Higher
Three-phase extraction with single step	Simple stirrer and centrifugal equipment	Without pretreatment	The liquid and solid mixture of mycelium and dark color matter gather in the top aqueous phase with small volume	Equal to the present techniques of filtered supernatant (Water < 1.2%, contamination index < 0.28, color degree ≤ 5)	Higher than 73% in single stage

## CONCLUSIONS

The three-phase extraction with a single step has been shown at the laboratory scale to greatly improve the product quality of penicillin and simplify the present complex techniques. The novel three-phase extraction can be recognized as an advanced method for complex systems such as purification of bioproducts from fermentation broth and Chinese medicine.

## ACKNOWLEDGEMENT

This paper was financially supported by the Outstanding Young Scientist Foundation of China (No. 29925617) and the National Nature Science Key Foundation of China (No. 29836130).

## REFERENCES

1. T. A. Hatton (1985), Comprehensive Biotechnology: Liquid-liquid Extraction of Antibiotics, Vol. 2, M. Moo-Young (ed.), Pergamon Press, New York, pp. 439-449.
2. R. E. Treybal (1980), Mass-transfer Operations, 3rd edn., McGraw-Hill, New York.
3. C. J. King (1980), Separation Processes, 2nd edn., McGraw-Hill, New York.
4. Z. F. Yang, S. Q. Yu and J. Y. Chen (1990), C. N. Pat., No. 1047293B (Nov. 28).
5. Z. F. Yang, S. Q. Yu and J. Y. Chen (1991), C. N. Pat., No. 1052862B (Jul. 10).
6. P. Y. Qi, Y. Y. Dai and Y. Miao (1999), C. N. Pat., No. 1228434B (Sep. 15).
7. S. Z. Li (1996), *Proc. Int. Solvent Extraction Conf., ISEC '96*, Vol. 2, University of Melbourne Press, Melbourne, pp. 1511-1515.
8. J. Pan, Z. H. Li and D. H. Qin (1999), *Biol. Eng. Proc. (Chinese)*, **19**(3), 48-51.
9. P. A. Albertsson (1986), Partition of Cell Particles and Macromolecules, 3rd edn., John Wiley and Sons, New York.



## EXTRACTION OF DRUG TRACES WITH LIQUID MEMBRANE SYSTEMS

Manfred Grote, Bedia Haciosmanoglu, Jürgen Nolte\*

University of Paderborn, Paderborn, Germany

\* Institute of Spectrochemistry and Applied Spectroscopy, Dortmund, Germany

Bulk-membrane experiments were carried out in a three-compartment transport cell. The liquid membrane system consists of an aqueous feed solution containing drugs of environmental concern (Ibuprofen, Diclofenac, Carbamazepin and Sulfamethoxazol) as analytes, a liquid membrane (organic solvent combined with a mobile carrier) and an aqueous stripping solution (e.g., mineral acids, salts or alkalies). Different solvents, admixed organic amines or acids as well as a pH-gradient between feed and strip-phase have been used to optimize the efficiency and selectivity of the transport of drugs across the bulk membrane. Complementary permeation studies are carried out applying biological flat sheet membranes such as the small intestine of sheep.

### INTRODUCTION

Pharmaceuticals are released into the environment mostly through sewage. The concentrations of drugs and their metabolites found in sewage treatment plant's effluents or rivers are in the range of micrograms to nanograms per liter [1]. As a consequence there is an urgent need to improve the purification of water and waste-water and to monitor the drug input of the waterways particularly of surface and groundwater.

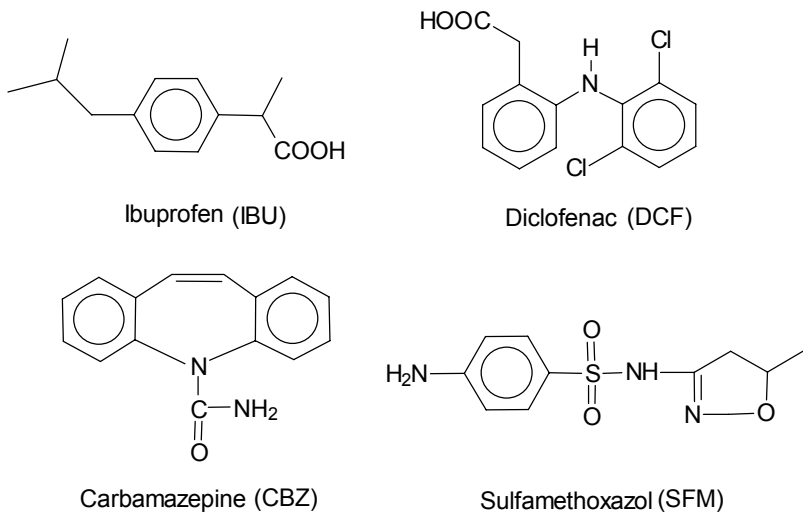


Figure 1. Drugs used for liquid membrane transport.

For this purpose reliable and efficient sample separation and preconcentration methods must be developed, which enable the reliable determination of trace amounts of drugs in complex matrices. As has been demonstrated in the analysis of herbicides in natural water samples by means of HPLC, liquid membrane techniques offer a more selective sample pretreatment compared to solid-phase extraction [2,3]. Furthermore, supported liquid-liquid extraction or membrane systems (SLP) can be used on-line with liquid chromatography [2,4]. Also badge-type passive samplers have been constructed applying different liquid trapping media for trace amounts of analytes in complex aqueous matrices [5].

The purpose of the present study is to examine the applicability of certain bulk three-phase liquid membrane-systems and also biological membranes for the separation of various basic and acidic drugs of environmental concern from dilute aqueous solution. The compounds selected were (Figure 1): *Ibuprofen*, *Diclofenac* (anti-inflammatory), *Carbamazepin* (antiepileptic) and *Sulfamethoxazol* (human and veterinary antibiotic).

The mass transfer of the analytes through the liquid phases (feed / membrane / strip) was carried out in a three-compartment cell equipped with an agitator. Such a bulk membrane cell was already operated for carrier facilitated transport of precious metal ions [6]. The results of these investigations are compared with the permeability of the drug mixtures through solid flat sheet membranes of biological origin. Details of this part of current research will be described elsewhere.

## EXPERIMENTAL

### Chemicals, Reagents and Stock Solutions

Carbamazepine (CBZ), Ibuprofen (IBU), Diclofenac (DCF) sodium salt and Sulfamethoxazol (SFM) were purchased from Sigma (Deisenhofen, Germany). The purity of the drugs was > 98%. The organic solvents used for the liquid-membrane-systems were decane, decanol and dihexylether (Sigma, Germany). Sodium octanesulfonic acid, tri-*n*-octylamine and tetrahexylammonium chloride used as carrier were of analytical-reagent grade (Merck, Darmstadt). Sodium dihydrogen phosphate monohydrate was used for mobile phase and was of analytical grade. Acetonitrile and methanol used for liquid chromatography were of HPLC grade.

Stock solutions of drugs were prepared in methanol. A series of standard solutions for calibration in the range 0.25-10 mg/dm<sup>3</sup> was obtained by diluting of aliquots of the appropriate stock solution with bi-distilled water.

### HPLC Analysis

Drug concentrations of the different liquid phases were determined by high performance liquid chromatography (HPLC). The samples were introduced into the chromatographic system by an autosampler (Gilson-Abimed Model 231 equipped with Dilutor 401) and an isocratic pump (Waters Model 590). A variable ultraviolet-visible detector 655 Å was connected to a chromato-integrator 2000-D (Merck-Hitachi). The analytical column used was LichroCART RP 18 (5µm, 250 x 4 mm; Merck). The flowrate of the mobile phase was 1.0 cm<sup>3</sup>/min with an average operating pressure of 130 bar. Detection was performed at 225 nm. The mobile phase consisted of a mixture of 60 mmol/dm<sup>3</sup> NaH<sub>2</sub>PO<sub>4</sub>: acetonitrile (50:50 v/v). Retention data (*t*<sub>R</sub>) of the analytes: SFM: 3.3 min, CBZ: 4.60 min, DCF: 10.68 min, IBU: 12.81 min.

### Membrane Equipment and Procedure

The liquid membrane system consisted of an aqueous feed solution containing the analyte, a liquid bulk-membrane (organic solvent with and without a dissolved mobile carrier) and an aqueous stripping solution (e.g., mineral acids, salts or alkalies). As shown schematically in Figure 2, the three-phase system was established in a home-made glass cell equipped with an agitator (PTFE). The cell consisted of two concentric chambers dividing it into separate compartments. Thus, the feed is allowed to contact the bulk-membrane and the strip solution to contact the membrane. The whole cell was covered by a fitting glass lid in order to minimize loss of solvent by evaporation.

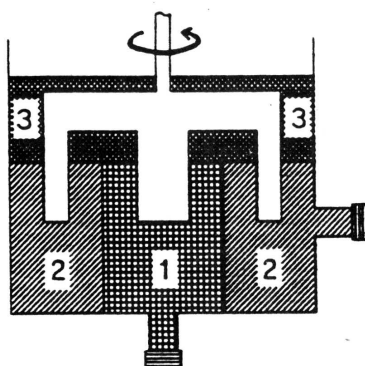


Figure 2. Three-phase liquid membrane system (1: Strip phase, total volume: 25 cm<sup>3</sup>; 2: Feed phase: 32 cm<sup>3</sup>; 3: Membrane phase, 20 cm<sup>3</sup>).

After careful loading of the cell with the three liquids the experiment was started under synchronously and continuously stirring at a fixed frequency of 60 rpm, so that the transport reactions were predominantly controlled by diffusion. In order to monitor the transport of the drugs through the membrane system by HPLC, aliquotes were taken from the phases in intervals by means of a microliter syringe which was introduced through self-closing seals and analyzed.

### RESULTS

In this work the transport of the acidic or basic drugs *Ibuprofen*, *Diclofenac*, *Carbamazepin* and *Sulfamethoxazol* (Figure 1) across different liquid membranes was measured. The membrane configuration employed (Figure 2) allows extraction and back-extraction in one unit. The experimental conditions were chosen by taking into account the following basic considerations. Among other factors the efficiency and selectivity of the bulk membrane is markedly influenced by the composition of the organic phase through which permeation will occur. Using common water-immiscible organic solvents the distribution of the analyte molecules governs the extent of extraction from the sample matrix. However, the mass transfer across the two feed/organic and organic/strip interfaces can be facilitated by mobile carriers. In such a case formation and dissociation reactions of ion-pair complexes near the interfaces are important for both the forward and back-extraction and, hence, the pH-gradient between the aqueous feed and strip phase will also influence the overall transport process. As a consequence for the present study the composition of each of the three liquid phases employed was adjusted to basic properties of the analytes such as their solubility in water and organic solvents, polarity and acid-base behaviour.

The extraction of the weak acid Ibuprofen and the amphoteric Diclofenac was determined by applying decane, decanol or dihexyl ether as membrane solvents, individually or combined. These solvents were used with and without admixed organic amines (tri-*n*-octylamine, TOA; tetrahexylammonium chloride, THAC) or octane-1-sulfonic acid (OcSA) as mobile carriers.

Furthermore a pH-gradient between feed and strip-phase has been used to optimize the effectivity of the extraction processes. As examples, the following results were obtained for the drugs investigated. If not otherwise stated, the concentration of each analyte in the aqueous feed was 10 mg/dm<sup>3</sup>.

### Transport of Ibuprofen

Complete extraction of Ibuprofen from dilute aqueous solution was achieved within 1 hour simply by applying 1-decanol as the bulk-membrane (Table 1). Not unexpectedly, the rate of transport of the weak acidic analyte ( $pK_a = 4.41$ ) was markedly enhanced by adding of basic liquid surfactants such as tri-*n*-octylamine, TOA, or tetrahexylammonium chloride, THAC [7].

**Table 1:** Transport of Ibuprofen: effect of membrane composition on forward extraction.  
(Feed: 10 mg/dm<sup>3</sup> Ibuprofen; carrier: 1g/dm<sup>3</sup>; strip: 2 mol/dm<sup>3</sup> HClO<sub>4</sub>).

Membrane phase	Carrier	Time [min] to achieve ~100% extraction
1-decanol	-	~120
1-decanol	THAC	~60
1-decanol	TOA	~30
decane/decanol (8 : 2 v/v)	THAC	~30

Particularly, the presence of the tertiary amine TOA increases the effectivity of forward-extraction drastically. However, the THAC-modified systems behave similarly when a mixture of 1-decanol and an excess of non-polar decane was used as the membrane solvent.

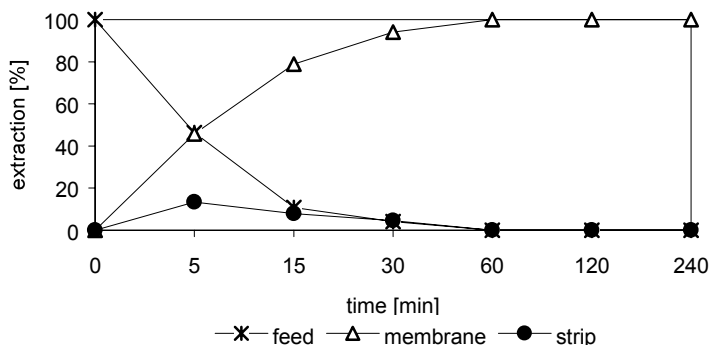


**Figure 3:** Carrier-facilitated transport of Ibuprofen across a three-phase membrane.  
(Feed: 10 mg/dm<sup>3</sup> Ibuprofen in water, membrane: 1g/dm<sup>3</sup> THAC in 1-decanol,  
strip: 2 mol/dm<sup>3</sup> HClO<sub>4</sub>).

It is assumed that the formation of ion-pairs between the mono-carboxylic acid and the carrier-amines proceeds rapidly at the feed/organic interphase compared to diffusion across the liquid membrane (Figure 3).

Stripping of Ibuprofen from the loaded membranes is not possible by the action of dilute hydrochloric acid. Perchloric acid (2 mol/dm<sup>3</sup>) displaces the extracted analyte to some extent due to the strong competing effect of the perchlorate anion (Figure 3). Obviously, re-extraction occurs which is particularly pronounced when TOA dissolved in 1-decanol was used as bulk-membrane and sodium perchlorate as the stripping agent: after 4 hours ~ 25% of the loaded Ibuprofen were back-extracted and 8 hours later this value was diminished to 5%. However, the most efficient membrane transport was observed from a 0.1 mol/dm<sup>3</sup> HCl feed by using octane-1-sulfonic acid, OcSA, as liquid ion exchanger dissolved in dihexyl ether and sodium carbonate solution as the stripping phase (Figure 5).

### Transport of Diclofenac

Diclofenac an amphoteric compound ( $pK_a = 4.18$ ) is sparingly water-soluble, therefore its sodium salt was used for preparing the aqueous feed [7]. Various membrane phases were composed utilizing decanol, decane and also dihexyl ether as solvents. Furthermore, amine based membrane-carriers were used and also OcSA, as an acidic ion-pairing reagent. In Table 2 some of the membrane systems employed are listed.

Figure 4 reveals clearly an order of extraction efficiency showing the carrier mediated transport by means of TOA and THAC dissolved in decanol or decane to be the most efficient one. Addition of the acidic carrier did not result in a higher extractability. By contrast, the transport of Diclofenac into the dihexyl ether phases proceeds much more slowly and to a lower extent compared to the latter systems.

*Table 2: Transport of Diclofenac: composition of three-phase membrane systems. (Feed: 10 mg/dm<sup>3</sup> Diclofenac sodium, basic carrier: 1g/dm<sup>3</sup> of amine, acidic carrier: 0.25 g/dm<sup>3</sup> OcSA).*

No.	Membrane phase	Carrier	Strip phase
1	Decanol	TOA	2 mol/dm <sup>3</sup> HClO <sub>4</sub>
2	decane:decanol (8:2 v/v)	THAC	2 mol/dm <sup>3</sup> HClO <sub>4</sub>
3	decane:decanol (11:1 v/v)	OcSA	0.1 mol/dm <sup>3</sup> NaOH
4	dihexyl ether	-	0.1 mol/dm <sup>3</sup> NaOH
5	dihexyl ether	OcSA	0.1 mol/dm <sup>3</sup> NaOH

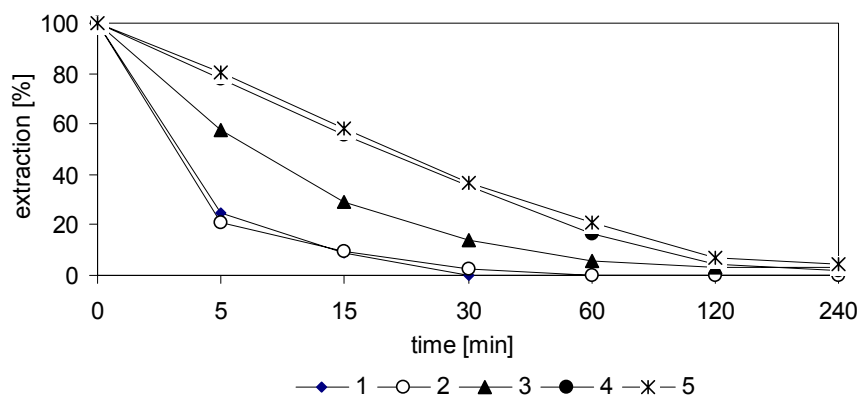


*Figure 4. Forward-extraction of Diclofenac as a function of time: effect of membrane composition (membrane components: see Table 2).*

The affinity of these organic phases to the drug molecules seems to be very high as none of the acidic and alkaline stripping phases listed in Table 2 result any detectable traces of back-extracted analyte. However, by adjusting of a more pronounced pH-gradient between feed and strip phase remarkable transport effects were obtained for Diclofenac as Figure 5 demonstrates.

### Transport of Carbamazepine

In order to utilize the weak base character of Carbamazepine ( $pK_a = 13.94$ ) the membrane solvents used (Table 3) were modified by the liquid cation exchanger OcSA [7]. The highest efficiency of the carrier was achieved in the decan-decanol mixture. However, compared to the transport of Diclofenac (Figure 4) the course of forward-extraction of Carbamazepine is retarded. The extent of loading of the ether based membranes was always low.

It was found that the influence of feed acidity is small as the rates of extraction from 0.1 mol/dm<sup>3</sup> HCl are quite equal to those determined from water. However, rate and yield of stripping from the loaded decane/decanol membrane phase (Tab. 3: No. 1) by dilute sodium hydroxide solution can be increased up to ~20% (4 h) when the aqueous feed is acidified.

**Table 3. Transport of Carbamazepine: effect of membrane composition on extraction yields.**  
(Feed: 10 mg/dm<sup>3</sup> Carbamazepine in water, carrier: 0.25 g/dm<sup>3</sup> OcSA, strip phase: 0.1 mol/dm<sup>3</sup> NaOH; extraction time: 4h).

No.	Membrane phase	Carrier	Forward-extraction [%]	Back-extraction [%]
1	decane:decanol (11:1 v/v)	OcSA	73.2	11.0
2	dihexyl ether	-	31.0	20.3
3	dihexyl ether	OcSA	36.6	16.3

It was found that the influence of feed acidity is small as the rates of extraction from 0.1 mol/dm<sup>3</sup> HCl are quite equal to those determined from water. However, rate and yield of stripping from the loaded decane/decanol membrane phase (Table 3: No. 1) by dilute sodium hydroxide solution can be increased up to ~20% (4 h) when the aqueous feed is acidified.

### Transport of Sulfamethoxazol

Because Sulfamethoxazol, a highly water-soluble drug, contains both acidic and weak basic groups ( $pK_{a1} = 2$ ,  $pK_{a2} = 5.7$ ) transport facilitating interactions with acidic and basic carrier compounds may be possible [8]. In general, the extractability of the polar compound is poor. E. g., employing OcSA dissolved in dihexyl ether the maximum extraction yield obtained was only 13% (for comparison without acidic carrier: 5%, in decane-decanol (11:1 v/v) with OcSA: 3%). Under these conditions the extent of back-extraction by 0.1 mol/dm<sup>3</sup> NaOH was also negligible (< 3%). In contrast with Carbamazepine, Sulfamethoxazol was extracted less effectively into the liquid membrane.

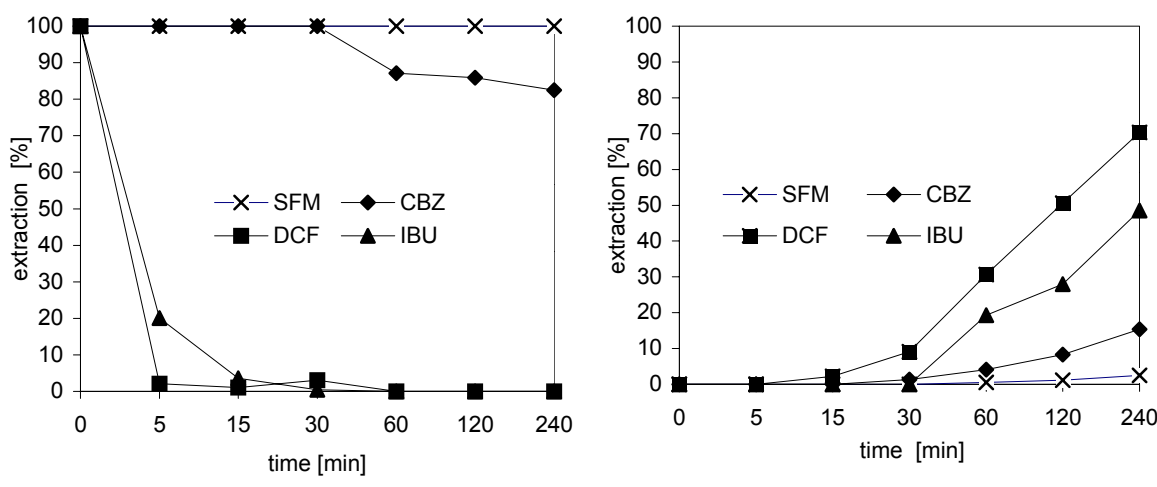


**Figure 5: Transport of a drug mixture a) forward-extraction b) back-extraction.**  
(Feed phase: 10 mg/dm<sup>3</sup> of each drug in 0.1 mol/dm<sup>3</sup> HCl, membrane phase: 0.25 g/dm<sup>3</sup> OcSA in DHE; strip phase: 0.1 mol/dm<sup>3</sup> Na<sub>2</sub>CO<sub>3</sub>).

The results were improved by using TOA dissolved in decane-decanol (8 : 2 v/v) as the membrane, thus the yield of extraction could be raised to 29 %. In the alkaline strip liquor small amounts of the sulfonamide (~ 5%, 4h) were detected which were partly re-extracted after an extended time of reaction.

### **Simultaneous Transport of Drug Mixtures**

Based on the results described some three-phase membrane systems were selected for application to the transport of drug mixtures. Figure 5 reveals that the carrier mediated system based on OcSA and dihexyl ether enables the simultaneous and complete separation of Ibuprofen and Diclofenac from the acidic aqueous feed while the extractability of Sulfamethoxazol and Carbamazepin is negligible. It is striking that the extracted carboxylic acids can be stripped to a large extent by means of sodium carbonate solution.

Complementary experiments realized that the combined drugs permeate simultaneously but with different rates, however, through *biological flat sheet membranes* (e.g., the small intestine of sheep or the internal membrane of the appendix of cattle, both preconditioned by a special treatment).

### **CONCLUSIONS**

Certain types of three-phase bulk membranes employed offer a tool to separate selectively and efficiently various acidic and basic drug traces from aqueous solution. Most efficiently the carboxylic acids Ibuprofen and Diclofenac were extracted from neutral aqueous feed by combining amine based carriers and 1-decanol as the appropriate solvent. Also octane-1-sulfonic acid dissolved in dihexyl ether separates both drugs from acidic feed and makes stripping possible by alkaline liquor. This membrane phase also enables the enhanced forward-extraction of the weak base Carbamazepin from aqueous solution. In general, the extractability of Sulfamethoxazol in presence of acidic or basic carriers compound is rather restricted. The stripping of drugs from the loaded bulk-membranes by means of alkaline or acidic reagents show some differences that can be attributed to their different acid/base-behaviour.

The investigations aiming for sample preparation techniques in environmental analysis are continued including main metabolites of the drugs in order to optimize the membrane compositions and, thus their efficiency and selectivity. Developments of membrane systems based on supported liquid membranes and also solid natural and synthetic membranes are in progress.

### **ACKNOWLEDGEMENTS**

Financial support of the Environment Ministry of North Rhine-Westphalia, Germany (Minsterium für Umwelt und Naturschutz, Landwirtschaft und Verbraucherschutz NRW) is gratefully acknowledged.

### **REFERENCES**

1. E. Möhle, S. Horvath, W. Merz and J. W. Metzger (1999), *Vom Wasser*, **92**, 207-223.
2. G. Nilve, M. Knutsson and J. A. Jönsson (1994), *J. Chromatogr.*, **688**, 75-82.
3. Y. Shen, L. Grönberg, J. A. Jönsson (1994), *Anal. Chim. Acta*, **292**, 31-39.
4. R. C. Martinez, E. R. Gonzalo, E. H. Fernandez and J. H. Mendez (1994), *Anal. Chim. Acta*, **304**, 323-332.
5. J. Namieśnik, T. Górecki (2000), *LC.GC Europe*, September 2000, 678-683.
6. M. Sanchez Loredo (1996), PhD Thesis, University of Paderborn, Germany.
7. ACD-Physico-Chemical Laboratory, [Internet]. Available from [http://www.acdlabs.com/products/phys\\_chem\\_lab/pka/exp.html](http://www.acdlabs.com/products/phys_chem_lab/pka/exp.html). [Accessed 21.05.2001].
8. M. J. B. Mengelers, M. B. M. Oorsprong, H. A. Kuiper, M. M. L. Aerts, E. R. Van Gogh and A. S. J. p. A. M. Van Miert (1989), *J. Pharm. Biomed. Anal.*, **7**, 1765-1776.



## SELECTIVITY IN THE EXTRACTION OF CARBOXYLIC ACIDS BY AMINE-BASED EXTRACTANTS

Aharon M. Eyal, Betty Hazan, Riki Canari, Asher Vitner and Tali Reuveny

Casali Institute of Applied Chemistry, The Hebrew University of Jerusalem, Jerusalem, Israel

The selectivity of extraction from a solution containing both succinic and propionic acid by tertiary amine-based extractants was examined. The distribution coefficients for propionic acid at 30°C and 75 °C are about 2 and 0.94, while those for succinic are about 0.5 and 0.12, respectively. These values are true for all of the mixtures except for the case where the succinic acid level is the highest.  $K_{75C}$  for propionic acid is significantly lower,  $K = 0.71$ , and that of succinic acid is slightly higher,  $K = 0.15$ . The mutual influence of the addition of one acid to the extraction system of another was analyzed.

### INTRODUCTION

Fermentation broth solutions, like those in carboxylic acid production, are characterized by a large amount of various impurities. The most difficult impurities to separate from the product are other carboxylic acids, produced by the microorganisms or introduced with the nutrients. Hence, the selectivity in extraction of acids from aqueous solutions containing their mixture is an important issue. Only a few publications have dealt with the selectivity of extraction from a mixture of acids. Jagirdar and Sharma [1] studied the selectivity of extracting carboxylic acids by tri-n-octylamine in xylene (and in 2-ethyl-hexanol). Selectivity values (for the stronger acid) in the case of a mixture containing acetic and monochloroacetic acid were found to be in the range of 23.2 to 37.8; for monochloroacetic + dichloroacetic acid, 4 to 6.7; for dichloroacetic + trichloroacetic acid, 15.3 to 16.8; for formic + oxalic acid, 9.2 to 9.5, and for glycolic and oxalic acid, 2.3 to 4.8. Jagirdar and Sharma's conclusion was that the technique of "dissociation extraction" proposed by Anwar *et al.* [2,3] can be successfully adopted to separate dilute aqueous mixtures of organic acids. Anwar *et al.* used the dissociation extraction technique to selectively separate a stronger acid from a mixture of two acids present in an organic solvent by adding an aqueous medium containing a stoichiometric deficiency of a strong base. In their articles, they explain the advantage of using this technique in industry, and give a long list of examples for mixtures made up of two acids or two bases which can be separated successfully with the dissociation extraction technique.

Kirsch and Maurer [4] studied the distribution of citric, acetic and oxalic acids between their binary aqueous mixtures and an organic solution of tri-n-octylamine in a diluent. They found that when there is an excess of a carboxylic group in the feed over the amine, the stronger acid is preferably extracted. Moreover, based on a model which they developed for a single acid extraction, they calculated the extraction of citric and oxalic acid and found it to be in reasonable agreement with the experimental results. However, when acetic acid is one of the extracted acids, the extraction results are higher than predicted. They assumed that the higher extraction is a result of "mixed complexes" formation, *i.e.*, acetic acid molecules bind to an ion-pair of the stronger acid.

Malmary *et al.* [5] studied the extraction of tartaric and malic acids from their binary aqueous solution at several pH values. The extractants were tributylphosphate (TBP) in dodecane and triisooctylamine (TOA) in 1-octanol. They found that the weaker extractant (TBP) selectively extracts the weaker acid (malic acid) and that the amine-based extractant preferably extracts the stronger acid (tartaric acid). Their explanation was that TBP binds the undissociated acid, preferring, therefore, the weakest acid in the mixture. In the case of amine-based extractant, an ion exchange reaction take place so that the stronger acid is preferred.

The present paper adds to research done in our laboratory [6]. The selectivity of extraction from a solution containing both succinic acid and propionic acid was examined and compared with the extraction from their separate solutions.

## MATERIALS AND METHODS

### Materials

The extractant used was 0.5 mol/kg trilauryl amine - Alamine 304 (Henkel, 95%) + 10% 1-octanol (Merck, 99%) in a low aromatics kerosene, Isopar K (Exxon). The acids used were: propionic acid (BDH, 99%) and succinic acid (BDH, Analytical grade).

### Methods

2.5 g aliquots of the organic phase were mixed at 25°C for 30 min with 1 g aliquots of aqueous phases containing various concentrations of the carboxylic acids. The organic and aqueous phases were separated and centrifuged. The organic phases were washed with 1 N NaOH solution. The wash solutions and the aqueous phases were injected to the HPLC at 42°C where the column was Polyspher<sup>R</sup> OA KC (Merck), the mobile phase was 0.01 N H<sub>2</sub>SO<sub>4</sub> and the flow rate was 0.4 ml/min.

## RESULTS

Figure 1 shows the distribution of succinic acid at 30°C between the aqueous phase and the extractant, which contains 0, 0.01, 0.04 or 0.3 mol/kg propionic acid at equilibrium. In addition, it shows the distribution of succinic acid at 75°C where the organic phase contains 0 or 0.3 mol/kg propionic acid at equilibrium. This figure shows that the presence of the propionic acid in the system, up to 0.3 mol/kg in the organic phase, does not affect the distribution of succinic acid at both temperatures.

Figure 2 shows the distribution of propionic acid at 30°C in the presence of various concentrations of succinic acid (0.34 -1.3 mol/kg succinic acid in the aqueous phase and 0.17 - 0.65 mol/kg in the organic phase). It also shows the distribution of propionic acid at 75°C in systems where the succinic acid concentrations in the phases were 0.88 - 5.2 mol/kg in the aqueous phase and 0.1 - 0.78 mol/kg in the organic phase. Table 1 summarizes the data presented in Figure 2 (except for propionic acid distribution in the absence of succinic acid), as well as the calculated distribution coefficients ( $K = [acid]_{org}/[acid]_{aq}$ ) and the selectivity to propionic acid ( $K_{propionic}/K_{succinic}$ ).

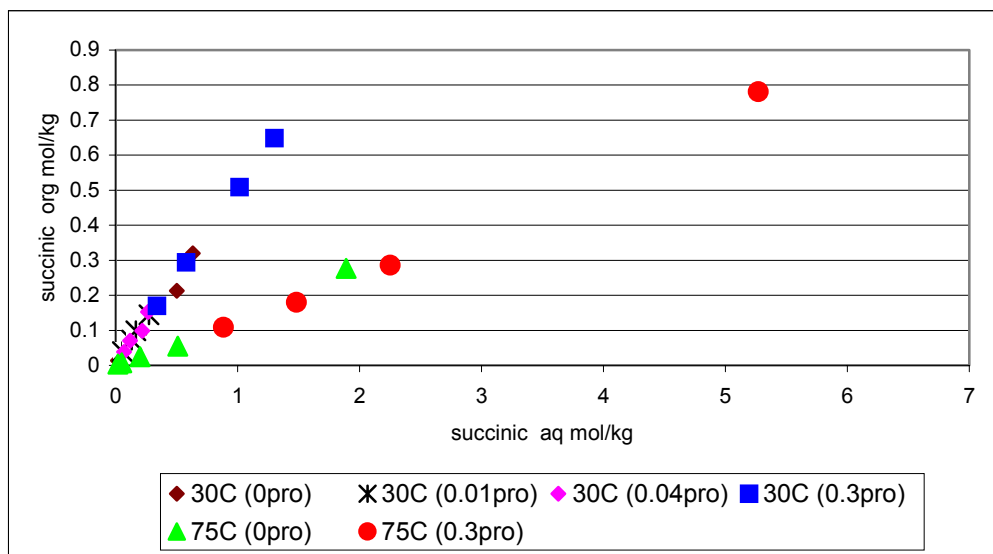


Figure 1. Extraction of succinic with or without propionic acid by Alamine 304 + 10% 1-octanol in kerosene.

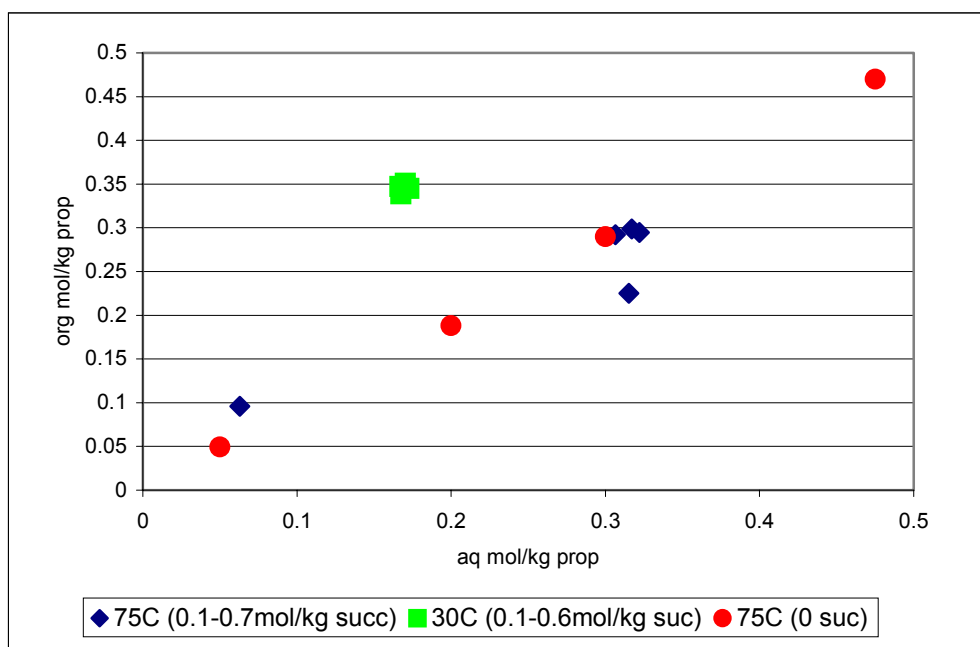


Figure 2. Extraction of propionic with or without succinic acid by Alamine 304 + 10% 1-octanol in kerosene.

Figure 2 and Table 1 show that:

1. The values of the distribution coefficients ( $K$ ) for propionic acid extraction at 30°C are about 2, while those for succinic acid at that temperature are about 0.5.
2. The  $K$  values of propionic acid at 75°C are about 0.94 and those for succinic acid at that temperature are about 0.12. These values are true for all of the cases except for the case where the succinic acid level in the system is the highest.
3. In that case (Exp. 4, 75°C, 0.78 and 5.27 mol/Kg succinic acid in the aqueous and organic phase, respectively) the propionic acid extraction is significantly lower,  $K = 0.71$  (compared with 0.94), and that of succinic acid is a slightly higher,  $K = 0.15$  (compared with 0.12).
4. Selectivity to propionic acid is about 4.0 at the lower temperature and about 7.6 at the higher one, except for case of the highest succinic acid level where it is 4.8.

*Table 1. Extraction of succinic and propionic acid by Alamine 304+ 10% 1-octanol in kerosene.*

75°C							
Exp.	Propionic acid mol/kg		Succinic acid mol/kg		K (org/aq)		S (Kpr/Ksuc) to propionic
No.	Aqueous	Organic	Aqueous	Organic	Propionic	Succinic	
1	0.322	0.295	0.88	0.108	0.92	0.12	7.47
2	0.317	0.299	1.48	0.180	0.94	0.12	7.74
3	0.306	0.292	2.25	0.286	0.95	0.13	7.51
4	0.315	0.225	5.27	0.781	0.71	0.15	4.82

30°C							
Exp.	Propionic acid mol/kg		Succinic acid mol/kg		K (org/aq)		S (Kpr/Ksuc) to propionic
No.	Aqueous	Organic	Aqueous	Organic	Propionic	Succinic	
5	0.167	0.348	0.340	0.170	2.1	0.50	4.17
6	0.170	0.351	0.58	0.294	2.1	0.51	4.05
7	0.167	0.339	1.01	0.509	2.0	0.50	4.04
8	0.173	0.345	1.30	0.649	2.0	0.50	4.01

## DISCUSSION

### Propionic Acid Extraction

The extraction of propionic acid by tertiary amine-containing extractants was examined in the past in our laboratory [7]. The IR spectrum of the loaded organic phase (where the amine:propionic acid molar ratio was 2:1) showed a large peak that refers to the undissociated acid (at about  $1720\text{ cm}^{-1}$ ). This result indicates that, although free amine molecules were present in the organic phase, ion pair formation is not the dominant mechanism and that the acid is preferably extracted through H-bond and/or dipole-dipole interactions in the organic phase. This conclusion was supported by the results of Yang and his co-workers [8] who found that propionic acid extraction by 100% Alamine 336 is similar to its extraction by 100% 2-octanol. The results presented here show that although the propionic acid is preferably extracted through H-bond or/and dipole-dipole interactions in the organic phase, its distribution constants are high,  $K(30^\circ\text{C}) \sim 2$ . This high distribution is due to its hydrophobic properties.

### Succinic Acid Extraction

The pH of half neutralization with HCl ( $\text{pH}_{\text{hn}(\text{cl})}$ ) of extractants containing the tertiary amine and low octanol content was determined to be about 4.5 [7]. Based on our conclusions (in the same publication), in a case where the  $\text{pH}_{\text{hn}}$  is higher than the  $\text{pK}_{\text{a}1}$  of the acid, ion pair formation will take place preferably over H-bond or/and dipole-dipole interactions. This is also true for the present case, since the  $\text{pK}_{\text{a}1}$  of succinic acid is 4.2 and since that acid is quite hydrophilic. Yet, since succinic acid is a relatively weak acid, its distribution constants, as found here, are relatively low -  $K(30^\circ\text{C}) \sim 0.5$ .

### Selectivity

In those cases where the presence of one acid does not affect the extraction of the other, the selectivity of extraction from a two-acids solution is equal to the ratio of their distribution constants in single-acid systems. That is the case in most of the extraction systems tested here and, as a result, the extraction is selective for the propionic acid ( $S(\text{propionic } 30^\circ\text{C}) \sim 7.6$ ).

### Mutual Influence

Adding an acid (II) to an extraction system of another acid (I) may affect both phases in various ways (see Table 2). The acids may compete with each other for their interaction with the amine and, as a result, the extraction of acid (I) will decrease. On the other hand, the extraction of acid (I) may increase since the organic phase hydrophilicity increases by the

addition of acid (II). In this case, acid (II) may act as a polar diluent (enhancer) in the system. Still another possible effect in the organic phase is increasing the above-stoichiometric extraction. Tamada *et al.* [9] showed that, in the case of propionic acid extraction by trioctylamine, the above-stoichiometric extraction is energetically favored over the stoichiometric extraction,  $K_{(1,1)} < K_{(2,1)}$  (where  $K_{(1,1)}$ ,  $K_{(2,1)}$  are the association constants for the stepwise reaction of 1:1 and 2:1 acid to amine in the organic phase). Thus, addition of another acid in the case of propionic acid extraction may increase the propionic extraction.

*Table 2. The effects of the adding acid (II) into solutions containing acid (I).*

	The effects of the adding acid (II) into solutions containing acid (I)	The effect on extraction of acid (I)
1	<b>Organic phase</b> Competition for the interaction with the amine	decrease
2	Increasing the hydrophilicity of the organic phase	increase
3	Increasing the over-stoichiometric extraction	increase
4	<b>Aqueous phase</b> decreasing the hydrophilicity of the aqueous phase	decrease
5	Salting out- reducing water activity	increase
6	Reducing the pH	increase

The addition of acid (II) at high concentrations also affects the properties of the aqueous phase. This addition decreases the hydrophilicity of that phase and thereby increases the interaction of organic acid (I) there. As a result, the extraction of acid (I) is expected to decrease. On the other hand, salting out affects the extraction in the opposite direction. Water molecules of hydration of acid (II) release acid (I) to transfer into the organic phase, increasing, thereby, the extraction of acid (I). Another effect may be on the pH of the aqueous phase. Harris and Geankoplis [10] showed that addition of sulfuric acid increases the propionic acid extraction by methylisobutyl ketone. Kertes and King [11] explained the increase by the suppressing of the dissociation of the weak carboxylic acid due to the pH decrease. In each extraction system, all these effects apply simultaneously. The net effect on the extraction is determined by the relative contribution of each effect.

The results here show that, in the system where the succinic acid concentration was the highest, propionic acid extraction was significantly lowered,  $K = 0.71$  (compared with 0.94), and that of succinic acid was slightly increased,  $K = 0.15$  (compared with 0.12). Therefore, the dominant effects in the case of propionic acid may be analyzed based on Table 2. The only two effects resulting in decrease of the extraction are No. 1 and 4: competition for the interaction with the amine and increase of the aqueous phase hydrophobicity. Which of these effects dominate our system? Based on the extraction mechanism of propionic acid, the first does not seem to be the main one since the propionic acid is preferably extracted through H-bond or/and dipole-dipole interactions and not through ion pair formation (see above). Moreover, the succinic acid loading in the organic phase at 30°C was very close to that at 75°C. Therefore, one would expect that, if the competition was the main effect, the same tendency of decrease in the propionic acid extraction would be seen. By elimination, in our case the main effect seems to be the increase of the aqueous phase hydrophobicity. One should keep in mind that at 75°C the acid solubility in the aqueous phase is extremely high and, that in the case discussed here, the succinic acid concentration in the aqueous phase was 5.27 mol/kg which is about 62%. A simple calculation shows that the concentration of the water in this aqueous phase is about 20 mol/kg (100% - 62% (succinic) - 2% (propionic)/18) and that of the carboxylic groups is about 11 equivalent COOH groups per kg aqueous solution (5.27 (succinic) \* 2 + 0.3 (propionic)). In this case, the molar ratio is less than two water molecules per one carboxylic group, which is a relatively hydrophobic medium.

## REFERENCES

1. G. C. Jagirdar and M. M. Sharma (1980), *J. Sep. Proc. Technol.*, **1** (2), 40.
2. M. M. Anwar, C. Hanson and M. W. T. Pratt (1971), *Trans. Instn. Chem. Engr.*, **49**, 9.
3. M. M. Anwar, C. Hanson, M. W. T. Pratt and A. N. Patel (1973), *Trans. Instn. Chem. Engr.*, **51**, 151.
4. T. Kirsch and G. Maurer (1996), *Ind. Eng. Chem. Res.*, **35**, 1722.
5. G. Malmay, A. Vezier, A. Robert, J. Mourguès, T. Conte and J. Molinier (1994), *J. Chem. Tech. Biotechnol.*, **60**, 67.
6. R. Canari and A. M. Eyal (2001), *Ind. Eng. Chem. Res.*, in press.
7. R. Canari and A. M. Eyal (2001), *Ind. Eng. Chem. Res.*, in press.
8. S. T. Yang, S. A. White and S. T. Haso (1991), *Ind. Eng. Chem. Res.*, **30**, 1335.
9. J. A. Tamada, A. S. Kertes and C. J. King (1990), *Ind. Eng. Chem. Res.*, **29**, 1319.
10. R. D. Harris and C. J. Geankoplis (1962), *J. Chem. Eng. Data*, **7**, 218.
11. A. S. Kertes and C. J. King (1986), *Biotechnol. Bioeng.*, **XXVIII**, 269.



# OPTIMISATION OF PROCESS CONDITIONS FOR INDUSTRIAL SEPARATION OF AMINO ACID ENANTIOMERS BY FRACTIONAL REACTIVE EXTRACTION

Maartje Steensma, Norbert J.M. Kuipers, André B. de Haan and Gerard Kwant\*

University of Twente, Enschede, The Netherlands  
\*DSM Research, Geleen, The Netherlands

The influence of process parameters on the chiral separation of amino acids by reactive extraction has been investigated experimentally. Compared to literature results for this separation, the process capacity can be increased substantially without much effect on the separation factor by increasing the concentration level of enantiomer and limiting the excess of extractant to a minimum. A slightly higher temperature, a pH of 6 and a polar solvent also have a positive effect on the process capacity. The separation factor could not be optimised much further. Careful selection of process conditions results in a potential productivity increase of 10-50 times.

## INTRODUCTION

In the life science industry, there is an increasing demand for optically pure substances. Direct synthesis of the pure enantiomers is desirable, but often impossible or difficult. As the current chiral resolution methods are either inflexible or not suitable for large-scale production, there is a need for a flexible industrial-scale chiral separation method. On lab scale, reactive fractional extraction has been shown to be a promising concept, but the productivity is yet far too low for commercial production [1-4]. From these studies, it has become clear that temperature, pH and solvent are important in process design, and it can be expected that concentration ratios and absolute concentrations of enantiomer and extractant also play an important role. Systematic study of the influence of these process parameters is therefore necessary for further development of this technique.

The aim of the current study is to determine experimentally the influence of parameter changes (concentrations, pH, temperature, and solvent composition) on selectivity and capacity in a single extraction step. The results can subsequently be used in process development and may be helpful in screening of new extractants for chiral separations. It will be shown that optimisation of process conditions results in a much more productive process.

The extraction operation proposed for this separation is fractional extraction. In this scheme, a stripping section and an additional wash section are present. In this way, two solutes can be separated completely from each other, so both enantiomers can be obtained at the desired purity. For low concentrations, the fractional extractor can be described with two Kremser equations [5], one for each section, and a feed stage mass balance. This model has been used to assess the influence of selectivity and process parameters on the number of stages and solvent requirements. A model valid for higher concentrations is under development.

## THEORY

The enantiomers to be separated are racemic amino acids and racemic amino alcohols. For the initial part of the study, the amino acid model system also reported by other authors was used: separation of leucine enantiomers with the copper(II) complex of N-dodecyl-L-hydroxyproline ( $C_{12}$ -Hyp, or 'HL') in systems of water and an organic solvent [3,4,6]. The copper complex which serves as enantioselective extractant consists of two chiral ligands 'HL' and a copper(II) ion (eq. 1. The overbar denotes organic-phase species). The ligands and the complex remain in the organic phase due to the long alkyl tail on the ligand [4,6]:



The separation mechanism is usually described as a reversible ligand-exchange mechanism. One of the organic ligands is exchanged for an amino acid enantiomer ( $HAA^+$  or  $HAA^-$ ) resulting in a mixed-ligand complex. In formula:



Enantioselectivity is obtained if one reaction equilibrium constant is larger than the other. The leucine enantiomers also partition between the aqueous and the organic phase. This is a physical, non-selective process, represented by a partition ratio  $P$ , which may vary with solvent composition and temperature. The total amount of extracted leucine by both mechanisms is characterised by the distribution ratio  $D$ .

In general, a fair number of other complex species may be present in the liquid phases and the complexation constants for reactions (2) and (3) cannot be determined easily. Under certain circumstances, namely at a large extractant/enantiomer ratio, a large ligand/copper ratio and a phase ratio of unity, free ligand HL is present (eqn. 1), no copper is left in the aqueous phase and virtually all copper in the organic phase is present in the form of  $CuL_2$ . In this situation, the distribution ratio for each HAA enantiomer can be expressed as [4,6]:

$$D = \frac{[\overline{HAA}] + [\overline{AACuL}]}{[\overline{HAA}]} = P(1 + R \cdot K) \quad (4)$$

The value of  $K$  can be obtained from a plot of  $D$  versus  $R$  ( $R < 0.5$ ). The partition ratio  $P$ , reaction equilibrium constant  $K$  and an additional variable  $R$  are defined as:

$$K_{AA} = \frac{[\overline{AACuL}][\overline{HL}]}{[\overline{HAA}][\overline{CuL_2}]} \quad P = \frac{[\overline{HAA}]}{[\overline{HAA}]} \quad \text{and} \quad R = \frac{[\overline{Cu}]_{total}}{[\overline{HL}]_0 - 2[\overline{Cu}]_{total}} \quad (5)$$

$[\overline{Cu}]_{total}$  denotes the total copper concentration, in all forms. The separation factor  $\alpha$  is the ratio of the distribution ratios for both enantiomers. The upper limit of this separation factor is the intrinsic selectivity  $\alpha_{int}$ , which equals the ratio of the reaction equilibrium constants. It is approached if only the enantioselective complexation process determines the total extraction.

## EXPERIMENTAL METHODS

The chiral ligands N-dodecyl-L-hydroxyproline ( $C_{12}$ -Hyp) and N-octyl-L-hydroxyproline ( $C_8$ -Hyp) were synthesised from dodecanal (98%, Merck) or octanal (99%, Acros) and L-hydroxyproline (99%, Fluka) according to a slightly adapted method from Takeuchi [6]. All other reagents were also obtained from Fluka or Merck. Distribution ratios were determined from equilibrium measurements. The aqueous solution was prepared by dissolving copper(II) acetate ( $Cu(Ac)_2$ ), sodium acetate ( $NaAc$ ) and DL-leucine in Q2-filtered water (Millipore) that was presaturated with the organic solvent to obtain a 0.2 M  $Ac^-$  solution with  $[\overline{Cu^{2+}}]_0$  ranging from 2.5-50 mM and  $[\overline{DL\text{-leucine}}]_0$  from 0-10 mM. The organic phase was prepared by

dissolving the chiral ligand C<sub>12</sub>-Hyp (0-100 mM) in the appropriate organic solvent, butanol or butanol/hexane, presaturated with water. The equilibrium measurements were carried out in jacketed 25-ml vessels at a constant temperature. 10 ml of both phases were mixed for 1-3 hrs with a magnetic stirrer to reach equilibrium and allowed to settle. Samples were taken from the aqueous phase with a syringe via a septum and analysed by HPLC. In initial experiments, the closure of the mass balance was confirmed. The HPLC set-up consisted of a Crownpak (+) chiral column (Daicel), post-column derivatisation with OPA/MCE reagent and fluorescence detection [7]. The Cu(II) concentrations in some of the aqueous samples were determined by AAS (Solaar 939, Unicam). The pH of the aqueous phase was determined at equilibrium (Inolab pH level 1, WTW) and was always between 5.5 and 6.

## RESULTS

### Influence of Copper Concentration

From the copper-ligand reaction combined with the ligand-exchange reaction, one may expect that an excess of copper ( $[Cu^{2+}]_0 > 0.5 [HL]_0$ ) will result in a very low free ligand concentration  $[HL]$ . Thus, the enantioselective equilibria are shifted to the right, resulting in formation of more mixed-ligand complexes. However, Takeuchi [1] showed for valine that the optimum copper concentration is  $[Cu^{2+}]_0 = 0.5 [HL]_0$ . From the experimental results in Figure 1, the same conclusion is obtained for DL-leucine: an excess of copper (copper present in the aqueous phase) causes a decrease in the distribution ratios and the separation factor. No straightforward explanation for this phenomenon has been found. Other complex species will have to be considered. All further experiments were carried out at the 'stoichiometric' copper concentration, except those for the determination of the complexation constant.

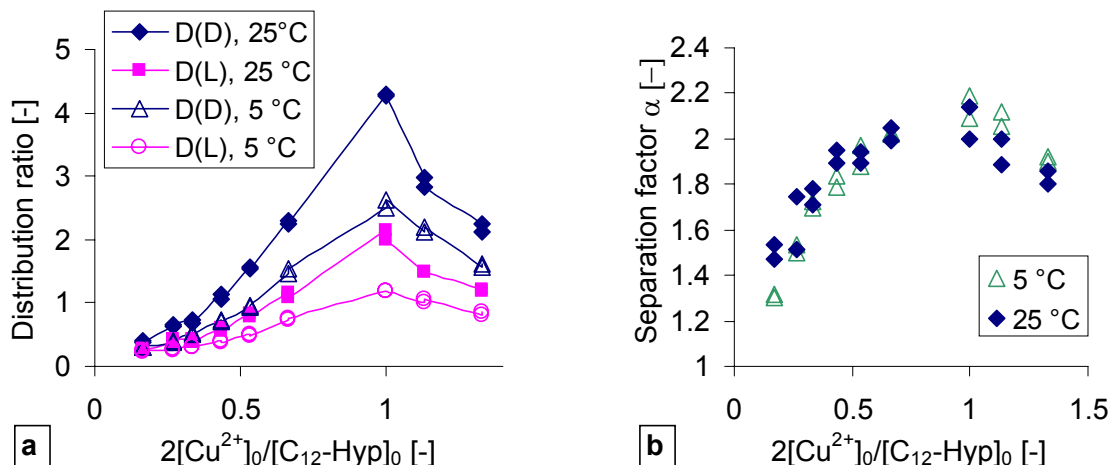


Figure 1. Influence of  $[Cu^{2+}]_0$  on (a) distribution ratio and (b) separation factor of DL-leucine. 5 and 25°C, butanol/water,  $[C_{12}\text{-Hyp}]_0 = 30 \text{ mM}$ ,  $[DL\text{-leucine}]_0 = 1 \text{ mM}$ ,  $[Cu^{2+}]_0 = 2.5\text{-}20 \text{ mM}$ .

### Influence of Excess Extractant and Concentration Level

In most studies reported so far, the enantioselective extraction has been investigated at a very large excess of extractant with respect to the enantiomers. This way of operation is not very economical and probably unnecessary. A series of experiments at constant enantiomer concentration and increasing chiral ligand concentration ( $[HL]_0$ ), with  $[Cu^{2+}]_0 = 0.5 [HL]_0$ , has been carried out. Figure 2a shows that there is no significant increase in D or  $\alpha$  once the excess extractant is large enough, i.e.  $[CuL_2]_0/[leucine]_0 > 3$ . Therefore, the large excess extractant (10-50) used by a number of authors [3,6] is not necessary.

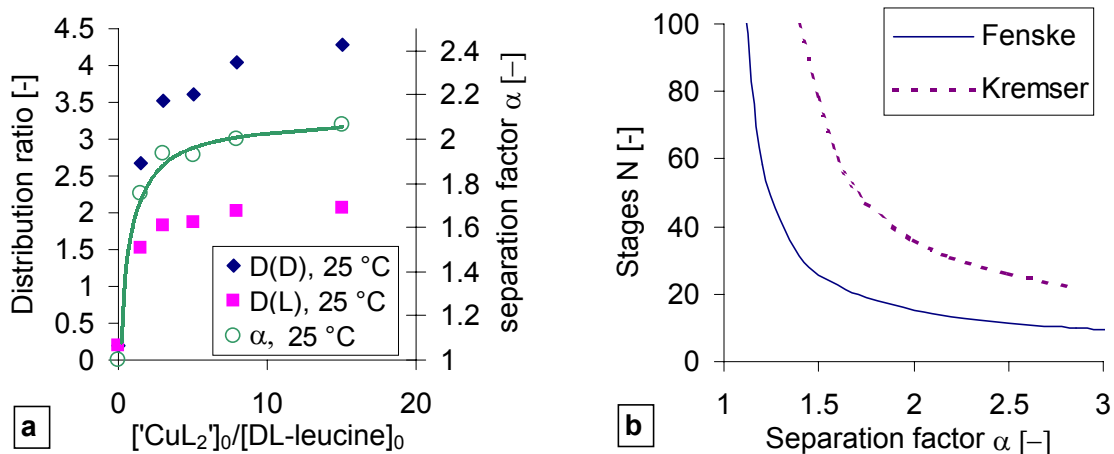


Figure 2. (a) Influence of excess extractant on  $D$  and  $\alpha$  at 25 °C; water/butanol,  $[DL\text{-leucine}]_0 = 1 \text{ mM}$ ,  $[C_{12}\text{-Hyp}] = 0\text{-}30 \text{ mM}$ ,  $[Cu^{2+}] = 0\text{-}15 \text{ mM}$  (stoichiometric) (b) Influence of  $\alpha$  on minimum number of stages, predictions by Fenske and Kremser equation [5], 99% purity.

Secondly, many studies are carried out at very low enantiomer concentrations (down to 0.1 mM). Higher concentrations of all components will increase the process capacity. The upper limit is the solubility. In our system, the leucine solubility decreases from > 50 mM in water to about 10 mM in 0.1 M Cu(Ac)<sub>2</sub>. Using less concentrated buffer solutions may partially prevent this. The ligand solubility varies with the solvent and the nature of the organic tail. In butanol, the solubility at 25 °C is about 0.1 M for C<sub>12</sub>-Hyp and 0.5 M for C<sub>8</sub>-Hyp. As expected, it can be concluded from the experimental data in Table 1 that a higher absolute concentration results in an almost unchanged separation factor but higher distribution ratios. Thus, a concentration level 10 times higher results in a process capacity 13-14 times higher.

Table 1. Influence of absolute concentrations (constant ratios), 25 °C, water/butanol.

$[leucine]_0 \text{ [mM]}$	$[Cu^{2+}]_0 \text{ [mM]}$	$[C_{12}\text{-Hyp}]_0 \text{ [mM]}$	$D(D) \text{ [-]}$	$D(L) \text{ [-]}$	$\alpha \text{ [-]}$
1	5	10	3.6	1.9	1.9
5	25	50	4.4	2.3	1.9
10	50	100	5.2	2.7	1.95

### Influence of Temperature

For chiral recognition systems, the enantioselectivity often increases with decreasing temperature [8,9]. Abe reports for a different system a decrease in  $D$  with increasing temperature [8].  $D$  and  $\alpha$  were determined at four temperatures at fixed concentrations (Table 2). Secondly, two data series were used to estimate  $K$  and  $P$  according to the 'R-method' (theory section). As expected,  $\alpha_{int}$  is slightly higher at the lower temperature.  $P$  varies slightly, but its value is small compared to the overall distribution ratios. At higher temperature,  $K$  and  $D$  for both enantiomers are higher. This is in contrast with the trend in Abe's results.

Table 2. Influence of temperature on leucine separation, water /butanol.

$D$  and  $\alpha$ :  $[leucine]_0 = 1 \text{ mM}$ ,  $[Cu^{2+}]_0 = 15 \text{ mM}$ ,  $[C_{12}\text{-Hyp}]_0 = 30 \text{ mM}$   
 $K$  and  $P$ :  $[leucine]_0 = 1 \text{ mM}$ ,  $[Cu^{2+}]_0 = 0\text{-}8 \text{ mM}$ ,  $[C_{12}\text{-Hyp}]_0 = 30 \text{ mM}$

	$D(D) \text{ [-]}$	$D(L) \text{ [-]}$	$\alpha \text{ [-]}$	$K_D \text{ [-]}$	$K_L \text{ [-]}$	$\alpha_{int}=K_D/K_L \text{ [-]}$	$P \text{ [-]}$
5 °C	2.6	1.2	2.1	7.9	3.3	2.35	0.17
25 °C	4.3	2.1	2.1	16.2	7.5	2.17	0.15
25 °C [5]				10.1	4.0	2.5	0.21
35 °C	5.0	2.5	2.0				
45 °C	5.9	2.9	2.0				

### Influence of pH

The pH has a complex influence on the performance of this process. From literature, it can be concluded that copper extraction by ligand L is favoured by a higher pH ( $> 5.5$ ) [4] and that the distribution ratios increase about five times when the pH increases from 4 to 6, but  $\alpha$  is not severely affected [1,3]. Therefore, all experiments were carried out at pH = 5.5-6. No further experiments at different pH values were performed at this stage.

### Influence of the Solvent

In the literature, several organic solvents and solvent mixtures have been applied. The solvent influences the solubility of all solutes, the partition ratios and possibly the reaction by acting as a ligand itself. It is reported that all solubilities are lower and the partition ratio is lower in a less polar solvent [4,6]. As an illustration, experimental results with two solvent mixtures are represented in Table 3. It can be seen that the separation factors are similar, but that the distribution ratio is lowered considerably in a less polar solvent mixture.

Table 3. Influence of solvent, 25 °C, [leu] = 1 mM,  $[Cu^{2+}] = 1.5\text{-}15 \text{ mM}$ ,  $[C_{12}\text{-Hyp}] = 3\text{-}30 \text{ mM}$ .

$[Cu^{2+}]_0 \text{ [mM] in 4:1 butanol/hexane}$	D(D) [-]	D(L) [-]	$\alpha$ [-]	$[Cu^{2+}]_0 \text{ [mM] in butanol}$	D(D) [-]	D(L) [-]	$\alpha$ [-]
1.5	1.6	0.9	1.7	1.5	2.7	1.5	1.75
5	2.9	1.5	1.9	5	3.6	1.9	1.9
15	3.1	1.5	2.0	15	4.3	2.1	2.05

### Reaction Kinetics

Preliminary time-dependent measurements were carried out in the equilibrium vessels in a totally dispersed system by interrupting the stirring movement at chosen intervals. It was observed that in some cases the equilibrium was approached more quickly at 25 °C than at 5 °C. This result indicates that reaction kinetics may be rate-limiting in this process, especially at low temperature. This deserves further investigation. For this purpose, a stirred cell of the adapted Lewis-type with constant interfacial area has been constructed.

## OPPORTUNITIES FOR OPTIMISATION & CONCLUSION

The focus of chiral extraction research in the past has been mostly on improving the separation factor and on designing lab-scale and pilot-scale extractors. For an industrial application, increasing the capacity without decreasing the selectivity is the most important issue. From previous studies, it is known that selectivities for chiral separations are usually below 2. From the Kremser model or the Fenske equation [5], the influence of the separation factor on the number of stages can be estimated (Figure 2b). For  $\alpha > 2$ , small changes in  $\alpha$  have a much smaller effect on the number of stages than if  $\alpha < 2$ . So, it is unwise to spend much effort on raising  $\alpha$  slightly if  $\alpha$  is already larger than 2. For the current model system at 25 °C, it can be concluded from Figure 2a that using an excess extractant [ $CuL_2$ ] larger than three is not justified. Accordingly, the process should not be carried out at 5 °C but at 25° or higher temperatures because the larger distribution ratios and the faster extraction kinetics at 25 °C more than compensate for the slightly higher separation factor at 5 °C. However, a too large temperature may cause other problems, such as extractant losses.

The required solvent flow and thus the process capacity increase proportionally with the enantiomer concentration and the absolute value of the distribution ratio. Therefore, the process should be carried out at the highest concentrations possible. For the model system, the leucine solubility is limiting (<10 mM at 0.1 M  $Cu(Ac)_2$ ). The solubility of the extractant is in the range of 0.1-0.5 M, which is much higher than applied in lab-scale experiments so far, and non-limiting given the low solubility of leucine. In most of the chiral fractional extraction

studies, large wash-to-feed and solvent-to-feed ratios have been applied. This practice has several drawbacks: dilution of the feed stream results in lower distribution ratios (table 1) and a large solvent flow causes much coextraction of the undesired enantiomer, thus requiring also a large wash stream. For two representative literature cases, the effects of parameter changes on the number of theoretical stages (N), the volumetric flow rate of feed (F), solvent (S) and wash fluid (W) and on the extractant inventory (C) have been estimated for a given capacity (kg/hr DL-leucine, product purity 99%) with the Kremser model, using the experimental results from this study (Table 4). It can be seen that both the total liquid volume (thus the extractor volume) and the extractant requirements can be decreased considerably.

*Table 4. Effect of process condition changes for two literature cases.*

Case	Proposed changes	N/N <sub>0</sub>	F/F <sub>0</sub>	S/S <sub>0</sub>	W/W <sub>0</sub>	C/C <sub>0</sub>	VR <sup>1</sup>
Takeuchi [1]: butanol, pH 6	[valine] <sub>0</sub> 2.4 → 24 mM [C <sub>12</sub> Hyp] 10 → 100 mM	1	0.1	0.07	0.1	0.7	
F <sub>0</sub> = 1, S <sub>0</sub> = 10, W <sub>0</sub> = 10	4* smaller S (adjust W)	1.15	1	0.25	0.2	0.25	
	<b>Overall effect</b>	1.15	F=0.1	S=0.18	W=0.2	<b>0.18</b>	<b>38</b>
Ding [3]: octanol, pH 4	[leucine] <sub>0</sub> 4.9 → 9.8 mM [C <sub>12</sub> -Hyp] 20 → 40 mM	1	0.5	0.5	0.5	1	
F <sub>0</sub> = 1	pH → 6, switch to butanol	1.05	1	0.091	1	0.091	
S <sub>0</sub> = 40	3* smaller S (adjust W)	1.15	1	0.333	0.25	0.333	
W <sub>0</sub> = 10	<b>Overall effect</b>	1.2	F=0.5	S=0.61	W=1.25	<b>0.03</b>	<b>18</b>

<sup>1</sup>VR= total extractor Volume Reduction = [m<sup>3</sup> liquid hr<sup>-1</sup>]<sub>0</sub>·N<sub>0</sub> / [m<sup>3</sup> liquid hr<sup>-1</sup>]<sub>new</sub>·N

Concluding, fractional extraction of chiral components with copper-based extractants can be made much more efficient by working with high concentrations of enantiomers, using a stoichiometric amount of copper, working with a slight excess of extractant in a polar solvent, at a sufficiently high temperature and pH. Compared with literature results reported so far, an extractor volume reduction of 10-50 times maintaining the same productivity can be obtained without changing existing chemistry. We are currently increasing the extractor volume reduction to > 100 times and extending this work to the separation of amino alcohols.

## ACKNOWLEDGEMENT

This project is financially supported by PiT (Procestechnological Institute Twente) and DSM Research. The authors would like to thank Henny Bevers for his aid in setting up the chiral analysis and Anita Podt and Thijs van Delden for their assistance in experimental work.

## REFERENCES

1. T. Takeuchi, R. Horikawa, T. Tanimura, Y. Kabasawa (1990), *Sep. Sci. Tech.*, **25** (7&8), 941-951.
2. A.B. de Haan, B. Simandi (2001), *Ion Exchange and Solvent Extraction*, Vol. 15, Y. Marcus and A SenGupta (eds.), Marcel Dekker, New York, pp. 255-294.
3. H.B. Ding, P.W. Carr, E.W. Cussler (1992), *A.I.Ch.E.J.*, **38** (10), 1493-1498.
4. P.J. Pickering, J.B. Chaudhuri (1997), *Chem. Eng. Sci.*, **52** (3), 377-386.
5. C.J. King (1980), *Separation Processes*, 2nd edn., McGraw-Hill.
6. T. Takeuchi, R. Horikawa, T. Tanimura (1984), *Anal. Chem.*, **56**, 1152-1155.
7. A.L.L. Duchateau, M.G. Hillemans, I. Hindrikx (1997), *Enantiomer*, **2**, 61-67.
8. Y. Abe, T. Shoji, S. Fukui, M. Sasamoto, H. Nishizawa (1996), *Chem. Pharm. Bull.*, **44** (8), 1521-1524
9. V. Prelog, Z. Stojanac, K. Kovacevic (1982), *Helv. Chim. Acta*, **65** (1), 377-384.



## EXTRACTION OF BORAGE SEED OIL BY COMPRESSED CARBON DIOXIDE: EFFECT OF PROCESS PARAMETERS

Filipe Gaspar, Tiejun Lu, Regina Santos, Bushra Al-Duri

School of Chemical Engineering, University of Birmingham, Birmingham, United Kingdom

The extraction of oil from borage seeds using compressed CO<sub>2</sub> was studied. The effect of process parameters on the extraction rate and yield was investigated. In the first set of tests the effect of seed pre-treatment was considered, where mechanical and physical pre-treatments were applied. Both crushing and grinding under atmospheric conditions to particle sizes of 0.6 mm yielded the best results. On a second set of experiments, the effects of pressure and temperature were studied. The decrease in temperature led to a faster extraction rate when pressure was less than 200 bar. At 300 bar the reverse was observed. The trend observed was related to the solubility behaviour with pressure and temperature. Finally, the effect of solvent flow rate was studied. With the increase in the flow rate, a faster extraction was observed. The oil load, however, decrease with the increase in flow rate. This proves that extraction is not only controlled by solubility but also by the rate of mass transfer from the seeds.

### INTRODUCTION

The interest in oils from seeds arises from their high content of important unsaturated fatty acid constituents, some of which are in very short supply. The extraction of these oils from seed materials has traditionally been performed by cold pressing or by hexane extraction. However, the use of compressed CO<sub>2</sub> as the extracting agent presents significant advantages as opposed to the conventional methods. Compared to cold pressing, higher recovery of the oil is obtained, eliminating the need for further processing to recover the residual oil. On the other hand, the oil extracted by CO<sub>2</sub> routes presents a higher quality than that obtained by hexane extraction, since it is free of degradation artefacts and of hexane contamination. At present hexane-extracted oils have been subjected to severe market resistances such as stringent legislation regarding the residual contents of hexane that can be left in the product. For example, the maximum permitted residue for hexane in fats, oils and cocoa butter was reduced to 1 ppm to comply with Directive 97/60/EC.

For an efficient extraction of seed oil with compressed CO<sub>2</sub> some process parameters have to be optimised. The seed pre-treatment, extraction pressure and temperature and CO<sub>2</sub> flow rate are among the most important ones, since they severely affect the extraction rate. In the present work the effect of these parameters on the extraction yields and rates was investigated. The model seed material used was borage (*Borago officinalis*), which is a recognised source of essential fatty acids, specifically gamma-linolenic acid.

## EXPERIMENTAL PROCEDURE

### Seed Pre-Treatment

In addition to untreated seeds, seeds were subjected to different pre-treatment methods before extraction. These were:

Grinding – Seeds were grinded on a commercial blender (Kenwood BL 350 – dry grinder mill). Different degrees of grinding were obtained by varying the exposure to the blender. Two exposure times were applied namely 20 and 60 s, leading to average particle sizes of 0.8 and 0.6 mm, respectively. In addition, the grinding of cryogenically frozen seeds for 60 s led to a particle size of 0.4 mm.

Crushing – Seeds were mechanically crushed for 5 min using a pestle and mortar. The average particle sizes obtained were 0.6 mm and 0.5 mm for non-frozen and cryogenically frozen seeds, respectively.

Cryogenic freezing – Seeds were frozen under liquid nitrogen for a 10 min period before applying the mechanical treatments.

Fast decompression – Seeds were subjected to compressed CO<sub>2</sub> at 300 bar and 25 °C for 60 min, after which the bed was suddenly expanded to atmosphere. The decompression rate, measured as the rate of CO<sub>2</sub> density drop in the bed, was 4 kg.m<sup>-3</sup>.s<sup>-1</sup>. The technique employed during the fast decompression treatment is described elsewhere [1].

### Extraction Equipment

The CO<sub>2</sub> extraction equipment is shown in Figure 1.

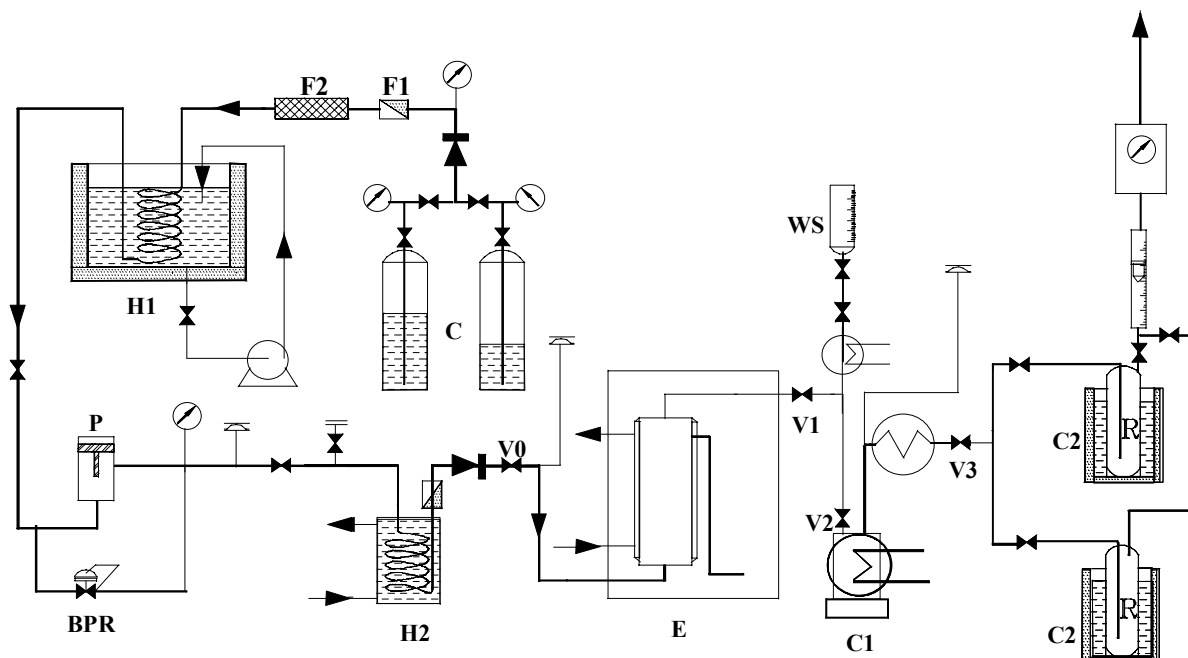


Figure 1. CO<sub>2</sub> extraction apparatus.

A bed of seed material was charged into extractor E. Carbon dioxide (industrial grade) was supplied from the storage cylinders (C) and was cooled in a refrigerator (H1) before pressurisation by a liquid pump (P). A backpressure regulator (BPR) and a heat exchanger (H2) controlled solvent pressure and temperature. The solvent, fed at the bottom of the extractor, passed through the bed of seed material. The stream containing dissolved material from the bed left E and was decompressed in two stages at valves V2 and V3. Expansion at V2 to 8-10 bar deposited most of the extract in the first collector (C1). The outlet stream of

C1 was heated to 40–45 °C before expansion to atmosphere at V3 and entered one of the two collectors in parallel (C2). These collectors were immersed in a mixture of acetone/dry-ice (-85 °C) and retained the water and any volatile components that may have escaped from C1. Valve V3 was adjusted to the desired flow rate that was monitored by a rotameter and a gas flow meter before the CO<sub>2</sub> discharged.

The mass of sample used in each test was 20 g and the diameter and height of the bed were 25 mm and 95 mm, respectively. The extract was collected at intervals as extraction proceeded. For each collection, valve V1 was closed and the downstream pipe to C1 was quickly washed with hot acetone from burette WS. The dissolved extract from C1 was mixed with that from C2 in a given volume of acetone and retained so that the oils contained in it could subsequently be analysed. The extract collectors at C1 and C2 were then replaced and the extraction resumed within 2 to 3 min.

After the dynamic extraction was completed, the extractor was slowly depressurised and the residue from the compressed CO<sub>2</sub> extraction was extracted by hexane in a Soxhlet apparatus in order to estimate the residual oil in the sample. This procedure allows the evaluation of the CO<sub>2</sub> extraction curves to be made in terms of degree of extraction, minimising errors from deviations in sample mass and in oil content. The mean oil content in the borage seeds was 26.7% with a standard deviation of 0.8%.

## RESULTS AND DISCUSSION

### Effect of Seed Pre-Treatment

The aim of the pre-treatment of seeds is to reduce the intraparticle resistance, invoked by the closed structure of the seeds (see Figure 2). A more ‘open’ structure would provide easier ‘access’ for CO<sub>2</sub> to diffuse within the pores and dissolve the oil entrapped in the cells.

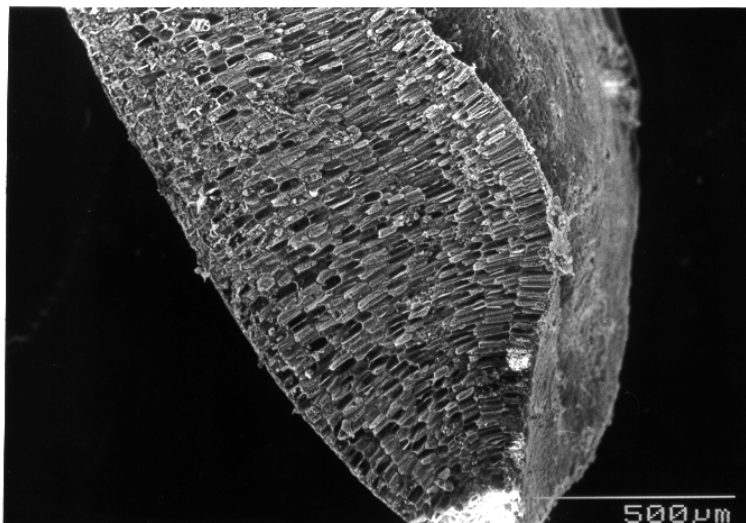


Figure 2. Scanning electron micrograph of a borage seed kernel (longitudinal cut).

The pre-treatment study was performed by extracting seeds, which have been pre-treated by different techniques, with compressed CO<sub>2</sub> at standard conditions (300 bar, 25 °C, 0.5 kg/h). The effect of seed pre-treatment on the extraction curves is shown in Figure 3. It can be seen that a remarkable increase on the rate of extraction and final yields was obtained when the seeds were either ground or crushed. Among the ground seeds it is noticeable that the rate and yields of extraction increased with the decrease of the particle size. Both crushed and

ground seeds to 0.6 mm yielded very high extraction rates and yields. On the other hand the effect of the fast decompression treatment (FD treatment) on the extraction curve was small but noticeable. The compact structure of the oil cells within the seed must have been able to withstand the pressure gradient formed during the decompression without disrupting the majority of the cells.

Figure 4 shows the effect of freezing the seeds cryogenically prior to grinding and crushing. In previous literature, cryogenic grinding has shown significant advantages over ambient milling for the extraction of volatile and/or thermal sensitive compounds [2]. This is due to lower grinding temperatures and smaller particle size. In the case of oil from borage seeds, however, and despite the leading to smaller particle sizes, there was no improvement on the extraction of oil from such material. In fact, the rate and yield of extraction from previously frozen seeds was lower. This is likely to result from the brittle state of the seeds after freezing; the smaller particles obtained contained most likely a higher fraction of intact oil cells.

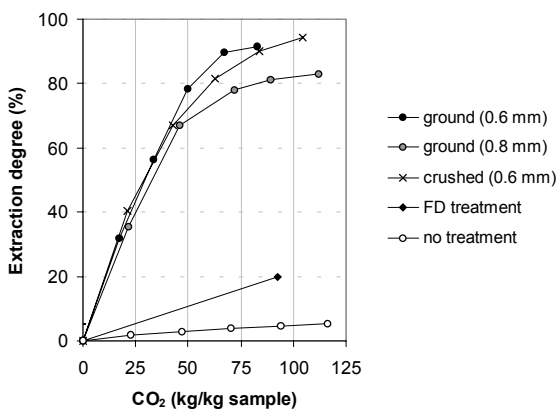


Figure 3. Effect of seed pre-treatment on the extraction curves.

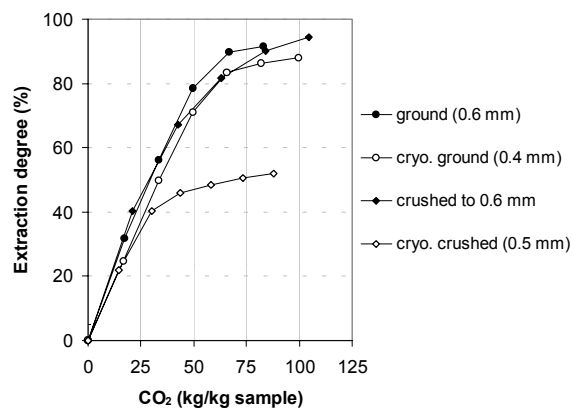
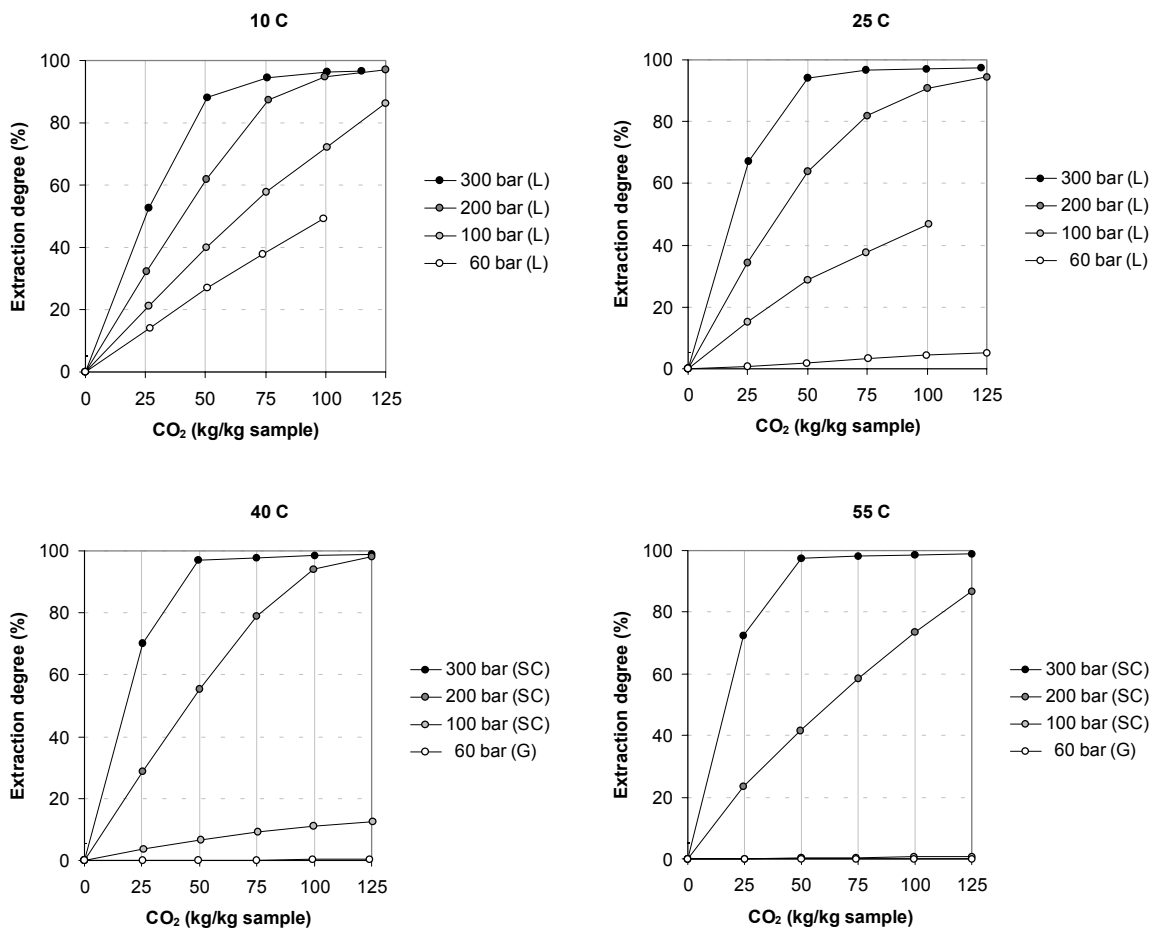


Figure 4. Effect of cryogenic freezing prior to comminution of the seeds on the extraction curves.

### Effect of Extraction Pressure and Temperature

The extraction pressure and temperature were varied from 60 to 300 bar and from 10 to 55 °C, respectively, covering within these ranges gas (G), liquid (L) and supercritical (SC) carbon dioxide. The extraction curves are illustrated in Figure 5. It can be seen that for all temperatures there was a clear improvement of the extraction rate with the increase of pressure. The effect of temperature, however, has shown two distinct behaviours. For pressures lower than 200 bar an increase of temperature lead to a decrease on the extraction rate but the inverse was observed at higher pressures. For pressures lower than 200 bar, the effect observed may be attributed to the reduction in density associated with the increase of temperature and consequently to decrease of oil solubility in CO<sub>2</sub>. For higher pressures the increase of oil volatility with the increase of temperature must have compensated the reduction in solvent density and consequently led to a higher solubility. The fastest extractions were consequently obtained with high pressure and high temperature supercritical CO<sub>2</sub>.



*Figure 5. Effect of pressure and temperature on the extraction curves (seeds ground to 0.5 mm).*

### Effect of Solvent Flow Rate

The effect of solvent flow rate can be used to determine whether the extraction is limited primarily by solubility and chromatographic retention or by the rate of transport of solutes from the matrix to the bulk of the extraction fluid [3]. In the first case increase of the flow rate results in a clear increase in the extraction rate. Moreover if the extraction is controlled only by solubility, the rate of extraction is directly proportional to the solvent flow rate. On the other extreme, if intraparticle is the only restriction, the rate of extraction is only dependent on the kinetics of the intraparticle transport and consequently little or not dependent on the solvent flow rate.

In our tests, performed using liquid CO<sub>2</sub> at 200 bar and 25 °C, the solvent flow rate was varied from 0.1 to 1.0 kg/h. The experimental extraction curves, presented in Figure 6, show that the rate of extraction is both dependent on the extraction time and amount of solvent used. This is an indication that extraction is not only controlled by solubility but also by mass transfer resistance. The film resistance is likely to predominate in the earlier stages of extraction whereas internal diffusion controls the extraction of the last fraction of oil.

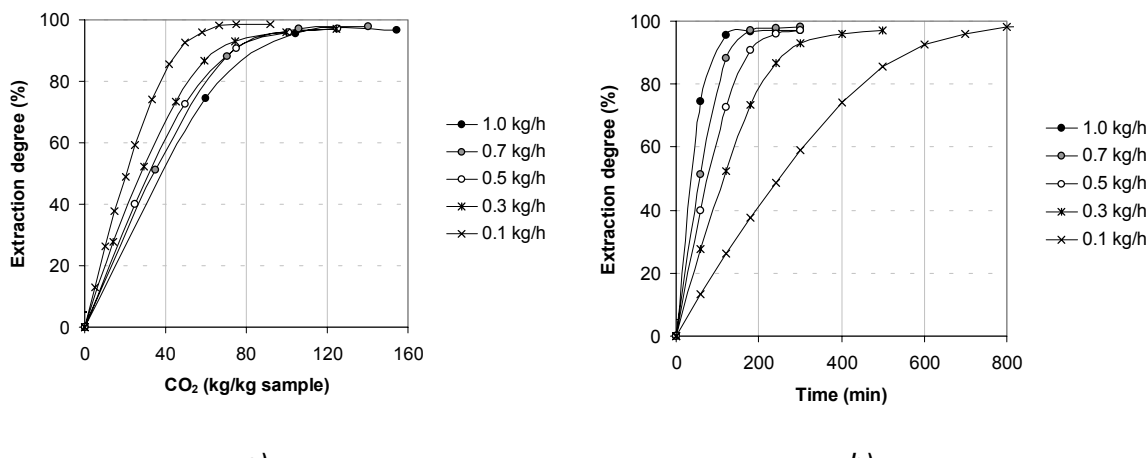


**Figure 6. Effect of solvent flow rate on the extraction curves (seeds ground to 0.5 mm)**  
**a) In terms of mass of solvent, (b) in terms of extraction time.**

## CONCLUSIONS

The extraction of oil from borage seeds using compressed  $\text{CO}_2$  greatly depends on seed pre-treatment, extraction pressure and temperature and on solvent flow rate. Pre-treatments leading to extensive disruption of the oil cells within the seed, such as grinding and crushing, were found to yield remarkable improvements on the extraction rates and ultimate yields of extraction. In preliminary tests grinding and crushing under atmospheric conditions to a particle size of 0.6 mm yielded the best results. Freezing the seeds cryogenically prior to comminution resulted in lower extraction rates and yields.

The use of supercritical  $\text{CO}_2$  at high pressures and high temperatures yielded the best extraction rates, most likely due to a greater solubility of the oils at such conditions.

The extraction rate was also found to be affected by both extraction time and mass of solvent used. This indicates that film resistance plays a role in the extraction process.

## ACKNOWLEDGMENTS

This paper is published by permission of John K King & Sons Ltd, Botanix Ltd and Croda Leek Ltd. We express our gratitude to the Link Programme: Competitive Industrial Materials from Non-Food Crops, to the Biotechnology and Biological Sciences Research Council (BBSRC) and the Engineering and Physical Sciences Research Council (EPSRC) for their financial support.

## REFERENCES

1. F. Gaspar, R. Santos, M. B. King (2000), *Ind. Eng. Chem. Res.*, **39** (12), 4603.
2. C. A. Pesek, L. A. Wilson, E. G. Hammond (1985), *J. Food Sci.*, **50**, 599.
3. S. B. Hawthorne, A. B. Galy, V. O. Schmitt, D. J. Miller (1995), *Anal. Chem.*, **57**, 2723.



## LIQUID-LIQUID EQUILIBRIUM DATA FOR THE CORN OIL / OLEIC ACID / AQUEOUS ETHANOL SYSTEM

Cintia B. Gonçalves and Antonio J. A. Meirelles

Faculty of Food Engineering, State University of Campinas, Campinas, Brazil

Deacidification of vegetable oils can be performed by liquid-liquid extraction. The present paper reports data for the system corn oil + oleic acid + ethanol + water at 298.15 K and different water contents. The addition of water to the solvent reduces the loss of neutral oil in the alcoholic phase and improves the solvent selectivity. The experimental data were correlated by the UNIQUAC model with a global deviation of 0.92%.

### INTRODUCTION

Crude vegetable oils consist predominantly of triacylglycerols and free fatty acids, with mono and diacylglycerols also present in lower level. The removal of free fatty acids (deacidification) is the most important stage of the purification process of oils, mainly because the yield of neutral oil in this operation has a significant effect in the cost of refining [1]. Besides, the presence of these compounds can adversely affect oil quality and stability to oxidation.

Deacidification of oils is usually performed by chemical or physical refining. However, for oils with high acidity, chemical refining causes high losses of neutral oil due to saponification and emulsification. Physical refining is also a feasible process for deacidification of highly acidic oils, since it results in less loss of neutral oil than the traditional process, but more energy is consumed. Moreover, in some cases, the refined oil is subject to undesirable alterations in color and a reduction of stability to oxidation [2]. Thus, it is important to develop alternative processes for the deacidification of edible oils.

The deacidification of oils by liquid-liquid extraction using an appropriate solvent has been receiving attention due to its advantages in comparison to the physical and chemical refining. Kale *et al.* [3] studied the deacidification of crude rice bran oil by extraction with methanol. Turkay and Civelekoglu [4] investigated the liquid-liquid extraction of sulfur olive oil miscella in hexane with aqueous ethanol solutions. As this process is carried out at room temperature and atmospheric pressure, less energy is consumed and the oil is subjected to milder treatments. Besides, liquid-liquid extraction has the advantages of avoiding the formation of waste products and reducing the loss of neutral oil. Furthermore, solvent stripping from refined oil and solvent recovery from the extract stream can be easily carried out, because of the high difference between the boiling points of the solvent, fatty acids, and triacylglycerols. In fact, these operations can be accomplished by evaporation or distillation at relatively low temperatures, in most cases lower than 80°C [5].

Liquid-liquid equilibrium data for systems containing vegetable oils and fatty acids are relatively scarce in the literature, yet such information is essential for studying the deacidification of edible oils by solvent extraction. The present paper reports liquid-liquid equilibrium data for the system corn oil + oleic acid + ethanol + water at 298.15 K and different water contents. The addition of water to the solvent reduces the loss of neutral oil and improves the solvent selectivity [5]. The experimental data set was used for adjusting the parameters of the UNIQUAC model.

## MATERIALS

Refined corn oil of the Mazzola brand (Brazil) was utilized as a source of triacylglycerols, and commercial oleic acid of Riedel de Haen as the source of fatty acids. The chemical composition of these reagents was determined by gas chromatography of fatty acid methyl esters (these data are published in Batista *et al.* [6]). Corn oil contains 12 different isomer sets with molecular weights varying in the range 831.35 - 887.46 g/mol. The commercial oleic acid contains 83.13 mass% oleic acid, 5.82 mass% palmitoleic acid, 5.05 mass% linoleic acid, 4.05 mass% palmitic acid and linolenic, stearic and myristic acids as minor components. The average molecular weight was 872.6131 g/mol for the corn oil, and 278.5868 g/mol for the oleic acid.

The solvent used was ethanol, from Merck, with purity greater than 99.5%. Distilled water was used to obtain the aqueous solvent at different water contents (5, 8, 12, 18 wt%).

## EXPERIMENTAL PROCEDURE

Equilibrium cells similar to those of Silva *et al.* [7] were used for the determination of liquid-liquid equilibrium data. The cell temperature was controlled with a thermostatic bath (Cole-Parmer, Model 12101-15, accurate to 0.1 °C). Thermometers (Cole-Parmer Instrument Co) with subdivisions of 0.1°C were used for monitoring the cell temperature. The component quantity was determined by weighing on a Sartorius analytical balance (Model A200 S, accurate to 0.0001 g). The mixture was stirred vigorously with a magnetic stirrer (FISATOM, Model 752A) for 20 min and left to rest for 12 h at least. This led to the formation of two clear and transparent phases, with a well-defined interface.

The oleic acid concentration in each phase was determined using potentiometric titration (Modified AOCS Method Ca 5a-40) [8] with an automatic burette (METROHM, Model Dosimat 715); the solvent was determined by evaporation in an EDG vacuum oven (Model EIV-1). The water concentration was determined by Karl Fisher titration, according to AOCS method Ca 23-55 [9]. Having determined the fatty acids concentration, solvent and water, the tryacylglycerols concentration was obtained by difference. The uncertainties of the concentrations varied within the following ranges: 0.06 – 0.24% for oleic acid, 0.02 – 0.11 % for ethanol, 0.02 – 0.18% for water and 0.06 – 0.26% for corn oil, being the lowest figures obtained for the lowest concentrations.

## MODELLING

The experimental equilibrium data determined in this work and the data for corn oil + oleic acid + anhydrous ethanol reported by Batista *et al.* [6] were used together to adjust the parameters of the UNIQUAC model [10]. Due to the large difference in molecular weights of the components, mass fractions were used as unity of concentration in the UNIQUAC model [11].

The adjustments were made by treating the system as a pseudoquaternary one, composed by a single triacylglycerol having the corn oil average molecular weight, a representative fatty acid with the molecular weight of the commercial oleic acid, ethanol and water. The values of  $r'_i$  and  $q'_i$  for the UNIQUAC model were calculated via Equation 1, which considers the composition of the oil and the commercial oleic acid.

$$r'_i = \frac{1}{\bar{M}_i} \sum_j^C x_j \sum_k^G \tilde{\iota}_k^{(i)} R_k; \quad q'_i = \frac{1}{\bar{M}_i} \sum_j^C x_j \sum_k^G \tilde{\iota}_k^{(i)} Q_k \quad (1)$$

where  $x_j$  is the molar fraction of the triacylglycerols of the corn oil or the fatty acids of the commercial oleic acid and  $\bar{M}_i$  is the average molecular weight of the corn oil or the commercial fatty acid. C is the number of compounds in the oil or in the commercial fatty acid and G the number of groups. As already mentioned, the compositions of the corn oil and the commercial oleic acid used in the present paper are reported by Batista *et al.*[6]. The values for  $r'_i$  and  $q'_i$  are furnished in Table 1. The parameters  $R_i$  and  $Q_i$  were obtained from Magnussen *et al.* [12].

*Table 1. Parameters  $r'_i$  and  $q'_i$  for corn oil, Riedel de Haen oleic acid, ethanol and water.*

Compound	$r'_i$	$q'_i$
corn oil (1)	0.044023	0.035675
commercial oleic acid (2)	0.045142	0.037157
ethanol (3)	0.055905	0.056177
water (4)	0.051069	0.077713

The parameter estimation procedure was based on the minimization of the objective function of composition, following the procedure developed by Stragevitch and d'Avila [13].

$$S = \sum_m^D \sum_n^N \sum_i^{C-1} \left[ \left( \frac{w_{inm}^{I,ex} - w_{inm}^{I,calc}}{\sigma_{w_{inm}^I}} \right)^2 + \left( \frac{w_{inm}^{II,ex} - w_{inm}^{II,calc}}{\sigma_{w_{inm}^{II}}} \right)^2 \right] \quad (2)$$

where D is the total number of groups of data, N is the total number of tie lines, and C is the total number of components in the group of data  $m$ .  $w$  is the mass fraction, the subscripts  $i$ ,  $n$  and  $m$  are component, tie line and group number, respectively, and the superscripts I and II are the phases; ex and calc refer to experimental and calculated concentrations.  $\sigma_{w_{inm}^I}$  and  $\sigma_{w_{inm}^{II}}$  are the standard deviations observed in the compositions of the two liquid phases.

Adjusted parameters are shown in Table 2.

*Table 2. UNIQUAC parameters for the systems corn oil (1) + commercial oleic acid (2) + ethanol (3) + water (4) at 25 °C.*

Pair $ij$	$A_{ij}/K$	$A_{ji}/K$
12	273.64	-212.27
13	246.94	-54.214
14	3032.0	-148.81
23	56.468	-80.240
24	235.76	49.931
34	337.46	-279.92

The deviations between experimental and calculated compositions in both phases for each system can be found in Table 3. These deviations are calculated according to Equation 3:

$$\Delta w = 100 \sqrt{\frac{\sum_{n=1}^N \sum_{i=1}^C \left[ (w_{i,n}^{I,ex} - w_{i,n}^{I,calc})^2 + (w_{i,n}^{II,ex} - w_{i,n}^{II,calc})^2 \right]}{2NC}} \quad (3)$$

Table 3. Mean deviations in phase compositions.

System	$\Delta w$ (%)
corn oil + oleic acid + anhydrous ethanol	0.84
corn oil + oleic acid + 5% aqueous ethanol	1.39
corn oil + oleic acid + 8% aqueous ethanol	0.79
corn oil + oleic acid + 12% aqueous ethanol	0.79
corn oil + oleic acid + 18% aqueous ethanol	0.79
Global deviation	0.92

Figures 1 shows the experimental points and calculated tie-lines for the system corn oil/ oleic acid/ 5% aqueous ethanol. The equilibrium diagram was plotted in triangular coordinates. For representing the pseudoquaternary system in triangular coordinates, ethanol + water was admitted as a mixed solvent. The middle points represent the overall compositions, while the extreme points represent the phases composition in the equilibrium.

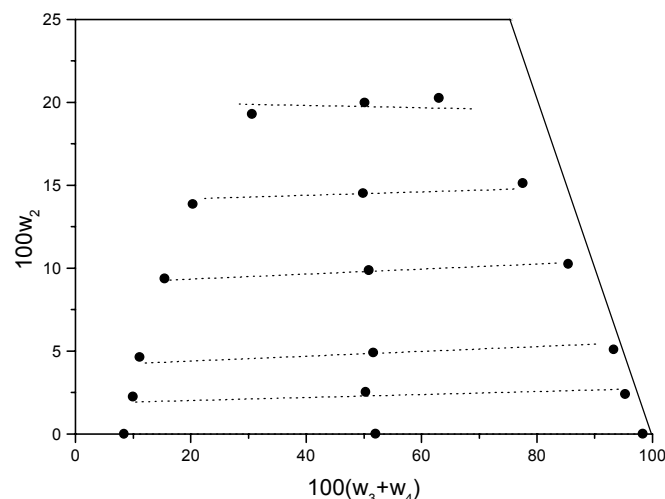
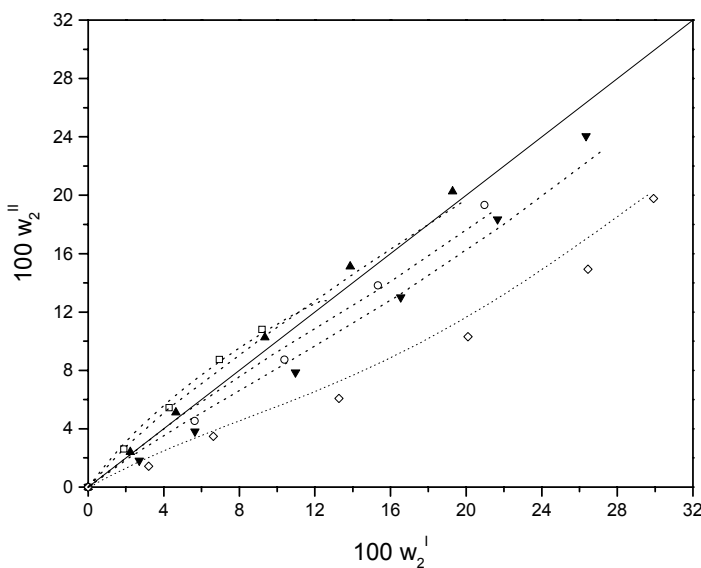


Figure 1. System of corn oil (1) + oleic acid (2) + 5% aqueous solvent [ethanol (3) + water (4)] at 298.15 K: experimental (●); (---) UNIQUAC.

Figure 2 presents the distribution of oleic acid between the phases at 298.15 K for the systems studied. As can be observed, the addition of water in the solvent decreases the fatty acid distribution coefficient, which is calculated according to Equation 4. These results indicate that aqueous ethanol has a lower capacity for extraction of fatty acids. Otherwise, the addition of water increases the solvent selectivity and consequently reduces the loss of neutral oil in solvent extraction. Solvent selectivity is calculated by Equation 5.

$$k_i = \frac{w_i''}{w_i'} \quad (4)$$

$$S = \frac{k_2}{k_1} \quad (5)$$



*Figure 2. Distribution diagram at 298.15 K for oleic acid ( $w_2$  = acid mass fraction):  
 (□) anhydrous ethanol; (▲) 5% aqueous ethanol; (○) 8% aqueous ethanol;  
 (▼) 12% aqueous ethanol; (◊) 18% aqueous ethanol; (- - -) UNIQUAC.*

In order to have a better insight about the influence of the water content on the performance of the solvent, flash calculations using the UNIQUAC model were performed for two levels of free fatty acids in the crude oil and different water concentrations in the solvent. The mass ratio between crude oil and aqueous solvent was fixed at the value 1:1. The results are given in Figure 3. As can be seen, the distribution coefficients exhibit a relatively slight decrease with the water content until values in the range 4-7 wt% of water in the aqueous ethanol, but the solvent selectivity shows a very significant increase.

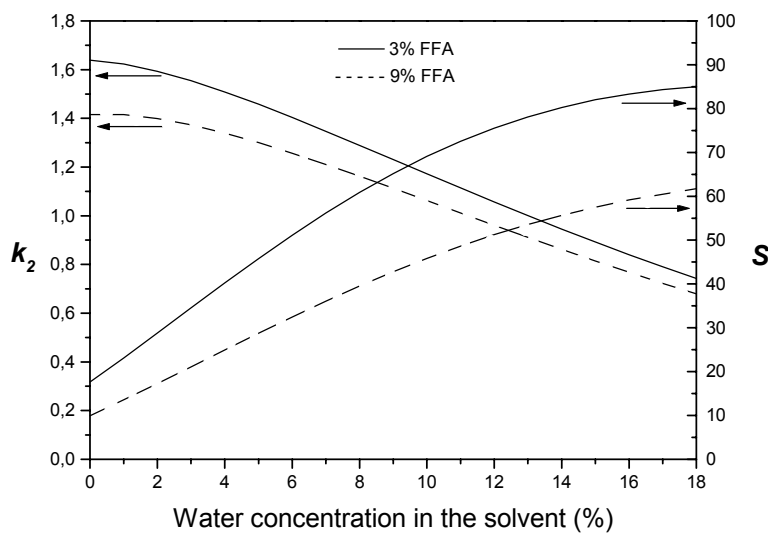


*Figure 3. Fatty acid distribution coefficient and selectivities for systems of corn oil (1) + oleic acid (2) + ethanol (3) + water (4): (—) 3 wt% free fatty acid in crude oil;  
 (---) 9 wt% free fatty acid in crude oil.*

## CONCLUSION

Liquid-liquid equilibrium data for systems containing corn oil + oleic acid + ethanol + water were experimentally determined at 298.15 K. The addition of water in the solvent causes a decrease in the fatty acid distribution coefficient and an increase in the selectivity.

Despite the complexity of the studied systems, the estimated parameters for the UNIQUAC model are representative, since the description of the liquid-liquid equilibrium for all the systems had presented mean deviations lower than 1.39% in relation to experimental data. These parameters enable the modeling and simulation of liquid-liquid extractors using the proposed solvents.

Moreover, the results obtained allow one to conclude that a water content in the range of 4-7 wt% in the aqueous ethanol is appropriate for deacidification by solvent extraction, as it still provides high values of fatty acid distribution coefficient (larger than 1), and very significant values for the solvent selectivity (larger than 40).

## ACKNOWLEDGEMENTS

The authors wish to acknowledge FAPESP (Fundação de Amparo à Pesquisa do Estado de São Paulo), CNPq (Conselho Nacional de Desenvolvimento Científico e Tecnológico), FINEP (Financiadora de Estudos e Projetos) and CAPES (Coordenação de Aperfeiçoamento de Pessoal de Nível Superior) for the financial support.

## REFERENCES

1. T. C. Lo, M. H. Baird and C. Hanson (eds.) (1983), *Handbook of Solvent Extraction*, John Wiley & Sons, New York, pp. 980.
2. R. Antoniassi, W. Esteves and A. J. A. Meirelles (1998), *J. Am. Oil Chem. Soc.*, **75** (10), 1411-1415.
3. V. Kale, S. P. R. Katikaneni and M. Cheryan (1999), *J. Am. Oil Chem. Soc.*, **76** (6), 723-727.
4. S. Turkay and H. Civelekoglu (1991), *J. Am. Oil Chem. Soc.*, **68** (2), 83-86.
5. C. G. Pina and A. J. A. Meirelles (2000), *J. Am. Oil Chem. Soc.*, **77** (5), 553-559.
6. E. Batista, S. Monnerat, L. Stragevitch, C. G. Pina, C. B. Gonçalves and A. J. A. Meirelles (1999), *J. Chem. Eng. Data*, **44** (6), 1365-1369.
7. L. H. M. Silva, J. S. Coimbra and A. J. A. Meirelles (1997), *J. Chem. Eng. Data*, **42**, 398-401.
8. A.O.C.S. (1993), *Official and Tentative Methods of the American Oil Chemists' Society*, Press, 3rd edn., Vol. 1, Champaign.
9. A.O.C.S. (1988), *Official Methods and Recommended Practices of the American Oil Chemists' Society*, Press, 3rd edn., Vol. 1-2, Champaign.
10. D. S. Abrams and J. M. Prausnitz (1975), *AIChE J.*, **21** (1), 116-128.
11. E. Batista, S. Monnerat, K. Kato, L. Stragevitch and A. J. A. Meirelles (1999), *J. Chem. Eng. Data*, **44** (6), 1360-1364.
12. T. Magnussen, P. Rasmussen and A. Fredenslund (1981), *Ind. Eng. Chem. Process Des. Dev.*, **20**, 331-339.
13. L. Stragevitch and S. G. d'Avila (1997), *J. Chem. Eng.*, **14**, 41-52.



## LIQUID-LIQUID EXTRACTION FOR DEACIDIFICATION OF VEGETABLE OILS

Eduardo Batista, Rosemar Antoniassi\*, Maria Regina Wolf Maciel\*\*  
and Antonio J. A. Meirelles

Faculty of Food Engineering, State University of Campinas, Campinas, Brazil

\*EMBRAPA, Rio de Janeiro, Brazil

\*\*Faculty of Chemical Engineering, State University of Campinas, Campinas, Brazil

Crude vegetable oils contain undesirable components, such as free fatty acids. They can be removed by alkali refining as well as physical refining. Liquid-liquid extraction is an alternative process that reduces the energy consumption for the oil refining without losses of natural components. This work aims to study the simulation of corn oil deacidification by liquid-liquid extraction using aqueous ethanol as the solvent. The results obtained indicate the best conditions for the deacidification by solvent extraction. The solvent to crude oil flow ratio, the number of stages and the water percent in ethanol could be selected to guarantee the minimum free fatty acids content in the refined oil with a minimum loss of neutral oil.

### INTRODUCTION

In the food and pharmaceutical industries, liquid-liquid extraction can be used in the recovery of vitamins, in the separation of caffeine, penicillin, aromas and fragrances, in the separation of lecithin, in the deterpenation of orange essential oil and in the deacidification of vegetable oils [1,2]. In the conventional refining process of edible oils, the deacidification is conducted by neutralization of free fatty acids with alkali. This process is applied to any vegetable oil, but high concentrations of free fatty acids cause a high loss of neutral oil. Leibovitz and Ruckenstein [3] reported losses of neutral oil in the range 15 to 25 % for the neutralization of crude corn oil containing 8-14 % of free fatty acids. In the Brazilian edible oil refining industry, the losses of neutral oil are proportionally higher, 14 % for crude corn oil with only 4 % of free fatty acids [4].

The deacidification of vegetable oils using solvents is based on the difference of the solubility of free fatty acids and neutral triglycerides in the solvent and on the difference of the boiling points of the solvent and fatty acids [5]. This process can be performed using several solvents: acetone, ethyl acetate, furfural, propanol, isopropanol, butanol, ethanol, methanol, ethyl methyl ketone, etc. Batista *et al.* [6] tested different solvents (methanol, ethanol, *n*-propanol, isopropanol, aqueous ethanol) for deacidification of canola oil. They verified that ethanol and aqueous ethanol were the best solvents for the deacidification process. The presence of water in ethanol increases the solvent selectivity, decreases the mutual solubility of the oil/ethanol mixture and reduces the loss of neutral oil in the final extract. This work is focused on the simulation of the deacidification process by solvent extraction and its optimization using surface response analysis. Batista *et al.* [7] used surface response analysis for optimizing a SRV distillation process and concluded that the factorial design is a powerful tool for analyzing the effects of the selected variables. For this reason this technique was employed in the present work to analyze the variables used in liquid-liquid extraction.

## CHARACTERIZATION OF VEGETABLE OILS

The first step in the chemical characterization of a edible oil is to determine its fatty acid composition by gas chromatography of fatty acid methyl esters. The fatty acid composition of corn oil is presented in Table 1.

*Table 1. Fatty acid composition of refined corn oil.*

n	Symbol	Fatty Acid	M (g.mol <sup>-1</sup> )	% molar	% mass
1	M	Miristic	C14:0 <sup>(1)</sup>	228.38	0.0365
2	P	Palmitic	C16:0	256.43	13.7943
3	Po	Palmitoleic	C16:1	254.41	0.0874
4	S	Stearic	C18:0	284.48	2.0333
5	O	Oleic	C18:1	282.47	32.6848
6	Li	Linoleic	C18:2	280.45	49.2415
7	Le	Linolenic	C18:3	278.44	1.3782
8	A	Arachidic	C20:0	312.54	0.6050
9	B	Behenic	C22:0	340.49	0.1388

<sup>(1)</sup> Cx:y - x = number of carbons, y = double bonds      M = molecular weight

From this fatty acid composition it is possible to estimate the triglyceride composition of the oil (Table 2) by using the computational method developed by Antoniosi Filho *et al.* [8]. The main triglyceride (Table 2) represents the component of greatest concentration in the isomer set with x carbons and y double bonds.

*Table 2. Estimated triglyceride composition of corn oil.*

n	Group	Main Triglyceride	M (g.mol <sup>-1</sup> )	% molar	% mass
1	50:1 <sup>(1)</sup>	POP	833.37	1.9072	1.8226
2	50:2	PLiP	831.35	2.9092	2.7735
3	52:1	POS	861.45	0.5616	0.5548
4	52:2	POO	859.40	5.3611	5.2836
5	52:3	POLi	857.39	13.6558	13.4267
6	52:4	PLiLi	855.37	10.7136	10.5090
7	52:5	PLiLe	853.37	0.6435	0.6298
8	54:2	SOO	887.46	0.9815	0.9988
9	54:3	OOO	885.44	5.5765	5.6623
10	54:4	OOLi	883.43	17.6755	17.9068
11	54:5	OLiLi	881.41	24.8117	25.0789
12	54:6	LiLiLi	879.43	13.5542	13.6694
13	54:7	LiLiLe	877.38	1.0442	1.0506
14	56:3	OLiA	913.52	0.6045	0.6333
Total				100.0000	100.0000

<sup>(1)</sup> X:Y - X number of carbons (except carbons of glycerol) and Y double bonds

The diglyceride composition can be estimated taking into account the probability of partial hydrolysis of each triglyceride (Table 2). For example, the partial hydrolysis of POS in the position 1 or 3 produces the diglycerides PO<sub>2</sub> or SO<sub>2</sub> and in position 2, the diglyceride P<sub>2</sub>S, all diglycerides in equal molar proportion. The estimated diglyceride composition for corn oil is presented in Table 3.

*Table 3. Estimated diglyceride composition of corn oil.*

n	Group	Diglyceride	M (g.mol <sup>-1</sup> )	% molar	% mass
1	34:1	PO_ and P_O	595.00	9.5850	8.2143
2	32:0	P_P	568.96	16.0500	13.1528
3	34:2	PLi and P_Li	592.98	13.8490	11.8283
4	34:3	PLe_	590.94	0.2150	0.1830
5	36:1	SO_ and S_O	623.05	0.8410	0.7547
6	34:0	PS_ and P_S	597.01	0.1870	0.1608
7	36:2	OO_ and O_O	621.04	13.5820	12.1491
8	36:3	LiO_ and Li_O	619.02	33.0790	29.4930
9	36:4	LiLi_ and Li_Li	617.01	25.7440	22.8787
10	36:5	LeLi_ and Le_Li	614.99	0.9110	0.8070
11	38:2	ALi_	649.06	0.2020	0.1888
12	38:1	O_A	651.08	0.2020	0.1894
Total			100.0000	100.0000	

## PROCESS SIMULATION

The algorithm developed by Naphtali and Sandholm [9], in the form proposed by Fredenslund *et al.* [10], was adapted for simulating the liquid-liquid extraction. The phase equilibrium estimation in such a complex system, containing 14 triglycerides, 12 diglycerides, 9 fatty acids, a short chain alcohol and water, is a very difficult task. Phase equilibrium was predicted using the new parameters of UNIFAC adjusted by Batista *et al.* [11] for ternary systems composed by a pure triglyceride, a pure fatty acid and anhydrous ethanol.

The extractor feed stream was composed by triglycerides, diglycerides and free fatty acids in a proportion of 92 / 4 / 4, respectively. All triglycerides and diglycerides of corn oil (Tables 2 and 3, respectively) were used in the feed stream. The free fatty acids were composed of the fatty acids presented in Table 1. It was considered that the free fatty acids present in crude corn oil have the same proportion of the fatty acid composition of refined corn oil (Table 1). Aqueous ethanol was used as solvent. A good deacidification by solvent extraction must provide a content of free fatty acids in refined oil lower than 0.3 mass% [12], without a great loss of neutral oil in final extract.

## SURFACE RESPONSE ANALYSIS

The optimization study was carried out by surface response analysis based on the results from factorial design and regression analysis [13]. The experimental design, which requires the use of coded variables (Table 4), was used as a tool to evaluate the influence of the main process variables on the free fatty acids content of refined oil (in a solvent free basis) and on the loss of neutral oil in final extract. Three levels were considered: 15 ( $2^3 + \text{star}$ ) process simulations were necessary for optimizing the liquid-liquid extraction by surface response analysis.

*Table 4. Coded variables.*

	-1.68179	-1	0	+1	+1.68179
Solvent to Crude Oil Ratio (S/O)	0.93182	0.90000	1.00000	1.10000	1.26818
Number of Stage (NS)	4	5	7	9	10
% Water in Solvent (W)	2.477	3.500	5.000	6.500	7.523

From the simulation results in the above-mentioned range, a mathematical model for each type of response was obtained. This permits the formulation of the following models, expressed in terms of coded variables (Table 4):

Free fatty acids in refined oil:

$$\% \text{ FFA} = 0.511081 - 0.187174 (\text{S/O}^*) + 0.028290 (\text{S/O}^*)^2 - 0.140224 (\text{NS}^*) + \\ + 0.034990 (\text{NS}^*)^2 + 0.290702 (\text{W}^*) + 0.046958 (\text{W}^*)^2 - 0.050325 (\text{S/O}^*) (\text{W}^*) \quad (1)$$

Loss of neutral oil:

$$L = 2.51473 + 0.25968 (\text{S/O}^*) + 0.04090 (\text{NS}^*) - 1.18148 (\text{W}^*) + 0.24230 (\text{W}^*)^2 - \\ - 0.08250 (\text{S/O}^*) (\text{W}^*) \quad (2)$$

where superscript \* defines coded variable.

With these models, it is possible to generate surfaces that represent the influence of the specific variables on each response. In the first analysis with the variables S/O and NS, the value for NS that guarantees a fatty acid concentration of 0.3 % and a lower loss of neutral oil was 10. The next step was to generate a surface with NS equal to 10 (Figure 1) for representing the effect of the solvent to crude oil flow ratio (S/O), as well as the water percent in that solvent (W), on the free fatty acid concentration in refined oil and on the loss of neutral oil. The variables, S/O and W, have a significant effect on the responses. The free fatty acids in refined oil decreases with the increase of solvent/oil flow ratio. At high W-values, in this case ethanol with 7.523 % water, the deacidification is affected because the solvent has a lower capacity of extracting free fatty acids, nevertheless the solvent becomes more selective with the water increase, reducing expressively the loss of neutral oil. The effect of W is much more significant than that of S/O. The loss of neutral oil in the final extract decreases as the S/O ratio decreases and also decreases, but much more significantly, with the increase of the water content in solvent. In fact, the addition of water to ethanol has a very significant influence on the mutual solubility of oil and the mixed solvent, reducing its value. When the surfaces are superimposed, the maximum concentration of free fatty acids permitted by legislation (0.3 %), with a minimum loss of neutral oil, is obtained for a S/O-value equal to the maximum one (1.26818).

The surface for NS and W with S/O equal to 1.26818 was then generated (Figure 2). The free fatty acid concentration decreases with the increase in NS and with the decrease of W, but the effect of W is higher than the effect of NS. When these figures are superimposed, the operating condition that permits a minimum loss of neutral oil and assures 0.3 % of free fatty acids in final product is NS = 10 and W = 5.75 %.

Using this procedure the optimal condition for solvent extraction can be found (Table 5). These values guarantee a concentration of free fatty acids in refined oil lower than 0.3 % [12] as well as a minimum loss of neutral oil in final extract. To check these optimal conditions a rigorous simulation was conducted using their values. The simulation results indicate that for these optimal conditions the concentration of free fatty acid in the refined oil is 0.27 %, the loss of neutral oil is equal to 2.40 % and 60.7 % of diglycerides was extracted. This loss of neutral oil is much lower than the loss presented in the literature, 15-25 % [3] and 14 % [4]. Batista *et al.* [14] found 8.11% of neutral oil loss in the deacidification of canola oil with 4 % of free fatty acids. In this case the authors employed anhydrous ethanol as solvent. This result proves that the maximum concentration of free fatty acids in neutral oil, 0.3%, can be obtained with a significant decrease in the loss of neutral oil in the final extract using aqueous ethanol as solvent.

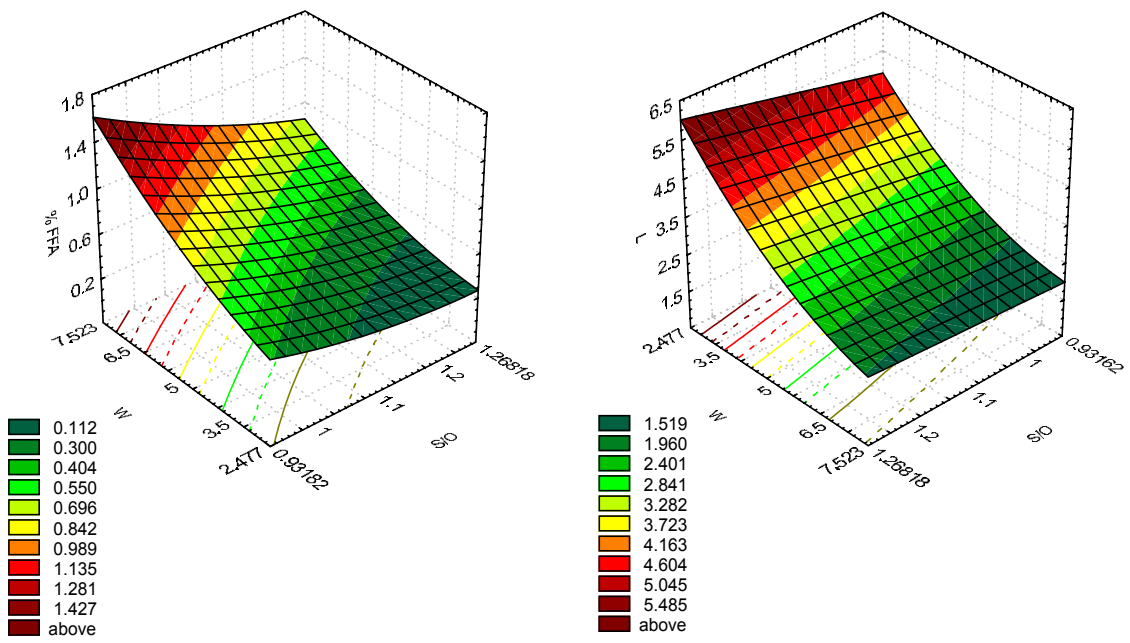


Figure 1. Effect of S/O and W on % FFA and on L (NS = 10).

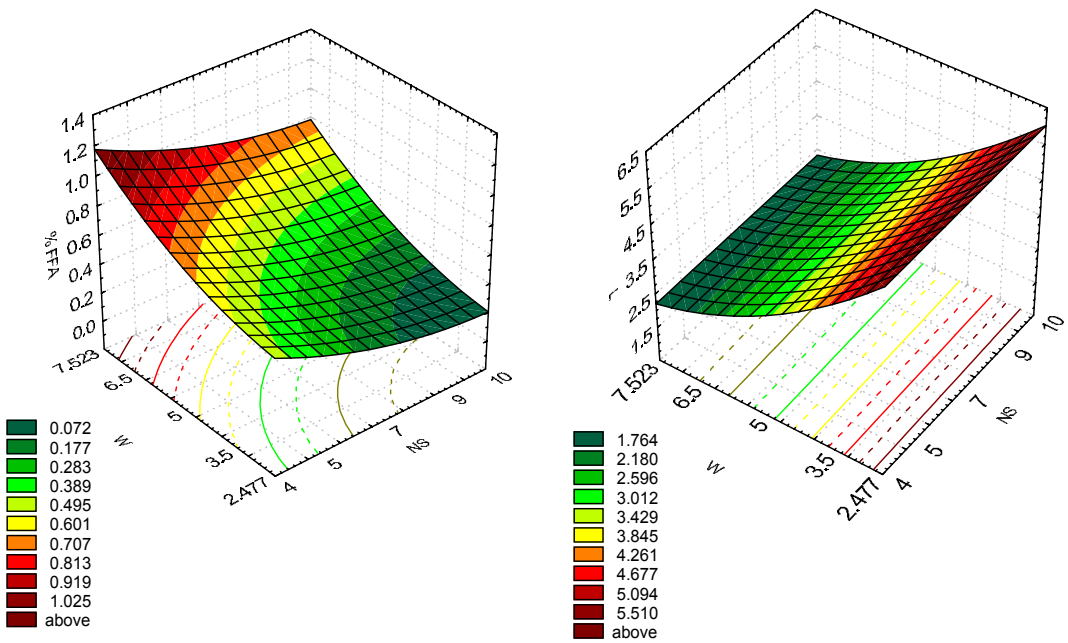


Figure 2. Effect of NS and W on % FFA and on L (S/O = 1.26818).

It should also be noted that experimental results reported in the literature [2] indicated that mechanically agitated extractors could be employed in oil deacidification using relatively high solvent to crude oil ratios without hydrodynamic problems, such as phase inversion.

*Table 5. Optimal conditions for deacidification by solvent extraction.*

Solvent to Oil Ratio (S/O) 1.26818	Number of Stages (NS) 10	Water Percent in Solvent (W) 5.75 %
---------------------------------------	-----------------------------	--

## CONCLUSION

The new parameters of the modified UNIFAC as well as the program developed allows to simulate liquid-liquid extraction of a complex multicomponent system. All components of corn oil (Tables 1, 2 and 3) were considered in the extractor feed stream without compromising the program convergence. The surface response analysis help us to find the optimal condition to operate the extractor with a concentration of free fatty acids in the refined oil lower than 0.3 % and a minimum loss of neutral oil. The presence of water in ethanol guarantees losses of neutral oil substantially lower.

## ACKNOWLEDGEMENTS

This work was supported financially by research grants from FAPESP, CNPq and FINEP.

## REFERENCES

1. E. Haypek, L. H. M. Silva, E. Batista, D. S. Marques, M. A. A. Meireles and A. J. A. Meirelles (2000), *Brazilian J. Chem. Eng.*, **17**, 705-712.
2. C. G. Pina and A. J. A. Meirelles (2000), *J. Am. Oil Chem. Soc.*, **77**, 705-712.
3. Z. Leibovitz and C. Ruckenstein (1983), *J. Am. Oil Chem. Soc.*, **60**, 347A - 351A.
4. R. Antoniassi, W. Esteves and A. J. A. Meirelles (1998), *J. Am. Oil Chem. Soc.*, **75**, 1411-1415.
5. C. Thomopoulos (1971), *Revue Française des Corps Gras*, **18**, 143-150.
6. E. Batista, S. Monnerat, K. Kato, L. Stragevitch and A. J. A. Meirelles (1999), *J. Chem. Eng. Data*, **44**, 1360-1364.
7. E. A. C. Batista, M. I. Rodrigues and A. J. A. Meirelles (1998), *Comp. Chem. Eng.* **22**, Suppl., S737-S740.
8. N. R. Antoniosi Filho, O. L. Mendes and F.M. Lanças (1995), *Chromatographia*, **40**, 557-562.
9. L. M. Naphtali and D. P. Sandholm (1971), *AIChE J.*, **17**, 148-153.
10. Fredenslund, J. Gmehling and P. Rasmussen (1977), Vapor-Liquid Equilibria using UNIFAC: a Group Contribution Method, Elsevier Scientific, New York.
11. E. Batista, S. Monnerat, L. Stragevitch, C. G. Pina, C. B. Gonçalves and A. J. A. Meirelles (1999), *J. Chem. Eng. Data*, **44**, 1365 - 1369.
12. Codex Alimentarius (1993), Fats, Oils and Related Products, Vol. 8, Joint FAO/WHO Food Standards Programme - Codex Alimentarius Commission, Rome, pp. 29-32.
13. G. E. P. Box, W. G. Hunter and J. S. Hunter (1978), Statistic for Experimenters - an Introduction to Design, Data Analysis and Model Building, John Wiley & Sons, New York.
14. E. Batista, M. R. Wolf Maciel and A. J. A. Meirelles (1999), *Proc. Press '99*, Budapest, pp. 163-168.



## INFLUENCE OF OPERATING FACTORS ON THE RHUBARB EXTRACTION PROCESS

Y. C. Lu, G. S. Luo and Y. Y. Dai

Tsinghua University, Beijing, China

Chinese traditional medicines are commonly produced from active ingredients extracted from herbs using solid-in-liquid extraction processes. These are often inefficiently operated and are poorly researched. The rhubarb extraction system has been used in this study to investigate various factors that influence the extraction process. These include choice of solvent, temperature, phase ratio and particle size. Based on the experimental findings and on an investigation of various modes of operation an improved extraction process is proposed.

### INTRODUCTION

Local Chinese herbs are commonly treated to provide the active ingredients that are used in the production of traditional medicines. Normally a solid-in-solvent extraction process is employed. These processes are in general inefficient and are not well researched [1].

For this study rhubarb extraction was chosen as the experimental system to investigate factors that influence the extraction process [2]. Rhubarb, the rootstock of the species *polygonaceae*, has highly compacted tissue that makes the extraction of active compounds difficult. In addition the presence of the suite of active ingredients provided by this system enabled the issues relating to complex extraction systems to be addressed. Factors investigated include solvent choice, temperature, phase ratio and particle size. Co-current and counter-current modes of operation were also investigated and a multiple extraction series was tested.

### EXPERIMENTAL PROCEDURES

#### Materials

All the chemicals (NaOH, ammonia, FeCl<sub>3</sub>, ethyl ester, 1,8-dioxyanthraquinone) were of analytical grade purity and used without any further purification.

Rhubarb slices, purchased from Beijing medical material service station, were pulverized with pulverizer, then classified by a series of screens (20, 40, 80 mesh/inch). Particle sizes were defined in following way: particles remaining between 40 mesh and 80 mesh screens were said to belong to 40 mesh size fraction, the rest might be deduced in the same way. All the particles in the same fraction were mixed well before use.

#### Equipment and Procedure

Except for soxhlet extractions, all experiments were done in a batch extractor with a water jacket and magnetic stirrer. The extraction chamber was a cylinder with height of 4 cm and 3 cm in diameter. For all the experiments a fixed stirring speed was used. Initial solvent volume was 20 ml. Before experiments, solvents were infused into the extractor first and pre-heated to the required temperature. The extract was separated from solid residues immediately by filtration when experiments finished. In multi-staged extraction, residues were returned to the extractor for next operation cycle. The pre-experimental results showed that the extract concentration tended to be constant after three hours of extraction in batch extractor. Three hours was therefore chosen as the time for each experiment.

### **Analytical Procedure**

The concentration of total anthraquinone in solution was determined using a HP8452 UV-vis spectrophotometer at wavelength of 512 nm. A standard curve was plotted using 1,8-dioxyanthraquinone as standard [3]. The anthraquinone compounds extracted are composed of a number of individual compounds (such as emodin and rheinic acids) that were determined using HPLC when required.

Phase ratio, denoted with S, is defined as proportion of the mass of initial medicine material and added solvent volume. The extraction ratio is defined as the mass ratio of the extracted anthraquinone and raw material.

## **RESULTS AND DISCUSSION**

### **Effect of Temperature**

Figure 1 gives final extraction ratio of total anthraquinone at a certain phase ratio for various extraction temperatures. It was clear that temperature had prominent effect on final extraction ratio. This effect was more pronounced for higher phase ratios. The variation of temperature changed the reaction environment and thus affected the equilibrium dissolution and adsorption/desorption conditions. A higher temperature was favorable for dissolution and desorption. From an extraction temperature of 60°C, there was no further benefit to extraction with an increase of temperature. Overly high temperature may in fact destroy some of the heat sensitive components.

### **Effect of Solvent Mixture**

Figure 2 shows the extraction results for the different solvent mixtures tested. These were water, various water/ethanol mixtures and pure ethanol. All experiments were done at the phase ratio of 1:200 and 60°C. The choice of solvent plays a key role in the technology optimization. Ethanol-containing solvent mixtures were better than pure water. The extraction ratio did not increase linearly with ethanol volume fraction as was expected but declined after 40 vol % ethanol. The results indicated that solvent mixtures from 40 to 60 vol % ethanol would be adequate. The concentrations of specific components of the extracts, emodin and rheinic acid, were determined by HPLC, the results are shown in Table 1.

*Table 1. Extraction ratio of emodin or rheinic acid with various solvents.  
(0.4 g medicine material, 20 mesh size fraction, 20 ml solvent).*

Solvent	Temperature (°C)	Extraction Ratio	
		Emodin	Rheinic acid
Water	60	0.06	0.38
25% Ethanol	40	0.13	0.32
50% Ethanol	40	0.36	0.59
Ethanol	40	0.29	0.25

It was found that the extraction behaviour of the various solvent mixtures with respect to the two components differed, even though both were anthraquinonic compounds. Solvent mixtures with higher content of water favored the extraction rheinic acid, while those with higher content of ethanol favored the extraction of Emodin. Solvent selection should therefore be based on the target component.

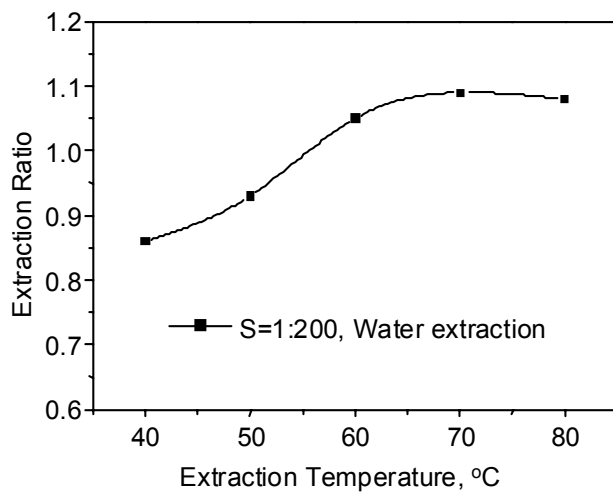


Figure 1. Influence of temperature on extraction ratio.

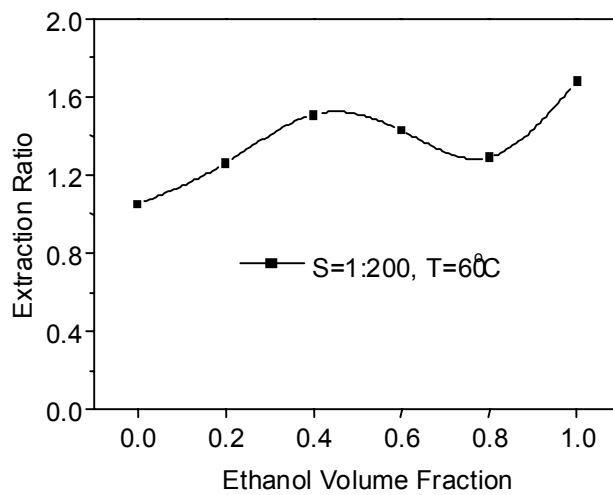


Figure 2. Influence of solvent on extraction ratio.

### Effect of Particle Size

Particles in various size fractions were treated in the batch extractor and a soxhlet extractor (for 8 hours), and the results are given in Tables 2 and 3, respectively.

Table 2. Single stage extraction ratios for various size fractions.  
(0.4 g medicine material, 20 ml solvent, 60°C).

Solvent	Size Fraction (mesh)	Extraction Ratio
Water	40	0.82
Water	80	0.85
Water	160	0.64

**Table 3. Soxhlet extraction ratios for various size fractions.  
(3 g medicine material, 150 ml solvent).**

Solvent	Size Fraction (mesh)	Extraction Ratio
Water	40	0.44
Water	80	0.68
Water	120	0.44
Water	160	0.39

Lower extraction ratios were obtained in the soxhlet extraction experiments, even when the same size fractions were compared. In soxhlet extraction, there is no stirring and the actual phase ratio varies, deviating from the nominal value. This could account for poor mass transfer from the surface of the particles to the bulk solution. These dynamic effects meant that equilibrium conditions had not been achieved by the interruption of the experiment. The optimal extraction was obtained for the 80-mesh size fraction. Commonly, smaller particle size implies larger specific area. While this will favor mass transfer it will also favor granular adsorption, with the net effect that lower extraction efficiencies would be obtained for both oversize and undersize particles. The extraction ratios observed for the various particle sizes could be related to the method of preparation. The tissue or structures of the plant vary with respect to the concentration of active components. Under specific pulverizing conditions, the degree of pulverization could differ with the degree of compactness of the plant tissue and thus account for the differences observed for the extraction ratios.

### Phase Ratio

Figure 3 shows the relationship of the extraction ratio and extract concentration with the phase ratio. The extract concentration increased with an increase in phase ratio. All of active compounds come from the raw material, and are conserved in the system. The slightly downward curve trend observed for the extraction ratio shows that the fraction of the active components in the bulk solution went down. This could be due to the effects of entrainment in the residue that are in turn related to the swelling characteristics of the tissue. The extraction ratio decreases with an increase of the phase ratio but this effect is less pronounced for  $S > 0.005$ . It is better to optimize the phase ratio to reduce solvent consumption and at the same time to assure an acceptable extraction ratio.

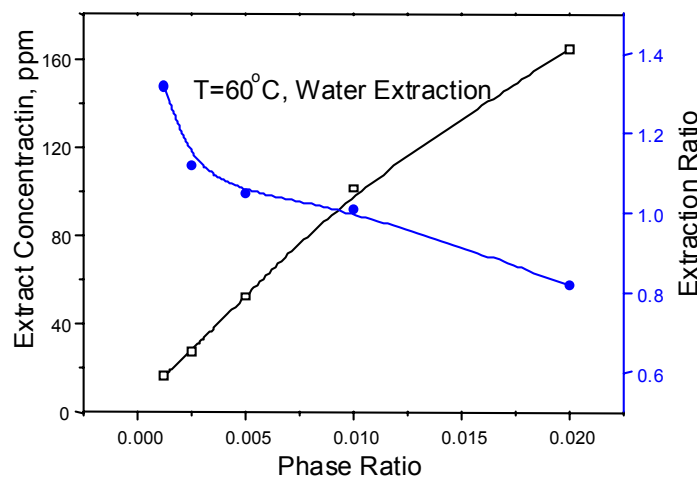


**Figure 3. Influence of phase ratio on extraction ratio and extract concentration.**

### **Co-current and Counter-current Extraction**

As we know, the maximum extraction ratio in any stage is limited by its thermodynamic properties. A three-stage co-current extraction process is usually adopted to assure high extraction ratios in traditional production. This process was simulated and the results are given in Table 4. For comparison a three-stage counter-current process was simulated and the results are given in Table 5. For the co-current extraction the per-stage extraction ratio decreases rapidly with progress to successive steps in the series for each experimental phase ratio. It is therefore important to select a suitable series by considering both total solvent consumption and accumulative extraction ratio.

*Table 4. Extraction ratio for co-current extraction.*

Solvent	Per Stage Solvent volume(ml)	Mass of medicine material (g)	Temperature (°C)	Size Fraction (mesh)	Serie s no.	Extraction Ratio
Water	20	0.4	60	20	1	0.60
					2	0.22
					3	0.08
					4	0.06
					Σ	0.97
Water	20	0.1	60	20	1	1.19
					2	0.22
					3	0.10
					Σ	1.51

*Table 5. Extraction ratio for counter-current extraction.*

Solvent	Solvent volume (ml)	Mass of medicine material (g)	Temperature (°C)	Size Fraction (mesh)	Extraction ratio
Water	20	0.4	60	20	1.06
	20	0.4	60	40	0.97

For the same solvent consumption the extraction ratio was observed to be some 20% greater for counter-current than co-current extraction.

### **Extraction with Different Solvents in Series**

Since the results shown in Table 1 indicated that the extraction of the different active components varied with solvent mixture an experiment was performed using different solvent mixtures in series. The results are given in Table 6. Compared with the extraction obtained with any single solvent, the extraction ratios were much higher. It is also found that the solvent order in the series had a distinct effect. Extraction with ethanol followed by water was best. The affinity of ethanol with the matrix material is better than for water, and this could therefore provide a better environment for the following extraction step.

*Table 6. Results of extraction with different solvent mixtures in series.*

Solvent	Per stage solvent volume (ml)	Mass of medicine material (g)	Size Fraction (mesh)	Extraction Ratio
Water first, then ethanol	20	0.4	20	1.79
Ethanol first, then water	20	0.4	20	2.05

## **CONCLUSIONS**

The experimental results indicated that solvent, temperature and raw material dimension were significant factors that affected the dynamic and thermodynamic performance of the rhubarb extraction system. Solvent and temperature should be chosen according to the active component targeted. Pulverizing raw material properly could decrease extraction time greatly. Increasing the series in co-current extraction to improve recovery ratio is not feasible. To maximize extraction of all of the active components a multiple solvent series is proposed. Multi stage counter-current extraction and extraction with different solvents in series achieved higher extraction ratios than for single-stage extraction, with less solvent consuming relatively. It is proposed that to extract target components more efficiently and to thus improve the utilization of resources and equipment a continuous counter-current extraction process be employed with solvent shifting.

## **REFERENCES**

1. A. W. Ding (1997), *J. Nanjing College Traditional Chinese Medicine*, **13** (4), 195-197.
2. X. C. Li (1998), *Chin. Pharm. J.*, **33** (10), 581-584.
3. F. L. Wei, M.C. Qi and J.S. Zhong (1998), *Chin. J. Chin. Mater. Medica*, **23** (10), 609-611.



## EXTRACTION OF LYSOZYME WITH REVERSE MICELLES USING A CONTACTOR AGITATED BY AUTOMATIC SUCTION OF LIQUID TYPE STIRRER

W. Zhang, H. Z. Liu, and J. Y. Chen

Young Scientist Laboratory of Separation Science and Engineering,  
State Key Laboratory of Biochemical Engineering, Institute of Chemical Metallurgy,  
Chinese Academy of Sciences, Beijing, China

Although the extraction and purification of proteins using reverse micelles has received wide attention in recent years, this method is not used in commercial practice. One major problem is the difficulty of phase separation because of easy emulsification owing to the presence of surfactant, especially using surfactants with a high hydrophile/lipophile balance value or dealing with intracellular proteins. In this paper, a novel contactor agitated with automatic suction of liquid type stirrer was used to disperse the aqueous phase or organic phase into another phase. Lysozyme was extracted to the reversed micellar phase with high extraction efficiency without emulsification even at low ionic strength (0.02 M KCl). The novel contactor can be used for a continuous process with integration of the mixer-settler contactor. The fixed and operating costs of the contactor are low and it can be used for reverse micelle extraction.

### INTRODUCTION

The extraction and purification of proteins using reverse micelles is a liquid-liquid extraction operation that has received wide attention. Most work has focused on the distribution of proteins and has been performed in a batch mode with little consideration given to the process itself or to the selection of equipment. The continuous extraction of protein using reversed micellar systems has been limited to a few examples, namely, the extraction of  $\alpha$ -amylase using two mixer-settler units [1], the extraction of a recombinant cutinase with a perforated rotating disc contactor [2,3], the recovery of intracellular proteins from *Candida utilis* in a spray column [4], the extraction of BSA using a centrifugal extractor [5] and the extraction of  $\alpha$ -amylase using two centrifugal extractors [6].

One major problem in the application of this method is the difficulty of phase separation owing to emulsification in the presence of surfactant, especially using surfactants with a high hydrophile/lipophile balance (HLB) value, such as AOT (sodium bis (2-ethylhexyl) sulfo-succinate) and SDS (sodium dodecyl sulphate) or dealing with intracellular proteins. It seems that static mixer-settler units and rotating disc contactor cannot be used to solve this problem [4]. Although spray column and centrifugal extractors can decrease the degree of emulsification during the extraction process, the extraction efficiency of the spray column is too low, while the fixed and operating costs of centrifugal contactors are too high. Therefore, a novel contactor that allows the efficient separation of the two phases with low cost and high extraction efficiency needs to be developed. In this study, we designed a novel contactor stirred by an automatic suction type stirrer at low speed, which can disperse an aqueous phase or organic phase into another phase. It was used to extract lysozyme from an aqueous phase to an AOT/ petroleum ether reverse micellar phase without emulsification.

## EXPERIMENTAL

### Experimental Apparatus

Two kinds of contactor stirred by automatic suction type stirrer were provided, as shown in Figure 1(a) and (b). The contactor consists of a cylindrical vessel and an automatic suction type stirrer. The vessel with four vertical baffles is 80 mm in inner diameter and 120 mm in height. As shown in Figure 1(c) and (d), the suction type stirrer consists of a hollow shaft, a hollow cylinder and a disc. The hollow shaft is 8.0 mm in inner diameter with four holes of 5.0 mm diameter drilled in the middle part. The hollow cylinder is 40 mm in diameter and 10 mm in height with 12 holes of 3.0 mm diameter on the wall. The function of the hollow shaft is to transport the solution. The disc is 40 mm in diameter and 5 mm in height. The function of the hollow cylinder is to stir the aqueous or organic phase and disperse the solution into small drops. The function of the disc is to stir the aqueous or organic phase.

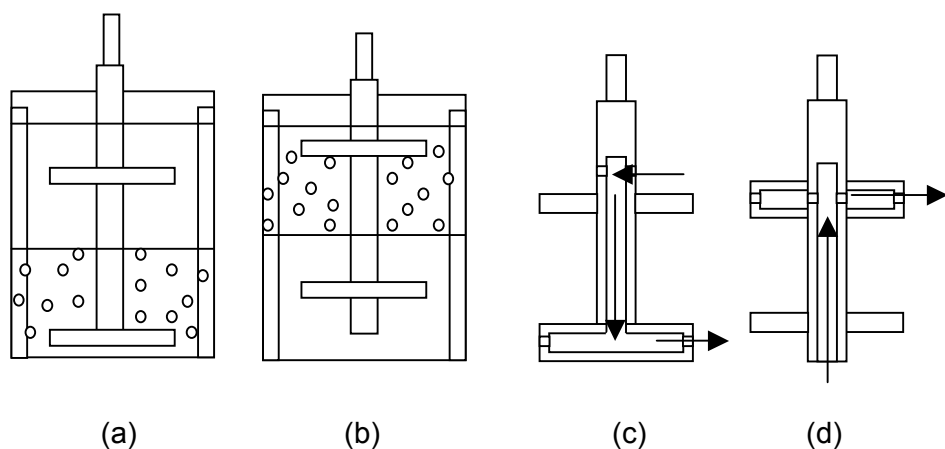


Figure 1. Experimental apparatus.

(a) contactor of light phase dispersed; (b) contactor of heavy phase dispersed; (c) stirrer of light phase dispersed; (d) stirrer of heavy phase dispersed.

### Reverse Micelle Extraction

The organic phase system used was 50 mM AOT/petroleum ether (b.p.: 90-120°C). The aqueous phase was 1.0 mg/ml lysozyme in 0.0125 M borax-HCl buffer at pH 9.0. Potassium chloride was used to control the ionic strength of the aqueous phase. Equal volumes (200 ml each) of aqueous and organic solutions were poured gently into the vessel. The suction stirrer rotated at a speed high enough to suck the dispersed phase and maintain a clear aqueous/organic interface. Samples of equal volumes (3 ml each) of aqueous and organic phase solutions were collected every 2 minutes and the amount of protein in each phase was measured. The protein concentration was determined from the UV absorption at 280 nm (UV-7542 spectrophotometer). Experiments were performed at  $25.0 \pm 0.5^\circ\text{C}$ . The protein mass balance was within the experimental error of  $\pm 5\%$ .

## RESULTS AND DISCUSSION

### The Effect of Rotation Speed

At the proper rotation speed, the aqueous/organic interface remains clear. When using the suction stirrer to disperse the organic phase (Figure 1(c)), the organic solution entered into the holes on the wall of the shaft under the suction pressure, then organic phase drops exited out of the cylinder of suction stirrer. They rose through the aqueous phase and coalesced at the aqueous/organic phase interface (Figure 1(a)).

The effect of rotation speed on lysozyme transfer was investigated using the suction stirrer for dispersion of organic phase (Figure 1(c)), as shown in Figure 2. Lysozyme transfer is relatively slow at low rotation speed such as 350 rpm, while the lysozyme transfer is relatively fast at a high rotation speed such as 580 rpm. For rotation speeds above 600 rpm, the aqueous/organic phase interface was destroyed. Solutions must be settled for a long time to obtain phase separation. For rotation speeds below 300 rpm, the organic solution cannot be dispersed into the aqueous phase due to low suction pressure arising from the rotation.

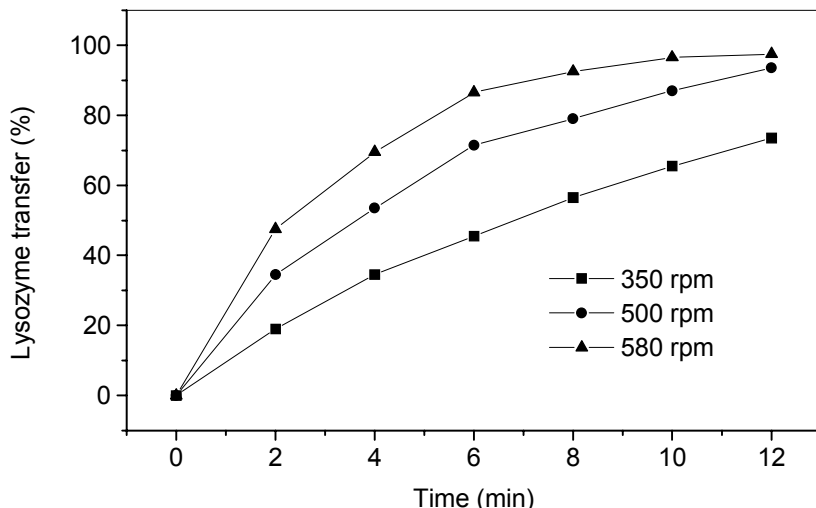


Figure 2. Effect of rotation speeds on lysozyme transfer using automatic suction type stirrer with organic phase dispersed. Aqueous phase: 1.0 mg/ml lysozyme, 0.10 M KCl.

### The Effect of Ionic Strength

The effect of ionic strength of the aqueous phase on the lysozyme transfer was studied using the automatic suction type stirrer to disperse organic phase at 500 rpm, as shown in Figure 3. The balance transfer of lysozyme at 0.02, 0.05 and 0.10 M KCl is close to 60%, 100% and 100%, respectively. Lysozyme transfer could be performed at different low KCl concentrations such as 0.10, 0.05, 0.02 M. The aqueous/organic phase interface remained clear and the organic phase remained transparent. A stable microemulsion was formed when the concentration of KCl in aqueous phase was zero. Lysozyme was extracted to the reverse micellar phase with high extraction efficiency without the emulsification problem of phase separation even with solutions having low ionic strength (0.02 M KCl).

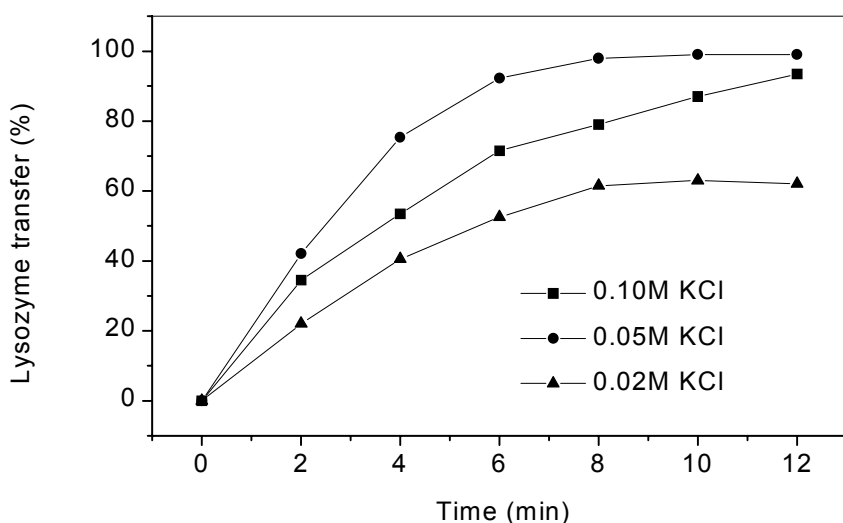


Figure 3. Effect of ionic strength on lysozyme transfer using automatic suction type stirrer with organic phase dispersed at rotation speed of 480 rpm.

### The Direction of Dispersion

The effect of the direction of dispersion on lysozyme transfer was studied, as shown in Figure 4. Mass transfer could be carried out with either phase dispersed. When using suction stirrer dispersing aqueous phase (Figure 1(d)), aqueous solution entered the holes at the bottom of shaft under the suction pressure, then drops of aqueous phase exited out of the cylinder of suction stirrer. They dropped through the organic phase and coalesced at the aqueous/organic phase interface. Finally, they entered into the aqueous phase and mass transfer was performed (Figure 1(b)). The lysozyme transfer for aqueous phase dispersion is faster than for organic phase dispersion. The experimental result could be explained that the reversed micelles were W/O emulsion. However, the highest rotation speed of 500 rpm for dispersion of aqueous phase to maintain a clear aqueous/organic interface is lower than that of 600 rpm required for dispersion of organic phase.

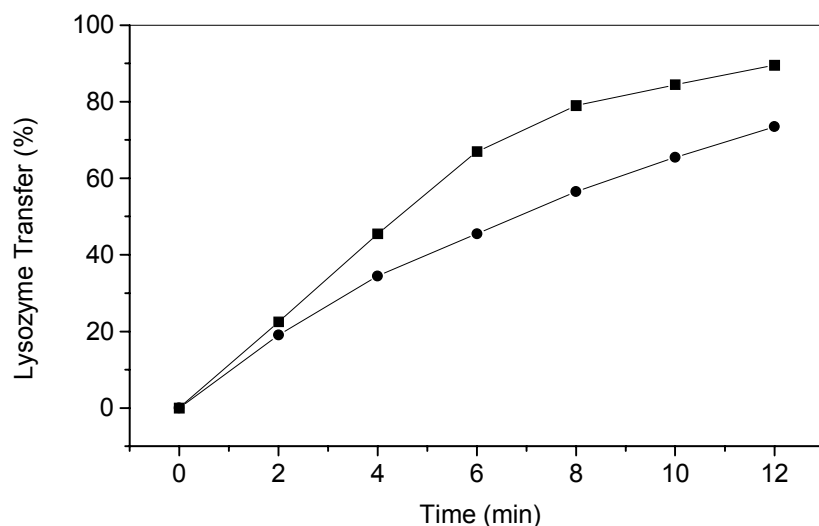


Figure 4. Effect of direction of dispersion on lysozyme transfer at rotation speed of 350 rpm.  
Aqueous phase: 0.10 M KCl, -■- aqueous phase dispersed; -●- organic phase dispersed.

### Comparing with a Traditional Mixer-settler Unit

The efficiency of the contactor agitated by automatic suction of liquid type stirrer was compared with that of a traditional mixer-settler unit. The effect of rotating speed of traditional stirrer on lysozyme transfer is shown in Figure 5. Lysozyme transfer reached 100% when stirred for 1 min and then settled to reach phase separation at relatively high rotating speed such as 580 rpm or 700 rpm. But lysozyme transfer reached 100% when stirred for 4 min and then settled to reach phase separation at relatively low rotating speed such as 480 rpm. The settling times at rotating speed of 480, 580 and 700 rpm were 8.5, 9.5 and 10.8 min, respectively. More than 10 min was needed to reach high efficiency and phase separation when using traditional mixer-settler unit.

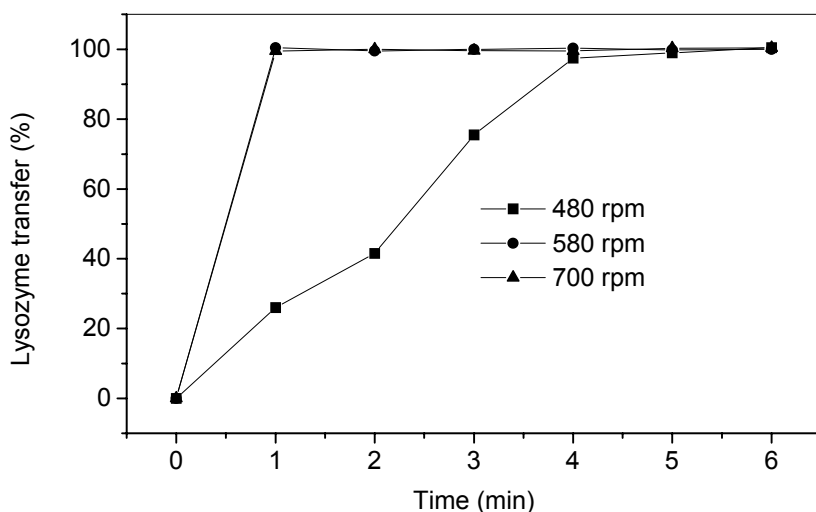


Figure 5. Effect of rotating speed on lysozyme transfer when using mixer-settler unit.

### The Character of the Contactor

The new contactor agitated by automatic suction of liquid type stirrer has several advantages. It can efficiently extract the protein using reverse micelles without emulsification problems even with solutions having low ionic strength (0.02 M KCl). The gentle rotation, which can avoid excessive shear, probably is good for maintaining the activity of proteins, while drastic agitation will cause the denaturation of proteins. The novel contactor can be used for a continuous process with integration of the mixer-settler contactor, as shown in Figure 6. The fixed and operating costs of the contactor may be low and it can be used for either phase dispersed. However, the advantages are not very notable since the total time for 100% extraction plus settling is the same for the new system or a traditional mixed-settler (near 10 min).

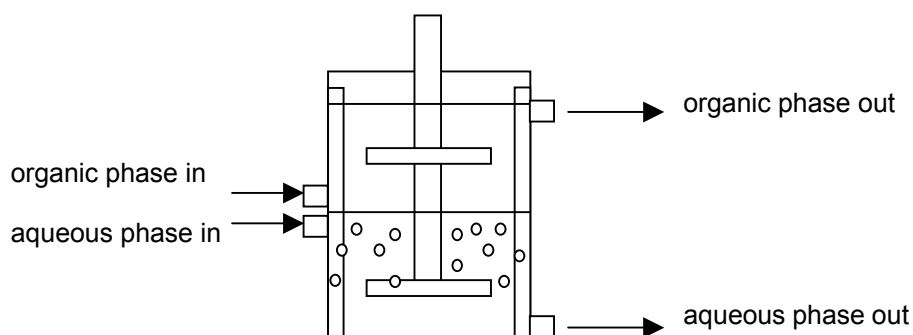


Figure 6. Apparatus for a continuous process when organic phase is dispersed.

### CONCLUSION

A novel contactor agitated with automatic suction type stirrer under low rotation speed to disperse the aqueous phase or organic phase into another phase could be efficiently used for the extraction of proteins using reversed micelles. Lysozyme was extracted to the reversed micellar phase without emulsification even at low ionic strength (0.02 M KCl).

## **ACKNOWLEDGEMENTS**

This work is supported by the National Natural Science Foundation of China, No. 29836130.

## **REFERENCES**

1. M. Dekker, K. Van't Riet, S. R. Weijers, J. W. A. Bultussen, C. Lanne and B. H. Bijsterbosch (1986), *Chem. Eng. J.*, **33**, B27-B33.
2. M. G. Carneiro-da-Cunha, M. R. Aires-Barros, E. B. Tambourgi and J. M. S. Cabral (1994), *Biotechnol. Tech.*, **8** (6), 413-418.
3. M. G. Carneiro-da-Cunha, M. R. Aires-Barros, E. B. Tambourgi and J. M. S. Cabral (1996), *Bioprocess Eng.*, **15**, 253-256.
4. D. H. Han, S. Y. Lee and W. H. Hong (1994), *Biotechnol. Tech.*, **8** (2), 105-110.
5. Q. Lu, K. Li, M. Zhang and Y. Shi (1998), *Sep. Sci. Technol.*, **33** (15), 2397-2409.
6. M. Dekker, K. Van't Riet, J. J. Van Der Pol, J. W. A. Baltussen, R. Hilhorst and B. H. Bijsterbosch (1991), *Chem. Eng. J.*, **46**, B69-B74.



## EXTRACTION OF LYSOZYME BY REVERSED MICELLAR SOLUTION IN A SIEVE-TRAY COLUMN

Yasuhiro Nishii, Chiemi Hara, Takumi Kinugasa,  
Susumu Nii\* and Katsuroku Takahashi\*

Niihama National College of Technology, Niihama, Japan  
\*Nagoya University, Nagoya, Japan

A sieve-tray column was designed and applied for reversed micellar extraction of lysozyme. Two-phase flow and mass-transfer characteristics were studied under various operating conditions. No effect of flow velocities was found on both overall mass-transfer coefficient and droplet diameter. Dispersed phase holdup increased with increasing velocity of continuous and dispersed phase. The column performance was compared with that of a spray and a packed column of similar size in terms of height equivalent per a theoretical stage. The sieve-tray column worked better at high throughput conditions. No significant activity change was observed for lysozyme in feed solution and that in raffinate or extract.

### INTRODUCTION

Reversed micellar extraction has attracted our attention as an emerging technology of bioseparation from 1980s. After the pioneering works by Luisi *et. al.* [1], Goklen and Hatton [2] and Dekker *et. al.* [3], research has been actively carried out to clarify the separation mechanism, equilibrium and kinetics of protein inclusion and release. With a rapid growth of pharmaceutical industries, efficient processes are eagerly desired for bioseparations. The technique of reversed micellar extraction is potentially applicable to a large-scale operation. Because of differences in properties between reverse-micellar solution systems and conventional liquid-liquid systems, special considerations are required for designing equipments for reversed micellar extraction. Only limited research has been carried out on column-type contacting devices.

Lye *et. al.* [4] reported individual mass-transfer coefficients in a spray column operation. The present authors conducted experiments on reversed micellar extraction of lysozyme with a packed column and found that the organic phase flows in the form of droplets even for PTFE packing which is highly wettable for organic phase [5]. This flow behavior was specifically observed for reversed micellar systems. Furthermore, the activity of lysozyme was successfully kept at high value during the operation. When a rotating disc contactor was used, sufficiently large holdup of dispersed phase could be attained. However at the same time, a large shear stress caused a loss of protein activity [6]. The present study focuses on a sieve-tray column which is typically used in various extraction processes for large scale operations. Flow and mass-transfer characteristics were examined in a laboratory scale apparatus and the performance was compared with other columns.

## EXPERIMENTAL

Aerosol-OT (bis (2-ethylhexyl) sodium sulfosuccinate, AOT) was supplied from Nacalai Tesque, Inc. and used without further purification. Organic solution as dispersed phase was prepared by dissolving AOT into 2-2-4 trimethylpentane at 0.05 kmol/m<sup>3</sup>. Lysozyme (M.W.14300, pI=11) was dissolved into 0.3 kmol/m<sup>3</sup> KCl aqueous solution and used as a feed solution of continuous phase. Concentration of lysozyme in feed solution was 0.1 kg/m<sup>3</sup>. It was adjusted to pH 7 with aqueous solutions of KOH and HCl. Prior to the experiment, the organic solution was saturated with protein-free feed solution for further use. Physical properties of both phases are listed in Table 1. Lysozyme was obtained from Sigma Chemical Co. and other chemicals from Wako Pure Chemical Industries, Ltd. or Katayama Chemical. Extraction equilibrium of the solution system was reported by Kinugasa *et al.* [7]. Within the range of operational condition of this work, linear equilibrium relation between  $C_d$  and  $C_c$  was obtained. Distribution ratio of lysozyme, which is defined as  $C_d / C_c$ , is as high as about 50.

*Table 1. Physical properties.*

	Density (kg/m <sup>3</sup> )	Viscosity (Pa.s)	Interfacial tension (mN/m)
Continuous phase	998	$0.90 \times 10^{-3}$	2
Dispersed phase	692	$0.47 \times 10^{-3}$	

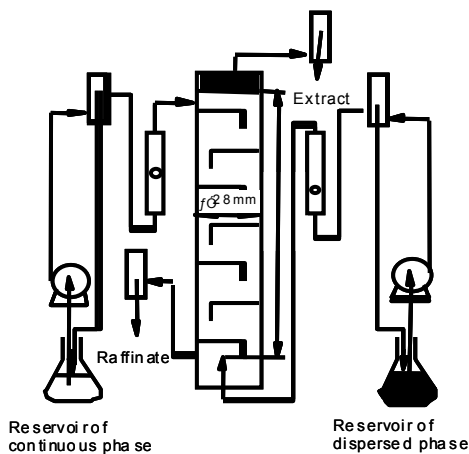


*Figure 1. Schematic diagram of experimental setup.*

Figure 1 shows a schematic diagram of the sieve-tray extraction column. Within a glass tube of 28 mm in i.d. and 210 mm long, 7 plates of PTFE were mounted at 25 mm clearance. PTFE was chosen as a tray material to provide a surface that is preferentially wetted by organic solvents. Such a surface can work twofold: one is to enhance the coalescence of organic phase droplets and the other is to enhance the droplet formation. The tray was fabricated from a circle plate. A part of the plate was bended down along with a chord to make an opening space for downcomer. Holes formed are on horizontal part of the plate. Detailed specification of the tray is given in Table 2.

The column operation was started with supplying both solutions slowly. After finding the continuous phase reaches a level, flow rates of both phases were adjusted at respective values to keep a constant level of water/oil interface. Samples of both solutions were taken out from the outlet after reaching steady state. Concentrations of lysozyme in each phase were determined with UV-Visible spectrophotometer (Shimadzu UV-1600) from an absorption at 280 nm. Sizes of dispersed droplets were measured from close-up images taken by a digital video camera. Behavior of two-phase flow above a tray was also monitored by the camera. Activity of lysozyme in extract and raffinate was measured by the method developed by Imoto and Yagishita [8].

Change in rising velocity of droplet,  $U_d$ , with  $V_d$  for various  $V_c$  is presented in Figure 5. Because of a constant drop size for any flow velocities examined (referred in Figure 7), the  $U_d$  can be interpreted as the velocity of circulation flow. Obviously, the increase of  $V_d$  leads to an increase of circulation flow velocity and a decrease of  $V_c$  causes an increase of  $U_d$ .

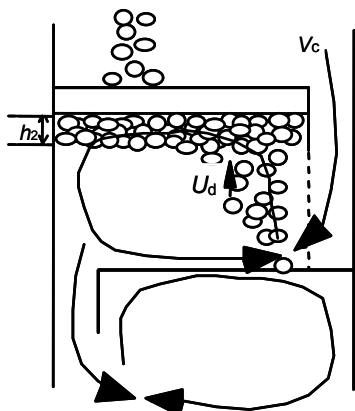


Figure 4. Flow pattern above a tray.

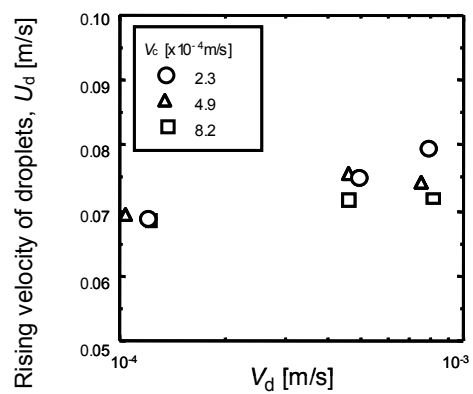


Figure 5. Rising velocity of droplets.

Figure 6 shows the effect of  $V_c$  on thickness of accumulated drop layer,  $h_2$ . The balance of rates between droplet supply and coalescence determines the thickness. Values of  $h_2$  increase with the increase in both  $V_c$  and  $V_d$ . The effect of  $V_d$  on  $h_2$  is straightforward. The increase of  $V_c$  leads to slow down the circulation and to suppress the movement of droplets in the accumulated layer. In such a way, increasing  $V_c$  may result in decreasing the rate of droplet coalescence.

### INTERFACIAL AREA AND MASS-TRANSFER COEFFICIENT

Average diameter of dispersed phase droplets is determined as follows. Since the shape of droplets is ellipse, the size is given as an equivalent diameter of a sphere which has the same volume as the body of ellipse revolution. For more than 100 droplets, the size is measured from their images and the average droplet diameter was determined. Effects of both flow velocities on droplet size are shown in Figure 7. The size is about 3 mm and is independent of both  $V_d$  and  $V_c$ .

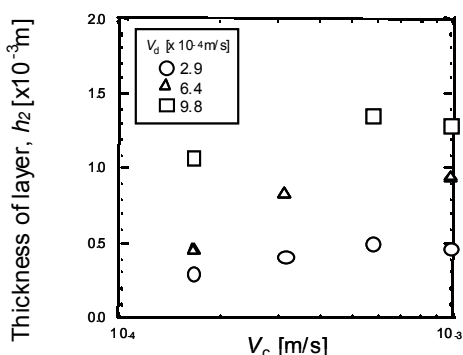


Figure 6. Thickness of layer of accumulated droplets.

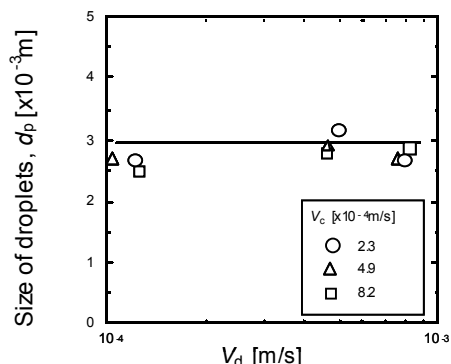


Figure 7. Size of droplets.

Since the organic phase mainly exists as a form of droplet, interfacial area is calculated from the following equation when holdup,  $\phi$ , is known.

Change in rising velocity of droplet,  $U_d$ , with  $V_d$  for various  $V_c$  is presented in Figure 5. Because of a constant drop size for any flow velocities examined (referred in Figure 7), the  $U_d$  can be interpreted as the velocity of circulation flow. Obviously, the increase of  $V_d$  leads to an increase of circulation flow velocity and a decrease of  $V_c$  causes an increase of  $U_d$ .

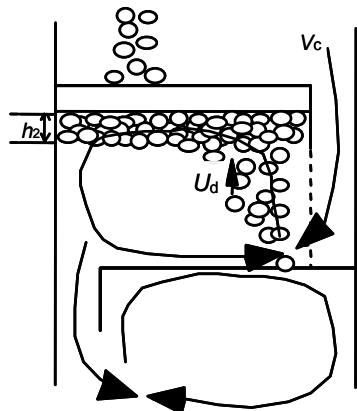


Figure 4. Flow pattern above a tray.

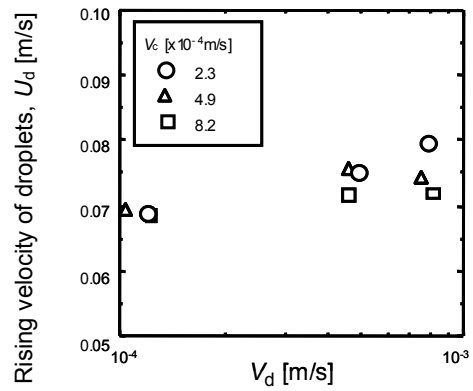


Figure 5. Rising velocity of droplets.

Figure 6 shows the effect of  $V_c$  on thickness of accumulated drop layer,  $h_2$ . The balance of rates between droplet supply and coalescence determines the thickness. Values of  $h_2$  increase with the increase in both  $V_c$  and  $V_d$ . The effect of  $V_d$  on  $h_2$  is straightforward. The increase of  $V_c$  leads to slow down the circulation and to suppress the movement of droplets in the accumulated layer. In such a way, increasing  $V_c$  may result in decreasing the rate of droplet coalescence.

### INTERFACIAL AREA AND MASS-TRANSFER COEFFICIENT

Average diameter of dispersed phase droplets is determined as follows. Since the shape of droplets is ellipse, the size is given as an equivalent diameter of a sphere which has the same volume as the body of ellipse revolution. For more than 100 droplets, the size is measured from their images and the average droplet diameter was determined. Effects of both flow velocities on droplet size are shown in Figure 7. The size is about 3 mm and is independent of both  $V_d$  and  $V_c$ .

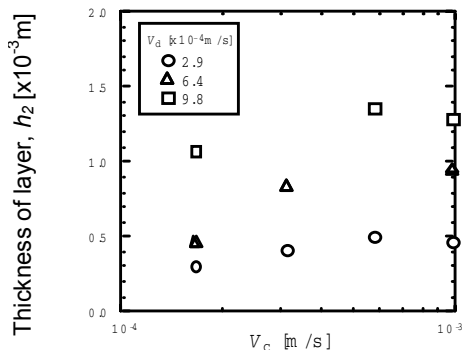


Figure 6. Thickness of layer of accumulated droplets.

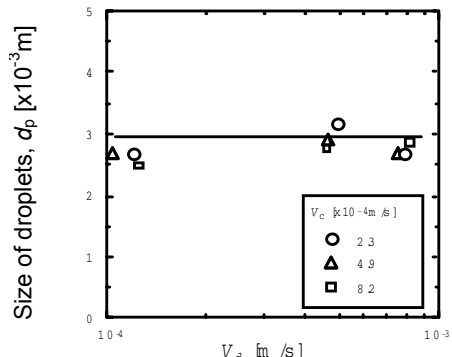


Figure 7. Size of droplets.

Since the organic phase mainly exists as a form of droplet, interfacial area is calculated from the following equation when holdup,  $\phi$ , is known.

$$a = \frac{6\phi}{d_p} \quad (2)$$

In Figure 8, interfacial area,  $a$  is plotted against  $V_d$  and  $V_c$ . Because  $d_p$  is constant under the present condition, interfacial area is proportional to holdup of dispersed phase. As mentioned above, the increase in  $V_c$  leads to the increase in holdup, thus the  $a$  increased with increasing  $V_c$ . Once interfacial area is determined, the overall mass-transfer coefficient,  $K_c$  can be separated from  $K_c a$ .

Overall mass-transfer coefficient,  $K_c$ , is presented in Figure 9. Values of  $K_c$  are constant with varying  $V_d$  and  $V_c$ , which suggests the mass-transfer coefficient of lysozyme is independent of flow conditions. Interestingly, values of  $K_c$  are in the same order of those values obtained for metal ion extraction in a mixer-settler column. Furthermore, those values are almost constant for the change of flow velocities under strong agitation [9]. This fact implies that a change of interfacial area predominates the extraction rate in column operations rather than a change of mass-transfer coefficient.

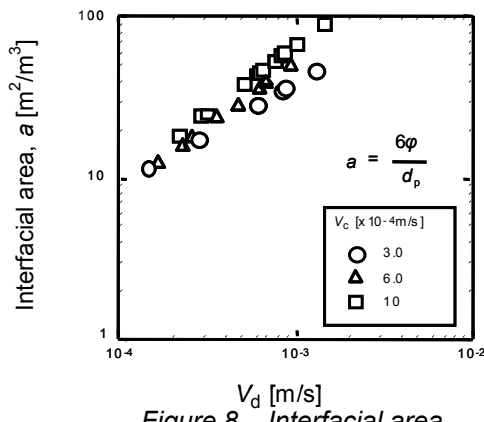


Figure 8. Interfacial area.

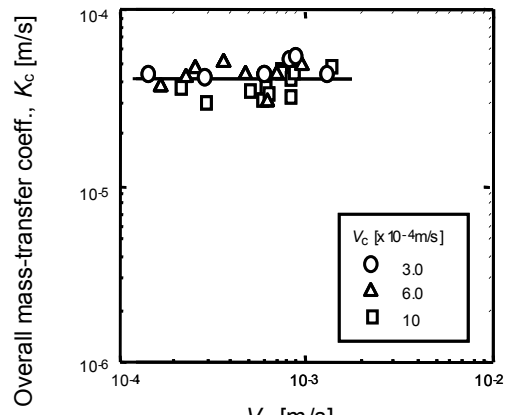


Figure 9. Overall mass-transfer coefficient.

## COMPARISON WITH OTHER COLUMNS

Performance of the sieve-tray column is compared with that of a spray or a packed column in terms of height equivalent per a theoretical stage (HETS). These three columns have similar height and diameter. Size of the spray column is the same as the sieve-tray column, and the packed column is of 35 mm i.d. and the height of packing is 200 mm.

Figure 10 represents values of HETS against total throughput,  $V_t$  which is defined as  $V_c + V_d$ . Better performance of the sieve-tray column is found at large  $V_t$ . Although the packed column gives the best HETS in the range of small  $V_t$ , the performance becomes worse with increasing the throughput. The use of sieve-tray column is recommended for the operation at a large throughput condition.

## ACTIVITY CHANGE OF LYSOZYME

Relative activity of lysozyme in the extract and the raffinate is given in Table 3. No significant change was observed for the activity during the experiment. Under a mild mixing condition in the sieve-tray column, lysozyme was extracted into reversed micelles without denaturation. Repeating of droplet coalescence and re-dispersion give no effect on the protein activity.

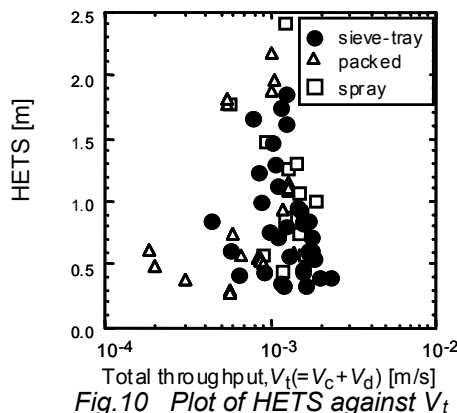


Fig. 10 Plot of HETS against  $V_t$

Table 3. Relative activity of lysozyme.

	$V_c$ (m/s)	$V_d$ (m/s)	Relative activity (%)
Extract *	$5.8 \times 10^{-4}$	$9.4 \times 10^{-4}$	99
Raffinate	$5.7 \times 10^{-4}$	$2.6 \times 10^{-4}$	108

\* Lysozyme was back-extracted from extract into aqueous solution.

## CONCLUSION

Extraction of lysozyme in a sieve-tray column was studied under various operating conditions and the column performance was compared with other columns. Droplet size was independent of flow velocities. A large circulation flow of continuous phase was observed above the tray and the effects of  $V_c$  and  $V_d$  on the circulation velocity was discussed. The holdup of dispersed phase, which is closely related to the interfacial area, changed with the circulation velocity. No effect of flow velocities was found on the overall mass-transfer coefficient. Performance of the sieve-tray column was compared with that of a spray and a packed column of similar size in terms of HETS. The sieve-tray column had an advantage of the operation at high throughput conditions. Activity of lysozyme was perfectly kept during the experiment.

## NOMENCLATURE

$a$ = interfacial area per unit volume	[ $m^2/m^3$ ]	$z$ = stage clearance	[m]
$C$ = lysozyme concentration	[ $kg/m^3$ ]	$\phi$ = holdup of dispersed phase	[-]
$E_{oc}$ = overall stage efficiency	[-]		
$d_p$ = drop diameter	[m]	<Subscripts>	
$h_2$ = thickness of accumulated layer	[m]	c = continuous phase	
$K$ = overall mass-transfer coefficient	[ $m/s$ ]	d = dispersed phase	
$U_d$ = rising velocity of droplets	[ $m/s$ ]	t = total	
$V$ = superficial velocity of phases	[ $m/s$ ]		

## REFERENCES

1. P. L. Luisi, F. J. Bonner, A. Pellegrini, P. Wiget and R. Wolf (1979), *Helv. Chim. Acta*, **62**, 740-753.
2. K. E. Goklen. and T. A. Hatton (1985), *Biotech. Prog.*, **1**, 69-74.
3. M. Dekker, K. V. Riet and S. R. Weijers (1986), *Chem. Eng. J.*, **33**, B27-B33.
4. J. Tong and S. Furusaki (1995), *J. Chem. Eng. Jpn.*, **28**, 582-589.
5. G. J. Lye, J. A. Asenjo and D. L. Pyle (1996), *AICHE J.*, **42**, 713-726.
6. Y. Nishii, S. Nii, K. Takahashi and H. Takeuchi (1999), *J. Chem. Eng. Jpn.*, **32**, 211-216.
7. T. Kinugasa, S. Tanahashi and H. Takeuchi (1991), *Ind. Eng. Chem.*, **30**, 2470-2476.
8. T. Imoto and K. Yagishita (1971), *Agr. Biol. Chem.*, **35**, 1154-1156.
9. S. Nii, J. Suzuki, K. Tani and K. Takahashi (1997), *J. Chem. Eng. Jpn.*, **30**, 1083-1089.



## MODELING OF SOLUBILITIES OF ESSENTIAL OILS IN LIQUID CARBON DIOXIDE PRESENT IN THREE ODORIFEROUS PLANTS

E. M. B. D. Sousa, D. N. Silva, O. Chiavone-Filho and M. A. A. Meireles\*

UFRN, Dept. de Engenharia Química, Natal, Brazil

\*UNICAMP, Faculdade de Engenharia de Alimentos, Campinas, Brazil

This work discusses a methodology to estimate the solubility for systems formed of an odoriferous plant + CO<sub>2</sub>. To develop the estimation method, experimental solubility data for three different odoriferous plants, whose volatile oils have several pharmacological applications, are used. The estimation method proposed uses the volatile oil composition obtained by supercritical fluid extraction. Based on the chemical composition of the volatile oil and the use of a group contribution method, a pseudo pure component is defined. The solubilities of the volatile oils for the systems are calculated using the Peng-Robinson equation of state with one adjustable parameter. The results demonstrate that, in spite of the simplifying assumptions, the method quantitatively describes the experimental data.

### INTRODUCTION

The worldwide energy crises and the consumer's choice for products made from natural resources have stimulated the search for new technologies. Supercritical fluid extraction (SFE) is known as a clean technology because it presents no harm to either man or the environment. SFE using CO<sub>2</sub> requires no additional treatment of the product and of the residues since the solvent (CO<sub>2</sub>) is not toxic. In addition, due to the use of relatively low temperatures, the solute maintains its original characteristics.

For the process design of SFE systems, reliable methods to calculate the phase equilibrium parameters of the extraction step (odoriferous plant + CO<sub>2</sub>) and the separation step (volatile oil + CO<sub>2</sub>) must be available. The multicomponent mixture that forms the volatile oil is generally composed of substances from different chemical classes such as aldehydes, alcohols, terpenes, sesquiterpenes, oxygenated and phenolic compounds, etc. Such systems have a behavior that is appreciably far from the ideal, to make thermodynamic modeling difficult. In addition, the strong asymmetry of the system, due to differences of size and polarity of the substances, and the proximity of the solvent critical point would require thermodynamic modeling using a complex equation of state. This would need a considerable amount of experimental data, not yet available. Therefore, simplified models are presently used to assess some of the information of the system. This work proposes a model for the measured solubilities of the, odoriferous plant + CO<sub>2</sub>, system using the chemical compositions of the volatile oils and the Peng-Robinson equation of state with one adjustable parameter for the attractive term.

The following odoriferous plants were selected for this work: Clove buds (*Eugenia caryophyllus*), Eucalyptus-NE (*Eucalyptus tereticornis* Smith), and *Lippia sidoides* Cham. The solubility data for the system odoriferous plant + CO<sub>2</sub> were obtained using the dynamic method [1].

## CHARACTERIZATION OF THE VOLATILE OIL

Volatile oils are multicomponent mixtures composed of substances from several chemical classes, for which the thermophysical properties are mostly unknown. For the solubility modeling, the volatile oil was considered a pseudo-component formed by the multicomponent mixture. The compositions of the multicomponent mixtures were determined by gas chromatography coupled to mass spectrometry [2, 3]. Although the response factor of the various substances for the GCMS analysis may not be the same, the area percent was used directly as a mass fraction. This information was used to obtain the mixture composition in terms of molar fractions. The thermophysical properties of CO<sub>2</sub> and of some volatile oil components were obtained from AIChE-DIPPR [4]. When the thermophysical properties of the substances were missing, their values were estimated using the group contribution method of Joback [5]. The needed vapor pressures  $P$  were estimated using the Wagner equation as modified by Vetere [6]:

$$A = -\alpha_c ; \quad \alpha_c = -0.294 + 1.1708 \frac{T_{br} \ln P_c}{1 - T_{br}} ; \quad (1)$$

$$\frac{\alpha_b}{\alpha_c} = 3.0042 - 2.4211 T_{br} ; \quad B = \frac{\alpha_b + 2\alpha_c - 3H - \ln P_c}{1.5(1 - T_{br})^{0.5}} ; \quad (2)$$

$$C = \frac{\alpha_c - H - B(1 - T_{br})^{0.5}}{(1 - T_{br})^{0.5}} ; \quad H = \frac{T_{br} \ln P_c}{1 - T_{br}} \quad (3)$$

where  $A$ ,  $B$ ,  $C$ ,  $\alpha$  and  $H$  are constants evaluated from the reduced ( $r$ ) and critical ( $c$ ) and boiling ( $b$ ) properties. The acentric factor  $\omega$  was determined using the Edmister [7] expression:

$$\omega = \frac{3}{7} \left( \frac{T_b}{T_b - T_c} \right) \log \left( \frac{1.01325}{P_c} \right) - 1 \quad (4)$$

Once the thermophysical properties of each compound were known, the Kay rule [8] was used to calculate the pseudo-component properties ( $M$ ):

$$M = \sum x_i M_i \quad (5)$$

The molar volume of each volatile oil ( $V_1^{sat}$ ) was experimentally determined using a digital densimeter (DMA 602 ANTON PAAR, Austria) for temperatures from 283.15 to 298.15 K, with a 5 K interval. The volatile oil densities varied linearly with the temperature, and this information was used to evaluate the Poynting correction.

## THERMODYNAMIC MODEL

The solubility was modeled using the following isofugacity criterion:

$$\hat{f}_i^S(T, P, X_i) = \hat{f}_i^F(T, P, Y_i) \quad (i = 1, N) \quad (6)$$

where the superscripts  $S$  and  $F$  refer to the solid (odoriferous plant) and the fluid (liquid, gas, or supercritical), respectively.  $X_i$  and  $Y_i$  correspond to the solid and fluid phase composition, respectively.

If the solid phase is said to be formed by a cellulosic structure (inert to the action of the solvent) and a solute, *i.e.*, the volatile oil, then we have  $\hat{f}_1^s(T, P, X_1) = f_1^s(T, P)$ . Recalling that the volatile oil is treated as a pseudo-component, designated by the subscript 1, the fluid phase can also be treated as a binary mixture, where the molar fraction of component 1 is the volatile oil solubility ( $Y_1$ ), so that equation (6) may be re-written as:

$$f_1^S(T, P) = \hat{f}_1^F(T, P, Y_1) \quad (7)$$

Therefore, the fugacities ( $\hat{f}_i^F$  and  $f_i^S$ ) of the volatile oil in the fluid and in the solid phases are given, in terms of the pseudo-component, by:

$$\hat{f}_1^F = Y_1 \hat{\phi}_1^F P \quad (8)$$

$$f_1^S = P_1^{sat} \phi_1^{sat} \exp \left[ \frac{V_1^{sat} (P - P_1^{sat})}{RT} \right] \quad (9)$$

Combining equations (8) and (9) and remembering that the vapor pressure values are low ( $\phi_1^{sat} \approx 1$  and  $P - P_1^{sat} \approx P$ ) and that so are the oil concentration ( $\hat{\phi}_1^F \approx \hat{\phi}_1^{F,\infty}$ ), the solubility can be evaluated from:

$$Y_1 = \frac{P_1^{sat} \exp \left( \frac{V_1^{sat} P}{RT} \right)}{\hat{\phi}_1^{F,\infty} P} \quad (10)$$

The fugacity coefficient at infinite dilution was calculated using the Peng-Robinson equation [9] and the computer routines from Sandler [10]. The values of  $K_{12}$  were estimated for every pair of temperature and pressure, considering that the solute is at infinite dilution in the solvent phase, i.e.,  $Y_{oil} = Y_1 = 10^{-6}$ , and using the experimental value of the solubility to establish the optimum value of the interaction parameter. Next, the average with respect to temperature and pressure of  $K_{12}$  for each oil or system was evaluated. These values were used to estimate the solubility and compared to the experimental value. Therefore, the procedure just described makes the parameter  $K_{12}$  correct both the non-ideal behavior of the fluid phase and the interaction between the oil components and the cellulosic structure. Actually, the parameter  $K_{12}$  is defined as a correction of the geometric average for the attractive term (a), using the quadratic mixing rule. For the repulsive term (b), the linear mixing rule was used, without additional parameter.

$$a = \sum \sum x_i x_j a_{ij} \quad (11)$$

when  $i$  is different to  $j$ , for instance  $i = 1$  and  $j = 2$ :

$$a_{12} = \sqrt{a_{11} a_{22}} (1 - K_{12}) \quad (12)$$

## RESULTS AND DISCUSSION

The thermophysical properties of the volatile oils are given in Table 1. Although the volatile oils compositions are very different from each other [1-3] their thermophysical properties are similar. For instance, clove oil contains 79.7% of eugenol, 10.1% of  $\beta$ -caryophyllene, 9.40% of Eugenyl acetate, and 0.80% of humulene. These values were obtained by averaging the composition of clove oil given in literature [1, 2]. The *L. sidoides* oil contains 24 compounds, the major ones being thymol (48.3 %), trans-caryophyllene (13.8%), 1,8-cineole (8.6%),  $\alpha$ -terpineol (2.3%) [3]. The eucalyptus-NE oil contains 26 substances [3], the major ones being aromadendrene (21.1%), globulol (13.8%), 1,8 cineole (11.0%), and 4-terpineol (4.4%). The volatile oils compositions given above are expressed in area percentage. Nonetheless, as previously discussed, they were directly used as a mass fraction in order to express the oils compositions in terms of molar fraction. The other substances found in the volatile oil of these three odoriferous species were polar, thus adding to the difficulties of characterizing and modeling the phase equilibria.

*Table 1. Thermophysical properties of clove oil, eucalyptus oil, and L. sidoides oil.*

Volatile oil	<i>MW</i> (g/mol)	<i>T<sub>b</sub></i> (K)	<i>T<sub>c</sub></i> (K)	<i>P<sub>c</sub></i> (bar)	$\omega$	<i>A<sub>p</sub></i> *	<i>B<sub>p</sub></i> *
Clove	172.38	530.11	737.60	32.44	0.6397	1.4254	-0.0014
Eucalyptus-NE	184.00	541.31	762.38	24.93	0.4435	1.4897	-0.0017
<i>L. sidoides</i>	159.66	533.24	755.71	30.90	0.5145	1.3933	-0.0015

$*\rho$  (g/cm<sup>3</sup>) =  $A_p + B_p T$  (K), from 283 to 298 K.

Tables 2 to 4 report the estimated values of the binary interaction parameter  $K_{12}$ , along with the experimental and the calculated solubilities.

*Table 2. Solubilities of clove oil [1] in CO<sub>2</sub> [2] as a function of temperature and pressure. Solubility values were calculated using  $K_{12} = 0.019$ .*

Experimental data	Pressure (bar)	Temperature (K)	Calculated solubility	Experimental solubility	Relative deviation (%)
[2]	66.7	283.15	0.0746	0.0618	20.8
	66.7	288.15	0.0555	0.0625	11.3
[1]	66.0	288.15	0.0548	0.0536	2.2
	70.0	288.15	0.0586	0.0561	4.3
	72.0	288.15	0.0604	0.0573	5.4
	80.0	288.15	0.0675	0.0586	15.1
	100.0	298.15	0.0514	0.0638	19.4
Mean deviation					11.2

*Table 3. Solubilities of L. sidoides oil [1] in CO<sub>2</sub> [2] as a function of temperature and pressure. Solubility values were calculated using  $K_{12} = 0.234$ .*

Experimental data	Pressure (bar)	Temperature (K)	Calculated solubility	Experimental solubility	Relative deviation (%)
[2]	66.7	288.15	0.0050	0.0053	6.7
	66.7	293.15	0.0050	0.0062	20.0
[1]	66.7	295.65	0.0047	0.0052	9.1
	66.7	283.15	0.0047	0.0036	31.3
	66.7	298.15	0.0042	0.0036	17.5
	78.5	288.15	0.0051	0.0049	4.9
	78.5	293.15	0.0053	0.0055	3.9
Mean deviation					13.4

*Table 4. Solubilities of Eucalyptus-NE oil [1] in CO<sub>2</sub> [2] as a function of temperature and pressure. Solubility values were calculated using  $K_{12} = 0.296$ .*

Experimental data Ref.	Pressure (bar)	Temperature (K)	Calculated solubility	Experimental solubility	Relative deviation (%)
[2]	66.7	288.15	0.00089	0.00094	5.1
	66.7	288.15	0.00089	0.00098	8.7
	66.7	283.15	0.00064	0.00049	32.0
	66.7	293.15	0.00120	0.00097	23.8
	78.5	288.15	0.00082	0.00118	30.0
Mean deviation					19.9

The mean deviations in Tables 2 to 4 are relatively large, but we should recall that several simplifications were made in order to treat a very complex system as a two-phase binary system. In addition, the majority of the experimental data used were taken close to the solvent critical point, thus making modeling even harder. Notwithstanding, from the designing point of view the calculated solubility can be satisfactorily used for initial scale-up calculations. In addition, the results can be used as a guide to experimental design for solubility isotherms determinations.

Figures 1 and 2 show the dispersion between calculated and experimental values of the solubility. The spread of the values observed for the system clove + CO<sub>2</sub> is partially due to the fact that two independent data sets were used. Nevertheless, for the other two systems (eucalyptus + CO<sub>2</sub> and *L. sidoides* + CO<sub>2</sub>) the deviations were even higher, although in both cases the experimental data came from a unique data set.

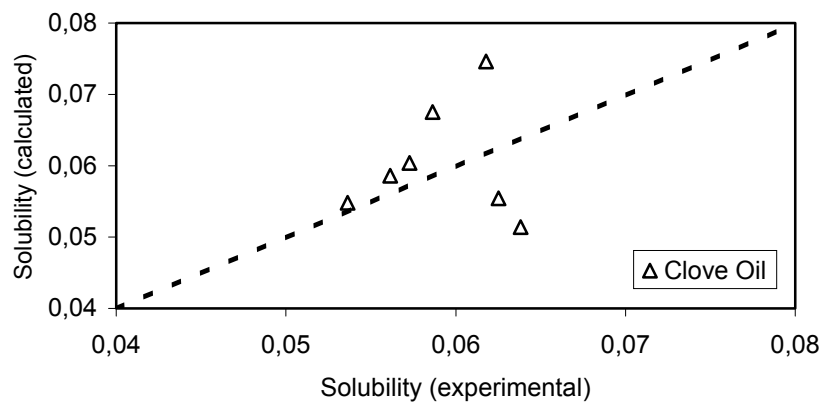


*Figure 1. Solubility of clove oil in CO<sub>2</sub> in mole fraction.*

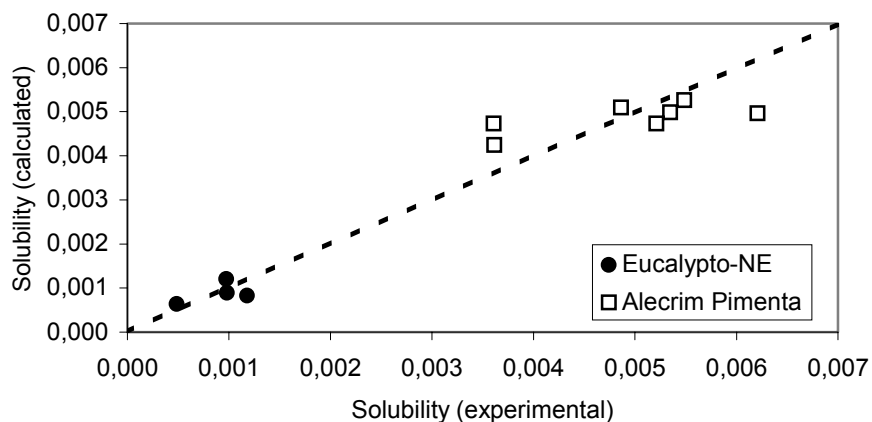


*Figure 2. Solubilities of Eucalyptus-NE and *L. sidoides* oils in CO<sub>2</sub> in mole fraction.*

## CONCLUSIONS

The methodology employed to estimate the solubility for systems containing odoriferous plant + CO<sub>2</sub> provided satisfactory results. They were satisfactory if we consider both the simplifications made to treat the multicomponent mixture that forms the volatile oil as a pseudo-component and the need to assess the thermophysical properties using a group contribution method, which was developed with information for substances that belongs to other chemical classes.

The parameter  $K_{12}$  embodies both the non-ideal behavior of the fluid phase and the interaction of the volatile oil with the cellulosic structure. Nevertheless, in order to obtain a quantitative description of the system, the cubic equation of state that was used would have to be substituted by relations that are more accurate, so that the polarity of the substances are better considered [11]. However, we should keep in mind that the phase equilibrium of the major volatile oil compounds with CO<sub>2</sub> has to be studied in order to understand the true nature of the interaction between the various substances. Another suggestion, is to optimize  $K_{12}$  with a least square procedure, instead of using the average value.

It must be added that for the scale up of processes the results are very important and satisfactory, since up to now scaling up is performed using the overall extraction curves, thus treating the SFE extracts as a pseudo-component.

## ACKNOWLEDGEMENTS

The authors would like to thank the financial support granted by the Brazilian National Science Foundation, CNPq (Conselho Nacional de Desenvolvimento Científico e Tecnológico) and FAPESP (1999/01962-1).

## REFERENCES

1. V. M. Rodrigues, M. A. A. Meireles and M. O. M. Marques (2000), *Proc. 5th Int. Symp. Supercritical Fluids*, Atlanta, Georgia, USA, CD-ROM.
2. V. M. Rodrigues, E. M. B. D. Sousa, A. R. Monteiro, O. Chiavone-Filho, M. A. A. Meireles and M. O. M. Marques (2001), *J. Supercrit. Fluids*, submitted.
3. E. M. B. D. Sousa, O. Chiavone-Filho, M. T. Moreno, H. N. M. Oliveira and M. A. A. Meireles (2001), *Proc. 2nd Int. Meet. High Pressure Chemical Engineering*, Hamburg, CD-ROM.
4. T. E. Daubert and R. P. Danner (1995), DIPPR Data Compilation Version 12.0, AIChE, New York.
5. R. C. Reid, J. M. Prausnitz and B. E. Poling (1987), *The Properties of Gases and Liquids*, 4th edn., McGraw Hill, New York.
6. A. Vetere (1991), *Fluid Phase Equilibria*, **62**, 1-10.
7. W. C. Edmister and B. I. Lee (1983), *Applied Hydrocarbon Thermodynamics*, Vol. 1, Gulf Publishing Company Book Division, Houston.
8. W. B. Kay (1936), *Ind. Eng. Chem.*, **28** (9), 1014-1019.
9. D. Y. Peng and D. B. Robinson (1976), *Ind. Eng. Chem. Fundam.*, **15**, 59-64.
10. S. I. Sandler (1989), *Chemical and Engineering Thermodynamics*, 2nd edn., John Wiley & Sons.
11. R. Stryjek and J. H. Vera (1986), *Can. J. Chem. Eng.*, **64**, 334-340.

## EVALUATION OF IMPROVED SOLVENTS FOR CAPROLACTAM EXTRACTION

Mathijs L. van Delden, Norbert J.M. Kuipers, André B. de Haan and Oded Lerner\*

University of Twente, Enschede, The Netherlands  
 \*Bateman Advanced Technologies Ltd., Yokneam, Israel

For environmental reasons conventional solvents such as benzene and chlorinated hydrocarbons are not desired for the industrial extraction of caprolactam. Therefore, alternative solvents and solvent mixtures have been investigated. Based on solvent design calculations using an extended UNIFAC group contribution model, mixtures of organic alkanes (hexane) with small amounts of alcohols (hexanol) as a co-solvent show caprolactam partition ratios equal or better than with benzene. These and other solvent mixtures will be tested on pilot plant scale in the Bateman Pulsed Column (BPC) and other types of columns.

### INTRODUCTION

Caprolactam, C<sub>6</sub>H<sub>11</sub>NO, the monomer of nylon 6, is produced in a multi-step process, shown schematically in Figure 1. More detailed descriptions of the available commercial processes are available elsewhere [1-4].

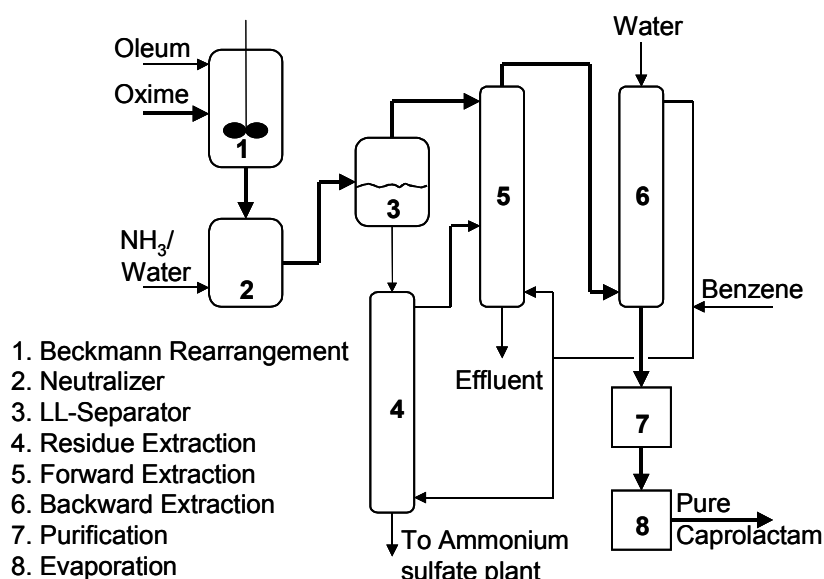


Figure 1. Schematic representation of the caprolactam process.

Crude caprolactam is first obtained by neutralizing the sulphuric acid containing reaction mixture from the Beckman rearrangement with aqueous ammonia. The neutralization results in the formation of two immiscible phases consisting of a highly concentrated, 65-70 wt%, crude aqueous caprolactam phase in equilibrium with a nearly saturated ( $\pm$  40 wt%) aqueous ammonium sulphate solution. After separating the two phases the caprolactam from both streams is recovered and purified by solvent extraction. Finally the crude caprolactam is re-extracted with water followed by chemical treatment and vacuum distillation. The extraction of caprolactam is commonly carried out with solvents such as benzene, toluene, nitrobenzene and various chlorinated hydrocarbons [1-8] in rotating disc contactors and pulsed packed columns.

Problems associated with equipment inefficiencies and toxicity of the solvents used have lead to the development of several options to improve existing caprolactam extraction technology by different process layouts [9, 10] or by a more accurate description of the effect of high ammonium sulphate concentrations on the phase behaviour in the caprolactam/water/ benzene system [11,12]. A possible option is the replacement of currently used contactors by the Bateman Pulsed Column technology. Other significant technology breakthroughs concern the development of new extraction schemes. Essential for the success of creating new extraction processes is the availability of suitable solvents. Introduction of alternative solvents can offer the opportunity of the development of environmentally benign caprolactam extraction technology in combination with enhanced selectivity's and capacities.

Evaluation of solvents can be based on predictive calculations using the UNIFAC group contribution approach, as presented in [13]. In this study an extended UNIFAC model was used to first verify it's applicability to predicting the effect of solvent structure on caprolactam distribution and then to evaluate solvent mixtures. It is intended that in future studies the most suitable solvent mixtures will be evaluated in pilot-plant investigations where the performance of various columns will be compared to that of the Bateman Pulsed Column.

## **DESIGN OF CAPROLACTAM SOLVENTS USING EXTENDED UNIFAC MODEL**

A study on the design of alternative, environmentally benign solvents for caprolactum extraction was performed. The UNIFAC group contribution model with linearly temperature dependent interaction parameters [14-17] was used to evaluate the effect of solvent structure on the selectivity as well as the capacity. Before this was possible the UNIFAC parameter matrix had to be extended to include more specific amide groups such as those present in caprolactam. According to the division used to characterize amine groups, the original, single UNIFAC amide group (-CO-NH-) was split up into 3 formamide and 3 new amide groups. An extensive amount of new vapour-liquid equilibrium and excess enthalpy data, using n-methylacetamide as the model component, was measured [18-22] and combined with data available in literature to determine interaction parameters for the amide group (-CH<sub>n</sub>-CO-NH-).

After demonstrating that the extended UNIFAC model was able to predict the effect of solvent structure on the distribution of caprolactam, the next step was to evaluate possible solvents and solvent mixtures that might be suitable for the extraction of caprolactam. For this evaluation two techniques were used. Firstly a pre-selection of potential solvent classes (alkanes, aromatics, ketones, alcohols, amines) was made using the principle component method [23]. Secondly, use was made of the knowledge that aromatics, chlorinated hydrocarbons and nitrobenzene were suitable solvents with respect to their capability of extracting caprolactam from an aqueous solution.

Combining this information leads to the following preliminary directions to find suitable alternative pure solvents.

1. Non-polar solvents such as alkanes and cycloalkanes are not suitable for the extraction of caprolactam because of their unfavourable caprolactam partition ratio. Other non-polar solvents such as secondary amines are also expected to be unsuitable.
2. Polar solvents, such as ketones, ethers, alcohols (see Figure 2), phenols, acids and amines exhibit strong and specific interactions with caprolactam. This results in a much more favourable caprolactam partition ratio compared to non-polar solvents. The main disadvantage of polar solvents is their relatively high solubility in the aqueous phase. Using polar solvents with a long hydrocarbon tail can counteract this. However, in that case solvent recovery is difficult because of the high boiling point. Another disadvantage of polar solvents is that a large fraction of polar impurities will be co-extracted resulting in a decreasing product quality.

Both polar and non-polar pure solvents are not suitable for the extractive recovery of caprolactam. However, by using tailor-made mixtures of polar and non-polar solvents the positive properties of both solvent classes can be combined to produce suitable solvents.

### **Experimental Procedure**

To obtain experimental data the following procedure was followed. A stirred glass equilibrium cell, controlled by thermostat to maintain the temperature within  $\pm 0.1$  K, was used. For each experiment an aqueous feed mixture, consisting of the desired amount of caprolactam in water, was prepared. After adding the organic solvent(s) and obtaining the desired temperature, the cell was stirred continuously for 30 minutes to ensure that equilibrium was attained. The stirring was stopped and the mixture was allowed to settle for the required time, generally 2 or more hours, to obtain full separation into two completely clear liquid phases. Samples were taken from both phases and analysed. Liquid chromatography was used to measure the caprolactam concentration, Karl-Fisher titration for the water concentration, and gas chromatography for the organic solvent concentration. The concentrations of caprolactam, water and organic solvent were obtained with a relative accuracy of  $\pm 1\%$ .

## **RESULTS**

### **Results For Pure Solvents**

In the caprolactam recovery processes one of the most important parameters is the distribution of the caprolactam between the solvent and aqueous phase. Figure 2 shows a comparison of the extended UNIFAC predictions with experimental data for the distribution of caprolactam between benzene and the aqueous phase. Considering the fact that the predicted distribution curves shown were produced using no information on caprolactam containing systems, their agreement with the quantitative results was quite good. The figure also illustrates that the predictions agreed quite well with the experimentally observed trend that at equal concentrations in the aqueous phase the solubility of caprolactam decreases in the order: benzene > toluene > cyclohexane. Further a solvent with strong specific interactions such as cyclohexanol shifts the caprolactam partition ratio (wt% in solvent phase / wt% in aqueous phase) by 1 to 2 orders of magnitude.

### **Results For Solvent Mixtures**

Instead of replacing benzene with a pure solvent, an environmentally benign solvent mixture can be used to modify the solvent character to such an extent that a more favourable caprolactam partition ratio is combined with minimal changes in the impurity partition ratios. Figure 3 illustrates that by adding small amounts of polar co-solvents, such as 1-hexanol to toluene, the caprolactam partition ratio became more favourable than for pure benzene.

Furthermore even for poor solvents, such as cycloalkanes and alkanes, the partition ratio was shown to increase rapidly to values comparable with those for pure benzene. Experimental results for hexane confirmed the increase of the partition ratio caused by adding 1-hexanol. However, deviations from the model predictions occurred, even for pure hexane. Figure 2 shows that such a deviation was also observed for cyclohexane.

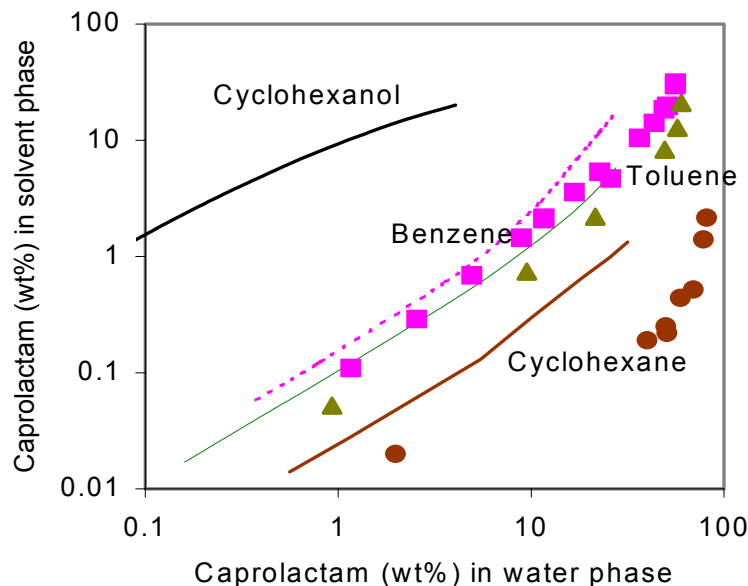


Figure 2. Distribution of caprolactam between various solvents and water at 20 °C.

■ = benzene; ▲ = toluene and ● = cyclohexane.

The curves are predicted with the extended UNIFAC group contribution model.

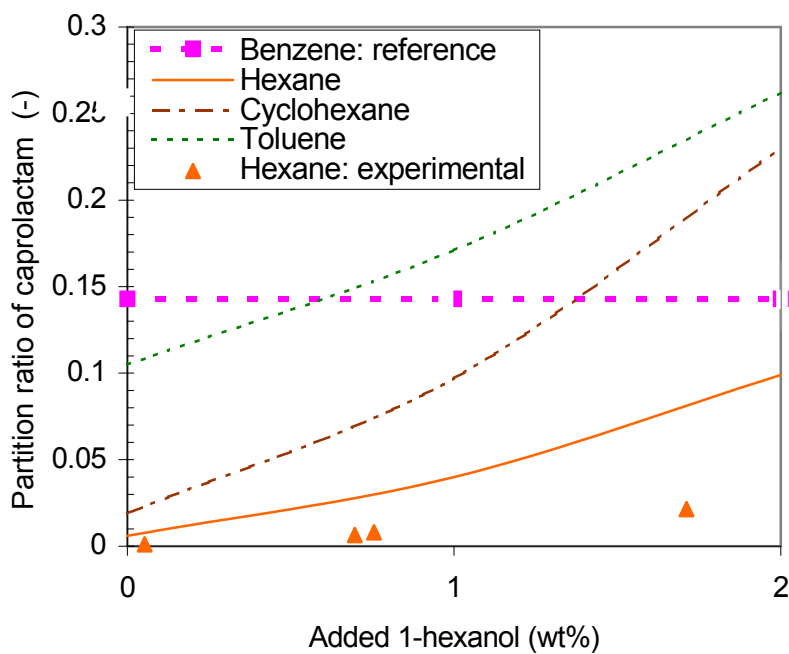


Figure 3. Calculated (lines) and experimental (for hexane) effect of adding 1-hexanol as a co-solvent to various solvents on the caprolactam partition ratio between the solvent and aqueous phase at 20 °C.

## INTENDED PILOTING WORK

Pilot plant trials are necessary to establish operating parameters, to obtain data for risk free scale-up and provide process guarantees. In the near future we want to be able to run various pilot plant scale extraction columns (Rotating Disc Contactor, Centrifugal Extractor, Membrane Extractor, Pulsed Packed Column) simultaneously using the same feed solutions. This enables direct comparisons between the various contactors. A recently erected contactor is a 40 mm diameter Bateman Pulsed Column with its characteristic alternating disks and doughnut-shaped baffles. This column promises to have improved extraction efficiency relative to other types of pulsed solvent extractors. Other advantages are the high mass transfer rates, the ease of operation with any desired phase continuity, and a closely controlled energy of mixing by varying the pulse intensity.

## CONCLUSIONS

For environmental reasons conventional solvents such as benzene and chlorinated hydrocarbons are not desired for the industrial extraction of caprolactam. Therefore, alternative solvents and solvent mixtures have been investigated. Both polar and non-polar pure solvents are not suitable for the extractive recovery of caprolactam due to an unfavourable caprolactam partition ratio and a high solubility in the aqueous phase, respectively. Based on solvent design calculations using an extended UNIFAC group contribution model, mixtures of organic non-polar alkanes (hexane) with small amounts of alcohol (hexanol) as a polar co-solvent show caprolactam partition ratios to be equal or better than with benzene. Experiments for the hexanol/hexane system confirm an increase in the caprolactam partition ratio by hexanol addition, though its absolute value is less than predicted. Promising types of solvent mixtures will be tested on pilot plant scale in the Bateman Pulsed Column and other types of extraction columns.

## ACKNOWLEDGEMENT

Bateman Advanced Technologies Ltd., Yokneam, Israel, financially supports this project.

## REFERENCES

1. A.J.F. Simons and N.F. Haasen (1983), *Handbook of Solvent Extraction*, T.C. Lo, M.H.I. Baird, C. Hanson (eds.), John Wiley, New York, pp. 557-566.
2. J. Ritz, H. Fuchs, H. Kieczka and W.C. Moran (2001), *Caprolactam*: Ullmann's Encyclopedia of Industrial Chemistry, 6th electronic edn.
3. H.C. Ries and R.G. Muller (1965), *Caprolactam: Part I and II*, Process Economics Program, Stanford Research Institute, Stanford.
4. H.C. Ries and K.K. Ushiba (1968, 1976), *Caprolactam, Supplement A and B*, Process Economics Program, Stanford Research Institute, Stanford.
5. A.C. Morachevskii and V.E. Sabinin (1960), *J. Appl. Chem. USSR*, **33**, 1775.
6. K. Tettamanti, M. Cogradi and J. Sawinsky (1960), *Period. Polytech.*, **4**, 201.
7. H.P. Pandya (1994), *Adv. Chem. Eng. Nucl. Process Ind.*, 504-516.
8. H.P. Pandya and S.A. Puranik (1995), *J. Inst. Eng. (India), Chem. Eng. Div.*, **76**, 1-4.
9. V. Alessi, R. Penzo, S. Pattaro, R. Tessari and M.J. Slater (1996), *Proc. ISEC '96*, University of Melbourne Press, Melbourne, pp. 1673-1678.

10. V. Alessi, R. Penzo, M.J. Slater and R. Tessari (1997), *Chem. Eng. Technol.*, **20**, 445-454.
11. A.B. de Haan and S.H. Niemann (1999), *Proc. ISEC '99*, Society of Chemical Industry, London, pp. 1537-1542.
12. A.B. de Haan and S.H. Niemann, *Sep. Purif. Techn.* (in preparation).
13. A.B. de Haan and A.J.F. Simons (1999), Presented at AIChE Annual Meeting, Dallas.
14. A. Fredenslund, J. Gmehling and P. Rasmussen (1977), *Vapor-Liquid Equilibria Using UNIFAC*, Elsevier, Amsterdam.
15. A. Fredenslund (1989), *Fluid Phase Equil.*, **52**, 135-140.
16. H.K. Hansen, P. Rasmussen, A. Fredenslund, M. Schiller and J. Gmehling (1991), *Ind. Eng. Chem. Res.*, **30**, 2351-2355.
17. H.K. Hansen, B. Coto and B. Kuhlmann (1992), IVC-SEP Report 9212, Lyngby.
18. A.B. de Haan, A. Heine, K. Fischer and J. Gmehling (1995), *J. Chem. Eng. Data*, **40**, 1228-1232.
19. A.B. de Haan and J. Gmehling (1996), *J. Chem. Eng. Data*, **41**, 474-478.
20. A.B. de Haan, R. Bolts and J. Gmehling (1996), *J. Chem. Eng. Data*, **41**, 1155-1159.
21. A.B. de Haan, K. Fisher, M. Haacke and J. Gmehling (1997), *J. Chem. Eng. Data*, **42**, 597-602.
22. A.B. de Haan, K. Fisher, M. Haacke, Oliver Aufderhaar, M. Petri and J. Gmehling (1997), *J. Chem. Eng. Data*, **42**, 875-881.
23. A. Henrion, R. Henrion, W. Abraham and D. Kreysig (1990), *Z. Phys. Chem.*, **271**, 29-34.



# EXTRACTION AND ENRICHMENT OF PHYSIOLOGICALLY ACTIVE LIPIDS AND NUTRIENTS FROM PLANT MATERIALS USING SUPERCRITICAL FLUID EXTRACTION

Darren Westerman, Bushra Al-Duri, Regina Santos, and John Bosley\*

Supercritical Fluids Group, School of Chemical Engineering,  
University of Birmingham, Birmingham, England  
\*Unilever Research, Bedford, England

Supercritical carbon dioxide solvent extractions were carried out on whole grain seed material over the range of temperatures 313K – 323K and pressures 100 barg – 300 barg. The aim was to isolate in an enriched fraction the commercially valuable compound squalene.

Milling of the seed was found to be the most effective sample pre-treatment as the physical nature of the seed was such that crushing and flaking were ineffective to complete commutation. Extraction yields were determined gravimetrically as a percentage of exhaustive Soxhlet hexane extraction.

Solubility studies of squalene were performed over the temperature and pressure range of interest with good agreement to predictions from the Adachi-Lu modification of the Chrastil Equation and Empirical Equations.

## INTRODUCTION

The properties of compressed gases as solvents and reaction mediums have been reported for over 100 years [1]. Intensified research into the solvating powers of compressed gases in the supercritical (sc) region, most notably carbon dioxide, has been undertaken since the mid 1970s, and is gaining favour as an alternative to processes requiring traditional organic solvents. The high initial capital investments required for the use of highly compressed gases have been difficult to justify in many cases. However, as environmental restraints continue to become more stringent, the commercial viability of the process is becoming more appealing.

The aim of this work is to investigate the extraction of essential oils from seed material (subject to confidentiality agreement) with a squalene, C<sub>30</sub>H<sub>50</sub>, as a major component whilst leaving the extracted seed material as a saleable food product.

The therapeutic properties of the squalene stem from its antioxidant nature, oxidative cell damage being a major cause for the development and spread of certain types of tumours. The natural presence of squalene in human skin tissue promotes cell oxygenation and so has both prophylactic and anti-oxidant anti-carcinogenic properties. It is also used in the cosmetic industry as a carrier for lipid soluble components through the skin. Since the principal uses of squalene are in the food, cosmetic and pharmaceutical industries, the use of organic solvents for its extraction must be avoided. Traditional steam distillation techniques are also unfavourable, as thermal degradation occurs.

## **Selection of Carbon Dioxide as Solvent**

From a material standpoint, CO<sub>2</sub> is a cheap, inert, non-flammable, non-corrosive, non-toxic by-product of many natural and industrial processes. It is intrinsically safe in use, has no residual taste, odour, colour or toxicity and is easily recycled and purified with minimal capital expenditure. As a solvent scCO<sub>2</sub> is non-polar and will therefore solubilise other non-polar molecules (oils, waxes etc.), however, the addition of small amounts of modifiers, entrainers or co-solvents such as water have a dramatic effect on the ability of the fluid to selectively solubilise more polar molecules. Patents exist for the extraction of compounds from acid hydrolysed plant materials using SCFs and co-solvents [2]. In addition to these benefits, the thermodynamic properties of CO<sub>2</sub> are such that the T<sub>c</sub> (31.1°C) and P<sub>c</sub> (73.8 bar) are sufficiently low and easily achieved compared to other SCFs as to make it the ideal sc solvent for the extraction of thermally labile molecules. Finally, since CO<sub>2</sub> is gaseous at atmospheric conditions the solute product is easily isolated upon venting and is completely free from solvent contamination.

## **Limitations of Distillation Techniques**

Distillation techniques are among the oldest methods for the extraction of oils. They rely on the relative volatility and hydrophilicity of the extracts and can be sub-divided into four main categories, each having its own specific advantages and disadvantages.

### ***Steam distillation***

Steam is applied at atmospheric pressure to the sample, the compounds extractable by this process are carried up with the steam flow to a condenser where the steam condenses to a liquid and the extracted components are collected. The major disadvantages to this process are that the superheated water vapour destroys thermo labile components in the extract (with associated thermal artefact production), also the extract requires further separation from the aqueous phase collected in the condenser.

### ***Hydrodistillation***

This process is similar to steam distillation except that the material to be extracted is immersed in water to which heat is applied. The extract is collected as a condensate as before but the process carries with it the same problems with regard to thermal decomposition and product separation. A small advantage over steam distillation is gained however as the material to be extracted is in continual motion within the extractor, thereby presenting a greater surface area to the 'solvent'.

### ***Steam injection***

This little-used technique is in principle identical to steam distillation except that high pressure steam is injected into the base of the material bed. The advantage of particle motion within the extractor gained by hydrodistillation is present with this technique, but the same disadvantages apply.

### ***Vacuum distillation***

This process is analogous to all the above processes with the advantage of lower temperatures being required. The boiling point of a liquid decreases with pressure and so the relative volatility increases. This is exploited where thermal degradation of extract is problematic with ambient pressure techniques. The advantage of this process is offset however by the higher capital and running cost of a vacuum system. The problem of extract separation in the condenser still applies however.

## **Limitation of Organic Solvents**

Organic solvent extraction techniques rely on a chemical affinity of the solute to the solvent. The selection of solvent for a specific component is not always possible and so oleoresin extracts typically contain both volatile and non-volatile components. The problem of solvent

removal from the extract persists (as in distillation techniques) however the more volatile components extracted can be lost due to entrainment during solvent evaporation. As mentioned elsewhere in the text the residual organic solvent traces permitted in the extract are typically <1 ppm for food and pharmaceutical use.

## EXPERIMENTAL

### Brief Discussion of Continuous Extraction Rig Capabilities

An extraction rig was constructed that was capable of extracting natural oils from solid materials. The rig was capable of obtaining a working pressure of 300 barg and a working temperature of 343 K, with carbon dioxide solvent flow rates ranging from 1 l/min to 5 l/min for extraction experiments and collection of the solute product by a two-stage decompression.

The basic principle of the 'once through' continuous extraction process involves the compressing of liquid carbon dioxide beyond its  $P_c$  (73.78 bar) and then heating this compressed liquid beyond its  $T_c$  (304.04K). At the cp the fluid departs from liquid or gas like properties and above this point becomes supercritical, the solvent used in this work. For  $\text{CO}_2$  a density of 0.47 g  $\text{cm}^{-3}$  is attained at this point.

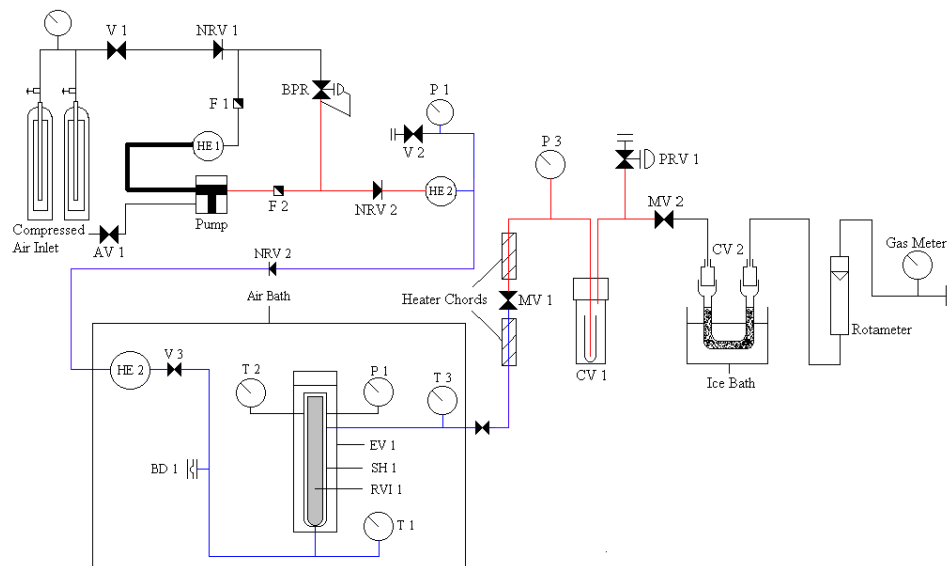


Figure 1. Schematic diagram of extraction rig.

The fluid, now in a supercritical state, entered an extraction vessel and contacted the material to be extracted. After passing through the material bed the extract loaded sc $\text{CO}_2$  stream left the extraction vessel and was slowly depressurised across a throttling device to 10 barg where the bulk of the extract was collected. The sub-critical  $\text{CO}_2$  stream, though still above the triple point ( $tp$ ) of  $\text{CO}_2$ , was then reduced to atmospheric pressure across a second throttling device where the more volatile components were collected in a chilled receptacle.

The prepared sample was loaded into the sample holder in such a way that the  $\text{CO}_2$  stream contacted the entire surface of the sample bed. This was accomplished by the insertion of a diffuser frit set into a hollow machined into the base of the sample holder. The loaded sample was also tamped down slightly to ensure the maximum  $\text{CO}_2$  contact through the sample bed.

The intact shell of the seed was impervious to SCF extraction, therefore, prior disruption of the shell was necessary. Flouring of the seeds in a Tema Mill (Siebtechnik) for 1 minute was selected as both crushing and blending proved less effective due to the physical nature of the seeds.

### **Solid seed material**

Solubility determinations enabled the solvent to be repeatedly re-circulated through the material bed at a known flow rate (~2 l/h) until saturation of the vapour was attained. A sample size of 250 ml was used to ensure it was always in excess. Make-up carbon dioxide was supplied as required from the solvent delivery section to maintain pressure during the experiment. Appreciable make-up was necessary in the early stages of the experiment to replace carbon dioxide lost to absorption into the material bed. Initial experiments were 12 hours in duration to ensure complete saturation of the solvent. After 4 hours the re-circulation pump was stopped and a measured volume of solvent (~10 l STP) was depressurised from the equilibrium cell through a throttling device, the solute was collected and weighed. The precipitated solute was left to stand in order to allow any absorbed CO<sub>2</sub> to desorb until a constant weight was achieved. The re-circulation was resumed and collections were repeated at 2 hour intervals. When the mass of successive solute collections ceased to increase the solvent was deemed saturated. The mass of the solute was then determined and used to calculate its solubility in scCO<sub>2</sub> at a given temperature and pressure.

### **Squalene liquid**

Liquid solubility experiments were essentially the same as for those of solid material using the same apparatus and duration. An excess sample volume of 100 ml was used as literature values of between approximately 0.3 g kg<sup>-1</sup> and 48 g kg<sup>-1</sup> have been reported over the range of temperatures and pressures used in this study [3]. Pure standard oil was used (Sigma 98% pure) and each fraction tested for molecular degradation by Infra-red Spectroscopy (Perkin Elmer 1600 series FTIR). No decomposition was observed from that of the pure standard.

## **RESULTS AND DISCUSSION**

Squalene solubilities in scCO<sub>2</sub> compare favourably to predictions from the 2 equations tested [4], these were:

### *Adachi-Lu Modification of the Chrastil Equation*

$$c = \rho^e \exp(a / T + b) \quad (\text{where the exponent } e = e_0 + e_1\rho + e_2\rho^2)$$
$$a(K) = -4545 \quad b = 39345, e_1 = -6.224, e_2 = 5.421 \times 10^3(\text{kg}^{-1}\text{m}^3), e_3 = -2.20 \times 10^{-6}(\text{kg}^{-2}\text{m}^6)$$

### *Catchpole Empirical Equation*

$$\ln(S_o) = K_s \ln(\rho_v) + A - B / T \quad (\text{where } K_s = 6.54, A = -28.24, B = 3936.6)$$

The Adachi-Lu modification of the Chrastil equation and Catchpole empirical equations adequately show the predicted vapour phase solubility concentration of squalene as a pure component in scCO<sub>2</sub> with good agreement (Figure 2). The experimental results follow the predicted solubility curve trend however there is a closer correlation to the Adachi-Lu equation at lower temperatures. It is assumed that the slight reduction in solute concentration experimentally observed was due to insufficient time between sample collections not allowing total re-saturation of the solvent.

Results of initial extraction experiments on milled seed material show that for a given temperature the rate of extraction increases with pressure. It can also be seen that the effect of pressure on the rate of extraction is more enhanced at higher temperatures as the result of

the combined effect of solvent density and vapour pressure of the extract. At low pressures, the increase on temperature leads to a significant decrease of solvent density and consequently on its dissolving power. However, at high pressure, the decrease in solvent density due to the increase of temperature is much less dramatic and is compensated for by the increase in the volatility of the extract, justifying the stronger dissolving power.

Figure 3 shows the four isobaric seed extraction curves at three temperatures. The rate of extraction increases with an increase of temperature for extraction pressures of 300 barg, this trend is reversed for pressures below 200 barg. This indicates that the cross-over pressure from density to volatility dependency of the total extract is between 200 and 300 barg.

## FUTURE WORK

The ultimate commercial goal of the project is to produce a squalene rich extract while leaving a saleable product in the flour. It is necessary therefore to extract only that component fraction to the exclusion of the majority of extractable matter, mainly diglycerides, triglycerides and fatty acids. To this end it is necessary to investigate the fractionation of squalene and the effect of co-solvent from the solute firstly:- directly from the seed matrix and secondly:- from the extracted material with a view to re-infusion of the flour with the residue.

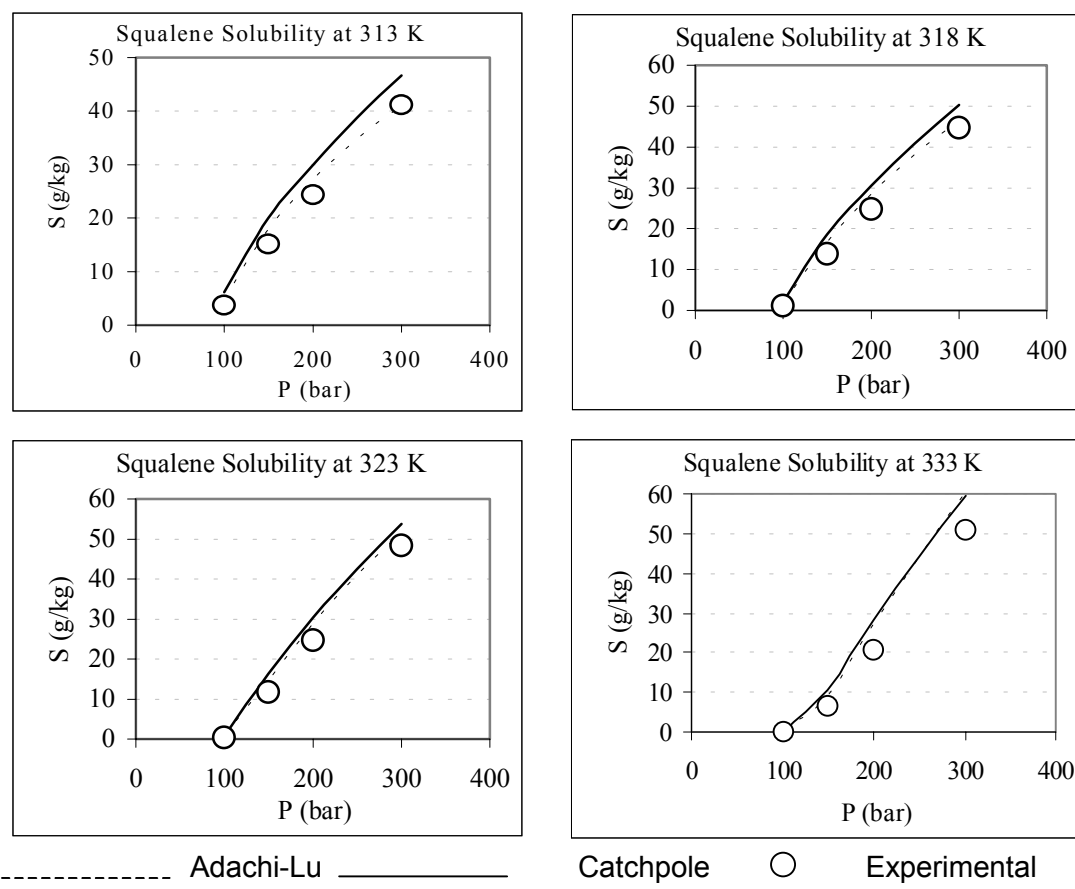


Figure 2. Experimental and empirical solubilities of squalene in  $\text{scCO}_2$ .

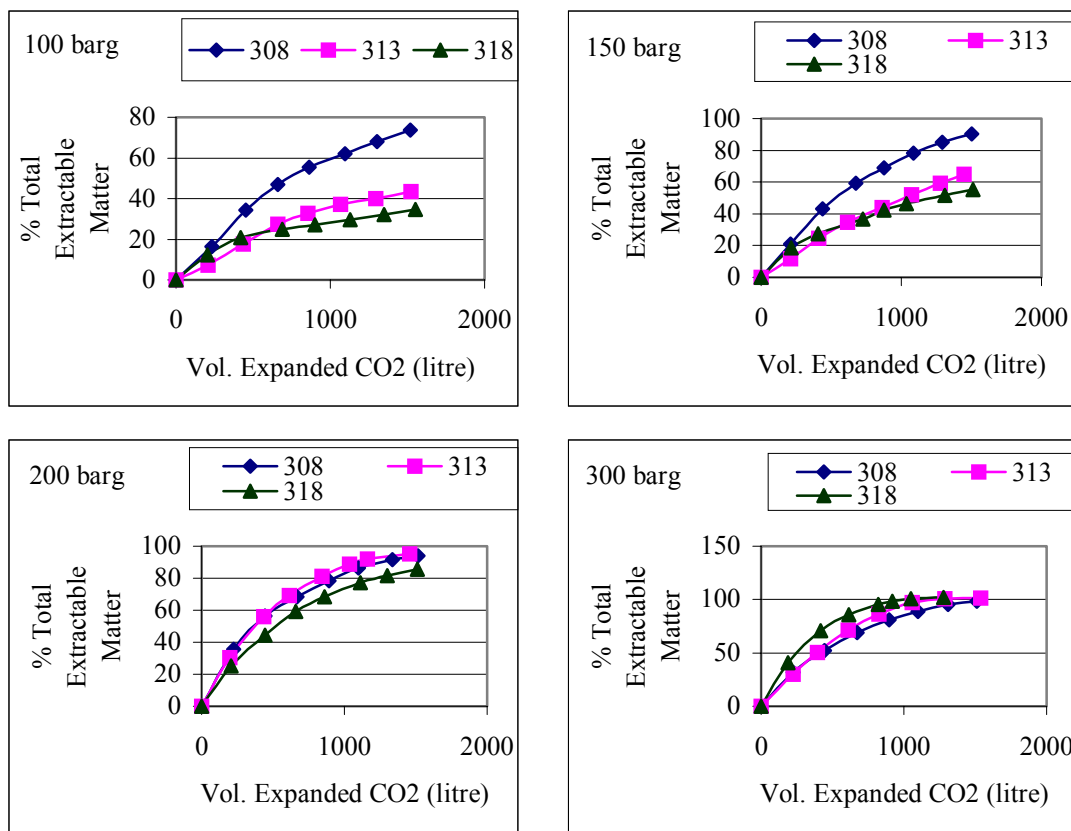


Figure 3. Experimental seed extraction curves at different temperatures.

Modification of the extraction rig to incorporate a temperature gradient controlled oven has been completed. The oven houses a 50 ml pressure vessel so that extractions can be performed over a solvent density gradient with controlled addition of co-solvents via a HPLC pump. The extract will be monitored on-line in the SCF phase by a Milton Roy UV detector fitted with a supercritical pressure cell. This system is similar in design and operation to a Supercritical Chromatography Instrument.

## ACKNOWLEDGEMENTS

This work was co-sponsored by The University of Birmingham School of Chemical Engineering and Unilever Research, Colworth.

I would like to thank my supervisors Dr. Bushra Al-Duri and Dr. Regina Santos (University of Birmingham), Dr. John Bosley, Dr. Scott Barclay and Mr. Gary Sassano (Unilever Research, Colworth) for their help and support throughout this work. I would also like to acknowledge the support of the staff of the Supercritical Fluids Technology Group, Birmingham for their technical expertise in the field.

## REFERENCES

1. J.B. Hannay, J. Hogarth (1879), *Proc. Royal Soc.*, **29**, 324.
2. M.A. Crosta, P. Kabasakalian, F.J.F. Snr. Honold (1993), *U.S. Pat.*, No. 5252729.
3. O.J. Catchpole, J.B. Grey, K.A. Noermark (1998), *J. Chem. Eng. Data*, **43**, 1091-1095.
4. O. J. Catchpole, J.B. Grey, K.A. Noermark (2000), *J. Supercrit. Fluids.*, **19**, 25-37.



## FORWARD AND BACKWARD EXTRACTION OF BSA USING MIXED REVERSE MICELLAR SYSTEM OF CTAB AND 4-METHYL-2-PENTANONE

W. Zhang, H. Z. Liu and J. Y. Chen

Young Scientist Laboratory of Separation Science and Engineering,  
State Key Laboratory of Biochemical Engineering, Institute of Chemical Metallurgy,  
Chinese Academy of Sciences, Beijing, P. R. China

The forward and backward extraction of bovine serum albumin (BSA) has been studied using the mixed reverse micellar system of cetyl trimethyl ammonium bromide (CTAB) and 4-methyl-2-pentanone (methyl isobutyl ketone, MIBK). The addition of 4-methyl-2-pentanone to 50 mmol/L CTAB/20%(v/v) hexanol/ petroleum ether reversed micellar system can significantly improve the BSA transfer into the reverse micelles. The mixed reverse micellar system formed with CTAB and 4-methyl-2-pentanone exhibits excellent backward extraction behavior for BSA. The mixed reverse micelles can obviously enhance the recovery of BSA under conditions such as in a wide pH range and low salt concentration of backward aqueous phase. The mixed reverse micellar system requires much less time to achieve higher BSA recovery in comparison with reverse micellar systems with CTAB only. It was deduced that the addition of 4-methyl-2-pentanone to CTAB reversed micellar system could decrease the hydrophobic interaction between protein molecules and surfactants. Petroleum ether, which is much cheaper than pure straight chain hydrocarbons such as iso-octane and hexane, could be used as solvent in protein extraction with reverse micelles.

### INTRODUCTION

The separation and recovery of proteins using reverse micelles is one type of liquid-liquid extraction operation which may keep the activity of proteins in the organic continuous phase [1]. The separation using reverse micelles is easy to scale up and operate continuously [2].

Recently, the application of a synergistic effect by adding a secondary surfactant for protein extraction has been reported. Kinugasa has reported that mixed reverse micelles formed with AOT (sodium bis(2-ethylhexyl)sulfosuccinate) and DEHPA (di(2-ethylhexyl)phosphoric acid) could be used to extract hemoglobin with transfer yield about 80% [3]. Goto has reported that the AOT and DOLPA (dioleylphosphoric acid) mixed reversed micelles showed a high selectivity between the active  $\alpha$ -chymotrypsin and denatured proteins [4]. Yan [5] and Zhang [6] reported that mixed reversed micelles formed with AOT or CTAB and TBP (tributyl phosphate) or TRPO (trialkylphosphine oxide) exhibited obvious advantage over the reversed micelles formed with AOT or CTAB only. Spirovská (1998) reported that the addition of sucrose in forward aqueous phase increased both protein recovery and activity of the protein [7]. It is clear that mixed reverse micelles exhibited some advantages over reverse micelles formed with one surfactant only.

In order to improve the forward and backward extraction behavior of CTAB reverse micelles, we studied the extraction of model protein BSA using the mixed reverse micellar system formed with CTAB and 4-methyl-2-pentanone (MIBK). The extraction of BSA using mixed reverse micellar systems formed with CTAB and heptylaldehyde or *n*-butyl acetate was carried out, which will be reported in another article.

## MATERIALS AND METHODS

### Materials

BSA (molecular weight 68,000, isoelectric point pl 4.8) was purchased from Beijing Baitai Biochemical Reagents Company. CTAB (>99%, analytical grade), hexanol (>98%, chemical grade), petroleum ether (b.p.: 90~120 °C, analytical grade), MIBK (>99%, analytical grade), were purchased from Beijing Chemical Reagents Company. Other reagents used were all commercially available reagents of analytical grade and were used as received.

### Forward Extraction and Backward Extraction Procedures

Forward extraction procedures for BSA were conducted by contacting petroleum ether solution containing a weighed amount of CTAB with an aqueous solution containing BSA. Equal volumes (usually 5 ml each) of aqueous and organic solutions were poured gently into a 50-ml flask, which was stoppered to prevent the evaporation of the solution. The flasks were shaken at the rate of agitation of 3.5 s<sup>-1</sup> at room temperature (22.0 ± 0.5 °C) for 20 minutes. After centrifugation (4000 rpm, 5 min), the protein concentration in the reversed micellar phase was determined by spectroscopy at 280 nm (UV-7542 spectrophotometer). The amount of BSA recovered in aqueous phase was determined by the Bradford method [8].

Backward extraction of BSA was conducted by contacting the reverse micellar solution that loaded BSA before with a fresh aqueous phase of desired pH and ionic strength at room temperature (22.0 ± 0.5 °C). Equal volumes (usually 5 ml) of aqueous and organic solutions were poured gently into a 50-ml stoppered flask. The flasks were shaken at the rate of agitation of 4.0 s<sup>-1</sup> at room temperature (22.0 ± 0.5 °C) for 60 minutes. The mixture was then centrifuged (4000 rpm, 5 min), and the protein concentration of the stripped aqueous phase was determined by Bradford method. The yield of the backward transfer of BSA was based on the percentage of BSA recovered from the aqueous phase divided by the amount of BSA extracted into the reverse micellar phase. The protein mass balances for a pair of forward & backward extractions were generally within the experimental error (± 5%).

## RESULTS AND DISCUSSION

### Effect of pH on the Forward Transfer of BSA

BSA with isoelectric point, pl, of 4.8 carries an overall negative charge under the conditions where the aqueous pH is higher than 4.8. Under such conditions, both CTAB and CTAB-MIBK reverse micellar systems could extract BSA completely as shown in Figure 1. The addition of MIBK to CTAB reverse micelles could significantly improve the forward transfer of BSA. On the other hand, with pH below pl of BSA, extraction into the reverse micellar phase was inhibited by the unfavorable electric repulsion. BSA transfer of mixed reversed micelles formed with CTAB and MIBK is higher than that of reverse micelles formed with CTAB only because of the addition of MIBK to CTAB reverse micelles resulted to the increase of the size of CTAB reverse micelles.

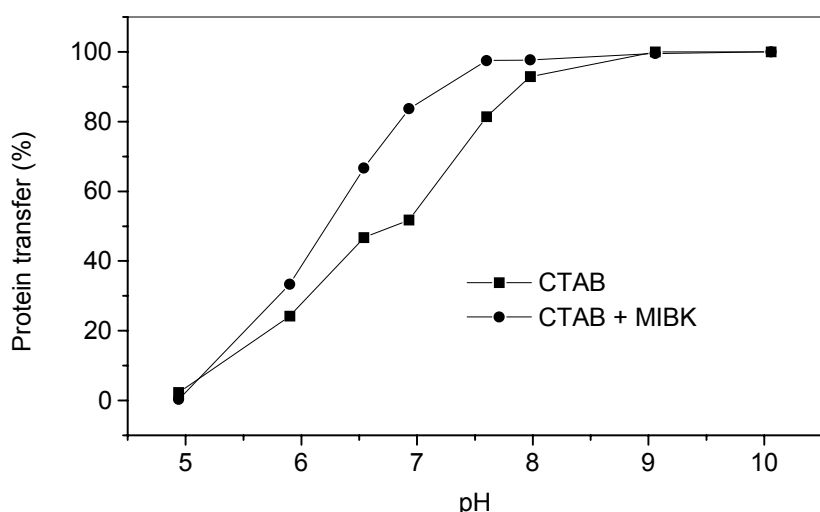


*Figure 1. Effect of aqueous phase pH on BSA transfer.*

Aqueous phase: 1.0 mg/ml BSA, 0.1 mol/L KCl.

Organic phase: 50 mmol/L CTAB/20%(v/v) hexanol/5%(v/v) MIBK/petroleum ether.

### Effect of Ionic Strength on the Forward Transfer of BSA

The ionic strength of the aqueous phase influences the degree of shielding of the electrostatic potential imposed by a charged surface. The effect of salt concentration on BSA transfer was investigated by varying the KCl concentration at pH 9.0, as shown in Figure 2. The BSA transfer to the reversed micellar phase decreased for reverse micellar systems formed by CTAB only or by CTAB and MIBK with increasing KCl concentration. The BSA transfer to the reverse micelles phase with the addition of MIBK is higher than that with CTAB only as surfactant, which indicated the improvement of BSA transfer with the presence of MIBK.

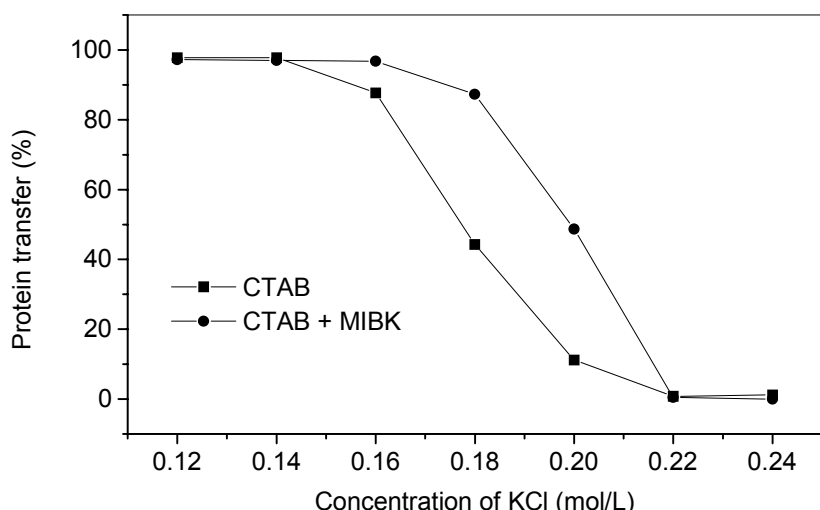


*Figure 2. Effect of concentration of KCl in aqueous phase on BSA transfer.*

Aqueous phase: 1.0 mg/ml BSA, pH = 9.0.

Organic phase: 50 mmol/L CTAB/20%(v/v) hexanol/5%(v/v) MIBK/petroleum ether.

### Effect of Aqueous Phase pH on the Backward Transfer of BSA

The protein extracted into the reverse micelles can be recovered through backward transfer either as a result of electrostatic repulsion of the surfactant by changing the solution pH, or through size exclusion by increasing the salt concentration in the aqueous phase used for

backward transfer. The recovery of BSA could carry out when using KBr as salt, while the recovery of BSA was difficult when using KCl. This might be due to the effect of different anionic on protein extraction. The effect of aqueous phase pH for backward transfer on BSA recovery was shown in Figure 3. The mass balance of protein was within the experimental error of  $\pm$  5%. BSA could be recovered only under conditions with pH below pI when using CTAB or CTAB-MIBK reverse micelles. The recovery curve of the reverse micelles formed with CTAB and MIBK is higher than that of the reverse micelles formed with CTAB only. Obviously, the addition of MIBK to CTAB reverse micelles improved the backward transfer behavior of CTAB reverse micelles. The result may be explained that the addition of MIBK to CTAB reversed micellar system could decrease the hydrophobic interaction between protein molecules and surfactants. Both of the recovery of BSA from CTAB and CTAB-MIBK reverse micelles shows optimum pH near pI.

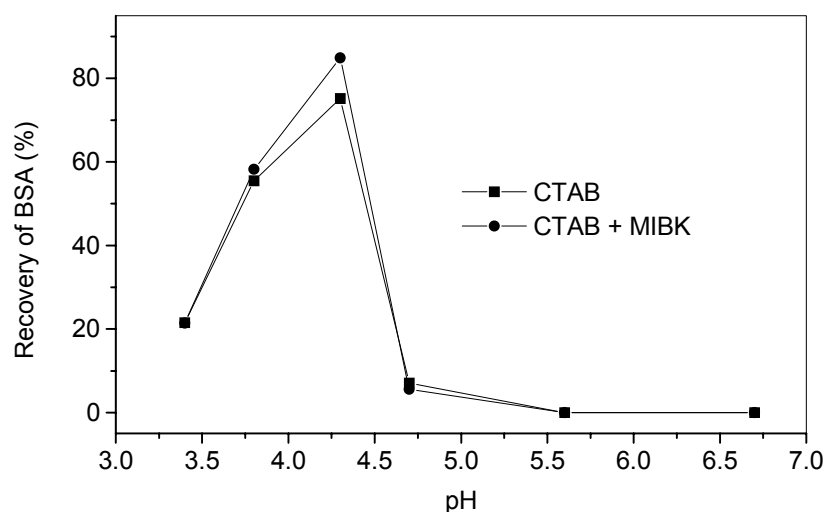


*Figure 3. Effect of aqueous phase pH on backward transfer of BSA recovery.*

Forward transfer aqueous phase: 1.0 mg/ml BSA, 0.1 mol/L KCl, pH = 9.0.  
Organic phase: 50 mmol/L CTAB/20%(v/v) hexanol/5%(v/v) MIBK/petroleum ether.  
Backward transfer aqueous phase: 1.0 mol/L KBr.

#### **Effect of Solution Ionic Strength on the Backward Transfer of BSA**

The salt concentration in the aqueous phase can affect the efficiency of protein transfer through the size exclusion effect. The effect of ionic strength of aqueous phase in backward extraction on BSA back-transfer was shown in Figure 4. The mixed reverse micelles formed by CTAB and MIBK exhibit higher backward transfer behavior for BSA than reverse micelles formed by CTAB only. The mixed reverse micelles formed with CTAB and MIBK obviously improve the BSA back-transfer. The reaction rate is also influenced by the ionic strength, because the extraction contains an electrostatic interaction in the reaction mechanism. However, one hour is long enough to achieve or close to backward extraction balance.

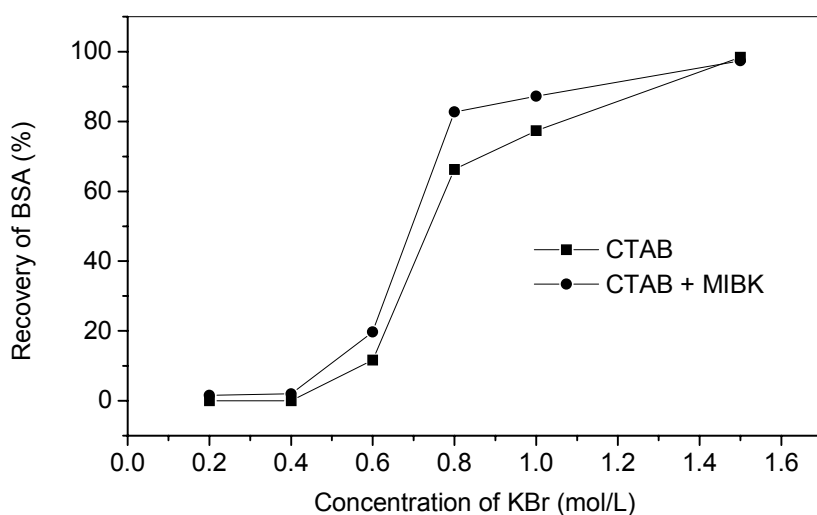


**Figure 4. Effect of concentration of KBr of backward transfer aqueous phase on BSA recovery.**

Forward transfer aqueous phase: 1.0 mg/ml BSA, 0.1 mol/L KCl, pH = 9.0.  
 Organic phase: 50 mmol/L CTAB/ 20%(v/v) hexanol/ 5%(v/v) MIBK/petroleum ether.  
 Backward transfer aqueous phase: pH = 4.3, KBr.

#### Time of Backward Extraction

It is well known that the rate of backward transfer of proteins from reverse micelles to an aqueous phase is relatively slow because of rather strong interaction resistance in mass transfer. The effect of time on BSA recovery when using CTAB or CTAB-MIBK reversed micellar systems was studied as shown in Figure 5. The mixed reverse micellar systems require less time to achieve higher BSA recovery in compare with reverse micellar systems with CTAB only.

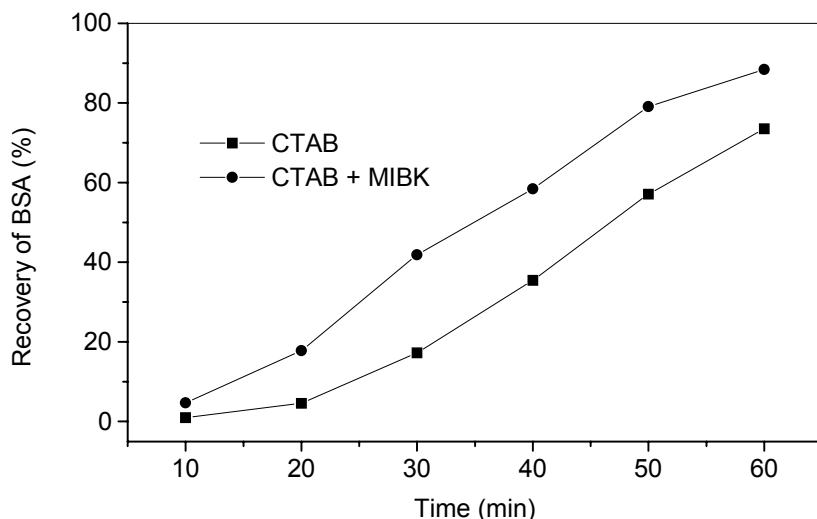


**Figure 5. Effect of backward transfer time on BSA recovery.**

Forward transfer aqueous phase: 1.0 mg/ml BSA, 0.1 mol/L KCl, pH = 9.0.  
 Organic phase: 50 mmol/L CTAB/ 20%(v/v) hexanol/ 5%(v/v) MIBK/petroleum ether.  
 Backward transfer aqueous phase: 1.0 mol/L KBr, pH = 4.30.

## CONCLUSIONS

The forward and backward extraction of BSA was investigated using mixed reversed micellar systems formed with CTAB and MIBK. The experimental results indicate that the addition of MIBK to CTAB reversed micelles could improve the extraction behavior of reversed micelles for BSA. The mixed reverse micelles can obviously enhance the recovery of BSA under the conditions such as in a wide pH region, at low salt concentration of backward aqueous phase. The mixed reverse micellar systems formed with CTAB and MIBK require less time to achieve a higher BSA recovery in comparison with reverse micellar systems with CTAB only. It was deduced that the addition of MIBK to CTAB reversed micellar system could decrease the hydrophobic interaction between protein molecules and surfactants.

## ACKNOWLEDGEMENTS

This paper is supported by National Natural Science Foundation of China, No. 29836130.

## REFERENCES

1. K. E. Golken and T. A. Hatton (1985), *Biotechnol. Prog.*, **1**, 69-74.
2. M. J. Pires, M. R. Aires-Barros and J. M. S. Cabral (1996), *Biotechnol. Prog.*, **12**, 290-301.
3. T. Kinugasa, A. Hisamatsu, K. Watanabe and H. Takeuchi (1994), *J. Chem. Eng. Jpn.*, **27** (5), 557-562.
4. M. Goto, T. Ono, F. Nakashio and T. A. Hatton (1996), *Biotechnol. Tech.*, **10** (3), 141-144.
5. Y. C. Yan (1997), PhD Thesis, Chinese Academy of Sciences, Beijing.
6. T. X. Zhang, H. Z. Liu and J. Y. Chen (1999), *Biochem. Eng. J.*, **4**, 17-21.
7. G. Spirovska and J. B. Chaudhuri (1998), *Biotechnol. Bioeng.*, **58** (4), 374-379.
8. M. M. Bradford (1976). *Anal. Biochem.*, **72**, 248-254.



## OPTICAL SENSOR FOR CHROMIUM(VI) MONITORING: OPTIMISATION OF CHROMIUM(VI) TRANSPORT THROUGH LIQUID MEMBRANES

Elianna Castillo, Mercè Granados and José Luis Cortina\*

Analytical Chemistry Department, Universitat de Barcelona, Barcelona, Spain

\*Chemical Engineering Department, Universitat Politècnica de Catalunya, Barcelona, Spain

Flat-sheet liquid-supported membranes have been evaluated as interface between the sample and the sensor head of an optosensor for chromium(VI). The sensor uses 1,5-diphenylcarbazide as spectrophotometric reagent for optical detection through optical fibers. One of the key parameters for sensor performance is the effective transport of Cr(VI): thus, this is an important issue to optimise. The effect of experimental variables such as nature of solvent, carrier, carrier concentration, pH and concentration of 1,5-diphenylcarbazide on the Cr(VI) transport are presented.

### INTRODUCTION

In the last few years, chromium determination has received considerable attention because of the element's toxicity even at low concentrations. This is highly relevant, as there are a considerable number of pollution sources responsible for the presence, accumulation and mobility of Cr in the different compartments of the environment. The major uses of chromium are metal finishing and corrosion control, pigments and leather tanning. Chromium is found in two oxidation states in natural systems, namely Cr(III) and Cr(VI). Whereas Cr(III) is considered relatively nontoxic, Cr(VI) causes both acute and chronic toxic effects.

Cr(VI) determination is of particular interest in industrial wastewater treatment plants and in environmental compartments, and new trends in Cr(VI) analysis are oriented towards continuous *in situ* monitoring. Optical sensing is an attractive approach to reach these objectives and in particular sensors based on reagent renewal [1,2] seem to fulfil the requirements for continuous monitoring.

The sensor uses a membrane as an interface between the sample and the detection cell. A chemical reaction occurs between the analyte that has diffused through the membrane and a chromogenic or fluorogenic reagent, and a strongly absorbing or fluorescent species is produced and is detected through optical fibers connected to the detector (spectrophotometer or fluorimeter). The reagent is continuously pumped, and the solution inside the detection cell continuously renewed, thus avoiding irreversibility problems, one of the main limitations of sensors based on immobilised reagents. The key parameters for the success of the sensor are the proper selection of the chemical reaction for the optical detection, and the membrane, which should allow an efficient transport of the analyte from the sample to the detection chamber, be not permeable to interferences, and prevent reagent leakage from the chamber to the sample.

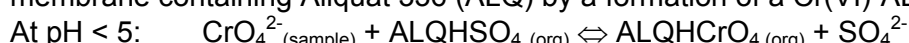
In this particular case, 1,5-diphenylcarbazide (DPC) was selected as the chromogenic reagent, because it is a very selective and sensitive reagent for Cr(VI) [3]. On the other hand previous studies on membranes have pointed out that flat-sheet liquid-supported membranes (FSLSM) using Aliquat 336 (ALQ) as a carrier are a good option as sensor interface [4]. In this paper we present the results of the optimisation of transport conditions directed towards Cr(VI) optical sensing.

## SENSOR TRANSDUCTION MECHANISMS

The sensor transduction mechanism of Cr(VI) can be described by the following steps [5,6]:

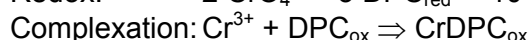
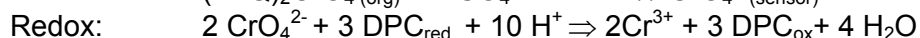
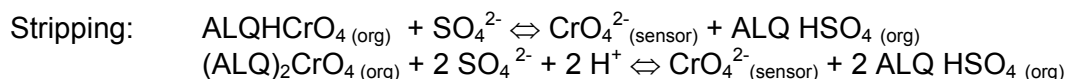
*Transport step I:* Cr(VI) (sample)  $\Rightarrow$  Cr(VI) (membrane).

Cr(VI) anions ( $\text{HCrO}_4^-$  and/or  $\text{CrO}_4^{2-}$ ) are extracted into the anion-exchange liquid supported membrane containing Aliquat 336 (ALQ) by a formation of a Cr(VI)-ALQ complexes.



*Transport step II:* Cr(VI) (membrane)  $\Rightarrow$  Cr(VI) (sensor detection chamber).

This is accomplished by the combination of Cr(VI) stripping and redox and complexation reactions between chromium and DPC. Thus, the stripping process is facilitated by the combination of chemical reactions leading to the formation of the absorbing species.



## EXPERIMENTAL

### Reagents and Solutions

All the chemicals used were A.R grade unless stated otherwise. Hexane (Fluka), kerosene (Fluka), toluene (Merck) and *n*-decanol (Fluka) were used as received. 1 g L<sup>-1</sup> Cr(VI) standard solution was prepared by dissolving sodium chromate (Merck) in water. 0.4 % (w/v) DPC solutions were prepared by dissolving 0.25 g of DPC (Merck) in 10 ml of ethanol and diluting to 100 ml with water. Working DPC solutions were prepared by appropriate dilution of 0.4% solutions with sulfuric acid solutions. ALQ, a quaternary ammonium salt ((CH<sub>3</sub>)R<sub>3</sub>N<sup>+</sup>Cl<sup>-</sup>), from Henkel was used as received.

### Apparatus

A 640 Varian atomic absorption spectrophotometer (AAS) was used for chromium measurements in the source phase and the stripping phase. A Metrohm AG 9100 glass combined electrode connected to a Digilab 517 pH-meter (Crison) was used for pH measurements.

Spectrophotometric measurements in the stripping phase were made with a Hewlett Packard diode array spectrophotometer HP 5483, coupled to a fiber-based transmittance probe from Photonetics.

### **FSSLM Preparation**

Millipore Durapore GVHP 4700  $12.5 \times 10^{-3}$  cm thick, a microporous polyvinylidenefluoride film with a nominal porosity of 75% and effective pore size of 0.22  $\mu\text{m}$ , was used as the polymeric support for the FSLSMs.

The FSLSMs were impregnated with ALQ solutions containing the extractant dissolved in hexane, kerosene, toluene and mixtures with n-decanol by immersion for 48 h, and then leaving it to drip for a few seconds before being placed in the transport cell.

### **Transport Experiments**

The batch transport experiments were carried out in a permeation cell consisting of two compartments made of methacrylate and separated by a FSSLM. The geometrical membrane area was  $19.50 \text{ cm}^2$  and the volume of the feed and stripping solution was 200 ml. The experiments were performed at  $20^\circ\text{C}$  at a mechanical stirring speed of 1300 rpm in the feed and the stripping phase except in the experiments where the stirring speed was varied. The aqueous feed solutions contained different concentrations of Cr(VI) and pH varied between 2 and 12.

The chromium permeation was monitored by periodically sampling the feed and the stripping phase, and chromium was analysed after appropriate dilution by AAS.

Continuous Cr monitoring in the stripping solution was performed using a transmission probe connected *via* optical fiber to the diode array spectrophotometer.

## **RESULTS AND DISCUSSION**

### **Optimisation of Cr(VI) Transport**

Series of experiments were performed in order to find the optimum conditions for chromium transport, which was evaluated in terms of extraction efficiency ( $E$ ),  $E$  being determined as the ratio between [Cr] in the stripping solution and the initial [Cr] in the feed solution. The stirring speed was fixed to 1300 rpm, since preliminary studies pointed out that above 1000 rpm the aqueous resistance to the mass transfer process was minimised.

The selection of the diluent used to prepare the ALQ FSLSMs is an important issue. Initial assays showed that, among the solvents tested to prepare the membranes, kerosene provided the best results. The use of n-decanol as a modifier has been proposed to improve Cr recoveries in liquid-liquid extraction [7]. Thus, n-decanol was added to kerosene to increase the polarity of the organic phase (*i.e.*, the FSSLM) and it was observed that 10% n-decanol in kerosene provided a significative improvement in Cr transport (Figure 1). The effect of the concentration of ALQ in the membrane phase on the extraction efficiency is shown in Figure 2. An increase is observed from 0.1 M to 0.2 M, and above this value  $E$  remains constant. From these results it was decided to prepare FSLSMs with 0.2 M ALQ in kerosene:n-decanol (90:10).

On the other hand it was observed that Cr(VI) transport improves with increases in the pH of the feed phase, which has important implications in Cr(VI) sensing. That is, calibration of the sensor system must be performed with Cr(VI) standards adjusted to the same pH that the sample to be monitored.

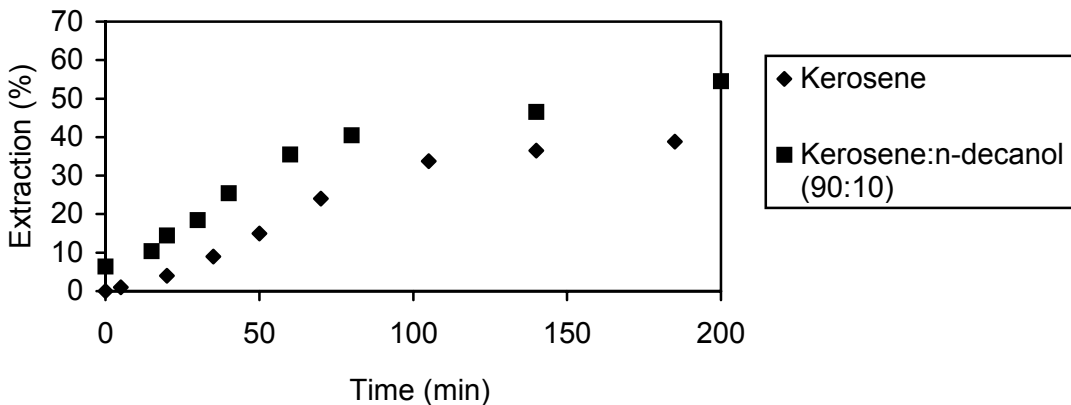


Figure 1. Effect of *n*-decanol. Feed phase:  $[Cr]=20\text{ mg L}^{-1}$ ,  $pH=3.0$ . Stripping phase:  $[DPC]=0.1\%$ ,  $pH=1.0$ . FSLSMs:  $0.1\text{ M ALQ}$  in kerosene.

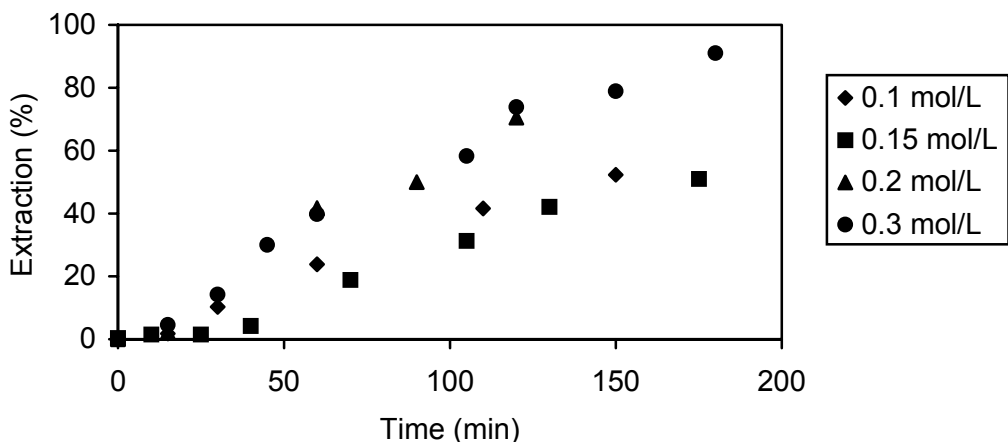


Figure 2. Effect of ALQ concentration. Feed phase:  $[Cr]=20\text{ mg L}^{-1}$ ,  $pH=3.0$ . Stripping phase:  $[DPC]=0.1\%$ ,  $pH=1.0$ . FSLSMs: ALQ in kerosene:*n*-decanol (90:10).

The effect of the stripping phase composition was also considered. It is in the stripping phase solution that optical sensing takes place, and this requires the presence of DPC in  $\text{H}_2\text{SO}_4$  medium. Therefore there are some constraints on the suitable range for the variables. pH of the phase was kept constant at 1. When DPC concentration was varied from 0.05% to 0.1% there was a clear improvement on the Cr(VI) transport, but increasing DPC concentration up to 0.2% did not contribute to any significative raise of transport (Figure 3). Higher DPC concentrations were not suitable because the reaction between Cr(VI) and DPC took place into the membrane, and complex immobilisation occurred. 0.1% was selected as the optimum value to assure the reduction and complexation reactions, which act as driving forces of the Cr transport and lead to the formation of the absorbing species.

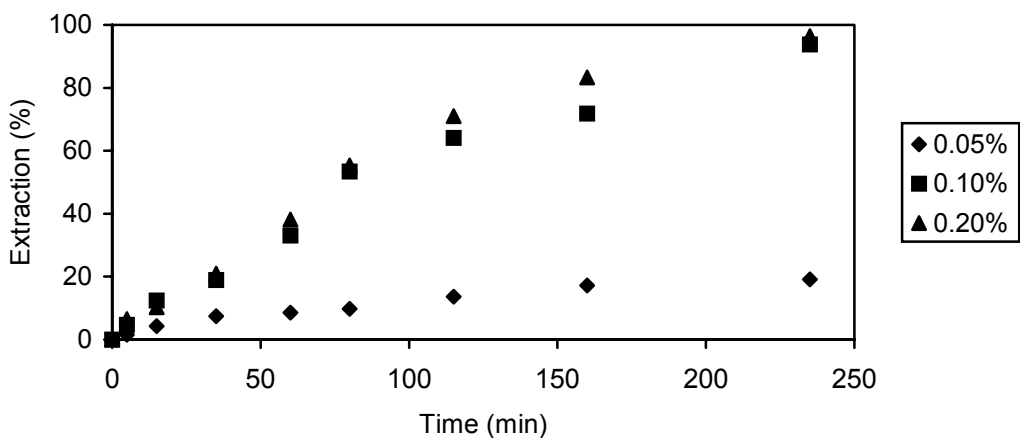


Figure 3. Effect of DPC concentration. Feed phase:  $[Cr] = 20 \text{ mg L}^{-1}$ ,  $pH = 3.0$ . Stripping phase:  $pH = 1.0$ . FSLSMs: 0.2 M ALQ in kerosene:*n*-decanol (90:10).

### Optical Sensing of Cr(VI)

Once the optimum conditions for Cr(VI) transport are established, (*i.e.*, the composition of both the FSLSM and the stripping phase), experiments were performed with a transmittance-based probe to check the feasibility of the *in situ* chromium monitoring with signal transmission through optical fibers. Thus, the probe was immersed into the stripping solution, and connected to a diode array spectrophotometer. Absorption spectra were acquired at elapsed times, and it was observed that light intensity was modulated by absorption changes in the visible range that occur when chromium(VI) diffuses across the FSLSM (Figure 4) and forms the violet Cr-DPC complex. Different Cr(VI) concentrations in the feed phase lead to different absorbance surfaces, indicating that the optical signals can be correlated to Cr(VI) concentration, through a calibration model, which will enable Cr(VI) quantitative monitoring.

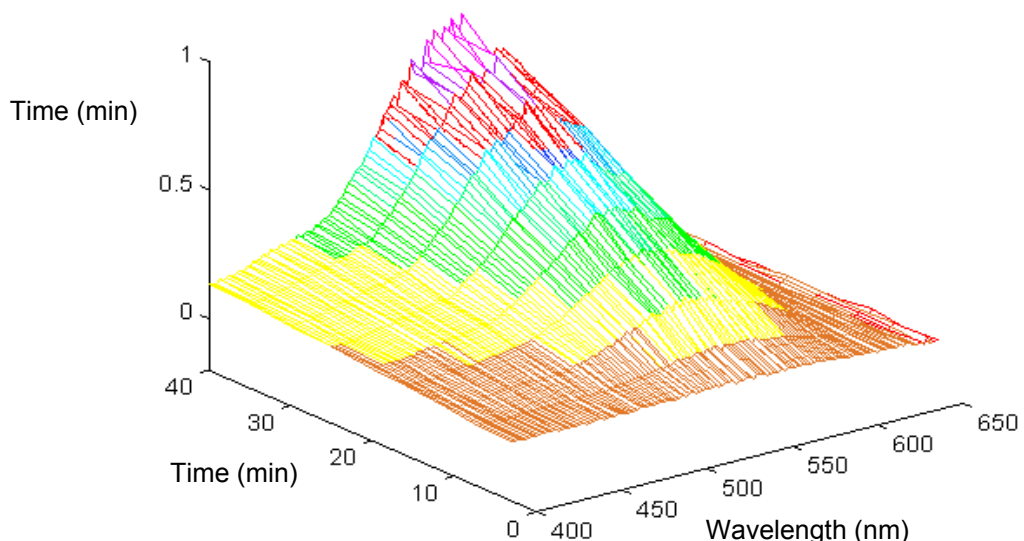


Figure 4. Chromium(III)-DFC<sub>ox</sub> complex spectra collected with a transmission probe in the stripping solution. Feed solution:  $Cr 15 \text{ mg L}^{-1}$ ,  $pH=3$ . FSLSM: ALQ 0.2 M in kerosene-*n*-decanol 90:10. Stripping solution: DPC 0.01%,  $pH 1.0$ .

## CONCLUSIONS

Flat-sheet liquid-supported membranes based on Aliquat 336 have been shown to be appropriate interfaces for a Cr(VI) optical sensor based on the chemical reaction between chromium(VI) and diphenylcarbazide and the spectrophotometric detection of the violet complex obtained. This chemical reaction simultaneously acts as a driving force for Cr(VI) transport. Optimisation of the chemical composition of the liquid membrane as well as that of the stripping solution allows achievement of a satisfactory Cr(VI) diffusion through the membrane.

The nature of the diluent used to prepare the membrane, Aliquat 336 concentration and diphenylcarbazide concentration have been identified as key parameters for successful Cr(VI) transport.

## ACKNOWLEDGEMENTS

This research was supported by CICYT projects AMB98-0327, HY99-1147-CO2-01 and QUI99-0749-C03-02, and SGR99-00049 project of the Generalitat of Catalonia. The authors wish to thank Cognis A.G. for kindly donating Aliquat 336.

## REFERENCES

1. R.J. Berman, G.D. Christian and LW. Burgess (1990), *Anal. Chem.*, **62**, 2066-2071.
2. J.L. Cortina, E. Castillo and M. Granados (2000), *Quím. Anal.*, **19**, 68-74.
3. K.L. Cheng, K. Ueno and I.T Imamura (1982), Handbook of Organic Analytical Reagents, CRC Press, Boca Raton FL, pp. 277.
4. E. Castillo, M. Granados, M.D. Prat, A.M. Sastre, A. Kumar and J.L. Cortina (2001), Solvent Extraction in the XXI Century, M. Cox, M. Valiente and M. Hidalgo (eds.), Society of Chemical Industry, London, pp. 47-52.
5. S.L. Lo and S.F. Shiue (1997), *Water Res.*, **32**, 174-178.
6. A.I. Alonso, B. Galan, J.A. Irabien and M.I. Ortiz (1997), *Sep. Sci. Tech.*, **32**, 1543-1555.
7. E. Salazar, M.I. Ortiz, A.M. Urtiaga and J.A. Irabien (1992), *Ind. Eng. Chem. Res.*, **31**, 1516-1522.



## APPLICATION OF NOVEL EXTRACTANTS FOR ACTINIDE(III)/ LANTHANIDE(III) SEPARATION IN HOLLOW FIBER MODULES

Andreas Geist, Michael Weigl, Udo Müllrich, Klaus Gompper

Forschungszentrum Karlsruhe, Institut für Nukleare Entsorgung, Karlsruhe, Germany

Separation tests in hollow fiber modules were performed regarding the difficult selective extraction of trivalent actinides over fission lanthanides from acidic media. With 2,6-di(5,6-dipropyl-1,2,4-triazin-3-yl)pyridine as extractant, up to 94% americium could be extracted from 1.0 kmol/m<sup>3</sup> HNO<sub>3</sub>, with minimal lanthanide co-extraction. Using a synergistic mixture of bis(chlorophenyl)dithiophosphinic acid and tri-*n*-octyl phosphine oxide, tests were performed on extraction, lanthanide scrubbing and stripping. In the extraction test, up to 99.99% americium could be extracted from 0.5 kmol/m<sup>3</sup> HNO<sub>3</sub>, with approximately one third of the lanthanides being co-extracted. Mass transfer calculations using a consistent set of input data showed good agreement with the experiments.

### INTRODUCTION

The radiotoxicity of spent nuclear fuel is governed by its content of plutonium and the Minor Actinides (neptunium, americium, curium) for several 10<sup>5</sup> years. The *Partitioning and Transmutation* strategy [1] aims at minimizing the long-term radiotoxicity by separating these elements (Partitioning) and fissioning them to short-lived and eventually stable nuclides (Transmutation). The separation of trivalent actinides (americium, curium) from the fission lanthanides is the key step of Minor Actinide Partitioning due to the chemical similarity of the two groups. To make this step process compatible, a feed acidity in the range of 0.1 to 1 kmol/m<sup>3</sup> HNO<sub>3</sub> must be processed.

Two of the most promising extractants for this separation task are:

- A synergistic mixture of bis(chlorophenyl)dithiophosphinic acid and tri-*n*-octyl phosphine oxide (TOPO) [2]. Depending on the diluent used, this mixture extracts actinides(III) from 0.5 kmol/m<sup>3</sup> HNO<sub>3</sub> with an Am(III)/Eu(III) separation factor of approx. 30 [3]. The so called SANEX-/I process (**s**elective **a**ctinide **e**xtraction) [3] is based on this extractant.
- 2,6-di(5,6-dipropyl-1,2,4-triazin-3-yl)pyridine (*n*-Pr-BTP), a solvating extractant which was developed in our laboratory [4]. It is able to extract actinide(III) nitrates from 1-2 kmol/m<sup>3</sup> HNO<sub>3</sub> with usable distribution coefficient and an Am(III)/Eu(III) separation factor of approx. 135. This extractant is used in the SANEX-III process [3].

These extractants have already proven their potential in mixer-settler and centrifugal extractor battery tests performed in other laboratories [3].

Instead of utilizing multistage contactors, we have performed tests on americium(III)/lanthanide(III) separation in hollow fiber modules (HFM) using these extractants. Basically, a HFM is a differential column contactor. Aqueous and organic phases are macroscopically separated by a micro-porous membrane. Phase contact is maintained within the pores by the application of an appropriate pressure difference. This yields a wide flexibility towards hydrodynamic conditions, overcoming restrictions encountered with conventional extractors, e.g., entrainment, flooding [5, 6].

The experiments were accompanied by predictive computer code calculations yielding stationary outlet concentrations. The calculations take into account relevant processes and use a consistent set of input data, making them applicable to scale-up and process design.

## EXPERIMENTAL

### Reagents and Feed Solutions

A solution of 0.5 kmol/m<sup>3</sup> bis(chlorophenyl)dithiophosphinic acid (bought from an external laboratory) + 0.25 kmol/m<sup>3</sup> TOPO in tert.-butylbenzene was used in the SANEX-IV experiments. *n*-Pr-BTP was synthesized according to [4]. A solution of 0.04 kmol/m<sup>3</sup> *n*-Pr-BTP in kerosene/1-octanol (70:30 vol.) was used in the SANEX-III extraction experiment.

Aqueous feed was a solution of inactive trivalent fission lanthanides (La, Ce, Pr, Nd, Sm, Eu, Gd + Y) in either 1.0 kmol/m<sup>3</sup> HNO<sub>3</sub> (SANEX-III) or 0.5 kmol/m<sup>3</sup> HNO<sub>3</sub> (SANEX-IV) tracered with <sup>241</sup>Am(III) (see Table 1). The loaded organic effluent from the SANEX-IV extraction experiment was used as feed in the scrubbing experiment into 1.0 kmol/m<sup>3</sup> HNO<sub>3</sub>, the organic effluent of which was then treated in the stripping experiment into 2.0 kmol/m<sup>3</sup> HNO<sub>3</sub>.

*Table 1. Aqueous feed compositions for the SANEX-III and -IV extraction experiments.*

compound	SANEX-III	SANEX-IV
HNO <sub>3</sub>	1.0 kmol/m <sup>3</sup>	0.5 kmol/m <sup>3</sup>
<sup>241</sup> Am	0.49 MBq/L	0.88 MBq/L
Y	89 mg/L	221 mg/L
La	294 mg/L	756 mg/L
Ce	566 mg/L	1460 mg/L
Pr	264 mg/L	699 mg/L
Nd	998 mg/L	2512 mg/L
Sm	199 mg/L	457 mg/L
Eu	36 mg/L	91 mg/L
Gd	28 mg/L	55 mg/L

### HFM Setup and Procedure

We set up a single HFM extractor inside a glove box. The HFM setup is shown schematically in Figure 1. Both phases were passed through the module in quasi-counter-current, single-pass mode, i.e., phases were not recycled. The modules used were Celgard LiquiCel Extra-Flow type modules (10,000 hollow fibers (HF), membrane material polypropylene, HF inner diameter = 0.24 mm, HF outer diameter = 0.30 mm, average pore size 0.02 µm, porosity 40%, tortuosity 2.6, active length = 0.15 m).

The HFM was filled with aqueous and organic phases and appropriate flow rates and pressures were set up. Static pressure in the aqueous phase was kept approx. 0.5 bar higher than in the organic phase to maintain proper phase separation. Aqueous and organic effluent samples were taken at appropriate intervals until steady state was reached. Then, flow rates were changed and the sampling procedure repeated.

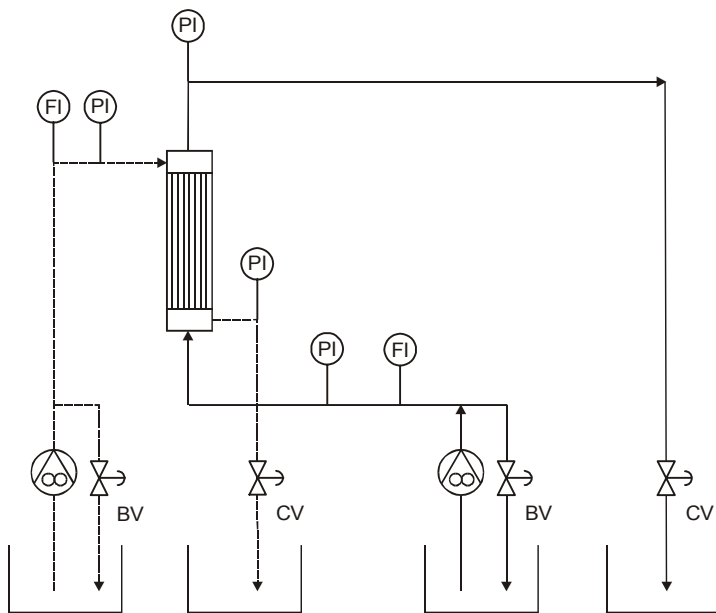


*Figure 1. Single-pass HFM setup (schematic). — organic phase, - - - aqueous phase, PI = pressure gauge, FI = flow meter (rotameter), CV = control valve, BP = bypass valve.*

Americium-241 activity in both effluent phases was measured on a gamma-counter (Packard Cobra Auto-Gamma). Lanthanide concentrations were measured with ICP-AES after appropriate dilution in nitric acid (aqueous samples) or stripping into nitric acid (organic samples). Stationary outlet concentrations were plotted vs. flow rate.

### MASS TRANSFER CALCULATIONS

A modeling was performed to predict experimental data. The calculations take into account fundamental physical and chemical processes (flow of phases, mass exchange according to experimentally determined equilibrium and kinetic data). The nature of the calculations allows to use them for scale-up. The modeling, which is described in detail in [7, 8], was adapted to the extraction systems and HFMs used here [9]. Mass fluxes were calculated from input concentrations, equilibrium and kinetic data, and diffusivities. With a hydrodynamic description of the module and a cell-wise calculation, outlet concentrations were calculated.

Mass transfer rate in the SANEX-IV system (dithiophosphinic acid) is controlled by diffusion in the range of hydrodynamic conditions relevant [9, 10]. Hence, the above mentioned modeling of mass transfer systems controlled by diffusion [7, 8] was adapted by using equilibrium data from [3]. Aqueous diffusion coefficients were taken from the literature, organic diffusion coefficients were estimated using the Wilke-Chang correlation [11].

In the SANEX-III system (n-Pr-BTP), extraction of metal nitrates and nitric acid was taken into account. Corresponding equilibrium data was taken from [3]. Kinetic investigations revealed that the rate of americium mass transfer is controlled by the chemical reaction [10]. A forward reaction rate constant was derived,  $k_{fwd} = 3 \cdot 10^{-5}$ . The additional (and dominating) mass transfer resistance due to the chemical reaction was implemented in the calculations.

## RESULTS

For all experiments performed, operation was stable and dispersion-free. Calculations agreed well with the experimental results. Extraction efficiency is strongly dependent on flow rate,  $Q$ , and hence residence time.

In the SANEX-IV extraction test, the aqueous phase was flowing inside the hollow fibers. Aqueous flow rate was varied,  $Q_{aq} = 300 \text{ mL/h}, 490 \text{ mL/h}, 800 \text{ mL/h}$ . Organic flow rate was kept constant at  $Q_{org} = 300 \text{ mL/h}$ .

Mass balances were 100-103% (americium) and (100±5)% (lanthanides). Aqueous effluent concentrations normalized to aqueous feed concentrations,  $[Me^{3+}]_{out}/[Me^{3+}]_{in}$ , as a function of aqueous flow rate,  $Q_{aq}$ , are shown in Figure 2: At  $Q_{aq} = 300 \text{ mL/h}$ , 99.99% americium could be removed from the feed phase. Approx. 30% of the lanthanide inventory was co-extracted.

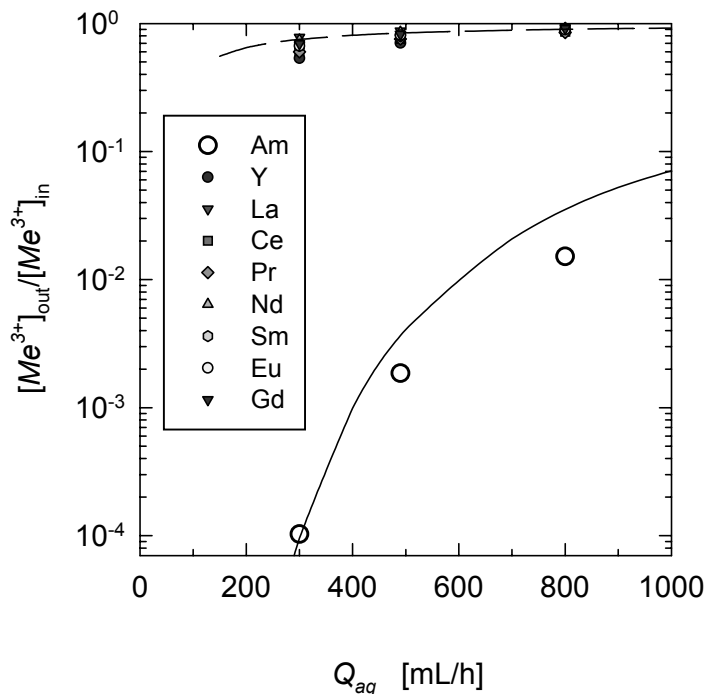


Figure 2. SANEX-IV extraction experiment. Flow rate dependency of extraction efficiency. Aqueous phase, in HF: Am(III) + Ln(III) in  $HNO_3$  0.5 kmol/m<sup>3</sup> (see Table 1). Organic phase, shell-side: Bis(chlorophenyl)dithiophosphinic acid 0.5 kmol/m<sup>3</sup> + TOPO 0.25 kmol/m<sup>3</sup> in tert.-butylbenzene.  $Q_{org} = 300 \text{ mL/h}$ . Symbols: experiment, lines: calculated.

A lanthanide scrubbing experiment was performed, contacting the loaded organic phase from the SANEX-IV extraction test with 1.0 kmol/m<sup>3</sup>  $HNO_3$ . Erroneously, the organic phase was led shell-side. Aqueous and organic flow rates were varied, 300 mL/h, 490 mL/h, 820 mL/h.

Mass balances were (100±1)% for americium, (100±5)% for yttrium and 89-94% for the other lanthanides. At 300 mL/h, approx. 70% of the lanthanides were scrubbed. 45% of americium was also scrubbed, see Figure 3. The dotted line shows the calculated lanthanide scrubbing efficiency if the organic phase was led inside the hollow fibers (americium scrubbing is not influenced by operating mode). The reason for the improved efficiency is explained in [9].

Finally, the organic effluent from the SANEX-IV scrubbing experiment was stripped into  $2.0 \text{ kmol/m}^3 \text{ HNO}_3$ . The organic phase was led in the lumen of the hollow fibers. Aqueous and organic flow rates were varied, 320 mL/h, 490 mL/h, 810 mL/h, with  $Q_{\text{aq}} = Q_{\text{org}}$ .

Mass balances were 97-99% for americium and  $(100 \pm 5)\%$  for the lanthanides. At 320 mL/h, 88% of americium and 93-95% of the lanthanide inventory could be stripped from the organic phase, see Figure 4. This is an improvement over a stripping experiment performed into  $1.5 \text{ kmol/m}^3 \text{ HNO}_3$  [9]. To reach 99% americium stripping efficiency, stripping would have to be performed at a flow rate of 100 mL/h, as suggested by the calculations.

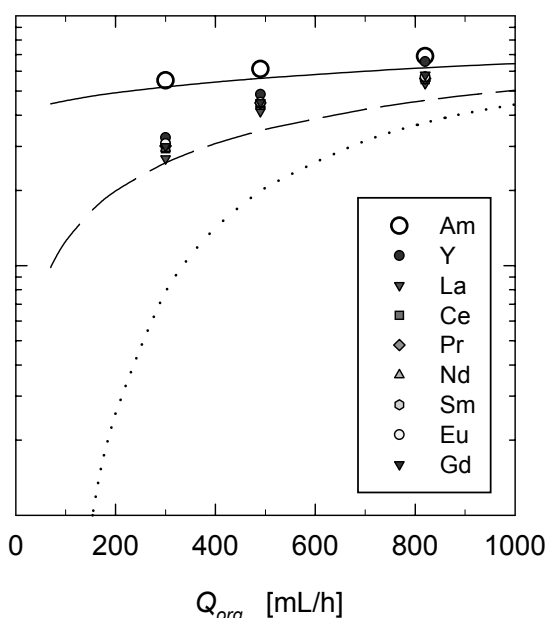


*Figure 3. SANEX-IV scrubbing experiment,  
organic phase shell-side,  
 $\text{HNO}_3 = 1.0 \text{ kmol/m}^3$ .*

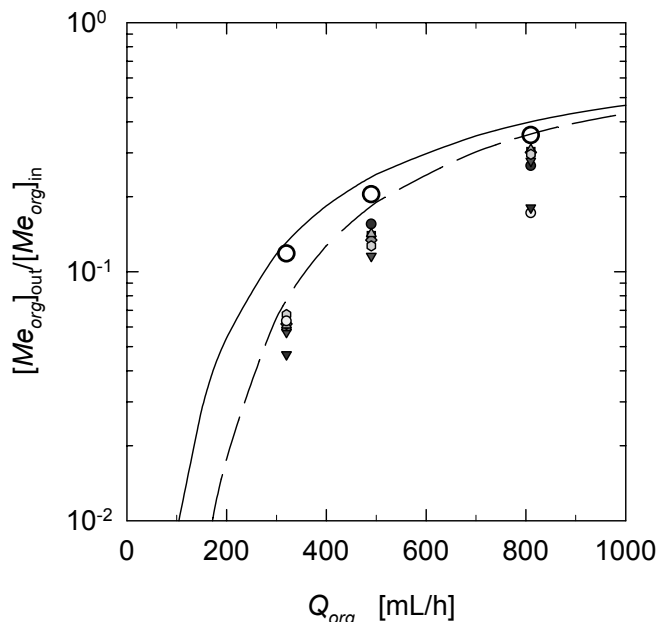


*Figure 4. SANEX-IV stripping experiment,  
organic phase in HF,  
 $\text{HNO}_3 = 2.0 \text{ kmol/m}^3$ .*

*Loaded organic phase: Bis(chlorophenyl)dithiophosphinic acid  $0.5 \text{ kmol/m}^3$  + TOPO  $0.25 \text{ kmol/m}^3$  in tert.-butylbenzene.  $Q_{\text{org}} = Q_{\text{aq}}$ . Symbols: experiment,  
— americium calculated, - - - lanthanides calculated.*

With the SANEX-III system, we have performed one extraction experiment yet. Aqueous phase was flowing on the shell-side of the HFM. Aqueous flow rate was varied,  $435 \text{ mL/h} \leq Q_{\text{aq}} \leq 1740 \text{ mL/h}$ , organic flow rate was kept constant at  $Q_{\text{org}} = 500 \text{ mL/h}$ . Except with an aqueous flow rate of 435 mL/h, mass balances were  $(100 \pm 2.5)\%$  for lanthanides, and 90-98% for Am(III). With an aqueous flow rate of 435 mL/h, americium mass balance was 66%, lanthanide mass balances were approx. 88%. This is a sign that, at this flow rate, the experiment was not run sufficiently long to reach steady state.

The results are shown in Figure 5. With an aqueous flow rate of 435 mL/h, 94% of americium could be removed from the aqueous phase. Lanthanide co-extraction, determined from the organic phase, was in the range of 1%. This is a result of the very high selectivity of n-Pr-BTP. However, to reach almost quantitative americium extraction, flow rates would have to be significantly lower.

## CONCLUSIONS

The performance of two novel extraction systems for the selective extraction of trivalent actinides over lanthanides was tested in HFM experiments. The SANEX-IV system shows excellent extraction efficiency. On the other hand, the extraction efficiency of the SANEX-III system is impeded by a slow chemical reaction. To achieve comparable Am(III) decontamination, flow rates must be substantially lower. However, the high separation factor of n-Pr-BTP could possibly simplify subsequent lanthanide scrubbing in a coupled extraction-scrubbing-stripping process.

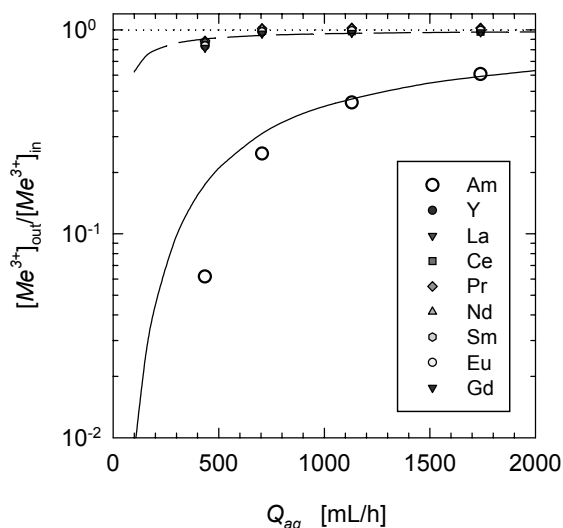


*Figure 5. SANEX-III extraction experiment. Flow rate dependency of extraction efficiency.*  
*Aqueous phase, shell-side: Am(III) + Ln(III) in  $\text{HNO}_3$  1.0 kmol/m<sup>3</sup> (see Table 1).*  
*Organic phase, in HF: n-Pr-BTP 0.04 kmol/m<sup>3</sup> in kerosene/1-octanol (70:30 vol.).*  
 $Q_{\text{org}} = 500 \text{ mL/h}$ . Symbols: experiment, lines: calculated.

## ACKNOWLEDGEMENT

The authors are grateful for the financial support from the Commission of the European Community (contract FIKW-CT2000-00087).

## REFERENCES

1. OECD Nuclear Energy Agency (1999), Actinide and Fission Product Partitioning and Transmutation, Status and Assessment Report, Paris.
2. G. Modolo and R. Odoj (1999), *Solvent Extr. Ion Exch.*, **17** (1), 33-53.
3. C. Madic, M.J. Hudson, J.O. Liljenzin, J.P. Glatz, R. Nannicini, A. Facchini, Z. Kolarik and R. Odoj (2000), New Partitioning Techniques for Minor Actinides, EUR 19149, European Commission, Luxembourg.
4. Z. Kolarik, U. Müllrich and F. Gassner (1999), *Solvent Extr. Ion Exch.*, **17** (5), 1155-1170.
5. B. M. Kim (1984), *J. Membr. Sci.*, **21**, 5-19.
6. G.W. Stevens and H.R.C. Pratt (2000), *Solvent Extr. Ion Exch.*, **18** (6), 1051-1078.
7. U. Daiminger, A. Geist, W. Nitsch and P. Plucinski (1996), *Ind. Eng. Chem. Res.*, **35**, 184-191.
8. A. Geist, P. Plucinski and W. Nitsch (2001), submitted to *J. Membr. Sci.*
9. A. Geist, M. Weigl and K. Gompper (2001), *Proc. GLOBAL 2001*, Paris, to be published.
10. M. Weigl, A. Geist, U. Müllrich and K. Gompper, (unpublished data).
11. C.R. Wilke and P. Chang (1955), *AIChE J.*, **1** (2), 264-270.



## HOLLOW FIBER MEMBRANE-BASED NON-DISPERSIVE EXTRACTION OF SILVER(I) FROM ALKALINE CYANIDE MEDIA USING LIX 79

Anil Kumar Pabby\*, A. Melgosa, R. Haddad and A. M. Sastre

Department of Chemical Engineering, Universitat Politecnica de Catalunya, Barcelona, Spain

\*PREFRE, Nuclear Recycle Group, Bhabha Atomic Research Center, Tarapur, India

This investigation is concerned with applications of hollow fiber non-dispersive solvent extraction (HFNDSX) of silver(I) from alkaline cyanide media using microporous hydrophobic hollow fiber contactors. LIX79 dissolved in *n*-heptane (Cognis Corporation) has been employed as extractant. The HFNDSX operation was carried out with 12% LIX79/*n*-heptane by passing alkaline feed  $\text{Ag}(\text{CN})_2^-$  through the tube side and organic extractant through the shell side in counter-current mode. The different hydrodynamic and chemical parameters such as linear flow velocity of the feed aqueous phase ( $3.07 \text{ cm/s} \geq v_f \geq 0.39 \text{ cm/s}$ ), linear velocity of organic phase ( $1.18 \text{ cm/s} \geq v_f \geq 0.92 \text{ cm/s}$ ) and pH variation of aqueous feed were evaluated. The mass transfer coefficients were calculated under different hydrodynamic and chemical conditions.

### INTRODUCTION

During the past few years, more attention has been focused on techniques pertaining to the recovery of precious metals [1]. Silver has gained pronounced importance owing to special interest in new technological applications. Moreover, because the market value of precious metals in many cases are very high, their full recovery from hydrometallurgical solutions (primary sources like ores, etc.) and via recycling are justified from an economic point of view. Although several conventional methods are tried for silver recovery no attempt has been made to use the hollow fiber non-dispersive solvent extraction (HFNDSX) technique for silver recovery.

HFNDSX is simply a liquid-liquid extraction in a hollow fiber contactor in which aqueous and organic streams flow through the capillary shell side and contact each other in the pore mouth without dispersion, which minimizes the possibility of forming emulsion/third phase or crud formation with this extractor. Hollow fiber modules may be connected in series or in parallel, and the length and diameters of fibers and modules can be varied to provide the required interfacial area. Such membrane processes not only remove the required compounds from the streams but can also concentrate these species simultaneously on the product side for possible further processing [2-3]. HFNDSX is also characterized by being rapid in separation, high in efficiency, low in power consumption and adaptable to diverse uses, in addition to being suitable for industrial applications due to a large area-to-volume ratio which can approach a value of  $10^4 \text{ m}^2/\text{m}^3$  [2, 4-5]. Furthermore, HFNDSX techniques have been extensively deployed in separation science applications such as metal recovery from leaching and waste waters, extraction of precious and strategic metals from neutral waters, and treatment of large volumes of the effluents including toxic and hazardous wastes generated by industries [2, 6-8].

In order to develop the HFNDSX scheme for silver extraction, LIX79 was selected as extractant based on the previous published work [9]. The aim of this paper is to evaluate design parameters in order to optimize performance of hollow fiber modules for the HFNDSX of Ag(I) from alkaline cyanide media.

## EXPERIMENTAL PROCEDURE

### Reagents

A stock solution of Ag(I) (5 g/L) was prepared from pure solid KAg(CN)<sub>2</sub> [Johnson Matthey Chemicals (Karlsruhe, Germany)] was dissolved in NaCN (Merck). The organic solvent used in HFNDSX studies was *n*-heptane, which is a commercially available solvent. All chemicals were used as received. LIX 79 (N,N'-bis(2-ethylhexyl) guanidine) was kindly provided by Cognis Corp. The HFM is manufactured by Hoechst Celanese, Charlotte, NC (Liqui-Cel, 8x28 cm 5PCG-259 contactor and 5 PCS-1002 Liqui-cel laboratory LLE) and specified as below.

Type of module	Number of fibers	Module diameters (cm)	Module length(cm)	Active interfacial area (m <sup>2</sup> )
5PCG-259 (contactor)	10,000	8	28	1.4

### Hollow Fiber Membrane

Fiber I.D. (cm)	$24.0 \cdot 10^{-3}$	Fiber O.D.(cm)	$30.0 \cdot 10^{-3}$	Fiber wall thickness (cm)	$3.0 \cdot 10^{-3}$
Fiber length (cm)	15	Porosity (%)	30	Pore size ( $\mu\text{m}$ )	0.03
Polymeric Material	polypropylene	Hydraulic diameter (cm)	0.1	Area per unit volume ( $\text{cm}^2/\text{cm}^3$ )	29.3

### Partition Coefficients of Ag(I)

The procedure adopted for determining Ag(I) partition coefficient is described elsewhere [10].

### The Non-Dispersive Membrane Extraction Set-up

A schematic view of the membrane-based extraction process of Ag(I) using a hollow fiber contactor in recirculation mode is shown in Figure 1. Both aqueous and organic phases were contacted counter-currently in a hollow fiber module for carrying out extraction or stripping run under recirculating mode. In the extraction module, the feed aqueous phase flows through the lumen of the fibers, while the organic phase circulates through the shell side, wetting the wall of the hydrophobic fibers. The pressure of the aqueous phase was held at 0.2-0.5 bar higher than the pressure in the organic phase.

In the stripping run, loaded organic extractant (LIX 79 with silver complex) flowed through the shell side, whereas NaOH flowed through the tube side in counter-currently in recirculation mode.

The Ag(I) concentration in the feed varied between  $4.64 \cdot 10^{-4}$  mol/dm<sup>3</sup>. The solution of 0.4 M to 1 M NaOH was used as the stripping phase when back extraction of Ag(I) was carried out in the hollow fiber module. At known times during the procedure, small aliquots of the stripping stream and from organic the solution were taken and analyzed for metal concentration by standard atomic absorption spectrophotometry (2380 Perkin Elmer Absorption Spectrometer).

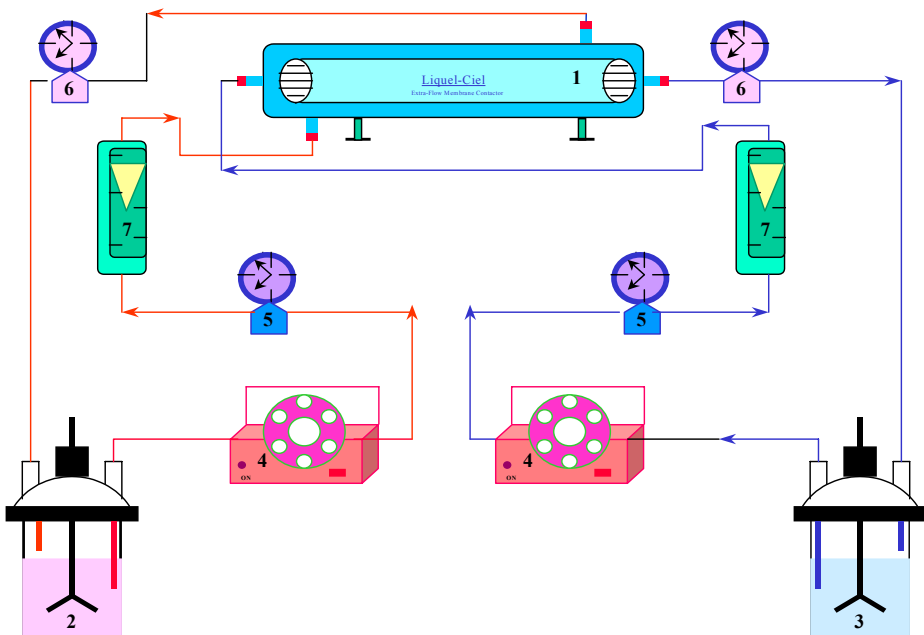


*Figure 1. A schematic view of the membrane-based extraction process of Ag(I) from cyanide media using hollow fiber contactor. (1) hollow fiber contactor; (2,3) organic extractant and feed; (4) feed and organic pump; (5,6) Inlet and outlet pressure gauge respectively for organic and feed; (7) Flow meters for feed and organic.*

## THEORETICAL BACKGROUND

### Extraction Equilibrium

The extraction mechanism for silver with LIX 79 is based on the ion-pair type. The extraction of Ag(I) from the process stream takes place at the interface of the feed and membrane. The Ag(I) ions in alkaline cyanide media (present as  $\text{Ag}(\text{CN})_2^-$ ) form a complex with the extractant LIX 79 ( $\text{N,N}'\text{-bis}(2\text{-ethylhexyl})\text{ guanidine}$ , R), which is protonated between pH 10.0-10.5, and is expressed as:



and similarly for stripping, the chemical reaction is presented as



The extraction equilibrium can be described by the following reactions and extraction constants:

$$K_{\text{ex}} = \frac{[\text{Ag}(\text{CN})_2(\text{HR}) \bullet 2\text{R}]_{\text{org}}}{[\text{Ag}(\text{CN})_2^-]_{\text{aq}} [\text{H}^+] [\text{R}]_{\text{org}}^3} \quad (3)$$

where R is the organic extractant. The value of  $K_{\text{ex}}$  for Ag(I) with LIX 79 was found to be  $7.41 \pm 0.5 \cdot 10^{+15}$   $\log K_{\text{ext}} = 15.87$  [10] and is related to the partition coefficient (H) through the following expression:

$$\log H = \log K_{\text{ex}} + \log[H^+] + 3\log[R]_{\text{org}} \quad (4)$$

## Mass Transfer Coefficient Evaluation

As derived by Delia *et al.* [11], the equation for the calculation of  $K_{Ag}^E$  for countercurrent flow is

$$\ln \left[ \frac{\left( C_{e/s}^0 / H - C_f^0 \right)}{\left( C_{e/s}^0 / H - C_f^0 \right) + \left( V_f / HV_{e/s} \right) \left( C_f^0 - C_f \right)} \right] = t \frac{\left[ 1 - \exp \left( -4 K_{Au}^E V_m / d \left( 1 / Q_f - 1 / Q_{e/s} H \right) \right) \right] \left[ 1 / V_f + 1 / V_{e/s} H \right]}{\frac{1}{Q_f} - \frac{1}{Q_{e/s}} \exp \left[ -\frac{4 K_{Au}^E V_m}{d} \left( \frac{1}{Q_f} - \frac{1}{Q_{e/s} H} \right) \right]} \quad (5)$$

where  $Q_f$  and  $Q_{e/s}$  are the feed and extract/strip flows;  $V_f$  and  $V_{e/s}$  are the feed and extract/strip volumes;  $C_f^0$  and  $C_{e/s}^0$  are the concentrations of the solute in the feed and in the extract/strip solutions at time zero;  $C_f$  is the concentration of the solute in the feed at time  $t$ ;  $V_m$  is the volume of all the hollow fibers; and  $d$  is the diameter of one fiber.

## RESULTS AND DISCUSSION

### Optimisation of Hydrodynamics and Chemical Parameters

In the HFNDSX technique, it is well established [2] that, in order to keep the interface within the pores of a hydrophobic membrane, it is necessary to maintain a higher local pressure in the aqueous phase. Figure 2 shows a typical plot of mass transfer coefficient versus aqueous linear flow velocity predicted by Equation 5 for extraction of Ag(I) into LIX 79. The results of these calculations are given in Table 1 which show the mass transfer coefficients  $K_{Ag}^E$  for the extraction varied from  $2.6 \cdot 10^{-7}$  to  $1.7 \cdot 10^{-6}$  cm/s. In extraction module, the Ag(I) extraction ranged from 95 to 100% in around 1-2 h for counter-current contact. As seen in Figure 2, the overall mass transfer coefficient increased with the feed flow rate and its value was maximum at  $13.88 \text{ cm}^3/\text{s}$ . For example, when linear flow velocity ( $v_f$ ) varied by a factor of 3, the overall mass transfer coefficient ( $K_{Ag}^E$ ) increased by 6 times.

*Table 1. Mass transfer coefficients for extraction of Ag(I) from aqueous alkaline cyanide media (pH=10.3) with 18% LIX 79 in n-heptane using HFNDSX technique in counter-current mode as a function of aqueous flow rates.*

Experiment No.	$Q_e$ ( $\text{cm}^3/\text{s}$ )	$Q_f$ ( $\text{cm}^3/\text{s}$ )	$v_f$ ( $\text{cm}/\text{s}$ )	$K_{Ag}^E \cdot 10^{-6}$ ( $\text{cm}/\text{s}$ )	$r^2$	Extraction (%)
1	4.72	4.16	0.92	0.26	0.99	93
2	4.72	6.94	1.53	0.60	0.97	100
3	4.72	11.11	2.46	0.70	0.99	100
4	4.72	13.88	3.07	1.70	0.99	100

Figure 3 shows the effect of changing the shell side organic-phase flow rate and keeping the aqueous flow rate constant for 18% v/v LIX 79/n-heptane. Table 2 presents the mass transfer coefficient of silver as a function of organic phase flow rate. Module extraction efficiency changes dramatically below  $2.77 \text{ cm}^3/\text{s}$  of organic flow rate. This means that most silver cyanide can be easily transferred into the organic phase through the interfacial reaction when the concentration of the LIX 79 is in excess due to an increase in the organic phase flow rate, since the aqueous inlet concentration of silver is only  $4.63 \cdot 10^{-4} \text{ mol}/\text{dm}^3$  and the aqueous stream flow rate,  $Q_f$ , is around  $11.1 \text{ cm}^3/\text{s}$  ( $v_f=2.5 \text{ cm}/\text{s}$ ).

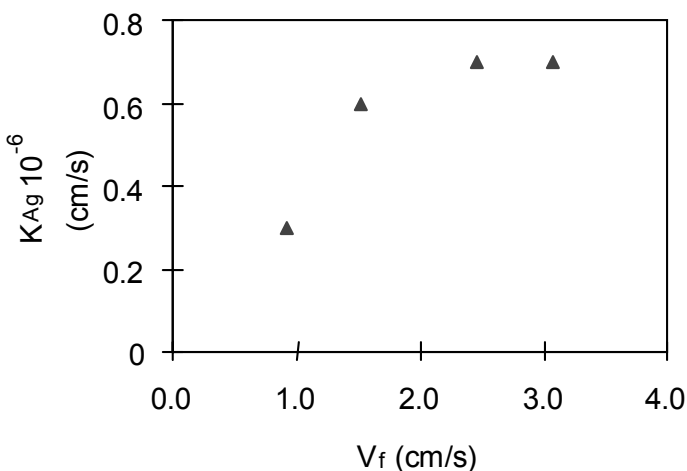


*Figure 2. Effect of feed flow rate on mass transfer coefficient of silver cyanide with LIX 79 in extraction module in counter-current mode.*

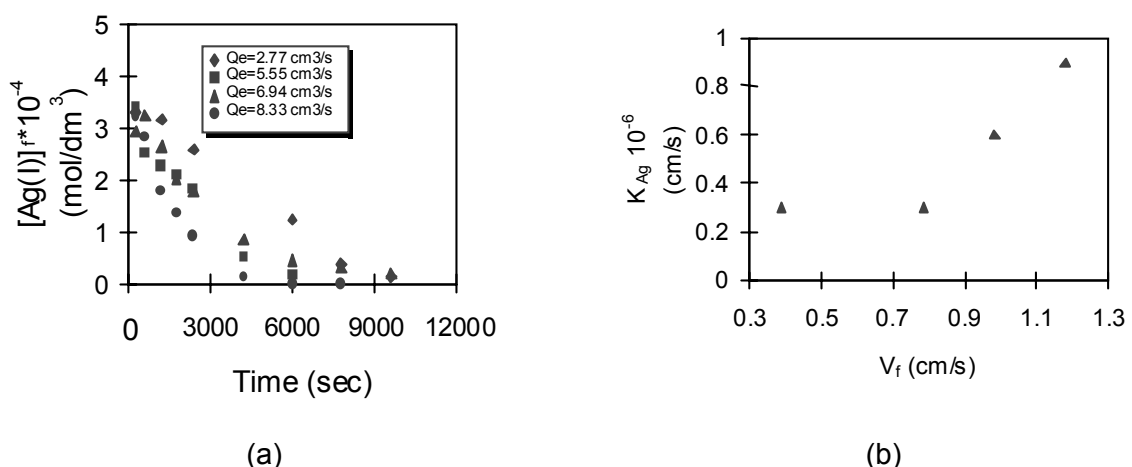


*Figure 3. Effect of organic flow rate in counter-current mode (a) plot of concentration of silver vs. time as a function of flow rate (b) mass transfer coefficient as a function of linear flow velocity.*

The effect of pH on the overall mass transfer coefficient is presented in Table 3. The initial pH of 10.0 to 10.5 was observed to be optimum for mass transfer when experiments were performed in counter-current mode maintaining the aqueous flow rate at  $6.94 \text{ cm}^3/\text{s}$ . The overall mass transfer coefficient decreased to  $0.09 \cdot 10^{-6} \text{ cm/s}$  at pH 11 and practically no extraction at pH 12 was observed, as suggested by the extraction mechanism (Figure 4).

*Table 2. Mass transfer coefficients for extraction of Ag(I) from aqueous alkaline cyanide media ( $\text{pH}=10.3$ ) with 18% LIX 79 in *n*-heptane using HFNDSX technique in counter-current mode as a function of organic flow rates.*

Experiment No.	$Q_f$ ( $\text{cm}^3/\text{s}$ )	$Q_e$ ( $\text{cm}^3/\text{s}$ )	$v_f$ ( $\text{cm}/\text{s}$ )	$K_{Ag}^E \cdot 10^{-6}$ ( $\text{cm}/\text{s}$ )	$r^2$	Extraction (%)
1	11.11	2.77	0.39	0.30	0.99	92
2	11.11	5.55	0.79	0.30	0.98	96
3	11.11	6.94	0.98	0.60	0.96	94
4	11.11	8.33	1.18	0.90	0.96	100

*Table 3. Mass transfer coefficients for extraction of Ag(I) from aqueous alkaline cyanide media as a function of initial feed pH with 18% LIX 79/ *n*-heptane in counter-current mode using the HFNDSX technique.*

Experiment No.	pH	$K_{Ag}^E \cdot 10^{-6}$ ( $\text{cm}/\text{s}$ )	$r^2$	Extraction (%)
1	9	0.20	0.96	95
2	10	0.60	0.97	100
3	11	0.09	0.91	37
4	12	--	---	0

The stripping studies were performed by passing 1 M NaOH in tube side and loaded LIX 79 / *n*-heptane in shell side. More than 95% silver recovery was obtained in less than 90 minutes. This work is still continued and integrated process for recovering silver in presence of base metals is being developed from alkaline hydrometallurgical solutions.

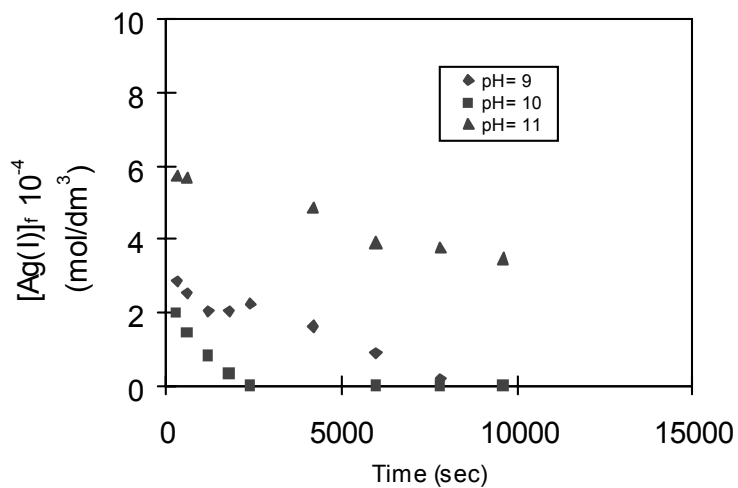


*Figure 4. Plot of concentration of silver vs. time as a function of initial aqueous feed pH in extraction module in counter current mode.*

## **ACKNOWLEDGEMENTS**

This work was supported by the CICYT (QUI 99-0749) and CIRIT (SGR-98-0082). Dr. Anil Kumar acknowledges the financial support from the Comisión Interministerial de Ciencia y Tecnología, Spain, through the award of the Visiting Scientist Fellowship. R. Haddad acknowledges the support from ICMA for a fellowship. The authors gratefully acknowledge Cognis Corporation, U.S.A. for supplying the LIX 79.

## **REFERENCES**

1. F. Z. El. Aamrani, A. Kumar, L. Beyer, M. Petrich and A.M. Sastre (2000), *J. Chem. Tech. Biotech.*, **75**, 701.
2. A. Kumar and A.M. Sastre (2001), Ion Exchange and Solvent Extraction, Vol. 15, Y. Marcus and A.K. SenGupta (eds.), Marcel Dekker, New York, pp. 331-469.
3. U.A. Daiminger, A.G.Geist, W. Nitsch, and P.K. Plucinski (1996), *Ind. Eng. Chem. Res.*, **35**, 184-191.
4. M.-C. Yang and E. L. Cussler (1986), *AIChE J.*, **32**, 1910.
5. Hoechst-Calanese Corporation(1996), Product information.
6. W. S. Ho and K. K. Sirkar, K.K. (1992), Membrane Handbook, Van Nostrand Reinhold, New York.
7. A. Kumar and A.M. Sastre (1998), *Spanish Patent*, 98 01736.
8. A. Kumar, R. Haddad and A. M. Sastre (2000), *AIChE J.*, **47**, 328.
9. M. J. Virnig and G. A. Wolfe (1992), *Proc. ISEC '96*, Vol. 1, University of Melbourne Press, Melbourne, pp. 311-316.
10. R. Haddad, A. Kumar and A.M. Sastre (2001), *J. Chem. Tech. Biotech.*, submitted.
11. N.A. D'Elia, L. Dahuron and E. L. Cussler (1986), *J. Membr. Sci.*, **29**, 309.



## SELECTIVE EXTRACTION OF LITHIUM ION WITH NOVEL LIPOPHILIC PHTHALOCYANINE DERIVATIVES AND ITS PERMEATION THROUGH SUPPORTED LIQUID MEMBRANE

Kazuo Kondo, Michiaki Matsumoto, Takashi Yoshida and Eiji Kamio

Doshisha University, Kyotanabe, Japan

New types of lipophilic phthalocyanine derivatives, hexadeca(2,2,2-trifluoroethoxy)-phthalocyanine and hexadeca(2,2,3,3,3-pentafluoropropoxy)phthalocyanine (abbreviated as H<sub>2</sub>Pc(TFE)<sub>16</sub> and H<sub>2</sub>Pc(PFP)<sub>16</sub>, respectively), were prepared. The extraction equilibria of alkali metals with H<sub>2</sub>Pc(TFE)<sub>16</sub> and H<sub>2</sub>Pc(PFP)<sub>16</sub> were investigated, and the extracted complexes and extraction equilibrium constants of the metals were estimated. The extraction rate of lithium with H<sub>2</sub>Pc(TFE)<sub>16</sub> was measured. The extraction process is considered to be limited by the diffusion of the extractant. The permeation rates of alkali metals through a supported liquid membrane containing H<sub>2</sub>Pc(TFE)<sub>16</sub> were measured. The transport selectivity of lithium was enhanced by increasing temperature and showed the value of 1.61 at 318K against potassium. Sodium permeation is limited by the reaction process at the interface. For lithium and potassium permeation the diffusion of complex in the membrane accompanying the reaction is considered to be the rate-controlling step.

### INTRODUCTION

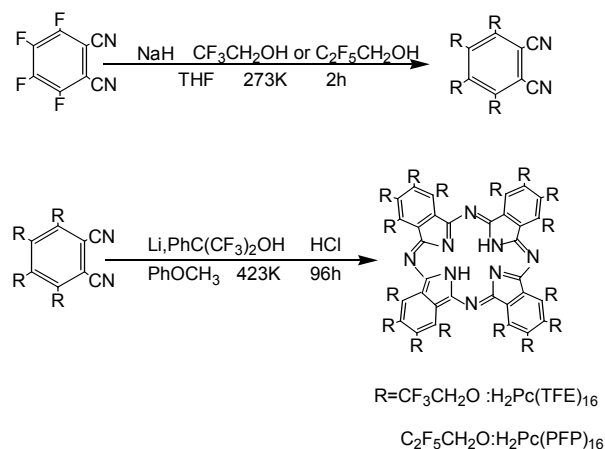
Lithium, which is used as a chargeable secondary battery for personal computers, is a scarce resource. Its use is expected to increase due to the realization of power stations with nuclear fusion and development of fuel cells [1]. In recent years, the recovery of lithium from sea, spa and waste water from geothermal power generation has been actively studied.

In this study, two types of phthalocyanine derivatives (hexadeca(2,2,2-trifluoroethoxy)-phthalocyanine and hexadeca(2,2,3,3,3-pentafluoropropoxy)phthalocyanine) were synthesized as novel macrocyclic extraction reagents. Phthalocyanine derivatives, which are stable to heat and chemical materials, have strong  $\pi$ - $\pi$  bonds. On account of the stacking effect by  $\pi$ - $\pi$  interaction, it is generally difficult to dissolve them in organic solvents. The phthalocyanine derivatives synthesized in this study have bulky alkoxy group containing fluorine, so the stacking is prevented and the solubility into organic solvents is increased. In addition, lithium is expected to be selectively extracted due to its high charge-to-radius ratio. No research has been done on the extraction kinetics of alkali metal ions except for that with crown ethers [2]. In our study, the extraction equilibrium and kinetic behaviour of alkali metals ( $\text{Li}^+$ ,  $\text{Na}^+$ ,  $\text{K}^+$ ) with the synthesized phthalocyanine derivatives are investigated and each extraction mechanism is discussed.

## EXPERIMENTAL

### Synthesis of Lipophilic Phthalocyanine Extractant

Lipophilic phthalocyanine derivatives used in this study were prepared by the two-step reactions shown in Scheme 1.



*Scheme 1. Synthesis of novel lipophilic phthalocyanine derivatives.*

### Synthesis of Phthalocyanine Containing Fluorine

4.4 g of 60% lipophilic sodium hydride ( $\text{NaH}$ ) was suspended in  $100 \text{ cm}^3$  of tetrahydrofuran (THF) in a flask.  $8.0 \text{ cm}^3$  of trifluoroethanol ( $\text{CF}_3\text{CH}_2\text{OH}$ ) or  $12.4 \text{ g}$  of pentafluoropropanol ( $\text{C}_2\text{F}_5\text{CH}_2\text{OH}$ ) was added under nitrogen atmosphere at 273 K. After that, they were agitated for 30 minutes. Subsequently,  $20 \text{ cm}^3$  of THF solution containing  $5.0 \text{ g}$  of tetrafluorophthalonitrile ( $\text{C}_6\text{F}_4(\text{CN})_2$ ) was dropped and suspended for 30 minutes at room temperature. After separating the solution by decantation, the aqueous phase was extracted with ethylether, dried with magnesium sulfate, and the ether was evaporated. The THF phase was also evaporated. The solids obtained from both phases were recrystallized from THF-*n*-hexane solution and purified with column chromatography. The obtained solution was then evaporated, and the resulting solid was again recrystallized from THF-*n*-hexane solution to obtain pure crystals.

5.2 g of tetrakis (2,2,2-trifluoroethoxy) phthalonitrile prepared above, 0.1 g of lithium powder and  $2.5 \text{ cm}^3$  of hexafluorocumin alcohol ( $\text{PhC}(\text{CF}_3)_2\text{OH}$ ) were added in  $30 \text{ cm}^3$  of anisole ( $\text{C}_6\text{H}_5\text{OCH}_3$ ) and agitated for 4 days under nitrogen atmosphere at 413- 418K. The aqueous phase was extracted with ethylether. Both the resulting aqueous and organic phases were distilled. The obtained solid was recrystallized from acetone-*n*-hexane mixture, thus green crystalline (hexadeca(2,2,2-trifluoroethoxy) phthalocyanine;  $\text{C}_{64}\text{F}_{48}\text{H}_{34}\text{N}_8\text{O}_{16}$ ) was prepared. By the same method, green crystalline (hexadeca(2,2,3,3,3-pentafluoropropoxy)-phthalocyanine;  $\text{C}_{80}\text{F}_{80}\text{H}_{34}\text{N}_8\text{O}_{16}$ ) was also prepared from tetrakis(2,2,3,3,3-pentafluoropropoxy)phthalonitrile. These were identified by IR and NMR.

### Extraction Equilibria of Alkali Metals

Extraction equilibrium experiment of alkali metal ions ( $\text{Li}^+$ ,  $\text{Na}^+$ ,  $\text{K}^+$ ) was carried out by a conventional method. Aqueous solutions were prepared by dissolving each alkali metal chloride in deionized water. The pH of aqueous solutions was adjusted with  $1 \text{ mol}/\text{dm}^3$  HCl-diethanolamine buffer solution using a pH meter. Butyl acetate was used as an organic solvent. The lithium- and sodium-ion concentrations were measured by inductively coupled plasma spectrometer (ICPS) and the potassium concentration was measured by atomic absorption spectrophotometry.

### Extraction Rate of Lithium

The extraction rate was measured using the stirred transfer cell reported in the previous paper [3] at 303 K. Equal volume of the aqueous and organic phases was contacted and they were stirred at 100 rpm. 1 cm<sup>3</sup> of the organic phase was collected at appropriate intervals. The metal complex concentration in the organic phase was determined from the absorption spectra at 699 and 733 nm measured by a spectrophotometer.

### Permeations of Alkali Metals Through a Supported Liquid Membrane

A membrane material, porous tetrafluoroethylene film (thickness 47 μm; porosity 0.77) was kindly supplied by Japan Gore Tex. The supported liquid membrane (SLM) was prepared by impregnating the porous film with 0.2 mol/m<sup>3</sup> butyl acetate containing H<sub>2</sub>Pc(TFE)<sub>16</sub>. The experimental apparatus used is the same as that in the previous work [3]. The feed and stripping solutions were fed concurrently. The stripping solution was collected at appropriate intervals and the metal concentration was measured by ICPS.

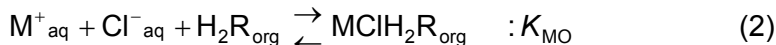
## RESULTS AND DISCUSSION

### Extraction Equilibria of Alkali Metals

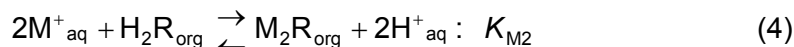
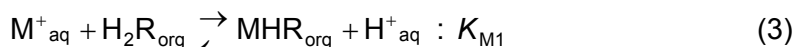
Figure 1 shows the effect of pH on the distribution ratio,  $D$ , defined as follows:

$$D = \frac{C_{M,aq}^0 - C_{M,aq}}{C_{M,aq}} \quad (1)$$

The distribution ratio does not depend on pH in low pH range for all metals. This suggests that phthalocyanine derivatives form ion-pair complex in the organic phase like crown ether. If it is assumed that the ligand and alkali metal ion form an extracted complex with a stoichiometric ratio of 1:1, the extraction equilibrium equation is written as follows:



The extraction equilibrium constant based on Eq. (2) was determined for the two extractants and they were listed in Table 1. In Figure 1, the distribution ratios increase with increasing pH for lithium and potassium extraction. It is found that the slope is unity between pH 8 and 9, and two over pH 9 for Li-H<sub>2</sub>Pc(TFE)<sub>16</sub> system. For Li-H<sub>2</sub>Pc(PFP)<sub>16</sub> system, the slope is unity over pH 8. These results suggest that the extraction progresses according to the following two-step cation-exchange reaction:



For Li-H<sub>2</sub>Pc(PFP)<sub>16</sub> system, the second step reaction does not occur due to the steric hindrance of side chain. For potassium extraction, the slopes were 2 and 1 over pH 8 for H<sub>2</sub>Pc(TFE)<sub>16</sub> and H<sub>2</sub>Pc(PFP)<sub>16</sub>, respectively. From the definitions of equilibrium constant and distribution ratio based on Equations (3) and (4), the following equations were established:

$$\log D = \log K_{M1} + \log \frac{[H_2R]_{org}}{[H^{+}]_{aq}} \quad (5)$$

$$\log D = \log (2K_{M2}) + \log \frac{[M^{+}]_{aq}[H_2R]_{org}}{[H^{+}]_{aq}^2} \quad (6)$$

Figure 2 shows the plots based on Eqs. (5) and (6) with the correlation coefficient  $\alpha$ . From the result, approximately straight line with slope 1 was obtained for all systems and the equilibrium constants were determined from the intercepts. They are also listed in Table 1.

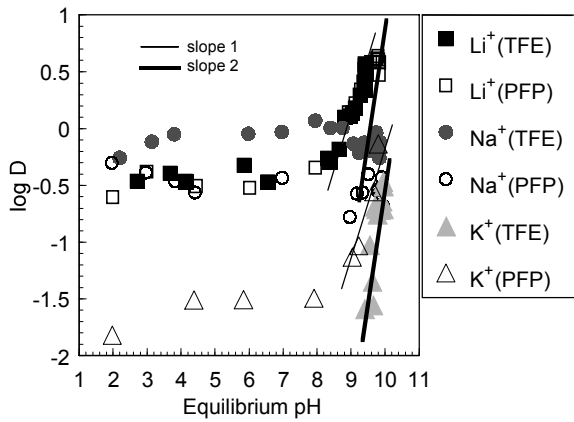


Figure 1. Relationship between  $\log D$  and pH.

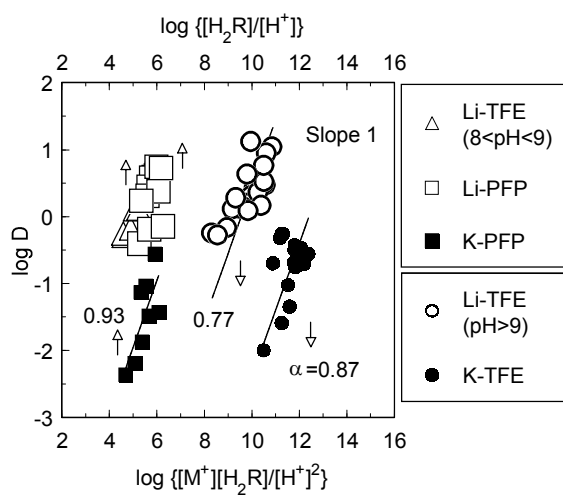


Figure 2. Determination of extraction equilibrium constants.

Table 1. Extraction equilibrium constants (logarithm values).

	Li-TFE	Na-TFE	K-TFE	Li-PFP	Na-PFP	K-PFP
$\log K_{M0}$	$1.45 \pm 0.15$	$2.14 \pm 0.16$	n.d.	$1.42 \pm 0.16$	$1.35 \pm 0.12$	$0.70 \pm 0.11$
$\log K_{M1}$	$-4.98 \pm 0.18$	-	-	$-5.46 \pm 0.13$	-	$-6.95 \pm 0.15$
$\log K_{M2}$	$-9.85 \pm 0.31$	-	$-12.7 \pm 0.26$	-	-	-

n.d. not determined

### Extraction Rate of Lithium

It was found that lithium was efficiently extracted at high pH range. So, the extraction rate of lithium was measured in the range of pH>9 with  $H_2Pc(TFE)_{16}$  as an extractant. Extraction rate was evaluated as an initial extraction rate,  $R_0$ , defined as follows:

$$R_0 = \frac{V_{org}}{A_s} \left( \frac{dC_{Li,org}}{dt} \right)_{t=0} \quad (7)$$

where,  $V_{org}$ ,  $A_s$  and  $C_{Li,org}$  denote volume of organic phase, interfacial area and lithium concentration in organic phase, respectively. The effect of extractant concentration on  $R_0$  is shown in Figure 3. From this result, the mass transfer of the extractant could be considered as the rate-determining step. Assuming that mass transfer of the extractant is the rate-determining step, the equation  $R_0 = 2k_{H2R}([H_2R]_0 - 0)$  is held. So the mass transfer coefficient of extractant,  $k_{H2R}$ , is evaluated from the following equation:

$$k_{H2R} = \frac{R_0}{2[H_2R]_0} \quad (8)$$

From Equation (8),  $k_{H2R}$  was determined as  $2.6 \times 10^{-6}$  m/s. From this result, it is suggested that the diffusion coefficient would become small because of the large cyclic structure of the phthalocyanine derivatives. Assuming that the mass transfer coefficient of complex,  $k_c$ , is approximately the same as  $k_{H2R}$  and using  $k_M$  for samarium ( $k_M = 2.2 \times 10^{-5}$  m/s) [3], the experimental results were analyzed. The solid lines in Figure 3 are the calculated results according to these assumptions.

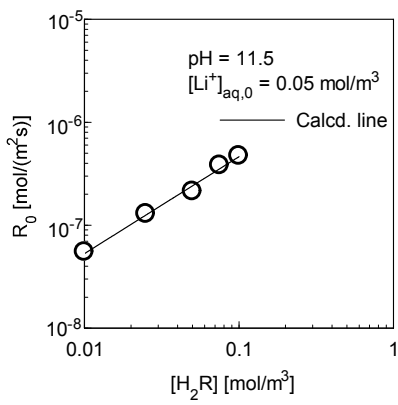


Figure 3. Relationship between initial extraction rate and extractant concentration.

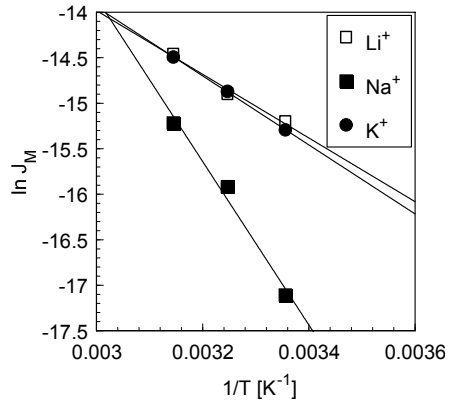


Figure 4. Arrhenius plot for permeations of alkali metal ions through SLM.

### Permeations of Alkali Metals Through Supported Liquid Membrane

The permeation rate of alkali metal ion,  $J_M$ , is defined as follows:

$$J_M = \frac{(C_{MS} \cdot Q_s)}{A_s} \quad (9)$$

The Arrhenius equation is expressed as the following equation:

$$J_M = A' \cdot \exp\left(-\frac{E_a}{RT}\right) \quad (10)$$

where  $A'$ ,  $E_a$ ,  $R$  and  $T$  represent apparent frequency factor, apparent activation energy, gas constant and temperature, respectively. Figure 4 shows the Arrhenius plots of  $J_M$  for  $\text{Li}^+$ ,  $\text{Na}^+$  and  $\text{K}^+$ . From the slope of the straight lines,  $E_a$  was determined as 29.1, 74.7 and 30.9 kJ/mol for lithium, sodium and potassium, respectively. It is generally said that the activation energy for diffusion process is under about 30 kJ/mol while that for reaction process is over about 60 kJ/mol. Therefore, it is suggested that  $\text{Na}^+$  permeation is limited by the reaction process at the interface. For  $\text{Li}^+$  and  $\text{K}^+$  permeation the diffusion of complex in the membrane phase accompanying the reaction may be considered to be the rate-controlling step.

The selectivity in the competitive transport experiment was also measured using the mixtures of alkali metals at various temperatures. The characteristic of permeation selectivity of alkali metals,  $\gamma_{M1/M2}$  was defined as follows:

$$\gamma_{M1/M2} = \frac{J_{M1}}{J_{M2}} \quad (11)$$

where subscripts M1 and M2 denote each alkali metal. The  $\gamma_{M1/M2}$  values of lithium calculated based on Equation (11) against potassium and sodium were increased with increasing temperature. This would occur because of the difference in permeation mechanisms for each alkali metal. The value of  $\gamma_{\text{Li}/\text{K}}$  was 1.61 at 318K, which showed a good selectivity for lithium.

### CONCLUSIONS

In this study, hexadeca(2,2,2-trifluoroethoxy)phthalocyanine and hexadeca(2,2,3,3,3-pentafluoropropoxy)phthalocyanine were synthesized as selective extractants for lithium. From metal-distribution experiments, the extraction equations and the equilibrium constants were determined for lithium, sodium and potassium. In addition, kinetic experiments were carried out, and it was suggested that the extraction process was limited by the diffusion of the extractant. From the obtained activation energy and the diffusion coefficient, it was

suggested that  $\text{Na}^+$  permeation was limited by the reaction process at the interface and for  $\text{Li}^+$  and  $\text{K}^+$  permeations the diffusion of complex in the membrane phase accompanying the reaction might be considered to be the rate-controlling step. The permeation selectivity of lithium against potassium and sodium was increased with increasing temperature.

### NOMENCLATURE

$A_s$	= interfacial area	[m <sup>2</sup> ]
$C_M$	= analytical concentration	[mol/m <sup>3</sup> ]
$D$	= distribution ratio of metal defined by Equation (1)	[-]
$E$	= extent of metal extracted	[-]
$J_M$	= permeation rate of alkali metal ion	[m/s]
$k_j$	= mass transfer coefficient of species i	[m/s]
$K_{M,0}$	= extraction equilibrium constant of Equation (2)	[m <sup>6</sup> /mol <sup>2</sup> ]
$K_{M,1}$	= extraction equilibrium constant of Equation (3)	[-]
$K_{M,2}$	= extraction equilibrium constant of Equation (4)	[-]
$R_0$	= initial extraction rate	[mol/m <sup>2</sup> s]
$\alpha$	= correlation coefficient	[-]
$\gamma_{M1/M2}$	= characteristic of permeation selectivity of alkali metals	[-]

#### <Subscript>

aq	= aqueous phase
b	= bulk
org	= organic phase
0	= initial state

### REFERENCES

1. T. Nishiyama (1989), Kobutsu Shigen no Genjyo, Arumu Shuppan, Tokyo, pp. 185-191.
2. M.Tanigawa, S. Nishiura, S. Tsuruya and M. Masai (1988), *Chem. Eng. J.*, **39**, 157-168.
3. K. Kondo, T. Hashimoto, H. Sumi and M. Matsumoto (1995), *J. Chem. Eng. Japan*, **28**, 511-516.



## EXTRACTION OF CADMIUM FROM PHOSPHORIC ACID WITH AN EMULSION LIQUID MEMBRANE: WATER TRANSPORT AND MEMBRANE RUPTURE

T. Gallego Lizon\* and E. Susana Pérez de Ortiz

Department of Chemical Engineering and Chemical Technology,  
Imperial College of Science, Technology and Medicine, London, UK

\*Environmental Research Laboratory, GlaxoSmithKline, Old Powder Mills, Tonbridge, UK

Emulsion swelling and membrane rupture were measured during the extraction of cadmium from phosphoric acid with an emulsion liquid membrane containing the reagent Cyanex 302 and stabilised with the surfactant Arlacel C with the aim of including their effect in the process modelling. The extraction was carried out in a stirred tank over a wide range of values of surfactant concentration, homogeniser speed and emulsion phase ratio. Emulsion swelling was significant and depended on all the parameters studied, whereas rupture remained low at all conditions except at very low surfactant concentrations. Comparison of cadmium extraction rate data with swelling indicated that the mechanisms of water and cadmium transfer were independent.

### INTRODUCTION

Mechanistic modelling of solvent extraction processes in stirred vessels requires the knowledge of the interfacial area between the dispersed and the continuous phases and of the dependency of the extraction flux on chemical, physical and hydrodynamic parameters. The interfacial area is usually calculated from correlations that relate the dispersion Sauter mean diameter with the operating parameters and the physical properties of the phases. In the case of extraction with emulsion liquid membranes (ELM) the dispersed phase is an emulsion, in which the continuous phase is called the liquid membrane. During extraction, the transfer of the solute from the external phase into the liquid membrane and from there into the emulsion internal droplets is usually accompanied by water transfer to the emulsion and by emulsion rupture. This reduces the extraction efficiency through dilution of the emulsion internal phase and leakage of the extract into the feed, affects the size of the dispersed emulsion globules and changes the physical properties of the emulsion. Therefore quantification of swelling and rupture is central to ELM extraction modelling.

This paper examines the effect of surfactant concentration, emulsion phase ratio and the homogeniser speed used in the preparation of the emulsion on emulsion swelling and rupture during the extraction of cadmium from phosphoric acid with an ELM containing the extractant Cyanex 302 and stabilised with the surfactant Arlacel C. Results are compared with those of the Cd extraction in order to clarify the extraction mechanisms. The incorporation of the swelling coefficient on a model of the emulsion dispersion Sauter mean diameter is presented elsewhere [1, 2].

Reports in the literature relate membrane breakage to a series of factors that include composition of the membrane phase and stirring speed [3-5]. Emulsion swelling, on the other hand, has been attributed to three different mechanisms: occlusion, secondary emulsification of the entrained solvent and external solvent permeation (osmosis). These are affected by the presence of electrolytes in the external phase, surfactant and extractant type and concentration, temperature, permeation time, solvent nature, and globule size distribution [6-9]. Here emulsion rupture and swelling are examined for a wide range of surfactant and extractant concentrations, emulsion phase ratios and homogeniser speeds.

## EXPERIMENTAL

### Reagents

The feed was a solution of CdSO<sub>4</sub> in H<sub>3</sub>PO<sub>4</sub> (30% wt P<sub>2</sub>O<sub>5</sub>). The organic phase of the water-in-oil emulsion was a solution of the reagent Cyanex 302 (Cytec Inc.) and surfactant Arlacel C (ICI Surfactants) in low odour kerosene (Aldrich Chemical Co.).

The emulsion aqueous phase (the stripping phase) contained NaCl (3 M) and HCl (1 M). Reagents 3CdSO<sub>4</sub>.8H<sub>2</sub>O (99% wt) and H<sub>3</sub>PO<sub>4</sub> (95% wt) were supplied by Aldrich Chemical Co. All reagents were used without further purification.

### Method

The experiments were conducted in a stirred tank (dimensions are given in Table 1). The emulsion was produced by blending the organic and stripping phases under intense shear (3000 rpm) using a Silverson homogeniser. The volume ratio of feed, V<sub>1</sub>, and emulsion, V<sub>e</sub>, or treat ratio (V<sub>1</sub>/V<sub>e</sub>), was held constant at a value of 20, whereas the emulsion phase ratio (V<sub>2</sub>/V<sub>3</sub>) was changed within 1 and 2.33. Surfactant concentrations ranged between 1 and 10% v/v and the reagent concentration between 0.15 and 0.91 M.

*Table 1. Tank dimensions.*

Internal diameter of vessel	0.09 m
Liquid height in vessel	0.125 m
Impeller diameter	0.0365 m
Impeller type	flat blade turbine
No. of blades	6
Blade length	0.009 m

The feed and the emulsion were placed in the tank and the impeller was carefully placed at the interface. Stirring was started and samples of the continuous and emulsion phases were taken and analysed for cadmium and sodium concentrations. The concentrations of Cd<sup>++</sup> and Na<sup>+</sup> in the continuous and internal phases were measured by atomic absorption spectrophotometry using a Perkin-Elmer premix burner spectrophotometer. Emulsion swelling was calculated from the emulsion volume change with time. Water content in the organic phase was measured using Karl Fisher titration after separation of the emulsion phases using a known volume of *n*-butanol (10%). Emulsion rupture was calculated by analysing the continuous phase for the presence of Na<sup>+</sup>, initially only present in the stripping phase. In order to check the possibility of Na<sup>+</sup> transport across the membrane by hydration of the carrier rather than by emulsion rupture, experiments were conducted in a quiescent cell, as described below.

## RESULTS AND DISCUSSION

In all experiments, results were evaluated by using the following relations:  
Swelling,

$$Sw(\%) = \frac{(V_3^t - V_3^o) + V_3^R + (V_2^t - V_2^o)}{V_3^o + V_2^o} \cdot 100 \quad (1)$$

where  $V$  is the volume of the phase, subscripts 2 and 3 indicate membrane and internal phases and superscripts  $t$ ,  $o$  and  $R$  denote given time  $t$ , initial conditions, and variations due to rupture respectively.  $V_3^R$  is the internal phase volume loss due to rupture.

Percentage membrane rupture ( $R\%$ ) was calculated from the sodium concentrations in the external phase using the equation:

$$R(\%) = \frac{[Na^+]_1^t V_1^t}{[Na^+]_3^o V_3^o} \cdot 100 \quad (2)$$

where  $[Na^+]$  is the concentration of sodium, subscripts 1 and 3 denote the continuous and internal phase respectively and superscripts  $t$  and  $o$  denote time  $t$  and the initial conditions. In order to check if there was  $Na^+$  transport across the membrane experiments were conducted in a non-dispersive quiescent cell (Figure 1). Results showed no significant variations in  $Na^+$  concentration in either phase over a period of 11 hours. This indicated that there was no  $Na^+$  transport through the membrane due to reaction, osmosis or hydration.

The standard experimental conditions are given in Table 2.

*Table 2. Standard experimental conditions.*

$[Cd]_{feed}$	$0.00042 \pm 0.00002 M$	$N_{homogeniser}$	$3000 \pm 30$ rpm
[Arlacel C]	$5\% \pm 0.1\% v/v$	$N_{stirrer}$	$300 \pm 1$ rpm
[Cyanex 302]	$0.3 \pm 0.01 M$	$V_1/V_e$	20
		$V_2/V_3$	1.0

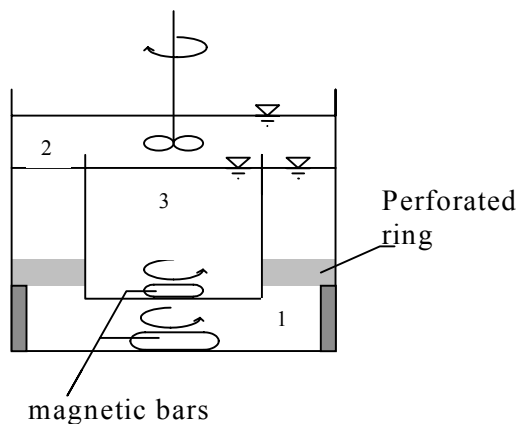


*Figure 1. Non-dispersive cell containing phases 1, 2 and 3.*

### Effect of Surfactant Concentration

Figure 2 shows the effect of the surfactant concentration on water transport for Arlacel C concentrations between 1% and 10% v/v at Cyanex 302 concentration of 0.3 M. As can be seen, increasing the surfactant concentration resulted in a practically linear increase in emulsion swelling, with a slope of 3.75. This is likely to be the result of water transport by the hydrated surfactant, or to the formation of surfactant reversed micelles. The calculated molecular ratios of water to surfactant in the membrane of 3.5, 2.9 and 1.6 for surfactant

concentrations of 3, 5 and 10 %, respectively, are lower than those expected for reversed micelles. However, either structure of the hydrated surfactant molecules can provide a shuttle mechanism for the osmotically induced water transport. Thus the higher the surfactant concentration, the higher the amount of water transferred during a fixed time. This is not the case for Cd (Figure 4), as the transfer of Cd is mediated by Cyanex 302 and not by the surfactant. However, although surfactants in general decrease the rate of transfer, in some cases they are reported to enhance extraction rate due to the formation of mixed reversed micelles. The possibility of increased swelling due to secondary emulsification of the external phase into the emulsion at the higher values of surfactant concentration was also examined from the results in Figure 4. It was concluded that this is unlikely since this would lead to increased Cd extraction with surfactant concentration.

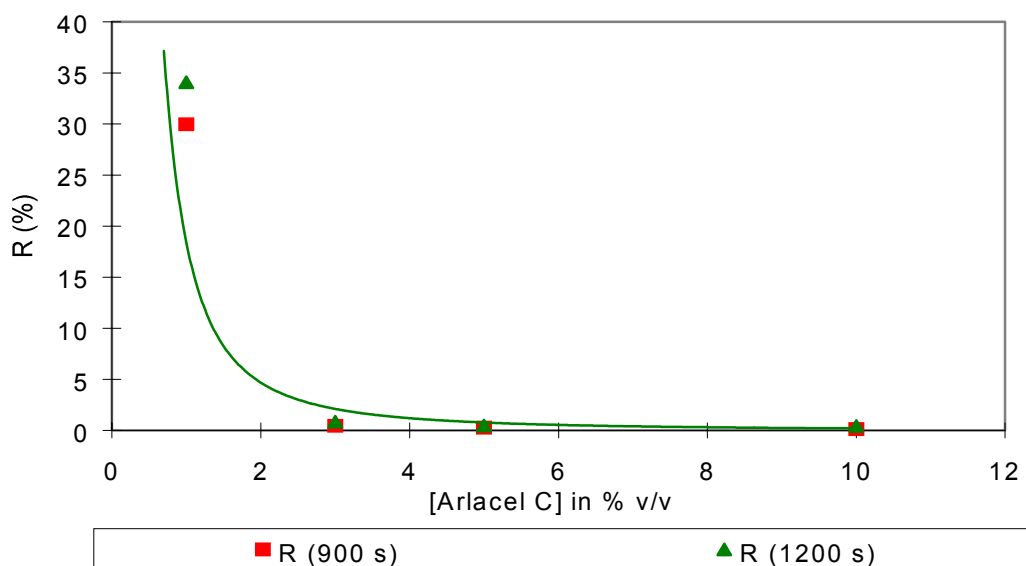


Figure 2. Effect of surfactant concentration on swelling and water content in the membrane after 1200s. Cyanex 302 concentration: 0.3 M.

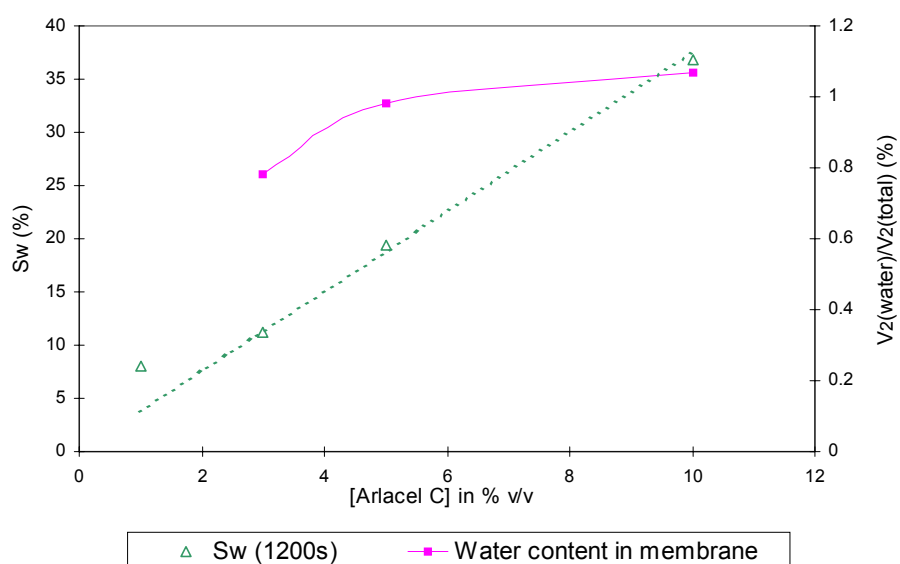
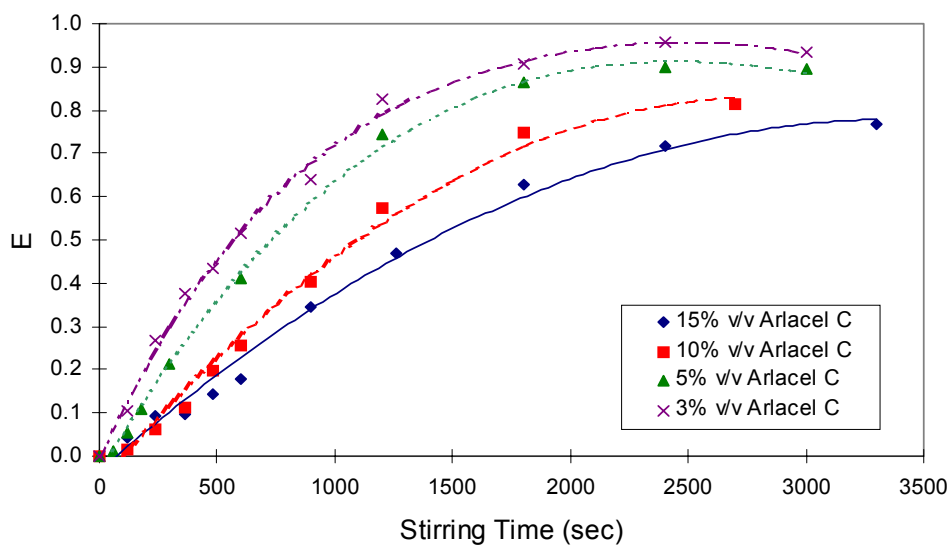


Figure 3. Effect of surfactant concentration on rupture.



*Figure 4. Effect of surfactant concentration on Cd<sup>2+</sup> extraction, where E is the ratio of Cd extracted over the initial Cd concentration.*

#### **Effect of Emulsion Phase Ratio ( $V_2/V_3$ )**

As shown in Figure 5, changing the phase ratio between 1 and 2.33, which corresponds to an increase in the organic phase volume fraction, resulted in an increase in swelling from 24 to 87% and also an increase in rupture. This would confirm that the water transport mechanism across the membrane is carrier mediated since the amount of surfactant in the membrane increases with phase ratio. In this case the rate of Cd extraction also increased [10] due to the increase in the amount of reagent.

Phase ratio also increased membrane rupture from 0.5 to 1.6 %, probably due to the large increase in swelling leading to droplet coalescence.

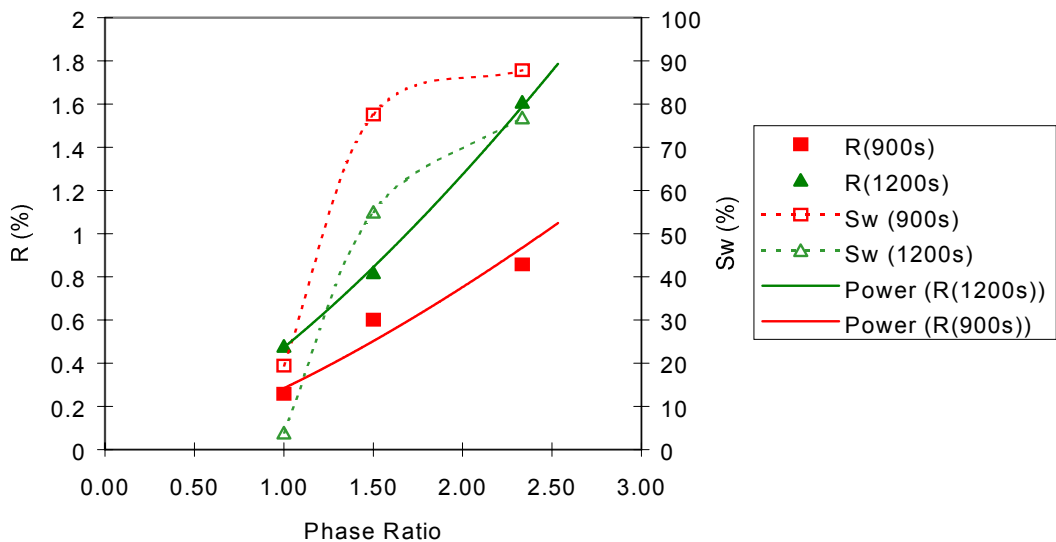


*Figure 5. Effect of phase ratio on swelling and rupture.*

### Effect of Homogeniser Speed

Results obtained at a permeating time of 1200 s have been plotted in Figure 6. As can be seen, increasing the homogeniser speed from 2000 to 5000 rpm resulted in a substantial increase in swelling. The viscosity of the emulsion measured at a shear rate of  $9\text{ s}^{-1}$  increased by 100% from 0.15 Nm/s for an emulsion prepared at 2000 rpm to 0.30 Nm/s for one at 4000 rpm probably due to the decrease in droplet size with increasing homogeniser speed. This increased the emulsion globule sizes in the tank with the consequent decrease in total interfacial area between the emulsion and the external phase. This was reflected by a decrease in Cd extraction rate [10]. The increase in swelling is more difficult to explain as results show an increase in the rate of water transfer, thus suggesting that this is controlled by the extent of the interface between the stripping phase, i.e., by phenomena taking place at the internal interface and not by diffusional resistances in the membrane.

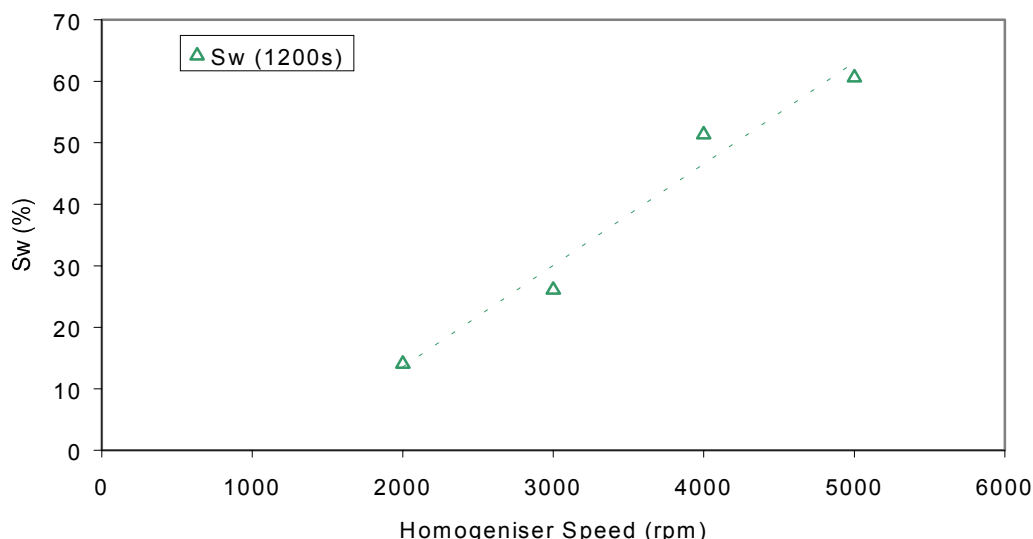


Figure 6. Effect of homogeniser speed on swelling at a stirring time of 1200 s.

### CONCLUSIONS

From the work presented above it has been observed that, for the conditions investigated, membrane rupture was considered unimportant for a surfactant concentration above 1% v/v. Similarly, it was determined that surfactant concentration was unlikely to increase Cd extraction through the membrane.

### REFERENCES

1. T. Gallego Lizon and E.S. Perez de Ortiz (2000), *Ind. Eng. Chem. Res.*, **39**, 5020-5028.
2. T. Gallego-Lizon and E.S. Perez de Ortiz (1997), Int. Symp. Liquid-Liquid Two-Phase Flow and Transp. and Phenom., D. M. Maron (ed.), Begell House, New York, pp. 301.
3. H. Itoh, M.P. Thien, T.A. Hatton and D.I.C. Wang (1990), *J. Membr. Sci.*, **51**, 309-322.
4. I. Abou-Nemeh and A.P. Van Peteghem (1993), *Ind. Eng. Chem. Res.*, **32**, 1431-1437.
5. J.Q. Shen, W.P. Yin, Y.Y. Zhao and L.J. Yu (1996), *J. Membr. Sci.*, **120**, 45-53.
6. T. Kinugasa, K. Watanabe and H. Takeuchi, H. (1989), *J. Chem. Eng. Jpn.*, **22** (6), 593-597.
7. P. Colinart, S. Delepine, G. Trouve and H. Renon (1984), *J. Membr. Sci.*, **20**, 167-187.
8. Y.S. Mok and W.K. Lee (1994), *Sep. Sci. Technol.*, **29** (6), 743-746.
9. M.T.A. Reis and J.M.R. Carvalho (1994), *Chem. Eng. Technol.*, **17**, 242-248.
10. T. Gallego Lizon (1998), Cadmium Separation from Phosphoric Acid using the Emulsion Liquid Membrane, Ph. D. Dissertation, University of London, UK.



## TRANSFER PROPERTIES OF CADMIUM(II) AND ZINC(II) FROM HYDROCHLORIC ACID WITH HEH/EHP USING MICROPOROUS HOLLOW FIBER MEMBRANE

F. Luo, Q. Jia, D. Q. Li and Y. L. Wu

Laboratory of Rare Earth Chemistry and Physics, Changchun Institute of Applied Chemistry, Chinese Academy of Sciences, Changchun, China

In this work, 2-ethylhexyl phosphonic acid mono-2-ethylhexyl ester in kerosene is used to extract the transition elements Zn and Cd from hydrochloric acid solution in a hollow fiber membrane extractor. The effects of  $H^+$  concentration, extractant and metal ion concentrations and different ammoniation rates of extractant on the total mass transfer coefficients based on the water phase ( $K_w$ ), have been investigated. The results show that the mass transfer coefficient decreases with the increase of  $H^+$  concentration, but that the value of  $K_w$  for  $Cd^{2+}$  is smaller than that for  $Zn^{2+}$ . This means the mass transfer resistance of  $Cd^{2+}$  is larger than that for  $Zn^{2+}$ . When the value of  $K_w$  reaches  $1.0 \times 10^{-6} \text{ m.s}^{-1}$ , the difference of pH between Zn and Cd ( $\Delta pH^{Zn}_{Cd}$ ) is 1.49. The mass transfer coefficient increases slightly with the increase of extractant concentration and decreases with the increase of the ammoniation rate of extractant. It is possible to carry out the separation of  $Zn^{2+}$  and  $Cd^{2+}$  by properly controlling the acidity of the aqueous solution because of the existence of this kinetics competition.

### INTRODUCTION

With the development of chemical industry, removing and refining the valuable metals in dilute solutions or difficult separation systems has become an important aspect of research. With the higher demands on environmental protection, it is necessary to find clean and effective processes. The extraction technique using hollow fiber membrane is a new separation method that combines the processes of liquid-liquid extraction and membrane extraction. Extraction with hollow fiber modules (HFM) is fast because of a large surface area per unit volume. The extractant and feed can be contacted at high speed, even if their densities are identical. There are no problems with 'flooding' or 'loading', and no direct contact of water phase and organic phase. As a result, HFM may offer advantages over conventional extraction equipment [1]. In addition the method is an environmentally friendly process.

It is well known that cadmium and zinc coexist because cadmium ore is often found intergrown with zinc ore. Because of the toxicity of Cd it is important to separate Cd from Zn in solution. This paper examines liquid-liquid extraction in a hollow fiber membrane module. Typically, feed solution containing the solute of interest flows through the lumen of the fibers, and extractant flows outside the fibers, on the shell side. Solute diffuses out of the feed solution, through the fibers' porous wall, and into the extractant. 2-ethylhexyl phosphonic acid mono-2-ethylhexyl ester (HEH/EHP) is an effective extractant for separating rare earths, and has been widely used in hydrometallurgy. In this paper, an investigation into the use of HEH/EHP-kerosene to extract the transition elements Zn and Cd from hydrochloric acid solution in a hollow fiber membrane extractor is presented.

## EXPERIMENTAL

The HEH/EHP used was dissolved in sulfured kerosene, supplied by the Jiangxi Fengxin Chemical factory. A stock solution of  $Zn^{2+}$  and  $Cd^{2+}$  was prepared by dissolving  $ZnCl_2$  and  $CdCl_2 \cdot 2.5H_2O$  respectively. The pH values of the aqueous solutions were measured with pHs-3C model acidity meter (made in Shanghai). The concentrations of  $Zn^{2+}$  and  $Cd^{2+}$  were determined by EDTA titration. For solution flow, BT01-100 model Lange static flow pumps (made in Hebei) were used. Hollow fiber membrane, made of polyvinylidene fluoride and polytetrafluoroethylene was provided by the Changchun Institute of Applied Chemistry. The extractor was composed of a glass tube and two HFMs [2]. The characteristics of a hollow fiber and the membrane extractor are summarized in Table 1.

*Table 1. Specifications of a hollow fiber and the membrane extractor.*

Membrane polymer	polyvinylidene fluoride and polytetrafluoroethylene
Length of module (mm)	300
No. of fibers in a module	2
Inner diameter of module (mm)	8.00
Inner fiber diameter (mm)	0.70
Outer fiber diameter (mm)	1.20
Average pore size ( $\mu m$ )	0.06
Membrane wall porosity (%)	81
Flexibility of membrane	Good
Acid resistance of membrane	General

The aqueous solution was fed circularly into the lumen of the fiber at a flow rate of  $11.5 \text{ cm}^3 \cdot \text{min}^{-1}$ , while the organic solution was fed circularly into the annulus of the extractor in a counter-current mode at a flow rate of  $6.0 \text{ cm}^3 \cdot \text{min}^{-1}$  [3]. Since the fibers are hydrophobic, the pores of the membrane were filled with organic solution. The aqueous-phase pressure was maintained higher than the organic-phase pressure to prevent leakage of the organic phase from the pores into the aqueous phase. The aqueous solution was sampled at intervals until equilibrium was achieved. The mass transfer coefficient was calculated using the following:

$$\begin{aligned} & \left\{ \frac{1/Q_w - 1/(m \cdot Q_s) \exp\{-4K_w V_m / d\}[1/Q_w - 1/(m \cdot Q_s)]}{1/V_w + 1/(m \cdot V_s)} \right\} \ln \left[ \frac{\Delta C_A}{C_A^o} \right] \\ & = -t \left\{ 1 - \exp \left[ -\frac{4K_w V_m}{d} \left( \frac{1}{Q_w} - \frac{1}{m \cdot Q_s} \right) \right] \right\} \end{aligned} \quad (1)$$

where,

$$\ln \left[ \frac{\Delta C_A}{C_A^o} \right] = \ln \left\{ \frac{C_A \left[ 1 + \frac{V_w}{m V_s} \right] - C_A^o \frac{V_w}{m V_s} - C_A^{s,o} / m}{C_A^o - V_A / m} \right\} \quad (2)$$

$C_A^0$  and  $C_A^{s,o}$  denote the initial solute concentrations in the aqueous and organic phases respectively. In these experiments,  $C_A^{s,o}$  was equal to zero.  $Q_w$  and  $Q_s$  are the flows of the aqueous and organic phases.  $V_w$  and  $V_s$  are the volumes of the aqueous and organic phases, which were always 40 ml in these experiments.  $V_m$  is the fiber volume;  $d$  the fiber diameter and  $m$  the partition coefficient. In the Eq. (1) and (2),  $C_A$  is the parameter that varies with time and all the other parameters related to the device or its operation are kept constant in each experiment.  $K_w$  can be obtained by interpolation with the slope of the curve of  $\ln[\Delta C_A / C_A^o]$  vs.

time,  $\ln[\Delta C_A/\Delta C_A^0]$  being calculated according to Equation (2).

Experimental temperature was controlled at  $25\pm1^\circ\text{C}$ .

## RESULTS AND DISCUSSION

### Reaction Mechanism of Membrane Extraction

The mass transfer process of  $\text{Zn}^{2+}$  and  $\text{Cd}^{2+}$  in two phases was assumed as a false first-order reaction, so that the extraction reaction could be simplified to:



where (a) denotes species in the aqueous phase, (o) species in the organic phase and M stands for metal ion. Eq. (3) can be expressed as follows:

$$q_f = \frac{C_o - C_e}{C_o} \ln\left(\frac{C_o - C_e}{C_t - C_e}\right) \quad (4)$$

$$q_b = \frac{C_e}{C_o} \ln\left(\frac{C_o - C_e}{C_t - C_e}\right) \quad (5)$$

where,  $C_o$ ,  $C_t$  and  $C_e$  are the initial, t and equilibrium concentration of metal ion respectively. t is the reaction time,  $q_f$  and  $q_b$  are positive and inverse apparent rate constants, respectively. If the assumption of Equation 3 is correct, the plots of  $\ln[(C_0 - C_e)/(C_t - C_e)]$  vs. t should be straight lines. Plots shown in Figure 1 show linear relationships and therefore the membrane extraction can be assumed to obey the false first-order reaction mechanism proposed.

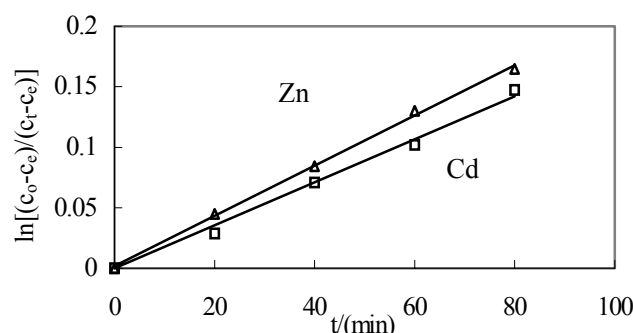


Figure 1. Plots showing the false first-order reaction for  $\text{Zn}^{2+}$  and  $\text{Cd}^{2+}$ .

### Effect of the Aqueous Phase Acidity on the Mass Transfer Coefficient

The acidity of the aqueous phase, being the main factor influencing the separation of metal ions, was investigated first. The results are shown in Figure 2. The results showed that  $K_w$  decreased with the increase of  $\text{H}^+$  concentration and those values of  $K_w$  for  $\text{Cd}^{2+}$  were smaller than for  $\text{Zn}^{2+}$ . Therefore the mass transfer resistance for  $\text{Cd}^{2+}$  was greater than for  $\text{Zn}^{2+}$ . When the value of  $K_w$  reached  $1.0 \times 10^{-6}$  m/s, the  $\Delta\text{pH}_{\text{Cd}}^{\text{Zn}}$  measured was 1.49. This provides a theoretical basis for the separation of  $\text{Zn}^{2+}$  and  $\text{Cd}^{2+}$ .

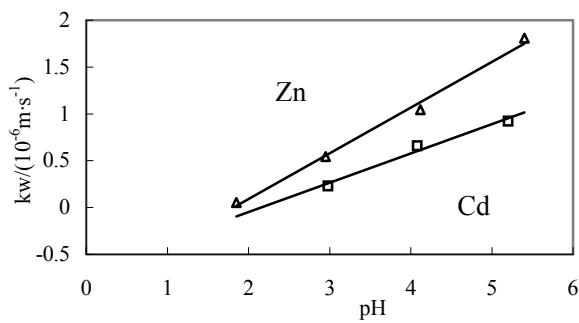


Figure 2. Effects of acidity of aqueous phase on the mass transfer coefficient.  
 $[Cd^{2+}] = 0.948 \times 10^{-3} \text{ mol L}^{-1}$ ;  $[Zn^{2+}] = 1.012 \times 10^{-3} \text{ mol L}^{-1}$ ;  $[HEH/EHP] = 0.1151 \text{ mol L}^{-1}$ .

### Controlling Step of Membrane Extraction

From previous experimental results [5,6], it was concluded that the rate of extraction is controlled by a chemical reaction in the lower region of pH and by diffusion in the higher region of pH. So the extraction mechanism of a hollow fiber membrane can be explained using a diffusion model accompanied by an interfacial reaction.

In the hydrophobic membrane, oil phase penetrates into the micropores of membrane and reaction takes place at the inside surface of a hollow fiber. In the hydrophilic membrane, aqueous phase penetrates into the membrane and reaction takes place at the outer surface [4].

$$\text{For hydrophobic membrane: } \frac{1}{K_w} = \frac{1}{k_w} + \frac{d_i}{mk_m d_{lm}} + \frac{d_o}{mk_o d_o} \quad (6)$$

where  $k_w$ ,  $k_m$  and  $k_o$  are mass transfer coefficients in aqueous film, membrane phase and oil film, respectively.  $d_i$ ,  $d_o$  and  $d_{lm}$  are the inner and outer diameter of a hollow fiber and their logarithmic mean, respectively.  $m$  is the distribution coefficient, which was obtained from the equilibrium study at each experimental condition of hollow fiber runs.

Because the hollow fibers used are hydrophobic membranes and their distribution coefficient  $m \approx 1$ , so the mass transfer resistance across the oil film could not be neglected in the analysis. The results are shown in Figure 3.

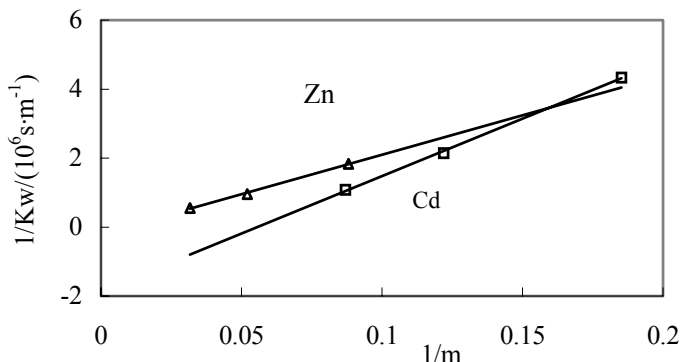


Figure 3. Plots of membrane resistance for  $Zn^{2+}$  and  $Cd^{2+}$ .

The first terms of Equation (6) for  $Zn^{2+}$  and  $Cd^{2+}$  ( $1/k_w$ ) are intercepts of the lines and because they were less than zero this indicates negligible mass transfer resistance of the aqueous film. The slopes of lines were  $(d_i/(k_m d_{lm}) + d_i/(k_o d_o))$  and were higher than that in the aqueous film. Because the slope for Cd was larger than that for Zn, the mass transfer resistance for  $Cd^{2+}$  was bigger than that for  $Zn^{2+}$ . It can therefore be concluded that the mass transfer rates for  $Zn^{2+}$  and  $Cd^{2+}$  are controlled simultaneously by the mass transfer resistance of the membrane and the organic phase.

### Effect of Extractant Concentration on the Mass Transfer Coefficient

The effect of extractant concentration on mass transfer coefficient is shown in Figure 4. The mass transfer coefficient was shown to increase with an increase in extractant concentration.

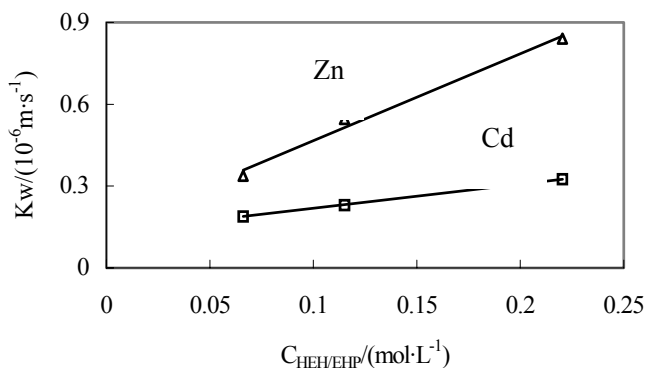


Figure 4. Effects of extractant concentration on the mass transfer coefficient.  
 $[Cd^{2+}] = 0.948 \times 10^{-3} mol \cdot L^{-1}$ ;  $[Zn^{2+}] = 1.012 \times 10^{-3} mol \cdot L^{-1}$ ;  $pH = 2.95$ .

### Effect of Ammoniation Rate of Extractant on the Mass Transfer Coefficient

Ammoniation rate of extraction was defined as follows:

$$AmmoniationRate = \frac{[NH_4^+]_0}{[HEH / EHP]_0} \quad (7)$$

Increasing the ammoniation rate of the extractant is expected to favor the extraction of rare earths [7]. From Figure 5 it was seen that the mass transfer coefficients in fact decreased with an increase in the ammoniation rate of the extractant. It is speculated that this may be because the mass transfer of  $NH_4^+$  was faster than that for the metal ion [7], and the ammonium compound formed in the aqueous phase, thus restrained the mass transfer of metal ions. These results show that it would be possible to separate  $Zn^{2+}$  and  $Cd^{2+}$  from rare earths by changing the ammoniation rate of the extractant.

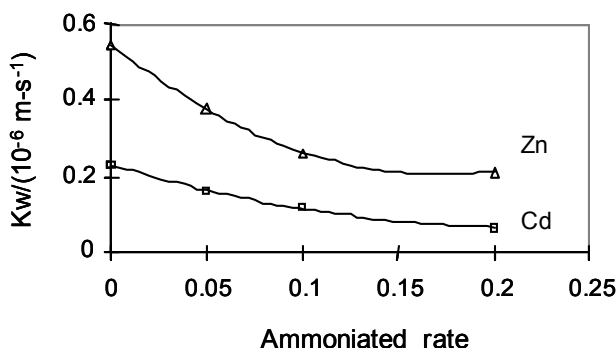


Figure 5. Effects of ammoniation rate of extractant on the mass transfer coefficient.  
 $[Cd^{2+}] = 0.948 \times 10^{-3} mol \cdot L^{-1}$ ;  $[Zn^{2+}] = 1.012 \times 10^{-3} mol \cdot L^{-1}$ ;  $[HEH/EHP] = 0.1151 mol \cdot L^{-1}$ ;  $pH=2.95$ .

## CONCLUSIONS

In this paper the extraction mechanism of metal ions in hollow fiber membrane extractor was explained as a false first order reaction. The mass transfer rates for Zn<sup>2+</sup> and Cd<sup>2+</sup> are controlled simultaneously by the resistance of aqueous phase and membrane and organic phase. The mass transfer coefficient decreased with the increasing of H<sup>+</sup> concentration and the ammoniation rate of the extractant and increased slightly with an increase in extractant concentration. When the value of kw arrived at 1.0×10<sup>-6</sup> m.s<sup>-1</sup>, ΔpH<sup>Zn</sup><sub>Cd</sub> was 1.49. It is possible to separate Zn<sup>2+</sup> and Cd<sup>2+</sup> by controlling the acidity of the aqueous solution properly because of the existence of the kinetics competition.

## ACKNOWLEDGEMENT

State Key Project of Fundamental Research (G1998061301) and the National Natural Science Foundation of China (29771028, 29801004) supported this work.

## REFERENCES

1. Y. Y. Dai (1992), *Membr. Sci. Tech.*, **12** (1), 1-7.
2. P. R. Alexander, R. W. Callahan (1987), *J. Membr. Sci.*, **35**, 57-71.
3. A. D'Elia Nancy, D. Lise, E. L. Cussler (1986), *J. Membr. Sci.*, **29**, 309-319.
4. T. Hano, M. Matsumoto, M. Hirata, T. Tohda, F. Kubuta, M. Goto and F. Nakashio (1996), *Proc. ISEC '96*, University of Melbourne Press, Melbourne, p. 1387.
5. M. Goto, F. Kubota, M. Miyata and F. Nakashio (1992), *J. Membr. Sci.*, **74**, 215-221.
6. T. Tsuneyuki, T. Hashizume, M. Goto and F. Nakashio (1993), *Proc. ISEC '93*, Society of Chemical Industry, London, pp. 878-882.
7. F. J. Zhang, D. Q. Li, Y. L. Wu (1998), *Chem. J. Chin. Univ.*, **19** (4), 514-516.



# A KINETIC STUDY OF THE EXTRACTION OF ZINC FROM HYDROCHLORIC ACID SOLUTIONS BY A SURFACTANT LIQUID MEMBRANE CONTAINING TRIOCTYLAMINE

S. Pérocheau, M. Stambouli, D. Pareau and G. Durand

Laboratoire de Chimie et Génie des Procédés  
Ecole Centrale Paris, Châtenay-Malabry Cedex, France

The surfactant liquid membrane extraction (SLM) is very promising for environmental uses but its application to industrial effluents is very reduced due to the complexity of the transfer phenomena. A more accurate comprehension of them will lead hopefully to an industrial development of this process.

The single drop method has been used to study the transfer of zinc from an hydrochloric solution into a W/O emulsion containing a tertiary amine. The main result is a surprising amount of extraction during the drop formation. Both extraction reactions (during the drop formation and during its rise in the column) have been carefully studied leading to the identification of the limiting steps. During the drop formation zinc transfer is controlled by an interfacial chemical reaction involving two extractant molecules; on the contrary during the drop rise, the extraction regime is mixed, suggesting a diffusion limitation in addition to the chemical reaction. These original results can be used to design new contactors for SLM extraction, better adapted than the classical solvent extraction devices commonly used.

## INTRODUCTION

SLM extraction is derived from solvent extraction. Due to the extremely high interfacial areas and the interesting volume ratios this process is a very promising separation technique for treatment of diluted polluted effluents as for pollutant concentration in order to valorise it [1,2]. SLM industrial development however needs a very accurate comprehension of the transfer phenomena occurring within the emulsion.

This kinetic study is based on the choice of a model chemical system and a specific experimental device. Zinc extraction in chloride solutions by trioctylamine (TOA) in xylene [3] has been studied. The single drop method, commonly used in solvent extraction [4], has been selected for this study because of many advantages: moderate agitation to prevent emulsion breakage, high specific interfacial area in contrast with a diffusion cell where the interfacial area is saturated with surfactant molecules preventing the solute transfer [5].

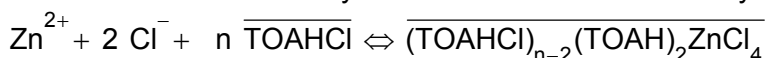
## EXPERIMENTAL

The aqueous solutions were prepared by dissolving zinc chloride (Acros, >98%) in the presence of hydrochloric acid (Labosi, 36%). TOA (Acros, 98%) was previously purified with activated carbon and diluted in xylene ( Aldrich). SPAN 80 ( sorbitan monooleate from Labosi) was chosen as a surfactant. Zinc analyses were performed by atomic absorption spectrometry ( Varian AA300) and by plasma emission (Jobin Yvon Y32). Emulsions were prepared with a mixer Ultra Turrax ( 6000 rpm). Size distribution was determined by a laser granulometer (Mastersizer X, Malvern). Droplet diameters vary between 1.6 and 2.6  $\mu\text{m}$ .

Solvent extraction studies were performed in thermostated reactors. The single drop experiments were realised in four thermostated columns with 30, 45, 95 and 135 cm heights. The injection device is a capillary at the bottom of the column; by varying the capillary diameter, droplets of various sizes are obtained. Droplets are collected at the top of the column, zinc is analysed in the internal phase of the emulsion after electrocoalescence.

## PRELIMINARY STUDY IN SOLVENT EXTRACTION

The extraction reactions of zinc by TOA in chloride solutions may be written as follows :



where TOAHCl stands for the amine salt.

The distribution ratio of zinc may be expressed by the following equation, taking into account the existence of more than one extracted complex:

$$D = \frac{[\text{Cl}^-]^2 \cdot \sum_n K_{\text{ex},n} [\overline{\text{TOAHCl}}]^n}{(1 + \sum_{i=1}^4 \beta_i [\text{Cl}^-]^i)} \quad (1)$$

$K_{\text{ex},n}$  is the equilibrium constant of formation of  $(\text{TOAHCl})_{n-2} (\text{TOAH})_2 \text{ZnCl}_4$ ;  $\beta_i$  is the formation constant of  $\text{ZnCl}_i^{(2-i)}$ .

By taking into account the dimerisation of TOAHCl [5] (dimerisation constant = 83) and by assuming the existence of a single extracted complex, the slope method allows to estimate  $n$ , by plotting  $\log D$  versus  $\log [\text{TOAHCl}]$ . The slope of the straight line obtained is  $n$ . The concentration of TOA has been varied between  $10^{-3}$  and  $10^{-1}$  mol/L with:  $[\text{Cl}^-] = 0.5$  mol/L ;  $[\text{Zn}] = 10^{-4}$  and  $5.10^{-4}$  mol/L. The results are illustrated in Figure 1.

The slope value suggests the existence of two different organic complexes with  $n = 2$  and 3. By exploiting the results with the two reactions, the extraction constants have been determined with a good accuracy:

$$K_{\text{ex},2} = (2.6 \pm 0.6) 10^5 \quad ; \quad K_{\text{ex},3} = (2.9 \pm 0.3) 10^7$$

The influence of SPAN 80 on the extraction of zinc has been investigated, because of its necessary use for the preparation of the emulsion. Equal volumes of aqueous phase ( $[\text{ZnCl}_2] = 10^{-3}$  mol/L ;  $[\text{HCl}] = 0.50$  mol/L) and organic one ( $[\text{TOAHCl}] = 10^{-2}$  mol/L ;  $[\text{SPAN}] : 0 - 3$  % ; xylene) have been contacted; more than 2% SPAN ( 0.028 mol/L) leads to a decrease in the extraction which is attributed to interactions between extractant and surfactant and formation of micelles. This phenomenon will not be observed in SLM because the surfactant molecules will be in majority adsorbed at the much greater interface and the extractant is continuously regenerated by rapid stripping [2].

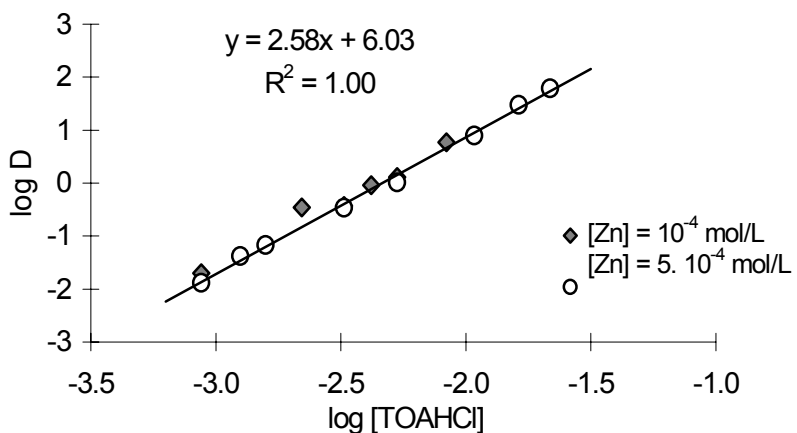


Figure 1. Determination of the extracted complexes stoichiometry.

The stripping phase is a strong acid:  $\text{HNO}_3$ ,  $\text{H}_2\text{SO}_4$ ,  $\text{HCl}$ , giving a rapid ( $< 2$  min) and quantitative stripping of zinc. In order to simplify the phenomena, it has been preferred to limit the number of chemical species and then to adopt  $\text{HCl}$  for stripping reagent.

The breakage rate of the emulsion has been measured by a tracer method; lithium has been added to the internal phase of the emulsion; its presence in the external phase after contact of it with the emulsion is only due to the emulsion breakage. An optimal concentration of SPAN of 3% has been adopted in order to minimize the breakage of the emulsion; by increasing the SPAN concentration above 3%, the extraction rate significantly decreases.

The optimal formulation of the emulsion for equal volumes of organic and aqueous phases is:

Internal phase :  $\text{HCl}$  (0.1 mol/L)

Organic membrane : TOA ( $2 \cdot 10^{-2}$  mol/L) ; SPAN 80 (3%) in xylene.

In these conditions the stability of the emulsion is satisfactory and the parasite phenomena of osmosis and inclusion are not observed within 15 minutes.

## KINETIC STUDY OF THE TRANSFER DURING THE DROP RISE

### Modeling

The following hypotheses have been adopted [3, 6] :

- The transfer resistance is limited in the external phase (phase 3): the transfer flux  $\Phi$  is expressed by  $\Phi = k_3 \cdot (C_3^0 - C_3^i)$ ,  $C_3^0$  and  $C_3^i$  being zinc concentrations in the external phase, in the bulk and at the interface respectively
- The transfer across the membrane is rapid and the stripping reaction is very rapid: there is no accumulation of zinc in the membrane (phase 2)
- The chemical extraction reaction takes place at the external interface with a rate expressed as follows:  

$$r = k_n \cdot [\text{Zn}^{2+}]_i \cdot [\text{Cl}^-]_i^m \cdot [\text{TOAHCl}]_i^n = k_{cn} \cdot C_3^i \cdot C_e^n$$
 $[\text{Cl}^-]_i$  is constant and has been introduced in  $k_{cn}$ ; TOA being in great excess,  $[\text{TOAHCl}]_i$  is constant too and noted  $C_e$ .

In pseudo stationary state, equality of the fluxes leads to:

$$C_3^i = \frac{k_3}{k_{cn} \cdot C_e^n + k_3} \cdot C_3^0 \quad (2)$$

The material balance is then:

$$d(V_1 C_1) = S_3 k_c C_3^i C_e^n dt \quad (3)$$

where  $S_3$  is the external interfacial area,  $V_1$  is the internal phase volume and  $C_1$  is the concentration in the internal phase (phase 1).

Integrating equation (3) gives:

$$C_1(t) = \left( \frac{S_3}{V_1} \cdot C_3^0 \cdot K \right) \cdot t + C_x \quad (4)$$

$C_x$  is the concentration of zinc in the internal phase after the drop formation and  $K$  is the global transfer conductance (diffusion + reaction):

$$\frac{1}{K} = \frac{1}{k_3} + \frac{1}{k_{cn} \cdot C_e^n} \quad (5)$$

Two limiting cases are considered:

- i.  $k_3 \ll k_{cn} \cdot C_e^n$  (diffusion regime):  $K \approx k_3$   $C_3^i \rightarrow 0$
- ii.  $k_3 \gg k_{cn} \cdot C_e^n$  (chemical regime):  $K \approx k_{cn} \cdot C_e^n$   $C_3^i \rightarrow C_3^0$

### Validation of the Model

The emulsion drop diameter is equal to  $(4.3 \pm 0.1)$  mm; their mean velocity is 7.0 cm/s. The results are gathered in Figure 2.

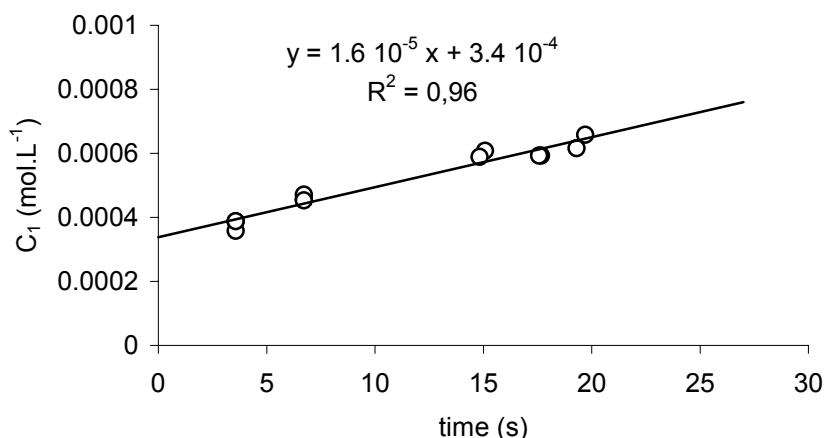


Figure 2. Experimental validation of the kinetic model.

The validity of the model is attested by the linearity of the curve (Figure 2). The slope of this straight line is proportional to  $K$  and the amount of the metal extracted during the drop formation is given by the origin ordinate. Here  $C_x$  is surprisingly high compared to  $SX$  common results. This phenomenon is quite original.

### Influence of Hydrodynamic Parameters

The chemical parameters being constant, the drop diameter has been varied from 2.5 to 5.1 mm. There is a slight effect on  $K$  suggesting a diffusion participation in the limiting step.

### Influence of chemical parameters

The TOA concentration has been varied from  $7.8$  to  $14.7 \cdot 10^{-3}$  mol/L; for example results for a diameter 2.6 mm are given in Figure 3.

These results show that the extraction reaction involves three TOA molecules; the kinetic constants have been estimated:

$$k_3 = 2.4 \cdot 10^{-4} \text{ (cm/s)} ; \quad k_{c3} = 3.0 \cdot 10^2 \text{ (cm/s)(mol/L)}^{-3}$$

In the concentration range explored these two constants are of the same order of magnitude: the regime is then mixed.

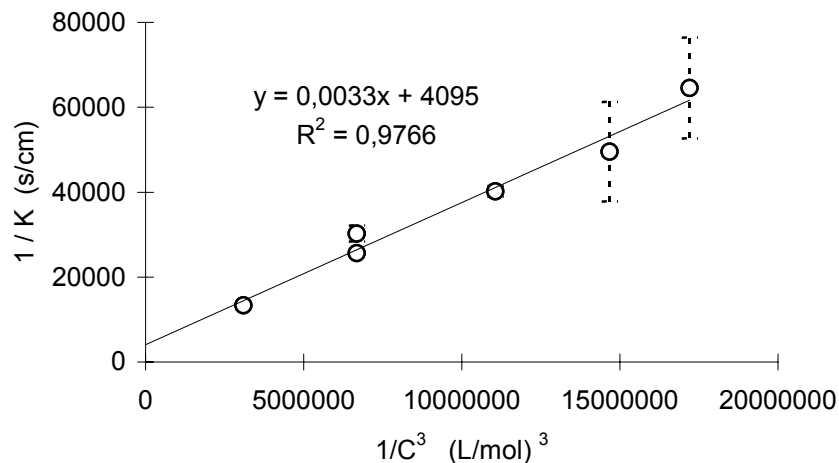


Figure 3. Influence of TOA concentration on  $K$ .

## KINETIC STUDY DURING THE DROP FORMATION

### Modeling

Considering the small formation times transfer is described by Higbie model. The growth of the emulsion drop is described by the model of progressive addition of fluid elements at the drop surface [8].

By integrating equation (3), identical equations are obtained for both limiting cases:

$$C_x = \alpha_1 \cdot K_{g1} \cdot C_3 \cdot t_f \cdot d^{-1} \quad \text{with } t_f \text{ formation time, } d \text{ final diameter.}$$

For the two different cases:

- i. diffusion regime :  $K_{g1} \approx k_3 \text{ moyen}$        $\alpha_1 = 8,9$
- ii. chemical regime :  $K_{g1} \approx k_{cn} \cdot C_e^n$        $\alpha_1 = 7,2$

### Nature of the Transfer Regime

It was not experimentally possible to vary significantly the drop diameter. So only the influence of TOA concentration may give information on the nature of the kinetic regime.

As can be seen in Figure 4, zinc transfer is controlled by a chemical reaction involving two TOAHCl molecules (slope 1.96). The kinetic constant  $k_{c2}$  is equal to  $180 \text{ (cm/s)(mol/L)}^{-2}$ .

### Interpretation

A quite original mechanism is proposed allowing to describe all the experimental results, insisting on the specific behaviour of the emulsion drop during its formation.

The limiting step of the whole process is the replacement at the interface of the adsorbed complex  $(TOAHCl)ZnCl_2$  by a molecule of free TOAHCl.

The rate is then written :

$$r = k_c^* \cdot [\text{TOAHC}]^2 \cdot [\text{TOAHC}]_{\text{ads}}$$

During the drop formation, the surfactant is located at the internal interface. The external interface is saturated by TOAHC so:  $[\text{TOAHC}]_{\text{ads}} = \text{constant}$ ; the second order with respect to TOA is explained. Progressively the surfactant migrates to the external interface replacing then TOAHC. Adsorbed TOAHC becomes minor and  $[\text{TOAHC}]_{\text{ads}} = \alpha_2 \cdot [\text{TOAHC}]$ ; the third order is then explained. A such mechanism is totally original.

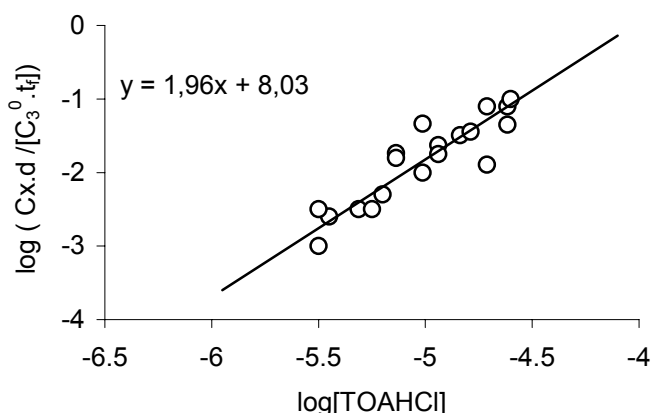


Figure 4. Influence of TOA concentration on the extraction during drop formation.

## CONCLUSION

The single drop method is suitable for the kinetic study of transfer for the extraction of zinc by SLM. A kinetic model has been proposed and discussed.

Whereas the side effects are in SX always negligible, they are here surprisingly high (during drop formation). An original mechanism has been established taking into account all the experimental results. It is based on a drastic change in the transfer process on both points of view (diffusion and reaction) between the drop formation and its rise in the column. These specific results will be exploited to conceive a new type of contactor, better adapted to SLM process, *i.e.*, favouring many steps of drop formation.

## REFERENCES

1. D. Pareau, M. Stambouli, G. Durand (1996), *Proc. Int. Solvent Extr. Conf. ISEC '96*, Vol. 1, University of Melbourne Press, Melbourne, pp. 653-658.
2. G. Durand, D. Pareau, M. Stambouli, M. Coste (1996), *Proc. Int. Solvent Extr. Conf. ISEC '96*, Vol. 2, University of Melbourne Press, Melbourne, pp. 1553-1558.
3. S. Pérocheau (1999), Thèse Université Paris VI.
4. S. Colombani (2000), Thèse Ecole Centrale Paris.
5. R. Ally, D. Pareau, M. Stambouli, G. Durand (1996), *Proc. Int. Solvent Extr. Conf. ISEC '96*, Vol. 2, University of Melbourne Press, Melbourne, pp. 911-916.
6. M. Aguilar (1974), *Chem. Scripta*, **5**, 213-213.
7. D. Lorbach, R. Marr (1987), *Chem. Eng. Proc.*, **21**, 274-281.
8. A. H. Skelland (1974), *Diffusional Mass Transfer*, Wiley Interscience, pp. 398-402.



## **EXTRACTION AND SEPARATION OF NICKEL AND COBALT BY ELECTROSTATIC PSEUDO LIQUID MEMBRANE (ESPLIM)**

**P. S. Heckley, D. C. Ibana and C. McRae\***

Nickel Hydrometallurgy Group, WA School of Mines,

Curtin University of Technology, Kalgoorlie, Australia

\*School of Chemistry, Macquarie University, Sydney, Australia

The extraction and separation of nickel and cobalt using Electrostatic Pseudo Liquid Membrane (ESPLIM) was investigated. An ESPLIM reactor was constructed and extraction tests were undertaken to determine the effects of various experimental variables on the extraction and separation of nickel and cobalt. At optimum conditions, devised as a result of this investigation, a nickel/cobalt ratio of 1000 in the raffinate from a synthetic feed solution containing 10,000 ppm nickel and 1000 ppm cobalt was achieved. Separation of nickel and cobalt from a pregnant leach solution (PLS) was achieved in two stages.

### **INTRODUCTION**

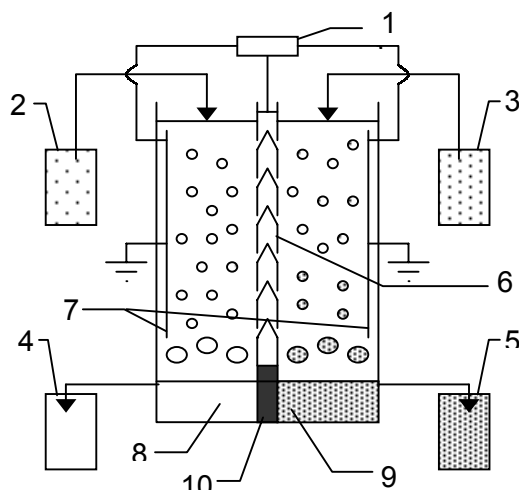
The extraction and separation of nickel and cobalt from pressure acid leach (PAL) solutions is currently a major research interest particularly in Western Australia where three new nickel laterite projects have recently commenced operation. These new generation nickel laterites projects have an initial combined output of approximately 63,000 t of nickel and 4000 t of cobalt. Although their process flowsheets have significant differences, all use PAL technology to dissolve the nickel and cobalt, and solvent extraction to separate and purify the nickel and cobalt.

Electrostatic pseudo liquid membrane is a novel separation technique, which combines the advantages of solvent extraction, liquid membrane and electrostatic dispersion. Like liquid membrane, extraction and stripping in ESPLIM occurs simultaneously and thus operate under non-equilibrium conditions. Agitation is by means of electrostatic dispersion, which provides a more efficient phase dispersion leading to higher mass transfer rates than mechanical agitation. Pioneered by Gu [1], the technique has since been applied in the extraction of, among others, nickel from rinse water [2], europium [3], and the separation of aluminium, lanthanum, samarium and yttrium [4] in bench scale studies.

This study is part of a project to develop the technique in separating and purifying nickel and cobalt from PAL generated leach solutions of nickel laterites by the direct solvent extraction route. This involves extracting Co together with the Mn, Cu, and Zn leaving a nickel SX feed (NSF) containing the Ni, as practised in Bulong Nickel Operation.

## DESCRIPTION OF THE ESPLIM REACTOR

The reactor used in the present study (Figure 1) is similar to the one developed by Gu [6] except for some modifications in the baffle and electrode design to improve extraction efficiency. The reactor consists of a rectangular tank separated into two compartments—extraction and stripping cells—by a perforated baffle plate. The baffle was constructed from a 6 mm wide plastic sheet with  $\Delta$ -shaped grooves cut into it and was sandwiched between two PTFE-coated stainless steel perforated plates (1 mm wide), which act as electrodes. Below the baffle plate is a blank plate separating the extraction and striping settlers. On the walls of the tank opposite the baffle are mounted steel plate electrodes insulated with a PTFE jacket. Except for the electrodes, the entire unit was constructed out of acrylic.



- (1) High voltage power supply (2) Feed solution (3) Strip solution (4) Raffinate  
(5) Concentrate solution (6) Baffle plate/electrode (7) Wall mounted electrode  
(8) Extraction settler (9) Stripping settler (10) Blank separation plate.

Figure 1. Schematic diagram of the ESPLIM cell.

The tank is filled with the extractant and the feed and stripping solutions are pumped onto the top of their respective cells. Under the influence of high voltage electrostatic charge these aqueous droplets break into fine droplets as they fall by gravity facilitating high mass transfer rates between the two phases.

The reaction in the extraction cell leads to a concentration gradient, which acts as the driving force for the diffusion of the extracted metal complexes towards the stripping cell. In the stripping cell, the reaction is reversed resulting in an increase in the concentration of the regenerated extractant, which drives its diffusion back into the extraction cell. Once out of the influence of the electrostatic field, aqueous droplets begin to coalesce and then fall into their respective settlers.

## MATERIALS AND METHODS

The reactor used in this study had an internal dimension of 50 mm W  $\times$  40 mm L  $\times$  140 mm H. The power supply, capable of supplying between 0.5 to 15.0 kV of AC, as well as the syringe pumps used were purpose built.

All extraction tests were carried out using Cyanex 272<sup>®</sup> (10%) dissolved in Solvent HF<sup>®</sup>. The Cyanex 272 was supplied by Cytec<sup>®</sup> and Solvent HF was supplied by Mobil Oil (Australia); both were used as supplied. Tributylphosphate (TBP) was added when a phase modifier was used. Sodium acetate (AR) was used as pH modifier. The strip solution was prepared from analytical grade sulfuric acid (1 M). The synthetic feed solutions were prepared using AR grade CoSO<sub>4</sub>.7H<sub>2</sub>O and NiSO<sub>4</sub>.6H<sub>2</sub>O. The actual leach solutions were taken from Bulong Nickel Operation.

Each extraction test was started by filling the reactor with the extractant. The electrodes were connected to the power supply, the desired voltage was selected and the power was turned on. The feed and stripping solutions were pumped in and the timer was started. The raffinate and stripping solutions were initially allowed to accumulate until the respective settlers were filled and these levels were maintained by opening their respective valve to allow excess volume to flow to their respective reservoirs.

All metal assays were carried out by atomic absorption spectrophotometry (Varian SpectrAA 50).

## RESULTS AND DISCUSSION

### The Effect of Applied Voltage

The effect of applied voltage on extraction efficiency was investigated using synthetic cobalt feed (1000 ppm) solution and 1 M H<sub>2</sub>SO<sub>4</sub> strip solution. It was found that increases in the applied voltage from 3.0–5.5 kV resulted in increases in extraction efficiency from ~40 to 98% (Figure 2). This trend is consistent with the theory of electrostatically enhanced mass transfer. Accordingly, imposing an electrostatic field on an electrolyte droplet falling through a continuous non-conducting phase causes its deformation and increases its horizontal velocity component. At sufficiently high field intensity, the interfacial tension is overcome and the droplets disintegrate into smaller droplets resulting in an increase in surface area and thus mass transfer. This was confirmed by determining the effect of applied voltage on the droplet size (Figure 3).

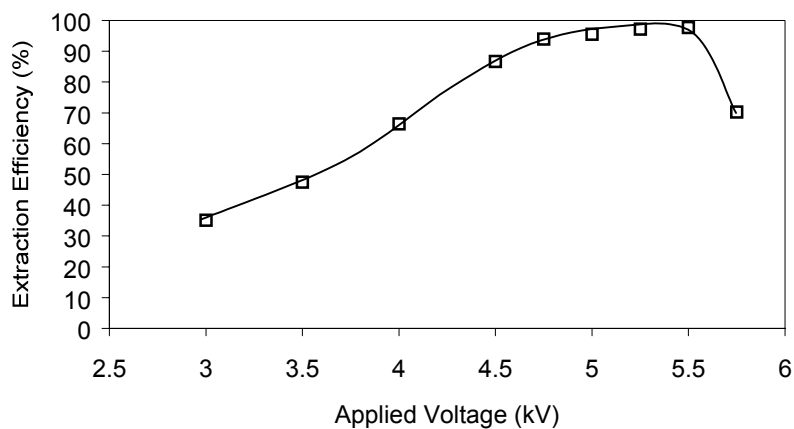


*Figure 2. The effect of applied voltage on cobalt extraction.  
(Feed flow rate: 60 mL/h; Strip flow rate: 14 mL/h)*

In addition, the increases in the horizontal velocity component of the droplets associated with the increases in applied voltage resulted in increases in hold up. Similarly the associated increases in interfacial turbulence promoted internal mixing resulting in continuous replenishment of interface with the reacting metal ions. Clearly, both contributed to the observed increases in mass transfer.

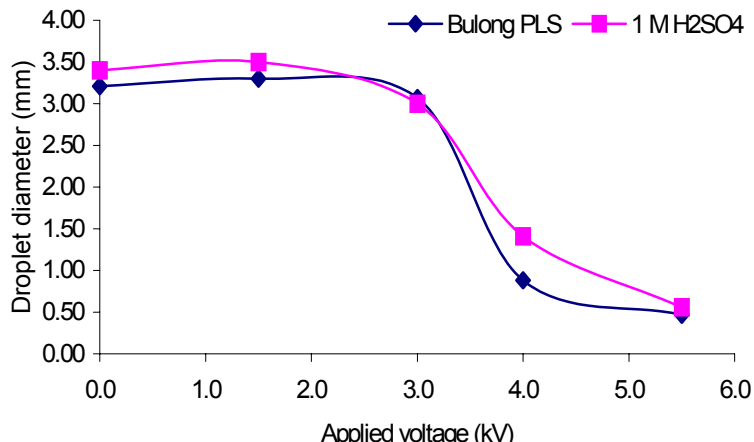


Figure 3. The effect of applied voltage on droplet size.  
(Feed flow rate: 60 mL/h; Strip flow rate: 14 mL/h).

The decrease in extraction associated with a further increase in applied voltage to 5.75 kV appeared to be due to leakage and swelling. That is, under this field strength, much smaller droplets were produced. Coupled with an increase in their horizontal velocity component, crossing over of these droplets, *i.e.*, strip droplets to extraction cell (leakage) or feed droplets to stripping cell (swelling) occurred leading to a decrease in extraction efficiency.

#### The Effect of pH

The effect equilibrium pH on the extraction of nickel and cobalt was investigated using separate solutions using 1000 ppm solutions of each metal. The feed flow rate was maintained at 64 mL/h while the strip flow rate was maintained at 12 mL/h. The results (Figure 4) were found to be comparable with the established isotherms of these metals, which were determined by conventional shake out tests. These results indicated that the chemical factors in the extraction process by means of ESPLIM are similar to those by conventional SX technique.

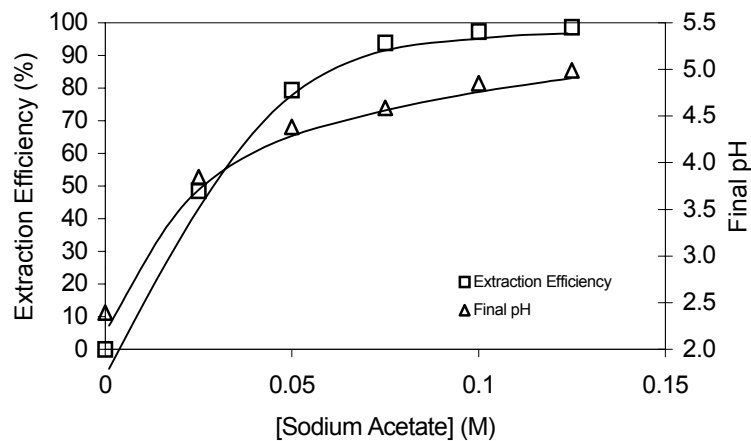


Figure 4. The effect of pH on the extraction of cobalt.

### The Effect of Feed and Strip Flow Rates

To determine the effect of the feed flow rate on the extraction of cobalt, several extraction tests were carried out under comparable conditions (feed solution containing 1000 ppm  $\text{Co}^{2+}$ , 13 mL/h, applied voltage of 5.5 kV) except that different feed flow rates were used (60-141 mL/h). The results (Figure 5) showed that, at constant strip flow rate (13 mL/h), substantial increases in the feed flow rate (60-141 mL/h) resulted in a slight decrease in extraction efficiency (<10%). This was accompanied by substantial increases in the concentration of the stripped cobalt. This indicated that as the rate of extraction increases, the rate of stripping also increases leaving only a small difference in the free extractant concentration. This is significant as it offers some flexibility in the practical application of the process. For instance, in a multi-stage extraction application, it is possible to use a much higher feed rate in the first stage to increase the throughput but a lower feed rate in the succeeding stage when the aim is high extractions and low raffinate values.

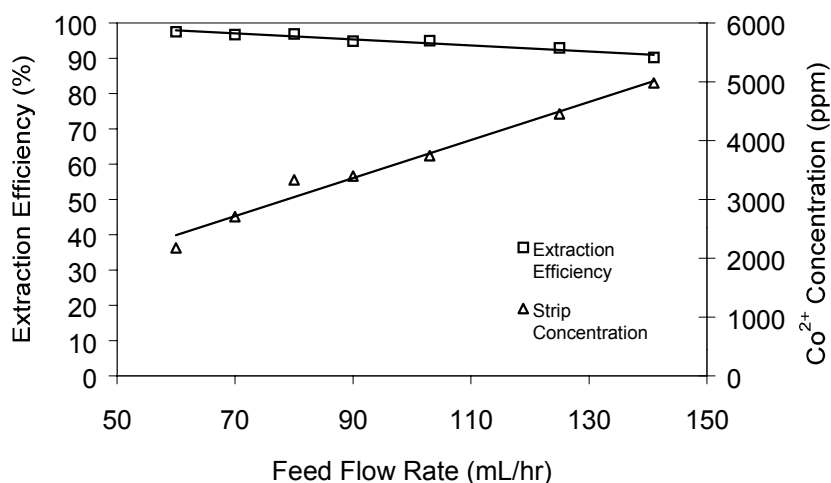


Figure 5. The effect of feed flow rate on cobalt extraction.

Consistently, increases in strip flow rates (13-26 mL/h) at constant feed flow rate (141 mL/h) resulted in slight increases in extraction efficiency (Figure 6). This indicated slightly faster stripping rates than extraction rates and thus higher free extractant concentration. The decrease in the strip concentration was due to dilution. In practical application, this can be upgraded by recirculation.

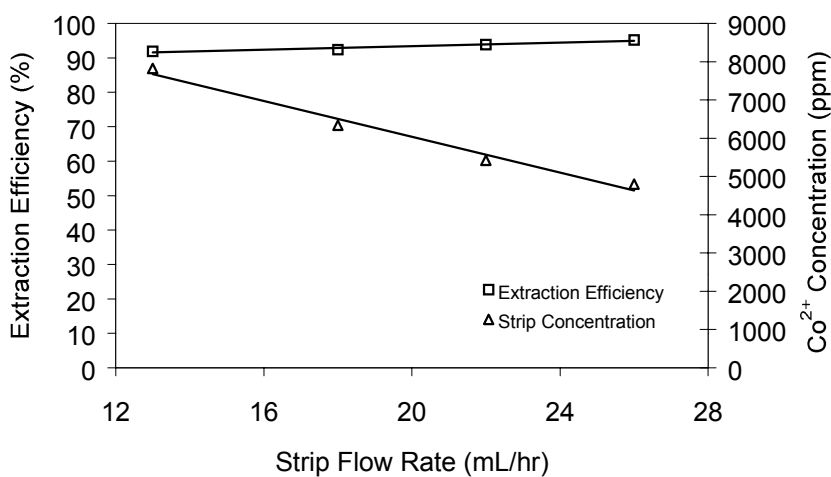


Figure 6. The effect of strip flow rate on cobalt extraction.

### **Separation of Cobalt from Nickel**

Separation of nickel and cobalt was attempted first by using a synthetic feed solution containing 10,000 ppm nickel and 1000 ppm cobalt. The experiment consisted of passing the feed through the ESPLIM reactor once, collecting the raffinate, adjusting the pH if necessary and then passing it through the ESPLIM again. The objective was to produce a nickel raffinate with a low cobalt content (*i.e.*, high Ni/Co ratio) to simulate the direct extraction of nickel and cobalt route as practised in Bulong Nickel Operation. The extraction tests were carried out under the following conditions as previous tests indicated that they provide optimum cobalt extraction: feed flow rate of 60 mL/h, strip flow rate of 14 mL/h, applied voltage of 5.5 kV and a slanted pH profile of ~4.9 to >5.

Typical results, summarised in Table 1, showed that a raffinate nickel/cobalt ratio of 1000 can be achieved in a 2-stage extraction. Consistent with established isotherm for cobalt, the pH of the raffinate after two stages should be over pH 5.0 to ensure satisfactory cobalt removal.

*Table 1. Separation of cobalt from nickel.*

Test number	Stage number	Feed pH	Feed Ni conc. (ppm)	Feed Co conc. (ppm)	Raffinate pH	Raffinate Ni/Co ratio
3a	1 <sup>st</sup> Stage	6.50	10610	977	4.85	49
3b	2 <sup>nd</sup> Stage	5.65	10588	203	5.03	1000

The application of the technique in the separation of nickel and cobalt from actual pregnant leach solutions (PLS) was attempted using PLS from Bulong Nickel Operation. Under comparable conditions to the above experiments, a 60 ppm cobalt raffinate was achieved after one stage. Second stage extraction resulted in cobalt raffinate values of 1 ppm or less in the nickel feed solution (NSF) clearly indicating a 2-stage extraction is sufficient. A comparable testwork, undertaken elsewhere, showed that a similar separation of Bulong PLS required 5 stages when using a conventional mixers-settlers.

### **CONCLUSIONS**

The separation of nickel and cobalt by Electrostatic Pseudo Liquid Membrane (ESPLIM) was attempted. It was found that the main variables that affect the extraction and separation are the applied voltage, feed and strip flow rates and pH. The optimum conditions devised as a result of this investigation were an applied voltage of 5.5 kV, feed flow rate of 60 mL/h, strip flow rate of 14 mL/h, pH of ~ 5.0. Under these conditions, cobalt raffinates with a nickel:cobalt ratio 1000 is achieved in a 2-stage extraction from a typical PLS solution used in the direct extraction route of nickel and cobalt.

### **ACKNOWLEDGEMENTS**

The authors thank Kalgoorlie Metallurgical Laboratories and MERIWA for the postgraduate scholarship of one of the authors (P. Heckley), Bulong Nickel Operation for supplying PLS and Cytec and Mobil Oil (Australia) for supplying Cyanex 272 and Solvent HF, respectively.

### **REFERENCES**

1. Gu, Z. (1988), *J. Membrane Sci.*, **52**, 77-88.
2. Gu, Z. M., Wasan, D. T. and Li, N. N. (1986), *J. Membrane Sci.*, **26**, 129-142.
3. Zhou, Q. and Gu, Z. (1988), *Water Treatment*, **3**, 127-135
4. Yang, X. J., Gu, Z. M. and Fane, A. G. (1998), *Hydrometallurgy*, **49**, 275-288.



## MEMBRANE SELECTION IN MEMBRANE ASSISTED METAL EXTRACTION AND STRIPPING PROCESSES

Karin H. Soldenhoff and Jennifer K. McCulloch

Australian Nuclear Science & Technology Organisation, Sydney, Australia

This study investigates the transport of three, industrially relevant metal extraction systems, using a flat sheet bulk liquid membrane technique. The systems tested are:

- i) Cerium extraction with di-2-ethylhexyl phosphoric acid and stripping with sulfuric acid;
- ii) Neodymium extraction with 2-ethylhexyl phosphonic acid mono-2-ethylhexyl ester and stripping with hydrochloric acid; and
- iii) Copper extraction with a ketoxime/aldoxime reagent and stripping with sulfuric acid.

The metal ions, Cu, Ce and Nd, are transported from feed to receiver solution by a counter-current coupled transport mechanism. It has been shown that in all cases, for membranes of similar thickness and porosity, the transport of metal ion from feed to solvent is favoured by a hydrophobic membrane rather than a hydrophilic membrane at the feed interface. The highest fluxes are obtained for membrane combinations of hydrophobic at the feed interface and hydrophilic at the strip interface for the Ce and Nd systems. The membrane hydrophilicity at the receiver interface was found to have no significant effect on the overall flux for the Cu system.

### INTRODUCTION

Liquid membranes have inherent advantages over solvent-extraction processes, such as lower solvent inventories and no mixing between two phases. The most commonly studied liquid membrane systems are the emulsion and supported liquid membranes. The third category, broadly termed as bulk liquid membrane, differs from the other two in that the membrane is not a thin film, but consists of a bulk phase. The bulk solvent phase can be sandwiched between two microporous membranes to form a contained liquid membrane, with pressure controls ensuring that the two interfaces remain at the membrane pore surface. The membranes can be flat sheets or hollow fibres. Hollow fibre membrane contactors are favoured for their very high surface area to module volume ratios. When both feed and receiver solutions are fed through a single hollow fibre module, the technique is known as hollow fibre contained liquid membrane [1]. Two separate membrane contactors can also be used for dispersion-free extraction and stripping, with the solvent circulating between the two modules. The greatest advantage of the bulk-liquid membrane technique is that, in principle, it solves the problem of solvent loss experienced by supported liquid membranes. However, the overall mass transfer rates are lower due to greater resistance caused by the addition of an extra membrane and the presence of the bulk solvent.

The bulk liquid membrane technique, where flat sheet microporous membranes are used as phase separators between three liquid phases is the subject of the present paper. This technique is used to investigate the effect of membrane hydrophilicity on the metal transport from feed to solvent and from solvent to receiver solutions. Most studies dealing with membrane assisted metal extraction processes have used hydrophobic membranes. In this work the effect of both hydrophobic and hydrophilic membranes are tested.

## EXPERIMENTAL

Extractants used were di-2-ethylhexyl phosphoric acid (DEHPA) and 2-ethylhexylphosphonic acid mono-2-ethylhexyl ester (EHEHPA), supplied by Albright & Wilson. LIX 984 was supplied by Henkel. Diluents used were Shellsol 2046 and Shellsol D70 (supplied by Shell), Escaid 300 (supplied by Exxon) and n-heptane. Solutions of Cu, Ce and Nd were prepared by dissolution of copper sulfate, cerium(IV) sulfate tetrahydrate and neodymium carbonate respectively.

The transport of Cu, Ce and Nd was measured using a three-compartment cell containing feed, solvent and receiver solutions. Flat sheet microporous membranes were used to separate the three bulk phases, which were stirred using magnetic stirrers at constant rpm. Metal concentrations in the feed and receiver solutions were monitored continuously with a UV-VIS spectrophotometer using wavelengths (795 nm) for Cu, (575 nm) for Nd and (795 nm) for Ce. Readings were taken at intervals ranging from 2 to 10 minutes. Millipore membranes used were GVHP, GVWP and VVLP with 0.2  $\mu\text{m}$  pore size and 125  $\mu\text{m}$  thickness. Care was taken to ensure that the pores of the GVHP hydrophobic membranes were filled with solvent phase, and the pores of the hydrophilic membranes, GVWP and VVLP, were filled with aqueous phase. The experiments were run for up to 113 hours. Mass balances, calculated from concentration measurements of final solutions by ICP, were between 93 and 104%.

Equilibrium distribution coefficients ( $m$ ) in two-phase liquid-liquid systems were measured by contacting the same volume of solvent and aqueous phase, and determining the ratios of the total metal concentrations in the solvent over the metal concentrations in the aqueous phase.

## RESULTS AND DISCUSSION

### Transport of Ce with DEHPA

The transport of Ce from a feed to a receiver solution via a bulk solvent phase was measured with a three-compartment batch permeation cell. The three phases, aqueous feed, solvent and aqueous receiver solutions were physically separated by two flat sheet microporous membranes. The solvent used was 0.2 M DEHPA in n-heptane. The feed consisted of a solution of 0.0014 M Ce in 0.55 M  $\text{H}_2\text{SO}_4$  and the receiver solution was 5.5 M  $\text{H}_2\text{SO}_4$ . These conditions were chosen to maximise extraction of Ce in the feed and stripping to the receiver solution, according to reaction (1).



where  $\overline{(\text{HR})_2}$  denotes the dimeric form of DEHPA in the solvent phase.

Concentration profiles in the three bulk phases during a permeation experiment are shown in Figure 1. In the initial stages of the experiment, the decrease in Ce concentration in the feed solution was accompanied by a corresponding increase in the solvent concentration. There was a lag time before the Ce was transferred from the solvent to the receiver solution. The receiver solution concentration then increased with time and after approximately 10 hours, Ce was being transported "uphill" against its concentration gradient, driven by the counter-current coupled transport of acid from receiver to feed solution. The overall initial flux  $J_{\text{Receiver}}$  and the flux of Ce transfer from feed to solvent  $J_{\text{Feed}}$  was determined from the slope of the linear part of the curves according to equations (2) and (3).

$$J_{\text{Receiver}} = \frac{V_R}{A_R} \frac{\partial [Ce]_R}{\partial t} \quad (2)$$

$$J_{\text{Feed}} = \frac{V_F}{A_F} \left| \frac{\partial [Ce]_F}{\partial t} \right| \quad (3)$$

where  $V_F$  and  $V_R$  are the volumes of feed and receiver solutions, respectively and  $A$  is the membrane area.

Both hydrophobic and hydrophilic membranes were tested on the feed/solvent and solvent/receiver interfaces and results are shown in Table 1. The Ce flux  $J_{\text{Feed}}$  measured from feed to solvent was 3.7 times faster for the hydrophobic GVHP membrane, compared to the hydrophilic VVLP membrane. Fluxes  $J_{\text{Receiver}}$  measured at the solvent/receiver interface, were 2.5 times faster with the VVLP hydrophilic membrane than with the GVHP hydrophobic membrane.

*Table 1. The effect of membrane type on Ce flux with DEHPA.*

Membrane interface feed/solvent		Flux ( $\text{mol m}^{-2} \text{s}^{-1}$ )	
	solvent/receiver	$J_{\text{Feed}}$	$J_{\text{Receiver}}$
hydrophobic – GVHP		$7.4 \times 10^{-6}$	
hydrophilic – VVLP		$2.0 \times 10^{-6}$	
hydrophobic – GVHP	hydrophobic – GVHP		$8.4 \times 10^{-7}$
hydrophobic – GVHP	hydrophilic – VVLP		$2.1 \times 10^{-6}$

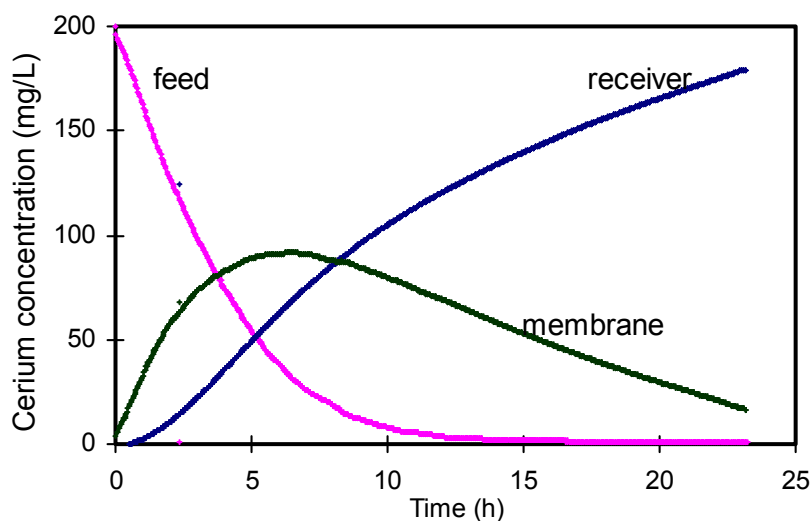


*Figure 1. Ce concentration profiles in permeation experiment.*  
 $[\text{DEHPA}] = 0.2 \text{ M}$ , Feed:  $[\text{Ce}]_{\text{initial}} = 1.4 \text{ mM}$ ,  $0.55 \text{ M H}_2\text{SO}_4$ , Receiver:  $5.5 \text{ M H}_2\text{SO}_4$   
 Membranes: GVHP at feed interface, GVWP at receiver interface.

These results are explained by analogy to a membrane based solvent extraction system. Although these permeation experiments were undertaken with simultaneous stripping, the solvent volume was sufficiently large so that the initial stage of the permeation experiment, was essentially independent of the stripping reaction. Overall mass transfer coefficients for flat sheet, membrane based extraction are described by equations (4) and (5), for extraction with hydrophobic and hydrophilic membranes, respectively, assuming instantaneous chemical reaction at the interface [2].

$$\text{extraction with hydrophobic membrane} \quad \frac{1}{K_a} = \frac{1}{mk_o} + \frac{1}{mk_{mo}} + \frac{1}{k_a} \quad (4)$$

$$\text{extraction with hydrophilic membrane} \quad \frac{1}{K_a} = \frac{1}{mk_o} + \frac{1}{k_{ma}} + \frac{1}{k_a} \quad (5)$$

where  $m$  is the distribution coefficient,  $k_a$  and  $k_o$  are the mass transfer coefficients for the aqueous and organic diffusion layers and  $k_{mo}$  and  $k_{ma}$  are the mass transfer coefficients for hydrophobic and hydrophilic membrane diffusion, respectively.  $K_a$  is the overall mass transfer coefficient based on the aqueous phase.

The difference between equations (4) and (5) lies in the middle term. Under extraction conditions, where  $m \gg 1$ , the terms containing  $m$  in the denominator are relatively small. The term  $1/k_{ma}$  for hydrophilic membrane extraction then tends to be greater than the term  $1/mk_{mo}$  for hydrophobic membrane extraction, provided the membranes being compared have similar properties in terms of membrane thickness ( $\delta_m$ ), porosity ( $\varepsilon$ ) and tortuosity ( $\tau$ ). Under such conditions, the overall resistance to mass transfer is greater with hydrophilic membranes than with hydrophobic membranes. Since the resistance due to chemical reaction at the feed/solvent interface is independent of membrane type, it follows that similar conclusions can be drawn for mass transfer with chemical reaction, provided the resistance to mass transfer due to diffusion processes is greater than that provided by chemical reaction.

The mass transfer from solvent to receiver solution is similarly interpreted by analogy to membrane based stripping as per equations (6) and (7), where  $K_o$  is the overall mass transfer coefficient based on solvent. Again the difference between these two equations lies in the middle term. For effective stripping  $m$  must be  $\ll 1$  and therefore the terms containing  $m$  in the nominator are relatively small, (i.e., the term  $1/k_{mo}$  for hydrophobic membrane stripping is likely to be greater than the term  $m/k_{ma}$  for hydrophilic membrane stripping). The overall mass transfer resistance for stripping is therefore likely to be higher for hydrophobic membranes.

$$\text{stripping with hydrophobic membrane} \quad \frac{1}{K_o} = \frac{1}{k_o} + \frac{1}{k_{mo}} + \frac{m}{k_a} \quad (6)$$

$$\text{stripping with hydrophilic membrane} \quad \frac{1}{K_o} = \frac{1}{k_o} + \frac{m}{k_{ma}} + \frac{m}{k_a} \quad (7)$$

In the case of tetravalent Ce transfer from 0.55M H<sub>2</sub>SO<sub>4</sub> to a solvent phase containing 0.2 M DEHPA, the distribution coefficient for extraction ( $m$ ) was equal to 6.1. The values for the membrane mass transfer coefficients were calculated from equation (8), using theoretically calculated diffusivity values ( $D$ ) for Ce in sulfuric acid solution and Ce-DEHPA complex in n-heptane [3]. These calculations support the above discussion and expectation that under comparable extraction conditions, the hydrophobic GVHP membrane flux is greater than that of the hydrophilic VVLP membrane, as was observed experimentally. Similarly for stripping with a 5.5 M H<sub>2</sub>SO<sub>4</sub>, where the distribution coefficient was  $< 0.005$ , the use of hydrophilic

VVLP membrane at the receiver interface resulted in a faster overall flux than when the hydrophobic GVHP membrane was used, as shown in Table 1.

$$\text{membrane mass transfer coefficient} \quad k_m = \frac{D\varepsilon}{\delta_m \tau} \quad (8)$$

### Transport of Nd with EHEHPA

The transport of Nd was also studied in the three-compartment permeation cell. The feed solution contained 0.013 M Nd chloride at pH 1.6. The solvent used was a 0.6 EHEHPA in Shellsol D70. The receiver solution contained 1.5 M HCl. EHEHPA is an acidic extractant commonly used for the separation of rare earths. Nd is extracted from acidic solutions according to reaction (9). The measured equilibrium distribution coefficient for this system was  $m = 7.6$  for extraction, and  $m = 0.004$  for stripping.



where  $HL$  represents EHEHPA.

The effect of membrane type at the feed and receiver interface is shown in Table 2. The highest flux was obtained with a combination of hydrophobic GVHP membrane at the feed interface and hydrophilic GVWP membrane at the strip interface. The Nd flux measured from feed to solvent was 1.4 times faster for the hydrophobic GVHP membrane, compared to the hydrophilic GVWP membrane. Fluxes measured at the receiver solution were 2.8 times faster with the GVWP hydrophilic membrane than with the GVHP hydrophobic membrane. These trends are similar to those observed for the Ce system and similar arguments as those presented above apply.

*Table 2. The effect of membrane type on Nd flux with EHEHPA.*

Membrane interface		Flux ( $\text{mol m}^{-2} \text{s}^{-1}$ )	
feed/solvent	solvent/receiver	$J_{Feed}$	$J_{Receiver}$
hydrophobic – GVHP	hydrophilic – GVWP	$1.5 \times 10^{-5}$	$9.2 \times 10^{-6}$
hydrophobic – GVHP	hydrophobic – GVHP		$3.3 \times 10^{-6}$
hydrophilic – GVWP	hydrophilic – GVWP	$1.1 \times 10^{-5}$	$6.7 \times 10^{-6}$

### Transport of Cu with LIX 984

The third system tested was copper transport using LIX 984, a reagent widely used in commercial copper solvent extraction circuits. The feed solution contained 0.03 M Cu sulphate at an initial pH of 2.5. The solvent used was a 10 vol.% solution of LIX 984 in either Escaid 300 or Shellsol 2046. The receiver solution contained 2 M  $\text{H}_2\text{SO}_4$ . LIX 984 is an oxime based chelating extractant consisting of a mixture of 5-nonylacetophenoneoxime and 5-dodecylsalicylaldomixe. Cu is extracted from acidic sulfate solutions according to reaction (9). The equilibrium distribution coefficient for extraction for this system was diluent dependent with measured values  $m = 7.6$  (Escaid 300) and  $m = 71$  (Shellsol 2046).



where  $HR$  represents the ketoxime or aldoxime.

The effect of membrane type at the feed and receiver interfaces is shown in Table 3. The membrane hydrophilicity had a dramatic effect on the copper flux measured from feed to solvent. The measured  $J_{Feed}$  using Escaid 300 diluent was 14 times faster for the hydrophobic GVHP membrane, compared to the hydrophilic GVWP membrane. In contrast, the membrane hydrophilicity at the receiver interface did not have a significant impact, with measured  $J_{Receiver}$  differing by only 10% for hydrophilic and hydrophobic membranes at the receiver interface, as shown in Table 3 (test carried out using Shellsol 2046 diluent).

The fluxes measured from feed to solvent ranged between  $1\text{--}3 \times 10^{-5}$  mol m $^{-2}$  s $^{-1}$ , values which are of the same order of magnitude as fluxes measured for similar Cu systems using supported liquid membranes [4]. In the supported liquid membrane system the main resistance is reported to be due to diffusion of the extracted Cu complex through the hydrophobic membrane support. It would seem therefore that the chemical extraction reaction rate is not an important parameter in Cu transport from feed to solvent, with a hydrophobic membrane. However, the overall flux for Cu measured in the three-compartment cell was very low compared to the Cu flux measured from feed to solvent and compared to the overall flux measured at the receiver solutions for the Nd and Ce systems discussed above. The low  $J_{Receiver}$  measured for both hydrophobic and hydrophilic membranes at the receiver interface suggest that membrane resistance is not important and that the stripping reaction kinetics may play a significant role in the transport of Cu in a flat sheet contained liquid membrane system.

*Table 3. The effect of membrane type on Cu flux with LIX.*

Diluent	Membrane interface		Flux (mol m $^{-2}$ s $^{-1}$ )	
	feed/solvent	solvent/receiver	$J_{Feed}$	$J_{Receiver}$
Escaid 300	hydrophobic – GVHP	hydrophilic – GVWP	$1.2 \times 10^{-5}$	$7.1 \times 10^{-7}$
	hydrophilic – GVWP	hydrophilic – GVWP	$8.6 \times 10^{-7}$	$1.3 \times 10^{-7}$
Shellsol 2046	hydrophobic – GVHP	hydrophilic – GVWP	$2.9 \times 10^{-5}$	$7.0 \times 10^{-7}$
	hydrophobic – GVHP	hydrophobic – GVHP		$7.7 \times 10^{-7}$

## CONCLUSIONS

The flat sheet bulk liquid membrane technique was found to be particularly useful in studying the effect of membrane hydrophilicity on the Cu, Ce and Nd fluxes from feed to solvent and from solvent to receiver solution. It has been shown that in all cases the transport of metal ion from feed to solvent is favoured by the presence of a hydrophobic membrane rather than a hydrophilic membrane at the feed interface. The highest fluxes were obtained for membrane combinations of hydrophobic at the feed interface and hydrophilic at the strip interface for the Ce/DEHPA/H<sub>2</sub>SO<sub>4</sub> and Nd/EHEHPA/HCl systems. The membrane hydrophilicity at the receiver interface was found to have no significant effect on the overall flux for the Cu/LIX/H<sub>2</sub>SO<sub>4</sub> system.

## REFERENCES

1. A. Sengupta, R. Basu and K.K. Sirkar (1988), *A/ChE J.*, **34**, 1698.
2. R. Prasad and K.K. Sirkar (1992), Membrane Handbook: Membrane-Based Solvent Extraction, W.S. Winston Ho and K.K. Sirkar (eds.), Van Nostrand Reinhold, New York, pp. 727-763.
3. K. Soldenhoff (2000), PhD Thesis, University of New South Wales, Australia.
4. C. Wijers (1996), PhD Thesis, Universiteit Twente, The Netherlands.



## AXIAL DISPERSION CHARACTERISTICS IN HOLLOW FIBER MODULES FOR MEMBRANE EXTRACTIONS

Wang Yujun, Luo Guangsheng, Wang Yan and Dai Youyuan

Department of Chemical Engineering, Tsinghua University, Beijing, P.R. China

In hollow fiber modules, non-ideal flow caused by channeling and dead zones can greatly influence the mass transfer characteristics. The flow characteristics in hollow fiber modules have been studied by measuring shell-side and tube-side residence time distribution curves. The axial diffusion model is applied to describe the non-ideal flow. It is found that the actual flow conforms to neither the ideal plug flow nor the complete mixed flow models. The residence time distribution curves calculated using the axial diffusion model agree well with those measured. The studies show that the axial diffusion model can be applied to describe the mass transfer characteristics in hollow fiber modules. In addition, a study of the sulfanilic acid/triethylamine system, shows that mass transfer performance is significantly decreased due to axial dispersion effects.

### INTRODUCTION

A hollow fiber module (HFM) is one of the typical membrane contactors in membrane extraction, in which hundreds or even thousands of hollow fibers are usually packed in random. Chen *et al.* [1] showed by theoretical calculation that the random packing had a great effect on the uneven flow in the shell. Their experimental results indicated that 50% of the fluid flowed through only 20% of the total cross-area. Park *et al.* [2] have shown that a significant degree of non-uniformity occurs in the flow distribution in the lumen side of a HFM by a finite-difference numerical calculation method and by tracer experiments. The non-uniformity of velocity reduced the efficiency of mass transfer in the hollow fiber modules. The complicated calculation methods in the work mentioned above, has prompted the search for a simple mathematical model to describe the effects of the non-uniformity of velocity on mass transfer performance.

In the work discussed in this paper, tracer tests were used to examine flow characteristics and an actual membrane extraction process was used to study the influence of non-ideal flow on mass transfer characteristics.

### EXPERIMENTAL PROCEDURE

#### Determination of Flow Status

Figure 1 shows a schematic of the experimental setup used for the determination of residence time distribution (RTD) curves. A step-trace method using saturated KCl solution as tracer was applied to examine the flow status in the hollow fiber modules. For the determination of shell-side flow the tracer solution was pumped through the shell side of the module and the tube side was filled with solvent. For the determination of tube-side flow the tracer solution was pumped through the tube side and the shell side was filled with solvent. The concentration at the module inlet and outlet was monitored on-line with electro-conductivity meters.

The polypropylene hollow fiber modules used in this work were manufactured by Seawater Desalting Center of National Ocean Agency in Tianjin, China. The characteristics of these modules are shown in Table 1.

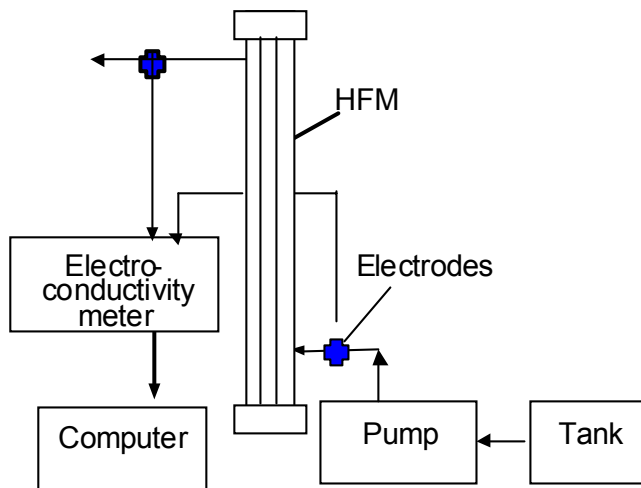


*Figure 1. Schematic of experimental setup for RTD curve determination.*

*Table 1. Characteristics of hollow fiber modules.*

No.	Module length (cm)	Module diameter (cm)	Fiber number	Fiber inner diameter $d_i$ (mm)	Membrane wall thickness (mm)	Porosity of fiber $\varepsilon$
A	33.5	3.32	3400	0.40	0.04	0.55
B	33.5	3.32	2500	0.40	0.04	0.55

#### Membrane Extraction Procedure

The actual membrane extraction system used was 20% triethylamine + 30% octanol + 50% kerosene / sulfanilic acid / water.

When extraction was carried out in a module, the aqueous phase flowed through the tube side, and the organic phase flowed counter-currently in the shell side. To avoid the breakthrough of the solvent, the pressure of the aqueous phase was 10 kPa higher than that of the organic phase. Samples at the module inlet and outlet under steady state were collected and the concentration was determined. The concentration of the sulfanilic acid was determined using a HP8452 UV spectrophotometer at 215 nm. The loaded solvent was regenerated with 10%(w/w) sodium hydroxide solution.

#### Calculation of Axial Diffusion Coefficient Pe without Mass Transfer

According to the mass conversation principle, the axial diffusion equation can be written as equation (1).

$$\frac{\partial C}{\partial \theta} = \left( \frac{E_2}{uL} \right) \frac{\partial^2 C}{\partial Z^2} - \frac{\partial C}{\partial Z} = \frac{1}{Pe} \frac{\partial^2 C}{\partial Z^2} - \frac{\partial C}{\partial Z} \quad (1)$$

where

$$C = \frac{c}{c_0}, \theta = \frac{t}{\tau}, Z = \frac{z}{L} \quad (2)$$

Pe being the only unknown parameter was determined using the stimulus-response curves.

### Calculation of True Mass Transfer Coefficients by Axial Diffusion Model

According to the axial diffusion model, equation (3) is the differential equation group for the two phases [3].

$$\begin{aligned} \frac{d^2 X}{dZ^2} - Pe_x \frac{dX}{dZ} - N_x Pe_x (X - X^*) &= 0 \\ \frac{d^2 Y}{dZ^2} + Pe_y \frac{dY}{dZ} + N_y \cdot \frac{u_y}{u_x} Pe_x (X - X^*) &= 0 \end{aligned} \quad (3)$$

The boundary conditions are:

$$\begin{aligned} Z = 0 &\quad Z = 1 \\ -\frac{dC_x}{dZ} &= Pe_x B (1 - C_{x0}) \quad -\frac{dC_x}{dZ} = 0 \\ -\frac{dC_y}{dZ} &= 0 \quad -\frac{dC_y}{dZ} = Pe_y (C_{y1} - C_y) \end{aligned} \quad (4)$$

The finite-difference method was used to solve the above equation group. When  $Pe_x$ ,  $Pe_y$ ,  $C_{x0}$ ,  $C_{x1}$ ,  $C_{y0}$  and the distribution coefficient  $m$  are known, the true mass transfer unit can be obtained. The parameters  $m$ ,  $C_{x0}$ ,  $C_{x1}$  and  $C_{y0}$  were determined by experiments and  $Pe_x$  and  $Pe_y$  were obtained from the resident time distribution curve. According to our previous work, the average distribution coefficient for the experimental system was 21.1 [4].

### Calculation of Apparent Mass Transfer Coefficients

The apparent mass transfer coefficients are the overall mass transfer coefficients obtained under the condition of plug flow. These can be obtained from the following correlation.

$$K_{aq} = \frac{Q_{aq}}{A} \frac{1}{1 - \frac{Q_{aq}}{mQ_o}} \ln \frac{c_{x0} - c_{x0}^*}{c_{x1} - c_{x1}^*} \quad (5)$$

The inlet and outlet concentration of aqueous phase was measured, and the distribution coefficient  $m$ , was 21.1.

## RESULTS AND DISCUSSION

### Typical Tube and Shell-Side RTD Curves

The RTD curves given in Figure 2, showed that the actual flow status in the tube side conformed to neither an ideal plug flow nor a complete mixed flow model. In fact back mixing and forward mixing resulted from drag associated with the inner wall of the fibers. The randomly packed and twisted fibers resulted in resistance gradients through the fiber bundles. The distribution of velocity on the tube side was therefore non-uniform. The RTD curves given in Figure 3 showed more complicated flow characteristics for the shell side than for the tube side. Compared to the case for ideal plug flow, "dead zones" and channelled flow were observed. The locations of the inlet and outlet of the module means that fluid has to flow across the fiber bundles to be evenly distributed at the cross section. As a result of the larger resistance across than along the fibers, the fluid tended to flow along the fibers thereby causing an uneven cross sectional velocity profile. In addition the non-uniform packing of the modules means that the fibers are not all straight and parallel. This arrangement, by causing channel variations along the length of the fiber bundle resulted in cross flow. The fluid tended to favor passage through the channels with large equivalent diameters. The uneven flow observed was clearly a result of the random packing of fiber bundles.

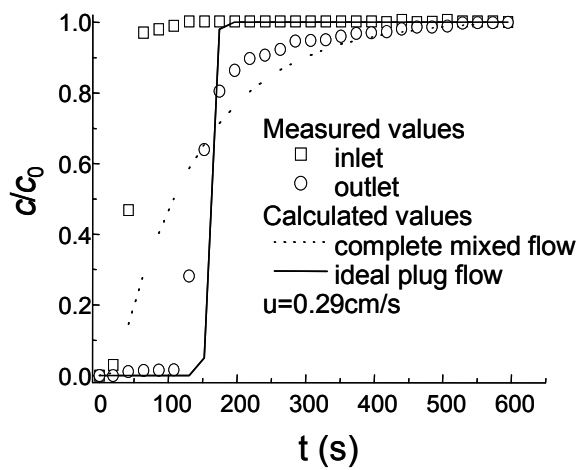


Figure 2. The RTD curves of tube side in Module B

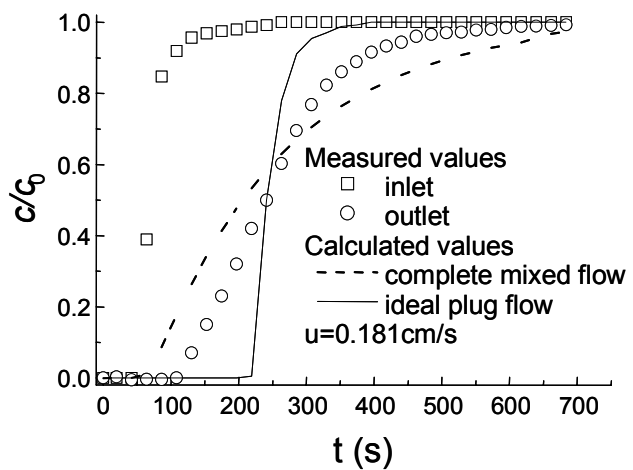


Figure 3. The RTD curves of shell side in Module A.

### Comparison of Calculated and Experimental Curves

Figure 4 showed that there was good agreement between the experimentally determined curves and those calculated using the diffusion model. The axial diffusion model in which all the non-ideal factors contribute to axial dispersion has been widely applied for the design of reactors and extraction columns. These results show that this model can be used to describe the flow characteristics in hollow fiber modules.

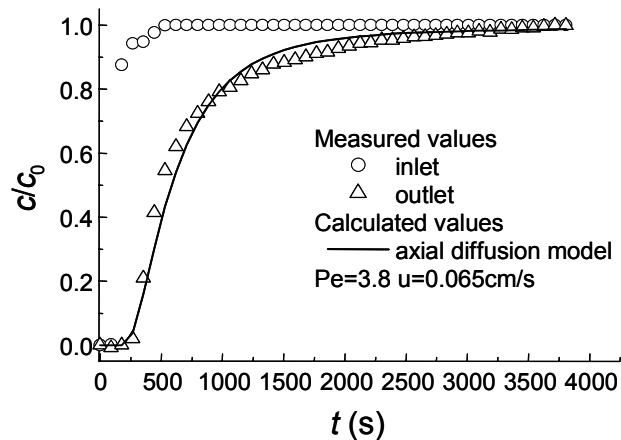


Figure 4. Comparison of experimental and calculated RTD curves of shell side in Module B.

### Influence of Velocity on Axial Dispersion

Figure 5 shows that velocity significantly affects axial dispersion. On the shell side, the resistance to flow of the fluid across the fibers increased with increasing velocity. For paths far from the inlet, lower velocities caused severe bypassing, resulting in an increase in axial dispersion. On the tube side, the influence of the drag associated with the fiber inner wall was reduced as the velocity increased. At the same time the increase in the radial mixing in each fiber, giving a more even flow distribution, resulted in a decrease in axial dispersion.

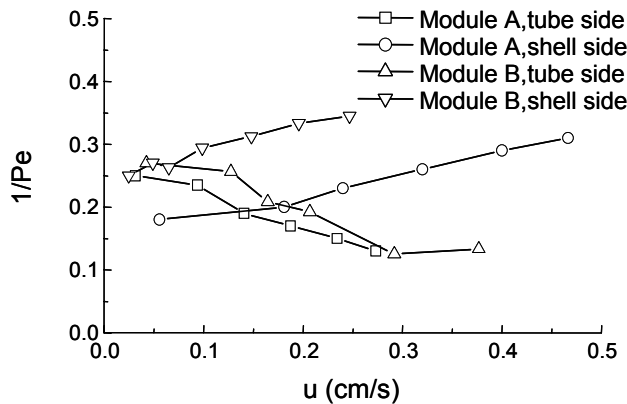


Figure 5. Influence of velocity on axial dispersion.

#### Comparison of the True and the Apparent Mass Transfer Coefficient

Figure 6 shows that the true mass transfer coefficient obtained by solving the axial diffusion equation was larger than the apparent coefficient. This indicated that the mass transfer performance was inhibited by axial back mixing. This is borne out by examination of an actual concentration profile in a hollow fiber module, given in Figure 7. The observed concentration jump at the module inlet and outlet would reduce the concentration driving force and thus reduce mass transfer performance.

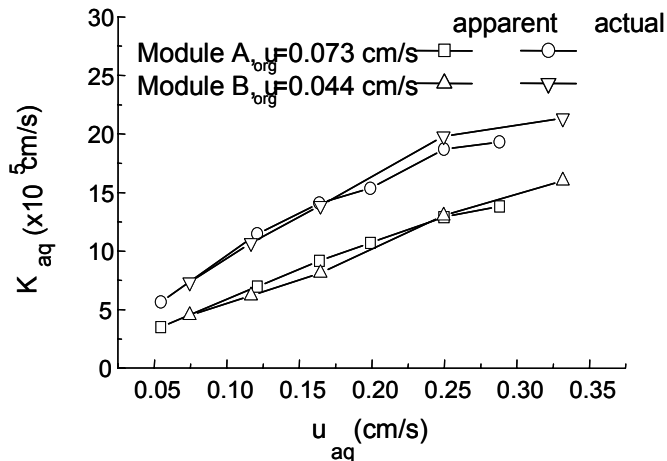


Figure 6. Comparison of the apparent and the actual mass transfer coefficients.

#### CONCLUSIONS

The flow characteristics in hollow fiber modules were studied using resident time distribution curves. They showed that the actual flow was non-ideal and conformed to neither the ideal plug flow nor the complete mixed flow models. Axial dispersion was found to decrease with an increase in flow velocity on the tube side and to increase with an increase in flow velocity on the shell side. Good agreement between the curves calculated using an axial diffusion model and experimentally determined RTD curves showed that the diffusion model can be used to describe the mass transfer characteristics in hollow fiber modules.

In a study using an actual extraction process, it was found that axial dispersion was the cause of the significant decrease in mass transfer performance.

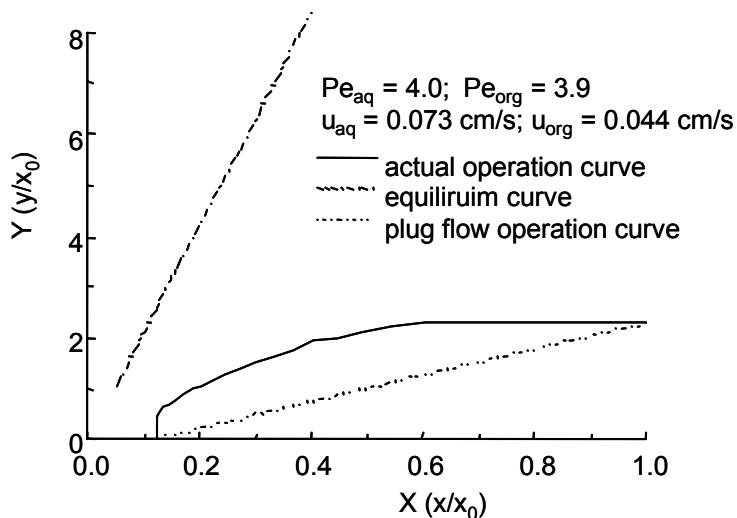


Figure 7. Actual concentration profile in Module B.

## ACKNOWLEDGEMENT

This work was supported by the National Natural Science Foundation of China (No.29836130) and Tsinghua University Science Foundation.

## NOMENCLATURE

$A$  = mass transfer surface area,  $\text{cm}^2$   
 $c$  = concentration,  $\text{mg/L}$   
 $C$  = dimensionless concentration  
 $d$  = diameter,  $\text{cm}$   
 $E$  = axial diffusion number,  $\text{cm}^2/\text{s}$   
 $L$  = length of the module,  $\text{cm}$   
 $K$  = overall mass transfer coefficients,  $\text{cm/s}$   
 $N$  = number of mass transfer unit  
 $Q$  = the flow rate,  $\text{ml/s}$   
 $t$  = time,  $\text{s}$   
 $u$  = velocity,  $\text{cm/s}$   
 $x$  = concentration of the aqueous phase,  $\text{mg/L}$   
 $X$  = dimensionless concentration,  $x/x_0$   
 $y$  = concentration of the organic phase,  $\text{mg/L}$   
 $Y$  = dimensionless concentration  $y/x_0$   
 $z$  = axial direction  
 $Z$  = dimensionless length,  $Z = z/L$

*Greek Symbols*  
 $\varepsilon$  = porosity of fibers  
 $\theta$  = dimensionless time  
 $\tau$  = average residence time,  $\text{s}$

*Subscripts*  
 $0$  = inlet  
 $1$  = outlet  
 $\text{aq}$  = aqueous phase  
 $\text{org}$  = organic phase  
 $x$  = aqueous phase  
 $y$  = organic phase  
 $z$  = axial direction  
 $*$  = equilibrium

## REFERENCES

1. V. Chen and M. Hlavacek (1994), *AIChE J.*, **40**, 606-612.
2. J.K. Park and H.N. Chang (1986), *AIChE J.*, **32**, 1937-1947.
3. Z. Li, Y.G. Li, W.Y. Fei and J.C. Yang (1993), *Processes and Equipment of Solvent Extraction*, Nuclear Energy Press, Beijing, pp. 288 (in Chinese)
4. Y.J. Wang, G.S. Luo, W.B. Cai, Y. Wang and Y.Y. Dai (2000), *Modern Chem. Indus.*, **20** (10), 31-33 (in Chinese).



## **SWELLING AND STABILITY OF EMULSIONS IN LIQUID MEMBRANE EXTRACTION**

**Marina Yu. Koroleva and Eugene V. Yurtov**

Mendeleev University of Chemical Technology, Moscow, Russia

Water diffusion during liquid membrane extraction often leads to emulsion swelling. The main causes of this unfavorable phenomenon are the differences of water activities in the internal and external phases. The investigation of the mechanisms of this process showed that nanodispersion droplets were carriers of water in the liquid membrane. Photomicrographs of swelling emulsions indicated the presence of nanodispersion droplets. Diffusion coefficients of nanodispersion water droplets were to a marked degree lower than that of water molecules. The velocity of water diffusion depends greatly on the gradient of electrolyte concentration and to a lower extent on the surfactant concentration in the liquid membrane.

### **INTRODUCTION**

Transmembrane water transfer in multiple emulsion leading to the emulsion swelling is a negative phenomenon, which takes place during the liquid membrane extraction. As known, such process takes place in a great extent in emulsion with Span 80 [1, 2]. The cause of this phenomenon is the difference in water activities between the internal and external water phases.

The water activity in the drop of internal phase depends on the forces that act on this drop or the pressure caused by these forces. The total pressure in the internal water phase of emulsion consists of the osmotic pressure of the brine and the Laplace pressure in the opposite direction. Laplace pressure is proportional to the interfacial tension and inversely proportional to the mean drop radius. The gravity force, water drops deformation, etc. are very small contributors to the total pressure and need not be considered in the model calculation for the liquid membrane extraction.

The scheme of varieties of water transfer in the three-phase system are shown in Figure 1. In the first case the electrolyte concentration ( $C$ ) in the internal water droplets is much higher than in the external water phase. This situation is typical for the extraction of inorganic or organic substances from dilute solutions and concentrating them in the internal water phase. Such conditions are the most negative from the point of view of emulsion swelling.

In the second case (Figure 1) electrolyte concentrations are high and equal in both water phases, so water diffusion is negligible. Such systems are seldom used for extraction.

They can be applied for recovery of substances, which adsorb on the interface in emulsion. For example, for the extraction of cholesterol from biological fluids [3] the isotonic buffer solution is used as the basic component of the internal phase in order to balance of pressures between blood and water drops in emulsion.

The two last variants are not typical for liquid membrane extraction. If the concentrations of electrolytes are very low in the external and in the internal water phases, water diffusion is extensive. As the Laplace pressure is inversely proportional to the drop radius, water diffuses from small drops to large ones. At the same time water diffusion takes place from large drops out of the emulsion to the external water phase.

If the electrolyte concentration in water drops is less than in the external phase, water diffuses out of emulsion. In the last two cases water fraction in the emulsion diminishes.

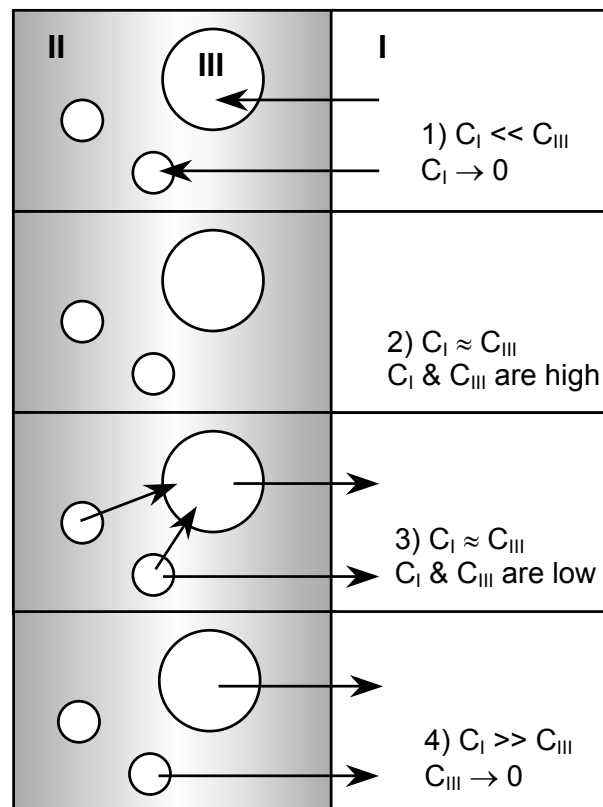


Figure 1. The directions of water diffusion at different electrolyte concentration in water phase. I, & III - external and internal water phases, II - organic liquid membrane.

### MECHANISM OF WATER TRANSFER IN THE LIQUID MEMBRANE

Water diffusion in the organic liquid membrane can be carried out by surfactant and extractant or carrier molecules. In addition to molecular mechanism, dispersed particles, such as micelles, microemulsions, and nanodispersions, can solubilize water and promote water transfer in the emulsion. These dispersed structures can be formed by surfactant and extractant. All types of water transportation take places in multiple emulsions, but their contributions are different.

Several articles were published in this field, and the related points of view can be divided into two groups: water can be transported by either microemulsion or nanodispersion [3, 4], and water can be transported by single surfactant and extractant-carrier molecules [2, 5].

The formation of microemulsion or nanodispersion droplets is promoted by the disequilibrium between the phases of the extracting emulsion, *i.e.*, by the mass transfer of the components and the solvents through the interface. Diffusion coefficients of microemulsion are much lower than those of the monomers or individual surfactant molecules [6]. To clear up the mechanism of this phenomenon we investigated transmembrane transfer of different substances in multiple emulsion.

Rhodamine C is a substance which dissolves well in water, does not dissolve in the mineral oil in the liquid membrane, does not interact with single surfactant molecules, but can be solubilized in micelles and water droplets of nanodispersion. So such dye can only be transported through the liquid membrane by surfactant micelles or nanodispersion, or as a result of coalescence of internal phase droplets leading to water phase separation.

Emulsion W/O was prepared from 3.4 M NaCl solution, mineral oil, and surfactant - sorbitanmonooleate. This emulsion was placed on a flat surface with area of  $6.5 \times 10^{-3} \text{ m}^2$ , and contacted with distilled water. Rhodamine C was added in the internal or in the external water phase.

Diffusion coefficient of water was calculated using the data from the kinetic curves of internal water phase fraction in emulsion. The diffusion coefficients of rhodamine C were obtained from the kinetic curves of rhodamine C concentration in the external water phase by means of the equation of non-stationary diffusion.

For the comparison of experimental diffusion coefficients of water and rhodamine C molecular diffusion coefficients were calculated of by Willke-Chang equation. The results are in Table 1.

*Table 1. Diffusion coefficients of water and rhodamine C.*

D experimental, $\text{m}^2/\text{s}$		D calculated, $\text{m}^2/\text{s}$	
Water	Rhodamine C	Water	Rhodamine C
$0.3 \times 10^{-14}$	$(1.4-5.6) \times 10^{-14}$	$5.4 \times 10^{-11}$	$0.7 \times 10^{-11}$

Calculated diffusion coefficients are approximately 1000 times higher than the experimental values. This fact points out that these substances are preferably transported in the form of nanodispersion.

To confirm the formation of nanodispersion droplets during water diffusion we obtained photomicrographs of emulsions. Pt/C replicas of emulsion were prepared by the freeze-etching method. Figure 2a illustrates the emulsion with nanodispersion in organic phase. The space around drops is so rough and rippled that the interface is blurred. Some droplets ( $d = 17 \sim 25 \text{ nm}$ ) are arranged near the interface of the large water drop (Figure 2b).

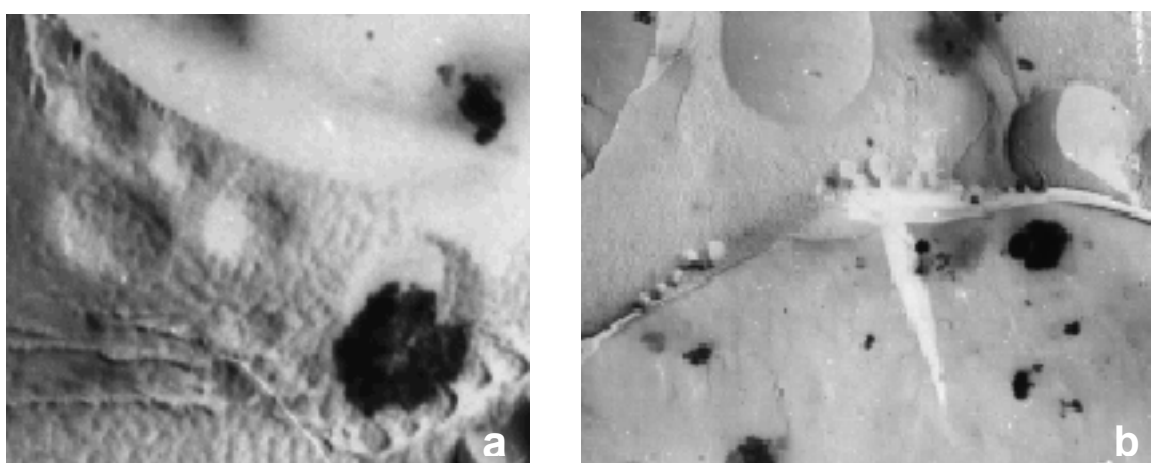


*Figure 2. Photomicrographs of emulsions with nanodispersion in organic phase:  
a) magnification - 80 000; b - 120 000.*

The formation of nanodispersion is confirmed by the photomicrographs and by the diffusion coefficient calculations. The main form of water diffusion in the liquid membrane is by nanodispersion droplets or solubilized micelles. Water can be also transported by molecules of surfactant or extractant-carrier, but the first mechanism is more significant.

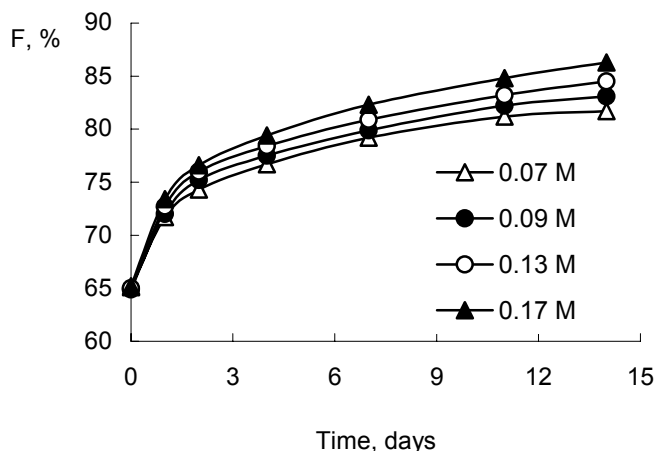


Figure 3. Kinetic curves for water transfer at different sorbitanmonooleate concentrations in emulsions.

#### INFLUENCE OF SURFACTANT ON EMULSION SWELLING

The presence of surfactant is necessary for nanodispersion droplet formation. Emulsions with sorbitanmonooleate swell in a great extent, so we investigated the kinetics of swelling in this system. Emulsion with the initial NaCl concentration of 3.4 M and different surfactant concentrations were contacted with distilled water as described above.

Figure 3 shows the kinetic curves of the alteration of  $F$ , the internal water phase fraction, in emulsions with different initial sorbitanmonooleate concentration. Water transfer continued for approximately 20-25 days, and the internal water phase concentration reached 87-92 %. Kinetics of emulsion swelling depends on surfactant concentration, but not significantly.

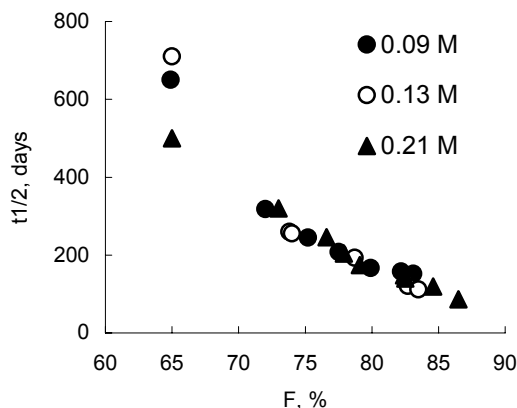


Figure 4. Half-separation of period of the water phase vs. internal phase fraction at different initial surfactant concentrations.

As published [7], raising the surfactant concentration increases the emulsion stability against coalescence. When the surfactant is present in an amount sufficient for the stabilization of all internal phase droplets formed as a result of the dispersing, a maximum stability of the emulsion is reached (0.13 M sorbitanmonooleate). With a greater concentration of the surfactant, the excess of the latter can dissolve in liquid membrane with the formation of different types of micelle structures.

So at low surfactant concentrations (up to 0.13 M) the velocity of water diffusion increased by 20% due to the increase of interfacial area, due to the gain of surfactant micelles in the liquid membrane. Surfactant amount in emulsion does not affect the velocity emulsion swelling strongly. The considerable difference in osmotic pressure between internal and external water phases leads to the formation of great water flux. In such conditions certain amount of surfactant molecules leaves the interface in emulsion for the outward emulsion surface and takes part in nanodispersion formation.

Emulsion stability against coalescence decreases sharply because of the increasing of interface area and the insertion of surfactant partly in nanodispersion (Figure 4). The half-separation periods ( $t_{1/2}$ ) of water phase in emulsions with high internal phase fractions turn almost equal in spite of the difference in surfactant concentration.

### INFLUENCE OF ELECTROLYTE ON EMULSION SWELLING

For increasing of capacity emulsions contain the concentrated solution of complexing agent or precipitant in the internal water phase. In the case of the high difference in osmotic pressure between water phases the velocity of emulsion swelling is considerable.

We investigated this process on the model emulsion with a NaCl solution in the internal phase. Sorbitanmonooleate concentration was 0.13 M. Emulsions were contacted with distilled water. The kinetic curves of emulsions swelling are showed in the Figure 5.

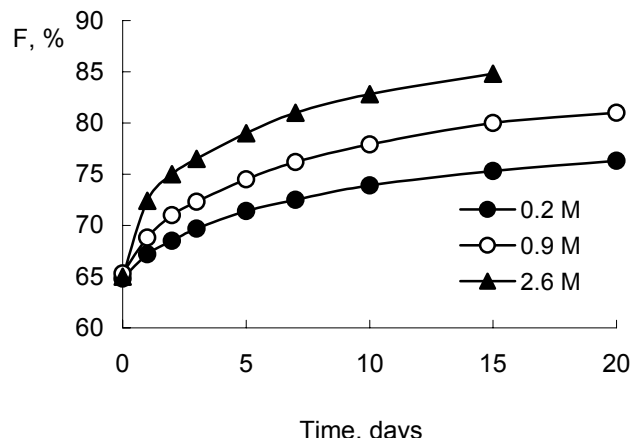


*Figure 5. Kinetic curves for water transfer at different initial NaCl concentrations in the internal phase of the emulsions.*

Half-separation periods of water phase in these emulsions only differ before mass transfer. The more stable emulsions against coalescence corresponds to the higher NaCl concentration in the internal phase. Swelling of emulsions results in diminishing of half-separation periods (Figure 6). These relationships are analogous to the curves in Figure 4.

The velocity of extraction is usually greater than the velocity of emulsion swelling. Often the efficiency of extraction diminishes at approaching to quasi-equilibrium in the multiple emulsion. This connected with the dilution of the solution in water drops because of emulsion swelling. Mathematical optimization of the mass transfer process makes it possible to achieve best results in concentrating or separating of substances in the internal water phase.

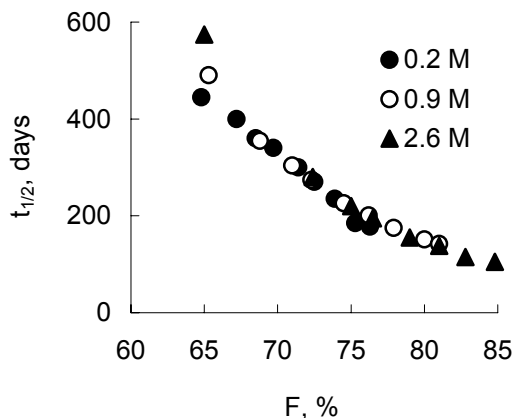


Figure 6. Half-separation of period of the water phase vs. internal phase fraction at different initial NaCl concentrations.

## CONCLUSIONS

Photomicrographs and diffusion coefficient calculation showed that the main form of water diffusion in the liquid membrane is by nanodispersion droplets or solubilized micelles. Water can be transported by surfactant or extractant-carrier in molecular form, but the first way is preferable.

Water diffusion through the liquid membrane leads to the emulsion swelling. Emulsion stability against coalescence decreases dramatically at high internal phase fractions and cannot be improved by the increasing of surfactant concentration. Mathematical modeling of the kinetics of extraction and emulsion swelling allows forecasting the optimum time of extraction process.

## ACKNOWLEDGEMENTS

Various aspects of the research presented in this paper were supported by Russian Federal Program "Integration" (grant A0078/3,5).

## REFERENCES

1. J. Draxler, R. Marr (1982), *Ber. Bunsenges Phys. Chem.*, **86** (1), 64-68.
2. P. Colinart, S. Delepine, G. Trouve, H. Renon (1984), *J. Memb. Sci.*, **20** (2), 167-187.
3. E.V. Yurtov, M. Yu. Koroleva (1991), *Russ. Chem. Rev.*, **60** (11), 1255-1270.
4. P. Plucinski (1985), *J. Memb. Sci.*, **23** (1), 105-109.
5. K. Tsuboi, S. Akita, T. Takahashi, H. Takeuchi (1987), *Kagaku Kogaku Ronbunshu*, **13** (1), 110-113.
6. H.F. Eike (1987), *Interfacial Phenomena in Apolar Media*, Marcel Dekker, Inc., New York, pp. 41-92.
7. E.V. Yurtov, M.Yu. Koroleva (1996), ACS Symp. Ser., **642**, Washington, DC, pp. 89-102.



## COMMERCIAL-SCALE RECOVERY OF HEXAVALENT CHROMIUM FOR RECYCLE WATER BY ANION LIQUID-LIQUID EXTRACTION (A-LLX)

Bruce Monzyk, H. Nicholas Conkle, J. Kevin Rose and Satya P. Chauhan

Battelle, Columbus, OH, USA

Commercial-scale liquid-liquid extraction recovery of hexavalent chromium from surface finishing process water has been successfully demonstrated. Cr(VI) levels in the raffinate were low enough for discharge to surface waters. Less than three years' payback is expected and depends on feed chromium concentration, flow rate, and chromium concentrate recycle value. Landfill disposal is avoided. Chromium recycle enables continued use of high performance chromium especially in aerospace applications. Testing has been performed at two sites. About 1,135,200 liters of feed were processed at site 1. Hexavalent chromium removal using three extraction stages was consistently 99% or greater with residuals  $\leq 0.1$  mg/l. Entrained organics were 30-120 mg/l. Solids and stable emulsion formation were controlled using pH.

### INTRODUCTION

Hexavalent chromate [Cr(VI)] is widely used within the military and industry to meet critical high corrosion control and other metal surface finishing [SURFIN] requirements. Cr(VI) is toxic and its control generates hazardous, costly waste. Alternatives for the most demanding applications have not been found. Cr(VI) recovery technology is needed to enable continued chromium use in these critical SURFIN processes.

The current process to control Cr discharge produces large amounts of metal hydroxide sludge. Disposal of this type of hazardous waste at US military maintenance facilities [1,2], can cost over \$440/ton, and poses a continuing environmental liability. Anion liquid-liquid exchange [A-LLX] offers a way to avoid disposal by providing Cr(VI) recycle.

In previous Battelle studies, A-LLX removal technology [3-5] was shown to consistently reduce Cr(VI) levels to below 0.05 mg/l, and that further reductions were possible. A-LLX would allow the SURFIN industry to meet future, more stringent discharge requirements via "continuous improvement" techniques.

Battelle was asked [6] to: (a) construct a portable, commercial-scale A-LLX process and demonstrate it at Warner-Robins Air Logistics Center, GA, (WR-ALC) maintenance depot and the Watervliet Army Arsenal (WAA) and to (b) develop detailed cost and performance results. This paper provides the first test results using the WAA feed material.

## PROCESS DESCRIPTION

Alamine 336<sup>®</sup> is a selective extractant for Cr(VI), even over sulfate ion. Ion pairing is the primary extraction mechanism involving the capture of the bichromate anion, HCrO<sub>4</sub>. The extractant phase is 5 vol.% Alamine 336<sup>®</sup> (Cognis Corp.), 5 vol.% isodecanol (Exxon Chemical Corp.), and 90 vol.% Conoco 170 ES aliphatic diluent (Conoco, Inc.). The Cr(VI)-loaded extractant is continually regenerated and recycled, keeping working capital low and achieving low raffinate Cr(VI) levels. The high interfacial surface area provides fast kinetics even with feed Cr(VI) levels as low as 1 mg/l. Figure 1 illustrates a projected A-LLX process flow diagram. Discharge at the WAA SURFIN shop over a seven-month period was ~87,000 l/day with a Cr(VI) concentration of 13 to 52 mg/l [7]. Discussions with chemical suppliers indicate that 20,000-mg/l Cr(VI) concentrates would be viable for commercial use.

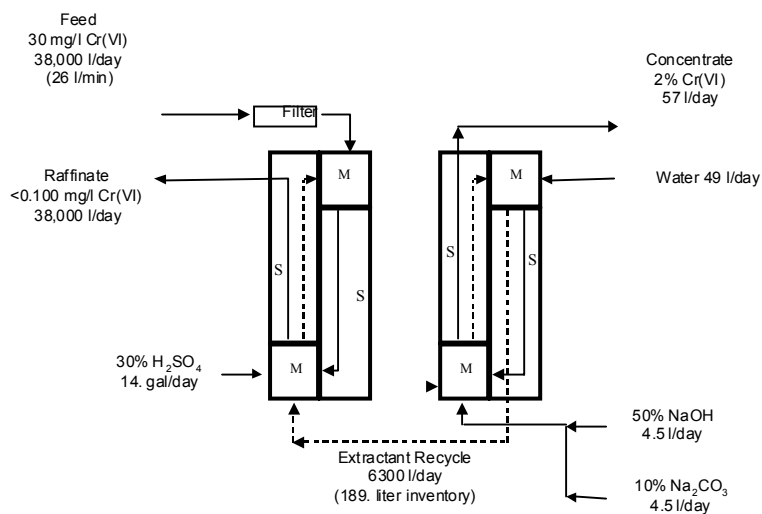


Figure 1. Full-scale A-LLX system design

## COMMERCIAL-SCALE TEST OBJECTIVES

The objectives of the program were to construct and operate a portable, commercial-scale LLX device to validate the technical and economic basis for metal SURFIN operations. To meet this goal it was necessary to reduce Cr(VI) concentrations in the raffinate to <0.3 mg/l, and to produce a useful Cr(VI) concentrate for recycle. The economic goal was a payback period of less than 3 years.

## EQUIPMENT AND PROCEDURES

### Equipment and Design Parameters

Extraction hardware was constructed by Versatile Industries (Tucson, AZ, USA) according to Battelle's specifications based on the pilot-plant work [4-6]. All mixer settlers are constructed of polyvinylchloride and have the same dimensions: mixers (18" x 18" x 16" L x W x H) and settlers (66.5" x 18" x 16"), or 11.08 ft<sup>3</sup>. Each mixing chamber has a 12" diameter impeller attached to a variable speed  $\frac{1}{3}$  hp motor. Mixer tip speed and interface levels were adjusted to minimize entrainments. Flow was counter-current. Strippers were internally recycled. Design feed flow rate was 7 gal/min and the extractant/aqueous (E/A) ratio was 1/6. The raffinate is passed through an oil/water separator prior to discharge. Figure 2 shows the equipment layout, and Figures 3 and 4 show external and internal views of the plant.

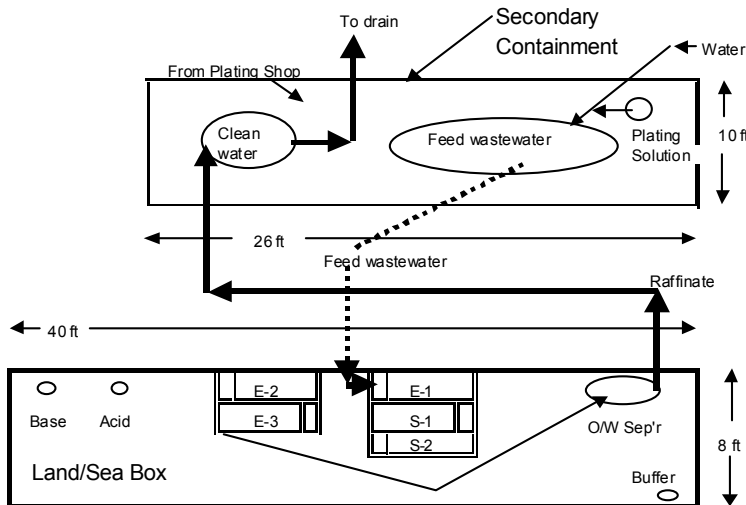


*Figure 2. Equipment layout.*

The commercial unit was constructed with three extraction stages to take advantage of the more favorable economics of higher Cr(VI) concentrations due to the reduced total feed flow rate.

The key process control parameters, which affect acceptability of the LLX technology are:

1. Operability and reliability: As SURFIN shop and IWTP staffing is limited, the need for operator intervention was minimized.
2. Control: For pH control, individual controllers were used to deliver sulfuric acid or sodium hydroxide to E1 and E3 (acid) or to S1 (base). Water was added to S2 for water balance.
3. Extractant losses: Extractant make-up rate is an important economic consideration. An oil/water (o/w) separator was used to capture inadvertent releases of extractant.
4. Concentrate value: The Cr(VI) concentrate needs to be recycled for the objectives of the program to be met. At least one recycler indicates recycling will be attractive.
5. Economic estimates: The pilot testing indicated that payback periods of less than three years with 2-10 mg/l Cr(VI) feed levels, and shorten as the Cr(VI) levels increase and feed flow rate decrease. Full-scale operating information will be used to estimate capital and operating costs compared to conventional treatment.

The demonstration/validation tests were accomplished using the following steps:

1. A Technology Demonstration-Validation Plan [7] was prepared to communicate and guide all aspects of the field testing. It established the objectives, site preparation, operations, sampling, analyses, data collection and analysis, performance criteria, and quality assurance. This plan was reviewed by the host site organizations and site personnel involved in the testing, and covered both general and specific issues.
2. Two field tests were run, one completed and one underway as of mid-May. The first used hard chrome plating bath feed water from WAA and was performed at Battelle (Columbus, OH, USA). The second test site was WR-ALC.
3. Results of the test will be published along with appropriate guidance to assist in the full commercial implementation of the technology, including development and benefit of a standard A-LLX.
4. New permits were not required for commercial scale A-LLX testing. No special exemptions or treatability study exemptions were needed.



Figure 3. Test site photo: tanks and portable box.



Figure 4. Mixer-settlers, chemical feed tanks, surge tanks, and control.

A total of 8 runs were made to assess the viability of the A-LLX process with the WAA feed:

- Runs W-1 to W-5 established process operating conditions;
- Run W-6 determined continuous operation capability;
- Run W-7 examined process chemistry and hardware robustness performance over 20 days 24 h/day test at high Cr(VI) concentrate levels in the strip circuit;
- Run W-8 evaluated the effect of higher feed rate on performance.

Entrainment levels were determined as oil and grease values (US EPA Procedure 413.1). Cr(VI) assays were determined to 10 ppb on location using a Hach, Inc. test kit colorimetric method. Acidity, as pH, was monitored using standard industrial glass electrodes. Operations ran 24 hours per day during each extended run. It is critical that the pH values be controlled at about 3 for the extraction and about 12 for the strip circuit to avoid formation of chromium(III) hydroxide and stabilized emulsions, respectively.

Cr(VI) contaminated feed water was provided by the commercial test sites. For WAA the source was a used hard chrome plating bath {73.3 g total Cr/L [17.4 g/L Cr(VI) and 55.9 g/L Cr(III)]}. This very high Cr(III)/Cr(VI) ratio did not pose a selectivity problem for the A-LLX process. This concentrate was used to prepare Cr(VI) feed for the A-LLX process by diluting with water to make a simulated rinse water with Cr(VI) concentration ranging from 2-20 mg/l.

All acids and bases were of industrial technical grade. The water used in the process was filtered city water from Columbus, Ohio, USA.

## RESULTS

The commercial-scale testing using WAA depot feed processed about 300,000 gallons (4.2 million liters) of feed during the eight runs with the following results:

- Runs W-1 – W-5 established the primary operating conditions; feed rate; E/A flow ratio; stirrer tip speeds; and pH control.
- Run W-6 demonstrated good operability and extraction performance over 5 day 24 h/day test (Figure 5) with excellent Cr(VI) removal, even with variable levels in the Cr(VI) feed water (6-16 mg/l). Table 1 provides the specific run parameters and results.
- Run W-7 demonstrated robustness and consistent performance over 20 days at 24 h/day operation with the strippers at high Cr(VI) concentrate levels (10,000 to 15,000 mg/l) (Table 1 and Figure 6). Very steady operation over the entire period is clearly illustrated. The impact of run conditions on raffinate Cr(VI) residual levels correlate well. Gradual

extractant losses, were made up at day 14. Raffinate entrainment and turbidity levels (Figure 7) were acceptable and similar to W-6.

- Run W-8 evaluated the effect of higher feed flow rate on performance, which was found to be acceptable.

The yellow Cr(VI) color of the feed is removed across the process, giving a clear and colorless raffinate. The raffinate analyzed sufficiently low in Cr(VI) for direct discharge (Table 1).

Entrainment losses were higher than desired but expected based on the water solubility of the protonated extractant. The turbidities were excellent, <7 NTU. It is believed that the extractant is dissolved in the raffinate as the cationic (protonated) species,  $R_3NH^+$ . The fully operational plant may adjust the pH of the raffinate to produce neutral  $R_3N^-$ , which will reduce its water solubility substantially. The IWTP already makes such a pH adjustment.

*Table 1. Results Summary for Runs W-6 and W-7.*

Parameter	Run W-6 Results	Run W-7 Results
Feed	22.7 l/min; 12.8 mg/l Cr(VI)	26.5 l/min; 16 mg/l Cr(VI)
E/A	1/6	1/6
pH	2.7 (E); 12.9 (S)	2.7 (E); 13.4 (S)
Cr(VI) E-1	0.86 mg/l (93%)	1.71 mg/l (89%)
Cr(VI) E-2	0.16 mg/l (84%)	0.40 mg/l (66%)
Cr(VI) E-3	0.11 mg/l (31%)	0.19 mg/l (53%)
Cr(VI) Composite Raffinate (overall % extraction) <sup>a</sup>	0.04 mg/l (99.7%)	0.23 mg/l (98.6%); 0.11 mg/l (99.4%) over days 14-18
Cr(VI) S-1	4000 mg/l (300X concentration)	12,000 mg/l (800X)
Raffinate Entrainment	76 mg/l	119 mg/l

<sup>a</sup> Every 10 minutes, 20.00 ml of raffinate was withdrawn and pumped to a composite tank. After 24 hr, this tank was mixed, sampled and analyzed.

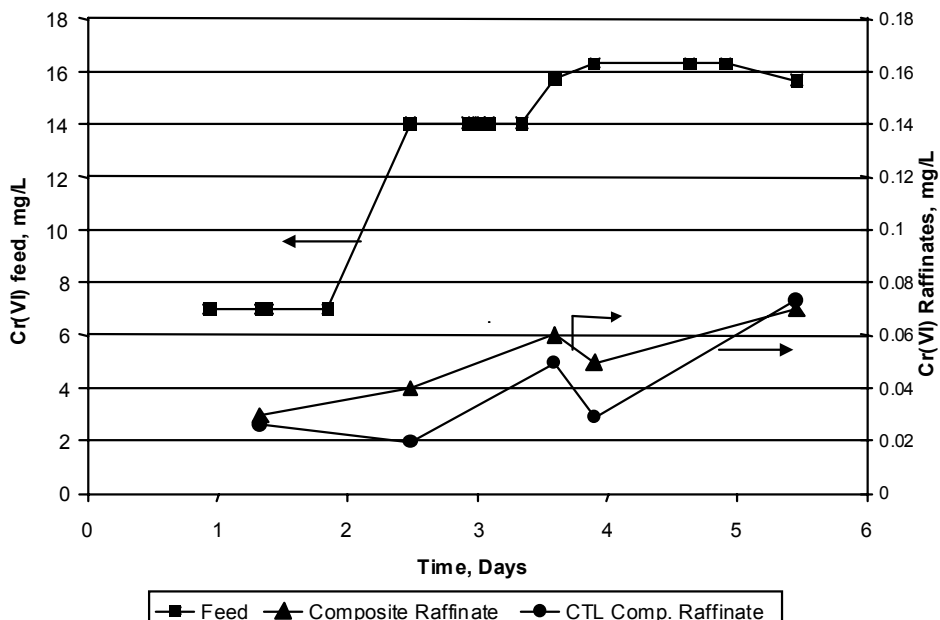


*Figure 5. Results from Run # W-6. Hexavalent chromium [Cr(VI)] in mg/l with run time.*

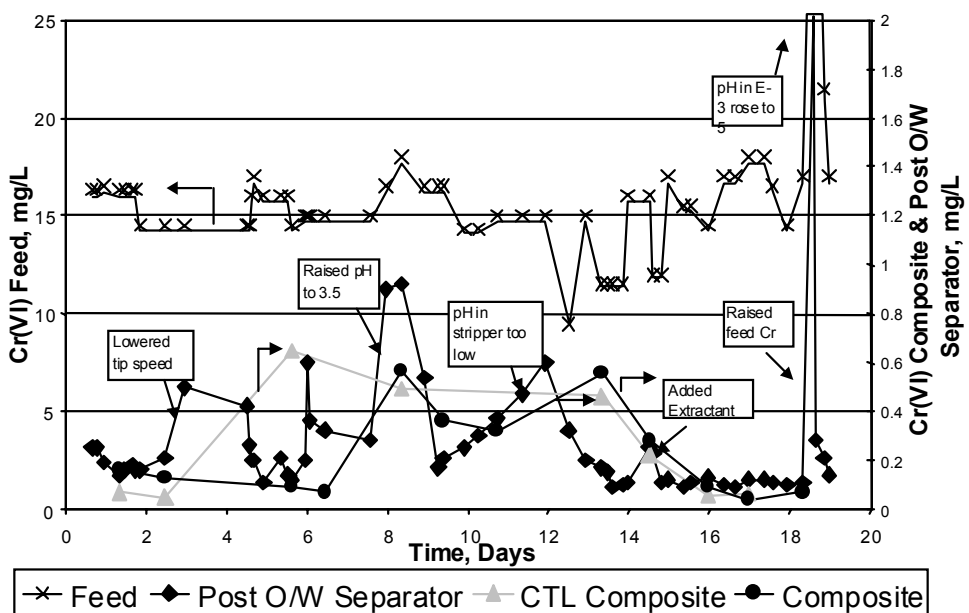


Figure 6. Run W-7: Cr(VI) concentration vs. time.

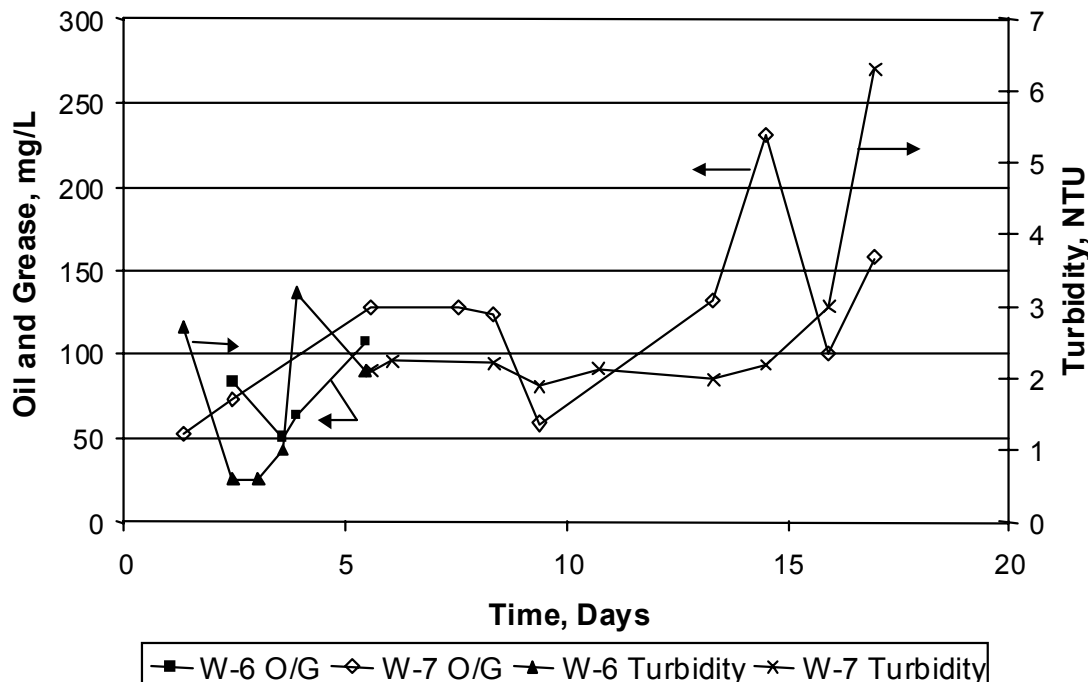


Figure 7. Entrainment losses (as oil and grease analysis), and raffinate clarity vs. time.

Figure 8 shows the clear yellow concentrated Cr(VI) product solution. The 10,000-20,000 mg/l Cr(VI) concentration is acceptable feedstock for production of Cr(VI)-based chemicals. Seven 208-liter drums of this material were produced for recycle process demonstration. Samples have been submitted to the recycler for evaluation.

As expected due to the low ionic strength of the feed water, the extractant phase picked up a fine aqueous emulsion giving it a turbid coloration, though the phases broke adequately and cleared overnight. Hence the o/w separator is beneficial.

## **CONCLUSIONS**

A-LLX was demonstrated to provide excellent Cr(VI) reduction, normally 99%+, and robust removal of Cr(VI) from SURFIN process water at economically attractive flow rates. A high selectivity for Cr(VI) over other contaminants, and the capability to substantially concentrate the Cr(VI) from very dilute feed were demonstrated, making a Cr(VI) product suitable for recycle. Therefore, landfill disposal avoidance is possible.

## **ACKNOWLEDGEMENTS**

The support from the following organizations and persons are gratefully acknowledged. The Air Force Research Laboratory [AFRL] is the lead organization: Capt. Gina Graziano and 1<sup>st</sup> Lt. Larry Cook (AFRL/MLQL) were the project managers. Lt. Joshua Knowles and Mr. Dave Bury of Robins AFB provided applications guidance and are hosting the second (ongoing) field test. Alice Fish of Watervliet Arsenal represented US Army interests and applications and provided the plant field material for the first (completed) field test. We all gratefully acknowledge funding by the US Environmental Security Technology Certification Program (ESTCP).

## **REFERENCES**

1. S. P. Chauhan, D. W. Folsom, P. J. Ucinoswicz and T. L. Tewksberry (1998), *Proc. 3<sup>rd</sup> Annual Joint Service Pollution Prevention Conference and Exhibition*, San Antonio, TX.
2. H. N. Conkle, P. J. Ucinoswicz, and S. P. Chauhan (2000), Contract Summary Report prepared by Battelle for WR-ALC/EM, Contract No. F09603-95-D-0180/D.O. 0080.
3. "Chromium", technical data sheet from Cognis Corporation (Tucson, AZ, USA), commercial supplier of Alamine® 336 liquid-liquid extractant.
4. T. M. Werner, R. D. Litt, S. P. Chauhan, and B. F. Monzyk (1998), *Proc. 3<sup>rd</sup> Annual Joint Services Pollution Prevention Conference and Exhibition*, San Antonio, TX, pp. 72-477.
5. T. M. Werner, S. P. Chauhan, and B. F. Monzyk (1998), *USAF Topical Report*, Contract No. F08637-95-D6003/DO 5300, Battelle.
6. G. M. Graziano, H. N. Conkle, S. P. Chauhan (2000), *Proc. 5<sup>th</sup> Annual Joint Services Pollution Prevention & Hazardous Waste Management Conference and Exhibition*, San Antonio, TX.
7. H. N. Conkle, S. P. Chauhan (2001), Demonstration/Validation Plan for "Removing Chromium(VI) from Wastewater by Anion Liquid Ion Exchange (A-LIX)," Contract No. F08637-00-C-6011, Submitted to ESTCP March 22, 2001.



## OPERATION OF A NDSX PILOT PLANT FOR RECOVERY OF Cr(VI) FROM GROUND WATERS

Inmaculada Ortiz, Berta Galán, David Castañeda and Angel Irabien

Dpto. de Ingeniería Química y Química Inorgánica, Universidad de Cantabria,  
Santander, Spain

This work has focused on the study of the viability of Cr(VI) removal from ground waters and the simultaneous concentration for its reuse in chromate baths. The experimental analysis has been carried out in a non-dispersive solvent extraction pilot plant that incorporated two hollow fibre modules and used Aliquat 336 as the organic carrier and NaCl as the back-extraction agent. Ground waters with a variable concentration of chromium(VI) were pumped, collected in a high volume reservoir and conducted to the pilot plant after dilution. The results of the continuous operation of the pilot plant are reported and compared to predictions using the mathematical model previously reported by the authors.

### INTRODUCTION

Chromium(VI) is a highly toxic metal that is widely used in industrial processes such as electroplating [1,2]. Besides the huge amount of waste waters generated during rinsing steps of metal finishing industries, leaks and deposits of different forms of the metal in the ground, may lead to filtration and transport of the pollutant to ground water sites. This situation needs efficient separation technologies that in the application to effluent treatment minimize the environmental impact of waste water discharges and that can also be used for remediation of ground waters.

The extraction and concentration of Cr(VI) from rinse waters, using hollow fiber membranes and Aliquat 336 as the extractant, has been previously studied by the authors working at a laboratory scale, and the mathematical model and design parameters have been obtained [3-5]. Taking into account the good results obtained at the laboratory level, the scale-up of the process to pilot plant level was achieved and reported previously [6]. In NDSX processes, the main scale-up variable is the mass transfer area [7] that was increased almost 20 times, *i.e.*, from 1.2 m<sup>2</sup> corresponding to laboratory scale to 20 m<sup>2</sup> in the pilot plant set-up. In that work, experimental tests in the NDSX pilot plant were carried out using rinse waters of galvanic processes of a local industry, that contained an average inlet chromium(VI) concentration of 0.064 g/l [6]. These rinse waters were successfully treated in the pilot plant operating in a semi-batch mode, reducing the concentration of chromium in the extraction phase below 5 x 10<sup>-4</sup> g/l, and concentrating the metal in the back-extraction solution. The experimental results were checked against data predicted by the mathematical model previously developed, confirming that the model and the values of the design parameters estimated from laboratory- scale experiments were accurate enough for the description of the separation-concentration process at pilot-plant scale.

In this work, the NDSX pilot plant previously developed has been used for the in-situ remediation of ground waters containing chromium(VI) as main pollutant and having also the objective of chromate concentration in a back-extraction solution.

## EXPERIMENTAL SYSTEM

Table 1 gives the physico-chemical characterization of the ground waters.

*Table 1. Physico-chemical characterization of the ground waters.*

Species	Concentration (mg/l)
$\text{Cr}^{+6}$	700-2000
$\text{Ca}^{+2}$	550
$\text{Al}^{+3}$	60
$\text{SO}_4^{=}$	1750
$\text{Cl}^-$	1200
DQO	170
COT	50

Due to the high content of calcium it was necessary to reduce its concentration ahead of the NDSX process in order to avoid precipitation of calcium sulfate in the hollow fibers. Thus, a cationic ion-exchange column was incorporated to the pilot plant in order to eliminate the presence of  $\text{Ca}^{+2}$  in the feed waters. The cationic ion-exchange column was filled with Lewatit Monoplus S-100 resin.

The plant included also two hollow fibre modules, the main components of the separation process, one for the extraction and the second one for the back-extraction process. The hollow fiber modules were Liqui-Cel Extra-Flow 4"x28" membrane contactors purchased from Hoechst Celanese Corporation [6]. In the modules, the aqueous phases run through the lumen of the hollow fibres and the organic phase flows through the shell side.

Four homogenisation tanks were also necessary: one for the organic phase, one for the feed aqueous phase, and two tanks for the back-extraction aqueous streams. The tank for the organic solution had 90 l capacity and was made of stainless steel. The tanks for the aqueous solutions: feed, back-extraction and purge, had capacities of 5000 l, 100 l and 60 l, respectively, and were made of polyethylene. The aqueous-phase pipes were made of teflon and polypropylene and the organic-phase pipes were made of stainless steel.

Initially, ground waters were stored in 1000 l containers. When necessary, the ground waters were passed through the ion-exchange column and, after calcium removal, they were sent to the extraction homogenisation tank where, if necessary, a dilution process was carried out in order to decrease the initial concentration of chromium(VI) to a value of around 1 g/l. The feed solution was then filtered through a sand filter to remove remaining suspended solids and passed through a 10  $\mu\text{m}$  filter before entering the modules to prevent fouling in the hollow fibres. The feed ground waters flowed through the extraction module in a continuous mode.

The organic solution was a mixture of Aliquat 336 (0.6 M), and isodecanol and kerosene that were used as modifier and diluent, respectively. The organic phase coming out of the extraction module was sent to the back-extraction module to accomplish two different objectives: i) concentration of the removed chromium, and ii) regeneration of the organic phase.

In the back-extraction module, chromium was transported from the organic solution to the BEX solution ( $\text{NaCl}$ , 1 M) that flowed to the storage tank. A continuous purge was applied to the tank receiving the concentrated chromate solution and the tank volume was kept constant by continuous addition of fresh BEX solution.

Hollow fibre modules were thermostatized, working at a temperature of 40°C (the maximum temperature allowed by the fibres). Three heater systems were included in the plant. An on-line system for pipes and tubes and electrical resistances were placed inside the organic and BEX tanks. Due to the hydrophobic nature of the fibres, the pressure of the aqueous phase was maintained higher than the pressure of the organic phase, ensuring that no displacement of the organic phase from the pores of the hollow fibres took place. The working differential pressure between phases was 2.5 psi.

Samples were taken out at the module outlet or in the aqueous tanks and prepared for analysis. The concentration of Cr(VI) in the feed and stripping solutions was measured in a Lange LP2W photometer.

## RESULTS AND DISCUSSION

Two different tests were carried out in the pilot plant: i) analysis of the viability of chromium concentration in the back-extraction solution up to a level that would allow reuse of the compound in chromate baths, and ii) analysis of the stability of the plant at long working times.

The first experiment was carried out working in a semicontinuous mode, *i.e.*, ground waters flowed continuously, but the organic and back-extraction solutions flowed in a recycling mode. The experiment was run for 170 hours until a concentration of 20 g/l was reached; this value was considered acceptable by the chromate salts industry.

Figure 1 shows the results of this first experiment and Table 2 shows the experimental conditions. It is observed that the concentration of Cr(V) in the back-extraction solution increased with time and reached a value around 20 g/l at 170 hours. The resulting solution was analysed by a local industry that used chromate baths, confirming its suitability.

*Table 2. Experimental conditions of experiments I and II.*

		Experiment I	Experiment II
Ground waters	Cr (VI) conc. (g/l)	0.78	0.60 → 0.8
	Cl <sup>-</sup> conc. (g/l)	0.45	0.45 → 1.2
	Ca conc. (g/l)	0.04	0.04 → 0.2
	Flow rate (l/h)	60	60
	pH	7.5	9 → 10
BEX solution	CINa conc. (g/l)	35	35 → 38
	pH	7.5	10 → 11

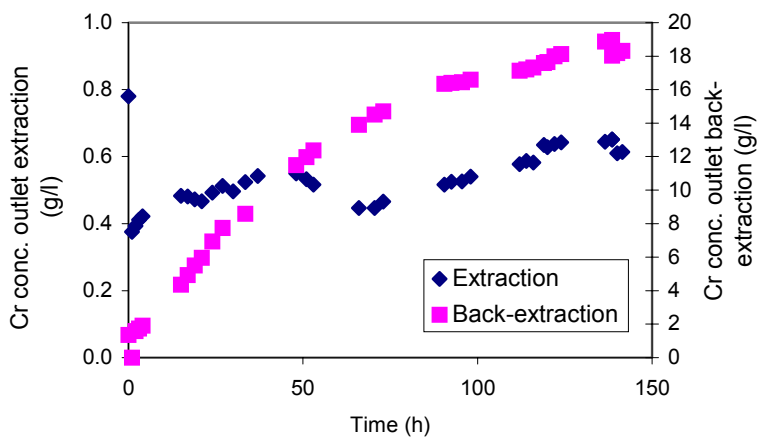


Figure 1. Extraction and back-extraction evolution of experiment I.

Once the viability of chromium concentration had been checked, the following experiment focused on the analysis of the stability of the system. Figure 2 represents the evolution of the Cr(VI) concentration in the extraction and back-extraction solutions with time.

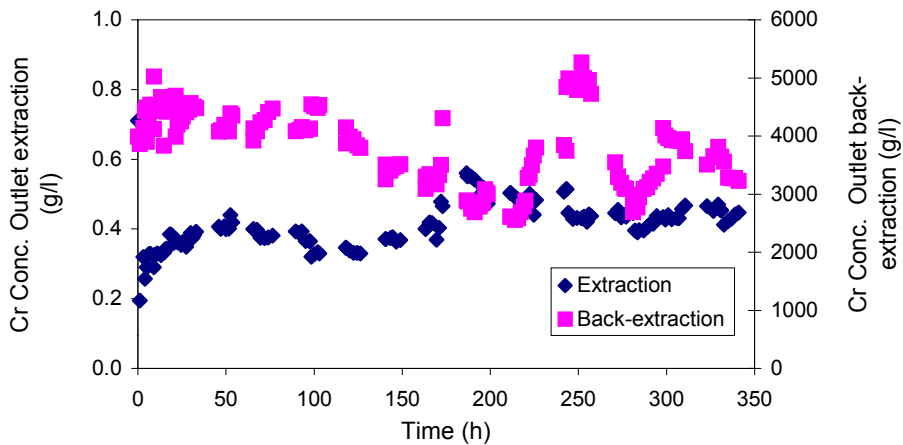


Figure 2. Extraction and back-extraction evolution in experiment II.

It is observed that the average outlet concentration of Cr(VI) in the extraction process is around 0.4 to 0.45 g/l, and the average outlet concentration in the back-extraction solution is around 4 g/l.

In both experiments, the outlet concentration of chromium in the extraction module was too high to consider that the ground waters were clean enough. Thus, further reduction of chromium concentration would be needed and would require either to flow the feed solution at lower flow rates or to carry out a second NDSX step. Both possibilities have been analysed in this work through simulation tasks. The mathematical model used in order to describe NDSX processes consisted of six nonlinear partial differential equations describing the mass transport through the membrane modules and two algebraic equations describing the equilibrium reactions. The mathematical model required also the knowledge of three characteristic parameters, two chemical equilibrium parameters of the interfacial reactions and the membrane mass transport coefficient [6]. The incorporation of additional NDSX steps required duplication of the number of differential equations but the design parameters remained the same.

After incorporation of a second NDSX step a new separation process was defined with the following steps:

- i. *Ion exchange with cationic resin Lewatit Monoplus S-100*, in order to reduce the concentration of  $\text{Ca}^{2+}$  to avoid precipitation of calcium salts in the porous hollow fiber membranes. Regeneration was carried out with NaOH.
- ii. *First NDSX step*, that incorporates two membrane modules: one for the extraction and a second one for the back-extraction process. Ground waters flow continuously from the ion-xchange column to the extraction module and then towards the third step. The organic phase circulates in a recycling mode from the extraction module to the back-extraction module. In the BEX tank a purge stream takes out the concentrated solution and the volume is kept constant by feeding fresh back-extraction solution. In the first NDSX step, a reduction of  $\text{Cr}^{+6}$  concentration below 50% of the initial value is searched whereas the stripping phase works with a concentration of 20 g/l.
- iii. *Second NDSX step*, that incorporates also one module for the extraction and a second one for the back-extraction. Ground waters come from the first NDSX step. The organic and the stripping phases work in a similar manner to the first step but the concentration of the BEX solution is kept at a lower value equal to 4 g/l. The concentration of  $\text{Cr}^{+6}$  is reduced to less than 0.1 g/l. The temperature of both NDSX steps was kept constant at 40 °C.

Figure 3 represents the flow sheet diagram of the analysed process.

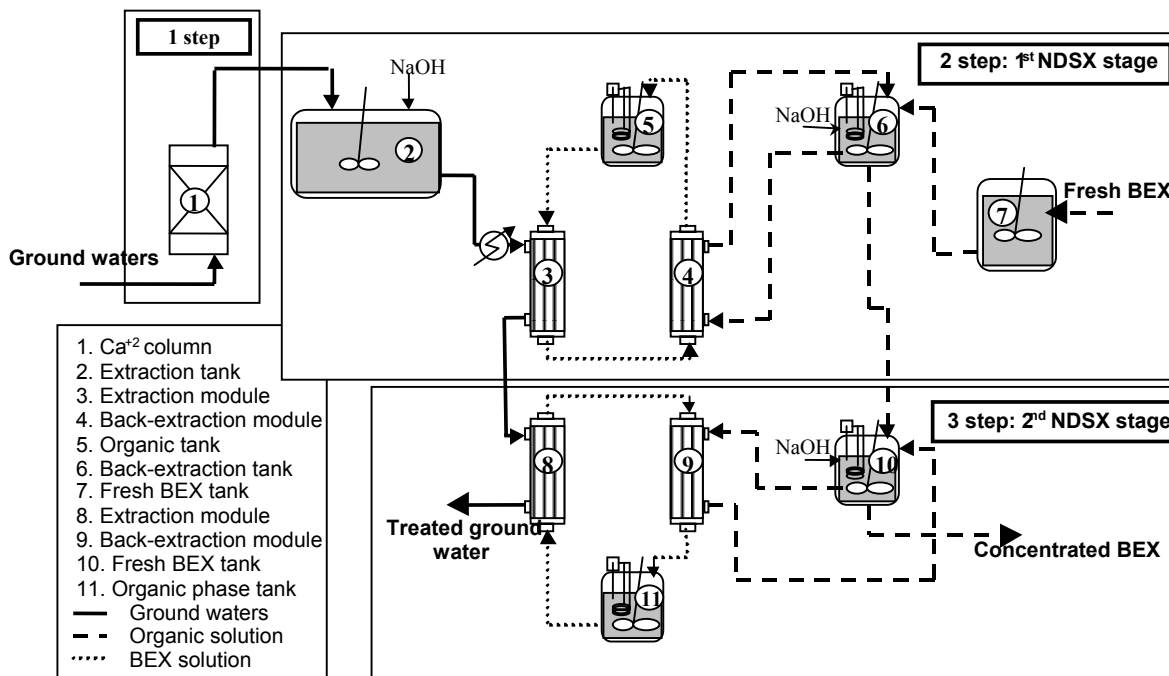


Figure 3. Flow sheet diagram of the separation process.

A sensitivity analysis of the process concentrations to the feed flow rate was performed. Table 3 reports a summary of the results obtained.

*Table 3a. Inlet and outlet conditions of the integrated process.*

Ground waters	Cr (VI) conc. (g/l) Cl <sup>-</sup> conc. (g/l) Ca <sup>2+</sup> conc. (g/l)	0.7 0.45 0.04
1 step NDSX	BEX conc. (g/l) pH	20 10.5
2 step NDSX	BEX conc. (g/l) pH	4.0 10.5

*Table 3b. Sensitivity of the concentration results to feed flow rate.*

Flow rate (l/h)	60	40	30	20	10	5
1 stage NDSX outlet conc. (g/l)	0.439	0.3339	0.259	0.156	0.072	0.050
2 stage NDSX outlet conc. (g/l)	0.231	0.1111	0.053	0.018	0.005	0.002

## CONCLUSIONS

In this work the theoretical and experimental analysis of the behaviour of a non-dispersive extraction process at pilot-plant scale has been carried out in the application to the separation and concentration of hexavalent chromium contained in ground waters.

The experimental tests working with different initial conditions checked the stability of the membrane process for times of 350 hours. Taking into account the experimental results and in order to achieve two main separation objectives, *i.e.*, cleaning of ground waters reducing the concentration of chromium and at the same time concentration of the metal in the back-extraction phase up to a level that enables reuse in chromate baths (20 g/l), an integrated process with three different steps has been defined. The sensitivity of the integrated process to changes in the feed flow rate has been analysed using the mathematical model and parameters obtained in a previous work at laboratory scale; this task was carried out working with gPROMS process software. Further work will include optimisation of the operation variables and optimum process design.

## ACKNOWLEDGEMENTS

This work has been financially supported by project 1FD97-2193.

## REFERENCES

1. H. H. Guyer (1989), *Industrial Processes and Waste Stream Management*, John Wiley, New York.
2. A. K. Guha, C. H. Yun, R. Basu, and K. K. Sirkar (1994), *AIChE J.*, **40**, 1223.
3. M. I. Ortiz, B. Galán, and A. Irabien (1996), *Ind. Eng. Chem. Res.*, **35**, 1369.
4. A. I. Alonso, B. Galán, M. I. Ortiz, and A. Irabien (1997), *Sep. Sci. Tech.*, **32** (9), 1543-1555.
5. I. Ortiz, B. Galan, and A. Irabien (1996), *J. Membr. Sci.*, **31**, 46.
6. A. I. Alonso, B. Galán, M. González, and M. I. Ortiz (1999), *Ind. Eng. Chem. Res.*, **38**, 1666.
7. A. F. Seibert and J. R. Fair (1997), *Sep. Sci. Tech.*, **32** (1-4), 573.



## SCREENING OF REAGENTS FOR RECOVERY OF ZINC(II) FROM HYDROCHLORIC ACID SPENT PICKLING SOLUTIONS

Magdalena Regel-Rosocka, Ireneusz Miesiac, Ana Maria Sastre\* and Jan Szymanowski

Institute of Chemical Technology and Engineering, Poznan University of Technology,  
Poznan, Poland

\*Departament d'Enginyeria Quimica, Universitat Politècnica de Catalunya, E.T.S.E.I.B.,  
Barcelona, Spain

The extraction of zinc and iron ions, water and hydrochloric acid was studied. The extraction studies permitted to select tributyl phosphate as the most convenient reagent. Due to a high transfer of hydrochloric acid, amines were not convenient for the extraction of zinc(II) from solutions containing below 5% HCl. Moreover, the HOE® F2562 caused relatively high oxidation of Fe(II) to Fe(III). Such oxidation was also observed when ALAMINE® 336, ALIQUAT® 336 and CYANEX® 923 were used. Bulk liquid membrane experiments supported the conclusions from extraction studies demonstrating a good extraction performance of tributyl phosphate.

### INTRODUCTION

Zinc protective layers are commonly used today to protect steel goods from corrosion. Zinc layers are deposited by immersing steel goods in molten zinc at about 450°C. Good quality zinc layers need appropriate pre-treatment of surface, including washing, degreasing, removal of rust and fluxing. 20% hydrochloric acid solution is usually used for pickling carried out at room temperature. Zinc accumulates also in the pickling solution. In the batch process steel goods are hang on hooks on which zinc is also deposited. The hooks are used again and zinc dissolves in the hydrochloric acid. Such a solution contains only few g/L Zn(II) or even less. Spent pickling solutions are also used to deplete zinc layers of insufficient quality. In such a case, the concentration of zinc(II) in the spent solution may increase to few tens g/L.

Only spent pickling solution containing less than 0.5 g/L Zn(II) is processed by Ruthner process in which the hydrochloric acid is evaporated and granules of iron oxide are formed in fluidised bed at temperature above 600°C. Therefore the spent pickling solution is often neutralised with lime and disposed to the environment together with toxic zinc ions.

Solvent extraction [1-7] can be used to remove toxic zinc(II) from spent pickling solutions. The use of various extractants was proposed but detailed studies have not been published. The aim of this work was to screen various reagents and to perform more detailed studies with selected extractants. Taking into account high concentrations both of proton and chloride ions, the studies were narrowed to selected solvating (tributyl phosphate and trialkylphosphine oxides) and basic extractants (tri- and dialkylamines and quaternary ammonium salts). The selection of reagents was narrowed to industrial extractants that could be used in practice.

## EXPERIMENTAL

The following reagents were used as extractants:  
tributyl phosphate (TBP), Hoechst, Germany,  
HOE® F2562 (diisotridecylamine), Hoechst, Germany,  
ALAMINE® 304 (tridodecylamine), Cognis, Germany,  
ALAMINE® 308 (triisooctylamine), Cognis, Germany,  
ALAMINE® 310 (triisododecylamine), Cognis, Germany,  
ALAMINE® 336 (trialkylamine, C<sub>8</sub>:C<sub>10</sub> = 2:1), Cognis, Germany,  
CYANEX® 923 (trialkylphosphine oxides), CYTEC, Canada,  
CYANEX® 925 (trialkylphosphine oxides), CYTEC, Canada,  
CYANEX® 302 (trialkylmonothiophosphinic acid), CYTEC, Canada,  
triisoctylamine, Windsor Laboratories Limited, UK,  
AMBERLITE LA-2 (N-dodecyl-N-trialkylmethylamine), Fluka, Germany,  
and ALIQUAT® 336 (trialkylmethylammonium chloride, C<sub>8</sub>:C<sub>10</sub> = 2:1), Cognis, Germany.  
Decanol was used as a modifier and low aromatic kerosene Exxsol D220/230, Deutsche  
Exxon Chemical GmbH, ESSO A.G. (Germany) as a diluent.

Extraction was carried out at room temperature using 1:1 phase volume ratio. Water was usually used for stripping. A double Lewis cell described in the previous paper [8] was also used to check the performance of reagents in membrane processes. The aqueous phase contained various amounts of zinc(II), iron(II) and iron(III). The concentration of hydrochloric acid was adjusted to 1.8 or 10%, and the chloride concentration was usually constant and equal to 5 M. Analytical procedures were described in the previous paper [7].

## RESULTS AND DISCUSSION

### Classical Extraction

The screening tests in which the aqueous feed contained simultaneously Zn(II), Fe(II) and Fe(III) showed that ALAMINE® 304, ALAMINE® 308 and ALAMINE® 310 were not useful because a precipitation occurred or strong emulsions were formed. It also concerned ALIQUAT® 336, although high extractions both of Zn(II) and Fe(II) were observed. An emulsion was also formed when CYANEX® 923 was used and aqueous phase contained 10% HCl. TBP and ALAMINE® 336 extracted iron(III) very strongly. Dialkylamine (HOE F2562 and AMBERLITE® LA-2) extracted less iron(III) than trialkylamine and tributyl phosphate. Extraction isotherms for zinc(II) and iron(III) extraction given in Figures. 1 and 2 indicated high extraction abilities of the considered amines and trialkylphosphine oxides. TBP was a weak extractant when used in kerosene. However, the reagent could be used without dilution and highly loaded both with zinc(II) and iron(III). CYANEX® 302, being an acidic extractant, extracted only small amounts of Zn(II) and Fe(III) and was not used in further studies.

The results indicated that iron(III) had to be reduced to iron(II) prior to extraction. It could be achieved by depletion of bad quality zinc layers. The presence of iron(II) did not disturb the extraction of zinc(II) with TBP and amine extractants. However, some co-extraction of iron(II) was observed. The co-extraction was strong for CYANEX reagents (Figure. 3). It could be explained by the oxidation of iron(II) to iron(III) and/or the transfer of iron(II) to the organic phase together with water, e.g. in the form of reverse micelles. The latter phenomenon seemed important when undiluted or highly concentrated TBP was used. The organic phase contained about 7% of water after extraction-stripping process. The hypothesis was supported by the presence of iron(II) in the aqueous solution phase after stripping with water. The oxidation of iron(II) seemed very important in the case of trialkylphosphine oxides. It was reported that some species, including hydrophosphate and some metal cations catalyse the oxidation [9].

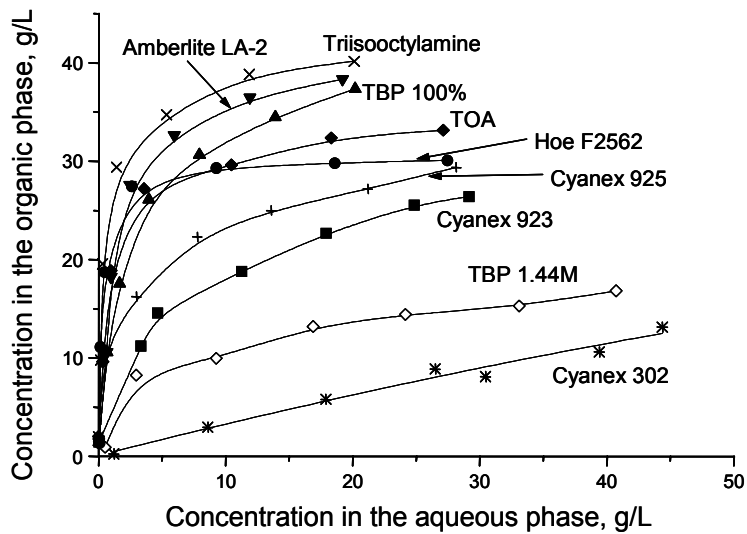


Figure. 1. Isotherms of zinc(II) extraction from 10% HCl with 1.44 M extractant solutions.

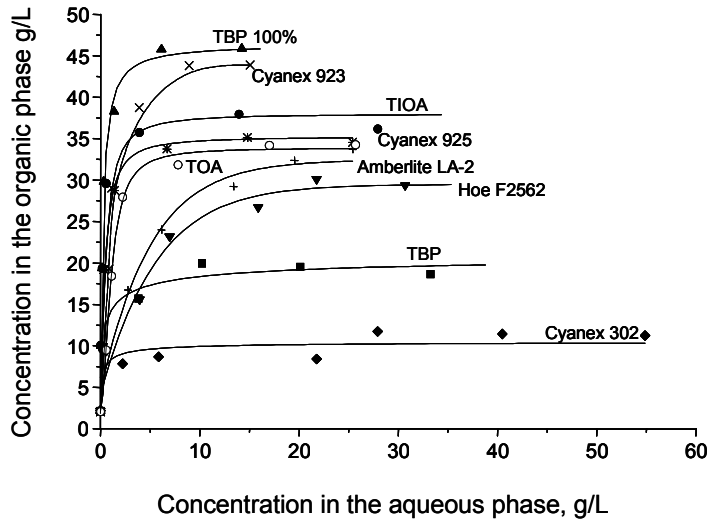


Figure. 2. Isotherms of iron(III) extraction from 10% HCl with 1.44 M extractant solutions.

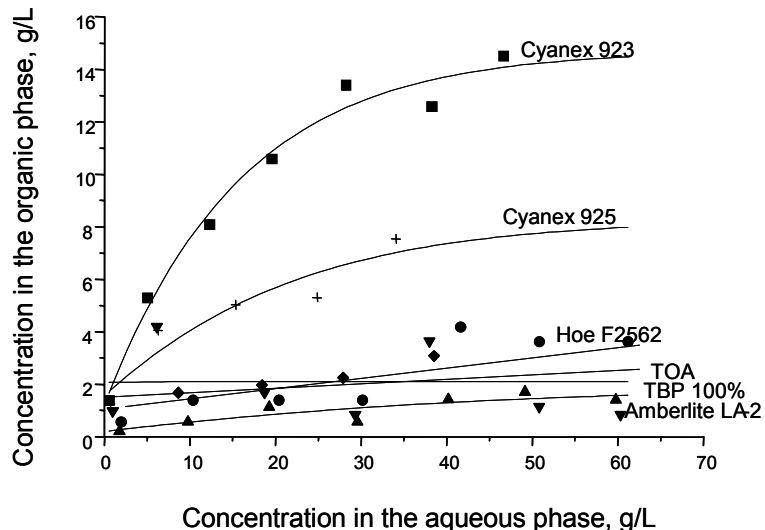


Figure. 3. Isotherms of iron(II) extraction from 10% HCl with 1.44 M extractant solutions.

The effective extraction of metal species from the aqueous feed had to be followed by effective stripping. The results shown in Table 1 indicated that both zinc(II) and iron(II) could be effectively stripped from the loaded TBP. Three stages were necessary. However, zinc(II) was inefficiently stripped from CYANEX® 923 and ALAMINE® 336. The efficiency of iron(III) stripping depended on HCl concentration and was higher for initial aqueous feed containing 10% HCl. Higher stripping of zinc(II) was achieved from HOE® F2562 and AMBERLITE® LA-2. However, the process was less effective than from loaded TBP.

The extraction and stripping experiments permitted to select TBP as the most appropriate extractant. The secondary amines could be also used.

*Table 1. Stripping of zinc(II) and iron from loaded organic phases with water in three stages (loaded zinc(II), app. 5 g/L).*

Reagent	%S <sup>Zn</sup>	%S <sup>Fe</sup>
TBP 100%	98.0	98.4
1.44 M CYANEX 923	5.4 15.5*	50.1** 42.7***
1.44 M ALAMINE 336	4.9 12.5*	70.3** 38.6***
30% ALAMINE LA-2	84.8	5.3
30% HOE F2562	100.0	7.7

\*diluted organic phase contained over 10 g/L iron ions

\*\*10% HCl in the aqueous feed

\*\*\*1.8% HCl in the aqueous feed

### Membrane Extraction

The bulk membrane experiments showed that only TBP could be used as a carrier (Figure 4). However, a great accumulation of zinc(II) in the membrane phase was observed. Maximum of zinc(II) concentration in the strip was observed. It was caused by a strong co-extraction of hydrochloric acid and back-transfer of zinc(II) from the strip phase to the membrane. That atypical phenomenon was caused by a competition of zinc(II) and hydrochloric acid transfer. The HCl content in the strip phase increased monotonically with time and achieved 0.5 M after 90 minutes. That concentration was high enough to stop further transfer of zinc(II) to the strip. Moreover, the back extraction of zinc(II) from the strip to the membrane was observed after 110 minutes. The transfer of water to the membrane phase also occurred and at the end of the process the content of water in TBP was 6.5-8.1% depending on zinc(II) concentration in the feed. The problem was overcome when the hydrochloric acid in the aqueous strip was neutralised. The transfer of zinc(II) and HCl from the aqueous feed to the strip phase depended on the concentration of chloride ions. An increase of the Cl<sup>-</sup> concentration affected positively the extraction of zinc(II) but negatively the stripping.

It was also possible to use AMBERLITE® LA-2 (Figure. 5) but as in the case of TBP zinc(II) accumulated in the membrane phase and its transfer to the aqueous phase was slow.

HOE® F2562 extracted only small amounts of zinc(II) to the membrane phase and transferred negligible amounts to the strip. The transfer was retarded by the interfacial phase, which could be clearly observed. Thus, the reagent showing good extraction performance was not suitable for the membrane process.

The experiments permitted to select TBP and AMBERLITE® LA-2 as appropriate extractants/carriers.

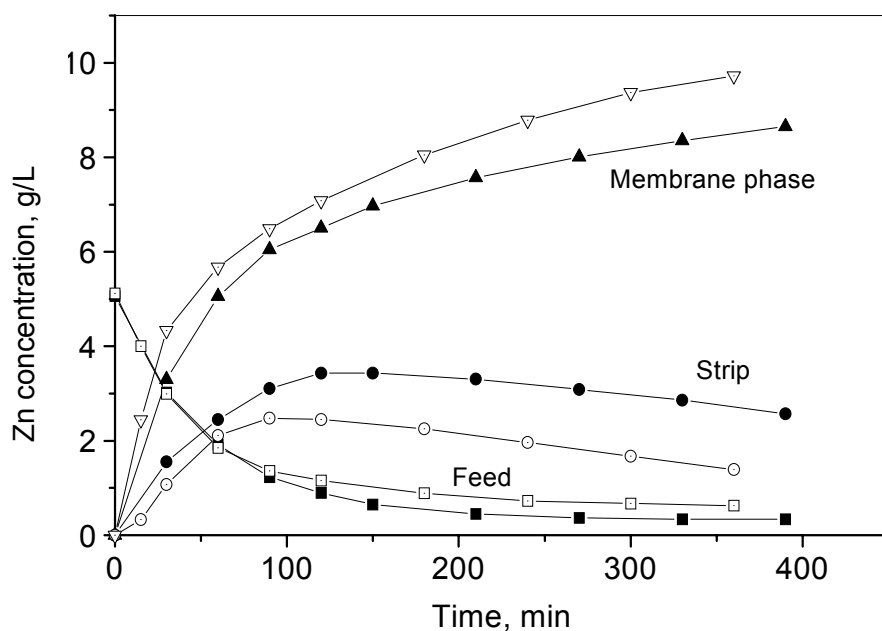


Figure. 4. Extraction-stripping of zinc(II) by TBP (undiluted) in bulk liquid membrane process (aqueous feed: 5 g/L Zn(II) and 10% HCl, chloride concentration: 3.40 M (full points) and 5.00 M (empty points), squares – feed, triangles – membrane and circles – strip).

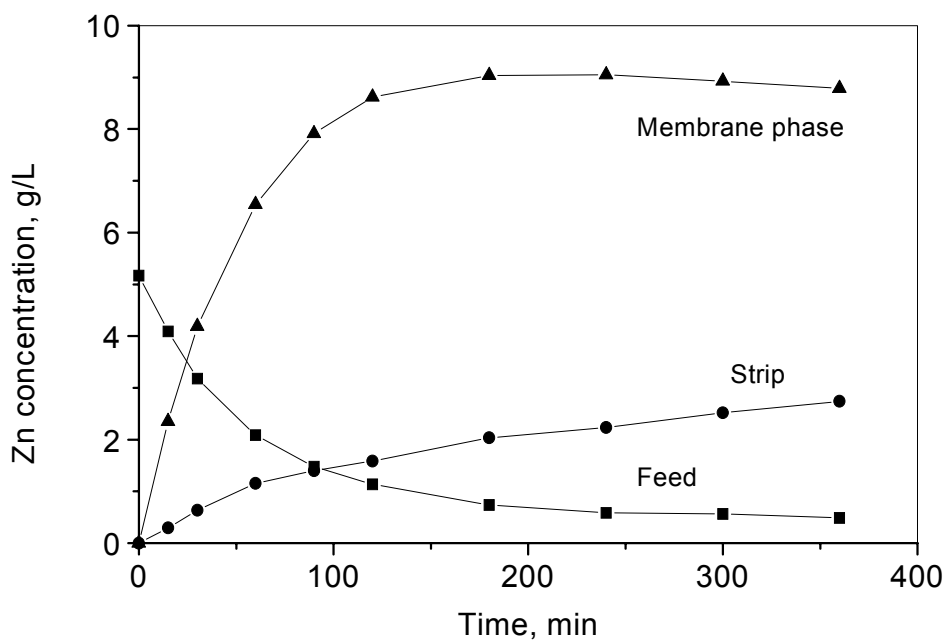


Figure. 5. Extraction-stripping of zinc(II) by 1.44 M AMBERLITE® LA-2 in bulk liquid membrane process (aqueous feed: 5 g/L Zn(II) and 10% HCl, chloride concentration: 3.40 M).

## ACKNOWLEDGEMENT

The work was supported by the NATO grant Science for Peace SfP 972398 Hydrochloric Acid.

## REFERENCES

1. F. J. Alguacil, A. Cobo and C. Caravaca (1992), *Hydrometallurgy*, **31**, 163-174.
2. V. M. P. Forrest, D. Scargill and D. R. Spichernell (1969), *J. Inorg. Nucl. Chem.*, **31**, 187-197.
3. T. Sato (1965), *J. Appl. Chem.*, **15**, 10-16.
4. K. Schuegerl, A. Larm and M. Gudorf (1996), *Proc. ISEC '96*, Vol. 2, University of Melbourne Press, Melbourne, pp. 1543-1547.
5. D. C. F. Morris and E. L. Short (1962), *J. Chem. Soc.*, 2662-2671.
6. W. W. Schulz, J. D. Navratil and T. Bess (1987), *Science and Technology of Tributyl Phosphate*, Vol. 2, CRC Press Inc., Fl.
7. M. Regel, A. M. Sastre and J. Szymanowski (2001), *Envir. Sci. Technol.*, **35**, 630-635.
8. W. Cichy, S. Schlosser and J. Szymanowski, *Solvent Extr. Ion Exch.* (in press).
9. W. Stumm and J. J. Morgan (1981), *Aquatic Chemistry – An Introduction Emphasizing Chemical Equilibria in Natural Waters*, 2nd edn., John Wiley & Sons, New York, Chap. 7.6.



## A CONTINUOUS SOLVENT EXTRACTION PROCESS FOR REFINING OF PICKLING BATHS

L. Caron, D. Pareau, M. Stambouli and G. Durand

Laboratoire de Chimie et Génie des Procédés, Ecole Centrale Paris,  
Chatenay-Malabry Cedex, France

A process flowsheet for the elimination of copper contained in sulphuric acid pickling baths of steel pieces has been developed. A preliminary study of solvent extraction options has lead to the choice of a suitable extracting system containing both Cyanex 302 and LIX 860. With this extractant mixture, copper is quantitatively and selectively extracted in a few minutes. The stripping step has been optimised with the use of thiourea as stripping agent. A regeneration step of the extractant is necessary because of the degradation of Cyanex 302. The feasibility of copper deposition from the strip solution has been demonstrated. A continuous micro-pilot scale test has been performed with good results (constant and low copper concentration in the pickling bath and electrowinning of copper) and a model has been developed for the design of the industrial process.

### INTRODUCTION

After use the pickling baths of interest in this study contain sulphuric acid (2 mol/L), iron (Fe(II) for the major part) and traces of other metals such as copper that can cause problems in the pickling process. These baths must be changed periodically, leading to the loss of residual acid and the formation of sludges. The development of a process that would allow better utilization of the baths by maintaining the copper concentration constant is therefore of interest and forms the subject of this paper.

### SOLVENT EXTRACTION OF COPPER

Oximes are well known extractants for copper, but they usually have a low efficiency in acid solutions. Salicylaldoximes on the contrary offer more promise: LIX 860 ( 5-salicylaldoxime) is able to extract copper by chelation in sulphuric acid [1,2]. The extractant is selective for copper over iron(III) and iron(II) [3,4,5].

Among the organophosphoric extractants, only thiophosphoric agents extract copper at high acidity. Tait [6] and Sole [7] confirmed the copper extraction efficiency of Cyanex 301 and 302 (bis 2,4,4-trimethylpentylidithiophosphinic acid and bis 2,4,4-trimethylpentylmonothiophosphinic acid, respectively). While iron(III) is also slightly extracted, iron(II) is not extracted at all. Copper stripping is however very difficult.

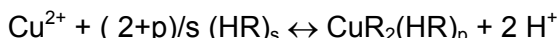
Laboratory batch experiments were then performed using these extractants to identify a suitable extractant system for further continuous test work.

## Experimental

Aqueous and organic phases were contacted in an agitated vessel at a constant temperature (varying from 25 to 80°C, because industrial baths operate at 60-70°C). The aqueous solutions contained 2 mol/L sulphuric acid, 5 to 100 mg/L copper and 1.5 g/L iron(III) (Prolabo reagents). Iron(II) being not extracted at all was not used in these batch laboratory experiments. LIX 860 (Henkel) and both Cyanex (Cyanamid) reagents were diluted in dodecane (Prolabo). Iron and copper were analysed by atomic absorption spectrometry (Varian AA 300).

### Copper Extraction with LIX 860

The extraction can be represented by the following equation:



where s is the aggregation number of LIX 860 (HR).

The concentration of copper has no influence on its distribution ratio D: so the extracted complex contains only one atom of copper. The extraction efficiency is however rather low: D is about 0.5 for 0.5 mol/L LIX 860 and 2 mol/L H<sub>2</sub>SO<sub>4</sub>.

The concentration of LIX 860 was varied between 0.1 and 1.6 mol/L; the major form of the oxime under these conditions is the dimer [1,2]. In addition the sulphuric acid concentration was varied from 1 to 4 mol/L. The results are presented in Figure 1, where ln D/[H<sup>+</sup>]<sup>2</sup> is plotted versus ln [(HR)<sub>2</sub>]. A straight line is obtained with a slope 1.1; then (2+p)/s = 1 and as s = 2, p = 0. The extracted complex is therefore CuR<sub>2</sub>.

The selectivity for copper over iron is quite good; under the same conditions the distribution ratio of iron is indeed lower than 0.007.

Despite its good selectivity LIX 860 is not efficient enough to extract copper quantitatively.

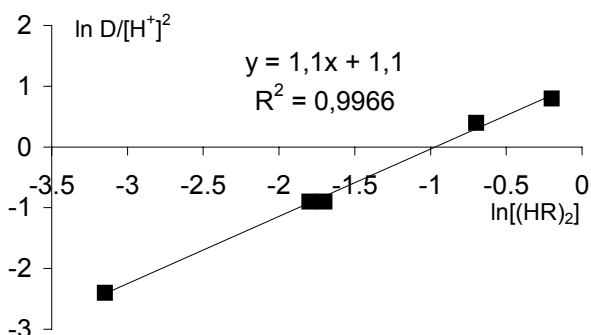


Figure 1. Determination of the extracted complex stoichiometry for the LIX 860/Cu system.

### Copper Extraction with Cyanex 301

At room temperature copper is quantitatively extracted in less than 30 seconds when Cyanex 301 is in excess over Cu. Solution conditions tested were: 48 mg/L Cu, 1500 mg/L Fe(III), 2 mol/L H<sub>2</sub>SO<sub>4</sub> and 0.076 mol/L Cyanex 301. Iron (III) extraction is both low and slow: only 30 mg/L is extracted in 3 hours.

The variation of temperature has no effect on these results; between 40 and 80°C, copper is quantitatively extracted in 10 minutes along with less than 0.2 mg/L Fe(III) (for 0.076 mol/L Cyanex 301).

Cyanex 301 is clearly an excellent extractant for copper in the presence of iron.

The stripping is however very difficult; the only possible solution is a mixture of thiourea and sulphuric acid. Many other stripping solutions were tested without success [8]. The concentrations of both reagents were varied and the results are given in Table 1 (10 minutes contact time, 0.076 mol/L Cyanex 301).

*Table 1. Influence of thiourea and sulphuric acid concentrations on copper stripping from Cyanex 301.*

H <sub>2</sub> SO <sub>4</sub> , mol/L	0	0.5	1	2	1	1	1	1
Thiourea, mol/L	0.1	0.1	0.1	0.1	0.2	0.3	0.4	0.5
Stripping, %	<1	11	21	33	82	88	90	97

Copper stripping is therefore possible provided thiourea and sulphuric acid are present in sufficient concentration.

### **Copper Extraction with Cyanex 302**

Like with Cyanex 301 the extraction of copper is quantitative, but much slower. To reach 90% extraction, 17 and 48 minutes are needed for 0.074 and 0.028 mol/L Cyanex 302, respectively. By comparison quantitative extraction is achieved in 3 minutes for 0.076 mol/L Cyanex 301.

By plotting  $\ln C/C_0$  versus time, where C and  $C_0$  are the copper concentrations at t and t = 0, straight lines were obtained, confirming that the limiting reaction is first order with respect to the metal. The slope p of these straight lines show linear dependence to Cyanex 302 concentration. The reaction is therefore first order with respect to Cyanex 302.

Efficient copper stripping is achieved for the same strip solution mixtures that proved efficient for Cyanex 301.

### **Degradation of Cyanex 301 and Cyanex 302**

Both molecules are oxidised into disulfide by contact with the aqueous solution. The rate of degradation is greater for Cyanex 301 than for Cyanex 302 (8 days compared to 40 days); Cyanex 302 was therefore selected for further study. The degradation product is a disulfide having poor extracting properties. This degradation is however reversible by contacting degraded organic solution with reducing agents such as hydrogen, nickel, iron or zinc [9].

### **Copper Recovery with Mixtures of Cyanex 302 and LIX 860**

LIX 860 extracts copper quickly, but poorly. On the contrary Cyanex 302 extracts it quantitatively, but slowly. By mixing both extractants, a rapid and quantitative extraction may be expected, as tested below.

#### **Copper extraction**

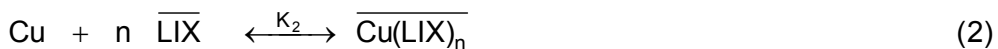
A positive effect on the extraction kinetics was observed in preliminary experiments, copper was quantitatively extracted as for Cyanex 302, but the extraction is quicker. A kinetic study was performed in an agitated vessel (stirrer speed - 1500 rpm). For each experiment  $\ln C/C_0$  was plotted versus time, resulting in a straight line (slope -p). Several chemical parameters were varied and their influence on p was studied. The results are given in Table 2.

Table 2. Influence of LIX 860 and Cyanex 302 concentration on  $p$  at 70°C.

LIX 860 mol/L	0	0.025	0.050	0.150	0.250	0.150	0.150	0.150
Cyanex 302 mol/L	0.028	0.028	0.028	0.028	0.028	0.038	0.052	0.080
$p$ min <sup>-1</sup>	0.06	0.10	0.15	0.32	0.54	0.20	0.28	0.41

$p$  is proportional to the LIX 860 concentration when the Cyanex 302 concentration is constant ( $r^2 = 0.997$ ).

A reaction scheme is proposed with three reactions: the first is the first order reaction observed for Cyanex 302, the second, the rapid extraction equilibrium of copper by LIX 860 and the third, the substitution in the extracted complex, of LIX 860 by Cyanex 302.



$k_1$  and  $k_3$  are the kinetic constants of (1) and (3) and  $K_{2\text{is}}$  the equilibrium constant of (2).

The reaction rate can be written as:

$$r = k_1 [\text{Cx}] [\text{Cu}] + k_3 K_2 [\text{Cu}] [\text{LIX}]^n [\text{Cx}]^m,$$

$r$  being the copper quantity extracted by volume and time unities.  $p$  is then proportional to  $[\text{Cx}] \{ k_1 + k_3 K_2 [\text{LIX}]^n [\text{Cx}]^{m-1} \}$ .

By plotting  $p/[\text{Cx}]$  versus  $[\text{LIX}]$  (Figure 2), a straight line is obtained; moreover  $p/[\text{Cx}]$  does not depend on  $[\text{Cx}]$ . So both  $n$  and  $m$  are equal to 1.

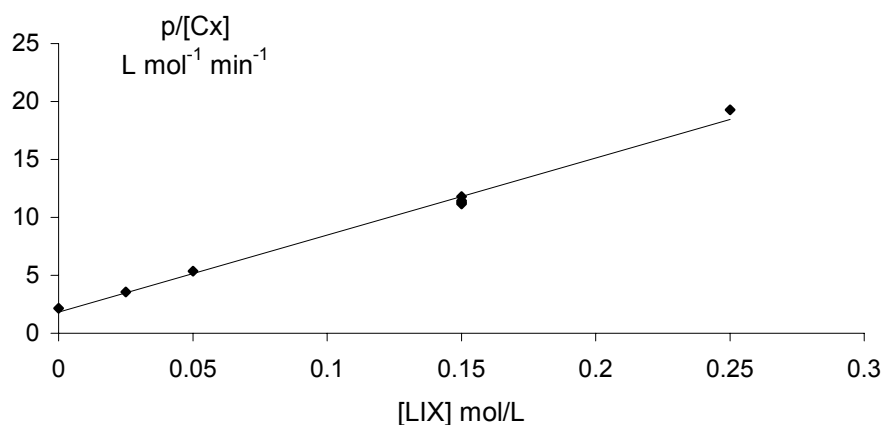


Figure 2. Testing of the kinetic model.

LIX 860 then acts as a catalyst for phase transfer.

### Stripping of copper

Again various mixtures of thiourea and sulphuric acid were studied. The concentration of LIX 860 was found to have no influence on the distribution ratio of copper:  $D = 0.09 \pm 0.006$  for LIX 860 between 0 and 0.05 mol/L. This result was obtained for a strip solution containing 0.1 mol/L thiourea and 1 mol/L sulphuric acid and for 0.028 mol/L Cyanex 302. The inference is that LIX 860 is not included in the stripping mechanism.

The results of stripping experiments for constant LIX 860 concentration (0.025 mol/L) are given in Table 3.

Table 3. Influence of various parameters on copper stripping from LIX 860/Cyanex 302.

Acid, mol/L	0.1	0.25	0.45	0.70	1	1	1	1	1	1	1
Thiourea, mol/L	0.1	0.1	0.1	0.1	0.1	0.05	0.075	0.15	0.2	0.1	0.1
Cyanex 302, mol/L	0.074	0.074	0.074	0.074	0.074	0.074	0.074	0.074	0.028	0.25	
D	4.6	2.5	1.1	0.8	0.6	5.0	1.5	0.16	0.07	0.09	3.2

The extracted complex is  $\overline{\text{CuA}_p(\text{HA})_q}$  with Cyanex 302 being mainly dimer,  $(\text{HA})_2$ .  $p$  may be equal to 1 or 2, depending whether copper is Cu(I) or Cu(II) in the organic phase. The complex of thiourea (TU) with copper involves only copper(I). So if the extracted complex contains Cu(II), this latter is reduced by thiourea during stripping, leading to the formation of formamidine disulfide (FDS).

The reaction equations for stripping may be written as follows:



Finally the distribution ratio of copper is expressed as follows:

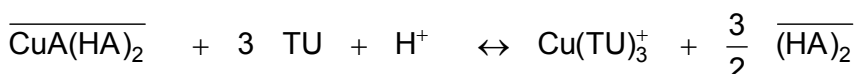
$$D = K \frac{\overline{[(\text{HA})_2]}^{\frac{p+q}{2}}}{[\text{TU}]^{r-p+1}} \frac{[\text{FDS}]}{[\text{H}^+]^p}^{\frac{p-1}{2}}$$

The slope method has given the following results:

- In  $D$  versus  $\ln [\text{H}^+]$  is a straight line of slope  $-1$
- In  $D$  versus  $\ln [\text{Cyanex 302}]$ : slope  $1.5$
- In  $D$  versus  $\ln [\text{TU}]$ : slope  $-3$

Then:  $p = 1$ ;  $q = 2$ ;  $r = 3$ .

The stripping equilibrium is then:



Copper is monovalent in the organic complex; it is reduced and extracted by Cyanex 302 at the same time. Cyanex 302 is oxidised to disulfide.

## COPPER ELECTRODEPOSITION

Electrodeposition was examined as a means of recovering copper from the loaded strip solution. The electrolysis device had a cathode consisting of a fixed bed of graphite pellets and two DSA anodes. Tests varying the thiourea concentration were performed using a current density of  $1.1 \text{ mA/cm}^2$  and a solution containing  $400 \text{ mg/L}$  copper and  $1 \text{ mol/L}$  sulphuric acid. For thiourea concentrations above  $0.2 \text{ mol/L}$ , there is no deposition. For lower concentrations, the rate of deposition is greater when the thiourea concentration is smaller. After 30 minutes the deposition yield is 25% for thiourea  $0.15 \text{ mol/L}$  and 60% for thiourea  $0.1 \text{ mol/L}$ . The feasibility of the process is then demonstrated.

A solution containing  $0.1 \text{ mol/L}$  thiourea and  $1 \text{ mol/L}$  sulphuric acid may be chosen; the copper electrodeposition is feasible, the stripping efficiency with such a solution is also convenient ( $> 90\%$ ). The solution coming from the electrodeposition step is optimally recycled to the stripping step provided thiourea is not reduced in the electrodeposition step; further experiments are needed to verify the feasibility of this recycling.

## PROCESS FLOWSHEET

The flowsheet shown in Figure 3 was tested at a micro-pilot scale in a continuous operation. The bath was agitated and the temperature maintained at  $60^\circ\text{C}$ . A concentrated copper solution ( $10 \text{ g/L}$ ) was continuously added to simulate the dissolution of copper from metal pieces. The bath composition was:  $2 \text{ mol/L}$  sulphuric acid,  $60 \text{ g/L}$  Fe(II),  $0.9 \text{ g/L}$  Fe(III) and  $9 \text{ mg/L}$  Cu. An aqueous phase (A) was withdrawn from the bath and sent to the extraction step (a single stage) from which it returned less concentrated in copper.

The stripping solution (L) comprised  $0.075 \text{ mol/L}$  thiourea and  $1 \text{ mol/L}$  sulphuric acid. This solution entered the stripping section (4 stages) without copper and leaves it with a rather high metal concentration.

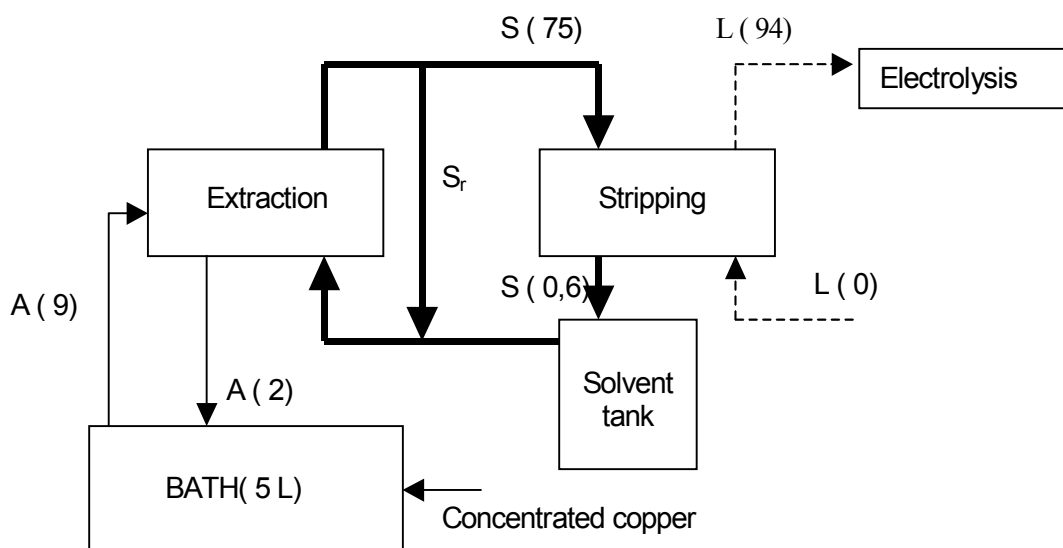


Figure 3. Flowsheet of the proposed process  
(the numbers in parentheses give the copper concentrations in mg/L).

The organic solution contained  $0.037 \text{ mol/L}$  Cyanex 302 and  $0.15 \text{ mol/L}$  LIX 860. Only a small part of this flow (S) goes to the stripping section; the major part ( $S_r$ ) is directly recycled to the extraction stage in order to increase the interfacial area in it.

For operation at the following flowrates: A = 160 mL/min; S = 15 mL/min;  $S_r$  = 85 mL/min; L = 13 mL/min, the steady-state (after 5 hours) copper concentrations (mg/L) indicated in parentheses in Figure 3 were obtained. The results show that only two stages of the stripping section are efficient; the flowrate of the stripping solution might therefore be reduced. The stripping solution contains only 10 mg/L Fe(III) which will be a very little nuisance for the electrolysis if the compartments of the device are separated.

A degradation of Cyanex 302 has been observed after 28 hours leading to a reduced extracting power. Cyanex 302 is oxidised by copper(II) during its extraction, this reaction being irreversible in the conditions of the process; this degradation is however reversible in reducing chemical conditions. It is then necessary to add in the process a Cyanex 302 regeneration by means of a reducing agent (nickel (0) or hydrogen) as proposed by Rickelton *et al.* [9].

## CONCLUSION

Technical viabilities of the proposed SX process for elimination of copper in pickling baths have been successfully demonstrated. At steady state the copper concentration of the bath is maintained to a low level (2 mg/L) as required; copper is recovered in the electrolysis step. Due to the degradation of Cyanex 302 a supplementary step of regeneration is necessary.

## REFERENCES

1. B. Raghuraman, N. Tirmizi and J. Wiencez (1994), *Environ. Sci. Technol.*, **28**, 1090-1098.
2. M. Yoshisuka, R. J. Nichols and K. Inoue (1990), *Hydrometallurgy*, **23**, 247-261.
3. N. Ocana and F. J. Alguacil (1998), *Hydrometallurgy*, **48**, 239-249.
4. J. Simpson, P. Navarro and F. J. Alguacil (1996), *Hydrometallurgy*, **42**, 13-20.
5. T. Zhu and Z. Xuexi (1996), *Proc. Int. Solvent Extr. Conf. ISEC '96*, University of Melbourne Press, Melbourne, pp. 581- 586.
6. B. Tait (1993), *Solvent Extr. Ion Exch.*, **10**, 799-809.
7. K. C. Sole and J. B. Hiskey (1992), *Hydrometallurgy*, **30**, 345-365.
8. G. R. Rapaumbya (1989), PhD Thesis, Paris.
9. W. A. Rickelton, I. O. Mihaylov, B. J. Love, P. K. Louie and E. Krause (1998), *U.S. Pat.*, No. 5,759,512.



## COPPER RECOVERY FROM SPENT AMMONIACAL ETCHING SOLUTIONS

M. Rosinda, C. Ismael and Jorge M. R. Carvalho

Dep. Eng. Química, Instituto Superior Técnico, Lisboa, Portugal

The extraction of copper using LIX 84-I was investigated. It was established the extraction isotherm for the system LIX 84-I ( $\text{HR} = 0.72 \text{ M}$ ) in Shellsol T/ etching effluent ( $\text{Cu}^{2+} = 121.6 \text{ g.L}^{-1}$ ,  $\text{NH}_4\text{Cl} = 4 \text{ M}$  and  $\text{NH}_3 = 3 \text{ M}$ ). The stripping of a loaded organic phase (LIX 84-I =  $0.74 \text{ M}$ ,  $\text{Cu}^{2+} = 19.9 \text{ g.L}^{-1}$ ) was carried out with an aqueous solution of sulphuric acid ( $150 \text{ g.L}^{-1}$ ) and the stripping isotherm was produced. For both process (extraction and stripping) the number of stages required for an industrial situation was determined.

Copper extraction from acidic sulphate solutions using LIX 84-I was studied in order to define the stoichiometry of copper extraction and to calculate the value of 1.7 for the thermodynamic equilibrium constant.

### INTRODUCTION

Today because of environmental concerns there is a general trend to recycle resources and to minimize the discharge of effluents containing hazardous metals. Effluents from the printed circuit board industry contain  $130\text{-}160 \text{ g.L}^{-1}$  Cu and  $7\text{-}9 \text{ M}$  ( $\text{NH}_4\text{Cl} + \text{NH}_3$ ). The recovery of copper from such effluents is advantageous due to the economic value of the copper and to the effluent recycling possibilities the removal of copper presents.

The extraction of copper from ammoniacal media can be carried out with hydroxyoxime extractants [3-6]. In this study LIX 84-I (2-hydroxy-5-nonyacetophenone oxime) is used. To be able to simulate the solvent extraction process requires data relative to the equilibrium constants of the extracted metal. The values found in literature are valid only for specific extraction conditions [7,8]. It was therefore decided to introduce the thermodynamics of solutions, mainly the non-ideal behaviour of the aqueous phase (Pitzer's model [9]) in order to establish the thermodynamic equilibrium constants of the copper/LIX 84-I system.

The stoichiometry of the extraction equilibrium of copper with hydroxyoximes can be expressed as follows [10,11,12]:



The thermodynamic equilibrium constant (non-ideal aqueous solution) for this reaction is equal to:

$$K^o = \frac{c_{CuR_2.nHR,org} a_{H_{aq}^+}^{2+n}}{a_{Cu_{aq}^{2+}} c_{(HR)_m}^m} = \frac{c_{CuR_2.nHR,org} c_{H_{aq}^+}^{2+n}}{c_{Cu_{aq}^{2+}} c_{(HR)_m}^m} \frac{\gamma_{H^+}^2}{\gamma_{Cu^{2+}}} \quad (2)$$

where  $a$  is the activity,  $c$  the concentration and  $\gamma$  the activity coefficient.

The application of logarithms to this expression leads to:

$$\log D' = \log K^o - 2 \log a_{H_{aq}^+} + \frac{2+n}{m} \log c_{(HR)_m} \quad (3)$$

where  $D' = \frac{c_{CuR_2.nHR,org}}{a_{Cu_{aq}^{2+}}}$ . The expression (3) can be used.

## EXPERIMENTAL

### Reagents

LIX 84-I was kindly supplied by Cognis (Ireland) and was received diluted in an aliphatic hydrocarbon diluent (kerosene). The organic phases used, in this work, were obtained by dilution of LIX 84-I solution in Shellsol T (aliphatic hydrocarbon from Shell). A Portuguese printed circuit board producer supplied real effluent. Other aqueous solutions were prepared using pro-analysis chemical reagents.

### Equipment and Procedure

The organic and aqueous phases were contacted by vigorous mixing in a mechanical mixer with temperature control for at least 12 h. The concentrations of copper in both phases were analysed directly by atomic absorption spectrophotometry.

## RESULTS AND DISCUSSION

### Extraction and Stripping of Copper with LIX 84-I

Table 1 presents data relative to the loading capacity of LIX 84-I solutions achieved after two consecutive contacts of the organic phase with the real effluent (phase ratio A:O = 3:1, T = 25°C).

*Table 1. Loading capacity of LIX 84-I solutions.*

LIX 84-I* in Shellsol T (% (v/v))	Cu <sub>org</sub> (M)
5	0.051
10	0.107

\* LIX 84-I solution as received from Cognis

If it is assumed that copper exists in the loaded organic phase as the  $\text{CuR}_2$  complex, the Cognis solution contains 2.10 M LIX 84-I (*HR*). Taking this result into account it was decided to continue the extraction of copper from the real effluent with an organic phase containing 0.72 M hydroxyoxime. Figure 1 shows the extraction isotherm for the system copper/LIX 84-I. As can be observed, more than 99% of copper can be removed from the effluent in three stages at A:O phase ratio of 1:7.

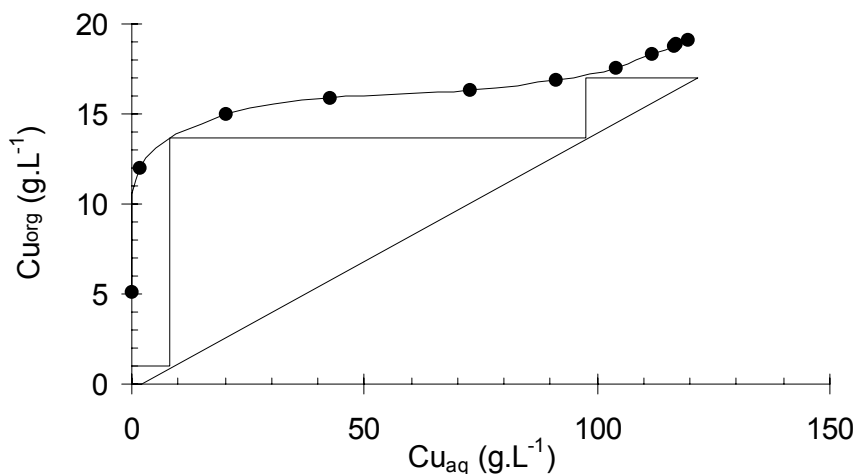


Figure 1. Equilibrium isotherm for copper extraction. (Aq. phase –  $\text{Cu} = 121.6 \text{ g.L}^{-1}$ ,  $\text{NH}_3 = 3 \text{ M}$ ,  $\text{NH}_4\text{Cl} = 4 \text{ M}$ ; Org. phase – LIX 84-I(*HR*) = 0.72 M in Shellsol T;  $T = 25^\circ\text{C}$ ).

Stripping of loaded organic phase ( $\text{Cu}^{2+}_{\text{org}} = 19.9 \text{ g.L}^{-1}$ ) was investigated using different concentrations of sulphuric acid solution and contacting at an A:O phase ratio 3:1. Copper removal of 75, 83, 86, 85, 85% was obtained for 50, 100, 130, 150, 200  $\text{g.L}^{-1}$  of  $\text{H}_2\text{SO}_4$ . The use of 150  $\text{g.L}^{-1}$   $\text{H}_2\text{SO}_4$  is adequate, this being the typical concentration in copper tank house electrolyte. Figure 2 shows that 99% copper stripping from loaded organic phase can be achieved in three counter-current stages at the A:O phase ratio of 1:2.5.

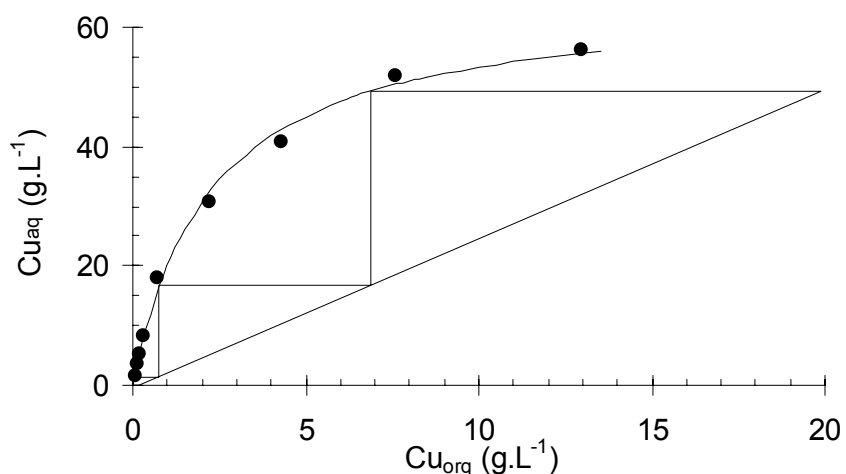


Figure 2. Equilibrium isotherm for copper stripping. (Aq. phase –  $\text{H}_2\text{SO}_4 = 150 \text{ g.L}^{-1}$ ; Org. phase – LIX 84-I(*HR*) = 0.74 M in Shellsol T,  $\text{Cu}^{2+} = 19.9 \text{ g.L}^{-1}$ ;  $T = 25^\circ\text{C}$ ).

These results allow the conclusion that the removal of copper with LIX 84-I, from ammoniacal media, is efficient. In consequence, there is a logical interest in the simulation of the extraction process. To achieve this purpose, different parameters are needed, including the equilibrium constant for the system copper/LIX 84-I.

### Equilibrium Studies in the System LIX 84-I/CuSO<sub>4</sub>/Na<sub>2</sub>SO<sub>4</sub>/H<sub>2</sub>SO<sub>4</sub>

The equilibrium studies were performed in sulphate/sulphuric acid media. In the CuSO<sub>4</sub>/Na<sub>2</sub>SO<sub>4</sub>/H<sub>2</sub>SO<sub>4</sub> system, assuming complete dissociation of Na<sub>2</sub>SO<sub>4</sub>, the species Cu<sup>2+</sup>, Na<sup>+</sup>, H<sup>+</sup>, SO<sub>4</sub><sup>2-</sup>, CuSO<sub>4</sub> and HSO<sub>4</sub><sup>-</sup> remain in solution. The calculus of the respective activities involves the following system of equations:

$$m_{HSO_4^-} + m_{SO_4^{2-}} = m_{(CuSO_4+H_2SO_4+Na_2SO_4)_{total}} \quad (4)$$

$$m_{Cu^{2+}} + m_{CuSO_4} = m_{(CuSO_4)_{total}} \quad (5)$$

$$m_{H^+} + m_{Na^+} + 2m_{Cu^{2+}} = m_{HSO_4^-} + 2m_{SO_4^{2-}} \quad (6)$$

$$Cu^{2+} + SO_4^{2-} \leftrightarrow CuSO_4 ; K_{CuSO_4}^o = \frac{\gamma_{CuSO_4}}{\gamma_{Cu^{2+}} \gamma_{SO_4^{2-}}} \times \frac{m_{CuSO_4}}{m_{Cu^{2+}} m_{SO_4^{2-}}} = 229 \quad (7)$$

$$HSO_4^- \leftrightarrow H^+ + SO_4^{2-} ; K_{a2}^o = \frac{\gamma_{H^+} \gamma_{SO_4^{2-}}}{\gamma_{HSO_4^-}} \times \frac{m_{H^+} m_{SO_4^{2-}}}{m_{HSO_4^-}} = 0.0105 \quad (8)$$

for m the molar concentration. The activity coefficients were estimated using Pitzer's model [9].

In order to define the stoichiometry and thermodynamic equilibrium constant for copper extraction studies, the influence of pH and extractant concentration on the equilibrium were studied. The use of equation 3 is helpful to define the stoichiometry of copper/LIX 84-I reaction. As shown in Figure 3, slopes of straight lines are ~ 2, which confirms the dependence of copper extraction on pH.

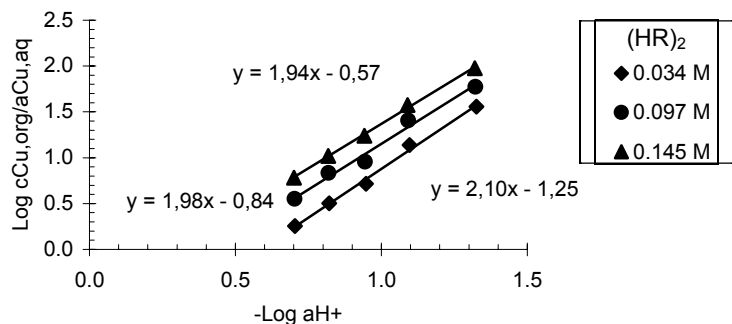
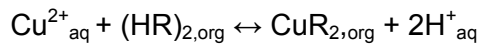


Figure 3. Influence of H<sup>+</sup> on copper extraction. (Aq. phase: CuSO<sub>4</sub> = 4.58 × 10<sup>-3</sup> mol/kg H<sub>2</sub>O; Na<sub>2</sub>SO<sub>4</sub>; H<sub>2</sub>SO<sub>4</sub> (Ionic strength = 0.70 M); Org phase: LIX 84-I ((HR)<sub>2</sub>) in Shellsol T; T=25°C).

The *log-log* plot of  $D_{\text{Cu}}$  versus  $(\text{HR})_2$  is shown in Figure 4. A straight line with slope equal to 1 was obtained, indicating the formation of  $\text{CuR}_2$ . Hence, the overall stoichiometry of the extraction equilibrium can be written as:



The extraction equilibrium constant,  $K^\circ$ , was determined from the intercept of straight lines shown in Figures 3 and 4. A value of 1.7 was obtained. This value is lower than the value of 13.2 obtained by Hu and Wiencek [12]. This discrepancy can be related to their use of a different diluent (tetradecane). Otherwise they assumed that LIX-84 molecules are monomers.

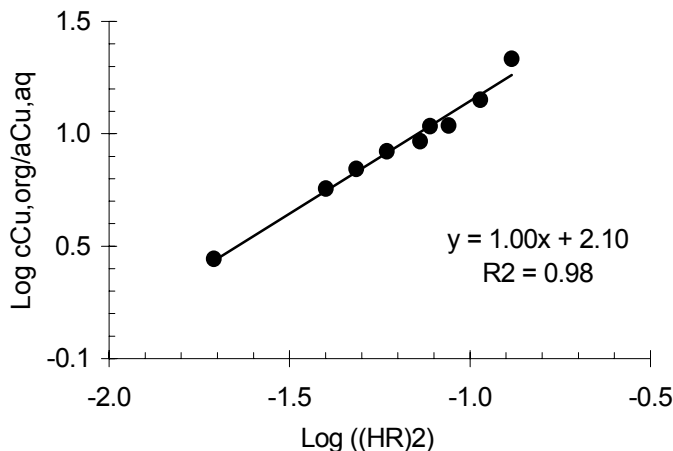


Figure 4. Influence of extractant concentration on copper extraction.  
(Aq. phase:  $\text{CuSO}_4 = 4.40 \times 10^{-3}$  mol/kg  $\text{H}_2\text{O}$ ;  $\text{Na}_2\text{SO}_4 = 0.184$  mol/kg  $\text{H}_2\text{O}$ ;  $\text{H}_2\text{SO}_4 = 0.207$  mol/kg  $\text{H}_2\text{O}$  (Ionic strength = 0.70 M); Org phase: LIX 84-I in Shellsol T;  $T = 25^\circ\text{C}$ ).

The effect of temperature on copper extraction was studied in the range  $19.5^\circ\text{--}60^\circ\text{C}$ . The results are shown in Figure 5.

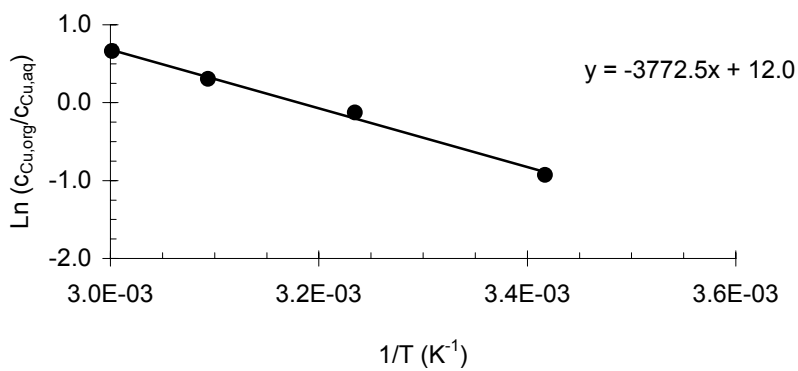


Figure 5. Influence of temperature on copper extraction. (Aq. phase:  $\text{CuSO}_4 = 4.37 \times 10^{-3}$  M;  $\text{Na}_2\text{SO}_4 = 0.181$  M;  $\text{H}_2\text{SO}_4 = 0.202$  M; Org phase:  $(\text{HR})_2 = 0.146$  M in Shellsol T; A/O = 1).

Analysing Figure 5 it is concluded that an increase in temperature reduces the extraction efficiency. Using the value of straight-line slope the  $\Delta H^\circ$  was calculated. This is  $31.3 \text{ kJ.mol}^{-1}$  indicating that the extraction process is endothermic.

## CONCLUSIONS

The extraction of copper from ammoniacal etching solution with LIX 84-I is very effective. The thermodynamic equilibrium constant for copper was determined to be 1.7. In the organic phase copper is in the form of CuR<sub>2</sub>.

Three stages are necessary to carry out either extraction or stripping, for 99% efficiency, under the following conditions:

- extraction of copper from an effluent from printed circuit board plant (copper = 121.6 g.L<sup>-1</sup>, NH<sub>4</sub>Cl = 4 M, NH<sub>3</sub> = 3 M using 0.72 M of LIX 84-I(HR) in Shellsol T) at A:O phase ratio of 1:7.
- stripping of loaded organic phase (LIX 84-I(HR) = 0.74 M, Cu<sup>2+</sup> = 19.9 g.L<sup>-1</sup>) with aqueous sulphuric acid solution (150 g.L<sup>-1</sup>) at A:O phase ratio of 1:2.5.

## ACKNOWLEDGEMENTS

The authors wish to thank to Helena Ribeiro, André Pereira, Ivo Reia, Miguel Pereira and Rodrigo Lourenço who carried out the experimental studies. Dr Werner Schwab (Cognis – Germany) and Cognis Ireland are thanked for providing the extractant used in this work.

## REFERENCES

1. W. Schwab and R. Kehl (1997), *Proc. XX International Mineral Processing Congress*, Vol. 4, Aachen, pp. 285-292.
2. M. Cox (1992), Principles and Practices of Solvent Extraction, J. Rydberg, C. Musikas, G.R. Chopin (eds.), Marcel Dekker, New York, pp. 357-412.
3. G. Kyuchoukov, M.B. Bogacki and J. Szymonowski (1998), *Ind. Eng. Chem. Res.*, **37**, 4084-4089.
4. F.J. Alguacil (1999), *Hydrometallurgy*, **52**, 55-61.
5. F.J. Alguacil and M. Alonso (1999), *J. Chem. Tech. Biotechnol.*, **53** (2), 1171-1175.
6. C. Parija and P.V.R.B. Sarma (2000), *Hydrometallurgy*, **54**, 195-204.
7. H. Aminian and C. Bazin (2000), *Miner. Eng.*, **13** (6), 667-672.
8. D. Doungdeethaveeratana and H.Y. Sohn (1998), *Miner. Eng.*, **11** (9), 821-826.
9. K.S. Pitzer (1991), Activity Coefficients in Electrolyte Solutions, 2nd edn., CRC Press, Boca Raton, FL.
10. K. Yoshizuka, H. Arita, Y. Baba and K. Inoue (1990), *Hydrometallurgy*, **23**, 247-261.
11. J. Piotrowicz, M.B. Bogacki, S. Wasylkiewicz and J. Szymonowski (1989), *Ind. Eng. Chem. Res.*, **28**, 284-288.
12. S.-Y. Hu and J. Wiencek (2000), *Solvent Extr. Ion Exch.*, **35** (4), 469-481.



## RECOVERY OF NICKEL FROM SPENT ELECTROLESS NICKEL PLATING BATHS BY SOLVENT EXTRACTION

Mikiya Tanaka, Mikio Kobayashi and Tsutomu Seki\*

National Institute of Advanced Industrial Science and Technology, Tsukuba, Japan  
\* Chiba Institute of Technology, Tsudanuma, Japan

For the purpose of establishing a recycling process for an electroless nickel plating bath, the solvent extraction and stripping of nickel from spent baths has been investigated using LIX 84I as the extractant. It is shown that nickel can be extracted with good selectivity at a pH greater than 6. A concentrated nickel sulfate solution ( $\text{Ni} > 100 \text{ kg/m}^3$ ) is obtained using 1 kmol/m<sup>3</sup> sulfuric acid, nickel sulfate ( $\text{Ni} 50 \text{ kg/m}^3$ ) solution as the stripping reagent. Organophosphorus extractants such as di(2-ethylhexyl)phosphoric acid and PC-88A are applicable to remove iron and zinc as impurities before the extraction of nickel with LIX 84I. PC-88A is more advantageous because the co-extraction of nickel is lower.

### INTRODUCTION

With the increasing importance of electroless nickel plating technology in many fields such as the electronic and automobile industries, the treatment of the spent baths is becoming a serious problem. These spent baths contain iron and zinc as impurities, organic acids as complexing reagents, and phosphonate ions as the oxidized species of the reducing reagent, as well as several grams per liter of nickel. The spent baths are currently treated by a conventional precipitation method, but a method with no sludge generation is desired. With this in mind, we are tackling the development of a nickel recycling process from the spent baths using solvent extraction and have recently reported the possibility of recovering nickel from a weakly acidic spent bath using a typical chelating reagent, LIX 84I [1-3].

In this paper, the applicability of LIX 84I for the recovery of nickel from three kinds of spent baths is studied together with the detailed stripping conditions. Removal of iron and zinc as impurities from the spent baths with organophosphorus acids [4] is also discussed.

### EXPERIMENTAL

#### Spent Baths and Reagents

Three kinds of spent baths (A, B, and C) discharged from an electroless nickel plating plant in Japan were used for the extraction experiments. Chemicals used in this experiment were all reagent grade except for the extractants and diluent. LIX 84I (Cognis), di(2-ethylhexyl)phosphoric acid (D2EHPA, Daihachi), and PC-88A (Daihachi) were used as received. These were respectively dissolved in Shellsol D70 (Shell Chemicals) in order to prepare the working organic phases. The concentrations of the extractants were 20 vol% for LIX 84I and 10 vol% for D2EHPA and PC-88A. Various concentrations of sodium hydroxide and hydrochloric acid as well as ion exchange-distilled water were used as pH adjusting reagents.

### **Extraction, Stripping, and Analysis**

In the experiment investigating the pH dependency of the extraction, the working organic phase, spent bath, and pH adjusting reagent were poured into a stoppered conical flask at a volume ratio of 5:4:1, and shaken in a water bath maintained at  $298 \pm 0.1\text{K}$  for more than 24 hours to ensure equilibrium. After shaking, the mixture was centrifuged, and the organic phase was pipetted out. In the nickel stripping experiment, the organic phase containing  $8.77\text{ kg/m}^3$  was first prepared by contacting 20 vol% LIX 84I with  $1.00\text{ kmol/m}^3 (\text{NH}_4)_2\text{SO}_4$ - $0.1\text{ kmol/m}^3 \text{NiSO}_4$ - $0.4\text{ kmol/m}^3 \text{NaOH}$  solution at a volume ratio of 1:3 in a separatory funnel at room temperature followed by washing with water. The organic phase obtained was then contacted with  $0.92\text{ kmol/m}^3 \text{NiSO}_4$ - $1.00\text{ kmol/m}^3 \text{H}_2\text{SO}_4$  solution (nickel concentration was  $54.0\text{ kg/m}^3$ ) at different volume ratios in the same manner as in the extraction experiment. The metal contents in the aqueous phases after extraction and stripping were determined by ICP-AES (Seiko SPS4000). The metal contents in the organic phase after extraction and stripping were determined by ICP-AES after stripping the metals in the organic phases using an excess volume of  $1\text{-}2\text{ kmol/m}^3$  hydrochloric acid. The pH values in the aqueous phases were measured by a pH meter (Toa HM-50AT). Sulfate, phosphinate, and phosphonate ions as well as the organic acids in the spent baths were determined by a capillary electrophoresis apparatus (Otsuka CAPI-3200).

## **EXPERIMENTAL RESULTS AND DISCUSSION**

### **Compositions of the Spent Baths**

The compositions and pH values of the spent baths were measured, and the results are shown in Table 1. Spent bath A is a typical weakly acidic bath with a high accumulation of phosphonate and sulfate ions. Spent bath B is also weakly acidic; however, the concentrations of the phosphonate and sulfate ions are low and that of zinc is the highest among these three baths. Spent bath C is almost neutral and contains boron with a high accumulation of phosphate and sulfate ions.

*Table I. The compositions ( $\text{kg/m}^3$ ) and pH values of the spent baths A, B, and C.*

Component	A	B	C	Component	A	B	C
Sodium	66	24	90	Lactic acid	31	3	8
Nickel	4	6	6	Propionic acid	2	0	35
Iron	0.1	0.003	0	Malic acid	0	24	0
Zinc	0.01	0.07	0.007	Succinic acid	0	7	0
$\text{SO}_4^{2-}$	48	7	64	Boron	0	0	0.8
$\text{H}_2\text{PO}_2^-$	16	19	12	Glycine			30
$\text{HPO}_3^{2-}$	98	17	100	pH	4.5	4.8	6.0

### **Extraction with LIX 84I**

Figures 1, 2, and 3 show the extraction percentages of nickel, iron, and zinc with LIX 84I as a function of the equilibrium pH values from the spent baths A, B, and C, respectively.

In spent baths A and B, when water is used as a pH adjusting reagent (that is, the extraction was done substantially without pH adjustment), the extraction percentages of nickel are only 34% (pH 4.1) and 43% (pH 4.4), respectively. However, when the pH is increased to greater than 6, the extraction percentages of nickel are enhanced to more than 99.9% (99.94% at pH 6.2 and 99.97% at pH 6.1 for spent baths A and B, respectively). Since the extraction percentages of iron and zinc are low throughout the pH range in this experiment, it is expected to selectively extract nickel leaving most of iron and zinc in the raffinate.

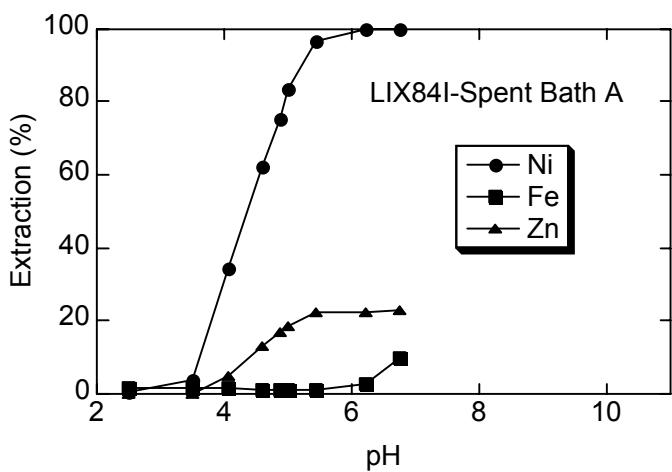


Figure 1. The effect of equilibrium pH on the extraction of metals from spent bath A with 20 vol% LIX 84I dissolved in Shellsol D70 at 298K.

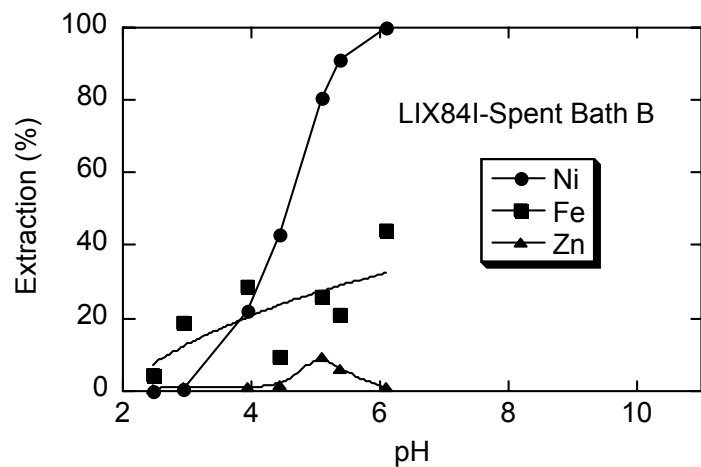


Figure 2. The effect of equilibrium pH on the extraction of metals from spent bath B with 20 vol% LIX 84I dissolved in Shellsol D70 at 298K.

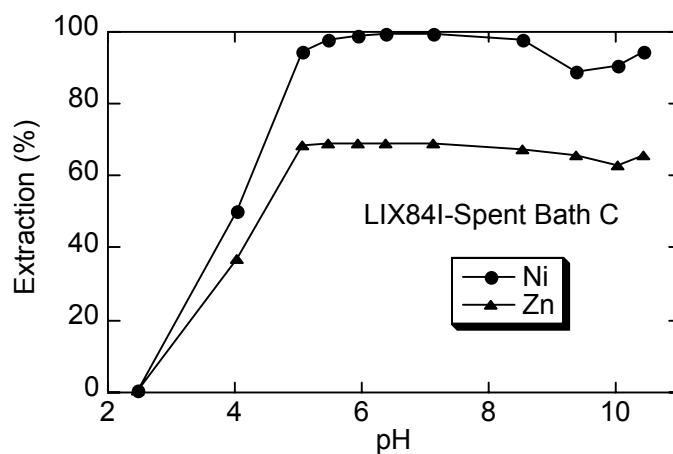


Figure 3. The effect of equilibrium pH on the extraction of metals from spent bath C with 20 vol% LIX 84I dissolved in Shellsol D70 at 298K.

In spent bath C, when the extraction is done substantially without pH adjustment, the extraction percentage is greater than 99.0% (pH 5.9). About 70% of the zinc was also extracted when the pH is greater than 5; however, the concentration of zinc in the spent bath C is so low that the coextraction of zinc would cause little problem when the recovered nickel is reused in the electroless plating process.

The McCabe-Thiele analysis of the nickel extraction isotherm of spent bath A at the initial pH of 6.4 reveals that when the ratio of the flow rates (aqueous to organic) is 2, the number of stages necessary to completely extract the nickel by countercurrent contact is 2. By using the two-stage extraction, 4 kg/m<sup>3</sup> nickel in spent bath A would be reduced to 0.0006 kg/m<sup>3</sup> [2, 3].

### Stripping of Nickel from LIX84I with Sulfuric Acid

In our previous studies [2,3], the effect of pH on the nickel stripping percentage with sulfuric acid was studied at 298K using 20 vol% LIX 84I dissolved in Shellsol D70 containing 9.1 kg/m<sup>3</sup> of nickel. As a result, more than 99% of the nickel was stripped at the equilibrium pH of less than 2.7 (the initial sulfuric acid concentration was greater than 0.17 kmol/m<sup>3</sup>). The concentration of nickel in the obtained aqueous phase after stripping was low, because the phase ratio in that experiment was unity. For the reuse of the recovered nickel sulfate solution as a source of nickel for the electroless nickel plating baths, the concentration of nickel should be as high as possible, and the free sulfuric acid remaining in the solution should be as low as possible.

In order to assess the operational conditions for obtaining such a solution, the stripping isotherm of nickel from nickel-loaded LIX 84I was constructed using the 0.92 kmol/m<sup>3</sup> NiSO<sub>4</sub>-1.00 kmol/m<sup>3</sup> H<sub>2</sub>SO<sub>4</sub> solution as the stripping reagent (Figure 4). The stoichiometric relation of the stripping of nickel from LIX 84I by acid is known to be expressed by the following equation [2,3].



Here, HR and the bar denote the monomer of the active component of LIX 84I and the organic phase species, respectively. As seen in this equation, one nickel ion in the organic phase exchanges with two hydrogen ions in the aqueous phase during stripping. The dotted line in Figure 4 signifies the theoretical maximum nickel concentration after stripping calculated by assuming that all of the hydrogen ions in the sulfuric acid are exchanged with the nickel ion in the organic phase when the amount of nickel in the initial organic phase stoichiometrically exceeds that of the hydrogen ion in the initial aqueous phase.

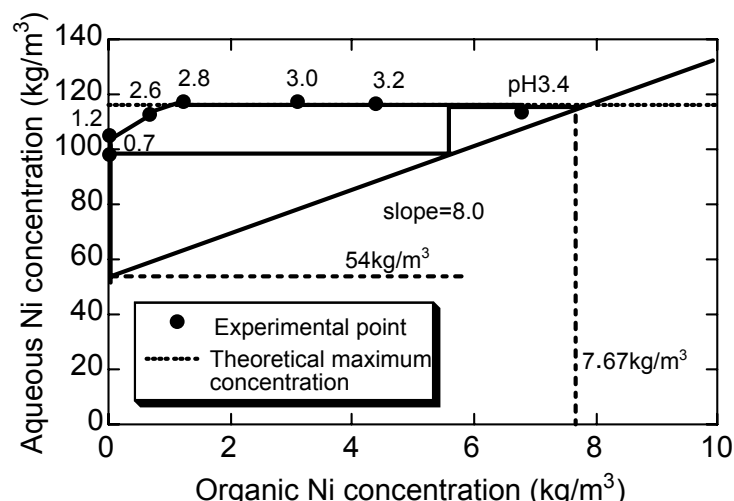


Figure 4. Stripping isotherm of nickel from 20 vol% LIX 84I dissolved in Shellsol D70 containing 8.77 kg/m<sup>3</sup> of nickel with 0.92 kmol/m<sup>3</sup> NiSO<sub>4</sub>-1.00 kmol/m<sup>3</sup> H<sub>2</sub>SO<sub>4</sub> solution.

According to the experimental results, with the increasing nickel concentration in the organic phase, the nickel concentration in the aqueous phase is enhanced, reaches the theoretical maximum value ( $117 \text{ kg/m}^3$ ) when the nickel concentration in the organic phase is  $1.21 \text{ kg/m}^3$ , and remains almost constant thereafter. The pH value continues to increase after the nickel concentration in the aqueous phase becomes almost constant and seems to approach 4.99, which is the pH value of the  $1.92 \text{ kmol/m}^3$  nickel sulfate solution ( $117 \text{ kg/m}^3$  nickel). This suggests that a small amount of hydrogen ion in the aqueous phase is exchanging with nickel in the organic phase even after the nickel concentration in the organic phase becomes almost constant.

The McCabe-Thiele analysis reveals that when the ratio of the flow rates (organic to aqueous) is 8 and the nickel concentration in the feed organic phase is  $7.67 \text{ kg/m}^3$ , two stage countercurrent contact can reduce the nickel concentration in the organic phase to a trace level and concentrate the nickel in the aqueous phase from  $54 \text{ kg/m}^3$  to  $117 \text{ kg/m}^3$ .

As shown here, it is possible to obtain concentrated nickel sulfate solution (nickel concentration  $> 100 \text{ kg/m}^3$ ) at pH 3.3. The impurity contents in this solution would be sufficiently low and thus can be used as a nickel source for the electroless nickel plating process.

Although the use of the concentrated nickel sulfate solution as the stripping reagent would depress the stripping efficiency as shown in equation (1), it enables one to obtain very concentrated nickel sulfate solution which is convenient for recycling to electroless nickel plating process.

### **Extraction with D2EHPA and PC-88A**

In order to recover nickel with a higher purity and simplify the treatment of the aqueous raffinate after the extraction with LIX 84I, the application of D2EHPA and PC-88A has been investigated by using spent bath B to remove iron and zinc before extracting the nickel with LIX 84I.

Figures 5 and 6 present the extraction percentages of nickel, iron, and zinc as a function of the equilibrium pH values with D2EHPA and PC-88A, respectively. When water is used as the pH adjusting reagent; that is, the extraction is substantially done without any pH adjustment, the extraction percentages of nickel, iron, and zinc with D2EHPA were 20%, 100%, and 90%, respectively (pH 4.3), while those with PC-88A were 1%, 100%, and 95% (pH 4.6). Thus, both extractants exhibit a high extraction ability for iron and zinc without pH adjustment. Since the extraction percentage of nickel with PC-88A is lower than that with D2EHPA, PC-88A is more suitable for the selective extraction of iron and zinc.

## **CONCLUSIONS**

LIX84I is capable of extracting nickel from spent electroless nickel plating baths with good selectivity at pH values greater than 6. Nickel extracted by LIX84I can be stripped with  $1 \text{ kmol/m}^3$  sulfuric acid solution. When nickel sulfate ( $50 \text{ kg/m}^3$  nickel) is added to the stripping reagent, it is possible to obtain a concentrated nickel sulfate solution ( $> 100 \text{ kg/m}^3$  nickel) containing a very low amount of free sulfuric acid by countercurrent contact with 2 stages. This nickel sulfate solution could be reused in the electroless nickel plating process.

Iron and zinc as impurities in the spent baths can be removed with an organophosphorus acid extractant such as D2EHPA and PC-88A before the nickel extraction with LIX84I. The pH adjustment is not necessary in this case. PC-88A is more suitable for this purpose than D2EHPA because the co-extraction of nickel is lower. This process will simplify the treatment of the raffinate after nickel extraction and will contribute to produce higher purity nickel sulfate.

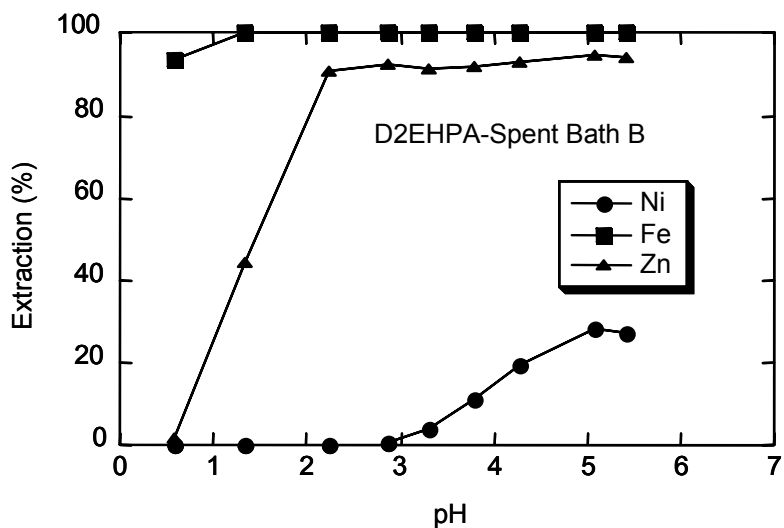


Figure 5. The effect of equilibrium pH on the extraction of metals from spent bath B with 10 vol% D2EHPA dissolved in Shellsol D70 at 298K.

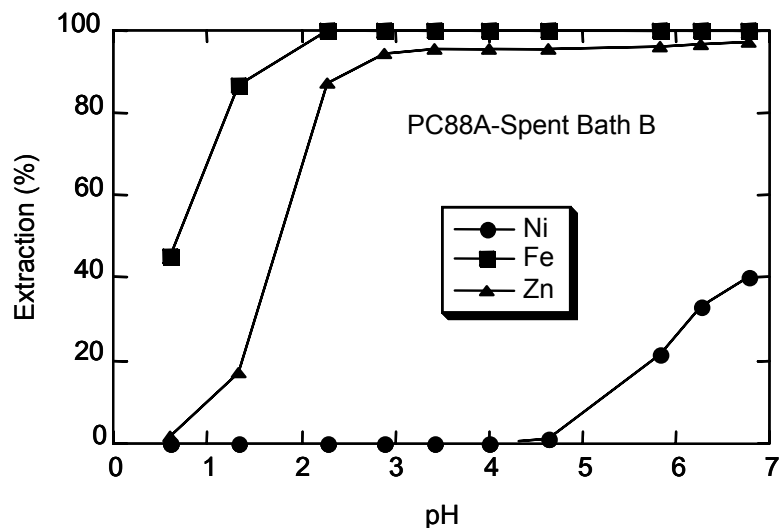


Figure 6. The effect of equilibrium pH on the extraction of metals from spent bath B with 10 vol% PC-88A dissolved in Shellsol D70 at 298K.

## REFERENCES

1. J. Szymanowski (1993), Hydroxyoximes and Copper Hydrometallurgy, CRC, Boca Raton, pp. 61-90
2. M. Tanaka, M. Kobayashi, M. A. S. AlGhamdi, K. Tatsumi, H. Senba and Y. Saiki (2000), *Proc. Second Int. Conf. Processing Materials for Properties*, B. Mishra and C. Yamauchi (eds.), TMS, Warrendale, pp. 737-740.
3. M. Tanaka, M. Kobayashi, M. A. S. AlGhamdi and K. Tatsumi (2001), *Shigen Sozai*, **117**, 507-511.
4. G. M. Ritcey and A. W. Ashbrook (1984), Solvent Extraction: Principles and Applications to Process Metallurgy, Part I, Elsevier, Amsterdam, pp. 90-110.



## RECOVERY OF COBALT AND NICKEL FROM SPENT CATALYSTS USING CYANEX 923

Bina Gupta, S. N. Tandon and Akash Deep

Department of Chemistry, University of Roorkee, Roorkee, India

The present communication reports the extraction behaviour of Co(II) and Ni(II) along with Cr(VI), Mo(VI), Al(III), Fe(III), Mn(II), Cu(II), Zn(II) and Pb(II) from HCl medium in Cyanex 923. Co(II) is quantitatively extracted while Ni(II) remains in the aqueous phase. The effect of extractant and metal ion concentration on the partition of Co(II) is investigated and the recycling capacity of Cyanex 923 determined. Based on the extraction data it has been possible to achieve some topical separations involving Co(II) and Ni(II). The commercial utility of the extractant is demonstrated by recovering high purity cobalt and nickel from spent catalysts.

### INTRODUCTION

Cobalt and nickel are two very vital metals because of their diverse industrial applications. There has been a rapid depletion in their mineral reserves resulting in to increasing interest in their recovery from the secondary sector. Liquid-liquid extraction has been commonly used for the said purpose and from time to time a variety of commercial extractants have been explored. Carboxylic acids, high molecular weight amines, oximes,  $\beta$ -diketones and aromatic hydroxyoximes suffer from the problem of solvent loss or require a strict control of aqueous-phase parameters for attaining the separations involving these metals. Among the alkylphosphorus extractants, D2EHPA [1,2] has been more frequently employed for recovering these metals but its use is limited because of emulsion formation at a higher pH and its hydrolytic stability. Of organophosphines of the Cyanex series, Cyanex 272 [3] and Cyanex 301 [4] have been applied for the mutual separation of Co(II) and Ni(II) and their isolation from commonly associated metal ions. The authors found that Cyanex 923 (a mixture of four trialkylphosphine oxides namely  $R_3P=O$ ,  $R_2R'P=O$ ,  $RR'_2P=O$ ,  $R'_3P=O$ , where R and R' represent *n*-octyl and *n*-hexyl groups, respectively) offers a convenient alternative for separations involving cobalt and nickel. The present communication embodies the extraction behaviour of Co(II) and Ni(II) in a toluene solution of Cyanex 923 from hydrochloric acid medium. The stoichiometry of the extracted Co(II) species is assessed and loading capacity of Cyanex 923 determined. The extraction of a number of commonly associated metal ions, namely Cr(VI), Mo(VI), Al(III), Fe(III), Mn(II), Cu(II), Zn(II) and Pb(II), has also been investigated. Based on the distribution data, the conditions for some important binary separations involving Co(II) and Ni(II) are optimized. This background has been used for the recovery of high purity cobalt from spent Co-Mn and Co-Mo catalysts and nickel from hydrogenation catalyst. The extractant can be recycled for use.

## EXPERIMENTAL

Stock solutions of metal ions were prepared by dissolving their salts of analytical purity in double-distilled water containing a minimum amount of the acid. The chemicals and organic solvents were analytical reagent grade materials from E.Merck/Thomas Baker, Mumbai, India. Cyanex 923 was received as a gift sample from Cytec Inc., Canada, and used without further purification. The spent catalysts were procured from the concerned industries in India.

Atomic absorption spectrometry (Perkin Elmer, 3100 USA) or inductively coupled plasma atomic emission spectrometry (Plasmalab, 8440 Australia) were used for the determination of metal ion concentrations.

For the partition studies, equal volumes of aqueous (metal ion solution in mineral acid) and organic phases were shaken for five minutes to ensure complete equilibration. After separation the two layers were isolated and the concentration of metal in the aqueous phase was assayed. The experimental conditions for the various studies are mentioned along with the corresponding data. The value of percent extraction of Co(II) at about 60% exhibits a coefficient of variance  $\pm 3\%$ .

About 1 g of powdered material was treated with  $2 \times 40$  mL of 8 mol/L HCl. The contents were heated, cooled and filtered. The final volume of the solution was made up to 100 mL keeping the overall acidity to 8 mol/L. The initial solutions of spent Co-Mn, Co-Mo and Ni hydrogenation catalysts were marked as Ai, Bi and Ci, respectively. In order to get a representative value three different samples of each matrix were processed by following the proposed extraction steps. The different results reported are an average of a minimum of two determinations.

## RESULTS AND DISCUSSION

### Extraction Behaviour of Metal Ions ( $1 \times 10^{-3}$ mol/L) from 1-10 mol/L HCl using 0.5 mol/L Cyanex 923

The variation in the percent extraction of Co(II) and Ni(II) along with Cr(VI), Mo(VI), Al(III), Fe(III), Mn(II), Cu(II), Zn(II) and Pb(II) with varying HCl concentration is shown in Figure 1. Co(II) shows an increasing trend in its extraction with an increasing HCl molarity whereas the extraction of Ni(II) is negligible (<3%) over the entire range of acidity investigated. Cu(II) and Pb(II) also show an increasing extraction with increasing acidity. A quantitative extraction (>95%) of Mo(VI), Fe(III) and Zn(II) is observed over a fairly wide range of acidity. The percent extraction of Cr(VI) decreases with increasing HCl molarity. Al(III) and Mn(II) show negligible (<3%) extraction in Cyanex 923 and their behaviour is not shown in the plot. The studies on the extraction behaviour of Co(II) and Ni(II) from 1-10 mol/L H<sub>2</sub>SO<sub>4</sub> and HNO<sub>3</sub> revealed that both of these metal ions are very poorly extracted (<3%) from these media. The subsequent studies were carried out using a  $1 \times 10^{-3}$  mol/L solution of Co(II) in 5 mol/L HCl using 0.5 mol/L Cyanex 923, unless stated otherwise.

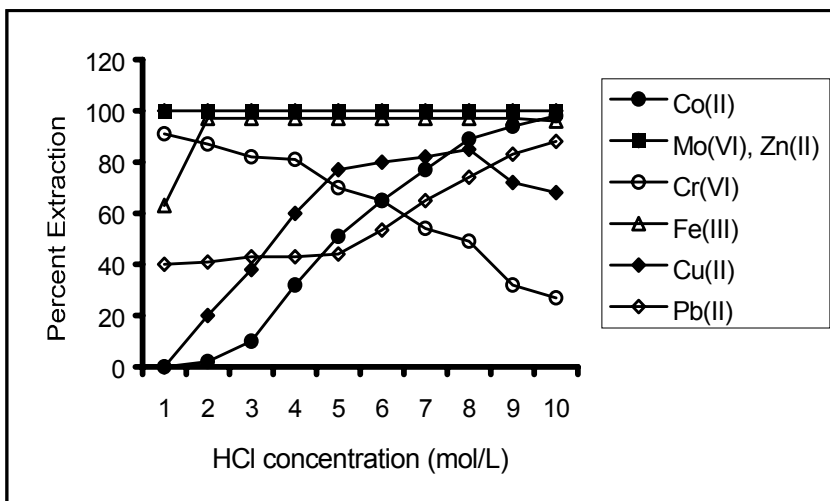


Figure 1. Extraction behaviour of metal ions.

#### Effect of Cyanex 923 Concentration

The effect of Cyanex 923 concentration (0.05-0.5 mol/L) on the partition of Co(II) was investigated. The results are shown in Figure 2. This gives a straight line with the slope around 2, thus suggesting the involvement of two Cyanex 923 molecules in the formation of the extracted Co(II) species.

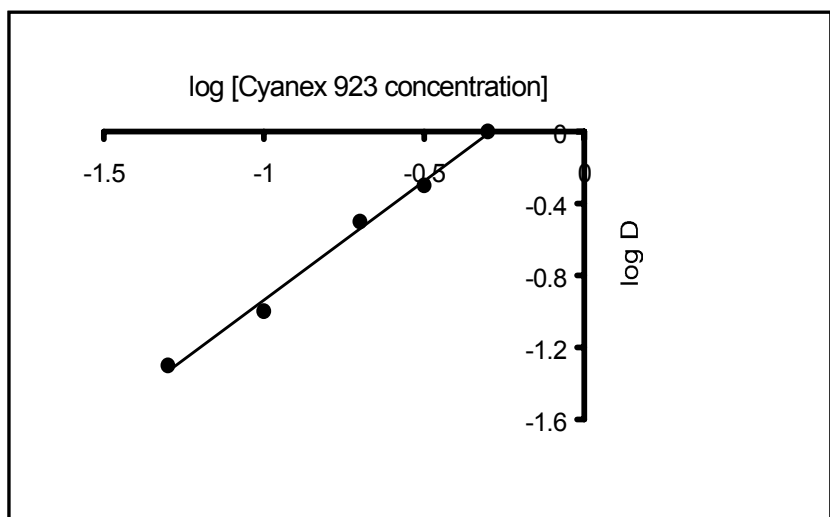


Figure 2. Effect of Cyanex 923 concentration on the extraction of Co(II).

#### Effect of Metal Ion Concentration

The effect of variation in the metal ion concentration ( $1 \times 10^{-5}$  – 0.6 mol/L) on the distribution of Co(II) from 6 mol/L HCl employing 0.4 mol/L Cyanex 923 gives a linear relation in the concentration range  $1 \times 10^{-5}$  – 0.2 mol/L Co(II). This indicates that the partitioning species of Co(II) does not change in this range of metal ion molarity. Beyond 0.2 mol/L, loading conditions start setting in. The percent extraction of Co(II) at the loading conditions is around 60% and therefore the metal concentration in the organic phase is calculated to be around 0.12 mol/L. It may be proposed that Cyanex 923 molecule can hold Co(II) up to a maximum of one half of its molar concentration.

### Stripping

A number of aqueous solutions were employed for the quantitative recovery of Co(II) from the organic layer. A minimum of four volumes of water, 1 mol/L HCl / H<sub>2</sub>SO<sub>4</sub> / HNO<sub>3</sub>, 8 mol/L H<sub>2</sub>SO<sub>4</sub> / HNO<sub>3</sub>, 0.3 mol/L EDTA and 0.2 mol/L oxalic / citric / tartaric acid can be used for the quantitative stripping of Co(II). Mo(VI) is stripped by employing 5% (NH<sub>4</sub>)<sub>2</sub>CO<sub>3</sub> solution in 10% NH<sub>3</sub>.

### Recycling Capacity of Cyanex 923

Successive extraction-stripping cycles were carried out to study the recycling power of Cyanex 923. Co(II) was extracted using 0.5 mol/L Cyanex 923 followed by stripping employing 8 mol/L H<sub>2</sub>SO<sub>4</sub>. The organic phase after stripping was washed with water until the washings were neutral. The recovery of each step was calculated from the amount of Co(II) was extracted in the organic phase in that particular cycle. It was observed that there was no significant decrease in the percent extraction (62-60%) / stripping (99-98%) of Co(II) up to fifteen cycles.

### Separtions

The partition data have been utilized to assess the separation of Co(II) and Ni(II) from other associated metals. The experimental conditions and recovery of metal ions are given in Table 1. Co(II) was separated from Ni(II) / Mn(II) by extracting the former at 8 mol/L HCl. Cr(VI) / Mo(VI) / Fe(III) / Zn(II) was separated from Co(II) / Ni(II) by extracting the first metal ion selectively over Co(II) / Ni(II) from 2 mol/L HCl. The extracted metal ions except Mo(VI) were recovered using 0.2 mol/L oxalic acid. The stripping of Mo(VI) was carried out by using 5% (NH<sub>4</sub>)<sub>2</sub>CO<sub>3</sub> in 10% NH<sub>3</sub>. The isolation of Ni(II) from Cu(II) was attained by achieving the selective extraction of Cu(II) from 8 mol/L HCl.

Table 1. Separation of Co(II) and Ni(II) ( $1 \times 10^{-3}$  mol/L) from Cr(VI) / Mo(VI) / Al(III) / Fe(III) / Mn(II) / Cu(II) / Pb(II) using (2 x vol) 0.5 mol/L Cyanex 923.

Metal ions	HCl conc. (mol/L)	Recovery of Co(II) <sup>a</sup> (%)	Ni(II) / Co(II) / Al(III) / Mn(II) remaining in aqueous phase (%)	Recovery of Cr(VI) <sup>b</sup> / Mo(VI) <sup>c</sup> / Fe(III) <sup>b</sup> / Cu(II) <sup>b</sup> / Zn(II) <sup>b</sup> (%)
Co(II)-Cr(VI)	2		97	95
Co(II)-Mo(VI)	2		96	96
Co(II)-Fe(III)	2		95	97
Co(II)-Zn(II)	2		97	98
Co(II)-Al(III)	8	94	97	
Co(II)-Mn(II)	8	93	98	
Co(II)-Ni(II) / Ni(II)- Cr(VI) / Ni(II)-Fe(III)	8	92	98	
Ni(II)-Cu(II)	2		98	90
	2		96	95
	8		97	93

a Recovered using 4(vol) x 1 mol/L H<sub>2</sub>SO<sub>4</sub>

b Recovered using 4(vol) x 0.2 mol/L oxalic acid

c Recovered using 4(vol) x 5% (NH<sub>4</sub>)<sub>2</sub>CO<sub>3</sub> in 10% NH<sub>3</sub>

### Recovery of Cobalt and Nickel from Spent Catalyst

10 mL of Ai, Bi and Ci were separately equilibrated with two volumes of 0.5 mol/L Cyanex 923. It quantitatively extracted Co(II) along with other metal ions, namely Mo(VI), Cr(VI), Fe(III) and Zn(II). In case of spent Ni hydrogenation catalyst solution (Ci), the above operation leaves pure Ni(II) in the aqueous solution and this was labeled as (Cf). The Co(II) content present in the organic layers of (Ai) and (Bi) was stripped by using 8 mol/L H<sub>2</sub>SO<sub>4</sub> and 2 mol/L HCl, respectively. The final recovered cobalt solutions were labeled as (Af) and (Bf). For recycling, the organic phase was washed with water, 0.5 mol/L oxalic acid, 5% (NH<sub>4</sub>)<sub>2</sub>CO<sub>3</sub> in 10% NH<sub>3</sub> (to recover pure Mo, if present) and water. Table 2 gives the compositions of (A), (B) and (C) before and after extraction.

*Table 2. Composition of spent Co-Mn (A), Co-Mo (B), and Ni hydrogenation (C) catalysts before and after extraction steps.*

Sample	Metal ions present	Concentration in initial solution (mg/L)	Concentration in final solution (mg/L)	Co purity (%)	Co recovery (%)
Spent Co-Mn catalyst	Co	497	469	$99.7 \pm 0.1$	$94 \pm 3$
	Al	32.2	< 0.01		
	Ni	13.3	< 0.01		
	Cr	5.53	0.25		
	Cu	5.8	1.14		
Spent Co-Mn catalyst	Co	155	147	$99.7 \pm 0.1$	$95 \pm 3$
	Mo	331	0.34		
	Al	291	< 0.01		
	Fe	35.2	0.13		
	Zn	8.52	0.04		
Spent Ni catalyst	Ni	2656	2598	$99.5 \pm 0.2$	$98 \pm 1$
	Fe	802	3.56		
	Cu	57.2	4.71		
	Zn	5.67	< 0.01		
	Cr	2.74	0.12		
	Mn	1.78	1.82		
	Co	1.32	0.03		

## CONCLUSIONS

The present investigations highlight the potential of Cyanex 923 for achieving a number of topical separations involving cobalt and nickel. The methods are convenient and require no strict control on phase variables. The extractant is easy to recycle and offers quicker phase separation. The loading capacity of Cyanex 923 for Co(II) is also good. The recovery process is simple and a fewer number of counter-current extraction steps will be sufficient to obtain high purity metals.

## ACKNOWLEDGMENTS

The authors are thankful to Cytec Canada, Inc. for providing the Cyanex 923 extractant. Financial support of Council of Scientific and Industrial Research and University Grant Commission, India, is gratefully appreciated.

## REFERENCES

1. M. Vladulescu, T. Vela, C. Revencu and I. Constantinescu (1981), *Ser. Chim. Metal.*, **43** (1), 65.
2. N. V. Thakur and S. L. Mishra (1998), *Hydrometallurgy*, **49** (3), 277.
3. K. Soldenhoff, N. Heward and D. Wilkins (1998), *Proc. TMS Annual Meeting*, Warrendale, PA, pp. 153.
4. B. K. Tait (1993), *Hydrometallurgy*, **31** (1-3), 345.



## CYANIDE RECOVERY BY SOLVENT EXTRACTION

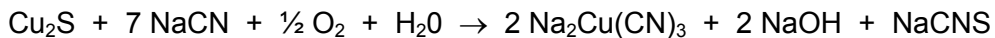
David Dreisinger, Berend Wassink, Keren Ship\*, James King\*,  
Marilyn Hames\* and Ralph Hackl\*

The University of British Columbia, Vancouver, Canada  
\*Placer Dome Technical Services, Vancouver, Canada

Cyanide is the preferred reagent for gold extraction from ores and concentrates. Cyanide is used in dilute concentration in solution so as to minimize cost and potential environmental impact. Residual cyanide in waste slurries or solutions is conveniently destroyed using either a chemical or biological process. Some ores and concentrates require higher concentrations of cyanide for leaching due to the presence of cyanide soluble copper or other species in solution. For these ores, it may be desirable to introduce cyanide recovery to reduce the net cost of gold extraction. Many of the current cyanide recovery processes (e.g., acidification/volatilization/re-neutralization (AVR) or sulfidization/acidification/ recycle/ thickening (SART)) produce acidic solutions containing soluble HCN. Soluble HCN can be recycled by direct neutralization or by volatilization/re-neutralization. The volatilization of HCN with air is undesirable due to the potential safety hazard of handling gaseous HCN and the high cost of air stripping/scrubbing columns. In this work, a solvent extraction alternative to HCN volatilization has been studied. The organophosphorus solvating extractants Cyanex 923, di-butyl-butyl-phosphonate and tri-butyl phosphate strongly extract HCN from aqueous solution. HCN may be conveniently stripped with any suitable alkali to reconstitute a strong cyanide solution for recycle.

### INTRODUCTION

The cyanidation of copper-gold ores containing the common oxide and secondary sulfide copper minerals results in irreversible cyanide degradation (to  $\text{CNO}^-$  and  $\text{CNS}^-$ ) and copper solubilization as cuprous cyanide complexes. Some of the possible reactions are shown below.

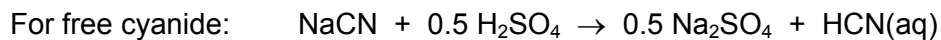


In conventional gold processing, the copper and complexed cyanide are not recovered after the gold is removed from solution (for example by carbon adsorption). This results in a significant economic penalty in excess cyanide consumption (beyond that converted to

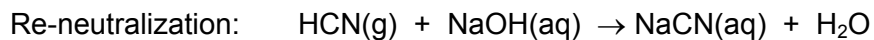
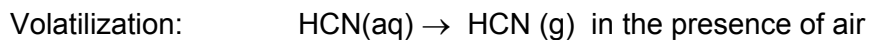
cyanate and thiocyanate or to other metal cyanide complexes) and loss of a potentially valuable copper by-product. A variety of approaches have been investigated for copper and cyanide recovery including solvent extraction of copper cyanide, ion exchange methods and electrowinning of copper [1-5]. Unfortunately none of these processes have found commercial application.

The SART process is often selected for cyanide recovery. The SART process has basically two chemical steps – sulfidization/acidification and re-neutralization. The re-neutralization may be performed directly on the acidified solution (after copper sulfide filtration) or may be linked to a volatilization step. In either case, the chemistry of re-neutralization is identical.

#### Step 1. Acidification in the presence of NaSH



#### Step 2. Volatilization/Re-neutralization



The SART process is inherently very simple and effective. Unfortunately, volatilization and re-neutralization of HCN is potentially dangerous and expensive. In this study [6], the use of solvent extraction for HCN recovery was investigated. The organophosphorus extractants were selected for investigation.

## EXPERIMENTAL

Cyanex 923, di-butyl-butyl-phosphonate (DBBP) and tri-butyl phosphate (TBP) were used in this study. Cytec Inc. (Niagara Falls, Canada) and Albright and Wilson (USA) provided the extractant samples. The extractants were used at full strength or diluted with a kerosene diluent (Exxsol D-80 from Exxon Chemicals Canada). Organic liquids containing TBP, DBBP and Cyanex 923 were prepared at 100%, 50% and 25% extractant strength.

Synthetic solutions containing HCN were prepared. Aqueous cyanide solutions for treatment were prepared to contain about 0.0077 M NaCN (0.377 g/L NaCN and 0.200 g/L CN) and 0.001 M NaOH. A known sample volume was titrated with 0.125 M H<sub>2</sub>SO<sub>4</sub> to pH 4.00+/-0.05 to determine the required amount of acid to add to convert NaCN to HCN. A mildly acid pH is preferably maintained to improve the equilibrium of extraction of the neutral HCN species into the organic solvent, and to avoid polymerization of HCN in the presence of CN<sup>-</sup>. Upon acidification the solution contained about 200 mg/L HCN and 600 mg/L Na<sub>2</sub>SO<sub>4</sub>.

Various phase ratios of aqueous and organic solutions were tested, using flasks or separatory funnels. Acid was added to the solutions for extraction to maintain an acid pH in the aqueous media. In the examples, the vessels were sealed and the mixtures were shaken or stirred vigorously for 20 minutes and then allowed to settle. To assay samples for cyanide content, aqueous phase samples were added to a NaOH solution and titrated with a known AgNO<sub>3</sub> solution (about 0.018 M) using rhodamine as the titration end-point indicator. Loaded organic solution samples (*i.e.*, the organic phase loaded with HCN following extraction) were stripped with 1 M NaOH, usually at an aqueous to organic (A/O) ratio of 1. Samples of the stripped aqueous solutions were titrated with AgNO<sub>3</sub>. Blank tests were also performed in which the aqueous phases were deionized water.

## RESULTS AND DISCUSSION

The equilibrium loading results are shown in Figures 1 to 4 and summarized in Table 1.

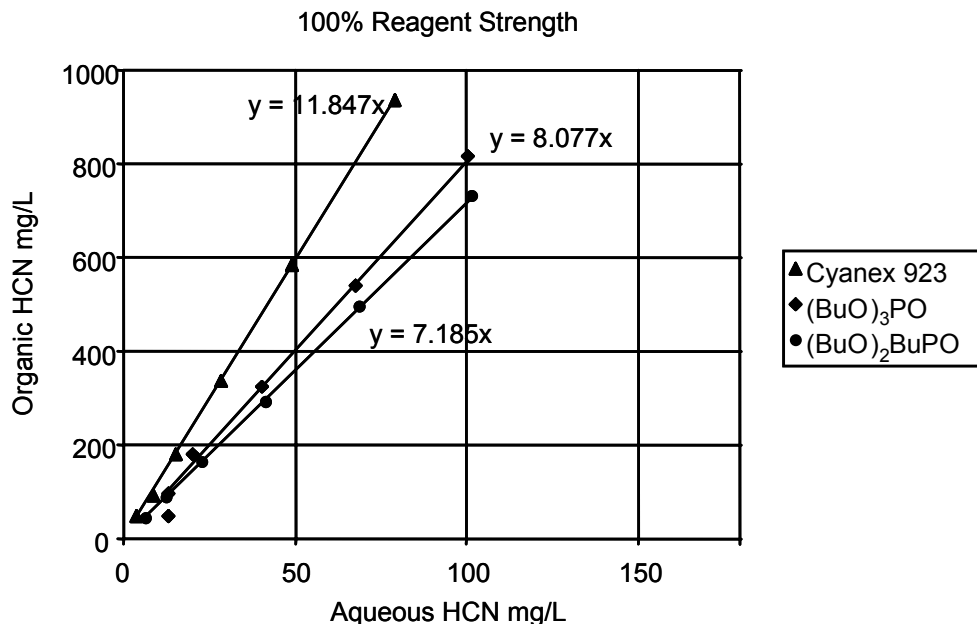


Figure 1. Cyanide extraction with 100% extractant solutions.

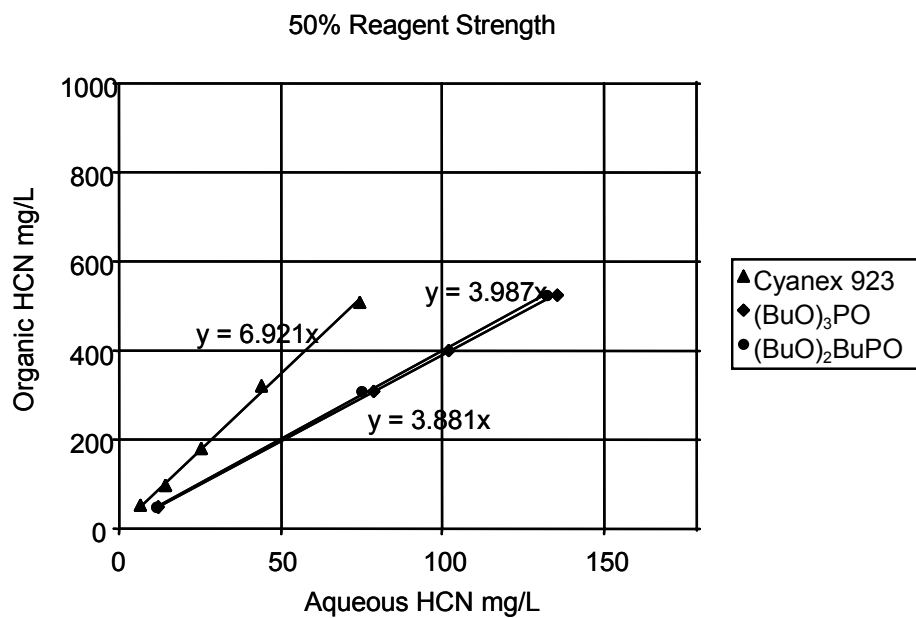


Figure 2. Cyanide extraction with 50% extractant solutions with Exxsol D-80 diluent.

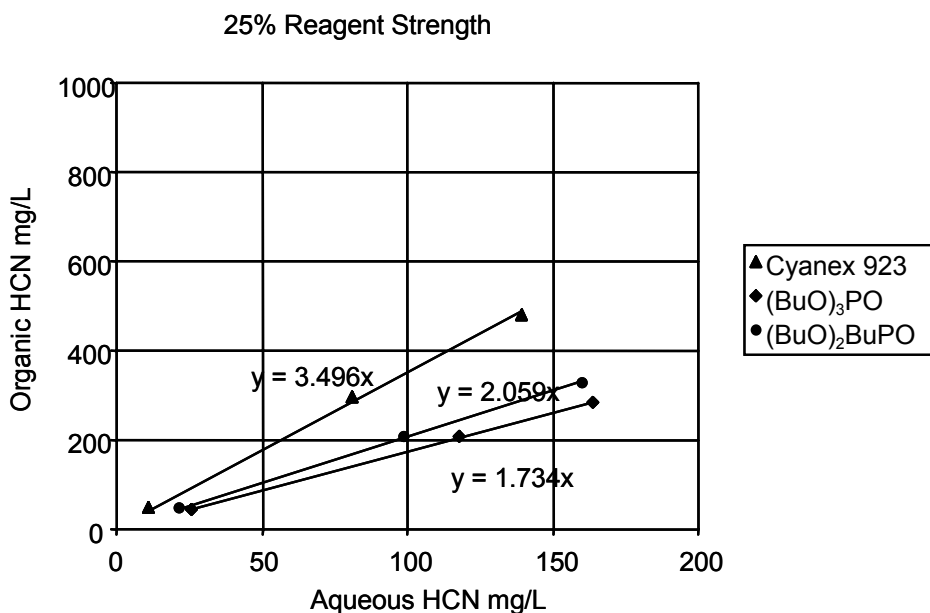


Figure 3. Cyanide extraction with 25% extractant solutions with Exxsol D-80 diluent.

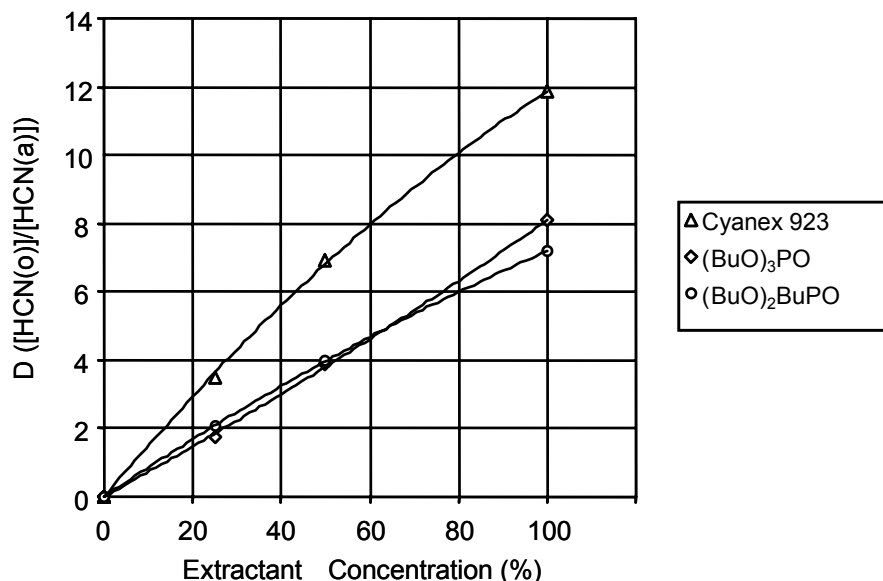


Figure 4. Comparison of the distribution values for various extractants as a function of extractant concentration.

Each of the solvents extracts HCN strongly from solution. Cyanex 923 is the strongest extractant in the series followed by DBBP and TBP. Dilution of the extractant with Exxsol D-80 weakens extraction of HCN in direct proportion to the dilution.

In the case of 100% TBP, the aqueous phases after loading were clear. These were analyzed without further clarification. A test was done to confirm that there was no interference from organic entrainment. In all other tests, the aqueous phases were centrifuged prior to analysis.

*Table 1. Distribution values for extraction.*

Organic reagent	Concentration (%)	$D_{HCN}$
Cyanex 923	25	3.5
	50	6.92
	100	11.85
$(BuO)_2P(O)Bu$	25	2.06
	50	3.99
	100	7.19
$(BuO)_3P(O)$	25	1.73
	50	3.88
	100	8.08

The lowest aqueous HCN levels detected (for single contact) were found for tests at A/O 0.25. For Cyanex 923 this was 4 mg/L, for dibutylbutylphosphonate, 7 mg/L and for tributylphosphate, 13 mg/L. These results indicate the tremendous potential of the solvent extraction system to remove HCN from solution and decontaminate discharge solutions from gold mine sites.

Figure 5 shows a simple McCabe-Thiele construction for HCN extraction. This diagram indicates that about 4 stages of extraction would be sufficient to recover cyanide to less than 10 mg/L residual cyanide from a starting concentration of 200 mg/L cyanide at an A/O ratio of 5:1. Figure 6 shows the potential integration of cyanide solvent extraction into a cyanide recovery circuit.

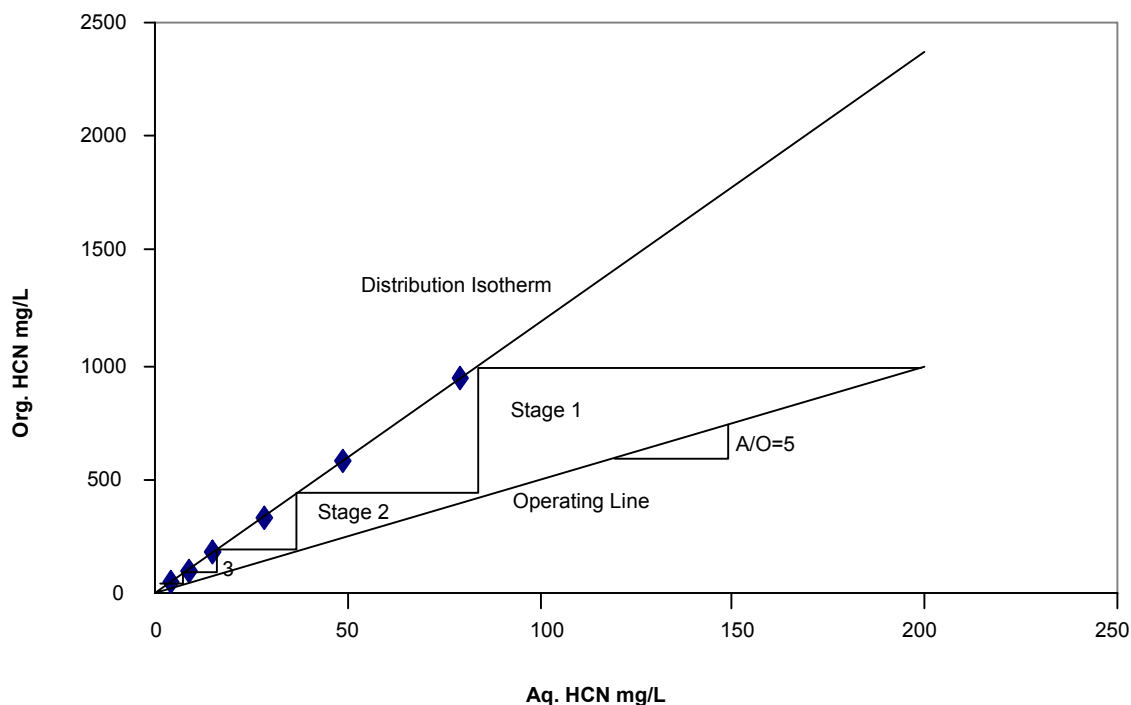


*Figure 5. McCabe – Thiele diagram for HCN extraction. 100% Cyanex 923.*

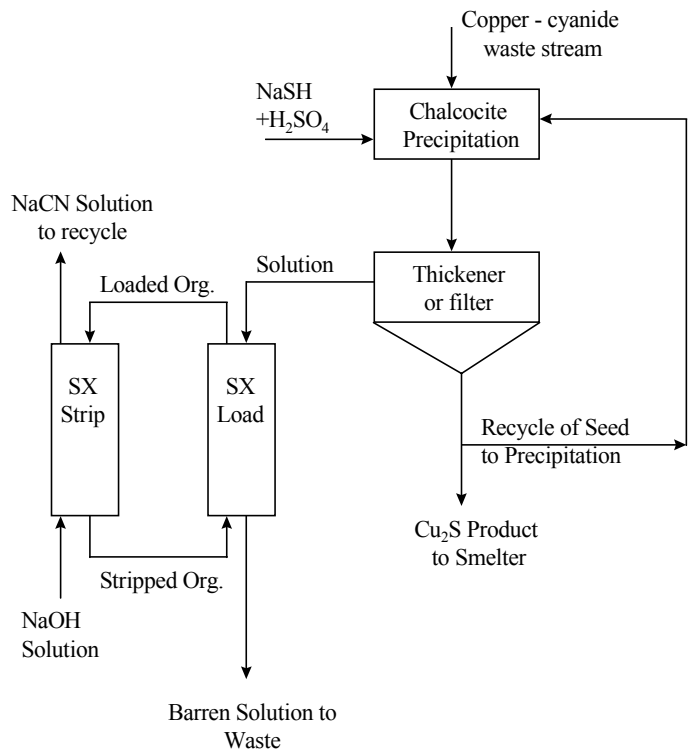


*Figure 6. Process flow diagram for cyanide recovery using solvent extraction.*

The extraction kinetics of HCN are fast and at least 4 stages of extraction are required for effective cyanide removal from solution. In this case, a column contactor such as the Bateman Pulsed Column system is ideal for application. The Bateman Pulsed Column system allows for high flow, low stage height contact of aqueous and organic solutions to effectively recover cyanide. Pilot scale testing of this system using a Bateman Pulsed Column will be the subject of a future publication.

## CONCLUSIONS

The solvent extraction recovery of cyanide from acidified solutions using organophosphorus solvating extractants has been demonstrated. Distribution factors for cyanide loading increase in the series TBP – DBBP – Cyanex 923 and even with dilution with Exxsol D-80 are favourable for effective HCN loading. Stripping of the organic loaded solvent can be accomplished by organic phase “neutralization” with an alkali solution (e.g., NaOH). The solvent extraction process for HCN appears to be a viable alternative to conventional volatilization/reneutralization in which air is the transfer medium.

## REFERENCES

1. G. W. Lower (1969), *U.S. Pat.*, No. 3,463,710 (Aug. 26).
2. C. A. Fleming, W. G. Grot and J. A. Thorpe (1995), *U.S. Pat.*, No. 5,411,575 (May 2).
3. G. R. Maxwell, J. A. Thorpe, K. M. Schall and K. A. Brunk (1997), Global Exploration of Heap Leachable Gold Deposits, D. M. Hausen (ed.), TMS, Warrendale, PA, pp. 141-149.
4. D. B. Dreisinger, J. Ji, B. Wassink and J. King (1995), *Proc. Randol Gold Forum - Perth '95*, Randol, Golden, CO, pp. 239-244.
5. D. B. Dreisinger, B. Wassink, J. Lu, F. De Kock, J. Ji, P. West-Sells and R. Dunne (2001), Cyanide: Social, Industrial and Economics Aspects, C. Young (ed.), TMS, Warrendale, PA, pp. 347-360.
6. D. B. Dreisinger (2001), *U.S. Pat.*, No. 6,200,545 (March 13).



## MERCURY RECOVERY FROM DENTAL AMALGAMS USING SOLVENT EXTRACTION

L. A. Silva De Lima, C. Pereira De Souza, J. Y. Pereira Leite and A. I. Curbelo Garnica\*

\*Universidade Federal do Rio Grande do Norte, Natal, Brasil

This paper presents the study of a leaching process of dental amalgam as well the solvent extraction of Hg ions from this waste. HCl, HNO<sub>3</sub> and HCl / HNO<sub>3</sub> (3:1) were used in the digestion process and the temperature, concentration of the solution and the time of contact between the phases were investigated. In the solvent extraction process tri-ethanoamine and tri-isooctilamine were used as extractant agent. The pH, mass ratio of the organic and aqueous phases and the time of contact between the phases were optimized. The tri-isooctilamine is more efficient than the tri-ethanoamine at lower pH at 25 °C.

### INTRODUCTION

Environmental pollution in the form of heavy metals at high concentrations generates a series of problems that can affect biological natural cycles. A source of this pollution is the dental amalgam from clinics that is discharged into sewer streams. The average composition used by dentists in the amalgam preparation is 50-55% Hg, 32.5-35% Ag, 12-14.5% Sn, 0-3% Cu and 0-1% Zn. Contamination by mercury represents a danger to the environment as the discharge enters the natural aquatic environment that in turn provides a food source (fish and mollusks) for the local population.

Statistical studies show that the amount of amalgam can reach approximately 150 kg/year in the State of Rio Grande do Norte [5,6] and this material is discharged in the sewer stream of the Potengi River in Natal city. The Hg is present in the inorganic form and the digestion process takes place in the organic form as methyl mercury. This process occurs by the action of the microorganisms contained in the flora of the river that are consumed by fish and mollusks. The toxicity of this metal can affect the nervous system and promotes other diseases. According to Klaassen [1,3], it can also change the genetic code of the humans.

The study of technical routes to solve this problem requires the investigation of new processes of recycling and recovery of the mercury contained in the dental amalgams collected from the clinics. In the present work various conditions of the digestion process have been optimized. These include the type and concentration of the leaching agent, contact time and temperature of the system [7,8]. In the second stage, two types of extractant agents, tri-ethanoamine (TEA) and tri-isooctilamine (TIOA) and the pH of the solution containing the Hg [2,4,9] were investigated.

## EXPERIMENTAL PROCEDURES

The experimental procedure developed in this work is shown in Figure 1.

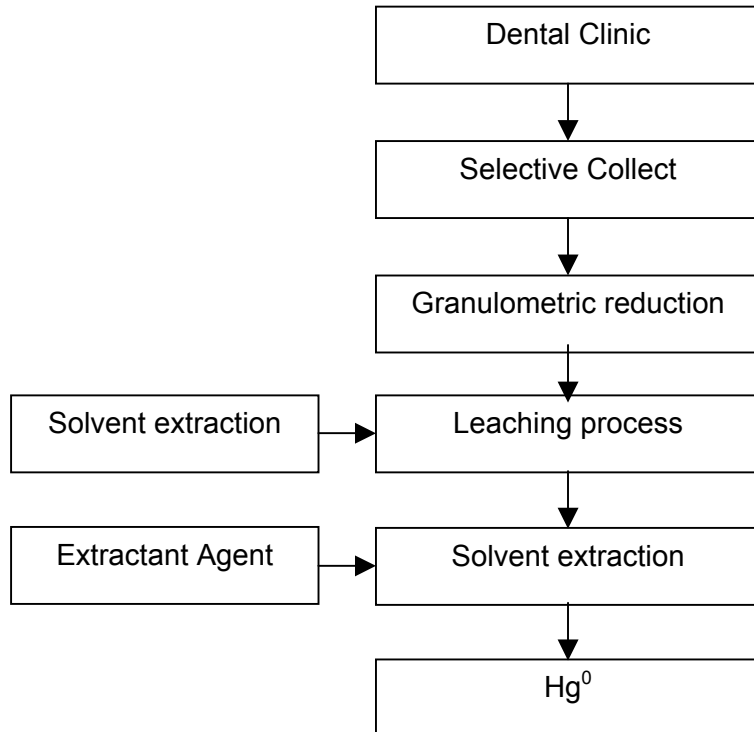


*Figure 1. Process flowsheet for the recovery and recycling of dental amalgams.*

Samples were collected from the Odontology Clinic of the CEFET – RN and then subjected to granulometric reduction using special ball mills (8'x 8') with balls that were coated with refractory ceramic to avoid the contamination of the material. The milling process reduced the particle size of the waste to lower than 105 µm. The samples were dissolved in HCl, HNO<sub>3</sub> and HCl/HNO<sub>3</sub> (3:1) using the following concentrations (vol.-%): 20%, 25%, 30% and 35%. The time of digestion was 2, 4 and 5 hours and the temperature was 25 and 50°C. The temperature of the system was controlled using a thermostatic bath.

In the solvent extraction process, the experiments were carried out using a synthetic solution of HgCl<sub>2</sub> containing 400ppm of Hg. The influence of the pH on the extraction process was studied for the mass relation between the Organic phase (OP)/Aqueous phase (AP) of 1:1. The composition of the organic phase was 95% kerosene, 4% octanol and 1% amine. The solution was stirred for 5 minutes using a glass extractor at 25°C. When the equilibrium was reached, the aqueous phase was separated and the Hg concentration was determined using an atomic absorption spectrophotometer. The efficiency of the process was calculated using equation 1:

$$\% E = \frac{[Hg]_E}{[Hg]_E + [Hg]_R} \times 100 \quad (1)$$

where [Hg]<sub>E</sub> and [Hg]<sub>R</sub> were the concentration of mercury in the extract and raffinate phases, respectively.

## RESULTS

### Dissolution

In the digestion process of the dental amalgam three different types of acids were used: HCl,  $\text{HNO}_3$  and HCl/ $\text{HNO}_3$  (3:1). The phases were shaken for 1.5, 3.0 and 4.5 hours and the temperature of the system was maintained at 25 and 50°C. The results are shown in Figures 2 to 4.

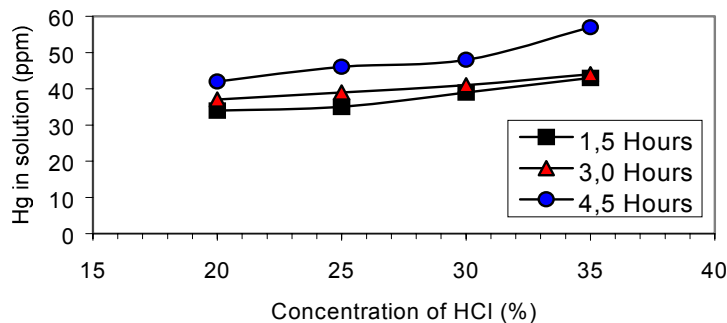


*Figure 2. Dissolution of Hg from amalgam waste using HCl at 25°C.*

Dissolution efficiency with HCl was low and increasing the time of contact and the concentration of acid did not improve the dissolution significantly.

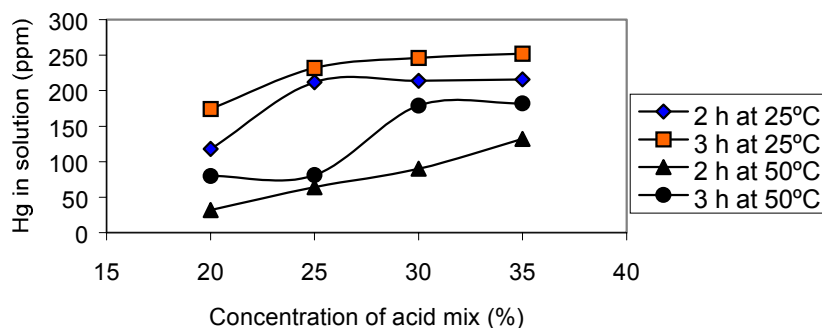


*Figure 3. Dissolution of Hg from amalgam waste using HCl / $\text{HNO}_3$  (3:1) mixture.*

Figure 3 shows that, for the acid mixture, an increasing amount of amalgam dissolved when the time of contact increased and a larger quantity of the amalgam dissolved for a temperature of 25°C than for 50°C.

The experiments using  $\text{HNO}_3$ , presented in Figure 4, show the total dissolution (400 ppm) of the Hg for a low concentration of  $\text{HNO}_3$  at 25°C. The HCl/ $\text{HNO}_3$  (3:1) mixture dissolves 250 ppm, while the HCl dissolves only 60 ppm at the same temperature, according to the Figures 3 and 2, respectively.

In summary, HCl is an inefficient lixiviant, while the HCl/ $\text{HNO}_3$  (3:1) mix gives better results at 25°C. This phenomenon can be explained by the gathering of the ions of  $\text{Hg}^{2+}$  as a function of the heat of solvation. When the temperature increases the increased solvation heat promotes the agglomeration of these ions that can therefore not be read by the molecular absorption instrument. Dissolution efficiencies were high for low concentrations of  $\text{HNO}_3$  that promotes the total dissolution of the amalgam. The temperature changing did not influence the process. The efficiency of the digestion process using the three different acids follows the sequence: [HCl] < [HCl/ $\text{HNO}_3$  (3:1)] < [ $\text{HNO}_3$ ].

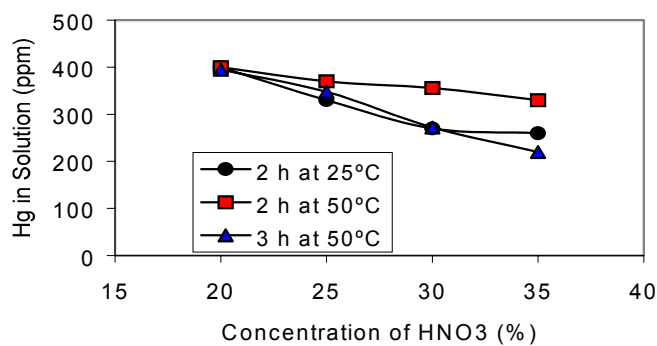


*Figure 4. Dissolution of Hg from amalgam waste using HNO<sub>3</sub>.*

### Solvent Extraction

In the study of the pH of the aqueous phase of the solvent extraction process, the experiments were carried out using TEA. The results are presented in Figure 5.

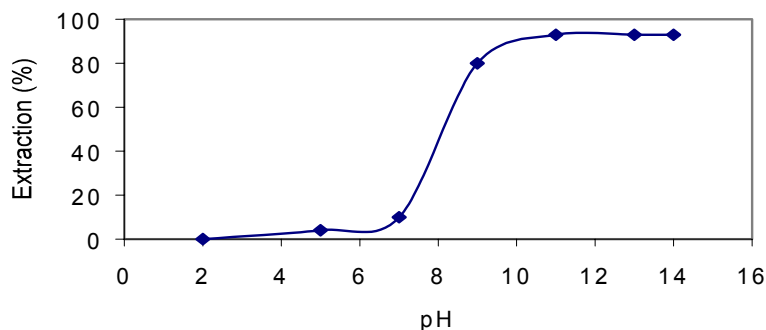


*Figure 5. Influence of pH on the solvent extraction of Hg using TEA.*

The curve presented in Figure 5 shows that the extraction reaches equilibrium with approximately 93% Hg extracted at the pH = 11.07. This phenomenon is explained by the saturation of the TEA with Hg.

Experiments varying contact time were carried out using TIOA. The pH was 2.55 and the mass ratio AP/OP of the phases was 1. The phases were stirred at 25 °C and samples were removed every 5 minutes for analysis. The results of the effect of contact time on the extraction efficiency are shown in Figure 6.

Figure 6 shows that extraction efficiency with TIOA at 25 °C increases with increasing time of contact. After 35 minutes of contact between the phases 74.44% of Hg was extracted from the solution.

The relative extraction efficiency of the two solvents can be compared using data from Figures 5 and 6. For the same pH (pH = 2) and 5 minutes of stirring, TIOA extracted 20% while TEA never extracted Hg ions.

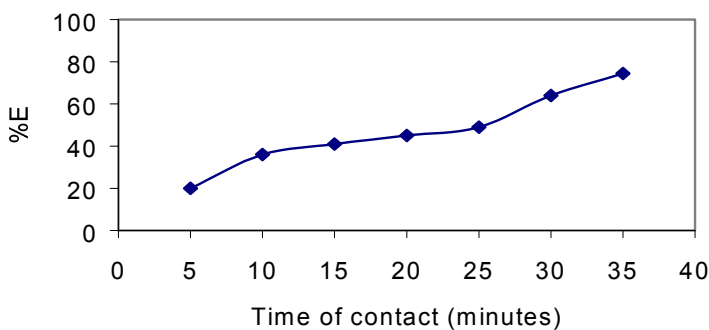


Figure 6. Influence of contact time on extraction efficiency of Hg using TIOA.

## CONCLUSIONS

The efficiency of the digestion process for the three acids used increased in the order: [HCl] < [HCl/HNO<sub>3</sub> (3:1)] < [HNO<sub>3</sub>]. The use of the nitric acid (20 vol.%) allows the total dissolution of the amalgam residues resulting in a solution containing 400 ppm of Hg at 25°C or 50 °C. In the next step of this work, the influence of the other species present in dental amalgam on the leaching process will be investigated.

Solvent extraction with TEA as the extractant presented better results as the pH increased (93% extraction at pH = 11) for a mass ratio between the phases of 1:1. The solution was stirred for 5 minutes at 25°C. For the same conditions of pH (pH = 2) and contact time (5 minutes) TIOA extracted 20% Hg while TEA extracted no metal. TIOA is therefore a more efficient extractant than TEA under these conditions. Further studies will be performed using the solution generated from the leaching of amalgam as will experimental studies of the phase diagram of the ternary system: Hg<sub>2</sub>(NO<sub>3</sub>)<sub>2</sub> – TIOA – Water at 25°C.

## ACKNOWLEDGEMENTS

The authors thankfully acknowledge the financial support provided by CNPq (National Council for Scientific and technological Development) for this work and the scholarships given to the student.

## REFERENCES

1. D. B. Filho (1983), Toxicologia Humana e Geral, LITEL, Paraná, Brazil.
2. A. I. C. Garnica (1999), MSc. Thesis, Natal, Brazil.
3. C. D. Klaassen, M. O. Amdur, M. D. J. Doull (1986), Toxicology: The Basic Science of Poisons, Macmillan Publishing Company, New York, USA.
4. G. S. Laddha, T. E. Degaleesan (1976), Transport Phenomena In Liquid Extraction, Tata McGraw-Hill Publishing Co. Ltd, New Delhi.
5. J. Y. P. Leite, M. J. V. F. Leite (2001), Avaliação Do Programa De Coleta Seletiva E Reciclagem De Resíduos De Amálagma No Estado Do Rio Grande Do Norte-Brasil ,VI SHMMT / XVIII ENTMH, Rio de Janeiro, Brazil.
6. J. Y. P. Leite, C. P. Souza, A. D. Araújo (1996), 51º Congresso Nacional da Associação Brasileira de Metalurgia e Materiais, Porto Alegre, Brazil, pp. 226-236.
7. L. A. S. De Lima, C. P. Souza, J. Y. P. Leite (1999), II ENPROMER, Vol. 1, Florianópolis, Brazil, pp. 459.
8. L. A. S. De Lima, C. P. Souza, J. Y. P. Leite (1998), 50ª SBPC, Natal, Brazil, pp. 1172.
9. G. Villanueva (1996), Aspectos Fundamentales Acerca De Las Operaciones De Extracción, UCLV, Cuba.



## SUPERCritical FLUID EXTRACTION-OXIDATION TECHNOLOGY TO REMEDIATE PCB CONTAMINATED SOILS/SEDIMENTS

Wu Zhou, Gheorghe Anitescu and Lawrence L. Tavlarides

Syracuse University, Syracuse, USA

Systematic studies conducted on PCB contaminated site samples to investigate both the technical and economic feasibilities of supercritical fluid extraction technology for remediation of soil/sediments are discussed. In support of the extraction process, partition equilibrium data of targeted solutes between contaminated samples and supercritical CO<sub>2</sub> with and without 5 mol % methanol are reported. Laboratory scale desorption experiments reveal that PCB concentrations in sediments can be reduced from ~2200 ppm to <5 ppm (99.7% extraction efficiency) in 60 minutes when CO<sub>2</sub> - MeOH (5 mol %) is used. Follow-up experiments conducted with a 2-liter fixed bed bench scale unit confirm the laboratory scale findings. A linear driving force model, developed on the laboratory scale desorption data, predicts the bench scale results well. An economic analysis of a two-stage process of supercritical fluid extraction and supercritical water oxidation of the sediment extracts shows that the cost range of 142-175 USD/m<sup>3</sup> is competitive with other remediation technologies.

### INTRODUCTION

It has been estimated that about 175 million kg of polychlorinated biphenyls (PCBs) exist in landfill and other storage, and another 11 million kg exist in sediments, soil, and biosystems [1]. The environmental threat of the large amount of PCBs has called for the development of effective PCB cleanup techniques. However, methods to extract and destroy PCBs from contaminated soils/sediments (S/S) are facing unusual challenging problems due to the wide spreading areas, strong molecular interactions with S/S pores, very high chemical stability, low water solubility, and slow kinetics. Extraction and destruction methods include *in situ* thermal desorption, liquid solvent extraction, supercritical fluid extraction (SFE) and incineration and chemical reduction/oxidation, respectively.

Studies regarding a two-stage supercritical fluid technology (SFT) for S/S remediation process consisting of SFE of PCBs and supercritical water oxidation (SCWO) of the extracted pollutants are in progress at Syracuse University [2-3]. SFE is seen as an appropriate method to remove both organics [4] and metals (through chelating agents) [5] from different solid matrices. The unique property of supercritical fluids (SCFs) that makes them technically enticing is that they show enhanced ability to dissolve organic compounds which can be easily tuned by changing temperature and/or pressure [6], leading to simple solute-solvent separation. Further, low viscosity and high diffusivity of SCFs are essential to reduce mass transfer resistance during the desorption process. The most popular SCF is the non-toxic, non-flammable, readily available, and inexpensive CO<sub>2</sub>. Using this “green” solvent to replace liquid organic solvents offers important health and environmental advantages and the cleaned, unaltered S/S are returned to the site.

## PROCESS DESCRIPTION

The two-stage SFT process we advance at Syracuse University consists of SFE of PCBs/PAHs from the contaminated S/S and SCWO of the extracts (Figure 1) [2-3]. In the first step, the contaminated materials are contacted in a multistage SFE system and the extracted pollutants are separated from the supercritical fluids by pressure letdown and can be concentrated by distillation. Residual methanol can be stripped from the clean S/S by switching to pure CO<sub>2</sub>. Different options of the technology propose different levels of methanol recovery and recycle. The cleaned S/S are returned to the site. In the second stage, the extracted solutions are oxidized in a SCWO unit to mineral products such as CO<sub>2</sub>, H<sub>2</sub>O, and HCl, which can be easily transformed in NaCl. The oxidation can occur at the end or at intermediate points in the separation step to recover high pressure CO<sub>2</sub>. Both steps of the technology are contained processes and use recycle loops. The methanol in the second step is fully reacted and contributes to the PCB rate reaction enhancement and acts as fuel for the SCWO process.

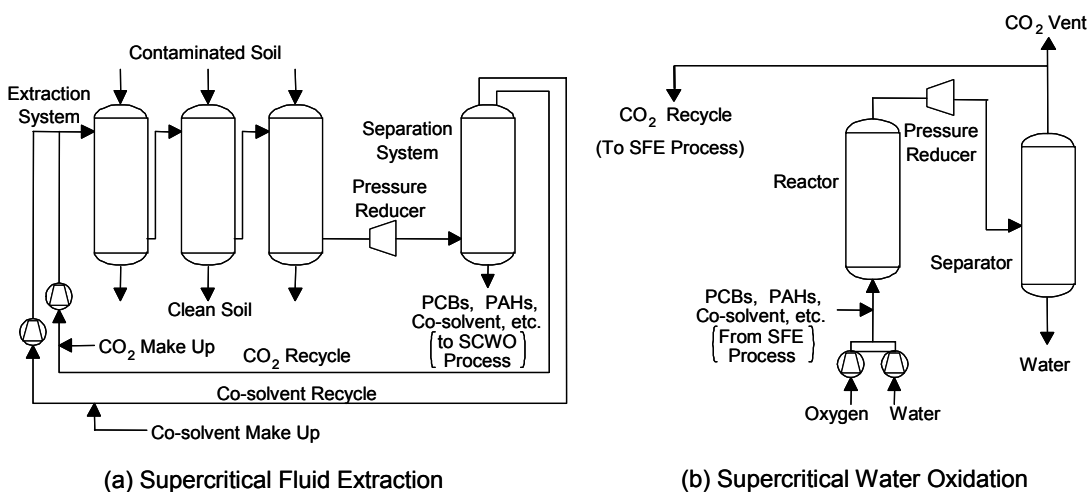


*Figure 1. Supercritical fluid technology process for soil / sediment cleanup*

## SCREENING, SOLUBILITY, SORPTION, AND DESORPTION STUDIES

Three real world St. Lawrence River sediment (SLRS) samples obtained from a contaminated site near Massena, NY, exhibit similar properties and PCB congener distribution patterns but different PCB concentration levels. These requirements are needed to conduct cohesive studies for a comprehensive and systematic evaluation of the SFE process. The three sediments were prepared by air-drying and sieving. Mineral properties, total organic carbon (TOC), and initial PCB concentrations of the three sediments given in Table 1 indicate that the three samples have similar properties yet different levels of PCB concentrations.

### Screening Desorption Rate Studies

Effects of pressure, temperature, cosolvent, soil moisture, initial PCB concentration, and soil type on PCB desorption efficiencies have been investigated to determine proper desorption conditions [7]. Table 2 summarizes the results of the systems studied and shows that sub 5 ppm PCB residual concentration can be achieved in approximately 60 minutes of desorption of 2200 ppm real world SLRS. Contact time for desired levels of desorption is seen to depend upon these conditions and vary between 15 to 60 minutes.

*Table 1. Properties of real world St. Lawrence River sediments.*

Sediment samples	Composition (%)			TOC (%)	PCB Conc. (ppm)
	Sand	Clay	Silt		
St. L. R. Sediment #1	37.67	32.72	29.60	1.34	130
St. L. R. Sediment #2	55.73	23.21	21.06	1.21	710
St. L. R. Sediment #3	58.38	22.1	19.53	1.76	2200

*Table 2. Laboratory scale desorption data with spiked soils and contaminated sediments.*

Sample	Initial Conc. (ppm)	P (atm)	T (°C)	Cosolvent (mol.%)	Moisture (wt.%)	Contact Time (min)	Residual Conc. (ppm)
Till <sup>a</sup>	1150	200	40	5	10	45	3.2
Sediment <sup>b</sup>	370	200	40	5	10	60	15.1
Sediment <sup>c</sup>	71	100	40	5	20	45	5.7
Surficial <sup>a</sup>	4257	200	40	5	10	30	6.7
Sand <sup>a</sup>	950	100	40	5	10	15	1.2
Sediment <sup>b</sup>	2200	116	50	5	0	60	<5

<sup>a</sup>Laboratory spiked samples;

<sup>b</sup>Real world contaminated St. Lawrence River sediment;

<sup>c</sup>Real world contaminated Hudson River sediment.

Initial PCB concentration effects indicate that, even though there exist more than three fold differences of initial concentrations, the desorption rates of PCBs are essentially identical for the same sample. Regarding the effects of S/S moisture content and cosolvent on PCB desorption rates from two different samples, experimental data show that the presence of 10 - 20 wt % water retards the initial PCB extraction rate sharply. In contrast, the addition of methanol in SC-CO<sub>2</sub> enhances PCB desorption rates and reduces the ultimate PCB residual levels in S/S. Among all the cosolvents studied (methanol, *n*-butane, *n*-propanol, and hexane) [7], the polar and water-soluble methanol is the most effective for the extraction of PCBs from S/S. Other factors studied show the system pressure effects on PCB desorption efficiencies. It is found that pressure affects PCB desorption much more significantly for wet samples than for air-dried samples, and that for extraction from wet samples the enhancement of PCB desorption rate was not proportional to pressure increment [7]. Also comparisons between real world contaminated and spiked sediments show that laboratory prepared samples have more rapid PCB desorption rates and lower final residual concentrations than real world samples. These results underscore the need to conduct laboratory tests with samples from the site to be remediated.

### Thermodynamic Solubility Studies

These data permit one to assess the most desirable SCF from a capacity and selectivity standpoint. Research efforts at Syracuse University have resulted in the generation of a substantial database of PCB solubilities in SC-CO<sub>2</sub> and SC-CO<sub>2</sub> modified with *n*-butane and methanol over a range of conditions [8]. Solubility data of PCBs are correlated by semiempirical equations over the experimental ranges of pressure and temperatures. Both *n*-butane and methanol were found to enhance the solubilities of PCB congeners compared to those in pure SC-CO<sub>2</sub>. For the entire data set, an enhancement of 5-91% of the solubilities is observed.

### **Partition Equilibrium Studies**

During extraction processes, the PCB concentrations in SC phase are less than their saturation solubilities due to the interactions between PCBs and soil matrices and relatively long contact time needed to reach equilibrium. For a SCF to effectively remove PCBs from soil, it must have high PCB dissolving capacities and proper interaction properties with the soil matrices and PCBs, such as competing with solute for active sites and swelling the soil matrices to improve solute accessibility. Therefore, to select a proper cosolvent and to provide information for desorption data modeling, the equilibrium partition behavior of PCBs between SCFs and S/S needs to be studied. PCB partitioning equilibrium studies between SLRSs and both SC-CO<sub>2</sub> and CO<sub>2</sub> - MeOH (5 mol %) were conducted at 40, 50, and 60 °C and different SCF density levels (5.5, 8.0, 10.5, 13, and 15.5 mol/L) requiring a pressure range of 76.3-177.5 bar. These results are used to model PCB desorption rates.

The partition equilibrium data were analyzed for both totals PCBs and 12 major individual congeners detected in the sediments. All the isotherms show good linearity except for those at lower density (5.5 and 8.0 mol/L) in pure CO<sub>2</sub> system. Preferential desorption was found among the PCB congeners analyzed. The partition coefficients increase roughly in the order of molar weight increase of PCB congeners. The increase of either temperature or density while one of them is kept constant results in the decrease of partition coefficients (favor PCB desorption) for both SCFs. Temperature and density effects appear to be more significant for the CO<sub>2</sub>-MeOH system than for pure CO<sub>2</sub>. All the isotherms are fitted with a linear model. The correlation between the partition coefficients (*K*) and system temperature and pressure is established for each PCB-sediment-SCF system. The AARD values of the models are in the range of 10-14% for all PCBs in the CO<sub>2</sub> system and 14-20% for CO<sub>2</sub>/MeOH. These models have been used in the analysis of PCB desorption data. The model analysis reveals that PCB adsorptions onto sediments from both SCFs are exothermic and physical processes with the adsorption energy of ~4 kcal/mol in pure CO<sub>2</sub> and ~8 kcal/mol in CO<sub>2</sub>/MeOH system. The larger adsorption energy in CO<sub>2</sub>/MeOH system suggests stronger interactions between sediment active sites, PCB molecules, and this SCF.

### **Desorption Studies from Real World St. Lawrence River Sediments**

These studies were conducted to develop a consistent set of data with real world samples at laboratory scale. The air-dried SLRS #3 samples (Table 1) are extracted 60 minutes at 50 °C and 117.8 bar (corresponding to a CO<sub>2</sub> density of 10.5 mole/L) to determine flow-rate effects. Both pure CO<sub>2</sub> and CO<sub>2</sub> with 5 mole % MeOH were used as SCFs. With the former, larger CO<sub>2</sub> flow rate (1.35 versus 0.76 g/min) increases the desorption rate and reduces the final PCB residual concentration. With the latter, it is found that PCB concentration in sediment can be reduced from approximately 2200 ppm to less than 10 ppm (+99.5% extraction efficiency) in 25 minutes of extraction time and to less than 5 ppm (99.77% extraction efficiency) in 60 minutes. These flow rate effects are not significant after ~7.5 minutes of extraction time in the presence of 5 mole % methanol in the SCF. These results demonstrate that the use of methanol as cosolvent induces more rapid desorption rates and lower PCB residual concentrations compared to SC-CO<sub>2</sub> alone.

PCB desorption from a fixed bed of sediments was modeled employing the transient desorption material balance and assuming negligible axial dispersion effects. The governing equation can be given as:

$$\varepsilon \frac{\partial C}{\partial t} + u \frac{\partial C}{\partial z} + (1-\varepsilon) \rho_p \frac{\partial q}{\partial t} = 0 \quad (1)$$

where  $\varepsilon$  is void fraction of the soil bed; C is PCB concentration in the SCF phase; t is processing time;  $u$  is SCF superficial velocity; z is axial dimension of the bed;  $\rho_p$  is the density of S/S; and q is solid phase PCB concentration. A linear relationship can relate the partition equilibrium of PCBs between SCF and solid phase,

$$q = KC \quad (2)$$

and the PCB diffusion rate is governed by a linear driving force,

$$\frac{\partial q}{\partial t} = \frac{15D_s}{R_p^2}(KC - q) \quad (3)$$

where  $R_p$  is the soil particle radius and  $D_s$  is a “lumped” diffusion coefficient for PCBs. Combined with equations (2) and (3) and a set of initial and boundary conditions, equation (1) is solved and the two parameters,  $D_s$  and K, are determined by regression analysis on the experimental desorption data when partition equilibrium data are not available for K values. This model is used to fit PCB desorption data from spiked till under various conditions [9].

Bench-scale desorption experiments have been conducted on SLRS #3 (Table 1). Based on the results of laboratory desorption and partition equilibrium studies, the conditions of bench-scale desorption studies are determined as: CO<sub>2</sub> and CO<sub>2</sub>/5 mol % MeOH as SCFs; sample size of ~1500 g; CO<sub>2</sub> flow rates of 450 and 250 g/min (2.11 and 4.22 mol CO<sub>2</sub>/min); temperature of 50 °C; pressure of 118 bar; SCF densities of 10.5-15.0 mol/L. Bench-scale desorption experiments show that PCB concentration in SLRSs can be reduced from ~1840 ppm to less than 5 ppm (more than 99.73% extraction efficiency) in 40 minutes. The final PCB concentrations after 60 minutes of extraction are around 3 ppm which is comparable with the final PCB concentrations of ~4 ppm for the laboratory-scale experiments when CO<sub>2</sub>-MeOH are used as SCF, suggesting that the scale-up effect is not significant on the desorption processes. The modeling analysis produces comparable parameters with those obtained from the laboratory-scale studies. The parameters obtained from laboratory-scale desorption data predict the bench-scale data and give reasonably good results, validating the linear driving force model.

## ECONOMIC ANALYSIS

The base case of the proposed remediation process for PCB contaminated S/S using SFT consists of three 2.5 m<sup>3</sup> extractors operated in a 30-minute cycle time (the time for each extractor to be exposed to fresh SCF) and in a 60-minute processing time (cycle- plus exposing-time of PCB/SCF from a previous extractor). It can treat 36,000 m<sup>3</sup> contaminated S/S each year. The total processing cost for the SFE-SCWO process includes the cost for S/S handling, SFE of the PCBs from the S/S, and the cost of oxidizing the extracted PCBs using SCWO. The excavation costs are estimated to be \$50/m<sup>3</sup> and the SCWO costs for the extracts are estimated to be \$15/m<sup>3</sup>-sediment. Purchase costs are estimated for all of the major process units. The total operating cost is estimated from the costs of operating labor, utilities, raw materials, the fixed capital investment, S/S processing, and SCWO. The total processing cost consists of the total operating cost plus the depreciation of the plant over 10 years. Capital cost factors are used for each process unit to account for installation, engineering and construction expenses, and contingency funds and the contractor's fee. The utilities costs used are \$0.06/kwh, \$31.00/kwh for cooling at -18 °C cooling and \$6.62/1000 kg of low pressure steam (160 °C steam). Raw materials costs are \$0.30/gal for methanol and \$65/ton for CO<sub>2</sub>. Allowance of \$54/hr was made for the replacement and treatment of the carbon in the filter unit. Using the costs outlined above, the total treatment cost including depreciation is \$175/m<sup>3</sup> of S/S for the base case.

Two alternatives to the base process were also evaluated. In the first alternative, the cycle time for the extraction of the soil is decreased from 30 minutes to 20 minutes. Another extraction unit is added and each canister is exposed to CO<sub>2</sub> and methanol for three cycles instead of two, increasing the rate of S/S treatment from 5 m<sup>3</sup>/hr to 7.5 m<sup>3</sup>/hr. For this alternative, the capital cost is increased by the cost of the extra unit, but labor and other operating costs for the process are essentially the same. The estimated total treatment cost for this alternative is \$142/m<sup>3</sup>. In the second alternative, the CO<sub>2</sub> and methanol stream used to extract the S/S is assumed to leave the extraction units at 70 % of the equilibrium PCB concentration. To assure this higher PCB concentration an additional extraction unit is also added and the cycle time is kept at 30 minutes. This concentration ( $\sim 2.9 \times 10^5$  µg/mol-SCF) is approximately four times the average concentration of PCBs ( $6.7 \times 10^4$  µg/mol-SCF) leaving the extractor units in the base case. Accordingly, the capacities of all the operation units, except the extractors and the PCB storage tank, are reduced by a factor of four. The resulting capital costs of these equipments are scaled down using a factor of 4<sup>0.6</sup>. The utilities and raw materials costs are also reduced by a factor of 4<sup>0.6</sup> while the labor costs are kept as constant. The estimated total treatment cost for this alternative is \$144/m<sup>3</sup>.

Economic analysis of these processes reveals that the operation costs for the proposed process are in the range of \$142-175/m<sup>3</sup> of S/S. Comparison of these costs with the costs of other alternative technologies shown in the introduction section, suggests that the SFE-SCWO process is economically promising and attractive for the remediation of PCB contaminated S/S.

## CONCLUSIONS

A new PCB remediation process using supercritical fluid technology has been systematically evaluated based on real world PCB contaminated St. Lawrence River sediments. Major research areas include the PCB partition equilibrium, both laboratory and bench scale PCB desorption experiments, and the economic analysis of the proposed process. The results show that the proposed process is both technically and economically feasible for the remediation of PCB contaminated soil/sediment. The significance of our work is that we have demonstrated that the SFE of CO<sub>2</sub> – MeOH (5 mol %) can achieve <5 ppm residual PCBs in real St. Lawrence River sediments and soils from initial concentrations of ~2200 ppm (4300 ppm with lab spiked soils) in 45-60 minutes processing time for 99.8% removal.

An updated preliminary economic analysis indicates this SCF technology costs of \$142-175/m<sup>3</sup> soil processed is economically competitive.

These studies suggest that a multistage semi-batch process with CO<sub>2</sub> and methanol recycle and SCWO of the PCB extract is an efficient process configuration. Other downstream process configurations may prove more effective. Additional process information is needed to define an operable and economic process configuration to implement this technology.

## ACKNOWLEDGEMENTS

The financial support from the National Institute of Environmental Health and Sciences through Superfund Basic Research Program, Grant P42 ES-04913 is acknowledged.

## REFERENCES

1. L. J. Amend and P. B. Lederman (1992), *Environ. Prog.*, **11**, 173-181.
2. W. Zhou (2000), PhD Thesis, Syracuse University, NY.
3. L. L. Tavlarides, W. Zhou and G. Anitescu (2000), *Proc. Hazardous Waste Research 2000 Conference: Environmental Challenges and Solutions to Resource Development, Production, and Use*, Denver, CO, pp. 239-255.
4. C. Thibaud-Erkey, Y. Guo, C. Erkey and A. Akgerman (1996), *Environ. Sci. Technol.*, **30**, 2127-2137.
5. M. Z. Ozel, K. D. Bartle, A. A. Clifford and M. D. Burford (2000), *Anal. Chim. Acta*, **417** (2), 177-184.
6. M. A. McHugh and V. J. Krukonis (1994), *Supercritical Fluid Extraction: Principles and Practice*, 2nd edn., Butterworths-Heinemann, Boston.
7. P. Chen, W. Zhou and L. L. Tavlarides (1997), *Environ. Prog.*, **16**, 227-236.
8. G. Anitescu and L. L. Tavlarides (1999), *J. Supercrit. Fluids*, **14**, 197-211.
9. P. Chen (1997), PhD Thesis, Syracuse University, Syracuse, NY.



# SUPERCritical CO<sub>2</sub> EXTRACTION OF HALOGENATED FLAME RETARDANTS FROM POLYMER MATERIALS USING DIFFERENT MODIFIERS

T. Gamse and R. Marr

Institute of Thermal Process and Environmental Engineering,  
Graz University of Technology, Graz, Austria

Electronic waste materials contain flame retardants to protect the plastic material in case of fire. These compounds cause problems during incineration because of the formation of dioxines. Solubility measurements and calculations were performed for two widely used flame retardants, hexabromocyclododecane (HBCD) and tetrabromobisphenyl-A (TBBA). Supercritical CO<sub>2</sub> extraction experiments were carried out for the polymer polybutylene-terephthalate (PBT) containing either TBBA or HBCD. With pure CO<sub>2</sub>, extraction yields up to 100 % could be achieved at the highest conditions of 500 bar and 100°C. Using CO<sub>2</sub>-modifier mixtures (methanol, isopropyl alcohol, toluene, water-methanol mixturea) reduces the necessary extraction pressure for complete separation to 200 bar. For TBBA, a small amount of water positively influences the extraction results.

## INTRODUCTION

New techniques are urgently required in the field of polymer recycling and/or disposal, especially for polymer composites of mass consumer products like electronic waste which contain flame retardants in concentrations up to 30%. As flame retardants, special inorganic compounds, halogenated organic compounds, organophosphorus and halogenated organic phosphorus compounds are used. One main recycling process for plastics is the incineration and there the formation of halogenated dibenzodioxines and dibenzofurans due to the halogenated compounds cannot be avoided.

One promising way to separate the halogenated flame retardants from polymer matrices is the extraction by supercritical fluids like supercritical carbon dioxide (SC-CO<sub>2</sub>). The advantage of this process is that the polymer as well as the flame retardant can be recycled. This gives an economic benefit because flame retardants are relatively high price products.

Before starting extraction experiments, the solubility behaviour has to be known. To date, only limited data on flame retardants in combination with supercritical CO<sub>2</sub> are available in literature [1, 2]. For this reason, solubility data in supercritical CO<sub>2</sub> for two widely used flame retardants, hexabromocyclododecane (HBCD) and tetrabromobisphenyl-A (TBBA), were performed for a wide range of pressure and temperature. The experimental data and the fitted parameters for the Chrastil equation are published [3, 4].

Based on these solubility data, supercritical CO<sub>2</sub> extraction experiments were carried out for different polymers (ABS, PS, PBT) containing either TBBA or HBCD. Preliminary tests showed that the polymers ABS and PS are not suitable for CO<sub>2</sub> extraction. They have a relatively low melting point (below 60°C) under CO<sub>2</sub> pressure, so the removal from the vessel after extraction is difficult to handle because the polymer is then a sticky material. Furthermore, the polymers ABS and PS are partly soluble in CO<sub>2</sub> and therefore a separation of flame retardant and polymer is not possible. The extractions were therefore performed with PBT + TBBA and PBT + HBCD using firstly pure CO<sub>2</sub> and then adding different modifiers (methanol, isopropyl alcohol, toluene and water-methanol mixtures).

## MATERIALS AND METHODS

### High Pressure Apparatus

A Speed-SFE apparatus from Applied Separations Co. with a 300 ml extractor designed for 690 bar and of 250°C was used for all extraction tests. The apparatus and procedure are described in [6-9].

### Gas Chromatographic Method

The flame retardant-solvent mixture of the CO<sub>2</sub> sample was analysed in a gas chromatograph (HP 5890 Series II) with electron capture detector (GC-ECD) using a capillary column (type HP-1, 12 m x 0.2 mm x 0.2 µm). The injector temperature was held constant at 290°C, the detector temperature at 300°C and oven temperature constant at 290°C.

### CO<sub>2</sub> Density Calculation

The dependence of the density of pure CO<sub>2</sub> on pressure and temperature was calculated using the equation of Bender [4, 5].

### Materials

HBCD with a purity of 97% was purchased from Sigma Aldrich and TBBA with a purity of 98% from Riedel de Haen. Methanol, isopropyl alcohol and toluene were purchased from Merck. The CO<sub>2</sub> with a purity > 99.94% and a dew point lower than -60°C was purchased from Linde (Graz) and stored in a tank with 3200 L capacity. The polymers ABS, PS and PBT spiked with HBCD and TBBA were purchased from Celabor, Belgium. The polymer particle size had to be reduced before extraction which was performed by cryogenic milling adding CO<sub>2</sub> snow to the polymer to avoid melting of the material and to give better size reduction. After milling the polymer was separated by sieving in three fractions (< 500 µm, 500 – 1000 µm and 1000 – 2000 µm).

## RESULTS

### Solubility of TBBA and HBCD in CO<sub>2</sub>

Detailed results of the determined solubility data are already published [6, 7].

### CO<sub>2</sub> Extraction With Pure CO<sub>2</sub>

Preliminary CO<sub>2</sub> extraction tests showed that the polymers ABS and PS are partly soluble in CO<sub>2</sub> so insufficient separation of the flame retardants can be achieved as these polymers melt in the presence of CO<sub>2</sub> below 60°C, giving a sticky product at the end of extraction. Therefore only the polymer polybutyleneterephthalate PBT spiked with 20 wt% TBBA or 26 wt% HBCD was used for the extraction tests. Extraction time was set constant at 4 hours for extracting 4 g polymer material with a CO<sub>2</sub> flow rate of 4.6 l/min. The best extraction yields result at the highest pressure (500 bar), highest temperature (100°C) and smallest particle size (< 500 µm) tested [8, 9].

## CO<sub>2</sub> Extractions Using Different Modifiers

To reduce the necessary extraction pressure and temperature for a complete extraction, different modifiers (methanol, isopropyl alcohol and toluene) and different modifier amount were added to the CO<sub>2</sub> stream.

Figure 1 shows the influence of different methanol concentrations on the extraction yield of TBBA. It is obvious that increasing modifier amount increases the extraction yield. With a modifier content of 10 % methanol the same efficiency can be reached at 200 bar as with pure CO<sub>2</sub> at 500 bar. The other modifiers tested also increased the efficiency but not to the extent that methanol does (see Figure 2).

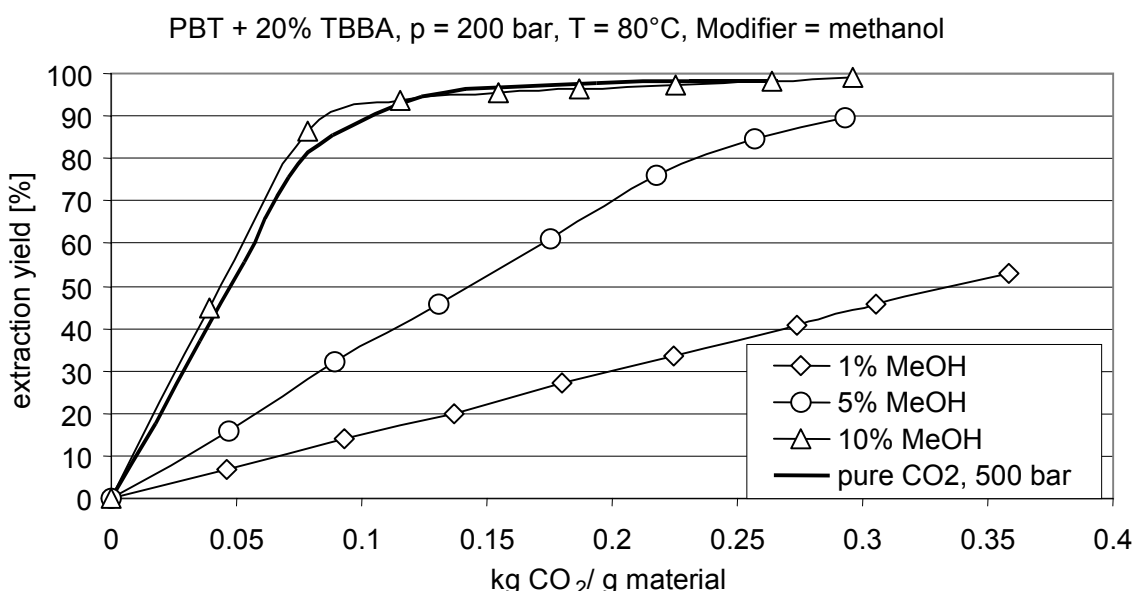


Figure 1. Influence of methanol concentration on extraction yield of TBBA.

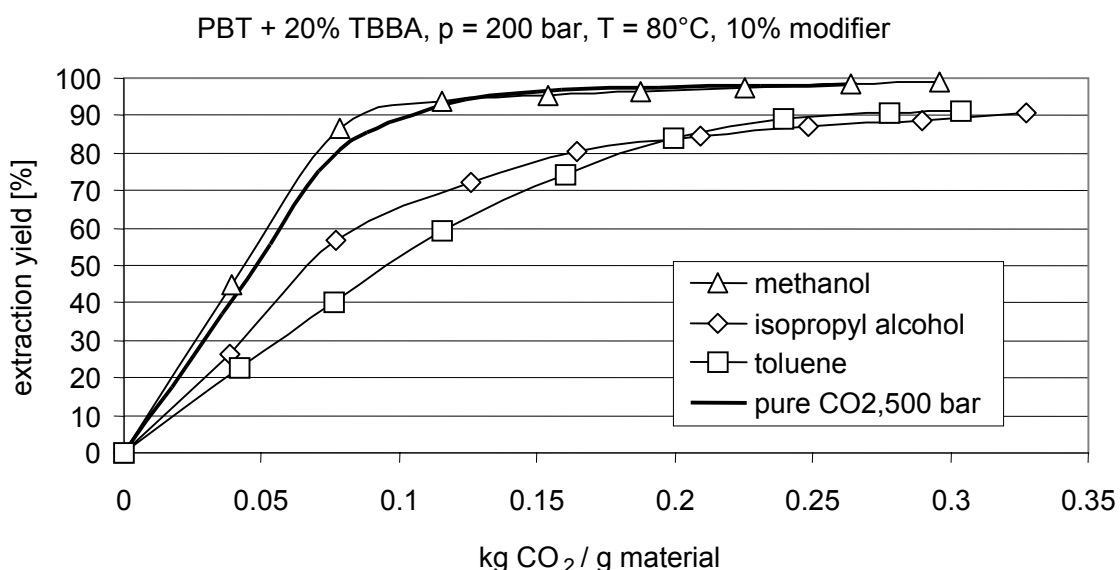


Figure 2. Influence of different modifiers on extraction yield of TBBA.

For the extraction of HBCD, methanol also gives the best results as shown in Figure 3. It is obvious that with a concentration of 10% methanol nearly the same extraction efficiency arises at 200 bar as with pure CO<sub>2</sub> at 500 bar.

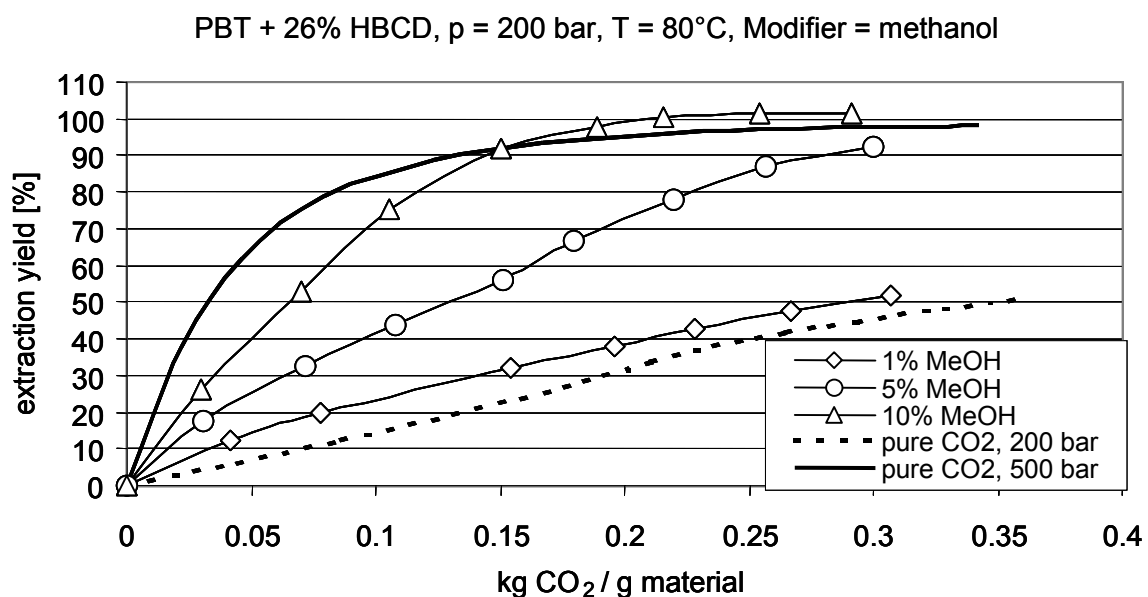


Figure 3. Influence of methanol content on extraction yield of HBCD.

The results at 40°C and 80°C are nearly the same but normally an increase in temperature results in better extraction yield. For this reason, the influence of temperature on the extraction yield using 10% methanol as modifier was determined. From Figure 4 it can be seen that a temperature increase starting at 40°C increases the extraction yield and at 70°C an optimum exists. Higher temperatures result in a decrease of the extraction yield.

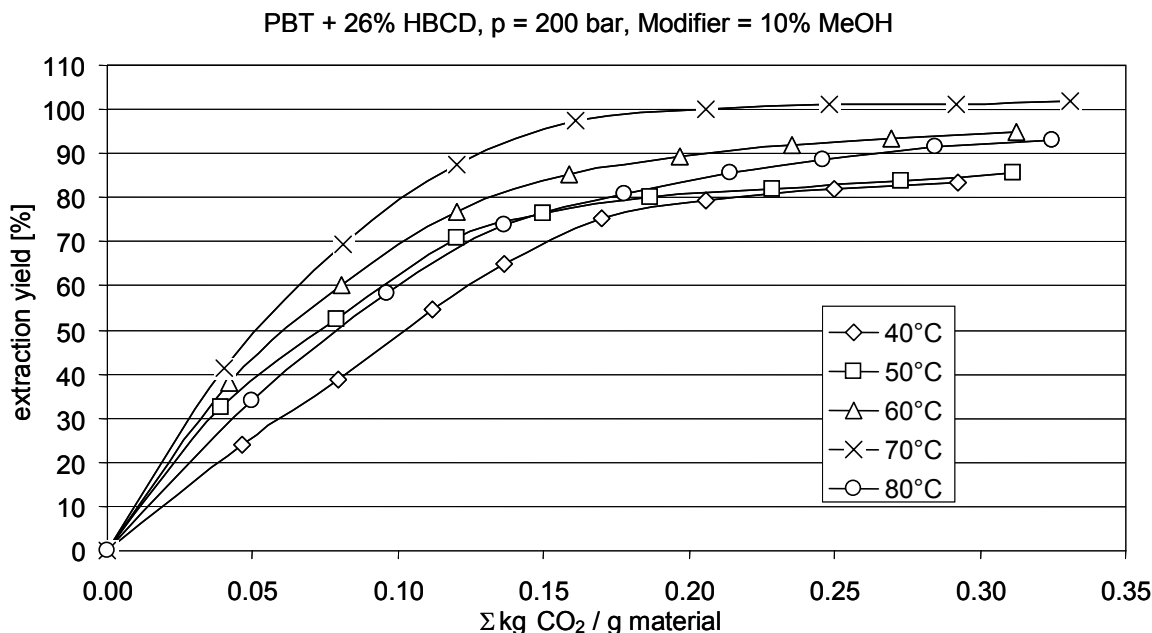


Figure 4. Temperature influence on extraction of HBCD using 10% methanol as modifier.

### CO<sub>2</sub>-Extractions Using Water-Methanol Mixtures As Modifier

To increase the polarity of the modifier, different amounts of water were added to the methanol. Figure 5 shows the influence of water concentration on the extraction yield of TBBA, where a modifier mixture of 5% water and 95% methanol gives the best extraction. Pure water was also used as modifier and it is obvious that this has a negative effect on the extraction rate.

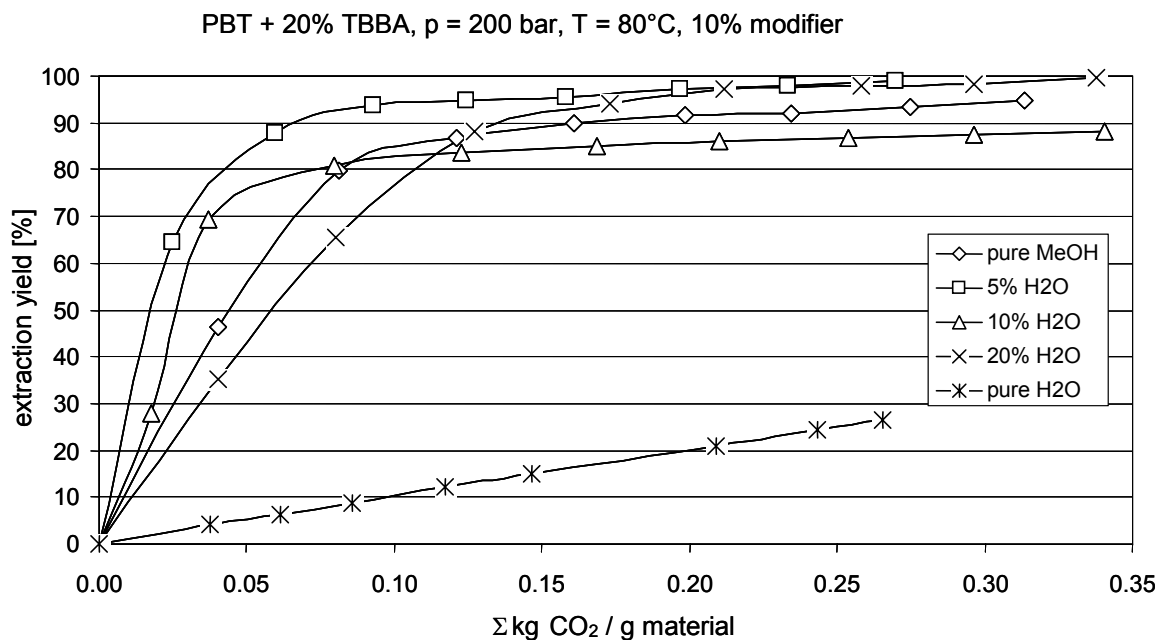


Figure 5. Influence of water-methanol mixture on extraction rate of TBBA.

In contrast to the extraction of TBBA, a water-methanol mixture has no positive influence for the removal of HBCD, as shown in Figure 6. For HBCD, pure methanol is the best modifier at an optimal extraction temperature of 70°C.

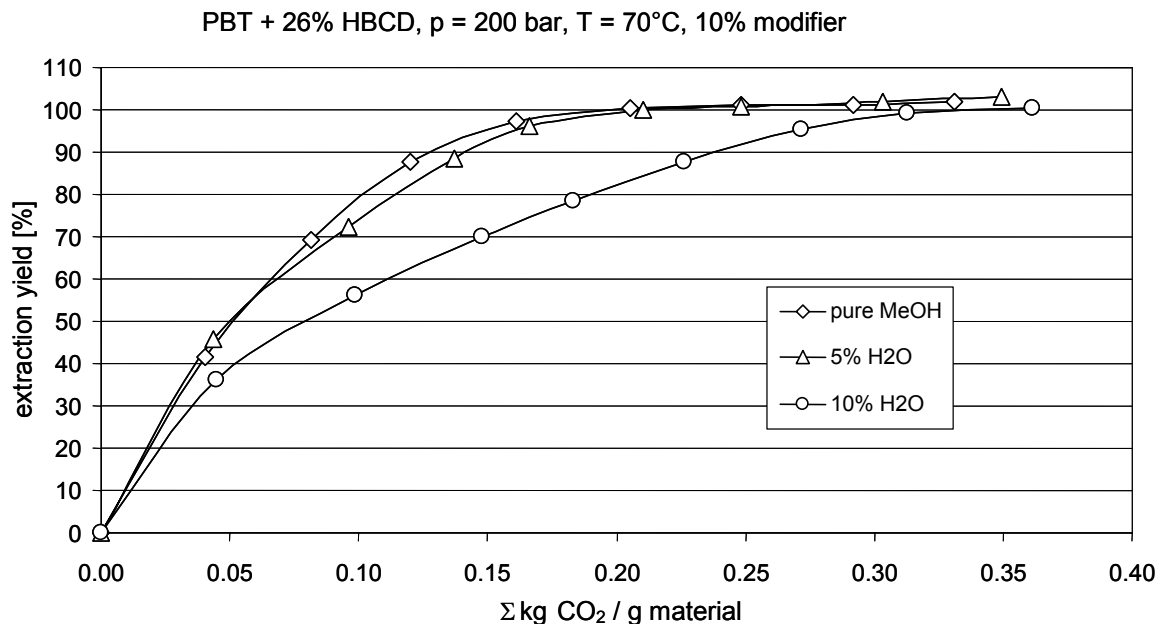


Figure 6. Influence of water-methanol mixture on extraction yield of HBCD.

## CONCLUSION

Supercritical CO<sub>2</sub> extraction is a promising process to get rid of the problem of flame retardants in polymers. A complete removal of TBBA and HBCD from the PBT polymer is possible, especially if higher temperatures, small particle sizes and modifiers are used. Best results for TBBA could be achieved using methanol with small amounts of water as a modifier. For HBCD, pure methanol as modifier gives the best results and the optimal temperature is 70°C at 200 bar.

To develop an economic process, the separation step has to be taken into account because a great amount of CO<sub>2</sub> is necessary for a complete removal of the flame retardants. Using absorption or adsorption as separation method will give the advantage of running this process isobarically or using only a small pressure decrease and therefore reducing investment and running costs for the CO<sub>2</sub> pump. Furthermore, a separation by absorption in a stripping column will result in modifier-saturated CO<sub>2</sub> entering the extraction vessel and the saturation concentration is much higher than the concentrations determined in these experiments. With increasing amount of modifier, the extraction yield also increases at shorter extraction times, so an industrial plant will run under much better conditions.

## ACKNOWLEDGEMENT

This project is funded by the European Commission within the EU project SCOW, project number BE 97 4675.

## REFERENCES

1. E. Marioth, G. Bunte, Th. Hardle (1996), *Polym. Recycl.*, **2** (4), 303-308.
2. G. Bunte, Th. Hardle, H. Krause, E. Marioth (1996), *Process Technol. Proc.*, **12**, 535-539.
3. E. Bender (1970) *Proc. Fifth Symposium on Thermophysical Properties*, American Society of Mechanical Engineers, New York, pp. 227-235.
4. U. Sievers (1984), *VDI-Fortschr.-Ber.*, **6/155**, VDI-Verlag, Düsseldorf.
5. J. Chrastil (1982), *J. Phys. Chem.*, **86**, 3016-3021.
6. T. Gamse, F. Steinkellner, R. Marr, P. Alessi, I. Kikic (2000), *Ind. Eng. Chem. Res.*, **39**, 4888-4890.
7. F. Steinkellner, T. Gamse, R. Marr, P. Alessi, I. Kikic (2000), *Proc. 5<sup>th</sup> Int. Symp. Supercrit. Fluids*, Atlanta, CD-ROM 5340939.pdf.
8. T. Gamse, R. Marr (2001), *Proc. 2<sup>nd</sup> Int. Meeting on High Pressure Chemical Eng.*, Hamburg, CD-ROM I-b11.pdf.
9. T. Gamse, R. Marr (2001), *Proc. 3<sup>rd</sup> European Congress of Chemical Engineering*, Nürnberg, CD-ROM 441.htm.



## METAL ION AND DYE EXTRACTION FROM TEXTILE WASTEWATER BY MICROEMULSIONS

L. T. Cordeiro Beltrame, E. L. Barros Neto, A. A. Dantas Neto, T. N. Castro Dantas

Universidade Federal do Rio Grande do Norte-Natal, Rio Grande do Norte, Brazil

The coloration resulting after conventional wastewater treatment in textile industries has been spurring the development of processes of color removal. This study presents a new extraction method to remove colors, dyes and metals by microemulsion. The wastewater used in this study was obtained by a real disperse dye bath containing the dyes Dianix Rubine S-2G (CI Disperse Red 167:1), Palanil Dark Blue 3RT (CI Disperse Blue 148) and Dianix Yellow Brown SE-R (CI Disperse Orange 29) and a real reactive dye bath containing the dyes Procion Yellow H-E4R (CI Reactive Yellow 84), Procion Blue H-ERD (CI Reactive Blue 160) and Procion Red H-E3B (CI Reactive Red 120). The optimized method was very efficient in removing all dyes and metals contained in the effluent.

### INTRODUCTION

Modern textile dyes are required to have a high degree of chemical and photolytic stability in order to maintain their structure and color. The stability and resistance of dyes to degradation have made color removal from textile wastewater difficult by biological treatment plants [1].

Many studies have been accomplished trying to help the textile industry to eliminate this problem [2-7]. Nowadays, the processes employed are few and the installation and operational costs are very high, making its utilization economically unviable.

The aim of this study was to develop a new method that is economically viable and observes the toxicological and environmental aspects, to remove the color present in textile effluent.

In recent years, attention has been given to the development of novel surfactant-mediated separation processes. Among the various new methods, the application of microemulsions for the separation, concentration and purification of proteins, for the extraction of metals, as drug-delivery systems, etc. seems to be one of the most exciting and promising techniques [8].

A microemulsion is a liquid-liquid dispersion, formed by two liquids of different polarities (most commonly water and oil) and a mixture of surfactant agents (surfactant and/or co-surfactant). Macroscopically it exhibits a monophase liquid (homogeneous), which has a translucent and isotropic appearance. Within the known proportions of its constituents this liquid is able to equilibrate with other phases, either aqueous or organic. In the case of extraction by microemulsions, one can work with the equilibrium between the microemulsion and the aqueous phase, which is called the Winsor II system.

Characteristic solvent effects of microemulsions, as reported in the stability of acids and bases and the reactivity of metal ions, are beneficial to various separation methods using microemulsions as media [9].

Metals have been found in textile wastewater [10] and some dyes are formed by chemical bonds between the metal and the organic molecule of the dye. Utilization of microemulsion systems in metallic cations extraction has been a good alternative [11-14], because they have some characteristics which make them profitable and safe, when compared to the conventional techniques.

This work presents the first application of microemulsion in color extraction from textile wastewater.

## EXPERIMENTAL METHODOLOGY

### **Composition and Preservation of the Samples**

The wastewater used in this study was obtained from a dyeing house, from the first discharge after dyeing with reactive dyes (hydrolyzed dyes) and from the first discharge after dyeing with disperse dyes. As simulating a real final wastewater, the mix of these baths together in the proportion of 1:1 was studied.

The dye baths had all the auxiliaries normally used, and the dyes are presented in Tables 1 and 2. All the extractions were carried out at room temperature (26°C) and after extraction the samples were preserved at 10°C.

*Table 1. Disperse dyes.*

Dye	Color Index	Chemical Characteristic	Concentration in the bath (g/L)
Dianix Rubine 2-2G	Disperse Red 167:1	Azoic	0.1805
Dianix Yellow Brown SE-R	Disperse Orange 29	Azoic	0.3888
Palanil Dark Blue 3RT	Disperse Blue 148	Azo	0.8333

*Table 2. Reactive dyes.*

Dye	Color Index	Chemical Characteristic	Concentration in the bath (g/L)
Procion Yellow H-E4R	Reactive Blue 84	Azoic - bismonochlortriazin	0.5902
Procion Blue H-ERD	Reactive Blue 160	Copper formazan bismonochlortriazin	0.4721
Procion Red H-E3B	Reactive Red 120	Azo - bismonochlortriazin	0.1062

### **Extraction Method**

A microemulsified system composed of a long chain amine (as surfactant), *n*-butanol (as co-surfactant), kerosene (as oil) and water was used as an extractor agent. This system was mixed in a 1:1 proportion with the disperse dye bath, the reactive dye bath and the mix of reactive and disperse baths, as it occurs in the effluent. The process was carried out in one stage by magnetic agitation (5 – 10 minutes) and immediate decantation. The two phases formed were easily separated: the superior phase, formed by the oil phase of the microemulsion, which is strongly colored and the colorless aqueous phase, formed by the water from the microemulsion and from the bath.

## **Methods of Analysis**

The samples from the dyes baths and the aqueous phases obtained after extraction were analyzed. The presence of metals was determined according to APHA [15], by flame atomic absorption spectrometry. The metals analyzed were Cd, Cu, Cr and Fe. The equipment used was a VARIAN SpectrAA – PLUS.

Color determination used the spectrophotometric method. In this method, absorbance was determined and the measures were compared to the Typical Color Consent [1]. The equipment used for color measurement was a molecular absorption spectrophotometer UV – Visible VARIAN CARY-1 E.

## **RESULTS AND DISCUSSION**

### **Choosing the Extraction Point**

Using a pseudo ternary diagram, three points were chosen from the microemulsion region. The initial chosen points were: w (rich in oil), z (rich in water) and k (same quantities of water and oil) as shown in Figure 1.

Extraction tests at these points with the disperse bath, reactive bath and disperse and reactive bath were realized. The best results were obtained at point z.

### **Study of the Best Concentration of Cosurfactant/Surfactant (C/S)**

With the objective of knowing the best concentration of the active matter, the points a, b and c, in which the same amounts of oil used in the point z were maintained, were tested (Figure 1). The points b and c presented better results but, as point b used smaller amounts of active matter, it was the chosen point. At this point, 20% of C/S, 79% of water and 1% of kerosene were used.

### **Study of the Optimum pH of Extraction**

The pH of the samples were 10.97 (reactive bath), 10.97 (disperse and reactive bath) and 5.25 (disperse bath). At these pH values, no extraction on the disperse bath, a good color extraction on the reactive bath and an excellent color extraction on the disperse and reactive bath, were observed.

It was observed that by varying pH, color extraction could be improved. The reactive dyes bath has better extraction when the sample is acidified at pH 9 or less, before extraction. In this case, aqueous phase is completely colorless. It is due to the high salinity of this kind of bath, in which Winsor II microemulsion formation is favored. The disperse dyes bath has an excellent extraction at pH 13., with colorless aqueous phase; above this pH the extraction still happens, but the aqueous phase becomes more colored as the pH increases. The mix of reactive and disperse dyes baths has the best extraction at pH 10 – 12. It is due to the high salinity of the mix (from the reactive bath) and the facility of extraction at high pH (from the disperse bath).

### **Dyes Baths Concentration**

The concentrations of the reactive bath and disperse bath are not possible to determine due to different exhaustion curves of the dyes used to dye. According to O'Neill *et al.* [1], the description of textile effluent in terms of absorbance is more useful in terms of describing a pollutant than its dye concentration, as different dyes give rise to different intensities and colors. As absorbance changes with the types of dye used, there is not a direct relationship between these values and dye concentrations.

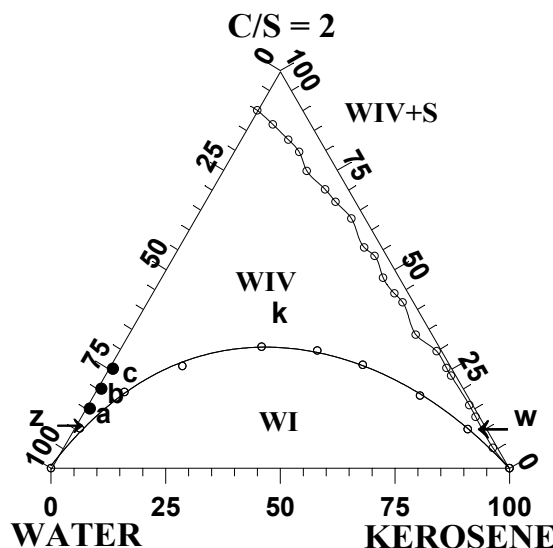


Figure 1. Ternary pseudo diagram with the chosen points for extraction tests.

#### Determination of COD (Chemical Oxygen Demand)

The determination of COD from the samples was not possible due to the high chloride concentration, over than 2000 mg Cl/L [15].

#### Extraction of Metals

Cd, Cu, Cr and Fe have been found in the wastewater from the industry where samples were collected [10]. In the samples of disperse and reactive baths, Cd, Cr and Fe quantities were under the detection limits of the equipment used. But copper was found in the reactive bath and in the mix of reactive and disperse baths. The quantities are shown in Table 3.

Table 3. Metals in the dyeing bath and in the extracted aqueous phase.

Metals	Dyeing bath			Extracted aqueous phase		
	Reactive	Disperse / reactive	Disperse	Reactive	Disperse / reactive	Disperse
Cu (mg/l)	1.34	0.58	-	0.05	0.02	-
Cr (mg/l)	-	-	-	-	-	-
Fe (mg/l)	-	-	-	-	-	-
Cd (mg/l)	-	-	-	-	-	-

According to the results obtained, the extraction of copper was 96.27% from the reactive bath and 96.55% from the mixture of reactive and disperse baths. It is important to say that these values were obtained without any correction of pH, which would improve the extraction and that the extraction was carried out in a single stage of agitation and decantation.

#### Color Removal

To date there is no environmental quality standard (EQS) for color, and therefore the practice is to determine an acceptable color for the river to which effluent is to be discharged by taking samples of the river and assessing which samples are acceptable to the eye [1]. Consent limits are usually expressed as absolute limits for the wavelength within a particular range. Consent limits [1] are expressed in Table 4, for comparing the results obtained after color extraction from the baths.

With the samples from reactive bath and from the mix of disperse and reactive baths, pH correction wasn't used. For the sample from disperse bath the pH was correct to 13.2.

*Table 4. Color consent standard for Sewage Treatment Works comparing to the dyeing bath absorbance and extracted aqueous phase absorbance.*

Color wavelength (nm)	Dyeing bath			Extracted aqueous phase			Typical color consent *
	Reactive	Disperse / reactive	Disperse	Reactive	Disperse / reactive	Disperse	
400	0.5356	1.4125	2.3875	0.0350	0.0422	0.0353	0.115
450	0.5494	0.9010	1.6250	0.0379	0.0239	0.0153	0.085
500	0.5765	0.9702	2.4501	0.0291	0.0133	0.0128	0.065
550	0.5000	0.8958	2.5998	0.0166	0.0076	0.0116	0.055
600	0.1482	0.4375	0.6875	0.0018	0.0031	0.0080	0.040
650	0.1053	0.2754	0.3750	0.0004	0.0001	0.0066	0.028
700	0.0333	0.0993	0.0113	0.0000	0.0000	0.0064	0.013

\* Environmental Agency in: O'Neill *et al.* [1]

These results show that aqueous phases obtained after extraction present very low absorbance and the new method used to color removal from textile effluent was very efficient.

## CONCLUSIONS

The system used was very efficient in color removal. Disperse dyes should be extracted in a strongly alkaline medium (pH 13.2). Reactive dyes and the mix of disperse and reactive dyes can be extracted at the normal pH of the samples. The extraction of reactive dyes is optimized as the sample is acidified and under pH 9, the aqueous phase is completely colorless. The mix of disperse and reactive dyes presents best extraction at pH 10 – 12.

The extraction of metals, in the case of copper, was 96.27% in the reactive dye bath and 96.53% in the mix of reactive and disperse dyes baths. For the extraction, simple agitation (magnetic agitation) was used, followed by decantation. In this determination, pH correction was not used.

Looking to verify possible interference from the dyeing auxiliaries, a real effluent was studied. The system was shown to be indifferent to any interference.

## REFERENCES

1. C. O'Neill, F. R. Hawkes, D. L. Hawkes, N. D. Lourenço, H. M. Pinheiro and W. Delée (1999), *J. Chem.Tech. Biotech.*, **74**, 1009-1018.
2. C. Crossley (1998), *J. Soc. Dyers Colour.*, **114**, 194-196.
3. P. Cooper (1993), *J. Soc. Dyers Colour.*, **109**, 97-100.
4. W. D. Kermer and I. S. Richter (1995), *Melland Textilberichte*, **76**, E116-E120.
5. W. S. Perkins (1998), *Am. Textiles Int.*, **27**, 62-64.
6. C. Moran (1998), *J. Soc. Dyers Colour*, **114**, 117-118.
7. A. K. Mukherjee, B. Gupta and S. M. S. Chowdhury (1999), *Am. Dyestuff Rep.*, **February**, 25-28.
8. S. P. Moulik and B. K. Paul (1998), *Adv. Coll. Interf. Sci.*, **78**, 99-195.

9. H. Watarai (1997), *J. Chromat. A*, **780**, 93-102.
10. L. T. Cordeiro Beltrame (2000), Caracterização de Efluente Têxtil e Proposta de Tratamento, Master of Science Thesis, UFRN, Brazil.
11. T. N. Castro Dantas, A. A. Dantas Neto and K. R. Forte (1997), *Pollution Control' 97. Study of the Selectivity of Heavy Metals by Microemulsions*, Bangkok, Thailand, cd-rom.
12. T. N. Castro Dantas, A. A. Dantas Neto, and M. C. P. A. Moura (1999), Urban Pollution Control Technology, Use of Impregnated Natural Clay With Microemulsion In The Treatment of Effluents Containing Heavy Metals, Hong Kong, China, pp. S1-S6.
13. T. N. Castro Dantas, A. A. Dantas Neto and M. C. P. A. Moura (1999), *Proc. Int. Solv. Extr. Conf. ISEC 99*, Society of Chemical Industry, London, pp.195-200.
14. T. N. Castro Dantas, A. A. Dantas Neto and M. C. P. A. Moura (2001), *Water Res.*, **35**, 2219-2224.
15. APHA (1995), Standard Methods For The Examination of Water and Wastewater, American Public Health Association, Washington.



## RECOVERY OF POLYPHENOLS FROM OLIVE MILL WASTE-WATERS BY PRECIPITATION AND LIQUID-LIQUID EXTRACTION

Jorge Rodrigues de Carvalho, Celina Santos, Rosinda Ismael, Licínio Ferreira

Departamento de Engenharia Química, Instituto Superior Técnico, Lisboa, Portugal

Olive mill waste-waters (OMWW) are rich in polyphenols. In order to remove polyphenols from OMWW, an integrated process including precipitation and polyphenol removal by liquid-liquid extraction is proposed. The precipitation was required to avoid crud formation during liquid-liquid extraction. Different concentrations of  $\text{FeCl}_3$  and lime were tested, with or without a flocculant. Several commercial extractants were tested to remove polyphenols from pre-treated OMWW. The raffinates were analysed by HPLC. None of extractants were selective for polyphenols. However, combination of two extractants, in a sequential extraction resulted in the recovery of an organic solution rich in hydroxytyrosol, which could be stripped with caustic soda. Synthetic polyphenol solutions extractions were also experimented.

### INTRODUCTION

The extraction of olive oil, accomplished in small, seasonally operated agro-industrial units, results in the production of high-density waste water. Their high levels of organic substances and, consequently, their highly pollutant nature pose a serious environmental problem. Such effluents have established low commercial values. Olive mill waste waters (OMWW), however, may also be a possible source of substances of possible technological interest, such as polyphenols. Polyphenol levels in OMWW are in the range of 453 ppm up to 7624 ppm [1]. Hydroxytyrosol, tyrosol, catechol, 4-methylcatechol and caffeic acid are the main polyphenols in OMWW [2]. Because of their high antioxidant effect, polyphenols are increasingly being used by pharmaceutical industries. As a recovery process, liquid extraction should be considered an attractive process to recover polyphenols from OMWW. However, the high turbidity of OMWW presents considerable liquid extraction problems, mainly due to crud formation. To avoid this crud formation, turbidity removal must be accomplished by coagulation and precipitation as a pre-treatment prior to liquid-liquid extraction. The purpose of the present work was to explore the different selectivities of four extractants for polyphenol extraction. Pre-treatment prior to the liquid-liquid extraction process was also studied by coagulation and precipitation processes. The efficacy of this pre-treatment was demonstrated.

## MATERIALS AND METHODS

### Chemicals

Ferric chloride, lime and other common reagents were analytical grade. Aliquat 336 and Alamine 336 were purchased from Cognis, tri-*n*-butylphosphate (TBP) and Primene JMT were from BDH Chemicals, Ltd. and Rohm and Haas Company, respectively. Cyanex 923 and TOPO were purchased from Cytec Canada Inc. Hostarex 327 was from Hoechst. ShellSol T (SST) and ShellSol A (SSA) were purchased from a local market. Flocculants non-ionic Praestol 2500, anionic polyacrylamide A100 (Cyanamide Superfloc) and cationic polyacrylamide C472 (Cyanamide Superfloc) were purchased from a local market. JMT and Hostarex 327 were sulphated as in [3]

### Effluent Characterization

OMWW in this study has a total polyphenol content of about 3300 ppm and a pH value of 4.9. Total solids and turbidity levels are 86 g/l and 16100 NTU, respectively. COD and BOD levels are 130 g O<sub>2</sub>/l and 13 g O<sub>2</sub>/l, respectively.

### Analytical Method

Total polyphenols were determined according to the method proposed in Standard Methods, which is based on the Folin-Ciocalteau reagent [4]. HPLC has been used to analyse aqueous phase for polyphenols. A Dionex system was used, equipped with a GINA auto sampler, a P 580A LPG gradient pump and a UV-Vis diode array UVD340S detector. A RP18 column from Merck was used. Turbidity was measured on a LP 2000 turbidity meter, from Hanna Instruments, and calibrated against formazin standards. COD and BOD concentrations were measured on a Aqualytic® Pcompact COD/CSB photometer and on a BOD-Sensor and Aqualytic inductive stirring system, respectively.

## RESULTS AND DISCUSSION

### Solvent Extraction Applied to OMWW

The following extractants were mixed with diluent (50% SST, 50% SSA): Cyanex 923, TOPO, Aliquat 336, TBP, sulphated JMT and sulphated Hostarex. These extractants represent different characteristics and therefore interact by a different mechanism with polyphenols. The results of these experiments, expressed as removal percentage, are given in Table 1, for pH 2 and pH 12. These results were obtained using the Folin-Ciocalteau method to analyse total polyphenols removal.

*Table 1. Removal of polyphenols from OMWW by liquid-liquid extraction by several extractants (%).*

pH	Cyanex 923	TOPO	Aliquat 336	TBP	sulphated JMT	sulphated Hostarex
2	26	8	44	12	8	20
12	-	0	53	8*	-	-

\* pH 11.

(10% v/v) in a 40% (v/v) SST + 40% (v/v) SSA diluent.

Volume of aqueous phase = Volume of organic phase.

The chromatographic determination of polyphenols, after their extraction with those extractants was also performed. These results showed no selectivity for all the extractants. Aliquat 336 extracted all the compounds existing in the range of retention time 35 to 75 min.

Solvent extraction applied directly to OMWW produced crud. Precipitation was, therefore, applied to OMWW in order to clarify this effluent.

### **Coagulation/Precipitation**

The experimental results, were carried out in terms of the effect of effluent dilution, iron(III) and CaO concentration on residual COD and turbidity, during the coagulation process. Furthermore, the use of different flocculants was experimented. This precipitation, as already was referred, is essential before applying liquid-liquid extraction because it can substantially reduce the turbidity and at the same time reduce the COD, as presented below.

#### **Effect of iron(III) concentration on turbidity and COD residual**

The addition of ferric chloride resulted in a black mass that tended to form amorphous aggregates. Above the poorly settling flocs, the supernatant was very dark brown in colour.

For undiluted effluent, 2000 ppm of iron(III) is required to reduce almost 60% of the initial COD and almost 97% of the turbidity. This concentration decreases with increasing effluent dilution (Figures 1 and 2).

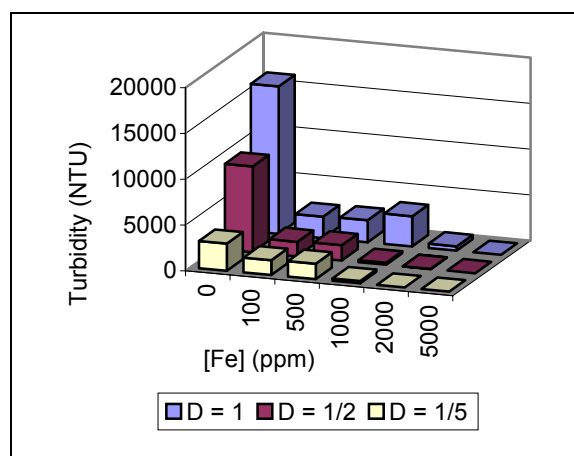


Figure 1. Residual turbidity (after 24 h) after addition of ferric chloride for different effluent dilutions (D). pH 5.5.

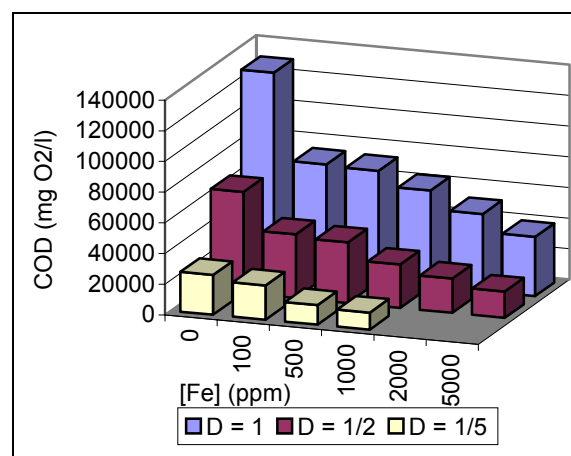


Figure 2. Residual COD (after 24 h) after addition of ferric chloride for different effluent dilutions (D). pH 5.5.

#### **Effect of lime concentration on turbidity and COD removal**

Lime coagulation led to an orange-yellow supernatant and a fine brown floc, which settled very slowly. To elucidate the effect of lime on OMWW, pure calcium oxide was used. When hydrated, it generated calcium hydroxide. It was shown that removal efficiency increased with increasing lime concentration. With lime treatment, 70% of COD and 99% of turbidity removal may be reached using 28 g/l of calcium oxide, but, for economical considerations, treatment with 10 g.dm<sup>-3</sup> calcium oxide was sufficient. For ½ effluent dilution, the calcium oxide concentration required to remove about 94% of turbidity and about 50% of COD was only 5 g/l.

#### **Effect of flocculant**

To further agglomerate coagulated particles, forming larger flocs and thus accelerating the sedimentation process, addition of a flocculant (synthetic polymer) is needed to decrease the amount of salt required and to improve the precipitation with trivalent salts.

The best result of flocculation was obtained with the flocculant Cyanamid C472 at a concentration value of 50 ppm.

### Solvent Extraction applied to Clarified OMWW

Before a solvent extraction process is applied, a pre-treatment with 5g/l CaO must be used. To remove the excess of calcium, an ion exchange process, using a Dowex 50W-X8 ion exchange resin, was used. During ionic exchange fouling was not detected. After these two steps, the polyphenol content of the effluent was 486 ppm hydroxytyrosol, 19 ppm protocatechuic acid, 473 ppm tyrosol, 11 ppm caffeic acid, 13 ppm of p-coumaric acid, 10 ppm of rutine, being the total polyphenols content of 758 ppm. For solvent extraction of OMWW, four extractants were assayed for polyphenols removal. The chromatographic determination of polyphenols, after their extraction with those extractants was also performed. The results in Table 2 show the percentage of removals of the main polyphenols with 0.18 M of different extractants in 50% SSA/SST.

*Table 2. Removal of polyphenols by liquid-liquid extraction by several extractants (%).*

Extractants	Hydroxy-tyrosol	Protocatechucic acid	Tyrosol	Caffeic acid	p-coumaric acid	Sinapinic acid	Rutine	Total
Initial aqueous phase at pH 1								
Cyanex 923	57	100	2	100	100	100	91	42
Aliquat 336	60	100	18	99	100	94	100	52
Alamine 336	49	100	0	99	98	89	100	42
TBP	4	50	0	73	90	61	20	24
Initial aqueous phase at pH 8								
Cyanex 923	52	68	7	90	93	29	91	37
Aliquat 336	62	100	30	96	96	80	100	64
Alamine 336	9	0	10	7	15	18	68	24
TBP	11	0	11	14	13	42	39	24

Aqueous phase/Organic phase (v/v) = 1.

Aqueous phase pre-treated with 5 g/l CaO and through a cation exchange resin.

As can be seen, neither of the extractants could selectively remove any polyphenols. Only Aliquat 336 was capable of extracting polyphenols better at pH 8 than at pH 1. Nearly equal removals were obtained with Cyanex and Alamine 336. Both of them showed poor extraction of tyrosol from the effluent. The best results were obtained with the quaternary ammonium compound Aliquat 336, which had a total polyphenol removal of about 51% and 64% at pH 1 and pH 8, respectively.

The combination of several consecutive extraction stages will result in the recovery of hydroxytyrosol. In the first extraction stage, Cyanex 923 can remove, at pH 1, almost all the polyphenols leading a raffinate rich in tyrosol and with 48% of hydroxytyrosol. This aqueous solution can again be extracted with fresh Cyanex 923 to remove the remaining hydroxytyrosol. This organic phase can then be stripped by caustic soda leading a solution rich in hydroxytyrosol.

Other studies of solvent extraction of p-coumaric acid with Aliquat 336 were performed. In order to reduce the amount of SSA in the diluent. Since aromatic compounds are toxic and soluble in aqueous phase, several diluent compositions were studied. Composition selection or rejection was based on third phase formation when the organic phase is loaded with the solute. The results are presented in Table 3 using p-coumaric acid as the solute.

Three systems are successful for liquid-liquid extraction of p-coumaric acid without third phase formation. The system with the solvent composition Aliquat 336 10% + 1-decanol 10% + SST 80% must be the best due to environmental considerations. Stripping was also studied for Aliquat 336. Only basic solutions in the presence of sodium chloride could strip the organic phase. However, it was observed that significant polyphenol dissociation or

degradation occur with this basic solution. This was shown by the disappearance of almost all polyphenols when the pH solution was increased to 10 and to 13. However, when the pH was readjusted to the initial value with concentrated H<sub>2</sub>SO<sub>4</sub> some polyphenols (hydroxytyrosol, tyrosol, p-coumaric acid and p-hydroxybenzoic acid) reappear, indicating that the reaction with NaOH is reversible for these four compounds. In Figure 3, spectra for hydroxytyrosol and tyrosol are overlaid to accentuate spectral changes.

*Table 3. Different compositions for organic phase and respective p-coumaric concentration attained after several contacts of organic and aqueous phases.*

Organic phase	[p-coumaric acid] in organic phase (not saturated) (ppm)	Third phase formation
Aliquat 336 1% + (SST+SSA) 99%	5337	Yes
Aliquat 336 10% + (SST+SSA) 90%	9959	Yes
Aliquat 336 10% + SST 30% + SSA 60%	9917	Yes
Aliquat 336 10% +1-decanol 10%+SST 40%+SSA 40%	13683	No
Aliquat 336 10% +1-decanol 10%+SST 80%	10530	No
Aliquat 336 10% +1-decanol 10%+SSA 10%+SST 70%	13477	No
Aliquat 336 10% +1-decanol 5%+SSA 10%+SST 75%	8537	Yes
Aliquat 336 10% +1-decanol 5%+ SST 85%	8324	Yes
Aliquat 336 5% +1-decanol 5%+ SST 90%	7976	Yes

Aqueous phase feed: P-coumaric concentration 700 ppm.

Phase ratio of 2/1.

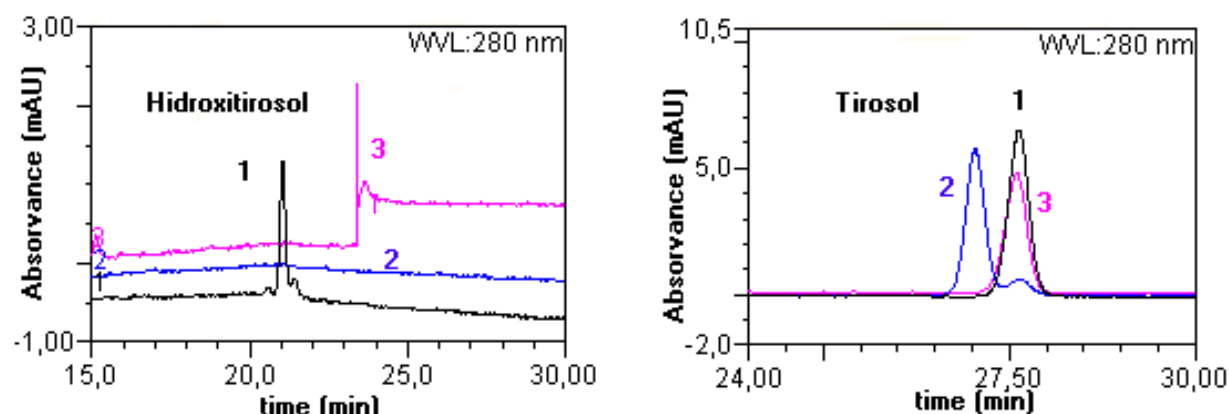


*Figure 3. Overlay of chromatographic spectra for hydroxytyrosol and tyrosol at different pH values; 1- Solution of 10 ppm of the compound at natural acidic pH, 2- Solution 1 after addition of NaOH, 3- Solution 2 after readjusting the pH for initial value of solution 1.*

These results led us to consider the stripping with basic solution efficient for tyrosol, hydroxytyrosol, p-coumaric acid and p-hydroxybenzoic acid. However, for the other polyphenols, degradation products will be obtained, leading to their poor recovery. Several basic stripping solutions were assayed for p-coumaric acid (Table 4).

*Table 4. Efficiency of different strip solution compositions for stripping of p-coumaric acid.  
Aqueous phase/Organic phase of 1 (v/v).*

Strip liquor	Strip efficiency (%)	Strip liquor	Strip efficiency (%)
NaCl 1 M, pH 2	1	NaOH 2 M, pH14	13
NaCl 1 M, pH 10	4	NaOH 0.5 M + NaCl 0.1 M	31
NaCl 3 M + NaOH 2 M, pH 14	94	NaOH 0.5 M + NaCl 0.3 M	59
NaOH 0.01 M, pH 12	2	NaOH 0.5 M + NaCl 0.5 M	75
NaOH 0.5 M, pH 14	7	NaOH 0.5 M + NaCl 1 M	91
NaOH 1 M, pH 14	11	NaOH 0.5 M + NaCl 3 M	95

## CONCLUSIONS

COD and turbidity from OMWW were efficiently removed by a precipitation/coagulation process with iron(III) or lime, followed by sedimentation. Dilution is needed to decrease the amount of ferric chloride or lime added to the effluent. Also, flocculant improved the coagulation performance. From the results reported above, it is possible to conclude that addition of about 5g/l of lime, to the ½ diluted effluent, are sufficient to produce a treated effluent with very low turbidity and suspended solids contents. This supernatant is suitable for solvent extraction application. Consecutive extraction steps resulted in the recovery of a solution rich in hydroxytyrosol.

If Aliquat 336 was used for a synthetic solution of p-coumaric acid extraction, the system Aliquat 336 10%+ 1-decanol 10% + SST 80% allow a concentration of p-coumaric acid in organic phase above 10g/l without third phase formation. Stripping with NaOH 0.5 M + NaCl 0.5 M was efficient for tyrosol, hydroxytyrosol, p-coumaric acid and p-hydroxybenzoic acid without polyphenol degradation. However, for the other polyphenols, degradation products were obtained, leading to their poor apparent recovery, in spite of the solvent being stripped.

## REFERENCES

1. G. Lолос, A. Skordilis and G. Parissakis (1994), *J. Environ. Sci. Health*, **A29** (7), 1349-1356.
2. R. Capasso, G. Cristinzio, A. Evidente and F. Scognamiglio (1992), *Phytochemistry*, **31** (12), 4125-4128.
3. G. Braun, W. Grünbein, B. Mayer and B. Wojtech (1986), *Proc. ISEC '86*, Vol. III, pp. 885-891.
4. Standard Methods for the Examination of Water and Wastewater (1998), 20<sup>th</sup> edn.



## METHYL TERT-BUTYL ETHER - A NEW SOLVENT FOR PHENOL AND ACETIC ACID EXTRACTION FROM WASTEWATER

Costică Strătulă, Florin Oprea, Casen Panaiteșcu, Mihaela Petre and Gheorghe Botoc\*

Universitatea Petrol-Gaze Ploiești, Romania

\*S. C. Carom S.A., Onești, Romania

In order to remove phenol from wastewater several solvents are used: aromatics, butyl acetate, and diisopropylether. Liquid-liquid experimental data in the system water-phenol-methyl *t*-butyl ether (MTBE) shows a much higher distribution coefficient for this solvent than other solvents. Similarly, the liquid-liquid experimental data show the same high distribution coefficient for this solvent in the water-acetic acid-MTBE system. Based on these experimental data, industrial plants for phenol and acetic acid extraction with MTBE have been designed. The industrial plants have two parts: the liquid-liquid extraction column and solvent recovery from the two phases: the extract phase (MTBE phase) and the water phase. Solvent recovery from water phase is necessary as the solubility of MTBE in water is nearly 4% by mass. Economic calculations show that in the case of phenol, the annual operating cost is under the value of the recovered phenol and a profit is obtained. In the case of acetic acid, even with two recovery columns, the process is much more advantageous than ordinary distillation or azeotropic distillation with butyl acetate.

### INTRODUCTION

In the phenol production process (cumene hydroperoxide method) wastewater with a phenol content of 0.5-2% by mass is produced. Such waters also result from NOVOLAC fabrication, wood distillation and in the thermocatalytic process in refineries, in which the phenol concentration is much lower (600-1000 ppm by mass). To avoid river and underground water pollution it is necessary to remove phenol from this water. For this is necessary to: (1) design and construct the wastewater treatment plant at the same time as the phenol production plant and, (2) choose a process with minimum phenol content in wastewater and with a minimum flow rate of such water. For existing processes, the flow rate of wastewater with phenol can be reduced by water recycling (totally or partially) after treatment and conditioning.

There are several processes for phenol removal from waste water, depending on the initial and final phenol contents required: (1) liquid-liquid extraction with several solvents, (2) distillation in presence of electrolytes, (3) adsorption on active carbon, and (4) biochemical process. In order to remove phenol from waste water using liquid-liquid extraction it is necessary to solve two problems: (1) proper liquid-liquid extraction using different solvents, and (2) solvent regeneration and phenol recovery.

## PHENOL EXTRACTION FROM WASTEWATER WITH MTBE

### Experimental Concerning Liquid-Liquid Extraction Data

In the liquid-liquid extraction of the phenol, different solvents are used: aromatics (benzene, toluene, xylenes, cumene), diisopropylether, butylacetate, and methyl *t*-butyl ether (MTBE). The most important property of a solvent is its solving power (capacity) for the component that is extracted, in our case phenol. This power can be expressed by the distribution coefficient, K, defined as the ratio of solute concentrations in both liquid phases:

$$K = \frac{Y}{X}, \quad (1)$$

where Y represents the phenol concentration in solvent (kg phenol/kg solvent or kg phenol/m<sup>3</sup> solvent);

X is the phenol concentration in wastewater (kg phenol/kg water or kg phenol/m<sup>3</sup> water).

As the distribution coefficient increases, the solving power of the solvent improves, and the performance of the process is better, requiring fewer equilibrium stages, a lower solvent ratio, and giving a higher degree of extraction. From this point of view, the solvents like diisopropyl ether butyl acetate and MTBE, having higher distribution coefficients, are better than aromatics.

In the case of phenol extraction with MTBE, liquid-liquid equilibrium data are presented in Figure 1. Experimental values were fitted and resulted in the fit of a Nerst-Shilov equation:

$$Y = a \cdot X^b, \quad (2)$$

where a has the value 1547.23411 and b = 1.39004.

The distribution coefficient of phenol in MTBE (80 to 110) is greater than the distribution coefficient of phenol in benzene, which has the value 3, and is comparable with those of butyl acetate and diisopropyl ether. On the other hand, the price of MTBE is much lower than that of the latter solvents (around US\$ 200 per tonne).

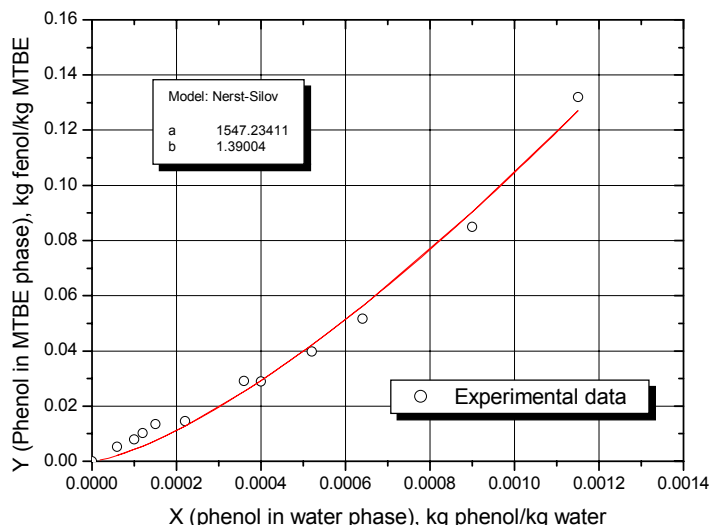


Figure 1. Liquid-liquid equilibrium data for the water-phenol-MTBE system.

### The Design of the Liquid-Liquid Phenol Extraction Column

With these data the principal parameters of the phenol extraction column can be calculated (number of theoretical trays and solvent ratio). In the extraction column presented in Figure 2,  $S_1$  represents water flow rate (kg/h);  $S_2$  – MTBE flow rate (kg/h);  $X_i$ ,  $X_e$  – phenol content in aqueous solution, input and output from the column (kg phenol/kg water);  $Y_i$ ,  $Y_e$  – phenol content in MTBE stream, input and output from the column (kg phenol/kg MTBE).

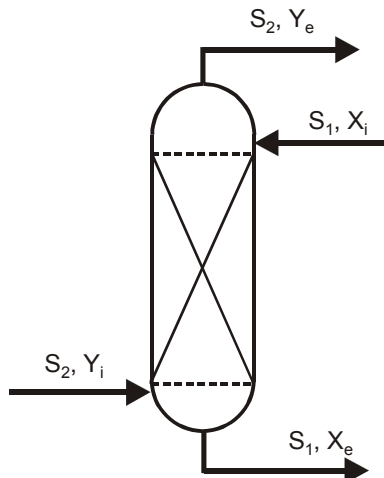


Figure 2. Extraction column configuration.

For a practical example it can be considered that in order to reduce phenol content in stream  $S_1$  from an input value  $X_i = 0.031$  kg phenol/kg water to an output value  $X_e = 0.0003$  kg phenol/kg water, the MTBE stream  $S_2$  enriches from the input concentration  $Y_i = 0.005$  kg phenol/kg MTBE (see next section) to several output concentrations  $Y_e$ . Using a simplified graphical method in rectangular diagram [1] the solvent ratios,  $S_2/S_1$ , were calculated for different numbers of necessary equilibria (number of theoretical trays),  $N_{tt}$ . The pairs ( $S_2/S_1$ ,  $N_{tt}$ ) are presented in Figure 3.

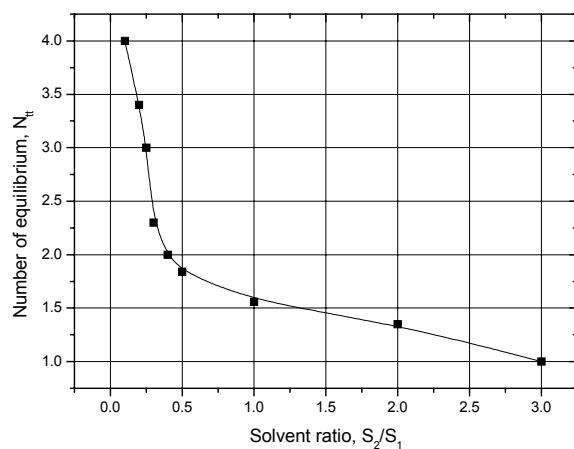


Figure 3. Number of theoretical trays versus solvent ratio for phenol extraction.

### Design of the Recovery Solvent System (Phenol Case)

In order to design a continuous phenol extraction system, with the correct number of extraction stages, it is necessary to include a solvent regeneration stage, simultaneously with extracted phenol recovery. In this way, the solvent can be recycled to the extraction stage. For these reasons, the regeneration stage has the same importance as the extraction

stages, and the design of this stage often is more difficult. In the case of phenol extraction with MTBE, because of the mutual solubility of water and MTBE, water stream  $S_1$  from the bottom of extraction column will contain MTBE at the solubility limit, and MTBE stream  $S_2$  from the top of extraction column will contain some water at the solubility limit. Therefore, the regeneration system for the solvent, MTBE (see Figure 4), will have two stages: one stage (column 2) for phenol separation from MTBE stream  $S_2$ ; and one stage (column 3) for MTBE separation from water stream  $S_1$ . Using this installation, the MTBE losses are substantially reduced.

The analysis of such a process leads to the utilities consumption presented in Table 1 for a feed flow rate (wastewater) of 1500 kg/h and for 20 ppm by mass maximum MTBE content in the wastewater [2, 3].

*Table 1. Main utilities consumption.*

Utility	Annual consumption	Cost (US\$)
Steam (tonne)	2776	15.6
Cooling water ( $m^3$ )	43 120	0.024
Electric power (kWh)	6160	0.042

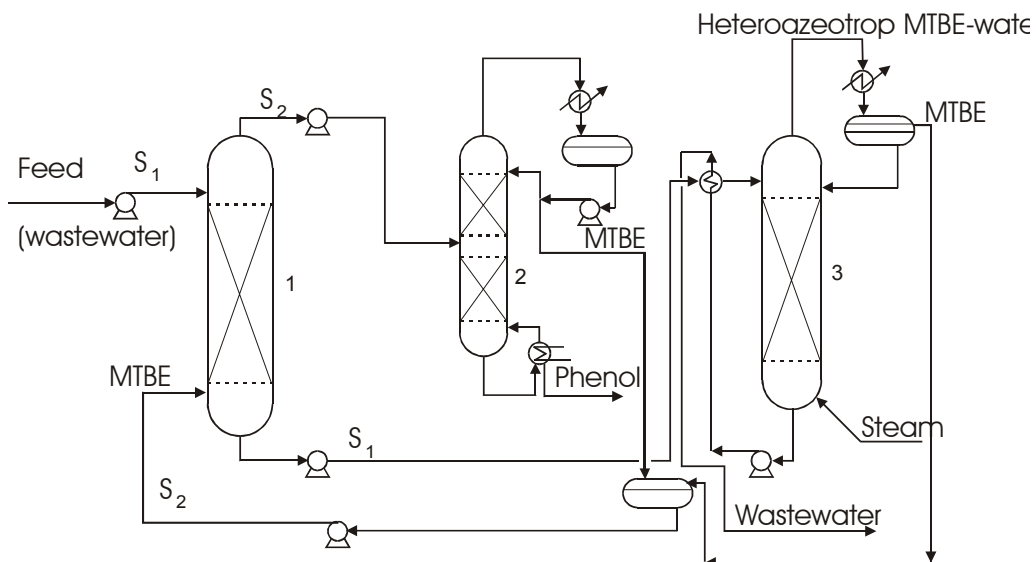


*Figure 4. Phenol extraction with MTBE installation.*

Considering the utilities prices in Table 1, this process results an annual total utilities cost of US\$25089. This process recovered 353.6 t/a phenol at a phenol price of US\$800/t, resulting in an operational cost of this process of only 8% of the value of the recovered phenol, even if the main goal of this process is cleaning wastewater with high phenol content.

## ACETIC ACID EXTRACTION FROM WASTEWATER WITH MTBE

### Experimental Concerning Liquid-Liquid Extraction Data

In order to recover acetic acid from wastewater streams (resulting from production of acetic acid, dimethyl terephthalate, etc.) different processes can be used: (1) liquid-liquid extraction with different solvents, (2) distillation, and (3) azeotropic distillation. There are two conditions for the use of solvents: (1) high distribution coefficient, and (2) a high enough boiling

temperature to ensure easy solute separation. The good results obtained for phenol extraction with MTBE led to the idea of using MTBE as a solvent for acetic acid extraction. Experimental data in this case are presented in Figure 5.

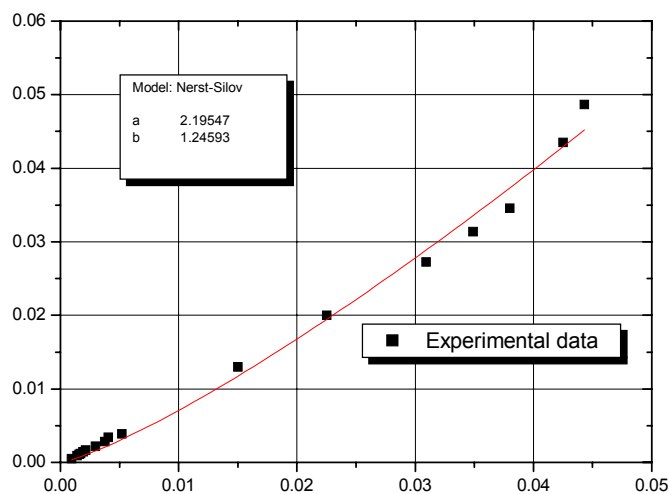


Figure 5. Liquid-liquid equilibrium data for the water- acetic acid - MTBE system.

The experimental values were fitted and a Nerst-Shilov equation obtained similar to Equation (2), where  $a$  has the value 2.19547 and  $b = 1.24593$ .

#### The Design of the Liquid-Liquid Extraction Column and Solvent Recovery System (Acetic Acid Case)

The same analysis as for the phenol case phenol was carried out in order to determine  $S_1/S_2$  for different numbers of theoretical trays,  $N_{tt}$ . The results are presented in the Figure 6.

The flowsheet of the process, with the recovery solvent system is the same as that presented for the phenol case. An economic comparison between this system and acetic acid removal using ordinary distillation was done in the case of a wastewater flow rate of 1500 kg/h with 9% weight acetic acid (Table 2).

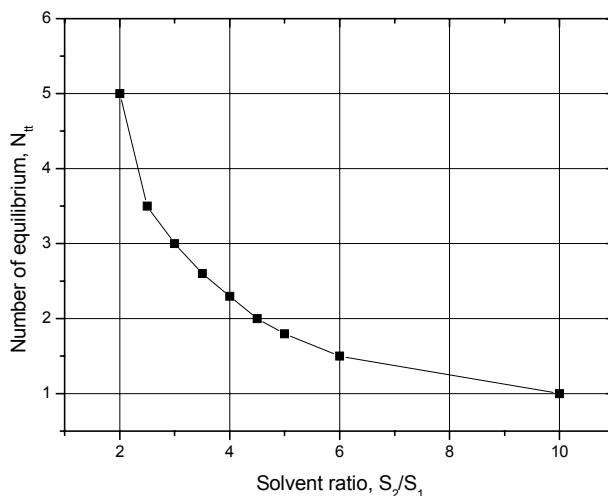


Figure 6. Number of theoretical trays versus solvent ratio for acetic acid extraction.

*Table 2. Economic comparison between two acetic acid removal processes: extraction and ordinary distillation. (Acetic acid product flow rate = 140 kg/h.)*

	Solvent ratio	$N_{tt}$	Steam consumption (t/h)	Water consumption (t/h)
Extraction followed by solvent recovery	2	5	1.2	35.4
	3	3	1.86	50.4
	4.5	2	3.54	93
Ordinary distillation	Reflux ratio: 2:1		5.52	142.8

## CONCLUSIONS

The liquid-liquid equilibrium data for system water-phenol-MTBE and for the system water-acetic acid-MTBE were experimentally obtained. These data were fitted to an equilibrium curve corresponding to the Nerst-Shilov equation.

Commercial processes for phenol and acetic acid removal were proposed. These include an extraction column, a column to separate MTBE from phenol/acetic acid, and a column to separate MTBE from water.

Technical and economical viability of the proposed processes has been successfully demonstrated. In the case of phenol removal, the economic analysis shows that the operating costs of this process represent only 8% of the value of the recovered phenol. In the case of acetic acid removal, the economic analysis shows that the steam consumption is 4.6 times lower and the water consumption 4 times lower than for ordinary distillation.

## REFERENCES

1. C. Taran and C. Strătulă (1978), Procese Difuzionale de Separare, Vol. II, IPG, Ploiești.
2. Agency for Toxic Substances and Disease Registry, ATSDR, Methyl Tert-Butyl Ether, CAS # 1634-04-4.
3. US Environmental Protection Agency (1999), EPA 420-R-99-021, Achieving Clean Air and Clean Water.



## POINT SOURCE RECOVERY OF HYDROCARBONS FROM WASTEWATERS BY SOLVENT EXTRACTION

Marc Halevy and Peter Jones

Universite de Sherbrooke, Quebec, Canada

An industrial liquid-liquid extraction process prototype is under development for the recovery of selected industrial solvents that are characterized by a limited but non-negligible aqueous miscibility, including phenol, and low molecular weight chlorinated organics and petroleum hydrocarbons. Process development activities presented in this paper were pursued on industrial wastewaters generated during routine aircraft maintenance operations. Aircraft coatings removal and application operations were targeted in order to recover solvents used in painting/paint stripping operations. Process development activities are pursued on an extraction process that relies on phosphine chemistry, on the use of a multi stage internal centrifugal mixer separator for phase contacting and separation, and on distillation/solvent washing for product and extractant separation and recovery.

### INTRODUCTION

Aircrafts are constantly subjected to hostile environments. Corrosion control operations ensure safety and lifespan. Wastewaters generated during coatings removal and/or application operations to aircraft surfaces are characterized by high concentrations of hazardous organics and inorganics that originate from the:

- usage of complex, maintenance formulations, based on petroleum-based and synthetic solvents, including dichloromethane, phenol, ketones, and benzoyl alcohol.
- paints, primers, and conversion coatings being removed from aircraft surfaces.
- aircraft metal and/or composite surfaces.

The majority of aircraft maintenance facilities surveyed or audited throughout Canada, United States, and Western Europe, generate wastewaters very similar in characteristics. Typical characterization data is summarized in Table 1 for organic parameters pertinent to this process development segment. This data is typical of a wastewater that was collected in a maintenance hangar where good housekeeping practices and waste segregation measures were implemented.

The wastewater was pre-treated to remove contaminants detrimental to the cyclic performance of the extraction process under development. These contaminants were shown, in earlier process development extraction runs, to have a noticeable impact on coalescence rates, solutes partitioning, hydration and free (entrained) water content in the loaded extractant, on crud formation in the solvent extraction and washing circuits, and on solvent poisoning.

*Table 1. Analytical characterization data highlights.*

Parameter Type	Concentration (mg/L)
Biochemical Oxygen Demand (BOD)	59
Chemical Oxygen Demand (COD)	15 100
Total Organic Carbon (TOC)	3 760
Phenol	4 670
Total Petroleum Hydrocarbons (TPH)	318
Dichloromethane	67
(Other) Volatile Organics (VOC)	< 10
Alcohols (C <sub>1</sub> – C <sub>6</sub> )	97
(Other) Semi-Volatile Organics	< 10

## EXPERIMENTAL SET-UP AND WORKPLAN

Stringent protocols were established for sampling, shipment, storage, preparation, equipment clean up and set-up, materials preparation, treatability, and analytical characterization. Aircraft paint stripping wastewaters were collected from selected Canadian aircraft maintenance hangars. The extractant formulation was based on Cyanex 923™, manufactured by Cytec Canada. Throughout the pursuit of the bench and pilot scale process development studies, phenol was selected as the main monitoring parameter. Occasional monitoring of organics by GC/MS, TOC, TPH (dichloromethane-extractables) and O&G (n-hexane extractables) was also conducted. The 4-amino-antipyrine Standard Method 5530 was retained for the spectrophotometric determination of phenol concentrations.

All chemicals used were reagent-grade. High detergency solutions and hot caustic solutions were used for the cleaning of equipment and peripherals. Hot tap water was used for rinsing. Treatability was conducted at 20–25°C. Solution pH for the wastewater was adjusted to a neutral to slightly acidic range (5<pH<7) that was previously shown to optimize the extraction process.

Bench scale experimentation was initially pursued to assess phenol partitioning in the extractant formulation. Aqueous and solvent phases were contacted until equilibrium conditions were reached. Reaction kinetics were studied to assess the:

- kinetics of the complexing reaction.
- rates of diffusion of the specie(s) that control the chemistry of the process.
- effect of reaction temperature and ionic strength on extraction performance.

Bench scale runs were either pursued in one litre, high shear (20000 rpm) mixer/homogenizer, for the thermodynamic studies, or in a two litre baffled vessel equipped with a variable shear mixer (600–2750 rpm) for the kinetic studies. Proper agitation was consistently realized to ensure that spatial composition gradients were minimized. Absolute liquid-liquid phase separation was achieved by using a phase separation inert microfiltration membrane.

In order to capture kinetic data, additional phenol needed to be added to the wastewater to increase the 4–7 g/L concentration range typically observed to 17–20 g/L. Very high aqueous-to-organic ratios (A:O) were retained, typically 100:1.0 (100) to 100:0.5 (200). A time lapse of five seconds was set to turn off the mixer, transfer the solution to the microfiltration unit, and collect the filtrate. In cases where an insufficient volume of filtrate was collected, the run was discarded, and repeated.

The bench scale treatability studies included the simulation of an ideal countercurrent process for several phase ratios. The following procedure was retained to simulate an ideal two-stage countercurrent process:

1. Feed, F, was contacted with virgin extractant, E. Extract, E2', was discarded. Raffinate, R1', was kept.
2. R1' was contacted with virgin extractant, E. Raffinate, R2', was discarded. Extract, E1', was kept.
3. E1' was contacted with Feed, F. Extract, E2', was discarded. Raffinate, R1', was kept.
4. R1' was contacted with virgin extractant. Raffinate, R2', was sent for analysis and discarded. Extract, E1', was kept.
5. Feed, F, was contacted with E1', and the cycle was repeated two additional times, to reach steady state.

## BENCH SCALE RESULTS AND DISCUSSION

Table 2 presents the distribution data for all five different 200 L batches collected for the conduct of the bench scale treatability program. Partition coefficients showed a strong concentration dependency: a range of 260 to 1457 was observed for phase ratios, A:O, of 100 to 1, and corresponding equilibrium phenol concentrations in the extract of 5 g/L to 372 g/L, respectively. In addition to the concentration dependency observed for phenol, the non-linear data collected suggests that other solute(s) might also be competing. From earlier trials on pure phenol systems where similar behavior was observed, water is known to be one of the competing solute. The partition data were retained for subsequent graphical and numerical analysis.

*Table 2. Partitioning data summary.*

A : O	Individual Distribution Coefficients	Mean and Standard Variation
100:1.0	255; 262; 263	260 and 4.7
100:2.0	474; 454; 441	456 and 16.6
100:2.5	350; 357; 222; 282	303 and 63.6
100:5.0	926; 901; 901; 955; 940; 792; 784	886 and 69.5
100:10	1162; 1136; 1136; 1160; 1142; 1208; 1196	1163 and 28.9
100:50	685; 685; 605	658 and 46.2
100:100	1718; 1718; 1169; 1151; 1718; 1217; 1507	1457 and 271.1

Initial Phenol Conc. Range 5.156 g/L - 6.030 g/L.

Table 3 presents the partitioning data generated for an ideal two-stage countercurrent extraction process. The empirically derived data confirms that a raffinate phenol concentration of 5 mg/L (and a corresponding 99.9 % phenol reduction) can be met for a A:O phase ratio of 20, resulting in a phenol loading in the extractant of 114 g/L. It should be noted that this treatability segment was pursued not to maximize phenol concentration in the extract, which was shown to be as high as 364 g/L under some of the higher A:O phase ratio runs presented, but to empirically derive ideal phase contacting/separating distribution data for a countercurrent, multi-phase process.

Tables 4 to 7 present extraction rate regime data. This kinetic study was conceived to distinguish the effect of the chemical reactions involved in solute partitioning from the effect of rate limiting diffusional processes. No temperature effect was noted in the range of 20 C to 70 C. When sodium chloride was retained to modify the aqueous ionic strength of the wastewater, no impact on partitioning values was observed for a range up to 100 g (NaCl)/L.

*Table 3. Ideal two stage countercurrent process performance summary.*

A:O	Mean (Standard Variation) Aqueous Phenol Conc. in Feed (g/L)	Mean (Standard Variation) Aqueous Phenol Conc. @ Stage 1 (g/L)	Mean (Standard Variation) Aqueous Phenol Conc. @ Stage 2 (g/L)
100 :1.0	5.156	4.21 (0.17)	1.56 (0.06)
100:2.0	5.156	1.69 (0.09)	0.19 (0.00)
100:2.5	5.59 (0.12)	0.87 (0.08)	0.030 (0.00)
100 : 5.0	5.45 (0.24)	0.144 (0.001)	0.005 (0.00)

Initial phenol conc. range 5.156 g/L - 5.687 g/L.

*Table 4. Effect of temperature on partitioning data.*

Temperature (K)	Phenol Concentration (mg/L) @ Reaction Time (min)				
	@ 0.5	@ 1.0	@ 2.0	@ 3.0	@ 5.0
322	140	131	128	126	138
331	147	127	120	127	129
343	140	134	129	121	138

Initial Phenol Conc. = 5.889 g/L; A:O = 100:5.

*Table 5. Impact of ionic strength on partitioning data.*

$\text{Na}^+\text{Cl}^-$ Concentration (g/L)	Phenol Conc. (g/L) @ reaction time (sec)				
	@ 5	@ 10	@ 15	@ 30	@ 150
3 g/L	3.09	3.11	3.03	3.19	3.23
100 g/L	3.06	3.14	3.01	3.06	-

Initial Phenol Conc. = 5.460 g/L; A:O = 100:0.5.

*Table 6. Kinetic regime extraction data.*

Phenol Conc. (g/L)	Reaction time (s)							
	2	2	3	4	5	10	60	120
	12.82	12.83	12.08	11.78	11.76	11.78	11.71	11.76

Initial Phenol Conc. = 19.430 g/L; A:O = 100:1.

*Table 7. Diffusional regime extraction data.*

Reaction Time (sec/min)	Aqueous Phenol Conc. (g/L) @ Stirring Rate (rpm)					
	@ 600	@ 800	@ 1 000	@ 1 500	@ 2 000	@ 2 750
0 (initial)	18.7	18.8	17.2	19.2	19.1	20.0
2 s	-	-	-	-	15.8	15.9
5 s	-	-	16.1	15.6	14.1	14.7
15 s	17.1	-	15.5	14.3	13.3	13.4
30 s	16.5	16.7	14.8	13.1	12.8	13.0
1 min	15.4	15.5	14.0	12.1	12.6	12.8
2 min	-	14.2	12.6	12.7	-	-
5 min	12.8	12.4	11.1	12.4	-	-
10 min	12.2	-	-	-	-	-

The kinetic data showed very fast reaction kinetics, and the following linear regression was derived:

$$\ln(C - C_{eq}) = -1.36(t) - 1.66$$

Next, diffusion-controlled kinetic data as a function of stirring rate was analysed. A linear regression was undertaken for each set of stirring rate data set. First order reaction rate constants were derived, and the following regression analysis relating individual reaction rate constants to the corresponding stirring rates is presented:

$$\ln(k) = 1.53 \ln(\text{rpm}) - 14.51$$

The kinetic data clearly shows the notable increase in kinetic rate constant values with increasing mixing energies. A significant increase in the rate constant by two orders of magnitude was observed when the system was operated in a kinetic regime (at 20000 rpm).

Based on the bench scale treatability data generated, a pilot scale program was undertaken with the wastewater as the continuous phase, as it is mass transfer controlling. Very high A:O phase ratios were experimented with, without any extract recycle. A kinetic operating regime operation and short residence time for partitioning and phase disengagement and separation were investigated.

The extractant-based formulation had already been modified in earlier trials to provide effective droplet coalescence in order to achieve rapid and clean phase separation even at high phenol loading in the extract when using a static settler/decanter. Consequently, short phase-separation times of the order of only a few seconds under several hundred g-force factors could conceivably be sufficient to simulate near ideal plug flow dynamics in a discrete multi-stage contactor. For those reasons, the use of an industrial multistage internal centrifugal mixer-separator contactor was chosen for the upcoming pilot scale development activities (to be presented in the oral or poster presentation). Figure 1 presents the schematics for the solvent extraction process under development.

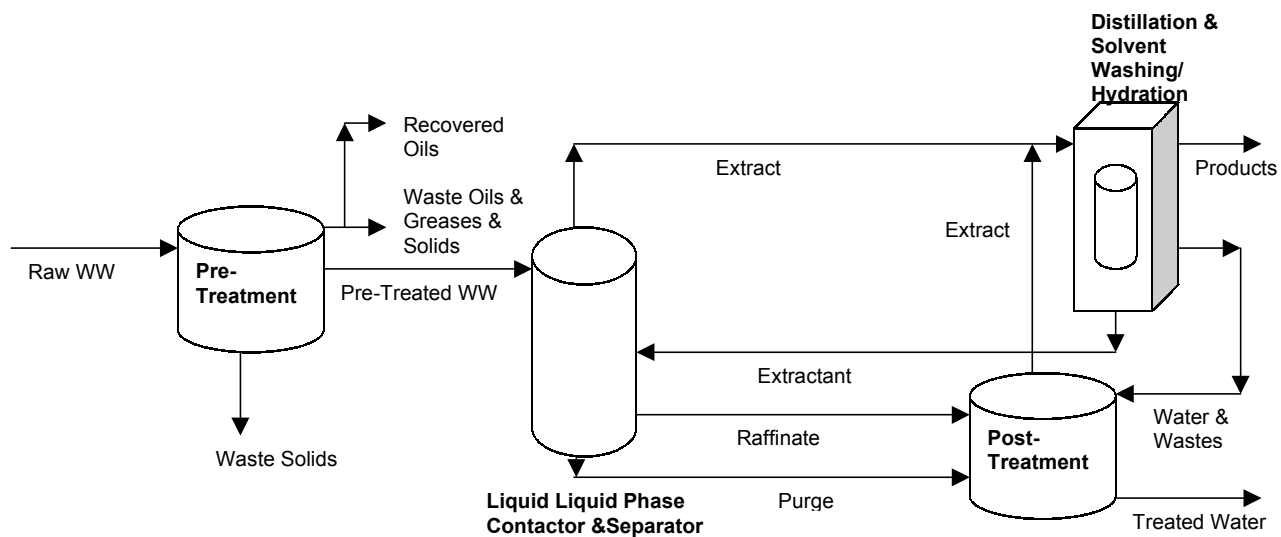


Figure 1. Solvent extraction circuit.

## **SUMMARY AND CONCLUSIONS**

Process development studies pursued at bench scale confirmed the strong affinity between Cyanex 923 and the targeted solvents and hydrocarbons in the wastewaters, including phenol, dichloromethane,  $\geq 4$ -C linear aliphatic alcohols, and residual concentrations of dissolved petroleum-based hydrocarbons. Phenol partitioning coefficients were observed to show a strong concentration dependency over the concentration range studied. Very high phenol loading in the extract was achievable and could exceed 370 g/L. Reaction kinetics were very fast. This almost instantaneous chemical reaction and/or partitioning confirm the possibility of conceiving the operation of a commercial process under a kinetic regime.

## **ACKNOWLEDGEMENTS**

The authors need to acknowledge the contributions of S.A. Zaidi, J. Neate and B. Jank from the Wastewater Technology Center/WTI Corp. (ON, Canada), of the late W.A. Rickleton from Cytec Canada, and of E. Chornet from l'Universite de Sherbrooke.



## CATALYST RECOVERY FROM THE WET PEROXIDE OXIDATION PROCESS BY MEANS OF NON-DISPERSIVE SOLVENT EXTRACTION

A. M. Urtiaga, C. Muela and I. Ortiz

Departamento de Ingeniería Química y Química Inorgánica, Universidad de Cantabria,  
Santander, Spain

In this work we analyse the recovery of a mixture of Fe(III), Cu(II) and Mn(II) used as a catalyst in the Wet Peroxide Oxidation Process by means of non-dispersive solvent extraction. The performance of different solvent extraction reagents was tested: D2EHPA, LIX 622N and Cyanex 272. LIX 622N was selected as a selective extractant for Cu(II) recovery, and Cyanex 272 for the selective recovery of Fe(III) and Mn(II). Extraction selectivity was achieved by working at different pH values in the feed solution. The three metals were stripped using sulphuric acid.

### INTRODUCTION

Chemical oxidation of refractory organic pollutants is an attractive method for industrial waste reduction because of its high efficiency and simplicity. Of these methods, hydrogen peroxide treatment has emerged as a viable alternative. It does not form harmful by-products and H<sub>2</sub>O<sub>2</sub> is a non-toxic chemical [1]. However the methods for oxidation of wastewaters with hydrogen peroxide are mostly based on homogeneous catalysis by metal ions. In the novel Wet Peroxide Oxidation (WPO) process a catalytic mixture of Cu(II), Mn(II) and Fe(II) is used [2]. But the use of metallic salts as catalysts induces additional pollution. When the oxidation is complete the metal catalysts are precipitated to form a sludge that must be managed as a toxic waste.

In this work, the viability of the recovery by means of membrane-based non-dispersive solvent extraction (NDSX) of Fe(III), Cu(II) and Mn(II) from the oxidised wastewater stream is analysed, as an alternative to the metals precipitation step.

### EXPERIMENTAL

The schematic representation of the experimental system that has been used for individual metal recovery is shown in Figure 1. The NDSX experimental set-up consisted of two hollow fibre contactors, having the following characteristics: 10,000 porous polypropylene fibres; internal diameter  $2.4 \times 10^{-4}$  m; wall thickness  $3.0 \times 10^{-5}$  m; mass transfer area  $1.4 \text{ m}^2$ .

As the feed phase, synthetic aqueous solutions of Fe<sub>2</sub>(SO<sub>4</sub>)<sub>3</sub>, CuSO<sub>4</sub> and MnSO<sub>4</sub> were used; initial metal concentrations simulated the average values in the aqueous stream after the Wet Peroxide Oxidation Process, *i.e.*, Cu, 250 mg/l; Fe, 170 mg/l and Mn, 170 mg/l. The performance of several extractants was studied: bis(2-ethylhexyl)phosphoric acid (D2EHPA) (Merck), LIX 622N (Cognis) and Cyanex 272 (Cytec). All the extractants were used as supplied. Experiments were performed at room temperature.

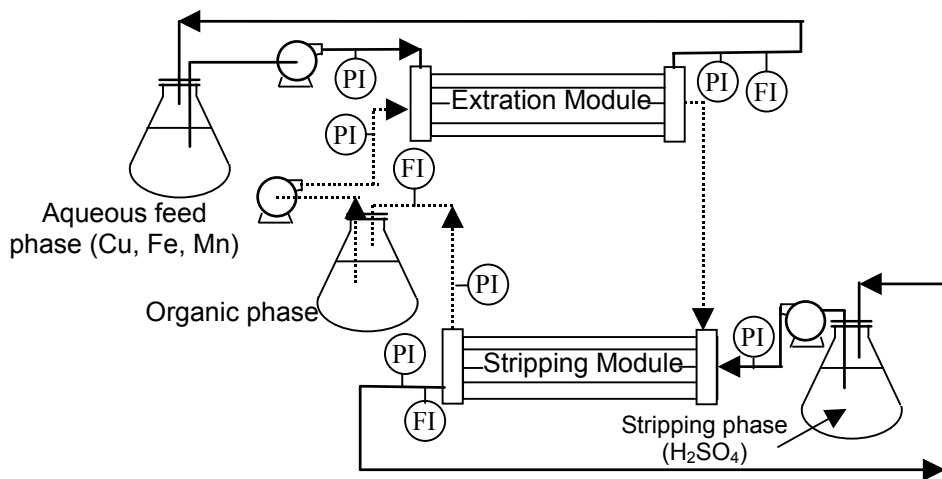


*Figure 1. Schematic diagram of the NDSX experimental system.*

## SELECTION OF EXTRACTANTS

The work started with selection of extractants for the removal and recovery of Fe, Cu and Mn from the oxidised aqueous stream. A review of the possibilities of solvent extraction in order to achieve metals separation from aqueous solutions containing iron is given by Ritcey [3]. Using the phosphinic acid Cyanex 272 together with tri-butyl phosphate (TBP) as the modifier, iron can be readily stripped from the loaded organic phase with sulphuric acid [3]. The solvent extraction of copper is a well-established hydrometallurgical process. The extractants with hydroxyoxime functional groups for chelation are in use in commercial solvent extraction-electrowinning plants. Chelating extractants are known to be selective for copper over Fe(III), the selectivity being based on the relative rates of extraction of copper and Fe(III).

In order to check the viability of the selective removal of copper from an aqueous solution containing Cu, Fe and Mn, the behaviour of LIX 622N was investigated. Results are given in Figure 2. It is observed that the concentration of Cu in the feed tank decreased with time while the concentrations of Fe and Mn remained at the initial value. According to these results it was thought that the separation of copper could be performed in a first step using LIX622N as a selective extractant.

A series of iron extraction/stripping experiments using D2EHPA and concentrated sulphuric acid and hydrochloric acid as stripping agents did not permit stripping efficiencies of Fe higher than 25% to be obtained. Thus the use of D2EHPA was discarded. Next the performance of Cyanex 272 was tested. As shown in Figure 3, Fe(III) is extracted and recovered in the stripping phase while Mn(II) remains in the feed phase. According to the information of the manufacturer (Cytec), the effect of the pH of the feed phase permits the selective separation of Fe and Mn from a sulphate media using Cyanex 272. Figure 4 shows the results of Mn extraction and stripping.

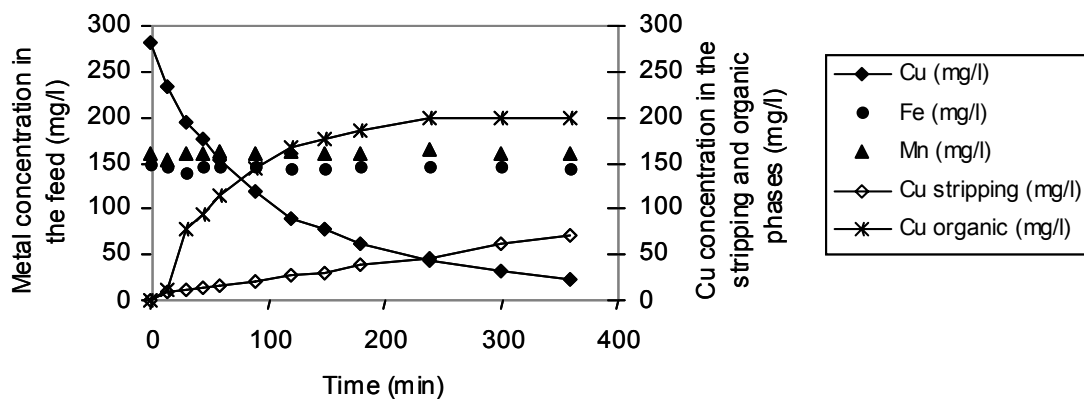


Figure 2. NDSX of Cu using LIX 622N. Organic phase: 10% v/v LIX 622N, 10% v/v TBP in kerosene. Initial pH of the feed phase pH=2. Stripping phase: sulphuric acid 2 M.

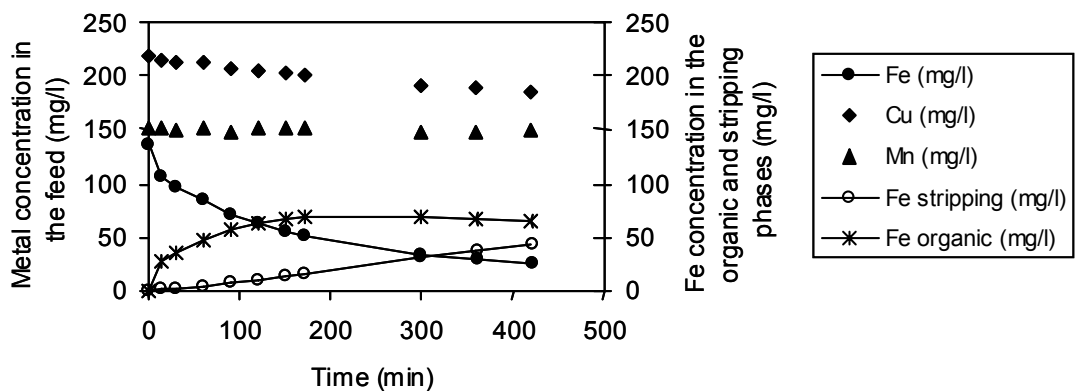


Figure 3. NDSX of Fe. Organic phase: 7.5% v/v Cyanex 272, 7.5% v/v TBP in kerosene. Initial pH of the feed phase pH=2.75. Stripping phase: sulphuric acid 2 M.

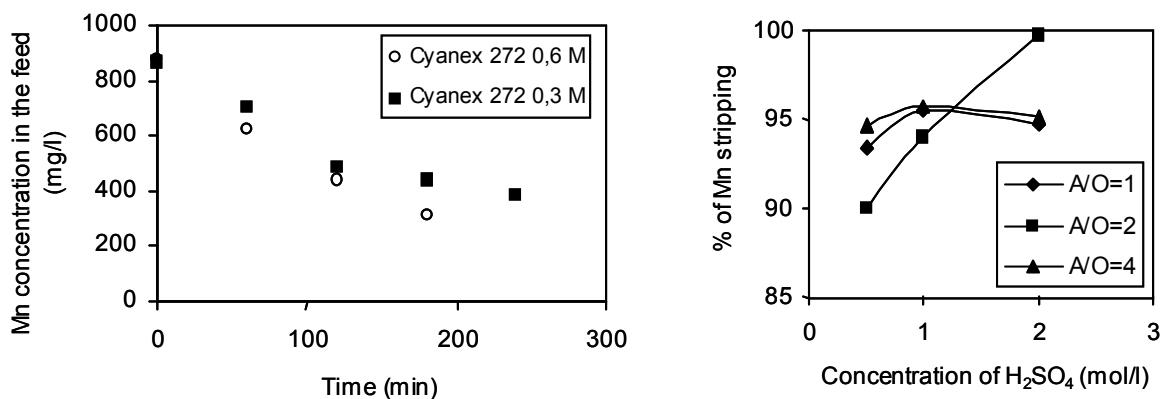


Figure 4. NDSX of Mn using Cyanex 272. Organic phase: Cyanex 272 0.3 M and 0.6 M, 10% v/v TBP in kerosene. pH of the feed phase pH=5.25. Stripping tests performed in perfect mixing experiments.

From the results obtained, the flowsheet proposed for the NDSX recovery of the WPO catalyst is shown in Figure 5.

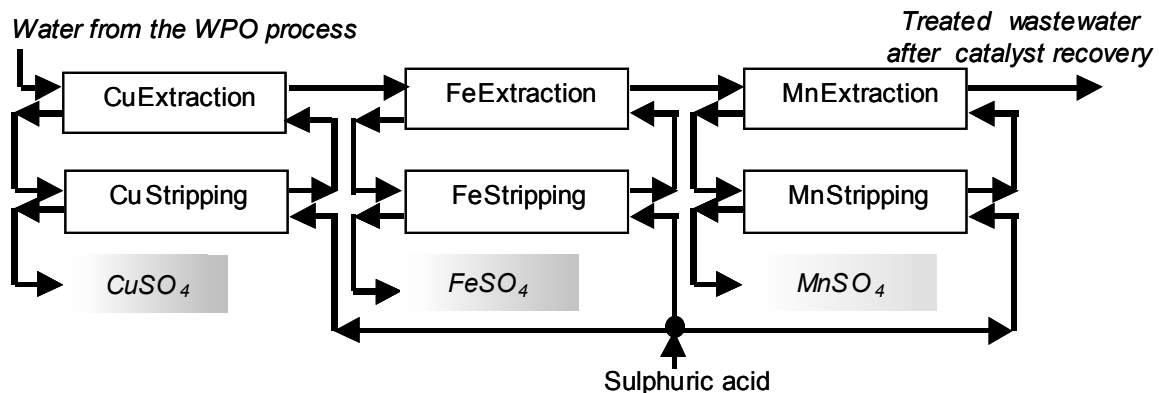


Figure 5. Flowsheet of the NDSX process for the recovery of the WPO catalyst.

### KINETICS OF COPPER EXTRACTION AND STRIPPING

Following the preliminary experiments for the selection of extractants, the NDSX process for the recovery of Cu was studied in detail. Kinetic experiments were performed working with a synthetic feed solution with an initial Cu concentration of 200 mg/l. Results are shown in Figure 6. In order to increase the concentration of Cu in the stripping solution, a set of experiments were carried out replacing the feed solution by a fresh one after 90 minutes running, while the organic and feed solutions were maintained the same.

It can be seen that the Cu concentration in the feed phase reaches values lower than 0.5 mg/l in the cycles 1, 2 and 3. In the stripping phase the Cu concentration increases linearly with time up to a value higher than 2 g/l. The concentration of Cu in the organic phase is maintained under 110 mg/l during all the experimental time. However, the rate of the extraction step is lower as time is increased, probably due to the influence of the loading of the stripping phase. Figure 7 shows the results of a similar experiment with two longer extraction cycles and using 10 litres of feed phase.

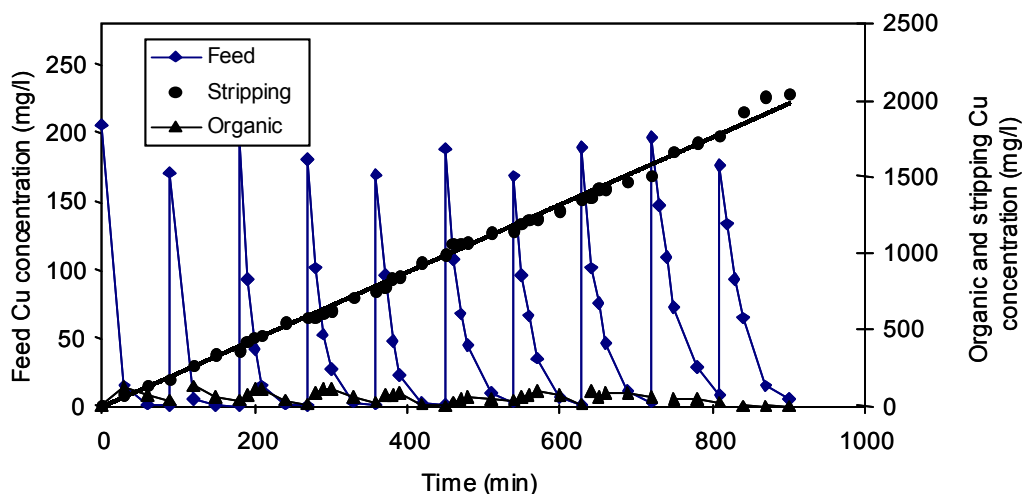


Figure 6. Evolution of the Cu concentration in the feed, stripping and organic tanks. Organic phase: 10% LIX 622N; 10% TBP in kerosene. Stripping phase:  $H_2SO_4$  1M. Constant feed pH = 2.5.  $V_{feed} = V_{org} = V_{stripping} = 1$  litre.

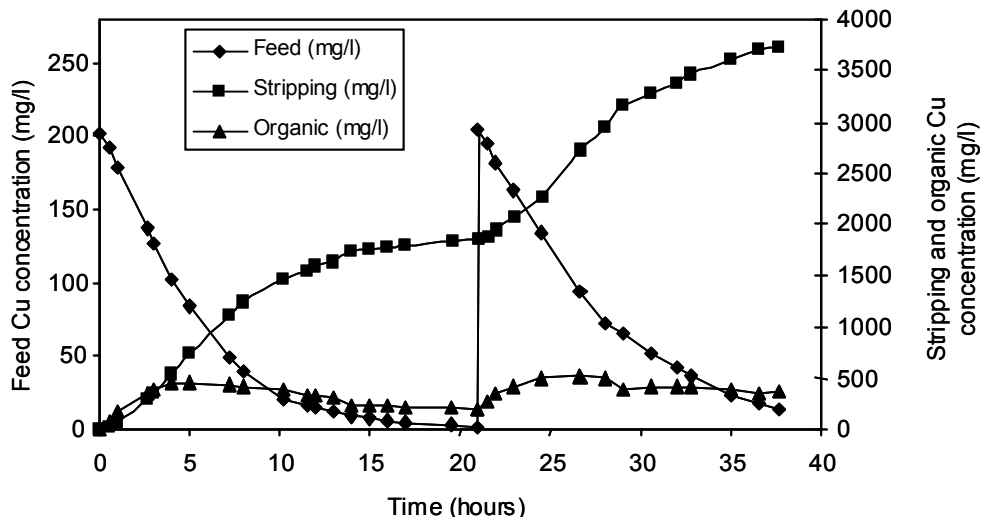
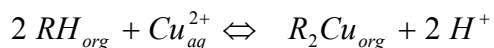


Figure 7. Evolution of the Cu concentration in the feed, stripping and organic tanks. Organic phase: 10% LIX 622N; 10% TBP in kerosene. Stripping phase:  $H_2SO_4$  1M. Constant feed pH = 2.5.  $V_{feed}$  = 10 litres.  $V_{org} = V_{stripping}$  = 1 litre.

### MATHEMATICAL SIMULATION OF THE NDSX OF Cu

The dynamic response of the process has been determined by the solution of the system of differential equations describing the evolution of the concentration of Cu in the feed, organic and stripping phases when flowing along the extraction and stripping modules together with the mass balances for the three tanks considered as ideal stirred vessels. This type of mathematical description has been previously employed to describe the NDSX separation of Cr(VI), Cd(II), and Ni-Cd mixtures [4].

Assuming that the mass transfer rate is limited by the transfer of the complex  $R_2Cu$  in the organic phase immobilised in the porous membrane, the parameters needed for the simulation are the diffusion coefficient of the complex  $R_2Cu$  in the organic phase and the equilibrium constant of the extraction reaction. The stoichiometry of the extraction of Cu with LIX 622N can be described by the expression:



As a first approximation, the values of the parameters were obtained from the literature [5] for the system LIX84-Cu(II):  $D_{CuR2} = 1.46 \times 10^{-10} \text{ m}^2/\text{s}$ ;  $K_{eq} = 1.7$ . Figure 8 shows the comparison of the experimental and simulated evolution of Cu concentration in the feed and stripping phases.

Further work will deal with the kinetic modelling of the selective recovery of Fe and Mn as necessary steps in process design; the methodology applied to the recovery of Cu will be applied to the rest of the metals.

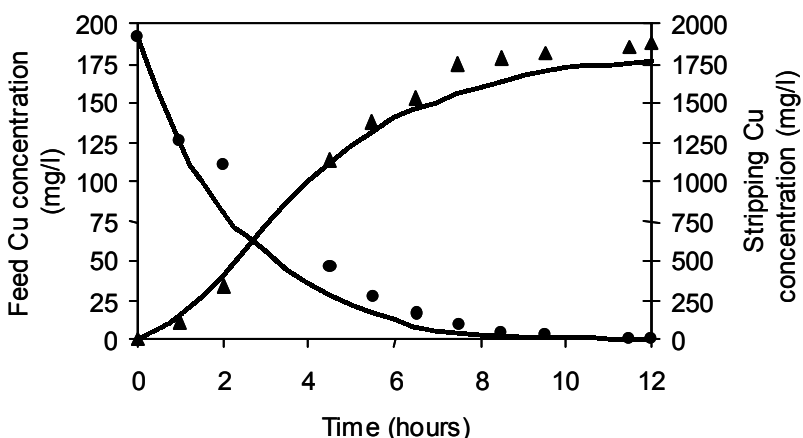


Figure 8. Experimental and simulated concentrations of Cu in the feed and stripping tanks.  
Organic phase: 10% LIX 622N; 10% TBP in kerosene. Stripping phase:  $H_2SO_4$  1M.

## CONCLUSIONS

This work focused on the recovery of the metallic catalyst used in wet peroxide oxidation processes constituted of mixtures of Fe(III), Cu(II) and Mn(II) by means of non-dispersive solvent extraction. It started with the selection of the suitable commercial extractants that would allow selective recovery of the three metals. Preliminary experiments led to the selection of LIX622N and Cyanex 272. Next, the development of the metal separation models and parameters was accomplished starting with the selective recovery of copper. Kinetic experiments were successfully described by means of a mathematical model previously developed for similar systems and using as characteristic parameters,  $D_{CuR2} = 1.46 \times 10^{-10} \text{ m}^2/\text{s}$ ;  $K_{eq} = 1.7$  [5]. Further work will deal with determination of the necessary parameters for the selective recovery of the three metals and definition of the integrated separation process.

## ACKNOWLEDGEMENTS

Financial support of the Ministry of Science and Technology (Spain) and European Commission under the project 1FD97-1189 is gratefully acknowledged. Cytec and Cognis are thanked for providing the extractants used in this work.

## REFERENCES

1. K. Fajerwerg, J. N. Foussard, A. Perrard and H. Debellefontaine (1997), *Wat. Sci. Tech.*, **35**, 103-110.
2. M. Falcon, K. Fajerwerg, J. N. Foussard, E. Puech-Costes, M. T. Maurette and H. Debellefontaine (1995), *Environ. Technol.*, **16**, 501-513.
3. G. M. Ritcey (1986), Iron Control in Hydrometallurgy, J. E. Dutrizac and A. J. Monhemius (eds.), Ellis Horwood, Chichester, pp. 247-281.
4. I. Alonso, A. M. Urtiaga, S. Zamacona, A. Irabien and I. Ortiz (1997), *J. Membr. Sci.*, **130**, 193-203.
5. Z.-F. Yang, A. K. Guha and K. K. Sirkar (1996), *Ind. Eng. Chem. Res.*, **35**, 1383-1394.



# COPPER RECOVERY USING LEACH / SOLVENT EXTRACTION / ELECTROWINNING TECHNOLOGY: FORTY YEARS OF INNOVATION, 2.2 MILLION TONNES OF COPPER ANNUALLY

Gary A. Kordosky

Cognis Corporation, Tucson, USA

The concept of selectively extracting copper from a low grade dump leach solution followed by stripping the copper into an acid solution from which electrowon copper cathode could be produced occurred to the Minerals Group of General Mills in the early 1960s. This simple, elegant idea has resulted in a technology by which about 2.2 million tonnes of high quality copper cathode was produced in year 2000. The growth of this technology is traced over time with a discussion of the key plants, the key people and the important advances in leaching, plant design, reagents and electrowinning that have contributed to the growth of this technology. Some thoughts on potential further advances in the technology are also given.

## INTRODUCTION

A keynote paper for solvent extraction (SX) applications in hydrometallurgy should “set the stage” for the papers that follow by discussing a commercially successful application of SX in hydrometallurgy. In addition the paper needs to discuss a complete metal recovery process for the simple reason that an SX process for metal recovery does not stand alone, it is always part of an overall metal recovery process. The SX process must be compatible with, and complimentary to, the metal leaching process that precedes it and the metal recovery process that follows. The paper should acknowledge that most of the advances in a metal recovery technology are made for economic reasons. This discussion of the leach / solvent extraction / electrowinning (L/SX/EW) process for copper recovery, considered by some to be one of the great advances in copper recovery technology of the last 100 years [1], satisfies these criteria.

## HISTORICAL BACKGROUND

When the sulfuric acid copper L/SX/EW flow sheet (Figure 1) was put forth by the Minerals Development Group of General Mills in 1960 solvent extraction had been known for over 100 years [2]. It was used extensively on a very small scale in analytical chemistry [3] and on a large scale for the recovery of uranium from sulfuric acid leach solutions [4]. General Mills had already developed and commercialized Alamine® 336 as an SX reagent for the recovery of uranium from sulfuric acid leach liquors [5] and believed that a similar technology for copper recovery would be welcome. However, an extensive market survey showed that the industry reception for copper recovery by L/SX/EW technology was almost hostile. The R&D director of a large copper producer predicted at an AIME annual meeting that there would never be a pound of copper recovered using solvent extraction and his comment prompted applause [5].

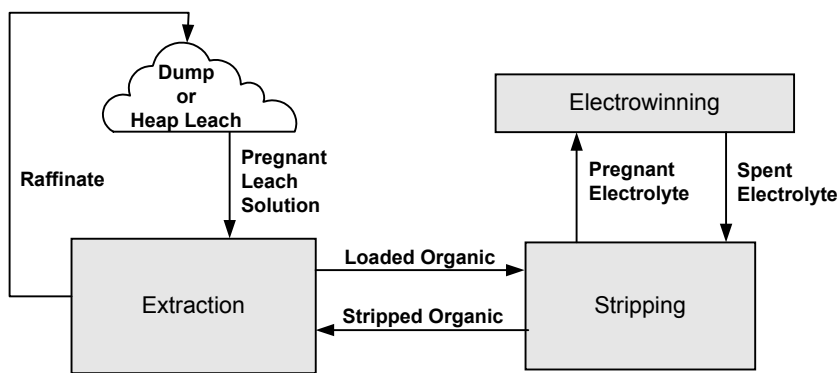


*Figure 1. Conceptual Leach / Solvent Extraction / Electrowinning flow sheet.*

Fortunately, the Minerals Development Group of General Mills, in the person of Joe House, Don Agers and Ronald Swanson, believed so much in the copper L/SX/EW process that they kept the development of this technology alive as a “bootleg” project, that is, a project where the three individuals had other primary work duties and could only work on this project when they found time or on their own time. By late 1962 this group had identified and formulated an organic soluble molecule containing a hydroxy-oxime functionality as the reagent LIX® 63. While LIX 63 had many of the properties required for a reagent to be successful in the proposed L/SX/EW flow sheet, LIX 63 was not compatible with the copper leaching process because it did not extract copper below pH ~ 3 [6].

Technically this problem could be solved by neutralizing the acid leach liquor or by leaching oxide copper with ammonia, but neither solution was economical. A molecule that extracted copper well from typical dump leach liquors (pH ~1.8) had to be built. The reagent LIX 64, containing the ketoxime LIX 65 (Figure 2) and a catalytic amount of LIX 63, was introduced in 1965 [7] and in March 1968 the first commercial copper L/SX/EW operation, the Bluebird plant of Ranchers Exploration and Development Corporation, came on line [1].

REAGENT	R	A	TYPE
LIX 65	C <sub>12</sub> H <sub>25</sub>	C <sub>6</sub> H <sub>5</sub>	Ketoxime
LIX 65N	C <sub>9</sub> H <sub>19</sub>	C <sub>6</sub> H <sub>5</sub>	Ketoxime
SME 529, LIX 84-I	C <sub>9</sub> H <sub>19</sub>	CH <sub>3</sub>	Ketoxime
LIX 860-I, LIX 622	C <sub>12</sub> H <sub>25</sub>	H	Aldoxime
P1, LIX 860N-I	C <sub>9</sub> H <sub>19</sub>	H	Aldoxime

*Figure 2. General structure of oxime molecules used for copper recovery.*

### Copper Recovery by L/SX/EW in 1968

In 1968 there was only two widely practiced copper leaching processes using dilute sulfuric acid. The first process, vat leaching of high-grade copper oxide ore followed by EW of copper from the leach solution, produced low quality copper cathode at relatively high cost. In 1968 the tonnage of high-grade oxide ores was decreasing and vat leaching was on the decline.

The second process, heap and dump leaching of low-grade oxide and/or sulfide ore followed by precipitation of low quality copper from the leach solution on scrap iron, was practiced on oxide ore that was too low grade for vat leaching, or low grade sulfide ore that had to be mined in order to expose the underlying high grade sulfide ore. Copper recovered from leaching low grade copper ores was considered a bonus and little effort had been made to fully understand the leaching process or to maximize copper recovery. While some fundamental leaching studies had taken place [8, 9], on the whole leaching was a poorly practiced art and little had been done to make it a well-practiced science.

Solvent extraction for copper was not yet proven commercially so most copper companies were taking a wait and see attitude. Furthermore LIX 64, the only reagent available, had significant limitations with respect to extractive strength, metal transfer kinetics and copper/iron selectivity and it could only be used up to a maximum copper loading of about 3 g/l because of entrainment problems. These properties restricted copper leach solutions which could be effectively treated by SX using LIX 64 to  $\leq$  3 g/l Cu at a pH  $\geq$  1.8.

In 1968 the copper industry as a whole did not believe large quantities of high quality copper could be produced by hydrometallurgy and at the time the Ranchers plant came on line, expectations for the eventual success of copper L/SX/EW technology were rather modest.

#### **Ranchers' Bluebird Sulfuric Acid Leach / Solvent Extraction / Electrowinning Plant**

Ranchers leached run of mine copper oxide ore ( $> 0.5\%$  Cu) placed in a sealed canyon in 20 foot layers (heaps) by distributing dilute sulfuric acid over the fresh ore via spray emitted from needle valves with pipes and needle valves placed to ensure complete coverage of the ore. New heaps were built over old heaps. Pregnant leach solution flowing from the bottom of the heap was collected in a pond created by placing a dam downstream from the leach area. The Bluebird copper SX plant was built similar to existing uranium SX plants with tall, single baffled mixers and long narrow settlers. Dispersion exiting the mixer was pumped to the opposite end of the settler and the phases flowed back toward the mixers.

In electrowinning rich electrolyte with  $\sim$ 36 g/l Cu, 3 g/l Fe and 145 g/l H<sub>2</sub>SO<sub>4</sub> entered one end of the EW cells and spent electrolyte with  $\sim$ 32 g/l Cu and 151 g/l H<sub>2</sub>SO<sub>4</sub> exited the other end. Cathodes weighing 60 kilograms were grown on copper starter sheets at a current density of about 180 A/m<sup>2</sup> with a current efficiency of 80 to 85%. The anode was 6 % Sb in Pb.

Design production at Ranchers was 30,000 pounds of copper daily. In its first fiscal year of operation, July 1968 – June 1969, the Bluebird plant produced 9 million pounds of copper (82% of design), a remarkable achievement for a metallurgical plant using new technology. By later adding only rectifier capacity the plant often exceeded its design production by 50%.

Ranchers' Bluebird plant proved that L/SX/EW technology could produce large quantities of good quality cathode copper on a consistent day to day basis at a profit [1]. This raised the awareness and sparked the interest of the industry in copper L/SX/EW. Improvements in the technology quickly followed from many sources including consultants, copper producers, engineering companies, chemical companies and metallurgical testing laboratories.

## **IMPROVEMENTS IN COPPER L/SX/EW TECHNOLOGY**

#### **Solvent Extraction Reagents**

The first improvement in copper SX reagents came when LIX 64N was added as makeup to the Ranchers plant in late 1968. LIX 64N had greater extractive strength, faster kinetics, faster phase separation, lower entrainment, increased copper/iron selectivity and lower viscosity than

LIX 64 [10]. These improved reagent properties broadened the range of copper leach liquors which could be successfully treated by solvent extraction, allowed for less staging thereby reducing the capital cost of the SX plant, and lowered operating costs by decreasing organic losses and tankhouse bleeds. LIX 64N is LIX 65N (Figure 2) with a catalytic amount of LIX 63.

In 1968 Ashland Chemical introduced Kelex® Reagents along with the idea of using varying amounts of modifier, either nonylphenol or isodecanol, to facilitate the stripping of copper from the loaded reagent with normal tankhouse electrolytes [11,12]. Kelex reagents have not been used commercially for copper SX, but the use of modifiers to shift the extraction ↔ stripping equilibrium of copper extractants represents a significant, widely used advance in copper SX.

Shell International Chemicals brought the reagent SME®529 (Figure 2) to the market in the mid-1970s as an alternative to LIX 64N. This reagent found only limited commercial use because the poor properties of the side products from the manufacture of this reagent overrode the very good properties of the extractant molecule, a molecule in wide use today.

At ISEC '74 Birch reported the reagent P1 (Figure 2) from Acorga Ltd. had rapid kinetics, excellent Cu/Fe selectivity and fast phase separation [14]. However, P1 was such a strong copper extractant that efficient stripping required nearly 250 g/l sulfuric acid, an acid content not compatible with normal EW practice. In 1977 the Acorga P-5000® series of reagents was described [15,16]. These reagents combined P1 with various amounts of nonylphenol to give reagents having tailored extraction ↔ stripping properties. These modified aldoxime reagents brought a significant advance to copper SX because they allowed solutions with a high copper content and/or a low pH to be effectively treated in 2 instead of 3 or 4 extraction stages.

In 1979 the tridecanol modified aldoxime reagent LIX 622 (Figure 2), was made available by the Henkel Group which had purchased General Mills Chemicals in 1977. LIX 622 was the first tridecanol modified reagent to be commercialized when the Pinto Valley copper SX plant came on line in 1981. Tridecanol is still a widely used modifier in copper SX reagents.

Aldoxime/ketoxime blends were introduced in 1982 by Henkel as the LIX 860 reagent series. This reagent series combines the fast kinetics and extractive strength of the aldoximes with the stability and good physical performance of the ketoximes, without the detrimental properties of added modifier [17]. The addition of LIX 860-I (Figure 2) to existing plants using LIX 64N allowed these plants to quickly upgrade their plant performance and flexibility if needed or desired. Today aldoxime/ketoxime blends are widely used in copper SX.

Henkel purchased the SME 529 technology from Shell in late 1984 and 2 years later, using a new manufacturing process, began producing LIX 84-I, a much improved version of SME 529 (Figure 2). LIX 84-I replaced LIX 64N and LIX 65N in the LIX Reagent line and led to the LIX 900 Reagent series of LIX 84-I/LIX 860-I blends.

The use of hindered, high molecular weight alcohols and esters as modifiers was reported in 1986 with the claim that ester modifiers increase both Cu/Fe selectivity and oxime stability when compared to other modifiers [18]. Since then the ester modified reagents such as M5640 and LIX 664N have become the most popular of the modified reagents.

Improvements in reagent properties for the extraction of copper from dilute sulfuric acid leach solutions are summarized in Table I. These improvements have come about for 3 reasons:

1. New molecules: LIX 65N, SME 529, P-1 and LIX 860-I are examples.
2. Improved processes to produce cleaner reagents: LIX 65N and LIX 84-I are examples.
3. Manipulation of reagent properties: modified aldoximes and aldoxime/ketoxime blends are examples.

*Table 1. Trends in reagent properties.*

Property	1965	1970	Late 1970s	Today
Extractive Strength	Moderate	Moderate	Strong	Tailored
Cu/Fe Selectivity	Fair	Good	Good	Excellent
Kinetics	Slow	Moderate	Fast	Fast
Stability	Excellent	Excellent	Good	Very Good
Crud Generation	Moderate	Low	Moderate	Low
Versatility	Poor	Marginal	Good	Excellent

There are two distinct classes of modern extractants: ketoximes and aldoximes. A general comparison of their properties as well as mixtures of the two is given in Table 2.

*Table 2. Properties for reagents based on ketoximes, modified aldoximes, and ketoxime-aldoxime mixtures.*

Property	Ketoxime	Aldoxime	Mixtures
Extractive Strength	Moderate	Strong	Customized
Stripping	Very Good	Reasonable	Customized
Cu/Fe Selectivity	Excellent	Excellent	Excellent
Copper Kinetics	Very Good	Very Fast	Fast
Phase Separation	Fast	Fast	Fast
Stability	Excellent	Very Good*	Very Good
Crud Generation †	Low	Variable	Low

\* Dependent upon the particular modifier used.

† Dependent upon the leach liquor and modifier.

Ketoximes are moderately strong copper extractants which operate best when the leach liquor is relatively warm and the pH is ~1.8 or above. Modified aldoximes have good metallurgical properties even at low temperatures and low pH. The properties of aldoxime/ketoxime blends reflect the ratio of the components. Today the metallurgist can select the best reagent or reagent blend for his/her leach liquor, plant design and operating conditions. For example, one plant used an aldoxime/ketoxime blend of 55/45 when the pH of the leach liquor was ~1.5, but, today the plant adds a 50/50 blend because the pH of the leach liquor has risen to ~1.7. Metallurgical performance, entrainment, crud generation, mixer stability, price and the performance of the various reagents in plants having a similar design and/or operating with a similar leach liquor should all be considered when making a reagent choice.

### Leaching

Once solvent extraction proved to be a cost-effective way to purify and concentrate copper from leach liquors, copper producers began to regard leaching as a much more important source of copper. Two early advances in leaching include the distribution of large drops of leach solution over the ore at Bagdad in 1970 [19] and the use of drip irrigation by Johnson Camp in 1976 [20]. These improvements resulted in decreased water consumption, increased temperature in the heaps or dumps and higher copper recovery.

The "Thin Layer" (TL) acid cure leaching process reported in 1978 is to date the single greatest advance in copper leaching [21]. The first plant practice of TL leaching for copper was in 1980 at Sociedad Minero Puduhuel (SMP) [22]. SMP obtained high copper recovery from both the oxide and sulfide portions of their ore, low soluble silica in the pregnant leach liquor, and an overall water / acid balance to give a zero discharge plant. The important role of bacteria in leaching metal sulfides had been known [9] and some of the practical aspects of biological leaching had been discussed [23]. However, copper recovery from a high-grade sulfide ore by bacteria assisted heap leaching was not considered economically viable until SMP showed that

the total copper recovery from the chalcocite/bornite portion of their mixed oxide sulfide ore could reach 85% by leaching the tails from their TL operation for another 45 days [22]. Inspiration Copper in Arizona was testing with good results a similar technique called "ferric cure" on heaps of 100% minus four inch mixed oxide/sulfide ore [8].

In 1984 BHAS began agitation leaching copper matte from a lead blast furnace with a sulfuric acid leach solution having about 1 molar chloride ion [24]. This leaching system is reported to be effective for leaching copper sulfide ores and concentrates. Also in 1984 Sunshine Mining company installed a batch plant to pressure leach copper sulfide concentrate with sulfuric acid containing a catalytic amount of sodium nitrite [25].

In the late 1980s low-grade chalcopyrite dumps at Toquepala were wetted with 10 g/l H<sub>2</sub>SO<sub>4</sub>. Naturally occurring bacteria multiplied, oxidized the sulfide minerals and warmed the dumps. When copper SX started in 1995 the initial flush of copper from these dumps was much greater than anticipated and copper recovery over the first five years has been much higher than expected based on the leaching history of other low-grade chalcopyrite dumps.

Forced aeration to increase bacterial activity in heaps and dumps was field tested in the 1970s and successfully commercialized in the mid to late 1990s [26]. Of particular note is the Quebrada Blanca operation in Chile where bacterially assisted heap leaching of chalcocite, aided by forced aeration, is successfully practiced at an elevation of 4,400 meters [27]. The leaching of high-grade chalcocite ore in an autoclave at relatively low temperature and pressure was commercialized at Mt. Gordon in mid-1998 by Western Metals Copper Ltd. [28].

"From an poorly practiced art to a near science" describes the changes in leaching practice since the late 1960s. Heaps and dumps are constructed to retain heat, wet all the ore evenly, and for sulfide ore, to encourage air circulation through the dump or heap. Advances in heap leaching include blasting techniques which size ore to optimize copper recovery, crushing to the optimum size, agglomeration techniques, agglomeration aids, curing methods, heat retention and bacteria augmentation. Copper recoveries of 85% are being reported at several oxide heap operations and many chalcocite heap leaches report 75% to 80% copper recovery.

Sulfuric acid leach solutions treated successfully by copper SX range from < 1 g/l Cu up to about 35 g/l Cu with a pH range of ~0.8 to ~2.5. Leach solutions contain a variety of impurities at various concentrations depending on the ore, available water and evaporation rate. The SX plant must produce an electrolyte from which Grade A copper can be plated and most plants do, some from very difficult leach solutions. For example, the Michilla plant in Chile treats a leach solution having 55 g/l chloride while Lomas Bayas in Chile has treated a leach solution having 35 g/l nitrate and 15 g/l chloride. Both plants consistently produce high quality copper.

### **Electrowinning**

In 1968 Ranchers installed flotation cells to remove entrained organic from the pregnant electrolyte resulting in improved copper quality. In the late 1970s Anamax installed an electrolyte filter to clean the electrolyte of both solids and organic. A major breakthrough in EW came when Bagdad cathode was registered on the Comex in 1975 followed several years later with the registration of Anamax cathode on the London Metal Exchange.

Other important EW developments include: plating hard bright copper consistently onto starter sheets at 320 A/m<sup>2</sup> [29], the addition of cobalt in the electrolyte to reduce lead anode corrosion [30] and the use of water soluble polymers as smoothing agents. Rolled anodes of Pb-Ca and Pb-Sr-Sn are now the anode of choice because of their dimensional stability, lower rate of corrosion and the fact that anode cathode spacing in the cell is slightly less than when a cast anode is used [31]. The use of a cathode press to straighten 2-day cathodes grown on copper starter sheets results in higher current efficiencies and improved copper quality [32].

Capital Wire and Cable plated full size cathodes on stainless steel blanks in the early 1970s while Magma Copper was the first Cu EW tankhouse to use the CRL ISA Process where full size cathodes are grown on stainless steel blanks and then mechanically stripped. Plating copper on stainless steel blanks improves copper quality and increases current efficiency. The use of a manifold to evenly distribute electrolyte to every cathode in a cell was installed at Magma Copper in the late 1980s and was a key factor in their ability to produce LME quality copper at current densities up to  $320 \text{ A/m}^2$  [33].

A modern copper EW tankhouse coupled with copper SX achieves 93 - 95% current efficiency while producing 60% to 80% more copper per unit of tankhouse area than the early EW tankhouses. Full size cathodes are deposited on stainless steel blanks at  $240 - 320 \text{ A/m}^2$  from a solution containing 32 to 37 g/l Cu and 160 to 180 g/l  $\text{H}_2\text{SO}_4$ . Most large tankhouses mechanically strip the copper from the blanks while most small tankhouses combine some automation with hand stripping. The electrolyte stream is cleaned by column flotation followed by filtration through garnet sand and anthracite. Special grades of guar are used as smoothing agents, and acid mist suppressants, either chemical, mechanical or a combination of both, are common. Most EW tankhouses coupled with a copper SX plant consistently produce Grade A copper.

### **Mixer Settler Design**

In 1972 General Mills suggested the addition of one or more properly designed “picket fences” in settlers to distribute the dispersion exiting the mixer evenly across the full width of the settler [34]. This results in improved settler throughput and much lower entrainment.

A major advance in mixer settler design is the low profile concept from P. Paige of Holmes and Narver [35]. The mixer consists of several shallow boxes separated by over/under baffles. A pumping impeller is used in the primary mix box while axial impellers designed to maintain the dispersion are used in the secondary mixers. The settlers have a length to width ratio  $\leq 1$  and are built on the ground, usually at grade. The advantages of this design included lower capital, high mixer efficiency, slower linear flow down the settler resulting in less entrainment, and an overall smoother operation. Most copper SX plants built in the past 25 years are of the low profile design. Typically copper SX plants are designed so that the dispersion exits the mixer directly into the mixer end of the settler with the flow of the phases away from the mixer. Recently several plants have been built where the dispersion is carried to the opposite end of the settler by a side launder as this design offers the potential to reduce capital.

A key improvement in mixer design that reduces entrainment is the swept vane impeller. The Lewis type baffled settler [36] and the Krebs design [37] while commercialized are not considered standard practice in the copper industry. Two recent innovations in mixer design are very promising, the Outokumpu Vertical Smooth Flow mixer [38] and the new Lightnin mixer system at ASARCO Silver Bell. Both have relatively small primary mixers and much larger secondary mixers. It is claimed these mixer systems give lower entrainment and less crud generation because the dispersion spends less time in the highly agitated primary mixer and more time in the more gently agitated secondary mixers. Reagent losses at Silver Bell are among the lowest in the industry suggesting the claims have merit.

Other important design innovations include well designed coalescers on the loaded organic stream, filter presses for crud treatment, clay treatment [39] to keep the organic clean and large flotation settling tanks that recapture organic entrained in the raffinate.

## INSTALLED PRODUCTION CAPACITY FOR SULFURIC ACID COPPER L/SX/EW

The installed capacity for copper production by sulfuric acid L/SX/EW is given in Table 3. Note that from a rather modest beginning in 1968 the installed capacity for copper production by L/SX/EW is today about 2.8 million tonnes annually. This represents about 20% of the primary copper produced. The major reason for the large increase in L/SX/EW capacity is its lower cost, both capital and operating, when compared to the traditional flotation / smelting route. An important feature of the economics is that both large and small plants can achieve low costs. For example, the Dos Amigos operation in Chile (10,000 MT Cu/year) has about the same cash cost to produce copper as the Zaldivar operation in Chile (140,000 MT Cu annually). In addition EW copper from copper SX plants obtains a premium in the market place over most cathode copper produced by the flotation/smelting route. Furthermore, L/SX/EW technology allows plants to obtain copper at a low incremental cost from low-grade overburden that needs to be mined but otherwise would not be processed. Copper SX technology also has great flexibility allowing plants to achieve design production under a variety of conditions. Finally, copper L/SX/EW provides a home for sulfuric acid produced by smelters.

*Table 3. Installed capacity for copper production by sulfuric acid L/SX/EW.*

Year End	Installed Capacity (MT Cu annually)
1970	11,250
1975	108,912
1980	255,122
1985	355,954
1990	800,857
1995	1,563,205
2001	2,844,200

Today there are more than 55 locations (China excluded) with SX plants recovering copper from dilute sulfuric acid leach solutions. The number of SX trains and the complexity of the SX/EW installation range from the simple 2E, 1S single train installation at Mt. Cuthbert in the Australian outback producing 5,500 MT Cu annually, to the Phelps Dodge L/SX/EW complex at Morenci, Arizona, where about 16,500 m<sup>3</sup>/h of heap and dump leach liquors are treated in four separate, multi-train, 1E, 2E, 1W, 1S stage SX plants placed strategically on the property. The SX plants at Morenci feed 3 EW tankhouses that produce a total of about 365,000 MT Cu annually. Copper SX mixer-settlers range in size from the very small treating about 100 m<sup>3</sup>/h of leach solution, to large modules treating about 2,000 m<sup>3</sup>/h of leach solution.

## FUTURE IMPROVEMENTS IN L/SX/EW TECHNOLOGY

There may be incremental advances in today's leaching practice for oxide and chalcocite ores. However, the most abundant copper mineral is chalcopyrite and heap leaching this mineral with dilute sulfuric acid gives recoveries of only 25 to 30%. Obtaining high recoveries by heap leaching chalcopyrite with dilute sulfuric acid would be a truly revolutionary advance that would change the copper industry dramatically. There is ongoing work in this area and, while there has been some progress, much work remains.

In recent years there has been significant progress in leaching copper sulfide concentrates as an alternative to smelting [40]. Both pressure leaching (without nitrite catalysis) and bacteria assisted leaching in stirred tanks have been demonstrated for copper sulfide concentrates in pilot plants and small demonstration plants and both technologies are likely to be commercially installed within 2-4 years.

While revolutionary improvements in the properties of reagents for the extraction of copper from sulfuric acid leach solutions are not likely, small improvements in the blending of reagents and in the processes to produce reagents may come. The reagents of today are very good and the investment required to produce better reagents would not likely pay the needed return.

Increases in the current density at which high quality copper can be plated will be incremental with the current EW cell design. A new cell design that plates high quality copper at high current density from low grade solutions has recently emerged [41] and if certain problems can be solved this design could represent a significant advance in copper EW technology.

## CONCLUSION

By any standard of measurement L/SX/EW technology has made an important contribution to the copper industry. Initially the availability of LIX 64N and the success of Ranchers sparked interest to improve leaching and electrowinning techniques. Since that time a synergistic push-pull mechanism has emerged where an improvement in one aspect of the technology drives improvement in the other aspects. This synergistic push-pull mechanism will continue to advance copper L/SX/EW technology, but not likely at the pace of the past 34 years. The close working relationships between suppliers, engineering companies and copper producers that developed over the years have also contributed significantly to the improvements in the technology and it is important that these relationships continue.

The most fitting way to close this paper is to quote two early believers in copper L/SX/EW technology. Maxie Anderson, president of Ranchers, at the dedication of the Bluebird copper L/SX/EW plant said: "Not often does a small company have the opportunity to change the course of an industry and add to new technology..." In 1970 Ken Power closed his paper describing the operation of the Bluebird copper L/SX/EW plant with the words: "The applicability of liquid ion exchange to the treatment of dilute impure copper solutions has been irrefutably demonstrated, both technically and economically. The field of application in the hydrometallurgical treatment of copper minerals and products appears limitless" [1]. Today, more than 3 decades later, these prophetic words ring with clarity.

## ACKNOWLEDGEMENTS

The author is grateful to Cognis group for the opportunity to write this paper and to the staff of the Mining Chemicals Technology Division of Cognis for their contributions to this paper. The author acknowledges every individual and company that has contributed to the success of copper L/SX/EW technology and apologizes for not being able to cite all of them in this paper.

Alamine<sup>®</sup>, LIX<sup>®</sup> and SME<sup>®</sup> are registered trademarks of the Cognis Group.  
Acorga<sup>®</sup> is a registered trademark of Avecia.

## REFERENCES

1. K.L. Power (1970), AIME Annual Mtg., Denver, February.
2. Peligot (1842), *Ann. Chim. Phys.*, **5** (3), 1.
3. G. Morrison and H. Freiser, Solvent Extraction in Analytical Chemistry, John Wiley and Sons, Inc., New York, 1957.
4. A.M. Ross (1957), AIME Annual Meeting, New Orleans, February.
5. J.E. House (1981), Gaudin Lecture, AIME Annual Mtg., Chicago, February.

6. R.R. Swanson and D.W. Agers (1964), AIME Annual Mtg., New York, February.
7. D.W. Agers, J.E. House, R.R. Swanson and J.L. Drobnick (1965), *Min. En.*, (12), 76-80.
8. E.A. Bilson, "Hydrometallurgy at Inspiration", Spring Meeting Arizona Section AIME, Miami, Arizona, June 5, 1982
9. L.C. Bryner and A.K. Jameson (1958), *Appl. Microbiol.*, **6**, 281-287.
10. E.R. Dement and C.R. Merigold (1970), AIME Annual Mtg., Denver, February.
11. Ashland Chemical Company (1968), Preliminary Technical Data Sheet, "Copper Solvent Extraction Reagents".
12. J.A. Hartlage and A.D. Cronberg (1973), CIM Conference of Metallurgists, Quebec City.
13. A.J. van der Zeeuw (1975), Symposium on Hydrometallurgy, Inst. of Chem. Eng., Manchester, April 1975, Inst. of Chem. Eng., Symposium Series No. 42, p. 161.
14. C.P. Birch (1974), *Proc. Int. Solv. Extr. Conf., ISEC '74*, Lyon.
15. J.A. Tumilty, R.F. Dalton and J.P. Massam (1977), Advances in Extractive Metallurgy, The Institution of Mining and Metallurgy, London.
16. A. Tumilty, G.W. Seward and J.P. Massam (1977), *Proc. Int. Solv. Extr. Conf., ISEC '77*, CIM Special Volume 21.
17. G.A. Kordosky, J.M. Sierakoski and J. House (1983), *Proc. Int. Solv. Extr. Conf., ISEC '83*, Denver, pp. 90-91.
18. R. F. Dalton, K.J. Severs and G. Stephens (1986), *Proc. IMM's Mining Latin America Conference*, Chile.
19. R. L. Jones (1977), *Min. Eng.*, (9), 38-42.
20. W. Rudy (1978), AZ. Conf. of AIME Spring Hydrometallurgy Meeting.
21. E.O. Brimm and P. E. Johnson (1978), *Proc. Conference of Metallurgists*, Montreal.
22. E.M. Domic (1981), *Proc. 10th Annual AIME Meeting*, Chicago, TMS paper A81-46.
23. A. Bruynesteyn and D.W. Duncan (1977), *Proc. XIth Int. Min. Proc. Congress*, Sao Paulo.
24. N.E. Meadows and M. Valenti (1989), *Proc. Non Ferrous Smelting Symp.*, Australian Institute of Min. and Met., Victoria, Australia, p. 153.
25. C. Anderson (2000), *Proc. ALTA 2000 Copper-6*, ALTA Metallurgical Services, Adelaide.
26. W.J. Schlitt (2000), *Proc. ALTA 2000 Copper-6*, ALTA Metallurgical Services, Adelaide.
27. H. Salomon-De-Friedberg (1997), LIX Reagent Users Conference, Iquique, Chile.
28. G.D. Richmond and M.A. Christie (1999), *Proc. ALTA Copper 99*, ALTA Metallurgical Services, Adelaide.
29. J.A. Holmes, A.D. Deuchar, L.N. Stewart and J.D. Parker (1976), *Int. Symp. on Extr. Met. of Copper*, Vol. II, J.C. Yannopoulos and J.C. Agarwal (eds.), pp. 907-942.
30. S.K. Mwenechanya and I. Sadig (1987), *Copper 87*, Vol. 3, Hydrom. and Electromet. of Copper, W.C. Cooper, G.E. Lagos and G. Ugarte (eds.), pp. 403 - 417.
31. R.D. Prengaman (1984), Anodes for Electrowinning, D.J. Robinson and S.E. James (eds.), The Metallurgical Society of AIME, Warrendale, PA.
32. Private Communication, S. Lynch, Phelps Dodge, Tyrone, New Mexico.
33. J.G. Jenkins and M.A. Eamon (1990), *20th Annual Hydromet. Mtg. of CIM*, Montreal.
34. D.W. Agers and E.R. Dement (1972), AIME Annual Meeting, New York, TMS paper A72-87.
35. P.M. Paige (1975), Annual Hydromet. Mtg., Canadian Institute of Mining and Metallurgy, Sudbury.
36. I.E. Lewis (1977), *Proc. Int. Solv. Extr. Conf. ISEC '77*, CIM Special Volume 21.
37. A.A. Sonntag, I. Szanto and D.A. Goodman (1989), SME Annual Meeting, Las Vegas.
38. Outokumpu VSF Solvent Extraction (1996), Outokumpu Engineering Contractors, Finland.
39. P.L. Mattison, G.A. Kordosky and W.M. Champion (1983), *Hydrometallurgy: Research Development and Plant Practice*, K. Osseo-Asare and J.D. Miller (eds.), *Proc. 3rd Int. Symp. on Hydrom.*, The Metallurgical Society of AIME, Warrendale, PA.
40. M. Jansen and A. Taylor (2000), *Proc. ALTA 2000 Copper-6*, ALTA Metallurgical Services, Adelaide.
41. P.A. Treasure (2000), *Proc. ALTA 2000 Copper-6*, ALTA Metallurgical Services, Adelaide.



## SOLVENT EXTRACTION IN THE PRIMARY AND SECONDARY PROCESSING OF ZINC

Peter M. Cole and Kathryn C. Sole\*

Hydrometallurgy Consultant, Johannesburg, South Africa

\*Anglo American Research Laboratories (Pty) Ltd, Johannesburg, South Africa

An unprecedented expansion of the global zinc industry is currently underway. While most new projects and plant upgrades remain committed to traditional processing technologies, recent advances in zinc solvent extraction (SX) have created opportunities for new process routes for both primary and secondary materials. The first commercial plant to use zinc SX for the mainstream processing of a low-grade ore is under construction and promises to become one of the lowest cost zinc producers. Several other oxide and sulphide projects in various stages of feasibility are considering the inclusion of SX in their process flowsheets. Zinc SX has also proved advantageous in the reprocessing of secondary materials, particularly for the treatment of zinc residues and furnace dusts. This review focuses on recent installations and projects under development that feature zinc SX as the key separation step.

### INTRODUCTION

The traditional roast-leach-electrowin (RLE) zinc production route was developed for the processing of sulphide ores. It can prove inefficient for some complex sulphides and is not readily applicable to the treatment of other ore types. Inherent to this route is the generation of SO<sub>2</sub> gas that has to be fixed for environmental reasons, usually resulting in the production of sulphuric acid. These limitations have encouraged the search for alternative processing routes for both sulphides and other ores.

Approximately 30% of global zinc production arises from recycled zinc. With increasing awareness of secondary zinc materials as a valuable resource and stricter environmental legislation that restricts dumping of these hazardous materials, interest in their recycling has increased [1]. Direct retreatment of such materials *via* the process of origin is not always cost effective and can deleteriously affect the operation of the primary plant due to high levels of impurity species.

The development of process routes for the treatment of both primary and secondary sources of zinc has been hindered by the very stringent requirements for production of high-purity zinc by electrowinning (EW) [2]. Zinc EW from sulphate medium is extremely sensitive to the presence of trace impurities and requires a highly purified electrolyte. The selectivity of modern solvent extractants, an improved understanding of the process chemistry, and engineering innovations, have today enabled SX to provide unique advantages as a purification step ahead of the EW circuit in hydrometallurgical process flowsheets.

In most of the new applications involving SX processing in sulphate media, di(2-ethylhexyl)-phosphoric acid (D2EHPA) is used. This extractant is selective for zinc over most of the species deleterious to EW (Cu, Cd, Co, Ni, and the halides) and is readily stripped by acid concentrations typical of the spent tankhouse electrolyte (~ 180 g/L H<sub>2</sub>SO<sub>4</sub>). Circuit configurations generally include an organic-phase scrub to further ensure electrolyte purity. Iron build up in the organic phase is controlled by a concentrated HCl treatment. The selectivity of D2EHPA for zinc over selected base metal and alkali cations is illustrated in Figure 1.

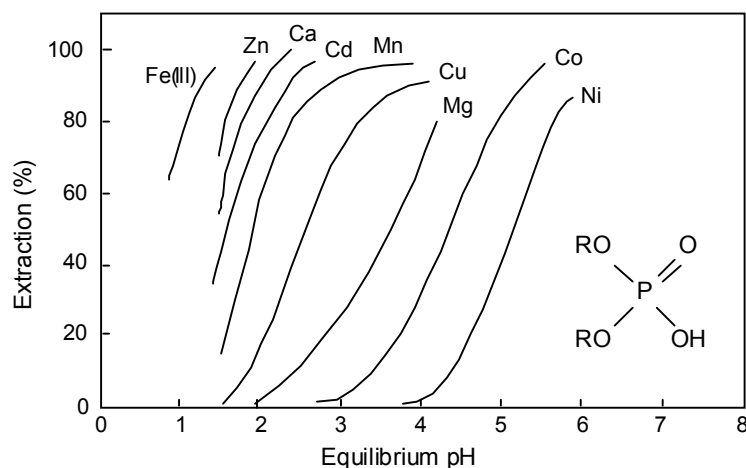


*Figure 1. pH dependence of the extraction of selected cations by D2EHPA [3].*

In contrast to the zinc industry itself, zinc SX has found wider application in the refining of other base metals, providing an efficient means for the removal of zinc as an impurity species. These applications are surveyed elsewhere [4]. This review focuses on recent installations and developmental projects featuring zinc SX. Some historical perspective is provided by brief descriptions of earlier processes.

## PRIMARY PROCESSING OF ZINC

Flowsheets involving zinc SX for the primary processing of zinc sulphides have been the subject of investigation for some time. Interestingly, however, the first commercial application of zinc SX on the mainstream process liquor will be for the exploitation of an oxide ore body.

### Sulphide Ores and Concentrates

Most zinc ores occur as sulphides and, as such, are amenable to upgrading by flotation. The traditional treatment route includes smelting of the concentrates, followed by hydrometallurgical processing to produce electrolytic zinc metal. Direct ore processing *via* a hydrometallurgical route could enable the economic exploitation of complex ores that yield low upgrading recoveries, while hydrometallurgical processing of concentrates would avoid the generation of SO<sub>2</sub> and would be more flexible with respect to the grade of feed material that can be treated. The inclusion of an SX separation step in potential process flowsheets could also accommodate difficult-to-treat concentrates, such as those with high lead or halide contents.

### Chloride routes

Chloride routes for the treatment of sulphides have been known for over a century, however few have been commercialised because of the associated corrosion problems. Although modern materials of construction have improved this situation considerably, there are currently no known plants that use this technology for zinc. There have, however, been several process developments that have made use of SX for the treatment of zinc sulphides.

The Zinclor Process was developed by Técnicas Reunidas (TR), for the treatment of concentrates [5]. Leaching with ferric chloride was followed by SX with pentylpentylphosphonate and EW in their patented Metclor cell. Another process for the treatment of concentrates proposed leaching in concentrated ammonium chloride, followed by zinc SX using D2EHPA modified with isodecanol [6]. The ammonia fixed in the metal-ammine complex provided neutralisation of the acid released during extraction.

More recently, a detailed engineering design for a plant based on ferric chloride leaching of a complex sulphide New Brunswick ore was reported [7]. The process featured zinc SX using the zinc-selective bisbenzimidazole extractant, ZNX 50, developed by Zeneca (now Aevia). Zinc metal was electrowon in a divided cell in which chlorine gas was also generated for recycle. Interestingly, this process route was reported to be more cost effective for treating the whole ore than for treating the concentrate, generating approximately 10% more revenue.

### **Sulphate routes**

Pressure leaching for the hydrometallurgical processing of zinc sulphides has been applied commercially for many years but purification of these liquors has, to date, relied on a series of precipitation steps to achieve the electrolyte purification required for the production of high-purity zinc. Indications are, however, that SX may be used in future installations, with pilot-plant studies having been carried out by TR on pressure leach liquors using D2EHPA [1].

An alternative approach to the hydrometallurgical treatment of sulphides is the use of bacterial leaching for solubilising the valuable metals. Following a bulk iron-removal step (typically by precipitation), SX has been shown to be successful in producing ultrapure electrolytes suitable for the production of special high-grade (SHG) zinc metal (>99.995% purity) from a variety of bioleach liquors. In pilot-plant studies, MIM Holdings of Australia have proved the feasibility of this route for treating concentrate, demonstrating that the simplified zinc-recovery flowsheet can provide low capital and operating costs with high overall zinc recoveries (96%) [8]. For the development of the Lanping deposit in China, BHP Billiton have proposed bacterial leaching of the sulphide concentrate, an atmospheric leach of the oxide material, and the treatment of the combined leach liquor by SX for the recovery of zinc [9]. A process for the treatment of Mexican polymetallic (Cu/Zn) and chalcopyrite copper concentrates, developed by BacTech and Mintek, includes bioleaching, copper recovery by SX/EW, and zinc recovery by SX/EW [10].

### **Non-Sulphide Zinc Ores**

Extensive feasibility studies have shown that oxide, silicate, and carbonate-based zinc ores, not amenable to conventional processing, can be viably treated using zinc SX technology in a purely hydrometallurgical processing route [9]. A key feature that contributes significant economic advantage to these projects is that SHG zinc cathode is produced at the mine site. This is rarely seen for the processing of sulphide ores. Use of SX enables the entire process stream to be treated for the selective recovery of zinc, with a single SX circuit capable of processing in excess of 150 000 t/a zinc [1]. This means that the impurity-removal operations are small, treating only a bleed stream of the main circuit, rather than the entire process stream as in traditional flowsheets.

### **Skorpion project**

Anglo American's Skorpion project will be the first commercial application of zinc SX for primary zinc processing, involving a capital investment of US\$ 454 million to develop the mine and refinery near Rosh Pinah in southern Namibia [11]. A simplified flowsheet of the proposed process is given in Figure 2 [12].

Following atmospheric leaching in sulphuric acid, iron, aluminium, and silica are removed from solution by precipitation. Zinc is then selectively extracted by SX with D2EHPA, enabling the electrowinning of SHG zinc. The selection of SX as the purification step serves several

purposes. The ore is a low-grade oxidised silicate containing soluble chloride and fluoride minerals. The choice of D2EHPA as the extractant and the inclusion of a scrubbing circuit ensure the rejection of the halides, as well as the base metals that are deleterious to zinc EW. SX also successfully upgrades the rather dilute leach liquor (30 g/L Zn) (produced as a consequence of the leach conditions dictated by the elevated silica content (~26%) of the ore) to an advance electrolyte containing 90 g/L Zn that is suitable for EW. Soluble losses of zinc in the filtration step are minimised by employing a dilute leach liquor, and the problematic formation of silica gel is avoided. Operation with a high extractant concentration ensures minimal calcium co-extraction and allows high zinc transfer in the extraction circuit without the need for neutralisation. The acid generated by the extraction reaction is then available for leaching on recycle of the raffinate.

TR was responsible for providing the SX technology [11] and the plant will be the largest yet built for zinc SX. The circuit comprises three extraction, three scrubbing, and two stripping stages, and an organic regeneration stage. Zinc transfer of 20 g/L across the extraction circuit is achieved, yielding a raffinate of 10 g/L Zn. The first two stages of the scrubbing circuit use demineralised water to wash out physically entrained impurity species; spent electrolyte is employed as the scrub liquor in the third wash stage to ‘crowd off’ co-extracted impurity species from the loaded organic phase. Treating a bleed stream with 6 M HCl controls iron build up in the organic phase. Residual HCl is removed from the regenerant solution by distillation, producing concentrated  $\text{FeCl}_3$  liquor, which is neutralised prior to disposal to tailings.

Construction of the full-scale plant commenced in May 2001, and the first metal is expected in December 2002. The feasibility study conducted for the planned capacity of 150 000 t/a zinc showed that the Skorpion project will be the most profitable zinc facility in the world [9], with an expected production cost of US\$ 0.25/lb.

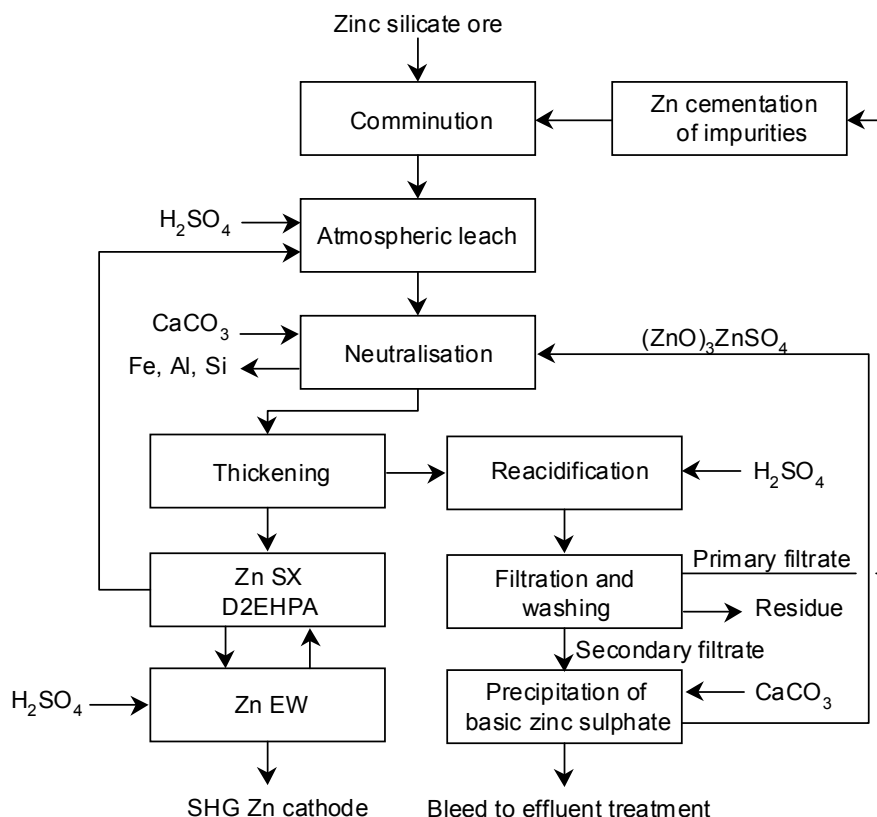


Figure 2. Simplified flowsheet for the Skorpion zinc project [12].

### **Projects under development**

Several non-sulphide ore projects in various stages of development and feasibility studies intend to use zinc SX for primary ore processing (Table 1).

*Table 1. Non-sulphide primary ore processing projects under development that use zinc SX.*

Project	Capacity (t/a Zn)	Ore type	Process route
Shairmerden, Kazakstan [13]	100 000	oxide, silicate, carbonate	Sulphate leach, zinc SX
Angouran, Iran [14]	100 000	carbonate, silicate	Sulphate leach, zinc SX
Sierra Mojada, Mexico [15]	-	oxide	Sulphate leach, zinc SX
Accha, Peru [16]	-	oxide, carbonate	Chloride leach, zinc SX

### **Zinc Recovery from Geothermal Brines**

A process originally developed by BHP for the recovery of zinc from geothermal brine that has been used for power generation is currently being commissioned by Kvaerner Metals for CalEnergy Minerals in the Imperial Valley of California. High-temperature underground brine is brought to the surface and flashed down in pressure vessels to produce steam to drive electricity-generating turbines. Zinc is recovered from the brine before it is pumped back underground. Very hot geothermal brine (19 t/h) is passed through an ion-exchange column to adsorb zinc. A conventional anion-exchange resin (DOWEX 21K XLT) selectively complexes zinc, as it is unique among the species present in forming multivalent anionic complexes in brine solution; other elements remain in solution as cations. The resin is eluted with water. The application of reverse osmosis to the eluate produces a concentrated zinc solution that is purified by SX using D2EHPA, prior to EW to produce zinc cathode. The operation is expected to yield 30 000 t/a zinc [17] in one of the cleanest zinc-recovery operations ever undertaken.

## **SECONDARY PROCESSING OF ZINC**

Several pyrometallurgical processes have been implemented for the treatment of secondary materials, however these are generally only efficient for a constant composition feed and need to have a high production capacity to be economically viable [18]. Some materials are not amenable to treatment by these routes, and environmentally acceptable discharges are not always assured. Hydrometallurgical processes are potentially less sensitive to these constraints; the most successful of these include an SX step to purify and upgrade the zinc.

TR has been at the forefront of developments in the processing of secondary zinc materials. Recycling plants, now closed, were built in Spain and Portugal based on their Zincox process [19,20]. This was superseded by the Modified Zincox Process (MZP), which has found application and is the instrument of numerous new investigations into the treatment of secondaries such as Waelz oxides, galvanizing residues, and electric arc furnace dusts (EAFD) [18,21]. The process uses D2EHPA for the selective extraction of zinc from the acidic sulphate liquor produced on the leaching of these materials. Advantages claimed for the MZP include the high selectivity over species such as halides and magnesium, the production of an electrolyte from which SHG zinc can be produced, high zinc recoveries, and safe and environmentally friendly operation. Gypsum precipitation in the SX circuits remains a problem, with the production of 80 to 150 kg per tonne of material treated. However, by using a source of pure lime for neutralisation in the SX circuit, 'white gypsum' can be produced, which may be sold for certain applications in the plasterboard industry.

### **Reprocessing of Furnace Dusts**

Electric arc furnaces produce 10 to 15 kg of dust per tonne of steel produced, representing one of the more contaminated zinc residues. The steel industry has approved the MZP as "technically, economically and environmentally suitable for the solution of the EAFD problem" [21]. A project for the treatment of 82 000 t/a EAFD in Spain has been proposed, but to date this has not been implemented, despite several successful pilot-plant trials on different EAFD compositions.

Dust generated from blast and reverberatory furnaces at the Met-Mex Peñoles lead smelter in Torreón, Mexico, has since 1998 been treated in a zinc SX plant built at the site [22]. The material was previously recycled, causing saturation of undesirable species such as cadmium, arsenic, and halides in the main circuit. Installation of the SX plant is reported to offer operating, economic, and environmental advantages: greater flexibility now allows the treatment of 'dirty' lead concentrates; increased revenues are realized from the sale of impurity species recovered; and airborne dust generation has decreased. Production is 5000 t/a zinc cathode of 99.99% purity. Table 2 compares the composition of the high-impurity feed material with an assay of the upgraded zinc solution produced by SX.

*Table 2. Composition of furnace dusts and upgraded zinc solution produced by SX at Met-Mex Peñoles [22].*

Element	Blast furnace dust (%)	Reverberatory furnace dust (%)	Upgraded zinc SX solution (mg/L)
Zn	10.6	15.6	95 000
Cd	23.8	1.1	128
As	1.1	8.8	< 1
Pb	39.1	30.2	< 2
Fe	0.1	0.1	< 2
Cl	4.3	0.4	7
F	0.5	0.3	2

Italian trials to recover zinc from EAFD by SX have also been reported [23]. In this process, iron was not removed from the leach liquor prior to SX. Zinc and iron were co-extracted using D2EHPA; zinc was stripped with 1 M H<sub>2</sub>SO<sub>4</sub> and iron was periodically removed from the organic phase by treatment with HCl. It was reported, however, that HCl stripping introduced partial degradation of the extractant, and a reductive stripping process for iron was under development.

Fluor Daniel Wright has also carried out development of an SX process to recover zinc from EAFD. The extraction of zinc chloride by ZNX 50 was evaluated [24].

### **Process Residues and Tailings**

In 1988, Española del Zinc in Cartagena, Spain, integrated SX into a conventional zinc refinery flowsheet for the recovery of water-soluble zinc from stockpiled and fresh leach residues [25,26]. The main refinery treats a mixed sulphide concentrate to produce 40 000 t/a zinc via a RLE circuit. The iron hydroxide precipitate exiting the primary leach circuit contains about 20% zinc. These solids are leached, along with previously dumped material, in a secondary leach using sulphuric acid and the loaded strip liquor generated in the SX plant. Iron is removed as ammonium jarosite. The secondary filtrate from the washing of the jarosite solids (containing 14 g/L Zn, 0.03 g/L Fe, 0.7 g/L Cu, 0.3 g/L Cd, pH 3) is not suitable for EW and is treated by SX to upgrade and purify the zinc into a concentrated (120 g/L Zn) strip liquor for recycle.

### **Zinc Tankhouse Bleeds**

Most operating zinc refineries use precipitation methods for zinc purification, followed by metal recovery by EW. In such processes, there is usually a gradual accumulation of impurities in the electrolyte, especially of species such as magnesium and manganese. Since zinc EW is extremely sensitive to the presence of impurities, it is necessary to bleed the electrolyte to control the composition. Several studies have looked at the use of SX for the recovery of both sulphuric acid and zinc from this bleed. These have involved recovery from both sulphate media with D2EHPA [27] and from chloride media using tri-*n*-butylphosphate [28].

### **Zinc Recovery from Spent Batteries**

The R.F. Procés plant, commissioned in the Spanish province of Cataluña in 1997, is the only plant in the world applying a hydrometallurgical process to the recycling of spent domestic batteries. The MZP is applied as the core separation step, producing a high-purity zinc sulphate solution suitable for electrowinning SHG zinc metal [29]. The loaded strip liquor is transported to Espanola del Zinc for zinc recovery.

A similar process for the recovery of zinc and other hazardous elements from spent batteries has been investigated in Switzerland. The initial flowsheet used D2EHPA for the purification of the leach liquor [30], however it was found that the process was too difficult to operate continuously because of the fine pH control required. CYANEX 301 was also tested for this application [31], and, although the extraction behaviour of this system was appropriate, the difficulties of stripping the irreversibly loaded copper and iron from the organic phase mitigated against it. The process has not been commercialised.

Another hydrometallurgical scheme for recycling of battery waste was developed by PIRA GmbH, Germany [32]. The BATENUS process, which also used D2EHPA SX for the recovery of zinc, was fully piloted and commercialisation was expected in 1995; the reason why this did not go ahead is unknown.

## **CONCLUSIONS**

The advantages afforded by hydrometallurgical processes that feature SX have only recently been realised in the zinc recovery industry. The commissioning of the Skorpion refinery, as the first plant to use SX for the recovery of zinc from a primary source, will add further impetus to this development. An increase in the application of zinc SX technology can be expected during the next decade, particularly in the processing of non-sulphide primary materials and for the treatment of an increasing variety of secondary materials.

## **ACKNOWLEDGEMENTS**

Appreciation is extended to Dr Doug Flett for his thoughtful comments on this manuscript. This review is published by permission of Anglo American Research Laboratories (Pty) Ltd.

## **REFERENCES**

1. D. Martín, G. Díaz, M. A. García, and F. Sánchez (2002), *Proceedings ISEC 2002*, K. C. Sole *et al.* (eds.), South African Institute of Mining and Metallurgy, Johannesburg, pp 1045-1051.
2. G. M. Ritcey and A. W. Ashbrook (1984), Solvent Extraction: Principles and Applications to Process Metallurgy, Part II, Elsevier, Amsterdam, p. 535.
3. K. C. Sole and P. M. Cole (2001), Ion Exchange and Solvent Extraction, Vol. 15, Y. Marcus and A. SenGupta (eds.), Marcel Dekker, New York, pp. 143-195.

4. P. M. Cole and K. C. Sole (2002), *Min. Proc. Ext. Met. Rev.*, submitted.
5. E. D. Nogueira, L. A. Suarez-Infanzon, and P. Cosmen (1983), Zinc '83, Canadian Institute of Mining, Metallurgy and Petroleum, Montreal, Paper 7.
6. S. Amer, J. M. Figueiredo, and A. Luis (1995), *Hydrometallurgy*, **37**, 323-337.
7. W. M. Smith, P. J. Brooks, and R. A. May (1997), *CIM Bull.*, **90** (1009), 57-63.
8. M. I. Steemson, F. S. Wong and B. Goebel (1997), *Proceedings Biomine '97*, Australian Mineral Foundation, Glenside, South Australia, Paper M1.4.
9. M. A. García, A. Mejias, D. Martín, and G. Díaz (2000), Lead-Zinc 2000, J. E. Dutrizac et al. (eds.), The Minerals, Metals and Materials Society, Warrendale, PA, pp. 751-761.
10. P. J. van Staden (2000), Colloquium: Bacterial Oxidation for the Recovery of Metals, South African Institute of Mining and Metallurgy, Johannesburg.
11. Anglo American Corporation (2000), *Press Release*, 7 September.
12. K. C. Sole (2001), *Proceedings 6<sup>th</sup> World Congress of Chemical Engineering*, Melbourne, Australia.
13. Anon (1999), *Metal Bull.*, (8 July), 5.
14. Cominco Ltd (2000), *Canada Newswire Press Release*, 14 June.
15. Metalline Mining Company (2000), *BusinessWire Press Release*, 28 November.
16. Southwestern Gold Corporation (2001), *CNN Press Release*, 7 May.
17. Anon (1998), *Min. J.*, October 30, 347.
18. G. Díaz, D. Martín, and C. Lombera (1994), *Resources, Conserv. Recycl.*, **10** (1-2), 43-57.
19. E. D. Nogueira, J. M. Regife, and P. M. Blythe (1980), *Chem. Ind.*, (2), 63-67.
20. E. D. Nogueira, J. M. Regife, and M. P. Viegas (1982), Chloride Electrometallurgy, P. D. Parker (ed.), The Metallurgical Society, Warrendale, PA, pp. 59-76.
21. G. Díaz, D. Martín, and C. Lombera (1995), *Proceedings 3<sup>rd</sup> International Symposium Recycling of Metals and Engineered Materials*, P. B. Queneau and R. D. Peterson (eds.), The Minerals, Metals and Materials Society, Warrendale, PA, pp. 623-635.
22. I. S. Fernández del Río (2000), Lead-Zinc 2000, J. E. Dutrizac et al. (eds.), The Minerals, Metals and Materials Society, Warrendale, PA, pp. 677-686.
23. C. Lupi, M. Cavallini, A. Ferone, D. Pilone, P. P. Milella, and R. Mussapi (1999), EPD Congress 1999, B. Mishra (ed.), The Minerals, Metals and Materials Society, Warrendale, PA, pp. 621-629.
24. SX Kinetics, Projects [Internet]. Available from <<http://www.sxkinetics.com/projects.htm>> [Accessed 3 January 2001].
25. R. Heng., R. Lehmann, and D. J. García (1986), *Proceedings ISEC '86*, Vol. 2, Dechema, Frankfurt, pp. 613-619.
26. A. Selke and D. de Juan García (1989), Productivity and Technology in the Metallurgical Industries, M. Koch and J. C. Taylor (eds.), The Minerals, Metals and Materials Society, Warrendale, PA, pp. 695-703.
27. D. Buttinelli, C. Lupi, E. Beltowska-Lehman, and A. Riesenkampf (1989), Extraction Metallurgy '89, Institute of Mining and Metallurgy, London, pp. 1005-1016.
28. B. Buttinelli, C. Giavarini, and A. Mercanti (1984), *Proceedings Mintek 50*, Vol. 2, L. F. Haughton (ed.), The Council for Mineral Technology, Randburg, pp. 619-625.
29. D. Martín, M. A. García, G. Díaz, and J. Falgueras (1999), *Proceedings ISEC '99*, M. Cox (ed.), Society of Chemical Industry, London, pp. 201-206.
30. L. Steiner, X. Miaoling, and S. Hartland (1988), *Proceedings First Conference on Hydrometallurgy*, Z. Yulian and X. Jiazhong (eds.), International Academic Publishers, Beijing, pp. 399-403.
31. L. Steiner, X. Miaoling, and S. Hartland (1992), Solvent Extraction 1990, T. Sekine (ed.) Elsevier Science Publishers, Amsterdam, pp. 1175-1180.
32. W. Lindermann, Ch. Dombrowsky, D. Sewing, M. Müller, S. Engel, and R. Joppien (1994), Iron Control and Disposal in Hydrometallurgical Processes, Canadian Institute of Mining, Metallurgy and Petroleum, Montreal, pp. 197-204.



## SOME DESIGN AND OPERATING PROBLEMS ENCOUNTERED IN SOLVENT EXTRACTION PLANTS

Gordon M. Ritcey

G.M. Ritcey & Associates Inc., Ottawa, Ontario, Canada

During the past 35 years the author has been involved with many solvent extraction plants. Some were projects of personal involvement in the process design, scale-up, commissioning, training, and trouble-shooting. Others were examined critically for improvements in the overall operation and improvements to the performance, solvent loss reduction, product quality, etc. Additionally, numerous plants were visited during that period to maintain a technical knowledge of new developments in solvent extraction processing—the reagents, contactors, methods of control, and problems in the design and operation. The paper is a summary of typical design and operating problems that were encountered in several types of metal recovery operations, including Cu, Ni, Co, U, Zr, rare earths. The causes and remedy to the problems are stated. No specific extraction systems or specific contactors are cited, and so the presentation is generic.

### INTRODUCTION

Solvent extraction (SX), as one of several unit operations in hydrometallurgy processing and refining, has now been operative for over 50 years. The development started with the nuclear industry, first with the refining of uranium using ether as the extractant in the late 1940s, soon followed by TBP as the safer extractant. Then the extraction process was taken to the uranium mills in the mid 1950s to provide an up-graded uranium product using essentially tertiary amines. Plants and refineries to that date were not large. Then with the copper industry recognizing the potential benefits of the solvent extraction process, the first large copper SX plant went on-stream in 1969. Thus the SX process became generally accepted and larger copper plants were to be placed in operation, using various chelating extractants.

Since that time there have been a considerable number of SX operations, of all sizes in the mining/metallurgical industry from the very small precious metals circuits and the radionuclide and reprocessing circuits, the medium size rare and less common base metals, and to the larger base metal plants. Now there are processes developed for virtually every metal in the periodic table of elements. Some of the processes are in operation; some have reached the pilot plant stage, while others are still in the development and optimization stage.

There are many aspects to be considered in the design and subsequent successful operation of the SX process, and include the following important areas:

- Chemistry--Extractants, Modifiers, Diluents
- Mass transfer--Dispersion and Coalescence
- Equipment-- Selection and Operation
- Economics
- Environmental and Solvent Losses

All impact on the possibility of the successful process, and if some are partially ignored then problems in the plant operation can be anticipated.

In this paper, a summary is presented of typical problems that have been personally encountered in a number of SX plants and refineries over the past 35 years. These include U, Zr, Nb, Cu, Co, Ni and Rare Earths plants. Practical solutions to those problems were often successfully implemented.

## DESIGN AND COMMISSIONING PROBLEMS

The following are some of the problems encountered in the commissioning and early running of some of the plants. It should be noted that other areas than SX, upstream and downstream, often have the greater problems in commissioning.

- excessive mixing in both mixers, with the result that the mixed flow entering the launder from mixer 2 was very turbulent and considerable air was drawn into the mixture to form emulsions. Return eddies travelled back as far as one-half the launder length;
- the launder distributor of the mixed phases (several split flows) appeared to provide for different flow velocities for the 5 flows; short-circuiting could result;
- No. 1 mixer was running slow in all units, as evidenced by the appearance of organic droplets on the surface;
- No. 2 mixer was running with excessive shear and turbulence causing extremely small droplets that were difficult to settle;
- no evidence of improved mass transfer occurred with a second stage mixer;
- the cause of some excessive turbulence encountered was due to the location of the turbine impeller in the mix tank (located about 1/3 down into the tank). A depth of perhaps greater than 2/3 would be better;
- some of the agitator shafts were not running "true";
- there was no provision for capturing any oil leaks that may result from running the agitator motors, which if permitted to enter the system could result in affecting the rate of coalescence;
- on the organic overflow there was considerable drawing in of air as the organic phase overflowed the weir and hit the bottom of the settler;
- stable emulsions-cruds were in all the settlers;
- stable gels formed and plant became inoperative;
- none of the mixers or settlers were covered. Even though there was a roof over the settlers, one or both ends of the "building" were open. The air velocity was therefore high over the settlers. Consequently, the SX circuit was susceptible to dust and bugs that will cause stable emulsions and cruds. Also, air entrainment of the solvent can be very high;
- piping diameters from strip to electrowinning (EW) were not compatible with flows;
- Jameson cell for entrainment removal was installed higher than circuit;
- interface control in the settler was not adequate and had to be improved. Evidence of considerable air entrainment causing stable emulsions and crud;
- inadequate flow control on the recycle streams;
- air locks in mixers had occurred on start-up: overcome by quick stopping of mixing and re-starting at high mixed flow;
- due to either dirty tanks or excessive fines in the PLS, cruds were formed;
- double salts formed in the case of some Ni circuits;
- solvent that was entrained and entered the tank house resulted in cathode pitting;
- darkening and gradual increased viscosity of solvent, and decreased loading;
- crystals in the carbon column (solvent removal prior to EW);
- impurities such as Cu, Co, Mg accumulated in product with solvent recycle.

## OPERATING PLANT PROBLEMS

Common problems that have occurred in many of the operating SX plants can be summarized as follows:

- metallurgical performance was poor (high raffinates, poor discrimination, and/or low loading as compared to the original McCabe-Thiele diagram);
- degradation of certain extractants occurred at high temperatures;
- poor phase separation; high solvent losses;
- excessive agitation (often in both mix stages) and often running under the design flow causing extremely fine droplets, emulsions, poor phase separation, and cruds;
- air entrainment and foam generation – due to over mixing, high shear, weir design, presence of surfactants. The total throughput will be adversely affected as stable emulsions are formed;
- cruds – many types (voluminous, spongy, stringy, gel, crystalline, precipitates) will have adverse effects on throughput and general performance in settlers. Generally an accumulation behind the picket fences in the settler; at the interface, on the bottom of the settler, as well as in the solvent phase;
- gel formation (different from an emulsion) and decreased settling and throughput;
- poor clarification and solids in feed – results in crud and decrease in throughput;
- third-phase formation;
- gypsum scaling and other precipitates – results in poor phase separation, stable emulsions, and crud formation. Settler capacity and total throughput is reduced; Scaling within the total circuit may occur;
- inadequate pH control during extraction / stripping resulted in formation of precipitates;
- formation of double salts, such as Ni ammonium sulphate – creates emulsions-cruds and decreases settler capacity, as well as reduction in total throughput;
- high solvent entrainment losses in the extraction raffinate;
- high solvent entrainment in strip raffinate and reduced EW performance;
- high evaporation/misting losses of solvent;
- solvent degradation and gradual decreased plant performance;
- inadequate control: phase continuity; equilibrium pH; interface; agitation; cross-contamination (solvents + extracted metals) in 2-SX circuits as well as in a single circuit.

## SOME SOLUTIONS TO THE PROBLEMS

### Dealing with Low Mass Transfer Efficiency

- verify extractant concentration, as a low concentration will result in high raffinates and low loading;
- if the solvent concentration analyses appears higher than was added, this would indicate a preferential high evaporation loss of the diluent and possibly the diluent has to be changed;
- poor stripping may be a result of the solvent still partially loaded after the previous stripping cycle;
- inadequate pH control (affects efficiency; promotes precipitation in either phase);
- inadequate control of acidity/alkalinity;
- check for solvent poisoning (by non-strippable organic acids and/or metal contaminants such as Zr, Mn);
- determine whether the PLS metal(s) concentration has changed, and if so, the calculated stages from a McCabe-Thiele plot will then be incorrect;

- determine possible contamination from water used in the circuit by bacteria, and organic acids from recycled pond water;
- continued poor performance may require a change in extractant.

### **Dealing with Excessive Phase Separation Time In the Settler**

The coalescence rate may be increased by:

- decreasing the shear and small droplet formation in mixing; running the process at the design flow to the mixer, based on rate of mass transfer required, so as to prevent excessive mixing under high shear conditions which create extremely fine droplets;
- elimination of a second stage mixer or reduction in agitation in that mixer;
- decrease in the turbulence of the mixed phases exiting mixer, possibly by baffles;
- reduction in entrained air: may be accomplished by better weir control;
- improved entry from the launder to the settle, possibly by increasing the number of split flows to the settler;
- use of wetting properties of dissimilar materials in construction of the picket fences;
- elimination or change/decrease of surfactant chemicals in the liquid-solids separation stage;
- ensuring that the circuit contains no oil leaks from pump motors that may be getting into the SX process;
- ensuring that minimum organic acids are present in the PLS,
- minimize the possible production of bacteria, yeast, mould;
- minimize colloidal silica and be aware of possible adverse effects of amphoteric compounds which may cause gels;
- control phase continuity;
- decrease in the linear velocity down the length of the settler.

### **Dealing with Solvent Losses**

#### **Entrainment**

- improved control in mixing to eliminate small droplets;
- check whether diluent choice is the best;
- check whether a modifier is required;
- contactor design and operation may be improved;
- examine the solvent for possible poisoning, which results in increased surface tension and increased entrainment losses;
- improve coalescing in settler (baffles location and design);
- minimize settler linear velocity;
- use of an external settler;
- eliminate air bubble formation as much as possible;
- phase continuity control may aid in minimizing losses by entrainment;
- examine circuit for the presence of possible surfactants that may have been added upstream of SX;
- examine the circuit for presence of organic acids (e.g., humic acids), bacteria, fungus, mould; and,
- minimize presence of crud, stable emulsions, colloids, and suspended solids.

#### **Evaporation/misting**

- eliminate any high air velocity over mixer-settlers;
- keep the covers over the mixer-settlers closed as much as possible;
- evaporation/misting can be severely enhanced as the temperature is increased, and misting can be higher than evaporation at times;

- creation of aerosols will result in loss of all components of the solvent, whereas evaporation losses will discriminate as regards the temperature. Thus the diluent will probably be lost first;
- recovery may be partially successful by installation of a vacuum scrubber over the mixer-settlers. Activated carbon as well as various coalescers and flotation will have various degrees of success in solvent recovery. If there are inorganic salts or precipitates present in the aqueous solution to be treated, then blocking of the carbon can occur.

#### ***Crud formation and abatement***

- requires the characterization, identification, and analyses of cruds;
- tests to verify mode of formation before crud reduction and possible elimination can be contemplated;
- Any other treatment before considering the above can only be a “band-aid” approach to the solution;
- minimize presence of suspended solids; as well as precipitates in either phase (often due to Ca, colloids of Al, Si and many amphoteric elements. The solids and colloids help to stabilize the crud; Improved clarification is a start and may minimize the amount of crud in the extraction circuit but may not prevent the carry-over of crud to the strip circuit;
- minimize high shear and extended time in mixing;
- minimize formation of air bubbles; weir adjustments can help;
- certain impurities may have to be removed or reduced in concentration;
- flocculants, organic acids in the PLS and solvent degradation products in certain plants can have adverse effects on the solvent and plant performance, such as emulsions and crud formation. Excessive flocculent may cause serious crud problems, particularly in the presence of silica colloids and other amphoteric compounds that may also cause gels;
- reduction/removal of surfactants (chemical and organic acids, e.g., humic, fulvic, degraded reagents, bacteria);
- maximize rate of coalescence;
- a wash stage, perhaps with water, may overcome crud carry-over into the strip circuit.

#### ***Third-phase formation***

- could be caused by several factors, including loading of organics (e.g., organic acids, bacteria), over-loading, stable emulsions;
- may be overcome by the addition of a modifier or the change in the diluent (increase the aromatic content). aromatic content will provide increased solvency of the extracted complex as well as can act as a bactericide;
- addition of a bactericide has a similar effect as an increase in the aromaticity;

#### ***Degradation of solvent***

- the extractant may be degraded, usually under severe oxidation conditions, forming compounds that may be detrimental to the process either in phase separation rates or also in the discrimination over impurities. This is common in some extractants and modifiers. Alcohol modifiers can degrade to carboxylic acids for example, thus forming an extractant that will adversely affect the ultimate purity of the strip product;
- in addition to decreased metallurgical performance due to degradation, the degradation products can have adverse effects on phase separation.

### **Solvent replacement and treatment**

- before reusing entrained solvent determine whether it has had an opportunity for degradation to occur if stored in ponds for subsequent reclamation. Long storage, especially at elevated temperatures, will rapidly degrade the solvent which may produce a number of oxidized products which can adversely affect the performance if not treated before re-use. It may not always be sensible to re-treat, and better to provide fresh solvent make-up to the process.
- periodically the solvent may have to be treated if contaminants are known to be present. These treatment processes to remove the accumulated contaminants include dilute alkali wash ( $\text{NaOH}$  or  $\text{Na}_2\text{CO}_3$  or a mixture); and treatment with clay and may be performed on the entire inventory periodically or on a "bleed" stream continually
- if the extractant is problematic, resulting in overall poor performance in extraction and, stripping, poor phase separation, and increased losses: it may have to be replaced.

### **Dealing with Phase Continuity**

- many plants attempt to control phase continuity at about 1:1 phase ratio. This can be most difficult, particularly as the respective densities change as loading or stripping occurs. There should be a larger difference in the ratio, and determined by conducting some tests and noting where "flipping" of the phases occur.
- flipping of phases can occur due to:
  - surfactants and poisons;
  - extreme phase ratios;
  - extremely fine droplets;
  - solvent concentration;
  - density of phases;
  - stable emulsions/cruds/gels.

### **Dealing with Stable Emulsions and Gels**

- often due to colloids, such as Si and Al and other amphoteric compounds. Often overcome by change in leaching conditions as well as a change of operating conditions, e.g., phase continuity, wetting characteristics, phase ratios in the case of recycles;
- poor contactor choice in original selection in spite of successful pilot plants on other contactor design with less shear; operation protocol changed, 5-day operation and 2-days for cleaning (different contactor was selected but not installed because of increased capital costs that would be incurred);
- because of poor phase separation and emulsions, contactor changed; result was ideal in extraction but insufficient shear mixing for mass transfer in the stripping stage. That is, only the extraction stage contactor should have been changed.

### **Dealing with Reagent and Impurity Carry-Over**

- between stages
  - interstage washing (scrub) required;
- into second circuit
  - solvent wash of the raffinate with diluent.

### **Dealing with Sustained Product Purity**

A gradual decrease in product purity can be caused by:

- entrainment from one stage to next; a wash stage would be required;
- entrainment of extractants from one circuit to a second circuit;
- accumulation of trace metals over time on the solvent;

- accumulation of degraded organics and other organic compounds that become “extractants”;
- steps taken to install scrub stages and/or impurity removal stages (e.g., removal of chloride to prevent entering tank house);
- equipment selection and operation.

### **Oxidation Problems**

One general comment relevant to the leaching and subsequent solvent extraction is that of the oxidation potential of the feed solution to solvent extraction. An overdose of the oxidant that might be necessary during leaching, or the production of an highly oxidized species during leaching or electrowinning, and the high operating temperature of the circuit have caused serious degradation of some extractants. Typical of the metals that can be expected to cause oxidation-degradation of the organic are  $\text{Co}^{3+}$ ,  $\text{V}^{5+}$ ,  $\text{Cr}^{6+}$ , and  $\text{Mn}^{7+}$ . The higher the valency state, together with high operating temperatures, and longer contact time than required for mass transfer, all lead to degradation problems.

### **Some Problems Due to Silica**

It was evident in many examples that Si, in its various forms, could provide a problem, and enhance the possibility for the formation of cruds. Following are some conclusions [1-4]:

- 1) The presence of Si can cause or enhance the formation of cruds and emulsions.
- 2) Most cruds are composed of Si as the major constituent, together with Fe, Mg, Ca, Al and the metal being extracted.
- 3) Unless there is a scrub stage between extraction and stripping, Si and other impurities may carry-over and appear in the strip product.
- 4) Organic continuous operation appears to minimize emulsion formation in the presence of Si.
- 5) The presence of humic acids together with Si enhances emulsions and cruds, as does high shear.
- 6) Solutions containing colloidal silica, in the aqueous continuous system, are severely retarded in phase separation rates and tend to form stable emulsions. Noticed in amines, alkylphosphates and oxime systems.
- 7) Colloidal silica and low molecular weight amines result in slower phase disengagement than higher molecular weight amines.
- 8) Most emulsions are produced by a third phase emulsifier consisting of a colloidal substance (such as silica-alumina, hydrosols or clays, ferric or aluminium hydroxide or colloidal phosphate).
- 9) Each emulsion or crud has its own characteristics and require laboratory identification. Methods of identification include microscopic, X-ray diffraction, infrared and emission spectrographic techniques.
- 10) TBP emulsions are stabilized by silicic acid.
- 11) Temperature, acidity and nature of the aqueous phase influence the stability of the TBP emulsion in the presence of silicic acid.
- 12) Possible methods of prevention include:
  - changes in pH;
  - addition of flocculating agents to remove the emulsifier;
  - addition of dispersion agents to disperse the emulsifying phase;
  - change plant practice to avoid formation of the surface-active materials;
  - addition of fluoride or other complex to solubilize the silica colloid.

## SUMMARY

In most cases the problems could be attributed to a few or all of the following operating parameters, some of which were not being performed correctly, or others that were not considered as an important factor:

- loading to saturation,
- scrubbing to remove entrainment of feed PLS,
- selective scrubbing/stripping,
- extractant choice and concentration,
- modifier choice (or none at all),
- diluent selection,
- co-extraction vs. selective extraction,
- pH control,
- kinetics,
- contactor selection and operation protocol.

The plant assessments have indicated that there are numerous causes of plant inefficiency. However one of the common causes that has been demonstrated is that of the solvent being fouled resulting in decreasing rates of coalescence, decreased loading, and ultimately reduced throughput. The high shear of most of the contactors (high shear mixer settlers), together with colloids of Si, Al, and ore slimes and fines enhances the problems. More attention has to be paid during the process design, piloting and ultimate plant scale-up to ensure that such possible costly problems will not occur. Each plant will be site-specific, and therefore a good interface between the metallurgists involved in the process design and the engineers involved in the plant design is necessary.

## REFERENCES

1. G. M. Ritcey and E. W. Wong (1988), *Proc. ISEC '88*, Moscow.
2. G. M. Ritcey (1982), *Proc. 14<sup>th</sup> Int. Min. Processing Conf.*, Toronto.
3. G. M. Ritcey (1985), *Hydrometallurgy*, **15**, 55-61.
4. G. M. Ritcey (1986), *Can Met. Quart.*, **25** (1), 31-43.



## THE EXTRACTION OF COPPER, ZINC, CADMIUM AND LEAD FROM WASTE STREAMS IN THE ZINC-LEAD INDUSTRY

M. Cox, D. S. Flett and L. Gotfryd\*

University of Hertfordshire, Hatfield, UK

\*Institute of Non-Ferrous Metals, Gliwice, Poland

Extractants have been assessed for the extraction and recovery of zinc, cadmium, copper and lead from wastewaters generated in the zinc-lead industry with specific reference to Poland. Initial assessment of potential extractants for recovery of these metals either in bulk or individually resulted in the selection of di(2-ethylhexyl)phosphoric acid, the dialkylphosphinic acid CYANEX 272® and a mixture of a carboxylic acid (di-isopropylsalicylic acid) and tri-*iso*-butylphosphine sulphide (CYANEX 471X®) for in-depth assessment in experimental studies. The testwork was carried out using synthetic solutions containing appropriate concentrations of zinc, cadmium, copper and lead. The results from all these studies are presented, collated and assessed and conclusions drawn with regard to viable options for commercial treatment, using solvent extraction, of such waste liquors.

### INTRODUCTION

At the Miasteczko Slaskie zinc plant in Poland zinc and lead metal are produced by the Imperial Smelting Process. Resulting from this process there are two liquors that appear to be amenable to the application of solvent extraction for the recovery of metals. The first is an acidic effluent arising from the off-gas washing system of the sulphuric acid plant with the following composition 0.25 g/l Zn; 0.34 g/l Cd; 0.0023 g/l Pb; 1.92 g/l SO<sub>4</sub><sup>2-</sup> and 0.17 g/l SO<sub>3</sub><sup>2-</sup> at a pH of 1.86. The second solution will arise after a cadmium cementation process to be introduced by management and has been forecast to have the following approximate composition: 40 g/l Zn; < 1 g/l Cd; 0.005 g/l Pb; 0.01 g/l Cu; 0.03 g/l Fe; 0.006 g/l Sb; < 0.01 g/l Sn and < 0.003 g/l Bi.

Options for treatment of these two liquors differ. For the first acidic effluent bulk removal of Zn, Cd and Pb would provide an effluent requiring minimal treatment prior to discharge or recycle except perhaps for neutralisation. For the second liquor however it would appear to be more appropriate, if possible, to remove all the impurities from zinc with the subsequent recycle of the purified zinc liquor to an appropriate part of the flow-sheet at the Miasteczko Slaskie plant.

Initial assessment of potential extractants for recovery of these metals either in bulk or individually resulted in the selection of di(2-ethylhexyl)phosphoric acid (DEHPA), the dialkylphosphinic acid CYANEX 272® and a mixture of a carboxylic acid (di-isopropylsalicylic acid (DIPSA)) and tri-*iso*-butylphosphine sulphide (CYANEX 471X®) for in-depth assessment in experimental studies. The choice of DEHPA and CYANEX 272 is based on these extractants known properties in extracting zinc, lead and cadmium. The mixture of DIPSA and CYANEX 471X was selected based on the work of Preston *et al.* [1-4] where it was shown that this combination of reagents had a remarkable synergistic effect on the extraction of cadmium in the presence of zinc. This is of obvious interest in the treatment of the second liquor only.

## EXPERIMENTAL

DEHPA was purchased from SIGMA/Aldrich. This was ~95% pure and was used without further purification. CYANEX 272 and CYANEX 471X were kindly provided by Cytec Industries France and were used as received. DIPSA was prepared according to Desseigne [5]. Diluents used in this work were either Escaid 120<sup>®</sup> (Exxon) or Solvesso 150<sup>®</sup> (Exxon). All synthetic aqueous solutions were prepared from analytical grade chemicals. The determination of metal ion concentrations were made using ICP emission or atomic absorption spectrophotometry or by EDTA titration for single metal solutions. Adjustment to solution pH was made by additions of NaOH or H<sub>2</sub>SO<sub>4</sub> as appropriate. Solution 1 was used as received from the smelter. Solution 2 was a synthetic solution made up to the composition as forecast by smelter personnel.

## RESULTS AND DISCUSSION

### Solution 1

The variation in the extraction of Zn, Cd and Pb with 0.2 M DEHPA and 0.2 M CYANEX 272 with pH are shown in Figures 1 and 2.

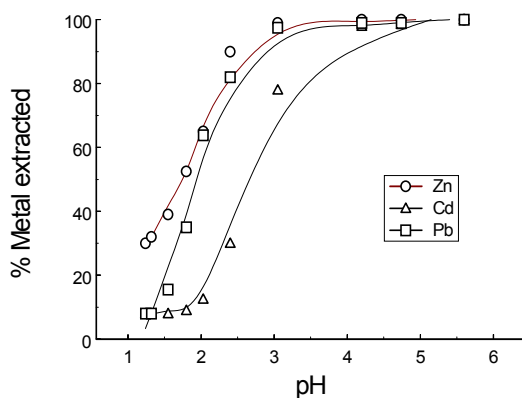


Figure 1. Extraction of Zn, Cd and Pb from solution 1 with 0.2 M DEHPA.

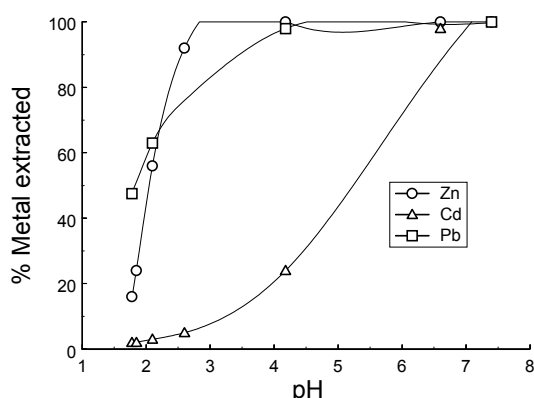
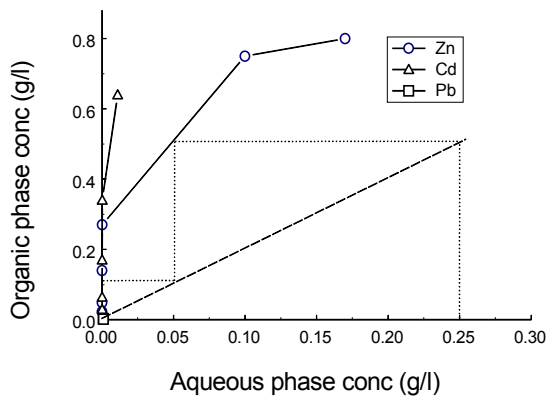


Figure 2. Extraction of Zn, Cd and Pb from solution 1 with 0.2 M CYANEX 272.

The figures show that removal of all three metals is essentially achieved at a pH value of >4.5 for DEHPA and ~7.0 for CYANEX 272. Both Zn and Pb are extracted strongly while Cd is less strongly extracted. These results show that there is no possibility of complete extraction of all metals at the natural pH of this effluent stream (pH 1.86) and that neutralisation is necessary to achieve full extraction of all the metal ions. Because of the significantly higher pH required for complete metal removal with CYANEX 272 all further work was based on DEHPA.

An extraction isotherm was developed for DEHPA partially converted to the sodium salt by contacting the DEHPA solution with Na<sub>2</sub>SO<sub>4</sub> at pH 5.0. This is shown in Figure 3 together with the appropriate McCabe-Thiele construction. This shows that complete removal of Zn, Cd, and Pb below 0.001 g/l is achievable in two counter-current stages at an O/A phase ratio of 2:1. The apparent anomalous selective extraction of Cd shown in Figure 3 is probably an artefact of the computer package and the actual zinc isotherm should be extended higher than depicted, which would then reflect the total extraction of Zn and Cd. The single point for Pb reflects its low concentration and thus the inability to include other points because of the scale required to plot the Cd and Zn results. Stripping of the metals from DEHPA is easy and tests have shown that a single stage using 2 M H<sub>2</sub>SO<sub>4</sub> can be used for this purpose.



*Figure 3. Extraction isotherm for Zn, Cd and Pb with 0.2 M NaDEHPA at pH ~ 5.0.*

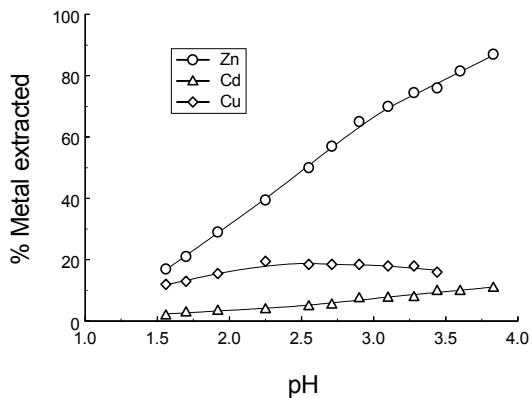


*Figure 4. Extraction of Cd, Cu and Zn from solution 2 with 0.5 M DEHPA.*

### Solution 2

The variation in extraction with pH for DEHPA, CYANEX 272 and DIPSA/CYANEX 471X is shown in Figures 4 to 6. Examination of the figures shows that it is not possible to extract all the metals, including zinc, without a significant degree of neutralisation. Furthermore, neither DEHPA nor CYANEX 272 can extract Cu and Cd selectively from Zn, a result that confirmed by the widely published behaviour of these extractants. Examination of Figure 6 however shows that both copper and cadmium can be extracted selectively from zinc with the DIPSA/CYANEX 471X mixed extractant system. This system was therefore selected for further study.

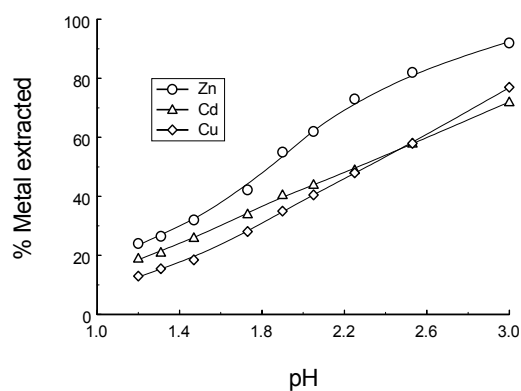


*Figure 5. Extraction of Cd, Cu and Zn from solution 2 with 0.5 M CYANEX 272.*

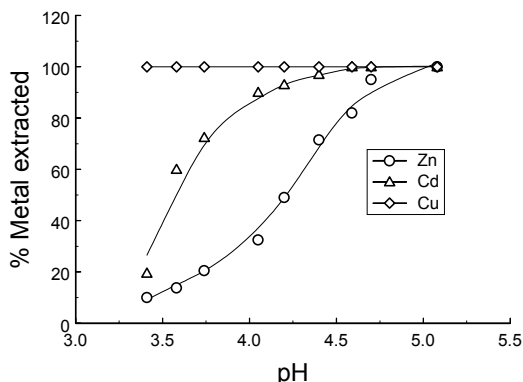


*Figure 6. Extraction of Cd, Cu and Zn from solution 2 with 0.5 M CYANEX 471X/0.5 M DIPSA.*

Extraction isotherms for Cu, Fe and Cd with a 0.1 M DIPSA/0.1 M CYANEX 471X reagent mixture at pH 5.5 are shown in Figure 7. These show that these metals and also Pb can be reduced to < 0.001g/l in 3 to 4 counter-current stages at an A/O ratio of 1.0 with only co-extraction of 5.5% of the zinc feed. Because of this co-extraction it will be necessary to scrub the loaded organic phase. Preliminary tests suggest that scrubbing with dilute H<sub>2</sub>SO<sub>4</sub> will readily remove the co-extracted Zn but detailed results are as yet incomplete.

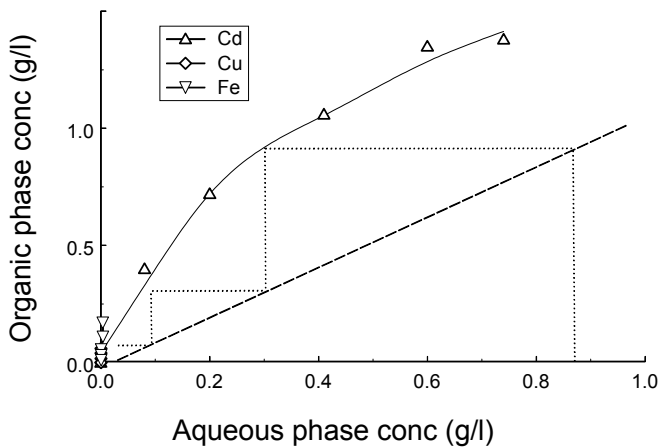


*Figure 7. Extraction isotherms for Cd, Cu and Fe with 0.1 M DIPSA/ 0.1 M Cyanex 471X at pH ~5.5.*

Stripping isotherms are shown in Figures 8a and b. These show that Cd and Fe can be readily removed in essentially one stage by 1 M H<sub>2</sub>SO<sub>4</sub> but neither Cu nor Pb are stripped with this concentration of acid. Further work is necessary to determine the appropriate stripping regime for these metals.

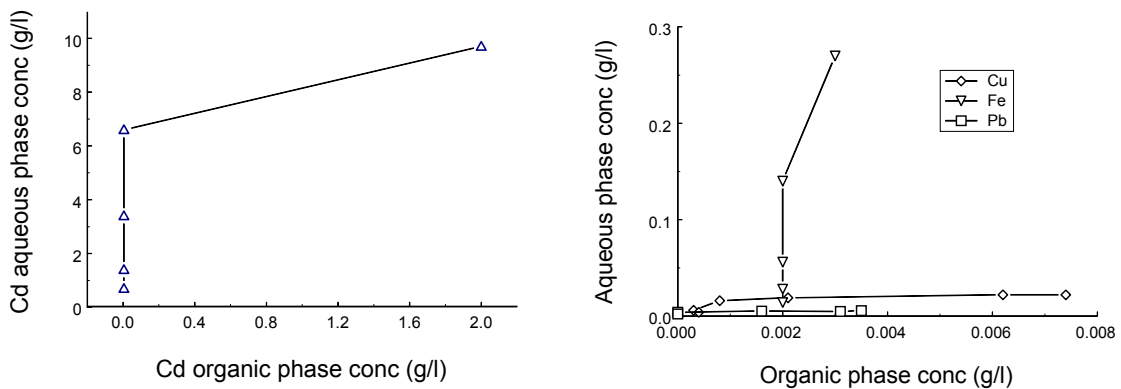


*Figure 8. Stripping isotherms of Cd, Fe, Cu and Pb from loaded 0.1 M DIPSA/ 0.1 M CYANEX 471X with 1 M H<sub>2</sub>SO<sub>4</sub>.*

## CONCLUSIONS

For solution 1, the contained metal ions can be successfully removed in two stages using 0.5 M DEHPA, with the possibility of either discharging the treated liquor or recycling within the plant. Stripping of the metals from DEHPA is easy, with only a single stage using 2 M H<sub>2</sub>SO<sub>4</sub> being required.

For solution 2, Cd, Fe, Pb and Cu can be selectively removed with the mixed extractant system DIPSA/CYANEX 471X from Zn in three to four stages, with possibly one to two stages of scrubbing with dilute H<sub>2</sub>SO<sub>4</sub> to minimise loss of zinc, although the stripping regime has not yet been finalised. The organic phase can be stripped of Cd and Fe with 1 M H<sub>2</sub>SO<sub>4</sub>. Neither Cu nor Pb are satisfactorily stripped with this acid concentration and a satisfactory stripping regime is yet to be determined. The purified zinc-containing raffinate can be recycled within the plant.

## **ACKNOWLEDGEMENTS**

Thanks are due to Cytec Inc for the supply of reagents and to the management of the Miasteczko Śląskie zinc plant for the supply of solutions and valuable discussions. This work formed part of a project under the EU INCO-Copernicus programme contract number ERB IC15 CT 98 0146.

## **REFERENCES**

1. J. S. Preston (1994), *Hydrometallurgy*, **36**, 61-78.
2. J. S. Preston, J. H. Patrick and G. Steinbach (1994), *Hydrometallurgy*, **36**, 143-160.
3. J. S. Preston and A. C. du Preez (1994), *Solvent Extr. Ion Exch.*, **12**, 667-685.
4. J. S. Preston, *European Patent*, No. 0 617 135 A1.
5. G. Desseigne (1948), *Bull. Soc. Chim. Fr.*, 68-70.



# THE EXTRACTION OF ARSENIC (V) AND SULPHURIC ACID FROM ACIDIC SULPHATE MEDIA BY TRI-N-BUTYL PHOSPHATE (TBP) IN SHELLSOL A OR T: I - AN EQUILIBRIUM STUDY

Afif Demirkiran, Nevill M. Rice and A. Ruth Wright

Department of Mining and Mineral Engineering, School of Process, Environmental and Materials Engineering, University of Leeds, Leeds, U.K.

The composition of the sulphuric acid and arsenic(V) species extracted by tri-*n*-butyl-phosphate (TBP), in either Shellsol A (aromatic) or Shellsol T (non-aromatic) diluent, from aqueous media, containing either H<sub>2</sub>SO<sub>4</sub> alone or both H<sub>2</sub>SO<sub>4</sub> and As(V) was studied by slope analysis. Other extractants, including amines, did not extract much As(V). The average compositions of the H<sub>2</sub>SO<sub>4</sub> species for 1.8-3.66 mol/L TBP from pure 1-5 mol/L H<sub>2</sub>SO<sub>4</sub> were (TBP)<sub>3</sub>(H<sub>2</sub>O)<sub>5</sub>H<sub>2</sub>SO<sub>4</sub> and (TBP)<sub>4</sub>(H<sub>2</sub>O)<sub>6</sub>H<sub>2</sub>SO<sub>4</sub> in Shellsol T or A, respectively. With As(V) present the extracted species were similar but less H<sub>2</sub>SO<sub>4</sub> was extracted. The As(V) species extracted from 0.25-4 mol/L H<sub>2</sub>SO<sub>4</sub> were (TBP)<sub>3</sub>H<sub>3</sub>AsO<sub>4</sub> in Shellsol T or (TBP)<sub>5</sub>H<sub>3</sub>AsO<sub>4</sub> in Shellsol A. The enthalpy of extraction was estimated to be -26.6 kJ/mol from the variation with temperature (12-33.5°C). As(V) extraction decreased slightly as the pH increased from 0.3 to 1.6.

## INTRODUCTION

Solvent extraction with tri-*n*-butyl phosphate (TBP) for the removal of arsenic from copper electrorefinery bleed streams has been applied in a number of refineries around the world including that operated by Mount Isa Mines Ltd. in Townsville, Queensland [1], who used results from the present study [2,3] in the development of their process. This paper reports a study of the composition of the organic phase species extracted from aqueous media with TBP dissolved in either Shellsol A (aromatic) or Shellsol T (non-aromatic) diluents[2].

## LITERATURE REVIEW

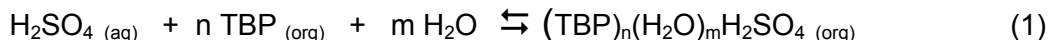
The TBP-H<sub>2</sub>SO<sub>4</sub>-water system has been studied extensively [4-11]. Much has been reported on methods for the removal and recovery of arsenic in process development, including solvent extraction and ion exchange (see part II) [12], but very little has been published on the nature of the arsenate species extracted by TBP [13-15]. Sealy and Freeman [11] reported a developmental study of a process for the extraction of As(V) from copper refinery electrolytes, including TBP-H<sub>2</sub>SO<sub>4</sub>-H<sub>2</sub>O ternary equilibria, based upon this earlier Soviet work [13-15]. The extraction of arsenic by other reagents, including carboxylic acids, Cyanex 301 and Cyanex 923, TOPO and Adogen 464 has been reported in the literature [16-19] but only neutral alkyl-phosphates showed any promise.

## THEORY

The overall composition of the extracted species was deduced by slope analysis of logarithmic plots of the distribution ratio as a function of varying reagent concentrations.

### Sulphuric Acid

The extraction reaction may be written as:



$$\text{for which the extraction equilibrium constant, } K_{\text{ex}} = \frac{[(\text{TBP})_n(\text{H}_2\text{O})_m\text{H}_2\text{SO}_4]_{\text{(org)}}}{[\text{H}_2\text{SO}_4]_{\text{(aq)}} [\text{TBP}]^n_{\text{(org)}} [\text{H}_2\text{O}]^m} \quad (2)$$

$$\text{whence } \log D_{\text{H}_2\text{SO}_4} = n \log [\text{TBP}]_{\text{(org)}} + \text{constant} \quad (3)$$

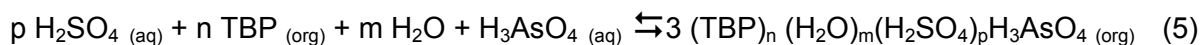
where  $D_{\text{H}_2\text{SO}_4}$  is the distribution ratio of  $\text{H}_2\text{SO}_4$ , assuming constant water activity and activity of TBP = mole fraction [20]. The value of m may be found [4, 6] using the equation:

$$(dN_w/dN_A) = m - n \quad (4)$$

where  $N_w$  and  $N_A$  are the respective number of moles of water and acid in the organic.

### Arsenic

Tserekova *et al.* [14] proposed  $(\text{TBP})_n(\text{H}_2\text{O})_m\text{H}_2\text{SO}_4 \text{ H}_3\text{AsO}_4$  as the organic phase species. composition. The extraction equilibrium may be generalised to:



$$\text{whence: } \log D_{\text{As}} = n \log [\text{TBP}]_{\text{(org)}} + p \log [\text{H}_2\text{SO}_4]_{\text{(aq)}} + \text{constant} \quad (6)$$

where  $D_{\text{As}}$  is the distribution ratio of As(V) assuming constant water activity and ideal TBP behaviour [20].

## EXPERIMENTAL

All reagents were A.R. grade (BDH) except Shellsol A and T diluents (Shell Chemicals Ltd.). Extraction equilibrium of As was achieved within 60 s. Normally 20 cm<sup>3</sup> of each phase were contacted for 10 minutes using a flask-shaker at ambient temperature (~ 20°C) followed by centrifuging at 2000 rpm, except when an AKUFVE mixer-centrifuge [21] was used to study the effect of varying temperature or pH.  $\text{H}_2\text{SO}_4$  concentrations were measured either by titration or (in the presence of both solutes) β-liquid scintillation counting of <sup>35</sup>S tracer with quenching corrected by the channels ratio method using an external <sup>226</sup>Ra standard. Distribution of As in both phases was determined by γ-scintillation counting of <sup>74</sup>As with a NaI well crystal. Organic water content was measured by Karl Fischer titration.

## RESULTS AND DISCUSSION

### Sulphuric Acid Extraction

Figures 1 to 4 show the results obtained for the extraction of sulphuric acid with TBP. From equations (3) and (4) and the results in Table 2 it was concluded that the average composition of the species extracted from sulphuric acid media were  $(\text{TBP})_3(\text{H}_2\text{O})_6\text{H}_2\text{SO}_4$  or  $(\text{TBP})_4(\text{H}_2\text{O})_6\text{H}_2\text{SO}_4$  in Shellsol T or A respectively in the absence of As(V) for concentrations of TBP from 1.8-3.66 mol/L (100% TBP) and  $\text{H}_2\text{SO}_4$  from 1-5 mol/L. Results were similar in the presence of 0.2 mol/L As (Figures 2 and 4) but slightly less sulphuric acid was extracted. However the slopes of 1.5 and 2 obtained for the variation with  $[\text{H}_2\text{SO}_4]$  indicate that reaction (1) may not fully represent the extraction equilibrium and that the composition of the extracted species depends on the concentrations of both acid and TBP in agreement with previous work [9]. From equation (4) the number of water molecules in the complex, m, was estimated between 5 and 6 in Shellsol T and 6 to 7 in Shellsol A, respectively.

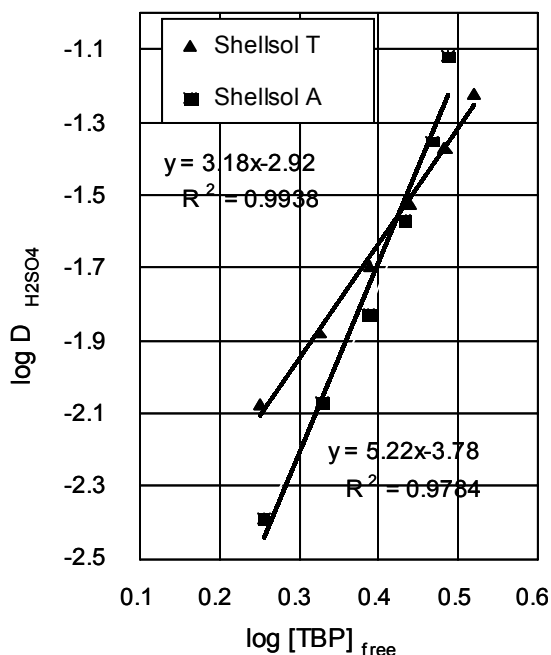


Figure 1. Variation of sulphuric acid extraction with free TBP concentration.

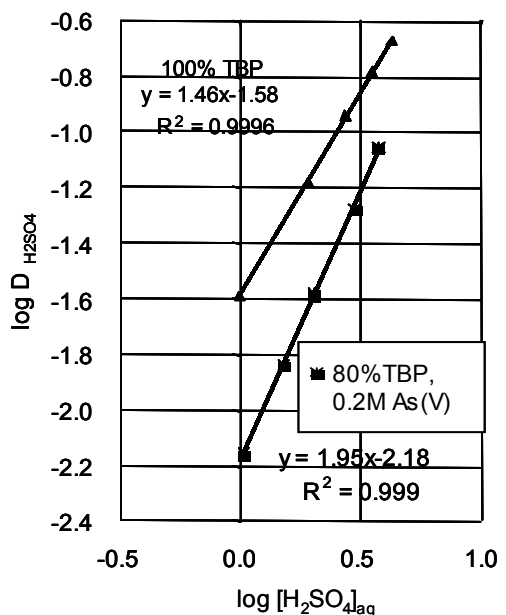


Figure 2. Variation of sulphuric acid extraction with aqueous sulphuric acid concentration.

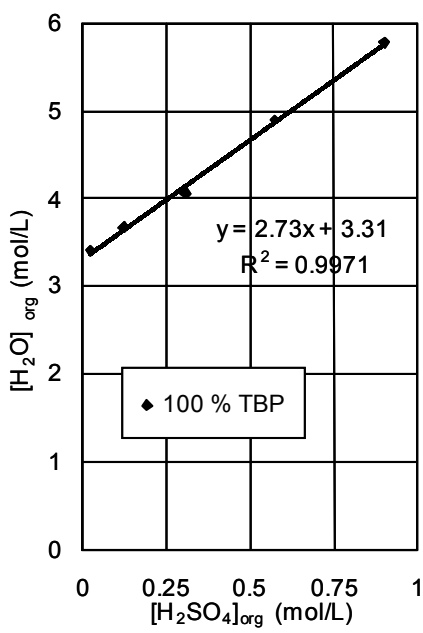


Figure 3. Water content of TBP phase as a function of organic  $H_2SO_4$  concentration.

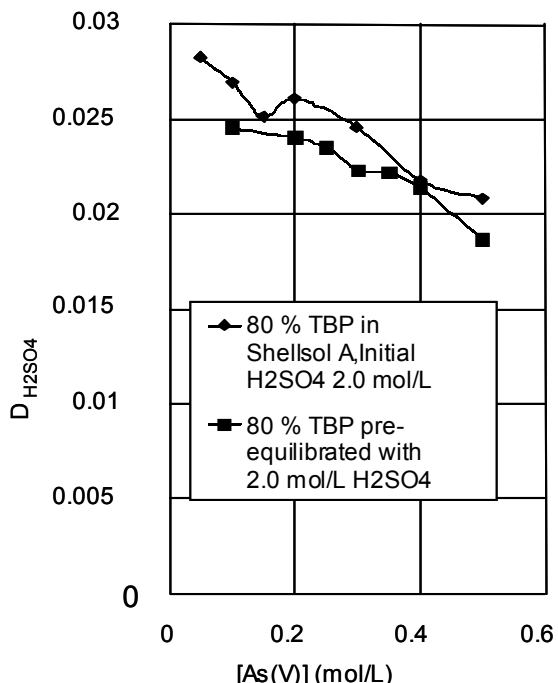


Figure 4. Effect of arsenic(V) concentration on sulphuric acid extraction.

### Arsenic(V) Extraction

Figures 5 to 8 shows the results obtained for the extraction of As (V). Table 1 shows results for the extraction of As(V) with a selection of other extractants. For 80% TBP in Shellsol T, variation of the As(V) concentration from 0.05 to 0.40 mol/L in 2.0 mol/L  $H_2SO_4$  increased the distribution ratio of As(V),  $D_{As}$ , from 0.347 to 0.418. With the same solvent pre-equilibrated with 2.0 mol/L  $H_2SO_4$ ,  $D_{As}$  varied from 0.404 to 0.442 for 0.10 - 0.40 mol/L As(V). Extraction of

As(V) from a copper refinery liberator bleed sample, that contained 2 mol/L H<sub>2</sub>SO<sub>4</sub>, gave comparable results to synthetic solutions with and without copper with D<sub>As</sub> = 0.405 and 0.412 respectively for 80 % TBP in Shellsol A.

Table 2 summarizes data for the slopes obtained from various plots of log D<sub>H<sub>2</sub>SO<sub>4</sub></sub> and log D<sub>As</sub> as a function of free and initial TBP concentrations and other variables. Values for the correlation coefficient, r<sup>2</sup>, are shown on the figures except where the plots were clearly non-linear and were mostly about 0.99. Free TBP concentrations were calculated using values of n estimated from the slopes of the plots with initial TBP concentration as a first approximation.

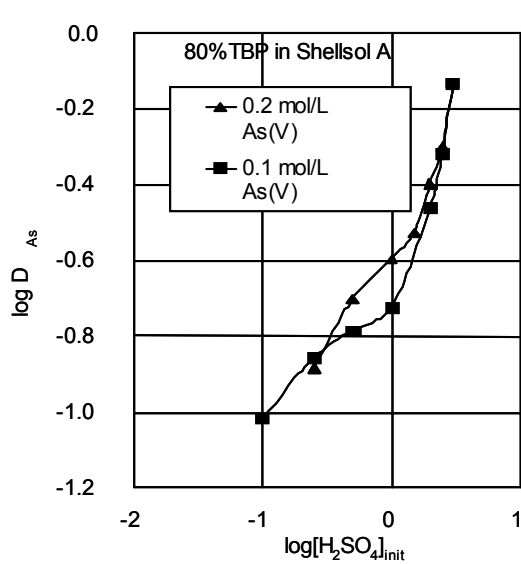


Figure 5. Variation of As(V) distribution with sulphuric acid concentration.

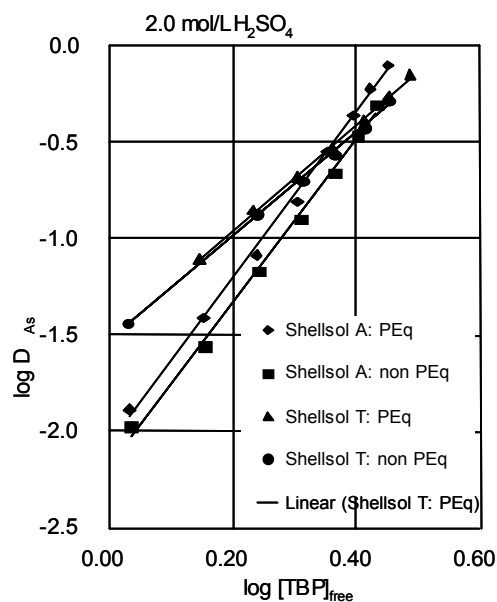


Figure 6. Variation of As(V) distribution with free TBP concentration.

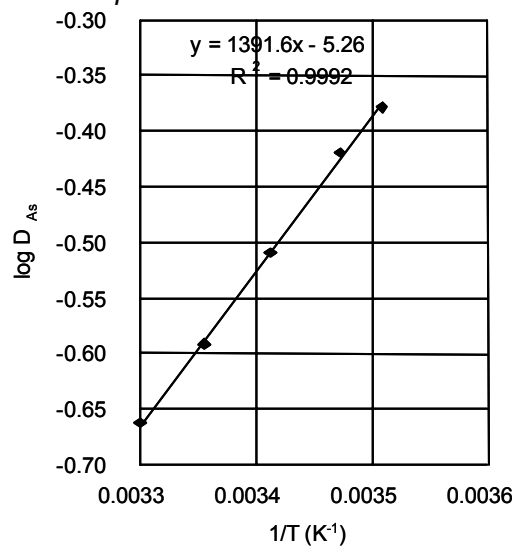


Figure 7. Variation of As(V) distribution with temperature (Arrhenius plot).

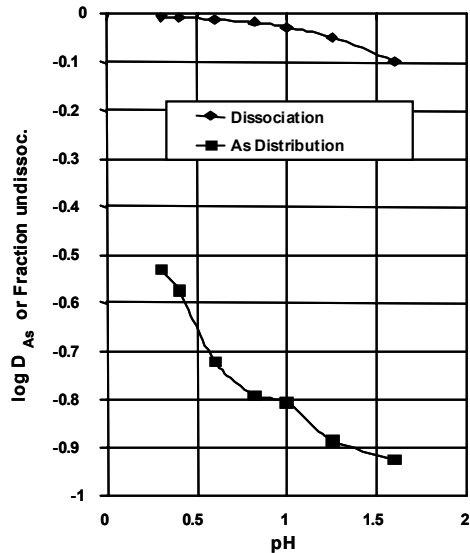


Figure 8. Variation of As(V) distribution and H<sub>3</sub>AsO<sub>4</sub> dissociation with pH.

From Table 1 it appears that TBP is the only reagent capable of extracting reasonable quantities of As(V) from acidic sulphate media though LIX X1-8A showed some extraction of As(V). Higher pH values were necessary for amine extractants to extract As(V). From Figure 5 and equation (6) the As(V) species extracted were found to be  $(TBP)_3H_3AsO_4$  in Shellsol T and  $(TBP)_5H_3AsO_4$  in Shellsol A but Figure 6 shows that the  $H_2SO_4$  composition varied over the concentration range 0.25-4 mol/L for both 0.1 and 0.2 mol/L As. Extraction increased rapidly above 2 mol/L  $H_2SO_4$  and increased slightly with pre-equilibrated TBP. From the slope of the Arrhenius plot (Figure 7) the enthalpy of extraction was estimated to be -26.6 kJ/mol in the temperature range 12 - 33.5°C. Extraction decreased with increasing pH from 0.3 to 1.6 (Figure 8) probably due to the increasing aqueous dissociation of the  $H_3AsO_4$  to  $H_2AsO_4^-$ . Figure 8 also shows the fraction of  $H_3AsO_4$  calculated taking  $pK_1 = 2.19$  [22]. This decreases with pH but less rapidly than  $\log D_{As}$  does.

*Table 1. Extraction of As(V) with various extractants.*

(All extractants 0.1 mol/L, pre-equilibrated twice with 1.5 mol/L  $H_2SO_4$  except as indicated)

Diluent	Kerosene (1% decanol)		Toluene	
Extractant	2 mol/L $H_2SO_4$	pH 1.8	2 mol/L $H_2SO_4$	pH 1.8
Primene JMT	-	-	0.040	0.055
Amberlite LA-1	0.010	0.046	0.004	0.070
Amberlite LA-2	0.007	0.053	0.004	0.113
Alamine 336S	0.009	0.034	0.006	0.085
Aliquat 336	0.017	0.086	0.025	0.117
Adogen 464 ( $Cl^-$ )	3 <sup>rd</sup> phase	emulsion	0.001	emulsion
Adogen 464 ( $SO_4^{2-}$ )	3 <sup>rd</sup> phase	emulsion	0.025	emulsion
Kelex-120	nil	nil	nil	Nil
LIX X1-8A	0.179	0.006	0.063	0.005
n-decanol(neat)	0.090	0.022	-	-
TBP (80%)	0.370	-	0.450	0.118

*Table 2. Slope analysis for the extraction of  $H_2SO_4$  and As(V) (trend lines).*

Plot	Figure no.	Shellsol A	Shellsol T
$\log D_{H_2SO_4} \text{ vs. } \log [TBP]_{\text{init}}$		4.17	2.85
$\log D_{H_2SO_4} \text{ vs. } \log [TBP]_{\text{free}}$	1	5.22	3.17
$\log D_{H_2SO_4} \text{ vs. } \log [H_2SO_4]_{\text{aq}}$	2	1.95	-
$\log D_{H_2SO_4} \text{ vs. } \log [\text{As(V)}]_{\text{init}}$		-0.06	-
$[H_2O]_{\text{org}} \text{ vs. } [H_2SO_4]_{\text{org}}$ (100% TBP)	3	2.73	-
$\log D_{As} \text{ vs. } \log [TBP]_{\text{init}}$		3.55	2.28
$\log D_{As} \text{ vs. } \log [TBP]_{\text{init}}$ (Pre-equilibrated)		3.36	2.38
$\log D_{As} \text{ vs. } \log [TBP]_{\text{free}}$	6	4.31	2.76
$\log D_{As} \text{ vs. } \log [TBP]_{\text{free}}$ (Pre-equilibrated)	6	4.22	2.69
$\log D_{As} \text{ vs. } \log [H_2SO_4]_{\text{aq}}$	5	Non-linear	-
$\log D_{As} \text{ vs. } \log [\text{As(V)}]_{\text{init}}$		0.09	-
$\log D_{As} \text{ vs. } \text{pH}$	8	-0.37	-
$\log D_{As} \text{ vs. } 1/T$	7	1391.6	-

## CONCLUSIONS

TBP is the best extractant for arsenic(V) from acid sulphate media. The extracted species contains both H<sub>2</sub>SO<sub>4</sub> and H<sub>2</sub>O to varying extents depending on concentration.

## ACKNOWLEDGEMENTS

Financial support from the SRC (now EPSRC) and RTZ (now Rio Tinto plc) is acknowledged with thanks. AD wishes to thank ETIBANK (Turkey) for a scholarship.

## REFERENCES

1. J. O'Kane, B. Middlin and D. Royston (1985), *Proc. Int. Symp. Extractive Metallurgy*, Institute of Mining and Metallurgy, London, pp. 951-965.
2. A. Demirkiran (1978), The Design of A Solvent Extraction Process for the Recovery of Arsenic From Copper Electrorefinery Bleed Streams, M.Phil. Thesis, University of Leeds.
3. A. Demirkiran, N.M. Rice and A.R. Wright (1981), *Proc. Symp. Hydrometallurgy 81*, Society of Chemical Industry, London, Poster P2/5.
4. E. Hesford and H.A.C. McKay (1960), *J. Inorg. Nucl. Chem.*, **13**, 156-164.
6. K. Naito and T. Suzuki (1962), *J. Phys. Chem.*, **66**, 983-988
7. S. Nishimura, R. Mitamura, Y. Kondo and N.C. Li (1968), *J. Inorg. Nucl. Chem.*, **30**, 3033-3037.
8. P. Biddle, A. oe, H.A.C. McKay, J.H. Miles and M.J. Waterman (1967), *J. Inorg. Nucl. Chem.*, **29**, 2615-2628.
9. C. Hanson and A.N. Patel (1969), *J. Appl. Chem.*, **19**, 20-24.
10. A. Apelblat (1973), *J. Chem. Soc. Dalton Trans.*, (11), 1198-1201.
11. C.J. Sealy and K.W. reeman (1973), Preprints of Informal Research Sem. Solv. Extr., Birmingham (SCI Solvent. Extraction and Ion Exchange Group) and (1974), Internal Rept. No. 5/CJS/6.5.74, Capper Pass and Sons Ltd., North Ferriby, Humberside, U.K.
12. A. Demirkiran and N.M. Rice (2002), *Proc. Int. Solv. Extr. Conf. ISEC 2002*, South African Institute for Mining and Metallurgy, Johannesburg, pp. 890-895.
13. G.P. Giganov and V.P. Ponomarev (1962), *Trud. Inst. Metall. Benefits Acad. Sci. Kazakh. SSR.*, **5**, 115-118.
14. A.M. Tserekova, G.P. Giganov, G.K. Kolomina and V.I. Fokina (1970), *Nauch. Tr. Vses. Nauch.-Issled. Gornemet. Inst.*, **19**, 119-124.
15. T.K. Tserekov, G.P. Giganov and G.L. Pashkov,(1972), *Tsvet. Met.*, **7**, 60-63.
16. I.M. Ivanov, L.M. Gindin, A.A. Vasil'eva and Z.A. Nel'kina (1969), *Izv. Sib. Otdel Akad. Nauk SSSR. Ser. Khim. Nauk.*, (6), 122-124, in *Chem. Abstracts*, **72**, 71213u.
17. W.A. Rickelton (1993), *Proc. Int. Solv. Extr. Conf. ISEC '93*, Society of Chemical Industry, London, pp. 731-736.
18. M. Kobayashi and T. Nagai (1977), *Proc. Ann. Meeting Min. Met. Inst. Japan*, pp. 243-246.
19. S. Facon, M. Avila Rodriguez, G. Cote and D. Bauer (1993), *Proc. Int. Solv. Extr. Conf. ISEC '93*, Society of Chemical Industry, London, pp. 557-564.
20. N.M. Rice and M.R. Smith (1973), *Proc. The Richardson Conf.*, Institute of Mining and Metallurgy, London, pp. 55-63.
21. H. Reinhardt and J. Rydberg (1966), *Solvent Extraction Chemistry*, North-Holland, Amsterdam, pp. 612-619.
22. G.H. Aylward and T.J.V. Findlay (1974), *S.I. Chemical Data*, 2nd edn., J. Wiley (Australasia), Sydney, p. 123.



## THE EXTRACTION OF ARSENIC (V) FROM COPPER REFINERY ELECTROLYTES WITH TRI-N-BUTYL PHOSPHATE: II - FLOWSHEET DEVELOPMENT

Afif Demirkiran and Nevill Matson Rice

Department of Mining and Mineral Engineering, School of Process, Environmental and Materials Engineering, University of Leeds, Leeds, U.K.

A preliminary laboratory study to define the parameters of a solvent extraction circuit for extracting arsenic from a bleed stream from the liberator cells of a copper electrorefinery is described. Equilibrium isotherms for arsenic(V) extraction with 80% tri-*n*-butyl phosphate (TBP) in Shellsol A diluent at various H<sub>2</sub>SO<sub>4</sub> concentrations were obtained by batch shake-out tests. Scrubbing isotherms with water or 0.2 mol/L Na<sub>2</sub>HAsO<sub>4</sub> were also obtained. The extraction of H<sub>2</sub>SO<sub>4</sub>, scrubbing of the acid from the loaded solvent and stripping of As(V) with water or 0.5% w/v Na<sub>2</sub>CO<sub>3</sub> solution were investigated. Batch counter-current simulation of the proposed circuit was carried out. A relatively high As concentration was necessary to recover As from the strip liquor by reduction to As<sub>2</sub>O<sub>3</sub> with SO<sub>2</sub>. Another possibility was the precipitation of a metal arsenate, e.g., bicupric arsenate (BCA), depending on local circumstances.

### INTRODUCTION

Solvent extraction with tri-*n*-butyl phosphate (TBP) for the removal of arsenic from copper electrorefinery bleed streams has been applied in a number of refineries around the world including that operated by Mount Isa Mines Ltd. in Townsville, Queensland [1-5], who used results of a preliminary laboratory study carried out at the University of Leeds [6,7] in the development of their process. This paper describes the results of that study.

### LITERATURE REVIEW

Biswas and Davenport [8] have described the electrolytic refining of copper. The nature of the sulphate and arsenate species extracted by TBP and the possible use of other extractants was reported in Part I [9] from which it appeared that TBP was the only reagent of those tested that was capable of extracting reasonable quantities of As(V) from acidic sulphate media and also that a relatively high pH was necessary for amine extractants to extract As(V). Much has been reported on methods for the removal and recovery of arsenic and on process development, including solvent extraction. Sealy and Freeman [10,11] were the first to report the development of a process for the extraction of As(V) from copper refinery electrolytes, based upon earlier basic Soviet work [12-14] but their company did not proceed further. However several other companies have also exploited this method [1-5,15-23] and

several patents were granted, e.g. [15,16,18]. Most of these processes exploited the extraction of As(V) by TBP but the  $\text{H}_2\text{SO}_4$  tenor varied. Figure 1 shows a flowsheet for a Cu electrolyte purification circuit. The main motivation for As removal is the danger of arsine gas evolution from the liberator cells when the copper tenor falls below about 15 g/L – generally during the 3<sup>rd</sup> stage. There are three points where solvent extraction of As can be applied, viz. (i) the feed to the liberator cells; (ii) the spent electrolyte from liberator stages 1 or 2; or (iii) the more concentrated liquor after evaporation for recovery and concentration of  $\text{H}_2\text{SO}_4$ . Because As(V) extraction is highly dependent on  $\text{H}_2\text{SO}_4$  tenor (figure 2) [9] the type of circuit depends on the acidity. Both points (ii) and (iii) but not (i) have been used before. Point (iii) leads to a smaller plant but requires more acid resistant construction materials. The MHO plant at Olen, Belgium is based on point (iii) [17] but that at Townsville uses (ii) [1-5].

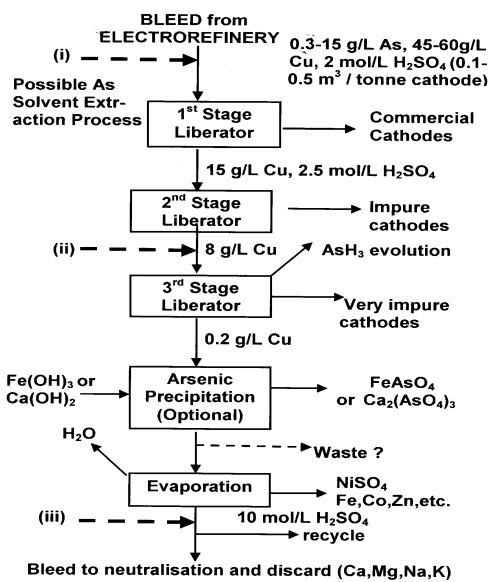


Figure 1. Purification of copper refining electrolytes

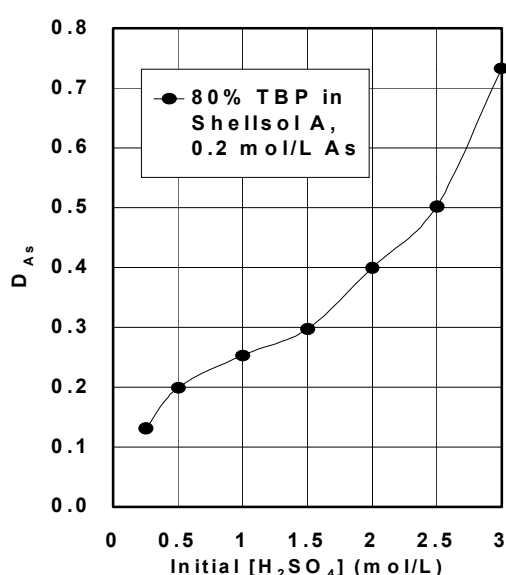


Figure 2. Variation of arsenic distribution with sulphuric acid concentration.

Studies of process chemistry have also been undertaken [6,9,20,24]. Other methods of As control or disposal used include periodic current reversal in the liberator cells [25,26] or precipitation of either sulphides or Fe(III) arsenates [27,28]. Improved As extraction with TBP plus various additives [29] or various alkyl-phosphonates [30] were reported recently.

## EXPERIMENTAL

For simplicity most of the test work was carried out using synthetic solutions containing only As and  $\text{H}_2\text{SO}_4$ , but a bleed stream of the following approximate composition:  $\text{H}_2\text{SO}_4$  2 mol/L, Cu 8.7 g/L; As 15 g/L; Sb 0.15 g/L; Fe 1 g/L; Ni 0.4 g/L; Zn 20 mg/L from the liberator cells of a copper electrorefinery (BICC, Prescott, Lancs, U.K) was also tested for comparison. Reagents were A.R. grade (BDH) except the Shellsol diluents (Shell Chemicals Ltd.). Shellsol A was the preferred diluent for the process development because of better phase disengagement and solubility of TBP. Extraction equilibrium of As was achieved within 60 s. 20 cm<sup>3</sup> of each phase were contacted for 10 minutes using a flask-shaker at ambient temperature ( $\sim 20^{\circ}\text{C}$ ) followed by centrifuging at 2000 rpm.  $\text{H}_2\text{SO}_4$  concentrations were measured by  $\beta$ -liquid scintillation counting of  $^{35}\text{S}$  tracer with quenching corrected by the channels ratio method using an external  $^{226}\text{Ra}$  standard. Distribution of As in both phases was determined by  $\gamma$ -scintillation counting of  $^{74}\text{As}$  with a NaI well crystal. Equilibrium isotherms were obtained by varying initial aqueous concentrations of reagents, volumetric phase ratios or crosscurrent loading of either the organic or aqueous phase with successive

contacts of the other phase. Similar procedures were followed for scrubbing using water or 0.2 mol/L Na<sub>2</sub>HAsO<sub>4</sub> and for stripping using water or Na<sub>2</sub>CO<sub>3</sub> solution. The McCabe-Thiele diagrams, that were plotted from shakeout test data were compared with batch counter-current simulation data for each step (separately) obtained after using 7 cycles of contacts to try to achieve steady state conditions.

## RESULTS AND DISCUSSION

Extraction of As(V) from the copper refinery liberator bleed sample gave comparable results to synthetic solutions with and without copper. D<sub>As</sub> = 0.405 and 0.412 respectively for 80 % TBP in Shellsol A. All subsequent work was undertaken using synthetic media.

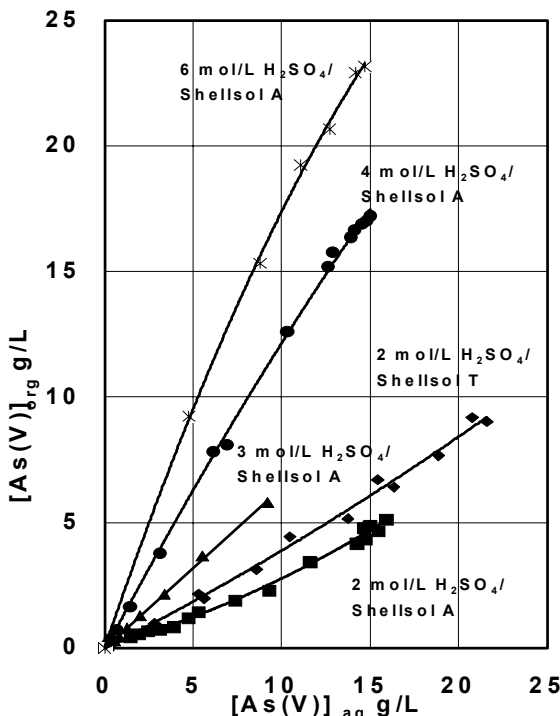


Figure 3. Extraction isotherms for As(V) at various sulphuric acid concentrations with Shellsol A or T, initial [As(V)] 15 g/L.

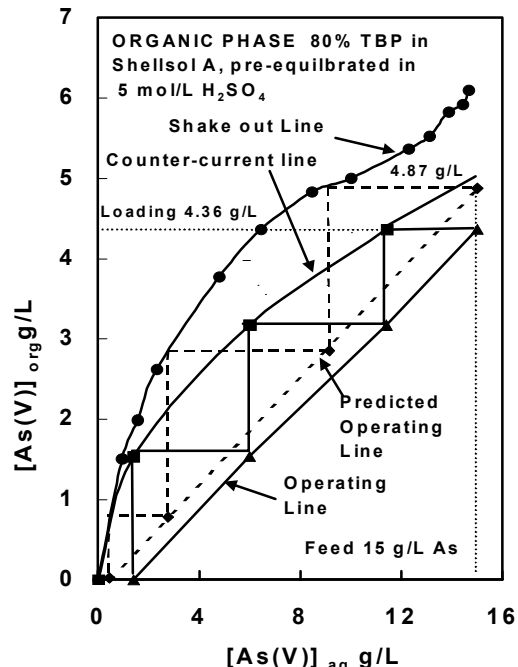


Figure 4. McCabe-Thiele diagram for loading of As(V) for 80%TBP 80% in TBP in Shellsol A from shake out and counter-current tests.

### Loading

Figure 3 shows the improvement in the extraction isotherms for As(V) with TBP (pre-equilibrated with 5 mol/L H<sub>2</sub>SO<sub>4</sub>) due to increased H<sub>2</sub>SO<sub>4</sub> concentration. Aliphatic Shellsol T is slightly better than aromatic Shellsol A at 2 mol/L H<sub>2</sub>SO<sub>4</sub>. Figure 4 shows the McCabe-Thiele plot, as predicted from shake out tests, for the loading of As from a feed containing 0.2 mol/L Na<sub>2</sub>HAsO<sub>4</sub> (15 g/L As) at an initial concentration of 2 mol/L H<sub>2</sub>SO<sub>4</sub> using 80% TBP in Shellsol A, pre-equilibrated in 1 stage 5 mol/L H<sub>2</sub>SO<sub>4</sub> at O/A = 0.5 as solvent. The recycled solvent was predicted to contain 0.17 g/L As. Data from a simulated batch counter-current run are also plotted. The difference in the plots was due to different H<sub>2</sub>SO<sub>4</sub> concentrations in each stage, which led to a slightly lower loading in the counter-current test. The simulation resulted in >90% reduction in As to 1.4 g/L with 3.4 mol/L H<sub>2</sub>SO<sub>4</sub> in the raffinate in 3 stages at O:A = 3.1. A further stage could be included if necessary. Figure 5 shows a McCabe-Thiele plot for H<sub>2</sub>SO<sub>4</sub> showing that back extraction of H<sub>2</sub>SO<sub>4</sub> occurs during loading. The operating line was not straight possibly due to varying phase ratio or the non-achievement of steady state or equilibrium for the sulphuric acid transfer.

## Scrubbing

Scrubbing of the extract to decrease the remaining  $\text{H}_2\text{SO}_4$  content was necessary for efficient stripping. A decrease from 0.07 to < 0.004 mol/L was achieved in 1 stage with either water or 0.2 mol/L As (which could be a strip liquor bleed) at O:A = 10 (Figure 6). The latter agent was preferred so as to decrease the loss of As from the extract, which fell from 4.3 to 4 g/L As. Scrub raffinate containing 16.75 g/L As would join the aqueous feed to the loading step after some dilution.

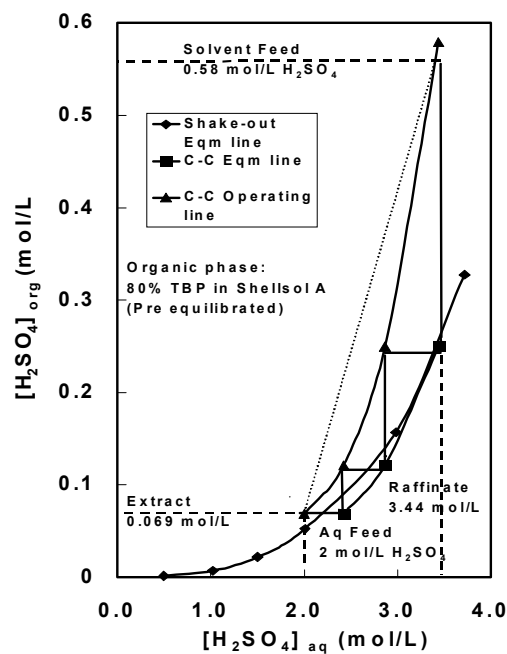


Figure 5. Behaviour of sulphuric acid during arsenic loading.

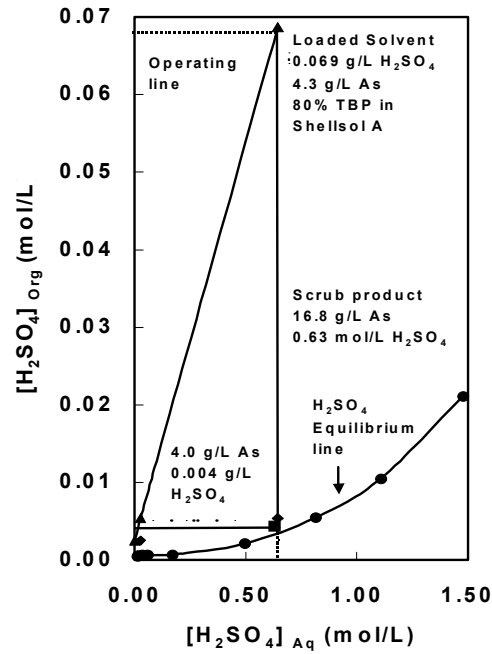


Figure 6. Sulphuric acid scrubbing with 15 g/L As(V) as  $\text{NaH}_2\text{AsO}_4$ .

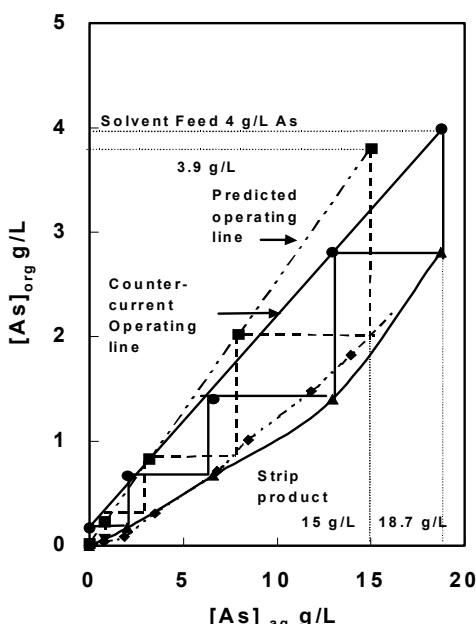


Figure 7. Stripping of scrubbed organic phase with water.

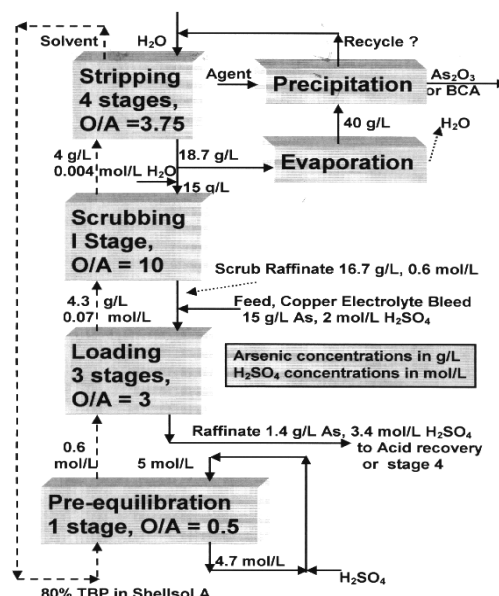


Figure 8. Proposed flowsheet for As recovery from Cu electrolytes.

### Stripping

Table 1 shows that As can be stripped by either water or dilute  $\text{Na}_2\text{CO}_3$  solution. If the residual acid is scrubbed from the organic phase water is the cheaper stripping agent. Figure 7 shows the McCabe-Thiele plots for stripping, both as predicted and from a batch counter-current simulation test. The results were in reasonably good agreement. Stripping with water in 4 stages at O:A = 3.75 gave an aqueous product that contained 18.7 g/L As with little  $\text{H}_2\text{SO}_4$  and a recycled solvent containing 0.17 g/L As.

Table 2 shows that the recycled solvent after stripping extracts As efficiently but that pre-equilibration in 1 stage with 5 mol/L  $\text{H}_2\text{SO}_4$  at O:A = 0.5 is required to maintain the  $D_{\text{As}}$  value.

Table 1. Stripping of As from 80% TBP in Shellsol A containing 4 g/L As(V) at O:A =1.

% $\text{Na}_2\text{CO}_3$ (w/v)	0 ( $\text{H}_2\text{O}$ )	0.25	0.5	1.0	2.0
$D_{\text{As}}$	0.14	0.1	0.05	0	0
% $\text{H}_2\text{SO}_4$ stripped	99	100	100	100	100

Table 2. Effect of recycling 80% TBP in Shellsol A after stripping on As extraction ( $D_{\text{As}}$ ).

Cycle	0.5% $\text{Na}_2\text{CO}_3$ strip	$\text{H}_2\text{O}$ strip	$\text{H}_2\text{O}$ strip/ Pre-equilibrate
1	0.346	0.391	0.391
2	0.292	0.355	0.41

### Arsenic Recovery and Overall Flowsheet

Figure 8 shows the proposed overall flowsheet for an arsenic recovery process based on the above results and gives data for the expected concentrations of As and  $\text{H}_2\text{SO}_4$  for each process step. A brief study of reduction to  $\text{As}_2\text{O}_3$  with  $\text{SO}_2$  indicated that concentration of As to about 40 g/L, perhaps by evaporation, might be needed at pH < 2. Arsenic can be recovered from the strip product either by reduction to  $\text{As}_2\text{O}_3$  with  $\text{SO}_2$ , or by precipitation of  $\text{As}_2\text{S}_3$  or as a metal arsenate, e.g., bicupric arsenate, BCA (Townsville), depending on local requirements and markets. Recycling of the strip liquor might also be necessary.

## CONCLUSIONS

A feasible solvent extraction circuit for the recovery of arsenic from copper refining electrolytes has been developed as illustrated in Figure 8.

## ACKNOWLEDGEMENTS

Financial support from the SRC (now the EPSRC) and RTZ (now Rio Tinto plc) and also from ETIBANK (Turkey) for a scholarship is acknowledged with gratitude.

## REFERENCES

1. D.W. Hoey, G.J. Leahy, B. Middlin and J. O'Kane (1987), Electrowinning and Winning of Copper, TMS, Warrendale, PA, pp. 271-293.
2. D. Royston and T.C. Hunter (1983), AIME 112<sup>th</sup> Annual General Meeting, Atlanta, GA, TMS Paper selection No. A83-30, 11 pp.
3. D. Royston, G.J. Sheehan, D.A. Winborne, F.S. Wong, R.W. Armstrong and P.G. Hall (1984), Proc. Chemeca, 12<sup>th</sup> Australian Chem. Eng. Conf., Melbourne, pp. 887-893.

4. J. O'Kane, B. Middlin and D. Royston (1985), *Proc. Int. Symp. Extractive Metallurgy*, Institute of Mining and Metallurgy, London, pp. 951-965.
5. S. Lallenec and D. Muir (1996), *Proc. Int. Solv. Extr. Conf. ISEC '96*, University of Melbourne Press, Melbourne, pp. 765-770.
6. A. Demirkiran (1978), The Design of a Solvent Extraction Process for the Recovery of Arsenic from Copper Electrorefinery Bleed Streams, M.Phil. Thesis, University of Leeds.
7. A. Demirkiran, N.M. Rice and A.R. Wright (1981), *Proc. Symp. Hydrometallurgy 81*, Society of Chemical Industry, London, Poster P2/5.
8. A.K. Biswas and W.G. Davenport (1994), Extractive Metallurgy of Copper, 3rd edn., Pergamon, Oxford, pp. 343-344.
9. A. Demirkiran, N.M. Rice and A.R. Wright (2002), *Proc. Int. Solv. Extr. Conf. ISEC 2002*, South African Institute of Mining and Metallurgy, Johannesburg, pp. 884-889.
10. C.J. Sealy and K.W. Freeman (1973), *Proc. Informal Research Sem. Solv. Extr. and Ion Ex. Group (SCI)*, Birmingham, U.K..
11. C.J. Sealy and K.W. Freeman (1974), Internal Report. No 5/CJS/6.5.74, Capper Pass and Sons Ltd., North Ferriby, Humberside, U.K.
12. G.P. Giganov and V.P. Ponomarev (1962), *Trud. Inst. Metall. Benef. Acad. Sci. Kazakh. SSR.*, **5**, 115-118.
13. A.M. Tserekova, G.P. Giganov, G.K. Kolomina and V.I. Fokina (1970), *Nauch. Tr. Vses. Nauch.-Issled. Gornemet. Inst.*, **19**, 119-124.
14. T.K. Tserekov, G.P. Giganov and G.L. Pashkov (1972), *Tsvet. Met.*, **7**, 60-63.
15. M. Takahashi, E. Itoh and T.Nagai (Nippon Mining) (1976), *German Pat.*, No. 2,603,874 (2 Aug.).
16. A. De Schepper and A. van Peteghem (MHO) (1977), *U.K. Pat.*, No. 1,473,825 (18 May).
17. A. De Schepper (1985), *Int. Symp. Extractive Metallurgy*, Institute of Mining and Metallurgy, London, pp. 167-189.
18. D.G.E. Kerfoot (Noranda) (1978), *U.S. Pat.*, No 4,115,512 (19 Sept.).
19. T. Nagai, N. Yamakazi and M. Kobayashi (1976), *Proc. Fall Meeting. Min. Met. Inst. Japan*, Hokkaido, pp. 1-3.
20. M. Kobayashi and T. Nagai (1977), *Proc. Ann. Meeting. Min. Met. Inst. Japan*, Tokyo, pp. 243-244.
21. M. Kobayashi and T. Nagai (1978), *Proc. Ann. Meeting. Min. Met. Inst. Japan*, Tokyo, pp. 427-428.
22. T. Nagai (1979), *Proc. Symp. Solv. Extr. Japan*, Tokyo, pp. 27-30.
23. P. Navarro and M.A.Solar (1982), *Proc. 1<sup>st</sup> Meeting Min. Proc. in Southern Hemisphere*, Rio de Janeiro, pp. 674-683.
24. J.M. Cohen (1983), *Proc. Int. Solv. Extr. Conf. ISEC '83*, Denver, CO, Poster No 19b.
25. G.J. Houllachi and P.L. Claessens (Noranda) (1978), *U.S. Pat.*, No. 4083761 (11 Apr.).
26. J. Thiriar, P.L. Claessens and G.J. Houllachi (1983), *Proc. 3<sup>rd</sup> Int. Symp. Hydrometallurgy*, AIME/SME, Atlanta, GA, pp. 705-720.
27. P.A. Bloom, J.H. Maysilles and H. Dolezai (1982), U.S. Bur. Mines, Report No. RI 8679.
28. P.M. Swash and A.J. Monhemius (1994), *Proc. Int. Symp. Hydrometallurgy '94*, Institute of Mining and Metallurgy, London, pp. 177-190.
29. Y. Jiaoyong, L. Daxing, Z. Huifang and J. Kaixi (1990), *Proc. Int. Solv. Extr. Conf. ISEC '90*, Kyoto, pp. 1205-1210.
30. D.B. Dreisinger, B.J.Y. Leong, B.J. Balint and M.H. Beyad (1993), *Proc. Int. Solv. Extr. Conf. ISEC '93*, Society of Chemical Industry, London, pp. 1271-1278.



# THE SOLVENT EXTRACTION PROPERTIES OF DI-*n*-HEXYL SULPHOXIDE IN RELATION TO THE REFINING OF PLATINUM-GROUP METALS

Anna C. du Preez and John S. Preston

Mintek, Randburg, South Africa

In this paper we describe some aspects of the solvent-extraction chemistry of di-*n*-hexyl sulphoxide (DnHSO) that are of relevance to the refining of platinum-group metals (PGMs). Although DnHSO is not used as such in the processing of PGMs, it can nevertheless be formed *in situ* by the oxidation of the parent di-*n*-hexyl sulphide (DnHS), which is used commercially as an extractant for palladium. The impact of the presence of DnHSO in PGM refining circuits may be favourable or unfavourable. Thus, the strong extraction of ferric iron from hydrochloric acid solutions by DnHSO results in this metal being co-extracted with palladium when DnHS is used in the recovery of the latter metal. Fortunately, however, the iron can be selectively washed out of the loaded organic phase by water, thereby providing a convenient exit from the process for this impurity. On the other hand, dialkyl sulphoxides are also able to extract rhodium from concentrated hydrochloric acid media, apparently by the formation of complexes such as  $(L_2 \cdot H_3O^+)RhCl_4L_2^-$ , where L = dialkyl sulphoxide. This complex is difficult to strip, and contributes to a gradual build-up of PGM values in the organic phase. Finally, the presence of small quantities of DnHSO in recycled organic solutions of DnHS causes a fortuitous increase in the extraction rate of palladium(II).

## INTRODUCTION

Recently, we carried out a study that entailed the dissolution of PGM scrap in hydrochloric acid sparged with chlorine, and the recovery of the individual metals by solvent-extraction techniques. During this work, we observed certain features that suggested the possibility that one of the extractants used (di-*n*-hexyl sulphide, R<sub>2</sub>S, where R = *n*-hexyl) might be undergoing gradual oxidation to the corresponding sulphoxide, R<sub>2</sub>SO. These features were:

- the co-extraction of considerable quantities of iron in the palladium extraction circuit;
- the build-up of rhodium in the stripped organic phase;
- a gradual increase in the extraction rate of palladium as the organic phase was recycled.

In this work, some aspects of the solvent extraction of iron(III), rhodium(III) and palladium(II) by dialkyl sulphoxides are examined in order to rationalize the above behaviour.

## EXPERIMENTAL METHODS

All the experimental procedures were as described previously [1,2]. Di-*n*-hexyl sulphide was prepared [1] and purified by distillation under reduced pressure (b.p. 69°C at 0.1 mm Hg,  $n_D^{20}$  1.4587,  $d_4^{20}$  0.8412). The sulphoxide was prepared and purified by recrystallization from petroleum ether as white needles (m.p. 59°C) [1]. Rhodium solutions were aged for several months before use. All extraction experiments were carried out using xylene as the diluent.

## RESULTS AND DISCUSSION

### Extraction of Iron(III) from Hydrochloric Acid Solutions

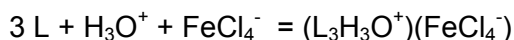
In its role as an extractant for palladium, di-*n*-hexyl sulphide (DnHS) is commonly used at high concentrations (e.g., 50 vol.%, equivalent to 2.08 M). At this concentration, even 5% oxidation of DnHS would produce 0.1 M di-*n*-hexyl sulphoxide (DnHSO). The presence of such quantities of DnHSO in recycled DnHS has been confirmed by infrared spectrophotometry [3]. Whilst DnHS (2.0 M in xylene) itself does not extract appreciable amounts of iron(III) from, for example, 0.02 M FeCl<sub>3</sub> in 4.0 M hydrochloric acid, increasing additions of DnHSO cause the extraction to increase markedly (Table 1).

*Table 1. Extraction of iron(III) from 4.0 M hydrochloric acid solutions by 2.0 M DnHS containing various concentrations of DnHSO in xylene at 20°C.*

Concentration of DnHSO (M)	Extraction of iron (%)
0.00	1
0.01	16
0.02	42
0.05	86
0.10	99

The effect of hydrochloric acid concentration on the extraction of iron(III) by DnHSO (0.20 M in xylene) is shown in Figure 1. It can be seen that extraction increases strongly over the region 2-4 M acid, and that extraction-stripping cycles could be carried out over this range.

With respect to the mechanism of extraction of iron(III) from hydrochloric acid solutions, Figure 2 shows the distribution coefficient of iron as a function of the concentration of DnHSO in the organic phase at a constant concentration of HCl (3.6 M) in the aqueous phase. The slope of this plot (3.2) is consistent with an extraction mechanism of the type in which an ion-pair is formed between a trisolvated hydronium ion and the iron(III) chloro-anion:



in which charged species are present in the aqueous phase, and neutral species (including ion-pairs) are in the organic phase.

This type of mechanism lends itself to a simple reversal by contacting the loaded organic phase with water, whereby both deprotonation of the solvated hydronium cation and aquation of the chloro-anion are favoured. The distribution isotherm for the stripping of iron(III) from 0.20 M DnHSO in xylene by water is shown in Figure 3. The McCabe-Thiele construction shows that, for example, iron can be effectively stripped (97%) from an organic phase containing 2 gL<sup>-1</sup> in 3 countercurrent stages at an organic-to-aqueous phase ratio of 15:1 to give an iron(III) chloride solution containing 30 gL<sup>-1</sup> Fe.

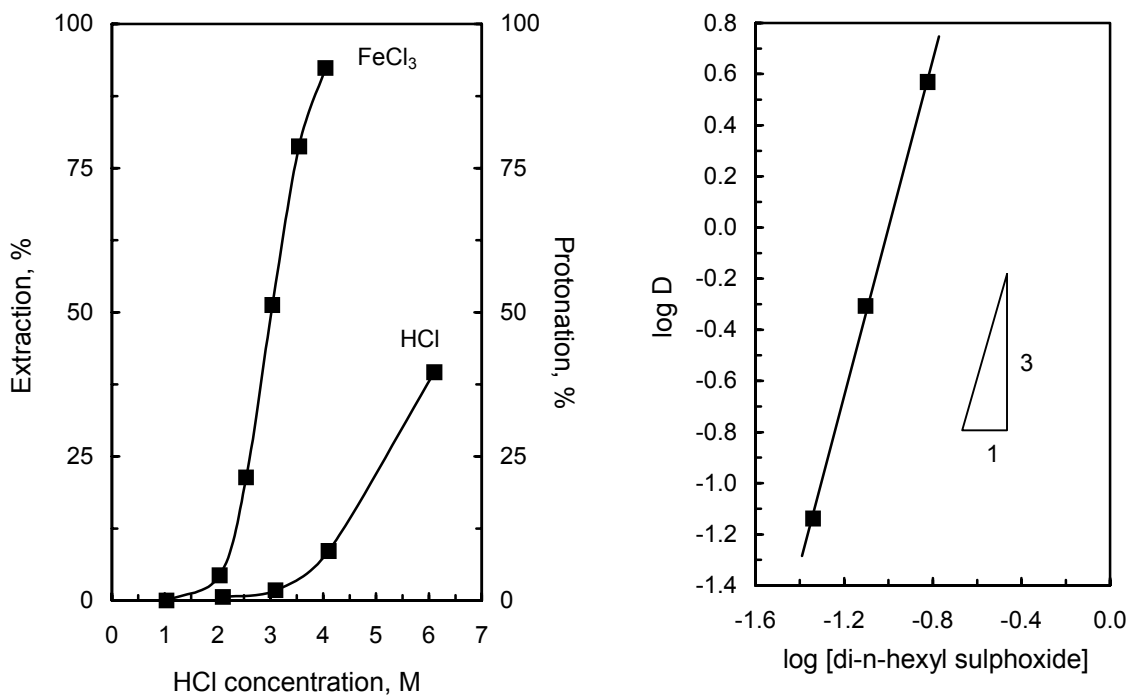


*Figure 1.* Dependence of extraction of iron(III) ( $0.02\text{ M}$ ) and protonation of  $\text{DnHSO}$  ( $0.20\text{ M}$ ) on aqueous concentration of  $\text{HCl}$  at  $20^\circ\text{C}$ .

*Figure 2.* Dependence of distribution ratio ( $D$ ) on  $\text{DnHSO}$  concentration for the extraction of iron(III) from  $\text{HCl}$  ( $3.6\text{ M}$ ) at  $20^\circ\text{C}$ .

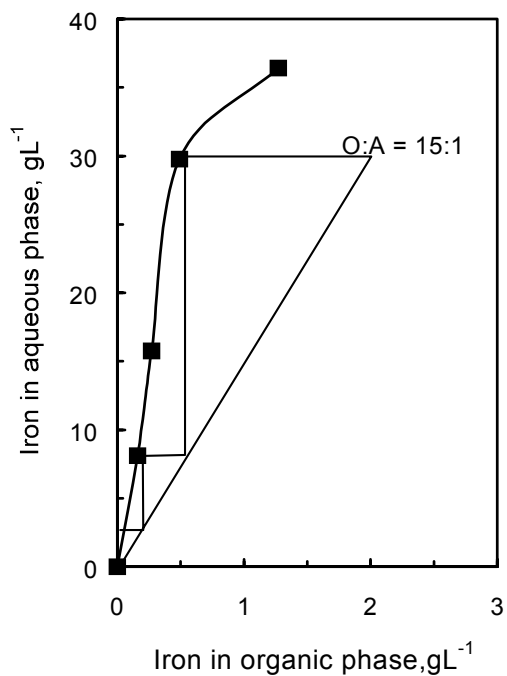


*Figure 3.* Distribution isotherm for the stripping of iron(III) from  $\text{DnHSO}$  ( $0.20\text{ M}$ ) in xylene by water at  $20^\circ\text{C}$ .

### Extraction of Rhodium from Hydrochloric Acid Solutions

Rhodium(III) is not extracted by dialkyl sulphides, yet appears to build up in organic phases that use these reagents for the recovery of palladium [3]. In contrast, dialkyl sulphoxides are reported to extract rhodium(III), albeit slowly [2,4]. The effect of hydrochloric acid concentration on the extraction of rhodium(III) by DnHSO (0.50 M in xylene) at 40°C is shown in Table 2. It can be seen that the extraction of rhodium(III) is low from dilute hydrochloric acid (under which conditions aquated cationic complexes such as  $\text{Rh}(\text{H}_2\text{O})_6^{3+}$  and  $\text{Rh}(\text{H}_2\text{O})_5\text{Cl}^{2+}$  are present), but is markedly enhanced in high concentrations of hydrochloric acid (where anionic complexes such as  $\text{RhCl}_6^{3-}$  and  $\text{Rh}(\text{H}_2\text{O})\text{Cl}_5^{2-}$  predominate). Nevertheless, the organic extracts (which are orange-yellow in colour, and show a molar absorptivity  $\varepsilon = 320$  at 424 nm) do not contain the  $\text{RhCl}_6^{3-}$  species (which is red in colour, and shows  $\varepsilon = 109$  at 529 nm and  $\varepsilon = 134$  at 417 nm when extracted into xylene solutions of trioctylammonium chloride (TOA.HCl), for example [2]).

*Table 2. Effect of hydrochloric acid concentration on extraction of rhodium(III) by 0.50 M DnHSO in xylene at 40°C.*

Concentration of HCl (M)	Extraction of rhodium(%)
0.0	0.4
1.0	7.2
2.0	13.6
4.0	51.7
6.0	95.9

A logarithmic plot of the distribution coefficient for rhodium against the concentration of DnHSO shows a linear slope of 3.9 [2], which is consistent with the formation of a species such as  $(\text{L}_2\text{H}_3\text{O}^+)(\text{RhCl}_4\text{L}_2^-)$ , as proposed earlier by Grant [5]. The dimethyl sulphoxide analogue of this compound has been characterized in the solid state [6]. The slow rate of extraction of rhodium(III) by DnHSO alone (curve 2 in Figure 4) is to be expected in view of the ligand substitution reaction required to form the  $\text{RhCl}_4\text{L}_2^-$  anion.

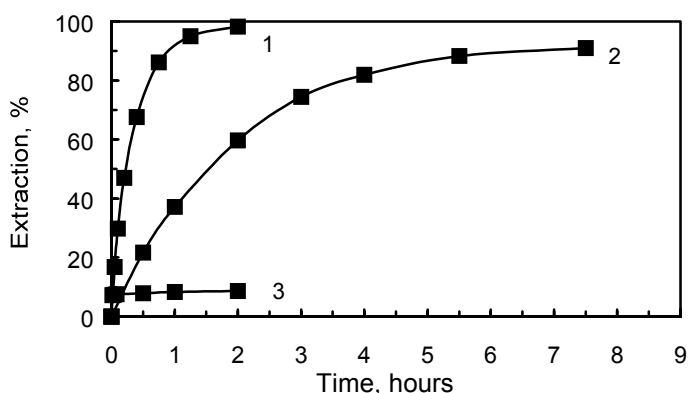
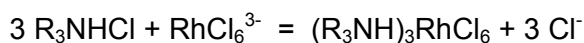
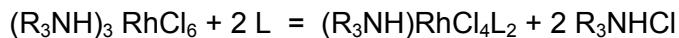


*Figure 4. Rate of extraction of Rh(III) (0.01 M) from HCl (6.0 M) by: (1) 0.25 M TOA + 0.25 M DnHSO, (2) 0.50 M DnHSO, and (3) 0.50 M TOA in xylene at 20°C.*

Interestingly, the rate of extraction of rhodium(III) is considerably enhanced in the presence of an amine salt, such as tri-*n*-octylammonium chloride ( $\text{R}_3\text{NHCl}$ , where  $\text{R} = n\text{-octyl}$ ). This effect (curve 1 in Figure 4) may result from a stepwise process starting with the weak, but rapid extraction of rhodium(III) by the amine salt (curve 3 in Figure 4):



which allows the ligand-substitution reaction to take place homogeneously in the organic phase:



It is pertinent that tri-*n*-octylammonium chloride (TOA.HCl) is commonly added to commercial DnHS in order to increase the rate of extraction of palladium [7].

At this stage, however, it has not been possible to confirm the suggested composition of the extracted rhodium complex by slope analysis, owing to the very slow reaction rates at concentrations low enough to result in less-than-quantitative metal extraction at equilibrium. With regard to stripping the extracted rhodium complex from the organic phase, various solutions such as hydrochloric acid (0.1 and 10 M), ammonia (2 M) and dimethyl sulphoxide (1.4 M) were ineffectual. However, nearly quantitative stripping (99%) was achieved using sodium nitrite solution (1 M) in 30 min. contacting at 45°C. The  $Rh(NO_2)_6^{3-}$  complex so formed can be re-converted to  $RhCl_6^{3-}$  by heating the strip liquor with an equal volume of concentrated hydrochloric acid to drive off nitrogen oxides.

### Extraction of Palladium(II) from Hydrochloric Acid Solutions

The extraction of palladium(II) from 4 M hydrochloric acid by pure DnHS (0.13 M) is shown in Figure 5 (curve 1). The rate of extraction is increased considerably by the addition of a relatively small concentration (0.01 M) of DnHSO (curve 2), although this concentration of the sulfoxide alone extracts palladium very weakly (curve 3).

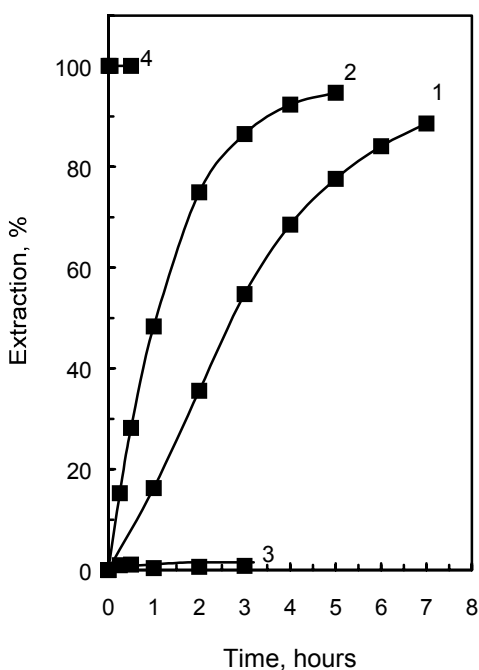


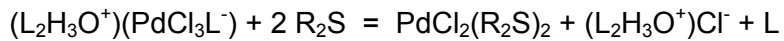
*Figure 5. Rate of extraction of Pd(II) (0.01 M) from HCl (4.0 M) by (1) 0.13 M DnHS, (2) 0.13 M DnHS + 0.01 M DnHSO, (3) 0.01 M DnHSO, and (4) 0.13 M DnHS + 0.01 M TOA.HCl.*

It was shown previously [2] that the distribution data for the extraction of palladium(II) by dialkyl sulfoxides are consistent with the extraction of the neutral complex  $PdCl_2L_2$  at low hydrochloric acid concentrations (1-2 M), and the ion-pair complex  $(L_2H_3O^+)(PdCl_3L^-)$  at higher concentrations (4-6 M). This change in the mechanism of extraction can be ascribed to the increasing extent of protonation of the weakly basic sulfoxide in the region above

about 3.5 M hydrochloric acid (shown in Figure 1). The presence of this ion pair in the organic phase evidently allows the normally slow interfacial reaction for the extraction of palladium(II) by DnHS [7],



to be replaced by the faster homogeneous process,



Since the formation of the  $(\text{L}_2\text{H}_3\text{O}^+)$  cation increases with increasing acidity, the enhancement in the rate of extraction of palladium would be expected to increase accordingly. This was found to be the case in the extraction of palladium by mixtures of DnHS (0.13 M) and DnHSO (0.01 M), the rate of which increased more than twofold over the range 4 to 6 M hydrochloric acid (times of 26 min and 61min to 50% extraction, respectively).

The catalytic effect is understandably less than that caused by the addition of the corresponding amount (0.01 M) of TOA.HCl (Figure 5, curve 4), since the TOA cation ( $\text{R}_3\text{NH}^+$ ) remains in the protonated form even at very low acidities.

## CONCLUSIONS

Some specific features that were observed when di-*n*-hexyl sulphide was used for the recovery of palladium from PGM chloride solutions (co-extraction of iron, build-up of rhodium on the organic phase, and increasing rate of palladium extraction) can be rationalized with reference to the presence of di-*n*-hexyl sulphoxide in the organic phase.

## ACKNOWLEDGEMENT

This paper is published by permission of Mintek.

## REFERENCES

1. J. S. Preston and A. C. du Preez (1996), *Solv. Extr. Ion Exch.*, **14**, 755-772.
2. J. S. Preston and A. C. du Preez (2001), *J. Chem. Tech. Biotechnol.*, submitted.
3. K. C. Sole (2000), Personal communication.
4. P. A. Lewis, D. F. C. Morris, E. L. Short and D. N. Waters (1976), *J. Less-Common Metals*, **45**, 193-214.
5. R. A. Grant (1990), Precious Metals Recovery and Refining, L. Manziek (ed.), International Precious Metals Institute, Allentown, PA, pp. 7-39.
6. B. R. James, R. H. Morris, F. W. B. Einstein and A. Willis (1980), *J.C.S. Chem. Comm.*, 31-32.
7. S. Daamach, G. Cote and D. Bauer (1987), Separation Processes in Hydrometallurgy, Pt. 2, G. A. Davies (ed.), Ellis Horwood, Chichester, pp. 221-228.



## RECOVERY OF AG AND AU FROM AQUEOUS THIOUREA SOLUTIONS BY LIQUID-LIQUID EXTRACTION

M. S. Dzul Erosa, R. Navarro Mendoza,  
T. I. Saucedo Medina, G. Lapidus Lavine\* and M. Avila-Rodríguez

Instituto de Investigaciones Científicas, Universidad de Guanajuato, Mexico

\* Depto. de Ing. de Procesos e Hidráulica, Universidad Autónoma Metropolitana, Mexico

In order to replace  $\text{CN}^-$  ions in the leaching of gold and silver, systems which employ thiourea have been investigated. In this paper, the results of silver and gold ion recovery, by liquid-liquid extraction, from aqueous thiourea solutions which originate from ore dissolution processes are discussed. The influence of thiourea on the extraction efficiency of the metal ions is studied. The highest extractions in the presence of thiourea were obtained when the alkylthiophosphinic acids Cyanex 302 and Cyanex 301 were used. To elucidate the nature of the species extracted into the organic phase, a simple thermodynamic model of extraction is proposed for the case of the extraction of gold(I) from  $\text{H}_2\text{SO}_4$ /thiourea media. In this model, the complexation of the metal ion with thiourea in the aqueous phase is taken into account through a side reaction coefficient.

### INTRODUCTION

Due to its toxicity, there has been a movement in the gold and silver industry to limit the use of cyanide in leaching systems. Leaching studies performed with thiourea solutions have shown satisfactory results [1, 2], and utilization on an industrial level may be possible if Ag(I) and Au(I) are recovered from the thiourea solution and passed on for electrowinning of both metals. Aqueous thiourea leaching solutions contain appreciable quantities of thiourea and Fe(III), which is used as an oxidant. The system is complex and requires the development of a process which permits gold and silver extraction, as well as the recycling of the thiourea solution back to the leaching step. Liquid-liquid extraction may be useful for this purpose since it is a versatile separation technique which may be easily adapted to industrial scale.

Diverse extraction systems in different acid media have been reported in the literature for Au(III). Extractants such as Cyanex 923, Cyanex 921 and Cyanex 471X have been used in HCl and cyanide media with favorable extraction results [3-6]. In the case of Ag(I), Cyanex 301 has been used in HCl and  $\text{H}_2\text{SO}_4$  media [7] and in nitrate media [8]. However, stripping of the silver was very difficult. Neutral ligands, such as acidic alkylthiophosphinic and alkylthiophosphinic esters, have been employed for silver extraction [9]. Cyanex 471 (triisobutyl phosphine) has also been studied as an extractant for Ag(I) in nitrate [10, 11] or concentrated HCl [12-14] media. The results obtained from these studies indicate that Cyanex 471 shows high affinity and selectivity for the Ag(I) ion in the different media. However, the extraction efficiency is limited in the presence of thiourea [14].

In the present work, results of gold and silver recovery from aqueous thiourea solutions by liquid-liquid extraction are presented. Different extractants were studied and the influence of the thiourea on the extraction efficiency was analyzed. In order to determine the nature of the extracted species in the organic phase, a simple thermodynamic model of extraction is proposed. In this model, the aqueous-phase metal ion (gold or silver)-thiourea complexes are considered using a side reaction coefficient.

## EXPERIMENTAL

All reagents used were analytical grade. The extractants studied in this paper were bis(2,4,4-trimethylpentyl)phosphinic acid (Cyanex 272), bis(2,4,4-trimethylpentyl)dithiophosphinic acid (Cyanex 301) and bis(2,4,4-trimethylpentyl)thiophosphinic acid (Cyanex 302), all of which were supplied by Cytec (Canada). The trioctylamine (Alamine 300) and the 7-(4-ethyl-1-methyloctyl)-8-hydroxyquinoline (LIX 26) were supplied by Cognis. The bis(2-ethylhexyl)-phosphoric acid (DEHPA), the 2-ethylhexyl phosphoric acid (EHPA) and the Ionquest 801 (2-ethylhexyl phosphoric acid, mono-2-ethylhexyl ester), were supplied by Rhodia. The organic phase consisted of the extractant diluted to different concentrations in kerosene containing 10% (V/V) of *n*-decanol. The aqueous phase consisted of the metal ion (Ag(I), Au(I), Fe(II) or Fe(III)) in HNO<sub>3</sub>, HCl or H<sub>2</sub>SO<sub>4</sub>. The volume ratio of the organic phase (*V*<sub>org</sub>) to the aqueous phase (*V*<sub>aq</sub>) was in each case equal to one (*V*<sub>aq</sub> = *V*<sub>org</sub> = 10 mL). The solutions (aqueous phase /organic phase) were shaken with a Cole Palmer 51502 ping-pong shaker at 150 rpm for 90 minutes (25°C), which was sufficient time to reach equilibrium. Once equilibrium was attained, the phases were separated and the concentration of metal ion in the aqueous phase was determined by atomic absorption spectrometry (AAS). The concentrations of metal ion in the organic phase were calculated by mass balance. The pH of the solutions were measured with a Titrino 716 (Metrohm) using a glass electrode.

## RESULTS AND DISCUSSION

### Selection of Extraction System

The affinity of the above mentioned 8 extractants were studied with respect to Au(I), Ag(I), Fe(II) and Fe(III), at pH 2, in the presence and absence of thiourea (0.06 mol/L). These conditions were similar to those originating from gold and silver leaching. Table 1 shows the results obtained.

*Table 1. Comparative extractions of Ag(I), Au(I), Fe(III) and Fe(II) with 0.1 mol/L of different extractants.*

Extractant	%E Ag(I)		%E Au(I)		Fe(III)		Fe(II)	
	NT	T	NT	T	NT	T	NT	T
Cyanex 301	99.0	99.0	91.2	98.2	99.6	95.8	99.7	98.5
Cyanex 302	99.9	99.1	92.6	99.5	98.7	51.7	17.6	11.26
Cyanex 272	41.0	2.9	92.6	6.5	99.6	99.51	99.7	97.3
Ionquest 801	43.8	5.5	89.7	12.9	98.7	73.8	19.4	70.7
LIX 26	54.8	3.33	86.8	2.5	70.3	56.6	97.9	60.8
EHPA	64.8	6.5	89.7	37.5	97.7	97.1	98.5	98.5
DEHPA	94.5	6.9	76.5	11.6	99.6	87.3	47.8	78.1
Alamine 300	50.1	12.9	89.7	11.6	3.0	< 1	14.6	13.11

NT = without thiourea; T = with thiourea

As may be observed, in the absence of aqueous phase thiourea, the extraction efficiencies obtained were all above 40%, except in the case of Fe(III) and Fe(II) extraction with Alamine 300, which were very low. In the presence of thiourea, the Au(I) and Ag(I) extraction efficiencies drastically decrease, except for Cyanex 301 and Cyanex 302, which maintained extractions of about 99%. The reduction in the extraction efficiency in the presence of thiourea may be explained considering the formation of strong Au(I) and Ag(I) complexes with the thiourea in aqueous solution, which impede the transport of the metal ions into the organic phase. Table 1 shows that the sulfur extractants, as electron donors, present a greater affinity for Au(I) and Ag(I) than the other extractants studied. This behavior may be explained by Pearson's hard and soft acids and bases empirical rule. Gold as well as silver show a strong covalent character in their complexes and they are also easily polarizable. Elements of this type are referred to as soft acids. On the other hand, sulfur is considered to be a soft base. Since soft acids form stable compounds with soft bases, stable compounds of Ag(I)/thiourea and Au(I)/thiourea result which reduces metallic ion transfer into the organic phase.

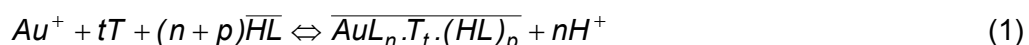
In the cases of Fe(III) and Fe(II) extraction in the presence of thiourea, a lesser influence on extraction efficiency is observed. These species behave as hard acids and the stability of their complexes with thiourea are less stable.

The results contained in Table 1 indicate that Cyanex 301 and Cyanex 302 may be employed for the recovery of Au(I) and Ag(I) from aqueous thiourea solutions. Additionally, for both extractants, selective extraction of gold and silver over iron has been shown in the presence of thiourea [15]. However, Cyanex 301 forms a complex so stable with the Ag(I) ion that stripping and extractant recovery are difficult.

With these results, a possible separation scheme could contemplate a first stage for the selective extraction of excess Fe with Cyanex 272, followed by the selective recovery of Ag(I) and Au(I) from aqueous thiourea with Cyanex 302. Finally, a stripping step would permit recovery of Au(I) and Ag(I).

### **Thermodynamic Extraction Modelling of Au(I) from H<sub>2</sub>SO<sub>4</sub> / Thiourea Media by Cyanex 302**

The extraction model of Au(I) from H<sub>2</sub>SO<sub>4</sub>/thiourea media considers the existence of the thiourea in the complex extracted into the organic phase. In this manner, the overall extraction reaction may be written as follows:



where  $HL$  = bis(2,4,4-trimethylpentyl)thiophosphinic acid (Cyanex 302)

$T$  = thiourea

The overlined species are present in the organic phase.

The above reaction may be represented by an apparent extraction constant,  $K_{ext}^{app}$ :

$$K_{ext}^{app} = \frac{[\overline{AuL_n.T_t.(HL)_p}][H^+]^n}{[Au^+][T]^t [\overline{HL}]^{(n+p)}} \quad (2)$$

Experimentally, one determines the distribution coefficient ( $D$ ), which is defined by the following expression:

$$D_{Au(I)} = \frac{[\overline{Au(I)}]}{[Au(I)]} \quad (3)$$

where  $[Au(I)]$  and  $\overline{[Au(I)]}$  denote the total concentration of metal ion in the aqueous and organic phases, respectively.

The thiourea forms a complex with Au(I) in the aqueous phase ( $\log \beta_2 = 21.5$ ). To consider its influence on the extraction process, the complex coefficient,  $\alpha_{Au(T)}$ , will be defined as follows:

$$\alpha_{Au(T)} = \frac{[Au(I)]}{[Au^+]} = 1 + \beta_2 [T]^2 \quad (4)$$

Introducing  $\alpha_{Au(T)}$  into equation (2) and considering that Au(I) is extracted into the organic phase principally as the complex  $\overline{AuL_n.T_t.(HL)_p}$ , equation (2) takes on the following form:

$$K_{ext}^{app} = \frac{D_{Au(I)} [H^+]^n \alpha_{Au(T)}}{[T]^t [\overline{HL}]^{(n+p)}} \quad (5)$$

Solving for  $D_{Au(I)}$  and  $\alpha_{M(T)}$ , and representing the equation in its logarithmic form:

$$\log D_{Au(I)} + \log \alpha_{Au(T)} = \log K_{ext}^{app} + t \log [T] + (n+p) \log [\overline{HL}] + npH \quad (6)$$

With equation (6) it is possible to determine, using slope analysis, the number of  $H^+$  ions ( $n$ ) involved in the extraction process, as well as the number of thiourea ( $t$ ) and extractant ( $n+p$ ) molecules in the extracted complex. Figure 1 shows the variation of  $\log D_{Au(I)} + \log \alpha_{Au(T)}$  as a function of pH (Figure 1a) and of  $\log [\overline{HL}]$  (Figure 1b).

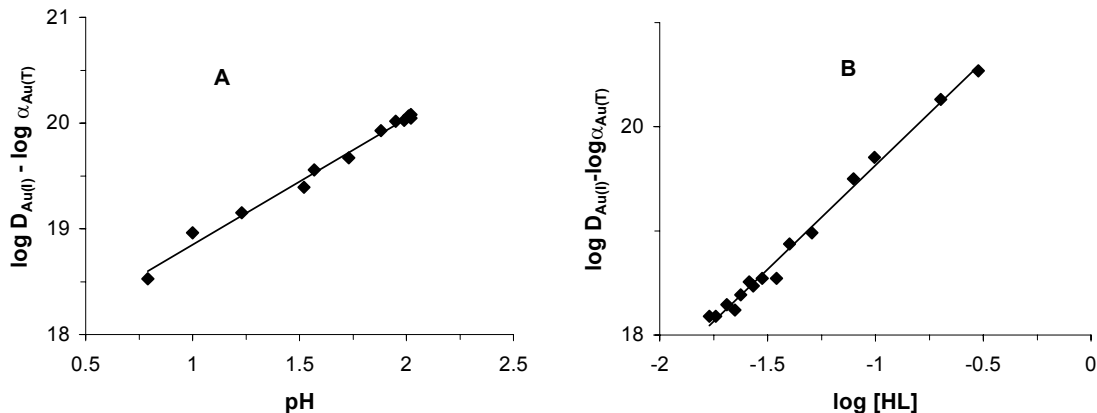


Figure 1. Variation of  $\log D_{Au(I)} + \log \alpha_{Au(T)}$  as a function of (A) pH ( $[Cyanex\ 302] = 0.1\ M$ );  $y = 1.19x + 20.45$ ; (B)  $\log [\overline{HL}]$  ( $pH = 1.7$ ),  $y = 1.99x + 16.48$ .

The analysis of this figure demonstrates that, in the case of the variation of  $\log D_{Au(I)} + \log \alpha_{Au(T)}$  with respect to pH, the experimental points denote a linear function whose slope is close to 1 ( $y = 1.19x + 20.45$ ). From this result, it may be concluded that the number of  $H^+$  ions involved in the extraction process is equal to one.

The variation of  $\log D_{Au(I)} + \log \alpha_{Au(T)}$  with respect to  $\log [\overline{HL}]$  indicates that the slope of the linear function which represents the experimental data is nearly two ( $y = 1.99x + 16.48$ ). For this reason, the number of extractant molecules ( $n+p$ ) in the complex is equal to two.

For the number of thiourea molecules ( $t$ ), the results of the slope analysis of the extraction of Au(I) with ethylhexylphosphoric acid (EHPA) were considered. In this study, the variation of  $\log D_{Au(I)}$  with respect to  $\log [T]$  was analyzed. The results indicate that there is one thiourea molecule in the complex extracted at the same conditions studied. Therefore, the proposed stoichiometry for the Au(I) complex in the organic phase is AuL.T.HL. If Cyanex 302 is considered to be dimerized in the organic phase, the formation of the extracted complex is in accordance with Au(I) complex geometries.

The value of the apparent extraction constant was determined by minimizing the function  $U = \sum (D_{exp} - D_{calc})^2$ . Different stoichiometries for the Au(I)/Cyanex 302/thiourea complex were tested, however the minimum of  $U$  was obtained considering the proposed complex. Therefore, the extraction reaction is proposed to be the following:



The value of the apparent extraction reaction constant is  $K_{ext}^{app} = 10^{21.13}$ .

The variations of  $D_{exp}$  and  $D_{calc}$  as a function of the extractant concentration are shown in Figure 2 in two different media,  $H_2SO_4$  ( $K_{ext}^{app} = 10^{21.13}$ ) and  $HNO_3$  ( $K_{ext}^{app} = 10^{21.31}$ ).

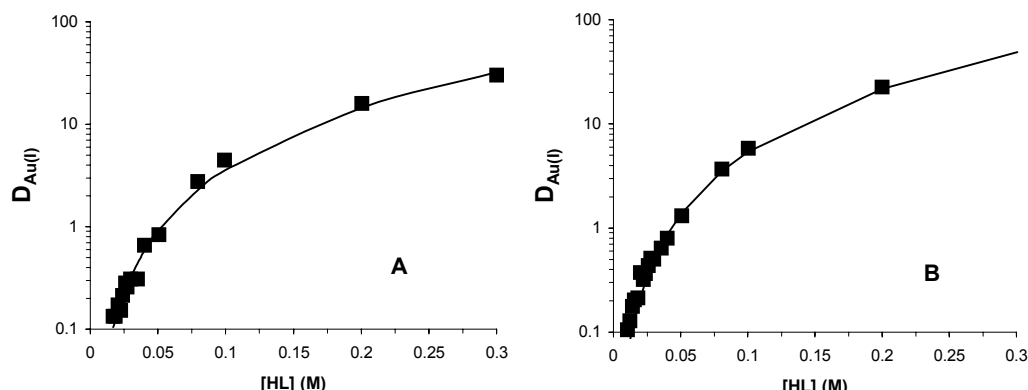


Figure 2. Distribution curves of Au(I). (A)  $H_2SO_4$ /thiourea and (B)  $HNO_3$ /thiourea.  $pH = 1.7$ . Experimental data (■), continuous lines represent those obtained from the model.

A satisfactory correlation may be observed between the experimental data and the distribution coefficient values obtained from the model developed in this work.

A similar study was performed for Ag(I) extraction in  $H_2SO_4$ /thiourea media. The variation of  $\log D_{Ag(I)} + \log \alpha_{Ag(T)}$  was analyzed as a function of the solution pH and  $\log [HL]$ . The value of the slope with respect to the pH was found to be close to 1 ( $y = 1.08x + 8.86$ ), showing behavior similar to that of Au(I). However, the function relative to the variation of  $\log [HL]$  showed a line whose slope was approximately 3 ( $y = 2.78x + 14.82$ ). As in the case of Au(I), the estimation of the thiourea participation in the Ag(I) organic phase complex was performed by slope analysis by EHPA.

The proposed stoichiometry for the Ag(I) complex in the organic phase is AuL.T.(HL)<sub>2</sub>. The values of the extraction constants of Ag(I) in the systems  $H_2SO_4$  / thiourea / Cyanex 302 and  $HNO_3$  / thiourea / Cyanex 302 obtained were respectively  $K_{extAg(I)}^{app} = 10^{13.01}$  and

$K_{extAg(I)}^{app} = 10^{13.16}$ . Figure 3 shows the correlation between the experimental data ( $D_{exp}$ ) and those obtained with the extraction model ( $D_{calc}$ ), for the two different media studied:  $H_2SO_4$ /thiourea and  $HNO_3$ /thiourea. As in the case of gold(I), a satisfactory correlation

between the experimental data and the theoretical distribution coefficient values was obtained.

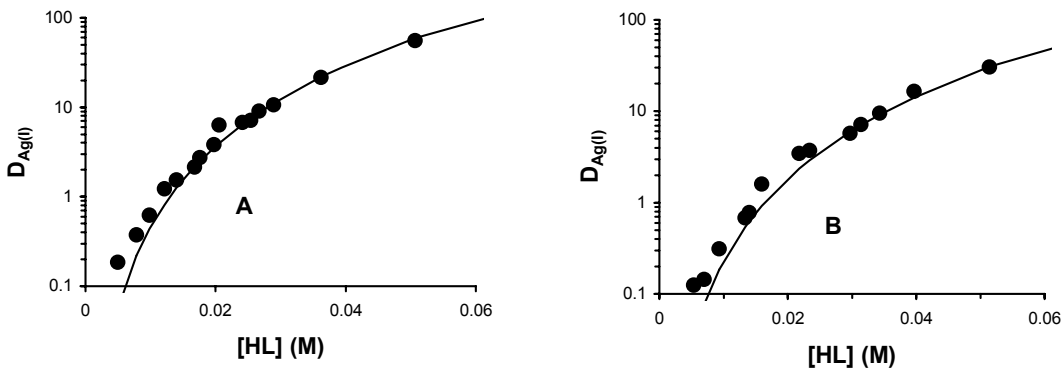


*Figure 3. Distribution curves of Ag(I). (A)  $H_2SO_4$ /thiourea pH = 3.3 and (B)  $HNO_3$ /thiourea. pH = 2.8. Experimental data (■), continuous lines represent those obtained from the model.*

## CONCLUSIONS

Au(I) and Ag(I) recovery from aqueous thiourea solutions is possible with liquid-liquid extraction using Cyanex 302. The extraction model developed, which considers the influence of the aqueous phase Au(I) and Ag(I) thiourea complexes, allows the determination of the nature of the extracted species. The stoichiometries of the complexes extracted into the organic phase were  $AuL.T.HL$  and  $AgL.T(HL)_2$ , in both  $H_2SO_4$  and  $HNO_3$  media.

## ACKNOWLEDGEMENT

This study was financed by CONACYT as part of project 32244-E.

## REFERENCES

1. L. Hernández, P. Mariel, Lapidus G. (1989), Avances en Metalurgia Extractiva No Ferrosa 1988, Universidad de Sonora, Hermosillo, Sonora, Mexico, pp. 248.
2. S. Ubaldini, P. Fornari, R. Massida, C. Abruzzese (1998), *Hydrometallurgy*, **48**, 113.
3. S. Martínez, A. Sastre, N. Miralles, F. J. Alguacil (1996), *Hydrometallurgy*, **40**, 77.
4. S. Martínez, P. Navarro, A. Sastre, F. J. Alguacil (1996), *Hydrometallurgy*, **43**, 1.
5. S. Martínez, A. Sastre, N. Miralles, F. J. Alguacil (1997), *Hydrometallurgy*, **46**, 205.
6. F. J. Aguacil, C. Caravaca, S. Martínez (1998), *J. Chem Techno. Biotechnol.*, **72**, 339.
7. S. Facon, M. Avila Rodríguez, G. Cote, D. Bauer (1993), *Proc. ISEC '93. Solvent Extraction in the Process Industries*, Society of Chemical Industry, London, pp. 557.
8. K. C. Sole, T. L. Ferguson, J. B. Hiskey (1994), *Solvent Extr. Ion Exch.*, **12** (5), 1033.
9. G. Cote, D. Bauer (1989), *Rev. Inorg. Chem.*, **10** (1-3), 121.
10. K. Ennassee, D. Pareau, M. Z. Benabdallah, G. Durand (1995), *Bull. Soc. Chim. France*, **132** (9), 985.
11. M. Muñoz, X. Ribas, M. Valiente (1991), *Quim. Anal.*, **10** (1), 11.
12. A.P. Paiva, L.M. Abrantes (1994), *Proc. 5th EPD Congress*, G.W. Warren (ed.), The Minerals, Metals and Materials Society, Warrendale, PA pp. 243.
13. A.P. Paiva, L. Lemaire (1996), *Sep. Sci. Technol.*, **31** (19), 2599.
14. L.M. Abrantes, M.C. Costa, A.P. Paiva (1994), *Proc. Hydrometallurgy '94*, Chapman and Hall, London, pp. 409.
15. E.D. Buendía-Cachu, N. Rodríguez-Saldivar, R.L. Vargas-Rivera, G.T. Lapidus (2000), UAM Report. Universidad Autónoma Metropolitana.



## OPPORTUNITIES AND CHALLENGES IN DEVELOPING A SOLVENT EXTRACTION PROCESS FOR RHODIUM BASED ON THE USE OF STANNOUS CHLORIDE

George P. Demopoulos, Yuxing Shang, Elyse Benguerel and Mark Riddle

McGill University, Montreal, Canada

Stannous chloride at a Sn(II)/Rh(III) ratio of (at least) 3 may be used to render rhodium 100% extractable via the formation of Rh(III)-Sn(II)-Cl complexes. A host of extractants may be used to effect the extraction. In this work Kelex 100 is used. The paper reports on the role of stannous chloride in effecting Rh extraction, its interaction with a great variety of impurities, such as Se, Te, Bi, As, Sb, Pb, Cu, Zn, Ni, Co, Fe, and ultimately its role in recovery-stripping of rhodium from the organic phase.

### INTRODUCTION

Rhodium has defied all past efforts to render itself amenable to recovery from refinery chloride solutions by conventional solvent extraction. Its complex coordination chemistry, and in particular its propensity to readily form mixed aquo-chloro complexes of the general formula  $[RhCl_{6-n}(H_2O)_n]^{(3-n)-}$ , has been held responsible for the poor response of rhodium to separation - particular by direct solvent extraction [1]. Hence, research efforts at McGill University have focused on converting these non-extractable mixed aquo-chloro complexes of Rh(III) to extractable ones via the use of "activating" agents. One such agent is stannous chloride [2,3]. In the McGill work the extractant used is Kelex 100 - an alkylated 8-hydroxyquinoline - however, other extractants may be used as well, such as dialkyl sulphides [5], TBP [6], amines [7] or other analogous anionic or solvating extractants. Depending on the amount of stannous chloride used two different Rh-Sn complexes are formed, either  $[RhCl_3(SnCl_3)_3]^{3-}$  at  $Sn/Rh < 6$  or  $[Rh(SnCl_3)_5]^{4-}$  for  $Sn/Rh > 6$  [4]. In an earlier communication [2] it was reported that despite the fact that rhodium may be quantitatively extracted with  $Sn/Rh > 2$  nevertheless it was only at molar ratio  $> 12$  that stripping was possible using a concentrated sulphuric acid medium ( $1.7\text{ M H}_2SO_4 + 1\text{ M Na}_2SO_4$ ) and this via cross-current contacts only. This stripping procedure was not satisfactory since it resulted in a large circulating load of stannous chloride (minimum  $Sn/Rh$  ratio = 12), lack of selectivity against tin and production of very dilute strip liquors. Since then further work was done focusing on the low  $Sn/Rh$  system ( $Sn/Rh = 3-4$ ) and in particular in the area of impurity behaviour and control and identification of alternate stripping methods. It is the object of this paper to outline the progress made in this regard and highlight the opportunities and challenges opened by the use of stannous chloride in the solvent extraction of rhodium.

## ACTIVATION AND EXTRACTION

### Rhodium and Tin

Prior to extraction the rhodium-containing feed liquor is activated by adding  $\text{SnCl}_2$  at a molar ratio  $\text{Sn(II)}/\text{Rh(III)} = 3\text{-}4$ . The selection of this ratio is justified on the basis of the data plotted in Figure 1. The respective activation reaction is:



Typical activation conditions (not optimized) are 15 min reaction at  $70^\circ\text{C}$  or 3 hours at  $25^\circ\text{C}$ . Activation works equally well for fresh or aged rhodium feed solution of a wide HCl/total chloride composition range. Since Sn(II) can be easily oxidized by air care should be exercised to prevent prolonged exposure of activated solutions to air. The rate of oxidation of Sn(II) by air at  $70^\circ\text{C}$  was determined to be  $6 \times 10^{-3}$  M/h while the rate at lower temperature is significantly lower. Finally, as discussed later, a number of impurities may react with stannous chloride hence the Sn(II)/Rh(III) ratio has to be appropriately adjusted.

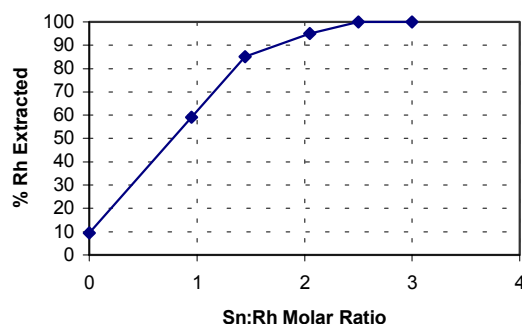


Figure 1. Effect of Sn(II)/Rh ratio on rhodium extraction  
(400 mg/L Rh, 1.5 M HCl - 4 M  $[\text{Cl}^-]_{\text{total}}$ , 2 vol. % Kelex 100).

The extractant used throughout this study was Kelex 100 along with tridecanol as modifier diluted in an aromatic diluent: Solvesso 150. Most of the tests were done with the following organic formulation (unless otherwise stated): 5 vol. % Kelex 100, 15 vol. % tridecanol, 80 vol. % Solvesso 150.

The extraction of the activated rhodium-tin species was found to be very fast and quantitative: 99% extraction in less than 5 minutes. Phase separation was also very fast with no incidence of third phase formation even after a 15 vol. % Kelex 100 solvent was fully loaded with 10 g/L Rh and 50 g/L Sn ( $\text{Sn/Rh} = 3.5$ ). Analysis of the extraction data by slope analysis and complex characterization [3] revealed the following extraction mechanism:



where HQ represents Kelex 100.

Extraction isotherms were obtained and McCabe-Thiele diagrams were constructed for 2 vol. % [3], 5 vol. % and 15 vol. % Kelex 100 solvents. The 5 vol. % extraction isotherm is shown in Figure 2(a). Batch-wise simulation [8] of a 3-stage counter-current extraction circuit (Figure 2(b)) yielded the following "steady-state" results: Rhodium in loaded organic = 2.7 g/L and rhodium in raffinate = 20 mg/L. The respective tin values were: 12.98 g/L and 4 mg/L. The residual rhodium in the raffinate was above the typical < 5 mg/l level due to the (accidentally) lower Sn/Rh ratio used (2.88 vs. the typical 3.5).

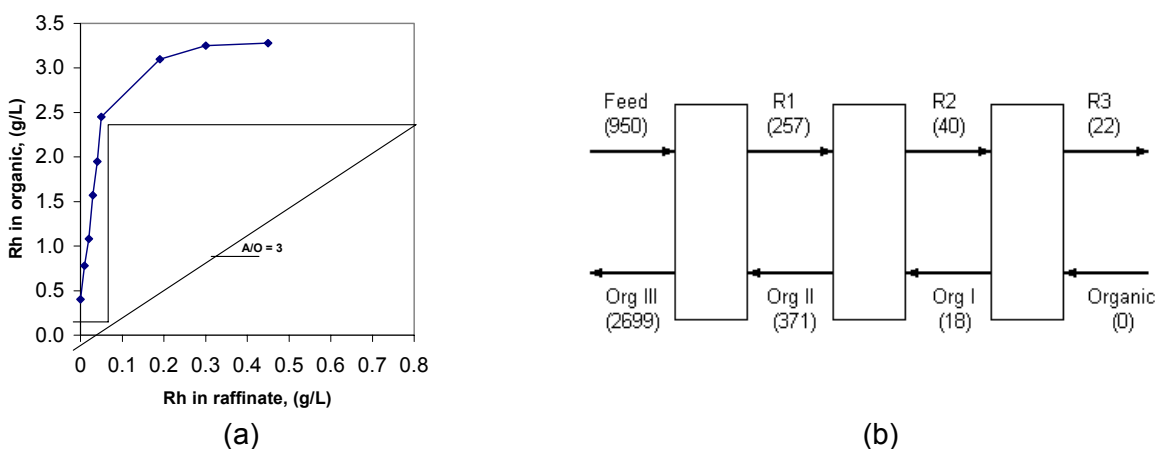


*Figure 2. (a) Rhodium extraction isotherm and McCabe-Thiele diagram for Sn/Rh = 3.57 and 5 vol. % Kelex 100.*

*(b) Batch-wise simulation of 3-stage continuous extraction circuit (AF = 0.95 g/L Rh, 3.17 g/L Sn, A/O = 3, CT = 3 min; numbers in brackets indicate rhodium concentration in mg/L).*

### Impurity Behaviour and Control

The behaviour of a large host of impurity elements that may potentially be present in refinery feedstocks was studied during both activation and extraction stages. The impurities investigated were: Se(IV), Te(IV), Sb(V), As(V), As(III), Bi(III), Cu(II), Fe(III), Zn(II), Pb(II), Ni(II) and Co(II). Since Sn(II) is a relatively strong reductant (the  $E_h$  for the couple Sn(IV)/Sn(II) 1 M HCl/4M total Cl<sup>-</sup> solution is estimated to be 0.0 V), some of the impurity elements were found to react with SnCl<sub>2</sub>. As a result, the concentration of Sn(II) available for the activation of Rh(III) is reduced. In order to understand the reaction between each impurity element and stannous chloride and consequently control impurity co-extraction, a number of titration-type tests were carried out at 70°C (under a nitrogen atmosphere to exclude air) by monitoring the solution potential. Some typical data are shown in Figure 3. Thus according to this work stannous chloride was found to react preferentially with a number of impurity elements such as Se(IV), Te(IV), Sb(V), Fe(III) and Cu(II) prior to formation of the stannous-rhodium complexes. The first two elements were found to precipitate in easily-filterable elemental forms with no rhodium losses by co-precipitation, while Sb, Fe and Cu remained in solution but in their lower oxidation states, i.e., Sb(III), Fe(II) and Cu(I). No reaction was observed between Sn(II) and the other impurity elements.

From a process point of view, the progress of these redox reactions can be controlled by the solution potential. The cut-point potential is 80 mV (vs. Ag/AgCl reference electrode). As soon as this potential is reached, the addition of SnCl<sub>2</sub> is stopped and the solution is filtered to remove the selenium and tellurium precipitates. Subsequent to this SnCl<sub>2</sub> is added to establish a Sn(II)/Rh(III) ratio of 3 hence to effect rhodium activation.

The potential for co-extraction of the various impurity elements after activation was tested by performing single contacts at A/O = 1. The obtained results are shown in Table 1. Scrubbing (single contact) with 1-2 M HCl proved effective in removing the small amounts of impurities extracted with the exception of antimony. It is noteworthy that no rhodium is lost from the loaded organic phase during scrubbing.

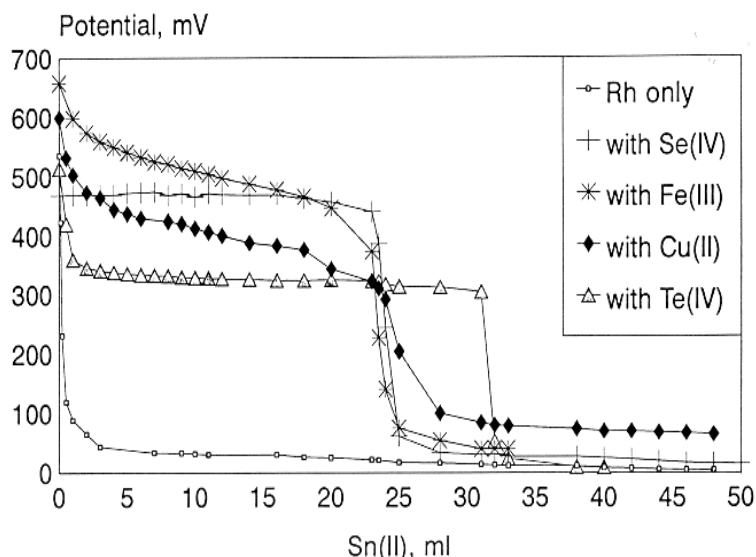


Figure 3. Potential variation during activation in the presence of reacting impurities (70°C, N<sub>2</sub> bubbling; the potential values are wrt Ag/AgCl electrode).

Table 1. Distribution of impurities during activation, rhodium extraction and scrubbing.  
 (Conditions: AF = 1.5 M HCl, 1.5 M MgCl<sub>2</sub>, activated at 70°C; Sn(II)/Rh(III) = 3.5 after the solution potential was reached to < 80 mV, 2 vol. % Kelex 100; A/O = 1 (in both extraction and scrubbing); scrub solution = 2 M HCl.)

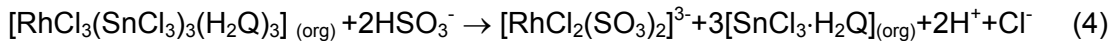
Impurity Species		Concentration (mg/L)		
Feed	After Activation	Activated Feed	Loaded Organic	Scrubbed Organic
Se(IV)	Se(0)	< 5	trace	nil
Te(IV)	Te(0)	< 5	trace	nil
Fe(III)	Fe(II)	210	4	nil
Cu(II)	Cu(I)	181	0	nil
Sb(V)	Sb(III)	794	556	417
As(V)	As(V)	315	23	trace
As(III)	As(III)	259	250	10
Bi(III)	Bi(III)	252	138	27
Pb(II)	Pb(II)	435	21	nil
Zn(II)	Zn(II)	117	23	nil
Ni(II)	Ni(II)	209	4	nil
Co(II)	Co(II)	123	2	nil

## STRIPPING AND RECOVERY

Various stripping approaches and media were tried. One approach was to use an oxidant (such as FeCl<sub>3</sub> in HCl) to cause stripping via destabilization of the extracted Rh(III)-Sn(II) complex by oxidation of Sn(II). Despite elevated temperatures (60°C) applied this approach proved ineffective. Use of stronger oxidants (such as Cl<sub>2</sub> as suggested by Zou *et al.* [6]) was not pursued due to fear of extractant decomposition - use of K<sub>2</sub>Cr<sub>2</sub>O<sub>7</sub> did indeed lead to such decomposition. The other approach tried was the use of sulphite (Na<sub>2</sub>SO<sub>3</sub>) in HCl due to the well-known reducing and complexing properties (including rhodium [9]) of sulphite ligands. This approach proved indeed effective initially when dilute solutions were used. However, as described below, when concentrated solutions were tried precipitation was observed to occur. Finally direct precipitation stripping was attempted with very encouraging results.

### Stripping with $\text{Na}_2\text{SO}_3$ - HCl

The effectiveness of sodium sulphite as rhodium stripping agent in HCl (2-2.5 M HCl is the optimum concentration range) is illustrated in Figure 4(a). Stripping times in the order of 20 to 30 min per contact had to be employed. Slope analysis and complex characterization led to the determination of the following stripping reaction stoichiometry:



The above reaction suggests 100% separation between Rh and Sn. In reality, however, a certain amount of Sn was found to co-strip with rhodium. The Sn/Rh ratio in the strip liquor was found to depend on the O/A ratio (see data in Table 2) and the type of modifier used. Unfortunately D2EHPA was found to form a stable emulsion in the downstream caustic tin scrub stage and could not be used further.

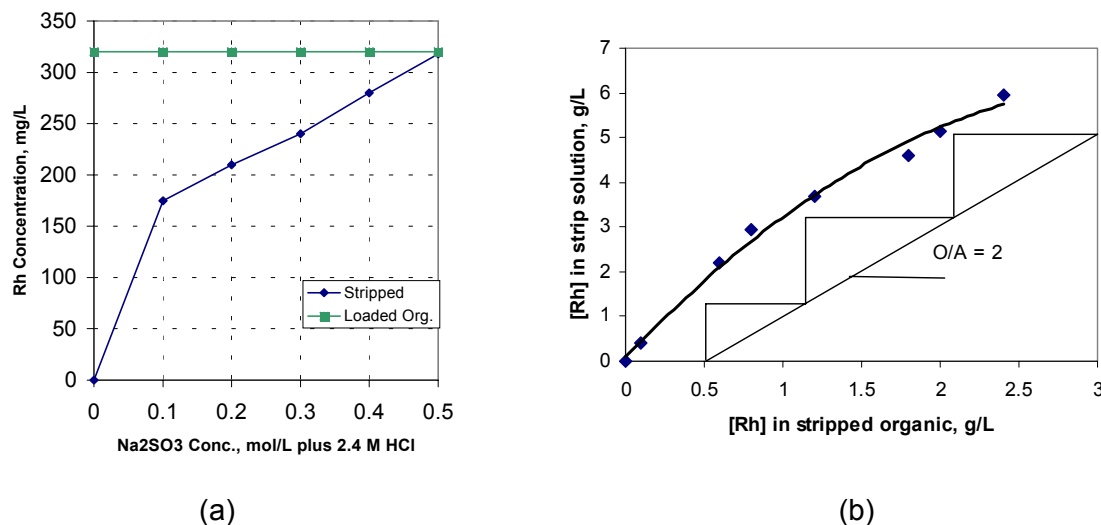


*Figure 4. (a) Effect of sodium sulphite concentration on rhodium stripping (2 vol. % Kelex 100, Sn/Rh = 3.4, CT = 20 min, A/O = 1, 2.4 M HCl).  
(b) Rhodium stripping isotherm and McCabe-Thiele diagram  
for 5 vol. % Kelex 100 (loaded organic = 3.02 g/L Rh, Sn/Rh = 3.2,  
Strip = 0.5 M  $\text{Na}_2\text{SO}_3$  and 2.4 M HCl, CT = 30 min.)*

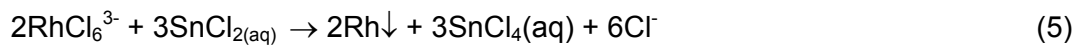
In addition to  $\text{Na}_2\text{SO}_3$  other forms of sulphite salts such as  $\text{Na}_2\text{S}_2\text{O}_5$  gave comparable results but gaseous  $\text{SO}_2$  was not as effective. The stripping isotherm for 5 vol. % Kelex 100 is shown in Figure 4(b). Batchwise simulation [8] of a 4-stage counter-current stripping circuit (based on the isotherm of Figure 4(b) with O/A = 2) yielded the following “steady-state” results: Rhodium in strip liquor = 3.3 g/L and rhodium in stripped organic = 0.65 g/L; rhodium in the loaded organic feed was 3.24 g/L. The respective tin values were 1.9 g/L and 10.12 g/L. This is clearly not a very satisfactory performance. Moreover upon standing for a few hours, rhodium started to precipitate out of the strip liquors. An extensive investigation of the precipitation problem revealed the  $\text{Rh(III)} - \text{SO}_3^{(II)} - \text{Cl}$  strip solutions to be metastable in nature with induction times varying from a few hours to a few days depending on the rhodium concentration and the Sn/Rh ratio in the strip liquor. The precipitate was determined to be a complex  $\text{Rh(III)} - \text{SO}_3 - \text{Cl} - \text{H}_2\text{O}$  salt.

*Table 2. Variation of Sn/Rh ratio in the strip liquor with O/A. (Conditions: 3 g/L Rh loaded in 5 vol. % Kelex 100 - 15 vol. % Modifier-Solvesso 150; 0.5 M Na<sub>2</sub>SO<sub>3</sub> in 2.4 M HCl Strip; Sn/Rh in loaded organic = 3.3).*

O/A	Sn/Rh Ratio in Strip	
	Tridecanol	D2EHPA
1/5	1.6	0.25
1/2	1.2	0.15
1/1	1.0	0.10
2/1	0.7	0.06
5/1	0.3	0.04

### Thermal Redox Stripping

From a thermodynamic point of view, SnCl<sub>2</sub> is capable of reducing RhCl<sub>6</sub><sup>3-</sup> to metal:



$$E^\circ = e_{\text{Rh(III)/Rh(0)}} - e_{\text{Sn/Cl2/SnCl2}} = 0.44 \text{ V}$$

Such reaction, however, was not observed under the conditions of activation applied due to apparently unfavorable kinetics - although partial reduction of Rh(III) to Rh(I) was indeed observed when a high Sn/Rh ratio (= 12) was used [3]. It was, therefore, decided to exploit this redox reaction for the purpose of recovering rhodium directly from the organic phase by thermal treatment in an autoclave. Through a few tests it was determined that this type of redox precipitation stripping is indeed feasible. Thus treating the loaded organic (containing ~1 g/L Rh and Sn/Rh = 3.5) in mixture with 0.2 M HCl (A/O = 1) at 150° for two hours resulted in quantitative precipitation of rhodium (> 95%) as a fine metallic black powder. No tin precipitation took place. No apparent signs of organic decomposition were noticed. To assess the potential for impurity co-precipitation with rhodium, an activated aqueous feed spiked with impurities was thermally treated at 150°C for 2 hours. The results obtained are shown in Table 3. Metal impurities such as Cu, Zn or Pb do not co-precipitate but metalloid impurities (Bi, Sb, As) do, hence they need to be recovered by scrubbing prior to stripping. Of interest are the results of platinum and iridium. No precipitation of iridium apparently occurs, opening the opportunity for Rh/Ir separation - more on this in a following section - but platinum does precipitate and needs to be absent from the feed.

*Table 3. Impurity behaviour during thermal redox precipitation of rhodium from activated aqueous solution (conditions: 150°C, Sn/Rh = 4.2, 2 hours).*

Element	Feed (mg/L)	After Treatment (mg/L)
Rh	908	47
Sn	4375	4413
Cu	700	750
Zn	576	585
Pb	213	226
Bi	180	120
Sb	111	35
As(III)	35	10
Pt	93	21
Ir	100	95

## TIN SCRUBBING AND ORGANIC RECYCLING

Following rhodium stripping/recovery the organic phase is subjected to caustic scrubbing with 1 N NaOH to remove tin. Attempts to recycle the tin-loaded organic directly into the activation stage failed hence the need for tin removal prior to recycling. Caustic scrubbing is effective for both tin species, i.e., Sn(II) and Sn(IV). Typically >80% of tin (and >30% of Sb if present) is recovered in a single contact of 60 minutes with 1 N NaOH at 20°C. Any rhodium left in the stripped organic follows tin, hence the importance of maximizing rhodium recovery during stripping.

Following tin scrubbing, the organic solvent is re-conditioned with 3 M HCl to remove any caustic prior to its recycling to activation. Recycling the same organic (2 vol. % Kelex 100 - 10% tridecanol - Solvesso 150) up to 4 cycles of activation-extraction-stripping with Na<sub>2</sub>SO<sub>3</sub> - tin scrubbing - reconditioning with HCl showed no sign of loss of rhodium extraction-stripping performance. The organic solvent was also subjected to long-term degradation tests in contact with simulated HCl feed and NaOH scrub solutions for up to 60 days with no signs of degradation.

## THE BEHAVIOUR OF IRIDIUM

Rhodium recovery is envisaged to be practiced following platinum/palladium extraction. Iridium may be present in the platinum raffinate liquor, hence its behaviour during extraction of rhodium following activation with SnCl<sub>2</sub> was briefly examined. Iridium in the form of Ir(III) - Sn(II) - Cl complexes was found to be co-extracted along with rhodium but to a lower extent (99% Rh vs. 65% Ir after one contact at A/O = 1 of an aqueous feed containing 988 mg/L Rh and 282 mg/L Ir with Sn/Rh = 4.2). The behaviour of iridium during stripping and scrubbing operations is exemplified with the data of Table 4. In general iridium stayed in the organic except in the case of the caustic scrub. A general deterioration of the phase separation characteristics was observed when iridium was present. Phase separation was facilitated at elevated temperature (50°C).

*Table 4. Iridium behaviour under various scrubbing and stripping operations.  
(Conditions: 5 vol. % Kelex 100, Sn/Rh = 4.2.)*

Loaded Organic (mg/L)	HCl Scrub A/O = 1 (1 contact) (mg/L)	Na <sub>2</sub> SO <sub>3</sub> Strip A/O = 1 (1 contact) (mg/L)	Thermally Stripped Organic 150°C, 2 hrs (mg/L)	NaOH Scrub A/O = 1 (1 contact) (mg/L)
433	<10	<20	420	<20

## CONCLUDING REMARKS

Stannous chloride at a molar Sn(II)/Rh(III) ratio of 3 renders rhodium(III) completely extractable from chloride feed liquors at very high loadings (10-12 g/L Rh(org)) and kinetics (3 min) via the formation of Rh(III)Sn(II)<sub>3</sub>Cl<sub>12</sub><sup>3-</sup> complexes. The extraction of rhodium(III) is selective against common impurities such as Se, Te, Bi, As, Pb, Cu, Zn and Fe but not against PGM (in particular iridium and platinum). Stripping of rhodium using a 0.5 M Na<sub>2</sub>SO<sub>3</sub> - 2.4 M HCl ratio was found to be only partly successful as the resultant Rh-rich strip liquor is metastable in nature causing rhodium to precipitate. An alternate promising stripping approach is the direct precipitation of rhodium in the organic phase via redox coupling of

Rh(III)/Sn(II) at elevated temperatures ( $> 150^{\circ}\text{C}$ ). This thermal redox treatment appears to be selective against tin and iridium. Tin is recovered from the stripped organic by caustic scrubbing. Any rhodium or iridium remaining in the organic phase following stripping reports in the tin caustic scrub solution.

Despite the significant progress made there remains a significant amount of work before the stannous chloride-assisted SX approach to rhodium refining proves successful. Further work is required to consider in detail (i) the behaviour and control of other PGMs and in particular that of iridium; (ii) the testing of new extractants; (iii) the further development of the thermal redox stripping and the determination-control of the rhodium metal purity, and finally (iv) the recovery for re-use of the stannous chloride from the caustic scrub liquor.

### ACKNOWLEDGEMENTS

The support of Inco Ltd., Noranda Inc and the Natural Sciences and Engineering Research Council of Canada is gratefully acknowledged.

### REFERENCES

1. E. Benguerel, G.P. Demopoulos and G.B. Harris (1996), *Hydrometallurgy*, **40**, 135.
2. E. Benguerel and G.P. Demopoulos (1993), *Proc. ISEC '93*, Vol. 1, D.H. Logsdail and M.J. Slater (eds.), Elsevier Applied Science, London, p. 326.
3. E. Benguerel and G.P. Demopoulos (1998), *J. Chem. Tech. Biotech.*, **72**, 183.
4. E. Benguerel, C. Cote, A. Lautie, G.P. Demopoulos and D. Bauer (1995), *J. Chem. Tech. Biotech.*, **62**, 380.
5. M. Sano, J. Shibata, S. Nishimura, S. Ichishi and H. Takao (1993), *Proc. ISEC '93*, Vol. 3, D.H. Logsdail and M.J. Slater (eds.), Elsevier Applied Science, London, p. 1407.
6. L. Zou, J. Chen and X. Pan (1998), *Hydrometallurgy*, **50**, 193.
7. I. Hall and K.R. Koch (1991), *Polyhedron*, **10**, 1721.
8. R.E. Treybal (1980), Mass-Transfer Operations, 3rd edn., McGraw-Hill Book Co., New York, NY, 518-520.
9. G. Newman and D.B. Power (1963), *Anal. Chim. Acta*, **19**, 213.



## EXTRACTION OF CHLOROCOMPLEXES OF Pt AND Pd BY DIAMINES AND THEIR SALTS WITH ORGANIC ACIDS

V.V. Belova, T.I. Jidkova\*, A.I. Kholkin, Yu.Yu. Brenno\* and L.L. Jidkov\*

Kurnakov Institute of General and Inorganic Chemistry of RAS, Moscow, Russia

\*Institute of Chemistry and Chemical Technology of SB RAS, Krasnoyarsk, Russia

The extraction of Pt and Pd from chloride solutions by binary extractants, salts of tetraoctylhexylenediamine with organic acids (di(2-ethylhexyl)phosphoric and di(2-ethylhexyl)dithiophosphoric acids), has been studied. Recovery of Pt from aqueous solutions decreases with increasing pH values in both extractant systems. The extraction of  $\text{PdCl}_4^{2-}$  by diamine dialkylphosphate proceeds through the formation of monomeric and dimeric extracted species in the organic phase depending on the Pd concentration. Palladium distribution in the diamine dialkyldithiophosphate system does not depend on the aqueous acidity. Under conditions of the loaded organic phase, the extracted species involving the diamine cation ( $\text{AmH}_2^{2+}$ ) and Pd complex anion with coordinated dialkyldithiophosphate is formed. With excess of the binary extractant, the dialkyldithiophosphate of palladium,  $\text{PdA}_2$ , is extracted into the organic phase. After separating, Pt and Pd can be stripped from the organic phase by  $\text{NH}_3$  solution in the diamine dialkylphosphate system.

### INTRODUCTION

Earlier we have studied the extraction of Pd chlorocomplexes by chlorides of diamines [1]. Tetraoctylalkylenediamines (Am) were found to be more effective extractants compared to diethylamine and triethylamine. In the extraction of Pd by tetraoctylalkylenediamine chlorides, monomeric  $(\text{AmH}_2)\text{PdCl}_4$  and dimeric  $(\text{AmH}_2)\text{Pd}_2\text{Cl}_6$  extracted species are extracted into the organic phase. Palladium extraction from solutions with high HCl concentration (extractant excess) occurs through an anion-exchange mechanism, forming monomeric extracted species.

Systems involving binary extractants based on monofunctional amines and quaternary ammonium bases are characterized by reversibility of the distribution process. As a result, platinum metals can be stripped from the organic phase more easily than for single extractant systems [2, 3]. We describe here the extraction characteristics of several systems involving diamines and their salts with organic acids.

## EXPERIMENTAL

The complex acids,  $H_2PtCl_6$  and  $H_2PdCl_4$ , were used as the initial compounds. Solutions of diamine chlorides ( $Am\cdot2HCl$ ), di(2-ethylhexyl)phosphate and di(2-ethylhexyl)dithiophosphate of tetraoctylhexylenediamine in toluene were used as extractants. The binary extractants,  $Am\cdot2HA$ , were prepared by mixing equimolar amounts of diamine and organic acid (HA) in toluene. Di-*n*-octylamine ( $R_2NH$ ), tri-*n*-octylamine ( $R_3N$ ), disubstituted ( $R_2N_2H_2(CH_2)_6$ ,  $R = C_8H_{17}$ ) and tetrasubstituted ( $R_4N_2(CH_2)_n$ ,  $R = C_8H_{17}$ ;  $n = 2; 4; 6$ ) diamines were employed. The compounds,  $R_3N$  and  $R_4N_2(CH_2)_n$ , were used as chlorides salts,  $R_3NHCl$  and  $R_4N_2(CH_2)_n\cdot2HCl$ , which were obtained by mixing organic solutions of amine and diamines with 3 M HCl solution for 10 min.

## EXTRACTION OF PLATINUM BY CHLORIDES OF DIAMINES

Disubstituted and tetrasubstituted diamines were used for the platinum extraction. Figure 1 shows that the extraction of Pt chlorocomplexes from 0.1 to 3 M HCl solutions by tetraoctylalkylenediamine chlorides gives percentage recoveries of platinum that are higher than those measured with  $R_2NH$  and  $R_3NHCl$  under comparable conditions. The extraction power of tetraoctylalkylenediamine chlorides was found to be well above that of dioctylhexylenediamine, as well as the extraction power of tertiary amines is higher than that of secondary amines.

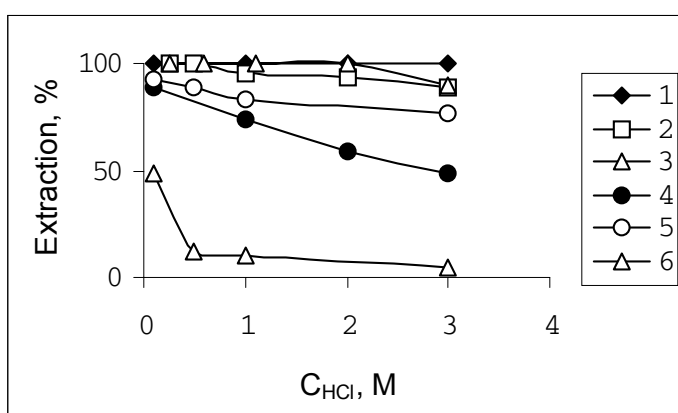


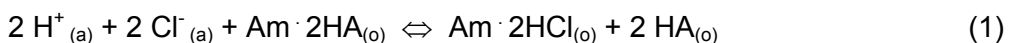
Figure 1. Extraction of Pt by 0.005 M solutions of  $R_4N_2(CH_2)_n\cdot2HCl$  (1-3);  $R_2NH$  (4);  $R_3NHCl$  (5) and  $R_2N_2H_2(CH_2)_6$  (6).  
 $C_{Pt\ init.} = 7 \times 10^{-4} M$ ;  $n = 2$  (1); 4 (2); 6 (3).

Thus, the experimental data showed that tetraoctylalkylenediamines are more effective extractants for platinum metals compared to monofunctional amines.

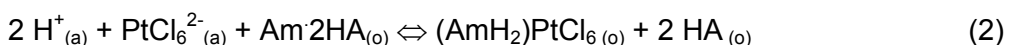
## EXTRACTION OF Pt AND Pd BY SALTS OF DIAMINE WITH ORGANIC ACIDS

In binary extractant systems, distribution of the chlorocomplex acids of platinum metals occurs through a binary or anion-exchange mechanism depending on the state of the binary extractant in the organic phase that is determined by the aqueous acidity and the nature of the extractant [2, 4]. Distribution of the chloride ion between  $Am\cdot2HA$  solutions in toluene and aqueous solutions with different concentrations of  $H^+$  at a constant chloride concentration ( $C_{Cl\ (aq)} = 3 M$ ) was studied. Experimental data showed that the dialkylphosphate of the diamine is mainly in the binary form at an equilibrium pH above 2, and that the

dialkyldithiophosphate is stable at equilibrium pH values above 1 because di(2-ethylhexyl)dithiophosphoric acid is stronger. With mixing of the binary extractant solution and acidic aqueous solutions, binary extraction of HCl occurs:



The extraction of platinum chlorocomplexes by binary extractants based on diamine was studied (Figure 2). The recovery of platinum was found to decrease with an increase in the pH values of the aqueous phase accordingly to the binary extraction regularities of mineral acids [5]. The data on spectrophotometrical studies showed that in the absorption spectra of the organic phases forming in the Pt extraction by binary extractants from aqueous solutions of different acidity, one absorption band at  $\lambda_{\max} = 475$  nm is observed in the visible range, which is characteristic for the spectrum of  $\text{PtCl}_6^{2-}$  complex anion [6]. Taking into account the state of binary extractants, the distribution of platinum in the systems involving salts of diamines with organic acids is described as binary extraction of  $\text{H}_2\text{PtCl}_6$ :



The platinum extraction by the diamine dialkyldithiophosphate proceeds with lower distribution coefficients (Figure 2, curve 2) in comparison with the dialkylphosphate system, due to higher stability of the first extractant.

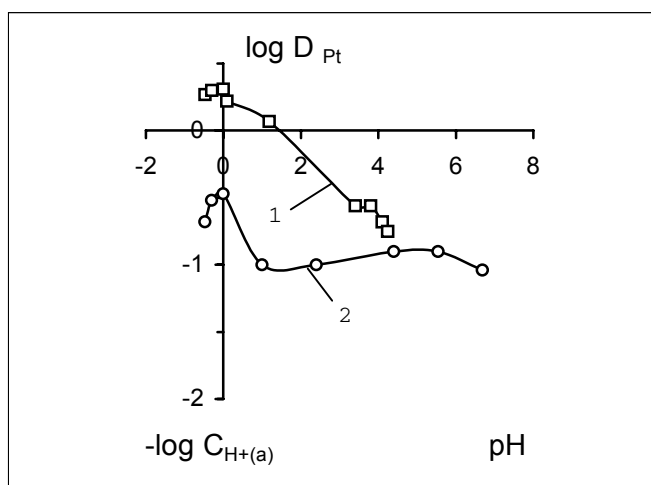


Figure 2. Extraction of Pt from chloride solutions by 0.005 M solutions of dialkylphosphate (1) and dialkyldithiophosphate (2) of tetraoctylhexylenediamine in toluene.  
 $C_{\text{Pt}} = 5.6 \times 10^{-3} \text{M}$ ;  $C_{\text{Cl}^-(\text{a})} = 3 \text{M}$ .

The reversibility of extraction and stripping is characteristic for binary extractant systems. The Pt stripping from the extracts forming in the dialkylphosphate diamine system by a 1 M ammonia solution was found to vary from 40 to 90%, depending on platinum concentration in the organic phase (Table 1).

*Table 1. Stripping of Pt and Pd from the organic phase by 1 M solution of NH<sub>3</sub> in the diamine dialkylphosphate system.*

$C_{M(o)} \times 10^3, M$		Recovery of metal into strip solution, %	
Pt	Pd	Pt	Pd
3.44	3.10	46.8	52.1
3.63	3.30	36.0	47.8
3.24	1.64	40.0	62.2
2.92	1.80	62.5	55.9
1.17		96.5	
1.23		86.7	

The data for the extraction of  $\text{PdCl}_4^{2-}$  by different salts of tetraoctylhexylenediamine are given in Figure 3. In the Pd extraction from acidic solutions ( $3\text{ M HCl}$  – pH ~ 1.5) the extraction power of diamine salts increases in the series: dialkylphosphate ~ chloride < dialkyldithiophosphate. With increasing pH values of the aqueous phase ( $\text{pH}_{\text{eq}} > 3$ ), the extraction of Pd by diamine dialkylphosphate decreases similar to in the binary extraction of mineral acids, while in the diamine dialkyldithiophosphate system,  $D_{\text{Pd}}$  does not change. Thus, in contrast to platinum extraction, palladium is more effectively recovered into the organic phase with diamine dialkyldithiophosphate.

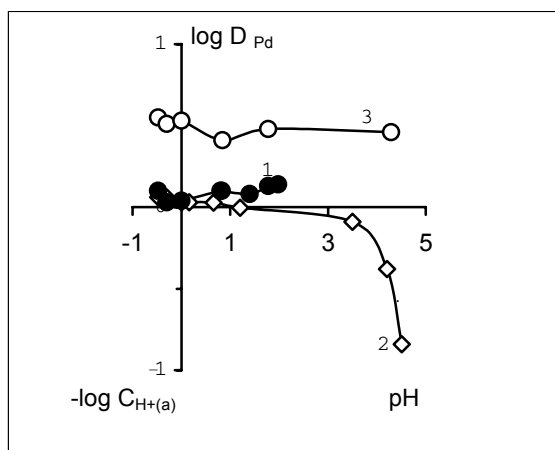
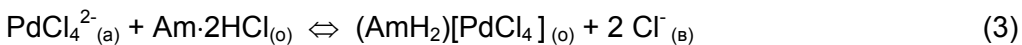
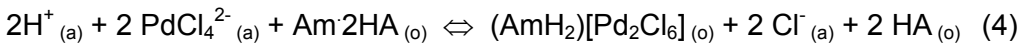


*Figure 3. Extraction of Pd from chloride solutions by 0.005 M solutions of chloride (1), dialkylphosphate (2) and dialkyldithiophosphate (3) of tetraoctylhexylenediamine in toluene.  $C_{\text{Pd}} = 5.6 \times 10^{-3} M$ ;  $C_{\text{Cl}(o)} = 3 M$ .*

The composition of the palladium extracted species was studied by a spectrophotometrical method. Spectrophotometrical data indicate that in the Pd extraction by dialkylphosphate from 3 M HCl solution, the  $\text{PdCl}_4^{2-}$  complex anion is distributed into the organic phase ( $\lambda_{\text{max}} = 476\text{ nm}$  [7]). With decreasing acidity of the aqueous phase, in the spectra of the corresponding extracts, the maximum of absorption is shifted to the low frequency spectra region. At pH > 3, an extracted species with  $\lambda_{\text{max}} = 440\text{ nm}$ , characterized as the spectrum of the dimeric anion,  $\text{Pd}_2\text{Cl}_6^{2-}$ , is extracted into the organic phase. Thus, the distribution of palladium from aqueous solutions of different acidity in the diamine dialkylphosphate system, taking into account the extractant state in the organic phase, can be described as follows:



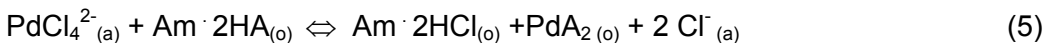
(extraction from acidic solutions)



(extraction from weak acidic solutions).

In the region of pH ~1 to 2, two extracted species of palladium are recovered into the organic phase because the spectra of the corresponding extracts have an intermediate character ( $\lambda_{\max} = 460$  to  $450$  nm). The influence of the concentrations of the binary extractant and palladium on the distribution of  $\text{PdCl}_4^{2-}$  in the diamine dialkylphosphate system was studied. Results obtained showed that with increasing Pd concentration in the organic phase ( $C_{\text{Pd(o)}} : C_{\text{ex.}} \geq 0.5$ ), both monomeric and dimeric species are also extracted ( $\lambda_{\max} \sim 460$  nm).

Unlike the Pd extraction by diamine dialkylphosphate, in the extraction of  $\text{PdCl}_4^{2-}$  by dialkyldithiophosphate, the distribution coefficients do not change with varying aqueous acidity from 3 M HCl to pH ~ 5 (Figure 3, curve 3). The spectra of the corresponding organic phases ( $C_{\text{Pd(o)}} : C_{\text{ex.}} \geq 1$ ) exhibit an absorption band at  $\lambda_{\max} = 415$  nm. In the extraction of Pd by diamine dialkyldithiophosphate under conditions of extractant excess, the extracted species has an absorption band at  $\lambda_{\max} = 466$  nm, which is characteristic for the  $\text{PdA}_2$  spectrum [8]. Thus, when the binary extractant is used in excess, the distribution of Pd from solutions with pH > 1 is described as follows:



Earlier we found that in the extraction of palladium from chloride solutions by dialkyldithiophosphates of tetraoctylammonium and amines under conditions of the loaded organic phase, extracted species involving the alkylammonium cation and the dialkyldithiophosphate anion, such as  $(\text{R}_4\text{N})[\text{PdCl}_2\text{A}]$  and  $(\text{AmH})[\text{PdCl}_2\text{A}]$ , are formed in the organic phase [8]. In the *d-d* spectra of such palladium complexes, the absorption band of the  $\text{PdCl}_4^{2-}$  complex anion ( $\lambda_{\max} = 476$  nm) shifts to lower frequencies. On the basis of these data, we supposed that the extracted species with  $\lambda_{\max} = 415$  nm also involves a complex anion with mixed ligands. Chemical analysis of the saturation product obtained in the Pd extraction by diamine dialkyldithiophosphate indicated the ratio of  $C_{\text{Pd (o)}} : C_{\text{e (init.)}}$  is close to 2. Thus, the composition of the extracted species can be presented as  $(\text{AmH}_2)[\text{PdCl}_2\text{A}]_2$ . The distribution of palladium chlorocomplexes from acidic and weak acidic solutions, taking into account the state of the binary extractant in the organic phase, can be represented respectively:



Table 2 shows compositions of the extracted species of Pt and Pd forming in the systems involving salts of diamines.

*Table 2. Pd(II) and Pt(IV) species extracted by salts of diamines from 1 M HCl.*

Extractant	Extracted species	
	Loaded organic phase	Excess of extractant
Am:2HCl	(AmH <sub>2</sub> )[PdCl <sub>4</sub> ] (AmH <sub>2</sub> )[Pd <sub>2</sub> Cl <sub>6</sub> ] (AmH <sub>2</sub> )[PtCl <sub>6</sub> ]	(AmH <sub>2</sub> )PdCl <sub>4</sub> (AmH <sub>2</sub> )[Pd <sub>2</sub> Cl <sub>6</sub> ] (AmH <sub>2</sub> )[PtCl <sub>6</sub> ]
Am:2HA	(AmH <sub>2</sub> )[PdCl <sub>2</sub> A] <sub>2</sub> (AmH <sub>2</sub> )[PtCl <sub>6</sub> ]	PdA <sub>2</sub> (AmH <sub>2</sub> )[PtCl <sub>6</sub> ]

## NOMENCLATURE

Am tetraoctylhexylenediamine ((C<sub>8</sub>H<sub>17</sub>)<sub>4</sub>N<sub>2</sub>(CH<sub>2</sub>)<sub>6</sub>)  
A<sup>-</sup> di(2-ethylhexyl)dithiophosphate anion ((C<sub>8</sub>H<sub>17</sub>O)<sub>2</sub>PSS<sup>-</sup>)

## ACKNOWLEDGEMENTS

Financial support from the Russian Foundation for Basic Research (grant N 00-03-32036) is gratefully acknowledged.

## REFERENCES

1. V. V. Belova, T. I. Jidkova, S. A. Vasilevich and A. I. Kholkin (1997), *Solv. Extr. Ion Exch.*, **15**, 1023-1042.
2. V. V. Belova and A. I. Kholkin (1998), *Solv. Extr. Ion Exch.*, **16**, 1233-1255.
3. A. I. Kholkin, V. V. Belova, G. L. Pashkov, I. Yu. Fleitlikh and V. V. Sergeev (1999), *J. Mol. Liquids*, **82**, 131-146.
4. V. V. Belova, A. I. Kholkin and T. I. Jidkova (1997), *Zh. Neorg. Khim.*, **42**, 1922-1926.
5. A. I. Kholkin and V. I. Kuzmin (1982), *Zh. Neorg. Khim.*, **27**, 2070-2074.
6. C. K. Jorgensen (1959), *Mol. Phys.*, **2**, 309-332.
7. L. I. Elding (1972), *Inorg. Chim. Acta*, **6**, 647-651.
8. V. V. Belova, A. I. Kholkin and T. I. Jidkova (1999), *Solv. Extr. Ion Exch.*, **17**, 1473-1491.



## COMMISSIONING OF THE NEW HARMONY GOLD REFINERY

**Angus Feather, Wendy Bouwer, Ronel O'Connell and Johan le Roux \***

Mintek, Randburg, South Africa

\*Harmony Gold Mining Company Ltd., South Africa

In 1997, a 24-tonne per annum gold refinery was commissioned at Harmony Gold Mine in South Africa making use of solvent-extraction technology to produce gold of 99.99% purity. Feed material for the refinery was cathode sludge arising from carbon-in-pulp/electrowinning circuits, zinc precipitate or atomised doré bullion.

Following Harmony's purchase of a further five gold mines, a larger refinery capable of producing 70 tonnes per year of high-purity gold, has been installed. Implementation of this process results in significant cost benefits compared with conventional smelting/toll-refining. Any premiums on the sale of high-purity gold products are realised. Harmony has established its own brand name.

### INTRODUCTION

The Minataur™ Process (Mintek Alternative Technology for Au Refining) is a solvent-extraction (SX) route for the purification of gold from chloride media. The process is capable of treating a range of gold-containing feed materials to produce refined gold of 99.99% purity. The process is selective for gold over silver, base metals, and minor quantities of platinum-group metals (PGMs). Following evaluation in two pilot-plant campaigns [1-3], a refinery with a production capacity of 24 tonnes of gold of 99.99% purity per annum was constructed at Harmony Gold Mine [4]. With the subsequent acquisition of other gold mines in South Africa by the Harmony group, a larger refinery was required to cope with the additional throughput of gold. A refinery to produce approximately 70 tonnes per annum has recently been constructed and commissioned.

### PROCESS DESCRIPTION

The gold plants that supply feed material to the Harmony Refinery operate conventional gold-processing plants, typical of most South African gold mining operations [5]. The ore is treated by run-of-mine milling followed by cyanidation in a carbon-in-pulp (CIP) circuit. Gold in the pregnant solution from elution of the loaded carbon is electrowon onto stainless-steel mesh cathodes, producing finely divided cathode sludge containing between 50 and 85% gold, or cemented from solution using zinc dust to produce a gold sludge containing approximately 40% gold.

The Minataur™ process as applied at the Harmony Refinery, uses dried cathode sludge or zinc precipitate as feed material, eliminating the traditional smelting and toll refining. The flowsheet of the Harmony Refinery is shown in Figure 1.

The gold content of the feed (~ 75%) is dissolved by leaching in HCl under oxidising conditions, using conventional technology [6]. The bulk of the base metals and PGMs are also solubilised under these conditions. Most of the silver precipitates as silver chloride and, along with any silica or fine carbon dust, is filtered off as a solid residue. This material is treated in a separate plant to recover residual gold and purify the silver using conventional anode casting followed by standard electro-refining technology.

Gold is selectively extracted from the leach solution by SX, while other soluble metal ions report to the raffinate. Small quantities of co-extracted impurities are scrubbed from the loaded organic phase before it is stripped to produce a purified, concentrated gold chloride solution. The stripped organic phase is recycled to the extraction circuit. Approximately 75% of the HCl-rich raffinate from the extraction section is returned to the leach, with a 25% bleed to control the build up of impurities in the leach/SX circuit and to preserve the solution balance in the plant.

Gold is recovered as a metal powder after reduction with sulphur dioxide from the loaded strip liquor. This step is relatively selective for gold over base metal impurities, and gold of 99.99% purity is produced.

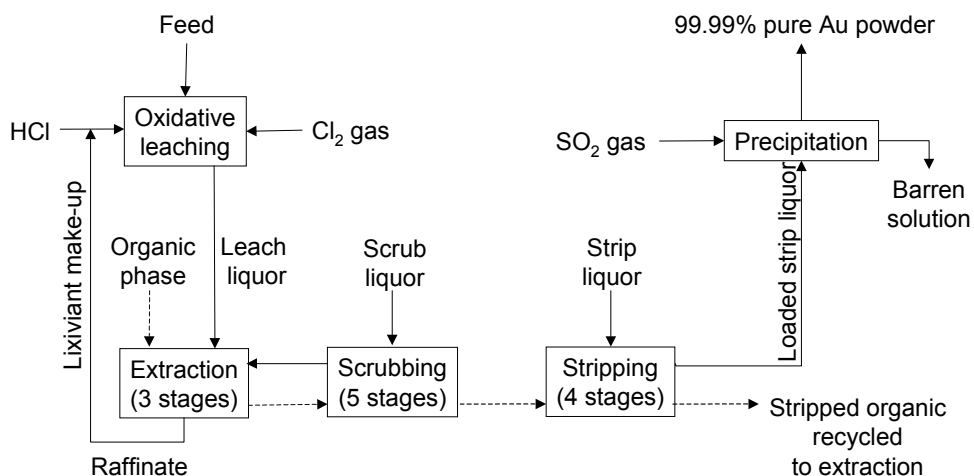


*Figure 1. Process flowsheet for the Harmony Refinery.*

## PLANT CONSTRUCTION

The Engineering Services Division of Mintek carried out the engineering, design and construction of the Harmony Refinery. The manufacture of some specialist items of equipment was contracted to local suppliers. Harmony Refinery is designed to treat approximately 70 tonnes of gold per year, operating a single 8-hour shift per day, with expansion capacity to accommodate 150 tonnes of gold per year.

The plant was constructed over a 7-month period. As the refinery staff at Harmony are highly skilled in the refining process, process and plant commissioning as well as the acceptance run was completed in three weeks. A new laboratory constructed to ISO 9001 standards is currently under consideration for the analysis of all samples for process control, and also to ensure the control of final product quality. Gold meeting the design specification for purity (99.99%) was produced from the second batch.

## OPERATING RESULTS

### Leaching

It is planned that Harmony Refinery will treat material from a variety of gold plants in South Africa. All feed materials are dried, passed through a sampling tower into a hopper for transfer into the leach reactor, using an overhead crane. There are currently two batch leach reactors, each capable of treating 100 kg of fine gold at a time.

The leach reactor is charged with approximately 100 kg of fine gold, irrespective of the impurities in the feed material. Based on the mass of gold in the feed material and the HCl concentration of the SX raffinate, appropriate volumes of fresh HCl and raffinate are added to the leach reactor. The liquid:solid ratio is calculated to produce leach liquor with a gold concentration of approximately 65 g/L. The reactor is pressurised at 0.4 bar with chlorine gas to provide the oxidising conditions necessary for gold dissolution. An inducing impeller is used to maintain the required gas dispersion in the leach reactor. The reactor is sealed using a standard double mechanical seal on the impeller shaft. The leach is done at ambient temperature with no provision for heating. The temperature increases to approximately 45 °C during the leach.

Any solids left at the end of the leach are mainly silver chloride, with minimal unleached gold, silica and carbon fines from the CIP process forming the remainder of the leach residue. The solids are removed from the leach liquor by filtration using a plate and frame filter press. Entrained leach liquor is washed from the filter cake with SX raffinate. The filter cake is refined using conventional electrolytic technology to recover the silver as high-purity crystals and any residual gold in the form of a finely divided powder. This can then be returned to the gold-refining leach circuit. A summary of the leaching conditions and typical results is shown in Table 1.

*Table 1. Batch leaching performance.*

Typical leaching time	2.5 – 5 h
HCl concentration	5.5 M
Average feed gold concentration	75%
Leaching efficiency	> 99%
Cl <sub>2</sub> consumption	0.7 kg per kg of gold

### Solvent Extraction

The SX plant both concentrates and purifies the gold. The SX plant comprises three extraction, five scrub and four strip stages. The stages are conventional box-type mixer settlers equipped with facility for the internal recycle of aqueous solutions. Solutions are fed to the SX plant by positive displacement peristaltic pumps. Table 2 shows the typical steady-state compositions of the leach liquor fed to the SX plant, with the corresponding loaded strip liquor and raffinate produced.

*Table 2. Typical compositions of leach liquor and loaded strip liquor.*

Sample analysis	Au	Ag	Cu	Fe	Pb	Se
Leach liquor (g/L)	65	0.5	8.3	0.2	1.3	0.02
Loaded strip liquor (g/L)	82	< 0.001	< 0.001	< 0.001	< 0.002	0.002
Raffinate (g/L)	0.1	0.5	8.2	0.2	1.2	0.02

Typical operating efficiencies for the SX circuit at steady-state conditions are given in Table 3. There is little incentive to reduce the gold concentration of the raffinate below 0.1 g/L, as 75% of this solution is recycled to the leach. Gold in the raffinate bleed (25%) is recovered from this stream in the CIP adsorption circuit.

Since treating a feed material with a high gold content minimises the proportion of the raffinate, which must be bled to control impurities, efforts are underway at Harmony to improve the operation of the upstream circuits and thereby increase the grade of the refinery feed material.

*Table 3. Operating efficiency of SX circuit.*

<i>Extraction</i>	
Extraction efficiency for gold (%)	> 99
Organic loading of gold (g/L)	64
Gold concentration of raffinate (g/L)	0.1
<i>Stripping</i>	
Stripping efficiency (%)	> 99.7
Au : impurities in loaded strip liquor (%)	> 99.97

### Precipitation

The precipitation of gold from the loaded strip liquor is carried out once per shift in a batch operation by sparging SO<sub>2</sub> gas through the solution. The reaction goes readily to completion and introduces a further degree of selectivity. Typical operating conditions and results are indicated in Table 4.

*Table 4. Operating efficiency of precipitation.*

Gold concentration in loaded strip liquor (g/L)	82
Gold concentration in precipitation barren (g/L)	0.002
Reduction efficiency (%)	> 99.9
Reaction time (h)	1.5 – 2

The gold powder is thoroughly washed with water to remove entrained waste solution from the reduction, then dried in a rotary drier at approximately 450 °C. The gold recovered has a powder morphology, and average particle size of < 100 µm, although some agglomeration does occur due to the nature of the material.

Analysis of the gold is carried out on site in the refinery using a spark spectrometer in SAFT mode (spark analysis for traces). Table 5 shows typical analyses of the major impurities of the gold produced at Harmony. The ASTM specification for 99.99% gold is shown for comparison (ASTM, 1986). All gold is produced to 99.99% purity. Some of the gold is then diluted for specialised products, such as the ten-tola bars, which are generally sold at a gold specification of 99.9%.

*Table 5. Typical analysis of Harmony PureGold.*

Element (ppm)	Ag	Bi	Cr	Cu	Fe	Mn	Ni	Pb	Pd	Sn	Au <sup>†</sup>
ASTM, 99.99%	90	20	3	50	20	3	3	20	50	10	99.99
Harmony	14	0.1	3	6	6	0.4	1.5	1.2	2	2.6	> 99.99

<sup>†</sup> Au calculated by difference

### Gold Products

The dried powder is weighed into batches of predetermined mass and melted in an induction furnace before being cast into products. All Harmony's gold products are marketed internationally by Pechiney, who have successfully established the Harmony brand in certain areas of the world. A variety of bars, including ten-tola, kilo, good-delivery bars and granules for the jewellery industry are produced. Market conditions determine the product range.

## PROCESS ECONOMICS

### **Capital and Operating Costs**

The capital and operating costs for the new Harmony Refinery are shown in Table 6. The battery limits for the refinery commence with the reception of impure gold material to the plant, and end with dry high-purity gold powder for bar casting or granule manufacture. The capital cost includes commissioning fees. In estimating the fixed costs, only labour costs directly attributable to the operation of the refinery are included. Infrastructure development, maintenance and insurance have been excluded. Effluent is discharged at the refinery battery limits. The operating costs do not include amortisation of the capital costs. All costs relate to South African conditions as at April 2001 and are quoted in South African Rands (R).

*Table 6. Capital and operating costs for Harmony Refinery.*

Item	Cost
Capital Cost	R 8 000 000
Operating Costs (per kg gold)	R 56
Fixed (per kg gold)	R 38
Variable (per kg gold)	R 18
Total Cost (per oz gold)*	US\$ 0.22

\*An exchange rate of R 8.00 = US\$ 1.00 is currently applicable.

The operating cost of the in-house refinery is approximately half the cost of the conventional smelting and toll-refining route. A payback period of the capital investment of less than 2.5 years has been calculated. If a premium can be obtained for gold of 99.99% purity (rather than 99.9%), the payback period is decreased further. These numbers are dependent on the tonnage of gold refined annually.

### **Variable Operating Costs**

The average reagent consumptions using the SX refining route are presented in Table 7. Reagent use in the two batch operations is close to the stoichiometric requirement. The major requirement is hydrochloric acid make-up from that lost to the circuit through the raffinate bleed stream.

*Table 7. Reagent consumption.*

Reagent	Consumption (kg / kg Au)
Chlorine	0.76
Hydrochloric acid	3.05
Solvent	0.001
Sulphur dioxide	0.65
Sodium hydroxide (off-gas neutralisation)	0.2

### **Gold Lock up**

As part of the refinery is operated on a batch basis, the lock-up time of the gold in the circuit depends largely on how the plant is operated. A small permanent inventory of gold is maintained in the SX circuit due to the continuous nature of its operation. This is typically between 40 to 50 kg gold. Pulsed columns to replace the mixer-settler plant will be tested in the near future. This will further reduce gold lock up if implemented.

### **FUTURE REFINERY EXPANSION**

As most of the unit operations are batch processes, expansion of the refining capacity is merely a case of adding extra modules to the plant. A further two leach reactors and two additional precipitation vessels are planned for the refinery. The SX plant from the old refinery may be refurbished to operate in parallel with the existing SX circuit. Once complete, the refinery will be capable of producing up to 1200 kg of gold powder per day if continuous operation is employed.

In addition to the ten-tola bars (116.64 g), kilogram bars, good delivery bars (12.5 kg), gold granules, and gold powder, The Minataur™ Process is also capable of producing gold of 'five nines' purity (99.999%) by introducing a greater degree of selectivity to the reduction process (1-3). As demand for this higher purity gold is appears to be on the increase, Harmony is considering the possibility of introducing this product line in addition to the 'four nines' product.

### **CONCLUSIONS**

The SX-based Minataur™ Process has been established as a commercially viable alternative to conventional gold-refining technologies. This process has made substantial savings for Harmony Gold Mine and allowed the company to establish its own branding on many of its products.

### **ACKNOWLEDGEMENTS**

The new Harmony Refinery was designed, constructed, and installed by Mintek under the site management of Allan Menton. This paper is published with the permission of Mintek and Harmony Gold Mining Company.

### **REFERENCES**

1. A. M. Feather, K. C. Sole, and L. J. Bryson (1997), *Randol Gold Forum '97*, pp. 181-185.
2. A. M. Feather, K. C. Sole, and L. J. Bryson (1997), *J. S. Afr. Inst. Min. Metall.*, **97**, 169-173.
3. A. M. Feather, K. C. Sole, and L. J. Bryson (1997), *Proc. XXII Convención Nacional de Minería*, Asociación de Ingieros de Minas, Metalurgistas y Geólogos de México, Acapulco, México.
4. K. C. Sole, A. M. Feather, J. Watt, L. J. Bryson, and P. F. Sorensen (1998), *Proc. EPD Congress 98*, The Minerals, Metals and Materials Society, Warrendale, PA, pp. 175-186.
5. G. G. Stanley (ed.) (1987), *The Extractive Metallurgy of Gold in South Africa*, Vol. 2, South African Institute of Mining and Metallurgy, Johannesburg, pp. 615-653.
6. N. P. Finkelstein, R. M. Hoare, G. S. James, and D. D. Howat (1966), *J. S. Afr. Inst. Min. Metall.*, **66** (12), 196-215.



## BEHAVIOUR OF Os(IV) AQUACHLORO AND AQUACHLOROHYDROXO COMPLEXES IN SOLVENT EXTRACTION FROM SULPHURIC ACID MEDIA

A. Mayboroda, H. Lang\*, I. D. Troshkina, and A. M. Chekmarev

D. Mendeleyev University of Chemical Technology, Moscow, Russia

\*Technische Universität Chemnitz, Chemnitz, Germany

The effect of chloride concentration on the composition of products resulting from osmium tetroxide reduction in sulphuric acid medium is described. The separation of the mixture of Os(IV) aquachloro and aquachlorohydroxo complexes was carried out by ion exchange chromatography. Three cationic complexes (cis- and trans-isomer of  $\{[\text{OsCl}_2(\text{OH})(\text{H}_2\text{O})_2]_2(\mu-\text{OH})\}^+$  as well as fac- $\{[\text{OsCl}_3(\text{OH})(\text{H}_2\text{O})_2](\mu-\text{OH})\}^-$ ) and one anionic species ( $[\text{OsCl}_5(\text{H}_2\text{O})]^-$ ) are shown to be present in solution at low chloride concentration. The increase of chloride concentration leads to an increase of the number of different osmium-containing species in solution. The behaviour of seven isolated Os(IV) complexes in solvent extraction with tri-n-octylamine (TOA) and tri-n-butyl phosphate (TBP) is also studied.

### INTRODUCTION

The promising sources for osmium recovery at nickel- and copper-producing plants are sulphuric acid solutions, which are used for wet cleaning (scrubbing) of gases from pyrometallurgical processes. During the smelting of the Ni or Cu concentrate and the blowing the matte, osmium is oxidised to its tetroxide and sublimes into gaseous phase [1]. The gases formed in the corresponding pyrometallurgicac processes pass dry and wet cleaning. In the wet cleaning step, the gases are generally scrubbed with dilute sulphuric acid. During the scrubbing,  $\text{OsO}_4$  is absorbed and reduced to a number of coordination species. The general osmium content in the scrub solutions of some plants is comparable with the osmium content in anode slims. The sulphuric acid solutions from scrubbers contain dissolved sulphur dioxide, chloride and fluoride ions, arsenic(III) oxide, ions of iron and non-ferrous metals. The presence of chloride in such solutions results in the formation of Os(IV) aquachloro and aquachlorohydroxo complexes, whose extraction chemistry is up to now only a less studied [2]. So far, only complex  $[\text{OsCl}_5(\text{H}_2\text{O})]^-$  could recently be isolated by solvent extraction with TBP [2]. Solvent extraction is used for recovery of rhenium from scrub sulphuric acid [3]. Data on solvent extraction of partly hydrolysed Os(IV) chloro complexes could be useful for explanation of the behaviour of osmium in the process of rhenium extraction from sulphuric acid scrub solutions.

## EXPERIMENTAL

Glass column having inner diameter of 35 mm was filled with diethylaminoethyl cellulose (DEAE 23 SS, Serva, Germany) as gel and used for ion exchange chromatography. The height of the ion exchanger layer was 500 mm. The sulphuric acid of  $1 \text{ mol} \cdot \text{L}^{-1}$  concentration was applied as eluent with flow rate of  $10 \text{ mL} \cdot \text{h}^{-1}$ .

UV-Vis spectra of the Os(IV) complexes were recorded on a Perkin Elmer Lambda 40 spectrophotometer in water solutions of sulphuric acid and in organic solutions (decane) in presence of TOA or TBP.

Electrodialysis of osmium-containing sulphuric acid solutions was carried out using a five chamber laboratory set (Figure 1) supplied with strong basic anion exchange AMX membranes and strong acidic cation exchange CMX membranes (Berghof, Germany). The volume of each chamber was 200 mL. Initial osmium-containing solutions were placed into the middle chamber *M*. Cathode chambers *K<sub>1</sub>*, *K<sub>2</sub>* and anode chamber *A<sub>1</sub>* was filled with 0.3 M  $\text{H}_2\text{SO}_4$ . Anode chamber *A<sub>2</sub>* was filled with 0.3 M  $\text{Na}_2\text{SO}_3$ . The time of an electrodialysis was 48 h at voltage of 12 V and current strength of 0.3 A.

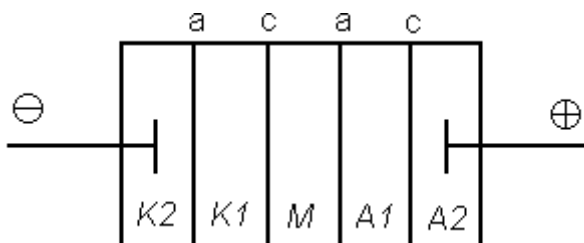


Figure 1. Schematic view of electrodialysis set.

*a* – anion exchange membranes; *c* – cation exchange membranes; *M* – middle chamber for initial solution; *K<sub>1</sub>*, *K<sub>2</sub>* – cathode chambers; *A<sub>1</sub>*, *A<sub>2</sub>* – anode chambers.

Experiments on solvent extraction of Os(IV) complexes were carried out at 20 °C. Tri-n-octyl amine and tri-n-butyl phosphate were supplied by Merck, Germany. n-Decane was used as diluent. To prevent the third phase formation, 10 % (vol.) of octanol-1 was added as modifier in a decane solution of tri-n-octylamine.

## RESULTS AND DISCUSSION

The key factors which determine composition of osmium complexes in industrial sulphuric acid scrub solutions are the concentrations of sulphur dioxide and chloride in such media. In the absence of chloride ions in the solution, the sulphur dioxide reacts with osmium tetroxide as reduction agent as well as the ligand. Sulphito complexes of Os(VI)  $[\text{OsO}_2(\text{SO}_3)_{4-x}(\text{HSO}_3)_x]^{2-}$  and  $[\text{OsO}_2(\text{SO}_3)_2(\text{H}_2\text{O})_2]^{2-}$  are formed in this instance [4]. However, such situation is never realised in industrial solutions, which always contain at least  $0.04 - 0.10 \text{ mol} \cdot \text{L}^{-1}$  of chloride. In the presence of chloride, sulphur dioxide acts as a reduction agent, and the reduction of  $\text{OsO}_4$  leads to Os(IV) complexes featuring chloride, hydroxide and aqua ligands.

Water solutions containing  $3 \text{ mol} \cdot \text{L}^{-1}$  of  $\text{H}_2\text{SO}_4$ ,  $0.04 \text{ mol} \cdot \text{L}^{-1}$  of  $\text{NaCl}$  and  $0.01 \text{ mol} \cdot \text{L}^{-1}$  of  $\text{Na}_2\text{SO}_3$  were used in preliminary experiments as a model of scrub sulphuric acid. Osmium tetroxide ( $2.3 \times 10^{-5} \text{ mol}$ ) was added to such solutions (100 mL) at 95 °C. The reaction mixture was heated for 20 min and afterwards cooled to 20 °C. For this mixture, a sharp absorption maximum was observed in the UV-Vis spectrum at 362 nm ( $\epsilon = 7.0 \times 10^3 \text{ L} \cdot \text{mol}^{-1} \cdot \text{cm}^{-1}$ ) (Figure 2a). The characteristic absorption for Os(VI) sulphito complexes in the area of 700 -

1000 nm [4] was not found in the UV-Vis spectrum. The obtained reaction mixture (*vide supra*) was contacted with 10 mL of a 0.1 M solution of TOA in decane in order to extract osmium. The extraction was relative low (12 %), but the osmium concentration in the organic extract allowed to record the UV-Vis spectrum of the extracted material. The absorption maximum observed at 349 nm (Figure 2c) indicates the presence of the anionic complex  $[\text{OsCl}_5(\text{H}_2\text{O})]^-$  in the organic phase. After extraction, the UV-Vis spectrum of the water phase (Figure 2 b) remained without variation in the position or intensity of the respective absorption band at 362 nm, which can be attributed to the Os(IV) aquachlorohydroxo complexes  $\text{cis}-[\{\text{OsCl}_2(\text{OH})(\text{H}_2\text{O})_2\}_2(\mu-\text{OH})]^+$  [5].

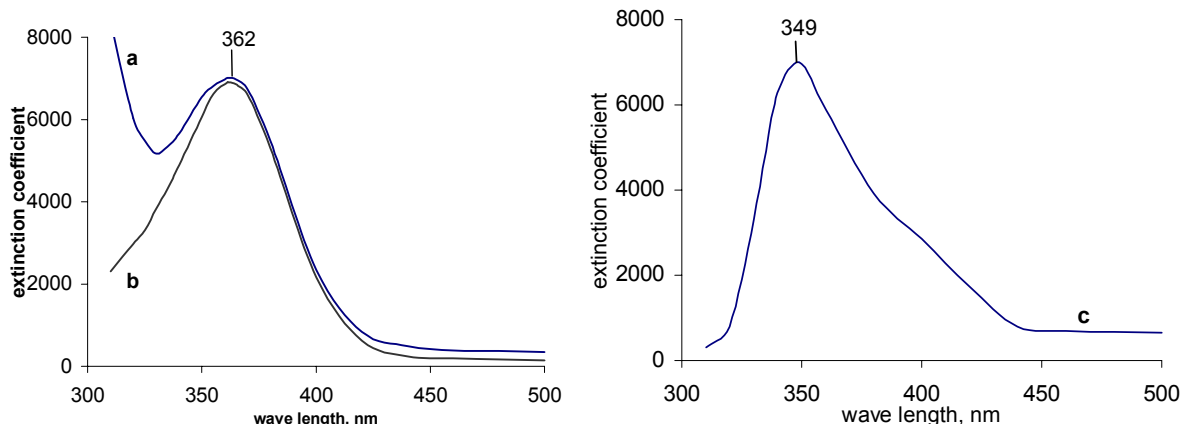


Figure 2. The electronic absorption spectra of initial osmium-containing model solution (a), raffinate after extraction with TOA (b), and organic extract (c).

The chloro complexes of Os(IV), e.g.,  $\text{cis}-[\{\text{OsCl}_2(\text{OH})(\text{H}_2\text{O})_2\}_2(\mu-\text{OH})]^+$  (1),  $\text{trans}-[\{\text{OsCl}_2(\text{OH})(\text{H}_2\text{O})_2\}_2(\mu-\text{OH})]^+$  (2),  $\text{fac}-[\{\text{OsCl}_3(\text{OH})(\text{H}_2\text{O})\}_2(\mu-\text{OH})]^-$  (3),  $\text{fac}-[\text{OsCl}_3(\text{OH})_2(\text{H}_2\text{O})]^-$  (4),  $\text{fac}-[\{\text{OsCl}_3(\text{OH})(\text{H}_2\text{O})\}_2(\mu-\text{O})]^{2-}$  (5),  $[\text{OsCl}_5(\text{H}_2\text{O})]^-$  (6) and  $[\text{OsCl}_6]^{2-}$  (7) were synthesized as described above by reduction of  $\text{OsO}_4$  in 3.0 M  $\text{H}_2\text{SO}_4$  in presence of 1.0 M  $\text{Na}_2\text{SO}_3$  and 0.5 or 1.0 M NaCl, respectively. To separate the diverse products from the reaction mixture, ion exchange gel chromatography was applied. The obtained chromatograms are shown in Figure 3. Seven different chloro complexes are found to be present in the reaction solution with concentration of NaCl being 1.0 mol $\times$ L $^{-1}$  (Figure 3a). The UV-Vis spectra of the appropriate fractions from the chromatographic separation were compared with literature data [5]. This allowed us to identify the structures of the formed osmium chloro complexes. The reaction solution obtained from the reduction of  $\text{OsO}_4$  with NaCl concentration of 0.5 mol $\times$ L $^{-1}$  shows four osmium chloro complexes, which could be separated by chromatographic technique (Figure 3b). The bulk of osmium is present as the *cis*- (1) or *trans*- (2) isomer of cationic  $[\{\text{OsCl}_2(\text{OH})(\text{H}_2\text{O})_2\}_2(\mu-\text{OH})]^+$ . However, the content of anionic species, e.g.,  $\text{fac}-[\{\text{OsCl}_3(\text{OH})(\text{H}_2\text{O})\}_2(\mu-\text{OH})]^-$  (3) and  $[\text{OsCl}_5(\text{H}_2\text{O})]^-$  (6) is significant lower than the cationic ones.

The charges of the corresponding Os(IV) aquachlorohydroxo complexes 1 – 5 were determined by Müller *et al.* on the base of the behaviour of these species in ion exchange chromatography processes [5]. To confirm this data, a separation of the respective complexes 1 – 6 using electrodialysis technique was carried out. The same osmium-containing solutions, which were applied for ion exchange chromatography (3.0 M  $\text{H}_2\text{SO}_4$ , 1.0 M  $\text{Na}_2\text{SO}_3$ , 0.5 or 1.0 M NaCl) were diluted 10 times with distilled water and treated by electrodialysis in a five chamber set (Figure 1). The dilution of the appropriate mixtures was necessary, since a transfer of osmium complexes through ion exchange membranes was completely inhibited in 3.0 M  $\text{H}_2\text{SO}_4$ . Such dilution seems to be admissible seeing that the UV-Vis spectra of the diluted solutions remain invariable at least for a weak. This indicates that a hydrolysis of the corresponding Os(VI) complexes does not take place in the diluted

solution and their structures remain without variation. The initial solution was placed in the chamber *M* of the electrodialysis set (*vide supra*). After 48 h of electrodialysis, only traces of osmium were found in this chamber. The solutions from chambers *K1* and *A1* were characterized by using UV-Vis spectroscopic methods. Spectroscopic data (Table 1) indicate that complexes **1** ( $\lambda_{\max} = 363$  nm) and **2** ( $\lambda_{\max} = 371$  nm) are indeed cationic; electrodialysis as well as ion exchange chromatography indicate the absence of neutral osmium complexes.

*Table 1. Absorption maxima of osmium-containing solutions from electrodialysis.*

[Cl] <sup>a)</sup> , mol·L <sup>-1</sup>	$\lambda_{\max}$ , nm		
	Initial solution	chamber <i>K1</i>	Chamber <i>A1</i>
0.5	360	364	355
1.0	376	371	380

<sup>a)</sup> Chloride concentration in solution, which was used as medium for  $\text{OsO}_4$  reduction.

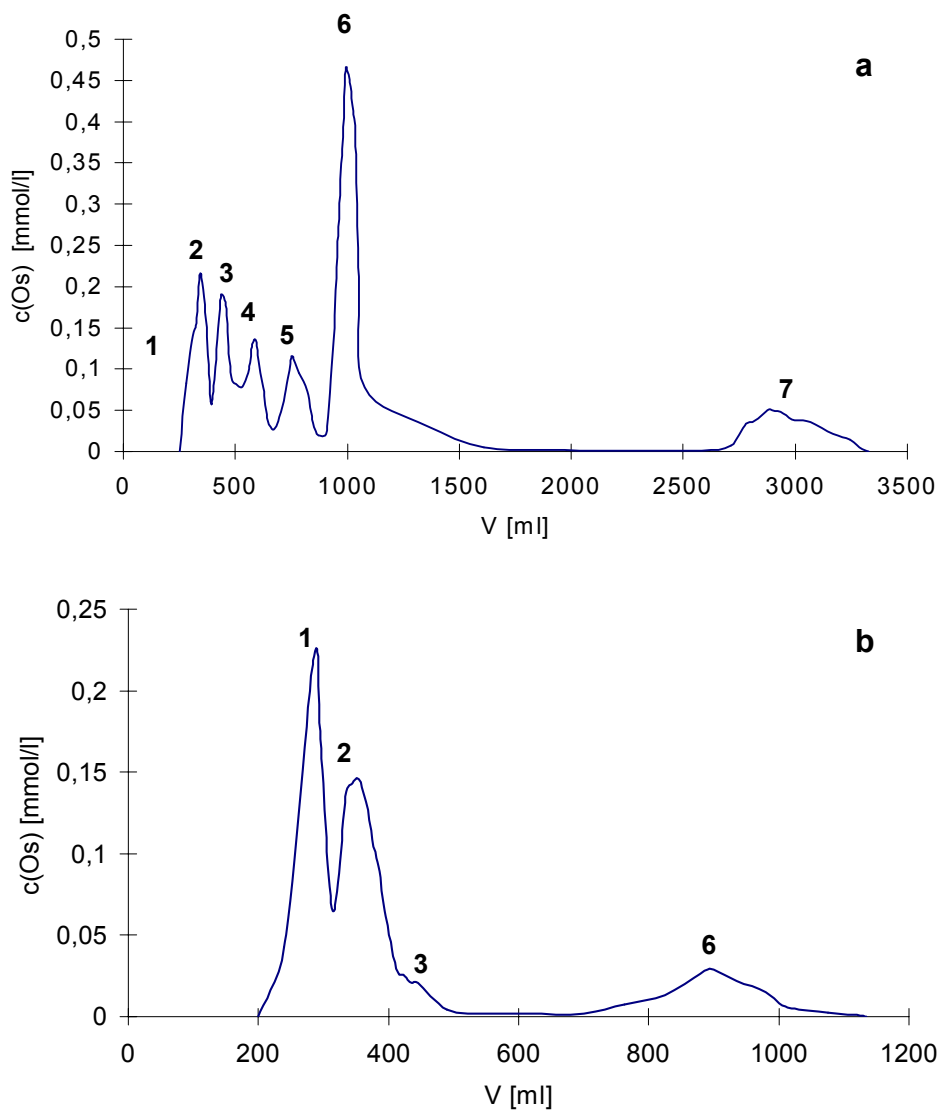


*Figure 3. Ion exchange chromatograms of products obtained by the  $\text{OsO}_4$  reduction in  $\text{H}_2\text{SO}_4$  solutions in presence of 1.0 M NaCl (a) or 0.5 M NaCl, respectively.*

The chromatographic fractions with maximal concentration of isolated complexes were used for the preparation of initial aqueous solutions for solvent extraction. Concentrations of H<sub>2</sub>SO<sub>4</sub> and NaCl in initial aqueous phase were adjusted using 5 M H<sub>2</sub>SO<sub>4</sub> and 3 M NaCl. The corresponding chloro complexes of Os(IV) **1 – 6** were extracted from sulphuric acid media with a 0.1 M TOA solution in decane or a TBP solution (50 % vol.) in decane. The data on the extraction conditions and on the distribution coefficients (D<sub>Os</sub>) are summarised in Table 2. Within this Table, the complexes are arranged in order of egress of the corresponding fractions from the chromatographic column. Complexes **1** and **2** could not be extracted with both extractant due to their positive charge.

It was found that the chloride concentration effects the extraction of complex **3**. The presence of extracted HCl in the organic phase is a condition of coextraction of complex **3**. In contrast, increasing the chloride concentration inhibits the extraction of complex **6** with TBP as well as with TOA. Anionic complexes **4** and **5** are not extracted with TBP but can be extracted with TOA.

## CONCLUSIONS

The reduction of OsO<sub>4</sub> in sulphuric acid solutions in the presence of chloride ions lead to the formation of cationic as well as anionic aquachlorohydroxo complexes of Os(IV). It appeared that the respective cationic complexes prevail in solution, having low concentration of chloride ions. The distribution coefficient of the corresponding osmium complexes **3 – 7** could be determined by solvent extraction with TOA or TBP.

## ACKNOWLEDGEMENT

This work was partly supported by the Deutschen Akademischen Austauschdienst (DAAD; A. M.) and the Deutschen Forschungsgemeinschaft (DFG). We also would like to express our appreciation to Degussa-Hülls AG for the very generous gift of OsO<sub>4</sub>.

## REFERENCES

1. V. D. Nagibin, S. K. Kalinin and L. I. Mekler (1974), *Vestnik AN KazSSR (News of Kasakh Academy of Science)*, (7), 53-55 (in Russian).
2. A. Maiboroda, G. Rheinwald and H. Lang (2000), *Inorg. Chem.*, **39**, 5725-5730.
3. A. N. Zagorodnyaya, E. I. Ponomareva, Z. S. Abisheva, E. G. Tarasova (1990), *Proc. Int. Solvent Extraction Conf., ISEC '90*, Kyoto, 170.
4. Z. S. Abisheva, N. M. Bodnar, T. N. Bukurov, T. M. Buslaeva and I. A. Blaida (1994), *Tsvet. Met. (Non-ferrous Metals)*, (9), 33-35 (in Russian).
5. H. Müller, H. Scheible and S. Martin (1980), *Z. Anorg. Allg. Chem.*, **462**, 18-34.

Table 2. Extraction behaviour of osmium(IV) chlorocomplexes.

N	$\lambda_{\text{max}}$ , nm (in water solution)	Complex	0.1 M TOA in decane				50% TBP in decane						
			c(OS) <sup>a)</sup> , mol×L <sup>-1</sup>	c[H <sub>2</sub> SO <sub>4</sub> ] <sup>b)</sup> , mol×L <sup>-1</sup>	c(Cl <sup>-</sup> ), mol×L <sup>-1</sup>	O:A <sup>b)</sup>	D <sub>Os</sub>	$\lambda_{\text{max}}$ , nm (in org. solution)	c(H <sub>2</sub> SO <sub>4</sub> ), mol×L <sup>-1</sup>	c(Cl <sup>-</sup> ), mol×L <sup>-1</sup>	O:A <sup>b)</sup>	D <sub>Os</sub>	$\lambda_{\text{max}}$ , nm (in org. solution)
1	363	cis-[{OsCl <sub>2</sub> (OH)(H <sub>2</sub> O) <sub>2</sub> } <sub>2</sub> (μ-OH)] <sup>+</sup>											
2	371	trans-[{OsCl <sub>2</sub> (OH)(H <sub>2</sub> O) <sub>2</sub> } <sub>2</sub> (μ-OH)] <sup>+</sup>											
			no extraction				no extraction						
3	377	fac-[{OsCl <sub>3</sub> (OH)(H <sub>2</sub> O) <sub>2</sub> (μ-OH)} <sup>-</sup>	0.194	1.0	0.01	1:1	0.03	381	0.201	1.0	0.01	1:1	0.04
4	381	fac-[{OsCl <sub>3</sub> (OH)(H <sub>2</sub> O) <sub>2</sub> (μ-O)} <sup>-</sup>	0.098	1.0	0.01	1:1	0.12	389	0.152	3.0	1.0	1:1	0.38
5	384	fac-[{OsCl <sub>3</sub> (OH)(H <sub>2</sub> O) <sub>2</sub> (μ-O)} <sup>2-</sup>	0.046	3.0	0.01	1:5	0.70	395					
			no extraction				no extraction						
6	345	[OsCl <sub>5</sub> (H <sub>2</sub> O)] <sup>-</sup>	0.055	3.0	0.01	1:10	50.2	351	0.056	3.0	0.5	1:5	21.1
			0.019	3.0	1.0	1:10	20.8	351	0.525	3.0	1.0	1:5	14.8
7	334; 370	[OsCl <sub>6</sub> ] <sup>2-</sup>	0.03	3.0	1.0	1:20	168	337; 374	0.015	3.0	0.04	1:10	10.0
								0.012	3.0	1.0	1:10	22.2	342,373

a) Concentration of osmium in raffinate.

b) Volumetric ratio of organic phase to aqueous one in extraction process.



## SOLVENT EXTRACTION AND HYDROCHEMICAL PREPARATION OF GOLD POWDERS WITH DITHIZONE DERIVATIVES

María Guadalupe Sánchez-Loredo and Manfred Grote\*

Universidad Autónoma de San Luis Potosí, San Luis Potosí, México

\*University of Paderborn, Paderborn, Germany

Solvent extraction of gold by S-decyldithizone **D-H** and its carboxylic acid derivatives was studied as a function of equilibration time, organic phase diluent, metal and hydrochloric acid concentrations. During the loading stage the chelating extractants were oxidized to the corresponding 2H-tetrazolium salts. Only from S-decyldithizone phases the loaded gold can be sufficiently re-extracted by thiourea. Both the non-acidic **D-H** and the ortho-carboxyl substituted extractant **D-oC** could be simultaneously stripped and fully regenerated by aqueous solutions of ascorbic acid or sodium borohydride. Gold was recovered as fine particles, which were characterised by means of scanning electron microscopy. The powder morphology was directly affected by the composition of the organic phases and the aqueous reducing media applied.

### INTRODUCTION

Solvent extraction has become an attractive alternative to traditional refining methods for the selective recovery of gold and other noble metals. Gold is normally removed from solution using solvating reagents [1]. Particularly reagents with incorporated sulphur have received much attention in the extraction of gold from chloride media [2,3]. According to Demopoulos, the metal could be recovered directly from the organic solvent by a precipitation method called hydrolytic stripping [4]. Also cementation or reduction with sulphur dioxide or hydrogen were applied [4]. Ultra-fine gold particles were obtained by utilising a water/oil micro-emulsion [5,6].

The present study on the behaviour of gold towards S-decyl derivatives of dithizone is based on results of earlier investigations: It was found that S-decyldithizone (**D-H**) and its ortho-, meta- and para-monocarboxyl substituted derivatives (**D-oC**, **D-mC** and **D-pC**, Figure 1) dissolved in organic solvents became progressively oxidised by mixtures of precious and base metal salt solutions when Au(III) was also present [7,8]. The molecular structure of the S-decyldithizone reagents represents the electrochemically reversible redox system of formazans (reduced form) and tetrazolium salts (oxidised form) [9]. It is to assume that the oxidation of the extractants by interactions with Au(III) could be reversed by reducing stripping agents.

Consequently in the present work the main characteristics of affinity of these dithizone derivatives towards Au(III) in acidic chloride medium were investigated. Stripping of gold by means of complexing and reducing agents was also studied.

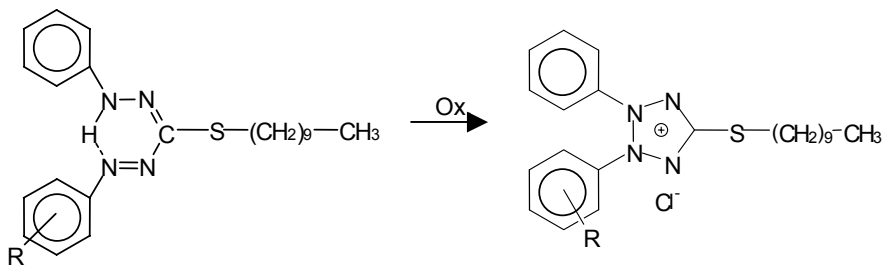


*Figure 1. Structures of S-decyldithizone **D-H** ( $R=H$ ), **D-oC** ( $R=o\text{-COOH}$ ), **D-mC** ( $R=m\text{-COOH}$ ) and **D-pC** ( $R=p\text{-COOH}$ ) and their corresponding oxidation products.*

## EXPERIMENTAL

### Reagents

The synthesis of the extractants is described elsewhere [7,8,10]. All chemicals used were of reagent grade quality. Gold feed solutions were prepared dissolving the required amount of the sodium salt of the tetrachloro complex (Degussa AG) in the selected acid medium. All aqueous phases used for extraction experiments were presaturated with the organic diluent *p*-xylene or chloroform. The standard solutions of Au(III) were prepared from commercial stock solution (Spex Industries Inc.).

### Extraction

Solvent extraction experiments were carried out at 20°C in 60 cm<sup>3</sup> separatory funnels shaken mechanically using a Bühler Co. shaker at a fixed frequency of 140 min<sup>-1</sup>. 10 cm<sup>3</sup> of the organic phase containing the extracting agent in the diluent were shaken with an equal volume of the aqueous phase containing the metal ion in 0.1, 1 or 3.5 mol/dm<sup>3</sup> HCl solutions. The metal ion and extractant concentrations were 0.1 mmol/dm<sup>3</sup> and 1 mmol/dm<sup>3</sup>, respectively. After a certain time of shaking (20 min, 1 h, 2 h, 4 h and 24 h), the two phases were allowed to separate and, if necessary, centrifuged. The metal concentrations of the aqueous phases were determined by DC-plasma emission spectrometry (Spectraspan 7, Thermo Jarrell Ash), and the organic phase metal content was calculated by mass balance.

### Stripping

In order to carry out the stripping experiments, metal loading was performed by shaking 50 cm<sup>3</sup> of gold salt solution (0.1 mmol/dm<sup>3</sup> in 0.1 mol/dm<sup>3</sup> HCl) with an equal volume of reagent solution (1 mmol/dm<sup>3</sup> in *p*-xylene) for 24 h. The metal loaded organic phase was separated and washed with 50 cm<sup>3</sup> of 0.1 mol/dm<sup>3</sup> HCl (15 min shaking). 10 cm<sup>3</sup> of the organic phase were transferred into a separatory funnel and contacted with an equal volume of 2 mol/dm<sup>3</sup> HClO<sub>4</sub>, 0.5 mol/dm<sup>3</sup> NaSCN or thiourea (Tu) solution (5% Tu (w/v) in 0.1 mol/dm<sup>3</sup> HCl).

Reductive stripping experiments were performed, firstly, by contacting 200 cm<sup>3</sup> of the organic phase (1 mmol/dm<sup>3</sup> of **D-H** and **D-oC** in *p*-xylene) with 100 cm<sup>3</sup> of the gold feed solution (5 mmol/dm<sup>3</sup> Au(III) in 0.1 mol/dm<sup>3</sup> HCl). In order to monitor the oxidation of the extracting reagents (spectrophotometrically, using a Lambda 13 Perkin Elmer Instrument), and the extraction process (by plasma emission spectrometry), 1 cm<sup>3</sup> aliquots of both phases were collected in intervals during the 24 h loading stage. A first fraction of elementary gold was formed during this stage. Therefore, prior to the subsequent reducing stripping procedure the phases were filtrated and allowed to separate.

The gold powders were filtered, washed with 500 cm<sup>3</sup> of acetone, 500 cm<sup>3</sup> of distilled water and weighed after drying. The residual gold was recovered from the loaded organic phase using one of the following reducing agents: oxalic acid (50 mmol/dm<sup>3</sup> in water), ascorbic acid (4, 50 and 100 mmol/dm<sup>3</sup> in water), or sodium borohydride (50 mmol/dm<sup>3</sup> in water, 0.1 mol/dm<sup>3</sup> HCl, 1 mol/dm<sup>3</sup> NaCl or 2.5 g/dm<sup>3</sup> NaOH). By 24 h shaking of 50 cm<sup>3</sup> of these solutions together with a 50 cm<sup>3</sup>-aliquot of gold-loaded organic phase in a separatory funnel elementary gold precipitated, which was isolated and finally treated as described above.

The morphology, size and purity of the gold powders obtained were determined by scanning electron microscopy (SEM) using an XL-30 microscope (Philips, Netherlands), and a DX-4I (EDAX) EDS analysis (energy-dispersive X-ray spectrometry).

## RESULTS AND DISCUSSION

### Solvent Extraction Experiments

Dissolved in *p*-xylene or chloroform, the originally deep red coloured, chelating S-decyldithizone compounds are oxidised by aqueous Au(III) solutions to the corresponding yellow tetrazolium salts, ion-pairing cationic heterocycles [8,10]. It seems that the extraction reaction involves some kind of metal reduction to the Au(I) oxidation state, and depending on the metal concentration, to elementary gold. The change from the dithizone to the tetrazolium salt was monitored by the *UV-Vis* spectrum of the organic phase (in *p*-xylene). On prolonged extraction time the intensities of the absorbances at 543 and 422 nm (**D-oC**) as well as 550 and 415 nm (**D-H**) diminishes while a concomitant rise at 324 (**D-oC**) and 321 nm (**D-H**) appears. In case of the extractant **D-oC**, the oxidation product formed was identified as S-decyl-[2-(2'-carboxyphenyl)-3-phenyl-2H-tetrazolium-5-thiolate], which was isolated and its structure confirmed spectroscopically [10]. Simultaneously formation of gold particles occurred at higher concentrations of Au(III) (>0.5 mmol/dm<sup>3</sup>). Most of the metallic powder was concentrated at the aqueous/organic interface. The precipitates obtained in both extractant systems consisted of dense, irregularly shaped particles, with significant differences in the shape and size [11]. It was found by SEM analysis that extracting gold with the reagent **D-H** leads to gold particles of around 20-40 µm in size, partly agglomerated. A change to the extractant **D-oC** resulted in finer particles (<10 µm) and agglomerates also. The precipitates were irregular containing platelet particles grown by coalescence. Some particles were pyramidal, a common morphology for this metal.

In order to avoid precipitation of the elementary metal the following extraction studies described were carried out by using a feed solution containing 0.1 mmol/dm<sup>3</sup> Au(III). The effect of the diluent on gold extraction was investigated using chloroform and *p*-xylene (Table 1). The yield of metal extraction does not differ significantly, however, for all the substituted dithizonates slightly higher extraction efficiencies were obtained when the aliphatic diluent was used. By using the non-acidic **D-H** in *p*-xylene the extraction proceeds quite fast as the equilibrium was achieved in less than 20 min. In chloroform much more time is necessary (4 h). By contrast, in case of the carboxyl-substituted derivatives faster extraction was achieved by means of the aliphatic diluent. As an example, for the extractant **D-oC** the extraction equilibrium was achieved in 4 h using CHCl<sub>3</sub> as diluent, by using *p*-xylene the equilibration time had to be extended to about 24 h.

*Table 1. Influence of the diluent on gold extraction by S-decyldithizonates.  
c(HCl)=0.1 mol/dm<sup>3</sup>, shaking time: 24 h.*

Diluent	<b>D-H</b>	<b>D-oC</b>	<b>D-mC</b>	<b>D-pC</b>
<i>p</i> -xylene	≈100	93.2	95.1	98.1
Chloroform	≈100	≈100	99.2	99.2

The influence of increasing HCl concentration was also studied (Figure 2). Generally, with increasing acidity the extraction yields drops off for the acidic S-decyldithiones. On the other side, the extraction yields for Au(III) obtained with the unsubstituted derivative **D-H** is not dependent on hydrochloric acid concentration in the range of acidity investigated.

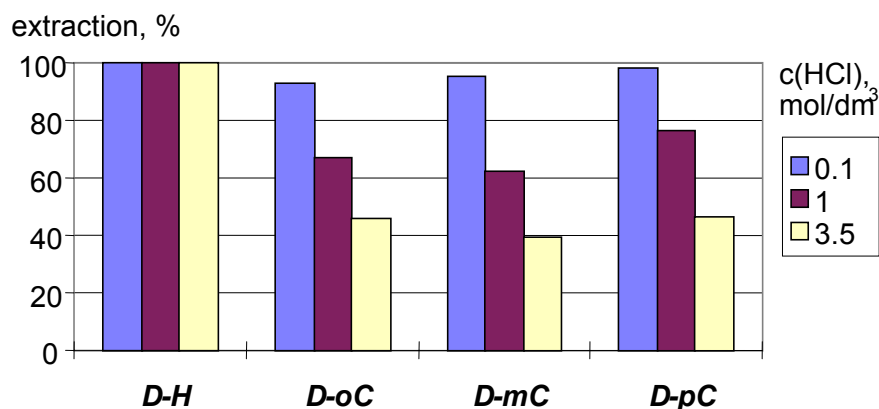


*Figure 2. Effect of hydrochloric acid concentration on extraction of Au(III). Diluent: p-xylene, shaking time: 24 h.*

### Stripping

Several reagents were tested for gold stripping. Coordinating ligands, like thiourea and thiocyanate, have been used, as well as perchloric acid, which displaces metal ions via ion exchange mechanism. However, stripping using perchloric acid solutions did not appear feasible as the extent of gold re-extraction was not higher than 1 %. Table 2 shows recovery data determined by using aqueous solutions of thiourea and thiocyanate. A sufficient recovery of gold from the loaded organic **D-H** phase was possible by applying a 5 % (w/v) thiourea solution in 0.1 mol/dm<sup>3</sup> HCl.

*Table 2. Recovery of gold using 5 % (w/v) thiourea-solution in 0.1 mol/dm<sup>3</sup> HCl and 0.5 mol/dm<sup>3</sup> NaSCN. Shaking time: 24 h.*

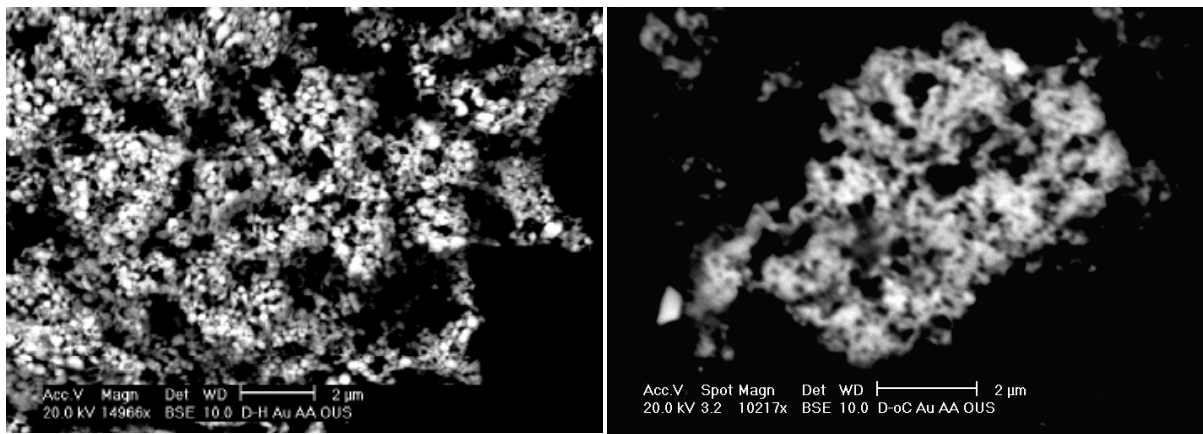
	<b>D-H</b>	<b>D-oC</b>	<b>D-mC</b>	<b>D-pC</b>
Thiourea	89.2	78.9	14.1	9.2
NaSCN	11.1	17.5	8.6	8.6

From the results obtained during the extraction and stripping experiments the superior effectiveness of **D-H** as extractant for gold is obvious.

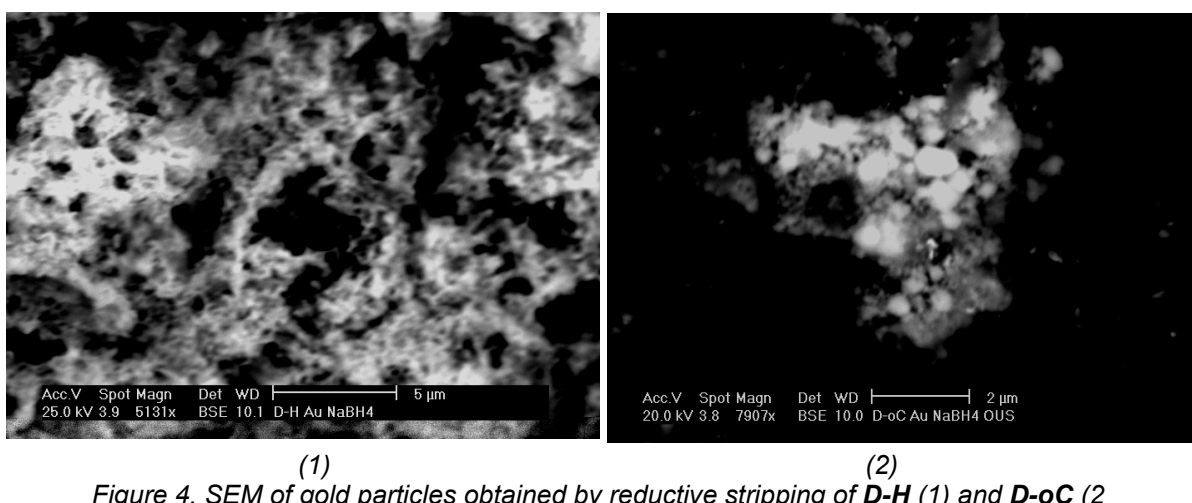
### Reductive Stripping

In order to perform the reductive stripping experiments, the extractant phases containing the S-decyldithiones **D-H** and **D-oC** in *p*-xylene were loaded with Au(III) for 24 h. As soon as the loaded organic extractants, being oxidised to tetrazolium salts, were contacted with aqueous reducing reagents a dramatic reaction occurred, indicated by a colour change of the yellow organic phase to deep red: the chelating molecules were reductively rebuilt and the precious metal extracted could be recovered as a black powder of elementary gold. When an oxalic acid solution was added, a part of the gold precipitated instantly as a very finely divided powder that is hard to handle, mostly plated on the internal walls of the funnel. UV/Vis-spectrophotometry revealed that regeneration was not complete even after 7 days shaking.

However, better results were obtained by using ascorbic acid as reducing agent. For example, 24 h were enough to reach an almost complete regeneration of the extractant **D-H** using 50 mmol/dm<sup>3</sup> of ascorbic acid dissolved in water. No residual amount of metal in the organic phase could be detected after chemical attack and analysis. The precipitates obtained were examined by SEM to determine their morphology and particle size and also data for determining the purity of the gold particles. Figure 3 shows SEM photographs of powders prepared by the ascorbic acid treatment of a loaded **D-oC** phase as mentioned above. A few particles are pyramidal, but most of them are spherical. The images obtained reveal aggregates consisting of nano-size subunits. The diameter of these subunits depends on the extractant applied. The values varied in the range of 220 to 280 nm (**D-H**) and 100 to 190 nm (**D-oC**).



Sodium borohydride has been widely used to reduce a variety of metal cations to the metallic state. In this work, optimum results were achieved by using NaBH<sub>4</sub> in alkaline solution. Particularly in the case of the non-acidic **D-H** precipitation of gold and regeneration of the organic extractant was extremely fast. Less than ten minutes were required for complete regeneration and quantitative metal recovery, compared to about eight hours when the carboxyl-substituted **D-oC** was used. In both cases the recovery of the metal was acceptable and no plating effects on the walls were observed. Figure 4 shows SEM-photographs of the gold particles, which revealed the powders to consist mostly of amorphous particles with some variation in size, composed from spherical subunits, which coalesced irreversibly and formed larger granules.



In general, the precipitation products were larger and showed broader size distribution. The size ranges of **D-H** and **D-oC** systems were 240 to 425 nm and 136 to 205 nm respectively, showing the strong influence of the acidic carboxyl group of the organic molecule on nucleation and growth and thus morphology and size of the gold particles.

## CONCLUSIONS

The extraction of gold by means of S-decyldithizone derivatives was studied. The extraction properties are significantly affected by substitution on one of the aromatic rings, and particularly the non acidic extractant **D-H** showed superior extraction and stripping properties. Ascorbic acid and sodium borohydride were used to prepare gold powders by reductive stripping. Almost quantitative gold recovery and good extractant regeneration was feasible. Particularly the use of the ortho-substituted **D-oC** as extractant, and ascorbic acid as reducing agent, allows to obtain nano-crystalline gold powders.

## ACKNOWLEDGEMENTS

M.G. Sánchez-Loredo is grateful to the Deutscher Akademischer Austauschdienst (Bonn, Germany) and to the Fondo de Apoyo a la Investigación (UASLP, México) for financial support. The assistance of Rodica Knaup, University of Paderborn, in performing careful analytical work is gratefully acknowledged.

## REFERENCES

1. G. P. Demopoulos (1986), *J. Met.*, **6**, 13.
2. M. Petrich, J. L. Cortina, J. Hartung, M. Aguilar, A. M. Sastre, L. Beyer, and K. Gloe (1993), *Solvent Extr. Ion Exch.*, **11** (1), 51.
3. F. Z. El Aamrani, A. Kumar, L. Beyer, J. L., Cortina, and A. M. Sastre (1998), *Solvent Extr. Ion Exch.*, **16** (6), 1389.
4. G. P. Demopoulos (1988), *J. Met.*, **6**, 46.
5. H. Majima, T. Hirato, Y. Awakura, and T. Hibi (1991), *Met. Trans. B*, **22**, 397.
6. J. B. Nagy (1999), *Handbook of Microemulsion Science and Technology*, P. Kumar, K.L. Mittel (eds.), Marcel Dekker, New York, Basel, pp. 499.
7. M. Grote, G. Pickert, and A. Kettrup (1989), *Productivity and Technology in the Metallurgical Industries*, M Koch and J.C. Taylor (eds.), TMS, Warrendale, pp. 613.
8. M. G. Sánchez-Loredo and M. Grote (2000), *Solvent Extr. Ion Exch.*, **18** (1), 55.
9. M. Grote and Th. Machate (1991), *New Developments in Ion Exchange*, M. Abe, T. Kataoka, T. Suzuki (eds.), Kodansha Ltd, Tokyo, Elsevier, Amsterdam, pp. 79.
10. M. Grote and U. Schumacher (1997), *React. Polym.*, **35**, 179.
11. M. G. Sánchez-Loredo, A. Robledo-Cabrera, and M. Grote (2001), to be published.



## THE APPLICATION OF SOLVENT EXTRACTION TO THE REFINING OF GOLD

Richard A. Grant and Valerie A. Drake

Johnson Matthey Technology Centre, Reading, United Kingdom

Gold is treasured for its colour, ductility and resistance to corrosion and appears to have been the first metal known and used by Mankind. Its uses in medicine, dentistry and decoration date back to the Ancient Egyptians and Chinese. Today, its principle uses are in investment, coinage, jewellery, electronics, dentistry and decorative coatings. This paper discusses the application of solvent extraction to the production of high-purity gold which has potential advantages over conventional refining techniques. A wide range of reagents have been reported in the literature for the extraction of gold but these have limitations particularly with selectivity and ease of stripping. We have identified the simple commercial alcohol, 2-ethylhexanol, as offering significant advantages including high selectivity over other metal impurities, the ability to be stripped with water at ambient temperatures, high capacity and low cost. The development of a continuous solvent extraction process is described and initial pilot plant results are presented.

### INTRODUCTION

Johnson Matthey is the world's largest refiner of gold and is also a major refiner of the Platinum Group Metals (PGM) and silver. The group is also the world's largest manufacturer of high purity small gold bar products for investment and jewellery manufacture. The Company both refines gold from mining operations around the world and recycles secondary (scrap) material. To serve this worldwide business, Johnson Matthey has refining operations located in the UK; Salt Lake City, USA; Toronto, Canada; Melbourne, Australia and Hong Kong.

Johnson Matthey Chemical Division's UK Refinery at Brimsdown in North London recovers Precious Metals (PM) from a wide variety of inputs and produces separate semi-refined concentrates containing gold, silver and the PGM. These are then transferred to a second Refinery at Royston near Cambridge for purification and subsequent conversion into either metallurgical or chemical products. The main gold concentrate comes from the Brimsdown Silver Process and has a typical composition of 89% Au, 9% Ag, 1% PGM and <1% Cu and BM. Other potential feeds are Dore bullion from mining operations (85% Au and 15% Ag), Carat Gold mostly from jewellery scrap (62% Au, 9% Ag, 1% PGM and 28% Cu) and "Good Delivery" gold bars for upgrading (>99.5% Au and <0.5% Ag).

The refining of gold traditionally relies on two processes which both date back to the 19<sup>th</sup> Century. The purification of molten gold by passing chlorine through it was first reported by Thompson [1] in 1838. A process based on this principle was patented by Miller in 1867 and put into commercial practice at the Sydney Mint [2]. As is often the case this technique is therefore known as the Miller Process. It exploits the fact that at around 1100°C gold chloride is not stable unlike most base metal (BM) chlorides. Some such as copper, iron, lead and

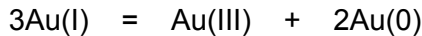
selenium are gaseous at this temperature and therefore volatilise. Others such as silver chloride are molten and collect as a slag layer on top. The PGM chlorides are unfortunately also unstable at these temperatures. Consequently the Miller Process is restricted to the refining of materials that do not contain these metals such as the gold from the Witwatersrand deposit in South Africa. The process also does not give a complete separation and so, without further purification, is limited to the production of "Good Delivery" gold (>99.5%). Its main advantages are that it is very quick and has quite low operating costs.

The second traditional process is the Wohlwill electrolysis. This was developed in 1898 at the Norddeutsche Affinerie in Hamburg [3]. Here the impure gold is cast into anodes which are electrorefined using an HCl/H[AuCl<sub>4</sub>] electrolyte. The gold dissolves and is then deposited in pure form on the cathode. Although high purity gold (>99.95%) can be readily achieved, the Wohlwill electrolytic process is slow and relatively inefficient. As a result it has a high inventory and is expensive to operate. Its major advantage, in addition to the production of high purity gold, is that it can be used to refine gold containing limited amounts of the PGM.

The introduction of solvent extraction for the refining of gold offers potential benefits over both the Wohlwill and Miller processes, particularly in terms of improved purity, a reduction in metal inventory and flowsheet simplification.

### SOLVENT EXTRACTION CHEMISTRY OF THE PRECIOUS METALS

Gold and the other PM (e.g., Pt, Pd, etc.) are most conveniently and effectively bought into aqueous solution in hydrochloric acid under oxidising conditions. In aqueous solution gold generally has two stable oxidation states, Au(I) and Au(III). In chloride media, however, Au(I) is unstable and slowly disproportionates to Au(III) and the metal.



The PM form stable chloro-complexes and the Au(III) is present in solution as [AuCl<sub>4</sub>]<sup>-</sup>. It can therefore be readily extracted by anion-exchangers. The PGM, however, also form anionic complexes ([PdCl<sub>4</sub>]<sup>2-</sup>, [PtCl<sub>6</sub>]<sup>2-</sup>, [RhCl<sub>6</sub>]<sup>3-</sup>, etc.) as do a number of the BM (e.g., [CuCl<sub>4</sub>]<sup>2-</sup>). The solvent extraction reagent used must therefore be selective for gold.

The extraction of anionic complexes by anion-exchangers is strongly influenced by the size to charge ratio of the metal anion[4]. Thus for the PM the order of extraction is



Anion-exchange solvent extraction reagents can be divided into two classes. The first are strong-base extractants which either have a fixed cationic charge, such as quaternary ammonium salts (e.g., R<sub>3</sub>NCH<sub>3</sub><sup>+</sup>Cl<sup>-</sup>), or amines which protonate readily in contact with weak acid (e.g., R<sub>3</sub>NH<sup>+</sup>Cl<sup>-</sup>). These not only extract gold extremely strongly but also palladium and platinum, and so are non-selective. Stripping can also be a problem due to the very strong extraction.

The other class of reagents are weak-base or solvating extractants. These generally do not "protonate" but instead solvate protons enabling these to transfer into the organic phase to give cationic groups. Almost any reagent with an oxygen containing group (P=O, S=O, C=O, C-O-) is capable of acting as a solvating extractant and therefore a very wide range of strength of extraction is available. Due to the fact that the singly charged [AuCl<sub>4</sub>]<sup>-</sup> ion is so strongly extracted by anion-exchangers, gold extractants are generally selected from the very weak solvating reagents. The other Precious Metals are not extracted to any appreciable extent by these systems and so provide an excellent means of separating gold from the PM.

These very weak solvating extractants are generally those containing carbon-oxygen functional groups such as ethers, esters and alcohols. A tri-functional ether, di(ethyleneglycol)dibutyl ether ( $C_4H_9OC_2H_4OC_2H_4OC_4H_9$ , BUTEX) has been successfully commercialised by INCO at their Acton Refinery in the UK [5]. Although BUTEX has a high selectivity it has a number of significant disadvantages. Due to the low ratio (4:1) of the hydrophobic ( $CH_2$ ) groups to the hydrophilic (O) groups, BUTEX has a high aqueous solubility ( $3\text{ g l}^{-1}$ ). It also cannot easily be stripped. The purified gold is therefore recovered by direct reduction from the loaded organic in a two-phase reaction with an oxalic acid solution. Appreciable amounts of reagent are occluded in the product and solvent losses approach 4% per cycle. BUTEX is a low volume speciality chemical and therefore expensive. As a result operating costs are high.

The ketone, 4-methyl-2-pentanone (methyl iso-butyl ketone), has been used for a number of years by both Johnson Matthey and Anglo American Platinum Corporation [6] for the extraction of gold in their PGM Refineries. Although this also has a high solubility and has to be stripped by direct reduction, it is a large tonnage industrial chemical and therefore extremely cheap. It is a stronger extractant than BUTEX and therefore also usefully removes a number of BM contaminants of the PGM feed such as Fe, Sb Se, Sn and Te. A significant drawback is its low flashpoint ( $13^\circ C$ ) that necessitates stringent plant safety control.

The extraction of gold by a wide range of alcohols (e.g., *i*-pentanol [7],  $C_7 - C_9$  alcohols [7], decanol [8], butanol [9] and 4-methyl-2-pentanol [10]) has been reported in the literature. The Council for Mineral Technology (Mintek) investigated a number of alternative reagents to BUTEX [11]. They found that the alcohol, *i*-decanol, offered several advantages over BUTEX including having a higher selectivity over base metals and, as an industrial chemical, was readily available and low cost. Furthermore, because *i*-decanol is a sufficiently weak extractant, it was possible to strip the gold from the organic phase with water as at low acidity the solvation of protons by the extractant is reversed. Subsequent to the commencement of our own studies, Mintek developed the Minataur<sup>TM</sup> Process for the solvent extraction of gold [12, 13]. Very few details about the solvent extraction section of the process have been published by Mintek and the reagent used has not been disclosed.

The extraction of gold with *i*-decanol appeared very attractive. However a significant potential drawback was that efficient stripping of the gold was reported to require elevated temperatures ( $\geq 50^\circ C$ ). A number of alternative alcohols were therefore examined at the Johnson Matthey Technology Centre.

## EXPERIMENTAL

Solutions of the alcohols (50% v/v) in Norpar 15 (Exxon Chemicals) were contacted for two minutes with an equal volume of a feed containing  $120\text{ g l}^{-1}$  Au(III) in 6 M hydrochloric acid. The raffinate was separated and contacted twice more with equal volumes of fresh organic. The loaded organic from the first extraction was then stripped three times by contacting with an equal volume of water at either 23 or  $50^\circ C$ .

## DISCUSSION

The analytical results for the extraction of gold by three representative alcohols are presented in Table 1. As can be seen, 2-ethylhexanol proved to be a far stronger extractant than *i*-decanol but gave similar results to the straight chain alcohol, *n*-octanol. Distribution isotherms were then determined for the extraction of gold by 2-ethylhexanol and *i*-decanol. These confirmed that 2-ethylhexanol was a significantly stronger extractant and had a ca. 50% greater capacity than *i*-decanol (Figure 1). This is 20% higher than would be expected from the higher molar concentration of the 2-ethylhexanol solution as a result of its lower molecular weight.

*Table 1. The extraction of gold(III) from 6M hydrochloric acid by 50% (v/v) solutions of different alcohols in Norpar 15.*

Alcohol	Initial feed (mg l <sup>-1</sup> )	1 <sup>st</sup> Raffinate (mg l <sup>-1</sup> )	2 <sup>nd</sup> Raffinate (mg l <sup>-1</sup> )	3 <sup>rd</sup> Raffinate (mg l <sup>-1</sup> )
<i>i</i> -decanol	120000	48700	1350	0.2
<i>n</i> -octanol	120000	25000	500	<0.1
2-ethylhexanol	120000	25100	299	<0.1

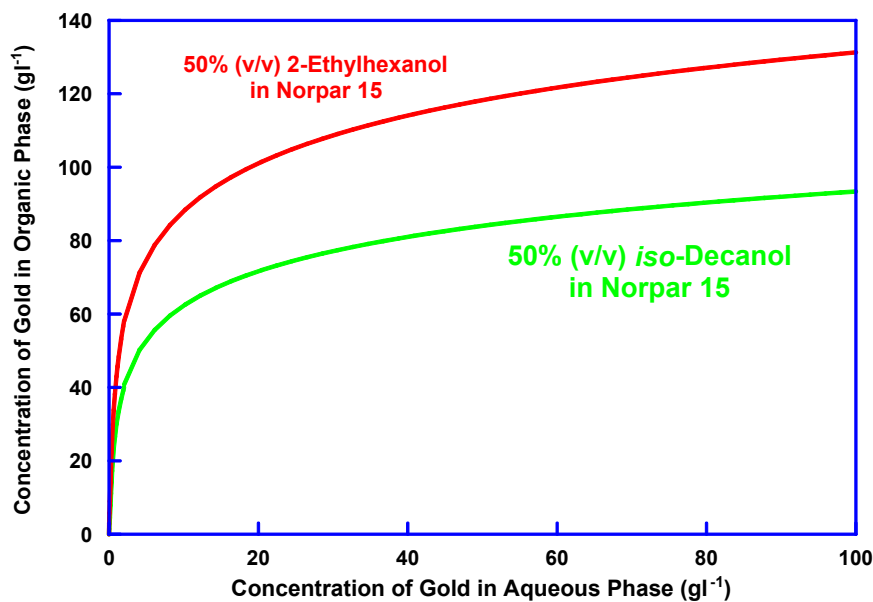


*Figure 1. Distribution isotherms for the extraction of gold(III) at 23°C.*

The results for the stripping of gold from the loaded organic from the first extraction are presented in Table 2. These showed that at ambient temperatures 2-ethylhexanol was easier to strip than *i*-decanol, whilst *n*-octanol was difficult to strip even at elevated temperatures.

*Table 2. The stripping of gold(III) from loaded 50% solutions of different alcohols in Norpar 15 using water at different temperatures.*

Alcohol	Temperature	Loaded organic (mg l <sup>-1</sup> )	Organic After 1 <sup>st</sup> Strip (mg l <sup>-1</sup> )	Organic After 2 <sup>nd</sup> Strip (mg l <sup>-1</sup> )	Organic After 3 <sup>rd</sup> Strip (mg l <sup>-1</sup> )
<i>i</i> -decanol	23°C	70800	12700	453	16
<i>i</i> -decanol	50°C	70800	7260	72	0.4
<i>n</i> -octanol	23°C	94500	33800	9630	1360
<i>n</i> -octanol	50°C	94500	24200	2990	85
2-ethylhexanol	23°C	94400	13600	348	1.8

Although the results confirmed that stripping would be more efficient at elevated temperatures, this has a number of potential disadvantages. Heating the strip section would complicate the design of equipment, not least because it would be operating at a much closer temperature to the flash point of the diluent. Loss of diluent by evaporation and the rate of possible degradation of the organic would also be significantly increased.

McCabe-Thiele constructions were therefore carried out to determine whether a gold extraction process based on 50% (v/v) 2-ethylhexanol could be successfully operated at ambient temperatures. These showed (Figure 2) that with a phase ratio of 1:1, the extraction of gold from a typical 90  $\text{g l}^{-1}$  Au(III) feed would require three equilibrium counter-current stages to produce a raffinate containing <1  $\text{mg l}^{-1}$  Au.

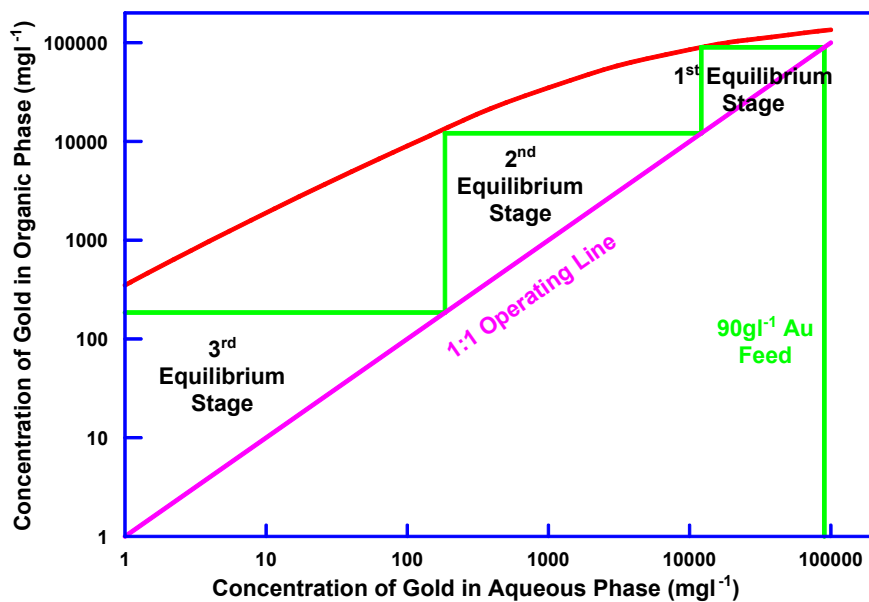


Figure 2. McCabe-Thiele construction for the extraction of gold by 50% 2-ethylhexanol.

Stripping the gold from this loaded organic to below 20  $\text{mg l}^{-1}$  Au (>99.98% strip) would require two equilibrium stages operating with a phase ratio of 1:2 (Figure 3). This level of gold recirculating in the stripped organic would not affect the number of extraction stages required.

Following further optimisation of the flowsheet, a series of pilot plant mixer-settler trials were carried out. These confirmed the promise of 2-ethylhexanol as a selective gold extractant. Typical analyses of the product streams are presented in Table 3. The level of extraction of gold achieved was >99.99%. The purity of the strip produced was >99.95%. Reduction of the gold from the strip using oxalic acid gave a further purification and produced a metal sponge of around 99.995% purity.

Table 3. Typical analyses of product streams from pilot plant trials.

	Feed ( $\text{mg l}^{-1}$ )	Raffinate ( $\text{mg l}^{-1}$ )	Strip ( $\text{mg l}^{-1}$ )
Au	150000	2.1	96000
Ag	200	95	< 2
Cu	30	16	< 2
Fe	170	86	< 2
Pd	248	125	< 2
Pt	630	320	< 2
Sb	20	10	< 2
Se	32	16	< 2
Te	125	67	< 2

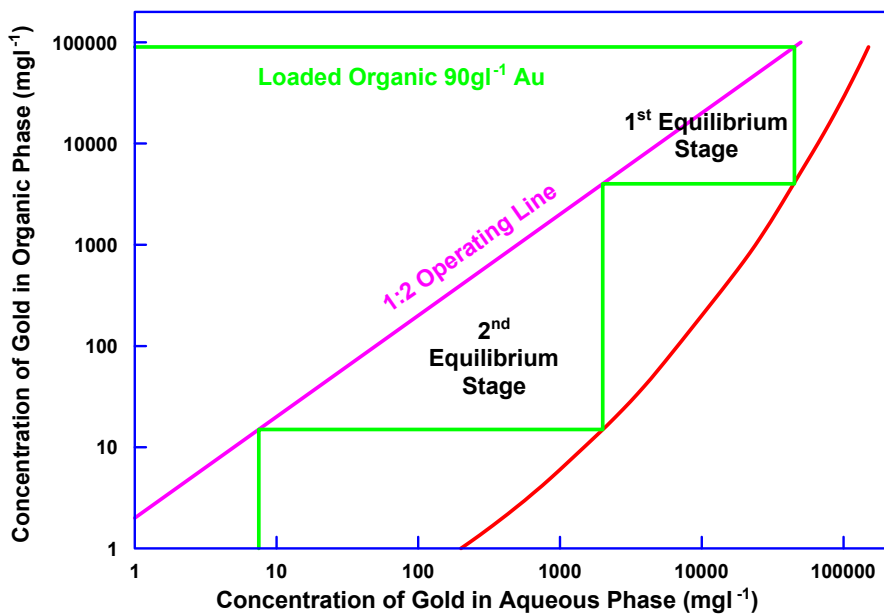


Figure 3. McCabe-Thiele construction for the stripping of gold from 50% 2-ethylhexanol.

## CONCLUSIONS

The refining of high purity gold by solvent extraction offers potential advantages over the traditional techniques such as the Miller and Wohlwill Processes. The industrial synthetic alcohol, 2-ethylhexanol, has been shown to have significant advantages over other potential gold extractants including high selectivity over other metals, the ability to be stripped with water at ambient temperatures, high capacity and low cost.

## REFERENCES

1. L. Thompson (1838), *J. Royal Soc. Arts*, **53**, 17.
2. F. B. Miller (1868), *J. Chem. Soc.*, **21**, 506.
3. E. Wohlwill (1898), *Zeit. Elektrochem.*, **4**, 379, 402, 421.
4. R. A. Grant (1990), Precious Metal Recovery and Refining Seminar, L. Manziek (ed.), International Precious Metal Institute, Allentown, PA.
5. B. F. Rimmer (1974), *Chem. Ind. (London)*, **2**, 63.
6. M. J. Cleare, R. A. Grant and P. Charlesworth (1981), Extraction Metallurgy '81, Institute of Mining and Metallurgy, London, p. 34.
7. G. S. Lopatin and I. N. Plaskin (1961), *Izv. Vyssh. Ucheb. Zavedenii, Tsvet. Met.*, **4** (4), 87.
8. N. M. Kuz'min, V. S. Vlasov and T. A. Bokova (1972), *Zh. Anal. Khim.*, **27** (9), 1807.
9. G. E. Baiulescu and I. Craciun (1974), *Rev. Chem. (Bucharest)*, **25** (7), 578.
10. S. P. Patil and V. M. Shinde (1975), *Sep. Sci.*, **10** (3), 323-9.
11. M. Fieberg, C. Connell and W. A. M. Te Riele (1978), *Mintek Report* 1996, Randburg, RSA.
12. A. Feather, K. C. Sole and L. J. Bryson (1997), *J. S. Afr. Inst. Min. Met.*, **97**, 169.
13. K. C. Sole, A. Feather, J. Watt, L. J. Bryson and P. F. Sorensen (1998), EPD Congress 1998, B. Mishra (ed.), The Minerals, Metals and Materials Society, Warrendale, PA, p. 175.



## PILOT-PLANT SOLVENT EXTRACTION OF COBALT AND NICKEL FOR AVMIN'S NKOMATI PROJECT

Angus Feather, Wendy Bouwer, Arnold Swarts\* and Vic Nagel\*\*

MINTEK, Randburg, South Africa

\*Anglovaal Mining Company Ltd., Johannesburg, South Africa

\*\*Bateman Engineering, Boksburg, South Africa

Avmin have developed a flowsheet for the refining of copper, nickel and cobalt from Nkomati concentrates. Cobalt is recovered from calcium-saturated solution using CYANEX® 272. Nickel is subsequently extracted using versatic acid. The loaded organic is stripped using spent electrolyte, producing advance electrolyte for recovery of nickel by electrowinning.

Cobalt was recovered with >99.5% extraction efficiency, reducing cobalt from 1.8 g/L to <10 mg/L. The cobalt/nickel ratio in the cobalt product solution was >1500. Nickel solvent extraction was optimised to recover 99%, reducing the nickel concentration from 32 g/L to <0.3 g/L, while minimising calcium deportment to the nickel electrowinning circuit.

### PROCESS DESCRIPTION

In the flowsheet developed by Avmin for the Nkomati base metal refinery, copper, nickel, and cobalt from a sulphide flotation concentrate are dissolved using fine grinding, followed by pressure leaching. Copper is recovered from the leach liquor by solvent extraction (SX). A bleed stream of the copper SX raffinate is treated to remove iron by oxidation/precipitation, and then to recover cobalt and nickel in sequential SX unit operations.

After precipitation of iron from the copper SX raffinate, cobalt is recovered from solution using a phosphinic acid extractant, CYANEX® 272. The cobalt concentration in the nickel solution is reduced to enable the cobalt specification in the downstream nickel electrowinning (EW) to be met. Co-extracted nickel, calcium, and magnesium are scrubbed from the loaded organic phase using a portion of the loaded strip liquor (cobalt concentration of approximately 25 g/L). The scrubbed organic phase is stripped with dilute sulphuric acid to produce a cobalt sulphate solution. The form of the final cobalt product has yet to be decided.

Nickel is extracted from the calcium-saturated solution by SX using versatic acid. Co-extracted calcium and magnesium are scrubbed from the loaded organic phase using a portion of the nickel loaded strip liquor diluted with water to a nickel concentration of 3 g/L and a pH of 5.6. The scrubbed organic phase is stripped with spent electrolyte from the nickel EW operation.

Both SX plants were operated at ambient temperature as this was considered to be a “worst case scenario” in terms of settling characteristics, reaction kinetics, and nickel ammonium sulphate precipitation. The circuit was continuously run for 400 hours. Nickel was recovered from the advance electrolyte by standard divided-cell EW technology. Figure 1 shows the overall process flowsheet.

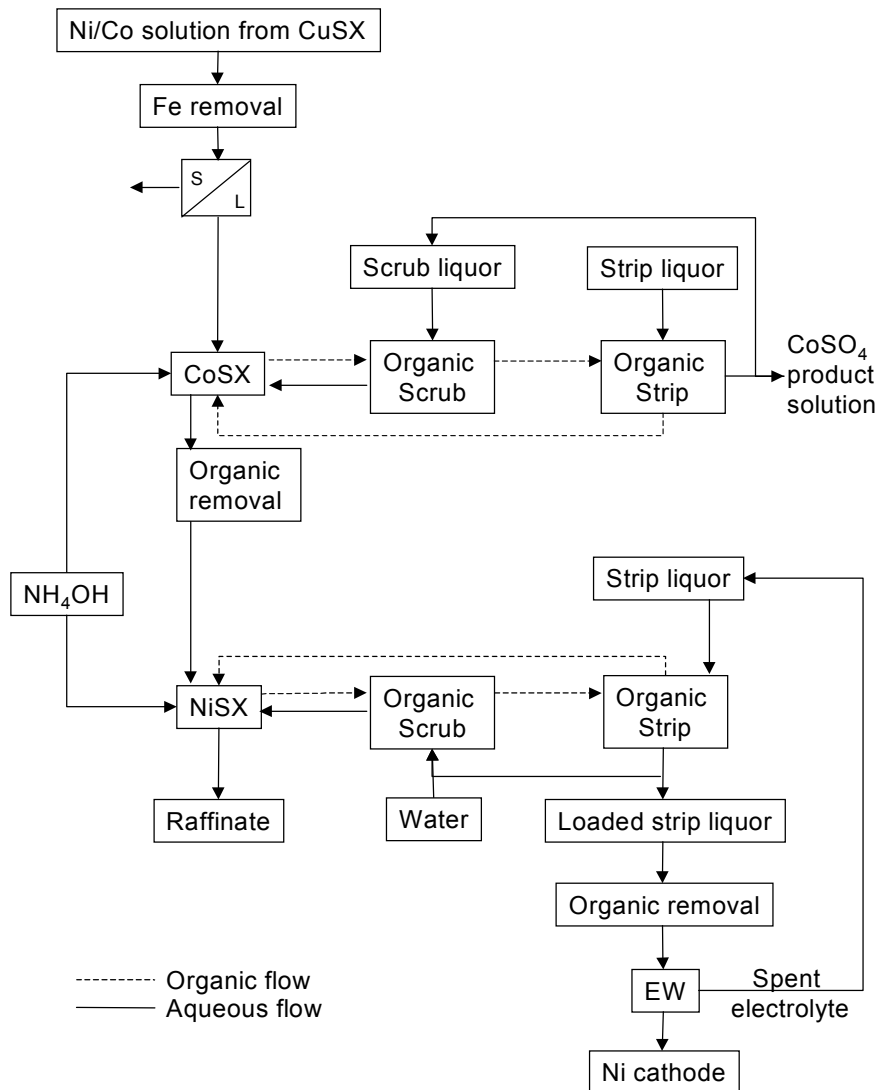


*Figure 1. Process flowsheet for treatment of Nkomati copper SX raffinate.*

## EQUIPMENT AND PROCEDURES

Conventional mixer-settler units, each with a mixer volume of 500 mL and settling area of 256 cm<sup>2</sup>, were operated in a countercurrent configuration. Solutions were pumped into the plant using peristaltic pumps. When required, stages were operated with internal recycle to maintain aqueous phase continuity in the mixers. Adjustment of pH in both SX circuits was achieved by the addition of 400 g/L NH<sub>4</sub>OH or 300 g/L H<sub>2</sub>SO<sub>4</sub> solution directly into the mixers. The NH<sub>4</sub>OH concentration was chosen based on Avmin's estimate of the concentration attainable from the lime boil ammonia recovery planned for the full-scale circuit. Control of pH in each stage was by the use of an ABB Commander 300 PID controller linked to a peristaltic pump and Foxboro pH meter and probe.

CYANEX 272 was supplied by Cytec, Canada, and versatic acid by Shell, South Africa. Both circuits used C<sub>12</sub>-C<sub>13</sub> *n*-paraffin (SasolChem, South Africa), an aliphatic hydrocarbon diluent.

## COBALT SOLVENT EXTRACTION

The feed solution to the cobalt SX was synthetically made up to represent Avmin's estimate of the cobalt SX feed. After 7 days operation, this was replaced by copper SX raffinate from a previous pilot campaign, which had been subjected to an iron removal step. The composition of the cobalt SX feed solution is shown in Table 1 and the circuit configuration in Figure 2.

*Table 1. Average composition of feed solution to cobalt SX.*

Element	Ni	Mn	Fe	Cu	Zn	Ca	Mg	Co
Concentration (g/L)	32.7	0.31	0.001	0.007	0.121	0.576	3.58	1.87

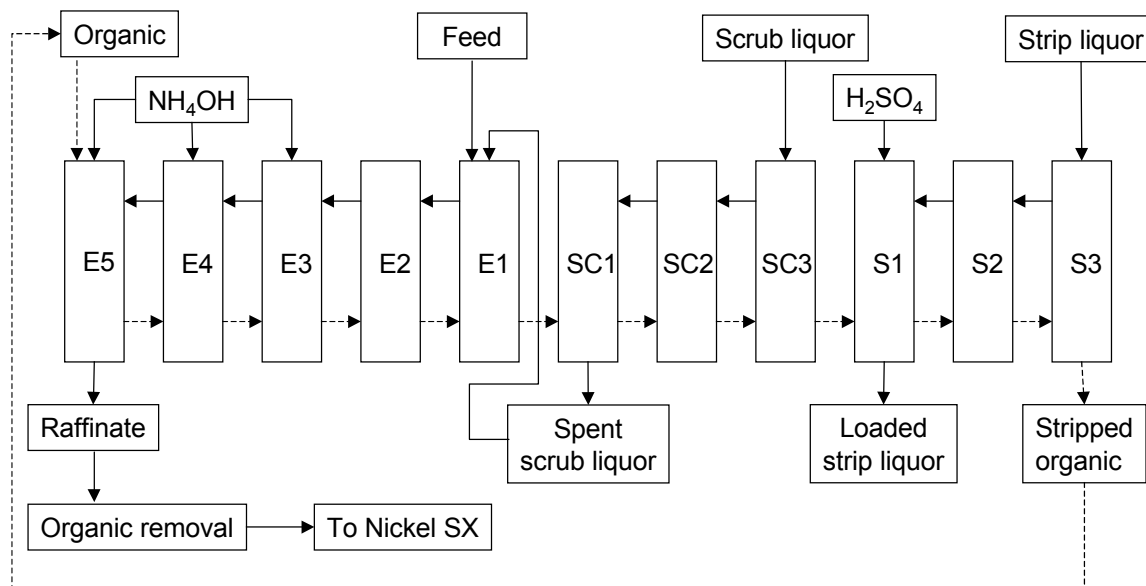


*Figure 2. Cobalt SX circuit configuration.*

### Extraction

The organic phase contained 7 vol.% CYANEX 272 and, with a phase ratio of 1, enabled the cobalt concentration to be consistently reduced to <10 mg/L. The pH was controlled in the last three stages to between 5.5 and 5.65, with the pH being slightly raised towards the end of the extraction bank to ensure low levels of cobalt in the raffinate. Some magnesium, calcium, and nickel were loaded in the last extraction stages, but progressively squeezed off the organic phase by cobalt in the incoming feed solution. Table 2 shows typical extraction efficiencies achieved for the various elements present in the feed solution.

*Table 2. Extraction efficiencies of major elements in the cobalt SX circuit.*

Element	Ni	Mn	Fe	Cu	Zn	Ca	Mg	Co
Extraction (%)	1.39	99.7	> 99.5	> 85	> 99.5	0.25	2.44	99.7

The  $\text{NH}_4\text{OH}$  consumption for cobalt extraction was 0.88 kg  $\text{NH}_4\text{OH}$  per kg of cobalt extracted, which represents 75% of the stoichiometric requirement. This low consumption has been noted during previous cobalt SX campaigns [1], and is thought to be due to the strong buffering effect of the high ionic strength of the aqueous solution. The consumption includes the  $\text{NH}_4\text{OH}$  required for the extraction of impurity elements such as copper, manganese, and zinc, as well as cobalt that is scrubbed off the organic phase in the scrubbing section and then re-extracted in the extraction stages.

### **Scrubbing**

The magnesium, calcium, and nickel in the loaded organic phase were scrubbed in three stages at an O/A ratio of approximately 52, using dilute cobalt (26 g/L) sulphate with a pH of 2.8. The scrub mixer-settler units were operated with internal recycle of aqueous phase, adjusted to ensure that the apparent phase ratio in the mixer was close to 1. This ensured that there was sufficient interfacial surface area for adequate mass transfer.

The optimised advance phase ratio and pH in the scrubbing section (pH 4.4 to 4.9) ensured that the following objectives were met:

- The magnesium, calcium, and nickel scrubbed from the loaded organic phase to meet the specification of the cobalt product solution;
- The cobalt in the spent scrub solution to be depleted by at least 50%; and
- Calcium concentration in the spent scrub solution to be below gypsum saturation level.

### **Stripping**

The scrubbed organic phase was stripped in three counter-current stages using dilute H<sub>2</sub>SO<sub>4</sub> (50 g/L). The pH in the first stage was controlled at 2 to ensure adequate stripping of impurities such as zinc, which are loaded in the extraction section and are not scrubbed off in the scrub section. Typical product solution composition is shown in Table 3.

*Table 3. Product solution from cobalt SX.*

Element	Concentration (g/L)	Element	Concentration (g/L)
Co	29.20	Fe	0.001
Ni	0.008	Zn	1.52
Cu	0.094	Si	0.001
Mn	3.98	Ca	0.003
Al	0.001	Mg	0.568

## **NICKEL SOLVENT EXTRACTION**

The raffinate from the cobalt SX plant was passed through a column of coal-based activated carbon (Montan Chemicals GRC 22) for the removal of dissolved organic from the solution. Table 4 shows the composition of a typical nickel SX feed, once the cobalt SX circuit had been optimised. The circuit configuration is shown in Figure 3.

*Table 4. Typical feed composition to nickel SX circuit.*

Element	Concentration (g/L)	Element	Concentration (g/L)
Ni	31.200	Zn	< 0.002
Co	0.005	Si	0.039
Cu	< 0.002	Ca	0.541
Mn	< 0.002	Mg	3.250

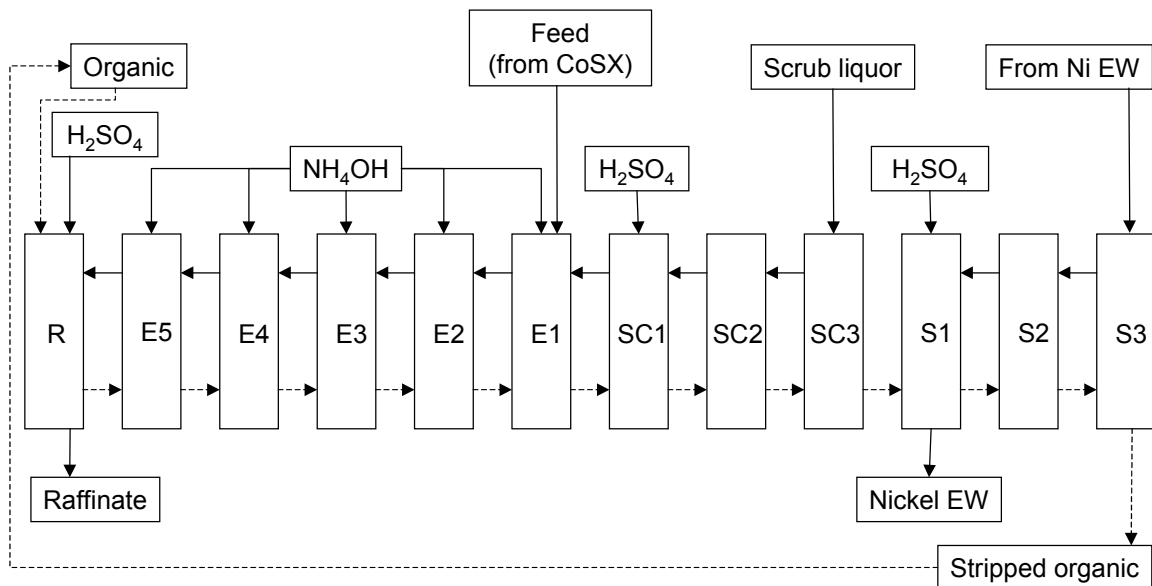


Figure 3. Nickel SX circuit configuration.

### Extraction

The objective in the extraction section was to achieve a nickel extraction efficiency of 99%, while minimising the co-extraction of calcium into the loaded organic phase to a level that could be scrubbed into a low scrub liquor flowrate without the precipitation of gypsum. No dilution was made to the extraction circuit, other than the neutralising base and the calcium-rich spent scrub liquor. The versatic acid concentration in the organic phase was 30 vol.%.

The nickel SX circuit was started with four extraction stages at the chosen pH profile. To achieve 99% extraction efficiency and improve nickel/calcium separation, a fifth extraction stage was added. The plant was operated to ensure that the calcium concentration in the aqueous phase of each stage was safely below the solubility limit of gypsum.

The main control mechanism was the organic-phase calcium profile. After optimisation of the pH profile, the target of 99% nickel extraction was achieved, and the co-extraction of calcium was limited to <3%. Figure 4 shows the aqueous and organic phase profiles of calcium and nickel across the extraction section.

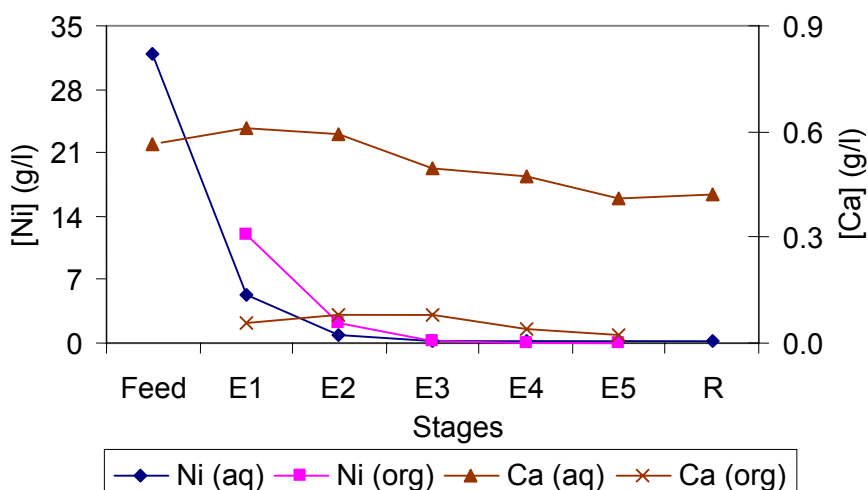


Figure 4. Nickel SX extraction profile.

Dissolved versatic acid was recovered from the raffinate by contacting the raffinate with the stripped organic phase. This operation was done in a separate reclamation mixer settler at a controlled pH of 3, reducing the versatic acid concentration in the raffinate to <25 mg/L.

### Scrubbing

The purpose of the scrubbing section was to minimise the transfer of calcium into the EW electrolyte circuit to such an extent that a bleed stream of <5% of the spent electrolyte would be sufficient to maintain the calcium concentration below the gypsum solubility limit. This meant that the calcium concentration on the scrubbed organic should be reduced to <9 mg/L. In order to scrub co-extracted calcium to this level, the correct pH profile across the scrubbing section is essential. To achieve this, the pH in the first scrubbing stage was maintained at 5.9 by the controlled addition of 300 g/L H<sub>2</sub>SO<sub>4</sub>.

### Stripping

The scrubbed organic phase was stripped in three stages using spent EW electrolyte. The steady-state compositions of the stripping solutions are shown in Table 5.

*Table 5. Composition of nickel SX stripping solutions.*

Element	Ni	Mn	Fe	Cu	Zn	Ca	Mg	Co
Spent (g/L)	66	0.003	0.001	0.001	0.001	0.21	0.29	0.05
Advance (g/L)	98	0.003	0.001	0.001	0.001	0.22	0.29	0.06

## CONCLUSIONS

The cobalt SX circuit was optimised to recover >99.5% of the cobalt in the feed stream with overall extraction of nickel <0.1%. The cobalt/nickel ratio of the loaded strip solution from this operation was >1500.

Nickel was recovered with >99% extraction efficiency in the second SX plant with overall calcium extraction into the nickel electrolyte circuit of <3%. Importantly, the nickel SX was optimised to prevent precipitation of gypsum or nickel salts in the extraction section.

## ACKNOWLEDGEMENTS

This paper is published by permission of Avmin and MINTEK. Start-up conditions for the nickel SX system were determined by John Preston. Pilot-plant control systems were optimised by Milton Summers. Cytec and Shell are thanked for providing the extractants.

## REFERENCES

1. A. M. Feather, K. C. Sole, and D. B. Dreisinger (1999), *Proc. International Solvent Extraction Conference ISEC '99*, Society of Chemical Industry, London, pp. 1443-1448.
2. V. Nagel, B. M. Davies, and P. M. Cole (1999), *Proc. International Solvent Extraction Conference ISEC '99*, Society of Chemical Industry, London, pp. 1437-1442.



# SEPARATION OF COBALT AND NICKEL BY SOLVENT EXTRACTION FROM SULFATE LIQUORS OBTAINED BY ACID LEACHING OF A PRODUCT FROM THE CARON PROCESS

**Elízabeth García Liranza, Aurora Moreno Daudinot, Roberto Viera Martínez,  
and Bernardo Rosales Bárzaga**

Laterite Research Center, Moa, Cuba

Laboratory-scale and miniplant studies have been conducted on the solvent extraction of cobalt from a liquor obtained by the sulfuric acid leaching of basic nickel - cobalt carbonate (a product of the Caron process for the treatment of lateritic ores).

Laboratory scale results showed that CYANEX 272 extracts 99% of cobalt and over 98% of zinc and manganese, with only 1.5% co-extraction of nickel. At miniplant scale, cobalt extraction was 99.7%, with nickel co-extraction below 1%, and over 98% extraction for other impurities. The Ni/Co ratio reached in the raffinate was 8166 and the Co/Ni ratio in the cobalt product solution was 528. Manganese was not separated from cobalt by solvent extraction.

## INTRODUCTION

Lateritic ore processing by reduction of the mineral and subsequent leaching in ammonium carbonate media (the Caron process) has been developed since the early 1940s at the Nicaro Plant in Cuba [1, 2]. Thereafter, similar processes were implemented at the Queensland Nickel plant in Australia (1974) [3, 4], at Companhia de Niquel Tocantins in Brazil (1981) [5, 6] and at the Punta Gorda Nickel plant in Cuba (1980s) [6].

The two Cuban plants currently running this process obtain nickel oxide as the main product in the form of sinter and a mixed nickel-cobalt sulfide, with a Ni/Co ratio of 2:1, as by-product.

Since the 1970s, studies have been carried out on the use of extraction by organic solvents for the separation of Ni, Co, Cu and Zn from sulfate and ammonium carbonate solutions, employing chelating and acidic extractants. A large amount of data has been obtained, serving as a basis for feasibility studies for the construction of a nickel-cobalt refinery based on the mixed sulfides from the ammoniacal process. By mid-1998, a small refinery with a capacity of about 30 t/y of cobalt as carbonate was designed and built at the Laterite Research Center, a product of reliable quality (99% purity) being obtained.

This paper presents a summary of the experimental results from laboratory and miniplant studies on a solvent extraction process for the selective recovery of cobalt from acid-leached basic nickel-cobalt carbonate.

## PROCESS DESCRIPTION

### Experimental

The laboratory and miniplant scale studies were carried out using an acid-leached basic nickel-cobalt carbonate solution obtained from the pilot-plant scale work. Impurities such as iron and copper were removed previously from the solution by precipitation using oxidation and neutralization methods. The chemical solution composition is shown in Table 1.

*Table 1. Chemical composition of the acid leached basic Ni-Co carbonate solution (g/L).*

Ni	Co	Fe	Zn	Cu	Mn	Ca	Mg	pH
92.63	3.53	0.004	0.193	0.001	0.643	0.12	0.628	4.3

Both studies were carried out with CYANEX 272 at 20% v/v (0.634 mol/L) in kerosene as hydrocarbon diluent. The sulfuric acid solutions employed were prepared from 98% reagent grade acid. Sodium hydroxide at 32% was used as the neutralizing agent.

Effect of pH, extraction isotherms, organic phase scrubbing, kinetics of cobalt extraction and stripping isotherms were determined in laboratory studies. All tests were carried out in beakers with mechanical agitation of the phases, after which the phases were separated in separating funnels. The pH control of the process was achieved by neutralizing the solvent with NaOH solution.

Once organic and aqueous phases were separated, stripping of the organic phase was carried out using 150 g/L sulfuric acid at unit phase ratio. Chemical analysis of the solutions was carried out by atomic absorption spectrophotometry. All the tests were done at room temperature (27- 29°C).

The miniplant consisted of ten mixer-settlers made of transparent acrylic. Each mixer was equipped with a digital speed control and a six-bladed turbine-type impeller to achieve the correct mixing of phases and pumping between stages. Aqueous and organic phases were pumped by using peristaltic pumps, and the flows were controlled by flowmeters. The dimensions of the mixer-settlers are given in Table 2.

*Table 2. Dimensions of the mixer-settlers.*

Dimensions	Mixer	Settler
Width	150 mm	150 mm
Length	96 mm	325 mm
Total height	228 mm	228 mm
Effective volume	2 736 cm <sup>3</sup>	9 360 cm <sup>3</sup>
Impeller diameter	55 mm	
Area	-	0.0487 m <sup>2</sup>

## RESULTS AND DISCUSSION

### Laboratory Test Work

#### *Effect of pH*

The variation in cobalt extraction with aqueous pH was studied at pH range from 1 to 6, O: A equal to 1, with 5 min. extraction time and 15 min. for stripping.

Figure 1 shows the extraction curves for the most relevant elements present in the feed solution. The maximum cobalt extraction is achieved at pH value 6, where 99.4% of cobalt is separated from the rest of the elements. Under these conditions about 3 % of nickel is co-extracted. The selectivity order showed by CYANEX 272 at pH 6 was:

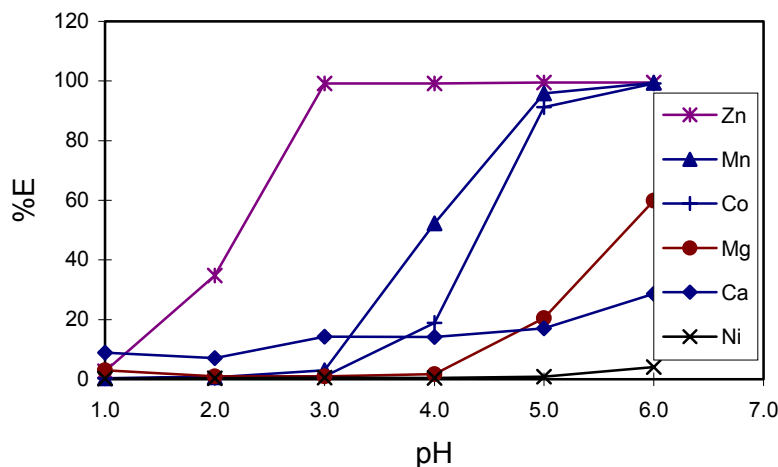


Figure 1. Extraction curves for CYANEX 272 at 20%, O:A = 1:1,  $t = 5\text{min}$ ,  $T = 28^\circ\text{C}$ .

#### Cobalt extraction isotherm

The extraction isotherm was obtained by contacting the phases at O:A ratios of 10, 5, 2, 1, 0.5, 0.25 and 0.1 (pH  $\sim 5.5$ ) at 5 min as extraction time. The results shown in Figure 2 indicate that three is the number of extraction stages required to separate more than 99% of cobalt.

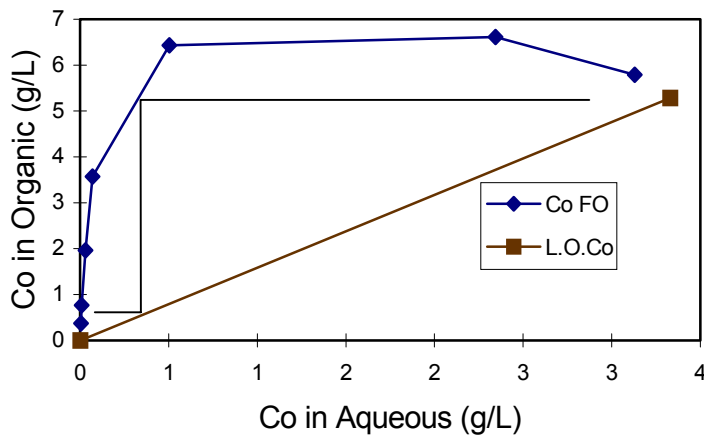


Figure 2. Extraction isotherm.  $T = 28^\circ\text{C}$ .

#### Organic phase scrubbing

To separate the co-extracted impurities (mainly nickel), tests for scrubbing of the organic phase with 20 g/L cobalt sulfate solutions were done at O:A ratios from 1 to 10. Under these conditions, the scrubbing efficiency for nickel was more than 98%. The scrubbing of calcium and magnesium was also effective, but manganese is scrubbed in smaller quantities. Figure 3 shows the effect of the phase ratios on the cobalt and nickel concentration in the loaded solvent.

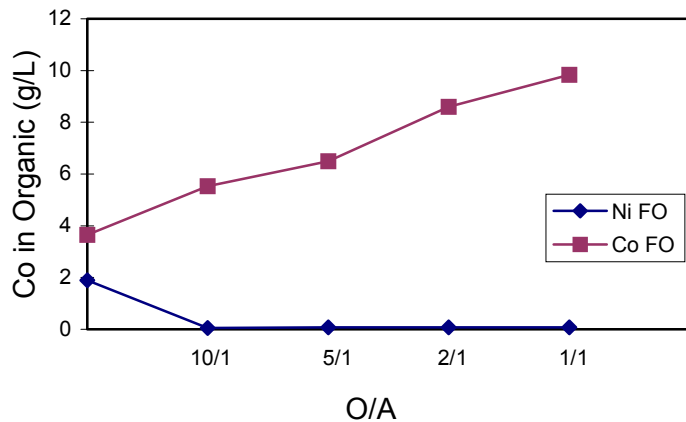


Figure 3. Effect of phase ratios O:A on organic scrubbing.

#### Kinetics of cobalt extraction

The effect of equilibrium time on cobalt extraction was studied at 1:1 phase ratio for times period of 30, 60, 90, 120 and 180 seconds. Figure 4 shows that cobalt extraction kinetics is very fast, reaching more than 97% extraction at pH values 5.4-5.5 in only 30 seconds. Nevertheless, there is no possibility of selecting cobalt extraction by controlling the extraction time, because all elements show rapid extraction kinetics.

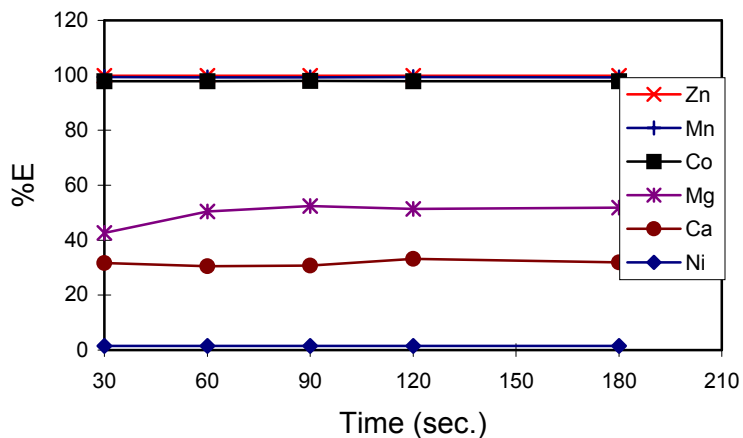


Figure 4. Extraction kinetics of elements. O:A = 1:1, T = 28°C.

#### Cobalt stripping isotherm

To determine the number of theoretical stages for cobalt stripping, experiments were carried out by using 10 to 1 O: A phases and 15 minutes of contact time. The cobalt-stripping isotherm (Figure 5) shows that two stages would recover more than 99% of loaded cobalt from the organic phase.

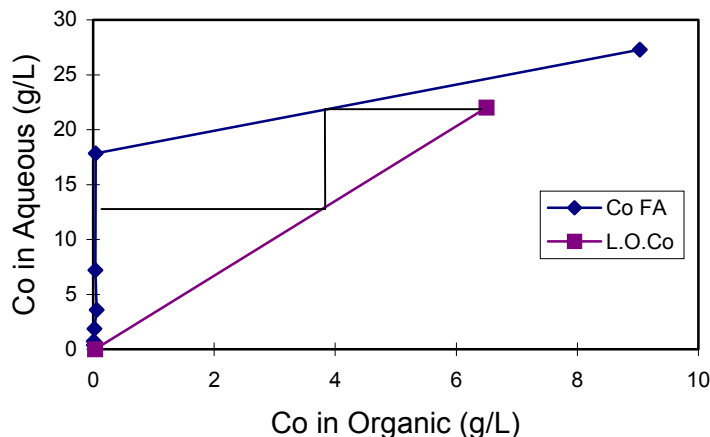


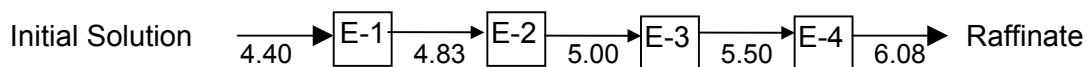
Figure 5. Cobalt stripping isotherm.  $T = 28^\circ\text{C}$ .

### Miniplant Run Test

The solvent extraction circuit was operated continuously for a total running time of 96 hours. This time  $2.13 \text{ m}^3$  of nickel-cobalt sulfate solution were treated. Organic and aqueous streams were sampled once every two hours. Chemical analyses were carried out by atomic absorption spectrophotometry.

### Extraction

The pH values across the extraction stages were controlled between 4.4 and 6.08 as shown in the following diagram:



Cobalt concentration in the raffinate was maintained below 0.012 g/L. The total extraction efficiencies for the elements are given in Table 3.

Table 3. Extraction efficiencies for the elements.

Elements	Ni	Co	Fe	Zn	Cu	Mn	Ca	Mg
Extraction (%)	0.23	99.67	92.7	99.6	98.7	99.3	3.7	25.6

### Organic phase scrubbing

Co-extracted nickel was scrubbed in two stages with 20 g/L cobalt sulfate solution, O: A  $\sim 8:1$  and at a pH of 5.5. Only nickel and part of the magnesium are scrubbed from the organic phase. Nickel and magnesium concentrations were reduced by 96.3 and 71.4%, respectively in the loaded organic phase, while iron, zinc, copper, manganese and calcium are reduced to a lesser degree, inferior to 30%. Table 4 shows the average concentrations of elements in the loaded and scrubbed organic phases.

Table 4. Chemical composition of loaded and scrubbed organic phases (g/L).

Elements	Ni	Co	Fe	Zn	Cu	Mn	Ca	Mg
Loaded phase	0.35	7.71	0.038	0.32	0.03	1.176	0.008	0.049
Scrubbed phase	0.013	7.84	0.03	0.29	0.021	1.13	0.007	0.014

### **Cobalt stripping**

Cobalt stripping was done by diluted sulfuric acid in three stages while iron, zinc, calcium and part of the others elements were stripped using a higher concentration of sulfuric acid than in the cobalt circuit. The total stripping efficiencies for the elements are given in Table 5.

*Table 5. Stripping efficiencies for the elements.*

Elements	Ni	Co	Fe	Zn	Cu	Mn	Ca	Mg
Stripping (%)	100	99.97	0.63	0.227	69.04	67.0	8.14	17.64

Table 6 shows the chemical composition of the final cobalt product solution from the run test.

*Table 6. Chemical composition of the final cobalt solution (g/L).*

Ni	Co	Fe	Zn	Cu	Mn	Ca	Mg
0.156	82.3	0.002	0.007	0.153	7.94	0.006	0.026

The manganese content was separated by treatment with sodium persulfate solution, giving 82 % manganese precipitation efficiency and only 0.5 % of cobalt co-precipitation.

## **CONCLUSIONS**

The results on the solvent extraction of cobalt from the nickel-cobalt sulfate leach liquor by CYANEX 272 shows the technical feasibility of this process. Impurity removal before and after the solvent extraction circuit is required, however.

Cobalt extraction was over 99% and nickel co-extraction was below 0.5%. The Ni:Co ratio was upgraded from 26.24 in the feed solution to 8 166 in the raffinate. In addition, a cobalt product solution with Co:Ni ratio equal to 528 was obtained.

## **REFERENCES**

1. Nichols Engineering and Research Corporation (1957), *Eng. Min. J.*
2. G. M. Ritcey (1991), *Proc. Int. Seminar on Laterite Ore Acid Leaching Technology*, Moa, Cuba.
3. J. G. Reid, M. J. Price (1993), *Proc. ISEC' 93*, York, England, pp. 225-231.
4. J. G. Reid (1995), *Proc. Aus. IMM Annual Conference*, AusIMM, Victoria, p.131.
5. R. F. Stauffer and R. M. Berezowski (1991), Sherritt Trip Report to Companhia Nickel Tocantins, Alberta, Canada, 9 pp.
6. G. M. Ritcey (1999), *ALTA '99 Nickel & Cobalt Pressure Leaching and Hydrometallurgy Forum*, Melbourne, 22 pp.



## MODELLING METHODOLOGY FOR THE SIMULATION OF SOLVENT EXTRACTION PROCESSES - COBALT/NICKEL

Jörg Leistner, Astrid Görge\*, Werner Bäcker\*\*, Andrzej Górkak and Jochen Strube\*\*

Chair for Thermal Process Engineering, University of Dortmund, Germany

\*H.C. Starck, Goslar, Germany

\*\*Fluid Process Development, Bayer AG, Leverkusen, Germany

A modelling basis for the description of reactive extraction processes has been developed. As an example, the separation of cobalt from nickel by a commercial cation exchanger has been chosen, to take manifold effects into account. Different models have been created that are based on a small number of parameters for the description of mass transfer and thermodynamic or chemical equilibrium respectively. Simulation studies of mixer-settler combinations as well as columns have been carried out to improve process comprehension.

### INTRODUCTION

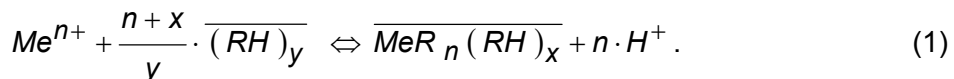
Process design in the field of multi-component extraction is strongly influenced by empirical procedures. Reasons for this are the strong ionic-interaction forces, high concentration ranges and several phenomena, which intensively affect the distribution in industrial applications. Therefore, the application of theoretical approaches to the separation of multi-component mixtures leads to failures in the prediction of phase equilibrium. Moreover, due to the complex flowsheet the amount of process and operating parameters that have to be optimised leads to a high number of experiments. In order to reduce experimental costs as well as expenditure for screening of process variants, detailed scale-up and process optimisation, simulation can be employed.

Either short cut or physico-chemical (rigorous) models are used in combination with numerical optimisation tools for a qualitative prediction of operating points based on lab scale experiments only. Short cut models are used for a first estimation of thermodynamic feasibility and economy evaluation of potential process alternatives and extraction media types. Rigorous models are applied for the next step in the design procedure in order to prove the experimental feasibility. The operating points simulated are validated during the first piloting studies and support than the quantitative prediction of further optimised operating points for a better process comprehension.

For this design strategy, the most important model parameters have to be determined by experiments like equilibrium data from shake out experiments, kinetic data from single drop apparatus and further investigations of drop behaviour. The complete model is used for the simulation of a continuous operating mixer-settler plant or a sequence of columns. The sensitivity of reactive extraction of cobalt and nickel with regard to individual model parameters will be illustrated by simulation studies. The complex separation behaviour of Co/Ni has been used as a test example.

## REACTIVE EXTRACTION OF COBALT AND NICKEL

The reactive extraction of n-valent metal cations,  $\text{Me}^{n+}$ , by ion exchangers, RH, is based on complex formation. Unfortunately, this complex formation is affected by many variables like the ionic strength and the concentration of the extractive agent. These dependencies complicate process modelling and simulation although the separation of cobalt and nickel by ion exchangers is a widely examined application in the field of hydrometallurgy [1-5]. Thus the complex structure or the number of associated extractive agent molecules can change due to the loading condition of the organic phase. At very high loading conditions even reversible polymerisation can occur [6]. To take these modifications into account the complex formation can be generalised as follows (Components in the organic phase are represented by a superscript bar.):



Depending on the solvent used, the cation exchanger usually forms dimers in aliphatic and monomers in aromatic dilutents, which is indicated by  $y$ . The number of additional ion exchanger molecules is represented by  $x$ , due to the coordination number of the complex formed. Nevertheless, equation 1 is still a simplification because possible formation of polynuclear or mixed complexes of cobalt and nickel are neglected as well as the saturation of coordination compounds by different anions or water molecules. However, this simplified description has been chosen because within certain operating ranges the influence of these parameters is constant and can be summed up as an assumption which has been proven.

Responding to equation 1 the reaction equilibrium can be described by the law of mass action for each metal by an equilibrium constant  $K_{\text{ex}}$ , if the stoichiometry is constant for the considered concentration range:

$$K_{\text{ex}} = \frac{\left[ \overline{\text{MeR}_n(\text{RH})_x} \right] \cdot [\text{H}^+]^n}{\left[ \text{Me}^{n+} \right] \cdot \left[ \overline{(\text{RH})_y} \right]^{n+x/y}}. \quad (2)$$

From equation 2 an expression for the distribution coefficient  $D$  can be derived:

$$D = K_{\text{ex}} \cdot \left[ \overline{(\text{RH})_y} \right]^{n+x/y} \cdot 10^{-n \cdot \text{pH}}. \quad (3)$$

This correlation connects the main regulating variables in reactive extraction processes with the distribution of metals in both phases. These are the equilibrium constant, the pH-value and the concentration of the free extractant.

## MODELLING

The equipment that is used in the field of extraction can be divided into two main groups: mixer-settlers and columns. In general there are two kinds of models for these equipments: stage models and models that take fluid dynamic non idealities into account.

**Mixer-settler combinations** have an overall stage efficiency near one. Therefore stage models can be used for feasibility studies with thermodynamic equilibrium, which is represented by equation 1, or in consideration of mass transfer resistance.

**Columns** can be described either by stage models or models which consider hydrodynamic behaviour, for example back-mixing, like the dispersive plug flow or drop population models. To take non idealities of fluid dynamic into account dispersive plug flow model has been chosen:

$$\frac{\partial}{\partial t} c_j^d = D_{ax}^d \cdot \frac{\partial^2 c_j^d}{\partial z^2} - u^d \cdot \frac{\partial c_j^d}{\partial z} - k_{eff} \cdot \frac{6}{d_{drop}} \cdot (c_j^d - c_j^{d,eq}) \quad (4)$$

$$\frac{\partial}{\partial t} c_j^k = D_{ax}^k \cdot \frac{\partial^2 c_j^k}{\partial z^2} + u^k \cdot \frac{\partial c_j^k}{\partial z} + k_{eff} \cdot \frac{\varepsilon}{(1-\varepsilon)} \cdot \frac{6}{d_{drop}} \cdot (c_j^d - c_j^{d,eq}) \quad (5)$$

The boundary conditions for this partial differential equation are derived by Danckwerts [7]. The models require several parameters depending on their complexity. They can be assigned to the following modelling phenomena: chemical and thermodynamic equilibrium, mass transfer, chemical reaction kinetic and hydrodynamics.

## DETERMINATION OF MODEL PARAMETERS

In order to simulate extraction processes the main regulating parameters, which are the equilibrium constant and the mass transfer coefficient, have to be determined.

### Equilibrium Constant $K_{ex}$

Shake out experiments were carried out under isothermal condition in closed Erlenmeyer flasks. Metal concentrations were analysed by atomic absorption spectroscopy as described by Manski [8]. The equilibrium constants are determined using the well-known slope-analysis method.

### Mass Transfer Coefficient $k_{eff}$

To determine the mass transfer coefficient a single drop cell was used (see [9] for a detailed description). The following photos (Figure 1) illustrate the dependency of the mass transfer of the relevant parameters of influence which are the concentration gradient, the drop diameter and its Reynolds number during one experiment with constant physical and chemical properties (density, viscosity, surface tension). The pH is adjusted in the feed solution and measured after exposition and removal.



Figure 1. Mass transfer experiment.

The intensive blue-coloured cobalt complex is formed at the interface. As the complexes are extracted by the continuous organic phase, the volume of the drop decreases. The experiments indicate a strong influence of pH to the drop size as well as simultaneous extraction of water into the unsaturated organic phase.

## VALIDATION

A countercurrent laboratory-scale mixer-settler cascade consisting of 8 extraction units, each with a mixer volume of 500 ml and settling area of 250 cm<sup>2</sup>, was used to validate the model. The pH was adjusted by addition of base into the mixers. A comprehension between simulated and measured Co and Ni concentrations of inlet and outlet as well as measured and simulated pH-values is represented by Figure 2. The model prediction corresponds within the accuracy of measurement. Therefore, the model is used for simulation studies as follows. Further validation studies with other sets of operating parameters will be done.

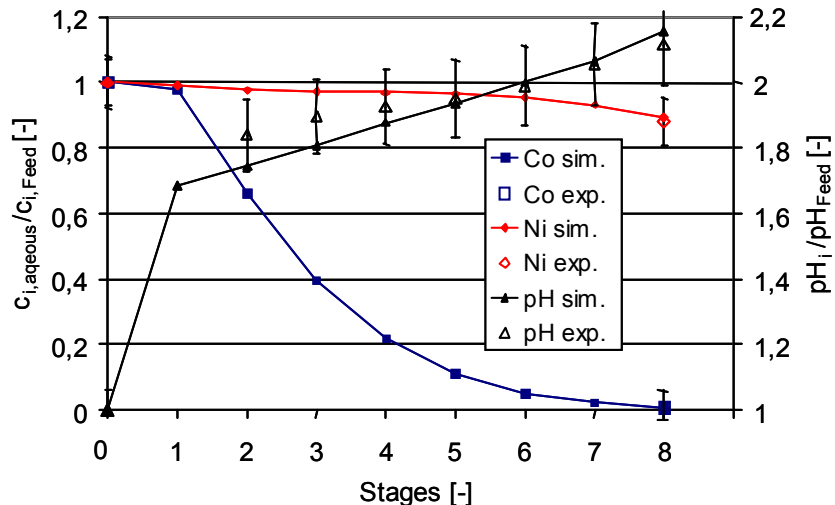


Figure 2. Experimental vs. simulated concentration profiles.

## SIMULATION STUDIES

A whole reactive extraction process with extraction, scrubbing and back-extraction units has been modelled within a flowsheet simulator to carry out the principal simulation studies. Under the condition that external streams like feed, scrub and back-extraction are constant, the pH-values in every stage of the extraction cascade have been optimised. Thus the constraints for special yields and a purity for cobalt of 99,5% in the re-extract are met. The results for these simulation studies are shown in Figure 3.

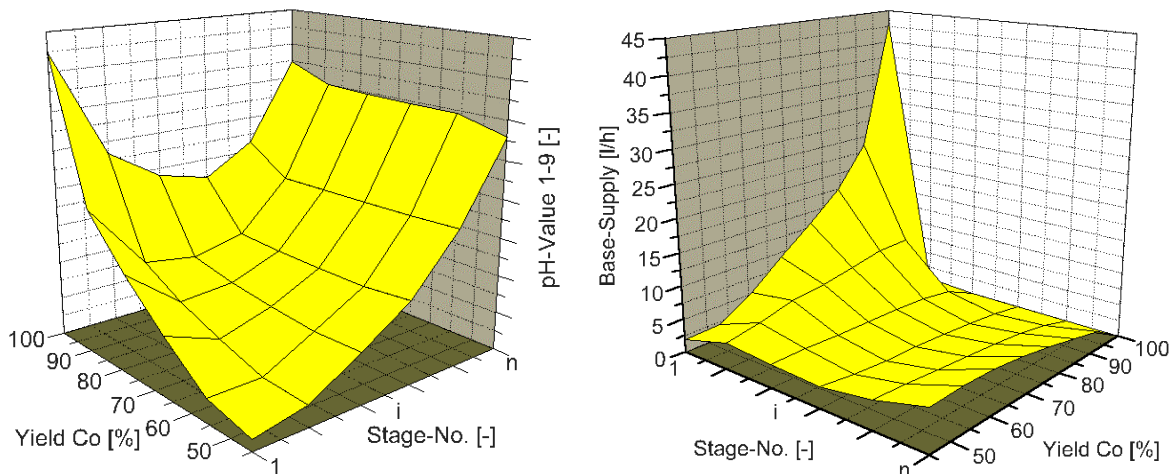


Figure 3. Comparison between optimised pH-values and required base volumes.

At a required yield for cobalt of 50 percent the pH-values increase linearly along the extraction cascade. If more cobalt should be extracted from the feed-solution the gradient in the cascade changes. The reason for this is that the mass transfer is shifted to the first stage, where the feed-solution is contacted for the first time with the extractant in the cascade.

To obtain these pH-values, different amounts of base must be fed to the single stages. The required base volumes are an indicator for mass transfer, since for every metal ion that is extracted, a stoichiometric amount of protons is released. That is the reason why the total amount of base increases linearly with the extraction yield.

At low yields the amount of base for every stage is almost equal. The small deviations are caused by different additional extractant flows to the stages. In the end, at a yield of 100 percent the whole amount of base is fed to the first stage, and the others lose importance.

The decisive difference between a mixer-settler cascade and a column is that the pH-values in a column can not be influenced as easily as in a mixer-settler cascade. To obtain a certain required yield, the pH-values at the entry have to be chosen high enough to ensure the neutralisation of released protons. In Figure 4 a simulation study for a laboratory scale column illustrates the concentration gradients of standardised component concentrations plotted against the column length. All concentrations are referred to the concentration of the leaving protons.

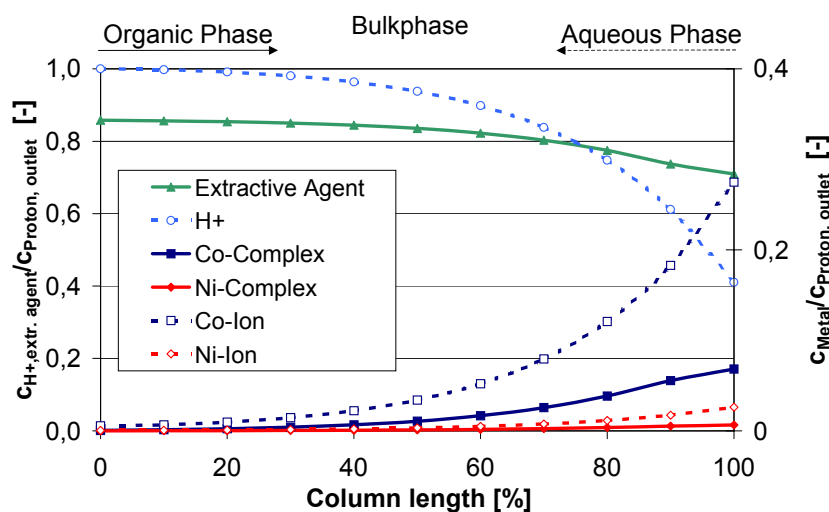


Figure 4. Simulated concentration profiles.

The solid lines represent the continuous phase concentrations and the broken lines the concentrations in the dispersed phase. At the first contact of aqueous and organic phase a large amount of metal cations is extracted and protons are set free equally. This amount of substance lowers the distribution coefficients due to the law of mass action, as can be seen in Figure 5.

Simultaneously the mass transfer decreases from its maximum value, at the top of the column to its minimum value at the bottom. The concentration gradients of both metals decrease in a very similar way, because no selective influence can be carried out inside the column. In a mixer settler cascade in which the amount of base or the concentration of the extractive agent can be changed easily at each stage, the separation factor can be modified in a much broader range than within an extraction column. Therefore, process parameters at the inlet like the selection of phase ratio, extractive agent concentration and pH-value become much more important in operating extraction columns than in mixer settler cascades, and have to be chosen carefully.

## CONCLUSIONS

A modelling approach for the complex separation of Co and Ni has been derived and implemented in models with different assumptions. Stage and dispersive plug flow models were used as an approximation for mixer-settlers and columns.

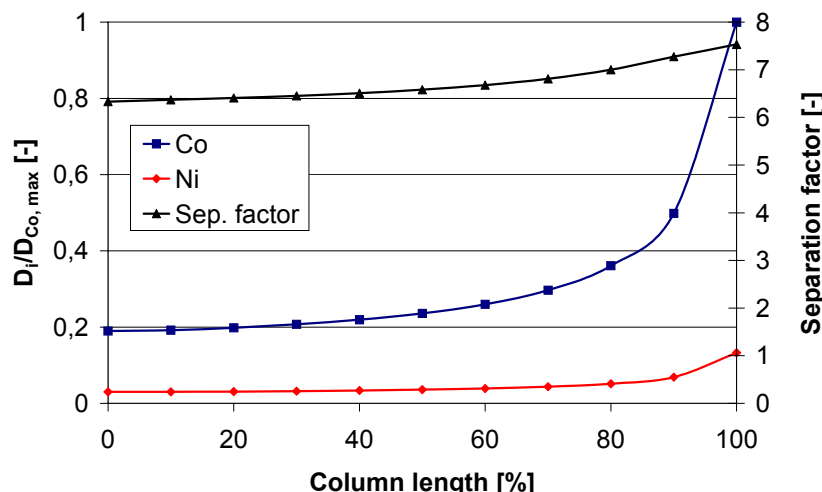


Figure 5. Distribution coefficients for cobalt and nickel.

The required model parameters were determined in laboratory-scale experiments. The objective of the described design strategy is to support feasibility studies and economy evaluation as well as piloting.

Furthermore, the design approach requires the knowledge on chemical equilibrium and mass transfer in multi-component and multi-reaction systems. The sensitivity analysis indicated that the equilibrium constant and the pH-values are the most important parameters. Experiments and simulations have proven the feasibility of the described simplified models as a first design approach. Further model validations and model improvements will be done.

Based on this modelling approach, process development and design are enhanced.

## ACKNOWLEDGEMENTS

The authors would like to thank H.C. Starck AG for support, and would like to acknowledge the support of the research groups from Bayer AG Technical Development, Leverkusen, especially Dr. M. Traving and Dr. E. Dikow, as well as R. Manski and Prof. H.-J. Bart of the chair of thermal separation technology at the University of Kaiserslautern for their collaboration in the project.

## REFERENCES

1. J.S. Preston (1982), *Hydrometallurgy*, **9**, 115-133.
2. D.B. Dreisinger (1984), PhD Thesis, Kingston, Ontario.
3. W.A. Rickelton, D.S. Flett and D.W. West (1985), *Proc. Second Congress on Cobalt Metallurgy and Uses*.
4. N.B. Devi, K.C. Nathsarma, and V. Chakravortty (1998), *Hydrometallurgy*, **49**, 47-61.
5. K. Sarangi, B.R. Reddy, and R.P. Das (1999), *Hydrometallurgy*, **52**, 253-265.
6. R. Grimm and Z. Kolarik (1976), *J. Inorg. Nucl. Chem.*, **38**, 1493.
7. P. V. Danckwerts (1951), *Ind. Eng. Chem.*, **43** (6), 1460-1477.
8. R. Manski and H.-J. Bart (2002), *Proc. ISEC '02*, Cape Town, South Africa, 161-166.
9. J. Schröter, W. Bäcker, and M.J. Hampe (1998), *Chem.-Ing. Tech.*, **70** (3), 279-283.



## COBALT-NICKEL SEPARATION BY SOLVENT EXTRACTION IN CUBA

Aurora María Moreno Daudinot and Elízabeth García Liranza

Laterite Research Center, Moa, Holguín, Cuba

In recent years, many plants have included solvent extraction in their processes to replace the cobaltic hydroxide or cobalt sulfide precipitation methods, due to the high selectivities and separation factors attainable.

In 1998 the Laterite Research Center introduced the results obtained during three years of research, and a small-scale plant was constructed at Moa, Cuba, in order to treat cobalt – nickel mixed sulfide by atmospheric and pressure leaching, purification, removal of cobalt by solvent extraction, and precipitation of cobalt and nickel carbonates.

The small-scale refinery treats a mixed sulfide, and produces Co 30 and Ni 60 ton/year contained in carbonates.

### INTRODUCTION

Several refineries in different countries throughout the world are in operation at present in order to obtain pure nickel and cobalt from matte, minerals or sulfides as raw material [1, 2].

Solvent extraction is the technology that is most advisable for carrying out the difficult process of separating metals with similar physicochemical characteristics contained in aqueous liquors. During the last twenty five years of the past century there has been a marked tendency to devise processes using solvent extraction such as: Nippon Hitachi Cobalt Refinery, Sumitomo's Niihama Nickel Refinery, Anaconda's Murrin Murrin, Bulong Nickel/Cobalt Project, and Cawse Nickel Operations [1, 3]. Solvent extraction technology has also been introduced into processes such as Falconbridge Nikkelverk a/s Kristiansand Refinery, Societe Le Nickel, and the Queensland Nickel Yabulu Refinery [1,4]; as well as replacing the hydroxide precipitation process at Companhia de Níquel Tocantins and Outokumpu Harjavalta Metals Oy [5, 6].

After three years of research and laboratory and bench scale experiments, the design criteria and the feasibility analysis were obtained. Then a small-scale refinery was erected in Cuba, in 1998, which started applying solvent extraction process at miniplant scale using nickel and cobalt mixed sulfide, obtained as a by-product from an ammoniacal leaching process.

## PROCEDURES

### Lab Scale

To separate cobalt from nickel, phosphoric (D2EHPA), phosphonic (PC 88A, P 507) and phosphinic solvents (CYANEX 272, CYANEX 301 and CYANEX 302) were tested with cobalt – nickel mixed sulfide leach liquors [7, 8]. Extraction pH curves and extraction isotherms were determined for all these reagents. Different solutions were used to scrub the extract to determine the optimum concentration and pH for the scrubbing, and stripping isotherms were also determined. Kinetic studies were also carried out for each of the stages: extraction, scrubbing, stripping, and solvent regeneration.

### Bench Scale

Once the lab scale researches were finished, CYANEX 272 was chosen as the organic reagent able to separate cobalt from nickel with a high separation factor (>7000) [9]. Calcium and magnesium were rejected and remained in the aqueous phase (raffinate). This solvent does not show any problems with stripping the extracted cobalt, and allows a cobalt product with a Co: Ni ratio of over 3000 to be obtained.

Experimental results obtained at lab scale such as extraction pH, number of stages, speed of stirring for aqueous and organic phases, extraction kinetics, speed of phase separation, and so on were introduced to bench scale. The necessary number of stages, flows rates and phase ratios, recycles, regenerated organic phase neutralization, and solvent losses were verified and fixed.

In this stage, the design parameters for the scaling of the bench results to miniplant scale were obtained. During operation at bench scale, cobalt and nickel liquors with high purity were obtained, to produce salts utilized in ceramics, military techniques and at the Animal Nutrition Institute in Cuba.

## DESCRIPTION OF CUBAN SMALL-SCALE REFINERY

The project for the construction of the refinery as such to small scale, capable of processing the nickel – cobalt mixed sulfide as a product of ammonium carbonate process in order to obtain basic cobalt and nickel carbonate of high purity, was performed with the parameters obtained at bench scale. The flowsheet of the Cuban small-scale refinery for nickel and cobalt is shown in Figure 1.

The mini-refinery was erected in the Investigations Area of the Laterite Research Center with the assistance and protection of Unión del Níquel. The investigators of this center carried out the calculations and design for the mini-refinery project, culminating in December 1998 with the Basic Industry minister's approval. Operations started in January 1999, reaching design capacity by the end of the first semester, and commercializing high purity nickel and cobalt carbonate.

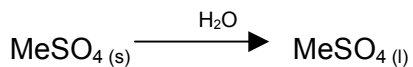
The mini-refinery is made up of three principal areas: leaching and purification, solvent extraction and final product.

### Leaching and Purification

Ni – Co mixed sulfide has the following composition (%):

Ni	Co	Fe	Mn	Cu	Zn	MgO	CaO
14 – 17	7 – 8.5	1 – 1.4	0.025 – 0.05	1.3 - 3	0.01 – 0.03	2.0	0.03

The following sulfate solution is obtained by atmospheric leaching with 80% efficiency:



The slurry containing solid sulfide is fed into a supplied compressed-air horizontal autoclave, and the following reactions take place for the different elements. Efficiency in this oxidation reaction is 99%.



### Removal of Impurities

The iron precipitation is carried out at 80°C by addition of limestone, thereby removing iron and copper from the liquor. Then the copper is separated from the liquor by means of sodium sulfide.

The efficiency of impurity removal is superior to 99%. The partially purified solution is filtered and adjusted with sodium hydroxide in order to feed to the solvent extraction circuit. The chemical composition in g/L is:

Ni	Co	Fe	Mn	Cu	Zn
25.2	12.8	0.005	0.002	0.001	0.018

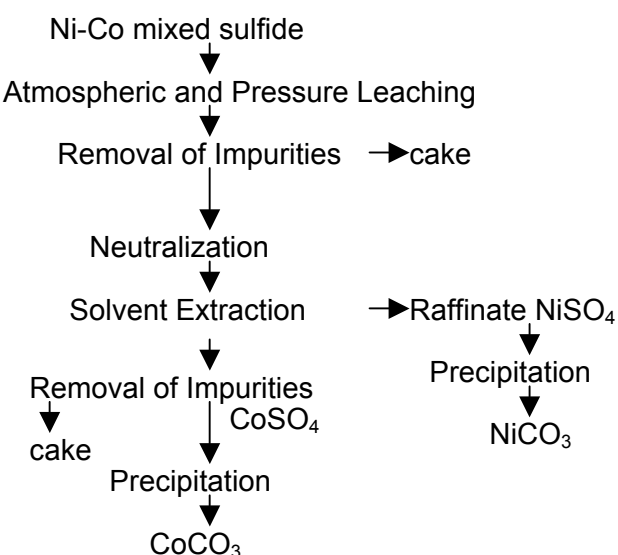


Figure 1. Flowsheet of the Cuban Nickel Refinery.

### Solvent Extraction

The system consisted of 9 stages. The extraction, scrubbing and stripping stages are performed in mixer settlers in countercurrent flow, and the organic phase: aqueous phase ratio in the settlers is 1 throughout the solvent extraction process.

CYANEX 272 is the organic reagent utilized at 20 % diluted in kerosene. The organic acid solution is neutralized with sodium hydroxide solution, as the following reaction:



The behavior of the individual metals in the organic phase through the solvent extraction circuit is shown in Figures 2 and 3.

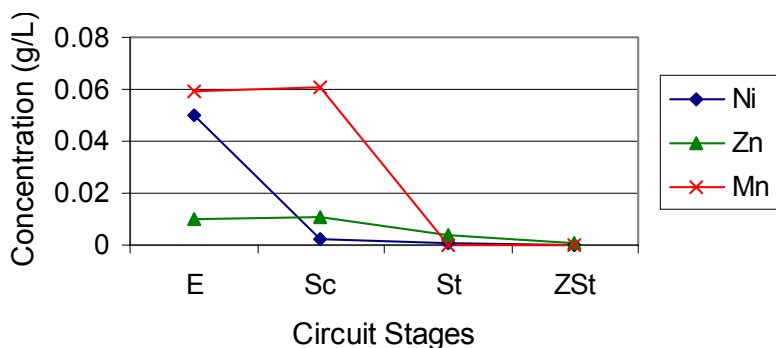


Figure 2. Metals behavior through the solvent extraction circuit.

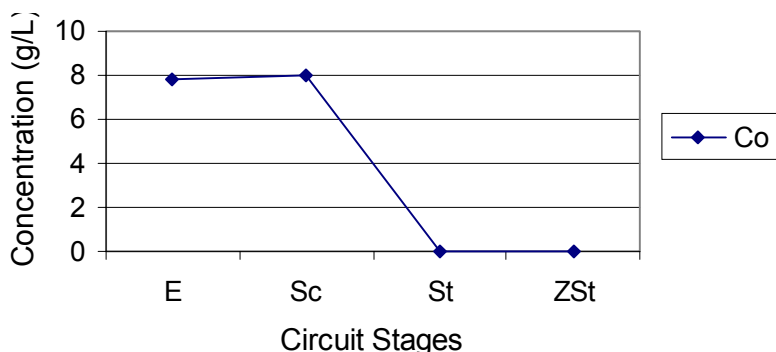
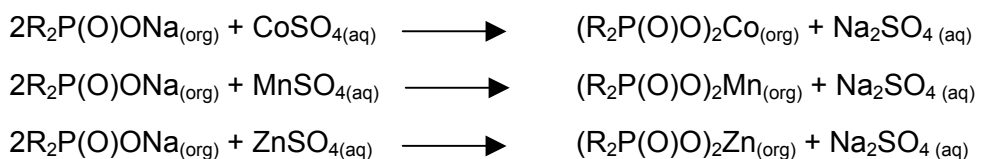


Figure 3. Cobalt behavior through the solvent extraction circuit.

### Extraction

The purified liquor enters the first mixer settler in the extraction stages of solvent extraction circuit. Solvent CYANEX 272 enters the last mixer settler. Three stages are sufficient to remove cobalt from nickel with pH 6.0, whilst nickel remains in the aqueous phase or raffinate. The extraction of manganese and cobalt in this stage is >99.5%.

The reactions for this manganese and cobalt extraction process are:



### Scrubbing

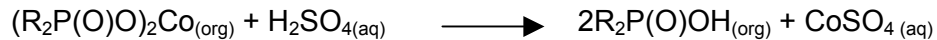
The extract containing over 99% of zinc, manganese and cobalt, and 0.35% of the coextracted nickel is scrubbed in two stages by a cobalt-containing solution in sulfate medium, to eliminate nickel, with an efficiency of 96%. This reaction is described as follows:



The spent scrubbing liquor is recycled to the extraction stages of the system, and the scrubbed extract continues to the stripping stages.

### Stripping

Stripping takes place at controlled pH, and the manganese and cobalt loaded during extraction are stripped in three stages with sulfuric acid, both metals are liberated due to the high hydrogen ion concentration in the aqueous phase.

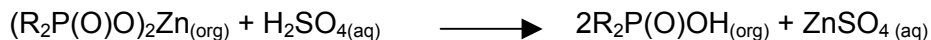


The cobalt liquor product contains manganese as an impurity. The composition in g/L of the cobalt sulfate product is as follows:

Co	Ni	Fe	Mn	Cu	Zn
62 - 65	0.005 – 0.01	0.01	0.06	-	0.01

### Zinc Stripping

The partially stripped organic phase contains zinc, and this is removed by means of concentrated sulfuric acid solution, giving a clean organic phase, ready again for neutralization. The reaction that takes place between partially stripped solvent and concentrated acid solution is:



The purified nickel and cobalt liquors pass through a carbon column, to clean off soluble solvent, then leave the solvent extraction area.

Manganese is removed by using a strong oxidant, separating 85% with 0.5% loss of cobalt. A product liquor of 99% purity and the following chemical composition in g/L is obtained:

Co	Ni	Fe	Mn	Cu	Zn
61.6 – 64.7	0.005 – 0.01	0.01	0.009	-	0.01

### Final Product

The carbonate in both cases (cobalt and nickel) is obtained in three stages by a precipitation process using sodium carbonate addition at elevated temperature. The obtained slurry is passed to the thickeners, and then the thickened slurry is filtered and washed to eliminate the entrained sodium sulfate.

Products containing 60 ton/year of nickel and 30 ton/year of cobalt are obtained with the following composition in percent.

Basic Nickel Carbonate					
Ni	Co	Fe	Mn	Cu	Zn
47-49	0.16	0.01	-	0.005	0.002
Basic Cobalt Carbonate					
Co	Ni	Fe	Mn	Cu	Zn
48-49	0.05	0.05	-	0.015	0.03

## REFERENCES

1. G. P. Tyroler and C. A. Landolt (1988), *117<sup>th</sup> TMS*, Phoenix, Arizona.
2. D. G. E. Kerfoot (1986), *25<sup>th</sup> CIM*, Toronto, Ontario, Canada, pp. 426-441.
3. M. Andoo, M. Takahashi and T. Ogata (1983), *112<sup>th</sup> AIME*, Atlanta, Georgia, pp. 463-474.
4. J. G. Reid M. J. Price (1993), *Proc. ISEC '93*, York, England, pp. 225-231.
5. R. F. Stauffer and R. M. Berezowski (1991), *Sherritt Trip Report to Companhia Nickel Tocantins*, Alberta, Canada, 9 pp.
6. K. Knuutila, S-E. Hultholm, B. Saxén and Leif Rosenback (1997), *ALTA Nickel/Cobalt*, Melbourne, Australia.
7. J. S. Preston (1982), *Hydrometallurgy*, **9**, 115-133.
8. B. K. Tait (1993), *Hydrometallurgy*, **32**, 365-372.
9. W. A. Rickelton, D. S. Flett and D. W. West (1984), *Solvent Extr. Ion Exch.*, **2**, 815-838.



## BATEMAN PULSED COLUMN PILOT-PLANT CAMPAIGN TO EXTRACT COBALT FROM THE NICKEL ELECTROLYTE STREAM AT ANGLO PLATINUM'S BASE METAL REFINERY

Victor Nagel, Mark Gilmore\* and Sean Scott\*\*

Bateman Engineering Limited, Boksburg, South Africa

\*Anglo Platinum, Rustenburg, South Africa

\*\*Mintek, Randburg, South Africa

An extended pilot-plant campaign was completed at Anglo Platinum's base metal refinery to evaluate the technical feasibility of using the Bateman Pulsed Column for the removal of cobalt from the nickel sulphate electrolyte produced at the refinery. A conventional Cyanex 272® solvent-extraction system was employed and the Bateman Pulsed Column was successfully evaluated for the extraction and stripping of cobalt.

The extraction of cobalt from the nickel feed solution was successfully evaluated at a flux of 50 m<sup>3</sup>/m<sup>2</sup>/h and the cobalt concentration in the feed was reduced from 250 to below 10 mg/L. The average Co:Ni and Co:Mg ratios on the loaded organic were 15.5 and 9.5, respectively.

The stripping of cobalt from the loaded organic was successfully evaluated at a flux of 25 m<sup>3</sup>/m<sup>2</sup>/h. The cobalt concentration of the loaded organic was consistently reduced from approximately 0.8 to 0.05 g/L (>95% stripping efficiency) and a loaded strip liquor containing approximately 12 g/L cobalt was produced.

### INTRODUCTION

Anglo Platinum declared a R12 billion expansion in February 2000 to increase its platinum production from 2 million to 5 million oz of platinum over a time period of 5 years. This expansion would include the establishment of a number of new mines, concentrators and a new smelter exploiting the eastern limb of the Bushveld Complex. Where appropriate, the existing operations would be de-bottlenecked to meet the increased production. The increase in platinum production would yield an associated increase in base metals, which will surpass the nominal capacity of the existing Rustenburg Base Metal Refinery (BMR), in the year 2003. It was decided that the BMR would be de-bottlenecked in line with the anticipated platinum expansion.

The BMR is a medium sized base metal refinery and has a nominal capacity of 21,000 tpa nickel, 12,000 tpa copper, 2000 tpa cobalt sulphate and 55,000 tpa sodium sulphate crystal. A simplified process flow diagram is indicated in Figure 1.

Currently the major bottlenecks in the production of nickel cathode are the nickel electrowinning operation as well as the cobalt removal stage. The process currently employed to remove cobalt from the nickel stream is an outdated Outokumpu process [1].

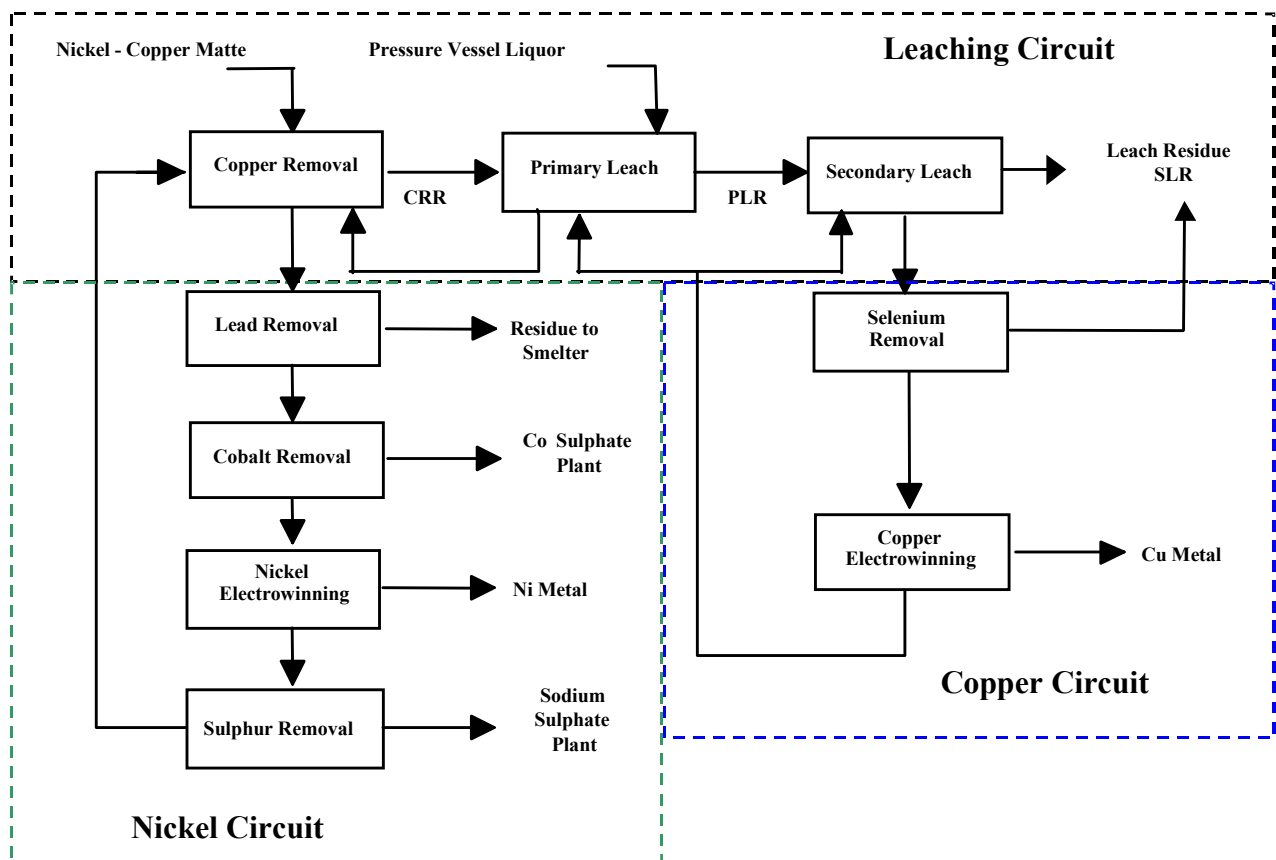


*Figure 1. Simplified process flow diagram of Anglo Platinum's BMR.*

The nickel hydroxide used in the separation process is manufactured internally by electrolytic means. This process is labour intensive, extremely costly and utilises approximately 7% of the potential nickel plating capacity. Anglo Platinum decided to evaluate the use of alternative technology for the removal of cobalt. A solvent extraction (SX) process using Cytec's organophosphinic acid reagent, Cyanex 272® was identified as the most likely technology.

Anglo Platinum commissioned Bateman and Mintek to run a 5-week pilot-plant campaign to evaluate the use of Cyanex 272®. The Bateman Pulsed Column (BPC) was identified as the preferred contacting equipment as it offered many advantages to Anglo Platinum when compared with conventional mixer settlers. Two main advantages are its limited footprint and reduced solvent inventory requirement. Space is currently a constraint at the BMR. The main perceived disadvantage of the BPC is that it has never been used before commercially in an industrial application for the extraction of cobalt using Cyanex 272®.

## PROCESS DESCRIPTION

The process tested during the campaign was a conventional Cyanex 272® cobalt SX circuit, comprising cobalt extraction, nickel and magnesium scrubbing, and cobalt stripping. As only one pilot BPC was available for the campaign, a combination of mixer settlers and the BPC were used for the evaluation of the individual extraction and stripping steps.

When evaluating the BPC for extraction, conventional mixer settlers were used for the scrubbing and stripping of the loaded organic. Co-extracted nickel was scrubbed from the loaded organic using a 45 g/L cobalt scrub solution originating from the BMR cobalt circuit, while the scrubbed organic was stripped with dilute sulphuric acid to produce a concentrated cobalt solution.

When the stripping performance of the BPC was being evaluated, three parallel banks consisting of three mixer settlers each were used for extraction. The mixer settlers were used to generate the cobalt-loaded organic while the BPC was used to strip the loaded organic and to produce the cobalt product solution. Dilute sulphuric acid was used as the strip liquor.

## EXPERIMENTAL

### Solutions and Reagents

The feed solution used during the campaign originated from the BMR, and is representative of the feed solution to be produced in the expanded refinery. A representative composition of the feed solution used during the campaign is shown in Table 1.

*Table 1. Average composition of the feed solution.*

Element	Concentration (g/L)	Element	Concentration (g/L)
Ni	67.5	Zn	< 0.005
Co	0.12 – 0.27	Ca	0.147
Cu	< 0.005	Mg	0.444
Mn	< 0.005	Na <sub>2</sub> SO <sub>4</sub>	120 – 140
Fe	< 0.005	pH	6.1 – 6.2

The organic phase used consisted of Cyanex 272<sup>®</sup> (2.2 – 4.5 vol.%) in an aliphatic diluent C<sub>12</sub>-C<sub>13</sub> *n*-paraffin (SasolChem). A 40 g/L H<sub>2</sub>SO<sub>4</sub> solution was used as strip liquor. Diluted product liquor originating from RBMR's cobalt recovery D<sub>2</sub>EHPA SX circuit was used as the scrub liquor to remove co-extracted nickel and magnesium from the loaded organic. The scrub liquor consisted of 45 g/L cobalt and trace amounts of nickel, calcium and magnesium.

### Equipment

The BPC used during the campaign consisted of two settlers, one passive and the other active depending on the phase continuity being tested and a 6-7 meter 100-mm ID contacting section. The contacting section was made up of 1-meter glass column lengths each fitted with PVDF (polyvinylidene fluoride) internals arranged in a disc-and-doughnut configuration. The pH along the length of the column was monitored and controlled by the addition of H<sub>2</sub>SO<sub>4</sub> or NaOH to various ports along the column. NaOH was also added directly into the organic phase before it entered the column during the extraction tests.

Conventional mixer settlers were used for the extraction, scrubbing and stripping duties as required.

## RESULTS AND DISCUSSION

### Extraction

Hydrodynamic tests were conducted to determine the conditions which would maximise the flux (combined flowrates divided by the flow area of the column), mixing intensity (combination of the frequency and stroke length of the mechanical pulsator) and the extraction efficiency attainable in the BPC. The hydrodynamic tests indicated that the BPC could be run at a higher mixing intensity at an equivalent flux without flooding, when the

continuity of operation was organic. This meant that the BPC could be run at higher fluxes in this continuity and a full-scale BPC would have a smaller diameter when compared with a BPC run in an aqueous continuity. As the extraction of cobalt is dependent on pH, the initial operating philosophy was to run the BPC aqueous continuous as this would facilitate the measurement and control of the pH along the length of the BPC.

The initial conditions tested were a flux of  $40 \text{ m}^3/\text{m}^2/\text{h}$ , an O:A of 0.4 and a mixing intensity of 126 cm/min. Initial results indicated that the cobalt concentration in the raffinate was high at 50 mg/l. To reduce the concentration, the operating flux was decreased to  $25 \text{ m}^3/\text{m}^2/\text{h}$ , the mixing intensified to increase the organic phase holdup and the height of the BPC lengthened to increase the residence time of the two phases in the column. The O:A ratio was also raised to ensure that there was sufficient capacity available on the organic phase. These attempts resulted in the cobalt concentration in the raffinate decreasing but it still exceeded the target of <10 mg/L. The initial conclusion drawn was that mass transfer was the limiting factor. No further testwork under aqueous-continuous conditions were done.

The initial concern with operating the organic continuity was that it would be difficult to control the pH along the length of the BPC. During the trials this was found not to be the case as the high aqueous hold ups achieved (~20-30%) ensured that sufficient aqueous phase was present to allow pH to be measured. Online measurements were regularly compared to aqueous samples taken along the length of the BPC to confirm the accuracy of the online readings.

During the extraction tests the extractant was converted to the sodium salt with approximately 400 g/L NaOH in a mixer settler to decrease the NaOH addition requirement to the BPC. During this preloading/conversion a brown wax-like substance formed. Analysis by Cytec of the substance indicated that it was an iron-contaminated sodium phosphinate gel and that its formation was reversible. This substance formed throughout the campaign and was attributed to the high concentration of NaOH used. Initially the Cyanex 272<sup>®</sup> concentration did not decrease but as the campaign progressed, the Cyanex 272<sup>®</sup> concentration decreased from 4.5 % to approximately 2.5 vol. %.

The results achieved during the organic continuous hydrodynamic tests did not give a clear indication of the conditions at which the BPC could be run at, as the Cyanex 272<sup>®</sup> concentration had decreased to 2.5 vol. % and there appeared to be insufficient capacity available on the extractant. The Cyanex 272<sup>®</sup> concentration was increased to 4.5 vol. % and the BPC was run under three different sets of conditions as indicated in Table 2.

*Table 2. Operating conditions for the extraction of cobalt – organic continuous.*

Flux ( $\text{m}^3/\text{m}^2/\text{h}$ )	30	40	50
Feed flowrate (L/min)	2.91	3.97	4.92
Organic flowrate (L/min)	1.02	1.27	1.62
Spent scrub flowrate (mL/min)	7.5	10.5	13
Mixing intensity (cm/min)	152	152	122-152

The increased concentration together with the organic continuity mode of operation resulted in the cobalt concentration in the raffinate decreasing to below 10 mg/L under all conditions tested. Once the raffinate specification was being met for the flux of 50 on a continuous basis, attempts were made to improve the Co:Ni and Co:Mg ratios in the loaded organic phase by controlling the pH in the top section of the column by the addition of 200g/L H<sub>2</sub>SO<sub>4</sub>. This was deemed necessary as the feed solution entering the column was at a pH of 6.2 and resulted in the pH in the upper sections of the BPC being around 5.8. A lower pH was deemed to be necessary as this would have increased the selectivity of the Cyanex 272<sup>®</sup> for cobalt over nickel and magnesium.

Large delay times between the point where the pH was measured and the point where the H<sub>2</sub>SO<sub>4</sub> was introduced resulted in the pH decreasing to levels as low as 5.2. This adversely effected the raffinate cobalt tenors achieved but did result in the selectivity of the system increasing. Before the addition, the average Co:Ni and Co:Mg ratios were 13 and 7; after the addition, these ratios increased to 25 and 14.5, respectively. This increase reduced the load on the scrubbing circuit and increased the overall selectivity of the circuit. Selected results produced during this period are shown in Table 3 and a typical profile along the length of the BPC is indicated in Table 4.

*Table 3. Selected results for extraction under organic-continuous conditions.*

Day	Time	Flux m <sup>3</sup> /m <sup>2</sup> /h	Co:Ni L.O.	Co:Mg L.O.	Co raffinate (g/L)
1	21:00	30	10.76	5.02	0.003
2	20:00	40	13.16	9.51	0.014
3	20:00	50	11.91	4.65	0.006
4	08:00	50	19.92	6.34	0.008
6	20:00	50	22.82*	16.87*	0.017*

\* indicates when H<sub>2</sub>SO<sub>4</sub> was added to port 7

*Table 4. A typical profile through the column (Flux 30 m<sup>3</sup>/m<sup>2</sup>/h, O/A ratio 0.35).*

Sample (aq)	Ni	Co	Mg	Sample (org)	Ni	Co	Mg
Feed	64.30	0.24	0.40	L.O.	53.40	0.893	0.18
Port 7	65.80	0.05	0.43	Port 7	0.06	0.52	0.20
Port 5	62.78	0.01	0.39	Port 5	0.19	0.20	0.25
Port 3	65.28	0.002	0.34	Port 3	0.19	0.05	0.22
Port 1	65.55	0.001	0.18	Port 1	0.22	0.003	0.06
Raffinate	64.20	0.003	0.27	S.O.	0.003	<d.l	0.006
SSL	23.32	22.87	2.07	% Extr.	0.16	98.8	31.6

Note: <d.l below detection limit

Extraction efficiencies = difference between feed and raffinate concentrations

SSL: Spent scrub liquor

The scrubbing of the organic phase was not successful during the campaign, as the residence time in the mixer settlers was inadequate to allow for sufficient scrubbing of the co-extracted nickel and magnesium. Further testwork after the campaign indicated that Co:Ni and Co:Mg ratios in excess of 1000 are achievable in three to four scrubbing stages with a residence time in the mixers in excess of 4 minutes.

### Stripping

The hydrodynamic tests indicated that the column could be run at a flux of 25 – 30 m<sup>3</sup>/m<sup>2</sup>/h - in an aqueous-continuous mode of operation, at various mixing intensities and at an O:A of approximately 20. The results of some of these tests are indicated in Table 5.

Following the optimisation test, the BPC was run for a period of 24 hours at a flux of 25, a mixing intensity of 176 and O:A of approximately 20. During this period an average cobalt stripping efficiency of 96% was achieved with the stripped organic phase exiting the column at between 17 - 40 mg/L cobalt. Typical loaded strip liquor (LSL) compositions are shown in Table 6. The high level of nickel and magnesium in the LSL can be attributed to the fact that the loaded organic was not scrubbed prior to being fed to the BPC for stripping.

*Table 5. Optimisation results.*

Test	Flux m <sup>3</sup> /m <sup>2</sup> /h	Mixing intensity (cm/min)	Dispersed phase hold-up (%)	[Co] (g/L)			Co Stripping (%)
				LO <sup>1</sup>	SO <sup>2</sup>	LSL <sup>3</sup>	
2	25	202.8	58	0.86	0.02	9.72	97.7
3	25	187.2	62	0.79	0.05	11.98	94.3
4	25	171.6	25	0.71	0.03	11.08	95.4
6	30	176.0	31	0.74	0.01	12.21	98.1 (flooded)

<sup>1</sup>Loaded organic entering the column

<sup>2</sup>Stripped organic exiting the column

<sup>3</sup>Loaded strip liquor

*Table 6. Typical LSL composition.*

Day	Analysis (g/L)							
	Ni	Co	Cu	Mn	Zn	Ca	Mg	Fe
1, 01h00	1.22	11.08	0.13	0.08	0.47	0.08	0.84	0.04
2, 02h00	1.26	11.44	0.23	0.13	0.55	0.03	0.32	0.62
3, 05h00	2.32	14.29	0.16	0.13	0.42	0.004	0.45	0.40

## CONCLUSION

The technical feasibility of using a BPC for the extraction of cobalt from the nickel feed solution and stripping of the cobalt loaded organic was successfully proven during an extended pilot-plant campaign.

The extraction tests indicated that the BPC could be operated at a higher flux at an equivalent mixing intensity when run organic continuous. An aqueous continuity favoured the measurement and control of pH in the BPC but a cobalt concentration of < 10 mg/L in the raffinate could not be consistently produced. When running the column organic continuous, the cobalt concentration of the raffinate was reduced to below 10 mg/L. The operating conditions used in the column were a flux of 50 m<sup>3</sup>/m<sup>2</sup>/h, an O:A ratio of 0.33, 3.5-4.5 vol. % Cyanex 272<sup>®</sup> in C<sub>12</sub>-C<sub>13</sub> n-paraffin and a 7 m contacting height. The average Co:Ni and Co:Mg ratios on the loaded organic phase were 15.5 and 9.5, respectively, and were increased to 25 and 14.5 when the pH at the top of the column was suitably controlled. On a full-scale plant 4-5 scrubbing stages would be necessary to achieve the required Co:Mg ratio of 500-1000:1.

The stripping tests conducted indicated that the BPC could be run at a higher flux at an equivalent mixing intensity when run organic continuous. However to ensure efficient stripping of the cobalt loaded organic, the column had to be run with an aqueous continuity. Operating the column at a flux of 25 m<sup>3</sup>/m<sup>2</sup>/h and an average O:A ratio of approximately 20, the cobalt concentration of the loaded organic was consistently reduced from approximately 0.8 g/L to 0.05 g/L (stripping efficiency of >95%) and a LSL was produced containing on average 12 g/L cobalt. This concentration can be raised to suit downstream process requirements by increasing the O:A ratio and the acid concentration in the strip liquor.

## REFERENCE

1. D. De J. Clemente, B. I. Dewar and J. Hill (1980), *Proc. Can. Inst. Min. Metall.*, 10th Annual Hydrometallurgical Meeting, Edmonton.



## EXTRACTION EQUILIBRIUM OF Zn(II) AND Ni(II) WITH LIX 984

M. T. Draa and M. Benamor

Department of Chemical Engineering, University of Bejaia, Bejaia, Algeria

The solvent extraction of Ni(II) and Zn(II) with LIX 984 dissolved in heptane was investigated. Extraction experiments were carried out varying the pH and metal concentration of the aqueous phase and the extractant concentration in the organic phase. The selectivity series for the extraction of these metals from nitrate media based on the  $\text{pH}_{50}$  was found to be Ni ( $\text{pH}_{50} = 3.75$ ) > Zn ( $\text{pH}_{50} = 5.5$ ).

The experimental data obtained were treated numerically. Ni(II) and Zn(II) extraction by LIX 984 could be explained by the formation of  $\text{NiR}_2$  and  $\text{ZnR}_2$  organic complex species. The values of the equilibrium constants for these extraction reactions were  $\log K_{\text{ex1}} = -5.69$  for Ni(II) and  $\log K_{\text{ex2}} = -9.50$  for Zn(II). Nickel stripping by acidic solution was also studied and it was found that 1 M  $\text{HNO}_3$  can strip Ni(II) to the extent of 99%.

### INTRODUCTION

Solvent extraction is widely used in the extraction of a number of non-ferrous metals. In the case of a multi-metal system, there are two basic process approaches for metal separation [1, 2]: sequential-selective extraction stripping and co-extraction-selective stripping. This latter is reported to be more economical [2]. Nickel and zinc are often present together in a number of raw materials, and liquid effluents. Thus, their recovery/separation presents an important industrial problem.

LIX reagents are powerful extractants for copper [3]. While there is ample published data on copper extraction with current LIX reagents such as LIX 860 (2-hydroxy-5-dodecylsalicylaldoxime), LIX 84 (2-hydroxy-5-nonylacetophenone oxime) and LIX 984 (equivolume mixture of the two) [4, 5], there is very little information on the extraction of nickel and zinc using these extractants.

The aim of this work is to study the extraction of these metals from nitrate solution using the commercially available LIX 984 as extractant. The influences of aqueous pH and extractant concentration are discussed, and a simple model explaining the extraction mechanism is developed.

### EXPERIMENTAL

#### Reagents

LIX 984, an equivolume mixture of 5-dodecylsalicylaldoxime and 5-nonyl-acetophenone oxime, was supplied by Cognis. It was used as received by diluting it to the desired concentration in heptane.

A stock solution (1 g/l) of zinc(II) and nickel(II) was prepared from  $\text{ZnNO}_3 \cdot 5\text{H}_2\text{O}$  and  $\text{NiNO}_3 \cdot 6\text{H}_2\text{O}$  (Prolabo) in double distilled water, respectively. Working solutions for extraction consisted of 0.1 M ( $\text{Na}^+$ ,  $\text{H}^+$ ,  $\text{Zn}^{2+}$ ) $\text{NO}_3^-$ . The total nitrate concentration was kept constant at 0.1 M. The aqueous pH was adjusted by changing different fractions of  $\text{HNO}_3$  and  $\text{NaNO}_3$  as required. All other chemicals used were of analytical grade.

A  $10^{-3}$  M solution of 4-(2-pyridylazo)resorcinol (PAR) (Fluka) was prepared for the spectrophotometric determination of Ni(II) and Zn(II).

### Apparatus

A Shimadzu UV-2101PC double beam UV-VIS spectrophotometer was used for absorbance measurement. For pH measurements, a 3420 electrochemistry analyzer (Jenway) with combined glass-saturated calomel electrode was used.

### Extraction Procedure

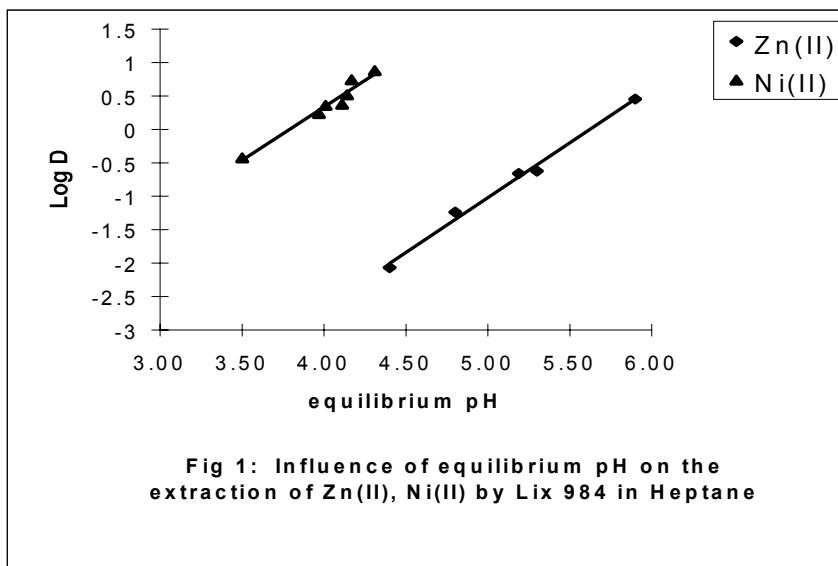
Suitable aliquots of the aqueous phase containing the desired concentration of the metal and sodium nitrate 0.1 M ( $\text{Na}^+$ ,  $\text{H}^+$ ,  $\text{M}^{2+}$ ) $\text{NO}_3^-$  were equilibrated with an organic phase containing the extractant LIX 984 dissolved in heptane. The initial pH of the aqueous phase was adjusted to the desired value by adding dilute  $\text{HNO}_3$  solution. Extraction was carried out in separating funnels at unit phase ratio for 20 min. Initial experiments indicated that a contact time of 10 min is sufficient to reach equilibrium. After phase disengagement, the aqueous phase was separated and its equilibrium pH was measured.

Metal concentration in the aqueous phase was estimated by spectrophotometric determination with PAR as follows. For both metals, the pH of the solution was adjusted by adding  $2\text{ cm}^3$  of a buffer of pH 6 (acetate buffer) and adding  $1\text{ cm}^3$  of  $10^{-3}$  M aqueous PAR. The absorbance of the complex was measured at 490 nm for zinc and 495 nm for nickel against a reagent blank prepared analogously. The concentration of metal in the organic phase was calculated from the difference between the metal ion concentration before and after extraction. All the extraction experiments were conducted at room temperature.

## RESULTS AND DISCUSSION

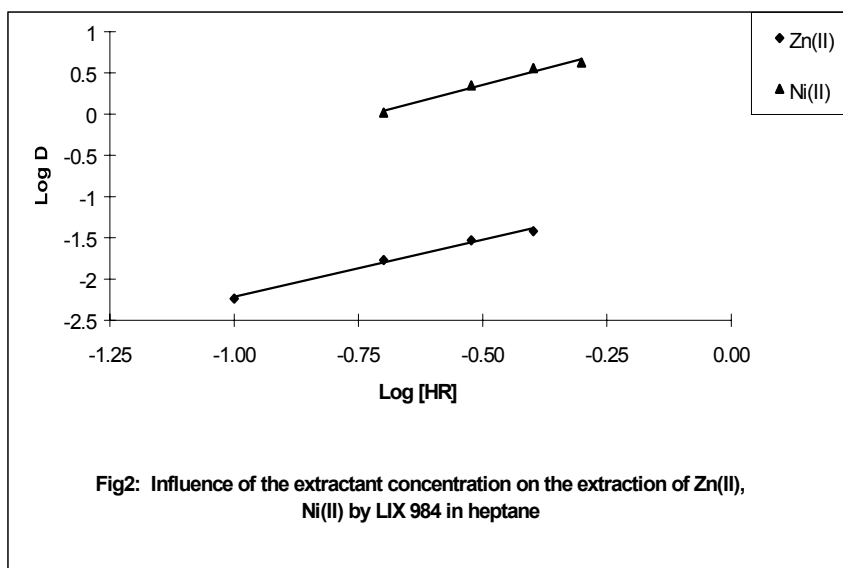
### Effect of pH

The effect of aqueous solution pH has been investigated by keeping the metal concentration constant (10 mg/l) using 10 % v/v LIX 984 in heptane. The results shown in Figure 1 indicate that Zn(II) is poorly extracted in comparison to Ni(II), the  $\text{pH}_{50}$  values corresponding to 50% extraction are equal to 3.75 and 5.5 for Ni(II) and Zn(II), respectively. For both metals, the extraction increases with increasing aqueous equilibrium pH. From the slope of the plot of  $\log D$  vs. pH, it is inferred that two protons are involved in the extraction of Zn(II) and Ni(II).



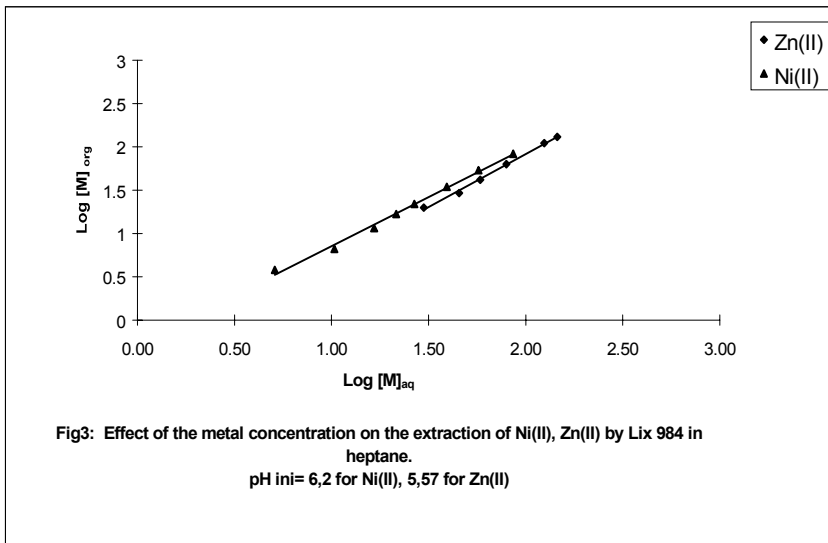
### Effect of Extractant Concentration

The effect of LIX 984 concentration (10%v to 50%v) on the extraction of Zn(II) and Ni(II) has been studied at constant metal ion concentration (10 mg/l), and a constant initial aqueous pH of 6 (Figure 2). In both cases, the distribution ratio D increases linearly with an increase in the concentration of LIX 984 and, from the slope of the log-log plot, it is inferred that two molecules of LIX 984 are associated with the extractable complexes.



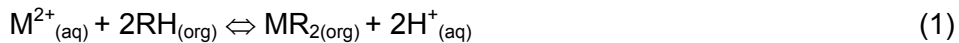
### Effect of Metal Ion Concentration

The effect of metal ion concentration on the extraction process has been investigated using 40% v LIX 984 in heptane for Zn(II) and Ni(II) (Figure 3). The metal concentration varied from 5 to 100 mg/l for Ni(II) and from 20 to 150 mg/l for Zn(II). The initial aqueous pH was maintained constant at 6.2 for Ni(II) and 5.57 for Zn(II). The plot of the equilibrium organic phase metal concentration  $\log [M]_{org}$  against the aqueous metal concentration  $\log [M]_{aq}$  is linear, with a slope close to unity for both metals, indicating that only mononuclear species are extracted into the organic phase for both cases.



### Extraction Equilibrium

It is generally accepted that the reaction between divalent metal and chelating molecules proceeds at the oil-water interface [6]. The chelating extraction is an acid-base reaction in which the oxime molecules donate protons in exchange of metal ions. The reaction is described by:



$$K_{ex} = \frac{[MR_2_{(org)}][H^+]^2}{[M^{2+}][RH]_{org}^2} \quad (2)$$

where RH represents hydroxime molecules, and the subscripts 'aq' and 'org' to the aqueous, and organic phase, respectively. From Equation (1), we can define the equilibrium constant  $K_{ex}$  as

This equilibrium constant is based on the assumption that both phases are ideal, and concentration could be used instead of activity. This assumption is only valid in the case of low species concentration [4].

Chelating extractants often form dimers, but only in nonsolvating diluents. They exist as monomers in solvating diluents such as aromatic hydrocarbon and chloroalkanes. The degree of hydroxime dimerization depends strongly on the extractant concentration. Hydroxime dimerization can be ignored in solution of aliphatic or aromatic hydrocarbon up to a concentration of 0.01 and 0.1 M, respectively [6].

The value of  $K_{ex}$  was obtained numerically through the minimization of the sum square of errors U defined by:

$$U = \sum (\log D_{exp} - \log D_{cal})^2 \quad (3)$$

where  $D_{exp}$  is the experimental metal distribution coefficient and  $D_{cal}$  is calculated by assuming the validity of Equation (1). The free extractant concentration  $[HR]$  is supposed to equal to total concentration  $[HR]_t$ . This calculation was carried out by using Microsoft Excel. The standard deviation is calculated by:

$$\rho(\text{Log D}) = (\text{U}/\text{N}_p)^{1/2} \quad (4)$$

where  $N_p$  is the difference between the total number of data points and the total number of equilibrium constants calculated.

In the first attempt, and following the slope analysis results, the value of  $n$  was varied between 0 and 2. Table 1 shows the best formulation for the metal/LIX 984 complexes, together with the calculated equilibrium constants obtained for both metals. This result partly agrees with the one obtained by Rodriguez *et al.* [7] who investigated the solvent extraction of some metals with LIX 984 dissolved in *n*-heptane and suggested the formation of  $\text{NiR}_2$  in the case of nickel and a mixture of  $\text{ZnR}_2$  and  $\text{ZnR}_2 \cdot 3\text{HR}$  in the case of zinc in the organic phase.

*Table 1. Results of the best formulation obtained in the Zn(II) / LIX 984 system and Ni(II) /LIX 984 system from various model species.*

Species	$\log K_{\text{ex}}$
$\text{ZnR}_2$	-9.5
$\text{NiR}_2$	-5.69

### **Effect of Acid Concentration on Stripping of Nickel from the Loaded Organic Phase**

Stripping studies were carried out to re-extract nickel from the loaded organic phase at varying concentrations of  $\text{HNO}_3$  (Table 2). The pH of the stripping phase ranged from pH 0.75 to pH 2.75. It was found that the percentage stripping of nickel increases with increasing acid concentration and reaches quantitative stripping for  $\text{HNO}_3$  concentration of 1 M.

*Table 2. Effect of  $\text{HNO}_3$  concentration on nickel stripping.*

$\text{HNO}_3$ (M)	0.001	0.01	0.03	0.10	0.17	0.31	0.56	1
Stripping (%)	14	52.1	63.4	80.6	90.54	95	98	> 99

### **CONCLUSION**

The solvent extraction of Ni(II) and Zn(II) with LIX 984 dissolved in heptane was studied. Extraction experiments were carried out varying the pH and metal concentration of the aqueous phase and the extractant concentration in the organic phase. These results show that zinc is poorly extracted in comparison to nickel. The selectivity series for the extraction of these metals from nitrate media based on the  $\text{pH}_{50}$  was found to be Ni ( $\text{pH}_{50} = 3.75$ ) > Zn ( $\text{pH}_{50} = 5.5$ ).

The experimental data obtained were treated numerically. Ni(II) and Zn(II) extraction by LIX 984 could be explained by the formation of  $\text{NiR}_2$  and  $\text{ZnR}_2$  organic phase complexes. The values of the equilibrium constants for these extraction reactions were  $\log K_{\text{ex1}} = -5.69$  for Ni(II) and  $\log K_{\text{ex2}} = -9.50$  for Zn(II).

Nickel stripping by acidic solution was also studied and it was found that 1 M  $\text{HNO}_3$  can strip Ni(II) to the extent of 99%.

## ACKNOWLEDGMENTS

We are grateful to Cognis (Germany) for kindly donating the LIX 984 sample.

## REFERENCES

1. C. Parija and P. V. R. Bhaskara Sarma (2000), *Hydrometallurgy*, **54**, 195.
2. A. M. Sastre and F. J. Alguacil (2001), *Chem. Eng. J.*, **81**, 109.
3. Henkel Corp. (1997), MID Redbook, Tucson.
4. B. H. Shih-Yao and J. M. Wiencek (2000), *Sep. Sci. Tech.*, **35** (4), 469.
5. B. Raghuraman, N. Tirmizi and J. M. Wiencek (1994), *Environ. Sci. Tech.*, **28**, 6.
6. J. Szymanowski (1995), *Crit. Rev. Anal. Chem.*, **25**, 142.
7. E. Rodriguez de San Miguel, J. C. Aguilar, J. P. Bernal, M. L. Balinas, M. T. J. Rodriguez, J. de Gyves and K. Schimmel (1997), *Hydrometallurgy*, **47**, 19.



# THE EFFECT OF ORGANOPHOSPHORIC EXTRACTANT CONCENTRATION AND INITIAL PHASE VOLUME RATIO ON COBALT(II) AND NICKEL(II) EXTRACTION

Darko Maljković and Zdenka Lenhard

Faculty of Metallurgy, University of Zagreb, Sisak, Croatia

Extraction and separation of cobalt(II) and nickel(II) with the commercial organophosphorus extractants MOOP, Cyanex 272 and Cyanex 302 were investigated. Within the scope of the investigations the effect of the initial extractant concentration (2.5 - 20 vol. %) and the initial phase volume ratio of the organic phase to the aqueous phase [0.5 and 1] on metal concentration in the organic phase was examined. Samples containing single metals or their mixture in sulphate solution were treated with the extractant, using kerosene as diluent, at initial pH = 8 and 25°C. Noticeable differences in dependence of metal extraction on extractant concentration and initial phase volume ratio as well as a significant mutual action of cobalt and nickel were observed. Under given experimental conditions the highest separation factors were found with Cyanex 302 at 2.5 and 20 % per volume.

## INTRODUCTION

Within the scope of study of application of commercial organophosphorus extractants for extraction and separation of cobalt(II) and nickel(II) from lateritic ore or from used hard metal the properties of Cyanex 272, Cyanex 302 and MOOP were examined. Extraction with those extractants was investigated previously by the authors, among others, extraction with Cyanex 272 from real and prepared samples, effect of different diluents and third phase appearance [1,2], mutual action of cobalt and nickel and third phase appearance for extraction with MOOP [3,4] as well as the behaviour of the extraction system containing Cyanex 302 [5]. All investigations were carried out with the extractant concentration 10 vol. % as a favoured level in literature. It seemed appropriate to investigate the influence of extractant concentration over a broader range than in the experiments of Tait with Cyanex 272 and Cyanex 302 [6]. Investigations were carried out with lower metal concentrations ( $c_{Co}^i = 0.09 - 0.7 \text{ g.dm}^{-3}$ ,  $c_{Ni}^i = 1.9 - 9.0$ ) and a lower nickel to cobalt ratio (16 - 21) than it was found in literature [6-9]. The cobalt concentrations reported in literature were from 0.4 to 2  $\text{g.dm}^{-3}$ , and those of nickel from 7 to 100  $\text{g.dm}^{-3}$  and the ratio of nickel to cobalt from 17 to 50. The experimental conditions as described in literature differed also in regard to diluent, use of modifier and pre-treatment of extractants (purification, conversion to Na-salt).

In this paper the results of investigation into the effect of extractant concentration on the behaviour of extraction systems containing commercial extractants, Cyanex 272, Cyanex 302 and MOOP, for low concentrations of cobalt and nickel, are presented.

## EXPERIMENTAL

### Materials

The extractants were Cyanex 272, Cytec, Canada, containing 85% bis (2,4,4-trimethylpentyl) phosphinic acid, Cyanex 302, Cytec, Canada, containing 84% bis (2,4,4-trimethylpentyl) mono thiophosphinic acid and Mono octyloctan phosphonate, MOOP, Bayer, Germany containing 97.5% of pure compound mono(2-ethylhexyl) phosphonic acid (2-ethylhexyl) ester. All extractants were used without further purification. Kerosene, INA, Croatia having a density (20°C) of 0.80 served as diluent in all experiments. All other chemicals were analytical reagent grade.

### Procedure

Samples containing a single metal, cobalt(II) or nickel(II), or a mixture of the two were prepared by dissolving metal sulphates in diluted sulphuric acid and by neutralisation with ammonium hydroxide to the required pH value. The examinations were carried out in graduated cuvettes (15 cm<sup>3</sup>). Cobalt(II) and nickel(II) concentrations were 0.15 g.dm<sup>-3</sup> (2.5x10<sup>-3</sup> M) and 2.3 g.dm<sup>-3</sup> (3.9x10<sup>-2</sup> M) and they corresponded to those in pre-treated leach liquors of lateritic ore. The initial pH value chosen on the basis of previous investigations was 8.0 in all experiments. The initial phase volume ratios of the organic phase to the aqueous phase (*r*) were 0.5 and 1.0. After the addition of the extractant (2.5 - 20 vol. % or approximately 0.08 - 0.6 M) diluted in kerosene samples were thermostated for 15 minutes at 25 ± 0.1°C, and after that, vigorously shaken four times for 30 seconds at 2-minute intervals. In between shakings the systems were thermostated.

### Methods of Analysis

Concentration of cobalt (using nitroso-R salt) and nickel (using dimethylglyoxime and K<sub>2</sub>S<sub>2</sub>O<sub>8</sub>) were determined by measurement of absorbance at 530 nm and 464 nm, respectively.

## RESULTS AND DISCUSSION

The effect of initial concentration of the extractant on cobalt(II) and nickel(II) concentrations in the organic phase ( $c_0^{\text{Co}}$ ,  $c_0^{\text{Ni}}$ ), as well as calculated distribution ratios ( $D_c$ ) and separation factors ( $\alpha$ ) at two different initial phase volume ratios were examined in samples containing a single metal or a mixture of metals.

In samples containing only cobalt, the best extraction was found with Cyanex 272 over Cyanex 302 and MOOP in the full range of extractant concentrations. In samples containing only nickel the metal was extracted better with MOOP than with Cyanex 302 and Cyanex 272. Concentration of metal in the organic phase was, as expected, always higher at the initial phase volume ratio 0.5 for all extractants, but for nickel, it always decreased with increase in extractant concentration, and for cobalt, it achieved a maximum value at extractant concentration between 5 and 15 vol. %.

Extraction of metals from samples containing a mixture compared to that from samples containing single metals differed.  $c_0^{\text{Ni}}$  obtained from a mixture with Cyanex 272 was significantly higher (e.g., at  $c_e = 10\%$  it was about 100 per cent higher), with Cyanex 302 significantly lower (Figure 1), and with MOOP slightly lower.  $c_0^{\text{Co}}$  obtained from a mixture was always higher than from samples containing a single metal, and the highest difference was observed with Cyanex 302 (e.g., at  $c_e = 10\%$  it was about 120 per cent higher). Additionally, for both metals, at the initial phase volume ratio 0.5, the difference increased with increase in extractant concentration. The effect of Cyanex 302 concentration on cobalt concentration in the organic phase is shown in Figure 2.

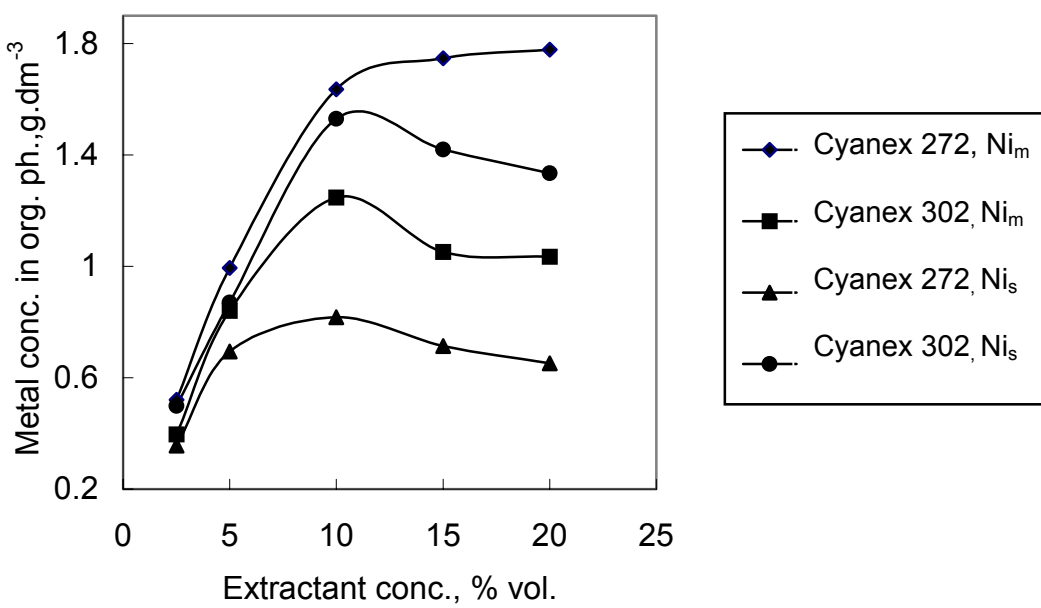


**Figure 1.** Effect of Cyanex 302 and Cyanex 272 concentration on nickel(II) extraction In the organic phase and comparison of extraction from samples containing a single metal ( $Ni_s$ ) and a mixture with cobalt(II) ( $Ni_m$ ) [  $pH^i = 8$ ,  $c^i_{Ni} = 2.3 \text{ g.dm}^{-3}$ ,  $c^i_{Co} = 0.15 \text{ g.dm}^{-3}$ ,  $r^i = 0.5$  ].

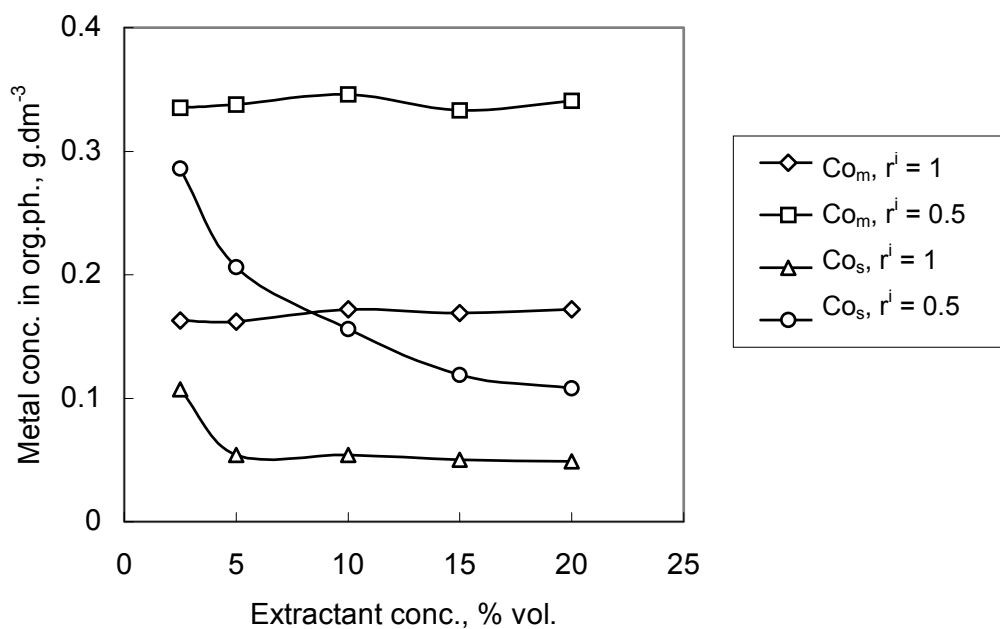


**Figure 2.** Effect of Cyanex 302 concentration on cobalt(II) concentration in the organic phase at different initial phase volume ratios and comparison of extraction from samples containing a single metal ( $Co_s$ ) and mixture with nickel(II) ( $Co_m$ ). [  $pH^i = 8$ ,  $c^i_{Ni} = 2.3 \text{ g.dm}^{-3}$ ,  $c^i_{Co} = 0.15 \text{ g.dm}^{-3}$  ].

In Figures 3. and 4 results of extraction from a mixture of metals with different extractants at two initial phase volume ratios are compared.

Extractant concentration produced a stronger effect on extraction of nickel than on extraction of cobalt at both investigated initial phase volume ratios. At the initial phase volume ratio 0.5, the highest nickel concentration in the organic phase was obtained with MOOP over Cyanex 272 and Cyanex 302 in the full range of extractant concentrations, except at 20 vol. % where MOOP and Cyanex 272 reached the same value. Significant influence of extractant concentration was observed. Under identical conditions cobalt concentration was not influenced by a change in extractant concentration, and higher concentrations were obtained with Cyanex 272 and Cyanex 302.

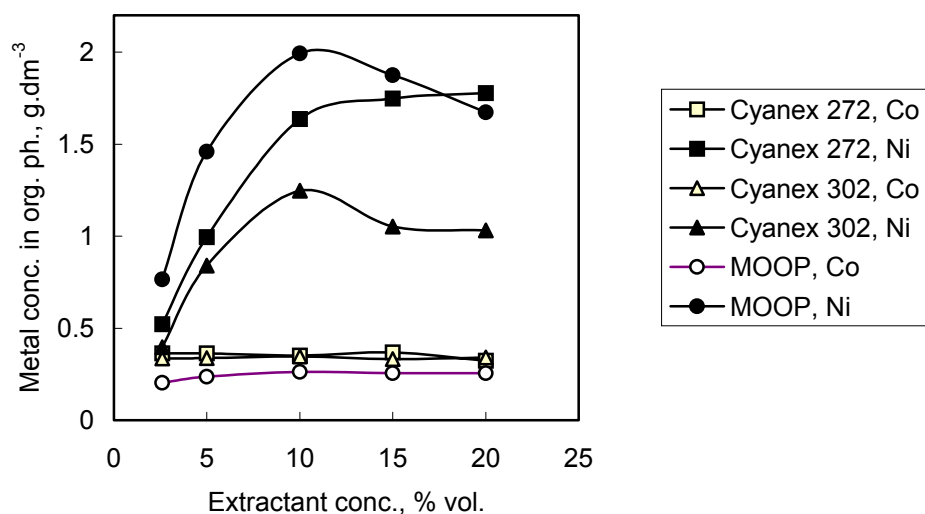


*Figure 3. Effect of concentration of different extractants on cobalt(II) and nickel(II) concentration in the organic phase  $r = 0.5$ . [  $pH^j = 8$ ,  $c_{Ni}^j = 2.3 \text{ g} \cdot \text{dm}^{-3}$ ,  $c_{Co}^j = 0.15 \text{ g} \cdot \text{dm}^{-3}$  ].*

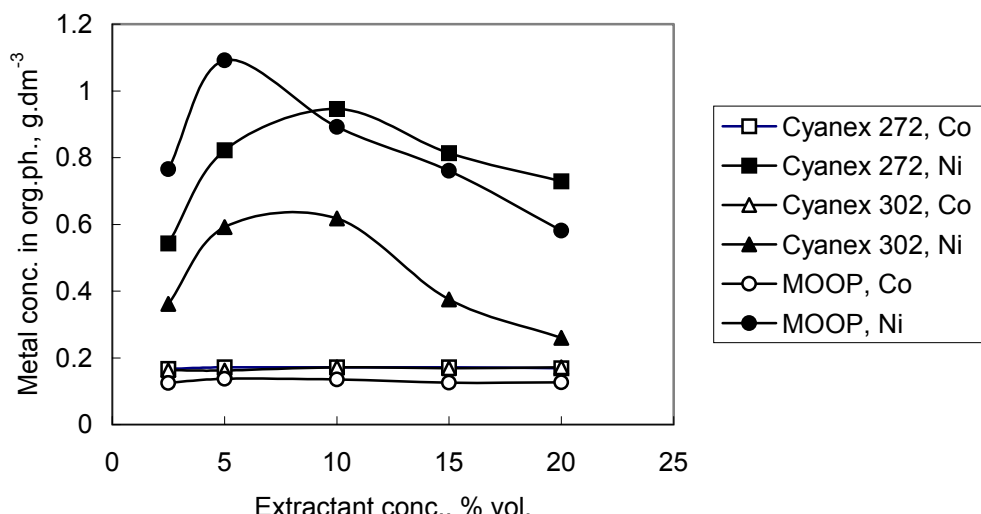


*Figure 4. Effect of concentration of different extractants on cobalt(II) and nickel(II) concentration in the organic phase at  $r = 1$ . [  $pH^j = 8$ ,  $c_{Ni}^j = 2.3 \text{ g} \cdot \text{dm}^{-3}$ ,  $c_{Co}^j = 0.15 \text{ g} \cdot \text{dm}^{-3}$  ].*

At the initial phase volume ratio 1, metal concentrations in the organic phase were generally lower than at initial phase volume ratio 0.5, and the effect of extractant concentration was similar, *i.e.*, it was present for nickel and absent for cobalt. The only difference concerned nickel extraction, as the highest nickel concentration in the organic phase at extractant concentrations over 10 vol. % was achieved with Cyanex 272.

Results obtained could be explained only partly by increase in the number of organic sites, by increase in extractant concentration, and, by a higher content of metal in the system at the initial phase volume ratio 0.5.

Presented results differ from those of Tait [6] who obtained increased concentration of both metals in the organic phase as a result of increase in extractant concentration. However, higher metal concentrations, a modifier and a different type of diluent were used.

The change in equilibrium pH in the systems prepared at initial pH 8, as a result of change in extractant concentration, was also measured. Decrease in equilibrium pH with increase of extractant concentration at constant initial pH depended not only on the extractant, but also on the type of the metals present, and on their concentration.

The highest distribution ratios of cobalt were achieved with Cyanex 302 at the initial phase volume ratio 0.5. At all extractant concentrations they were over 110. These distribution ratios were much lower than the maximum distribution ratio reported previously [4] for lower cobalt concentrations at the same initial pH. The distribution ratio of cobalt calculated for Cyanex 272 at the same initial phase volume ratio increased with increase in extractant concentration and achieved the highest value ( $D_c^{Co} = 108$ ) at extractant concentration 20 vol. %. In all other cases the effect of extractant concentration was evident to a greater or lesser extent, but highest distribution ratios of cobalt were below 60. As expected, on the basis of changes in metal concentrations in the organic phase, the distribution ratio of nickel was strongly influenced by extractant concentration. In all systems its maximum value was between extractant concentration 5 and 15 vol. %. The highest distribution ratios for nickel were achieved with MOOP ( $D_c^{Ni} = 1.45$ ,  $c_e = 20$  vol. %) and Cyanex 272 ( $D_c^{Ni} = 1.27$ ,  $c_e = 20$  vol. %) at the initial phase volume ratio 0.5.

The separation factors ( $\alpha$ ) as a result of changes of distribution ratios, mostly those of nickel, also show significant changes with increase in extractant concentration. In the case of Cyanex 272 and Cyanex 302, at both initial phase volume ratios, the minimum value of separation factor appeared at extractant concentration between 5 and 15 vol. %.

Table 1 shows the highest separation factors obtained with Cyanex 302 and Cyanex 272 and corresponding experimental conditions. The separation factors obtained with MOOP were between 15 and 36 in all cases.

*Table 1. Separation factors for Cyanex 302 and Cyanex 272.*

r	$C_e$ , % vol.	$\alpha_{Co/Ni}^{Co}$	
		Cyanex 272	Cyanex 302
0.5	2.5	233	558
	20.0	85	196
1.0	2.5	139	429
	20.0	122	330

## CONCLUSIONS

Comparison of metal extraction from samples containing a mixture of metals and those with a single metal confirmed the existence of a mutual effect of metals, noticed in our previous investigations of similar systems. Extraction was influenced by extractant concentration, but the extent and mode of that effect were different, and depended among others, also on the initial volume ratio and on the type of metal. Results showed that under given experimental conditions Cyanex 302 was a better extractant for the separation of cobalt from nickel at all extractant concentrations and both investigated initial volume ratios, than Cyanex 272 and MOOP.

## ACKNOWLEDGEMENT

Financial support of this investigation by the Ministry of Science and Technology of the Republic of Croatia Grant No 124003 is kindly acknowledged. Authors thank Prof. Dubravka Maljkovic for her useful discussions concerning the experiment design and the preparation of this paper. Supply of samples of extractants by Cytec Canada Inc. (Cyanex 272 and Cyanex 302) and Bayer AG, Germany, (MOOP) is greatly appreciated.

## NOMENCLATURE

### Symbols

c - concentration, g.dm<sup>-3</sup>

D<sub>c</sub> - distribution ratio

r - volume ratio of the organic to the aqueous phase

α - separation factor

### Subscripts and superscripts

Co - of cobalt

Ni - of nickel

e - of extractant

i - initial

m - extracted from mixture of both metals

o - in the organic phase

s - extracted from sample containing single metal

## REFERENCES

1. Da. Maljkovic, Z. Lenhard and M. Balen (1988), *Proc. Int. Solvent Extr. Conf., ISEC '88*, Moskow, Russia, Vol. 4, pp. 269-271.
2. Da. Maljkovic, Z. Lenhard and M. Balen (1991), *Proc. First European Metals Conf. EMC '91*, Brussels, Belgium, pp. 175-181.
3. Z. Lenhard, Da. Maljkovic and D. Hrsak (1998), *Kem. Ind.*, **47**, 357-359.
4. Da. Maljkovic, Z. Lenhard and Du. Maljkovic (2000), *Proc. Int. Solvent Extr. Conf. ISEC '99*, Barcelona, Spain, Vol. 2, pp.1177-1182.
5. Z. Lenhard and Da. Maljkovic (2000), *Proc. 15th Int. Conf. Ars Separatoria 2000*, Borowno n. Bydgoszcz, Poland, pp. 202-204.
6. B. K. Tait (1993), *Proc. Int. Solvent Extr. Conf., ISEC '93*, York, England, Vol. 3, pp. 1303-1310.
7. B. K. Tait (1993), *Hydrometallurgy*, **32**, 365-372
8. C. Bourget, M. Cox and D. S. Flett (1996), *Proc. Int. Solvent Extr. Conf. ISEC '96*, Melbourne, Australia, Vol. 1, pp. 505-510.
9. N. B. Devi, K. C. Nathsarma and V. Chakravorty (1998), *Hydrometallurgy*, **49**, 47-61.



## OPTIONS FOR COPPER(II) AND ZINC(II) EXTRACTION FROM CHLORIDE MEDIA WITH BI-FUNCTIONAL EXTRACTANTS

Aleksandra Borowiak-Resterna, George Kyuchoukov\* and Jan Szymanowski

Poznan University of Technology, Poznan, Poland  
\*Bulgarian Academy of Sciences, Sofia, Bulgaria

Extraction of copper(II) and zinc(II) from acidic chloride solutions with mixtures of two extractants: a basic or solvating one and a chelating extractants are discussed. The processes for recovery and separation of copper(II) from zinc(II) are proposed. The processes consist of the following steps: extraction from chloride media with the formation of metal chlorocomplex ion pair or solvate, scrubbing of chloride ions with an aqueous solution of appropriate pH with simultaneous transfer of the metal ion to the chelate, traditional stripping with sulphuric acid and conditioning of the basic extractant. Both effective recovery and separation of metal ions with simultaneous change of the system from the chloride to sulphate one can be achieved. A bi-functional extractant, such as derivatives of 8-hydroxyquinoline, can also be used in place of a mixed extractant system.

### INTRODUCTION

Hydroxyoximes are well known extractants and are widely used to recover copper(II) from dilute acidic sulphate solutions [1].  $\beta$ -diketones are used for the extraction of copper(II) from ammoniacal etching solutions obtained in circuit board manufacture [1]. Both hydroxyoximes and  $\beta$ -diketones are chelating reagents (HL). The stable chelate complexes are formed and extracted, but the reaction is reversible and equivalent amounts of protons are liberated.



As a result, the reagents are not convenient for the processing of concentrated copper(II) solutions which can be obtained by the leaching of sulphide ores, e.g., with  $FeCl_3$  or  $CuCl_2$ . In this case the leaching solution (pH 3) can contain 0.2-1.0 M copper(II) and ferric ions and 4-6 M  $Cl^-$ . Under such conditions copper(II) is mainly in the form of chlorocomplexes and can be effectively extracted with solvating reagents (S) [2].



Such a commercial reagent, ACORGA CLX 50, was produced by ZENECA (now Avecia) and the CUPREX process was developed based on it [3]. The main drawback of the extraction of copper(II) from chloride solutions with solvating reagents is the stripping with water and subsequent electrowinning from chloride media. Reactive granules of copper with well-developed surface area are produced instead of traditional copper sheets.

In this paper possibilities are explored to recover copper(II) from acidic chloride solutions with mixed extractants, or with a bi-functional extractant, to obtain loaded sulphate solution suitable for classical electrowinning of the metal. Leaching of copper sulphide ores and etching of copper covered goods can give such chloride solutions. In the first case the solution also contains large amounts of iron. Chloride leaching is also important for processing of ores and wastes containing zinc alone and alloys of copper and zinc. Thus, depending on the system the extractant must be selective for copper over iron or zinc and effectively extract metal species from highly concentrated chloride solutions at appropriate acidity of the aqueous feed. Proprietary extractants and model compounds synthesised mainly by the authors are considered. The proposed processes and conditions are the results of the author's own investigations.

### CONCEPTUAL FLOWSHEET FOR RECOVERY OF METAL CHLORO-COMPLEXES

A conceptual flowsheet for a process based on the use of mixed extractants (one basic or solvating and one chelating reagent) or a bi-functional extractant is shown in Figure 1.

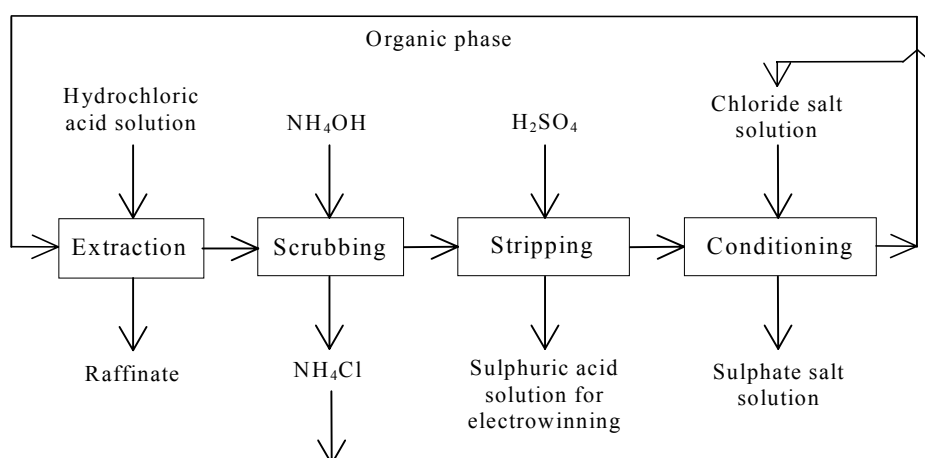


*Figure 1. Flowsheet of the process proposed for metal(II) recovery from chloride media with simultaneous change of the system from chloride to sulphate.*

In the extractant systems the basic or solvating reagent can extract metal ions present in the form of anionic chloro-complexes or neutral chloro-complex, respectively. When the organic phase is then scrubbed with an aqueous solution the complex is decomposed and liberated chloride anions are transferred to the aqueous phase, while the metal cations remain in the organic phase as complexes with the chelating reagent. In such a case, a traditional stripping with sulphuric acid of appropriate concentration and then conventional electrowinning can be carried out. Depending on the type of reagent used to extract copper from chloride solutions the process can be selective (a solvating reagent) or not-selective (a basic reagent) with respect to iron(III) or zinc(II). Depending then on the type of the chelating reagent and the type of metal, water at different adjusted pH must be used for scrubbing of chloride ions to prevent the simultaneous stripping of metal ions.

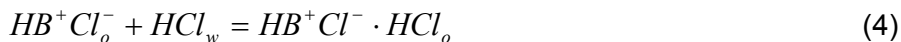
## SOLVENT-EXTRACTION CHEMISTRY

Most of the common metal ions form chloro-complexes in chloride media. At comparable conditions the chloro-complex formation constants change in the following order:  $\beta_i(\text{Fe}) > \beta_i(\text{Zn}) > \beta_i(\text{Cu})$ . This means that negatively charged chloro-complexes are more readily formed with iron(III) and zinc(II) than with copper(II). This results in a poor selectivity for zinc(II), and especially for copper(II) extraction from highly concentrated chloride media with basic extractants carried out in the presence of iron(III). However, it also reveals some possibilities for separation of zinc(II) from copper(II).

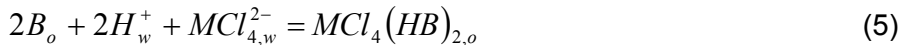
The basic extractant is easily protonated in a contact with an acidic aqueous chloride solution:



This means that the amine hydrochloride can be decomposed by a decrease of the acidity and/or chloride content in the aqueous phase. The amine hydrochloride can bind the second molecule of the hydrochloric acid transferring it to the organic phase:



The reaction is favoured by a high concentration of the hydrochloric acid [4]. A basic extractant can also be protonated in a contact with aqueous acidic solutions containing metal chloro-complexes. The reaction can occur even more readily than reaction (4), especially for  $\text{ZnCl}_4^{2-}$ :



A basic extractant treated with a sulphuric acid solution gives two products:

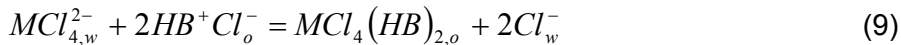


The equilibrium of these two reactions depends on the concentration of sulphuric acid. In low acidity, depending on the basicity of amine, reaction 7 is favoured. However, when treated with 1 *M* sulphuric acid ammonium hydrogensulphate is mainly formed. It can bind the second molecule of sulphuric acid.

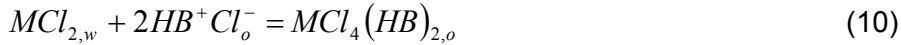
Hydrogensulphate or sulphate forms can be readily transferred to the chloride form by treating with a chloride solution, e.g., with 2.8 *M* NaCl solution:



Metal chlorocomplexes can be extracted by the amine hydrochlorides according to reaction:

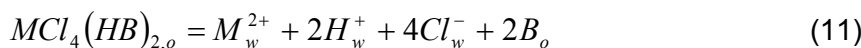


The reaction with  $\text{MCl}_3^-$  and the neutral chlorocomplex  $\text{MCl}_2$  are also possible, e.g.:

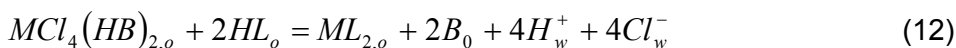


The amine metal chlorocomplex can also bind one additional molecule of hydrochloric acid, i.e.,  $\text{MCl}_4(\text{HB})_2 \cdot \text{HCl}$  [5].

The amine metal chlorocomplex can be decomposed by treating with an aqueous solution of low concentration of chloride ions. The extractant can also undergo deprotonation.



The scrubbing of the metal cation to the aqueous phase can be neglected when the organic phase contains appropriate quantities of a chelating extractant (or an acidic extractant); and the acidity of the aqueous phase is low enough to permit the formation of the chelate according to reaction similar to Equation (1). The process can be described as follows:



When a solvating extractant is used instead of an amine the protonation of the reagent can be avoided but the extraction must be carried out from weakly acidic solutions (Equation (2)).

### TECHNOLOGICAL ASPECTS

Various extractants can be selected for extraction (Table 1). The following parameters should be considered: compatibility of structure and properties, including the mutual reactivity and extraction capacity, selectivity and kinetics of extraction, compatibility of extractants to the composition and acidity of the aqueous phase in each step of the separation process, physicochemical properties of solutions in each separation step, molar ratio of extractants, their concentrations in the solvent and the phase volume ratio.

*Table 1. Extractants and process conditions.*

Extractants	Extraction	Scrubbing	Stripping
ALAMINE 336/LIX 54 Synergistic mixture	Up to 130 g/L Cu(II), 3 M HCl and 7 M Cl <sup>-</sup>	Equilibrium pH 6 - 7	Even 0.04 M H <sub>2</sub> SO <sub>4</sub>
ACORGA CLX 50/LIX 54	pH 3, 4-6 M Cl <sup>-</sup> Selective in respect of Fe(III)	Equilibrium pH ≥ 6 - 7	Even 0.04 M H <sub>2</sub> SO <sub>4</sub>
N,N,N',N'-tetrahexyl- pyridine-3,5-dicarboxamide /2-hydroxy-5-t-octylbenzo- phenone oxime	pH 3, 0.1 - 6 M Cl <sup>-</sup> Selective in respect to Fe(III)	Water	1.7 M H <sub>2</sub> SO <sub>4</sub>
N,N,N',N'- tetrahexylpyridine-3,5- dicarboxamide/1- phenyldecane-1,3-dione	pH 3, 5 - 6 M Cl <sup>-</sup> Selective in respect of Fe(III)	Equilibrium pH ≥ 3.8	0.25 M H <sub>2</sub> SO <sub>4</sub>
KELEX 100 or LIX 26 Zn/Cu separation	Up to 130 g/L Cu(II), 3 M HCl and 7 M Cl <sup>-</sup>	Equilibrium pH 2 - 9 for Cu(II) and 7 - 8 for Zn/Cu separation	2.8 M H <sub>2</sub> SO <sub>4</sub>

The extractants used must not react with each other. Their co-association via hydrogen bonding should also be avoided. A mixture of ALAMINE 336 and LIX 860 can be given as an example of an incompatible pair of extractants. Using this mixture for extraction of copper(II) from acidic chloride solutions an important drop in extraction capacity is observed [4]. Reagents having an appropriate selectivity, especially with respect to iron(III) should be used, *i.e.*, the use of a solvating reagent instead of alkylamines is favoured, permitting the selective extraction of copper(II) and zinc(II) in the presence of iron(III).

Kinetics of extraction should not be worse with the mixed extractants. Again, it means that the concentrations of the active forms of extractants should not be decreased. A good compatibility of reagents should also be assured in the scrubbing and stripping steps.

In scrubbing, chloride ions must be qualitatively washed out but metal ions should be completely transferred from the metal ion pair, or solvate, to the chelate. The removal of chloride ions can be easily accomplished using an aqueous solution at relatively broad range of acidity. However, to obtain full chelation the acidity of the scrubbing solution must be adjusted to the extraction ability of chelating extractant. The limiting pH of the scrubbed solution depends both on extractant and on the metal ion considered, and a higher and lower pH is needed for the scrubbing of chloride ions from the organic phase containing zinc(II) and copper(II), respectively.

In stripping, besides the transfer of the metal ions to the acidic sulphate solution, the undesired protonation of the basic extractant occurs. The solvating extractant (e.g., ACORGA CLX 50) can also be protonated depending on the basicity of the nitrogen atom in the pyridine moiety and the concentration of sulphuric acid. The phenomenon should not result in any precipitation of the extractant and emulsification of the system. A good and quick separation of phases must be obtained in each step of the process.

Molar ratio of extractants, their concentrations and volume phase ratio are important for two reasons. First, the chelating reagent must be able to bind the metal ion released in the scrubbing from the metal ion pair, or from the solvate. Moreover, the chelation must compete kinetically with the scrubbing. A use of a small excess of the chelating reagent (10 mol%) is recommended. Second, the separation of metal ions is easier near the capacity of extractants. The crowding effect permits the dismissal of metal ions weakly bound by the extractant. The concentration of the extractants and/or the phase volume ratio can be adjusted to achieve a high loading of the organic phase.

## EXTRACTION WITH MIXED REAGENTS

### **ALAMINE 336-LIX 54 [4, 6-8].**

ALAMINE 336 and LIX 54 are the basic and chelating extractants, respectively. The extractants are mutually compatible and useful for the recovery of copper(II) from hydrochloric acid etching solutions obtained in circuit printed board manufacture (130 g/L copper(II), 2.8-2.9 M HCl and 7 M Cl<sup>-</sup>). A strong synergistic effect is observed. 30% solution of ALAMINE 336 in kerosine extracts about 16 g/L copper(II) from the etching solution. LIX 54 does not extract copper(II), but a 30:70 mixture of ALAMINE 336 and LIX 54 extracts ~20 g/L copper(II). The synergistic effect is especially strong when copper(II) is extracted from 1 M HCl. In such a case, the mixture of reagents permits the extraction 10 g/L copper(II), whilst individual components extract only negligible amounts of copper(II). Scrubbing must be carried out with an ammoniacal solution to obtain the equilibrium pH 6-7. The stripping can be carried out with a very diluted sulphuric acid (even 0.04 M at the equilibrium). However, the concentration of 1.5 M is recommended to obtain the acidity typical for electrowinning. The mixture can also be used to separate copper(II) from zinc(II) [9].

### **ACORGA CLX 50-LIX 54 [10]**

ACORGA CLX 50 acts as a solvating reagent at pH 3 and efficiently extracts neutral chloro-complex of copper(II) from solutions containing 4 - 6 M Cl<sup>-</sup>. An equimolar mixture of ACORGA CLX 50 and LIX 54 extracts copper(II) in comparable amounts to ACORGA CLX 50 from aqueous chloride solutions above 2 M at pH 3. At lower concentrations of chloride ions an important coextraction of copper(II) by LIX 54 is also observed. The scrubbing of chloride ions must be carried out with an ammonia solution to neutralise hydrogen cations liberated in chelation with LIX 54. The equilibrium pH cannot be lower than 6. The system is suitable for practical applications in the presence of large amounts of iron(III).

### **N,N,N',N'-tetrahexylpyridine-3,5-dicarboxamide (a) / 2-Hydroxy-5-t-octylbenzophenone oxime (b) [11]**

The equimolar mixture of an amide analogue of CLX 50 (a, above) and a LIX 65 type oxime (b, above) permits effective extraction of copper(II) from chloride media and the transfer of copper from solvate ( $\text{CuCl}_2\text{B}_2$ ) to the chelate ( $\text{CuL}_2$ ) by scrubbing with water. The effect of chloride concentration on the extraction of copper(II) is almost negligible. However, at low ( $0.1 \text{ M}$ ) chloride concentration copper is mainly bound with the oxime in the chelate (74 %) and at high ( $5 - 6 \text{ M}$ ) chloride concentration with the amide in the solvate (92 %). The oxime is a strong enough extractant to bind copper(II) when the organic phase is scrubbed with water. In this case only 5 - 16 % of copper(II) with respect to that present in the aqueous feed is transferred back with chloride ions to the aqueous phase, while 58 - 51 % remains in the organic phase in the form of the chelate, and the rest in the form of the chloro-complex solvate. Although copper is successfully transferred from the solvate to the chelate the system needs additional washing of the organic phase before recycling for extraction. Sulphuric acid (170 g/l) must be used for stripping. In such a case some protonation of the pyridine function and its deprotonation must be obtained before recycling the organic phase. In another case the reagent would complex iron chloro-complexes in the form of an ion pair. As a result, the system is not suitable for recovery of copper(II) in the presence of iron(III).

### **N,N,N',N'-tetrahexylpyridine-3,5-dicarboxamide (a) / 1-Phenyldecane-1,3-dione (c) [11]**

The equimolar mixture of (a, above) and a LIX 54 type dione (c, above) permits effective extraction of copper(II) from chloride media and the transfer of copper(II) from the solvate to the chelate; by scrubbing with an ammoniacal solution. In this case, when the ammoniacal solution is used for scrubbing only small amounts of copper(II) (3 - 6 %) are transferred back to the aqueous phase. The equilibrium pH after scrubbing cannot be lower than 3.8 and 5.7 for the concentration of chloride ions in the initial feed equal to  $5 - 6$  and  $0.1 - 1 \text{ M}$ , respectively. Copper(II) can be then stripped with dilute sulphuric acid solutions containing at least 25 g/L  $\text{H}_2\text{SO}_4$ . At such concentration of sulphuric acid a significant protonation of the pyridine function is not observed. The use of the system for recovery of copper(II) from chloride solutions is proposed.

## **EXTRACTION WITH BIFUNCTIONAL EXTRACTANTS KELEX 100 AND LIX 26**

The 8-hydroxyquinoline derivatives, KELEX 100 and LIX 26, can act as a chelating extractant (Equation (1)), or as a basic extractant after protonation (Equation (9)). The reagent must be used with a modifier (about 15 v/v% octanol) to avoid the formation of the third phase. The process was developed to recover copper(II) from etching solutions containing 120 g/L copper(II),  $2.9 \text{ M HCl}$  and  $6.8 \text{ M Cl}^-$  [5, 12-14]. The recovery of copper(II) and zinc(II) from brass leaching solutions is also possible. An ammonium solution must be used for scrubbing of chloride from organic solution containing copper(II) with the equilibrium pH changed in the broad range from 2 to 9. In the case of the organic phase loaded with zinc(II) the equilibrium pH must be adjusted to 7-8 [13, 14]. Stripping of copper(II) and zinc(II) can be carried out in one stage with  $2.8 \text{ M H}_2\text{SO}_4$ . A lower concentration of sulphuric acid can be also used, especially for the stripping of zinc(II), e.g.,  $0.5 \text{ M}$ . In such a case KELEX 100 is only slightly protonated. The organic phase must then be treated with waste hydrochloric acid solution to obtain full protonation and the scrubbing of sulphate ions. Thus, it is more convenient to use more concentrated sulphuric acid for stripping and then  $4.7 \text{ M NaCl}$  or  $\text{NH}_4\text{Cl}$  for the replacement of sulphate by chloride anion.

The separation of copper(II) from zinc(II) can be accomplished at the stage of extraction, scrubbing or stripping. The separation at the extraction stage, chemically easier to accomplish, is technologically less attractive because two parallel loops for copper and zinc streams have to be considered for the next stages. Thus, technologically and economically

the most attractive option is the separation in the stripping stage. The separation can be accomplished by the selective stripping of zinc(II) with the equilibrium sulphuric acid concentration in the range of 0.1 - 0.5 M. The stripping of zinc(II) is not complete below 0.1 M, while the stripping of copper(II) is observed above 0.75 M. Thus, the initial concentration for the stripping of zinc(II) should be in the range 0.25 - 0.8 M. Copper(II) can be stripped with 3 M sulphuric acid. Two stages for complete stripping are needed. Sulphuric acid of lower concentration can also be used but more stages are needed.

## CONCLUSION

Mixed extractants containing a basic or solvating extractant with a chelating extractant permits the recovery of copper(II) and zinc(II) from acidic chloride solutions with the change from a chloride to a sulphate system. As a result, the traditional electrowinning from the sulphate solution can be carried out. The method is also suitable to separate copper(II) from zinc(II) that can be achieved at the stage of extraction, scrubbing or stripping. The use of ALAMINE 336 and LIX 54 is proposed when iron(III) is absent or ACORGA CLX 50 and LIX 54 when Fe(III) is present in the aqueous feed. KELEX 100 and LIX 26 can be considered as bi-functional extractants (a basic and chelating extractant) and can be used in place of mixed extractants to recover both copper(II) and zinc(II) from chloride acidic solutions in the absence of iron(III) and to separate these metal ions at the stage of extraction, scrubbing or stripping.

## ACKNOWLEDGEMENTS

The work was supported by KBN Poland for the Institute activity (DS/32/049/2001 and DS 32/044/2001).

## REFERENCES

1. J. Szymanowski (1993), *Hydroxyoximes and Copper Hydrometallurgy*, CRC Press, Boca Raton, FL.
2. A. Borowiak-Resterna and J. Szymanowski (2000), *J. Radioanal. Nucl. Chem.*, **246**, 657-663.
3. R.F. Dalton, R. Price, P.M. Quan and D. Steward (1982), *Eur. Pat.*, No. 57,797 (Aug. 18).
4. G. Kyuchoukov and I. Mishonov (1999), *Solvent Extr. Res. Dev., Jpn.*, **6**, 1-11.
5. M. B. Bogacki, S. Zhivkova, G. Kyuchoukov and J. Szymanowski (2000), *Ind. Eng. Chem. Res.*, **39**, 740-745.
6. G. Kyuchoukov and I. Mihajlov (1991), *Hydrometallurgy*, **27**, 361-369.
7. G. Kyuchoukov and I. Mishonov (1993), *Solvent Extr. Ion Exch.*, **11**, 555-567.
8. I. Mishonov and G. Kyuchoukov (1996), *Hydrometallurgy*, **41**, 89-98.
9. G. Kyuchoukov, M.B. Bogacki and J. Szymanowski (1998), *Ind. Eng. Chem. Res.*, **37**, 4084-4089.
10. R. Cierpiszewski and J. Szymanowski, *Solvent Extr. Ion Exch.*, in press.
11. A. Borowiak-Resterna and J. Szymanowski (2000), *Solvent Extr. Ion Exch.*, **18**, 77-91.
12. G. Kyuchoukov and R. Kounev (1994), *Hydrometallurgy*, **35**, 321-342.
13. G. Kyuchoukov, A. Jakubiak and J. Szymanowski (1997), *Solvent Extr. Res. Dev., Jpn.*, **4**, 1-11.
14. G. Kyuchoukov, A. Jakubiak, J. Szymanowski and G. Cote (1998), *Solvent Extr. Res. Dev., Jpn.*, **5**, 172-188.



## IMPURITY REMOVAL FROM COPPER TANKHOUSE LIQUORS BY SOLVENT EXTRACTION

M. Cox, D. S. Flett, T. Velea\* and C. Vasiliu\*

Department of Physical Sciences, University of Hertfordshire, UK  
\*IMNR SA, Bucharest, Romania

A possible flowsheet for the removal of As, Sb and Bi from copper electrorefinery electrolytes has been developed for the Allied Deals Phoenix SA plant at Baia Mare in Romania where the feed to the smelter is a complex ore containing quite high levels of As, Sb and Bi. From a literature survey three commercial solvent extraction reagents, namely LIX 1104®, CYANEX 923® and Acorga SBX 50® were selected for screening. From this preliminary work, CYANEX 923 was selected as the preferred reagent. This paper describes the results of the screening tests and the further work undertaken to develop a workable process for the removal of As, Sb and Bi from the copper tankhouse electrolyte at Baia Mare with CYANEX 923.

### INTRODUCTION

In copper refineries, the total monthly volume of bleed electrolyte from the tankhouse is quite high and the flowrate of the bleed stream is determined by impurity levels of which the most important is As, with lesser importance put on Sb and Bi. At the Allied Deals Phoenix plant at Baia Mare in Romania, quite high amounts of As, Sb and Bi arise from the complex ore feed. According to the company, the maximum impurity concentration at which the electrolyte is removed is 4 g/l As; 1.2 g/l Sb and 0.008 g/l Bi. Solvent extraction has been shown by several authors to be a promising technique for As, Sb and Bi removal from copper tankhouse electrolytes [1-3], and was chosen in this study for application to the problem of impurity control at Baia Mare.

Impurity control by solvent extraction in copper electrorefining has been demonstrated in numerous studies and also in plant practice. Thus tributylphosphate (TBP) is employed to extract arsenic at several copper electrorefineries around the world [1]. This extractant only extracts As(V). Dreisinger *et al.* [2, 3] investigated a large number of extractants and found that, among the solvating extractants, dibutylbutylphosphonate (DBBP) and dipentylpentylphosphonate (DPPP) were stronger extractants for arsenic than TBP and that Sb could be extracted by a mixed reagent (2EHAPo<sub>4</sub>, Albright and Wilson). The extraction of As, Sb and Bi with a commercial hydroxamic acid (LIX 1104®, Cognis) has been described by Schwab and Kroke [4] and others [2, 3]. Stripping of arsenic was difficult and H<sub>2</sub>S or anhydrous sodium sulphide were proposed as strippers. Iron is also co-extracted but can be stripped with HCl. The trialkylphosphine oxide reagent CYANEX 923® (Cytec Inc.) has been studied by Wisniewski and co-workers as an extractant for both As(III) and As(V) [5-8]. These authors have compared this reagent with ENIM 100®, TBP, 2-methylhexanol [7] and neodecanohydroxyamic acid [8]. Extraction equilibrium was established in 5 minutes with CYANEX 923 compared to 15 minutes for the hydroxamic acids; arsenic extraction increased with increasing H<sub>2</sub>SO<sub>4</sub> concentration and H<sub>2</sub>SO<sub>4</sub> was co-extracted. Choice of diluent was important for CYANEX 923 with toluene being a better diluent than Exxsol D 220/230® [8].

Arsenic could be stripped with water, and four extraction and three stripping stages were concluded to be sufficient to effectively extract and strip As [8] although the reported results for water stripping do not bear this out. Removal of arsenic from a copper speiss leach liquor using CYANEX 923 has been reported by Newell [9] who obtained results similar to Wisniewski's but did not address arsenic stripping. Using an actual speiss leach liquor containing 28.5 g/l As; 44.9 g/l Cu; 0.06 g/l Fe; 1.25 g/l Sb and 8.6 g/l Ni, it was also shown that Fe but not Cu and Sb was co-extracted. Zeneca (now Avercia) developed a new alkylphosphonic acid (Acorga SBX 50<sup>®</sup>) for the extraction of Sb and Bi, but not As from copper tankhouse electrolytes [10].

Based on the above literature survey it was decided to screen LIX 1104, CYANEX 923 and SBX 50 for the removal of As, Sb and Bi from the Baia Mare copper refinery electrolyte. TBP was not selected as it only extracts As(V) and not As(III).

## EXPERIMENTAL

The extractants LIX 1104 SM<sup>®</sup>, CYANEX 923 and SBX 50 were kindly supplied by Cognis Mining Chemicals, Cytec Industries B.V. and Avercia, respectively. These were used as received. The diluents used were Orform SX 7<sup>®</sup> from Philips Petroleum and kerosene from Combinatul Petrochimic Pitesti, Romania. Synthetic solutions of As, Sb and Bi were prepared from analytical grade arsenic acid, bismuth chloride and antimony oxide by dissolution in H<sub>2</sub>SO<sub>4</sub>. An actual liquor from Baia Mare assaying 1.3 g/l As; 0.16 g/l Sb; 0.063 g/l Bi, 0.073 g/l Cl<sup>-</sup>, 0.33 g/l Fe, 38.5 g/l Cu and 172 g/l H<sub>2</sub>SO<sub>4</sub> was also used in the testwork.

For the work carried out in the UK, metal ion analyses were carried out using a Perkin Elmer ICP spectrophotometer. For the analyses at IMNR an OES-DCP Beckman (SUA) Spectaspan V was used. As appropriate, H<sup>+</sup> and Cu<sup>2+</sup> were analysed electrochemically and SO<sub>4</sub><sup>2-</sup> was determined gravimetrically.

## ALLIED DEALS PHOENIX (BAIA MARE) OPERATIONS

Currently the flash furnace at Baia Mare is undergoing refurbishment. However on start-up the maximum levels of impurities anticipated by the company in the tankhouse bleed will be 5-6 g/l As; 1.2 g/l Sb and 0.01 g/l Bi. An operating level of 2 g/l As; 0.8 - 1 g/l Sb and 0.005 g/l Bi has been chosen as the goal for this study.

## RESULTS AND DISCUSSION

### Screening Tests

Screening tests with the three selected extractants were carried out on individual synthetic solutions of 100 ppm As, Sb and Bi in 2 M H<sub>2</sub>SO<sub>4</sub> using 50 v/o CYANEX 923 and 10 v/o LIX 1104.

As and Sb extraction with CYANEX 923 was fast (< 2 minutes), decreased with increasing temperature but increased with increasing H<sub>2</sub>SO<sub>4</sub> concentration as reported by Wisniewski for As [8]. Bi was not extracted from the 100 ppm solution of the element. Sb could be stripped readily with water but As was less easily stripped requiring elevated temperature (60 °C).

With LIX 1104, As extraction was very slow, 90 minutes at 60 °C for >90% extraction. Extraction increased with increasing temperature in agreement with literature data [4]. LIX 1104 also extracted Sb and Bi well and faster than As. Increasing temperature decreased the degree of extraction of Sb and Bi. Because of the poor As extraction kinetics; the need to use H<sub>2</sub>S or CuSO<sub>4</sub> for As stripping and a chloride solution for Sb and Bi stripping, which then required a water wash to remove organic phase chloride to avoid transfer to the refinery electrolyte, no further work was carried out with LIX 1104.

With 10 v/o SBX 50 good extraction of Sb and Bi was obtained at ambient temperature (18 °C). Sb and Bi extraction decreased with increasing temperature. From the literature [10], stripping of Sb and Bi can only be sensibly carried out with acid chloride liquors. Stripping tests in this work confirmed this.

With real electrolyte solutions however, CYANEX 923 extracted all three impurities well. The extraction of Bi is probably due to the presence of chloride in this liquor compared with the synthetic liquor. For Sb, where addition of chloride was required to prevent hydrolysis in the synthetic solution, it appeared that Sb extraction from this liquor was probably as an antimony chloro-complex. Co-extraction of sulphuric acid [2, 5] and water [8], as expected, also occurred.

Tests were also carried out on real solutions with SBX 50. It was found that Sb extraction was better than from the synthetic solutions. This may be due to the higher concentration of chloride in the synthetic solutions. Stripping tests with 2.5 M CaCl<sub>2</sub> and 1 M HCl showed excellent recovery of Sb, but Bi was not totally stripped. According to Cupertino *et al.* [10] Bi removal requires 0.5 M HCl and 6 M Cl<sup>-</sup> to strip 195 ppm from the organic phase so better Bi stripping should be possible with higher chloride concentrations.

From these results it was concluded that the best extractant for all three impurities was CYANEX 923, and so further work was carried out with this reagent.

### Extraction Isotherms

Extraction isotherms (Figures 1 to 3) have been obtained for As, Sb and Bi at different temperatures (20, 40 and 60 °C) for the refinery electrolyte enriched in arsenic by addition of As(V) to 17.2 g/l. The As isotherms in Figure 1 show that As(V) extraction decreases with increasing temperature. From McCabe-Thiele construction it can be seen that two stages at 60 °C at an O/A ratio of 10:1 are required to remove arsenic to the required level of 2 g/l or below.

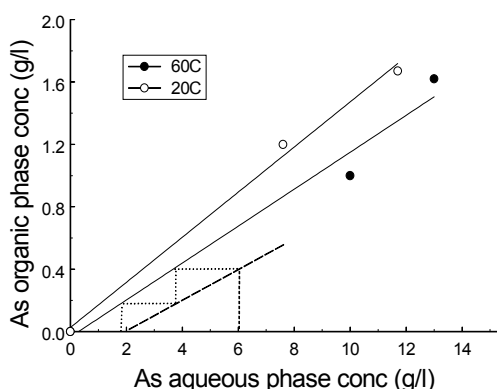


Figure 1. As extraction isotherm with 50% CYANEX 923 in kerosene.

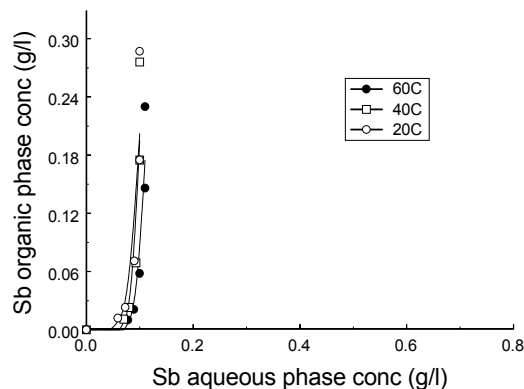


Figure 2. Sb extraction isotherm with 50% CYANEX 923 in kerosene.

Figure 2 shows that Sb extraction decreases slightly with increasing temperature. From the shape of the curves it is obvious that the conditions for As extraction would be more than sufficient to remove Sb to the required level of 0.8 - 1 g/l.

Figure 3 also shows that Bi extraction decreases slightly with increasing temperature. From the diagram it seems that it might be difficult to remove Bi to < 0.005 g/l but, at these levels, analysis of Bi is at the limit of determination.

Co-extraction of sulphate from the same feed as for Figures 1, 2 and 3 is also shown in Figure 4. This shows that significant amounts of sulphate are co-extracted. As sulphate ion is not believed to be involved to any significant degree with the extraction of As, Sb and Bi, this verifies the large co-extraction of sulphuric acid reported by other authors [2, 3, 5]. From Figures 1 and 2 the value of the separation factor for As over  $\text{SO}_4^{2-}$  is 0.75. This may be compared with the value of 6.25 obtained by Wisniewski [5] for 50% CYANEX 923 from 150 g/l  $\text{H}_2\text{SO}_4$  but at 50 °C. While the  $D$  values for  $\text{SO}_4^{2-}$  obtained in this work and that for  $\text{H}_2\text{SO}_4$  in Wisniewski's study are similar, i.e., 0.2 and 0.18, respectively, thus corroborating the conclusion that sulphate extraction is identical with  $\text{H}_2\text{SO}_4$  extraction, the  $D$  values for As (V) are very different, i.e., 0.15 in this work at 60 °C compared with 1.125 at 50 °C by Wisniewski [5]. For comparison, Dreisinger *et al.* [2] obtained a separation factor of 3.7 for neat CYANEX 923 also at 50 °C but from 200 g/l  $\text{H}_2\text{SO}_4$  in the presence of 30 g/l Cu. The respective  $D$  values for As (V) and  $\text{H}_2\text{SO}_4$  were 1.74 and 0.47. The reason for the apparently anomalously low distribution of arsenic found in the current study is unknown.

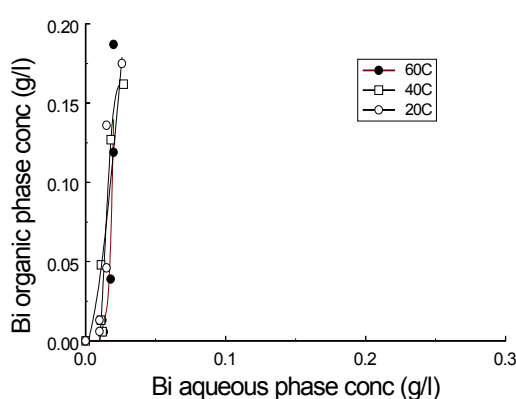


Figure 3. Bi extraction isotherms with 50% CYANEX 923 in kerosene.

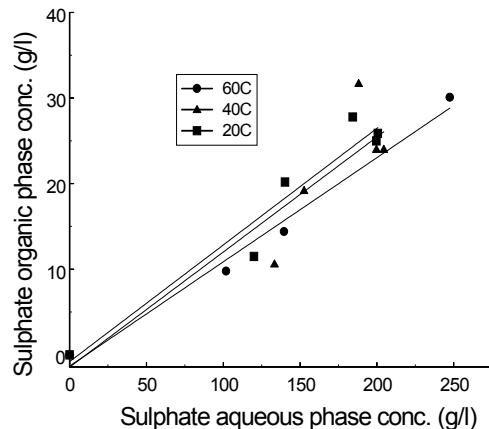
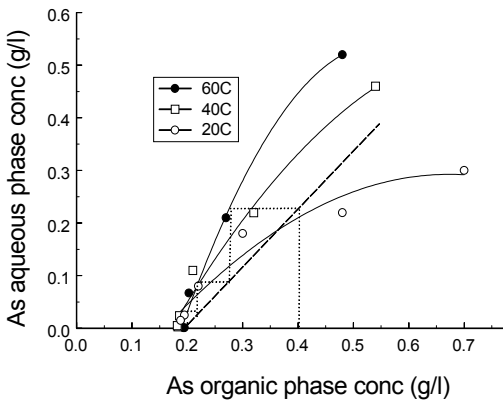


Figure 4. Sulphate extraction isotherms with 50% CYANEX 923 in kerosene.

### Stripping Isotherms

Stripping isotherms for As and Sb are shown in Figures 5 and 6, respectively. The residual concentrations of As and Sb in the organic phases were calculated by difference from aqueous solution analyses. Figure 5 shows that it is not possible to fully strip As from the loaded organic phase with water and a residual concentration of ~0.2 g/l is the limit at 60 °C. This contradicts the results of Wisniewski [8] who showed that As at a concentration of ~1.4 g/l could be stripped to a residual organic phase concentration of ~0 g/l with water. It has not yet been possible to reconcile these differences.

Figure 6 shows that Sb stripping varies considerably with temperature and satisfactory stripping is only achieved at 20 °C. Even at that temperature, a residual concentration of 0.4-0.5 g/l can be expected. It is anticipated that stripping with a chloride solution will improve this performance but no results are available yet.



*Figure 5. As stripping isotherms with water.*

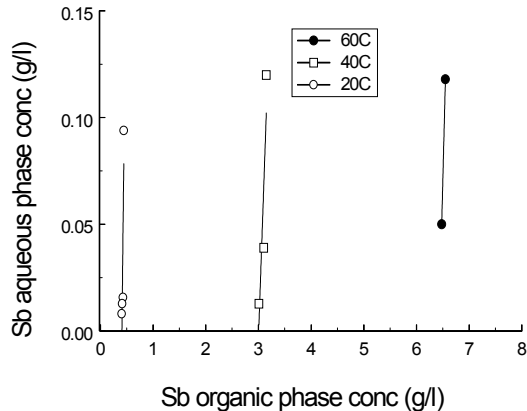


*Figure 6. Sb stripping isotherms with water.*

Although not shown here, Bi strips well with water and can be expected to be stripped with As.

## FLOWSCHEET DEVELOPMENT

Based on the above results the best extraction and stripping conditions for the removal of As, Sb and Bi from the Baia Mare copper refinery electrolyte are:

- a) extraction: two stages at 60 °C at an O/A ratio of 10:1;
- b) stripping: As and Bi: three stages at 60 °C with water at an A/O ratio of 2:1, Sb: stripping with a chloride solution, results awaited.

## CONCLUSIONS

Of all the extractants tested for the removal of As, Sb and Bi from the copper refinery electrolyte at Baia Mare, CYANEX 923 was shown to provide most promise for the development of a single extractant-based process. Tests on real electrolytes and electrolytes with an enhanced As content showed that, using 50 v/o CYANEX 923 in Romanian kerosene, the required operating levels of As, Sb and Bi could be achieved by extraction of the tankhouse bleed in two counter-current stages at 60 °C at an O/A ratio of 10:1. However anomalies remain with regard to the As extraction results obtained in this study and earlier published data in the literature and further work is required to resolve these. Stripping of the impurities can be achieved with water, although with the following reservations:

- a) it appears impossible to strip As below ~0.2 g/l although the indications are that Bi strips easily;
- b) Sb stripping with water is very temperature dependent with the best stripping performance being achieved at 20 °C, albeit with a residual concentration of 0.4-0.5 g/l Sb in the organic phase;
- c) two strip circuits may have to be contemplated, one at 60 °C for As and Bi and the second at 20 °C for Sb;
- d) improved Sb stripping at temperature is anticipated using a chloride solution.

## ACKNOWLEDGEMENTS

The authors would like to thank Cytec Inc, Cognis and A vecia for the supply of reagents and Philips Petroleum and Combinatul Petrochimic Pitesti for diluents. The management of Allied Deals Phoenix, Baia Mare, are also thanked for their help and the supply of electrolyte solution. Ms Auta Guta is thanked for valuable technical assistance.

This work was supported by the EU under the INCO-Copernicus Programme contract number ERB IC15 CT 98 0146.

## REFERENCES

1. D. S. Flett (1992), *Hydrometallurgy*, **30**, 327-344.
2. D. B. Dreisinger, B. J. Y. Leong, B. R. Saito and P. G. West-Sells (1993), *Hydrometallurgy Fundamentals, Technology and Innovation*, J. B. Hiskey and G. W. Warren (eds.), SME, Littleton, Colorado, pp. 801-815.
3. D. B. Dreisinger, B. J. Y. Leong and I. Grewal (1994), *Impurity Control and Disposal in Hydrometallurgical Processes*, B. Harris and E. Krause (eds.), CIMM, Canada, pp. 71-89.
4. W. Schwab and H. Kroke (1988), *Arsenic Metallurgy Fundamentals and Applications*, R. G. Reddy, J. L. Hendrix and P. B. Queneau (eds.), TMS-AIME, Warrendale, PA, pp. 249-262.
5. M. Wisniewski (1998), *Hydrometallurgy*, **46**, 235-241.
6. M. B. Bogacki, M. Wisniewski and J. Szymanowski (1997), *J. Radioanal. Nuclear Chem.*, **228**, 57-61.
7. M. Wisniewski (1997) *J. Radioanal. Nuclear Chem.*, **228**, 105-108.
8. M. Wisniewski, L. Iberhan and J. Szymanowski (2000), *Solvent Extraction for the 21<sup>st</sup> Century*, Vol. 2, M. Cox, M. Hidalgo and M. Valiente (eds.), Society of Chemical Industry, London, pp. 1261-1266.
9. R. Newell (2000), *Proc. ALTA 2000 SX/IX-1*, Melbourne, Australia, pp. 9.
10. D. C. Cupertino, P. A. Tasker, M. G. King and J. S. Jackson (1994), *Hydrometallurgy '94*, Chapman & Hall, pp. 591-600.



# STUDIES OF COPPER EXTRACTION USING THE SYSTEM SCO / ISOAMYL ALCOHOL / KEROSENE / COPPER SULFATE SOLUTION

E.L. de Barros Neto, A.A. Dantas Neto, T.N. Castro Dantas,  
L. J. N. Duarte and A.C.M. de Araújo\*

\*Universidade Federal do Rio Grande do Norte, Campus Universitário, Natal, Brazil

The purpose of this work is to carry out studies on the equilibrium curves and handling of a microemulsified system containing saponified coconut oil (SCO), isoamyl alcohol, kerosene and copper sulfate solution, so as to feasibly develop a process in a countercurrent extraction column. The equilibrium data were analyzed with the aid of Langmuir and Freundlich isotherms. Better fitting was obtained with the Freundlich isotherm and as this model deals with the multilayer adsorption of the substance on the adsorbent, it can be assumed that the adsorption of copper by the surfactant within the microemulsion phase occurs on multilayers. The minimum solvent rate and the number of transfer units were determined for a column operating at a level of 30% higher than the minimum solvent rate.

## INTRODUCTION

The process of heavy metal recovery with the use of microemulsions has been studied in the laboratories of Surfactant Technology and Separation Processes at Federal University of Rio Grande do Norte (UFRN) [1-5]. Such works have proven the great efficiency of microemulsions in extracting heavy metals, close to 100 %. The representation of microemulsion extraction equilibrium through pseudophases [6-9] is based upon the fact that a microemulsion formed of micelles, water in oil or oil in water, is microscopically structured according to three domains: polar domain, formed of water and some surfactant; interfacial amphiphilic domain, formed of surfactant and co-surfactant molecules; and an non-polar domain, formed of oil, cosurfactant and a small amount of water. They are called aqueous, membrane and oil pseudophases, respectively.

In adsorption, Langmuir and Freundlich isotherms can be used to represent equilibrium data. Langmuir model [10] can be written in the following way:

$$\frac{C_e}{q} = \frac{1}{bq_m} + \frac{C_e}{q_m} \quad (1)$$

where:

$$q = \frac{V(C_0 - C_e)}{W} \quad (2)$$

For Freundlich model [10], the theoretical representation for the experimental data is done through equation (3).

$$q = K C_e^{1/n} \quad (n > 1,0) \quad (3)$$

where K and n are equilibrium constants inherent to the system under study. The value of ln K is a measure of the capacity of the adsorbent, whilst the term 1/n gives an indication about the intensity of adsorption.

Studies on adsorption of metals onto surfaces coated with surfactants [11,12] show that the interaction among them can be represented by adsorption isotherms. Since the extraction process with microemulsions occurs from interactions between the surfactant polar head group and the copper ion, one can consider that the interaction between metal (solute) and surfactant (adsorbent) behaves like an adsorption process. Moreover, in the pseudophases model, the surfactant layer that coats the microemulsion droplets can be considered as a phase. These concepts were employed to apply Langmuir and Freundlich isotherms in the representation of the equilibrium curve of the microemulsified system.

## METHODOLOGY

Firstly, equilibrium data that relate the concentrations on copper in the microemulsion phases (extract) to those in the aqueous solution (raffinate) were determined. The system studied in this part was constituted of a solvent (a microemulsion formed of isoamyl alcohol, SCO, kerosene and water) and the copper sulfate aqueous solution with concentrations ranging between 1 720 and 8 600 ppm in Cu<sup>+2</sup>, regarded as the feed materials to be treated.

The equilibrium between the phases was determined from the analyses of evolution of the concentration on copper in the phases, and takes about 1 minute to be reached. Nevertheless, the samples were allowed to stir for 10 minutes, so as to assure that the equilibrium was attained. The mixture points were kept under a controlled temperature of 30°C. After phase separation, samplings of each phase were performed, after which the samples were analyzed in a SPECTRA-10A atomic absorption spectrophotometer, thus quantifying the amount of copper present in the microemulsion and aqueous phases.

The microemulsion diagram was obtained through successive titration of the samples among its several points. This allowed for the determination of the best regions and extraction conditions, and also the point S.

After obtaining the equilibrium curve, operational conditions were simulated for a countercurrent extraction column. Since the microemulsion density is lower than the aqueous solution density, it is inserted at the bottom of the column, whilst the feed aqueous solution is inserted at the top of the column.

## RESULTS AND DISCUSSION

### Microemulsion Diagram

The microemulsion diagram is composed of three pseudoconstituents: isoamyl alcohol / SCO at a ratio of 4.0, water and kerosene. Such pseudoconstituents were selected from previous studies [2,4] that report excellent copper recovery percentages in microemulsion extraction. Figure 1 shows the diagram and the microemulsion region (Winsor IV), evidencing the point S, which is the mixture considered as the solvent for the study of the equilibrium curve.

The choice of point S was based on the fact that, at such point, one has a water-in-oil microemulsion, which provides a good phase separation after interacting with a copper solution [1-5]. Thus, such microemulsion is considered to allow only the mass transfer of solute (copper), previously contained in the aqueous phase, towards the microemulsified phase.

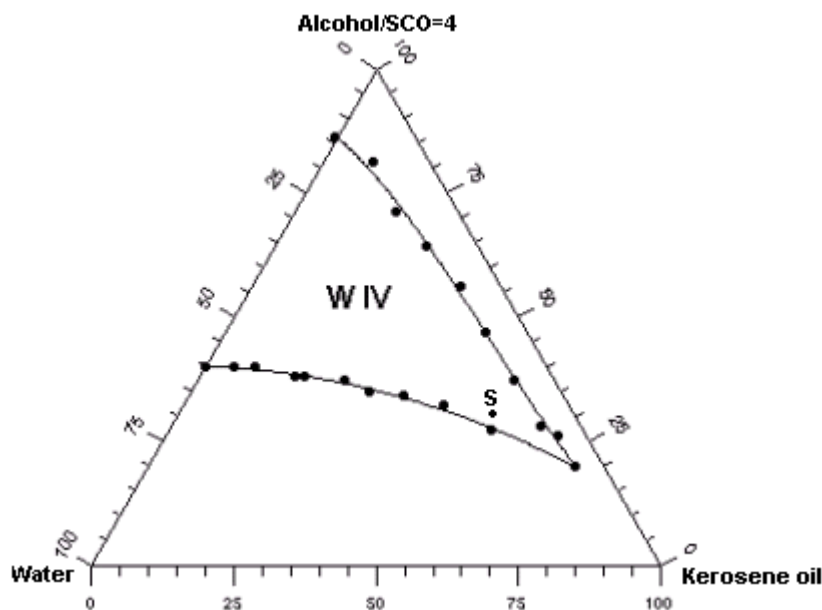


*Figure 1. Pseudoternary diagram showing the Winsor IV region for the system water-kerosene-isoamyl alcohol and saponified coconut oil (SCO).*

### Equilibrium Curve

The equilibrium curve was built from mixtures of the solvent (microemulsion solution with the composition shown in Table 1) with copper sulfate aqueous solutions at various concentrations. Table 2 presents the concentrations of copper in the feed line, in the microemulsion and in the treated solution. The volumes of the microemulsion and aqueous phases are equal to 1 mL and 50 mL, respectively.

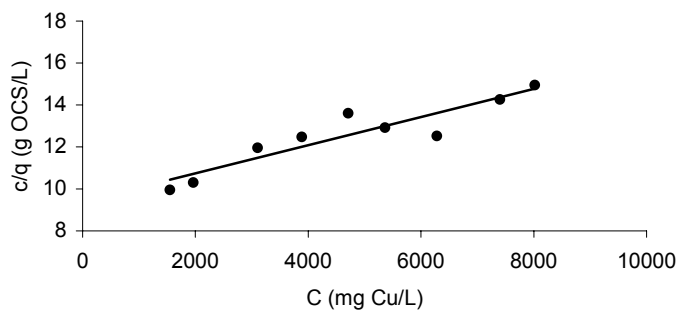
*Table 1. Composition of the microemulsion used.*

Component Composition (%)	SCO	Alcohol	Kerosene	Water
	6.0	24.0	55.0	15.0

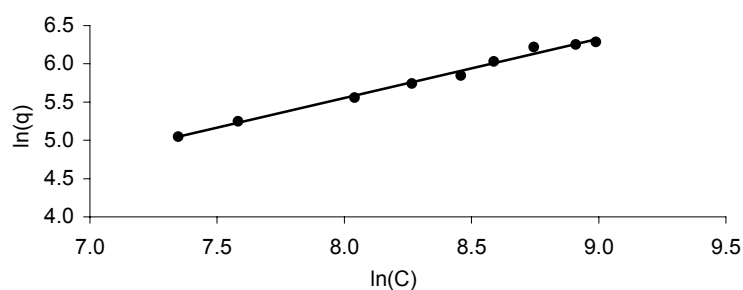
*Table 2. Concentrations of the phases.*

Cu feed (mg/L)	Cu micro (mg/L)	Cu water (mg/L)
1720.0	9347.7	1551.7
2168.7	11425.0	1963.0
3383.9	15579.5	3103.4
4225.2	18695.4	3888.7
5085.2	20772.7	4711.2
5814.3	24927.2	5365.6
6823.8	30120.4	6281.7
7964.3	31159.1	7403.4
8599.9	32197.7	8020.3

The equilibrium data in Table 2 were used to carry out a study of copper adsorption to the surfactant once both are present in the microemulsion. This study regards the surfactant as a coating that directly interacts with the copper ions. The presence of the surfactant itself is a condition to make possible the extraction by microemulsions. Equations (1) and (3) were used with this purpose, and they describe the Langmuir and Freundlich adsorption models. Figures 2 and 3 show the adjustment of such isotherms.



*Figure 2. Langmuir isotherm for the system SCO / Cu<sup>+2</sup> solution.*



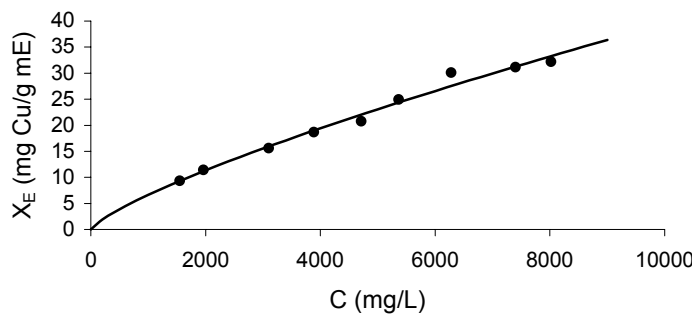
*Figure 3. Freundlich isotherm for the system SCO / Cu<sup>+2</sup> solution.*

Table 3 presents the parameters and the correlation coefficients provided by Langmuir and Freundlich models.

*Table 3. Parameters and correlation coefficients for the adsorption models.*

T(°C)	Langmuir			Freundlich		
	R <sup>2</sup>	q <sub>m</sub> (mg Cu/g OCS)	b	R <sup>2</sup>	n	ln K
30	0.854	1492	7.1·10 <sup>-5</sup>	0.991	0.7749	-0.648

From Table 3, it is noted that the Freundlich model better represents the extraction phenomenon, since it provides a correlation coefficient closer to 1.0. Figure 4 shows the adjustment for this model, applied for the microemulsion system.



*Figure 4. Adjustment of Freundlich model for the system SCO / Cu<sup>+2</sup> solution in the microemulsified system.*

From equation (3), it was possible to develop a model that represents the equilibrium between the microemulsion phases and the copper sulfate aqueous solution for the studied system, thus originated equation (4).

$$X_E = 0.0314 \cdot C^{0.7749} \quad (4)$$

#### Simulation of the Process in a Countercurrent Column

From the equilibrium relationship (equation (3)), the behavior of a countercurrent-operated column was simulated. The copper-containing aqueous solution enters the column from its top at a concentration  $C$  and in a flow rate  $D_T$ , and leaves from its bottom at a concentration  $C_B$  and flow rate  $D_B$ . The microemulsion enters the column from its bottom at a concentration  $X_0 = 0$  and flow rate  $S_B$ , leaving the column at a concentration  $X$  and flow rate  $S_T$ . Since the amount of solute transferred between the phases is negligible when compared to the flow rates, the latter can be considered as unaltered. Therefore, one can say that  $D_B = D_T = D$  e  $S_B = S_T = S$ , and the mass balance can be expressed in the following way:

$$C_o D_T + X_o S_B = C_B D_B + X S_T \quad (5)$$

$$X = \frac{D}{S} (C - C_B) \quad (6)$$

Thus:

$$\left( \frac{S}{D} \right)_{min} = \frac{(C - C_B)}{X} \quad (7)$$

For an aqueous solution with a concentration equal to 8 000 mg/L in Cu<sup>+2</sup>, to be treated in a way as to reach the final concentration of 500 mg/L, a minimum solvent rate of 225.9 g μE/L of aqueous solution is required. The number of transfer units (NTU) [13] is given by equation (8):

$$NTU = \int_{33.22}^{0.0} \frac{dX}{X - X_E} = \int_{33.22}^{0.0} \frac{dX}{X - 0.0314 \cdot \left[ \left( \frac{S}{D} \right) X + C_B \right]^{0.7749}} \quad (8)$$

If a solvent rate 1.3 times higher than the minimal rate is employed, equation (8) can be used with a number of transfer units equal to 4.76.

## CONCLUSIONS

The results obtained in this work show that it is possible to represent the equilibrium data of extraction processes by microemulsions through the Freundlich equation. This model deals with the multilayer adsorption of the substance on the adsorbent; it can be assumed that the adsorption of copper by the surfactant within the microemulsion phase occurs on multilayers. When the behavior of a countercurrent-operated extraction column is simulated, a minimum solvent rate is obtained and the number of transfer units (NTU) can be calculated through an equation determined as a function of the equilibrium and operation equations.

## NOMENCLATURE

b – Langmuir equilibrium constant

C – concentration of copper in aqueous solution (mg of Cu/L)

$C_e$  – equilibrium concentration

$C_o$  – initial concentration

D – aqueous phase flow rate

k – Freundlich constant, provides the capacity of the adsorbent

n – dimensionless equilibrium constant inherent to the system

q – adsorbed amount

$q_m$  – maximal adsorbed amount

$R^2$  – correlation coefficient

S – microemulsion phase flow rate

V – phase volume

W – amount of adsorbent (SCO)

$X_E$  – composition of copper in the microemulsion phase (mg Cu/g  $\mu$ E)

## REFERENCES

1. R. H. L. Leite (1995), Master of Science thesis, DEQ/PPGEQ/UFRN, Natal.
2. E. L. Barros Neto (1996), Master of Science thesis, DEQ/PPGEQ/UFRN, Natal.
3. A. C. S. Ramos (1996), Master of Science thesis, DEQ/PPGEQ/UFRN, Natal.
4. K. R. Forte (1998), Master of Science thesis, DEQ/PPGEQ/UFRN, Natal.
5. M. C. P. A. Moura (1997), Master of Science thesis, DEQ/PPGEQ/UFRN, Natal.
6. P. Bothorel, J. Biais, B. Clin, P. Lalanne and P. Maelstaf (1979), *C. R. Acad. Sci., Sér. C*, **289**, 409-412.
7. J. Biais, P. Bothorel, B. Clin and P. Lalanne (1981), *J. Dispersion Sci. Technol.*, 67-95.
8. V. Nieuwkoop and G. Snoei (1985), *J. Colloid Interface Sci.*, **103** (2), 400-406.
9. F. J. Ovejero Escudero (1987), Extraction de Cations Metaliques avec des Microémulsions: Diagramme de Phases, Modélisation des Equilibres, Simulation des Procéde, INPT, Toulouse.
10. P. W. Atkins (1994), Physical Chemistry, 5th edn., Oxford University Press, Oxford, pp. 961-1006.
11. T. N. Castro Dantas, A. A. Dantas Neto, M. C. P. Moura, E. L. Barros Neto and E. P. Telemaco (2001), *Langmuir*, **17**, 4256-4260.
12. T. N. Castro Dantas, A. A. Dantas Neto and M. C. P. Moura (2001), *Wat. Res.*, **35** (9), 2219-2224.
13. R. E. Treybal (1980), Mass-Transfer Operations, 3rd edn., McGraw-Hill, Inc., USA.



# COPPER HYDROMETALLURGY PROCESS EVOLUTION: CHANGING OPERATING PARAMETERS AND PHILOSOPHIES THROUGHOUT THE LIFE OF GIRILAMBONE COPPER COMPANY'S SOLVENT EXTRACTION CIRCUIT

Kym A. Dudley, David J. Readett, Phillip A. Crane\* and J. Murdoch W. Mackenzie\*

Straits Resources Ltd, West Perth, Australia

\*Cognis Australia Pty Ltd, Broadmeadows, Australia

Ore mineralogy has a major influence on the quality of the leach solution that is presented to a solvent extraction plant, and many operations see a change in the pregnant leach solution quality as the ore mineralogy changes over the project life.

This paper uses as an example the course of the solvent extraction circuit developments at Girilambone Copper Company in illustrating how changes in pregnant leach solution quality can be managed through appropriate selection of solvent extraction circuit operating conditions.

## INTRODUCTION

The Girilambone Copper Company (GCC) has utilised solvent extraction (SX) to process copper-bearing liquors produced from heap leaching since 1993. During this time the initial low-grade oxide leach has progressed, with the changing ore types from the open-cut mine, to a predominately bacterial assisted chalcocite leach operation resulting in leach liquor composition changes throughout the life of the operation. This has required continual SX investigation, test work and plant optimisation to consistently produce an electrolyte suitable for copper electrowinning (EW); and much of this work has been presented in detail elsewhere [1-6].

This paper serves as a collective summary and update of these events to illustrate the importance of understanding the various parameters that affect the copper SX and EW process and to demonstrate the degree of versatility that copper SX offers under changing conditions.

### Ore Mineralogy

From 1993 to 2000, almost 10M tonnes of ore containing approximately 138,000 tonnes of contained copper was mined and placed on the leach heaps at GCC, with the approximate composition shown in Table 1.

### Leach Solution Quality

Changing ore mineralogy and subsequent heap leach performance through the life of the mine resulted in changes in the composition of the pregnant leach solution (PLS) treated through the solvent extraction circuit. Figure 1 shows PLS composition throughout the mine life.

Table 1. Typical composition of GCC ore.

Ore type	Grade (% Cu)	Cu metal (tonnes)	Principal copper minerals (order of abundance)
Oxide	0.75	25,900	Malachite / Azurite
Transition	1.38	13,350	Malachite / Cuprite / Native Copper
Sulphide	2.05	98,800	Chalcocite / Chalcopyrite/(Pyrite)

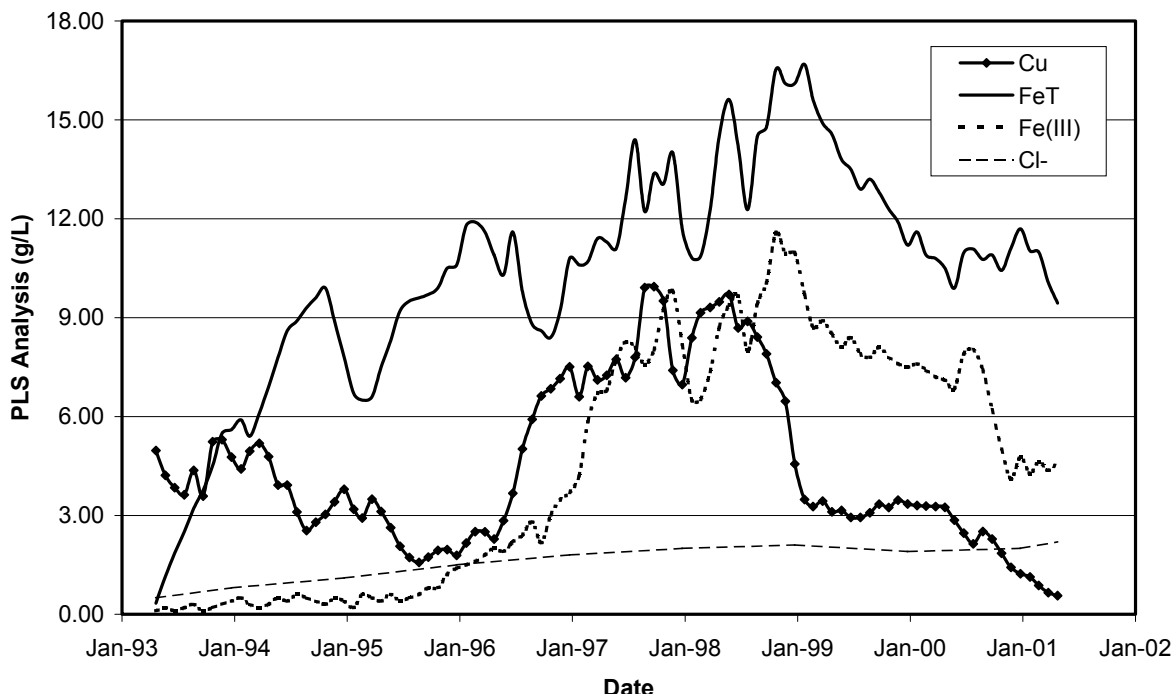


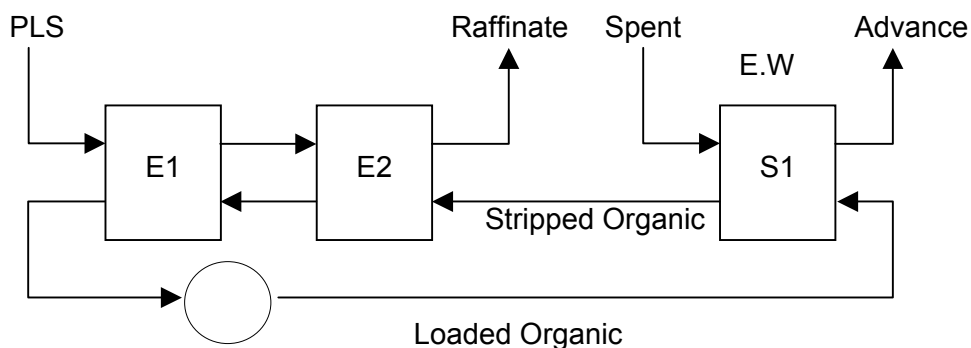
Figure 1. Historic GCC PLS composition trend.

Figure 1 displays the interesting chemical changes that occurred during the transition of GCC from a predominantly oxide leach since 1993 to the predominantly sulphide bioleach operation commencing in 1995. Most notable is that the PLS copper tenor increased shortly after PLS ferric iron generation was initiated primarily through the implementation of heap aeration methods to promote bacterial activity. Also interesting to note is that the levels of both the total iron and iron(III) remain reasonably high despite the decline in copper tenor towards the latter stages of the operational life. PLS chloride concentration, a major EW impurity element requiring control shows a gradual increase throughout the project life.

### Solvent Extraction Plant Design

The initial SX plant at Girilambone was designed as a conventional two extract and one strip circuit (2E x 1S) capable of producing 14,500 tonnes of copper cathode per annum. SX circuit configuration is shown in Figure 2 and typical design parameters in Table 2.

Initially, LIX 984 was selected as the copper extractant for Girilambone, an equimolar mixture of dodecyladoxime (LIX 860-I) and ketoxime (LIX 84-I). This reagent was chosen for its compatibility with the expected PLS solutions to be produced from the oxide heap leach. During 1995, the dodecylaldoxime was replaced with salicylaldoxime (LIX 860N-I), a C9 aldoxime, as it was believed that this offered slightly improved copper extraction kinetics with cooler leach solutions. The resultant extractant mixture is commonly called LIX 984N.



*Figure 2. Configuration of 2E x 1S SX circuit.*

*Table 2. Design parameters of 2E x 1S SX circuit.*

Parameter		Value
PLS	Cu tenor (g/L)	4.8
	Flow (m <sup>3</sup> /h)	400
	Recovery (%)	93
	pH	1.8-2.0
	Fe <sup>2+</sup> / Fe <sup>3+</sup>	2.8 / 0.2
Loaded Organic	LIX 984 conc. (%/v/v)	14.0
	Flow (m <sup>3</sup> /h)	400
	Transfer (kg Cu/h)	1,730
	Cu:Fe selectivity	>2,000:1

## OXIDE ORE TREATMENT PHASE

Throughout the first year of operation, the designed SX plant performed well at design volumetric flow rates. However, the PLS copper tenors were not as high as anticipated, so the PLS and organic flows were increased to maintain design copper transfer to electrowinning. The SX parameters obtained during the initial year of operation are shown in Table 3.

*Table 3. Operational parameters of 2E x 1S SX circuit.*

Parameter		Value
PLS	Cu tenor (g/L)	4.5
	Flow (m <sup>3</sup> /h)	420
	Recovery (%)	85
Loaded Organic	LIX 984N conc. (%/v/v)	14.7
	Flow (m <sup>3</sup> /h)	420
	Transfer (kg Cu/h)	1,730

During this first year of operation, several important lessons were learnt relating to the performance and control of the SX plant.

Shortly after commissioning of the SX circuit, extensive entrainment of PLS in the loaded organic occurred, transferring considerable quantities of manganese and chloride into the EW cells [4]. The initial effect of this created significant cathode stripping problems. A secondary effect was that, in the absence of sufficient ferrous iron, the manganese oxidised at the anode and increased the electrochemical potential of the electrolyte. This, in turn, oxidised the organic in the loaded organic stripping stage, producing by-products, which retarded phase separation rates and extraction kinetics. A vicious circle was established with increasing entrainments accelerating the degradation process [7].

Henkel (now Cognis) and GCC examined extractant performance and implemented clay treatment (developed by Henkel) to rectify the problem [8]. CMPS&F (now Egis) and GCC developed an understanding of coalescing media in the SX circuit to assist with phase disengagement. Both a loaded organic coalescer tank and in-settler coalescing media were commissioned [9]. Problems associated with high soluble silica levels in the PLS were also predominant during this period, and the importance of mixer phase continuity was also established [2].

### TRANSITION ORE TREATMENT PHASE

As leaching of ore progressed into the secondary sulphides (predominately chalcocite, Cu<sub>2</sub>S), leach kinetics remained low, resulting in PLS copper tenors well below design. The immediate action was to increase the PLS flow until the SX plant became hydraulically limited to maintain production. At this point, specific settler flow throughputs were being achieved at 7 m<sup>3</sup>/m<sup>3</sup>/h, whereas the design was around 4.5 m<sup>3</sup>/m<sup>3</sup>/h. Despite the reduced mixer residence time under the high flow conditions, the organic phase maintained high extraction kinetics.

The continued effect of slow leach kinetics during 1994 was such that the solvent extraction circuit required upgrading in December 1994 to accommodate a fourth mixer settler [1], shown in Figure 4.

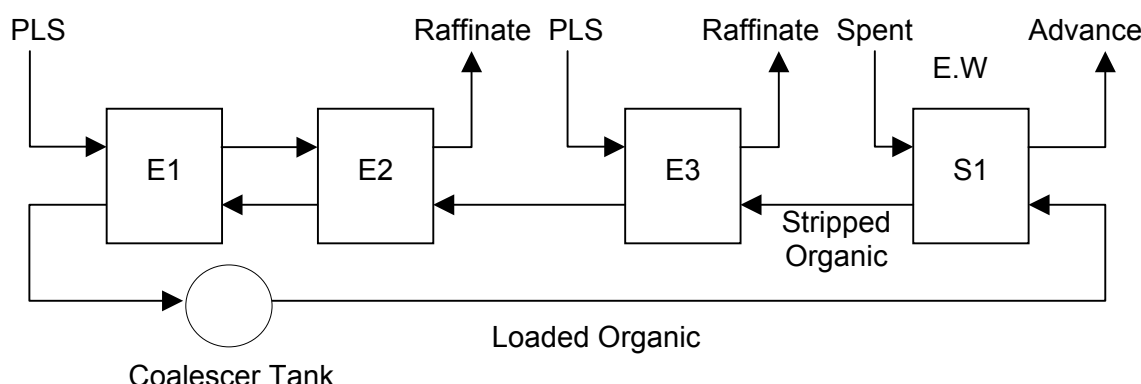


Figure 4. Series-parallel circuit.

The additional settler enabled the operation of a series parallel circuit, consisting of two extract stages in series, one parallel extract stage and one strip stage (2E x 1E(P) x 1S). PLS flowrates could now be pushed to 850 m<sup>3</sup>/h total flow, split equally into E3 and E1 extraction mixer-settlers. Typical operating parameters encountered during this period are outlined in Table 4.

*Table 4. Operational parameters of 2E x 1P x 1S SX circuit.*

Parameter		Value
PLS	Cu tenor (g/L) Flow (m <sup>3</sup> /hr) Recovery (%) Fe <sup>2+</sup> / Fe <sup>3+</sup>	1.95 - 3.20 580 - 860 90 8.3 / 0.6
Loaded Organic	LIX 984N conc. (%/v/v) Flow (m <sup>3</sup> /h) Transfer (kg Cu/h) Cu:Fe selectivity	18.0 - 14.0 320 - 460 1,730 >1,500:1

## SULPHIDE ORE TREATMENT PHASE

### Pre-Aeration

A PLS grade below 2 g/L continued during the second half of 1995, as most of the ore under leach at this point was chalcocite and the leach rates were slower than expected.

In early 1996, in order to counter the effects of the low PLS grade, another modification was made to the SX circuit, shown in Figure 5 below. Conversion to a 3 - Parallel circuit (3P x 1S, or 1P x 1P x 1P x 1S) allowed the SX plant input to be increased to 1200m<sup>3</sup>/h total PLS flow, offsetting the low PLS grades and lifting productivity. Typical operating parameters encountered during this period are outlined in Table 5.

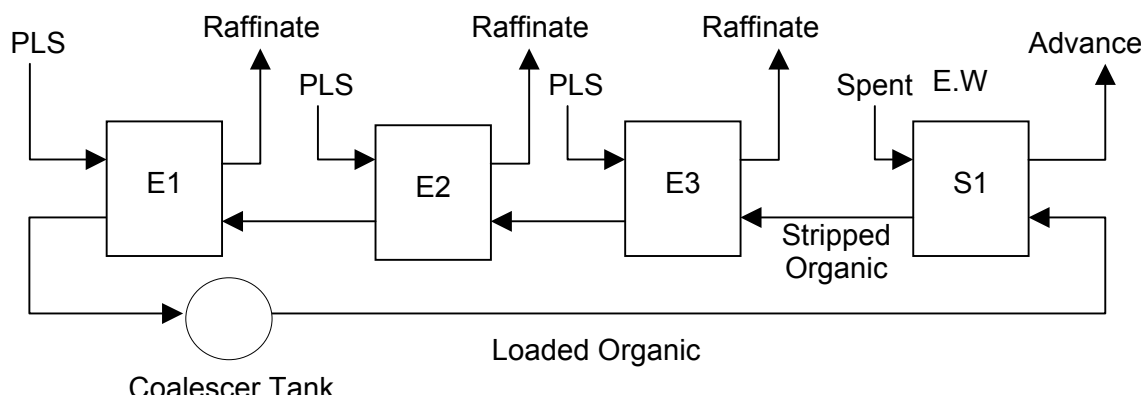


*Figure 5. The 3-parallel SX circuit.*

### Post-Aeration

With the advent of heap forced-aeration, and the subsequent improvement in bioleaching and chalcocite leach kinetics, the PLS copper grade rose dramatically during 1996, from 1.71 g/L in January to over 8.5 g/L in December that year. The increase in the copper content of the PLS allowed the circuit to be returned to series-parallel operation, as depicted in Figure 4. A simultaneous increase was obtained in the PLS iron content due to accelerated iron mineral leach kinetics and a change in the ratio of iron(II) to iron(III). This resulted in an increase in the transfer rate of iron to the electrolyte, (decreased organic Cu:Fe selectivity) adversely affecting the EW current efficiency [5, 6, 10].

*Table 5. Operational parameters of 3P x 1S SX circuit.*

Parameter		Value
PLS	Cu tenor (g/L)	1.75 - 2.84
	Flow (m <sup>3</sup> /h)	810 - 1140
	Recovery (%)	80
	Fe <sup>2+</sup> / Fe <sup>3+</sup>	9.2 / 1.7
Loaded Organic	LIX 984N conc. (%/v/v)	14.0 - 17.0
	Flow (m <sup>3</sup> /h)	390 - 450
	Transfer (kg Cu/h)	2,500
	Cu:Fe selectivity	>1,800:1

*Table 6. Operational parameters of 2E x 1P x 1S SX circuit (post aeration).*

Parameter		Value
PLS	Cu tenor (g/L)	3.65 - 9.70
	Flow (m <sup>3</sup> /h)	510 - 720
	Recovery (%)	40 - 80
	Fe <sup>2+</sup> / Fe <sup>3+</sup>	5.0 / 11.6
Loaded Organic	LIX 984N conc. (%/v/v)	14.0 - 17.0
	Flow (m <sup>3</sup> /h)	240 - 400
	Transfer (kg Cu/h)	2,500
	Cu:Fe selectivity	< 500:1

### ADVENT OF THE WASH / SCRUB STAGE

In June 2000, the production of ore from the Girilambone pits ceased. Thereafter, the PLS copper content commenced a controlled decline, which impacted upon copper output, and also EW impurity transfer, particularly chloride and iron.

In pilot plant tests conducted on site, a number of extractant and circuit combinations were evaluated with the aim of minimising impurity transfer. The most effective solution was found to be a conversion of one of the extract stages to an organic wash/scrub stage [11]. This was implemented in February 2001. Figure 6 shows the circuit layout and Table 7 shows the operating parameters before and after the conversion.

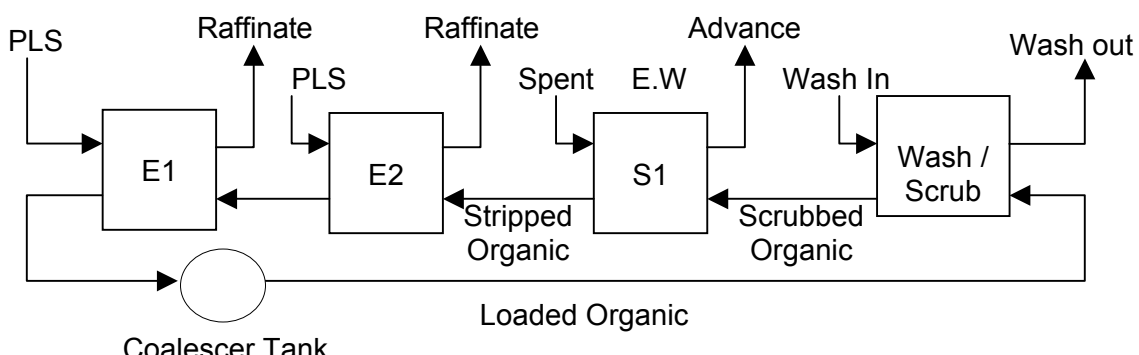


*Figure 6. 2P x 1W x 1S SX circuit.*

*Table 7. Operational parameters of 2P x 1W x 1S SX circuit (post aeration).*

Parameter		Value	
		Before	After
PLS	Cu tenor (g/L)	< 2	< 2
	Flow (m <sup>3</sup> /h)	700 - 850	700 - 850
	Recovery (%)	>95	>95
	Fe <sup>2+</sup> / Fe <sup>3+</sup>	5.0 / 11.6	5.0 / 11.6
Loaded Organic	LIX 984N conc. (%/v/v)	>11.0	<11.0
	Flow (m <sup>3</sup> /h)	350 - 400	350 - 400
	Transfer (kg Cu/h)	500	500
	Cu:Fe selectivity	< 100:1	> 500:1

## CONCLUSIONS

It is expected that many projects that employ Leach/SX/EW to recover copper from an orebody comprising both oxide and sulphide mineralisation will see variations in PLS composition as ore mineralogy changes over time. The SX process is shown to possess a significant degree of flexibility as PLS compositions change and the experiences gained here and elsewhere may assist existing and new SX projects with managing these changes to maximise productivity.

## ACKNOWLEDGEMENTS

The authors would like to acknowledge the permission from Straits Resources Ltd., and Girilambone Copper Company to prepare and present this information.

## REFERENCES

1. D. Readett, G. Miller, and H. Holle (1996), *Proc. Chemeca 96*, Sydney, pp. 71-76.
2. D. Readett, and G. Miller (1995), *Proc. Copper-Cobre 95*, Vol. 3, Santiago, pp. 679-690.
3. K. Dudley (1996), The Cobar Mineral Field – A 1996 Perspective, W. Cook, A. Ford, J. McDermott, P. Standish, C. Stegman and T. Stegman (eds.), AusIMM, Carlton, pp. 431-438.
4. G. Miller, D. Readett and P. Hutchinson (1997), *Miner. Eng.*, **10** (5), 467-481.
5. A. Moroney and K. Dudley (1997), *Proc. ALTA 1997 Copper Hydrometallurgy Forum*, Brisbane.
6. K. Dudley, A. Moroney, D. Readett and M. Braaksma (1999), *Proc. Copper-Cobre 99*, Vol. 4, Phoenix, AZ, pp. 247-262.
7. G. Miller (1995), *Proc. Copper-Cobre 95*, Vol. 3, Santiago, pp. 649-663.
8. P.L. Mattison, G.A. Kordosky, and W.H. Champion (1983), *Hydrometallurgy: Research, Development, and Plant Practice*, K. Osseo-Asare and J.D. Miller (eds.), The Metallurgical Society of AIME, pp. 617-628.
9. G. Miller, D. Readett and P. Hutchinson (1996), *Value Adding through Solvent Extraction*, D.C. Shallcross *et al.* (eds.), The University of Melbourne Press, Melbourne, pp. 795-800.
10. A. Moroney, K. Dudley, P. Crane and G. Wolfe (1999), *Proc. ALTA 1999 Copper Hydrometallurgy Forum*, Gold Coast.
11. G. Kordosky, S. Olafson and C. Hahn (2000), *Proc. ALTA 2000 Copper Hydrometallurgy Forum*, Adelaide.



## APPLICATION OF TWO TYPES OF COMMERCIAL EXTRACTANTS FOR COPPER IN CHINA

Yang Jiaoyong

Beijing Extractive Metallurgy and Technology Development Co., Ltd., Beijing, China

The applications of two types of commonly used solvent extraction reagents, *i.e.*, aldoximes with modifier (Acorga M5640) and the mixture (LIX 984) of modifier-free aldoximes and ketoximes (LIX 84), in China's copper SX plants are discussed in this paper. The paper details the effects of modifier on the extraction performance. Operational data and results from some plants are given. Laboratory experiments with the two types of reagents are also discussed. Data such as loading capacity, sensitivity to pH value, phase disengagement, entrainment, as well as the formation of crud were obtained and are illustrated. Results from both the experiments and the plants operation show that the over-all performances of aldoximes with modifier (Acorga M5640) are preferable.

### INTRODUCTION

Aldoxime reagents, as well known, are the new generation strong copper extractants. However, since their copper complex is difficult to strip with conventional spent sulphate electrolyte, the aldoxime extractants must be blended with modifiers to improve the stripping performance. Acorga M5640, a product of Avera Inc. (formerly Zeneca Specialties), is ester modified with a branched chain ester, whereas LIX 984, a product of Cognis Co. (formerly Henkel), is a blend of aldoxime and ketoxime. Conventionally, the former is called modified aldoxime extractant, and the latter is regarded as extractant without modifier. In some articles the authors [1] hold that the modified extractants are not as good as the unmodified ones because the modifier will cause the formation of excess crud. This is debatable. In fact, it is the emergence of the aldoxime extractants that resulted in the change of the global solvent extraction technology of copper. The much stronger aldoxime reagent makes it possible to reduce the number of stages in the SX circuit, hence reducing the capital investment of the SX plant and lowering the operating costs. Moreover, the reagent can be adopted for feed solutions with a much higher copper content and/or at lower pH. As regards the mechanism of crud formation during extraction and the performance comparison between M5640 and LIX 984, there have already been detailed reports [2,3]. The application of these two types of extractants in China's SX plants is discussed in this paper, and the performance comparison is presented as well. The results produced over a period of 10 years show that Acorga M5640 is much more adaptable compared with LIX 984.

## APPLICATION OF THE TWO TYPES OF EXTRACTANTS IN CHINA

The two types of commonly used extractants in the world, LIX 984 and M5640 have been supporting China's copper SX industry since the early 1990s. At present, cathode copper produced by SX process in China exceeds 20000 t/a. The market share of each reagent in China is about 50 %. Because the identified copper resources are scattered, it is difficult to find copper mines that have adequate reserves and are suitable for SX technology. There are dozens of SX plants with capacities ranging from 200 t/a to 300 t/a cathode copper, among them the largest one so far is only 4000 t/a capacity. The reserves are distributed throughout China including Tibet, that is on the roof of the world, Heilongjiang Province, in the high-latitude cold area (the lowest temperature is 50 °C below zero), and the southern part of Xinjiang Uygur Autonomous Region, at the edge of the arid Taklamakan Desert. Yunnan has smaller SX plants than other provinces. Some typical plants are listed in Table 1. In most plants the real production is lower than the designed capacity due to the shortage of ore supply.

*Table 1. Typical SX plants in China.*

Name of plants	Designed capacity (t/a)	Ore type and grade (Cu)	Leaching method	Extractant	Location of plant	Remarks
Guangtong Copper Plant	1000	Oxide, 1%	Heap	M5640	Lufeng, Yunnan	**
Makuang Fuli Plant	500	Oxide, 2%	Agitating	M5640	Gejiu, Yunnan	
Baoping Copper Co.	1000	Oxide, 0.6-1%	Heap	M5640	Yongsheng, Yunnan	
Chuxiong Copper Mine	2500	Sulphide concentrate, 25%	Roasting-agitating	M5640	Chuxiong, Yunnan	Closed down
Fute Copper Co.	1000	Earthy oxide, 1%	Agitating/heap	M5640	Yuanjiang, Yunnan	Temporarily closed
Yuanjiang Copper Mine	600	Oxide, 1%	Heap	LIX 984	Yuanjiang, Yunnan	
Limin Copper Mine	600	Oxide, 1.2%	Heap	M5640	Jinggu, Yunnan	
Xingkang Co.	1000	Oxide, 1%	Heap	LIX 984	Dayao, Yunnan	
Purina Copper Plant	500	Oxide, 1%	Heap	LIX 984	Baoshan, Yunnan	
Mill Copper Mine	500	Oxide, 1.2%	Heap	M5640	Yongsheng, Yunnan	
Pingchuan Copper Mine	1000	Oxide, 1.1%	Heap/agitating	M5640	Yanyuan, Sichuan	
Yaxi Copper Co.	600	Oxide, 1%	Heap/agitating	M5640	Yanyuan, Sichuan	
Dexing Copper Mine	2000	Waste dump, 0.1%	Dump	LIX 984	Dexing, Jiangxi	Actual Production 600 t/a
Tongkuangyu Copper Mine	500	Oxide, 0.3-1%	In situ	LIX 984	Yuanqu, Shanxi	
Duobaoshan Copper Mine	1500	Oxide, 0.7%	Heap	M5640	Nenjiang, Heilongjiang Province	
Neymu Copper Mine	1000	Oxide, 1.1%	Heap	M5640	Neymu, Tibet	
Kunlun Copper Co.	1000	Oxide, 1.5-2%	Agitating/heap	M5640	Jiashi, Xinjiang	Under reform
Zhongyuan Gold Smelter	2500	Gold concentrate 1-3%	Roasting/agitating	LIX 984/M5640	Sanmenxia, Henan Province	
Lingbao Gold Smelter	4000	Gold concentrate 1-3%	Roasting/agitating	LIX 984	Lingbao, Henan Province	
Guoda Gold Smelter	3500	Gold concentrate 1-3%	Roasting/agitating	LIX 984/M5640	Zhaoyuan, Shandong	
Dongfang Gold Smelter	1000	Gold concentrate 1-3%	Roasting/agitating	LIX 984	Mouping, Shandong Province	
Chaoyang Gold Smelter	1000	Gold concentrate 1-3%	Roasting/agitating	LIX 984/M5640	Chaoyang, Liaoning Province	

\*\* It was the first plant with capacity of 1000 t/a in China. It was put into operation in 1992 and was shut down in 2000 due to the depletion of copper resource.

It can be seen from Table 1 that M5640 is widely used especially in areas with tough environmental conditions. In Duobaoshan Copper Mine, Heilongjiang Province, the SX circuit with M5640 can run normally in winter time despite the fact that the temperature of feed solution (PLS) is only 3.0 °C. LIX 984 has been more widely used in gold recovery plants in recent years. However, it has gradually been replaced by M5640 due to such disadvantages as lower loading capacity and the vulnerability to pH of PLS. This will be demonstrated by the comparative results of the operational data with these two types of extractants in Guoda Gold Smelter in Zhanyuan, Shandong province.

## TEST RESULTS AND DISCUSSION

Performance tests comparing between M5640 and LIX 984 were conducted at plants and mines, respectively. Tests were carried out using Averia Inc.'s special apparatus for determining extraction equilibrium and kinetics. The results of the tests are described below.

### Extraction Equilibrium and Stripping Kinetics

Extraction equilibrium and stripping kinetics of the two extractants are shown in Figure 1 and Figure 2. The data indicates that in the case of M5640 the 90% maximum loading capacity can be achieved after 20 seconds of mixing, whereas for LIX 984, 30 seconds are needed. Regarding the stripping kinetics, LIX 984 also shows correspondingly a 10~20 seconds delay. This phenomenon is not only because LIX 984 contains some LIX 84, which is a weaker ketoxime-based extractant, but also due to the fact that the aldoxime of LIX 984 is based on a C<sub>12</sub> alkyl, a long carbon chain compound that may bring about steric hindrance, depressing the extraction equilibrium and stripping kinetics.

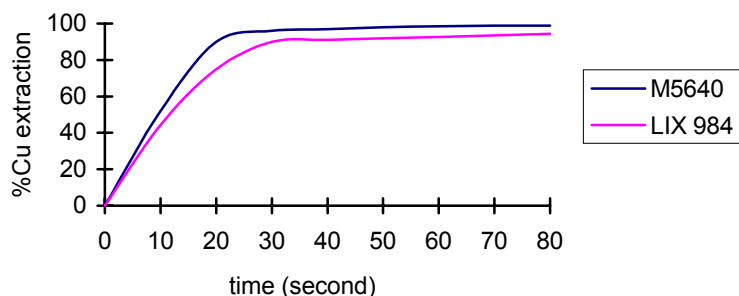


Figure 1. Extraction equilibrium.

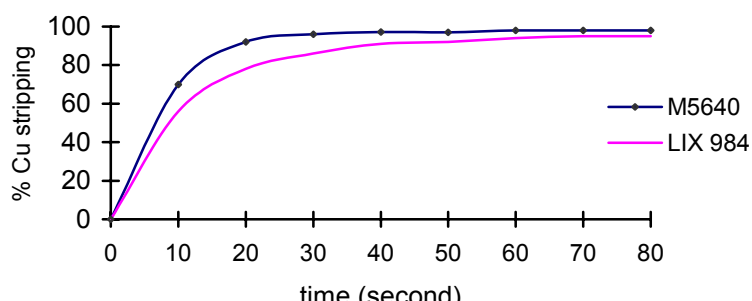
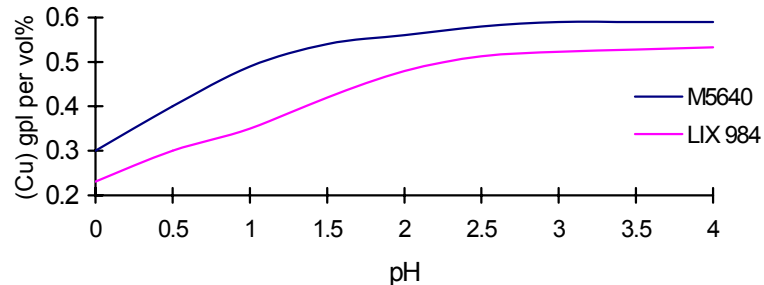


Figure 2. Stripping kinetics.

### **Effect of Feed Solution pH on Copper-loading Capacity**

The variation of copper loading capacity of the two extractants at different pH is shown in Figure 3. It is seen that with regards to copper loading performance, M5640 has higher adaptability to pH variation than LIX 984, especially at pH < 2. This pH-dependent nature is more important in the case of PLS with higher copper content, because acid will be liberated during copper extraction, which will cause the pH to drop further decreasing the extraction recovery of copper. Fortunately, M5640 can reduce this impact to a minimum.



*Figure 3. Effect of pH on copper loading capacity.*

It can also be seen from the curve that both extractants reach their maximum loading capacity at pH 2.5. The maximum loading per volume percent of M5640 is 0.59 g/l Cu, while that of LIX 984 is 0.51 g/l Cu.

### **Phase Disengagement**

The phase disengagement curve is plotted in Figure 4, in which the phase disengagement time is plotted on the horizontal axis and the depth of clear aqueous phase is on the vertical axis. The cross points D and D' represent the depth of aqueous phase at complete phase disengagement for M5640 and LIX 984, respectively, while t and t' represent the final time at which phase disengagement completed. The complete phase disengagement time for M5640 is 48 seconds, and for LIX 984 is 60 seconds.

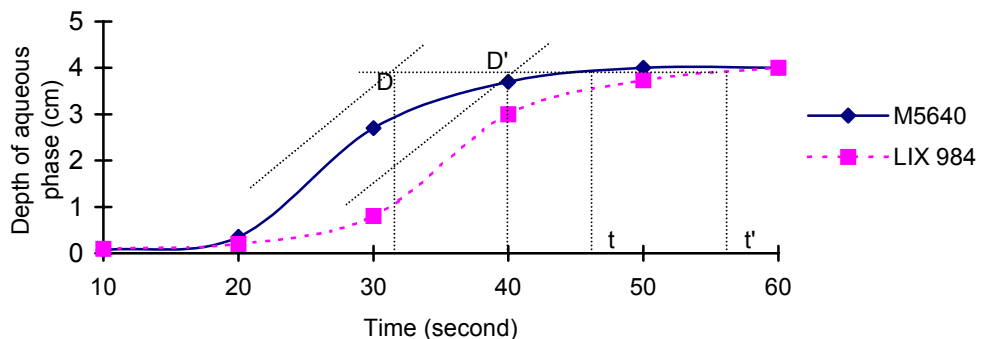


*Figure 4. Phase disengagement.*

### **Copper/Iron Selectivity**

The plant PLS contains 1.3 g/l Cu and 24.1 g/l Fe at pH 2. The organic phase is 5 % v/v M5640 and 5 % v/v LIX 984, respectively. Test results are given in Table 2.

*Table 2. Copper / iron selectivity.*

M5640			LIX 984		
Cu <sub>org</sub> (g/l)	Fe <sub>org</sub> (g/l)	Cu / Fe	Cu <sub>org</sub> (g/l)	Fe <sub>org</sub> (g/l)	Cu / Fe
1.196	0.001	1196	1.091	0.02	546
1.274	0.001	1274	1.039	0.02	320
1.143	0.001	1143	1.139	0.02	520

It can be seen that the Cu / Fe selectivity of M5640 is much higher than that of LIX 984 when extracting copper from PLS with high iron content (Cu / Fe = 18.5). The Cu/Fe selectivity (or, rejection ratio) of M5640 is about twice as high as that of LIX 984.

### COMPARISONS OF ACTUAL PRODUCTION DATA BETWEEN TWO EXTRACTANTS

Copper-bearing solution derived from the roasting-leaching process of gold concentrate is treated at the copper SX plant of Guoda Gold Smelter in Shandong Province. There are two SX circuits: one employs M5640 and the other, LIX 984. The operational data of the two SX circuits from 16 February to 8 March are listed in Table 3. Based on these data, the actual copper uptake per volume percent of extractant is calculated and is shown in Figure 5. Table 3 and Figure 5 indicate that with a PLS containing about 7 g/l Cu, a copper recovery of 96 % and actual copper net transition of 0.4 g/l can be achieved for 1 % (v) M5640. Whereas 92 % and 0.2 g/l are achieved with 1 % (v) LIX 984, though the organic concentration of LIX 984 is 9.1 percentage points higher than that of M5640. Moreover, the pH of PLS in M5640 circuit and LIX 984 circuit is 1.7 and 2.7, respectively. That means that M5640 not only has stronger copper loading capacity and higher copper net transition, but also is more suitable to higher acidity of the PLS than LIX 984.

### CRUD

Like in other countries, all SX plants in China, using either M5640 or LIX 984, have had problems with crud. However, most of the plants can run normally by removing the crud regularly, except in certain cases where production had to be temporarily suspended for specific treatment due to heavy crud.

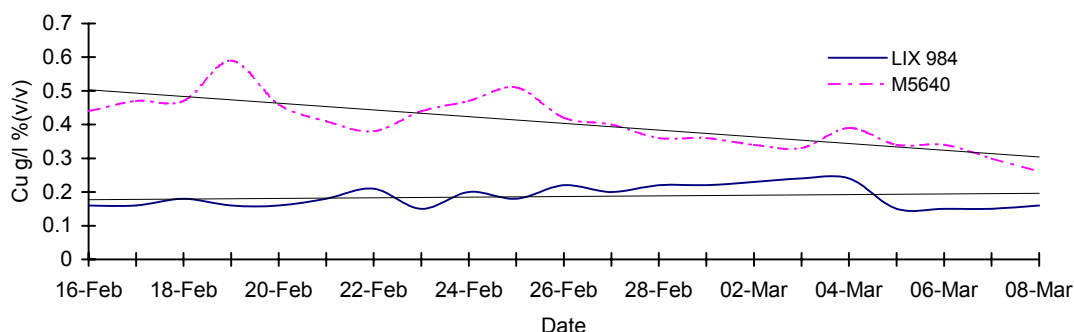


*Figure 5. Copper net transition comparison of the two operation circuits.*

*Table 3. Plant comparison data from 16 February to 8 March.*

Circuit	Item	Date																				
		6/Feb	17	18	19	20	21	22	23	24	25	26	27	28	1/Mar.	2	3	4	5	6	7	8
LIX984 27.3%(v)	PLS (pH2.7) Cu g/l	4.9	5.2	5.2	4.6	4.6	5.2	5.9	4.2	5.7	5.1	6	5.8	6.2	6.7	7.4	7.2	7	4.5	4.7	4.7	4.5
	Raffinate, Cu g/l	0.5	0.8	0.3	0.2	0.1	0.2	0.2	0.1	0.1	0.1	0.1	0.4	0.3	0.7	1.2	1.2	0.6	0.3	0.5	0.2	0.2
	recovery, %	89	85	95	96	97	97	96	98	98	98	98	93	95	90	86	86	92	94	89	95	96
	net transfer, Cu g/l 1%(v)	0.16	0.16	0.18	0.16	0.16	0.18	0.21	0.15	0.2	0.18	0.2	0.2	0.2	0.2	0.2	0.2	0.2	0.2	0.2	0.15	0.16
M5640 18.2%(v)	PLS (pH1.7) Cu g/l	8.5	10	11	12	9.1	8.3	7.8	8.4	9.6	11	9.4	8.5	7.4	7.3	6.6	6.2	7.4	6.5	6.4	5.5	4.8
	Raffinate, Cu g/l	0.5	1.8	2	1.4	0.8	0.9	0.8	0.4	1.1	1.5	1.7	1.2	0.9	0.8	0.4	0.3	0.3	0.2	0.2	0.1	0.1
	recovery, %	95	83	81	88	92	89	89	96	89	86	82	86	88	89	94	96	96	96	97	98	99
	net transfer, Cu g/l 1%(v)	0.44	0.47	0.47	0.59	0.46	0.41	0.38	0.44	0.5	0.51	0.42	0.4	0.4	0.4	0.3	0.3	0.4	0.3	0.3	0.26	

### **Plant 1**

Excessive humic acid contained in the feed solution formed grumos that could hardly decompose. The feed solution was mine wastewater containing 0.5-1.2 g/l Cu and 9-24 g/l Fe, at pH 1.5-2. 5 %(v/v) LIX 984 was used as extractant. In the previous semi-industrial tests the SX circuit ran normally and no problems with crud were observed. However, several days after putting into commercial operation grumos formed heavily. As the whole organic layer of the settler turned into emulsion, clear organic phase could not be obtained. Later, it was found that the feed solution was seriously contaminated by humus. Organic carbon content in the feed was as high as 40 ppm, while that in the uncontaminated copper-bearing mine water was less than 5 ppm. It was also found that two years earlier there was a house refuse heap on the mine waste dump. The humic acid produced by the decayed garbage flowed into the feed solution pond, contaminating the copper bearing mine water. After the contaminated waste dump water was bypassed, the SX plant has been operating normally.

### **Plant 2**

Entrained manganese ions caused degradation of the organic reagent, producing large quantity of floating crud. This plant employed mixer-settlers designed by in-house technical personnel. The inappropriate selection of parameters resulted in excessive entrainment of PLS in the loaded organic phase, which went into the stripping system. The Mn<sup>2+</sup> in the PLS was later oxidized to higher valence manganese ions during electrolysis. When the spent electrolyte recycled to the stripping stage, it contacted with organic phase and caused the degradation of the organic reagent. Thus, huge amounts of floating crud were produced and the plant had to be shut down for clean up. The PLS treated in this plant contained 1.2 g/l Cu, 1.5 g/l Fe and 1.6 g/l Mn<sup>2+</sup>, at pH 2. The organic phase was 7%(v) LIX 984 in kerosene. After two months of operation the LIX 984 content was decreased to 2 %(v). This resulted in the sharp decrease of copper extraction recovery. Later, the mixer settlers were modified and the pipelines for loaded organic were changed. The loaded organic phase flowed to the organic holding tank, and was then pumped to the stripping stage, so that the entrainment of PLS in organic phase could be reduced. After modifications, M5640 has been employed as the extractant. The plant has been operating normally since then.

### **Plant 3**

Excessive solid suspensions in the PLS resulted in serious crud. The plant adopted agitated leaching process. Due to lack of effective clarifying and filtering equipment, the PLS entering the SX circuit contained suspended solids as high as 2000 mg/L. Heavy crud resulting from the suspended solids caused the operation shut down. Later, a sand filter pond of large area was added to the leaching section and the suspended solids in the PLS have been reduced to less than 100 mg/L. At the same time, by keeping the organic phase continuous, the solids settle

down at the settler and are discarded together with raffinate, another measure is to draw regularly the aqueous solution containing solids from the bottom of the settler into the raffinate pond.

Nowadays, SX plants in China can easily handle the crud problem. They remove regularly the crud from the oil/water interface in the settler and put it into the crud storage pond for natural phase disengagement. Subsequently, the crud is washed with kerosene. Finally, the concentrated crud is blended with natural sandy bentonite. The exuded organic is further treated with activated clay before recycling to the extraction system. The residue is stockpiled after being solidified. This treatment is fairly effective, though simple. Eighty percent of organic in the crud can be recovered after kerosene washing. As is known to all, the crud is an unstable emulsion composed of organic phase, water and solid particles. Bentonite absorbs water. It can break the stability of the emulsion by soaking in water, hence attaining the goal of separating organic phase from the crud. In order to speed up the separation of the absorbed organic phase from bentonite, sand particles are added, which can lower the viscosity of bentonite and improve the permeability. The years of experience indicate that both type extractants will not generate, or accelerate the formation of crud. Instead, suspended solids, humic acid, silica gel and oxidative metal ions, like  $Mn^{2+}$ , in the PLS, as well as the impurities in kerosene are the real cause of the crud formation.

## CONCLUSIONS

LIX 984 and M5640 have been commercially used in China for about ten years, and have greatly facilitated the development of China's copper SX industry. In most heap (dump) leaching SX-EW plants with PLS containing 1-3 g/l Cu, at pH 2, there is no obvious difference in the performance of both extractants. The nature of both reagents has no special influence on the formation of crud. Nevertheless, when copper extraction is carried out from PLS with higher copper content and lower pH, M5640 shows clear superiority over LIX 984. Loading capacity, copper net transfer and adaptability to acidity variation of PLS of M5640 is better than of LIX 984. Because of that, M5640 is more adaptable to such areas with adverse environment conditions as in the very cold region. This has been proved by long plant runs in Tibet, Xinjiang, Heilongjiang, etc.

## ACKNOWLEDGEMENTS

The author wishes to extend thanks to Guoda Gold Smelter, Shandong, for giving permission to publish their production data, and to Zhongyuan Gold Smelter for assistance in the comparison tests of the two types of extractants.

## REFERENCES

1. M. J. Virnig, S. M. Olafson, G. A. Kordosky and G. A. Wolfe, *Proc. Int. Conf. Hydrometallurgy of Copper*, Vol. IV, Phoenix, Arizona, USA, pp. 291-303.
2. R. F. Dalton and C. Maes (1996), Randol, Vancouver Conference, pp. 313-317.
3. D. C. Cupertino, M. H. Charlton, D. Buttar and R. M. Swart, *Proc. Int. Conf. Hydrometallurgy of Copper*, Vol. IV, Phoenix, Arizona, USA, pp. 263-276.



## PILOT COPPER SOLVENT-EXTRACTION TESTING USING THE BATEMAN PULSED COLUMN

Eliyahu M. Buchalter, Rafi Kleinberger, Baruch Grinbaum\* and Curtis Nielson\*\*

Bateman Projects Ltd, Yokneam, Israel

\*IMI (TAMI) Institute for R&D, Haifa, Israel

\*\*Bateman Engineering Inc., USA

Testwork has been performed using 40 mm and 100 mm diameter pilot Bateman Pulsed Columns as part of an integrated pilot plant investigation at a processing facility of a leading copper producer. Both extraction and stripping were tested.

The target extraction recovery of 90-95% was achieved with 0.1 – 0.15 g/l copper in the raffinate. The required 47-51g/l copper in the advance electrolyte was obtained. Organic-in-aqueous entrainments in the raffinate as low as 1 ppm were obtained without the use of coalescers, flotation columns or other additional separation equipment. No major crud problems were encountered with the operation of the column. The design flux for extraction was found to be  $45 \text{ m}^3/\text{m}^2/\text{h}$  and for stripping  $40 \text{ m}^3/\text{m}^2/\text{h}$ .

### INTRODUCTION

Copper purification by solvent extraction (SX) is one of the largest applications of this technology in the hydrometallurgical industry. The copper SX process consists of extraction, scrubbing (sometimes) and stripping. In general extraction can be achieved in 2 or 3 stages and stripping in one stage. Kinetic requirements often lead to more than one mixer box per stage. Due to phase separation difficulties, settlers are often very large; design fluxes being of the order of  $4 \text{ m}^3/\text{m}^2/\text{h}$ . This results in high solvent evaporative losses. In addition, when crud forms, long down times are required for cleaning the settlers. The fine droplets formed during mixing also result in organic entrainment losses. This often requires the inclusion of expensive additional equipment (such as flotation columns like Jameson cells and after-settlers) into flowsheets. The Bateman Pulsed Column (BPC) has been designed to overcome these and other difficulties experienced with conventional mixer settlers. In addition the floor space occupied by the BPC is relatively small.

Previous work on copper extraction in BPC has been reported by Buchalter [1,2] while comparisons of BPC and mixer settlers has been reported by Fox [3] and Movsowitz [4]. Scale up and application of BPC to uranium, cobalt and nickel has been reported by Movsowitz [5,7], Klienberger [6] and Parkes [8].

To investigate the application of the BPC for copper, SX exploratory tests were conducted using a 40 mm diameter pilot BPC installed at IMI (TAMI) Institute for R&D. Scale-up design parameters were deduced from operating a 100 mm diameter pilot BPC in parallel with a client's mixer-settler pilot plant at the mine site. This paper discusses both sets of tests and the resulting conclusions.

## PILOT BATEMAN PULSED COLUMNS

All BPC units consist of a vertical cylindrical active section containing internals (usually disc and doughnut). Sampling points are situated at regular intervals along the column. Upper and lower settlers are connected to ends of the active section. A mechanical pulsator with adjustable amplitude and frequency is used for pulse generation. Mass transfer takes place in the active section and phase separation in the two settlers. When operating organic continuous, the interface between the two phase will be in the lower settler and in the upper settler for aqueous continuous operation.

### The 40 mm BPC

This all-glass column was tested with two active section heights (2 m & 4 m) and several different configurations of internals (disc/doughnut (d/d), sieve plate (s/p), Polyethylene (PE), polypropylene (PP), stainless steel (SS) and plate spacing: 5, 10 & 23 mm). The column is used to perform go/no-go tests on processes for which limited quantities of solutions are available.

### The 100 mm BPC

The column had a 7 m active section made from 1 m PVDF lengths with sight glasses between them. PVDF disc/doughnut internals were used (plate spacing 23 mm). The column is used to generate data for scale up to industrial-size BPC. Sample points (labeled SP) are equally spaced from the bottom to the top of the active section.

## EXPERIMENTAL

Extraction was tested in the 40 mm BPC while both extraction and stripping were tested in the 100 mm BPC. Actual solutions from an operating plant were used. The pregnant leach solution (PLS) copper concentration varied around 3 g/l. The strip solution was tankhouse spent electrolyte. Two types of tests were conducted: Hydraulic and mass transfer.

### Hydraulic Tests

These tests are done in order to determine the flooding and hold-up characteristics of the system. Flowrates, pulse frequency and amplitude are varied in order to determine the conditions at which flooding occurs. Flooding is defined as the condition in which a phase accumulates at the end of the column at which it enters. Hold-up, determined by sampling, is defined as the percentage of dispersed phase at a specific point in the column.

### Mass Transfer Tests

These tests are performed at selected conditions under which flooding did not occur. After establishing stable operation, the BPC is operated for at least 2 hours before sampling the in and out flows, as well as two-phase samples along the active section.

## RESULTS

### The 40 mm BPC

For this run the organic phase consisted of 16 vol.% LIX 84 in Conoco 170 ES diluent, the A:O ratio was 1.7:1 and the temperature was 21°C. Maximum fluxes achieved for a 2 m active section with various internals are shown in Table 1.

*Table 1. The maximum non-flooding flux achieved with the 2 m active section.*

Internals Type		Flux (m <sup>3</sup> /m <sup>2</sup> /h)	Recovery (%)
PE	d/d with 23mm spacing	55	20
PE	d/d with 5mm spacing	<10	
PE	d/d with 10mm spacing	40	50
SS	d/d with 23mm spacing	55	
SS	s/p with 23mm spacing	40	

With the 4 m active section, using PE disc/doughnut internals with 7.5 mm spacing, the maximum non-flooding flux was 30 m<sup>3</sup>/m<sup>2</sup>/h. At this flux the recovery of copper was 75%. The process is kinetically controlled, therefore the increased height and reduced flux results in an increased recovery. The tests with the 40 mm BPC achieved the objective of proving that the BPC technology was viable for copper extraction. Further in-depth testing was required using the 100 mm BPC.

### The 100 mm BPC

The work using this column was done in two phases. The hydraulic and mass transfer tests were done during the first phase by a combined Bateman and client team. During the second phase, the client ran the column for an extended period for both extraction and stripping. The optimum result for extraction during the first phase was found with an O:A of 1.2:1, at a flux of 45 m<sup>3</sup>/m<sup>2</sup>/h and a temperature of 27°C. Under these conditions, an extraction recovery in excess of 90% was achieved during continuous operation over a 20 hour period. Figure 1 is the flooding curve for extraction.

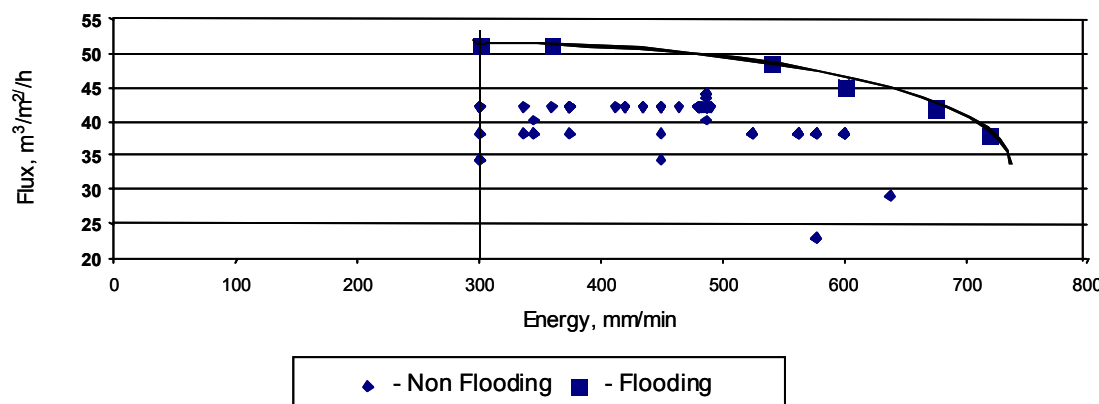


*Figure 1. Flooding curve for extraction stage.*

The optimum stripping result was found at an O:A Of 3.5:1, using a flux of 40 m<sup>3</sup>/m<sup>2</sup>/h and a temperature of 32°C. This produced an advance electrolyte of 47-51 g/l copper. Both these results met the client's operational criteria. The entrainment of solvent in the raffinate and in the advance electrolyte varied between 1 and 12 ppm. The recommended dispersion for both batteries is organic continuous. It was found that the bottom portion of the column was always organic continuous, while, the top was aqueous continuous. These dispersions are stable and co-exist in the column over long periods. This has the benefit of improving mass transfer while minimizing organic entrainment in the aqueous outlet. In industrial BPC both these interface levels are measured and the distance between them controlled by adjusting the energy input. The purpose of the second phase of testing was to confirm the above design parameters and for the client to become familiar with the operating ease of the BPC for his application.

Comparison of the extraction recovery for the pilot BPC and the client's mixer-settler pilot plant, operated at the same time, is shown in Figure 2. In the first period high PLS concentrations resulted in low (and comparable) recoveries for both plants. In the second period reduced PLS concentrations resulted in both plants meeting the operating criteria. In the third period reduced pulsation intensity (energy) resulted in lower recoveries from the BPC. Comparison of organic entrainment in the raffinate is shown in Figures 3 and 4.

The entrainment from the BPC was consistently and significantly lower than for the mixer settlers. This translates into significant savings in OPEX (of the order of \$110,000 pa). Flooding the column in order to drain crud caused the entrainments to temporarily increase. The column nevertheless remained on-line and recoveries were not affected.

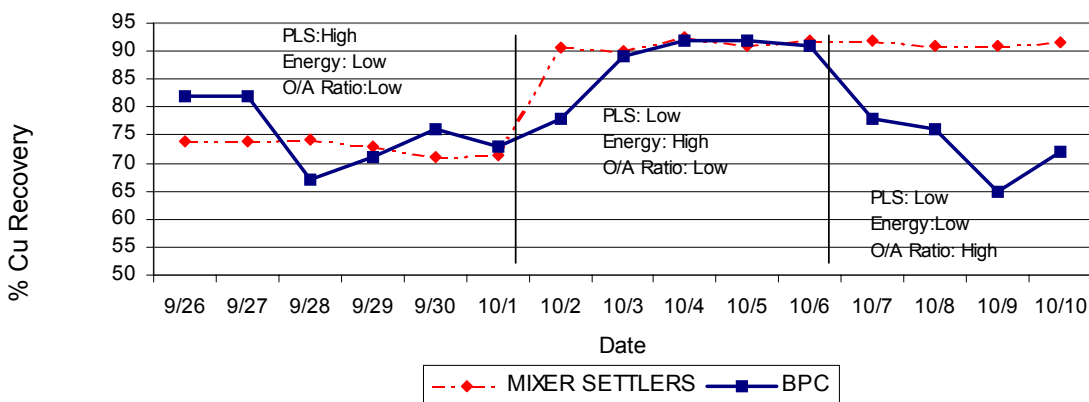


Figure 2. Comparison of Cu extraction in BPC and mixer-settler pilot plants.

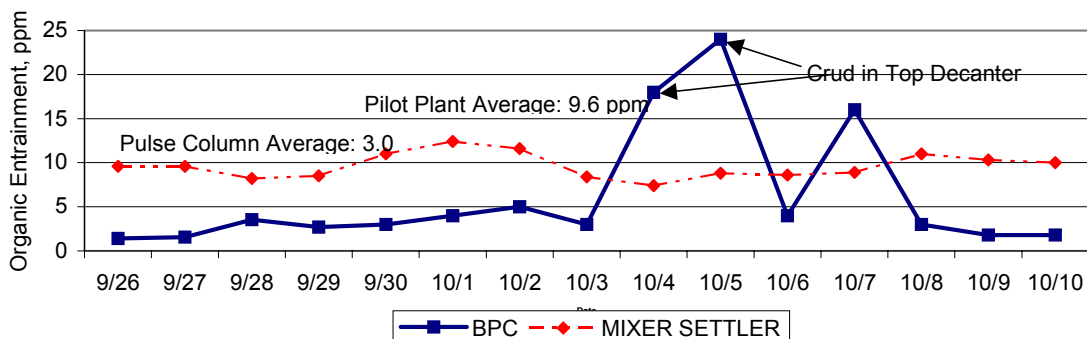


Figure 3. Organic entrainment in raffinate for BPC and mixer-settler pilot plants.

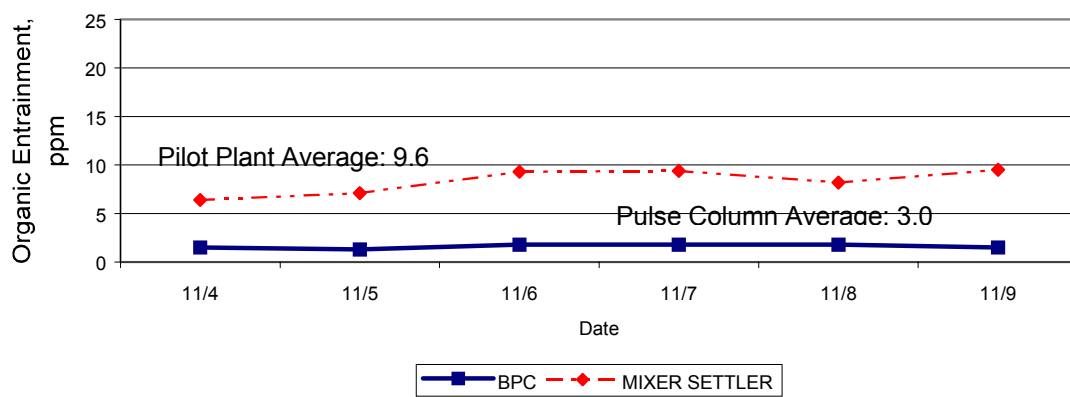


Figure 4. Organic entrainment in raffinate for BPC and mixer-settler pilot plants.

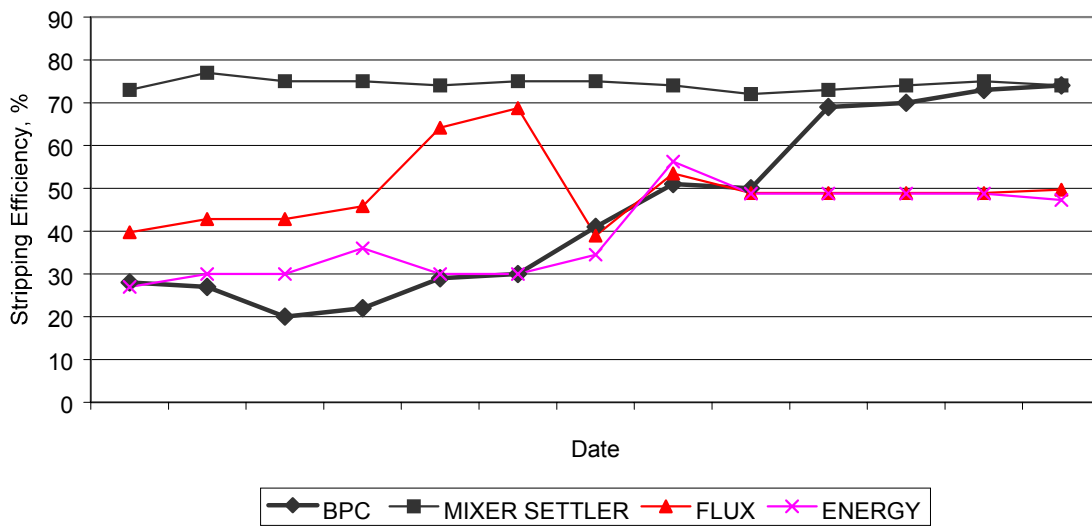


Figure 5. Stripping efficiency for BPC and mixer-settler pilot plants.

The results obtained for the pilot BPC and mixer-settler plants are shown in Figure 5. During the first period, the operation of the column was optimized by testing various fluxes and pulsation parameters. It is clear that at reasonable flux and increased energy, the operation of the two plants was similar.

It was consistently found (both in extraction and stripping) that increased temperature improved the hydraulics in the column and permitted operation at increased flux. A stripping flux of  $40 \text{ m}^3/\text{m}^2/\text{h}$  was achieved at  $21^\circ\text{C}$  and  $60 \text{ m}^3/\text{m}^2/\text{h}$  at  $40^\circ\text{C}$  (above  $40^\circ\text{C}$ , fluxes up to  $75 \text{ m}^2/\text{m}^3/\text{h}$  were achieved). This results from the decrease in viscosity with increasing temperature. It was not always possible to maintain temperature during the testwork. This was the main cause of operational problems during the second phase of stripping.

## CONCLUSIONS

### Extraction

- A copper recovery of 90% was achieved and maintainable.
- The BPC was easy to operate and required minimal operator attention.
- The organic entrainment in the raffinate was 55 to 80% lower than the mixer-settler pilot plant. This translates into savings of about \$110 000 pa.
- The optimal flux was  $42\text{-}45 \text{ m}^3/\text{m}^2/\text{h}$ .
- Crud was removable without shutting down.

### Stripping

- A rich electrolyte of 50 g/l was obtained with a copper increase of 15 g/l.
- The flux was  $40 \text{ m}^3/\text{m}^2/\text{h}$  at  $21^\circ\text{C}$  and  $60 \text{ m}^3/\text{m}^2/\text{h}$  at  $40^\circ\text{C}$ .

These design results were used to design an industrial plant. Comparative Capex with a mixer-settler plant showed a 15% saving (including first fill).

### Operator comments

- “Easy to operate”.
- “Just leave it alone and it works”.
- “Set it and forget it, except when it gets cold”.

## REFERENCES

1. E. M. Buchalter, R. Kleinberger and B. Grinbaum (1998), *Alta 1998 Copper Hydrometallurgy Forum*, Brisbane, Australia.
2. E. M. Buchalter, R. Kleinberger and B. Grinbaum (1998), *SAIMM Extraction Metallurgy Africa 1998*, Johannesburg, South Africa.
3. M. H Fox, S. J Ralph, N. P. Sithebe, E. M. Buchalter and J. J. Riordan (1998), *Alta Nickel/ Cobalt Forum*, Perth, Australia.
4. R. L. Movsowitz, R. Kleinberger, E. M Buchalter, B. Grinbaum and S. Hall (1999), *Proceedings of ISEC 99*, Barcelona, Spain, pp. 1455-1460.
5. R. L. Movsowitz, R. Kleinberger and E. M. Buchalter (1997), *SAIMM Conference Extraction Metallurgy Africa 1997*, Randburg, South Africa.
6. R. Kleinberger (1998), Application of Bateman Pulsed Columns for Uranium SX. Australian Uranium Summit.
7. R. L. Movsowitz, R. Kleinbereger and E. M. Buchalter (1997), *Alta 1997 Nickel/Cobalt Forum*, Perth, Australia.
8. D. Parkes, B. Armall, B. Grinbaum and R. Kleinberger (2000), *Alta 2000 Nickel/Cobalt Conference*, Australia.



## AMMONIA LEACH-SOLVENT EXTRACTION-ELECTROWINNING PROCESS FOR TREATMENT OF HIGH ALKALINE GANGUE-CONTAINING COPPER ORES

Daxing Liu, Kaixi Jiang, Chunyun Wang\* and Peiwen Zhang\*

Beijing General Research Institute of Mining & Metallurgy, Beijing, P. R. China  
\*Dongchuan Bureau of Mine, Dongchuan, Yunnan, P. R. China

Tangdan copper mine, which is located in Yunnan Province, China, has a deposit of 1.16 million metric tons of copper. The copper mineral is a high alkaline gangue containing oxide and sulfide copper with CaO and MgO accounting for 40% weight in the ore. The copper concentrate produced from the mixed ore has a relatively low content of 14~16% copper and 3~4% S while CaO and MgO contents are higher than 20%, respectively. The concentrates are not suitable for direct treatment by a smelter, and are therefore used as supplementary concentrates. A process combining roasting, ammonia leaching, solvent extraction and electrowinning has been developed for treatment of the concentrates. The laboratory tests, process development and pilot operation results are discussed in this paper. A pilot plant with a capacity of 500 t copper cathode per annum was built in 1997 and it has been running well since being brought on line. LIX 54-100 is employed to extract copper from ammonia leach liquors. The effects on the extraction and electrowinning, especially the ammonia concentration, are discussed in this paper. The operational measures for the pilot plant are also given. The economical feasibility of this pilot plant is reviewed.

### INTRODUCTION

Tangdan Copper Mine is located near Dongchuan City, Yunnan Province. The copper deposit is 1.16 million t with an average grade of 0.64% Cu. About 50% of the copper is oxide (malachite and chrysocolla) with the remainder being secondary copper sulphides such as chalcocite and bornite. However, the copper ore contains high alkaline gangue with CaO and MgO up to 40%. Furthermore, the copper minerals are finely divided in the ore body and as a result flotation only achieves a copper recovery of 75~78%. The copper concentrate produced contains 14~16% Cu, 3~4% S, 15% CaO and 15% MgO. This type of concentrate is not readily accepted by smelters and therefore it would have to be sold at a discounted price.

Tangdan also has 300,000 t copper contained as copper oxide in high alkaline gangues. The acid leach of this ore is uneconomical due to the high acid consumption. Previous development work on the Tangdan copper deposit focused on treatment of the whole ore either by ammonia pressure leaching, or by converting copper oxides to sulphides, followed by flotation to produce a copper concentrate. These processes operated at relatively high temperature and pressure (150°C and 1.5 MPa). The unit ammonia consumption was high because of the low copper grade of the ore.

In the early 1990s, Beijing General Research Institute of Mining & Metallurgy (BGRIMM) concentrated on the development of a leach-SX-EW process in order to produce copper cathodes from both the low copper/low sulphide concentrates and the copper oxide ore. Roasting-ammonia pressure leach-SX-EW was adopted for the treatment of the low grade copper concentrates while ammonia leach-SX-EW was adopted for the treatment of the copper oxide ore. A pilot plant with a capacity of 500 t/a copper cathode was built on site in 1996 and put into production in 1997. The plant run well since start-up, thus, providing a technology for the treatment of high alkaline gangue containing copper ores.

## EXPERIMENTAL

### Raw Materials

Two kinds of raw materials were used in the laboratory tests, the low quality copper concentrates and the copper oxide ore mentioned above. The chemical assay of raw materials is shown in Table 1.

*Table 1. Chemical assays of copper concentrates and oxide ores (%).*

	Cu	Fe	S	CaO	MgO
Concentrate	14~16	5~6	3~4	8~10	7~10
Oxide ore	1.5~4	7~8	0.4~0.6	3~5	4~6
	SiO <sub>2</sub>	Al <sub>2</sub> O <sub>3</sub>	As	Au (g/t)	Ag (g/t)
Concentrate	22~25	4~5	0.1~0.15	0.1	100
Oxide ore	60~65	8~10	0.1	0.06	5~6

The copper in the concentrates is present as follows: 30% malachite, 50~60% chalcocite and bornite, and 5% chalcopyrite. The gangue materials are carbonates with the copper minerals finely disseminated in the gangue material. The copper in the copper oxide ore is present as 80% malachite, 10% chalcocite and covellite, and 3~4% chalcopyrite. The gangue materials are also carbonates. Because of the high content of oxide gangue materials in the concentrate and in the oxide ore, direct leaching with sulfuric acid is not economical and for this reason the ammonia leach route was adopted.

### Ammonia Leach

The most important feature of ammonia leaching is that the oxides of Ca, Mg, Al, Si, Mn, and Fe are not leached. This simplifies the downstream treatment of the leach liquor, especially for Fe removal, thus helping ensure a pure copper product is obtained.

Direct ammonia leaching of the low grade copper concentrate without air introduction achieves only 80% copper recovery even at 140~150°C. Roasting under the proper conditions converts copper sulphide to copper sulfate and copper oxide, both of which are easily leached with ammonia under mild conditions. Temperature control is very important in the roasting. Too low a temperature results in low converting efficiency while too high a temperature gives difficult to leach copper silicates or ferric oxides. The preferred roasting temperature is 550~600°C.

The percent copper recovery in leach for the roasted concentrate was studied as a function of the: roasting temperature, particle size, ammonia concentration, NH<sub>3</sub> / CO<sub>2</sub> ratio, leach temperature, pressure and time. The recommended conditions follow: particle size: 80% minus 0.074mm; ammonia concentration 5 molar; NH<sub>3</sub>/CO<sub>2</sub> ratio 2.5:1; liquid / solid ratio in leach is 4; leach temperature is 90~100°C; leach time 1.5 to 2.0 h. Under the proper conditions about 92% copper recovery can be achieved across roast / ammonia leach.

It is critical to control the ammonia concentration in leaching to achieve a proper balance in the total copper recovery process. A high ammonia concentration will improve copper recovery in leach, but it will also increase ammonia losses and negatively impact the solvent extraction process that follows leaching.

### Solvent Extraction

Two reagents were tested for copper extraction from ammonia media, LIX 54-100, a beta-diketone and LIX 84, a ketoxime, both supplied by Cognis Corp. LIX54-100 has a very high copper loading capacity of 100 g/l Cu. Copper can be stripped from LIX 54 with relative ease and 80 to 100 g/l H<sub>2</sub>SO<sub>4</sub> will quantitatively strip the copper from a fully loaded 30 v/v % solution of LIX 54-100. The copper extraction was studied as functions of pH, aqueous ammonia concentration, temperature, and phase ratio.

Equal volumes of 30% v/v LIX 54-100 and liquor containing 20.56 g/l Cu was contacted at 25°C for different aqueous ammonia concentrations. The result is shown in Figure 1. Copper extraction decreased with increasing aqueous ammonia concentration. To ensure a good copper extraction, the aqueous ammonia concentration should be controlled in the ranges of 40 to 60 g/l.

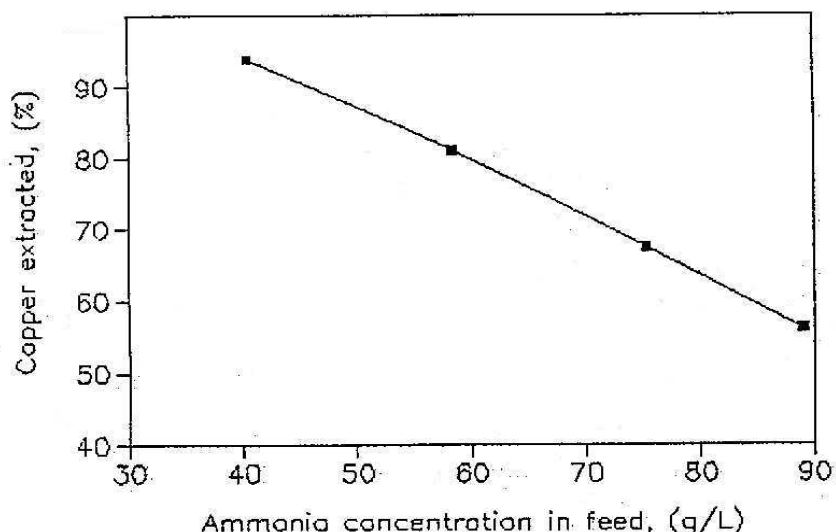


Figure 1. Effect of aqueous ammonia concentration on copper extraction.

The McCabe-Thiele curve is shown in Figure 2. 99% copper extraction can be achieved in 2 stages.

LIX 84 also exhibits a good extraction and stripping performance. However, at a same extractant concentration, LIX 84 extracts less copper than LIX 54-100 does. Considering 20-25 g/l copper in the leach liquor contains, and LIX 54-100 has a higher copper loading capacity and better stripping performance, 30% v/v LIX 54-100 thus was adopted as an extractant for the pilot plant.

### Electrowinning

The quality of the copper cathode as a function of the ammonia concentration in the copper electrolyte was studied at current density of 150 A/m<sup>2</sup>. The results indicate that the cathode quality will not be adversely affected when the ammonia concentration of the electrolyte is less than 2 g/L. To ensure a smooth dense cathode, a portion of Guarfloc 66 is added into the copper electrolyte. The presence of Guarfloc 66 in the electrolyte also reduces the ammonia impact on copper cathode quality.

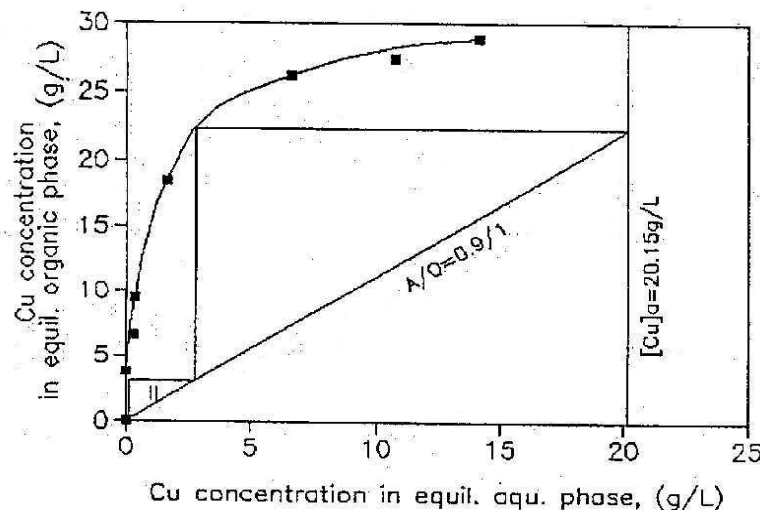


Figure 2. McCabe-Thiele curve of copper extraction.

Aqueous phase: 20.15 g/L Cu and 43.2 g/L ammonia. Organic phase: 30% v/v LIX 54-100.

### Pilot plant

The recommended process flowsheet is shown in Figure 3. Based on this process, a pilot plant with a capacity of 500 t/a copper cathode was built in the end of 1996. The pilot plant has been running for five years and a great deal of operation experience in the running of a roast / ammonia leach / SX / EW plant has been gained.

Two kinds of raw materials are processed at the pilot plant, a low copper / low sulphide / high gangue containing concentrate and a high gangue / high grade copper oxide ore. The copper concentrate is roasted in a rotary kiln 1.2 m in diameter and 16 m in length. The rotary rate is adjustable. The roasting temperature is controlled in the range of 500~600°C. The retention time of concentrates in the kiln is 2 h. Because the low grade sulphide in the concentrate is converted into oxide and sulphate small amounts of sulphur dioxide is given off during the roasting. The sulphur dioxide is absorbed into water so that it is not emitted to the atmosphere. The floatation reagent remained in the copper concentrates will have a bad impact on solvent extraction operation. The problem can be solved effectively via the roasting operation.

After roasting the calcine is mixed with raffinate in a pulping tank at solid to liquid ratio of 1, then flowed into a ammonia concentration adjusting tank, where ammonia is made up to a desired level. The pulp is pumped by a pressure pump into a heat exchanger, then a serial column style autoclave. The autoclave is built by connecting 10 steel pipes of 300 mm in diameter and 5.7 m in length. The ammonia leach is operated at 90~100°C and 0.2 MPa. After leaching the pulp is taken into 3 stages of count-current thickeners. The overflow from the thickeners is pumped to the solvent extraction circuit.

The SX circuit is configured with 2 stages of extraction, 2 stages of scrubbing, and 2 stages of stripping. The residence time in the mixer is 3 min. The flow rates of aqueous and organic phases are 4.5 m<sup>3</sup>/h and 3.5-3.7 m<sup>3</sup>/h, respectively. The specific flow is 3.8 m<sup>3</sup>/m<sup>2</sup>.h. The top of mixer-settler was covered to reduce ammonia evaporation and its impact on operation environment. The scrubbing stages are very important in order to minimize ammonia transfer from the leach solution to the electrolyte. The loaded organic phase is scrubbed with water to remove entrained and co-extracted ammonia. Spent electrolyte can be added to the scrub liquor to adjust the acidity of the scrub stages. The pH of outlet scrub liquor is controlled at 5~6 to ensure that 90% of ammonia in the loaded organic phase is removed. The scrub liquor is recycled to the thickener which follows pressure leaching. Spent electrolyte, containing 30~35 g/l Cu and 80~100 g/l H<sub>2</sub>SO<sub>4</sub>, is used as a stripping agent.

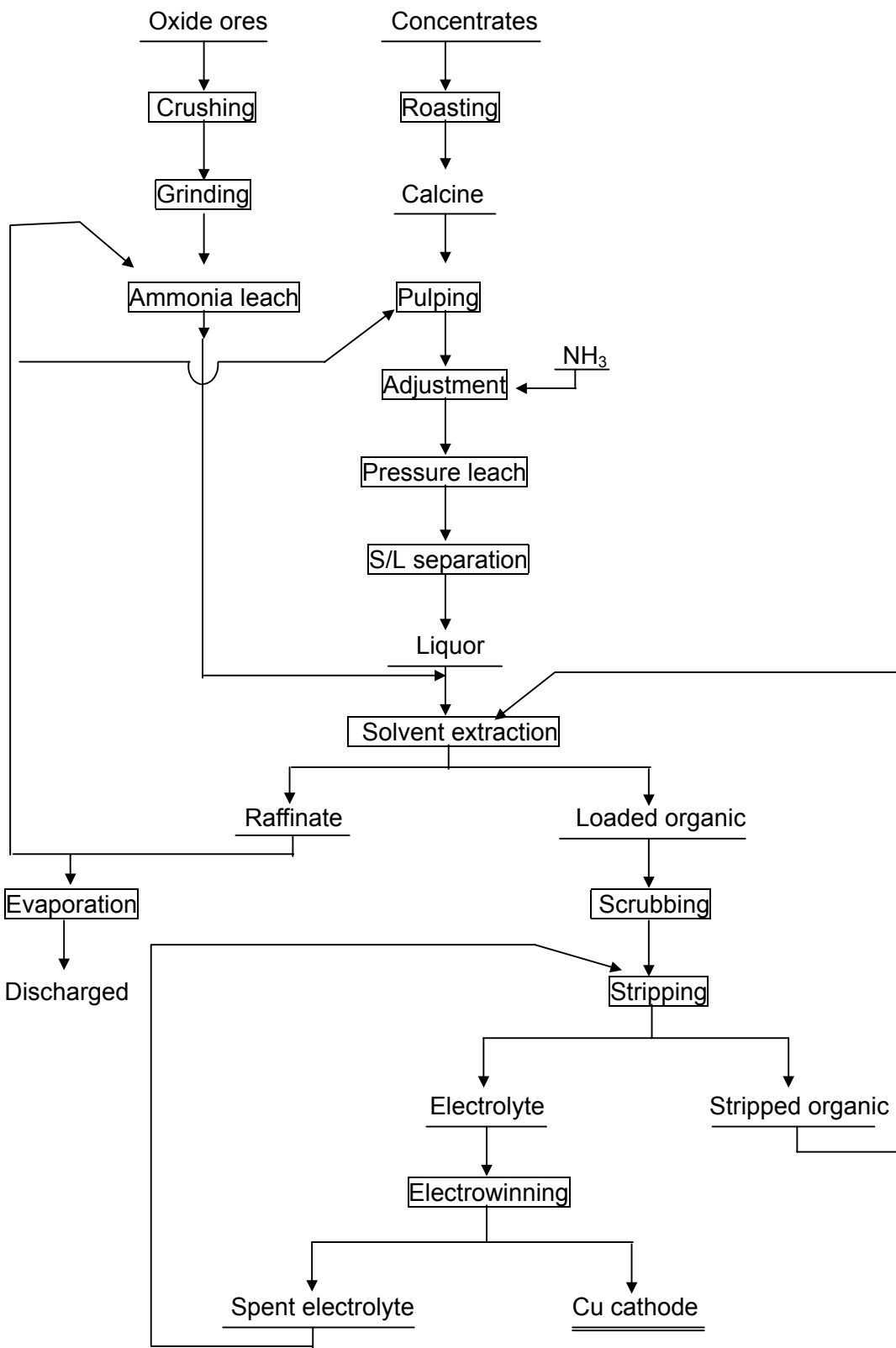


Figure 2. Principle flowsheet of ammonia leach-SX-EW process for treatment of high alkaline gangue containing copper ores.

Organic entrained in the strip liquor is removed by a flotation tank prior to electrowinning. The ammonia build up in the electrolyte is very slow, 6 kg of ammonia is transferred to the tankhouse per 1000 m<sup>3</sup> leach liquor. 0.5 m<sup>3</sup> of copper electrolyte is bleed off per day to control the ammonia in the electrolyte at 2 g/L. There are 30 cells in the tankhouse each containing 17 cathodes and 18 anodes. The dimensions of each cell are 920 by 2300 by 1060 mm. The anode is a Pb-Ag-Ca-Sr alloy and cathodes are grown on copper starting sheets.

The raffinate from extraction, containing less than 0.1 g/l Cu, is taken back to leaching and thickening. To keep water balance of the whole process, 10-12 m<sup>3</sup>/d of raffinate is bleed off to ammonia evaporation, then discharged.

In the pilot operation the ammonia consumption for the processing of copper concentrate is 102 kg/t Cu while for copper oxide ore processing it is 250 kg/t Cu. The operation cost is US\$ 650~700/t Cu.

## CONCLUSIONS

The laboratory tests and pilot plant operation prove that ammonia leach-SX-EW is a practical technology for the treatment of Tangdan's high alkaline gangue containing copper ores.

- 1) Copper concentrates are converted to sulphate or oxide by roasting at 550~600 °C, the calcine is pressure leached using ammonia at relatively low pressure and temperature, e.g., 90~100°C, 0.2M Pa. The pressure leach is conducted in a column style autoclave, a small and cheap equipment with high capacity.
- 2) Ammonia leaching is adopted for the treatment of high alkaline gangue containing copper ores. Impurities such as Ca, Mg, Al, Si, Mn and Fe in the ore are not leached, the leach liquor purification is thus simplified resulting in high quality copper cathodes.
- 3) LIX54-100 has high copper loading capacity, good kinetics and phase disengagement performance. Stripping can be achieved using a low acidic liquor. The SX circuit is configured with 2 stages of scrubbing in order to remove entrained and co-extracted ammonia from the loaded organic phase and ensure copper cathode quality.

## REFERENCES

1. W.Hopkin (1981), Recovery of Copper From Copper-Lead Dross, *37<sup>th</sup> Meeting of The Lead Technical Committee*.
2. Anon (1995), Escondida's New Cathode Plant, *Eng. Min. J.*, 24-28.



## SOLVENT EXTRACTION OF COPPER FROM HIGH CONCENTRATION PRESSURE ACID LEACH LIQUORS

Kathryn C. Sole

Anglo American Research Laboratories (Pty) Ltd, Johannesburg, South Africa

Hydrometallurgical processes for the recovery of copper from sulphide concentrates are under evaluation for the Konkola Deep project in Zambia and for a copper-gold ore deposit. The process flowsheets involve copper dissolution from the concentrate by pressure leaching in sulphuric acid, followed by purification of the leach liquor by solvent extraction, and metal recovery by electrowinning. The autoclave discharge liquors contain 50 to 90 g/l Cu and, under appropriate operating conditions, minimal residual free acid. The choice of extractants and operating conditions for the recovery of copper from such solutions is discussed, and selected results from laboratory and pilot-scale studies are presented.

### INTRODUCTION

Pressure acid leaching (PAL) can offer technical and economic advantages in base metal flowsheets and is now being considered for the treatment of sulphide concentrates [1]. Flowsheets that integrate PAL with solvent extraction (SX) for the downstream processing of autoclave discharge liquors present interesting opportunities for efficient metal recovery.

Significant advances in copper SX have been made over the past thirty years [2], with almost 30% of world copper production today via this route. Most applications involve the relatively dilute liquors (1 to 4 g/l Cu) arising from the dump or heap leaching of low-grade material. In contrast, autoclave discharge liquors from the partial or total oxidation of copper sulphides have tenors ranging from 50 to 90 g/l Cu.

Modern copper extractants (HA) employ the hydroxyoxime functionality for the complexation of copper, the schematic reaction for which can be written:



The reaction stoichiometry shows that 1.54 g H<sub>2</sub>SO<sub>4</sub> is generated per g Cu extracted. The purification of leach liquors with high copper concentrations provides challenges in designing flowsheets to accommodate the substantial quantities of acid produced by the extraction reaction. Limited studies on the processing of such liquors have been documented [3].

This paper examines two case studies (the recovery of copper from a copper-gold deposit and the hydrometallurgical option for the Konkola Deep expansion project in Zambia) in which these challenges are met by innovative process integration. The choice of extractants and operating conditions for the purification of copper from the high-concentration PAL liquors are discussed, and selected results from laboratory and pilot-scale studies presented.

## SELECTION OF EXTRACTANTS

### **Simulation Modelling**

Potential extractant systems for achieving the high copper transfers required ( $\Delta\text{Cu} = 50 \text{ g/l}$ ) for the processing of PAL pregnant leach solutions (PLS) were identified using the *Isocalc* (Cognis) and *MEUM* (Avecia) simulation models. There was excellent agreement between experimental data and the model predictions, confirming the validity of using modelling for the preliminary selection of extractant compositions and operating conditions.

Selected results are presented in Table 1. Various combinations of circuit configurations and organic-to-aqueous (O:A) flowrate ratios will achieve similar objectives; the particular choice of conditions will be governed by capital and operating costs, as well as by site-specific considerations.

*Table 1. Modelling of copper extraction from high-concentration liquors.*

Extractant	Concn. (vol.%)	PLS Cu (g/l)	Circuit configuration	Advance O:A	Raffinate Cu (g/l)	$\Delta\text{Cu}^*$ (g/l)
LIX 984N	32	60	3E, 2S** 2E, 2S	4.2 5.5	8.8 9.88	51.2 50.1
		80	2E, 2S 3E, 1S	6 6	30.0 28.7	50.0 51.3
	32	60	3E, 2S 3E, 2S	6 5	8.47 10.0	51.5 50.0
		60	4E, 2S 3E, 2S	4.5 3.76	9.1 15.0	50.9 45.0
Acorga M5640	32	70	3E, 2S	5 6	15.2 12.6	54.8 57.4
		70	3E, 2S	5 6	15.8 13.3	54.2 56.6
	35	70	3E, 2S	5 6	14.1 12.4	55.9 57.6

\* PLS acid: 5 g/l H<sub>2</sub>SO<sub>4</sub>; SE: 35 g/l Cu, 180 g/l H<sub>2</sub>SO<sub>4</sub>; AE: 45 g/l Cu; Mixer efficiency: 98%

\*\* 3E, 2S = three extraction stages, two stripping stages

### **Extraction Isotherms**

The extractants chosen for the experimental study are described in Table 2. The partially aromatic diluent was Shellsol 2325, supplied by Shell Chemicals.

*Table 2. Copper extractants.*

Supplier	Extractant	Functionality	Modifier
Avecia  Cognis	Acorga M5640	aldoxime	ester
	Acorga M5774	aldoxime	ester
	LIX 664N	aldoxime	ester
	LIX 84-I	ketoimine	none
	LIX 984N	50:50 aldoxime:ketoimine	none
	LIX 973N	70:30 aldoxime:ketoimine	none

Figure 1 shows the extraction of copper from an autoclave discharge liquor containing 70 g/l Cu. Both Acorga extractants, LIX 664N and LIX 984N will produce a raffinate of < 10 g/l Cu under appropriate operating conditions. LIX 84-I and LIX 973N were also tested, but their extraction capability dropped significantly in the presence of too much acid, so they are not suitable for the treatment of autoclave discharge liquors. In general, aldoximes have a higher loading capacity for copper than ketoximes, but, since they form stronger complexes, are typically less readily stripped; hence the need to include a stripping modifier in the formulation of aldoximes.

The effect of extractant concentration is shown in Figure 2. Higher concentrations increase copper transfer due to higher loadings, thereby reducing the equipment size for a given PLS throughput. Higher concentrations usually require higher temperature operation due to viscosity and settling limitations, however even at ambient temperature, the use of 48 vol.% extractant did not pose visible problems, and loadings up to 25 g/l Cu were measured.

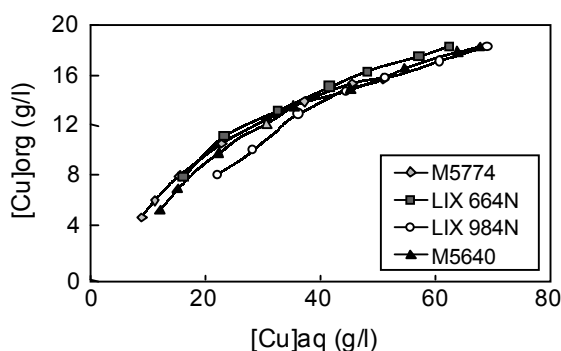


Figure 1. Extraction of copper from PAL liquor (70 g/l Cu, 2.8 g/l Fe, 6 g/l  $H_2SO_4$ ) by 32 vol.% extractant in Shellsol 2325.

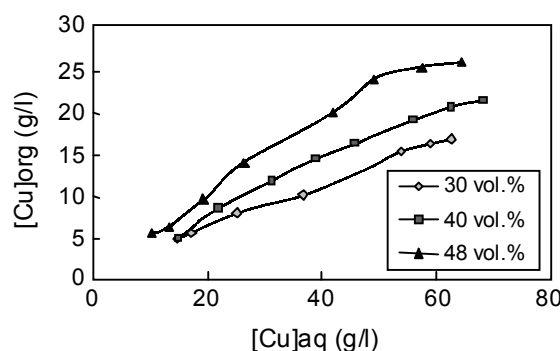


Figure 2. Effect of extractant concentration on copper extraction from PAL liquor by Acorga M5774 in Shellsol 2325.

## RECOVERY OF COPPER FROM A COPPER-GOLD DEPOSIT

A hydrometallurgical process is under development for the recovery of copper from a copper-gold deposit. Copper is liberated from the finely ground concentrate by pressure leaching under conditions that minimise the free acid and iron in solution. The clarified leach solution contains 60 g/l Cu which is treated by SX to maximise copper recovery. The raffinate, containing significant quantities of acid liberated in the extraction reaction, is recycled to the leach. The flowsheet also includes a second conventional SX circuit to recover copper from the filtrate wash water. A single electrowinning (EW) circuit provides a recycle of electrolyte between the two SX strip circuits. Gold is recovered from the leach residue.

Following modelling simulations and initial screening of extractants, LIX 984N and Acorga M5774 were chosen for further evaluation using leach liquor generated from the pressure leaching testwork. The SX performance of the high-tenor circuit (32 vol.% extractant) is summarised in Table 3.

Table 3. Extraction and stripping performance of the high-tenor SX circuit.

Stream	Acorga M5774	LIX 984N
Stripped organic (SO) (g/l Cu)	3.58	3.94
Loaded organic (LO) (g/l Cu)	18.58	16.18

McCabe-Thiele constructions were used to determine the staging requirements and operating conditions for the high-tenor SX circuit (Figure 3). An advance O:A of 5.4 will produce a raffinate of 10 g/l Cu in three extraction stages from a PLS containing 60 g/l Cu at pH 1.4. Using a spent electrolyte (SE) of 35 g/l Cu and 180 g/l H<sub>2</sub>SO<sub>4</sub>, a stripping ratio of O:A = 1.1 will upgrade the advance electrolyte (AE) to 45 g/l Cu in two stages.

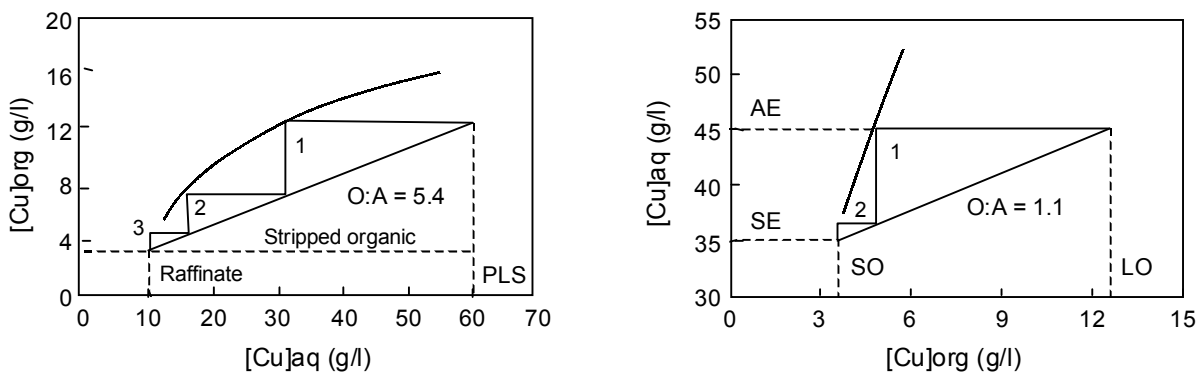


Figure 3. McCabe-Thiele constructions for (a) extraction and (b) stripping of copper in the high-tenor SX circuit (32 vol.% Acorga M5774 in Shellsol 2325).

### KONKOLA DEEPS EXPANSION PROJECT

A hydrometallurgical flowsheet (Figure 4) for the combined treatment of the Konkola Deep sulphide deposit and Chingola refractory ore (CRO) has been proposed. The sulphide concentrate (40-45% Cu) is pressure leached under conditions that maximise recovery of copper and cobalt while rejecting iron as hematite. The autoclave discharge contains 60 g/l Cu and the acid tenor is minimised to 5 g/l, allowing the liquor to be purified directly by SX. The high-tenor SX1 circuit removes the bulk of the copper, the extraction of 50 g/l Cu generating a raffinate containing ~80 g/l H<sub>2</sub>SO<sub>4</sub>. This acid is used to leach copper from the CRO, the aggressive conditions necessitated by the high aluminium, magnesium, and calcium oxides and carbonates in this material. The atmospheric leach liquor is treated for copper recovery in the low-tenor SX2 circuit. Both SX circuits are integrated with EW to produce a high-grade copper cathode product.

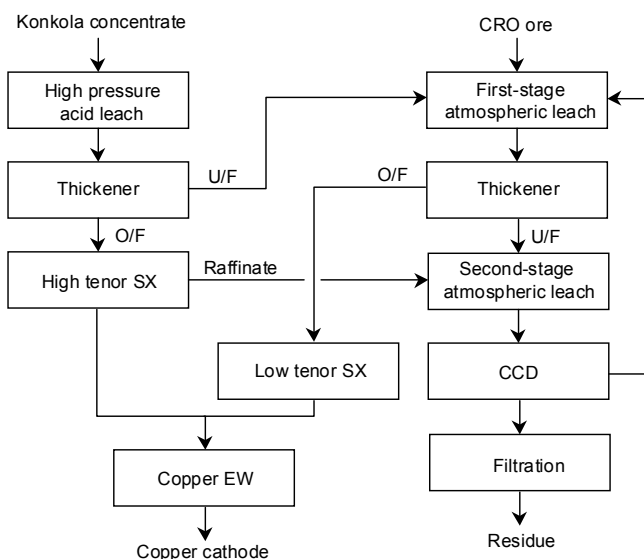


Figure 4. The hydrometallurgical flowsheet for the Konkola project.

This flowsheet capitalises on the synergy between the leaching of the sulphide concentrate (acid producing) and the oxide ore (acid consuming), which provides a convenient way of ‘transferring acid’ from the sulphide to the oxide circuit. Key to the concept is the high copper transfer ( $\Delta\text{Cu} = 50 \text{ g/l}$ ) of the SX1 circuit which generates a raffinate of sufficient acid strength to leach the refractory CRO minerals. SX1 maximises copper extraction using a high extractant concentration and high O:A; SX2 generates a low copper raffinate (< 0.5 g/l).

### Pilot-Plant Evaluation

An eight-week, integrated pilot-plant campaign producing 24 kg/h cathode copper was carried out at AARL [4]. The pilot plant treated 27 tons of CRO and 2.5 tons of Konkola concentrate, and produced 940 kg of LME Grade A copper cathode.

Both SX circuits comprised three extraction and two strip stages, configured for counter-current flow. Two extractants were tested: Acorga M5640 and LIX 984N. The diluent was Shellsol 2325. The operating conditions are shown in Table 4.

*Table 4. Konkola pilot-plant SX operating conditions.*

Parameter	SX1	SX2
Extractant concentration (vol.%)	32	16
PLS	Clarified autoclave discharge	Clarified CRO liquor
PLS composition	60 g/l Cu, 6.5 g/l H <sub>2</sub> SO <sub>4</sub>	5.3 g/l Cu, 2.7 g/l H <sub>2</sub> SO <sub>4</sub>
Extraction advance O:A	4.9	1.0
Target extraction $\Delta\text{Cu}$ (g/l)	50	4.8
Strip advance O:A	0.91	1.76
Strip liquor (SE)	37 g/l Cu, 170 g/l H <sub>2</sub> SO <sub>4</sub>	37 g/l Cu, 170 g/l H <sub>2</sub> SO <sub>4</sub>
Loaded strip liquor (AE)	46.1 g/l Cu, 156 g/l H <sub>2</sub> SO <sub>4</sub>	45.4 g/l Cu, 157 g/l H <sub>2</sub> SO <sub>4</sub>

SX1 consistently achieved copper extractions of 50 g/l. SX2 exceeded the performance specifications, with average raffinates of 0.25 g/l Cu. Typical results are shown in Table 5. Comparison of the plant data with laboratory isotherms generated from the plant solutions showed excellent correlation (Figure 5), indicating optimal operation of both SX circuits. Both extractants performed well and little differentiation of metallurgical performance could be quantified under the pilot-plant operating conditions. LME Grade A copper was produced throughout the campaign, with all cathodes meeting the BSI standard 6017:1981.

*Table 5. Typical performance of SX circuits during the Konkola pilot-plant campaign.*

Element (g/l)	SX1			SX2		
	PLS1	LO1	SO	PLS	LO	SO
Cu	59.29	15.6	6.2	5.81	8.85	3.8
Co	1.23	< 0.001	< 0.001	0.61	< 0.001	< 0.001
Fe	1.22	< 0.001	< 0.001	1.77	< 0.001	< 0.001
Al	1.12	< 0.001	< 0.001	1.31	< 0.001	< 0.001
Mg	7.95	< 0.001	< 0.001	6.83	< 0.001	< 0.001
Ca	0.65	< 0.001	0.001	0.69	< 0.001	< 0.001
Mn	1.31	< 0.001	< 0.001	1.22	< 0.001	< 0.001
Zn	0.10	0.001	< 0.001	0.05	< 0.001	0.001

## CONCLUSIONS

Pressure leaching technologies currently under development for the treatment of copper sulphide concentrates yield leach liquors that contain 50 to 90 g/l Cu. Purifying such liquors by SX requires an integrated flowsheet in which the large quantities of acid produced by the extraction reaction can be accommodated. This work has demonstrated that extractant

concentrations up to 45 vol.% can achieve copper transfers of 50 g/l in three stages. Adequate stripping is achieved in two stages with a conventional SE composition, producing an AE from which LME Grade A copper cathode can be electrowon.

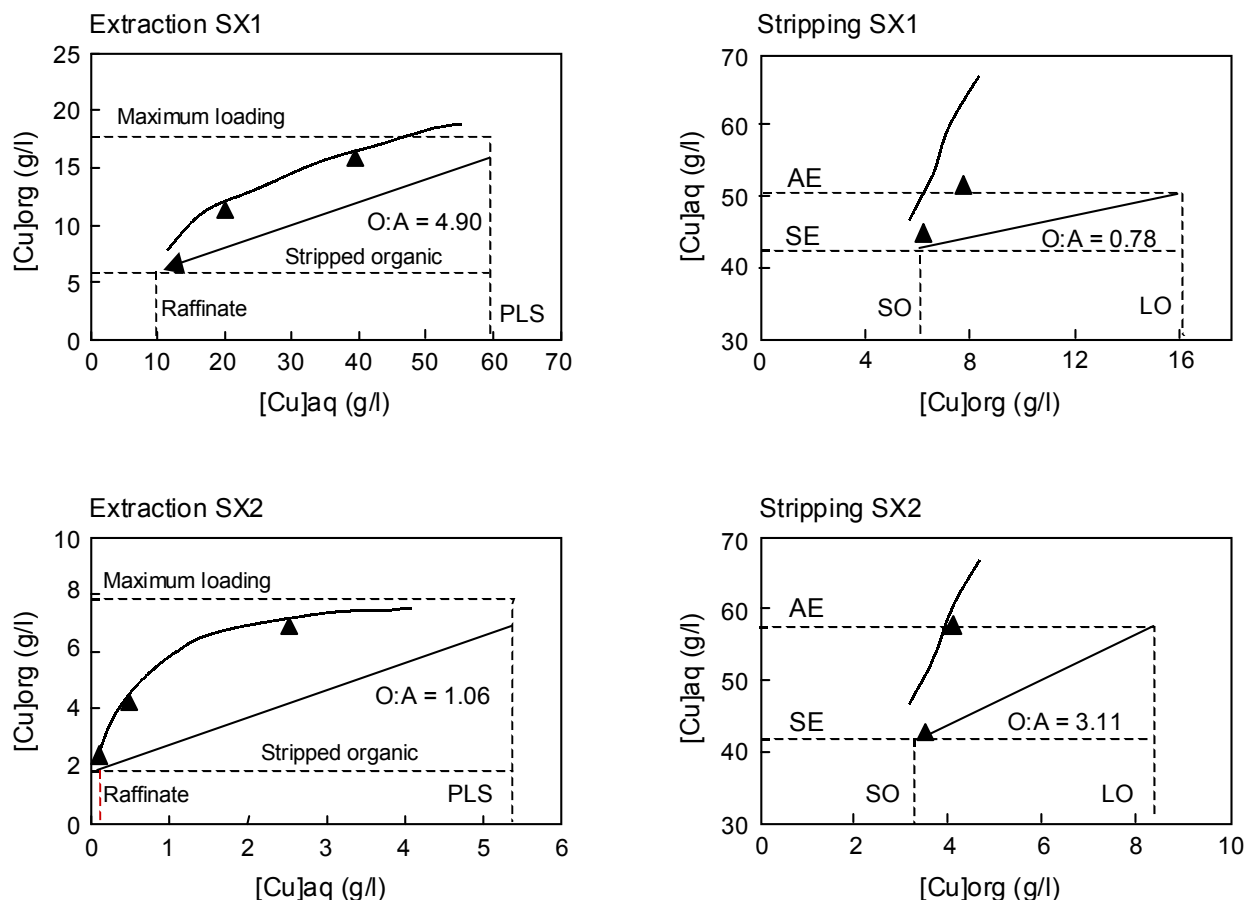


Figure 5. Comparison of laboratory extraction and stripping isotherms (solid lines) with typical pilot-plant operating conditions ( $\blacktriangle$  and dotted lines) for SX1 and SX2.

The performance of conventional extractants and circuit configurations for transferring such high amounts of copper has not been previously documented for continuous trials. The successful completion of the Konkola pilot plant demonstrated that existing extractants can be used in non-traditional applications without problems.

## ACKNOWLEDGEMENTS

The extractants and modelling packages were kindly made available by Avecia and Cognis. Anglo Base are thanked for permission to discuss details of the two development projects. This paper is published by permission of Anglo American Research Laboratories (Pty) Ltd.

## REFERENCES

1. R. McElroy, W. Young (1999), Copper Leaching, Solvent Extraction and Electrowinning, G. V. Jergensen (ed.), Society for Mining, Metallurgy and Exploration, Littleton, pp. 29-40.
2. G. Kordosky (2002), *Proc. International Solvent Extraction Conference ISEC 2002*, South African Institute of Mining and Metallurgy, Johannesburg, pp. 853-862.
3. T. Moore, B. Townson, C. Maes, O. Tinkler (1999), ALTA 1999 Copper Hydrometallurgy Forum, ALTA Metallurgical Services, Melbourne.
4. R. M. Whyte, N. Schoeman, K. G. Bowes (2001), Copper, Cobalt, Nickel and Zinc Recovery, South African Institute of Mining and Metallurgy, Johannesburg, 15 pp.



## PURIFICATION OF COPPER ELECTROLYTE WITH CYANEX 923

Chun Wang\*, Kaixi Jiang, Daxing Liu and Haibei Wang

Beijing General Research Institute of Mining and Metallurgy, Beijing, P. R. China

Comparative extraction tests on a range of extractants for the removal of impurities from actual copper electrolyte has revealed Cyanex 923 to be the most effective extractant. The extraction of As, Sb and Bi was studied as functions of aqueous acidity, concentrations of chloride ion and Cyanex 923, and contact time. The loading capacities were determined. Organic entrainment and residual antimony in the raffinate were further removed by absorption using activated carbon. A novel process was proposed, which uses Cyanex 923 combined with subsequent absorption using activated carbon to remove As, Sb and Bi from a copper electrolyte. The process can be used as a supplement for producing high quality copper cathode, especially for plants whose Bi and Sb contents in the electrolyte are high.

### INTRODUCTION

In the electrorefining of copper, the impurities in the electrolyte, particularly As, Sb and Bi, will reduce the quality of the cathode copper. Therefore the concentration of Bi and Sb is generally maintained at 0.3-0.5 g/l and As at 0.5-10 g/l [1, 2]. To maintain these impurity levels, a portion of the electrolyte is bled continuously to a purification circuit where both the copper and impurities are co-deposited as a mixed cathode. This conventional process has several disadvantages, such as the potential risk of evolution of toxic arsine gas and recycling of the impurities in the process.

The application of solvent-extraction and ion-exchange techniques for the selective removal of As, Sb and Bi from copper electrolyte has been recently reviewed along with descriptions of plant operations [2, 3]. The solvent extraction of arsenic with tributylphosphate (TBP) is well documented [4] and employed at several refineries for electrolyte purification, such as MHO Hoboken Refinery in Belgium [5 - 7].

Studies on the use of organophosphorus reagents for the extraction of impurities from copper electrolytes have revealed several trends [8]. Arsenic was extracted best by dibutylbutylphosphate (DBBP) followed by DPPP and TBP. Sb and Bi were extracted with an equimolar mixture of mono(2-ethylhexyl)phosphoric acid (M2EHPA) and di(2-ethylhexyl)-phosphoric acid (DEHPA). The use of Cyanex 923 for the extraction of As and the mineral acids has been studied [9, 10]. Another study showed that 1.6 g/l As and 0.15 g/l Sb could be loaded by 50% v/v Cyanex 923, and that Bi was quantitatively extracted [11]. These studies were performed on a synthetic copper electrolyte and in tests by the authors using actual electrolyte, indications were that Bi extraction performance was different from that reported [12].

In the present study, a number of extractants were screened for electrolyte purification. Of those tested, Cyanex 923 was found to be the most promising and a stronger extractant than TBP. The parameters studied in further extraction tests with Cyanex 923, were aqueous acidities, concentrations of chloride ion and extractant, and contact time.

## EXPERIMENTAL

### Reagents

Aqueous solutions used were copper electrolytes obtained from operating Chinese refineries. For tests where acid concentration was varied, either water or concentrated sulphuric acid was added to the electrolyte. Chloride was added where required.

The extractants, Cyanex 923 (mixture of straight chain alkylated phosphine oxides) and Cyanex 925 (mixture of branched chain alkylated phosphine oxides), were supplied by Cytec Industries Co. TBP, DEHPA, mono-alkylphosphoric acid (P538), and a primary amine (N1923) were obtained from domestic chemical plants. N1923 was converted into the sulphate form. Kerosene was used as diluent.

### Extraction and Analytical Procedures

All the batch experiments were conducted by equilibrating measured volumes of the feed and organic solutions in separation funnels and shaking for 1-10 min at room temperature. Aqueous solutions were analyzed by atomic absorption spectrophotometry (AAS) using a Perkin-Elmer model TC5100 instrument or inductively coupled plasma atomic emission spectrometry (ICP-AES) using a Perkin-Elmer model Optima 3000 instrument. The metal contents in the loaded organic phases were determined by mass balance. The absorption with activated carbon was performed by adding a measured portion of activated carbon into the copper electrolyte (2-3 g powder carbon/liter of solution) and stirring for an hour. The total organic content in solution was analyzed as previously described [12].

## RESULTS AND DISCUSSION

### Extraction of As, Sb and Bi with Various Solvents

Neutral organophosphorus reagents (TBP, Cyanex 923 and Cyanex 925); acidic organophosphorus reagents (P538 and DEHPA); primary amine reagent (N1923) and their binary mixtures were compared in extraction tests. The results are summarized in Table 1.

*Table 1. Extraction of As, Sb and Bi with various solvents.*

Aqueous: As 3.50 g/l, Sb 0.21 g/l, Bi 1.20 g/l and H<sub>2</sub>SO<sub>4</sub> 190.1 g/l.  
Phase contact: 5 min at O/A = 1.

Solvent Composition v/v	% Extraction		
	As	Sb	Bi
50% TBP	10.28	0.00	0.00
50% Cyanex 923	70.00	50.48	23.33
50% Cyanex 925	46.28	22.86	7.50
50% P538	0.00	47.62	15.00
10% N1923	0.00	14.28	76.67
40% TBP - 10% DEHPA	32.26	0.40	0.00
37.5 Cyanex 923 - 1.5% DEHPA	58.00	28.57	17.50
25% Cyanex 923 - 3% DEHPA	48.57	19.05	13.33
33% Cyanex 923 - 6.7% P538	46.57	42.86	26.67
16.7% Cyanex 923 - 13.3% P538	13.14	47.62	22.50
37.5% Cyanex 923 - 12.5% TBP	61.43	9.52	11.67
25% Cyanex 923 - 25% TBP	53.42	19.05	8.31
12.5% Cyanex 923 - 37.5% TBP	36.86	4.76	3.33
5% N1923-25% Cyanex 923	56.86	14.28	12.50

For the three neutral organophosphorus reagents, the extraction performance decreases in the order: Cyanex 923 > Cyanex 925 > TBP. Of the other extractants or mixtures tested, no better extraction of As, Sb and Bi was demonstrated.

A more extensive study on the extraction of As, Sb and Bi by Cyanex 923 for different sulphuric acid and chloride concentrations was then undertaken.

### Effect of Sulphuric Acid Concentration

The results of the extraction of impurity elements for different concentrations of sulphuric acid are shown in Figure 1. The extraction of As, Sb and Bi is shown to first increase with increasing sulphuric acid concentration and then to decrease. The observed decrease is due to the competitive extraction of sulphuric acid by Cyanex 923. It has been shown that the extraction of sulphuric acid increases with increasing acid concentration and that 30 g/l sulphuric acid is loaded at an aqueous acidity of 200 g/l  $H_2SO_4$ .

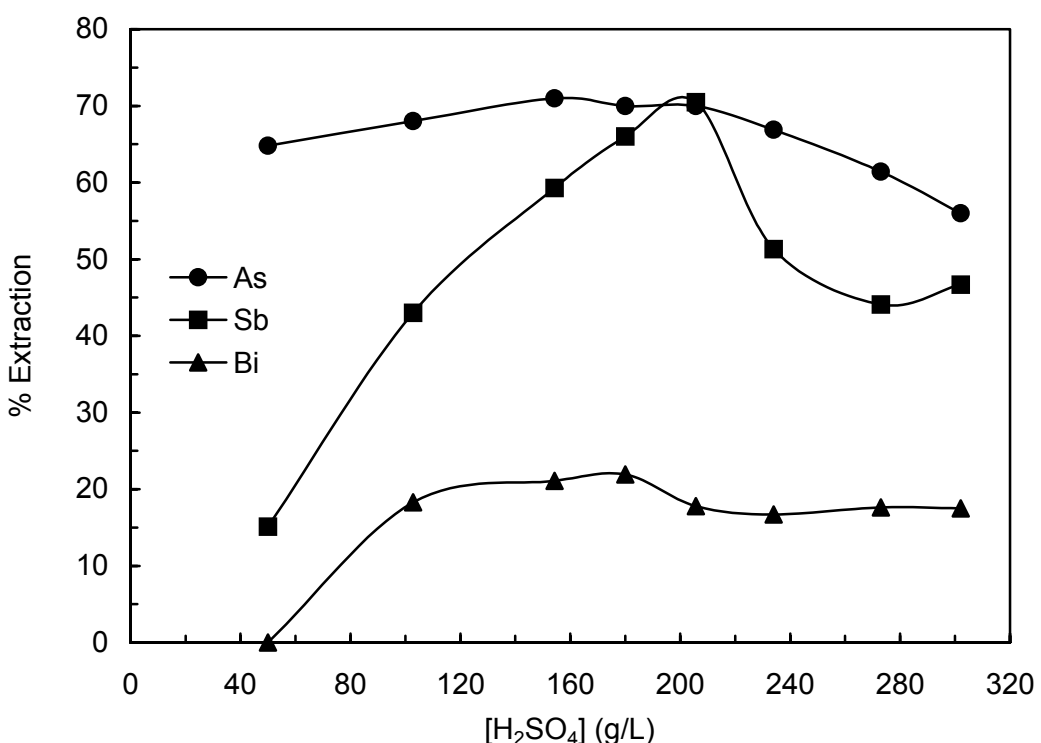


Figure 1. Extraction of As, Sb and Bi at different aqueous acidities.  
Organic phase: 50% v/v Cyanex 923; aqueous phase: As 3.50 g/l, Sb 0.21 g/l, Bi 1.20 g/l.

### Effect of Chloride Ion Concentration

As shown in Figure 2, the chloride has a significant impact on the extraction of Bi and Sb. For all the chloride ion concentrations studied Bi was extracted well, while Sb extraction improved at higher concentrations. Arsenic extraction was less affected, ranging from 50 to 60%. The aqueous chloride ion concentrations before and after the extraction were analyzed and are shown in Table 2.

Table 2. Aqueous chloride ion concentrations before and after extraction.

Sample No.	$[Cl^-]_{feed}$ (g/l)	$[Cl^-]_{raffinate}$ (g/l)
1	0.34	0.14
2	0.51	0.18
3	0.89	0.41

After the extraction, 50-60% of chloride ion in the aqueous phase was loaded into the organic phase. This result indicates that Bi and Sb are extracted in the form of chloride complexes.

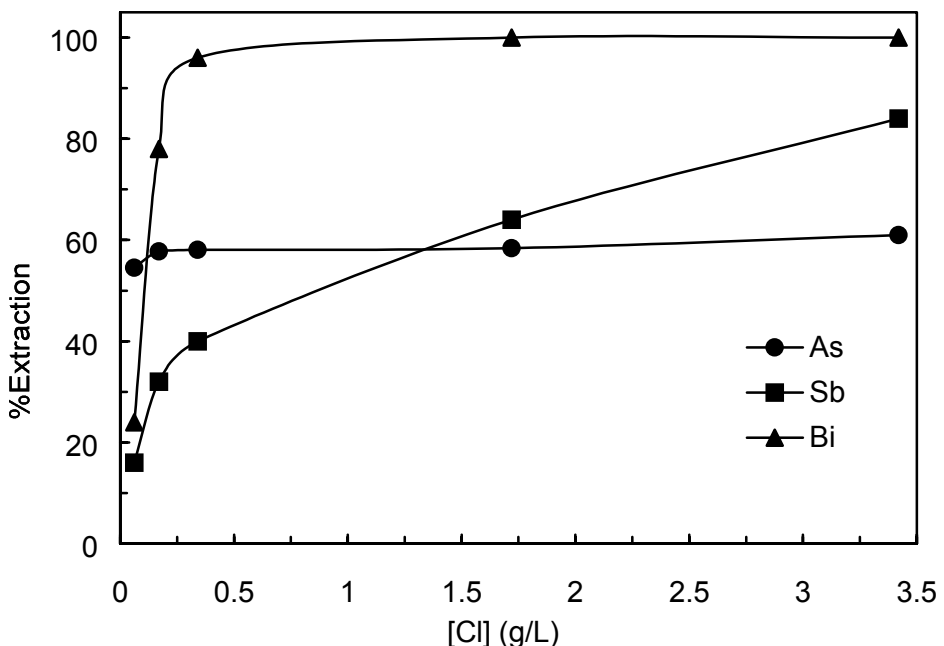


*Figure 2. Extraction of As, Sb and Bi at different chloride ion concentrations.*

Organic phase: 50% v/v Cyanex 923; aqueous phase: As 3.10 g/l, Sb 0.25 g/l, Bi 0.50 g/l and H<sub>2</sub>SO<sub>4</sub> 190.1 g/l. Phase ratio: O/A=1.

### Effect of Contact Time and Extractant Concentration

For the following tests, the chloride concentration in the copper electrolyte was adjusted to 0.4 g/l, and the extraction of As, Sb and Bi was studied as functions of contact time and extractant concentration.

The variation of contact time between 2-10 minutes had no effect on the extraction of arsenic, antimony and bismuth. 56% As, 21% Sb and 98% Bi can be extracted within 1 min and no further increase is observed with time. Therefore, extraction equilibrium is reached quickly.

Extraction of impurity elements increases with increasing extractant concentration, with 55.8% As, 28.0% Sb and 100% Bi extracted by 50% v/v Cyanex 923.

### Loading of As, Sb, Bi, Cu, H<sub>2</sub>SO<sub>4</sub> and Chloride ion onto Cyanex 923

In these repeated loading tests equal volumes of the organic phase and copper electrolyte were first contacted and after equilibrium had been reached, the loaded organic phase was re-contacted with a further sample of fresh electrolyte for subsequent loading cycles. Extraction results are shown in Figure 3.

In the repeated loading cycles, Bi is very strongly extracted, with 90% of the Bi in the electrolyte being extracted even at the tenth cycle. Cyanex 923, thus, has a very high bismuth loading capacity. As and Sb extraction decrease significantly with increasing cycles and neither are extracted at the end of the tenth cycle. Between 50~70% of the chloride ion can be extracted into the organic phase, which may correspond mainly to the extraction of bismuth. However, copper is not extracted in the test cycles. Nearly 30 g/l of sulphuric acid is extracted in the first cycle and then rapidly decreases to zero. At the end of the test, As, Bi, Sb and chloride in the organic phase amounted to 4.09 g/l, 3.70 g/l, 0.12 g/l and 2.56 g/l, respectively. The co-extracted sulphuric acid could be scrubbed with water.

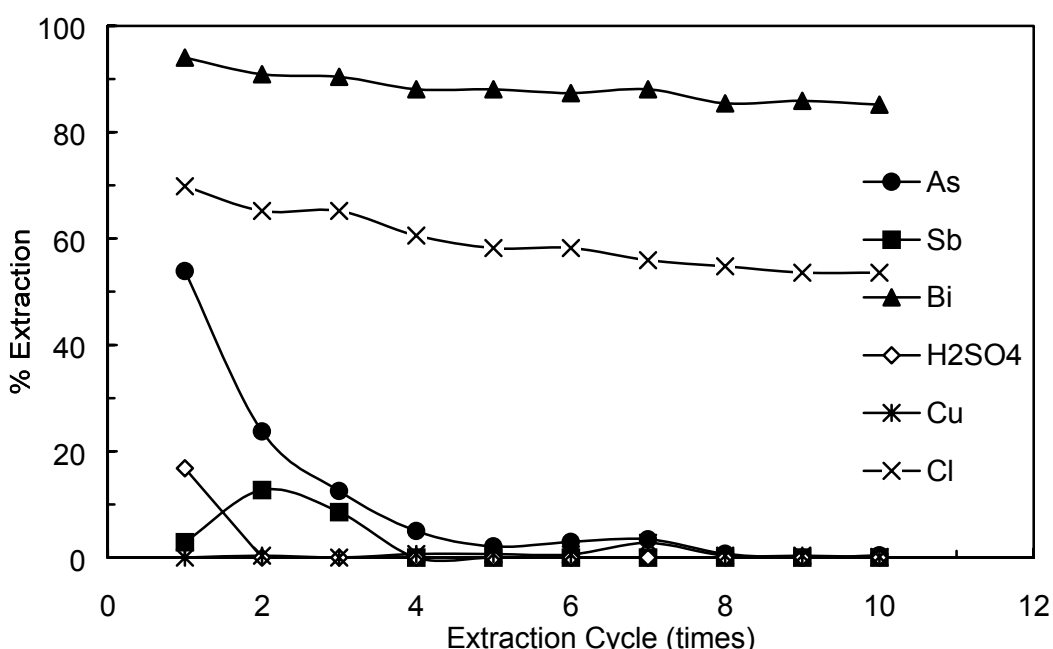


Figure 3. Loading of As, Sb, Bi, Cu, H<sub>2</sub>SO<sub>4</sub> and chloride ion onto Cyanex 923.

Organic phase: 50% v/v Cyanex 923; aqueous phase: As 3.91 g/l, Sb 0.48 g/l, Bi 0.42 g/l, H<sub>2</sub>SO<sub>4</sub> 177.1 g/l and 0.43 g/l Cl.

#### Absorption of Organic, As and Sb in the Raffinate using Activated Carbon

Organic phase from soluble loss or entrainment present in the raffinate after extraction would cause organic burn or cathode surface roughening when returned to the copper electrorefining circuit. The removal of organic from typical raffinate was therefore examined using activated carbon and the results, together with those for As and Sb adsorption, are shown in Table 3.

Table 3. Absorption of organic phase, As and Sb by activated carbon.

Raffinate: As 1.6~2.3 g/l, Sb 0.34~0.48 g/l, total organic phase content 200~410 mg/l.

Test No.	Organic phase content (mg/l)		% Absorption	
	Before absorption	After absorption	As	Sb
R-A-1	411	7.3	13.63	48.87
R-A-2	350	6.5	11.84	48.42
R-A-3	281	2.4	10.05	50.33
R-A-4	220	5.6	13.38	61.24
R-A-5	208	4.0	8.35	55.50

Most of the organic phase can be removed by carbon absorption. The residual solvent level in the treated electrolyte is less than 5 to 7 mg/l, which will not cause deterioration of copper deposit quality [1]. It is also found that arsenic (8 - 13%) and antimony (40 - 60%) could be further removed by absorption on activated carbon. This may be attributed to the absorption of fine slimes (mainly the mixed oxides of arsenic and antimony) from the electrolyte.

#### Stripping of As, Sb and Bi from the Loaded Organic Phase

Water can be used to strip arsenic from the loaded organic phase, with 50% of the As stripped in one stage. However, Sb and Bi are difficult to strip. Reagents including: sodium sulphide, sodium thiosulphate, sulphourea, sodium tartrate, sodium citrate, ethylene diamine tetraacetic acid disodium salt, and sodium oxalate were tested [12]. Sodium tartrate was shown to be the most effective stripping agent, especially for Bi.

Stripping for different sodium tartrate concentrations showed that the stripping of As, Sb and Bi improved with increasing sodium tartrate concentration. Using 80 g/l sodium tartrate solution, 70.9% As, 80.0% Sb and 83.3% Bi can be stripped in one stage.

### Regeneration of Stripping Reagent

The stripping reagent can be regenerated in a two-step process: (1) precipitation of As, Sb and Bi using 30 g/l sodium sulphide, followed by filtration; and (2) pH adjustment of the filtrate using solid sodium hydroxide, pH adjustment to 7-8.

In tests where the regenerated stripping reagent was re-used three times the results indicated that the stripping of As, Sb and Bi using regenerated reagent decreased slightly, but was comparable to that using fresh reagent.

### CONCLUSIONS

Cyanex 923 has been shown to be an effective extractant for removing As, Sb and Bi from actual copper electrolyte. Cyanex 923 has a high bismuth loading capacity when a small portion of hydrochloric acid is added to the electrolyte. The application of this solvent-extraction technology for copper electrolyte purification with Cyanex 923 has resulted in a Chinese patent [13]. The process involves the adjustment of chloride concentration in the copper electrolyte to 0.4-0.6 g/l with 36.5% hydrochloric acid, then three stages of extraction with 50% v/v Cyanex 923; two stages of scrubbing with water; and two stages of stripping with 80 g/l sodium tartrate, followed with absorption of raffinate using activated carbon powder, and regeneration of stripping agent using 30 g/l sodium sulphide.

This process can remove 80% As, 95% Bi and 40%-60% Sb from a copper electrolyte solution and thus can be considered as a supplement to copper plants, especially those whose bismuth and antimony content in the electrolyte is high.

### REFERENCES

1. A. K. Biswas and W. G. Davenport (1976), Extractive Metallurgy of Copper, Pergamon Press, Oxford, pp. 291-331.
2. J. Szymowski (1998), *Miner. Proc. Extr. Metall. Rev.*, **18**, 389-418.
3. T. Nagai (1997), *Miner. Proc. Extr. Metall. Rev.*, **17**, 143-168.
4. M. Cox (1992), Principles and Practice of Solvent Extraction, J. Rydberg, G. R. Choppin and C. Musikas (eds.), Marcel Dekker Inc., New York, pp. 357-412.
5. A. De Schepper (1985), *Proc. Extraction Metallurgy*, London, pp. 167-188.
6. O. Kane, J. Middlin, B. Royston (1985), *Proc. Extraction Metallurgy*, London, pp. 951-965.
7. J. Yang, D. Liu, H. Zhan and K. Jiang (1992), *Proc. Int. Conf. Solvent Extraction*, Vol. B, Amsterdam, pp. 1205-1210.
8. D. B. Dreisinger, B. J. Y. Leong, B. J. Balint and B. H. Byyard (1993), *Proc. Int. Conf. Solvent Extraction*, Vol. 3, York, U. K., pp. 1271-1278.
9. M. Wisniewski (1997), *Hydrometallurgy*, **46**, 235-241.
10. F. J. Alguacil and F. A. Lopez (1996), *Hydrometallurgy*, **42**, 245-255.
11. W. A. Rickelton (1993), *Proc. Int. Conf. Solvent Extraction*, Vol. 3, York, U. K., pp. 731.
12. C. Wang and K. Jiang (1998), *BGRIMM Research Report*, No. KY-03-328, Beijing, pp. 11-13 pp.
13. C. Wang, K. Jiang, D. Liu and H. Wang (2000), *Chinese Pat.*, CN1297067A (May 30).



## EXTENDING ZINC PRODUCTION POSSIBILITIES THROUGH SOLVENT EXTRACTION

D. Martín, G. Díaz, M.A. García and F. Sánchez

Técnicas Reunidas. R&D División, Madrid, Spain

The Modified ZINCEX® Process, developed by Técnicas Reunidas, is highly flexible dealing with a wide range of pregnant leach solutions. No matter if those solutions are produced from primary or secondary raw materials, and/or are based on conventional leaching, pressure leaching, heap leaching or bio leaching the result is always high-purity zinc product. The zinc solvent extraction unit within the process is a very effective barrier for impurities and a buffer for the composition of the pregnant liquor. This unit achieves an extremely pure aqueous extract that can be converted into different final products. All of them are characterised by fulfilling the highest purity standards. Also, there is the possibility to adapt the global process to a wide range of pregnant liquor compositions and various production capacities up to a zinc production limit over 150000 t/a with a single solvent extraction plant.

### INTRODUCTION

Traditionally zinc production from zinc sulphide concentrates is based on the roasting, leaching and electrowinning (RLE) process [1]. The concentrates containing around 50% Zn as zinc sulphide and about 30% sulphur are roasted to give zinc oxide calcine. The gaseous SO<sub>2</sub> outlet requires an annexed sulphuric acid plant. Zinc oxide calcines are leached with sulphuric acid solution generating a pregnant leach solution (PLS). In this process there is one single circuit between leaching and electrowinning (EW), therefore a high grade PLS is required and successful EW must carefully control impurities removal stages to avoid impurities passing to the pregnant electrolyte to achieve a high-grade zinc product.

Técnicas Reunidas, S.A. (TR) has developed, at commercial level, the “Modified ZINCEX® Process” (MZP) where the solvent extraction (SX) unit behaves as a very effective barrier for impurities and a buffer for changes in the composition of the PLS. In this way not only zinc concentrates, but different raw materials can be processed to produce special high-grade (SHG) zinc or other zinc compounds.

### THE MODIFIED ZINCEX® PROCESS DESCRIPTION

The former ZINCEX® process [2, 3] was developed by TR in Spain and first introduced in commercial operation at the 8,000 t/a MQN plant in Bilbao (Spain) in 1976. The MQN plant treats secondary zinc materials and after proven success, another ZINCEX® plant with a capacity of 11,500 t/a was built in 1980 for Quimigal at Lisbon (Portugal). This plant treats high-chloride leach liquors from various sources.

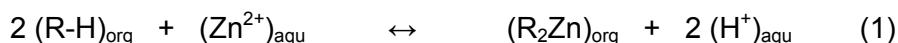
The Modified ZINCEX® Process [4-6] is a further developed and simplified version of the ZINCEX® Process, specifically adapted to treat solid oxidised materials or impure sulphate solutions. In 1997 a plant near Barcelona, Spain, was commissioned to recover zinc from 2,800 t/a of spent zinc batteries containing mercury and manganese as the main impurities [9].

ZINCEX® processes have the ability to treat primary and/or secondary zinc materials [10-13] for the recovery of zinc in circumstances where significant amounts of impurities are present. Solvent extraction is the key step used to concentrate and purify the zinc solution, which is then available for a number of products. Whilst the product can be slab zinc, it is equally possible to produce pure zinc sulphate and zinc oxide. In Table 1 flexibility and versatility of the MZP is briefly described.

*Table 1. Flexibility & versatility of the Modified Zincex® Process.*

<b>PLS SOURCES</b>	<ul style="list-style-type: none"> <li>➤ Primary ores (acid leaching, pressure leaching, bio-leaching, heap-leaching, etc)</li> <li>➤ Secondary raw materials (EAFD, Waelz oxides, galvanisation ashes, tyre ashes, spent batteries, etc.)</li> </ul>
<b>COMPOSITION RANGE</b>	<ul style="list-style-type: none"> <li>➤ Zn: 5 or less to 160 g/l</li> <li>➤ Metallic Impurities: Cu, Cd, Co, Ni, As, Sb, etc. (g/l levels)</li> <li>➤ Anionic impurities: Cl, F, etc (g/l levels)</li> <li>➤ Alkali and Alkali earth: Ca, Mg, Na, K, etc. (g/l levels)</li> </ul>
<b>MEDIA</b>	<ul style="list-style-type: none"> <li>➤ Sulphate</li> <li>➤ Chloride</li> <li>➤ Others</li> </ul>
<b>PRODUCTS</b>	<ul style="list-style-type: none"> <li>➤ Zn<sup>0</sup> SHG (by electrowinning)</li> <li>➤ ZnSO<sub>4</sub> X H<sub>2</sub>O ultra pure (by crystallisation)</li> <li>➤ ZnO ultra pure (by precipitation/calculations), other Zn salts and solutions</li> </ul>
<b>OPERATION FLEXIBILITY</b>	<ul style="list-style-type: none"> <li>➤ All production capacity</li> <li>➤ No shut down problems &amp; Buffer for perturbances</li> <li>➤ Suitability for other process (installed or not) combination</li> </ul>

A conceptual block diagram for the Modified ZINCEX® process SX section, applied to different PLS to generate a zinc solution able to produce the desirable product, is shown in Figure 1. The process steps included in the MZP are extraction, washing, and stripping and organic phase regeneration. A solution of di-2-ethylhexyl phosphoric acid (DEHPA) as extractant reagent in kerosene base is used as the organic phase. This organic phase (RH) has a high affinity to extract the zinc at MZP conditions according to the reaction.



Due to the process conditions applied by TR, impurities such as Co, Ni, Cd, Mg, Mn, Ca, etc. are not allowed to pass to the next process step. Under these conditions, the selectivity of the organic for the zinc is extremely high. Besides, in the washing stage the aqueous entrainment and the last residual co-extracted impurities are physically and chemically removed from the organic extract. Finally, in the stripping stage, an ultra-pure zinc sulphate solution is produced, able to be processed into the appropriate zinc compound (SHG-Zinc,

$\text{ZnSO}_4$ ,  $\text{ZnO}$ ). Additionally a bleed of the organic phase is treated with HCl solution, in the regeneration stage, to avoid the build up of co-extracted impurities (such as Fe) that are not stripped. A comparative diagram for impurities behaviour is presented in Figure 2, as a summary of the MZP ability to deal with any kind of zinc PLS to generate a commercial zinc product.

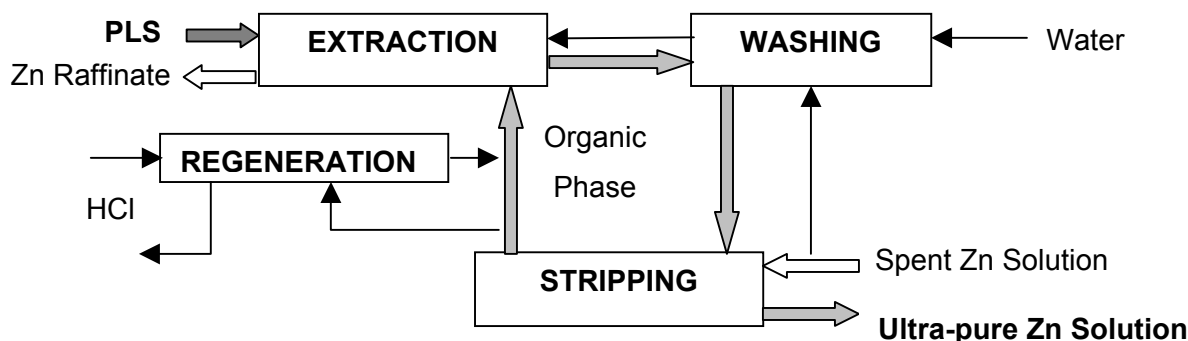


Figure 1. MZP: Conceptual scheme of solvent extraction section.

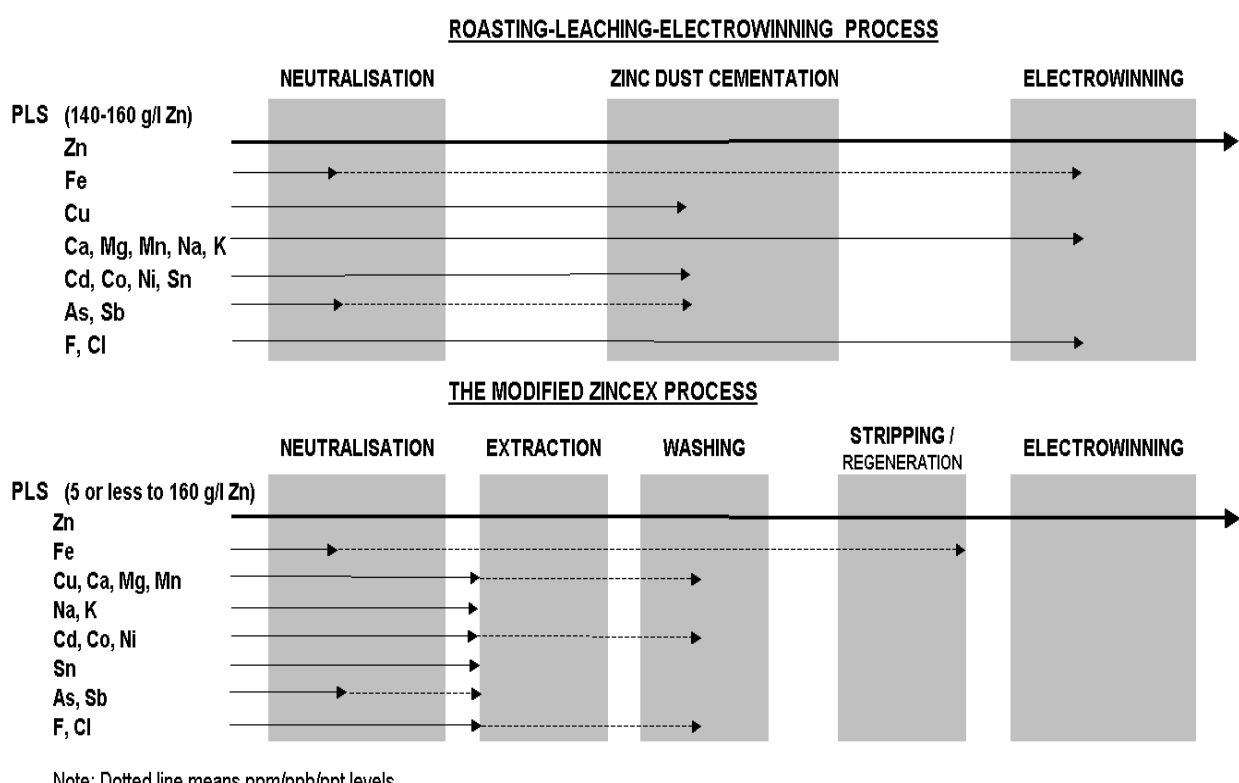


Figure 2. Comparison between RLE and MZP. Concentrations and impurities.

As can be observed Figure 2, and because of the physical and chemical separation between the PLS and the electrolyte, SX is a more effective barrier to impurities than the conventional RLE process. This is true for both steady and disturbed operation.

## RANGE OF APPLICATIONS FOR MODIFIED ZINCEX PROCESS

PLS quality and zinc product could be taken to define the range of application for MZP. Several experimental investigations and industrial plant projects performed during the last 25 years have demonstrated the viability of the MZP to treat any PLS (see Table 2).

### Zinc Concentration in PLS

#### **Low zinc concentration in PLS**

To date many primary zinc ores have not been treated due to their low zinc content that does not allow processing by the traditional RLE process. With the MZP [11-15] it is possible to treat these raw materials because the MZP solvent extraction circuit will produce an electrolyte that can be processed in any EW tankhouse. A general application is shown in Figure 3, where a zinc oxide ore is treated by means of the proper leaching process, producing a PLS zinc concentration between 5-50 g/l Zn and Cu, Cd, Co, Ni, Fe, Ca and Mg as impurities, independent of the source.

Table 2. Typical selected cases of PLS composition (g/l) fed to MZP SX section.

PRIMARY	Zn	Main Impurities	Project Case
Oxidised ores from acid leaching	30	Cd, Cu, Ni, Co, Cl, F, Mg	Skorpion
Sulphides ores from Bio leaching	120	Cd, Cu, Cl, F, Mg	Confidential
Sulphide ores from Bio + Acid leaching	50	Cd, Cu, Ni, Co, Cl, F, Mg	Confidential
Sulphide ores from Indirect bio-leaching	10	Cd, Cu, Ni, Co, Mg	RTM, S.A.
Sulphide ores from Pressure leaching	150	Cd, Cu, Ni, Co, Cl, Mg	Confidential
SECONDARY	Zn	Main Impurities	Project Case
EAFD from acid leaching	25	Cd, Cu, Cl	Elansa
Cu SX PLS Bleed from heap leaching	33	Cu, Ni, Co, Cl, Mg	Sanyati
Spent domestic batteries from acid leaching	20	Cd, Cu, Ni, Cl	Proces
Waelz O./Galv. Ashes from acid leaching	32	Cd, Cu, Ni, Co, Cl, F	Comm. of EU

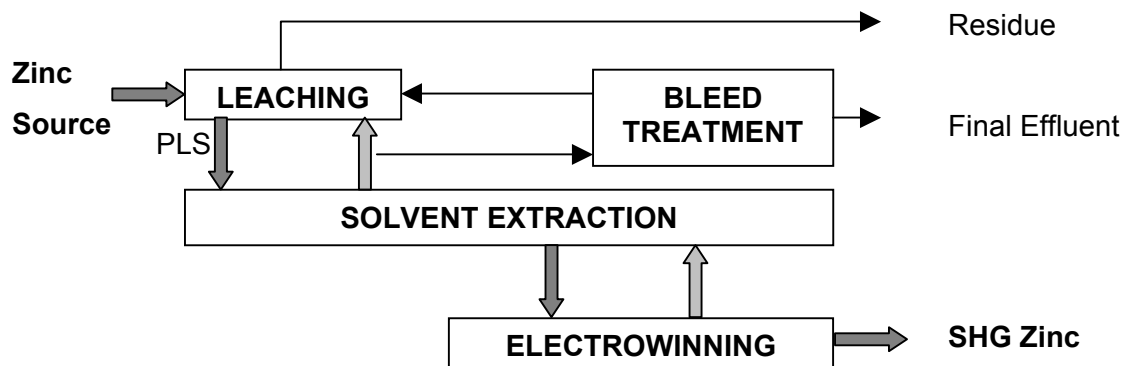


Figure 3. MZP applied on primary & secondary zinc materials.

A bleed of the raffinate is treated in a bleed-treatment unit, in order to avoid impurities building up in the system, and to then allow the EW unit to produce SHG zinc from the electrolyte.

### **High zinc concentration in PLS**

Some zinc ore treatments (pressure, heap and bio leaching) are capable of producing high zinc concentrated PLS. In this way the associated impurity levels are too high and present difficulties for the traditional process route. Thus the benefits due to the reduction in equipment sizes in the leaching unit can be impaired by a major complexity in the purification unit. The use of the MZP for this PLS is technically and economically viable. Figure 4 shows an example of processing by bio leaching. In the bio-leaching unit a PLS with 120 g/l Zn is produced and impurities such as Cu, Fe, Co, Ni, Cd, Ca, Mg are present in high levels. The SX unit, in the MZP conditions, produces an electrolyte without impurities that can be processed by EW to obtain SHG zinc ingots.

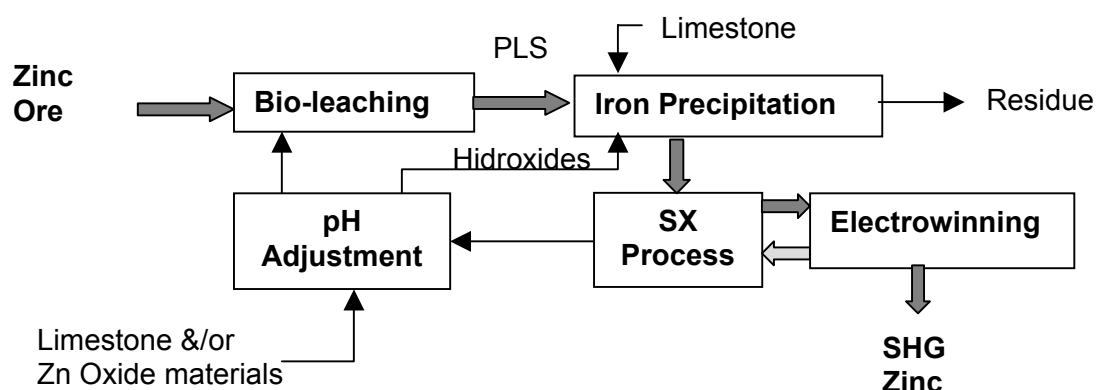


Figure 4. Example of MZP applied to zinc sulphide ores.

### **Impurities in PLS**

Primary and secondary zinc raw materials contain different impurities that produce a negative effect in the traditional RLE zinc processing. These impurities are Sb, As, Cl, Co, Cu, F, Ge, Ni, Fe, Se, Te, Hg, Sn, Mn, Ca, K and Mg and the effect is produced mainly during the EW stage. While some of them are difficult to remove by cementation using RLE conventional process, others cannot be avoided (Cl, F, Mg, etc.) or make operation difficulties (Ca, Mn, etc.). The MZP is not conditioned by this fact, as these impurities are not allowed to pass to the electrolyte. It is possible to find two kinds of contaminated PLS, a lot of impurity compounds in the PLS and a high concentration of impurities of some of them. Typical examples for these types of PLS are described below.

### **Variety of impurities**

Secondary zinc sources such as Electric Arc Furnace Dust (EAFD), Waelz Oxides, Galvanizing A, Tyre Ashes, Spent Batteries, etc. are becoming, nowadays, more a zinc source than a residue. MZP applied on these raw materials [4-10] has been demonstrated to be a viable solution to recover the zinc content. The MZP copes with the negative effect of the impurities being a fully effective barrier.

Electric Arc Furnace Dust (EADF) can be processed by MZP (Figure 3) and this treatment has been successfully tested [6, 7]. Technical, environmental and economical feasibility has always been proven through several studies at all levels. PLS contain 30 g/l Zn, 25 g/l Cl, 0.9 g/l Cu, and produces an electrolyte with 90 g/l Zn suitable to produce SHG Zinc by EW process.

### **High concentration of impurities**

Hydrometallurgical processing of metals, such as Cu, Ni, etc. can require a bleed to avoid build up of impurities such as Zn. This results in losses of the desirable metal as well as the zinc content is not valued anymore. A profitable solution to avoid this is the use of MZP to recover the zinc content in the bleed that is a Zn PLS and at the same time returning a solution able to be recycled to the main process. In this way the value of the zinc is realized and the desirable metal is not lost from the PLS. The high level of impurities (for Zn processing) is not a problem for MZP while other processes to remove zinc from this impure solution means high costs and reagent consumption and without any zinc valorisation.

Application of the process on a Cu PLS in a conventional leaching, SX, and EW circuit is shown in Figure 5. The feasibility of treating PLS containing 1-2 g/l Cu, 16 g/l Mn, 33 g/l Zn, 0.5 g/l Co, 2.4 g/l Mg, 0.1 g/l Ca, etc. has been demonstrated by Técnicas Reunidas.

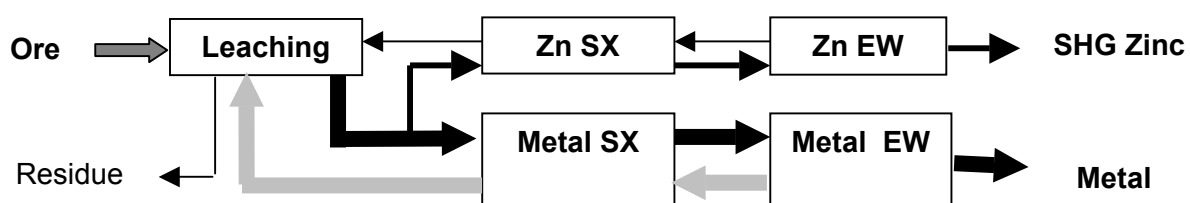


Figure 5. MZP applied on PLS bleeds of other metals production.

### **Zinc Product Alternatives**

MZP has the flexibility to produce zinc solutions able to be converted to any desired zinc product. This is possible due to the SX circuit that can be designed for every operation specifically to reach the desired zinc solution quality. Figure 6 shows a case of zinc sulphate salt production using MZP.

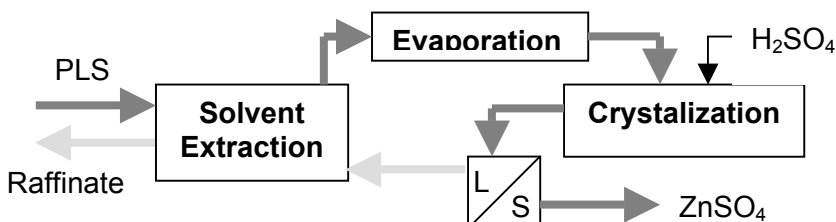


Figure 6. Zinc Sulphate production from MZP.

In Figure 7 we can see different alternatives for MZP applications regarding the zinc product.

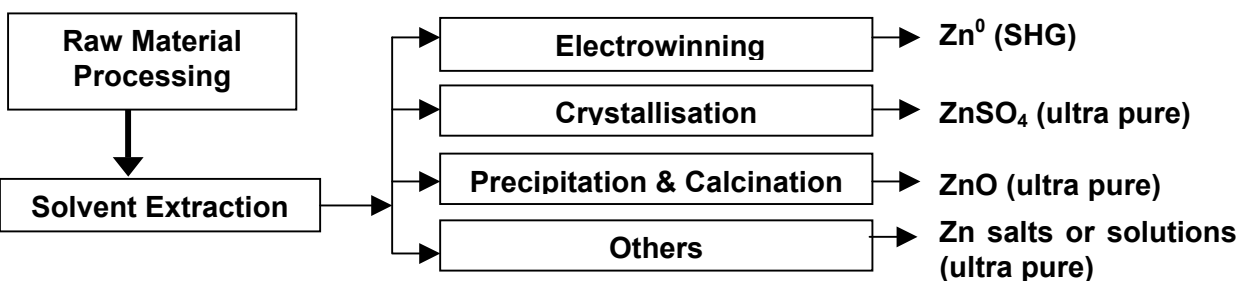


Figure 7. MZP zinc product alternatives.

## CONCLUSIONS

In conclusion the statement can be made that the viability of the Modified Zinced® Process to deal with any kind of PLS and to produce different zinc products has been demonstrated. Irrespective of the raw material source, the zinc content in the PLS and the variety and quantity of impurities present, the MZP is the most suitable, efficient and reliable application. In this process the Solvent Extraction stage, using appropriate operation conditions, is able to produce ultra-pure zinc solutions that can be processed to obtain the desired final zinc product.

## REFERENCES

1. C.B. Hill (1980), Nonferrous Extractive Metallurgy, John Wiley & Sons.
2. E.D. Nogueira, J.M. Regife and P.M. Blythe (1980), *Chem. Ind.*, (2) 19, 63-67.
3. E.D. Nogueira, J.M. Regife and M.P. Viegas (1982), *111<sup>th</sup> AIME Annual Meeting*, Dallas, Texas, pp. 59-76.
4. D. Martín, J.M. Regife and E.D. Nogueira (1983), *U. S. Pat.*, No. 4401531.
5. E.D. Nogueira, J.M. Regife, D. Martín and G. Díaz (1985), Zinc' 85. International Symposium on Extractive Metallurgy of Zinc, Tokyo, Japan, pp. 763-781.
6. G. Díaz and D. Martín (1992), *3<sup>rd</sup> European East-West Conference on Materials. Symposium E: Recycling of Materials in Industry*, Strasbourg (France), pp. 43-57.
7. G. Díaz, D. Martín and C. Lombera (1992), *4th European Electric Steel Congress*. Madrid, Spain, pp. 511-517.
8. G. Díaz, D. Martín and C. Lombera (1995), *3<sup>rd</sup> International Symposium on Recycling of Metals and Engineering Materials*, Alabama, USA, pp. 623-635.
9. D. Martín, M.A. García, G. Díaz and J. Falgueras (1999), *ISEC'99 – Solvent Extraction for the 21<sup>st</sup> Century*, Barcelona, Spain, pp. 353-361.
10. D. Martín, J. Falgueras and M. A. García (1997), *Spanish Pat.*, No. P9701296.
11. M.A. García, A. Mejías, D. Martín and G. Díaz (2000), Lead-Zinc 2000 Symposium, Pittsburg, PA, pp. 751-762.
12. D. Martín, M.A. García and G. Díaz (2001), *International Symposium on Recycling and Reuse of Used Tyres*, Dundee, UK, pp. 141-148.
13. D. Martín, G. Díaz and M.A. García (1999), *Spanish Pat.*, No. P9902777.
14. D. Martín, G. Díaz and M.A. García (1999), *Namibian Pat.*, No. P/00/78248.
15. D. Martín, G. Díaz and M.A. García (2001), *Pat.*, No. PCT/ES01/00060.



## EFFECT OF TBP AS A MODIFIER FOR EXTRACTION OF ZINC AND CADMIUM WITH A MIXTURE OF DEHPA AND MEHPA

E. Keshavarz Alamdari, D. Darvishi, S. K. Sadrnezhaad\*, Z. Mos'hefi Shabestari,  
A. O'hadizadeh and M. Akbari

Dept. Mining and Metallurgical Engineering, Amirkabir University of Technology, Tehran, Iran

\* Dept. Materials Science and Engineering, Sharif University of Technology, Tehran, Iran

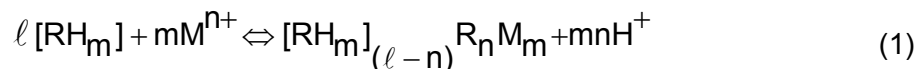
The simultaneous extraction of zinc and cadmium by a mixture of di(2-ethylhexyl)phosphoric acid (DEHPA) and mono-2-ethylhexylphosphoric acid (MEHPA) in the presence of tri-*n*-butylphosphate (TBP) as a modifier was investigated. The effects of temperature, pH and TBP concentration on extraction of zinc and cadmium were determined. It was shown that the extraction reaction for zinc is endothermic, while that for cadmium is exothermic. An increase in the TBP concentration caused greater synergistic shifts than when TBP was not dissolved in the organic phase. Separate formulae were deduced from the experimental data for the distribution factors of both zinc and cadmium.

### INTRODUCTION

Zinc and cadmium usually occur together in the nature. During leaching of low-grade ores, zinc and cadmium dissolve simultaneously into the leach liquor. The level of impurities in the electrolyte is generally high. The purification process is, therefore, very necessary, especially if production of ultra-high purity (UHP) zinc or cadmium is required.

Cadmium is one of the most toxic constituents of industrial wastes and effluents. It should, therefore, be totally removed from wastes and effluents before disposal to the outdoor environment [1]. Approximately half of the world's total consumption of cadmium is utilized in alkaline storage batteries. Cadmium recycling is, therefore, an important subject both economically and environmentally [2].

The method of solvent extraction may be used for selective extraction of impurities from leach liquors. The extractants can be considered as molecules that are chained together with hydrogen bonds [3]. The number of bonds depends on the acidic nature of the extractant. So  $\ell$  extractant molecules, each having  $m$  hydrogen ions, bond together to make a structure that can extract metal ions. The stoichiometric equation describing the solvent extraction process can, therefore, be written as:



where  $[RH_m]$  is an organic extractant molecule,  $[RH_m]_{(\ell-n)}$   $R_nM_m$  is the extracted metallic complex and  $H^+$  is the proton released by the organic extractant in exchange for the cationic metal species,  $M^{n+}$ . The equilibrium constant of the reaction, expressed in terms of the concentration of the reactants, can be defined as:

$$K_C = \frac{[RH_m]_{(\ell-n)} R_n M_m \cdot [H^+]^{m.n}}{[RH_m]^\ell [M^{n+}]^m} \quad (2)$$

where the concentration equilibrium constant  $K_C$  depends on temperature and concentration. Assuming the effect of concentration to be negligible, and taking logarithms of both sides of Equation (2) yields:

$$\log D = \frac{\Delta H_{app.}}{2.3 RT} + \frac{\Delta S_{app.}}{2.3 R} + m.n \text{ pH} + \ell \log [RH_m] + (m - 1) \log [M^{n+}] + \log m \quad (3)$$

in which the distribution coefficient,  $D$ , is defined as  $D = \sum[M_{org.}] / \sum[M_{aq.}]$ .

The thermodynamics of solvent extraction of some metals has recently been investigated by the same authors [4]. We report in this paper the effect of TBP as a modifier for the separation of zinc and cadmium from mixtures of DEHPA and MEHPA serving as suitable organic extractants. Coefficient factors mathematically obtained for quantifying the distribution ratio that prevails in the extraction system are also reported.

## EXPERIMENTAL METHODS AND MATERIALS

Organic phases containing 12% DEHPA and 8% MEHPA as extractant plus 0%, 2.5%, 5% and 10% TBP as modifier were prepared by dissolving the materials into pure kerosene. Initial metals concentrations in the aqueous solution were both 5 g/l. NaOH and sulfuric acid were used for adjusting pH of the system. Around 20 ml of aqueous solution was mechanically stirred with equal volume of organic phase in a jacketed vessel for one hour. The mixture was then allowed to disengage into two separate phases. The metal content of the aqueous phase was determined by titration against a standard solution of EDTA (0.09 M) using Eriochrom Black T as the indicator. These experiments were carried out at three temperatures (25, 40 and 60°C) using a thermostatic reaction bath.

## RESULTS AND DISCUSSION

### Effect of TBP as a Modifier

Experiments were carried out to study the effect of pH on the extent of extraction and determination of the maximum recovery. Extraction curves are presented in Figure 1. It is seen that zinc extraction occurs at  $0.6 < \text{pH} < 1.7$ , while cadmium extraction occurs at  $-0.05 < \text{pH} < 1.1$ . The extraction of cadmium occurs, therefore, under more acidic conditions than that of zinc. Figure 1 also shows that addition of TBP has a small effect on the  $\text{pH}_{0.5}$  (the equilibrium pH value at which 50% extraction of metal occurs) of zinc and cadmium extraction. Other experiments have, however, shown that at higher TBP concentrations, the rate of extraction of cadmium increases more rapidly with pH.

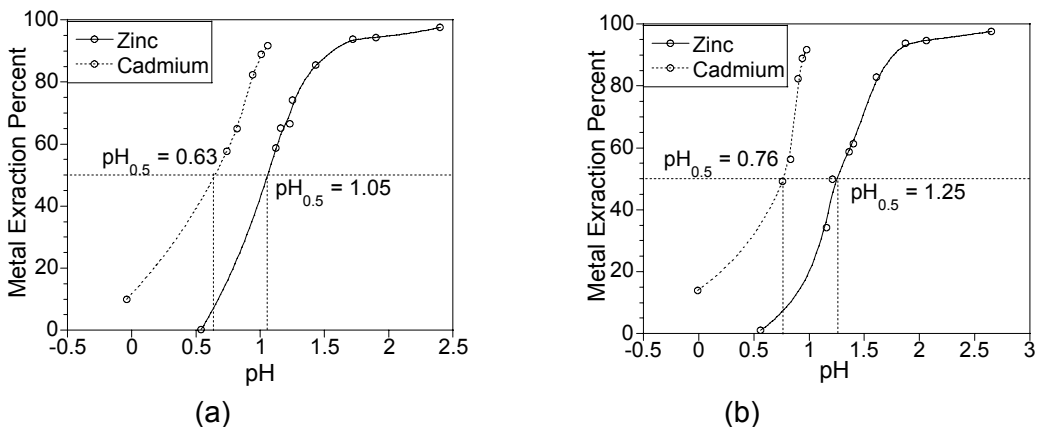


Figure 1. Extraction of zinc and cadmium at 25°C. a) 0% TBP; b) 10% TBP.

The effect of TBP on extraction of zinc and cadmium was investigated at different extractant concentrations. The extraction curves obtained show a synergistic shift to the right by increasing the relative amount of TBP with respect to the extractants (DEHPA and MEHPA). As is seen in Figure 1, the extraction percentage of cadmium and zinc varied from 0% to 90% depending on the pH and the relative amount of the organic modifier. The selectivity of the mixture can be expressed by the difference between the  $pH_{0.5}$  values of the two metals. The data obtained for  $pH_{0.5}$  and  $\Delta pH_{0.5}$  of the metals are illustrated in Table 1.

Table 1.  $pH_{0.5}$  for zinc and cadmium and  $\Delta pH_{0.5}$ .

TBP (%)	$pH_{0.5}$		$\Delta pH_{0.5}$ Zn-Cd
	Zn	Cd	
0	1.05	0.63	0.42
2.5	1.13	0.65	0.48
5	1.02	0.56	0.46
7.5	1.19	0.74	0.47
10	1.25	0.76	0.49

The values given in Table 1 show that the presence of TBP facilitates the separation of zinc from cadmium due to its  $\Delta pH_{0.5}$  enhancing effect. Figure 2 shows that at constant pH,  $\log D$  varies linearly with  $\log [TBP]$  with a slope of  $-1.00$  for zinc and  $-0.35$  for cadmium. A possible reason for this effect is that TBP, DEHPA and MEHPA molecules form hydrogen bonding with each other; hence they reduce the possibility of polymerization of DEHPA and MEHPA molecules to extract metallic ions. This causes diminution of the equivalent extraction potential and decreasing of the distribution ratio for zinc and cadmium extraction reactions. However it increases the gap between the required pH for extraction of Zn and Cd and it can, therefore, improve the selectivity of the extraction process.

As was mentioned before, the reason for synergistic shifts returns to the formation of new bonds in organic media. An equivalent organic value can, thus, be defined and the concentration of extractants can be considered as a function of TBP so that the equivalent concentration of extractant reagents can be estimated from the expressions defined for this purpose at TBP concentrations around  $[TBP]=0$ :

$$\begin{cases} [RH_m] = \sum [RH] + \sum [RH_2] = 0.66 \\ [RH_m]_{eqv} = 0.66 - a[TBP] \end{cases} \quad (4)$$

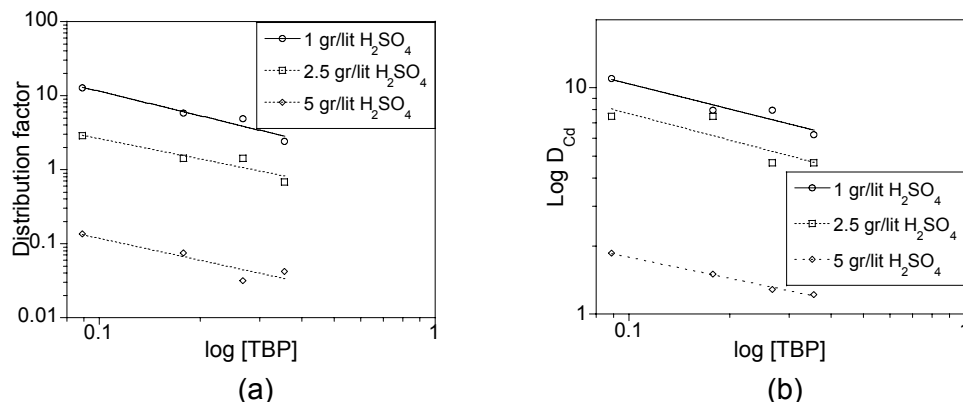


Figure 2. Variation of  $\log D$  vs.  $\log [TBP]$  at constant initial pH for a) zinc; b) cadmium.

So that:

$$\ln [RH_m] = \ln 0.66 - \frac{a[TBP]}{0.66} - \frac{a^2[TBP]^2}{2 \times 0.66^2} - \frac{a^3[TBP]^3}{3 \times 0.66^3} - \frac{a^n[TBP]^n}{n \times 0.66^n} \quad (5)$$

Substituting (6) in (3) and eliminating the terms with the order of 3 and more, one can obtain:

$$\begin{aligned} \log D = & \frac{-\Delta H_{app}}{2.3RT} + \frac{\Delta S_{app}}{2.3R} + m.n \text{pH} + \frac{I \times \ln 0.66}{2.3} - \frac{I \times a[TBP]}{2.3 \times 0.66} \\ & - \frac{I \times a^2[TBP]^2}{2 \times 2.3 \times 0.66^2} - \frac{I \times a^3[TBP]^3}{3 \times 2.3 \times 0.66^3} - \frac{I \times a^n[TBP]^n}{n \times 2.3 \times 0.66^n} \\ & + (M-1) \log [M^{n+}] + \log m \end{aligned} \quad (6)$$

Variation of  $\log D$  versus  $[TBP]$  is shown in Figure 3. As was assumed before, the relationship between  $\log D$  and  $[TBP]$  is of polynomial form. The coefficients used in Equation (6) can thus be evaluated by a curve-fitting method. The coefficient of the ( $\log [RH_m]$ ) term in Equation (3) can also be obtained by substituting the coefficients of the TBP terms into Equation (6).

### Effect of Temperature

The effect of temperature on the distribution coefficients of Zn and Cd was determined at three different temperatures (25, 40 and 60 °C). The results obtained are shown in Figure 4. As shown, by increasing the temperature (decreasing the inverse of temperature) the distribution factor of zinc increases, while that of cadmium decreases. So the extraction of zinc and cadmium are endothermic and exothermic, respectively. The apparent enthalpies of the reactions can be calculated from the slopes of the plots of  $\log D$  against  $1/T$ .

### Devising a Correlation for Estimation of the Distribution Factor

The data obtained at different conditions for both zinc and cadmium were analyzed by SPSS for Windows Ver. 8. The following equations were obtained for prediction of the distribution factors of both zinc and cadmium:

$$\begin{aligned} \log D_{Zn} = & -0.66 - \frac{501.86}{T} + 0.63 \text{pH} + 0.36 [TBP] - 5.00 [TBP]^2 \\ & + 8.94 [TBP]^3 - 1.03 \log [Zn^{2+}] \end{aligned} \quad (7)$$

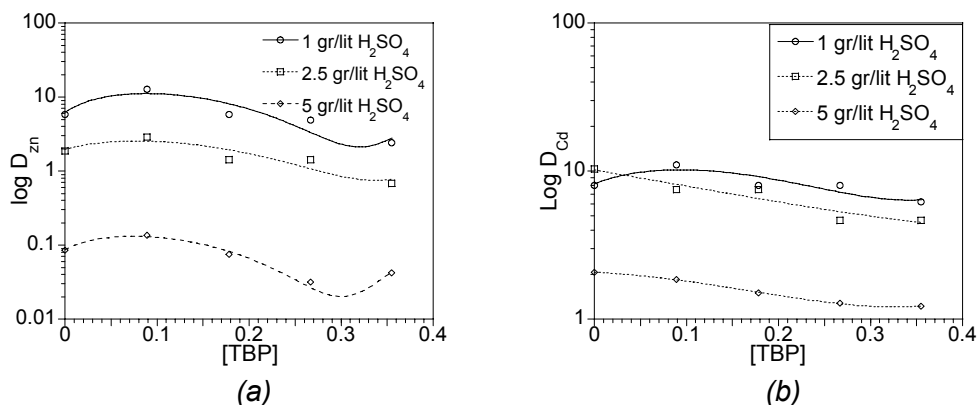


Figure 3. Variation of  $\log D$  vs. [TBP] at constant initial pH for a) zinc; b) cadmium.

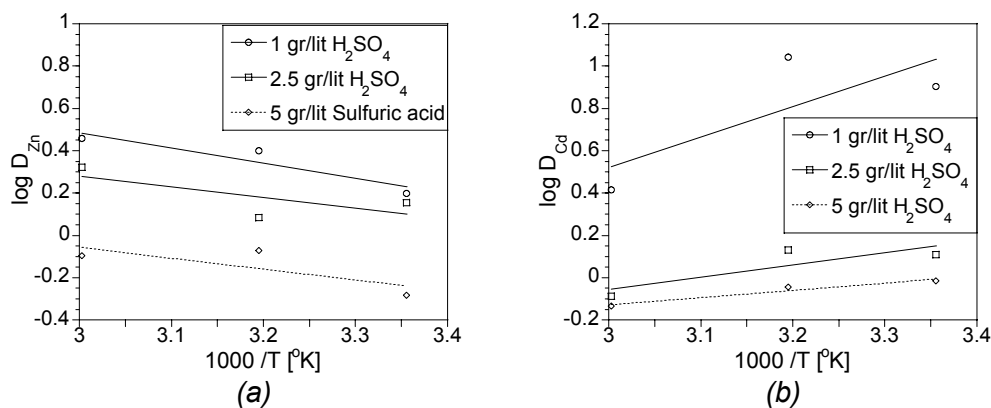


Figure 4. Effect of temperature on  $\log D$ . a) zinc; b) cadmium.

and

$$\begin{aligned} \log D_{Cd} = & -2.34 + \frac{195.98}{T} + 0.55 \text{ pH} - 0.27 [\text{TBP}] + 2.23 [\text{TBP}]^2 \\ & - 5.50 [\text{TBP}]^3 - 0.90 \log [\text{Cd}^{2+}] \end{aligned} \quad (8)$$

The experimental values for the distribution factors are compared with those predicted from formulae in Table 2. The values show that the estimated distribution factors for zinc and cadmium are very close to those obtained from the experiments. The values predicted from Equations (7) and (8) are plotted against the experimental values of Figure 5. The slope of the data equals one with a confidence factor of 95% and 96% for zinc and cadmium extraction, respectively.

## CONCLUSIONS

The extraction of metal ions by DEHPA and MEHPA in presence of TBP was modelled based on theoretical concepts of polymerization reactions of the extractant reagents and utilization of the experimental data. Equations obtained for zinc and cadmium distribution coefficients were assessed through comparison of their results with the experimental data. These equations can be utilized to estimate the extent of the zinc and cadmium extraction reactions and evaluation of  $\log D$  against  $\log [\text{TBP}]$  as two applicable correlations. The experimental results show that TBP can influence the extraction mechanism and rate of reaction. Proposing the new idea of polymerization of DEHPA and/or MEHPA by TBP helped the modification of Equation (2) and turned out to be useful. TBP caused the

extraction curves to shift to the right of the diagram. However, in the case of cadmium, its shifting effect was not very significant. From the equations given, the apparent enthalpy of extraction of zinc was obtained to be 9.6 kJ and that of cadmium was found to be -3.75 kJ.

*Table 2. Comparison of estimated and experimental values of zinc and cadmium distribution factors.*

TBP (%)	Experiment		Estimated	
	D <sub>Zn</sub>	D <sub>Cd</sub>	D <sub>Zn</sub>	D <sub>Cd</sub>
2.5	3.83	10.99	3.77	8.69
	4.55	7.99	4.03	8.16
	2.23	4.82	1.95	5.18
	1.21	1.36	1.21	1.11
5	2.87	8.6	2.7	7.05
	2.89	4.59	2.42	5.34
	1.28	1.50	1.14	1.00
	0.76	1.03	0.83	.98

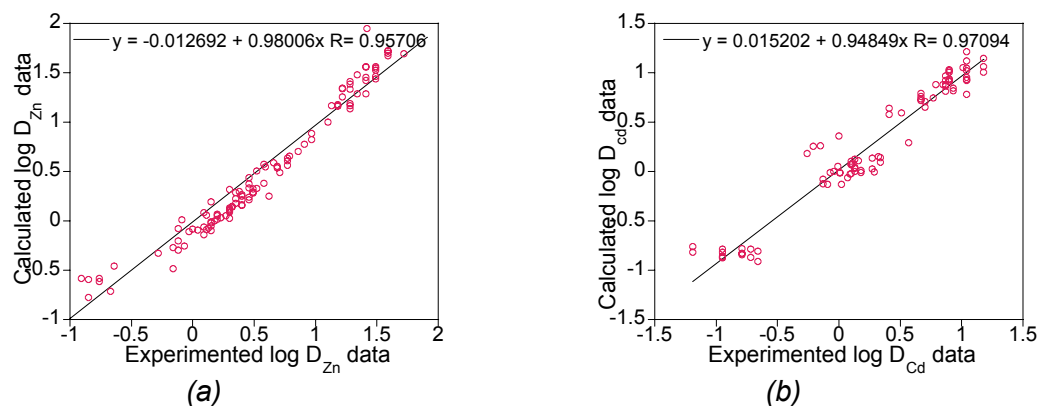


*Figure 5. Comparison of the measured and the calculated data for distribution factors for a) zinc and b) cadmium, treated with a mixture of DEHPA and MEHPA in kerosene with TBP as a modifier from aqueous sulfuric acid media.*

## ACKNOWLEDGEMENT

The authors wish to express their gratitude to Iranian Zinc Mines Development Company, and to the Ministry of Industry and Mining of The Islamic Republic of Iran for their financial support of this project.

## REFERENCES

1. S. Zielinski, M. Buca, and M. Famulski (1998), *Hydrometallurgy*, **48** (3), 253-263.
2. J.S. Preston, J. H. Patrick, and G. Steinbach (1994), *Hydrometallurgy*, **36** (2), 141-158.
3. M. Salimi, S. K. Sadrnezhaad, and E. Keshavarz Alamdari (2000), *Proc. 4th Conf. Metal. Eng. Iran*, 17-19 Oct. 2000, Tehran, Iran, pp. 559-566 [in Farsi].
4. S. K. Sadrnezhaad, E. Keshavarz Alamdari, Z. Mos'hefi shabestari, M. Abbaspoor, M. salimi, and M. Akbari (2002), unpublished data.



## ZINC EXTRACTION AND STRIPPING WITH D2EHPA: FURTHER CONSIDERATION AS A TEST SYSTEM

D. Antonelli, F. Vegliò, M.B. Mansur\*, E.C. Biscaia Junior\*\*\* and M.J. Slater\*\*

Dip. Ing. Chim. e Mat., University of L'Aquila, Italy

\* Dep. Eng. Química, Universidade Federal de Minas Gerais, Brazil

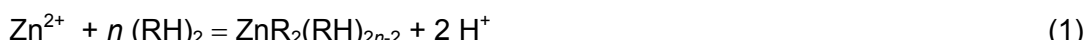
\*\* Dept. of Chem. Eng., University of Bradford, Bradford, UK

\*\*\* Programa Eng. Química (COPPE), Universidade Federal do Rio de Janeiro, Brazil

Equilibrium in the Zn/H<sub>2</sub>SO<sub>4</sub>/D2EHPA system has been studied in order to establish how stoichiometry varies as D2EHPA becomes progressively loaded with zinc to its maximum extent. Modelling assuming one- and two-zinc complexes taking into account the non-ideal behaviour of liquid phases has been investigated. The mechanism seems to be complicated by thermodynamic non-idealities in concentrated solutions, whether aqueous or organic, but applications of the models of Pitzer to the aqueous species and van Laar, Wilson, NRTL and UNIQUAC to the organic species were not able to reproduce data for loaded conditions assuming only one-zinc complex. A reasonable model for the extraction and stripping processes with constant mechanism can be proposed assuming two-zinc complexes in equilibrium.

### INTRODUCTION

The European Federation of Chemical Engineering has encouraged the adoption of test systems for liquid-liquid extraction studies and over recent years the reactive system Zn/H<sub>2</sub>SO<sub>4</sub>/D2EHPA has been investigated by many workers. Various diluents have been used but models proposed so far seem to be limited to certain concentration domains due to changes in stoichiometry as conditions change from extraction to stripping. The overall reaction is



For extraction conditions the value of  $n$  is near 1.5 when aliphatic diluents are used but near 1.0 for stripping. The observed dependence of  $n$  with concentration of the reactive species may be a consequence of incorrect modelling and/or non-ideality of the liquid phases. Sainz-Diaz *et al.* [1] modelled Zn/D2EHPA equilibrium using the Hildebrand-Scott theory assuming three species in the organic phase: dimeric-D2EHPA, ZnR<sub>2</sub>RH complex ( $n = 1.5$  from FT-IR analysis) and diluent. The Hildebrand-Scott model is based on symmetric convention (Lewis-Randall rule), *i.e.*,  $\gamma_i \rightarrow 1$  for very concentrated solution to pure; consequently, the zinc-complex is assumed liquid at the same T and P. The model is able to reproduce extraction data within 10% deviation but it has not been evaluated for stripping conditions. Loading of D2EHPA experiments have shown that  $n$  takes a value of 1.5 (for *n*-heptane diluent) and decreases slightly as D2EHPA loading increases towards about 50-60% [2].

In this work, the Zn/D2EHPA equilibrium is investigated assuming the existence of (a) one zinc complex with non-ideal behaviour of liquid phases accounted for by thermodynamic models, and (b) two zinc complexes with all activity coefficients equal 1.0. The kinetics of extraction and stripping have been examined because during extraction of zinc the back reaction becomes increasingly important as the extractant D2EHPA becomes loaded beyond about 20%.

## DESCRIPTION OF THE $\text{ZnSO}_4/\text{D2EHPA}$ SYSTEM EQUILIBRIA

### Single Mechanism with Thermodynamic Models

The equilibrium constant value depends on the convention assumed to describe the non-ideality of the organic phase species; due to the presence of dissolved salts, aqueous phase species are described by asymmetric convention (Henry's law), *i.e.*,  $\gamma_i^* \rightarrow 1$  for very dilute solution. Therefore, writing the equilibrium relation in terms of the asymmetric convention,

$$K_a = \frac{a_C a_H^2}{a_A a_{BD}^n} = \frac{\gamma_C \gamma_H^2}{\gamma_A \gamma_{BD}^n} \frac{C_C C_H^2}{C_A C_{BD}^n} = \frac{\gamma_C^\infty (\gamma_H^\infty)^2}{\gamma_A^\infty (\gamma_{BD}^\infty)^n} \frac{\gamma_C^* (\gamma_H^*)^2}{\gamma_A^* (\gamma_{BD}^*)^n} \frac{C_C C_H^2}{C_A C_{BD}^n} = K_\gamma^\infty K_\gamma^* \frac{C_C C_H^2}{C_A C_{BD}^n} \quad (2)$$

with  $K_\gamma^\infty$  as a function of temperature only. For very dilute systems,  $K_\gamma^* \rightarrow 1$ , so

$$K_a^\infty = \frac{K_a}{K_\gamma^\infty} = \frac{C_C C_H^2}{C_A C_{BD}^n} \quad (3)$$

Much of the equilibrium data found in the literature is commonly adjusted using Equation (3). However, Equation (3) is valid only at infinite dilution conditions; for example, the Pitzer model [3, 4] predicts  $\gamma_A^* \approx 0.75$  for 0.01 mol/m<sup>3</sup>  $\text{ZnSO}_4$  in aqueous solution! As experimental data usually involve higher concentrations,  $K_\gamma^*$  is unlikely to be near unity. The same conclusions are valid if data obtained from experiments with excess of D2EHPA relative to zinc are fitted by Equation (3), except if  $\gamma_B^* \approx 1$  for the whole range of  $C_B$ .

More reliable description is obtained assuming the standard state of all species in the organic phase as the pure component state (Lewis-Randall rule). Thermodynamic models such as van Laar, Wilson, NRTL and UNIQUAC were fitted to extraction and stripping equilibrium data by (1) slope analysis and (2) minimisation of the following objective function  $g(n, K_{eq}$  and model parameters) by Newton's method:

$$\min g = \log(K_{eq}) - \log \left[ \frac{\gamma_C (\gamma_H^*)^2}{\gamma_A^* \gamma_{BD}^n} \right] - \log \left( \frac{C_C C_H^2}{C_A C_{BD}^n} \right) \quad (4)$$

where  $K_{eq}$  is a new equilibrium constant; note that the ratio of activity coefficients is no longer unity at infinite dilution. Activity coefficients for aqueous phase species were estimated by Pitzer [3, 4] considering the formation of aqueous hydrogen sulphate. In contrast to Sainz-Diaz *et al.* [1], the  $n$  coefficient is assumed to be an adjustable parameter. Extraction data from Bart and Rousselle [5] and stripping data from Zimmermann and Robl [6] were fitted using Equation (4). Fitting results for extraction are shown in Table 1. Both slope analysis and optimisation procedures show that the regular solution model of van Laar is able to describe the  $\text{ZnSO}_4/\text{D2EHPA}/\text{isododecane}$  equilibrium. UNIQUAC and van Laar models showed similar results (parameters are listed in Table 2) while the NRTL and Wilson models did not show comparable results. Model equations are available in Sandler [7]. Extraction

data fitting including  $n$  as an optimisation parameter confirms the constant mechanism ( $n = 1.5$ ) obtained by Sainz-Diaz *et al.* [1] using the FTIR spectra technique. Activity coefficients at infinity dilution of extractant and complex shown in Table 3 were obtained by extrapolation of models at null concentration with parameters from Table 2.

*Table 1. Comparative mechanism and equilibrium constant for the extraction of zinc with D2EHPA using different thermodynamic models.*

Model	Optimisation			Slope Analysis		
	$n$	$\log(K_{eq})$	min*	$n$	$\log(K_{eq})$	$R^2$
van Laar	1.50	-2.146	8.95 (56 pt)	1.52	-2.093	0.94
UNIQUAC	1.44	-2.220	12.14 (52 pt)	1.44	-2.213	0.91
Wilson	1.40	-2.060	19.67 (55 pt)	1.75	-1.170	0.86
NRTL	1.28	-2.439	16.41 (55 pt)	1.59	-1.858	0.83

\* Number of valid points used from a total of 72 data points (pt).

*Table 2. Optimised parameters of van Laar and UNIQUAC models for extraction conditions.*

van Laar	UNIQUAC	
$\Lambda_{BC} = 0.2971$	$\tau_{BC} = 1.8740$	$r_B = 25.460$
$\Lambda_{BD} = 0.3292$	$\tau_{BD} = 1.1076$	$r_C = 25.460$
$\Lambda_{CB} = 2.3581$	$\tau_{CB} = 1.9927$	$r_D = 8.546$
$\Lambda_{CD} = 3.2021$	$\tau_{CD} = 1.0568$	$q_B = 22.358$
$\Lambda_{DB} = 1.3180$	$\tau_{DB} = 0.8718$	$q_C = 30.494$
$\Lambda_{DC} = 0.0022$	$\tau_{DC} = 0.7161$	$q_D = 7.096$

*Table 3. Equilibrium parameters at infinite dilution for van Laar and UNIQUAC models.*

	$\gamma_B^\infty$	$\gamma_C^\infty$	$\log(K_a^\infty)$ by optimisation	$\log(K_a^\infty)$ by slope analysis
van Laar	1.388	10.938	-2.971	-2.915
UNIQUAC	0.254	0.800	-2.980	-2.973

Short-cut correlations for the activity coefficients of extractant and complex in the asymmetric convention have been derived for fast calculations (Pitzer for aqueous phase species):

$$\gamma_{BD}^* = 1 \quad \text{for all } C_B \quad (5-a)$$

$$\gamma_C^* = 1 \quad \text{for } C_C < 0.00007 \text{ mol/L} \quad (5-b)$$

$$\gamma_C^* = 0.0312C_C^{-0.3604} \quad \text{for } C_C \geq 0.00007 \text{ mol/L} \quad (24.5\% \text{ relative error}) \quad (5-c)$$

Stripping data were fitted by the van Laar model only and, as shown in Table 4, poor fitting was obtained. It was found that  $1.0 < n < 1.5$  is suitable to reproduce stripping data if one single zinc-complex is assumed. Therefore, it seems that thermodynamic models are not suitable to describe the Zn/D2EHPA equilibrium with constant mechanism for high loading conditions. Unless some change in mechanism occurs, the slightly lower  $n$  value compared to extraction may indicate inadequate modelling.

*Table 4. Estimated equilibrium parameters for stripping (van Laar model).*

Optimisation			Slope Analysis		
$n$	$\log(K_{eq})$	min	$n$	$\log(K_{req})$	$R^2$
1.33	-2.400	1.36 (19 pt)	1.38	-2.305	0.77

### Parallel Mechanism with Activity Coefficients equal 1.0

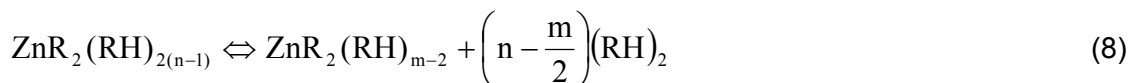
If splitting of the free-D2EHPA molecules from dimeric to monomeric form really occurs as loading of the organic phase increases, so Equation (1) and the following additional reaction with constant mechanism could be assumed to compete for zinc ions at the liquid-liquid interface



and five species are then supposed to exist in the organic phase: free dimeric and monomeric D2EHPA, dimeric and monomeric zinc-D2EHPA complexes and the diluent. Under these conditions, the equilibrium model is a non-linear algebraic equation with five parameters to be estimated by data fitting ( $K_D$ ,  $K_M$ ,  $K_{RH}$ ,  $m$  and  $n$ ). Assuming all activity coefficients equal unity, the following equilibrium relationships

$$K_D = \frac{C_{CD} C_H^2}{C_A C_{BD}^n} \quad K_M = \frac{C_{CM} C_H^2}{C_A C_{BM}^m} \quad K_{RH} = \frac{C_{BM}^2}{C_{BD}} \quad (7)$$

and respective mass balance equations of reactive species were solved by Newton's method with initial concentrations as initial guesses. The parameters were estimated by the direct search method of Hooke and Jeaves in order to minimise the difference between experimental and calculated zinc concentrations in aqueous phase. Extraction [5, 8] and stripping [2, 6] data were fitted to the model and convergence to a singular solution was achieved independently of the initial value of the parameters. Two zinc complexes produced by competitive reactions with  $n = 1.46 \pm 0.10$  and  $m = 1.99 \pm 0.07$  are indicated. Furthermore, statistical analysis of the results revealed strong correlation between  $K_M$  and  $K_{RH}$  parameters indicating that Equation (6) is not representative of the system, i.e., as commonly ascertained in the literature, no partial break-down of the dimer-D2EHPA to monomer-D2EHPA occurs in the investigated range of concentrations. Information concerning the second zinc complex is obtained by elimination of  $K_{RH}$  and  $K_M$  constants resulting in the following homogeneous reaction:



$$K_C = \frac{C_{CM} C_{BD}^{n-m/2}}{C_{CD}} \quad (9)$$

According to this new model, the dimeric zinc complex produced in Equation (1) (heterogeneous reaction) could break down producing free dimer D2EHPA as in Equation (8) (homogeneous reaction) as loading of the organic phase increases. The following mass balance equations were used in further fitting calculations to find  $K_C$ ,  $K_D$ ,  $n$  and  $m$ :

$$C_{CM} + C_{CD} = C_{CM}^o + C_{CD}^o + \left( C_A^o - C_A \right) \frac{V_{aq}}{V_{org}} \quad (10)$$

$$C_{BD} = C_{BD}^o - n \left( C_A^o - C_A \right) \frac{V_{aq}}{V_{org}} - \left( n - \frac{m}{2} \right) \left( C_{CM}^o - C_{CM} \right) \quad (11)$$

$$C_H = C_H^o + 2 \left( C_A^o - C_A \right) \quad (12)$$

Final fitted parameters including 95% confidence levels are shown in Table 5. No correlation between pairs of parameters was found by statistical analysis. As shown in Figure 1, extraction and stripping data were reproduced within 11% total error. Figure 2 shows the behaviour of the  $n$  coefficient with loading in the absence of monomer zinc-complex ( $m = 2n = 3$ ). Further detailed discussion is presented by Mansur *et al.* [9].

*Table 5. Final fitting results for Zn/D2EHPA equilibrium.*

$K_D \text{ (mol/L)}^{2-n}$	$0.278 \pm 0.001$
$K_C \text{ (mol/L)}^{n-m/2}$	$0.010 \pm 0.003$
$n$	$1.457 \pm 0.003$
$m$	$2.06 \pm 0.08$

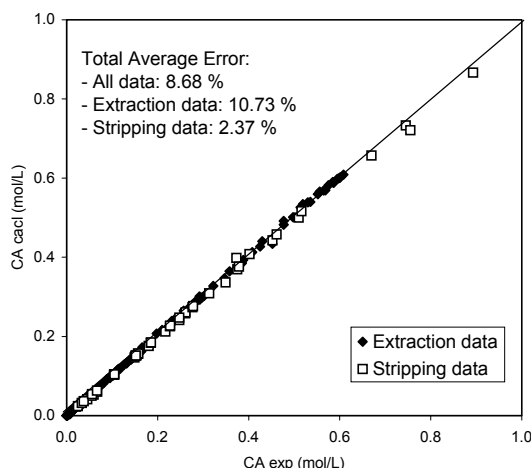


*Figure 1. Fitted extraction and stripping data.*

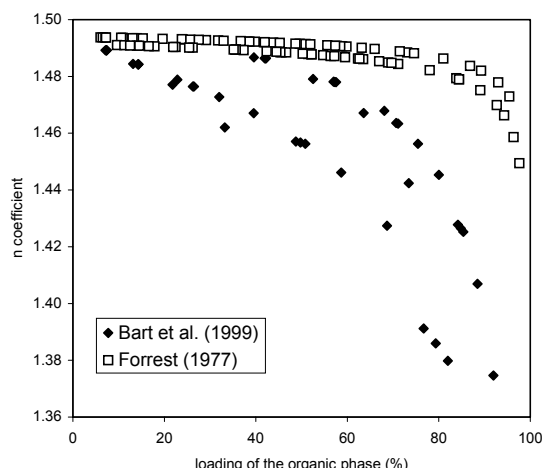


*Figure 2. Behaviour of  $n$  for single zinc complex model.*

## CONCLUSIONS

Much work on the Zn/D2EHPA possible test system has been done in order to find a unifying theory to describe extraction and stripping conditions. Models available in the literature are only accurate for specific concentration domains because a change in mechanism is found as loading of organic phase increases. The use of thermodynamic models was not able to explain data assuming a single-complex mechanism. The origin of the problem may reside in the existence of an additional zinc complex formed according to Equation (8). Thermodynamic models are not necessary to describe equilibrium when competitive zinc complexes are considered; extraction and stripping data are reproduced within 11% average error. Maybe the inclusion of thermodynamic theories to estimate activity coefficients will improve predictions for this new model.

## ACKNOWLEDGMENTS

The experimental work done at the University of Bradford was made possible by financial support received from the Coordenação de Aperfeiçoamento de Pessoal de Nível Superior (CAPES, Brazilian Government Agency, PICDT/UFMG and PDEE Doctorate Grant nº 0299/99-5), which is gratefully acknowledged. M. B. Mansur would also like to record his appreciation for financial support from Conselho Nacional de Desenvolvimento Científico e Tecnológico (CNPq), Brazil and Fundação de Amparo a Pesquisa do Estado de Minas Gerais (FAPEMIG), Brazil, to attend this Conference.

## NOMENCLATURE

$a_j$	activity of specie j
$C_j$	concentration of specie j
K	concentration-based equilibrium constant reaction
$m, n$	stoichiometric coefficients
V	volume

### Subscripts

A	zinc ion
BD	dimer-D2EHPA
BM	monomer-D2EHPA
CD	dimer-D2EHPA complex
CM	monomer-D2EHPA complex
D	diluent
H	hydrogen ion

### Greek

$\gamma$	activity coefficient
$\Lambda, \tau$	UNIQUAC parameters

### Superscripts

$\infty$	at infinite dilution
*	assymetric convention

## REFERENCES

1. C.I. Sainz-Diaz, H. Klocker, R. Marr and H.-J. Bart (1996), *Hydrometallurgy*, **42**, 1-11.
2. M.B. Mansur (2000), *PDEE/CAPES Report*, No. 0299/99-5, Brasília, Brazil, 68 pp.
3. K.S. Pitzer and G. Mayorga (1973), *J. Phys. Chem.*, **77**,(19), 2300-2308.
4. K.S. Pitzer and G. Mayorga (1974), *J. Solution Chem.*, **3**, (7), 539-546.
5. H.-J. Bart and H.-P Rousselle (1999), *Hydrometallurgy*, **51**, 285-298.
6. W. Zimmermann and S. Robl (1997), Kinetics and equilibrium of the stripping process in the Zn/D2EHPA/n-heptane system, Diploma Thesis, University of Bradford, UK.
7. S.I. Sandler (1999), Chemical and Engineering Thermodynamics, John Wiley & Sons, 3<sup>rd</sup> Ed., New York.
8. C. Forrest (1977), The modelling of equilibrium data for the solvent extraction of metals, PhD Thesis, University of Bradford, UK.
9. M.B. Mansur, M.J. Slater and E.C. Biscaia Jr (2001), Equilibrium analysis of the reactive liquid-liquid test system ZnSO<sub>4</sub>/D2EHPA/n-heptane. Accepted by *Hydrometallurgy* in May, 2001.



# THE INTEGRATED RECOVERY OF RARE EARTHS FROM APATITE IN THE ODDA PROCESS OF FERTILIZER PRODUCTION BY SOLVENT EXTRACTION. A PLANT EXPERIENCE

**Abdulla W. Al-Shawi, Svein E. Engdal, Ole B. Jenssen, Tom R. Jørgensen  
and Morten Røsæg**

Norsk Hydro ASA, Porsgrunn, Norway

An integrated method to recover rare earths from apatite within the Odda process of fertilizer production was commissioned by Norsk Hydro, Norway, in 1996. The method involves selective precipitation of a rare earth phosphate concentrate by partial neutralization of a fertilizer solution stream. The phosphate concentrate is re-dissolved in nitric acid, partially neutralized, filtered and fed into a Cyanex 923 extraction circuit, where rare earths were separated from phosphate and calcium ions. Loaded Cyanex 923 was stripped with HNO<sub>3</sub>, and in order to meet a stringent specification levels, further purification by a tributylphosphate extraction circuit ensured rare earths are free from ammonium and other impurity ions. The rare earth nitrate solution leaving the tributylphosphate circuit was evaporated to generate a 470 g/L rare earths oxide trading solution.

## INTRODUCTION

Apatites, also called phosphate rocks, are virtually the sole raw material for phosphate fertilizers. Fluorapatite, with a simplified chemical formula Ca<sub>5</sub>(PO<sub>4</sub>)<sub>3</sub>F, represents the most common form of apatite. Fluorapatites are further divided into sedimentary apatites (phosphate rocks precipitated from seawater and bones), which represent the primary source of apatite, and magmatic (igneous) apatites, which are also considered important. The total worldwide consumption of apatite in 1989 was 160 million tonnes. About 90% of mined apatite is used in fertilizer production, being divided almost equally among superphosphates, ammonium phosphates and compound fertilizers, including those produced by the Odda process [1].

The abundance of rare earths in the earth's crust is 0.015%. Monazite (55% REO), bastnasite (70% REO) and xenotime (42% REO) are considered to be the principal raw materials [2]. Igneous apatites on the other hand often contain much lower but appreciable concentrations of rare earths substituted in the apatite lattice for calcium ions [3,4].

Sulphuric acid attack on apatite for phosphoric acid production is termed the 'wet process', and represents between 85-90% of the world production. In this process, sulphuric acid attacks apatite to produce phosphoric acid and calcium sulphate (phosphogypsum), which separates as an insoluble salt. Unfortunately, up to 70% of the apatite's rare earth content is retained by the phosphogypsum, which complicates their recovery. Attempts on the recovery of rare earths from the phosphogypsum and the phosphoric acid have been reported both in patents and on laboratory scale [5-7].

Table 1. Rare earths content of some apatites.

Apatite (Origin)	Rare earth oxides, % <sub>w/w</sub>
Kola/Russia (Igneous)	0.8-1.0
Phalaborwa/South Africa (Igneous)	0.4-0.9
Florida/USA (Sedimentary)	0.06-0.29
BouCraa/Morocco (Sedimentary)	0.13-0.18

Nitric acid attack on apatite on the other hand is known as the Odda process for fertilizer production; it is also referred to as the nitrophosphate route [8] (Figure 1).

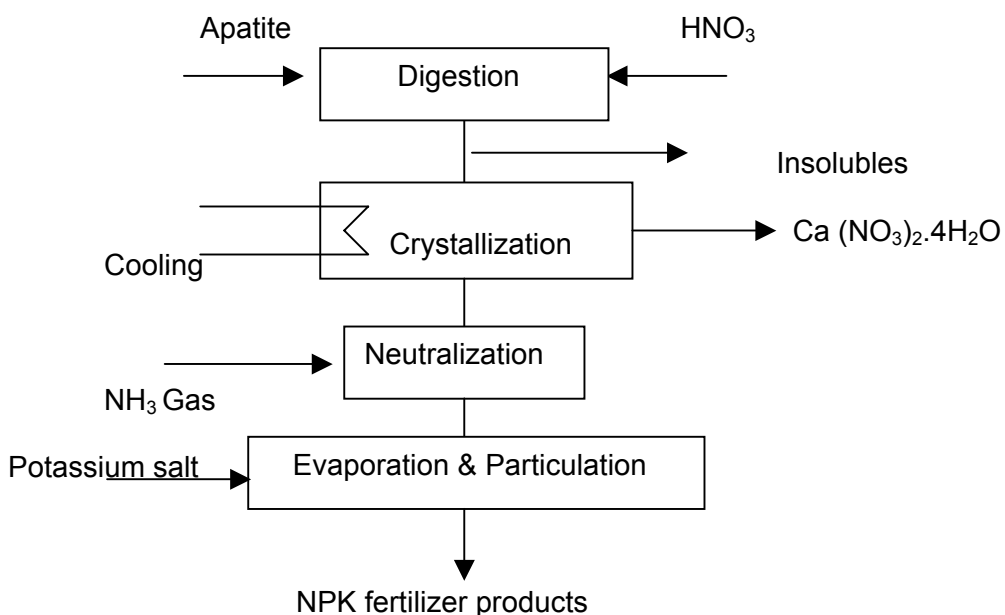


Figure 1. The Odda process for fertilizer production.

In the Odda process all the rare earths are completely solubilized and report to the mother liquor solution after the calcium nitrate crystallisation stage. There is no loss of rare earths with the calcium nitrate crystals. On this basis, their recovery from the Odda process is more suitable than from the wet process [9,10].

Kemira Oy, Finland, has operated a full-scale industrial plant based on solvent extraction technology to recover rare earths from Kola apatite at the Oulu fertilizer plant, Finland between 1965-1972. Tributylphosphate was utilized as the organic solvent for that production plant, which operated on 100 000 tonnes of apatite per year with REO content of 1%, producing a rare earth hydroxide/oxide mixture [11].

## PROCESS DESCRIPTION

Norsk Hydro's rare earths recovery is inserted after the calcium nitrate crystallization in the Odda process of fertilizer production. The recovery process consists of three main separation stages:

1. Selective precipitation of rare earths from post calcium nitrate crystallization solution.
2. Cyanex 923 extraction circuit for rare earths separation from Ca and  $\text{PO}_4$  ions.
3. Tributylphosphate extraction circuit for rare earths separation from ammonium ion and other impurities.

The overall process is illustrated in Figure 2.

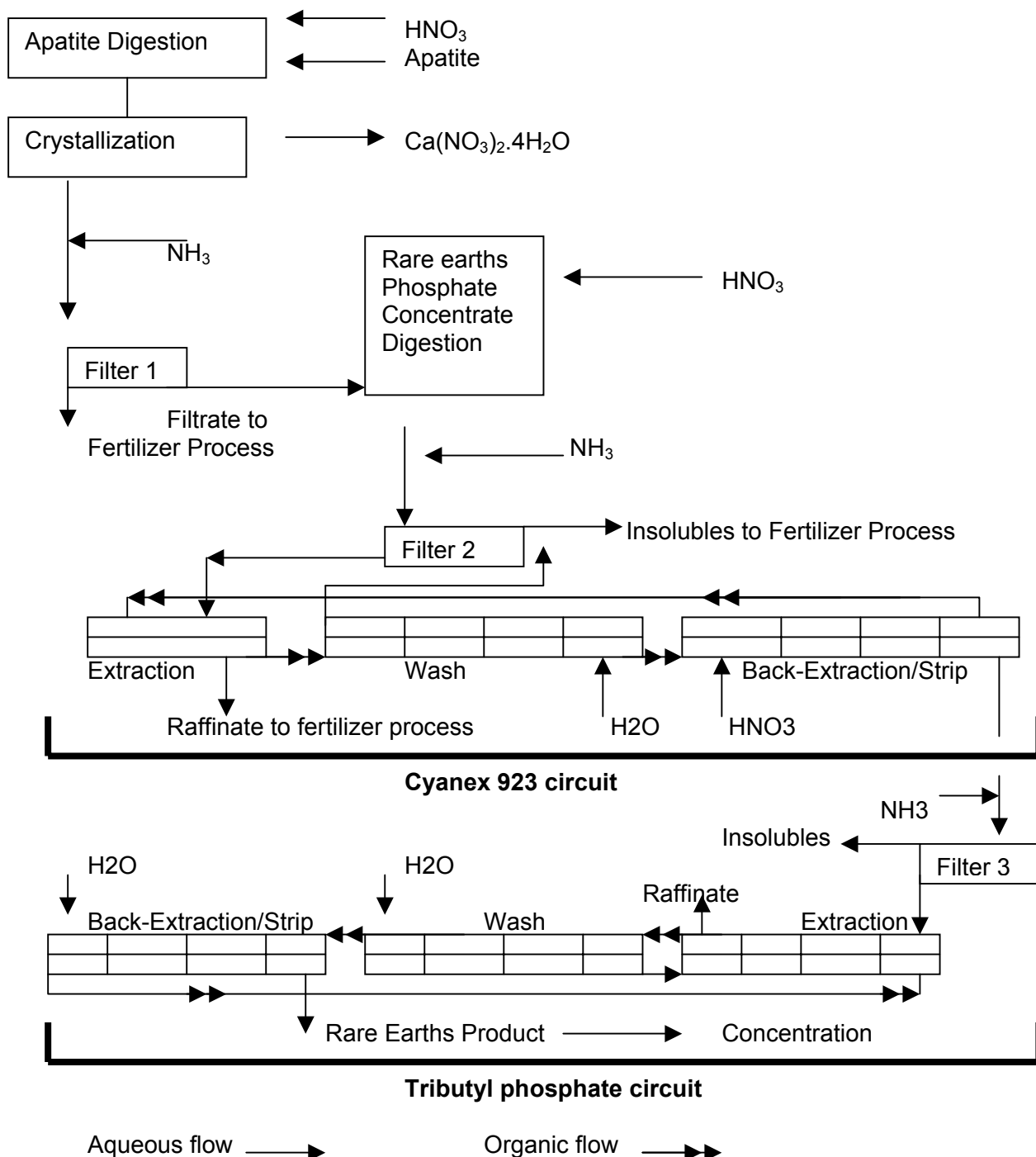


Figure 2. Rare earth extraction circuits.

### Selective Precipitation of Rare Earths from Mother Liquor Solution

The initial stage of the recovery involves a selective precipitation of rare earth phosphate concentrate (cake) from calcium nitrate crystallization mother liquor. This selective precipitation was performed by partial neutralization of the mother liquor with ammonia to a pH of 1.6-1.9 (1+13), where (1+13) denotes the dilution of 1 part of the process solution with 13 parts water prior to pH measurement (Table 2).

At this pH range, rare earths phosphates precipitate out of solution (> 85%) with minimum co-precipitation of dicalcium phosphate (DCP). The rare earths phosphate concentrate is then separated on filter 1.

The rare earth phosphate concentrate was then digested with fresh nitric acid, and the solution was then neutralized to a pH of 1.0 (1+13) with ammonia, filtered on filter 2, and fed into the Cyanex 923 extraction circuit.

*Table 2. Precipitation of rare earths at pH 1.8(1+13) from mother liquor solution.*

Stream	Amount	Density, kg/L	[RE]	[Ca]	[PO <sub>4</sub> ]
Mother liquor pre-filter 1	32 m <sup>3</sup> /h	1.52	5.7 g/L	60-70 g/L	400 g/L
Mother liquor post-filter 1	30 m <sup>3</sup> /h	1.51	0.8 g/L	65 g/L	380 g/L
RE phosphate concentrate	1.31 t/h	2.10	6.2 %	5.3 %	21.6 %
Feed solution post-filter 2	2.20 m <sup>3</sup> /h	1.50	70 g/L	50 g/L	120 g/L

### Cyanex 923 Extraction Circuit

Cyanex 923 is a mixture of four phosphine oxides, that extract rare earth nitrates by a solvating mechanism [12]. The Cyanex 923 circuit (50% with Exxol D80) is intended to separate the rare earths from both calcium and phosphate ions. As Cyanex 923 extracted both nitric acid and rare earth nitrates, the distribution ratios increased with the reduction of the total acidity at equilibrium (Table 3).

*Table 3. Rare earth distribution ratios with 50% Cyanex 923.*

Post extraction pH / Element	La	Ce	Pr	Nd	Y
Raffinate pH 0.90 (1+13)	0.09	0.17	0.25	0.34	2.30
Raffinate pH 1.20 (1+13)	0.74	1.40	2.36	4.25	> 10
Raffinate pH 1.35 (1+13)	1.29	3.89	6.82	7.16	> 10
Raffinate pH 1.80 (1+13)	15.6	12.90	31.2	51.50	> 10

The Cyanex 923 circuit consisted of the streams shown in Table 4.

*Table 4. Cyanex 923 circuit streams.*

Stream	Volume, m <sup>3</sup> /h	pH (1+13)	Total RE, g/L	Ca, g/L	PO <sub>4</sub> , g/L
Feed solution	2.20	0.9 - 1.0	70	50	120
Raffinate solution	2.00	1.7	5.4	45	110
50% Cyanex , in extraction	8.50	0.4 M HNO <sub>3</sub>	0.0	0.0	0.0
50% Cyanex , out extraction	8.50	0.8 M HNO <sub>3</sub>	15-17	1.2	2.8
Strip solution out	4.20	8 M HNO <sub>3</sub>	30-33	0.02	0.01

### **Tributylphosphate (TBP) Extraction Circuit**

The strip solution from the Cyanex 923 circuit is neutralized with ammonia to pH 3.0, filtered on filter 3, and fed into the TBP extraction circuit (Table 5). At this pH other metallic impurities precipitate. Rare earth distribution ratios from nitrate solution with 100% TBP are well documented in the chemical literature [13]. The ammonium ion concentration in the feed solution of this circuit salts-out the rare earths extraction which enables their concentration in the strip solution to be doubled.

*Table 5. Tributylphosphate circuit streams.*

Stream	Volume, m <sup>3</sup> /h	pH	Total RE, g/L	NH <sub>4</sub> , g/L	Ca, g/L	PO <sub>4</sub> , g/L
Feed	4.3	3.0 - 3.2	30 - 33	110	0.015	0.005
Raffinate	4.1	6.2 - 6.4	< 1.0	120	0.007	0.0020
100% TBP, in extraction	2.0	5.0 - 6.0	<1.0	0	0	0
100% TBP, out extraction	2.1	4.0	70 - 80	5	0	0
Strip solution out	2.0	3.0 - 4.0	70 - 80	0.1	0.007	0.0025

The strip solution from the TBP circuit is then concentrated to produce a rare earth nitrate solution, which is 470 g/L in REO.

### **PLANT EQUIPMENT AND PROCEDURES**

Conventional mixer-settler units were employed in both extraction circuits, and were all operated in a counter-current configuration. Membrane pumps were utilized to pump aqueous and organic solutions into the plant. All neutralizations were performed by ammonia gas, and all pH measurements were taken after dilution of 1 part process solution with 13 parts water.

The Cyanex 923 circuit has 1 extraction stage (0.515 m<sup>3</sup> mixer, 3.6 m<sup>3</sup> settler), 4 washing and 4 back-extraction (strip) stages (0.515 m<sup>3</sup> mixer, 1.2 m<sup>3</sup> settler). The TBP circuit consisted of 4 extraction, 4 washing and 4 back-extraction (strip) stages (0.515 m<sup>3</sup> mixer, 1.2 m<sup>3</sup> settler). Both extraction circuits were maintained at ambient temperature and were operated in parallel.

Cyanex 923, manufactured by Cytec, Canada, diluted with Exxol D80 (aliphatic hydrocarbon), Exxon, USA, to 50% in volume concentration, and 100% TBP, Bayer, Germany were used.

Plant control was installed by ABB Master process-system, Sweden. The control system has many measurement devices like flow amount (46), temperature (13), tank level (28), pH (10), and pressure (4).

### **SPECIFICATION**

Norsk Hydro's rare earths recovery process from apatite is designed to produce a pure rare earths nitrate solution with stringent specification, the process was also fully integrated with the main fertilizer production process. Environmental issues were fully implemented by ensuring that the rare earth process has no waste streams or products. The product specification is shown in Table 6.

*Table 6. Market specifications of the rare earth nitrate solution.*

Total rare earths oxides (TREO)	> = 470 g/L
Ce <sup>3+</sup> /TREO	> 50 %
Total free Acidity (HNO <sub>3</sub> )	< 0.7 mol/L
Phosphorus/TREO	< 0.001 wt.%
Fluoride/TREO	< 0.003 wt %
Calcium/TREO	< 0.007 wt %
Aluminium/TREO	< 0.0025 wt %
Iron/TREO	< 0.005 wt %
Ammonium/TREO	< 0.005 wt %
Vanadium	< 0.0003 wt %
Ce <sup>4+</sup> / total Ce	= 0
Yttrium/TREO	> 2.0 % wt %
Radioactivity	< 10 Bq/Kg

## REFERENCES

1. G. Kongshaug *et al.* (1991), Ullmann's Encyclopedia of Industrial Chemistry: Phosphate Fertilizers, **A19**, Chap. 5, Verlagsgesellschaft, Weinheim, Germany, pp. 425-427.
2. R. J. Callow (1967), The Industrial Chemistry of the Lanthanons, Yttrium, Thorium and Uranium, Pergamon Press, London, Chap. 4, pp. 58-93.
3. F. Habashi, M. Zailaf and F. T. Awadalla (1986), *Fresenius Z. Anal. Chem.*, 479-480.
4. F. Habashi and F.T. Awadalla (1989), *Ind. Eng. Chem. Res.*, 1101-1103.
5. R. Kijkowska (1983), *Phosphorus Potassium*, pp. 24-26.
6. D. A. Clur and K. R. N. Hansen (1981), *South African Pat.*, No. ZA 8005,318.
7. J. Kwiecien *et al.* (1967), *Polish Pat.*, No. 54, 179.
8. G. Kongshaug *et al.* (1991), Ullmann's Encyclopedia of Industrial Chemistry: Phosphate Fertilizers, Vol. A19, Chap. 11, Verlagsgesellschaft, Weinheim, Germany, pp. 448-455.
9. F. Habashi (1985), *J. Chem. Tech. Biotechnol.*, **34A**, 4-14.
10. F. Habashi (1981), *Proc. Inter. Congr. Phosphorus Compounds*, Paris, pp. 629-660.
11. V. P. Judin and H. E. Sund (1981), *Proc. Int. Congr. Phosphorus Compounds*, Paris, pp. 759-768.
12. W.A. Rickelton and R.J. Boyle (1988), *Sep. Sci. Technol.*, **23**, 1227-1250.
13. D. Scargill, K. Alcock, J.M. Fletcher, E. Hesford and H.A. McKay (1957), *J. Inorg. Nucl. Chem.*, **4**, 304-314.



## EXTRACTION OF LANTHANIDES AND YTTRIUM WITH PC-88A FROM AQUEOUS PHOSPHATE MEDIA

Ahmed A. Abdeltawab, Susumu Nii, Fumio Kawaizumi, and Katsuroku Takahashi

Department of Chemical Engineering, Nagoya University, Nagoya, Japan

The extraction of lanthanides (La, Gd, Yb) and yttrium from an aqueous phosphate medium with 2-ethylhexyl phosphonic acid mono-2-ethylhexyl ester (PC-88A) was studied. Different concentrations of PC-88A in *n*-dodecane were studied for the separation of lanthanides and yttrium ions from both single and multi-component systems. Heavy lanthanides ions were extracted with low concentrations of PC-88A from phosphoric acid aqueous solutions of low concentration. The extraction distribution ratios of all lanthanides and yttrium ions were found to decrease with increasing H<sub>3</sub>PO<sub>4</sub> concentration. The extraction distribution ratio increased with increasing pH value up to 2. The experimental results supported an extraction mechanism different from that in the case of nitrate medium.

### INTRODUCTION

A great deal of attention has been directed to phosphate deposits as a secondary source for lanthanides and yttrium [1]. This attention arises from the importance of studying the recovery of lanthanides and yttrium from phosphoric acid solutions produced during processing of phosphate ores.

Although solvent extraction techniques have been extensively applied to the practical separation of lanthanides using acidic organophosphorus extractants [2], the separation of lanthanides from phosphoric acid media has not been studied intensively. In most cases, production of lanthanides and yttrium have been carried out by using dialkylphosphonates such as 2-ethylhexyl phosphonic acid mono-2-ethylhexyl ester (PC-88A), particularly from chloride and nitrate media [3].

In this work, the extraction behavior of lanthanides and yttrium with PC-88A from phosphoric acid aqueous solution has been studied.

### EXERIMENTAL

#### Reagents

The commercial extractant, PC-88A, was supplied by Daihachi Chemical Industry Co., Ltd. Japan (Lot No.: N-10102) and used without further purification. Lanthanide nitrates and *n*-dodecane were supplied by Wako Pure Chemical Industries, Ltd. Japan. All inorganic chemicals used were of analytical grade.

### Extraction Equilibrium Procedure

Organic solutions were prepared by diluting PC-88A with *n*-dodecane to the desired concentration. Aqueous solutions were prepared by dissolving lanthanides and yttrium nitrates in phosphoric acid. The concentration of each metal ion was 0.2 mol/m<sup>3</sup>. Solution pH was adjusted with 1000 mol/m<sup>3</sup> sodium hydroxide. The pH values were measured with a Horiba F-22 pH meter (probe no. S8721) with a measuring range: pH 0-14 ± 0.01. Equal volumes of aqueous and organic phases, 10 cm<sup>3</sup>, were equilibrated in 30 cm<sup>3</sup> screwed cap vials by vigorously shaking for 30 min at 25 ± 1°C. After reaching equilibrium, the aqueous phase was separated, and lanthanide and yttrium concentrations were determined by ICP-atomic emission spectroscopy (IRIS Plasma Spectrometer, Thermo Jarrell Ash Corporation).

## RESULTS AND DISCUSSION

### Effect of PC-88A Concentration

The effect of PC-88A concentration, *C*, on the extraction distribution ratios of lanthanides (La, Gd, Yb) and yttrium from phosphoric acid aqueous solutions (500, 1000 mol/m<sup>3</sup>) is shown in Figures 1 and 2. Extraction of Yb and Y was increased considerably by increasing the PC-88A concentration, while the extraction of La and Gd slightly increased, which indicates the possibility of separating the heavy lanthanides and yttrium from the lanthanides mixture with low concentrations of PC-88A.

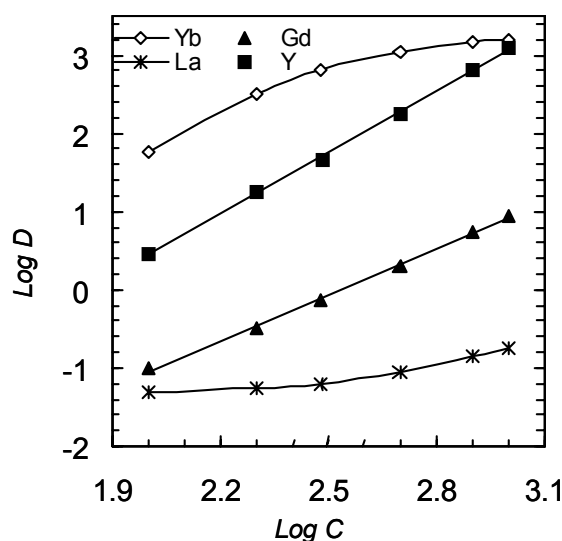


Figure 1. The effect of PC-88A concentration on extraction of lanthanides and Y from 500 mol/m<sup>3</sup> H<sub>3</sub>PO<sub>4</sub>.

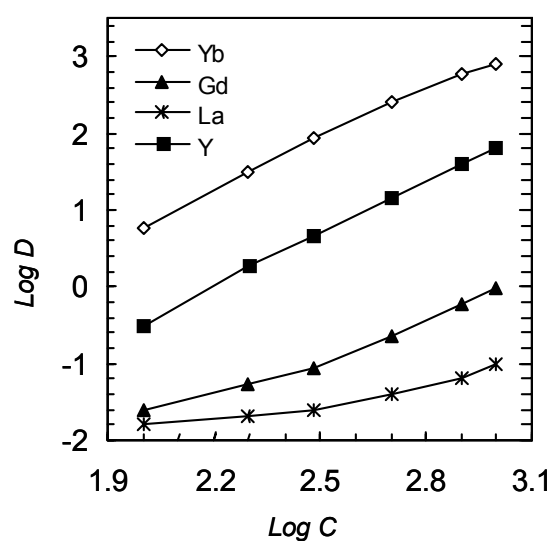


Figure 2. The effect of PC-88A concentration on extraction of lanthanides and Y from 1000 mol/m<sup>3</sup> H<sub>3</sub>PO<sub>4</sub>.

This increase of the extraction distribution ratio with increasing atomic number of the light to heavy lanthanides was also reported by Koopman *et al.* [4] for the extraction of lanthanides with di(2-ethylhexyl)phosphoric acid (D2EHPA) from phosphoric acid solution. This tendency was explained by the order of polarizability sequence POO<sup>-</sup> > H<sub>2</sub>O, the phosphate carrier D2EHPA replaces water ligands from the cations, resulting in an increasing affinity with increasing charge density of the bare cation [4]. On the other hand, as the bare ionic radius decreases with increasing atomic number from 1.061 Å for La to 0.858 Å for Yb and 0.88 Å for Y [5], the affinity also increases. The extraction distribution ratios of La, Gd, Yb and Y decreased considerably when phosphoric acid concentration increased from 500 mol/m<sup>3</sup> (Figure 1) to 1000 mol/m<sup>3</sup> (Figure 2) for the same PC-88A concentration values.

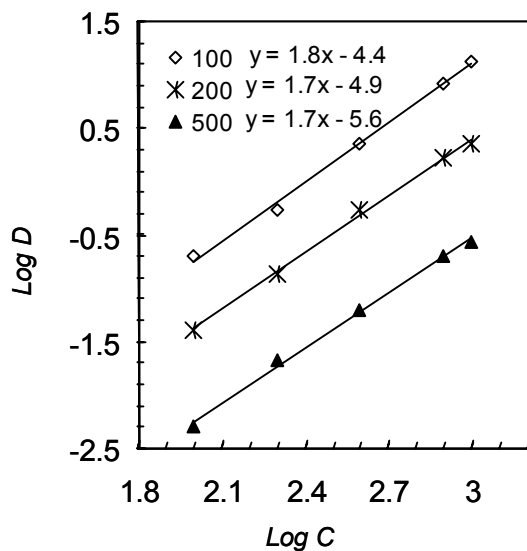


Figure 3. The effect of PC-88A concentration on extraction of La from (100, 200, and 500 mol/m<sup>3</sup>) H<sub>3</sub>PO<sub>4</sub>.

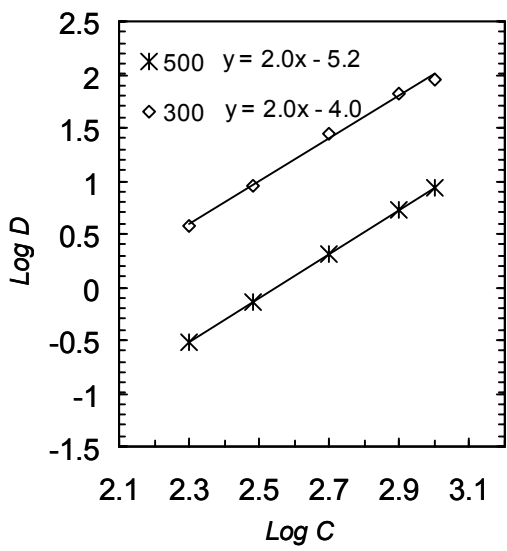


Figure 4. The effect of PC-88A concentration on extraction of Gd from (300, and 500 mol/m<sup>3</sup>) H<sub>3</sub>PO<sub>4</sub>.

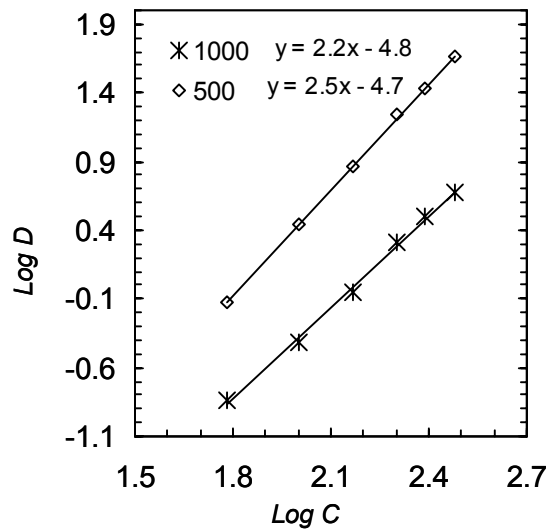


Figure 5. The effect of PC-88A concentration on extraction of Y from (500, and 1000 mol/m<sup>3</sup>) H<sub>3</sub>PO<sub>4</sub>.

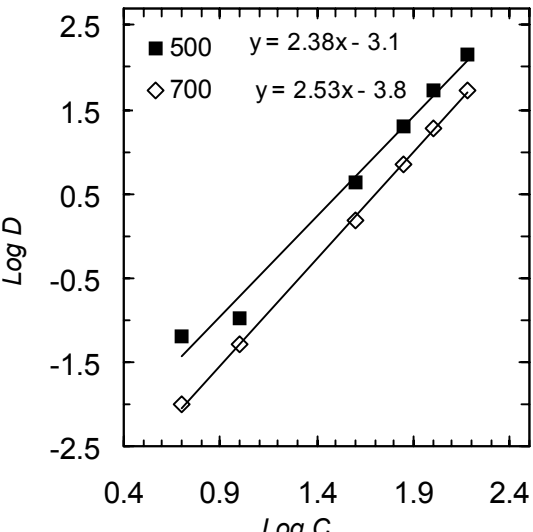


Figure 6. The effect of PC-88A concentration on extraction of Yb from (500, and 700 mol/m<sup>3</sup>) H<sub>3</sub>PO<sub>4</sub>.

The effect of PC-88A concentration on the extraction behavior of individual metal ions in single component systems of different phosphoric acid concentrations are shown in Figures 3 to 6. Figure 3 shows the effect of PC-88A concentration on extraction of La from phosphoric acid solutions of different concentrations (100, 200, 500 mol/m<sup>3</sup>). By increasing the PC-88A concentration, the extraction distribution ratio of La increased considerably at all phosphoric acid concentrations up to 500 mol/m<sup>3</sup>. The slope is approximately 2. At higher phosphoric acid concentrations (1000 to 2000 mol/m<sup>3</sup>) the extraction of La was very low and no valuable increase in the extraction distribution ratio when increasing PC-88A concentration. Figures 4, 5 and 6 show the results of Gd, Y and Yb systems, respectively. In all cases the observed values were close to straight lines with a slope of approximately 2; in contrast with the previously reported results for extraction from nitrate media [3], which suggests that in phosphate media, the charges of the Yb and Y ions (= +3) are not completely neutralized by

the deprotonated anionic species of the extractant but partly by some coexisting anionic species in the aqueous phase such as  $[H_2PO_4^-]$ . Similar extraction behavior was reported by Inoue *et al.* [6], for the extraction of calcium with PC-88A. Consequently the extraction reaction may be expressed as following:



where HR is PC-88A.

### Effect of pH

The effect of aqueous phase pH on the extraction distribution ratio of lanthanides (La, Gd, Yb) and Y from  $1000 \text{ mol/m}^3$  phosphoric acid solution is shown in Figure 7 (100  $\text{mol/m}^3$  PC-88A) and Figure 8 (200  $\text{mol/m}^3$  PC-88A). The extraction distribution ratios of La, Gd, Yb and Y increased considerably with increasing aqueous phase pH. At low pH values (pH 1-1.2) the extraction distribution ratios of La and Gd were very low, which indicates the possible separation of heavy lanthanides and yttrium at those low pH values.

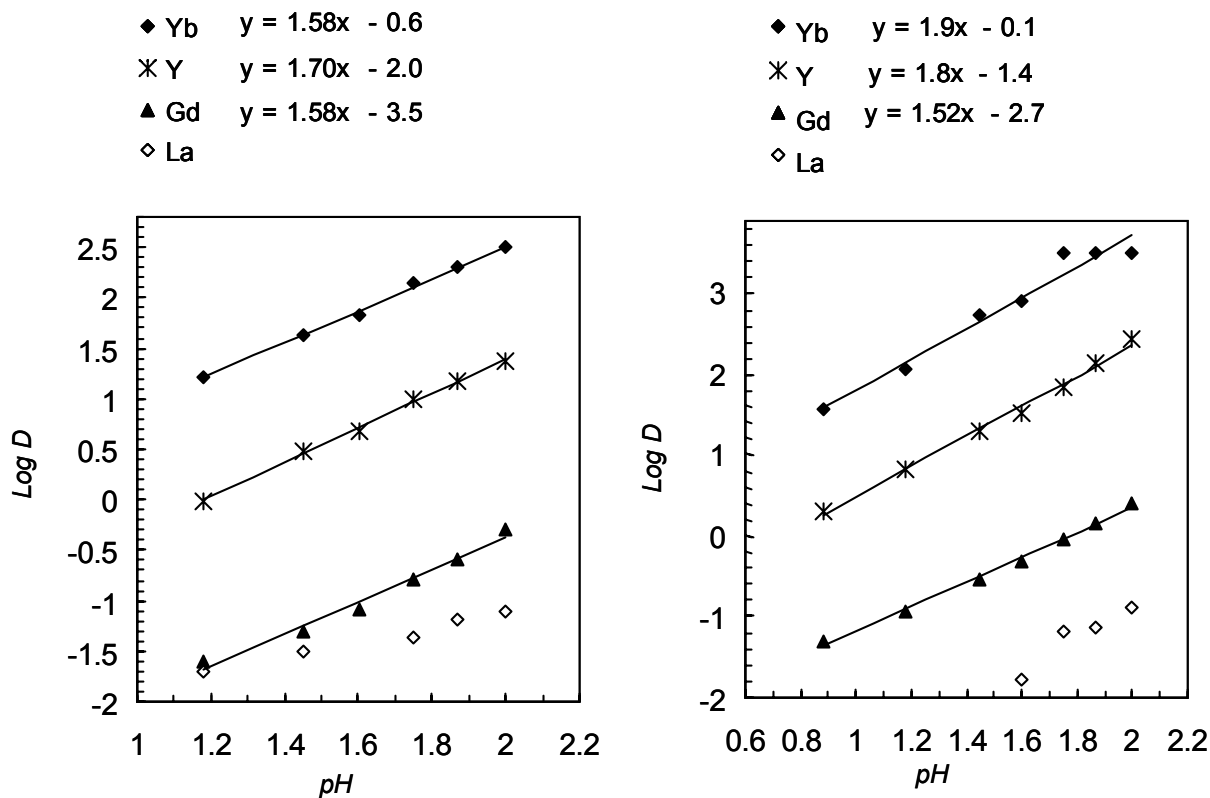


Figure 7. The effect of pH on extraction of lanthanides and Y from  $1000 \text{ mol/m}^3 H_3PO_4$  with  $100 \text{ mol/m}^3$  PC-88A.

Figure 8. The effect of pH on extraction of lanthanides and Y from  $1000 \text{ mol/m}^3 H_3PO_4$  with  $200 \text{ mol/m}^3$  PC-88A.

The effect of aqueous phase pH on the extraction behavior of individual metal ions from 1000 mol/m<sup>3</sup> phosphoric acid in single component systems with different PC-88A concentrations are shown in Figures 9 to 11.

The experimental points lie on straight lines with a slope of approximately 1.5, which confirms that lanthanide(III) ions are not extracted as +3 ions but extracted as lanthanide phosphate ionic species as shown in equation 1.

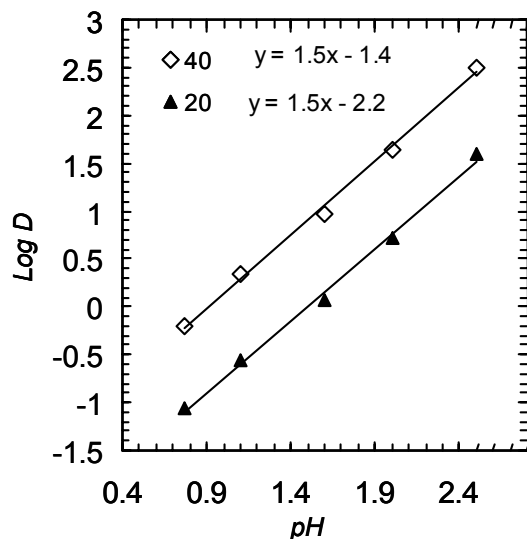


Figure 9. The effect of pH on extraction of Yb from 1000 mol/m<sup>3</sup> H<sub>3</sub>PO<sub>4</sub> with 20 and 40 mol/m<sup>3</sup> PC-88A.

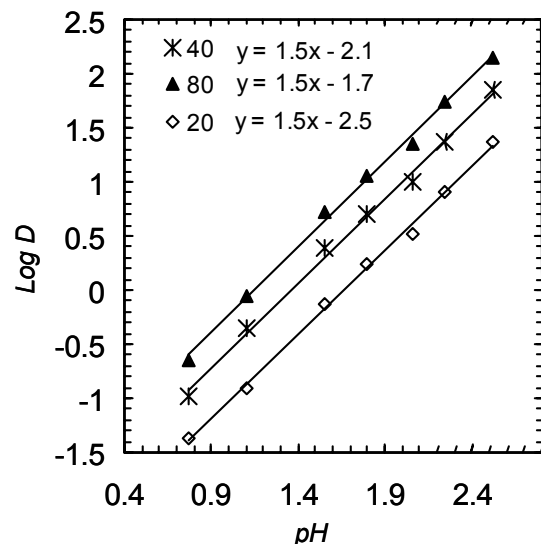


Figure 10. The effect of pH on extraction of Y from 1000 mol/m<sup>3</sup> H<sub>3</sub>PO<sub>4</sub> with 20, 40, 80 mol/m<sup>3</sup> PC-88A.

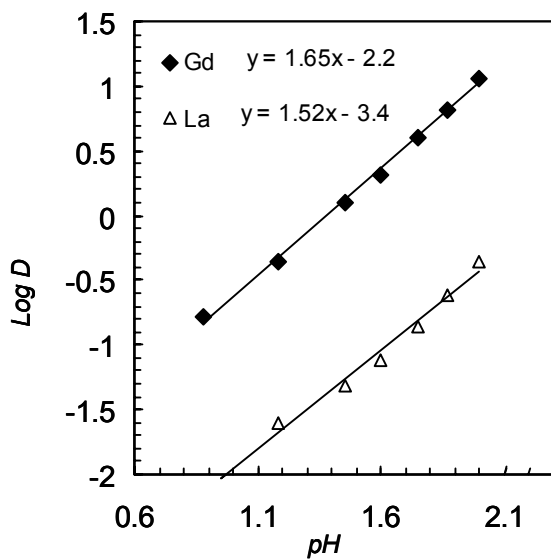


Figure 11. The effect of pH on extraction of Gd and La from 1000 mol/m<sup>3</sup> H<sub>3</sub>PO<sub>4</sub> with 400 mol/m<sup>3</sup> PC-88A.

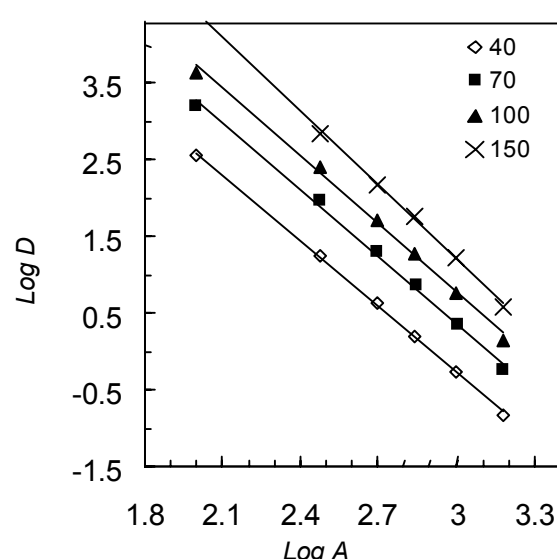


Figure 12. The effect of H<sub>3</sub>PO<sub>4</sub> concentration on extraction of Yb with 40, 70, 100 and 150 mol/m<sup>3</sup> PC-88A.

### **Effect of Phosphoric Acid Concentration**

The effect of phosphoric acid concentration on the extraction of Yb with different concentrations of PC-88A is shown in Figure 12. The extraction distribution ratio of Yb decreased considerably with increasing phosphoric acid concentration. This may be because the formation of the complex: M ( $H_2PO_4$ )<sub>3</sub>, where M is the metal ion, increases in the aqueous phase with increasing  $H_3PO_4$  concentration and this complex is a neutral complex and not extracted. This negative effect of high concentrations of phosphoric acid on the extraction efficiency of lanthanides agrees with the results reported by Krea *et al.* [1].

### **CONCLUSIONS**

The extraction of lanthanides (La, Gd, Yb) and yttrium from an aqueous phosphate medium with PC-88A was studied. Heavy lanthanide ions were extracted with low concentrations of PC-88A from phosphoric acid aqueous solutions of low concentration. The extraction distribution ratios of all lanthanides and yttrium ions were found to decrease with increasing  $H_3PO_4$  concentration. The extraction distribution ratio increased with increasing the pH value up to 2. The experimental results strongly supported the suggested extraction mechanism.

### **REFERENCES**

1. M. Krea and H. Khalaf (2000), *Hydrometallurgy*, **58**, 215-225.
2. K. Kondo and M. Matsumoto (1995), *Solv. Extr. Res. Develop., Japan*, **2**, 213-220.
3. A. Hino, T. Hirai and I. Komatsuwa (1996), *J. Chem. Eng. Japan*, **29** (6), 1041-1044.
4. C. Koopman, G. J. Witkamp, and G. M. van Rosmalen (1999), *Sep. Sci. Technol.*, **34** (15), 2997-3008.
5. J. Rydberg, C. Musikas, and G. R. Choppin (1992), *Principles and Practices of Solvent Extraction*, Marcel Dekker, New York, p. 394.
6. K. Inoue, K. Ohto and A. Mori (1998), *Solv. Extr. Res. Develop., Japan*, **5**, 16-24.



## EXTRACTIVE LEACHING IN THE TECHNOLOGY OF RARE METAL RAW MATERIALS: PROBLEMS AND PERSPECTIVES

Svetlana Chizhevskaya, Alexander Chekmarev and Michael Cox\*

D. Mendeleyev University of Chemical Technology of Russia, Russia

\*University of Hertfordshire, United Kingdom

Industrial processing of comparatively low-grade raw materials results in a considerable increase in the cost of rare metals production. Non-traditional techniques can decrease the negative influence of such raw materials on the overall economic efficiency. In this review the opportunities and limitations of replacement of such common techniques as acid leaching, solvent extraction or extraction-in-pulp to the direct recovery of metal values from the solid phase by organic solvents (extractants), in a process known as extractive leaching, are discussed, with examples of several types of oxide and silicate raw materials containing rare metals. Mechanical activation of the raw materials is shown to be a promising method for improving process efficiency.

### INTRODUCTION

The current situation regarding the resources of raw material containing rare shows, with a few exceptions, that the process of depletion of ores steadily continues [1]. The involvement of comparatively low-grade ores increases the processing, energy and transport expenses, which, together with increasingly rigorous environmental requirements, negatively affects the overall economics. To reduce the effect of this tendency on the economical efficiency of rare metal production new techniques need to be developed.

The development of integrated processes by the combination of leaching with solvent extraction (SX) seemed to be a promising route to improve the economics of hydrometallurgical processing. Thus, solvent-in-pulp (SIP) processing for uranium allows the elimination of the expensive process of filtration, however formation of interfacial cruds, stable extraction emulsions and, frequently, considerable losses of the extractant nullify the advantages of this technique [2]. These complications are largely related to the presence of silica in the ore. Thus in the course of acid leaching the silica forms polysilicic acids of various compositions and structures [3-6].

The recovery of metal values directly from the solid phase by an organic solvent (extractant) allows these difficulties to be avoided and simultaneously increases the economic efficiency of hydrometallurgical processing of raw materials containing rare metals, especially those with high silica contents [5,7-18].

It is worth mentioning that, in contrast to SIP processing, there is no clearly defined terminology in the literature devoted to such solid phase–organic solvent (extractant) processes. Terms such as extractive leaching, non-aqueous leaching, direct leaching with organic solvent, and extractive dissolution can be found. Extractive leaching (EL) seems to be the most suitable term to designate processes that involve direct recovery of metal values from solids by organic solvents or mineral acid-containing extractants in absence of water as a macro-phase.

A tolerable level of the extractant loss is one of the most important indices that determines the economics of uranium recovery in the SIP process [2]. The loss of the extractant in this process generally occurs by:

- solubility in the aqueous phase;
- entrainment with the strip solution;
- adsorption on the surface of the solid phase;
- formation of stable emulsions and cruds.

In EL processes, the loss of organic solvents will be probably be mostly associated with adsorption on the surface of the solid phase. The nature of the solvent (extractant) used is also of great importance [2,7]. In contrast to liquid-liquid systems, the rate of recovery of the target components in the system mineral-organic solvent depends on numerous factors, which are difficult to generalise. The processes in these systems are very complicated and, as a rule, are limited by the kinetics of interfacial interaction and by diffusion in solid phase. Therefore, the acceleration of such processes is achievable mainly by improving the reactivity of the solid phase. Mechanical activation could be a promising technique for this purpose [19-22].

The aim of the present review is to discuss the opportunities and limitations of EL for several types of oxide and silicate raw materials of rare metals as an alternative to conventional hydrometallurgical techniques, and to show the influence of preliminary mechanical treatment of solid phase on the process efficiency.

## EXTRACTIVE LEACHING OF OXIDE RAW MATERIALS

The studies on EL of uranium from various raw materials were the first in this field, originating in the late 1940s from a desire to minimise the cost of hydrometallurgical processing, first at the leaching stage [7-14].

Sulphating treatment of the ores of the Colorado plateau was associated with high consumption of  $H_2SO_4$  (sometimes exceeding 250 kg/t) [7]. The replacement of acid leaching by EL with alkylphosphoric acids for the recovery of uranium from carnotite and uranite ores resulted in a significant decrease of acid consumption (from 180 to 15-20 kg/t) [8]. Concentrated  $H_2SO_4$  added to the extractant or to its pulp with the ore before contact resulted in the formation of a gypsum layer that coated the calcite particles thus preventing excessive acid consumption. Stripping of uranium was carried out by HCl solution. The extractant captured and separated from the solid residue by flushing with a fresh portion of solvent, which was recycled from the tailings by distillation. In the absence of added  $H_2SO_4$  to isoctylphosphoric acid, the extractant loss with tailings increased considerably because of the formation of the insoluble calcium salt. Fine grinding of the ore (up to –50 mesh) promoted recovery, especially for uranite ore, however this sometimes caused further problems associated with precipitation of fine particles and subsequent filtering. The authors indicated that EL was an effective technique only in case U(VI)-containing minerals with large amounts of calcite as well as for the ores forming the pulps, which are difficult to thicken and to filter.

Similar EL processes for uranium using tri-*n*-butylphosphate (TBP) in hexane combined with preliminary mixing with concentrated H<sub>2</sub>SO<sub>4</sub> and then with HNO<sub>3</sub> [9-11] or by acetone combined with mixing with a concentrated HCl/H<sub>2</sub>SO<sub>4</sub> mixture were tested on a pilot-industrial scale [12,13]. According to Magnér [7], these versions have no advantages in minimising acid consumption in comparison with acid leaching.

A percolating leach of uranium from the product of a mixture of ground superphosphate by 1 to 2% octylpyrophosphoric acid (OPPA) solution in hexane (O:A = 1:1) resulted in a 30 to 40% increase in recovery in comparison with SX from phosphoric acid [14]. The extractant captured by the residue was washed with hexane, which was then distilled from the residue at 80°C. Uranium was stripped by HF, HCl, etc., and the OPPA recycled. It was also noted that the recovery increased with a decrease of superphosphate particle size.

Total dissolution of uranium dioxide in 0.1 mol dm<sup>-3</sup> TBP and di(2-ethylhexyl)phosphoric acid (DEHPA) kerosene solutions and 0.1 mol dm<sup>-3</sup> tri-octylamine solution in xylene, all saturated with concentrated HNO<sub>3</sub>, under conditions allowing oxidation of the metal was shown by Filippov and Strelkov [15]. The higher oxidative ability of HNO<sub>3</sub> in the organic phase was attributed to occurrence of the acid predominantly in the non-dissociated form.

EL using organophosphorous compounds of niobium and tantalum from a microlite concentrate (31.4% Ta<sub>2</sub>O<sub>5</sub>, 16.5% Nb<sub>2</sub>O<sub>5</sub>) that was resistant to decomposition was shown by Mineev *et al.* [16]. The extractants dibutyl methylphosphonate (DBMP), dioctyl butylphosphonate (DOBp) and TBP were first saturated with 20% HF (O:A = 1:1). Maximum recovery (81% Ta and 74% Nb) was obtained on initially ground (-200 mesh) concentrate by 100% DBMP (A:O=1:10, 20°C, 4 h). Multistage processing (A:O=1:5, 55-60°C, 4 h) resulted in practically total recovery of both metals (80 to 90 g dm<sup>-3</sup> Me<sub>2</sub>O<sub>5</sub>). Some impurities (Si, Sn, Fe and Ti) also partially passed into the organic phase and were separated in the course of subsequent washing. Niobium and tantalum were stripped using NH<sub>4</sub>NO<sub>3</sub> and NH<sub>4</sub>F solutions, respectively. The combination of stages led to a two-fold decrease in the amount of HF required and the use of H<sub>2</sub>SO<sub>4</sub> was avoided. Grinding the concentrate allowed a two-fold increase of Nb and Ta recovery into DOBp.

Extractive leaching of molybdenum (60°C, 5 h) from a molybdenite concentrate, as received and mechanically activated in an EI-2 planetary mill (60 g, 10 min), using organic solvents containing 1 mol dm<sup>-3</sup> acids (HClO<sub>4</sub>, H<sub>2</sub>SO<sub>4</sub>, HCl, HNO<sub>3</sub>) has been discussed [17]. Propylene carbonate (PC), acetonitrile (AN), dimethylsulfoxide (DMSO) and dimethylformamide (DMFA) were tested as the organic solvents. Maximum recovery was achieved for the mechanically activated concentrate using a HNO<sub>3</sub>-containing solvent; the acid acting as an oxidant. According to increasing molybdenum recovery, these solvents were put into the following series: AN > PC > DMSO > DMFA. The following phenomena were observed in the course of this extractive leaching of the molybdenite concentrate:

- a significant increase in the viscosity of PC solutions as a result of propyleneglycol formation, that also impeded subsequent filtration and analysis of the products;
- destruction of the solvent lead to formation of resin-like products under long-term contact with H<sub>2</sub>SO<sub>4</sub>;
- stratification of the organic phase into two because the products formed mixed badly with AN.

At the same time, in the opinion of the authors, slight hydrolysis of PC by nitric acid leading to propyleneglycol formation may promote the leaching of Mo(VI) from molybdenite. The possibility of EL of molybdenum from molybdenite concentrate using alcohols (allyl, propyl, butyl, heptyl) and esters such as ethyl acetate, butyl acetate, and TBP containing HNO<sub>3</sub> was also established [17]. The maximum Mo(VI) recoveries (60°C, 5 h) were observed for the mechanically activated concentrate using propanol (23.6%) and ethyl acetate (42.3%), whereas the values for the non-activated concentrate were 1.8 and 0.7%, respectively.

Studies on the effect of mechanical treatment on the efficiency of EL processes are for the most part phenomenological. Frequently even those authors who use the term mechanical activation (MA) do not discuss the influence of mechanical treatment on transformations in the structure of main and admixture minerals, their morphology, particle size and other factors that determine reactivity to organic solvents as well as losses of the latter. In the last 30 to 40 years, a considerable number of studies illustrating the efficiency of MA for increasing of reactivity of solids have been published (a number of them have been cited, e.g., monographs [19,20]). MA not only increases the specific surface of solids but also significantly affects the structure by deformation and partial destruction of the crystal lattice forming various types of defects thus influencing the kinetics of the leaching processes. The efficiency of MA is to a large extent determined by the type of device used as well as by regime of action on the material subjected to the treatment: attrition, vortex and impact. The material of construction and geometry of the equipment and the acting bodies, the medium of the process, the mass ratio of acting bodies and the material being treated are also of considerable importance. The planetary type apparatus has been shown to be efficient for mechanical activation of resistant raw materials. Depending on the aim of the treatment, each material requires an optimum selection of specific activation conditions.

## EXTRACTIVE LEACHING OF SILICATE RAW MATERIALS

Extractive leaching is a very effective technique for selective recovery of metal values (Zr, REE) from low-grade high-silica mineral raw materials such as eudialyte [5,6,21-26]. Eudialyte is a complex zirconosilicate containing, along with rare elements (Zr, Hf, Nb, Ta, REE), large amounts of silica ( $\geq 50\%$  SiO<sub>2</sub>). Considerable resources of this mineral are available in Russia, USA, Canada, Greenland, Sweden, Australia and the Republic of South Africa. The use of this mineral resource is limited by the absence of an economically suitable technology. All known methods of acid leaching of eudialyte proposed its "total dissolution", associated with large amounts of silica passing into solution and characterised by high cost of leaching agents, energy and lengthy processing.

EL of eudialyte by 100% TBP saturated with concentrated HNO<sub>3</sub> practically eliminates the dissolution of silica and the phases are easy to separate [5,6]. Preliminary short-term mechanical activation (1 min) in a high-energy AGO-2 activator under regimes that preserve the main structure of the mineral results in a three-fold increase of the recovery of metal values (Zr, REE) in the organic phase and a reduction by half of the organic phase capture by the solid cake. Combination of mechanical activation and EL actually allows total selective recovery of REE and 50% of zirconium in 10 min [5].

It was shown with quantitative IR spectroscopy that the extracts obtained by EL from eudialyte using 100% TBP ( $C_{HNO_3}^{org} = 4$  to 5.5 mol/l) contain the complex  $[TBP \cdot H_3O^+ \cdot (H_2O)_n]Zr(NO_3)_5^-$  as a major product [27]. This complex is formed from  $[TBP \cdot H_3O^+ \cdot (H_2O)_2] \cdot NO_3(HNO_3)_p^-$  ionic pairs and  $Zr(NO_3)_5^-$  anions through an ion-exchange mechanism.

Regrettably, it is not possible to discuss in the scope of this review interesting results of other recent studies on EL of rare and non-ferrous metals from, for example, intermediate products of chlorinating or sulphating of ores (concentrates) [18], secondary raw materials [28], as well as the studies on adsorption of extractants on solid particles related to the problem of crud formation and our own studies, in particular, on the effect of the nature of eudialyte concentrate on extractant losses.

## CONCLUSIONS

This review illustrates that very interesting results of the studies on EL of uranium from ores performed in 1950s, which regrettably have not been further applied to industry, promoted studies on recovery of rare and non-ferrous metals from natural and secondary raw materials, products of decomposition of ores and concentrates as well as investigations into the problems of extractant losses.

EL is a complex process, whose efficiency depends on a number of factors such as: the nature of the ore; the amount of admixture minerals (first of all, silicates); extent of embedding of the minerals into barren rock; particle size; the nature of the organic phase used, hydrodynamics of the process, temperature as well as some other less obvious factors. Nevertheless, in our opinion, the accumulated experience on SIP processes as well as in the field of intensification of mineral raw material treatment by mechanical activation enables the consideration of EL techniques as an alternative to conventional hydrometallurgical processes to solve the problems of extractant losses.

EL provides a significant decrease in the consumption of chemicals and energy; reduces the number of stages in the process by recovering target components directly from solid phase; permits the change of redox equilibria in the system thus controlling the mechanism and kinetics of the recovery processes; and enables the recycling of organic solvents thus protecting the environment.

In connection with the increasing use of relatively low-grade raw material resources, the EL technique will be of growing importance. Therefore, in our opinion, it seems reasonable to include this technique into the group of solvometallurgical methods [1,29]. Solvometallurgy gathers together the recovery of metal values from raw materials using chemical reactions in organic, inorganic or mixed non-aqueous media in absence of water as the macro-phase. The comprehensive development of the theoretical and applied aspects of solvometallurgy will provide the basis for development of principally new techniques for treating primary and secondary raw materials as an alternative to those currently in use.

## ACKNOWLEDGEMENT

The studies of mechanical activation on EL of eudialyte have been supported by ISTC (Grant 1332-99).

## REFERENCES

1. A. M. Chekmarev, S. V. Chizhevskaya and E. P. Buchikhin (2000), *Khim. Tekhn.*, **10**, 2-7.
2. G. M. Ritcey, and A. W. Ashbrook (1983), Solvent Extraction: Principles and Applications to Process Metallurgy, Part II, Metallurgia, Moscow, pp. 308-350.
3. G. M. Ritcey (1986), *Can. Met. Q.*, **25**, 31-43.
4. G. M. Ritcey (1996), *Proc. ISEC '96*, Vol. 1, University of Melbourne, Melbourne, pp. 17-24.
5. S. V. Chizhevskaya, A. M. Chekmarev, M. Cox, O. M. Klimenko *et al.* (1994), *Proc. Hydrometallurgy '94*, Society of Chemical Industry, London, pp. 219-228.
6. S. V. Chizhevskaya, O. A. Sinegribova, A. M. Chekmarev, and M. Cox (1996) *Proc. ISEC '96*, Vol. 1, University of Melbourne, Melbourne, pp. 683-687.

7. J. E. Magner and R. H. Bails (1959), *Proc. 2<sup>nd</sup> Int. Conf. on Peaceful Applications of Nuclear Energy*, Publ.: Atomizdat, Moscow, p. 307.
8. J. E. Magner (1957), *DOW-156*, (cited in [7]).
9. P. Galvanek and D. Kaufman (1949), *MITG-A74*, (cited in [7]).
10. P. Galvanek and D. Kaufman (1950), *MITG-225*, (cited in [7]).
11. P. Galvanek and M. S. Pelland (1955), *WIN-31*, (cited in [7]).
12. R. A. Ewing *et al.* (1955), *BM1279-280*, (cited in [7]).
13. D. R. Foley and R. B. Filbert (1957), *Paper at American Nuclear Congress*, Philadelphia, (cited in [7]).
14. R. S. Long, D. A. Ellis and R. H. Bails (1955), *Proc. Int. Conf. on Peaceful Applications of Nuclear Energy*, Publ.: Chemistry of Nuclear Fuel, GNTI Khim. Lit., Moscow, 1956, pp. 7-16.
15. A. P. Filippov and L. A. Strelkov (1971), *Radiokhimia*, **13**, 52-57.
16. G. G. Mineev, A. S. Chernyak and T. A. Skogoreva (1972), *Trudy Irgiredmeta: Development and Research of Metallurgical Processes of Noble and Rare Metals Recovery from Ores and Concentrates*, **27**, pp.184-189.
17. I. Ya. Schevtcova, A. S. Chernyak and A. A. Khalzov (1992), *J. Appl. Chem.* **65**, 1966-1972.
18. A. S. Chernyak (1998), Processes of Dissolution: Leaching, Solvent extraction, Irkutsk University Publ., Irkutsk, 407 pp.
19. E. G. Avvakumov (1986), Mechanical Methods of Activation of Chemical Processes, Nauka, Novosibirsk, 304 pp.
20. V. I. Molchanov, O. G. Selezneva and E. N. Zhirnov (1988), Activation of Minerals in Course of Grinding, Nedra, Moscow, 208 pp.
21. S. V. Chizhevskaya, A. M. Chekmarev, M. V. Povetkina *et al.* (1999), *Proc. Indo-Russian Microsym. Nonferrous Extractive Metallurgy in the New Millennium. A Compendium of Invited Papers*, Nat. Metall. Lab., Jamshedpur, India, pp. 21-28.
22. S. V. Chizhevskaya, A. M. Chekmarev, V. A. Michailov and E. G. Avvakumov (2001), *Proc. VI SHMMT/XVIII ENTMME*, Vol. 2, Rio de Janeiro, Brazil, pp. 323-328.
23. S. V. Chizhevskaya, M. V. Povetkina, A. M. Chekmarev, and M. Cox (1996), *Proc. ARS Separatoria*, Minikovo, Poland, pp. 69-71.
24. S. V. Chizhevskaya, A. M. Chekmarev, M. V. Povetkina M.V. *et al.* (1998), *Proc. of the IV Int. Conf. on Clean Technologies for the Mining Industry*, Vol. 2, Santiago, Chile, pp.523-532.
25. S. V. Chizhevskaya, A. M. Chekmarev, M. Cox *et al.* (2000), *Proc. ISEC '99*, Society of Chemical Industry, London, pp. 805-809.
26. S.V. Chizhevskaya, A.M. Chekmarev, O.M. Klimenko and M. Cox (2001), *Proc. XII Romanian Int. Conf. on Chemistry and Chem. Eng.*, Bucharest, Romania, (in press).
27. S. V. Chizhevskaya, E. S. Stoyanov and A. M. Chekmarev *et al.* (1990), *Sbornik Nauchn. Trudov RCTU*, Physico-chemical problems of chemical plants, Moscow, pp. 7-12.
28. G. Thorsen, H. F. Svendsen, and A. Grislingas (1982), *Proc. NATO Advanced Research Institute on Hydrometallurgical Process Fundamentals*, Vol. VI, Cambridge, UK, pp. 269-292.
29. A.M. Chekmarev, S.V. Chizhevskaya, E.P. Buchikhin and M. Cox (2001), *Proc. VI SHMMT/XVIII ENTMME*, Vol. 2, Rio de Janeiro, Brazil, pp. 441-444.



# DEVELOPMENT OF A SOLVENT EXTRACTION PROCESS FOR THE PRODUCTION OF PURE NEODYMIUM OXIDE FROM SYNTHETIC MT WELD PROCESS LIQUOR

**Chu Yong Cheng, Karin Sodenhoff\*** and **Mike Vaisey†**

AJ Parker CRC for Hydrometallurgy / CSIRO Minerals, Australia

\*Australian Nuclear Science and Technology Organisation, Australia

†Lynas Corporation Pty Ltd, Australia

The objective of the current project was to develop a solvent extraction process for the production of pure Nd oxide (98%) from Mt Weld leach liquor. Ionquest 801 was chosen as extractant and Shellsol D70 as diluent. pH isotherms were obtained from batch tests. Semi-continuous tests were carried out to develop the solvent extraction process in three separate circuits. In circuit 1, almost all middle and heavy rare earths were extracted. The co-extracted light rare earth metals were effectively scrubbed. In circuit 2, the Nd/(La-Nd) ratio increased from 15% in the feed to 44% in the loaded strip solution. In circuit 3, the Nd/(La-Nd) ratio was further increased to 71% by extraction and from 71% to 97.5% by scrubbing. The goal to obtain a Nd/(La-Nd) ratio of 98%, is thought to be achievable with the present flowsheet by increasing the number of scrub stages in Circuit 3.

## INTRODUCTION

The Mt Weld Rare Earths Project is based upon a world-class resource of rare earths near Laverton in Western Australia. The resource contains approximately 2 million tonnes at 18% rare earth oxide in phosphate mineralisation [1]. The Mt Weld deposit is unique in that it has a low level of radioactivity compared to other monazite concentrates. Lynas Corporation and its joint venture partners expect project development to commence in 2002. The Australian Nuclear Science and Technology Organisation (ANSTO) was contracted to carry out the pilot plant program. One of the objectives of the program was to develop a solvent extraction (SX) process for the separation of rare earths from a chloride solution. In February 2000, ANSTO, in partnership with the AJ Parker Cooperative Research Centre for Hydrometallurgy, was commissioned to develop an SX process for the production of pure neodymium oxide (98%).

A comprehensive literature review was conducted. The emphasis was to review commercial processes [2-5] and research work with D2EHPA (di-2-ethylhexyl phosphoric acid) [6-7] and EHEHPA (2-ethylhexyl phosphonic acid mono-2-ethylhexyl ester) [8-10] for the production of pure rare earth products, especially Nd oxide [11]. EHEHPA was found to be a better extractant compared with D2EHPA due to the reduced tendency for gel formation, lower acid concentration required for stripping, and larger separation factors for the separation of Nd from other light rare earths (LRE). Based on the literature review and assessment of previous ANSTO work [12], Ionquest 801 (EHEHPA) was chosen as the extractant with Shellsol D70 as the diluent.

## EXPERIMENTAL

The synthetic rare earth chloride solution contained (in g/L) La (41.6), Ce (1.21 in circuit 1 and 41.2 in circuit 2), Pr (6.82), Nd (22.4), Sm (3.67), Eu (0.32), Gd (1.30), Tb (0.09), Dy (0.27), Y (0.56) and Er (0.04). The organic solution contained 0.6 M Ionquest 801 in Shellsol D70.

### Batch Tests

Shakeout tests were conducted using plastic rectangular boxes and overhead stirrers. Hydrochloric acid (100 g/L) and ammonia solution (10%) were used to adjust the solution pH as required. Aqueous solution sample and organic strip raffinate were analysed.

### Semi-continuous Tests

The term "semi-continuous" is relative to "fully-continuous". In a semi-continuous counter-current solvent extraction test, extraction, scrubbing and stripping circuits are operated independently. Two mini rigs of 10 mixer-settlers each with mixer volume of 0.16 litre and settler volume of 0.38 litre were used to conduct semi-continuous tests. All tests were conducted at 22°C.

## SEPARATION OF LIGHT FROM MIDDLE AND HEAVY RARE EARTHS (CIRCUIT 1)

### pH Isotherms

pH isotherms of the rare earth metals (Figure 1) were obtained from batch tests. It was found that:

- The pH for the separation of light from middle and heavy rare earths should be around 1.0.
- The pH for the separation of Nd from La, Ce and Pr should be around 1.4.
- The separation of Nd from Ce and Pr would require many extraction and scrubbing stages.

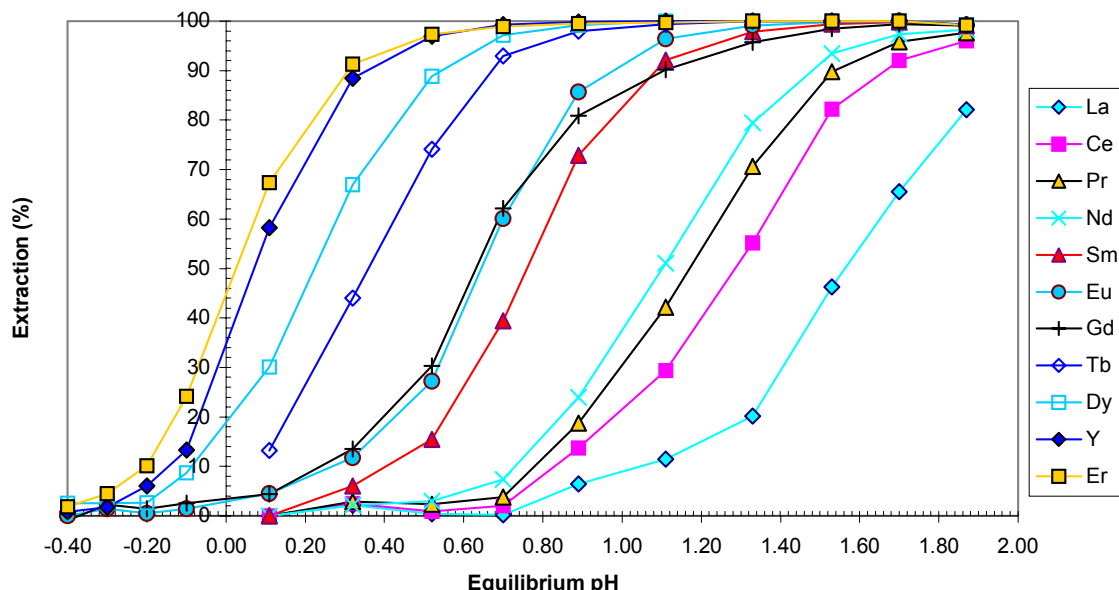


Figure 1. pH isotherms of rare earths with 0.6 M (20% v/v) Ionquest 801 in Shellsol D70.

### Semi-continuous Extraction

Distribution isotherms were determined and the McCabe Thiele diagrams indicated that four theoretical stages were needed to separate Sm and Nd. Therefore in circuit 1, a total of six extraction stages were used. The pH in stages 1, 3 and 6 was controlled at 1.0 and the A/O flowrate ratio was 1:1.5. Almost all middle and heavy rare earths were extracted. The Sm concentration in the raffinate was as low as 17 mg/L with a 99.5% extraction (Table 1). Some 18% Nd, 11% Pr, 5.5% Ce and 1.7% La were co-extracted. Figure 2 shows that some Nd extracted was crowded out by middle and heavy rare earths in stages 2 and 1 where the concentration of middle and heavy rare earths was high.

*Table 1. Metal concentration and extraction in circuit 1.*

Element	Concentration (g/L)			Extraction (%)
	Feed	Raffinate	Loaded organic	
La	41.6	37.6	0.445	1.74
Ce	1.21	1.04	0.040	5.45
Pr	6.82	5.58	0.465	11.11
Nd	22.4	16.7	2.47	18.13
Sm	3.67	0.017	2.37	99.53
Eu	0.315	0.000	0.205	100.00
Gd	1.30	0.000	0.855	100.00
Tb	0.090	0.000	0.055	100.00
Dy	0.270	0.000	0.165	100.00
Y	0.560	0.000	0.340	100.00
Er	0.040	0.000	0.035	100.00

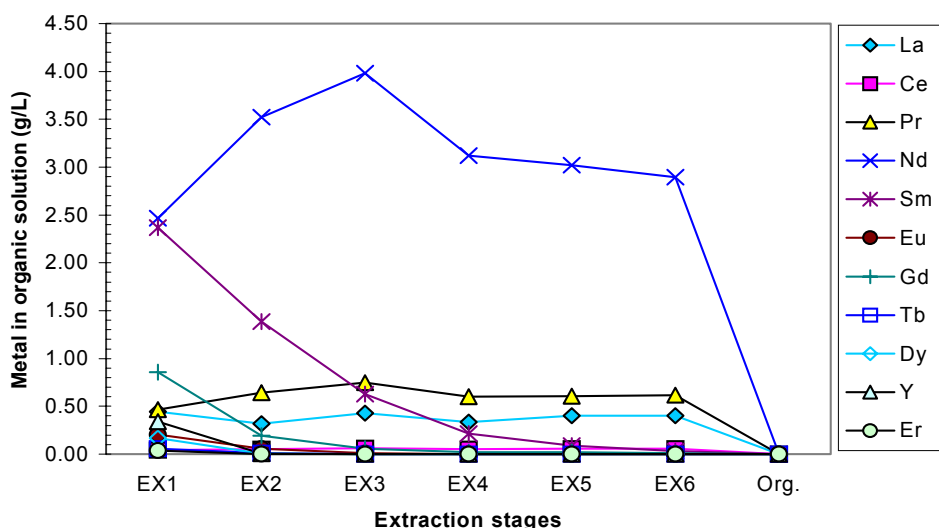


*Figure 2. Metal concentration in organic solution in extraction stages in circuit 1.*

### Semi-continuous Scrubbing

Pre-loaded organic phase was scrubbed at an A/O flowrate ratio of 1:5 using a scrub solution containing 12 g/L HCl, 5 g/L Sm and 2 g/L Gd. Almost all LRE were scrubbed with the concentration of La, Ce, Pr and Nd in the scrubbed organic phase being 2, 2, 1 and 4 mg/L respectively (Table 2). Figure 3 shows that displacement of Nd by Sm occurred in the first two stages. In stages 3-6, the concentration of both Sm and Nd in the organic phase dropped due to the higher acidity in the scrub solution.

Table 2. Metal concentration and scrubbing efficiency in circuit 1.

Element	Concentration (g/L)				Total scrub efficiency (%)
	Scrub solution	Loaded organic	Scrubbed organic	Spent scrub liquor	
La	0.034	0.330	0.002	1.62	97.39
Ce	0.000	0.045	0.002	0.204	96.22
Pr	0.003	0.555	0.001	2.65	99.76
Nd	0.020	2.89	0.004	13.3	99.71
Sm	4.83	2.63	2.25	4.05	10.57
Eu	0.001	0.230	0.190	0.106	17.38
Gd	2.03	1.01	1.45	0.309	-31.54
Tb	0.000	0.065	0.060	0.008	7.69
Dy	0.003	0.200	0.200	0.008	0.00
Y	0.000	0.415	0.400	0.001	3.61

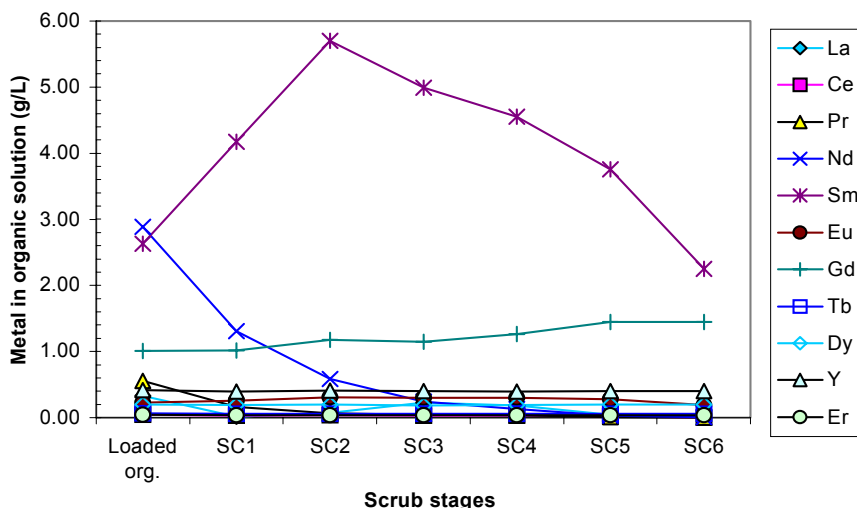


Figure 3. Metal concentration in organic solution during scrubbing in circuit 1.

### Semi-continuous Stripping

The semi-continuous stripping test in circuit 1 was conducted in 6 stages of which the first three stages were used for selective stripping to obtain a Sm, Eu and Gd product, and the remaining three stages were used for bulk stripping. The strip test was conducted at an A/O flowrate ratio of 1:5. HCl solutions of 1 M and 3 M were used in the selective and bulk stripping, respectively. In the selective strip stages, over 96% Sm, 98% Eu and 94% Gd were stripped and smaller fraction of heavy rare earths were stripped, indicating the possibility of obtaining a Sm, Eu, Gd product via selective stripping (Table 3). All middle and heavy rare earths were stripped with 3 M HCl in bulk stripping.

Table 3. Metal concentration and stripping efficiency in circuit 1.

Element	Concentration (g/L)			Strip efficiency (%)	
	Scrubbed organic	Loaded strip liquor 1	Loaded strip liquor 2	Selective	Total
Sm	4.44	20.7	0.863	96.15	100.00
Eu	0.230	1.01	0.048	98.08	100.00
Gd	1.72	6.91	0.387	94.58	100.00
Tb	0.100	0.226	0.066	75.09	100.00
Dy	0.195	0.188	0.330	34.48	100.00
Y	0.420	0.097	1.24	5.24	100.00
Er	0.040	0.004	0.118	7.86	100.00

## SEPARATION OF NEODYMIUM FROM OTHER LRE (CIRCUIT 2)

During the course of this work, the projected Ce concentration in the feed was increased from 1.2 g/L to 41.2 g/L. Therefore, the Ce concentration in the extraction raffinate of circuit 1 (feed for circuit 2) was similarly affected, increasing the difficulty in the separation of Nd from the light rare earths, due to the closeness of the pH isotherms of Nd and Ce (Figure 1).

### **Semi-continuous Extraction**

The semi continuous extraction test in circuit 2 was conducted at pH 1.4 with an A/O flowrate ratio of 1:3. A total of 10 stages were used and the pH was controlled at stages 1, 5 and 10. The ratio of Nd/(La-Nd) increased from 15% in the aqueous feed solution to 44% in the loaded organic solution (Table 4). This indicates that it would be very difficult to scrub the organic solution to obtain a Nd/(La-Nd) ratio of 98% in the scrubbed organic solution. A decision was made to strip the loaded organic solution and to re-load it with the strip raffinate in a third circuit.

*Table 4. Metal concentration and extraction in circuit 2.*

Element	Concentration (g/L)			Extraction (%)	Separation factor ( $\beta_{Nd/M}$ )
	Feed	Raffinate	Loaded		
La	33.3	24.2	0.45	4.01	179.7
Ce	41.2	20.0	4.05	29.49	16.3
Pr	4.90	1.20	0.98	59.69	4.1
Nd	14.8	1.30	4.30	87.06	1.0
Nd/(La-Nd) (%)	15.7	2.8	43.9		

## SEPARATION OF NEODYMIUM FROM OTHER LRE (CIRCUIT 3)

### **Semi-continuous Extraction**

The semi continuous extraction in circuit 3 was conducted, again, at pH 1.4 with an A/O ratio of 1:3. A total of 15 stages were used with pH controlled in stages 1, 13 and 15. After 15 stages of extraction, the ratio of Nd/(La-Nd) increased from 50% in the synthetic feed to 71% in the loaded organic, with 97% Nd extraction (Table 5). The cumulative separation factor of Nd/La (359) and Nd/Ce (32) was much larger than Pr (5.7), indicating that in the extraction stages, Nd was mainly separated from La and Ce. Figure 4 shows that the Nd concentration increased constantly from stage 15 to stage 1 while the Ce concentration increased initially and then dropped, indicating that the Nd crowded out the Ce from the organic solution.

*Table 5. Metal concentration and extraction in circuit 3.*

Element	Concentration (g/L)			Extraction (%)	Separation factor ( $\beta_{Nd/M}$ )
	Feed	Raffinate	Loaded organic		
La	3.01	2.54	0.08	7.48	359.0
Ce	14.0	5.24	1.77	37.82	31.5
Pr	4.36	0.53	0.99	67.78	5.7
Nd	21.1	0.67	7.05	96.95	1.0
Nd/(La-Nd) (%)	49.7	7.4	71.4		

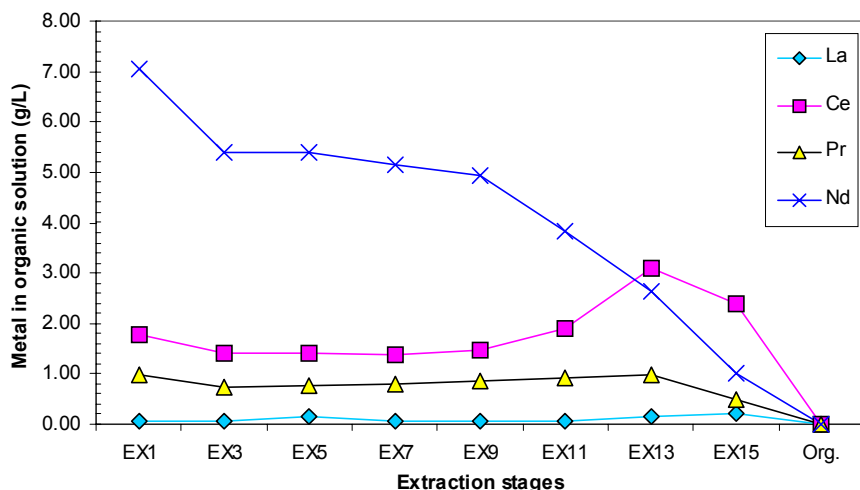


Figure 4. Metal concentration in organic solution in extraction stages in circuit 3.

### Semi-continuous Scrubbing

The semi continuous scrub test was conducted without pH control. The scrub solution, made from a very pure Nd oxide (99.9%), contained 15 g/L Nd at pH 1.4. A total of 20 scrub stages were used at an A/O flowrate ratio of 1:5. The Nd/(La-Nd) concentration ratio in the scrubbed organic reached 97.5% with the total concentration of the other three LRE (La, Ce and Pr) being 0.215-0.225 g/L (Table 6).

Table 6. Metal concentration and scrubbing efficiency in circuit 3.

Element	Concentration (g/L)				Scrub efficiency (%)
	Loaded organic	Scrub solution	Spent scrub liquor	Organic scrubbed	
La	0.075	0.002	0.311	0.015	80.00
Ce	1.77	0.005	7.53	0.100	94.33
Pr	0.985	0.038	4.24	0.110	88.83
Nd	7.05	15.5	7.37	8.80	-24.82
Nd/(La-Nd) (%)	71.4	99.7	37.9	97.5	

### CONCLUSIONS

pH isotherms of the rare earth elements were obtained with 0.6 M lonquest 801 (EHEHPA) in Shellsol D70 by shakeout tests to determine the pH for the separation of Sm from Nd (1.0) and the pH for the separation of Nd from other LRE (1.4). Semi-continuous extraction tests in circuit 1 showed that almost all middle and heavy rare earths were extracted at pH 1.0 in six stages at an A/O ratio of 1:1.5. The raffinate contained only 17 mg/L Sm. After six stages of scrubbing with a solution containing middle rare earths, almost all co-extracted light LRE were scrubbed, indicating an over 99% LRE recovery in the raffinate in circuit 1. The Nd/(La-Nd) ratio increased from 15% in the feed to 44% in the loaded organic solution in circuit 2 by extraction at pH 1.40 in 10 stages. In circuit 3, the Nd/(La-Nd) ratio was further increased to 71% in the organic solution by extraction at pH 1.4 in 15 stages and from 71% to 97.5% by scrubbing with pure Nd solution in 20 stages. This work has shown that the goal of obtaining a 98% Nd/(La-Nd) ratio is achievable and pilot trials were conducted to confirm the technical feasibility of the process.

## **ACKNOWLEDGEMENTS**

The provision of Ionquest 801 by Albright and Wilson Australia Limited and Shellsol D70 by The Shell Company of Australia Limited is acknowledged. The authors thank the management and staff of ANSTO and The AJ Parker CRC (CSIRO Minerals and Murdoch University) for carrying out and supporting the project.

## **REFERENCES**

1. K. Soldenhoff, D. Kingsnorth and M. Vaisey (2000), *ALTA 2000 SX/IX-1*, ALTA Metallurgical Services, Melbourne, Australia.
2. H. G. Li (1979), *The Principles and Technologies of Rare Metal Metallurgy*, Metallurgical Industry Publisher (in Chinese), pp. 65-158.
3. G.M. Ritcey and A.W. Ashbrook (1984), *Solvent Extraction: Principles and Applications to Process Metallurgy*, Part I, Elsevier, Amsterdam, pp.106-107.
4. L. Sherrington (1983), *Handbook of Solvent Extraction*, T.C. Lo, M.H.I. Baird and C. Hanson (eds.), Krieger Publishing Company, Florida, pp. 717-723.
5. M.L.P. Reddy, T.P. Rao and A.D. Damodaram (1995), *Min. Proc. Ext. Met. Rev.*, **12**, 91-113.
6. J.S. Preston, A.C. du Preez, P.M. Cole and M.H. Fox (1996), *Hydrometallurgy*, **42**, 131-149.
7. N.V. Thakur, D.V. Jayawant and K.S. Koppiker (1992). *Proc. International Solvent Extraction Conference 1990*, T. Sekine (ed.), Kyoto, Japan, pp.1003-1008.
8. D. Q. Li, Z.H. Wang, Y.F. Xie, C.L. Shen, C.P. Zhang and S.N. Le, (1985), *International Conference: Rare earth Development and Application*, Beijing, China, **1**, pp.463-467.
9. T. Sato (1989), *Hydrometallurgy*, **22**, 121-140.
10. J.S. Preston (1996), *Hydrometallurgy*, **42**, 151-167.
11. N.V. Thakur, D.V. Jayawant, N.S. Tyer and K.S. Koppiker (1993), *Hydrometallurgy*, **34**, 99-108.
12. K. Soldenhoff (2000), *Australian Nuclear Science and Technology Organisation Commercial Report*, ANSTO/C627, Sydney, Australia, 81 pp.



## SEPARATIONS AND RECOVERY OF URANIUM, THORIUM AND LANTHANIDES FROM MONAZITE USING CYANEX 923

Bina Gupta, Poonma Malik and Akash Deep

Department of Chemistry, University of Roorkee, Roorkee, India

The extraction behaviour of uranium, thorium and lanthanides, represented by cerium and ytterbium, has been investigated in Cyanex 923. Effect of different variables like the concentration of acids, metal ion and extractant, nature of diluent and temperature has been studied. The composition of the extracted U(VI) and Th(IV) species has been proposed. Based on the partition data some important ternary separations involving the aforesaid metal ions have been achieved. The proposed procedure has been applied for the recovery of uranium, thorium and lanthanide fraction from monazite sand. Stability and regeneration capacity of the extractant have been evaluated.

### INTRODUCTION

Uranium and thorium are the two most vital elements for nuclear energy programme. Their natural sources generally contain a sizeable fraction of lanthanides which in their own right have diverse technological applications. Thus the methodology adopted for the separation of these metal ions from different ores has always attracted the attention of separation scientists. Over the years a variety of extractants such as high molecular weight amines, carboxylic acids, tributylphosphate (TBP), di-2-ethylhexylphosphoric acid (DEHPA) and tri-*n*-octylphosphine oxide (TOPO) have been more frequently used for the attainment of these separations. However, they have their own limitations such as aqueous miscibility, low hydrolytic stability, interference from  $\text{CO}_3^{2-}$ ,  $\text{SO}_4^{2-}$  and  $\text{PO}_4^{3-}$  anions, emulsion formation and poor selectivity. Lately Cyanex 923, a mixture of four tri-alkylphosphine oxides ( $\text{R}^1\text{P}=\text{O}$ ,  $\text{R}_3\text{P}=\text{O}$ ,  $\text{R}^1\text{R}_2\text{P}=\text{O}$ ,  $\text{R}^1\text{R}_2\text{P}=\text{O}$  where  $\text{R}^1 = n\text{-octyl}$  and  $\text{R} = n\text{-hexyl}$ ) has come up on the forefront as a good extractant [1-3] because of its poor aqueous solubility and resistance to hydrolysis. Its major advantages over the widely used Cyanex 921(TOPO) are that it is completely miscible with all common hydrocarbon diluents even at low ambient temperatures, is liquid whereas TOPO is solid at room temperature and shows better selectivity than TOPO because it is structurally more hindered than TOPO. The present paper embodies the extraction behaviour of U(VI), Th(IV) and the lanthanides being represented by Ce(III), Ce(IV) and Yb(III) in toluene solution of Cyanex 923 from  $\text{HNO}_3$  and  $\text{H}_3\text{PO}_4$  media. Phosphate is an integral part of one of the enriched sources of these elements namely monazite, its effect on the extraction of said metal ions has also been studied. The effect of equilibration time, nature of diluent, temperature and concentration of acids, extractant and metal ion on the extraction has been investigated. Loading and recycling capacities of the extractant are assessed. Based on the partition data some important ternary separations involving U(VI), Th(IV) and Ce(III)/Ce(IV)/Yb(III) have been achieved. The practical utility of the proposed procedure has been demonstrated by separating uranium, thorium and the lanthanide fraction from the solution of monazite sand.

## EXPERIMENTAL

Equal volumes (10.0 ml) of the aqueous phase ( $1.0 \times 10^{-4} M$  or any other concentration of metal ion) and organic phase (appropriate concentration of Cyanex 923 in toluene) were shaken at room temperature ( $25 \pm 2^\circ C$ ) for five minutes to ensure complete equilibration. The two phases were separated and suitable aliquots of each phase were assayed for gamma activity or the aqueous phase was employed for determination by ICP-AES. Based on five observations the value of percent extraction for U(VI) ( $0.008 M$  Cyanex 923) and Th(IV) ( $0.01 M$  Cyanex 923) at about 60 % extraction exhibits a coefficient of variation of  $\pm 3\%$ .

About 0.1 g sample of monazite sand was digested with 25 ml mixture of concentrated HF,  $HNO_3$  and  $HClO_4$  (3:1.5:0.5) in a teflon vessel for twenty four hours at  $80^\circ C$  [4]. After complete evaporation to dryness, the mass was dissolved in 100.0 ml solution of  $5.0 M$  nitric acid and the solution was labelled as (A).

## RESULTS AND DISCUSSION

### Extraction Behaviour

The extraction behaviour of U(VI), Th(IV), Ce(III), Ce (IV) and Yb(III) from  $1.0 \times 10^{-3}$  to  $10.0 M$   $HNO_3 / H_3PO_4$  in a  $0.10 M$  toluene solution of Cyanex 923 is given in Table 1. The extraction of U(VI) and Th(IV) is almost quantitative ( $\approx 99\%$ ) in the entire investigated range of  $HNO_3$  molarity, while with increasing  $H_3PO_4$  molarity it shows a decreasing trend. Ce(III) and Ce(IV) show maximum extraction at  $0.5 M$  nitric acid but are negligibly extracted ( $\leq 5\%$ ) over the entire range of  $H_3PO_4$  concentration. It is interesting to note that at  $5.0 M$   $HNO_3$  Th(IV) is quantitatively extracted into  $0.1 M$  Cyanex 923 solution leaving Ce(IV) un-extracted. This is probably due to the reduction of Ce(IV) to Ce(III) by commercial grade Cyanex 923 as reported by Jun *et al.* [3] also. The extraction of Yb(III) is around 45 % at  $1.0 \times 10^{-3} M$   $HNO_3$  and  $H_3PO_4$ . It decreases with the increasing  $H_3PO_4$  molarity, however, in case of nitric acid medium the percent extraction of Yb(III) again increases to around 30 % at  $0.5 M$ .

From Table 1 it is apparent that U(VI) and Th(IV) can be separated from the lanthanide fraction beyond  $2 M$   $HNO_3$  by extracting them selectively in Cyanex 923 and leaving the lanthanide fraction in the aqueous phase. The effect of phosphate ions on the extraction of U(VI) and Th(IV) from nitric acid medium was also investigated using  $Na_3PO_4$  to maintain  $PO_4^{3-}$  ion concentration. The phosphate ion concentration was varied from  $1.0 \times 10^{-3}$  to  $0.80 M$  keeping nitric acid concentration constant at  $5.0 M$  and using  $1.0 \times 10^{-4} M$  U(VI) / Th(IV). The extraction of U(VI) and Th(IV) remains quantitative ( $\approx 99\%$ ) in this investigated range of  $PO_4^{3-}$  ion concentration. Monazite generally contains around 26 % phosphate, 0.3 % uranium and 8.1 % thorium [5] therefore it can be concluded that the extraction of U(VI) and Th(IV) from  $5.0 M$   $HNO_3$  will not be affected at the phosphate ion concentration in ratio to the metal ion expected to be encountered in the solution of the monazite sand. The effect of different parameters on the extraction of U(VI) and Th(IV) was investigated from  $0.50 M$   $HNO_3$  at  $25 \pm 2^\circ C$  employing a  $1.0 \times 10^{-4} M$  metal ion and  $0.10 M$  toluene solution of Cyanex 923 unless otherwise stated.

*Table 1. Percent extraction of metal ions in 0.1 M Cyanex 923 at different molarities of HNO<sub>3</sub> and H<sub>3</sub>PO<sub>4</sub>.*

Metal ion	Acid molarity (M)															
	1 × 10 <sup>-3</sup> M		1 × 10 <sup>-2</sup> M		1 × 10 <sup>-1</sup> M		5 × 10 <sup>-1</sup> M		1.0 M		2.0 M		5.0 M		10.0 M	
	a	b	a	b	a	b	a	b	a	b	a	b	a	b	a	b
Ce(IV)	-	-	0.0	0.0	2.0	0.0	26	0.0	0.0	0.0	0.0	0.0	0.0	0.0	0.0	0.0
Ce(III)	4.0	5.0	0.0	0.0	7.0	0.0	26	0.0	0.0	0.0	0.0	0.0	0.0	0.0	0.0	0.0
Yb(III)	46	46	40	46	10	5.0	28	0.0	0.0	0.0	0.0	0.0	0.0	0.0	0.0	0.0
Th(IV)	-	-	100	60	100	48	100	24	100	0.0	100	0.0	100	0.0	100	7.0
U <sup>VI</sup>	100	68	100	56	100	19	100	10	100	0.0	100	0.0	100	0.0	100	5.0

(a = HNO<sub>3</sub> and b = H<sub>3</sub>PO<sub>4</sub>)

### Diluent Effect

Cyclohexane, xylene, toluene, chloroform and cyclohexanone were employed as diluents for investigating their effect on the distribution ratio. There is a decreasing trend in the distribution ratio with increasing dielectric constant of the diluent. Toluene, xylene, and cyclohexane show almost quantitative extraction and toluene was used for all further studies.

### Effect of the Temperature and Equilibration Time on the Partition of U(VI) and Th(IV)

The effect of temperature (10 – 70 °C) on the extraction of U(VI) and Th(IV) was investigated. There is a decrease in extraction with increasing temperature indicating the process to be exothermic. Studies further reveal that two minutes equilibration time is necessary to achieve the limiting extraction and prolonged shaking has no adverse effect on the extraction.

### Composition of the Extracting Species and Loading Capacity

The effect of concentration of Cyanex 923 (1.0 × 10<sup>-3</sup> – 5.0 × 10<sup>-2</sup> M) on the extraction of U(VI) and Th(IV) (Figure 1) was studied. The distribution ratio increases with the increasing concentration of the extractant. A slope of around two for U(VI) and three for Th(IV) suggests the involvement of two and three molecules of Cyanex 923 in the formation of the extracting species which may be proposed as UO<sub>2</sub>(NO<sub>3</sub>)<sub>2</sub>.2R and Th(NO<sub>3</sub>)<sub>4</sub>.3R (R = Cyanex 923). A similar species for the extraction of Th(IV) in Cyanex 923 has been proposed by Lu *et al.* [6]. The extraction equilibrium can be written as



Partition studies carried out with varying U(VI) and Th(IV) concentrations (1.0 × 10<sup>-6</sup> M – 0.10 M) using 0.01 M toluene solution of Cyanex 923 show maximum loading at 0.005 M U(VI) and 0.003 M Th(IV), i.e., 0.34 g U(VI) and 0.20 g Th(IV) can be loaded per gram of the extractant.

### Stripping Reagents for Uranium and Thorium

Various stripping reagents were examined for the back extraction of Th(IV) and U(VI) from the organic phase. The results of the efficiency of stripping reagents are given in Table 2. 2 M HCl (5 volumes) and 0.5 M H<sub>2</sub>SO<sub>4</sub> (4 volumes) were found effective for the quantitative stripping of Th(IV) whereas U(VI) is stripped almost completely with 0.5 M H<sub>2</sub>SO<sub>4</sub> (5 volumes).

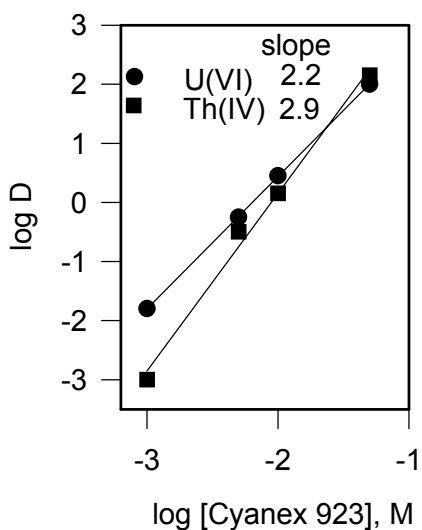


Figure 1. Effect of Cyanex 923 concentration.

Table 2. Stripping efficiency of different reagents for Th(IV) and U(VI).

Reagent	Recovery (%)		Reagent	Recovery (%)	
	Th(IV)	U(VI)		Th(IV)	U(VI)
0.5 M malonic acid	0.0	2.6	0.1 M HCl	0.0	0.0
0.1 M citric acid	24.6	17.6	1.0 M HCl	30.0	0.0
0.1 M EDTA	6.2	2.0	2.0 M HCl	50.0	0.0
1.0 M NH <sub>4</sub> NO <sub>3</sub>	1.5	0.0	0.5 M H <sub>2</sub> SO <sub>4</sub>	68.0	55.0
0.1 M tartaric acid	0.0	0.0	1.0 M H <sub>2</sub> SO <sub>4</sub>	30.0	0.0

[Metal ion] = 1.0 × 10<sup>-4</sup> M, [HNO<sub>3</sub>] = 5.0 M, [Extractant] = 0.1 M.

### Stability and Regeneration Capacity of the Extractant

The stability of Cyanex 923 towards nitric acid was determined by keeping a toluene solution of the extractant in contact with 5.0 M HNO<sub>3</sub> solution and checking the percent extraction of U(VI) and Th(IV) periodically after a gap of five days. No significant decrease in the extraction of either of the metal ions is observed even after a contact of 50 days. Experiments were also carried out to determine the recycling capacity of the extractant by first loading it with a mixture of Th(IV) and U(VI) and then stripping them with 2.0 M HCl (5 volumes) and 0.5 M H<sub>2</sub>SO<sub>4</sub> (5 volumes), respectively. The organic phase after stripping was regenerated by washing it with water till the washings were neutral. The recovery at each step is calculated from the amount of metal ions which get extracted in that particular cycle. No significant change was observed in the percent extraction and recovery of U(VI) and Th(IV) solutions up to fifteen cycles.

### Separtions

Based on the partition data some important ternary separations involving U(VI), Th(IV) and lanthanides were attained. The lanthanide fraction (represented by cerium and ytterbium) was separated from U(VI) and Th(IV) at 5.0 M HNO<sub>3</sub>. However, the mutual separation of U(VI) and Th(IV) was feasible at 2.0 M HCl. Table 3 illustrates the conditions and results of these separations.

*Table 3. Ternary separations of uranium, thorium and lanthanides from 5.0 M HNO<sub>3</sub> using 0.10 M Cyanex 923.*

Metal ions separated	Molar ratio (10 <sup>-4</sup> M)	Ce(III)/Ce(IV)/Yb(III) remaining in aqueous phase	Th(IV) <sup>a</sup> recovered from organic phase	U(VI) <sup>b</sup> recovered from organic phase
Ce(III):Th(IV):U(VI)	10:1:1	99.6	99.	99.6
	1:10:1	99.2	99.4	99.8
	1:1:10	99.5	99.6	99.7
Ce(IV):Th(IV):U(VI)	10:1:1	99.9	99.5	99.6
	1:10:1	99.8	99.6	99.6
	1:1:10	99.7	99.7	99.5
Yb(III):Th(IV):U(VI)	10:1:1	99.7	99.3	99.4
	1:10:1	99.6	99.2	99.7
	1:1:10	99.5	99.6	99.9

a - Stripped using 5(volumes) x 2.0 M HCl, b - Stripped using 5(volumes) x 0.5 M H<sub>2</sub>SO<sub>4</sub>.

#### **Recovery of Uranium, Thorium and Lanthanides from Monazite**

Ten milliliters of (A) were equilibrated with an equal volume of 0.10 M Cyanex 923. Thorium and uranium were quantitatively ( $\approx$ 99 %) extracted in the organic phase leaving behind the lanthanide fraction ( $\approx$ 99 %) in the aqueous phase. The organic layer was then washed with double distilled water till the washings were neutral. Th(IV) was recovered from the organic phase using 2.0 M HCl (5 volumes). The organic phase was again washed with double distilled water till the washings were neutral and then U(VI) was recovered employing 0.5 M H<sub>2</sub>SO<sub>4</sub> (5 volumes). (B) and (C) refer to the recovered solutions of thorium and uranium. The organic phase after stripping was regenerated by washing it with double distilled water. Table 3 presents the composition of (A), (B) and (C). The overall recovery and purity of each fraction is more than 98%. In order to show the efficacy of the above procedure for separation of uranium and thorium from lanthanides from monazite solution, the initial and final concentration of other lanthanides namely lanthanum, neodymium, europium and gadolinium is also shown in Table 4.

#### **CONCLUSIONS**

The present investigations have resulted in offering a convenient liquid-liquid extraction method for separating uranium, thorium and lanthanides. The presence of phosphate ions does not affect the separations from nitric acid medium. The recovery of metals is almost quantitative and the purity of each fraction is also high. Strict control of the acidity, of the aqueous phase is not required to achieve the separations. The extractant offers a good loading and recycling capacity. The stripping agents used for U(VI) and Th(IV) are simple and convenient for the subsequent processing of the recovered metal ions.

*Table 4. Separation of uranium, thorium and lanthanides from monazite.*

Metal ion	Conc. in (A) (mg/L)	Conc. in remaining aqueous layer (mg/L)	(B)			(c)		
			Conc. (mg/L)	Recovery (%)	Purity (%)	Conc. (mg/L)	Recovery (%)	Purity (%)
<i>Lanthanide fraction</i>								
La	82.31	82.31	0.01			< 0.01		
Ce	196.90	196.70	0.12			0.10		
Nd	42.31	42.20	0.10			< 0.01		
Eu	1.50	1.50	< 0.01			< 0.01		
Gd	1.80	1.79	0.04			< 0.01		
Yb	0.72	0.72	< 0.01			< 0.01		
Th	55.31	0.03	55.20	99.8	99.5±0.2	0.10		
U	10.62	< 0.01	< 0.01			10.58	99.6	98.1±0.3

(B) - Th(IV) recovered using 5(volumes) x 2.0 M HCl

(C) - U(VI) recovered using 5(volumes) x 0.5 M H<sub>2</sub>SO<sub>4</sub>

#### ACKNOWLEDGEMENTS

Thanks are due to Cytec Inc. Canada for providing Cyanex 923 sample as a gift. Financial support of Council of Scientific and Industrial Research and Department of Science and Technology, New Delhi, India is gratefully acknowledged.

#### REFERENCES

1. M.L.P. Reddy, R.L. Varma, T.R. Ramamohan, S.K. Sahu and V. Chakaravortty (1998), *Solvent Extr. Ion Exch.*, **16** (3), 795.
2. C. Dequiang, M. Genxiang and L. Deqian (1998), *Fenxi Huaxue*, **26** (11), 1346.
3. L. Jun, W. Zhenggui, L. Deqian, M. Gengxiang and J. Zucheng (1998), *Hydrometallurgy*, **50** (1), 77.
4. H.J. Forster and D. Rhede (1995), *Third Hutton Symposium on the Origin of Granites and Related Rocks*, M. Brown and P.M. Piccoli (eds.), US Geological Survey Circular **1129**, pp. 54.
5. M.D.N. Wadia (1966), Minerals of India, National Book Trust, India, pp. 168.
6. J. Lu, D.Q. Li and Z.C. Jiang (1999), *Acta Metall. Sin.*, **12** (2), 191.



# SOLVENT EXTRACTION PILOT PLANT RESULTS FOR RECOVERY OF COPPER AND NICKEL FROM AN AMMONIACAL LEACH OF DEEP-SEA MANGANESE NODULES

Gale L. Hubred

Retired, Brea, California, USA

A LIX-64N® solvent extraction pilot plant was operated for 20 days to co-extract nickel and copper from an ammonium carbonate leach liquor. Data includes: trace element monitoring, a steady state balance, and individual stage equilibrium approach measurement. Ammonia extraction and stripping were measured. All extractions and copper stripping were fast and complete. Nickel stripping was slower and further study is needed. The feed solution contained 90 g/l NH<sub>3</sub>, 6.2 g/l Ni, 5.7 g/l Cu, and was pregnant liquor from a deep-sea manganese nodule leach. The pregnant liquor contained 200 mg/l cobalt, some of which extracted, and accumulated on the organic. Thallium leached from the nodules, extracted and was stripped in the acidic ammonia strip. Boron extracted from the nickel strip solution and stripped into the raffinate.

## INTRODUCTION

In the 1970s, Kennecott Corporation developed a deep-sea manganese nodule extraction process [1]. This paper presents the solvent extraction data gathered in 1974 during extensive pilot-plant operations. Most of the other aspects of the process development program and description and operation of the complete pilot plant are not available. The data is old, and interest in manganese nodules has subsided, but the trace element tracking and stage equilibrium data might be useful.

## PROCESS DESCRIPTION

Figure 1 shows the solvent-extraction process. The process co-extracted copper and nickel in three stages. Extraction conditions determined the copper and nickel recoveries. The process stripped ammonia in two sections, one basic to allow ammonia recovery and the second acidic to allow thorough ammonia removal. Nickel was stripped using nickel electrowinning acid concentrate and copper was stripped in an analogous way. The nickel/copper separation was controlled by the acidity of the nickel stripping solution. All stages operated at 40 C. in acrylic mixer settlers with a cubic mixer box and a settler volume three times the mixer volume. Flows determined the external phase ratio. The internal phase volume phase ratio was forced to 1 by recycle from the settler to the mixer of some of the aqueous phase.

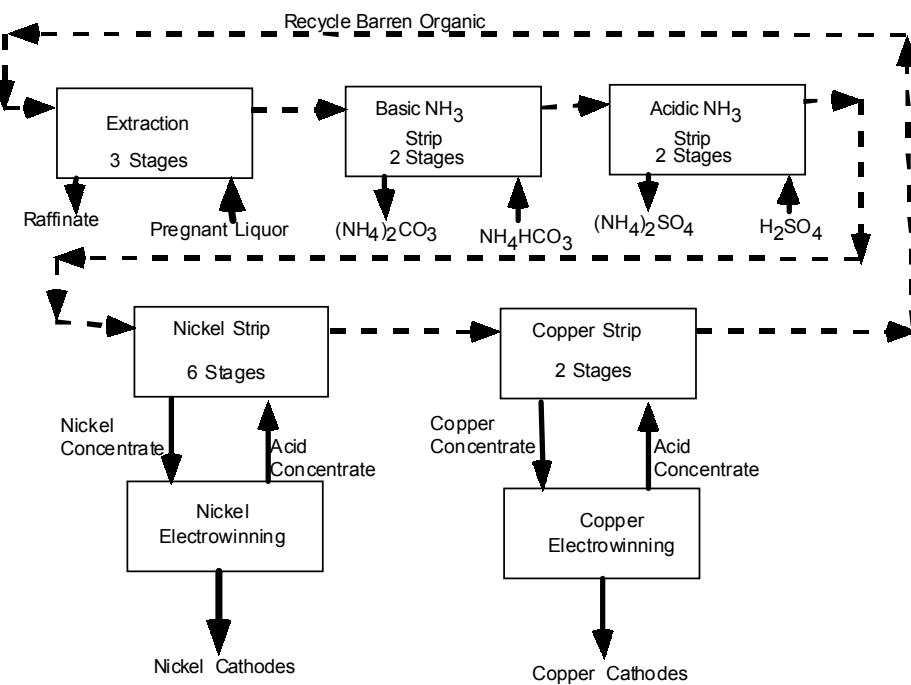


*Figure 1. Solvent extraction process.*

### Extraction

The Kennecott Cuprion Process was a reducing ammonia carbonate leach to dissolve manganese nodules. Copper, as Cu(I), reduced the tetravalent manganese oxide of the nodule. Copper, nickel and cobalt were dissolved as divalent ammines. Mn(II) precipitated as manganese carbonate. The Co(II) ion was air oxidized to Co(III) that was known to extract little or slowly. The ammonia concentration was a key parameter to the liquid ion exchange process. Some of the ammonia extracted. Extraction consisted of three stages, each with 3 minutes contact time and  $1.3 \text{ m}^3/\text{h}/\text{m}^2$  settler flux.

### Ammonia Stripping

Ammonia was stripped with two stages of basic  $1 \text{ M } \text{NH}_4\text{CO}_3$  solution. This ammonia was then recovered by distillation. Contact time was 3.75 min and settler flux was  $1.0 \text{ m}^3/\text{h}/\text{m}^2$ . Ammonia left on the organic was stripped with two stages of pH 2  $\text{H}_2\text{SO}_4$  solution. Contact time was 3 minutes and settler flux was  $1.3 \text{ m}^3/\text{h}/\text{m}^2$ . A trace of ammonia left on the organic is stripped with nickel and leads to the accumulation of nickel ammonium sulfate, often a contaminant in nickel extractive metallurgy.

### Nickel Stripping

Nickel was produced by electrowinning. Semi-batch nickel electrowinning was operated in parallel to the pilot plant to remove the nickel from the nickel concentrate solution and to provide a nickel acid electrolyte to drive nickel stripping. Nickel was stripped in preference to copper by controlling the nickel concentrate between pH 2.9 to 3.0. The pH controlled the flow of the nickel acid electrolyte to nickel stripping. Contact time was 3 minutes in each of six stages. The approach equilibrium is slow, relative to copper stripping. A Ni:Cu ratio of about 25,000:1 was achieved while stripping 98.8% of the nickel. Interstage samples showed three stages should be adequate.

### Copper Stripping

The copper-loaded organic containing 0.04 g/l Ni passed to two copper stripping stages with contact times of 3.75 minutes and specific settler flux of  $1.0 \text{ m}^3/\text{h}/\text{m}^2$ . Copper was produced by electrowinning. Semi-batch copper electrowinning was operated in parallel to the pilot

plant to remove copper from the copper concentrate and to provide a copper acid concentrate to drive copper stripping. A Cu:Ni ratio of about 75:1 was achieved while stripping > 99.9% of the copper which had been extracted in a particular cycle or organic.

## RESULTS

Table 1 summarizes the process performance during the pilot plant operation.

*Table 1. Pilot-plant steady-state profile.*

	Extraction				Basic ammonia strip		
	Pregnant liquor	Raffinate	Barren organic	Loaded organic	Organic out	HCO <sub>3</sub> feed	CO <sub>3</sub> out
Cu (g/l)	5.7	0.002	0.5	3.8	3.8	0	0
Ni (g/l)	6.2	0.007	0.008	3.6	3.6	0	0
NH <sub>3</sub> (g/l)	90	85	0	2.49	0.09	17	25
CO <sub>2</sub> (g/l)	55	55					
Co (g/l)	0.2	0.194	0.07	0.07	0.07	0	0
Flow (ml/min)	432	432	746	746	746	224	224
Flow (g/min)	453	453	625	631	631	230	232
	Acidic ammonia strip			Nickel strip			Copper strip
	Organic out	Acid feed	Acid out	Organic out	Acid feed	Ni con.	Acid feed
Cu (g/l)	3.8			3.8	0.0008	0.0011	37
Ni (g/l)	3.6	0.55	0.55	0.04	50	77	1.4
NH <sub>3</sub> (g/l)	0.005	27	27	0	0.31	0.39	0.15
CO <sub>2</sub> (g/l)							
Co (g/l)	0.07			0.07	0.0027	0.0042	0.012
Flow (ml/min)	746	746	746	746	98	98	237
Flow (g/min)	631	783	783	627	119	121	277
							237
							279

### Mass Balance

With few exceptions, flows throughout the LIX® plant were held constant for the entire 20-day run. The flows were measured by volumetric calibration and were maintained by positive displacement pump with hourly rotameter checks. Metal concentrations were obtained by atomic absorption. In some cases, such as the cobalt on the barren organic, steady state was not achieved. Values for the nickel stripping were taken from the last two days of the run because they were closest to the run plan. Most of the mass balances were within 1%, reflecting careful planning of the operation and close attention by the operators. Only a few of the calculated values require further comment.

### Ammonia mass balance

The results depend upon which analysis is trusted and if entrainment is considered. For example, the ammonia loss from the raffinate (2.16 g/min) is compared to the calculated ammonia gain by the organic (1.86 g/min) showing a 13.9% loss. The loss would be even larger if the ammonia analysis of the loaded organic were used directly. Instead, 2.49 g/l was calculated based upon the ammonia transferred to the basic NH<sub>3</sub> strip. Alternatively, the organic analysis could have been retained and the excess ammonia deposited in the aqueous basic ammonia strip solution could have been attributed to entrainment. However, there was no recycle of this basic solution making it difficult to estimate entrainment based on a tracer element build-up. Therefore, no entrainment was assumed. The NH<sub>3</sub> entering nickel strip is off balance 11.8% based upon accumulation of ammonia in the nickel strip solution. This is equivalent to an acidic ammonia strip organic effluent of 0.01 g/l NH<sub>3</sub> as compared to the reported 0.005 g/l. Entrainment seems likely but could not be estimated because the acidic strip solution contained no element useful as a tracer. Ammonia absorption from the air was considered by assuming the absorption for the six stages of

nickel strip solution could be at the most three times the ammonia accumulation in the more acid two-stage copper system. Such an assumption will not account for the imbalance and seems unlikely because the mixers and settlers were covered.

#### **Nickel mass balance in copper stripping**

The mass balance on the nickel entering the copper stripping unit has been forced to balance by adjusting the nickel concentration of the organic from 0.026 g/t to 0.04 g/t Ni. This value is based on the nickel accumulation in the copper electrolyte. Entrainment was estimated to be insignificant based on the sodium accumulation in the copper strip electrolyte.

#### **Cobalt mass balance over-all**

A small fraction of the cobalt (6 of 200 mg/l) extracted from the pregnant liquor and accumulated on the organic. The barren organic cobalt loading increased from 24 to 76 mg/l over the 20 day run. The reductive Cuprion leaching process leached cobalt in a cobaltous ammine state. We did not investigate whether the cobalt extraction was due to the rapid extraction of some remaining cobaltous ammine or due to slow extraction of cobaltic ammine. The stability of cobalt on the organic is probably due to the cobaltic-LIX® compound whether directly extracted or formed by oxidation of the organic phase as it passes through the system. Further study is needed to deal with this issue. 65 g cobalt was extracted over the 20-day run; 40 g accumulated on the barren organic; 11.5 g deposited as nickel cathode and 4.5 g deposited as copper cathode. This result means a cobaltic removal step needs to be found and tested [2]. It is expected to include: reduction of cobaltic complex on a slip stream of barren organic, followed by cobalt stripping and return of the cleaned organic to the barren organic.

#### **Trace Element Analysis**

The results for the trace element analysis are shown in Table 2.

*Table 2. Trace elements balance.  
Total amount transferred during 20 day pilot plant run (g).*

Metal	Extraction circuit	Strip circuit				
		Basic strip	Acidic strip	Nickel strip	Copper strip	Other
Co	65	0	3	4.5	4.5	4.0*
Mn	828	0	31	770	16.2	
Zn				3.1		
Fe	31	0	0	0	30	
Pb	0					
Mo	0					
Tl	83	43	43	7	0	
B	-560			-128		293*

\* Accumulated on barren organic phase

\*\* Based on a later set of analyses

\*\*\* Stripped from loaded organic: Analyses suspect.

#### **Thallium**

Mass spectrophotometry revealed that significant amounts of thallium leached from manganese nodules and was extracted into the SX circuit. All of the thallium (7 mg/l) in the pregnant liquor extracted, but only a little more than half (4.6 mg/l) could be accounted for. 1.3 mg/l and 2.8 mg/l, stripped in the basic and acidic NH<sub>3</sub> strips. About 0.5 mg/l was found in the nickel concentrate electrolyte and it all deposited on the nickel cathode. The thallium was unexpected so little analysis was done. The results suggest that thallium can be stripped in the acidic ammonia circuit and removed there. We suspect the thallium in the nickel circuit is due to entrainment of the ammonia strip solution in the loaded organic and carryover into the nickel electrolyte.

### **Boron**

Boric acid is typically used in nickel electrowinning for cathode control. Some boron extracted from the nickel electrolyte. The mass balance was not good, but the evidence indicated that more than 200 g B left the nickel circuit in the raffinate. The copper circuit also contained 0.6 g B at the end of the run but it is suspected this is due to entrainment.

### **Manganese**

A small amount of manganese was present in the pregnant liquor and was completely extracted at the rate of .030 g/min. Most of this manganese was recovered in nickel stripping (0.028 g/min) based on daily electrolyte analysis. About 0.002 g/min accumulated in the acidic ammonia strip based upon the total accumulation during the run. An even smaller amount (0.0006 g/min) reported to copper stripping, based on daily electrolyte analysis. The manganese mass balance thus shows 0.030 g/min extracted and 0.031 g/min stripped. The manganese stripped in the nickel circuit subsequently precipitates at the anode and will be an issue there.

### **Iron**

The pregnant liquor contained about 0.0025 g/l Fe that extracted and accumulated in copper strip during the run. The total iron extracted, 31 g, is in good agreement with that accumulated in the copper strip circuit. The iron would probably not be a problem in the operation because the nickel bleed from the copper circuit would limit the accumulation.

### **Zinc**

The zinc content of the pregnant liquor increased from 0.15 g/l to 0.18 g/l during the 20-day run. Zinc extraction increased with zinc concentration. Only a small amount of the zinc was extracted so that rather than a mass balance over the entire LIX section, only the increment in the nickel strip circuit, 0.001 g/l, was detectable. This increment is equivalent to a cathode content of about 40 mg/l that is in good agreement with the cathode analysis. The first cathode was 43 mg/l Zn and the second cathode 50 mg/l. No accumulation of zinc was noted in the acidic ammonia strip. Zinc extraction is probably sensitive to the extraction conditions and bears watching in future evaluation runs.

### **Molybdenum**

Molybdenum concentration of the pregnant liquor increased throughout the pilot plant run, but none was extracted because it is present an anion.

### **Crud**

Crud accumulated at the interface and was measured and sampled at the end of the run. All crud samples represent the accumulation from all pilot plant runs. Attempts to analyze the crud by mass spectrometer and x-ray fluorescence failed. The total crud was not enough to affect the mass balance of the major components. Atomic absorption analysis for Cu, Ni, Co indicated that the sum of these metals constituted about 0.5 wt % of the various cruds.

### **Interstage Equilibrium**

One goal of the pilot plant run was to obtain interstage equilibrium data. Samples of all interstage streams were taken at least once and analyzed. Then the samples of streams exiting a stage were contacted together with the proper O/A ratio for 30 minutes (to obtain equilibrium), separated, and analyzed again. The measurement then indicates how close to equilibrium any particular stage operated. The results are provided in Table 3 based on the organic analysis. Some impossible values of greater than 100% are tabulated, but these were obtained in stages where only a small amount of the mass transfer took place. The efficiency can be based on organic analysis, aqueous analysis, or the position of the operating point relative to the equilibrium line. All methods should be equivalent, but due to analytical and sampling problems, differences will exist. The efficiencies are better when based on the organic analysis than when based on the aqueous. This is evidently due to erroneous analytical results for some of the values, but a systematic error is not evident. The

following considerations were made to identify the source of the problem but were unsuccessful. Entrainment, if it were a serious problem, should decrease the organic based efficiencies in the stripping sections as the aqueous stream contains more than 10 times as much metal as the organic. An improper duplication of the O/A ratio would be detectable from the ratio of the incremental mass transfer to each phase during the equilibrium shakeout. There is scatter in the data, but the values do not indicate a consistent error. Usually each Interstage stream was sampled twice, once during the run and once at the end of the run. Only one stage was sampled at a time to insure that samples were not distorted because of upsets in adjacent stages. Samples were withdrawn directly from the settler with a 50-ml pipette and placed directly in screw cap glass bottles. Some samples were accidentally broken after the first analysis so an equilibrium shakeup was not possible. In these cases the equilibrium value was determined by contacting the two feed streams to that stage in the appropriate A/O ratio or a sample from another time was used.

*Table 3. Interstage equilibrium.*

Operation	Stage	Approach to equilibrium (%)	Transferred in stage (%)	Operation	Stage	Approach to equilibrium (%)	Transferred in stage (%)
Extraction	1	<b>Ni/Cu</b> 90/100	<b>Ni/Cu</b> 34/98	Nickel strip	1	<b>Ni</b> 150	<b>Ni</b> 0.9
	2	93.5/100	58/0.9		2	106	20
	3	108/100	8.3/0.9		3	59	3/8
					4	71	30
					5	86	10
					6	58	0.5
Basic NH <sub>3</sub> strip	1	<b>NH<sub>3</sub></b> 98.3	<b>NH<sub>3</sub></b> 92.5	Copper strip	1	<b>Cu</b> 92	<b>Cu</b> 85
	2		7.7		2	86.7	13
Acid NH <sub>3</sub> strip	1	91.5	98				
	2	31	1.9				

### ***Extraction***

Nearly all (98%) of the copper extraction occurs in the one stage, but some nickel extraction occurs in all three stages; 34%, 58%, and 8.3% respectively. It may be possible to shorten the contact time and this should be evaluated.

### ***Ammonia stripping***

Most of the mass transfer occurs in the first stage in both the basic and acidic strip sections. The efficiency is over 90% in those stages. Elimination of the second stage basic strip should be considered. It is considered essential to lower the NH<sub>3</sub> content organic as low as possible because this concentration determines the size of the bleed stream on the nickel electrolyte. The calculated efficiency of the second stage is low probably because of entrainment of the aqueous stream that contains 27 g/l NH<sub>3</sub>. Nearly half of the analyzed organic ammonia is entrained judging from analysis after deentrainment.

### ***Nickel stripping***

Most of the mass transfer takes place in the middle stages. This is because the mass transfer is pinched on both ends. In the first stages there is almost no hydrogen ion left in the aqueous phase to transfer to the organic phase. In the last stages there is very little nickel left in the organic to transfer into the aqueous. Stage efficiencies are low in the main mass transfer stages. This is interpreted as evidence that more contact time is needed in the mixing stage. In the laboratory equilibrium studies, it was evident that the nickel strip needs considerably longer contact times. The necessary contact time varied with the O/A ratio, but significant mass transfer occurred for up to 12 minutes. The first stage in the nickel strip operation may be better viewed as a part of the control system as opposed to a mass transfer stage. It is in the first stage where the copper loaded onto the aqueous is squeezed back onto the organic and the copper to nickel ratio in the nickel strip solution is determined.

The McCabe Thiele stage calculation indicates only two equilibrium stages of nickel stripping are necessary. The nickel strip operation should be simulated using three stages with variable minutes contact time in each stage.

### **Copper stripping**

85% of the copper stripping mass transfer occurs in the first stage with a 92% approach to equilibrium based on the organic analysis. The second stage is nearly as efficient in completing the mass transfer. Residual copper is recycled in the barren organic and is not lost. The copper strip staging and contact time seem to be close to optimum.

## **CONCLUSIONS AND RECOMMENDATIONS**

1. Greater than 99.9% extraction of copper and nickel was achieved.
2. Critical nickel copper separation was achieved by means of a pH control process with a Ni to Cu transfer ratio of greater than 25,000 to 1.
3. Cobalt extraction did occur, resulting in accumulation of 0.076 g/l Co in the organic phase.
4. Approach to equilibrium was generally better than 90% except in nickel stripping, where it was much less.
5. The quantitative behavior of several trace elements (Fe, Pb, Zn, Mn, Mo, Cd, B, Ti, and Zr) was measured.
6. The mass balance closed to less than 1% for copper and nickel.
7. The fundamentals of cobalt extraction and stripping should be studied and a method devised to deal with cobalt accumulation.
8. Nickel stripping should be studied with a goal of reducing the number of stages to as few as three.

Processes using solvent extraction from ammonia liquor have since started up [3].

## **ACKNOWLEDGEMENTS**

Many individuals contributed to the effort, but only the leaders will be acknowledged here: Dr. J. Agarwal (Ledgemont Laboratory Development Division Director), Dr. N. Beecher (Manganese Nodule Team Manager), and Dr. H. Barner, Dr. R. Kust, and Mr. D. Davies who headed the engineering, chemistry and pilot plant teams. Mr. R. Skarbo and Mr. D. Natwig did most of the solvent extraction process development and piloting. I had the good fortune to arrive in time to help run the pilot plant and to write the report on the solvent extraction results.

## **REFERENCES**

1. J. C. Agarwal, N. Beecher, D. S. Davies, G. L. Hubred, V. K. Kakaria, and R. N. Kust (1976), *J. Metals*, (4), 24-31.
2. G. L. Hubred (1986), *Proc. 25th Annual Conference of Metallurgists*, Canadian Institute of Mining and Metallurgy, Toronto.
3. M. J. Price and J. G. Reid (1993), *Proc. ISEC '93: Solvent Extraction in the Process Industries*, Society of Chemical Industries, London, pp. 159-166.



# POSSIBLE APPLICATION OF OFFSHORE OIL & GAS PHASE SEPARATION TECHNOLOGY TO HYDROMETALLURGICAL SOLVENT EXTRACTION

David Stanbridge and John Sullivan\*

CDS Engineering, Arnhem, The Netherlands

\*J. D. Sullivan & Associates, Perth, Australia

This paper explores the potential for extending high efficiency separator design as applied in the oil and gas industry to improve the equivalent processes within minerals processing. Test cases from both Oil and Gas and Hydrometallurgy applications will be compared to illustrate some of the weaknesses of current minerals processing designs. Computational Fluid Dynamics (CFD) techniques have been used to model both applications. The CFD approach used in this paper was presented at the 1999 World CFD conference in Melbourne.

There are many offshore oil and gas applications requiring very efficient liquid from liquid separation in order to meet strict environmental limitations. These applications involve both the reduction of water in the hydrocarbon phase and the process of reducing the hydrocarbon content within the water prior to the disposal of it to sea. In these disposal applications an entrainment level below 40 ppm is required.

## INTRODUCTION

CFD techniques have been used widely within the oil and gas market to troubleshoot under performing processes/equipment. One of the specialised areas in which CDS Engineering are involved is that of equipment used for both liquid from gas and liquid from liquid separation.

This paper outlines the modifications to main line separation equipment that led to a substantial reduction in the hydrocarbon within the water phase. A comparison will then be drawn between this process and a settler tank within a copper production circuit in order to show the savings that could be made if a similar oil and gas market approach was adopted.

## BACKGROUND TO OFFSHORE PROBLEM

The offshore application that is to be considered is summarised in Figure 1. The system is typical of an offshore oil production application with 3 stages of pressure let down. Within these systems it is then also general for the HP and LP separators to be 3 phase, that is separating the oil, water and gas. The water streams from these separators can then be treated with further equipment in order to meet the environmental constraints prior to disposal to the sea. Currently this limit in the North Sea is 40 mg/l.

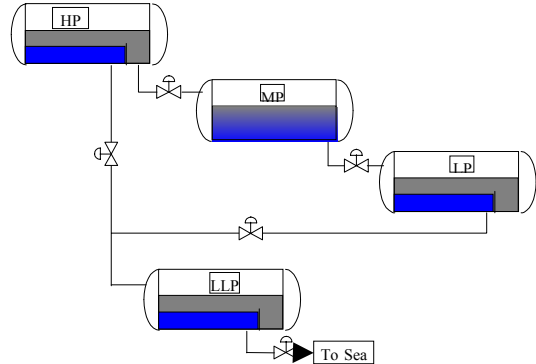


*Figure 1. Typical offshore water processing scheme.*

For the actual system covered by this paper this environmental constraint was not being met without further treatment of the water. It was thus decided to see if something could be done to better the performance. For this system the main loading to the water treatment facility came from the HP Separator with typical figures in the range 300-950 mg/l oil in water entrainment. In order to find the causes of this poor performance a three-dimensional CFD simulation of the liquid section of the vessel was carried out; the results of which are presented below.

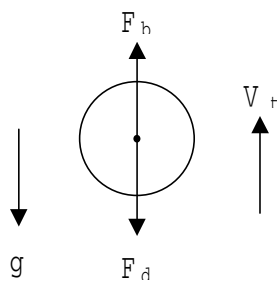
### FINDINGS FROM THE CFD SIMULATION

Figure 2 summarises the results obtained from the three-dimensional CFD model. In summary, the vessel had a cluster of four inlet cyclones followed by a perforated distribution baffle. However, the perforated plate did not extend fully to the bottom of the vessel and so an even distribution was not found down stream of it. It is easy to see that with the flow distribution shown Figure 2 optimal conditions for separation have not been set up and therefore better performance should be achievable.

In order to improve the performance of the separator then the jet of liquid flowing inside of the vessel needs to be removed. In this way the theoretical residence of the fluids will increase thereby maximising the droplet separation within the vessel. Also by removing the jet from the vessel the re-circulation will also disappear that again contributes to an increased residence time of the fluids.

### Effect of Increased Residence Time

Reviewing the equations governing the removal of a dispersed phase from a continuous one can see the benefit of increasing the residence time of the fluid. Ignoring the effects of turbulence and surface tension the forces governing the gravity settling of a droplet are shown in the diagram below. The directions of  $F_b$  and  $F_d$  relate to whether the droplet is rising or falling. However when determining if a droplet can be separated it is usual only to find the terminal velocity of the droplet. This being the point at which  $F_b = F_d$  where steady state conditions exist.



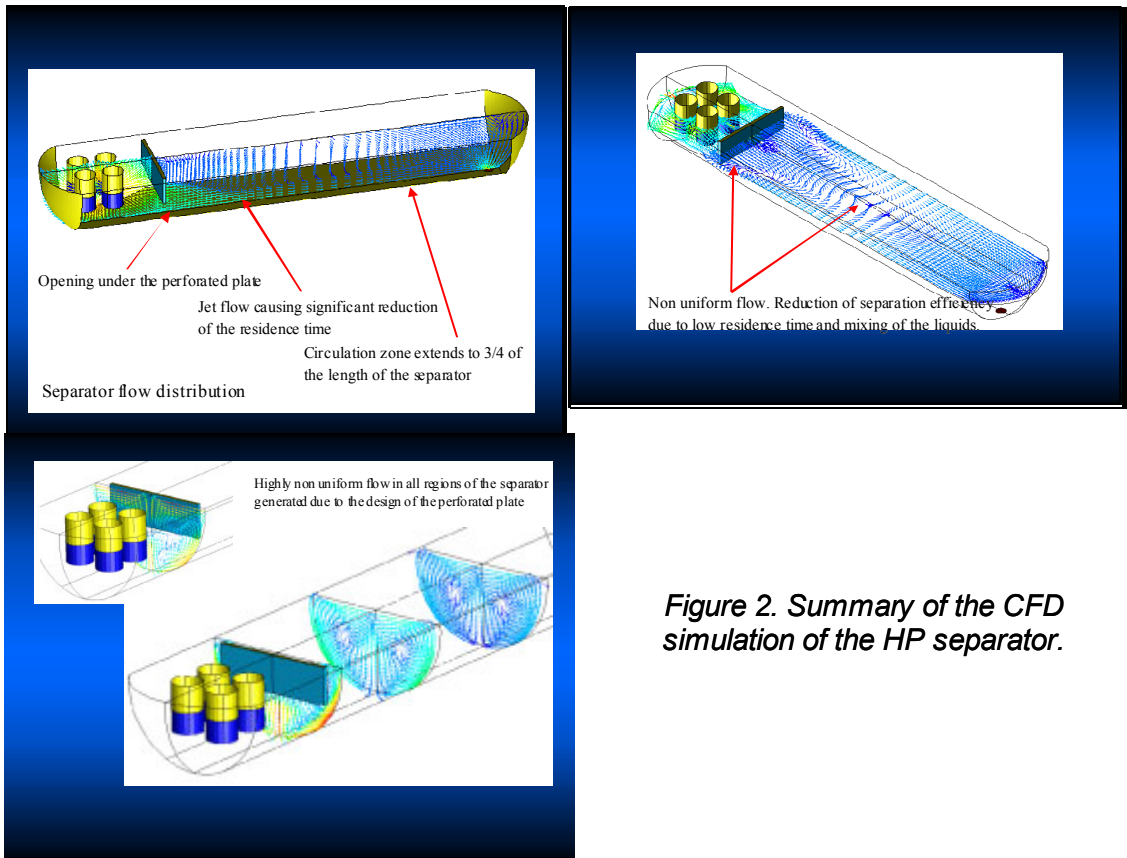


**Figure 2. Summary of the CFD simulation of the HP separator.**

$$F_b = \frac{M_d |(\rho_c - \rho_d)| g}{\rho_d} \quad (1)$$

$$F_d = \frac{1}{2} C' \rho_c V_t^2 A_d \quad (2)$$

If the droplet is assumed to be a solid sphere then the drag coefficient can be determined from the Reynolds number. Equating the above gives:

$$V_t = \sqrt{\frac{2gM_d |(\rho_c - \rho_d)|}{\rho_c \rho_d A_d C'}} \quad (3)$$

Or in terms of droplet diameter:

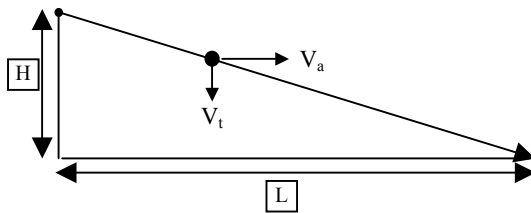
$$V_t = \sqrt{\frac{4gD_d |(\rho_c - \rho_d)|}{3\rho_c C'}} \quad (4)$$

Rearranging to determine the droplet diameter gives

$$D_d = \frac{3\rho_c C' V_t^2}{4g |(\rho_c - \rho_d)|} \quad (5)$$

For a vessel of a given length the minimum available  $V_t$  is determined by the following equation assuming that there is no slip between the continuous and dispersed phase:

$$V_t = \frac{HV_a}{L} \quad (6)$$



The minimum available  $V_t$  enables the calculation of the minimum droplet size that can be separated. Assuming that the Reynolds number of the droplet is less than 1 then Stokes Law gives the following:

$$C' = \frac{24}{Re} \quad (7)$$

Combining equations (5), (6) and (7) leads to the following relationship:

$$D_d = \sqrt{\frac{0.018\mu_c HV_a}{gL(\rho_c - \rho_d)}} \quad (8)$$

Therefore assuming that all parameters in the RH side of equation (8) are the same other than  $V_a$  then  $D_d = k\sqrt{V_a}$ . So if a liquid jet has a velocity 10 times higher than that of the theoretically attainable velocity then the droplet size removed will be approximately 3.2 times as large.

### Modifications made to the Vessel

In order to remove the jet flow from the liquid section the perforated plate was extended to the bottom of the vessel. However due to the location of the liquids entering the vessel, at the bottom of the inlet cyclones, the pressure drop over the perforated plate also had to be increased to ensure that an even distribution was achieved.

With an even flow distribution, the next consideration was to determine the droplet size that can be separated within the vessel. As shown in equation (8) above the main parameters that are changeable to achieve a specified droplet removal are the separation height H, the separation length L and  $V_a$ , the axial velocity. However, for this vessel all of these parameters were set by the existing design. Although the performance would have improved just by the amendments to the perforated distribution baffle it was decided to maximise the achievable separation.

Since a better degree of separation was required than could be given by the existing design further internals were needed within the vessel. These took the form of parallel plates. As

shown in equation (8),  $D_d = k\sqrt{\frac{H}{L}}$ . So if the ratio H/L is reduced then so is the droplet size

removed within the vessel. For the existing vessel H/L was in the order of 0.08. With parallel plates of 10 mm spacing and a length of 2000 mm H/L becomes 0.005 thus providing a 4 times reduction in the droplet size removed. Figure 3 shows the arrangement of these parallel plates.

### Results after the Modification

After the new equipment had been fitted into the separator results typically in the range 18-25 mg/l oil in water entrainment. As can be clearly seen these results show a considerable improvement compared to the original design. This led to the disposal of the water directly to sea, without further treatment.



*Figure 3. Photograph of parallel plate arrangement.*

## APPLICATION TO HYDROMETALLURGY

One of the areas that we see can benefit from the approach described above is within the mixer / settler combinations of existing hydrometallurgy plants. In this part of the process substantial savings can be made if the carryover of both the organic and aqueous can be minimised from the settler. Generally, these settler tanks are large with a volume approximately 10 times higher than those installed offshore in order to achieve the same degree of separation. Unfortunately as shown above this large volume does not always guarantee adequate separation.

It should also be noted that within the combined mixer / settler process the mixer tank is providing a sufficiently fine droplet size distribution to ensure that a high degree of mass transfer occurs. The design of the settler therefore must ensure that the droplet size distribution generated within the mixer will be separated within the settler.

In order to see if such improvements are possible within Hydrometallurgy we shall review the design of the new Cu SX settler tanks at the WMC Olympic Dam location. The design comprises a large rectangular vessel with vertical mounted pickets at the inlet end of the tank to act as a distribution device. An outline sketch of this part of the vessel is given in Figure 4. The sketch is split in two parts, the upper half showing the top view of the vessel whilst the lower gives the relative location of the inlet from the upstream mixer. Towards the back of the vessel there is a bucket weir arrangement in order for the organic to leave the vessel followed by an overflow weir for the removal of the aqueous phase.

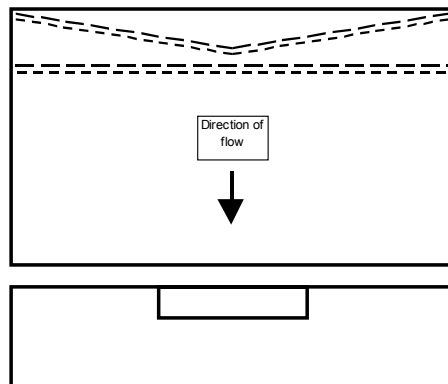


*Figure 4. Sketch of the settler inlet configuration.*

### CFD Analysis of the Settler Vessel

As this vessel is essentially a two-phase separator then a two-phase CFD model is preferred allowing for the flow of both the organic and aqueous liquids. However since little is known regarding the flow in these settler vessels a single-phase model will initially be solved in order to see the general flow patterns that are created within the vessel. After this stage then a strategy shall be developed in order to model the vessel with two liquid phases, if necessary.

In order to investigate this vessel in detail a three-dimensional model has been set up using Gambit. The solution itself will be found using the Fluent 5 CFD code. It should be noted that only one half of the vessel has been modelled since the central vertical axis can be taken as a symmetry plane. The whole model is shown in Figure 5. The grey areas depict the wall of the vessel, the inlet from the upstream mixer is shown in blue whilst the symmetry is in yellow. What is not clear in the above picture is that each individual picket has been modelled. In this way a very accurate representation of the inlet flow distribution can be achieved within the model, something that is beneficial if any optimisations are to be performed. A close up of the pickets is shown in Figure 6.

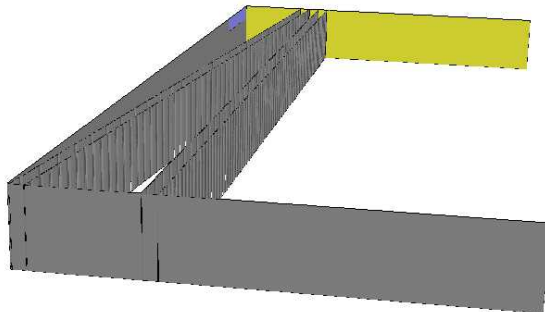


Figure 5. Picture of the settler model generated within Gambit.

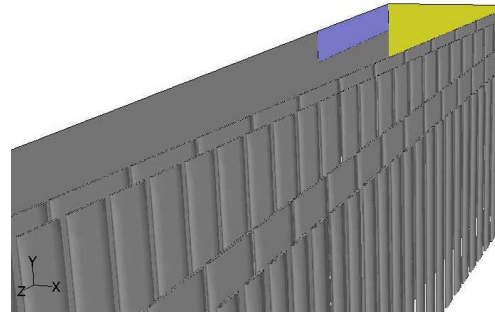


Figure 6. Close up of the pickets clearly showing that each was modelled individually.

### Findings from the CFD Simulation of the Settler Vessel

The result from the simulation shows that the flow in the vessel is not distributed well. What is seen at the inlet is that the flow enters the vessel, strikes the pickets opposite and subsequently starts rotating (Figure 7). Although the pickets then show a distributing effect the overall effect is not optimal with the simulation showing a velocity range of  $-0.93 \text{ m/s}$  to  $1.0 \text{ m/s}$  in the flow direction.

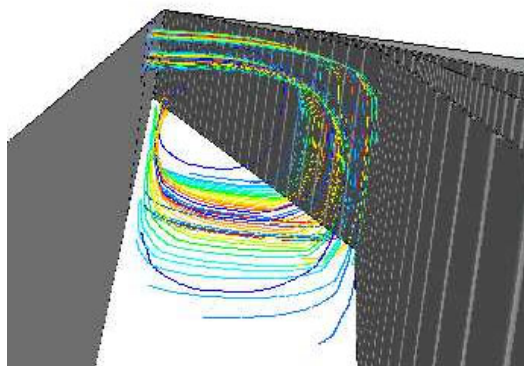
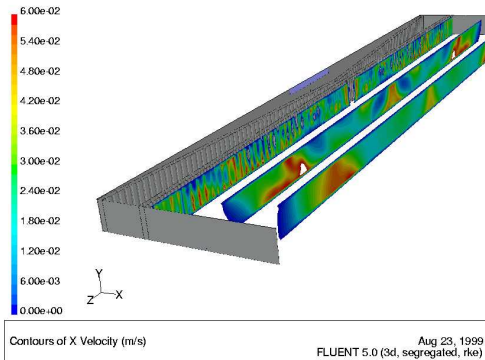


Figure 7. Picture showing the path lines of the fluid after it enters the vessel. A corkscrew motion is clearly seen.

Figures 8 to 10 show further distributions in the vessel. In all cases the velocity range has been restricted between 0 m/s to 0.06 m/s in the flow direction. Although these findings are true only of a single-phase flow we would expect that a similar profile would be found in a two-phase flow simulation of both the organic and aqueous phase. A single-phase simulation was performed initially both due to a quicker convergence and also if the flow distributes evenly for a single-phase it is generally found that it will do so also for a multiphase flow.

In order to prevent the maldistribution shown above then it will be necessary to firstly simulate the settler but with a two-phase flow. After this then a definitive upgrade strategy can be determined in order to solve the maldistribution and hence optimise the gravity separation from the settler.



*Figure 8. Picture showing the x velocity profile along the length of the vessel.*

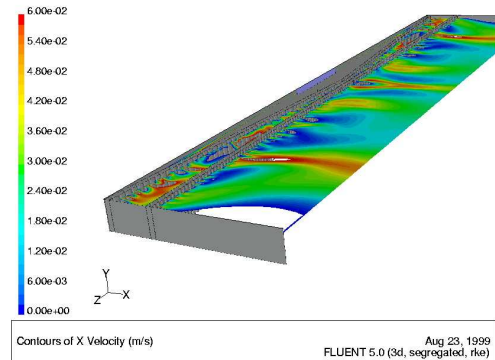


*Figure 9. Picture showing the x velocity profile in the plane through the centre of the inlet.*

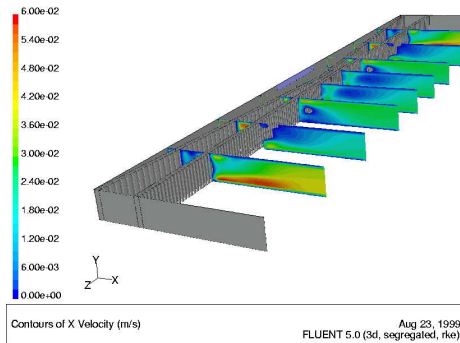


*Figure 10. Picture showing the x velocity profile along the length of the vessel.*

## CONCLUDING REMARKS

From this preliminary investigation it is seen that the flow distribution within the settler is not optimal. This means that increased separation should be achievable if a different arrangement to the currently installed picket arrangement is used. In order to quantify this further is will be necessary to perform a two-phase simulation of the settler and from there determine a suitable upgrade strategy.

## NOMENCLATURE

C'	Drag Co-efficient	(dimensionless)	M <sub>d</sub>	Mass of dispersed droplet	(kg)
D <sub>d</sub>	Droplet Diameter	(m)	V <sub>a</sub>	Axial velocity of fluid	(m/s)
F <sub>b</sub>	Buoyancy Force	(N)	V <sub>t</sub>	Terminal settling velocity	(m/s)
F <sub>d</sub>	Drag Force	(N)	ρ <sub>c</sub>	Density of continuous phase	(kg/m <sup>3</sup> )
g	Acceleration due to gravity	(m/s <sup>2</sup> )	ρ <sub>d</sub>	Density of dispersed phase	(kg/m <sup>3</sup> )
H	Separation height	(m)	μ <sub>c</sub>	Viscosity of continuous phase	(cP)
L	Separation length	(m)			



## VIRTUES AND VICES OF REAGENTS FOR ACTINIDE PARTITIONING IN THE 21<sup>ST</sup> CENTURY

Kenneth L. Nash

Chemistry Division, Argonne National Laboratory, Argonne, Illinois, USA

The viability of nuclear power as an electricity generation technology in the 21<sup>st</sup> Century depends to a great degree on the development of efficient new separations technologies that conform to contemporary requirements for protection of the environment. Both the high throughput of solvent extraction and the more than 50 years of accumulated experience for processing of radioactive materials ideally qualify this science and technology for solving the problems of actinide and fission product isolation, recycle, and disposal. In this report, the continuing development of new reagents and processes for the isolation of actinides from nuclear fuels will be discussed with emphasis on how they respond to the demands for environmental stewardship in the 21<sup>st</sup> Century.

### INTRODUCTION

During the first half century of large-scale actinide production, recovery, and recycle, the combined influence of incomplete understanding of the chemistry of the byproducts of nuclear energy and the political imperatives of the arms race led to the creation of some daunting environmental cleanup challenges. In response, the past decade has seen a considerable emphasis, both scientific and financial, on developing new technologies to clean up the aftermath of the Cold War. These environmental insults, combined with continued difficulties in siting and licensing a high level waste repository, stand as significant obstacles to the continued development and application of nuclear energy in the U.S.

While the research establishment in the U. S. has expended considerable effort during the past decade on environment restoration, the rest of the world has continued to research techniques for actinide recycle. Some of this work is based on fundamental studies conducted at ANL on CMPO extractants and the TRUEX process during the 1980s and 1990s. Others have elected to develop alternatives for hydrometallurgical separations of actinides. Some new reagents (and classes of reagents) have been developed. A number of process flowsheets based on a variety of different extractant molecules (some new, some old) have been demonstrated [1]. In this report, selected characteristics of a variety of different classes of reagents designed for enhancing the efficiency of actinide separations by solvent extraction (and related methods) are discussed. The emphasis will be on highlighting the positive features of new reagents for actinide partitioning while simultaneously recognizing the limitations of the new compounds and their application. Coverage of the subject area will not attempt to be comprehensive but rather will focus on selected reagents and processes.

## EXTRACTANT MOLECULES

While the PUREX extractant, tributylphosphate (TBP), has provided exemplary performance for selective isolation and partitioning of Pu and U from dissolved spent fuel, it exhibits little ability to extract trivalent actinides (Am and Cm) from an acceptable aqueous solution. During the first 30 years or so of actinide processing, this was not considered a fault of the system, as the minor actinides (Np, Am, Cm) simply were routed to the waste. Unfortunately, the comparatively long radioactive lifetime of these elements and their radiotoxicity greatly complicates efforts to provide assurance that a geologic repository will adequately isolate high level radioactive wastes from the hydrosphere for a sufficient time to protect the biosphere (and thus the human food chain). Substantial research has been conducted over the past 20 years seeking to develop new extractants for isolation of the minor actinides.

The most extensively developed class of reagents for recycle and isolation of the minor actinides are the carbamoyl phosphonates and phosphine oxides [2], whose existence can be traced to the seminal work of Siddall in the mid-1960s [3]. Nearly 100 different derivatives of these bifunctional extractants have been prepared and characterized. The TRUEX extractant, octyl(phenyl)-N,N-diisobutylcarbamoylmethyl phosphine oxide (CMPO) is the most studied of these reagents. The positive features of CMPO-class reagents are their moderate affinity for trivalent actinides, comparatively flat acid dependencies for extraction of tri-, tetra-, and hexavalent actinides, adaptability to a variety of different acid media, and the extent of their process/pilot-scale demonstration. On the other hand, the reagents tend to be moderately expensive to synthesize, experience some limitations in their phase compatibility, and introduce phosphate into the waste stream. This latter feature is considered somewhat problematic at present because of the tendency of metal phosphates to form crystalline inclusion in radioactive waste glasses, thus decreasing their long-term stability. Continuing research on alternate waste forms for actinide isolation indicate the possible utility of phosphate glasses and crystalline ceramics [4], which could reduce the importance of this feature.

Two other organophosphorus extractant molecules have also received substantial interest during the past several years. To overcome the comparative expense of the CMPO-class extractants, Chinese researchers have developed a total actinide recovery system based on a trialkylphosphine oxide extractant (commercially available as Cyanex 923) [5]. The TRPO system can readily accommodate extraction of tri-, tetra-, and hexavalent actinide ions in a comparatively straight-forward flowsheet. The principal negative feature of this extraction system is the narrow range of nitric acid concentration in which the extraction of trivalent actinides is most efficient. This feature of TRPO reflects the high affinity of phosphine oxide extractant molecules for nitric acid, which compete with the actinide. The bifunctional extractant CMPO was designed to overcome this limitation. For recycle of actinides from dissolved spent fuel, the process flowsheet requires both dilution of feedstock (by a factor of 10) and denitration. Each of these requirements amplifies the volume of wastes created. Researchers at the Japan Atomic Energy Research Institute (JAERI) have demonstrated a total actinide recycle process based on di(isodecyl)phosphoric acid (DIDPA), an acidic extractant [6]. Among the current solvent extraction processes for actinide partitioning, this one is unique in that it incorporates into the basic separation scheme a reverse TALSPEAK separation for partitioning of trivalent actinides from lanthanides. Aside from the phosphate waste issue, this extraction system suffers the principle defect of requiring lower nitric acid concentrations than are typically produced during fuel dissolution, hence must include denitration as a first step. As was noted for the TRPO system, denitration can amplify the volume of wastes created during processing.

To accommodate a desire for waste volume reduction within a total actinide recycle fuel cycle, Musikas [7] initially proposed the CHON (carbon, hydrogen, nitrogen, oxygen) concept for extractant design. The idea is to only employ reagents containing these elements to minimize the amount of ash produced when the extractant is incinerated upon the conclusion of its useful life. Subsequent research has led to the development of a series of extractant molecules based on amides of carboxylic acids. Both mono- and diamide reagents have been synthesized and their extraction characteristics profiled. Presently, the most investigated reagent is N,N'-dimethyl-N,N'-dibutyltetradecyl malonamide, DMDBTDMA. This reagent extracts tri-, tetra-, and hexavalent actinides from nitric acid solutions more concentrated than 4 M into conventional (normal or branched alkane) diluents. Among the advantages of this class of reagents are the relatively innocuous nature of extractant degradation products and their "ash-free" incineration character. Drawbacks of the malonamides are the comparative complexity of the reagent (similar to CMPO's), and the somewhat narrow range of nitric acid concentrations from which trivalent actinides are extractable. Recent reports from Japan indicate some interesting variations in actinide selectivity for the tetraoctyl diamide of diglycolic acid, though this reagent has been subject to only laboratory-scale investigations [8].

In addition to these more mature extractant systems, research continues around the world on the development of new extractant systems for actinide partitioning. Dozol and co-workers [9] have initiated studies on the development of actinide-specific extractants based on calixarenes. These molecular-inclusion reagents can be functionalized to enhance their affinity for actinide metal ions. One possible drawback of these compounds is their comparatively large molecular size which may inhibit phase compatibility and thus limit solubility. They have the advantage of being synthesized in moderately high yields of relatively pure compounds from inexpensive starting materials. Another class of extractants that have been known for a number of years but not extensively investigated for their actinide separation efficiencies are the mono- and bis-phosphine oxides of pyridine-N-oxides synthesized by Paine and coworkers [10]. We have recently initiated a program at ANL to evaluate the actinide partitioning potential of this class of extractants. We have also examined the actinide extraction performance of dialkyl esters of diphosphonic acid chelating agents in various potential metal ion coordination geometries [11]. These extractant molecules exhibit high affinity for actinide ions in the important oxidation states, though they are typically too strong to be applied as the principal extractant in an actinide partitioning scheme. Another class of special-purpose "extractants" are the functionalized polyethylene-imine ultrafiltration polymers reported by Jarvinen and coworkers [12]. Applications of cation binding ultrafiltration polymers for the cleaning of aqueous waste streams has been demonstrated.

## AQUEOUS COMPLEXANTS

In hydrometallurgical separations of actinides, strong mineral acids (nitric, hydrochloric, sulfuric) are the most common media from which actinides are extracted. The respective electroneutral actinide complexes are carried into the extractant phase by solvating extractants like TBP. The electroneutral actinide complexes are not usually present in the aqueous solution. In operation of the PUREX process, oxalic and hydrofluoric acids have been employed as holdback reagents to prevent extraction of zirconium and molybdenum, which can be present at sufficiently high concentrations to interfere with actinide extraction. For solvent reconditioning prior to recycle, sodium carbonate is typically employed to remove traces of uranium that are not stripped by the dilute acid contact. A report on the development of a TRUEX flowsheet in Japan relies on the use of hydrazine oxalate and hydrazine carbonate for reductive stripping of TRUEX process solvent prior to recycle [13]. The TALSPEAK process for trivalent actinide-lanthanide separation relies on both lactic acid

and diethylenetriamine-N,N,N',N'',N''-pentaacetic acid (DTPA) as aqueous complexing agents to accomplish this difficult separation. DTPA has been proposed for actinide selective stripping of trivalent actinides in a CMPO-based extractant system (SETFICS) [14]. Other aminopolycarboxylic acids (HEDTA, EDTA, NTA) have been employed in various operations within the Department of Energy complex to enhance selectivity for some separations. This latter group of complexing agents have proven somewhat problematic, as they are moderately resistant to degradation (their presence is associated with the generation of H<sub>2</sub> in underground waste tanks at Hanford [15]) and have been associated with radionuclide mobility in the environment [16].

To respond to the need for actinide complexing agents in processing, we have characterized the actinide complexing characteristics of a series of derivatives of water-soluble diphosphonic acids ((X,Y)C(PO<sub>3</sub>H<sub>2</sub>)) [17]. These chelating agents exhibit exceptional affinity for actinide cations (even in moderately acidic media) making them particularly useful as potential stripping or decontaminating reagents for actinide processing. By altering the composition of the X and Y substituents on the methylene backbone, we have demonstrated that these reagents can be made to readily decompose (called Thermally Unstable Complexants or TUCS) producing H<sub>2</sub>O, CO<sub>2</sub>, and H<sub>3</sub>PO<sub>4</sub> as byproducts. For actinide processing, this can be expected to lead to generation of an actinide phosphate solid that could in principle be incorporated into an appropriate waste form. Though these reagents do not conform to the CHON principle of complexant design, their actinide complexing ability in strong acid qualifies them as uniquely capable reagents for stripping of extractant solutions prior to their recycle in a process.

## APPROACHES TO ACTINIDE OXIDATION STATE CONTROL

With most classes of extractants employed for actinide partitioning, tetra- and hexavalent actinide ions are considerably more strongly extracted than the trivalent actinides which in turn are extracted much more strongly than the pentavalent actinide ions. For acidic extractants like DIDPA, An(IV) is most strongly extracted, while for solvating extractants like TBP the hexavalent nitrate complexes are most strongly partitioned to the organic phase under most process conditions. The moderate differences in extractability of the oxidation states can be used to selectively partition actinide ions from a loaded extractant solution. In the PUREX process, as in most actinide recycle streams, U(VI) and Pu(IV) are co-extracted away from most fission products. Pu is selectively stripped by introducing a reagent that takes Pu(IV) to the considerably less extractable trivalent state, which reports to the aqueous medium. In PUREX, either Fe(II) or U(IV) are used for the reduction. Efficient separation of U from Pu is attained in practice.

In contrast to plutonium, neptunium oxidation state control at process scale has proven moderately difficult. Neptunium is typically found in dissolved fuel initially in the hexavalent oxidation state, which is readily extractable by typical reagents. However, Np(VI) is a moderately strong oxidant, and so readily reduced during processing to the poorly extracted pentavalent oxidation state, which can disproportionate in acidic aqueous solutions producing Np(IV) and Np(VI). As a result neptunium is often observed to distribute between phases in a somewhat irregular fashion. In a combined PUREX-TRUEX flowsheet, researchers in India have introduced K<sub>2</sub>Cr<sub>2</sub>O<sub>7</sub> to improve consistency in Np extraction then stripped Np and Pu together using H<sub>2</sub>O<sub>2</sub> and ascorbic acid for reduction [18]. In this process, the separation of Np and Pu is accomplished using extraction chromatography on a CMPO-based resin. In the TRPO process, Np is electroreduced to the tetravalent state and subsequently stripped with oxalic acid [5].

Two water-soluble organic reagents have been tested for Np oxidation state control in recent years. Taylor *et al.* [19] have reported that the combined complexation and redox action of formo- and acetohydroxamic acids ( $\text{HC}=\text{O}(\text{NHOH})$ ,  $\text{H}_3\text{CC}=\text{O}(\text{NHOH})$ ) can effectively assist in the control of neptunium partitioning in PUREX (and presumably in other nitric acid based) processing. Butyraldehydes have been known for some time to have an impact on actinide oxidation state control in PUREX processing. A more recent report from Japan has revealed a difference in redox chemistry for *n*-butyl and isobutyl derivatives [20].

## TRIVALENT ACTINIDE-LANTHANIDE SEPARATIONS REAGENTS

Within the broad concept of actinide recycle, there is not universal agreement on the desirability of isolating and transmuting the trivalent transplutonium actinides. The argument in favor of transmutation is that it will reduce the long-term radiotoxicity of the wastes from spent fuel. The principal argument against transmutation is the difficulty of efficiently separating trivalent lanthanides and actinides. The several examples of successful group separations (chloride based ion exchange or alkylamine solvent extraction, TALSPEAK) succeed based on the slight enhancement in covalency in the bonding of trivalent actinides relative to lanthanides [21]. Such effects are not manifested in oxygen-donor extractant systems, presumably because of the strongly electrostatic nature of their bonding. In these “reference” extraction systems, group separation factors average about 10.

During the past two decades of research on actinide-lanthanide separations, new examples of extraction systems have been reported in which higher group separation factors are observed. Ensor *et al.* [22] reported Am/Eu separation factors of about 100 for the synergistic extraction of these metal ions using a combination of 4-benzoyl-2,4-dihydro-5-methyl-2-phenyl-3H-pyrazol-3-thione (BMPPT) and 4,7-diphenyl-1,10-phenanthroline (DPPHEN), neither of which reagents extracts either of these metal ions significantly separately. Musikas separately reported separation factors of nearly 100 for the thiolated analog of HDEHP, though the hydrolytic instability of the extractant compromised the utility of the extraction system [7]. While these extraction systems have not received substantial attention due to reagent instability or low solubility, the importance of the separations target has precipitated a moderate amount of research seeking suitable materials for this inherently difficult separation.

The Musikas report was the first to enunciate the CHON principle, introducing the polyaza ligand trimethylpyridyltriazine (TPTZ) as a potential usable extractant that in principle yielded no ash upon incineration. In the final analysis, TPTZ proved too hydrophilic to be truly useful as an actinide/lanthanide separations reagent. A European consortium has conducted additional research on the efficacy of polyaza ligands as extractants. Kolarik *et al.* have identified the compound 2,6-di-(5,6,-dipropyl-1,2,4-triazin-3-yl)pyridines (DPTP) as a reagent providing Am/Eu separation factors of 100-120 in extraction from an aqueous medium of 1.9 M  $\text{HNO}_3/\text{NH}_4\text{NO}_3$  [23]. The *n*-propyl derivative self-associates (dimers and trimers) in a solution of branched alkanes with 2-ethyl-1-hexanol as a phase modifier. The extracted complexes have the stoichiometry  $\text{M}(\text{NO}_3)_3 \cdot \text{HNO}_3 \cdot 3\text{DPTP}$ . The extraction and separation efficiency is strongly dependent on the diluent. Jensen *et al.* have examined the complexation thermodynamics and structural details of complexes of trivalent lanthanide and actinide complexes with tetramethylpyridyl-N,N,N',N'-ethylene diamine (TPEN) [24]. This structural analog to EDTA forms hexadentate complexes with six metal-nitrogen bonds to both lanthanides and actinides. The actinide complex is 100-fold stronger than that of the lanthanide of comparable cation radius with a more exothermic complexation enthalpy, possibly indicating greater covalency in the actinide-nitrogen bonds. In both the DPTP and TPEN systems, the 6 M-N bonds can account for only 11-12 kJ/mol of enhanced selectivity, indicating that the separation is derived from a very subtle bonding difference between the lanthanides and actinides.

The largest trivalent actinide/lanthanide separation factors have been reported for systems based on dialkyldithiophosphinic acids. Zhu *et al.* [25] reported Am/Ln separation factors between  $2 \times 10^3$  and  $1 \times 10^4$  for the commercially available extractant Cyanex 301 (bis(2,4,4-trimethylpentyl)dithiophosphinic acid). The extractant must be rigorously purified from all acidic oxygenated impurities and the extraction reaction must be run from dilute acid media. Numerous derivatives of dialkyldithiophosphinic acid extractants have been prepared and evaluated, though to date few exceed the capabilities of Cyanex 301. The substitution of C-P for C-O-P bonds in the extractant greatly enhanced hydrolytic stability of the extractant (relative to the dialkyldithiophosphoric acids originally reported by Musikas. Recently completed research in our laboratories has apparently resolved some inconsistencies in the literature regarding extracted complex stoichiometries in extracted complexes [26].

## PHASE COMPATIBILITY, DILUENTS AND PHASE MODIFIERS

Because solvent extraction is fundamentally a mass transfer process, developing an understanding of the basic chemistry of metal complex formation and ligand design is in actuality only a small (but necessary) component of the overall picture. Even with appropriately designed and proven reagents, a solvent extraction separation can still fail if the solutes prove incompatible with the matrix or if the reagents prove incompatible with the mixing equipment. In hydrometallurgical processing of spent nuclear fuels, the most common media of choice are nitric acid (stainless steel is more-or-less inert toward HNO<sub>3</sub>) and low-volatility normal alkane solvents (e.g., kerosine). As extracted complexes and extracting reagents are often quite polar, maintaining these solutes in the non-polar organic solution can be a challenge, particularly at higher loading of solutes in the extractant phase. Maintaining phase compatibility in nuclear separations is particularly important, as it is possible to unintentionally assemble a critical mass of either <sup>239</sup>Pu or highly enriched uranium with potentially disastrous consequences.

Extractant molecules for such applications are usually designed to maintain good compatibility with the organic medium. Occasionally, the ideal metal ion coordination environment cannot be created in a geometry fully compatible with the diluent. In this case, polar phase modifiers are employed to assist in maintaining phase integrity. The most common phase modifiers employed in nuclear separations are TBP, long-chain alcohols (e.g., octanol), and trialkyl amines. Addition of phase modifiers can increase the capacity of the organic phase for the polar species being separated, but not without limits. Even with such additives, occasionally the organic phase will split, forming a "third" liquid phase. Though third phase formation has been studied for more than 40 years, laboratory investigations of the phenomenon have focused on identifying those characteristics that lead to phase splitting so that they can be avoided. Because of the variety of materials that can be made to undergo phase splitting, no universal description of third phases has emerged. Recent advances in analytical methodologies have created an opportunity to investigate the physical and chemical characteristics of this phenomenon in greater detail than was possible in prior studies. It is expected that a more complete understanding of the phenomenon will emerge from these ongoing studies [27,28].

## CONCLUSION - A VIEW TO THE FUTURE?

Under the potentially critical threat of global warming to modern society, nuclear power should be viewed as perhaps the most environmentally friendly technology for electricity production. However, the longevity of the radioactive wastes (more than  $10^5$  years at higher levels than that in natural uranium ore without processing and transmutation of actinides) and the absence of a clear disposal pathway that can be "guaranteed" to protect the environment

(atmosphere, hydrosphere, biosphere) stand in the way of this solution. Closing the loop on nuclear fuel and transmuting actinides and long-lived fission products using the proven technology of solvent extraction could improve the acceptability of this technology if we can learn to do it cleaner than we did during the past 50 years. The continuing development of new reagents and processes for their use, combined with new techniques for waste minimization, environment restoration, and waste form development could make important contributions toward this goal. Some of these new technologies have been described above. Others are found in the literature dedicated to environment cleanup and protection. There is also a major opportunity for computational science to contribute to both ligand/process design and to on-line monitoring of processes for improved efficiency. All that is required is to think somewhat outside of the box and apply the new ideas to solving the outstanding issues of hydrometallurgical separations. Opportunities abound for improved waste handling procedures.

## ACKNOWLEDGEMENT

The submitted manuscript has been created by the University of Chicago as Operator of Argonne National Laboratory ("Argonne") under contract No. W-31-109-ENG-38 with the U.S. Department of Energy. The U. S. Government retains for itself, and others acting on its behalf, a paid-up, non-exclusive, irrevocable worldwide license in said article to reproduce, prepare derivative works, distribute copies to the public, and perform publicly and display publicly, by or on behalf of the Government.

## REFERENCES

1. J. N. Mathur, M. S. Murali and K. L. Nash (2001), *Solvent Extr. Ion Exch.*, **19** (4), 357.
2. E. P. Horwitz and W. W. Schulz (1999), Metal Ion Separation and Preconcentration: Progress and Opportunities, *ACS Symposium Series*, No. 716, A. H. Bond, M. L. Dietz and R. D. Rogers (eds.), American Chemical Society, Washington D.C., pp. 20-50.
3. T. H. Siddall, Jr. (1963), *J. Inorg. Nucl. Chem.*, **25**, 883.; T. H. Siddall, Jr. (1964), *J. Inorg. Nucl. Chem.*, **26**, 1991.
4. I. W. Donald, B. L. Metcalfe and R. N. J. Taylor (1997), *J. Mater. Sci.*, **32** (22), 5851.
5. Y. Zhu and R. Jiao (1994), *Nucl. Technol.*, **108**, 361.
6. Y. Morita, I. Yamaguchi, Y. Kondo, K. Shirahashi, I. Yamagishi, T. Fujiwara and M. Kubota (1995), Safety and Environmental Aspects of Partitioning and Transmutation of Actinides and Fission Products, IAEA-TECDOC-783, IAEA, Vienna, p. 93.
7. C. Musikas (1985), *Proc. Int. Symp. Actinide/Lanthanide Separations*, Honolulu, Hawaii, G. R. Choppin, J. D. Navratil and W. Schulz (eds.), World Scientific Publishing, Singapore, p.19.
8. Y. Sasaki, Y. Sugo, S. Suzuki and S. Tachimori (2001), *Solv. Extr. Ion Exch.*, **19**, 91.
9. J. F. Dozol, A. G. Carrera, H. Rouquette and V. Lamare (1999), *Proc. Int. Conf. Future Nuclear Systems, Global '99, Nuclear Technology Bridging Millennia*, pp. 605-612.
10. E. M. Bond, U. Engelhardt, T. P. Deere, B. M. Rapko, R. T. Paine and J. R. Fitzpatrick (1997), *Solvent Extr. Ion Exch.*, **15**, 381.
11. R. Chiarizia, A. W. Herlinger, Y. D. Cheng, J. R. Ferraro, P. G. Rickert and E. P. Horwitz (1998), *Solvent Extr. Ion Exch.*, **16**, 505, and references therein.
12. G. D. Jarvinen, B. F. Smith, T. W. Robison, K. M. Kraus and J. A. Thompson (1999), *Proc. Symp Metal Separations Technologies Beyond 2000*, sponsored by the United Engineering Foundation, Kuhuku, Oahu, Hawaii, K. C. Liddell and D. J. Chaiko (eds.), pp. 131-138.

13. M. Ozawa, Y. Koma, K. Nomura and Y. Tanaka (1998), *J. Alloys Compds.*, **271-273**, 538.
14. Y. Koma, M. Watanabe, S. Nemoto and Y. Tanaka (1998), *Solvent Extr. Ion Exch.*, **16**, 1357.; Y. Koma, T. Koyama and Y. Tanaka (1999), *J. Nucl. Sci. Tech.*, **36**, 934.
15. D. M. Strachan, L. R. Pedersom, S. A. Bryan, E. C. Ashby, C. L. Liotta, E. K. Barefield, H. M. Neumann, F. Doctorovich, A. Konda, K. Zhang, D. Meisel, C. D. Jonah and M. C. Sauer (1993), *Proc. ACS Symp. Chemical Pretreatment for Nuclear Waste Disposal*, E. P. Horwitz and W. W. Schulz (eds.), Plenum Press, New York, pp. 71-79.
16. J. M. Cleveland and T. F. Rees (1981), *Science*, **212**, 1506.
17. K. L. Nash and P. G. Rickert (1993), *Sep. Sci. Technol.*, **28**, 25-41.
18. D. S. Deshingkar, R. R. Chitnis, P. K. Wattal, T. K. Theyyunni, M. K. T. Nair, A. Ramanujam, P. S. Dhami, V. Gopalakrishnan, M. K. Rao, J. N. Mathur, M. S. Murali, R. H. Iyer, L. P. Badheka and A. Bannerji (1994), Partitioning of Actinides from Simulated High Level Wastes Arising from Reprocessing of PHWR Fuels: Counter-current Extraction Studies Using CMPO, Report BARC/E-014/1994.
19. R. J. Taylor, I. May, A. L. Wallwork, I. S. Denniss, N. J. Hill, B. Ya. Galkin, B. Ya. Zilberman and Yu. S. Fedorov (1998), *J. Alloys Compds.*, **271-273**, 534.
20. G. Uchiyama, T. Asakura, S. Hotoku and S. Fujine (1998), *Solvent Extr. Ion Exch.*, **16**, 1191.
21. K. L. Nash (1993), *Solvent Extr. Ion Exch.*, **11** (4), 729.
22. D. D. Ensor, G. D Jarvinen and B. F. Smith (1988), *Solvent Extr. Ion Exch.*, **6**, 439.
23. Z. Kolarik, U. Mullich and F. Gassner (1999), *Solvent Extr. Ion Exch.*, **17**, 23, 1155.
24. M. P. Jensen, L .R. Morss, J. V. Beitz and D. D. Ensor (2000), *J. Alloys Compds.*, **303-304**, 137.
25. Y. Zhu, J. Chen and R. Jiao (1996), *Solvent Extr. Ion Exch.*, **14**, 61; Y. Zhu, J. Chen and R. Jiao (1996), *Sep. Sci. Technol.*, **31**, 2723.
26. M. P. Jensen, R. Chiarizia and V. Urban (2001), Aggregation of the Nd Complexes of HDEHP, Cyanex 302, and Cyanex 301 in toluene, Abstract IEC-067, American Chemical Society 221<sup>st</sup> meeting, Manuscript in preparation.
27. L. Lefrancois, J.-J. Delpuech, M. Hebrant, J. Chrisment and C. Tondre (2001), *J. Phys. Chem. B*, **105**, 2552.
28. M. P. Jensen, R. Chiarizia, J. R. Ferraro, M. Borwoksi, K. L.Nash, P. Thiagarajan and K. C. Littrell (2002), *Proc. Int. Solvent Extr. Conf. ISEC 2002*, Cape Town, South African, pp. 1137-1142.



## UPDATE ON THE SCIENCE AND TECHNOLOGY OF TRIBUTYL PHOSPHATE

James D. Navratil

Department of Environmental Engineering and Science, Clemson University,  
Anderson, South Carolina, USA

Although tri-*n*-butyl phosphate (TBP) has a dominant position in solvent extraction applications in the nuclear industry, it is also an important reagent in many non-nuclear hydrometallurgical applications. Since the first work on TBP research was conducted as part of the U.S. Manhattan Project in 1944, numerous scientists and engineers in many countries have examined almost every aspect of TBP. Many of the results of these studies have been published in the open literature, but there has also been a great deal of useful knowledge about TBP whose availability is difficult to locate. To solve this problem, various authors over the last 55 years have reviewed parts of the science and/or technology of TBP, including a four-volume set of books containing a systematic, comprehensive, and critical account of all aspects of TBP. This paper provides a selected update on the science and technology of TBP since this set of books was published.

### INTRODUCTION

Since World War II, tri-*n*-butyl phosphate (TBP) has been the subject of continuous research and development. During this time a vast scientific literature has accumulated dealing with all aspects of TBP related to the science and technology of solvent extraction processes. Although most review articles on solvent extraction, which are quite numerous, devote considerable space to a description of the more common properties and reactions of TBP, there has been no single monograph until 1984 devoted solely to an extensive review of TBP. Between 1984 and 1991 CRC Press, Inc., Boca Raton, Florida, published a four-volume set of books containing a comprehensive account of all available data on the science and technology of TBP [1-4]. The purpose of these books was to bring together in an organized form as much as possible of the then-known accumulation of facts pertaining to the properties, reactions, and uses of TBP.

*Science and Technology of Tributyl Phosphate*, Volume I, reviews the fundamental chemistry of TBP (analysis, behavior in nuclear solvent extraction systems, physical properties, reactions with various inorganic reagents, and synthesis), diluents (types, properties and reactions of various organic compounds) and radiolysis of TBP. Volume II, published in 1987, gives a detailed account of TBP in hydrometallurgical process applications, miscellaneous non-nuclear industrial uses, and analytical applications. Volume III, published in 1990, is devoted to various aspects of nuclear applications: PUREX and THOREX processes, French experience in recovering plutonium from metallurgic scrap, and the development and application of computer codes to simulate PUREX process operations; miscellaneous nuclear applications are also covered in Volume III. Volume IV addresses the extraction of water and mineral and organic acids from aqueous media by TBP-diluent solutions.

This paper provides an update on the science and technology of TBP since this series of volumes was published; selected advances in the nuclear and non-nuclear applications of TBP for solvent extraction processes are highlighted. This review is dedicated to the late Professor A. Steven Kertes. Dr. Kertes was on the editorial board of the TBP books and served as a co-editor of Volume IV. The following quote is from his Foreword to Volume I: "The Editors should be congratulated for conceiving this project and for their success to recruit as contributing authors many top experts in the field, most of whom with many years of first-hand experience in basic and applied research involving this important extractant. I believe that the compact and authoritative chapters written by them will orient and stimulate chemists and technologists in many branches of research in the general field of solvent extraction [1]."

### NUCLEAR APPLICATIONS OF TBP

In the nuclear field, spent nuclear fuel reprocessing plants employ the PUREX process to separate plutonium and uranium from fission products as well as to purify the separated uranium and plutonium. PUREX (Plutonium Uranium Recovery by EXtraction) typically uses TBP in a hydrocarbon diluent. TBP is applied similarly, but much less widely, to the reprocessing of spent nuclear fuels containing thorium. Recovery of plutonium from nuclear weapons scrap materials has also utilized the PUREX process.

Oak Ridge National Laboratory (ORNL), faced with the problem of recovering uranium from wartime reprocessing plant wastes, initially developed the PUREX process. Several PUREX process flowsheets were investigated around 1950 at ORNL, with varying proportions of TBP to diluent. As a result of these investigations, 30% TBP-diluent flowsheets were operated at ORNL and in large plants at Savannah River from 1954 and at Hanford from 1956 [1-4].

In addition, there are many other applications of TBP in the nuclear industry including the production of nuclear-grade uranium from "yellow cake," the separation of neptunium and the separation of an actinide-lanthanide fraction from reprocessing wastes. Owing to its many uses, and also the stringent requirements of the nuclear industry, TBP has been thoroughly researched [1-4].

The first paper on the use of TBP, based on work performed in 1944 as part of the U.S. Manhattan Project, was published by Warf in 1949 [5]. At that time there were no citations in *Nuclear Science Abstracts* (NSA) under the heading "butyl phosphate." In 1961 there were over 210 entries under this heading in the indices of Volumes 11 to 15 of NSA. The replacement of NSA, the International Nuclear Information System (INIS), compiled and published by the International Atomic Energy Agency, has 252 and 245 entries under the heading of TBP for the last two respective decades, indicating a sustaining research and development interest in TBP.

Table 1 summarizes the various TBP subject areas found in the INIS citations from 1990 to the present. Since these citations came from INIS, they mainly relate to TBP science and technology in the nuclear field and related areas. The only significant review published in this period outlined the current status of the chemistry of nuclear fuel reprocessing [6].

*Table 1. Number of papers cited in INIS 1990-2000 by major subject area.*

Nuclear waste processing/partitioning	43
Purex solvent degradation/stability/clean up	28
Non-nuclear	27
General chemistry	27
Analytical applications	22
Miscellaneous	18
New diluents/solid supports	16
Purex development	15
Health and safety	10
General chemistry of TBP	6
Equipment	4
Analysis of TBP	3

Table 1 shows that the major area of TBP publication during the last decade involved high-level nuclear waste treatment and partitioning, *i.e.*, the separation of long-lived actinides from shorter life fission products. TBP has been utilized as a phase modifier in several new organic systems. Amines and bifunctional organophosphorous extractants, mixed with TBP, have mostly been reported [7,8]. The chemistry of these extractant systems has been studied for not only actinides, but also fission products including technetium and rhenium [9,10]. No further details on nuclear waste partitioning processes will be given here since they are extensively reviewed by Nash [8].

The second highest publication area noted in Table 1 deals with TBP solvent degradation/stability/cleanup [11-15]. Some of these studies were a result of safety concerns relating to TBP degradation products [16,17]. Several studies have been reported on third phase formation caused by saturation of plutonium species in the organic phase [18,19]. A noteworthy advance deals with the regeneration of PUREX solvent by vacuum distillation, developed and implemented in a French reprocessing plant [20].

Other work on Purex process improvements has involved new redox reagents for partitioning actinides [21]. An improved Purex process, Impurex, was reported based on the extraction of U(VI) and Pu(IV) from 5M nitric acid at elevated temperature (50C) [21]. Reports also appeared for processing highly burned fuel, better U/Th separation and neptunium separation [22-25]. Further, troublesome fission product decontamination continues to be studied, in particular zirconium, niobium and ruthenium; recent work showed that Zr(IV) present in the fuel solution causes extraction of technetium from the solution [26].

Alternative reagents continue to be tested to find an improved extractant for the PUREX process. Various amines and organophosphorous compounds have recently been tested but none have come close to matching all the excellent properties of TBP [7,27]. These favorable solvent properties include suitable extraction of Pu and U with good fission product decontamination, reasonable stability, good physical properties, and no requirement for salting agents other than nitric acid [1].

Another active area related to Purex process improvement has been diluent development and testing. Besides fluorinated solvents, supercritical carbon dioxide shows promise for selected applications [28-31]. Various solid supports have been utilized for both process development and analytical separations; the sorbents have employed various materials, such as commercial styrene divinyl benzene resins, inorganic materials, etc. [32]. Work on membranes as solvent supports continues to be reported [33].

Analytical applications in the nuclear area have included a variety of pre-analysis separation methods utilizing supported TBP. One report used reverse phase chromatography for uranium analysis [34]. New analysis methods for TBP and its degradation products have also been reported [35,36].

In this review, uranium was found to be the most common element studied in nuclear technology during the past decade, including recent work on improvements to processes for the recovery of uranium from ores [37]. Plant-scale use of TBP to purify crude uranium recovered from its ores began in the U.S. in 1953; similar uranium refineries based upon the use of TBP were also constructed in Canada and the U.K. in the early 1950s. Today, TBP extraction technology and processes continue to be applied worldwide for purification of crude uranium as well as thorium. The extraction of zirconium into TBP is also in use as a purification step in the production of high-purity zirconium metal from its ores.

### NON-NUCLEAR APPLICATIONS OF TBP

TBP first became available as a commercial product because of its use in the plastics industry as a plasticizer. TBP also has important industrial applications as an antioxidant, an antifoaming agent, a catalyst and a corrosion inhibitor. There are few operating plants designed for the use of TBP in the extraction of non-nuclear metals and other materials. Perhaps one of the main reasons for this is that TBP operates through a solvating mechanism of extraction, and, therefore extraction is highly dependent upon the ionic strength of the anion. Major process metallurgy flowsheets utilizing solvent extraction involve extraction from a sulfate medium. Very few plants have gone on-stream employing chloride or nitrate systems, even though TBP is an excellent reagent from aqueous chloride and nitrate media. Non-nuclear industrial-scale hydrometallurgical applications of TBP include its use in the preparation of individual rare earths, the separation of zirconium and hafnium, and the removal of iron from chloride liquors containing copper, nickel, and cobalt [1,3].

The extent of early non-nuclear research and development on TBP can be represented by citations in *Chemical Abstracts* (CA). The CA Decennial (1937 to 1946) Index (Volumes 31 to 40) lists 13 entries under the heading “(BuO)<sub>3</sub>PO”, none of which pertain to use of TBP in solvent extraction systems. By contrast, the CA subject index of Volumes 51 to 55, 1957 to 1961, contains almost 400 entries for TBP, two-thirds of them concerning solvent extraction applications. During the past decade there have been over 700 citations of TBP with almost 300 of them relating to separations science and technology.

The recovery and purification of scandium, yttrium, and lanthanides continue to be the most cited research area during the past 10 years [38,39]. During the TBP extraction of scandium from industrial HCl solutions containing aluminum and iron, the loaded TBP is stripped with 1 M HCl to provide 100% scandium recovery. Recent work on yttrium has been reported [40]. For the separation of rare earths, generally alkylphosphorus acids have been used for extraction in chloride, nitrate, or sulfate media. However, in the past decade there has been much research on the use of TBP to extract rare earth elements, mostly from nitrate or chloride systems; in addition, attempts to enhance the separation of the chemically similar rare earths have been carried out, using TBP mixed with other extractants, such as acidic organophosphorous reagents, to promote synergistic interactions [38,39].

Only limited work has been reported on TBP extraction of alkali metals, and there are no industrial plants in operation. More attention has been given to TBP extraction of Group IIA metals, mainly because the alkaline earths are present in many minerals with important metallic values; TBP extraction of alkaline earth metals in nitrate systems follows the pattern Ca > Sr > Ba, but distribution coefficients are low [2]. Out of the Group IIIB elements (Al, Ga, In, Ti) only an excellent review of indium has recently appeared in the literature [41]. However, research activity is strong with Group IVB (Ti, Zr, Hf) as well as with vanadium,

niobium and tantalum [42-44]. New work with TBP extraction of Group VIB (Cr, Mo, W) and base metals, such as copper, nickel and zinc, from chloride media, has been reported [45-47]. Considerable attention has been given to the use of TBP for extraction and recovery of precious metals (Ag, Au, Platinum Metals Group), but currently there are only three known plants using this technology [48,49]. Other significant studies with metals have involved the extraction kinetics of iron [50].

In addition to being an excellent extractant for metallic species from aqueous solutions, TBP also extracts a number of other chemicals including organic compounds, mineral acids, etc. The use of TBP for the extraction of different phenolic compounds from aqueous effluents from various manufacturing processes has been reported [51]. TBP associates with phenols through a hydrogen bond, and the stability of the extracted species increases with increasing phenol acidity.

## CONCLUSIONS

TBP continues to be the dominant solvent extractant in nuclear and non-nuclear applications. Although more is known about TBP than any other metal liquid-liquid extraction reagent, new work continues to be reported at a sustained level of activity during the past decade. The future continues to look bright for the science and technology of tributyl phosphate.

## REFERENCES

1. W. W. Schulz and J. D. Navratil (eds.) (1984), *Science and Technology of Tributyl Phosphate*, Vol. I. *Synthesis, Properties, Reactions and Analysis*, CRC Press, Boca Raton, FL.
2. W. W. Schulz and J. D. Navratil (eds.) (1987), *Science and Technology of Tributyl Phosphate*, Vol. II. *Selected Technical and Industrial Uses*, CRC Press, Boca Raton, FL.
3. W. W. Schulz, L. L. Burger and J. D. Navratil (eds.) (1990), *Science and Technology of Tributyl Phosphate*, Vol. III, *Applications of Tributyl Phosphate in Nuclear Fuel Reprocessing*, CRC Press, Boca Raton, FL.
4. W. W. Schulz, J. D. Navratil and A. S. Kertes (eds.) (1991), *Science and Technology of Tributyl Phosphate*, Vol. IV, *Extraction of Water and Acids*, CRC Press, Boca Raton, FL.
5. J. C. Warf (1949), *J. Amer. Chem. Soc.*, **71**, 3257.
6. D. D. Sood and S. K. Patil (1996), *J. Radioanal. Nucl. Chem. Articles*, **203** (2), 547-573.
7. C. Musikas, C. Condamines, C. Cuillerdier and L Nigond (1991), *Proc. Int. Symp. Radiochemistry and Radiation Chemistry*, Bombay, IT 16.1.
8. K. L. Nash (2002), *Proc. Int. Solvent Extraction Conf., ISEC 2002*, Cape Town, South Africa, pp. 1110-1117.
9. M. Takeuchi, S. Tanaka and M. Yamawaki (1993), *Radiochim. Acta*, **63**, 97-100.
10. M. Takeuchi, S. Tanaka and M. Yamawaki (1994), *Solv. Extr. Ion Exch.*, **12** (5), 987-1000.
11. J. Mailen and O. K. Tallent (1984), *Proc. ANS Int. Topical Meeting Fuel Reprocessing and Waste Management*, Jackson, Vol. I, p. 431.
12. G. S. Markov, M. M. Moshkov and V. A. Shcherbakov (1993), *Proc. Int. Solvent Extraction Conf., ISEC '93*, Society of Chemical Industry, York.
13. M. V. Krishnamurthy and R. Sampathkumar (1992), *J. Radioanal. Nucl. Chem.*, **166** (5), 421-429.
14. P. R. V. Rao and Z. Kolarik (1996), *Solv. Extr. Ion Exch.*, **14** (6), 955-993.
15. S. C. Tripathi, S. Sumathi and A. Ramanujam (1999), *Sep. Sci. Technol.*, **34** (14), 2887-2903.
16. M. L. Hyder, D. F. Paddleford and M. C. Thompson (1995), *Emerging Technologies in Hazardous Waste Management VII*, D. W. Tedder (ed.), American Chemical Society, Washington, DC, pp. 387-390.

17. G.S . Barney and T. D. Cooper (1995), Emerging Technologies in Hazardous Waste Management VII, D. W. Tedder (ed.), American Chemical Society, Washington, DC, pp. 391-393.
18. Z. Kolarik (1991), Handbook on the Physics and Chemistry of the Actinides, A. J. Freeman and C. Keller (eds.), Vol. 6, Elsevier Science Publishers, Amsterdam, p. 511.
19. P. R. V. Rao (1994), *IANCAS Bull.*, **10** (2), 16.
20. C. Ginisty and B. Guillaume (1990), *Sep. Sci. Technol.*, **25**, 1941.
21. D. O. Campbell and W. D. Burch (1990), *J. Radioanal. Nucl. Chem. Articles*, **142**, 303.
22. B. Ya. Zil'berman (2000), *Radiokhim.*, **42** (1), 3-15.
23. H. Schmieder and G. Petrich (1989), *Radiochim. Acta*, **40**, 181.
24. Z.-M. Zhou, Y.-X. Sun, S.-N. Yu and H.-F. Du (1996), *J. Radioanal. Nucl. Chem.*, **214** (5), 369-379.
25. May, R. J. Taylor, G. C. Brown and N.J. Hill (1999), *Radiochim. Acta*, **83** (3), 135-138.
26. C. Phillips (1989), *Atom*, **394**, 13.
27. J. P. Shukla (1997), *Proc. Nucl. Radiochem. Symp.*, K. L. Ramakumar, P. K. Pujari, R. Swarup and D. D. Sood (eds.), Bhabha Atomic Research Centre, Mumbai, pp. 196-197.
28. Y. Lin, C. M. Wai, F. M. Jean and R. Brauer (1994), *Environ. Sci. Technol.*, **28** (6), 1190-1193.
29. K. E. Laintz and E. Tachikawa (1994), *Anal. Chem.*, **66** (13), 2190-2193.
30. N. G. Smart, Z. Yoshida, Y. Meguro, S. Iso, A. A. Clifford, Y. Lin, K. Toews and C. M. Wai (1997), *Proc. Internat. Conf. Future Nucl. Systems*, Atomic Energy Society of Japan, Tokyo, pp. 350-354.
31. R. S. Addleman and C. M. Wai (2001), *Radiochim. Acta*, **89** (1), 27-33.
32. H. Akcay, S. Kilinc and R. Karakas (1998), *Sep. Sci. Technol.*, **33** (13), 2025-2037.
33. J. S. Gill, U. R. Marwah and B. M. Misra (1994), *Sep. Sci. Technol.*, **29** (2), 193-203.
34. Z. Falian and L. Zhiyuan (1995), *J. East China Geo. Inst.*, **18** (1), 70-76.
35. M.A. Ali and A.M. Al-Ani (1991), *Analyst*, **116** (10), 1067-1069.
36. K. E. Grant, G. M. Mong, S. A. Clauss, K. L. Wahl and J. A. Campbell (1997), *J. Radioanal. Nucl. Chem.*, **220** (1), 31-35.
37. R. A. Nagle, S. V. Parab, S. S. Gharat, A. B. Girivalkar and K. S. Koppiker (1991), *Proc. Int. Symp. Uranium Technol.*, Vol. 2, Bhabha Atomic Research Centre, Bombay, pp. 570-581.
38. M. Majdan and Z. Kolarik, Z. (1993), *Solv. Extr. Ion Exch.*, **11** (2), 331-348.
39. G. Gaikwad and A. D. Damodaran (1992), *J. Radioanal. Nucl. Chem.*, **163** (2), 277-288.
40. S. A. Semenov, I. F. Poletaev, A. M. Reznik and V. V. Vygovskij (1991), *Zh. Neorg. Khim.*, **36** (10), 2711-2717.
41. P. Paiva (2001), *Sep. Sci. Technol.*, **36**, 1395-1419.
42. Siriudomratana (1984), Thesis, Chulalongkorn University, Bangkok, 56 pp.
43. V. G. Majorov, A. I. Nikolaev and V. K. Kopkov (1999), *Zh. Priklad. Khim.*, **72** (6), 929-932.
44. L. D. Kurbatova, T. A. Sinitsyna, L. N. Garidulich and L. M. Sharygin (1991), *Zh. Neorg. Khim.*, **36** (10), 2708-2710.
45. H. A. El-Naggar, H. Someda and A. Abdel-Gawad (1992), *J. Radioanal. Nucl. Chem. Articles*, **157** (1), 159-168.
46. W. Sanad, H. Flex and S. Marei (1993), *J. Radioanal. Nucl. Chem.*, **170** (1), 235-241.
47. V. A. Prokuev and V. S. Kurguzova (1989), *Zh. Neorg. Khim.*, **34** (9), 2289-2295.
48. M. Parent, R. Cornelis, R. Dams and F. Alt (1993), *Anal. Chim. Acta*, **281** (1), 153-160.
49. M. Rozen, N. A. Kartasheva and Z. N. Nikolotova (1995), *Radiokhimiya*, **37** (3), 232-238.
50. W. Sanad, H. Flex and S. A. Marei (1992), *J. Radioanal. Nucl. Chem. Articles*, **157** (1), 185-192.
51. W. Cichy and J. Szymanowski (2001), Abstracts of the 9th International Conference SIS 01, Slovakia, 108.



## COMPOUNDS OF HEXAVALENT URANIUM AND DIBUTYL PHOSPHATE IN NITRIC ACID

Brian A. Powell, James D. Navratil, and Major C. Thompson\*

Department of Environmental Engineering and Science, Clemson University, Anderson, USA

\*Westinghouse Savannah River Company, Aiken, USA

Storage tanks at the Savannah River Site contain highly enriched uranyl nitrate and dibutyl phosphate (DBP), which can precipitate together as yellow solids. Accumulation of solids in these waste tanks presents a criticality hazard and must be avoided. In this work, uranium dibutylphosphate compounds were formed from batch reactions in 0.2 to 6.0 M HNO<sub>3</sub> and DBP concentrations both above and below its aqueous solubility limit. UO<sub>2</sub>(DBP)<sub>2</sub> precipitates from 0.2 M HNO<sub>3</sub> with DBP below its aqueous solubility limit. In 0.2 M HNO<sub>3</sub>, with DBP above its aqueous solubility limit, UO<sub>2</sub>(DBP)<sub>2</sub>(HDBP)<sub>x</sub> precipitates (where x = 1 or 2). Indications of nitrate complexation appear in precipitates from 0.8M HNO<sub>3</sub> for both DBP concentrations, however a 1:1 uranium:nitrate ratio is not reached until higher acid concentrations are used. UO<sub>2</sub>(NO<sub>3</sub>)(H(DBP)<sub>2</sub>)(HDBP)<sub>2</sub> precipitates from  $\geq$  3.0 M HNO<sub>3</sub> for high DBP concentrations. This compound is not formed until 6.0M HNO<sub>3</sub> is used for lower DBP concentrations. It is assumed that the change in physical characteristics of the compounds and addition of nitrate coincides with the breakdown of the UO<sub>2</sub>(DBP)<sub>2</sub> polymer. Supporting data for these findings are presented.

### INTRODUCTION

The purpose of this research was to gain a better understanding of the chemistry of solid uranyl dibutyl phosphate compounds forming within solutions in storage tanks located at the Savannah River Site (SRS) in South Carolina. These tanks were originally constructed for temporary storage of enriched uranium solutions that had gone through the second uranium cycle of the plutonium and uranium recovery by extraction (PUREX) process. Trace levels of the organophosphorus reagent tributyl phosphate (TBP), used in the PUREX process, present in the solutions undergo hydrolysis to form dibutyl phosphate (DBP) that facilitates the precipitation of uranium solids, thus causing a possible nuclear criticality hazard.

Analysis indicated DBP concentrations of 30-50 mg/L in the storage tanks [1]. It was inferred that all of the TBP has not yet hydrolyzed because of the slow hydrolysis reaction at ambient temperature and high acid concentrations. For complete hydrolysis of the TBP present an estimate of 158 mg/L was obtained using a psuedo-first-order rate constant for the decomposition of 30% (vol%) TBP in kerosene (reported as  $7.2 \times 10^{-8} \text{ h}^{-1}$  in water at ambient temperature [2]). Pierce *et al.* [3] noted that precipitation could occur from a solution containing 110 mg/L DBP. All compounds formed regardless of acid concentration have a limited solubility, but there is a slight increase in the solubility observed in compounds extracted from high acid concentrations [3].

Several areas governing the general solution chemistry between uranium and DBP remain unclear. Solids precipitated out of 0.2 M HNO<sub>3</sub> have been determined to have the formula UO<sub>2</sub>(DBP)<sub>2</sub>, which is present as a polymer structure [4-8]. Addition of nitrate and HDBP (dibutyl phosphoric acid) to UO<sub>2</sub>(DBP)<sub>2</sub> occurs when solids are prepared from 6.0 M HNO<sub>3</sub> [6]. UO<sub>2</sub>(DBP)<sub>2</sub> precipitates as a yellow powder, but as the acid concentration increases the precipitates become an oily mass. Krutikov and Solovkin reported that two compounds are extracted from 6.0 M HNO<sub>3</sub> with the formulas UO<sub>2</sub>(NO<sub>3</sub>)(H(DBP)<sub>2</sub>) and UO<sub>2</sub>(NO<sub>3</sub>)(H(DBP)<sub>2</sub>)(HDBP)<sub>2</sub> [6]. These compounds were both described as a "vitreous mass." DBP has the ability to dimerize so it could be present in these compounds as a dimer.

## EXPERIMENTAL METHODS

Four methods were employed in order to prepare uranium DBP compounds from 0.2, 0.5, 0.8, 1.0, 2.0, 3.0, 4.0, 5.0, and 6.0 M HNO<sub>3</sub>. All DBP additions were done with a 4:1 DBP:uranyl nitrate ratio. The samples are cited as UDBP-XXM-Suffix, where XX is the acid concentration from which the solids were prepared and the suffix refers to the method of preparation.

UO<sub>2</sub>(DBP)<sub>2</sub> was prepared by adding purified DBP (Acros Organics, New Jersey) to a stirring uranyl nitrate hexahydrate (UNH) (reagent grade, Alfa-Asear, Ward Hill, MA) solution and filtering the precipitate with a cellulose nitrate membrane filter. This solid was divided into nine portions that were added to the acid solutions listed above. After stirring for two hours, the solids were filtered, washed with isopropanol, and air-dried. These solids will be referred to as addition (-ADD) in the suffix.

Two sets of samples were prepared by adding purified DBP directly to a UNH solution dissolved in the acid concentrations listed above. One set used an aqueous volume where DBP could exist as a separate phase above its aqueous solubility limit. These solids will be referred to as extracted solids (-EXT) in the suffix. The second set of samples used a larger reaction volume where any residual DBP could be completely dissolved in the aqueous acid medium. These solids will be referred to as precipitated (-PPT) in the suffix. In both cases, the solids were washed with cold water and the solids were either filtered or the free liquid was decanted and the solids were allowed to dry on a watchglass overnight. Solids in three special cases (UDBP-0.2 M-EXT, UDBP-3.0 M-EXT, and UDBP-6.0 M-EXT) were re-crystallized from 2-ethylhexanol (Mallinckrodt, reagent grade, used as received, Paris, KY). The re-crystallized solids were filtered and the filtration apparatus was left overnight in order to remove all remaining 2-ethylhexanol.

Roughly 100 mg/L solutions of each sample were prepared for analysis. The solutions were analyzed using ion chromatography for nitrate concentrations (Dionex DX-100 IC, Sunnyvale, CA), liquid scintillation counting for uranium concentrations (Packard LS 2550 TR/AB Model B2555, Downers Grove) using Hi Safe III liquid scintillation cocktail (Wallac, Akron, OH) and a persulfate digestion followed by reduction of molybdophosphoric acid with stannous chloride for DBP concentrations [9]. Infrared spectra (IR) were obtained using a Nicolet IR-550 FT-IR (Masidon, WI) with KBr plates at 4 cm<sup>-1</sup> resolution and 64 scans. <sup>31</sup>P NMR was obtained in d2-methylene chloride (EM Science, Darmstadt, Germany) using a Bruker AC 300 MHz NMR at 129.49 MHz. UV-Vis spectroscopy was performed, by first dissolving the solids in chloroform, and then using a Beckman 640 DU (Schaumburg, IL) for analysis.

## RESULTS

Table 1 shows nitrate:uranyl and DBP:uranyl molar ratios for all synthesized compounds along with the main factor in the preparation of each compound. These ratios can be used to infer an empirical formula for each compound.

*Table 1. Molar ratios of uranyl DBP solids from chemical analysis.*

Sample	Preparation	DBP/UO <sub>2</sub>	SD (±)	NO <sub>3</sub> /UO <sub>2</sub>	SD (±)
All –ADD	Isopropanol	2.0-2.2	0.1	0.0	0.00
UDBP-0.2M-EXT	Extracted	3.0	0.1	0.0	0.00
UDBP-0.5M-EXT	Extracted	2.9	0.1	0.0	0.00
UDBP-0.8M-EXT	Extracted	3.2	0.1	0.2	0.00
UDBP-1.0M-EXT	Extracted	3.3	0.1	0.2	0.00
UDBP-2.0M-EXT	Extracted	4.2	0.1	0.3	0.00
UDBP-3.0M-EXT	Extracted	4.1	0.1	0.5	0.01
UDBP-4.0M-EXT	Extracted	4.2	0.2	0.7	0.01
UDBP-5.0M-EXT	Extracted	4.1	0.1	0.9	0.02
UDBP-6.0M-EXT	Extracted	3.8	0.1	0.9	0.01
All-REC	2-ethylhexanol	1.9-2.1	0.1	0.0	0.00
UDBP-0.2M-PPT	Precipitated	2.2	0.1	0.0	0.00
UDBP-0.5M-PPT	Precipitated	2.5	0.1	0.0	0.00
UDBP-0.8M-PPT	Precipitated	2.4	0.1	0.0	0.00
UDBP-1.0M-PPT	Precipitated	2.5	0.1	0.1	0.00
UDBP-3.0M-PPT	Precipitated	2.7	0.1	0.1	0.00
UDBP-6.0M-PPT	Precipitated	3.7	0.1	0.9	0.01

### Solids Prepared via Addition

The chemical analysis of all –ADD compounds showed there was no nitrate present and the DBP:uranyl ratio was  $2.0-2.2 \pm 0.1$ , corresponding to UO<sub>2</sub>(DBP)<sub>2</sub> that has been well characterized as a polymer [5-7]. However, it is not consistent with other reported compounds where nitrate and additional DBP/HDBP modify UO<sub>2</sub>(DBP)<sub>2</sub> at higher acid concentrations. A pale yellow powder, characteristic of UO<sub>2</sub>(DBP)<sub>2</sub>, was initially added to each acid solution. As the experiments progressed a breakdown in the physical structure of the powder was observed. At acid concentrations  $>3.0\text{ M HNO}_3$  the yellow powder took on a viscous gel-like appearance. However, after filtration and washing with isopropanol, all solids changed back to a pale yellow powder. If the change in the visual appearance observed in some experiments is taken to represent the addition of nitrate groups, this could indicate that the solids were changed back to UO<sub>2</sub>(DBP)<sub>2</sub> when washed with an inert solvent like isopropanol. IR analysis of these compounds showed no evidence of nitrate coordination or –OH stretching (which would represent HDBP). There was a strong peak at  $1120\text{ cm}^{-1}$  corresponding to bound P=O, which is present in the polymer structure, and no evidence of unbound P=O at  $1234\text{ cm}^{-1}$ .

### Solids Prepared via Extraction (-EXT) and RE-Crystallization (-REC)

Table 1 indicates that UO<sub>2</sub>(DBP)<sub>2</sub>(HDBP) is present between  $0.2-0.8\text{ M HNO}_3$ , from the molar ratio 2.9 to  $3.2 \pm 0.1$ . Another shift occurs at  $1.0-2.0\text{ M HNO}_3$  acid to a DBP:uranyl ratio of  $3.2-3.3 \pm 0.1$ . This shift corresponds to the point where nitrate begins adding to the compound. The final shift occurs from  $3.0$  to  $6.0\text{ M HNO}_3$  when the DBP:uranyl ratio varies

from  $3.8 \pm 0.1$  to  $4.2 \pm 0.2$ , where four DBP molecules are present on each compound. Extraction data corresponding to the compound  $(\text{UO}_2(\text{DBP})_2(\text{HDBP})_x$ , with  $x = 1$  or  $2$ , have been previously reported, without rigorous chemical analysis [10]. The data presented here show that additional HDBP can add to the solids if DBP is initially present in a significant concentration. IR analysis of these compounds showed the presence of both bound and unbound P=O stretching at  $1120\text{cm}^{-1}$  and  $1234\text{ cm}^{-1}$  [7,11], respectively. There was also evidence of strong –OH stretching observed at  $2272\text{ cm}^{-1}$ ,  $2655\text{ cm}^{-1}$ , and  $>3200\text{ cm}^{-1}$ .

Nitrate groups begin to add to the solids extracted from  $0.8M\text{ HNO}_3$ , then increases until a 1:1 nitrate:uranyl ratio is reached. Nitrate begins adding with molar ratios significantly less than one ( $0.2 \pm 0.01$ ) from  $0.8\text{-}1.0 M\text{ HNO}_3$ . Then the nitrate:uranyl ratio steadily increases with acid concentration until it reaches  $0.9 \pm 0.02$  from  $5.0 M\text{ HNO}_3$ . The stepwise addition of nitrate as the acid concentration increases may indicate the constant breakdown of the polymer structure with an end group attack of nitrate. It is a possibility that some nitrate is extracted by DBP through hydrogen bonding but data on this extraction are unavailable. The molar ratios indicate the compound  $\text{UO}_2(\text{NO}_3)(\text{H}(\text{DBP})_2(\text{HDBP})_2$  in accordance with the previous work [6,7].

Nitrate coordination was observed in IR spectra at  $1529\text{ cm}^{-1}$  [7,11,12] for compounds extracted from  $0.8\text{-}2.0 M\text{ HNO}_3$ . When  $\geq 3.0 M\text{ HNO}_3$  was used, a peak began to appear at  $1636\text{ cm}^{-1}$  and the  $1529\text{ cm}^{-1}$  peak began to lose intensity. The free nitrate ion has two doubly degenerate fundamentals that split upon nitrate coordination [12]. There is also a corresponding shift in the asymmetric uranyl stretch from  $929\text{ cm}^{-1}$  to  $933\text{ cm}^{-1}$  at the same point where the nitrate shift occurs [7]. UV-Vis spectra also showed a change in the uranyl environment at UDBP-3.0 M-EXT through indications of nitrate complexation with uranyl [13].  $^{31}\text{P}$  NMR spectra indicated a very broad single peak that consistently shifted from  $6.2\text{ ppm}$  (UDBP-0.2 M-EXT) to  $3.5\text{ ppm}$  (UDBP-3.0-EXT) and remained steady as the acid concentration increased. A very small shoulder appeared around  $5.0\text{ ppm}$  for samples extracted between  $2.0\text{-}6.0 M\text{ HNO}_3$ . This shoulder is assumed to be present, but hidden, for other samples and was unable to be characterized.

As the acid concentration from which the solids were extracted increased, the transition from a pale yellow powder to a bright yellow gel progressed stepwise with nitrate addition. Therefore, if the visual changes in the solids are assumed to represent nitrate addition, then the solids formed via addition in higher acid concentrations were augmented but returned to  $\text{UO}_2(\text{DBP})_2$  after washing the solids with isopropanol or 2-ethylhexanol. All IR evidence of nitrate and –OH presence disappeared from the spectra after re-crystallization.

### Solids Prepared via Precipitation (-PPT)

$\text{UO}_2(\text{DBP})_2$  is precipitated from  $0.2 M\text{ HNO}_3$ , but the solids from higher acid concentrations have DBP:uranyl molar ratios  $>2$ . They also took on the visual changes as the extracted compounds, corresponding to the increasing nitrate:uranyl ratio. However at  $6.0 M\text{ HNO}_3$ ,  $\text{UO}_2(\text{NO}_3)(\text{H}(\text{DBP})_2)(\text{HDBP})_2$  was found for both compounds regardless of DBP concentration.

## DISCUSSION

When solids are extracted from solutions containing DBP in a separate organic phase and in nitric acid concentrations between  $0.2\text{-}0.5 M$ , the sticky compound  $\text{UO}_2(\text{DBP})_2(\text{HDBP})$  results. The additional DBP molecule must be protonated in order to maintain electro-neutrality of the extracted solids. The presence of –OH groups in these compounds is seen by the strong absorption of the IR regions  $1250\text{-}950\text{ cm}^{-1}$ ,  $2250\text{ cm}^{-1}$ , and  $2650\text{ cm}^{-1}$ . IR spectra of these solids also indicate that there is a mixture of bound and unbound DBP

groups because of a strong absorbance at  $1124\text{ cm}^{-1}$  in all spectra and a shoulder at  $1234\text{ cm}^{-1}$ , indicating unbound P=O. The presence of unbound P=O bonds indicates that HDBP could be adsorbed to the particle surface, present as an outer sphere complex, or it could be coordinated to uranyl by neutral ligand complexation. A possible explanation is that it represents resonance structures of HDBP, through O-P=O bonds, coordinated as a neutral ligand.

Nitrate ions begin adding to the extracted solids from  $0.8\text{ M HNO}_3$  and four DBP/HDBP molecules are present at  $\geq 2.0\text{ M HNO}_3$ , as the nitrate:uranyl ratio increases. The solids extracted between  $0.8\text{-}4.0\text{ M HNO}_3$  have the formula  $\text{UO}_2(\text{H(DBP)})_2(\text{NO}_3)_y(\text{HDBP})_2$ , where  $y$  steadily increases to one at high acid concentrations. The IR peaks corresponding to P=O bonding are the same as those observed for the lower acid extractions showing DBP remaining bound to uranyl. The IR spectra of the solids with nitrate:uranyl ratios  $<1$  show direct complexation of the nitrate group via a sharp peak at  $1528\text{ cm}^{-1}$  that decreases in intensity as the acid concentration increases. This decrease of the  $1528\text{ cm}^{-1}$  peak is in conjunction with an increase in the intensity of a  $1636\text{ cm}^{-1}$  peak, which corresponds to coordinated nitrate or free nitric acid. It is assumed that the  $1636\text{ cm}^{-1}$  peak represents a uranyl nitrate complex because of the indication of uranyl nitrate complexes observed in UV-Vis spectra for the same compounds where the  $1636\text{ cm}^{-1}$  peak is present. There is no observable change in the uranyl ion because the  $929\text{ cm}^{-1}$  peak, representative of  $\text{UO}_2\text{-O-P}$  bonding in  $\text{UO}_2(\text{DBP})_2$ , does not shift. Also, UV-Vis spectra were unable to resolve any effects of nitrate addition to uranyl for the solids formed between  $0.8\text{-}2.0\text{ M HNO}_3$ . Therefore, nitrate is only influencing a portion of the uranyl ions for those acid concentrations. This could represent a point where there is insufficient breakdown of the polymer to influence the uranyl bonding environment. The shift in the uranyl peak, when the nitrate:uranyl ratio is  $\geq 0.5$ , indicates the shift in the uranyl environment when a majority of uranyl ions are coordinated with nitrate, giving a strong indication that the increasing amounts of nitrate correspond to a breakdown of the polymer structure. The similarities in uranyl spectra for nitrate:uranyl ratios  $<0.5$  show that the majority of uranyl ions are still effected only by DBP/HDBP molecules. As the polymer breakdown occurs, then more uranyl ions are coordinated with nitrate, and there is a shift in the uranyl-bonding environment in  $3.0\text{ M HNO}_3$  loading, observed through IR and UV-Vis spectra.

$\text{UO}_2(\text{NO}_3)(\text{H(DBP})_2)(\text{HDBP})_2$  is extracted from  $>5.0\text{ M HNO}_3$ . This compound shows a shift in the uranyl chemical environment, via IR spectra, and a single DBP chemical environment via a single broad  $^{31}\text{P}$  NMR peak. A neutral ligand complexation of HDBP and rapid proton exchange with the one bound DBP molecule fit the interpretation of one DBP environment because the bound and unbound DBP could participate in the rapid proton exchange through its resonance structures. Therefore, the coordination number of uranyl could be increasing with HDBP binding as an inner sphere ligand and as the polymer structure breaks down, there is less steric hindrance around the uranyl ion.

$\text{UO}_2(\text{DBP})_2$  was precipitated from  $0.2\text{ M HNO}_3$  in accordance with the literature. However, there was a decrease in the extent of nitrate and HDBP addition to precipitated compounds when compared to extracted compounds, except for solids from  $6.0\text{ M HNO}_3$ . The excess HDBP present on extracted compounds could be causing stress on the P-O-U bond and making nitrate infiltration easier for extracted compounds. When  $6.0\text{M HNO}_3$  was used in both methods, solids with identical spectra and empirical formula were found.

The addition of DBP and nitrate, as well as the transition of the physical nature of the compounds from a solid to a gel are proposed to represent the breakdown of the  $\text{UO}_2(\text{DBP})_2$  polymer structure. This was also an assumption of other researchers [6]. The polymer may be initially forming in solution followed by a nitrate attack on the end of the molecule, where bulky DBP molecules that remain complexed with the uranyl ion will not cause hindrance.

However, further studies are required to verify the polymer breakdown. There is indication of DBP remaining complexed with uranyl because of the strong absorption at  $1124\text{ cm}^{-1}$  in the IR spectra of these samples. At least one DBP molecule must be bonded with uranyl in order to maintain electro-neutrality of the solid, since a maximum of one nitrate coordinates with each uranyl ion.

The IR spectra indicate that DBP can be present as a neutral ligand (indicated by  $-\text{OH}$  peaks), causing an increased coordination number in uranyl than that observed in the polymer structure. There is evidence of bound and unbound DBP presence but if it was present in both inner and outer sphere coordination then two strong  $^{31}\text{P}$  NMR peaks would appear. Therefore, it is proposed that any additional DBP is present as a neutral ligand capable of resonance structures, represented by the very broad NMR peak. Mono- or bidentate nitrate coordination has not been ascertained. However, the increased degree of splitting of the degenerate fundamental peaks in free nitrate observed in this research provide some indication of a further decrease in symmetry that would be caused by bidentate coordination.

## CONCLUSIONS

The formation of uranium DBP solids is highly dependent on the nature of the solution in which they are formed. At lower acid concentrations and lower DBP loadings, the well-characterized polymer  $\text{UO}_2(\text{DBP})_2$  precipitates as a pale yellow powder.  $\text{UO}_2(\text{DBP})_2(\text{HDBP})_x$  ( $x = 1$  to  $2$ ) precipitates with higher DBP loadings. However, when extracting from  $6.0\text{ M HNO}_3$ ,  $\text{UO}_2(\text{NO}_3)(\text{H}(\text{DBP})_2)(\text{HDBP})_2$  is formed, regardless of the initial DBP concentration, as a sticky solid or gel. The similarities in IR spectra indicate that the same  $\text{UO}_2(\text{DBP})_2$  monomer is present in all compounds and adds new ligands with increasing acid or DBP concentrations.

Nitrate addition to compounds can be detected in nitric acid concentrations as low as  $0.8\text{ M HNO}_3$ . However, nitrate does not add in a 1:1 stoichiometric ratio with uranium until  $5.0\text{ M HNO}_3$  is used with high DBP concentrations and  $6.0\text{ M HNO}_3$  in lower DBP concentrations. The addition of nitrate may affect DBP bonding to uranyl but there is still a strong complexation of DBP to a central uranyl ion, indicated by IR data. This addition of nitrate is assumed to accompany the breakdown of the polymer structure observed for  $\text{UO}_2(\text{DBP})_2$ . This phenomenon can be observed through changes in the physical appearance of the solids as they become more viscous with increasing acid concentrations. This change in physical appearance corresponds with the increasing nitrate: uranyl ratio, which is most likely responsible for the polymer structure breakdown. The increasing nitrate:uranyl ratio is also accompanied by a shift in the uranyl IR stretch, which corresponds to an increase in the ionic character of the uranyl bond. The coordination number of uranyl is most likely increased with nitrate and HDBP addition through neutral ligand coordination of HDBP. This will be an inner sphere complexation because phosphorous is indicated to be in one chemical environment from  $^{31}\text{P}$  NMR data. Compounds containing nitrate and additional DBP molecules can be easily converted to  $\text{UO}_2(\text{DBP})_2$  by re-crystallizing from 2-ethylhexanol or washing with isopropanol.

## ACKNOWLEDGEMENT

The authors would like to acknowledge financial support from the SRS and the U.S. Department of Energy.

## REFERENCES

1. R. A. Pierce, M. C. Thompson, and R. J. Ray (1999), Solubility Limits of Dibutyl Phosphoric Acid in Uranium Nitric Acid Systems, No. WSRC-MS-99-00321, SRS Aiken, SC, USA, 22 pp.
2. W. W. Schulz and J. D. Navratil (1984), The Science and Technology of Tributyl Phosphate, Volume 1, CRC Press, Boca Raton, 249-251.
3. R. A. Pierce, M. C. Thompson, and R. J. Ray (1998), Solubility Limits of Dibutyl Phosphoric Acid in Uranium Solutions at SRS, No. WSRC-TR-98-00188, SRS, Aiken, SC USA, 11 pp.
4. W. H. Baldwin and C. E. Higgins (1961), *J. Nucl. Inorg. Chem.*, **17**, 334-336.
5. V. A. Mikhailov and E. F. Grigor'eva (1964), *Russ. J. Inorg. Chem.*, **9**, 477-481.
6. P. G. Krutikov and A. S. Solovkin (1970), *Russ. J. Inorg. Chem.*, **15**, 825-827.
7. E. G. Teterin, N. N. Shestervikov, P. G. Krutikov, and A. S. Solovkin (1971), *Russ. J. Inorg. Chem.*, **16**, 416-418.
8. J. H. Burns (1983), *J. Am. Chem. Soc.*, **22**, 1174-1178.
9. A. E. Greenburg, L. S. Clesceri, and A. D. Eaton (1992), Standard Methods for the Examination of Water and Wastewater, 18th edn., Vol. 4, American Public Health Association, Washington D.C., pp. 4-139-4-147.
10. I May, R. J. Taylor, A. J. Wallvork, J. J Hastings, Y. S. Federov, B. Y. Zilberman, E. N. Mishin, S. A. Arkhipov, I. V. Blazheun, L. Y. Powerkova, F. R. Livens, and J. M. Charnock (2000), *Radiochim. Acta*, **88**, 283-290.
11. H. G. Edwards, E. Hickmolt, and M. A. Huges (1997), *Spectrochim. Acta A*, **53**, 43-53.
12. J. I. Bullock (1967), *J. Inorg. Nucl. Chem.*, **29**, 2257-2264.
13. M. D. Marcantonatos, M. Deschaux and F. Celardin (1981), *Chem. Phys. Lett.*, **69**, 144-150.



## EFFECT OF U(VI) CONCENTRATION ON EQUILIBRIUM AND KINETICS IN FLOW-EXTRACTION OF U(VI) IN HNO<sub>3</sub> / SUPERCRITICAL CO<sub>2</sub> + TBP SYSTEM

Yoshihiro Meguro, Shuichi Iso and Zenko Yoshida

Advanced Science Research Center, Japan Atomic Energy Research Institute,  
Tokai, Japan

The distribution ratio  $D$  of U(VI) was determined in the supercritical CO<sub>2</sub> extraction system with the nitric acid solution containing  $10^{-3}$  –  $10^{-1}$  M U(VI) and the supercritical CO<sub>2</sub> containing 0.1 – 0.5 M tributylphosphate (TBP) at 60 °C and 15 MPa. The distribution behavior was found to be practically independent on the U(VI) concentration, though the  $D$  decreased slightly with an increase of U(VI) concentration, which was attributed to a decrease of the equilibrium concentration of free TBP in the supercritical CO<sub>2</sub> phase. The solubility of UO<sub>2</sub>(NO<sub>3</sub>)<sub>2</sub>(TBP)<sub>2</sub> in the supercritical CO<sub>2</sub> phase was determined to be higher than  $7 \times 10^{-2}$  M and a suppression of the  $D$  due to the solubility limitation of the extracted complex in the supercritical CO<sub>2</sub> was unlikely to occur under the extraction condition examined. The extraction-rate curve was measured in the flow-extraction system. The distribution ratio  $D_{\text{flow}}$  of U(VI) in the flow-extraction system was calculated and compared with the  $D$ . The  $D_{\text{flow,max}}$  agreed well with the  $D$  indicating that the extraction equilibrium of U(VI) was attained rapidly even in the flow-extraction performance.

### INTRODUCTION

Supercritical fluid extraction (SFE) using the supercritical CO<sub>2</sub> instead of an organic solvent has several fundamental and practical advantages that the extraction efficiency or rate is enhanced due to the rapid mass transfer in the supercritical fluid phase, the rapid and complete recovery of the extracted substances from CO<sub>2</sub> is attained by gasification of CO<sub>2</sub>, and the solvent properties can be optionally changed by tuning pressure [1-3]. The use of SFE in the field of nuclear technology exhibits a particular significance for minimizing the amount of the radioactive solvent waste [4]. The authors have developed the SFE of U(VI) and Pu(IV) from nitric acid solution using the supercritical CO<sub>2</sub> containing tributylphosphate(TBP) [2, 4-7].

For the assessment of a feasibility of the SFE to the process-scale separation of a large amount of an objective metal, e.g., the separation of uranium for reprocessing the spent nuclear fuel, the distribution behavior of the metal of high concentration needs to be elucidated. In this connection, the distribution behavior of the metal of a large amount is suppressed due to the solubility limitation of the metal-extractant complex in the supercritical CO<sub>2</sub>, which is observed in the SFE of the metal [8] and is considered to be one of the main disadvantages with the SFE process. In addition, the extraction behavior of the metal in the flow SFE system, in which the metal is extracted into a stream of the supercritical CO<sub>2</sub> phase flowing through the aqueous solution, needs to be studied, since the flow extraction system will be adopted in a practical SFE process [9].

In the present study, the equilibrium distribution ratio  $D$  of U(VI) of relatively high concentration was determined by the batchwise extraction procedure with the  $\text{HNO}_3$  solution containing  $10^{-3}$  -  $10^{-1}$  M U(VI) and the supercritical  $\text{CO}_2$  phase containing 0.1 - 0.5 M TBP, for the elucidation of the dependence of  $D$  on the concentration of U(VI). The extraction behavior of U(VI) in the flow SFE system was also investigated for the elucidation of the parameters determining the flow-extraction rate.

## EXPERIMENTAL

### SFE Apparatus and Procedure

#### *Batchwise extraction*

The batchwise extraction experiment for the determination of the distribution ratio  $D$  under SFE equilibrium condition was conducted using the apparatus identical to that reported previously [6]. The main part of the apparatus consisted of a stainless steel extraction vessel of ca. 50 ml of inner volume, a sampling vessel, a restrictor and a pump. Twenty five ml of  $\text{HNO}_3$  solution containing U(VI) was taken in the extraction vessel. An appropriate volume of TBP was added to the extraction vessel to which the  $\text{CO}_2$  was introduced using the syringe pump. The volume of the  $\text{CO}_2$  phase was 25 ml. The two phases were allowed to stand for 60 min at  $60^\circ\text{C}$  (extraction temperature,  $T_{\text{ex}}$ ) and 15 MPa (extraction pressure,  $P_{\text{ex}}$ ) with stirring by the use of a magnetic stirrer. After the SFE equilibrium was attained, 5 ml of the aqueous phase was taken quickly using the sampling vessel. The concentration of U(VI) in the sampled solution was determined by ICP-AES and the  $D$  of U(VI) was calculated as the ratio of the concentration of U(VI) in the supercritical  $\text{CO}_2$  phase to that in the aqueous phase.

#### *Flow extraction*

The flow extraction experiment was conducted with the apparatus which was essentially identical to that reported previously [6] but with the extraction vessel of approximately 40 ml of inner volume, 500 mm of inner height and 10 mm of inner diameter. Thirty ml of the  $\text{HNO}_3$  solution was taken in the extraction vessel through which a mixture of the supercritical  $\text{CO}_2$  and TBP was forced to flow at a constant flow rate,  $f$ . The  $T_{\text{ex}}$  and  $P_{\text{ex}}$  were  $60^\circ\text{C}$  and 15 MPa, respectively. The supercritical  $\text{CO}_2$  phase eluted from the extraction vessel was introduced into the collection vessel kept at ca.  $60^\circ\text{C}$  and an ambient pressure. The extracted substances were collected on the quartz wools packed in the collection vessel. The collection vessel was replaced by new one at intervals of 10 min during the continuous flow SFE. The amount of uranium in each 10 mins' fraction was determined by ICP-AES after the U(VI) recovered as the  $\text{UO}_2(\text{NO}_3)_2(\text{TBP})_2$  complex was completely decomposed and dissolved into the aqueous solution by mixing the  $\text{UO}_2(\text{NO}_3)_2(\text{TBP})_2$  complex with 1 M  $(\text{NH}_4)_2\text{CO}_3$  aqueous solution. The extraction-rate curve was established by plotting the extraction efficiency (E%) calculated from the integrated amount of U(VI) collected against the integrated amount of  $\text{CO}_2$  employed for the flow SFE.

## RESULTS AND DISCUSSION

### Distribution Ratio D of U(VI)

The distribution ratio  $D$  of U(VI) was determined in the SFE at  $60^\circ\text{C}$  and 15 MPa using 3 M  $\text{HNO}_3$  solution containing  $2 \times 10^{-3}$  -  $1 \times 10^{-1}$  M U(VI) and the supercritical  $\text{CO}_2$  containing 0.1 - 0.5 M TBP. The logarithmic plots of  $D$  and the initial concentration of TBP in the supercritical  $\text{CO}_2$ ,  $C_{\text{TBP,SF}}$ , are shown in Figure 1. The slope of the plot is  $2.0 \pm 0.2$  indicating that the extracted species involves two TBP molecules, i.e.,  $\text{UO}_2(\text{NO}_3)_2(\text{TBP})_2$  [5,6], independently on the concentration of U(VI) in the range examined.

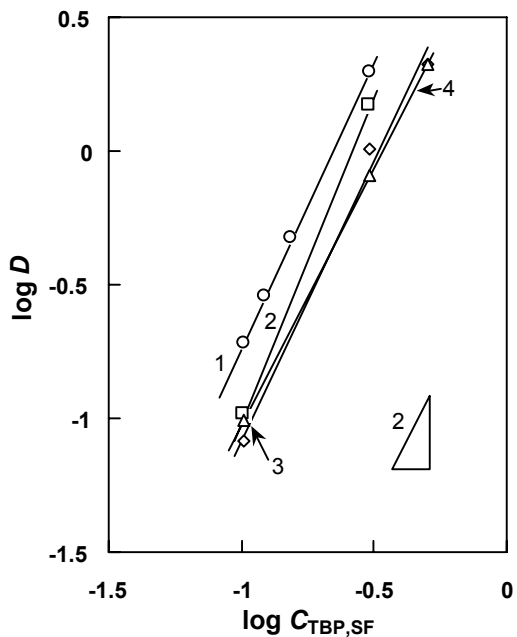


Figure 1.  $\log D$  vs.  $\log C_{TBP,SF}$  plots in the SFE of U(VI).

Aqueous phase; 3 M  $HNO_3$  + (1)  $2 \times 10^{-3}$  M U(VI),  
 (2)  $1 \times 10^{-2}$  M U(VI), (3)  $5 \times 10^{-2}$  M U(VI), (4)  $1 \times 10^{-1}$  M U(VI),  
 $C_{TBP,SF}$ ; 0.1 – 0.5 M,  $T_{ex}$ ; 60 °C,  $P_{ex}$ ; 15 MPa.

With an increase of the initial concentration of U(VI) in the aqueous solution,  $C_{U(VI)}$ , the  $D$  decreases gradually. This is attributable to the decrease of the concentration of free TBP in the supercritical  $CO_2$  phase after the extraction equilibrium of a large amount of U(VI) is attained. It is concluded that the solubility of  $UO_2(NO_3)_2(TBP)_2$  complex into the supercritical  $CO_2$  phase is enough high and the solubility limitation of the complex does not disturb the SFE equilibrium. The SFE condition under which the highest  $D$  and the highest U(VI) concentration in the supercritical  $CO_2$  were obtained was  $C_{U(VI)} = 1 \times 10^{-1}$  M and  $C_{TBP,SF} = 0.5$  M ( $T_{ex} = 60$  °C,  $P_{ex} = 15$  MPa). The solubility of  $UO_2(NO_3)_2(TBP)_2$  in the supercritical  $CO_2$  is estimated from these results to be still higher than  $7 \times 10^{-2}$  M.

### Flow SFE of U(VI)

The extraction-rate curve for the flow SFE of U(VI) was measured with the 3 M  $HNO_3$  solution containing  $1 \times 10^{-2}$  M or  $5 \times 10^{-2}$  M U(VI) and the supercritical  $CO_2$  phase containing 0.1, 0.3 or 0.5 M TBP which was forced to flow through the aqueous solution in the extraction vessel at  $f = 2.0$  ml/min. The results are shown in Figure 2. The extraction rate increases with an increase of  $C_{TBP,SF}$  and does not depend strongly on  $C_{U(VI)}$ . The increase of the extraction rate with  $C_{TBP,SF}$  is attributable to the increase of  $D$  of U(VI).

In order to clarify whether or not the distribution equilibrium is attained in the flow SFE of U(VI), an apparent distribution ratio in the flow system,  $D_{flow}$ , was defined and compared with the  $D$  determined under the equilibrium condition. The  $D_{flow}$  is expressed by the ratio of the concentration of U(VI) in the supercritical  $CO_2$  phase,  $C_{U(VI),SF,flow}$ , to the concentration of U(VI) in the aqueous phase,  $C_{U(VI),aq,flow}$ , at a given period of time during the continuous flow SFE and calculated from the results of the amount of U(VI) extracted,  $m_{U(VI),SF}$  (in mole), as expressed by eq. (1).

$$D_{flow} = C_{U(VI),SF,flow} / C_{U(VI),aq,flow} = m_{U(VI),SF} / (V_{CO_2} C_{U(VI),aq,flow}) \quad (1)$$

where  $V_{\text{CO}_2}$  denotes the total volume (in liters) of the supercritical  $\text{CO}_2$  fed to the flow SFE system for a given time. In the present work, the results shown in Figure 2 were used for the calculation of  $D_{\text{flow}}$ . The average of the concentrations of U(VI) remaining in the aqueous solution before and after each 10 mins' flow SFE was employed as  $C_{\text{U(VI),aq,flow}}$ .

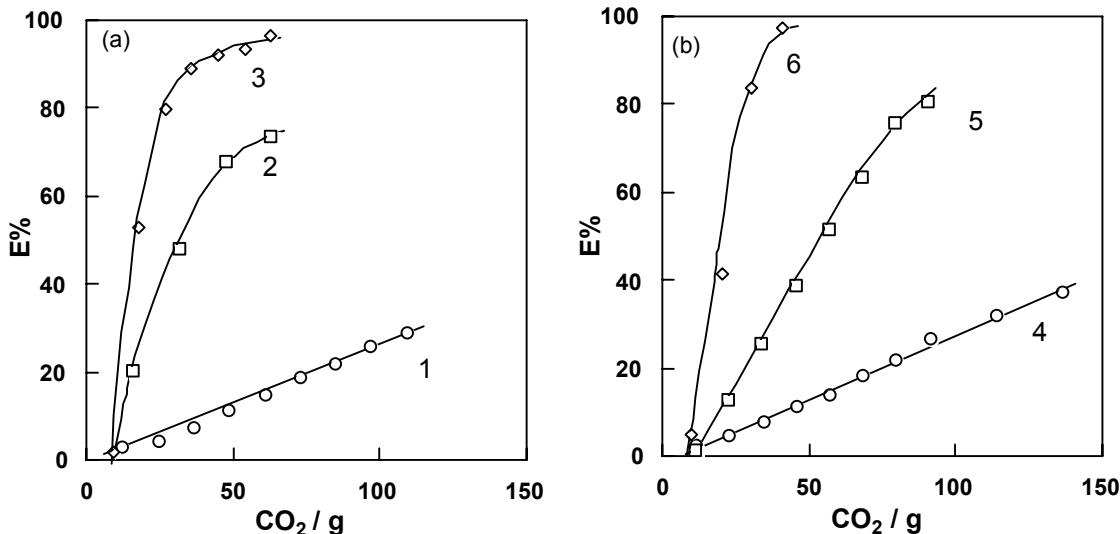


Figure 2. Extraction-rate curve for the SFE of U(VI).  
Aqueous solution; 3 M  $\text{HNO}_3$  + (a)  $1 \times 10^{-2} \text{ M}$  U(VI), (b)  $5 \times 10^{-2} \text{ M}$  U(VI),  
 $C_{\text{TBP,SF}}$ ; (1,4)  $1 \times 10^{-1} \text{ M}$ , (2,5)  $3 \times 10^{-1} \text{ M}$ , (3,6)  $5 \times 10^{-1} \text{ M}$ ,  $f$ ; 2.0 ml/min,  
 $T_{\text{ex}}$ ;  $60^\circ\text{C}$ ,  $P_{\text{ex}}$ ; 15 MPa.

The  $D_{\text{flow}}$  calculated using the results given in Figure 2 exhibits a general tendency which reflects a situation varying through the flow SFE. The  $D_{\text{flow}}$  calculated from the results in the earlier stage of the flow SFE were slightly smaller than those in the successive stages. This results from the situation that a steady-state condition is not attained yet at the earlier stage of the flow SFE. The  $D_{\text{flow}}$  increases gradually as the flow SFE proceeds and shows a maximum,  $D_{\text{flow,max}}$ . Further proceeding of the flow SFE leads to a decrease of the U(VI) concentration in the aqueous phase; under this condition,  $D_{\text{flow}}$  becomes smaller than  $D_{\text{flow,max}}$ , which is due to the situation that a diffusion of U(VI) in the aqueous phase controls partly the extraction rate of U(VI).

The  $D_{\text{flow,max}}$  determined at various  $C_{\text{U(VI)}}$  and  $C_{\text{TBP,SF}}$  are listed in Table 1. The  $D_{\text{flow,max}}$  and the  $D$  under the identical conditions of  $C_{\text{U(VI)}}$  and  $C_{\text{TBP,SF}}$  are compared with each other in Figure 3.

Table 1. The distribution ratio  $D_{\text{flow,max}}$  of U(VI) in the flow SFE.

$C_{\text{U(VI)}} / \text{M}$	$C_{\text{TBP,SF}} / \text{M}$	$D_{\text{flow,max}}$
$2 \times 10^{-3}$	0.1	0.163
$1 \times 10^{-2}$	0.1	0.073
$1 \times 10^{-2}$	0.3	0.562
$1 \times 10^{-2}$	0.5	1.39
$5 \times 10^{-2}$	0.1	0.092
$5 \times 10^{-2}$	0.3	0.60
$5 \times 10^{-2}$	0.5	1.73
$1 \times 10^{-1}$	0.1	0.080

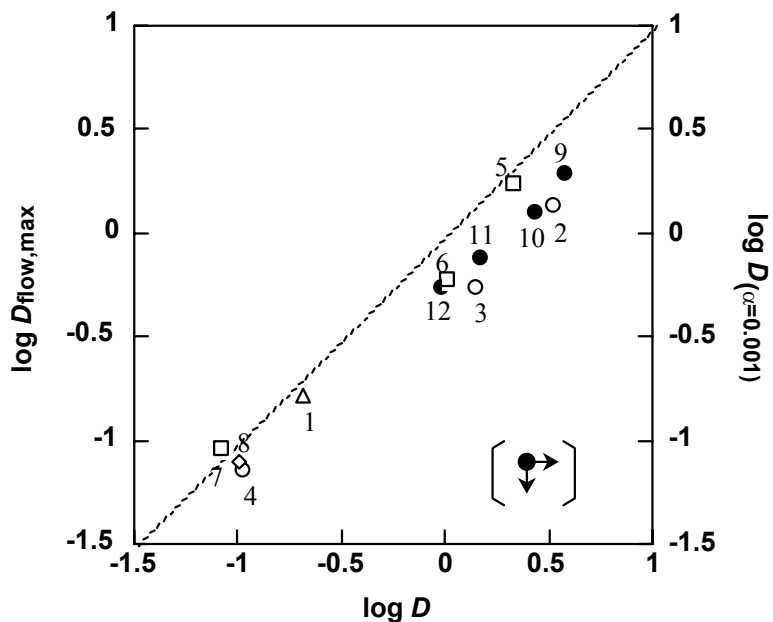


*Figure 3. Comparison between  $D_{\text{flow},\text{max}}$  and  $D$  for the SFE of U(VI) in 3 M  $\text{HNO}_3$  solution.*

$C_{\text{U(VI)}}$ ; (1)  $2 \times 10^{-3}$  M, (2, 3, 4)  $1 \times 10^{-2}$  M, (5, 6, 7)  $5 \times 10^{-2}$  M, (8)  $1 \times 10^{-1}$  M.

$C_{\text{TBP,SF}}$ ; (1, 4, 7, 8) 0.1 M, (3, 6) 0.3 M, (2, 5) 0.5 M.

●;  $D_{(\alpha=0.001)}$  calculated for SFE of U(VI) with  $C_{\text{TBP,SF}} = 0.5$  M.

$C_{\text{U(VI)}}$ ; (9)  $5 \times 10^{-2}$  M, (10)  $1 \times 10^{-1}$  M, (11)  $2 \times 10^{-1}$  M, (12)  $3 \times 10^{-1}$  M.

The dotted line in the figure indicates a complete agreement between  $D_{\text{flow},\text{max}}$  and  $D$ . The  $D_{\text{flow},\text{max}}$  is slightly smaller than the  $D$ .

In principle, the distribution ratio  $D$  can be expressed by eq. (2) using the extraction constant  $K_{\text{ex}}$ .

$$D = K_{\text{ex}} [\text{NO}_3^-]^2 [\text{TBP}]_{\text{SF}}^2 \quad (2)$$

where  $[\text{NO}_3^-]$  and  $[\text{TBP}]_{\text{SF}}$  are activities of  $\text{NO}_3^-$  in the aqueous phase and TBP in supercritical  $\text{CO}_2$  phase, respectively, at the SFE equilibrium and given by eqs. (3) and (4) using the initial concentration,  $C_{\text{U(VI)}}$ ,  $C_{\text{NO}_3}$ , and  $C_{\text{TBP,SF,eq}}$  and the ratio of the volume of the supercritical  $\text{CO}_2$  phase to that of the aqueous phase,  $\alpha$ . Here the activity coefficients of U(VI) and TBP in both phases are approximated to be unity for simplicity.

$$[\text{NO}_3^-] = C_{\text{NO}_3} - C_{\text{U(VI)}} \{ x \alpha D / (1 + \alpha D) \} \quad (3)$$

$$[\text{TBP}]_{\text{SF}} = C_{\text{TBP}} - C_{\text{U(VI)}} \{ (yD / (1 + \alpha D)) \} \quad (4)$$

where  $x$  and  $y$  are the number of  $\text{NO}_3^-$  ions and TBP molecules involved in the SFE reaction, and  $x = 2$  and  $y = 2$  for the SFE of U(VI) studied in the present work. In the flow SFE system, the distribution reaction occurs between the aqueous phase and the supercritical  $\text{CO}_2$  phase which is a small bubble dispersed in the aqueous phase. Under such extraction condition, the ratio of the phase volume  $\alpha$  affects the distribution behavior appreciably. The  $D$  at  $\alpha = 0.001$ , as an example, was calculated using eqs. (2) – (4) and the results are plotted by closed circle in Figure 3. The value of  $K_{\text{ex}}$  used for the calculation was 2.35 which was determined from the experimental  $D$  value in the batchwise extraction of 0.002 M U(VI) from the 3 M  $\text{HNO}_3$  solution into the supercritical  $\text{CO}_2$  containing 0.1 M TBP (cf. Figure 1). The  $D_{(\alpha=0.001)}$  is obviously

smaller than the  $D$  which is obtained usually at  $\alpha = 1$ . The experimental  $D_{\text{flow,max}}$  scatters around the plots of  $D_{(\alpha=0.001)}$ . Therefore, the smaller  $D_{\text{flow,max}}$  than  $D$  can be also attributable to the effect of  $\alpha$ , which is very small in the flow SFE, on the distribution ratio. Finally, it is concluded that the distribution equilibrium of U(VI) is attained almost completely even in the flow SFE system examined in the present work.

## CONCLUSION

The distribution ratio  $D$  for the SFE of U(VI) between 3 M  $\text{HNO}_3$  and supercritical  $\text{CO}_2 + 0.1 - 0.5$  M TBP does not depend on the concentration of U(VI) upto 0.1 M. The solubility of  $\text{UO}_2(\text{NO}_3)_2(\text{TBP})_2$  to be extracted in the supercritical  $\text{CO}_2$  is sufficiently high. These results imply that the SFE using TBP is feasible to the separation of a large amount of U(VI) in the aqueous sample solution. The distribution equilibrium is attained efficiently even in the flow SFE of U(VI). The larger extraction rate of the flow SFE of U(VI) can be attained using the supercritical  $\text{CO}_2$  containing TBP of higher concentration, which enhances the distribution ratio of U(VI).

## REFERENCES

1. Y. Lin, N. G. Smart and C. M. Wai (1995), *Trends Anal. Chem.*, **14**, 123-132.
2. Y. Meguro, S. Iso and Z. Yoshida (1998), *Anal. Chem.*, **70**, 1262-1267.
3. K. W. Hutchenson and N. R. Foster (1995), Innovations in Supercritical Fluids, Science and Technology, ACS Symp. Sers. 608, ACS, Washington, DC.
4. S. Iso, Y. Meguro and Z. Yoshida (1997), *Proc. Workshop on Actinides Solution Chemistry, Wasc '94*, Z. Yoshida, T. Kimura and Y. Meguro (eds.), World Science Publishers, Singapore, pp. 238-246.
5. S. Iso, Y. Meguro and Z. Yoshida (1995), *Chem. Lett.*, 365-368.
6. Y. Meguro, S. Iso, H. Takeishi and Z. Yoshida (1996), *Radiochim. Acta*, **75**, 185-191.
7. S. Iso, S. Uno, Y. Meguro, T. Sasaki and Z. Yoshida (2000), *Prog. Nucl. Energ.*, **37**, 423-428.
8. A. V. Yazdi and E. J. Beckman (1997), *Ind. Eng. Chem. Res.*, **36**, 2368-2374.
9. N. G. Smart, Z. Yoshida, Y. Meguro, S. Iso, A. A. Clifford, Y. Lin, K. Toews and C. M. Wai (1997), *Proc. Int. Conf. Future Nucl. Systems (Global '97)*, Yokohama, Japan, pp. 350-354.



## NEW INSIGHTS IN THIRD PHASE FORMATION IN THE U(VI)-HNO<sub>3</sub>, TBP-ALKANE SYSTEM

Mark P. Jensen, Renato Chiarizia, John R. Ferraro, Marian Borkowski,  
Kenneth L. Nash, Pappanan Thiagarajan\* and Ken C. Littrell\*

Chemistry Division, Argonne National Laboratory, Argonne, Illinois, USA  
\*IPNS Division, Argonne National Laboratory, Argonne, Illinois, USA

In this work, the system U(VI)-HNO<sub>3</sub>-tributylphosphate (TBP)-*n*-dodecane has been revisited with the objective of gaining coordination chemistry and structural information on the species that are formed in the organic phase before and after third phase formation. Chemical analyses, spectroscopic and EXAFS data indicate that U(VI) is extracted as the UO<sub>2</sub>(NO<sub>3</sub>)<sub>2</sub>•2TBP adduct, while the third phase species has the composition UO<sub>2</sub>(NO<sub>3</sub>)<sub>2</sub>•2TBP•HNO<sub>3</sub>. Small-angle neutron scattering (SANS) data reveal the presence in the organic phase, both before and after phase splitting, of ellipsoidal aggregates whose formation seems to depend more on the extraction of HNO<sub>3</sub> than that of U(VI).

### INTRODUCTION

The phenomenon of third phase formation in solvent extraction is well known and has been investigated in a number of studies. Excellent reviews, one of which is quite recent, have summarized the most important aspects of this phenomenon [1,2]. The main focus in previous works has been on the conditions under which third phase formation is observed and avoided, and on the composition of the species present in the heavy organic phase. Very little information is available on structural aspects of third phase formation.

A recent work has reported that, in the case of HNO<sub>3</sub> extraction by a diamide extractant in *n*-dodecane, small-angle X-ray scattering measurements revealed the onset of extensive aggregation of the organic phase species when phase splitting was approached [3]. Similar observations have been reported by some of the present authors in small-angle neutron scattering studies (SANS) of metal extraction by dialkyl-substituted alkylidendiphosphonic acids [4]. Large cylindrical aggregates form in toluene solutions of the extractants when they are loaded with progressively higher concentrations of certain metal ions such as Fe(III) and Th(IV). The aggregation eventually leads to the separation of a gelatinous material that can be considered a particular case of third phase formation.

In an attempt to verify that the formation of large aggregates in the organic phase before phase splitting is a general feature shared by most if not all solvent extraction systems, we have revisited the U(VI)-HNO<sub>3</sub>-tributylphosphate (TBP)-*n*-dodecane system from the standpoint of third phase formation. We chose this system because, in spite of its technological importance, very few detailed studies are available on third phase formation when U(VI) is extracted by alkane solutions of TBP [5-7]. The objective of this work was to gain information on coordination chemistry and morphology of the species present in the organic phase before and after third phase formation.

## SAMPLE PREPARATION AND CHARACTERIZATION

*n*-Dodecane solutions containing 20% (v/v) TBP (0.73 M) and varying concentrations of HNO<sub>3</sub> and U(VI) were prepared by contacting at 23 ± 1 °C a small volume of the TBP solution, preequilibrated twice with 10 M HNO<sub>3</sub> (phase ratio = 1), with an equal volume of 10 M HNO<sub>3</sub> solutions containing progressively increasing concentrations of UO<sub>2</sub>(NO<sub>3</sub>)<sub>2</sub> (from 0.040 to 0.66 M). When contacting the 20% TBP organic phase with an aqueous solution that was 0.66 M in UO<sub>2</sub>(NO<sub>3</sub>)<sub>2</sub> and 10.5 M in HNO<sub>3</sub>, a third phase was obtained having a volume of about 13% of the original organic phase volume, and a density of 1.26 g/mL. The solutions containing the U(VI) limiting organic concentration (LOC), that is, the highest metal concentration in the organic phase that could be achieved under the selected experimental conditions without phase splitting, was obtained by first causing formation of the third phase and then adding very small amounts of lean organic phase and/or water until the third phase disappeared, as indicated by the absence of turbidity in the organic phase. The samples for the SANS measurements were prepared by following an identical procedure, with the exception that the diluent was *d*<sub>26</sub>-deuterated dodecane.

After centrifugation and phase separation, aliquots of the various phases were analyzed. The aqueous phase HNO<sub>3</sub> concentrations were determined by titration to pH ~6 with standard base after appropriate dilution and after making the solution 0.2 M in (NH<sub>4</sub>)<sub>2</sub>C<sub>2</sub>O<sub>4</sub>. The aqueous U(VI) concentration was determined by ICP-AES. The organic HNO<sub>3</sub> and U(VI) were first stripped by contacting an aliquot of the organic phases diluted 10-fold with dodecane with a larger and known volume of 0.1 M (NH<sub>4</sub>)<sub>2</sub>C<sub>2</sub>O<sub>4</sub>. HNO<sub>3</sub> and U(VI) in the stripping solution were then determined as above. The TBP concentration in the heavy and light organic phases resulting from phase splitting were determined, after HNO<sub>3</sub> and U(VI) stripping, from the distribution ratio (D) of <sup>233</sup>U between the organic phase and 3 M HNO<sub>3</sub> by using an *ad hoc* calibration curve of D<sub>U</sub> vs. TBP concentration.

Table 1 summarizes the composition of the organic phases investigated in this work. The table also reports the concentration of TBP bound to U(VI) (assuming that the U(VI) exists as UO<sub>2</sub>(NO<sub>3</sub>)<sub>2</sub>•2TBP in the organic phase), the concentration of the excess TBP, (that is, the TBP not bound to U(VI)), and the ratio of the HNO<sub>3</sub> to the excess TBP.

*Table 1. Composition of the U(VI)-TBP samples investigated.*

Sample	[TBP] mol/L	[U] mol/L	[HNO <sub>3</sub> ] mol/L	[TBP] <sub>bound to U</sub> mol/L	[TBP] <sub>excess</sub> mol/L	[HNO <sub>3</sub> ] / [TBP] <sub>excess</sub>
1	0.73	-	-	-	-	-
2	0.73	-	0.74	-	-	-
3	0.73	0.032	0.72	0.064	0.67	1.1
4	0.73	0.23	0.27	0.47	0.26	1.0
5	0.73	0.26	0.22	0.52	0.21	1.0
6 (LOC)	0.73	0.26	0.19	0.52	0.20	0.95
7 (Third Ph.)	2.1	1.02	0.92	2.04	~ 0	-
8 (Light Ph.)	0.51	0.18	0.19	0.35	0.16	1.2

TBP is known to form complexes with HNO<sub>3</sub> having the composition TBP•(HNO<sub>3</sub>)<sub>n</sub>, with *n* equal to 1 through 4 [8]. Under our experimental conditions (equilibrium aqueous phase 10 M in HNO<sub>3</sub>), the data in Table 1 indicate that HNO<sub>3</sub> exists in the organic phase predominantly as the 1:1 HNO<sub>3</sub>:TBP complex. Also, as more and more U(VI) is extracted from 10 M HNO<sub>3</sub>, the data in Table 1 show that U(VI) displaces the acid from the phosphoryl group of TBP, forming the well-known UO<sub>2</sub>(NO<sub>3</sub>)<sub>2</sub>•2TBP adduct [9], while the excess TBP remains in the form of TBP•HNO<sub>3</sub>. Finally, the data in Table 1 indicate that the third phase is highly concentrated in TBP and U(VI). Karl Fisher titrations of the third phase samples provided a

water concentration of 0.4 M. Based on the results shown in Table 1, the composition of the third phase species can be expressed as  $\text{UO}_2(\text{NO}_3)_2 \cdot 2\text{TBP} \cdot \text{HNO}_3$  (neglecting water), in agreement with previous findings [6].

## RESULTS AND DISCUSSION

### Infrared Spectroscopy

IR spectra of the samples in Table 1 were collected using a Nicolet Nexus 870 FTIR Spectrometer equipped with a HATR Attenuated Total Reflectance accessory containing a diamond resolution element. The results will be treated in more detail elsewhere [10]. However, several important features of the IR spectra that give insight into the nature of the third phase are summarized here. Overall, the shifts of the P=O stretching vibration upon U(VI) extraction by TBP ( $\sim 100 \text{ cm}^{-1}$ ) provide clear evidence that the P=O oxygen is strongly coordinated to U(VI). Also, the magnitude of the frequency separation ( $\sim 250 \text{ cm}^{-1}$ ) between the asymmetric and symmetric stretching vibrations of the  $\text{NO}_2$  group of the nitrate ion indicates a bidentate coordination of the nitrates in the organic complex [11].

A marker band for molecular  $\text{HNO}_3$  ( $1672 \text{ cm}^{-1}$  [12]) is present in the spectra of samples 2 through 8. This band exhibits two peaks indicating that two forms of  $\text{HNO}_3$  occur in these solutions: the lower energy vibration ( $1648 \text{ cm}^{-1}$ ) can be attributed to strongly hydrogen-bonded acid, while the higher energy one ( $1671 \text{ cm}^{-1}$ ) is associated with unbonded or weakly bonded acid. Sample 7 (third phase) exhibits a much stronger  $1671 \text{ cm}^{-1}$  band than the other samples, thus providing support to the conclusion that in  $\text{UO}_2(\text{NO}_3)_2 \cdot 2\text{TBP} \cdot \text{HNO}_3$ , the third phase species, the  $\text{HNO}_3$  molecule is not in the primary coordination sphere of the uranyl ion, in agreement with previous results [5]. Other studies, however, concluded that the trinitrato complex,  $\text{HUO}_2(\text{NO}_3)_3 \cdot 2\text{TBP}$ , exists in the third phase [6,7].

### Visible Spectroscopy

Spectra of the organic phases (Figure 1) were obtained using a Cary-14 spectrophotometer and quartz cells of various pathlengths. Before phase splitting (Samples 3-6), the shape, energy, and intensity of each of the absorption bands is invariant and in complete agreement with literature reports of the spectrum of  $\text{UO}_2(\text{NO}_3)_2 \cdot 2\text{TBP}$  [13]. After phase splitting, the light phase (Sample 8) displays the same spectrum as the pre-splitting samples (represented in Figure 1 by Sample 6). However, the spectrum of the third phase (Sample 7) is distinctly different from the rest, indicating that the coordination of U(VI) is unique in the heavy phase. The intensity differs for most of the heavy phase absorption bands, the shape and energy of each peak change, and a weak new band appears at 494 nm. Taken together, this indicates that the U(VI) complex in the third phase has a lower symmetry [14,15] than  $\text{UO}_2(\text{NO}_3)_2 \cdot 2\text{TBP}$ . This could be accounted for by any number of complexes, not only the trinitrato complex  $\text{HUO}_2(\text{NO}_3)_3 \cdot 2\text{TBP}$ , as previously postulated based on the modest resemblance of the spectra of the third phase and  $\text{UO}_2(\text{NO}_3)_3^-$  [6,7]. The abrupt change in the spectrum on phase splitting suggests that in this system, third phase formation is *not* driven by progressive assembly of discrete molecules of the extracted complex into large aggregates that are insoluble in the original organic solvent.

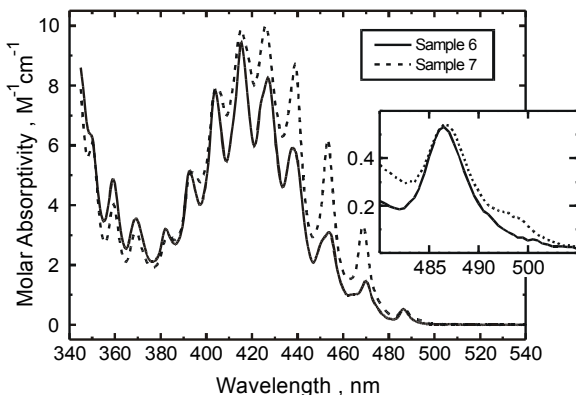


**Figure 1.** Visible absorption spectra of the limiting organic concentration (LOC) and third phase samples.

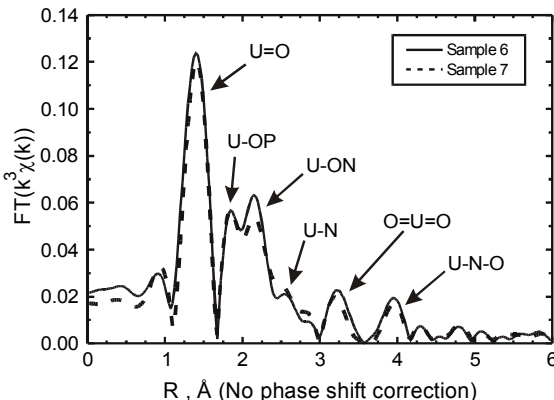


**Figure 2.** Fourier transformation of  $k^3$  weighted uranium  $L_3$  edge EXAFS for the LOC and third phase samples.

### EXAFS Measurements

Extended X-ray absorption fine structure (EXAFS) measurements of the organic phases were made on the BESSRC-CAT bending magnet beamline of the Advanced Photon Source at the uranium  $L_3$  edge. The data were fit using the program EXAFSPAK [16] to the theoretical phase and amplitude functions generated by FEFF 7.02 [17].

The results show similar patterns to those observed in each of the other experiments. The third phase is distinctly different from each of the other samples, which are identical to each other regardless of U(VI) loading or TBP concentration. Figure 2 shows the radial distribution of the shells of atoms about the U(VI) center (without phase shift correction). The EXAFS of the samples before phase splitting (Samples 4-6) and the light phase after splitting (Sample 8) are indistinguishable. The two “-yl” oxygen atoms are observed at  $1.765 \pm 0.005$  Å in all of the samples. Two TBP oxygen atoms at  $2.35 \pm 0.02$  Å and 4 oxygen atoms from bidentate nitrate groups at  $2.50 \pm 0.01$  Å can be partially resolved in the equatorial coordination sphere. These results agree well with previous work [18, 19].

None of the uranium-oxygen bond distances change significantly upon formation of the third phase. In addition, the number of inner sphere TBP oxygen atoms (2) observed in the third phase (Sample 7) is exactly the same seen for the other samples. The primary difference in the U(VI) inner coordination sphere of the heavy phase is a significant decrease (from 4.0 to 3.5) in the average number of nitrate oxygen atoms (when the Debye-Waller factor,  $\sigma^2$ , for the equatorial oxygen atoms is held constant). This decrease in the number of coordinated nitrate oxygen atoms with no change in the number of coordinated TBP groups is entirely inconsistent with the formation of even small amounts of  $UO_2(NO_3)_3^-$  in the heavy phase, given the bicoordinate nature of the nitrate groups demonstrated by the IR data. The additional equivalent of  $NO_3^-$  present in the third phase cannot be present in the U(VI) inner coordination sphere.

All of our results are consistent with some of the bidentate nitrate ligands of  $UO_2(NO_3)_2 \cdot 2TBP$  becoming monodentate with respect to a single U(VI) in order to bridge two uranyl centers or possibly to form a strong hydrogen bond with the water or nitric acid present in the heavy phase. Such behavior would lower the symmetry of the complex, accounting for the change in the UV-visible spectrum for the heavy phase without requiring the presence of an inner sphere trinitrato complex. Nevertheless, the changes in the U(VI) inner coordination sphere that induce, or are a result of, third phase formation in the uranyl/nitrate/TBP system are subtle.

## SANS Measurements

SANS measurements on samples similar to those in Table 1, but prepared in deuterated *n*-dodecane, were made using the small-angle neutron diffractometer SAND at the Argonne National Laboratory Intense Pulsed Neutron Source (IPNS) as previously described [4]. Figure 3 shows the neutron scattering data for selected samples together with their fit to an elliptical form factor. Table 2 reports the values of the perpendicular (a) and parallel (b) semiaxis resulting from the elliptical form factor fit for all samples investigated, together with the gyration radius ( $R_g$ ) of the scattering entities present in solution.

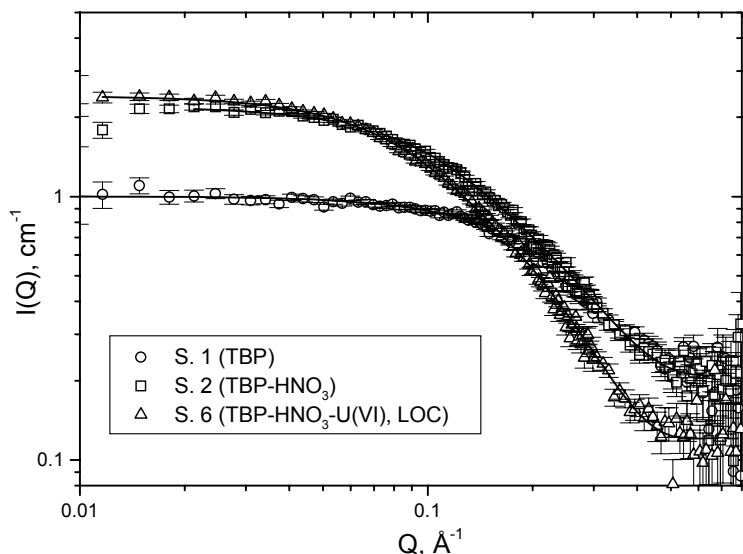


Figure 3. SANS data and fit to elliptical form factor for samples 1, 2 and 6.

Table 2. Elliptical form factor fit for U(VI)-TBP samples.

Sample no.	a Å	b Å	$R_g$ Å
1	$7.0 \pm 0.4$	$12.2 \pm 0.6$	$7.0 \pm 0.5$
2	$6.7 \pm 0.2$	$25.9 \pm 0.3$	$12.3 \pm 0.3$
3	$6.7 \pm 0.1$	$27.1 \pm 0.2$	$12.8 \pm 0.2$
4	$7.4 \pm 0.1$	$28.8 \pm 0.3$	$13.7 \pm 0.3$
6 (LOC)	$7.5 \pm 0.1$	$32.1 \pm 0.3$	$15.1 \pm 0.3$
8 (Light Ph.)	$7.1 \pm 0.2$	$25.2 \pm 0.3$	$12.1 \pm 0.3$

From the data in Table 2 it appears that growth of the solute particles along the parallel axis occurs when  $HNO_3$  is extracted by TBP. When extracted U(VI) progressively replaces  $HNO_3$  in the aggregates, only modest further growth takes place. The largest aggregates exist, as expected, in sample 6 (LOC), with the parallel axis  $b$  equal to approximately 3 times that for the TBP species in sample 1. Somewhat smaller aggregates exist in the light phase after phase splitting. The third phase sample presents a more complex scattering profile. Because the third phase is a highly concentrated sample, interpretation of the SANS data requires a different approach. Attempts to this effect are in progress.

## CONCLUSIONS

Chemical analyses, spectroscopic and EXAFS evidence indicate that, under the experimental conditions of this work, U(VI) is extracted by 20 % TBP in *n*-dodecane as  $\text{UO}_2(\text{NO}_3)_2 \cdot 2\text{TBP}$ , while the third phase species has the composition,  $\text{UO}_2(\text{NO}_3)_2 \cdot 2\text{TBP} \cdot \text{HNO}_3$  where both of the TBP oxygen atoms are in the inner coordination sphere. Aggregation of the organic phase species occurs upon  $\text{HNO}_3$  extraction in the absence of metal. Coextraction of U(VI) promotes only modest additional growth. Based on these results, it seems reasonable to conclude that formation of a third phase in this system is probably not caused by extensive solute aggregation. More likely, a dramatic change in solution leading to phase splitting takes place when one molecule of  $\text{HNO}_3$  becomes part of the U(VI)-adduct. At this point, the solute probably becomes too polar to exist in the alkane diluent and collects in a separate phase.

## ACKNOWLEDGMENTS

The authors acknowledge the infrastructure support of the Argonne Actinide Synchrotron Facility and BESSRC-CAT. This work was funded by the U. S. Department of Energy, Office of Basic Energy Science, Divisions of Chemical Science (support of the ANL Chemistry Division), Material Science (support of the work at the IPNS), and Office of Energy Research (support of the Advanced Photon Source) under contract No. W-31-109-ENG-38.

## REFERENCES

1. P. R. Vasudeva Rao and Z. Kolarik (1996), *Solvent Extr. Ion Exch.*, **14**, 955-993.
2. A. S. Kertes (1965), Solvent Extraction Chemistry of Metals, McMillan, London, pp. 377-399.
3. C. Erlinger, D. Gazeau, T. Zemb, C. Madic, L. Lefrançois, M. Hebrant and C. Tondre (1998), *Solvent Extr. Ion Exch.*, **16**, 707-738.
4. R. Chiarizia, V. Urban, P. Thiagarajan and A. W. Herlinger (1998), *Solvent Extr. Ion Exch.*, **16**, 1257-1278; *ibidem* (1999), **17**, 113-132 and (1999), **17**, 1171-1194.
5. T. V. Healy and H. A. C. McKay (1956), *Trans. Faraday Soc.*, **52**, 633-642.
6. A. S. Solovkin, N. S. Povitskii and K. P. Lunichkina (1960), *Russian J. Inorg. Chem. (English Transl.)*, **5**(9), 1026-1028.
7. N. Boukis and B. Kanellakopoulos (1983), *KfK Report*, No. 3352, Karlsruhe, 29 pp.
8. J.M. Schaekers (1991), Science and Technology of Tributyl Phosphate, W. W. Schulz, J. D. Navratil and A. S. Kertes (eds.), CRC Press, Boca Raton, FL, vol. IV, pp. 71-204.
9. H. A. C. McKay (1956), *Proc. Int. Conf. Peac. Uses At. En.*, Geneva, vol. 7, pp. 314-317.
10. J. F. Ferraro, Manuscript in preparation.
11. N. K. Curtis and Y. M. Curtis (1965), *Inorg. Chem.*, **4**, 804-809.
12. S. A. Stern, J. T. Mullhaupt and W. B. Kay (1960), *Chem. Rev.*, **60**, 185-207.
13. Yu. S. Fedorov and B. Yu. Zilberman (2000), *Radiochem.*, **42** (3), 242-246.
14. C. Gorller-Walrand and S. De Jaegere (1972), *Spectrochim. Acta*, **28A**, 257-268.
15. V. M. Vdovenko, A. Skoblo, and D. Suglobov (1967), *Soviet Radiochem.*, **11**,(1), 30-36.
16. I. J. Pickering and G. N. George (1995), *Inorg. Chem.*, **34**, 3142-3152.
17. A. L. Ankudinov and J. J. Rehr (1997), *Phys. Rev. B*, **56**, R1712.
18. C. Den Auwer, C. Lecouteux, M. C. Charbonnel, C. Madic and R. Guillaumont (1997), *Polyhedron*, **16**, 2233-2238.
19. C. Den Auwer, M. C. Charbonnel, M. T. Presson, C. Madic and R. Guillaumont (1998), *Polyhedron*, **17**, 4507-4517.



## SUPERCritical CO<sub>2</sub> FLUID LEACHING (SFL) OF URANIUM FROM SOLID WASTES USING HNO<sub>3</sub>-TBP COMPLEX AS A REACTANT

Osamu Tomioka, Yoshihiro Meguro\*, Shuichi Iso\*, Zenko Yoshida\*, Youichi Enokida\*\*, Ichiro Yamamoto

Department of Nuclear Engineering, Nagoya University, Nagoya, Japan

\*Advanced Science Research Center, Japan Atomic Energy Research Institute,  
Tokai, Japan

\*\*Research Center for Nuclear Materials Recycle, Nagoya University, Nagoya, Japan

A new method, which is based on the efficient and selective dissolution of uranium oxides with supercritical CO<sub>2</sub> containing HNO<sub>3</sub>-tributylphosphate (TBP) complex and is referred to as supercritical CO<sub>2</sub> fluid leaching (SFL) method, has been developed for the removal of uranium from the solid waste contaminated by uranium oxides. It was found that uranium oxides, UO<sub>2</sub> or U<sub>3</sub>O<sub>8</sub>, could be dissolved almost completely in supercritical CO<sub>2</sub> phase at 60 °C and 20 MPa. The feasibility of the SFL method for the decontamination of uranium from the solid wastes was demonstrated using a synthetic waste, *i. e.*, a mixture of the standard sea sand (*ca.* 50 g) and UO<sub>2</sub> or U<sub>3</sub>O<sub>8</sub> powders (*ca.* 100 mg of U). The decontamination factor of UO<sub>2</sub> or U<sub>3</sub>O<sub>8</sub> of 10<sup>2</sup> or 10<sup>4</sup>, respectively, were attained by the recommended procedure.

### INTRODUCTION

Removal of radioactive contaminants from various solid wastes such as mine tailings, ash and sludge products from the nuclear processes leads to safe and economical storage and disposal of these wastes. The decontamination treatment of the solid wastes, however, is not commonly conducted because of the following methodological limitations; methods feasible for a large-scale treatment of the wastes are very limited and a large amount of the secondary wastes is often generated from the decontamination process. A method based on a new principle, which can be applied to the contaminated solid of a large amount and generates less process waste, is required to be developed.

Recently, much attention has been paid to a novel method for the separation of metals using the supercritical CO<sub>2</sub> fluid as a medium [1-12]. Supercritical fluid extraction (SFE) with the supercritical CO<sub>2</sub> instead of an organic solvent has several advantages as follows. The extraction efficiency and rate are expected to be enhanced due to rapid mass transfer in the supercritical fluid phase. The rapid and complete recovery of the extracted substances from CO<sub>2</sub> is attained by gasification of CO<sub>2</sub>. The extraction efficiency or selectivity can be optimized by changing optionally the properties of the CO<sub>2</sub> medium by tuning pressure or temperature [3,11]. The use of SFE in the field of nuclear technology exhibits a particular significance for minimizing the amount of the radioactive solvent waste [13]. The authors have developed the SFE of U(VI) and Pu(IV) from nitric acid solution using supercritical CO<sub>2</sub> containing tributylphosphate(TBP) [1-4,13]. An alternative and more attractive method based on the SFE is "direct leaching (extraction)" of the metals from the solid samples. Neither organic solvent nor acid for the pretreatment of the samples are necessary to be used in this method, which leads to a total minimization of the secondary wastes generated from the metal separation process.

The present study aims at the development of a method, *i.e.*, the supercritical CO<sub>2</sub> fluid leaching (SFL), for the decontamination of uranium from the solid wastes containing uranium oxides, UO<sub>2</sub> or U<sub>3</sub>O<sub>8</sub>. The HNO<sub>3</sub>-TBP complex was employed as a reactant to dissolve the uranium oxides efficiently and selectively into supercritical CO<sub>2</sub> phase.

## EXPERIMENTAL

Apparatus for the SFL, which was essentially identical to that used for the supercritical CO<sub>2</sub> fluid extraction of the metal from an aqueous solution [2], is shown in Figure 1. The main part of the apparatus consisted of a stainless steel reaction vessel (50 ml), which was installed in a thermostat oven (60°C), a reactant mixing vessel and a collector. Stainless balls of 3.2 mm in diameter were packed in the collector which was made of Pyrex glass cylinder of 300 mm in height and 10 mm in diameter with water jacket to keep temperature at 60 °C. A syringe pump was used to flow CO<sub>2</sub>.

The HNO<sub>3</sub>-TBP complex was prepared by mixing vigorously 100 ml of 70% HNO<sub>3</sub> (Wako Pure Chemicals Co.) with 100 ml of TBP (Koso Chemical Co.) in a conventional extraction tube for 30 min. The HNO<sub>3</sub>-TBP complex liquid thus obtained was determined to contain HNO<sub>3</sub> and TBP at mole ratio of 1.4 ~ 1.5 : 1 as the mixture of (HNO<sub>3</sub>)<sub>2</sub>(TBP) and HNO<sub>3</sub>(TBP) complexes[14]. The water content of the HNO<sub>3</sub>-TBP complex was determined to be 1.6 mol/l by Karl-Fischer titration method.

A synthetic solid waste sample was a mixture of ca. 100 ~ 200 mg of UO<sub>2</sub> or U<sub>3</sub>O<sub>8</sub> powders and 50 g of the standard sea sand (Wako, 20-30 mesh). The UO<sub>2</sub> powder was obtained by grinding mechanically the UO<sub>2</sub> nuclear fuel pellet and the U<sub>3</sub>O<sub>8</sub> was prepared by heating the UO<sub>2</sub> powder at 480 °C in air for 2 hrs.

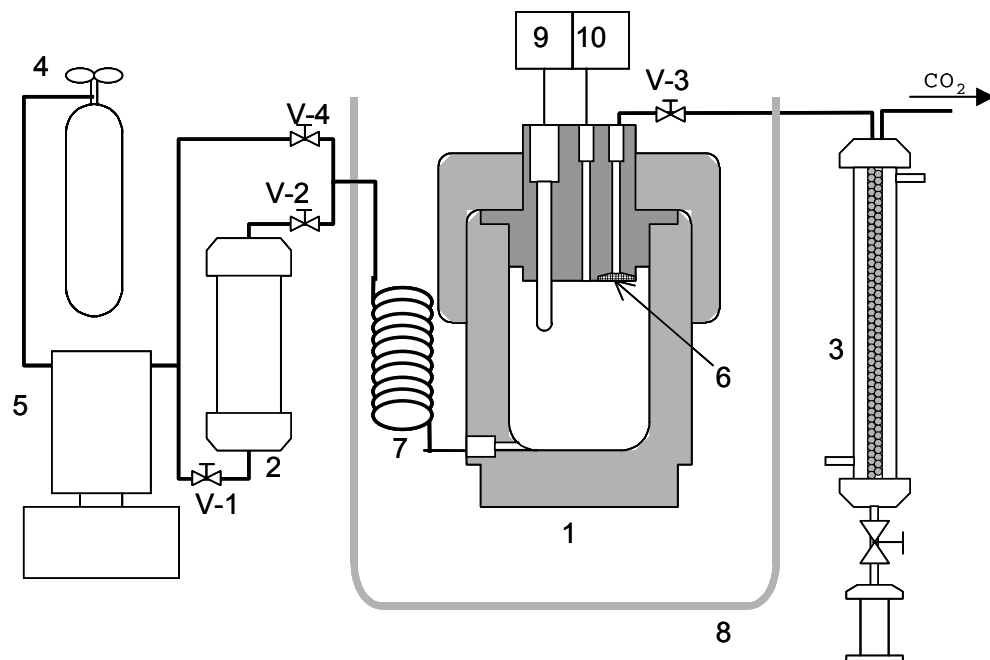


*Figure 1. Apparatus for the SFL for the decontamination of uranium from contaminated solid waste.*

- 1; reaction vessel, 2; reactant mixing vessel, 3; collector, 4; liquid CO<sub>2</sub> cylinder,
- 5; syringe pump, 6; filter, 7; preheating coil, 8; water bath, 9; thermometer,
- 10; pressure gauge.

## RECOMMENDED PROCEDURE

Place the solid waste sample (*ca.* 50 g) in the reaction vessel (1) and keep the temperature inside the vessel at 60°C. Take an aliquot of HNO<sub>3</sub>-TBP complex (2.2 ml) in the reactant mixing vessel (2) of 15.7 ml in inner volume which is kept at 25°C. Close all valves V-1 to V-4. Open valve V-1 and introduce the CO<sub>2</sub> into the reactant mixing vessel by means of the syringe pump (5) until the pressure in the vessel becomes 20 MPa. Open V-2 to introduce a mixture of the HNO<sub>3</sub>-TBP complex and the CO<sub>2</sub> into the reaction vessel through the pre-heating coil using the syringe pump until the pressure becomes 20 MPa. Close V-2 and allow the system to stand for an appropriate time (30 to 180 mins) to leach uranium from the solid sample [static SFL procedure]. After the static SFL, open V-4 and V-3 and flow the CO<sub>2</sub> at a given flow rate (3.0 ml/min at the syringe pump and 3.6 ml/min at the outlet of the reaction vessel) for an appropriate time (30 to 180 mins) to transport such CO<sub>2</sub>-soluble contents of the reaction vessel as the uranium-TBP complex and the HNO<sub>3</sub>-TBP complex unreacted into the collection vessel through a restrictor and to wash the solid wastes [washing procedure].

## RESULTS AND DISCUSSION

Fundamental studies have been performed on the dissolution behavior of UO<sub>2</sub> or U<sub>3</sub>O<sub>8</sub> in supercritical CO<sub>2</sub> containing HNO<sub>3</sub>-TBP complex as a reactant. The results obtained are summarized as below, and will be published [15] in more detail.

- (i) The UO<sub>2</sub> and U<sub>3</sub>O<sub>8</sub> powders react with HNO<sub>3</sub>-TBP complex in the supercritical CO<sub>2</sub> medium to form U(VI)-TBP complex, UO<sub>2</sub>(NO<sub>3</sub>)<sub>2</sub>(TBP)<sub>2</sub>, which is soluble in the CO<sub>2</sub> phase. The UO<sub>2</sub> or U<sub>3</sub>O<sub>8</sub> solids can be thus dissolved (leached) in the supercritical CO<sub>2</sub> phase.
- (ii) The rate of the dissolution of UO<sub>2</sub> or U<sub>3</sub>O<sub>8</sub> is high enough when the content of HNO<sub>3</sub> in the HNO<sub>3</sub>-TBP complex is high. In particular, when the ratio of the mole fraction of HNO<sub>3</sub> to that of TBP is larger than unity, *i.e.*, the content of 2 : 1 complex (HNO<sub>3</sub>)<sub>2</sub>TBP becomes large, the dissolution rate increases remarkably.
- (iii) The dissolution of UO<sub>2</sub> or U<sub>3</sub>O<sub>8</sub> is facilitated by the presence of the water which is dissolved in the CO<sub>2</sub> phase at the concentration more than *ca.* 0.2 mol/l.
- (iv) The dissolution rate is not strongly dependent on the temperature in the range of 40 to 60°C, and is dependent on the pressure so that the dissolution rate decreases with an increase of the pressure in the range of 12 to 25 MPa.
- (v) The UO<sub>2</sub>(NO<sub>3</sub>)<sub>2</sub>(TBP)<sub>2</sub> complex dissolved into the supercritical CO<sub>2</sub> can be completely recovered in the collector. The UO<sub>2</sub>(NO<sub>3</sub>)<sub>2</sub>(TBP)<sub>2</sub> is decomposed by mixing with 1 M (NH<sub>4</sub>)<sub>2</sub>CO<sub>3</sub> solution and U(VI) is dissolved into the aqueous solution.

The reactant HNO<sub>3</sub>-TBP complex was found to be enough effective to dissolve UO<sub>2</sub> or U<sub>3</sub>O<sub>8</sub> and to play multi-functions as follows in the dissolution of the uranium oxides. (i) H<sup>+</sup> contained in HNO<sub>3</sub>-TBP complex dissociates the U-O bond, (ii) NO<sub>3</sub><sup>-</sup> in the complex plays roles both as an oxidant to convert U(IV) to U(VI) and as the counter anion to neutralize the uranium ion, and (iii) TBP acts as a complex forming agent to result hydrophobic complex UO<sub>2</sub>(NO<sub>3</sub>)<sub>2</sub>(TBP)<sub>2</sub>, being soluble into supercritical CO<sub>2</sub> phase [2].

The decontamination of the synthetic uranium-containing solid wastes, the mixture of UO<sub>2</sub> or U<sub>3</sub>O<sub>8</sub> and the standard sea sand, was conducted according to the recommended procedure. The sand sample after the decontamination procedure was washed to remove uranium using concentrated nitric acid at boiling point for 30 min. The concentration of uranium in the nitric acid solution was analyzed by an ICP-AES (Shimadzu, ICPS-8000E). The results are shown in Table 1.

*Table 1. Decontamination efficiency of synthetic uranium-containing solid wastes by SFL using the supercritical CO<sub>2</sub> + HNO<sub>3</sub>-TBP complex.*

Synthetic solid wastes	Total amount of U remaining in the solid after the SFL (mg)	Decontamination factor (DF) <sup>1)</sup>
120 mg UO <sub>2</sub> powder + 50 g sea sand	0.3	3.5 × 10 <sup>2</sup>
120 mg U <sub>3</sub> O <sub>8</sub> powder + 50 g sea sand	0.009	1.1 × 10 <sup>4</sup>

SFL condition; 60 °C, 20 MPa, the static SFL for 150 mins and washing for 100 min (flow-rate of CO<sub>2</sub>; 3.5 ml/min).

<sup>1)</sup>DF = (U before SFL) / (U after SFL)

The solid sample after the SFL treatment was in a form of dried solid which contains neither acid and organic solvent nor reactant. It was found also that most of uranium (95-99%) was recovered in the collector. This allows the further treatment or management of the solid waste more easily. Uranium(VI) was quantitatively stripped as U(VI)-carbonate from the UO<sub>2</sub>(NO<sub>3</sub>)<sub>2</sub>(TBP)<sub>2</sub> using (NH<sub>4</sub>)<sub>2</sub>CO<sub>3</sub> aqueous solution and the TBP recovered can be reused.

The synthetic solid waste employed in the present work was the simple physical mixture of uranium oxides and sand. Many real wastes generated from the nuclear-fuel production processes are in the form of the simple mixture of the uranium oxides and a variety of solid substances. The recommended procedure can be applied to these solid wastes. On the other hand, a waste containing uranium which is strongly bound to the solid matrices is also present. Further investigation is now in progress to optimize the SFL condition for the practical use of the method for the treatment of such wastes of more complicated form.

## CONCLUSION

A supercritical CO<sub>2</sub> fluid leaching (SFL) method for the decontamination of uranium oxides from uranium-containing solid wastes has been developed. The UO<sub>2</sub> or U<sub>3</sub>O<sub>8</sub> in the solid wastes can be removed and recovered using the supercritical CO<sub>2</sub> containing HNO<sub>3</sub>-TBP reactant. The most distinguished advantages with the proposed SFL method are that (i) the highly efficient removal of U(VI) is attained, (ii) a generation of the secondary wastes from the decontamination process is totally minimized, and (iii) CO<sub>2</sub> and even HNO<sub>3</sub>-TBP reactant can be easily reused.

## REFERENCES

1. S. Iso, Y. Meguro and Z. Yoshida (1995), *Chem. Lett.*, **1995**, 365.
2. Y. Meguro, S. Iso, H. Takeishi and Z. Yoshida (1996), *Radiochim. Acta*, **75**, 185.
3. Y. Meguro, S. Iso and Z. Yoshida (1998), *Anal. Chem.*, **70**, 1262.
4. S. Iso, S. Uno, Y. Meguro, T. Sasaki and Z. Yoshida (2000), *Prog. Nucl. Energ.*, **37**, 423.
5. C. M. Wai, S. Wang, Y. Liu, V. Lopez-Avila and W. F. Beckert (1996), *Talanta*, **43**, 2083.
6. K. L. Toews, N. G. Smart and C. M. Wai (1996), *Radiochim. Acta*, **75**, 179.
7. O. Tomioka, Y. Enokida and I. Yamamoto (1998), *J. Nucl. Sci. Technol.*, **35**, 515.
8. O. Tomioka, Y. Enokida, I. Yamamoto and T. Takahashi (2000), *Prog. Nucl. Energ.*, **37**, 417.
9. A. A. Murzin, V. A. Babain, A. Yu. Shadrin, I. V. Smirnov, V. N. Romanovskii and M. Z. Muradymov, *Radiochem.*, **40**, 47.
10. M. D. Burford, M. Z. Ozel, A. A. Clifford, K. D. Bartle, Y. Lin, C. M. Wai and N. G. Smart (1999), *Analyst*, **124**, 609.
11. Y. Lin, N. G. Smart and C. M. Wai (1995), *Trends Anal. Chem.*, **14**, 123.
12. C. Erkey (2000), *J. Supercrit. Fluids*, **17**, 259.
13. S. Iso, Y. Meguro and Z. Yoshida (1997), Recent Progress in Actinides Separation Chemistry, Proc. Workshop on Actinides Solution Chemistry, Wasc '94, Z. Yoshida, T. Kimura and Y. Meguro (eds.), World Science Publishers, Singapore, pp. 238-246.
14. D. J. Chaiko and G. F. Vandergrift (1988), *Nucl. Technol.*, **82**, 52.
15. O. Tomioka, Y. Meguro, Y. Enokida, I. Yamamoto and Z. Yoshida (2001), *J. Nucl. Sci. Technol.*, in press.



## STRUCTURAL STUDIES BY NMR AND MOLECULAR DYNAMIC CALCULATIONS OF LANTHANIDE COMPLEXES WITH ETHOXY MALONAMIDES IN SOLUTION

Claude Berthon, Philippe Guilbaud, Maryline Bousquet and Chantal Gimenez

CEA – Marcoule, Bagnols-sur-Cèze, France

<sup>17</sup>O NMR spectra obtained with TEEEMA (2-(2-ethoxyethyl)-N,N,N',N'-tetraethylmalonamide) in solution are consistent with solid state results: there is a direct carbonyl oxygen interaction with the metal ion that is not observed with the ether oxygen. Structural information such as the ratio of average distance between metal and carbon atoms of the ligand are determined from the <sup>13</sup>C NMR longitudinal relaxation time. The experimental data are used as constraints for molecular dynamic simulations. Calculations performed with the TEEEMA/La<sup>3+</sup>/H<sub>2</sub>O system show that the more water molecules there are in the system, the better the agreement between experimental and calculated results. <sup>1</sup>H NMR spectra of malonamides obtained at low temperatures in a H<sub>2</sub>O/acetone/CBr<sub>2</sub>F<sub>2</sub> mixture show a water molecule in the first coordination sphere of La(III). This water molecule appears able to bind with the metal and the ether oxygen, in good agreement with molecular dynamic simulations.

### INTRODUCTION

In studies related to nuclear fuel reprocessing, malonamides have been proposed as extractants [1] able to separate trivalent actinides from most fission products with the exception of the trivalent lanthanides, which are coextracted with actinides(III). Extensive data have been compiled to understand the extraction mechanisms. A large number of molecules with the general formula RR'N-COCHR"-CO-NRR' have been evaluated. Malonamides with the ethoxy alkyl chain R" are molecules of interest because they lead to higher extraction [2] of both actinides(III) and lanthanides(III) than those with an alkyl chain R". In order to explain this behavior, it was suggested that the ether O atom present in the R" radical participates in complexation. However, it has been established that this potential donor atom is not bound to the metal ion in the solid state [3, 4]. Because there is no straightforward answer concerning such systems in liquid media, the present study attempts to elucidate the structure of a malonamide ligand complexed to a lanthanide nitrate in a liquid phase. NMR experimental data combined with theoretical calculations yielded significant data about the TEEEMA/Nd(NO<sub>3</sub>)<sub>3</sub>/CH<sub>3</sub>CN system.

### EXPERIMENTAL DESCRIPTION

Among the malonamides, TEEEMA (Figure 1) was chosen in this study for <sup>17</sup>O NMR and theoretical calculation purposes. Light molecules yield narrower NMR signals than the conventional malonamide extractant, with long hydrophobic alkyl chains. Moreover, short alkyl or alkyl ethoxy chains make dynamic calculations less time consuming. TEEEMA was provided by Panchim, Lisses (91), France, and used without further purification.

DMDOHEMA (2-[2-(hexyloxy)ethyl]-*N,N'*-dimethyl-*N,N'*-dioctylmalonamide) was also provided by Panchim. Acetonitrile, the liquid medium of the system, and lanthanide nitrates  $\text{La}(\text{NO}_3)_3 \cdot 6\text{H}_2\text{O}$  or  $\text{Nd}(\text{NO}_3)_3 \cdot 6\text{H}_2\text{O}$  (Aldrich) were all at least reagent grade and were used as received. Acetonitrile-d3 and acetone-d6 (Euriso-Top) provided a deuterium lock signal. The  $\text{CBr}_2\text{F}_2$  (Aldrich) was used as received (97% purity) to prepare a mixture with acetone for low-temperature NMR experiments.

The NMR spectra were recorded on a Varian 300 VXR-s spectrometer equipped with a 5 mm broadband probe. Quantum mechanics calculations were carried out with the Gaussian 98 program [5], molecular dynamic (MD) simulations with Amber [6,7] release 5, and programs for imaging or analysis of molecular trajectories in solution with MDS and Draw [8]. All calculations were performed with R12000 Silicon Graphics processors.

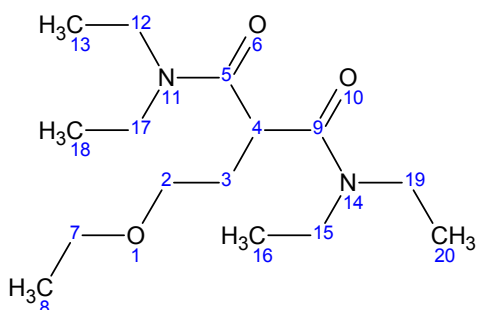


Figure 1. TEEEMA molecule (2-(2-ethoxyethyl)- $N^1,N^1,N^3,N^3$ -tetraethylmalonamide) with atom numbering.

## EXPERIMENTAL RESULTS: $^{17}\text{O}$ NMR SPECTRA

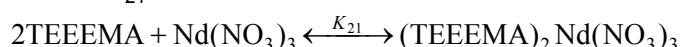
One of the easiest ways to check oxygen binding with lanthanide(III) ion in solution is to examine  $^{17}\text{O}$  NMR spectrum variations due to the presence or absence of a paramagnetic cation. From a TEEEMA solution in  $\text{CD}_3\text{CN}$ , it can be seen (Figure 2A) that the carboxyl O atoms ( $\text{O}_6$  and  $\text{O}_{10}$ ) are 327 ppm and the ether O atom ( $\text{O}_1$ ) is 9 ppm from the  $\text{D}_2\text{O}$  reference signal. When Nd(III) nitrate is added to this solution, only the carboxyl signal is enlarged (590 Hz to 1445 Hz) and shifted up field. There is, in fact, a direct interaction between the carboxyl oxygen atoms and the metal ion, while the ether O atom is not directly bound to the paramagnetic ion.

This straightforward answer is in agreement with solid state results. However, we carried out further NMR and MD structural investigations in solution.

## STRUCTURAL STUDIES

### NMR Investigation

The malonamide:metal ion stoichiometry of the complexes formed is commonly 1:1 and/or 2:1 depending on the lanthanide nitrate and ionic strength of the medium [9-11]. After  $^1\text{H}$  and  $^{13}\text{C}$  NMR assignments of the TEEEMA in  $\text{CD}_3\text{CN}$ , the binding constant and stoichiometry were determined for the TEEEMA/ $\text{Nd}(\text{NO}_3)_3 \cdot 6\text{H}_2\text{O}/\text{CH}_3\text{CN}$  system by chemical shift analysis. The concentration of neodymium nitrate was kept constant during the experiments, with variable TEEEMA concentrations. From  $^1\text{H}$  and  $^{13}\text{C}$  NMR signal analysis, the best results were obtained for 2:1 stoichiometry and the binding constant corresponding to the following equilibrium was found to be  $K_{21}=1.3 \pm 0.1 \text{ mol} \cdot \text{L}^{-1}$ .



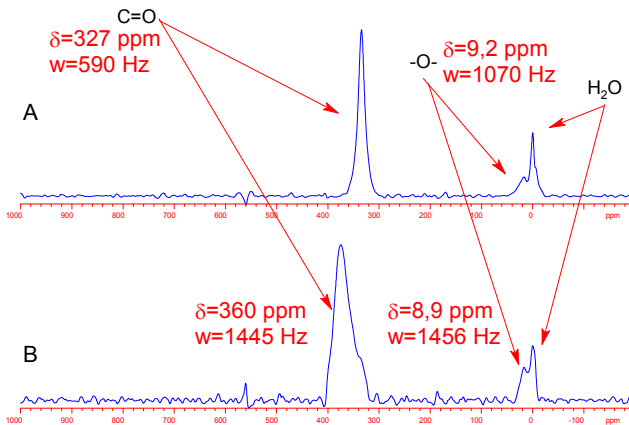


Figure 2.  $^{17}\text{O}$  NMR spectra of TEEEMA  $0.1\text{mol}\cdot\text{L}^{-1}$  in  $\text{CD}_3\text{CN}$  with (bottom) and without (top)  $\text{Nd}(\text{NO}_3)_3$   $0.045\text{mol}\cdot\text{L}^{-1}$ .

At room temperature, it has been established that a fast exchange occurs for this system on the NMR time scale. Because of this fast exchange, the observed relaxation times  $T_{1\text{obs}}$  are the sum of the contributions from each  $T_1$  TEEEMA species: free and bound TEEEMA (respectively  $T_{1f}$  and  $T_{1b}$  in Eq. 1;  $x$  is the molar fraction of the complex). In order to extract the  $\text{TEEEMA}_2\text{Nd}(\text{NO}_3)_3$  complex longitudinal relaxation time from  $^{13}\text{C}$  NMR  $T_1$  measurements, further analysis was performed using the binding constant determined earlier.

$$\frac{1}{T_{1\text{obs}}} = \frac{1}{T_{1f}} + x \frac{1}{T_{1b}} \quad (1)$$

We paid special attention to  $^{13}\text{C}$  atoms 2 and 7, which neighbor on the ether oxygen, and to carbon atom 4, which is in a central position within the malonamide. These three nuclei are far enough from the complex metallic center so that the contact interaction term is negligible. The main contribution to the  $T_1$  relaxation time in the paramagnetic complex ( $T_{1b}$ ) thus comes from dipole-dipole interactions from which structural information can be deduced. The ratio of the induced relaxation rates of the nuclei  $i$  and  $j$  is given as:

$$\frac{T_{1b}(i)}{T_{1b}(j)} = \left( \frac{R_i}{R_j} \right)^6 \quad (2)$$

where  $R_i$  and  $R_j$  are the average distances between the Nd(III) metal ion and the  $^{13}\text{C}$  nuclei  $i$  and  $j$  of the ligand. The experimental ratios obtained from the relaxation time values of the selected carbon atoms were then used for molecular dynamic simulations.

### Theoretical Calculations

After TEEEMA partial charge calculation of the atoms, the structure was optimized by *ab initio* quantum mechanics calculations using the 6-31G<sup>\*\*</sup> basis set. MD studies were performed on a system composed of two TEEEMA molecules and one lanthanum cation with 0 to 5 H<sub>2</sub>O molecules, in a vacuum and in a water box. For convenience, the Nd(III) were replaced by the La(III) metallic ion because a consistent published set of La<sup>3+</sup>, Eu<sup>3+</sup> and Lu<sup>3+</sup> parameters was available [12]. We verified later that the choice of La<sup>3+</sup> instead of Eu<sup>3+</sup> to simulate experimental results with the Nd<sup>3+</sup> did not induce any significant change in our study.

The  $R_4$  distance was determined for various complexes using MD simulations. From the NMR relaxation time ratios determined above,  $R_{2(NMR)}$  and  $R_{7(NMR)}$  distances were obtained and compared with  $R_{2(MD)}$  and  $R_{7(MD)}$  from MD simulations. In the gas phase without  $\text{H}_2\text{O}$  molecules, the O ether atom may or may not be coordinated with the metal, in which case the  $R_{2(MD)}$  and  $R_{7(MD)}$  values are either too short or too long. From MD simulations with 1 to 5 water molecules, we noted that the more  $\text{H}_2\text{O}$  molecules in the first coordination sphere of  $\text{La}^{3+}$ , the closer  $R_{2(MD)}$  and  $R_{7(MD)}$  are to  $R_{2(NMR)}$  and  $R_{7(NMR)}$ . In a water box, at least one TEEEMA molecule is bidentate and the other malonamide may be dissociated or monodentate. The  $\text{La}^{3+}$  ion may also be coordinated with 6 to 7 water molecules.

Another series of MD simulations was performed with  $R_{2(MD)}$  and  $R_{7(MD)}$  constrained to  $R_{2(NMR)}$  and  $R_{7(NMR)}$ . From gas phase simulations with water molecules, the number of hydrogen bonds with the O ether atom was found to increase with the number of  $\text{H}_2\text{O}$  molecules in the system. However, in a water box, one TEEEMA molecule is monodentate.

Thus, for bidentate coordination of TEEEMA ligands, the agreement between the experimental and calculated distance ratios improves as the number of water molecules in the system increases. More interestingly, from the simulated trajectories, the analysis of the Radial Distribution Functions (RDF) of water protons around the O ether (Figure 3) reveals that one water molecule is bound to one malonamide. According to the second malonamide RDFs and visual inspection of the trajectories, it can be seen that the aforementioned water molecule temporarily bridges the TEEEMA ether oxygen. The other molecules are at least 5 Å from the TEEEMA ethoxy chain.

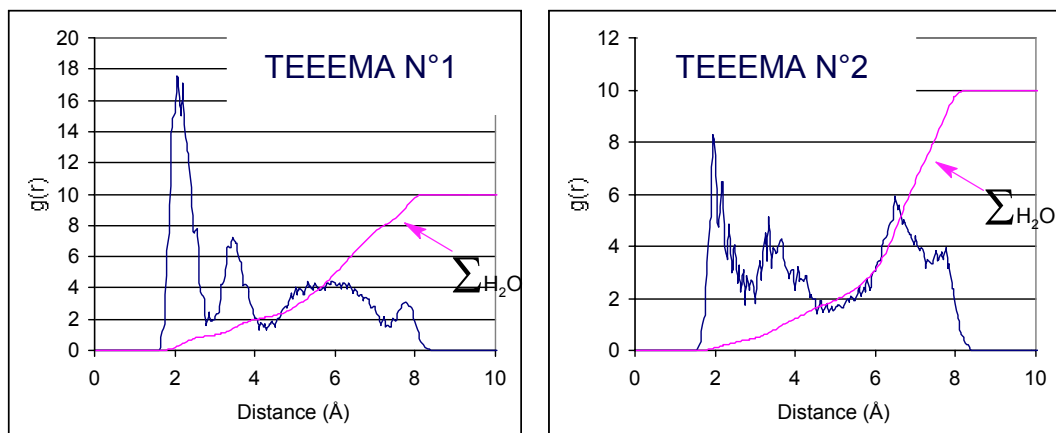


*Figure 3. Water-ether oxygen radial distribution function (RDF) for both malonamides from simulated trajectories in the case of a MD with five water molecules. Pink curves characterize the sum of the  $\text{H}_2\text{O}$  hydrogens ( $\Sigma_{\text{H}_2\text{O}}$ ).*

One of the most typical structures during MD simulations with five water molecules in the gas phase is shown in Figure 4. Note that the oxygen atom of the ethoxy chain may be bound to the metal atom via a water molecule.

Further NMR experiments were carried out at low temperatures to check these interesting results.

### LOW-TEMPERATURE $^1\text{H}$ NMR SPECTRA

The low-temperature NMR technique allows the metal-ion solvation shell to be studied directly. Extensive research has been done in this field recently [13]. At temperatures below -100°C, proton and ligand exchange are slow enough to permit direct observation of  $^1\text{H}$

resonance signals for coordinated and free water molecules, leading to an accurate measure of the  $\text{La}(\text{NO}_3)_3$  hydration number. Such temperatures require an acetone/ $\text{CBr}_2\text{F}_2$  mixture to preserve a liquid phase.

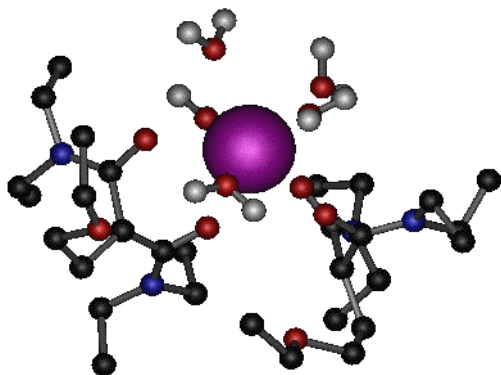


*Figure 4. Image of the  $(\text{TEEEMA})_2/\text{La}^{3+}/(\text{H}_2\text{O})_5$  system during the molecular dynamic simulation with  $R_{2(\text{NMR})}$  and  $R_{7(\text{NMR})}$  constraints of 5 kcal·mol<sup>-1</sup>.*

Because of the small amount of TEEEMA available in our laboratory, NMR experiments were carried out with DMDOHEMA. In a way, this hydrophobic malonamide brought us closer to the extraction process. A diamagnetic cation, La(III), was used in preference to a paramagnetic one (Nd(III)) to prevent a broad <sup>1</sup>H signal especially for the bound water.

<sup>1</sup>H NMR spectra were obtained from three kinds of solutions:

- DMDOHEMA/acetone/ $\text{CBr}_2\text{F}_2$
- $\text{La}(\text{NO}_3)_3 \cdot 6\text{H}_2\text{O}$ /acetone/ $\text{CBr}_2\text{F}_2$
- $\text{La}(\text{NO}_3)_3 \cdot 6\text{H}_2\text{O}$ /DMDOHEMA/acetone/ $\text{CBr}_2\text{F}_2$

The first one allowed us to determine the amount of free water in the DMDOHEMA sample (3  $\text{H}_2\text{O}$  molecules per malonamide). The second spectrum showed two  $\text{H}_2\text{O}$  signals: coordinated water at low field (2 water molecules per lanthanum cation) and free water (4 water molecules). The La(III) hydration number of two is in agreement with other studies [14]. According to the two previous spectra, Figure 5, showing the third spectrum, suggests that the water molecule is bound to the lanthanum cation.

The first coordination sphere of the metal ion thus comprises two DMDOHEMA molecules directly bonded via the carbonyl groups and one water molecule.

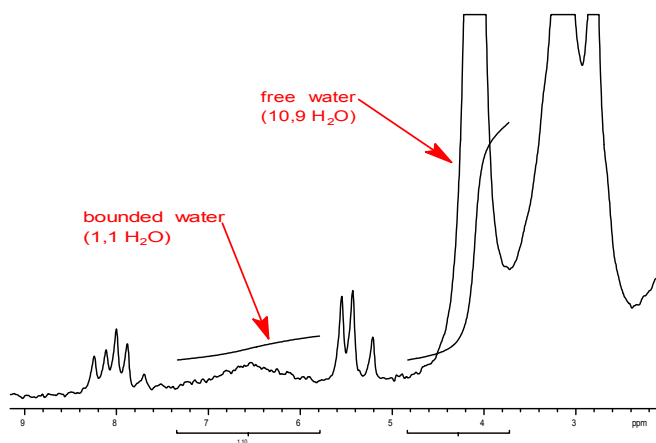


*Figure 5. <sup>1</sup>H NMR spectrum of DMDOHEMA 0.06 mol·L<sup>-1</sup> with  $\text{La}(\text{NO}_3)_3 \cdot 6\text{H}_2\text{O}$  0.03 mol·L<sup>-1</sup> in an acetone: $\text{CBr}_2\text{F}_2$  mixture (molar ratio 2:1) at -112°C.*

## CONCLUSION

MD simulations and experimental distances ( $R_2$  and  $R_7$ ) suggest that a water molecule may be bound to the ether oxygen via a hydrogen bond; a direct ether oxygen bond to the metal would have given short  $R_2$  and  $R_7$  values. Low-temperature NMR experiments clearly validate these results by showing there is only one water molecule in the first coordination sphere of the metal which is in fast exchange with free water.

The enhanced extraction properties of malonamide with an ethoxy chain may be explained, in part, by the ability of a water molecule to be extracted in the organic phase. Consequently, the hydration sphere of the lanthanum does not need to be completely removed to allow extraction of the metal.

One of our future projects will be to check whether water molecules are involved in alkyl malonamide complexed with lanthanide(III) nitrates. The number and the position of the oxygen atoms in the oxyalkyl chain will be studied in solution. In addition, the MD simulations will be improved by adding nitrates.

## ACKNOWLEDGEMENTS

The authors are grateful for the financial support from the Commission of the European Communities (Contract PARTNEW – FIKW-CT2000-00087).

## REFERENCES

1. C. Musikas (1987), *Inorg. Chim. Acta*, **140**, 197.
2. L. Nigond (1992), Ph.D. Thesis, Université Blaise Pascal, Clermont-Ferrand II, France.
3. P. Thuéry, M. Nierlich, M.C. Charbonnel and J.P. Dognon (1999), *Acta Cryst.*, **C55**, 1434-1436.
4. P.B. Iveson, M.G.B. Drew, M.J. Hudson and C. Madic (1999), *J. Chem. Soc., Dalton Trans.*, 3605-3610.
5. Gaussian, Inc. (1998), Gaussian 98, Revision A.7, Pittsburgh, PA.
6. D.A. Pearlman, D.A. Case, J.W. Caldwell, W.S. Ross, T.E. Cheatham III, S. DeBolt, D. Ferguson, G. Seibel, P. Kollman (1995), *Comp. Phys. Comm.*, **91**, 1-41.
7. D.A. Case *et al.* (1997), AMBER, University of California, San Francisco.
8. E. Engler and G. Wipff (1994), MDS, DRAW: Programs for Analysis of Molecular Trajectories in Solution, Université Louis Pasteur, Strasbourg.
9. P. Byers, M.G.B. Drew, M.J. Hudson and N.S. Isaacs (1994), *Polyhedron*, **13**, 349-352.
10. T. Nakamura, C. Miyake (1995), *J. Alloys Comp.*, **225**, 334-337.
11. P. Thuéry, M. Nierlich, M.C. Charbonnel, C. Den Auwer and J.P. Dognon (1999), *Polyhedron*, **18**, 3599-3603.
12. S. Durand, J.P. Dognon, P.G. Guilbaud, C. Rabbe and G. Wipff (2000), *J. Chem. Soc. Perkin Trans. 2*, 705-714.
13. A. Fratiello, V.Kubo-Anderson, R.A. Lee, M. Patrick, R.D. Perrigan, T.R. Porras, A.K. Sharp and K. Wong (2001), *J. Solution Chem.*, **30**, 77-97.
14. A. Fratiello, V. Kubo-Anderson, S. Azimi, T. Flores, E. Martinez, D. Matjka, R. Perrigan and M. Vigil (1990), *J. Solution Chem.*, **19**, 811-829.



## EXTRACTION OF Ln(III) AND Am(III) FROM NITRATE MEDIA BY MALONAMIDES AND POLYDENDATE N-BEARING LIGANDS

M.C. Charbonnel, J.L. Flandin, S. Giroux, M.T. Presson, C. Madic and J.P. Morel\*

CEA/Valrho, Marcoule, Bagnols-sur-Cèze, France

\* Université Blaise Pascal, Aubière, France

Malonamides and polydendate N-bearing ligands are promising extractants for the partitioning of actinides from high-level active nuclear wastes. This study focuses on the stoichiometry of their extracted complexes of actinides(III) and lanthanides(III) and on some related thermodynamic properties.

The extraction of Nd(III) from 2.5 M NaNO<sub>3</sub> by the malonamides DMDBTDMA and DMDOHEMA in dodecane has been studied in the range of temperature 10 to 40°C. The stoichiometry of the extracted complexes Nd(NO<sub>3</sub>)<sub>3</sub>L<sub>x</sub> is influenced by temperature for both extractants. Consequently the classical van't Hoff method should be used with care to determine the extraction enthalpy  $\Delta_{ext}H$ ; microcalorimetric titration seems to be more appropriate for such a complex chemical system.

The extraction of Eu(III) and Am(III) from 2.5 M NaNO<sub>3</sub> into *pr*-BTPs in octanol-1 has also been studied. The specie ML<sub>3</sub>(NO<sub>3</sub>)<sub>3</sub> is the dominant extracted complex under all experimental conditions and the extraction enthalpies and entropies have been calculated from the temperature dependence of the metal ion distribution ratios. The driving force for Am(III) or Eu(III) extraction by *pr*-BTPs from aqueous nitrate solution is the enthalpic term of the Gibbs free energy. The extraction is more exothermic for Am(III) than for Eu(III) which is an indication of the enhanced Am-BTP bond strength.

### INTRODUCTION

This study was carried out under the CEA programme for the partitioning of long-lived radionuclides, particularly the minor actinides, contained in high-level radioactive liquid waste (HAW) generated by reprocessing nuclear spent fuel. The first step of the separation strategy is the DIAMEX process, designed to coextract trivalent actinides and lanthanides from the HAW using a diamide extractant. The malonamide DMDBTDMA (N,N'-dimethyl-N,N'-dibutyltetradecylmalonic diamide) was the first reference extractant; extensive data were therefore collected to understand its extraction behaviour and to define a computer model of the DIAMEX process [1]. The extractant has been optimized to improve the extraction properties [2]; since 1997, the reference molecule is DMDOHEMA (N,N'-dimethyl-N,N'-diethyl-hexylethoxymalonic diamide). The second step of the strategy is the SANEX (Selective ActiNide(III) EXtraction) process, designed to separate actinides(III) from lanthanides(III). Among numerous nitrogen polydendate ligands, BTP molecules (2,6-bis(5,6-alkyl-1,2,4-triazin-3-yl)pyridines) were found promising [3,4] because the Am(III)/Ln(III) separation could be performed from highly acidic liquid waste. Counter-current hot tests with genuine high-level liquid waste confirmed the feasibility of the DIAMEX and SANEX concepts [1,3].

Although extraction and structural studies have been performed on both systems [1,3], very few basic data on the complexes present in the organic phases have been published to date. Some results obtained in this field are briefly presented here.

## EXPERIMENTAL

### Materials

The malonamides DMDBTDMA and DMDOHEMA were provided by Panchim, Lisses, 91029 EVRY Cedex, France. Their purity, determined by mass spectrometry, was better than 99%. The diamide DMDBTDMA was further purified on a alumina column to eliminate surface-active compounds [1]. The extractants 2,6-bis(5,6-bis-*iso*-propyl-1,2,4-triazin-3-yl)-pyridine and 2,6-bis(5,6-di-*n*-propyl-1,2,4-triazin-3-yl)-pyridine (designated *iPr*-BTP and *nPr*-BTP, respectively) were synthesized in our laboratory [4]. The purity of the BTP molecules was checked by NMR and mass spectrometry. Lanthanide(III) nitrates, lithium nitrate, sodium nitrate, *n*-dodecane and *n*-octanol-1 were reagent grade with purity better than 99% .

### Procedure and Apparatus

Organic phases were systematically pre-equilibrated with suitable aqueous solutions a few hours before the tests. The rare earth concentration in each phase was determined either by arsenazo III visible spectrophotometric analysis, X-ray fluorescence measurements or Inductive Coupled Plasma analysis. The radionuclides  $^{152}\text{Eu}$  and  $^{241}\text{Am}$  were used as tracers for some experiments and were measured by gamma spectrometry (at 121.8 keV and 59.54 keV, respectively).

For measurements at variable temperatures, a Haake bath was used with a temperature control of  $\pm 0.1^\circ\text{C}$ .

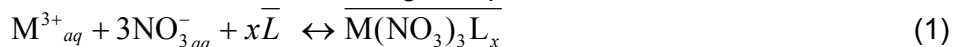
Microcalorimetric titrations were performed with a Thermal Activity Monitor (TAM) microcalorimeter from Thermometric. This modular system with a highly stable temperature-controlled bath ( $\pm 0.2 \text{ mK}$ ) could contain up to four calorimetry vessel units. The aqueous phase was loaded in a 2 mL glass ampoule and the organic phase was delivered through a fine bore cannula. The volume of titrant delivered was controlled by a programmable motor-driven syringe pump.

## RESULTS AND DISCUSSION

### Extraction of Ln(III) Nitrates by Malonamides in Neutral Aqueous Conditions

#### *Stoichiometries of extracted complexes*

Experiments were conducted to determine the enthalpy of Ln(III) and An(III) nitrates extraction by DMDBTDMA noted L hereafter. The extraction of Ln(III) or An(III) proceeds through the formation of solvates according to Equation 1:



Of course, the knowledge of the nature of all species present in the organic phases is a prerequisite condition to allow a correct interpretation of the extraction data and for the determination of the extraction thermodynamic properties.

The first measurements were related to the extraction of Nd(III) from aqueous phases ( $\text{NaNO}_3$ ) without acid. The pH was measured and the concentration of the lanthanide ion was checked before and after extraction. The pH was equal to 5.9 which is sufficient at conditions of  $2.5 \text{ mol.L}^{-1}$  ionic strength to prevent metal ion hydrolysis and precipitation [5].

The experimental conditions were selected to have a constant ionic strength in the aqueous phases and thus to ignore the variation of the aqueous activity coefficients. As a first approximation, we also considered the ratio  $\gamma_{M(NO_3)_3L_x}/\gamma_L^x$  as constant. The apparent equilibrium constant  $K'$  can then be written as follows:

$$K' = \frac{[M(NO_3)_3L_x]}{[M^{3+}][NO_3^-]^3[L]^x} \quad (2)$$

The experimental distribution ratio  $D_M$  is the ratio of the concentrations of the extracted complex to the metal species in the aqueous phase, *i.e.*, the aquo  $M^{3+}$  and the 1/1  $M^{III}$  nitroso complex  $M(NO_3)_{aq}^{2+}$  with  $\beta_1$  stability constant:  $D_{Nd} = [M(NO_3)_3L_x] / [M^{3+}](1+\beta_1[NO_3^-])$ .

This equation combined with equation (2) gives an expression of  $D_M \cdot (1+\beta_1[NO_3^-])$  versus  $[L]$ . The slope of the log-log plot allows the determination of the stoichiometry of the extracted complex.  $[L]$  has been calculated as  $[Diamide]_{tot} \cdot x[Nd]_{org}$ . A first value for  $x$  was selected and then corrected if the slope obtained was not consistent with the hypothesis.

At 25°C, the average slope for the log-log plot was  $5.1 \pm 0.2$ . The involvement of five molecules of diamide in the extracted complex can be explained by the aggregation of diamide in the second sphere of coordination around the inner-sphere complex  $Nd(NO_3)_3L_2$  [6]. Numerous extraction studies by the classical slope method corresponding to aqueous acidic conditions indicate a metal/ligand stoichiometry close to 1/2 for the extracted complex. This result is consistent with most of the crystal structures published related to the complexes formed between Ln(III) nitrates and diamide ligands [4,7]. Nevertheless, some authors mentioned also conditions where  $x > 2$  [8] or  $x = \text{non-integer number}$  [9]. The authors often attributed these results to the existence of molecules of ligand in the second sphere of coordination of the metal ion. Metal/diamide stoichiometries close to five have also been pointed out in our laboratory by recent ESI-MS measurements.

In these experimental conditions, the main extracted complex seems to be  $Nd(NO_3)_3L_5$ .

In order to determine Nd(III) extraction thermodynamic parameters, we measured Nd(III) distribution ratios for different temperatures. The curves of  $\log D_{Nd}(1+\beta_1[NO_3^-])$  against  $\log [L]$  were plotted. The variation of  $\beta_1$  of the Nd(III) mononitroso complex with temperature can be neglected ( $\Delta H = 1.7 \text{ kJ.mol}^{-1}$  [10] at ionic strength 2.0 mol.kg $^{-1}$ ). We obtained surprising results because it was shown that the slopes of the log/log plots depend on the temperature, as presented in Figure 1: at 10 and 15°C, the slope is close to 3; at 20°C, the slope is close to 4, and at 25-30-35 and 40°C, the slope is close to 5.

The number of diamide molecules in the second sphere of co-ordination of Ln(III) increases with the temperature of extraction.

The same behaviour has also been observed for the diamide DMDOHEMA though the slopes are lower in this case: 2 at 10°C and 4 at 40°C, for example. So, one can conclude that the number of diamide molecules involved in the extraction of Ln(III) nitrates decreases for malonamides with a central group containing an ether oxygen.

The crystal structures of Ln(III) nitrate solvate of malonamide with an ethyl ethoxy chain indicated the absence of coordination of the ether oxygen with the metal ion [4,11].

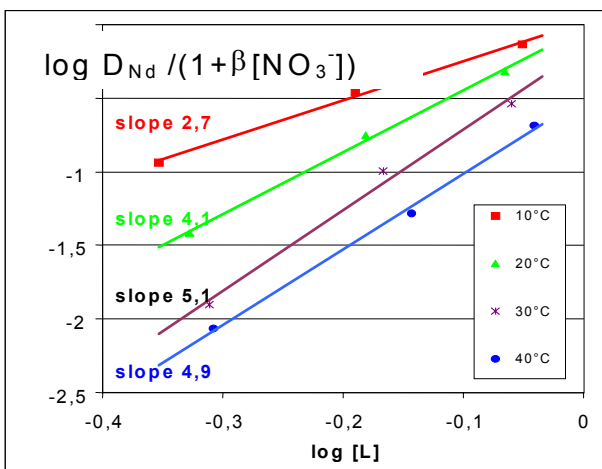


Figure 1. Effect of DMDBTDMA concentration on the extraction of neodymium(III) nitrate from 2.5 M NaNO<sub>3</sub> aqueous solution (pH 5.9-6.0) as a function of temperature.

Previous studies pointed out that the water concentration in the organic phases is higher for malonamides bearing an ethoxy group [1]. Water concentration measurements were done for both diamides DMDBTDMA and DMDOHEMA to compare the number of H<sub>2</sub>O molecules involved in the extraction of neodymium(III) nitrate. When neodymium(III) nitrate is extracted by a diamide, the concentration of water in the organic phase is higher than observed in the absence of Nd(III) (organic phase pre-equilibrated with NaNO<sub>3</sub>). From the data obtained it appears that Nd(III) nitrate is extracted by DMDBTDMA with one molecule of H<sub>2</sub>O and by DMDOHEMA with two molecules of H<sub>2</sub>O. The important role of H<sub>2</sub>O molecules was also pointed out for these systems by molecular modelling and NMR experiments [12] where the presence of a bridging H<sub>2</sub>O molecule between the metal ion and the oxygen ether in the Ln(III) nitrate extracted complex(es) could be an explanation for the better affinity of malonamides possessing an ethoxy group in their central substituent. At a molecular scale, the behaviour of the two diamide extractants seems to present some differences: the presence of more H<sub>2</sub>O molecules can possibly explain the lower number of ligands involved in the extraction of neodymium(III) nitrate by DMDOHEMA.

#### Determination of thermodynamic extraction properties

The Gibbs free energy related to this reaction,  $\Delta_{ext}G' = -RT \cdot \ln K'$  lead to the average value of  $2.4 \pm 0.2 \text{ kJ.mol}^{-1}$  (see some selected values in Table 1).

Table 1. Apparent constant of extraction of Nd(III) nitrate from 2.5 mol.L<sup>-1</sup> aqueous NaNO<sub>3</sub> solution by DMDBTDMA-dodecane solution (25°C ; [Nd]<sub>init</sub> = 0.1 mol.L<sup>-1</sup>).

[diamide] (mol L <sup>-1</sup> )	D <sub>Nd</sub>	K (L <sup>8</sup> .mol <sup>-8</sup> )	$\Delta_{ext}G'$ (kJ.mol <sup>-1</sup> )
0.42 ± 0.01	0.028	0.388	2.34
0.50 ± 0.01	0.056	0.368	2.42
0.66 ± 0.01	0.166	0.391	2.32
1.18 ± 0.05	1.22	0.385	2.36

If we assume that the slopes of the lines presented in Figure 1 are related to a single complex present in the organic phase, we can calculate K<sub>ext</sub> and ΔG'<sub>ext</sub> for each temperature. The corresponding data are presented in Table 2.

*Table 2. Values of  $K'$  and  $\Delta G'$  related to the extraction of Nd(III) nitrate from  $\text{NaNO}_3$  2.5 mol.L<sup>-1</sup> by DMDBTDMA in dodecane (0.5 to 1.1 mol.L<sup>-1</sup>).*

Temperature (°C)	Stoichiometry Nd(III)/diamide	$K'$ (L <sup>8</sup> .mol <sup>-8</sup> )	$\Delta G'$ (kJ.mol <sup>-1</sup> )
10	3	0.48 ± 0.03	+1.7 ± 0.2
15	3	0.35 ± 0.02	+2.5 ± 0.1
20	4	0.34 ± 0.05	+2.6 ± 0.3
25	5	0.37 ± 0.02	+2.4 ± 0.2
30	5	0.22 ± 0.05	+3.8 ± 0.4
35	5	0.21 ± 0.03	+4.0 ± 0.3
40	5	0.11 ± 0.02	+5.6 ± 0.4

The van't Hoff method can be applied only for determinations between 25 and 40°C for which the stoichiometry of complexes is similar: 1/5. The plot  $\log K'$  versus  $1/T$  gives straight lines and the slope gives the value  $\Delta H = -56 \pm 6 \text{ kJ.mol}^{-1}$ .

The microcalorimetric approach is certainly more appropriate here because each determination can be realised for one temperature (here 25°C) and thus for only one stoichiometry of the extracted complex. The quantity of heat measured after each addition of aliquot of organic phase has been divided by the amount of formed complex (*i.e.* organic neodymium transferred to the organic phase) to calculate  $\Delta H$ .

*Table 3. Microcalorimetric determination of enthalpy variations for the extraction of Nd(III) nitrate from  $\text{NaNO}_3$  aqueous solution by DMDBTDMA-dodecane solution.*

(Experimental conditions: 25°C; aqueous phase in vessel: 0.8 mL of  $[\text{Nd}]_{\text{init}} = 0.1 \text{ mol.L}^{-1}$  in 2.5 mol.L<sup>-1</sup>  $[\text{NO}_3^-]$ ; addition of aliquot of DMDBTDMA in dodecane pre-equilibrated with  $\text{NaNO}_3$ .)

[diamide] (mol.L <sup>-1</sup> )	Number and volume of aliquots added	Average heat (mJ)	$n_{\text{Nd}} / \text{each aliquot added (mol)}$	$\Delta_{\text{ext}}H$ (kJ.mol <sup>-1</sup> )
$0.50 \pm 0.01$	9 * 5 $\mu\text{L}$	-1.5 ± 0.1	$2.48.10^{-8}$	-63 ± 5
	20 * 10 $\mu\text{L}$	-3.4 ± 0.1	$5.04.10^{-8}$	-68 ± 5
$0.60 \pm 0.01$	9 * 5 $\mu\text{L}$	-3.3 ± 0.4	$5.0.10^{-8}$	-65 ± 8
$0.82 \pm 0.02$	9 * 5 $\mu\text{L}$	-9.1 ± 0.5	$1.52.10^{-7}$	-58 ± 3
$1.00 \pm 0.03$	9 * 5 $\mu\text{L}$	-12.3 ± 0.5	$3.17.10^{-7}$	-39 ± 3
$1.30 \pm 0.03$	9 * 5 $\mu\text{L}$	-24 ± 0.4	$8.36.10^{-7}$	-29 ± 1
	20 * 10 $\mu\text{L}$	-46.5 ± 1.5	$1.55.10^{-6}$	-30 ± 1

The  $\Delta H_{\text{ext}}$  values presented in Table 3 exhibit important variations with the DMDBTDMA concentration when  $[\text{diamide}] > 0.8 \text{ mol.L}^{-1}$ . This effect may be due to the supramolecular organisation of the Nd(III)-malonamide solvate at high diamide concentrations observed in third phases but also in organic phases in the absence of third phase [4].

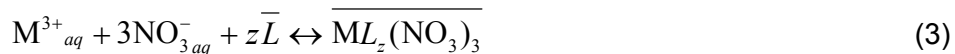
In the diamide concentration range 0.5 to 0.9 mol.L<sup>-1</sup>, the results are the following:  $\Delta H = -63 \pm 5 \text{ kJ.mol}^{-1}$  by microcalorimetry and  $\Delta H = -56 \pm 5 \text{ kJ.mol}^{-1}$  by the classical van't Hoff method in the temperature range 25-40°C. The calculated values of  $\Delta H$  obtained by two different approaches give values that are quite similar. We think that microcalorimetry is certainly the best method for such a complex chemical system and we will try to optimize the experimental conditions to reduce the uncertainties. Moreover, we have to check our first assumption since the slopes of the log/log plots (Figure 1) can represent average values of the stoichiometries of different  $\text{Nd}(\text{NO}_3)_3\text{L}_x$  complexes present in the organic solutions.

However, we can estimate, for [diamide] < 0.9 mol.L<sup>-1</sup>, the variation of entropy for Nd(III) nitrate extraction by DMDBTDMA  $\Delta S = (\Delta H - \Delta G)/T$ :  $\Delta S = -220 \pm 20$  J.K<sup>-1</sup>.mol<sup>-1</sup>.

### Extraction of Eu(III) and Am(III) Nitrates by BTPs

Experiments were conducted with *n*- and iso-BTPs, which exhibited promising efficiency for the separation of Am(III) versus Eu(III) [3,4]. For this system, preliminary determinations were conducted to check the stoichiometry of the reaction (no data were published to date in absence of nitric acid and for a diluent of 100 % octanol-1).

We assumed that the extraction of Eu(III) proceeds in neutral conditions through the formation of solvates according to the following equation:



The ratio of the activity coefficients of the organic species is considered constant, and the thermodynamic activities of the aqueous species were calculated using the Mikulin relation:  $a_{M^{3+}(NO_3)_3} = \gamma_{st}^4 [M(III)][NO_3]^3$  [13]. It was necessary to work with different nitrate concentrations in order to avoid precipitation in organic phase. We then obtained the following apparent extraction constant:

$$K'_{ex} = \frac{[M(III)]_{org}}{[BTP]^z \cdot \gamma_{stoch}^4 \cdot [M(III)].[NO_3]^3} \quad (4)$$

The slope analysis method was applied to treat the distribution ratio data. The log/log plots related to the influence of [free BTP] on  $D_{Eu}$  give straight lines and the slopes obtained are closed to 3 (2.97 for the variation of [free *i*Pr-BTP] from  $1.9 \cdot 10^{-3}$  to  $3.10^2$  mol.L<sup>-1</sup>). These results, compared to previous ones, pointed out that the absence of proton has no influence on the stoichiometry of the reaction:  $x = 3$ . This stoichiometry is not influenced by temperature (measurements were realised at 10 and 40°C).

The second step of this study was the determination of the thermodynamic data related to the M(III) extraction reactions:  $K_{ex}$ ;  $\Delta G_{ex} = -RT \ln K_{ex}$ ;  $\Delta H_{ex}$  and  $\Delta S_{ex}$ , using the van't Hoff method, with  $D_{Eu}$  and  $D_{Am}$  determined for several temperatures.

*Table 4. Gibbs free energy, enthalpy and entropy variations for the extraction of Eu(III) and Am(III) nitrate from aqueous NaNO<sub>3</sub> 2.2 ± 0.2 mol/L solution by BTPs in octanol-1 solution.*

Ligand	Aqueous phase	[BTP] (mol.L <sup>-1</sup> )	$D_{M(III)}$	log $K'$	$\Delta G'$ (kJ.mol <sup>-1</sup> )	$\Delta H'$ (kJ.mol <sup>-1</sup> )	$\Delta S'$ (J.mol <sup>-1</sup> .K <sup>-1</sup> )
<i>n</i> Pr-BTP	Eu as traces	0.01	0.078	6.7 ± 0.1	-38.5 ± 1	-31 ± 6	+25 ± 15
	Am as traces		0.101 5.59 6.69	6.8 ± 0.1 8.5 ± 0.2 8.6 ± 0.2	-	-	+6 ± 10
<i>i</i> Pr-BTP	Eu as traces	0.01	50.3 42.6	9.4 ± 0.3 9.4 ± 0.3	-53 ± 2	-	-
	[Eu] <sub>init</sub> = $10^{-2}$ mol.L <sup>-1</sup>		0.286 0.293	8.7 ± 0.3 8.9 ± 0.3	-50 ± 2	-	-
	0.03	3.38 3.29 4.34	8.8 ± 0.2 8.8 ± 0.2 9.1 ± 0.2	-51 ± 1	-53 ± 8	-7 ± 10	

The main results obtained are presented in Table 4. The behaviours of *n*Pr-BTP and *i*Pr-BTP are similar from a thermodynamic point of view: the extraction reaction is governed by the enthalpy for both BTP extractants. The ligand *i*Pr-BTP exhibits a greater affinity for Eu(III) owing to a more favorable entropic term. The reaction is more exothermic for Am(III) extraction, which can be an indication of the formation of stronger M-N bond between BTP molecules and Am(III) compared to those between BTP and Eu(III). But in the same time, the entropic term becomes less favorable. It could be noticed that  $\Delta S$  is very low compared to results related to the extraction by malonamides.

## CONCLUSION

The preliminary results for the determination of thermodynamic parameters of the extraction of trivalent lanthanide and actinide nitrates showed the complexity of the thermodynamic properties, which involve numerous parameters.

The driving force for the M(III) nitrate extraction by malonamides and *pr*-BTPs from aqueous nitrate solution was always the enthalpic term.

## ACKNOWLEDGEMENTS

The authors are grateful for the financial support from the European Communities Research Programme (Contract PARTNEW - FIKW-CT2000-00087). The BTP molecules were synthesised by D. Guillaneux and S. Garcia-Argote (CEA/DEN/DRCP Marcoule). We warmly thank the referee for his remarks and helpful advice.

## REFERENCES

1. C. Madic and M.J. Hudson (1998), Report EUR n°18038, 208 pp.
2. P. Baron, L. Berthon, M-C. Charbonnel, C. Nicol (1997), *Proc. GLOBAL '97 - Int. Conf. Future Nuclear Systems*, Yokohama, Japan.
3. Z. Kolarik, U. Müllrich, F. Gassner (1999), *Solv. Extr. Ion Exch.*, **17** (5), 1155-1170.
4. C. Madic, M.J. Hudson, J.O. Liljenzin, J.P. Glatz, R. Nannicini, A. Facchini, Z. Kolarik and R. Odoj (2000), Report EUR No. 19149, 287 pp.
5. E.N. Rizkalla, G.R. Choppin (1994), *Handbook on the Physics and Chemistry of Rare Earths*, Vol.18, A.J.Freeman, C.Keller (eds.), North Holland, Amsterdam, pp. 525-529.
6. C. Erlinger, L. Belloni, T. Zemb, C. Madic (1999), *Langmuir*, **15** (7), 2290-2300.
7. P. Byers, M. G. B. Drew, M. J. Hudson N. S. Isaacs, C. Madic (1993), *Polyhedron*, **13** (3), 349-352
8. B.K. McNamara, G.J. Lumetta, B. Rapko (1999), *Solv. Extr. Ion Exch.*, **17** (6), 1403-1421.
9. L. Spjuth, J.O. Liljenzin, M. Skalberg, M.J. Hudson, G.Y.S. Chan, M.G.B. Drew, M. Feaviour, P.B. Iveson, C. Madic (1997), *Radiochim. Acta*, **78**, 39-46.
10. C. Bonnal, J-P. Morel, N. Morel-Desrosiers (1998), *J. Chem. Soc., Faraday Trans.*, **94** (10), 1431-1436.
11. P. Thuery, M. Nierlich, M.C. Charbonnel, J.P. Dognon (1999), *Acta Cryst.*, **C55**, 1434-1436.
12. P. Guilbaud, C. Berthon (2000), Proceedings of Atalante 2000, Avignon, France.
13. B. Mokili (1992), PhD Thesis, University of Paris VI, France.



# AGGREGATION OF THE SOLVATES FORMED IN LIQUID-LIQUID EXTRACTION OF METALLIC CATIONS BY MALONAMIDES: STUDY OF THE Nd(NO<sub>3</sub>)<sub>3</sub> / H<sub>2</sub>O / LiNO<sub>3</sub> / DMDBTDMA / DODECANE SYSTEM

L. Martinet, L. Berthon, N. Peineau, C. Madic\* and T. Zemb\*\*

CEA VALRHO, DEN/DRCP/SCPS/LCSE, Bagnols sur Cèze cedex, France

\*CEA Saclay, DEN, Gif-sur-Yvette cedex, France

\*\*CEA Saclay, DSM/DRECAM/SCM, Gif-sur-Yvette cedex, France

In the framework of the research of a physical model to predict the occurrence of third-phase formation in liquid-liquid extraction, we investigated the malonamide extractant used in the so-called DIAMEX process for partitioning of minor actinides from high-level liquid radioactive wastes. Third-phase transition was studied from a fundamental point of view. The organisation of the organic phases of the system DMDBTDMA / *n*-dodecane / water / neodymium nitrate / lithium nitrate was studied at three levels: 1/ at a macroscopic scale: the phase transition boundaries were determined and quantified by the LOC (limit organic concentration) of solute; 2/ at a molecular scale: the composition(s) of the extracted complex(es) was determined and this give information about the stoichiometry of the organic phase species; 3/ at a supramolecular scale: the critical micellization concentration was measured and the aggregation number was determined. Small Angle Neutron Scattering (SANS) measurements were used to give qualitative information about the size and interactions between the organic aggregates. The observable macroscopic effect, *i.e.*, the phase split of the organic phase with the formation of the third phase, results from an increase of the aggregation number of the DMDBTDMA in the organic phase and an increase of the interactions of these aggregates with the increase of the concentration of the extracted neodymium(III) nitrate.

## INTRODUCTION

In liquid-liquid solvent extraction, the stability of the organic phase, composed at least of two components, *i.e.*, the solvent (diluent) and the extractant, is fundamental for the definition of industrial processes. For a particular extraction system, the risk that the organic phase splits into two layers - phenomenon known as *third-phase formation* - depends essentially on the concentration of the extractant and solutes and of the temperature. This risk can possibly be reduced, by the optimisation of the extractant formula.

In the frame of the research of a physical model to predict the occurrence of third-phase formation, we investigated the malonamide extractant used in the so-called DIAMEX process for partitioning of minor actinides from high-level liquid radioactive wastes. The feasibility of the DIAMEX process has been demonstrated during counter-current "hot" tests with (*N,N'*-dimethyl *N,N*'-dibutyltetradecyl malonamide, (C<sub>4</sub>H<sub>9</sub>(CH<sub>3</sub>)NCO)<sub>2</sub>CH(C<sub>14</sub>H<sub>29</sub>) (DMDBTDMA), which was the first reference molecule of the process [1, 2]. Since few years, studies have been started to consider third phase transition on a fundamental point of view [3-7]. The objectives of the present investigation were to demonstrate the link between the composition boundaries where third-phase formation occurs and the supramolecular interactions between aggregates in the organic phase.

This paper deals with the organisation of the organic phases of the system DMDBTDMA / *n*-dodecane / water / neodymium (III) nitrate / lithium nitrate at three levels:

- At a macroscopic scale, the phase transition boundaries were determined and quantified by the LOC (limit organic concentration) of solutes, before the third phase formation.
- At a molecular scale, the compositions of the extracted complexes were determined and give information about the stoichiometry of the organic phase species.
- At a supramolecular scale, the critical micellization concentration was measured. It represents a change in the organisation of the organic phase. The aggregation number was quantified by vapour pressure osmometry. The organisation of the species in the organic phases was analysed by Small Angle X-Ray Scattering (SAXS) and Small Angle Neutron Scattering (SANS).

## EXPERIMENTAL

### Reagents

DMDBTDMA was provided by Panchim, Lisses, 91, France. Its purity, determined by mass spectrometry, was better than 99%. The diamide was then purified on a silica column to eliminate traces of surface-active compounds [8]. Neodymium nitrate hexahydrate, lithium nitrate and dodecane were reagent grade with purity better than 99%.

### Procedure and Apparatus

The diamide concentrations in organic solutions were determined by pHmetric titration with  $\text{HClO}_4$  in anhydride acetic media. The water content of the organic phases was determined using a Karl Fischer Metrohm KF737 coulometer. The neodymium concentration in each phase was determined by X-ray Fluorescence (Nd  $\text{K}\alpha$  ray at 35-45 keV).

The organic/aqueous interfacial tension measurements were carried out using the drop-weight technique. The organic phases have been systematically pre-equilibrated before measurement with the appropriate aqueous solutions.

The osmometric measurements were carried out using a Knauer Model K7000 vapour pressure osmometer (VPO). The temperature is fixed at 60°C to obtain accurate vapour pressure osmometry measurements. The calibration of the osmometer was performed using bromotetradecane diluted in dodecane because it does not aggregate and using myristic acid because this compound is present as dimers in the dodecane diluent. A period of 20 min was sufficient to reach equilibrium. The organic phases have been systematically pre-equilibrated with the appropriate aqueous solutions. The aggregation of the DMDBTDMA (noted E) can be represented by the general equation :  $n \cdot E = E_n$ , where E corresponds to the momomeric species and  $E_n$  corresponds to the *n*-mere. The average number of aggregation  $N_{\text{average}}$  was determined by the procedure proposed by Buch [9], defined as follows :

$$N_{\text{average}} = \sum (n \cdot [E_n]) / \sum [E_n].$$

Small Angle X-ray Scattering (SAXS) experiments were performed on the Huxley-Holmes, High Flux camera of the small-angle X-ray laboratory in the Service de Chimie Moléculaire, at CEA Saclay. Small Angle Neutron Scattering (SANS) experiments were carried out in the Laboratoire Léon Brillouin, at CEA Saclay. The characteristics of these instruments and the procedure to place the data in a two-dimensional spectra have been reported in previous studies [4, 5, 10].

## RESULTS AND DISCUSSION

### Macroscopic Scale

The phase transition boundaries during neodymium(III) nitrate extraction were determined. Figure 1 shows the phase transition line between the single organic phase (2 phases: *i. e.*, one aqueous and one organic) and the biphasic system (3 phases) issued from its split into a intermediate phase (third phase) and an upper one. Figure 2 presents the LOC (limiting organic concentration) of neodymium nitrate as a function of the DMDBTDMA concentration in the initial organic phase. The LOC value increases strongly with the diamide concentration.

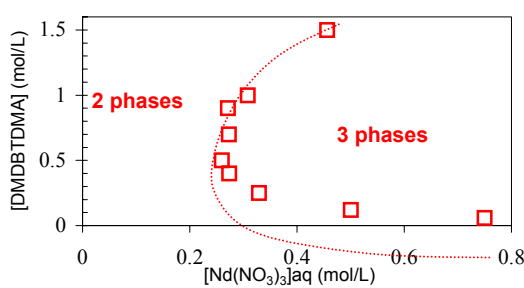


Figure 1. Third phase boundary for neodymium(III) nitrate extraction by DMDBTDMA diluted in dodecane. Aqueous phase: neodymium nitrate in lithium nitrate 1 mol/L, pH=2. Temperature: 23°C.

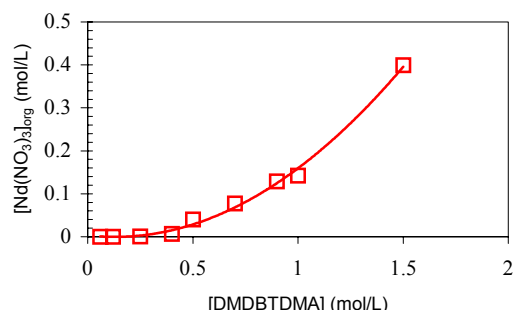


Figure 2. Limiting organic concentration (LOC) of neodymium(III) nitrate as a function of DMDBTDMA concentration in dodecane contacted with neodymium (III) nitrate in lithium nitrate 1 mol/L pH=2. Temperature: 23°C.

### Molecular Scale

Macroscopic variations (splitting of the organic phase into two layers) may have an explanation at molecular scale. Indeed, a modification in the neodymium(III) nitrate extraction mechanism when the apparition of the third phase could account for changes of organic solutes concentrations and thus for third phase formation.

Figure 3 represents the ratio R and R' of neodymium(III) ion *per* DMDBTDMA molecule and water molecule *per* DMDBTDMA molecule corresponding to the LOC values in the organic phases. Thus, it can be concluded that the splitting of the organic phase does not appear for a fixed value of the ratio R or R' of neodymium(III) ion or water molecule *per* extractant molecule. These ratios related to the LOC are dependent on the DMDBTDMA concentration: the slopes of the straight lines  $[\text{Nd}]_{\text{org}}/[\text{DMDBTDMA}]$  and  $[\text{H}_2\text{O}]_{\text{org}}/[\text{DMDBTDMA}]$  as a function of the DMDBTDMA concentration are respectively equal to 0.19 and 0.38. From these data, it is evident that water molecules are co-extracted with neodymium nitrate.

To study the transition between the biphasic and triphasic systems, an organic solution of DMDBTDMA was contacted with several aqueous phase containing increasing neodymium(III) nitrate concentration. Each organic and aqueous phase was analysed and its composition was determined for the two-phase system as well as the three-phase system. Figure 4 represents the ratio of neodymium(III) ion or water molecule (R and R') *per* extractant molecule during the extraction of neodymium(III) nitrate in the organic phase (two-phase system) or in the middle phase (three-phase system). In the upper phase, the concentration of diamide, water and neodymium are not represented because they are very low.

Before third-phase formation, water molecules are coextracted with neodymium(III) nitrate. The ratios  $[Nd]_{org}/[DMDBTDMA]$  R and  $[H_2O]_{org}/[DMDBTDMA]$  R', increase strongly just before the splitting of the organic phase, and after the splitting the ratio  $[Nd]_{org}/[DMDBTDMA]$  R in the third phase continues to increase while the  $[H_2O]_{org}/[DMDBTDMA]$  ratio R' decreases. Thus, one can conclude that the neodymium(III) nitrate extracted species are reorganized in the third phase with the elimination of water.

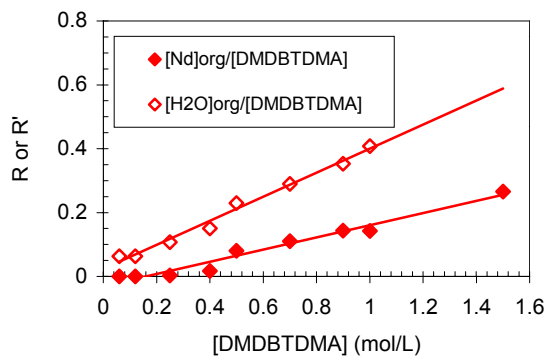


Figure 3.  $[Nd(NO_3)_3]_{org}/[DMDBTDMA]$  and  $[Nd(NO_3)_3]_{org}/[H_2O]$  ratios, R and R', corresponding to the LOC values as a function of DMDBTDMA concentration. Organic phase: DMDBTDMA in solution in dodecane contacted with neodymium(III) nitrate in lithium nitrate 1 mol/L, pH=2. T: 23°C.

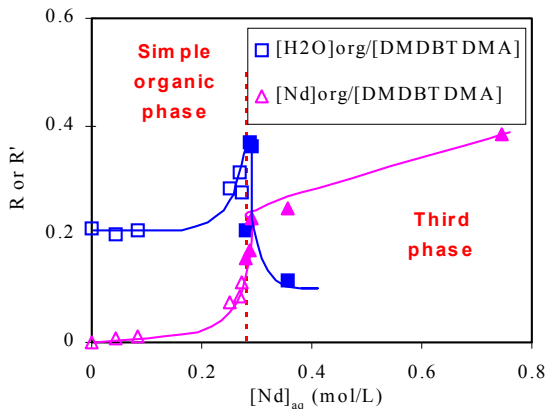


Figure 4.  $[Nd(NO_3)_3]_{org}/[DMDBTDMA]$ ;  $[H_2O]_{org}/[DMDBTDMA]$  ratios, R and R', as functions of  $[Nd(NO_3)_3]_{aq}$ . Organic phase :  $[DMDBTDMA]_{initial}$  0.7 mol/L in dodecane. Aqueous phase: neodymium(III) nitrate in lithium nitrate 1 mol/L pH = 2. T: 23°C.

### Supramolecular Scale: Formation, Size and Interactions of Aggregates

Supramolecular organisation (aggregates formation), if present, could also possibly explain the macroscopic variations of the third phase boundary. Formation of aggregates is characterised by the critical micellization concentration (cmc), above which extractant molecules coexist as monomers and aggregates. Figure 5 represents the interfacial tension at the aqueous / organic interface as a function of the DMDBTDMA concentration for a given aqueous phase containing neodymium(III) and lithium nitrate. The slope rupture indicates the presence of aggregates with a cmc value equal to 0.18 mol/L.

The average aggregation number  $N_{average}$  was determined by VPO. Figure 6 represents the VPO measured signal as a function of the DMDBTDMA concentration for organic solution equilibrated with a given aqueous phase : neodymium nitrate 0.2 mol/L in lithium nitrate 1 mol/L, pH = 2. This signal is compared with those measured for bromotetradecane (monomeric solute) and for myristic acid (dimeric solute). For total DMDBTDMA concentration lower than 0.2 mol/L, the DMDBTDMA does not form aggregates and for total diamide concentration larger than 0.2 mol/L, the average aggregation number is lower than 2: few aggregates are probably present in organic phases.

To understand the role of the neodymium(III) concentration in organic phase on the observed phenomena, we determined by VPO the average aggregation number of different organic solutions of diamide issued from a two-phase system as well as from a three-phase system (Table 1). Figure 7 represents these average aggregation number as a function of the organic neodymium concentration. The aggregation number is slightly dependent on the amide concentration, but it depends of the organic neodymium concentration whatever the amide concentration.

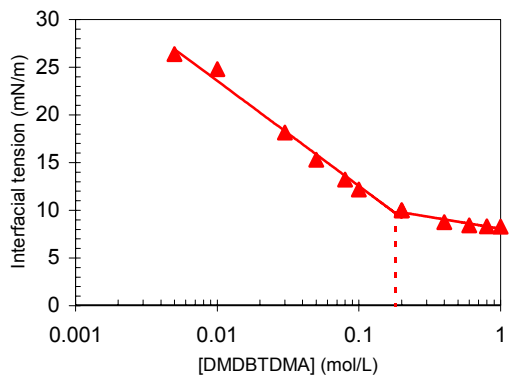


**Figure 5.** Organic / aqueous interfacial tension as a function of [DMDBTDMA].  
Organic phase: DMDBTDMA in solution in dodecane. Aqueous phase: neodymium nitrate 0.2 mol/L, lithium nitrate 1 mol/L, pH=2. T : 23°C.

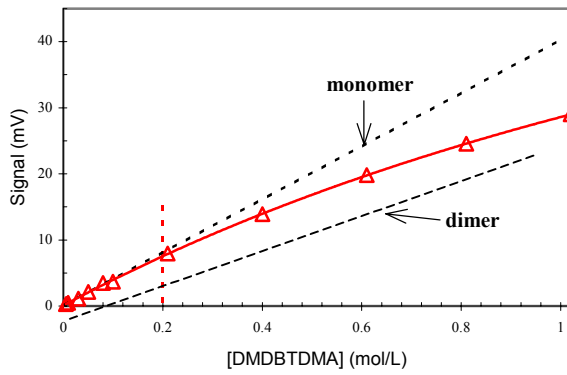


**Figure 6.** Measured signal by vapour pressure osmometry as a function of [DMDBTDMA] at 60°C. Organic phase: DMDBTDMA in solution in dodecane contacted at 23°C with an aqueous phase with the composition: neodymium nitrate 0.2 mol/L, lithium nitrate 1 mol/L, pH=2.

**Table 1.** Average aggregation number determined by vapour pressure osmometry at 60°C.

	[DMDBTDMA] (mol/L)	[Nd] <sub>org</sub> (mol/L)	N <sub>average</sub>
Organic phase	0.1	0.013	1.2
	0.4	0.013	1.2
	0.61	0.015	1.2
	0.81	0.021	1.3
	1.02	0.025	1.4
	0.7	0.003	1.4
	0.7	0.04	1.5
Third phase	0.227	0.02	1.1
	0.93	0.14	2.7
	1.1	0.25	2.9
	1.3	0.4	6.5

Organic phase : DMDBTDMA in solution in dodecane contacted with an aqueous solution containing neodymium nitrate and lithium nitrate 1mol/L, pH=2.

The aggregates were then characterised by SANS experiments to determine interactions and the size of aggregates in the organic phases. The scattered intensity  $I(q)$  of organic phase samples was registered as a function of the scattering vector  $q = (4\pi/\lambda) * \sin\theta$ , where  $2\theta$  is the scattered angle. The scattered intensity  $I(q)$  is relative to the interactions between aggregates for low values of  $q$  [0.001 to 0.1 Å<sup>-1</sup>] and to the shape and size of aggregates for high values of  $q$  [0.1 to 1 Å<sup>-1</sup>].

Qualitative information about the size and their interactions can already be deduced from experimental data. Experimental scattered intensities  $I(Q)$  are represented for [DMDBTDMA] 0.7 mol/L in dodecane contacted with various neodymium(III) aqueous solutions on Figure 8. For high values of  $q$  (from 0.1 to 1 Å<sup>-1</sup>), the intensities spectra are converging towards the same curve. Without even numerical evaluation of models, we know that it is the consequence of constant surface/volume ratio of aggregates. Considering these aggregates

in the first approximation as spheres, we can conclude that the aggregation number is independent on neodymium(III) concentration. This is agreement with the osmometry measurements because the corresponding average aggregation number is about 1.5 for the whole SANS curve.

For low values of  $q$  (0.001 to 0.1  $\text{\AA}^{-1}$ ), the intensities, relative to interactions between aggregates, are increasing with the neodymium(III) concentration. It can thus be concluded that an increase in neodymium concentration induces an increase of attractive interactions between aggregates.

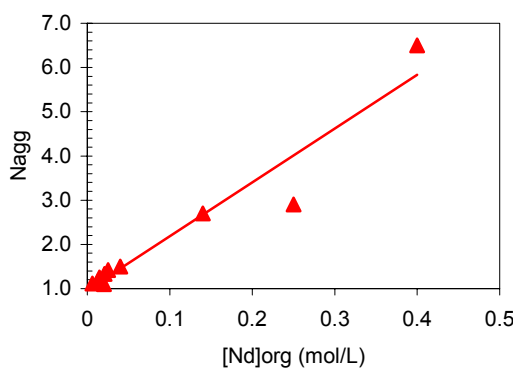


*Figure 7. Average aggregation number determined by vapour pressure osmometry at 60°C as a function of neodymium (III) concentration in organic phase. Organic phase: DMDBTDMA in solution in dodecane contacted with an aqueous solutions of neodymium nitrate and lithium nitrate 1 mol/L, pH=2 at 23°C.*

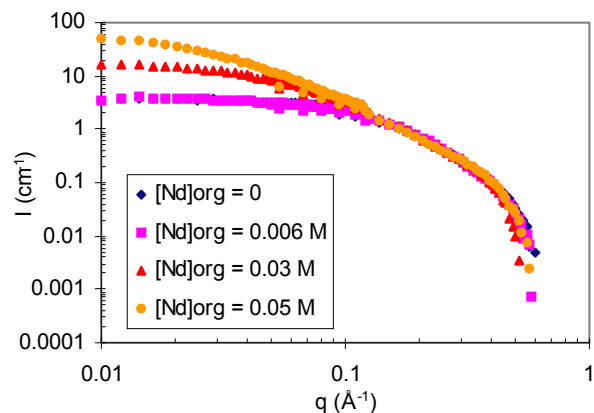


*Figure 8. SANS spectra: experimental scattered intensity  $I(q)$  of organic solutions of DMDBTDMA 0.7 M in dodecane contacted with an aqueous solution of neodymium (III) nitrate and lithium nitrate 1 mol/L, pH=2. Room temperature. The neodymium organic concentrations are reported in the legend.*

## CONCLUSION

This study shows that DMDBTDMA in solution in dodecane does not form aggregates when its concentration is lower than 0.2 mol/L. When the DMDBTDMA concentration is higher than 0.2 mol/L, small aggregates can be formed, the aggregation number being dependent of the concentration of the neodymium(III) nitrate in the organic phase. The increase of the neodymium(III) concentration in the organic phase leads also to an increase of the interactions between aggregates. A thermodynamic model of attractive spheres at short distances (Baxter's model) will be used to quantify aggregate interactions. This model is based on the use of an attractive interaction potential  $U$  that can account for three known interactions that come into play: 1/ the destabilising van der Waals interaction, 2/ the stabilising hard sphere repulsion, and 3/ a repulsive steric contribution from the aliphatic chains of the extractant molecules.

The observable macroscopic effect, namely the phase split of the organic phase with the formation of the third phase, results from an increase of the neodymium(III) concentration in the organic phase which induces an increase of the aggregation number of the DMDBTDMA and an increase of the interactions between these aggregates.

## ACKNOWLEDGEMENTS

The authors are grateful for the financial support from the Commission of the European Communities (Contract PARTNEW – FIKW-CT2000-00087).

## REFERENCES

1. C. Madic, P. Blanc, N. Condamines, P. Baron, L. Berthon, C. Nicol, C. Pozo, M. Lecomte, M. Philippe, M. Masson, C. Hequet and M.J. Hudson (1994), *Proc. Int. Conf. RECOD'94*, London.
2. L. Nigond (1992), Thèse de doctorat, University Clermont-Ferrand II and *Report CEA R5610*.
3. C. Erlinger (1999), Thèse de doctorat, University Parix XI – Orsay and *Report CEA R5834*.
4. C. Erlinger, L. Bellono, T. Zemb and C. Madic (1999), *Langmuir*, **15**, 2290-2300.
5. C. Erlinger, D. Gazeau, T. Zemb, C. Madic, L. Lefrancois, M. Hebrant, C. Tondre (1998), *Solv. Extr. Ion Exch.*, **16** (3), 707-738.
6. L. Lefrancois, F. Belnet, D. Noel and C. Tondre (1999), *Sep. Sci. Technol.*, **34** (5), 755-770.
7. L. Lefrancois, J.J. Delpuech, M. Hebrant, J. Chrisment and C. Tondre (2001), *J. Phys. Chem. B*, **105**, 2251-2564.
8. C. Madic and M.J. Hudson (1998), *Report EUR 18038*.
9. A. Buch, D. Pareau, M. Stambouli and G. Durand (2001), *Solv. Extr. Ion Exch.*, **19** (2), 277-299.
10. J.P. Cotton (1991), Neutrons, X-rays and Light Scattering, P. Lindner and T. Zemb (eds.), North Holland, Amsterdam, p. 3.



# EXTRACTION OF TRIVALENT ACTINIDES AND LONG-LIVED FISSION PRODUCTS BY DIFFERENT CLASSES OF FUNCTIONALIZED CALIXARENES

Jean François Dozol, Alejandro Garcia-Carrera, Véronique Lamare  
and Hélène Rouquette

CEA Cadarache, Saint Paul Lez Durance, France

High and medium level activity liquid wastes arising from nuclear fuel reprocessing contain important concentrations of transplutonium elements (Am, Cm) and fission products including cationic species, such as cesium and strontium, and anionic species, such as pertechnetate or selenate. A strategy developed by CEA is the separation of these long-lived nuclides from these highly acidic solutions. Calixarenes represent a class of cyclic oligomers, offering nearly unlimited possibilities of chemical modification. Several new classes of functionalized calixarenes were synthesised. These compounds, diluted in nitrophenylalkylether, at concentrations ranging from  $10^{-3}$  to  $10^{-2} M$ , display distribution coefficients comparable to those of their podand counterparts used at a hundredfold higher concentration. This improvement of extraction strength is essential to remove the targeted element among many other elements arising from fission.

## INTRODUCTION

Nuclear spent fuels contain both fissile and fertile residues of significant energy value and radioactive products, alpha, beta, gamma and neutron emitters, which make them very irradiant and which release an important amount of heat (mainly due to  $^{90}\text{Sr}$  and  $^{137}\text{Cs}$ , after a five years of cooling process). The radio-toxicity of these fuels can last for millions of years. Reprocessing is of great interest to recover uranium and plutonium, which can be recycled in the form of new nuclear fuels, and to optimise the conditioning of waste.

Acidic solutions arising from the PUREX process contain minor actinides (neptunium, americium, curium) and 99 % of the non-gaseous fission products. Some of these radionuclides have long half-lives:  $^{93}\text{Zr}$  ( $1.5 \times 10^6$  y),  $^{107}\text{Pd}$  ( $7 \times 10^6$  y),  $^{129}\text{I}$  ( $1.7 \times 10^7$  y),  $^{135}\text{Cs}$  ( $3 \times 10^6$  y),  $^{237}\text{Np}$  ( $2.14 \times 10^6$  y). The present strategy is to vitrify these high level activity wastes for disposal or long-term storage. An alternative strategy, studied in France, Japan and Russia, is to separate the minor actinides and the long-lived fission products from these wastes and destroy them by transmutation or dispose of them in specific matrixes. This would also involve the recovery of other fission products,  $^{90}\text{Sr}$  (27.7 y) and  $^{137}\text{Cs}$  (30 y), which would remove about 90 % of the heat released by high activity wastes, allowing their volume to be reduced and thereby facilitating their disposal or their intermediate storage.

## CALIXARENES

Calix[*n*]arenes, cyclic compounds constituted by *n* phenolic units linked by methylene groups, are conformationally mobile. Calix[4]arenes which display four conformations: cone, partial cone, 1-3 alternate, 1-2 alternate, can be tailored for the removal of the different long-lived elements (Figure 1). On this structure, different functions can be substituted for the hydrogen of the phenolic units (narrow rim) or to *p* *tert* butyl groups (wide rim). The different calixarenes studied were synthesised by the Universities of Parma (calix[4]arenes-crown-6, calix[*n*]arenes amides) and Mainz (calixarenes CMPO) within the framework of projects granted by Commission of European Communities.

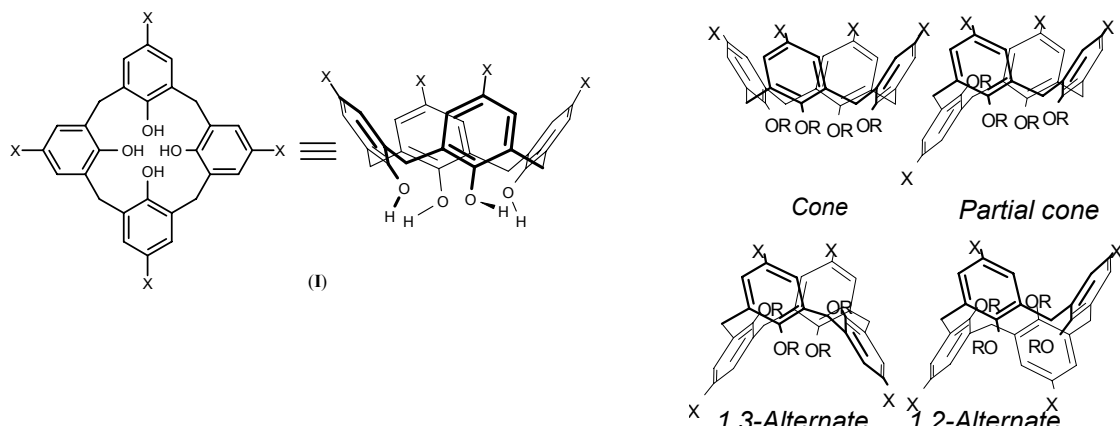


Figure 1. Calix[4]arene and its four conformations.

These calixarenes are exceptionally efficient for the extraction of cesium, specially from high concentration soda media. They allow a quantitative extraction of cesium ( $10^{-3} M$ ) from near saturated soda solutions (NaOH 15 M) (Table 1).

Table 1. Sodium and cesium distribution (*D*) coefficients of *t*-butyl-calix[4]arene,  $10^{-2} M$  in NPHE.

	Composition of different aqueous phases				
	NaOH $10^{-2} M$ NaNO <sub>3</sub> 4 M CsNO <sub>3</sub> $10^{-3} M$	NaOH 2 M NaNO <sub>3</sub> 2 M CsNO <sub>3</sub> $10^{-3} M$	NaOH 4 M CsNO <sub>3</sub> $10^{-3} M$	NaOH 10 M CsNO <sub>3</sub> $10^{-3} M$	NaOH 15 M CsNO <sub>3</sub> $10^{-3} M$
<i>D</i> <sub>Na</sub>	< $10^{-3}$	< $10^{-3}$	< $10^{-3}$	< $10^{-3}$	< $10^{-3}$
<i>D</i> <sub>Cs</sub>	$8 \cdot 10^{-2}$	3.4	11	50	75

## DI ALKOXY CALIXARENES CROWN 6

Crown ethers or cyclic polyethylene glycol being the most efficient extractants of cesium, it seemed interesting to graft this polyethylene glycol moiety on calix[4]arene (Figure 2). Calix[4]arene-crown-*n* compounds consist of a calix[4]arene frame, maintained in the 1-3 alternate conformation by a polyethylene glycol bridge containing *n* oxygen atoms. The two remaining phenolic units are derived with alkyl chains (Figure 3).

Distribution coefficient values and extraction of efficiency of the different compounds are summarized in Table 2. To be efficient, the calixarene crown 6 must adopt the 1-3 alternate conformation; dihydroxy- and diethoxy-calix[4]arenes which are conformationally mobile are less efficient than calix[4]arenes bearing alkyl groups bulkier than ethoxy (such as dipropoxy, diiso-propoxy, dioctyloxy). The latter are much more efficient than benzo or dibenzo 21-crown-7-ethers.

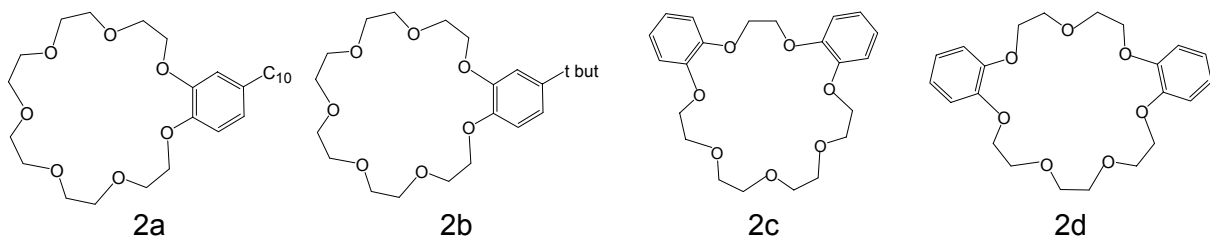


*Figure 2. a: Decyl-benzo-21-crown-7, b: t-butyl-benzo-21-crown-7, c: 2,5-benzo-21-crown-7, d: 3,4-benzo-21-crown-7.*

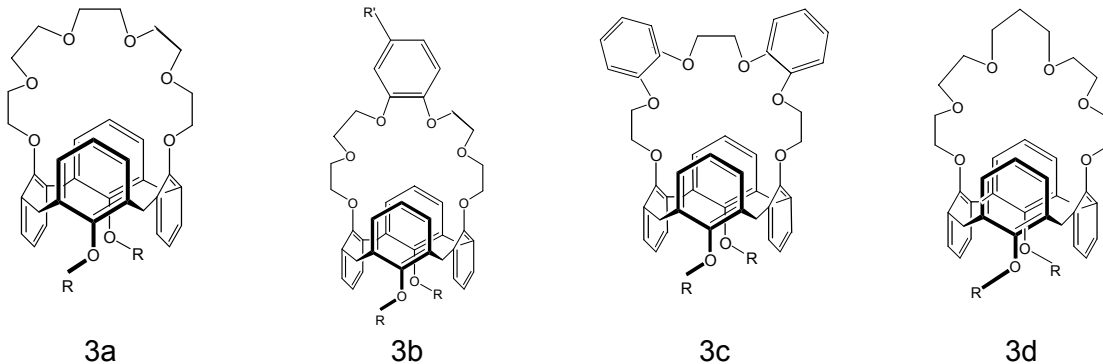


*Figure 3. a: Di-alkoxy-calix[4]arene-crown-6, b: di-alkoxy-calix[4]arene-benzocrown-6, c: di-alkoxy-calix[4]arene-di-benzo-crown-6, d: di-alkoxy-calix[4]arene-propylene-crown-6.*

*Table 2. Cesium distribution (D) coefficients and extraction efficiency (E) for different di-alkoxy-calix[4]arene-crown-6 and 21-crown-7. Aqueous solution :  $MNO_3 5 \times 10^{-4} M$ ,  $HNO_3 1 M$ . Organic solution :  $1 \times 10^{-2} M$  calixarene or crown ether in NPHE.*

Compounds	DCs	E (%)
Di-hydroxy-calix[4]arene-crown-6	$1.2 \times 10^{-2}$	1.2
Di-methoxy-calix[4]arene-crown-6	$4 \times 10^{-2}$	3.8
Di-ethyleneglyco-calix[4]arene-crown-6	4.2	80.8
Di-propoxy-calix[4]arene-crown-6	19.5	95.1
Di-iso-propoxy-calix[4]arene-crown-6	28.5	96.6
Di-iso-propoxy-calix[4]arene-(propylene crown-6)	2.5	71.4
Di-n-octyloxy-calix[4]arene-crown-6	33	97.0
Di-n-octyloxy-calix[4]arene-benzo-crown-6	24	96.0
Di-iso-propoxy-calix[4]arene-(t-oct benzo crown-6)	34	97.1
Di-n-octyloxy-calix[4]arene-dibenzo-crown-6	31	96.9
Di-iso-propoxy-calix[4]arene-(dibenzo-propylene-crown-6)	0.78	43.8
Di-iso-propoxy-calix[4]arene-(di-t-butyl dibenzo-crown-6)	$1.7 \times 10^{-2}$	1.7
Di-methoxy-calix[4]arene-crown-7	$7 \times 10^{-3}$	0.7
n-decylbenzo-21-crown 7	0.3	23
t-butylbenzo-21-crown 7	0.3	23
2,5-dibenzo-21-crown 7	0.52	34.2
3,4-benzo-21-crown 7	0.3	23

Calix[4]arene-crown-4 and calix[4]arene-crown-5 are selective respectively for sodium [1] and for potassium [2], whereas calix[4]arene-crown-6 [3] is selective for cesium, while the size of calix[4]arene-crown-7 is too large for this cation. Increasing the size of the crown by adding one carbon in the polyethylene glycol chain of the crown leads to an important decrease of extracting ability of calixarene-propylene-crown-6. All these trends can be explained by molecular modeling [4].

Like crown ethers, the crowns of calixarenes can include one or two benzene units. Introduction of these units in the crown strongly increases the cesium extraction and reduces that of nitric acid. The very low distribution coefficients displayed by di-iso-propoxy-calix[4]arene-(di-*t*-butyl dibenzo-crown-6) are explained by the presence of four bulky *t*-butyl groups which lead to strains on the crown, which are detrimental to the preorganization of the crown. For all the calixarenes-crowns, extraction of cesium is enhanced as the nitrate concentration increases and reaches a maximum (for a nitric acid concentration ranging between 2 and 3 M) then decreases due to a competitive extraction of nitric acid. For a nitric concentration of 3 M, the distribution coefficients values are respectively for di-octyloxy-calix[4]arene-crown-6, di-octyloxy-calix[4]arene-benzo-crown-6 and di-octyloxy-calix[4]arene-dibenzo-crown-6, 24, 105 and 200 whereas they are 2.2 for the best crown ether (2,5-dibenzo-21-crown 7).

### CALIX[n]ARENES AMIDES

Starting from the observation that Sr<sup>2+</sup>/ Na<sup>+</sup> selectivity in calixarene-amides increases going from calix[4] to calix[6]arenes (Table 3), Parma University prepared a series of calix[6]arene-hexamides and calix[8]arene-octamides which present different substituents at the wide rim (Figure 4).

*Table 3. Sodium and strontium distribution (D) coefficients for different *t*-butyl calix[n]arene-amides. Aqueous solution: MnO<sub>3</sub> 5 × 10<sup>-4</sup> M, HNO<sub>3</sub> 1 M. Organic solution: 10<sup>-2</sup> M for calix[n]arene (n = 4, 5), 5 × 10<sup>-3</sup> calix[6]arene in NPHE.*

Compounds	D <sub>Na</sub>	D <sub>Sr</sub>	D <sub>Sr</sub> /D <sub>Na</sub>
p- <i>t</i> -butyl-calix[4]arene-tetra-di-N-ethyl-amine	12.3	0.11	0.089
p- <i>t</i> -butyl-calix[5]arene-penta-di-N-butyl-amine	0.82	2.3	2.8
p- <i>t</i> -butyl-calix[6]arene-hexa-di-N-ethyl-amine	510 <sup>-3</sup>	3.8	760

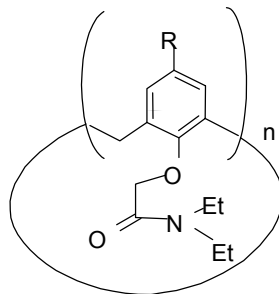


*Figure 4. Calix[n]arene-di-N-ethyl-amine.*

Trends observed when the size of calixarenes increases from tetramer to hexamer are confirmed by the larger calix[8]arene-octa-di-N-ethyl-amine. Some bearing benzyloxy, pentyloxy, octyloxy functionality display an efficiency towards strontium much higher than its counterpart hexamer or than usual extractants of strontium: di-cyclohexano-18-crown-6 or the more lipophilic di-*t*-butyl-di-cyclohexano-18-crown-6. The distribution coefficients depend on the para substituent of calix[8]arene-octa-di-N-ethyl-amine (Table 4). Crowns have to be used at a concentration higher than 10<sup>-2</sup> M in NPHE to be able to remove strontium from

acidic solutions. One has to point out that this efficiency observed for pentyloxy calix[8]arene-octa-di-N-ethyl-amine for a nitric acid concentration of 1 M is maintained for acidities ranging between 1 and 3 M.

*Table 4. Strontium distribution (*D*) coefficients for different calix[8]arene-di-N-ethyl-amide. Aqueous solution:  $MNO_3$   $5 \times 10^{-4}$  M,  $HNO_3$  1 M. Organic solution:  $10^{-2}$  M for calix[n]arenes amide and DC18-crown 6 in NPHE.*

Extractants	$D_{Sr}$
benzyloxy calix[8]arene-octa-di-N-ethyl-amide	20
entyloxy calix[8]arene-octa-di-N-ethyl-amide	30
octyloxy calix[8]arene-octa-di-N-ethyl-amide	24
octyloxy calix[6]arene-hexa-di-N-ethyl-amide	0.80
di-cyclohexano-18-crown-6	0.28
di-t-butyl- di-cyclohexano-18-crown-6	0.43

### CALIX[4]ARENES CMPO

The TRUEX process was developed in the United States for the extraction of actinides and lanthanides, whatever their valence, from high salinity or acidic media. The process uses CMPO or octylphenyl N,N diisobutyl carbamoyl methyl phosphine oxide. It was decided to synthesize calixarenes CMPO in order to combine the extracting ability of CMPO and the preorganization of calixarene (Figure 5). Various compounds were synthesized. All the "CMPO-like" calixarenes were soluble at a very low concentration in NPHE ( $10^{-3}$  M). None of the classical extractants are able to remove actinides from acidic media at this concentration, whereas the dimer extracts plutonium and the trimer extracts americium, in agreement with the stoichiometries of the corresponding CMPO complexes [5].

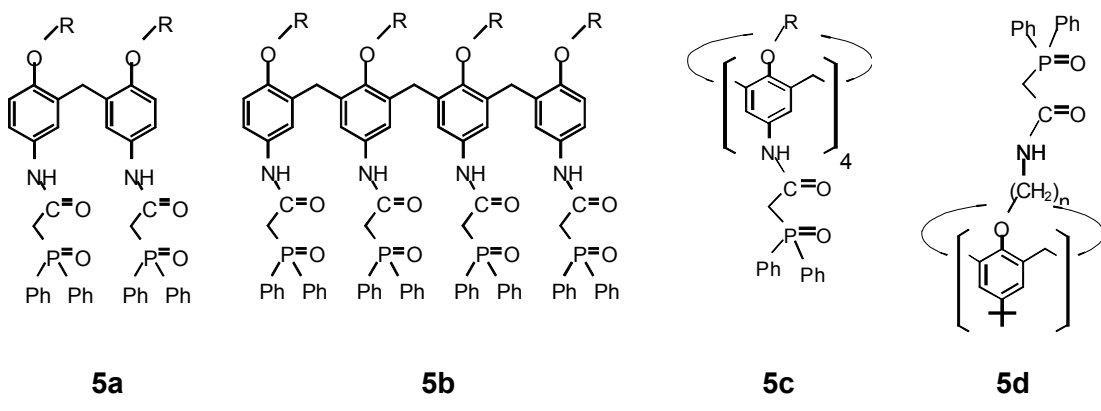


*Figure 5. a: Dimer, b: tetramer, c: wide rim calixarenes CMPO, d: narrow rim calixarenes CMPO.*

Measurements carried out in acidic medium with CMPO, wide rim calixarenes CMPO and the tetramer, acyclic counterpart of the latter show that to obtain comparable distribution coefficients for lanthanides or trivalent actinides (americium, curium), CMPO has to be used at a concentration of 0.25 M while calixarene and tetramer were applied at a concentration of  $10^{-3}$  M. Whereas CMPO and tetramer display a low selectivity among lanthanides, a marked decrease of the distribution coefficients along the lanthanide series is observed for calixarene CMPO. Many other fission products are present in raffinate arising from Purex process (Zr, Nb, Mo, Ru, Rh, Pd...). Some of these elements are significantly extracted by CMPO. Extraction kinetics of some of these elements being slow, organic and aqueous phases were put in contact for three days. On the contrary, except for palladium, where distribution was comparable for CMPO and calixarene CMPO, distribution coefficients for these elements are

very low (Table 5). Calixarenes CMPO are much more selective and enable minor actinides to be separated from most of the fission products except palladium and lightest lanthanides.

One has to also emphasize that calixarenes bearing CMPO on the narrow rim display a different behaviour: distribution coefficients are lower and selectivity is not so marked as for wide rim calixarene CMPO [6]. An other important factor is the length of the arm linking CMPO moieties and calixarene cavity. Increasing the length of the arm ( $n$  varying from 2 to 5) leads to inversion of the order of selectivity among lanthanides.

*Table 5. Zr, Nb, Mo, Ru, Rh, Pd distribution coefficients for CMPO and wide rim calixarene CMPO. Aqueous solution: HNO<sub>3</sub> 1 M, MnO<sub>3</sub> 10<sup>-5</sup> M. Organic solution: 0.25 M for CMPO, 10<sup>-3</sup> M for calix[n]arenes CMPO in NPHE.*

Extractants	Zr	Nb	Mo	Ru	Rh	Pd
CMPO	85	5.5	6	0.09	0.03	185
Calixarene CMPO	0.2	0.1	0.08	0.02	0.03	170

## CONCLUSIONS

Synthesis of many calixarenes demonstrates the interest of this very lipophilic structure, well adapted to liquid-liquid extraction. The comparison of different calixarenes (di-alkoxy-calixa[4]rene-crown-6, calixarene-CMPO ...) with their non-calixarene counterparts (crown-ether, CMPO...) shows an enhancement of extracting abilities and, above all, an exacerbation of selectivity—indispensable properties to remove specific nuclides from solutions containing large amounts of nitric acid and many ionic species often present at higher concentrations. Examples given show that there are many possibilities of synthesis and that in some cases minor changes (size, conformation, rigidification of calixarenes, grafting on one or other rim...) in the structure of calixarenes induce large modifications of extraction properties and selectivity. Moreover, dialkoxy calixarenes crown 6 display good chemical and radiochemical stability. A process was defined for the removal of cesium from acidic high liquid waste and tested on genuine waste arising from PUREX and DIAMEX (actinide removal) processes.

## ACKNOWLEDGEMENTS

The authors thank Prof. Rocco Ungaro (University of Parma) and Prof. Volker Böhmer (University of Mainz) and their teams who synthesized the calixarenes, and the European Commission for financial support under projects EUR 17615 EN and EUR 19605 EN.

## REFERENCES

1. H. Yamamoto, S. Shinkai (1994), *Chem. Lett.*, 1115-1118.
2. Casnati, A. Pochini, R. Ungaro, C. Bocchi, F. Ugozzoli, R.J.M. Egberink, H. Struijk, R. Lugtenberg, F. de Jong, D.N. Reinhoudt (1996), *Chem. Eur. J.*, **2** (4), 436-445.
3. R. Ungaro, A. Casnati, F. Ugozzoli, A. Pochini, J.F. Dozol, C. Hill and H. Rouquette (1994), *Angew. Chem. Int. Ed. Engl.*, **33** (14), 1506-1509.
4. V. Lamare, J.F. Dozol, S. Fuangswasdi, F. Arnaud-Neu, P. Thuéry, M. Nierlich, Z. Asfari, J. Vicens (1999), *J. Chem. Soc., Perkin Trans. 2*, 271-284.
5. F. Arnaud-Neu, V. Böhmer, J.F. Dozol, C. Grütter, R.A. Jakobi, D. Kraft, O. Mauprivel, H. Rouquette, M.J. Schwing-Weill, N. Simon., W. Vogt (1996), *J. Chem. Soc., Perkin Trans. 2*, 1175-1182.
6. S. Barbosa, A. Garcia Carrera, S. E. Matthews, F. Arnaud-Neu, V. Böhmer, J.F. Dozol, H. Rouquette, M.J. Schwing-Weill (1999), *J. Chem. Soc., Perkin Trans. 2*, 719-723.



## MODELLING OF NITRIC ACID AND ACTINIDE / LANTHANIDE EXTRACTION BY CMPO-LIKE CALIXARENES

A. Garcia-Carrera, J.F Dozol,\* P. Dannus, V. Böhmer\*\* and A.M. Sastre-Requena\*\*\*

Commissariat à l'Energie Atomique, CEA-Saclay, Gif-sur-Yvette, France

\* Commissariat à l'Energie Atomique, CEA-Cadarache, Saint Paul lez Durance, France

\*\* Institut für Organische Chemie, Johannes-Gutenberg-Universität, Mainz, Germany

\*\*\* Dept. Chemical Engineering, Universitat Politècnica de Catalunya, Barcelona, Spain

CMPO-like calixarenes are potential alternative extractants for the trivalent actinide/lanthanide separation in nuclear fuel reprocessing. Extraction mechanisms of HNO<sub>3</sub> and actinide/lanthanide cations (Am(III), Cm (III), Eu(III) and Ce(III)) from nitric acid media are investigated for the calix[4]arenes-CMPO. Spectrometric techniques (infrared spectroscopy and mass spectrometry / electrospray ionisation) give information about the way extraction is carried out (chemical groups implied in complexation, complexes formed during cation extraction). Using this information and liquid-liquid extraction results, the extraction of nitric acid and cations have been modelled.

### INTRODUCTION

Nuclear fuel reprocessing is important to reduce the toxicity and volume of waste for disposal. Following PUREX processing, the acidic effluent contains numerous long-lived radionuclides, such as transplutonium elements. Selective extraction of the actinides from lanthanides is a critical step in order to transmute them into short lived or non-radioactive radionuclides. Calix[4]arenes substituted by acetamidophosphine oxide groups (CMPOs) are powerful extractants for trivalent actinides and lanthanides from aqueous nitric acid media. They could be used for the treatment of PUREX effluent.

The substitution of calixarenes on their wide or narrow rim modifies extraction efficiency and separation factors between actinides and lanthanides. Wide rim calixarenes are more efficient extractants than narrow rim congeners for actinides and lanthanides. However the stripping and acid hydrolysis behaviour of calixarenes substituted on their narrow rim make them interesting molecules for study.

### EXPERIMENTAL

Calix[4]arenes-CMPO were synthesised by V. Böhmer's group (University of Mainz, Germany). These extractants (Figure 1) were diluted in NPHE (1,2-nitrophenylhexylether). Extraction experiments were performed by shaking equal volumes of aqueous solutions and organic solvents for one hour at 20°C (equilibrium was reached in a few minutes). Samples were taken for analysis after centrifugation. Acidities were measured by titration with NaOH in aqueous media for respectively aqueous and organic solutions. <sup>241</sup>Am(III), <sup>152</sup>Eu(III), <sup>144</sup>Ce(III) concentration were analysed by  $\gamma$  counting ( $\gamma$  spectrometry). <sup>244</sup>Cm(III) concentration was measured by  $\alpha$  counting (liquid scintillation).

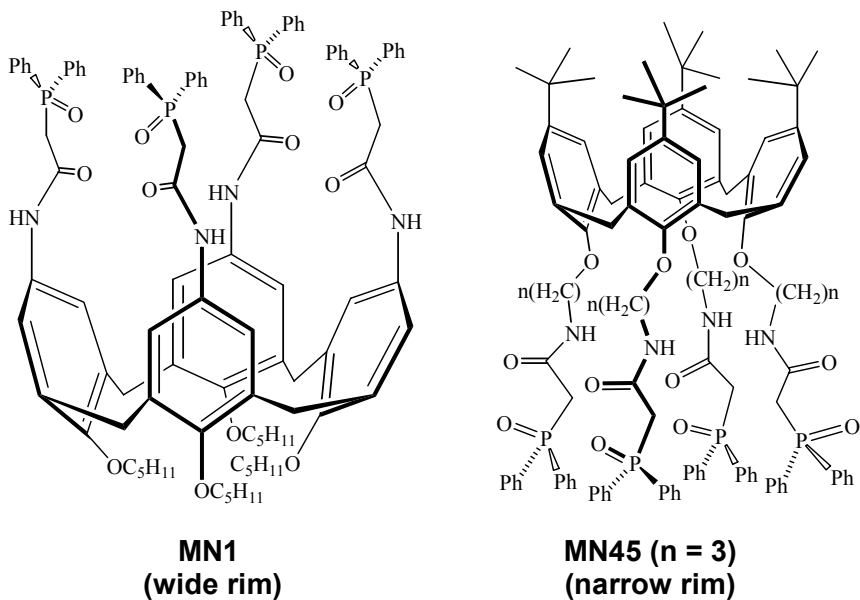


Figure 1. Wide and narrow rim calix[4]arenes-CMPO.

## RESULTS AND DISCUSSION

### Nitric Acid Extraction

The  $\text{HNO}_3$  extraction isotherms for MN1 and MN45 are plotted in Figure 2. This feature shows the presence of species such as  $[(\text{HNO}_3)_n \cdot \text{Calix}]_{\text{org}}$  ( $n = 1 - 6$ ) since the  $\text{HNO}_3$  concentration extracted by the calixarene is  $n$  times higher than that of the extractant, (the nitric acid extraction by the diluent (NPHE) is subtracted).

MN45 extracts more acid than MN1 at high nitric acid concentrations, due to the higher mobility of the structure (alkyl chains linking calixarene platform with the CMPO moieties).

To gain insight into the  $[\text{calix}-\text{HNO}_3]_{\text{org}}$  bonds, the infrared (IR) spectra of  $[\text{calix}(\text{HNO}_3)_n]$  adducts in the organic phase were investigated. Diluents other than NPHE were used to carry out the acid extractions to avoid interferences between diluent and adducts IR bands. Trichlorethane, octanol and chloroform were selected.

For the free calixarene MN1, two main C=O stretching bands at  $1680$  and  $1603 \text{ cm}^{-1}$  were identified (Table 1). A new band was observed ( $\sim 1675 \text{ cm}^{-1}$ ) for the samples after  $\text{HNO}_3$  extraction ( $[\text{HNO}_3] > 1 \text{ M}$ ). In the same way, P=O functions are involved in the nitric acid complexation at high nitric acid concentration. New bands (at lower wave numbers than those of free calixarene) are well defined for  $[\text{HNO}_3] > 4 \text{ M}$ .

The band at  $1550 \text{ cm}^{-1}$  belongs to the aromatic groups (calixarene platform). For nitric acid concentrations ( $[\text{HNO}_3]_{\text{aq},\text{init}}$ ) higher than  $4 \text{ M}$ , a shoulder at lower wave numbers ( $1535 \text{ cm}^{-1}$ ) appeared, becoming a new band at  $[\text{HNO}_3]_{\text{aq},\text{init}} 7 \text{ M}$ . This drift could indicate that aromatic units are involved in the nitric acid extraction at high acid concentration.

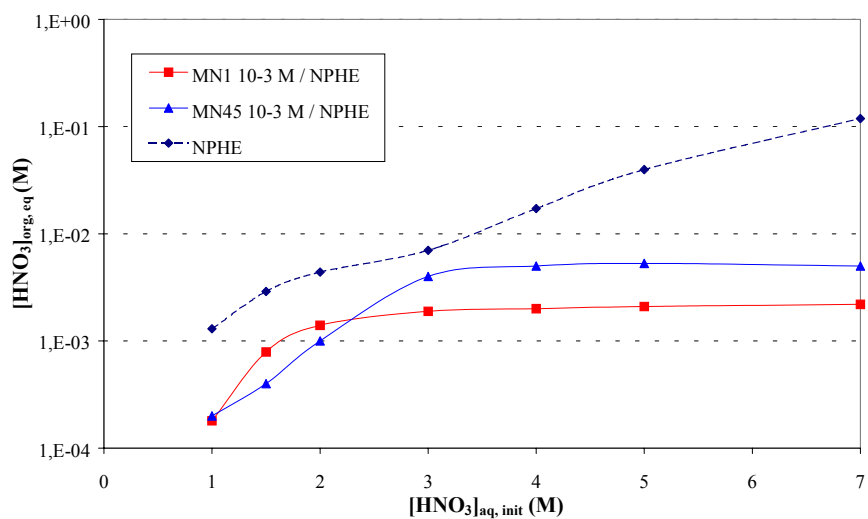


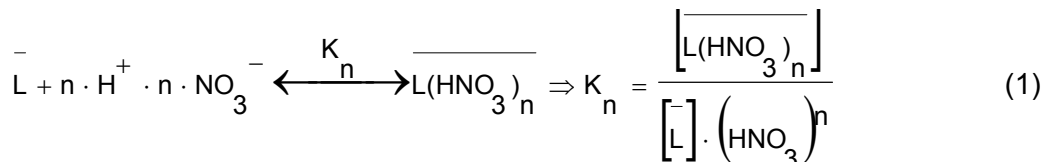
Figure 2. Nitric acid extraction by MN1, MN45 and NPHE.  
[MN1] = [MN45] = 10<sup>-3</sup> M in NPHE (T = 20°C).

Taking into account the IR results (C=O (mainly), P=O and aromatic groups involved in the acid extraction at high nitric acid concentration), numerous complexes [calix(HNO<sub>3</sub>)<sub>n</sub>]<sub>org</sub> are formed in the organic phase during extraction (Table 1).

Table 1. IR Spectra of MN1. Nitric acid extraction.  
[MN1] = 10<sup>-2</sup> M in CHCl<sub>3</sub> // [HNO<sub>3</sub>] variable (T = 20°C)  
Solid sample (evaporation of CHCl<sub>3</sub>)/ KBr pellet.

IR bands (wave numbers, cm <sup>-1</sup> )						
	MN1	0.1 M HNO <sub>3</sub>	1 M HNO <sub>3</sub>	3 M HNO <sub>3</sub>	5 M HNO <sub>3</sub>	7 M HNO <sub>3</sub>
$\nu_{PO}$	1218	1215	1215	1216	1219 (1203)	1203
	1180	1180	1180	1180	1160	1160
$\nu_{CO}$	1680	1680	1680 (1670)	1680 (1670)	1680 (1670)	1653 (1680)
	1603	1603	1603	1603	1603 (1590)	1590
$\nu_{Ph}$	1552	1552	1552	1552	1552 (1533)	1532

The general extraction equilibrium can be written in which bars indicate organic species (assuming that the activity coefficients are constant in the organic phase),



where parenthesis indicate activities and brackets concentrations. Activity coefficients for aqueous HNO<sub>3</sub> solutions were taken from [1]. Assuming constant activity coefficients in the organic phase. Total extractant concentration is constant. The organic acid concentration is very low compared with the “diluent concentration”, so, all the organic species were mainly surrounded with diluent molecules.

The free extractant concentration can be written,

$$[\bar{L}] = \frac{[L]_0}{1 + K_1 \cdot (HNO_3) + K_2 \cdot (HNO_3)^2 + \dots + K_n \cdot (HNO_3)^n} \quad (2)$$

Introducing values of the effective constants,  $K_n$ , we obtain the free calixarene concentration, which may be used to calculate the organic  $HNO_3$  concentration. This calculated concentration is compared with the experimental value.

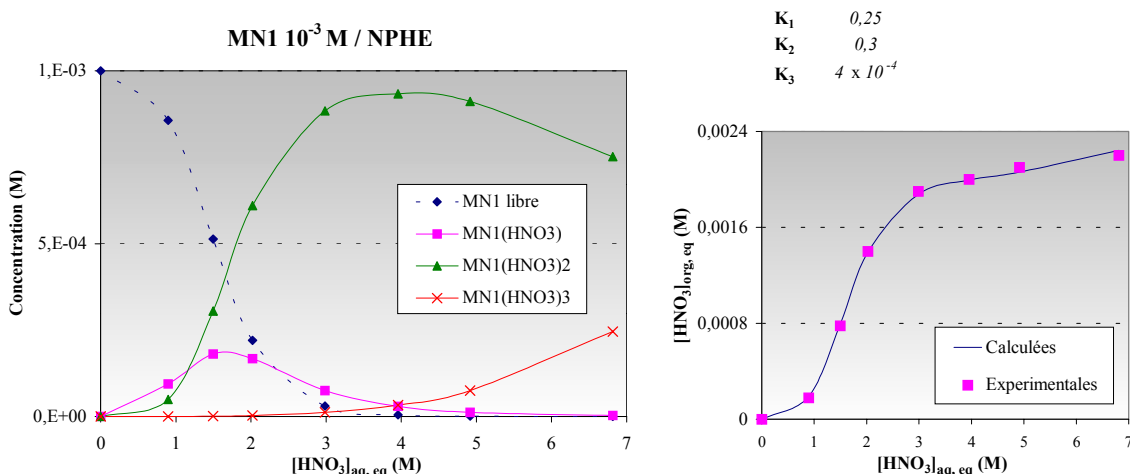


**Figure 3. Extraction of  $HNO_3$  by  $[MN1] = 10^{-3} M$  in NPHE ( $T = 20^\circ C$ ).**  
*Distribution of organic species with respect to the aqueous acidity.*  
*Calculated and experimental  $HNO_3$  extraction isotherms.*

The concentration of each species, for MN1, as a function of  $[HNO_3]_{aq, eq}$ , and the fit of calculated and experimental values, are illustrated in Figure 3. It can be seen that free MN1 was the main species for nitric acid concentration lower than 1.5 M, but for higher  $HNO_3$  concentrations,  $[MN1(HNO_3)_2]_{org}$  predominated.

In the case of MN45, for low nitric acid concentrations, results were similar to those for MN1, but for  $HNO_3$  concentrations higher than 2.5 M, the main species was  $[MN45(HNO_3)_5]_{org}$ , and  $[MN45(HNO_3)_6]_{org}$  was not negligible for high acidities. A good fit of the model to the experimental data was obtained.

### Cation Extraction

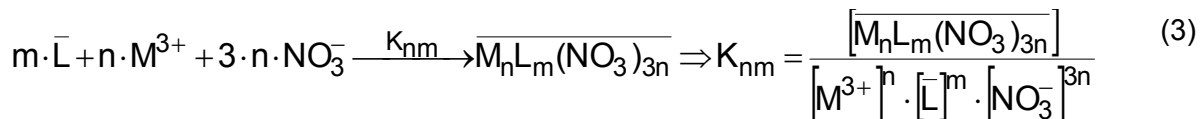
The study of the extraction of the different lanthanides from a highly acidic medium by CMPO like calixarenes demonstrates the ability of these compounds to extract these cations. A sensible discrimination occurs between trivalent actinides and lanthanides and among the trivalent lanthanides [2,3,4].

The IR spectra results illustrated that calixarene coordination sites were the oxygen of P=O (mainly) and C=O groups. Table 2 shows the changes of the C=O and P=O vibration bands as a function of the lanthanide. For the best extracted (i.e. the lightest) cations, a shift of the C=O and P=O IR bands, towards lower wave numbers, appears in comparison with the free calixarene IR spectrum.

*Table 2. IR Spectra of MN1. Lanthanide extraction.*  
 $[MN1] = 10^{-2} M$  in  $CHCl_3 // [Ln(NO_3)_3] = 10^{-2} M // [HNO_3] = 1M$  ( $T = 20^\circ C$ ).  
 Solid sample (evaporation of  $CHCl_3$ ) / KBr pellet.

	MN1	La	Ce	Nd	Sm	Eu	Gd	Dy	Er	Lu
$\nu_{PO}$ ( $cm^{-1}$ )	1183		1162	1163	1164	1163	1164	1162	1182	1184
$\nu_{CO}$ ( $cm^{-1}$ )	1678	1675	1676	1677	1678	1678	1678	1679	1676	1679
		1617	1617	1614	1612	1611	1610	1606	1605	1606
		1653	1653	1653	1653	1653				

The extraction of a metallic cation,  $M^{3+}$ , by a calixarene, L, is described by the equilibrium,



Taking into account the ES/MS spectra, three different stoichiometries, 1:1, 1:2 and 2:1, (calixarene : cation) can be considered. So, the equilibrium extractant concentration can be written,

$$[L]_{eq} = [L]_0 - [L]_{acid} - \left\{ K_{11} \cdot [M^{3+}] \cdot [L]_{eq} \cdot [NO_3^-]^3 + 2 \cdot K_{12} \cdot [M^{3+}] \cdot [L]_{eq}^2 \cdot [NO_3^-]^3 + K_{12} \cdot [M^{3+}]^2 \cdot [L]_{eq} \cdot [NO_3^-]^6 \right\} \quad (4)$$

We consider that certain acid species,  $[(HNO_3)_n \text{ Calix}]$  (with  $n < 5$ ), extract cations in the same way that free calixarene. After protonation of the four carbonyl functions, phosphoryl groups can be protonated. We assume that phosphoryl protonation prevents cation extraction.

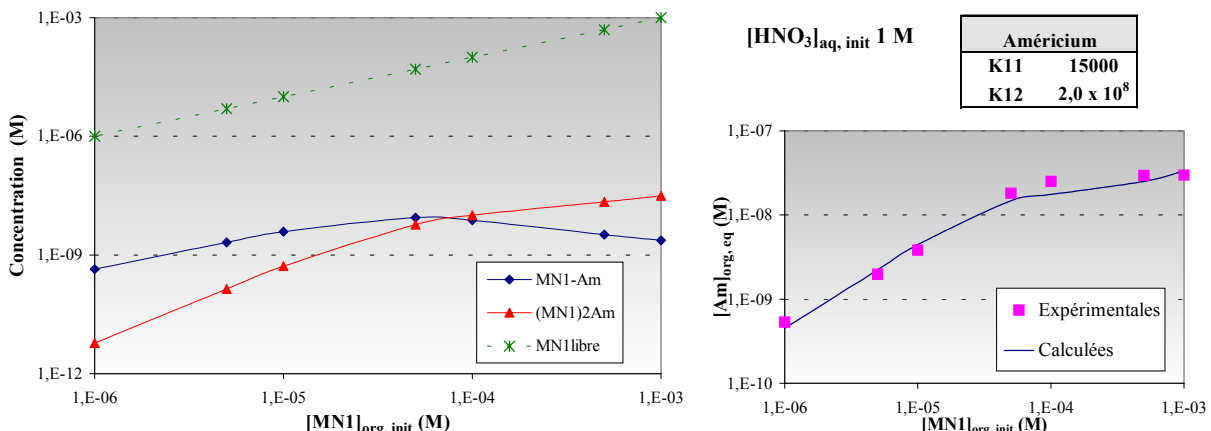


*Figure 4. Extraction of Am by  $[MN1] = 10^{-3} M$  in NPHE ( $T = 20^\circ C$ ).*  
*Distribution of organic species with respect to calixarene concentration.*  
*Calculated and experimental americium extraction values.*

When the cation concentration is very low in comparison with the calixarene concentration, two main species are involved in the extraction  $[(\text{calix})_n M]_{\text{org}}$  ( $n=1,2$ ), for every cation (lanthanide or actinide) and calixarene (MN1 or MN45). The proportion of  $[(MN1)_2 M]_{\text{org}}$  increased with the calixarene concentration. A good fit of the model with the experimental data was obtained (Figure 4).

When the cation concentration is comparable to or higher than that of calixarene, the species  $[MN1(M)_2]_{\text{org}}$  can dominate. Also, when the aqueous solution contains two different cations, the species  $[MN1(M_1)(M_2)]_{\text{org}}$  were taken into account to fit the model to the experimental data. These species were identified by ES/MS.

On the other hand, for high cation and nitric acid concentration, nitric acid extraction can compete with that of the cation. Figure 5 illustrates the fit of the model to the experimental data for the joint extraction of  $\text{Eu}^{3+}$  and  $\text{Ce}^{3+}$  by MN45 taking into account the following three hypotheses in relation to the ability of the acid species  $[\text{MN45}(\text{HNO}_3)_n]$  to extract cations: (1) All the acid species  $[\text{MN45}(\text{HNO}_3)_n]$  behave like free MN45, (2)  $[\text{MN45}(\text{HNO}_3)_n]$  ( $n = 1 - 4$ ) behave like free MN45, but not for  $n = 5, 6$  and (3) No acid species  $[\text{MN45}(\text{HNO}_3)_n]$  behaves like free MN45.

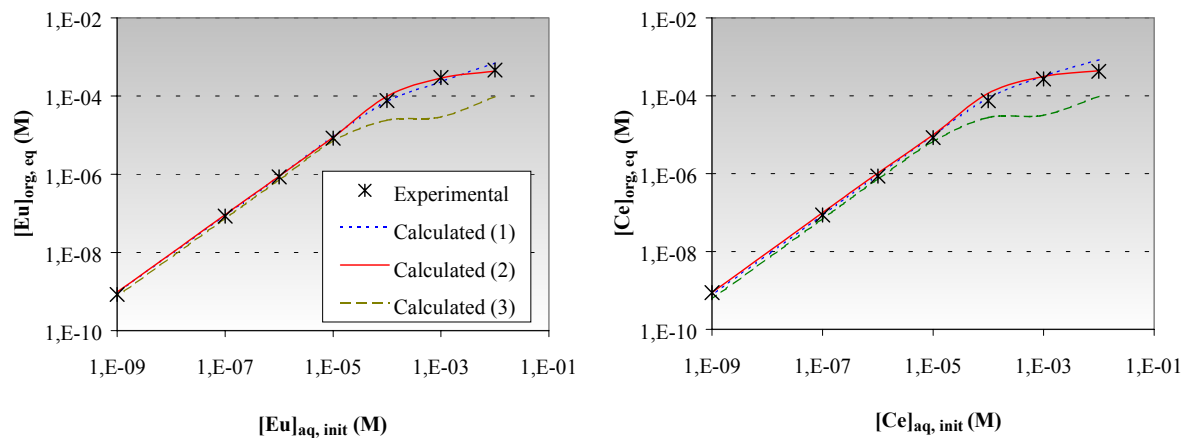


Figure 5. Extraction of  $\text{Eu}^{3+}$  and  $\text{Ce}^{3+}$  by MN45.  
 $[\text{MN45}] = 10^{-3} \text{ M}$  in NPHE /  $[\text{Eu}^{3+}] = [\text{Ce}^{3+}]$  variable /  $[\text{HNO}_3] = 3 \text{ M}$  ( $T = 20^\circ\text{C}$ ).  
 Calculated and experimental Eu and Ce extraction isotherms.

Model (1) performs better than Model (2), but for the highest cation concentration, it overestimates the calculated concentration. Modelling of cation extraction at higher nitric acid concentration could help to elucidate if only certain acid species,  $[\text{MN45}(\text{HNO}_3)_n]$ ,  $n < 5$  can extract cations like free MN45 – assuming that carbonyl groups are protonated but the phosphoryl groups are available for cation complexation.

## CONCLUSIONS

The extraction of  $\text{HNO}_3$  by CMPO-like calixarenes occurs through the formation of numerous organic species. Nitric acid is linked by hydrogen bonds to the carbonyl functions. Moreover, phosphoryl and phenyl groups seem to be implicated in the complexation of  $\text{HNO}_3$  at high nitric acid concentrations.

On the other hand, the extraction of the trivalent lanthanides and actinides by the wide rim calixarenes is more efficient than that of the narrow rim ones. Nitric acid complexation prevents cation extraction, when coordination sites, mainly phosphoryl groups, are “taken up” by  $\text{HNO}_3$  molecules.

A good fit of the model with the experimental data was obtained for  $\text{HNO}_3$  and cation extraction by CMPO-like calixarenes.

## REFERENCES

1. W. Davis and J. H. de Bruin (1968), *J. Inorg. Nucl. Chem.*, **26**, 1069-1083.
2. S. Barboso, A. Garcia Carrera, S. E. Matthews, F. Arnaud-Neu, V. Böhmer, J. F. Dozol, H. Rouquette and M. J. Schwing-Weill (1999), *J. Chem. Soc., Perkin Trans.*, 2, 719-723.
3. L. Delmau, N. Simon, M. J. Schwing-Weill, F. Arnaud-Neu, J. F. Dozol, S. Eymard B. Tournois, C. Grütter, C. Musigmann and A. Tunayar (1998), *Chem. Comm.*, 1627-1628.
4. S. E. Matthews, M. Saadioui, V. Böhmer, S. Barboso, F. Arnaud-Neu, M. J. Schwing-Weill, A. Garcia Carrera and J. F. Dozol (1999), *J. Prakt. Chem.*, **341** (3), 264-273.



## **EXTRACTION OF ACTINIDES AND LANTHANIDES WITH DIPHENYL[DIBUTYLCARBAMOYLMETHYL]PHOSPHINE OXIDE IN THE ABSENCE OF A SOLVENT**

**B. F. Myasoedov, Yu. M. Kulyako, D. A. Malikov, T. I. Trofimov and M. K. Chmutova**

V. I. Vernadsky Institute of Geochemistry and Analytical Chemistry,  
Russian Academy of Sciences, Moscow, Russia

It is established for the first time that solid diphenyl[dibutylcarbamoylmethyl]phosphine oxide (DPBCMPO) forms liquid phases ("liquid reagent") non-miscible with acid solutions on contact with mineral acids. It is found that the compositions of liquid reagent correspond to DPBCMPO· $\text{HNO}_3 \cdot n\text{H}_2\text{O}$  and 2DPBCMPO· $\text{HAn} \cdot n\text{H}_2\text{O}$ , where HAn is  $\text{HClO}_4$  or HCl. The compositions of nitrate and perchloric complexes of liquid reagent with U(VI) and Nd(III) are found. Extraction of a number of actinides in various oxidation states as well as extraction of some lanthanides by liquid reagent in the absence of organic solvent is studied. It is shown that in case of extraction by liquid reagent, distribution ratios increase in comparison with usual solvent extraction. It is established that the complex of the reagent with nitric acid has redox properties resulting in a change of valence states of some actinides in the process of extraction. The use of inert matrices containing DPBCMPO is suggested for isolation and immobilization of actinide and rare-earth elements by vitrification.

### **INTRODUCTION**

Solvent extraction is a simple, effective, express and selective method of isolation and separation of the elements. Nevertheless, the most serious deficiency in this method is the necessity to use large volumes of organic solvents, many of which are volatile, combustible, flammable, toxic and explosive liquids. A number of untraditional systems were developed to avoid the use of organic solvents. Two-phase aqueous systems based on polyethylene glycol, where the second aqueous phase enriched by the polymer is formed as a result of influence of salts on water structure, are such systems [1]. Aqueous systems, aliquation of which is conditioned by chemical interaction of the constituents of aqueous solution being in definite molar ratios, were suggested [2, 3]. The systems "water–antipyrine-pyrocatechol" [2], "water-antipyrine-monochloracetic acid" [3] and others are examples. Solvent-free extraction systems using liquid reagent (for example, 100% tributylphosphate [4]) as an extracting phase are known.

Earlier [5] the study on solubility of such bidentate neutral organophosphorus compounds (BNOC) such as diphenyl[dibutylcarbamoylmethyl]phosphine oxide (DPBCMPO) in nitric acid solutions has shown that the solid like-powder reagent changed its aggregative state from solid to liquid on contacting with the acid. The liquid phase formed, which is immiscible with water ("liquid reagent"), was a complex of the reagent with the acid, and it had high extraction capability with respect to Am(III), Cm(III) and Pr(III) [6, 7]. In further works [8-11] we studied an influence of various factors on both changes of aggregative state of the reagent and its extraction capability with respect to lanthanides and actinides in various valence states. The results of these works, as well as new data regarding the systems DPBCMPO –  $\text{HClO}_4$  and DPBCMPO – HCl are presented in this work.

## RESULTS

### Interaction of DPBCMPO with Mineral Acids

Visual examination of the processes occurring in the system solid DPBCMPO–mineral acid has shown that an irregular lump covered by an oily layer is formed immediately after mixing the components. On subsequent stirring the lump becomes gel-like and develops into a drop on centrifuging. The formation of a "liquid reagent" is observed at acid concentrations  $\geq 0.8$  M  $\text{HClO}_4$ ,  $\geq 2$  M  $\text{HNO}_3$  [6] and  $\geq 4$  M HCl. Transformation of the solid reagent into a liquid one is accompanied by an increase of its weight. The correlation coefficient, which takes into account this increase, is equal to  $1.266 \pm 0.015$ . The density of nitrate "liquid reagent" is equal to  $1.163 \pm 0.012$  g/cm<sup>3</sup> [7]. Thus, for nitric acid solutions one can determine the weight of liquid reagent and its volume, knowing the weighed portion of dry reagent.

The compositions of liquid reagent formed on contacting DPBCMPO with  $\text{HNO}_3$ ,  $\text{HClO}_4$  and HCl solutions were determined (Table 1). The results show that the average molar ratio of the reagent to bound acid is close to 1 in the case of nitrate liquid reagent. Therefore, composition of nitrate liquid reagent corresponds to the formula  $\text{DPBCMPO} \cdot \text{HNO}_3 \cdot n\text{H}_2\text{O}$  [7, 8]. For perchloric and hydrochloric acids, the reagent/acid ratio is close to 2 and compositions of liquid reagents in this case are expressed as  $2\text{DPBCMPO} \cdot \text{HAn} \cdot n\text{H}_2\text{O}$ , where An is the acid anion. The formation of bi-solvate was noticed earlier during extraction of perchloric acid by the solutions of carbamoylmethylphosphine oxides [12], dioxides [13] and carbamoylmethylphosphonates [14] in organic solvents.

*Table 1. Composition of "liquid reagent" formed on contacting DPBCMPO with  $\text{HNO}_3$ ,  $\text{HClO}_4$  and HCl solutions.*

HAn (acid)	Initial concen- tration of HAn, M	Weighed portion of DPBCMPO, mole	Quantity of absorbed HAn, mole	Ratio DPBCMPO:HAn
$\text{HNO}_3$	3.947	$8.11 \times 10^{-4}$	$6.99 \times 10^{-4}$	1
	6.464	$8.54 \times 10^{-4}$	$8.82 \times 10^{-4}$	
	8.143	$10.98 \times 10^{-4}$	$11.69 \times 10^{-4}$	
$\text{HClO}_4$	0.868	$2.79 \times 10^{-4}$	$1.37 \times 10^{-4}$	2
	1.742	$2.77 \times 10^{-4}$	$1.38 \times 10^{-4}$	
	3.012	$2.85 \times 10^{-4}$	$1.30 \times 10^{-4}$	
HCl	4.685	$6.16 \times 10^{-4}$	$2.93 \times 10^{-4}$	2
	6.130	$7.77 \times 10^{-4}$	$3.91 \times 10^{-4}$	
	7.124	$8.85 \times 10^{-4}$	$4.35 \times 10^{-4}$	

The solubility of  $\text{DPBCMPO} \cdot \text{HNO}_3 \cdot n\text{H}_2\text{O}$  in 3 M nitric acid solution, where  $n = 2-3$ , is 1.76 g/L [5, 7]. The solubility of perchloric DPBCMPO as liquid reagent in 3 M  $\text{HClO}_4$  solution ( $2.5 \pm 0.5$  g/L) is higher than it is in 3 M  $\text{HNO}_3$  solution.

### Solvent-free Extraction of Np, Pu and Am in Various Oxidation States by "Liquid Reagent" (LR) from $\text{HNO}_3$ Solutions

Solvent-free extraction of the actinides in various oxidation states by liquid reagent (LR) from nitric acid solutions was studied. In all the cases, a weighed portion of dry reagent (DPBCMPO) was introduced into the solution containing the actinides. The heterogeneous system was stirred for 3 minutes followed by centrifuging for 10 minutes to separate the phases. Time of contact of the reagent with acid solution was sufficient for its transformation into a liquid. The data obtained are presented in Table 2. It is seen, that the efficiency of actinides extraction depends on their valence state and decreases in the following order: IV > VI > III > V. The concentration factor of actinides varies from 20 to 66.

*Table 2. Solvent-free extraction of the actinides in various oxidation states by “liquid reagent” from 4 M HNO<sub>3</sub> solutions.*

M <sup>n+</sup>	[M <sup>n+</sup> ], M		V, mL (aq. ph.)	DPDPCMPO, mole	V, mL (org. ph.)	D*	E*, %
	Initial solution	Aqueous phase					
Np(IV)	1.50×10 <sup>-3</sup>	6.20×10 <sup>-6</sup>	1.2	4.4×10 <sup>-5</sup>	0.018	1.6×10 <sup>4</sup>	99.96
Np(V)	1.47×10 <sup>-3</sup>	8.44×10 <sup>-4</sup>	1.2	3.6×10 <sup>-5</sup>	0.015	59.3	42.60
Np(VI)	1.72×10 <sup>-3</sup>	2.10×10 <sup>-5</sup>	1.2	4.4×10 <sup>-5</sup>	0.018	5.4×10 <sup>3</sup>	98.78
Pu(III)	3.01×10 <sup>-3</sup>	4.44×10 <sup>-5</sup>	1.5	8.1×10 <sup>-5</sup>	0.033	3.0×10 <sup>3</sup>	98.53
Pu(IV)	3.30×10 <sup>-3</sup>	8.80×10 <sup>-6</sup>	1.5	8.1×10 <sup>-5</sup>	0.033	1.7×10 <sup>4</sup>	99.73
Pu(VI)	3.59×10 <sup>-3</sup>	9.90×10 <sup>-5</sup>	1.5	8.1×10 <sup>-5</sup>	0.033	1.6×10 <sup>3</sup>	97.23
Am(III)	0.81×10 <sup>-3</sup>	1.50×10 <sup>-5</sup>	1.2	8.1×10 <sup>-5</sup>	0.033	1.9×10 <sup>3</sup>	98.15
Am(V)	1.55×10 <sup>-3</sup>	0.72×10 <sup>-3</sup>	1.2	8.1×10 <sup>-5</sup>	0.033	41.9	53.54
U(VI)	1.50×10 <sup>-3</sup>	9.10×10 <sup>-6</sup>	1.0	1.0×10 <sup>-4</sup>	0.050	3.3×10 <sup>3</sup>	99.40

(\*) – distribution ratio (D) and extraction efficiency (E) were calculated according to the formulas: D = C<sub>org.</sub>/C<sub>aq.</sub>; E = [D/(D+V<sub>aq.</sub>/V<sub>org.</sub>)].100.

Np(IV), Np(VI), Pu(IV) and Pu(VI) do not change valence state during extraction by the liquid reagent. At the same time Pu(III), Np(V) and Am(VI) change valence state to Pu(IV), Np(VI) and Am(III), Am(V), respectively. Therefore, the reagent has redox properties. Taking into account the values of formal redox potentials of Pu(IV)/Pu(III), Np(VI)/Np(V) and Am(VI)/Am(V) pairs equal to +0.982 V, +1.37 V and +1.60 V, respectively [15], its redox potential may be evaluated as about +1.5 V.

### Solvent-free Extraction and Solvent Extraction of Actinides and Lanthanides by DPDPCMPO from Nitric Acid Solutions

It was of interest to compare efficiency of extraction of the elements from nitric acid solutions by DPDPCMPO as LR with the efficiency of extraction with the same quantity of DPDPCMPO in organic solvent (liquid-phase extraction – “LPE”). In the case of Pr(III) extraction, the concentration of DPDPCMPO is less than is required for maximum extraction of the metal ([Pr(III)] = 8·10<sup>-3</sup> M, [HNO<sub>3</sub>] = 5.8 M, V<sub>(aq. phase)</sub> = 2 mL, quantity of DPDPCMPO was equal to 18.5 mg for both types of extraction). Dichloroethane and fluoropol (“ftoropol”), in which DPDPCMPO has a maximum extraction capability [16], were used as a solvent for solvent extraction. In case of extraction of Np(IV) and Np(VI) the quantity of DPDPCMPO was sufficient for maximum extraction of the metal ([Np(IV)] = 1.51·10<sup>-3</sup> M, [Np(VI)] = 1.72·10<sup>-3</sup> M, [HNO<sub>3</sub>] = 4 M, V<sub>(aq. phase)</sub> = 1.2 mL, quantity of DPDPCMPO was equal to 16.3 mg for both types of extraction, dichloroethane was used for solvent extraction as a solvent). The data obtained are presented in Table 3. It is seen that the use of DPDPCMPO as liquid reagent for extraction of the metals from nitric acid solutions is more effective than extraction by the solutions of DPDPCMPO in organic solvents.

**Table 3. Extraction of Pr(III), Np(IV) and Np(VI) by DPBCMPO as “liquid reagent” (LR) and by the solution of the same quantity of DPBCMPO in organic solvent (liquid-phase extraction – “LPE”).**

Type of extraction	Element	D*	E*, %
LR	Pr(III)	1.61	62
LPE (dichloroethane)		0.11	10.4
LPE (fluoropol)		0.48	32.5
LR	Np(VI)	242	99.6
LPE (dichloroethane)		20	95.2
LR		81	98.8
LPE (dichloroethane)		8	88.4

(\*) – distribution ratio (D) and extraction efficiency (E) were calculated according to the formulas:

$$D = C_{\text{org}} / C_{\text{aq}}, E = [D/(D+1)] \cdot 100$$

### **Compositions of U(VI) and Nd(III) Complexes with Nitrate and Perchloric “Liquid Reagent”**

It is known, that americium (III) is extracted by organic solutions of diaryl[dialkylcarbamoylmethyl]phosphine oxides from perchloric acid solutions as tri- and tetra-solvates [17] and from nitric acid solutions as bi-solvates[18, 19].

We determined the molar ratio of the reagent to metal cation belonging to the complex formed as a result of extraction of U(VI) and Nd(III) by nitrate LR. The composition of extracted compounds of Nd(III) with perchloric LR was determined as well. The data obtained are presented in Table 4. In all cases, the extraction of cations of the metals by LR from acid solutions was complicated by solidification (cementing) of formed complexes of U(VI) and Nd(III) with liquid reagents. Increasing the temperature of heterogeneous systems to about 80°C allowed us to carry out the extraction processes further. Heated phases were separated by centrifugation. Analysis of residual contents of U(VI) and Nd(III) was carried out at room temperature. The extraction process was completed, when the content of metal cations in the aqueous solution was constant after the next extraction. The quantity of the extracted element was determined and a ratio between constituents in formed complex was calculated. Melting points of complex compounds of Nd(III) with nitrate and perchloric liquid reagent were evaluated as 65-70C and 110-120C, respectively.

The composition of Nd(III) complexes with LR under study was determined at room temperature as well. In this case, LRs were deposited onto the matrix of silicon oxide (Chromatron, 100-150 µm, DMSC, weight content of DPBCMPO in matrix is equal to 6.06%). Thus, Nd(III) is extracted by LR as tetra-solvate from 3- 7 M HNO<sub>3</sub> solutions and it is extracted as tri-solvate from 0.87 – 3.01 M HClO<sub>4</sub> solutions. Uranium (VI) is extracted by nitrate LR as bi-solvate. A comparison of compositions of extracted complexes obtained by us in the absence of organic solvents with the results reported in literature [17-19] shows, that the compositions of extracted compounds of actinide and lanthanide elements with DPBCMPO depend on composition of both organic (solvent-free or solvent extraction) and aqueous (acid nature) phases.

**Table 4.** The compositions of complexes formed as a result of U(VI) and Nd(III) extraction by “liquid reagent” from nitric acid and perchloric acid solutions.

HAn (acid)	[HAn], (initial) M	Element (M <sup>n+</sup> )	Quantity of DPDBCMPO in “LR”, mole	Quantity of extracted M <sup>n+</sup> , mole	Ratio DPDBCMPO : M <sup>n+</sup>
HNO <sub>3</sub>	2.82	Nd(III)	1.68×10 <sup>-4</sup>	0.429×10 <sup>-4</sup>	3.9
	7.22		1.97×10 <sup>-4</sup>	0.500×10 <sup>-4</sup>	
	3.23	U(VI)	2.75×10 <sup>-4</sup>	1.46×10 <sup>-4</sup>	1.9
HClO <sub>4</sub>	0.87	Nd(III)	8.21×10 <sup>-5</sup>	2.73×10 <sup>-5</sup>	3.0
	3.01		8.29×10 <sup>-5</sup>	2.80×10 <sup>-5</sup>	

The composition of Nd(III) complexes with LR under study was determined at room temperature as well. In this case, LRs were deposited onto the matrix of silicon oxide (Chromatron, 100-150 μm, DMSC, weight content of DPDBCMPO in matrix is equal to 6.06%). Thus, Nd(III) is extracted by LR as tetra-solvate from 3- 7 M HNO<sub>3</sub> solutions and it is extracted as tri-solvate from 0.87 – 3.01 M HClO<sub>4</sub> solutions. Uranium (VI) is extracted by nitrate LR as bi-solvate. A comparison of compositions of extracted complexes obtained by us in the absence of organic solvents with the results reported in literature [17-19] shows, that the compositions of extracted compounds of actinide and lanthanide elements with DPDBCMPO depend on composition of both organic (solvent-free or solvent extraction) and aqueous (acid nature) phases.

#### Recovery and Separation of Uranium and Lanthanides by DPDBCMPO Immobilized on an Inert Matrix from Acid Solutions.

The use of DPDBCMPO immobilized on inert matrices is one of the alternatives for separation of actinide and lanthanide elements and for isolation of those from radioactive waste for their subsequent underground disposal.

#### Separation of uranium and lanthanides by DPDBCMPO immobilized on SiO<sub>2</sub>

A certain quantity of DPDBCMPO (about 10% by weight with respect to SiO<sub>2</sub>) was dissolved in CHCl<sub>3</sub> and mixed with SiO<sub>2</sub> (30-60 mesh) with simultaneous evaporation of the solvent. The mixture obtained was thoroughly stirred until the solvent was evaporated. The necessary quantity of SiO<sub>2</sub> with DPDBCMPO immobilized on its surface and 1.5-2.0 mL of aqueous nitric acid solution containing the element under study were used in the each experiment. Extraction was carried out for 3 minutes at room temperature for achievement of equilibrium. After centrifugation and phase separation, concentrations of the elements involved were determined by spectrophotometry. The data obtained were used for calculation of distribution ratios and extraction percentages. The results obtained are presented in Table 5.

**Table 5.** Extraction of U(VI) and lanthanides by DPDBCMPO immobilized onto SiO<sub>2</sub> from 3 M HNO<sub>3</sub> solution. [Me] = 0.01 M, V<sub>ag. phase</sub> = 2.0 mL, [Me] : [DPDBCMPO] = 1 : 2.

Ion	λ, nm	A <sub>0</sub>	A <sub>1</sub>	E, %	D*, mL/g	S <sub>U/Ln</sub>
U(VI)	415	0.165	0.008	95.2	230.9	-
Pr(III)	444	0.142	0.092	35.2	6.4	36.1
Nd(III)	794	0.179	0.117	34.6	6.2	37.2
Ho(III)	450	0.103	0.071	31.1	5.3	43.6
Er(III)	379	0.102	0.072	29.4	4.9	47.1

\* - D = c<sub>s</sub> × V / (c<sub>aq</sub> × m) (mL/g), where c<sub>s</sub> and c<sub>aq</sub> denote equilibrium concentrations of the element in phases of SiO<sub>2</sub> (DPDBCMPO) and aqueous solution, respectively, V is the volume (mL) of the aqueous phase, m is the amount (g) of SiO<sub>2</sub>(DPDBCMPO). The concentrations c<sub>s</sub> and c<sub>aq</sub> were calculated, using the expressions: c<sub>s</sub> = (A<sub>0</sub> - A<sub>1</sub>) / εl and c<sub>aq</sub> = A<sub>1</sub> / εl, where A<sub>0</sub> and A<sub>1</sub> are optical absorbances of aqueous phase before and after the extraction, respectively.

As seen in Table 5, the distribution ratio of U(VI) considerably exceeds the distribution ratios of the lanthanides. The separation factor,  $S_{U/Ln}$ , achieves a value of 40. The separation factor,  $S_{U/Ln}$ , was found to be higher in case of heavy lanthanides than that of light ones. Quantitative isolation of the lanthanides from the solid phase of the reagent can be performed by twice repeated re-extraction with 2 mL of water. Unlike lanthanides, very little uranium is stripped with  $H_2O$ . However, it can be easily stripped with 0.01 M sodium carbonate.

#### ***Isolation of Pr(III) with DPDBCIM immobilized on powder-like matrix of aluminum phosphate glass for subsequent vitrification of the product obtained***

A 0.01 M solution of Pr(III) in 3 M  $HNO_3$  was used in the experiment. A sample of molten aluminum phosphate glass was powdered. Immobilization of the reagent onto a glass powder was done as follows. A measured amount of DPDBCIMPO was dissolved in acetone and this solution was mixed with a weighed portion of a glass powder. Acetone was then evaporated carefully, while stirring, and the product was dried at ambient temperature. The matrix of aluminum phosphate glass (2.5 g) contained 0.3 g of DPDBCIMPO. The prepared powder-like mass (1.73 g) containing  $5.0 \times 10^{-4}$  moles of the reagent was placed into a chromatographic column (5 mm i.d. and 40 mm h). Initially, 1 mL of 3 M  $HNO_3$  solution was passed through the column to transform DPDBCIMPO into LR. Next, 5 mL of  $HNO_3$  solution containing  $5 \times 10^{-5}$  moles of praseodymium were passed through the column, followed by washing with 2 mL of 1 M  $HNO_3$  solution at the rate of about 0.18 mL/min. The concentration of Pr(III) was measured by spectrophotometry. The residual concentration of Pr(III) in the solution collected after sorption and washing was equal to  $3 \times 10^{-4}$  M. Thus, more than 96% of the initial amount of Pr was isolated from the solution. The column content was transferred quantitatively into a glass-graphite test-tube and dried. This test-tube was placed into a muffle, where praseodymium-containing glass powder was melted at  $1100^{\circ}C$  for 4-5 hours. The final weight of the vitrified matrix was 1.3 g. Weight loss compared to the initial matrix weight (1.73 g) can be explained by partial dissolution of the matrix in  $HNO_3$  solution.

## **CONCLUSIONS**

The data obtained show that on contact with mineral acid solutions DPDBCIMPO powder changes its aggregative state, being transformed into a liquid colorless viscous substance immiscible with aqueous solutions. Acidity of the solution and interaction of the reagent with mineral acid are the factors determining both physical state of the product of their interaction and extraction capacity of the compound formed. The use of "liquid reagent" allows extracting the metals in question more effectively in comparison with extraction by the DPDBCIMPO solutions in organic solvents. It is promising for the processing of acidic high-level wastes because the use of toxic and environmentally hazardous organic solvents can be avoided.

## **REFERENCES**

1. T. I. Zvarova, V. M. Shkinev, B. Ya. Spivakov, Yu. A. Zolotov (1983), *Dokl. Akad. Nauk SSSR*, **273** (1), 107-110.
2. B. I. Petrov, G. Yu. Afendikova (1985), *Russ. J. Appl. Chem.*, **58** (10), 2194-2199.
3. B. I. Petrov, S. I. Rogoschnikov (1985), *Radiokhim.*, **27** (3), 293-296.
4. V. I. Zemlyanukhin, G. P. Savos'kin, M. F. Pushlenkov (1964) *Radiokhim.*, **6** (6), 694-702.
5. M. K. Chmutova, L. A. Ivanova, B. F. Myasoedov (1995), *Radiokhim.*, **37** (5), 427-429.

6. Yu. M. Kulyako, D. A. Malikov, M. K. Chmutova, B. F. Myasoedov (1997), *Mendeleev Commun.*, (4), 135-137.
7. Yu. M. Kulyako, D. A. Malikov, M. K. Chmutova, B. F. Myasoedov (1997), *Mendeleev Commun.*, (5), 193-195.
8. Yu. M. Kulyako, D. A. Malikov, M. K. Chmutova, M. N. Litvina, B. F. Myasoedov (1998), *J. Alloys Comp.*, **271-273**, 760-764.
9. M. K. Chmutova, Yu. M. Kulyako, M. N. Litvina, D. A. Malikov, B. F. Myasoedov (1998), *Radiokhim.*, **40** (3), 241-247.
10. Yu. M. Kulyako, T. I. Trofimov, B. F. Myasoedov, Chien M. Wai (2000), *Proc. 5<sup>th</sup> Int. Conf. on Nuclear and Radiochemistry*, Pontresina, Switzerland, pp. 114-117.
11. M. N. Litvina, M. K. Chmutova, Yu. M. Kulyako, B. F. Myasoedov (2001), *Radiokhim.*, **43** (1), 61-65.
12. M. K. Chmutova, M. N. Litvina, N. P. Nesterova, B. F. Myasoedov (1990), *Radiokhim.*, **32** (5), 88-95.
13. A. M. Rosen, Z. I. Nikolotova, N. A. Kartashova (1977), *Dokl. Akad. Nauk SSSR*, **237**, (1), 148-151.
14. T. Mitsugashira, M. Maki, S. Suzuki (1984), '84 *Symposium on Actinide-Lanthanide Separation Int. Chem. Congr. Pacif. Basin Soc.*, Honolulu.
15. Ch. F. Metz, G. R. Waterbury (1967), *Analiticheskaya Khimiya Transuranovykh Elementov*, Atomizdat, Moscow, p. 69.
16. B.F. Myasoedov, M.K. Chmutova, I.V. Smirnov and A.Yu. Shadrin (1993), *Proc. Int. Conf. Future Nuclear Systems: Emerging Fuel Cycles and Waste Disposal Options*, GLOBAL '93, Vol. 1, Seattle, Washington, pp. 581-583.
17. M. K. Chmutova, M. N. Litvina, N. P. Nesterova, B. F. Myasoedov, M. I. Kabachnik (1992), *Solv. Extr. Ion Exch.*, **10** (3), 439-458.
18. M. K. Chmutova, M. N. Litvina, G. A. Pribylova (1995), *Radiokhim.*, **37** (5), 430-435.
19. M. K. Chmutova, L. A. Ivanova, N. E. Kochetkova, N. P. Nesterova, B. F. Myasoedov, A. M. Rosen (1995), *Radiokhim.*, **37** (5), 422-426.



# DISSOLUTION OF ACTINIDE OXIDES IN SUPERCRITICAL FLUID CARBON DIOXIDE MODIFIED WITH VARIOUS ORGANIC LIGANDS

M. D. Samsonov, T. I. Trofimov, S. E. Vinokurov, S. C. Lee\*,  
B. F. Myasoedov and C. M. Wai\*

Laboratory of Radiochemistry, V.I. Vernadsky Institute of Geochemistry and Analytical Chemistry, Russian Academy of Sciences, Moscow, Russia

\* Department of Chemistry, University of Idaho, Moscow, ID, USA

The dissolution of actinide oxides in supercritical fluid carbon dioxide containing a complex of tri-*n*-butyl phosphate with nitric acid was investigated. It was shown for the first time that milligram amounts of uranium dioxide can be quantitatively dissolved in supercritical carbon dioxide containing this reagent and efficiently separated from plutonium, neptunium, and thorium on its supercritical fluid extraction from a mixture of their oxides. The quantitative dissolution of milligram amounts of uranium trioxide in supercritical carbon dioxide containing thenoyltrifluoroacetone and tri-*n*-butyl phosphate was first performed using ultrasonication. The separation of uranium (VI) and cerium (IV) in the system involved was demonstrated.

## INTRODUCTION

A key chemical process in the nuclear industry is the extraction and purification of uranium and plutonium in the initial production of fuel for nuclear reactors and in reprocessing of spent nuclear fuel. The most widely used commercial process to achieve this objective is the PUREX (Plutonium Uranium Reduction Extraction) process, which involves the dissolution of spent nuclear fuel in strong nitric acid followed by solvent extraction of uranium from the acid solution using tri-*n*-butyl phosphate (TBP) as an extractant [1,2]. The extracted uranium and plutonium nitrate-TBP complexes are further separated by chemical steps to yield pure uranium and plutonium dioxides. The PUREX process, though highly efficient, has the inherited drawbacks of liquid-liquid extraction including generation of large volumes aqueous and organic high-level radioactive wastes. So a search for new alternative techniques for reprocessing of spent nuclear fuels, which will allow minimizing waste generation, is a major task challenging the future of the nuclear industry.

The possibility of using supercritical fluid carbon dioxide as a solvent for reprocessing of spent nuclear fuels was suggested recently in the literature [3]. Of particular interest is the idea of direct dissolution of the spent nuclear fuel in supercritical carbon dioxide utilizing a suitable complexing agent. Supercritical CO<sub>2</sub> is considered a green solvent because it is non-toxic and environmentally benign. Carbon dioxide is also cheap, readily available in relatively pure form, and has moderate critical constants ( $T_c = 31.3^\circ\text{C}$ ,  $P_c = 72.8$  atm, and  $\rho_c = 0.47 \text{ g/cm}^{-3}$ ) [4]. A major advantage of using supercritical CO<sub>2</sub> for reprocessing spent nuclear fuels is elimination of the acid and organic solvent required in the conventional PUREX process. A major problem of developing this new process is to identify a complexing agent that will form a supercritical CO<sub>2</sub>-soluble complex with the main component of the spent nuclear fuel, basically uranium dioxide.

The hexavalent uranyl ion ( $\text{UO}_2^{2+}$ ) is known to form  $\text{CO}_2$ -soluble complexes with a number of complexing agents including TBP and  $\beta$ -diketones [5,6]. It has been demonstrated that uranium trioxide  $\text{UO}_3$  can be dissolved in supercritical  $\text{CO}_2$  with thenoyltrifluoroacetone (HTTA) and TBP [7,8]. Recent studies have also demonstrated the possibility of lanthanide extraction from their oxides using supercritical  $\text{CO}_2$  containing TBP- $\text{HNO}_3$  complex [2]. However the extraction efficiency of all elements involved did not exceed 40%. Thus it was of interest to develop a procedure for the quantitative extraction of uranium from its oxides simultaneously with its separation from other actinides, such as Pu, Np, and Th. The results obtained are presented below.

## PROCESS DESCRIPTION

Figure 1 shows a schematic diagram of the set-up employed for SFE is shown. A syringe pump was used to deliver liquid  $\text{CO}_2$  through a pre-heating coil to the extraction system placed in a chromatographic oven for heating the system to the required temperature. A known amount of either an actinide oxide sample or a mixture of those were put into a glass tube and plugged at both ends with glass wool. After weighing, the tube was placed in a 3.5 mL extraction cell.

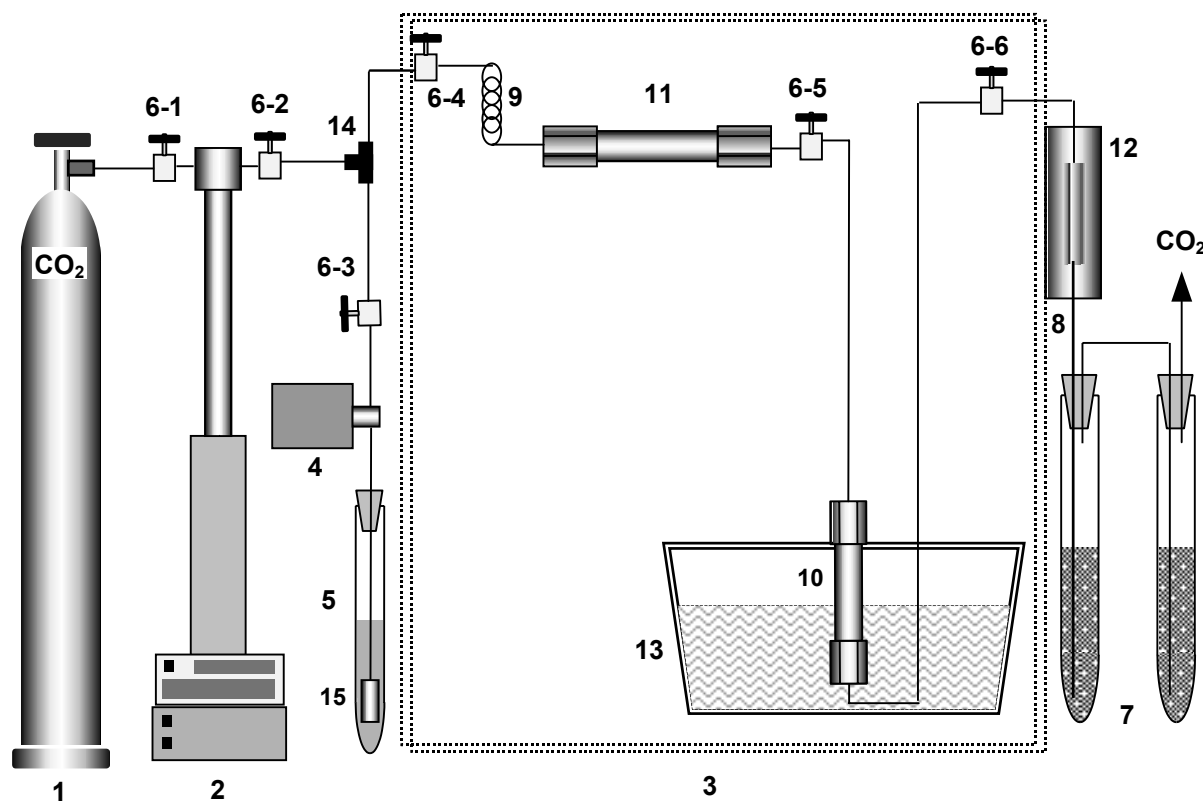


*Figure 1. Schematic diagram of the experimental system for uranium oxides dissolution in supercritical carbon dioxide. 1,  $\text{CO}_2$  cylinder; 2, syringe pump; 3, oven; 4, HPLC pump; 5, test-tube with TBP; 6-1 – 6-6, volumeless valves; 7, collection system; 8, restrictor; 9, fluid preheating coil; 10, extraction cell; 11, ligand cell; 12, restrictor heater; 13, ultrasonic cleaner; 14, T-joint; 15, filter.*

The saturation of supercritical CO<sub>2</sub> with the ligands (TTA or TBP-HNO<sub>3</sub> complex) was performed in a 10.4 mL ligand cell connected upstream of the extraction. Pure TBP was injected into the system through a T-end joint using a HPLC pump. The flow rate of TBP injected into the system was about 0.02 mL/min, which corresponded to its concentration in supercritical CO<sub>2</sub> of about 5% v/v. The extractions were performed in static (a sample and supercritical CO<sub>2</sub> are allowed to interact for a given amount of time), dynamic (supercritical CO<sub>2</sub> is allowed to flow continuously through the extraction cell containing the sample), and combined modes (a static mode followed by dynamic mode). The time of the static mode was about 10 min in all runs, and that of dynamic one was varied from 15 to 60 min. Supercritical CO<sub>2</sub> flow rates through the system were maintained at 0.2-0.6 mL/min. Faster flow rates tend to decrease the extraction efficiency of uranium thanks to incompleteness of the interaction of the TBP-HNO<sub>3</sub> complex with an oxide involved. After extraction, the system was allowed to depressurize for about 1 hour. Extracted actinide complexes were collected in a trap solution (chloroform) through the restrictors made of deactivated fused silica, about 25 cm in length and 50 μm in internal diameter. Actinides were back extracted from the trap solutions with 50% nitric acid in the case of using TTA and TBP as the ligands or with 0.1 M (NH<sub>4</sub>)<sub>2</sub>CO<sub>3</sub> in the case of the TBP-HNO<sub>3</sub> complex. The actinide content in the solutions obtained was determined by alpha-radiometry (Pu, Np, and U), luminescence (U), and ICP-MS (Th, Ce). The extraction efficiency E (%) was calculated according to the formula (1).

$$E = \frac{m_1}{m_0} \times 100\% \quad (1)$$

where  $m_1$  and  $m_0$  are the amounts of actinides found in the trap solution and taken in to the run correspondingly (mg). The powder-like oxides of ThO<sub>2</sub>, UO<sub>3</sub>, U<sub>3</sub>O<sub>8</sub>, NpO<sub>2</sub>, and PuO<sub>2</sub> were used as supplied. UO<sub>2</sub> sample was prepared by milling a real, nonirradiated, uranium fuel pellet.

### DISSOLUTION OF THE ACTINIDE OXIDES USING SUPERCRITICAL CO<sub>2</sub> CONTAINING THE TBP-HNO<sub>3</sub> COMPLEX

It is known that uranyl ions in strong nitric acid solutions can be extracted by supercritical CO<sub>2</sub> containing TBP [10]. The extracted uranyl complex UO<sub>2</sub>(NO<sub>3</sub>)<sub>2</sub>•2TBP has an unusually high solubility in supercritical CO<sub>2</sub>, of the order of 4.2×10<sup>-1</sup> mol/L at 40°C and 200 atm [11]. HNO<sub>3</sub> is known to be extracted with TBP forming a complex  $n$ HNO<sub>3</sub>•TBP, where  $n$  = 1, 2, 3, depending on HNO<sub>3</sub> concentration [12]. It was found that this complex is very soluble in the supercritical CO<sub>2</sub> phase [9]. In addition, the TBP-HNO<sub>3</sub> complex may be an effective reagent for dissolution of UO<sub>2</sub> because HNO<sub>3</sub> is an oxidizing agent.

To obtain the TBP-HNO<sub>3</sub> complex, a 100% TBP was treated with concentrated nitric acid (13.8 M, density 1.37 g/cm<sup>3</sup>). After separating phases by centrifuging, the necessary amount of the complex obtained was placed in the ligand cell, where supercritical CO<sub>2</sub> was saturated with the TBP-HNO<sub>3</sub> complex for 15 min.

The results on SFE of actinides from their individual oxides and from a mixture of those using supercritical CO<sub>2</sub> modified with the TBP-HNO<sub>3</sub> complex are presented in Tables 1 and 2, respectively. The chosen SFE conditions were found previously to be optimal for this system. As is seen from the data presented, uranium can be quantitatively extracted from all its oxides tested. It was shown by spectrophotometry, that uranium is present only in the +6 valent state in the trap solution. Thus, as one would expect, it was demonstrated that on interaction of the TBP-HNO<sub>3</sub> complex with UO<sub>2</sub>, oxidation of tetravalent uranium to the hexavalent state proceeds, leading to the formation of the highly soluble UO<sub>2</sub>(NO<sub>3</sub>)<sub>2</sub>•2TBP

complex in the supercritical CO<sub>2</sub> phase. At the same time, the extraction efficiencies of Pu, Np, and Th are extremely poor from both the individual oxides and the mixture with uranium dioxide (Table 2). Of course, the common mixture of oxides is not identical to the real nuclear fuel which is a solid solution of uranium and plutonium dioxides. Nevertheless, the demonstration of effective dissolution of uranium in supercritical CO<sub>2</sub> modified with the TBP-HNO<sub>3</sub> complex and its separation from the actinides tested is very promising for further development of a supercritical CO<sub>2</sub>-based process for reprocessing spent nuclear fuel.

*Table 1. SFE of actinides from their individual oxides using supercritical CO<sub>2</sub> modified with the TBP-HNO<sub>3</sub> complex. T = 65°C, P = 250 atm. SFE mode – thrice-repeated alternation of static (10 min) and dynamic (15 min) modes. \* - not milled uranium fuel pellet.*

Oxide	Actinide added, m <sub>0</sub> (mg)	Molar ratio An : complex	Extraction efficiency E (%)
UO <sub>2</sub>	61.5	1 : 50	> 99
	334.4	1 : 10	90 ± 5
	367.9*	1 : 10	65 ± 3
UO <sub>3</sub>	175.1	1 : 20	92 ± 5
U <sub>3</sub> O <sub>8</sub>	177.3	1 : 20	85 ± 3
PuO <sub>2</sub>	8.1	1 : 250	< 0.1
	50.1	1 : 50	< 0.1
NpO <sub>2</sub>	5.6	1 : 250	< 0.1
	55.0	1 : 50	< 0.1
ThO <sub>2</sub>	52.9	1 : 50	< 0.1

*Table 2. Separation of U from the Pu, Np, and Th using supercritical CO<sub>2</sub> modified with the TBP-HNO<sub>3</sub> complex. T = 65°C, P = 250 atm. SFE mode – thrice-repeated alternation of static (10 min) and dynamic (15 min) modes.*

Mixture of oxides	Actinide added, m <sub>0</sub> (mg)	Molar ratio (U+An) : complex	Extraction efficiency E (%)
UO <sub>2</sub> PuO <sub>2</sub>	430.0	1 : 10	79 ± 4
	37.4		< 0.1
UO <sub>2</sub> NpO <sub>2</sub>	120.6	1 : 20	91 ± 5
	11.5		< 0.1
UO <sub>2</sub> NpO <sub>2</sub> PuO <sub>2</sub> ThO <sub>2</sub>	133.5	1 : 20	89 ± 4
	15.4		< 0.1
	13.0		< 0.1
	58.5		< 0.1

## DISSOLUTION OF URANIUM OXIDES IN SUPERCRITICAL CO<sub>2</sub> CONTAINING HTTA AND TBP USING ULTRASONICATION

The hexavalent uranyl ion (UO<sub>2</sub>)<sup>2+</sup> is known to form supercritical CO<sub>2</sub>-soluble complexes with a number of complexing agents including TBP and HTTA [7,10,13]. It has been demonstrated that uranium trioxide can be dissolved in supercritical CO<sub>2</sub> with a fluorinated β-diketone thenoyltrifluoroacetylacetone (HTTA) and TBP according to the following reaction:



However, the extraction efficiency of uranium did not exceed 40% [8].

It is well known that ultrasonication can accelerate many heterogeneous processes. We used an ultrasonic cleaner with a heater (model FS30, Fisher scientific, PA, USA) with working frequency 44-48 kHz (Figure 1). The SFE conditions applied were found previously [8] to be optimal for the UO<sub>3</sub>-HTTA-TBP system. Table 3 shows the effect of ultrasonication on the SFE of uranium from its oxides with supercritical CO<sub>2</sub> containing TTA and TBP.

*Table 3. Dissolution of uranium oxides in supercritical CO<sub>2</sub>, containing HTTA and TBP using ultrasonication. SFE conditions is P = 150 atm and T = 60°C. SFE mode – thrice-repeated alternation of static (10 min) and dynamic (15 min) modes. \* without ultrasonication.*

Oxide	Uranium added, m <sub>0</sub> (mg)	Uranium trapped	
		m <sub>1</sub> (mg)	E (%)
UO <sub>3</sub>	22.9	8.5 ± 0.3	37.0*
UO <sub>3</sub>	25.2	24.3 ± 0.6	96.4
U <sub>3</sub> O <sub>8</sub>	30.9	0.7 ± 0.1	2.3
UO <sub>2</sub>	23.9	1.2 ± 0.2	5.0

As can be seen from the data obtained, ultrasound allows uranium to be quantitatively extracted from UO<sub>3</sub> with the above system. Unfortunately its application does not result in an essential increase of both UO<sub>2</sub> and U<sub>3</sub>O<sub>8</sub> dissolution in supercritical CO<sub>2</sub> containing TTA and TBP. This fact may be explained by structural differences between UO<sub>2</sub>, U<sub>3</sub>O<sub>8</sub>, and UO<sub>3</sub> (UO<sub>2</sub> – face-centered, U<sub>3</sub>O<sub>8</sub> orthorhombic and UO<sub>3</sub> – octahedral), as well as by steric hindrances in the U(IV) complexation with TTA and TBP. The effect of ultrasound can be attributed to the cleaning of the oxide surface by removing the complex formed. As a result, the reaction with TTA takes place more effectively.

The data in Table 4 show that the suggested system can be successfully applied to the separation of uranium and cerium in the SFE from a mixture of UO<sub>3</sub> and CeO<sub>2</sub>. The molar ration [U]:[Ce] in the trap solution is about 30 times higher than that in the starting mixture.

*Table 4. Separation of the U(VI) and Ce(IV) using supercritical CO<sub>2</sub>, containing TTA and TBP under ultrasonication. SFE conditions is P = 150 atm and T = 60°C. SFE mode – thrice-repeated alternation of static (10 min) and dynamic (15 min) mode.*

Oxide	Metal added, $m_0$ , (mg)	Metal trapped	
		$m_1$ (mg)	E (%)
UO <sub>3</sub>	23.0	21.3±0.4	92.7
CeO <sub>2</sub>	13.6	0.4±0.1	3.1

## CONCLUSIONS

The study conducted has demonstrated that milligram amounts of uranium can be quantitatively extracted from UO<sub>2</sub>, UO<sub>3</sub>, and U<sub>3</sub>O<sub>8</sub> with supercritical CO<sub>2</sub> containing the TBP-HNO<sub>3</sub> complex, and efficiently separated from plutonium, neptunium, and thorium in the SFE from the mixture of their oxides. Also milligram amounts of uranium can be quantitatively extracted from UO<sub>3</sub> with supercritical CO<sub>2</sub> containing HTTA and TBP under ultrasonication. The enhanced dissolution of UO<sub>3</sub> by means of ultrasound is, probably, caused by removing the UO<sub>2</sub>(TTA)<sub>2</sub>•H<sub>2</sub>O complex from the oxide surface, hence facilitating the complexation process. Demonstration of effective dissolution of uranium oxides in supercritical CO<sub>2</sub> is of great importance for developing a new alternative environmentally benign process for reprocessing spent nuclear fuel. Application of the SFE technique may be very promising for spent nuclear fuel reprocessing thanks to minimizing of environmentally hazardous liquid radioactive waste generation associated with the currently used PUREX process.

## ACKNOWLEDGEMENTS

This work was supported by British Nuclear Fuel Ltd. (BNFL), Contract Number A80153, and by the Russian Foundation for Basic Research, Grants # 99-03-32819 and 00-15-97391.

## REFERENCES

1. F. Weigel, J. J. Katz, and G. T. Seaborg (1986), *The Chemistry of Actinide Elements*, Vol. 1, 2nd edn., J. J. Katz, G. T. Seaborg and L. R. Morss (eds.), Chapman and Hall, London, p. 525.
2. I. S. Denniss and A. P. Jeapes (1998), *The Nuclear Fuel Cycle: From Ore to Waste*, P. D. Wilson (ed.), Oxford University Press, Oxford, p. 123.
3. N. G. Smart, C. L. Phelps and C. M. Wai (1998), *Chem. Brit.*, **34**, 34.
4. S. B. Hawthorn (1990), *Anal. Chem.*, **62**, 633A.
5. Y. Lin, C. M. Wai, F. M. Jean, and R. D. Brauer (1994), *Environ. Sci. Technol.*, **28**, 1190.
6. Y. Lin and C. M. Wai (1994), *Anal. Chem.*, **66**, 1971.
7. C. L. Phelps, N. G. Smart and C. M. Wai, (1996), *J. Chem. Educ.*, **73**, 1163.
8. C. L. Phelps (1997), *Recycling Uranium: Hello SFE, Goodbye PUREX?*, PhD Thesis, University of Idaho, Department of Chemistry.
9. O. Tomioka, Y. Enokida, and I. Yamamoto (1998), *J. Nucl. Sci. Technol.*, **35**, 515.
10. Y. Lin., N. G. Smart, and C. M. Wai (1995), *Environ. Sci. Technol.*, **29**, 2706.
11. M. J. Carrott, B. E. Waller, N. G. Smart, and C. M. Wai (1998), *J.C.S. Chem. Commun.*, 377.
12. V. I. Zemlyanukhin, G. P. Savoskina, and M. F. Pushlenkov (1964), *Radiokhim.*, **6**, 714.
13. Y. Lin., N. G. Smart, and C. M. Wai (1995), *Trends Anal. Chem.*, **14**, 123.



## MODELLING THE INFLUENCE OF ORGANIC PHASE COMPOSITION ON THE EXTRACTION OF TRIVALENT ACTINIDES

M. Nilsson, J-O. Liljenzin, C. Ekberg and S. Wingefors\*

Department of Nuclear Chemistry, Chalmers University of Technology, Göteborg, Sweden

\* Swedish Nuclear Power Inspectorate, Stockholm, Sweden

A model for description of solvent influence on extraction of Am, Cm and Pm is proposed. The model comprises an extension of the Scatchard-Hildebrand theory for regular solutions employing Hansen's 3-D solubility parameters to describe interactions in the organic phase. The model was tested by performing a number of extraction experiments with 2,2':6',2''-terpyridine and 2-bromodecanoic acid as complexing agents in different combinations of organic solvents. The results obtained were used for fitting the parameters in the model and another set of experiments was performed to validate the model. The model shows good agreement between experimental and calculated distribution ratios for most of the extraction cases tested. From this analysis it can be concluded that the choice of solvent has a negligible effect on the selectivity of the studied extraction system.

### INTRODUCTION

One major concern regarding nuclear power production is management of the long-lived radioactive nuclear waste. Through transmutation by neutron irradiation, long-lived waste can be converted into short-lived or stable nuclides. This means that the long-lived waste from the nuclear fuel cycle has to be isolated from the biosphere only for a couple of hundred years instead of, as in the case of direct disposal of spent nuclear fuel, for hundreds of thousands of years. Another benefit from this process is that the released energy may be utilised. This means that the nuclear fuel is more efficiently used, which is a step towards a more sustainable society. A transmutation process must be connected to a partitioning process, where transmutable elements, e.g., Am, Cm and Np, are separated from other elements that will reduce the transmutation efficiency. Sufficient separation of the different elements can be achieved with solvent extraction using a selective extraction system. In order to find a suitable extraction system, a large number of different combinations of organic solvents and extracting reagents must be studied. In an attempt to reduce the time needed for this investigation, a model that can predict the extraction of some trivalent actinides and lanthanides is being developed. The model is based on the Scatchard-Hildebrand solubility parameter theory and its extension to describe dispersion, polar and hydrogen bonding interactions according to Hansen's 3-D solubility parameter concept.

## THEORY

### Solubility Parameters

The relation between intermolecular attraction forces and solubility is reflected in the Hildebrand solubility parameter,  $\delta$ , defined approximately as [1]

$$\delta = \left[ \frac{\Delta H_m - RT}{v} \right]^{\frac{1}{2}} \quad (1)$$

where  $\Delta H_m$  and  $v$  are the molar heat of vaporisation and molar volume respectively. The heat of vaporisation is the energy required to separate the molecules in a liquid from each other, turning the liquid into a gas. This energy can be referred to the amount of energy that holds the molecules together. Thus the Hildebrand solubility parameter is based on the assumption that the same intermolecular attractive forces have to be overcome to vaporise a liquid as to dissolve it. Similar to the miscibility problems with components of different intermolecular attraction forces, immiscibility will occur if the solubility parameters of the compounds differ too much.

The original Scatchard-Hildebrand model was based on the assumption of only weak molecular attraction, dominated by dispersion forces. Higher accuracy in describing non-ideal solutions can be achieved if the total attraction between molecules in a solution is considered as a sum of dispersion, polar and hydrogen bonding forces. The most widely used three-parameter system has been developed by Hansen 1967 [2]. Hansen split the Hildebrand parameter into three parts according to

$$\delta_t^2 = \delta_d^2 + \delta_p^2 + \delta_h^2 \quad (2)$$

$\delta_t^2$  = total Hildebrand parameter

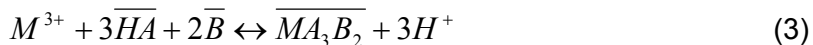
$\delta_d^2$  = dispersion parameter

$\delta_p^2$  = polar parameter

$\delta_h^2$  = hydrogen bonding parameter

### Applications of Solubility Parameters

The extraction is assumed to follow the reaction



$M^{3+}$  is the metal ion that is to be extracted ( $Am^{3+}$ ,  $Cm^{3+}$  or  $Pm^{3+}$ ). HA is the dimerised form of 2-bromodecanoic acid and B is 2,2':6',2''-terpyridine. The bars denote quantities relevant to the organic phase. The thermodynamic equilibrium constant for the extraction reaction in terms of activities is expressed as:

$$K_D = \frac{\overline{M} \overline{H^+}^3}{\overline{M}^{3+} \overline{HA}^3 \overline{B}^2} \quad (4)$$

In equation 4 and subsequently, the extracted complex,  $\overline{MA_3B_2}$ , is written as  $\overline{M}$ . It is assumed that this equilibrium is applicable for all organic solvents. The metal is present in tracer amounts so the concentrations of HA, B and  $H^+$  are assumed constant and equal to starting concentrations,  $\overline{C}_{HA}$ ,  $\overline{C}_B$  and  $C_H$ . With the assumption that the dominating species are trivalent metal ion and non-charged metal complex in the aqueous and organic phase respectively, equation 4 can be transformed into:

$$D \cdot \frac{\left(\frac{x_M}{C_M}\right)}{\left(\frac{x_{HA}}{C_{HA}}\right)^3 \left(\frac{x_B}{C_B}\right)^2} \frac{C_H^3}{C_{HA}^3 \cdot C_B^2} = K_D' \frac{\gamma_{HA}^{-3} \cdot \gamma_B^{-2}}{\gamma_M} \quad (5)$$

where  $x$  is molar fraction and  $K_D'$  the thermodynamic equilibrium constant,  $K_D$ , referred to a standard state of infinite dilution of the organic solvent. The activity factors,  $\gamma$ , are found using the Scatchard-Hildebrand equation

$$RT \ln \gamma_i = v_i [(\delta_{d,i} - \delta_{d,tot})^2 + (\delta_{p,i} - \delta_{p,tot})^2 + (\delta_{h,i} - \delta_{h,tot})^2] \quad (6)$$

If the solubility parameters and molar volume of the extracted complex are known as well as  $K_D'$ , equation 5 together with equation 6 can be used for estimating the distribution ratio.

## EXPERIMENTAL

### Materials

The organic solvents used, 2,2':6,2''-terpyridine (terpy) and 2-bromodecanoic acid along with their solubility parameters are listed in Table 1.

*Table 1. A list of substances used in the experiments.  
All parameter values were found in [3], if not stated otherwise.*

Different organic substances	Hansen solubility parameters in $(J/cm^3)^{1/2}$			Supplier	Purity (%)
	$\delta_d$	$\delta_p$	$\delta_h$		
2,2':6,2''-Terpyridine	22.3 <sup>a</sup>	10.3 <sup>a</sup>	6.93 <sup>a</sup>	Aldrich	98
2-bromodecanoic acid	19.3 <sup>a</sup>	4.99 <sup>a</sup>	3.17 <sup>a</sup>	Fluka	98
Xylene	17.6	1.84 <sup>b</sup>	2.45 <sup>b</sup>	Merck	99.8
Toluene	18.0	1.40	2.00	R.-de-Ha��n	99.7
Cyclohexane	16.8	0.00	0.20	FSA lab.suppl.	99.8
<i>n</i> -Hexane	14.9	0.00	0.00	LAB-scan	99
Nitrobenzene	20.0	8.60	4.10	Fisher	99.9
Chloroform	17.8	3.10	5.70	Merck	99.2
<i>tert</i> -Butylbenzene	17.08 <sup>c</sup>	0.65 <sup>c</sup>	0.00 <sup>c</sup>	Aldrich	99
Benzene	18.4	0.00	2.00	Merck	99.7
Carbon tetrachloride	17.8	0.00	0.60	Merck	99.8
Chlorobenzene	19.00	4.30	2.00	Fisher	99.9
Ethyl benzene	17.8	0.60	1.40	Fluka	99

<sup>a</sup>: Parameter value calculated from group molar contributions[4]

<sup>b</sup>: Parameter value from Charles Tenant & Company Ltd[5]

<sup>c</sup>: Parameter value calculated using equations found in [6]

### Procedure and Apparatus

Solvent extraction of Am, Cm and Pm was investigated. The aqueous phase was the same during all experiments and consisted of about 1.7 kBq per cm<sup>3</sup> each of <sup>241</sup>Am, <sup>244</sup>Cm and <sup>147</sup>Pm in 0.05 M HNO<sub>3</sub>. The organic phase was made up of one or more organic solvents with 1 M 2-bromodecanoic acid and 0.1 M terpy. If more than one organic solvent were

present in the organic phase the volume ratio between the solvents was 1. 2.5 ml of each phase was added to a test tube, which was vigorously shaken for 5 minutes and then the phases were allowed to settle. Aliquots from each phase were taken for radiometric analysis. This process was repeated five times to minimise fluctuations. The  $\gamma$ -energy at 59.5 keV for  $^{241}\text{Am}$  was measured using an Intertechnique Gamma Counter 4000 NaI(Tl) detector. For detection of  $\alpha$ - and  $\beta$ -radiation a LKB Wallac 1219 Rackbeta liquid scintillator was used.

## RESULTS AND DISCUSSION

The experimental data show that there is a distinct difference in the distribution of the metals when different organic solvents are used. Am and Cm have higher distribution ratios than Pm, about ten times as high in most extraction cases tested. This actinide-lanthanide separation has been observed in earlier experiments [7]. No specific separation between Am and Cm could be observed.

### Fitting a Model to the Experiments

Experimental distribution ratios (D-values) obtained for a number of pure solvents employed for fitting of the proposed model to find the 5 unknown parameters in equation 5 and 6 (*i.e.*,  $K_D$ ,  $\bar{v}_M$ ,  $\bar{\delta}_{d,M}$ ,  $\bar{\delta}_{p,M}$ ,  $\bar{\delta}_{h,M}$ ). In order to make the model work, the number of unknown parameters must be minimized. Thus, the molar volume of the extracted complex,  $\bar{v}_M$ , can be expressed as a sum of the molar volumes of its components [8].

$$\bar{v}_M = 3 \cdot \bar{v}_{HA} + 2 \cdot \bar{v}_B \quad (7)$$

Also the dispersion parameter of the complex,  $\bar{\delta}_{d,M}$ , can be derived from the dispersion parameters of the organic ligands.

$$\bar{\delta}_{d,M} = \sqrt{\frac{3 \cdot \bar{v}_{HA} \cdot \bar{\delta}_{d,HA}^2 + 2 \cdot \bar{v}_B \cdot \bar{\delta}_{d,B}^2}{3 \cdot \bar{v}_{HA} + 2 \cdot \bar{v}_B}} \quad (8)$$

Hence only three unknown parameters must be found. Data from extraction experiments with solvent mixtures was used for testing the model. The solvent mixtures are displayed in Table 2. Hansen solubility parameters for the total organic phases were calculated using the formula [9]

$$\delta_{i,tot} = \frac{\delta_{i,1} \cdot V_1 + \delta_{i,2} \cdot V_2 + \dots + \delta_{i,n} \cdot V_n}{V_1 + V_2 + \dots + V_n} \quad (9)$$

$i = d, p$  or  $h$

$n =$  number of components

$V =$  volume of each component in the mixture

*Table 2. Combinations of organic solvents used in the experiments where more than one solvent was present in the organic phase.*

Combinations of organic solvents tested
Chloroform / <i>tert</i> -Butylbenzene
Chlorobenzene / Xylene
Ethyl benzene / Chlorobenzene
Cyclohexane / Toluene
Nitrobenzene / <i>n</i> -Hexane
Benzene / Carbon tetrachloride
Benzene / Carbon tetrachloride / Toluene
Cyclohexane / Chloroform / Chlorobenzene

Comparison between experimental and calculated distribution ratios are plotted in graphs, see Figure 1. Parameters obtained by fitting equation 5 are shown in Table 3. Statistical uncertainties in Table 3 were estimated using the chi-square method [10]. The standard deviations presented in Figure 1 were based on five replicate measurements on different samples.

Table 3. Constants used in equation 5 and 6, obtained from fitting and calculations.

Constant parameters for equation 5 and 6	M = Am-complex	M = Cm-complex	M = Pm-complex
$\bar{v}_M$ (cm <sup>3</sup> /mole)	1597.18	1597.18	1597.18
$\bar{\delta}_{d,M}$ (cal/cm <sup>3</sup> ) <sup>1/2</sup>	9.78	9.78	9.78
$\bar{\delta}_{p,M}$ (cal/cm <sup>3</sup> ) <sup>1/2</sup>	2.83 ± 0.06	2.81 ± 0.05	2.75 ± 0.07
$\bar{\delta}_{h,M}$ (cal/cm <sup>3</sup> ) <sup>1/2</sup>	1.99 ± 0.10	1.95 ± 0.09	1.99 ± 0.11
$K_D'$ (mole/dm <sup>3</sup> ) <sup>2</sup>	1.10 ± 0.84	0.83 ± 0.50	0.053 ± 0.05

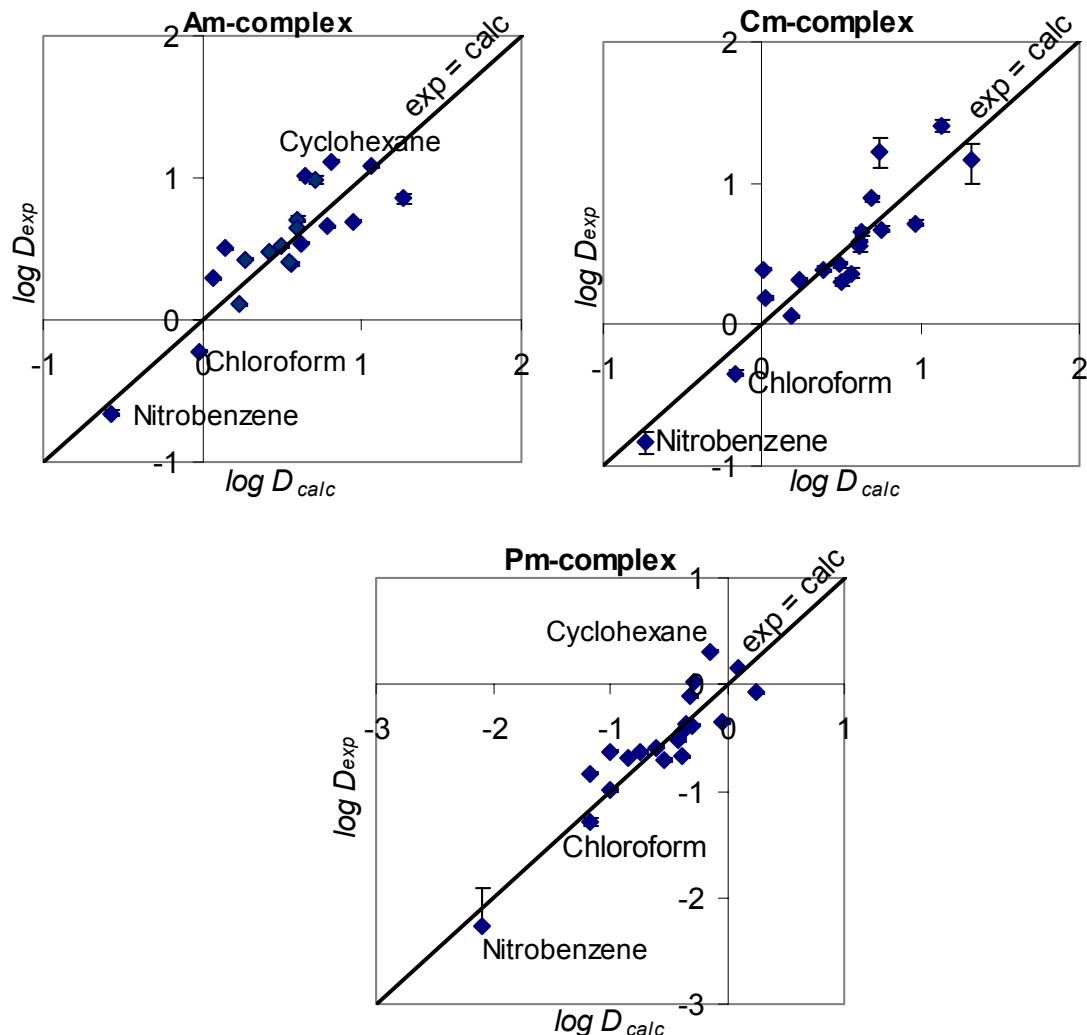


Figure 1. Comparison between experimental and calculated  $D$ -values, with one standard deviation included for the experimental values. A few interesting points are indicated. For most of the experimental  $D$ -values the standard deviation is so small that it is covered completely by the dots.

## CONCLUSIONS

The model gives reasonably good agreement with experiments in most of the extraction cases tested. However, the real merit of this analysis lies more in the possibilities to draw conclusions about the effects of different solvents. Inspection of the fitted polar and hydrogen bonding solubility parameters strongly indicates that there is no significant difference between the three metal complexes in their solvent interactions. This confirms and provides an explanation of why the choice of solvent is of no significance to the selectivity. The separation between lanthanides and actinides is most likely dominated by the complex formation as indicated by the big difference in  $K_D$ -values.

Nevertheless, a careful selection of solvent is still necessary, e.g., with respect to phase flows in a multistage process, chemical and radiolytical stability, ease of phase separation and kinetics.

In future work the viability of still more refined extensions of the Scatchard-Hildebrand theory will be tested, e.g., by inclusion of induced dipole interactions. Similar concepts of this kind have been applied at this department quite some time ago [11].

## ACKNOWLEDGEMENTS

We wish to thank the Swedish Nuclear and Waste Management Co., SKB and the European Union (PARTNEW FIKW-CT2000-00087) for financial support.

## REFERENCES

1. J. Burke (1984), The Book and Paper Group Annual / Washington D.C Book and Paper 1982, **3**, 13-58.
2. C. Hansen (1967), *J. Paint. Tech.*, **39** (505), 104-117.
3. C. Hansen (2000), Hansen Solubility Parameters: A Users Handbook, CRC Press, pp. 167-185.
4. A. F. M. Barton (1991), CRC Handbook of Solubility Parameters and Other Cohesion Parameters, CRC Press, pp. 182-185.
5. Charles Tenant & Company (London) Ltd [*Internet*]. Available from: <http://www.ctenant.co.uk/proddata/tp00006a.htm> [Accessed 28 May 2001].
6. C. Hansen and K. Skaaup (1967), *Dansk Kemi*, **48**, 81-84.
7. I. Hagström, L. Spjuth, Å. Enarsson, J-O. Liljenzin, M. Skålberg, M.J. Hudson, P.B. Iveson, C. Madic, P.Y. Cordier, C. Hill and N. Francois (1999), *Solvent Extraction and Ion Exchange*, **17** (2), 221-242.
8. M. Tanaka (1971), *Proc. ISEC '71*, The Hague, the Netherlands, paper 66, 18-24.
9. H. Jobst (1972), *Farbe und Lack*, **78** (9), 813-822.
10. G. Meinrath, C. Ekberg, A. Landgren and J-O. Liljenzin (2000), *Talanta*, **51** (2), 231-246.
11. S. Winge fors, J-O. Liljenzin, E. Saalman (1980), *Proc. ISEC '80*, Liege, Belgium, paper 3-15A-80-116.

### Editors' Note:

Please note that this is the corrected version of this paper, and replaces that which appears in the published version of the Proceedings of ISEC 2002.



## APPLICATION OF SISAK FOR FAST CONTINUOUS SOLVENT EXTRACTION PROCESSES TO STUDY EXOTIC NUCLIDES

G. Skarnemark, J. Alstad\*, K. Eberhardt\*\*, K.E. Gregorich\*\*\*, D.C. Hoffman\*\*\*,  
M. Johansson\*, U. Kirbach\*\*\*, G. Langrock\*\*, M. Mendel\*\*, V. Ninov\*\*, H. Nitsche\*\*\*,  
A. Nähler\*\*, J.P. Omtvedt\*, L.A. Omtvedt\*, L. Stavsetra\*, R. Sudowe\*\*,  
N. Trautmann\*\* and N. Wiehl\*\*

Department of Nuclear Chemistry, Chalmers University of Technology, Göteborg, Sweden

\*Department of Chemistry, University of Oslo, Oslo, Norway

\*\*Institut für Kernchemie, University of Mainz, Mainz, Germany

\*\*\*Nuclear Science Division, Lawrence Berkeley National Laboratory, Berkeley, CA, USA

SISAK (Short-lived Isotopes Studied by the AKUFVE technique) enables on-line studies of exotic nuclides chemically separated from complex nuclear reaction product mixtures. The technique applies multistage liquid-liquid extraction steps, where rapid phase separation is achieved by using specially designed centrifuges with short hold-up times. The technique has been successfully applied to nuclear spectroscopic investigations of short-lived fission products, but in the recent years focused on studies of the chemical properties of the heaviest elements, the transactinides. The chemical properties that can be investigated with the SISAK system include distribution coefficients and complex formation, as well as the kinetics of solvent extraction processes and redox reactions.

### INTRODUCTION

During the last decades there has been a growing interest in studying chemical properties of the heaviest elements, the transactinides (atomic number  $\geq 104$ ). These investigations are of great interest, because the comparison of the chemical properties of the transactinides with the behavior of their lighter group homologs allows the examination of trends within the periodic table and an assessment of the influence of relativistic effects. The transactinides are synthetic, radioactive elements with short half-lives, usually in the range of seconds. They can be produced at suitable accelerators only in extremely small amounts, typically less than a few atoms per hour. The nuclear reaction products, from which they are to be isolated, comprise a very complex mixture of more or less the rest of the elements of the periodic table. This makes the chemical separation a difficult task. The technique used must be fast, selective and also suitable for one-atom-at-a-time chemistry. The latter statement indicates that the transactinide atoms are likely to arrive at the chemical separation system one at a time, which means that many of the normal chemistry laws are not valid. Examples are that polynuclear complexes cannot be formed, and with only one atom present normal chemical equilibrium does not exist. Instead of concentrations, the probability that the atom exists in a certain chemical state must be used.

The fast chemical separation technique SISAK [1-3] has been developed for studies of exotic nuclides. In this paper, "exotic" refers to nuclides with half-life shorter than a few seconds or nuclides which can only be produced on a one-atom-at-a-time scale. SISAK was originally used for on-line nuclear spectroscopy studies of short-lived  $\gamma$ -emitters. Recently the technique has been successfully adopted to studies of transactinides [4,5]. Below, the method is described together with the application to studies of short-lived isotopes of protactinium and rutherfordium ( $^{104}\text{Rf}$ ).

## EQUIPMENT

In a typical SISAK experiment, see Figure 1, radionuclides are continuously transported from the production site in an accelerator or a research reactor to the SISAK equipment attached to aerosol particles ("clusters") in a gas-jet transport system [6,7]. The nuclides carried by the gas-jet are dissolved in an aqueous phase in a static mixer, and then a specially designed degassing centrifuge [3,8] is used to separate the carrier gas and volatile products from the liquid. The solution is usually heated to  $\sim 70$  °C to enhance the dissolution of the aerosol particles delivered by the gas-jet, to increase the efficiency of the degassing centrifuge and to speed up the solvent extraction kinetics in the subsequent separation steps.

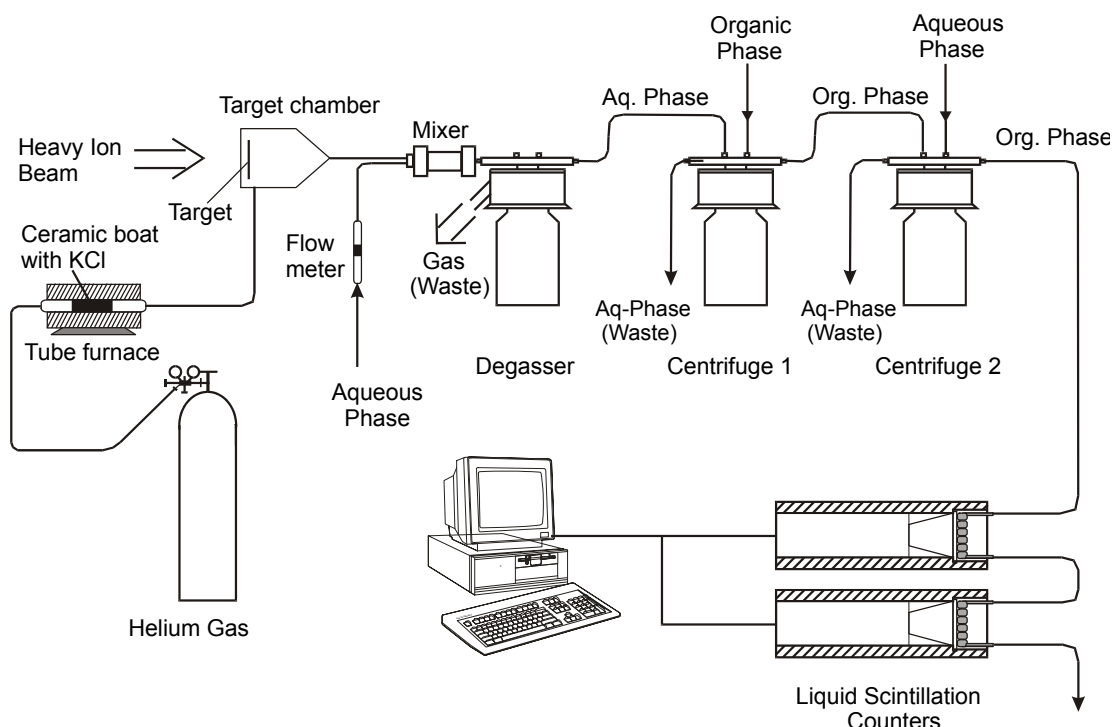


*Figure 1. A typical SISAK set-up for transactinide studies.*

The effluent from the degasser is fed into a battery with a number of H-centrifuges [3,9]. The centrifuges used in the third version of SISAK, the equipment presently in use, are made of PEEK (polyetheretherketone), a material that withstands organic solvents and all common acids except concentrated sulfuric acid. The rest of the equipment is made of Kel-F, PTFE (polytetrafluoroethylene), PVDF (polyvinylidenefluoride) and PEEK. The centrifuges have been thoroughly described elsewhere [3,9], and the technical details will not be further discussed here.

Monitoring the purity of the phases leaving the centrifuges is performed by measuring the optical transmittance through the liquid. In a phase containing entrainment of the opposite phase light will be refracted at the boundaries between the two phases. The measuring devices, which consist of a small light emitting diode (LED) and a photo transistor, are connected to a personal computer. There, the phase purity and its fluctuations with time can be easily displayed. It is also possible to let the computer intervene if the phase purity falls below a selected value, e.g., by switching the valve between the SISAK equipment and the nuclear detection system to a bypass position. The phase purity is adjusted manually by valves affecting the counter-pressure on the phases leaving the centrifuge. Usually the system runs very steadily when pure phases have been achieved, and there has been no urgent need to computerize the valve operation.

The feed pumps used in the equipment are cog-wheel pumps with a flow capacity that can be continuously varied up to ~3 ml/s. Several types of pumps are used: all PEEK pumps, pumps with a house of titanium and cog-wheels of Kel-F and pumps with a house of stainless steel and cog-wheels of carbon. The flowrates of the pumps are measured with mass flow meters, and the flow-rates are displayed on the same computer screen as the phase purity. The computer is also used to regulate the speed of the pumps.

## SOLVENT EXTRACTION PROCEDURES

Rapid SISAK solvent extraction procedures have so far been developed for 20 elements: copper, arsenic, bromine, zirconium, niobium, technetium, ruthenium, palladium, iodine, lanthanum, cerium, praseodymium, hafnium, tantalum, tungsten, neptunium, rutherfordium, dubnium, seaborgium, and bohrium, see Table 1. These procedures are described in detail in [10-23].

One of the most important issues when designing chemical separation procedures for SISAK is the need for fast solvent extraction kinetics. The flow-rates are typically ~1 ml/s, and under these circumstances the contact time of the two phases is ~40 ms. Under ideal conditions solvent extraction is a fast process. An example is the transfer of nitric acid from water to tributylphosphate (TBP) which is complete in about 12 ms [24]. This time is, however, close to the contact time available in the SISAK 3 system. Thus it is necessary to choose separation procedures with rapid chemical kinetics or with a distribution ratio that is high enough to extract a sufficient amount of the element to be investigated, even if the extraction is terminated under non-equilibrium conditions. The first type of procedures can be exemplified by the extraction of inorganic species like Br<sub>2</sub>, AsI<sub>3</sub> or RuO<sub>4</sub> into a pure organic solvent [10,11] and by extraction of ion pairs [11,18]. The second type of systems can be illustrated by the extraction of zirconium or hafnium from 6 M nitric acid into 0.25 M HDBP (dibutyl phosphoric acid) in toluene. In this system the distribution coefficient has been measured to be 10 in SISAK experiments, while the corresponding value in test tube experiments with 5 s contact time is ~1.5·10<sup>4</sup> [20]. A chelate extraction with β-diketones is usually too slow to be used in SISAK experiments, but there are exceptions, e.g. the extraction of short-lived palladium isotopes that is made possible by a fast isotopic exchange with a pre-formed palladium complex [15].

## APPLICATIONS TO STUDIES OF EXOTIC NUCLIDES

The application of SISAK to nuclear spectroscopic studies of short-lived fission products has been described elsewhere [13,14,23,25], and will not be further discussed here. Instead, the application to studies of <sup>224</sup>Pa ( $T_{1/2} = 0.85$  s) and <sup>257</sup>Rf ( $T_{1/2} = 4.0$  s) will be described.

*Table 1. SISAK separation systems available 2001.*

Element	Procedure	References
Cu	Cu extracted from 6 M ZnCl <sub>2</sub> at pH = 3-3.5 into LIX64 in kerosene. Backextraction into 0.5 M HCl	1
As	Extraction as AsI <sub>3</sub> from 3 M HCl and 1 M HI into CHCl <sub>3</sub> . Back-extraction into 0.1 M HCl	10
Br	Oxidation to Br <sub>2</sub> by KBrO <sub>3</sub> followed by extraction into CCl <sub>4</sub> . Back-extraction into 0.1 M H <sub>2</sub> SO <sub>4</sub> and 0.1 M Na <sub>2</sub> SO <sub>3</sub> , re-oxidation, re-extraction into CHCl <sub>3</sub>	11
Zr	Extraction of Zr and Nb from 1 M H <sub>2</sub> SO <sub>4</sub> into tertiary amine in kerosene. Back-extraction into 0.1 M HNO <sub>3</sub> , addition of HNO <sub>3</sub> until 5 M, addition of H <sub>2</sub> O <sub>2</sub> , re-extraction of Zr into 1 M HDEHP in kerosene	11
Nb	See Zr procedure; Nb remains in aqueous phase after the final Zr extraction	11
Tc	Extraction from 0.1 M H <sub>2</sub> SO <sub>4</sub> and 0.01 M Ce(SO <sub>4</sub> ) <sub>2</sub> into 0.005 M TPAC in CHCl <sub>3</sub>	11,12-14
Ru	Extraction from 0.1 M H <sub>2</sub> SO <sub>4</sub> and 0.015 M Ce(SO <sub>4</sub> ) <sub>2</sub> into CCl <sub>4</sub>	10,15,16
Pd	After isotopic exchange of fission product Pd with a pre-formed Pd-acetylacetone complex, Pd is extracted into toluene.	15
I	Extraction from 0.1 M HNO <sub>3</sub> and 0.1 M NaNO <sub>2</sub> into CCl <sub>4</sub> , back-extraction into 0.1 M H <sub>2</sub> SO <sub>4</sub> and 0.1 M Na <sub>2</sub> SO <sub>3</sub>	11
La	Extraction from HNO <sub>3</sub> (pH = 1.4) into 0.3 M HDEHP in kerosene, back-extraction into 1 M HNO <sub>3</sub> and 0.05 M K <sub>2</sub> Cr <sub>2</sub> O <sub>7</sub>	2,13,14
Ce	Extraction from 1 M HNO <sub>3</sub> and 0.05 M K <sub>2</sub> Cr <sub>2</sub> O <sub>7</sub> into 0.3 M HDEHP in kerosene, back-extraction into 1 M HNO <sub>3</sub> , 0.05 M H <sub>2</sub> O <sub>2</sub> and 0.02 M sulfamic acid	2,13,14
Pr	Extraction from 1 M HNO <sub>3</sub> and 0.05 M K <sub>2</sub> Cr <sub>2</sub> O <sub>7</sub> into 0.3 M HDEHP in kerosene, back-extraction into 1 M HNO <sub>3</sub> and 0.05 M K <sub>2</sub> Cr <sub>2</sub> O <sub>7</sub>	13,14
Hf	Extraction from 3 M HNO <sub>3</sub> into 0.2 M HDBP in toluene	17
Ta	Extraction from 1 M $\alpha$ -hydroxyisobutyric acid into 0.047 M TOA in toluene	18
W	See Ta	18
Np	Reduction to Np(IV) by TiCl <sub>3</sub> followed by extraction of contaminants into HDEHP in CCl <sub>4</sub> . Np re-oxidized to Np(V) by HNO <sub>3</sub> , extraction into 0.2 M HDEHP in kerosene, back-extraction into 5 M H <sub>3</sub> PO <sub>4</sub>	19
<sup>104</sup> Rf	Extraction from 6 M HNO <sub>3</sub> into 0.05 M TOA in toluene, wash with 2 M NaNO <sub>3</sub>	4,5,20
<sup>105</sup> Db	See Ta	18
<sup>106</sup> Sg	Extraction from 0.5 M lactic acid into 0.05 TOA in toluene. For enhanced radiochemical purity a back-extraction into 0.2 M NaClO <sub>4</sub> and 0.5 M H <sub>3</sub> PO <sub>4</sub> , and a re-extraction into 0.37 M TOA in toluene can be added.	19,21
<sup>107</sup> Bh	Extraction from 0.05 M HNO <sub>3</sub> and 0.05 M KBrO <sub>3</sub> into 0.05 M TOA in toluene	22

<sup>224</sup>Pa was studied in an experiment to verify that the SISAK technique can be used to identify short-lived  $\alpha$ -decaying radionuclides on a one-atom-at-a-time basis [26]. The protactinium isotope was produced by bombarding a bismuth target with oxygen ions. The production rate was about 60 atoms/s, *i.e.* much higher than in an experiment on a transactinide but nevertheless so low that the protactinium atoms arrived one at a time in the chemical separation equipment. The nuclear reaction products were transported to the SISAK equipment by the gas-jet system, and dissolved in 1 M lactic acid (HLac). Since considerable amounts of polonium were formed in the nuclear reaction, the aqueous phase was put in contact with 1 M Cyanex 471X (tri-isobutylphosphine sulfide) in toluene in the first solvent extraction step. Otherwise polonium would be co-extracted with protactinium in the following step.

In the second step, the aqueous phase was put in contact with 0.047 M tri-n-octyl amine (TOA) in toluene. The organic phase also contained a scintillator, and the solution was fed straight into a liquid scintillation detection system [27] where the radioactivity was measured. In order to make the identification of  $^{224}\text{Pa}$  unambiguous, the entire  $\alpha$ -decay chain  $^{224}\text{Pa} - ^{220}\text{Ac} - ^{216}\text{Fr} - ^{208}\text{Bi}$  was measured. The result of the experiment showed that  $^{224}\text{Pa}$  could be extracted and identified [26], *i.e.* it proved that SISAK can be applied to one-atom-at-a-time separations of short-lived  $\alpha$ -emitters.

Recently, an experiment to study chemical properties of rutherfordium was performed [5]. A lead target was bombarded with titanium ions to produce  $^{257}\text{Rf}$ . The production rate of rutherfordium was a few atoms per hour. To improve the chemical purity of the measured solution, the Berkeley Gas-filled Separator (BGS) [28] was used as a pre-separator to remove polonium and other potential contaminants prior to the chemical separation. The separated rutherfordium was then transferred to the SISAK equipment via a specially designed gas-jet system [29].

The radionuclides were then dissolved in 6 M nitric acid. The acid solution was then contacted with 0.25 M dibutyl phosphoric acid (HDBP) to extract rutherfordium. The organic phase was then washed with 2 M sodium nitrate to back-extract nitric acid that would otherwise disturb the subsequent liquid scintillation measurement. After washing, scintillation chemicals were added and the solution was purged with argon before being pumped into the liquid scintillation system.

So far the experiment, however not fully evaluated, showed that rutherfordium was extracted and the estimated distribution ratio is comparable to those of the homologs zirconium and hafnium, *i.e.*, it shows the expected behavior of a group 4 element.

A general conclusion from the experiment is that rapid on-line liquid-liquid extraction can be used for one-atom-at-a-time separations. Thus it should be possible to obtain distribution curves for transactinides and to deduce information about complex formation. By applying more specific chemical separation systems, it should also be possible to distinguish between different valency states and thus investigate redox properties of the heaviest elements.

## REFERENCES

1. P.O. Aronsson, B.E. Johansson, J. Rydberg, G. Skarnemark, J. Alstad, B. Bergersen, E. Kvåle and M. Skarestad (1974), *J. Inorg. Nucl. Chem.*, **36**, 2397-2403.
2. G. Skarnemark, P.O. Aronsson, K. Brodén, J. Rydberg, T. Bjørnstad, N. Kaffrell, E. Stender and N. Trautmann (1980), *Nucl. Instrum. Methods*, **171**, 323-328.
3. H. Persson, G. Skarnemark, M. Skålberg, J. Alstad, J.O. Liljenzin, G. Bauer, F. Haberberger, N. Kaffrell, J. Rogowski and N. Trautmann (1989), *Radiochim. Acta*, **48**, 177-180.
4. J.P. Omtvedt, J. Alstad, K. Eberhardt, K. Fure, R. Malmbeck, M. Mendel, A. Nähler, G. Skarnemark, N. Trautmann, N. Wiehl and B. Wierczinski (1998), *J. Alloys Compounds*, **271-273**, 303-306.
5. J.P. Omtvedt, the SISAK collaboration, and the LBNL Heavy Element Group (2000), Ernest Orlando Lawrence Berkeley National Laboratory, Nuclear Science Division Annual Report. Available from <<http://ydcmac.lbl.gov/>>.
6. N. Trautmann, P.O. Aronsson, T. Bjørnstad, N. Kaffrell, E. Kvåle, M. Skarestad, G. Skarnemark and E. Stender (1975), *Inorg. Nucl. Chem. Lett.*, **11**, 729-735.
7. E. Stender, N. Trautmann and G. Herrmann (1980), *Radiochem. Radioanal. Lett.*, **42**, 291-296.
8. K. Brodén, H. Persson, J. Rydberg and G. Skarnemark (1982), *Nucl. Instrum. Methods*, **195**, 539-542.

9. J. Alstad, G. Skarnemark, F. Haberberger, G. Herrmann, A. Nähler, M. Pense-Maskow and N. Trautmann (1995), *J. Radioanal. Nucl. Chem.*, **189** (1), 133-139.
10. G. Skarnemark, K. Brodén, M. Yun, N. Kaffrell and N. Trautmann (1983), *Radiochim. Acta*, **33**, 97-100.
11. K. Brodén, G. Skarnemark, T. Bjørnstad, D. Eriksen, I. Haldorsen, N. Kaffrell, E. Stender and N. Trautmann (1981), *J. Inorg. Nucl. Chem.*, **43**, 765-771.
12. T. Altzitzoglou, J. Rogowski, M. Skålberg, J. Alstad, G. Herrmann, N. Kaffrell, G. Skarnemark, W. Talbert and N. Trautmann (1990), *Radiochim. Acta*, **51**, 145-150.
13. G. Skarnemark, M. Skålberg, J. Alstad and T. Bjørnstad (1986), *Phys. Scripta*, **34**, 597-607.
14. G. Skarnemark, J. Alstad, N. Kaffrell and N. Trautmann (1990), *J. Radioanal. Nucl. Chem.*, **1**, 145-158.
15. N. Kaffrell, J. Rogowski, H. Tetzlaff, N. Trautmann, D. De Frenne, K. Heyde, E. Jacobs, G. Skarnemark, J. Alstad, M.N. Harakeh, J.M. Schippers, S.Y. van der Werf, W.R. Daniels and K. Wolfsberg (1988), *AIP Conference Proceedings*, **164**, 286-295.
16. G. Lhersonneau, B. Pfeiffer, J. Alstad, P. Dendooven, K. Eberhardt, S. Hankonen, I. Klöckl, K.-L. Kratz, A. Nähler, R. Malmbeck, J.P. Omtvedt, H. Penttilä, S. Schoedder, G. Skarnemark, N. Trautmann and J. Äystö (1998), *Europ. Phys. J A*, **1**, 285-297.
17. M. Pense-Maskow, J. Alstad, K. Eberhardt, G. Herrmann, A. Nähler, A.V.R. Reddy, G. Skarnemark, N. Trautmann and B. Wierczinski (1994), *University of Mainz Report IKMz* 94-1, p. 4.
18. B. Wierczinski, J. Alstad, K. Eberhardt, B. Eichler, H. Gäggeler, G. Herrmann, D. Jost, A. Nähler, M. Pense-Maskow, A.V.R. Reddy, G. Skarnemark, N. Trautmann and N. Türler (1995), *Radiochim. Acta*, **69**, 77-80.
19. H. Tetzlaff, G. Herrmann, N. Kaffrell, J.V. Kratz, J. Rogowskil, N. Trautmann, M. Skålberg, G. Skarnemark, J. Alstad, M.M. Fowler, K.J. Moody, W. Brüchle, H. Gäggeler, M. Schädel and K. Sümmerer (1986), *J. Less Comm. Met.*, **122**, 441-444.
20. J.E. Dyve (2000), Diploma Thesis, University of Oslo, Norway.
21. M. Johansson, J. Alstad, J.E. Dyve, K. Eberhardt, A. Nähler, J.P. Omtvedt, G. Skarnemark and N. Trautmann (2001), submitted to *J. Radioanal. Nucl. Chem.*
22. R. Malmbeck, G. Skarnemark, J. Alstad, K. Fure and J.P. Omtvedt (2000), *J. Radioanal. Nucl. Chem.*, **246** (2), 349-353.
23. B. Wierczinski, J. Alstad, K. Eberhardt, J.V. Kratz, R. Malmbeck, M. Mendel, A. Nähler, J.P. Omtvedt, G. Skarnemark, N. Trautmann and N. Wiehl (1998), *J. Radioanal. Nucl. Chem.*, **236** (1) 193-197.
24. K.K. Lunes and R.P. Wishow (1985), *USAEC Report TID-11414*.
25. G. Skarnemark (2000), *J. Radioanal. Nucl. Chem.*, **243** (1), 219-225.
26. B. Wierczinski, K.E. Gregorich, B. Kadkhodayan, D.M. Lee, L.G. Beauvais, M.B. Hendricks, C.D. Kacher, M.R. Lane, D.A. Keeney-Shaughnessy, N.J. Stoyer, D.A. Strellis, E.R. Sylwester, P.A. Wilk, D.C. Hoffman, R. Malmbeck, G. Skarnemark, J. Alstad, J.P. Omtvedt, K. Eberhardt, M. Mendel, A. Nähler and N. Trautmann (2001), *J. Radioanal. Nucl. Chem.*, **247** (1), 57-60.
27. B. Wierczinski, K. Eberhardt, G. Herrmann, J.V. Kratz, M. Mendel, A. Nähler, F. Rocker, U. Tharun, N. Trautmann, K. Weiner, N. Wiehl, J. Alstad and G. Skarnemark (1996), *Nucl. Instrum. Methods Phys. Res. A*, **370**, 532-538.
28. T.N. Ginter, K.E. Gregorich, U.W. Kirbach, V. Ninov, J.B. Patin, D.A. Strellis, P.A. Wilk and P.M. Zielinski (1999), Ernest Orlando Lawrence Berkeley National Laboratory, Nuclear Science Division Annual Report. Available from <<http://ydcmac.lbl.gov/>>.
29. U.W. Kirbach, K.E. Gregorich, V. Ninov, D.M. Lee, J.B. Patin, D.A. Shaughnessy, D.A. Strellis, P.A. Wilk, D.C. Hoffman and H. Nitsche (1999), Ernest Orlando Lawrence Berkeley National Laboratory, Nuclear Science Division Annual Report. Available from <http://ydcmac.lbl.gov/>.



## SANEX-BTP PROCESS DEVELOPMENT STUDIES

Clément Hill, Denis Guillaneux and Laurence Berthon

Commissariat à l'Energie Atomique, Marcoule, France

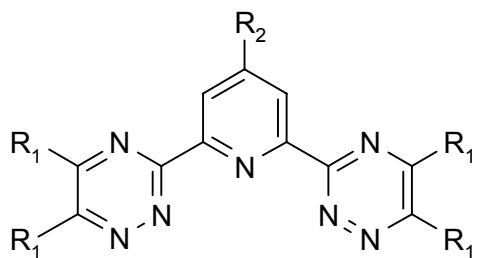
*Bis*-triazinyl-pyridines have been developed at CEA-Marcoule to separate actinides(III) from lanthanides(III). Although high separation performances were observed in the counter-current hot test carried out in 1999 on a highly active effluent, the extraction and back-extraction yields of actinides(III) were lower than expected from calculation. A strong sensitivity of the extractant towards air oxidation and acidic hydrolysis was actually pointed out. Therefore, the hydrolysis of *bis*-triazinyl-pyridines has been thoroughly investigated (qualitative determination of the degradation products) under different experimental conditions. It appeared that the branching of the alkyl groups on the  $\alpha$  position of the triazine rings hindered the hydrolysis of the extractant. The formulation of the solvent was thus optimized and tested again during year 2001 on a genuine DIAMEX back-extraction solution in the ATALANTE facility.

### INTRODUCTION

The separation of trivalent minor actinides ( $An(III) = Am(III)$  and  $Cm(III)$ ) from trivalent lanthanides ( $Ln(III)$ ), accounting for about one third of the total amount of fission products), is a key step for the partitioning of long-lived radionuclides from the highly active effluents issuing from the reprocessing of nuclear spent fuels. However, this separation is very difficult because  $An(III)$  and  $Ln(III)$  exhibit similar chemical properties.

Several studies in media of low acidity have shown already that nitrogen-containing polydendate ligands were able to separate  $An(III)$  from  $Ln(III)$  when mixed with lipophilic anions [1,2]. However, a new family of extractants -*bis*-triazinyl-pyridines- (Btp, Figure 1) has been developed by Dr. Z. Kolarik [3] in the framework of the European contract NEWPART led by CEA-Marcoule. These molecules appeared to be very efficient extracting agents: they remained selective towards  $An(III)$  even in very acidic conditions ( $[HNO_3] \geq 2 \text{ mol/L}$ ).

Various BTP molecules were synthesized and studied at CEA-Marcoule. Among them, the 2,6-bis(5,6-*n*-propyl-1,2,4-triazin-3-yl)-pyridine (*nPr*-Btp) was chosen in 1999 to perform a counter-current hot test in the ATALANTE facility on a genuine radioactive effluent. The performances of the flowsheet were very satisfactory ( $1,400 < DF_{Ln(III)} < 450,000$ ), but the extraction and back-extraction yields of  $Am(III)$  and  $Cm(III)$  were lower than expected from calculation. *nPr*-Btp showed up to be sensitive to air oxidation and to acidic hydrolysis.



with R<sub>1</sub> = H, Methyl, *n*-Propyl,  
*i*-Propyl, *n*-Butyl, *i*-Butyl  
and R<sub>2</sub> = H, *i*-Nonyl

*Figure 1. General formula of Btp.*

## DEGRADATION OF nPr-BTP UNDER OXIDATIVE AND HYDROLYZING CONDITIONS

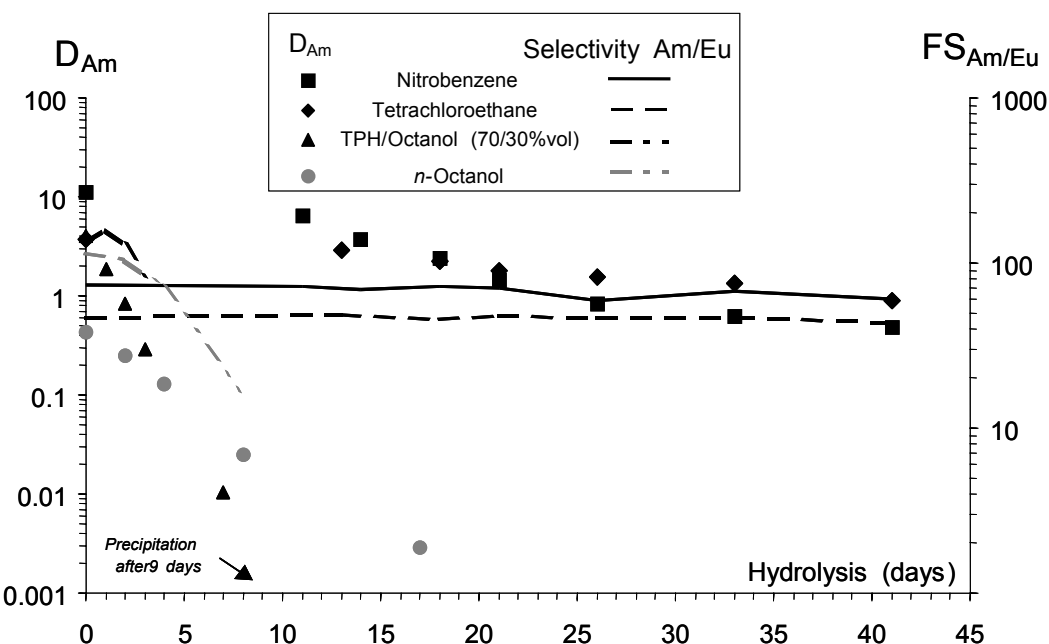
A systematic measurement of the distribution ratios of Am(III) and Eu(III), when hydrolyzing *n*Pr-Btp with nitric acid (with or without nitrous acid), revealed that its extraction properties steadily decreased when the atmosphere was rich in oxygen or when [HNO<sub>3</sub>] exceeded 0.5 mol/L (D<sub>Am</sub> decreased by 80% after 2 days when [HNO<sub>3</sub>] = 1 mol/L). Furthermore, the extraction properties of *n*Pr-Btp quickly decreased when [HNO<sub>2</sub>] exceeded 0.005 mol/L (D<sub>Am</sub> decreased by 50% after 2 hours when [HNO<sub>3</sub>] = 1 mol/L + [HNO<sub>2</sub>] = 0.01 mol/L).

Gas Phase Chromatography and/or Electro-spray Ionization Mass Spectrometry qualified the main degradation products of *n*Pr-Btp. The influence of several parameters such as: (i) the nature of the atmosphere above the Btp solution (e.g.: air or inert argon), (ii) the nature of the diluent (e.g.: dodecane/octanol (70/30%<sub>vol</sub>) mixture or chloroform), (iii) the presence or absence of an acidic aqueous phase, has been studied on the degradation of *n*Pr-Btp. It appeared that the degradation products of *n*Pr-Btp were the same whatever the experimental conditions, only their quantities varied. From these studies, the first step of *n*Pr-Btp degradation was assumed to be the attack of one CH<sub>2</sub> group, on the  $\alpha$  position of the triazinyl rings, resulting in the formation of a nitro compound (observed by <sup>15</sup>N NMR). Thereafter, the compound would degrade into an alcohol (which was the main degradation product observed in the absence of an hydrolyzing aqueous phase) or into a ketone (which was the main degradation product after the hydrolysis of *n*Pr-Btp by nitric acid). In the same way, the attack of a second CH<sub>2</sub> group would result in the formation of bifunctional compounds (dialcohols and diketones). The alcohol compounds could also loose one propyl chain. Another reaction was the breaking of the triazinyl ring leading to cyano compounds.

The nature of the organic diluent affected the stability of *n*Pr-Btp: as compared to aliphatic, alcoholic or aromatic diluents, nitrobenzene and chlorinated diluents seemed to prevent *n*Pr-Btp from degrading (Figure 2). However, since these organic diluents were not acceptable for an industrial separation process development, further investigations were carried out to strengthen *n*Pr-Btp towards hydrolysis. Thus, the formulation of the solvent has been improved and optimized.

## OPTIMIZATION OF THE BTP SOLVENT FORMULATION

Other substituted Btp molecules, especially those bearing branched groups on the  $\alpha$  position of the triazinyl rings (such as Cy-Btp-Me and *i*Pr-Btp), proved to be much more stable in acidic conditions than *n*Pr-Btp or *n*Bu-Btp, bearing linear alkyl groups. Although Cy-Btp-Me and *i*Pr-Btp were not chosen for the implementation of the hot test in 1999, because of several practical reasons (*i.e.*: tedious synthesis, low solubility in organic diluent, slow kinetics of extraction), they actually showed a favorable stability over 30 days of acidic hydrolysis (Figure 3).



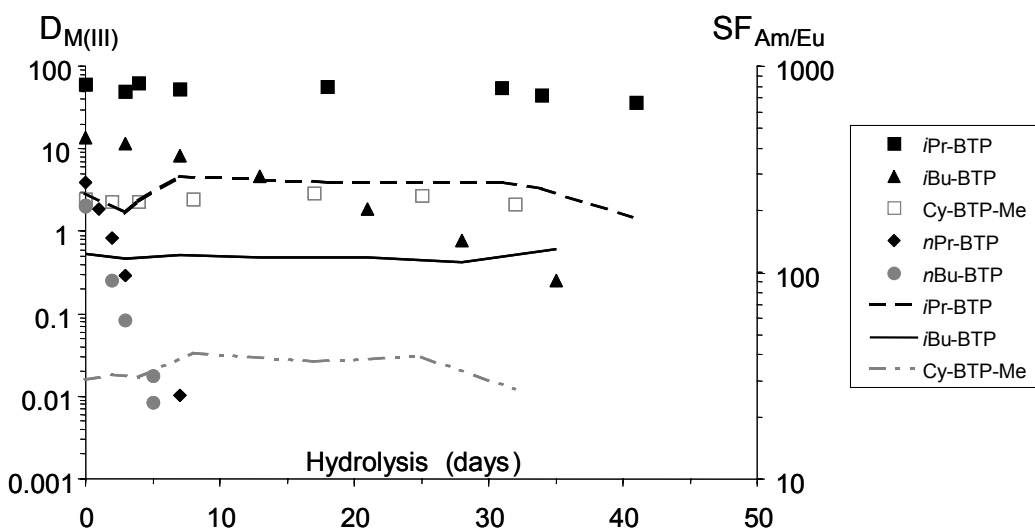
Hydrolysis cycles: 1 hour mixing followed by 2 hours settling (24 hours/day);  $\theta = 25^\circ\text{C}$ .

Hydrolyzing aqueous solution:  $[\text{HNO}_3] = 1 \text{ mol/L}$ .

Hydrolyzed organic solutions:  $[\text{nPr-Btp}] = 0.02 \text{ mol/L}$  in various organic diluents.

Extraction tests:  $[\text{HNO}_3] = 1 \text{ mol/L}$ , spiked with  $^{152}\text{Eu}$  and  $^{241}\text{Am}$ ;  $\theta = 25^\circ\text{C}$ .

Figure 2. Influence of the nature of the organic diluent on the stability of nPr-Btp under acidic hydrolysis/oxidation.



Hydrolysis cycles: 1 hour mixing, followed by 2 hours settling (24 hours/day);  $\theta = 25^\circ\text{C}$ .

Hydrolyzing aqueous solution:  $[\text{HNO}_3] = 1 \text{ mol/L}$ .

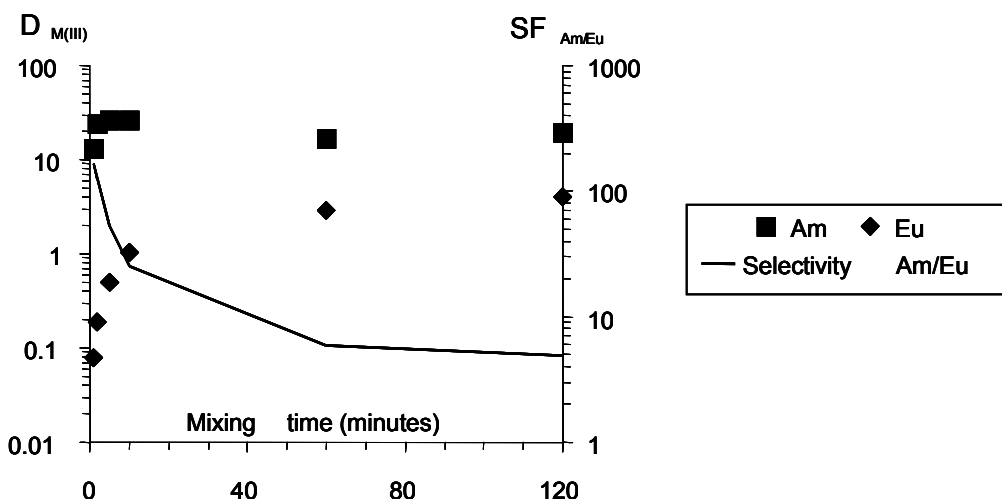
Hydrolyzed organic sol.:  $[\text{Btp}] = 0.005$  or  $0.01 \text{ mol/L}$  in n-octanol or "n-octanol /TPH" mixture.

Extraction tests:  $[\text{HNO}_3] = 1 \text{ mol/L}$ , spiked with  $^{152}\text{Eu}$  and  $^{241}\text{Am}$ ;  $\theta = 25^\circ\text{C}$ .

Figure 3. Comparison of the stability of different Btps under acidic hydrolysis.

Several attempts were made to accelerate the kinetics of extraction of these Btps, by mixing them with other co-extractants, such as: TBP, monoamides or diamides. In some cases, the latter modifiers increased the kinetics of extraction of the Btps, and in other cases, they enhanced their extraction performances or their stability under acidic hydrolysis, but lowered their selectivity towards An(III).

For instance, the case of *i*Pr-Btp was rather peculiar. As compared to *n*Pr-Btp, when *i*Pr-Btp was diluted in a mixture of *n*-octanol and TPH and when the feed solution was only spiked with radio-tracers  $^{241}\text{Am}$  and  $^{152}\text{Eu}$ , the observed extraction kinetics were fast for Am(III) and very slow for Eu(III) (Figure 4a). When concentrated solutions simulating genuine DIAMEX back-extraction effluents were used, a precipitate occurred with the "*n*-octanol/TPH" mixtures. However, no precipitate was observed when dissolving *i*Pr-Btp in pure *n*-octanol, tetrachloroethane or nitrobenzene, but the extraction kinetics became very slow both for Am(III) and Eu(III).



(a) Aqueous solution:  $[\text{HNO}_3] = 1 \text{ mol/L}$ , spiked with  $^{152}\text{Eu}$  and  $^{241}\text{Am}$ .  
Organic solution:  $[\text{iPr-Btp}] = 0.01 \text{ mol/L}$  in an "*n*-octanol / TPH" mixture;  $\theta = 25^\circ\text{C}$ .  
(b) Aqueous solution: synthetic solution simulating a DIAMEX back-extraction effluent.

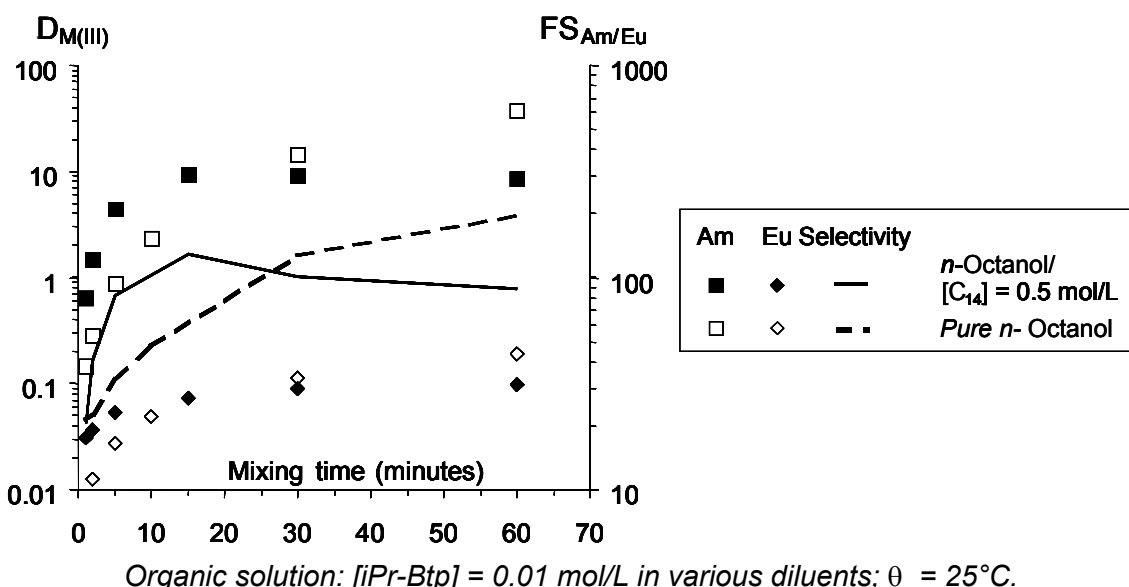


Figure 4. Comparison of the kinetics of extraction of *i*Pr-Btp in various diluents and experimental conditions.

Therefore, a phase transfer catalyst, such as a diamide ( $C_{14}$  = dimethyl-dibutyl-tetradecyl-malonamide) had to be mixed with *i*Pr-Btp to increase the kinetics of extraction and decrease the time required to reach equilibrium (Figure 4b). Other diamides have been tested as co-extractants of *i*Pr-Btp in *n*-octanol. Very good results were observed with dimethyl-diethyl-hexylethoxy-malonamide ( $C_2OC_6$ ). However, although the kinetics of extraction of An(III) and Ln(III) were fast with these binary mixtures, the kinetics of back-extraction of the latter two cations appeared to be easy but too slow in diluted nitric acid to develop a process flowsheet (the equilibrium was only reached after 2 hours of mixing). That is why, hydrophilic complexing agents, such as citric acid or glycolic acid, have been tried to enable and increase An(III) and Ln(III) back-extraction.

Prior to the hot test, numerous series of experiments have been carried out in micro-tubes on synthetic aqueous solutions simulating DIAMEX back-extraction solutions. The influence of the composition of the organic solvent (concentration of *i*Pr-BTP or  $C_2OC_6$  in *n*-octanol) on the extraction yields and extraction kinetics of Ln(III) and An(III) was assessed. A process flowsheet has been designed and first tested on a battery of eight centrifugal-contactors, using a synthetic nitric acid solution containing Nd(III) and Eu(III) at 2 g/L and 100 mg/L, respectively. The hydrodynamic behavior of the solvent was very satisfactory.

A 32-stage process flowsheet should be tested in the ATALANTE facility on a genuine highly active effluent at the end of June 2001. The results of this hot test will be discussed later on.

## CONCLUSION

The SANEX hot test carried out at CEA-Marcoule in 1999 with the 2,6-bis(5,6-*n*-propyl-1,2,4-triazin-3-yl)-pyridine pointed out the strong sensitivity of this extractant towards air oxidation and acidic hydrolysis. Qualitative determination of the degradation compounds of *n*Pr-Btp allowed a better understanding of its degradation mechanism: *n*Pr-Btp mainly degraded into alcoholic derivatives through the oxidation of its propyl substituents (probably through radical reactions). Therefore, many efforts were put forward to strengthen the stability of *n*Pr-Btp under hydrolysis and to optimize the formulation of the solvent. 2,6-bis(5,6-*i*-propyl-1,2,4-triazin-3-yl)-pyridine (*i*Pr-Btp), mixed with dimethyl-diethyl-hexylethoxy-malonamide ( $C_2OC_6$ ) in *n*-octanol, has been chosen to carry out the hot test on a genuine DIAMEX back-extraction solution at the end of June 2001.

## ACKNOWLEDGEMENTS

This work has been partially financially supported by the European Union Nuclear Fission Safety Program (Contract FI41-CT-96-0010).

## REFERENCES

1. P.Y. Cordier, C. Hill, P. Baron, C. Madic, M.J. Hudson and J.O. Liljenzin (1998), *J. All. Comp.*, **271**, 738-741.
2. I. Hägström, L. Spjuth, A. Enarsson, J.O. Liljenzin, M. Skälberg, M.J. Hudson, P.B. Iveson, C. Madic, P.Y. Cordier, C. Hill, and N. François (1999), *Solv. Extr. Ion Exch.*, **17**, 221-242.
3. Z. Kolarik, U. Müllrich and F. Gassner (1999), *Solv. Extr. Ion Exch.*, **17**, 23-32.



## AUTOMATICALLY CONTROLLED SOLVENT EXTRACTION CYCLE FOR ADVANCED CO-DECONTAMINATION PROCESS

Claudio Andaur, Marcelo Falcón, Alberto Gauna, Fernando Granatelli, Analía Russo,  
Jorge Vaccaro and Vanesa Balmaceda

UAMyCN, Centro Atómico Ezeiza, Comisión Nacional de Energía Atómica,  
Buenos Aires, República Argentina

A modified IMPUREX process for the co-decontamination of uranium and plutonium from spent nuclear fuel has been developed. The process involves the co-decontamination of uranium and plutonium as a whole, excluding their mutual separation, thus making it a non-proliferating process. An automatically controlled laboratory scale plant is described. The results of a typical extraction run are presented.

### INTRODUCTION

IMPUREX (IMproved PUREX) process was first published by Schmieder and Petrich from the Institut für Heiße Chemie, Kernforschungszentrum Karlsruhe, in 1989 [1]. This is a solvent extraction process for the reprocessing of spent nuclear fuel elements that are dissolved in nitric acid and extracted with a suitable organic extractant like tri-butylphosphate (TBP). In the original publication it includes the partition of uranium and plutonium enabling their recovery separately.

A modified process, avoiding the later U-Pu partition (which would have made it a proliferating process) but keeping the IMPUREX main guidelines unchanged, has been developed and tested in facilities of the Ezeiza Atomic Center (CAE) [2, 3].

Following these guidelines, an automatically controlled laboratory-scale extraction plant has been designed and operated using a nitric acid solution of natural U (0.7% U235) as feed to simulate the spent fuel.

In this paper experimental data and cycle performance calculations are presented.

### PROCESS DESCRIPTION

The main goal of this process is the separation of uranium and plutonium from other fission products generated in a spent nuclear fuel. The process basically consists of two blocks, namely the extraction and the re-extraction blocks (Figure 1).

In the first block, a highly acidic aqueous phase (FEED) carrying uranium (U), plutonium (Pu) and several fission products (FP) is fed and contacted with a 30% tri-butylphosphate solution in hydrocarbon (TBP). An extra aqueous stream (SCRUB) ensures the FP scrubbing.

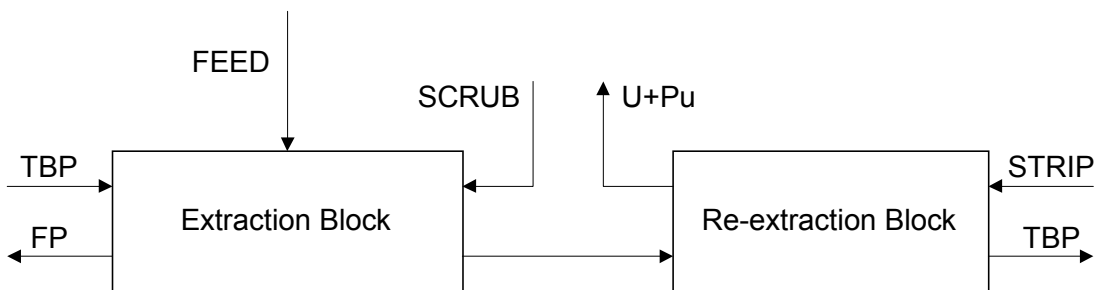


*Figure 1. Schematic of a modified IMPUREX process.  
Uranium and plutonium are extracted without further partition.*

While FP remain in the aqueous phase and leave the system, U and Pu are extracted to the organic stream and therefore conducted to the second block. In the re-extraction block the organic stream is contacted with a fresh low-acid aqueous phase (STRIP). Due to the different acidity, U and Pu are extracted from the TBP to the aqueous stream. The TBP can be recycled for reuse.

While room temperature is high enough to achieve a reasonably high separation of U-Pu from fission products in the extraction block, a higher temperature is needed when dealing with re-extraction.

## LABORATORY-SCALE PLANT DESCRIPTION

Mixer settlers were chosen as suitable extraction equipment for the two main blocks. Mixer-settler prototypes were used in both the extraction and re-extraction blocks. These devices were designed and constructed after information gathered from repeated extraction experiments. In the extraction block, a 7-stage mixer settler was installed, while in the re-extraction block a 9-stage mixer settler was preferred due to the lower mass transfer rate of the re-extraction process.

Mixing in both mixer-settlers is achieved by air pulse injection. The air injection performs both the mixing of the organic and aqueous phases and the generation of a pulse in the liquid which is mainly responsible for the organic phase flowing. While organic phase flows by gravity and mixing generated pulses, the aqueous phase is pumped through air lifts drilled in the mixer-settler's body. In this way the aqueous phase does not obstruct the normal flow of the lighter organic phase. Streams are pumped by automatically controlled diaphragm pumps.

Uranium concentration is sensed in a separate cell connected to the extraction mixer-settler. This cell is made out of glass or any other suitable transparent material which allows light transmission. A 435 nm light beam corresponding to a uranium maximum absorption peak, is taken from a spectrophotometer and conducted through a bundle of optical fibres to the cell's wall. An additional optical fibre bundle in the opposite wall receives the diminished light beam and transmits it back to the spectrophotometer where its decrease in intensity is measured. This decrease is a function of uranium concentration in the aqueous phase contained in the cell. Optical fibres are attached to the cell with its face parallel to the glass wall, to ensure minimum light losses.

## AUTOMATIC CONTROL LOOP PERFORMANCE

Concentration vs. time curves were plotted to evaluate the mixer-settler's response to a concentration step input (Figure 2). Following these results it was obvious that the system had a slow response to changes and that a simple on-off control system was enough to keep the high uranium concentration front between desirable bounds and at the same time avoid uranium losses in the raffinate.

PC control software was developed and installed. Control parameters are minimum and maximum aqueous phase uranium concentration limits, and corresponding minimum and maximum TBP flow rates. The aqueous phase flow rate was kept constant.

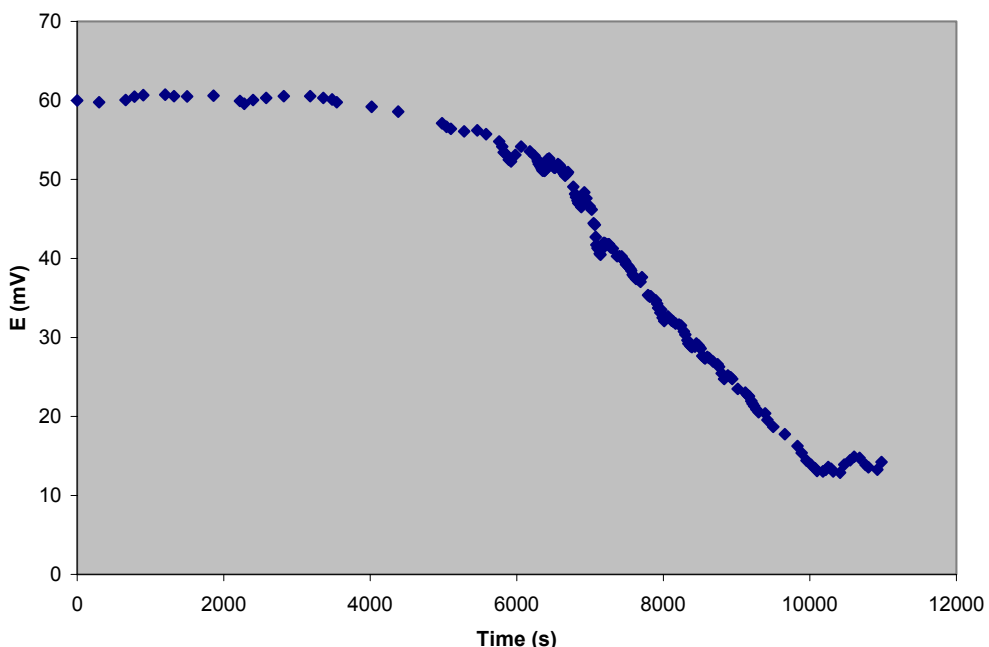


Figure 2. Concentration proportional  $E$  plotted against time in a mixer-settler stage without control action. Concentration input step took about 2 hours to completely leave the stage.

When the sensed aqueous uranium concentration reaches the maximum, the TBP flow rate is increased to a suitable value to reduce aqueous uranium concentration to the minimum. Inversely when a minimum limit is reached, TBP flow rate is decreased to let the uranium concentration in the mixer-settler raise. A control loop set this way proved to be suitable for 12-14 hours/day of continuous operation.

## EXPERIMENTAL

In the extraction block, there are three input streams: the uranium feed solution ( $[H^+] = 5 M$ ), the organic extractant, and an additional aqueous scrubbing stream ( $[H^+] = 5 M$ ) which is used to "wash" the aqueous phase and helps to scrub it from fission products. In the re-extraction block, there are only two input streams: the organic extractant carrying uranium, and an aqueous stripping stream ( $[H^+] = 0.05 M$ ) which is used to re-extract uranium back to the aqueous phase.

Settings for all the streams are listed in Table 1.

*Table 1. Process settings. Indicated TBP flow rates are the control flow rate limits.*

Stream	Flowrate (mL/h)	[U] (g/L)	[H <sup>+</sup> ] (M)	T (°C)
Feed	150	247	5	25
Strip	400	0	0.05	50
TBP	240-400	0	0.1	25
Scrub	50	0	5	25

According to the IMPUREX guidelines, a front with high uranium concentration is required to gain proper cycle performance. This condition is reached through a control loop as described earlier (see Tables 2 and 3).

*Table 2. Uranium concentration (g/L) in extraction mixer-settler.*

Stage	1	2	3	4	5	6	7
Aqueous	0.0	0.36	4.4	15.62	63.2	60.9	61.3
Organic	0.0	0.0	13.2	35.3	103.6	121.9	122.1

*Table 3. Uranium concentration (g/L) in re-extraction mixer-settler.*

Stage	1	2	3	4	5	6	7	8	9
Aqueous	67.2	49.5	31.6	17.7	8.10	0.59	0.32	0.0	0.0
Organic	85.6	44.6	31.2	16.3	5.3	0.0	0.0	0.0	0.0

Tables 2 and 3 were plotted to show typical concentration profiles in both mixer-settlers (Figures 2 and 3, respectively). These profiles were taken under controlled operation and therefore concentration steps are somewhat expected to occur.

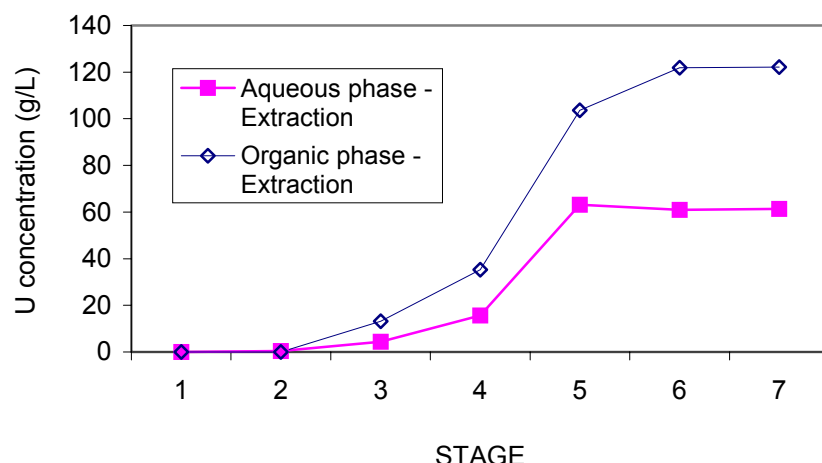


*Figure 3. Uranium concentration profile in extraction mixer-settler under automatic control action. Uranium is fed in stage 5. Uranium concentration is sensed in stage 2.*

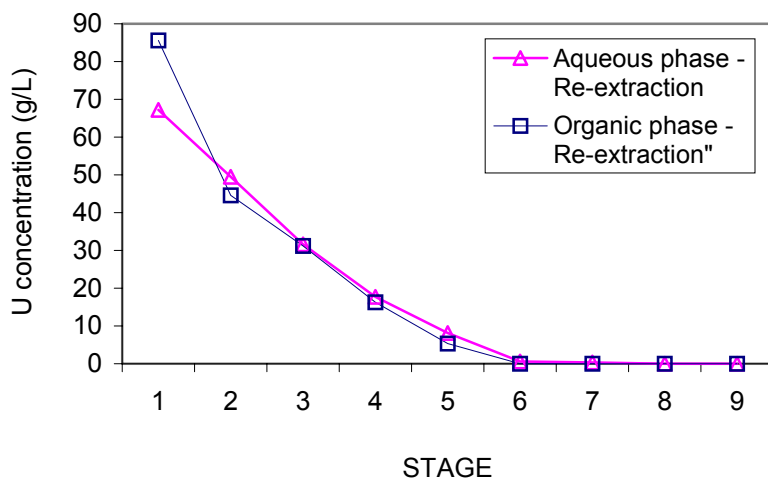


Figure 4. Uranium concentration profile in re-extraction mixer-settler.  
This mixer-settler is not under automatic control.

Equilibrium curves calculated by software were traced for the process experimental conditions. Operation points in extraction and re-extraction were also plotted. Operation lines were fitted to help visualisation of the process, even when they should not necessarily be straight due to the scales used (non free solvent). The slope of the lines should approximate to the flow rate relationship.

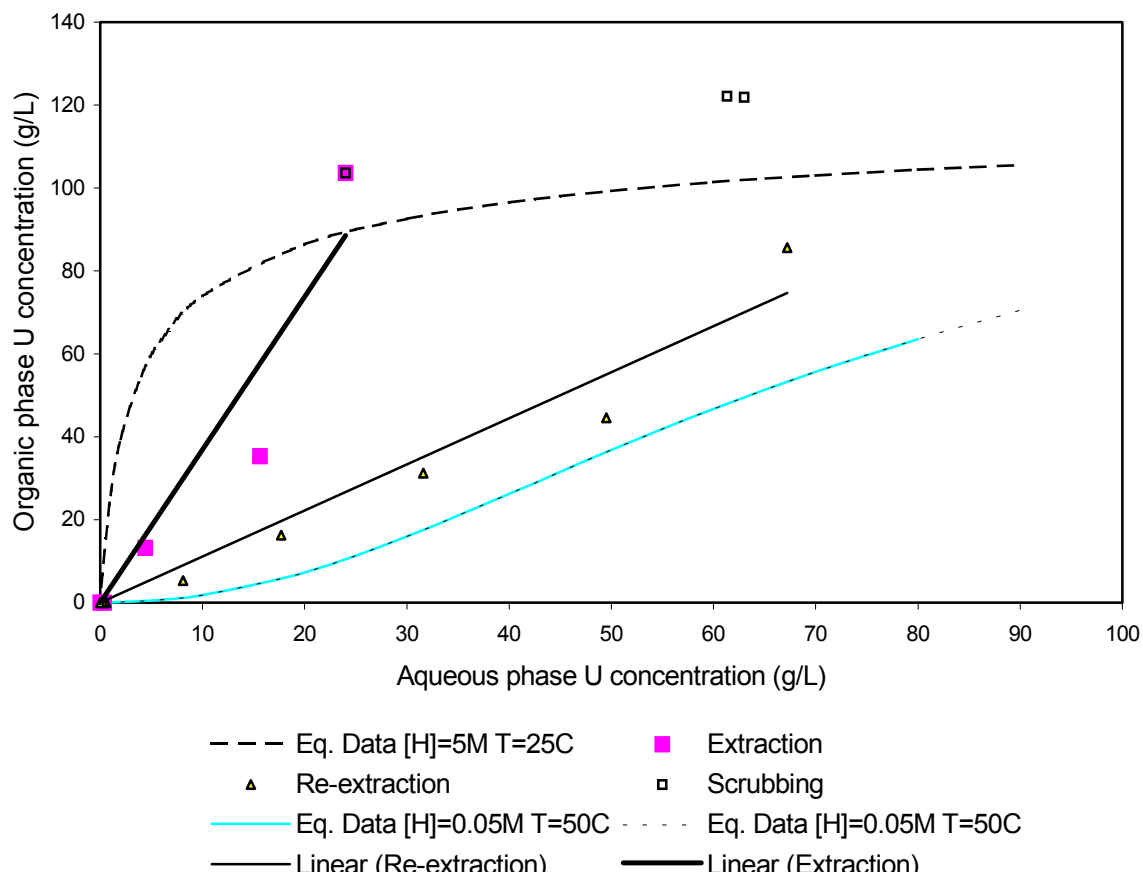


Figure 5. Equilibrium curves and operation points for both extraction and re-extraction mixer-settlers. Fitting lines were traced to suggest operation lines.

## **CONCLUSIONS**

Continuous operation has demonstrated reliability of an automatic control loop in keeping the process variables within the desired bounds for several hours.

No uranium losses were detected in the aqueous waste streams (raffinates).

Analytical results confirm an overall good cycle performance under high uranium concentration process conditions such as IMPUREX process.

## **REFERENCES**

1. H. Schmieder and G. Petrich (1989), *Radiochim. Acta*, **48** (3/4), 181-192.
2. C. Andaur, M. Falcón, A. Gauna, A. Russo and J. Vaccaro (1998), *Proc. XXV Reunión Anual Asociación Argentina de Tecnología Nuclear*, Buenos Aires, pp. 15.
3. C. Andaur, M. Falcón, F. Granatelli, A. Russo, J. Vaccaro and A. Gauna (1999), *Proc. XXVI Reunión Annual Asociación Argentina de Tecnología Nuclear*, Bariloche. Available from <<http://www.cab.cnea.gov.ar/AATN99/Actas/Docs/R4D09.pdf>> [Accessed 17 Sept. 2001].



# DEVELOPMENT AND CHARACTERIZATION OF A UNIVERSAL SOLVENT MIXTURE FOR THE SEPARATION OF CESIUM, STRONTIUM, ACTINIDES AND RARE EARTH ELEMENTS FROM ACIDIC RADIOACTIVE WASTE

T. A. Todd, J. D. Law, R. S. Herbst, V. N. Romanovskiy\*, I. V. Smirnov\*, V. A. Babain\*,  
V. M. Esimantovski\*, B. N. Zaitsev\*, E. G. Nazin\*\* and G. F. Egorov\*\*\*

Bechtel BWXT Idaho LLC, Idaho Falls, Idaho, USA

\*V. G. Khlopin Radium Institute, St. Petersburg, Russia

\*\*Military University of Radiological, Chemical and Biological Protection, Moscow, Russia

\*\*\*A. N. Frumkin Electrochemistry Institute, Russian Academy of Science, Moscow, Russia

The Universal Extraction process was developed to facilitate removal of all major radionuclides from acidic waste, simultaneously in a single process. The solvent composition developed for the Universal Extraction process is 0.08 M chlorinated cobalt dicarbollide, 0.35 to 0.5 vol.% polyethylene glycol-400, and 0.01 to 0.02 M diphenyl-N,N-dibutylcarbamoylphosphine oxide in phenyltrifluoromethyl sulfone. Numerous solvent diluents and extractants, as well as extractant concentrations were evaluated to develop an optimal solvent composition. Results of numerous evaluations indicate the solvent is highly resistant to thermal, chemical or radiological degradation and meets safety criteria for flammability.

## INTRODUCTION

Treatment of highly radioactive wastes may require the removal of cesium, strontium, actinides (AN), and rare earth elements (RE) to allow contact handling and economic disposal of the bulk (inert) constituents of the waste. Numerous processes have been demonstrated to effectively remove a single element, or group of related elements, from the waste in a single unit operation. However, decontamination of a highly radioactive waste stream would require two or three discrete processes. For example, cesium can be effectively removed from acidic waste using inorganic ion exchange technology, strontium can be removed using a solvent extraction process and the AN/RE fraction can be removed using another solvent extraction process [1-3]. Simultaneous separation of cesium, strontium, AN and RE elements in a single process offers significant potential capital and operating cost savings over the use of multiple unit operations. A universal extraction (UNEX) solvent was developed to provide such a capability.

The UNEX solvent is based on the chemistry of chlorinated cobalt dicarbollide (CCD). The extraction properties of cobalt dicarbollide were first described by Rais *et al.* [4]. Chlorinated cobalt dicarbollide (CCD), shown in Figure 1, is a large hydrophobic anion which exhibits the properties of a strong acid. Chlorinated cobalt dicarbollide selectively extracts cesium through a cation-exchange mechanism with dissociation of the solvated species in the organic phase. Dipicrylamine, tetraphenylborate, polyiodide, and heteropolyacids extract cesium by the same mechanism, but only CCD is simultaneously a strong acid, such as

heteropolyacids, and extremely hydrophobic, such as tetraphenylborate. This combination of properties enables CCD to extract cesium from strongly acidic media and provides low solubility of CCD in aqueous solutions. Chlorinated cobalt dicarbollide and its salts are highly polar compounds. They are essentially insoluble in low-polar solvents such as saturated and aromatic hydrocarbons. Furthermore, solutions of CCD in polar solvents like alcohols, ketones, ethers, or esters have very low extraction abilities. Aromatic and aliphatic nitrocompounds are the best diluents for CCD [4,5].

Halogenated derivatives of cobalt dicarbollide, especially chlorinated cobalt dicarbollide, exhibit high resistance to acid hydrolysis, reductants, and radiation, was well as excellent thermal stability [6]. Therefore, in the majority of studies, especially in radiochemistry, the hexachloro-derivative of cobalt dicarbollide, as indicated in Figure 1, is the preferred choice.

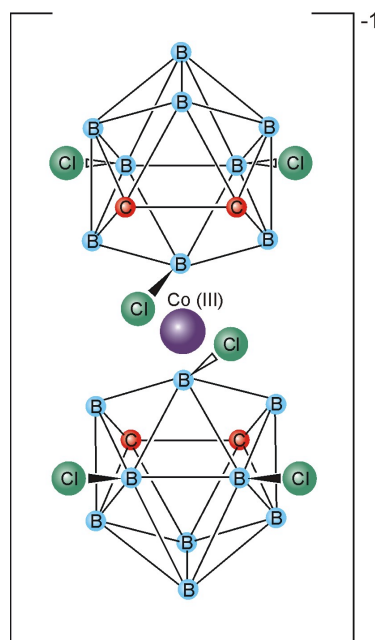


Figure 1. Structure of hexachlorocobalt dicarbollide anion.

The co-extraction of strontium, and other alkaline earth elements has been shown by the addition of polyethylene glycols (PEG) to the CCD solvent [7]. This process has been implemented in Russia to process approximately 750 m<sup>3</sup> of highly radioactive waste, and recover megacurie quantities of cesium and strontium.

The development of a universal solvent required addition of an AN/RE extractant to the CCD/PEG solvent, and development of a non-nitroaromatic diluent, suitable for use in the United States. An appropriate diluent for radiochemical waste treatment must have high chemical and radiation stability, low aqueous solubility, low viscosity, and a density substantially different than the aqueous process solutions. Furthermore, the extractant and the solvated metal complex must be readily soluble in the diluent to prevent formation of an immiscible third phase.

## SELECTION OF ACTINIDE/RARE EARTH EXTRACTANT

Several bifunctional neutral organophosphorus compounds, known to be effective AN/RE extractants, were studied. These included substituted diphosphine dioxides, triphosphine trioxides and substituted carbamoylphosphine oxides (CMPO). All extractants exhibited high AN/RE distribution coefficients, but carbamoylphosphine oxides were selected because their synthesis is less complex, they are more soluble in polar diluents, and they have been demonstrated to extract actinides in combination with CCD [8]. There has also been a significant amount of work with CMPO in the development and testing of the transuranic extraction (TRUEX) process. Distribution coefficients, measured from 3 M HNO<sub>3</sub>, are indicated in Table 1 for a constant solvent composition of 0.06 M CCD, 1 vol % Slovalfol-909, and 0.02 M CMPO oxide in *m*-nitrobenzotrifluoride (MNBTF).

*Table 1. Extraction of metals from 3 M HNO<sub>3</sub> by 0.06 M CCD, 1 vol % SLOVAFOL-909, and 0.02 M CMPO in MNBTF.*

CMPO	Distribution coefficient				
	Cs	Sr	Eu	Pu	Np
Ph <sub>2</sub> Bu <sub>2</sub>	4	12	300	700	> 500
OctPhBu <sub>2</sub>	5	15	4	200	80
OctO <sub>2</sub> Bu <sub>2</sub>	3	9	0.4	60	10

Ph<sub>2</sub>Bu<sub>2</sub> = diphenyl-N,N-dibutylcarbamoylmethylphosphine oxide

OctPhBu<sub>2</sub> = octyl(phenyl)-N,N-diisobutylcarbamoylmethylphosphine oxide

OctO<sub>2</sub>Bu<sub>2</sub> = dioctyl-N,N-dibutylmethylcarbamoyl phosphonate

The use of diphenyl-N,N-dibutylcarbamoylmethylphosphine oxide (Ph<sub>2</sub>Bu<sub>2</sub>CMPO) exhibits the best overall extraction properties based on Eu, Pu and Np distributions. Additional studies using simulated radioactive wastes, indicate that the solvent mixture containing Ph<sub>2</sub>Bu<sub>2</sub>CMPO provided higher solubility of metal complexes, reducing the likelihood of forming a third phase. Distribution measurements were also made over Ph<sub>2</sub>Bu<sub>2</sub>CMPO concentrations ranging from 0.01 to 0.06 M. Increasing the Ph<sub>2</sub>Bu<sub>2</sub>CMPO concentration in the solvent mixture obviously provides for higher AN/RE distribution ratios, but decreases cesium and strontium distribution ratios. Therefore, concentrations of Ph<sub>2</sub>Bu<sub>2</sub>CMPO in the range of 0.01 – 0.02 M were determined to be adequate.

## SELECTION OF POLYETHYLENE GLYCOL (STRONTIUM EXTRACTANT)

As mentioned earlier, PEG added to CCD has been demonstrated to synergistically extract strontium. The mechanism of this extraction process has not yet been established, but it is believed that the PEG and CCD form a complex with a crown-like cavity providing solvation of the strontium cation. Substituted PEGs are less soluble in the aqueous phase, but do not sufficiently extract Sr in the CCD/PEG/CMPO mixture. Unsubstituted PEGs exhibit adequate Sr extraction in the CCD/PEG/CMPO mixture, as shown in Table 2. Increasing the molecular weight of PEG reduces metal distributions, and decreases solubility in the aqueous phase.

*Table 2. Extraction of radionuclides by a mixture of 0.15 M CCD, 0.025 M Ph<sub>2</sub>Bu<sub>2</sub>CMPO, and 1 vol % PEG in MNBTf from simulated acidic waste.*

Polyethylene glycol	Distribution coefficients		
	Cs	Sr	Eu
Slovafol-909	8.9	0.46	37
OP-10	9.1	0.3	7.2
PEG-1500	6.3	0.6	41
PEG-400	4.5	4.1	43
PEG-300	6.7	4.0	60

Increasing PEG concentration in the solvent mixture suppresses Cs extraction; therefore, it is necessary to minimize the concentration of PEG. Concentrations of PEG-400 in the range of 0.35 to 0.5 vol % were determined to be optimal.

### SELECTION OF DILUENT FOR THE UNIVERSAL SOLVENT

Nitrobenzene and its derivatives, are the most widely used diluents for cobalt dicarbollide-based extraction systems. Regulatory, environmental and health issues make the use of nitro-aromatic diluents impractical in the United States. The high chemical and radiation stability of fluoro-organic compounds, coupled with their highly polar nature and favorable hydrodynamics, make them promising substitutes for nitro-aromatic diluents. A detailed description of the compounds evaluated and test results is provided by Romanovskiy *et al.* [9,10]. A new class of compounds, showing promise as diluents was introduced-fluorinated sulfones. Polyfluoroalkyl sulfones with different substituents were synthesized, and the main characteristics in the UNEX solvent were defined. These data indicate the introduction of polyfluoroalkyl substituents in the sulfone molecule decreases the basicity and significantly increases the extraction ability of CCD. The effect of sulfone substituents on the Cs extraction ability of CCD follows the order: HCF<sub>2</sub>CF<sub>2</sub> ≈ CF<sub>3</sub> > HCF<sub>2</sub> > HCF<sub>2</sub>CF<sub>2</sub>CH<sub>2</sub> >>Aryl, Alkyl. The extraction of cesium, strontium and europium in universal solvents utilizing different sulfone diluents as compared to MNBTf is shown in Table 3.

*Table 3. Extraction of Cs, Sr and Eu from simulated INEEL acidic tank waste by mixtures of 0.08 M CCD, 0.02 M PH<sub>2</sub>Bu<sub>2</sub>CMPO, and 0.6 vol % PEG-400 in different diluents.*

Diluent	Distribution coefficients		
	Cs	Sr	Eu
MNBTf	4.0	3.2	4.1
40 vol% S-612 & 60 vol% toluene	2.8	2.6	1.4
100% FS-24	2.0	2.2	1.1
100% FS-13	1.0	1.7	2.7

S-612 = hexyldifluoromethyl sulfone

FS-24= phenyltetrafluoroethyl sulfone

FS-13= phenyltrifluoromethyl sulfone

From Table 3, it can be seen that the sulfones have lower extraction ability than *m*-nitrobenzotrifluoride, but given the complexity of the waste stream, which contains molar quantities of alkali metals, the distribution coefficients shown are acceptable. Considerations other than extraction ability (diluent synthesis, cost, extractant and metal solubilities, physical properties) led to the selection of phenyltrifluoromethyl sulfone as the diluent for the UNEX process. The solvent composition: 0.08 M chlorinated cobalt dicarbollide, 0.35-0.5 vol.%

Polyethylene glycol-400, and 0.01-0.02 M diphenyl-N,N-dibutylcarbamoylphosphine oxide in phenyltrifluoromethyl sulfone provides the needed recovery of Cs, Sr, AN and RE, with suitable physio-chemical properties of the solvent. The distribution of Cs, Sr, AN and RE elements is dependent on temperature, which allows for enhancement of the extraction operation by cooling and of the strip section by heating. Stripping of the extracted metals is accomplished using a solution containing 1 M guanidine carbonate and 20 g/L diethylene triamine pentaacetic acid (DTPA).

### PROPERTIES OF THE UNIVERSAL SOLVENT

The universal solvent has a density of 1.417 g/cm<sup>3</sup> and a viscosity of 4.6 mPa-s at 20 °C. As for explosion and fire safety, the UNEX solvent greatly surpasses the typical PUREX solvent of 30% tri-*n*-butyl phosphate in *n*-dodecane. The flash point of the UNEX solvent is above 90 °C, while that of the PUREX solvent is about 70 °C. The UNEX solvent exhibits high chemical stability in that it does not react with 14 M HNO<sub>3</sub> at temperatures up to 120 °C. Gas evolution above 120 °C proceeds uniformly without the presence of an exotherm. At higher temperatures (about 120-150 °C) weak uniform gas evolution is observed without any heat release. At about 160 °C, a weak exotherm is observed, with self-heating of 15-17 °C for a duration of 10-15 minutes. The thermal stability of the UNEX solvent is much higher than for the PUREX solvent, which exhibits a strong exotherm at about 90 °C.

Gamma irradiation of the universal solvent, in both one and two-phase systems was conducted using a Co-60 source at a dose rate of 10 kGy and at 25-27 °C. The universal solvent was exposed to an absorbed dose of 20 W·h/L. This equates to the expected dose for about 350 extraction cycles of contact with Idaho National Engineering and Environmental Laboratory (INEEL) tank waste. The total yield of phenyltrifluoromethyl sulfone radiolytic decomposition products is 4.5 to 5.0 molecules/100 eV (loss of sulfone in 350 cycles is less than 1%). The primary radiolysis products include hexafluoroethane and benzenesulfonic acid, which do not accumulate in the organic phase. The radiolytic gas-evolution rate does not exceed 4.5 mL/h·L at a dose rate of 10 kGy/h. The extraction and hydrodynamic properties of the UNEX solvent did not change with absorbed doses of 20 W·h/L.

The universal solvent losses due to solubility do not exceed 0.02% vol. in a 3 M HNO<sub>3</sub> aqueous phase. Phenyltrifluoromethyl sulfone solubility in INEEL tank waste and the proposed stripping reagents is even lower. These data indicate the plausibility of using the UNEX solvent for radiochemical waste processing.

### CONCLUSIONS

A universal extraction solvent has been developed that allows for the simultaneous extraction and recovery of cesium, strontium, actinides and rare earth elements from acidic radioactive wastes. A new class of polar diluent has been introduced, replacing nitroaromatic diluents commonly used in cobalt dicarbollide extraction systems. The solvent is composed of 0.08 M chlorinated cobalt dicarbollide, 0.35 to 0.5 vol.% polyethylene glycol-400, and 0.01 to 0.02 M diphenyl-N,N-dibutylcarbamoylphosphine oxide in phenyltrifluoromethyl sulfone. This solvent composition has favorable physical/hydrodynamic properties, which allow its use in centrifugal extraction equipment, and has been shown to have chemical and thermal stability far exceeding the well known PUREX solvent. Radiation doses expected in 350 cycles of operation have no deleterious effect on the solvent's extraction or hydrodynamic properties. The combination of extraction properties as well as thermal, chemical and radiation stability make it technically feasible for the universal solvent to be utilized for the treatment of highly radioactive acidic wastes.

## **ACKNOWLEDGEMENTS**

This work was supported by the U. S. Department of Energy Office of Science and Technology's Efficient Separations and Processing Crosscutting Program and Tanks Focus Area under the auspices of the Joint Coordinating Committee for Environmental Management (JCCEM).

## **REFERENCES**

1. T. A. Todd *et al.* (2001), *Sep. Sci. Tech.*, **36** (5&6), 999-1016.
2. E. P. Horwitz *et al.* (1985), *Sol. Extr. Ion Exch.*, **3** (1&2), 75-109.
3. E. P. Horwitz, M. L. Dietz and D. E. Fisher (1990), *Sol. Extr. Ion Exch.*, **8** (4&5), 557-572.
4. J. Rais, P. Selucky and M. Kyrs (1976), *J. Inorg. Nucl. Chem.*, **38**, 1376.
5. E. Makrlik and P. Vanura (1985), *Talanta*, **32**, 423.
6. J. Rais *et al.* (1991), *J. Radioanal. Nucl. Chem.*, **148**, 349.
7. J. Rais, E. Sebestova, P. Selucky and M. Kyrs (1976), *J. Inorg. Nucl. Chem.*, **38**, 1742.
8. J. Rais, S. Tachimori, P. Selucky, L. Kadlecova (1994), *Sep. Sci. Tech.*, **29**, 261.
9. V. N. Romanovskiy *et al.* (2001), *Sol. Extr. Ion Exch.*, **19** (1), 1-21.
10. V. N. Romanovskiy, T. A. Todd *et al.* (2001), *Russian Federation Patent*, No. 2163403.



# DEVELOPMENT AND PILOT SCALE TESTING OF SOLVENT EXTRACTION FLOWSHEETS FOR THE SEPARATION OF RADIONUCLIDES FROM ACIDIC RADIOACTIVE WASTE

J. D. Law, T. A. Todd, and R. S. Herbst

Idaho National Engineering and Environmental Laboratory, Idaho Falls, Idaho, USA

The presence of long-lived radionuclides presents a challenge to the management of radioactive wastes. Separation of the radionuclides from the waste solutions has the potential of significantly decreasing the costs associated with the immobilization and disposal of the waste by minimizing waste volumes. Several solvent extraction processes have been developed for the separation of transuranic elements (TRUs),  $^{90}\text{Sr}$ , and/or  $^{137}\text{Cs}$  from acidic radioactive waste solutions. These processes have been tested at the Idaho National Engineering and Environmental Laboratory using pilot scale centrifugal contactor equipment ranging in size from 2.2-cm to 5.5-cm diameter, including contactors installed in a shielded cell facility for testing with actual radioactive wastes. The most recent results of the flowsheet testing are summarized and information on the centrifugal contactor equipment used for the testing is provided.

## INTRODUCTION

The Idaho National Engineering and Environmental Laboratory (INEEL) previously reprocessed spent nuclear fuel to recover enriched uranium. The radioactive raffinate stream from reprocessing was stored and subsequently solidified at 500°C in a fluidized bed calciner. The INEEL currently has approximately 4,400 cubic meters of radioactive calcine stored onsite in above ground stainless steel bins enclosed in concrete vaults. The average composition of the two most prevalent types of this calcine are given in Table 1. A secondary acidic aqueous waste was generated during equipment decontamination between processing campaigns and from solvent cleanup activities. Currently, approximately 4.8 million liters of liquid acidic radioactive tank waste are stored in underground, concrete enclosed stainless steel tanks at the INEEL. This liquid waste is not directly amenable to calcination due to its high sodium content which causes agglomeration of the fluidized bed. The average composition of this tank waste is given in Table 2.

Separation processes are being evaluated as alternatives to calcination for treating the remaining liquid tank waste. Additionally, separation processes are being developed for treatment of INEEL calcine (after dissolution in nitric acid solution). The goal of the separation processes is to remove fission products and/or actinides from the calcine and liquid wastes so the bulk of the treated waste can be disposed of as a contact handled transuranic (TRU) or non-TRU waste. It is anticipated that the combined low-activity waste (LAW) raffinate streams resulting from the separation unit operations would be grouted for near surface disposal. The high-activity waste (HAW) resulting from separation processes would be vitrified for disposal at a geological repository.

*Table 1. Average compositions of INEEL calcine wastes.*

Component	Al Calcine (wt%)	Zr Calcine (wt%)
Al <sub>2</sub> O <sub>3</sub>	90.6	14.4
NaO <sub>2</sub>	3.1	---
ZrO <sub>2</sub>	---	23.4
CaF <sub>2</sub>	---	54.3
CaO	---	3.9
B <sub>2</sub> O <sub>3</sub>	0.6	3.0
Fe <sub>2</sub> O <sub>3</sub>	0.6	0.1
Hg	2.9	---
SO <sub>4</sub>	1.2	---
Other (volatile nitrates)	1.0	0.9
Radionuclides	<1	<1

*Table 2. Average composition of INEEL liquid wastes.*

Component	(M)	Component	(M)
Acid	1.59	Na	1.9
Al	0.64	NO <sub>3</sub>	5.07
B	0.018	Pb	0.0012
Ca	0.054	SO <sub>4</sub>	0.05
Cr	0.003	Zr	0.002
Fe	0.022	Alpha (nCi/g)	369.4
Hg	0.0011	<sup>137</sup> Cs (Ci/m <sup>3</sup> )	41
K	0.206	<sup>90</sup> Sr (Ci/m <sup>3</sup> )	38

Solvent extraction processes are being developed worldwide for the treatment of acidic high-level liquid waste [1]. At the INEEL, several solvent extraction technologies have been developed for the separation of the transuranic elements (TRUs), <sup>137</sup>Cs, and/or <sup>90</sup>Sr from INEEL radioactive waste solutions (liquid wastes and dissolved calcine solutions) in centrifugal contactor pilot plants. The solvent extraction technologies developed include the Transuranic Extraction (TRUEX) process, the Strontium Extraction (SREX) process, a chlorinated cobalt dicarbollide (ChCoDiC) process, a chlorinated cobalt dicarbollide/polyethylene glycol process, a phosphine oxide (POR) process, and a universal solvent extraction process (UNEX). For each of these solvent extraction processes, considerable experimental development and flowsheet testing was performed in order to develop the flowsheets. In order to test the solvent extraction technologies with the solid calcines, the calcines are dissolved in 3.0 M to 5.0 M nitric acid at 95 °C for 60 minutes. Under these conditions, approximately 95% of the calcine is dissolved. It should be noted that the separation of <sup>99</sup>Tc is not required for treatment of INEEL waste since the activity of <sup>99</sup>Tc (~0.01 Ci/m<sup>3</sup> in liquid waste) is well below the NRC Class A LLW limit of 0.3 Ci/m<sup>3</sup>. However, it has been determined that the TRUEX and POR processes extract the majority of the <sup>99</sup>Tc with the flowsheets tested. The ChCoDiC and UNEX processes do not extract <sup>99</sup>Tc to any appreciable extent.

## EQUIPMENT DESCRIPTION

Liquid-liquid extraction processes have been utilized in nuclear fuel reprocessing for over 40 years. There have been three types of solvent extraction contacting equipment successfully used in the nuclear industry: pulsed columns, mixer-settlers, and centrifugal contactors. All solvent extraction flowsheet development work at the INEEL is being performed using centrifugal contactors.

There are three centrifugal contactor pilot plants at the INEEL. The rotor diameters and the basic design of each set of centrifugal contactors is different, as shown in Table 3. The 3.3-cm and 5.5-cm contactor pilot plants are set up for testing with non-radioactive solutions. The 2.0-cm contactors are located in a shielded cell facility, which allows for testing with highly radioactive solutions.

*Table 3. Description of the centrifugal contactor pilot plants.*

Size	2.0-cm rotor diameter	3.3-cm rotor diameter	5.5-cm rotor diameter
Manufacturer	Argonne National Lab.	NIKIMT, Moscow, Russia	Oak Ridge National Lab.
Number of stages	24	26	16
Rotor rpm	3,600 rpm (not adjustable)	2,780 rpm	0 – 4,000 rpm
Maximum throughput	40 mL/min	250 – 400 mL/min	3,000 mL/min
Weir system	Not adjustable	Adjustable light phase	Not adjustable
Configuration	Single stage units. Stages are connected using U-tubes.	Single stage units. Stages are connected using U-tubes.	Block of four contactors (4-pack) machined from a single block of metal.

Each of these centrifugal contactor pilot plants have been used to develop flowsheets for the treatment of INEEL wastes. Typically, initial flowsheet development work is performed using non-radioactive waste simulants in the 5.5 or 3.3-cm centrifugal contactor pilot plants. Testing then progresses to the 2.0-cm centrifugal contactors where the flowsheets are demonstrated with actual waste solutions and/or waste simulants spiked with radiotracers.

## RESULTS AND DISCUSSION

For each of the flowsheets developed for the treatment of INEEL liquid and dissolved calcine waste solutions, the status of the development work and a summary of the results obtained are given below. In addition, removal efficiencies for the components of interest are presented for each of the technologies in Table 4.

### Transuranic Extraction Process

The TRUEX process was developed at Argonne National Laboratory for the separation of TRUs from acidic waste solutions [2]. The process uses octyl(phenyl)-N,N-diisobutylcarbamoylmethyl phosphine oxide (CMPO) as the active extractant, tributyl phosphate (TBP) as a phase modifier, and a hydrocarbon diluent. A research program began in 1993 to develop the TRUEX process for the removal of TRUs from acidic radioactive wastes at the INEEL. Numerous countercurrent pilot-scale flowsheet tests with simulated liquid waste and dissolved pilot plant calcine solution have been performed [3,4], including extended operation integrated with the SREX process and cesium ion exchange [5]. TRUEX flowsheets have also been demonstrated using actual liquid waste in a 2-cm centrifugal contactor pilot plant [6,7], including integrated testing with the SREX process and cesium ion exchange (CSIX) [5].

**Table 4. Summary of the removal efficiencies obtained from demonstrations of various solvent extraction processes with actual or simulated acidic radioactive waste.**

Comp	TRUEX[5,7] (liq. waste) (%)	SREX[5,15] (liq. waste) (%)	POR[24] ChCoDiC/ (liq. waste) (%)	PEG[24] (liq. waste) (%)	ChCoDiC[24] (liq. waste) (%)	UNEX[27] (liq. waste) (%)	UNEX (calcine) (%)	TRUEX[4] <sup>c</sup> (calcine) (%)	SREX[24] <sup>c</sup> (calcine) (%)
Alpha	99.8/ 99.2 <sup>a</sup>	94.0/93.1 <sup>b</sup>	98.9	d	d	99.96	99.9	d	d
<sup>241</sup> Am	99.8/99.95	2.0/d	56.4	d	d	>99.9	>99.9	>96.4	d
Pu	99.97/99.9	99.95/d	99.97	d	d	99.994	99.97	d	d
U	99.8/d	99.6/d	d	d	d	d	d	d	d
<sup>90</sup> Sr	d/ 0.1	99.994/99.997	0.03 <sup>c</sup>	96.2	0.09	99.995	99.7	d	99.6
<sup>137</sup> Cs	d/d	0.4/d	0.03 <sup>c</sup>	99.3	>99.998	99.4	99.99	d	d
<sup>99</sup> Tc	89/63	d/d	66.4	d	d	<0.14	b	d	d
Al	d/<0.01	0.4/0.03	0.01 <sup>c</sup>	0.03 <sup>c</sup>	d	d	0.14	d	<0.5
B	d/<1.8	<23/d	1.3 <sup>c</sup>	d	d	d	d	d	3.6
Ba	d/<2.7	63.6/81.3	d	d	d	>99.0	>99.8	d	d
Ca	d/<0.08	d/<0.1	0.08 <sup>c</sup>	1.4	<28	2.2	2.9	d	0.007
Ce	d/d	d/d	68 <sup>c</sup>	d	d	>89.0	d	>98.7	d
Cr	d/<0.2	d/<0.4	<15	d	d	d	1.3	1.1	<1.7
Fe	0.7/<0.02	1.7/0.4	2.1 <sup>c</sup>	<2.1	<40	8.3	12.8	1.3	<2.6
Hg	73.7/94.7	>89.2/87.2	92	26.4	37.5	<1.0	d	d	d
K	d/0.5	31.5/16.4	d	45.2	50	27.9	42.1	d	6.4
Na	0.07/13	0.4/2.6	d	2.1	0.7	0.14	d	d	d
Pb	d/<0.7	>94/97.9	0.6 <sup>c</sup>	98.5	d	98.8	>99.4	d	d
Zr	42/28.5	>82/d	28 <sup>c</sup>	<5.8	d	87.0	7.4	0.01	<0.25

a. (x/y) where x is data from a TRUEX test and y is data from the TRUEX portion of an integrated CSIX/TRUEX/SREX test.

b. (x/y) where x is data from a SREX test and y is data from the SREX portion of an integrated CSIX/TRUEX/SREX test.

c. Data from flowsheet testing with simulated waste.

d. d = Data were not obtained.

A TRUEX flowsheet has been demonstrated with actual liquid tank waste several times, most recently as part of an integrated TRUEX/SREX/CSIX process. With these tests, the removal efficiencies ranged from 99.2% to 99.8% for the total alpha activity. Also, 74% to 95% of the Hg and 29% to 42% of the Zr were extracted and exited with HAW strip product.

A TRUEX flowsheet has also been developed for the treatment of dissolved zirconium calcine. This flowsheet has been tested using simulated dissolved calcine spiked with <sup>241</sup>Am and <sup>95</sup>Zr. With this flowsheet, a removal efficiency of >96.4% was obtained for <sup>241</sup>Am. An ammonium fluoride scrub was effectively used to back-extract the Zr from the TRUEX solvent. Less than 0.25% of the <sup>95</sup>Zr was extracted and exited with the strip product. Cerium was extracted from the calcine (>98.7%); however, the expected concentration of Ce in the dissolved INEEL calcine is ~1.3E-04 M which will not impact the capacity of the extractant.

### Strontium Extraction Process

The SREX process uses the crown ether 4,4'-(5')di-(t-butylcyclohexano)-18-crown-6 (DtBuCH18C6) which has been determined to be a selective and efficient extractant for Sr [8-10]. A research program began in 1993 to develop the SREX process for the removal of <sup>90</sup>Sr from liquid wastes and dissolved calcine solutions at the INEEL. This research has focused on the use of DtBuCH18C6 with a TBP phase modifier in a hydrocarbon diluent. Numerous countercurrent pilot-scale flowsheet tests have been performed with simulated liquid waste and dissolved calcine solutions [10-14], including extended operation integrated with the TRUEX process and cesium ion exchange [5]. A SREX flowsheet has also been demonstrated with actual liquid waste solution in a 2-cm centrifugal contactor pilot plant [15].

The SREX flowsheet that was demonstrated several times with actual liquid tank waste resulted in  $^{90}\text{Sr}$  removal efficiencies ranging from 99.994% to 99.997%. With these flowsheets, >94% to 98% of the Pb, >82% of the Zr, 16% to 31% of the K, 87% to >89% of the Hg, and 64% to 81% of the Ba were extracted and exited with the HAW strip product. It should be noted that U and Pu are extracted by the TBP present in the SREX solvent.

A SREX flowsheet has also been developed for the treatment of dissolved zirconium calcine. This flowsheet has been tested using simulated dissolved calcine spiked with  $^{85}\text{Sr}$ . With this flowsheet, a removal efficiency of 99.6% was obtained for  $^{85}\text{Sr}$ . An efficiency of 60% in the extraction section of the flowsheet reduced the removal efficiency for Sr. A sodium nitrate scrub was effectively used to back-extract the K from the SREX solvent resulting in only 6.4% of the K exiting with the strip product.

### **Phosphine Oxide Process**

A phosphine oxide solvent extraction process has been developed for the treatment of acidic radioactive waste at the INEEL [16]. The solvent consists of an alkylated phosphine oxide in a hydrocarbon diluent. A joint research program with the Khlopin Radium Institute in St. Petersburg, Russia was initiated in 1993 to develop the POR process for the removal of TRUs from acidic radioactive waste at the INEEL. Countercurrent pilot-scale flowsheet testing with simulated liquid waste has been performed [16,17]. This testing has culminated in the development of a POR flowsheet which has been demonstrated using actual liquid waste solution in a 2-cm centrifugal contactor pilot plant [17].

The POR flowsheet that was demonstrated with actual liquid tank waste resulted in a total alpha removal efficiency of 98.9%. With this flowsheet, 92% of the Hg, 28% of the Zr, and 2.1% of the Fe were extracted and exited with the high-activity waste strip product. A POR flowsheet has not been developed for the treatment of dissolved zirconium calcine.

### **Cobalt Dicarbollide-Based Processes**

Chlorinated cobalt dicarbollide (ChCoDiC) has been developed as an extractant for Cs from acidic waste solutions [18-21]. With the addition of polyethylene glycol (PEG) to the solvent, Sr can also be partitioned from acidic waste streams [22,23]. A joint research program with the Khlopin Radium Institute in St. Petersburg, Russia was initiated in 1993 to develop ChCoDiC based processes for the removal of  $^{137}\text{Cs}$  and  $^{90}\text{Sr}$  from acidic radioactive waste at the INEEL. Numerous countercurrent pilot-scale flowsheet tests with simulated liquid waste have been performed [17]. This testing has culminated in the development of ChCoDiC flowsheets (with and without PEG for the extraction of Sr) which have been demonstrated using actual liquid waste solution in a 2-cm centrifugal contactor pilot plant [24].

The ChCoDiC/PEG flowsheet that was demonstrated with actual liquid tank waste resulted in removal efficiencies of 96.2% for  $^{90}\text{Sr}$  and 99.3% for  $^{137}\text{Cs}$ . Also, 98.5% of the Pb, 45.2% of the K, 26.4% of the Hg, 2.1% of the Na, 1.4% of the Ca, <5.8% of the Zr, and <2.1% of the Fe were extracted and exited with the high-activity waste strip product.

The ChCoDiC flowsheet that was demonstrated with actual liquid tank waste resulted in a removal efficiency of >99.998% for  $^{137}\text{Cs}$ . Also, 50% of the K and 37.5% of the Hg were extracted and exited with the high-activity waste strip product. A ChCoDiC flowsheet has not been developed for the treatment of dissolved zirconium calcine.

The use of a single solvent extraction process to remove the desired radionuclides, as opposed to a combination of processes in separate unit operations that remove these same radionuclides in sequential steps, evolved from the previous collaborative work with the Khlopin Radium Institute. The development of a universal solvent extraction (UNEX) process containing ChCoDiC with PEG to remove  $^{137}\text{Cs}$  and  $^{90}\text{Sr}$ , and a carbamoylmethylphosphine

oxide derivative (diphenyl CMPO) to remove the TRUs was initiated in 1996. Numerous countercurrent pilot-scale flowsheet testing with simulated liquid waste have been performed [24,25], including extended operation of the UNEX process [26]. A universal solvent extraction flowsheet has also been demonstrated using actual liquid waste and actual dissolved calcine solution in a 2-cm centrifugal contactor pilot plant [24,27].

The UNEX flowsheet that was demonstrated with actual liquid tank waste resulted in removal efficiencies of 99.995% for  $^{90}\text{Sr}$ , 99.4% for  $^{137}\text{Cs}$ , and 99.96% for the actinides. Also, 87% of the Zr, 98.8% of the Pb, 28% of the K, >99% of the Ba, and 8% of the Fe were extracted and exited with the high-activity waste strip product.

The UNEX flowsheet that was demonstrated with actual dissolved calcine resulted in removal efficiencies of 99.7% for  $^{90}\text{Sr}$ , 99.99% for  $^{137}\text{Cs}$ , and 99.9% for the actinides. Also, 99.4% of the Pb, 42% of the K, >99.8% of the Ba, 7% of the Zr, and 13% of the Fe were extracted and exited with the high-activity waste strip product.

## ACKNOWLEDGEMENTS

This work was supported by the U.S. DOE Assistant Secretary for Environmental Management under DOE Idaho Operations Office contract DE-AC07-94ID13223. It was also supported by the U. S. DOE Office of Science and Technology's Tanks Focus Area and the U. S. DOE Office of Science and Technology's Efficient Separations & Processing Program.

## REFERENCES

1. EP Horwitz and W. W. Schulz (1999), Metal Ion Separation and Preconcentration: Progress and Opportunities, A.H. Bond, M.L. Dietz and R.D. Rogers (eds.), pp. 20.
2. E. P. Horwitz, D. G. Kalina, H. Diamond, G. F. Vandegrift, and W. W. Schulz (1985), *Solvent Extr. Ion Exch.*, **3** (1&2), 75.
3. J. D. Law, and R. S. Herbst (1995), INEL-95/0130, Idaho Falls, ID.
4. J. D. Law, R. S. Herbst, K. N. Brewer, and T. A. Todd (1998), *Proc. SPECTRUM '98*, Denver, CO, pp. 566-570.
5. J. D. Law, R. S. Herbst, and T. A. Todd (2001), *Sep. Sci. Technol.*, in press.
6. J. D. Law, K. N. Brewer, R. S. Herbst, T. A. Todd (1996), INEL-96/0353, Idaho Falls, ID.
7. J. D. Law, K. N. Brewer, R. S. Herbst, T. A. Todd, and L. G. Olson (1998), INEEL/EXT-98-00004, Idaho Falls, ID.
8. E. P. Horwitz, M. L. Dietz, and D. E. Fisher (1990), *Solvent Extr. Ion Exch.*, **8** (4&5), 557.
9. E. P. Horwitz, M. L. Dietz, and D. E. Fisher (1991), *Solvent Extr. Ion Exch.*, **9** (1), 1.
10. M. L. Dietz , E. P. Horwitz, and R. D. Rogers (1995), *Solvent Extr. Ion Exch.*, **13** (1), 1.
11. J. D. Law, D. J. Wood, and R. S. Herbst (1995), INEL-95/0314, Idaho Falls, ID.
12. J. D. Law and D. J. Wood (1996), INEL-96/0437, Idaho Falls, ID.
13. J. D. Law, D. J. Wood, and R. S. Herbst (1997), *Sep. Sci. Tech.*, **32** (1-4), 223.
14. D. J. Wood, and J. D. Law (1007), *Sep. Sci. Tech.*, **32** (1-4), 241.
15. J. D. Law, D. J. Wood, and T. A. Todd (1997), INEEL/EXT-97-00832, Idaho Falls, ID.
16. K. N. Brewer, R. S. Herbst, A. L. Olson, T. A. Todd, and T. J. Tranter (1994), WINCO-1230, Idaho Falls, ID.
17. J. D. Law, R. S. Herbst, T. A. Todd and K. N. Brewer (1996), *Proc. Spectrum '96*, Seattle, WA.
18. E. Makrlik and P. Vanura (1985), *Talanta*, **32**, 423.
19. S. D. Reilly, C. P. Mason, and P. H. Smith (1992), LA-11695, Los Alamos, NM.
20. V. A. Babain, A. Y. Shadrin, L. N. Lazarev, R. N. Kiseleva, (1993), *Radiokhimiya*, **35**, 81.

21. J. Rias, P. Selucky, and M. Kyrs (1976), *J. Inorg. Nucl. Chem.*, **38**, 1376.
22. V. Koprda and V. Scasnar (1979), *Radioanal. Chem.*, **51**, 245.
23. P. Selucky, P. Vanura, J. Rais, M. Kyrs (1979), *Radiochem. Radioanal. Letters*, **38**, 397.
24. J. D. Law, R. S. Herbst, K. N. Brewer, T. A. Todd and D. J. Wood (1999), *Waste Management*, **19** (1), 17-27.
25. J. D. Law, R. S. Herbst, T. A. Todd, V. N. Romanovskiy, V. M. Esimantovskiy, I. V. Smirnov, V. A. Babain, and B. N. Zaitsev (2001), *Proc. Waste Management 2001*, Tucson, AZ.
26. J. D. Law, R. S. Herbst, T. A. Todd, V. N. Romanovskiy, V. M. Esimantovskiy, I. V. Smirnov, V. A. Babain, B. N. Zaitsev, and S. B. Podoynitsyn (2000), INEEL/EXT-2000-01328, Idaho Falls, ID.
27. J. D. Law, R. S. Herbst, T. A. Todd, V. N. Romanovskiy, V. M. Esimantovskiy, I. V. Smirnov, V. A. Babain, and B. N. Zaitsev (1999), INEEL/EXT-99-00954, Idaho Falls, ID.



## EXTENDED FLOWSHEET TESTING OF THE UNIVERSAL EXTRACTION (UNEX) PROCESS FOR THE SIMULTANEOUS SEPARATION OF Cs, Sr AND ACTINIDES FROM ACIDIC WASTE

J. D. Law, R. S. Herbst, T. A. Todd, V. N. Romanovskiy\*, V. M. Esimantovskiy\*,  
I. V. Smirnov\*, V. A. Babain\*, and B. N. Zaitsev\*

Idaho National Engineering and Environmental Laboratory, Idaho Falls, Idaho, USA

\*V. G. Khlopin Radium Institute, St. Petersburg, Russia

The universal solvent extraction (UNEX) process has been developed as a collaborative effort between the Idaho National Engineering and Environmental Laboratory (INEEL) and the Khlopin Radium Institute in St. Petersburg, Russia for the simultaneous separation of Cs, Sr, and the actinides from acidic radioactive waste. The UNEX process was recently tested for an extended length of time at the INEEL to evaluate the UNEX process for the treatment of acidic tank waste at the INEEL. The UNEX flowsheet tested was operated continuously for 66 hours using 26 stages of 3.3-cm diameter centrifugal contactors and a tank waste simulant. The UNEX process solvent used for this testing contained chlorinated cobalt dicarbollide (Cs extractant), polyethylene glycol-400 (Sr extractant), and diphenyl-N,N-dibutylcarbamoylphosphine oxide (actinide extractant) in a diluent consisting of phenyltrifluoromethyl sulfone. The UNEX solvent was recycled a total of 89 times during the testing. The buildup of metals in the solvent was not observed. Removal efficiencies of 97.5% to 98.6% were obtained for Cs, >99.993% were obtained for Sr, and 17.2% to 34.1% were obtained for Eu (Am surrogate). Loading of the actinide extractant with Fe, Zr, and Mo resulted in the low removal efficiency for Eu. Laboratory experiments using individual stage process solutions and Am and Pu tracers indicate >99.99% of the Pu and very little of the Am (<2%) would be removed from actual waste solutions with this flowsheet. With minor adjustments, the UNEX process was subsequently successfully tested with actual dissolved calcine waste solution, resulting in removal efficiencies of 99.99%, 99.7%, 99.9% and >99% for <sup>137</sup>Cs, <sup>90</sup>Sr, total alpha, and <sup>241</sup>Am, respectively.

### INTRODUCTION

The Idaho National Engineering and Environmental Laboratory (INEEL) previously reprocessed spent nuclear fuel to recover enriched uranium. The radioactive raffinate stream from reprocessing was stored and subsequently solidified at 500 °C in a fluidized bed calciner. The INEEL currently has approximately 4,400 cubic meters of radioactive calcine stored onsite in above ground stainless steel bins enclosed in concrete vaults.

A secondary acidic aqueous waste was generated during equipment decontamination between processing campaigns and from solvent cleanup activities. Currently, approximately 4.8 million liters of liquid acidic radioactive tank waste are stored in underground, concrete enclosed stainless steel tanks at the INEEL. This liquid waste is not directly amenable to calcination due to its high sodium content, which causes agglomeration of the fluidized bed.

Separation processes are being evaluated as alternatives to calcination for treating the remaining tank waste. The goal of the separation processes is to remove fission products and/or actinides from the calcine and liquid wastes so the bulk of the treated waste can be disposed of as a contact handled transuranic (TRU) or non-TRU waste. It is anticipated that the combined low-activity waste (LAW) raffinate streams resulting from the separation unit operations would be grouted for near surface disposal. The high-activity waste (HAW) resulting from separations processes would be vitrified for disposal at a geological repository.

Several separation technologies (TRUEX [1], SREX [2], trialkylphosphine oxide [3], cobalt dicarbollide [3,4], and Cs ion exchange [5,6]) have been demonstrated at the INEEL using actual tank waste and 2-cm centrifugal contactors. The use of a single process to remove the desired radionuclides, as opposed to a combination of the above mentioned unit operations that remove these same radionuclides, evolved from the previous collaborative work with the scientists from the KRI. A process based on a universal solvent may provide a more simple and cost effective method for waste treatment than a method that utilizes two or three separate processes. Development and batch contact testing of a universal solvent was performed in 1997 using actual INEEL tank waste [7], a countercurrent flowsheet test of the Universal Solvent Extraction (UNEX) process using simulated tank waste was performed in 1997 [8], and countercurrent flowsheet tests using actual tank waste were performed in 1998 and 1999 [9,10], all with very positive results. The most recent flowsheet demonstration resulted in removal efficiencies of 99.4%, 99.995% and 99.96% for Cs, Sr, and total alpha activity, respectively [10].

After this highly successful flowsheet demonstration with actual tank waste, testing was performed at the KRI in which the process flowrates and solution compositions were optimized in order to reduce the volumes of the waste streams. The resulting flowsheet was tested at the INEEL with simulated tank waste over approximately 66 hours of operation with continuous recycle of the UNEX solvent. This document reports the results of this extended flowsheet testing of the UNEX process with simulated tank waste. Removal efficiencies of the Cs, Sr, and Eu (Am surrogate), as well as some of the other metals present in the tank waste are reported.

## EQUIPMENT DESCRIPTION

Flowsheet testing was performed using 26 stages of 3.3-cm diameter centrifugal contactors. The 3.3-cm contactors were designed and fabricated in Moscow, Russia by the Research and Development Institute of Construction Technology (NIKIMT).

Heat tape was wrapped around the strip section centrifugal contactors in order to operate the strip section at an elevated temperature. The temperature of the solution in these contactors was maintained at approximately 60 °C by monitoring the temperature of the solution in the stages and adjusting the current to the heat tape as necessary. In addition, the strip feed solution was heated to approximately 60 °C by pumping the solution through a heating coil submerged in a heated water bath. Solvent exiting the strip section was cooled prior to recycle to the extraction section by pumping the solvent through a cooling coil submerged in an ice water bath.

## EXPERIMENTAL PROCEDURE

### Concentrated Tank Waste Simulant

Approximately 45 liters of a simulant of the INEEL tank waste were prepared as feed for this flowsheet testing. This simulated waste was diluted by 10 vol.% with 3.3 M HF. The feed is diluted to reduce the concentration of metals, thus decreasing the loading of the actinide extractant in the solvent. Fluoride is added to the feed to complex Fe and Zr, thus minimizing the extraction of these bulk matrix components. Also, additional stable Cs, Sr, and Eu were added to the feed to facilitate analysis of these components in the aqueous raffinate. Two feeds were used for this testing, each for approximately half of the operational time. The differences in the two feed simulants is primarily the Eu concentration, which was decreased by approximately one order of magnitude in Feed #2 due to concerns that the Eu in Feed #1 was loading the UNEX solvent resulting in reduced Eu removal (*vide infra*). The compositions of the adjusted tank waste simulant feeds are shown in Table 1.

Table 1. Tank waste simulant feed compositions after 10% dilution with 3.3 M HF.

Component	Feed #1	Feed #2	Component	Feed #1	Feed #2
Acid (M)	2.0	2.0	K (M)	0.16	0.17
Al (M)	0.63	0.62	Mn (M)	0.012	0.013
Ba (M)	5.4E-05	5.2E-05	Mo (M)	6.1E-04	6.1E-04
Ca (M)	0.051	0.050	Na (M)	1.45	1.53
Ce (M)	2.5E-05	2.0E-05	Nd (M)	1.9E-05	1.7E-05
Cl (M)	0.028	0.029	Ni (M)	2.1E-03	2.0E-03
Cr (M)	5.2E-03	5.0E-03	Pb (M)	1.0E-03	9.8E-04
Cs (M)	8.9 E-04	9.1E-04	Pr (M)	1.2E-05	2.9E-06
Eu (M)	5.8E-03	5.6E-04	Ru (M)	1.8E-05	1.7E-05
F (M)	0.39	0.47	Sr (M)	8.7E-04	9.0E-04
Fe (M)	0.021	0.021	Zr (M)	0.013	0.011
Hg (M)	1.6E-03	1.8E-03			

### Solvent

The UNEX process solvent used in this testing is a “universal extraction mixture” which was developed to remove all of the radionuclides of concern, both fission product and actinides, in a single solvent extraction unit operation. The target solvent composition was 0.08 M chlorinated cobalt dicarbollide, 0.35 vol.% polyethylene glycol-400 (PEG-400), and 0.008 M diphenyl-N,N-dibutylcarbamoylphosphine oxide ( $\text{Ph}_2\text{Bu}_2\text{CMPO}$ ) in a diluent consisting of phenyltrifluoromethyl sulfone (FS-13). The solvent was continually recycled during the testing.

### Flowsheet Configuration and Testing

Based on the results of universal solvent development studies performed at the KRI and at the INEEL, a flowsheet was developed and recommended for extended countercurrent flowsheet testing in the 3.3-cm diameter centrifugal contactors. This flowsheet tested is shown in Figure 1.

The duration of the flowsheet testing was 66 hours. Samples were taken from each of the effluent streams every hour for the first five hours, then every five hours until the end of the test. The contactors were then shut down by simultaneously stopping the contactor motors and feed pumps. Each stage remains approximately at steady-state operating conditions with this type of shutdown. This allowed aqueous and organic samples to be taken from each stage and, therefore, distribution coefficients to be determined for any of the 26 stages. Each

effluent was collected in an individual product vessel for the duration of the testing. At the end of the test, each product vessel was mixed and sampled to obtain a composite analysis. Two sets of product composite solutions were collected and sampled, one while operating with Feed #1 and one while operating with Feed #2.

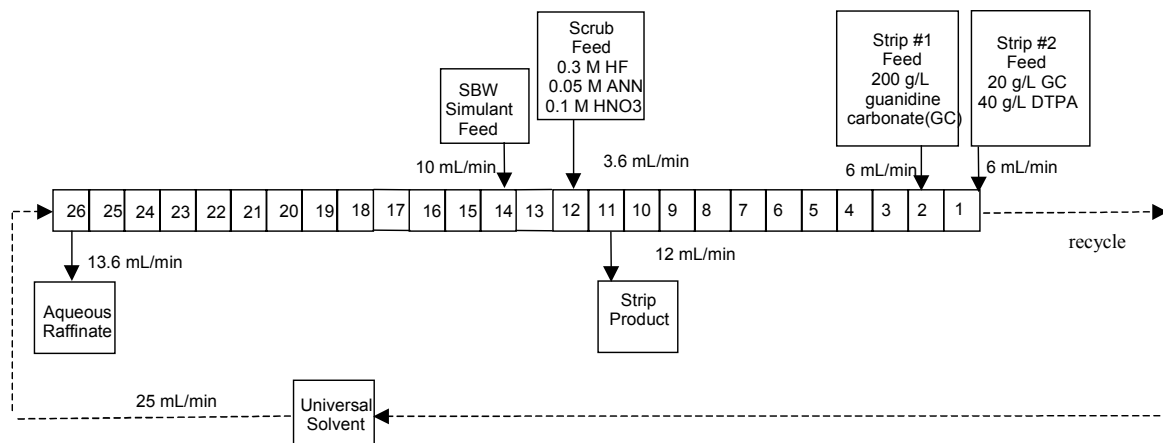


*Figure 1. Flowsheet for UNEX extended testing.*

## RESULTS AND DISCUSSION

The primary species of interest for evaluating UNEX flowsheet characteristics were Cs, Sr, and Eu (Am surrogate). Composite samples were obtained from the product tanks after concluding the experiment. Concentrations of the target metals, e.g., Cs, Sr, and Eu, and the percentage of each component in the various composite products are indicated in Table 2. A discussion of each of the components evaluated with this testing follows.

*Table 2. Percentages of components in the composite effluents for the extended UNEX testing.*

Effluent	Cs		Sr		Eu	
	Feed #1	Feed #2	Feed #1	Feed #2	Feed #1	Feed #2
Raffinate	2.5%	1.4%	0.007%	<0.007%	83%	70.4%
Strip	98.3%	91.4%	107.0%	101.0%	17.2%	34.1%
Solvent	<0.19%	0.35%	0.56%	0.47%	<0.05%	<0.5%
Material Balance	100.8%	92.8%	107.0%	101.0%	100.2%	104.5%

### Cesium

As shown in Table 2, 97.5% Cs removal was obtained with Feed #1 and 98.6% Cs removal was obtained with Feed #2. These removal efficiencies are greater than the required removal efficiency of 95% necessary to reduce the activity of  $^{137}\text{Cs}$  in the average tank waste to below the NRC Class A LLW requirement of 1.0 Ci/m<sup>3</sup> in a grout waste form.

The removal efficiency for Cs varied throughout the test due to fluctuations in ambient temperature. The Cs removal efficiencies were highest during the coolest part of the day and lowest during the hottest part of the day. Removal efficiencies for Cs ranged from 97.2% to 99.3% during the test, and are all above the required 95% removal efficiency.

### **Strontium**

As shown in Table 2, 99.993% Sr removal was obtained with Feed #1 and >99.993% Sr removal was obtained with Feed #2. These removal efficiencies are greater than the required removal efficiency of 99.98% necessary to reduce the activity of  $^{90}\text{Sr}$  in the average tank waste to below the NRC Class A LLW requirement of 0.04 Ci/m<sup>3</sup> in a grout waste form.

The effect of temperature on the Sr removal efficiencies could not be evaluated since the concentrations of Sr in the raffinate stream were below analytical detection limits throughout the test, resulting in removal efficiencies which ranged from >99.94% to >99.993%.

### **Europium**

As shown in Table 2, 17% Eu (Am surrogate) removal was obtained with Feed #1 and 29.6% Eu removal was obtained with Feed #2. With Feed #1, the amount of Eu present is sufficient to completely consume the Ph<sub>2</sub>Bu<sub>2</sub>CMPO in the UNEX solvent. Therefore, at approximately the midpoint of the test the Eu concentration in the feed was reduced by an order of magnitude (Feed #2) in order to prevent the loading of the Ph<sub>2</sub>Bu<sub>2</sub>CMPO. The Eu removal efficiency did increase when the feed was switched to Feed #2; however, a much greater increase was expected. The extraction distribution coefficients for Eu ranged from 0.62 to 0.16, decreasing steadily from the solvent feed stage (stage24) to the scrub section. These low Eu distribution coefficients, combined with the fact that they decreased as the solvent contacted the aqueous feed, indicates the Ph<sub>2</sub>Bu<sub>2</sub>CMPO was still being consumed, likely by other extractable metals such as Fe, Mo, and Zr.

The total alpha activity in the average tank waste is 579 nCi/g (511 nCi/g Pu, 65 nCi/g Am and 2.6 nCi/g Np). The total alpha activity must be reduced to below 100 nCi/g in order to be classified as a non-TRU waste. Therefore only Pu removal is required in order to be classified as non-TRU. Europium (III) is a surrogate for Am (III). The low removal efficiencies obtained for Eu, which indicate Am removal efficiencies will be low with this flowsheet, are not applicable to Pu (IV). Laboratory testing with solutions from this flowsheet test and Pu tracers were performed to determine what the Pu distribution coefficients would have been and, therefore, what total alpha removal efficiency could be expected. The aqueous and organic stage samples taken at the completion of the test were spiked with  $^{239}\text{Pu}$  or  $^{241}\text{Am}$ , re-equilibrated, and the two phases analyzed to determine distribution coefficients. The resulting  $^{239}\text{Pu}$  and  $^{241}\text{Am}$  distribution coefficients correspond to >99.99% Pu removal and <2%  $^{241}\text{Am}$  removal with the tested flowsheet, which is sufficient to reduce the total alpha activity in a grouted LAW form to approximately 30 nCi/g. Although it appears the flowsheet tested is adequate to achieve the non-TRU limit, it is desirable to prevent the loading of the Ph<sub>2</sub>Bu<sub>2</sub>CMPO by the metals and increase the extraction of  $^{241}\text{Am}$ . The flowsheet would then be capable of treating wastes which vary significantly above the average activity of  $^{241}\text{Am}$ . Increasing the concentration of Ph<sub>2</sub>Bu<sub>2</sub>CMPO in the UNEX solvent and/or reducing the amount of Zr extracted by adding additional F to the feed would prevent the loading of Ph<sub>2</sub>Bu<sub>2</sub>CMPO. It should be noted that the UNEX process, with minor adjustments, was subsequently tested using actual dissolved calcine waste, resulting in removal efficiencies of 99.99%, 99.7%, 99.9% and >99% for  $^{137}\text{Cs}$ ,  $^{90}\text{Sr}$ , total alpha, and  $^{241}\text{Am}$ , respectively.

### **Other Matrix Components**

The samples of the composite products were analyzed for a variety of matrix metals to evaluate or further confirm their behavior in the UNEX process. Ba, and Pb were nearly completely extracted from the feed. In addition, Ca, Ce, Fe, K, Pb, Mo, Ni, Pr, and Zr were partially extracted. Al, Cr, Na, Mn, and Hg were essentially inextractable. The results obtained for Feed #1 were very comparable to the results for Feed #2. Note that the amount of Ce, Mo, and Zr extracted increased with Feed #2. This is consistent with having a lower Eu concentration in Feed #2, resulting in less of the Ph<sub>2</sub>Bu<sub>2</sub>CMPO being consumed by Eu. A buildup of metals in the UNEX solvent was not observed.

## CONCLUSIONS

The universal solvent extraction process was successfully operated for an extended period of time using simulated waste solution. The UNEX flowsheet was operated for 66 continuous hours and the solvent was recycled 89 times. Based upon this testing it can be concluded that 1) components extracted from the tank waste will not build up in the UNEX solvent and adversely effect operation of the UNEX process during extended operation, 2) cesium and strontium were effectively separated from the concentrated tank waste simulant. An average removal efficiency of >99.993% was obtained for Sr. The average Cs removal efficiency was 98.6% while operating with Feed #1 and 97.5% with Feed #2, and 3) europium (Am surrogate) was not effectively removed from the tank waste simulant due to loading of the Ph<sub>2</sub>Bu<sub>2</sub>CMPO in the UNEX solvent with metals. However, results of testing using actual stage solutions spiked with Pu tracers indicate >99.99% Pu separation can be expected with this flowsheet. The activity of <sup>241</sup>Am expected in the average tank waste is 65 nCi/g, which is already below the 100 nCi/g non-TRU limit. Flowsheet modifications are necessary to prevent the loading of the Ph<sub>2</sub>Bu<sub>2</sub>CMPO in the UNEX solvent in order to effectively process batches of concentrated waste with higher <sup>241</sup>Am activity. The UNEX process was subsequently tested using actual dissolved calcine waste, resulting in removal efficiencies of 99.99%, 99.7%, 99.9% and >99% for <sup>137</sup>Cs, <sup>90</sup>Sr, total alpha, and <sup>241</sup>Am, respectively.

## ACKNOWLEDGEMENTS

This work was supported by the U. S. Department of Energy Assistant Secretary for Environmental Management under DOE Idaho Operations Office contract DE-AC07-99ID13727. This work was also supported by the U. S. Department of Energy Office of Science and Technology's Efficient Separations and Processing Crosscutting Program under the auspices of the Joint Coordinating Committee for Environmental Management.

## REFERENCES

1. J. D. Law, K. N. Brewer, R. S. Herbst, T. A. Todd, and L. G. Olson (1998), INEEL/EXT-98-00004, Idaho Falls, ID.
2. J. D. Law, D. J. Wood, L. G. Olson, and T. A. Todd (1997), INEEL/EXT-97-00832, Idaho Falls, ID.
3. J. D. Law, K. N. Brewer, T. A. Todd, E. L. Wade, V. N. Romanovskiy, V. M. Esimantovskiy, I. V. Smirnov, V. A. Babain and B. N. Zaitsev (1997), INEL/EXT-97-00064, Idaho Falls, ID.
4. J. D. Law, R. S. Herbst, T. A. Todd, K. N. Brewer, V. N. Romanovskiy, V. M. Esimantovskiy, I. V. Smirnov, V. A. Babain and B. N. Zaitsev (1999), INEL-96/0192, Idaho Falls, ID.
5. K. N. Brewer, T. A. Todd, P. A. Tullock, V. M. Gelis, E. A. Kozlitin, and V. V. Milyutin (1999), INEEL/EXT-99-00663, Idaho Falls, ID.
6. T. A. Todd, K. N. Brewer, D. J. Wood, P. A. Tullock, N. R. Mann and L. G. Olson (2001), *Sep. Sci. Tech.*, **36**, in press.
7. K. N. Brewer, T. A. Todd, J. D. Law, D. J. Wood, V. N. Romanovskiy, V. M. Esimantovskiy, I. V. Smirnov, V. A. Babain, and B. N. Zaitsev (1998), INEEL/EXT-98-00094, Idaho Falls, ID.
8. J. D. Law, R. S. Herbst, K. N. Brewer, T. A. Todd, V. N. Romanovskiy, V. M. Esimantovskiy, I. V. Smirnov, V. A. Babain, B. N. Zaitsev, G. I. Kuznetsov, and L. I. Shklyar (1998), INEEL/EXT-98-00544, Idaho Falls, ID.
9. J. D. Law, R. S. Herbst, K. N. Brewer, T. A. Todd, V. N. Romanovskiy, V. M. Esimantovskiy, I. V. Smirnov, V. A. Babain, B. N. Zaitsev, and Y. Glagolenko (1998), INEEL/EXT-98-01065, Idaho Falls, ID.
10. J. D. Law, R. S. Herbst, T. A. Todd, V. N. Romanovskiy, V. M. Esimantovskiy, I. V. Smirnov, V. A. Babain, and B. N. Zaitsev (2001), *Solvent Extr. Ion Exch.*, **19** (1), 23-36.



# COMPARISON OF SOLVENT EXTRACTION PROCESSES AND ION EXCHANGE RESINS FOR REPROCESSING ACTINIDE EFFLUENTS

L. Pescayre, C. Douche and C. Thiébaut

CEA, DTMN, Centre de Valduc, Is sur Tille, France

Nuclear recycled materials which are generated at the Valduc Centre have been chemically reprocessed since the 1970s. Solvent extraction and ion exchange resin processes have been used at large scale to separate plutonium from the other actinides and inert materials. Technologies have evolved in recent decades to contend better with cost, safety and environment.

However, major differences in criteria between these two purification processes exist and this study aims to point out the advantages and drawbacks of each. Significant results deal with the performance (degree of purification with various fuels to be reprocessed), the chemical and radiolytic stabilities, the control of the operating point and the generation of waste.

## INTRODUCTION

The activities of the Valduc Nuclear Centre generate various plutonium-contaminated residues (such as glass containers, impure scraps, etc.) and plutonium metal which does not meet the required purity specifications to be directly reused. A nitric acid-based process enables the recovery of plutonium in a purified form. It consists of four main stages:

- Dissolution of the nuclear materials,
- Purification of plutonium nitrate,
- Conversion into plutonium dioxide,
- Reduction treatment.

The efficiency of the entire process is mainly characterised by the purification stage of the plutonium nitrate solution, which determines the recovery rate as well as the volume of the waste generated. Two different technologies can be used to perform the purification: liquid-liquid solvent extraction and ion exchange resin processes [1]. Each one has specific characteristics and operating conditions.

The objectives of this study are to present the background of the Valduc Centre concerning several decades of exploitation of successive resin and solvent extraction facilities. A description of the two processes is followed by a comparison of the results obtained in order to point out general choice criteria for optimal operating conditions.

## PROCESSES

### Ion Exchange Resin Process

Plutonium is one of the few metals that forms stable anions in nitric acid solutions, inducing the creation of the Pu(IV) complex  $\text{Pu}(\text{NO}_3)_6^{2-}$  [1]. For an acid concentration of about 7 M, the Pu(IV) anions preferentially sorb to the resin by displacing or exchanging with nitrate anions.

Porous beads made from resin are packed into a column through which the 7 M nitric acid solution flows. The plutonium sorbs to the resin while impurity elements wash away (U, Am and inert materials). Once the resin has been sufficiently loaded with plutonium, the solution conditions are changed (0.5 M nitric acid). The plutonium is released from the resin and is recovered as pure plutonium solution (Figure 1).

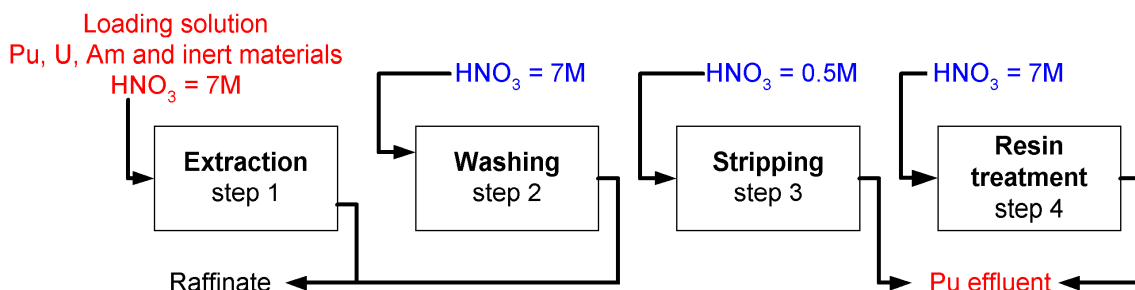


Figure 1. Flowsheet for the recovery of plutonium with an anionic resin.

For several decades, studies have focused on the resin to improve the efficiency of the process. During the 1980s, gel-type resins were used (such as Dowex 21K from Dow Chemical). They were replaced in early 1990s by macroporous resins which are cross-linked (e.g., Lewatit MP 500 from Bayer) with extra large pores that greatly increase the effective surface area and consequently the kinetics. More recently, studies have been performed using a macroporous polyvinylpyridine resin (mono or bifunctional) which offers better sorption and desorption kinetics, greater capacity and higher resistance to nitric acid and radiation damage (Reillex HPQ from Reilly Industries) [2].

### Liquid Extraction Process

Tetravalent plutonium is extracted from nitric acid by an organic phase (tributylphosphate: TBP) and forms a neutral, unhydrated complex  $(\text{PuNO}_3)_4 \cdot (\text{TBP})$  [1]. The well-known Purex process, based on this principle, has widely supplanted the other solvent extraction processes because 30% TBP in an aliphatic diluent (like dodecane) presents good selectivity and radiolytic stability [3].

Various equipment is suitable to perform the extraction. However, major constraints have led to the choice of mixer-settlers as contactors: pulsed columns can not be used in a glove box because of their height, while multistage centrifugal contactors are not suitable for use during normal working hours only because the starts and stops need many processes and controls.

After a nitric acid adjustment to 4 M, plutonium solution is fed to the center of the extraction mixer-settler. The organic phase, containing plutonium and uranium, overflows from the first mixer-settler battery into the center of the second mixer-settler battery. An aqueous acid stream, containing ferrous sulfamate, enters from the opposite end and strips the plutonium(III). The organic phase, containing uranium, overflows into the end of the third mixer-settler battery. A dilute acid stream strips the uranium. At the end, alkaline sodium reagents partially strip the degradation products from the solvent in mixer-settlers with an internal recycle of the aqueous phase (Figure 2). Mechanical barriers perform the destruction of micro-emulsion of each aqueous solution before storage.

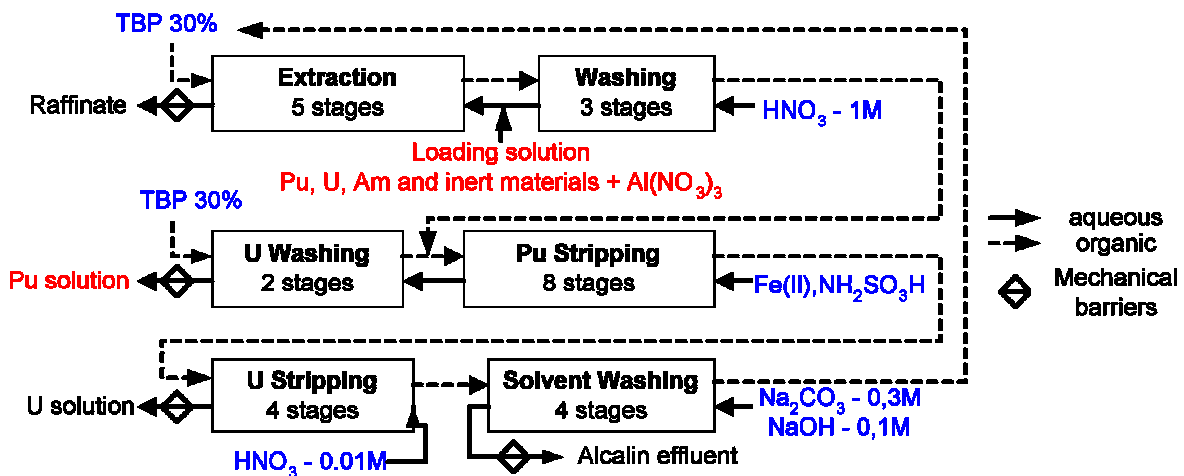


Figure 2. Flowsheet for the recovery of plutonium by extraction with 30% TBP.

## COMPARISON OF THE PROCESSES

These two plutonium extraction processes can be characterised by three main guidelines:

- the efficiency: to meet the end-product specifications (classified information) and to achieve high recovery of these products,
- the environmental consideration: to comply with radioactive release restrictions, to reduce the volume of wastes and to reprocess these wastes for final disposal,
- the engineering aspect: to take into account the objectives of an industrial approach (cost, safety, reliability and operating availability).

### Efficiency of the Processes

The efficiency of the anionic resin is determined by the  $Kd$  coefficient which characterises the sorption affinity. It is defined as:

$$Kd = \left( 1 - \frac{[B]}{[A]} \right) \frac{V}{M} \quad (1)$$

where  $[A]$  and  $[B]$  are the concentrations of the element in solution before and after contact respectively,  $V$  is the volume of solution (l) and  $M$  is the mass of resin (kg).

The characteristics of the solutions to be purified have evolved during the years but the  $Kd$  value of Pu was always near 100, that is 30 times higher than for Am. Consequently the extraction is extremely efficient and selective. Moreover, the recovery rate is high; an average value of 98 % is obtained in Valduc facilities, but a large volume of stripping solution is needed (see next section).

Nevertheless, the average plutonium concentration in the raffinate is not negligible. This might be due to a local channelling effect which considerably lowers the efficiency of the operation. This effect could be linked with a chemical swelling of the resin and its weight loss due to radiolysis. A specific arrangement which packs the resin in the column has been developed to decrease this phenomenon but the plutonium concentration is still about 50 mg/l.

The use of resin allows the reprocessing of solutions for which plutonium concentrations vary significantly (between 1 to 60 g/l).

The efficiency of the Purex process is determined by the extraction coefficient  $D$ , defined as:

$$D = \frac{\text{concentration of the element in solvent after contact}}{\text{concentration of the element in solution after contact}} \quad (2)$$

The  $D(\text{Pu})$  values decrease quickly between the first and the subsequent mixer-settlers, and can be as low as 10 for the first mixer-settler, and 2 for the last one. This is linked with the presence of strong complexants in the solution. However, introducing  $\text{Al}(\text{NO}_3)_3$  to the feed solution increases the  $D(\text{Pu})$  value (Figure 3).

With a five-stage mixer-settler battery, and after  $\text{Al}(\text{NO}_3)_3$  introduction, the plutonium concentration in raffinate is measured near 5 mg/l (see the evolution during the process in Figure 4). Both in the raffinates and in the unloaded solvent, the plutonium losses are extremely low (recovery rate higher than 98 %). The modification of feed concentration implies a need to change the operating parameters.

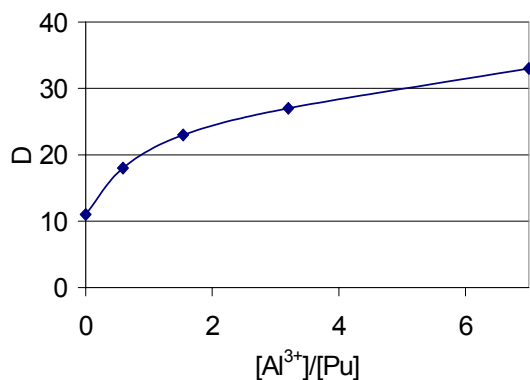


Figure 3.  $D(\text{Pu})$  versus  $[\text{Al}^{3+}]/[\text{Pu}]$  ratio in the first mixer-settler.

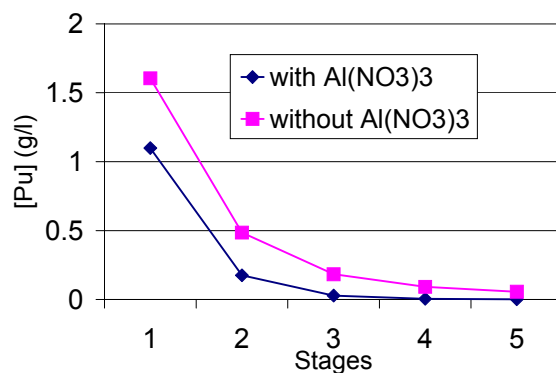


Figure 4. Pu extraction with and without  $\text{Al}(\text{NO}_3)_3$ .

### Environmental Considerations

The effluent management system of the Valduc Nuclear Centre aims to decrease the amount of waste solutions sent to the effluent treatment station and to reprocess all wastes for final disposal.

Two significant aspects differ between the solvent and resin processes. The first one is the volume of aqueous effluent introduced during the process. Concerning the resin extraction, two types of solutions have to be introduced: the 7 M nitric acid solution which is necessary for the washing and resin treatment and the 0.5 M nitric acid used for Pu stripping. For the solvent extraction treatment, various solutions are introduced: nitric acid with various concentrations, sulfamate ferrous solution, and alkaline sodium solution.

The total volume introduced for the solvent extraction process is one half of the volume introduced for the resin process (Figure 5). Liquid-liquid extraction thus presents an advantage over the resin process, but the nature of the waste effluents is more diversified and impurities are introduced.

Instead of Fe and sulfamate as the back-extraction agents, a mixture of hydroxylamine/hydrazine could be used and later eliminated as gases. However, this is not used at the Valduc centre because it presents a safety hazard and increases the costs due to the hydroxylamine/hydrazine treatment.

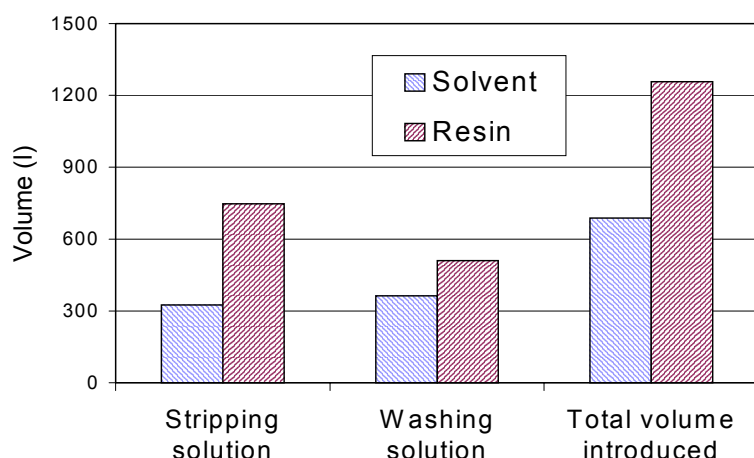


*Figure 5. Comparison of the solution volumes introduced for solvent and resin processes to purify 1 m<sup>3</sup>.*

The second significant difference between the two processes is the nature of the organic wastes. The nuclear aqueous solution induces radiolytic and chemical degradation of the solvent and the resin. The degradation products of the solvent or the resin process are responsible for the loss of efficiency of the extraction.

Concerning the solvent process, a widely used scrubbing solution containing sodium carbonate and caustic soda eliminates solvent degradation products which can combine with metal ions. However, efficiency is partial and after one year interfacial sludge is observed which contributes to the clogging of the extraction battery. The sludge is currently stored and could be mineralised in the future [4].

In case of the resin process, no specific treatment is realised. However anionic resins have evolved for several decades to offer superior resistance to degradation. The current resins have to be replaced after two years. The irradiated resins are stocked and we plan to reprocess them by an oxidising cobalt or silver dissolution treatment [5].

### **Engineering Aspects**

Every new reprocessing facility set up at the Valduc Centre has been an opportunity for technological progress and a step to reach an industrial maturity.

The liquid-liquid extraction process is a continuous process whereas the resin process is a semi-continuous process. The facilities operate five days a week during the usual working hours (8 h/day).

Suitable automation makes these processes easier to control. In particular, in-line analysers enable the operator to monitor the plutonium residual content in the aqueous streams as well as organic streams in the case of the solvent extraction facility. A germanium gamma spectrometer and a neutron measurement station are used for monitoring the processes.

Concerning the throughput range, the liquid-liquid extraction offers a significant advantage over the resin extraction process. For this second one, the strong influence of the throughput on the pressure in the bottom of the column requires operation at a flow below 15 l/h.

Regulatory constraints must be respected to avoid safety hazards. The mixer-settlers were built with reduced height to make them geometrically safe but wide enough to handle the throughputs. In the same manner, the diameter of the resin glass column, which is surrounded by a stainless steel grid, forms geometrically safe equipment. Furthermore, to avoid explosion hazards, a stripping step is necessary after each week of operation. The resin has to be kept in a nitrate solution between the cycles and maintained at room temperature.

The investment costs are higher for the solvent extraction process (150 %) as well as maintenance costs because this process needs more complex equipment (volumetric pumps, electric motors and agitators have to be regularly replaced). The highest reliability has been achieved with the resin extraction process, for which the equipment is simpler.

## CONCLUSIONS

Close attention is paid to the reliability and flexibility of the plutonium purification process to avoid rework of out-of-spec products. This implies efficient processes and adequate safety margins during usual operation as well as a suitable process control system. The advantages and drawbacks of the two processes tested at Valduc Centre are summarised in Table 1.

*Table 1. Advantages and drawbacks of the two processes.*

Process	Advantages	Drawbacks
Liquid-liquid extraction	<ul style="list-style-type: none"> <li>• High decontamination factor</li> <li>• Large throughputs</li> <li>• Continuous process</li> </ul>	<ul style="list-style-type: none"> <li>• Waste generation due to solvent</li> <li>• Modification of operating parameters</li> </ul>
Ion exchange resin	<ul style="list-style-type: none"> <li>• Low investment costs</li> <li>• Simple maintenance</li> <li>• Simple technology</li> <li>• Wide range of plutonium concentrations</li> </ul>	<ul style="list-style-type: none"> <li>• Waste generation due to resin</li> <li>• Waste generation due to the large volume of solutions introduced (Figure 5)</li> <li>• Limited throughputs</li> </ul>

The resin extraction process offers more advantages at low throughput (lower than 15 l/h), but for higher values liquid-liquid extraction can not be overlooked.

In the future, the variety of generated wastes has to be reduced and a choice should be made between the two processes. It is recommended that solvent extraction processes be utilized for future processing because higher throughputs can be handled, which is a major criterion in an industrial context.

## REFERENCES

1. J. M. Cleveland (1979), *The Chemistry of Plutonium*, American Nuclear Society, La Grange Park, IL, pp. 148-156 and pp. 161-178.
2. S. F. Marsh, G. D. Jarvinen and R. A. Bartsch (2000), *Proc. Pu Futures - the Science*, Santa Fe, USA, pp. 233-234.
3. B. Boullis, M. Germain, J. P. Goumondy and H. Rouyer (1994), *Proc. 4th Int. Conf. on Nuclear Fuel Reprocessing and Waste Management*, London, UK.
4. J. P. Moulin, C. Redonnet, V. Blanc (1998), *Proc. 5th Int. Conf. on Recycling, Conditioning and Disposal*, Nice, France, pp. 505-508.
5. D. F. Steele, J. P. Wilks and W. Batey (1992), *Therm. Treat. Radioact., Hazard Chem., Mixed Med. Wastes, Proc. 11th Incineration Conf.*, AEA Technology Doureay, Thurso/ Caithness, UK, pp. 167-174.



## PREPARATION OF N, N'-DIACYLPIPERAZINES AND THEIR EXTRACTION PROPERTIES FOR U(VI)

Yang Xing-Cun, Bao Bo-Rong<sup>\*</sup> and Cao Wei-Guo<sup>\*</sup>

Shanghai Institute of Nuclear Research, Chinese Academy of Sciences,  
Shanghai, P.R. China

\* Department of Chemistry, Shanghai University, Shanghai, P.R. China

Four amide extractants of the type N,N'-diacylpiperazine (DAPEZ), including N,N'-dihexanoylpiperazine (DHPEZ), N,N'-dioctanoylpiperazine (DOPEZ), N,N'-didecanoylpiperazine (DDPEZ), and N,N'-dilauroylpiperazineare (DLPEZ), were synthesized and characterized for the first time. Their extraction of U(VI) from aqueous nitric acid media has been studied. The relation between structure and property of the extractant has also been investigated. From the experimental results, it is shown that the extraction performance of DAPEZ for U(VI) is good compared to other diamides and that the longer acyl chain benefits the extraction. The extracted complexes were  $\text{UO}_2(\text{NO}_3)_2(\text{DAPEZ})_2$  and  $\text{UO}_2(\text{NO}_3)_2\text{DAPEZ}$ .

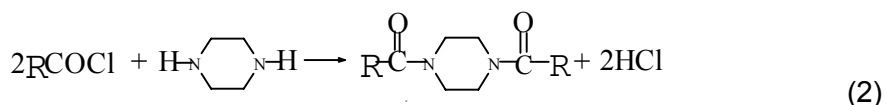
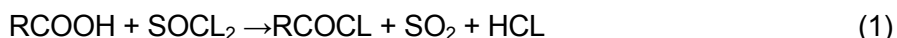
### INTRODUCTION

During the last forty years there have been numerous publications concerning amides. Amides have been proposed as an alternative to tri-n-butylphosphate (TBP) for the reprocessing of spent nuclear fuel [1-5]. They not only selectively extract U(VI) effectively from nitric acid media, but also have other advantages compared with TBP, such as their complete incinerability, innoxious degradation products, easier preparation and back extraction. However, when the acidity or the U(VI) content is higher, third-phase formation usually appears [6,7]. In order to modify the chemical structure of the amide and improve the extraction properties, a series of amides of the type N,N'-diacylpiperazine (N,N'-dihexanoylpiperazine (DHPEZ), N,N'-dioctanoylpiperazine (DOPEZ), N,N'-didecanoylpiperazine (DDPEZ), and N,N'-dilauroylpiperazine (DLPEZ)) were synthesized and characterized. Some physical properties of the four amides are given and the U(VI) extraction properties studied.

### EXPERIMENTAL

#### Preparation of N, N'-Diacylpiperazine

The synthesis of DAPEZ can be expressed as follows:



where R=C<sub>5</sub>H<sub>11</sub>, C<sub>7</sub>H<sub>15</sub>, C<sub>9</sub>H<sub>19</sub>, C<sub>11</sub>H<sub>23</sub>.

DAPEZ was synthesized by adding a stoichiometric quantity of chloride dropwise into a round-bottomed flask containing a mixture of piperazine and triethylamine in dichlorethane, being cooled to 0°C. After the addition, the mixture was heated under reflux for 10 hours at 75–80°C. On cooling, the contents in the flask were washed three times with distilled water, twice each with 5 % hydrochloric acid and 5 % sodium hydroxide, and finally with distilled water until free from alkali. The thick brown liquid obtained was dried overnight with an excess of anhydrous sodium sulfate. The solvent was evaporated under vacuum and the rough product was recrystallized in ether and then the noncolored (or light yellow) crystal was obtained with higher yields.

### Characterization of DAPEZ

The purity of DAPEZ was checked by IR spectrometry, elemental analysis and <sup>1</sup>H NMR spectrometry.

The elemental analyses for C, H, N were obtained. They are, respectively, for DHPEZ: 68.34% (68.04%), 10.58% (10.71%), 9.90% (9.92%); for DOPEZ: 70.86% (70.91%), 11.52% (11.31%), 8.15% (8.27%); for DDPEZ: 72.97% (73.04%), 11.47% (11.75%), 7.15% (7.09%); and for DLPEZ: 74.85% (74.61%), 11.87% (12.08%), 6.16% (6.21%). The theoretical values (in brackets) agree well with the experimental values, indicating that the products are sufficiently pure.

The data of IR spectra of DAPEZ help us to observe the  $\nu(\text{C=O})$  stretching band. Strongly absorptive peaks are found at 1643.3, 1646.5, 16544.8, 1643.1  $\text{cm}^{-1}$ , respectively for the four amides, in the IR spectra. They are the characteristic peaks of  $\nu(\text{C=O})$  of amide.

The data of <sup>1</sup>H NMR spectra fit the structure of diacylpiperazine well.

### Extraction Procedure

Extraction was performed by shaking 1 ml of benzene solution containing DAPEZ and 1 ml nitric acid solution containing uranyl nitrate in a stopper tube at  $298 \pm 1$  K for 40 minutes. After centrifugation and phase disengagement, the concentration of U(VI) in aqueous phase was analyzed by the arsenazo-III spectrophotometric method, and that in organic phase was calculated according to the difference between initial and final concentration of U(VI) in the aqueous phase. The distribution ratio,  $D$ , was then calculated.

## RESULTS AND DISCUSSION

### Effect of Nitric Acid Concentration

Figure 1 denotes the dependence of the distribution ratio on nitric acid concentration in the range of 1~9 mol/L. The values of  $D$  first increase rapidly with increasing concentration of nitric acid, then decrease gradually at higher acidity after a maximum value at the concentration of  $\text{HNO}_3$  about 6.2 mol/L. This is because DAPEZ not only extracts U(VI), but also extracts  $\text{HNO}_3$  from the aqueous phase especially at higher acidity. Accordingly the concentration of free extractant decreases greatly, which decreases the distribution ratios at higher acidity.

For all the extractants, owing to the similar chemical structures, the variation trends of plots of  $D$  versus  $C_{\text{HNO}_3}$  are similar and the acidities of nitric acid at the maximum values of  $D$  are almost same. But the maximum values of distribution ratios are different due to the different length of the acyl chain. That of DLPEZ is the highest and the others are nearly equal. The longer substituted groups not only enhance the solubility of the complex in the organic phase leading to an increase of extraction ability, but also increase the steric hindrance resulting in a decrease of extraction ability. The value of  $D$  is effected by both factors at the same time. In the case of DLPEZ, the effect of the former dominates, and for the others the both effective degrees are nearly equivalent.

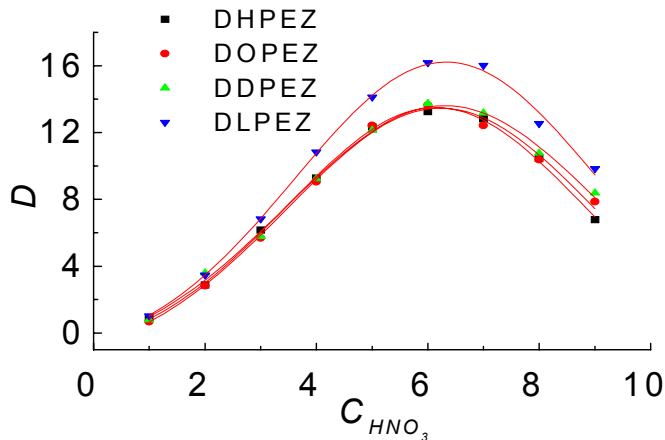


Figure 1. Dependence of distribution ratio on initial aqueous nitric acid concentration for the extraction of U(VI) by DAPEZ in benzene.

$[UO_2^{2+}] = 5.0 \times 10^{-3} \text{ mol/L}$ ;  $[DAPEZ]_{(o)} = 0.5 \text{ mol/L}$ ;  $T = 298 \text{ K}$ .

### Effect of Extractant Concentration

The dependence of distribution ratio on extractant concentration is shown in Figure 2. The plots of  $\log D$  versus  $\log [DAPEZ]_{(o)}$  are all straight lines with slopes of 1.46, 1.44, 1.46, 1.35, respectively. Although the substituted groups of DAPEZ are different, the values of slopes are near, being non-integer and close to 1.5. This suggests that there are probably two kinds of extracted species. The number of  $NO_3^-$  ions in the extracted species could be proved to be 2 by IR spectra [10], viz.,  $UO_2(NO_3)_2(DAPEZ)_2$  and  $UO_2(NO_3)_2DAPEZ$ . The extraction reactions were given as follows:



where the subscript (o) refers to the species in organic phase. For the above reactions, the distribution ratio,  $D$ , is

$$D = K_1[NO_3^-]^2[DAPEZ]_{(o)} + K_2[NO_3^-]^2[DAPEZ]_{(o)}^2 \quad (5)$$

The values of  $K_1$  and  $K_2$  were calculated by the curve-fitting method [8,9], for the given values of  $[NO_3^-]$  and  $[DAPEZ]_{(o)}$ , as shown in Table 1.

Table 1. Equilibrium constants of U(VI) by different extractants in benzene.

Extractant	DHPEZ	DOPEZ	DDPEZ	DLPEZ
$K_1$	0.98	1.07	1.07	0.93
$K_2$	1.65	1.01	1.16	2.40

$[UO_2^{2+}] = 5.0 \times 10^{-3} \text{ mol/L}$ ;  $[HNO_3] = 3.0 \text{ mol/L}$ ;  $T = 298 \text{ K}$ .

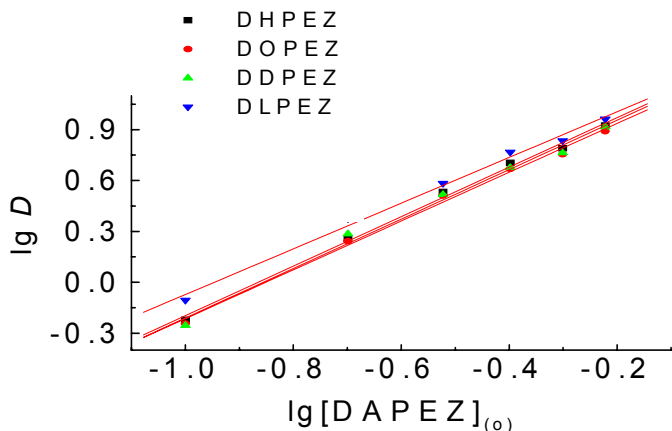


*Figure 2. Effect of DAPEZ concentration in benzene on distribution ratio of U(VI).  $[UO_2^{2+}] = 5.0 \times 10^{-3} \text{ mol/L}$ ;  $[HNO_3] = 3.0 \text{ mol/L}$ ;  $T = 298 \text{ K}$ .*

According to the results above, it implies that the acyl length of DAPEZ influences the values of  $K_1K_2$ , but there is no relationship between the  $K_1K_2$  value and carbon number of the acyl moiety. The carbon number of the acyl moiety does not influence the composition of the extracted species under the conditions studied.

## CONCLUSIONS

A series of novel amide extractants have been synthesized for the first time. The preparation procedures for DAPEZ are reliable. The extraction properties of DAPEZ are better than other extractants of this class. The carbon number of the acyl group affects the extraction ability and the longer acyl benefits extraction for U(VI).

## REFERENCES

1. C. H. Shen and B. R. Bao (1993), *J. Nucl. Radiochem.*, (in Chinese), **15** (4), 246-249.
2. T. H. Siddall (1963), *J. Inorg. Nucl. Chem.*, **26**, 883-887.
3. G. X. Sun, J. T. Han and B. R. Bao (1998), *J. Radioanal. Nucl. Chem.*, **232** (1), 245-250.
4. C. Musikas (1998), *Sep. Sci. Technol.*, **23**, 1211-1216.
5. C. Musikas and Hubert (1993), *Sol. Extr. Ion. Exch.*, **17**, 1007-1011.
6. C. H. Shen, B. R. Bao and Y. Z. Bao (1994), *J. Radioanal. Nucl. Chem.*, **178** (1), 91-99.
7. J. P. Shukla, S. A. Pai and M. S. Subramanian (1979), *Sep. Sci. Tech.*, **14** (10), 883.
8. L. G. Sellen (1956), *Acta Chem. Scand.*, **10**, 186-189.
9. D. Dyrssen (1957), *Acta Chem. Scand.*, **10**, 1771-1774.
10. Y. Zang, D. F. Wang and G. X. Wang (1978), *Acta Inorg. Chem.*, **3**, 66-69.



## DESIGNER SOLVENTS FOR LIQUID-LIQUID EXTRACTION

Braam van Dyk and Izak Nieuwoudt

The University of Stellenbosch, Stellenbosch, South Africa

A method is proposed for the computer-aided molecular design of solvents for liquid-liquid extraction. The method is based on a genetic algorithm and uses group contribution methods to predict solvent properties. Modified UNIFAC is used to estimate the selectivity of the proposed solvent. Any number of properties may be specified simultaneously. The basic genetic algorithm is enhanced by the addition of biased gene selection, viability checks, evolving fitness functions and seeding.

The method is applied to a system of industrial significance. The proposed solvents compare favourably with those recommended in literature.

### INTRODUCTION

The effectiveness of a liquid-liquid extraction (LLX) process depends greatly on the choice of solvent. As the technology of LLX has developed, a number of methods have been proposed to help in the selection of solvents. Unfortunately, these methods are mostly qualitative.

In recent years, a number of methods for Computer-Aided Molecular design (CAMD) have been proposed [1-14]. In these methods the required properties for a molecule are specified and using group-contribution methods, a molecular structure is then found that will satisfy these requirements.

Many different CAMD algorithms have been proposed. They may be broadly classified as interactive, combinatorial, knowledge-based and mathematical programming methods. In this work a genetic algorithm is used. This retains the efficiency of the mathematical programming methods, whilst performing well in difficult search-spaces. Genetic algorithms are also not as susceptible to local minima traps as are other mathematical programming methods. A detailed description of the method may be found in [13-15].

### GENETIC ALGORITHMS AND CAMD

#### **The Basic Algorithm**

A genetic algorithm is an optimisation method based on the theory of evolution. The method was first proposed by Holland in 1975 [16] and has been applied to numerous types of problems since [17, 18]. The method relies in the principle of survival of the fittest. Individuals that are better suited to their environment will have a better chance of passing their genetic material on to the next generation.

To apply this principle in molecular design, molecules are encoded as strings of sub-molecular groups. These groups are often referred to as genes, in reference to their biological equivalents. Similarly, the molecules are referred to as chromosomes.

The properties of each chromosome are calculated using group-contribution methods and measured against the required values for these properties. Each chromosome is then assigned a fitness, based on how well it matches the requirements.

The algorithm typically starts with a randomly created population of chromosomes. New generations are then created through mutation and recombination of parent chromosomes in the current generation. Once a new generation has been created, it replaces the current generation in its entirety. The probability of any chromosome to be used as a parent chromosome is directly proportional to its fitness. To prevent the loss of good candidates to random mutations, an elitist policy is followed in which the best 10% of each generation is copied to the next generation unchanged.

Genetic algorithms require that the chromosomes be encoded as linear data structures. This does not limit the search space to linear molecules. Genes of arbitrary complexity may be constructed by combining structural groups.

To satisfy the octet rule two types of genes are constructed. These are start/end genes with one free bond each and middle genes with two free bonds each. To construct cyclic molecules, only middle genes are used.

The use of these predefined genes has a number of advantages:

1. Physically unfeasible combinations of structural groups can be avoided to a large extent.
2. It allows the construction of more complex molecules than through the simple linear combination of structural groups, such as those used by UNIFAC.
3. It allows for the simultaneous design of aromatic and aliphatic molecules.

As molecules may vary greatly in size, the chromosomes must also be able to vary in length. This type of genetic algorithm is often called a 'messy' genetic algorithm [18].

The process may be summarised as follows (See Figure 1):

1. Initialise a population of chromosomes
2. Evaluate each chromosome against the property requirements.
3. Copy best 10% unchanged to new generation.
4. Create new chromosomes through mutation and recombination to fill up the remaining 90% of the population.
5. Replace the old generation with the new chromosomes.
6. Repeat the process a specified number of times.
7. Evaluate the final generation.
8. Return a list of best chromosomes.

### **Improvements to the Algorithm**

Although the basic algorithm described above gives satisfactory results, there are a number of ways in which it may be improved upon.

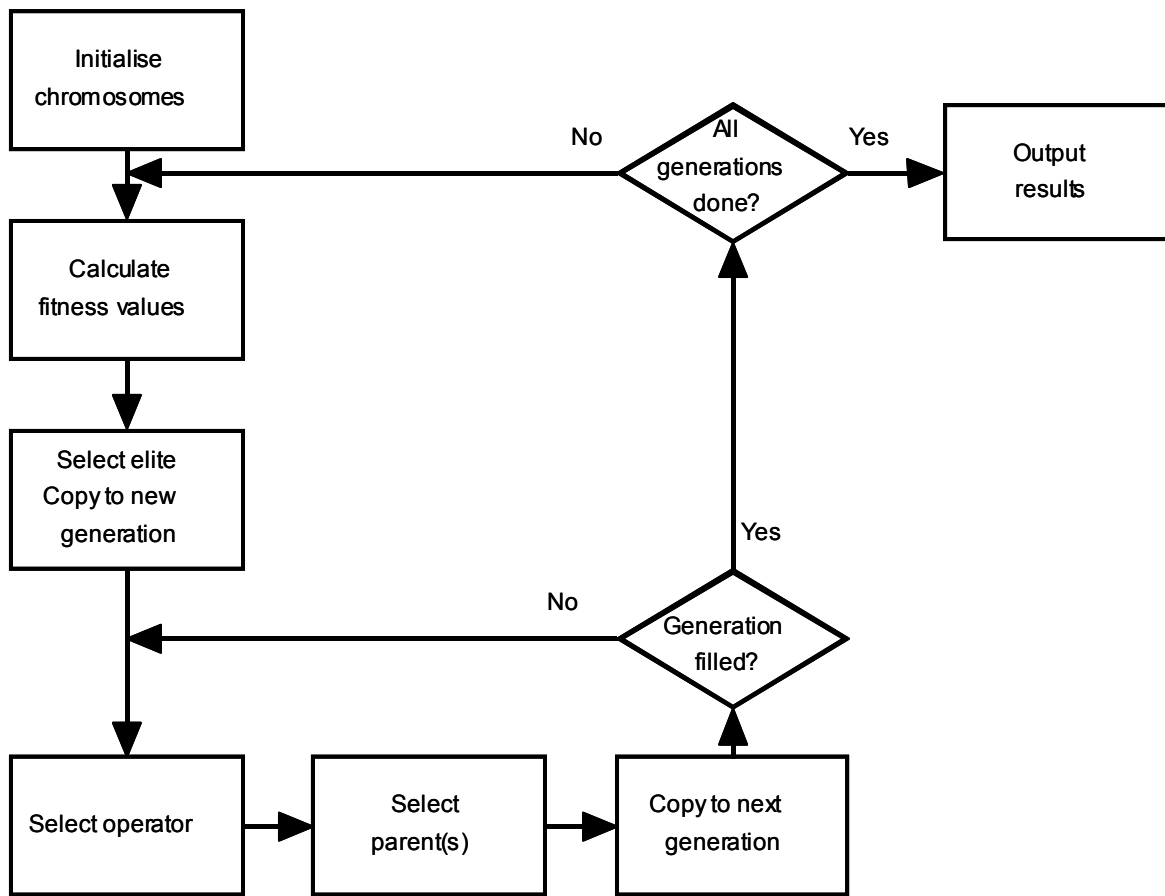


Figure 1. The basic genetic algorithm.

### **Missing interaction parameters**

As CAMD algorithms rely on group-contribution methods to estimate the macroscopic properties of candidate structures, these methods are sensitive to the accuracy and generality of these methods. As the principal property of a solvent is its ability to assist the separation, the UNIFAC method is of great importance in the design of solvents. The availability of UNIFAC interaction parameters is especially important.

Since the introduction of the UNIFAC method in 1975 [19], the matrix of interaction parameters has been greatly extended through the work of Gmehling and others [20]. Gmehling has also published a modified version of UNIFAC [21, 22] that offers improved estimation of liquid-liquid equilibria. Unfortunately, it may still be some time before the current matrix is complete. This leaves the problem of dealing with missing interaction parameters.

Missing interaction parameters may be set to zero [23], but this may lead to gross errors in the calculation of activity coefficients and is not acceptable. One could disqualify all chromosomes that require these missing parameters, or as a less harsh alternative, introduce a penalty system. A small value is then subtracted from the fitness for each missing interaction parameter it requires. This will cause these chromosomes to be eliminated through natural selection within a few generations, while still allowing any good traits of these chromosomes to be passed on to future generations.

### ***Biased gene selection***

The many heuristics that have been developed to assist in solvent selection are based on experimental observation and experience. A good example of this is the Robbins chart [24]. This knowledge should not be discarded out of hand and can be used to speed up the convergence of the genetic algorithm. This is achieved by using these heuristics to adjust the selection probability for each gene. The selection probability of a gene is increased whenever a heuristic indicates that a functional group in the gene will aid the separation and vice versa.

This biasing of gene selection also allows genes containing certain functional groups to be excluded from the design process. This can be done for safety or environmental reasons, or because a certain functional group may cause the solvent to react with the feed.

### ***Physical feasibility***

Although the use of predefined genes will help prevent physically impossible combination of functional groups within a gene, it is still possible that certain combinations of genes will result in infeasible structures. Physical viability is tested against a simple set of rules and a penalty is applied for each violation. These rules are mostly concerned with the number of heteroatoms bonded to a carbon atom.

### ***Incorporating the user's experience***

A great advantage of the interactive design methods is that the user's knowledge and experience is available to the program. This is also possible when using a genetic algorithm. The initial population may be seeded with candidate solvents that are either known or suspected to perform well in the specific separation. As these solvents should perform better than the randomly generated initial population, the algorithm will spend more time in these areas of the search space in the initial generations. As the functional groups that allow these solvents to assist the separation will be present in the population from an early stage, the speed of convergence will be greatly increased.

### ***Automatic tuning of operator selection***

The selection probabilities of the genetic operators (insertion, deletion, mutation and recombination) may be determined so as to optimise the speed of convergence and the quality of the final result. Unfortunately the optimal values for these probabilities vary depending on the system under consideration.

It is possible to determine the optimal parameters for the algorithm run-time through automatic parameter tuning. Whenever a new chromosome is created, the fitness of the new chromosome is compared with that of its parent chromosome. If the new chromosome has a higher fitness, the selection probability of the operator that created the chromosome is increased and vice versa. This method allows the selection probabilities to quickly converge to the optimal values for the specific system.

## **CASE STUDY**

The power of CAMD in solvent design may be illustrated through a case study. The genetic algorithm discussed here was implemented in a Windows application – SolvGen. [13-15]. The SolvGen program uses a set of 531 start/end genes and 368 middle genes. Each gene may consist of up to six types of UNIFAC groups and each chromosome may contain up to eight genes. This gives a total solution space in the order of  $10^{20}$  molecules. Each generation contains 10 000 chromosomes.

A problem of industrial significance is the separation of phenolics from nitrogen bases. Although such mixtures would normally consist of numerous components, for purposes of illustration the problem may be simplified by using only representative species. In this example phenol and aniline represent the phenolics and nitrogen bases respectively.

The use of co-solvents and anti-solvents is common practice in industry. To assure a liquid-liquid split, it was decided to use water and hexane as the co- and anti-solvents respectively. The feed composition used is given in Table 1

*Table 1. The feed composition (combined with water and hexane).*

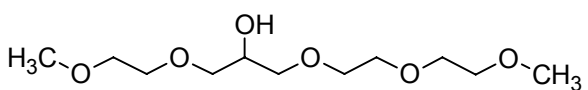
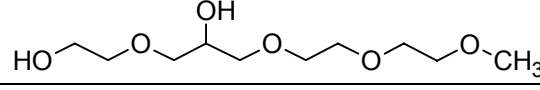
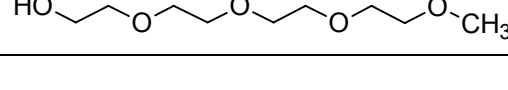
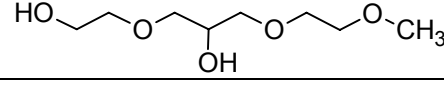
Component	Mass Fraction	Molar Fraction
Phenol	0.148	0.084
Aniline	0.019	0.011
Water	0.167	0.492
Hexane	0.666	0.413

The algorithm was allowed to run for 15 generations (approx. 10 minutes on a Pentium II desktop PC). The molar fraction of the solvent was set to 0.15 and a temperature of 315K was specified. Table 2 lists some of the chromosomes from the final generation and their estimated selectivities, as calculated according to equation (1) with Modified UNIFAC (Dortmund) [21].

These solvents are very similar in structure to the polyethylene glycols. Polyethylene glycols are relatively easily obtainable and as such much cheaper than solvents that have to be specially synthesised. Using the interactive mode of SolvGen we find that the predicted selectivity for triethylene glycol, using the same solvent fraction, is 7.475, for tetraethylene glycol it is 7.840 and for pentaethylene glycol it is 8.141.

Venter and Nieuwoudt did a detailed study on the separation of phenolics from neutral oils and nitrogen bases [25-27], using complex feeds so as to accurately represent industrial streams. They report that the polyethylene glycols, combined with water and hexane, are indeed very effective solvents for this separation. They recommend triethylene glycol, based on their experimental results, some of which are summarised in Figure 2.

*Table 2. Some candidate solvents.*

Solvent Structure	Selectivity $\alpha$ Phenol / Aniline
	8.322
	8.447
	7.652
	8.177

$$\alpha_{ij} = \frac{x_i^I}{x_j^I} / \frac{x_i^{II}}{x_j^{II}} \quad (1)$$

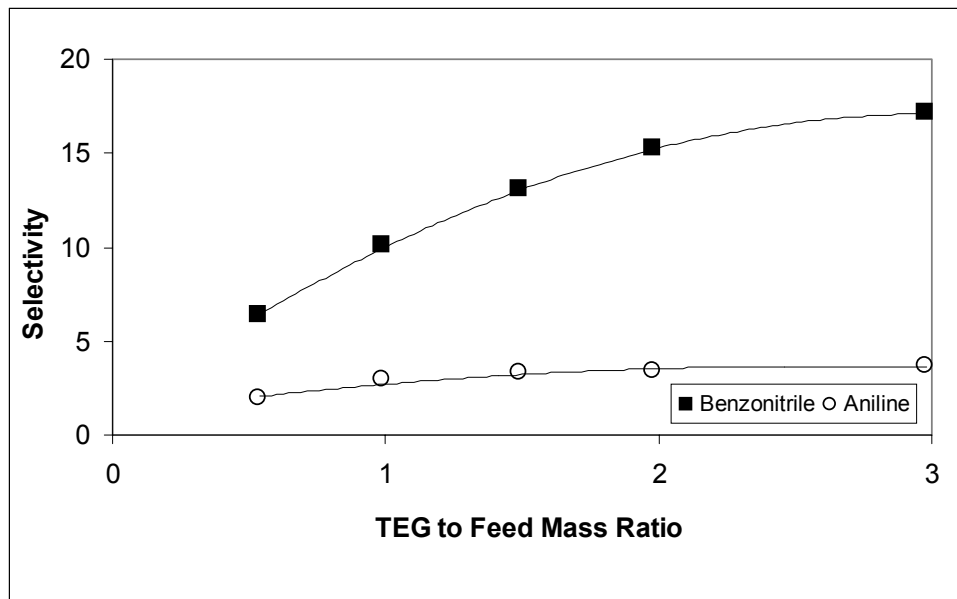


*Figure 2. Selectivity of phenol over neutral oils and nitrogen bases in the presence of triethylene glycol (TEG), water and hexane at 40°C [27].*

## NOMENCLATURE

$\alpha_{ij}$	Selectivity for component i over component j
$x_i^I$	Mass/molar fraction of component i in phase I
$x_i^{II}$	Mass/molar fraction of component i in phase II
$x_j^I$	Mass/molar fraction of component j in phase I
$x_j^{II}$	Mass/molar fraction of component j in phase II

## REFERENCES

1. E. A. Brignole, *et al.* (1986), *Fluid Phase Equilibria*, **29**, 125.
2. N. Churi and L. E. K. Achenie (1996), *Ind. Eng. Chem. Res.*, **35**, 3788.
3. R. Gani and E. A. Brignole (1983), *Fluid Phase Equilibria*, **13**, 331.
4. R. Gani, *et al.* (1991), *AIChE J.*, **37** (9), 1318.
5. K. G. Joback and G. Stephanopoulos (1989), Proc. FOCAPD '89, Snowmass, CO.
6. S. Macchietto, *et al.* (1990), *Trans. IChemE.*, **68**(A), 429.
7. C. D. Maranas (1996), *Ind. Eng. Chem. Res.*, **35**, 3403.
8. S. F. Naser and R. L. Fournier (1991), *Comp. Chem. Eng.*, **15** (6), 397.
9. B. Nielsen, *et al.* (1990), *Comp. App. Chem. Eng. Process Technology Proc.*, Elsevier, Vol. 9, p. 227.
10. E. J. Pretel, *et al.* (1994), *AIChE J.*, **40** (8), 1350.
11. R. Vaidyanathan and M. El-Halwagi (1996), *Ind. Eng. Chem. Res.*, **35**, 627.
12. V. Venkatasubramanian, *et al.* (1994), *Comp. Chem. Eng.*, **18** (9), 833.
13. B. Van Dyk and I. Nieuwoudt (2000), *Ind. Eng. Chem. Res.*, **39** (5), 1423.
14. B. Van Dyk and I. Nieuwoudt (2001), Ion Exchange and Solvent Extraction, Vol. 15, Y. Marcus and A. Sengupta (eds.), Marcel Dekker, New York, pp. 221-253.
15. B. Van Dyk (1998), Master's Thesis, University of Stellenbosch, South Africa.
16. J. H. Holland (1975), Adaptation in Natural and Artificial Systems, The University of Michigan Press Ann Arbor.
17. L. Davis (ed.) (1991), Handbook of Genetic Algorithms, Van Nostrand Reinhold, New York.
18. J. R. Koza (1992), Genetic Programming: On the Programming of Computers by Means of Natural Selection, M.I.T. Press, Cambridge, MA.
19. A. Fredenslund (1975), *AIChE J.*, **21** (6), 1086.
20. H. K. Hansen, *et al.* (1991), *Ind. Eng. Chem. Res.*, **30**, 2352.
21. J. Gmehling, *et al.* (1993), *Ind. Eng. Chem. Res.*, **32** (1), 178.
22. J. Gmehling, *et al.* (1998), *Ind. Eng. Chem. Res.*, **37** (12), 4876.
23. R. C. Reid, *et al.* (1987), The Properties of Gasses and Liquids, 4th edn., McGraw-Hill, New York.
24. L. A. Robbins (1980), *Chem. Eng. Prog.*, **76** (10), 58.
25. D. L. Venter and I. Nieuwoudt (1998), *J. Chem. Eng. Data*, **43** (4), 676.
26. D. L. Venter and I. Nieuwoudt (1998), *Ind. Eng. Chem. Res.*, **37** (10), 4099.
27. D. L. Venter and I. Nieuwoudt (1999), Proc. Int. Solvent Extr. Conf. ISEC '99, Society of Chemical Industry, London, pp. 1319-1324.



## REVAMP OF AN AROMATICS EXTRACTION COMPLEX USING HIGH PERFORMANCE MASS TRANSFER INTERNALS

Jose Bravo and Sergio Bergerman

Shell Global Solutions International BV, Amsterdam, The Netherlands

This paper discusses the reconfiguration of an Aromatics Extraction Unit that uses Sulfolane technology, to enable it to process segregated feeds in two extractors in parallel. The existing RDC extraction columns were retrofitted with Shell HiFi Extraction trays to provide about 10% more hydraulic capacity and about 20% more stages for separation. The design was based on a process model that was tuned to actual plant performance based on test run data, and later modified to reflect the new unit line up and operating conditions. The process design also required to increase the lean solvent purity, in order to achieve the necessary extraction performance within the capacity of the equipment. Special measures were undertaken in the design of equipment modifications to ensure this stringent solvent quality.

### INTRODUCTION

Sieve trays are often used for continuous extraction processes in the chemical and petrochemical industries. The sieve tray extractor is simple in design, requires no moving parts, reforms drops at every tray, reduces backmixing, and can handle some slurries. The extraction column consists of a series of perforated plates that are connected by downcomers (or upcomers). The perforations are designed to pass the dispersed phase and the downcomers (or upcomers) are to pass the continuous phase. A completely coalesced layer is supposed to exist underneath the tray (light phase dispersed) for the purpose of reforming drops and preventing backmixing of the continuous phase.

Two studies using larger equipment to examine extraction column flooding have been reported by Seibert and Fair [1] and Eldridge and Fair [2]. Sieve tray flooding studies [4] that have been carried out using 10.2 and 42.8 cm diameter columns, often with "actual" industrial mixtures, indicate that there are several mechanisms that can limit tray capacity, among them

- Spray column flood (ultimate capacity);
- Cross-flow velocity of the continuous phase;
- Length of flow path.

This paper will address a revamp of a column that removes the three limitations mentioned above.

### **Spray and Rotating Disc Contactor (RDC) Column Flood**

The capacity of the spray column is generally limited by entrainment of dispersed phase by the continuous phase and high dispersed phase hold-up. As a result of a distribution in drop sizes, entrainment of smaller drops is the most common mechanism of flooding in a spray column. In larger diameter columns, tray capacity may exceed that of a large diameter spray column depending on the phase flow ratio and the degree of continuous phase recirculation. Spray column axial mixing experiments at the Separations Research Program have indicated that the actual velocity of the continuous phase can be increased by backmixing [4]. Nevertheless one would expect the maximum capacity of a sieve tray extractor to approach that of a spray column free of backmixing but in reality, backmixing will always be present in industrial scale spray extractors. The capacity of RDCs is even more limited than that of spray columns due to the additional dispersed phase holdup present due to shear and the higher velocity flow across baffles. Many RDCs in Sulfolane aromatics extraction service operate as simple baffle columns since the operators have found empirically that stopping the rotation of the discs increased extractor capacity with no detriment to separation performance. In this case the capacity of the static RDCs is limited by the smaller effective cross section available between the discs and the stators. Revamps of RDCs with sieve trays often have yielded more capacity and efficiency, as this paper illustrates.

## **PROCESS DESIGN**

### **Process Description**

The Sulfolane Extraction Unit (SEU) is an industrial process applied in oil refineries and chemical complexes to separate aromatic-containing feedstocks in the gasoline range (platformate, pygas) into two fractions: the extract (mainly consisting of benzene and toluene), and the raffinate (mainly consisting of the non-aromatics components). A liquid-liquid extraction process is used for this purpose, using sulfolane as extraction solvent, in view of its selectivity for dissolving aromatics and its significant density difference with hydrocarbons. The SEU process consist of three main steps: liquid-liquid extraction (aromatics recovery from the feedstock), extractive stripping of the rich solvent (separation of the extract from the rich solvent), and solvent recovery by distillation (purification of the solvent). The raffinate stream is routed to other refinery processes for further processing, while the extract is routed to a fractionation section to separate and purify a benzene and a toluene stream, what is done in a number of conventional distillation columns.

In the SEU unit under consideration in this paper, two different feedstocks (reformate and pygas) coming from other refinery/chemical processes, were mixed together and processed as a single stream in two RDC extractor columns lined up in series. In this way, a maximum number of separation stages were available for the extraction step of the process, but of course a single raffinate stream was resulting from the unit.

### **Project Objective**

The revamp project that was developed for this SEU unit had two main objectives: the segregation of the processing of pygas and reformate feedstocks, and an increase in the unit throughput. The segregated processing of the two feedstocks is achieved by using one of the existing extractor columns for pygas processing, and the other one for reformate processing, thus operating these two columns in parallel (both on the feed side and also within the solvent circulation loop) rather than in series as in previous operation. In this way, two separate raffinate streams would be resulting ("reformate raffinate" and "pygas raffinate"), one from each extractor column, while a single extract stream (mainly benzene and toluene) will still be produced (since the rich solvent streams from each extractor would be combined together before routing them to the extractive stripper).

The economic incentive of obtaining segregated raffinate streams out of the two feedstocks is resulting from the possibility to select different processing routes for each of these streams. The pygas raffinate has much higher content of naphthenic components than the reformate raffinate, thus making it a high quality feedstock for the catalytic reformer unit (in this refinery process unit, naphthenes are converted to high-valued aromatics with high yields). The reformate raffinate, in view of its low content of naphthenic components, is not an attractive feedstock for the catalytic reformer, and thus would be routed as feedstock to the ethylene cracker unit in the chemicals area of the complex. Overall, the segregated processing of the feedstocks to the SEU unit represented a significant improvement to the economic margin of the refinery.

In addition to the feed segregation, an increase of 13% in the total feed intake to the unit was also considered in the project, in order to take full advantage of the potential economic benefits of the unit revamp.

### **Process Modelling and Process Design Considerations**

As a starting point for the process design of the revamp project, a process simulation model of the unit was prepared, representing the existing line up and typical process operating conditions. A key feature for an accurate representation of the process in this model was the selection of suitable thermodynamic package data to predict the L-L equilibrium in the extractor columns, and the V-L-L equilibrium in the extractive stripper and solvent recovery column. The characterisation of the different feedstocks was done based on a set of 48 individual chemical components, for all of which the relevant interaction parameters for the prediction of L-L and V-L-L equilibria were available.

The simulation model was tuned against actual operating data from a unit test run, and the number of theoretical stages in each of the RDC extractor columns was varied until a good match between predicted and actual extraction performance was obtained.

After establishing in this way the base case for the project (both the existing operating conditions and unit line up), the simulation model was adjusted to reflect the required / expected changes in the unit. The main changes are summarised as follows:

- parallel line up of the two extractor columns in the solvent circulation loop;
- segregated line up of the two feedstocks, one to each extractor;
- increased number of theoretical stages in each extractor column, due to higher mass transfer efficiency of sieve trays vs. RDCs;
- new feed flows and composition;
- addition of a tertiary (lean) solvent stream to the pygas extractor;
- addition of a new reformate raffinate water wash column;
- optimised line-up / split for the backwash recycle from the extractive stripper to extractors, and from the top of reformate extractor to the pygas extractor;
- general tuning of the different process conditions for the new requirements.

As a result of the higher total feed intake and the reduced number of theoretical stages available for the solvent extraction step, as compared to the existing conditions (due to the parallel line-up of the extractors instead of in series), a significant increase in the solvent circulation flow was required. In order to limit this increase, and thus the required modifications to existing equipment, an improved quality (*i.e.*, concentration of benzene + toluene) of the lean solvent was specified in the revamp process design. In this way, a larger driving force for mass transfer resulted in the extractors, and the additional solvent circulation was cut down. For this purpose, additional separation stages were added in the (steam) stripping section of the solvent recovery column, so as to reduce the aromatics content of the lean solvent without increasing the reboiler duty or operating temperature in the column.

A summary of the key process parameters of the unit, both for the pre- and post- revamp conditions, is shown in Table 1.

*Table 1. Comparison of process parameters pre- and post- revamp.*

		Previous operation Extractors in series	Revamp design Extractors in parallel
<b>Unit feed</b>			
Total unit intake		100% (base)	113% of base
Pygas feed		100% (base)	95% of base
Reformate feed		100% (base)	173% of base
<b>Solvent properties</b>			
Total lean solvent circulation		100% (base)	143% of base
Solvent / feed ratio	w/w	2.19	<sup>(1)</sup> 2.37 <sup>(2)</sup> / 3.01
Benzene + toluene in lean solvent	%w	0.42	0.30
Benzene + toluene in rich solvent	%w	23.7	<sup>(1)</sup> 22.1 / 19.4
Hydrocarbon load in rich solvent	%w	28.1	<sup>(1)</sup> 27.2 / 23.6
<b>Product quality &amp; recovery</b>			
Benzene in raffinate	%w	1.12	<sup>(1)</sup> 0.81 / 0.95
Toluene in raffinate	%w	1.82	<sup>(1)</sup> 0.91 / 1.14
Benzene recovery	%	98.9	99.1
Toluene recovery	%	93.0	93.9

(1): values for pygas extractor / reformate extractor, respectively

(2): includes primary + tertiary solvent

## EQUIPMENT MODIFICATIONS

### Extractor Columns

In order to accommodate the higher feed and solvent flows resulting from the desired revamp process conditions, an increase in the hydraulic capacity of the existing extractor columns was required. On the other hand, the reduced number of theoretical stages available for the extraction of each feedstock as compared to the existing conditions (due to the parallel line-up of the extractors instead of in series), represented also an incentive to find alternatives to increase the mass transfer efficiency of the column.

The conversion of the existing columns from RDC type to trayed extractors, equipped with high capacity Shell HiFi™ extraction trays, fulfilled both requirements, as is further described later on in this article.

The conversion of both columns from a RDC to a trayed extractor involved the following main hardware modifications:

- removal of all existing elements associated with RDC operation (motor, shaft, rotor discs, bearings, supports, etc.);
- dismantling/cutting of existing stator discs to make them suitable as support rings for the new sieve trays;
- new (radial) inlet nozzles for feed, solvent and backwash recycles at suitable locations;
- blanking of existing (tangential) inlet nozzles;
- installation of new sieve trays, on existing support rings;
- installation of new spider-type inlet devices for feed, solvent and backwash recycles;
- required modifications to instrument connections, external piping, etc.

The rating of the hydraulic capacity of the extractor columns, when equipped with the new sieve trays, was done with the help of a computer design program for L-L extractors named LLE 5.07, that was developed by the Separation Research Program, of the University of Texas at Austin, based on extensive research and development work. This program allows the determination of the hydraulic capacity of extractor columns, as it is determined from the physical properties of the system and the type of contacting device.

The interfacial tension of the system is a key parameter in this respect, both because it has a large influence in the hydraulic capacity itself, and also because its value is very difficult (when not impossible) to determine under actual plant conditions. Nevertheless, this uncertainty can be solved to some extent by performing a hydraulic rating of the extractors under the existing (pre-revamp) conditions, and using the interfacial tension as tuning parameter to let the columns be just below the flooding point. This approach will result with the lowest value for the interfacial tension that prevents the columns to flood under present conditions, and thus can be used conservatively for the revamp design.

An additional (new) extractor column was specified as part of the revamp project, for the service of reformate raffinate wash. This column is also equipped with high capacity Shell HiFi™ extraction trays, although the service is less critical than the sulfolane extractors, in view of the much higher interfacial tension and lower impact in the overall process.

Relevant hardware details on the extractor columns are shown in Table 2 below.

*Table 2. Hardware details.*

		Column C-8210	Column C-8211
Extractor service previous operation revamp design		Reformate + Pygas extractor Pygas extractor 3200 19782	Reformate + Pygas extractor Reformate extractor 3500 16250
Column diameter	mm		
Column T-T length	mm		
Number of stages previous operation revamp design		56 RDC compartments 55 trays	30 RDC compartments 32 trays

### Distillation Columns

The distillation columns associated with this process were also revamped for more solvent recovery capacity at a higher purity since the solvent purity is the key process variable for aromatics recovery in extraction. These modifications are not discussed in this paper.

## FEATURES OF THE HIGH PERFORMANCE EXTRACTION TRAYS

The Shell HiFi Extraction sieve trays combine several features that make them achieve larger capacities when compared with RDCs and conventional sieve trays:

- a) Short flow paths for the continuous phase. This feature reduces the amount of intertray recirculation of the continuous phase and thus allows for more hydraulic capacity without loss of tray efficiency. Large diameter conventional sieve trays are prone to this intertray recirculation of the continuous phase. The typical flow path length of a Shell HiFi extraction tray in the order of 300 to 600 mm which is the same as that tested in pilot columns. This allows for very reliable scale-up of capacity information.

- b) Higher efficiency than RDCs. Trays significantly reduce the amount of axial mixing of both the continuous and dispersed phases when compared to spray columns and RDCs. This leads to higher volumetric efficiency and larger numbers of theoretical stages achieved.
  - c) Better flow distribution and avoidance of high velocity zones. As can be seen from Figures 1, 2 and 3, the Shell HiFi Extraction trays are designed to provide a close approach to pure plug flow of both phases that translate to better capacity and efficiency.

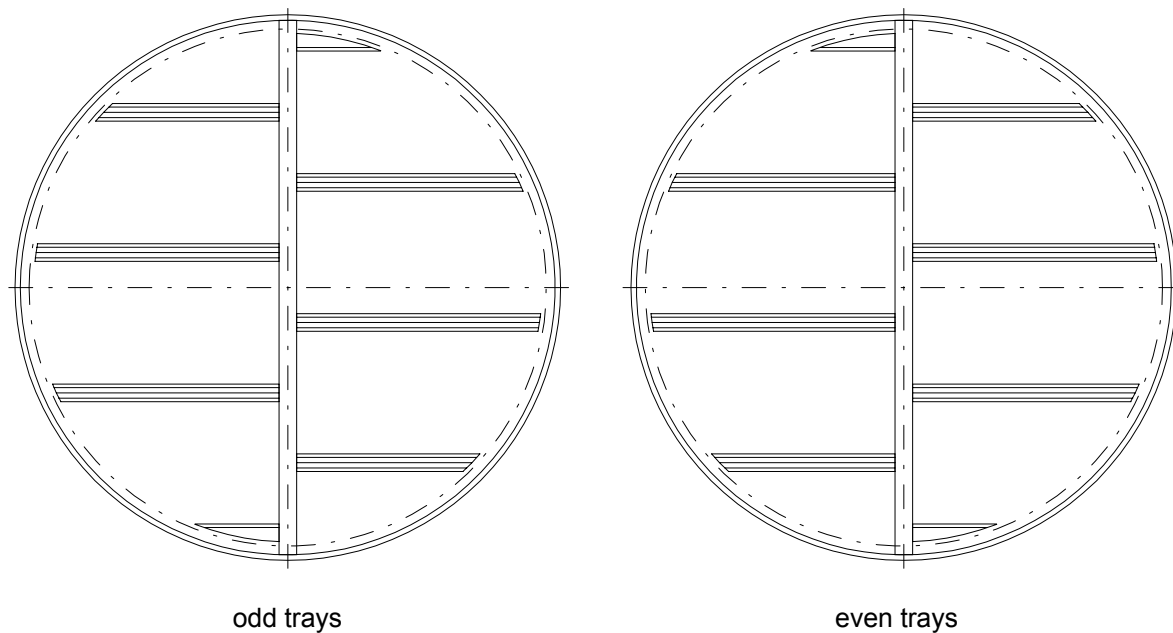


*Figure 1. Layout of a Shell HiFi™ extraction tray.*

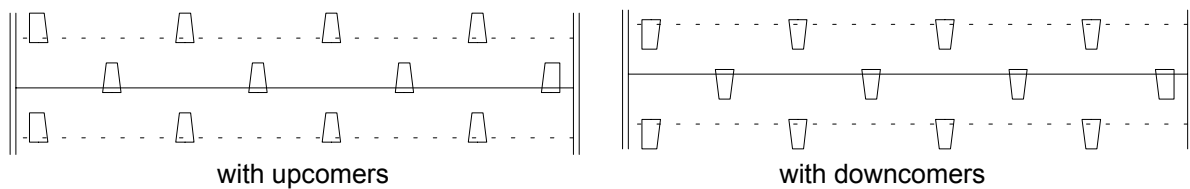


*Figure 2. Side view of Shell HiFi™ extraction trays.*



Figure 3. Picture of a Shell HiFi™ extraction tray with upcomers.

#### REFERENCES

1. A. F. Seibert and J.R. Fair (1993), *Ind. Eng. Chem. Res.*, **32**, 2213-2219.
2. R. B. Eldridge and J.R. Fair (1999), *Ind. Eng. Chem. Res.*, **38**, 218-222.
3. D. Mewes and W. Kunkel (1978), *Ger. Chem. Eng.*, **1**, 111-115.
4. O. Becker and A. F. Seibert (1999), *Chemie-Ing-Tech.*, **72**, 359-364.



## A NEW APPROACH TO IMPROVE THE SULFOLANE AROMATIC EXTRACTION COLUMN

Weiyang Fei and Xiaoming Wen

Department of Chemical Engineering, Tsinghua University, Beijing, China

Sieve tray columns are widely used for aromatics extraction with sulfolane. However, they suffer from limited mass transfer efficiency due to the very low interfacial tension of the system in the feedstock inlet section and the serious axial mixing inside the column. As an alternative approach to improve column performance, the use of Super Mini Ring (SMR) packing has been investigated. The hydrodynamics and mass transfer of SMR have been studied in the laboratory using a 30% tri-*n*-butylphosphate (kerosene) / acetic acid / water system and in a pilot plant using a real pyrolysis gasoline / sulfolane system. The results show that the mass transfer efficiencies for SMR packing are more than 30% higher than for the sieve trays. A reliable scale-up approach based on the characteristic velocity and diffusion model has been formulated for the retrofit design of an aromatic extraction column that contains SMRs. In a case study, an existing sieve tray extraction column, after being retrofitted with SMR packing, is shown to have significantly improved capacity and mass transfer efficiency characteristics.

### INTRODUCTION

The Sulfolane Extraction Process is widely used because of its ability to produce high purity BTX (benzene, toluene and xylene) products with high recoveries [1,2]. However, technological developments and changing feedstocks have forced many existing units to be retrofitted to meet the demands of higher capacity and aromatic recovery. For example, if the feedstock is changed from the reform liquid to pyrolysis gasoline, the solvent ratio has to be increased significantly to ensure the proper aromatic recovery but the capacity declines.

Most of the extraction columns used for aromatic extraction with sulfolane are sieve tray columns. They have several advantages, such as being simple to manufacture, easy to maintain, and at low cost, etc. However, a commercial operation that uses sieve plates has been shown to suffer from limited mass transfer efficiency problems. The column's tray efficiency was as low as 17% [3]. There is clearly a need for development of new column internals for the Sulfolane Process to increase the mass transfer efficiency and to ensure high aromatics recovery, high capacity and a lower solvent ratio.

The SMR (Super Mini Ring), shown in Figure 1, was developed for liquid-liquid extraction, high-pressure distillation and absorption with high liquid loading at the Tsinghua University in 1989 [4]. The small height/diameter ratio (about 0.3) ensure that most of the rings orient themselves at less than 30° from the horizontal in the columns. They have no flanges and their inner space is divided into 4 spaces by three arc stripes. These features of the packing enhance the dispersion-coalescence recycle, control the non-ideal flow in the packed bed and thus increase column capacity and efficiency. Extensive experiments have shown that

the new packing has superior characteristics for solvent extraction and gas-liquid mass transfer with high liquid loading both in term of capacity and mass transfer efficiency. For example, when the SMR is used for the solvent extraction of low and middle interfacial tension systems, its mass transfer efficiency is much high than those of Intalox Saddle, Pall Ring and Mellapak structure packing while the capacity is almost the same [5]. More than 50 SMR packed columns have been put into operation successfully for lube-oil refining, aromatic separation, waste water treatment, LPG desulfurization, gasoline desulfurization, methanol recovery, deasphalt by propane and so on [6]. The excellent performance of commercial applications has demonstrated the superior characteristics and the reliability of scale up of the SMR.



*Figure 1. SMR packing.*

In this paper the results of laboratory and pilot-plant investigations on the comparative use of SMR packing and sieve trays for the Sulfolane Aromatics Extraction Process are presented. In addition a case study of the retrofitting of an existing sieve-plate column with SMR packing is described.

## EXPERIMENTAL PROCEDURES

### Laboratory Tests

The hydrodynamics and mass transfer of SMRs and sieve trays were tested in the laboratory using a 30% tri-*n*-butylphosphare (TBP) in kerosene / acetic acid / water system. Their physical properties are shown in Table 1. The experimental column had an internal diameter of 100 mm and an effective height of a mass transfer unit of 1000 mm. The geometries of two kinds of SMR packing tested are shown in Table 2. The sieve tray column used had the same geometry as that used in the commercial sulfolane process (Table 3) [7,8].

*Table 1. Physical properties of the system tested.*

	Continuous phase	Dispersed phase
Density (kg/m <sup>3</sup> )	837	997
Viscosity (Pa.s)	0.00172	0.00094
Diffusivity (m <sup>2</sup> /s)	7.8x10-10	1.04x10-9
Interfacial tension (N/m)		0.000929

*Table 2. Properties of the SMR.*

Size (mm)	$\varepsilon$	A ( $m^2/m^3$ )
16	92.3%	348
25	93.6%	228

*Table 3. Properties of sieve-plate extraction column.*

Hole diameter	Free area of holes	Free area of up upcomer	Upcomer height
0.007 m	7 %	10 %	0.055 m

### Pilot-Plant Tests

The pilot-plant tests were carried out in a 150 mm internal diameter column using a real pyrolysis gasoline / sulfolane system. Both the pyrolysis gasoline feedstock and solvent were taken from the commercial units. The 16 mm SMR and the sieve tray with the geometry shown in Table 3 were used in the tests. The working section of the column was 1 m high into which five sieve trays or SMR packing were installed. The distributors for the two phases were appropriately designed for each of the internals. According to the hydrodynamic experiments, the capacities of both kinds of column internals were very high because of the large density difference of the two phases. The special capacities of both internals were more than  $45 \text{ m}^3/\text{m}^2/\text{h}$  and the flooding velocities could not be reached due to the limitations of the pumping systems.

## RESULTS

### Laboratory Tests

Typical results of laboratory mass transfer experiments are shown in Figure 2. It was clear that the HTUs for SMRs were far lower than for the sieve trays, demonstrating the superior mass transfer efficiency of SMRs. When comparing the two kinds of SMRs tested, the smaller the nominal diameter of the SMR, the higher was its mass transfer efficiency.

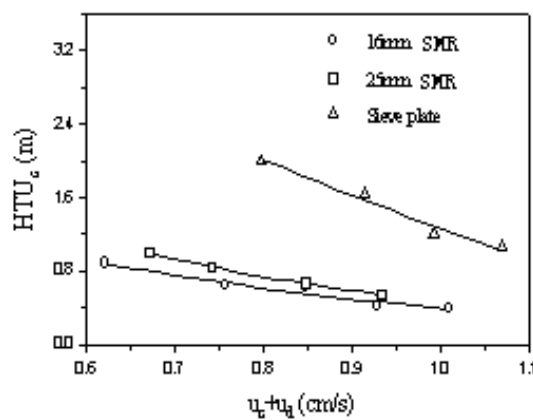


*Figure 2. Laboratory comparison of SMR and sieve tray performance.*

## Pilot-Plant Tests

The performance of the SMR and sieve tray pilot-plant systems tested is compared in Figure 3. The superiority of SMRs was confirmed for the real system [9,10].

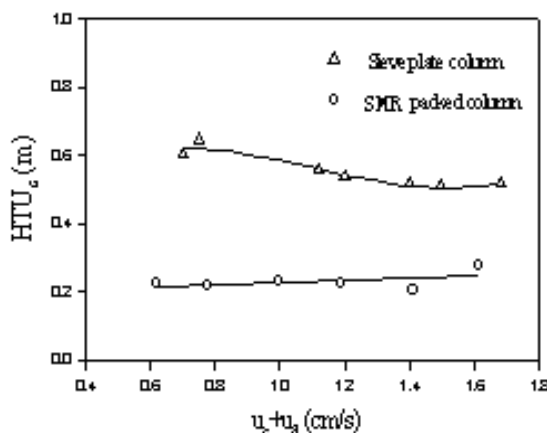


Figure 3. Pilot-plant comparison of SMR and sieve tray columns.

## CASE STUDY

Based on the laboratory and pilot-plant experiments and on previous studies, a reliable scale-up approach of SMR packed column for sulfolane process was worked out. The flooding velocity was calculated from the characteristic velocity and the mass transfer efficiency was estimated according to a diffusion model [11]. This was used to design the retrofit for a commercial sieve-tray extraction column.

### Trouble Shooting

It was shown from a troubleshooting exercise, based on the non-equilibrium stage model, that the main problems of the existing extraction column were as follows [12]:

1. The tray efficiency for the benzene was only 17% while that for C8 and C9 aromatics was much lower. This was because of the significant difference between the diffusivities and drop mass transfer coefficients of benzene, toluene, xylene and C9 aromatics.
2. The flow rates of the two phases varied tremendously along the column. However, the sieve tray geometry was kept the same right through the column. Therefore, many trays were operating in the wrong regime. This was one of the main reasons for the low tray efficiency.
3. The sieve tray number in the extraction section of the column was not enough for the recovery of C8 and C9 aromatics.
4. The nozzle velocities of the feed and solvent distributors were too high, causing emulsions and localized flooding.

### Retrofitting

According to the laboratory and pilot-plant tests, the mass transfer efficiency of the SMRs was more than 30% higher than for sieve trays. Therefore, it was decided to replace 50 sieve trays with SMR packing in the extraction section of the column in order to increase the number of theoretical stages and to thus meet the separation demands. The distributors were redesigned using CAD software to ensure the optimal jet velocity through the nozzles and uniform distribution of drop swarm across the column cross section.

## The Benefits of Retrofitting

The retrofitting exercise was completed successfully. The total aromatic concentration in the raffinate was reduced by more than 6.0 % (from 10% to less than 4 %), while the solvent to feed ratio and the purity of the aromatic products remained the same. The recovery of the aromatics increased significantly and the capacity of the unit increased by 10% after the revamping. It is clear from the simulation that the mass transfer efficiency of the SMR packed extraction is more than 30% higher than that of the traditional sieve tray column [12,13]. The total economic benefit of the revamp is US\$ 700,000 per year with an investment recovery period of less than three months [14].

## CONCLUSION

1. It is shown from the comparison of SMR packing and sieve trays, using 30% TBP (kerosene) / acetic acid / water system that the mass transfer efficiency of the SMR is much higher than that of the sieve tray.
2. The pilot-plant tests using real pyrolysis gasoline / sulfolane system have demonstrated the superior characteristics of SMR packing.
3. The revamping of an existed aromatic extraction column by replacing 50 sieve trays with SMR packing in the extraction section was completed successfully. The economic benefit is significant and the simulation results of the commercial column have confirmed the advantage of the SMR packed extraction column.

## ACKNOWLEDGEMENTS

This work was completed in the Solvent Extraction Laboratory, State Key Laboratory of Chemical Engineering (China), and was supported by the Nature Science Foundation of China who is gratefully acknowledged.

## REFERENCES

1. H. Voetter and W.C.G. Kosters (1963), *Proc. 6<sup>th</sup> World Petroleum Congress*, Frankfurt, Sec.III, p.131.
2. W.C.G. Kosters (1983), *Handbook of Solvent Extraction*, T.C. Lo *et al.* (eds.), Chap. 18.2.3, Wiley, New York.
3. W.Y. Fei (1990), *Petroleum Refinery (Chinese)*, (8), 19.
4. W.Y. Fei, X.M. Wen, and S.H. Fang (1989), *Chinese Patent*, No. ZL 89 1 091521.
5. W. Fei, X. Wen, S. Fang and H. Mao (1993), *Proc. ISEC '93*, Vol.1, Society of Chemical Industry, London, p. 49.
6. W.Y. Fei and X.M. Wen (1995), *Chem. Eng. (Chinese)*, **23** (3), 24.
7. H. Mao (1991), M Sc Thesis, Tsinghua University, China.
8. Q.J. Ye (1989), M Sc Thesis, Tsinghua University, China.
9. R.X. Xie (1992), M Sc Thesis, Tsinghua University, China.
10. F.H. Li (1994), M Sc Thesis, Tsinghua University, China.
11. D.H. Chen, H. Mao and W.Y. Fei (1997), *Chem. Eng. (Chinese)*, **25** (4), 13.
12. W.Y. Fei, X. M. Wen and R.X. Xie (1993), *Proc. ISEC '93*, Vol. 2, Society of Chemical Industry, London, p. 1253.
13. W.Y. Fei, X.M. Wen, and R.X. Xie (1996), *Tsinghua Sci. Tech.*, **1** (4), 332.
14. W.Y. Fei *et al.* (1998), *Chem. Ind. Eng. Prog. (Chinese)*, (4), 28.



## NON-EQUILIBRIUM STAGE MODELLING OF LUBE EXTRACTION PROCESSES

A. K. Jain, P. K. Sen and S. J. Chopra

Research and Development Division, Engineers India Limited, Gurgaon, India

A non-equilibrium stage model has been developed to simulate the lube extraction column using *n*-methyl-2-pyrrolidone as solvent. The equilibrium constants and overall mass transfer coefficients are estimated at each cell for each component. The complex feed to the column was characterised in terms of pseudo components representing each hydrocarbon class. The model provides the detailed flow and composition profile along the column and can be used to analyze data from pilot-plant or bench-scale columns. The model along with a regression method can also be used to determine mass transfer coefficients and back mixing coefficients for carrying out scale up to commercial scale extraction column.

### INTRODUCTION

Solvent extraction of raw lube distillates to manufacture base oils for lubricant formulation continues to be an integral step in the conventional process sequence. The straight run lube oil fractions and deasphalted oil contain naturally occurring unstable lower viscosity index constituents such as condensed aromatics and other polar components. Solvent extraction partially removes these components and improves viscosity index, oxidation stability, colour and oxidation inhibitor response. The present day solvent for the purpose is *n*-methyl-2-pyrrolidone (NMP).

The lube extraction units are operated in blocked-out mode with different vacuum distillate cuts and deasphalted oil as feed. Each feedstock requires specific extraction operating conditions like solvent-to-oil ratios, solvent-water content, etc., to maximise throughput and raffinate yield. Multistage simulation models based on the equilibrium stage concept accomplish the detailed design of extraction columns. Normally, five to eight theoretical stages are required to achieve the desired separation. Packed extraction columns filled with modern random packings are now well proven in this service. The design is preceded by detailed laboratory and bench-scale column studies with individual feedstocks to evaluate the extraction performance against different process variables. Due to the complex nature of feedstocks, the end composition of the phases from single-stage and multi-stage experimental runs is rarely available and performance is evaluated based on the physical characteristics of the products.

The evaluation of bench-scale column data is a critical step in the process development. The simulation of bench-scale data with conventional models based on equilibrium concepts is of limited success since fractional stages cannot be simulated and detailed behaviour of components as they flow along the column is not estimated. To overcome these limitations, a non-equilibrium stage model has been developed for lube extraction process and is presented in this paper.

The non-equilibrium stage model concepts are now well established. Krishnamurthy [1] developed the detailed generalized model for simulation of a counter-current multi-component distillation column. Commercial simulators like Aspen have also incorporated non-equilibrium module 'RATEFRAC' for distillation processes. For liquid-liquid extraction processes, the non-equilibrium models are also available [2-6]. In this work, the calculation method proposed by Spencer [4] was selected for the development of a model for the lube extraction process.

## THE APPROACH

The feed to the solvent-extraction process is characterised in terms of the pseudo components, *i.e.*, paraffins, naphthene and aromatic compounds which are assigned carbon and hydrogen numbers. This characterisation is based on the prediction of experimentally determined liquid-liquid equilibrium data using the UNIFAC group contribution model and feed physicochemical characteristics like distillation, detailed Z-no analysis and specific gravity. The model compounds are defined in terms of UNIFAC groups, such as CH<sub>3</sub>–, CH<sub>2</sub>–, ACH–, etc., that are then used for carrying out non-equilibrium multi-stage extraction computations. The packed extraction column is divided into an arbitrary number of cells. The mass transfer coefficients were estimated from the correlations available in literature. Isothermal operation of the liquid-liquid extraction process is assumed so that the enthalpy balance equations and other associated variables can be eliminated from the calculations.

The cell back mixing model with mass transfer rate approach of a counter-current extractor is shown schematically in Figure 1. Solvent and hydrocarbon feed phases are assumed to enter stages 1 and N respectively. Back mixing between cells k and k+1 is represented by  $f^{k+1}U^{k+1}$  for the hydrocarbon phase and rate g<sup>k</sup>. V<sup>k</sup> represents the extract or solvent phase. f<sup>k</sup> and g<sup>k</sup> are back mixing coefficients of individual flow rates U<sup>k</sup> (raffinate phase flow) and V<sup>k</sup> (extract phase flow). The mass transfer direction is from raffinate to extract phase while the mass transfer rate r<sub>j</sub><sup>k</sup>, in mass flow unit is expressed as

$$r_j^k = K_j^k (m_j^k x_j^k - y_j^k) \quad (1)$$

where, K<sub>j</sub><sup>k</sup>, the overall mass transfer coefficient for the j<sup>th</sup> species, is the product of the conventional mass transfer coefficient, the interfacial area and mass of each cell. The equilibrium constant, m<sub>j</sub><sup>k</sup> is estimated from the UNIFAC group contribution model with pseudo components. It has been observed that the equilibrium constants can be defined as a function of the solvent composition in the extract phase (Figure 2). The following function was found to mimic the behaviour accurately.

$$\ln m_j^k = a_j + \frac{b_j}{s^k} + c_j s^k + d_j (s^k)^2 \quad (2)$$

where, s<sup>k</sup> is mole fraction of solvent in extract phase at cell k. a<sub>j</sub>, b<sub>j</sub>, c<sub>j</sub>, and d<sub>j</sub> are constants regressed for each component from equilibrium values calculated from UNIFAC. The incorporation of this equation makes the model efficient.

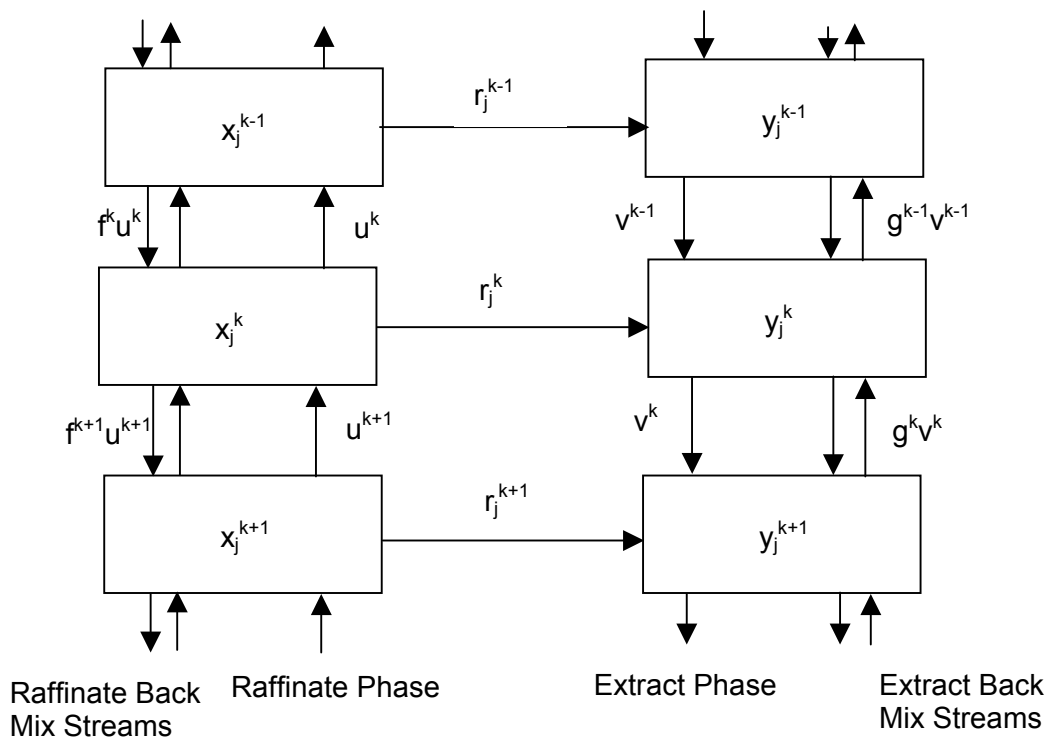


Figure 1. Non-equilibrium model with cell back mixing representation.

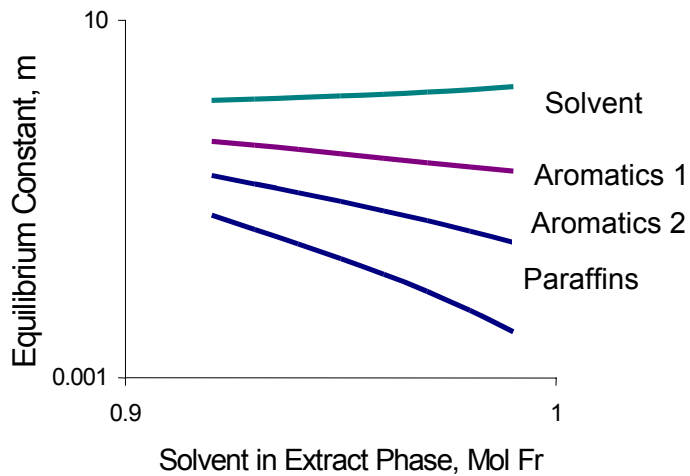


Figure 2. Equilibrium constants as function of solvent composition in extract phase.

Mass balance equations for raffinate phase and extract phase were developed separately for each component at each cell except paraffin components in the extract phase and solvent components in the raffinate phase. For cell k and component j, the mass balance in the raffinate phase is

$$f^k U^k x_j^{k-1} - (1+f^k)U^k x_j^k - f^{k+1}U^{k+1}x_j^k - r_j^k + (1+f^{k+1})U^{k+1}x_j^{k+1} = 0 \quad (3)$$

For the extract phase, the mass balance for component j in cell k is

$$(1+g^{k-1})V^{k-1}y_j^{k-1} - (1+g^k)V^k y_j^k - g^{k-1}V^{k-1}y_j^k + r_j^k + g^k V^k y_j^{k+1} = 0 \quad (4)$$

The overall balance for the k<sup>th</sup> cell, raffinate phase is

$$U^k = U^{k+1} - \sum_{j=1}^C r_j^k \quad (5)$$

and for the extract phase is

$$V^k = V^{k-1} + \sum_{j=1}^C r_j^k \quad (6)$$

These are 2NC independent nonlinear algebraic equations, which determine the 2NC variables, represented by U<sup>k</sup>, V<sup>k</sup> and 2N(C-1) composition vector.

The generalized equation in matrix form for 2(C-1) components in the extract and raffinate phases for the k<sup>th</sup> stage can be expressed as

$$A^k W^{k+1} + (B^k + R^k)W^k + C^k W^{k+1} = a^k \quad (7)$$

where A<sup>k</sup>, B<sup>k</sup>, R<sup>k</sup> and C<sup>k</sup> are 2(C-1)\*2(C-1) matrices, W<sup>k</sup> are 2(C-1) composition matrices for both phases and a<sup>k</sup> is a 2(C-1) dimensional vector. It may be noted that A and C are diagonal matrices. The set of equations described above can be solved using the Thomas algorithm [7] in conjunction with a Gaussian reduction. The developed extraction model incorporates the back mixed flow as well as the true mass transfer coefficient. Thus it can be used directly to evaluate the actual number of stages for staged counter-current extractors. For differential contactors, which is the current application, the number of stages called cells are chosen arbitrarily and mass transfer rates are estimated for each cell, thus, providing detailed composition and flow profiles.

## APPLICATION OF THE MODEL TO LUBE EXTRACTION

One of the refineries located in the Eastern part of India is processing a vacuum distillate, known as "wide cut" in an extraction unit to produce high waxy raffinate. The unit is being revamped to NMP solvent from present highly toxic phenol solvent. The feed characteristics of the vacuum distillate [8] are provided in Table 1.

*Table 1. Feed analysis of vacuum distillate obtained from Indian Eastern Region crude.*

Parameter	Value
Density @ 15 C, g/ml	0.9313
Kinematics viscosity, cst @ 100 C	9.54
Saturates, % wt	50.9
Aromatics, % wt	49.1
ASTM D 1160, Deg C	
IBP/ 50% / EP	315/ 430/ 505

The estimation of pseudo components (Table 2) is based on the prediction of experimentally determined liquid-liquid equilibrium data as explained in the previous section.

*Table 2. Characterisation of vacuum distillate obtained from Eastern Sector Region.*

Component	Wt%	Z No	UNIFAC groups
Paraffins	21.07	2	CH3-1, CH2-29
Naphthenes	29.07	-4	CH2-16, CH-1, CH2r-12, CHr-3
Monoaromatic	20.55	-10	CH2-12, CH-1, CH2r-10, CHr-2, ACH-5, AC-1
Diaromatics	15.07	-24	CH2-1, CH2r-6, CHr-1, ACH-9, AC-5
Polyaromatics	14.24	-30	CH2-1, CH2r-6, CHr-1, ACH-11, AC-7

The details of experimental studies carried out for extraction column design are provided elsewhere [9]. Table 3 provides the experimental data generated in a glass-packed column with the above feed at a solvent-to-feed ratio close to 1.0 (by volume) and compares these data with the results obtained from the present non-equilibrium model. For calculation purposes, the column was divided in 10 cells of equal volume. The back-mixing coefficients were ignored since velocities of both phases were on the lower side. The diffusivity for estimating the mass transfer coefficients was estimated based on the group contribution model of Fei [10]. The continuous phase and dispersed phase mass transfer coefficients were estimated with Seibert [11] Model. The composition profile so obtained, could not be validated, as the experimental profile is not available. However, end properties agree well with the measured values.

*Table 3. Comparison of model results with laboratory scale experimental data.*

Parameter	Experimental	Predicted with model
Solvent in extract phase, wt%	71.7	71.8
Raffinate yield, wt%	64.4	62.4
Raffinate Density @15C, g/ml	0.8781	0.8782

Figure 3 shows the column profiles for mono aromatics (long chain alkyl aromatics) and condensed aromatics along the column. While condensed aromatics in the raffinate continue to decrease as they go up, mono aromatics behave differently. Mono aromatics being the desired component in lube due to their high viscosity index characteristics, needs to be maximized in the raffinate. These mono aromatics reach their maximum composition in the raffinate at close to the upper end of the column and then decrease slightly. Packing above this height is required for reducing condensed aromatics to meet product specification.

The model developed for lube extraction can also be used to estimate mass transfer coefficients from bench-scale or pilot-scale data [12]. For this purpose, a non-linear regression technique is incorporated in the model. These coefficients can then be used for scale up/trouble shooting of commercial-size columns.

## CONCLUSIONS

A non-equilibrium stage model has been developed and is applied to the lube extraction process. The model provides detailed composition and flow profile along the length of the column, which helps in better understanding the column performance. The model is especially useful for analyzing the bench-scale extraction column data where equilibrium model simulates the performance with fractional stages.

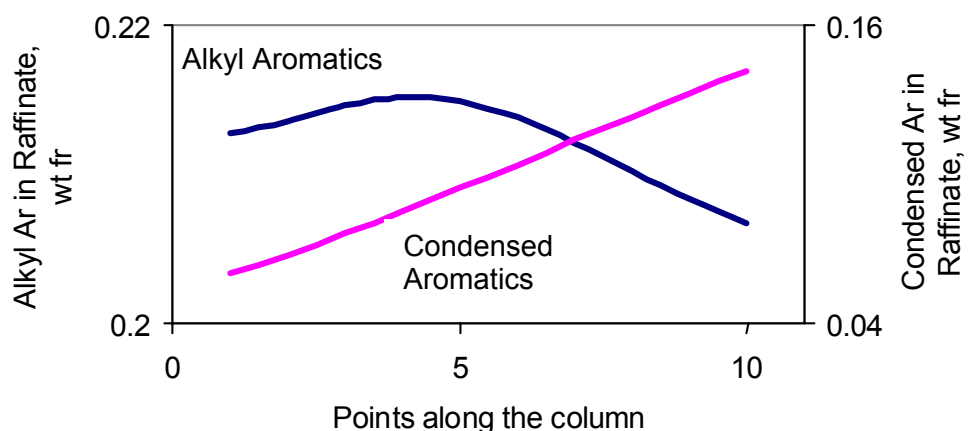


Figure 3. Column profile.

#### ACKNOWLEDGEMENT

Thanks are due to the management of Engineers India Limited, New Delhi, for permission to publish this work.

#### REFERENCES

1. R. Krishnamurthy and R. Taylor (1985), *AIChE J.*, **31** (3), 449-456.
2. A. H. P. Skelland and W. L. Conger (1973), *IEC Proc. Des. Dev.*, **12** (4), 448-454.
3. N. L. Ricker, N. Fumiuki and C. J. King (1981), *AIChE J.*, **27** (2), 277-283.
4. J. L. Spencer, L. Steiner and S. Hartland (1981), *AIChE J.*, **27** (6), 1008-1016.
5. A. Zimmermann, C. Gourdon, X. Joulia, A. Gorak and G. Casamatta (1992), *Proc. ESCAPE-1*, Elsinore, Denmark, pp. S403-410.
6. W. Y. Fei, X. M. Wen and R. X. Xie (1993), *Proc. ISEC '93*, Society of Chemical Industry, London, pp. 1253-1259.
7. E. J. Henley and J. D. Seader (1981), *Equilibrium-Stage Separation Operations in Chemical Engineering*, John Wiley, New York, pp. 563-565.
8. A. K. Jain, L. Hariharan, R. Padmini, M. O. Garg, S. J. Chopra, H. Singh, M. Anwar, G. S. Chaudhary, R. S. Kaushik, K. S. Balaraman and A. Varadarajan (1994), *Proc. Int. Symp. Prod. and Appl. of LOBS*, New Delhi, India, pp. 113-121.
9. H. Singh, M. Anwar, G. S. Chaudhary, R. S. Kaushik, K. Manoj, T. S. R. Prasada Rao, A. K. Jain, S. J. Chopra and K. S. Balaraman (1999), *Proc. Third Int. Pet. Conf. & Exbn-Petrotech 99*, Vol. II, New Delhi, India, pp. 383-388.
10. M. Ye, W.Y. Fei, Y. Dai and J. Wang (1996), *Proc. ISEC '96*, University of Melbourne Press, Melbourne, pp. 69-74.
11. A. F. Seibert (1986), *Hydrodynamics and mass transfer in spray and packed liquid-liquid extraction columns*, PhD Thesis, The University of Texas at Austin, USA.
12. A. K. Jain, L. Hariharan and S. J. Chopra (1996), *Proc. ISEC '96*, University of Melbourne Press, Melbourne, pp. 1097-1101.



## SELECTIVE RECOVERY OF ALDEHYDES AND KETONES FROM HYDROCARBON MIXTURES BY REACTIVE EXTRACTION WITH AQUEOUS SALT SOLUTIONS

Boris Kuzmanović, Rimon Jallo, Norbert JM. Kuipers, André B.de Haan, Gerard Kwant\*

University of Twente, Enschede, The Netherlands

\*DSM Research, Geleen, The Netherlands

Reactive extraction of carbonyl compounds (aldehydes, ketones) from hydrocarbon mixtures applying aqueous solutions of several amino and bisulfite salts was studied. Results obtained for hydrazone formation salts and sodium bisulfite show an increase of distribution ratio of benzaldehyde of up to 1000 times. For Schiff base formation salts the exhibited increase of the distribution ratio compared to the no-salt conditions is up to 50 times. The regeneration of chemically extracted aldehyde by a simple temperature shift was also considered. The Schiff base formation salts showed a change of the distribution ratio of up to 3 times when increasing the temperature from 25°C to 75°C. For other salts the influence of temperature was weaker.

### INTRODUCTION

Aldehydes and ketones are often present in relatively small concentrations in organic solutions from which they should be recovered. Very common industrial examples are the hydrocarbon oxidation processes, in which carbonyl compounds are present as solutes in an apolar hydrocarbon solvent (toluene, cyclohexane or p-xylene oxidation processes [1]). Although large amounts of energy are required for evaporation of the solvent, the most commonly applied methods for the recovery of a carbonyl compound from such systems are still based on distillation [2]. Other options are reported, for example use of ion-exchange membranes [3], adsorption or absorption on a polymeric reagent [4] or electrophoresis [5], but industrial applications are rare.

The low concentrations of an aldehyde or a ketone and the difference in chemical structure of a carbonyl and the solvent justify the consideration of extraction technology for the recovery of carbonyls. In the case when large amounts of solvent are evaporated in distillation process, the superiority of extraction compared to the distillation in respect to the energy efficiency is obvious. On the other hand, the use of common organic extraction solvents that would be adequate for extraction of carbonyls is usually not acceptable when carbonyls are going to be applied in the food or pharmaceutical industry. An alternative is to use water as a solvent. Concerning its immiscibility with apolar organic solvents, its environmental acceptability and the fact that does not cause contamination of the system since it is generated in the oxidation process this seems to be a feasible option. Nevertheless, its potential as a pure solvent is limited due to the poor capacity and selectivity towards the most of the carbonyl products.

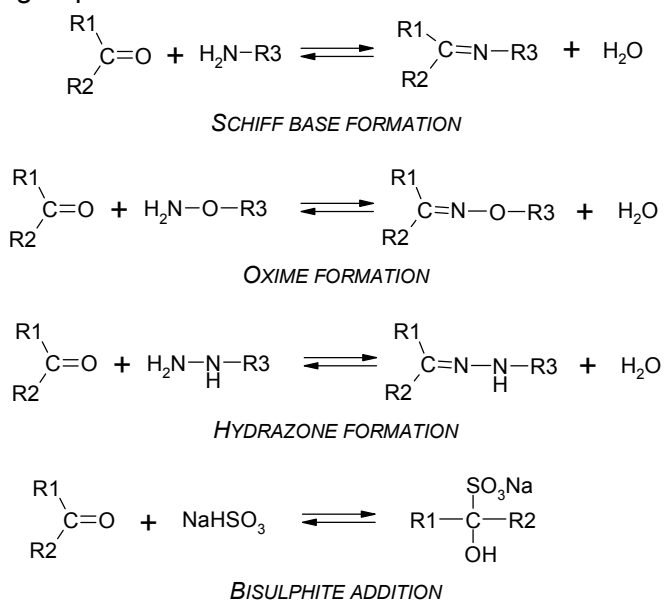
To overcome these disadvantages an environmentally benign modifier that can significantly and selectively improve solubility of carbonyl in water without contaminating the organic solution can be used. An option to satisfy those requirements is to introduce a charged compound in water, which will be able to complex or react with carbonyl product selectively, producing another charged species. Being charged, *i.e.*, salt generally implies good solubility in water and insolubility in apolar organic media. Furthermore, the environmental acceptability of the compound has to be satisfied. Hence, the aqueous solutions containing appropriate salts as extractants can be a feasible option for the recovery of carbonyl compounds from the apolar hydrocarbon mixtures.

To prove technical feasibility of the proposed principle we considered the recovery of benzaldehyde from toluene solution, as a typical industrial case of carbonyl compound present in apolar organic solvent.

## EXTRACTION OF CARBONYLS WITH AQUEOUS SALT SOLUTIONS

### Characteristic Reactions of Carbonyl Compounds

Several reversible chemical reactions are evaluated for use in the reactive extraction of aldehydes or ketones using aqueous salt solutions. All reactions are based on the nucleophilic addition mechanism that is highly characteristic for carbonyl groups. Condensation of carbonyl compounds with nitrogen bases, *i.e.*, Schiff base formation, hydrazone formation and oxime formation, as well as bisulfite addition (Figure 1), are typical examples [6]. For our purpose, the reactant has to be a salt, *i.e.*, R3 in Figure 1 has to be a charged hydrocarbon group.

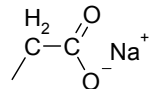
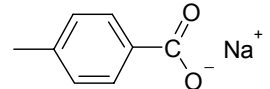
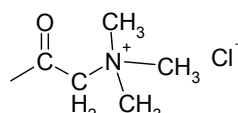
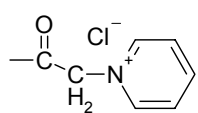
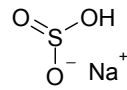


*Figure 1. Reactions characteristic for carbonyl compounds [6, 7].*

### Evaluated Salt Solutions

Several suitable and commercially available amino and bisulfite salts are evaluated experimentally. These are listed in Table 1. To investigate the influence of the structure of the R3 hydrocarbon group, both, an aromatic and an aliphatic group for Schiff base formation salt, as well as for hydrazone formation salt, were considered. Salts able to perform oxime formation with a carbonyl are not evaluated up till now because the oxime formation reaction is considered comparable to the hydrazone formation. The assumption on comparability is based on similar characteristics of the oxygen (oxime) and nitrogen (hydrazone) atom that are bonded to the primary amino group, as well as on the findings given in [6]. Hence, the results obtained for hydrazone are expected to be indicative for oxime as well.

Table 1. Salts evaluated as carbonyl compound extractants.

	Aliphatic R3	Aromatic R3
Schiff base formation salt ( $\text{H}_2\text{N}-\text{R}3$ )	Sodium glycine: 	Sodium p-aminobenzoate: 
Hydrazone formation salt ( $\text{H}_2\text{N}-\overset{\text{H}}{\underset{\text{N}}{\text{N}}}-\text{R}3$ )	Carbazoylmethyl-trimethylammonium chloride (Girard T): 	1-(carbazoylmethyl)pyridinium chloride (Girard P): 
Bisulfite adduct formation salt	Sodium bisulfite: 	

### Definition of the Evaluated Extraction Parameters

The distribution ratio of a component  $i$  ( $D_i$ ) is defined as the ratio of its equilibrium concentrations in the aqueous and organic phase. When the chemically modified form is a charged molecule, its concentration in the apolar organic phase is negligible and the distribution ratio can be defined as:

$$D_i = \frac{c_i^{\text{aq}} + c_{i^*}^{\text{aq}}}{c_i^{\text{org}}} = (K_D)_i + \frac{c_{i^*}^{\text{aq}}}{c_i^{\text{org}}} \quad (1)$$

$c_i$  represents the concentration of original component and  $c_{i^*}$  the concentration of  $i$  in its chemically modified form. The distribution constant  $(K_D)_i$  represents the physical distribution in the aqueous/organic system. The separation factor ( $\alpha_{A,B}$ ) is the ratio of the distribution ratios of two components, A and B:

$$\alpha_{A,B} = \frac{D_A}{D_B} \quad (2)$$

### EXPERIMENTAL PROCEDURE

Benzaldehyde (purity 99%), toluene (purity 99%), Girard P (purity 98%), Girard T (purity 99%) and sodium bisulfite (39% solution in water) were supplied by Merck, Germany and sodium glycine (purity 99%) and sodium p-aminobenzoate (purity 99%), by Acros Organics, Belgium. The chemicals were used as received.

As mentioned before, the principle of reactive extraction of carbonyls with aqueous salt solutions was evaluated on a single solute hydrocarbon solution. A solution of benzaldehyde in toluene was used as the model system. The initial concentration of benzaldehyde in the solution was 1.5 wt% in all experiments. This concentration of benzaldehyde is typical for the industrial toluene oxidation process in combined production with other products [11]. Aqueous salt solutions were prepared by dissolving a salt in demineralised water in the whole range of its solubility in water.

The experiments were performed in 100 ml jacketed glass vessels. Equal volumes (40 ml) of organic and aqueous salt solutions were introduced in the thermostated ( $\pm 0.04^\circ\text{C}$  at  $30^\circ\text{C}$ ) vessel, stirred vigorously for 30 minutes and left to settle for 1.5 hours that phase splitting and equilibrium can occur. By monitoring concentration change in time, it was found that in the system when no salt was present the equilibrium is reached in less than 30 minutes. When sodium glycine salt solution is contacted with the organic solution, concentrations reached their equilibrium values after settling of approximately 90 minutes. Furthermore, it is reported that reaction equilibrium in case of bisulfite adduct formation is reached in not more than 5 minutes [7], for hydrazone formation a period of not longer than 2 hours is required (for benzaldehyde itself), while for Schiff base formation with benzaldehyde it takes one hour [7]. Considering all these facts, a contact time of 2 hours (30 minutes mixing and 1.5 hours settling) is adopted as sufficient. For the experiments with sodium p-aminobenzoate, the vessels were covered with aluminium foil to prevent decomposition to aniline and benzoate, which would take place during exposure to light.

Samples of both phases were taken through side sampling ports. The samples were dissolved in ethanol to prevent possible phase splitting due to a temperature difference between experimental and sampling vessel. In case of ethanol-insoluble salts, the dissolution was done by water. The samples were analysed by HPLC, using dibenzofuran as an internal standard or resorcinol for water diluted samples. By analysing a sample of known concentration of benzaldehyde for 15 times, it has been determined that the deviation of the arithmetic mean value of measurements from the true value was 1.8%, with a maximum of around 6%. The repeatability of the analysis, quantified by the relative standard deviation in percentage (coefficient of variation), was just above 2%.

## RESULTS AND DISCUSSION

### Distribution Ratio and Selectivity

Figure 2 presents the distribution ratios for the analysed salt extractants, as a function of the initial salt concentration ( $C_s^0$ ) in the aqueous solution. At the higher salt concentrations, Girard P, Girard T and sodium bisulfite increased the benzaldehyde distribution ratio approximately 1000 times comparing to the no-salt conditions. Under the same conditions, an increase of 10 to 20 times for sodium glycine and sodium p-aminobenzoate was found.

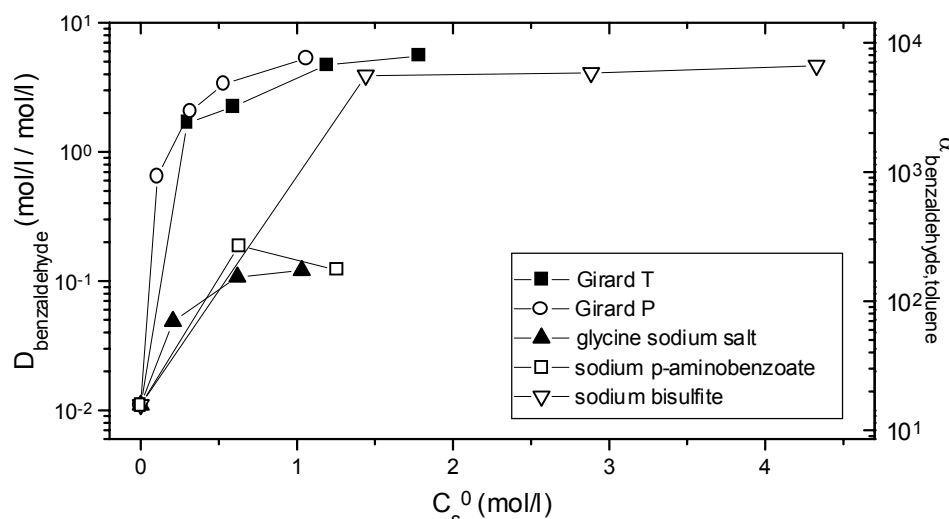


Figure 2. Distribution ratio of benzaldehyde and selectivity compared to toluene as a function of initial salt concentration in the aqueous phase ( $25^\circ\text{C}$ ).

The significant difference in distribution ratios of Schiff base and hydrazone formation salts, although the mechanisms of reactions are very similar, can be explained by the fact that the condensation reaction, in comparison with the reverse, hydrolysis reaction is much more favourable in the case of hydrazones than in the case of Schiff bases [6, 8]. For example, results given in [8] indicate that the equilibrium constant for acetone in a hydrazone formation reaction is 20 times higher than for Schiff base formation at the same conditions.

In the case of nitrogen bases (Schiff base or hydrazone formation) the reaction mechanism involves nucleophilic addition followed by elimination of water, while only an addition step is involved in the reaction of bisulfite. Since bisulfite addition does not involve water elimination, good extraction performance of sodium bisulfite in the aqueous system may be expected.

No strong influence of the structure of the hydrocarbon group R<sub>3</sub> was noticed. As a confirmation of this finding, the values of equilibrium constants (yields) given in [9] for the same carbonyl compound, but different primary amine, can be mentioned. Certain differences exist, but no systematic dependence could be established.

The selectivity of the extraction solvent towards benzaldehyde compared to toluene ( $\alpha_{\text{benzaldehyde}, \text{toluene}}$ ) is also shown in Figure 2. A 1000 fold increase, from around 10 for no-salt conditions up to the values of around 10000 for higher salt concentration of Girard T, Girard P or sodium bisulfite, was achieved. A salting-out effect of the salts on the toluene distribution was noticed, but since it was minor comparing to the influence on the distribution of benzaldehyde, its influence on the selectivity is neglected.

### **Regeneration of Chemically Modified Carbonyl by Temperature Shift**

Although different methods for regeneration of modified carbonyl compounds back to its original form are reported in the literature, regeneration by a simple temperature shift would be the most convenient for a large-scale industrial application. The use of a pH shift [8, 7] as commonly done in organic chemistry or microwave irradiation [10] can be mentioned as interesting alternatives. A temperature shift does not involve introduction of any contaminant, as required for a pH shift, and could be performed with the most common process equipment. Hence, the influence of the temperature on the distribution of benzaldehyde between aqueous and organic phase was investigated.

Figure 3 shows the distribution ratio as function of the initial salt concentration ( $C_s^0$ ) at temperatures of 25°C and 75°C. For both Schiff base formation salts noticeable differences in the distribution ratio exist for different temperatures, while for hydrazone formation salts or bisulfite such differences are small.

## **CONCLUSIONS**

Aqueous solutions of hydrazone formation and bisulfite salts show good extraction capacity for extraction of aldehydes present in the small concentrations in an apolar organic solvent. Schiff base formation salt solutions exhibit a much poorer performance due to lower values of the reaction equilibrium constants. On the other hand, reconversion of the chemically extracted aldehyde by a temperature shift is feasible for the Schiff base formation salt solutions, but not for the other two cases. Other options of reconversion, like pH shift for example, should be considered.

Although the extraction behaviour of oxime formation salt solutions is considered to be very similar with the hydrazone case, their performance should be evaluated experimentally. Extraction of other carbonyl compounds should be undertaken to generalise conclusions about the application of analysed aqueous salt solutions for the recovery of aldehydes and ketones.

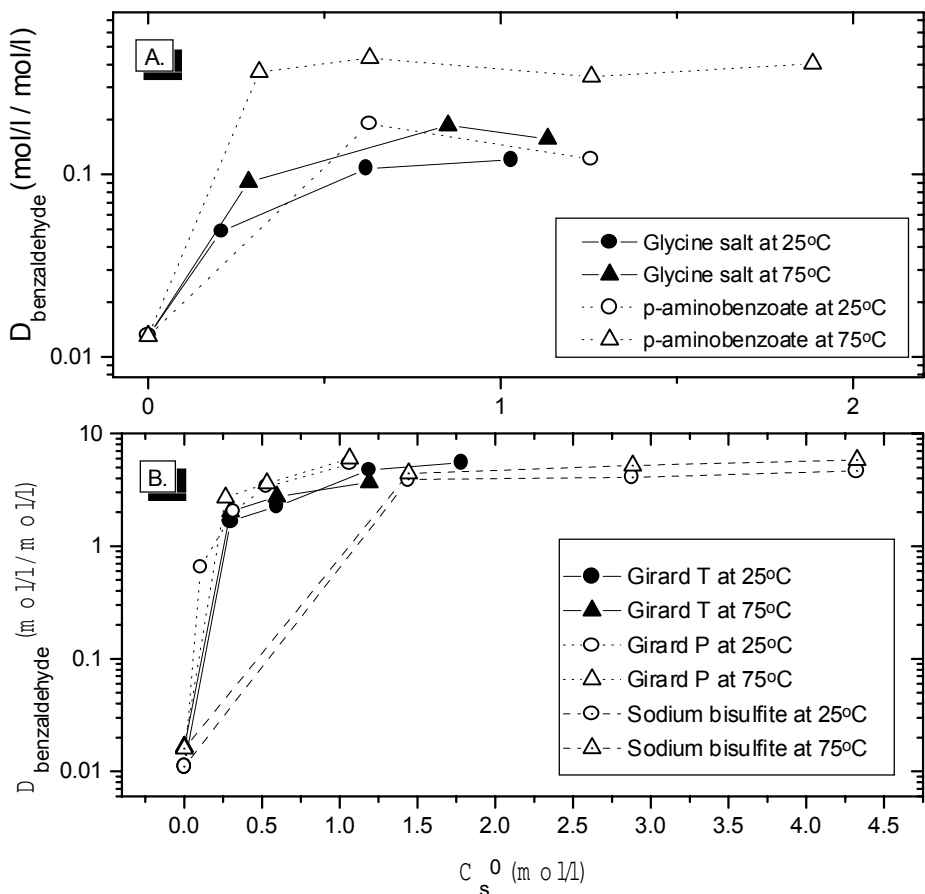


Figure 3. Temperature dependence of the distribution ratio of benzaldehyde for A. Schiff base formation salts, B. hydrazone formation salts and sodium bisulfite.

#### ACKNOWLEDGEMENTS

We would like to thank Mr. Henny Bevers and Mr. Jaap van Soolingen for their support in the area of chemical analysis, as well as Mr. Chris Stoelwinder for useful suggestions and comments. Furthermore, we are grateful for the financial support of DSM, NWO-CW (Netherlands Organisation for Scientific Research - Chemical Science) and Novem (Netherlands Agency for Energy and Environment).

#### REFERENCES

1. F. Ullmann (2001), Ullmann's Encyclopedia of Industrial Chemistry, Oxidations, 6th edn.
2. Stamicarbon B.V. (1980), *G.B. Pat.*, No. 1.570.858 (Jul. 9).
3. M. Igawa *et al.* (1990), *Ind. Eng. Chem. Res.*, **29**, 857-861.
4. S. Lieberman, V.V.K. Prasad and P.A. Warne (1984), *U.S. Pat.*, No. 4.461.876 (Jul. 24).
5. M. Lores Arguin, J. Vindevogel and P. Sandra (1993), *Chromatographia*, **37**, 451-454.
6. S. Patai (1966), The Chemistry of the Carbonyl Group, Interscience Publishers, New York, pp. 600-614.
7. S. Siggia and J.G. Hanna (1979), Quantitative Organic Analysis via Functional Groups, John Wiley And Sons, New York, pp. 95-160.
8. S. Patai (1970), The Chemistry of the Carbon-Nitrogen Double Bond, Interscience Publishers, New York, pp. 468-485.
9. R.W. Layer (1963), *Chem. Rev.*, **63**, 489-508.
10. A.K. Mitra, A. De and N. Karchaudhuri (1999), *J. Chem. Res.*, **9**, 560-561.
11. F. Ullmann (2001), Ullmann's Encyclopedia of Industrial Chemistry, Benzoic Acid Production, 6th edn., electronic form.



# EXTRACTION OF SULPHONATED TRIPHENYLPHOSPHINES FROM OLEUM AND SEPARATION OF REAGENTS FROM HYDROFORMYLATION OF HEXENE CARRIED OUT IN MICROEMULSION

Ireneusz Miesiac, Wilhelm Tic\*, Anna Sobczynska and Jan Szymanowski

Institute of Chemical Technology and Engineering, Poznan University of Technology,  
Poznan, Poland

\*Institute of Heavy Organic Synthesis, Kedzierzyn-Kozle, Poland

Sulphonated triphenylphosphines used for the manufacture of the hydrophilic rhodium-based catalysts are separated from excess oleum by extraction with tributyl phosphate. Sodium salts of mono-, di- and trisulphonated triphenylphosphines could be then recovered as precipitates and further separated by crystallisation. The extraction gave separated phosphines with higher purity (by 5-10%) and yield (by 3-6%) than the direct crystallisation from different solvents. The conditions for the formation and separation of microemulsion in six component system, containing water, sodium tri(m-sulphophenyl)phosphine (Na-TPPTS), hydridocarbonyl tris[sodium tri(m-sulphophenyl)phosphine]rhodium, hexene or heptanal, sodium dodecylsulphate (SDS) and butanol, were elaborated.

## INTRODUCTION

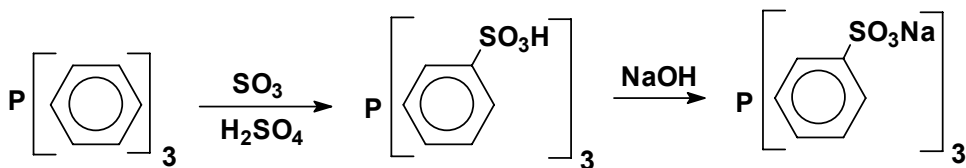
The hydroformylation of olefins, including propylene, is an important industrial process used to synthesise various alcohols and aldehydes. The synthesis is usually carried out using rhodium type catalysts dissolved in the reaction medium. The products are separated by distillation [1]. The use of water-soluble rhodium-based complexes allows the hydroformylation of olefins to be carried out in an aqueous-organic system. Hydroformylation can be also carried out in microemulsion [2].

Water solubility of the catalytic complexes can be obtained when sulphonated triarylphosphines are used both for the preparation of the rhodium-based complexes and as the free ligand present in an excess in the reaction system [3, 4]. Among the water-soluble phosphines, hydrophilic trisodium salt of tri(m-sulphophenyl)phosphine (NaTPPTS) is advantageous as a modifying ligand. The sulphonation of triphenylphosphine gives mono-, di- and trisulphonated derivatives which are usually separated by crystallisation.

The aim of this work was i) to use solvent extraction to separate sulphonated triphenylphosphines from the post-reaction mixture containing concentrated sulphuric acid, ii) to separate mono-, di- and triderivatives and iii) to formulate microemulsion suitable to carry out hydroformylation of hexene and to separate into two phases with the extraction of the products to the organic phase.

## EXTRACTION OF SULPHONATED TRIPHENYLPHOSPHINES FROM OLEUM

Triphenylphosphine was first dissolved in concentrated sulphuric acid and then treated with oleum, containing 60% free sulphur trioxide, at temperature below 15°C under argon atmosphere. The sulphonation occurred at 3 position of the phenyl ring giving subsequently derivatives containing 1, 2 and 3 sulphonyl groups.



Both sulphonated phosphines and sulphuric acid could be extracted with solvating and basic extractants, including tributyl phosphate, trialkylphosphine oxides (CYANEX reagents) and trialkylamines (ALAMINE reagents). The use of trialkylphosphine oxides was disregarded because compounds containing phosphorus(V) could be introduced as undesirable impurities in NaTPPDS and NaTPPTS. Some separation problems (hazy phases and/or formation of emulsion) are also observed with these extractants. Trialkylamines were protonated with sulphuric acid and strongly extracted mineral acids, even above typical mole ratio. They had to be used in a hydrocarbon diluent and an addition of the hydrophobic modifier was necessary to avoid the formation of stable emulsions. As a result, the use of tributyl phosphate (TBP) was selected. Undiluted TBP without any solvent and modifier was used. However, this reagent underwent slow hydrolysis giving butanol and di- and monoesters. The negative effect of this process on the purity of Na TPPDS and NaTPPTS was not observed.

Sulphonated phosphines were less hydrophilic than sulphuric acid and their extraction with TBP was preferred. The distribution coefficient, calculated as the ratio of P<sup>3+</sup> content in the TBP phase and sulphuric acid phase, amounted to nearly 30 for SO<sub>3</sub>/TPP ratio corresponding to 10-15 mol/mol (Table 1). It meant that about 97% of sulphonated phosphines was transferred to the TBP phase. However, the distribution coefficient decreased to 0.75 for a SO<sub>3</sub>/TPP ratio = 35 mol/mol, indicating that the extraction of sulphuric acid instead of sulphonated phosphines occurred. A high value of the distribution coefficient was obtained for an SO<sub>3</sub>/TPP ratio equal to 5 mol/mol, but this ratio did not permit high yields of the desired di- and tri sulphonated phosphines to be obtained. Actually sulphonated phosphines were extracted twice, each time with new portions of TBP using 80 ml TBP per 12 g of triphenylphosphine used for sulphonation.

*Table 1. Extraction of sulphonated triphenylphosphine with undiluted tributyl phosphate.*

SO <sub>3</sub> /TPP ratio (mol/mol)	SO <sub>3</sub> content (%)	P <sup>3+</sup> content (%)		Distribution coefficient*
		TBP phase	Sulphuric acid phase	
5	5	0.920	0.00	high
10	10	0.900	0.030	30.0
15	15	0.950	0.035	27.1
25	20	0.485	0.088	5.5
35	25	0.220	0.220	0.75

\*calculated as the ratio of phosphorus(III) content.

Stripping of the sulphonated phosphines was achieved by washing TBP phase with 50% NaOH. Sulphonated phosphines precipitated as sodium salts (equilibrium pH of the aqueous phase = 11). It was also possible to precipitate both sodium sulphate and sodium salts of sulphonated phosphines. Sodium sulphate was then separated from phosphines by the dissolution of the precipitate in water and the precipitation of the inorganic salt with methanol.

The sodium salt of diphenyl(m-sulphophenyl)phosphine (NaTPPMS) was isolated with a low yield of 5% up to the SO<sub>3</sub>/TPP ratio equal to 6 mol/mol. No important difference between crystallisation and solvent extraction-crystallisation was observed. The chemical purity calculated as the ratio P<sup>3+</sup>/P<sub>total</sub>, was estimated as high as 94 and 96.5% for crystallisation and extraction-crystallisation, respectively. Products of the higher sulphonation degree were not isolated from such mixture.

At the SO<sub>3</sub>/TPP ratio above 6 mol/mol, sodium salts of both phenyl(di(m-sulphophenyl))phosphine (NaTPPDS) and tri(m-sulphophenyl)phosphine (NaTPPTS) were isolated. The maximum yield of NaTPPDS was about 70% and 75% for crystallisation and extraction-crystallisation procedure, respectively at the SO<sub>3</sub>/TPP ratio equal to 6 mol/mol and it monotonously decreased to 4% at the SO<sub>3</sub>/TPP ratio equal to 48 mol/mol. The yield of the separated NaTPPTS increased from 5 to 33 and 43% % for crystallisation and extraction-crystallisation procedure, respectively, when the SO<sub>3</sub>/TPP ratio increased from 6 to 30 mol/mol. However, at higher SO<sub>3</sub>/TPP ratio the post-reaction mixture became brown and lower amounts of sulphonated phenylphosphines (about 5 and 20% of NaTPPDS and NaTPPTS ) were separated.

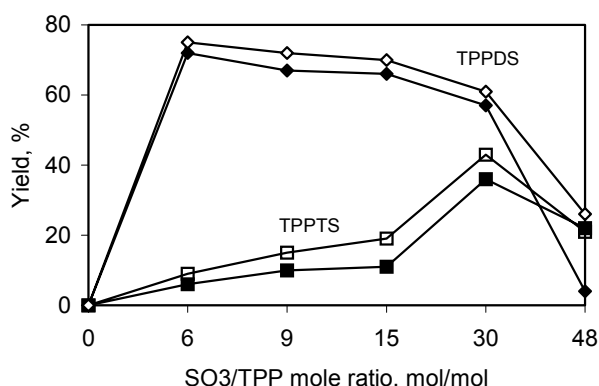


*Figure 1. Effect of the SO<sub>3</sub>/TPP ratio on the yield of the separated sodium salts of phenyl(di(m-sulphophenyl))phosphine (NaTPPDS) and tri(m-sulphophenyl)phosphine (NaTPPTS) (crystallisation technique, time of sulphonation 20 h, full and empty symbols denote crystallisation and extraction-crystallisation, respectively).*

Besides higher yields the products isolated by extraction had the purity higher by about 5% in respect to those isolated only by crystallisation. Thus, the undesired oxidation of phosphines to phosphine oxides was significantly retarded.

## FORMATION OF MICROEMULSION

Two phase hydrocarbon-water system exhibited a high interfacial tension, e.g., 51.2 and 50.8 mN m<sup>-1</sup> for hexene and hexane, respectively. An addition of sodium dodecylsulphate to the aqueous phase permitted to decrease the interfacial tension only to few mN m<sup>-1</sup> and typical emulsions could be formed. An addition of butanol up to 25% had relatively a small effect on the interfacial tension although some decrease of the interfacial tension was observed. Ultralow values, characteristic for microemulsions, were first observed for systems containing

above 25% butanol and above 7% SDS. They varied in the range of few  $\mu\text{N m}^{-1}$ . Only in the case of 2-ethylhexanol higher values of the interfacial tension were registered. 60-120 minutes were necessary to achieve these low values. The interfacial tension changed in the order: heptanal < hexane < hexene < 2-ethylhexanol. Somewhat lower values were observed at 50°C in comparison to those registered at 20°C.

The solubilisation of hexene in the aqueous phase depended both on the content of butanol and SDS (Figure 2). The concentration of SDS in the aqueous phase should exceed 7% to make the butanol containing solution homogeneous. The solubility of hexene in pure water was negligible, while the solubility of butanol amounted to 6.4% at 20°C. Thus, an addition of surfactant was needed to obtain homogeneous solutions. A further solubilisation of hexene was very specifically related to butanol content. In the range of 10-40% butanol in the aqueous phase, solubilisation increased monotonically with increased SDS concentration and also with increased butanol content. In the range of 43-47% butanol in the aqueous phase, the hexene solubilisation increased very slowly with SDS concentration up to 18-21 g SDS/100 g of the aqueous phase. In such system an abrupt increase of solubilisation was observed up to the values over 130-150 g/100 g of the aqueous phase. The formed transparent system, as being a true bicontinuous microemulsion, accepted not only large quantities of hexene, but also small quantities of water, without any phase separation. It was interesting to note that the solubilisation was not observed for aqueous solutions containing 50% of butanol, even for a high SDS concentration of 26 g/100 g aqueous phase. It meant that the bicontinuous microemulsion region was strictly limited to butanol content of 43-47%.

The solubilisation efficiency of the examined system depended on the polarity of solubilised species and the content of sodium tri(m-sulphophenyl)phosphine (Figure 3). The following order of solubilisation was observed: hexane > hexene > heptanal = benzene. 16-18% and 25% SDS were needed to solubilize nonpolar hydrocarbons and polar heptanal and benzene, respectively. An addition of sodium tri(m-sulphophenyl)phosphine caused a decrease of solubilisation and shifted the curves towards higher quantities of SDS (26 and 32%, respectively). The microemulsion was homogeneous when heated to 60°C (a heating to higher temperatures needed a pressure system) but separated after addition of 1% NaCl.

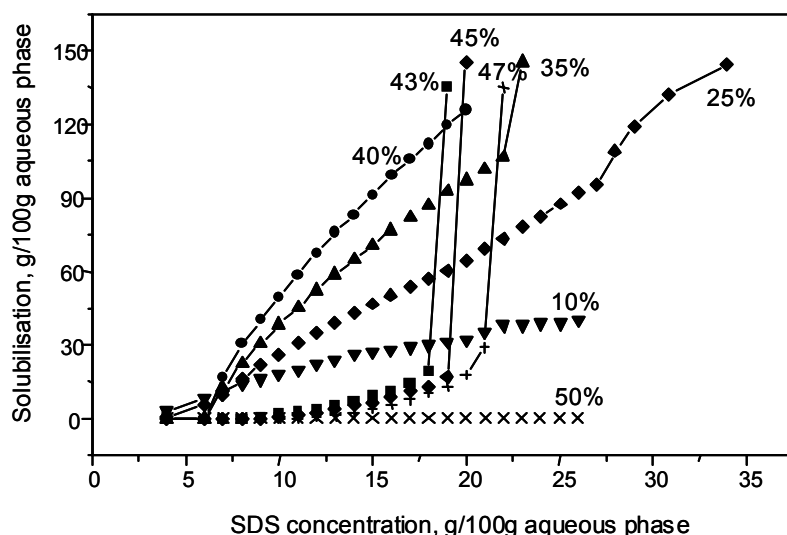
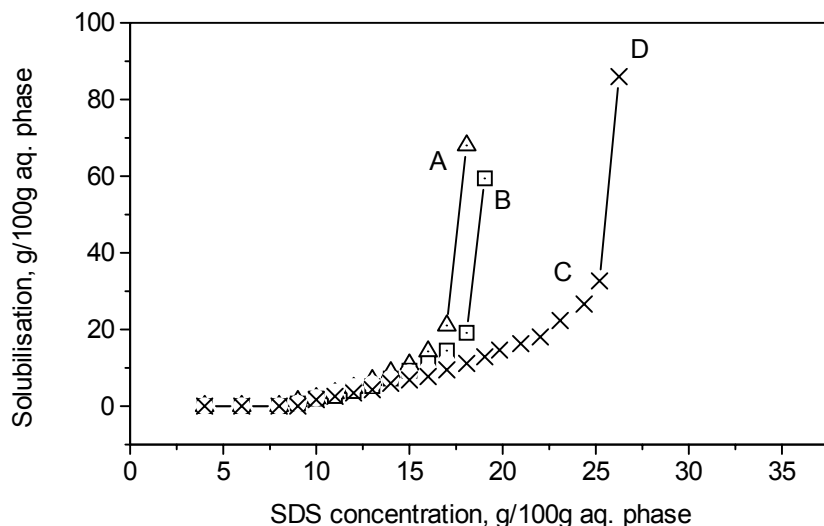


Figure 2. Solubilisation of hexene in sodium dodecylsulphate-butanol-water system for various concentrations of butanol (percents given on curves denote the concentration of butanol in aqueous phase without SDS).

## HYDROFORMYLATION AND SEPARATION OF MICROEMULSION

The separation of the post-reaction mixture (after hexene hydroformylation) was achieved by the addition of butanol (43%)-water solution to decrease the concentration of SDS to about 13 and 14-17.5% in systems without and with Na-TPPTS, respectively (Table 2). Aldehydes were transferred into the organic phase with the distribution coefficient equal to 1.6 and 2.5 in the systems without and with 3% Na-TPPTS, respectively. SDS remained in the aqueous phase together with the whole amount of catalyst used.



*Figure 3. Solubilisation of various components in sodium dodecylsulphate-butanol (43%)-water system (A, hexane; B, hexene; C, heptanal, D, benzene).*

*Table 2. Separation of the post-reaction mixture after hydroformylation (43% butanol and 57% water).*

Content of SDS (%)	Content of Na-TPPTS (%)	SDS conc. in aqueous phase (%)	O/W phase ratio	Distribution coefficient
20	0.0	12.5	1 : 1.8	1.6
30	0.0	12.8	1 : 2.6	1.5
20	3.0	14.0	1 : 1.2	2.5
30	3.0	17.5	1 : 1.6	2.4

The use of microemulsion for hydroformylation of hexene permitted to achieve a high conversion of hexene equal to about 97% and the yield of heptanals above 94%, in the reaction time below 40 minutes (Table 3). 50% conversion of hexene was obtained already after 11-13 minutes. It was the main advantage of the microemulsion use in comparison to the heterogeneous micellar systems applied for hydroformylation. However, the ratio of isomers (n/iso) having straight and branched alkyl chain was not enough high and changed in the range of 2.2-2.5.

An addition of 3% Na-TPPTS to the aqueous medium had a small but positive effect on the olefin total conversion. A small increase in n/iso isomer ratio was also observed. It was accompanied by a little decrease in kinetics as regards the increasing values of half-conversion time. Evidently, an increase of ligand (or electrolyte) concentration improved reaction selectivity expressed as n/iso ratio equal to 2.8-2.9.

*Table 3. Hydroformylation of hexene in sodium dodecylsulphate-butanol-water system.*

SDS (%)	Content Na-TPPTS (%)	n/iso ratio (mol/mol)	Reaction time (min)	Half conversion time (min)	Total conversion (%)	Aldehyde yield (%)
0.0	0.0	-	60.0	-	0.0	0.0
20	0.0	2.2	37.0	11.0	96.7	94.6
30	0.0	2.5	37.5	11.3	96.9	94.2
20	3.0	2.9	30.0	12.6	98.0	95.8
30	3.0	2.8	33.0	13.0	99.2	96.8

Experimental conditions: pressure, 2 MPa; temperature, 100°C; catalyst 500 ppm Rh as RhH(CO)(Na-TPPTS)<sub>3</sub>; hexene 0.02 mol; contact liquid 10 g; synthetic gas H<sub>2</sub>:CO=1:1 mol/mol, 43% butanol in respect to water.

## CONCLUSIONS

Solvent extraction was a suitable technique to separate sulphonated triphenylphosphines from oleum with the purity and yield higher than that obtained by crystallisation from various solvents. Tributyl phosphate was a suitable extractant. Sodium salts could be then recovered as precipitates by treating the organic phase with sodium hydroxide solution. The solvent extraction simplified the separation process. About 90% of sulphate ions remained in the aqueous phase after extraction with TBP. As a result, an increase of the yield (5-10%) and purity (3-6%) was observed in comparison to the separation only by crystallisation. The separation could be obtained more quickly using less chemicals and producing less wastes.

Microemulsions could be easily obtained in the systems containing hydrocarbons, water, butanol, sodium dodecylsulphate and tri(m-sulphophenyl)phosphine and could be separated in organic and aqueous phases by addition of aqueous butanol solution. SDS remained in the aqueous phase together with the whole amount of catalyst used and could be recycled.

The hydroformylation carried out in microemulsion occurred rapidly in comparison to the classical system and high yields of reaction were obtained. However, the selectivity of reaction was lower.

## ACKNOWLEDGEMENT

The work was supported by KBN donation for the University activity DS No. 32/006/2000.

## REFERENCES

1. R. L. Pruet and J. A. Smith (1975), *U. S. Pat.*, No. 3,917,661.
2. W. Herrmann, C. Kohplaintner, L. Tinucci, and E. Platone (1990), *E.P. Pat.*, No. 380,154.
3. E. Wiebus and B. Cornils (1996), *Hydrocarbon Process*, **3**, 63-68.
4. B. Cornils, W. A. Herrmann, and R. W. Eckl (1997), *J. Mol. Catal.*, **116**, 27-32.



## DEVELOPMENT OF A NOVEL PROCESS FOR PURIFICATION OF PHENOLIC DERIVATIVE

Oldrich Mikus and Bridget M. Hutton\*

AECI Ltd., Modderfontein, South Africa

\*CSIR, Bio/Chemtech, Modderfontein, South Africa

A novel process for purification of a phenolic derivative using liquid-liquid extraction was developed as an alternative to a three-stage re-crystallisation. The extraction process operates at a high aqueous to organic ratio and at elevated temperature. The process development was performed on two different scales. Initially, a bench-scale study was conducted on 1:133 scale. This gave an indication of the process characteristics and provided engineering data for design of the commercial process. Subsequently, the commercial-scale process was specified and the equipment was designed. This was followed by a pilot-plant study on the system at a scale-down ratio of 1:9. The process was successfully commercialised using a compact mixer-settler unit with a capacity of 8 m<sup>3</sup>/h. This novel process enables the product to be effectively purified using fewer unit operations and features higher product recovery, shorter batch cycle and less solvent consumption than the original crystallisation purification process.

### INTRODUCTION

Recent experience in the development of fine chemical processes has shown that the isolation of products from crude post reaction mixtures to the required purity typically represents about 80% of the overall effort. This purification typically requires a complex set of unit operations, some of which have to be performed under very specific conditions.

Catalytic alkylation of an aromatic hydrocarbon yields a post-reaction product containing both *mono-* and *di*-alkyl derivatives, where the *mono*-alkyl derivative is the required product and the *di*-alkyl derivative is an undesirable impurity to be removed in the purification process. Even after optimisation of the reaction conditions, the concentration of the *di*-alkyl derivative in the crude product is still approximately 10% by mass. The final product specification, however, requires that the concentration of the *di*-alkyl derivative should not exceed 0.03% by mass. The original process to achieve a final product with less than 0.03% impurities was *via* a three-stage re-crystallisation. The three stage re-crystallisation entailed complete dissolving of the crude product firstly in water, filtering the hot solution followed by crystallisation of an intermediate, which contained about 0.3% of impurities. Further reduction of the impurities was achieved by another re-crystallisation from an organic solvent, followed by re-crystallisation of the product from water. The final re-crystallisation from water was used to remove the organic solvent from the product, since the solvent would contaminate the product.

Another possible purification method considered was distillation under high vacuum, however, the relative volatility of the components to be separated indicated that a rectification column with many stages and high reflux ratio would be required. Another problem would be that operation under high vacuum and high temperature could allow oxygen to enter the distillation column, which would cause oxidation of the product.

The application of solvent extraction as a possible purification process was investigated. It was found that despite the similar solubility of the both *mono*- and *di*-derivative in an organic solvent, the partition coefficients of both species differed by two orders of magnitude in favour of the component to be removed. This phenomenon, which was previously employed only as an analytical technique [1], facilitated an opportunity for replacement of multiple crystallisation with solvent extraction. Figure 1 compares the original three stage re-crystallisation process with the newly developed extraction process.

### **INITIAL EVALUATION OF THE NOVEL PROCESS**

Initial evaluation of the system on a laboratory scale indicated that the organic solvent could effectively remove the impurities using a single stage extraction operated at elevated temperature. However, it was also evident, that should the quantity of solvent remain the same as or similar to that used for re-crystallisation, a large percentage of the required product would be extracted along with the impurities. The ratio of solvent to feed required for the extraction was found to range between 1: 60 and 1:120. Further tests on a laboratory scale indicated that at these extreme ratios, the system was not operable, due to problems both with mixing and settling of the two phases. Another problem encountered was that it was impossible to effectively replicate the continuous extraction system. In addition, the concentrations of impurities monitored in the raffinate were ppm levels and the actual success of the novel process could only be evaluated as per the quality of the final product crystallised from sufficient quantity of raffinate. The laboratory tests also showed that due to the small amount of material used and the accuracy of the analytical technique employed, it was impossible to achieve mass balance closure. Consequently the decision was made to conduct the next development stage on a bench scale, operating the process continuously.

### **BENCH-SCALE INVESTIGATION (1:133)**

Two options were considered for the bench-scale investigation, namely application of an extraction column or a single-stage mixer settler. The latter option was employed due to equipment availability and in-house experience with mixer-settler extraction.

A rectangular, polypropylene mixer-settler with a total volume of 10 litres was used for the bench-scale development. The unit comprised four compartments, a mixer, a settler, an extract compartment and a raffinate compartment. The volume of the mixer was 1.8 litres. The mixer was furnished with a pumping agitator connected to a variable speed drive. All the compartments were furnished with stainless steel heating coils to enable the required temperature to be maintained. Equipment was furnished with a glass lid in order to minimise losses of solvent by evaporation and to allow visual inspection of the behaviour of the phases in the individual compartments. To achieve the required high aqueous to organic ratio and yet to allow a reasonable phase ratio in the mixer the extract was recycled from the extract compartment to the mixer in external tubing *via* a peristaltic pump. In terms of throughput, the bench-scale unit operated at a 1:133 scale-down ratio as compared to the commercial equipment. The unit was installed and operated at a pilot plant facility since large vessels were required to support the extraction operation on a continuous basis, for the duration of at least 10 hours.

During the bench-scale experiments, the effect of feed to solvent ratio on the extraction efficiency of both the impurities and the product was studied, at a predetermined temperature and hydrodynamic conditions. In addition, the effect of changing the temperature was tested. Large samples of raffinate were collected and crystallised to allow evaluation of the product quality. Several bench-scale experiments were performed which allowed determination of the system characteristics and facilitated identification of possible operability and scale-up problems. The results produced mass balance data for the novel process design and enabled integration of the design into the original flow-sheet. Of greater importance was the fact that the bench-scale process demonstrated that the required quality of the product was achievable on a consistent basis. A complete component mass balance was performed which allowed calculation of the extraction efficiencies of both the product and impurities. The effect of the phase ratio on the extraction efficiency of both species is shown in Figure 2.

Because of the limited solubility of the product in water, an attempt was made to maximise the concentration of the product in the feed by operating at as high a temperature as possible. Continuous extraction trials have, however, revealed that the organic phase in equilibrium to the feed composition represents a supersaturated solution, which solidifies on cooling and thus accurate temperature control is essential. Because of solidification, the handling of extract at low flow rates was identified as a major operability problem and it was found that standard extraction equipment readily available was not suitable for the novel process. Consequently specialised equipment was designed, specifically for the novel process.

Figure 3 illustrates an example of the liquid-liquid equilibrium of the product and the effect of different feed to solvent ratios on the operability of the process.

The bench-scale study confirmed that a single-stage continuous extraction was an effective alternative to the three-stage re-crystallisation. Dissolved solvent was flashed off from the raffinate, which was then cooled and crystallised to produce product that was of the required specification. Furthermore, it was found that an optimum mass ratio of solvent to feed of 1:100 was required in order to achieve the lowest possible extraction efficiency (loss) of the product (preferably <15%), while simultaneously maintaining an extraction efficiency on impurities greater than 94%. It was also found that the extract represents a supersaturated solution and that even a small temperature drop resulted in immediate solidification.

### PILOT-PLANT STUDY (1:9)

Based on the results of the bench-scale study the commercial extraction unit was conceptually designed. A geometrically similar pilot plant unit was fabricated on a scale-down ratio of 1:9. The unit was a horizontal cylinder of an internal diameter of 0.3 m and length of 2.5 m. It was fabricated from stainless steel and glass segments to enable visual monitoring of the process. The internal space comprised five compartments, namely a mixer, a settler, an extract recycle compartment, an extract accumulation compartment and a raffinate compartment. The extract was circulated from the extract recycle compartment to the mixer via an internal pipe using the pumping effect of the agitator. Fresh solvent was injected directly into the recycle line. The mixer was furnished with two baffles and a straight-blade pump turbine impeller.

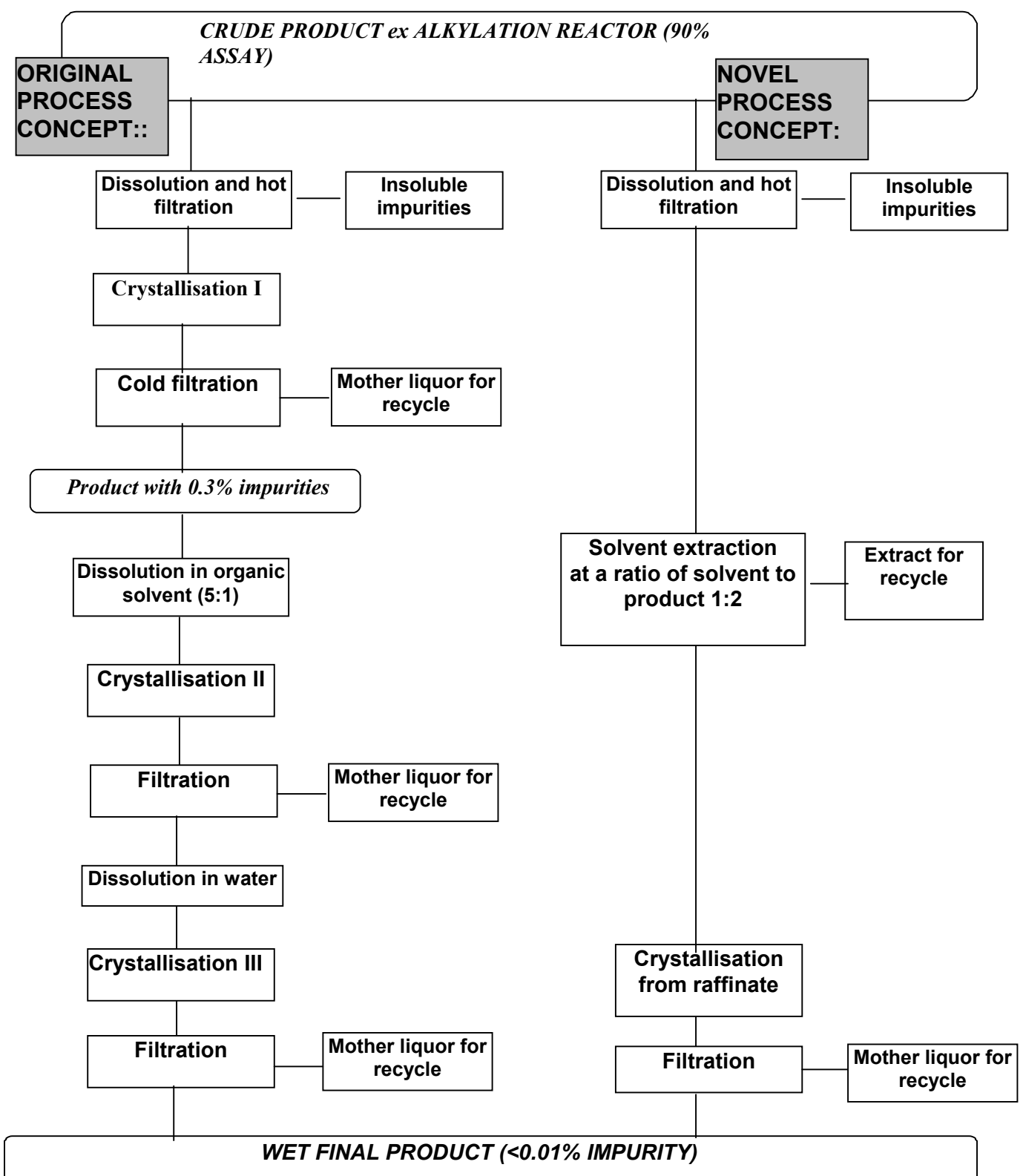


Figure 1. Comparison of the original and the novel process.

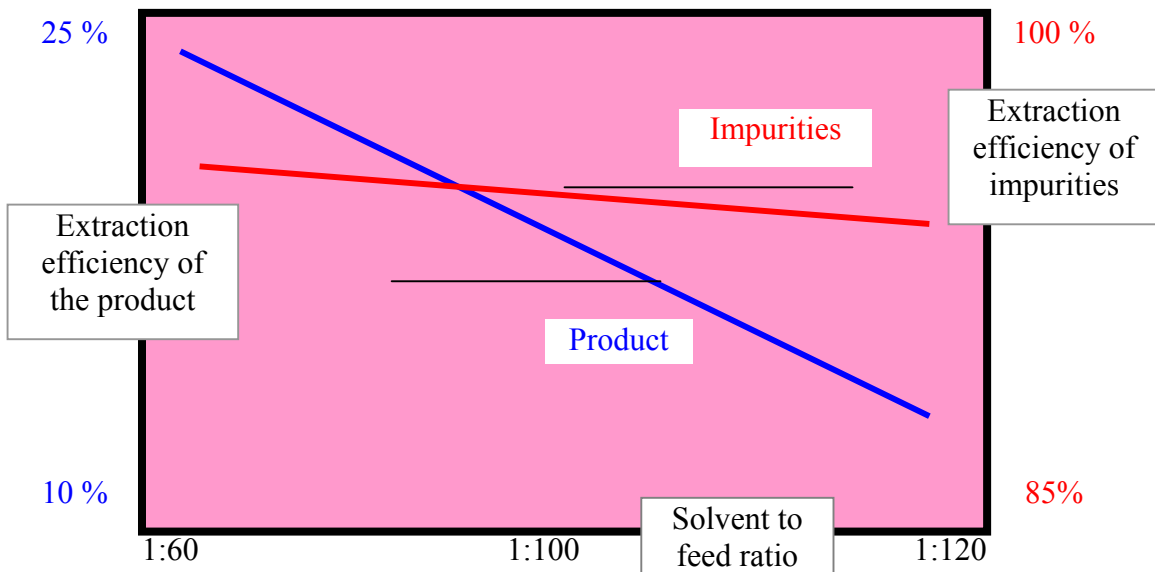


Figure 2. Effect of solvent to feed ratio on the extraction efficiency of product and impurities.

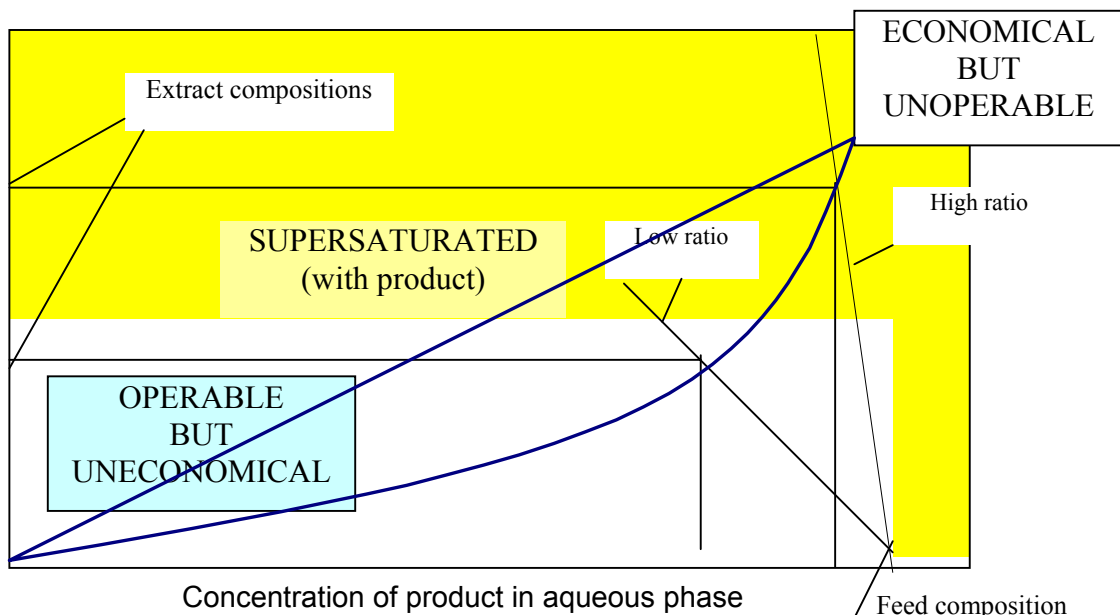


Figure 3. Partitioning of the product between phases at elevated temperature.

The pilot-plant unit was installed at the commercial plant and operated. In terms of performance, the extraction efficiency results obtained compared favourably with those obtained from the bench-scale studies. Additional information was obtained for modification of the commercial unit design in terms of the hydrodynamic condition in the mixer, settling characteristics, temperature control, start-up and shut-down, as well as sizes of the individual compartments.

## NOVEL PROCESS COMMERCIALISATION

Based on the results obtained from the pilot-plant study the original design of the commercial unit was modified and the recommended changes implemented. The unit was then fabricated, installed and integrated into the existing process.

Because of the non-standard geometry of the mixer, very little information was available to scale-up the mixing, namely the agitator speed. The factor used to adjust the small-scale (1:9) speed to the commercial-scale operation was a scale ratio as defined in Eq. (1), raised to an exponent,  $n$ :

$$N_2 = N_1 (1/R)^n = N_1(D_1/D_2)^n \quad (1)$$

The value of the exponent,  $n$  generally depends on the type of agitation problem and typically ranges between  $n = 2/3$  and  $n = 1$  [2]. The mixing problem in this case was actually three fold. Firstly, reasonably equal liquid motion was required in order to prevent emulsification (recommended  $n = 1$ ). Secondly, equal mass transfer between the liquid phases was required (recommended  $n = 2/3$ ). In addition, the agitator needed to provide a sufficient pumping effect, in order to recycle the extract. Based on experimental observation of the mixing and settling characteristics, as well as the volumetric mass transfer coefficient, a value of  $n \sim 0.8$  was found to be a reasonable compromise for scale-up [3].

Performance tests were completed using the commercial unit which proved that product complying with the specification was produced on a consist basis. A comparison of the novel process with the original purification process is summarised in Table 1.

*Table 1. Comparison of major features of original and novel process.*

	Original process	Novel process
Number of process steps	10	5
Number of recycle stream	3	2
Batch cycle time	40 hours	16 hours
Consumption of solvent	5 kg /kg of product	0.5 kg/kg of product
Product recovery	66%	71%
Product quality	complies with specification	complies with specification

## CONCLUSION

Application of the scale-up/scale-down approach to commercialisation of the novel process was found to be very beneficial despite the increased total development time and costs. It allowed identification of the process problems affecting the design of the equipment and facilitated changes prior to the fabrication and commissioning of the commercial-scale unit. The pilot-plant study using 1:9 geometrically similar unit, installed and operated at the commercial plant, gave engineering information on the process hydrodynamics, settling characteristics, process operability and instrumentation required. It also enabled the full-scale process to be accurately replicated and the proposed operating procedures tested including the start-up and shut-down. Furthermore operation of the pilot-plant unit contributed to better understanding of the novel process by the plant operating staff, which made a valuable contribution to the novel process commercialisation.

## REFERENCES

1. M. C. Goldberg, L. DeLorg and M. Sinclair (1973), *Anal. Chem.*, **45**, 89.
2. R. R. Rautzen and R. R. Corpstein (1976), *Chem. Engr.*, **10**, 64 – 71.
3. O. Mikus, B. Hutton and E. Chemaly (1997), *Proc. 7<sup>th</sup> National Meeting S. Afr. Inst. Chem. Eng.*, Cape Town.



## THE SEPARATION OF PHENOLIC COMPOUNDS FROM NEUTRAL OILS AND NITROGEN BASES

Denise L. Venter and Izak Nieuwoudt

Department of Chemical Engineering, University of Stellenbosch, Stellenbosch, South Africa

Liquid-liquid extraction with a solvent system consisting of triethylene glycol as selective solvent, water as co-solvent and hexane as countercosolvent is proposed for the separation of phenolic compounds from neutral oils and nitrogen bases. Solvent selection was by means of computer-aided molecular design. Liquid-liquid equilibria for the solvent system plus phenolic compounds, neutral oils and nitrogen bases were determined. The effect of solvent ratios on the desired separation are illustrated on the basis of separation factors and percentage recoveries of phenolic compounds. The three-parameter NRTL model was fitted to the equilibrium data and was used in the optimisation of a multistage countercurrent extraction process. Pilot-plant tests performed on an industrial heavy naphtha stream yielded a final phenolic product purity of 99.75% and phenolic recovery in excess of 91%.

### INTRODUCTION

Coal pyrolysis liquors are a major source of valuable phenolic compounds. The separation of phenolic compounds from the neutral oils and nitrogen bases also present in the pyrolysis liquors is difficult due to low relative volatilities and the formation of azeotropes and eutectics [1]. The desired high phenolic recovery and phenolic product purity of 99.5% cannot be achieved by means of conventional distillation processes.

Alternative processes such as liquid-liquid extraction with various low-boiling solvents [2-5], mixtures of high-boiling solvents [5-7] and extractive distillation [8] have been extensively investigated. Disadvantages of these processes include the high solvent ratios required, low recovery of the higher substituted phenolic compounds, inability to treat a wide-boiling feedstock in one process step and complex post-purification of the phenolic product. A solvent system consisting of a selective solvent, water as a co-solvent, and hexane as a countercosolvent, is proposed as an alternative.

A computer-aided molecular design program identified glycols as suitable commercial selective solvents. The suitability of the proposed solvent system for the separation of phenolic compounds from neutral oils and nitrogen bases was evaluated by means of batch extraction and pilot plant tests.

## SOLVENT SELECTION

Three synthetic feed streams were compiled to represent a typical industrial coal pyrolysis liquor namely:

- phenol (71 wt%) + benzonitrile (6.67 wt%) + aniline (6.67 wt%) + mesitylene (9 wt%) + 5-et-2-me-pyridine (6.67 wt%)
- m-cresol (53.33 wt%) + o-tolunitrile (6.67 wt%) + o-toluidine (6.67 wt%) + pseudocumene (6.67 wt%) + undecane (6.67 wt%) + indene (20 wt%)
- 2,4-xlenol (13.33 wt %) + 3,5-xlenol (6.67 wt%) + 3,4-xlenol (6.67 wt%) + indane (6.67 wt%) + dodecane (26.67 wt %) + naphthalene (40 wt%)

Solvent selection was based on the phenol containing feed stream. Of the neutral oils and nitrogen bases present in the pyrolysis liquor, benzonitrile was identified as the neutral oil potentially most difficult to separate from phenol. A computer aided molecular design program based on a genetic algorithm, using the modified Unifac model, was used to predict a suitable solvent for the separation of phenol from benzonitrile [9]. Favourable phenol-benzonitrile separation factors were predicted for ethylene glycol as well as for a variety of high molecular weight molecules containing ether, carbonyl and hydroxyl functional groups. Of the commercially available solvents tested on batch extraction scale, triethylene glycol achieved the highest phenol-benzonitrile, phenol-aniline and phenol-5-et-2-me-pyridine separation factors as well as the highest phenol recovery.

From the solvent selection process it was concluded that effective solvents for the separation under investigation were those containing hydroxyl groups positioned on the molecule backbone in such a way as to facilitate hydrogen bonding with more than one phenolic molecule at a time. Two commercially unavailable solvents, 1,3-(ethoxy-2-hydroxy)-propane-2-ol and 1,3-(diethoxy-4-hydroxy)-propane-2-ol were therefore synthesised from ethylene glycol and diethylene glycol respectively [10].

The performance of the synthesised and commercially available solvents with respect to phenolic recoveries as well as m-cresol-o-tolunitrile, 2,4-xlenol-o-tolunitrile, and 2,4-xlenol-o-toluidine separation factors was tested in batch extraction experiments. The results obtained are listed in Table 1.

*Table 1. Batch extraction test results for the comparison of synthesised and commercial solvent performance at constant solvent molar ratios.*

Solvent	Functional groups		$\beta_{m\text{-Cresol-o-Toluonitrile}}$	$\beta_{2,4\text{-Xlenol-o-Toluonitrile}}$	$\beta_{2,4\text{-Xlenol-o-Toluidine}}$	Recovery (%)		$n_{m\text{-Cresol}} / n_{\text{Solvent}}$	$n_{2,4\text{-Xlenol}} / n_{\text{Solvent}}$
	-C-O-C-	-O-H				m-Cresol	2,4-Xlenol		
EGd*	2	2	8.9	n/a	n/a	88.2	n/a	1.2	n/a
DiEGd**	4	4	19.1	12.5	3.5	95.1	86.7	1.2	0.4
TEG	2	2	13.1	9.6	3.5	93.9	90.8	1.6	0.6
Tetra EG	3	3	16.5	11.1	3.6	95.3	90.7	1.3	0.5
Glycerol	0	3	3.8	10.1	1.1	60.1	2.1	0.7	0.02
Tetraglyme	4	1	3.3	n/a	n/a	83.2	n/a	1.3	n/a

\*1,3-(ethoxy-2-hydroxy)-propane-2-ol    \*\*1,3-(diethoxy-4-hydroxy)-propane-2-ol

As can be seen from Table 1, 1,3-(diethoxy-4-hydroxy)-propane-2-ol yielded higher phenolic recoveries and separation factors than triethylene glycol. However, the difference in solvent performance is small and triethylene glycol is relatively inexpensive and readily available. Triethylene glycol was therefore selected for further process development.

## EXPERIMENTAL

Batch extraction tests were executed on each of the three synthetic feed streams in order to determine the effect of solvent ratios on separation efficiency. Ratios of solvent (triethylene glycol) to feed, water to solvent (triethylene glycol) and countercosolvent (hexane) to feed were varied from 0.5 to 3.0, 0.0 to 0.7 and 0.5 to 5.0, respectively. The concentrations of the components in each resulting liquid phase, with the exception of water, were determined by means of capillary gas chromatography with an FID detector. The water concentrations were determined by means of Karl-Fischer titrations.

The separation factor  $\beta_{ij}$  for a phenolic compound  $i$  relative to a neutral oil or nitrogen base  $j$  is defined as follows :

$$\beta_{ij} = (x_i^E / x_i^R) / (x_j^E / x_j^R) \quad (1)$$

where  $x_i^E$  and  $x_i^R$  are the molar concentrations of component  $i$  and  $x_j^E$  and  $x_j^R$  are the molar concentrations of component  $j$  in the extract and raffinate phases respectively.

Separation factors obtained for phenolic compounds relative to paraffins, alkyl-substituted benzenes, indane, indene and naphthalene are listed in Table 2. Figure 1 illustrates the effect of the solvent (TEG) to feed, water to solvent (TEG) and hexane to feed ratios on the separation factors obtained for phenolic compounds relative to aromatic amines, nitriles and 5-*et*-2-me-pyridine. Figure 2 illustrates the effect of the various solvent ratios on the phenolic recoveries. The mass compositions of the resulting phases and corresponding separation factors and phenolic recoveries are reported elsewhere [11].

*Table 2. Separation Factors,  $\beta_{ij}$ , for phenolic compounds,  $i$ , relative to neutral oils,  $j$ .*

$i$	$j$	$\beta_{ij}$ (minimum)	$\beta_{ij}$ (maximum)
Phenol	Mesitylene	81	1600
m-Cresol	Pseudocumene	34	3100
m-Cresol	Undecane	79	4600
m-Cresol	Indene	20	172
Xylenol	Dodecane	204	6300
Xylenol	Indane	50	2950
Xylenol	Naphthalene	36	170

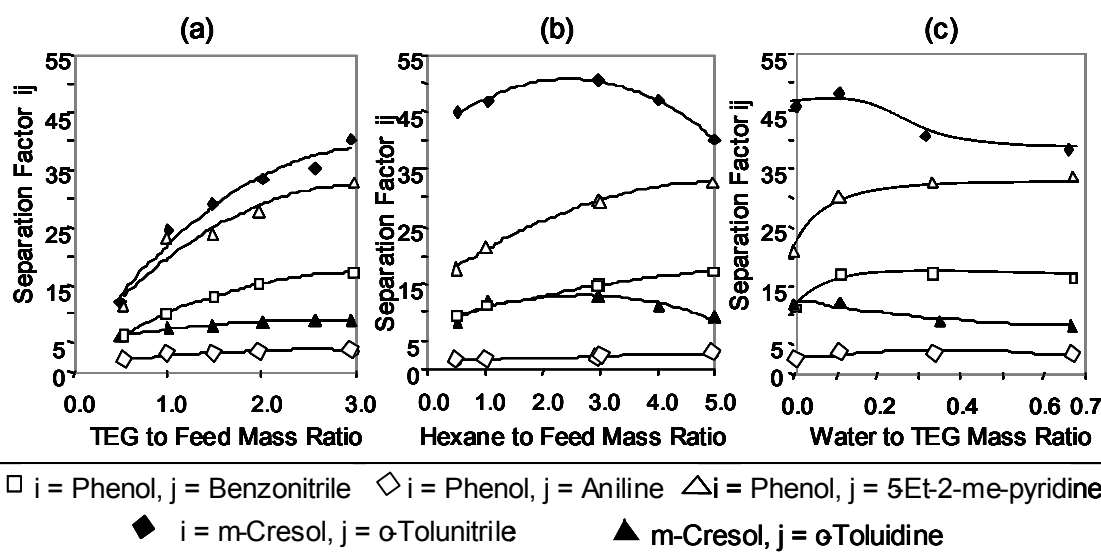


*Figure 1. Effect on the separation factor  $\beta_{ij}$  of the (a) solvent to feed mass ratio at a constant water to solvent mass ratio of 0.3 and a constant hexane to feed mass ratio of 5.0; (b) hexane to feed mass ratio at a constant solvent to feed ratio 3.0 and a constant water to solvent mass ratio of 0.3. (c) water to solvent mass ratio at a constant solvent to feed ratio 3.0 and a constant hexane to feed ratio of 5.0.*

It is clear from Table 2 that the separation of phenolic compounds from paraffins, naphthalene, indene, indane and the alkyl-substituted benzenes is trivial using the proposed solvent system. Figure 1 shows that excellent separation factors are obtained for phenolic compounds relative to aromatic nitriles and 5-et-2-me-pyridine. The separation factors obtained for phenol relative to aniline are satisfactory.

It can further be seen from Figure 2 that excellent phenol and m-cresol recoveries are obtained for all solvent ratios tested. For phenol and m-cresol, recoveries in excess of 99% may be obtained in a single stage. Recoveries in excess of 98% may be obtained for the xylenol isomers at solvent ratios in excess of 2 and water to solvent ratios smaller than 0.25.

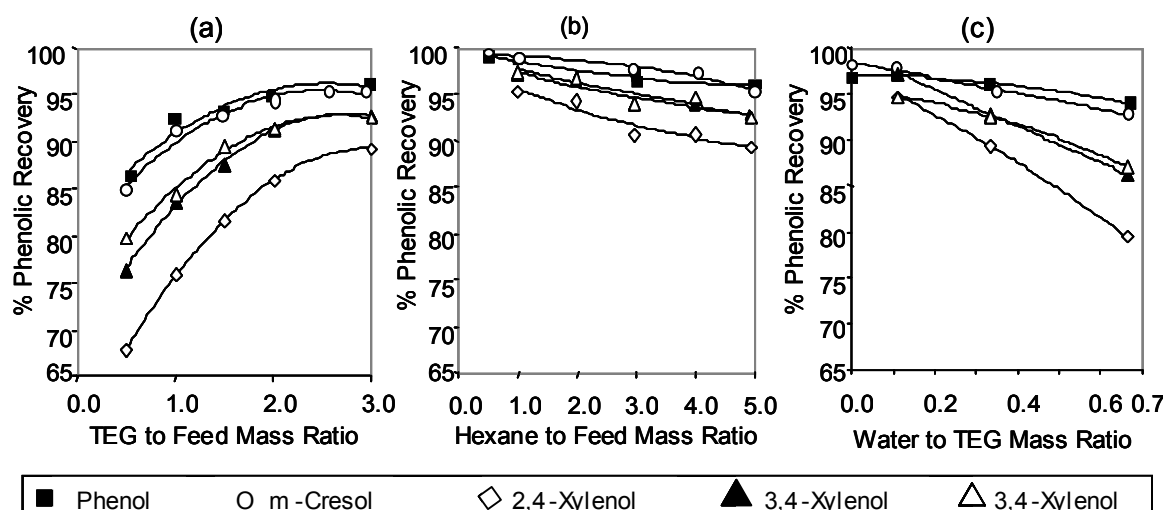


*Figure 2. Effect on the percentage recovery of phenolic compounds of (a) the solvent to feed mass ratio at a constant water to solvent mass ratio of 0.3 and a constant hexane to feed mass ratio of 5.0; (b) the hexane to feed mass ratio at a constant water to solvent mass ratio of 0.3 and a constant solvent to feed mass ratio of 3.0; (c) the water to solvent mass ratio at a constant solvent to feed ratio 3.0 and a constant hexane to feed ratio of 5.0.*

It is clear from Figures 1a and 2a that while an increase in the solvent to feed ratio from 0.5 to 3.0 results in an increase in both the phenolic recoveries and the separation factors, a further increase will have a negligible effect on either separation efficiency or recovery.

It can be seen from Figure 1b that an increase in the hexane to feed ratio from 1.0 to 3.0 results in an increase in all the separation factors. As the hexane to feed ratio is increased further, the separation factors of phenol relative to benzonitrile, aniline and 5-et-2-me-pyridine increase while those of m-cresol relative to o-tolunitrile and o-toluidine decrease. It can be concluded from Figure 1 that, using the proposed solvent system, the most difficult separation is that of phenol from aniline. It can further be seen from Figure 2b that the effect of the hexane to feed ratio on phenolic recovery is small. The optimum hexane to feed ratio is therefore determined as that at which the separation of phenol from aniline is optimum.

From Figure 1c it can be seen that an increase in the water to solvent ratio from 0.0 to 0.2 results in an increase in the separation factors of phenol relative to aniline, benzonitrile and 5-et-2-me-pyridine and a decrease in those of m-cresol relative to o-toluidine and o-tolunitrile. A further increase in the water to solvent ratio results in a decrease in the all the separation factors. It can further be seen from Figure 2 that an increase in the water to solvent ratio results in a decrease in the phenolic recovery. The effect of the water to solvent ratio becomes more significant with a progression in the phenolic homologous series.

It is concluded that the optimum solvent to feed, water to solvent and hexane to feed ratios, with respect to phenolic recovery and separation efficiency, are 3.0, 5.0 and 0.2 respectively.

## THERMODYNAMIC MODELLING

For a multicomponent two-phase liquid-liquid extraction system at equilibrium, the distribution coefficient may be expressed in terms of either the activity coefficients or equilibrium molar concentrations of component  $i$  in both phases:

$$K_i = x_i^E / x_i^R = \gamma_i^R / \gamma_i^E \quad (2)$$

where  $\gamma_i^E$  and  $\gamma_i^R$  are the activity coefficients of component  $i$  in the extract and raffinate phases respectively.

The activity coefficients for a two-phase liquid-liquid extraction system may be modeled with the three-parameter Non-Random Two-Liquid (NRTL) model [12] using an appropriate set of binary interaction parameters,  $b_{ij}$  and  $\alpha_{ij}$ .

Each batch extraction was simulated with the process simulator, PRO/II version 5.11, (Simulation Sciences Inc. 1999), using the sets of binary parameters obtained through regression of the equilibrium data [10]. The root-mean-square deviation (RMSD) for each multicomponent system was calculated from the experimental and simulated equilibrium molar fractions of each component in the two resulting liquid phases according to the following equation:

$$\text{RMSD} = \left[ \sum_n \frac{\sum_i (x_{i,\text{exp}}^E - x_{i,\text{sim}}^E)^2 + \sum_i (x_{i,\text{exp}}^R - x_{i,\text{sim}}^R)^2}{2kn} \right]^{1/2} \quad (3)$$

where  $n$  is the number of data points,  $k$  is the number of components,  $x_{i,\text{exp}}^E$  and  $x_{i,\text{sim}}^E$  are the experimental and simulated molar fractions of component  $i$  in the extract phase and  $x_{i,\text{exp}}^R$  and  $x_{i,\text{sim}}^R$  are the experimental and simulated molar fractions of component  $i$  in the raffinate.

The experimental and simulated distribution coefficients for the system hexane + water + triethylene glycol + mesitylene + 5-et-2-me-pyridine + aniline + benzonitrile + phenol are shown in Figures 3 and 4. The RMSD value calculated for the system is 0.0037. The experimental and simulated distribution coefficients for the systems hexane + water + triethylene glycol + pseudocumene + undecane + indene + o-tolunitrile + o-toluidine + m-cresol and hexane + water + triethylene glycol + indane + dodecane + 2,4-xylenol + 3,4-xylenol + 3,5-xylenol are reported elsewhere [11]. The RMSD values calculated for the two systems are 0.010 and 0.0058 respectively.

From Figures 3 and 4 and it can be concluded that the equilibrium data can accurately be correlated with the NRTL model.

## MULTISTAGE EXRACTION

The proposed solvent system was tested in an agitated glass column containing 28 mixing stages. Mixing was by means of six-blade Rushton turbines. Two perforated stator plates with a free cross-sectional area of 36% separated each mixing stage. Knitted wire mesh was installed between the stator plates to induce coalescence and settling of the dispersed phase liquid droplets. The pilot plant extraction column was configured for countercurrent extraction with the light countercurrent phase as the continuous phase and the heavy solvent phase as the dispersed phase.

Pilot-plant tests using a synthetic feed stream consisting of aniline, o-tolunitrile, m-cresol and p-cresol were performed in order to determine the impeller rotation speed, feed entry point position and solvent ratios required to obtain the highest possible phenolic product purity and recovery.

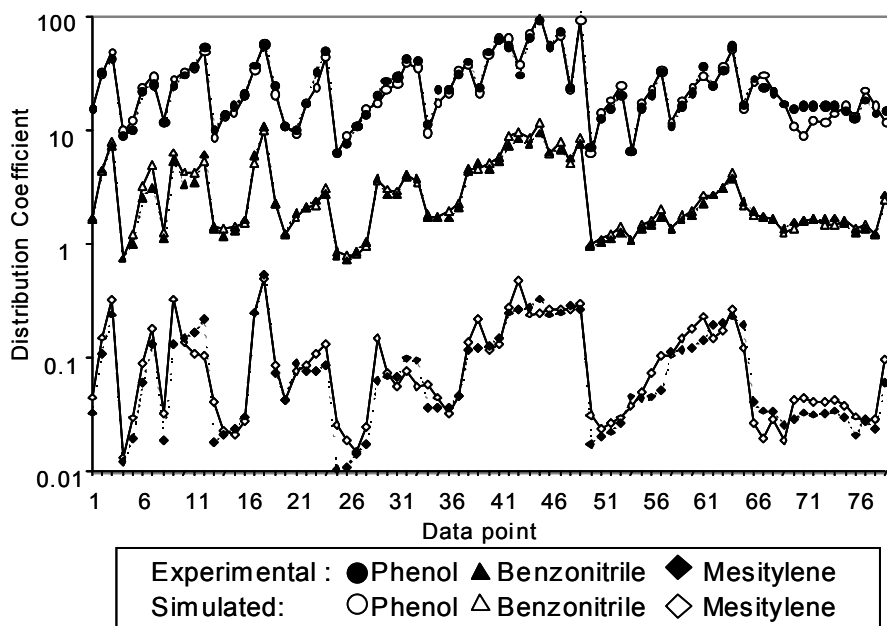


*Figure 3. Experimental and simulated distribution coefficients obtained for phenol, benzonitrile and mesitylene for the system phenol + benzonitrile + aniline + 5-ethyl-2-methyl pyridine + mesitylene + triethylene glycol + water + hexane at 313.15 K and 101.3 kPa.*

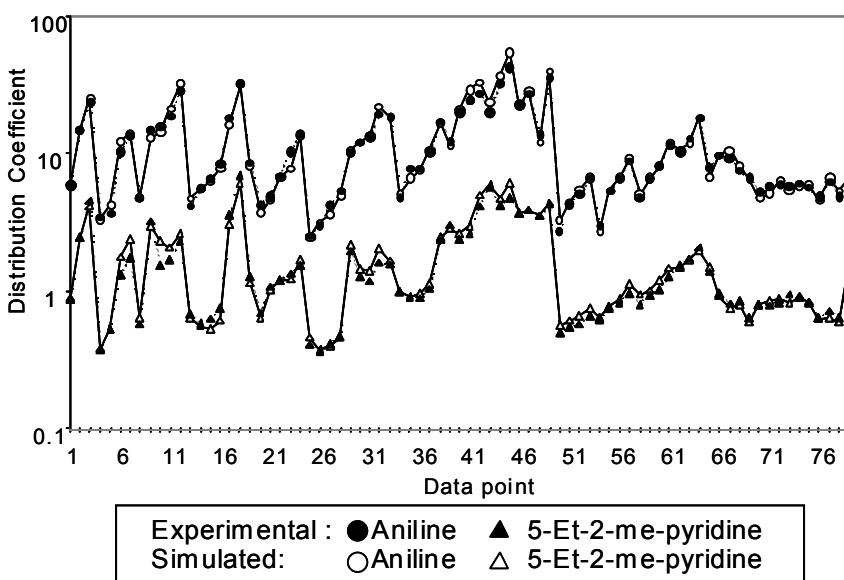


*Figure 4. Experimental and simulated distribution coefficients obtained for aniline and 5-ethyl-2-methyl pyridine for the system phenol + benzonitrile + aniline + 5-ethyl-2-methyl pyridine + mesitylene + triethylene glycol + water + hexane at 313.15 K and 101.3 kPa.*

The optimum solvent to feed, hexane to feed and water to solvent ratios with respect to product purity and phenolic recovery were determined as being 3.0, 5.0 and 0.25 respectively. The optimum phenolic product purity and recovery were yielded using a feed point at the top of the extraction column and an impeller speed of 250 rpm.

Implementation of these optimum operating conditions on an industrial heavy naphtha stream yielded a phenolic product purity of 99.75% after solvent recovery. The corresponding phenolic recovery was in excess of 91 %. Under these conditions, seven equilibrium stages were obtained in the extraction column.

The proposed separation process, including solvent recovery, was simulated with using the NRTL model with the experimentally determined interaction parameters. A single stream consisting of all the components used in the batch extraction tests was specified as the feed stream to the simulated process. A final simulated phenolic product purity of 99.5% and recovery in excess of 94% was obtained after solvent recovery. The optimum simulated solvent ratios were identical to those obtained for the pilot-plant tests.

## CONCLUSIONS

Liquid-liquid equilibria for the solvent system triethylene glycol, hexane and water plus phenolic compounds plus neutral oils and nitrogen bases were determined at 313.15 K in order to evaluate its suitability in separating phenolic compounds from neutral oils and nitrogen bases.

The separation of phenolic compounds from paraffins, indane, indene, naphthalene and trimethylbenzene isomers is trivial using the proposed solvent system. The selectivities obtained for phenol with regards to benzonitrile, aniline and 5-et-2-me-pyridine as well as those obtained for m-cresol with regards to o-tolunitrile and o-toluidine are highly satisfactory. The proposed solvent system was implemented in a multistage countercurrent extraction column with an industrial heavy naphtha stream as feed. The final phenolic product purity after solvent recovery was 99.75% and the phenolic recovery in excess of 91%.

It can therefore be concluded that the triethylene glycol, hexane and water are effective solvents for the separation of phenolic compounds from neutral oils and nitrogen bases.

## NOMENCLATURE

x	equilibrium molar fraction	<i>Subscripts</i>
K	distribution coefficient (defined in eq. 1)	i component i
$\beta$	separation factor (defined in eq. 2)	j component j
$\gamma$	liquid phase activity coefficient	
k	number of components	<i>Superscripts</i>
n	number of data points	E extract (water-rich) phase
		R raffinate (hexane-rich) phase

## ACKNOWLEDGEMENTS

The authors would like to thank Braam van Dyk for assistance in the selection of a solvent by means of computer-aided molecular design.

## REFERENCES

1. H. Fiege and A.G.Bayer (1987), *Ull. Encyc. Ind. Chem.*, **A8**, 25-59.
2. E. Gorin and M. B. Neuwirth (1954), *U.S. Pat.*, No. 2666796 (Jan 19).
3. C.S.B. Nair, D.K. Sen and A.N. Basu (1967), *J. Appl. Chem.*, **17**, 113-117.
4. P. Raj, M.A. Akmal, Y.V.S. Rao and S.M. Ahmed (1970), *J. Appl. Chem.*, **20**, 252-255.
5. T.J. Bhaduri, K.K. Tiwari and A.N. Basu (1965), *Ind. J. Tech.*, **3**, 93-97.
6. A.P.C. Cumming and F. Morton (1952), *J. Appl. Chem.*, **2**, 314-323.
7. D. Duncan, G. Baker, D. Maas, K. Mohl and A. Kuhn (1991), *Eur. Pat.*, No. 0901998A1.
8. D. Duncan, G. Baker, D. Maas, K. Mohl and R. Todd (1996), *Eur. Pat.*, No. 0545814A1.
9. B. van Dyk and I. Nieuwoudt (2000), *Ind. Eng. Chem. Res.*, **39**, 1423-1429.
10. D.L. Venter and I. Nieuwoudt (2001), *J.C.E.D.*, **46**, 813-822.
11. D.L. Venter (2001), Ph.D Thesis, University of Stellenbosch.
12. J.M. Prausnitz, R.N. Lichtenthaler and E.G. De Azevedo (1986), Molecular Thermodynamics of Fluid-Phase Equilibria, PTR Prentice-Hall Inc., New Jersey.



## WAX FRACTIONATION WITH SUPERCRITICAL FLUID EXTRACTION

I. Nieuwoudt, J. C. Crause, M. du Rand and C. E. Schwarz

The University of Stellenbosch, Stellenbosch, South Africa

Supercritical fluid processing offers an attractive alternative for the processing of paraffin waxes. Supercritical fluid phase equilibria for wax systems were experimentally determined and equations of state models were fitted to the data. These models were used to optimise the supercritical fluid fractionation process. Pilot-plant experiments were done to confirm the model predictions. It was shown that superior wax products could be produced with supercritical fluid fractionation and that the processing costs are comparable with that of competing processes.

### INTRODUCTION

Supercritical fluid extraction has been around for almost a century and has several times been hailed as a miracle cure for several problems. However, it often looks like an elegant solution looking for a suitable problem. In 1935 Van Dijck [1] alluded to the use of supercritical solvents in the fractionation of oligomers. Although he used thermal instability as the reason for doing the work, no technical or economic comparison with other methods was presented.

A systematic study was made to identify the wax products for which supercritical fluid extraction is the technically and economically superior fractionation method.

In order to cut down on R&D time and costs, the following route was followed. Accurate phase equilibrium data was measured and equation of state models fitted to the data. The models were used to explore the possibilities of the process. Models were also developed for the competing processes namely short path distillation and fractional crystallization. Pilot plant experiments were done to confirm the model predictions. Conceptual designs were done to compare the economics of the various processes.

### PHASE EQUILIBRIUM MEASUREMENTS

Although several papers have been published on the phase equilibria of supercritical solvents and high molecular weight n-alkanes[2], several of the data sets are incomplete in the mixture critical region whilst some other data sets are highly unreliable. High pressure static equilibrium cells were constructed with which it was possible to measure accurate phase equilibrium data that encompasses the mixture critical region [2,3]. Some of the data sets are shown in Figures 1 and 2. To keep the operating pressures in a comfortable range, ethane is recommended for waxes with carbon numbers of up to 35 whereas propane is recommended for higher molecular weight waxes.

From Figures 1 and 2 it is evident that the solvents can be loaded to approximately 10 % wax. This is important since it determines the solvent:feed ratio which in turn has a dramatic effect on the operating and capital costs. It is also clear that the solubilities of the wax components (at constant pressure and temperature) are a strong function of the chain length. This is important to get good selectivity.

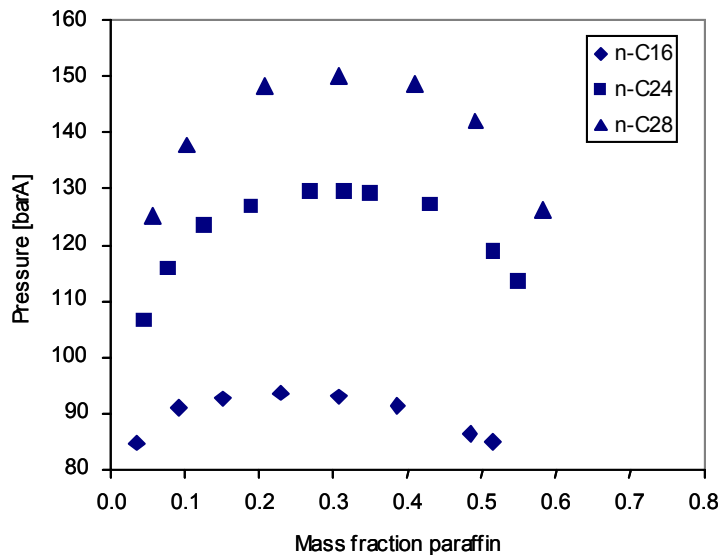


Figure 1. Phase equilibrium data for ethane binaries at 69.7 °C [2].

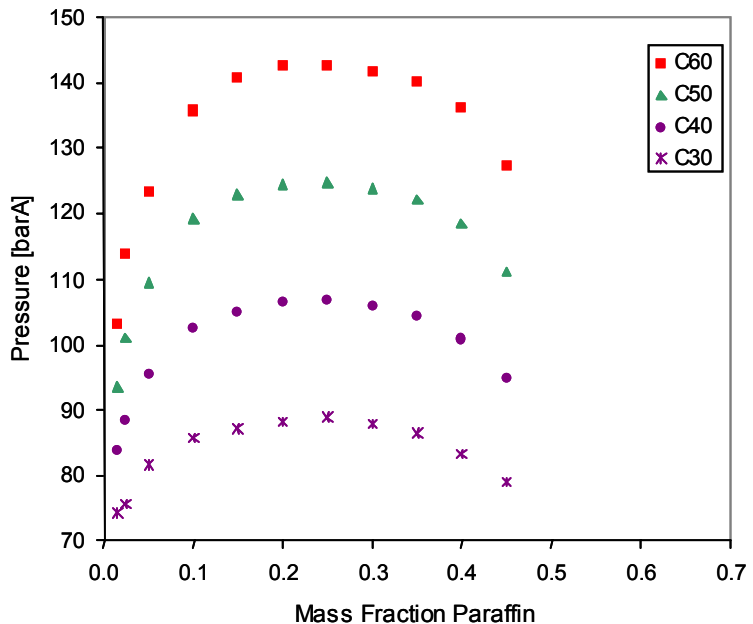


Figure 2. Phase equilibrium data for propane binaries at 135 °C [3].

Equations of state are fitted to the equilibrium data. An example is given in Figure 3. It was found that by using multiple interaction parameters, the cubic equations of state better reproduced the phase diagrams than the more complex equations of state based on statistical mechanics.

These cubic equation of state models were used to optimise the conceptual design of a supercritical fluid wax fractionation unit.

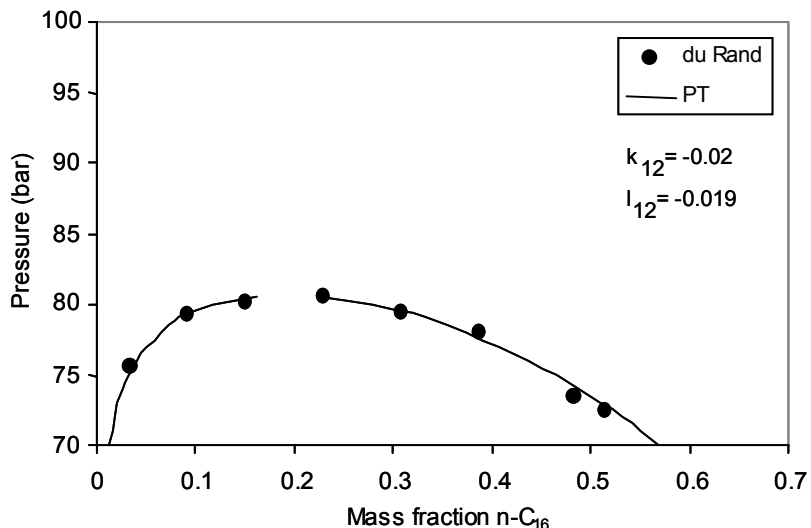


Figure 3. Ethane-hexadecane phase equilibria fitted with Patel-Teja EOS at 59.7°C [2].

### MEDIUM WAX FRACTIONATION

The Patel-Teja model was used to find the optimal conditions for fractionating medium wax ( $C_{16} - C_{36}$ ) with ethane. Supercritical fluid extraction experiments (with ethane as solvent) were conducted at the conditions predicted by the model [4]. The same fractionation was also experimentally done with short path distillation [4]. From Figure 4 it can be concluded that the fractionation in an optimised supercritical fluid extraction column is much better than in a single short path distillation unit.

Based on the experimental results, a conceptual design was done for a supercritical fluid extraction unit and a series of short path distillation units. The final product specifications of the units were identical. A model was also developed to model a wax crystallization unit [5]. A conceptual design of a crystallization unit, with the same product specifications, was also done. Whilst keeping an eye on the capital costs, energy integration was used to minimize the operating costs.

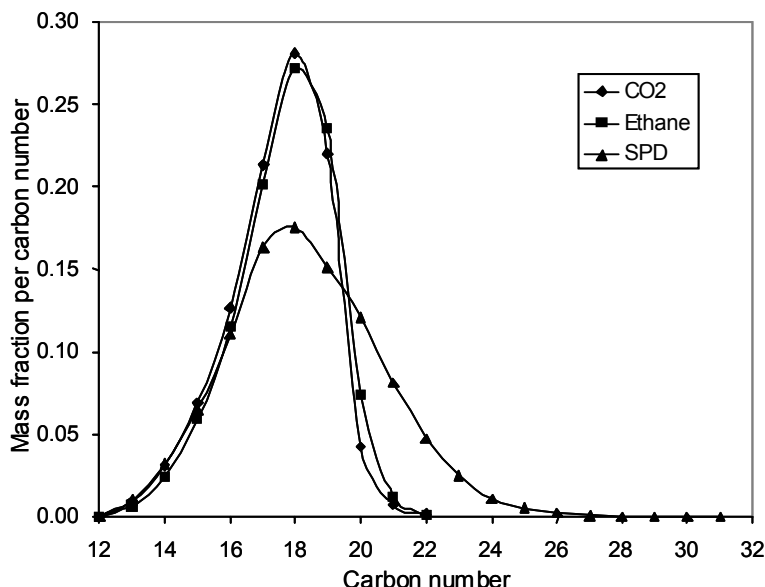


Figure 4. Comparison between the distillate cut sharpness of SCF with ethane or  $CO_2$  and Short Path Distillation.

The following results were obtained for a plant that fractionates 60 000 tons/a of medium wax into two products.

*Table 1. Cash Flow Analysis of Medium Wax Fractionation Conceptual Plant Designs.*

	SCFE	Crystallization	SPD
No of stages(units)	45	5	5
Feed Position	Mid. Column	3	2
Reflux Ratio	10.5	2	0.27
Capital Cost (million \$)	8.7	22.0	13.6
Utilities Cost (\$/ton product)	19	13	10
Internal Rate of Return	32.1	15.7	24.8
Pay Back Period	3.2	5.0	3.8

Both the supercritical fluid extraction and crystallization units are operated at approximately the melting point of the wax, which means that no thermal degradation takes place. The short path distillation unit is operated at approximately 160 °C (and a pressure of 40 Pa abs.). However, due to the high heat capacity of the ethane and the high ethane:feed ratio, the energy consumption of the supercritical extraction process is rather high. The energy consumption of the crystallization process is high as a result of the high heat of fusion and the limited opportunities for heat integration in a solids handling plant.

It is clear that the economics of the supercritical fluid extraction process is sound. The crystallization process has the advantage that it can preferentially remove the oily iso-paraffins from medium wax. However, if the aim is to fractionate n-paraffins, supercritical extraction must certainly be a contender.

## HARD WAX FRACTIONATION

As the molecular weight of the waxes become higher, the iso-paraffin content becomes less, which takes away the advantages of the crystallization process. In this case a comparison between supercritical fluid extraction and short path distillation is required. Models were fitted to equilibrium data, as well as to experimental supercritical fluid extraction and short path distillation data. These models were used to do a conceptual design of the two processes. The products from a single short path distillation unit and from a single supercritical fluid extraction column are shown in Figure 5. The supercritical extraction unit uses propane at 125°C (just above melting point) and 95 bar whereas the short path distillation unit uses a heat transfer fluid at 330°C and operates at a pressure of 20 Pa abs.

It is evident that the products from the supercritical extraction unit are superior to that of a single short path distillation unit. The high temperatures in the SPD unit may also cause degradation of the wax. The high temperature also has a negative impact on the utility consumption of the SPD unit. The economics of supercritical extraction of hard waxes will thus even be more favourable compared to that of short path distillation than is the case with medium wax (Table 1).

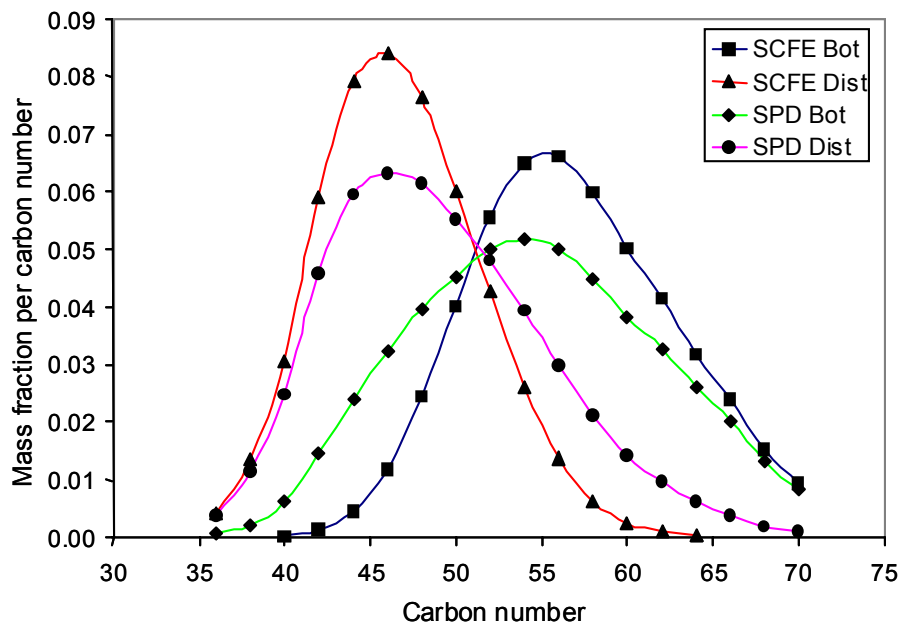


Figure 5. Comparison between the cut sharpness of SCF with propane and Short Path Distillation.

## CONCLUSIONS

The following conclusions can be drawn from this study:

- Several short path distillation or crystallization units are needed to give the same fractionation as a single supercritical extraction column.
- Crystallizations have an edge in waxes with a high iso-paraffin content since it fractionates based on melting points.
- The profitability of supercritical fluid wax fractionation units improve relative to that of the competing processes as the carbon number of the wax increases.
- For high molecular weight waxes supercritical fluid extraction should be the fractionation method of choice based on technical and economic considerations.

## REFERENCES

1. W. J. D. Van Dijck (1942), *US Patent*, 2,281,865.
2. M. Du Rand (2000), M.Sc.Ing. Thesis, University of Stellenbosch, South Africa.
3. I. Nieuwoudt, M. Du Rand and C. Schwarz (2001), *Proc. 76th International Bunsen Discussion Meeting "Global Phase Diagrams"*, Walberberg, Germany.
4. I. Nieuwoudt, C. Crause and M. Du Rand (2001), *J. Supercrit. Fluids*, submitted.
5. C. Crause (2001), Ph.D.Ing. Thesis, University of Stellenbosch, South Africa.



## NOVEL APPLICATION PERSPECTIVES FOR METAL EXTRACTANTS: OLEFIN SEPARATIONS

Bart A.E. Wentink, Patrick W.T. Krooshof, Norbert J.M. Kuipers,  
André B. de Haan and Harko Mulder\*

University of Twente, Enschede, The Netherlands  
\*Sasol Technology, Sasolburg, South Africa

Olefin separations are industrially important but energy intensive separations. Application of metal ligand complexes, based on ligands developed for the hydrometallurgy industry, can reduce the energy consumption of such separations. This concept is investigated experimentally by gravimetical measurement of the ethylene solubility. Silver complexed with the commercial ligand di(2-ethylhexyl)phosphoric acid diluted in dodecane, more than triples the ethylene solubility, compared to the situation without silver. However, the ethane solubility remained unaffected. Commercially viable separation factors are around 1.2, so the achieved selectivity of 2.4 is sufficient. Another ligand, Cyanex 301, diluted in dodecane and complexed with either copper(I) or silver(I) did not enhance the ethylene solubility.

### INTRODUCTION

The recovery and purification of olefins (e.g., ethylene, propylene or 1-butene) from hydrocarbon streams is a difficult and expensive operation. Selective and reversible olefin complexation by (transition) metal ions has been put forward as a possible alternative for conventional separations. In most cases, aqueous silver salt or organic copper(I) solutions are employed [1]. Disadvantages of these are the high vapour pressure of the applied solvent, the low metal solubility in hydrocarbons and an insufficient metal ion stability. This restrains the application on an industrial scale. These disadvantages can be overcome by complexation of the metal ion with an organic ligand. In this way the solubility in organic solutions and metal ion stability are increased, whereas the vapour pressure is reduced by application of a low boiling solvent.

In hydrometallurgy many complexing ligands have been developed for the recovery of metal ions from aqueous streams. These ligands are commercially available, widely applied, diverse and have a low vapour pressure. The right combination of metal ion, diluent and ligand is expected to yield a new range of olefin complexing media.

The feasibility of the proposed concept will be demonstrated in this paper by measurement of the ethylene solubility in dodecane containing the metal ion ligand complex. The investigated ligands are Cyanex 301 [di(2,2,4-trimethylpentyl)dithiophosphinic acid,  $(C_8H_{17})_2P(S)SH$ ] and D2EHPA [di(2-ethylhexyl)phosphoric acid,  $(C_8H_{17}O)_2P(O)OH$ ]. The metal ions used in this investigation are silver(I) and copper(I).

## $\pi$ -COMPLEXATION BETWEEN METAL IONS AND OLEFINS

The complexation of olefins by transition metal ions is described by the Dewarr-Chatt-Duncanson or  $\pi$ -complex model. A  $\pi$ -complex is composed out of two bonds, a  $\sigma$  and  $\pi$ -bond. The  $\sigma$ -bond is formed between the vacant  $s$ -orbital of the metal ion and the  $\pi$ -molecular orbital of the olefin, as illustrated in Figure 1. The empty metal ion  $s$ -orbital acts as a Lewis acid by accepting an electron from the olefin. The metal ion also acts as a Lewis base by back-donating electrons from its full  $d$ -orbital in the empty  $\pi^*$ -orbital of the olefin [1]. In principle, all transition metal ions can be used, but copper(I) and silver(I) ions exhibit a strong but reversible reaction.

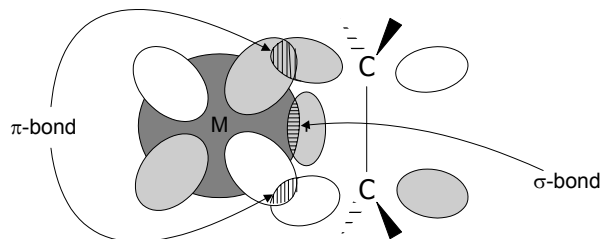


Figure 1.  $\pi$ -Complex formation between transition metal ion (M) and olefin [1].

## GAS ABSORPTION

The overall ethylene ( $C_2^-$ ) solubility ( $S_{C_2^-}$ ) in solvents containing metal ion ligand complexes that are capable of  $\pi$ -complexation is equal to the sum of the physical solubility and the solubility as a result of the  $\pi$ -complexation reaction. The physical solubility of ethylene is described by means of a Henry coefficient ( $H_{C_2^-}$ ). The  $\pi$ -complexation of ethylene with the metal ion ligand complex is described as a equilibrium reaction ( $K_r^{C_2^-}$ ), as indicated in Figure 2.

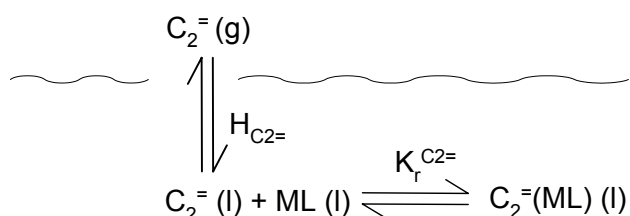


Figure 2. Ethylene solubility in liquids with  $\pi$ -complexation with metal ligand complexes.

Based on the processes shown in Figure 2, Equation (1) has been derived, describing the ethylene solubility as a function of the ethylene pressure ( $P_{C_2^-}$ ) and initial metal ion complex concentration  $[\text{ML}]_0$ . It is assumed that the reaction stoichiometry between ethylene and metal ion-ligand complex is 1:1.

$$S_{C_2^-} = \frac{P_{C_2^-}}{H_{C_2^-}} \left( 1 + \frac{K_r^{C_2^-} [\text{ML}]_0}{1 + (K_r^{C_2^-} P_{C_2^-}) / H_{C_2^-}} \right) \quad (1)$$

The model parameters were determined from the experimentally observed ethylene solubilities of two experiments. Henry's coefficient was estimated using a solution of metal free ligand in dodecane. From the determined Henry coefficient, the equilibrium constant was determined by fitting equation (1) to the experimental solubilities.

## EQUIPMENT AND PROCEDURES

All silver complexes were synthesised by liquid-liquid extraction. In the liquid-liquid extraction, equal volumes of the organic ligand (in dodecane) and aqueous silver nitrate solution were mixed for approximately 1 h using a magnetic stirrer. The equilibration time differed from ligand to ligand, but is well below the time used. Samples of the organic phase were taken ( $\pm 5$  ml) for analysis of the metal content by atomic absorption spectrophotometry (AAS).

The copper complexes were synthesised by liquid-liquid extraction or by reacting an (acidic) ligand with solid copper(I) oxide. The liquid-liquid extraction for copper is similar to the method described for silver. In the oxide method, a molar excess of cuprous oxide ( $Cu_2O$ ) was reacted with an acidic ligand in dodecane under continuous flowing nitrogen. After the reaction, the excess oxide settled and liquid samples were taken to determine the metal content.

The ethylene ( $C_2H_4$ ) solubility was determined with an Intelligent Gravimetric Analyser (IGA, model 003, Hiden Analytical). The IGA was originally designed to measure the gas uptake by solids, but was adapted to study gas absorption (for more details on the IGA, see [2, 3]). Typically a sample of 0.5 g metal ion ligand complex (in dodecane) was used, held in a Pyrex-glass sample holder. Pressure steps of approximately 0.6 bar were used at a constant temperature ( $25^\circ C$ ) to determine the absorption isotherms. The temperature was controlled by a Julabo (F32 MP) water bath to within  $\pm 0.2^\circ C$ . A typical IGA run lasted around 4000 min.

Ethylene (99.95%) was acquired from Praxair,  $AgNO_3$ ,  $Cu_2O$ ,  $CuSO_4$  and dodecane ( $C_{12}H_{26}$ ) from Aldrich, and D2EHPA (95%) from Merck. Cyanex 301 (77.2%) was a gift from Cytec Industries Europe. All chemicals were reagent grade, except when noted, and used as received. In the reported Cyanex 301 concentration the impurities were neglected.

## SELECTION OF ORGANIC EXTRACTANTS (LIGANDS)

In hydrometallurgy many complexing ligands have been developed that have the potential to be used in olefin complexation. The main criterion for a first selection was that the organic ligand must be able to complex either copper(I) or silver(I). Additional criteria were that the organic ligand must be thermally stable and if possible form a strong bond with the metal. The selected ligands are shown in Figure 3.

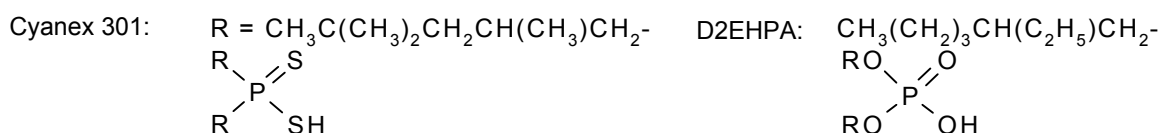


Figure 3. Selected ligands.

Cyanex 301 exists in the organic phase as a monomer, forms strong bonds with copper and silver and reacts with a metal:ligand ratio of 1 [5, 6]. It is claimed that Cyanex 301 reduces copper(II) to copper(I) upon extraction [5]. This is advantageous, because copper(I) complexes olefins and copper(II) does not. Furthermore, Cyanex 301 easily extracts copper(II) or silver(I) at a pH below 2, that facilitates the synthesis of complexes with these metals. D2EHPA forms dimers in the organic phase because of hydrogen bonding [10]. Therefore the metal:ligand molar ratio is 1:2 [10]. D2EHPA extracts silver(I) at a pH of approximately 5, due to its higher  $pK_a$  value. This complicates the synthesis of these complexes. The bond between metal and oxygen is weaker compared to the metal-sulphur bond, possibly resulting in a lower metal ion-ligand complex stability. The extraction of Cu(I) by D2EHPA or Cyanex 301 is not described in the literature.

## RESULTS

### IGA Method Verification

Figure 4 presents the ethylene solubility in pure dodecane as a function of pressure. The results from the IGA accurately correspond with the literature results. The calculated Henry coefficient for both the literature and IGA solubility data is reported in Table 1 and deviates approximately 1%.

### Oxygen-Containing Ligands

The effects of  $\pi$ -complexation on the ethylene solubility are illustrated in Figure 4. The silver/D2EHPA-complex almost triples the ethylene solubility, compared to the situation of only D2EHPA in dodecane, and more than doubles the solubility compared to pure dodecane. The ethane solubility, however, remained unaffected by the silver complex. The curved nature of the ethylene solubility isotherm is indicative for the  $\pi$ -interaction between silver and ethylene and is typical for a system with a combination of chemical complexation and physical solubility [9]. The addition of D2EHPA to dodecane reduced the ethylene solubility. It is believed that this is due to the enlarged liquid polarity, as a result of the functional group of the D2EHPA. The absorption curves of ethylene and ethane in D2EHPA/dodecane are straight, typical for only physical solubility and in accordance with Henry's law [8]. The selectivity of ethylene over ethane varied with pressure and was between 1.9 and 1.4.

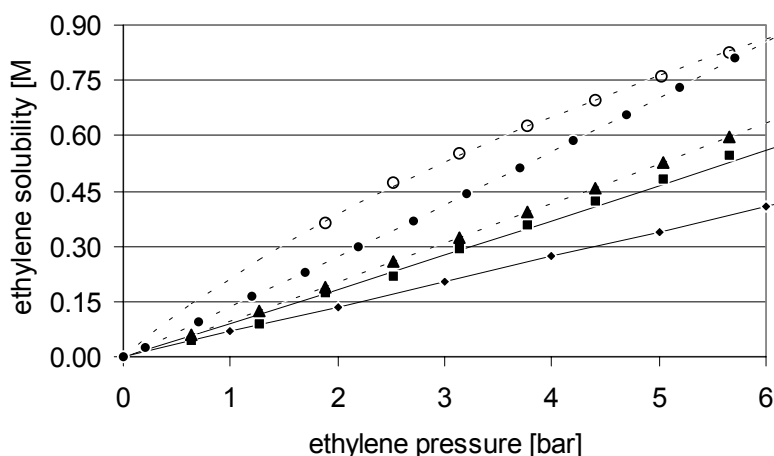


Figure 4. Ethylene and ethane solubility isotherm at 298 K. Ethylene in: (■) pure dodecane; (—) pure dodecane literature [4]; (—◆—) 2 M D2EHPA/dodecane; (○), (···) 0.79 M Ag/2 M D2EHPA/dodecane experimental & model. Ethane in: (··●··) pure dodecane literature [11]; (··▲··) 0.79 M Ag/2 M D2EHPA/dodecane.

### Model Results

The model can accurately describe the ethylene solubility, for the reactive and non-reactive situation, as displayed in Figure 4. The corresponding parameters are given in Table 1.

Table 1. Henry coefficients and equilibrium constant of ethylene and ethane.

	$H_{C_2^=}$ [bar·M <sup>-1</sup> ]	$K_r^{C_2^=}$ [M <sup>-1</sup> ]
ethylene dodecane [4]	10.8	--
ethylene dodecane	10.7	--
ethylene 2 M D2EHPA/dodecane	14.7	--
ethylene 0.79 M Ag/2 M D2EHPA/dodecane	14.7	3.4
ethane 2 M D2EHPA/dodecane	9.6	--

## Sulphur-Containing Ligands

Figure 5 presents the ethylene solubility in solutions of Cyanex 301 complexed with or without copper or silver in dodecane. Two copper-containing solutions were measured, a solution with 0.44 M copper synthesised by liquid-liquid extraction and a solution with 0.88 M copper synthesised by the oxide method.

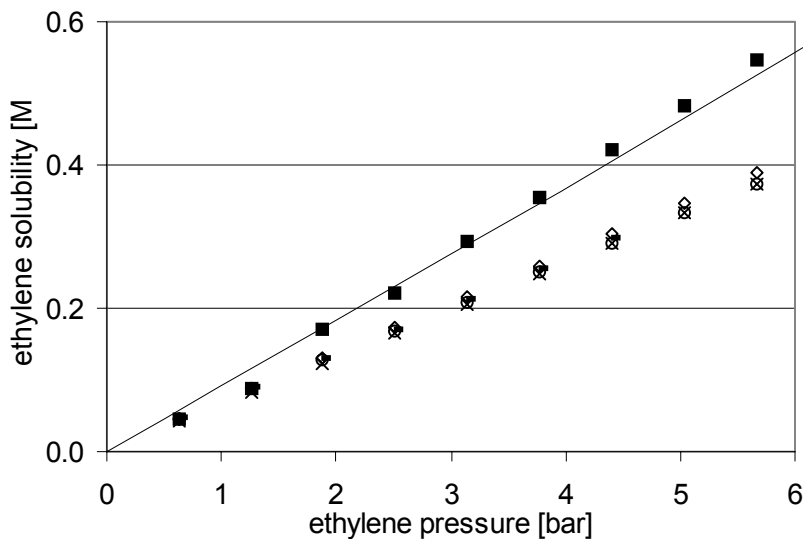


Figure 5. Ethylene solubility at 298 K in: (■) pure dodecane; (—) pure dodecane literature [4]; (◊) 1 M Cyanex 301/dodecane; (×) 0.44 M Cu/1 M Cyanex 301/dodecane; (○) 1.0 M Ag/1 M Cyanex 301/dodecane; (∗) 0.88 M Cu/1 M Cyanex 301/dodecane.

Again, the solubility of ethylene is reduced by the presence of the organic ligand. However, in contrast to the silver/D2EHPA-complex, the introduction of copper(I) or silver(I) complexed with Cyanex 301 does not enhance the ethylene solubility. Apparently, the metal ion is inhibited by Cyanex 301 from forming a  $\pi$ -bond with the olefin. The reasons for this could be the redistribution of electrons around the metal ion, steric hindrance of the ligand or a combination of both.

The complexation of copper(I) involves  $\pi$ -bonding of metal *d*-orbitals and sulphur atom orbitals that alter the electron structure of copper(I) [7]. It is claimed, however, that for silver(I),  $\pi$ -bonding does not play a significant role [7]. So, in case of copper the electron delocalisation might lead to a reduced affinity towards ethylene, but for silver it can be expected that this is of less importance. Another possibility is the formation of multinuclear complexes of Cyanex 301 with copper or silver [5, 6], as shown in Figure 6.

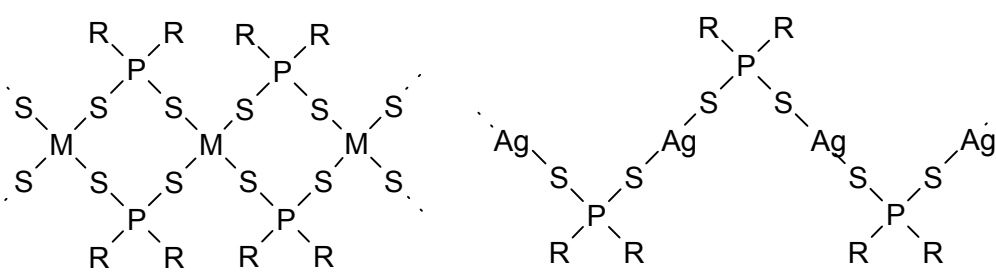


Figure 6. Metal-Cyanex 301 complex structure ( $M = \text{Cu}(\text{I})$  or  $\text{Ag}(\text{I})$ ) [5,6].

Copper(I) forms tetrahedral complexes, as is shown in the left part of Figure 6. Opposite to copper(I), silver(I) forms four-coordinate tetrahedral complexes less readily than two-coordinate linear ones [12]. Consequently, the linear complex structure as shown in the right

part of Figure 6 was suggested [6]. However, the formation of a four-coordinated complex with silver can not be excluded. The formation of these multinuclear complexes could result in steric hindrance of the metal ion that inhibits the formation of  $\pi$ -complexes between metal ion and ethylene. It is a phenomenon that occurs for both metals, which is in accordance with the observed ethylene solubility. Further investigation of sulphur-containing complexes that do not form multinuclear complexes might clarify this.

## CONCLUSIONS

It has been demonstrated that olefin/paraffin separations are a novel application for ligands that were developed for extractive hydrometallurgy. If the ligand is complexed with a suitable metal ion, the olefin solubility can be increased by selective  $\pi$ -complexation. The metal ion is stabilised by the ligand and can be solvated in a useful (high) concentration. The effects of such complexes on the ethylene solubility were investigated experimentally, using a gravimetical method.

Pure dodecane already has an intrinsic selectivity for ethane over ethylene, due to differences in polarity. The achieved selectivity is approximately 0.7, based on the ratio of the physical solubility of ethylene over ethane. The addition of the silver/D2EHPA complex, however, raises the solubility of ethylene by a factor of almost three without affecting the ethane solubility. The increase in selectivity between the presence and absence of the complex is more then three. The achieved selectivity of ethylene over ethane is 2.4, which is sufficient for the separation of ethylene from ethane with the developed metal ligand complex.

The use of ligands is not always beneficial, as is the case with Cyanex 301 that is complexed with copper(I) or silver(I). The ligand inhibits the metal ion from forming  $\pi$ -complexes with silver and consequently the ethylene solubility is not enhanced. Metal complexes with this ligand are therefore unsuitable for the separation of ethylene from ethane.

## ACKNOWLEDGEMENTS

Sasol Technology is thanked for their financial support of the project and permission to publish this paper. Cyanex 301 was a gift from Cytec Industries.

## REFERENCES

1. D.J. Safarik and R.B. Eldridge (1998), *Ind. Eng. Chem. Res.*, **37**, 2571-2581.
2. M. Benham and P. Stonadge (1993), IGA Systems Guide.
3. Available from: <http://www.hiden.co.uk>.
4. IUPAC Solubility Data Series (1994), Ethene, **57**, 78-98.
5. K.C. Sole and J.B. Hiskey (1995), *Hydrometallurgy*, **37**, 129-147.
6. K.C. Sole, T.L. Ferguson and J.B. Hiskey (1994), *Solvent Extr. Ion Exch.*, **12**, 1033-1050.
7. F.A. Cotton and G. Wilkinson (1980), Advanced Inorganic Chemistry, 4th edn., Wiley Interscience, pp. 970.
8. R.C. Reid, J.M. Prausnitz and B.E. Poling (1987), The Properties of Gases and Liquids, pp. 332-337.
9. C.J. King (1987), Handbook of Separation Process Technology, R.W. Rousseau (ed.), John Wiley & Sons, pp. 760-775.
10. S.C. Lee, B.S. Ahn and W.K. Lee (1996), *J. Membr. Sci.*, **114**, 171-185.
11. IUPAC – Solubility Data Series (1982), Ethane, Vol. 9, 133-134.
12. N.N. Greenwood and A. Earnshaw (1997), Chemistry of the Elements, Pergamon, pp. 1196.



# HYDRODYNAMIC BEHAVIOUR IN PACKED COUNTERCURRENT COLUMNS FOR SUPERCRITICAL FLUID EXTRACTION

Gerd Brunner and Ron Stockfleth

Technische Universität Hamburg-Harburg, Hamburg, Germany

The hydrodynamic behavior, *i.e.*, flooding, liquid holdup, and pressure drop of countercurrent columns with two random packings, Raschig Rings and Berl Saddles, and two gauze packings, Sulzer CY and Sulzer EX, is scrutinized at temperatures between 313 K and 373 K and pressures between 8 MPa and 30 MPa using carbon dioxide as supercritical solvent and water and olive oil deodorizer distillate as liquid phases. The behaviour of falling films at high pressures is examined. A general predictive approach to flooding based on sophisticated mechanistic models is developed. Parameters in this correlation have to be fitted for each packing. Therefore, a more general empirical approach has been employed. The resulting correlation represents measured flooding point data for a variety of packings, fluid substances and mixtures within a standard deviation of 19%.

## INTRODUCTION

In recent years supercritical fluids have been introduced as a mass-separating agent for various separation processes. For liquid feeds, supercritical fluid extraction can most effectively be carried out using a continuous countercurrent process. For the design of countercurrent columns knowledge about the hydraulic capacity and the flow regimes of the packed column is required. Correlations would enable the reduction in number of experiments. The objective was the examination of the hydrodynamic behaviour, that is, flooding, liquid holdup, and pressure drop of columns with random and regular packing. The falling film on the packing is of major importance and was therefore investigated in true liquid-fluid countercurrent flow. The influence of mass transfer was eliminated by equilibrating the phases before contacting them countercurrently. Knowledge about the hydraulic capacity of the packed column is important to determine the inner diameter that will be needed for the countercurrent throughput of the required amounts of solvent and feed without flooding the column.

## EXPERIMENTAL

### Apparatus

The apparatus shown in Figure 1 is operated at pressures between 8 and 30 MPa and temperatures between 313 and 373 K. It consists of two main parts: the 1.89 m high column with four long windows filled with up to 0.9 m packing and an equilibrium autoclave, equipped with a stirrer. The bottom segment of the column is also equipped with a long window to allow the continuous monitoring of the liquid level [1].

## Methods, Substances And Experimental Conditions

The coexisting phases are brought into equilibrium by circulating and stirring to observe the hydrodynamic phenomena independently of mass transfer phenomena. Three high-pressure gear pumps (two for the supercritical phase and one for the liquid phase) convey the two phases from the autoclave to the column and back into the autoclave after passing through the packing [2].

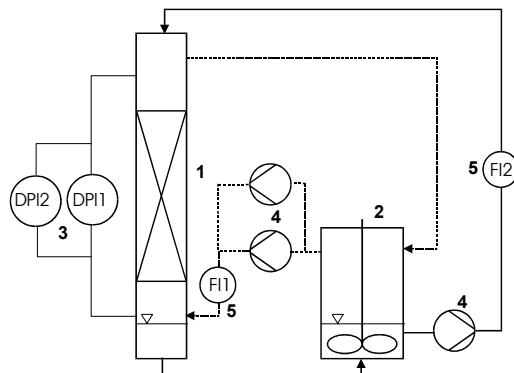


*Figure 1. Flowsheet of the experimental apparatus. 1, column; 2, autoclave; 3, differential pressure transducers; 4, gear pumps; 5, flow meters; full line, liquid cycle; dashed line, supercritical fluid cycle.*

The hydrodynamic behaviour, *i.e.*, flooding, liquid holdup, and pressure drop of countercurrent flow in the column was investigated for two random packings, Raschig Rings and Berl Saddles, and two gauze packings, Sulzer CY and Sulzer EX, at temperatures between 313 K and 373 K and pressures between 8 MPa and 30 MPa using carbon dioxide as supercritical solvent and water and olive oil deodorizer distillate as liquid phases.

With respect to the behaviour of falling films at high pressures, film thickness, flow regimes, and flooding points for countercurrent annular flow of corn oil (Mazola<sup>TM</sup>) and carbon dioxide at 338 K and pressures between 7.6 and 20.6 MPa were examined experimentally. The film flows down a stainless steel rod with a diameter of 10 mm and a length of 1000 mm that is inserted in a glass tube with an internal diameter of 15 mm yielding an annulus of 2.5 mm. The glass tube is placed within the high-pressure column.

## A UNIVERSAL PREDICTIVE APPROACH TO FLOODING

At constant gas velocity the pressure drop as a function of the superficial liquid velocity first rises slightly and then abruptly with increasing liquid velocity. This abrupt change in pressure drop is a typical indicator for flooding. Liquid holdup as a function of the superficial liquid velocity exhibits the same behavior.

There are numerous possible definitions and criteria for the flooding point of a countercurrent column. Throughout this paper a liquid layer of 50 mm height on the uppermost packing element is the indicator for a flooding point. Most sophisticated semi-mechanistic models for the hydraulic capacity use the interdependence of liquid holdup and pressure drop to quantify the flooding point. These models follow a modular approach. First, the dry pressure drop and the holdup below the loading point are described. That means the interaction of a single phase with the packing is modeled. Then, the holdup beyond the loading point and the pressure drop of the irrigated packing are specified. These two phenomena are coupled, *i.e.*, pressure drop depends on holdup since this determines the free area available to the gas flow and the holdup depends on the pressure drop because this is a measure for the shear

force the gas flow exerts on the liquid. A consequence of the coupled equations is, that the solution is cumbersome because it involves iterations. With these equations the flooding point can be determined as the point where the derivative of the holdup with respect to the dry pressure drop, which is a measure for the gas velocity, becomes infinity.

### Dry Pressure Drop

Experimental studies [3] of the single-phase flow through fixed beds of varying porosity (0.3 – 0.75) suggest that the friction factor  $\psi$  is proportional to  $\varepsilon^{4.55}/(1-\varepsilon)$ . This is slightly different from Ergun's result [4] stating that  $\psi \sim \varepsilon^3/(1-\varepsilon)$ . Since the latter did not vary the porosity to the extent of the former, the following friction factor as suggested by Stichlmair *et al.* [5] according to Rumpf is used.

$$\psi = \frac{4}{3} \frac{\Delta P_0 \varepsilon^{4.65} d_p}{H(1-\varepsilon) \rho_G u_G^2} = f \left( \text{Re}_G = \frac{u_G d_p \rho_G}{\eta_G} \right) = \frac{K_1}{\text{Re}_G} + K_2, \quad (1)$$

with  $\Delta P$  as the pressure drop,  $H$  the height of the packing,  $\rho_G$  the density of the gas,  $\eta_G$  its viscosity, and  $u_G$  its velocity. Due to the limited accuracy and quantity of the experimental data a simple function of the Ergun-type was chosen to describe the dependence of the friction factor on the Reynolds number of the gaseous phase. The correlations obtained are:

$$EX : \psi = \frac{155}{\text{Re}_G} + 3.4, \quad Raschig, Berl : \psi = \frac{23}{\text{Re}_G} + 1.2, \quad CY : \psi = \frac{23}{\text{Re}_G} + 0.2 \quad (2)$$

### Holdup below the Loading Point

The loading point is the point at which the two phases flowing through the packing start to interact. Below the loading point the liquid flows through the packed bed as if there was no other phase flowing countercurrently. So, the holdup below the loading point describes the sole interaction of the liquid with the packing in the same way as the dry pressure drop describes the sole interaction of the gas with the packing. The total liquid holdup consists of two contributions: the dynamic or operating holdup and the static holdup. The static holdup is liquid trapped in gussets and attached to the packing by adhesive forces. It will not drain from the packing and remain there until removed by some other means. The dynamic or operating holdup is the liquid that will drain if the liquid pump is shut off. The following function was used to correlate the holdup to  $\text{Re}_L$  and  $Fr_L$ :

$$h_0 = C_1 \left( \frac{Fr_L^2}{\text{Re}_L} \right)^{C_2}, \quad Fr_L := Fr_L^* \frac{\rho_L}{\Delta \rho} = \frac{u_L^2 a \rho_L}{g \Delta \rho} \quad (3)$$

where  $h_0$  denotes the dynamic liquid holdup below the loading point. The Reynolds number relates the inertial force to the viscous force and the Froude number rates the inertial force to the gravitational force.  $C_1$  and  $C_2$  are parameters obtained by fitting calculated to measured data. This approach contains already a simplification; the more general approach would raise each dimensionless number to a different unknown power. The holdup below the loading point correlated with the modified Froude number  $Fr_L$  taking the buoyancy into account results in an absolute standard deviation of 1.8 % with  $C_1 = 1.6$  and  $C_2 = 0.23$  for Raschig rings, Berl saddles and Sulzer EX. The Sulzer CY packing requires a correlation different from the one valid for the other packings:  $C_1 = 1.1$  and  $C_2 = 0.25$  with an absolute standard deviation of 0.5 %.

### Holdup and Pressure Drop beyond the Loading Point

Above the loading point the holdup and pressure drop are no longer independent of each other. The liquid holdup decreases the available free cross-sectional area available for the gas flow thereby increasing the local gas velocity and the pressure drop. The pressure drop is a measure for the interfacial shear force the gas exerts on the liquid – the higher this force the higher the liquid holdup. In this paper the authors follow the suggestion of Stichlmair *et al.* [5] for the interdependence of holdup and pressure drop.

$$h = h_0 \left[ 1 + C_3 \left( \frac{\Delta P}{H \Delta \rho g} \right)^{C_4} \right] \quad (4)$$

$$\frac{\Delta P}{\Delta P_0} = \frac{\left\{ \left[ 1 - \varepsilon \left( 1 - \frac{h}{\varepsilon} \right) \right] / (1 - \varepsilon) \right\}^{2+c}}{\left( 1 - \frac{\varepsilon}{h} \right)^{4,65}} \quad (5)$$

$$c := \frac{-K_1}{\psi} \quad (6)$$

$K_1$  is the constant from equation 1 and  $\psi$  the friction factor that would result if there were no liquid flow, *i.e.*, the dry friction factor. Equation 6 relates the holdup beyond the loading point to the holdup below the loading point and the reduced pressure drop. The reduced pressure drop is the ratio of the force the gas flow exerts on the liquid to the total static head of the liquid. In analogy to fluidized beds a force balance yields that the upper limit for the reduced pressure drop is the liquid holdup, because this would mean that the force the gas flow exerts on the liquid suspends the entire liquid in the column. As already pointed out earlier, the difference of the densities has to be used instead of the liquid density to account for the significant buoyancy force exerted on the liquid by the dense gas.  $C_3$  and  $C_4$  are parameters obtained by fitting calculated to experimental data. Since pressure drop and holdup have also been measured above the loading point,  $C_3$  and  $C_4$  can be obtained directly. The fitting procedure yielded a relative standard deviation of 17.15 % for  $C_3 = 4.1$  and  $C_4=2.0$  with constant  $C_4$  and a relative standard deviation of 17.05 % for  $C_3 = 5.5$  and  $C_4=2.3$  with variable  $C_4$ . However, since these parameters have a significant impact on the calculation of the flooding point, it was also tried to fit  $C_3$  and  $C_4$  to the measured flooding points, as described in the following.

### Flooding

The flooding point is reached if a finite change in gas or liquid velocity leads to an infinite change in pressure drop or holdup. The dry pressure drop is a measure for the gas velocity and the flooding criterion can be formulated as [5]:

$$\frac{\partial \Delta P}{\partial \Delta P_0} = \infty \quad \Leftrightarrow \quad \frac{\partial \Delta P_0}{\partial \Delta P} = 0 \quad (7)$$

Substituting equation 6 for the holdup into equation 7 then inverting it and taking the derivative, yields:

$$\left(\frac{\Delta P}{H\Delta\rho g}\right)^{-C_4} - \frac{4,65C_3C_4h_0}{\varepsilon - h_0 \left[1 + C_3 \left(\frac{\Delta P}{H\Delta\rho g}\right)^{C_4}\right]} - \frac{\frac{2+c}{3}C_3C_4h_0}{1 - \varepsilon + h_0 \left[1 + C_3 \left(\frac{\Delta P}{H\Delta\rho g}\right)^{C_4}\right]} = 0 \quad (8)$$

Equation 8 has to be solved iteratively. The flowsheet for the calculation of a flooding point is displayed in Figure 2. Considering the limited success of the universal predictive approach outlined in the previous paragraphs, an alternative empirical approach is presented as well.

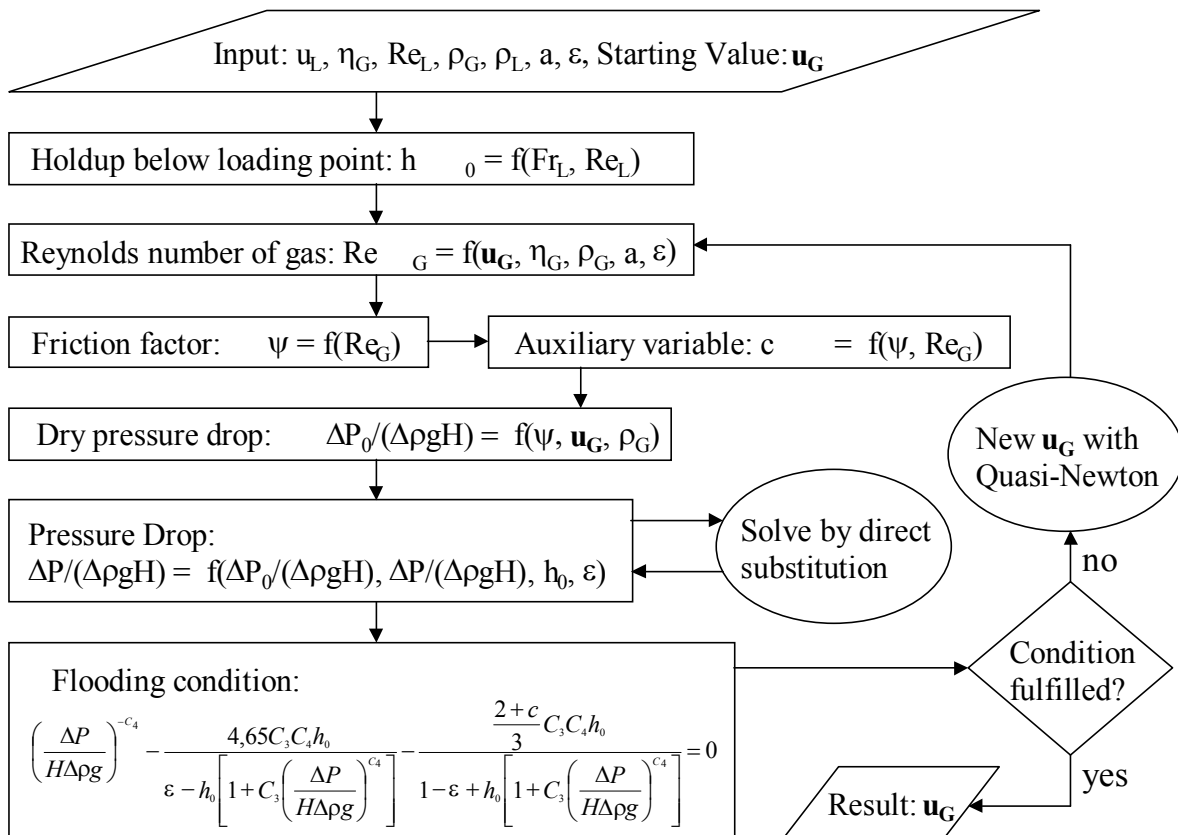


Figure 2. Flowsheet for the calculation of the flooding point.

## A UNIVERSAL EMPIRICAL APPROACH TO FLOODING

### A Falling Film At High Pressures

The flow regime of a falling film is an important asset for the design of gas-liquid contacting devices, because it determines the interfacial area, the rate of its renewal, and the mixing and backmixing of the liquid phase. In countercurrent annular flow the liquid flows downwards in different flow regimes: smooth, waves, crests, or droplets. The gas flows upwards and exerts a shear force on the liquid. The magnitude of this force depends on the momentum of the gas flow, its physical properties and the topology of the interfacial area. Both phases interact and this may lead to flooding if the annular area is too small to allow the countercurrent flow of both phases.

Film thickness, flow regimes, and flooding points for countercurrent annular flow of corn oil (Mazola<sup>TM</sup>) and carbon dioxide at 338 K and pressures between 7.6 and 20.6 MPa are examined experimentally. The film flows down a stainless steel rod with a diameter of 10 mm and a length of 1000 mm that is inserted in a glass tube with an internal diameter of 15 mm yielding an annulus of 2.5 mm. The film thickness adheres to Nusselt's equation [6] for smooth water films. With increasing liquid flow rate the falling film exhibits the following flow regimes: wavy film, troughs/crests on the film, drop formation, and flooding. The countercurrent gas flow affects the flow regime of the liquid film. The flooding points for the falling film column can be correlated with the same equation as the flooding points for packed columns with various packings and fluids at different states (high and ambient pressure).

### Film Thickness And Transition Between Different Flow Regimes

Nusselt's equation [6]  $\psi_L = \frac{6}{Re_L}$  describes the measured film thickness with acceptable accuracy. The borderlines between the flow regimes waves - troughs/crests and troughs/crests - drops can be shown in a  $Re_L$ - $K_F$ -diagram as suggested by Grimley [7]. The data for the crest-drop-transition can be described with decent accuracy using Moser's correlation [8]:

$$Re_L = 0.84 K_F^{0.18} \quad . \quad (9)$$

It is obvious that the gas flow has a significant impact on the flow regime of the liquid film. The gas flow exerts a shear force on the liquid film and this affects the shape of the interface, i.e., the flow regime.  $F_{shear} \approx \tau H d_H$ , where  $\tau$  is the shear stress,  $H$  the height of the film and  $d_H$  its hydraulic diameter, in this case the difference between rod diameter and inner diameter of the glass tube (5 mm). The gas flow exerts the following force on the liquid surface:

$F_{gas} \approx \Delta P d_H^2$ , where  $\Delta P$  is the pressure drop. If the shear force the gas exerts on the inner wall of the glass tube is neglected, a force balance yields:  $F_{gas} = F_{shear} \Rightarrow \tau \approx \Delta P \frac{d_H}{H}$ .

The shear stress in the liquid surface is proportional to the pressure drop. Rating the pressure drop to the impact pressure of the gas flow gives the dimensionless gas resistance

factor  $\psi_G$ :  $\psi_G = \frac{\Delta P d_H}{\rho_G (u_G - u_L)^2 H}$ , where  $u_G - u_L$  is the slip velocity. The influence of the gas

flow on the flow regime was taken into account by using the property  $Re_L(1+\psi_G)^n$  instead of  $Re_L$  as in Figure 3. For the exponent the value of  $n = 1/3$  yielded the best coincidence between transition points with and without countercurrent gas flow. The newly introduced ordinate appropriately accounts for the impact of the gas flow on the transition of the flow regimes.

### Flooding

For the correlation of the flooding points an approach dating back to Wallis [10] was employed.

$$j_G^* = f(j_L^*); \quad j_G^* = \frac{u_G}{\varepsilon} \sqrt{\frac{\rho_G}{g d_H (\rho_L - \rho_G)}}; \quad j_L^* = \frac{u_L}{\varepsilon} \sqrt{\frac{\rho_L}{g d_H (\rho_L - \rho_G)}} \quad (10)$$

With  $u_L$  for the superficial liquid velocity and  $\varepsilon$  the fractional void volume which is unity for a falling film column but smaller than unity for packed columns.  $j_G^*$  and  $j_L^*$  are modified Froude numbers rating the respective impact pressure to the difference between liquid head and buoyancy. Figure 6 shows that flooding diagram, which is only marginally different to that proposed by Sherwood *et al.* [9] where  $j_G^*$  is a function of  $\phi$ . Figure 4 displays various flooding data for packed columns for a variety of packings (Sulzer CY, Sulzer EX, Sulzer Mellapak, 5 x 5 x 0.5 mm Raschig rings, and 4 mm Berl saddles) and substances (water, air, carbon dioxide, olive oil deodorizer distillate, soybean oil deodorizer distillate, fatty acid methyl esters, and tocopherols) and the flooding data of the falling film column. A flooding point correlation as suggested by Wallis [10] was employed.

$$\sqrt{j_G^*} + K_1 \sqrt{j_L^*} = \sqrt{K_2} \Leftrightarrow j_G^* = \frac{K_2}{(1 + K_1 \sqrt{\Phi})^2} \quad (11)$$

with  $K_1$  and  $K_2$  as dimensionless parameters.

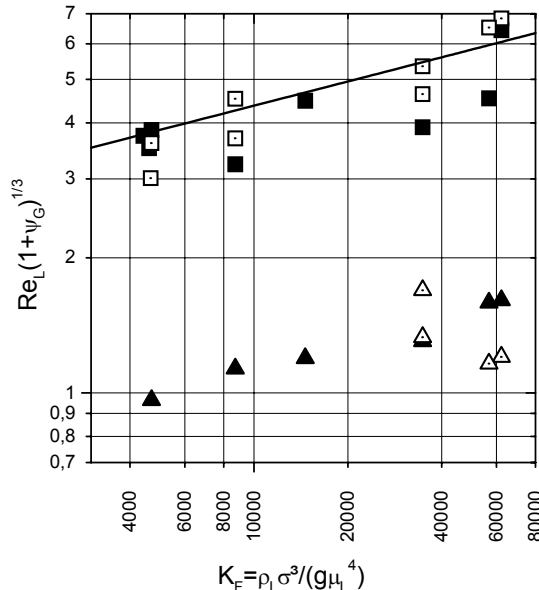
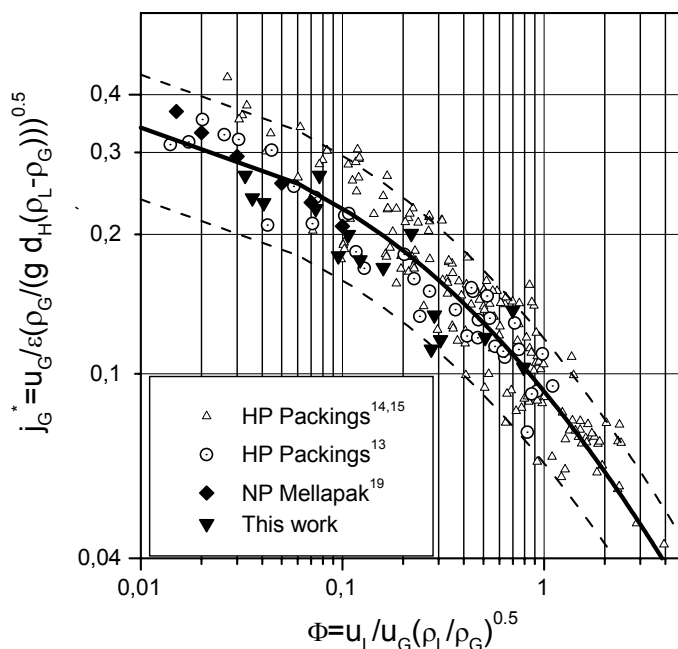


Figure 3. Flow regimes: New diagram accounting for shear stress. ■, drop formation without gas flow; □, drop formation with gas flow; ▲, crest formation without gas flow; △, crest formation with gas flow; line, Moser's correlation [8].

For the correlation of the data displayed in Figure 4, the values  $K_1 = 0,4222$  and  $K_2 = 1,1457$  resulted in a relative standard deviation of 19 %. This is an acceptable value, especially if considering that only one set of parameters for Equation 11 correlates the flooding points for a wide variety of geometries (structured packings, random packings and falling film columns), substances and states (temperature, pressure).

## CONCLUSIONS

Hydrodynamic behaviour of countercurrent columns at high pressure can be described with models developed for normal pressure if density of the gaseous phase is taken into account. This phase produces significant buoyancy that reduces the static head of the liquid. Dry pressure drop can be modeled with an Ergun-type equation. Liquid holdup below the loading point is correlated with one set of parameters of a two-parameter expression using the Reynolds and Froude numbers of the liquid phase. Falling film thickness can be described with the Nusselt's equation. Flooding points could not be predicted in general with a mechanistic model of solid physical background. A modified empirical flooding diagram from Sherwood, Shipley and Holloway and the flooding equation proposed by Wallis for vertical pipes are suitable to correlate the measured flooding points with sufficient accuracy.



*Figure 4. Flooding diagram. Thick line, correlation; dashed lines,  $\pm 30\%$  interval;  $\Delta$ , structured and random packings at high pressures;  $\circ$ , structured packings at high pressures;  $\blacklozenge$ , Mellapak<sup>TM</sup> at normal pressure;  $\blacktriangle$ , falling film flooding at high pressures.*

## REFERENCES

1. R. Stockfleth and G. Brunner (1999), *Ind. Eng. Chem. Res.*, **38**, 4000 - 4006.
2. R. Stockfleth and G. Brunner (2001), *Ind. Eng. Chem. Res.*, **40**, 347 - 356.
3. H. Rumpf and A. R. Gupte (1971), *Chem. Ing. Techn.*, **43**, 367 - 375.
4. S. Ergun (1952), *Chem. Eng. Progr.*, **48**, 89 - 94.
5. J. Stichlmair, J. L. Bravo and J. R. Fair (1989), *Gas Sep. Purif.*, **3**, 19 - 28.
6. W. Nusselt (1916), *Z. Verein Deutscher Ingenieure*, **60** (27), 151.
7. S. S. Grimley (1945), *Trans. Inst. Chem. Eng.*, **23**, 228.
8. M. Moser and C. Trepp (1997), *Chem. Eng. Technol.*, **20**, 612.
9. T. K. Sherwood, G. H. Shipley and F. A. L. Holloway (1938), *Ind. Eng. Chem.*, **7**, 765 - 769,
10. G. B. Wallis (1969), *One-Dimensional Two-Phase Flow*, McGraw-Hill, New York.



## A CASE STUDY OF AN INDUSTRIAL PACKED COLUMN DESIGN USING SINGLE DROP MASS TRANSFER DATA

P. Barnard, M. J. Slater\* and X.-P. Wu

A.H. Marks and Company Ltd., Bradford, United Kingdom  
\*University of Bradford, Bradford, United Kingdom

Drop mass transfer coefficients have been measured for an industrial extraction system in a rising drop column and a counter-current packed bed of 150 mm diameter, 1.8 m packing height. The drop interaction, break-up and coalescence in a packed column can all be expected to enhance the mass transfer coefficients by virtue of mixing of drop contents and because of shortening of drop life-times. However in this case drop mass transfer coefficients for the packed column had values corresponding to those for drops with long life-time with no evidence of enhancement. A marked sensitivity of calculations of coefficients to assumed average drop size is demonstrated. A model for mass transfer coefficients allowing for interfacial contamination suggested that rigid drop conditions were suffered. The design of a large diameter column was made more certain by the results obtained.

### INTRODUCTION

An industrial process has previously been successfully operated using several mixer-settlers. It was required to determine the possibility of using a packed column to reduce ground space requirements and to contain solvent safely. A programme of work on single drop mass transfer measurements and preliminary column design calculations to assess feasibility and costs was undertaken. This led to further limited pilot work on a counter-flow packed column.

### PRELIMINARY WORK

Equilibrium data were obtained at 32 and 50°C and were found to be favourable and independent of temperature. The distribution coefficient for the component to be recovered (solute concentration in solvent/concentration in aqueous, in g/L) was about 16 at low solute concentrations but much less at higher concentrations.

In order to carry out performance calculations various physical properties were measured – densities and viscosities at the two temperatures and interfacial tension at 30°C (Table 1). There was no reason to believe that any problems were posed by these properties.

Table 1. Physical properties.

Temperature	32°C	50°C
Aqueous density kg/m <sup>3</sup>	1168	
Solvent density kg/m <sup>3</sup>	874	
Aqueous viscosity, g/m.s	1.56	1.02
Solvent viscosity, g/m.s	0.53	0.45
Interfacial tension, mN/m	8.4	

Drop sizes were then estimated for the packed column using [1]

$$d_{32} = 1.0 (\gamma / g \Delta\rho)^{0.5} \quad (1)$$

giving a value of 1.7mm (at 32°C) with an uncertainty of about ± 20%. There will of course be a size distribution – the largest drops are not expected to exceed twice d<sub>32</sub>.

Drops of about this size were produced from glass needles at the base of an empty rising drop column. Drop terminal velocities were measured and for a drop of 1.9 mm the velocity was 67 mm/s. Using the correlation [2]

$$V_T = 0.249 d_{32} (g^2 \Delta\rho^2 / \rho_c \mu_c)^{0.33} \quad (2)$$

this value was adjusted to 60 mm/s for a drop of 1.7 mm. The characteristic velocity is less than the terminal velocity due to hindrance and was obtained using [3]

$$V_K = V_T [ 1 - (d_{32}/d_p)^{0.7} ]^{1.5} \quad (3)$$

assuming 25 mm Raschig ring packing, hence V<sub>K</sub> = 47 mm/s. Using the simplest possible slip velocity relationship [4]

$$V_{\text{slip}} = V_K (1 - x) \quad (4)$$

and a suitable flow ratio V<sub>d</sub> / V<sub>c</sub> = 0.33, a flooding hold-up of x<sub>f</sub> = 0.25 was determined. At 60% approach to flooding superficial velocities of V<sub>c</sub> = 8.2 mm/s and V<sub>d</sub> = 2.7 mm/s can be used. The full-scale column diameter calculated using the expected flow rate of aqueous phase was 0.6 m which was acceptable. Under these conditions the actual dispersed phase hold-up, x, would be 0.075 and the specific interfacial area 200 m<sup>2</sup>/m<sup>3</sup>.

The calculation of column height depends on having realistic kinetic data and specification of degree of extraction.

### SINGLE DROP MASS TRANSFER COEFFICIENTS

An empty jacketted column was set up for single drop rise mass transfer experiments. The column had three different rise heights, (305, 450 and 1200 mm) and a collection point 20 mm above the drop formation needle so that drop formation mass transfer was excluded. Several heights are needed to establish the time-dependency of the mass transfer coefficient. Two solvent drop sizes of 1.9 and 2.5 mm were used (it being difficult to produce small drops of exactly the right size, especially when small). Data were obtained at 32 and

50°C (Figure 1). The feed composition was altered from 8.3 wt% down to 1.5 wt% for some runs; a small reduction in the overall solvent-based mass transfer coefficient  $K_{os}$  was apparent as feed concentration decreased. Higher temperature gave significantly higher  $K_{os}$  values. The strong variation of  $K_{os}$  with contact time indicated that circulation conditions inside the drop dominate the mass transfer process since diffusion in spheres is an unsteady-state process. There was little dependence on drop size. The small degree of scatter is an indication of the reliability of the data.

Assuming a worst case and using  $K_{os}$  values expected for long contact times (> 20 s); the overall solvent-based transfer unit height  $H_{os}$  was estimated to be about 2.4 m at 32°C and 1.6 m at 50°C. (The drop contact time per transfer unit height is far longer than 20 s). If repeated drop break-up and coalescence were obtained in a packed column much smaller transfer unit heights would be anticipated but this effect cannot be predicted.

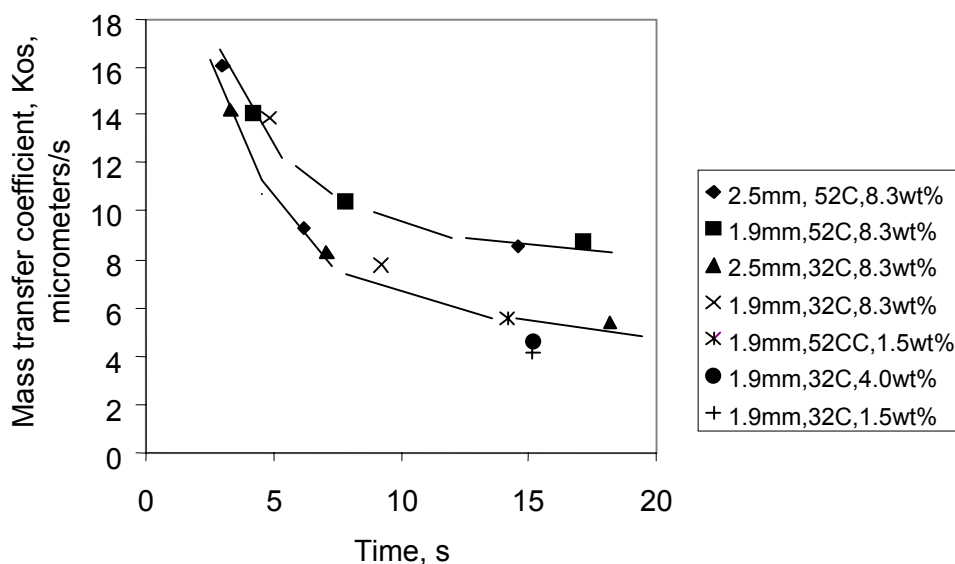


Figure 1. Rising drop mass transfer coefficients.

## NUMBER OF TRANSFER UNITS

For a feed of 8.3 wt% and a solvent/aqueous flow ratio of 1/3 the number of transfer units based on the solvent phase was calculated by graphical integration. For 98% extraction  $N_{os} = 2.25$  and for 99% extraction  $N_{os} = 3.24$ . The column heights estimated on the basis of single drop results ( $H_{os}$  values) were acceptable and gave reasonable column height/diameter ratios.

## PILOT COLUMN RESULTS

The packed column of 150 mm diameter, 1.8 m packed height initially contained stainless steel Mini-rings. The feedstock was taken from the production plant but cooling during transport caused solutes to crystallize out of solution. The feed was therefore reheated to 32°C prior to extraction. The first few trials at lower than the required flow rate showed sensible degrees of extraction with  $H_{os}$  of 3 to 4 m and calculated  $K_{os}$  values of 2 to 4  $\mu\text{m/s}$ . These  $K_{os}$  values were however lower than those indicated for single drops. There was also an unexpected problem with phase separation.

The phases disengaged at the top interface with a normal thickness of dispersion band of a few centimetres but above that a foam developed, carrying aqueous feed into the solvent product stream. Mild agitation with a simple paddle broke this foam. Foam formation was presumed to be due to the presence of interfacially active contaminants or solutes in the feed.

A further four runs at higher flow rate using ceramic packing were then carried out with better control over the feed condition and excellent mass balances. Transfer unit heights ranged from 3.6 to 4.6 m for different flow rates and ratios (Table 2). The derived overall mass transfer coefficients are shown in Table 3. Again it was found that values of  $K_{os}$  were much lower than for single drops when using the average drop size of 1.7 mm in calculations.

*Table 2. Mass transfer results for packed column  
1.8m ceramic packing, 32°C.*

Run	Aqueous flowrate L/min	Solvent flowrate L/min	$N_{os}$	$H_{os}$ m
1	3.3	1.00	0.46	3.9
2	5.5	3.25	0.39	4.6
3	10.4	3.89	0.50	3.6
4	8.3	3.09	0.50	3.6

## DISCUSSION

In view of the uncertainty over drop size estimation, calculations were also made using physical property data that were more accurately determined for liquids at each end of the column. Densities and viscosities varied slightly with composition and interfacial tension had dropped to 6.8 mN/m from 8.4 mN/m. Visually drops appeared to be in the 1 to 3 mm size range; average drop sizes of 1.4 and 2.0 mm were arbitrarily assumed (with adjustments to  $V_T$  and  $V_K$ ) and column  $K_{os}$  values recalculated. The values are rather sensitive to average drop size and for an assumed value of 2 mm they were close to single drop values for long contact time (Table 3 and Figure 1).

*Table 3. Mass transfer coefficients for packed bed.*

Run	$V_c$ , mm/s	$V_d$ , mm/s	$K_{os}$ , $\mu\text{m}/\text{s}$		
			$d = 1.4 \text{ mm}$	$d = 1.7 \text{ mm}$	$d = 2.00 \text{ mm}$
1	3.06	0.92	2.0	3.0	5.5
2	5.06	3.00	1.5	2.4	4.3
3	9.58	3.58	1.5	2.4	4.7
4	7.64	2.85	1.9	2.8	5.1

The prediction of drop size is clearly an important issue in estimating performance of the column. The data for this case suggested that little internal drop mixing was present and that drop life-time was long enough to allow the assumption that any break-up / coalescence that occurred did not enhance the mass transfer coefficients.

Arbitrary variation of an index on the term  $(1-x)$  in the slip velocity relationship as proposed by Godfrey and Slater [4] has no impact on calculations since the hold-up  $x$  is less than 0.15.

Axial mixing in both phases has been neglected since in a column of 150 mm diameter the effects are small and other uncertainties noted above are more significant. Correction for the adverse effects of axial mixing should be made in designing a large diameter column, particularly if a very high degree of extraction is to be specified.

Fitting of a combined mass transfer coefficient model [5] to the data indicated that there was a high degree of "contamination" with near-stagnant drops in the size range used. This could explain the observed lack of extensive coalescence between drops.

## CONCLUSIONS

From the data obtained prediction of column height for 98% and 99% extraction can be made with confidence. However, the prediction of a packed column performance depends sensitively on average drop size estimation. To make better predictions study of the drop breakage rate in packed columns is desirable and feasible; measurement of coalescence rate is also needed but is not easily done. The comparison of single drop mass transfer coefficients and those in a packed bed is perhaps the best, if pragmatic, approach to understanding the exceedingly complex role of drop break-up and coalescence processes. In the particular case studied there seemed to be no evidence of mass transfer enhancement by packing; modelling of the single drop mass transfer coefficient data suggests that drops are rigid in condition and so not amenable to coalescence.

The combination of limited work on single drops and a pilot column is very helpful in giving confidence in design and the use of the column can reveal unsuspected operating problems. In future similar work the replacement of pilot column tests with two-phase counter-flow tests with batch circulation of phases to equilibrium using a short section of column is advocated as a sensible approach so that relevant data can be obtained and problem-resolving can be achieved at low cost.

## ACKNOWLEDGEMENTS

We gratefully acknowledge the permission of A.H. Marks and Company Ltd. to publish the generic results of this commercial investigation.

## NOMENCLATURE

d	drop diameter, m	$V_c$	continuous phase superficial velocity, m/s
$d_{32}$	Sauter mean drop size, m	$V_{slip}$	slip velocity, m/s
$d_p$	packing size, m	$V_K$	terminal velocity, m/s
g	gravitational acceleration, m/s <sup>2</sup>	$V_T$	characteristic velocity, m/s
$H_{os}$	height of transfer unit based on solvent phase, m	x	dispersed phase hold-up
$K_{os}$	overall solvent phase mass transfer coefficient, m/s	$x_f$	dispersed phase hold-up at flooding
$N_{os}$	number of transfer units based on solvent phase	$\Delta p$	density difference, kg/m <sup>3</sup>
$V_d$	dispersed phase superficial velocity, m/s	$\rho_c$	continuous phase density, kg/m <sup>3</sup>
		$\mu_c$	continuous phase viscosity, kg/m.s
		$\gamma$	interfacial tension, N/m

## REFERENCES

1. P. J. Bailes, J. Gledhill, J. C. Godfrey and M. J. Slater (1986), *Chem. Eng. Res. Des.*, **64**, 43-55.
2. T. Misek and J. Marek (1970), *Brit. Chem. Eng.*, **15**, 202-207.
3. Z. Fan, J. O. Olöidi and M. J. Slater (1987), *Chem. Eng. Res. Des.*, **65<sub>1</sub>** (3), 243-250.
4. J. C. Godfrey and M. J. Slater (1991), *Trans. Inst. Chem. Eng., Part A*, 130-141.
5. M. J. Slater (1995), *Can. J. Chem. Eng.*, **73**, 462-469.



## INDUSTRIAL APPLICATIONS OF CENTREK CENTRIFUGAL EXTRACTORS

Kuznetsov G.I., Pushkov A.A. and Kosogorov A.V.

Research and Development Institute of Construction Technology (NIKIMT), Moscow, Russia

This paper describes the design and technical characteristics of CENTREK centrifugal extractors and their industrial applications. These include enriched uranium purification, natural uranium, Zr, Hf, Sm, Re production, copper electrolyte purification, copper extraction from ammonical etching solutions and medicine production. The processes tested on pilot scale are also discussed.

### CENTREK CENTRIFUGAL EXTRACTORS

In centrifugal extractors intense mixing is combined with subsequent separation of the emulsions under the action of centrifugal forces hundred times that of gravity to make it possible to achieve a high capacity with a relatively small piece of equipment. Therefore they are applied in industry for processes requiring short residence time of solutions because of radiolytic solvent decomposition or changing product properties with time, for processes requiring the restriction of the solvent volume (for reasons of nuclear safety, expense and fire hazard), for processes which use viscous liquids with small difference in density that are prone to emulsification and for processes where it is possible to use the difference in the extraction rate of components to improve their separation.

The NIKIMT have developed various modifications of CENTREK centrifugal extractors for fast and slow mass transfer rate processes (EC type), in single-stage and blocks, with phase recirculation, for radiochemical processes remotely controlled by manipulators or robots (ECR type), and for operation with solutions containing solid contaminants (ECK type) [1]. The units most extensively used in industry are centrifugal extractors with a conical rotor (Figure 1). The technical characteristics of these ECK type extractors are given in Table 1.

The extractor operates as follows: feed solutions are fed to the mixing chamber (1) where they are mixed by stirrer (2). The emulsion thus formed is transferred by screw conveyer (3) to a rotor (7) where it is separated under the action of centrifugal forces. Separated liquids are directed into circular collectors (5) of the fixed body (4) and then gravitate out of the extractor. The conical shape of the rotor and special design hydrolock (6) with activator (5) promote the continuous removal of solid contaminants from the rotor together with heavy phase. The apparatus design allows the change of phase contact time by changing the volume of the mixing chamber. Engineering design of extraction processes requires the combination of single stage centrifugal extractors in multistage cascades with commutating tubes.

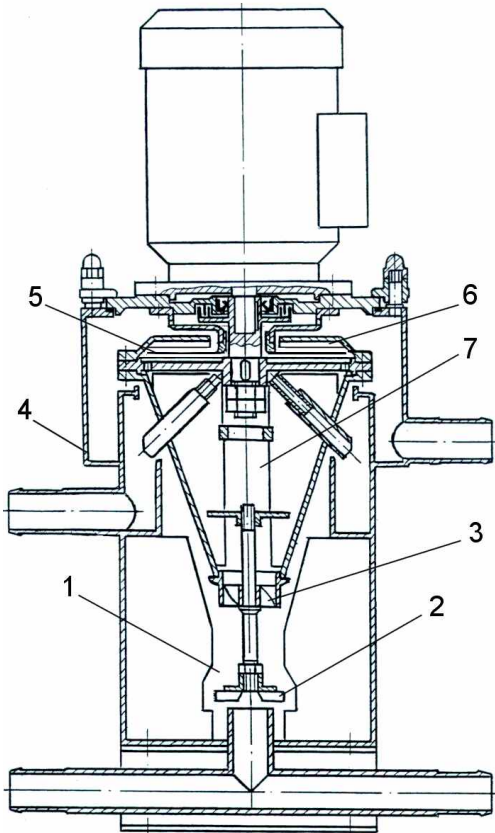


*Figure 1. CENTREK centrifugal extractor.*

*Table 1. Specifications of ECK type CENTREK centrifugal extractors.*

	ECK100	ECK 125	ECK 140	ECK 160	ECK 200T <sup>**</sup>	ECK 280	ECK 320
D*, mm	100	125	140	160	200	280	320
N, s <sup>-1</sup>	25	25	25	25	25	25	25
Q, m <sup>3</sup> /h	0.40	0.60	0.9	1.3	2.5	7.0	10
V <sub>s</sub> , L	0.35	0.90	1.2	2.1	3.5	7.0	11
V <sub>m</sub> , L	0.73	0.7	1.25	2.2	2.3	6.0	18
P, W	180	370	370	750	1500	3 000	3 000
I, mm	300	260	294	333	420	513	620
B, mm	240	265	240	280	365	500	675
H, mm	590	590	618	727	900	1 350	1 648
M, kg	18	20	24	50	37	260	340

\*D- rotor diameter; N-rotation speed; Q-capacity for system of 1 M TBP in kerosene – 2 M HNO<sub>3</sub>, for the ratio of flow rate equal to 1 and emulsion type – “oil in the aqueous phase”; V<sub>s</sub>, V<sub>m</sub>-volume of the separation and mixing chambers, respectively; P-drive output; I,b,h-length, width, height, respectively; m-mass of the extractor; \*\* - made of titanium.

To assemble the cascades easier the modules of three and more single stage extractors were developed. The block design was also developed [1]. Commutating channels between stages and mixing chambers are integrated into the apparatus body. The block extractor is designated for processes with slow mass transfer rates.

CENTREK centrifugal extractors are simple in service and reliable in operation. This is achieved making use of vibroinsulators, the application of conical shape of rotor and the related location of the center of the rotating mass in the zone of the bearing support.

### PURIFICATION OF ENRICHED URANIUM FOR FUEL ELEMENT FABRICATION [2,3]

For more than 30 years enriched uranium purification, especially for high grade, has been carried out with centrifugal extractors. They are also used for the recovery and purification of enriched uranium from scrap and residue of fuel element fabrication. A process flow sheet with EC100 extractors is shown on Figure 2. Presently, more than 200 extractors are in operation at several plants. An automated process control system is used in their operation. The use of centrifugal extractors together with the process control system allows a reduction to one tenth of the normal solution volume inventory and thereby to improve nuclear safety.

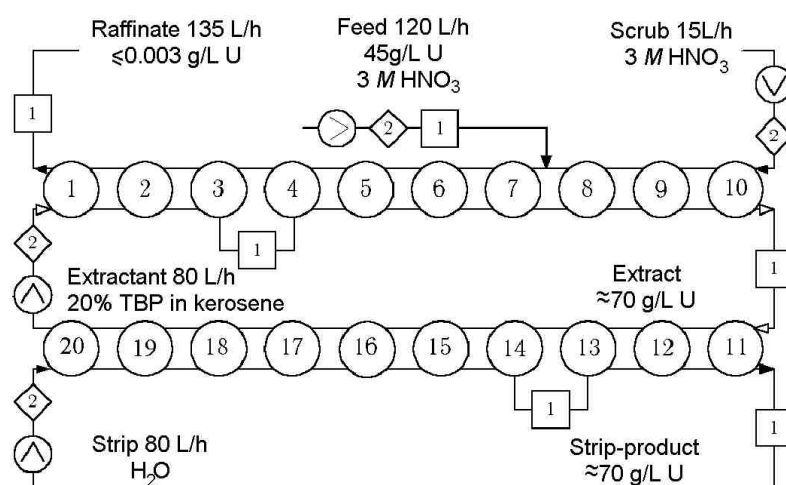


*Figure 2. Flow sheet of enriched uranium purification: [1] – concentration detector, [2] - flowmeter, (>) – pneumatic valve.*

### PROCESSING URANIUM ORE SOLUTIONS [1]

The four-stage block type extractor with a 400 mm rotor diameter is used for this process. During the commercial tests 10 000 m<sup>3</sup> sulfuric acid desorption solutions were processed. They contained 4 000 kg solid contaminants and an average flowrate was 22 m<sup>3</sup>/h. Extractant: Di(2-ethylhexyl)phosphoric acid (DEHPA) – 50 g/l, TBP – 25 g/l, Trialkylamine (TAA) – 12 g/l.

During the operation dynamic equilibrium is established in the apparatus. The quantity of contaminants in solutions on entrance to the apparatus is equal to their quantity on exiting. The use of centrifugal extractors allows the reduction of the working area, volume of solutions in the process as well as to considerably improve fire safety.

### RARE-EARTH ELEMENTS PRODUCTION [2,4]

The technology is complicated by the difficult conditions of separation of the emulsions because of the high viscosity (up to 0.04 Pa·s) and a small difference in the densities (not over 0.02 g·cm<sup>-3</sup>) of the solutions, as well as the low separation coefficients of adjacent rare-earth (RE) elements (about 1.5-2.0), which necessitates a large number of stages (up to

100). For example, a cascade of EC125 type centrifugal extractors have been used for more than 15 years for samarium production from a middle-group RE-concentrate (Figure 3). It was necessary to take into account the effect of phase entrainments on process performance. Increasing entrainments are observed in the parts of the cascade where the difference in phase densities is smallest. Admissible entrance on extraction should not exceed 1%, but on strip stage entrainments more than 1% have no effect on technological performances of the process, as samarium purification is ended on the scrub stage.

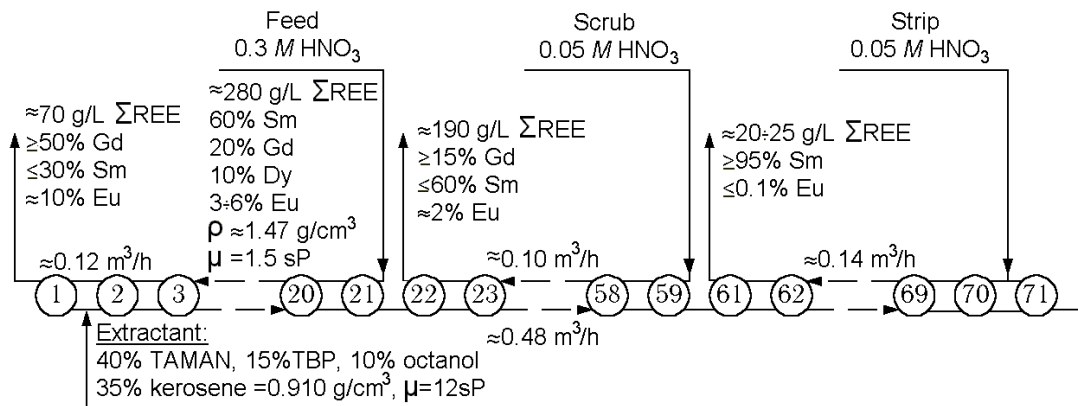


*Figure 3. Flow sheet of samarium production from RE concentrate.*

Fifteen-year experience of industrial operation showed high reliability of centrifugal extractors and their stable operation in very complicated conditions of given technological processes.

## ZIRCONIUM AND HAFNIUM PRODUCTION [2,5]

A flow sheet for nuclear-grade zirconium production that has been used for more than 25 years is shown as Figure 4. The primary removal of Zr and Hf from bulk impurities is achieved in their co-extraction (stages 1-8) and the removal of Hf and a number of limiting contaminants (Al, Cr, Cu, Ti, Fe, Si and others) is achieved with scrubbing (stages 9-23). EC250 extractors are used in all operations except stages 33-38 where EC125 extractors are used for complete Zr extraction. The Zr decontamination factor in the scrubbing operation notably depends on the flow ratio of organic to scrubbing solutions, as well as on the entrainments of aqueous phase. For example, decreasing flow ratio O/A from 5 to 4 increases the decontamination factor from 200 to 1 800, and increasing the entrance of aqueous phase to organic one from 0.005 to 0.5% decreases the decontamination coefficient from 1 600 to 300, when O/A=4. The proper choice of value and direction of entrainments allows the capacity of the extractors to be increased without deterioration of overall performance. The flow sheet of Hf production differs negligibly from the Zr one. Hf strip product solution is used as feed solution and ECK160 extractors are used.

## RHENIUM EXTRACTION [6]

For the extraction and concentration of rhenium three EC250 units are used for extraction and one EC125 unit is used for stripping. Extractant: 30% TAA, 10% octanol and kerosene. Ammonium hydroxide solution is used for stripping. A concentrating ratio of more than 100 is achieved. Extraction from sulfuric acid solutions has also been successfully tested [7].

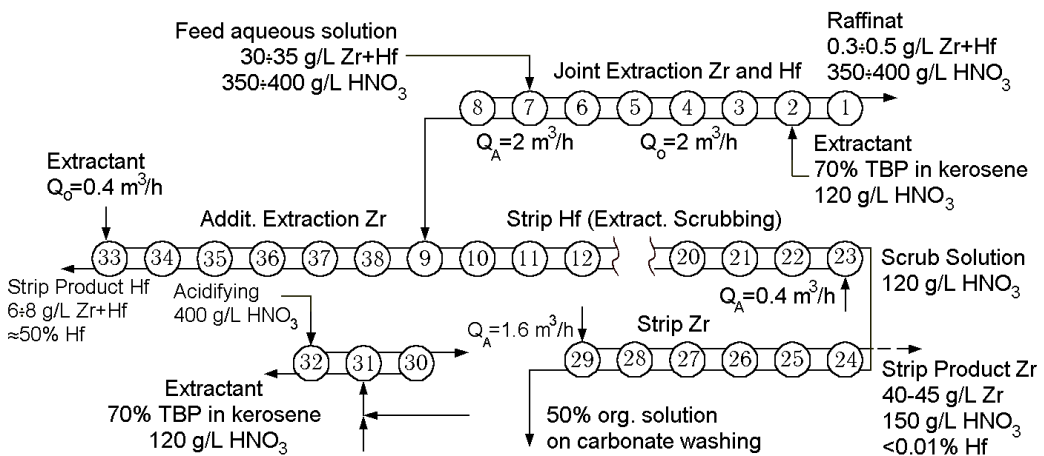


*Figure 4. Flow sheet of production of nuclear grade zirconium.*

### ARSENIC REMOVAL FROM COPPER ELECTROLYTE [8]

For this process 6 centrifugal extractors (4 on extraction and 2 on stripping) are used for arsenic removal to purify copper electrolyte. Electrolyte after correction of  $\text{H}_2\text{SO}_4$  concentration to 170-180 g/l is decontaminated by 100% TBP. Water is used for stripping. TBP is periodically scrubbed from its hydrolysis products with soda solution. Fine electrolytic copper is prepared from the strip product solution.

### COPPER EXTRACTION FROM AMMONIACAL ETCHING SOLUTIONS (MECER-PROCESS) [9]

Copper extraction and keeping its concentration in etching solutions up to optimal limits of 100-130 g/l is carried out by the MECER-process in which the expensive extractant LIX-54 is used. The replacement of mixer-settlers with CENTREK centrifugal extractors of type ECK140 (titanium construction) allows a ten-fold decrease in the extractant volume and improves the compactness of the MECER unit. Six MECER units with CENTREK centrifugal extractors have been in operation in France, Slovenia and Norway since 2000.

### MEDICINE PRODUCTION [10,11]

In antibiotic production a number of problems have to be overcome concerning the formation of poorly separating emulsions, the use of extractant easily dissolved in water, the decomposition of products in time, and, the presence of solid contaminants in solutions. These problems have been successfully solved by employing CENTREK centrifugal extractors. In these solid contaminants are removed together with the aqueous phase, and emulsification and phase contact time are kept to a minimum. Besides considerably improved working conditions of the operation staff due to the hermetic nature of the apparatus and the decreased frequency of their cleaning from precipitates. Compared with the existing process the use of the cascade of 6 CENTREK centrifugal extractors allows a decrease of the consumption of extractant by half and an increase of the antibiotic concentration by 6 times (to 30 000 mg/l). Therefore the evaporation stage has been eliminated. The product yield increased, its quality improved and technological time shortened by half. Similar positive results have been obtained in the extraction and purification of flaminium and kaleflonium from vegetable sources [12]. The industrial production of amino acids was started in July 2001 [13].

## PILOT-SCALE INVESTIGATIONS

The industrial applications of CENTREK centrifugal extractors are testimony to the success of this technology. Pilot-scale tests that have been conducted show that there is a good potential for further applications of CENTREK centrifugal extractors in industry. The processes tested include: reprocessing fast breeder reactor spent fuels [14,15], UNEX process for long-lived fission products, cesium, strontium, transplutonium elements from liquid radioactive wastes [16], sewage purification [17] and nickel and cobalt separation [18,19].

## REFERENCES

1. G. I. Kuznetsov, A. A. Pushkov and A.V. Kosogorov (2000), CENTREK Centrifugal Extractors, Mendeleev University of Chemical Technology of Russia, Moscow, 213 pp.
2. G. I. Kuznetsov, A. V. Kosogorov, A. A. Pushkov, A. V. Savin and N.N. Trusilov (1992), *Proc. 2nd Int. Conf. Hydrometallurgy. ICHM '92*, Vol. 2, Changsha, China, pp. 801-806.
3. G. I. Kuznetsov, A. V. Kosogorov, A. A. Pushkov, A. M. Belintsev and L. V. Maslov (1999), *Czech. J. Phys.*, **49**. Suppl. S1., 937-941.
4. G. I. Kuznetsov, A. V. Kosogorov, A. M. Chekmarev and A. A. Pushkov (1995), *Proc. Int. Conf. Rare-earth metals*, Krasnoyarsk, pp. 161-165.
5. G. I. Kuznetsov, V. S. Skachkov, A. V. Kosogorov, A. M. Chekmarev and A. A. Pushkov (1996), *Proc. ISEC '96*, Vol. 2, University of Melbourne Press, Melbourne, pp. 1257-1261.
6. G. I. Kuznetsov, A. A. Pushkov, V. T. Soldatenkov and A. D. Fedotov (1993), *Proc. Conf. Intensification of Processes of Chemical and Food Industry. Processes – 93*, Vol. I, Tashkent, pp. 40-44.
7. V. P. Lanin, E. I. Chebrikina, A. A. Pushkov, G. I. Kuznetsov, Yu. M. Nikolaev, A. V. Savin, A. K. Zhalimbetov and A. K. Tulekbaeva (1993), *ISEC '93*, Vol. 1, Society of Chemical Industry, London, pp. 218-224.
8. V. V. Kalujta, G. I. Kuznetsov, A. N. Kravchenko, V. P. Lanin, G. P. Miraevsky, A. A. Pushkov, V. F. Travkin and L. I. Shklyar (1988), *ISEC '88*, Vol. IV, Moscow, pp. 252-254.
9. S.O.S. Andersson and H. Reinhardt (1983), Handbook of Solvent Extraction, John Wiley & Sons, Inc., pp. 751-763.
10. G. I. Kuznetsov, A. A. Pushkov, A. V. Kosogorov and M. I. Semenov (1993), *J. Appl. Chem.*, **6** (10), 2258-2262.
11. G. I. Kuznetsov, A. A. Pushkov, A. V. Kosogorov and M. I. Semenov (1994), *Proc. Int. Conf. Separations for Biotechnology 3*, London, pp. 255-259.
12. L. I. Shklyar, G. I. Kuznetsov, A. A. Pushkov, V. I. Emeljanov and I. S. Chernishov (1992), *Proc. ISECOS' 92*, Voronezh, pp. 413-414.
13. Z. I. Kuvaeva (1999), PhD thesis, Byelorussian Academy of Sciences.
14. G. I. Kuznetsov, N. V. Glasunov, A. A. Pushkov and E. V. Renard (1991), *Proc. RECOD'91*, Vol. 2, Sendai, Japan, pp. 770-774.
15. A. S. Nikiforov, B. S. Zacharkin, E. V. Renard, A. M. Rosen, V. S. Vlasov, E. A. Filippov, A. A. Pushkov, G. I. Kuznetsov and E. Ya. Smetanin (1988), *Proc. ISEC '88*, Vol. IV, Moscow, pp. 168-174.
16. J. D. Law, R. S. Herbst, K. N. Brewer, T. A. Todd, V. N. Romanovskiy, V. M. Esimantovskiy, I. V. Smirnov, V. A. Babain, G. I. Kuznetsov and L. I. Shklyar (1998), Report INEL/EXT-98-00544, Lockheed Martin Idaho Technologies Co.
17. G. I. Kuznetsov and A. A. Pushkov (1993), *Proc. XV Mendeleev Congress of Common and Applied Chemistry*, Nauka and Technica, Minsk, pp. 175-176.
18. V. P. Lanin, A. A. Pushkov, G. I. Kuznetsov, V. T. Soldatenkov, L. I. Shklyar, A. N. Kravchenko and V. F. Travkin (1986), *Proc. Mendel. Inst. Chem. Techn.*, (143), 48-54.
19. A. A. Pushkov, V. P. Lanin and V. F. Travkin (1985), *J. Nonferr. Met.*, (11), 1-26.



## SIEVE TRAY EXTRACTORS: A CLOSER LOOK AT CAPACITY LIMITATIONS

Frank Seibert, James R. Fair and Jose L. Bravo\*

Separations Research Program (SRP), The University of Texas at Austin, TX, USA

\*Shell Global Solutions International, Amsterdam, The Netherlands

Sieve tray extractors continue to be highly utilized in the chemical and petrochemical industries. The trays are inexpensive, simple and have demonstrated the ability to handle very high throughputs. Their mass transfer efficiency, while somewhat limited, is often adequate and may be compensated for by a modest increase in the solvent to feed ratio. However, the tray hydrodynamics are very complex and not well understood, especially in large diameter columns. As a result, expected throughputs may not be realized. Unfortunately, use of a single model or correlation developed from laboratory-scale equipment to predict sieve tray flooding velocities would likely be unreliable. A close look reveals that there are six significant and distinct mechanisms that limit capacity. These mechanisms have been observed in the Separations Research Program (SRP) 10.2- and 42.8-cm diameter extractors and have also been reported by SRP industrial sponsors. The objective of this paper is to address briefly the important mechanisms that limit capacity of sieve tray extractors. A collateral objective is to familiarize process engineers with these mechanisms.

### INTRODUCTION

Sieve trays are often used for continuous extraction processes in the chemical and petrochemical industries. The sieve tray extractor is simple in design, requires no moving parts, reforms drops at every tray, reduces backmixing and can handle some slurries. The extraction column consists of a series of perforated plates that are connected by downcomers (or upcomers). The perforations are designed to pass the dispersed phase and the downcomers (or upcomers) are to pass the continuous phase. A completely coalesced layer is supposed to exist underneath the tray (light-phase dispersed) for the purpose of reforming drops and preventing backmixing of the continuous phase.

The hydraulic mechanisms involved in flooding of sieve tray extractors are not clearly understood, especially for larger diameter columns. While very little has been reported on the hydraulic performance of large-scale sieve tray extractors, three studies using larger equipment have been reported by Ololidi *et al.* [1], Seibert and Fair [2] and Eldridge and Fair [3]. An example of sieve tray flooding data is illustrated in Figure 1. Sieve tray flooding studies have been carried out at the SRP using 10.2- and 42.8-cm diameter columns, often with mixtures of industrial importance, indicate that there are six distinct mechanisms that can limit tray capacity:

- Spray column flood (ultimate capacity);
- Large height of coalesced layer at one or more trays (from high orifice and/or downcomer pressure drop, or entrainment into downcomer);
- Inadequate drop coalescence at main operating interface;
- Cross-flow velocity of the continuous phase/length of flow path;
- Poor interface control.

This paper addresses briefly each of the flooding mechanisms.

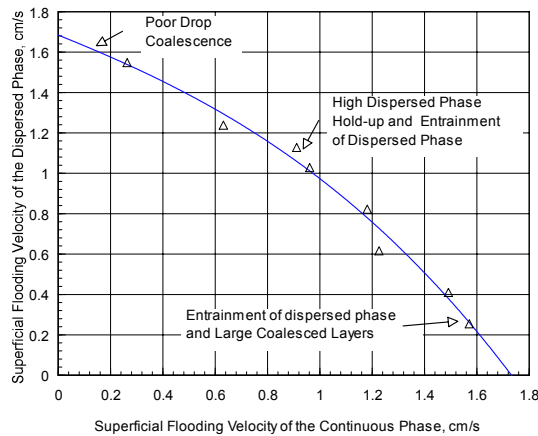


Figure 1. Sieve tray flooding data. System: toluene (d) / water (c). Tray spacing = 30.5 cm. Column diameter = 42.8 cm.

## FLOODING MECHANISMS

### Spray Column Flood

The ultimate capacity of a tray extractor will approach that of a spray column. A flooding model developed at the SRP with supporting experimental data is provided in a previous publication [2]. The capacity of the spray column is generally limited by entrainment of dispersed phase by the continuous phase, or vice versa. As a result of a distribution in drop sizes, entrainment of smaller drops is the most common mechanism of flooding in a spray column. In larger diameter columns, tray capacity may exceed that of a large diameter spray column depending on the phase flow ratio and the degree of continuous phase recirculation. Spray column axial mixing experiments at the SRP have indicated that the actual velocity of the continuous phase can be increased by backmixing [4]. These experimental studies indicate that the interstitial continuous phase velocity can be increased by a factor of 25 for  $U_c/U_d$  of 0.05. Nevertheless one would expect the maximum capacity of a sieve tray extractor to approach that of a spray column free of backmixing.

### Large Height of the Coalesced Layer

The performance of a sieve tray extractor is strongly influenced by the height of the coalesced layer below (light-phase dispersed) or above (heavy-phase dispersed) the tray. The height will depend on the pressure drop through the sieve holes and downcomer along with the density difference. As discussed in the paper by Mewes and Kunkel [5], the height also depends on the dispersed phase hold-up in the drop rise region, downcomer length, and possible dispersed phase hold-up in the downcomer. Their generalized model assuming no dispersed phase in the downcomer is given in Equation 1.

$$h = \frac{(\Delta P_o + \Delta P_{dow})}{(\rho_c - \rho_d)g(1-\phi_d)} - \frac{\phi_d}{(1-\phi_d)} Z_d \quad (1)$$

The pressure drop through the sieve holes may be estimated using the model of Pilhofer [6]. The downcomer (or upcomer) pressure drop may be estimated using the model of Major and Hertzog [7]. In addition, the rigorous model developed by the SRP, which not only accounts for expansion and compression but also for frictional losses, may be used. Experimental verification of the coalesced height model is provided in an SRP Technical Report [8]. The two downcomer pressure drop models are very similar except the SRP model includes frictional losses that are important for viscous systems and with trays having long downcomers (upcomers). The SRP downcomer pressure drop model is also applicable when the inlet and outlet areas are different.

$$\Delta P_{dow} = \rho_c \left[ 0.75U_1^2 + U_2^2 + 0.5 \left( \frac{f_1 L_1 U_1^2}{d_1} + \frac{f_2 L_2 U_2^2}{d_2} \right) \right] \quad (2)$$

$$Z_d = L_1 + L_2 \quad (3)$$

$$Re \left( \frac{\rho_c U_{dow} d}{\mu_c} \right) < 3,000 \quad (\text{laminar flow}) \quad f = \frac{64}{Re} \quad (4)$$

$$Re \left( \frac{\rho_c U_c d}{\mu_c} \right) > 3,000 \quad f = -0.0071 \ln\{Re\} + 0.1 \quad (5)$$

Large coalesced layer heights will result in reduced mass transfer and control of the main operating interface. Ideally, for commercial-scale columns, the design height should be limited to approximately 2.5 cm. In addition, the designer should be careful to include an allowance for flow variations in the column and their effect on coalesced layer height fluctuations and on interface control.

### Inadequate Drop Coalescence

The capacity of a tray extractor may be limited by insufficient drop coalescence at the main operating interface, which results in significant carryover of continuous phase. Generally, an uncoalesced layer will cause problems for the interface sensor and will likely exit the column carrying with it a significant quantity of continuous phase trapped between the uncoalesced drops. This method of flooding has become common with columns having high dispersed-to-continuous phase flow ratios and whose rates have increased significantly beyond their original design point. The presence of surface-active contaminants can also promote the formation of an uncoalesced layer. Studies at the SRP show that the critical superficial dispersed phase velocity ( $U_{df,uncoal}$ ), which may result in the formation of a large uncoalesced layer, can be estimated from the characteristic drop velocity ( $U_{so}$ ) obtained using the model of Grace and co-workers [9].

$$U_{df,uncoal} \approx 0.12 \bullet U_{so} \quad (6)$$

The formation of the uncoalesced layer is a result of the rate of drop coalescence being slower than the rate of drop arrival at the interface. One method of eliminating or minimizing the height of the this layer is to use a larger column diameter section in the region of the main operating interface, to create additional interface area for coalescence. A more cost-

effective remedy may be to add structured packing to the interface region. However, to promote coalescence the packing must be preferentially wetted by the dispersed phase and should be relatively open to allow counterflow of the coalescing phases. In a hydrocarbon/water system, hydrocarbon will generally preferentially wet a hydrophobic surface like Teflon while water will generally preferentially wet a less-hydrophobic material such as stainless steel. The effectiveness of a Type 2 Teflon structured packing to reduce the height of uncoalesced layer and extend column capacity is shown in Figure 2 [10]. Additional experimental data may be found in the study of Schober [10]. In the example, n-hexane is dispersed into a continuous water phase.

### High Cross Flow of the Continuous Phase

Pilot tests of sieve tray extractors are often performed prior to final design of the commercial-scale column. The design is often scaled-up based on superficial velocities of the dispersed and continuous phases calculated from the volumetric flow rates and the column cross-sectional area. However, in scaling up one must be careful about the cross-flow velocity ( $U_{c\text{flow}}$ ) of the continuous phase, the value of which may be estimated by Equation 7.

$$U_{c\text{flow}} \approx \frac{D_{\text{col}}}{Z - h} U_c \quad (7)$$

With regard to scale-up, larger diameter extractors will exhibit a greater amount of internal circulation within a tray. A high degree of continuous phase circulation was observed and reported in the larger-scale study of Eldridge and Fair (3). These effects were especially pronounced at high dispersed-to-continuous phase flow ratios. The high cross-flow continuous phase velocity will lead to a velocity vector associated with the drop as shown in Figure 3.

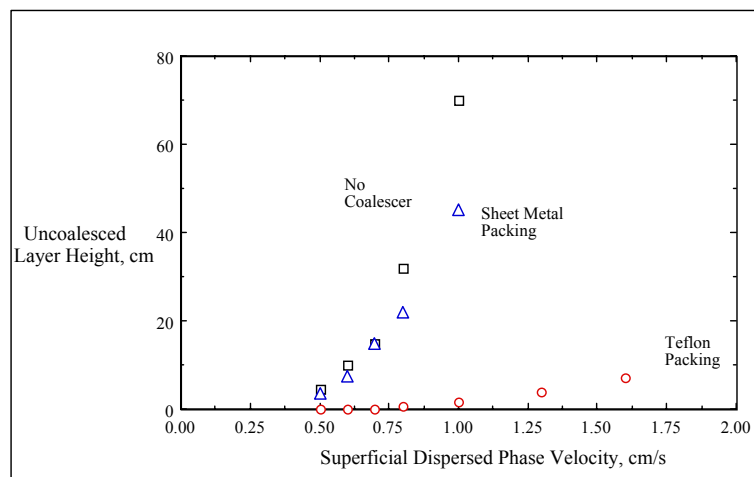


Figure 2. Effects of a teflon coalescer [10]. System: hexane (d) / water (c).

The cross flow velocity and the additional drag reduce the  $j$  component of the characteristic drop velocity. As a result the capacity will likely be equivalently reduced.

$$U_{so} = U_{so,i} + U_{so,j} \quad (8)$$

The characteristic drop velocity in the  $j$  direction may be calculated implicitly from

$$U_{so,j}^2 = U_{so}^2 \frac{1}{\sqrt{1 + \left(\frac{U_{so,i}}{U_{so,j}}\right)^2}} - U_{so,i}^2 \quad (9)$$

where:  $U_{so,i}$  = cross-flow velocity, cm/s

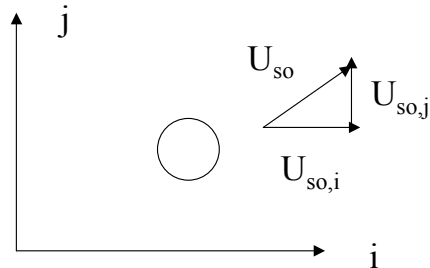


Figure 3. Characteristic drop velocity vector.

The effect of the flow path length phenomenon has been observed empirically in large-scale industrial extractors where more hydraulic capacity is achieved by shortening the flow path of sieve trays and increasing the number of passes. The use of multiple upcomers or downcomers will result in a lower cross-flow velocity and therefore reduce the overall drag force on the drop. Large diameter multiple upcomer trays have been shown to provide 10-15% greater capacity relative to the single pass tray.

#### Poor Interface Control

Poor control of the main operating interface is another cause of flooding. As shown in Figure 4, the position of this interface is often controlled by adjusting the heavy phase outlet flow from the extractor. If an adjustment of the interface level is required, the valve will open to lower the level or close to raise the level. As the valve changes, the internal flows change with resulting change in the coalesced layer height. Unfortunately, depending on the relative pressure drops (orifice versus downcomer), the height may increase or decrease until reaching a steady value. This results in a response lag which in many cases will cause the interface to move initially in the wrong direction. Such an inverse response may cause the operator to over-react and re-adjust the valve, which in turn can cause a coalesced layer flood as discussed earlier. The ability to measure the heavy phase outlet flow rate can be extremely beneficial in controlling the interface position and preventing an accidental flood.

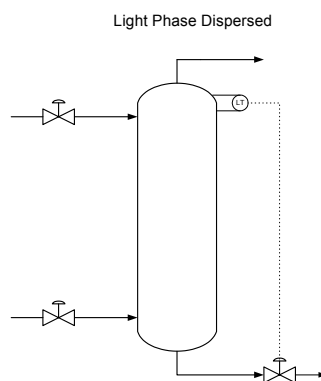


Figure 4. Typical interface control of a sieve tray extractor.

## CONCLUSIONS

There are many mechanisms that can limit the capacity of a sieve tray extractor. Six of the most common are addressed in this paper. While it may comprise complex hydrodynamics, the sieve tray extractor still provides reliable and cost effective efficiency for a large number of chemical and petrochemical applications. Trays such as UOP's multiple upcomer/downcomer or Shell's new Hi-Fi tray are modified versions of the conventional sieve tray that have demonstrated reliable performance and 10-15% higher capacities.

## NOMENCLATURE

d	Downcomer diameter, cm
$d_1$	Inlet diameter of downcomer, cm
$d_2$	Outlet diameter of downcomer, cm
$f_1$	Friction factor associated with downcomer diameter $d_1$
$f_2$	Friction factor associated with downcomer diameter $d_2$
g	Gravitational constant, cm/s <sup>2</sup>
h	Height of the coalesced layer, cm
$L_1$	Length of downcomer having Velocity $U_1$ and Diameter $d_1$
$L_2$	Length of downcomer having Velocity $U_2$ and Diameter $d_2$
$\Delta P_o$	Pressure drop through sieve hole, g/cm-s <sup>2</sup>
$\Delta P_{dow}$	Pressure drop through downcomer, g/cm-s <sup>2</sup>
$U_c$	Superficial continuous phase velocity based on cross-sectional area, cm/s
$U_{cflow}$	Superficial crossflow velocity of the continuous phase based on the average projected area, cm/s
$U_1$	Inlet velocity in downcomer, cm/s
$U_2$	Outlet velocity in downcomer, cm/s
$U_{dow}$	Downcomer velocity, cm/s
$U_{so}$	Characteristic drop velocity calculated by the method of Grace et al., cm/s
$Z_d$	Length of the downcomer, cm
$\phi_d$	Dispersed phase hold-up
$\rho_c$	Density of the continuous phase, g/cm <sup>3</sup>
$\rho_d$	Density of the dispersed phase, , g/cm <sup>3</sup>
$\mu_c$	Viscosity of the continuous phase, g/cm-s

## REFERENCES

1. J. Ololdi, G.V. Jeffreys and C.J. Mumford (1987), *Inst. Chem. Eng. Symp. Ser.*, **103**, 117-132.
2. A. F. Seibert and J. R. Fair (1993), *Ind. Eng. Chem. Res.*, **32**, 2213-2219.
3. R. B. Eldridge and J. R. Fair (1999), *Ind. Eng. Chem. Res.*, **38**, 218-222.
4. O. Becker and A. F. Seibert (1999), *Chemie-Ing-Tech.*, **72**, 359-364.
5. D. Mewes and W. Kunkel (1978), *Ger. Chem. Eng.*, **1**, 111-115.
6. T. R. Pilhofer (1981), *Chem. Eng. Commun.*, **11**, 241.
7. C. J. Major and R. R. Hertzog (1955), *Chem. Eng. Progr.*, **51**, 17-21.
8. A.F. Seibert (1998), SRP Technical Report, October 20.
9. J. R. Grace, T. Wairegi and T. H. Nguyen (1976), *Trans. Instn. Chem. Eng.*, **54**, 167.
10. G. Schober (1996), Diploma Thesis, Technische Universität München and The University of Texas at Austin.



## HYDRODYNAMICS AND MASS TRANSFER OF A ROTATING DISC COLUMN

Manabu Yamaguchi, Haruo Yamashita and Hideo Noda

Department of Mechanical Engineering, Himeji Institute of Technology, Himeji, Japan

Characteristics of hydrodynamics and mass transfer in a rotating disc column, consisting of six stages separated by stator rings equipped with stainless steel mesh coated with teflon, has been investigated experimentally. Hydrodynamics: effects of the impeller speed, the flow rates of the continuous and dispersed phases on the drop size, the hold-up fraction and the flooding flow rate of the dispersed phase are examined using the system of toluene drops in water phase. Mass transfer: column performance for mass transfer is also examined using the system of toluene/acetone/water under various operating conditions and evaluated by the number of theoretical stages per unit column height.

### INTRODUCTION

A large number of contactors for liquid-liquid extraction have been developed and their characteristics have been reported [1]. Recently, we developed a multistage mixer-settler column with a novel impeller [2]. The impeller consisted of a special structure of static-mixers inside channels fixed on a disc and was named an active turbine impeller. When the dispersed and continuous phases flow with twist-shear force through the channels rotating together with the disc, the one phase is dispersed into the other phase and both phases are discharged from the channel into the column stage [3]. Consequently, it was shown that the column had excellent characteristics for the hydrodynamics as well as mass transfer in the lower revolution of the impeller [2].

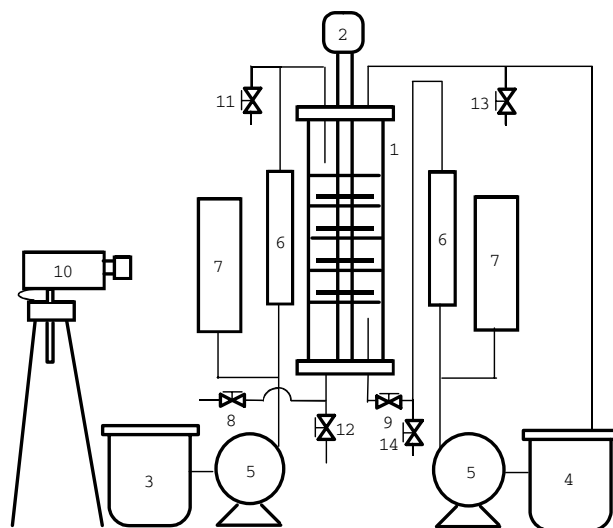
The aims of the present study were to examine the hydrodynamic and mass transfer characteristics of a rotating disc column and to compare the column performance with the novel impeller in the previous study [2] and that with disc impeller in the present study, which was taken off the channel with the static-mixer elements.

### EXPERIMENTAL

#### Experimental Apparatus

A schematic diagram of an experimental apparatus is shown in the Figure 1. The column consisted of a 150 mm diameter, 570 mm high glass column divided into 6 compartments; the top of the column 100 mm high, 4 stages each 70 mm high, and the bottom of the column 185 mm high (hereafter called the top stage, 1st stage, 2nd stage..., and bottom stage). The diameter of the disc, located 15 mm above the lower stator ring in each stage, was 110 mm and that of the stator opening was 110 mm. Each stator ring was equipped with a drop

coalescer made of a stainless steel mesh coated with teflon and with two downcomers of stainless steel bent into a U shape. Thus, the space in each stage was divided into a mixing zone and a coalescence zone except for the top and bottom of the column. In the experiment, fine droplets formed in the column were carried down with the continuous phase and accumulated at the bottom stage and, in the extreme case, they flowed out with the continuous phase as entrainment. Therefore, at the bottom stage, a stainless steel-like sponge layer was inserted to prevent these entrainments. Each stage in the column was equipped with probes to sample the liquid phases. The probes were set at a suitable position above the impeller.



- 1. rotating disc column; 3. continuous phase tank;
- 2. 4. dispersed phase tank; 5. Pump; 6. Flowmeter;
- 3. 7. air damper; 10. CCD camera; 8.9.11-14. valve

*Figure 1. Schematic of experimental apparatus.*

### **Experimental Procedure**

In the hydrodynamic experiment, the system of toluene drop in water phase was used. In the mass transfer experiment, the system of water/acetone/toluene recommended by European Federation of Chemical Engineering Working Party (EFChE) was used.

### **Drop size**

Drops in the 2nd stage were recorded on a personal computer through a CCD camera and later they were measured by reproducing their images. Drop size was determined as the Sauter mean diameter.

### **Hold-up fraction of dispersed phase**

The column was filled to a given level with water as the continuous phase, which was fed at a given flow rate through the flowmeter from the top of the column. The impellers were rotated at a given speed, and the air in the column was perfectly exhausted by rotating the impeller intermittently. Toluene as the dispersed phase was fed at a given flow rate through the flowmeter from the bottom of the column. Each of the phases flowed countercurrently at a constant flow rate. After steady-state flow of both phases was maintained, the hold-up was measured by the following two methods. For the first method, the liquid phase in each stage was sampled using a syringe from each sampling probe, and the volume of both phases was measured using a volumetric cylinder. The hold-up fraction was defined as the ratio of dispersed phase volume to total volume of both phases. For the second method, after the

feeding of both phases was simultaneously stopped, the dispersed phase was collected by intermittently rotating the impeller. A position of the dispersed phase/continuous phase interface was measured and the total volume of dispersed phase in each stage was obtained. In this way the ratio of dispersed phase volume to total volume of the 4 stage compartments was determined.

#### ***Flooding flow rate of dispersed phase***

When the feeding rate of the dispersed phase attained a critical value under a constant flow rate of the continuous phase and a constant impeller speed, the volume of the uncoalesced drops in the top stage increased and forced the dispersed phase/continuous phase interface down, and finally the interface entered into the 1st stage from the top one. This behavior made a steady state flow for both phases in the column impossible. Flooding was defined by this behavior.

#### ***Mass transfer***

Mass transfer experiments were carried out for different flow rates for both phases and different revolutions of the impeller. A specific operating condition was chosen to compare the mass transfer performance in the present column with those of conventional contactors in the literature; a constant throughput ratio of 1 to 1.5 (water to toluene phase) was used. The experimental procedures were essentially the same as those in the hold-up experiment except for the liquid-liquid system used. After a steady-state flow for both phases was achieved, the liquid phases at each stage were sampled using a syringe from each sampling probe. After both sampled phases were separated into the dispersed and continuous phases, they were rapidly moved by syringe into the covered sample bottles. Also, simultaneously the dispersed and continuous phases at the inlet and the outlet of the column were sampled. The acetone concentration in each phase was measured using a gas chromatograph with a packing of 1.2.3-Tris(2 cyanoethoxy) propane/Uniporto B.

## **RESULTS AND DISCUSSION**

#### **Drop Size**

Experimental drop sizes obtained under various operating conditions are shown in Figure 2. In the figure, RDC means a column with rotating disc impellers and ATC means a column with active turbine impellers. In the RDC, the dispersed phase (toluene phase) trapped by a disc impeller was discharged into the stage space as dispersed drops due to centrifugal force of the rotating disc. Therefore, it is considered that drop size is greatly influenced by impeller speed and the flow rate of the dispersed phase. In fact, in the case of low speed of the impeller, dispersed phase trapped widely by the disc moved about unsteadily together with rotation of the impeller. This was especially true in the case of around 100 rpm where bigger drops were formed irregularly as well as intermittently, and drop size could not be determined. The drops were formed regularly with increasing impeller speed and their sizes decreased, but effect of flow rates of the dispersed and continuous phases on their size was very small. At greater than 400 rpm impeller speed, drop size decreased significantly with flow rate of the dispersed phase. On the other hand, in the ATC, the drop sizes were small and nearly constant as shown in the Figure 2.

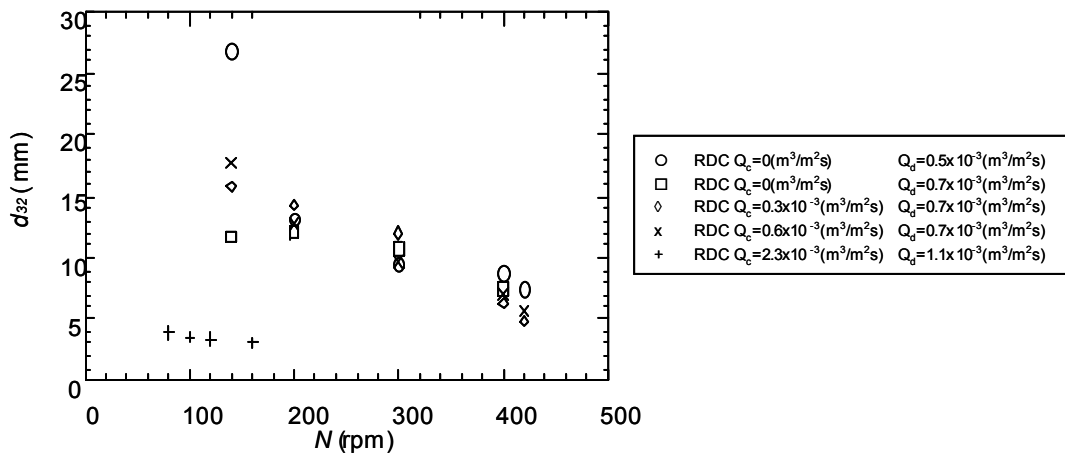


Figure 2. Relation between drop size and impeller speed.  
(RDC – Rotating Disc Impellers, ATC – Active Turbine Impellers).

### Hold-up Fraction of Dispersed Phase

A typical result of the experimental hold-up fraction for constant flow rates of both the phases is shown in Figure 3. The hold-up in the RDC were nearly constant values in the region of less than 400 rpm of impeller speed, but increased abruptly in the region of higher speed than 400 rpm. This was considered to be due to the marked decrease in the drop size for speeds of higher than 400 rpm that caused the rise velocity of the drops to decrease. Although the effect of the flow rate of the dispersed phase on the hold-up is not shown in the figure, the hold-up increased with increased flow rate of the dispersed phase. Their curves of the hold-up vs. impeller speed were similar to the circle symbols in Figure 3. On the other hand, the hold-up in the ATC was higher than in the RDC. As a result, the ATC predominates over the RDC in respect of operating conditions, e.g., lower impeller speed, easier operations etc.

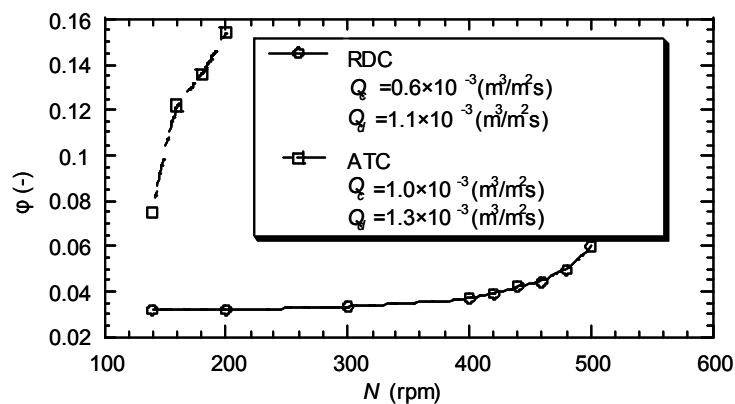


Figure 3. Relation between hold-up fraction and impeller speed.

## Mass Transfer

The stage efficiency for the system of water/acetone/toluene was close to 100% irrespectively of the impeller speed and flow rate of both phases. This is because the equilibrium constant of the test liquid system used is large. The column performance was evaluated using the Number of Theoretical Stages per Column Height which is often cited in the literature. NTS/H value was obtained by graphical stepwise construction using the concentration equilibrium line and column operating one. Figure 4 shows typical experimental results between NTS/H and impeller speed in the RDC. NTS/H values increased with impeller speed and significantly in the region of higher speed than 400 rpm. In the figure, the values of NTS/H in the ATC are also shown to compare with those in the RDC. NTS/H values in the ATC result in much higher than those in the RDC.

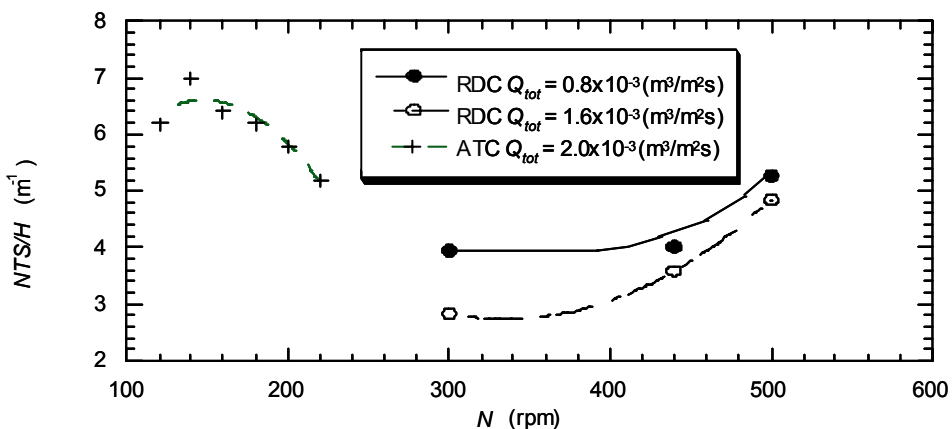


Figure 4. Relation between NTS/H and impeller speed.

## CONCLUSIONS

Droplet sizes in the present column (RDC) decreased with increasing rotating speed of the disc impeller and the flow rate of the dispersed phase, but were larger than those in the previous column (ATC). The Hold-up fractions of the dispersed phase were lower than those in the previous one. Mass transfer performance in the previous column was much better than that in the present one.

## REFERENCES

1. T. C. Lo, M. H. I. Baird and C. Hanson (1983), *Handbook of Solvent Extraction*, John Wiley & Sons, New York.
2. H. Yamashita, M. Yamaguchi, A. Kiyose, Y. Senba, M. Kaneda and H. Noda (1999), *Kagaku Kogaku Ronbunshu (Japanese)*, **25**, 707-713.
3. H. Yamashita, M. T. Tasaka, M. Yamaguchi and H. Noda (1999), *Kagaku Kogaku Ronbunshu (Japanese)*, **25**, 478-481.



## EXPERIMENTS WITH A SHORT KÜHNI COLUMN USED IN BATCH MODE

D. Antonelli, F. Vegliò, M.B. Mansur\*, E.C. Biscaia Junior\*\* and M.J. Slater\*\*\*

Dip. Ing. Chim. e Mat., University of L'Aquila, Italy

\* Dep. Eng. Química, Universidade Federal de Minas Gerais, Brazil

\*\* Programa Eng. Química (COPPE), Universidade Federal do Rio de Janeiro, Brazil

\*\*\* Dept. of Chem. Eng., University of Bradford, Bradford, United Kingdom

In recent years effort has been focussed on developing alternative experimental procedures to generate reliable design data for extraction columns at reduced costs. The study of single drop behaviour has been very fruitful but the problem remains of accounting for drop interaction, affecting hydrodynamics and mass transfer by drops coalescing and breaking up. An alternative technique is proposed in this work concerning the study of a 4-stage Kühni column with circulation of aqueous and organic phases until chemical equilibrium is reached. The hydrodynamic conditions in the column are realistic because normal flow rates are used. A model has been developed to describe the transient process of concentration changes in both phases assuming fixed hydrodynamic conditions and constant flow rates. Start-up results for the extraction and stripping of zinc with D2EHPA are presented. The procedure yields data immediately useful for column design at minimal cost.

### INTRODUCTION

In recent years, much work on single drops has been done in order to develop cheaper alternative experimental procedures with short columns [1-3]. The complex effects in a swarm of drops whose interaction affect hydrodynamics and mass transfer by drops coalescing and breaking up are not measured. Axial and radial mixing effects also arise in operation of industrial-scale columns, so direct application of single drop data is therefore of limited value [4,5]. The use of short columns with circulation of both phases at normal flow rates until equilibrium is reached is an alternative method. A drawback concerns the generation of a swarm of drops with sizes appropriate to a longer column. Several start-up procedures applied to reactive systems have been discussed by Mansur *et al.* [6]. Mathematical modelling complexities depend on the start-up strategy chosen to perform the experiments. The simplest cases involve fixed hydrodynamic conditions, for example, when one or both solute-free phases are fed to the column until hydrodynamic equilibrium is reached, then the pure phase(s) is(are) replaced at initial time by the real stream(s) containing the reactive species. A similar idea is a  $\delta$ -injection of solute as proposed by Wichterlova and Rod [7] to investigate mixer-settler performance.

In this paper, the transient start-up behaviour of a 4-stage Kühni column of 150mm diameter with circulation of both phases is investigated. Results for extraction and stripping of zinc with D2EHPA are presented. A stagewise model is proposed to describe the transient process of concentration changes in both phases assuming fixed hydrodynamic conditions and constant flow rates. Parameters have been estimated by data fitting.

## COLUMN MODELLING AND NUMERICAL SOLUTION

The stagewise backflow model [8] has been widely used to describe the non-ideal flow in extraction columns since the late 1960s. According to this model, both phases are assumed to behave as continua. In other words, this assumption presupposes that drops split and coalesce so frequently that any change in concentration spreads rapidly into neighbouring drops resulting in no differences in concentration in drops of different sizes. The model assumes an extractor with N perfectly mixed cells; circulating streams are characterised by a backmixing coefficient. Additional stages assuming no mass transfer are added to the extremes of the column to represent settling ( $i = 1$ ) and coalescence ( $i = N+2$ ) zones. The model has been evaluated using the reactive possible test system  $ZnSO_4/D2EHPA/n$ -heptane. Equilibrium and kinetics descriptions valid for extraction and stripping conditions have recently been proposed by Mansur *et al.* [9,10] assuming two consecutive reactions with all activity coefficients equal to unity with equilibrium constants as follows:

$$K_D = \frac{[ZnR_2RH][H^+]^2}{[Zn^{2+}][RH]^2} = 9.436(\text{mol}/\text{m}^3)^{0.5} \quad (1)$$

$$K_C = \frac{[ZnR_2][RH]^2}{[ZnR_2RH]} = 0.212(\text{mol}/\text{m}^3)^{0.5} \quad (2)$$

According to the equilibrium model, zinc ions and dimeric-D2EHPA molecules react reversibly at the liquid-liquid interface producing a  $ZnR_2RH$  complex and protons. However, at high loading conditions, part of the zinc-complex breaks down in the organic bulk solution [Equation (2)] producing  $ZnR_2$  and free dimeric-D2EHPA that reacts again with zinc [Equation (1)]. Therefore, the transient mass balances of the five reactive species in the stage  $i$  of the column are:

$$\frac{(1-\phi)V_i}{Q_c} \frac{dC_{A,i}}{dt} - (1+\alpha)C_{A,i+1} - \alpha C_{A,i-1} + (1+2\alpha)C_{A,i} + \frac{aV_i}{Q_c} R_i = 0 \quad (3)$$

$$\frac{(1-\phi)V_i}{Q_c} \frac{dC_{H,i}}{dt} - (1+\alpha)C_{H,i+1} - \alpha C_{H,i-1} + (1+2\alpha)C_{H,i} - \frac{2aV_i}{Q_c} R_i = 0 \quad (4)$$

$$\frac{\phi V_i}{Q_d} \frac{dC_{BD,i}}{dt} - (1+\beta)C_{BD,i-1} - \beta C_{BD,i+1} + (1+2\beta)C_{BD,i} + \frac{aV_i}{Q_d} \left( \frac{3R_i - S_i}{2} \right) = 0 \quad (5)$$

$$\frac{\phi V_i}{Q_d} \frac{dC_{CD,i}}{dt} - (1+\beta)C_{CD,i-1} - \beta C_{CD,i+1} + (1+2\beta)C_{CD,i} + \frac{aV_i}{Q_d} (R_i - S_i) = 0 \quad (6)$$

$$\frac{\phi V_i}{Q_d} \frac{dC_{CM,i}}{dt} - (1+\beta)C_{CM,i-1} - \beta C_{CM,i+1} + (1+2\beta)C_{CM,i} - \frac{aV_i}{Q_d} S_i = 0 \quad (7)$$

where  $R_i$  and  $S_i$  are reaction rate fluxes according to Equations (1) and (2), respectively. Assuming no significant effect on the diffusion of dimer-D2EHPA and protons [10]:

$$R_i = \frac{\frac{C_{A,i}C_{BD,i}}{C_{H,i}} - \frac{C_{CD,i}C_{H,i}}{K_D C_{BD,i}^{0.5}}}{\frac{C_{BD,i}}{k_A C_{H,i}} + \frac{1}{k_{F,i}} + \frac{C_{H,i}}{k_{CD} K_D C_{BD,i}^{0.5}}} \quad (8)$$

$$S_i = K_C C_{CD,i} - C_{CM,i} C_{BD,i}^{0.5} \quad (9)$$

so the balance between diffusional and chemical reaction control is determined not only by hydrodynamic conditions affecting the mass transfer coefficients but also by the concentrations of the reacting species and equilibrium considerations. The chemical reaction contribution depends on the ionic strength of aqueous phase with  $k_{F,i}$  given by [10]:

$$\log(k_{F,i}) = -5.597 - 3.211 \frac{\sqrt{I_i}}{1 + \sqrt{I_i}} \quad (10)$$

The organic phase from the coalescence zone ( $i = N+2$ ) is sent to an additional stage containing organic phase only ( $i = N+3$ ) which feeds the organic phase tank. Mass balances in this additional stage and in the tanks of aqueous and organic phases assume a first order delay to describe the dynamic response in these compartments. If long pipes between the tanks are used, the inclusion of a dead time in the circulation streams is required [6]. The model is a non-linear set of algebraic-differential equations, but substitution of Equations (8)-(9) into the mass balances Equations (3)-(7) results in an initial value problem with non-linear ordinary differential equations. Numerical solution has been obtained by the DASSL code [11]. Mass transfer and hydrodynamic parameters ( $\phi$ ,  $d_{32}$ ,  $k_A$ ,  $k_{CD}$ ,  $\alpha$  and  $\beta$ ) assumed to be stage and time independent have been estimated using the Hooke-Jeaves direct search optimisation method. In this work, the objective function is the total squared deviation between estimated and experimental concentrations of zinc and zinc-complex at the ends of the column at various times. The following start-up strategy has been adopted to initialise the numerical procedure: at  $t = 0^+$ , both phases circulate the entire plant but reaction is assumed to start only at  $t = 0^+$ . This physically unreal situation presumes an instantaneous hydrodynamic equilibrium and may not be valid for long columns.

## EXPERIMENTAL PROCEDURE

The experiments shown in Table 1 were carried out for 30 min with sampling at the ends of the column. Samples were analysed by atomic absorption. For extraction runs, the same liquor ( $10 \text{ mol/m}^3 \text{ Zn}^{2+} + 1 \text{ mol/m}^3 \text{ H}^+$ ) was contacted with  $75 \text{ mol/m}^3$  dimer-D2EHPA organic solution. For stripping runs, a fully loaded organic phase was contacted with sulphuric acid solutions at  $120 \text{ min}^{-1}$  and  $A/O = 2$ . Before each run, the column was circulated with continuous aqueous phase only, then dispersed organic phase was fed at  $t = 0$ . In all runs, the aqueous flow rate was kept constant at  $2 \text{ L/min}$ . The same total volumes of aqueous and organic phases were contacted (10 and 5 L, respectively).

*Table 1. Variable levels investigated to extraction and stripping runs.*

Run	Speed ( $\text{min}^{-1}$ )	A/O	Run	$C_{BD}^\circ (\text{mol/m}^3)$	$C_H^\circ (\text{mol/m}^3)$
E1	120	2	S1	75.0	100
E2	180	2	S2	75.0	1000
E3	120	4	S3	7.5	100
E4	180	4	S4	7.5	1000

## START-UP SIMULATIONS AND PARAMETER OPTIMISATION

Typical transient concentration outputs at the ends of the column are shown in Figure 1 (points are experimental data and lines are optimised concentration outputs). Labels AIC and OOC mean “Aqueous Input Column” and “Organic Output Column”, respectively. The zinc-complex concentration output at the end of the column for the extraction process exhibits a maximum at initial time due to the zinc-complex produced throughout the column that is accumulated and transported by the organic phase. A maximum at initial time is also observed for the stripping process, but the start-up strategy assumed to initialise the model is not realistic and led to failure in reproduce the OOC curve. Similar transient concentration outputs have been discussed in detail elsewhere [6].

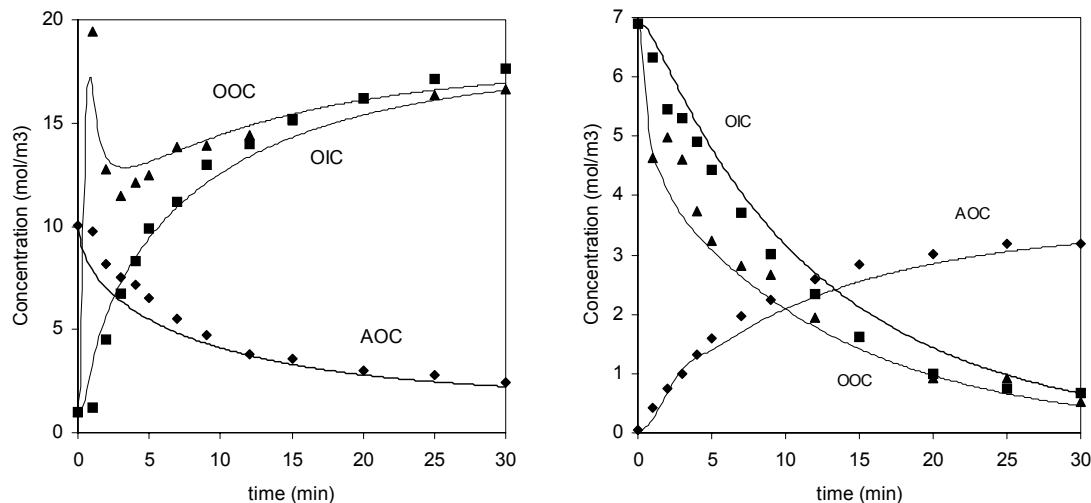


*Figure 1. Dynamic extraction and stripping of zinc (runs E1 and S4, respectively).*

The hydrodynamic and mass transfer parameters shown in Table 2 have been estimated by fitting data from measured solute concentrations with the transient backflow model. The procedure yields data immediately useful for column design at minimal cost because operating parameters can be obtained from one experiment by model-fitting, but data should accurately measured [13].

Estimated average drop sizes are smaller than predicted by empirical correlations [12]. This result could be explained at least in part to the mass transfer effect which results in gradients of interfacial tension that affect coalescence/splitting rate of drops. It is generally ascertained in the literature that  $c \rightarrow d$  transfer tends to produce smaller drops, so larger drops should be expected in stripping runs. However, a reduction in drop size stabilising with time was observed visually, indicating that drop splitting prevails for the investigated stirring conditions. Estimated sizes in Table 2 are average values with time and stage. Therefore, as any change in drop size results in a change in the mean drop velocity, the estimated hold-ups in Table 2 are average figures. Hold-up values are reasonable but three drop size values seem unrealistic, possibly due to low data quality. Furthermore, the optimisation results have shown that drop size and hold-up are very sensitive parameters with some degree of correlation, possibly because only end of column data have been used. A distributor has been used to get acceptable drop sizes because the initial drop size distribution seems to influence results; a drop size distribution has not been employed in the model. The results indicate also that axial mixing effects are more likely associated with continuous phase flow rate because a null value of  $\beta$  has been estimated in most cases; no backward movement of drops was detected visually. On the other hand, estimated axial mixing coefficients for the continuous aqueous phase in extraction runs indicate strong mixing effects compared to predictions from correlations [12]. Sampling along the column is therefore necessary to identify real axial mixing effects.

*Table 2. Estimated mass transfer and hydrodynamic parameters.*

Run	$\phi \times 10^2$	$d_{32}$ m	$k_A (x10^4)$	$k_{CD}$	$\alpha$	$\beta$
E1	$8.19 \pm 0.02$	$(1.06 \pm 0.01) \times 10^{-3}$	$1.42 \pm 0.02$	$(3.41 \pm 1.10) \times 10^{-6}$	$\infty$	0
E2	$8.68 \pm 0.03$	$(5.68 \pm 0.01) \times 10^{-6}$	$\infty$	$(1.69 \pm 0.01) \times 10^{-9}$	$\infty$	0
E3	$3.19 \pm 0.02$	$(9.68 \pm 0.14) \times 10^{-4}$	$\infty$	$(4.81 \pm 0.05) \times 10^{-6}$	$\infty$	0
E4	$10.48 \pm 0.01$	$(9.14 \pm 0.70) \times 10^{-6}$	$\infty$	$(1.57 \pm 0.12) \times 10^{-9}$	$\infty$	0
S1	$4.96 \pm 0.03$	$(7.00 \pm 0.16) \times 10^{-5}$	$\infty$	$(2.24 \pm 0.05) \times 10^{-7}$	0	0
S2	$8.19 \pm 0.03$	$(2.63 \pm 0.01) \times 10^{-4}$	$\infty$	$(4.40 \pm 0.01) \times 10^{-5}$	$\infty$	0
S3	$9.39 \pm 0.12$	$(9.56 \pm 0.33) \times 10^{-4}$	$\infty$	$(1.80 \pm 0.21) \times 10^{-5}$	$0.20 \pm 0.36$	0
S4	$9.37 \pm 0.11$	$(6.13 \pm 0.15) \times 10^{-4}$	$\infty$	$(3.07 \pm 0.09) \times 10^{-6}$	0	0

The aqueous phase mass transfer resistance seems to be significant only for extraction experiments at low stirring speed (below  $120\text{ min}^{-1}$ ). Except at high stirring speed ( $180\text{ min}^{-1}$ ), the extraction rate is mainly controlled by the kinetics of the reaction, while the stripping rate is mixed-rate controlled (chemical reaction and organic phase mass transfer resistances) for the range of operational conditions investigated.

In general terms, it has been found the equilibrium model is suitable for reproducing extraction and stripping equilibrium data of the Zn-D2EHPA system for practical conditions. The backflow model is able to reproduce the start-up behaviour reasonably well.

## CONCLUSIONS

- (a) Design data generated from start-up experiments in short columns with circulation of both phases are significantly cheaper to obtain compared to steady-state experiments in long columns, but the reliability of the parameter estimates obtained from solute profiles depends on the accuracy and location of the measurements. Operating parameters can be obtained from one experiment by model-fitting.
- (b) Empirical correlations found in the literature have been developed to predict operating variables in columns at steady-state conditions, so these equations do not necessarily predict parameters well for transient situations.
- (c) A better mathematical description of hydrodynamics in columns is required to reproduce better the adopted start-up strategy. Models assuming transient hydrodynamic characteristics (in population balance models, for example) may improve data description and minimise any parameter correlation effects.

## ACKNOWLEDGEMENTS

The experimental work done at the University of Bradford was made possible by financial support received from the Coordenação de Aperfeiçoamento de Pessoal de Nível Superior (CAPES, Brazilian Government Agency, PICDT/UFMG and PDEE Doctorate Grant n° 0299/99-5), which is gratefully acknowledged. M.B. Mansur would also like to record his appreciation for financial support from Conselho Nacional de Desenvolvimento Científico e Tecnológico (CNPq), Brazil and Fundação de Amparo a Pesquisa do Estado de Minas Gerais (FAPEMIG), Brazil, to attend this Conference.

## NOMENCLATURE

$a$	interfacial area ( $\text{m}^2$ )
$C_j$	concentration of specie $j$ ( $\text{mol}/\text{m}^3$ )
$d_{32}$	average drop size (m)
$I$	ionic strength ( $\text{kmol}/\text{m}^3$ )
$k_i$	mass transfer coefficient of specie $i$ (m/s)
$k_F$	concentration-based forward reaction rate constant (m/s)
$K_C$	concentration-based equilibrium constant reaction ( $\text{mol}/\text{m}^3$ ) $^{1/2}$
$K_D$	concentration-based equilibrium constant reaction ( $\text{mol}/\text{m}^3$ ) $^{1/2}$
$Q$	volumetric flow rate ( $\text{m}^3/\text{s}$ )
$R$	overall molar flux of the heterogeneous reaction ( $\text{mol}/(\text{s} \cdot \text{m}^2)$ )
$RH$	molecule of monomer-D2EHPA
$S$	overall molar flux of the homogeneous reaction ( $\text{mol}/(\text{s} \cdot \text{m}^2)$ )
$t$	time (s)
$V$	volume ( $\text{m}^3$ )

### Subscripts

A	zinc ion
BD	dimer-D2EHPA
c	continuous phase
CD	dimer-D2EHPA complex
CM	monomer-D2EHPA complex
d	dispersed phase
H	hydrogen ion

### Greek

$\alpha$	backmixing coefficient continuous phase
$\beta$	backmixing coefficient dispersed phase
$\phi$	hold-up of dispersed phase

## REFERENCES

1. Z. Fan, J. O. Ololdi and M.J. Slater (1987), *Chem. Eng. Res. Des.*, **65**, 243-250.
2. H. Bahmanyar, D. K. Chang-Kakoti, L. Garro, T.-B. Liang and M. J. Slater (1990), *Trans. IChemE.*, **68**, Part A, 74-83.
3. I. Seikova, C. Gourdon and G. Casamatta (1992), *Chem. Eng. Sci.*, **47** (15-16), 4141-4154.
4. M. J. Brodkorb (1999), Multicomponent kinetics in liquid-liquid systems, PhD thesis, University of Bradford, UK.
5. S. E. Kentish (1996), Forward mixing in a countercurrent solvent extraction contactor, PhD Thesis, University of Melbourne, Australia.
6. M. B. Mansur, M. J. Slater and E. C. Biscaia Jr (2001), Start-up behaviour of reactive systems in counter-current extraction columns. *Latin American Applied Research*, in press.
7. J. Wichterlova and V. Rod (1991), *Trans. IChemE*, **69**, Part A, 282-286.
8. C. A. Sleicher (1959), *AIChE J.*, **5**, 145-149.
9. M. B. Mansur, M. J. Slater and E. C. Biscaia Jr (2001), Equilibrium analysis of the reactive liquid-liquid test system  $\text{ZnSO}_4/\text{D2EHPA}/n\text{-heptane}$ . *Hydrometallurgy*, in press.
10. M. B. Mansur, M. J. Slater and E. C. Biscaia Jr. (2001), Kinetic analysis of the reactive liquid-liquid test system  $\text{ZnSO}_4/\text{D2EHPA}/n\text{-heptane}$ . *Hydrometallurgy*, in press.
11. L. Petzold (1989), *DASSL code*, Computing and Mathematics Research Division, Lawrence Livermore National Laboratory, L316, PO Box 808, Livermore, CA 94559.
12. A. Kumar and S. Hartland (1994), Empirical prediction of operating variables. In: Liquid-liquid extraction equipment, Vol. 17, J. C. Godfrey and M. J. Slater (eds.), Wiley, UK, pp. 625-735.
13. V. Rod, W-Y. Fei and C. Hanson (1983), *Chem. Eng. Res. Des.*, **61**, 290-296.



# THE IMPORTANCE OF HOLDUP IN PILOTING OF KINETICALLY CONTROLLED SX PROCESSES IN COLUMNS

Baruch Grinbaum

IMI(TAMI) Institute for Research and Development, Haifa, Israel

In chemical extraction, the residence time per theoretical stage must be at least equal to the time needed to complete the reaction. The holdup plays a crucial role in these processes, as the residence time of the dispersed phase increases linearly with the holdup. It is also important to run the pilot column at the minimum flux that yet allows high holdup. In many cases the residence time in the pilot may be too low to obtain the required recovery. In industrial columns this problem is less severe, as the HETS increases with the diameter of the column, and so for a similar residence time the flux may be higher. The experimental results should be analyzed, using the proposed scale-up procedures, to calculate the size of the industrial equipment.

## INTRODUCTION

Although a lot of work has been done on kinetic aspects of extraction, expressed usually through the rate coefficients [1], their impact on experimental procedures in columns is often neglected. The importance of the kinetics in SX process development is well known and the relevant models are widely documented in numerous papers and books, e.g., [1-3], to quote just a few. Yet, only few publications (e.g., [4]) mention the kinetic aspects in piloting of columns, and they are often left either disregarded or misinterpreted.

In chemical extraction, the time needed to complete the reaction, as a function of the temperature, must be known, from the literature, from previous experience or from simple batch kinitical experiments, prior to any piloting. The residence time per theoretical stage, of each phase, must be at least equal to this time.

### Residence Time

It is important to remember that the residence time of each phase in the column is different. For the dispersed phase, it is equal to:

$$\tau_d = Ah\phi e/F_d \quad (1)$$

and for the continuous phase:

$$\tau_c = Ah(1-\phi)e/F_c \quad (2)$$

where  $F_d$  and  $F_c$  are the flow rates of the dispersed and continuous phases,  $A$  is the cross-sectional area of the column,  $h$  is the total height of the column in which extraction takes place,  $\phi$  is the holdup, and  $e$  is the fractional free area in the column.

The residence time can also be expressed as a function of the flux J:

$$\tau_d = (1 + R)h\phi e/J \quad (3)$$

$$\tau_c = (1 + R)h(1-\phi)e/(RJ) \quad (4)$$

where R is the flow rate ratio,  $F_c/F_d$ , and is assumed constant through the column. The flux follows the standard definition:

$$J = F/A = 4F/\pi D^2 \quad (5)$$

where D is the diameter of the column.

To obtain the residence time per stage, h in Equations (1) to (4) should be substituted by the height equivalent to a theoretical stage (HETS). For most columns  $e \sim 1$ , and for the sake of simplicity it is omitted in the following discussion.

Figure 1 shows the residence times in the column, for each dispersion, at various fluxes and phase ratios, at constant holdup of 20%, and Figure 2 shows the influence of the holdup on the residence time.

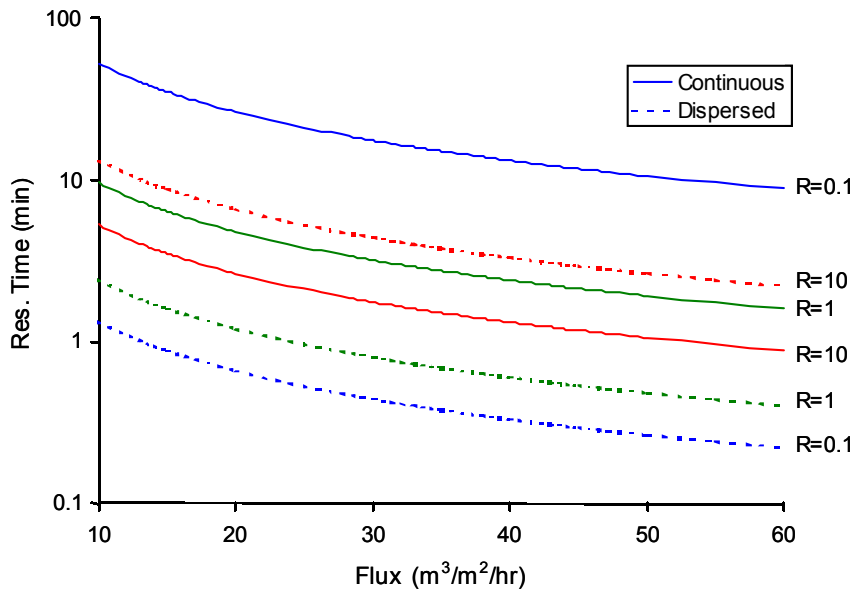
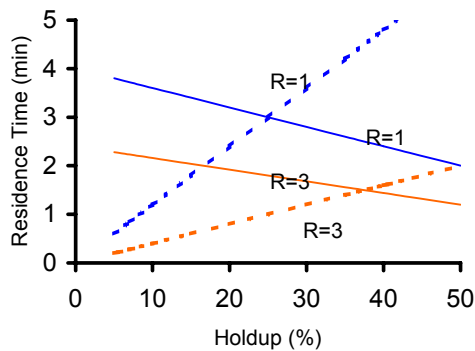


Figure 1. Residence time in a 1 m column vs. flux and phase ratio.

From Equations (3) and (4), the following equation is derived:

$$R = (1-\phi)/\phi \Leftrightarrow \tau_d = \tau_c \quad (6)$$

Equation (6) means that when the ratio of the flow rates R is equal to the relative volume of the phases in the column, both phases have the same residence time. As this condition ( $\tau_d = \tau_c$ ) assures the best kinetic performance of the column, for every R the best holdup  $\phi$  can be calculated. The graphical description of Equation (6) appears in Figure 3.



*Figure. 2. Influence of the holdup on the residence time (--- dispersed phase, - - - continuous phase).*

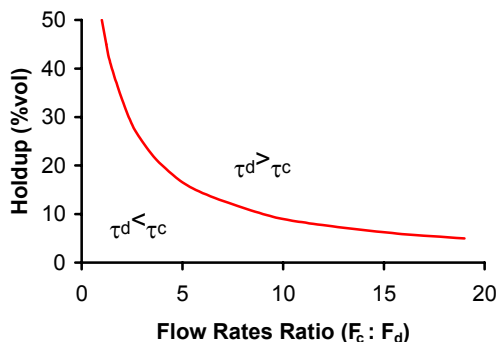


*Figure 3. Optimum holdup vs. the flow rates ratio.*

### **Which phase has a longer residence time?**

As one can see from both Figures 2 and 3, increasing the holdup, at constant phase ratio, eventually makes the dispersed phase the slow one, *i.e.*, with longer residence time. But this can happen only if the minor phase (*i.e.*, the phase with lower flow rate) is dispersed in the major one. As found by Arashmid and Jeffreys [5] and others, the holdup of the continuous phase is greater than (or at least similar to) the holdup of the dispersed one. When the major phase is dispersed, it always has the lower residence time, as its flow rate is higher and yet it occupies less than 50% of the active volume of the column.

### **When should the kinetics be considered?**

In pilot columns the HETS is usually below 100 cm, and in some agitated columns, *e.g.*, Karr or Scheibel, it may be even shorter than 20 cm. Substituting  $h = \text{HETS}$  in Equations (3) and (4), one finds directly the residence time per stage at given operating conditions, and may deduce whether kinetics should be considered.

For example, at phase ratio 1:1, holdup of 20% and a flux of 20-30 m<sup>3</sup>/m<sup>2</sup>/h, the residence time in a 20 cm length of a column is only 10-15 s, and in 100 cm – 50-80 s. At a flux of 50 m<sup>3</sup>/m<sup>2</sup>/hr or holdup of 10%, the residence time even in 100 cm drops below 30 s.

As a rule of thumb, kinetics should be considered for pulsed columns kinetics if the required residence time per stage exceeds 30 s, and in Karr or Scheibel columns, above 15 s.

### **Kinetic considerations in experimental procedure**

The standard procedure for SX process development, using columns (see [4]) is:

1. Determine the NTS and phase ratio, either from data given by the client or by simulation.
2. Determine the residence time for one equilibrium stage from batch experiments. This is the approximate residence time per stage needed for the quickest phase in the column.
3. Knowing the maximum height of your pilot column and the approximate HETS, calculate the maximum flux that provides the necessary residence time at both dispersions (O/W and W/O), using eqs. 3-4 and assuming holdup between 15-30%.

If this flux is within the normal range of the tested columns, no kinetic considerations are necessary. Otherwise, the special procedure for slow processes, which is given below, should be applied.

## PILOTING OF SLOW SX PROCESSES

### Hydrodynamic Tests

The piloting starts with the standard hydrodynamic tests, to find the flooding curve, *i.e.*, the flux as a function of the energy input. During these experiments the holdups are measured for every tested value of flux and energy.

Without kinetic constraints, the flooding curve is prepared for both dispersions, and the one that gives higher flux is chosen, unless there are special considerations to rule it out. For quick processes the holdup is of secondary importance, and any value above 5% is considered satisfactory.

For slow processes, there is a big incentive to keep the major phase continuous, in order to increase its residence time (the holdup of the continuous phase is always above 50% [5]). It is also very important to keep the holdup as near to the optimum calculated in Equation (6) as possible, to have similar residence time for both phases.

Sometimes, due to either process or hydrodynamic considerations, the major phase must be the dispersed one. From our experience, this is usually the rule at phase ratio above 1:10, as the mass transfer tends to be poor when the minor phase is dispersed. In this case it is important to achieve the highest possible holdup, above 30%. It should be kept in mind that holdup approaching 50% means that the maximum possible energy is applied, and further increase of the energy may cause flooding or phase inversion [5]. A holdup of 10% and below for such a process is often a no-go factor.

For a slow process, it is important to investigate the maximum holdup available at low fluxes. We noticed that the holdup tends always to drop at lower flow rates. The bottom line is that decreasing the flux may cause a lower residence time than at the higher flux. A comprehensive hydrodynamic test enables us to find the flux that yields maximum  $\tau$  of the quickest phase.

Knowing the holdups for a given flux, one can calculate the residence time of both phases,  $\tau_c$  and  $\tau_d$ , using Equations (3) and (4).

The available NTS of the experimental column, under the kinetic constraint, is:

$$\text{NTS} = \eta_s \cdot \min(\tau_c, \tau_d) / \tau_s \quad (7)$$

where  $\tau_s$  is the time needed to approach equilibrium, to the desired extend, on one theoretical stage, and  $\eta_s$  is the fraction of equilibrium achieved. It is important to remember that  $\tau_s$  does not have a unique value, and it depends on how near do we want to approach equilibrium. One may use an optimization technique over NTS in Equation (7), and find the residence time that yields the maximum overall number of transfer units. Often not enough data are available for such an optimization, and a reasonable guess is used instead. The author recommends residence time that enables ~90% of the equilibrium mass transfer.

The value of NTS from Equation (7) is always lower than one could expect, for similar column, without kinetic problems. It is often below the required NTS for the process.

### Mass Transfer Experiments

In a normal process, the mass transfer experiments enable the calculation of HETS and establish the recovery in the column. For a slow process, the feasibility of the process is proven in two stages:

1. The preferred dispersion and maximum flux are found in the hydrodynamic test.
2. The mass transfer experiments have to prove whether the NTS, calculated by Equation (7), and using the actual holdups, can be achieved. They should be carried out twice: once at the highest flux that enables working at the optimum holdup, and once under conditions that predict maximum recovery, *i.e.*, maximum NTS. If the experimental NTS is similar to the calculated one, in both cases, it means that there are no unexpected problems of mass transfer, and the extraction in the pilot is really kinetically controlled. Otherwise the kinetics is not the limiting constraint, and the diffusion should be addressed too, probably by using higher energy and lower flux.

### **Influence of temperature**

It is most important to carry out the experiments at the design temperature. In piloting normal process, a deviation of 5-10°C from the set temperature through the column may be tolerated, as its influence on the flux is within the accuracy of the experimental procedure. Kinetics are more sensitive to temperature than flux, as the reaction rate constant  $k$  is an exponential function of the temperature, through the Arrhenius law and an increase of 10°C may double the rate of the reaction [6]. It is very difficult to keep a constant temperature in a pilot scale column, with a diameter in the range of 25-100 mm. The problem is especially severe when the process temperature is above 50°C and a high phase ratio (>10:1) is applied. In this case, heating of the small flow is ineffective, and the heat losses from the column's surface cause a significant temperature drop over the column. As a rule, the large stream should be overheated, so that the temperature in the middle of the column is the desired one. From our experience, in long columns it is difficult, even if good insulation is used. The problem may be overcome by active insulation (*i.e.*, heating) of the column. If not feasible, the height of the column should be reduced, so that the temperature drop is as small as possible. The extrapolation of the results from a shorter column is more reliable than working with full-length column along wide range of temperature.

### **Next steps**

If the client believes in scale-up procedures based on extrapolation, then the experimental work is over, and the scale-up calculations, based on the experimental work, may be done – see next section.

Otherwise, experimental simulation of a longer column is needed. For extraction, the column is rerun with fresh solvent and the raffinate from the previous run is used as a feed. For purification/stripping, the purified/stripped solvent is rerun against fresh purification/strip solution. This procedure gives approximately the equivalent of a column with double length. It can be repeated again and again, so that with the existing column one can simulate a process that requires many stages. The rigorous procedure is described in [4]. The experiment becomes longer, but no extrapolation is needed.

Sometimes the piloting of columns is run in parallel to an existing plant with MS (mixer-settlers). This is usually done in order to test the feasibility of replacing MS with columns. In such a case, the experimental procedure is easier and more accurate. Assume that the tested battery has  $n$  MS stages: From Equations (3), (4) and (7) one can calculate  $j$  - the expected NTS of the pilot column. The column is first fed with the aqueous feed and a solvent from the  $j$ -th stage in the MSr battery. In the next experiment, the feed solvent and the aqueous phase from the  $(n-j)$  MS are used as feeds to the column. If the compositions of the outlet streams do not fit the results of the mixer-settler plant, our estimation of the NTS in the column must have been wrong, and the procedure is repeated for an updated value of  $j$ , until exact simulation with the column is obtained.

Is the second run really necessary? No, unless problematic mass transfer may be expected in the diluted end of the process, or if the client is reluctant to extrapolate and wishes to see the real thing coming out of the pilot plant.

One way or another, the pilot column enables the kinetic HETS in the pilot column to be calculated and the flux at which it was obtained  $J_k$ .

## SCALING UP

For an industrial column, in a kinetic-controlled process, the HETS must fulfill both the kinetic and the hydrodynamic constraints. The exact procedure of scaling up is done by the manufacturer of the equipment. But it is important for the researcher (and for his client) to make a rough estimation of the size of the industrial column - both diameter and height.

### **HETS – from Kinetic Considerations**

The recovery, at known flux and column length, is found from the piloting. A comparison to simulation or to known plant results yields the effective NTS, under the kinetic constraint. From here one can get the kinetic HETS or  $HETS_k$ , and the flux at which it was calculated  $J_k$ . These values determine the volume of the industrial column, as the residence time, *i.e.*, the speed of flow of both phases through the column, remains constant. Assuming that the holdup does not change in the scale up, it means that:

$$(HETS/J)_p = (HETS/J)_i \quad (8)$$

where the indexes  $i$  and  $p$  stand for industrial and pilot, respectively.

### **HETS - from Hydrodynamic Considerations**

In kinetically controlled process the true HETS in the pilot is not known. The safe guess is  $HETS = HETS_k$ , measured during the low flux mass transfer experiments.

In the industrial column the HETS is always larger than in the pilot one. For most columns it follows the empirical Equation (7):

$$HETS_i/HETS_p = K(D_i/D_p)^M \quad (9)$$

where  $K$  and  $M$  are efficiency scale factors.  $K$  is slightly greater than 1, and in some cases is omitted.  $M$  is in the range of 0.2-1.0, according to the type of the column, for example, for the Karr column  $M = 0.38$ .

Substitution of  $HETS_i$  from Equation (8) in Equation (9), using the value of  $J_i$  from Equation (5), yields:

$$D_i = \left( \frac{4F_i D_p^a}{\pi J_p} \right)^{\frac{1}{2+a}} \quad (10)$$

Knowing the diameter, it is possible to estimate the height of the industrial column and the flux in it, using Equations (8) and (9).  $J_i$ , obtained from these calculations, is always higher than  $J_p$ , the low flux at the pilot, that was used for the scale-up. But it must, of course, be smaller than the maximum value predicted by the hydrodynamic test.

Remark: The values obtained by these calculations are not necessarily the optimum, and they will be recalculated by the manufacturer. But they give an estimate about the size of the future plant, and a feeling whether columns are or are not feasible.

## CONCLUSIONS

The kinetic aspects in piloting of SX processes in columns are important, and sometimes overlooked. The holdup plays a crucial role in these processes, as the residence time of the dispersed phase increases linearly with the holdup. It is important to run the pilot at the minimum flux that yet allows high holdup. In many cases the residence time in the pilot may be too low to obtain the required recovery. In industrial columns the HETS increases with the diameter of the column, and so for similar residence time the flux may be much higher. Failure to get the required recovery in the pilot may lead to unjustified rejection of the column. The experimental results should be analyzed, using the recommended scale-up procedure, and only then the decision whether columns are yet an attractive option should be done.

## REFERENCES

1. M. J. Slater (1994), Liquid-liquid Extraction Equipment, J. C. Godfrey and M. J. Slater (eds.), Wiley, New York, pp. 48-89.
2. M. M. Sharma (1983), Handbook of Solvent Extraction, T. C. Lo, M. H. Baird and C. Hanson (eds.), Wiley, New York, pp. 37-52.
3. M. Cox and D. S. Flett (1983), Handbook of Solvent Extraction, T. C. Lo, M. H. Baird and C. Hanson (eds.), Wiley, New York, pp. 53-89.
4. B. Grinbaum (2001), Ion Exchange and Solvent Extraction, Vol. 15, Y. Marcus and A. SenGupta (eds.), Marcel Dekker, New York, pp. 1-106.
5. M. Arashmid and G.V. Jeffreys (1980), *AIChE J.*, **26**, 51.
6. M. J. Sienko, R. A. Plane (1961), Chemistry, McGraw Hill, New York, p. 241.
7. R.W. Cusack (1998), *Chem. Eng.*, (6), 1998.



## AXIAL MIXING IN A RECIPROCATING PLATE COLUMN

Alfredo I. C. Garnica, Márcia M. L. Duarte and Carlson P. de Souza

Departamento de Engenharia Química, Universidade Federal do Rio Grande do Norte,  
Natal, Brasil

The axial dispersion coefficient in the liquid phase has been measured by unsteady tracer response methods in a 5 cm internal diameter reciprocating plate column, using water as a continuous phase. The main variables studied were plate spacing (5-7, 5-10 cm), amplitude (2-4-6 cm) and frequency of reciprocation (0-1.85 Hz), superficial velocity (0.15-0.46 cm/s), and hole diameter (0.3-0.7 cm). Measured values of axial dispersion coefficient ranged from about 1 cm<sup>2</sup>/s to a maximum of 16 cm<sup>2</sup>/s. An empirical correlation for the axial dispersion coefficient is proposed by using the experimental results.

### INTRODUCTION

The efficiency of the reciprocating plate column is strongly affected by the axial dispersion, for this reason it is very important to determine the axial dispersion coefficient, which is the parameter that characterizes and quantifies the intensity with which this phenomena takes place.

The investigators have used two fundamental models for the determination of the axial dispersion coefficient. These models are: the dispersion model proposed by Levenspiel [1] and the backflow model proposed by Sleicher [2]. Other models were also proposed by Novotny [3] and Baird [4].

Using these models the investigators have proposed different correlations for the axial dispersion coefficient for counter current contactors mainly for extraction column [5]. Even though many correlations have been developed for predicting axial mixing there is a lack of agreement between these correlations regarding the form of the dependence of axial mixing upon the numerous parameters involved.

In this work the dispersion model was used according to the recent studies [6-9] carried out in this area where a tendency exists to use this model due to its reproducible results obtained by the other models. The purpose of this work, is to obtain a new correlation for the axial dispersion coefficients that provides a better knowledge on the dependence of some parameters of operation of the reciprocating plate column for this coefficient.

## COLUMN AND PLATE

The reciprocating plate column and ancillaries are schematically shown in Figure 1a. Water was fed to the base of the column by gravity. The column is made of a glass tube with 5 cm internal diameter. The reciprocating system is made of a motor with 370 W (0.5 Hp). The operating frequency can be varied up to 3 Hz and up to 6 cm amplitude. The measurements of the reciprocating plates (Figure 1b) used in this work are given in Table 1.

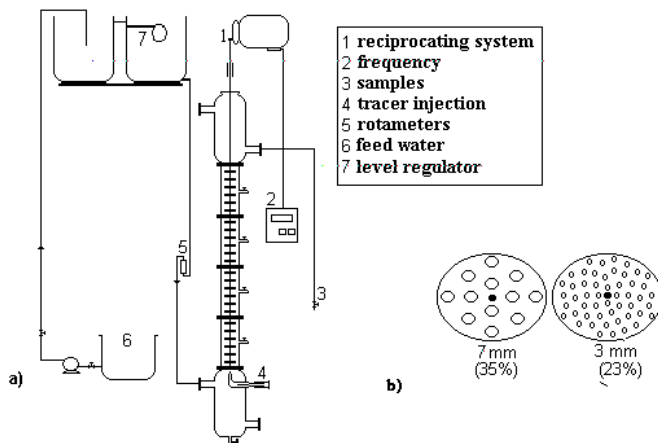


Figure 1. Reciprocating plate column and ancillaries.

Table 1. Column parameters, types of plates and ranges of operating conditions.

COLUMN	
Internal diameter (cm)	5
Active length (cm)	120
Total length (cm)	200
PLATES	
Material	stainless steel
Diameter (cm)	4.5
Hole diameter, (cm)	0.3 and 0.7
Thickness (cm)	0.12
% Fractional free area	23 and 35
OPERATING CONDITIONS	
Amplitude (cm)	0-4-6
Frequency (Hz)	0-1.85
Superficial water velocity (cm/s)	0.15-0.46
Plate spacing (cm)	5-7, 5-10
Number of plate (above spacings)	24-16-12

## AXIAL DISPERSION COEFFICIENT DETERMINATION

The dispersion coefficient ( $E$ ) was determined from a pulse tracer experiment. Here the tracer concentration of the column is measured as a function of time. The samples were collected each and every minute from the first plate on the top and then analyzed by spectrophotometry. Methylene blue was used as the tracer. From the tracer concentration data the mean residence time and variance were calculated and these values were then used to determine  $E$ . Using the equation of dispersion model in dimensionless form, we have

$$\frac{E}{UL} \frac{\partial^2 \Psi}{\partial \lambda^2} - \frac{\partial \Psi}{\partial \lambda} = \frac{\partial \Psi}{\partial \theta} \quad (1)$$

Using the boundary conditions for closed vessels, analytical solutions of equation (1) for the mean residence time,  $t_m$  and the variance are:

$$t_m = \tau \quad (2)$$

$$\frac{\sigma^2}{t_m^2} = \frac{2}{Pe} - \frac{2}{Pe^2} (1 - e^{-Pe}) \quad (3)$$

Using equations (2) and (3), the Peclet number ( $Pe$ ) can be calculated and hence the axial dispersion coefficient  $E$ .

## RESULTS AND DISCUSSION

The experimental values of the axial dispersion coefficient for a combination of three superficial velocities, three amplitudes and four frequency of reciprocation, three spacing plate, and two hole diameter, for a total of 216 data points, are separately presented in four figures. The diameter of the column was kept constant (Table 1).

The main variables affecting axial dispersion are the agitation level, which is determined by the product of the amplitude and frequency of reciprocation ( $Af$ ), and the superficial velocity ( $U$ ). In this work, when the axial dispersion coefficient has a significant value in the absence of agitation level, then it passes through a minimum as  $Af$  is increased. This tendency was also shown by Hafez [10], Karr [11] and Baird and Rama Rao [6]. This is due to the observed tendency of water flow to be poorly distributed across the column. The effect of the agitation level upon axial dispersion coefficient  $E$ , for three amplitudes is shown in Figure 2. It can also be seen that, when the values of the term  $Af$  increases, the value of  $E$  also increases. The same happens with the amplitude when the other parameters are kept constant.

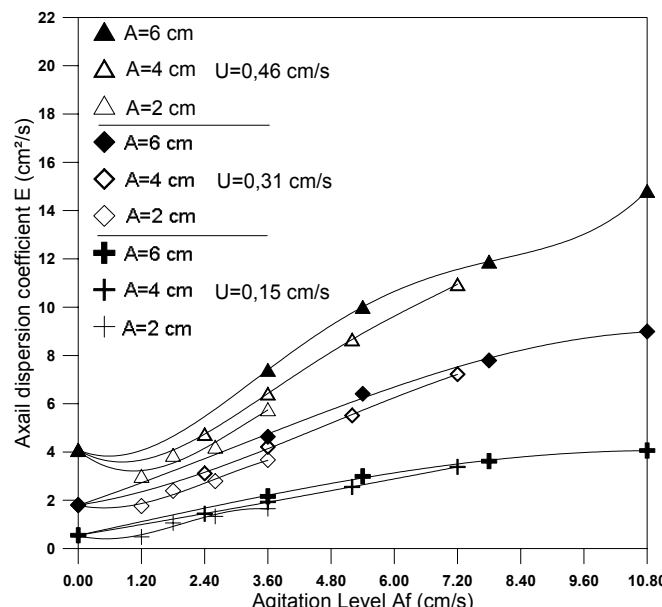


*Figure 2. Effect of agitation level ( $Af$ ) and amplitude upon axial dispersion coefficient for plate spacing  $h = 10$  cm and hole diameter  $d = 0.3$  cm.*

The effect of superficial velocity is shown in Figure 3. In all the experiments the axial dispersion coefficient increases with superficial velocity mainly for a higher level of agitation. This is possible because this behavior is associated with the increase of the turbulence caused by the elevation of the superficial velocity providing better indexes of mixture.

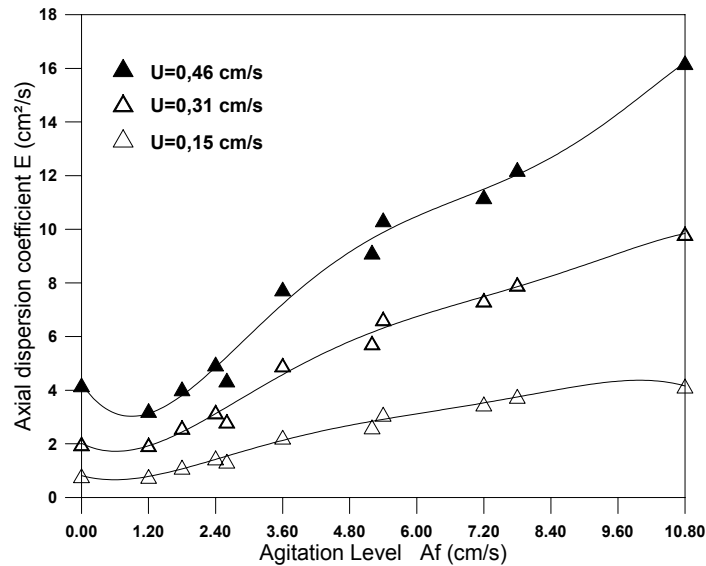


Figure 3. Effect of agitation level ( $A_f$ ) and superficial velocity ( $U$ ) for plate spacing  $h = 5 \text{ cm}$  and hole diameter  $d = 0.7 \text{ cm}$ .

The role of the plate spacing ( $h$ ) is examined in Figure 4. It was observed that the axial dispersion coefficient decreases when the spacing plate increases. This effect is more significant for higher values of the level agitation. This is possible because an increase in the numbers of plates produce a higher agitation and mixture hence the axial dispersion of the tracer in the continuous phase also increases. The effects of hole diameter ( $d$ ) are also shown in Figure 4. These results indicate that the axial dispersion coefficient increases when the diameter of the holes increases. This is due to the smaller eddy scale associated with the smaller holes.

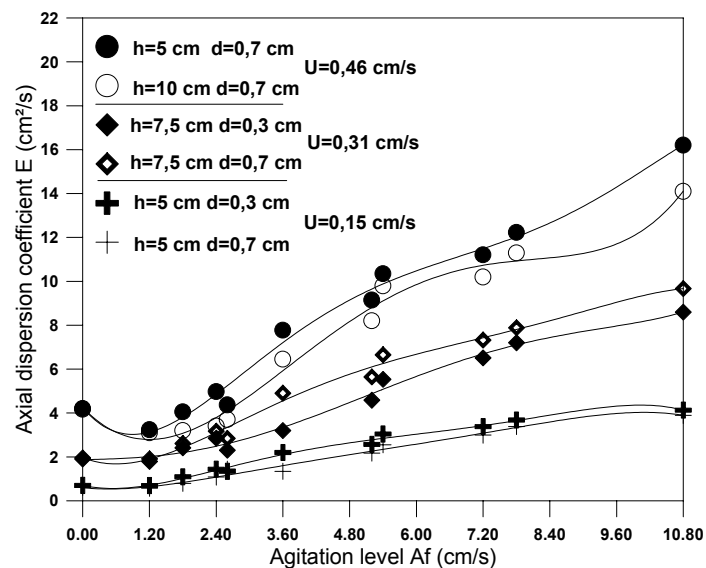


Figure 4. Effect of agitation level ( $A_f$ ), plate spacing ( $h$ ) and hole diameter ( $d$ ).

The experimental data were treated using non-linear estimation and an empirical correlation was proposed for the axial dispersion coefficient,  $E$  ( $\text{cm}^2/\text{s}$ ):

$$E = 5,6224 A^{0,867941} f^{0,650632} U^{1,109021} h^{-0,025506} d^{0,034861} \quad (4)$$

Comparison between observed and measured values of axial dispersion coefficient is shown in Figure 5.

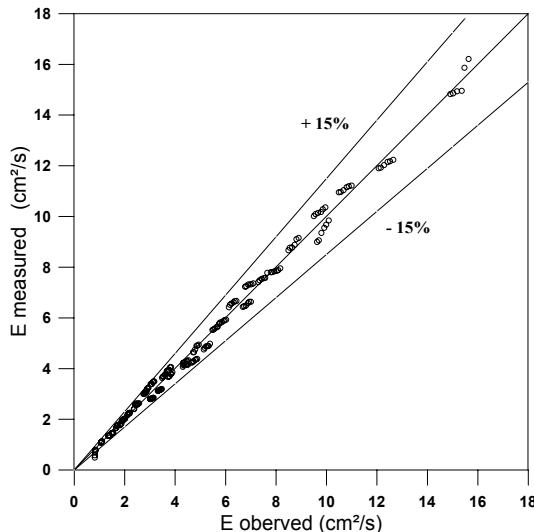


Figure 5. Comparison between observed and measured values of  $E$ .

## CONCLUSION

This paper discusses the determination of the axial dispersion coefficient in a reciprocating plate column. The values of  $E$  range from about  $1 \text{ cm}^2/\text{s}$  to a maximum of  $16 \text{ cm}^2/\text{s}$ . The amplitude, frequency of reciprocation and superficial velocity have an important impact on the axial dispersion coefficient. The axial dispersion coefficient has a significant value in the absence of agitation level ( $Af$ ) where it passes through a minimum as  $Af$  is increased. In general, the axial dispersion coefficient decreases when the plate spacing increases and hole diameter decreases. An empirical correlation is presented, giving  $E$  as a function of amplitude, frequency of reciprocation, superficial velocity of continuous phase, plate spacing and hole diameter.

## ACKNOWLEDGEMENTS

We thank CAPES (Coordenação de Aperfeiçoamento de Pessoal de Nível Superior) for providing scholarships for the authors and funding part of this research. We also thank the Chemical Engineering Department for providing technical assistance and support.

## NOMENCLATURE

$A$	amplitude of reciprocation, cm	$t_m$	mean residence time, s
$Af$	agitation level, $\text{cm}/\text{s}$	$U$	superficial velocity, $\text{cm}/\text{s}$
$d$	hole diameter, cm	$\Psi$	dimensionless concentration
$E$	axial dispersion coefficient, $\text{cm}^2/\text{s}$	$\lambda$	dimensionless distance
$f$	frequency of reciprocation, Hz	$\theta$	dimensionless time
$h$	plate spacing, cm	$\tau$	space time, s
$L$	active length of column, cm	$\sigma$	variance, s
$Pe$	Peclet number		

## REFERENCES

1. O. Levenspiel (1972), Chemical Reaction Engineering, 2nd edn., John Wiley and Sons, New York, pp. 281-282.
2. Sleicher (1959), *A/ChE J.*, **5** (2), 145-149.
3. P. J. Novotny, J. Prochazka and J. Landau (1970), *Can. J. Chem. Eng.*, **48**, 405-410.
4. M. H. I. Baird, and S. D. Kim (1976), *Can. J. Chem. Eng.*, **54**, 81-89.
5. H. R. Pratt and M. H. I. Baird (1983), Handbook of Solvent Extraction, T.C. Lo, M. H. I. Baird and C. Hanson (eds.), Wiley-Interscience, New York, Chapter 6.
6. M. H. I. Baird and N. V Rama Rao (1998), *Can. J. Chem. Eng.*, **76**, 370-378.
7. M. Lounes and J. Thibault (1996), *Can. J. Chem. Eng.*, **74**, 187-194.
8. G. W. Stevens and M. H. I. Baird (1990), *Chem. Eng. Sci.*, **45**, 457-465.
9. N. V Rama Rao and M. H. I. Baird (2000), *Can. J. Chem. Eng.*, **78**, 261-264.
10. M. M. Hafez, M. H. I. Baird and I. Nirdosh (1979), *Can. J. Chem. Eng.*, **57**, 150-158.
11. A. E. Karr, S. Ramanujam, T.C. Lo, and M. H. I. Baird (1987), *Can. J. Chem. Eng.*, **65**, 373-381.



## DESIGN OF PULSED EXTRACTION COLUMNS BASED ON LABORATORY-SCALE EXPERIMENTS

**Edwin Groß-Hardt, Martin Henschke, Sigrid Klinger and Andreas Pfennig**

Lehrstuhl für Thermische Verfahrenstechnik, RWTH Aachen, Germany

The design of pulsed extraction columns today still strongly relies on experimental investigations on pilot-plant scale with the specific system of interest. These experiments are time-consuming and expensive. We propose the ReDrop model (representative drops) for the simulation of extraction columns where about 2000 individual drops are followed as they move through the equipment. The effects considered acting on the drops are sedimentation, mass transfer, drop breakage and coalescence. The parameters of the models describing these effects are determined under very controlled conditions in laboratory-scale experiments with only some liters of liquid. The results of this prediction for pulsed sieve tray columns in the dispersion regime agree very well with experimental data for the coalescence inhibited system toluene + acetone + water.

### INTRODUCTION

In an extraction column many influencing factors are of roughly equal importance. Unfortunately these factors are strongly interrelated. Until now it has not been possible to identify any dominating influences and to describe them with sufficient accuracy. Thus for the safe design of extraction columns experiments on pilot-plant scale are still necessary. Such a design requires a large amount of substance and time and thus is expensive.

To improve the design procedure it is our goal to circumvent the expensive experiments on pilot-plant scale or at least to minimize them by substituting them with laboratory-scale experiments in standardized measuring cells with a small number of drops. These experiments are performed with a small amount of the original substances. Based on the results of laboratory-scale experiments the parameters determining the interplay between

- mass transfer to or from drops
- sedimentation of drops
- breakage of drops
- swarm behaviour

can then be determined. A method for the determination of coalescence parameters from these experiments is in progress. By suitably modelling this interplay additionally taking into account axial dispersion all basic effects acting on the droplets in a pulsed extraction column can be accounted for. Fortunately a variety of models is available for correlating the individual effects acting on the drops since the idea of describing extraction-column performance from single-drop behaviour is followed by several groups worldwide. The model we then use for the description of the entire extraction column is the ReDrop model [1, 2] which considers the individual behaviour of a sufficiently large number of drops in the column. The column behaviour is thus predicted from the single-drop behaviour characterized in the measuring cells.

## MASS-TRANSFER CELL

The laboratory-scale cell for the determination of mass transfer of single drops which was developed in collaboration with Bayer AG, Leverkusen, is shown in Figure 1 [3, 4]. A drop of the dispersed phase is generated with a computer controlled syringe. This drop then rises until it reaches a stable position in the thermostated conical part of the cell because of the counterflow of the continuous phase. If then the flow rate of the continuous phase is turned off for a short period of time, the drop rises further and reaches the withdrawal funnel which is also connected to a computer controlled syringe. Thus it is possible to generate a drop with a defined volume and contact it with the continuous phase for an arbitrary time span while it is virtually freely rising. For the generation of different drop volumes different syringes and nozzles have to be used.

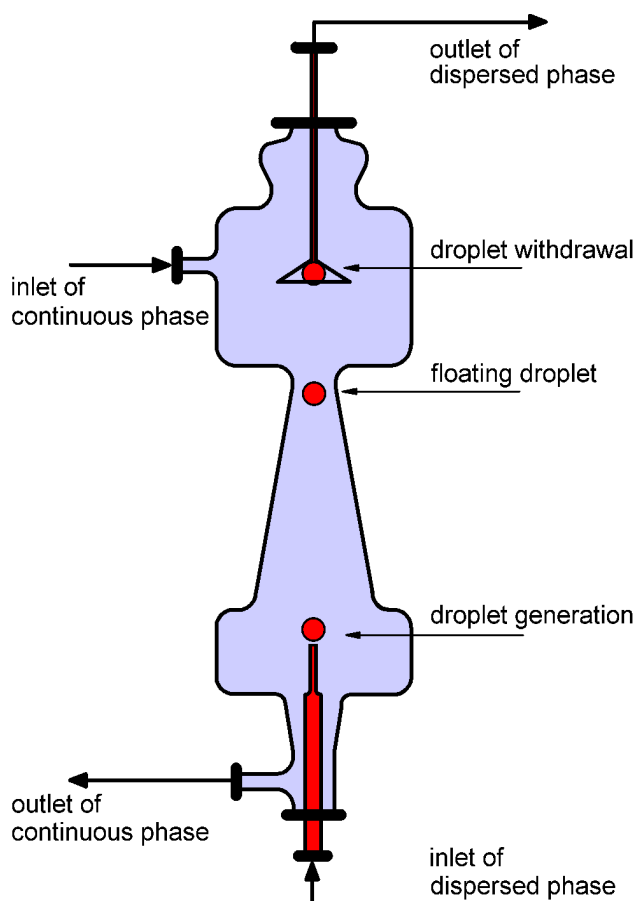
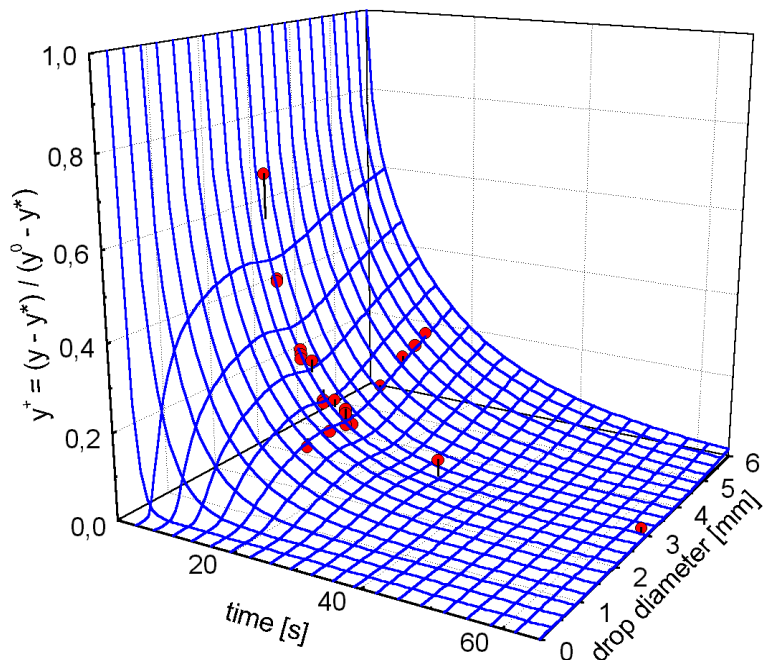


Figure 1. Schematic drawing of the laboratory-scale measuring cell for mass transfer.

Results obtained with this cell are presented in Figure 2. The dimensionless driving concentration difference which decays from unity at the start of the experiment to zero in equilibrium is plotted versus contact time and drop diameter. The specific slope of the surface obtained is a result of the various flow conditions of the drop as its diameter increases. While small drops behave like hard spheres a circulation is induced for larger drops. For even larger drops the shape begins to oscillate. This of course has direct influence on the mass-transfer rate. The model developed for the description of this behaviour takes these effects into account and additionally includes the enhancement of mass transfer by interfacial turbulence [4]. It can be seen that this correlation is able to describe the mass-transfer data with good accuracy. In further experiments the sieve-tray influence on mass transfer has been investigated in the same apparatus [5]. This correlation obtained for a single drop is later used directly for the simulation of an arbitrary large number of drops in an extraction column.



*Figure 2. Mass transfer of single drops in the system:  
n-butyl acetate (d) + acetone (t) + water (c), mass-transfer direction: c to d.*

Laboratory-scale cells of comparable size are used for the determination of sedimentation velocity also under the influence of mass transfer and the breakage [6] and coalescence probabilities. The sedimentation velocity is e.g. obtained from an evaluation of a video recording of drops sedimenting over 500 mm in a glass tube filled with continuous phase. Especially in the range of interest around 2.5 mm drop diameter it turns out that the sedimentation velocity is strongly affected by mass transfer, which compares well with literature [7].

### THE REDROP MODEL

The individual models obtained for a specific system with these laboratory-scale measuring cells are then joined together in the ReDrop model (representative drops). Additionally the axial dispersion of the continuous phase has to be taken into account. The idea of the ReDrop model is to follow a representative number of individual drops through the entire column with all the effects acting on them as quantitatively determined from the single-drop measurements. Typically 2000 drops are considered to obtain reliable results. The advantage of this approach is that all interactions between the different effects can be accounted for without problem.

A screenshot of the ReDrop model for a pulsed sieve-tray column is presented in Figure 3. On the left the column is shown with a representative number of individual drops and the sieve trays. As the simulation proceeds these drops are rising and it is then also indicated whether drops break or are coalescing in every time step. To the right of the column the drop size distribution is shown at all positions where it has been measured. In this case it has been measured only at the top of the column. Next the concentration and hold-up profiles (lines) are shown again in comparison with the experimental data (dots, for overall hold-up the straight line). It can be seen that the agreement of the concentration profiles is excellent while the hold-up shows slight deviation which is still in the range of experimental uncertainty. In the rightmost column some numerical data are shown which represent results as well as several control variables.

The ReDrop model for sieve-tray columns has then been tested against column data in our data base. This data base for pilot-plant scale columns has been collected with the support of several companies and universities and can be obtained from the authors.

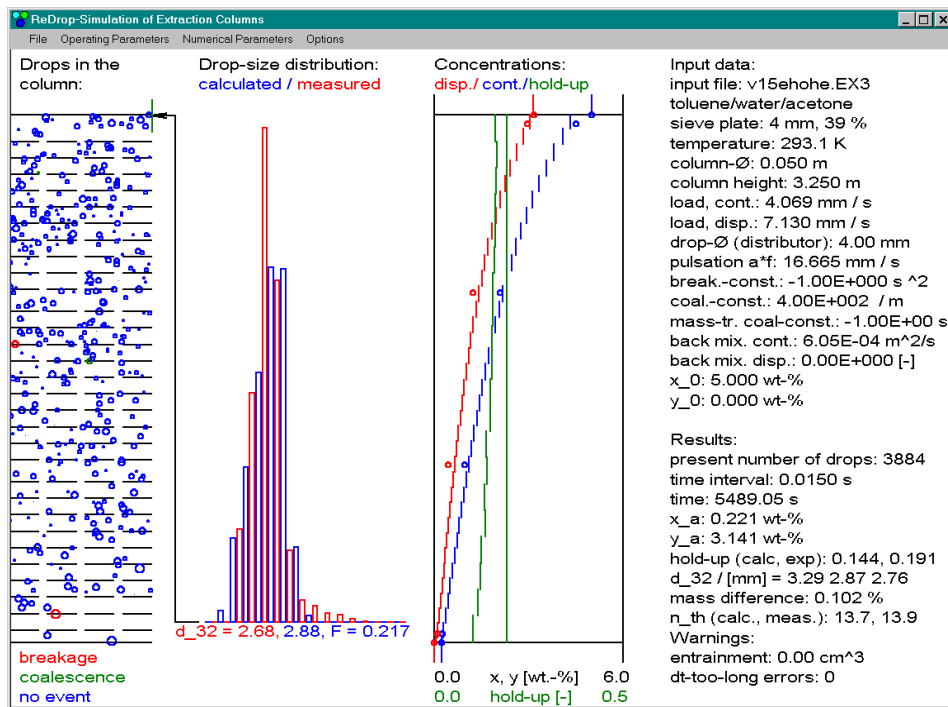


Figure 3. Screenshot of the ReDrop model.

## RESULTS

While coalescence is in principle taken into account already in the ReDrop simulation the coalescence parameters can not be determined until now. Thus only coalescence inhibited systems like toluene (d) + acetone (c → d) + water (c) can be simulated today. Another restriction is that only the dispersion regime is considered in the model equations. Furthermore only dual-flow sieve trays are investigated and the calculations are restricted to a single transfer component. Since these restrictions are no principle limitations progress is directed at extending the applicability of the ReDrop model beyond these limitations.

Some results obtained with the ReDrop model as it is available today are shown in Figure 4. Here the measured number of theoretical stages is compared with the predictions of the ReDrop simulation. This simulation is indeed a true prediction since only single drop data and available correlations for swarm behaviour [8], which are extended for liquid drops, are used and no column data have been applied in fitting the model parameters. The agreement between experiment and simulation is roughly 10% which is fully sufficient for a first design of an extraction column.

The simulations with ReDrop also describe the dynamic behaviour of the extraction column. Thus we investigated whether ReDrop is able to predict the dynamic limits of the extraction process, namely flooding. The corresponding results are shown in Figure 5 in comparison with experimental data [9]. It is obvious that ReDrop is in principle able to determine the limits of operation with high confidence.

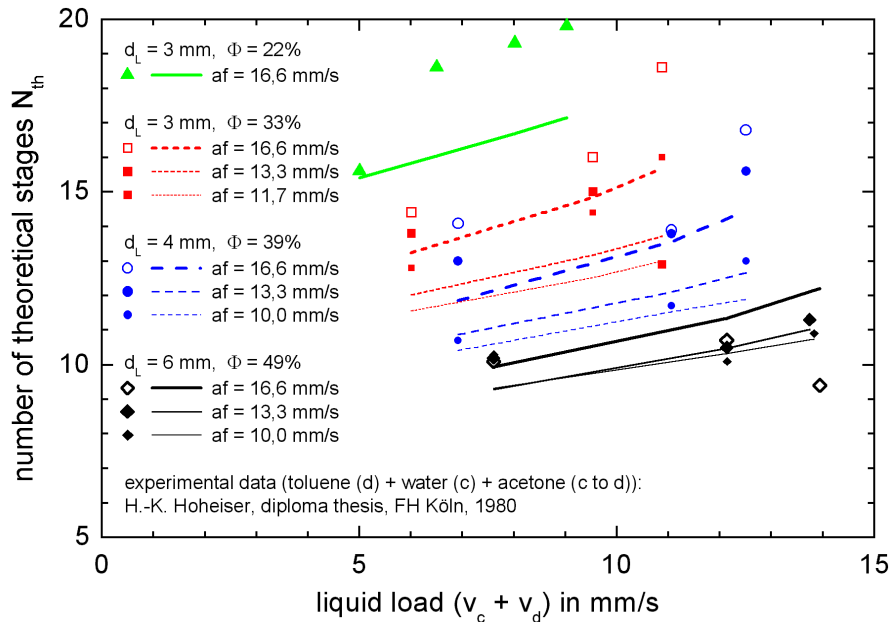


Figure 4. Comparison of experiment and ReDrop on the basis of column efficiency.

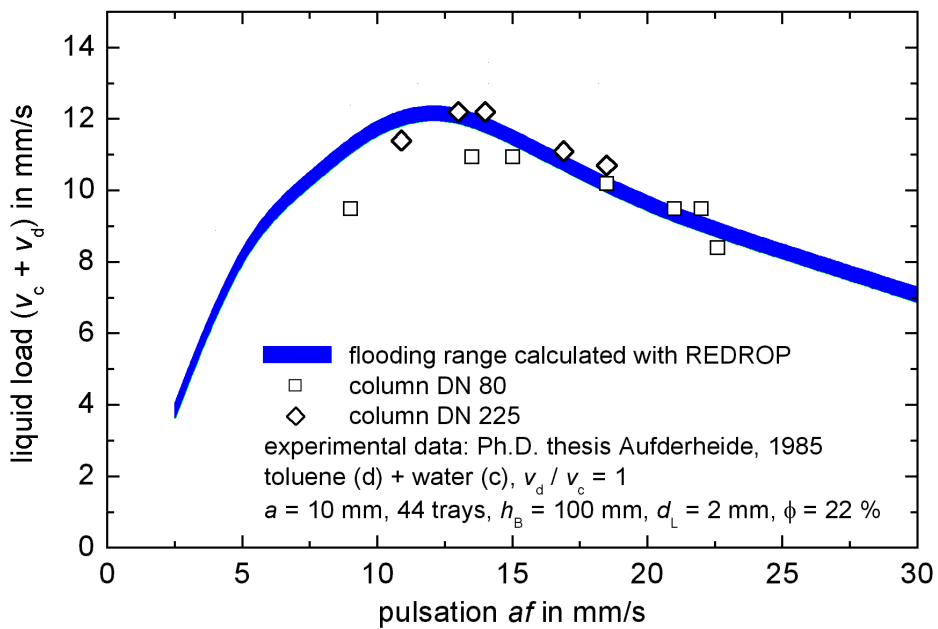


Figure 5. Flooding as predicted with the ReDrop model in comparison with experiment.

## CONCLUSIONS

It has been shown that based solely on the results of single-drop experiments it is possible to predict the behaviour of pulsed sieve-tray columns on pilot-plant scale. Even the dynamic limits of the operation of the column can be predicted with high confidence in the example shown. Future work will now be directed at extending the applicability of ReDrop to coalescing systems and to pulsed columns with packings. In a joint project with the groups of Professor Bart, Kaiserslautern, and Professor Stichlmair, Munich, all commonly used column types including those with rotating internals will be modelled based on laboratory-scale experiments. From these standardized experiments it is then possible to perform simulations for all column types and decide on the optimum design of the column in a knowledge based fashion.

## ACKNOWLEDGEMENTS

Financial support by the German Science Foundation as well as the Bayer AG are gratefully acknowledged. We also thank Mr. Schröter and Mr. Bäcker from the Bayer AG, Leverkusen, for many helpful discussions.

## REFERENCES

1. K. Arimont, M. Soika, and M. Henschke (1996), *Chem. Ing. Tech.*, **68** (3), 276-279.
2. M. Henschke and A. Pfennig (1996), *Proc. 12th Int. Congr. Chem. Proc. Eng.*, Chisa, Praha, Czech Republic, Paper 1130.
3. J. Schröter, W. Bäcker, and M. J. Hampe (1998), *Chem. Ing. Tech.*, **70** (3), 279-283.
4. M. Henschke and A. Pfennig (1999), *AICHE J.*, **45** (10), 2079-2086.
5. M. Henschke and A. Pfennig (2001), Influence of sieve trays on the mass transfer of single drops, *AICHE J.* (accepted for publication).
6. H. Haverland (1988), Untersuchungen zur Tropfendispersierung in flüssigkeitspulsierten Siebboden-Extraktionskolonnen, Ph.D. Thesis, TU Clausthal, Germany.
7. B. Hoting (1996), Untersuchung zur Fließdynamik und Stoffübertragung in Extraktionskolonnen mit strukturierten Packungen, Reihe III, No. 439 in Fortschr.-Ber. VDI, VDI-Verlag, Düsseldorf, Germany.
8. K. E. B. Andersson (1961), *Chem. Eng. Sci.*, **15**, 276-297.
9. E. Aufderheide (1985), Hydrodynamische Untersuchungen an pulsierenden Siebbodenextraktionskolonnen, Ph.D. thesis, TU Clausthal, Germany.



## A DISTRIBUTOR FOR LIQUID-LIQUID EXTRACTION COLUMNS

Alfons Vogelpohl and Jörg Koch\*

Technical University of Clausthal, Clausthal-Zellerfeld, Germany

\* RTM 2000 AG, Langelsheim, Germany

Extraction columns equipped with ordered packing allow for a large operating range between 10 and 90 % of the load at flooding. In order to take full advantage of this flexibility, a new distributor design and operating mode has been developed, which produces a very uniform drop-size distribution and allows control of the average drop size at changing throughputs.

The main feature of the new design is the use of a pressure pulse produced by a mechanically excited PTFE membrane attached to the distributor and operated at a frequency of up to 50 Hz. The pressure pulse serves to control the disengagement of the drops formed at the holes of the distributor independent of the velocity of the liquid exiting the holes of the distributor and thus of the liquid throughput.

### INTRODUCTION

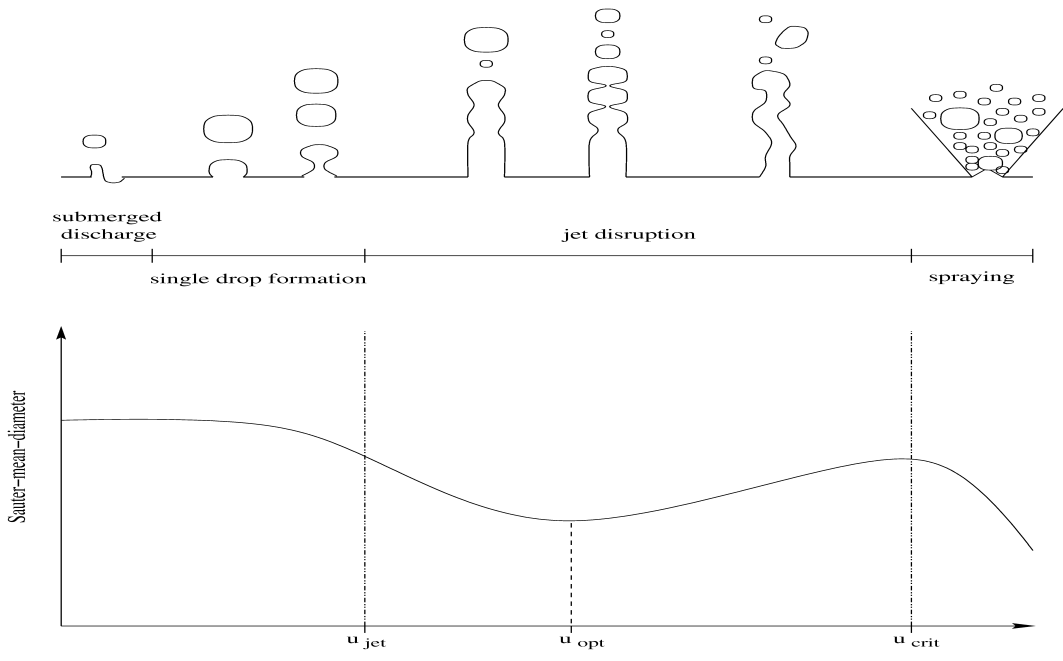
In liquid-liquid extraction one liquid is dispersed in a second immiscible liquid. The interfacial area required for mass transfer depends largely on the drop-size distribution generated by the primary distributor. Most conventional distributors generate the drops by the flow of the liquid through defined orifices and jet disruption. The drop size changes, however, with the liquid velocity in the orifices and, therefore, with the flowrate of the dispersed phase.

Figure 1 shows the different mechanisms of drop formation and the main dependency of the drop size on the velocity in the holes of the distributor. At very low velocities the drops are formed similar to a dripping water tap. This range is of no interest for technical use because of the low flowrate and the formation of very large drops. An increasing velocity leads to a periodic formation of single drops of equal size. In the medium range a jet is formed. The drops are generated by disruption at the top of the jet. With increasing velocity the jet length increases up to a maximum length and then decreases. At even higher velocities many small drops are formed by spraying.

For an economic operation of an extraction column and for modeling the mass transfer a narrow and constant drop-size distribution at all flowrates is desired. This requires an additional possibility of adjusting the drop size independent of the flow velocity through the orifice. This adjustment can be affected in several ways: by a multi-stage distributor [1], by the flow of continuous phase around a capillary in a two-phase nozzle [2], by pulsation of the total column content [3] or by pulsation of the dispersed phase [4, 5].

## EXPERIMENTAL PROCEDURE

In these experiments the pulsation of the dispersed phase inside the distributor was chosen for controlling the drop size. The experiments were carried out with a normal tubular distributor with 21 orifices of  $d_O = 2$  mm diameter. The dispersed phase was fed to one end of the distributor by a centrifugal pump. The opposite end of the distributor pipe was closed by a PTFE membrane. With a conventional electromagnet a periodic mechanical impulse was generated on the film and transferred to the liquid inside the distributor. The pulsation frequency was adjusted with a frequency generator [6]. The pulsed distributor was attached to the bottom of a laboratory scale extraction column with a diameter of 190 mm as shown in Figure 2.



*Figure 1. Mechanism of drop formation and drop-size for different velocities.*

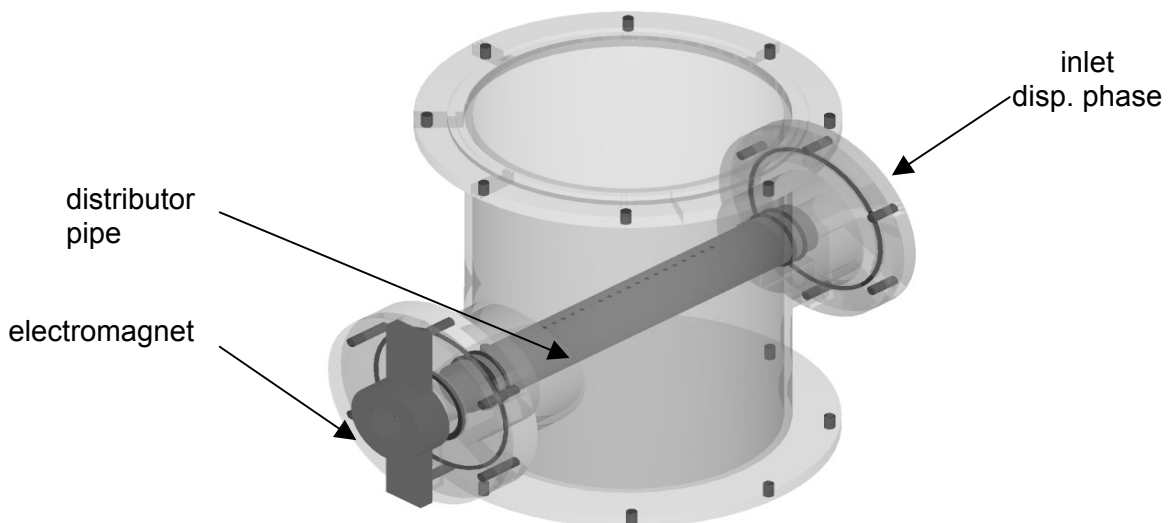


*Figure 2. Column section with the load independent distributor.*

Demineralized water was used as the continuous phase, the dispersed phase was ShellSol D70 ( $\rho_d = 798 \text{ kg m}^{-3}$ ,  $\eta_d = 1.7 \cdot 10^{-3} \text{ Pa s}$ ,  $\gamma = 34.3 \cdot 10^{-3} \text{ N m}^{-1}$ ). In all experiments the continuous phase was at rest. 350 mm above the distributor, the drop-size distribution was measured with the capillary suction method and the mean drop diameter was calculated. By changing the flowrate, the mean liquid velocity in the orifices was varied between 0.2 and  $1.15 \text{ m s}^{-1}$  in steps of  $0.1 \text{ m s}^{-1}$ . The pulsation frequency was changed between 0 and 45 Hz in steps of 5 Hz. At lower flowrates not every orifice was operating and at higher flowrates spraying started. A pulsation frequency higher than 45 Hz had no effect as the amplitude is too small due to the inertia of the oscillator.

## RESULTS AND DISCUSSION

Figure 3 shows the Sauter mean diameter for all combinations of liquid velocity and pulsation frequency in form of a fitted hyper surface. Without pulsation, corresponding to  $f_p = 0 \text{ Hz}$ , the well known dependency of the drop size on the velocity was observed with a distinct minimum at a velocity of  $0.4 \text{ m s}^{-1}$  and an increasing drop size at lower and higher velocities.

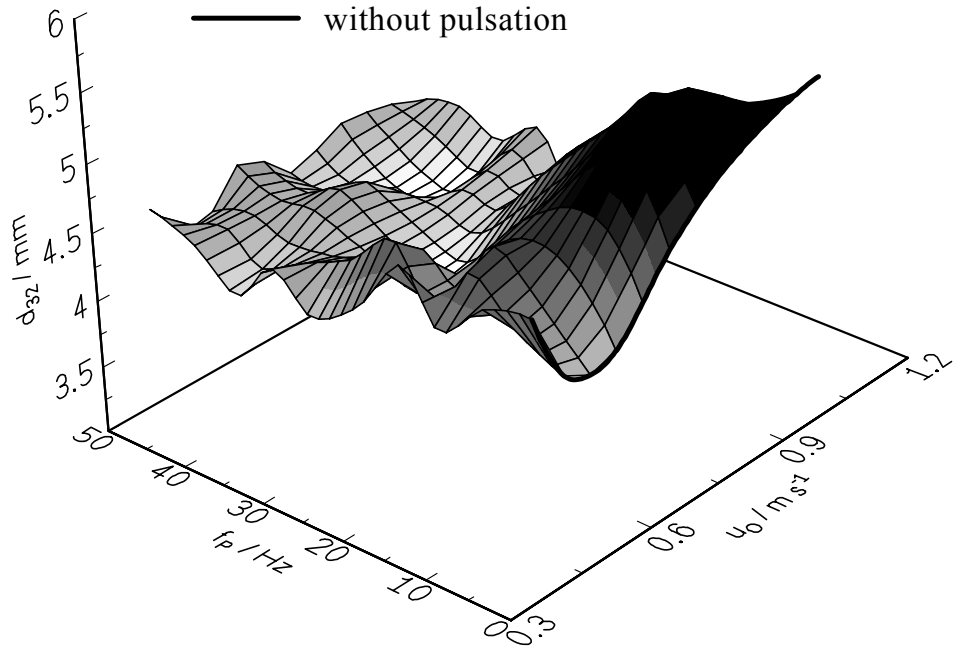


Figure 3. Sauter mean diameter vs. velocity and pulsation frequency.

The pulsation allowed the control of drop size. The diameter remained at the low level of the minimum in unpulsed operation and was independent of the liquid velocity and, therefore, of the flowrate of the dispersed phase. The operating range for a desired drop size of the distributor was widened substantially. If the distributor is designed for a velocity of  $0.4 \text{ m s}^{-1}$  without pulsation, with pulsation it can be operated between  $0.3$  and  $1.2 \text{ m s}^{-1}$  which corresponds to a load ratio of 1:4.

Besides the mean diameter the width of the drop-size distribution is an important criterion. Figure 4 shows the measured drop-size distribution for two different operating conditions. The upper part of the figure shows the drop-size distribution at unpulsed conditions, the lower part for a

pulsation frequency of  $f_P = 35$  Hz. In both experiments the mean liquid velocity was  $u_O = 0.53 \text{ m s}^{-1}$  which corresponds to a Weber number of  $We = 13$ . Without pulsation a bimodal distribution typical for drop formation by jet disruption was observed. A pulsation of  $f_P = 35$  Hz forced 80 % of all drops to be formed in a class of 0.2 mm width, i.e., the drop-size distribution was nearly monodisperse.

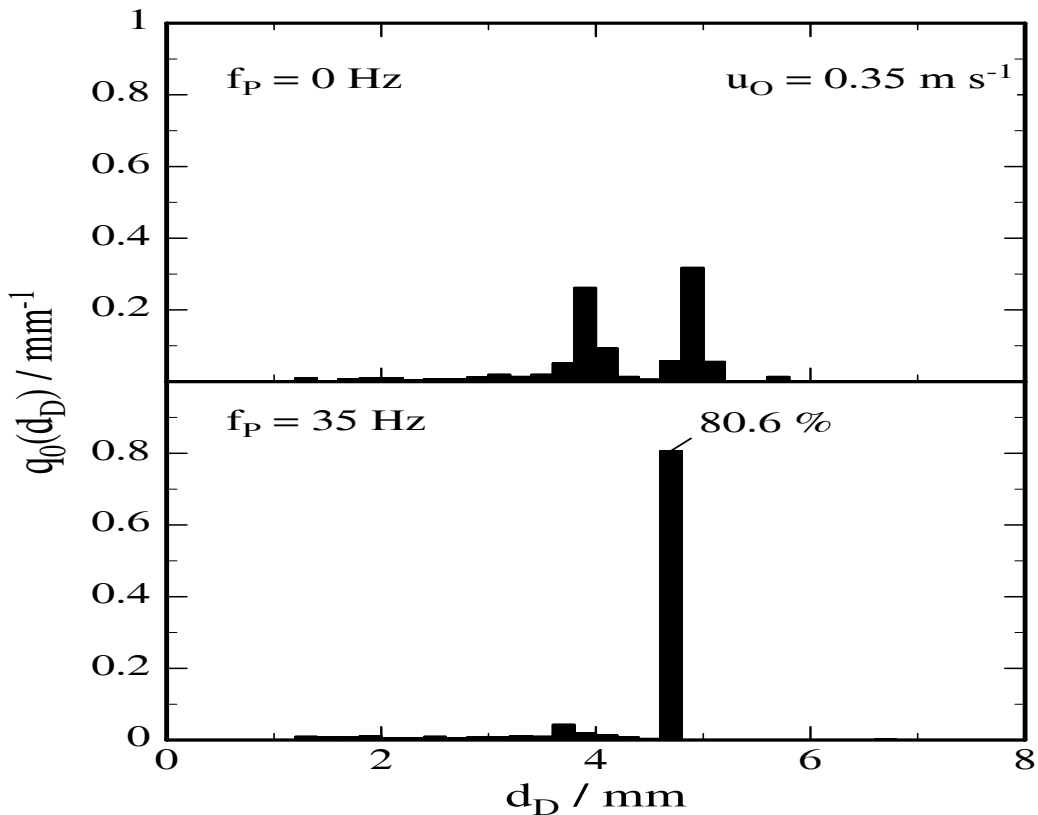
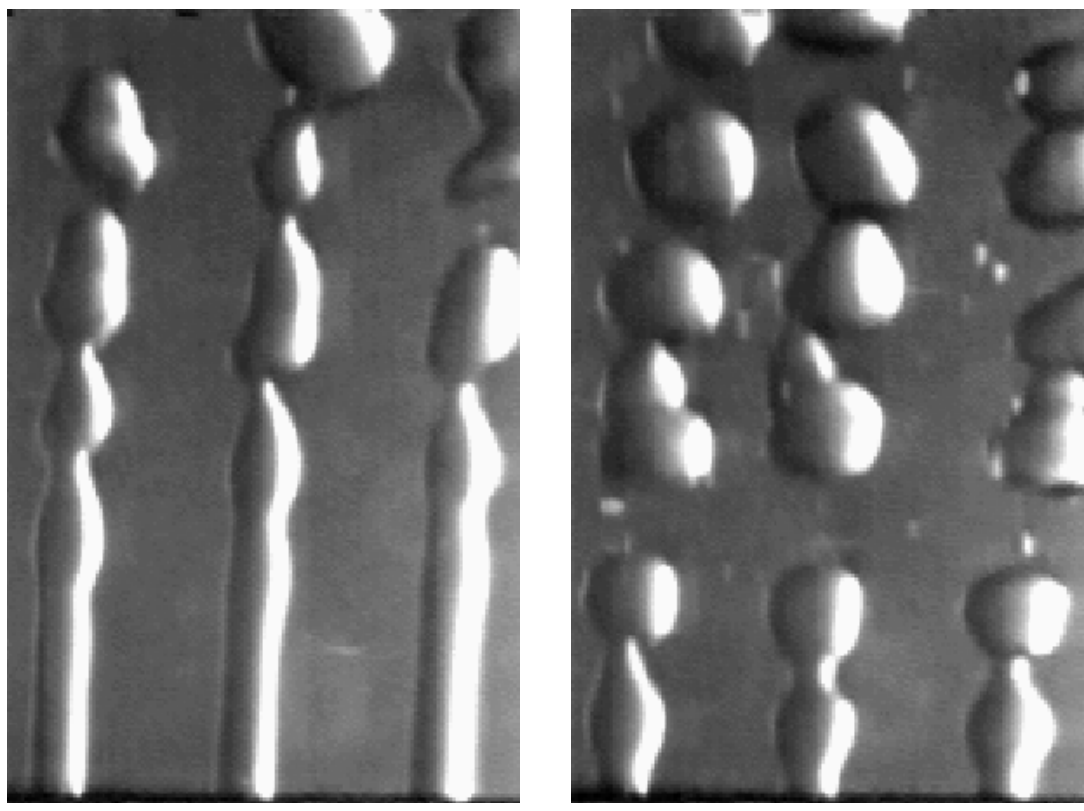


Figure 4. Drop-size distribution at pulsed and unpulsed conditions and a liquid velocity of  $u_O = 0.53 \text{ m s}^{-1}$ .

The pulsation triggers the detachment of drops from the jet at the pulsation frequency so that equally sized drops are formed. Figure 5 shows digitized still frames of a high-speed video sequence of both experiments. The drop formation under unpulsed conditions is shown in Figure 5a. Instabilities were forming waves on the surface of the jet. (The dark line at the bottom is the top surface of the distributor pipe.) If the length of the jet exceeded one wavelength of the disturbance, a drop was formed by disruption. If the jet length is not an integer multiple of the wavelength, Meister and Scheele [7,8] observed an alternation of the drop size and jet length between two stable states. This phenomenon was observed at the central jet in the picture. The two drops above the jet were of different size. The complete video sequence has clearly shown the alternation of the jet length. The bimodal drop-size distribution in Figure 5a proves this fact.

Figure 5b shows the drop formation at the same liquid velocity under pulsed conditions. The liquid jets were shorter than without pulsation, all drops formed being nearly the same size. The drop formation under pulsed conditions occurred by jet disruption, too, but the disturbance was generated by the pulsation and not by instability of the flow. Without pulsation such short liquid jets can be observed only at the transition from single drop formation to jet disruption at a lower liquid velocity. The pressure impact of the mechanical impulse from the electromagnet creates a much stronger disturbance as the natural disturbance generated by surface forces at the interface between the continuous phase and the jet.



a) without pulsation

b) at a pulsation of  $f_P = 35 \text{ Hz.}$

*Figure 5. High speed still frames of drop formation at a liquid velocity of  $u_O = 0.53 \text{ m s}^{-1}$ .*

## CONCLUSIONS

Mechanical pulsation of the liquid in a distributor allows control of the drop size independent of the flowrate in a wide load range. Very narrow, nearly monodisperse drop-size distributions are produced, which is not possible with conventional distributors. The operating range is much enlarged compared to unpulsed conditions.

For liquid-liquid extraction columns with structured packing this behavior is of particular advantage with respect to mass transfer as these columns may be operated in a wide load range. The narrow drop-size distribution also reduces the forward mixing of the dispersed phase because drops of the same size have the same rising velocity in the column. Since all the required additional equipment is installed outside the column, the free cross section in the distributor area of the column is not affected.

## ACKNOWLEDGEMENT

Financial support by the AiF (Association of Industrial Research Organisations) "Otto von Guericke e.V." is gratefully acknowledged.

## NOMENCLATURE

### Latin symbols

$d$	[m]	diameter
$f$	[Hz]	frequency
$u$	[m s <sup>-1</sup> ]	liquid velocity
$q_0$	[mm <sup>-1</sup> ]	number-density-distribution

### Greek symbols

$\gamma$	[N m <sup>-1</sup> ]	surface tension
$\eta$	[Pa s]	dynamic viscosity
$\rho$	[kg m <sup>-3</sup> ]	density

### Indices

d	dispersed phase
O	orifice
P	pulsation
D	drop

### Dimensionless numbers

$$We = \frac{\rho_d u_O^2 d_O}{\gamma} \quad \text{Weber number}$$

## REFERENCES

1. D. Möhring and S. Weiß (1997), *Chem.-Ing.-Tech.*, **69**, 812-816.
2. A. Eckstein and A. Vogelpohl (1998), *Chem.-Ing.-Tech.*, **70**, 1553-1556.
3. F. Widmer (1965), *Chem.-Ing.-Tech.*, **37**, 39-43.
4. P. Walzel (1979), *Chem.-Ing.-Tech.*, **51**, 525.
5. J.C. Yang, W. Chien, M. King and W.L. Grosshandler (1997), *Exp. in Fluids*, **23**, 445-447.
6. Patent Application No. 198 52 601.6, German Patent Office (1998).
7. B.J. Meister and G.F. Scheele (1969), *AIChE J.*, **15**, 700-706.
8. B.J. Meister and G.F. Scheele (1968), *AIChE J.*, **14**, 9-15.



## APPLICATION OF DRIFT FLUX THEORY TO PACKED EXTRACTION COLUMNS

Lintong S. Hutahaean, Vincent Van Brunt and Jeffrey S. Kanel\*

Department of Chemical Engineering, University of South Carolina, Columbia, USA  
\*Dow Chemical Company, South Charleston, USA

Wallis drift flux theory was used to develop flooding correlation for continuous-phase-wetted packed liquid-liquid extraction columns. The average absolute error associated with the new correlation is 21.7% for 295 data points, almost a factor of 2 less than previously developed correlations. The Wallis drift flux expression was modified to  $j_{dc} = V_\infty \alpha (1-\alpha) \exp(m\alpha)$ . Here,  $V_\infty$  is a characteristic velocity,  $m$  measures the deviation of slope of the square root superficial velocity plot from the theoretical value of -1, and  $\alpha$  is the dispersed phase holdup. The new correlation method predicts  $V_\infty$  and the maximum drift flux at flooding ( $j_{dc,max}$ ), through which the parameter  $m$  is then determined.

### INTRODUCTION

Wallis [1] developed a one-dimensional drift flux model to describe two-phase flow in a column. Equation 1 is the definition of drift flux ( $j_{dc}$ ) where  $\alpha$  is dispersed phase holdup while  $j_d$  and  $j_c$  are flux or superficial velocities of the dispersed and continuous phases respectively.

$$j_{dc} = (1-\alpha) j_d + \alpha j_c \quad (1)$$

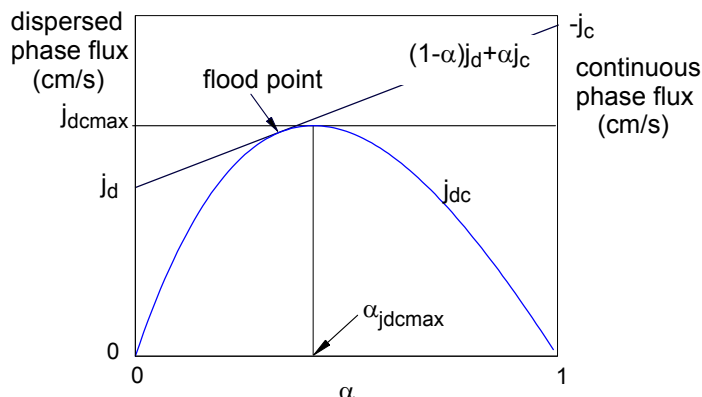


Figure 1. Relation between  $j_{dc}$ ,  $j_c$ ,  $j_d$ , and  $\alpha$ .

The right hand side of equation 1 represents a straight line connecting points  $(0, j_d)$  and  $(1, j_c)$  on plot of holdup versus flux that is tangent to  $j_{dc}$  curve as shown in Figure 1. Wallis [1] suggested equation 2 to approximate the relationship between  $j_{dc}$  and  $\alpha$ .

$$j_{dc} = V_\infty \alpha (1-\alpha)^n \quad (2)$$

Our previous investigation [2] revealed that a modification of equation 2 to the form shown by equation 3 was needed to improve the approximation.

$$j_{dc} = V_\infty \alpha (1 - \alpha) \exp(m \alpha) \quad (3)$$

Superficial velocities of both phases can be correlated in terms of  $V_\infty$ ,  $m$  and  $\alpha$  as follows. Equating equation 1 and equation 3, and inspecting the tangent results in

$$j_d = V_\infty \alpha e^{m\alpha} - \alpha / (1 - \alpha) j_c \quad (4)$$

$$j_c - j_d = dj_{dc}/d\alpha = V_\infty e^m [1 + (m-2) \alpha - m \alpha^2] \quad (5)$$

Combining equations 4 and 5 leads to the following explicit equations for  $j_d$  and  $j_c$ .

$$j_c = V_\infty e^{m\alpha} (1 - \alpha) [1 + (m-1) \alpha - m \alpha^2], \quad j_d = -V_\infty e^{m\alpha} \alpha [(m-1) \alpha - m \alpha^2] \quad (6), (7)$$

Thus, to determine  $j_d$  for a given  $j_c$ , one has to first solve for  $\alpha$  from equation 6 then calculate  $j_d$  using equation 7.

### Extracting $V_\infty$ and $m$ from Flooding Data

Most flooding data do not provide holdup values; thus it should be extracted from the data. For flooding data that form a straight line on  $j_c^{1/2}$  vs.  $j_d^{1/2}$  with slope  $k_2$ , the following relation can be derived and used to estimate holdup from flooding data.

$$\alpha = j_d^{1/2} / (j_d^{1/2} - k_2 j_c^{1/2}) \quad (8)$$

Thus a representative holdup for each data point and its corresponding drift flux (equation 1) can be calculated provided that a representative value of slope exists. Hence, the constants  $V_\infty$  and  $m$  can be extracted from each flooding data series by fitting the resulting  $j_{dc}$  and  $\alpha$  values to equation 3. Figure 2 shows representative flooding data and their respective holdups that were obtained using the above procedure.

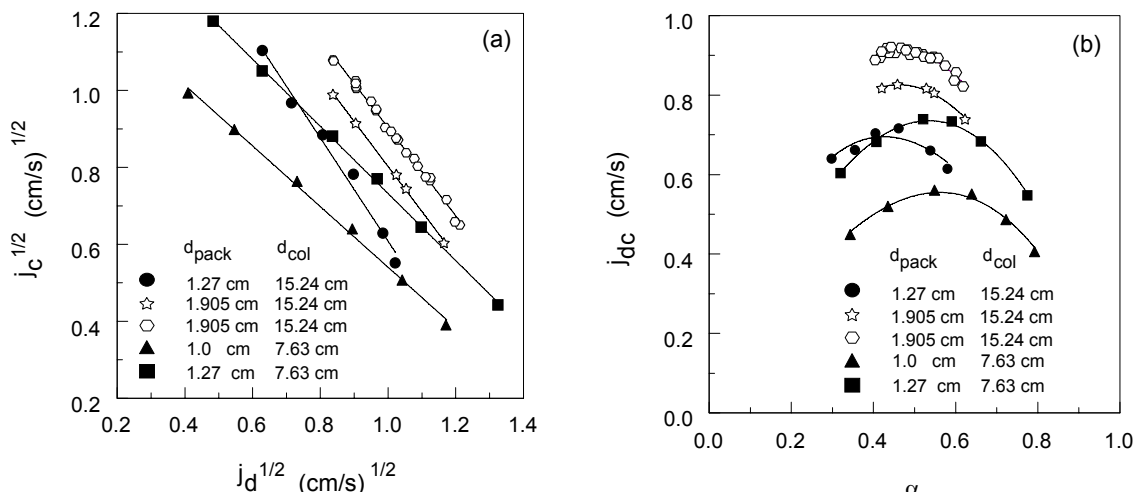


Figure 2. (a) Flooding data of methyl isobutyl ketone (*d*)-water systems with Raschig rings [7] and (b) their corresponding holdup and drift flux;  $d_{pack}$  and  $d_{col}$  are packing and column diameters, respectively.

## CORRELATION DEVELOPMENT

There are two constants,  $V_\infty$  and  $m$ , that need to be correlated in terms of physical and packing properties: densities ( $\rho_d$ ,  $\rho_c$ ), density difference ( $\Delta\rho$ ), viscosities ( $\mu_d$ ,  $\mu_c$ ), interfacial tension ( $\sigma$ ), packing void fraction ( $\varepsilon$ ), specific surface area ( $a_p$ ), and packing size ( $d_p$ ). Observation on the resulting  $V_\infty$  and  $m$  values and the values of the maximum drift flux ( $j_{dc,max}$ ), which corresponds to a condition where  $j_d = j_c$ , suggests that correlation be developed to predict  $V_\infty$  and  $j_{dc,max}$ . Once  $j_{dc,max}$  and  $V_\infty$  are predicted, the value of  $j_{dc,max}/V_\infty = f_\alpha = \alpha_{jdcmax}(1-\alpha_{jdcmax}) \exp(m\alpha_{jdcmax})$  can be calculated. Furthermore, since  $\alpha_{jdcmax}$  is also a function of  $m$ , that is (by solving  $d_{dc}/d_\alpha = 0$  for  $\alpha$ )

$$\alpha_{jdcmax} = \left( m - 2 + \sqrt{m^2 + 4} \right) / (2m) , \quad (9)$$

$m$  can be determined from  $f_\alpha$ . For convenience, the following explicit functions were developed and can be used as alternatives.

$$\text{For } f_\alpha \geq 0.25: m = 1.6648 [\ln(4 f_\alpha)]^{0.8695}. \quad (10)$$

$$\text{For } f_\alpha < 0.25: m = \ln(0.1211 - 4.5331 f_\alpha + 47.488 f_\alpha^2 - 61.3402 f_\alpha^3). \quad (11)$$

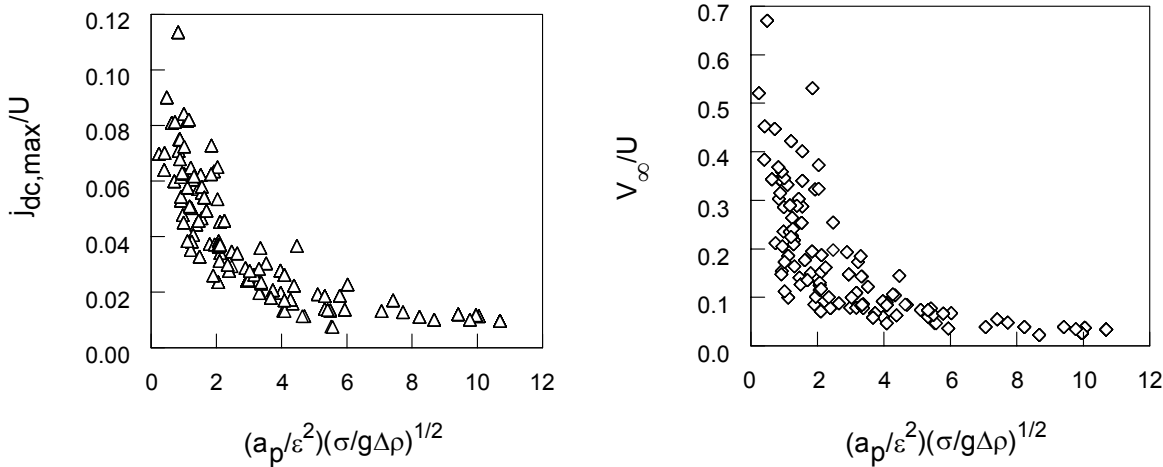


Figure 3. Maximum drift flux and characteristic velocity plotted against  $N_1$ . Both were made dimensionless by dividing them with terminal velocity calculated with equation 12.

For correlation development purposes,  $j_{dc,max}$  and  $V_\infty$  were made dimensionless by dividing them with the terminal rise velocity of a single drop in an infinite continuous phase,  $U$ , calculated using the recently published prediction of Jamialahmadi et al. [3] as shown by equation 12 below. By taking the drop characteristic length as  $(\sigma/(g\Delta\rho))^{1/2}$ ,  $U^{sp}$  is a modified Hadamard-Rybczynski [4,5] terminal velocity of a small sphere subject to internal circulation and  $U^w$  is a modified drop rise velocity from wave analogy for large drops.  $U^{sp}$  and  $U^w$  are given by equations 13 and 14, respectively. With this choice it is expected that the ratio of  $V_\infty$  to  $U$  will asymptotically approach unity as  $N_1 = (a_p/\varepsilon^2)(\sigma/(g\Delta\rho))^{1/2}$ , which measures the ratio of drop-size to the packing size, approaches zero; thus, it represents a measure of flow resistance due to the packing.

$$U = \frac{U^{sp} U^w}{\sqrt{(U^{sp})^2 + (U^w)^2}}, \quad U^{sp} = \frac{1}{18} \frac{\sigma}{\mu_c} \left[ \frac{3\mu_c + 3\mu_d}{2\mu_c + 3\mu_d} \right] \quad (12), (13)$$

$$U^w = \sqrt{\frac{2(g\sigma\Delta\rho)^{1/2}}{(\rho_c + \rho_d)} + \left(\frac{g\sigma}{4\Delta\rho}\right)^{1/2}} \quad (14)$$

Dimensionless forms of maximum drift flux ( $j_{dc,max}/U$ ) and characteristic velocity ( $V_\infty/U$ ) are plotted against  $N_1$  in Figure 3 for 130 data series representing 798 data points. Both figures show that the effects of various factors decrease as  $N_1$  increases. Although all previously correlated dimensionless groups used for development of flooding correlations by other researchers [6,7,8] were tried, only the following groups were found to significantly affect the correlation.

$$\begin{aligned} N_1 &= a_p/\varepsilon^2(\sigma/(\Delta\rho g))^{1/2} & N_2 &= a_p d_p & N_3 &= \rho_d/\Delta\rho & N_4 &= (\Delta\rho^2 g/\mu_c^2)^{1/3}/a_p \\ N_5 &= \Delta\rho/\rho_c & N_6 &= \mu_d/\mu_c & N_7 &= (\rho_d+\rho_c)/\Delta\rho \end{aligned}$$

### Flooding Correlation for Systems that meet Criteria

In practice, most commercial packed columns are designed to meet both of the packing size criteria; packing diameter should be larger than  $2.42[\sigma/(g\Delta\rho)]^{1/2}$  and the ratio of packing diameter to column diameter should be less than 1/8. Therefore, it is important that the correlation be developed only using data that meet both these criteria. Various combinations of equations involving the above dimensionless groups were tried; dependencies on influencing groups were evaluated graphically by examining the residuals and goodness of fit parameters. The following correlations were obtained using only data that meet both criteria whose physical property ranges are listed in Table 1. The average absolute relative error for predicting  $V_\infty$  and  $j_{dc,max}$  are 16% and 8%, respectively.

$$\ln\left(\frac{V_\infty}{U}\right) = \left(C_1 \varepsilon^{4.2} + C_2/N_2 + C_3/N_4 + C_4 N_5^{0.29}\right) N_1 + C_5 N_3 N_4^{-0.337} + \left(C_6 \varepsilon^{5.3}/N_2 + C_7 N_3^{0.55} + C_8\right) \ln(N_1 + 1) \quad (15)$$

$$\begin{aligned} C_1 &= -1.495 \pm 0.190 & C_2 &= -2.08 \pm 0.17 & C_3 &= 1.318 \pm 0.168 & C_4 &= 0.448 \pm 0.029 \\ C_5 &= -0.744 \pm 0.047 & C_6 &= 10.85 \pm 1.66 & C_7 &= 0.912 \pm 0.069 & C_8 &= -2.239 \pm 0.093 \end{aligned}$$

$$\ln\left(\frac{j_{dc,max}}{U}\right) = \left(P_1(1-\varepsilon)/\varepsilon + P_2 N_3^{-0.47}\right) N_1 + P_3 N_3 N_6^{0.1} + P_4 + \left(P_5/N_2 + P_6 N_7^{-8.4} + P_7/N_4 + P_8 N_5\right) \ln(N_1 + 1) \quad (16)$$

$$\begin{aligned} P_1 &= 0.146 \pm 0.014 & P_2 &= -0.319 \pm 0.034 & P_3 &= -0.110 \pm 0.004 & P_4 &= -1.618 \pm 0.025 \\ P_5 &= -2.725 \pm 0.137 & P_6 &= 26.02 \pm 2.20 & P_7 &= -1.093 \pm 0.150 & P_8 &= -0.574 \pm 0.053 \end{aligned}$$

The dimensionless number  $N_2$  in the correlations accounts for the differences in random packing shape; different types of random packings with the same nominal size have different specific surface areas. For structured packings the nominal diameter is approximated as  $5.5\varepsilon/a_p$  thus  $N_2=5.5\varepsilon$ .

Although no adjustable specific constants for each type and size of packing are used in the correlation, the prediction is significantly better than that of existing correlation. In Figure 4, all the prediction points have been moved, in  $j_d$  vs.  $j_c$  space, so they collapsed into a single curve of  $j_d^* = 1 + j_c^* - 2j_c^{*1/2}$  or  $j_d^{*1/2} + j_c^{*1/2} = 1$ . The average error for the predicted dispersed phase velocity is only 21.7% for 295 data that meet the criteria. This is compared to the approximate 35% error of the direct correlations of Kumar and Hartland [8], Dell and Pratt [7], and Hutahean, Van Brunt and Kanel [6]. When tested with all data that meet the packing to column diameter ratio criterion regardless of packing size (482 data), the correlation has a 24.3% prediction error. Comparison to other correlations is also presented in Table 2 where the error associated with each type of packing is presented.

*Table 1. Packing types and physical property ranges for 295 data that meet the criteria of  $2.42(\sigma/(g\Delta\rho))^{1/2} \leq \text{packing diameter} \leq 1/8 \text{ column diameter}$ .*

Physical properties	Range	Packing type	Size (cm)
Continuous phase density, g/cm <sup>3</sup>	0.985 - 1.58	Raschig rings	0.6 - 3.81
Dispersed phase density, g/cm <sup>3</sup>	0.697 - 13.6	Lessing rings	0.635
Continuous phase viscosity, cP	0.88 - 11	IMTP®	2.54 - 3.81
Dispersed phase viscosity, cP	0.50 - 70	Solid cylinder	0.635
Density difference ( $\Delta\rho$ ), g/cm <sup>3</sup>	0.114 - 12.6	Intalox 2T®	structured
Interfacial tension, dyne/cm	8.6 - 375	Filip®	structured
Flow ratio, $j_d/j_c$	0.02 - 19	Montz BI-300™	structured

*Table 2. Performance of different correlations in terms of percentage of AARE for each type of packing for flood data that meet criteria.*

Types of packing	No. of Data	Dell and Pratt <sup>7</sup>	Kumar and Hartland <sup>8</sup>	Correlations from our previous work <sup>6</sup>		This work
				Corr. 1	Corr. 2	
Intalox 2T®	5	9.0*	31.0	30.3	8.7	18.3
IMTP®	29	23.3*	44.2	34.2	38.2	21.3
Montz™	2	32.4*	24.0	38.4	31.8	34.8
Fillip®	4	21.6*	12.9*	14.2	21.9	19.4
Solid cylinder	4	17.3*	2.2*	38.1	29.8	22.0
Raschig rings	240	35.4	43.6	36.0	39.9	22.2
Lessing rings	11	82.0	15.5	25.5	11.2	13.0
All above types	295	35.1	41.3	35.1	37.7	21.7

\* Constant for the relevant correlation is determined in our previous work [6].

$$AARE = \frac{1}{NDP} \sum_{i=1}^{NDP} \frac{| \text{predicted value} - \text{observed value} |}{\text{observed value}}, \text{ NDP is number of data point.}$$

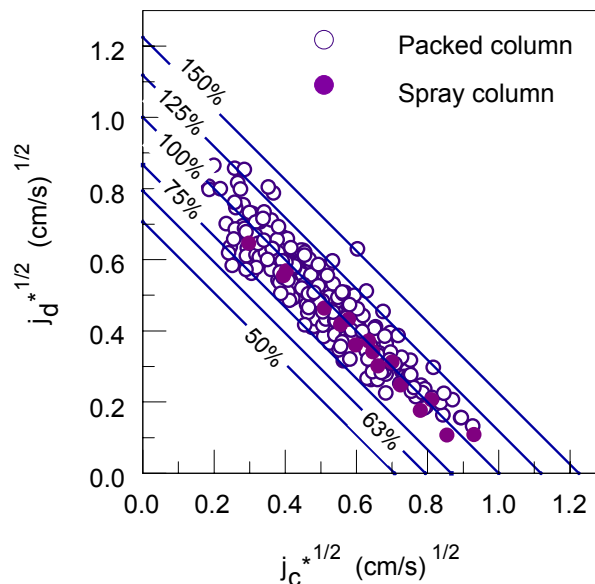


*Figure 4. Predicted and observed of flooding in terms of square root of superficial velocities for data that meet both criteria. The lines are relations based on corresponding percentage of predicted flooding. The prediction was calculated using equations 15, 16, 6, and 7.*

## CONCLUSIONS

New flooding correlations were developed, and they are the first ones for liquid-liquid systems derived using drift flux theory and without incorporating specific constants that depend on type or size of packing. The correlations, equations 15 and 16, have an average absolute relative error of 21.7% for 295 data points in predicting the dispersed phase velocity, very far below the errors possible with previously developed correlations using the same data set. They can easily be used with new packings since  $\varepsilon$ ,  $a_p$  and  $d_p$  are used in correlations. Most data fell within a band from 75% to 125% of predicted flooding. Using these correlations, design based on 50% of predicted flooding can be considered conservative.

## REFERENCES

1. B. G. Wallis (1969), One-dimensional Two-phase Flow, McGraw-Hill, New York.
2. L. S. Hutahaean, J. S. Kanel and V. Van Brunt (1999), *Proc. Int. Solvent Extr. Conf., ISEC '99*, Barcelona, Spain, pp. 1585-1592.
3. M. Jamialahmadi, C. Branch and H. Muller-Steinhagen (1994), *Trans. I. Chem. E.*, **72**, 119.
4. J. S. Hadamard (1911), *Compt. Rend. Acad. Sci. Paris*, **152**, 1735-1738.
5. W. Rybczynski (1911), *Bull. Acad. Sci. Cracovie*, **A**, 40-46.
6. L. S. Hutahaean, J. S. Kanel, and V. Van Brunt, Predicting Flooding in Continuous-Phase-Wetted Packed Extraction Columns; Part I, A Direct Correlation Using the Wallis Model. Submitted for publication in *Ind. Eng. Chem. Res.*
7. F. R. Dell and H. C. R. Pratt (1951), *Trans. I. Chem. E.*, **29**, 89-109.
8. A. Kumar and S. Hartland (1994), *Ins. Chem. Engr.*, **72**, 89-104.
9. E. Brunazzi and A. Paglianti (1997), *AIChE J.*, **43**, 317-327.
10. R. P. Chhabra and J. Bangun (1997), *Canad. J. Chem. Eng.*, **75**, 817.
11. R. Gayler, N. W. Roberts, and H. R. C. Pratt (1953), *Trans. I. Chem. E.*, **31**, 57-68.
12. A. F. Siebert and J. R. Fair (1988), *Ind. Eng. Chem. Res.*, **27**, 470-481.
13. J. H. Ballard and E. L. Piret (1950), *Ind. Eng. Chem.*, **42**, 1088-1098.
14. F. H. Blanding and J. C. Elgin (1942), *Trans. AIChE*, **38**, 305-335.
15. E. H. Hoffing and F. J. Lockhart (1954), *Chem. Eng. Prog.*, **50**, 94-103.
16. J. Mackowiak and R. Billet (1986), *Ger. Chem. Eng.*, **1**, 48-64.
17. J. W. Crawford and C. R. Wilke (1951), *Chem Eng Prog.*, **47**, 423-431.
18. B. C. Sakiadis and A. I. Johnson (1954), *Ind. Eng. Chem.*, **46**, 1229-1239.
19. J. S. Watson and L. E. McNeese (1973), *AIChE J.*, **19**, 230-237.
20. J. S. Watson and L. E. McNeese (1972), *Oak Ridge National Laboratory Report*, No. ORNL-TM-3259, Tennessee, 216-237.
21. J. S. Watson, L. E. McNeese, and J. Day (1975), *AIChE J.*, **21**, 1080-1086.
22. J. A. Rocha and J. L. Bravo (1993), *Ind. Eng. Chem. Res.*, **32**, 641-651.
23. S. Jayanti, A. Tokarz, and G. F. Hewitt (1996), *Int. J. Multiphase Flow*, **22**, 307-324.
24. J. H. Jeong and H. C. No (1996), *Int. J. Multiphase Flow*, **22**, 499-514.
25. Y. Koizumi and T. Ueda (1996), *Int. J. Multiphase Flow*, **22**, 31-43.
26. C. E. Lacy and A. E. Dukler (1994), *Int. J. Multiphase Flow*, **20**, 219-233.
27. C. E. Lacy and A. E. Dukler (1994), *Int. J. Multiphase Flow*, **20**, 235-247.



## A BACKFLOW MODEL TO DETERMINE BACKMIXING IN A VIBRATING PLATE EXTRACTION COLUMN FOR A DISSOCIATION EXTRACTION

Bridget Hutton, Ales Heyberger\*, Peter Myburgh\*\* and Ilse Godwin

CSIR Bio/Chemtek Speciality and Fine Chemicals Programme, Modderfontein, South Africa

\*Institute of Chemical Process Fundamentals, Czech Academy of Sciences,  
Prague, Czech Republic

\*\*Private Consultant, Johannesburg, South Africa

An industrial process was developed whereby a phenolic derivative and a semi-oxidised form of a phenolic derivative were separated using dissociation extraction. The large difference in the component de-protonation constants, and the fact that the ionic forms of both components are not soluble in the solvent, was exploited. The system characteristics were quantified by performing shake tests and then piloted using a mixer-settler and a vibrating plate extraction column. In order to quantify the axial mixing characteristics of the column, a specific backflow model was developed which accounted for the properties of the system.

### INTRODUCTION

A phenolic derivative (referred to as component B) was produced by preferential oxidation of a mixture of various constituents. The post oxidation mixture was subjected to various unit operations prior to the dissociation extraction, which was used to separate the product B from a residual phenolic reagent (component A). The components were separated by exploiting the large difference in the de-protonation,  $pK_a$  constants (9.8 and 7.7 respectively) and the fact that the ionic forms of neither A nor B were soluble in the solvent. The pH was adjusted to the required level by adding a stoichiometric deficiency of a mineral acid, thereby allowing selective protonation of component A and not component B. The re-protonated species of A was then extracted using an organic solvent, while the sodium salt of component B remained in the residual raffinate for subsequent processing. Downstream processing required significant removal of component A from the raffinate, while project economics constrained the allowable loss of component B in the extract. The extraction was piloted using a conventional mixer-settler and a vibrating plate extraction (VPE) column. Since the piloting was performed for the purposes of generating scale-up data for design of the commercial process, it was important to determine axial mixing in the extraction column. The use of a backflow model, as opposed to a diffusion model for quantifying axial mixing in VPE columns is well established.

## EXPERIMENTAL WORK

Shake tests were performed, whereby aqueous feed and solvent were mixed, the pH adjusted to the required value by addition of a mineral acid to allow selective protonation and extraction of component A, while component B remained in the residual raffinate. Extensive bench and pilot-scale testwork was performed on the system. The equipment used consisted of a single stage mixer-settler and a VPE column, set up in a counter-current manner, as depicted in Figure 1. Raffinate from the mixer settler was used as feed for the VPE and extract from the VPE as solvent for the mixer settler. The mixer-settler extract was subject to distillation to recover component A and the solvent, which was recycled back to the VPE.

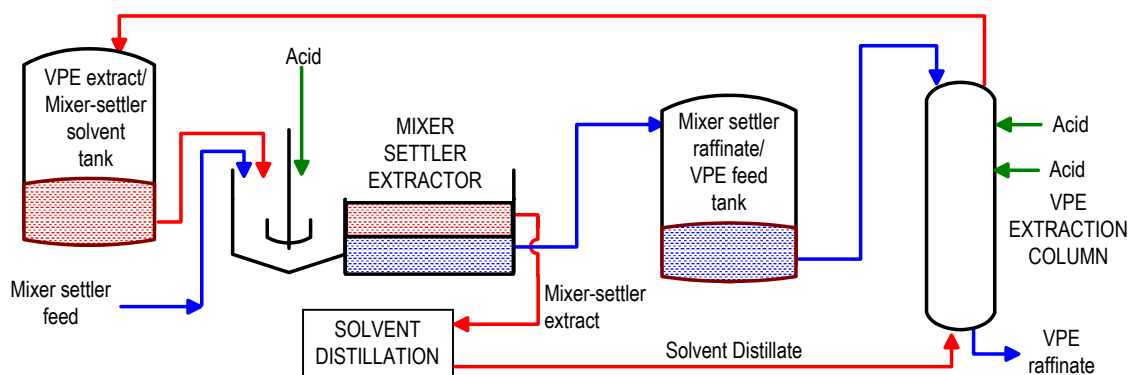


Figure 1. Set-up of the mixer-settler and VPE.

The VPE column is a type of reciprocating plate extractor, similar to the Karr column, but differing in plate design and mode of operation. The pilot-scale column of 50 mm diameter, was operated with 6 m of active height and stainless steel plates. The plates used had two types of holes; 3 mm holes for passage of the dispersed phase and 10 mm holes for the continuous phase. Acid requirements for each extraction test were pre-determined by performing acid titrations. The acid was added to the VPE at two positions; two thirds of the total acid required was added after 600 mm and the remaining third, 1 790 mm from the top of the VPE, respectively (to account for the decreasing concentration of component A in the aqueous phase). It was found that component A acted as a co-solvent for the extraction of component B - the higher the concentration of protonated component A in the solvent, the greater the loss of protonated component B. To minimise losses of component B, it was necessary keep the concentration of protonated B low in the mixer settler by maintaining a high pH of 10, while in the VPE, a low pH of 9 was required for sufficient removal of component A from the raffinate. In the VPE, any component B that was extracted in the region below the acid addition points was back extracted in the region above the first acid addition point, where the pH was high.

## THEORY

The de-protonation of any particular acid will have an equilibrium constant,  $K_A$  which is a measure of the extent of de-protonation in an aqueous solution:



By incorporating the definitions of the extent of de-protonation,  $pH$  and  $pK_A$ , it is possible to derive the following equation [1], which allows determination of the extent of de-protonation:

$$Dep = \frac{1}{10^{pK_a - pH} + 1} \quad (2)$$

Consider two components A and B, which exhibit an appreciable difference in their strengths as acids. Knowing the respective  $pK_a$  values and applying Equation (2), the theoretical extent of de-protonation versus  $pH$  can be plotted, as depicted below in Figure 2.

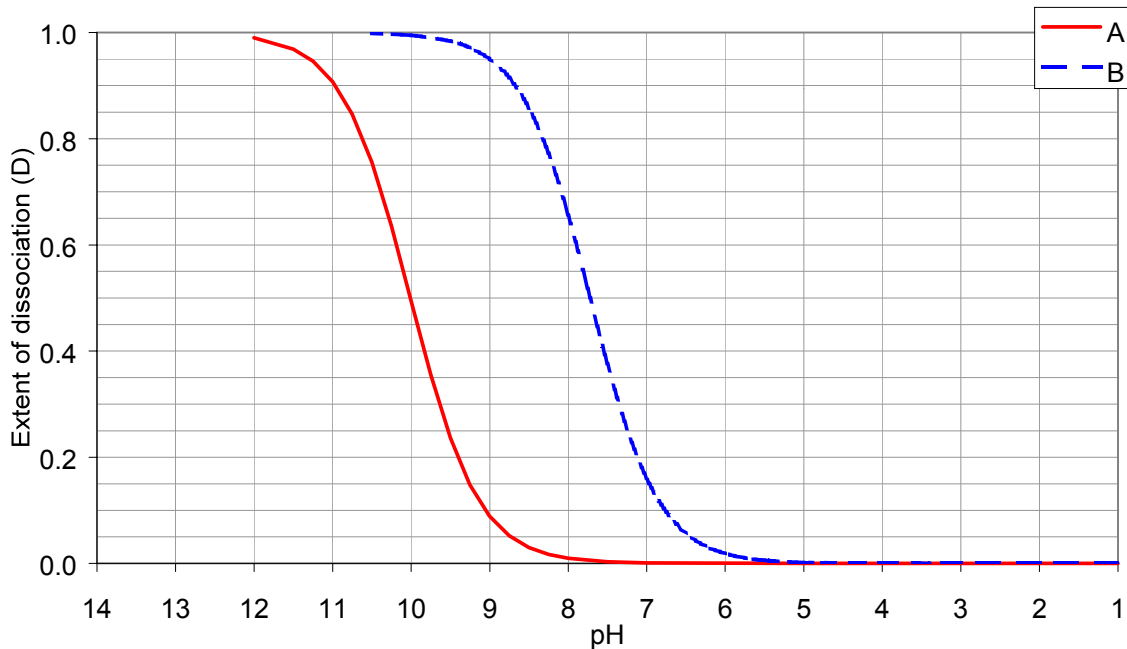


Figure 2. Extent of de-protonation versus  $pH$ .

The analytical method employed for determining the concentrations of components A and B does not differentiate between the protonated and de-protonated forms. Conventionally in solvent extraction, a distribution ratio is determined for one particular species and consequently when considering the distribution of component A, only the protonated species in each phase is considered. Not differentiating between the two species results in an average distribution ratio, which is strongly pH dependent (an overall distribution ratio), and which can be defined as follows (solubility of the de-protonated species of component A in a non-polar organic can be expected to be very low, and as such considered negligible, i.e.,  $C_{A,E} = 0$ ):

$$D_A = \frac{C_{A,E} + C_{A^-,E}}{C_{A,R} + C_{A^-,R}} \quad (3)$$

When calculating the true distribution ratio ( $D_A$ ) of component A between the aqueous and organic phases only the protonated species in each phase is considered, which results in a partition coefficient that is independent of pH. Using Equation 2 and the total concentration of component A (determined analytically), it is possible to distinguish between protonated and de-protonated forms of component A in the aqueous phase and calculate the distribution ratio:

$$m_A = \frac{C_{A,E}}{C_{A,R}} \quad (4)$$

## THE MODEL

The behaviour of the VPE is such that a layer of the dispersed phase forms above or below the reciprocating plates (depending on which phase is dispersed), the droplets coalesce and are then re-dispersed by the action of the plates. This partially stagewise mode of operation determines the applicability of a backflow model to determine axial mixing in the VPE. For the industrial process under consideration, it was necessary to modify the conventional models.

The characteristics of the process, which had to be taken into account by the model, included:

- only the protonated species of component A was extracted by the solvent, while the ionic species remained in the raffinate.
- acid was added at two points along the length of the column, resulting in re-protonation of component A,
- the equilibrium relationship of component A was non linear.

In order to account for the fact that only the protonated species was extracted, the model could be structured using one of two approaches:

- either using the pH profile through the length of the column to calculate the concentration of protonated component A,
- or, considering the addition of acid as addition of protonated component A to the column.

The second method was selected since it allowed a more simplified approach. Some acid was consumed by organic impurities in the system and it was necessary to estimate the proportion of the acid that was used to re-protonate component A. By considering the ratio of the moles of re-protonated component A to acid protons added it was found that approximately 53% of the acid was used to re-protonate component A.

The specific form of the backflow model applied to the system was the conventional "Mass Transfer Coefficient model" [2] where both forward and backmixing were taken into account. The backmixing coefficients of the continuous and dispersed phases were assumed constant through the length of the column. This assumption was adopted since it substantially simplified the mathematical description of the process. The model was set up in an Excel spreadsheet. Experimental steady state concentration profiles of component A in both the dispersed and continuous phases were measured. Using the theory described above and the sample pH measurements, it was possible to determine the concentration of protonated component A in the aqueous phase. The results were then interpreted by "force fitting" the model to the experimentally determined concentration profiles using the excel solver function. This allowed determination of the coefficients of backmixing and the overall mass transfer coefficient.

## RESULTS

The equilibrium data (total concentrations of component A) are plotted in Figure 3. The pH represents the pH of the raffinate after reaching equilibrium. Since only the protonated species is extracted into the organic solvent, the overall distribution ratio of component A (ionic and protonated) is dependent on pH (effectively is a measure of the extent of de-protonation). Using the total concentration of A and the measured pH, the concentration of de-protonated species in the aqueous phase was calculated (Equation 2), which allowed determination of the concentration of the protonated species in the aqueous phase. The equilibrium data of the protonated species is depicted in Figure 4. The distribution ratio of protonated species A is independent of pH, however it is not constant, but dependent on the concentration of protonated species A in the organic phase, probably as a result of the association of simple molecules into complex molecules in the organic phase.

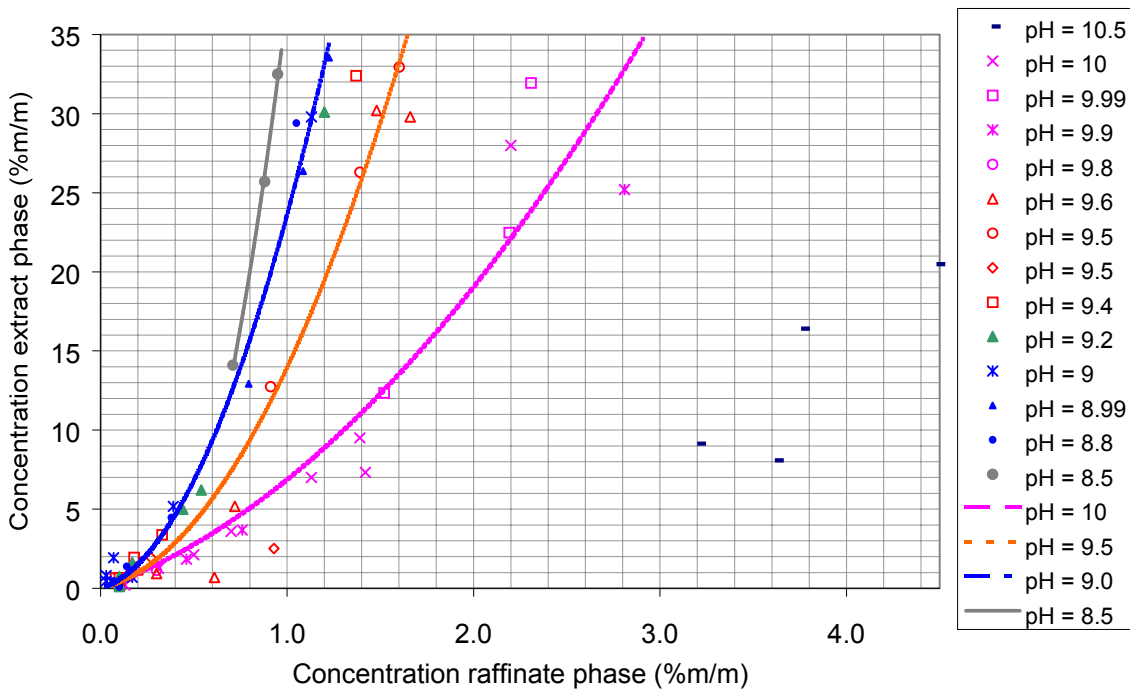


Figure 3. Analytical equilibrium data.

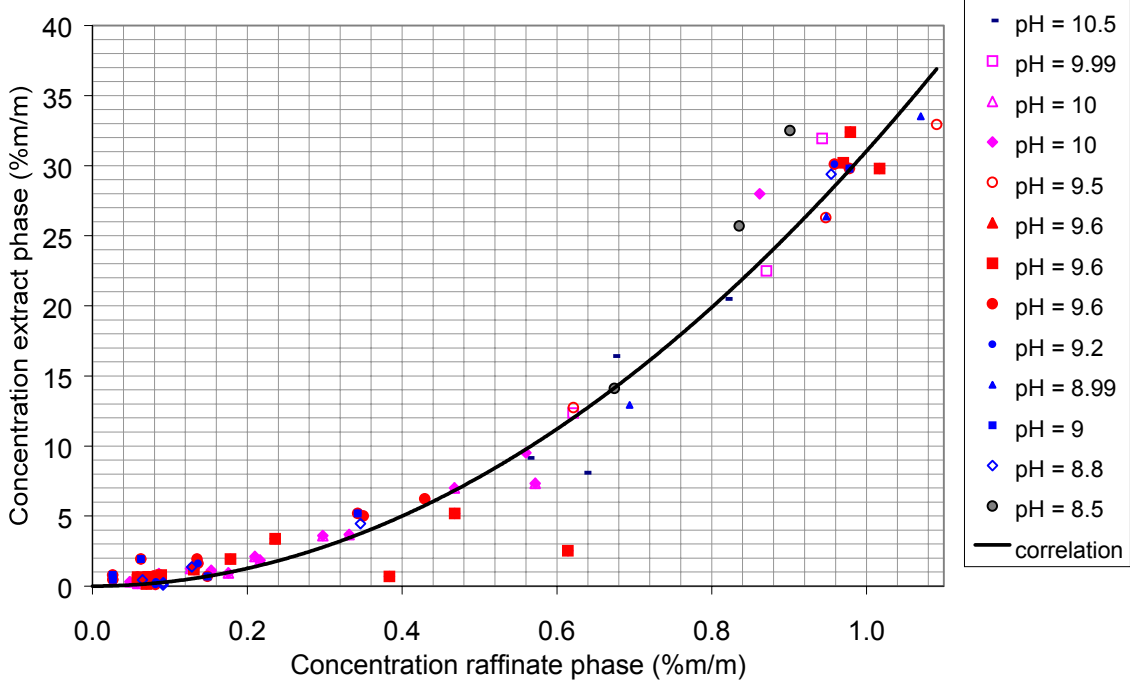


Figure 4. Protonated species equilibrium data.

During piloting the mixer-settler extracted 75% of component A, while the VPE extracted 92% of the residual component A. The entire extraction operation reduced the feed concentration of component A from 8.5% m/m to less than 0.2% m/m in the VPE raffinate, while losing only 2% of component B in the mixer-settler extract. The column concentrations profiles of protonated component A were “force fitted” with the model to evaluate the model parameters (backmixing ratios and the overall mass transfer coefficient). A typical operating line, as predicted by the model is depicted in Figure 5. The operating line discontinuities represented the points at which acid was added to the column, since the acid releases protonated component A, thereby

changing the protonated component A mass balance (essentially three operating lines exist). It was found that backmixing of the dispersed and continuous phases in the VPE was low, a property typical of the VPE.

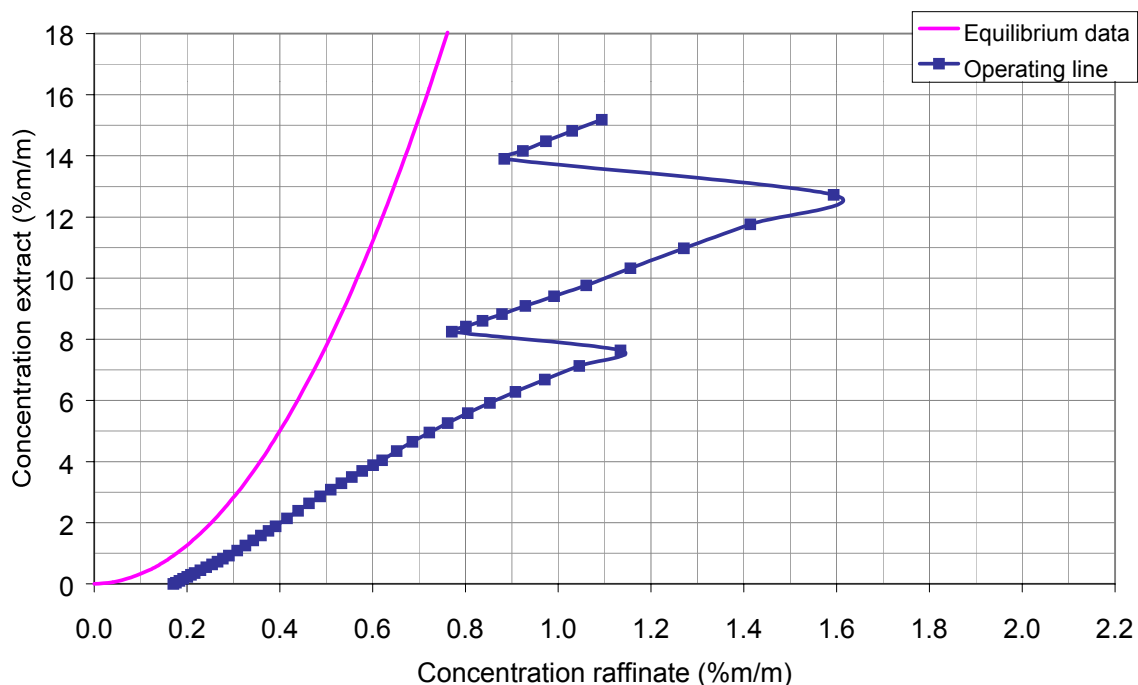


Figure 5. Typical equilibrium line and operating line predicted by the model.

## CONCLUSIONS

The novel use of a VPE to perform a dissociation extraction was proven. The theoretical methods of predicting the extent of protonation of component A allowed quantification of the equilibrium data. The general form of the Backflow model was modified to allow prediction of a dissociation extraction and axial mixing in the VPE was found to be low.

## NOMENCLATURE

$C_A$	: concentration of protonated component A
$C_{A-}$	: concentration of de-protonated form of component A
$C_{H^+}$	: concentration of hydronium ion,
$Dep$	: extent of deprotonation ,
$K_a$	: de-protontion equilibrium constant
$D$	: distribution ratio of component A,

### subscripts

$E$	- extract
$R$	- raffinate

## REFERENCES

1. S. Glasstone (1995), Textbook of Physical Chemistry, Macmillan and Co. Ltd., London.
2. H.R.C. Pratt and M. H. I Baird (1983), Handbook of Solvent Extraction, John Wiley, pp. 199 - 247.



## LIQUID-LIQUID MINIPLANT EXTRACTOR – A NOVEL TOOL FOR PROCESS DESIGN

Peter Kolb and Hans-Jörg Bart

Institute of Thermal Process Engineering, University of Kaiserslautern,  
Kaiserslautern, Germany

Experimental studies using a 32 mm diameter miniplant extractor are presented including a description of the auxiliary equipment and measuring techniques for hydrodynamic data acquisition. In single backmixing experiments linear relationships were found between the dispersion coefficient and stirrer agitation speed and the dispersion coefficient and the flow rate. Dispersion coefficients calculated using CFD agreed well with experimentally measured values. It was shown that CFD contributes to a better understanding of the basic mechanisms governing the hydrodynamics of liquid-liquid extraction.

### INTRODUCTION

For the development of new industrial processes in the chemical industry the use of lab-scale continuous plants (miniplants) without piloting, in combination with simulation tools, finds increasing application. The reasons are the reduction of costly and time consuming experiments in pilot plants, which leads to a cheaper and faster realisation of the industrial process.

Liquid-liquid-extraction is superior to distillation for special separation processes like the reconditioning of very dilute solutions or temperature sensitive products. Flow rates around 10-L/h can be used in laboratories without special permits. Such flow rates are in the range of 30 mm miniplant extractors [1,2]. Information on hydrodynamic parameters such as the axial dispersion, hold-up and throughput is important for the scale-up and design of extraction columns. This work reports on the hydrodynamic behaviour of such a miniplant extractor. The parameters studied include throughput (flooding), axial dispersion, hold-up and velocity profiles. The results are discussed and compared with computational fluid dynamics (CFD) simulations.

### EXPERIMENTAL SETUP

The Kühni miniplant extractor used is a glass unit with an internal diameter of 32 mm, equipped with four 6-bladed stirrers mounted on an axial shaft. The stirrers rotate inside 34 mixing compartments separated by stator rings which are electrically isolated. Four of those compartments are composed of stainless steel and can be used as sampling or injection ports. The general arrangement of the column and auxiliary equipment such as storage tanks, pumps etc. is shown in Figure 1.

Some of the physical design parameters of the miniplant unit are given in Table 1.

*Table 1. Miniplant specifications (mm).*

Column inside diameter $d_c$	32
Column total height	1545
Compartment height $H_c$	37
Stirrer diameter	20
Stator ring inside diameter	18.5

Axial mixing for single-phase flow was quantified by injecting 0.5 mL of aqueous 0.02 N KCl pulses through an inlet port in the upper part of the column, and measuring the electrical conductivity at two locations in the lower part of the column. In principle, only one measuring point is necessary if the tracer injection is in the form of a perfect delta pulse. However because of the difficulty in obtaining a perfect pulse and other experimental shortcomings it is usual to monitor the attenuated pulse at two sample points. The generated data plots were fitted to the analytic solution of the well-known dispersion model of Levenspiel [2] (open-open condition) using the "convolution" method:

$$C_2(t) = \frac{1}{2\sqrt{\pi\tau(D_{ax}/v_c L)}} \int_0^t \exp\left[-\frac{(D_{ax}/v_c L)[\tau - (t-\theta)]^2}{4\tau(t-\theta)}\right] d\theta \quad (1)$$

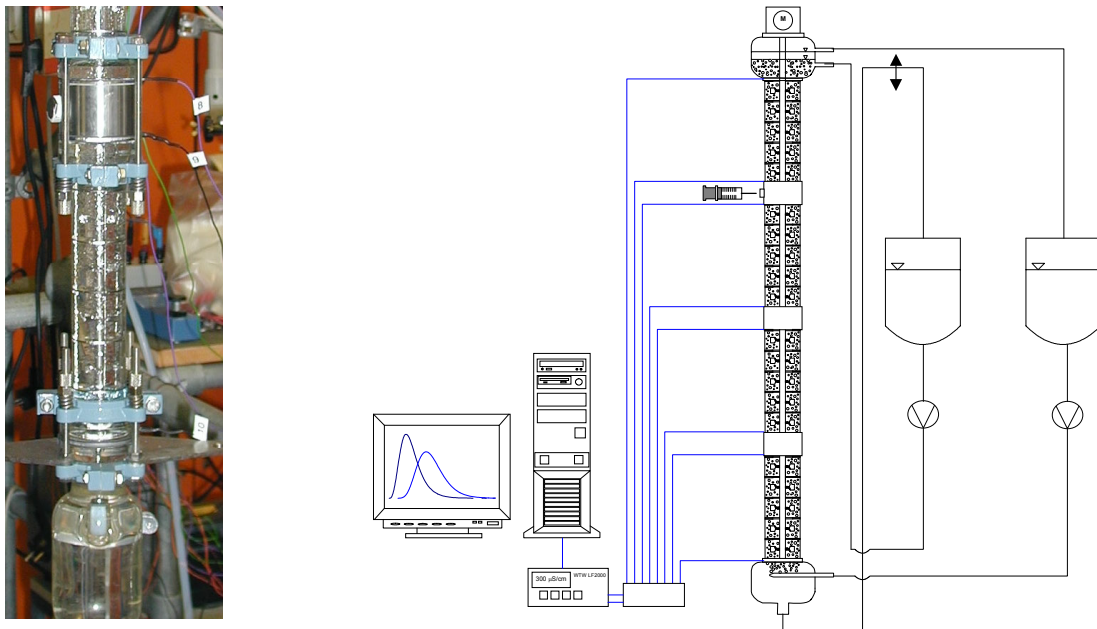


*Figure 1. Schematic experimental setup of the miniplant (left: lower part of the column with adapted stainless steel compartment).*

## CFD-MODELLING

One objective of this work was to examine the capabilities of CFD in the field of liquid-liquid extraction. This multidimensional approach can give deeper insight into the details of the flow structure [4], while it can also supply information required in the "classical" one-dimensional methods of column design. For the CFD-simulation the commercial software FLUENT, which is based on the finite volume method, was used. Due to the identical geometry of the compartments a periodically repeating flow pattern can be expected. Furthermore, the

symmetry of the geometry can be exploited to reduce the number of computational cells. Consequently, just two adjacent compartments of the column were modelled and a slice between two stirrer blades was assumed to be sufficient. The computational mesh, a structured-hexahedron mesh, consisting of approximately 200,000 cells, is shown in Figure 2. As boundary conditions the column wall and the stators were considered to be fixed walls and the shaft and the stirrers as moving walls (moving reference frame). In the axial and circumferential directions periodic boundary conditions were used. The turbulence was taken into account using the standard k- $\varepsilon$ -model.

## TWO-FLUID-MODEL: EULER-LAGRANGE

For the determination of the backmixing of the continuous phase the Euler-Lagrange model has been used [5]. In this model, the continuous phase is described by fields of velocity and pressure (Euler approach), whereas the 'dispersed' phase is represented as an ensemble of particles whose trajectories have to be computed (Lagrangian approach) by integration of equation (2) which results from a simple force balance at a particle.

$$\frac{du_i^P}{dt} = \frac{3\eta C_D Re_P}{4\rho_P d_P^2} (u_i - u_i^P) + f_i^P \quad (2)$$



Figure 2. Computational mesh.

Axial periodic boundary conditions normally do not allow the flow to be traced with Lagrangian particles. Therefore in a first step the stationary flow for a certain throughput and agitation speed has been calculated. In a second step the calculated velocity profile at the inlet has been taken for a change of the boundary condition from periodic to a standard velocity inlet. Afterwards, approximately 10,000 particles of 10  $\mu\text{m}$  in diameter and equal density to the continuous phase have been calculated to receive a residence time distribution curve (RTD) which is independent of the amount of particles. For single droplet behaviour, in particular 'inert' particles, the coupling between the particle and the continuous fluid flow field does not need to be considered [6]. To obtain a hydrodynamic parameter that is comparable to the 'classical' method of column design, these curves have also been fitted to the analytic solution (2) of Levenspiel. Because in the CFD-simulation the ideal Dirac delta function can be obtained, a direct fitting without the use of the convolution integral is possible.

## RESULTS AND DISCUSSION

The values of dispersion coefficient obtained for the miniplant column are illustrated in Figure 3. There is a linear relationship between the coefficient and the impeller speed. By increasing the number of stirrer blades the dependency becomes stronger. As usual the dispersion coefficient increases with increasing flow rate. Also for the continuous phase throughput and the dispersion coefficient a linear relationship can be observed (Figure 5). Similar results which take into account this linear relationship (3) have been published for Kühni columns [8]. The values determined in this study are in accordance with this correlation, which is now valid for a wide range of column diameters ( $d_c = 32$  to  $600$  mm).

$$D_{ax} = 0.046 \cdot n \cdot d_c \cdot h_c \cdot \varepsilon + 0.14 \cdot h_c \cdot v_c \quad (3)$$

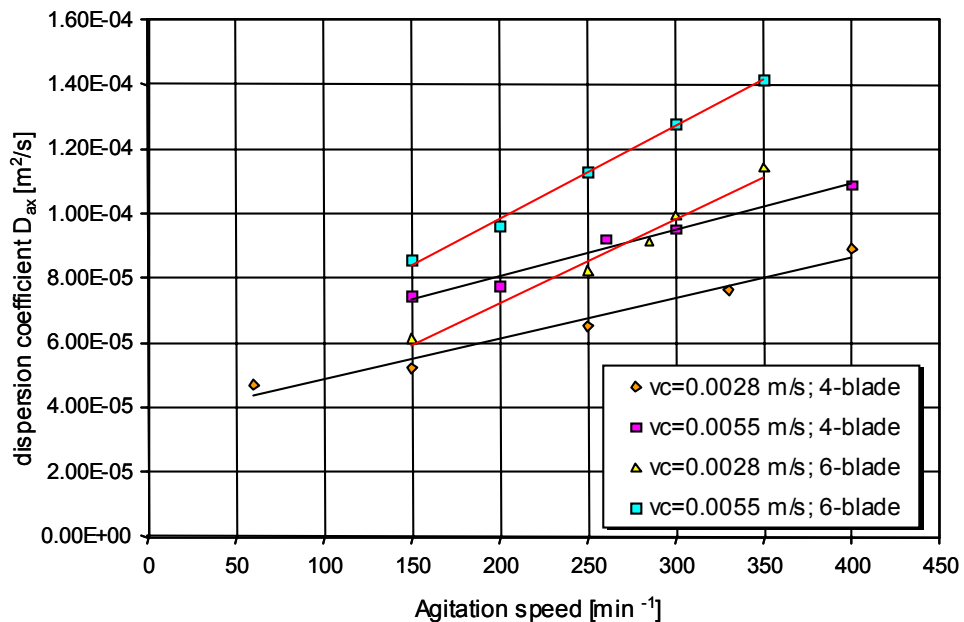


Figure 3. Relationship between dispersion coefficient and agitation speed.

Figure 4 illustrates the residence time distribution (RTD) for an ideal pulse of inert particles at the inlet of one compartment. The shapes of all C1-response curves (response after the first compartment) obtained in our CFD studies are well described by the dispersion model. For the C2-curves another result was obtained. Curve fitting of the data mostly gave poor results which were unable to describe the shape of the simulated curves. The only difference between the 'measuring' ports used to obtain the response curves is that for the C2 data, the tracers really leave the computation region and so multiple passing for them is not possible. In Figure 5 simulated dispersion coefficients were plotted against measured ones. If the assumptions of the CFD model, e.g., to neglect the baffles inside the column, are taken into account, good agreement is obtained.

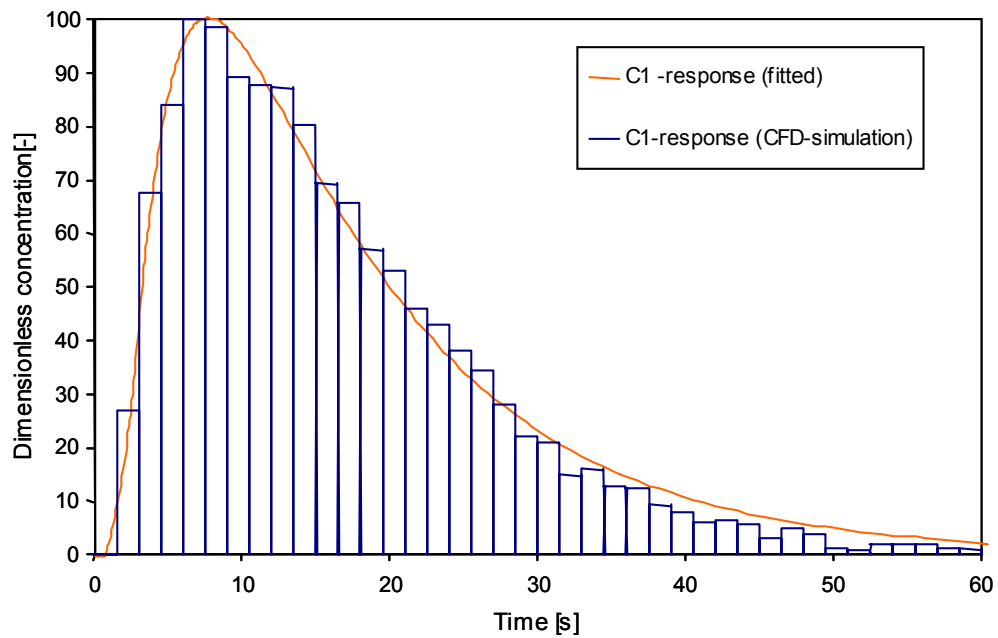


Figure 4. Response curve for an ideal pulse (agitation speed  $300\text{ min}^{-1}$ ,  $V_P=13.2\text{ L/h}$ ).

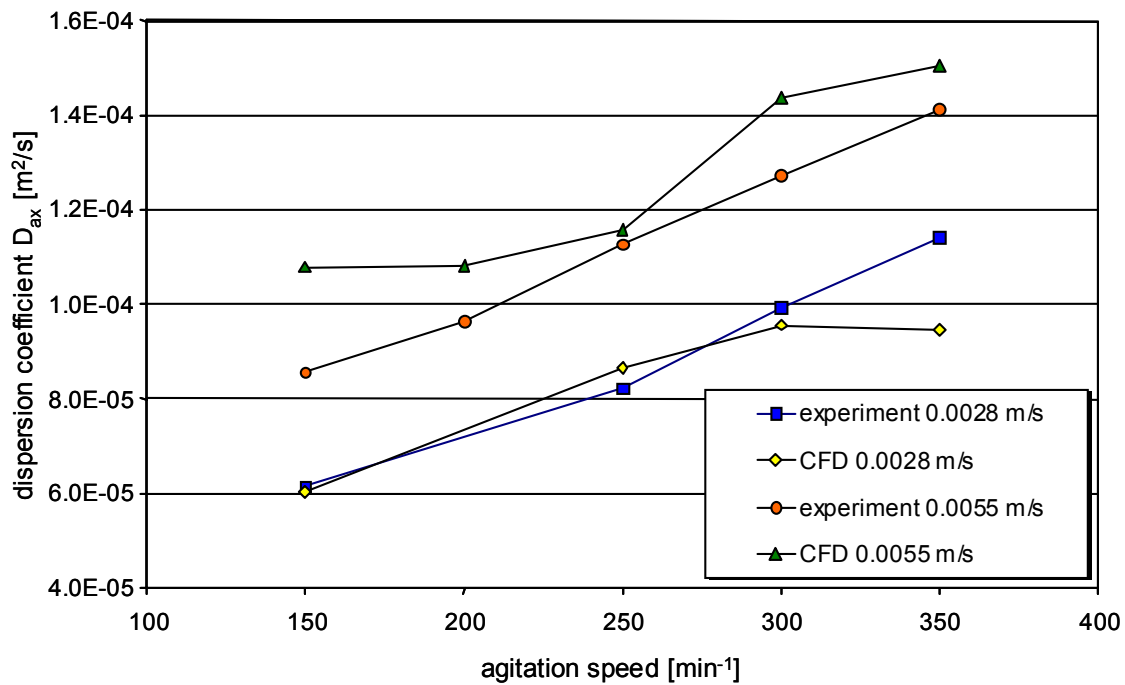


Figure 5. Comparison of measured and simulated dispersion coefficients.

## CONCLUSIONS

In single-phase backmixing experiments a linear relationship between the dispersion coefficient and the stirrer agitation speed was obtained. The relation between the dispersion coefficient and the throughput was also linear. In a theoretical analysis of the data, it has been shown, that it is possible to predict dispersion coefficients using CFD. Furthermore CFD can contribute to better understanding of the basic principles governing the hydrodynamics of a 3-D two phase flow (backmixing, channeling, etc.). Multidimensional computational approaches open the possibility of cross-checking against the conventional 1-D methods (which rely on empirical coefficients) and of improving the semi-empirical correlations making possible a more sound design of columns various geometries. Also the effect of different liquids could be easily investigated. However, the challenge remains to link disperse phase and mass transfer with this hydraulic design.

## ACKNOWLEDGEMENTS

The support of this research by the 'Kommission für Technologie und Innovation (KTI)', Bern and the companies Kühni, Novartis, Roche and Lonza (Switzerland) is gratefully acknowledged.

## NOMENCLATURE

B	[m <sup>3</sup> /m <sup>2</sup> h]	throughput	t	[s]	time
C <sub>D</sub>	[·]	particle drag coefficient	τ	[·]	reduced time
C	[·]	tracer response to an ideal pulse input	θ	[·]	integration variable
d <sub>C</sub>	[mm]	column diameter	u <sub>i</sub>	[m/s]	flow velocity in i-direction
d <sub>P</sub>	[mm]	particle diameter	u <sub>i</sub> <sup>P</sup>	[m/s]	particle flow velocity in i-direction
D <sub>ax</sub>	[m <sup>2</sup> /s]	dispersion or axial dispersion coefficient	η	[Pa s]	turbulent viscosity
ε	[·]	free surface area	ρ <sub>P</sub>	[kg/m <sup>3</sup> ]	particle density
f <sub>i</sub> <sup>P</sup>	[·]	forces affecting the particle e.g. buoyancy, centripetal force	Re <sub>P</sub>	[·]	particle Reynolds number
H <sub>C</sub>	[mm]	compartment height	v <sub>C</sub>	[m/s]	continuous phase velocity
L	[mm]	characteristic length	V <sub>P</sub>	[L/h]	flow rate

## REFERENCES

1. H. Steude, L. Deibele and J. Schröter (1997), *Chem.-Ing.-Techn.*, **69**, 623-631.
2. H.-J. Bart and A. Schöneberger (2000), *Chem. Eng. Technol.*, **8**, 653-660.
3. O. Levenspiel (1962), *Chemical Reaction Engineering*, John Wiley & Sons, 275-278.
4. G. Modes and H.-J. Bart (2001), *Chem.-Ing.-Techn.*, **73**, 332-337.
5. R. Rieger, C. Weiss, G. Wigley, H.-J. Bart and R. Marr (1996), *Computers Chem. Engng.*, **20**, 1467-1475.
6. V. Elogobashi (1991), *Appl. Sci. Res.*, **48**, 301-314.
7. D. H. Logsdail, J. D. Thornton and H. R. C. Pratt (1957), *Trans. Instn. Chem. Engrs.*, 301-315.
8. J. Breysse, U. Bühlmann and J. C. Godfrey (1983), *Proc. ISEC '83*, pp. 94-101.



## ADVANCED METHODS FOR DESIGNING TODAY'S OPTIMUM SOLVENT EXTRACTION MIXER SETTLER UNIT

Bernd Gigas and Michael A. Giralico

LIGHTNIN, Rochester, USA

Optimization of impeller designs, mixing and settler tank configurations, and the understanding of the mixing and separation process requirements, has resulted in optimized solvent extraction mixer settler designs.

The size and expense of the equipment and flow rates hamper experimental settler optimisation efforts. Computational Fluid Dynamics offers the opportunity of quick and relatively inexpensive settler design. The model consists of a steady state solution using a segregated solver in unstructured grids. Phase separation is analysed using multiple species for the aqueous and organic phase. Experimental validation shows good agreement between the computational and experimental solutions in both flow field and phase separation on small scale.

The model is used to show performance differences between various choices of settler geometry and flow rates, allowing the development of optimised settler designs. This paper focuses on major design components of the settler and how future technological advances of said components can lead to further improvements.

### INTRODUCTION

Solvent extraction processes in copper mining involve the use of kerosene based solvents and sulphuric acid to increase the copper concentration and purity of the copper rich electrolyte pumped to the electro-winning house. The complete solvent extraction chain typically involves two extraction steps (E1 & E2) where copper is extracted from the pregnant leach stream (PLS) into the organic stream, one or two stripping steps (S1 & S2) where copper is stripped from the organic phase into unladen sulphuric acid from the electro-winning house and finally a wash step (W1) where further impurities are removed from the PLS prior to being pumped to the electro-winning house.

While each of the process steps in the solvent extraction process sheet performs a unique function the design of the equipment is based on the same operational principles. The discussion of mixer-settler designs can thus be done in generic terms, independent of its application as an extraction, stripping or wash step. The focus of this paper is on the performance and optimisation of the settler portion of the process only.

The operational concept of the settler requires phase separation of the immiscible liquid-liquid dispersion of the organic (kerosene) and aqueous (sulphuric acid) components. Common configurations feed the dispersion through a launder at the centre of the settler, followed by an angled picket fence to evenly distribute the inlet stream and followed by a second picket fence located at approximately one third of the total settler length to assure even flow distribution

further downstream. The exit section of the settler consists of an overflow weir for the lighter organic phase and an underflow-overflow weir for the heavier aqueous phase. Typical volume ratios of organic to aqueous in the settler are 1:2 to 1:1. Conventional design methodology for rectangular settlers is based on hydraulic theory and empirical results from pilot plants and full scale installations. Generally speaking, the basic settler dimensions are derived from open channel flow theory to develop linear velocity targets, specific flow rate (total flowrate per settler footprint area) and picket fence design. Empirical results have refined the linear velocity, specific flowrate, and total settler depth guidelines derived from theory.

The commercial use of solvent extraction technology in copper mining application supports the claim that the simple rectangular arrangement commonly in use is successful both technically and economically. Nonetheless several issues remain that offer the opportunity for improvement in settler performance. Organic entrainment in the aqueous phase is a cost consideration. Organic lost into the aqueous phase during stripping and wash is sent to the tank house and lost during electro-winning. While there are several ancillary technologies available to recover the entrained organic after the settler, any improvement in the settler itself would be beneficial.

A second concern is the generation of crud or scum. This is a three phase semi-stable emulsion consisting of solid particulate, organic liquid and entrained air. Depending on the continuous phase of the dispersion this emulsion may collect at the organic weir between the organic and aqueous phases and block transport between the two layers [1]. It can thus lead to a shortened effective length of the settler, it also provides a source of organic material that erodes from the crud layer into the aqueous phase. As the degree of crud generation varies between mine sites there are multiple approaches to dealing with this problem ranging from doing nothing to regular removal using specialised suction devices.

A third and less obvious issue is the flow pattern in the settler itself. The flow in a settler is not completely laminar and channelling occurs. Specifically, the flow velocity in the centre of the settler can be different than at the edges and reverse flow can often be observed, particularly behind the second picket fence. It is difficult to assess the entrainment impact of this behaviour without major modifications to either the shape of the settler or its internals. At minimum however, reverse flow negates the assumption of plug flow used in coalescence review and indicates that for a given total design flow rate existing rectangular settlers exceed the minimum foot print requirement for process.

A number of authors have published papers covering design features to improve the operational efficiency of the solvent extraction settler [1, 2, 4, 5]. These cover the design requirements for the settler in terms of hydraulics, coalescence speed, phase inversion, etc. The approach in these developments is typically based on empirical correlations from literature followed by experimental validation in either pilot plant or full scale. This approach is valid for many of the design features such as overall dimensions, overflow weir sizing, basic picket fence designs etc. The drawback of purely experimental validation is however that most analysis is based on global values such as average linear velocity and average specific settler flowrate. Local values or phenomenon are not usually considered since observation of all but surface effects is very difficult due to the opaque nature of the lighter organic phase.

This paper reports on current efforts to incorporate computational fluid dynamic (CFD) analysis into the design process of solvent extraction settlers. CFD offers the opportunity of evaluating the conditions at local points of interest in the settler. This can be used to develop improved designs of the inlet launder, picket fences, coalescence rails and overflow weir structure. Overall settler models can be used to evaluate the impact of settler shape and flowrate variation. We will also report on early results of phase separation modelling and the associated complications with this type of model.

## SMALL SCALE MODEL

Giralico and Gigas [3] reported on CFD validation of a small scale settler using mineral oil and water as the organic and aqueous phase, respectively. The model consisted of a 32" wide by 34" long by 4.5 deep trapezoidal acrylic settler using a total flow rate of 2 gpm. To facilitate experimental validation of CFD results no picket fences were installed.

Computational model details were 43,000 cells in a structured mesh, operating through a coupled viscous solver, single phase, multiple species. A steady state laminar flow field is assumed since the Reynolds number is below 2000. The numerical approach was to model the organic and aqueous phase as different species with a diffusivity of 1E-08 m<sup>2</sup>/s in order to show phase separation of the inlet stream. A more rigorous approach is to model a two phase system using an Eulerian-Eulerian model such as Volume-of-Fluid. In consideration of the computational effort required to run this multiple phase, non-steady model the simpler approach was tried. The justification for this approach was that phase separation from gravitational effects are assumed to be controlling the overall performance, not primary or secondary coalescence.

The results of this study were encouraging. Overall flow predicted from CFD matched actual flow well in terms of the flow field in the model settler. The phase boundary location was also found to be in good agreement between the experimental and computational model. Phase separation in terms of predicted entrainment was however high and this particular model exhibited limitations that were difficult to quantify within the parameters of this study.

Figure 1 shows the results of the small scale computational work. The red/light grey areas represent pure organic flow, the dark blue/black represent pure aqueous flow. Notable in the results are the accurate prediction of the organic plume directed toward the left side of the settler in the direction of the weir outlet and the interfacial boundary location. The velocity field is not shown here but also correlated well. Validation of a full scale single phase, multiple species model was attempted using this approach.

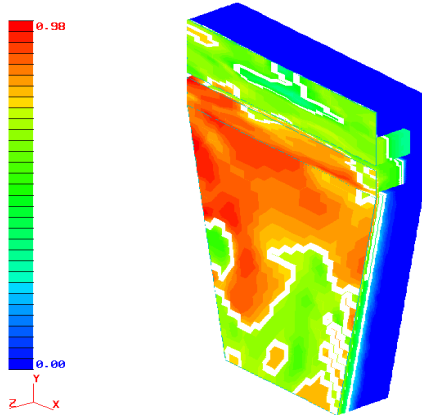


Figure 1. Small scale computational results.

## FULL SCALE MODEL

The next step in the development of CFD as a tool for overall solvent extraction settler design was to model a full scale operating settler and validate the results of the computational model with experimental data. The requirements from the model are to accurately predict the overall flow features of the settler and to locate the interfacial boundary between the aqueous and organic phases. At this time little emphasis was to be placed on accurately predicting the entrainment values. The operational settler has external dimensions of 28'-5" wide by 55'-3" overall inside length. It is equipped with two standard picket fences located near the entry zone and 9'-0" into the settler.

Computational details are similar to the small scale settler with the exception of the grid size which is now approximately 130,000 cells. Results of this overall settler analysis are not presented here as the current model shows severe convergence problems. This problem is rooted in the numerical sweep direction and is particularly notable in the picket fence region resulting in incomplete species separation. While the model continues to show promise for future overall settler analysis the current state of the technology does not readily permit the use of CFD for the expedient and practical optimisation of the overall solvent extraction settler design required for industrial application.

## INDIVIDUAL FEATURE DESIGN

The current inability to model the entire flow and process features of a settler requires a reassessment of the usefulness of CFD for application in this process. A number of observations in both small scale experimental modelling and full scale settler analysis indicate that CFD may offer the opportunity to optimise individual features of a settler. Observation of the flow pattern in the inlet region of the settler shows strong channelling toward the centre and inlet launder and first picket fence modelling from a fluid dynamic perspective appears useful. Recirculation in the flow field in the section after the second picket fence puts the overall settler shape and second picket fence design into question. Observation of the flow in front of the organic weir points to potential entrainment sources stemming from the weir shape. Finally, CFD allows relatively quick analysis of the flow pattern changes that can be expected from changes in operating flow rate.

### Inlet Launder

Figure 2 models a 9.3 m wide by 0.9 m deep settler from the 2 m wide inlet launder to the front end of first picket fence located 6.9 m into the settler. Inlet flow velocity is 1 m/s corresponding to common full scale application. The model is run 3-D, laminar steady state. Note that only a single phase is modelled. This represents a relatively accurate picture of the flow before the first and second fence as phase separation often has not occurred until after the second fence. Since the inlet launder is assumed to be located in the centre of the settler only one half is modelled, the mirror image half is inferred along the centreline symmetry axis.

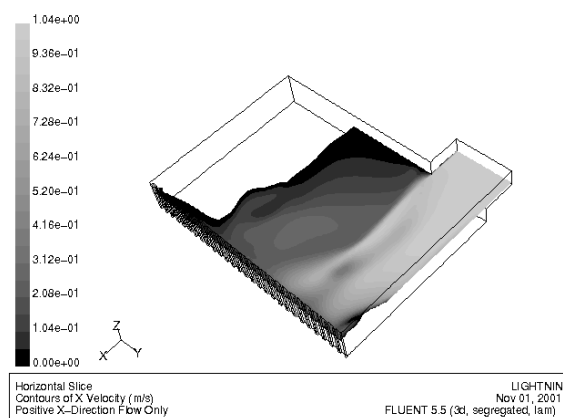


Figure 2. Horizontal slice, velocity magnitude – positive X.

The positive x-direction velocity field distribution of this arrangement is shown in Figure 2. Note that clear areas indicate reverse flow in the settler. Here, a plane located 0.35 m off bottom is highlighted showing strong recirculation of the flow within the front section of the settler not only in the horizontal plane but also vertically (plot not shown for brevity).

Clearly the assumption of plug flow does not hold in the front end of the settler and the degree of flow circulation further questions the validity of the laminar flow assumption. The axial distribution of the velocity field can be avoided either through the use of an inlet launder spanning the entire height of the settler (as shown in later sections) or by angling the launder from the inlet to the settler floor. The recirculation in the horizontal plane can be avoided through the use of inlet launder directional vanes or through modified picket fence design, or a combination of both.

### Overall Settler Shape

Figures 3 and 4 show two settler designs with identical overall settler length, launder width, weir width and liquid depth. The sole difference lies in the trapezoidal shape of the settler in Figure 4 where a significant portion of the foot print has been removed. The inlet velocity is set at 1 m/s, overall dimensions of the rectangular settler are appropriate for operating settler design.

Figures 3 and 4 show x-direction velocity field distribution in the horizontal plane located 0.35 m off bottom. Note that clear areas reflect flow in the negative x-direction, or flow reversal. Both designs show recirculation in the outside portion of settler thus necessitating picket fences for flow distribution. The trapezoidal settler shows a lesser degree of recirculation coupled with smaller foot print. While the average residence time of the trapezoidal settler will be shorter due to the reduced volume the distribution will be closer to plug flow than the rectangular settler of equal weir width. In order to fully qualify the concept of a reduced foot print settler experimental validation using tracer studies are required to evaluate residence time distribution in comparison to primary and secondary coalescence time.

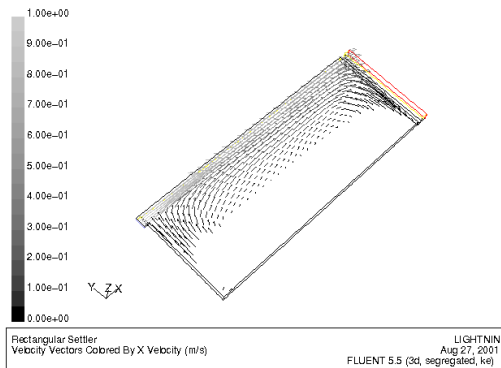


*Figure 3. Positive x-direction flow field in rectangular settler.*

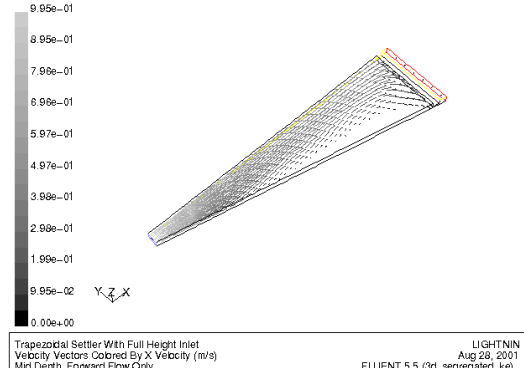
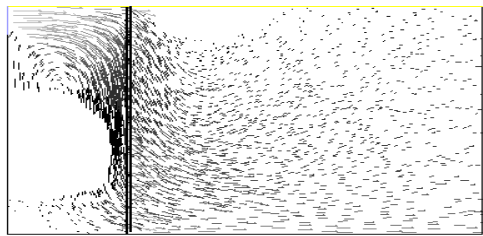


*Figure 4. Positive x-direction flow field in trapezoidal settler.*

### Fence Spacing & Design

In order to facilitate the evaluation of picket fence designs in a settler this section of the work is done in 2D. Due to the relatively small size of the pickets and inter-picket spacing in relation to the overall settler dimensions a 3-D analysis is computationally not reasonable for the scope of this paper.

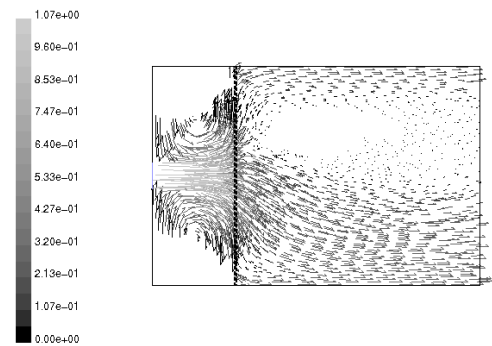
A 2-dimensional plot of a rectangular settler without picket fence is equivalent to Figure 3. Figure 5 adds a single picket fence located roughly 1/3 into the settler. The model pickets are 0.1 m wide with 0.025 m spacing. Overall settler dimensions are 25 m wide by 20 m long, inlet velocity is set at 1 m/s. The resultant flow pattern shows the distribution across the width of the settler. This particular picket arrangement is not optimised as the flow preferentially channels to the outside of the settler.



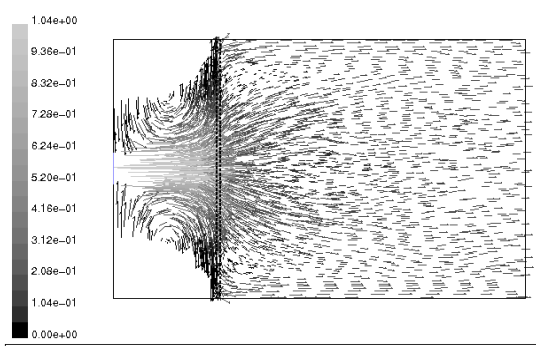
*Figure 5. Rectangular settler – single picket fence.*

Figure 6 refines the picket fence arrangement through the use a double picket fence to produce a more even flow field. Note that the x-direction flow field shown is not completely symmetric as the fence arrangement is slightly offset from centre. This represents a common arrangement of fence pickets since the design is typically started on one side of the settler and terminates with pickets cut to size on the opposite end. The resultant flow asymmetry is significant in that a large part of the settler flow behind the picket fence is reversed, i.e., toward the settler inlet.

Figure 7 represents the flow field generated in a settler with symmetric double picket fence. All parameters of the settler shown in Figure 7 are identical to that shown in Figure 6 with the exception of the picket locations. For Figure 7 all pickets are centred and completely symmetric. The resultant flow field is uniform and raises the question if single picket fence arrangements are feasible full scale installations.



*Figure 6. Rectangular settler double picket fence.*



*Figure 7: Rectangular settler double symmetric picket fence.*

### Weir Design

As we progress through the settler the final major feature in the design is the weir section. While the basic concept of an overflow weir is simple care must be taken to avoid cross phase entrainment as well as air entrainment. The modelling of air entrainment in the overflow section of the weir requires multiphase modelling that is not addressed here but other features of the weir can be evaluated using single phase modelling. Figure 8 shows a plain rectangular organic weir cross section. By nature of the design the organic-aqueous interface lies on the vertical wall thus forming a stagnation point some distance upstream of the weir itself. Transport of fluid from front to back in the settler locates any accumulated crud in the interfacial region right at this stagnation point.

Note the downward flow velocity of the liquid from the interfacial region toward the organic weir underflow. This phenomenon has been validated experimentally and can lead to crud layer erosion and entrainment losses of organic in aqueous. Specific design modifications to alleviate this problem are not addressed here but their evaluation via CFD is a logical starting place.

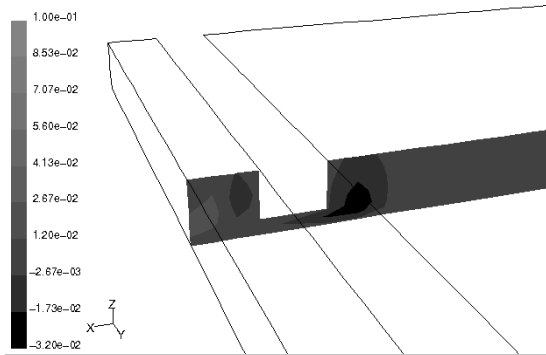


Figure 8. Organic weir cross section.

### Flow Rate Sensitivity

Once modelling has lead to an optimised settler configuration CFD offers the opportunity of evaluating various operating parameter changes. The most common is inlet flow rate change. The most effective way to model the impact of velocity step changes can be reviewed using an unsteady model. Figure 9 shows plots of velocity changes in the vertical plane six seconds after a step change of inlet velocity from 1 m/s to 3 m/s.

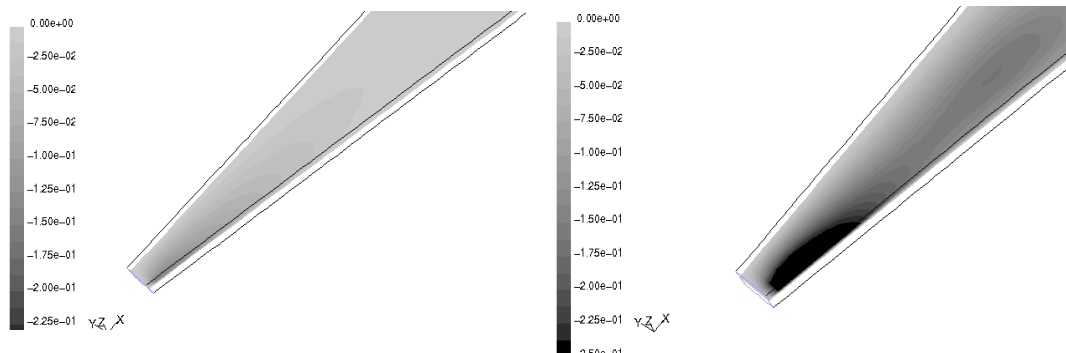


Figure 9. Vertical velocity field change after inlet velocity step change.

Note the steep increase in vertical velocity in the inlet region noted by the darker areas. Similar behaviour should be expected behind picket fences and helps to explain the entrainment surges often associated with inlet flowrate changes.

As has been pointed out by Miller [6] the full scale operating solvent extraction settler is not operating at a true steady state. Inlet surges of either liquid phase lead to transient behaviour in the settler and are at least partially responsible for entrainment losses in the settler. Unsteady CFD models allow a first glance at the impact of these transient flows and future two phase CFD work should lead to a better understanding of these transient flows and their impact on settler performance.

## CONCLUSIONS

To date attempts to develop a single comprehensive computational design tool for solvent extraction settlers have met with very limited success. A single phase, multiple species model has shown good agreement with experimental results in small scale open models. This concept has yet to be successfully validated on full scale copper mining solvent extraction processes due to numerical convergence difficulties.

Nonetheless, CFD can be used to develop optimised solutions for individual settler components such as inlet launders, picket fence design and location, overall settler shape and overflow weir design.

Generalised results are that a trapezoidal shape of the settler offers a reduction in overall foot print coupled with improved plug flow performance and reduced organic inventory. Pilot plant experiments are under way to validate small scale and computational results with respect to the flow field as well as to characterise the entrainment impact of CFD derived design modifications to the inlet launder, picket fences and overflow weirs.

## REFERENCES

1. J. R. Spence and M. D. Soderstrom (1999), Copper Leaching, Solvent Extraction, and Electrowinning Technology, G.V. Jorgensen (ed.), Society for Mining, Metallurgy, and Exploration, Inc., Littleton, CO, pp. 239.
2. Davy International (undated), Qualifications for Copper Leaching Solvent Extraction Elecrowinning Facilities, Section 4: Technology – SX-EW.
3. B. Gigas and M. Giralico (2000), *Proc. Randol Copper Hydromet Roundtable 2000*, Tucson, AZ.
4. Copper SX/EW Seminar: Basic Principles, Alternatives, Plant Design, ALTA Metallurgical Services, Melbourne, Australia, Section 13.
5. T. Lo, M. Baird and C. Hanson (eds.) (1991), Handbook of Solvent Extraction, Section 9, Krieger Publishing Company, Malabar, FL.
6. G. Miller (2001), *Proc. SME Annual Meeting*, Denver, CO.



## TESTING NOVEL FEATURES IN MIXER-SETTLER PROTOTYPES

Alberto Gauna, Claudio Andaur and Fernando Granatelli

Comisión Nacional de Energía Atómica, Buenos Aires, Argentina

A mixer-settler with novel qualities has been developed as part of an advanced non-proliferating PUREX process program to collect experimental data.

Some of its operating features are:

- Air pulsed mixing with two different height nozzles in each mixer. The nozzles and a special baffle in the mixing channel give a better mixing distribution and allow high viscosity mixture or crud to flow smoothly from the mixer to the settler.
- An independent aqueous-phase flow for each of the mixer-settler stages achieved by pumping of small air-lifts to get a very low overall pressure drop.

Some of its manufacturing features are:

- The mixing and settler cells and the air-lift channels were carved and drilled in the central plastic block.
- Materials such as high-density polythene and tempered glass were used to obtain a suitable watertightness and are a good option for hot cell operation.

These features could be applied to any kind of mixer-settler configuration.

### INTRODUCTION

A small high-performance mixer-settler specially suitable for use in high uranium concentration processes was developed as part of an advanced and non-proliferating PUREX process development program conducted in the Centro Atómico Ezeiza (C.A.E.) of the Comisión Nacional de Energía Atómica de la República Argentina. This experimental work is currently being carried out with natural uranium, but experimental works using tracers at an early stage and small quantities of spent nuclear fuel subsequently, are scheduled to begin at a new hot cell laboratory called LFR very soon. For this reason, our Department work team has decided to develop a small, simple and reliable mixer-settler prototype that could also be highly resistant to corrosion and opacity generation and also provides suitable watertightness.

### FEATURES OF THE MIXER SETTLER

#### Selection of Materials and Manufacturing Features

The results obtained from a thorough analysis of durability and visibility limitations in the equipment helped to solve some operating problems.

As is widely known today, materials such as polycarbonate, acrylic and other polymers typically used to manufacture prototypes for process development are not corrosion free and tend to get corroded under the action of nitric acid and tributyl phosphate, or are likely to show opacity as a result of cracking.

After their mechanical endurance and chemical resistance have been verified by means of calculations and tests, high density polythene charged with titanium dioxide and tempered glass were selected to manufacture the central block and the cover plate respectively.

Bibliographical and experimental data about the behaviour of high density polythene and tempered glass confirmed that such materials were the proper choice. Some experimental data about their endurance to radiation were collected in the C.A.E.'s hot cells, where <sup>99</sup>Mo is produced. The first one of these materials was found to be highly resistant and long lasting in a radiation field of 36 Sv/h during 8 hours a week and a permanent field of 0.054 Sv/h. Although the second material presented some fragility and opacity problems, this was only developed after several months of being exposed to the same conditions.

Experimental decontamination works with small quantities of spent nuclear fuel of irradiated material are under schedule in the C.A.E. They will be performed in the L.F.R. Laboratory hot cells, where the radiation field is much lighter than in the <sup>99</sup>Mo hot cells mentioned above.

The widely known configuration with oblique settlers was selected in this event, but other arrangements could be made under the same characteristics of this device.

The three most important pieces of the device are:

- A central block made of polythene where mixers, settlers, channels and holes were carved.
- Two tempered glass plates. One of them has the holes where special connections for the stream outlets pass through.
- A pair of stainless steel frames and screws to press the central block and the plates together in order to get enough watertightness (See Figure 1). The applied pressure is compatible with the compression resistance of polythene.

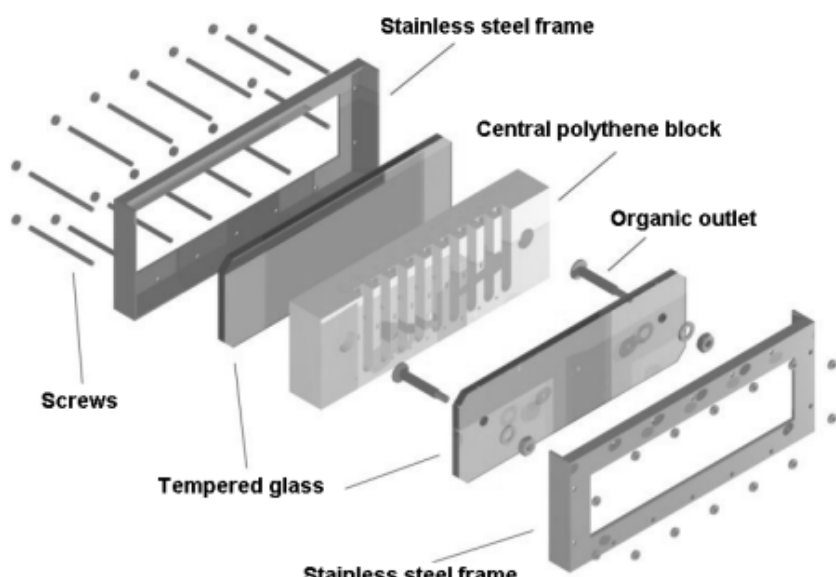


Figure 1. Mixer-settler prototype assembly.

## **Standard Operating Features**

This design includes standard and novel operating features. The standard operating features are:

- The input streams (organic phase, scrub solution, and uranium feed) could be directly fed in the correct mixers by any kind of dosage system. In this particular case, externally controlled diaphragm pumps were used.
- The organic phase flows by gravity from one settler to its corresponding mixer through a channel drilled in between every mixer and settler.
- The mixers are agitated by air pulses. The pulses are generated by diaphragm pumps and transmitted by means of typical liquid seals.

## **Novel Features**

Advanced and non-proliferating processes can involve high uranium concentration gradients with sharp density variations.

Three novel features were incorporated after a testing period in a small single-stage mixer-settler where the best geometrical and operating conditions were found:

- Different height and position of the two nozzle ends (one is at the top and the other at the bottom of the mixer), in order to gain a better mixing distribution. Classical air pulsed mixing systems have equal height and are placed at the top of the mixer [1].
- The upper ended nozzle makes the mixed phase flow smoothly from mixer to settler through the mixed-phase channel, because the stream pulsed by this nozzle is directed to a specially orientated baffle placed in the mixing channel. Each pulse of mixing phase crashes into the baffle and goes into the settler. As a result, it is possible to break off the high viscosity mixture or crud, which are formed under certain conditions, and to let the mixed phase flow easily from mixer to settler. The best angle for the baffle was determined in the single-stage mixer-settler.
- The aqueous phase flows from a settler to the corresponding mixer through a combination of holes made in each stage. A small tube is inserted for each stage into one of these holes. This tube is supplied with compressed air so that a small air-lift is generated to pump the aqueous phase to the corresponding mixer. (See Figure 2). This pumping eliminates the accumulation of pressure drop along the device and eases the aqueous phase circulation if a density step is formed at the bottom of the settler. The achieved effect is similar to pump-mixer-settler behaviour.

The flow rate of the small air-lifts was adjusted in the single mixer-settler. It must be five to ten times the aqueous phase flow fed to the mixer-settler.

The organic phase flows by gravity conventionally from one settler to its corresponding mixer through a channel drilled in between every mixer and settler.

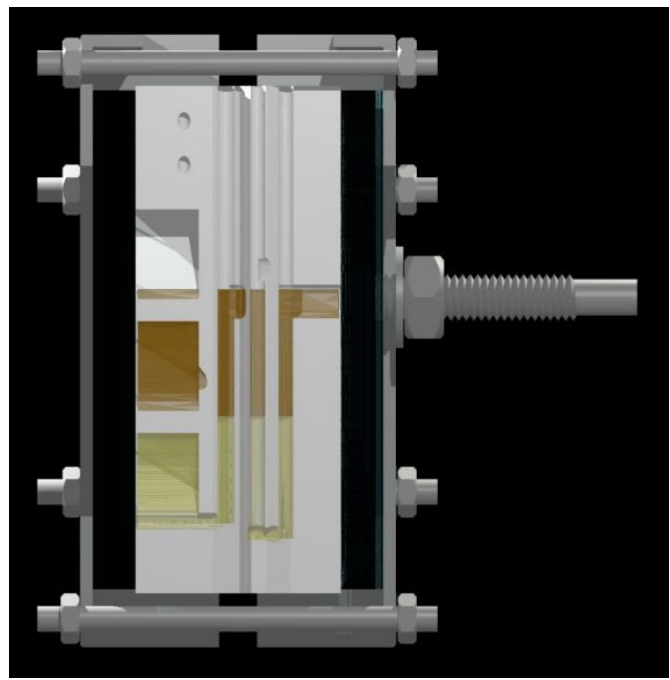


Figure 2. Computer generated mixer-settler section. Air-lifts holes are visible in the central area. Modelized organic and aqueous phases were coloured in brown and yellow respectively. The organic outlet is also visible.

## EXPERIMENTAL WORK

The device was tested in an extraction-scrubbing and stripping cycle consisting of seven-stage and nine-stage mixer-settlers respectively, under two different process conditions.

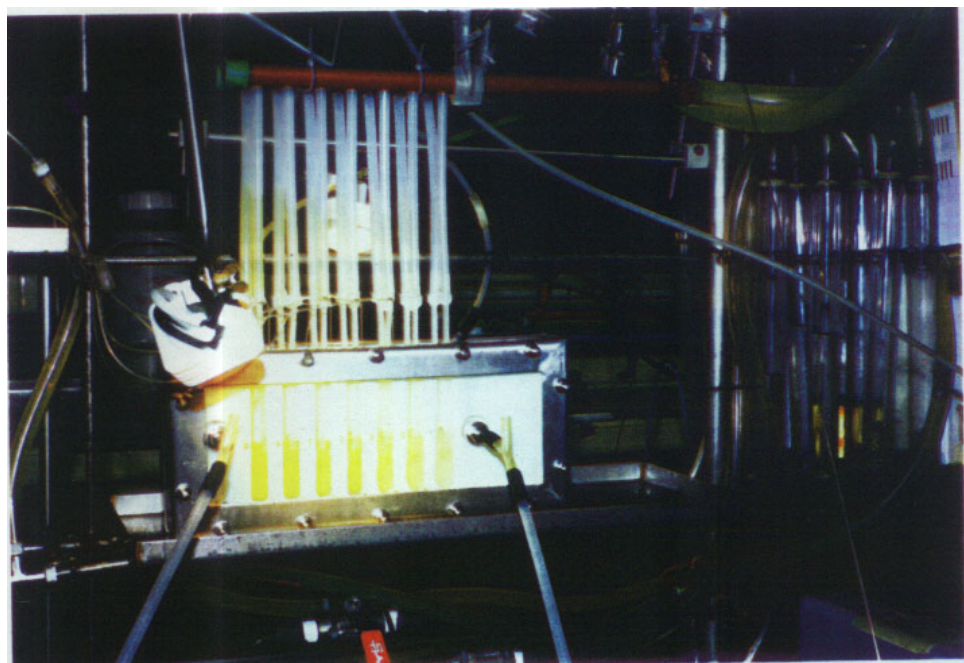


Figure 3. Mixer-settler prototype during extraction tests in laboratory.

At first, PUREX process conditions were tested during several continuous periods of 14 hours. Considering the flow rate and the uranium concentration of the fed solution into the corresponding mixer and its volume, values as 3.52 g U/h.cm<sup>3</sup> and 0.50 g U/h.cm<sup>3</sup> for the extraction feeding mixer and for the 7 stages mixers of the device respectively were obtained, as a measurement of production capacity. An average stage efficiency of 81 % and an overall efficiency of 73 % were obtained. A typical concentration profile obtained in one of these experiments can be seen in Table 1.

*Table 1. Typical uranium concentration profile for PUREX process conditions.*

Stage	Organic U concentration [g/L]	Aqueous U concentration [g/L]
1	32.8	104.2
2	38.5	105.1
3	45.5	105.6
4	10.4	43.5
5	4.5	13.5
6	2.5	1.17
7	0.156	0.47
8	0.01	0.065

Then, a high concentration uranium process like IMPUREX [2] was tested during several continuous periods of 14 hours too. The cycle was automatically controlled by means of a loop integrated by an optical measurement of uranium concentration, a PC software specially designed and externally operated pumps. A typical concentration profile [3] obtained in one of these experiments can be seen in Table 2.

*Table 2. Typical uranium concentration profile for IMPUREX process conditions.*

Stage	Organic U concentration [g/L]	Aqueous U concentration [g/L]
1	0	0
2	0	0.36
3	13.2	4.4
4	35.3	15.62
5	103.6	63.2
6	121.9	60.9
7	122.1	61.3

Watertightness, stability, perfect mixing, correct circulation of phases and high mass transfer rate were observed.

## CONCLUSIONS

Materials such as high density polythene and tempered glass have been demonstrated to be highly resistant to corrosion and radiation, they have a long lasting visibility, and when pressed together, they perform within suitable watertightness values. They can be used in hot cells, so they are a good option for use as experimental mixer-settlers.

The different height of the two air-mixing nozzles produces an optimum mixing.

The upper ended nozzle directed to a special baffle placed in the mixing channel allows any high viscosity mixture or crud to flow easily from the mixer to the settler. Back mixing was not observed.

A small air-lift placed in every stage eliminates the overall pressure drop and breaks aqueous phase density steps, as a result of sufficient pumping of aqueous phase from settler to mixer.

The data collected from the test series have demonstrated the following advantages: high stage and overall efficiency and high mass transfer per unit of time and mixer volume, to become this device in a good option for hot cell operation.

## REFERENCES

1. N. Venturini (1974), Estudio de un reactor tanque agitado por boquillas pulsantes. DSc. Thesis, Universidad de Buenos Aires, F.C.E. y N.
2. H. Schmieder and G. Petrich (1989), *Radiochim. Acta*, **48**, 3-4.
3. C. Andaur, M. Falcon, F. Granatelli, A. Russo, J. Vaccaro and A. Gauna (1999), *Proc. Asociación Argentina de Tecnología Nuclear*, Bariloche, República Argentina.



## THE INFLUENCE OF EXPERIMENTAL DROP SIZE ERRORS ON LIQUID-LIQUID EXTRACTION MODELLING EVALUATION

M.L.A.C.N. Gomes, M.M.L. Guimarães, J.M.M. Cardia Lopes, C.M.N. Madureira\*,  
J. Stichlmair\*\* and J.J.C. Cruz-Pinto\*\*\*

Depº. Engª Química, CIEA, Instituto Superior de Engenharia do Porto, Porto, Portugal

\*Faculdade de Engenharia, Universidade do Porto, Porto, Portugal

\*\*Lehrstuhl für Fluidverfahrenstechnik, Technical University of Munich, Germany

\*\*\*Depº. Química, Universidade de Aveiro, Aveiro, Portugal

Improved performance of modern computers has added pertinence to the possibility of testing the predictions of complex theoretical models of liquid-liquid extraction processes against experimental data. However, a search of the available literature has shown that comprehensive studies of the errors in the measurement of drop size distributions have never been performed. Analysis is performed in this work of the random errors of experimental data from a pilot-scale Kühni-type column at the Technical University of Munich.

Also, although several hydrodynamic simulation models have been developed in the past, their authors seem never to have felt the need to take experimental error into consideration when evaluating their proposed models. As gauged by our random error estimates, simulation results for the Coulaloglou-Tavlarides' interaction model exhibit excellent agreement with our drop size distribution experimental data and fair conformity with those concerning dispersed phase hold-ups.

### INTRODUCTION

Mass transfer of solute between two liquid phases (one being dispersed into the other in a contactor) is known to be highly dependent on the hydrodynamics of the drop interaction occurring within the dispersed phase. This interaction consists of break-up and coalescence of individual drops, which take place as a consequence of the chaotic movements of the fluids, which are known to greatly affect the hydrodynamic and mass transfer / reaction performance of liquid-liquid contactors/reactors, through their influence on the drop size distribution and the redistribution of solutes/reactants among the dispersed phase drops.

In the last decades, mechanically agitated devices for liquid-liquid contact in extraction equipment have acquired great importance, due to their capacity to create and maintain large interfacial areas, which accelerate mass transfer. The efficient behaviour of these columns has been shown to be due, not only to these large interfacial areas, but also to the mixing effects caused by drop interactions (breakage and coalescence). Thus, it is obviously necessary to describe both physically and mathematically those interaction processes, in addition to the actual mass transfer fluxes, in order to simulate the behaviour of such systems and predict the effect of the process variables on the extraction efficiency.

In recent years, many authors have spent great effort in modelling such contactors and attempting experimental validation of their models. Models such as those of Cruz-Pinto [1], Casamatta and Vogelpohl [2], Laso *et al.* [3], Tsouris *et al.* [4] and, more recently, Gerstlauer *et al.* [5], have been reported as able to describe with reasonable accuracy the results of their authors' experiments, even though most of them adopted drastic simplifications in order to ensure time-effective computation.

Recently, a simplified version of an algorithm previously developed by Ribeiro [6], and further streamlined by Regueiras *et al.* [7], has been proved able to accurately describe the transient behaviour of a continuous ideally agitated vessel, requiring only modest computer resources and very low computation times. This algorithm, further adapted to model an agitated column by solving the population balance equations in dynamic conditions, was designed to obtain the drop size distribution, solute concentrations and local dispersed phase hold-up profiles along the column height. However, the evaluation of such models so far has never benefited from a detailed assessment and quantification of the experimental errors with which local drop size distribution and dispersed phase hold-up experimental data are obtained. To our knowledge, only one previous study [1] attempted to consider the similar, but much simpler, problem of the consequences of the experimental variability in measured overall (average) dispersed phase hold-ups and Sauter-mean drop diameters on both the experimental and model-predicted column (RDC – Rotating Disc) mass transfer efficiencies.

## EXPERIMENTAL WORK

The experimental work was carried out by Gomes [8] at the TUM in a Kühni pilot-plant column (150 mm inside diameter, active height 2520 mm, divided into 36 stirred compartments with free passage area of 25%). The equilibrated (no mass transfer) standard high interfacial tension toluene (dispersed phase) – water (continuous phase) system was used in these studies.

The extraction column was equipped with measurement devices that allow the investigation of the hydrodynamic conditions along the column. A photoelectric technique initially developed by Pilhofer (Genenger *et al.* [9]) was used to measure the axial profile of drop size distributions at steady state. This was installed in five compartments (2<sup>nd</sup>, 5<sup>th</sup>, 11<sup>th</sup>, 21<sup>st</sup> and 35<sup>th</sup>) of the column. It should be noticed that the experimental set-up does not provide for the acquisition of the feed drop size distribution or even of the drop size distribution at the first column stage. Samples of 1000 drops were collected for each measurement of the local drop size distribution. Local hold-ups were dynamically monitored (at four compartments: 4<sup>th</sup>, 10<sup>th</sup>, 16<sup>th</sup> and 22<sup>nd</sup>) using a non-invasive ultrasonic technique described by Yi and Tavlarides [10]. Simultaneously, the global hold-up was measured using the pressure difference between the top and bottom of the active part of the column. All these data as well as intensity of agitation and flow rates of the dispersed and continuous phases were recorded on-line on a personal computer.

Under normal industrial or pilot-plant experimental conditions, the drop size distribution may be influenced by fluid contamination, which in turn induces variations in the interfacial tension, a key variable affecting the drop interaction dynamics. It is almost impossible and highly uneconomical to stop an industrial installation in order to perform fluid cleaning operations, although periodical removal of impurities accumulated at the top and bottom interfaces may be adopted as routine procedure. Further, interfacial tension is highly dependent upon temperature, an environmental variable that is uneconomical to try to stabilise.

Several experiments were planned and performed, under both steady and transient states. Since, in the experimental set-up, environment conditions were not either controlled or measured, repeated runs, were planned in order to study the reproducibility of the hydrodynamic performance, as well as the measurement and sampling errors. These, including those directly resulting from slightly varying (drifting) interfacial tension, were later used to assess the quality of the model's predictions.

The standard operating conditions (labelled B16-standard in Gomes [8]) used in this paper were ( $F_d = 160 \text{ L.h}^{-1}$ ;  $F_c = 125 \text{ L.h}^{-1}$ ; rpm = 140). For these conditions, six measurements of drop size distributions and thirty measurements of global and local hold-ups were obtained, in two different work periods. The reason for the selection of these specific measurements was the critical importance of the corresponding variables / operating conditions on the contactor's performance [1, 8].

## ERROR ANALYSIS

In any experimental work two kinds of errors, systematic and random, are to be expected. Ideally, systematic errors should be identified and then corrected. During the experiments carried out with the extraction column, we have detected some evidence of systematic errors affecting the drop size measurements at the fifth column stage. Unfortunately, we were not able to identify and correct their source(s).

Random errors, however, cannot be totally avoided, so that a statistical treatment must be performed in order to assess their magnitude. The meaning of results quality is, of course, quite subjective: what may be thought of as good quality in one instance may be quite unacceptable in another one. In order to have some assessment of measurement quality we used the 98% probable width of the random error interval of the experimental results. In order to do this, we must estimate not only the average,  $\mu$ , but also the mean square deviation,  $\sigma$ . Under favourable circumstances, normal (gaussian) sampling theory will be adequate for this purpose. We, however, came across time and expense limitations, which limited the maximum size of the drop sample to be taken. In this case, small-sample theory must be invoked, the uncertainty introduced by the poor estimation ( $\bar{x}, s$ ) of the population parameters ( $\mu, \sigma$ ) must be accounted for, and the confidence interval must be calculated as

$$\bar{x} \pm \frac{t.s}{\sqrt{n}} \quad (1)$$

where

$n$  = Number of available samples

$t$  = Student's statistic  $t$  for the appropriate significance level (98% in our case) and number of degrees of freedom ( $n - 2$ , because two of them have been spent in the estimation of the average and the mean square deviation). The values for Student's  $t$  may be found in any standard statistical hand- or textbook.

## CONFIDENCE CHANNELS

The absolute instrumental error implicit in the size class-by-class drop counts impinges upon the relative error, because drops may be assigned to one class when they should be assigned to a neighbouring one. Figure 1 (left) shows the relative error as computed from the Student's  $t$ -distribution for six runs performed under the operating conditions designated B16-standard. The graph is typically *U*-shaped, both small and large size-classes exhibiting anomalous high relative errors.

In the case of small sizes, this may be ascribed to small-diameter drops not being stretched enough by the capillary, and thus not presenting enough length to be individually counted. The fact of the error being minimal for drop diameters just above the capillary diameter (0.8 mm) seems to confirm this interpretation. According to this analysis, the anomalous high errors in the smaller size classes must be thought of as systematic, or instrument-related, and cannot be removed or decreased by statistical means.

In the case of large sizes, which are characteristically infrequent, the sampling error is expected to be correspondingly higher since even one misplaced drop translates into a large relative error. This interpretation seems to be confirmed by the error increasing upwards along the column, the direction along which, under the present conditions, the number size distribution becomes narrower and narrower, as Figure 1 (right) shows.

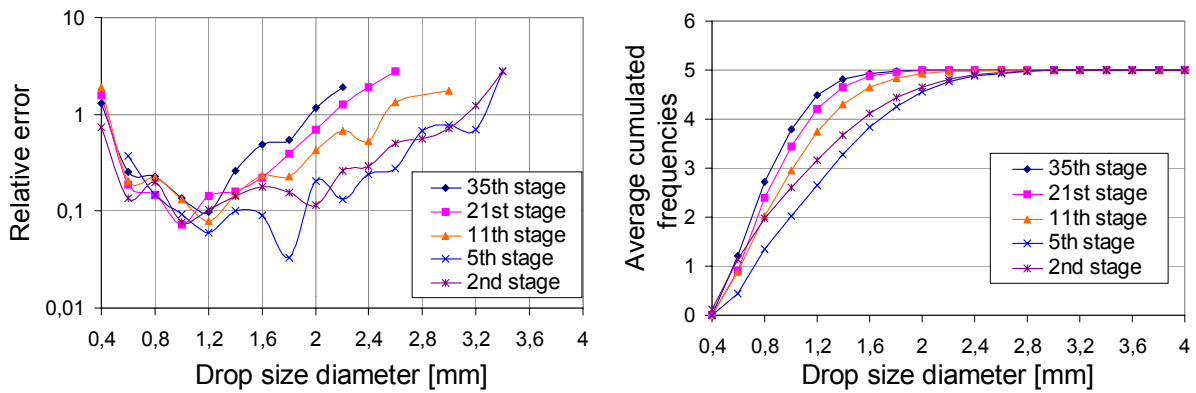


Figure 1. Left: Relative error calculated from number drop size distributions for the different stages of the column, under B16-standard operating conditions.

Right: Average cumulated frequencies for the number drop size distributions for the different stages of the column, under B16-standard operating conditions.

For the assessment of model performance, we used the error in cumulative size distributions, in order to minimise the relative error for the larger size classes. In fact, by taking cumulated frequencies, *i.e.*, counting in each class all drops smaller than the upper limiting size of the class, instead of the individual frequencies, the error curves become significantly different because the larger size classes now contain a considerably larger number of drops, as Figure 2 (left) shows.

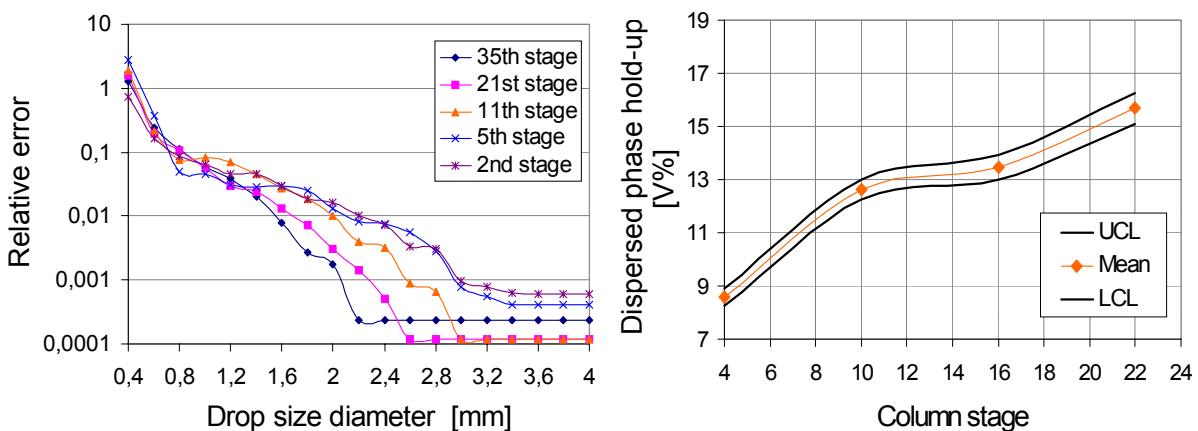


Figure 2. Left: Relative error for the cumulative number drop size distributions at different stages of the column, under B16-standard operating conditions.

Right: Confidence channel for the dispersed phase hold-up measured profile (UCL = Upper (98%) confidence limit; Mean = Average; LCL = Lower (98%) confidence limit).

The relative (random) error for the local hold-up measurements under B16-standard conditions was consistently about 4% of the average value, as shown in Figure 2 (right). This is remarkable, since mean drop sizes, temperature and illumination are bound to vary significantly along column height.

The relative (random) error for the global hold-up of the column has been estimated as 2.30% for the B16-standard operating conditions.

## CONFIDENCE INTERVALS AND MODEL PARAMETER ESTIMATION

The parameter optimisation algorithm selected was Levenberg-Marquardt's, for its recognised capability of handling highly multidimensional spaces (up to nine parameters were to be considered) and its frugality on function calls (the execution time of each call, involving the dynamic simulation of the process until it reaches steady-state, in a 300 MHz Pentium III, with 64 Mbytes of core memory, may, in certain cases, result in up to 2 hours of processor time). The objective function was defined as a weighed sum of the square deviations between calculated and experimental values of the overall and local dispersed phase hold-ups and of the local cumulative number-based drop size distributions. The C<sup>++</sup> code used was written by Regueiras [11] and based on Nash [12], using double precision in all critical number representations and special care in the estimate of derivatives.

In the absence of direct experimental measurements for the dispersed phase feed size distribution, this was assumed to be lognormal. In fact, preliminary runs have shown that, among several common distribution types, this was the most adequate to describe our data. The average and standard deviation of the feed drop size distribution have been adjusted together with the model parameters.

As seen in Figure 3, the simulated cumulative drop size distributions and local hold-up profiles globally fall within the experimental confidence limits of the data. The most important exceptions occurred in stages 2 (subject to influence of the unknown dispersed phase feed distribution) and 5 (where systematic errors, due to deficiencies in the column instrumentation, were suspected). Thus, evidence has been obtained that the minimized predicted to experimental data residuals are consistent with the experimental errors.

The present work extends the previous study by one of the authors [1], in which experimental overall dispersed phase dispersed phase hold-ups and local drop size distributions, and experimental and predicted extraction efficiencies (forward mixing model with no drop breakage/coalescence and rigid or oscillating mass transfer model, for the dispersed phase, and plug flow with axial mixing, for the continuous phase [1, 13]) were obtained for four sets of duplicate experimental runs, in an RDC column. This study highlighted the importance of the variability of experimental hydrodynamic data even for weakly interacting dispersions, and, when interaction rates are high, one can only expect much stronger effects, in view of the strong dependence of the drop breakage and coalescence frequencies on the local dispersed phase hold-ups and drop size distributions.

## CONCLUSIONS

An estimation of the (random) relative error of experimental data, as computed from Student's *t* for replicate data was shown to be important for checking the goodness-of-fit between simulated and experimental values. Model parameter values fitted by the Levenberg-Marquardt algorithm with the sum of squares of deviations as an objective function exhibited excellent agreement with experimental data concerning drop size distributions and fair conformity with those concerning hold-ups.

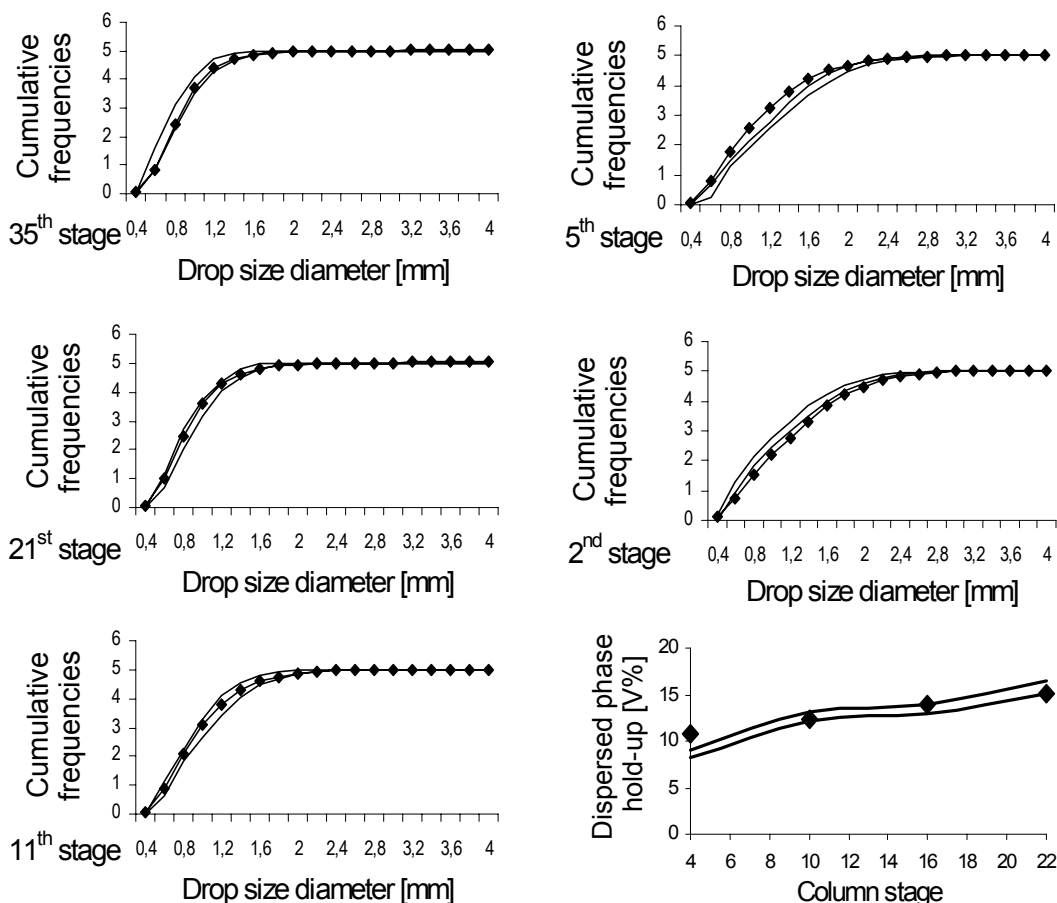


*Figure 3. Simulated values, together with confidence limits. Left: drop size distributions to 35<sup>th</sup>, 21<sup>st</sup> and 11<sup>th</sup> stages; Right: drop size distributions to 5<sup>th</sup> and 2<sup>nd</sup> stages and local dispersed-phase hold-up profile.*

## REFERENCES

1. J.J.C. Cruz-Pinto (1979), Experimental and Theoretical Modelling Studies of the Hydrodynamic and Mass Transfer Processes in Countercurrent-Flow Liquid-Liquid Extraction Columns, Ph.D. Thesis, The Victoria University of Manchester, England.
2. G. Casamatta, A. Vogelpohl (1985), *Ger. Chem. Engng.*, **8**, 96-103.
3. M. Laso, L. Steiner, S. Hartland (1987), *Chem. Engng. Sci.*, **42** (10), 2429-2437.
4. C. Tsouris, V. I. Kirou, L. L. Tavlarides (1994), *AIChE J.*, **40** (3), 407-418.
5. A. Gerstlauer, A. Mitrovic, E.D. Gilles, G. Zamponi, J. Stichlmair (1996), *Proc. ISEC '96*, University of Melbourne, Australia, pp.1091-1096.
6. L.M. Ribeiro (1995), Simulação Dinâmica de Sistemas Líquido-Líquido, Ph.D. Thesis, Universidade do Minho, Braga, Portugal.
7. P.F.R. Regueiras, L.M. Ribeiro, M.M.L. Guimarães, J.J.C. Cruz-Pinto (1996), *Proc. ISEC '96*, University of Melbourne, Australia, pp.1031-1036.
8. M.L.A.C.N. Gomes (1999), Comportamento Hidrodinâmico de Colunas Agitadas de Extracção Líquido-Líquido, Ph.D. Thesis, Universidade do Minho, Braga, Portugal.
9. B. Genenger, B. Lohrengel, M. Lorenz, A. Vogelpohl (1991), Hydromess-Meßsystem zur Bestimmung der Blasen – und Trpfengröße in Mehrphasenströmungen, Institut für Thermische Verfahrenstechnik der TU Clausthal, Germany.
10. J. Yi, L. L. Tavlarides (1990), *Ind. Engng. Chem. Res.*, **29**, 475-482.
11. P.F.R. Regueiras, Ph.D. Thesis in preparation.
12. J.C. Nash (1979), Compact Numerical Methods for Computers: Linear Algebra and Function Minimisation, A. Hilger (ed.), Bristol.
13. R. Chartres, W. J. Korchinsky (1975), *Trans. IChemE*, **53**, 247-254.



## VERIFICATION OF A PROCESS IN A DEMONSTRATION PLANT: HOW LONG DOES IT TAKE TO FIND ALL THE PROBLEMS?

**Baruch Grinbaum, Leni Kogan**

IMI(TAMI) Institute for Research and Development, Haifa, Israel

A demonstration plant is erected to fully simulate the future plant. Its configuration and type of equipment is similar to the full-scale plant, and it should be run in the designated site, using the real raw materials. Its main purpose is the verification of the process, which was developed on the bench-scale or pilot plant scale, regarding production rate, recovery, product quality and analysis of accumulation phenomena.

Quick accumulation phenomena can be detected and solved during the running-in of the bench or pilot plant. Slow phenomena, which are detected after a few weeks or months, are the more problematic ones. They are caused by solvent decomposition, oxidation, precipitation or extraction of traces of harmful elements. A crucial problem is to decide how long should the running-in be.

An example of a full follow-up of a process in a demonstration plant is given.

### INTRODUCTION

The most difficult problem in scaling up SX processes is to predict and solve various accumulation phenomena. All other scaling-up parameters can be successfully determined in an adequate process and/or equipment pilot plant, during relatively short running-in, typically a few weeks of experimental work. The accumulation phenomena, on the other hand, take a long time to be detected – typically a few months and more. One of their worst properties is that often they are quite unpredictable, and only after being discovered can one start thinking about a possible solution. Quick accumulation phenomena can be detected and solved during the running-in of the bench or pilot plant, if the pilot is run with the real raw material of the future plant. Slow phenomena, which are only detected after a few weeks or months, are the more problematic ones. They may be detected in a demonstration plant only. A demonstration plant is erected to fully simulate the future plant. Its configuration and type of equipment is similar to the full-scale plant, and it should be run in the designated site, using the real raw materials. Its main purpose is the verification of the process, which was developed on the bench-scale or pilot plant scale, regarding production rate, recovery, product quality and analysis of accumulation phenomena.

### What causes Accumulation Phenomena?

Accumulation phenomena are caused by solvent decomposition, oxidation, precipitation or extraction of traces of harmful elements. The common phenomena are: poisoning (by irreversible reaction with the solvent), precipitation of scale, decomposition of the solvent, foaming or deteriorating phase separation (due to creation of surface active compounds or very fine solid particles in the solvent).

The detection of the accumulation phenomena is slow. Every detected problem has to be solved and the running-in should be continued, until the next one is spotted and solved, and so on. In many cases, once an accumulation problem was detected and its cause understood, the solution is rather quick. Sometimes the solution is difficult, or even impossible. Often the symptoms of one problem mask the others, and only after solving the first problem, the other ones (sometimes more problematic) are detected and treated.

To find all of them requires a long verification run.

But how long should it be? Usually, the running-in of the demonstration plant goes on until one of the following conditions is satisfied:

***Full proof:***

The running-in was long enough to ensure a profitable process, even if the plant needs to be shut down for periodic cleaning or the solvent has to be totally exchanged in the future. In other words: the expected profit on the product is high enough to cover the cost of a periodical cleanup or total exchange of the solvent. Sometimes the deterioration of the solvent goes on slowly, despite all the direct or side-stream treatments, but the solvent remains good enough to enable profitable production.

***Time criterion:***

A period, set before the running-in started, passed without any new problem being discovered. A typical period of 2-6 month is recommended.

***The budget or time limit expired:***

There is no satisfactory proof that the solvent works “forever”, but on the other hand it did not fail during the time allocated to the experiment. The management has to use its best judgement and decide what to do.

## THE STORY OF THE LONGEST RUNNING-IN OF A DEMONSTRATION PLANT

The running-in of the demonstration plant for extraction of CaBr<sub>2</sub> from Dead Sea Brines demonstrates the methodology and problematics of the running-in.

**The Process**

The process for extraction of CaBr<sub>2</sub>, that was developed by IMI(TAMI) for Dead Sea Bromine (DSB), was a classic case for erection of a demonstration plant. The final product of the process is a clear solution of 52% CaBr<sub>2</sub>, with less than 0.5% Cl<sup>-</sup>.

The idea of the process is to extract the CaBr<sub>2</sub> directly from the brine, using a solvent that has high selectivity for both Br<sup>-</sup> over Cl<sup>-</sup> and Ca<sup>2+</sup> over Mg<sup>2+</sup>. The extraction process consists on 3 steps, each carried out in a separate battery. First, the Br<sup>-</sup>, together with Ca<sup>2+</sup> and some Cl<sup>-</sup> and Mg<sup>2+</sup> are extracted in the extraction battery. The extract, which contains relatively high concentration of Cl<sup>-</sup> and Mg<sup>2+</sup>, is purified in the purification battery by part of the product. Finally, the pure CaBr<sub>2</sub> is re-extracted from the purified extract by distilled water. The resulting solution is concentrated to 52 %, to make the final product.

The proprietary composite solvent was a mixture of amine and fatty acid in a diluent. The approximate composition of the Dead Sea end brine is: 0.75-0.95 % Br, 22-27 % Cl<sup>-</sup>, 2-5 % Ca<sup>2+</sup> and 5-7 % Mg<sup>2+</sup>. The concentrations are higher in the summer, and decrease in the winter. The distribution coefficients for all ions rise sharply with increasing ionic strength of the brine and drop with increasing temperature. The flux through the plant increases significantly with the temperature, as the viscosity decreases and the coalescence is quicker.

The overall performance of the plant was expected to be much better in the summer, and the production rate in summer was expected to be double relative to that in the winter.

The process was designed carefully, including good process simulation, and the only question marks, that convinced DSB to erect the demonstration plant, were the unknown accumulation phenomena.

### **The Demonstration Plant**

The most important strategic decision was to make a huge demonstration plant, with production rate about 10 % of the industrial plant, *i.e.*, flow rates above 100 m<sup>3</sup>/hr. Such a big plant makes the design of the industrial plant in the future much safer, as the total scale-up is just by factor of 10. Moreover, the product made by such a big plant can pay the variable costs of the operation, enabling a longer running-in without excessive budget limitations.

The plant consisted of mixer-settlers, arranged in three batteries: extraction, purification and washing.

### **The Running-in Design and Startup**

One of the most problematic features of the process is that it *practically never reaches steady state*. The composition of the brine changes between summer and winter, and so does of course the temperature. The influence of the ionic strength of the brine and of the temperature was known from the simulation to be very strong. The practical meaning for the running-in was that *variations in the flux and bromide recovery could be attributed to seasonal changes as well as to deterioration in the solvent performance*. The plant was started in the summer, when both the flux and the production rate are at maximum. So, any deterioration in the plant performance in autumn and winter could have been attributed to the seasonal changes just as well as to real deterioration due to accumulation problems. The direct conclusion was, that the running-in must take more than one year, to overcome this point and to get data about the expected performance in every season.

The running-in program was simple: operate the plant at maximum possible flux, while fine tuning the operational parameters that were calculated by the simulator, *e.g.*, phase ratio in the extraction, degree of washing, concentration and flow rate of the reflux stream etc. The product was to be sold, and, in addition to checking the market, had to cover most of the current costs of the operation. No *a priori* dead time for the running in was set, yet nobody expected that it would take six years.

The start-up was promising: after 3 weeks, the production rate of the plant was well above the design values. By then, the operating time of the demonstration plant was equal to the total period of the running of the bench scale, equipment and process pilot plant. However there remained the unavoidable question; what will strike first and when?

Over all, many accumulation phenomena were encountered and solved. The most interesting ones are listed below.

#### **Accumulation of ions**

The first, and quite unexpected problem, was the uneven loading of the solvent. After a few weeks significant deterioration in the washing of the solvent was observed. A crash research program revealed that under real process conditions either Br<sup>-</sup> or Ca<sup>++</sup> (depending on the pH of the brine) may accumulate on the solvent without a counter-ion, creating a stable amine bromide or calcium acid salt. As these ions cannot be washed out with water, they decrease the net loading of the solvent. Once detected and understood the problem was solved readily: an analytical method to determine the concentration of the bound ions was developed, and they were stripped by continuous addition of HBr or NaOH to the wash water.

### **Deposition of scale**

This was also an unexpected problem. After a month of successful running, some blockages of the pipes were observed. They were identified as  $\text{CaCO}_3$  and  $\text{CaF}_2$ . The precipitation of the carbonate could have been expected, as its presence in the brine, although in low concentration, was known, and the affinity of the amine to carbonate was common knowledge too. The presence of  $\text{F}^-$  was a surprise, as according to the solubility product its maximum concentration should not have exceeded 1 ppm. Yet, a concentration of 10 ppm  $\text{F}^-$  in the brine was detected, most of it being preferentially extracted by the solvent, and washed in the washing battery.

There was no way to prevent the extraction and creation of scale. The preventive treatment was to wash periodically the instrumentation, valves and narrow pipes with HCl.

The  $\text{CaF}_2$  was also the main culprit in the creation of crud – see below.

### **Solvent deterioration**

Early stability tests in the laboratory confirmed that the fatty acid and the diluent are stable, while the amine may undergo slow decomposition in the presence of oxygen. To avoid it, the plant was constructed with a nitrogen blanket. According to both the literature and laboratory tests this should have been more than enough (it was well known that, in many hydrometallurgical plants, amines are used without nitrogen blanketing and no deterioration was reported over years). Yet, after about 3 months a slow but steady deterioration in the performance of the plant was observed. It included lower yield on one hand and slower phase separation, which led to decreased flow rated on the other. As it was already autumn, the deterioration could have been attributed to the seasonal changes just as well as to problems with the solvent. The only reliable way was to compare the output of the plant with the results as predicted by the simulator. And this was really the way the problems with the solvent were detected. Once the problem was identified, the chemical decomposition of the amine was verified analytically. It was found, that at the summer temperature of the Dead Sea brines (close to 50 °C) even the small amount of oxygen, fed with the inlets or entering the vessels in spite of the nitrogen, was enough to oxidize the solvent. The solvent was used for another 6 month, with slow but irreversible deterioration. Meanwhile an efficient chemical additive, which could stop the oxidation, was developed and tested. Once the stability tests were positive, the entire batch of solvent (near to 100 m<sup>3</sup>) was removed, the plant was cleaned up and a new batch of solvent was introduced. In parallel, a device to strip the oxygen from both the feed brine and the wash water, using nitrogen, was installed in the plant. A year after the initial start-up the plant was restarted. The additive proved to be efficient, and practically zero oxidation was detected in the following years.

### **Crud**

Crud started accumulating at the interface after a few days, but a few months passed before it started affecting the plant performance. It caused increased thickness of the dispersion zone in the settler, and increased entrainment of both O/W and W/O, eventually decreasing the possible flow rates.

Initially the crud was attributed to the decomposition of the amine, which by then was already known. Only about three months *after* the new solvent was introduced, the crud was positively identified as a harmful accumulation phenomenon, and another six months passed until it was fully understood. Its main component was silica silt, which was readily identified. It was hardly a surprise, but the good news was that it caused no trouble and after a few months its accumulation stopped, i.e. the amount of silica in the feed and in the raffinate was equal. The real harm was done by  $\text{CaF}_2$  that precipitated in the washing battery as very fine crystals (<1μ in diameter), adsorbed molecules of the solvent, and created a colloidal gel that

traveled through the entire plant (its concentration was equal in all the batteries). To overcome it, two alternative side stream treatments were developed and tested.

The first one was chemical: it was found in the laboratory, that at pH<1 the colloid was broken, the captured solvent released and the CaF<sub>2</sub> precipitated on the bottom. HCl was the most convenient acid to use. But to get to this pH all of the amine had to react with the acid, to yield amine chloride. To complete the process, all the amine chloride had to be neutralized with NaOH. In the demonstration plant this operation was done batchwise, in a side-stream mixing vessel with a conical bottom, through which the fine solids were removed. This solution had harmless wastes (NaCl solution), but the cost of the reagents was relatively high.

When the chemical treatment was finally developed, the solvent was in a really bad condition, with a very low production rate. To speed up the cure, the entire batch of solvent – about 100 m<sup>3</sup> – was treated in a quite complex logistic operation. After two weeks the plant was restarted – and the solvent worked almost as new.

The other treatment was physical, and consisted of passing the solvent through a decanter centrifuge, in which the gel was separated. It was developed in order to save the cost of chemical reagents needed for the chemical treatment. This procedure was efficient but not really cheaper, mainly due to the solvent losses: the separated gel contained above 50 % amine and fatty acid. There was no economical way to recover them, and they were discarded, adding the cost of waste treatment to the solvent losses and direct cost of the decantation.

Both methods were tested, each for more than one year. Both were efficient in keeping the CaF<sub>2</sub> at a level, which caused no significant harm, and enabled continuous running of the plant.

#### ***Entrainment of aqueous phase***

As the O:W phase ratio in the purification and washing batteries exceeded 20, the aqueous entrainment in these batteries had to be very low. The plant was designed to meet this constraint, and all the settlers were “furnished” with partitions, to decrease entrainment. In the first few month the entrainment was well below the allowed 0.5 %. Yet, during the second winter (about six months after the plant was restarted with the new solvent) the entrainment rose sharply. The highest entrainment was in the last (i.e. the most diluted) stage of the washing battery – up to 4 %, which was unacceptable. It took a few months to realize that it was a combined problem of the lower temperature, which increased the viscosity, and the influence of the colloidal gel, which increased the width of the dispersion band. The immediate (and trivial) solution was to decrease the flow rates and to wait for the summer. During the summer, although the entrainment significantly decreased, it remained well above the design values. In the next winter the side-stream treatment was already operating, yet the entrainment was hardly smaller than in the previous year. The next attempt to solve the problem was to invert the phases, i.e. to disperse the major organic phase in the minor aqueous one. The mechanical changes, necessary for the phase inversion, were made only in the two critical stages, namely the end of both the purification and washing batteries, so that the solvent leaves the batteries with small entrainment. After suitable new turbine-pump-mixers (TPM) were designed and installed, both stages operated in aqueous continuous dispersion. The entrainment dropped below 0.5 % and the problem was practically solved. In other stages of these batteries the entrainment was between 1-2 %, and it was possible to live with it. In the extraction battery, where the phase ratio was near to 1:1, even 3 % of entrainment had hardly any influence on the process. During the remaining two years, the aqueous entrainment did not increase, and the phase inversion in the critical stages solved the problem.

### ***Entrainment of solvent***

Solvent entrainment was similar to the aqueous entrainment: it started with values about 100-150 ppm solvent in the raffinate, that are reasonable for mixer-settlers but too high for any SX process. The raffinate was sent to a continuous horizontal packed coalescer, where most of the entrained solvent was separated, leaving about 30 ppm to the waste. Over time, the entrainment went up to 300 ppm. Most of it was adsorbed onto the silica silt or CaF<sub>2</sub> particles, leaving the plant. This solvent was not separated in the horizontal coalescer. A sand filter was added, and it succeeded in decreasing the entrainment to 30 ppm.

### ***Long term durability of the equipment***

The long running-in enabled an excellent verification of the durability of the materials of construction, the reliability of the instrumentation, improvements in the analytical methods, sampling and control schemes etc. Nobody runs a demonstration plant for six year just to validate these parameters, but once such a long running-in period happens, it is an invaluable chance to check all these parameters on an experimental scale. Moreover, if after six years no functional or corrosion problems were detected, it may be considered as a full proof for the equipment. Such a long run minimizes the risk of failure in the commercial plant.

### **The Happy End**

The long story had a happy end: during the last 12 months no new phenomena were discovered, and there was an efficient treatment of the known ones. After six years both the managers and the researchers were convinced that the process is feasible, and the demonstration plant, that fulfilled its task, was shut down.

## **CONCLUSIONS**

The running-in of the CaBr<sub>2</sub> demonstration plant proved that in order to detect all the accumulation phenomena and overcome them, the running-in may take a few years. It supports the approach of making the demonstration plant large enough, so that the value of the product covers most of the operating costs, enabling a long run without excessive costs. It also proved, that once sufficient time is given, there is an economical solution for almost every accumulation problem.

Had the industrial plant been erected without any demonstration plant, its failure is almost certain, as nobody could afford the losses connected with long shutdowns and changes in the plant, caused by the accumulation phenomena.



## PERFORMANCE CHARACTERISTICS FOR A KARR RECIPROCATING PLATE EXTRACTION COLUMN

Angela Stella, H. R. Clive Pratt and Geoffrey W. Stevens

Department of Chemical Engineering, The University of Melbourne, Parkville, Australia

A program for the prediction of mass transfer performance in a Karr reciprocating plate column has been developed for two-phase, phenolic-based systems. Using correlations that have been verified for a 50 mm diameter column, the dispersed phase holdup, droplet size and the continuous phase backmixing coefficient were predicted for 100 and 450 mm diameter columns. Pilot-scale studies, using a solvent-alkaloid-aqueous alkali system were conducted to establish the optimum operating variables, including pulsation characteristics, with a high organic (continuous) to aqueous ratio. A robust model was obtained that enabled the mass transfer performance in a Karr reciprocating plate column to be determined for two-phase systems based on non-linear equilibrium data.

### INTRODUCTION

Since its development, the Karr column [1] has found application in many industries for the separation of the components of mixtures by liquid extraction. The contactor itself consists of a series of reciprocating perforated plates that provide up to 60% open area. Today, the Karr column is used in many areas such as the hydrometallurgical, pharmaceutical and petrochemical industries.

The counterflow of the dispersed phase drops in the continuous phase can induce significant deviations from ideal plug flow, thus leading to a fall in the effective driving force. Factors that contribute to backmixing include: -

- Entrainment of the continuous phase in the wakes of the dispersed phase droplets;
- Circulatory flow of the continuous phase caused by energy dissipation of the droplets;
- Molecular/turbulent eddy diffusion, as well as channelling and stagnant flow effects.

Novotny *et al.* [2], Kim & Baird [3] and Baird & Rao [4] have characterised the performance of various columns predominantly for single-phase operation. Prvcic *et al.* [5] later predicted axial dispersion for a two-phase system in a pulsed, perforated plate extraction column. To date, Stevens and Baird [6] have measured axial dispersion for a single-phase system via continuous tracer injection for a reciprocating plate column. Numerous correlations of mass transfer data to single droplets during formation and coalescence are available in liquid-liquid extraction [7, 8]. Their applicability to droplet swarms in real extractors is not apparent since little is known about the flow patterns of the continuous phase, the effect of throughput, contact area and distributor geometry. Harikrishnan *et al.* [9] have provided a correlation that enabled the prediction of mass transfer coefficients as a function of the dissipation energy for a reciprocating plate column to determinate the effective driving force.

## PROCESS DESCRIPTION

The flowsheet proposed for the alkaloid extraction in a Karr reciprocating plate column is shown in Figure 1. The experiments involved studies of a phenolic alkaloid system, whereby the solute was removed from the solvent mixture into an aqueous alkali solution by solvent extraction. The column consists of a dispersed phase inlet where fresh aqueous alkali was introduced into the column. At the bottom of the column the organic continuous phase was fed from the solvent header that was part of the stream intended to the production columns. The spent solvent was dispensed in the bottom stream that exited the agitated columns. The rich aqueous phase was then sent to the settler whereby the organic phase was later recycled. Further solvent extraction was required to improve the percent of recovery and the loaded liquor was then separated by changes in pH.

## EQUIPMENT AND PROCEDURES

Initial experiments were conducted in a 50 mm diameter column using a phenol - 10% tributyl phosphate/kerosene - water system. Plate frequencies and amplitudes of 2.0 and 3.0 Hz and 0.5 and 1.2 cm, respectively, were studied. The perforated plates with an open area of 45% had a hole size of 12.7 mm and plate spacing of 50 mm. The pulsing unit, driven by a variable speed motor, provided the reciprocating motion via a central shaft. The shaft supported the Teflon plates, which were fixed by three tie rods and positioned on a triangular pitch around the plate. Drainage was used to determine the dispersed phase holdup, while the drop size was found using a photographic technique. Pulse injection of a colour tracer, Waxoline Blue at the continuous phase inlet and measurement of the concentration response at two locations further down the column enabled the degree of continuous phase backmixing to be determined [10].

This was followed by work using an alkaloid system in 100 and 450 mm diameter columns, each constructed from 5m long Pyrex glass and stainless steel tubes. High-density polyethylene plates imparted a reciprocating motion by a variable speed motor with an adjustable yoke coupled to the motor. The plate geometry and plate spacing remained constant for all column diameters studied. Experiments involved the determination of the mass transfer coefficient, which was correlated in terms of the dispersed phase holdup, drop size and the continuous phase back mixing parameter.

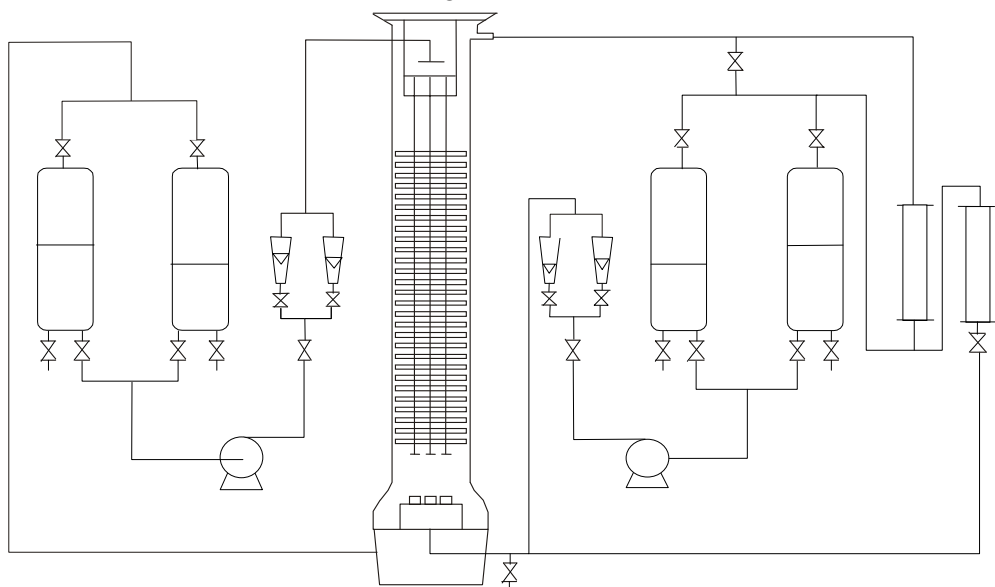


Figure 1. Schematic flow diagram for the alkaloid extraction in a reciprocating plate column.

## RESULTS

### Phenol Solvent Extraction

The properties of the feed and extractant solution for the phenol study are given in Table 1.

*Table 1. Typical properties for the phenol system.*

Element	Symbol	Properties
Dispersed phase	d	Tap Water
Continuous phase	c	10% TBP/Kerosene
Solute	—	Phenol
Interfacial tension	$\gamma$	11.8 mN/m
Continuous phase density	$\rho_c$	809 kg/m <sup>3</sup>
Continuous phase viscosity	$\mu_c$	1.76 cP

The holdup and Sauter mean droplet diameters were measured during mass transfer. Holdup data were in good agreement with predicted measurements using the Kumar & Hartland correlation [11], assuming plates wetted by the dispersed phase as given by,

$$x_d = [k_1 + k_2(Af)^{3.0}] V_d^{0.81} (V_d + V_c)^{0.32} \Delta \rho^{-0.98} \dots \dots \dots (1)$$

where  $k_1$  and  $k_2$  are  $7.2 \times 10^3$  and  $3.2 \times 10^6$  respectively. The relative deviation between predicted and experimental holdup values was  $\pm 10\%$ . Measurements of the Sauter mean diameter of the droplets enabled the predicted data to be expressed as a function of the pulsation intensity,  $Af$  (cm/s) for mass transfer in the direction from the continuous to the dispersed phase, thus,

$$d_{32} = -0.591(Af) + 3.434 \dots \dots \dots (2)$$

### Extraction

Extraction equilibria for the system were significantly improved due to the presence of tributyl phosphate in the solvent phase. The conditions were optimised by maintaining the pH of the extraction circuit between 6.0 and 7.5, and using a variable organic to aqueous volume phase ratio, (O:A). Increasing the phase ratio to 2.5 resulted in a lower backmixing coefficient and thus greater affinity for extraction.

### Stripping

Sodium hydroxide, of pH in excess of 13.0, effectively enabled the phenol to be stripped. Typical mass transfer coefficients based on the backflow model are shown in Figure 2.

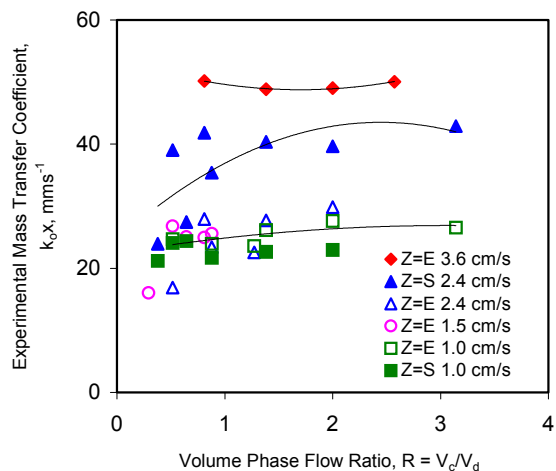


*Figure 2. Overall mass transfer coefficients obtained in the 50 mm diameter Karr column.*

## Alkaloid Solvent Extraction

The alkaloid system involved the comparable stripping of a phenolic alkaloid in a solvent solution with aqueous caustic soda using 100 and 450 mm diameter columns. The operating condition was to load the organic phase as fully as possible with alkaloid, using a high volume solvent to aqueous phase ratio and to collect samples from the spent solvent and aqueous phase outlets.

Measurements of the dispersed phase holdup were conducted in the 100 mm column to verify the correlated results for the 50 mm diameter column. The drop size, as for the phenol system, was derived using *equation 2*, while the continuous backmixing coefficient was found based on the model developed for a two-phase system in a pulsed, perforated plate extraction column [12]. Various phase flow ratios and pulsation velocities were used to determine optimal operating conditions.

Various single drop models were considered based on the assumption that the continuous organic phase was the governing resistance for mass transfer. Thorsen and Terjesen [13], for continuous phase mass transfer, and Rozen and Bezzubova [14], for dispersed phase mass transfer, were investigated as possible predictive techniques to determine the overall mass transfer coefficient. The resulting models for mass transfer coefficients for each phase,

$$k_c = \frac{D_c(-178 + 3.62 Re^{0.5} Sc_c^{0.33})}{d_{32}} \quad \dots \dots \dots \quad (3)$$

where  $D_c$  and  $D_d$  represent the molecular diffusivities of the continuous and dispersed phase respectively.

## ***Stripping***

When considering the effect of the pulsation frequency, it was evident that an optimum mass transfer rate was reached at 180 rpm and gradually fell with increasing agitation. Interpretation of this result was derived from analysis of the individual film coefficients. Table 2 shows the effects of the continuous and dispersed phase mass transfer coefficient for the various pulsation frequencies. Approach of high frequencies with increasing backmixing, resulted in the formation of rigid droplets of high specific interfacial area. This contrasted the presence of circulation eddies within the droplet at much lower frequencies. An optimal pulsation frequency for the 100 mm diameter column was determined at 180 rpm, with a pulsation velocity of 3.6 cm/s. As presented in Figure 3, the capacity for alkaloid mass transfer as derived using the back-flow model [15], peaked in the frequency range of 2.0 and 3.0 Hz as supported by earlier results [16].

Table 2. Hydrodynamic characteristics for various pulsation frequencies.

Property	Value obtained in 100 mm diameter column			
A, cm	1.2	1.2	1.2	1.2
f, rpm	120	180	210	240
$\alpha_c$	0.01	0.05	0.07	0.10
d <sub>32</sub> , mm	2.0	1.3	1.0	0.60
x <sub>d</sub> , %	3.5	9.9	15.2	22.0
k <sub>c</sub> , (eqn. 3), m/s	$1.7 \times 10^{-4}$	$1.5 \times 10^{-4}$	$1.1 \times 10^{-4}$	$8.1 \times 10^{-6}$
k <sub>d</sub> , (eqn. 4), m/s	$2.1 \times 10^{-8}$	$2.0 \times 10^{-8}$	$1.9 \times 10^{-8}$	$1.7 \times 10^{-8}$
R	16.7	16.7	16.7	16.7

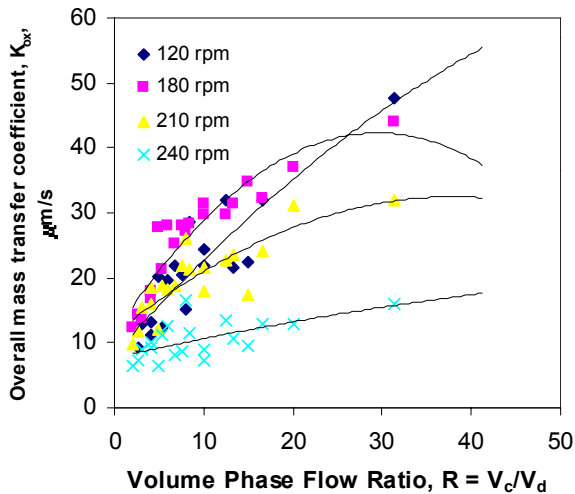


Figure 3. Experimental overall mass transfer coefficients for the 100 mm diameter column.

Results from the 450 mm diameter column confirmed an increase in backmixing with a lower phase flow ratio. The pH of the aqueous alkali was maintained at 13.0 to ensure that the alkaloid remained in solution. The percent of entrainment for Column 1 was measured as 0.74%, while a much lower value of 0.16% was found for Column 2. Table 3 gives the hydrodynamic and performance characteristics at a phase flow of 14.0 and 6.0 for Column 1 and 2 respectively. It shows the effect of the different volume ratios has on both the measured dispersed phase holdup and the predicted value for the continuous phase backmixing coefficient. By doubling the phase flow ratio, the extent of backmixing was significantly reduced. Figure 4 confirms that under negligible backmixing, as was the case in the 100 mm diameter column, the simple plug flow relationship is valid [17].

Table 3. Characteristics of the 450 mm diameter columns.

Column	Column 1	Column 2
A, cm	1.2	1.05
f, rpm	180	180
$\alpha_c$	0.4	1.5
$d_{32}$ , mm	0.9	0.95
$x_d$ , %	3.8	3.0
$K_c$ , m/s	$1.0 \times 10^{-4}$	$1.1 \times 10^{-4}$
$K_d$ , m/s	$1.9 \times 10^{-8}$	$1.9 \times 10^{-8}$
R	14.0	6.0

## CONCLUSIONS

Prediction of the hydrodynamic and mass transfer performance for a two-phase system in pilot-scale reciprocating plate columns was enabled via development of a program. Its viability was extended to existing production columns, wherein the optimum operating conditions were found. More importantly, comparisons were drawn between the performance coefficient found using the backflow model and that based on plug flow operation.

The present work highlights the effect of the phase flow ratio on the backmixing coefficient and the underlying result on the mass transfer coefficient. The optimised alkaloid circuit achieved stripping efficiencies of better than 95%, with losses to the raffinate of below 0.007 g/l, from a feed containing 2 g/l. This work has intended to enhance present understanding of the factors that control the performance of a Karr column and draw conclusions on the optimum throughput permissible and mass transfer efficiency.

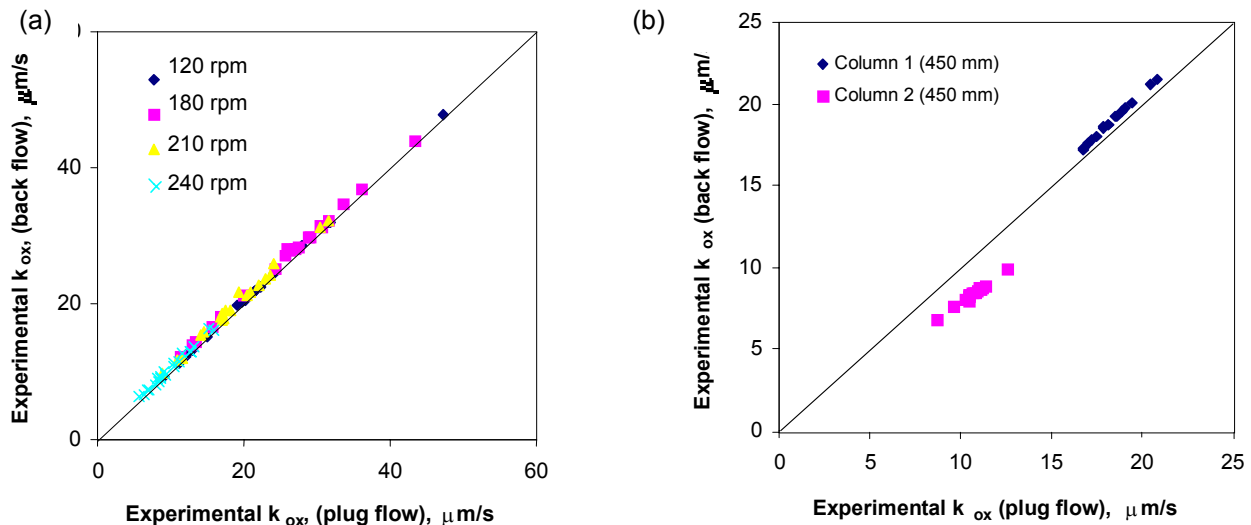


Figure 4. Overall mass transfer coefficient derived using the (non-ideal) back flow model and simple plug flow relationship for (a) 100 and (b) 450 mm diameter columns.

#### ACKNOWLEDGEMENTS

This paper is published by permission of GlaxoSmithKline. The process simulation was modelled using the software program *Mathematica*. Shell Australia and GlaxoSmithKline are thanked for providing the extractants used in this work. Successful completion of the pilot-plant studies was made possible with the significant contribution from Prof. G. W. Stevens and Prof. H. R. C. Pratt from The University of Melbourne.

#### NOMENCLATURE

A	amplitude, m
d	dispersed phase, m
$d_{32}$	Sauter mean drop diameter, mm
D	molecular diffusivity, $\text{m}^2/\text{s}$
E	mass transfer in the direction of the dispersed to continuous phase
f	frequency, 1/s
k	mass transfer coefficient, m/s
$k_o$	overall mass transfer coefficient, m/s
R	volume phase flow ratio, $V_c/V_d$
Re	Reynolds number, $d_{32}V_t \rho_c/\mu_c$
S	mass transfer in the direction of the continuous to dispersed phase
$Sc_c$	Schmidt number for the continuous phase, $\mu_c/(\rho_c D_c)$
$Sc_d$	Schmidt number for the dispersed phase, $\mu_d/(\rho_d D_d)$
V	superficial velocity, m/s
$x_d$	fractional holdup of dispersed phase
Z	pulsation velocity, Af, cm/s

### Greek Symbols

$\alpha_c$	backmixing ratio of continuous phase
$\gamma$	interfacial tension of phases, N/m (kg/s <sup>2</sup> )
$\mu$	viscosity, kg/ms
$\rho$	density, kg/m <sup>3</sup>

### Subscripts

c	continuous phase
d	dispersed phase
x	x-phase (continuous phase in present case)
y	y-phase (dispersed phase in present case)

## REFERENCES

1. A. E. Karr (1959), *AICHE J.*, **3**, 943.
2. P. Novotny, J. Prochazka, and J. Landau (1970), *Can. J. Chem. Eng.*, **48**, 405-410.
3. S. D. Kim and, M. H. I. Baird (1976), *Can. J. Chem. Eng.*, **54**, 81-89.
4. M. H. I. Baird and N. R. V. Rao (1988), *Can. J. Chem. Eng.*, **66**, 222-231.
5. L. M. Prvcic, H. R. C. Pratt, and G. W. Stevens (1989), *AIChE J.*, **35** (11), 1845-1855.
6. G. W. Stevens and M. H. I. Baird (1990), *Chem. Eng. Sci.*, **45** (2), 457-465.
7. A. E. Handlos and T. Baron (1957), *AIChE J.*, **3**, 127-136.
8. A. Kumar and S. Hartland (1999), *Trans. IChemE*, **A77**, 372-384.
9. T. L. Harikrishnan, N. K. Prabhavathy and Y. B. G. Varma (1994), *Chem. Eng. J.*, **54**, 7-16.
10. K. R. Dongaonkar, G. W. Stevens and H. R. C. Pratt (1993), *Ind. Eng. Chem. Res.*, **32**, 1169-1173.
11. A. Kumar and S. Hartland (1988), *Ind. Eng. Chem. Res.*, **27**, 131-138.
12. L. M. Prvcic, H. R. C. Pratt and G. W. Stevens (1989), *AIChE J.*, **35**, 1845-1855.
13. A. M. Rozen and A. I. Bezzubova (1968), *Theo. Found. Chem. Eng.*, **2**, 715-724.
14. G. Thorsen and S. G. Terjesen (1962), *Chem. Eng. Sci.*, **17**, 137-148.
15. H. R. C. Pratt and M. H. I. Baird, M. H. I. (1983), Axial Dispersion: Handbook of Solvent Extraction, Wiley-Interscience, New York, pp. 208-209.
16. A. K. Bensalem, L. Steiner and S. Hartland (1986), *Proc. Int. Solvent Extr. Conf. ISEC '86*, Munich, Germany, pp. III-191-198.
17. R. E. Treybal (1980), Mass Transfer Operations, McGraw-Hill, 3rd edn., New York, p. 551.



## GETTING THE BALANCE RIGHT – SOME PRACTICAL DESIGN CONSIDERATIONS FOR SOLVENT EXTRACTION CIRCUITS

Geoff Laing

Bateman Engineering, Perth, Western Australia

On scheduled commissioning and effective operation of a solvent extraction circuit relies on getting the design of both the core contact equipment and the peripheral plant right. Experience has shown that poor performance of new plants is frequently a result of 'utility' systems that do not match the requirements of the circuit, rather than the mass transfer equipment itself. Both the operator/owner and designer need to understand the 'complete requirements' for the circuit to get the balance of the design right. This paper reviews generic issues, frequently overlooked or altered during cost cutting exercises, which have a significant impact on plant performance.

### INTRODUCTION

The performance of a solvent extraction plant is affected by numerous factors ranging from the fundamental mass transfer characteristics of the system to the layout of the plant. Successful commissioning and operation of a solvent extraction circuit relies on getting all the detail right during the design stage. However, getting the detail right all too often becomes a process of trial and error during the commissioning and early operation of the plant. To satisfy the financial constraints of a project and design the optimum circuit a balanced approach to the plant specification needs to be adopted.

Naturally, the most complex issues receive the greatest attention at the piloting and design phases. However, it is not uncommon that the 'simpler issues' result in poor performance of such plants. Problems are often associated with ancillary equipment required to filter, heat, store etc liquors rather than the solvent extraction units themselves. Both the ancillary units and materials of construction tend to be the main focus of cost cutting exercises in the latter stages of design. Often the case is that the solvent extraction plant is given a higher priority than the utility equipment servicing that plant. This equipment must be considered part of the solvent extraction circuit and allocated the same level of importance as the contact equipment. This paper documents a list of factors, in addition to the extraction, scrubbing, and stripping detail, to be considered for any solvent extraction plant. These issues should be considered both prior to any piloting campaign, to enable a suitable test program to be established and then again during the detailed design. The discussion is generic, covering a range of issues relevant to conventional mixer settler type circuits.

## EVALUATING THE CIRCUIT REQUIREMENTS

Successful inclusion of a solvent extraction circuit in a hydrometallurgical flowsheet requires that the selected process operate under appropriate conditions. Suitable equipment will minimize the risk to both the organic reagents and the surrounding unit operations. The selection of appropriate equipment will depend on numerous factors such as the position of the solvent process in the overall flowsheet, the complexity of the aqueous solutions, likely deviations from normal conditions, solvent sensitivity, solvent cost, etc. Illustrated below is a generic block diagram of a solvent extraction process with some of the peripherals that may be necessary for smooth operation of the plant. Certain of the peripheral units are discussed in some detail in the following sections. While the contact equipment is not dealt with *per se*, details of selected issues within each of the extraction, scrub and strip circuits are also addressed.

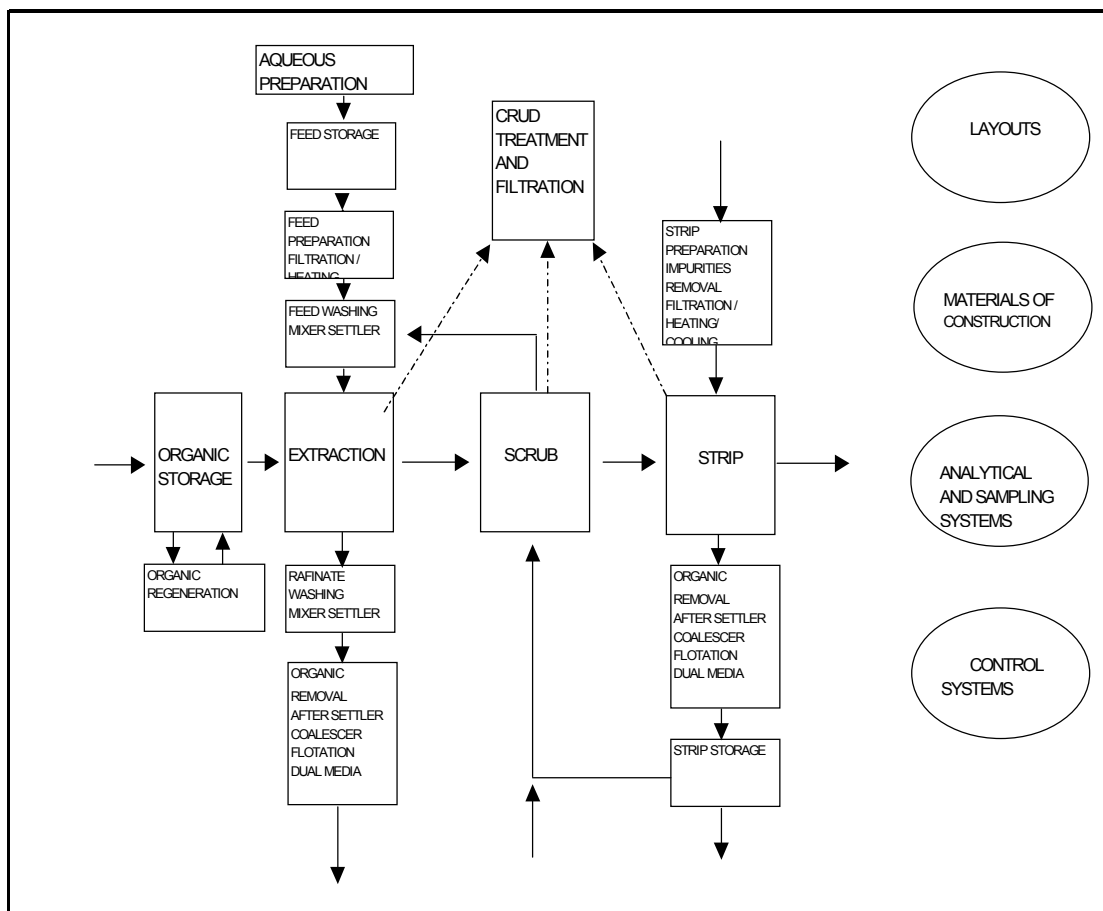


Figure 1. Typical solvent extraction circuit.

During the design of the process the risk associated with including a solvent extraction step in the flowsheet should be evaluated and quantified. The following factors should be considered in the evaluation.

- *Position of the solvent extraction plant in the process flowsheet:* - There are a number of issues to be considered. Firstly, the type of aqueous solution to be contacted with the solvents, this is discussed in more detail in the following point. Secondly, the likelihood of contamination to or from other solvent extraction circuits. Processes using more than one solvent in a series of circuits require careful consideration. Thirdly, the requirement to protect other unit operations linked with the solvent extraction circuit particularly with regard to organic contamination.

- *Exposure of the solvent to undesirable components:* - The more complex the aqueous feed to a solvent extraction circuit the greater the potential risk. The so-called direct solvent extraction circuits result in high exposure while circuits treating refined (relatively pure) process streams present relatively lower exposure. This is especially true in the case where the aqueous solution may vary considerably in composition particularly with regard to trace elements. A refined process stream having a well-defined composition presents far less risk.
- *Resilience of the solvent:* - The ranges of available solvents have quite different resistance characteristics to similar conditions and as such may have very different life expectancies. Understand whether solvent replacement will be to make up physical losses or to replace degraded material.
- *Cost of the solvent:* - Prices range by orders of magnitude, the organic inventory may represent a substantial portion of the plant capital, and replacement, a significant portion of operation.

The following example demonstrates two applications at opposite ends of the spectrum. Risk factors are on a scale of 1 to 5.

*Table 1. Risk ratings of two hypothetical solvent extraction plants.*

	<b>Case 1</b>	Risk	<b>Case 2</b>	Risk
Aqueous feed composition	Complex solution direct from a leach circuit	4	Refined solution containing well defined components	2
Downstream unit operations	Raffinate to second SX circuit in series. EW on strip circuit	5	Raffinate to effluent. Precipitation on strip circuit	2
Stability of solvent	Organic molecules susceptible to oxidation and poisoning by trace elements	4	Stable non oxidizing solvent composition easily regenerated	1
Cost of solvent	High cost, low availability solvent	4	Low cost solvent	1
Skill of potential operators and analytical staff	Poor skill, long term training required	5	Skilled staff from similar type operation	2
<b>Overall Risk</b>	<b>Very High</b>	<b>22/25</b>	<b>Low</b>	<b>8/25</b>

The numbers assigned to the above example are notional, however they demonstrate how a circuit may be evaluated in terms of the requirement for ancillary, or protective equipment. The cost of ancillary plant for case 1 may be similar to the cost of the contact equipment itself while that in case 2 may be only a small portion of the overall capital cost. Detailed understanding of the circuit requirements and realistic assumptions of operating conditions will minimize the need for retrofits and loss of production.

## **SOLVENT EXTRACTION PLANT FEED LIQUOR**

The feed solution to the solvent extraction (SX) plant must be compatible with the solvents and suitable for the selected equipment. This requires that potential solvent poisons, scaling compounds and solids be reduced to levels such that continuous, long-term operation of the plant is achieved. Removal of poisons and scale forming components will require suitable specialized processes. While it is beyond the scope of this paper to discuss such operations design of the SX circuit should make provision for "slippage" from such circuits. This may

involve developing a suitable operating strategy for such an event or provision of sufficient feed storage capacity to isolate the SX plant until the excursion has been rectified. Removal of solids requires some form of filtration system. Suitable filtration capacity for the unsteady state condition should be provided for. Designing to average expected solids loading may result in substantial plant downtime from crud formation because of solids breakthrough to the SX circuit.

## **CONTROL SYSTEMS – FLOW AND INTERFACE LEVEL**

Flow measurement and control within the solvent extraction circuit is critical to maintaining a stable and efficient operation. All instruments should be such that they may be removed for inspection and cleaning with the plant operational. The type of instrument should also be carefully reviewed in terms of suitability to the liquor being measured and constituents (e.g., dissolved solids, suspended solids, organics) that may be present in such liquors. Control valves should provide very smooth changes in flow, thus minimizing the likelihood of setting up cyclical patterns. As most solvent extraction applications rely on either gravity or inefficient pump mixers for liquor transfer, reduction in line size for flow measurement and control valves must be carefully reviewed. Cost savings realized by reducing valve sizes may be very attractive, however, they may cause long-term problems for the operator.

Interface level control in settlers may be affected in a number of ways. While the weir type system is most commonly utilized a level control loop acting on the aqueous discharge from the settler may also vary the interface. The interface is measured by float type instrument. The preferred method of operation will depend on the process as each system has both advantages and disadvantages. The factors governing the choice of level control should include not only steady state operation but how the system will react dynamically and under shutdown conditions. Overflow systems do not normally seal completely, and as a result, settler levels may change under reduced or zero flow conditions. The consequence of a settler level dropping may be severe as the separation of organic and aqueous may be lost and organic may be drawn into the aqueous system. The ability to 'freeze a circuit' on shutting down has very significant advantages. The ability to see an interface may be useful as a 'manual check' of instrumentation measurements. Sight glasses are obviously the most simple and efficient way to check an interface and should be considered where practical. They should also be accessible for in-situ cleaning. Automatic level control may be advantageous particularly in the situation where minimizing organic inventory is critical based on the high cost of the extractant. Once the method of level control has been selected, the task of engineering a fail-safe system needs considerable attention. Redundant valves, instruments and storage tanks should be allocated to ensure that slugs of organic are not lost from the system.

## **MEASUREMENT OF PROCESS DATA**

As temperatures and pressures in SX systems are typically benign, measurement of process data is relatively simple. However, this is complicated by the fact that instruments need to be resistant and may even need to operate in both aqueous and organic media. The equipment must be both robust and located in a suitable position for the required duty. As the processes are atmospheric, care should be taken to ensure that instruments can be withdrawn from tanks during operation for calibration and maintenance purposes.

## **MATERIALS OF CONSTRUCTION**

While this is an area that normally gets significant attention during the design of the plant, the materials of construction are frequently subject to change when the cost containment phase of a project arrives. Experience has demonstrated that compromising on materials of construction particularly in terms of settlers seldom pays off. Substitution of steels, fiberglass and polyconcrete with cheaper plastic materials may reduce the life expectancy of the plant to unacceptable levels. The effects of solvents on rubbers, plastics and the glues used to hold them together may not be adequately demonstrated in piloting trials! Prudent design will allow for some mechanical type cleaning of all surfaces in the plant.

## **CRUD HANDLING SYSTEMS**

From the outset, the crud handling system should be considered an integral part of a solvent extraction circuit, having equal importance to the contact equipment. Depending on the anticipated severity of the crud problem the system may be designed to operate continuously or in a batch wise fashion. As the formation of crud may occur rapidly and extensively the system should have sufficient capacity to store significant quantities of crud which may then be treated at a reasonable rate. Filtration systems should be sized conservatively providing for the poorest fluxes, as the types of crud formed may vary during the course of operation. Removal of crud from settlers may be achieved by a number of methods. In most cases, access to the settler, by the operator, is necessary to identify the location of the crud and in some instances physically remove the crud with a 'vacuum cleaner' type system.

The treatment system should include sufficient tankage to perform the necessary steps for separation of the crud from the organic and aqueous phases. This normally includes 'washing in diluent' followed by settling and filtration through an absorbent clay. There may be special requirements for acid treatment, etc.

## **TANKAGE AND STORAGE CAPACITY**

Solvent extraction circuits are normally coupled to a number of other unit operations that may operate quite independently of the circuit. Volumetric balance around the circuit may only be achieved by the inclusion of significant storage buffer around the plant. Dynamic scenarios should be considered when specifying storage capacity. The storage facilities should not be designed to accommodate two opposing requirements, that of the solvent extraction plant and that of the down/upstream unit operation. Generally, solvent extraction plants respond poorly to stop start situations and may take considerable time to settle down to steady state. Operating errors are far more likely to occur during start-up or shutdown of the plant. Adequate storage will in many cases provide the necessary buffer to prevent having to go through frequent start-up or shutdowns.

Design of tankage around a solvent extraction circuit should allow for the possibility of both aqueous, organic or both ending up in the vessel. Materials of vessels should be suitable for all liquors in the circuit and tanks should be designed in such a way that operators can easily determine the quantities of each phase in a particular tank. Pump discharge arrangements should be carefully designed to facilitate decanting of either phase from any tank without affecting the operation. While storage tanks should not be expected to perform the duties of after settlers, suitable design of feed systems may assist in facilitating significant phase separation in the vessel by minimizing the amount of agitation that occurs within the vessel.

## **ORGANIC RECOVERY FROM AQUEOUS AND STRIP LIQUORS**

The system of organic removal should include stages that remove organic within the SX circuit (such as a pH adjustment step) followed by recovery of 'bulk' organic (for upset conditions) followed by recovery of normal arisings from steady state operation. The equipment for example would include a mixer settler for pH adjustment, followed by an after settler to recover slugs of material, followed by coalescers, dual media filters and carbon columns. Suitable instrumentation should be included on the final settler or after settler to warn operators of organic in the aqueous stream. The plant should also be designed to operate organic continuous in the final stages (of extraction or stripping) to minimize organic entrainments in the aqueous stream. An organic wash stage in which aqueous is contacted only with diluent to reduce losses of extractant or to clean up the aqueous feed stream may be necessary.

Organic entrainments tend to be consistently high during a plant startup and having the facility to put the plant onto recycle may be an effective method of controlling entrainments until the plant 'settles down'. When the organic removal requirements have been specified, the media usage in the various units may be predicted. Time should be taken to design user friendly systems for change-out of media and in the case of high consumption there may be justification to look at regeneration methods for carbon and cleaning of media.

## **PIPING SYSTEMS**

Piping systems in solvent extraction plants need to be carefully designed as in many instances, the process relies on gravity or inefficient pump mixers to transport the liquors. The process engineer responsible for the design of the plant must be actively involved in the piping design and plant layout. Plant layouts should obviously allow for efficient operation of the equipment. Compressing of plant footprints to save on piping costs is a practice that should be avoided. Pipe sizing should be done on the basis that there will be some degree of scale formation on the surfaces – scale even adheres to plastic pipes. Restrictions in piping runs should be kept to a minimum and reduction in line diameters for installation of valves and instrumentation should be avoided.

## **ORGANIC REGENERATION**

A side stream that allows for treatment of the solvent externally to the main circuit may be necessary. This for example may include a high concentration acid strip to remove components that are not stripped under the normal stripping conditions. In the assessment of whether such a circuit is necessary prediction of likely excursions from steady state in upstream processes will be important

Where there are two or more solvent extraction processes in series, solvent, slipped from the primary circuit may need to be recovered from the secondary circuit in a side stream. This should be considered a last resort option, as fail-safe mechanisms should be included in the primary circuit to prevent the occurrence of organic slippage.

## **NEUTRALIZING OR pH ADJUSTMENT REAGENT ADDITION**

The mechanism of introducing the base to the process liquors is important and will result in operational problems if not properly designed. There are many options available ranging from injection of an aqueous solution of the base into the primary mixers to pre-equilibration of a pure organic stream by ammonia gas. Individual options are beyond the scope of this paper, however, in general terms the following should not be overlooked.

The use of strong and concentrated bases may result in the formation of an emulsion with certain extractants (notably Cyanex 272). Strong bases may also cause precipitation of metal species in localized high pH regions that may lead to the formation of cruds. Therefore, consider the strength of the reagent used and the mixing available (which tends to be mild and kept to a minimum) to introduce the material to the process. The neutralizing reagent may be added to the process based on the pH of the aqueous phase. In organic continuous systems it may not be possible to measure the pH in the mixer requiring some phase separation to take place before a measurement may be obtained. The location of the pH instrument is important, as lag time in the control loop should be minimized.

## SAMPLING AND ANALYTICAL

Like other hydrometallurgical processes, the successful operation of a solvent extraction plant is dependant on accurate and efficient analyses of representative samples. The multi component systems in solvent extraction plants make the sampling and analysis more challenging. Detailed design of plants should include allocation of the required sample points to effectively achieve the above. In certain configurations the aqueous phase may not be accessible to operators, for example when level control valves are used for interface control, in which case sample points in transfer lines may be necessary. Multiple sample points in mixer tanks and storage tanks should also be considered, as mixtures may not be homogeneous.

The analytical requirements will depend on the selected process and particularly the requirement to monitor organic composition, quality and entrainment values. Typically, the aqueous analytical requirements will fit in with the remainder of the process. In general terms the determination of entrainments and monitoring of solvent condition and quality, is non-trivial and may require special techniques or assistance from external organizations. The sample composition may also be time dependant requiring immediate attention. The requirements to accomplish the above should be quantified as early as possible and provision made for the associated equipment and training of relevant staff prior to commissioning of the circuit.

## CONCLUSIONS

Solvent extraction circuits are a combination of mass transfer equipment and appropriate process plant to maintain the specified conditions in the feed, discharge and within the circuit. Provision of a successful plant requires that the entire circuit be considered throughout flowsheet development, plant design and construction. Operators/owners and designers must avoid the trap of committing the majority of the resources to the mass transfer problems at the expense of potentially fatal 'side issues'. A balanced approach will ensure that the peripheral equipment services the solvent extraction equipment as required.

## ACKNOWLEDGEMENTS

This paper is published with the permission of Bateman Engineering. It has been compiled based on the combined experience of process engineers throughout the Bateman group. Special thanks to Mark Vancas who has provided significant material for this paper. Other contributors were Alan Langley, Tony Pavlides, Richard Mayze, Alan Lathwood, Geoff Montgomery and Graham Fisher.



## ORGANIC RECOVERY WITH COMATRIX™ FILTRATION

William A. Greene

SpinTek Filtration, LLC

This paper outlines a new method of coalescing and filtering electrolyte and raffinate streams that improves the performance and enhances the ability to recover the organic phase. Different methods of floatation have been tried in the last few years as a roughing coalescer to a media filter and this paper will present a new concept in treating electrolyte or raffinate. A 400 m<sup>3</sup>/h system has been successfully operating in Australia for over three years, with excellent results demonstrating the viability of the technology.

### INTRODUCTION

Most copper solvent-extraction (SX) plants today operate with a filter in the electrolyte stream to act as a coalescer for the small amounts of organic phase left entrained after settling and to filter out suspended solids. This practice has been adequate, but the loss of organic phase through the backwash step and the large quantities of waste generated during this backwash process have been the topic of studies to reduce the operating costs. Some smaller SX-EW plants do not have the funds to install these filters and are attempting to reduce the organic content by means of a flotation column alone with the capability to retrofit a filter at a later date should it be necessary.

We developed a two-stage coalescing filter, the CoMatrix™, to address these issues. This unit consists of a Matrix™ coalescing plate section in the upper zone of a pressure tank followed by a deep dual media bed. The combination allows operation at flow rates of 61 m<sup>3</sup>/h/m<sup>2</sup> (25 gpm/ft<sup>2</sup>), which is five times the flow rate of conventional filters, with a capital cost usually half that of conventional filters. The backwash volume is about one third that of conventional filters, with improved performance. The coalesced organic is recovered in the upper zone as a clean stream that is not tied up in the backwash waste tank requiring treatment for recovery.

### COMATRIX TOWER DESIGN

The conventional electrolyte filter, SX filter, is designed to operate at 12.3 m<sup>3</sup>/h/m<sup>2</sup> (5 gpm/ft<sup>2</sup>) in a pressure vessel containing a media bed. This bed consists of two active layers, a 300 mm (12") layer of fine anthracite above a 300 mm (24") bed of fine garnet.

The anthracite is crushed coal that has irregular surfaces to perform the coalescing portion of the filtration. The fine garnet is more uniform and performs the conventional filtration similar to a sand filter and removes suspended solids like fine clays. The organic phase in the feed stream coats on the surfaces of the anthracite and some of the organic is coalesced

in large enough droplets to rise to the upper zone of the tank. This bed becomes saturated in about 12 h of operation when exposed to normal levels of organic entrainment, requiring a backwash cleaning cycle to remove the material in preparation for the next cycle. This is a time-consuming process and a few steps are necessary to adequately clean the media. These are to lower the liquid level in the tank to a level just above the media and introduce air at  $55 \text{ m}^3/\text{h/m}^2$  ( $3 \text{ scfm/ft}^2$ ) for 10 minutes to completely scour and loosen the particles from the media. The entire bed is then backwashed at  $24\text{-}29 \text{ m}^3/\text{h/m}^2$  ( $10\text{-}12 \text{ gpm/ft}^2$ ) for 5-7 minutes to flush the particles from the bed and reclassify the media back into the two zones of heavier garnet on the bottom and lighter anthracite on top. There are many variations to this basic operation, depending upon each plant's operational preferences. Some of these consist of displacing the entire volume of the tank to recover the electrolyte and the use of water for backwashing. The entire sequence usually takes about 30 minutes.

The CoMatrix Tower is quite different from the SX filters, having a packed section 2.1 m (7') deep in the upper zone to perform the coalescing of usually 70% of the inlet organic. The openings in the Matrix plates are 12 mm (1/2") to reduce the possibility of fouling from crud. Just below the packing and before the anthracite/garnet media is a "quiet zone". This quiet zone allows organic that has coalesced but passed through the Matrix plates to rise back up through the plates and into the upper head of the tank. The CoMatrix automatically senses the presence of coalesced organic in the vessel head and discharges it from the filter for recovery.

The Matrix plates are made of PVC or polyethylene that is hydrophobic and acts as an excellent media for organic coalescing. The design of the plates is illustrated in Figure 1 and consists of corrugated plates at opposing angles that allow liquid to easily flow from one channel to the next, and do not limit the effective area of the tank as would be the case with conventional parallel plates. The arrows show that the direction of flow of the organic coalesced is opposite the flow of the main influent stream. These matrix plates are welded together, allowing for easy installation and removal, and are strong enough for a person to stand on during maintenance.

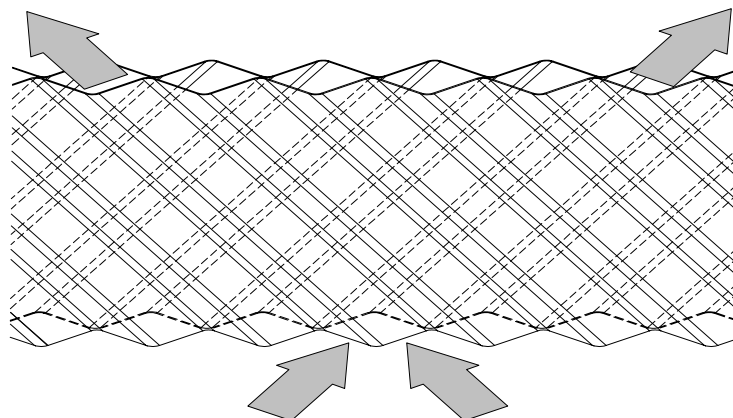


*Figure 1. Matrix plate design.*

The practice of coalescing liquids on plates has been used for some time and relies on supplying an increased surface area of a material compatible with the liquid being coalesced that has corrugations. These create low turbulence areas in the upper area of the corrugation for the lighter liquid to collect. These droplets have only a little vertical distance to rise to reach this area rather than an open tank. This area allows other droplets to combine with each other to form larger droplets that will then rise to the upper zone without the worry of being carried downward with the flow of electrolyte. This phenomenon is illustrated in Figure 2. The added benefit is that any organic that is carried down to the media bed, through the

plates, has already been partially coalesced which greatly reduces the load on the anthracite coalescing section of the media bed.

This organic can then combine with other organic droplets on the top of the anthracite bed and will rise back up to the plate zone and through the plates to the upper section of the tank. The result is a large reduction in the loading on the anthracite, allowing for an increased operating velocity. We should point out that velocity is very important to proper operation of the CoMatrix and that operation at lower flow rates does not improve performance. In our initial testing, we found that when we increased the flow rate from  $24 \text{ m}^3/\text{h/m}^2$  to  $61 \text{ m}^3/\text{h/m}^2$  ( $10 \text{ gpm/ft}^2$  to  $25 \text{ gpm/ft}^2$ ), we actually recovered more organic and had little effect on the loading of the media bed below.

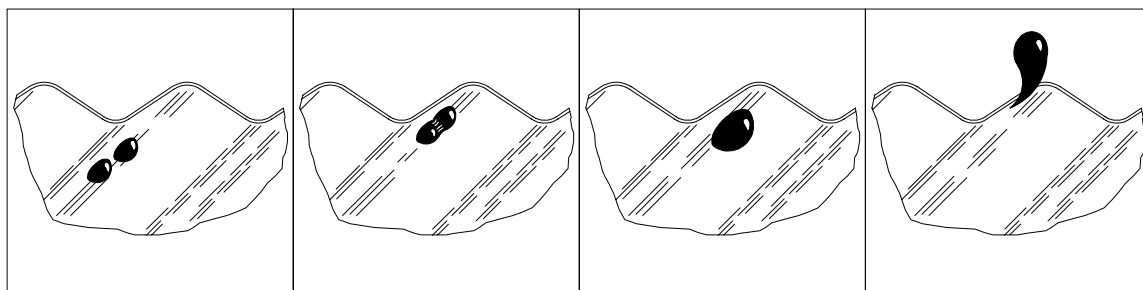


Figure 2. Coalescing droplets on Matrix plate surface.

The material of which the Matrix plates are made is crucial to performance. The PVC or polyethylene plates are hydrophobic upon which the non-aqueous organic adheres.

An important factor in coalescing is the micron size of the droplet. When using plates or air flotation, the size is more critical than when using an anthracite bed since the contact through a media bed offers far more surface area and more potential liquid contact. Generally a droplet size ranging from 10 micron and larger coalesces well in Matrix plates with 100% efficiency obtained at 30  $\mu\text{m}$  sizes and larger. When the size drops to 10  $\mu\text{m}$ , the efficiency is lower.

The media bed consists of anthracite as in the SX filters except that the level is increased to 600 mm (24") from 300 mm (12") for the anthracite. The garnet remains the same since the amount of suspended solids is not the controlling factor in a filtering cycle. The depth between the anthracite bed and the plates is high enough to allow for the air scour/backwash cleaning cycle to take place below the plates. A backwash distributor is installed below the plate section with laterals for proper collection of the backwash waste and allows the bed to expand sufficiently to remove the loosened particles. A cross section of the CoMatrix is shown in Figure 3.

The plates are not disturbed during the backwash step as they operate better with the organic coating left in place. The performance of the plates improves during the first cycle when the CoMatrix is initially placed into service. This is due to an organic coating being formed on the Matrix plates. New entrained organic will touch this organic coating on the plates and themselves coalesce. When sufficient organic droplet size is obtained on the plates, droplets will break free from the plates and rise to the top of the vessel.

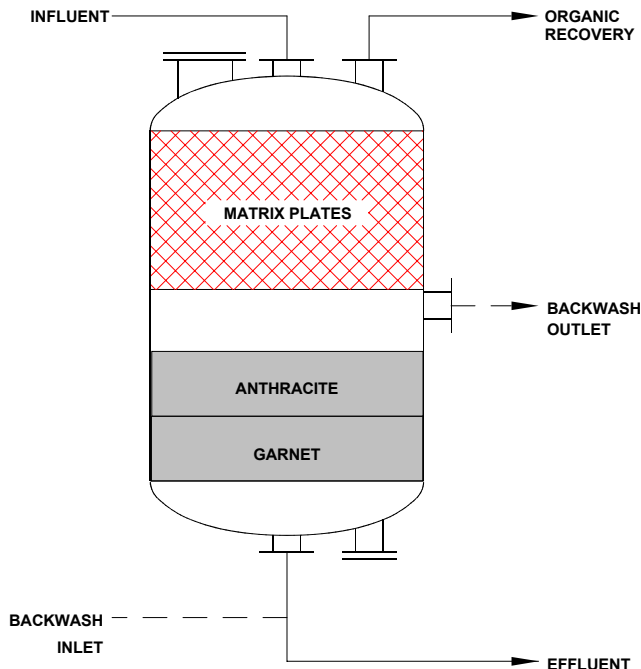


*Figure 3. CoMatrix Tower design.*

### COMATRIX TOWER TESTING

Testing was performed at a few plants in Arizona that operated existing SX filters and provided excellent models of well-run plants with organic levels normally around 30 ppm. Our test unit was 300 mm (12") in diameter and was installed parallel to the existing SX filters. The test unit has an area of 0.074 m<sup>2</sup> (0.8 ft<sup>2</sup>) and operates at 76 l/m (20 gpm). The feed was taken from the same pumps that supplied the SX filters and the performance was equal to the SX filters except that we were able to recover a pressurized stream of clean organic from the top of the CoMatrix tower as a result of the plate performance. We consistently obtained non-detectable organic (centrifuge test) from the lower portion of the media bed and we monitored the organic level at points within the tank to verify the recovery amounts in the Matrix plate zone.

Subsequent cycling of the CoMatrix demonstrated that the effluent from the filter maintained non-detectable organic levels (centrifuge test) and 1-2 ppm by Freon extraction.

The CoMatrix's operating cycle was 8 hours compared to 12 hours for the SX filter but the CoMatrix processed 333 % more electrolyte over the time period. Figure 4 shows the performance cycle for a typical electrolyte stream with 30 ppm (30 mg/l) organic. The upper Matrix plate section recovered 20 ppm or 66% of the inlet organic and the anthracite/garnet bed removed the remaining 10 ppm. Subsequent cycles obtained the same performance. An important factor was the reduction in backwash volume when using the CoMatrix.

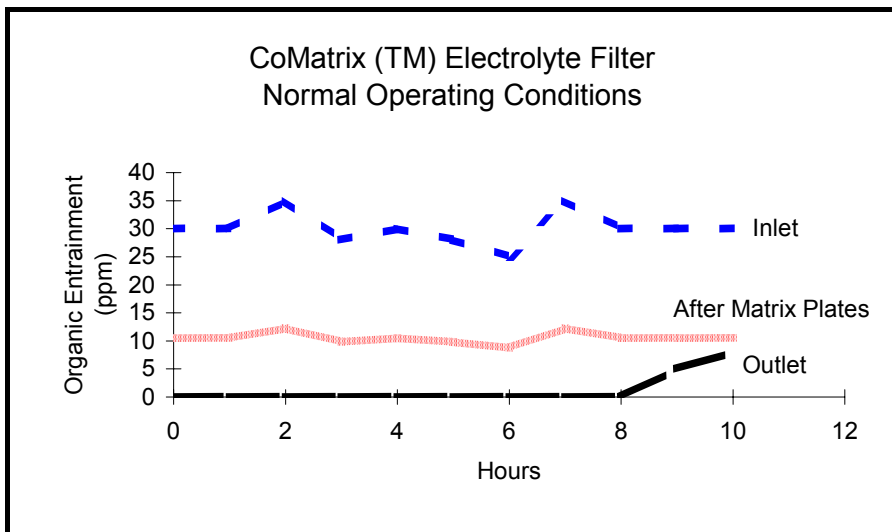


Figure 4. CoMatrix performance.

In an attempt to simulate an upset condition, we operated the CoMatrix from the effluent weir of the E1 settler and fed the unit with an average of 800 ppm organic. Figure 5 illustrates the performance when operated at these high levels. We were able to achieve the same non-detectable level (centrifuge test) of organic in the effluent of the unit and recovered about 75% of the organic in the upper Matrix plate zone. The service cycle in this case was 6 h, compared to 8 h at lower entrained organic levels

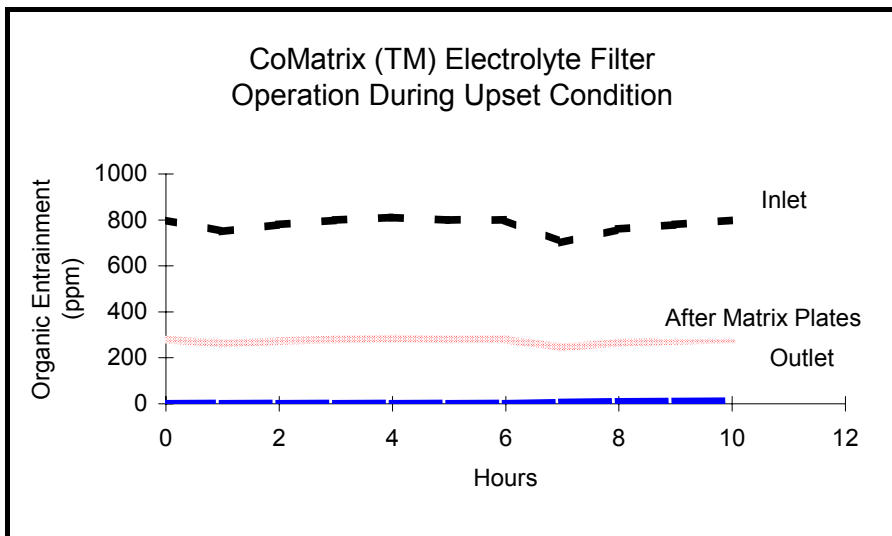


Figure 5. CoMatrix Tower performance.

## **BACKWASH COMPARISON**

Using the service cycle referenced in Figure 5 we can see that the CoMatrix tower will process 333% more electrolyte than a conventional SX filter. We must also compare the amount of backwash required to clean media beds. In actual operation, a 636 m<sup>3</sup>/h (2,800 gpm) electrolyte flow requires five 3.65 m (12') diameter filters while only a single 3.65 m (12') CoMatrix is required.

Using this comparison, in a one-year period, the backwash volume is 156,000 m<sup>3</sup> (41.2M gal) for the SX filter and 47,000 m<sup>3</sup> (12.4M gal) for the CoMatrix tower, or a savings of 70%. In addition, there is 70% less backwash waste to process to recover the organic.

Since the CoMatrix Tower recovers approximately 2/3 of the organic in a concentrated stream, less recovery time is lost for the retrieval of the organic. On a 636 m<sup>3</sup>/h (2800 gpm) electrolyte stream with 30 ppm of organic present, this represents 113 m<sup>3</sup> (30,000 gallons) each year of recovered organic that is not recovered as part of the backwash water. The remaining 38 m<sup>3</sup> (10,000 gallons) of organic recovered is part of the backwash water similar to conventional SX filters.

## **FULL-SCALE OPERATION**

We have installed several small CoMatrix filters on pilot-plant streams with the same results. In addition, a full scale 400 m<sup>3</sup>/h CoMatrix system has been in operation at an Australian copper mine with excellent results. In over three years of operation, the filter consistently produces an electrolyte stream containing 1-2 ppm (Freon extraction) entrained organic phase.

The performance of this large-scale CoMatrix will be the subject of a newly published report.

## **CONCLUSIONS**

We have demonstrated the CoMatrix through pilot studies and the operation of a full-scale 400 m<sup>3</sup>/h (1,760 gpm) unit. The benefits of this system are:

- Coalesces up to 70% of the entrained organic phase prior to the media bed;
- Allows for clean recovery of the coalesced organic phase;
- Improves the performance of the media bed;
- Flow rate of 61 m<sup>3</sup>/h (25 gpm/ft<sup>2</sup>) reduces organic less than 2 mg/l;
- Reduces the backwash flow rate to 20% that of SX filters;
- Reduces the backwash volume by 70% compared to SX filters;
- Reduces the cost of equipment significantly;
- Matrix plates alone are comparable to flotation columns without the need for air introduction that can emulsify the entrained organic phase.

## AUTHOR INDEX

Abdeltawab, AA	1070	Capela, RS	335
Adachi, K	576	Cardia Lopez, JMM	1402
Aguilar, M	506	Caron, L	774
Akbari, M	1052	Carvalho, JMR	781, 828
Al-Duri, B	626, 674	Casten��da, D	762
Al-Shawi, AW	1064	Castillo, E	687
Alstad, J	1199	Castro Dantas, TN	822, 1001
An, ZT	602	Chambliss, CK	396
Andaur, C	1210, 1396	Chang, Z-D	131
Andersson, S	549	Charbonnel, MC	1154
Anitescu, G	809	Charlesworth, P	14
Antonelli, D	1058, 1339	Chauhan, S	755
Antoniassi, R	638	Chayama, K	576
Avila-Rodriguez, M	902	Chekmarev, AM	441, 928, 1076
Azimi, A	167	Chen, J-Y	131, 602, 650, 680
		Chen, J	227
Babain, VA	1216, 1229	Cheng, CY	1082
B��cker, W	161, 958	Chiarizia, R	390, 408, 1137
Bacon, G	1	Chiavone-Filho, O	174, 662
Bailes, PJ	83	Chizhevskaya, SV	1076
Balmaceda, V	1210	Chmutova, MK	1180
Ban, T	89	Chopra, SJ	1265
Baptista, M	95	Cole, PM	863
Barnard, P	1316	Conkle, HN	755
Bart, H-J	45, 77, 101, 125, 161, 251, 524, 1382	Cordeiro Beltrame, LT	822
Batista, E	638	Cortina, JL	377, 493, 506, 687
Bauer, D	291	Costa, MC	371
Belhamel, K	307	Cote, G	155, 291
Belova, VV	341, 916	Cox, M	879, 995, 1076
Benamor, M	307, 500, 976	Crane, PA	1007
Benguerel, E	908	Crause, C	1296
Bergerman, S	1253	Cruz-Pinto, JJC	95, 1402
Berthon, C	1148	Cupertino, D	347
Berthon, L	1161, 1205	Curbelo Garnica, AI	804
Biscaia Jnr., EC	1058, 1339	Dahlgren, E	459
B��hmer, V	1174	Dai, Y	644
Bolton, GT	487	Dannus, P	1174
Bonnesen, PV	299, 396	Dantas Neto, AA	822, 1001
Borkowski, M	1137	Darvishi, D	1052
Bo-Rong, B	1241	De Ara��jo, ACM	1001
Borowiak-Resterna, A	988	De Barros Neto, EL	822, 1001
Bosley, J	674	De Haan, AB	589, 620, 668, 1271, 1301
Bosse, D	125	De Sousa, CP	1352
Bot��c, G	834	Deep, A	793, 1089
Bousquet, M	1148	Delmau, LH	299
Bouwer, W	922, 946	Demirkiran, A	884, 890
Bravo, J	1253, 1328	Demopoulos, G	908
Brenno, Yu Yu	916	Depalo, M	402
Brown, GM	396	D��az, G	1045
Brunner, G	1308	Dietz, ML	390
Buch, A	262		
Buchalter, EM	1021	Douche, C	1235
Bukowsky, H	313	Dozol, JF	1168, 1174
Camagong, GT	555	Draa, MT	500, 976
Campbell, J	347	Drake, VA	940
Canari, R	137, 614	Dreisinger, DB	798
		Du Preez, AC	896

Du Preez, JGH	319	Greene, WA	1428
Du Rand, M	1296	Gregorich, KE	1199
Duarte, LNJ	1001	Grinbaum, B	1021, 1345, 1408
Duarte, MML	1352	Groß-Hardt, E	1358
Dudley, KA	1007	Grote, M	607, 934
Durand, G	262, 724, 774	Guangsheng, L	742
Dzul Erosa, MS	902	Guilbard, P	1148
Dzung, NTK	307	Guillaneux, D	1205
Eberhardt, K	1199	Guimaraes, MML	95, 1402
Edalat, A	83	Gunn, DM	280
Egorov, GF	1216	Gupta, B	793, 1089
Ekberg, C	549, 1193	Haciosmanoglu, B	607
El-Hassan, Z	143	Hackl, RP	798
Emeleus, LC	347	Haddad, R	699
Engdal, SE	1064	Halevy, M	840
Enokida, Y	1143	Halpern, M	24
Esimantovkiy, VM	1216, 1229	Hames, M	798
Eyal, AM	137, 614	Hamley, PA	34
Fair, JR	1328	Hara, C	656
Falcón, M	1210	Harris, SG	347
Fang, R	459	Hasegawa, Y	149
Feather, A	922, 946	Hashem, MA	209
Fei, W	257, 1260	Hatton, TA	15
Ferraro, JR	1137	Havelock, TJ	299, 396
Ferreira, L	828	Hazan, B	137, 614
Fir Medelros, B	402	Heckley, P	730
Flandin, JL	1154	Helal, AA	558
Fleitikh, I Yu	341	Hendrawan, H	238
Flett, DS	879, 995	Henschke, M	1358
Galán, B	762	Herbst, RS	1216, 1222, 1229
Gallego Lizon, T	712	Herlinger, AW	390
Gamse, T	816	Hewitt, GF	70
Garcia Liranza, E	952, 964	Heyberger, A	1376
García, MA	1045	Hill, C	1205
Garcia-Carrera, A	1168, 1174	Hillhouse, J	402
Garnica, AIC	1352	Hirai, T	467
Gaspar, F	626	Hoffman, DC	1199
Gasperov, V	353	Hokura, A	425
Gauna, A	1210, 1396	Holbrey, JD	474
Geist, A	693	Holdt, H-J	313
Gigas, B	1388	Honjo, T	555
Gilmore, M	970	Hossain, KZ	555
Giminez, C	1148	Hosten, EC	319
Giralico, M	1388	Hubred, G	1095
Giroux, S	1154	Hughes, DV	581
Gloe, K	353	Hughes, MA	53
Gneist, G	101	Hutahaean, LS	1370
Godwin, I	1376	Hutton, B	1283, 1376
Gomes, MLACN	1402	Ibana, D	730
Gompper, K	693	Inagaki, A	149
Gonçalves, CB	632	Inoue, K	453
Górak, A	958	Irabien, A	762
Görge, A	161, 958	Ishikawa, I	366
Gotfryd, L	879	Ismael, MRC	781, 828
Granados, M	687	Iso, S	1131, 1143
Granatelli, F	1210, 1396	Jadhav, SB	570
Grant, RA	940	Jahim, J	215

Jain, A	1265	Laing, G	1421
Jakovljevic, B	402	Lamare, V	1168
Jallo, R	1271	Lang, H	928
Jensen, MP	1137	Langrock, G	1199
Jenssen, OB	1064	Lapidus Lavine, G	902
Jia, Q	718	Law, JD	1216, 1222, 1229
Jiang, K	1027, 1039	Lee, JS	512
Jiaoyong, Y	1014	Lee, SC	1187
Jidkov, LL	916	Leistner, J	958
Jidkova, TI	916	Lenhard, Z	982
Jin, MJ	436	Leong, AJ	353
Johansson, M	1199	Lerner, O	668
Jones, J	840	Levitskaia, TG	299, 396
Jørgensen, TR	1064	Li, CZ	436
		Li, DQ	268, 436, 537, 718
Kamio, E	274, 706	Li, S	192
Kanel, J S	1370	Liao, WP	268
Katsuzaki, M	565	Liljenzin, J-O	549, 1193
Kautzmann, RM	506	Lindoy, LF	353
Kavallieratos, K	299	Littrell, KC	1137
Kawaizumi, F	89, 1070	Liu, D	430, 1027, 1039
Keshavarz Alamdari, E	1052	Liu, H-Z	131, 602, 680
Khalifa, SM	558	Liu, JG	597
Kharchev, AE	441	Liu, QF	602
Kholkin, AI	341, 916	Lu, J	537
King, JA	798	Lu, T	626
Kinugasa, T	656	Lu, YC	644
Kirbach, U	1199	Ludwig, R	307
Kislik, V	108		
Kleinberger, R	1021	Luo, F	718
Klinger, S	1358	Luo, GS	597, 644
Knoetze, SE	319		
Kobayashi, M	787	MacKenzie, JMW	1007
Koch, J	1364	Madic, C	1161
Koch, KR	327	Madureira, CMN	1402
Kogan, L	1408	Mahinay, MS	353
Kojima, I	565	Malik, P	1089
Kolb, P	1382	Malikov, DA	1180
Komasawa, I	467	Maljković, D	982
Komatsu, Y	414, 518	Malve, SP	570
Kondo, K	274, 706	Manski, R	161
Kongas, M	581	Mansur, MB	1058, 1339
Korchinsky, WJ	245, 487	Mao, Z-S	227
Kordosky, G	360, 853	Marr, R	816
Koroleva, MY	748	Martín, D	1045
Korovin, V	377, 506	Martin, J-V	291
Kosogorov, AV	1322	Martinet, L	1161
Krooshof, PWT	1301	Matar, OK	70
Kuipa, PK	53	Materna, K	155
Kuipers, NJM	589, 620, 668,	Matsubayashi, I	149
	1271, 1301	Matsumoto, M	274, 706
Kokusen, H	518	Mattison, P	360
Kulyako, Yu	1180	Mayboroda, AB	928
Kumar Pabby, A	699	McAlister, DA	390
Kusakabe, S	425	McCulloch, JM	736
Kuzmanović, B	1271	McRae, C	730
Kuznetsov, G	1322	Meguro, Y	1131, 1143
Kwant, G	620, 1271	Meireles, MAA	662
Kyuchoukov, G	988		

Meirelles, AJA	632, 638	Omtvedt, LA	1199
Melgosa, A	699	Oprea, F	834
Mendel, M	1199	Ortiz, I	762, 846
Mendes-Tatsis, MA	221	Osseo-Asare, K	118, 530
Meng, SL	436	Otu, EO	408
Merzliak, T	233	Owens, S	347
Mickler, W	313		
Miesi, I	768	Paiva, AP	335, 371
Miesiac, I	1277	Pan, S	597
Mihaylov, I	1	Panaiteescu, C	834
Mikus, O	1283	Pareau, D	262, 724, 774
Miller, HA	280	Parsons, S	347
Monzyk, B	755	Pashkov, GL	341
Moreira, AS	174	Peineau, N	1161
Morel, JP	1154	Pereira de Souza, C	804
Moreno Daudinot, AM	952, 964	Pereira Leite, JV	804
Mori, T	576	Perez de Ortiz, ES	70, 143, 712
Moriya, Y	58	Pérocheau, S	724
Mos'hefi Shabestari, Z	1052	Pescayre, L	1235
Mottot, Y	291	Petre, M	834
Mourad, Gh A	558	Pfennig, A	233, 1358
Moyer, BA	299, 396	Poliakoff, M	34
Muela, C	846	Powell, B	1124
Mulder, H	1301	Pratt, HRC	1414
Müllich, U	693	Presson, MT	1154
Murashova, NM	197	Preston, JS	896
Muraviova, OV	180	Purcell, M	221
Myasoedov, BF	1180, 1187	Pushkov, A	1322
Myburgh, P	1376		
Nagel, V	946, 970	Readett, DJ	1007
Nähler, A	1199	Regel-Rosocka, M	768
Nakata, S	58	Reuveny, T	137, 614
Nash, KL	1110, 1137	Ribeiro, LM	95
Navarro Mendosa, R	902	Ribeiro, MM	95
Navratil, JD	1118, 1124	Rice, NM	167, 884, 890
Nazin, EG	1216	Riddle, M	908
Nielson, C	1021	Ritcey, GM	871
Nieuwoudt, I	1246, 1289, 1296	Rogers, RD	474
Nii, S	89, 656, 1070	Romanovskiy, VN	1216, 1229
Nilsson, M	1193	Røsæg, M	1064
Ninov, V	1199	Rosales Bárzaga, B	952
Nishihama, S	467	Rose, JK	755
Nishii, Y	656	Rouquette, H	1168
Nitsche, H	1199	Roux, J	922
Noda, H	1334	Russo, A	1210
Noguchi, Y	366	Sadrnezhaad, SK	1052
Nolte, J	607	Safiulina, AM	447
Noro, J	425	Saien, J	209
Nucciarone, D	402	Sakamoto, H	565
O'Connell, R	922	Saloheimo, K	581
O'hadizadeh, A	1052	Sampaio, CH	506
O'Keefe, M	459	Samsonov, MD	1187
O'Keefe, T	459	San Miguel, G	224
O'Neil, AS	34	Sánchez, F	1045
Ogawa, N	58	Sánchez-Loredo, MG	934
Ogura, K	420	Santamaría, MP	245
Ohto, K	453	Santos, C	828
Omtvedt, JP	1199	Santos, R	626, 674
		Sastre, AM	699, 768, 1174

Sato, K	366, 384	Tasker, PA	280, 347, 353
Sato, T	366, 384	Tavlarides, LL	512, 809
Saucedo Medina, TI	902	Texeira, P	95
Schaadt, A	524	Thiébaut, C	1235
Schmäh, M	233	Thiyagarajan, P	1137
Schott, R	233	Thompson, C	1124
Schwarz, CE	1296	Tic, W	1277
Scott, S	970	Tinkler, OS	347
Seibert, AF	1328	Todd, TA	1216, 1222, 1229
Seki, T	787	Tomioka, O	1143
Sekine, T	425	Trautmann, N	1199
Sen, PK	1265	Traving, M	161
Shang, Y	908	Trofimov, TI	1180, 1187
Shestak, Y	377, 506	Troshkina, ID	928
Shibata, S	543	Tsuji, H	576
Ship, K	798	Tsurubou, S	414, 518
Shkinev, VM	447	Umetani, S	414, 420
Silva de Lima, LA	804	Uribe-Ramirez, AR	245
Silva, DN	174, 662	Urtiaga, AM	846
Simon, M	77	Vaccaro, J	1210
Simonin, J-P	238	Vaisey, M	1082
Sinegribova, OA	180, 186, 447	Van Brunt, V	1370
Skarnemark, G	549, 1199	Van Delden, M	668
Slater, MJ	215, 1058, 1316, 1339	Van Dyk, B	1246
Smirnov, IV	1216, 1229	Varnek, A	481
Sobczynska, A	1277	Vasiliu, IC	995
Soeiro, JM	95	Vegliò, F	1058, 1339
Soldenhoff, K	736, 1082	Velea, T	995
Sole, KC	863, 1033	Venter, DL	1289
Solov'ev, V	481	Viera Martínez, R	952
Sousa, EMBD	662	Vinokurov, SE	1187
Stambouli, M	262, 724, 774	Virnig, M	360
Stanbridge, D	1102	Visser, AE	474
Stavsetra, L	1199	Vitner, A	137, 614
Steensma, M	589, 620	Vogelpohl, A	1364
Stella, A	1414	Voskhin, AA	341
Stepanov, SI	441		
Stephan, H	353		
Stevens, GW	1414	Wai, CM	1187
Stichlmair, J	1402	Wang, B	602
Stockfleth, R	1308	Wang, C	430, 1027, 1039
Strátulă, C	834	Wang, H	1039
Strube, J	161, 958	Wang, J	131
Su, Q	268	Wang, JD	597
Sudowe, R	1199	Wang, YG	436
Sullivan, J	1102	Warshawsky, A	493
Sun, J	459	Wassink, B	798
Suzuki, K	384	Watarai, H	64
Swart, RM	280, 347	Wei, H	257
Swarts, A	946	Wei, X-F	131
Szymanowski, J	155, 768, 988,	Weigl, M	693
	1277	Wei-Guo, C	1241
		Wen, X	1260
Takahashi, K	89, 656, 1070	Wentink, AE	1301
Takahashi, T	384	West, LC	280
Tanaka, M	787	Westerman, D	674
Tandel, SP	570	Westra, A	327
Tandon, SN	793	White, DJ	280, 347
Tang, S	221	Wichmann, K	353

Wiehl, N	1199	Yoshida, T	706
Wildberger, A	251	Yoshida, Z	1131, 1143
Wipff, G	481	Yoshizuka, K	453
Wolf Maciel, MR	638	Youyuan, D	742
Wright, AR	884	Yuan, C	192
Wu, X-P	1316	Yue, ST	268
Wu, YL	718	Yujun, W	742
		Yurtov, EV	197, 748
Xing-Cun, Y	1241		
Xu, Y	537	Zaitsev, BN	1216, 1229
		Zemb, Th	1161
Yamada, M	565	Zeng, X	530
Yamaguchi, M	565, 1334	Zhai, SL	597
Yamamoto, I	543, 1143	Zhang, J	430
Yamashita, H	1334	Zhang, P	1027
Yamazaki, S	420	Zhang, W	650, 680
Yan, W	742	Zhou, W	809
Yeo, LY	70	Zhu, T	203

The ISEC 2002 Organising Committee gratefully acknowledges the contributions  
of the following companies, professional societies and organisations



**ANGLO  
PLATINUM**



Anglo American Research  
Laboratories (Pty) Ltd



**Avecia**

**BATEMAN**



**SASOL**

**Rhodia**

**cognis.**



**ExxonMobil**



South African  
Institution of  
Chemical Engineers

**SCHÜMANN**  **SASOL**



THE SOUTH AFRICAN  
CHEMICAL INSTITUTE



  
**Shell Chemicals**

  
**CSIR**



'Click' on a logo for more information on company

# Avecia

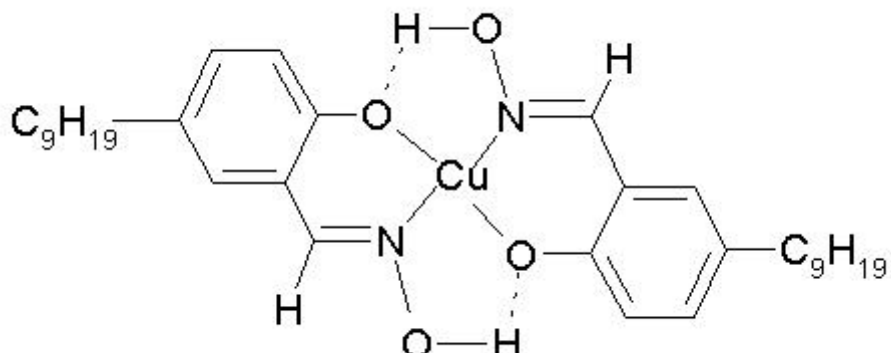
# Acorga

[www.acorga.com](http://www.acorga.com)

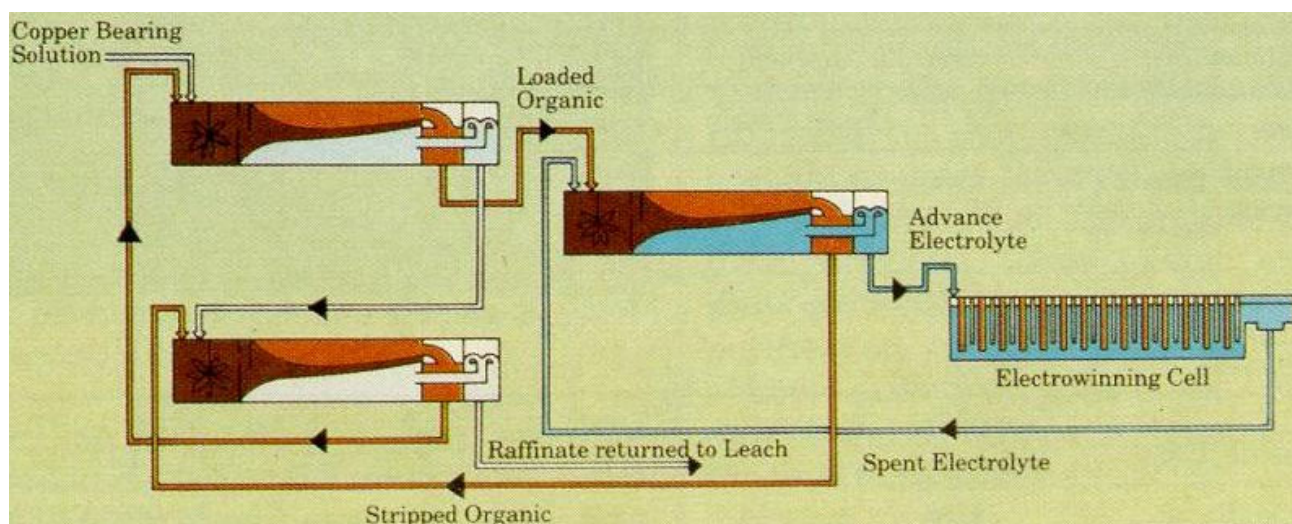
## METAL EXTRACTION PRODUCTS

**The Market Leading supplier of solvent extraction reagents for copper:** AVECIA's Acorga Metal Extraction Products business specializes in the supply of metal extractants to the mining industry. Acorga products have been used successfully in solvent extraction (SX) for the recovery of copper for over 20 years. We discovered and patented nonyl salicylaldoxime extractants for the recovery of copper over 20 years ago and this is now the basis of virtually all copper SX products in use around the world. In addition, Acorga introduced the first successful modified products to the industry and maintain our position as the industry's experts on reagent modification.

### 5-nonyl salicylaldoxime



### Leach – SX – EW Schematic





## METAL EXTRACTION PRODUCTS

### Contact Us!

If you're beginning or considering a solvent extraction operation, call us or visit our website at [www.acorga.com](http://www.acorga.com). Our Acorga extractants are of uncompromising quality and our technical expertise can be an invaluable asset to any operation. Our experienced scientists are located in every major copper mining center in the world and their wealth of experience is available to assist customers in maximizing production and reducing costs.

### AVECIA Metal Extraction Product Centers:

#### **Business Headquarters, USA**

Avecia Inc.  
Metal Extraction Products  
1405 Foulk Road  
P.O. Box 15457  
Wilmington, DE 19850-5457

#### **Phoenix, USA**

Avecia Inc.  
3259 E. Harbour Dr., Suite 100  
Phoenix, AZ 85034  
Tel: (1) 602 470 1446  
Fax: (1) 602 470 5030

#### **Santiago, Chile**

Avecia Inc.  
Andres de Fuenzalida 147  
Providencia, Santiago  
Tel (56) 2 336 5300  
Fax (56) 2 336 5310

#### **Manchester, UK**

Avecia PLC  
Research Center  
PO Box 42, Hexagon House  
Blackley, Manchester  
M9 8ZS, UK  
Tel: (44) 161 721 1208

#### **Sydney, Australia**

Stahl Australia  
15 Sammut Street  
PO Box 6187  
Wetherill Park 2164  
NSW, Australia  
Tel (61) 29 604 6666  
Fax (61) 29 604 6467



## METAL EXTRACTION PRODUCTS

### PRODUCTS

Solvent extraction (SX) is a chemical purification and concentration operation with wide use for production of pure copper metal. Acorga solvent extraction reagents provide a wide range of physical and chemical properties.

**Those "state-of-the-art" technical features of Acorga® reagents include:**

- **highest available Cu:Fe selectivity**
- **excellent hydrolytic stability**
- **excellent kinetics, even when treating solutions at temperatures as low as 3 degrees centigrade**
- **excellent extract efficiency over a wide pH range**
- **highest Cu recovery at low pH**
- **high recovery from concentrated feeds**
- **proven results against solids providing superior protection against crud.**

### Product Range

Product Data Sheets and MSDSs are available from any of our offices or on-line at [www.acorga.com](http://www.acorga.com).

**Acorga M5640**

**Acorga M5774**

**Acorga M5850**

**Acorga PT-5050MD**

**Acorga PT-5038**

**Acorga M5640 HS**

**Acorga M5397**

**Acorga PT-5050**

**Acorga PT-5034**

**Acorga P-5100**



## METAL EXTRACTION PRODUCTS

### Technical Service



At Avecia Metal Extraction Products, we have one very specific but far-reaching goal - to maximize the recovery of metal values at the lowest possible cost. It's a goal that directly benefits our customers, some of whom we've worked with to achieve flow rates of 120-130% of plant design. Stretching capacity like that can only mean a significantly better return on their mine investments.

To achieve results like this requires no small commitment from a reagents supplier. That's why we have chemical engineers, metallurgists, and chemists located in every major copper mining center in the world to provide our customers with all the technical support they need. We stay on-site with them for as long as it takes to help them use the reagents and equipment in a way that maximizes productivity and profitability.

Our technical support often begins even before a customer has broken ground for their solvent extraction facility. In fact, many of our relationships start at the feasibility studies stage, working with the engineering firms that design our customers' plants.

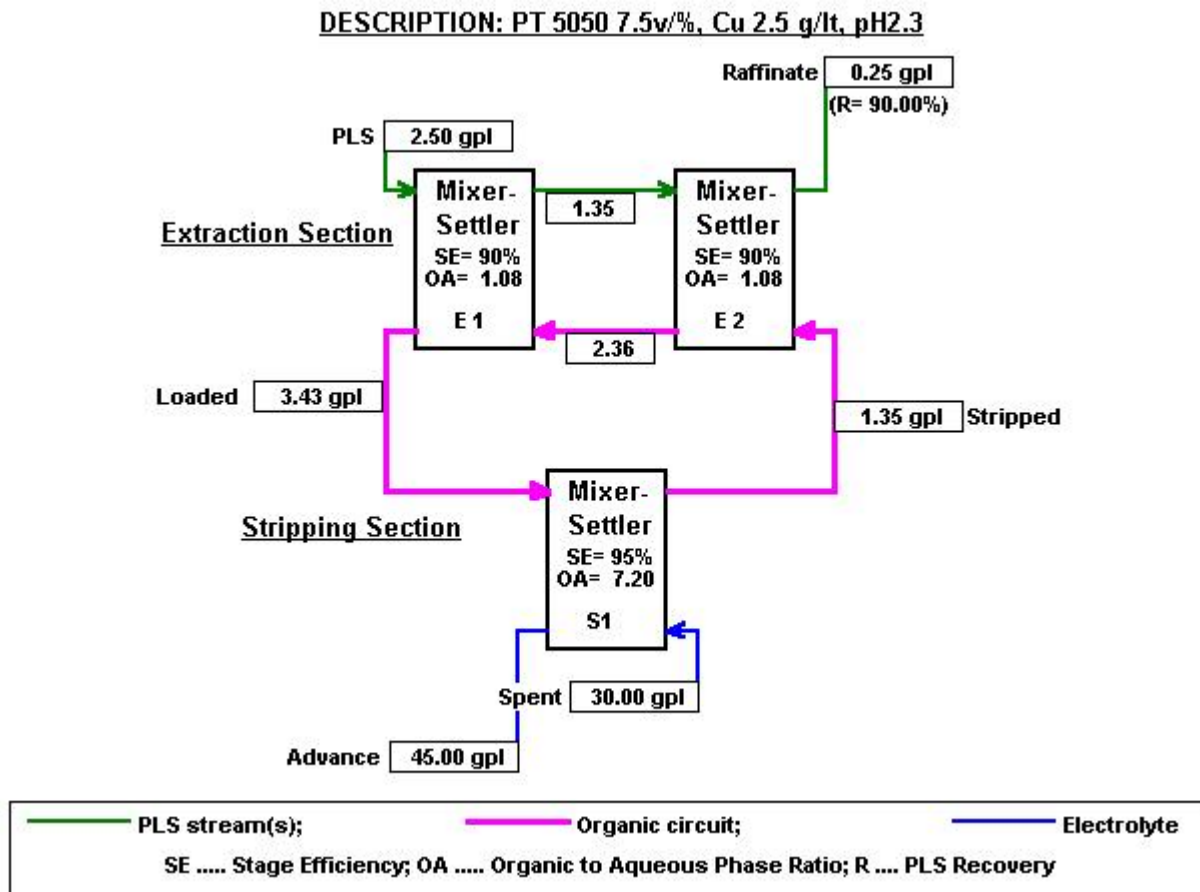
#### Minchem and MEUM computer process modeling:

When it comes to process optimization, we wrote the program. Using computer software programs for process optimization is nothing new to many industries. And it's not new to SX/EW. Thanks to the international scope of the computing and engineering expertise within Avecia, there's MINCHEM - the solvent extraction industry's first, and still most sophisticated, software program. MINCHEM is more than just a flowsheet/design package. It's Windows based system that allows Avecia to design solvent extraction circuits virtually on demand. With minimum information from mining companies or their engineering firms, we are able to evaluate circuit layouts, flow options, recovery options, reagent inventory, and make-up requirements. The end result - the achievement of optimum parameters to maximize plant performance.

What's more, MINCHEM's invaluable capability is available to customers, on their site, at no charge. The MINCHEM End User Module (MEUM), a streamlined version of the software, is user-friendly and enables customers to manipulate data as rapidly as binary file data exchange, via the Internet. For added customer value, the package includes expert system technology and data base and plant control capability.

MINCHEM/MEUM software, the only reagent supplier proprietary program in the industry, and only available from Avezia, is one more example of the unrivaled service capability the metallurgical Industry receives from the SX/EW leaders.

### Minchem Circuit Diagram





## METAL EXTRACTION PRODUCTS

### Manufacturing and Quality

Acorga products are manufactured at our world-class facility in Mt. Pleasant, Tennessee USA. It is the largest, most modern copper solvent extraction reagent plant in the world. Our patented manufacturing process insures consistently high-quality products, unmatched in the industry. In addition, our investment in and commitment to Safety, Health and the Environment insures our position as we enter the 21<sup>st</sup> century. As an example, our Mt. Pleasant plant recently celebrated 4 consecutive years of operation without a lost time accident.



Location:	Mount Pleasant, Tennessee, USA
Number of employees :	170
Main Activities:	'Acorga' metal extractants; 'PTZ' Stabilizer for acrylics 'Cosmocil' ; 'Almacryl' toner resin; Phosphines; 'Baquacil'
Contact:	PO Box 152, Mt. Joy Road, Mt. Pleasant, TN 38474 Phone: (615) 379 3257 Fax: (615) 379 7124

### **Never a quality rejection and we fully intend to keep it that way.**

Many factors contribute to a company's ability to maintain a leadership position throughout an industry's existence. Not the least of them is consistent product quality. And where some companies might define consistent quality as having "minimum" rejections, we define it as having zero. The Avecia standard for quality has become the industry's benchmark. How have we done it? And how will we continue to do it in the years to come? Quite simply, our manufacturing systems are fundamentally better than any other supplier in the SX industry.

Our unique, patented technology provides us with a "window" in which virtually all of the product we make is of exceptional quality. And our state-of-the-art process controls keep it that way. In-process and end-process quality control procedures simply don't allow us to make a bad batch. In all our years of supplying SX reagents to the copper mining industry, we've never had a quality rejection. Can any of our competitors make that claim? Ask them. Are we proud of that fact? You bet we are.

How important is consistent reagent supply in the SX/EW industry? At Avecia, our goal is to make sure it's something our customers can take for granted. We achieve this by being stationed in every major copper mining country in the world, and by applying decades of experience in cost-effectively servicing world markets.

In addition, our customer service staff is set up with in-home computers so they can respond to customers' needs, even if weather or some other condition prevents them from reporting to work. In both the U.S. and Chile, we also have a 24-hour emergency response system in place.

Also, where needed, we establish local warehouses to ensure uninterrupted supply to customers in remote locations.

When it comes to transportation of product, as part of a world class specialty chemical company, we are well versed in the world's regulatory requirements. Accordingly, we not only meet, but generally exceed those requirements. Avecia is also a member of SOCMA, a Responsible Care® partner association.

With our remote inventory Telemetering, we're there even when we are not.

In 1994, we introduced the first, and still the only, telemetering system in the industry to monitor a customer's bulk reagent supply. We know exactly how much is needed and when. Result: product always arrives in plenty of time.

The constant monitoring of bulk reagent levels is the logical "first step" in maintaining constant reagent supply. Avecia customers benefit from automatic (and accurate) 24-hour telemetric monitoring of their site's inventory - information which is analyzed and acted upon by the Avecia customer service support team. Instantaneously. The net result: reagent inventories become one less thing to worry about in an already demanding industry.

**In April 1999, MEP Business of Avecia was granted the prestigious Queen's Award for Environmental Achievement** for the development of a unique patented chemical process for producing Acorga metal extraction reagents. The award recognizes MEP's environmental improvements over older reagent manufacturing processes.

This unique process, developed by MEP's Research and Process Development staff in Manchester, UK, has enabled MEP to reduce effluent components by up to 85 percent. It is also significant that the composition of the effluent from the new process is essentially benign inorganic salts.

Development of the new process was key to justifying investment in MEP's world-scale production facility at Mount Pleasant, Tennessee, USA, where the process technology has been in commercial practice since commissioning of the Acorga plant in late 1994. The efficient and environmentally superior process reduces production costs (which we have passed along to our customers) and ensures our long-term viability, as our environmental compliance is fully assured.



## METAL EXTRACTION PRODUCTS

### Research and Innovation

Most of the improvements in copper solvent extraction reagents over the past 20 years have come out of our Research programs—e.g. 5-nonyl salicylaldoxime (the basis of virtually all copper SX reagents today) and ester-modified reagents.

Research and innovation - two words, one mission. By its very nature, Avecia is a company driven by research and innovation. Our key skill areas include all of the key chemistry disciplines - organic, physical, coordination, analytical - and molecular design. Expertise in these disciplines enables us to continually evolve and improve our copper SX/EW products. And to continue to invent new technologies, such as our low-cost route for oximes.

Additionally, we are constantly augmenting our knowledge base through our linkage with leading edge thinkers at universities pre-eminent in the metals recovery field.

Our Analytical department has been a pioneer in developing techniques for SX solution analysis. Avecia provides the most accurate and responsive analytical services available which is invaluable when your operation is experiencing a problem and days can mean millions of dollars to your bottom line.

Location:	Blackley, North Manchester, UK
Number of employees:	900+
Main Activities:	Avecia Research Avecia Limited HQ Biocides HQ Displays and Electrophotography HQ Ink Jet Printing Materials HQ LifeScience Molecules HQ
Contact:	PO Box 42, Hexagon House, Blackley, Manchester M9 8ZS Phone: (0161) 740 1460 Fax: (0161) 795 6005

# The MCT Redbook

## The MCT Redbook

is an introduction to the chemistry of metals recovery using LIX® reagents

Cognis LIX® Reagents fall into five different chemical classifications:

- **Ketoximes** such as [LIX® 84-I](#)
- **Aldoximes** such as [LIX® 860N-I](#)
- **Beta-Diketones** such as [LIX® 54-100](#)
- **Non- Modified Extractants**, which include [LIX® 984N](#), a 50:50 blend of [LIX® 84-I](#) and [LIX® 860N-I](#).  
Cognis supplies many different mixtures according to each customer's needs.
- **Modified Extractants**, which include [LIX® 622N](#), a blend of [LIX® 860N-I](#) and TDA, and [LIX® 664N](#).

Products manufactured for the MCT by Cognis Ireland Ltd. include:

<a href="#">LIX® 54-100</a>	<a href="#">LIX® 622N</a>
<a href="#">LIX® 664N</a>	<a href="#">LIX® 84-I</a>
<a href="#">LIX® 84-IC</a>	<a href="#">LIX® 860N-I</a>
<a href="#">LIX® 860N-IC</a>	<a href="#">LIX® 973N</a>
<a href="#">LIX® 973N-C</a>	<a href="#">LIX® 984N</a>
<a href="#">LIX® 984N-C</a>	

Cognis Alamine® and Aliquat® Products are manufactured at Cognis Corporation. Alamine® is the trade name for a series of tertiary amines produced with various alcohol raw materials. For example, Alamine® 336 is a tertiary amine chemical produced from C8 – C10 straight chain alcohol.

Products for Solvent Extraction include:

- [Alamine® 300](#) is tri-n-octyl amine.
- [Alamine® 304-1](#) is tri-n-laurylamine.
- [Alamine® 308](#) is tri-iso-octyl amine.
- [Alamine® 336](#) is tri-n-octyl/decyl amine.

**Aliquat®** is the trade name for a series of quaternary amines, made for Alamines. An example is Aliquat® 336.

- [Aliquat® 336](#) is a quaternary ammonium product made by methylation of Alamine 336.

The gold and silver ion exchange reagents include: [AuRIX® 100](#), [LIX® 79](#) and LIX® 7820.

To learn more about products manufactured by Cognis, go to <http://www.cognis-us.com/cognis/default.htm> or call (520) 622-8891

---

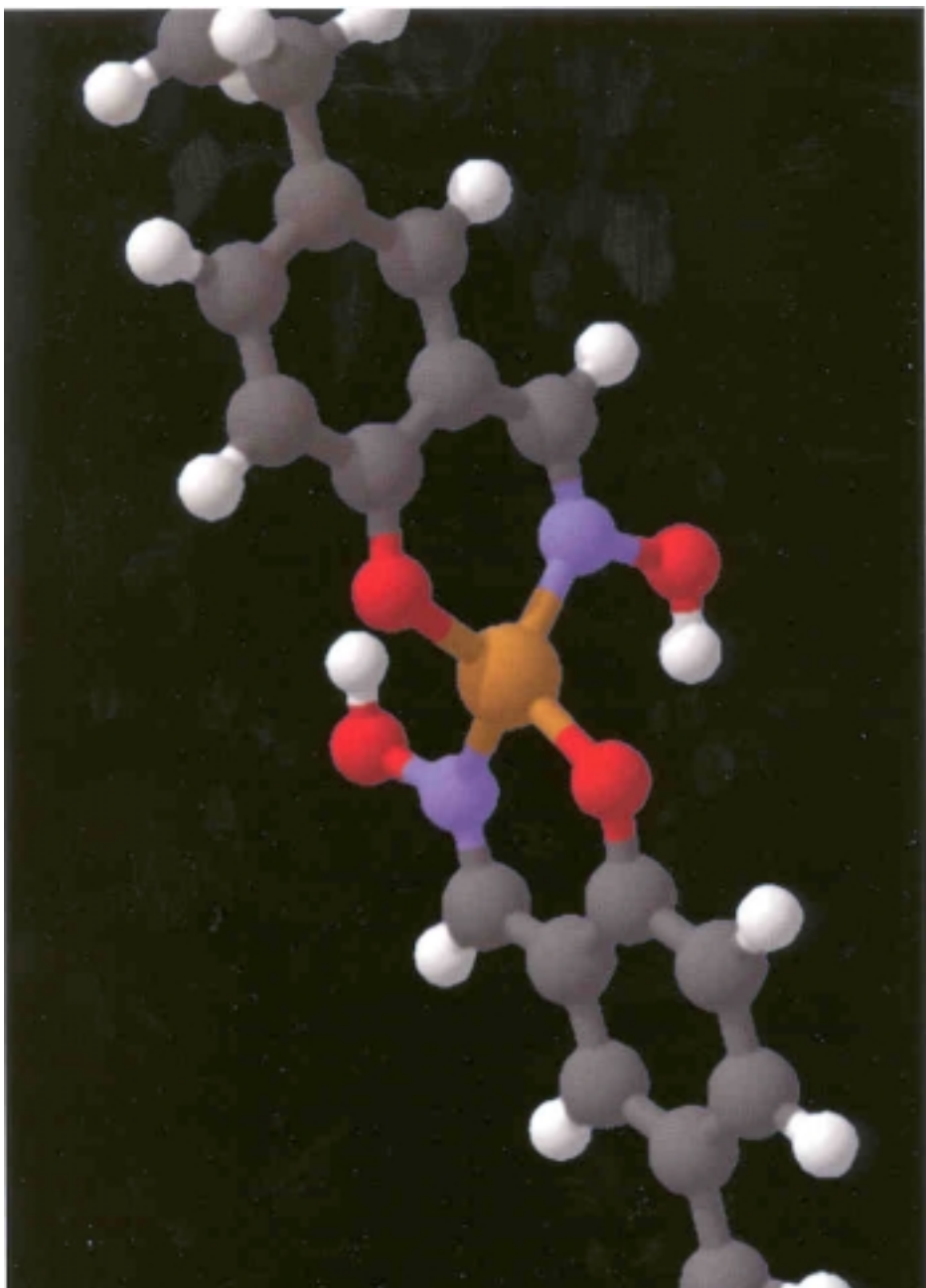
# The Chemistry of Metals Recovery Using LIX® Reagents

---

## MCT Redbook

Cognis Corporation  
Mining Chemicals Technology  
Division

Specialist in Applied  
Chemistry



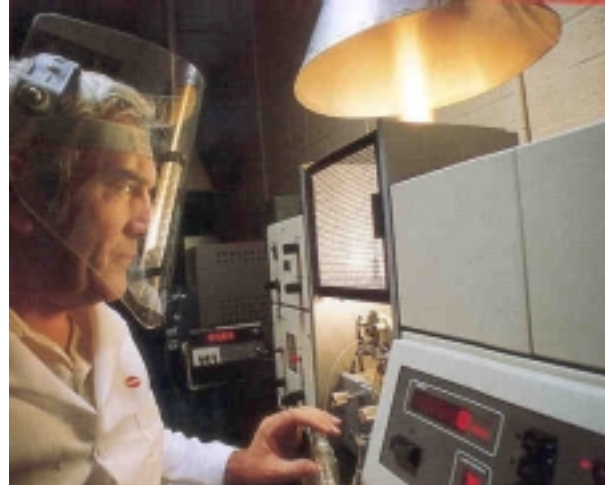
**Cognis.**  
**Meeting the needs of the mining industry,  
worldwide, for more than 40 years.**

Cognis has long been the acknowledged leader in solvent extraction technology. We provide technical support for plant operations, innovative solutions to the challenges of metals recovery and, of course, the best and most effective reagents in the world today. Our products are used on six continents, in more than 30 countries, at over 80 plants...for one very basic reason: they simply work better.

**Product Quality. Customer Service.  
Our highest priorities.**

Cognis products are designed to exhibit specific performance characteristics for specific metallurgical applications. Because we know that plant requirements vary from site to site, we offer more than 25 basic reagents and dozens of derivatives, all of which have a long and impressive track record. We are dedicated to production of the highest quality products because we believe that comprising quality, in the end, means compromising productivity.

That's also why Cognis engineers believe in the highest levels of customer service, and why we remain, continually, "at your service." To answer questions, to analyze plant performance, to help clients solve their unique problems. We work hard to make metals recovery more efficient *and* more profitable, for everyone.



# **Solvent Extraction Using Cognis Corporation Liquid Ion Exchange Reagents**

Edited by  
the staff of the  
Mining Chemicals Technology Division,  
Cognis Corporation



**Cognis Corporation**  
Mining Chemicals Technology Division

# Table of Contents

<b>Introduction</b>	<b>1</b>
<b>Description of the Solvent Extraction Process</b>	<b>2</b>
I. Extractable Metal Species	
II. Reagent Requirements	
 <b>Types of Extractants</b>	<b>3</b>
I. Chelation Agents	3
A. General Comments	
B. Laboratory Evaluation Program for a Copper Leach Solution	
C. Computer Generated McCabe-Thiele Diagrams for Copper	
D. Commercial Applications for Copper Recovery	
1. Sulfuric Acid Leach Solutions	
a. Commercial Copper Solvent Extraction Reagents	
b. Cognis Copper Solvent Extraction Reagents	
2. Ammonia Leach Solutions	
E. Cognis Chelating Reagents and Some of Their Possible Uses	
F. Capital Costs for Copper SX-EW	
II. Ion-Pair Extractants	13
A. Alamine® Series	
B. Aliquat® Series	
C. Laboratory Evaluation Program For Ion-Pair Extractants	
D. Present and Possible Future Uses of Amine Extractants	
III. Neutral or Solvating Type Extractants	15
IV. Organic Acid Extractants	15
 <b>Reagents in Development</b>	<b>16</b>
 <b>Solvent Extraction Diluents</b>	<b>17</b>
 <b>Conclusion</b>	<b>17</b>
 <b>Figures</b>	<b>19</b>
 <b>References</b>	<b>30</b>

## Introduction

An increasing demand for metals in general, and higher purity metals in particular, decreasing ore grades and more stringent environmental regulations have driven, and will continue to drive, research into finding more effective and efficient methods for processing the ores available to us, and recycling previously used metals. Hydrometallurgy has provided, and will continue to provide, many of the new processes and solvent extraction technology will certainly play an important role in many of these new processes.

Solvent extraction as a simplified technique to purify and recover a metal goes back to at least 1842 when Peligot extracted uranyl nitrate into ethyl ether<sup>1</sup>. The chemical literature has hundreds of references to the use of solvent extraction as a technique in analytical chemistry and a large amount of fundamental knowledge in solvent extraction, particularly in the areas of solution chemistry and organic based extractants, comes from analytical chemistry<sup>2</sup>.

Solvent extraction technology has been applied on a commercial scale to the recovery of uranium, vanadium and molybdenum for about forty years<sup>3</sup> and to copper and nickel for almost thirty years<sup>4</sup>. For this same length of time Cognis Corporation, (formerly General Mills Chemicals, Inc.), has been committed to the development of solvent extraction technology in general, and solvent extraction reagents in particular. This commitment has resulted in the development and successful marketing of the LIX®, Alamine® and Aliquat® Reagents used by numerous, commercially successful metal recovery operations around the world. These reagents are noted for the wide range of conditions in which they operate and for their pollution free flowsheets. It is within the realm of technical feasibility that one day the hydrometallurgist could have an unlimited selection of commercially available chemical reagents at his disposal in order to make efficient and economic separations of virtually all metals in solution.

It is important for the reader to understand that solvent extraction is only one unit process in a series of unit processes needed to win metal from ore. For this reason solvent extraction must be compatible with, and complimentary to, the leaching process

which precedes it and the final metal recovery process which follows (Figure 1). The success of the whole operation then is dependent of the success of each individual unit process.

This booklet is designed to familiarize the reader with some of the basic concepts of solvent extraction technology as well as with the LIX, Alamine and Aliquat Reagents and systems marketed by Cognis Corporation. More detailed information about specific reagents, metals, or process systems is available on request.

LIX®, Alamine® and Aliquat® are registered trademarks of Cognis Group.

Copyright© 1997 by Cognis Corporation

# Description of the Solvent Extraction Process

Solvent extraction (SX) is applicable in any instance where it is desirable to selectively remove or extract a species from one solution into another. This can apply either to the removal of a valuable component from contaminants or to the removal of contaminants from the valuable component. The solution originally containing the desired species and the solution into which this species or the contaminants are to be extracted must be immiscible to effect separation.

In metal recovery operations the valuable component is normally a metal ion or a metal ion complex contained in an aqueous solution. This aqueous solution is mixed with an immiscible organic phase containing the active extractant at which time the active extractant transfers the desired component from the aqueous phase into the organic phase. The aqueous / organic mixture, which is called a dispersion, then passes from the mixer to a settler where the phases disengage. The "loaded organic" phase, now containing the extracted metal, is then transferred from the extraction section to the stripping section where the extracted metal is stripped from the organic phase. The "stripped organic" is then recycled back to extraction. In most instances, stripping the extracted species from the loaded organic is accomplished by mixing the loaded organic with an aqueous solution. After the stripping operation final metal recovery takes place from the aqueous solution. The recovery of metal directly from the loaded organic phase is also possible, but, currently not commercially in use<sup>5,6</sup>. Because the solvent extraction process resembles metal extraction with solid ion exchange resins, it is sometimes called liquid ion exchange.

Figure 2 shows a typical counter-current, mixer-settler solvent extraction unit. An individual mixer-settler is known as a stage. In some systems specific problems make it desirable to add one or more organic "wash" or "scrub" stages in order to prevent the transfer of deleterious species from extraction to strip or vice versa.

Solvent extraction as part of an overall metal recovery process has three main objectives:

1. The purification of a metal(s) from unwanted impurities either by extracting the desired metal(s) from the impurities or by extracting the impurities from the desired metal(s).
2. The concentration of metal in order to reduce downstream processing costs.
3. The conversion of the metal values to a form which simplifies eventual recovery.

In any given solvent extraction process one, two or all three objectives may be accomplished.

These objectives can usually be met by choosing the proper reagent and operating under the optimum conditions. A variable number of mixer-settler stages, adjustable flow rates and the ability to use wash stages allows the optimization of operating conditions as well as design flexibility.

## I. EXTRACTABLE METAL SPECIES

If a metal is to be extracted from impurities or vice versa it is important to know what species are present in solution. With respect to metals, the extractable species can be divided into four categories:

1. Metal cations such as  $\text{Cu}^{2+}$ ,  $\text{Ni}^{2+}$ , and  $\text{Co}^{2+}$
2. Complex metal anions, for example  $\text{UO}_2(\text{SO}_4)_3^{4-}$ , and  $\text{Mo}_8\text{O}^{4-}$
3. Complex metal cations such as  $\text{MoO}_2^{2+}$
4. Neutral metal specials like  $\text{UO}_2(\text{NO}_3)_2$

The examples above represent metal species which are recovered by solvent extraction in commercial metal recovery plants. There are many others.

## II. REAGENT REQUIREMENTS

It is obvious that if a metal species is to be transferred from an aqueous leach solution into an organic solution, there must be some chemical interaction which causes this to happen. The component in the organic phase, which chemically interacts with the metal, is properly called the extractant, but is commonly called the reagent.

At the present time there are organic extractants known for virtually all metals in one form or another<sup>7</sup>. As stated previously, this body of knowledge is due in large part to analytical chemists, however, the requirements for a successful extractant in analytical chemistry are different than the requirements for a reagent to be successful in large scale metal recovery operations, especially as they relate to process continuity and economics. In order for a reagent to be commercially successful it must:

- a. Extract the desired metal(s) selectively from the metal-containing solution.
- b. Be strippable into a solution from which eventual metal recovery can take place.
- c. Be stable to the circuit conditions so it can be recycled many times.
- d. Be nonflammable, nontoxic, noncarcinogenic, etc.
- e. Be soluble in an inexpensive organic diluent or be able to function as the diluent.
- f. Load and strip metal at a rate fast enough to allow for the use of economical mixing times.
- g. Not promote stable emulsions.
- h. Not transfer deleterious species from strip to extraction.
- i. Have an acceptable cost.

Normally, reagent behavior with respect to the above list is not a black and white, pass or fail situation. No one reagent is the best with respect to all of the properties in the list; rather, successful reagents possess a good balance of all of the properties in the list.

There are misconceptions about the selectivity of reagents which merit discussion. It should be realized that no reagent is selective for only one metal under all conditions, but that many reagents are selective for only one metal under certain conditions. Selectivity is dependent upon conditions and the challenge is to match the conditions presented by a given leach solution to the selectivity characteristics of the reagents available. A perfect match is not always possible and is, in fact, rare. Most of the time, the researcher either settles for a reagent which, even though not perfect, functions well, or he tries to alter the leach procedure to give a leach solution from which a reagent will be more selective. In order to do this successfully, the chemistry of extraction processes must be understood.

## Type of Extractants

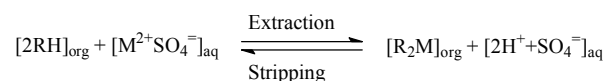
There are five classes of metal extractants as characterized by structure, extraction mechanism and the metal species extracted: chelation, organic acids, ligand substitution, neutral or solvating and ion pairing. Cognis markets chelation reagents and ion pairing reagents and has research interests in ligand substitution reagents.

### I. Chelation Extractants

#### A. GENERAL COMMENTS

Chelation refers to "claw" which is a graphic description of the way in which the organic extractant binds the metal ion in that the extractant chemically bonds to the metal in two places in a manner similar to holding an object between the ends of the thumb and the index finger. Upon bonding with the metal ion the extractant releases a hydrogen ion into the aqueous solution from which the metal was extracted. The simplified equation shown below is for the extraction of a +2 metal cation:

One of the important parameters controlling the equilibrium position of this reaction is the acid content of the aqueous phase. A graphic representation of this behavior is referred to as a pH isotherm, with some typical pH isotherms for the reagent LIX 84



shown in Figure 3. These pH isotherms can be used to predict the extraction characteristics of the reagent with respect to the metals shown under a variety of conditions. For example, at pH 2.0 copper(II) is strongly extracted, ferric iron is slightly extracted, while nickel(II) and cobalt(II) are not extracted. However, at pH 5 all four of these metals would be strongly extracted, except that this fact is not always important for iron(III) since it is only slightly soluble at pH 5.

It is important to realize that in order to make a direct comparison of the pH isotherms of two different reagents with the same metal, or of two different metals with the same reagent, the pH isotherms must be determined under exactly the same conditions.

A tabular method to express these extraction characteristics is shown in Table I.

**Table I Relative Extraction Power of LIX® 84-I for Metals at pH 2.0**

Metal	Relative Extractive Power
Cu(II)	Very strongly extracted
Fe(III)	Slightly extracted
Mo(VI)	Somewhat strongly extracted
V(V)	Slightly extracted
Zn(II)	Nil
Sn(II)	Nil
Ca(II)	Nil
Mg(II)	Nil
As(III)	Nil
Al(III)	Nil
Fe(II)	Nil
Si(V)	Nil
Co(II)	Nil
Ni(II)	Nil

\*The chemistry of Mo(VI) and V(V) is complex on the acid side, however, these metals do not present a problem to copper extraction.

The investigator screens the reagent against the metals most likely to be found in the aqueous feed solutions of interest under conditions similar to those expected in the solvent extraction process. This is normally referred to as selectivity data and holds only at the conditions under which it is determined. These conditions include the metal and reagent concentration, the oxidation state of the metal, the pH of the aqueous feed solution, and the organic-aqueous contact time. From Table I it is obvious that Cu(II) is the only metal listed which is strongly extracted by LIX 84 at pH = 2, and that only Fe(III) would present any potential problems to the preparation of a pure copper solution from a "normal" feed at pH = 2. This data is in agreement with the pH isotherms shown in Figure 3.

The extraction of metals from ammoniacal solution is also an area of interest, thus, the extractive behavior of some metals from ammoniacal solutions has been examined. In general, these data are expressed as ammonia dependent extraction isotherms, several of which are shown for LIX 84-I in Figure 4. The tendency for extraction to decrease with increasing ammonia concentration can readily be explained by the extraction/stripping equation for a typical +2 metal cation shown below:



In essence, the ammonia in solution functions as a coordinating ligand and competes with the organic extractant for the metal ion. The reaction is reversible and stripping with ammonia might be practical in some situations. The number of ammonia molecules coordinated to the metal will vary depending on the conditions; four being a favored number.

By looking at extraction isotherms and selectivity data, it is possible to develop metal separations schemes. For example, a look at the pH isotherms of LIX 84-I with Cu(II) and Ni(II) (Figure 3) suggests that a good Cu-Ni separation can be made with LIX 84-I by controlling the pH in the extraction stages. All of the copper can be extracted at low pH (1.5 to 2.0) before the system is adjusted with ammonia to higher pH (9.0 to 9.5) where the nickel is extracted. This type of scheme has been used on a commercial scale at the S.E.C. Corporation in El Paso, Texas, for the recovery of copper and nickel from a refinery bleed stream<sup>8</sup>.

The LIX 84-I ammonia dependent extraction curves in Figure 4 show that copper(II) is more strongly extracted from an ammoniacal solution than is nickel. Thus copper-nickel separations from ammonia leach solutions should be possible and indeed have been studied for a similar reagent<sup>9</sup>. The study concentrated on a flow scheme where copper is preferentially extracted from an ammonia solution containing copper and nickel before the nickel is extracted. A high copper / nickel ratio on the copper loaded organic is obtained by using an extra extraction stage in which copper crowds nickel from the loaded organic, i.e., the copper in an ammoniacal copper and nickel containing solution, when contacted with an organic loaded with nickel, will replace some of the loaded nickel. After the copper and nickel are loaded in separate extraction operations, each "metal loaded organic" is washed and then stripped to give a copper-rich and a nickel-rich electrolyte, respectively. Circuit complexity, overall operational ease and the number of stages required are dependent upon the aqueous feed.

A different separation scheme on the same type of feed has been reported<sup>10</sup> and has also been studied in this laboratory<sup>11</sup>. This scheme involves the coextraction of nickel and copper with the same organic stream, then washing followed by pH controlled,

selective stripping of each metal, to give copper-rich and nickel-rich electrolytes, respectively. This flow scheme is based on the ammonia isotherms, which show that copper and nickel are strongly extracted from ammoniacal solutions by LIX 84-I, and the pH isotherms, which show that while LIX 84-I loads copper very well at a pH of 2.5 to 3.0, nickel is readily stripped at that pH.

It is well indeed, that the study of pH isotherms, selectivity data and ammonia isotherms leads to the conceptual development of metal separation processes. However, this type of data does not tell in a detailed way how to do a given metal separation, nor the way the circuit must be set up in order to do the separation in the most effective and least costly manner. For this type of information some research effort is required.

## B. Laboratory Evaluation Program for a Copper Leach Solution

Assuming a metal containing solution is available, what is the next step? The first thing is that the contents of the solution must be known, (metals, pH, NH<sub>3</sub>, etc.) as well as whether that solution is typical of the feed solution to be treated. The evaluation of a feed solution, which is not typical of the solution to be treated, can at times be a wasted effort. Once the solution contents are known, judgments about which metals can be separated should be made based on the extraction isotherms available. If data on some of the contained metals is not available, the reagent(s) to be used should be screened against these metals. At this point it should be known which metals are considered desirable to recover, and which metals are possible to recover via solvent extraction, under the given set of conditions. The circuit development work can now begin with the realization that all parts of the total metal recovery scheme must fit together in a workable manner.

For example, consider a solution obtained from a typical copper leach operation containing 2.5 g/l Cu(II) and 1.30 g/l total Fe at a pH of 1.80. The overall goal of the laboratory evaluation program is to determine the conditions required so that about 90% copper recovery is realized. It is also important to generate data on copper over iron selectivity.

From experience it is known that LIX 984, a mixed aldoxime-ketoxime reagent, is a good reagent for the leach liquor under discussion. Previous work tells us

that in a 2 extraction - 1 strip stage circuit, where ~ 90 % copper recovery was obtained, LIX 984 transferred about .24 to .30 g/l Cu per volume percent reagent. Since the leach liquor of interest has a pH of 1.8 assume that LIX 984 will transfer in the middle to lower end of the range. The following simple calculation then gives the reagent concentration, which should be suitable:

$$\begin{aligned} 2.50 \text{ g/l Cu} \times (0.90) & / 0.26 \text{ g/l Cu per v/v\% reagent} \\ & = 8.7 \text{ v/v\% reagent} \end{aligned}$$

An organic solution containing 8.7 v/v% LIX 984 in a suitable diluent is prepared and then vigorously contacted once for about three minutes in a separatory funnel with the feed solution at an organic /aqueous (O/A) ratio of about 1. After the phases have separated and the aqueous phase is discarded the copper loaded organic phase is vigorously contacted twice, for about one minute each contact, with fresh pregnant strip solution (the aqueous solution expected to exit the strip stage of the circuit, 50 g/l Cu and 140 g/l H<sub>2</sub>SO<sub>4</sub> in this case), also at an O/A=1. This results in an organic solution which closely approximates the stripped organic (S.O.) to be expected in the actual continuous circuit operation. The newly prepared stripped organic and the leach solution are now equilibrated at various organic to aqueous volume ratios by vigorous shaking for 3-10 minutes in separatory funnels or by rapid stirring in mixer boxes. After phase separation the respective organic and aqueous layers are filtered and saved for analysis. The organic layer is analyzed for copper (and perhaps iron) and the aqueous layer for copper only. The data is shown in Table II and is plotted as illustrated in Figure 5.

Stripping isotherm data is generated in a similar fashion by equilibrating the stripping aqueous phase (S.E.), in this instance a typical copper electrowinning tankhouse electrolyte containing ~30 g/l Cu and 170 g/l H<sub>2</sub>SO<sub>4</sub>, with copper loaded organic (L.O.) at various O/A ratios (Table II, Figure 6).

**Table II. Equilibrium Extraction and Stripping Data for LIX® 984**

Analysis in g/l Cu

**Extraction**

O/A	Organic	Aqueous
10/1	2.04	0.07
5/1	2.28	0.09
2/1	2.96	0.17
3/2	3.26	0.26
1/1	3.70	0.51
1/2	4.19	1.24
1/5	4.35	1.94
S.O.	1.80	
Leach Solution		2.50

**Stripping**

O/A	Organic	Aqueous
10/1	1.76	51.3
5/1	1.38	43.2
2.5/1	1.21	37.7
1/1	1.07	33.8
1/2	1.01	32.3
1/4	0.98	31.2
L.O.	3.90	
S.E.		30.7

Isotherms are unique to the conditions under which they are generated. If one of the parameters is changed, for example, the reagent concentration, the copper concentration of the respective organic or aqueous phase, the pH of the leach liquor, the acid concentration of the strip liquor, etc., then a different isotherm will be generated. In instances where the change in one or two of the parameters is very small it may not be necessary to run a second isotherm.

Properly generated extraction and stripping isotherms represent equilibrium conditions and, as such, predict the best extraction and the best stripping which can be obtained. These isotherms can be used to set the staging in a circuit. Consider, for example, the extraction isotherm in Figure 5 and suppose that the stripped organic entering into the last extraction stage contains 1.80 g/l Cu and that the advance flowrates of the leach solution and the organic phase are equal. Knowing this, an operating line can be constructed by starting at the point where the stripped organic intersects the isotherm and

drawing the line up and to the right with a slope equal to the ratio of the organic/aqueous flow rates (one in this instance) until the operating line intersects the vertical line representing the copper content of the feed. Next, a horizontal line to the isotherm curve and then a vertical line to the operating line are drawn creating a "step". This process is repeated, creating a second step and completing a two stage "McCabe-Thiele" diagram. Each triangle represents a single stage of extraction. In this system, a raffinate of 0.22 g/l Cu and a loaded organic of 4.24 g/l Cu are predicted in two stages of extraction.

Even though the McCabe-Thiele diagram shown in Figure 5 does not represent true equilibrium, but only a first approximation, it is still quite useful. For example, if a third stage of extraction were to be added to the McCabe-Thiele diagram in Figure 5, (note the dotted line) a near perfect equilibrium McCabe-Thiele diagram would result. In addition, a more accurate two stage McCabe-Thiele extraction diagram can be drawn by taking the two stage McCabe-Thiele construction as shown in Figure 5 and choosing as the point from which a new operating line is to be drawn a distance about 1/2 way between the isotherm line and the raffinate line. When this is done, and then a second two stage McCabe-Thiele diagram constructed as described above, a raffinate of about 0.15 g/l Cu and a loaded organic of 4.17 g/l Cu are predicted. The construction of a true equilibrium McCabe-Thiele diagram is an iterative process. With the example under discussion the second step of iteration is all that is needed to produce a near equilibrium McCabe-Thiele diagram. This will not always be the case.

The construction of an equilibrium McCabe-Thiele diagram depicting one stage of stripping is very simple (Figure 6). A horizontal line is drawn from the loaded organic line (3.90 g/l Cu) to the isotherm line at the value of the pregnant electrolyte (P.E.) desired, 51 g/l Cu in this case. Then a vertical line is dropped from the point where the P.E. line intersects the isotherm to the horizontal axis. This gives the stripped organic (S.O.) to be expected (1.77 g/l Cu). Next, the strip electrolyte (S.E.) line, 30.7 g/l Cu, is drawn horizontally from the vertical axis of the graph to the S.O. line. The line connecting this point with the intersection of the loaded organic and pregnant electrolyte lines is the operating line. The slope of the operating line ( $2.13/20.3 = .105$ ) is equal to the ratio of the advance strip aqueous flow to the

advance organic flow needed to obtain the desired pregnant strip solution.

A two stage McCabe-Thiele strip diagram, constructed as described above for extraction, predicts a stripped organic of 1.12 g/l Cu when building a pregnant electrolyte of 51 g/l Cu and operating at an O/A of 7.3/1.

One of the important decisions the designer or builder of an SX plant must make is to decide on the staging requirements. The capital cost of a stage must be weighed against the benefits the stage provides. For example, consider the benefit of a second strip stage for the example cited above. Two stages of stripping will give a stripped organic of 1.12 g/l Cu and result in a net copper transfer for the organic (the difference between the loaded and stripped organic) of about 2.78 g/l Cu, while one stage of stripping gives a copper net transfer of about 2.13 g/l Cu. Because of the difference in net copper transfer, a one strip stage circuit requires a reagent concentration about 1.3 times greater than a two strip stage circuit in order to have equal copper extraction performance. Therefore, the organic losses expected in a one strip stage plant should be about 1.3 times greater than those in a two strip stage plant. By comparing the capital cost for a second strip stage with the increased operating cost (due to higher reagent usage) for the one strip stage plant, a purely economic decision on the strip stage requirements can be made.

In recent times most companies have opted to treat dump leach liquors in 2 extraction - 1 strip (2E-1S) stage plants rather than 2E-2S or 3E-2S plants. For this reason, a 2E-1S circuit was set up and operated at the advancing O/A ratios shown in the McCabe-Thiele diagrams in Figures 4 and 5. A mixer retention time of 2.6 minutes was used simply because most copper SX plants have two or three minute mixers, depending on the leach solution conditions, mixer design and company philosophy.

In order to run a circuit properly, resulting in good metallurgy and maximum information, several things are important. Flow rates must be accurately set and continually monitored. Mixer dispersions should have an O/A ratio near one in order to get proper mixing, thus, recycles should be employed where needed. The mixing turbines must rotate fast enough for good mixing, but, not so fast that heavy entrainment results<sup>12</sup>. Another important feature of

running a good circuit is frequent sampling with rapid and accurate analyses. This allows the operator to monitor the circuit closely, easily observing circuit behavioral differences as operating parameters are changed. Once an operator has changed operating conditions, the circuit should be allowed to run until circuit equilibrium is established. When a circuit is in equilibrium it means that there is a good metal balance and a good metal-acid balance across the whole circuit, as well as in each stage. Thus, the metal extracted from the aqueous phase in an extraction stage is equal to the acid equivalent gained by that same aqueous phase, and also equal to the metal loaded by the organic in that stage. In a stripping stage the metal stripped from the organic phase is equal to the metal gained, and to the acid equivalent lost, by the strip aqueous phase in that stage.

Obviously, in order to balance metal and acid values, solution analyses and solution flow rates must be known. Furthermore, solution samples for a given stage should be taken from the rear of the respective settler for that stage. When possible it is best to pull samples at those points easiest to access and least likely to upset the circuit.

It is important to realize that circuit behavior will reflect the interdependence of the extraction stripping operations. For example, a loss of stripping efficiency will result in a higher stripped organic which in turn leads to a higher raffinate. The circuit must then be operated with a slightly higher reagent concentration in order to maintain copper recovery or a slightly lower recovery must be accepted.

Because of the design of mixers currently used in copper solvent extraction plants, metal transfer in a stage is usually about 85 to 95% of theoretical. For this reason, the values predicted by equilibrium McCabe-Thiele diagrams for the aqueous and organic phases exiting a given stage are seldom realized in an operating circuit. For example, compare the organic and aqueous values which are predicted by the McCabe-Thiele diagram in Figure 5 with the values generated in a continuous laboratory circuit using the same aqueous, organic and strip aqueous solutions (Table III, Figure 7).

The circuit produced a raffinate of 0.28 g/l Cu and a loaded organic of 4.08 g/l Cu as compared to the raffinate of 0.22 g/l Cu and the loaded organic of 4.24 g/l Cu predicted by the first approximation McCabe-Thiele extraction diagram (Figure 5). The

stripped organic of 1.80 g/l Cu is close to the 1.77 g/l Cu predicted by the McCabe-Thiele strip diagram (Figure 6).

**Table III. Circuit Profile Data with 8.7 v/v% LIX® 984 in Escaid 110**

Sample	Organic g/l Cu	Aqueous g/l Cu	Organic g/l Fe	Aqueous g/l Fe
Extraction Stage One	4.08	0.0020	1.31	
Extraction Stage Two	2.88	0.0038	0.28	
Strip Stage	1.80	N.D.	51.2	0.026
Strip Aqueous			30.7	0.010
Leach Aqueous			2.50	1.30

The natural question arises: Why perform the work required for an equilibrium isotherm when the circuit will not produce the predicted results? There are several good reasons. First of all, generating an isotherm helps to develop a "feel" for the system. Secondly, if the system has any unusual metallurgical behavior characteristics, the isotherm will usually reflect them. Thirdly, a good idea of the actual circuit results can be obtained by drawing in the operating line as previously described. However, instead of filling in the horizontal and vertical lines to reflect 100% mixer efficiency, draw the horizontal lines in to represent only 95% efficiency. When this is done using Figure 5, a two stage raffinate of 0.28 g/l Cu is predicted - a value identical to that realized in the circuit operation.

The feed chosen for the above example is typical of many copper leach operations and represents one of the simplest feeds to treat. Copper recovery is very good, the selectivity for copper over iron is high (in the above circuit it is about 1100/1 on a transfer basis), and there is little tramp metal contamination. More complicated feed solutions are evaluated in a manner similar to that described above, but, the extraction and stripping isotherms and the staging in the circuit can be, and often are, more complicated. Thus, the initial circuit may have to be modified several times before the best recovery scheme is worked out.

### C. Computer-Generated McCabe-Theile Diagrams for Copper

Cognis has developed a computer program, called Isocalc®, which will generate isotherms for the extraction of copper from typical sulfuric acid leach solutions. This computer program is based on the equilibrium constants for the extraction of copper from aqueous acidic sulfate solutions with the Cognis reagents LIX 84-I, LIX 984, LIX 622 and LIX 860-I, respectively, according to the equation on page 3. The program also incorporates the effects of sulfate buffering, the initial pH of the leach liquor, the reagent concentration and the stripping conditions for the loaded organic.

After generating an isotherm, the program will use that isotherm to calculate McCabe-Thiele extraction diagrams under specified conditions. Finally, the program will calculate and print mass balances across both the extraction and stripping stages.

This program is useful for:

- a) predicting reagent behavior under varying conditions,
- b) comparing the performance of one reagent with another under varying conditions,
- c) predicting metallurgical changes as conditions in a circuit are changed, for example, staging, the pH of the leach liquor, reagent concentration, mixer efficiency and stripping conditions.

However, the computer program only predicts those circuit behaviors associated with the copper extraction \_ stripping equilibrium. It does not predict copper over iron selectivity nor does it address the physical properties of a circuit such as:

- d) phase separation - how fast the aqueous/organic dispersion exiting a mixer separates into organic and aqueous phases,
- e) entrainment - the very small droplets of one phase carried in the other phase after primary phase separation has taken place,
- f) crud generation - the term crud or gunk is used to describe an interfacial material which is present in almost all solvent extraction circuits. This material usually contains finely divided solids

(either carried into the circuit with the leach liquor or precipitated in the circuit), some stable emulsion, bulk leach solution and/or bulk organic, colloidal silica and at times bacteria. Crud is a very difficult thing to describe as crud in one plant may be quite different from crud in another plant.

The Isocalc program should be used in conjunction with, but, not as a total substitute for, laboratory evaluations. As such, it can save a lot of time by very quickly providing information on "what if" type questions. This is particularly true early in a project.

A version of the program is available for Cognis customers, but, it is not available for general distribution. Under certain conditions your Cognis solvent extraction specialist will be happy to run Isocalc programs for your projected sulfuric acid copper leach solutions.

## D. Commercial Applications for Copper Recovery

### 1. Sulfuric Acid Leach Solutions

The use of chelation type extractants in liquid ion exchange has enjoyed its greatest commercial success for the recovery of copper from dilute sulfuric acid leach solutions which are generated from the leaching of oxide and/or sulfide ores using a variety of leaching techniques including dump, heap, in-situ, vat, thin layer and agitation. The leach-SX-EW technology begins with leaching and Cognis advises that companies considering this technology thoroughly investigate the leaching characteristics of their ore. Money spent up front in leaching studies usually pays handsome dividends.

Typical leach solutions may contain less than 1 g/l Cu up to about 35 g/l Cu over a pH range of 1.1 to 3.0. The leach solution may also contain up to 50 g/l chloride and a host of other impurities depending on the ore, available water and evaporation rate. Typical sulfuric acid leach solutions successfully treated by solvent extraction are summarized in TABLE IV.

**Table IV. Typical Sulfuric Acid Leach Solutions**

Type	Cu (g/l)	pH
Dump, Heap, In-situ	< 1 to 6	1.3 to 2.2
Ferric Cure, Thin Layer	3 to 6	1.5 to 2.2
Vat	5 to 50	1.6 to 2.0
Agitation	1 to 35	1.4 to 2.0

Other common constituents: Fe, Mo, Mn, Al, Mg, Na, K, sulfate ions and at times chloride ions.

Typical solutions from which high purity copper is electrowon contain from 30 to 38 g/l Cu and 140 to 180 g/l H<sub>2</sub>SO<sub>4</sub>. Most copper tankhouses coupled with SX in the acid sulfate system will have copper and acid concentrations in these ranges.

At the present time (December 1996) there are forty seven commercial operations that recover copper from dilute sulfuric acid leach solutions and there are several plants under construction with several others planned. Actual operating costs for one of the largest of these, the tailings leach plant of the Chingola Division, Zambia Consolidated Copper Mines, Ltd., in Zambia, Africa<sup>13</sup>, and one of the smaller, the Cyprus Bagdad Copper Company plant in Bagdad, Arizona<sup>14</sup>, have been published. The advantages of solvent extraction-electrowinning (SX-EW) over the cementation process for the recovery of copper from these types of leach solutions is well documented in these papers. These papers also demonstrate the applicability of solvent extraction on a very large scale, since ZCCM produces over 7,000 tons per month of high quality cathode copper, and on a smaller scale, as Cyprus Bagdad produces about 1100 tons per month of superior quality cathode copper. In addition, the ability to forecast fairly accurate operating costs for the SX-EW operation, as reported in the above papers, is a great advantage to the parties involved during feasibility studies.

### a. Commercial Copper Solvent Extraction Reagents

Even though a large number of molecules with a wide variety of extractive functionality's have been proposed as extractants to be used for the recovery of copper from sulfuric acid leach solutions, only the

hydroxy oximes have been used in commercial copper SX-EW plants. The basic structure for these copper extractants is shown in Figure 8.

The extractants of the general structure can be subdivided into two distinct classes based on their structure and properties: the ketoximes, which are normally copper extractants of moderate strength and the salicylaldoximes, which are very strong copper extractants. The strength of a copper extractant is based on the degree to which the copper extraction stripping equilibrium previously shown is driven toward extraction by the reagent. In simple terms, very strong copper extractants extract substantial amounts of copper at pH values less than 1.0, while moderate strength copper extractants are most useful above a pH of 1.6-1.8.

Another class of extractant combines a salicylaldoxime with a ketoxime in an approximate 1/1 mole ratio. This "third" class is not based on structure, but rather on the distinct and advantageous properties the mixtures exhibit. These patented mixtures<sup>15</sup> are classified as strong copper extractants and as such are useful at pH values as low as ~1.2.

**Ketoximes:** A ketoxime was the first hydroxy oxime extractant to be used commercially for the extraction of copper from dilute sulfuric acid leach liquor<sup>2</sup> and ketoximes were used exclusively for about 11 years. The most outstanding feature of the ketoximes, as represented by LIX 84, is the good physical performance they display under a wide variety of conditions, especially with respect to solutions that are known to be sensitive to certain organic solutions. One example would be agitation leach solutions which contain colloidal silica, some solids and/or residual flocculent. A second example are leach solutions containing dissolved organics, often present due to rotting vegetation. The ketoximes show excellent phase separation, low entrainment losses to the raffinate, and do not promote excessive crud formation. Because ketoximes are only moderately strong copper extractants and kinetically slow at cold temperatures, the number of copper SX plants using a ketoxime extractant exclusively is limited. However, in the circuits which are designed to use ketoximes, the operator enjoys a low cost, trouble-free copper extractant.

**Salicylaldoximes:** The salicylaldoximes were developed to overcome the perceived shortcomings of the ketoximes. Their outstanding characteristics in-

clude rapid copper transfer kinetics and high extractive strength. However, the salicylaldoximes by themselves are such strong copper extractants that they are most often used in combination with an equilibrium modifier or with a ketoxime so that they can be efficiently stripped with an acidic copper solution from which high quality copper can be electrowon.

The use of equilibrium modifiers leads directly to certain shortcomings in that some modifiers are known to accelerate reagent degradation. It has also been reported that equilibrium modifiers contribute significantly to the amount of crud generated in some solvent extraction circuits<sup>16</sup>. Another problem sometimes associated with modified reagents is the contamination of electrolyte due to the excessive entrainment of leach liquor in the loaded organic stream. Finally, nonylphenol is known to have deleterious effects on certain materials of construction.

As a group salicylaldoximes are less stable than ketoximes and within the salicylaldoxime subgroup, the nonyl derivative is less stable than the dodecyl derivative. In operating circuits at normal temperatures, reagent degradation with 5-nonylsalicylaldoxime has been calculated to be equal to about 10% of the total reagent makeup. Actual degradation results on operating circuits have not been published, however, for some plants they are known to be higher than the calculated value depending on the modifier, the temperature and the acid content of the aqueous stripping solution. With heated circuits, reagent degradation could be even more significant and should be determined experimentally. Still, overall reagent loses are quite low in a well operated plant so the loses due to degradation are not excessive in any case.

In spite of their shortcomings, modified salicylaldoxime reagents such as LIX 622 have been quite successful in commercial circuits which are designed for their use, and where the leach liquor is compatible with the reagent.

**Ketoxime-Salicylaldoxime Mixtures:** The properties of ketoxime-salicylaldoxime mixtures containing no added modifier, such as LIX 984 and LIX 984N, reflect the most desirable characteristics of the components: the extractive strength and fast kinetics of the salicylaldoximes combined with the proven, excellent physical performance and stability of the ketoximes<sup>16</sup>.

Although the extractive strength of the mixtures is not quite as high as the modified salicylaldoximes, it is considerably greater than the ketoximes. Copper transfer kinetics are a little slower than salicylaldoximes, but are still very fast.

One interesting feature of these mixtures is the greater than expected copper transfer these mixtures give because of their lower than expected stripped organic value. It is felt this property results from the ketoxime component of the mixture functioning as a modifier for the salicylaldoxime component in the strip stages of the circuit. The mixtures were introduced to the industry in 1982 and are now the most widely used copper extractant system in the world. Since the ketoxime and salicylaldoxime components can be mixed in any ratio, a reagent mixture can be tailored to the demands of almost any leach liquor. Indeed, these mixtures could prove in time to be a universal reagent system for acid sulfate copper leach solutions since, in most instances, a properly tailored mixture will function both physically and chemically very well with virtually any leach solution of this type.

Since all three reagent classes of oxime extractants are commercially successful it follows that each class of extractant meets the reagent requirements previously given. In reading the successful reagent requirements it is obvious that they are somewhat general in nature. For example, the first requirement says that the reagent must extract the desired species selectively (in this case copper), but, it says nothing about how much copper must be extracted, nor the degree of selectivity the reagent must have. In fact, it is virtually impossible to be more specific because each leach liquor, each plant and each reagent is unique. Whereas a given reagent requirement may be critical in one situation, in another it can be relatively unimportant. What should be understood is that all three classes of hydroxy oxime reagents possess the successful reagent requirements to such an extent that all three classes are commercially successful, yet, no one reagent is the best for each and every copper leach liquor or copper solvent extraction circuit.

## b. Cognis Copper Solvent Extraction Reagents

Cognis produces three (3) oxime extractants: 5-nonylsalicylaldoxime, 5-dodecylsalicylaldoxime and 5-nonyl-2-hydroxyacetophenone oxime. These three oximes form the basis for a wide range of reagents which are derived by blending the oximes in a variety of ways, for example, with diluent, with one another or with a modifier, to give LIX Copper Solvent Extraction Reagents with properties that best fit the particular leach solution and plant design under consideration.

Furthermore, there are operating copper SX plants which purchase the individual reagent components separately and mix these components in a way that best meets the individual needs of the particular leach solution, plant or season. The ability to purchase the reagent components gives copper SX plant operators great flexibility in the operation of their plant to meet changing conditions, for example, summer versus winter operation, while still maintaining excellent physical properties.

Cognis makes available both normally formulated reagents and concentrated reagents. The concentrated reagents contain the same oximes as the normally formulated reagents. However, because the concentrated reagents are formulated with less diluent in order to save packaging, shipping and handling costs, the concentrated reagents are more viscous than normally formulated reagents and they do not flow well at temperatures less than about 5°C.

Table V shows the contents for some of the oxime copper extractants available from Cognis. If you would like more information about Cognis oxime copper solvent extraction reagents, or if you would like to discuss the extraction of copper from dilute sulfuric acid leach solutions in more depth, contact your local Cognis representative.

The oxime copper extractants marketed by Cognis Corporation, either alone or mixed, are highly selective for copper over iron when mixed with almost all copper leach solutions. As a result minimum tank-house bleeds are needed for iron control.

**Table V. Composition of some Hydroxy Oxime Copper Extractants, available from Cognis**

<u>Extractant/Catagory</u>	<u>Composition</u>
LIX® 84 /Ketoxime	A mixture of predominantly 2-hydroxy-5-nonylacetophenone oxime with a small amount of 5-dodecylsalicylaldoxime in a high flash point hydrocarbon diluent needed for handling purposes.
LIX® 860 /Aldoxime	A mixture of predominantly 5-dodecylsalicylaldoxime with a small amount of 2-hydroxy-5-nonylacetophenone oxime in a high flash point hydrocarbon diluent needed for handling purposes.
LIX® 860N /Aldoxime	A mixture of predominantly 5-nonylsalicylaldoxime with a small amount of 2-hydroxy-5-nonylacetophenone oxime in a high flash point hydrocarbon diluent needed for handling purposes.
LIX® 984 /Mixture	An equivolume mixture of LIX 84 with LIX 860.
LIX® 973 /Mixture	A 7 / 3 volume blend of LIX 860 with LIX 84.
LIX® 622 /Salicylaldoxime	A mixture of 5-dodecylsalicylaldoxime and tridecanol in a high flash point hydrocarbon diluent.

## 2. Ammonia Leach Solutions

The extraction of metal from ammoniacal leach solutions is a second commercial application for chelation type extractants. Ketoximes, such as LIX 84, and the beta-diketone reagent LIX 54 have both been used. In one example, a ketoxime was used as the extractant for a leach liquor derived from the ammonia leaching of copper sulfide concentrates in a process termed the "Arbiter Process"<sup>17</sup>. In another example, LIX 54 is used as the extractant for copper from a leach liquor derived from the ammonia leaching of copper-lead dross<sup>18</sup>.

LIX 54 was designed for the extraction of copper from ammoniacal leach liquors. Its ease of stripping, low ammonia loading, fast kinetics, good phase separation, high copper loading, and low viscosity when fully loaded, make it ideally suited for this task<sup>19</sup>. However, LIX 54 is not applicable to sulfuric acid leach solutions since it does not extract copper well below pH ~3.0.

## E. COGNIS CHELATING REAGENTS AND SOME OF THEIR POSSIBLE USES

**LIX 54:** A beta-diketone based reagent, used for the selective extraction of copper from ammoniacal leach solutions, which strips with very low concentrations of residual sulfuric acid and operates at a high net copper transfer<sup>18,19</sup>. It may be possible to strip copper from this reagent using concentrated ammonia solutions.

**LIX 63:** This hydroxy oxime has been proposed for germanium recovery<sup>20</sup>, for copper recovery from typical tankhouse electrolytes<sup>21</sup>, in synergistic mixtures with other reagents for cobalt and nickel recovery<sup>22, 23, 24</sup> and for the separation of molybdenum from uranium in dilute sulfuric acid solution.

**LIX 84:** This ketoxime based reagent requires about 150 g/l H<sub>2</sub>SO<sub>4</sub> for copper stripping and contains no added modifier. It is widely used for copper recovery from dilute sulfuric acid leach solutions, and has application for the recovery of copper and nickel from ammonia solutions<sup>9, 10, 11, 25</sup>.

**LIX 87QN:** A ketoxime based reagent developed specifically for the extraction of nickel from ammonia, followed by a stripping operation using a concentrated solution of ammonia and carbon dioxide<sup>26</sup>.

**LIX 860:** This aldoxime based reagent, containing no added modifier, has been proposed as a reagent for the coextraction and selective stripping of copper and zinc<sup>27</sup>. In addition, this reagent when coupled with a copper sulfate crystallization circuit can be used to extract copper efficiently at pH values less than 1.0.

Whereas the above list is impressive, it should not be considered as limiting. Cognis is constantly working on the development of new chelating functionalities, while Cognis, and others in the industry, are continually working on new applications for existing chelation type extractants.

## F. CAPITAL COSTS FOR COPPER SX-EW

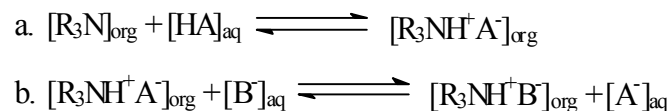
It is difficult to set out a formula by which to predict capital costs for solvent extraction-electrowinning plants. Raw material costs, local labor markets, the type of construction, the nature of the feed and the final plant designs are variables important in predicting capital costs. Cognis Corporation does try to keep current in these areas and will do some preliminary capital cost analysis for people interested in solvent extraction. To this end, Cognis has developed its Metcalc® computer program, which can be used in conjunction with the Isocalc program previously discussed, or by itself. The Metcalc program is not available for distribution, but, Cognis technical representatives will be happy to run the program according to customer needs.

## II. ION-PAIR EXTRACTANTS

A second class of extractants is based on the principle of ion association; whereby a large, positively charged organic moiety causes the extraction of a large, anionic metal complex into the organic phase, with concomitant expulsion of a small common anion to the aqueous phase. Cognis Corporation markets two classes of compounds which fall into this general classification.

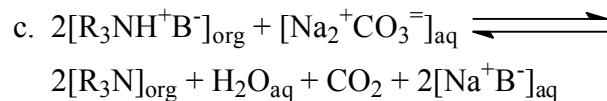
## A. ALAMINE® SERIES

The Alamine Series of Reagents all contain a basic nitrogen capable of forming amine salts with a wide variety of inorganic and organic acids. The amines which find the widest use in metals recovery processing by solvent extraction are the tertiary amines of the general formula R<sub>3</sub>N, where R can represent a variety of hydrocarbon chains. The equations below are representative of the extraction chemistry of the Alamine Series of Reagents:



Equation a represents simple amine salt formation while equation b represents true ion exchange. The extent to which B<sup>-</sup> will exchange for A<sup>-</sup> is a function of the relative affinity of the two anions for the organic cation and the relative stability of the anions in the aqueous medium. Since tertiary amines can form salts with a wide variety of acids, the choice of reagents for a liquid ion exchange process is quite large, i.e., the bisulfate salt, the chloride salt, etc., of any of the Alamine Reagents.

Amine type extractants can be stripped with a wide variety of inorganic salt solutions such as NaCl, Na<sub>2</sub>CO<sub>3</sub>, and (NH<sub>4</sub>)<sub>2</sub>SO<sub>4</sub>. The choice of stripping agent depends on the overall recovery process, but in general, basic stripping agents which deprotonate the amine, give the best stripping in the fewest stages. The equation below shows the stripping action of Na<sub>2</sub>CO<sub>3</sub> on an amine salt:



The greatest commercial acceptance for Alamine type reagents has been in uranium recovery processes, however, any metal capable of forming anionic complexes in aqueous solutions is a candidate for extraction by an amine type extractant. Figure 9 shows some of the extraction data which has been generated using Alamine 336 and/or similar amines<sup>28</sup>. The data is far from all-inclusive, but, it does show the wide variety of metal-aqueous systems which are amenable to treatment with amine type extractants.

## B. ALIQUAT® SERIES

The Aliquat Series of Reagents is based on the methyl chloride quaternization of a respective Alamine reagent. Because a quaternized amine is always positively charged, anion extraction with Aliquat Reagents is not pH dependent like it is with the tertiary amines. As a result, some basic metal leach solutions may be successfully treated by Aliquat type reagents without pH adjustment. The biggest disadvantage of using an Aliquat reagent is that these reagents will not deprotonate, therefore, stripping is usually more difficult than with the parent amine type reagent.

## C. LABORATORY EVALUATION PROGRAM FOR ION-PAIR EXTRACTANTS

Laboratory evaluation programs with amine type extractants are carried out much like those described earlier for chelating type reagents. Even though amine systems tend to be more complicated than chelating systems for a variety of reasons:

- a. the large number of aqueous anionic systems where an amine extractant may be applicable,
- b. the large variety of potential stripping agents as compared, for example, to copper loaded chelates, where stripping with sulfuric acid is the norm,
- c. the three variables: pH, the oxidation state of the metal and the concentration of the anion contributing to the anionic metal complex, all of which are important in metal separation schemes with amines,

The goals of the laboratory evaluation program remain the same; to develop the best conditions for the extraction, stripping and final product recovery consistent with the overall metallurgical flowsheet.

An example which illustrates the importance of the variables cited above is the separation of Co, Fe and Ni from an acidic chloride solution. Refer to Figure 10 and note that Ni(II) is only slightly extracted at 200 g/l chloride ion, Co(II) and Fe(III) are strongly extracted at 150-200 g/l chloride ion and Fe(III) is strongly extracted at 50 g/l chloride ion. As a result, an excellent Co, Ni, and Fe separation can be effected by taking an alloy of the metals into a con-

centrated HCl solution, oxidizing the iron to ferric, co-extracting the Co(II) and Fe(III) while leaving the Ni in the original solution, and then selectively stripping the Co(II) from the Fe(III) with water. This flowsheet has been studied in our laboratory. Several slightly different flowsheets have also been reported<sup>29, 30</sup>. The best flowsheet for this type of feed is dependent upon the relative amounts of Co, Ni and Fe present.

In general, the use of organic phase modifiers, normally polar organic molecules such as long chain alcohols, is required with amines in order to keep the amine metal complexes soluble, prevent third phase formation and/or to have acceptable phase separation.

## D. PRESENT AND POSSIBLE FUTURE USES OF AMINE EXTRACTANTS

One of the best ways to illustrate the value of amines as ion-pair metal extractants is to list the high purity amines commercially available from Cognis Corporation and some of their known uses:

1. Alamine®300 (tri-n-octylamine): cobalt extraction from chloride leach solutions<sup>31</sup>.
2. Alamine®308 (tri-isooctylamine): cobalt-nickel separation from hydrochloric acid liquors<sup>32</sup>.
3. Alamine®336 [tri-(C<sub>8</sub>C<sub>10</sub>)amine]: uranium recovery from sulfuric acid leach liquors<sup>33</sup> or sulfuric acid resin eluate solutions<sup>34, 35</sup>, cobalt-nickel separations from hydrochloric acid<sup>36</sup>, iron extraction from aluminum chloride solutions<sup>37</sup>, vanadium extraction<sup>38</sup>, chromium extraction<sup>39</sup>, platinum group metals separations<sup>40</sup> and tungsten recovery.
4. Alamine®310 (tri-isodecylamine): uranium and vanadium extraction from acidic sulfate leach liquors and platinum group metals separations<sup>40</sup>.
5. Alamine®304 (trilaurylamine): uranium and molybdenum extraction from acidic leach liquors, the advantage being that the molybdenum amine complex is highly soluble.
6. Aliquat®336 [tri-(C<sub>8</sub>C<sub>10</sub>)methylammonium chloride]: vanadium extraction<sup>38</sup>, separation of platinum group metals<sup>40, 41</sup>, rare earth extrac-

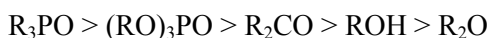
- tions<sup>42</sup>, rhenium recovery<sup>43</sup>, and arsenic extraction from refinery electrolytes<sup>44</sup>.
7. Aliquat®336 Nitrate: the nitrated salt of Aliquat 336, a specialty product for rare earth separations.

Future uses for these types of reagents may lie in the areas of:

- a) reclaiming metals from spent catalysts<sup>45</sup>,
- b) niobium, tantalum, titanium and zirconium separations<sup>46</sup>,
- c) inorganic acid purification<sup>47</sup>,
- d) separation of cobalt, copper and zinc from nickel<sup>48</sup>.

### III. NEUTRAL OR SOLVATING TYPE EXTRACTANTS

A third class of extractants are known as neutral or solvating type extractants. Extractants of this class are basic in nature and will coordinate to certain neutral metal complexes by replacing waters of hydration, thereby causing the resulting organo-metal complex to become aqueous insoluble, but, organic soluble. Solvating extractants have an atom capable of donating electron density to a metal in the formation of an adduct, and are classified according to that ability:



trialkylphosphine oxides > trialkylphosphates > ketones > alcohols > ethers.

It takes little imagination to see that the above list is only a brief representation of the organic compounds which could function as solvating extractants. In general, extractions with solvating extractants are limited by: 1) the metal's ability to form neutral complexes with anions, 2) the co-extraction of acid at high acid concentrations, and 3) the solubility of the organo-metal complex in the organic carrier.

An important extractant of this type is tri-n-octylphosphine oxide (TOPO),  $(\text{C}_8\text{H}_{17})_3\text{PO}$ . The extraction characteristics of TOPO with a wide variety of metals have been investigated<sup>49</sup> and are summarized (Figure 11). The most important commercial application of TOPO in solvent extraction is its synergistic combination with di-2-ethylhexyl-

phosphoric acid (D2EHPA) for the extraction of uranium from wet process phosphoric acid<sup>50, 51</sup>.

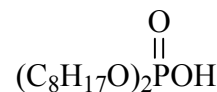
Other important extractants in this class are tributyl-phosphate (TBP), di-butyl butylphosphonate (DBBP) and 2,2'-dibutoxy diethyl ether (trade name dibutyl carbitol).

It is of interest to note that all of the equilibrium and phase modifiers commonly used come from this class of extractants. This is no surprise since both require a group having the ability to donate electron density and in some cases to be a hydrogen bond acceptor and/or donor.

Cognis Corporation does not currently market reagents of this type.

### IV. ORGANIC ACID EXTRACTANTS

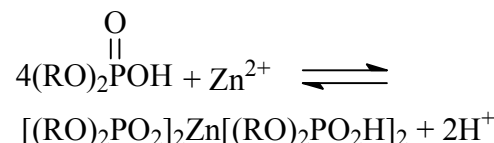
A fourth class of extractant is the so-called acid extractants. The chemistry of this type of extractant has some characteristics which resemble chelating extractants and some which are similar to neutral or solvating extractants. Di-2-ethylhexyl-phosphoric acid (D2EHPA), shown below, is representative of this class of extractant.



Di-2-ethylhexylphosphoric acid (D2EHPA)

Reagents which belong to this class are the organophosphoric, -phosphonic and -phosphinic acids, their respective mono- and di-thio derivatives, organosulfonic acids and carboxylic acids.

The following equation shows the dual behavioral characteristics:



Note that two of the D2EHPA molecules lose a proton much like a chelating extractant while two other D2EHPA molecules solvate the zinc similar to solvating type extractants. The pH extraction char-

acteristics of D2EHPA with respect to several metals is shown in Figure 12.

One of the more interesting characteristics of the extraction behavior of non thio acid extractants is their strong affinity for iron(III) over other base metals. This is unfortunate since it limits the use of these reagents for two reasons:

1. Insufficient selectivity for most base metal systems,
2. Iron is so strongly extracted that stripping the iron can be a problem.

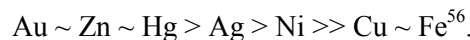
In spite of these limitations the acid extractants have found some actual and proposed use for metal recovery. D2EHPA has been used for the recovery of uranium<sup>3, 52</sup>, vanadium<sup>3, 52</sup>, and zinc<sup>53</sup>. All three types of acidic organo-phosphorous compounds have been used for the selective extraction of cobalt over nickel<sup>54, 55</sup>. There are remarkable selectivity differences for cobalt over nickel between certain types of these compounds resulting from very interesting and subtle chemical and steric differences.

## Reagents in Development, Gold

At the time this edition of the Red Book was published, development work on several new extraction reagents and/or metal recovery processes was taking place in our laboratories. A brief discussion about one of these developments follows. Inquiries from interested parties about the progress of these developments are invited.

### GOLD EXTRACTION

Cognis is developing a reagent for the extraction of gold from typical cyanide leach solutions which can be stripped with an aqueous solution of 2-4 w/v% NaOH and .5 w/v% of NaCN. The selectivity of this reagent for metal cyanide complexes has the following order:



The recovery of gold from clarified cyanide leach solutions may offer certain advantages over existing gold recovery processes, particularly:

1. Where very high gold recovery is needed or,
2. In the case of leach solutions carrying either high levels of copper or organic compounds which foul carbon.

In addition, the gold inventory carried in the SX-EW recovery process is less than that in typical carbon in column or Merrill Crowe recovery processes.

The functionality is also available as a solid ion exchange resin called Aurix® 100<sup>57</sup>. This resin has shown excellent gold extraction kinetics and high gold loading in laboratory and pilot plant tests. It has also been shown to be resistant to breakage in typical resin in leach or resin in pulp applications. Aurix 100 may show significant advantage over activated carbon for gold extraction from preg robbing pulps or from bio-leach liquors which foul carbon.

## SOLVENT EXTRACTION DILUENTS

The discussion to this point has been centered around the reagents used for metal extraction, yet, in many commercial SX plants the diluent used as a carrier for both the reagent and the reagent metal complexes is present in far larger amounts than the reagent. Furthermore, the diluent can alter both the chemical and physical properties of an SX system. Given this, a brief discussion on diluents is appropriate.

In many cases, the role of the diluent on the chemistry of the system is minor, and the choice of diluent is made simply on economics and on the diluents physical properties such as phase separation, flash point and the solubility of the reagent and the reagent metal complexes. It is fortunate that with many of the large SX systems, for example, the copper-oxime system, the above holds true. In other cases, where the diluent has a major role in the chemistry of the system, the choice of diluent depends on both chemical and physical properties. In either case, efforts to choose a proper diluent, and to monitor the quality of continuing supplies of the diluent, is important. These efforts must be included as part of any good laboratory evaluation program.

It should be noted that in this discussion, the function of the diluent is assumed to be separated from that of the modifier. In real systems this is not a valid assumption, but, solvent-modifier interactions are complex and for reasons of brevity this topic will not be discussed.

## CONCLUSION

The potential of solvent extraction is well documented by the wide variety of metal containing solutions, which are amenable to recovery, purification, and concentration, by solvent extraction. However, much work in both reagent synthesis and process development remains. Cognis plans to continue as an industry leader in this field via its vigorous research and development program. This program includes close working relationships with existing and potential customers in a joint effort to solve problems of common interest in metals recovery. Efforts in the area of technical service to existing

and potential customers have made a significant contribution to our overall success in solvent extraction. Cognis realizes it does not have all the answers nor it is aware of all the problems. But, Cognis firmly believes that by cooperating with the customer we can become aware of, and help find solutions to, many of these problems. Cognis' 40 years of experience in solvent extraction is an important asset to our problem solving ability.

*Information provided in this technical literature is believed to be accurate. However, Cognis assumes no liability and makes no warranty or representation that the information is correct or complete. Final determination of suitability of any material and issues of patent infringement are the sole responsibility of the user who alone knows the conditions of intended use.*



Figure 1. Generalized Metal Recovery Flowsheet Incorporating Solvent Extraction

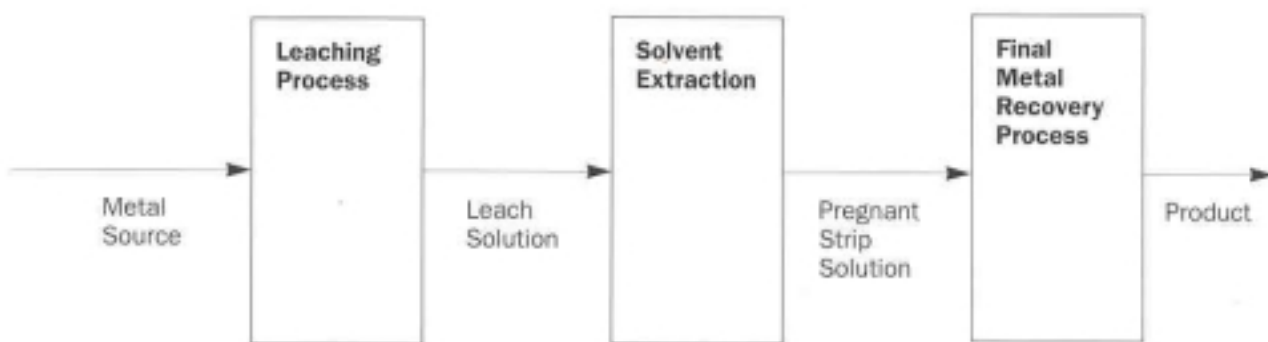
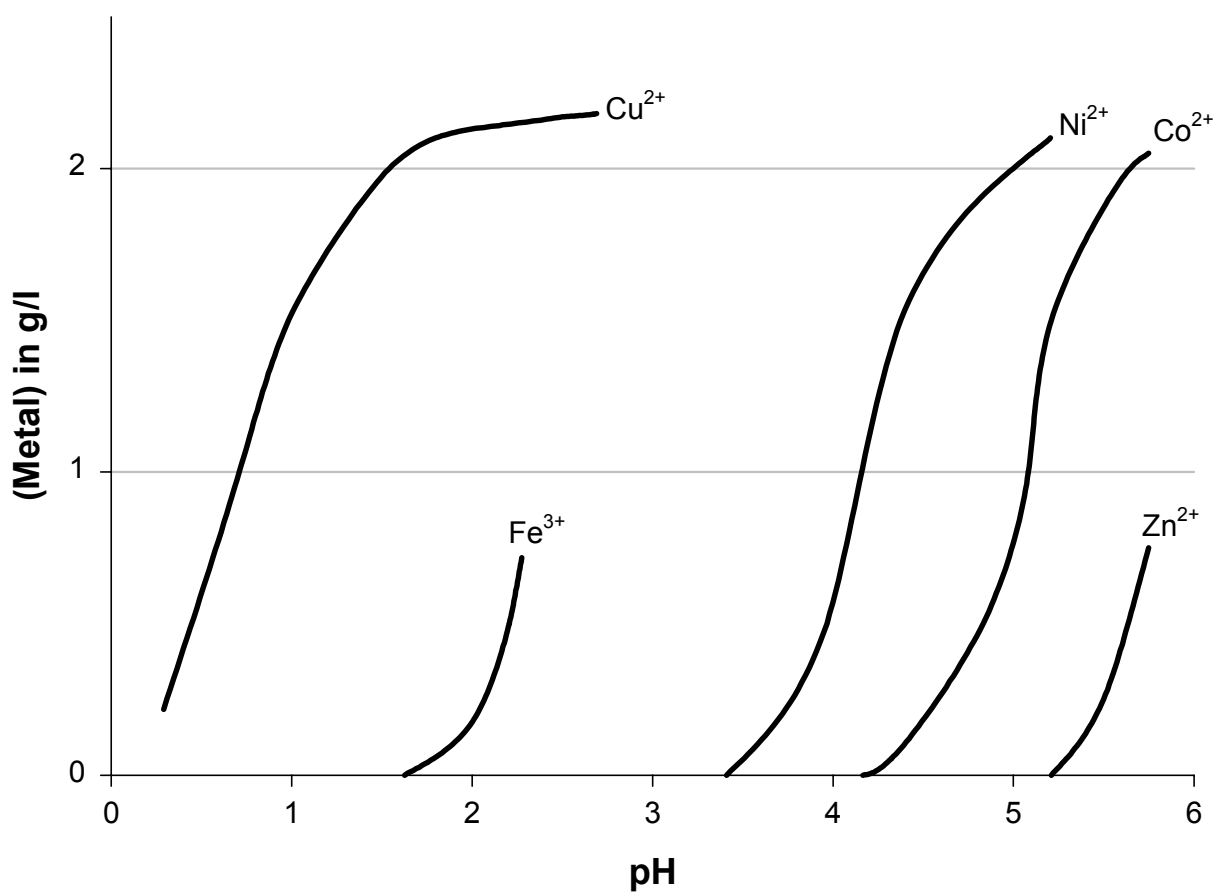


Figure 3. Some pH Isotherms for LIX® 84-I



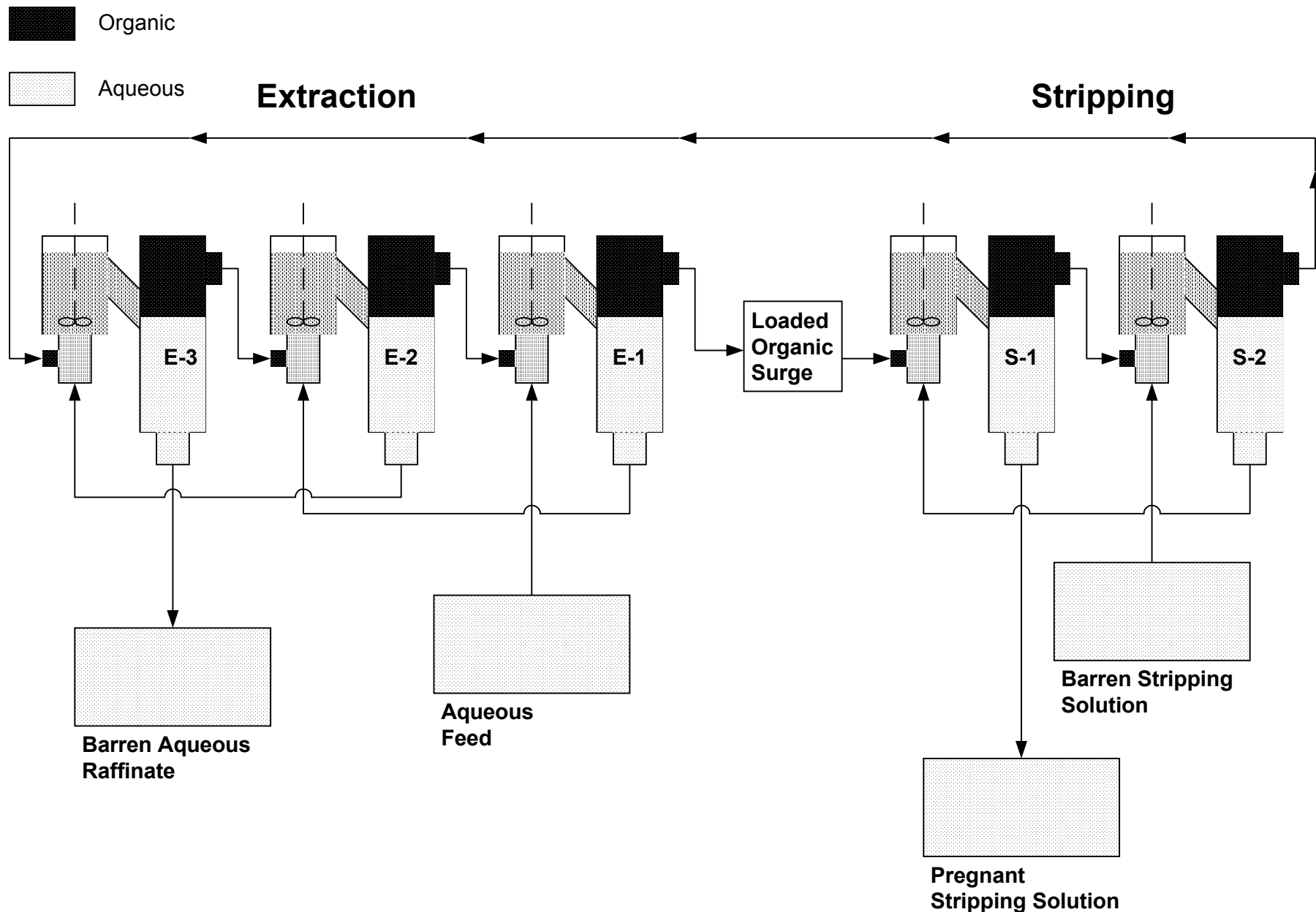
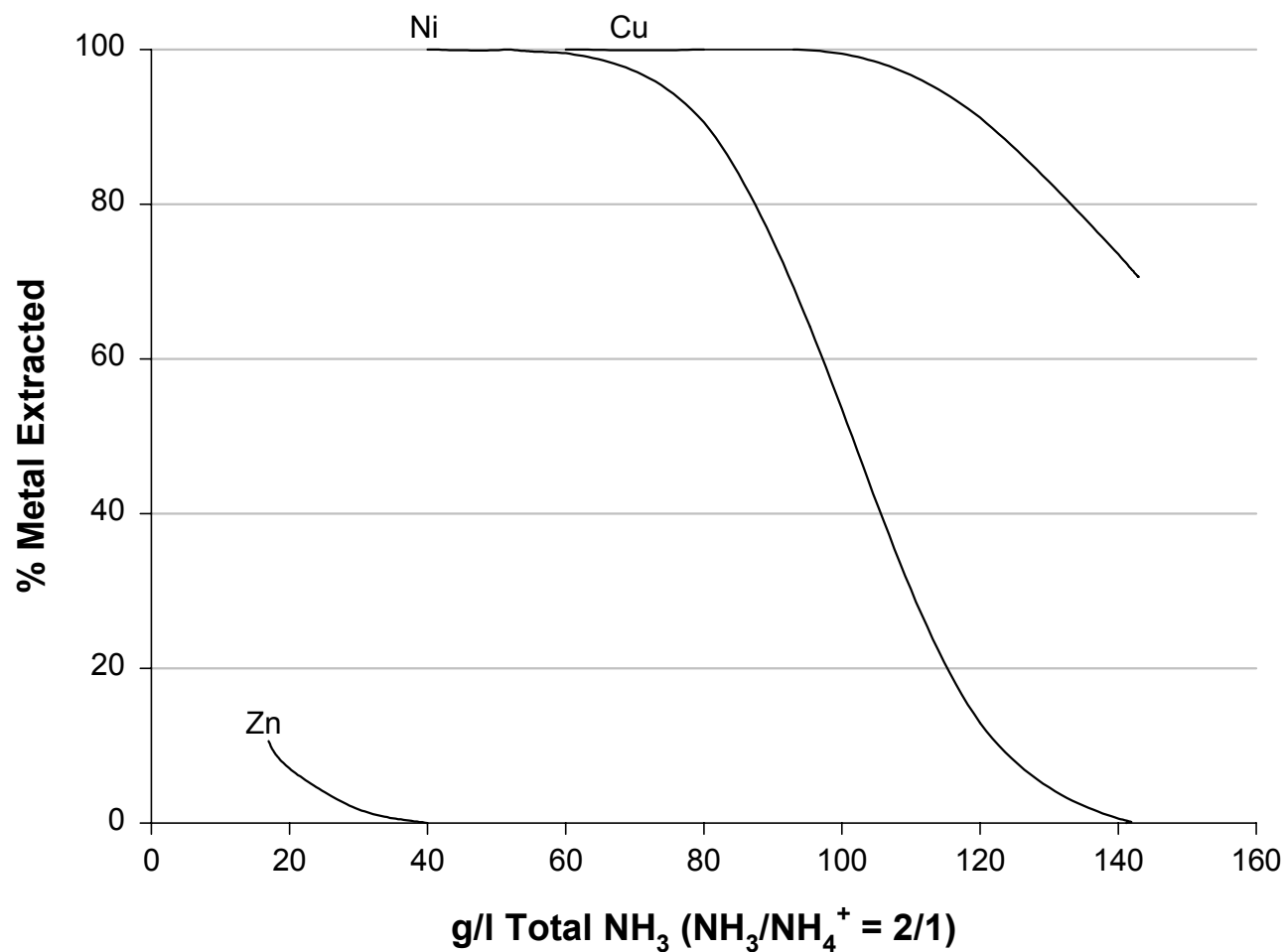


Figure 2. Continuous Liquid Ion Exchange Unit

**Figure 4. Some NH<sub>3</sub> Isotherms for LIX® 84**



**Figure 5. Equilibrium Extraction Isotherm**

Organic: 8.7 v/v% LIX<sup>®</sup> 984 in Escaid 110  
Aqueous: 2.50 g/l Cu, 1.30 g/l Fe (total), pH=1.80

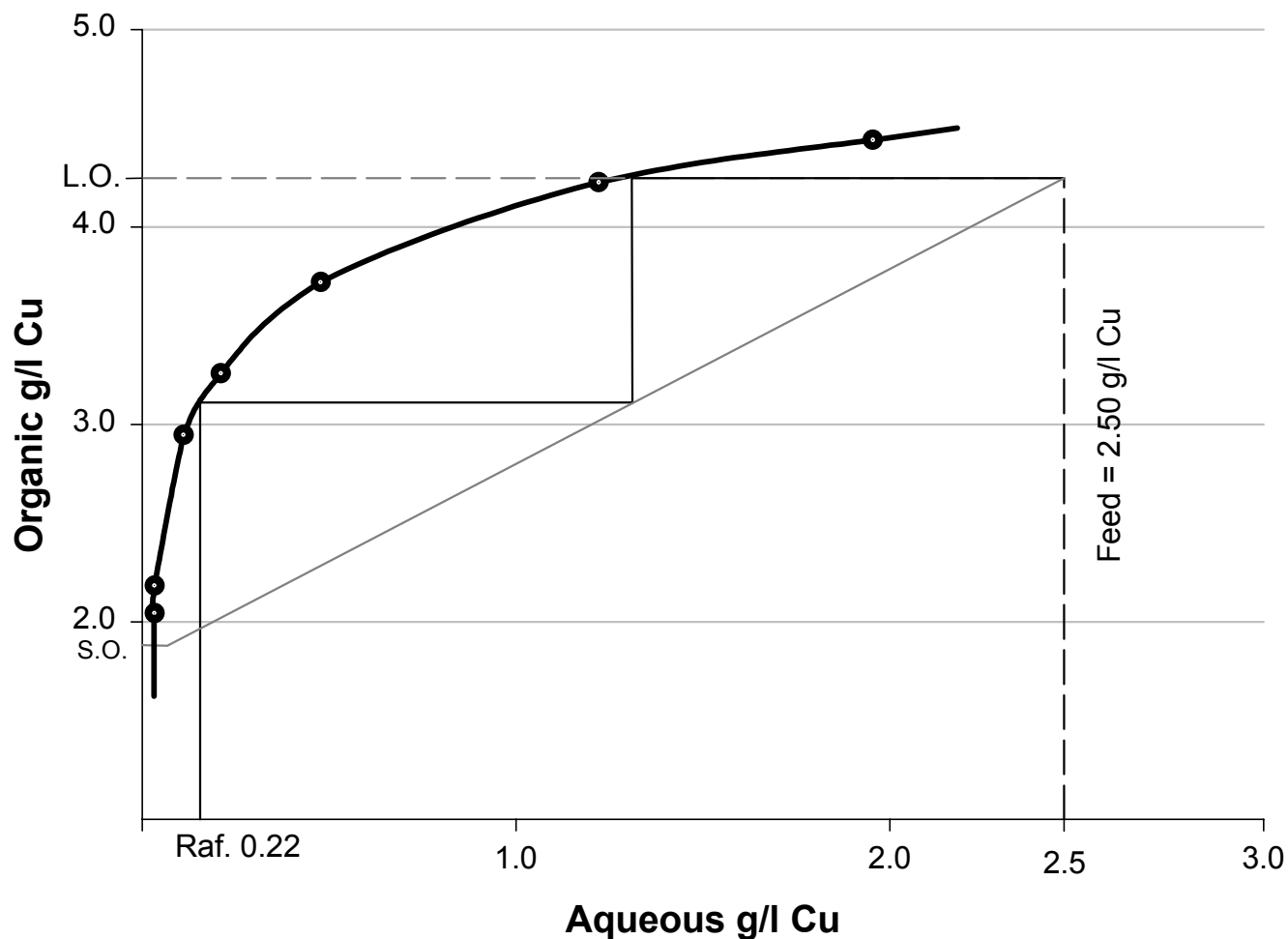


**Figure 6. Equilibrium Strip Isotherm**

Organic: 8.7 v/v% LIX® 984 in Escaid 110  
Aqueous: 30.7 g/l Cu, 170 g/l H<sub>2</sub>SO<sub>4</sub>

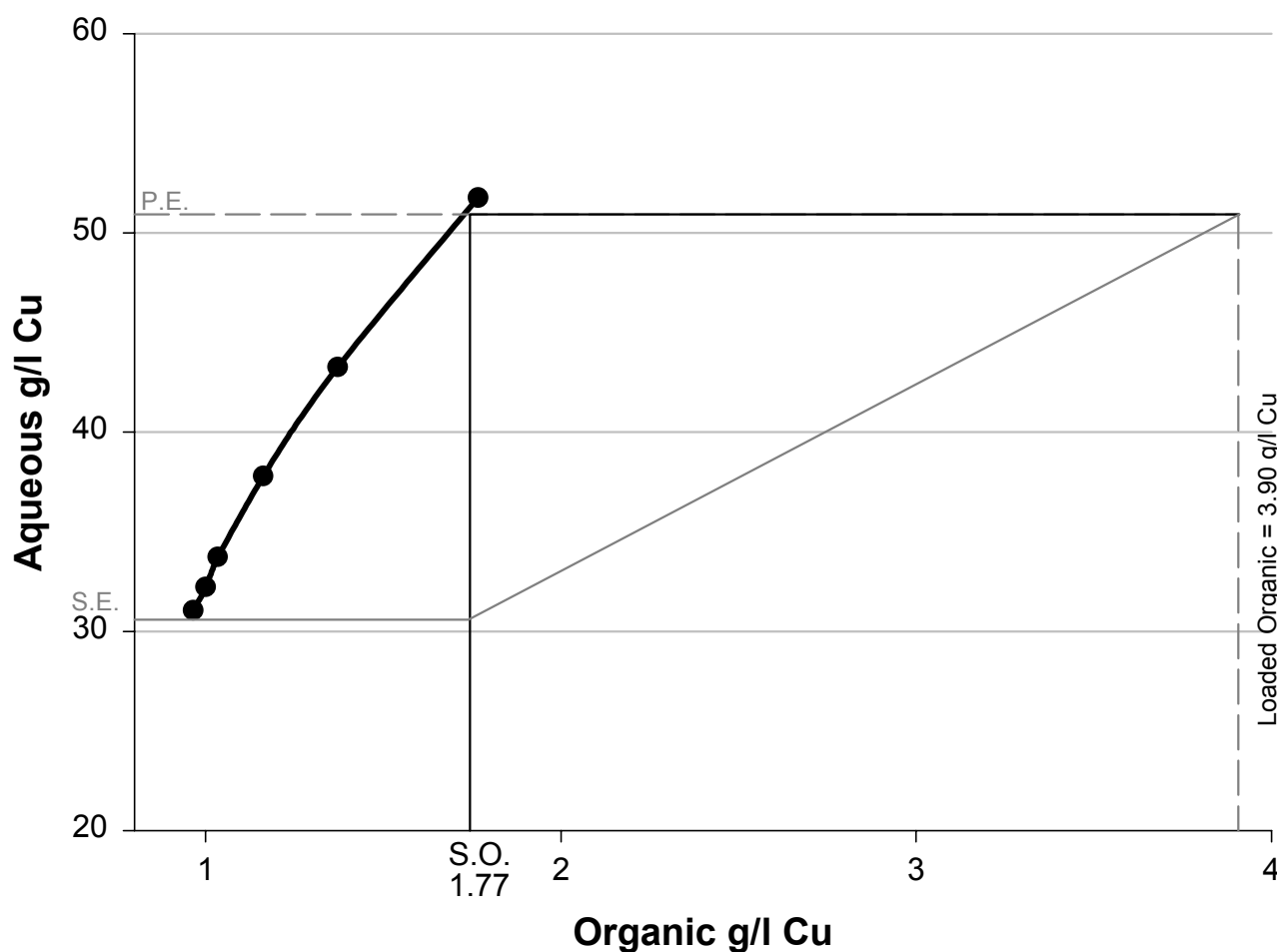


**Figure 7. Circuit Extraction Isotherm**

Organic: 8.7 v/v% LIX® 984 in Escaid 110

Aqueous: 2.50 g/l Cu, 1.30 g/l Fe (total), pH=1.80

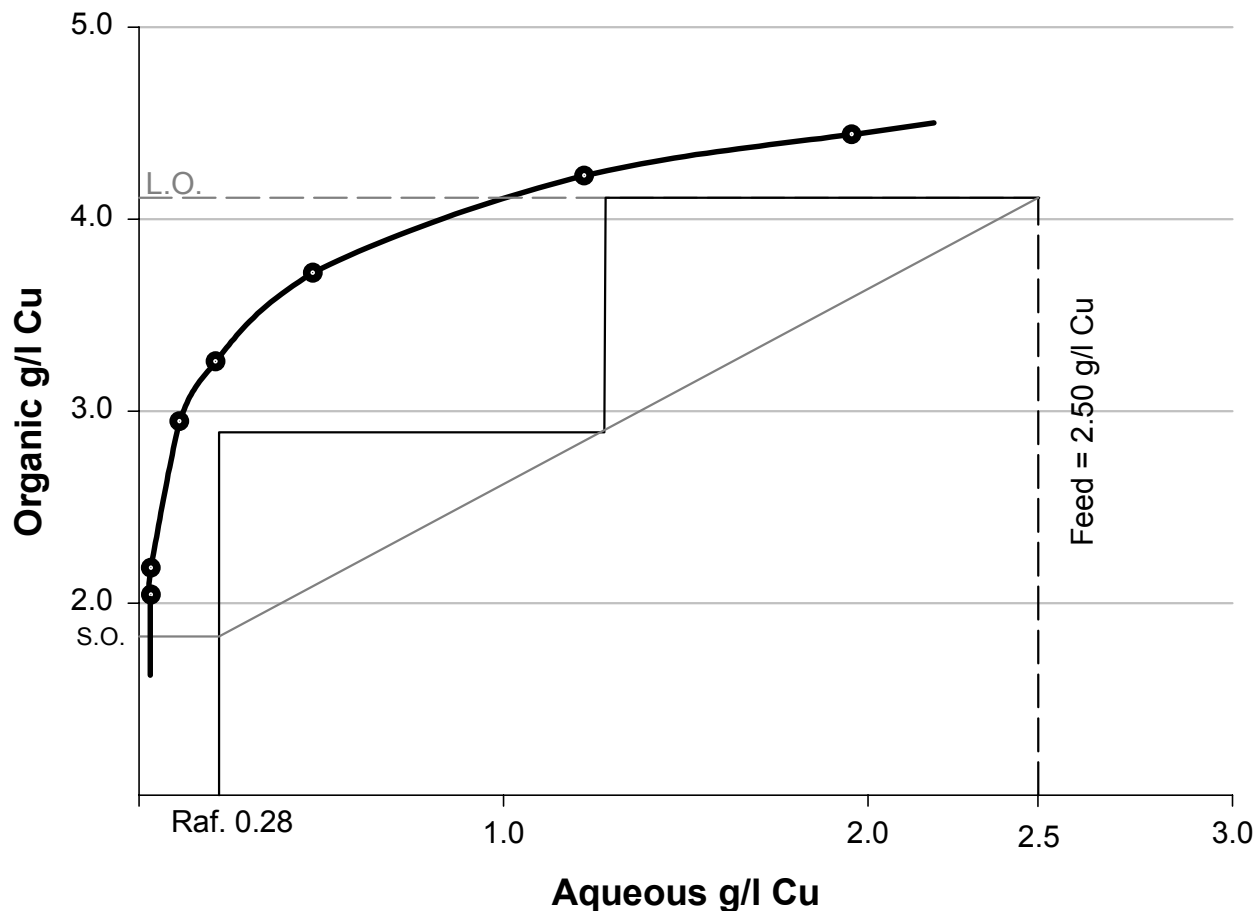


**Figure 8. General Chemical Structure of the Hydroxy Oximes  
Used Commercially for Copper Recovery**

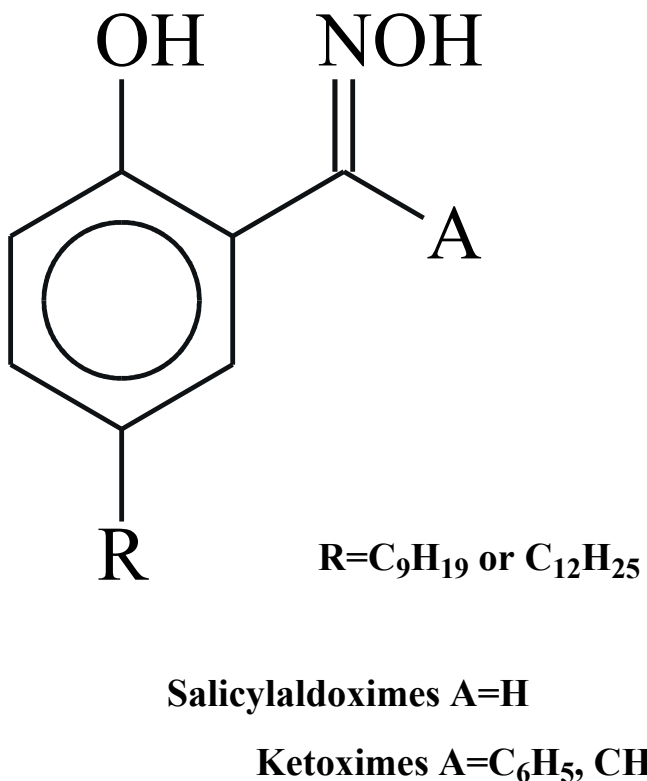


**Figure 9. Tertiary High Molecular Weight Amine Extraction of the Elements (a)**

Blocked elements are strongly extracted by one contact with .1M amine from the acid systems shown below:

Key

## Element Valence System

a) Taken from "Standard Methods of Chemical Analysis," volume II A, Sixth Edition, page 190. Van Nostrand Reinhold Company, 1963.

**Figure 10. Alamine 336 Extraction Isotherms from Chloride Solutions at 40°C and pH=2**

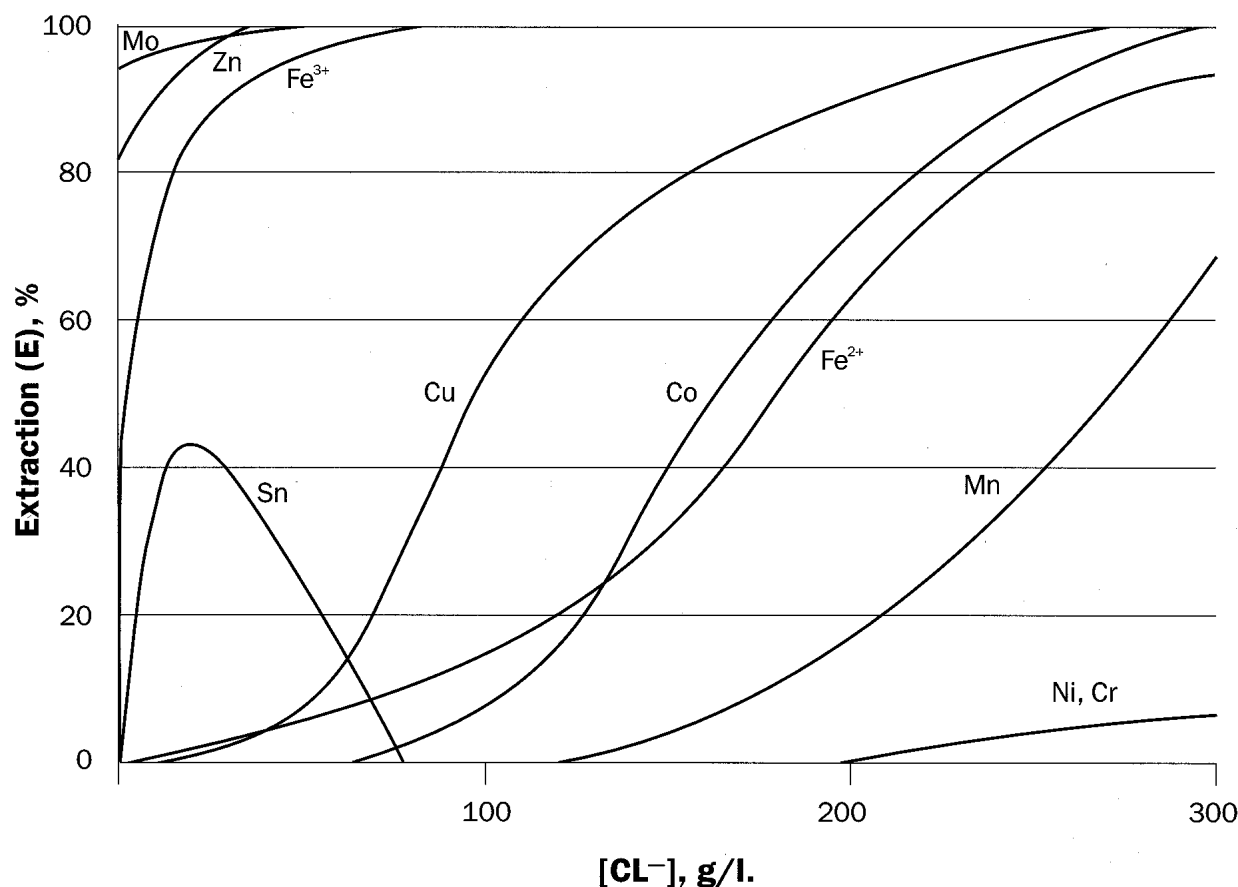
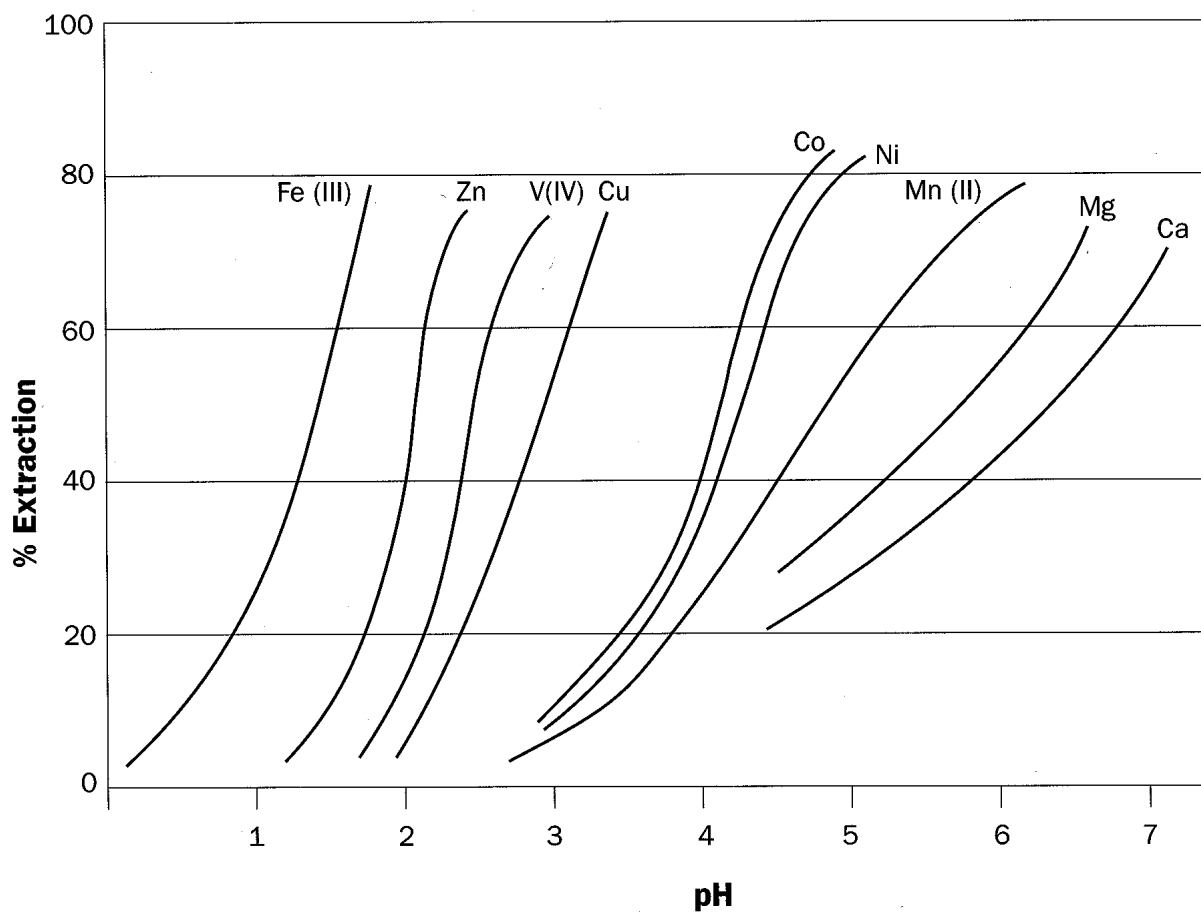


**Figure 11. Tri-n-Octylphosphine Oxide (TOPO) Extraction of the Elements<sup>(a)</sup>**

(a) Taken from "Standard Methods of Chemical Analysis," Volume II A, Sixth Edition, page 192. Van Nostrand Reinhold Company, 1963.

**Figure 12. Extraction of Metals by D2EHPA from Sulfate Solutions**



## References

- <sup>1</sup> Peligot, E., Ann. Chim. Phys., (3), Vol. 5, 1 (1842).
- <sup>2</sup> Morrison G., and Freiser, H, Solvent Extraction in Analytical Chemistry, John Wiley and Sons, Inc., New York, 1957.
- <sup>3</sup> Ross, A. M., "Solvent Extraction Newcomer to the Colorado Plateau", AIME Annual Meeting, New Orleans, Louisiana, February 27, 1957.
- <sup>4</sup> Power, K. L., "Operation of the First Commercial Copper Liquid Ion Exchange and Electrowinning Plant", AIME Annual Meeting, New York, New York, February, 1970.
- <sup>5</sup> Thorsen, G., and Monhemius, A. J., "Precipitation of Metal Oxides by Hydrolytic Stripping of Loaded Cation Exchangers in Solvent Extraction", AIME Annual Meeting, New Orleans, Louisiana, February 12, 1979.
- <sup>6</sup> Demopoulos, G., and Distin, P A., "Production of Copper Powder by Reaction Between Hydrogen and Loaded Extractants", AIME Annual Meeting, Las Vegas, Nevada, February 24-28, 1980.
- <sup>7</sup> De, A. K., Khopkar, S. M., and Chalmers, R. A., "Solvent Extraction of Metals," Van Nostrand, London, (1970).
- <sup>8</sup> "New Recovery Process Can Yield Both Electrolytic Nickel and Copper", Engineering and Mining Journal, January 1972, p. 94-95.
- <sup>9</sup> Merigold, C. R. and Suderth, R. B., "Recovery of Nickel by Liquid Ion Exchange Technology", AIME Annual Meeting, Chicago, Illinois, February 25-March 2, 1973.
- <sup>10</sup> Agarwal, J. C.; Beecher, N.; Hubred, G. L.; Natwig, D. L.; and Skarbo, R. R., "Metal Separation by Fluid Ion Exchange in the Processing of Ocean Nodules", AIME Annual Meeting, Las Vegas, Nevada, February 22-26, 1976.
- <sup>11</sup> Kordosky, G. A.; Champion, W. H.; Dolegowski, J. R. and Olafson, S. M., "The Use of pH Control in Solvent Extraction Circuits", AIME Annual Meeting, New Orleans, Louisiana, February 19-23, 1979.
- <sup>12</sup> Agers, D. W. and DeMent, E. R., "The Evaluation of New LIX® Reagents for the Extraction of Copper and Suggestions for the Design of Commercial Mixer-Settler Plants", AIME Annual Meeting, San Francisco, Calif. 1972 TMS Paper Selection A72-87.
- <sup>13</sup> Holmes, J. A.; Deuchar, A. D.; Stewart, L. N.; and Parker, J. D., "Design, Construction and Commissioning of the N'Changa Tailings Leach Plant", International Symposium on Copper Extraction and Refining AIME Annual Meeting, Las Vegas, Nevada, February 22-26, 1976.
- <sup>14</sup> Jones, R. L., "Cyprus Bagdad's LIX® Complex", SME Fall Meeting, Salt Lake City, Utah, September 10-12, 1975.
- <sup>15</sup> U.S. Patent 4,507,268; March 26, 1985  
U.S. Patent 4,544,532; October 1, 1985.
- <sup>16</sup> Kordosky, G. A.; Sierakoski, J. M.; and House, J. E., "The LIX®860 Series: Unmodified Copper Extraction Reagents", Proceedings of the International Solvent Extraction Conference (1983), Denver, Colorado, August 26-September 2, 1983.
- <sup>17</sup> "In Clean-Air Copper Production, Arbiter Process is First Off the Mark", E/MJ, February 1973, p. 74-75.
- <sup>18</sup> Hopkin, W.; Hunter, W. H.; Nakade, K.; Asaro, A.; and Kobayashi, S., "The Copper Recovery Plants of Commonwealth Smelting Limited and Mitsui Mining and Smelting Co. Limited", Hydrometallurgy: Research, Development, and Plant Practice, Proceedings 3rd International Symposium on Hydrometallurgy, K. Osseo-Asare and J. D. Miller, Ed., pp. 985-999, 1983.
- <sup>19</sup> Preliminary report "LIX®54 - A New Reagent for Metal Extractions From Ammoniacal Solutions", 1975. Available from Cognis Corporation, Tucson, AZ.
- <sup>20</sup> U.S. Patent 3,883,634; May 13, 1975  
U.S. Patent 4,432,952; February 21, 1984  
U.S. Patent 4,915,919; April 10, 1990.
- <sup>21</sup> Suderth, R. B.; and Jensen, W. H., "Utilization of LIX®63 in Some Liquid Ion Exchange Systems", CIMM, 1976 General Meeting, Montreal, Quebec, Canada, April 21-25, 1974.
- <sup>22</sup> U.S. Patent 4,081,865, "Solvent Extraction Process for Recovery and Separation of Metal Values", April 19, 1977.
- <sup>23</sup> Osseo-Asare, K.; Leaver, H. S.; Davis, P. K.; and Laferty, J. M., "Extraction of Nickel and Cobalt from Acidic Solutions Using LIX®63-DNNS Mixtures", AIME Annual Meeting, Denver, Colorado, Feb. 26-March 2, 1978.
- <sup>24</sup> British Patent 1,470,046, "Process for Liquid-Liquid Extraction of Cobalt", April 14, 1977.

- <sup>25</sup> Merigold, C. R.; Agers, D. W.; and House, J. E., "LIX®64N The Recovery of Copper from Ammoniacal Leach Solutions", Solvent Extraction, Soc. Chem. Ind., London (1971), pp. 1351-1355.
- <sup>26</sup> Price, M. J. and Reid, J. G., "Queensland Nickel to Commission New Nickel Solvent Extraction Plant", Tech/News, A Publication of the Mining Chemicals Technology Division of Cognis Corporation, September, 1988.
- <sup>27</sup> U.S. Patent 4,563,256, "Solvent Extraction Process for Recovery of Zinc", Jan. 7, 1986.
- <sup>28</sup> *Standard Methods of Chemical Analysis*, Vol. II A, Sixth Edition, p. 185, Van Nostrand Reinhold Company, New York, New York.
- <sup>29</sup> Brooks, P. T.; and Rosenbaum, J. B., Rep Invest. U.S. Bureau of Mines, 1969, No. 7316.
- <sup>30</sup> Ave, A.; Skjutare, L.; BJORLING, G.; Reinhardt, H.; and Rydberg, J., "Separation of Iron, Cobalt and Nickel from Scrap Alloy by Solvent Extraction", Proceedings of the International Solvent Extraction Conference (1971) Hague, Netherlands, April 18-24, 1971.
- <sup>31</sup> Monhemius, A. J. and Burkin, A. R., "Extraction of Cobalt by Tri-n-octylamine from Chloride Leach Solutions Containing Other Anions", AIME Annual Meeting, Washington, D.C., Feb. 16-20, 1969.
- <sup>32</sup> Magner, J. E., "Cobalt-Nickel Separation by Solvent Extraction", AIME Annual Meeting, New York, Feb. 15-18, 1960.
- <sup>33</sup> Tunley, T. H. and Faure, A., "The Purlex Process", AIME Annual Meeting, Washington, D.C., Feb. 16-20, 1969.
- <sup>34</sup> Faure, A. and Tunley, T. H., "Uranium Recovery by Liquid-Liquid Extraction in South Africa", Int. Atomic Energy Symposium, San Paulo, Brazil, August, 1970.
- <sup>35</sup> Cross, R., "A Note on Solvent Extraction of Uranium at Harmony Gold Mine", J. of South African Inst. of Min. and Met., Nov. 1968, (196-201).
- <sup>36</sup> Baggott, E. R., Fletcher, A. W., and Kirkwood, T. A. W., "Recovery of Valuable Metals from Nickel-Cobalt Alloy Scrap", Ninth Commonwealth Mining and Metallurgical Congress, London, 1969.
- <sup>37</sup> Eiseke, J. A.; Schultze, L. E.; Berinati, D. J.; and Bauer, B. J., "Amine Extraction of Iron from Aluminum Chloride Leach Liquors," USBM RI 8188, 1976.
- <sup>38</sup> Agers, D. W.; Drobnick, J. L.; and Lewis, C. J.; "The Recovery of Vanadium from Acidic Solutions by Liquid Ion Exchange", AIME Annual Meeting, New York, February 18-22, 1962 and references therein.
- <sup>39</sup> "Chromium", Technical Bulletin CDS 1-61, Henkel Corporation.
- <sup>40</sup> British Patent 1,418,391; December 17, 1975  
U.S. Patent 3,979,207; September 7, 1976  
U.S. Patent 4,105,442; August 8, 1978.
- <sup>41</sup> U.S. Patent 4,012,481; March 15, 1977  
U.S. Patent 4,107,261; August 15, 1978.
- <sup>42</sup> U.S. Patent 3,323,857; June 6, 1967.
- <sup>43</sup> U.S. Patent 3,244,475; April 1, 1966  
U.S. Patent 4,185,078; January 22, 1980.
- <sup>44</sup> U.S. Patent 4,115,512, "Method for Removing Arsenic from Copper and/or Nickel Bearing Aqueous Solution by Solvent Extraction," Sept. 19, 1978.
- <sup>45</sup> Millsap, W. A. and Reisler, N., "Cotter's New Plant Diets on Spent Catalysts", E/MJ, May, 1978, pp. 105-107.
- <sup>46</sup> Merrill, C. C. and Couch, D. E., "Separation of Columbium Tantalum, Titanium, and Zirconium from Titanium Chlorination Residues", U. S. Bureau of Mines, RPI 7671, 1972.
- <sup>47</sup> Agers, D. W.; House, J. E.; Drobnick, J. L.; and Lewis, C. J., "The Purification of Inorganic Acids by the Amine Liquid Ion Exchange Process", AIME Annual Meeting Dallas, Texas, February, 1963.
- <sup>48</sup> O'Neill, C. E.; Ettel, V. A.; Oliver, A. J.; and Itzkovitch, I. J., "Purification of Nickel-Containing Process Streams by Aliquat®336 Thiocyanate", CIM Conference of Metallurgists, August 22-26, 1976, Ottawa, Ontario, Canada.
- <sup>49</sup> White, J. C. and Ross, W. J., "Separation by Solvent Extraction with Tri-n-octylphosphine Oxide", 1961.  
Available from Office of Technical Services, Department of Commerce, Washington, D.C.
- <sup>50</sup> Hurst, F. J.; Crouse, D. J.; and Brown, K.B., "Recovery of Uranium from Wet-Process Phosphoric Acid", Ind. Eng. Chem. Process Des. Develop., 11(1), 122-128 (1972).

<sup>51</sup> Ross, R. C., "Uranium Recovery from Phosphoric Acid Nears Reality as a Commercial Uranium Source", E/MJ, Dec. 1972, p. 80-85.

<sup>52</sup> Blake, C. A.; Brown, K. B.; and Coleman, D. F., "The Extraction and Recovery of Uranium (and Vanadium) from Acid Sulfate Liquors with Di-2-ethylhexylphosphoric Acid and Some Other Organophosphorous Acids", USAEC Report ORNL-1903, May 13, 1955.

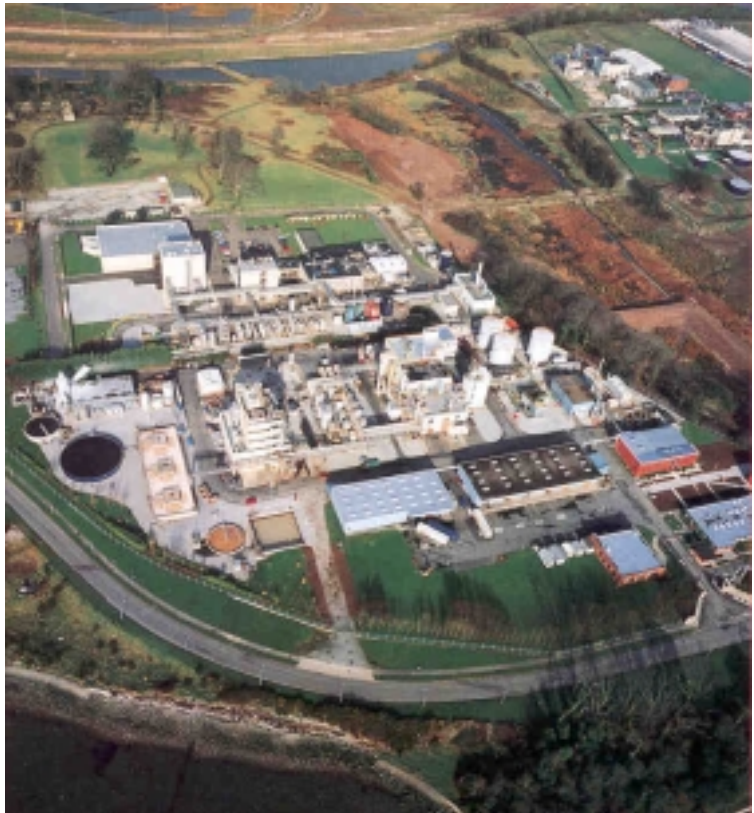
<sup>53</sup> Sudderth, R. B.; Clitheroe, J. B.; and Kordosky, G. A., "The Sulfite System - A New Hydrometallurgical Process for Zinc", AIME Annual Meeting, Denver, Colorado, February 26-March 2, 1978.

<sup>54</sup> Preston, J.S., "Solvent Extraction of Cobalt and Nickel by Organophosphorous Acids I. Comparison of Phosphoric, Phosphonic and Phosphinic Acid System", Hydrometallurgy, 9 (1982) pp. 115-133.

<sup>55</sup> Komasawa, I.; Otake, T. and Ogawa, Y., "The Effect of Diluent in the Liquid-Liquid Extraction of Cobalt and Nickel Using Acidic Organophosphorous Compounds", J. of Chem. Eng. of Japan, 17 (4) 1984, pp. 410-417.

<sup>56</sup> Kordosky, G. A., Sierakoski, J. M., Virnig, M. J. and Mattison, P. L., "Gold Solvent Extraction From Typical Cyanide Leach Solutions", Hydrometallurgy, 30 (1992) 291-305.

<sup>57</sup> Kordosky, G. A., Kotze, M. H., Mackenzie, J. M. W. and Virnig, M. J., "New Solid and Liquid Ion Exchange Extractants for Gold", XVIII International Minerals Processing Congress, Sydney, 23-28 May 1993.

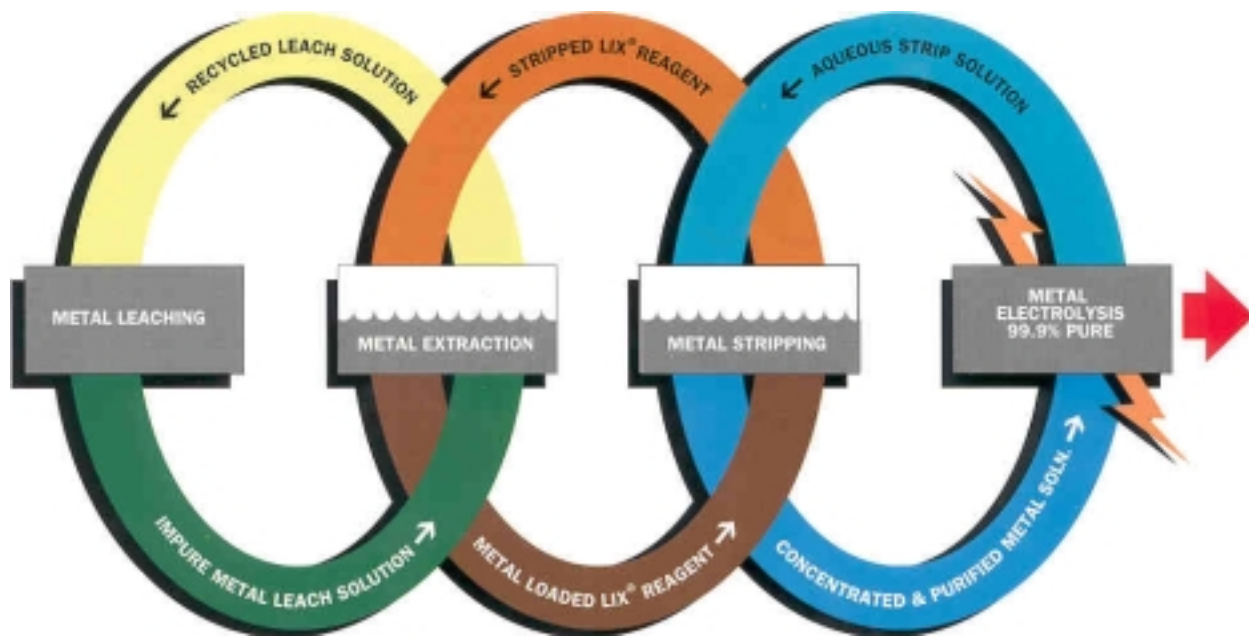


Cognis Mining Chemicals Technology is supported by our parent company, the \$3 billion Cognis GmbH, a specialty chemical company of international importance, headquartered in Roermond, Netherlands. An innovator in applied chemistry, Cognis GmbH is a major producer of industrial chemicals for the worldwide market.

Our Cork Ireland facility, the only certified ISO-9000 SX plant in the world, is also well known for its environmentally friendly products, such as solvent free adhesives and phosphate free detergents as well as a host of other specialty chemicals.

As a member of the Chemical Manufacturers Association, Cognis has been instrumental in the implementation of Responsible Care Initiative, and remains totally committed to the efficient, safe and responsible development of useful products the serve industry and the home.





### Cognis products and technical support will help you

- Yield high quality metals
- Secure more convenient and safer reagent handling
- Reduce reagent consumption
- Produce cleaner circuits
- Generate greater efficiencies
- Build better plant performance and throughput
- Lower cost of production
- Convert "waste ore" to a valuable resource
- Yield greater potential profits

### Solvent Extraction Technical Services

- On-site personnel training
- New plant start-up assistance
- Feasibility studies/design analysis
- Flow sheet analysis
- Monitoring of reagent behavior
- Physical and chemical analysis

**Cognis' development technology provides the world's best selection of efficient solvent extraction reagents for recovery of:**

- Cobalt
- Copper
- Germanium
- Gold
- Molybdenum
- Nickel
- Palladium
- Rhenium
- Silver
- Tungsten
- Uranium
- Vanadium



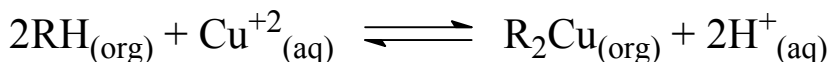
## Cognis Corporation

Mining Chemicals Technology Division

2430 N. Huachuca Drive, Tucson, Arizona 85745-1273; Telephone (520) 622-8891; Fax (520) 624-0912

# **LIX®84-I**

LIX 84-I solvent extraction reagent is water insoluble 2-hydroxy-5-nonylacetophenone oxime in a mixture with a high flash point hydrocarbon diluent. It forms water insoluble complexes with various metallic cations in a manner similar to that for copper which is described in the following equation:



Copper extraction from typical leach solutions is pH dependent. Stripping is accomplished with acid solutions such as a typical barren electrolyte from copper electrowinning.

### **TYPICAL PROPERTIES**

#### **A. Physical Properties:**

Extractant Appearance	Fluid Amber Liquid
Specific Gravity (25°/25°C)	0.90-0.92
Flash Point <sup>1</sup>	Greater than 160°F
Copper Complex Solubility	>30 g/l Cu at 25°C

#### **B. Performance Specifications<sup>2</sup>:**

Maximum Copper Loading	4.7 to 5.0 g/l Cu
Extraction Isotherm Point	≥ 3.65 g/l Cu
Extraction Kinetics	≥ 90% (60 seconds)
Extraction Cu/Fe Selectivity	≥ 2000
Extraction Phase Separation	≤ 60 seconds
Strip Isotherm Point	≤ 0.50 g/l Cu
Net Copper Transfer	≥ 3.30 g/l Cu
Strip Kinetics	≥ 90% (30 seconds)
Strip Phase Separation	≤ 80 seconds

<sup>1</sup>The flash point is determined by Setaflash closed cup.

<sup>2</sup>The performance parameters are determined using the Standard Cognis Quality Control Test dated 6/28/96.

# LIX®860N-I

LIX 860N-I, 5-nonylsalicylaldoxime in a high flash point hydrocarbon diluent, is a very strong copper extractant requiring more than 225 g/l H<sub>2</sub>SO<sub>4</sub> for stripping.

### SUGGESTED USES

LIX 860N-I can be blended with LIX 84-I over a broad range to give copper extraction reagents of variable extractive strength. It extracts copper according to the equation below:



LIX 860N-I will also extract zinc from ammoniacal solutions.

### TYPICAL PROPERTIES

#### A. Physical Properties:

Extractant Appearance	Fluid Amber Liquid
Specific Gravity (25°/25°C)	0.90-0.92
Flash Point <sup>1</sup>	Greater than 160°F
Copper Complex Solubility	>30 g/l Cu at 25°C

#### B. Performance Specifications<sup>2</sup>:

Maximum Copper Loading	5.5 to 5.9 g/l Cu
Extraction Isotherm Point	≥ 5.00 g/l Cu
Extraction Kinetics	≥ 95% (30 seconds)
Extraction Cu/Fe Selectivity	≥ 2500
Extraction Phase Separation	≤ 70 seconds
Strip Isotherm Point	≤ 3.50 g/l Cu
Strip Kinetics	≥ 95% (30 seconds)
Strip Phase Separation	≤ 80 seconds

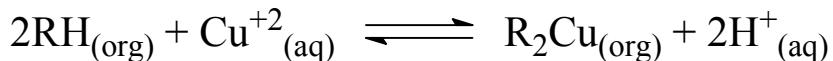
<sup>1</sup>The flash point is determined by Setaflash closed cup.

<sup>2</sup>The performance parameters are determined using the Standard Cognis Quality Control Test dated 6/28/96.



# LIX® 54-100

LIX 54-100 solvent extraction reagent is a water insoluble reagent, which forms hydrocarbon soluble complexes with various metal cations in a manner similar to that shown below for copper:



### TYPICAL USES

LIX 54-100 was designed and is most commonly used for the extraction of copper from aqueous ammonia leach solutions arising from the ammonia leaching of printed circuit boards, copper scrap, copper alloys, copper/lead dross and certain copper sulfide concentrates.

Because of its low viscosity LIX 54-100 can be operated at copper loadings up to about 35 g/l (35 v/v% reagent) resulting in relatively small solvent extraction circuits when compared to oxime copper extractants.

Copper can be stripped from LIX 54-100 with an aqueous solution whose equilibrium copper concentration is high, but, whose equilibrium acid concentration is low. This allows an operator to tailor the pregnant copper strip solution to the specific needs of the final copper recovery operation.

### TYPICAL PROPERTIES

#### A. Physical Properties:

Extractant Appearance	Fluid Amber Liquid
Specific Gravity (25°/25°C)	0.95-0.99
Flash Point <sup>1</sup>	Greater than 200°F
Viscosity @25°C (Kinematic)	10 centipoise
Copper Complex Solubility	≥ 40 g/l Cu

#### B. Performance Specifications<sup>2</sup>:

Maximum Copper Loading	Not less than 100 g/l Cu
Extraction Kinetics	≥ 95% (30 seconds)
Extraction Phase Separation	≤ 120 seconds
Strip Isotherm Point	≤ 0.10 g/l Cu
Strip Kinetics	≥ 90% (30 seconds)
Strip Phase Separation	≤ 90 seconds

<sup>1</sup>The flash point is determined by Setaflash closed cup.

<sup>2</sup>The performance parameters are determined using the Standard Cognis LIX 54 Quality Control Test dated 6/03/93.



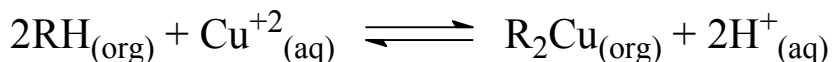
Cognis Corporation • 2430 North Huachuca Drive • Tucson, Arizona USA 85745-1273  
Telephone: (520) 622-8891 • FAX: (520) 624-0912 • Web site: [www.cognis-us.com](http://www.cognis-us.com)

Information provided in this technical literature is believed to be accurate. However, Cognis assumes no liability and makes no warranty or representation that the information is correct or complete. Final determination of suitability of any material and issues of patent infringement are the sole responsibility of the user who alone knows the conditions of intended use.

LIX® is a registered trademark of Cognis Group

# LIX®984N

LIX 984N reagent, a 1:1 volume blend of LIX 860N-I and LIX 84-I, is a mixture of 5-nonylsalicylaldoxime and 2-hydroxy-5-nonylacetophenone oxime in a high flash point hydrocarbon diluent which forms water insoluble complexes with various metallic cations in a manner similar to that shown below for copper:



Because this extractant contains no added modifier it may show advantages when used for copper extraction from solutions containing soluble silica or finely divided solids.

### TYPICAL PROPERTIES

#### A. Physical Properties:

Extractant Appearance	Fluid Amber Liquid
Specific Gravity (25°/25°C)	0.90-0.92
Flash Point <sup>1</sup>	Greater than 160°F
Copper Complex Solubility	>30 g/l Cu at 25°C

#### B. Performance Specifications<sup>2</sup>:

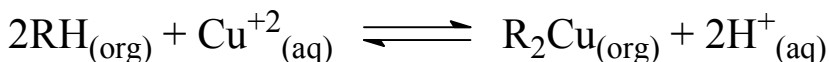
Maximum Copper Loading	5.1 to 5.4 g/l Cu
Extraction Isotherm Point	≥ 4.40 g/l Cu
Extraction Kinetics	≥ 95% (30 seconds)
Extraction Cu/Fe Selectivity	≥ 2000
Extraction Phase Separation	≤ 70 seconds
Strip Isotherm Point	≤ 1.8 g/l Cu
Net Copper Transfer	≥ 2.70 g/l Cu
Strip Kinetics	≥ 95% (30 seconds)
Strip Phase Separation	≤ 80 seconds

<sup>1</sup>The flash point is determined by Setaflash closed cup.

<sup>2</sup>The performance parameters are determined using the Standard Cognis Quality Control Test dated 6/28/96.

# LIX® 622N

LIX 622N solvent extraction reagent, which forms water insoluble complexes with various metallic cations, is a mixture of 5-nonylsalicylaldoxime with tridecanol and a high flash point hydrocarbon diluent. Its extraction-stripping reaction with copper can be described by the following equation:



Copper extraction from typical leach solutions is pH dependent. Stripping is accomplished with relatively strong acid solutions such as a typical barren electrolyte from copper electrowinning.

### TYPICAL PROPERTIES

#### A. Physical Properties:

Extractant Appearance	Fluid Amber Liquid
Specific Gravity (25°/25°C)	0.91-0.93
Flash Point <sup>1</sup>	Greater than 160°F
Copper Complex Solubility	>30 g/l Cu at 25°C

#### B. Performance Specifications<sup>2</sup>:

Maximum Copper Loading	5.5 to 5.9 g/l Cu
Extraction Isotherm Point	≥ 4.70 g/l Cu
Extraction Kinetics	≥ 95% (30 seconds)
Extraction Cu/Fe Selectivity	≥ 2500
Extraction Phase Separation	≤ 70 seconds
Strip Isotherm Point	≤ 2.30 g/l Cu
Net Copper Transfer	≥ 2.70 g/l Cu
Strip Kinetics	≥ 95% (30 seconds)
Strip Phase Separation	≤ 80 seconds

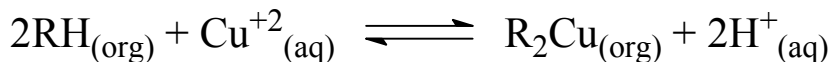
<sup>1</sup>The flash point is determined by Setaflash closed cup.

<sup>2</sup>The performance parameters are determined using the Standard Cognis Quality Control Test dated 6/28/96.



# LIX® 664N

LIX 664N solvent extraction reagent, which forms water insoluble complexes with various metallic cations, is a mixture of 5-nonylsalicylaldoxime with a proprietary ester modifier and a high flash point hydrocarbon diluent. Its extraction-stripping reaction with copper can be described by the following equation:



Copper extraction from typical leach solutions is pH dependent. Stripping is accomplished with relatively strong acid solutions such as a typical barren electrolyte from copper electrowinning.

### TYPICAL PROPERTIES

#### A. Physical Properties:

Extractant Appearance	Fluid Amber Liquid
Specific Gravity (25°/25°C)	0.935 - 0.955
Flash Point <sup>1</sup>	Greater than 160°F
Copper Complex Solubility	>30 g/l Cu at 25°C

#### B. Performance Specifications<sup>2</sup>:

Maximum Copper Loading	5.5 to 5.9 g/l Cu
Extraction Isotherm Point	≥ 4.70 g/l Cu
Extraction Kinetics	≥ 95% (30 seconds)
Extraction Cu/Fe Selectivity	≥ 2500
Extraction Phase Separation	≤ 70 seconds
Strip Isotherm Point	≤ 2.10 g/l Cu
Net Copper Transfer	≥ 2.70 g/l Cu
Strip Kinetics	≥ 95% (30 seconds)
Strip Phase Separation	≤ 80 seconds

<sup>1</sup>The flash point is determined by Setaflash closed cup.

<sup>2</sup>The performance parameters are determined using the Standard Cognis Quality Control Test dated 6/28/96.



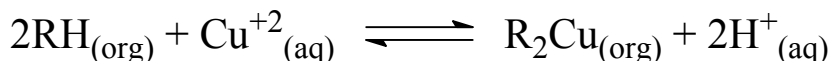
Cognis Corporation • 2430 North Huachuca Drive • Tucson, Arizona USA 85745-1273  
Telephone: (520) 622-8891 • FAX: (520) 624-0912 • Web site: [www.cognis-us.com](http://www.cognis-us.com)

Information provided in this technical literature is believed to be accurate. However, Cognis assumes no liability and makes no warranty or representation that the information is correct or complete. Final determination of suitability of any material and issues of patent infringement are the sole responsibility of the user who alone knows the conditions of intended use.



# LIX® 84-IC

LIX 84-IC solvent extraction reagent is water insoluble 2-hydroxy-5-nonylacetophenone oxime in a mixture with a high flash point hydrocarbon diluent. It forms water insoluble complexes with various metallic cations in a manner similar to that for copper, which is described in the following equation:



Copper extraction from typical leach solutions is pH dependent. Stripping is accomplished with acid solutions such as a typical barren electrolyte from copper electrowinning.

### TYPICAL PROPERTIES

#### A. Physical Properties:

Extractant Appearance	Fluid Amber Liquid
Specific Gravity (25°/25°C)	0.945-0.965
Flash Point <sup>1</sup>	Greater than 170°F
Copper Complex Solubility	>30 g/l Cu at 25°C

#### B. Performance Specifications<sup>2</sup>:

Maximum Copper Loading	4.7 to 5.0 g/l Cu
Extraction Isotherm Point	≥ 3.65 g/l Cu
Extraction Kinetics	≥ 90% (60 seconds)
Extraction Cu/Fe Selectivity	≥ 2000
Extraction Phase Separation	≤ 60 seconds
Strip Isotherm Point	≤ 0.50 g/l Cu
Net Copper Transfer	≥ 3.30 g/l Cu
Strip Kinetics	≥ 90% (30 seconds)
Strip Phase Separation	≤ 80 seconds

<sup>1</sup>The flash point is determined by Setaflash closed cup.

<sup>2</sup>The performance parameters are determined using the Standard Cognis Quality Control Test dated 6/28/96 except the dilution is 7.143 v/v%.

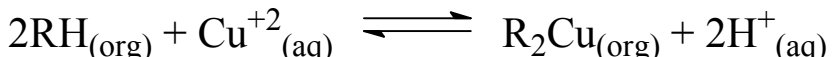


# LIX®860N-IC

LIX 860N-IC, 5-nonylsalicylaldoxime in a high flash point hydrocarbon diluent, is a very strong copper extractant requiring more than 225 g/l H<sub>2</sub>SO<sub>4</sub> for stripping.

### SUGGESTED USES

LIX 860N-IC can be blended with LIX 84-IC over a broad range to give copper extraction reagents of variable extractive strength. It extracts copper according to the equation below:



LIX 860N-IC will also extract zinc from ammoniacal solutions.

### TYPICAL PROPERTIES

#### A. Physical Properties:

Extractant Appearance	Fluid Amber Liquid
Specific Gravity (25°/25°C)	0.945-0.965
Flash Point <sup>1</sup>	Greater than 170°F
Copper Complex Solubility	>30 g/l Cu at 25°C

#### B. Performance Specifications<sup>2</sup>:

Maximum Copper Loading	5.5 to 5.9 g/l Cu
Extraction Isotherm Point	≥ 5.00 g/l Cu
Extraction Kinetics	≥ 95% (30 seconds)
Extraction Cu/Fe Selectivity	≥ 2500
Extraction Phase Separation	≤ 70 seconds
Strip Isotherm Point	≤ 3.50 g/l Cu
Strip Kinetics	≥ 95% (30 seconds)
Strip Phase Separation	≤ 80 seconds

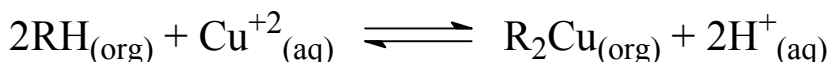
<sup>1</sup>The flash point is determined by Setaflash closed cup.

<sup>2</sup>The performance parameters are determined using the Standard Cognis Quality Control Test dated 6/28/96 except the dilution is 7.143 v/v%.



**LIX®973N**

LIX 973N solvent extraction reagent is a mixture of 5-nonylsalicylaldoxime and 2-hydroxy-5-nonylacetophenone oxime in a high flash point hydrocarbon diluent which forms water insoluble complexes with various metallic cations in a manner similar to that shown below for copper:



Because this extractant contains no added modifier it may show advantages when used for copper extraction from solutions containing soluble silica or finely divided solids.

**TYPICAL PROPERTIES****A. Physical Properties:**

Extractant Appearance	Fluid Amber Liquid
Specific Gravity (25°/25°C)	0.90-0.92
Flash Point <sup>1</sup>	Greater than 160°F
Copper Complex Solubility	>30 g/l Cu at 25°C

**B. Performance Specifications<sup>2</sup>:**

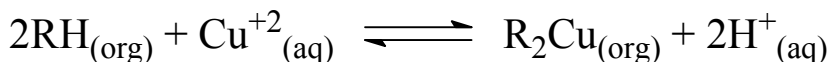
Maximum Copper Loading	5.2 to 5.6 g/l Cu
Extraction Isotherm Point	≥ 4.80 g/l Cu
Extraction Kinetics	≥ 95% (30 seconds)
Extraction Cu/Fe Selectivity	≥ 2300
Extraction Phase Separation	≤ 70 seconds
Strip Isotherm Point	≤ 2.25 g/l Cu
Net Copper Transfer	≥ 2.70 g/l Cu
Strip Kinetics	≥ 95% (30 seconds)
Strip Phase Separation	≤ 80 seconds

<sup>1</sup>The flash point is determined by Setaflash closed cup.

<sup>2</sup>The performance parameters are determined using the Standard Cognis Quality Control Test dated 6/28/96.

# LIX®973N-C

LIX 973N-C solvent extraction reagent is a mixture of 5-nonylsalicylaldoxime and 2-hydroxy-5-nonylacetophenone oxime in a high flash point hydrocarbon diluent which forms water insoluble complexes with various metallic cations in a manner similar to that shown below for copper:



Because this extractant contains no added modifier it may show advantages when used for copper extraction from solutions containing soluble silica or finely divided solids.

### TYPICAL PROPERTIES

#### A. Physical Properties:

Extractant Appearance	Fluid Amber Liquid
Specific Gravity (25°/25°C)	0.945-0.965
Flash Point <sup>1</sup>	Greater than 170°F
Copper Complex Solubility	>30 g/l Cu at 25°C

#### B. Performance Specifications<sup>2</sup>:

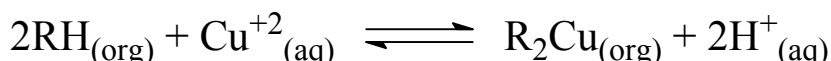
Maximum Copper Loading	5.2 to 5.6 g/l Cu
Extraction Isotherm Point	≥ 4.80 g/l Cu
Extraction Kinetics	≥ 95% (30 seconds)
Extraction Cu/Fe Selectivity	≥ 2300
Extraction Phase Separation	≤ 70 seconds
Strip Isotherm Point	≤ 2.25 g/l Cu
Net Copper Transfer	≥ 2.70 g/l Cu
Strip Kinetics	≥ 95% (30 seconds)
Strip Phase Separation	≤ 80 seconds

<sup>1</sup>The flash point is determined by Setaflash closed cup.

<sup>2</sup>The performance parameters are determined using the Standard Cognis Quality Control Test dated 6/28/96 except the dilution is 7.143 v/v%.

# LIX®984N-C

LIX 984N-C reagent, a 1:1 volume blend of LIX 860N-IC and LIX 84-IC, is a mixture of 5-nonylsalicylaldoxime and 2-hydroxy-5-nonylacetophenone oxime in a high flash point hydrocarbon diluent which forms water insoluble complexes with various metallic cations in a manner similar to that shown below for copper:



Because this extractant contains no added modifier it may show advantages when used for copper extraction from solutions containing soluble silica or finely divided solids.

### TYPICAL PROPERTIES

#### A. Physical Properties:

Extractant Appearance	Fluid Amber Liquid
Specific Gravity (25°/25°C)	0.945-0.965
Flash Point <sup>1</sup>	Greater than 170°F
Copper Complex Solubility	>30 g/l Cu at 25°C

#### B. Performance Specifications<sup>2</sup>:

Maximum Copper Loading	5.1 to 5.4 g/l Cu
Extraction Isotherm Point	≥ 4.40 g/l Cu
Extraction Kinetics	≥ 95% (30 seconds)
Extraction Cu/Fe Selectivity	≥ 2000
Extraction Phase Separation	≤ 70 seconds
Strip Isotherm Point	≤ 1.8 g/l Cu
Net Copper Transfer	≥ 2.70 g/l Cu
Strip Kinetics	≥ 95% (30 seconds)
Strip Phase Separation	≤ 80 seconds

<sup>1</sup>The flash point is determined by Setaflash closed cup.

<sup>2</sup>The performance parameters are determined using the Standard Cognis Quality Control Test dated 6/28/96 except the dilution is 7.143 v/v%.

# **ALAMINE®300**

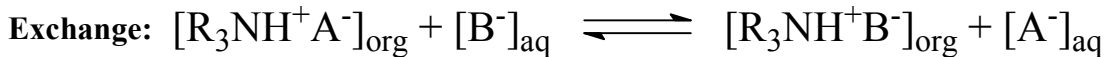
**Alamine 300** is a water insoluble, tri-n-octyl amine which is capable of forming oil soluble salts of anionic species at low pH.

### **APPLICATIONS :**

**Alamine 300** finds use as an agent for producing oil soluble salts of various anions or as a reagent in recovering and/or purifying organic or inorganic species which are capable of forming anions using a process known as solvent extraction.

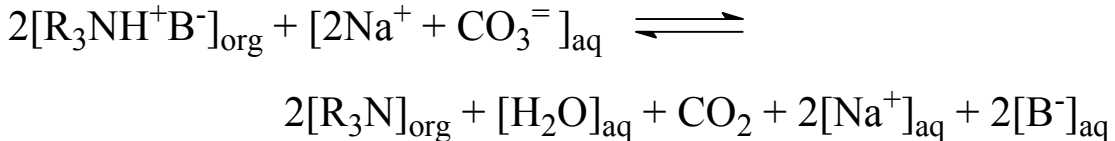
### **CHEMISTRY:**

Since **Alamine 300** contains a basic nitrogen atom, it typically can react with a variety of inorganic and organic acids to form amine salts, which are capable of undergoing ion exchange reactions with a host of other anions. The general reactions are shown below in two steps, protonation and exchange, describe this behavior.



The extent to which  $\text{B}^-$  will exchange for  $\text{A}^-$  is a function of the relative affinity of the two anions for the organic cation and the relative solvation energy of the anions by the aqueous phase.

When used as reagent in solvent extraction, the Alamine® 300 first extracts the target species from an aqueous solution and then must be regenerated ( stripped ) for recovery of the target species and reuse of the reagent. Amine type extractants can be stripped by a wide variety of inorganic salt solutions such as  $\text{NaCl}$ ,  $\text{Na}_2\text{CO}_3$  and  $(\text{NH}_4)_2\text{SO}_4$ . The type of stripping agent used depends on the overall recovery process, but in general basic stripping agents, which reverse the amine protonation reaction, give the best stripping in the fewest stages. The equation below shows the stripping action of  $\text{Na}_2\text{CO}_3$  on the amine salt:



Cognis Corporation • 2430 North Huachuca Drive • Tucson, Arizona USA 85745-1273  
Telephone: (520) 622-8891 • FAX: (520) 624-0912 • Web site: [www.cognis-us.com](http://www.cognis-us.com)

Information provided in this technical literature is believed to be accurate. However, Cognis assumes no liability and makes no warranty or representation that the information is correct or complete. Final determination of suitability of any material and issues of patent infringement are the sole responsibility of the user who alone knows the conditions of intended use.

Alamine® is a registered trademark of Cognis Corporation

In certain cases the formation of anionic complexes, and their subsequent extraction, is dependent upon the concentration of the anion contributing to the anionic complex. Examples include the chloride complexes of copper, cobalt and iron.

### **SUGGESTED USES:**

**Alamine 300** is effective for cobalt extraction from chloride leach solutions. **Alamine 300** is also effective for acetic acid recovery.

### **TYPICAL ANALYSIS:**

% Tertiary Amine Content .....	95.0-100.0
% Secondary Amine Content .....	0.0-5.0
Color (Gardner) .....	1-3
Clarity.....	Clear

### **AVAILABILITY:**

**Alamine 300** is available in bulk, totes (net 1700 pounds) drums (net 360 pounds) and five gallon pails (net 30 pounds), F.O.B. Kankakee, Illinois. Pint samples of **Alamine 300** are also available.

### **SAFETY:**

A Material Safety Data Sheet is available on request.



Cognis Corporation • 2430 North Huachuca Drive • Tucson, Arizona USA 85745-1273  
Telephone: (520) 622-8891 • FAX: (520) 624-0912 • Web site: [www.cognis-us.com](http://www.cognis-us.com)

Information provided in this technical literature is believed to be accurate. However, Cognis assumes no liability and makes no warranty or representation that the information is correct or complete. Final determination of suitability of any material and issues of patent infringement are the sole responsibility of the user who alone knows the conditions of intended use.

Alamine® is a registered trademark of Cognis Corporation

# ALAMINE® 304-1

**Alamine 304-1** is a water insoluble, tri-n-dodecyl amine which is capable of forming oil soluble salts of anionic species at low pH.

## APPLICATIONS :

**Alamine 304-1** finds use as an agent for producing oil soluble salts of various anions or as a reagent in recovering and/or purifying organic or inorganic species which are capable of forming anions using a process known as solvent extraction.

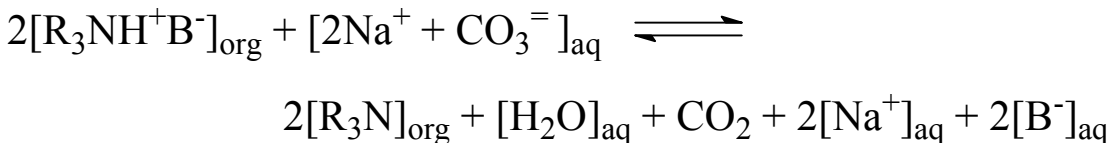
## CHEMISTRY:

Since **Alamine 304-1** contains a basic nitrogen atom, it typically can react with a variety of inorganic and organic acids to form amine salts, which are capable of undergoing ion exchange reactions with a host of other anions. The general reactions are shown below in two steps, protonation and exchange, describe this behavior.



The extent to which  $\text{B}^-$  will exchange for  $\text{A}^-$  is a function of the relative affinity of the two anions for the organic cation and the relative solvation energy of the anions by the aqueous phase.

When used as reagent in solvent extraction, the **Alamine 304-1** first extracts the target species from an aqueous solution and then must be regenerated (stripped) for recovery of the target species and reuse of the reagent. Amine type extractants can be stripped by a wide variety of inorganic salt solutions such as  $\text{NaCl}$ ,  $\text{Na}_2\text{CO}_3$  and  $(\text{NH}_4)_2\text{SO}_4$ . The type of stripping agent used depends on the overall recovery process, but in general basic stripping agents, which reverse the amine protonation reaction, give the best stripping in the fewest stages. The equation below shows the stripping action of  $\text{Na}_2\text{CO}_3$  on the amine salt:



Cognis Corporation • 2430 North Huachuca Drive • Tucson, Arizona USA 85745-1273  
Telephone: (520) 622-8891 • FAX: (520) 624-0912 • Web site: [www.cognis-us.com](http://www.cognis-us.com)

Information provided in this technical literature is believed to be accurate. However, Cognis assumes no liability and makes no warranty or representation that the information is correct or complete. Final determination of suitability of any material and issues of patent infringement are the sole responsibility of the user who alone knows the conditions of intended use.

Alamine® is a registered trademark of Cognis Corporation

In certain cases the formation of anionic complexes, and their subsequent extraction, is dependent upon the concentration of the anion contributing to the anionic complex.

### **SUGGESTED USES:**

**Alamine 304-1** is effective for acetic, citric, lactic and other organic acid recovery.

### **TYPICAL ANALYSIS:**

% Tertiary Amine Content .....	95.0-100.0
% Secondary Amine Content .....	0.0-0.5
Color (Gardner).....	1-3
Clarity.....	Clear

### **CHEMICAL AND PHYSICAL PROPERTIES:**

PROPERTIES		VISCOSITY (cps)		SOLUBILITY (g/100g)		
		4°C	solid	0°C	30°C	60°C
Specific Gravity	0.82					
Surface Tension (dyn.cm@25 C)	57	30°C	36	Benzene	100	100
Pour Point (ASTM)	10°C	60°C	12	Chloroform	100	100
Flash Point (ASTM)	190°C			Isopropanol	1	20
Fire Point(ASTM)	245°C			Hexane	100	100

### **AVAILABILITY:**

**Alamine 304-1** is available in bulk, totes (net 1700 pounds) drums (net 360 pounds) and five gallon pails (net 30 pounds), F.O.B. Kankakee, Illinois. Pint samples of **Alamine 304-1** are also available on request.

### **SAFETY:**

A Material Safety Data Sheet is available on request.



Cognis Corporation • 2430 North Huachuca Drive • Tucson, Arizona USA 85745-1273  
Telephone: (520) 622-8891 • FAX: (520) 624-0912 • Web site: [www.cognis-us.com](http://www.cognis-us.com)

Information provided in this technical literature is believed to be accurate. However, Cognis assumes no liability and makes no warranty or representation that the information is correct or complete. Final determination of suitability of any material and issues of patent infringement are the sole responsibility of the user who alone knows the conditions of intended use.

Alamine® is a registered trademark of Cognis Corporation

# **ALAMINE®308**

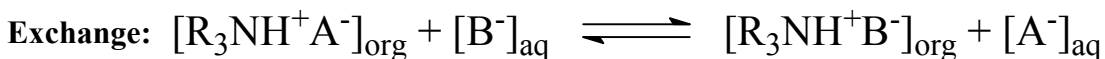
**Alamine 308** is a water insoluble, tri isoctyl amine which is capable of forming oil soluble salts of anionic species at low pH.

### **APPLICATIONS :**

**Alamine 308** finds use as an agent for producing oil soluble salts of various anions or as a reagent in recovering and/or purifying organic or inorganic species which are capable of forming anions using a process known as solvent extraction.

### **CHEMISTRY:**

Since **Alamine 308** contains a basic nitrogen atom, it typically can react with a variety of inorganic and organic acids to form amine salts, which are capable of undergoing ion exchange reactions with a host of other anions. The general reactions are shown below in two steps, protonation and exchange, describe this behavior.



The extent to which  $\text{B}^-$  will exchange for  $\text{A}^-$  is a function of the relative affinity of the two anions for the organic cation and the relative solvation energy of the anions by the aqueous phase.

When used as reagent in solvent extraction, the **Alamine 308** first extracts the target species from an aqueous solution and then must be regenerated (stripped) for recovery of the target species and reuse of the reagent. Amine type extractants can be stripped by a wide variety of inorganic salt solutions such as  $\text{NaCl}$ ,  $\text{Na}_2\text{CO}_3$  and  $(\text{NH}_4)_2\text{SO}_4$ . The type of stripping agent used depends on the overall recovery process, but in general basic stripping agents, which reverse the amine protonation reaction, give the best stripping in the fewest stages. The equation below shows the stripping action of  $\text{Na}_2\text{CO}_3$  on the amine salt:



Cognis Corporation • 2430 North Huachuca Drive • Tucson, Arizona USA 85745-1273  
Telephone: (520) 622-8891 • FAX: (520) 624-0912 • Web site: [www.cognis-us.com](http://www.cognis-us.com)

Information provided in this technical literature is believed to be accurate. However, Cognis assumes no liability and makes no warranty or representation that the information is correct or complete. Final determination of suitability of any material and issues of patent infringement are the sole responsibility of the user who alone knows the conditions of intended use.

Alamine® is a registered trademark of Cognis Corporation

In certain cases the formation of anionic complexes, and their subsequent extraction, is dependent upon the concentration of the anion contributing to the anionic complex. Examples include the chloride complexes of nickel and cobalt.

### **SUGGESTED USES:**

**Alamine 308** is effective for cobalt or nickel extraction from chloride leach solutions.  
**Alamine 308** is also effective for tungsten extraction.

### **TYPICAL ANALYSIS:**

% Tertiary Amine Content .....	95.0-100.0
% Secondary Amine Content .....	0.0-5.0
Color (Gardner).....	1-3
Clarity.....	Clear

### **AVAILABILITY:**

**Alamine 308** is available in bulk, totes (net 1700 pounds) drums (net 360 pounds) and five gallon pails (net 30 pounds), F.O.B. Kankakee, Illinois. Pint samples of **Alamine 308** are also available on request.

### **SAFETY:**

A Material Safety Data Sheet is available on request.



Cognis Corporation • 2430 North Huachuca Drive • Tucson, Arizona USA 85745-1273  
Telephone: (520) 622-8891 • FAX: (520) 624-0912 • Web site: [www.cognis-us.com](http://www.cognis-us.com)

Information provided in this technical literature is believed to be accurate. However, Cognis assumes no liability and makes no warranty or representation that the information is correct or complete. Final determination of suitability of any material and issues of patent infringement are the sole responsibility of the user who alone knows the conditions of intended use.

Alamine® is a registered trademark of Cognis Corporation

# ALAMINE®336

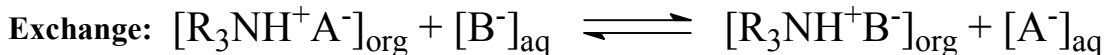
**Alamine 336** is a water insoluble, tri-octyl/decyl amine which is capable of forming oil soluble salts of anionic species at low pH.

## APPLICATIONS :

**Alamine 336** finds use as an agent for producing oil soluble salts of various anions or as a reagent in recovering and/or purifying organic or inorganic species which are capable of forming anions using a process known as solvent extraction.

## CHEMISTRY:

Since **Alamine 336** contains a basic nitrogen atom, it typically can react with a variety of inorganic and organic acids to form amine salts, which are capable of undergoing ion exchange reactions with a host of other anions. The general reactions are shown below in two steps, protonation and exchange, describe this behavior.



The extent to which  $\text{B}^-$  will exchange for  $\text{A}^-$  is a function of the relative affinity of the two anions for the organic cation and the relative solvation energy of the anions by the aqueous phase.

When used as reagent in solvent extraction, the **Alamine 336** first extracts the target species from an aqueous solution and then must be regenerated (stripped) for recovery of the target species and reuse of the reagent. Amine type extractants can be stripped by a wide variety of inorganic salt solutions such as  $\text{NaCl}$ ,  $\text{Na}_2\text{CO}_3$  and  $(\text{NH}_4)_2\text{SO}_4$ . The type of stripping agent used depends on the overall recovery process, but in general basic stripping agents, which reverse the amine protonation reaction, give the best stripping in the fewest stages. The equation below shows the stripping action of  $\text{Na}_2\text{CO}_3$  on the amine salt:



Cognis Corporation • 2430 North Huachuca Drive • Tucson, Arizona USA 85745-1273  
Telephone: (520) 622-8891 • FAX: (520) 624-0912 • Web site: [www.cognis-us.com](http://www.cognis-us.com)

Information provided in this technical literature is believed to be accurate. However, Cognis assumes no liability and makes no warranty or representation that the information is correct or complete. Final determination of suitability of any material and issues of patent infringement are the sole responsibility of the user who alone knows the conditions of intended use.

Alamine® is a registered trademark of Cognis Corporation

In certain cases the formation of anionic complexes, and their subsequent extraction, is dependent upon the concentration of the anion contributing to the anionic complex. Examples include the chloride complexes of copper, cobalt and iron.

### **SUGGESTED USES:**

**Alamine 336** is effective for Cadmium, Cobalt, Hafnium, Iron, Niobium, Rare Earths, Tungsten, Uranium, Vanadium and Zinc extraction. **Alamine 336** is also effective for recovery of organic acid recovery from process and waste streams.

### **TYPICAL ANALYSIS:**

Tertiary Amine Content.....	95.0-100.0%	Secondary Amine Content .....	0.0-5.0%
Color (Gardner).....	1-3	Clarity.....	Clear

### **CHEMICAL AND PHYSICAL PROPERTIES:**

PROPERTIES		SOLUBILITY (g amine/100 g solvent)	
Specific Gravity	0.81	Acetone	13
Surface Tension(dynes.cm@25°C)	53	Water	<5ppm
Pour Point (ASTM)	-54°C	Completely Miscible in:	
Flash Point (ASTM)	179°C	Benzene, Carbon Tetrachloride	
Fire Point(ASTM)	210°C	Chloroform, Cyclohexane	
Viscosity (CPS)	40°C	Diisobutyl Ketone, Ethanol,	
	86°C	#2 Fule oil, isopropanol,	
	140°C	Kerosene, n-Butanol,	
		n-Decanol.	

### **AVAILABILITY:**

**Alamine 336** is available in bulk, totes (net 1700 pounds) drums (net 360 pounds) and five gallon pails (net 30 pounds), F.O.B. Kankakee, Illinois. Pint samples of **Alamine 336** are also available on request.

**SAFETY:** A Material Safety Data Sheet is available on request.



Cognis Corporation • 2430 North Huachuca Drive • Tucson, Arizona USA 85745-1273  
Telephone: (520) 622-8891 • FAX: (520) 624-0912 • Web site: [www.cognis-us.com](http://www.cognis-us.com)

Information provided in this technical literature is believed to be accurate. However, Cognis assumes no liability and makes no warranty or representation that the information is correct or complete. Final determination of suitability of any material and issues of patent infringement are the sole responsibility of the user who alone knows the conditions of intended use.

Alamine® is a registered trademark of Cognis Corporation

# **Aliquat® 336**

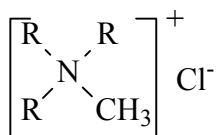
**Aliquat 336** is a water insoluble quaternary ammonium salt made by the methylation of mixed tri octyl/decyl amine, which is capable of forming oil soluble salts of anionic species at neutral or slightly alkaline pH.

### **APPLICATIONS:**

- 1) **Solvent Extraction:** **Aliquat 336** has been used to recover or purify the following ionic complexes: Cadmium, Cobalt, Iron, Molybdenum, the Rare Earths, Tungsten, Uranium, Vanadium and Zinc. **Aliquat 336** has also been used in acid purification.
- 2) **Waste treatment:** **Aliquat 336** has been used successfully to remove and recover acids or their salts or to remove certain heavy metals from wastewater. **Aliquat 336** is also effective in defoaming wastewater containing anionic surfactants.
- 3) **Adhesion promoter and surface curing aid** for fluorocarbon elastomers.
- 4) **Anti-static agent:** for textile fabrics and carpeting.
- 5) **Decolorization and deodorization:** of fermentation broths.

### **Chemistry:**

**Aliquat 336** is composed of a large organic cation associated with a chloride ion, as shown below.



Because the ammonium structure has a permanent positive charge, it can form salts with anions over a wider pH range than primary, secondary or tertiary amines. For this reason, **Aliquat 336** finds application in environments from acid to slightly alkaline pH.

When used as reagent in solvent extraction, the **Aliquat 336** first extracts the target species from an aqueous solution and then must be regenerated (stripped) for recovery of the target species



Cognis Corporation • 2430 North Huachuca Drive • Tucson, Arizona USA 85745-1273  
Telephone: (520) 622-8891 • FAX: (520) 624-0912 • Web site: [www.cognis-us.com](http://www.cognis-us.com)

Information provided in this technical literature is believed to be accurate. However, Cognis assumes no liability and makes no warranty or representation that the information is correct or complete. Final determination of suitability of any material and issues of patent infringement are the sole responsibility of the user who alone knows the conditions of intended use.

Aliquat® is a registered trademark of Cognis Corporation

and reuse of the reagent. Quaternary ammonium extractants are more difficult to strip than amines. Usually the stripping agent must be more strongly attracted to the quaternary than the anion to be stripped. In some cases, stripping can be accomplished by using a large anion, which will crowd off the anion to be stripped. Chloride ions are frequently effective stripping agents. In certain cases the formation of anionic complexes, and their subsequent extraction, is dependent upon the concentration of the anion contributing to the anionic complex. In other cases, the chloride ion in **Aliquat 336** prevents effective extraction. This is because different anions are bound more strongly than others. It may be desirable to exchange the chloride anion to some other anion. (Request bulletin "Converting **Aliquat 336** chloride to hydrogen sulfate")

### **TYPICAL ANALYSIS:**

% Quaternary salt content .....	90	Acid value .....	0-1.0
Amine value .....	1.0-2.0	Color (Gardner) .....	3-6
% Water.....	5	Appearance.....	amber colored, viscous liquid

### **Chemical and Physical Properties**

PROPERTY	PROPERTY				PROPERTY
Average Molecular Weight	442	Viscosity (Brookfield)			Thermal Stability*
Specific Gravity(25°C/25°C)	0.88	4° C	6300cps		Temp
Pour Point (ASTM)	-14°C	30° C	1450cps		4 hours
Flash Point (ASTM)	132°C	60° C	197cps		8 hours
Surface Tension (dynes/cm)	28	Solubility**	0°C	8°C	III°
<b>Interfacial Tension (dynes/cm)</b>			30°C	60°C	IV°
1.0% Nujol Solution	1.6	Benzene	-	100	25° C
0.1% Nujol Solution	3.1	Chloroform	100	100	60° C
0.01% Nujol Solution	20.6	Isopropanol	100	100	100° C
		Kerosene***	100	100	Control
		Water ****	-	0.12	(0 Hour)
				0.2	

\* Stability tests were done by stirring equal volumes of 10w/v% **Aliquat 336** in xylene and 50% aqueous NaOH at elevated temperatures. Samples were titrated for tertiary amine (III°) and quaternary salt (IV°) values.

\*\* (g/100g solvent)

\*\*\* Increasing aromatic content of kerosene results in increased solubility.

\*\*\*\* The distribution of **Aliquat 336** into an aqueous phase from kerosene would be much lower than the solubility of **Aliquat 336** in the aqueous phase.

### **Availability:**

**Aliquat 336** is available in bulk, totes (net 1800 pounds) drums (net 390 pounds) and five-gallon pails (net 30 pounds), F.O.B. Kankakee, IL or Charlotte, NC. Pint samples of **Aliquat 336** are also available.

**Safety:** Material safety data sheet (MSDS) available on request.



Cognis Corporation • 2430 North Huachuca Drive • Tucson, Arizona USA 85745-1273  
Telephone: (520) 622-8891 • FAX: (520) 624-0912 • Web site: [www.cognis-us.com](http://www.cognis-us.com)

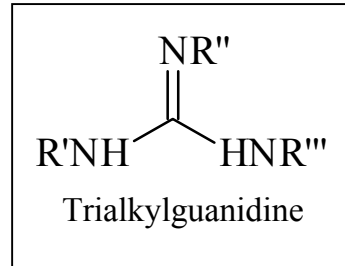
Information provided in this technical literature is believed to be accurate. However, Cognis assumes no liability and makes no warranty or representation that the information is correct or complete. Final determination of suitability of any material and issues of patent infringement are the sole responsibility of the user who alone knows the conditions of intended use.

Aliquat® is a registered trademark of Cognis Corporation

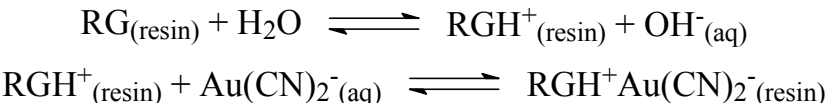
# AuRIX® 100

AuRIX 100 ion exchange resin is based on a styrene di-vinylbenzene based macroreticular resin bead functionalized with guanidine groups.

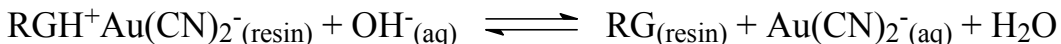
Guanidines are strong organic bases especially suited to the extraction of aurocyanide from typical alkaline cyanide leach liquors. Upon contact with an aqueous solution, the guanidine will extract a proton from water at pH's typically less than 11.5 to form a guanidinium cation, which can then form an ion pair with auro-cyanide resulting in extraction. At pH's above 13, the guanidinium cation gives up its proton to re-form the neutral guanidine group resulting in transfer of the aurocyanide back into the aqueous resulting in stripping. The overall process is described in the following equations:



### Extraction



### Stripping



## TYPICAL PROPERTIES

### A. Physical Properties:

Appearance	Tan Spherical Beads
Resin Bulk Density	
As shipped – wet	620-700 gpl
Dry basis	330 gpl
Moisture Retention (Cl) %	47-53 %
Particle Size (% < 0.60 mm)	0.01

### B. Performance Properties:

Volume Capacity	0.25-0.35 eq/l
Recommended Gold Loading in Extraction	2,000 – 10000 gm/ton
Typical Eluted Resin Values	300 gm/ton Au
Typical Elution Time	12-24 hours
Typical Residence Time per Stage in RIP	15-30 mins



Cognis Corporation • 2430 North Huachuca Drive • Tucson, Arizona USA 85745-1273  
Telephone: (520) 622-8891 • FAX: (520) 624-0912 • Web site: [www.cognis-us.com](http://www.cognis-us.com)

Information provided in this technical literature is believed to be accurate. However, Cognis assumes no liability and makes no warranty or representation that the information is correct or complete. Final determination of suitability of any material and issues of patent infringement are the sole responsibility of the user who alone knows the conditions of intended use.

AuRIX® is a registered trademark of Cognis Group



### Selectivity

While quite selective for gold, AuRIX 100 will extract other anionic metal cyanide complexes. The order of extraction is as follows:



The observed selectivity is to some extent dependent upon the pH of the incoming aqueous feed solution as might be expected for an ion pair extraction type mechanism.

### TYPICAL OPERATING CONDITIONS

AuRIX 100 ion exchange resin is ideally suited for recovery of gold from typical alkaline cyanide leach liquors having a pH of 9.0-11.5. AuRIX 100 is well suited for extraction of gold from clear solutions in the Resin-in-Solution(RIS) process and from pulps in the Resin-in-Pulp(RIP) process. Attrition tests in an Anglo American pump cell contactor have shown that no detectable break down of AuRIX resin beads occurred during the processing of 800 tons of pulp.

The resin is shipped as the hydrochloride form. Before beginning any test work to evaluate the effectiveness of AuRIX 100 on a given leach solution, it is recommended that the resin be first converted to the free base form by two contacts with 1 molar sodium hydroxide (2 volumes of aqueous caustic/volume of resin beads) followed by washing with water until the pH of the wash water is neutral. Resin amounts must be determined on a volume measurement basis. Drying the resin beads in an attempt to obtain a dry weight will result in destruction of the resin upon re-exposure to water.

Stripping is achieved by contacting the loaded resin with a caustic solution containing 0.5M sodium hydroxide, 0.5M sodium benzoate and 100 ppm of sodium cyanide at 55-60°C. The gold values are recovered from the eluent by electrowinning.

For assistance in developing a test program for evaluating the application of AuRIX 100 ion exchange resin to a particular leach solution, please contact your Cognis technical representative.

### TOXICITY

Material Safety Data Sheet available upon request.



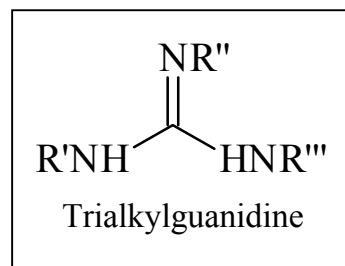
Cognis Corporation • 2430 North Huachuca Drive • Tucson, Arizona USA 85745-1273  
Telephone: (520) 622-8891 • FAX: (520) 624-0912 • Web site: [www.cognis-us.com](http://www.cognis-us.com)

Information provided in this technical literature is believed to be accurate. However, Cognis assumes no liability and makes no warranty or representation that the information is correct or complete. Final determination of suitability of any material and issues of patent infringement are the sole responsibility of the user who alone knows the conditions of intended use.

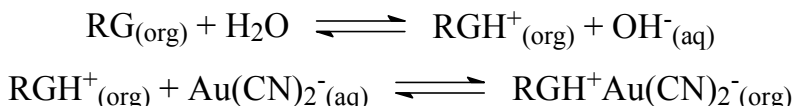
AuRIX® is a registered trademark of Cognis Group

# LIX®79

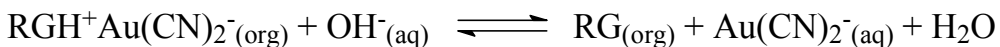
LIX 79 solvent extraction reagent is a water insoluble tri-alkylguanidine in a mixture with a high flash point hydrocarbon diluent. Tri-alkylguanidines are strong organic bases especially suited to the extraction of aurocyanide from typical alkaline cyanide leach liquors. Upon contact with an aqueous solution, the tri-alkylguanidine will extract a proton from water at pH's typically less than 11.5 to form a guanidinium cation, which can then form an organic soluble ion pair with aurocyanide resulting in extraction. At pH's above 13, the guanidinium cation gives up its proton to reform the neutral tri-alkylguanidine resulting in transfer of the aurocyanide back into the aqueous resulting in stripping. The overall process is described in the following equations:



### Extraction



### Stripping



## TYPICAL PROPERTIES

### A. Physical Properties:

Extractant Appearance	Fluid Yellow Liquid
Specific Gravity (25°/25°C)	0.80-0.85
Flash Point <sup>1</sup>	Greater than 155°F
Viscosity (20°C)	4.4 Centistokes
Pour Point	-18°C

### B. Performance Specifications:

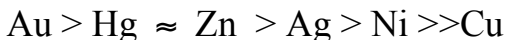
Maximum Au(CN) <sub>2</sub> <sup>-</sup> Loading <sup>2</sup>	410 – 430 mg/l
Extraction Kinetics	≥ 95% (30 seconds)

<sup>1</sup>The flash point is determined by Setaflash closed cup.

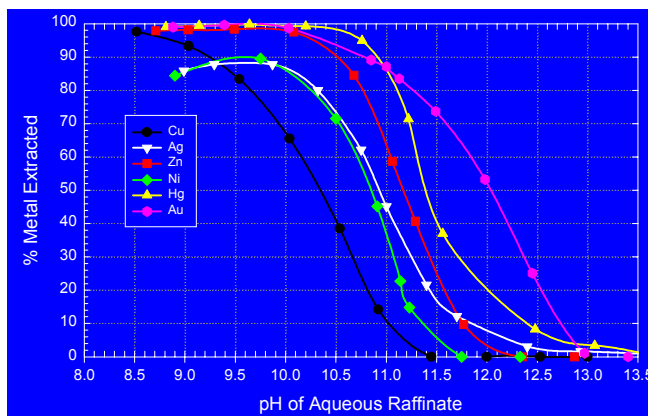
<sup>2</sup>Determined at a reagent concentration of 1.5 v/v% by four repetitive contacts at an O/A of 1/10 of the organic with an aqueous containing 25 ppm of gold as the aurocyanide and 100 ppm of free cyanide as sodium cyanide at a pH = 10.25.

### Selectivity

While quite selective for gold, LIX 79 will extract other anionic metal cyanide complexes. The order of extraction is as follows:



The observed selectivity is to some extent dependent upon the pH of the incoming aqueous feed solution as illustrated by the pH isotherms shown in the figure below:



### TYPICAL OPERATING CONDITIONS

Based on pilot plant experience with actual leach liquors having gold concentrations in the range of 0.65 to 1.3 ppm, it is suggested that initial lab shake out tests be carried out with reagent concentrations in the 10-15%(v/v) range. The reagent should be diluted in a mixture of a typical high quality solvent extraction diluent containing some aromatic character and a highly branched aliphatic alcohol, such as isotridecanol. Best results are typically achieved with an overall concentration of 75 gpl of isotridecanol in the organic phase. When working with diluents having lower levels of aromatic character, it may be necessary to add additional isotridecanol to insure good solubility of the complex in the organic phase.

Stripping is achieved by contacting the loaded organic with a caustic solution containing 0.8-1.0M sodium hydroxide. Depending on the metal values in the strip solution, stripping efficiency begins to fall off at sodium hydroxide concentrations much below 0.8M.

Using 15%(v/v) reagent in a 3Ex2S configuration, raffinates containing less than 0.01 ppm of gold have been achieved with greater than 99% gold recovery from a typical alkaline cyanide heap leach liquor.

**TOXICITY:** Material Safety Data Sheet available upon request.

## CYANEX® Solvent Extractant Database: Description and Documentation

The database of CYANEX solvent extractants contains bibliographic information on all publications from 1967 to the present in which CYANEX SX reagents are discussed. In order to use this database, you must have Microsoft ACCESS\* version 97 or greater. Copy the database file ([SXBIB.mdb](#)) to the ACCESS folder of your PC. Initially the file will be in a "Read Only" format and while you will still be able to search the database and view the results, changes cannot be made. The "Read Only" restriction can be removed as follows: From "Windows Explorer", highlight the database file name, right click and select "Properties" from the drop down menu. In the "General" form, remove the check mark from the "Read Only" box by left clicking on it. Select "Apply" and close the dialogue box.

The data fields consist of the following: Entry Number, Publication Year, Patent Number, Reagent Name, Title, Journal, Author, Patent Assignee, Corporate Source, Country and Abstract. The most useful way to access the data is through the "FORMS", of which, there are ten.

Two of the forms require no user interaction – "All Data" and "All Patents". Opening these forms will list every entry and every entry, which is a patent. All others will require one or two user inputs. The form titles are self-explanatory. For example, "Papers by Author" allows one to search the database for publications by a particular author and "Papers by Reagent" allows one to search for all publications on a particular reagent. "One Abstract Key Word plus Reagent" and "One Title Key Word plus Reagent" allows one to narrow the search somewhat.

When the forms are opened, the user is prompted for the type of entry. Each field has been entered as a string. To avoid not getting any hits, inputs to the prompts should be entered as string segments using "\*" before and after the entry as a multiple character "wild card". For example, there are several papers in the database with William A Rickelton as one or more of the authors. The name is also entered in more than one way. The surest way to retrieve all papers concerning this author is to enter \*Rickelton\*. The only time when it is not necessary to enclose the input with \*'s is when search by publication year.

The SX reagents are entered as CYANEX 272 extractant, CYANEX 301 extractant, etc. However, to retrieve entries for a particular reagent, it is only necessary to use the reagent number bracketed by \*'s. For example, when searching for CYANEX 272 extractant, either \*272\* or \*CYANEX 272\* will achieve the same results.

The one instance in which one **should not** enclose the prompt reply with an "\*" is when searching by "Publication Year" In this case, just enter the year – e.g. 1993 and not "\*1993\*".

The form "Papers by Metal" searches the title strings for the name of the metal supplied by the user input. In some cases, extraneous entries will be retrieved. For example, if the title contains the word "smelting" as well as \*tin\* or "environment" as well as \*iron\*, then those publications will appear as well as those containing "tin" or "iron".

Those users who are proficient in the use of ACCESS\* may modify the forms and associated queries as well as add additional records, provided that you have removed the "Read Only" restriction as indicated above.

While the information included in the database is thought to be reasonably inclusive and accurate, Cytec cannot be responsible for any errors or omissions.

\*product of Microsoft

# CYANEX® 272 Extractant

## Solvent Extraction Reagent

- Selective for cobalt over nickel from sulfate and chloride media.
- Selective for zinc in the presence of calcium and cobalt.
- Extracts other metal cations.

**CYTEC**

# CONTENTS

## INTRODUCTION

Chemical Structure	1
Typical Properties	1
Stability	1
Solubility Losses	2
Toxicity	2
Suitability of Construction Materials	2

## COBALT RECOVERY

Cobalt-Nickel Selectivity	3
Sulfate Solution (Table 1)	3
Chloride Solution (Table 2)	4
Calcium Rejection	4
Cobalt Extraction Isotherm	4
Cobalt Loading	4
Scrubbing Isotherm	5
Stripping Isotherms	
Using H <sub>2</sub> SO <sub>4</sub> (Table 7)	5
Using HCl (Table 8)	5
Continuous Separation of Cobalt from Nickel in Sulfate Solution	5
Effect of process Variables on Cobalt-Nickel Separation Factor	
Effect of Temperature (Table 9)	7
Effect of Equilibrium pH (Table 10)	7
Effect of Diluent Aromaticity (Table 11)	7
Effect of Phase Modifier (Table 12)	7
Diluent Oxidation and Prevention	8
Recovery from Ammoniacal Solutions (Table 13)	8

## OTHER POTENTIAL APPLICATIONS

Extraction from Single Metal Sulfate Solutions (Table 14)	8
---	---

## ANALYTICAL METHODS

In Organic Solvents	10
In Aqueous Solutions	11

## TECHNICAL PAPERS AND PATENTS

Technical Papers	13
Patents	18

## HEALTH AND SAFETY

20
----

# INTRODUCTION

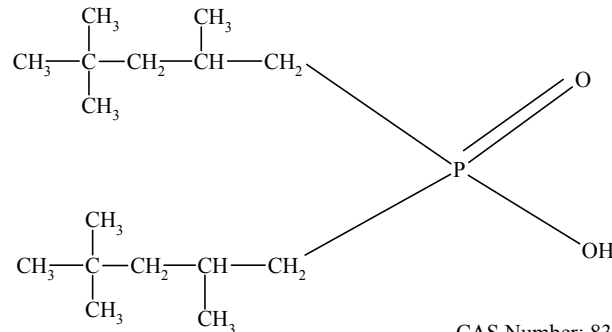
CYANEX® 272 extractant has proven to be the reagent of choice for the separation of cobalt from nickel from both sulfate and chloride media. It is now being used to produce a major portion of the world's cobalt.

Since the active component of CYANEX 272 extractant is a phosphinic acid, metals are extracted through a cation exchange mechanism. Although CYANEX 272 is selective for cobalt in the presence of nickel, a variety of other cations can also be extracted depending upon the solution pH.

CYANEX 272 extractant is totally miscible with common aromatic and aliphatic diluents, and is extremely stable to both heat and hydrolysis.

## Chemical Structure

The active component of CYANEX 272 extractant is bis(2,4,4-trimethylpentyl)phosphinic acid.



CAS Number: 83411-71-6

## Typical Properties

Bis(2,4,4-trimethylpentyl)phosphinic acid :	85%
Appearance	: Colourless to light amber liquid
Specific Gravity at 24°C	: 0.92
Viscosity, Brookfield at 25°C	: 142cp
50°C	: 37cp
Solubility in distilled H <sub>2</sub> O at pH 2.6	: 16 µg/ml
pH 3.7	: 38µg/mL
Boiling Point	: >300°C
Pour Point	: -32°C
Flash Point, closed cup	: >108°C
Specific Heat @ 52°C	: 0.48 cal/gm/°C
Thermal Conductivity	: 2.7 x 10 <sup>-4</sup> cal/cm/sec/°C

## Stability

The hydrolytic stability of CYANEX 272 extractant was examined in several tests which involved equilibrating the reagent with aqueous cobalt-nickel sulfate solutions at pH 5 and 50°C.

The experimental procedure involved contacting the aqueous and organic phases in a stirred vessel for one week and then stripping the organic phase with sulfuric acid. The solvent was subsequently returned to the vessel for a further one week contact with a fresh aqueous solution. The procedure was repeated for a total contact time of four weeks.

Analysis by titration and P<sup>31</sup> NMR failed to detect any degradation of the reagent, nor were any statistically significant changes in cobalt-nickel selectivity observed.

Furthermore, no degradation has been detected in plants which have been operating continuously for as long as ten years.

## Solubility Losses

Losses of CYANEX 272 extractant by distribution to aqueous cobalt-nickel sulfate solutions were determined in a number of shake-out tests. The effect of two variables, pH and aqueous phase salt concentration, was studied.

Aliquots of the organic and aqueous phases were contacted for 5 minutes at 50°C and A/O = 1. After coalescence, the aqueous phases were analyzed for CYANEX 272 extractant using a gas chromatographic procedure. The solvent was composed of 12 v/o CYANEX 272 extractant in Kermac\* 470B diluent. Ammonium hydroxide was used for pH adjustment. The results are given below.

Aqueous Composition (g/l)			Equilibrium pH	CYANEX 272 Extractant Solubility (µg/ml)
Ni	Co	Total Salt Conc.		
100 25	2 25	300 133	3.5	0.5-1.5
			4.6	2
			5.3	2
			6.2	2
5	5	27	4.6	3
			5.5	8
			6.5	25

The solubility losses follow the general pattern expected of an acidic extractant. Distribution to the aqueous phase was found to be proportional to pH and inversely proportional to salt concentration.

As can be seen, the losses are not excessive and this is corroborated by operating plant experience where total annual losses from both solubility and entrainment are approximately 10-15% of the solvent inventory.

## Toxicity

The acute oral (rat) and acute dermal (rabbit) LD50 values for CYANEX 272 extractant are 4.9 g/kg and >2.0 g/kg, respectively. The product produced only limited to mild eye and skin irritation during primary irritation studies with rabbits. The acute LC<sub>50</sub> (96 hr) for the bluegill sunfish and rainbow trout are 46 ppm and 22 ppm, respectively. When CYANEX 272 extractant was assayed for mutagenic potential in the Ames *Salmonella* Test, it was determined to be non-mutagenic.

## Suitability of Construction Materials

**Metals:** Samples of stainless steel (304 and 316), mild steel and aluminum in the form of coupons (approximate dimensions 50mm x 20mm x 3mm) were immersed in capped jars for 8-1/2 months at 50°C (temperature was maintained only during working hours). No corrosion was observed in the three steel samples but aluminum exhibited minimal corrosion at a rate of 1 mil/year.

**Plastics and Rubbers:** Samples of various plastics and rubbers were immersed in CYANEX 272 and kept at 50°C for a total of 424 hours. The following observations were made:

Material	Remarks
Butyl Rubber	Unsuitable. Increase in dimensions and softening.
Teflon fluorocarbon Film**	Suitable. No measured effect.
Polypropylene	Suitable. No measured effect.
Natural and Black Latex	Unsuitable. Complete dissolution in less than 192 hours
PVC Laboratory Grade	Short term suitability. Loss of plasticity in less than 192 hours.
PVC Solvent Grade	Suitable. Only small change in dimensions observed.
Red Gum Rubber	Unsuitable. 100% increase in weight and dimensions and softening.
Viton Fluoroelastomer*	Suitable. No measured effect.
Silicon	Unsuitable. Disintegrated after 56 hours.

\*\* E.I. Dupont de Nemours & Co.

\* A product of Kerr McGee Refining Corp.

# COBALT RECOVERY

## Cobalt-Nickel Selectivity

The results of batch shake-out tests showing the effect of pH on Co-Ni selectivity from both sulfate and chloride media are given in Tables I and 2, respectively.

**TABLE 1 - SULFATE SOLUTION**

Solvent (v/o)	:	12% CYANEX 272 extractant, 5% isodecanol in Kermac 470B diluent
Aqueous (g/l)	:	1.96 Co, 98.0 Ni as sulfates
Temperature	:	50°C
Contact Time	:	5 minutes
A/O	:	1
pH Control	:	NH <sub>4</sub> OH

Co	% Extraction		Equilibrium pH	Separation Factor
	Co	Ni		
21.5	0.04		3.8	700
43.7	0.08		4.2	1000
88.0	0.37		5.3	2000
96.7	1.05		5.7	2700
100	1.81		6.1	

**TABLE 2- CHLORIDE SOLUTION**

Solvent (v/o)	:	10% CYANEX 272 extractant, 5% isodecanol in Kermac 470B diluent
Aqueous (g/l)	:	0.88 Co, 1.76 Ni as chlorides
Temperature	:	50°C
Contact Time	:	5 minutes
A/O	:	1
pH Control	:	NaOH

Co	% Extraction		Equilibrium pH	Separation Factor
	Co	Ni		
2.9	0.1		3.2	40
54.2	0.3		4.0	370
98.1	7.0		5.1	680
99.7	30.0		5.5	680
99.9	72.9		6.2	650

## Calcium Rejection

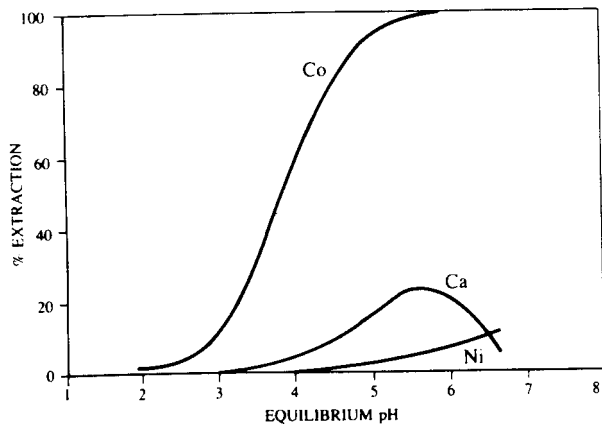
Unlike other organophosphorus cobalt extractants, CYANEX 272 extractant will extract cobalt preferentially to calcium when both are present in the same feed stream. This performance characteristic is demonstrated in Table 3 and Figure 1.

**TABLE 3- CALCIUM REJECTION IN THE PRESENCE OF COBALT AND NICKEL**

Solvent (v/o)	: 15% CYANEX 272 extractant, 10% p-nonylphenol in Kermac 470B diluent
Aqueous (g/l)	: 1.60 Co, 77 Ni, 0.31 Ca as sulfates
Temperature	: 50°C
Contact Time	: 5 minutes
A/O	: 1
pH Control	: NH <sub>4</sub> OH

Co	% Extraction		Equilibrium pH
	Ni	Ca	
3.1	0	0.95	1.99
17.2	0.04	1.24	3.34
54.3	0.17	3.33	3.85
91.7	1.03	12.0	4.84
98.3	3.95	25.7	5.72
100	13.4	5.16	6.63

**FIGURE 1**



## Cobalt Extraction Isotherm

Procedural details and results of our extraction studies are given in Table 4.

**TABLE 4**

Solvent (v/o)	: 12% CYANEX 272 extractant, 5% isodecanol in Kermac 470B diluent.
Aqueous (g/l)	: 5 Co as sulfate
Temperature	: 50°C
Equilibrium pH	: 5.0±0.1
pH Control	: 1N NaOH

A/O	Equilibrium Cobalt Concentration (g/l)	
	Solvent	Aqueous
10	6.32	4.68
5	6.13	4.13
2	5.54	2.58
0.5	2.72	0.06

The actual loading capacity of this solvent was 6 g/l cobalt, whereas the stoichiometric capacity is approximately 10 g/l cobalt.

## Cobalt Loading

Loading studies were carried out at 50°C and pH 6.0 -t 0. 1. The pH was controlled by the addition of ammonia. Other details and results are shown in Table 5.

**TABLE 5**

Solvent (v/o)	: 30% CYANEX 272 extractant in Kermac 470B diluent
Aqueous (g/l)	: 10 Co as sulfate
Theoretical Maximum (g/l)	: Approximately 24
Contact Time	: 5 minutes

A/O	Co in Solvent (g/l)	% of Theoretical Maximum	
		0.5	1.0
0.5	5	21	
1.0	10	42	
1.5	15	63	
3.0	23*	96	
5.0	23*	96	

\*At this loading the solvent was judged to be too viscous for practical use. The 15 g/l solvent did not exhibit this viscosity problem. The maximum practical loading for the conditions cited is probably about 65-75 % of theoretical

It should be noted that the loading capacity of CYANEX 272 extractant will vary depending upon several parameters, notably pH, temperature, and extractant concentration, and may be more or less than the figure cited. For example, with a 15% CYANEX 272 extractant solution at 50°C and pH 5-5 the solvent can be loaded to 100% of the theoretical maximum while remaining sufficiently mobile for practical use.

### Scrubbing Isotherm

As can be seen from the results in Table 6, even if a high quantity of nickel is co-extracted with the cobalt, it can be successfully scrubbed from the loaded solvent.

**TABLE 6**

Solvent (v/o)	: 12% CYANEX 272 extractant, 5% isodecanol in Kermac 470B diluent
Solvent Loading (g/l)	: 1.9 Co, 1.9 Ni
Scrub Feed (g/l)	: 30 Co (as sulfate), initial pH 3.7
Temperature	: 50°C

Equilibrium Concentration in Scrubbed Solvent ( $\mu\text{g/ml}$ )			
O/A	Co	Ni	Co-Ni Ratio
10	3820	4.5	850
5	3790	2.2	1720
2	3740	1.3	2900
1	3730	1.1	3400

### Stripping Isotherms

Stripping from a solvent modified with isodecanol tended to produce hazing. Substituting p-nonylphenol or TBP for the isodecanol essentially eliminated this problem.

Tables 7 and 8 show stripping isotherms obtained with a p-nonylphenol modified solvent.

**TABLE 7 -Using H<sub>2</sub>SO<sub>4</sub>**

Solvent (v/o)	: 12% CYANEX 272 extractant, 10% p-nonylphenol in Kermac 470B diluent
Solvent Loading (g/l)	: 3.26 Co (2 $\mu\text{g/ml}$ Ni)
Temperature	: 40°C
Contact Time	: 5 minutes
Strip Feed (g/l)	: 20.5 Co (as sulfate), 24.5 H <sub>2</sub> SO <sub>4</sub>

O/A	Equilibrium Cobalt Conc. (g/l)	
	Organic	Aqueous
6.67	0.58	38.4
5	0.22	35.7
4	0.19	32.5
3.33	0.03	31.3
2.86	0	29.8
2	0	27.0

**TABLE 8 - USING HCl**

Solvent (v/o)	: 12% CYANEX 272 extractant, 10% p-nonylphenol in Kermac 470B diluent
Solvent Loading (g/l)	: 9.26 Co
Temperature	: 50°C
Contact Time	: 5 minutes
Strip Feed (g/l)	: 19.4 Co (as chloride) 100 HCl

O/A	Equilibrium Cobalt Conc. (g/l)	
	Organic	Aqueous
2	0	37.9
3	0	47.1
5	0	65.7
7.5	0.01	88.8
10	0.35	108.5

### Continuous Separation of Cobalt from Nickel in Sulfate Solution

In continuous countercurrent tests (four extraction and two scrub stages) carried out at Warren Spring Laboratory (Stevenage, U.K.), more than 99.5% of the cobalt in the feed was recovered as a product containing a Co-Ni ratio of greater than 1000 to 1.

The experimental conditions are shown below. A circuit flowsheet and the relevant assays are given in Figure 2.

Solvent (v/o)	: 20% CYANEX 272 extractant (NH <sub>4</sub> salt)*, 10% p-nonylphenol
Aqueous Feed (g/l)	: 2 Co, 100 Ni as sulfates, 20 (NH <sub>4</sub> ) <sub>2</sub> O <sub>4</sub> , pH 5
Scrub Feed (g/l)	: 40 Co as sulfate, pH 3
Temperature	: 50°C
Phase Ratios	: Extraction A/O = 2 Scrubbing O/A = 32
Mixer Residence Time	: 3.5-4 minutes (Based upon total liquid flow)

\*The phosphinic acid contained in the solvent was converted 70% to the ammonium salt by reaction with concentrated ammonium hydroxide solution (S.G. = 0.88). A phase modifier was used since converting more than 50% of the free acid to a salt (NH<sub>4</sub> or Na +) usually requires a modifier to prevent third phase formation.

\*\*A product of Shell Chemical Co.

## Effect of Process Variables on Cobalt-Nickel Separation Factor

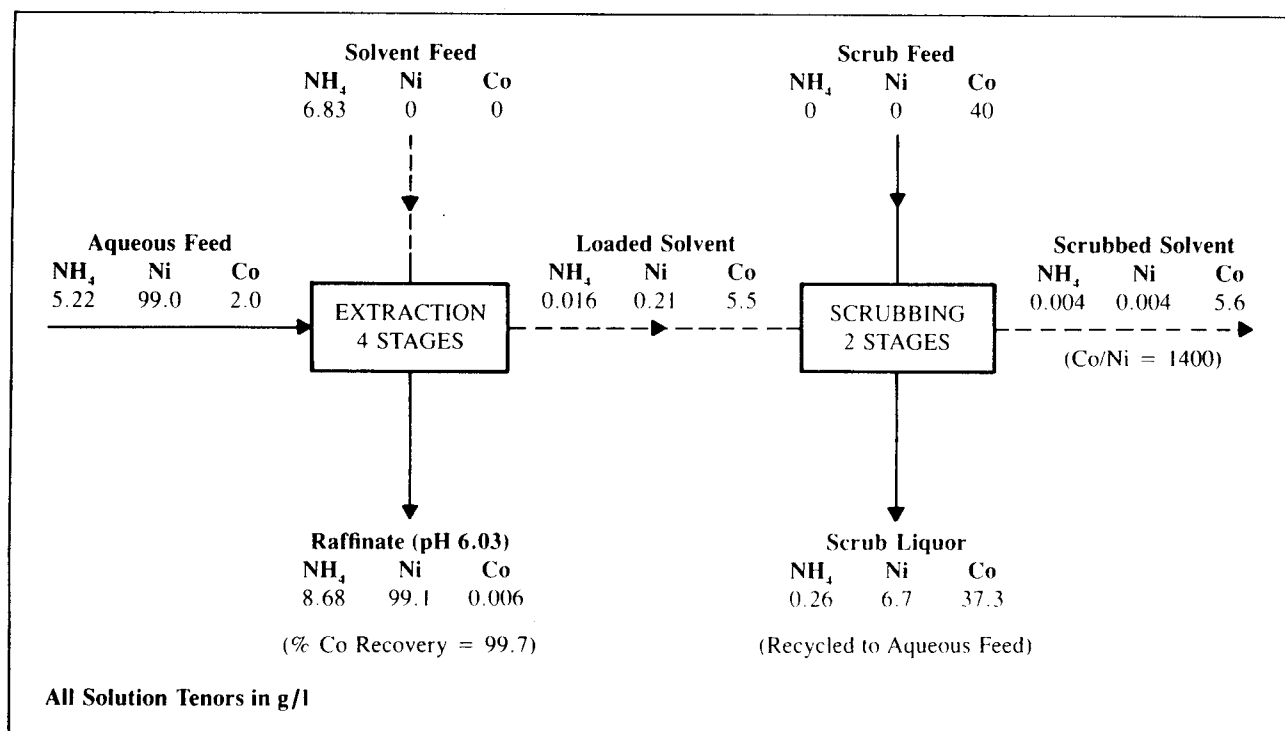
The effect of pH, temperature and diluent aromaticity on the cobalt-nickel separation factor in sulfate solutions was measured in a series of statistically designed tests and the data fitted to the following mathematical model:

$$\log_{10} S = 1.8827 + 0.0332T + 0.01249A + 0.0033PT - 0.002151PA = 0.0003405T^2$$

Where:

S = Co-Ni Separation Factor  
T = Temperature (°C)  
A = % Aromatics in diluent  
P = Equilibrium pH

FIGURE 2—CONTINUOUS TESTING OF CYANEX 272 EXTRACTANT



The effect of these process variables on the separation factor is shown in Tables 9 through 11.

**TABLE 9 - EFFECT OF TEMPERATURE**

Solvent (v/o) :	22% CYANEX 272 extractant in the diluent (95% MSB 210* diluent, 5% Aromatic 150**) diluent).
Aqueous (g/l) :	2 Co, 100 Ni as sulfates
pH :	5.5
A/O :	1

Co-Ni Separation Factor	Temperature °C
1320	30
1850	35
2480	40
3220	45
4000	50
4790	55
5510	60

\* A product of Shell Chemical Co.

\*\*A product of Exxon Co., USA.

**TABLE 10 - EFFECT OF EQUILIBRIUM pH**

Temperature :	50°C
Diluent (v/o) :	95% MSB 210, 5% Aromatic 150
Other Conditions :	See Table 9

Co-Ni Separation Factor	pH
2810	4.5
3010	4.7
3230	4.9
3470	5.1
3730	5.3
4000	5.5

**TABLE 11 -EFFECT OF DILUENT AROMATICITY**

Temperature	:	50°C
Diluent (v/o)	:	100% MSB 210 (aliphatic) to 100% Aromatic 150
pH	:	5.5
Other Conditions	:	See Table 9

Co-Ni Separation Factor	Aromaticity v/o
3970	0
4030	10
4090	20
4160	30
4220	40
4280	50
4350	60
4420	70
4480	80
4550	90
4620	100

The effect of the phase modifiers TBP, p-nonylphenol, isodecanol and TOPO (tri-n-octylphosphine oxide) on the separation factor is shown in Table 12.

**TABLE 12 -EFFECT OF PHASE MODIFIER**

Extractant (v/o)	:	22%
Modifier	:	10 v/o (TBP, isodecanol, p-nonylphenol) 10 w/o TOPO (solid)
Aqueous (g/l)	:	10 Co, 100 Ni as sulfates
A/O	:	1
Temperature	:	55°C
Equilibrium pH	:	5.5
Contact Time	:	5 minutes
Diluent	:	MSB 210

Co-Ni Separation Factor	Modifier
6700	None
3400	TBP
1800	p-Nonylphenol
1000	Isodecanol
1000	TOPO

# OTHER POTENTIAL APPLICATIONS

## Diluent Oxidation and Prevention

Hydrocarbon diluents oxidize readily to carboxylic acids in the presence of a cobalt ( $\text{Co}^{2+}$ ) catalyst. The formation of carboxylic acids, which are active nickel extractants, can seriously reduce the cobalt-nickel selectivity obtained with CYANEX 272 extractant. However, inhibitors such as BHT can be used to prevent this oxidation. Plants following this practice have run for many years without loss of selectivity.

## Recovery from Ammoniacal Solutions

CYANEX 272 can be used to recover cobalt from ammoniacal as well as acidic solutions. The data in Table 13 show that it outperforms other organophosphorus extractants.

**TABLE 13 - EXTRACTION FROM AMMONIACAL SOLUTIONS**

Solvent (v/o)	:	20% extractant, 5% isodecanol in Kermac 470B diluent
Aqueous (g/L)	:	0.97 $\text{Co}^{3+}$ , 0.95 $\text{Ni}^{2+}$ , $(\text{NH}_4)_2\text{O}_4$ for a total $\text{SO}_4^{2-}$ concentration of 16
Temperature	:	50°C
pH Control	:	11.6 with $\text{NH}_4\text{OH}$
Contact Time	:	5 minutes
A/O	:	1
Extractant	% Extracted	Co/Ni Separation Factor
	Co	Ni
CYANEX 272	91.5	15.6
PC-88A	91.4	22.0
D2EHPA	90.4	46.9

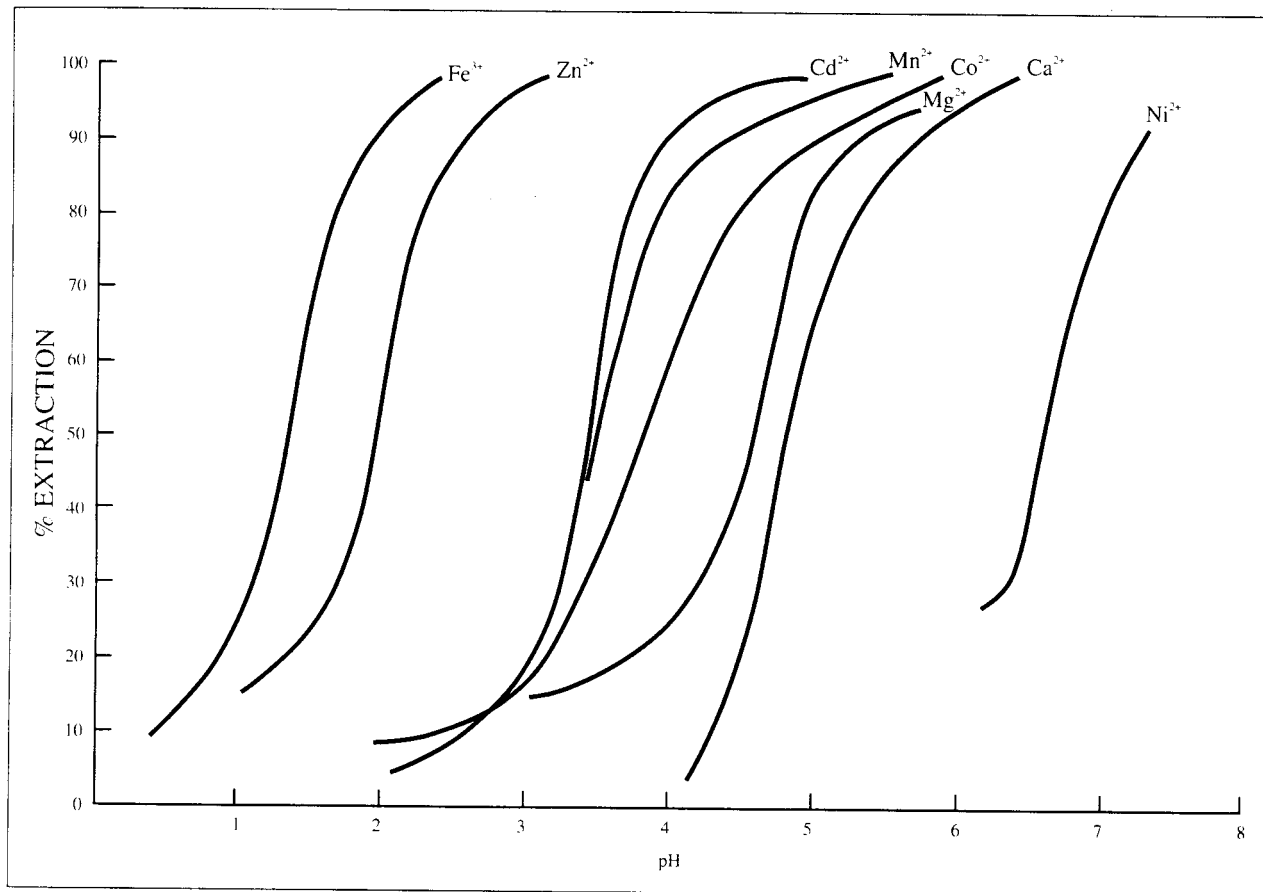
Although CYANEX 272 extractant is designed primarily for cobalt-nickel separations, the data in Table 14 and Figure 3 show that it will extract a variety of metal cations and indicate its potential for other selective separations.

**TABLE 14 - EXTRACTION FROM SINGLE METAL SULFATE SOLUTIONS**

Solvent	:	0.6 M CYANEX 272 extractant, 10 v/o p-nonylphenol in Kermac 470B diluent
Aqueous	:	0.015 M metal as sulfate
Temperature	:	50°C
pH Control	:	$\text{NH}_4\text{OH}$ or $\text{H}_2\text{SO}_4$ as appropriate
Contact Time	:	5 minutes
A/O	:	1

Metal	% Ext.	Final pH	Metal	% Ext.	Final pH
$\text{Fe}^{3+}$	8.8	0.25	$\text{Ni}^{2+}$	27.6	6.33
	23.6	0.85		36.0	6.59
	61.2	1.33		52.3	6.72
	88.1	1.75		84.0	7.22
	98.7	2.31		92.8	7.47
	14.6	0.90		14.5	3.00
$\text{Zn}^{2+}$	24.2	1.42	$\text{Mg}^{2+}$	29.7	4.20
	53.3	1.88		67.1	4.76
	87.7	2.40		82.0	4.99
	99.4	3.08		97.4	5.81
	6.4	1.73		23.9	1.11
$\text{Cu}^{2+}$	17.7	2.64	$\text{Al}^{3+}$	41.9	2.50
	21.7	2.90		87.5	2.92
	73.9	3.56		97.2	3.14
	9.2	1.78		42.3	3.40
$\text{Co}^{2+}$	19.0	3.34		86.1	3.96
	70.8	4.11		99.8	5.66
	99.8	5.98			
	3.4	4.15		7.9	1.11
$\text{Ca}^{2+}$	20.4	4.53	$\text{V}^{4+}$	21.1	1.34
	81.7	5.38		46.5	1.44
	99.6	6.52		85.1	1.81
	4.2	2.00			
$\text{Cd}^{2+}$	19.7	3.00	$\text{Cr}^{3+}$		
	63.1	3.51			
	91.0	4.00			
	99.5	5.00			
				Not extracted from sulfate solution	

### FIGURE 3 - EXTRACTION OF METALS BY CYANEX 272 FROM SULFATE SOLUTIONS



# ANALYTICAL METHODS

## Analysis for Active Component in CYANEX 272

### Extractant in Organic Solvents

The active component of CYANEX 272 extractant is bis(2,4,4-trimethylpentyl)phosphinic acid. Its concentration in an organic solvent is determined by titration with standard caustic solution.



The extractant contains small quantities of a dibasic impurity (2,4,4-trimethylpentyl phosphonic acid) which also titrates with caustic.



The endpoints are detected potentiometrically.

### Apparatus

pH meter

Magnetic stirrer

Standard laboratory glassware

### Reagents

75 v/o 2-propanol in distilled water

0.1N Standard NaOH solution in 75 v/o 2-propanol

100 g/l H<sub>2</sub>SO<sub>4</sub>

All reagents are AR grade.

### Procedure

1. Contact approximately 50 ml of the solvent to be analyzed with 50 ml of 100 g/l H<sub>2</sub>SO<sub>4</sub> for 5 minutes at 50°C. Separate the phases and allow to stand for 15-30 minutes. Centrifuge the solvent or filter through PS paper\* to remove entrained aqueous.
2. To prepare the analyte solution, pipette a 25 ml aliquot of the solvent and dilute to 200 ml in a volumetric flask with the appropriate diluent (Escaid\*\*, Kermac\*\*\* etc.). Alternatively, the 75 v/o solution of 2-propanol may be used for volume make-up.
3. Pipette 25 ml of the analyte solution into a 150 ad tall-form beaker. Dilute to approximately 50 ml with the 2-propanol solution. Insert the pH electrodes and begin stirring.

\* Phase separation paper available from Whatman Inc., Clifton, NJ.

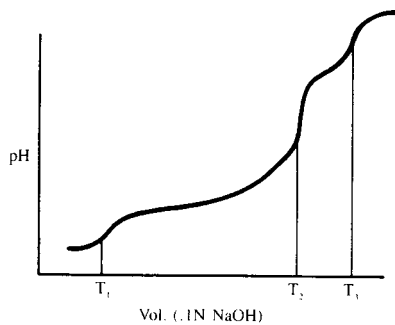
\*\* A product of Exxon Chemical Co., USA

\*\*\* A product of Kerr McGee Refining Corp.

4. Note the initial pH and begin to titrate with 0.1N NaOH. Record the pH as a function of the volume of NaOH added. Three endpoints should be observed. As each endpoint is approached, the incremental addition of NaOH should be reduced to 0.1 ml to facilitate calculation of the titer by the method of second differences.

### Calculation

A typical potentiometric curve is as follows:



The titer  $T_1$  corresponds to the neutralization of sulfuric acid dissolved in the solvent.  $T_2$  represents the neutralization of the phosphinic acid *plus* the reaction of the first of two replaceable hydrogen ions associated with the phosphinic acid. The phosphinic acid is totally neutralized at  $T_3$ .

ml 0.1N NaOH	pH	First Differential	Second Differential
9.8	7.50		
9.9	8.00	50	+40
10.0	8.90	90	+90
10.1	10.70	180	-130
10.2	11.20	50	-40
10.3	11.30	10	

$T_1$  and  $T_3$  may be calculated in an analogous manner.

When all three titers are known, the concentration of bis(2,4,4-trimethylpentyl)phosphinic acid may be determined.

$$\text{bis}(2,4,4\text{-trimethylpentyl}) \text{ phosphinic acid (g/l)} = \frac{[T_2 - (T_3 - T_2) - T_1] \times N(\text{NaOH}) \times 290 \times 1000}{1000 \times \frac{25}{200} \times 25}$$

Similarly the concentration of the phosphonic acid and dissolved sulfuric acid may also be calculated.

$$2,4,4\text{-trimethylpentyl phosphonic acid (g/l)} = \frac{T_2 - T_1 \times N(\text{NaOH}) \times 194 \times 1000}{1000 \times \frac{25}{200} \times 25}$$

$$\text{H}_2\text{SO}_4 (\text{g/l}) = \frac{T_1 \times 49 \times N(\text{NaOH}) \times 1000}{1000 \times \frac{25}{200} \times 25}$$

### NOTES

1. A minimum net titer, i.e.  $[T_2 - (T_3 - T_2) - T_1]$ , of 10 ml is recommended to obtain reproducible results. In this procedure, 10 ml of 01N NaOH is equivalent to approximately 100 g/l concentration of phosphinic acid. Where necessary, the size of the aliquots and dilutions may be varied to ensure a sufficient volume of titrant is consumed.
2. Approximate pH's corresponding to the  $T_1$ ,  $T_2$  and  $T_3$  endpoints are 4, 9 and 11, respectively. However these values may vary depending upon the composition of the solvent. After gaining experience with a system, the NaOH may be added rapidly until the particular endpoint pH is approached and then added in 0.1 ml increments to define the point of inflection in the curve.
3. The concentrations of sulfuric and phosphonic acids in the solvent are usually small and these endpoints may not be observed. In this case  $T_1$  and  $T_3$  should be assigned a value of zero in the calculations. Typically,  $T_1$  and  $T_3 - T_2$ ) will be  $< 0.2$  and  $< 0.1$  ml of 0.1N NaOH, respectively, corresponding to  $< 0.3$  g/l  $\text{H}_2\text{SO}_4$  and  $< 0.6$  g/l phosphonic acid.

$$\text{Then, } T_2 = (10.0 + 0.1) \frac{90}{90 + 130} = 10.04 \text{ ml}$$

## **Analysis for Active Component in CYANEX 272**

### **Extractant in Aqueous Solutions**

The concentration of the active component, bis(2,4,4-trimethylpentyl)phosphinic acid in water is determined by gas chromatography of its silyl derivative.

1. Transfer exactly 10 ml of the aqueous sample into a separatory funnel and acidify with 0.50 ml of 37% hydrochloric acid.
2. Extract this acidified sample with 10 ml of dichloromethane.
3. Concentrate the dichloromethane extract to about 0.5 ml in a Kontes tube concentrator at a temperature of 7-75°C.
4. Dilute the concentrate to exactly 1.5 ml with dichloromethane, add 0.40 ml of Regisil RC-2\*, and silylate at 70-75°C for 10 minutes.
5. Analyze the silylated sample by gas chromatography as described under chromatographic conditions.
6. Calculations:

Bis(2,4,4-trimethylpentyl)phosphinic acid ( $\mu\text{g}/\text{ml}$ )

$$= \frac{A_{\text{Spl}}}{A_{\text{Std}}} \times \frac{C_{\text{Std}}}{10/1.5}$$

Where  $A_{\text{Spl}}$  = area of phosphinic acid peak from sample.

$A_{\text{Std}}$  = area of phosphinic acid peak from standard.

$C_{\text{Std}}$  = concentration (Rg/ml) of phosphinic acid in standard.

\*Regisil-RC-2 is available from Regis Chemical Company, 8210 North Austin Avenue, Morton Grove, Illinois 60053.

### **Chromatographic Conditions**

Instrument	:	Hewlett-Packard 5840 or equivalent
Column	:	10' x $\frac{1}{4}$ " x 2 mm ID glass column packed with 3% SP 2100 on 100/120 mesh Supelcoport
Detector	:	FID
Carrier Gas	:	Helium (20 ml per minute)
Temperatures	:	FID Detector = 300°C Injection port = 250°C Column programmed from 120°C to 270°C at 5° per minute
Sample Injection		
Volume	:	4 microliters
Peak Areas	:	Electronic integration. The compound has
Calibration	:	a retention time of about 15.7 minutes. Calibrate the instrument using standard solutions in dichloromethane containing 2 to 50 micrograms per ml. Then silylate 1.5 ml of this standard solution in the manner described in Procedure 4.

# TECHNICAL PAPERS AND PATENTS

## Technical Papers (listed chronologically)

### 1. Vanadium-uranium extraction from Wyoming vanadiferous silicates

Hayashi, M; Nichols, J.L.; Huiatt, J.L.  
Rep. Invest. - U.S., Bur. Mines RI 8822 Pages 13; (1983)

### 2. Recent developments in the separation of nickel and cobalt from sulfate solutions by solvent extraction

Preston, J.S.  
J.S. Afr. Inst. Min. Metall. 83 6 Pages 126-32; (1983)

### 3. Separation of cobalt and nickel by liquid-liquid extraction and supported liquid membranes with bis(2,4,4-trimethylpentyl)phosphinic acid (CYANEX® 272 Extractant)

Danesi, P.R.; Reichley-Yinger, L.; Cianetti, C.; Rickert, P.G.  
Solvent Extr. Ion Exch. 2 6 Pages 781-814; (1984)

### 4. Extraction equilibria of ammonia with acidic organophosphorus extractants

Inoue, Katsutoshi; Nakayama, Daizo; Watanabe, Yasushi  
Proc. Symp. Solvent Extr. Pages 127-32; (1984)  
(Shizuoka Univ., Hamamatsu, Japan)

### 5. Cobalt-nickel separation by solvent extraction with bis(2,4,4-trimethylpentyl)phosphinic acid

Rickelton, W.A.; Flett, D.S.; West, D.W.  
Solvent Ext. Ion Exch. 2 6; (1984)

### 6. Separation and recovery of cobalt from copper leach solutions

Jeffers, Thomas H.  
J. Met. 37 1 Pages 47-50; (1985)

### 7. Cobalt recovery from copper leach solutions

Jeffers, TH.; Harvey, M.R.  
Rep. Invest. - U.S., Bur. Mines RI 8927 Pages 16; (1985)

### 8. Glycine enhanced separation of cobalt (II) and nickel (II) with bis(2,4,4-trimethylpentyl)phosphinic acid (CYANEX 272® Extractant) by liquid-liquid extraction and supported liquid membranes

Reichley-Yinger, L.; Danesi, P.R.  
Solvent Extr. Ion Exch. 3 1-2 Pages 49-60; (1985)

### 9. Selectivity-structure trends in the extraction of cobalt (II) and nickel (H) by dialkylphosphoric, alkyl alkylphosphonic, and dialkylphosphinic acids

Danesi, Pier R.; Reichley-Yinger, L.; Mason, G.; Kaplan, L.; Horwitz, E.P.; Diamond, H.  
Solvent Extr. Ion Exch. 3 4 Pages 435-52; (1985)

### 10. Determination of the equilibrium constants of organophosphorus liquid-liquid extractants by inductively coupled plasma-atomic emission spectroscopy

Li, Ke An; Muralidharan, S.; Freiser, Henry  
Solvent Extr. Ion Exch. 3 6 Pages 895-908; (1985)

### 11. Some observations on the performance of hollow-fiber supported liquid membranes for cobalt-nickel separations

Danesi, P.R.; Rickert, P.G.  
Solvent Extr. Ion Exch. 4 1 Pages 149-64; (1985)

### 12. Extraction equilibria of ammonia with acidic organophosphorus compounds

Inoue, Katsutoshi; Nakayama, Daizo; Watanabe, Yasushi  
Hydrometallurgy L6 1 Pages 41-53; (1986)

### 13. A composite supported liquid membrane for ultraclean cobalt-nickel separations

Danesi, Pier R.; Reichley-Yinger, L.  
J. Membr. Sci. 27 3 Pages 339-47; (1986)

### 14. Extraction of lanthanide metals with bis(2,4,4-trimethylpentyl)phosphinic acid

Li, Kean; Freiser, Henry  
Solvent Extr. Ion Exch. 4 4 Pages 739-55; (1986)

### 15. A possible use of photoreaction in liquid-liquid extraction of substitution-inert metal complexes.

Extraction of chromium (III) and cobalt (III) complexes  
Ohki, Akira; Fujino, Yasumitsu; Ohmori, Kiyoshi;  
Takagi, Makoto  
Solvent Extr. Ion Exchange 4 4 Pages 639-62; (1986)

### 16. Extraction and stripping of iron (III) in systems of sulfuric acid and monoacidic phosphates and phosphonates

Yu, Shugu; Wu, Zhichun  
Youse Jinshu 38 3 Pages 39-45; (1986)

### 17. Solvent extraction equilibria of neodymium and praseodymium with acidic organophosphorus compounds

Inoue, Katsutoshi; Fujino, Osamu; Arita, Hiroshi  
Nippon Kogyo Kaishi 103 1182 Pages 491-4; (1986)

### 18. Determination of the equilibrium constants of organophosphorus liquid-liquid extractants by inductively coupled plasma-atomic emission spectroscopy

Kean L.; Muralidharan, S.; Freiser, H.  
Report DOE/ER/04073-17; (1985)

### 19. Applications of solvent extraction in treatment of metal finishing wastes

Brooks, Clyde S.  
Met. Finish. 85 3 Pages 55-9; (1987)

### 20. Adsorption of nickel (II) and cobalt (II) from aqueous solutions on Levextrel resin containing acidic organophosphinic extractant and phosphorus-based chelating resins: comparative study on the selectivity of the resins

Inoue, Katsutoshi; Baba, Yoshinari; Sakamoto, Yumi,  
Egawa, Hiroaki  
Sep. Sci. Technol. 22 4 Pages 1349-57; (1987)

- 21. Extraction of nickel (II) from nitrate media by di-n-octylphosphinic acid dissolved in toluene**  
Elizalde, M.P.; Castresana, J.M.; Aguilar, M.; Cox, M.  
*Polyhedron* 6 Pages 1251-4; (1987)
- 22. Recovery of cobalt from spent copper leach solution using continuous ion exchange**  
Jeffers, T.H.; Gritton, K.S.; Bennett, P.G.; Seidel, D.C.  
*Rep. Invet. U.S., Bur. Mines RI 9084* Pages 17; (1987)
- 23. Solvent extraction of cobalt and nickel in bis(2,4,4-trimethylpentyl)phosphinic acid, "CYANEX® 272 Extractant"**  
Xun, Fu; Golding, J.A.  
*Solvent Extr. Ion Exch.* 5 2 Pages 205-26; (1987)
- 24. Extraction equilibria of indium (III) from nitric acid with acidic organophosphorus compounds**  
Inoue, Katsutoshi; Baba, Yoshinari; Yoshizuka, Kazuharu; Soejima, Kohichi; Nakamura, Hiroaki  
*Proc. Symp. Solvent Ext.* Pages 181-4; (1986)
- 25. Extraction and separation of metals with Levextrel resins**  
Baba, Yoshinari; Inoue, Katsutoshi; Yoshizuka, Kazuharu; Sakamoto, Yumi; Nakashirna, Hisashi  
*Proc. Symp. Solvent Extr.* Pages 79-84; (1986)
- 26. Measurement of self-diffusion coefficients in extractant systems using the FT-NMR technique**  
Waernheim, T.; Paatero, E.Y.O.  
*Hydrometallurgy* L9 I Pages 129-34; (1987)
- 27. Equilibria in the solvent extraction of indium (III) from nitric acid with acidic organophosphorus compounds**  
Inoue, Katsutoshi; Baba, Yoshinari; Yoshizuka, Kazuharu  
*Hydrometallurgy* 19 3 Pages 393-9; (1988)
- 28. Recovery of cobalt and copper from complex sulfide concentrates**  
Dannenberg, R.O.; Gardner, P.C.; Crane, S.R.; Seidel, D.C.  
*Rep. Invest. -U.S., Bur. Mines R19138* Pages 20; (1987)
- 29. Extraction of cobalt. XI. Relation between structure of organophosphorus acids and their properties in extraction separation of cobalt from nickel**  
Li, Jinshan; Zhu, Tun; Chen, Jiayong  
*Wuji Huaxue* 3 3 Pages 7-15; (1987)
- 30. Extraction of molybdenum oxyl cation by monoacidic phosphates and phosphonates**  
Yu, Shuqiu  
*Youkuangye* 6 2 Pages 27-33; (1987)
- 31. Investigation on the potential techniques to recover gold from thiourea solution**  
Deschenes, G.  
*Proc. Int. Symp. Gold Metall* Pages 359-77; (1987)
- 32. Equilibrium and mass transfer for the extraction of cobalt and nickel from sulfate solutions into bis(2,4,4-trimethylpentyl)phosphinic acid, "CYANEX® 272 Extractant"**  
Fu, Xun; Golding, J.A.  
*Solvent Extr. Ion Exch.* 6 5 Pages 889-917; (1988)
- 33. Diphasic acido-basic properties of organophosphorus acids**  
Sella, C.; Bauer, D.  
*Solvent Extr. Ion Exch.* 6 5 Pages 819-33; (1988)
- 34. Molecular modeling of organic extractants**  
Gtrone, Ralph C.; Horwitz, E. Phillip  
*Solvent Extr. Ion Exch.* 6-6 Pages 937-72; (1988)
- 35. Synergistic extraction of ferric iron in sulfate solutions by tertiary amine and 2-ethylhexyl 2-ethylhexylphosphonic acid (HEHEMP) or dialkylphosphinic acid**  
Yu, Shuqiu; Chen, Jiayong  
*Hydrometallurgy* 22 1-2 Pages 183-92; (1989)
- 36. Solvent extraction of gallium and indium with acidic extractants**  
Inoue, Katsutoshi; Baba, Yoshinari; Yoshizuka, Kazuharu  
*Proc. Symp. Solvent Extr.* Pages 31-6; (1988)
- 37. Extraction of uranium (VI) from hydrochloric acid solutions by dialkyl phosphinic acid**  
Sato, Taichi; Sato, Keiichi  
*Proc. Symp. Solvent Extr.* Pages 61-6; (1988)
- 38. Solvent extraction of indium (III) and gallium (III) with various acidic extractants**  
Inoue, Katsutoshi  
Shigen to *Sozai* 105 10 Pages 751-4; (1989)
- 39. Extraction mechanism of rare earth metals in the presence of diethylenetriaminepentaacetic acid in aqueous phase**  
Matsuyama, Hideto; Okamoto, Takahiro; Miyake, Yoshikazu; Teramoto, Masaaki  
*J. Chem. Eng. Jpn.* 22 6 Pages 627-35; (1989)
- 40. Equilibrium and kinetic studies for the extraction of nickel from sulfate solutions into CYANEX® 272 extractant**  
Fu, Xun; Zhao, Shujhen; Hu, Zhengshui; Sui, Suping; Hao, Jianmin; Golding, J.A.  
*Proc. Int. Conf. Sep. Sci. Technol. 2nd* I Pages 205-13; (1989)
- 41. Determination of some basic constants for bis(2,4,4-trimethylpentyl)phosphinic acid - CYANEX® 272 extractant**  
Fu, Xun; Hu, Zhengshui; Liu, Yide; Golding, J.A.  
*Proc. Int. Conf. Sep. Sci. Technol., 2<sup>nd</sup>* I Pages 214-21; (1989)

- 42. Extraction separation of tervalent lanthanide metals with bis(2,4,4trimethylpentyl)phosphinic acid**  
Komatsu, Y.; Freiser, H.  
Anal. Chim. Acta 227 2 Pages 397-404; (1989)
- 43. Purification of CYANEX® 272 extractant**  
Yang, Yonghui; Shen, Jinglan; Sun, Sixiu  
Huaxue Shiji 11 6 Pages 381; (1989)
- 44. Extraction equilibrium of molybdenum (VI) with CYANEX® 272 extractant**  
Cao, Yiming; Nakashio, Fumiyuki  
Mo Kexue Yu Jishu 9 4 Pages 6-12; (1989)
- 45. Immobilized extractants: selective transport of magnesium and calcium from a mixed chloride solution via a hollow fiber module**  
Belfer, S.; Binman, S.; Lati, Y.; Zolotov, S.  
J. Appl. Polym. Sci. 40 11-12 Pages 2073-85; (1990)
- 46. The effect of trioctylphosphine oxide on phase and extraction equilibria in systems containing bis(2,4,4-trimethylpentyl)phosphinic acid**  
Paatero, E.; Lantto, T.; Ernola, P.  
Solvent Extr. Ion Exch. 8 3 Pages 371-88; (1990)
- 47. Extraction of sodium in bis(2,4,4-trimethylpentyl)phosphinic acid "CYANEX® 272 extractant": basic constants and extraction equilibria**  
Fu, Xun; Hu, Zhengshui; Liu, Yide; golding, J.A.  
Solvent Extr. Ion Exch. 8 4-5 Pages 573-95; (1990)
- 48. Extraction of divalent metals with bis(2,4,4-trimethylpentyl)phosphinic acid**  
Sastre, A.M.; Miralles, N.; Figuerola, E.  
Solvent Extr. Ion Exch. 8 4-5 Pages 597-614; (1990)
- 49. Improved separation of closely related metal ions by centrifugal partition chromatography**  
Muralidharan, S.; Cai, R.; Freiser, H.  
J. Liq. Chromatogr. 13 18 Pages 3651-72; (1990)
- 50. Analytical utility of coupled transport across a supported liquid membrane**  
Cox, James A.; Bhatnagar, Atul  
Talanta 37 11 Pages 1037-41; (1990)
- 51. Study of uranium removal from groundwater by supported liquid membranes**  
Chiarizia, R.; Horwitz, E.P.  
Solvent Extr. Ion Exch. 8 1 Pages 65-98; (1990)
- 52. The selective recovery of zinc with new thiophosphinic acids**  
Rickelton, W.A., Boyle, R.J.  
Solvent Extr. Ion Exch. 8 6 Pages: 783-97; (1990)
- 53. The significance of diluent oxidation in cobalt-nickel separation**  
Rickelton, W.A., Robertson, A.J., Hillhouse, J.H.  
Solvent Extr. Ion Exch. 9 1/1 Pages 73-84; (1991)
- 54. An improved extractant for separation of ammonia from sour waters by combined stripping and extraction**  
Poole, Loree J.; King, C. Judson  
Solvent Extr. Ion Exch. 9 1 Pages 103-25; (1991)
- 55. Application of supported liquid membranes for removal of uranium from groundwater**  
Chiarizia, R.; Horwitz, E.P.; Rickert, Pg.; Hodgson, K.M.  
Sep. Sci. Technol. 25 13-15 Pages 1571-86; (1990)
- 56. The solvent extraction of europium by some organophosphorus and carboxylic acids**  
Preston, J.S.; Du Preez, A.C.  
Solvent Extr. Ion Exch. 9 2 Pages 237-57; (1991)
- 57. Mechanism of membrane extraction of Molybdenum (VI) with CYANEX® 272**  
CaO, Y and Nakashio, F.  
Huazue Fanying Gongcheng Yu Gongyi, 6, No. 3, Pages 67-73; (1990)
- 58. Organophosphorus compounds in extraction of metal ions**  
Gega, J. and Walkowiak, W.  
Rudy Met. Niezelaz, 36, No. 1, Pages 27-32; (1991)
- 59. Separation of thulium, ytterbium and lutetium by centrifugal partition chromatography with organophosphinic acids**  
Suzuki, Y. et. al.  
Anal. Sci., 7 Pages 249-52; (1991)
- 60. Transport of lanthanoid elements through liquid membrane with organophosphinic acid**  
Nakamura, S. et. al.  
Proc. Symp. Solvent Extr., Pages 45-52; (1991, Japan)
- 61. Solvent extraction of thorium, uranium and some metals from nitrate solution with organophosphinic acid**  
Kenichi, A. et. al.  
Ibid., Pages 181-6
- 62. Solvent extraction characteristics of thiosubstituted organophosphinic acid extractants**  
Sole, K.C. and Hiskey, J.B.  
Hydrometallurgy, 30, No. 1-3, Pages 345-65; (1992)
- 63. Separation of cobalt-zinc, cobalt-manganese and zinc-manganese systems from their binary solutions through supported liquid membrane containing organophosphorus acid as extractant**  
Mohapatra, R. et. al.  
Indian J. Chem., Sect. A., 31A, No. 31A, Pages 389-90; (1992)
- 64. Solvent impregnated resins containing CYANEX® 272. Preparation and application to the extraction and separation of divalent metals**  
Cortins, J. et. al.  
React. Polym., 18, No. 1, Pages 67-75; (1992)

- 65. Comparison of aggregates formed by acidic organophosphorus extractants and metals (nickel and cobalt) in solvent extraction**  
Zhou, N. et. al.  
Process Metals, 7A, Pages 165-70; (1990)
- 66. W/O microemulsions formed by acidic extractants and effect of lanthanides**  
Wu, J. et. al.  
Ibid. Pages 195-200
- 67. The recovery of cobalt and nickel from acidic sulfate solutions in the presence of aluminum**  
Orive, M. et. al.  
Solvent Extr. Ion Exch., 10, No. 5, Pages 787-97; (1992)
- 68. Solvent extraction of iron (111) by bis(2,4,4-trimethylpentyl)phosphinic acid: experimental equilibrium study**  
Miralles, N., et. al.  
Hydrometallurgy, 31, No. 1-2, Pages 1-12; (1992)
- 69. Modification of hollow fibers by impregnation and radiation**  
Belfer, S., et. al.  
Proc. Int. Conf. Ion Exch. (1991).  
Published by Kodansha, Tokyo
- 70. Extraction separation of scandium and iron from hydrochloric acid solutions with bis(2,4,4-trimethylpentyl)phosphinic acid**  
Ma, G., et. al.  
FenxiHuaxe, 20, No.10, Pages 1113-16; (1992)
- 71. Synergistic extraction of iron from sulfuric acid solutions with mixed Kelex 100 - alkyl phosphorus acid extractants**  
Demopoulos, G.P., et. al.  
Solvent Extr. Ion Exch., 11, No. 1, Pages 67-89; (1993)
- 72. Extraction of nickel from aqueous sulfate solution into bis(2,4,4-trimethylpentyl)phosphinic acid, CYANEX® 272. Equilibrium and kinetic studies**  
Golding, J.A., et. al.  
Ibid. Pages 91-118
- 73. The potential for recovery of cobalt from copper leach solutions**  
Sole, K.C.; Hiskey, J.B.  
Proc. Copper 91 - Cobre 91 Int. Symp.,  
Pages 229-43; (1991)
- 74. Extraction rates of terbium, thulium and lutetium with acidic organophosphorus reagents**  
Nakamura, Shigeto; Yamada, Kiyofumi; Akiba, Kenichi  
Proc. Symp. Solvent Extr., Pages 169-74; (1992)
- 75. Extractive separation of copper(II) and zinc(II) using emulsion liquid membrane**  
Cao, Yiming; Goto, Masahiro; Nakashio, Fumiuki  
Mo Kexue Yu Jishu, 12, No. 4, Pages 12016; (1992)
- 76. A spectrophotometric method for the determination of cobalt (11) in organic phases**  
Azimi, A.; Rice, N.M.  
Hydrometallurgy, 32, No.2, Pages 223-32; (1993)
- 77. Simultaneous characterization of extraction equilibria and back extraction kinetics: use of Arsenazo III to characterize lanthanide-bis(2,4,4-trimethylpentyl)phosphinic acid complexed in surfactant micelles**  
Inaba, Kazuho; Muralidharan, Subramaniam; Freiser, Henry  
Anal. Chem., 65, No. 11, Pages 1510-16; (1993)
- 78. Cobalt-nickel separation: the extraction of cobalt (11) and nickel(II) by CYANEX® 301, CYANEX® 302 and CYANEX® 272**  
Tait, Brian K.  
Hydrometallurgy, 32, No.3, Pages 365-72; (1993)
- 79. Solvent extraction of lanthanides by acidic organophosphorus compounds**  
Akiba, Kenichi; Yamada, Hiyofumi; Nakamura, Shigeto  
Nippon Kagaku Kaishi, No. 5, Pages 555-60; (1993)
- 80. Recovery of molybdenum, vanadium, nickel and cobalt from spent hydrodesulfurization catalysts**  
Inoue, Katsutoshi; Pingwei, Zhang; Tsuyama, Hiromi  
Prepr. - Am. Chem. Soc., Div. Pet. Chem., 38,  
No. 1, Pages 77-80; (1993)
- 81. Extraction of rare earth ions with bis(2,4,4-trimethyl pentyl)phosphinic acid**  
Zhang, Xiaofeng; Li, Deoian  
Yingyong Huaxue, 10, No. 4, Pages 72-4; (1993)
- 82. Extraction of metal (titanium, vanadium, molybdenum)oxyz cations by monoacidic phosphates and phosphonates**  
Fu, Xun; et.al.  
Rare Met. (Beijing), 12, No. 2, Pages 142-7; (1993)
- 83. Bioextraction of cobalt from cobaltite**  
Torma, A.E.; Wey, J.E.; Pesic, B.  
Metall (Berlin), 47, No. 7. Pages 648-51; (1993)
- 84. Dissociation constants of organophosphinic acid compounds**  
Maritinez, M.; Miralles, N.; Sastre, A.; Bosch, E.  
Talanta, 40, No. 9, Pages 1339-43; (1993)
- 85. Solvent extraction separation of cobalt(II) from nickel and other metals**  
Gandhi, M.N.; Deorkar, N.V.; Khopkar, S.M.  
Talanta, 40, No. 10, Pages 1535-9; (1993)

86. Solvent-impregnated resins containing di-(2,4,4-trimethylpentyl)phosphinic acid. II. Study of the distribution equilibria of zinc(II), copper(II) and cadmium(II)  
Crotina, J.L.; et. al.  
React. Polym., 21, No. 1-2, Pages 103-16; (1993)
87. Study on rare earth complexes with bis(2,4,4-trimethylpentyl)phosphinic acid  
Li, Qiongqing; et. al.  
JinshuXuebao, 29, No.4, Pages 13251-13257; (1993)
88. Solvent-impregnated resins containing di-(2,4,4-trimethylpentyl)phosphinic acid. I. Comparative study of di-(2,4,4-trimethylpentyl) phosphinic acid adsorbed into Amberlite XAD-2 and dissolved toluene  
Corina, J.L.; et. al.  
React. Polym., 21, No. 1-2, Pages 89-101; (1993)
89. Extraction of thorium(IV) by CYANEXI reagents, PC-88A and their mixtures from aqueous hydrochloric acid media  
Rout, K.C.; Mishra, P.K.; Chakravortty, V.; Dash, K.C.  
Radiochim. Acta, 62, No. 4, Pages 203-6; (1993)
90. Recovery of molybdenum, vanadium, nickel and cobalt from spent dehydrosulfurization catalysts  
Inoue, Katsutoshi; Zhang, Pingwei; Tsuyama, Hiromi  
Prepr. - Am. Chem. Soc., Div. Pet. Chem., 38, No. 1, Pages 77-80; (1993)
91. Thermodynamic function of microemulsions in sodium salt of dialkylphosphoric acid extractant systems  
Fu, Xun; Xin, Huizhen; Hu, Zhengshui; Liu, Zhixiang  
Huaxue Xuebao, 51, No. 12, Pages 1151-6; (1993)
92. Comparative study on kinetic behavior of solvent extraction of  $\text{Co}^{2+}$  and  $\text{Ni}^{2+}$  with organophosphorus extractants  
Zhu, Tun  
HuagongXuebao (Chin. Ed.), 44, No. 3, Pages 343-9; (1993)
93. Vibrational spectra of rare earth complexes of bis(2,4,4trimethylpentyl)phosphinic acid  
Li, Qiongqing; Zeng, Guangfu; Li, Deqian  
Guangpuxue Yu Guangpu Fenxi, 13, No. 6, Pages 19-24; (1993)
94. Sodium salts of D2EHPA, PC-88A and CYANEX® 272 and their mixtures as extractants for cobalt(II)  
Devi, N.B.; Nathsarma, K.C.; Chakravortty, V  
Hydrometallurgy, 34, No. 3, Pages 331-42; (1994)
95. Application of europium(III) extraction with organophosphinic acid to liquid membrane transport  
Nakamura, S.; Sato, A.; Akiba, K.  
J. Radioanal. Nucl. Chem., 178, No. 1, Pages 63-71; (1994)
96. Organophosphinic, phosphonic acids and their binary mixtures as extractants for molybdenum(IV) and uranium(VI) from aqueous HCl media  
Behera, P.; Mishra, S.; Mohanty, I.; Chakravortty, V.  
J. Radioanal. Nucl. Chem., 178, No. 1, Pages 179-92; (1994)
97. Purification of nickel sulfate solutions containing iron copper, cobalt, zinc and manganese  
Senapati, Dabasis; Chaudhury, G. Roy;  
Sarma, PXR. Bhaskara  
J. Chem. Technol. Biotechnol., 59, No. 4, Pages 335-9; (1994)
98. Extraction mechanism of Sc(III) and separation of Th(IV), Fe(III), and Lu(III) with bis(2,4,4-trimethylpentyl) phosphinic acid (A) in n-hexane from sulfuric acid solutions  
Wang, Chun; Li, Deqian  
Solvent Extr. Ion Exch., 12, No. 3, Pages 615-3 1; (1994)
99. Study on transport and separation of Zn(II) from Cd(II) and other metal ions through the emulsion liquid membrane system of CYANEX® 272-Span 80- toluene  
Zou, Changying; Li, Kean; Tong, Shenyang  
Gaochang Xuexiao Huacue Xuebao, 15, No. 2, Pages 185-8; (1994)
100. Synergistic extraction of rare earth elements (III) with BTMPPA and HPMBP  
Sun, Jing; Li, Deqian  
Yingyong Huaxue, 11, No. 3, Pages 49-53; (1994)
101. Extractive spectrophotometric determination of cobalt using CYANEX® 272  
Reddy, B.R.; Sarma, P.V.R. Bhaskara  
Talanta, 41, No. 8, Pages 1335-9; (1994)
102. Solvent extraction of silver by CYANEX® 272, CYANEX® 302 and CYANEX® 301  
Sole, Kathryn C.; Ferguson, Tonya L.; Hiskey, J. Brent  
Solvent Extr. Ion Exch., 12, No. 5, Pages 1033-50; (1994)
103. Effect of the kinetic factors on the efficiencies of centrifugal partition chromatographic separations of tervalent lanthanides with bis(2,4,4-trimethylpentyl)phosphinic acid as extractant  
Inaba, K.; et. al.  
Solvent Extr. Res. Dev., Jpn., 1, Pages 13-29; (1994)
104. Liquid membrane transport of lanthanoid elements using organophosphinic acid  
Nakamura, S., et. al.  
J. Radioanal. Nucl. Chem., 181, No. 2, Pages 281-9; (1994)
105. Kinetics of the extraction of cobalt (II) Using CYANEX® 272  
Liu, Ping; et. al.  
Shandong Daxue Xuebao, 29, No. 3, Pages 320-5; (1994)

- 106. Separation of Zn, Co and Ni using solvent extraction techniques**  
 Cho, E.H. and Dai, P.K.  
*Miner. Metall. Process.*, 11, No. 4, Pages 185-7; (1990)
- 107. Recovery of metals from spent hydrodesulfurization catalysts by liquid-liquid extraction**  
 Zhang, P.; et. al.  
*Energy Fuels*, 9, No. 2, Pages 231-9; (1995)
- 108. Two-phase potentiometric metal extraction titrations of silver (I), copper (II) and cadmium (II) using some cation-exchangers as extractants**  
 Tait, Brian K.  
*Talanta*, 42, No. 1, Pages 137-42; (1995)
- 109. Solvent extraction of copper by CYANEX® 272, CYANEX® 302 and CYANEX® 301**  
 Sole, Kathryn C. and Hiskey, Brent J.  
*Hydrometallurgy*, 37, No. 2, Pages 129-47; (1995)
- 110. Solvent extraction of zinc and cadmium by CYANEX® 272, 301 and 302 extractants**  
 Nayak, Al; et. al.  
*Indian J. Chem. Technol.*, 2, No. 2; (1995)
- 111. Solvent extraction of Sc (III), Zn (IV), Th (IV), Fe (III) and Lu (III) with thiosubstituted organophosphinic acid extractants**  
 Wang, C. and Li, D.  
*Solvent Extr. Ion Exch.*, 13, No. 3, Pages 502-23; (1995)
- 112. Metals recovery from hydrosulfurization catalysts**  
 Delmas, F; et. al.  
*Hydrometall.* '94, Pages 1075-86,  
 Chapman & Hall, London; (1994)
- 113. Sodium salts of D2EHPA, PC-88A and CYANEX®272 and their mixtures as extractants for nickel**  
 Devi, N.; et. al.  
*Scand. J. Metall.*, 23, No. 5/6, Pages 194-200; (1994)
- 114. Application of a new extractant, CYANEX® 272, to liquid membrane separation technology**  
 Zhang, R. and Chen, G.  
*Mo Kexue Yu Jishu*, 15, No. 1, Pages 8-13; (1995)

### Patents (listed chronologically)

- 1. Extraction process for the selective removal of cobalt (II) from aqueous solutions**  
 Rickelton, William Andrew; Robertson, Allan James, Burley, David Richard European Patent Appl. EP 46933 A2 (1982)
- 2. Extraction process for the selective removal of cobalt (II) from aqueous solutions**  
 Rickelton, William Andrew; Robertson, Allan James; Burley, David Richard European Pat. Appl. EP 46940 A2 (1982)
- 3. Selective removal of cobalt (II) from aqueous solutions with phosphinic extractants**  
 Rickelton, William Andrew; Robertson, Allan J.; Burley, David R. US Patent 4348367 (1982)
- 4. Selective extraction of cobalt (II) from aqueous solutions with phosphinic acid extractants**  
 Rickelton, William A.; Robertson, Allan J.; Burley, David R. US Patent 4353883 (1982)
- 5. Bis-(2,4,4-trimethylpentyl)phosphinic acid**  
 Robertson, Allan J.  
 US Patent 4374780 (1983)
- 6. Use of a synergistic extractant mixture for cobalt-nickel separation**  
 Michels, Bernd Dieter; Mathy, Wolfgang  
 German Patent DE 3411885 A1 (1985)
- 7. Separating rare earths by liquid-liquid extraction**  
 Sabot, Jean Louis; Rollat, Alain  
 European Patent Appl. EP 156735 A1 (1985)
- 8. Recovery of zirconium by solvent extraction**  
 Witte, Margaret Kent; Frey, Carla Corinne  
 European Pat. Appl; EP 154448 a 2 (1985)
- 9. Electroplating zinc utilizing primary and secondary zinc sources**  
 Duyvesteyn, Willem P.C.; Hogsett, Robert F.  
 US Patent 696985 (1985)
- 10. Method of solvent extraction of metal**  
 Babjak, Juraj  
 Belgium Patent 903209 A1 (1985)
- 11. Ion-exchange column**  
 Inco Ltd.  
 Japan Kokai Tokkyo Patent 8673842 A2 (1986)
- 12. Separation extraction process for immiscible liquids**  
 Lowenhaupt, Harris; Hollenbeck, Melinda European Pat. Appl. EP 183501 A1 (1986)

- 13. Purification of a nickel solution by two-stage liquid-liquid extraction**  
Ermirio de Moraes, Luis  
Brazil Patent BR 8404685 A (1986)
- 14. Purification of a nickel solution by liquid-liquid extraction for separation of high-purity electrolytic nickel and cobalt**  
Ermirio de Moraes, Luis  
Brazil Patent BR 8404686 A (1986)
- 15. Recovery of cobalt from ammoniacal solutions containing cobalt and nickel**  
Rickelton, William, A.  
US Patent 4619816 (1986)
- 16. Zirconium isotope separation process comprising photo-assisted solvent extraction**  
Peterson, Steven H; Laboda, Edward J. US Patent 4767513 (1988)
- 17. Recovery of metals from electroplating wastewaters by recycling of metals and of extractants**  
Magdics, Alex; Stain, Donald B. European Patent Appl. EP 332447 A1 (1989)
- 18. Separation of nickel and cobalt from sulfate solutions by solvent extraction**  
Chou, Eddie C.; Beckstead, Leo W. US Patent 4900522 (1990)
- 19. Aqueous-organic softening agents containing soluble salts for detergents for use in hard water**  
Lokkesmoe, Keith D.; Besse, Michael E.; Olsen, Keith E. US Patent 4911856 (1990)
- 20. Polymer beads containing immobilized metal extractant**  
Seidel, D.; Jeffers, T.  
US Patent Appl. 429326 AO (1990)
- 21. Germanium extraction from sulfate solution**  
Vliegen, Jean H.M.; Haesebroek, Guy G.L.B.; De Schepper, Achille J.M. PCT International Patent WO 9013677 (1990)
- 22. Extraction of rare earth metals from sulfurous acid solution using organophosphorus compounds**  
Fulford, George D.; Lever, Gordon; Sato, Taichi Canadian Patent 2,021,415 1991
- 23. Recovery of rare earth elements from red mud**  
Fulford, George Dennison; Lever, Gordon; Sato, Taichi Brazil Pedido; BR 9001453 A (1991)
- 24. Extraction of rare earth metals from sulfurous acid solution using organophosphorus compounds**  
Fulford, George D., et. al. Canadian Patent Application 2,021,415 (1991)
- 25. Cadmium and nickel recovery and recycling from spent batteries**  
Agh, J., et. al.  
Hungary Telges, HU 55451, (1991)
- 26. Solvent extraction of metals and selective redox stripping of cations for separation**  
O'Keefe, Thomas J.  
WO 9,116,465 (1991)
- 27. Manufacture of high purity nickel sulfate**  
Siekierski, Slawomir; et. al.  
Poland; PL 15 8842 B1 (1992)
- 28. Recovery of sulfuric acid from metal sulfate-containing waste sulfuric acid**  
Mikami, Yasuie; Iyatomi, Nabuyoshi  
European Pat. Appl.; EP 541002 A1 (1993)
- 29. Recovery of base metals from geothermal brines**  
Duyvesteyn, Willem P.C.  
United States; US 5229003 A (1993)
- 30. Prevention of formation of jarosite and ammonium and alkali double salts in solution extraction in acid leaching of valuable metals**  
Nyman, Bror Goeran; Hultholm, Stig Erik  
Germany Offen.; DE 4320314 A I (1993)
- 31. Extraction of vanadium using phosphinic acid compounds**  
Inoe, Katsutoshi; Cho, Hen; Tsuyama, Hiromi  
Japan Kokai Tokkyo Koho; JP 94192759 A2;  
JP 06192759 (1994)
- 32. Recovery of vanadium from aluminum-containing solutions**  
Inoe, Katsutochi; Cho, Hen; Tsuyama, Hiromi Japan Kokai Tokkyo Koho: JP 94092760 As: JP 06192760 (1994)
- 33. Recovery of molybdenum**  
Inoe, Katsutoshi; Cho, Hen; Tsuyama, Hiromi  
Japan Kokai Tokkyo Koho; JP 94192761 A2;  
JP 06192761 (1994)
- 34. Recovery of nickel and/or cobalt**  
Tsuyama, H.  
Japan Kokai Tokkyo Koho; JP 94264156 A2 (1994)
- 35. Process for the extraction of strontium from acidic solutions**  
Horwitz, E. Philip and Dietz, Mark L.  
U.S. Patent 5344623 (1994)
- 36. Solvent extraction process for the purification of cobalt sulfate as intermediate solution**  
Fittock, John; et. al.  
European Patent Application; EP 651062 A I (1995)

*As of July 24, 1995*

---

## **Health and Safety**

The oral and dermal toxicity of CYANEX 272 extractant is low. CYANEX 272 extractant produces moderate eye and skin irritation upon contact. CYANEX 272 extractant did not produce an allergic dermal reaction in guinea pigs after repeated dermal exposure. This product did not produce mutations in bacteria. CYANEX 272 extractant is toxic to fish and invertebrates and care should be exercised to avoid environmental exposure.

## **IMPORTANT NOTICE**

The information and statements herein are believed to be reliable but are not to be construed as a warranty or representation for which we assume legal responsibility. Users should undertake sufficient verification and testing to determine the suitability for their own particular purpose of any information or products referred to herein. NO WARRANTY OF FITNESS FOR A PARTICULAR PURPOSE IS MADE. Nothing herein is to be taken as permission, inducement or recommendation to practice any patented invention without a license.

FOR ADDITIONAL INFORMATION PLEASE CONTACT:

**Cytec Industries Inc.**  
West Paterson, NJ, USA  
Tele: 973-357-3100  
Fax: 973-357-3050

**Cytec Canada Inc.**  
Phosphine Technical Centre  
Niagara Falls, Ontario  
Tele: 905-356-9000  
Fax: 905-374-5939

**Cytec Australia Holdings Pty. Ltd.**  
Baulkham Hills, NSW 2153  
Tele: 61-2-9686-4188  
Fax: 61-2-9639-4248

**Cytec Industries France**  
Rungis-Cedex  
Tele: 33-1-4180-1700  
Fax: 33-1-4978-0780

**Cytec Industries B.V.**  
Botlek, The Netherlands  
Tele: 31-181-295400  
Fax: 31-181-295401



# **CYANEX®301 Extractant**

## **Solvent Extraction Reagent**

- Extracts zinc, cadmium and many other metals at low pH.
- Selective for heavy metals vs alkaline and alkali earths.

**CYTEC**

# CONTENTS

---

---

## INTRODUCTION

Chemical Structure	1
Typical Properties	1

## MATERIALS OF COMPATIBILITY

Plastics	2
Metals	2

## HYDROLYTIC STABILITY

3

## PERFORMANCE DATA

General Extraction Properties	4
Zinc-Calcium Separation	4
Zinc Extraction and Stripping	6
Continuous Countercurrent Testing	7
Load-Strip Cycle Tests	7
Recovery of Amino Acids	8

## ANALYTICAL METHODS

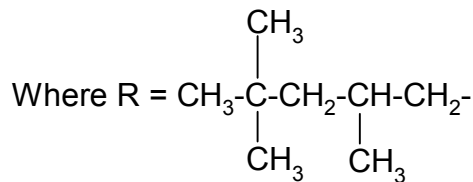
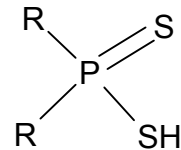
Analysis in Organic Solvents	10
Analysis in Aqueous Solution	10

# INTRODUCTION

CYANEX 301 is a dialkyl dithiophosphinic acid extractant. This sulfur-containing compound is a much stronger acid than its analogous oxy-acid, CYANEX 272. As such, it is capable of extracting many metals at lower pH (<2). CYANEX 301 extractant does not discriminate between heavy metals in this pH range, however, a high degree of selectivity of extraction of heavy metals vs the alkaline earths is observed. This reagent was originally developed for the selective extraction of zinc from effluent streams also containing calcium, such as those generated in the manufacture of rayon by the viscose process.

## Chemical Structure

The active component of CYANEX 301 extractant is bis(2,4,4-trimethylpentyl)dithiophosphinic acid.



Molecular Weight = 322

## Typical Properties

Appearance	:	Green mobile liquid
Odor	:	Faintly characteristic of hydrogen sulfide
Assay	:	75-80% Bis(2,4,4-trimethylpentyl) dithiophosphinic acid
Specific Gravity	:	0.95 at 24°C
Viscosity	:	78 centipoise at 24°C
Boiling Point	:	Decomposes at 220°C
Pour Point	:	-34°C
Flash Point (Closed Cup)	:	165°F(74°C)
Solubility in Water	:	7 mg/L*

\*Solubility will be lower in aqueous solutions containing dissolved salts.

# MATERIALS OF COMPATIBILITY

---

## Plastics

Samples of the following plastics and rubbers, in the form of tubing, were immersed for 1000 hours at 50°C in glass vessels containing CYANEX 301. The weights and dimensions of the test samples were determined before and after immersion. The following observations were made.

Material	Remarks
PVC (Solvent Grade)	No change in weight or dimensions. Loss of plasticity. Short-term suitability only.
PVC (Heavy Duty Chemical Grade)	15% loss in weight. Color change from transparent to black. Loss of plasticity. Short term suitability only.
PVC (Laboratory Grade)	20% loss in weight. Loss of plasticity. Short term suitability only.
Polyethylene	Suitable. No change significant changes in weight or dimensions
Polypropylene	Suitable. No change in weight or dimensions.
Teflon	Suitable. No change in weight or dimensions.
Fluorocarbon Film*	Suitable. No change in weight or dimensions.
Latex	Unsuitable. Twofold increase in dimensions.
Viton	15% increase in weight.
Fluoroelastomer*	Some loss of flexibility. Short term suitability only.

## Metals

Samples of stainless steel (316 and 304) and mild steel in the form of coupons (approximate dimensions 50 mm x 20 mm x 3 mm) were immersed for 24 hours at 50°C in glass vessels containing CYANEX 301. No detectable corrosion was observed in this period. However, the shiny surfaces of the test samples became dull and the CYANEX 301 was severely discolored. None of the test metals are recommended for extended service.

\*Product of E.I. du Pont de Nemours & Co.

# HYDROLYTIC STABILITY

Experiments were conducted to investigate the stability of CYANEX 301 extractant in contact with hydrochloric and sulfuric acid.

A solvent containing CYANEX 301 extractant was contacted with 75 g/L HCl or 300 g/L H<sub>2</sub>SO<sub>4</sub> in a stirred resin flask at A/O=1 and 50°C for a total of 411 hours (HCl) and 466 hours (H<sub>2</sub>SO<sub>4</sub>).

The flask was equipped with a condenser to minimize diluent evaporation.

Samples of the dispersed phase were removed periodically and the coalesced solvent analyzed by base titration. The results are given in Table 1 and Figure 1.

Although some degradation did occur, the rate appeared to decrease after approximately 300-350 hours in both sulfuric and hydrochloric acids. The observed degradation is approximately equivalent to a plant residence time of 200-250 days.

**FIGURE 1**  
**HYDROLYTIC STABILITY**

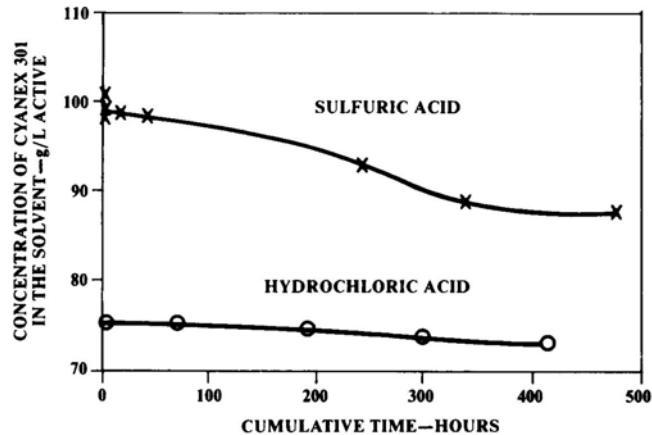


**TABLE 1 - STABILITY TESTING**

Solvent	:	CYANEX 301 extractant in Exxsol D-80 diluent*
Aqueous	:	75 g/L HCl or 300 g/L H <sub>2</sub> SO <sub>4</sub>
A/O	:	1
Temperature	:	50°C

	Cumulative Time (Hours)	Solvent Analysis (g/L Active)
Hydrochloric Acid	0	75.6
	62	75.3
	196	74.5
	300	73.8
	411	73.6
Sulfuric Acid	0	98.1
	1	100.3
	2	99.1
	4	98.3
	15	97.9
	52	97.4
	235	91.5
	338	88.4
	466	88.1

\*A product of Exxon Co., U.S.A.

# PERFORMANCE DATA

## General Extraction Properties

CYANEX 301 extractant is capable of the selective recovery of heavy metals at low pH in the presence of alkaline earths. This is illustrated by the data obtained in some batch, shake-out tests and given in Table 2.

It is also known that this type of compound is capable of extracting cadmium from wet process phosphoric acid<sup>1</sup> and amino acids from fermentation broths.<sup>2</sup>

**TABLE 2 -  
EFFECT OF pH ON METAL EXTRACTION**

Solvent	:	160 g/L CYANEX 301 extractant in toluene
Aqueous	:	0.015 M in Zn <sup>2+</sup> , Ca <sup>2+</sup> , Co <sup>2+</sup> , Ni <sup>2+</sup> , Cu <sup>2+</sup> Mg <sup>2+</sup> and Fe <sup>3+</sup> as their sulfate salts
Temperature	:	50°C
Time	:	5 minutes
A/O	:	1
pH Adjustment	:	H <sub>2</sub> SO <sub>4</sub> or NH <sub>4</sub> OH, as appropriate

## % Extraction

Equilibrium pH	Zn <sup>2+</sup>	Ca <sup>2+</sup>	Co <sup>2+</sup>	Ni <sup>2+</sup>	Cu <sup>2+</sup>	Mg <sup>2+</sup>	Fe <sup>3+</sup>
0.48	100	0.8	87.6	99.1	100	0	37.6
0.90	100	0.6	98.2	100	100	0	55.2
1.55	100	0.7	99.9	100	100	0	97.1
2.15	100	1.1	100	100	100	0	99.5
2.55	100	1.0	100	100	100	0	100

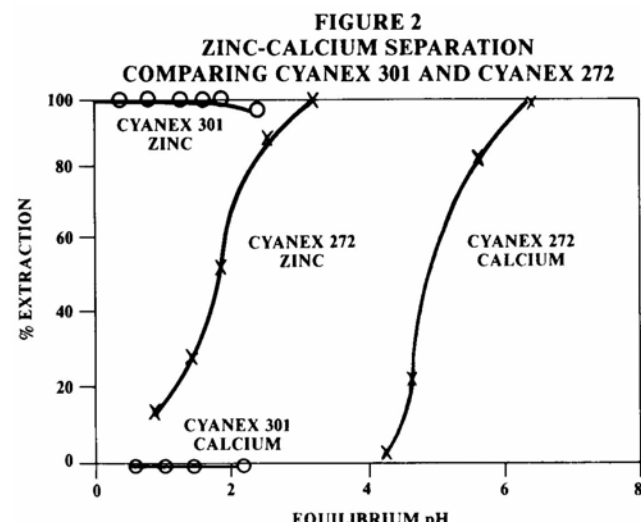
## Zinc-Calcium Separation

CYANEX 301 extractant was originally developed to recover zinc from the effluent streams of viscose rayon plants.<sup>3</sup> Zinc and calcium are present in this effluent in the form of their sulfate salts at a pH between one and two. The objective was to recover the zinc and recycle it for use in the viscose process acid bath.

It is important to make a highly selective zinc-calcium separation because, if calcium is recycled to the acid bath, gypsum forms and its precipitation has a deleterious effect on the rayon product. One further constraint is that the solvent extraction process must operate at the pH of the effluent. The low dollar value of the zinc and the comparatively low solution tenors, <1 g/L, make it uneconomical to adjust the pH.

Zinc-calcium separation can be effected by such organophosphorus extractants as CYANEX 272 but pH adjustment to approximately 3 is required for complete recovery. In contrast, CYANEX 301 is a stronger acid and complete zinc extraction is possible in the pH range 1-2. Additionally, this reagent exhibits a high selectivity for zinc versus calcium.

This is illustrated by the pH isotherms for CYANEX 301 and CYANEX 272 extractants which are shown in Figure 2. The corresponding data are given in Table 3.



<sup>1</sup> Process For the Recovery of Cadmium and Other Metals From Solution. L W Bierman, et al, U.S. Patent 4,511,541 (1985)

<sup>2</sup> Extraction of Amino Acids from an Aqueous Solution with Dithiophosphinates. C. Savides and J. H. Bright, U.S. Patent 4,536,596 (1985)

<sup>3</sup> Selective Removal of Metals From Aqueous Solutions With Dithiophosphinic Acids. R.J. Boyle, et al, U.S. Patent 4,721,605 (1988)

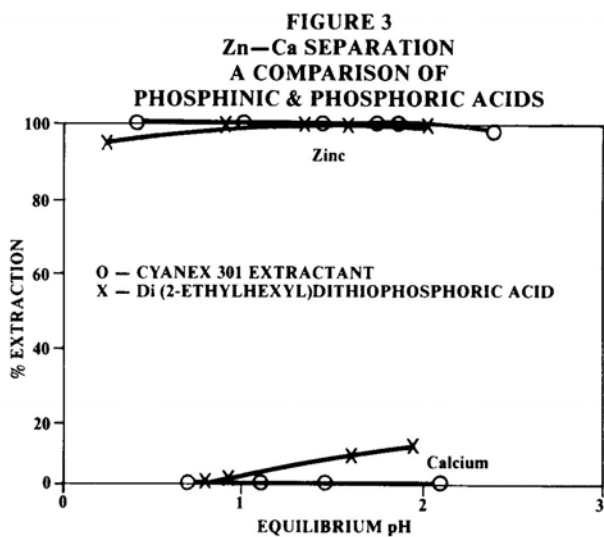
**Table 3**  
**ZINC-CALCIUM SEPARATION WITH CYANEX 301 AND CYANEX 272 EXTRACTANTS**

Solvent : 0.6 M extractant in Kermac 470B diluent\*  
 Aqueous : Single metal sulfate solutions, 0.015 M in metal ion  
 Temperature : 50°C  
 pH control : H<sub>2</sub>SO<sub>4</sub> or NH<sub>4</sub>OH appropriate  
 A/O : 1

CYANEX 301 Extractant				CYANEX 272 Extractant			
Zn	Equilibrium pH	% Extraction	Ca	Zn	Equilibrium pH	% Extraction	Ca
0.41	99.9	0.62	0	0.90	14.6	4.15	3.4
0.91	100	1.11	0	1.42	24.2	4.53	20.4
1.42	100	1.50	0	1.88	53.3	5.38	81.7
1.67	100	2.06	0	2.40	87.7	6.52	99.6
1.87	100			3.08	99.4		
2.35	97.5						

\* A product of Kerr-McGee Corp. U.S.A.

Dithiophosphoric acids are also commercially available. However, acids of this type do not exhibit the high selectivity for zinc versus calcium which is associated with CYANEX 301. This is illustrated by the pH isotherms for di(2-ethylhexyl) dithiophosphoric acid and CYANEX 301 which are plotted in Figure 3. The isotherms were obtained under the same conditions as outlined in Table 3.



## Zinc Extraction and Stripping

A zinc extraction isotherm for a solvent containing 100 g/L CYANEX 301 is plotted in Figure 4 using the data given in Table 4. The isotherm has an almost ideal shape; indicative of low staging requirements. For example, the McCabe-Thiele construction in Figure 4 implies complete recovery from a stream containing 6 g/L Zn in two theoretical stages at A/O=1.

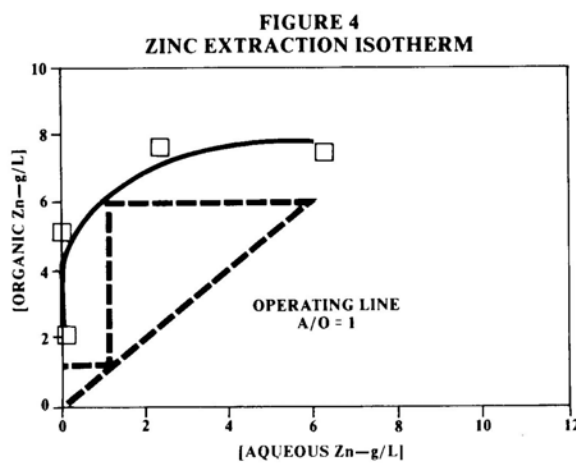


**TABLE 4 - ZINC EXTRACTION ISOTHERM**

Solvent	:	100 g/L CYANEX 301 extractant in Exxsol D-80 diluent
Aqueous	:	9.95 g/L Zn <sup>2+</sup> as the sulfate
Temperature	:	50°C
pH	:	Controlled to 1.50 ± 0.05 with 200 g/L NaOH
Time	:	2 minutes contact after obtaining a stable equilibrium pH

A/O	Equilibrium Zn Concentration (g/L)	
	Organic	Aqueous
0.2	1.99	0
0.5	4.98	0
1	7.58	2.37
2	7.64	6.13

CYANEX 301 is not readily stripped as indicated by the stripping isotherm obtained using 300 g/L H<sub>2</sub>SO<sub>4</sub> as the strip feed (Table 5 and Figure 5). Isotherms of this type are difficult to interpret using standard McCabeThiele constructions. However, a continuous, countercurrent, mini-plant test did reveal that a strip liquor containing in excess of 20 g/L Zn could be produced (Table 6 and Figure 6). A solution of this composition is suitable for recycle in the viscose process.

**TABLE 5 - ZINC STRIPPING ISOTHERM**

Solvent	:	100 g/L CYANEX 301 extractant in Exxsol D-80 diluent loaded to 7.29 g/L Zn by contact with a ZnSO <sub>4</sub> solution
Strip Feed	:	300 g/L H <sub>2</sub> SO <sub>4</sub>
Temperature	:	50°C
Time	:	5 minutes

A/O	Equilibrium Zn Concentration (g/L)	
	Organic	Aqueous
5	1.84	1.09
2	2.85	2.22
1	3.59	3.70
0.5	4.24	6.10
0.2	4.93	11.8
0.1	5.45	18.4
0.05	5.71	31.6

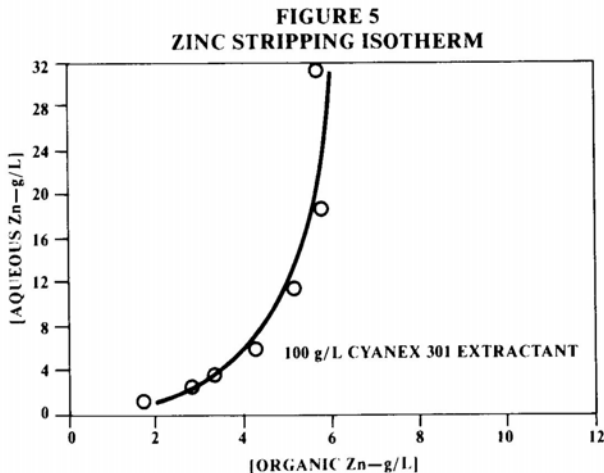
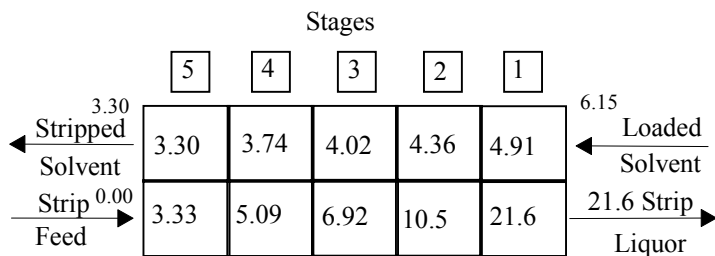


**TABLE 6 - CONTINUOUS, COUNTER CURRENT TESTING:  
EXPERIMENTAL CONDITIONS**

Stages	:	5
O/A	:	10
Solvent	:	100 g/L CYANEX 301 extractant In Exxsol D-80 diluent, loaded To 6.15 g/L Zn
Strip Feed	:	300 g/L H <sub>2</sub> SO <sub>4</sub>
Duration of Test	:	4 hours
Temperature	:	40°C

**Figure 6  
Continuous Stripping Test:  
Circuit Profile**

Strip Feed = 300 g/L H<sub>2</sub>SO<sub>4</sub>



Numbers Refer to Zinc Solution Tenors IN g/L

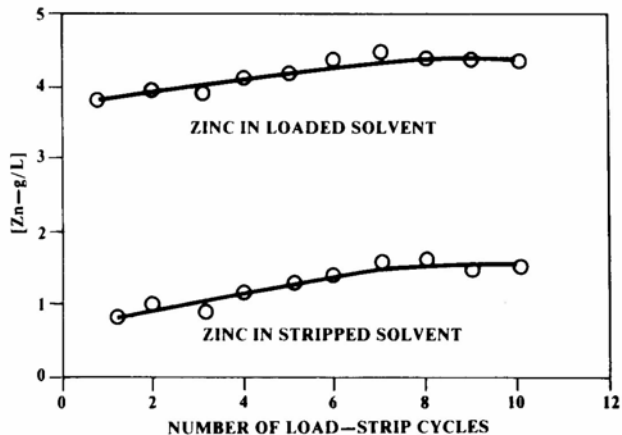
Although zinc is not readily stripped from CYANEX 301, there is no evidence of a zinc accumulation on the solvent which would lead to poisoning. This is illustrated by the results of some cycle tests where zinc was repeatedly loaded and stripped from a solvent containing CYANEX 301. The results are given in Table 7 and plotted in Figure 7.

**TABLE 7 - LOAD-STRIP CYCLE TESTS**

Solvent	:	50 g/L CYANEX 301 extractant In Exxsol D-80 diluent
Aqueous	:	10 g/L Zn as sulfate (loading)
pH	:	1.50±0.05 (loading): controlled with 200 g/L NaOH
Strip Feed	:	500 g/L H <sub>2</sub> SO <sub>4</sub>
Temperature	:	50°C (loading and stripping)
A/O	:	1 (loading and stripping)
Phase Continuity	:	Aqueous continuous (loading And stripping)

Load-Strip Cycle	Zinc In Loaded Solvent (g/L)	Zinc In Stripped Solvent (g/L)
1	3.90	0.78
2	3.95	0.89
3	3.92	0.84
4	4.08	1.06
5	4.18	1.21
6	4.35	1.33
7	4.45	1.44
8	4.42	1.46
9	4.35	1.40
10	4.32	1.39

**FIGURE 7  
LOAD-STRIP CYCLE TESTS**



## Recovery of Amino Acids

Dialkylthiophosphinic acids, or their salts, have been shown to be effective in extracting a number of  $\alpha$ -amino acids from fermentation broths. This will be illustrated with particular reference to the recovery of L-phenylalanine using CYANEX 301 extractant.

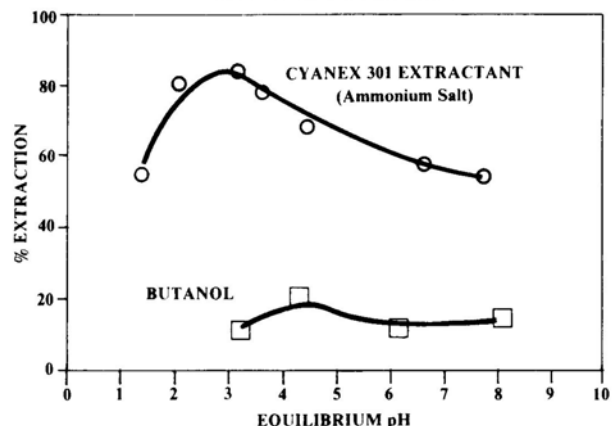
CYANEX 301 is more powerful and less water soluble than other extractants which might be used for the same purpose e.g. butanol. This can be seen by the results of shake-out tests (Table 8 and Figure 8) which show the effect of pH on the extraction of L-phenylalanine with CYANEX 301 and butanol.

**TABLE 8 - EFFECT OF pH ON THE EXTRACTION OF L-PHENYLALANINE**

Solvent	:	(1) 283 g/L CYANEX 301 extractant (ammonium salt) in decanol (2) butanol (undiluted) (3) decanol (undiluted)
Aqueous	:	25.5 g/L L-phenylalanine
Temperature	:	25°C
A/O	:	1
Contact Time	:	5 minutes

	<b>% Extraction</b>	<b>Equilibrium pH</b>
CYANEX 301	55	1.5
	80	2.3
	84	3.1
	80	3.5
	69	4.5
	58	6.5
	54	7.6
Butanol	13	3.4
	20	4.2
	15	6.1
	16	8.1
Decanol	2	3.0
	1	6.7

**FIGURE 8  
EFFECT OF pH ON THE EXTRACTION OF PHENYLALANINE**



Additionally, interpolations from an extraction isotherm obtained with CYANEX 301 (Table 9 and Figure 9) indicate essentially quantitative recovery at A/O=2 in five or six theoretical stages from a fermentation broth containing 20 g/L L-phenylalanine. A polar diluent, such as decanol, is required for good extraction performance. CYANEX 301 was used in its ammonium salt form in the above two series of tests.

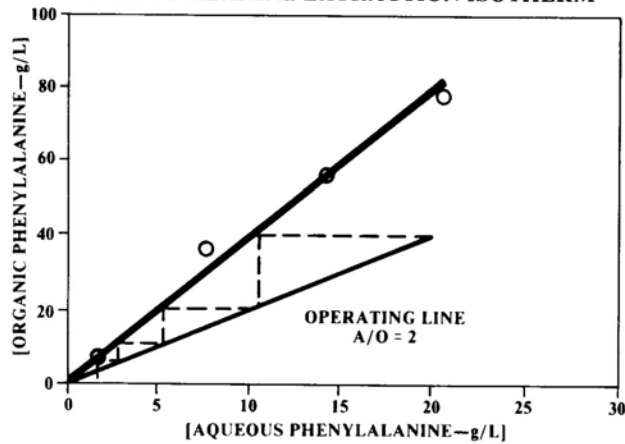
**TABLE 9 -L-PHENYLALANINE EXTRACTION ISOTHERM**

Solvent : 283 g/L CYANEX 301 extractant (ammonium salt) in decanol

Aqueous : 25.5 g/L L-phenylalanine  
Equilibrium pH : 3.0-3.3  
Temperature : 25°C  
Contact Time : 5 minutes

A/O	Equilibrium Concentration (g/L)	
	Organic	Aqueous
0.2	4.8	14.0
2	36.0	79.0
5	56.0	14.4
15	78.0	20.4

**FIGURE 9**  
**PHENYLALANINE EXTRACTION ISOTHERM**



Dialkyl dithiophosphinic acids extract  $\alpha$ -amino acids through a pH dependent mechanism. Extraction is favored at a pH of approximately 3 while stripping is favored at both higher and lower pH (Figure 8). Water, at a pH of approximately 1.3-1.7, has been used successfully to strip L-phenylalanine from reagents similar in composition to CYANEX 301 extractant. A salting-out agent in the strip feed, e.g. 10-20%  $(\text{NH}_4)_2\text{SO}_4$  or  $\text{NH}_4\text{Cl}$ , is required to maintain good phase disengagement characteristics. Data indicate that the amino acid may be selectively separated from the strip liquor by fractional crystallization due to its comparatively low aqueous solubility (approximately 30 g/ L at 25°C).

# ANALYTICAL METHODS

## ANALYSIS IN ORGANIC SOLVENTS

The gas chromatographic procedure described below is suitable for the accurate determination of the concentration of CYANEX 301 in organic solvents, typically containing 5-50 (v/o) CYANEX 301.

The active ingredient present in CYANEX 301 is bis(2,4,4-trimethylpentyl) dithiophosphinic acid. This acid is converted to the corresponding methyl ester for analytical purposes. Trioctylphosphine oxide (TOPO) is employed as an internal standard (ISTD).

### Reagents

1. TOPO (purified-see note 1)
2. Methyl-8® (dimethylformamide dimethylacetal, Pierce Chemical Co.)

### Calibration

The relative response factor of the dithioacid vs. TOPO must be determined. For the analytical conditions below, the RRF was found to have a value of 1.09 (see note 2).

### Procedure

1. Accurately weigh 0.10 g of TOPO and combine with a 1.0 mL aliquot of the organic solution of CYANEX 301 in a Pierce 3 mL Reacti-vial®.
2. Add 0.4 mL of Methyl-80 (see note 3) and maintain the mixture at 65°C, with occasional swirling, for 1 hour.
3. Allow the mixture to cool to ambient temperature, then analyze as described under "Gas Chromatographic Conditions".

### Calculations

$$\text{Concentration of } \text{R}_2\text{PSSCH}_3 = \frac{\text{Area of } \text{R}_2\text{PSSCH}_3 \times 1000 \times 1.09 \times \text{wt. ISTD}}{\text{Area of TOPO}}$$

Where wt. ISTD = wt. TOPO (g)

## Gas Chromatographic Conditions

Instrument	:	Perkin-Elmer Sigma 115 or equivalent
Column	:	Supelco SPB-1 (100% methyl silicone) fused silica capillary column, 30 m x 0.32 mm I.D., 0.25 μ film thickness
Injection Volume	:	0.1 μL
Detector	:	FID
Carrier Gas	:	Helium at 70 psi
Auxiliary Gas	:	Nitrogen at 16 psi
Column Flow	:	1.0 mL/min
Split Ratio	:	60.1
Temperatures	:	°C
Detector	:	290
Injector	:	290
Oven	:	220 (0 min.) programmed to 300 At 10°C/min
Peak Areas	:	Determined by electronic integration

### Notes

1. Pure TOPO can be obtained by recrystallizing commercial grade TOPO from hexane (three recrystallizations are necessary).
2. The RRF value for R<sub>2</sub>PSSH vs. TOPO used here was found to be constant for 5-50 (v/o) solutions of CYANEX 301 in Exxsol D-80.
3. Methyl-8® or equivalent methylation agent is employed to prepare the methyl ester of R<sub>2</sub>PSSH.
4. This method has not been validated.

## ANALYSIS IN AQUEOUS SOLUTION

The procedure is based upon extracting the reagent into methylene chloride and determining the concentration of bis(2,4,4-trimethylpentyl) dithiophosphinic acid by gas chromatography. Trioctylphosphine oxide (TOPO) is used as an internal standard (ISTD).

The solubility of CYANEX 301 extractant in water is 7 mg/L. Soluble losses to a raffinate may be expected to be lower.

### Reagents

1. Methyl-8® Concentrate. Pierce Chemical Co.
2. TOPO (purified-see note 1)

## Calibration

1. Prepare a stock solution of TOPO (ISTD) by accurately weighing ( $\pm 1$  mg) approximately 100 mg of TOPO into a 10 mL volumetric flask. Dilute to 10 mL with methylene chloride and dissolve the TOPO.
2. Determine the relative response factor of the dithiophosphinic acid with respect to the internal standard (TOPO). This is accomplished by accurately weighing these materials, combining with excess Methyl-8® Concentrate, and analyzing as described under "Gas Chromatographic Conditions".

## Procedure

1. A 100 mL aliquot of the aqueous solution is adjusted to pH 1.5 with concentrated HCl and extracted with methylene chloride (3 x 35 mL).
2. The organic extracts are combined and evaporated to 2 mL, transferred to a 3 mL Pierce Reacti-Vial and concentrated with nitrogen to 0.5 mL.
3. Add 70  $\mu$ L of Methyl-8® concentrate, followed by 100  $\mu$ L, of TOPO stock solution (ca. 100  $\mu$ g TOPO).
4. Inject 0.1  $\mu$ L of this solution and analyze as described under "Gas Chromatographic Conditions".

## Calculations

1. Concentration of dithiophosphinic acid in aqueous sample (g/L)

$$= \text{RRF} \times 1.25^* \times \frac{\text{area of methyl dithiophosphinate}}{\text{area of TOPO (ISTD)}} \times \text{wt. ISTD (g)} \times 10$$

\* See note 2

## Gas Chromatographic Conditions

Instrument	:	Perkin-Elmer Sigma 115 or equivalent
Column	:	Supelco SPB-1 (100% methyl Silicone) fused silica capillary Column, 30 m x 0.32 mm I.D., 0.25 $\mu$ film thickness
Detector	:	FID
Carrier Gas	:	Helium at 70 psi, flowrate 1.0 mL/minute
Temperatures	:	$^{\circ}$ C
FID	:	290
Injection Port	:	290
Oven	:	100 to 300 at 15 $^{\circ}$ C/minute, hold Final temp. for 2 minutes
Sample Injection	:	
Volume	:	0.1 $\mu$ L, splitless injection with septum Purge after 30 seconds
Peak Areas	:	Determined by electronic integration

## Notes

1. Pure TOPO can be obtained by recrystallizing commercial grade TOPO from hexane (three recrystallizations are necessary).
2. A factor (1.25) is used to correct for an incomplete extraction of the dithiophosphinic acid from aqueous solutions. If extraction efficiency is 100%, then the factor is unity. It may be determined by spiking the aqueous feed solution with a known quantity of CYANEX 301 and following the steps as described in "Procedure".
3. Retention times for TOPO and methyl dithiophosphinate are approximately 14 and 10 minutes, respectively.
4. The detection limit is approximately 1 mg/L.
5. This method has not been validated.

---

---

## **IMPORTANT NOTICE**

The information and statements herein are believed to be reliable, but are not to be construed as a warranty or representation for which we assume legal responsibility. Users should undertake sufficient verification and testing to determine the suitability for their own particular purpose of any information or products referred to herein. NO WARRANTY OF FITNESS FOR A PARTICULAR PURPOSE IS MADE. Nothing herein is to be taken as permission, inducement or recommendation to practice any patented invention without a license.

### **Trademark Notice**

The ® indicates a Registered Trademark in the United States and the TM or \* indicates a Trademark in the United States. The mark may also be registered, the subject of an application for registration or a trademark in other countries.



CYTEC INDUSTRIES INC.  
Five Garret Mountain Plaza  
West Paterson, NJ 07424  
973-357-3100

---

# CYANEX® 302 Extractant

## Solvent Extraction Reagent

- Extracts metal cations at low pH.
- Selective for zinc over calcium and magnesium.
- Selective for cobalt over manganese

**CYTEC**

# CONTENTS

---

---

## INTRODUCTION

Chemical Structure	2
Typical Properties	2

## MATERIALS OF COMPATIBILITY

Plastics	2
Metals	2

## HYDROLYTIC STABILITY

3

## PERFORMANCE DATA

General Extraction Properties	3
Zinc-Calcium Selectivity	4

## ANALYTICAL METHODS

Analysis in Organic Solvents	6
Analysis in Aqueous Solution	7

## HEALTH AND SAFETY

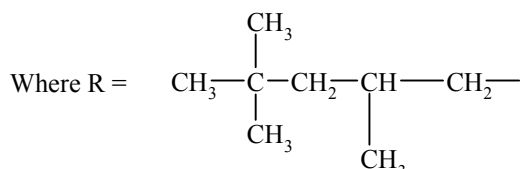
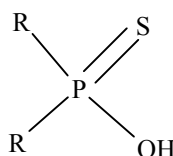
8

# INTRODUCTION

CYANEX 302 extractant is a monothiophosphinic acid. Selective metal separations can be performed at a lower pH than is possible with its oxy-acid analogue, CYANEX 272 extractant. This property is particularly useful when metals are present at low concentration and pH adjustment is uneconomical.

## Chemical Structure

The active component of CYANEX 302 extractant is bis(2,4,4-trimethylpentyl)monothiophosphinic acid.



Molecular Weight = 306

## Typical Properties

Appearance	: Pale yellow liquid
Odor	: Faintly characteristic of Hydrogen sulfide
Assay	: 84% Bis(2,4,4-trimethyl-Pentyl)-monothiophosphinic acid
Specific Gravity	: 0.93 at 24°C
Viscosity	: 195 centipoise at 24°C
Pour Point	: -20°C (approximately)
Flash Point (Closed Cup)	: .205°F (>96°C)
Autoignition Temperature	: 739°F (393°C)
Solubility in Water	: 3 mg/L at 50°C

## MATERIALS OF COMPATIBILITY

### Plastics

Samples of the following plastics and rubbers, in the form of tubing, were immersed for 800 hours at 50°C in glass vessels containing CYANEX 302 extractant. The weights and dimensions of the test samples were determined before and after immersion. The following observations were made.

Material	Remarks
PVC (Solvent Grade)	Loss of plasticity. Short term Suitability only.
Polyethylene	Suitable. No significant change in weight or dimensions.
Teflon*	Suitable. No significant change in weight or dimensions.
Fluorocarbon Film	
Latex	Unsuitable. Swelling with loss of mechanical strength.
Red and Black Gum Rubber	Unsuitable. Swelling with loss of mechanical strength.
Neoprene	Suitable. Small increase in weight and dimensions.

### Metals

Samples of the following metals in the form of coupons (approximate dimensions 50 mm x 25 mm x 3 mm) were immersed for 700 hours at 50°C in glass vessels containing CYANEX 302 extractant. The following observations were made.

Metal	Remarks
Stainless Steel (316)	No detectable corrosion.
Stainless Steel (304)	No detectable corrosion.
Mild Steel	Corrosion at approximately 2 mils per year. Although the corrosion rate was low the extractant became discolored and the use of mild steels is not recommended.

\*Product of El DuPont de Nemours & Co.

## HYDROLYTIC STABILITY

A solvent containing CYANEX 302 extractant was contacted for 640 hours in a stirred resin flask with 300 g/L H<sub>2</sub>SO<sub>4</sub> at 50°C and A/O=1. The flask was equipped with a condenser to minimize diluent evaporation.

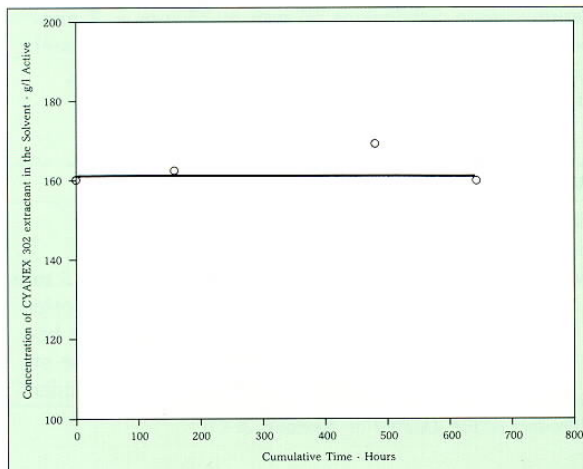
Samples of the dispersed phase were removed periodically and the coalesced solvent analyzed by gas chromatography. The results are given in Table 1 and Figure 1.

**TABLE 1**  
**Stability Testing**

Solvent	:	CYANEX 302 extractant in Exxsol*
		D-80 diluent
Aqueous	:	300 g/L H <sub>2</sub> SO <sub>4</sub>
Phase Contact	:	50°C at A/O=1
<u>Cumulative Time</u> <u>(Hours)</u>		<u>Solvent Analysis</u> <u>(g/L Active)</u>
0		160
160		162
480		169
640		160

\*Product of Exxon Co., U.S.A.

**FIG. 1 — HYDROLYTIC STABILITY**



No significant degradation of the extract was observed. The concentration of tris(2,4,4-trimethylpentyl)phosphine oxide in the solvent (approximately 20 g/L) did not change during the course of the experiment: indicating that diluent losses through evaporation were negligible. The latter compound is an impurity in CYANEX 302 extractant.

## PERFORMANCE DATA

### General Extraction Properties

The fundamental difference between CYANEX 302 extractant and its oxy analogue - CYANEX 272 extractant - is that metal separations can be carried out at lower pH. Displacement of the pH functionality of this extractant toward the acid side is derived from the presence of sulfur in the molecule. This is illustrated by the results of shake-out tests in Table 2 and Figure 2 showing the effect of pH on metal extraction. CYANEX 301 extractant, the dithio analogue, is an even stronger acid than CYANEX 272 or 302 extractants.

**TABLE 2**  
**Extraction From Single Metal Sulfate Solutions**

Solvent	:	0.6 M extractant in Exxsol D-89 diluent
Aqueous	:	0.015 M metal as the sulfate salt
pH Control	:	NH <sub>4</sub> OH or H <sub>2</sub> SO <sub>4</sub> as appropriate
Phase Contact	:	A/O = 1 at 50°C, aqueous continuous

Metal	% Extraction	Equilibrium pH	Metal	% Extraction	Equilibrium pH
Zn (2+)	37.2	0.48	Mn (2+)	1.85	1.99
	66.4	0.83		7.41	2.49
	86.2	1.10		20.4	3.13
	95.1	1.33		73.3	4.02
	99.5	1.82		98.9	5.28
Fe(3+)	45.9	0.68	Ni(2+)	5.81	1.86
	66.9	1.08		17.4	3.15
	73.2	1.18		32.6	4.08
	71.2	1.58		90.6	5.04
	64.3	2.08		99.4	6.08
Co(2+)	61.1	2.63			
	0	1.10			
	36.3	2.49			
	87.8	3.22			
	97.8	3.76			
	99.0	4.01			

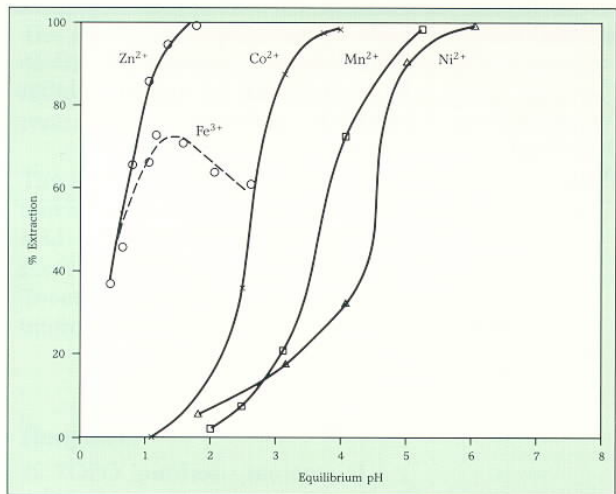
Ca(2+) No extraction detected in the pH range 0.98 to 5.01

Mg(2+) No extraction detected in the pH range 0.65 to 5.30

Cd(2+) quantitatively extracted: pH 0.85 to 4.98

Cu(2+) quantitatively extracted: pH 1.39 to 2.10

**FIG. 2 – EXTRACTION FROM SINGLE METAL SULFATE SOLUTIONS**



Another noteworthy difference between CYANEX 302 and 272 extractants is the ability of CYANEX 302 extractant to separate cobalt (2+) from manganese (2+).

### Zinc-Calcium Selectivity

As a result of its good hydrolytic stability, selectivity and comparatively low pKa, CYANEX 302 extractant is ideally suited to the recovery of metals from effluents or where these metals are present as impurities in process solutions.

This will be illustrated by reference to the selective recovery of zinc from low-pH sulfate solutions also containing calcium. Effluents of this composition are generated in the manufacture of rayon by the viscose process. Zinc can be recycled but must be free from calcium which is deleterious to the process (gypsum precipitates).

A series of shake-out tests was conducted to determine the effect of three process variables, (temperature, pH and diluent aromaticity) on zinc-calcium selectivity. The results are given in Tables 3, 4 and 5.

**TABLE 3  
Effect of Temperature on Zn-Ca Selectivity**

Solvent	:	0.6M extractant on Exxsol D-80 diluent
Aqueous	:	1.04 g/L Zn and 0.090 g/L Ca as sulfates
Phase Contact	:	5 mins at A/O=1
Temperature	:	20, 30, 40, 50 and 60°C
Equilibrium pH	:	1.70±0.01

Temperature °C	% Extraction	
	Zn	Ca
20	99.0	0
30	99.0	0
40	99.0	0
50	99.0	0
60	99.0	0

**TABLE 4  
Effect of pH on Zn-Ca Selectivity**

Solvent	:	0.6M CYANEX 302 extractant in a Mixture of Exxsol D-80 diluent and Toluene (50/50 v/o)
Aqueous	:	1.00 g/L Zn and 0.097 g/L Ca as sulphate
Phase Contact	:	5 mins at A/O = 1 and 24°C
pH	:	Between 1 and 3 (controlled with H <sub>2</sub> SO <sub>4</sub> or NH <sub>4</sub> OH, as appropriate)

Equilibrium pH	% Extraction	
	Zn	Ca
1.00	57.0	0
1.49	93.2	0
2.00	99.2	2.0
2.50	100	2.0
3.03	100	2.0

**TABLE 5  
Effect of Diluent Aromaticity on Zn-Ca Selectivity**

Solvent	:	0.6M extractant in Exxsol D-80 Diluent, toluene and a 50/50 volume Mixture of Exxsol D-80 diluent and Toluene
Aqueous	:	1.02 g/L Zn and 0.10 g/L Ca as sulfates
Phase Contact	:	5 mins at A/O = 1 and 24°C
Equilibrium pH	:	1.70 ± 0.02 (No control necessary)

Diluent Aromaticity (v/o)	% Extraction	
	Zn	Ca
100	96.1	0
50	98.0	0
0	99.0	0

Temperature in the range 20-60°C had no effect. Selectivity increased with increasing pH in the range 1-3. However, in the operating pH range (2.0-0.5), the effect was not significant. The presence of aromatics (toluene) in the diluent depressed zinc extraction without changing calcium extraction. Again, the magnitude of the effect was small.

Isotherms indicated low staging requirements in extraction (Table 6, Figure 3) and stripping (Table 7, Figure 4).

**TABLE 6**  
**Zinc Extraction Isotherm**

Solvent	: 0.6M extractant in Exxsol D-80 diluent
Aqueous pH	: 10.2 g/L Zn as $\text{ZnSO}_4$
pH	: 2.00 ± 0.05 controlled with 100 g/L NaOH
Phase Contact	: 50°C, 2 minute contact after pH stabilization

A/O	Equilibrium Concentration (g/L)	
	Organic	Aqueous
4	9.20	7.90
2	8.75	5.83
1	7.80	2.40
0.5	5.04	0.12
0.33	3.36	0.03

**FIG. 3 — ZINC EXTRACTION ISOTHERM**

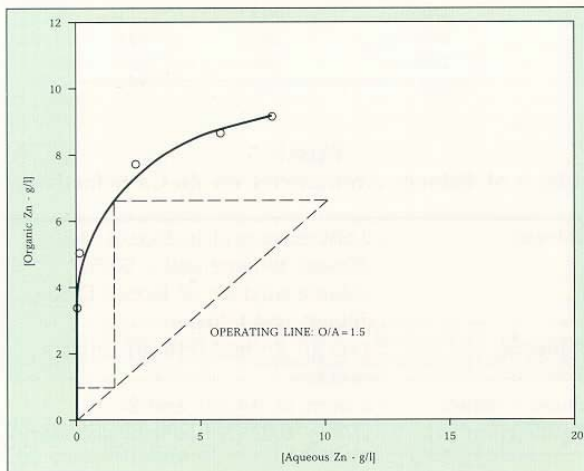
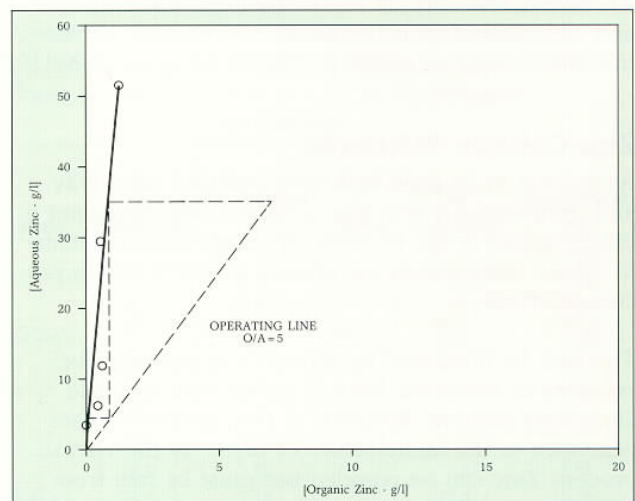


**TABLE 7**  
**Zinc Stripping Isotherm**

Solvent	: 0.6M extractant in Exxsol D-80 diluent. Solvent loaded to 6.4 g/L Zn by contact with an aqueous solution of $\text{ZnSO}_4$
Strip Feed	: 200 g/L $\text{H}_2\text{SO}_4$
Phase Contact	: 5 minutes at 50°C

A/O	Equilibrium Concentration (g/L)	
	Organic	Aqueous
2	0.04	3.18
1	0.40	6.00
0.5	0.55	11.7
0.2	0.50	29.6
0.1	1.24	51.6

**FIG. 4 — ZINC STRIPPING ISOTHERM**



# ANALYTICAL METHODS

## ANALYSIS IN ORGANIC SOLVENTS

The gas chromatographic procedure described below is suitable for the accurate determination of the concentration of CYANEX 302 extractant in organic solvents, typically containing 5-50 v/o CYANEX 302 extractant.

The active ingredient present in CYANEX 302 extractant is bis(2,4,4-trimethylpentyl)-monothiophosphinic acid -  $R_2P(S)OH$ . This acid is converted to the corresponding methyl ester for analytical purposes. Trioctylphosphine oxide (TOPO) is employed as an internal standard (ISTD).

### Reagents

1. TOPO (purified -see note 1)
2. Methyl-8 concentrate (dimethylformamide dimethylacetal, Pierce Chemical Co.).

### Calibration

The relative response factor of the monothioacid vs. TOPO must be determined. For the analytical conditions below, the RRF was found to have a value of 1.04.

### Procedure

1. Centrifuge the solvent to be analyzed or filter through PS paper to remove entrained aqueous or suspended solids.
2. Accurately weigh 0.10 g TOPO and combine with a 1.0 mL aliquot of the organic solution of CYANEX 302 extractant in a Pierce 3 ml Reacti-vial glass bottle.
3. Add 0.5 ml of Methyl-8 (see note 3) and maintain the mixture at 65°C, with occasional swirling, for one hour.
4. Allow the mixture to cool to ambient temperature, then analyze as described under "Gas Chromatographic Conditions." Perform the analysis within three hours after addition of the Methyl-8 reagent.

### Calculations

$$\text{Concentration of } R_2P(S)OH \text{ (g/L)} = \frac{\text{Area of } R_2P(S)OCH_3 \times 1000 \times 1.04 \times \text{wt. ISTD}}{\text{Area of TOPO}}$$

### Gas Chromatographic Conditions

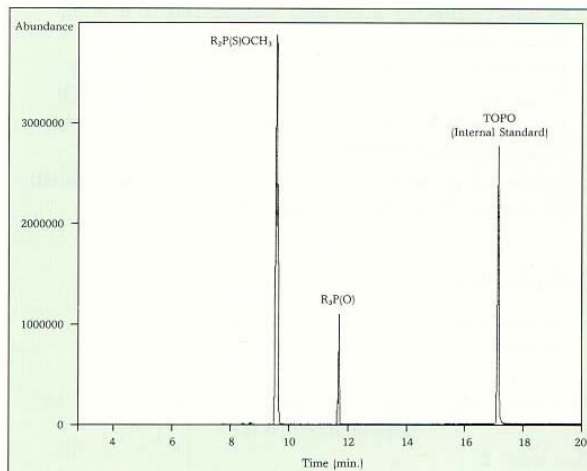
Instrument	:	Perkin Elmer Sigma 115 or equivalent
Column	:	Supelco SPB-5*, fused silica capillary column, 30 m x 0.32 mm x 0.25 $\mu$ film thickness
Injection Volume	:	0.2 $\mu$ L
Detector	:	FID
Carrier Gas	:	He, 70 psi
Auxilliary Gas	:	N <sub>2</sub> , 16 psi
Column Flow	:	1.5 mL/min.
Split Ratio	:	60.1
Temperatures	:	
Detector	:	290°C
Injector	:	290°C
Oven	:	200°C (0 min.) programmed to 300°C at 5°/min.
Peak Areas	:	Determined by electronic integration

\*Product of Supelco Canada, Ltd.

### Notes

1. Pure TOPO may be obtained by recrystallizing commercial grade TOPO from hexane (three recrystallizations are necessary).
2. The RRF value for  $R_2P(S)OH$  vs. TOPO used here was determined for a 10 v/o solution of CYANEX 302 extractant in toluene.
3. Methyl-8 or equivalent methylating agent is employed to prepare the methyl ester of  $R_2P(S)OH$ .
4. This method has not been validated.

FIG. 1A — TYPICAL CHROMATOGRAM OF CYANEX 302 EXTRACTANT



## ANALYSIS IN AQUEOUS SOLUTIONS

The procedure is based upon extracting the reagent into methylene chloride and determining the concentration of bis(2,4,4-trimethylpentyl)monothiophosphinic acid by gas chromatography. Trioctylphosphine oxide (TOPO) is used as an internal standard.

The solubility of CYANEX 302 extractant in water is 3 mg/L. Soluble losses to raffinates may be expected to be lower.

### Reagents

1. Methyl-8 concentrate. (Pierce Chemical Co.)
2. TOPO (purified - see note 1.)

### Calibration

1. Prepare a stock solution of TOPO (ISTD) by accurately weighing ( $\pm 1$  mg) approximately 200 mg of TOPO into a 10 ml volumetric flask. Dilute to the mark with methylene chloride and dissolve the TOPO.
2. Determine the relative response factor of the monothiophosphinic acid with respect to the internal standard (TOPO). This is accomplished by accurately weighing these materials, combining with excess Methyl-8 concentrate, and analyzing as described under "Gas Chromatographic Conditions."

### Procedure

1. Filter the aqueous solution to remove entrained organic.
2. A 100 mL aliquot of the aqueous solution is adjusted to pH 1.0 with concentrated HCl and extracted with methylene chloride (2 x 100 mL).
3. The organic extracts are combined and evaporated to approximately 2 ml and transferred to a 3 ml Pierce Reactivial.
4. Add 50  $\mu$ l of Methyl-8 concentrate, followed by 25  $\mu$ L of TOPO stock solution (ca. 0.5 mg TOPO). Let the solution stand at ambient temperature for approximately 15 minutes.
5. Inject 1.0  $\mu$ L of this solution and analyze as described under "Gas Chromatographic Conditions."

### Calculations

1. Concentration of monothiophosphinic acid in aqueous sample (g/L)

$$= \text{RRF} \times 1.18^* \times \frac{\text{area of } R_2P(S)\text{OCH}_3}{\text{area of TOPO (ISTD)}} \times \text{wt. ISTD (g)} \times 10$$

### Gas Chromatographic Conditions

Instrument	:	Perkin-Elmer Sigma 115 or Equivalent
Column	:	Supelco SPB-1* (100% methyl silicone) fused silica capillary column, 30 m x 0.32 mm ID x 0.25 $\mu$ film thickness
Detector	:	FID
Carrier Gas	:	Helium at 70 psi, flowrate 1.5 mL/min
Temperatures	:	
FID	:	290°C
Injection Port	:	290°C
Oven	:	150°C, programmed to 300°C at 10°/min., hold 5 minutes
Sample	:	
Injection Volume	:	1.0 $\mu$ L, splitless injection with septum purge after 30 seconds
Peak Areas	:	Determined by electronic integration

\*Product of Supelco Canada, Ltd.

### Notes

1. Pure TOPO may be obtained by recrystallizing commercial grade TOPO from hexane (three recrystallizations are necessary).
2. A factor (1.18) is used to correct for an incomplete extraction of the monothiophosphinic acid from aqueous solutions. If extraction efficiency is 100%, then the factor is unity. It may be determined by spiking the aqueous feed solution with a known quantity of CYANEX 302 extractant and following the steps described in "Procedure."
3. The detection limit is approximately 1 mg/L.
4. This method has not been validated.

\* See note 2

---

---

## **HEALTH AND SAFETY**

CYANEX 302 extractant has a moderate degree of oral and a low degree of dermal toxicity. Direct contact with this material may cause severe skin and mild eye irritation. CYANEX 302 extractant was determined to be nonmutagenic in the Ames test. For more detailed health hazard information and handling precautions, please consult the Material Safety Data Sheet.

## **IMPORTANT NOTICE**

The information and statements herein are believed to be reliable but are not to be construed as a warranty or representation for which we assume legal responsibility. Users should undertake sufficient verification and testing to determine the suitability for their own particular purpose of any information or products referred to herein. NO WARRANTY OF FITNESS FOR A PARTICULAR PURPOSE IS MADE. Nothing herein is to be taken as permission, inducement or recommendation to practice any patented invention without a license.



**CYTEC INDUSTRIES INC**

**Phosphine Chemicals**

Five Garret Mountain Plaza West Paterson, NJ 07424  
973-357-3468

---

---

# CYANEX® 471X Extractant

## Solvent Extraction Reagent

- Selective for silver.
- Separates palladium from platinum.

**CYTEC**

# CONTENTS

---

<b>INTRODUCTION</b>	
Chemical Structure	1
Typical Properties	1
Stability	1
Toxicity	1
<b>SILVER RECOVERY</b>	
Background	2
Effect of Acidity	2
Diluents and Phase Modifiers	2
Extraction Isotherm	3
Stripping Isotherm	3
Selectivity in Continuous Testing	5
Aqueous Solubility	5
<b>SEPARATION OF PALLADIUM FROM PLATINUM</b>	
Background	6
Extraction Isotherms	6
Selectivity	7
Kinetics	7
Stripping	7
<b>ANALYTICAL METHODS</b>	
Analysis in Organic Solvents	8
Analysis in Aqueous Solution	9
<b>APPENDIX A</b>	
Silver Recovery from Fixer Solution	11
<b>APPENDIX B</b>	
Purification of CYANEX 471X Extractant	11

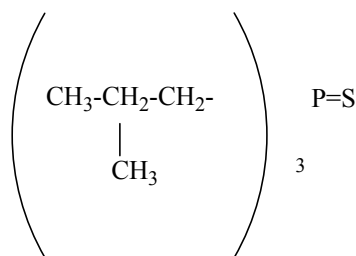
*Cytec Industries Inc. is the former  
Chemicals Group of American Cyanamid Company*

# INTRODUCTION

CYANEX 471X extractant is a new phosphine-based extractant developed by Cyanamid for the hydrometallurgical industry.

This reagent is particularly useful for the selective recovery of silver and in the separation of palladium from platinum.

## Chemical Structure



Triisobutylphosphine Sulfide (TIBPS)

## Typical Properties

Appearance	: Off-white crystalline solid
Specific Gravity at 22°C	: 0.91
Melting Point	: 58-59°C
Solubility in Distilled Water	: 43 µg/mL at 24°C

## Stability

Some hydrolysis of CYANEX 471X extractant (triisobutylphosphine sulfide) to the oxide or other oxygen bearing degradation products might be expected on continuous contact with sulfuric or hydrochloric acid systems. However, as can be seen in Tables 1 and 2, we found that no measurable degradation (detectable by gas chromatography) occurs even at elevated temperatures for 30-40 day exposure periods. Furthermore, gas chromatographic analysis of the aqueous phase at the completion of each test also failed to detect any degradation products.

Solvent : 25.9 g/L CYANEX 471X extractant  
5 v/o D2EHPA in Varsol\* DX-3641 diluent

Aqueous : 6N H<sub>2</sub>SO<sub>4</sub>  
Temperature : 50°C  
A/O : 1

Solvent Analysis		
Contact time (hr)	CYANEX 471X Extractant (g/L)	Oxide Concentration (g/L)
0	25.9	<0.1**
2	24.7	<0.1
336	25.1	<0.1
676	26.4	<0.1

TABLE 2 – IN CONTACT WITH HYDROCHLORIC ACID

Solvent : 142.7 g/L CYANEX 471X extractant, in Varsol DX-3641 diluent  
Aqueous : 1.1 g/L Pd (as PdCl<sub>2</sub>), 2N HCl  
Temperature : 50°C  
A/O : 1

Solvent Analysis		
Contact time (hr)	CYANEX 471X Extractant (g/L)	Oxide Concentration (g/L)
0	142.7	<0.1**
2	146.2	<0.1
158	142.7	<0.1
216	145.2	<0.1
844	143.9	<0.1
964	146.3	<0.1

\* A product of Exxon Co., USA

\*\* Detection limit of analytical method.

## Toxicity

The acute oral (rat) and acute dermal (rabbit) LD<sub>50</sub> values for the active phosphine sulfide contained in CYANEX 471X extractant are 10,000 mg/kg of body weight. No significant skin irritation and only mild eye irritation were produced during primary irritation studies with rabbits. The sulfide was determined to be non-mutagenic in the Ames *Salmonella* Assay.

TABLE 1 – IN CONTACT WITH SULFURIC ACID

# SILVER RECOVERY

## Background

CYANEX 471X extractant is a solvating reagent and will extract silver from sulfate, nitrate and chloride systems. Note that, although silver chloride is essentially insoluble in water, it does exhibit finite solubility in chloride solutions, as follows:

Temperature : 25°C

HCl (g/L)	AgCl(g/L)	Specific Gravity
235	1.12	1.10
372	3.91	1.16
443	4.44	1.19

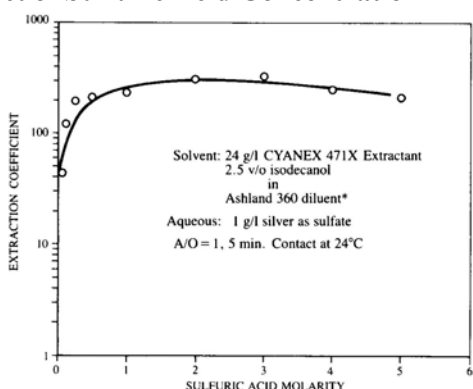
The majority of the world's silver is produced as a by-product from the mining of base metals. Silver may, therefore, form a component of many aqueous streams when the treatment of such ores or secondary sources involves hydrometallurgical processing.

While the source of silver may be a sulfate, chloride or nitrate liquor containing a combination of copper, lead, and other metals, the data cited describes specifically the selective recovery of silver from acid sulfate solutions of zinc or copper.

## Effect of Acidity

Since acidity has a significant impact on the extraction power of solvating reagents in many systems (e.g., TBP-uranyl nitrate), the effect of sulfuric acid concentration on silver extraction with CYANEX 471X extractant was studied. Results and experimental conditions are given in Figure 1.

**FIGURE 1**  
**Effect of Sulfuric Acid Concentration**



As can be seen, silver extraction was essentially quantitative for initial acid concentrations in excess of 0.015M. The small decrease in the extraction coefficient observed with the 4 and 5M acid solutions, may have resulted from a crowding effect due to co-extraction of sulfuric acid.

On the basis of these results the extraction of silver with CYANEX 471X extractant should not be affected by the different sulfuric acid concentrations which might be encountered in commercial practice.

Extraction tests with CYANEX 471X extractant dissolved in Ashland\* 360 diluent produced emulsions even when isodecanol was used as a modifier. For this reason, a number of other diluent-modifier combinations were examined under the following conditions.

Solvent	: 24 g/L CYANEX 471X extractant, 0 and 5 v/o modifier in the diluent
Aqueous	: 1 g/L Ag as $\text{Ag}_2\text{SO}_4$ , 10 g/L $\text{H}_2\text{SO}_4$
A/O	: 1
Contact Time	: 5 minutes
Temperature	: 24°C
Diluents	: Varsol DX-3641**, Kermac 470B***, Aromatic 150**
Modifiers	: Isodecanol, Tributylphosphate, D2EHPA

Silver extraction was essentially quantitative in all of the examined systems. However, only those solvents modified with D2EHPA solubilized the extracted complex. This may be due to the displacement of bonded water from the silver ion by the stronger OH ligand present in D2EHPA. The OH group in water is a stronger ligand than in isodecanol and, conceivably, could account for the failure of the alcohol modifier. In later experiments, p-nonylphenol, which like D2EHPA contains an acidic OH group, also proved to be an effective modifier.

\* A product of Ashland Chemical Co.

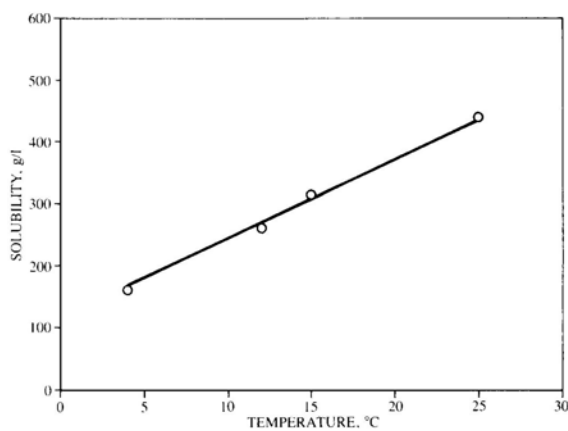
\*\* A product of Exxon Co., USA.

\*\*\* A product of Kerr McGee Refining Corp.

Solvent poisoning may occur in a system where the pH is sufficiently high to allow D2EHPA to extract cations such as  $\text{Fe}^{3+}$ . In this event, p-nonylphenol is the phase modifier of choice.

Based on its performance, availability and the general preference for aliphatic over aromatic diluents, Varsol DX3641 is recommended. The solubility of CYANEX 471X extractant in this diluent is shown as a function of temperature in Figure 2.

**FIGURE 2**  
**Solubility in Varsol DX-3641 Diluent**



### Extraction Isotherms

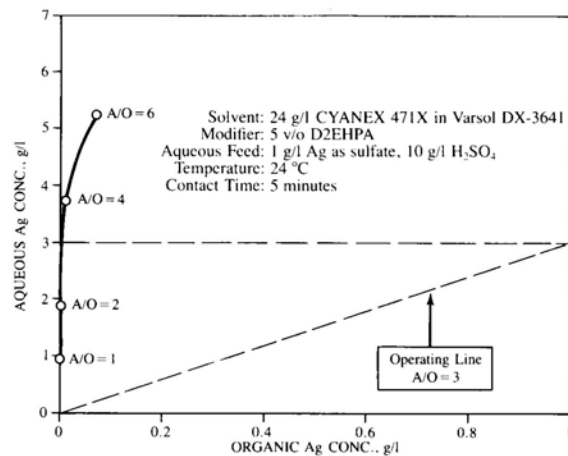
A silver extraction isotherm was generated by contacting an aqueous and solvent feed solution at several A/O ratios. This isotherm along with experimental conditions is shown in Figure 3.

McCabe-Thiele interpolations indicated essentially quantitative silver extraction in one theoretical stage at  $\text{A}/\text{O} = 3$  from an aqueous solution containing 1 g/L silver. The inflection in the isotherm suggested that the loading capacity of the solvent (0.1 M in extractant) was being approached at approximately 5.2 g/L Ag ( $0.024\text{M Ag}_2\text{S}_4$ ).

The solvent loaded to 5.2 g/L Ag darkened after several hours standing; possibly a result of the minimal amount of acid which would be expected to co-extract under these conditions and the consequent hydrolysis of the extracted silver complex.

The solvent loaded to 3.7 g/L Ag at  $\text{A}/\text{O} = 4$  was observed for five days and remained homogeneous.

**FIGURE 3**  
**Silver Extraction Isotherm**



### Stripping Isotherm

Theoretically, stripping may be achieved with any compound which forms a strong ligand with silver. However, reagents proposed in the past for laboratory use have been unsatisfactory for a number of reasons; e.g. cyanide solutions in acid systems are toxic and ammonia tends to form explosively unstable fulminates.

For this reason, it was necessary to find a new stripping system for this class of compounds. The discovery that thiosulfate fixer solutions were effective made possible the commercialization of CYANEX 471X extractant. These reagents are non-toxic and form stable complexes with silver from which silver metal may be recovered by well established processes (see Appendix A). The recovery of metallic silver regenerates the strip liquor which can be recycled. This contributes significantly to lowering process costs.

A silver stripping isotherm was constructed by contacting loaded solvents at various A/O ratios with a stabilized thiosulfate solution of the following composition:

COMPONENT	QUANTITY
Water (at 50°C)	600 mL
Sodium Thiosulfate, $\text{Na}_2\text{S}_2\text{O}_3 \cdot 5\text{H}_2\text{O}$	240 g
Sodium Sulfite $\text{Na}_2\text{SO}_3$	15 g
Acetic Acid (28%)*, $\text{CH}_3\text{COOH}$	48 mL
Boric Acid (Crystal)**, $\text{H}_3\text{BO}_3$	7.5 g
Aluminum Potassium Sulfate, $\text{A1K} (\text{SO}_4)_2 \cdot 12\text{H}_2\text{O}$	15 g
Cold Water to make	1 liter

The following procedure was adopted to prepare the solution from its components.

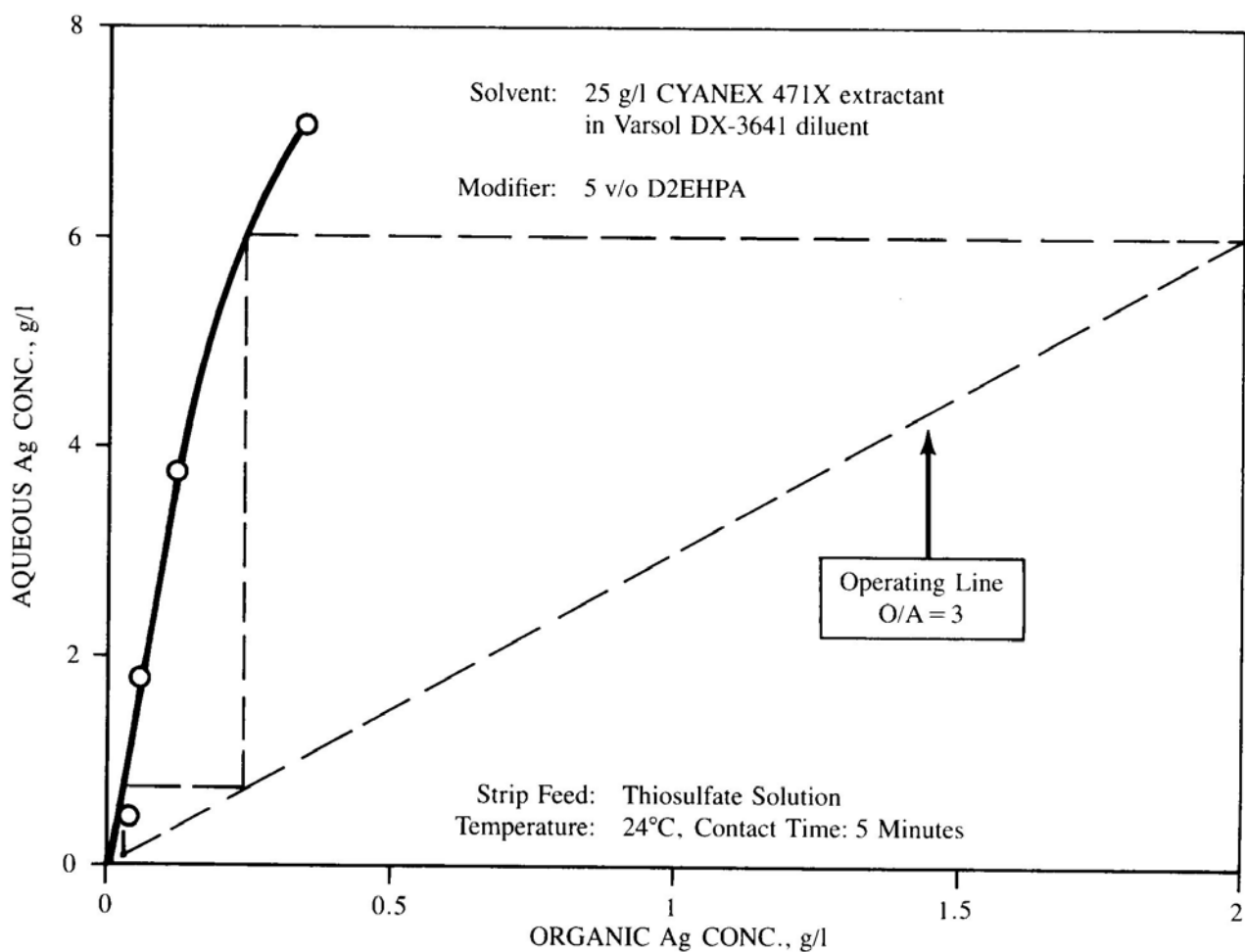
- Sodium thiosulfate was dissolved in the specified volume of warm water.
- The remaining components were added in the given order; ensuring that each was dissolved before adding the next.

The isotherm, plotted in Figure 4, indicates efficient stripping.

\* To make 28% acetic acid, dilute 3 parts of glacial acetic with 8 parts of water.

\* Crystalline boric acid should be used as specified. Powdered boric acid dissolves only with great difficulty and its use should be avoided.

**FIGURE 4**  
**Silver Stripping Isotherm**



## Selectivity in Continuous Testing

The selective extraction of silver from a copper-zinc sulfate solution was investigated in a continuous, counter-current, mini-plant test using a Bell Engineering mixer-settler apparatus. The solvent was recycled through two extraction and two stripping stages. The thiosulfate strip feed was not recycled. Operating conditions and results are given in Table 3.

**TABLE 3 - CONTINUOUS, COUNTER-CURRENT TESTING OPERATING CONDITIONS**

Mixer Volume	:	180 mL
Settler Volume	:	620 mL
Settler Area	:	88.5 cm <sup>2</sup>
Solvent	:	24 g/L CYANEX 471X extractant, 5 v/o D2EHPA in Varsol DX-3641 diluent
Aqueous Feed	:	0.97 g/L Ag <sup>+</sup> , 6.06 g/L Zn <sup>2+</sup> , 10.3 g/L Cu <sup>2+</sup> (as sulfates) 10 g/L H <sub>2</sub> SO <sub>4</sub>
Extraction Stages	:	2
Strip Stages	:	2
Solution Flow- rates (mL/min)		
Aqueous Feed	:	50
Solvent	:	50
Strip Feed	:	50
Continuous Phase	:	Organic (extraction and stripping)
Temperature	:	24°C
Duration of Test	:	4 hours

### Analysis

Raffinate	Ag Recovery	Strip Liquor (g/L)		
		Ag	Zn	Cu
<0.001 g/L Ag	99.9%	0.97	0.012	0.006
Separation Factors:	(Ag/Zn)=0.5 x 106 (Ag/Cu)=1.5x106			

The high separation factors are indicative of the extremely selective separations which can be achieved with CYANEX 471X extractant.

## Aqueous Solubility

Although CYANEX 471X extractant has very little solubility in water, there will be some losses and these will vary from system to system depending upon the composition of the aqueous phase and other operating parameters.

For example, losses to the raffinate and strip liquor described in the continuous test were determined to be 6 µg/mL and <1 µg/mL, respectively. Solubility of the corresponding triisobutyl oxide in water is approximately 40 g/L. If any long-term hydrolysis to the oxide does occur, this compound will be lost to the aqueous phase through preferential solubility.

# SEPARATION OF PALLADIUM FROM PLATINUM

## Background

CYANEX 471X extractant has potential in the separation of palladium from chloride solutions containing platinum (IV) and palladium (II). As with silver, palladium extraction occurs through a solvating mechanism. Similarly, stabilized thiosulfate solutions are an effective strip feed. If present, Ag, Hg (II), Au (III) will be co-extracted with palladium.

The following information on palladium extraction, stripping and palladium/platinum separation will be of use in the design of preliminary batch experiments.

## Extraction Isotherms

The results of two extraction isotherms are shown in Table 4. One was generated with an unmodified solvent and the other using a solvent modified with p-nonylphenol.

In the absence of the modifier, the extracted palladium complex precipitated as a dark brown solid at loadings of 11.2 and 22.4 g/L Pd. The p-nonylphenol solubilized the compound to at least 22.4 g/L Pd in the solvent. This represents an 87% stoichiometric loading; assuming that 2 moles of CYANEX 471X extractant react with 1 mole of palladium.

**TABLE 4 - EFFECT OF p-NONYLPHENOL ON THE LOADING CAPACITY**

Solvent	:	(A) 120 g/L CYANEX 471X extractant in Varsol DX-3641 diluent.
	:	(B) As above, modified with 10 v/o p-nonylphenol.
Aqueous	:	2.24 g/L Pd (as $\text{PdCl}_2$ ) in 2N HCl.
Temperature	:	50°C
Contact Time	:	20 minutes

Solvent	A/O	Organic [Pd] (g/L)	% Pd Extracted
A	1	2.24	100
	2	4.48	100
	5	11.20*	100*
	10	22.40*	100*
B	1	2.24	100
	2	4.48	100
	5	11.20	100
	10	22.40	100

\*Precipitation of the extracted complex occurred.

## Selectivity

Initial batch experiments to investigate Pd/Pt selectivity were made by contacting a solvent containing CYANEX 471X extractant with a Pd/Pt chloride solution. The results were as follows.

Solvent : 300 g/L CYANEX 471X extractant, 10 v/o p-nonylphenol in Varsol DX-3641 diluent.  
Aqueous : 1.23 g/L Pd (II) < 2.54 g/L Pt(IV) as chloride 2N in HCl.  
Contact Time : 10 minutes  
Temperature : 50°C

% Extraction		
A/O	Pd	Pt
1	100	11
2	100	13

Higher selectivities will be obtained by reducing the concentration of CYANEX 471 X extractant in the solvent.

## Kinetics

A study of the rate of Pd and Pt extraction has shown that the selective separation of these two metals is kinetically based; as illustrated in Figure 5. The results were obtained at 50°C and A/O = 2 by contacting an unmodified solvent (30g/L CYANEX 471X extractant in Varsol DX-3641 diluent) with an aqueous chloride

solution containing 1 g/L Pd (II) and 1 g/L Pt (IV) in 2N HCl

## Stripping

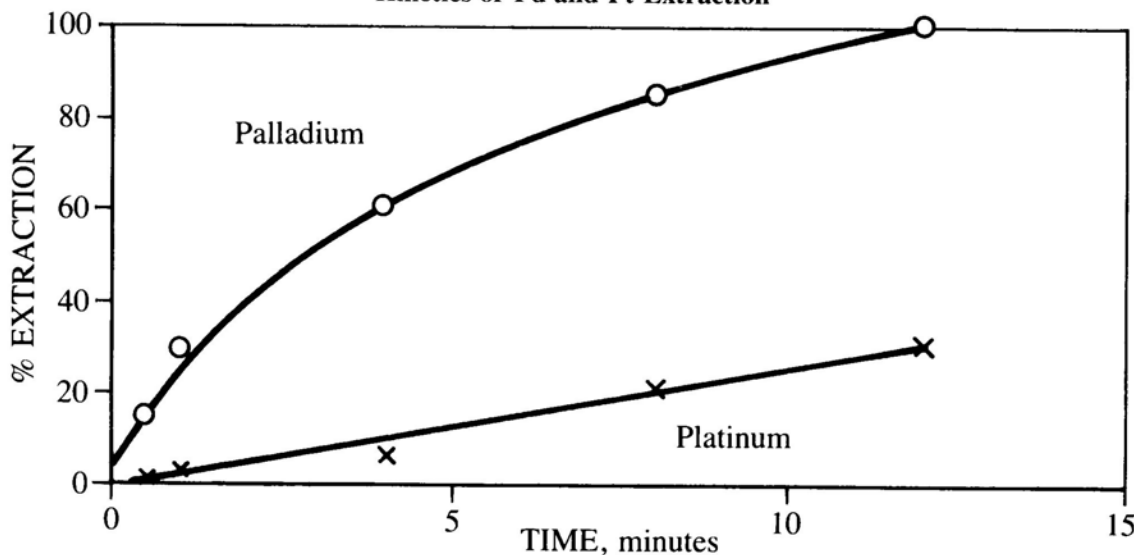
Palladium may be stripped from the loaded solvent using a sodium thiosulfate solution of the same composition as given in the section on silver recovery. The results of preliminary batch tests illustrating the utility of thiosulfates as strip feeds are as follows:

Solvent : 120 g/l CYANEX 471X extractant in Varsol DX-3641 diluent; loaded to 2.21 g/L Pd  
Strip Feed : Stabilized sodium thiosulfate solution  
Temperature : 50°C  
Contact Time : 20 minutes

A/O	% Pd Stripped
1	100
2	100

Ammonia has not been evaluated as a strip feed for palladium in our laboratories. However, its properties are such that it will probably be effective. Palladium-ammonia complexes are stable but care must be exercised to avoid complex formation with other metals which form explosively unstable fulminates; e.g. silver and mercury.

**FIGURE 5**  
**Kinetics of Pd and Pt Extraction**



# ANALYTICAL METHODS

Two gas chromatographic procedures have been developed for the determination of the active ingredient of CYANEX 471X extractant (triisobutylphosphine sulfide, or TIBPS). The first method is designed to analyze the concentration of TIBPS in process solvents and the second, to measure solubility losses in raffinates, strip liquors or other aqueous solutions.

Both procedures require the preparation of standard solutions of TIBPS. Typically, CYANEX 471X extractant will be 95% pure and this should be compensated for when preparing standard solutions from commercial product.

Alternatively and preferably, AR grade CYANEX 471X extractant may be prepared from CYANEX 471X by recrystallization from a 70 v/o solution of 2-propanol in distilled water. The recrystallization procedure is described in Appendix B.

## Analysis In Organic Solvents

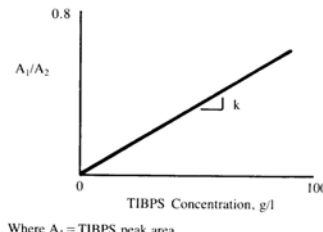
As described, the procedure is suitable for analyzing solvents containing between 20 and 100 g/L TIBPS. Other concentrations may be determined by making appropriate changes to the aliquots and/or dilutions which are cited.

## Reagents

1. 25 v/o solution of hexadecane (internal standard) in toluene.
2. AR grade TIBPS.

## Calibration

1. Make up 20, 40, 60, 80 and 100 g/L standard solutions of TIBPS in the appropriate diluent; e.g. Varsol DX-3641, Escaid 100, etc.
2. Prepare the analyte solutions by pipetting 10 mL of the hexadecane internal standard into a 50-mL volumetric flask and making up to volume with the standard solution. Analyze the solution as described under "Gas Chromatographic Conditions."
3. Plot the calibration curve as follows and determine the slope "k".



Where  $A_1$  = TIBPS peak area  
 $A_2$  = Hexadecane peak area

Hexadecane elutes before TIBPS. The calibration curve should be a straight line passing through the origin.

### Procedure

1. Centrifuge the solvent to be analyzed or filter through PS paper to remove any entrained aqueous or suspended solids.
2. Pipette 10 mL of the hexadecane internal standard into a 50-mL volumetric flask and make up to volume with the process solvent. Determine the hexadecane and TIBPS peak areas as described under "Gas Chromatographic Conditions."

### Calculation

$$\text{Concentration of TIBPS in the solvent (g/L)} = \frac{A_t}{A_h} \times \frac{1}{k}$$

Where  $A_t$  = TIBPS peak area

$A_h$  = Hexadecane peak area

$k$  = Slope of the calibration curve

### Gas Chromatographic Conditions

Instrument	: Perkin Elmer, Sigma 115 or equivalent
Column	: 6' x 1/8" stainless steel, packed with 3% OV 17 on 80/100 Chromasorb W (AW)
Detector	: FIX (Air at 30 psig, H <sub>2</sub> at 20 psig)
Carrier Gas	: Helium (22 mL/min)
Temperatures	: FID = 300°C Injection Port = 310°C
Program	: Column at 175°C for 4 min then raised to 250°C at 30°C/min and held for 5 min.
Sample Injection	
Volume	: 1 μL
Peak Areas	: Determined by electronic integration. hexadecane and TIBPS have approximate retention times of 3.6 and 5.6 min., respectively.

### Notes

1. PS (Phase Separation) paper is available from Whatman, Inc., Clifton, NJ.
2. Escaid 110 diluent is available from Exxon Company, USA.
3. Varsol DX-3641 diluent is available from Exxon Company, USA.
4. Organic compounds generally exhibit high coefficients of volumetric expansion. Care should be taken to maintain all organic solutions at a controlled temperature to avoid errors induced by volume changes.
5. This method has not been validated.

### Analysis in Aqueous Solution

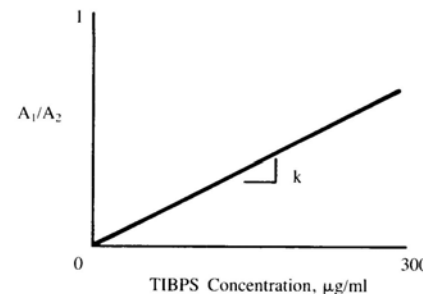
The procedure is designed for the analysis of raffinates or other aqueous solutions containing up to 15 μg/mL of TIBPS. Detection limit is approximately 1 μg/mL.

#### Reagents

1. Cyclohexane
2. 3500 μg/mL solution of hexadecane (internal standard) in cyclohexane.
3. 350 μg/mL solution of hexadecane in cyclohexane.
4. 2000 μg/mL solution of TIBPS in cyclohexane.
5. All reagents are AR grade.

#### Calibration

1. Pipette 1, 5, 10 and 15 mL aliquots of the 2000 μg/mL solution of TIBPS into 100-mL volumetric flasks. Pipette 10 mL aliquots of the 3500 μg/mL hexadecane solution into each of the flasks. Make up to volume with cyclohexane to prepare 20, 100, 200 and 300 μg/mL TIBPS standard solutions each containing 350 μg/ml of the internal standard, hexadecane.
2. Analyze the solutions as described under "Gas Chromatographic Conditions."
3. Plot the calibration curve as follows and determine the slope "k".



Where  $A_1$  = TIBPS peak area

$A_2$  = Hexadecane peak area

The calibration curve is a straight line passing through the origin.

### Procedure

1. Filter the aqueous solution to remove entrained organic.
2. Pipette 100 mL of the aqueous and 5 mL of the 350 μg/mL solution of hexadecane in cyclohexane into a 250 mL separatory funnel (or other suitable vessel) and equilibrate for 10 minutes at room temperature (24°C).
3. Allow 15 minutes to settle and transfer the organic (and any emulsion) to a glass vial and centrifuge for one hour at 1300 g to remove entrained aqueous. If no emulsion is present initially, filtration through PS paper is adequate.
4. Analyze the coalesced organic as described under "Gas Chromatographic Conditions".

## **Calculation**

Concentration of TIBPS in the Aqueous ( $\mu\text{g/mL}$ )

$$= \frac{A_t}{A_h} \times \frac{1}{k} \times \frac{O}{A}$$

Where  $A_t$  = TIBPS peak area

$A_h$  = Hexadecane peak area

$k$  = Slope of the calibration curve

$O/A$  = Organic/aqueous volume phase ratio for extraction (in this case 1/20)

## **Gas Chromatographic Conditions**

Instrument	: Perkin Elmer, Sigma 115 or equivalent
Column	: 6' x 1/8" stainless steel, packed with 3% OV 17 on 80/100 Chromasorb W (AW)
Detector	: FID (Air at 30 psig, $H_2$ at 20 psig)
Carrier Gas	: Helium (10 mL/min)
Temperatures	: FID = 300°C Injection Port = 310°C
Program	: Column at 175°C for 6 minutes then raised to 200°C at 10°C/min and held for 5 minutes
Sample Injection Volume:	0.5 $\mu\text{L}$
Peak Areas	: Determined by electronic integration. Hexadecane and TIBPS have approximate retention times of 6.9 and 10.3 minutes, respectively.

## **NOTES**

1. The solubility of TIBPS in distilled water is approximately 43  $\mu\text{g/mL}$  at 24°C.
2. The solubility in TIBPS in a 10 g/L  $H_2SO_4$  raffinate containing 6 g/L  $Zn^{2+}$  and 10 g/L  $Cu^{2+}$ , is 6  $\mu\text{g/mL}$  at 24°C. The solubility in a thiosulfate stripping solution (ibid) is <1  $\mu\text{g/mL}$  at 24°C. Solubilities will vary depending upon the composition of the solvent, aqueous feed, temperature etc.
3. PS (Phase Separation) paper is available from Whatman, Inc.
4. Organic compounds generally exhibit high coefficients of volumetric expansion. Care should be taken to maintain all organic solutions at a controlled temperature to avoid errors induced by volume changes.
5. This method has not been validated.

## APPENDIX A

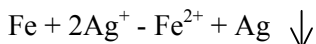
### SILVER RECOVERY FROM FIXER SOLUTIONS

Two methods are widely used in the photographic industry to recover silver from fixer solutions used in film and paper processing. These are:

Electrolysis

Cementation

Electrolysis produces high purity silver cathodes. However, it is the more costly of the two alternatives. In cementation the fixer solution is passed through a filter cartridge containing spun steel and silver metal is precipitated according to the reaction:



Both methods can and are operated on a continuous basis. Occasional make-up of the thiosulfate solution is required.

## APPENDIX B

### PURIFICATION OF CYANEX 417X EXTRACTANT

1. At 40°C, dissolve 500 g of CYANEX 471X extractant in 150-200 mL f a 70 v/o solution of 2-propanol in distilled water.
2. Cool to room temperature and vacuum filter to remove undissolved solids.
3. Cool the filtrate to approximately 0°C and maintain at this temperature for 1 hour. Vacuum filter the recrystallized TIBPS and wash the filter cake with 100 mL of the 70 v/o 2-propanol solution (at 0 to 10°C).
4. Repeat the procedure for a total of 3 recrystallizations. Vacuum dry the final TIBPS filter cake at 25-30°C for 24 hours.
5. The final product should be >98% pure by total GC peak integration and have a melting point of 58-59°C.

---

---

**IMPORTANT NOTICE:** The information and statements in this manual are believed to be reliable but are not to be construed as a warranty or representation for which we assume legal responsibility or as an assumption of a duty on our part. Users should undertake sufficient verification and testing to determine the suitability for their own particular purpose of any information or products or vendors referred to herein. NO WARRANTY OF FITNESS FOR A PARTICULAR PURPOSE IS MADE. Nothing in this manual is to be taken as permission, inducement or recommendation to practice any patented invention without a license.

**TRADEMARK NOTICE:** The ' indicates a Registered Trademark in the United States and the TM or \* indicates a Trademark in the United States. The mark may also be registered, the subject of an application for registration or a trademark in other countries.

---

**FOR ADDITIONAL INFORMATION PLEASE  
CONTACT:**

Cytec Industries, Inc.  
West Paterson, NJ, USA  
Tele: 973-357-3100  
Fax: 973-357-3050

Cytec Canada, Inc.  
Phosphine Technical Center  
Niagara Falls, Ontario  
Tele: 905-356-9000  
Fax: 905-374-5939

Cytec Australia Holdings Pty. Ltd.  
Baulkham Hills, NSW 2153  
Tele: 61-2-9686-4188  
Fax: 61-2-9639-4248

Cytec Industries France  
Rungis-Cedex  
Tele: 33-1-4180-1700  
Fax: 33-1-4978-0780

Cytec Industries B.V.  
Botlek, The Netherlands  
Tele: 31-181-295400  
Fax: 31-181-295401



*Technology ahead of its time*

---

[www.cytec.com](http://www.cytec.com)

# CYANEX®921 Extractant

## Solvent Extraction Reagent

- Selective for cobalt over nickel from sulfate and chloride media.
- Selective for zinc in the presence of calcium and cobalt.
- Extracts other metal cations.

**CYTEC**

# CONTENTS

---

## INTRODUCTION

Chemical Structure .....	1
Typical Properties .....	1
Compatible Materials .....	1
Stability .....	1
Solubility Losses .....	1
Organic Solubility .....	1
Toxicity .....	1

## COMMERCIAL APPLICATIONS

Uranium Recovery From Wet Process	
Phosphoric Acid .....	2
Acetic Acid Recovery From Effluent Streams .....	2

## POTENTIAL APPLICATIONS

METAL EXTRACTION .....	4
Niobium Tantalum Separation .....	4
Rhenium Recovery .....	4
Arsenic Extraction From Copper Electrolytes .....	4
Lithium Recovery .....	4
Additional Applications .....	4
ORGANIC EXTRACTION	
Phenol Recovery .....	5

## REFERENCES .....

---

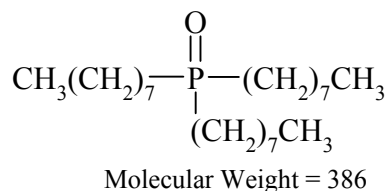
ANALYTICAL METHODS	
Analysis in Organic Solvents .....	9
Analysis in Aqueous Solution .....	9

# INTRODUCTION

CYANEX® 921 extractant, better known as trioctylphosphine oxide (TOPO), was the first member of a family of solvent extraction reagents developed by Cytec. This reagent has been used commercially for many years to recover uranium from wet process phosphoric acid. A more recent industrial application is in the extraction of acetic acid from effluent streams.

## Chemical Structure

The chemical structure of CYANEX 921 extractant is as follows:



## Typical Properties

Trioctylphosphine oxides	:	93%
Appearance	:	Off-white, waxy solid
Specific Gravity at 25°C	:	0.88
Specific Gravity at 61°C	:	0.84
Melting Point °C	:	47-52
Viscosity at 55°C	:	15.0 centipoise (15.0 mPa.s)
Brookfield Viscometer At 100°C	:	5.5 centipoise (5.5 mPa.s) (Viscosity is shown as a function of temperature in Figure 1)

## Compatible Materials

Stainless steel (304 and 316), mild steel and aluminum were found to corrode at <1 mil per year when in contact with a TOPO melt at 60-80°C.

## Stability

Trialkylphosphine oxides, of which CYANEX 921 is one example, are known to be the most stable members of the group of organophosphorus solvating reagents.<sup>(1,2,3,4)</sup>

Losses due to degradation are, therefore, likely to be lower than those associated with extractants such as tributylphosphate and dibutyl butylphosphonate.

## Solubility Losses

Losses of CYANEX 921 extractant by distribution to aqueous solutions of various composition were determined in some batch shake-out tests. The results are given below.<sup>(3)</sup>

Composition of Aqueous Phase	Extractant Solubility mg/L
Water	1.1±0.7
1 M HCl	0.2±0.07
0.5 M SO <sub>4</sub> <sup>2-</sup>	0.2±0.07
0.1 M HNO <sub>3</sub>	
2% Na <sub>2</sub> CO <sub>3</sub>	3.6±0.06
5% Na <sub>2</sub> CO <sub>3</sub>	3.6±1.3

The experimental conditions were as follows:

Solvent : 0.1 M extractant (38.6 g/L) in decane  
Temperature, °C : 25  
Equilibration Time : 10 minutes  
A/O : 1

The soluble losses are generally lower than those of other extractants in commercial use, e.g. losses of amines to acidic sulphate solutions are reported to be in excess of 10 mg/L.<sup>(4,5)</sup>

## Organic Solubility

The solubility of CYANEX 921 extractant in four typical commercial diluents is shown as a function of temperature in Figure 4. Solubility is higher in the aromatic diluents, - Aromatic 100\* and Aromatic 150\* diluents than in the two essentially aliphatic diluents Escaid 110\* diluent and Kermac 470B\*\* diluent.

## Toxicity

The acute oral (rat) and acute dermal (rabbit) LD50 values for CYANEX 921 extractant are >10.0 g/kg and 2.83 g/kg, respectively. Marked skin and eye irritation were produced during primary irritation studies with rabbits. Inhalation of airborne material may be irritating to the respiratory tract. CYANEX 921 was determined to be not mutagenic in the Ames Salmonella Assay.

\*Product of Exxon Co., U.S.A. "Product of Kerr-McGee Refining Corp.

\*\*Product of Kerr-McGee Refining Corp.

# COMMERCIAL APPLICATIONS

## Uranium Recovery From Wet Process Phosphoric Acid

Original work at the Oak Ridge National Laboratories led to the development of a solvent extraction process to recover the small quantities of uranium (0.1 to 0.2 g/L) present in wet process phosphoric acid.<sup>(6,7,8)</sup> The process, which is based on the extraction of hexavalent uranium using a synergic mixture of CYANEX 921 extractant and D2EHPA, is operating successfully in a number of commercial plants in the U.S., Canada and Belgium.

## Acetic Acid Recovery From Effluent Streams

Processes in petrochemical plants, wood pulp mills and other chemical facilities often generate aqueous effluent streams containing small concentrations of carboxylic acids; particularly acetic acid. Typically, the acids are present in concentrations of 1 to 50 gpl depending upon the source.<sup>(9)</sup>

The use of CYANEX 921 extractant and other reagents to recover acetic acid from these streams has formed the subject of several informative papers in recent years<sup>(10,11,12,13)</sup> and a number of patents have been issued in this area.<sup>(14,15)</sup> Briefly, the described processes consist of extracting the acid into a water-immiscible solvent, recovering or stripping the acid from the loaded solvent by distillation and recycling the solvent. One such plant, which recovers acetic acid and furfural, has been operated successfully by Lenzing AG in Austria since 1983.

The advantages of CYANEX 921 in this application lie in low solubility losses, stability during distillation at elevated temperatures and high extraction coefficients for acetic acid in comparison to other solvating reagents. These properties have the effect of minimizing plant operating and capital costs.

As an illustration of efficient performance characteristics, an acetic acid extraction isotherm obtained with a solvent containing 400 g/L CYANEX 921 extractant is shown in Figure 1. The corresponding experimental results and conditions are given in Table 1.

McCabe-Thiele interpolations from the isotherm indicate essentially quantitative recovery in three theoretical stages at O/A = 1.5; assuming an initial feed containing 10 g/L acetic acid.

Raffinates obtained from the above shake-out tests were analysed and found to contain <2 mg/L of CYANEX 921 extractant (detection limit of the method).

Rapid extraction kinetics play an important role in any solvent extraction process as good kinetic properties allow for the design of compact equipment and, consequently, have a favorable effect on capital expenditures. This property is

particularly important when differential (column) contactors are used because of the comparatively short contact times and low interfacial areas prevalent in this type of equipment.

Data on the rate of extraction of acetic acid with CYANEX 921 are presented in Table 2 and Figure 2 and indicate that extraction is essentially complete in <2 minutes. This rate is sufficiently high so as not to impose any kinetically based limitations on equipment selection for this process.

TABLE 1  
Acetic Acid Extraction Isotherm

Solvent	:	400 g/L CYANEX 921 extractant in DPA diluent*
Aqueous	:	10.0 g/L acetic acid
Temperature, °C	:	50
Contact Time	:	5 minutes

A/O	Equilibrium Acetic Acid Concentration (g/L)	
	Organic	Aqueous
2	8.40	5.80
1	7.50	2.50
0.5	4.48	1.05
0.2	1.92	0.40
0.1	0.92	0.20

\*DPA, a high boiling (330-379°C) diphenylalkene diluent, is a product of Conoco Chemicals Co. (a division of Conoco)

TABLE 2  
Acetic Acid Extraction Kinetics

Solvent	:	400 g/L CYANEX 921 extractant In DPA diluent
Aqueous	:	Synthetic solution containing 7.50 g/L acetic acid
Temperature, °C	:	50
A/O	:	1 (Organic continuous phase)

Time (mins)	Acetic Acid		
	Conc. In Raffinate (g/L)	% Extraction	Extraction Coefficient E <sup>o</sup> A
0	7.50	0	0
0.5	1.92	74.5	2.91
1	1.67	77.8	3.49
2	1.67	77.8	3.49

E<sup>o</sup> A = Concentration of Acetic Acid in Solvent at Equilibrium / Concentration of Acetic Acid in Aqueous

FIG. 1—ACETIC ACID EXTRACTION ISOTHERM

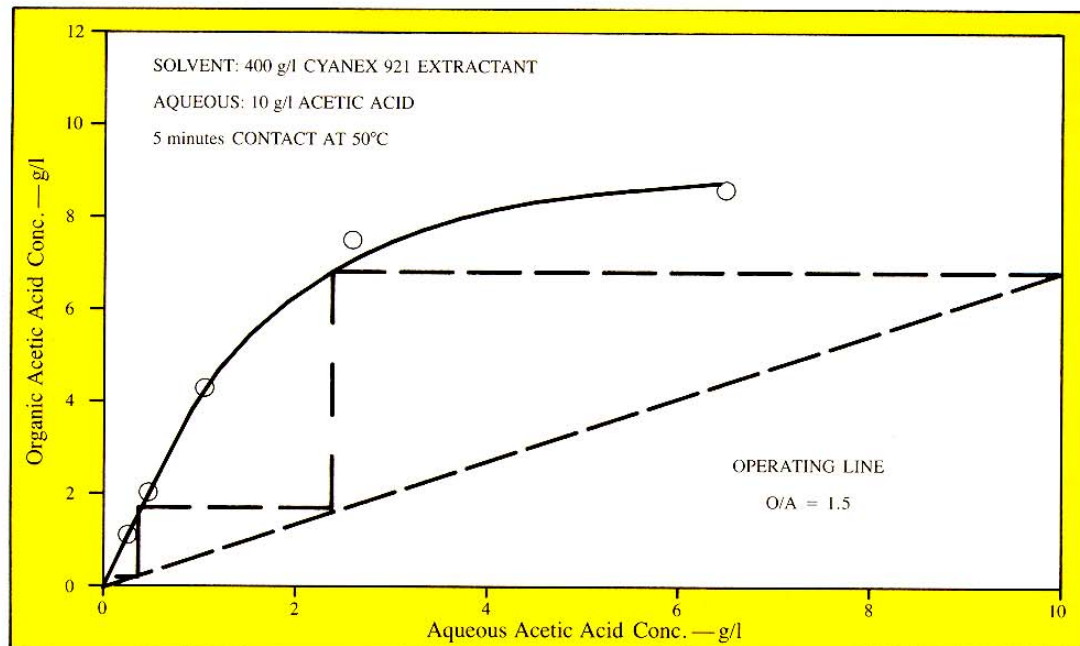
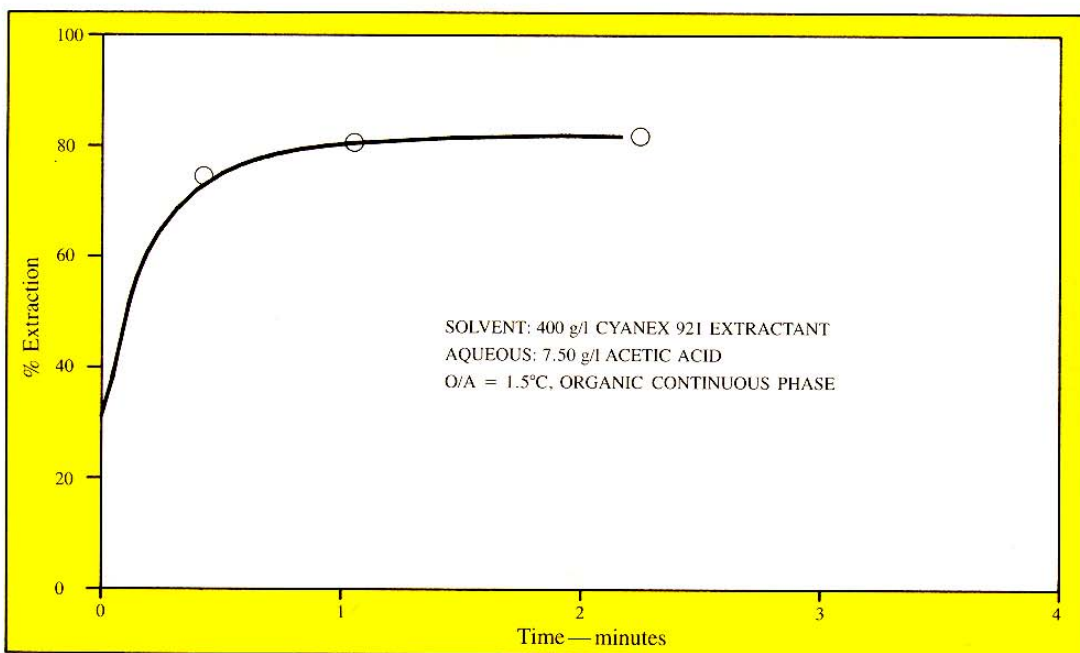


FIG. 2—KINETICS OF ACETIC ACID EXTRACTION



# POTENTIAL APPLICATIONS

## METAL EXTRACTION

### Niobium Tantalum Separation

A pilot-plant process using CYANEX 921 extractant to recover and separate niobium and tantalum has been demonstrated recently.<sup>(16,17)</sup> Both metals are extracted from a hydrofluoric-sulphuric acid leach liquor and then selectively stripped from the loaded organic. The advantages of CYANEX 921 extractant in comparison to the commercially used MIBK extractant were shown to be higher stability, lower aqueous solubility, rapid phase disengagement and, particularly, the production of high purity niobium oxide which meets the stringent specifications required for nuclear, optical and electronic applications.

Data comparing the impurities in niobium oxides derived by solvent extraction with MIBK and CYANEX 921 extractant are shown in Table 3 below.<sup>(16)</sup>

TABLE 3  
NIOBIUM OXIDE PURITY

COMPONENT	Concentration mg/L	
	CYANEX 921 EXTRACTANT	MIBK
Ta <sub>2</sub> O <sub>5</sub>	< 20	600
Fe <sub>2</sub> O <sub>3</sub>	< 5	< 500
CoO	1	10
CuO	1	5
MnO	1	10
MoO <sub>3</sub>	< 5	< 20
WO <sub>3</sub>	< 10	< 50
TiO <sub>2</sub>	< 5	< 200
SiO <sub>2</sub>	< 10	< 200
Cr <sub>2</sub> O <sub>3</sub>	< 3	< 50
P	< 10	< 200
Loss on Ignition	0.1%	0.1%

Table 3 reproduced by the kind permission of VCH Verlagsgesellschaft, Weinheim, Federal Republic of Germany.

### Rhenium Recovery

Rhenium is an essential element in the production of petroleum reforming catalysts. A recent patent granted to American Cyanamid Company<sup>(18)</sup> discloses the use of CYANEX 921 to recover rhenium from these source materials. The process involves leaching the spent catalyst with sulphuric acid, extracting rhenium and then stripping with ammonium sulphate. Excellent selectivity against typical impurity metals such as aluminum, calcium, magnesium and iron is achieved.

### Arsenic Extraction From Copper Electrolytes

The removal of arsenic impurities from copper electrolytes by solvent extraction with CYANEX 921 forms the subject of a recent European Patent issued to Vereinigte Metallwerke Ranshofen-Berndorf AG.<sup>(19)</sup> The process describes the selective extraction of arsenic followed by stripping with an acidic sodium sulphate solution and recovery of arsenic from the strip liquor by precipitation with H<sub>2</sub>S. CYANEX 921 is shown to be a stronger extractant for arsenic than tributylphosphate which is now used in two commercial arsenic solvent extraction plants. This property is claimed to result in lower staging requirements and solvent inventory.

### Lithium Recovery

The commercial significance of lithium has increased in recent years as a result of the development of new uses for this element, e.g. in batteries, and because of increased demand in established applications (ceramics, etc.).

A novel solvent extraction process using CYANEX 921 extractant to recover lithium from one of its sources (neutral brines) has been described<sup>(20)</sup>

### Additional Applications

CYANEX 921 is known to extract approximately 30 metals from aqueous solution as indicated in Table 4.<sup>(21)</sup>

Selective separations can be made depending upon a variety of factors, e.g. the valence state of the metal, the anionic nature of the solution (chloride, sulphate, etc.) and the concentration of the extractant in the solvent.

For example, one separation suggested by these data is the selective recovery of vanadium<sup>(5+)</sup> from chloride solutions containing aluminum, cobalt and nickel (these solutions may be derived from leaching spent catalysts used in the petroleum industry).

The reader is referred to two comprehensive reviews for more detailed information on the performance characteristics of TOPO.<sup>(22,23)</sup>

TABLE 4 TRI *n*-OCTYLPHOSPHINE OXIDE (TOPO) EXTRACTION OF THE ELEMENTS

Li	Be															B	C	N	O	P
Na	Mg															Al	Si	P	S	Cl
K	Ca	Sc	Ti	V	Cr	Mn	Fe	Co	Ni	Cu	Zn	Ga	Ge	As				Se	Br	
			IV	V	VI	VII	III			II	II	III	IV	III						
			ac	a	ac	abc	a			a	a	a	a	a						
Rb	Sr	Y	Zr	Nb	Mo	Tc	Ru	Rh	Pd	Ag	Cd	In	Sn	Sb				Te	I	
			IV	V	VI	VII				II	III	IV	III	V						
			ab	a	abc	acde				a	a	a	a	a						
Cs	Ba	La*	Hf	Ta	W	Re	Os	Ir	Pt	Au	Hg	Tl	Pb	Bi				Po	At	
			IV	V					IV	III	II			III						
			ab	a					a	a	a			b						
Fr	Ra	Ac†	Ce	Pr	Nd	Pm	Sm	Eu	Gd	Tb	Dy	Ho	Er	Tm	Yb	Lu				
* Elements 58-71			IV																	
† Elements 90-103			bc																	
			Th	Pa	U	Np	Pu	Am	Cm	Bk	Cf	Es	Fm	Md	No	103				
			IV		VI	IV	IV VI													
			ab		ab	bc	ab ab													
Key																				
Element																				
Valence																				
System																				

Elements enclosed in color are extracted. Acid system from which favorable or selective extraction can be effected:  
a-HCl; b-HNO<sub>3</sub>; c-H<sub>2</sub>SO<sub>4</sub>; d-HBr; e-H<sub>3</sub>PO<sub>4</sub>

## ORGANIC EXTRACTION

### Phenol Recovery

Phenol occurs in aqueous effluents from many processes, e.g. in the petroleum, steel and coal gasification industries. CYANEX 921 is a strong extractant for phenol and offers a lower cost alternative to conventional Phenosolvan technology for phenol recovery.

This new process<sup>(24)</sup> involves dissolving CYANEX 921 extractant in a high boiling point diluent, extracting phenol and then stripping the solvent by distillation.

Extraction isotherms given in Table 5 and plotted in Figure 5 show the efficient extraction properties of CYANEX 921.

McCabe-Thiele interpretations from the isotherms indicated the following theoretical staging requirements and A/O ratios for essentially quantitative phenol recovery.

Extractant Conc. (g/L)	Theoretical Stages	A/O Ratio
100	2	2
200	2	3
325	2	5

TABLE 5  
The Effect of Extractant Concentration on Phenol Recovery

Solvents	:	100, 200 and 325 g/L CYANEX 921 extractant in Nalkylene 500 diluent*
Aqueous	:	10 g/L phenol (nominal) and 30 g/L Na <sub>2</sub> SO <sub>4</sub>
Temperature, °C	:	50
Contact Time	:	5 minutes

A/O	Equilibrium Phenol Concentration (g/L)					
	100 g/L		200 g/L		325 g/L	
Org	Aq	Org	Aq	Org	Aq	
0.25	2.54	0.02	2.46	0.01	2.63	0.02
0.5	5.07	0.05	4.93	0.02	5.25	0.03
1	10.1	0.10	9.84	0.04	10.5	0.04
2	19.4	0.47	19.6	0.10	20.9	0.08
5	34.3	3.34	45.0	0.87	-	-
7	40.0	4.48	56.6	1.79	68.2	0.79
10	-	-	-	-	88.8	1.65

\*Nalkylene 500, a linear alkyl benzene diluent, is a product of Conoco Chemicals Company (a division of Conoco).

FIG. 3—EFFECT OF TEMPERATURE ON VISCOSITY

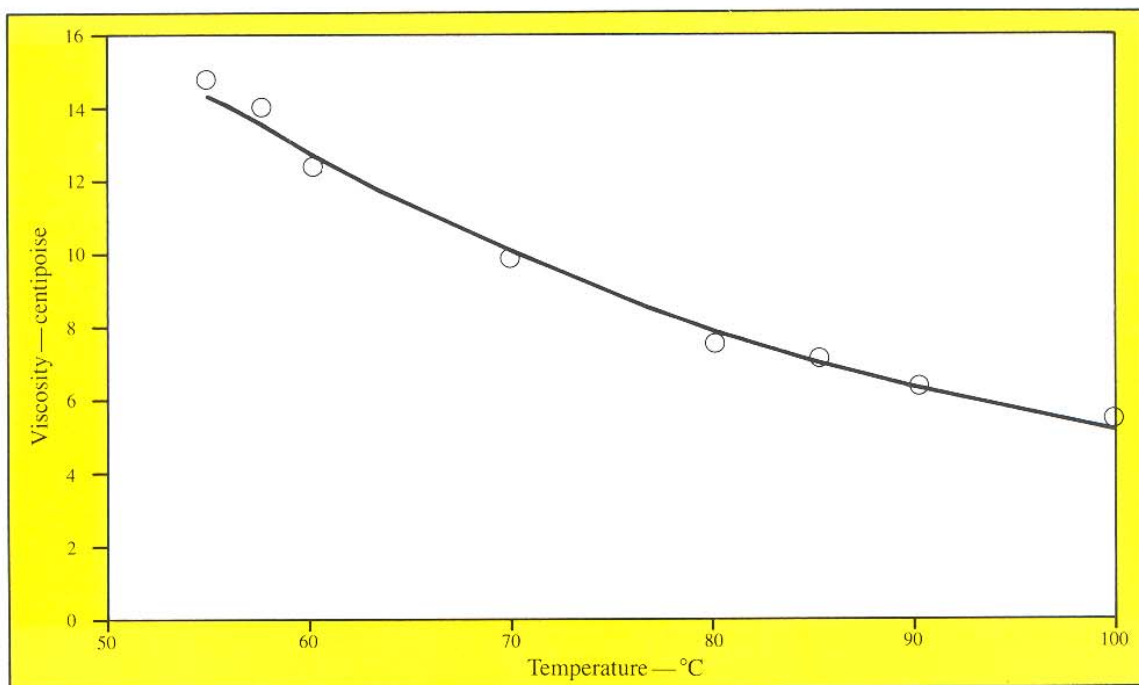


FIG. 4—EFFECT OF TEMPERATURE ON ORGANIC SOLUBILITY

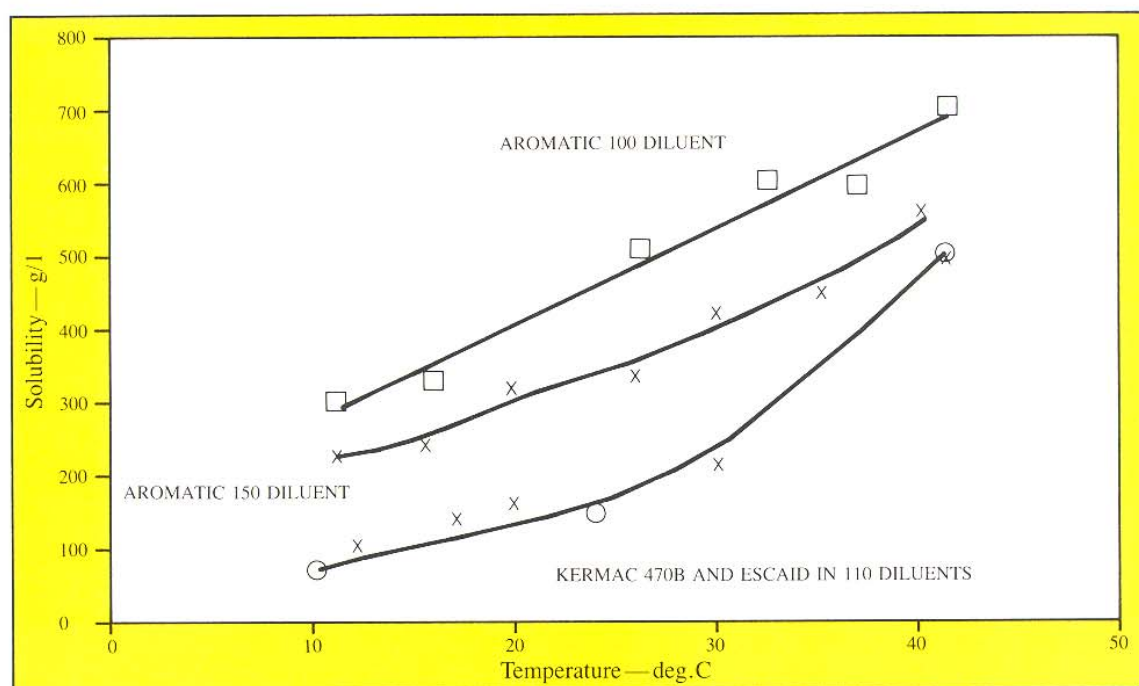
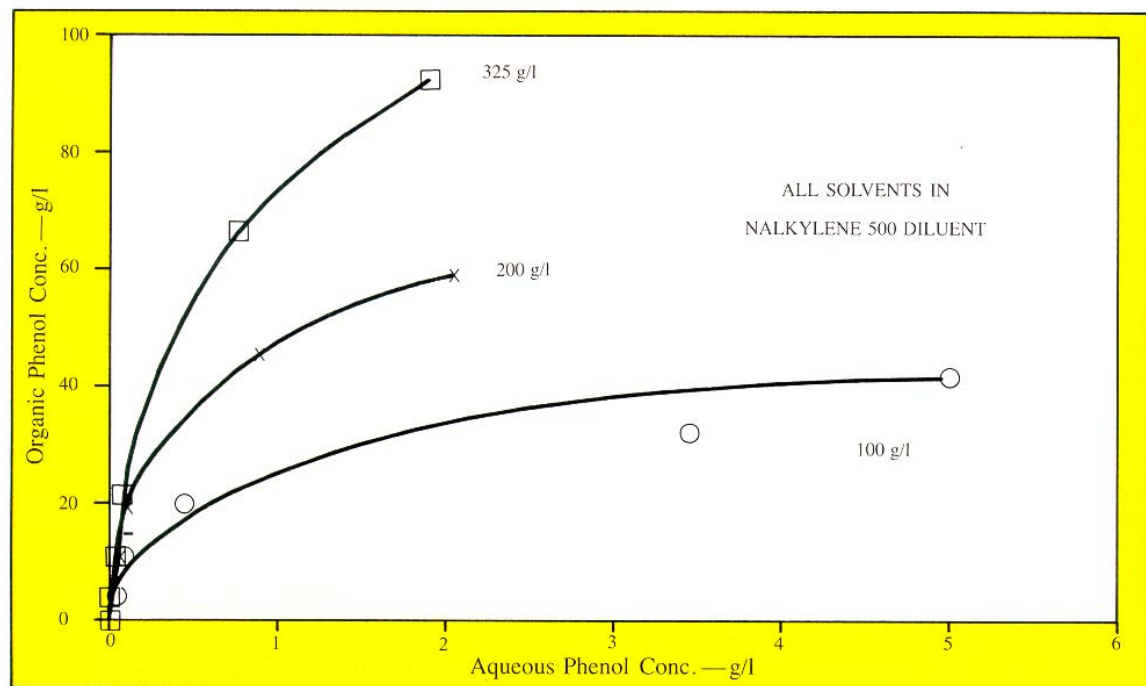


FIG. 5—EFFECT OF EXTRACTANT CONCENTRATION ON PHENOL RECOVERY



## REFERENCES

---

1. G.M. Kosolapoff. Organophosphorous Compounds. J. Wiley & Sons Inc. New York (1950).
2. Y. Marcus and A.S. Kertes. Ion Exchange And Solvent Extraction of Metal Complexes. Wiley Interscience, London (1968).
3. C. A. Blake et. al. Solvent Extraction of Uranium and Vanadium From Acid Liquors With Trialkylphosphine Oxides. Oak Ridge National Laboratory. Report No. 1964 (1955).
4. G.M. Ritcey and AW. Ashbrook. Solvent Extraction: Principles and Applications To Process Metallurgy. Part I Elsevier, Amsterdam (1984).
5. Ibid Part 11.
6. F.J. Hurst, D.J. Crouse and K.B. Brown. Solvent Extraction of Uranium From Wet-Process Phosphoric Acid. Oak Ridge National Laboratory. Report #ORNL-TM-2522 (1969).
7. F.J. Hurst, D.J. Crouse and K.B. Brown. Recovery of Uranium From Wet-Process Phosphoric Acid. Ind. Eng. Chem. Process Des. Develop., Vol. 11, No. 1, (1972) pp. 122-128.
8. Fred J. Hurst and David J. Crouse. Reductive Stripping Process For The Recovery of Uranium From Wet-Process Phosphoric Acid. U.S. Patent 3.711.591 (1973).
9. R.W. Helsel, Removing Carboxylic Acids From Aqueous Wastes, CEP May 1977.
10. J.M. Wardell and C. Judson King, Solvent Equilibria For Extraction of Carboxylic Acids From Water, Journal of Chemical and Engineering Data, Vol. 23, No. 2, 1978.
11. N.L. Ricker, J.N. Michaels and C.J. King, Solvent Properties For Organic Bases For Extraction of Acetic Acid From Water, J. Separ. Proc. Technol 1(1) 36-41 (1971).
12. N.L. Ricker, E.F. Pittman, C.J. King, Solvent Extraction With Amines For Recovery of Acetic Acid From Dilute Aqueous Industrial Streams, J. Separ. Proc. Technol 1(2) 23-30 (1980).
13. Janvit Golob, et. al., Extraction of Acetic Acid From Dilute Aqueous Solutions With Trioctylphosphine Oxide, Ind. Eng. Chem. Process Des. Dev. Vol. 20, No. 3, pp. 433-435 (1981).
14. R.R. Grinstead, U.S. Pat. 3.816.524 (1974).
15. W. Kantzler and J. Schedler, Verfahren Zur Extraktion Von Essigsäure, Ameisensäure, Gegebenfalls Furfural. Austrian Patent 365080 (1980).
16. R. Hahn & H. Retelsdorf. Production of Pure Niobium Using a New Extraction Process for Niobic Oxide and Optimal Reduction Processes. Erzmetall, 37, (9), 444-448(1984).
17. J. Eckert & J. Bauer. Use of a TOPO Solution for Separating and Producing High Purity Oxides of Tantalum and Niobium. German Offen 3241832 (1984).
18. J.H. Bright. Selective Recovery of Rhodium From Sulphuric Acid Solutions. European Patent 113912-A.
19. R. Marr, et. al. Verfahren zum Abtrennen von Arsen aus einem Kupferelectrolyten. European Patent 0 106 118 A1 (1983).
20. U.S. Patent 3.793.433.
21. Standard Methods of Chemical Analysis. Edited by F.J. Welcher© 1965 by Litton Educational Publishing Inc. Vol IIA, Sixth Edition. Table 4 reprinted by the kind permission of Van Nostrand Reinhold Company.
22. J.C. White and W.J. Ross. Separations by Solvent Extraction with Tri-n-octylphosphine Oxide. Oak Ridge National Laboratory. ORNL Central Files Number 61-2-19 (1961).
23. Ishimori T. et. al. Nippon Genshiyoku Gakkaishi. 4(2), 177(1962). CA 63, 141338f.
24. C. Savides and J.H. Bright. Extraction of Phenols from Aqueous Solutions. U.S. Patent 4.420.643 (1983).

# ANALYTICAL METHODS

## ANALYSIS IN ORGANIC SOLVENTS

As described, the gas chromatographic procedure is suitable for analyzing solvents containing  $120 \pm g/L$  TOPO. Other concentrations may be determined by making appropriate changes to the tenor of TOPO in the standard solution. (The method is based upon a single point standardization).

### Reagents

1. Didecylphthalate (AR grade-internal standard)
2. TOPO (purified-see note 1).
3. Process diluent (e.g. Escaid 110\* diluent, Aromatic 150\* diluent).

### Calibration

1. Accurately weigh ( $\pm 1$  mg)  $3 \pm 0.1$  g of pure TOPO and  $2 \pm 0.1$  g of didecylphthalate into a 50 mL volumetric flask. Dissolve and make up to volume using the process diluent.
2. Analyze the standard solution as described under "Gas Chromatographic Conditions" to determine the relative response factor of TOPO and didecylphthalate.

### Procedure

1. Centrifuge the solvent to be analyzed or filter through PS paper to remove entrained aqueous or suspended solids.
2. Accurately weigh ( $\pm 1$  mg)  $2 \pm 0.1$  g of didecylphthalate into a 50 mL volumetric flask and pipette 25 mL of the clarified solvent into the same flask. Make up to volume with the process diluent.  
Determine the relative response factor of TOPO and didecylphthalate as described under "Gas Chromatographic Conditions".

### Calculations

$$\text{Trioctylphosphine oxide (g/L)} = \frac{R_1}{R_2} \times 2 \times C_s$$

Where  $R_1$  = Relative response factor in standard solution

$R_2$  = Relative response factor in analyte solution

$C_s$  = TOPO concentration in standard solution (g/L)

### Gas Chromatographic Conditions

- Instrument: Hewlett Packard 5880A or equivalent
- Column: 30 m X 0.32 mm fused silica capillary column coated with  $0.25\mu m$  of SPB-1
- Detector: Thermal Conductivity
- Carrier Gas: Helium
- Temperature, °C
- Detector: 320
- Injector: 290
- Column: 270 (isothermal)

Column Flow:	1 mL/minute
Vent Flow:	60 mL/minute
Sample Injection	
Volume:	0.5 $\mu L$
Peak Areas:	Determined by electronic integration. Retention times for TOPO and didecylphthalate are approximately 6.5 and 10 minutes, respectively.

### Notes

1. Pure TOPO (>99.5%) can be obtained by recrystallizing commercial grade TOPO from hexane. (Three recrystallizations are necessary).
2. PS (Phase Separation) paper is available from Whatman, Inc.
3. Isomers of TOPO will also be detected using the subject method. These compounds may be assigned the same response factors as TOPO and determined accordingly. A typical chromatogram of commercial TOPO is shown in Figure 1A.
4. If the TOPO peak exhibits a leading tail this may effect the accuracy of the electronic integration. The effect can be minimized by increasing the column temperature by 10 to 20°C.
5. Megabore columns can be used as an alternative to capillary columns.

## ANALYSIS IN AQUEOUS SOLUTION

Two methods have been developed which allow trace quantities of TOPO to be determined. The first method is suited to solutions which contain small concentrations of dissolved salts, while the second method is appropriate for high salt concentrations.

Both methods are based upon gas chromatography. In general, the solubility of TOPO in aqueous process solutions will be <5 mg/L.

### Low Dissolved Solids

The concentration of trioctylphosphine oxide (TOPO) is determined by evaporating the aqueous solution to dryness, leaching the residue with chloroform and analyzing the leachate by gas chromatography.

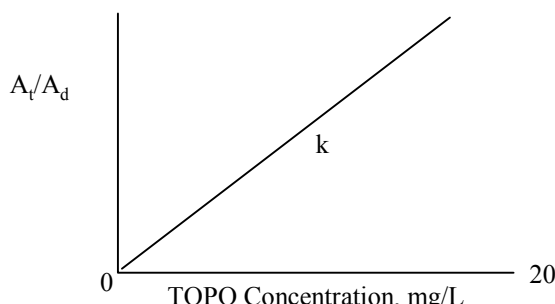
\*Product of Exxon Co., U.S.A.

## Reagents

1. Chloroform
2. Didecylphthalate
3. 25 mg/L solution of didecylphthalate (internal standard) in chloroform
4. TOPO (purified - see Note 1)
5. All reagents are AR grade

## Calibration

1. Prepare standard solutions containing 2, 5, 10 and 20 mg/L TOPO in chloroform. Each solution should also contain 25 mg/L didecylphthalate internal standard.
2. Analyze the solutions as described under "Gas Chromatographic Conditions".
3. Plot the calibration curve as follows and determine the slope "k".



Where  $A_t$  = TOPO peak area

$A_d$  = Didecylphthalate peak area

## Procedure:

1. Filter the aqueous solution to remove entrained organic.
2. Evaporate to dryness exactly 10 mL of the aqueous solution using a nitrogen-swept Pierce Reacti-Therm at 80°C.
3. At room temperature, leach the residue with exactly 1 mL of the chloroform solution containing 25 mg/L didecylphthalate.
4. Analyze the chloroform leachate as described under "Gas Chromatographic Conditions".

## Calculation

$$\text{Concentration of TOPO in the aqueous (mg/L)} = \frac{A_t}{A_d} \times \frac{1}{k} \times \frac{1}{10}$$

Where  $A_t$  = TOPO peak area

$A_d$  = Didecylphthalate peak area  
 $k$  = Slope of the calibration curve

## Gas Chromatographic Conditions

Instrument: Perking Elmer Sigma 115 or equivalent  
Column: 30 x 0.326 mm fused silica capillary column coated with 0.1 µm Durabond 1 (15 or 60 m columns with a film thickness of 0.10 or 0.25 µm may be substituted)

Split Ratio:	10 to 1
Detector:	FID
Carrier Gas:	Helium at 12 psig (30 m column)
Vent Flow:	2.0 mL/minute (23 cm/sec)
Temperatures, °C	
FID:	300
Injection Port:	300
Program, °C	
Isothermal:	270
Sample Injection Volume:	5 µl

## Notes

1. Pure TOPO can be obtained by recrystallizing commercial grade TOPO from hexane. (Three recrystallizations are necessary).
2. TOPO and didecylphthalate will elute at approximately 5.4 and 7.8 minutes respectively.
3. Detection limit approximately 1 mg/L.
4. This method has not been validated.

## High Dissolved Solids

Aqueous solutions containing TOPO are analyzed by direct injection gas chromatography.

## Reagents

1. Tetrahydrofuran (THF). "Baker Analyzed Reagent, 100%"
2. TOPO (purified - see Note 1)

## Calibration

1. Prepare a stock solution by accurately weighing (1±mg) approximately 0.5 g of TOPO into a 50 mL volumetric flask. Dilute to 50 mL with THF and dissolve the TOPO.
2. Dilute aliquots of the stock solution with distilled water to prepare standard solutions containing 2, 5, 10 and 30 mg/L of TOPO.
3. Analyze the solutions as described under "Gas Chromatographic Conditions".

## Procedure

1. Filter the aqueous solution to remove entrained organic.
2. Inject 3 µl of the analyte solution and analyze as described under "Gas Chromatographic Conditions".

## Calculation

\* Response Factor for TOPO (R)  
Conc. of TOPO in Standard (mg/L)

Area of TOPO, Standard Peak

Concentration of TOPO in the aqueous (mg/L) = Area of TOPO peak (Analyte)  $\times R$

\* Response factor for the standard closest in concentration to the sample.

## Gas Chromatographic Conditions

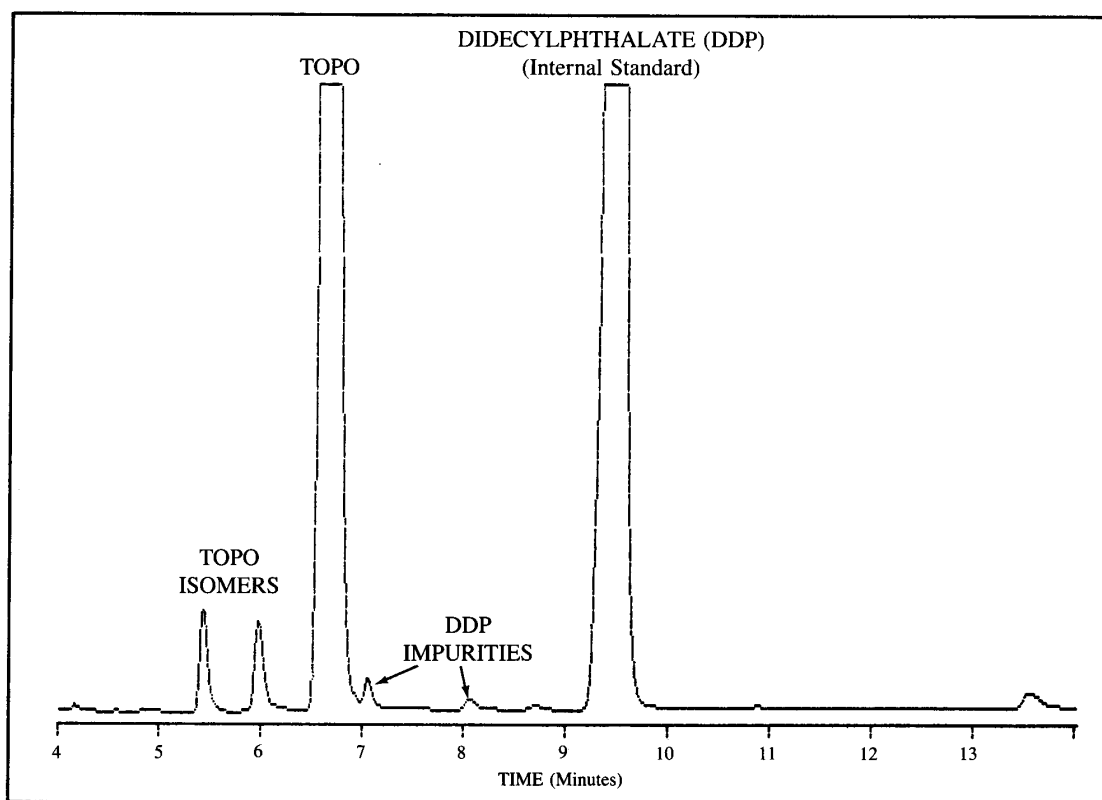
Instrument: Hewlett Packard 5730A or equivalent  
Column: 2 ft. x 1/4 inch OD x 2 mm ID glass  
Column packed with 9% OV-17 and 12% SP2401 on 80/100 mesh Supelcoport

Detector: FID  
Carrier Gas: Helium at 57 psi (flowrate 40 mL/minute)  
Temperatures, °C  
FID: 300  
Injection Port: 250  
Column: 230  
Program, °C  
Isothermal: 230  
Sample Injection Volume: 3  $\mu$ L

## Notes

1. Pure TOPO can be obtained by recrystallizing commercial grade TOPO from hexane. (Three recrystallizations are necessary)
2. Retention time for TOPO is approximately 12 minutes
3. Detection limit approximately 2 mg/L.

FIG. 1A TYPICAL CHROMATOGRAM OF COMMERCIAL TOPO



---

**IMPORTANT NOTICE**

The information and statements herein are believed to be reliable but are not to be construed as a warranty or representation for which we assume legal responsibility. Users should undertake sufficient verification and testing to determine the suitability for their own particular purpose of any information or products referred to herein. NO WARRANTY OF FITNESS FOR A PARTICULAR PURPOSE IS MADE.

Nothing herein is to be taken as permission, inducement or recommendation to practice any patented invention without a license.



Cytec Industries Inc.  
Five Garret Mountain Plaza  
West Paterson, NJ 07424  
Tel (973)357-3100  
Fax (973)357-3054

# CYANEX® 923 Extractant

## Solvent Extraction Reagent

A Liquid Phosphine Oxide

- Removes impurities from copper electrolytes.
- Separates niobium from tantalum.
- Extracts acetic acid and phenol from aqueous effluents.
- Separates ethanol from water.

**CYTEC**

---

---

# **CONTENTS**

## **INTRODUCTION**

Composition .....	2
Typical Properties .....	2
Suitability of Construction Materials .....	3

## **POTENTIAL APPLICATIONS**

### **ORGANIC SOLUTES**

Carboxylic Acid Recovery.....	4
Phenol Recovery .....	4
Ethanol Extraction .....	5

### **INORGANIC SOLUTES**

Impurity Removal From Copper Electrolytes.....	6
Uranium Extraction From Wet Process Phosphoric Acid .....	8
Niobium-Tantalum Separation.....	9

## **ANALYTICAL METHODS**

ANALYSIS IN ORGANIC SOLVENTS.....	12
ANALYSIS IN AQUEOUS SOLUTION.....	13
DETERMINATION OF WATER .....	14

## **TECHNICAL PAPERS**

AND PATENTS.....	15
------------------	----

<b>HEALTH AND SAFETY.....</b>	<b>16</b>
-------------------------------	-----------

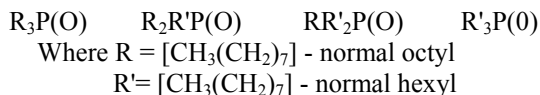
# INTRODUCTION

CYANEX® 923 extractant is a liquid phosphine oxide which has potential applications in the solvent extraction recovery of both organic and inorganic solutes from aqueous solution, e.g. carboxylic acids from effluent streams and the removal of arsenic impurities from copper electrolytes.

The major advantage of CYANEX 923 extractant over similar extraction reagents, e.g. TOPO (trioctylphosphine oxide), is that it is completely miscible with all common hydrocarbon diluents even at low ambient temperatures. The major benefit of high solubility lies in the ability to prepare concentrated, stable solvents which can recover solutes (e.g. acetic acid) that are normally only weakly extracted by this type of reagent.

## Composition

CYANEX 923 extractant is a mixture of four trialkyl-phosphine oxides as follows:



Average Molecular Weight = 348 (approximately)

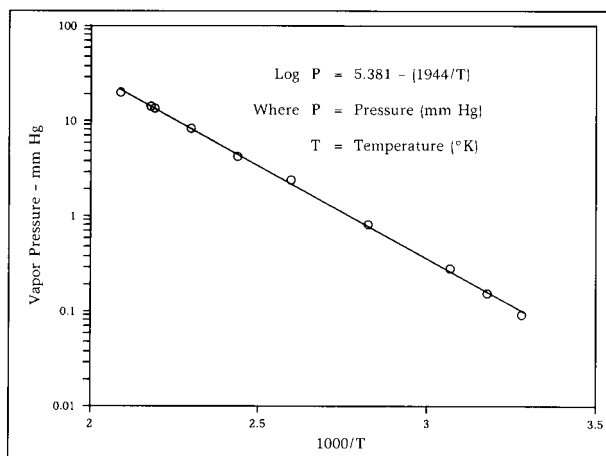
## Typical Properties

Trialkylphosphine oxides	:	93%
Appearance	:	Colorless mobile liquid
Specific Gravity	:	0.88 at 25°C
Freezing Point	:	-5 to 0°C
Viscosity	:	40.0 centipoise at 25°C
	:	13.7 centipoise at 50°C
Flashpoint	:	182°C
(Closed Cup Setaflash)		
Autoignition Temperature	:	281°C
Vapor Pressure*	:	0.09 mm. Hg at 31°C
Boiling Point	:	310°C at 50 mm Hg
Solubility in Water	:	> 10 mg/l
CYANEX 923 extractant	:	8 w/o

Surface Tension	@ 25°C	9.0 dynes/cm
	@ 100°C	7.5 dynes/cm
	@ 150°C	5.2 dynes/cm
Viscosity Kinematic	@ 25°C	51.6 cSt
	@ 50°C	18.9 cSt
	@ 100°C	4.2 cSt
Specific Heat	@ 25°C	0.45 cal/gm/°C
	@ 50°C	0.47 cal/gm/°C
	@ 100°C	0.51 Cal/gm/°C
Thermal Conductivity	@ 25°C	0.000302 cal/cm/sec/°C
	@ 120°C	0.000288 cal/cm/sec/°C
	@ 200°C	0.000274 cal/cm/sec/°C

\* Shown as function of temperature in Figure 1

FIG. 1 — EFFECT OF TEMPERATURE ON VAPOR PRESSURE



## **Suitability of Construction Materials**

Samples of the following plastics and rubbers (in the form of tubing) were immersed for 200 hours at 50°C in glass vessels containing CYANEX 923 extractant.

The results are summarized below:

<b>Material</b>	<b>Remarks</b>
Butyl Rubber	Unsuitable. Rapid swelling and softening.
Teflon Fluorocarbon Film*	Suitable. No detectable effect.
Polypropylene	Suitable. No detectable effect.
Natural & Black Latex Rubber	Unsuitable. Complete dissolution in less than 192 hours.
PVC (Laboratory Grade)	Short-term suitability. Loss of plasticity in less than 192 hours.
PVC (Solvent Grade)	Suitable. Only a slight increase in dimension observed.
Red Gum Rubber	Unsuitable: Rapid swelling and softening.
Viton Fluoroelastomer*	Suitable. No detectable effect.
Silicone	Unsuitable. Disintegrated after 56 hours.

Samples of the following metals in the form of coupons (approximate dimensions 50 mm x 20 mm. x 3 mm) were immersed for 1000 hours at 50°C in glass vessels containing CYANEX 923 extractant. The following observations were made.

<b>Metal</b>	<b>Remarks</b>
Mild Steel	No detectable corrosion.
Stainless Steel (316)	No detectable corrosion.
Stainless Steel (304)	No detectable corrosion.
Aluminum	No detectable corrosion.

\*Product of E.L DuPont de Nemours & Co.

# POTENTIAL APPLICATIONS

## ORGANIC SOLUTES

### Carboxylic Acid Recovery

Processes in petrochemical plants, wood pulping mills, and other chemical facilities often generate aqueous effluent streams containing carboxylic acids; particularly acetic acid. Typically, these acids are present in concentrations between 1 and 50 g/l.

A solvent extraction plant to recover acetic acid from an effluent stream has been operated successfully by Lenzing A.G. in Austria since 1983. Briefly, the process involves extracting acetic acid with a solvent containing TOPO and stripping the loaded solvent by distillation.

The advantage of using CYANEX 923 extractant in this application, as opposed to TOPO, lies in the ability to prepare a concentrated, low freezing point solvent.

This leads to lower staging requirements in extraction and virtually eliminates the problem of plant freeze-up during periods when the ambient temperature is low.

The potential for CYANEX 923 extractant in this application is illustrated by the acetic acid extraction isotherms shown in Figure 2. The isotherms were plotted from the data in Table 1.

FIG. 2 — ACETIC ACID EXTRACTION ISOTHERMS

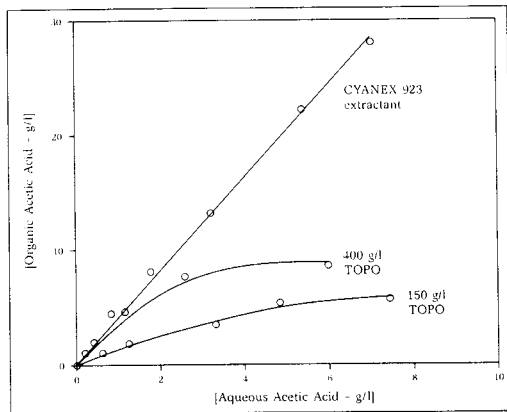


TABLE 1  
Acetic Acid Recovery

Solvents	:	CYANEX 923 extractant undiluted) 150 g/l and 400 g/L TOPO in DPA diluent*
Aqueous	:	10 g/l acetic acid (approx.)
Temperature	:	50°C
Contact Time	:	5 minutes

Equilibrium Acetic Acid Concentration (g/l)

A/O	150 g/l TOPO		400 g/l TOPO		CYANEX 923 extractant	
	Org.	Aq.	Org.	Aq.	Org.	Aq.
10	-	-	-	-	27.7	6.84
5	-	-	-	-	22.0	5.22
2	5.60	7.20	8.40	5.80	13.0	3.11
1	5.30	4.70	7.50	2.50	7.87	1.74
0.5	3.43	3.15	4.48	1.05	4.41	0.80
0.2	1.77	1.15	1.92	0.40	-	-
0.1	0.95	0.55	9.95	0.20	-	-

\* DPA, a high boiling (330-379°C) diphenylalkene diluent, is a product of Conoco Chemicals Co. (a division of Conoco).

### Phenol Recovery

Phenols, like carboxylic acids, are a common component of many aqueous effluents, e.g. waste streams produced during coal liquefaction, coal gasification (steel manufacture), and in the petrochemical industry.

Again, the potential benefit of recovering phenol by solvent extraction with CYANEX 923 extractant is the ability to construct plants with minimal staging requirements. Since phenol is strongly extracted by phosphine oxides, the advantages of CYANEX 923 extractant vs. TOPO are less marked than in the case of the more weakly extracted acetic acid. The major factor in choosing between the two in phenol systems will obviously depend upon the concentration of phenol in the effluent.

Phenol extractions isotherms are shown in Figure 3 and were plotted using the batch, shake-out data given in Table 2. Composition of the aqueous solution was chosen to approximate a real effluent. As with carboxylic acids, stripping is achieved by distillation.

Estimates indicate significant savings in capital and operating costs vs. the conventional Phenosolvan process.

**FIG. 3 — PHENOL EXTRACTION ISOTHERMS**

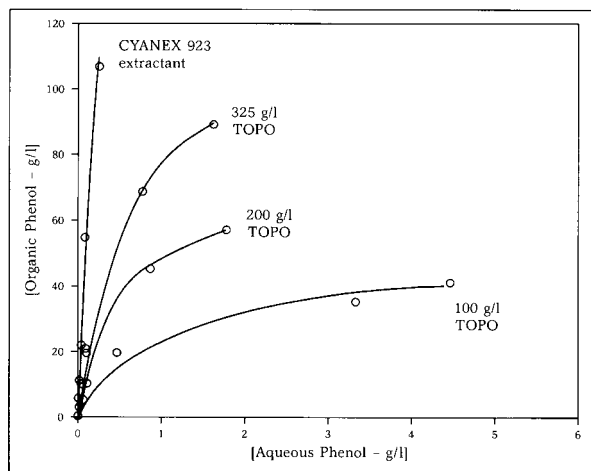


**TABLE 2**  
**Phenol Recovery**

Solvents	:	CYANEX 923 extractant (undiluted) 100, 200 and 325 g/l TOPO in Nalkylene 500 diluent*
Aqueous	:	10 g/l phenol (approx.) and 30 g/l Na <sub>2</sub> SO <sub>4</sub> . Initial pH = 5 (approx.)
Temperature	:	50°C
Contact Time	:	5 minutes

#### Equilibrium Phenol Concentration (g/l)

A/O	CYANEX 923							
	100 g/l		200 g/l		325 g/l		extractant	
A/O	Org.	Aq.	Org.	Aq.	Org.	Aq.	Org.	Aq.
10	-	-	-	-	88.8	1.65	107.2	0.28
7	40.0	4.48	56.6	1.79	68.2	0.79	-	-
5	34.3	3.34	45.0	0.87	-	-	54.6	0.089
2	19.4	0.47	19.6	0.10	20.9	0.08	21.0	0.028
1	10.1	0.10	9.84	0.04	10.5	0.04	11.0	0.013
0.5	5.07	0.05	4.93	0.02	5.25	0.03	5.50	0.005
0.25	2.54	0.02	2.46	0.01	2.63	0.02	2.75	0.002**

\* Nalkylene 500, a linear alkyl benzene diluent, is a product of Conoco Chemicals Co. (a division of Conoco.)

\*\*Detection limit of the analytical method.

#### Ethanol Extraction

CYANEX 923 extractant exhibits a separation factor in ethanol/water solutions near the maximum useful limit for recovery from continuous fermentation broths, typically containing 5% ethanol. Higher values do not further reduce extractor size or energy required in the downstream distillation. This is illustrated in Figure 4 where separation factors for CYANEX 923 extractant and for other candidate extractants are shown in relation to the upper and lower limits. Extraction coefficients, and their effect on extractor size, are also plotted in Figure 4. The coefficient for

CYANEX 923 extractant is well into the flat part of the curve. This excess capacity can be exchanged for increased separation factor, if needed, by dilution with inert diluents.

The principle advantage of CYANEX 923 extractant lies in its very low solubility in water. This obviates or minimizes extra processing of raffinate that would be required by more soluble extractants. The solubilities in water of CYANEX 923 extractant and of other candidate ethanol extractants are compared in Table 3.

**FIG. 4 — ETHANOL EXTRACTION**

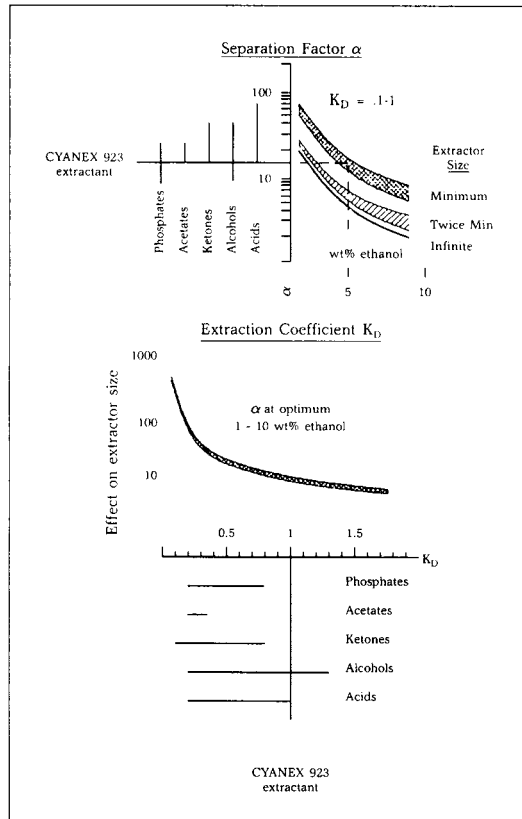


**TABLE 3**  
**Solubility in Water, WT%**

	Expt <sup>(1)</sup>	UNIFAC <sup>(4)</sup>
<b>CYANEX 923 extractant</b>	0.001 <sup>(2)</sup>	
<b>Phosphates</b>		
Tri-n-Butyl	0.042 <sup>(3)</sup>	
<b>Acetates</b>		
n-Butyl	0.64	
i-Butyl	0.85	
<b>Ketones</b>		
Methyl Isobutyl	1.9	
Diisobutyl	0.083	
Isophorone		0.19
<b>Alcohols</b>		
3-Phenyl-1-Propanol		0.15
2-Ethyl-1-Butanol		0.88
3-Methyl-3-Pentanol	4.3	
4-Methyl-2-Pentanol	1.6	
3-Ethyl-3-Pentanol	1.7	
2,4-Dimethyl-3-Pentanol	0.7	
1-Octanol	0.051	
2,2-Dimethyl-3-Octanol		0.017
3,7-Dimethyl-3-Octanol		0.017
1-Nonanol	0.013	
1-Decanol	0.0037	
4-Decanol		0.016
1-Dodecanol	0.00023	
1-Tridecanol		0.00072
<b>Acids</b>		
2-Ethyl-4-Methyl Pentanoic		0.24
n-Hexanoic	1.1	
2-Ethyl Hexanoic		0.24
n-Octanoic		0.24
Neodecanoic		0.032

(1) J.M. Sorenson and W. Arlt, "Liquid-Liquid Equilibrium Data Collection," DECHHEMA, Vol. V, Part 1 (1979)

(2) This work

(3) W.N. Schulz and J.P. Navratil, "Science and Technology of Tributyl Phosphate," CRC Press (1982)

(4) A. Fredenslund, et. al., "Group-Contribution Estimation of Activity Coefficients in Nonideal Liquid Mixtures," *AICHE Journal* 21, No. 6, (1975), pp. 1086-1099.

## INORGANIC SOLUTES

### Impurity Removal From Copper Electrolytes

Briefly, the advantages of removing arsenic, antimony and bismuth impurities from copper electrolytes by solvent extraction rather than conventional processes consist of improvements in current efficiency, the quality of electrolytic copper, and in the productivity of the tankhouse. Minimizing the formation of arsine gas is also an important consideration.

Data on the extraction of arsenic, antimony and bismuth from a synthetic, nickeliferous copper electrolyte are given in Table 4. The corresponding arsenic and antimony extraction isotherms are shown in Figure 5. McCabe-Thiele interpolations indicated a reduction in the electrolyte arsenic concentration from 6 g/l to 1 g/l in two theoretical stages at O/A = 4. Under these conditions, the data indicated quantitative extraction of bismuth, 30-40% extraction of the antimony and a solvent loaded to 10-20 g/l H<sub>2</sub>SO<sub>4</sub>. High selectivity against copper and nickel extraction was observed. Copper loading in the solvents varied from 3 to 5 mg/l while no nickel extraction was observed.

Scrubbing sulfuric acid from the loaded solvent was readily achieved with water. The data in Table 5 and Figure 6 implied essentially quantitative removal in 3 theoretical stages at O/A=8 to produce a scrub liquor containing 130 g/l H<sub>2</sub>SO<sub>4</sub> for recycle. The feasibility of a selective metal/acid scrub was also indicated.

Water proved to be an effective strip feed at a lower O/A ratio as shown by the data in Table 6 and the arsenic stripping isotherm plotted in Figure 7

Interpolations from the isotherm showed complete arsenic stripping in 5 stages at O/A = 2. Quantitative antimony stripping was estimated under these conditions while approximately 0.07 g/l bismuth remained loaded on the solvent.

Solubility losses of the extractant in this system varied from 1 mg/l in the electrolyte to 10 mg/l in the strip liquor.

**TABLE 4**  
**Arsenic, Antimony and Bismuth**  
**Extraction Isotherms**

Solvent	:	50 v/o CYANEX 923 extractant in Exxsol D-80 diluent*
Aqueous	:	31.3 g/l Cu, 8.4 g/l Ni (as sulfates), 7.30 g/l As, 0.35 g/l Sb, 1.10 g/l Bi, 167.4 g/l H <sub>2</sub> SO <sub>4</sub>
Contact Time	:	5 minutes
Temperature	:	50°C

---

<u>Equilibrium Metal Concentration (g/l)</u>				
O/A	Arsenic		Antimony	
	Organic	Aqueous	Organic	Aqueous
1	1.60	5.70	0.15	0.20
2	1.43	4.45	0.08	0.20
5	1.04	2.10	0.03	0.22
10	0.63	1.03	0.01	0.24

## *Bismuth quantitatively extracted at all O/A ratios*

**TABLE 5**  
**Sulfuric Acid Scrubbing Using Water**

Solvent : 50 v/o CYANEX 923 extractant in Exxsol D-80 diluent; loaded to 16.4 g/l H<sub>2</sub>SO<sub>4</sub> and 1.90 g/l As, 0.14 g/l Sb and 1.10 g/l Bi  
 Scrub Feed : Distilled Water  
 Contact Time : 5 minutes  
 Temperature : 50°C

---



<u>O/A</u>	<u>Organic</u>	<u>Aqueous</u>
0.5	0	9.1
1	0	17.4
5	0.7	78.4
10	5.4	110.0
20	9.9	130.2

\* A product of Exxon Co., U. S. A.

**TABLE 6**  
**Arsenic, Antimony and Bismuth Stripping Isotherms**

Solvent	:	50 v/o CYANEX 923 extractant in Exxsol D-80 diluent; loaded to 1.38 g/l As, 0.061 g/l Sb, 0.19 g/l Bi
Strip Feed	:	Distilled Water
Contact Time	:	5 minutes
Temperature	:	50°C

**FIG. 5 — ARSENIC AND ANTIMONY EXTRACTION ISOTHERMS**

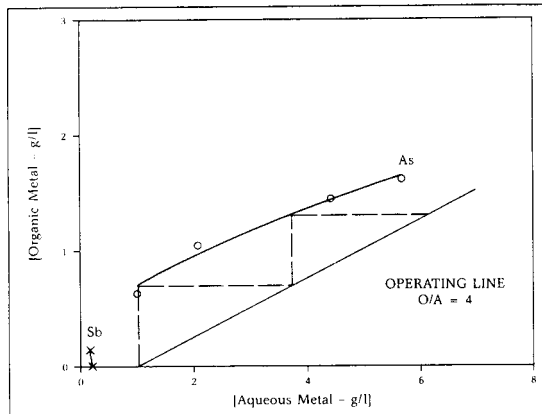


FIG. 6 – SULFURIC ACID SCRUBBING

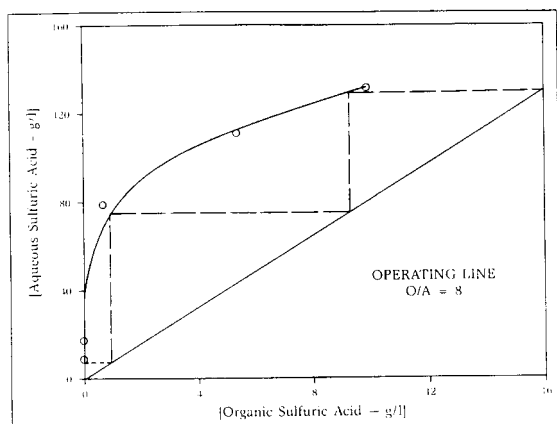
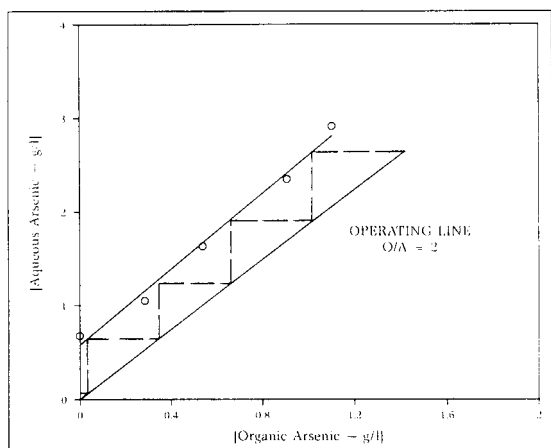


FIG. 7 – ARSENIC STRIPPING ISOTHERM



### Uranium Extraction From Wet Process Phosphoric Acid

The conventional process for recovering uranium from wet process phosphoric acid involves extraction with a synergistic mixture of D2EHPA and TOPO. CYANEX 923 extractant is a potential substitute for TOPO in this process and offers a materials handling advantage in that it is a liquid, while TOPO is a solid at normal temperatures (melting point approximately 50°C) and must be melted for ready removal from its container.

The feasibility of using CYANEX 923 extractant in this application is illustrated by the results of shake-out tests which are presented in Table 7 and Figure 8.

TABLE 7  
Uranium Recovery from Wet-Process Phosphoric Acid Using Synergistic Mixtures of Phosphine Oxides and D2EHPA

Solvent	:	All 0.5M D2EHPA in Ashland 140 diluent*. Varying in Phosphine Oxide concentration from 0 to 0.3M.
Aqueous	:	Florida WPPA 0.118 g/l U, oxidized with H <sub>2</sub> O <sub>2</sub> to + 370 mV (vs.SCE).
A/O	:	1
Temperature	:	40°C
Contact Time	:	10 minutes

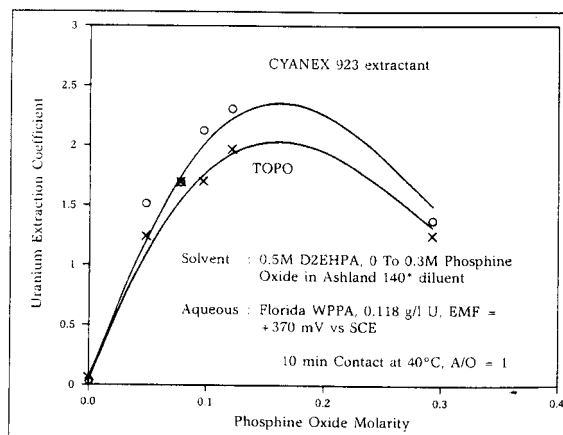
$$\text{Uranium Extraction Coefficient } (E_A^O)$$

Phosphine Oxide Molarity	TOPO	CYANEX 923 Extractant
0	0.08	0.05
0.05	1.26	1.54
0.08	1.73	1.72
0.10	1.73	2.16
0.125	2.00	2.34
0.3	1.26	1.39

$$E_A^O \frac{\text{Uranium Concentration In Solvent}}{\text{Uranium Concentration In Aqueous}} = \text{At Equilibrium}$$

\*Ashland 140, an aliphatic diluent, is a product of Ashland Chemical Co.

FIG. 8 – EFFECT OF PHOSPHINE OXIDE MOLARITY ON URANIUM EXTRACTION FROM WPPA



## Niobiurn - Tantalum Separation

Niobium - tantalum separation is normally effected using MIBK. The disadvantage here is the high aqueous solubility of the ketone (approximately 20 g/l) and the consequent need to treat the raffinate for recovery of the extractant. Recent work<sup>1</sup> has shown that TOPO has utility in niobium - tantalum separation and is reported to produce higher purity niobium oxide than MIBK.

The advantage of using CYANEX 923 extractant in place of TOPO is again related to its liquid state and higher organic solubility.

A strong diluent effect was observed in preliminary experiments on niobium extraction. This is illustrated by the results of extraction isotherms given in Table 8 and plotted in Figure 9. Aromatic 150\* proved to be the superior diluent in comparison to both Aromatic 100\* and Exxsol D-80.

The process for niobium - tantalum separation, as with MIBK and TOPO, consists of extracting both metals followed by a selective strip; first of niobium and then of tantalum. This is illustrated in Table 9 and Figure 10 where selective stripping of niobium from a niobium - tantalum loaded solvent was observed using a strip feed containing 0.1 N NH<sub>4</sub>OH and 1 % NH<sub>4</sub>F. Tantalum was subsequently stripped using a more basic strip feed of 0.4 N NH<sub>4</sub>OH and 4% NH<sub>4</sub>F.

\*A product of Exxon Co., U.S.A.

TABLE 8

### The Effect of Diluent Type on Niobium Extraction

Solvent	:	277 g/l (0.8M) CYANEX 923 extractant in the appropriate diluent.
Diluents	:	Exxsol D-80, Aromatic 100 and Aromatic 150
Aqueous	:	88.5 or 91.4 g/l Nb, 4N HF, 8N H <sub>2</sub> SO <sub>4</sub>
Temperature	:	24°C
Contact Time	:	5 minutes

### Equilibrium Nb Concentration (g/l)

O/A	EXXSOL D-80		Aromatic 100		Aromatic 150	
	Organic	Aqueous	Organic	Aqueous	Organic	Aqueous
2	43.8	66.6	38.7	72.0	61.3	60.7
1	36.6	51.9	39.7	51.7	61.9	29.5
0.5	36.6	15.3	36.5	18.5	44.8	1.86
0.3	-	-	-	-	27.2	0.73
0.2	17.4	1.53	18.2	0.30	18.2	0.56
	8.84	0.07	9.12	0.13	9.13	0.05

FIG. 9 — EFFECT OF DILUENT TYPE ON NIOBIUM EXTRACTION

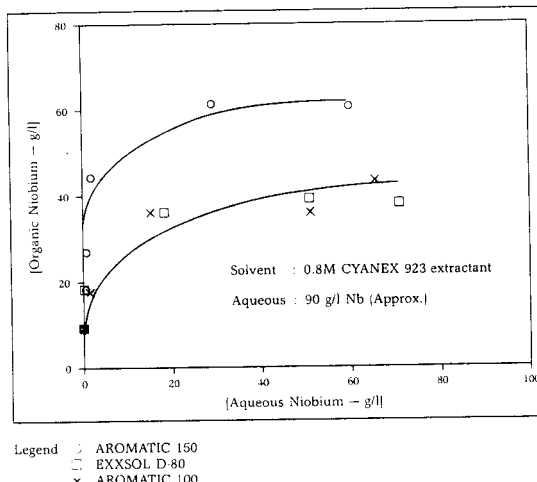


**TABLE 9**  
**Niobium Stripping From a Solvent Containing**

**Niobium and Tantalum**

Solvent	:	277 g/l (0.8M) CYANEX 923 extractant in Aromatic 150 diluent.
		Loaded to 22.4 g/l Nb and 3.61 g/l Ta.
Strip Feed	:	0.1N NH <sub>4</sub> OH, 1% NH <sub>4</sub> F
Contact Time	:	5 minutes
Temperature	:	24°C

Equilibrium Nb Concentration g/l

A/0	Organic	Aqueous
5	0	4.66
2	0	11.6
1	0	22.7
0.05	3.30	38.2
0.2	10.9	57.3
0.1	14.8	75.6

**FIG. 10 — NIOBIUM STRIPPING ISOTHERM**

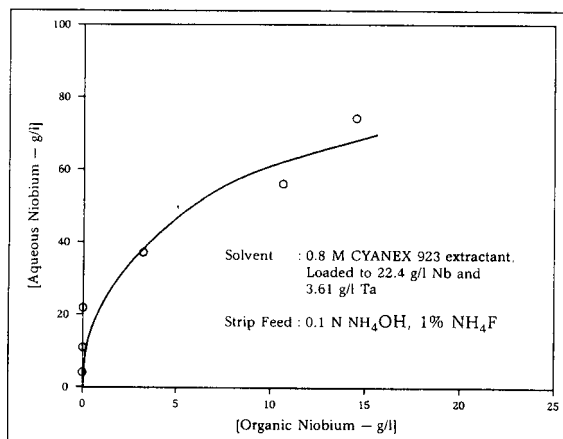


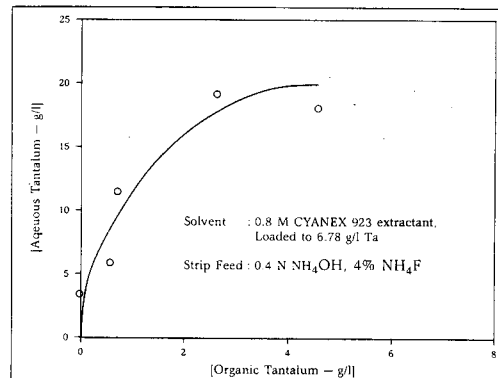
**TABLE 10**  
**Tantalum Stripping Isotherm**

Solvent	:	277 g/l (0.8M) CYANEX 923 extractant in Aromatic 150 diluent.
		Loaded to 6.78 g/l Ta.
Strip Feed	:	0.4N NH <sub>4</sub> OH, 4% NH <sub>4</sub> F
Contact Time	:	5 minutes
Temperature	:	24°C

Equilibrium Ta Concentration g/l

O/A	Organic	Aqueous
2	0	3.39
1	0.61	5.93
0.5	0.74	11.6
0.2	2.66	19.4
0.1	4.71	18.3

**FIG. 11 — TANTALUM STRIPPING ISOTHERM**



<sup>1</sup> R. Hahn and H. Retelsdorf. Production of Pure Niobium Using a New Extraction Process for Niobic Oxide and Optimal Reduction Processes. *Erzmetall*, 37, (9), 444-448 (1984).

## Cadmium Removal from Phosphoric Acid

Cadmium sometimes occurs as an undesirable impurity in phosphoric and other acids. The data given in Table 11 illustrate the ability of CYANEX 923 to readily reduce the concentration of cadmium from 10 mg/l to below a target of 2 mg/l; the specification in this particular application. McCabe-Thiele interpolations from the isotherm (Figure 12) indicate minimal staging requirements and that cadmium can be reduced from 10 mg/l to < 2 mg/l in two theoretical stages at A/O = 4.

Cadmium, as well as co-extracted acids, are efficiently stripped from the loaded solvent with water as shown by the data in Table 12. The stripping isotherm (Figure 13) again indicates minimal staging requirements.

**TABLE 11**  
**Extraction of Cadmium from**  
**HCl/H<sub>3</sub>PO<sub>4</sub> Using 2.5 v/o CYANEX 923**

Solvent	:	2.5 v/o CYANEX 923 in Exxsol D-80
Aqueous	:	10.2 mg/l Cd <sup>2+</sup> , 100 g/l HCl, 133 g/l H <sub>3</sub> PO <sub>4</sub>
Phase Contact	:	10 mins at 40°C

### Equilibrium Concentration

A/O	Cd(mg/l)		HCl (g/l)		H <sub>3</sub> PO <sub>4</sub> (g/l)	
	Organic	Aqueous	Organic	Aqueous	Organic	Aqueous
0.25	2.46	0.36	0.6	97.6	0.75	130
0.5	4.85	0.51	1.3	97.4	0.5	132
1	9.37	0.83	2.5	97.5	1	132
2	17.6	1.40	2.4	98.8	2	132
5	40.6	2.08	6.0	98.8	5	132

**FIG. 12 – CADMIUM EXTRACTION ISOTHERM:**  
**2.5 v/o CYANEX 923**

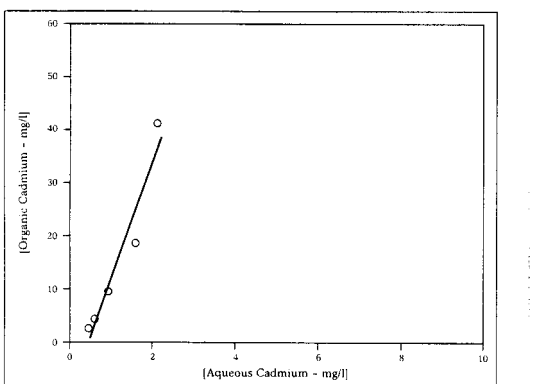


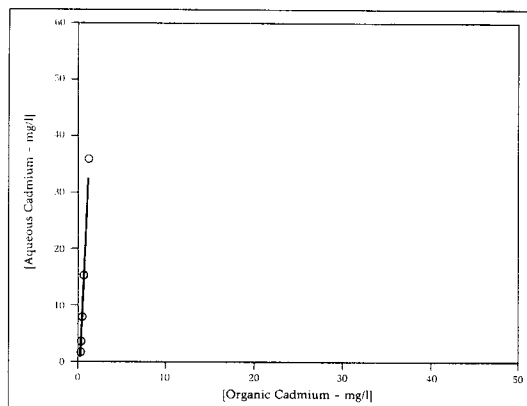
**TABLE 12**  
**Cadmium Stripping from 2.5 v/o CYANEX 923**

Solvent	:	2.5 v/o CYANEX 923 in Exxsol D-80 loaded to 8.05 mg/l Cd, 1.3 g/l HCl, 1.2 g/l H <sub>3</sub> PO <sub>4</sub>
Strip Feed	:	Water
Phase Contact	:	10 mins at 40°C

### Equilibrium Concentration

A/O	Cd(mg/l)		HCl (g/l)		H <sub>3</sub> PO <sub>4</sub> (g/l)	
	Organic	Aqueous	Organic	Aqueous	Organic	Aqueous
5	0.15	1.58	0	0.2	0	0.3
2	0.15	3.95	0	0.6	0	0.7
1	0.40	7.65	0	01.0	0	1.3
0.5	0.50	15.1	0	2.2	0	2.5
0.2	0.79	36.3	0	5.4	0	6.4

**FIG. 13 – CADMIUM STRIPPING ISOTHERM:**  
**2.5 v/o CYANEX 923**



# ANALYTICAL METHODS

## ANALYSIS IN ORGANIC SOLVENTS

As described, the gas chromatographic procedure is suitable for analyzing solvents containing approximately 120 g/l CYANEX 923 extractant. Other concentrations may be determined by diluting the solvent appropriately or adjusting the composition of the standard solution.

CYANEX 923 extractant is a mixture containing four major components, as follows: Trihexylphosphine oxide (1), dihexylmonoocetyl-phosphine oxide (2), dioctylmonohexyl-phosphine oxide (3) and trioctylphosphine oxide (4).

The method is based upon the fact that, within the limits of experimental error, the response factors for components 1, 2 and 3 are the same as for 4 and that 4 (TOPO) is readily available and may be easily purified to AR grade.

### Reagents

1. Didecylphthalate (AR grade - internal standard)
2. TOPO (purified - see note 1)
3. Process diluent (e.g. Escaid\* 110 diluent)

### Calibration

1. Accurately weigh 1g ( $\pm$  1 mg) of pure TOPO and 2g ( $\pm$  0.1 g) of didecylphthalate into a 50 ml volumetric flask. Dissolve and make up to volume with the process diluent.
2. Analyze the above standard solution as described under "Gas Chromatographic Conditions" to determine the relative response factor of TOPO vs. didecylphthalate.

### Procedure

1. Centrifuge the solvent to be analyzed or filter through PS paper" to remove entrained aqueous or suspended solids.
2. Accurately weigh 2g ( $\pm$  0.1g) of didecylphthalate into a 50 ml volumetric flask and pipette 25 ml of the clarified solvent into the same flask. Make up to volume with the process diluent.
3. Determine the relative response factor of each component of CYANEX 923 extractant vs. that of the internal standard as described under "Gas Chromatographic Conditions".

\* A product of Exxon Co., U.S.A.

\*\* Phase separation paper available from Whatman, Inc., Clifton, NJ

### Calculations

Total Concentration of Trialkylphosphine Oxides (g/1)

$$\sum \left[ \frac{R_{4S}}{R_{na}} \right] \times 2 \times C_{4S}$$

Where  $R_{4S}$  = Relative response factor for TOPO in the standard solution

$R_{na}$  = Relative response factor for the  $n^{\text{th}}$  component in the analyte solution.

$C_{4S}$  = Concentration of TOPO in the standard solution (g/1)

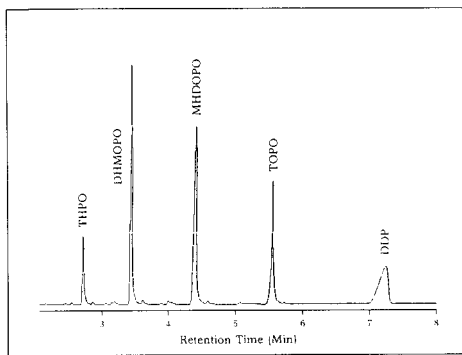
### Gas Chromatographic Conditions

Instrument	:	Perkin Elmer Sigma 115 or equivalent
Column	:	30 in x 0.32 mm fused silica capillary column coated with 0.25 $\mu$ m of DB1
Detector	:	FID
Carrier Gas	:	Helium at 18 psig
Vent Flow	:	100 ml/min
Column Flow	:	4.3 ml/min
Split Ratio	:	23/1
Temperatures °C		
Detector	:	340
Injection Port	:	340
Column	:	220 to 330 at 10°C/min
Sample		
Injection		
Volume	:	0.1 $\mu$ l
Peak Areas	:	Determined by electronic integration

### Notes

1. A chromatogram of commercial CYANEX 923 extractant is shown in Figure 1A.
2. Pure TOPO (>99.5%) can be obtained by recrystallizing commercial grade TOPO from hexane (three recrystallizations are necessary).
3. Megabore columns may be used as an alternative to capillary columns. A thermal conductivity detector may also be used in place of an FID.
4. The method is based upon a single point determination. If required, a calibration curve can be constructed by varying the concentration of TOPO in the standard solution while maintaining a constant concentration of the internal standard.
5. This method has not been validated.

FIG. 2A — CHROMATOGRAM OF CYANEX 923 EXTRACTANT CONTAINING DIDECYLPHTHALATE (DDP) AS AN INTERNAL STANDARD



## ANALYSIS IN AQUEOUS SOLUTION

The aqueous solubility of each component of CYANEX 923 extractant will normally be <2 mg/l. The method is based on analysis of the aqueous sample by gas chromatography. The response factors of the four active components are equal within the limits of experimental error.

### Reagents

1. Tetrahydrofuran (THF). "Baker Analyzed Reagent, 100%."
2. TOPO (purified - see note 1.)

### Calibration

1. Prepare a stock solution by accurately weighing ( $\pm$  1 mg) approximately 0.5 g of TOPO into a 50 ml volumetric flask. Dilute to 50 ml with THF and dissolve the TOPO.
2. Dilute aliquots of the stock solution with distilled water to prepare standard solutions containing 2, 5, 10 and 30 mg/l of TOPO.
3. Analyze the solutions as described under "Gas Chromatographic Conditions."

### Procedure

1. Filter the aqueous solution to remove entrained organic
2. Inject 3 $\mu$ l of the analyte solution and analyze as described under "Gas Chromatographic Conditions."

### Calculation

$$1. \text{ *Response Factor for TOPO (R)} = \frac{\text{Conc. of TOPO in Standard (mg/l)}}{\text{Area of TOPO Standard Peak}}$$

$$2. \text{ Concentration of Component in Aqueous (mg/l)} = \frac{\text{Area of Component Peak (analyte) x R}}{\text{Area of Component Peak (standard)}}$$

\*Response factor for the standard closest in concentration to the sample.

### Gas Chromatographic Conditions

Instrument	:	Hewlett Packard 5730A or equivalent
Column	:	2 ft x 1/4 inch x 2 mm ID glass Column packed with 9% OV-17 and 12% SP2401 on 80/100 mesh Supelcoport
Detector	:	FID
Carrier Gas	:	Helium at 57 psi (Flowrate 40 ml/minute)
Temperatures °C		
FID	:	300
Injection	:	
Port	:	250
Column	:	230 (Isothermal)
Sample		
Injection		
Volume	:	3 $\mu$ l

### Notes

1. Pure TOPO can be obtained by recrystallizing commercial grade TOPO from hexane. (Three recrystallizations are necessary).
2. Retention time for TOPO is approximately 12 minutes.
3. Detection limit approximately 2 mg/l.
4. This method has not been validated.

## **DETERMINATION OF WATER**

The method is based on distilling water from CYANEX 923 extractant in the form of an azeotrope with toluene. On contacting a condenser, the water and toluene separate and fall into a graduated trap. The volume of the distillate is then measured.

### **Apparatus**

1. 500 ml round-bottomed, short-necked glass flask with a 40/50 ground glass fitting.
2. Water-cooled condenser. Cold-finger type.
3. Dean and Stark type trap. 10 ml capacity graduated in 0.1 ml divisions with a 40/50 ground glass fitting.
4. Heating mantle controlled by a rheostat.

### **Reagents**

1. AR grade toluene (water-free)

### **Procedure**

1. Weigh 50 g of the sample ( $\pm 0.5$  g) into the 500 ml flask.
2. Add approximately 200 ml of toluene to the flask and assemble the apparatus.
3. Heat the contents of the flask to boiling and allow to reflux for 30 to 60 minutes or until the volume of water in the trap is constant.
4. Read the volume of water in the trap at room temperature.

### **Calculation**

$$\% \text{ Water} = \frac{\text{Volume of Water in Trap (ml)}}{\text{Sample weight (g)}} \times 100$$

### **Notes**

1. This method has not been validated.
2. Karl-Fisher titration is not recommended.

# TECHNICAL PAPERS AND PATENTS

## Technical Papers (listed chronologically)

1. **A Liquid Phosphine Oxide; Solvent Extraction of Phenol, Acetic Acid and Ethanol**  
Watson, E.K.; et.al.  
Solvent Extr. Ion Exch., 6, No. 2, Pages 207-20; (1988)
2. **Solvent Extraction Separation of Niobium and Tantalum at MHO**  
Haesebroek, G.; et.al.  
Process Metall., 7B, Pages 1115-20; (1992)
3. **Simulation of Countercurrent Multistage Extraction Process for Recovery of Titanium**  
Kagaku Kogaku Ronbunshu, 19, No. 2, Pages 214-19; (1993)
4. **Computer Modelling of Countercurrent Multistage Extraction for Titanium (IV) - Sulfuric Acid - CYANEX 923 System**  
Technal. Rep. Kansai Univ., 35, Pages 59-67; (1993)
5. **Phenol Recovery with SLM using CYANEX 923**  
Garea, A.; et.al.  
Chem. Eng. Commer., 120, Pages 85-97; (1993)
6. **Computer Modelling of Countercurrent Multistage Extraction for Ti(4+) – H<sub>2</sub>SO<sub>4</sub> CYANEX 923 System**  
Int. Conf. Process. Mater. Prob.  
Pages 521-4, Ed. Henein, H. Pub.  
Miner. Met. Mater. Soc., Warrendale PA; (1993)
7. **Gold (I) Extraction Equilibrium in Cyanide Media by the Synergic Mixture of Primene 81R-CYANEX 923**  
Coravaca, C.  
Hydrometallurgy, 35, No. 1, Pages 27-40; (1994)
8. **The Phosphine Oxides CYANEX 923 and CYANEX 923 as Extractants for Gold (I) Cyanide Aqueous Solutions**  
Alquacil, F.J.; et.al.  
Hydrometallurgy, 16, No. 3, Pages 369-84; (1994)

## Patents (listed chronologically)

1. **Liquid Phosphine Oxide Systems for Solvent Extraction**  
Robertson, A.J. and Rikelton, W.A.  
European Pat. Appl. EP 132700 A1 (1985)
2. **Procede de Separation des Terres Rares par Extraction Liquide-Liquide**  
Dellaye, T.; et.al.  
European Pat. Appl. 0284504 (1988)
3. **Recovery of Uranium from Wet Process Phosphoric Acid Using Asymmetrical Phosphine Oxides**  
Rikelton, W.A.  
U.S. Patent 4778663 (1988)
4. **Process for Solvent Extraction Using Phosphine Oxide Mixtures**  
Rikelton, W.A. and Robertson, A.J.  
U.S. Patent 4909939 (1990)
5. **Recovery of Indium from Acidic Solutions by Solvent Extraction Using Trialkylphosphine Oxide**  
Rikelton, W.A.  
Canadian Pat. Appl. CA 2077601 (1994)
6. **Method for Recovering Carboxylic Acids from Aqueous Solutions**  
Gentry, J.C.; et.al.  
U.S. Patent 5399751 (1995)

*As of July 26, 1995*

---

## **HEALTH AND SAFETY**

The oral and dermal toxicity of CYANEX 923 extractant is low. CYANEX 923 extractant produces mild eye irritation and severe skin irritation upon contact. Repeated dermal exposure for 28 consecutive days produced severe skin irritation, but no systemic toxicity. CYANEX 923 extractant did not produce dermal sensitization in guinea pigs after repeated dermal exposure. This product did not produce mutations in bacteria nor did it produce chromosomal effects in the mouse micronucleus or human lymphocyte aberration assays. CYANEX 923 extractant is highly toxic to fish and invertebrates and great care should be exercised to avoid environmental exposure.

### **IMPORTANT NOTICE**

The information and statements herein are believed to be reliable but are not to be construed as a warranty or representation for which we assume legal responsibility. Users should undertake sufficient verification and testing to determine the suitability for their own particular purpose of any information or products referred to herein. NO WARRANTY OF FITNESS FOR A PARTICULAR PURPOSE IS MADE. Nothing herein is to be taken as permission, inducement or recommendation to practice any patented invention without a license.

---

**FOR ADDITIONAL INFORMATION  
PLEASE CONTACT:**

**Cytec Industries, Inc.**  
West Paterson, NJ, USA  
Tele: 973-357-3100  
Fax: 973-357-3050

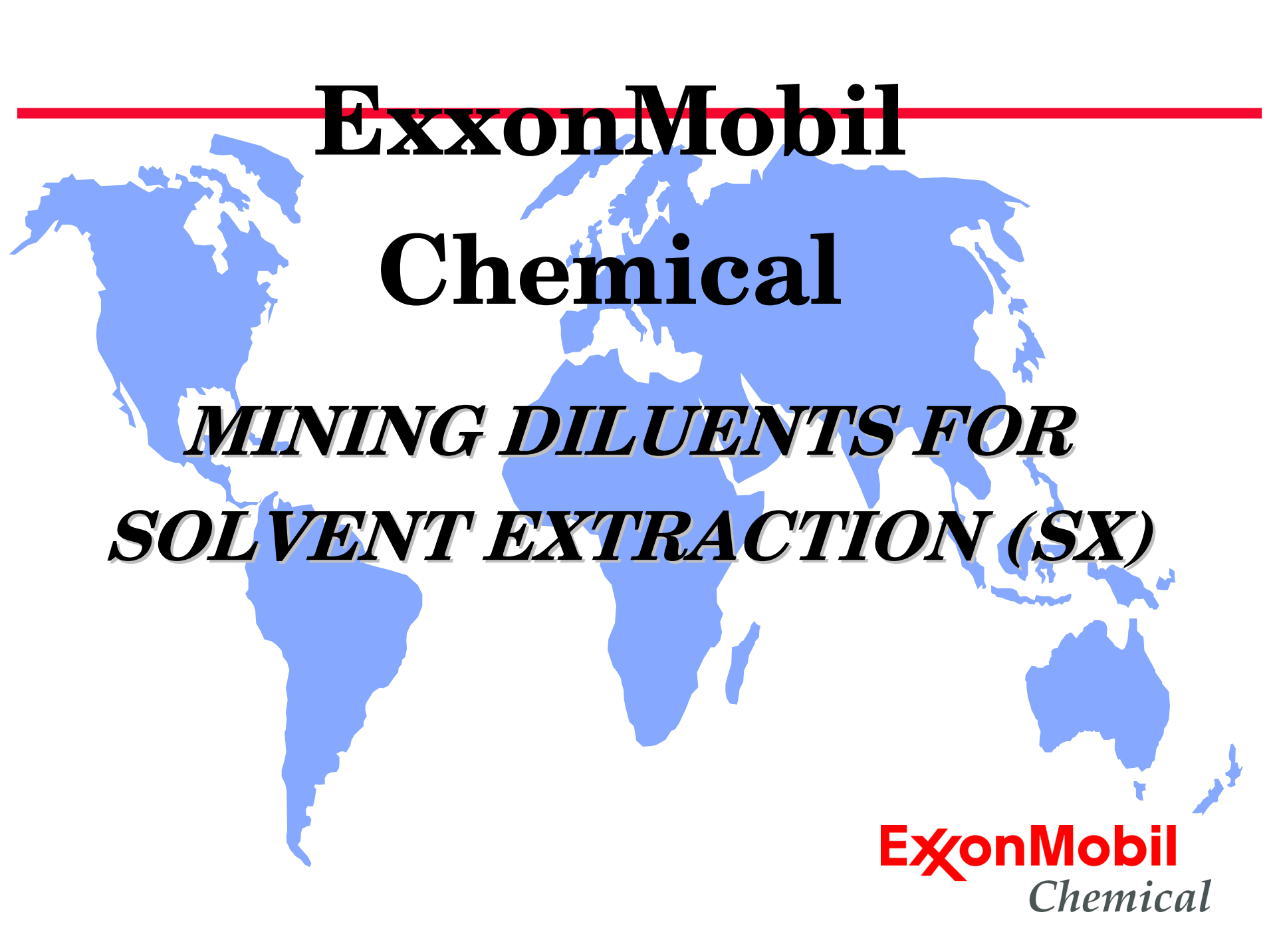
**Cytec Canada, Inc.**  
Phosphine Technical Centre  
Niagara Falls, Ontario  
Tele: 905-356-9000  
Fax: 905-374-5939

**Cytec Australia Holdings, Pty. Ltd.**  
Baulkham Hills, NSW 2153  
Tele: 61-2-9686-4188  
Fax: 61-2-9639-4248

**Cytec Industries France**  
Rungis-Cedex  
Tele: 33-1-4180-1700  
Fax: 33-1-4978-0780

**Cytec Industries B.V.**  
Botlek, The Netherlands  
Tele: 31-181-295400  
Fax: 31-181-295401

**CYTEC**



# **ExxonMobil**

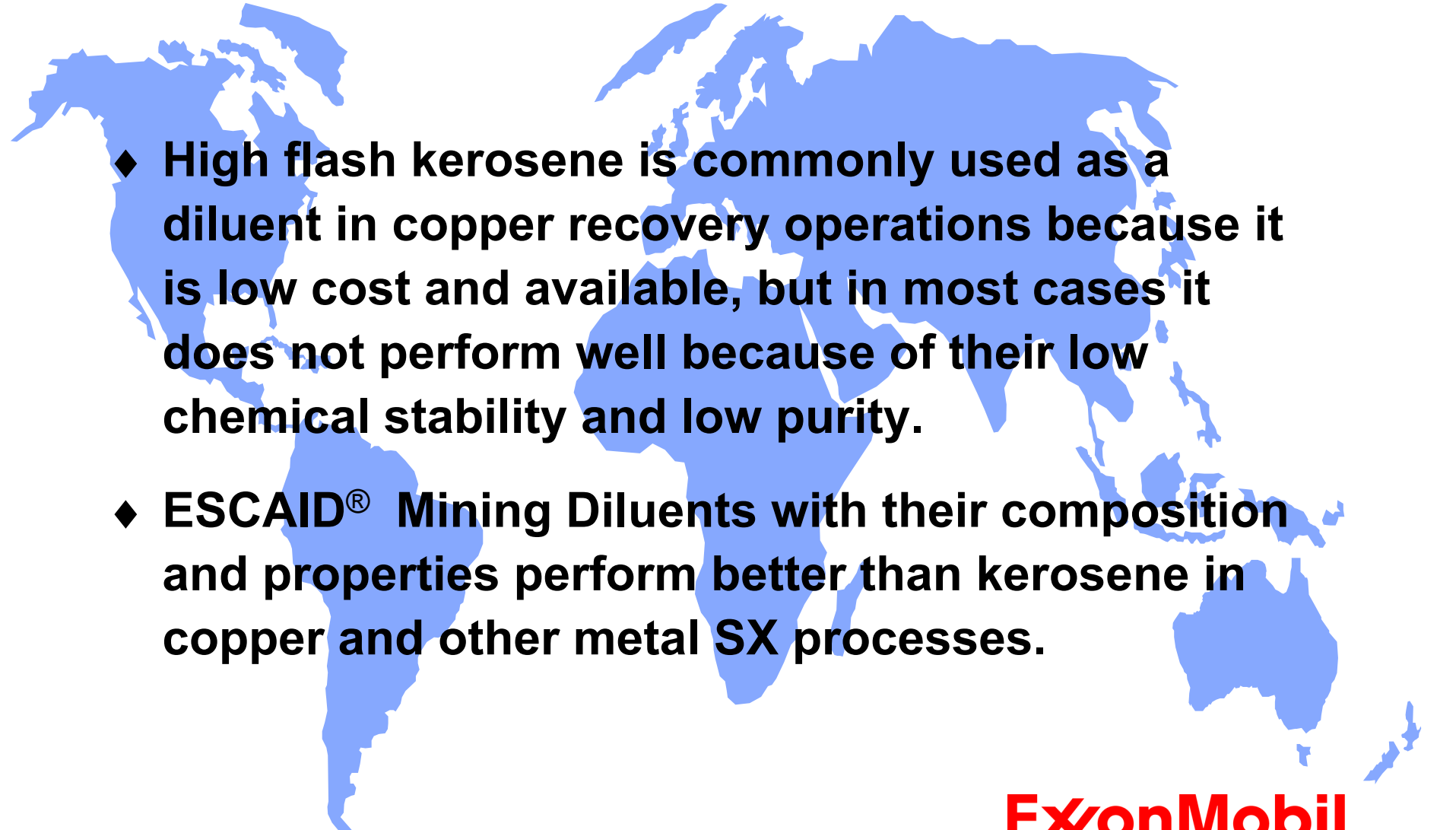
## **Chemical**

***MINING DILUENTS FOR  
SOLVENT EXTRACTION (SX)***

**ExxonMobil**  
*Chemical*

# Background

---

- 
- ◆ High flash kerosene is commonly used as a diluent in copper recovery operations because it is low cost and available, but in most cases it does not perform well because of their low chemical stability and low purity.
  - ◆ ESCAID® Mining Diluents with their composition and properties perform better than kerosene in copper and other metal SX processes.

# What Determines Whether a Diluent Performs Well?

---

- ◆ Phase Separation
  - Rate at which the organic (diluent, complexing agent and modifiers) and aqueous phases separate.
- ◆ Copper Loading Capacity
  - Loading or uptake refers to the maximum amount of copper that can be taken up by the organic phase. Loading capacity depends on several factors including diluent composition, solubility of the complexing agent and copper complex in the diluent, pH of the aqueous phase and competing ions, especially iron.
- ◆ Transfer Efficiency
  - Transfer efficiency refers to the percent of copper loading transferred between the organic and aqueous phases during the extraction and stripping operations. Most of the copper transfer occurs during mixing.
- ◆ Rate of Mass Transfer
  - Rate of mass transfer is the rate at which copper is transferred from one phase to the other.

# Summary

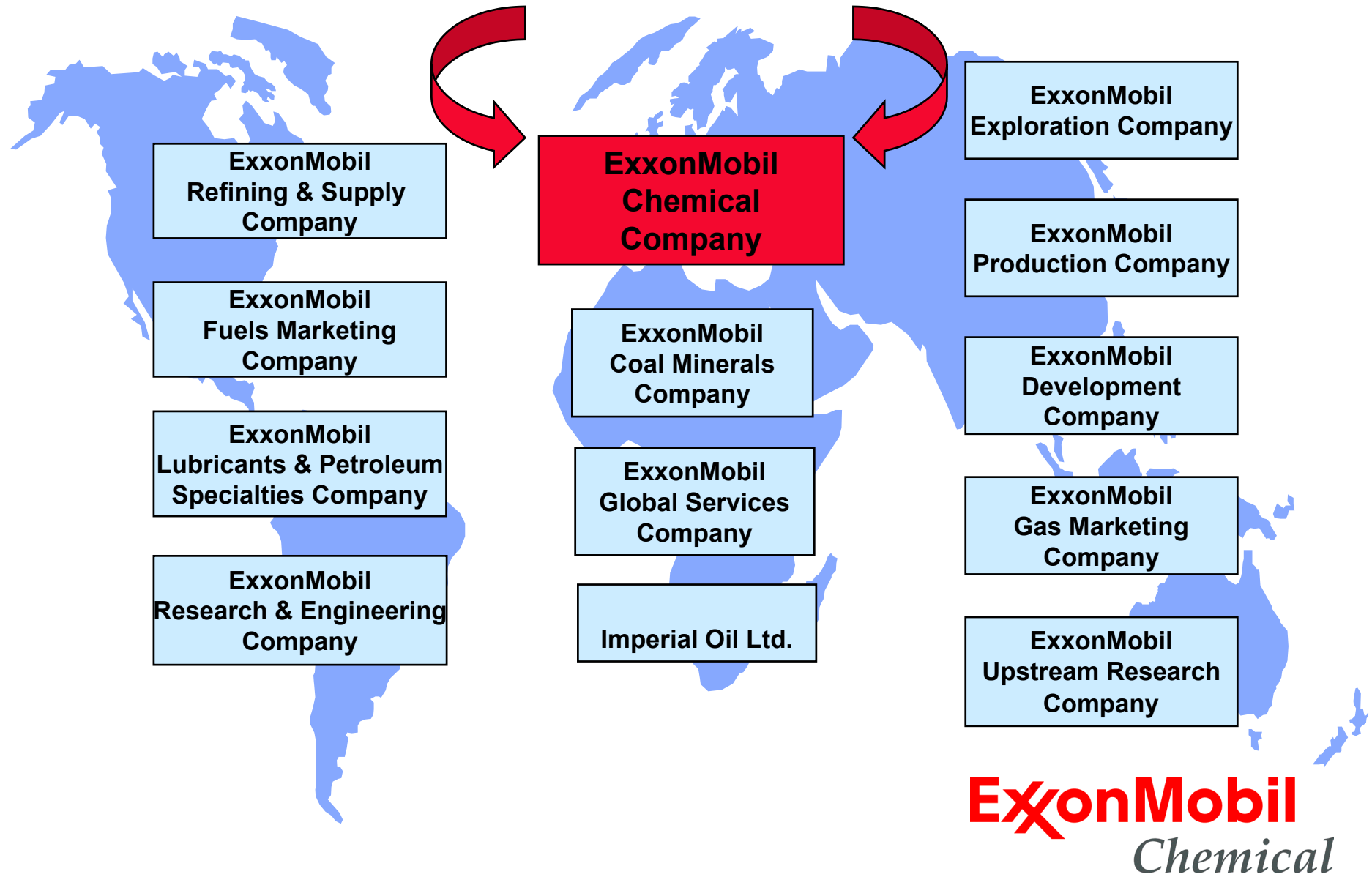
---

- ◆ ExxonMobil Chemical has mining diluents such as ESCAID 100, ESCAID 103, ESCAID 110 and ESCAID 120 that perform better than kerosene in copper recovery processes
- ◆ ESCAID 110 has become the diluent of choice in several mines in Africa and other continents. Close to diluent recommendation in composition and properties, ESCAID 110 offers increased copper loading and high flash point with lower diluent losses

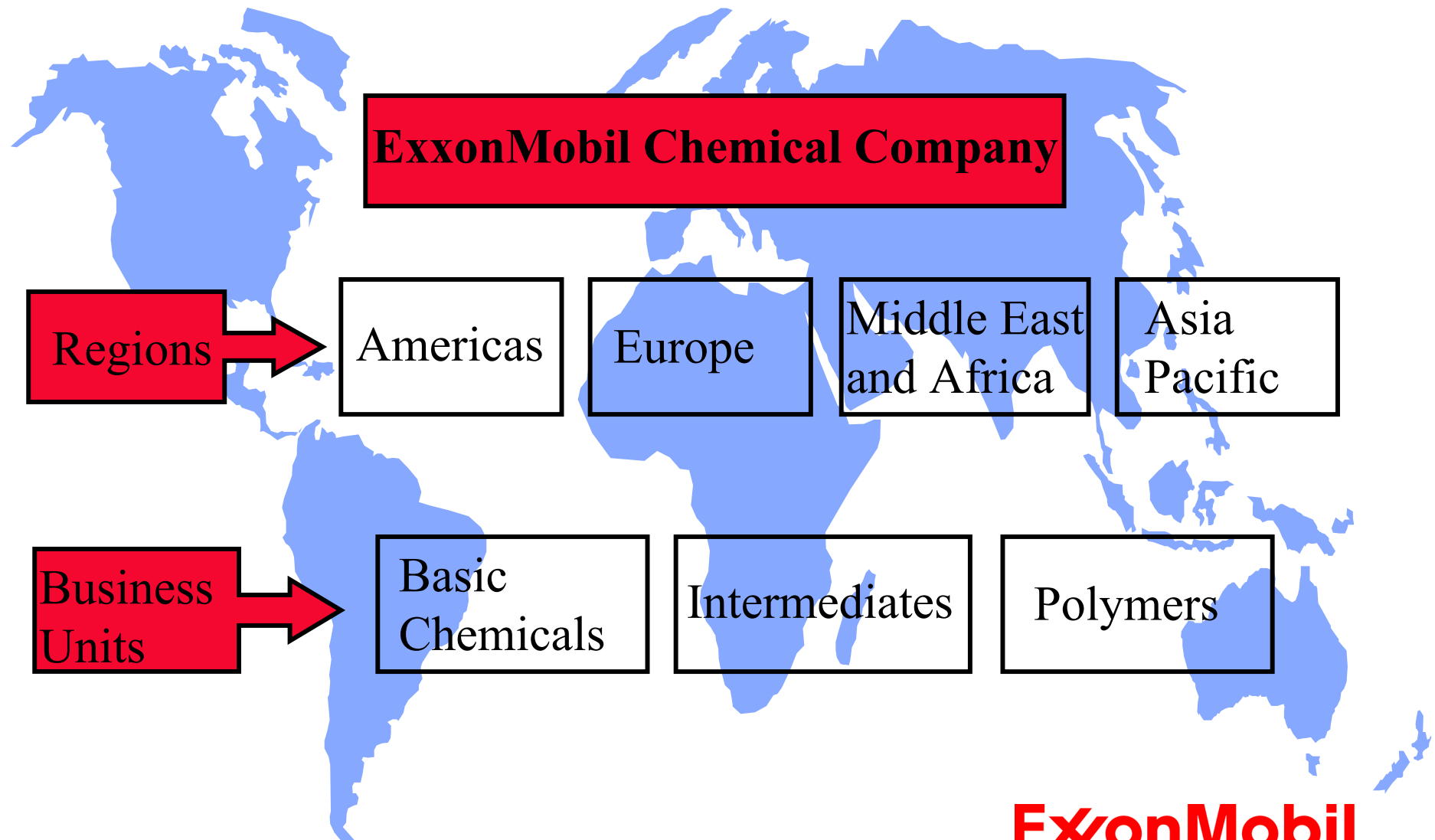
# Key properties of ESCAID® Mining Diluents

PROPERTIES	UNITS	Escaid 100	Escaid 103	Escaid 110	Escaid 120	Test Method
Distillation Range * Initial Boiling Point * Dry Point	°C	203 239	201 241	203 238	240 264	ASTM D 86
Flash Point	°C	77	76	78	103	ASTM D 93
Aromatic Content	wt%	25.0	12	< 0.4	< 0.9	EC-A-A07
Density 15°C	kg/dm <sup>3</sup>	0.814	0.811	0.795	0.817	ASTM D 4052
Viscosity at 25°C	mm <sup>2</sup> /s	1.98	2.02	2.01	3.2	ASTM D 445

# Exxon Mobil Corporation and Affiliated Companies



# ExxonMobil Chemical Company



**ExxonMobil**  
Chemical

# Company Overview

---

## ExxonMobil Chemical Worldwide

- ▶ One of three largest world-wide petrochemical companies
- ▶ 17.500 employees
- ▶ Manufacturing locations in more than 20 countries
- ▶ Products marketed in more than 100 countries

**ExxonMobil**  
*Chemical*

# Company Overview

## Our Commitment to Responsible Care®

Responsible Care® is the world-wide chemical industry's commitment to continuous improvement in all aspects of health, safety and environmental performance, and to openness in communication about its activities and achievements.

There are six areas providing clear improvement targets, each aimed at specific public concerns:

1. Community Awareness and Emergency Response
2. Process Safety
3. Distribution
4. Employee Health and Safety
5. Pollution Prevention
6. Product Stewardship

# Introduction to Mintek

*MINTEK, South Africa's national minerals-research organization that was founded in 1934 to assist the mining industry to operate more effectively and profitably, has achieved international recognition for its contributions. Our mining and minerals industry has been extremely innovative, and many notable advances in extraction, refining, and manufacturing technology that originated in South Africa have impacted on the minerals industry world-wide.*



*Aerial view of Mintek*

Mintek works with industry and other R&D organizations to research, develop, and implement new and improved technologies in the minerals and metallurgical sectors. South Africa has become a world leader in this technological niche, with a successful record of technology export, and Mintek itself has become an international player in the field.

## Location

Mintek's research complex is situated in Randburg, about 15 kilometres north of Johannesburg, within easy reach of Johannesburg International Airport.

## Expertise

With a total staff of more than 500, Mintek employs highly qualified and motivated people with a wide range of skills, including metallurgical, chemical, and electronics engineers, chemists, physicists, and

mineralogists. Many of our engineers and scientists are recognized as leaders in their fields of specialization.

## Products and breakthrough technologies

Mintek has been successful in the development of 'breakthrough' technologies that have transformed their industry sectors. Recent successes include the Minataur process for the refining of high-purity gold; gold and copper bioleaching; DC arc furnace technology for the fuming of magnesium, lead, and zinc from ores and wastes, and smelting of chromite, ilmenite, and cobalt-bearing slags; jigging technology for the recovery of ferroalloys from furnace slag; and a range of hardware and software for the stabilization and optimization of metallurgical plants, including submerged-arc furnaces and milling, flotation, and leaching plants. Technologies at an advanced stage of development

include new materials based on the precious metals (gold and platinum), ferronickel production from lateritic ores by pre-heating/reduction and smelting in a DC arc open bath furnace, and hydro-metallurgical techniques for recovering metals from waste streams.

### **Process development and services**

Mintek provides world-class R&D expertise, testwork, and process optimization for the precious and base metals, ferro-alloys, and industrial minerals sectors on an international basis. The activities range from initial investigations to process development, and the design, construction, and commissioning of industrial plants. Working closely with clients, and in conjunction with engineering partners, Mintek supplies a flexible package of technology for process development and optimization.

### **Facilities**

A full range of sophisticated facilities is available for sample preparation and characterization, comminution, flotation, physical separation, smelting, leaching, purification, and metal recovery. Some of these facilities were developed in-house and are unique to Mintek. Processes can be scaled up from initial exploratory batch tests to continuous pilot campaigns operating at feed rates up to 4 tons per hour involving several hundred tons of material, using bulk samples shipped to Mintek. In many cases, work can be carried out at the client's site using modular plant transported in containers. The extensive laboratories and pilot-plants are supported by specialist analytical, mineralogical, and information services, expertise in computer simulation and modelling, and techno-economic studies.

**MINTEK'S Analytical Science Division supports the research activities at Mintek, in particular pilot plant operations. We analyse greatly diverse samples from mining and metallurgical processes, following strict quality procedures and focusing on accuracy and timeous service. Critical operations can be supported by 24-hour standby service.**

The Division has excellent instrumental and laboratory facilities, and highly qualified and experienced staff. The versatility of the laboratory is illustrated by the availability of many different analytical techniques tailored to the needs of specific analyses.

## Equipment and scale of operation

### *Trace ICP section:*

An Elan 6000 ICP-mass spectrometer and an Elan DRC ICP-mass spectrometer are used in measuring a wide range of trace and minor elements in simple and complex sample types. The technique is particularly well suited to precious metals and rare-earth elements. It has great sensitivity, and can readily determine elements in the ppb concentration range. Semi-quantitative analysis of solution samples is generally done by this technique.

An Optima 3300 DV ICP-OES instrument is available for trace analysis of elements not suited to measurement by ICP-MS. A wide range of sample preparation techniques is available.

### *AAS section:*

A number of atomic absorption spectrometers, which work in flame or graphite furnace mode, are available. The technique is useful for the determination of a wide range of elements, and complements the other solution spectroscopic techniques available. Very low levels can be reached by graphite furnace AA. The AA technique is best used where only a few elements have to be determined in a sample.

### *Wet chemistry section:*

Many types of classical analysis are done by volumetric, gravimetric and spectrophotometric determination. These techniques are useful for high-precision work as well as for some difficult analyses.

Total carbon and sulphur determinations at high and low levels, and speciation analyses, are carried out using combustion instruments. A combustion instrument is available for the determination of oxygen and nitrogen in metal samples.

A dedicated water analyser is used for routine water quality analysis, and for the analysis of toxic contaminants in water.

A variety of instruments are available for the



*Emission spectrometer*



*Fire assay*

measurement of pH, TSS, TDS, conductivity and anions. The section also has excellent facilities for TCLP extractions according to US Environmental Protection Agency, Department of Water Affairs and Forestry, and other standards. This technique is used extensively for determining whether solids are acceptable from an environmental point of view. The solutions from TCLP extraction can be accurately analysed by a variety of techniques available in the Division.

### *Chromatography section:*

Ion chromatography, HPLC and FIA are used to determine a wide range of anions and metal complexes. The section has a great deal of experience in dealing with complex sample types. Specialised analysis of cyanide in environmental samples is carried out with a dedicated Skalar segmented flow analyser.

### *XRF section:*

An X-Lab 2000 energy-dispersive XRF instrument is used mainly for the quantitative determination of major and minor elements in geological-type materials and process samples, and for analysis of environmentally important samples such as environmental filter disks. A useful feature of the technique is its ability to provide semi-quantitative information regarding the composition of a wide variety of sample types.

### *ICP-OES section:*

The section uses four Spectroflame ICP-OES instruments, which can determine up to 40 elements simultaneously in the UV and the visible spectrum. The instruments have been set up to be complementary to one another in spectral line combinations. Scanning and background correction facilities are available.

Due to the broad applicability and outstanding analytical capabilities of this technique, a large proportion of the determinations in the Analytical Science Division is done by ICP-OES. A special feature is the capability to carry out accurate analyses at high concentration levels.

### *Fire assay:*

This classical technique is still applied to precious metal analysis, as it allows high-precision analyses for low-level elements in a variety of sample types. This section has excellent facilities for lead collection (mainly for Au, Pt, Pd, and Rh, either as individual elements or as a total figure), and for the nickel sulphide collection technique (Au, Pt, Pd, Rh, Ru, Ir and Os). Generally, a gravimetric finish is used, but individual PGE analysis requires an ICP-OES finish.

Much attention is given to careful control of the tests, so that high-precision results can be obtained. For this reason, electrically heated furnaces are used, lids are used during fusion, and it is preferred to do all samples in duplicate.

### **Quality system**

Mintek's Analytical Science Division has been accredited to ISO Guide 25 since 1995. As Guide 25 has been superseded by ISO 17025, the Division is in the process of converting to the new standard. Accreditation to this internationally accepted quality management system means that stringent standards

have to be followed to ensure reliable results for our clients. Regular internal and external audits, calibration of instruments, and participation in local and international proficiency testing programmes are requirements of the quality management system.

Supporting the quality management system and the operations of the Division is our Laboratory Information Management System (LIMS), which improves the reliable handling of analytical data, reporting of results, maintenance of quality standards, and allows archiving of results.

### **Reference materials**

Mintek has been the only local producer of internationally certified ore and processed material reference materials for over twenty years, and recently also took on the sales and distribution functions for these materials. Mintek has excellent facilities to produce reference materials according to clients' requirements if suitable materials cannot be sourced elsewhere.

### **Staff**

The Division is staffed with experienced and highly qualified personnel. Most members of the analytical and management staff have tertiary qualifications from technikons and universities, and are permanent employees to allow the building of high levels of expertise. Contract staff supplement them when necessary.

All members of staff are thoroughly trained in their fields of expertise, and their competence is tested before they are allowed to report results. The Division stresses all aspects of quality, safety and health and environmental awareness, and is a part of Mintek's QES management systems.

The heads of the various sections have extensive practical experience in the field of analytical chemistry in a mining and metallurgical environment, as well as research experience and proven expertise in their field. They act as consultants and actively participate in national and international conferences.

**Sandra Graham** (Trace ICP and XRF) - 15 years' experience in analytical chemistry, including several analytical techniques.

**Joe Baloyi** (AAS) - 11 years' experience in AA analysis, and 14 years' general analytical experience.

**Joseph Moepane** (ICP-OES) - 12 years' experience in analytical chemistry, specialising in fire assay and ICP-OES.

**Russell Vine** (Fire assay) - 25 years' experience in fire assay at Mintek and in industry.

Highly qualified specialists, supervisors and analysts support the heads of sections.

# Biotechnology

*AS near-surface oxide orebodies become depleted, more mines will have to process deeper, more complex and difficult-to-treat sulphide ores. These will require a modern, simple, environmentally sound technology. In many cases, bacterial oxidation will be the most suitable technique.*

Mintek, together with joint-venture partner BacTech Enviromet Corporation of Canada, offers the full range of services required for the evaluation and commercial implementation of bacterial leaching processes, including proprietary bacterial cultures, testwork and consulting, piloting, flowsheet design, and plant commissioning for gold and base-metal projects. Bioleach pre-oxidation of refractory gold ore concentrates containing sulphide minerals such as pyrite and arsenopyrite (the Bacox™ process) is established commercial technology, and technologies for the bioleaching of copper sulphide concentrates and complex base-metal sulphide concentrates are at the demonstration stage.

The bioleach technologies are supported by comprehensive analytical and mineralogical services, and established capabilities for development, optimization, piloting, and plant design in the areas of ore flotation, solvent extraction, electrowinning, and metal recovery.

## Equipment and scale of operation

- Extensive facilities to handle laboratory bioleach amenability testing.
- Six multi-stage fully instrumented continuous bioleach plants with a capacity of 1 to 5 kg concentrate per day, together with associated solvent extraction and electrowinning facilities.
- Bioleach column rigs for heap-leach simulation studies.

## Recent projects

Mintek and BacTech provided a licence to use the Bacox™ gold bio-oxidation technology for the 25 kt/a concentrate-treatment plant at the Beaconsfield joint venture, Tasmania. A 120 t/d commercial Bacox plant was commissioned at Laizhou Gold Metallurgy Plant in Shandong province, China in 2001. The plant is custom-treating refractory gold concentrates from a number of sources in Shandong, and will also be able to serve as a demonstration facility.

A demonstration pilot plant with integrated SX/EW facilities, with a capacity of 500 kg/d of copper was, commissioned in Mexico in mid-2001 for treating complex sulphide and chalcopyrite-containing concentrates. Together with Industrias Peñoles of



*Continuous bioleaching mini-plant at Mintek*



*Integrated demonstration plant for bioleaching base-metal sulphide, Monterrey, Mexico*

Mexico, Mintek and BacTech are conducting a feasibility study towards a jointly owned 25 kt Cu per annum commercial plant in Mexico.

A major R&D effort, supported by Noranda Inc. of Toronto, Canada, is under way to develop heap bioleaching for the recovery of copper from low-grade chalcopyrite ores. The two-year project aims to optimize the technology and establish its commercial viability.

## **Staff**

The Biotechnology Division includes graduate engineers and scientists qualified in chemical engineering, metallurgical engineering and microbiology, as well as experienced pilot-plant operators.

**Tony Pinches**, Manager: Biotechnology, has over 20 years' experience in biohydrometallurgy and biochemical engineering. He graduated from Cardiff University with a degree in microbiology and went on to obtain a PhD in minerals engineering at the same university, the subject of his thesis being the bioleaching of pyrite and arsenopyrite.

**Petrus van Staden** (Head: Bioprocess Engineering) has over 10 years' experience in hydrometallurgy. He graduated in chemical engineering from the University of Pretoria in 1986, and obtained his MSc (Chemical Engineering) in 1991 from the University of the Witwatersrand. Petrus has extensive experience in gold extraction techniques, and currently specializes in bioleach flowsheet design.

**John Neale** (Specialist: Biotechnology) has over 10 years' experience in chemical engineering and biohydrometallurgy. He joined Mintek in 1985 after obtaining a degree in chemical engineering from the University of Cape Town.

**Vishal Deepaul** (Head: Process Implementation) has 8 years' experience as a production metallurgist (including gold and copper operations) and in R&D. He obtained his BSc in extractive metallurgy and chemistry at Murdoch University in Perth, Western Australia.

**Mariekie Gericke** (Chief Scientist: Bioprocess Support) has 10 years' experience in microbiology. She joined Mintek in 1995. Mariekie graduated from the University of the Free State, and obtained a MSc (Microbiology) from the University of Pretoria.

**Paul Kruger** (Chief Engineer) has approximately ten years' experience in biohydrometallurgy. He joined Mintek in 1992 after obtaining a degree in chemical engineering from the University of Natal (1991).

# Electrowinning

**MINTEK has special expertise in the electrowinning of base metals such as cobalt, chromium, manganese (under exclusive contract), nickel, zinc and gold, and experience in the recovery of platinum-group metals (PGMs) from effluent streams, the production of electrolytic manganese dioxide (EMD), as well as the electrowinning and electrorefining of copper. Testwork is done on laboratory, pilot-plant and industrial scales. Reliable product and electrolyte sample analyses are provided by the Analytical Science Division.**

## Equipment and scale of operation

### Laboratory-scale electrowinning cells

Laboratory cells with a three-electrode configuration have been developed for testwork in electrowinning and electrorefining of most base metals. There are two main categories of cells – divided and undivided. The divided cell is used for metals such as cobalt, nickel, manganese and chromium, where the electrolytes surrounding the anode and cathode are separated by a porous diaphragm. The undivided cell has a common electrolyte, and is used for copper, cobalt, and zinc. The electrode configuration in both types of cell can be changed from a single cathode/two anodes to a single anode/two cathodes system; thus both cathodic and anodic processes can be investigated. There are two different sizes of divided and undivided cells. The smaller cells have a cathode area of approximately  $0.03\text{ m}^2$  and volume of approximately 3.5 - 5.5 l. The larger cells have a typical cathode area of  $0.1\text{ m}^2$  and a slightly larger volume of approximately 6.5 - 8.5 l.

The cells form part of a portable integrated rig that houses the cell and all ancillary equipment required for testwork. Each rig allows for the concurrent operation of two separate electrowinning cells under temperature control, utilising similar or different operating conditions and either synthetic or real plant solution. A total of six rigs have been commissioned for testwork purposes. Previous experience has shown that the performance of the laboratory cells compares favourably with that of well-operated industrial scale cells.

### Electrowinning cells for the production of EMD

Glass electrowinning cells have been developed for the production of electrolytic manganese dioxide (EMD), ranging from 800 g up to 8 kg. This is sufficient to fulfil in-house laboratory requirements and the battery manufacturers' sample requirements for initial testing. A discharge capacity rig has also been developed to quantify the EMD activity, and for comparison against IBA reference samples.

### Pilot-plant-scale electrowinning cells

Minetek has two types of electrowinning cells suitable for pilot-plant testwork on both synthetic and real



*Laboratory-scale electrowinning of EMD*



*Pilot-scale, portable electrowinning rig*

plant solutions - a full depth, full width cell housing up to two cathodes, and a deep (full depth, narrow width) cell, housing a single cathode. The full-scale cell is used to determine the effect of hydrodynamic forces on the deposit morphology, ease of stripping the deposit, impurity deportment, and typical performance data. The cathode area is approximately 1.8 m<sup>2</sup>. The deep electrowinning cell is designed to operate with a full depth, but narrow width, cathode. This allows the factors mentioned above to be examined on a slightly smaller scale, while still retaining the benefits of operating with a full-depth cathode.

Mintek has two deep cells, one with modular electrical, storage and pumping units that fit into a single shipping container. This allows for easy disassembly, transport, and re-assembly of the testing facility at distant locations throughout the world.

#### *Control and test cells in cell-houses*

Once specific recommendations have been made based on laboratory testwork, these can be tested on an industrial scale before implementation throughout the entire cell-house.

Two or three cells in the cell-house are prepared so as to operate with minimal mechanical or electrical faults (i.e. under ideal conditions). One cell (the control cell) is run according to the standard conditions in the cell-house. The other cells are designated as test cells, and are operated under conditions recommended from the laboratory testwork. Once these recommendations have been proved at this scale, they can be implemented successfully throughout the cell-house.

### **Recent projects**

#### *Cobalt*

With an increased international interest in cobalt, testwork has been done on the electrowinning of cobalt in divided and undivided cells has been conducted on laboratory, pilot plant and industrial scales. Clients include:

- Bulong., Australia
- Anglo American Corporation, Zimbabwe
- Kasese Cobalt Company, Uganda.

#### *Nickel*

Testwork on the electrowinning of nickel from standard and dilute solutions, including the effect of certain additives and organics, has been performed at laboratory and pilot scales. Clients include:

- Bulong., Australia
- Billiton Process Research, South Africa, and Queensland Nickel Industries, Australia
- Anglo American Corporation, Zimbabwe
- Anglovaal Mining, South Africa.

#### *Zinc*

Various aspects of zinc electrowinning have been optimised for Zincor Ltd, South Africa's only zinc producer. These include anode preconditioning, manganese removal, suppression of acid mist, the effects of additives, and anode evaluation. This work has been done on a laboratory and industrial scale.

#### *Manganese*

Various aspects of manganese metal production have been investigated on a laboratory scale under an exclusive contract between Mintek and Manganese Metal Company (MMC). Cell-house audits have been completed for both MMC and Zincor Ltd.

#### *Electrolytic manganese dioxide*

The production of EMD has been investigated on a laboratory scale. Clients include:

- Golden Tiger Resources, Australia
- Geometals Ltd., South Africa
- HiTec Energy, Australia (formerly Sovereign Resources)
- SA Mineral Resources Corporation Ltd, South Africa Gold.

Mintek recently provided the conceptual and detailed design for three gold refineries incorporating precious-metal chemical production. Electrochemistry is utilized in the gold refinery, gold potassium cyanide plant, and the silver cyanide production plant.

#### **Staff**

**Isaac Kappers** (Operator) - six years' experience

**Ephraim Mabusela** (Principal Operator) - eight years' experience

**Karen Matchett** (Senior Engineer) - six years' experience

**Ivan Greager** (Senior Engineer) - three years' experience.

**MINTEK'S gold process development programme provides a quick and cost-effective method of ensuring that gold recovery operations perform at their optimum level. Testwork may be carried out at both laboratory and pilot-plant scale, supported by well-proven computer-simulation design packages, so as to arrive at the most appropriate process route.**

The programme offers a complete gold process testing package for

- refereeing routine samples
- preliminary feasibility studies
- elucidation of problems occurring on existing operations
- development and evaluation of process flowsheets for new and existing operations
- evaluation and design of carbon-in-pulp (CIP) and resin-in-pulp (RIP) process flowsheets for gold recovery
- process consulting service.

The expertise base includes the skills of experienced mineralogists, analysts, and engineers with access to comprehensive analytical, laboratory, and pilot-scale facilities.

## Equipment and scale of operation

### Laboratory scale

- Batch cyanidation tests to optimize leaching parameters
- Batch tests to establish amenability of ore to heap leaching
- Batch gravity concentration tests to establish free gold occurrence and composition
- Batch amenability testing for chloride leaching of gold concentrates (Gravitaur process)
- Batch adsorption loading tests to establish the relative merits of activated carbon or ion-exchange resin, and process simulation
- Batch carbon elution testing
- Activated carbon quality assessment
- Quantification diagnostic leaching tests to characterize the mineral phases, establish gold deportment, gold/mineral associations, and thus determine the reasons for gold lock-up
- Cyanide speciation in process streams

### Pilot-plant scale

- Skid-mounted multi-stage contacting systems (5 litre, 150 litre) for continuous leaching and adsorbent-in-pulp process evaluation
- A range of percolation column sizes for heap leaching appraisals
- Minix resin elution and gold electrowinning facility.



*Skid-mounted adsorbent-in-pulp pilot plant at Kloof Gold Mine*

## Projects undertaken

Mintek has undertaken numerous gold processing appraisals on ore sources world-wide. Typical examples include the following:

### Process flowsheet development

Morilla - Mali  
Tirek - Algeria  
Tarkwa- Ghana  
Driefontein - South Africa  
Geita, Tanzania  
Syama - Mali  
Sino Mining - China  
Ararat Gold Recovery Co. - Armenia  
Hindustan Zinc Ltd - India

### Techno-economic evaluation of CIP vs RIP

Vaal Reefs - South Africa  
Hutti - India  
Western Areas - South Africa  
New Consort - South Africa  
CVRD - Brazil  
Millsite - South Africa

## **Staff**

The Gold Technology Group consists of 12 members, six of whom have tertiary qualifications, with the remaining members having extensive experience in metallurgical (and specifically gold) testing.

**Dennis Bosch** - BSc (Chem Eng), MSc (Mineral Process Design) *Head: Gold Technology*

Joined Mintek in 1999 after gaining 30 years' experience in mineral processing in South Africa and Canada, much of this in the gold mining industry. His involvement has been in operations, process development, plant design and consulting.

**Peter Tout** - HND (Extractive Metallurgy) *Principal Scientist*

More than 20 years' experience in gold and uranium processing. Was involved in Minetek's CIP and RIP development programmes, and has extensive experience in gold metallurgy at both laboratory and pilot scales.

**Peter Lotz** - Dipl (Chem) (Swiss) *Principal Scientist*

More than 10 years' experience at Mintek in various fields of process chemistry. Recently specialized in cyanide chemistry and its application to processing and the environment.

# Leaching and precipitation

**LEACHING** is the primary step in most hydrometallurgical processes. The overall recovery of the valuable species is thus directly affected by the efficiency of the leach, and optimization of the leach parameters is therefore of critical importance. Mintek is able to select and optimize leaching conditions for a variety of ores. Mintek's expertise in this field includes an understanding of the basic chemistry involved, mathematical modelling, and process optimization.

Precipitation techniques are often used to purify or concentrate process streams. In these cases, both purity and recovery need to be considered. Mintek's precipitation technology provides a number of techniques that can readily be integrated into new or existing processes. Special expertise is available in base metal precipitation and the removal of iron from process streams.

Mintek has facilities to undertake projects from basic flowsheet design through to laboratory testwork, piloting and full-scale plant commissioning. The services include process design, and optimization of process conditions and economics, based on computer simulation and experimental work.

## Equipment and scale of operation

- Laboratory-scale glass reactors ranging from 250 ml to 5 l for bench-scale batch tests. The vessels can be sealed, and are equipped with mechanical overhead stirrers and gas-dispersing impellers to ensure good agitation and induction of various gaseous reagents.
- A multipurpose six-stage pilot-scale continuous stirred-tank reactor cascade. The reaction vessels are of polypropylene which allows operating temperatures up to 90°C. The vessel sizes range from 10 l to 25 l. This plant is equipped with full PID control circuits for both temperature and pH control.
- A multipurpose five-stage miniplant scale continuous stirred-tank reactor cascade. The reaction vessels are of glass, and range in size from 250 ml to 5 l.
- Multipurpose batch-mode pilot-plant-scale stirred-tank reaction vessels of sizes ranging from 500 l to 2200 l.
- Process variables such as temperature, agitation speed, pH, and redox potential can be controlled.

## Recent Projects

Flowsheet conceptualization, process simulation, laboratory and pilot-scale testwork to develop a process for the production of high-purity electrolytic manganese dioxide from Woodie Woodie ore, Western



*Multipurpose continuous leach and precipitation facility*

Australia. The work was performed for HiTec Energy NL, of Perth. The feasibility study was recently completed, and the project is now at the design stage. Laboratory and pilot-scale testwork for the proposed expansion of Impala Platinum's base-metals refinery. This project implemented recently developed technology for the removal of manganese and iron from nickel and cobalt leach solutions.

Flowsheet conceptualization, process simulation, laboratory and pilot-scale testwork to develop a new process for the treatment of Merensky and UG2 PGM concentrates. This project was for a feasibility study undertaken by Lonmin Platinum to expand their current operations.

Laboratory-scale testwork for upgrading tantalum- and niobium-bearing ferro-alloys for Mamoré Mineração e Metalurgia, Brazil.

Flowsheet conceptualization, process simulation, laboratory and pilot-scale testwork to remove iron from BioNIC® nickel-cobalt bioleach process liquor.

## **Staff**

**George Benetis** (Chief Technician)

Fifteen years' experience in leaching, precipitation, and electrowinning technology. Specializes in intricate laboratory testwork and the management of pilot-plant operations.

**Danie Jacobs** (Chief engineer)

Four years' experience in leaching and precipitation technology. Specializes in the management of large projects and pilot-plant operations.

**Petrus Mafulako** (Senior Operator)

Ten years' experience in laboratory and pilot-plant operations.

**Sydney Mahlatsu** (Technician-in-training)

Three years' experience in leaching and precipitation technology. Specializes in laboratory testwork and the operation of pilot plants

**Michael Ramoipone** (Senior Operator)

Four years' experience in laboratory and pilot-plant operations.

**Patric Tshisikhawe** (Chief Operator)

Fourteen years' experience in laboratory and pilot-plant operations.

**MINTEK'S expertise in solvent extraction (SX) covers testwork requirements from initial laboratory studies through to a complete process design package and full-scale plant commissioning. This range of capabilities includes:**

- **development of solvent systems for individual applications**
- **laboratory shake-out tests and batch countercurrent tests**
- **small- and large-scale piloting**
- **process flowsheet development**
- **process flowsheet simulation modelling**
- **preliminary process design for contracting engineer**
- **auditing of process flowsheets and plant design**
- **commissioning**
- **troubleshooting.**

Mintek has a professional team of process chemists and engineers, supported by a wide range of in-house services such as costing engineers, analysts, mineralogists, and engineering workshops. Ongoing research in solvent extraction of base and precious metals, as well as equipment design, is undertaken to broaden our knowledge and to develop new technologies, as well as improve existing ones. Mintek also has excellent piloting facilities for upstream and downstream unit operations, allowing the continuous testing of solvent-extraction unit operations within integrated process flowsheets.

## Equipment and scale of operation

Mintek has a wide range of modern laboratory equipment for the development, evaluation, and understanding of fundamental SX process chemistry.

Mixer-settler equipment for continuous pilot-plant evaluations is available, with solution throughputs from 60 cm<sup>3</sup>/h up to 3 m<sup>3</sup>/h.

A Bateman pulsed column (BPC) with an internal diameter of 100 mm is also available for treating solution flowrates of 1 to 2 m<sup>3</sup>/day. A 40 mm diameter column will be available soon. Testing and scale-up of the BPC are done in a joint venture with Bateman Projects (South Africa and Israel).

Piloting is undertaken either in Mintek's well-equipped pilot bays or on site at the client's facility. Pilot campaigns have been carried out extensively both in southern Africa and internationally.

Mintek has designed and constructed several small full-scale SX plants.

## Recent projects

Harmony Gold Refinery (Virginia, South Africa). Design, installation, and commissioning of a refinery



*Integrated pilot plant*

to produce 99.99 per cent gold using the Minataur™ process. Similar 2 t/month refineries will be commissioned in Italy, South Africa, and Algeria during 2001. The Minataur (Mintek Alternative Technology for Au Refining) process uses a leach/solvent extraction/precipitation route to produce high-purity gold powder. The process can treat gold-containing materials ranging from jewellery scrap to cathode/anode sludges.

During 1999, Mintek and joint-venture partner Billiton successfully completed integrated pilot-plant campaigns in South Africa and Australia to produce nickel cathode from BioNIC® bioleach process liquor. Treating the sulphate liquor directly, the circuit comprised iron removal by precipitation, cobalt and nickel concentration and recovery by SX, followed by nickel purification by SX, and the electrowinning of LME-grade nickel cathode.

An integrated pilot plant operated in Zimbabwe for several months, treating 15 m<sup>3</sup>/d nickel sulphate electrolyte for the removal of cobalt by SX. The cobalt

stream was purified using ion exchange, followed by electrowinning of 99.9 per cent cobalt metal. LME-grade nickel cathode was produced from the purified nickel electrolyte.

Manganese removal and cobalt recovery from a copper SX raffinate bleed stream was piloted for a North American client as part of an integrated operation involving iron removal, purification by ion exchange, and cobalt electrowinning.

An integrated circuit was operated for the sequential solvent extraction of cobalt and nickel for subsequent electrowinning for a South African producer.

In collaboration with Mintek's bioleaching team, a SX miniplant was operated for recovering copper from chalcopyrite bioleach liquors. This integrated technology is being demonstrated in collaboration with technology partners Bateman (Australia) and Peñoles (Mexico).

An integrated flowsheet for the separation of platinum, palladium, rhodium and iridium from precious-metal alloy scrap has been piloted for a European client. In addition to SX, the flowsheet comprised leaching, precipitation, and effluent treatment.

Mintek has worked with contracting engineers on a number of projects involving the design of solvent-extraction plants to remove cobalt from nickel solutions.

## Specialist staff

**John Preston** (*Specialist Scientist*). More than 20 years' international experience in the development of solvent systems for base-metal, precious-metal, and rare-earth separations, with numerous publications in these areas. Currently process chemistry consultant to Mintek's SX engineers.

**Angus Feather**. Project leader, responsible for process flowsheet development, pilot-plant operations, and commissioning and troubleshooting on full-scale plants. Has spent 15 years in extractive metallurgy R&D, mainly in SX, with particular experience in base metals, gold, and several rare element and inorganic acid systems.

**Marthie Kotze** (*Head: Separation Technology*). Fifteen years' experience in solvent extraction, ion exchange, and resin-in-pulp processes. Currently heads a group of ten professional staff specializing in these areas.

**Rene du Preez**. Fifteen years' experience in developing solvent extraction systems for base metals, platinum-group-metals, and other commodities.

**Sean Scott**. Five years' experience in extractive metallurgy, focusing on SX systems for the recovery and separation of base and precious metals. Project leader, particularly for the BPC pilot-plant evaluation campaigns.

**Wendy Bouwer**. Two years' experience in solvent extraction for base-metals recovery and separation and gold refining.

**ION exchange is a hydrometallurgical technique that can be used to**

- **recover and upgrade valuable species in terms of purity and concentration**
- **remove impurities from a process liquor**
- **remove noxious species from process effluents.**

**Ion exchange can be effective at very low concentrations (ppm levels), and where other separation techniques fail, selective separations may be achieved by the correct choice of ion exchange resin. Ion exchange can potentially treat poorly clarified liquors or even pulps, thus eliminating costly solid/ liquid separations.**

## Applications

The best-known metallurgical application of ion exchange is in the recovery of uranium - a process developed in South Africa in which Mintek, with its patented NIMCIX contactor, played a major role. Other industrial applications include recovery of gold, purification of electrolytes for electrowinning, removal of heavy metals from waste streams, and water purification.

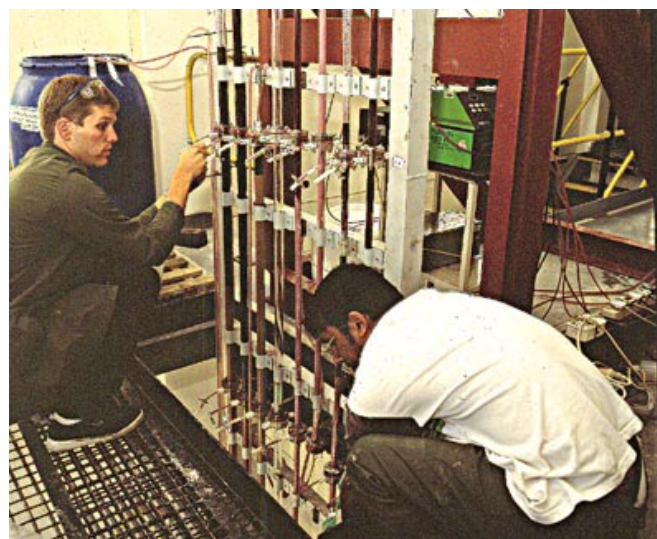
Mintek's biggest effort in ion exchange during the past decade involved the development of a resin-in-pulp (RIP) process for gold. A gold-selective resin (Dowex-Minx) developed at Mintek has been commercialised, and is used for the processing of a preg-robbing ore at the industrial scale. This resin is currently being evaluated by a South American gold producer for the recovery of gold and silver from a heap-leach liquor.

Recent developments in RIP technology have focused on the recovery of base metals from slurries. Evaluations have been carried out on the recovery of nickel, zinc, cobalt and copper at mini-plant scale, and zinc at pilot-plant scale. A final feasibility study using this technology has been completed for a South African client.

During the past 5 years, Mintek has been involved in a number of projects for the design and piloting of fixed-bed ion exchange operations for the removal of impurities such as copper, zinc and nickel from cobalt and copper and zinc from nickel electrolyte streams, as well as the recovery of metals from effluent streams such as solvent extraction raffinates.

## Facilities and scale of operation

Mintek has facilities to undertake projects from basic flowsheet design through to laboratory testwork, piloting, and full-scale plant commissioning. The service includes process design, and optimization of process conditions and economics based on computer simulation and experimental work. Personnel include chemists and engineers who work together in close collaboration throughout a project, and assist the



*Ion-exchange columns being used to remove impurities from a cobalt electrolyte*



*Pump-cell tests on a gold-selective resin*

engineering contractor with the final design and feasibility studies.

Mintek has a range of laboratory and pilot-plant equipment for:

- resin evaluation and comparison
- fixed-bed applications, including countercurrent circuits
- NIMCIX (fluidised-bed) evaluation
- resin-in-pulp evaluation.

All testwork, including piloting, can be carried out either at Mintek or at the client's site.

## Recent Projects

Recent projects in which processes were designed or evaluated for clients include:

- removal of base-metal impurities from cobalt and nickel electrolytes
- primary recovery of nickel from low-grade solutions to produce electrolyte for electrowinning of nickel
- recovery of nickel and cobalt from clear effluent streams such as solvent-extraction raffinates
- recovery of base and precious metals from slurries
- recovery of gold and silver from heap-leach liquor.

Preliminary laboratory testwork for these applications included evaluation of commercially available resins to determine the most suitable resin for a specific application.

## Staff

**Brian Green** (*Specialist Consultant: Hydrometallurgy*)

Twenty-five years' experience in process chemistry, particularly in ion-exchange technology and the development of speciality resins.

**Marthie Kotze** (*Head: Separation Technology and Project Co-ordinator of resin-in-pulp for gold*). Seventeen years' experience in ion-exchange technology.

**Peter Tout** (*Senior Chief Technician*). Twenty-six years' experience in gold metallurgy and the application of resins for gold and silver recovery.

**Jacolien Wyethe** (*Principal Engineer*). Seven years' experience in ion-exchange technology and its application in metallurgy.

**Ivan Greager** (*Senior Engineer*). Five years' experience in ion-exchange technology.

**Johanna van Deventer** (*Senior Technician*). Six years' experience in ion-exchange technology.

# Phosphorus and Performance Derivatives



**Rhodia**

## Contents

Phosphorus Derivatives ..... 4-8

Water Management ..... 9-12

Flame Retardants ..... 13-16

Phosphorus Specialties ..... 17-19

Directory ..... Back cover



## Rhodia - A Leader in Specialty Chemicals

*Rhodia, one of the world leaders in specialty chemicals, contributes to improving the quality of life by developing value-added solutions for the beauty, clothing, foodstuffs and healthcare markets, in addition to transport, industry and the environment.*

*To maintain our commanding market position and reinforce foundations for continued growth, Rhodia is committed to developing innovative new products and services, providing our customers with long-term competitive advantages.*

*Our Phosphorus and Performance Derivatives (PPD) enterprise is dedicated to bringing quality products based on phosphorus technology to our customers. Our extensive product portfolio provides solutions for water management, phosphorus derivatives and flame retardants for the textile and polyurethane markets.*

*The PPD group is a dynamic, technology-driven business that provides innovative solutions to meet customer needs. We work in partnership with our customers to develop new products and technologies, relying on close cooperation and detailed understanding of their processes.*

*We provide a high level of technical and analytical support to help customers overcome challenges and achieve their goals. Products are manufactured at our global production facilities which operate to the highest standards, with ISO 9002 and GMP accreditation.*

## Phosphorus Derivatives

*Rhodia produces a diverse range of organophosphorus compounds within the Phosphorus Derivatives product range, beginning with the basic building blocks of phosphorus trichloride ( $\text{PCl}_3$ ), phosphorus oxychloride ( $\text{POCl}_3$ ) and phosphorus pentoxide ( $\text{P}_2\text{O}_5$ ). Phosphorus Derivatives are a major growth area for Rhodia. Significant investment in research and development, equipment and capacity expansion is key to growing our business. Chemicals produced include organic phosphites, organic phosphates, organic alkylphosphonates, acid phosphates and organic pyrophosphoric acids which are used in a variety of applications. Also included in the range are phosphorous acids which are used in the production of agrochemicals and water treatment products.*

*Rhodia is the world's largest merchant producer of phosphorus trichloride and phosphorus oxychloride. Both products are available in DOT-approved drums or in bulk, utilizing the company's fleet of dedicated tank trailers and rail cars.*



## Primary Derivatives

PRODUCT	DESCRIPTION	APPLICATION
<b>PHOSPHORUS HALIDES</b>		
ALBRITE® $\text{PCl}_3$	Phosphorus trichloride	Basic building block for a range of organic phosphites, phosphates, phosphonates and chlorides, which are used to make a variety of end products, such as antioxidants, stabilizers, peroxides, agricultural chemicals, lubricant additives, water treatment chemicals, pharmaceuticals and flame retardants.
ALBRITE® $\text{POCl}_3$	Phosphorus oxychloride	
<b>PHOSPHORUS PENTOXIDE</b>		
$\text{P}_2\text{O}_5$	Phosphorus pentoxide	Raw material to synthesize acid phosphates which have a variety of end uses both in the acid and neutralized form.
<b>HYPOPHOSPHOROUS ACID</b>		
ALBRITE® 50%	50% aqueous solution	Used as antioxidant, catalyst, color inhibitor, reducing agent and chemicals intermediate.
<b>SODIUM HYPOPHOSPHITE</b>		
$\text{NaH}_2\text{PO}_2 \cdot \text{H}_2\text{O}$	Sodium hypophosphate	Reducing agent in electroless nickel plating, for producing nickel-phosphorus alloy coatings.
<b>PHOSPHOROUS ACID</b>		
ALBRITE® Phosphorous Acid Flake	Solid form of $\text{H}_3\text{PO}_3$ typically 99+ % purity	ALBRITE® phosphorous acids are used to manufacture a variety of inorganic phosphites and organic phosphonates which find use as agrochemicals, chelating agents, scale and corrosion inhibitors.
ALBRITE® 70% Phosphorous Acid	70% aqueous solution of $\text{H}_3\text{PO}_3$ ; contains up to 7% HCl	
ALBRITE® 70% Phosphorous Acid Low Chloride	70% aqueous solution of $\text{H}_3\text{PO}_3$ ; < 35 ppm Cl	

## Secondary Derivatives

PRODUCT	DESCRIPTION	APPLICATION
<b>ACID PHOSPHATES</b>		
ALBRITE® N-Butyl Acid Phosphate		
ALBRITE® N-Octyl Acid Phosphate		
ALBRITE® 2-Ethylhexyl Acid Phosphate		
ALBRITE® Amyl Acid Phosphate		
ALBRITE® N-Hexyl Acid Phosphate	Mixed mono and diesters of phosphoric acid	Organic acid phosphates and their salts are employed in many different applications, such as acid catalysts in coatings, dispersants, lubricants and antistatic agents in textile manufacture.
ALBRITE® Nonyl Acid Phosphate		
ALBRITE® Phenyl (PA-75) Acid Phosphate		
ALBRITE® Cetyl Acid Phosphate		
ALBRITE® Isooctyl Acid Phosphate		
ALBRITE® Octylphenyl Acid Phosphate		
<b>TRIARYL PHOSPHITES</b>		
ALBRITE® Triphenyl Phosphite	A clear, mobile fluid; chemical formula $(C_6H_5O_3P)$	Used as a chemical intermediate for the production of other phosphite esters and phosphonates, as a secondary stabilizer for polyvinyl chloride (PVC) and other polymers such as polypropylene. Also used as a viscosity modifier for epoxide resins, as a flame retardant for polyurethane foams, as an antioxidant for synthetic rubbers and as a lubricant oil additive.
<b>DIALKYL PHOSPHITES</b>		
Diisopropyl		
Dibutyl		
Bis(2-ethylhexyl)	Liquid products conforming to general formula $(RO)_2P(O)H$	Mobile, colorless liquids with mild odors and good thermal stability. Miscible with alcohol, ether and most common organic solvents. Uses include additives for extreme pressure lubricants, adhesives, antioxidants and organic phosphorus intermediates.
Bis(tridecyl)		
Dioleyl		Undergo oxidation, transesterifications and hydrolysis reactions. React with acid halides, acids, esters, amides, aldehydes, ketones, ethers, Grignards and certain unsaturated compounds.

PRODUCT	DESCRIPTION	APPLICATION
<b>TRIALKYL PHOSPHITES</b>		
Tris(2-chloroethyl)		
Triisopropyl		
Tributyl	Liquid products conforming to general formula $(RO)_3P$	Mobile, colorless liquids with characteristic odors. Miscible with alcohol, ether and most common organic solvents. Used as intermediates for insecticides and flame-proofing agents. Additives for lubricants and greases, speciality solvents, stabilizers and color inhibitors for resins.
Tri(2-ethylhexyl)		
Triisoctyl		Highly reactive. Readily oxidized, transesterified or hydrolyzed. Also react with organic acids, halides, ketones, aldehydes, ethers and many other functional groups.
<b>TRIALKYL PHOSPHATES</b>		
Tributyl		
Tributoxyethyl (TBEP)		
Tris(2-ethylhexyl) (TOF)	Liquid products conforming to general formula $(RO)_3P$	Clear mobile liquids with little odor or color. All are miscible in organic solvents. Only triethyl phosphate is soluble in water. Show good thermal and hydrolytic stability. Major uses include plasticizers, dispersants, flame retardants and antifoaming agents.
Triethyl**		
<b>DIALKYL ALKYLPHOSPHONATES</b>		
Dimethyl methyl		
Diethyl ethyl		
Dibutyl butyl	Liquid products conforming to general formula $R-P(O)(OR)_2$	Colorless liquids with mild odors. Stable organophosphorous compounds that are miscible with alcohol, ether and most organic solvents. Uses include heavy metal extraction and solvent separation, pre-ignition additives to gasoline, anti-foam agents in plasticizers and stabilizers, additives in solvents and low temperature hydraulic fluids, flame-proofing agents and to replace organic phosphates for improved stability. Also used as a flame retardant for polyurethane foam, as an antioxidant for synthetic rubbers and as a lubricant oil additive.
Bis(2-ethylhexyl)		
2-ethylhexyl		
Bis(2-chloroethyl)		
2-chloroethyl		

## Metal Extractants

<b>ALBRITE® DBBP</b>	Dibutyl butylphosphonate	Dibutyl butylphosphonate and di(2-ethylhexyl) phosphoric acid are mobile, colorless to light-yellow liquids which are soluble in kerosene-type organic diluents. DBBP exhibits a synergistic effect with di(2-ethylhexyl) phosphoric acid in the extraction of heavy metals.
<b>DEHPA®</b>	Di(2-ethylhexyl) phosphoric acid	Used commercially for the extraction of uranium from wet process phosphoric acid streams, beryllium, rare earths and other metals.
<b>ALBRITE® TBPO<sub>4</sub></b>	Tributyl phosphate	A colorless mobile liquid with low odor. TBPO <sub>4</sub> is an established product for the refining of uranium from yellow cake and is used for solvent extraction of a variety of other metals from aqueous streams.
<b>IONQUEST® 801</b>	2-Ethylhexylphosphonic acid, mono-2-ethylhexyl ester	Used for the extraction and separation of rare earth metals (lanthanides) and the separation of Co from Ni.

\*\* Available only in Europe

## Agricultural Intermediates

PRODUCT	DESCRIPTION	APPLICATION
ALBRITE® TMP	Trimethyl phosphite	Intermediate for monocrotophos, DDVP, NALED phosphamidon, mevinphos and other products.
ALBRITE® TEP	Triethyl phosphite	Intermediate for chlorfenvinphos, fosamine-ammonium, and other products.
ALBRITE® DMHP	Dimethyl hydrogen phosphite	Intermediate for glyphosate, trichlorfon, dimethon-methyl and other products.

## Phosphorus Based Lubricant Additives

DURAPHOS® DMHP	Dimethyl hydrogen phosphite	The dialkyl hydrogen phosphites and acid phosphates are used as intermediates in the formation of extreme pressure (EP) anti-wear (AW) and friction modifier (FM) additives in lubricating oils and greases.
DURAPHOS® DIPH	Disopropyl hydrogen phosphite	
DURAPHOS® DBHP	Diethyl hydrogen phosphite	
DURAPHOS® B(2EH)HP	Bis (2-ethylhexyl) hydrogen phosphite	
DURAPHOS® BTDHP	Bis tridecyl hydrogen phosphite	
DURAPHOS® AP-230	Dilauryl hydrogen phosphite	
DURAPHOS® AP-240	Dioleyl hydrogen phosphite	
DURAPHOS® TLP	Trilauryl phosphite	
DURAPHOS® TPP	Triphenyl phosphite	
DURAPHOS® AAP	Amyl acid phosphate	
DURAPHOS® 610**	C <sub>6</sub> -C <sub>10</sub> alkyl acid phosphate	
DURAPHOS® 2EHAP	2-ethylhexyl acid phosphate	
DURAPHOS® OAP	Octyl acid phosphate	
DURAPHOS® APO 128	Oleyl acid phosphate	
DURAPHOS® 178	Acid phosphonate-based corrosion inhibitor	Approved for use in food grade applications at up to 0.5% by weight. Can also pass EMCOR and ASTM D05969 at higher treat rates in grease formulations.
DURAPHOS® 1700	Low viscosity corrosion inhibitor	Imparts excellent wear protection and corrosion inhibition in grease and oil
DURAPHOS® 444	An effective FG EP for greasers	Anti-wear performance at low levels and good water resistance in both oils and greases.
DURAPHOS® 100**	Neutral phosphonate-based friction modifier	Imparts excellent anti-wear performance

## OTHER

N-Butylchloride*	Intermediate C <sub>4</sub> H <sub>9</sub> Cl	Used in the preparation of a Grignard reagent, in Butyllithium production and in organotin catalyst manufacture.
------------------	---	--

\* Available only in the USA

\*\* Available only in Europe

## Water Management Chemicals

The Water Management Chemicals business specializes in the manufacture and marketing of specialty chemicals designed to control scale, corrosion and microbiological fouling across a wide range of industrial applications. Our extensive product range is targeted at the oil, industrial water, paper, leather and desalination service industries and is supported by worldwide applications expertise.

Products are manufactured to ISO 9002 quality standards from primary locations in the US and UK

TOLCIDE® PS is an innovative product used in oilfield recovery, industrial water treatment and pulp and paper applications. TOLCIDE® PS combines broad spectrum anti-microbial activity with a favorable aquatic toxicity profile and to date has achieved several new registrations including:

- US Environmental Protection Agency registration
- US FDA approval for paper slimicide applications
- German BGW
- Offshore Chemical approvals

Rhodia has also received the US Presidential Green Chemistry Challenge Award in the category of Designing Safer Chemicals.

In addition, BRICORR® 288 is a completely new multi-functional corrosion inhibitor for use in industrial water treatment. BRICORR® 288 combines the benefits of outstanding performance and stability to oxidizing biocides with a favorable environmental profile.



PRODUCT	DESCRIPTION	APPLICATION
<b>BIOCIDES - Key Actives</b>		
TOLCIDE® PS	Series of aqueous solutions of tetrakis(hydroxymethyl) phosphonium sulphate (THPS)	Broad spectrum, fast acting, non-oxidizing biocide for industrial water treatment, oil recovery operations and pulp and paper production. Benefits include excellent performance profile with low environmental impact.
TOLCIDE® MBT	Series of technical active and formulated biocides based on methylene bis(thiocyanate)	Non-oxidizing biocide especially effective as a bactericide and fungicide in paper manufacturing and leather processing.
TOLCIDE® C80* *	Series of products comprising (2-thiocyanomethylthio) benzothiazole (TOMTB), a non-metallic organosulphur compound in liquid form	Used in various stages of leather processing and other preservation applications.
DAZOMET**	Non-metallic organosulphur compound in solid form	Good fungicidal and bactericidal activity effective over a wide pH range.

#### BRIQUEST PHOSPHONATES FOR WATER TREATMENT APPLICATIONS

BRIQUEST® ADPA-60A**	Aqueous solution of 1-hydroxyethane-1,1-diphosphonic acid (HEDP), 60% active acid	Useful in a variety of industrial applications (i.e. cooling water, oilfield, textile) for scale inhibition and metal ion control (sequestration).
BRIQUEST® ADPA-60AW*	Aqueous solution of 1-hydroxyethane 1,1-diphosphonic acid (HEDP), 60% active acid	
BRIQUEST® 301-50A	Aqueous solution of aminotri-(methyleneephosphonic acid), [ATMP], 50% active acid	
BRIQUEST® 301-30SH	Aqueous solution of the pentasodium salt of ATMP, pH10, 30% active acid	
BRIQUEST® 543-45AS	Aqueous solution of diethylenetriaminepentakis (methyleneephosphonic acid), 45% active acid	
BRIQUEST® 462-23K	Aqueous solution of the potassium salt of hexamethylene diaminetrakis (methyleneephosphonic acid), 23% active acid	
BRIQUEST® 5123-45A	Aqueous solution of bis(hexamethylene) triaminepentakis (methyleneephosphonic acid), 45% active acid	
BRIQUEST® 221-50A	Aqueous solution of 2-hydroxyethyliminobis (methyleneephosphonic acid), 50% active acid	
BRIQUEST® 3010-25K	Proprietary, phosphonate formulation as potassium salt solution, 25% active acid	
BRIQUEST® 3010-25KH	Proprietary aqueous phosphonate potassium salt, pH10, 25% active acid	
BRIQUEST® 422-25S	Aqueous solution of the sodium salt of ethylenediaminetetrakis (methyleneephosphonic acid), 25% active acid	
BRIQUEST® 543-25S	Aqueous solution of the sodium salt of diethylenetriamine-pentakis (methyleneephosphonic acid), 25% active acid	

\* Available only in the USA

\*\* Available only in Europe

PRODUCT	DESCRIPTION	APPLICATION
<b>BRIQUEST PHOSPHONATES FOR WATER TREATMENT APPLICATIONS</b>		
BRIQUEST® 281-25S	Neutral, aqueous solution of the sodium salt of 2-ethylhexyliminobis (methylenephosphonic acid), 25% active acid	
BRIQUEST® 2N81-25S	Neutral, aqueous solution of the sodium salt of n-octyliminobis (methylenephosphonic acid), 25% active acid	
BRIQUEST® 8106-25S	Neutral aqueous solution of the sodium salt of pentaethylenhexamineoctakis (methylenephosphonic acid) 25% active acid	Useful in a variety of industrial applications (i.e. cooling water, oilfields, paper manufacture and textiles) for scale inhibition and metal ion control (sequestration).
BRIQUEST® 684-30S	Proprietary phosphonate formulation, supplied as a neutral sodium salt, 30% active acid	
BRIQUEST® Blend B*	Patented synergistic formulation containing phosphonate, 55% active acid	
<b>BRIQUEST PHOSPHONATES FOR DETERGENT APPLICATIONS</b>		
BRIQUEST® 422-25S	Aqueous solution of the sodium salt of ethylenediaminetetrakis (methylenephosphonic acid), 25% active acid	
BRIQUEST® 422-34CS	Calcium/sodium salt of ethylenediaminetetrakis (methylenephosphonic acid), granular, free flowing powder, 34% active acid	
BRIQUEST® 543-25S	Aqueous solution of the sodium salt of diethylenetriaminopentakis (methylenephosphonic acid), 25% active acid	Important properties of sequestration, threshold scale inhibition and dispersion. Used in detergents, textile bleaching and allied applications.
BRIQUEST® ADPA-18SH	Aqueous solution of the tetrasodium salt of 1-hydroxyethane-1, 1-diphosphonic acid, 18% active acid	
BRIQUEST® ADPA-21SH	Aqueous solution of the tetrasodium salt of 1-hydroxyethane-1, 1-diphosphonic acid, 21% active acid	
BRIQUEST® ADPA-60SH	Tetrasodium salt of 1-hydroxyethane-1, 1-diphosphonic acid, free flowing powder, 60% active acid	

\* Available only in the USA



PRODUCT	DESCRIPTION	APPLICATION
<b>POLYMERS</b>		
BRISPERSE® 891*	50% aqueous solution of polymaleic acid	Useful in a variety of anti-scalant and dispersant applications including cooling water, mining, detergents and sugar processing.
<b>CORROSION INHIBITORS</b>		
BRICORR® 288	40% sodium salt solution of a phosphonocarboxylic acid mixture	New generation of environmentally friendly corrosion inhibitor for cooling water systems. Other advantages include stability to oxidizing biocides and scale inhibition properties.
BRICORR® 288B	Ready to use formulation for once through and open recirculating cooling water systems - soft, moderate water conditions	Cooling water treatment - multi functional scale and corrosion inhibitor.
BRICORR® 288C	Ready to use formulation for once through and open - recirculating cooling water systems hard water conditions	Cooling water treatment - high cycled, high hardness conditions.
<b>DESALINATION</b>		
Albrivap & Hagevap	Series of scale inhibitors and antifoams	Desalination chemicals for thermal evaporation processes.
Brinequest 2000*	Scale inhibitor	Desalination applications.

\* Available only in the USA

## Flame Retardants

Rhodia is a leading worldwide manufacturer of phosphorous-based flame retardant chemicals that delay or prevent combustion of materials in textiles, plastics, foams, timber, paper, coatings and adhesives.

The support provided by Rhodia's research and technical teams ensures that the flame retardant range meets both the current and future demands of customers. One of the leading worldwide textile flame retardants is PROBAN®, which is applied to fabrics by textile finishing companies through a license agreement with Rhodia. PROBAN® is used in protective clothing, bedding and furnishings in a wide range of industries.

We also offer the ANTIBLAZE® product line of flame retardants, which includes a series of ammonium polyphosphates, cyclic phosphonate esters and other phosphonates used on a wide range of fabrics and nonwovens containing both natural and synthetic fibers. These products are easily applied to fabric and nonwovens using the most common application methods, including padding, spraying and coating. Properties include binder compatibility, water solubility or insolubility, high efficiency thermal stability, minimal effect on hand and neutral pH. Selected ANTIBLAZE® polyurethane and textile flame retardants also provide innovative solutions to the automotive industry where low fogging performance is required.

The largest range of flame retardants designed for the polyurethane industry for flexible and rigid foam is phosphate esters. Applications in the flexible foam area include soft furnishings and car components. Rigid foams are most commonly used for insulation. A developing range of ANTIBLAZE® products is also available for plastics, coatings and timber.



PRODUCT	DESCRIPTION	APPLICATION
<b>TEXTILE FLAME RETARDANTS</b>		
<b>ANTIBLAZE™ CL</b>	Aqueous solution of ammonium polyphosphate	Non-durable flame retardant for cellulosic fabrics.
<b>ANTIBLAZE™ CU</b>	Cyclic phosphonate ester	
<b>ANTIBLAZE™ CT</b>	Low viscosity modification of <b>ANTIBLAZE™ CU</b>	Durable flame retardant for polyester fabrics. Used in back-coating applications.
<b>ANTIBLAZE™ BQ</b>	Ammonium salts of phosphoric and sulphuric acids	Non-durable flame retardant for cellulosic fabrics. Used in flame retardant paper applications.
<b>ANTIBLAZE™ FSD</b>	Aqueous-based ammonium polyphosphate blend	Non-durable flame retardant for a wide range of fabrics, including blends with high levels of synthetic fibres.
<b>ANTIBLAZE™ LR2</b>	Aqueous solution of polyphosphoric acid salts	Semi-durable flame retardant for cellulosic upholstery fabrics. Meets Furnishing Standard BS EN1021.
<b>ANTIBLAZE™ LR3</b>	Ammonium polyphosphate	
<b>ANTIBLAZE™ LR4</b>	Ammonium polyphosphate of low water solubility	Powder flame retardant used in combination with a binder system. Used in back-coating systems where limited durability is required (e.g. BS EN1021).
<b>ANTIBLAZE™ TR</b>	Aqueous solution of polyphosphoric acid salts	Non-durable flame retardant for cellulosic textiles. Used in flame retardant paper applications.
<b>ANTIBLAZE™ RD1*</b>	Organic phosphonate in aqueous solution	Non-hygroscopic, low-fogging flame retardant for use on a variety of fabrics. Compatible with binders. Non-durable.
<b>ANTIBLAZE® 37*</b>	Organic phosphonate blend	Versatile flame retardant for many fabrics, especially polyester and coatings. Minimal effect on fabric hand. Durable or non-durable, depending on application.
<b>ANTIBLAZE® N*</b>	Cyclic phosphonate ester	Flame retardant for fabrics and latex binder applications. High performance at reduced loadings in many systems.
<b>ANTIBLAZE® NT*</b>	Low viscosity modification of <b>ANTIBLAZE® N</b>	Flame retardant for thermosol application to polyester fabrics.
<b>ANTIBLAZE® NT D-1*</b>	High purity, low color, cyclic, phosphonate ester	Non-durable flame retardant for plastics, synthetics and a wide range of other uses.
<b>ANTIBLAZE® IS*</b>	Chlorinated diphosphate ester	Semi-durable flame retardant for a wide range of fabrics. Can be applied directly or incorporated into binder systems. Low water solubility makes it especially useful for passing leach tests such as BS 5851.
<b>ANTIBLAZE® XL</b>	Organic phosphonate in aqueous solution	Non-hygroscopic, low fogging flame retardant for use on a variety of fabrics. Compatible with binders. Non-durable.
<b>PROBAN® CC</b> <b>PROBAN® ST</b>	Tetrakis(hydroxymethyl) phosphonium chloride based pre-polymer	Cellulosic, cellulosic/polyester blends (durable finish) PROBAN® licensee only.

\* Available only in the USA

PRODUCT	DESCRIPTION	APPLICATION	%P	%Cl
<b>POLYURETHANE FLAME RETARDANTS</b>				
<b>ANTIBLAZE™ DMMP</b>	Dimethyl methylphosphonate	Flame retardant for rigid polyurethane foams.	25.0	0
<b>ANTIBLAZE® N*</b>	Neutral cyclic diphosphonate ester liquid	Flame retardant for all polyether foams where low volatility and high performance is required	21.0	0
<b>ANTIBLAZE™ TDCP</b>	Tris(Dichloropropyl) phosphate	Flame retardant for flexible polyether and polyester foam where hydrolytic stability is critical.	7.2	49.1
<b>ANTIBLAZE™ TDCP LV</b>	Low viscosity version of <b>ANTIBLAZE™ TDCP</b> <b>ANTIBLAZE® 195</b>	Flame redundant for flexible polyurethane foam.	7.4	47.0
<b>ANTIBLAZE™ TMCP</b>	Tris(2-chloropropyl) phosphate liquid	General purpose flame retardant for polyurethane foam including one and two component systems	9.3	33.0
<b>ANTIBLAZE™ 80</b>				
<b>ANTIBLAZE™ V6</b>	Chlorinated diphosphate ester	Flame retardant for polyether, high resilience and moulded foam	10.6	36.0
<b>ANTIBLAZE™ 100</b>				
<b>ANTIBLAZE™ V66</b>	Chlorinated diphosphate ester	Low fogging flame retardant for automotive polyether and moulded polyurethane foams	10.3	32.9
<b>ANTIBLAZE® 78</b>	Chlorinated diphosphonate ester	Flame retardant for rigid polyurethane foam and phenolic based laminates	12.0	34.0
<b>ANTIBLAZE™ V88</b>	Chlorinated diphosphate ester	Flame retardant for polyether, high resilience and moulded foam	10.4	36.1
<b>ANTIBLAZE® 125*</b>	Chlorinated phosphorus ester liquid	Low viscosity flame retardant for bonded flexible urethane foam	11.2	34.0
<b>ANTIBLAZE® 140*</b>	Mixture of chlorinated phosphate & chlorinated phosphonate esters	General purpose flame retardant for all flexible polyether based foams	9.8	39.0
<b>ANTIBLAZE™ 205*</b>	Mixture of alkyl and aryl phosphate esters	Low viscosity, low scorch flame retardant for flexible polyurethane foam	7.6	32.0
<b>ANTIBLAZE® 230*</b>	Mixture of aryl phosphate and phosphonate esters	Low fogging, high efficiency, flame retardant for flexible polyether based foams	13.4	0
<b>ANTIBLAZE™ V280</b>	Chlorinated phosphate ester	Low fogging flame retardant for polyester and polyether foam	7.3	44.2
<b>ANTIBLAZE™ V300</b>	Halogen-phosphate ester mixture	Low viscosity, mixed halogen containing flame redundant for polyether, high resilience rigid and moulded foam	4.7	16.2 (35.4 Br)
<b>ANTIBLAZE™ V490</b>	Organo phosphonate ester	Halogen free system stable flame retardant for rigid polyurethane foams	18.7	0
<b>ANTIBLAZE™ V500</b>	Chlorinated phosphate ester	Low fogging flame retardant for automotive polyether and moulded polyurethane foams	10.4	32.9
<b>ANTIBLAZE™ V610</b>	Mixture of chlorinated diphosphate and chlorinated phosphonate esters	Low viscosity, high efficiency flame retardant for moulded polyurethane foam	11.3	35.0
<b>ANTIBLAZE™ V650</b>	Chlorinated phosphate esters	General purpose flame retardant for polyether high resilience and moulded foams	10.0	34.5
<b>VIRCOL® 82</b>	Neutral phosphorus polyol	Polyol flame retardant for use in rigid polyurethane foam pre-polymers and pre-mixes	11.3	0

\* Available only in the USA

PRODUCT	DESCRIPTION	APPLICATION	%P
<b>PLASTICS ADDITIVES</b>			
<b>ANTIBLAZE™ 1045</b>	Neutral cyclic diphosphate ester	Flame retardant for polyester fibers, extrusions and engineering plastics.	20.8
<b>ANTIBLAZE™ NK</b>	Alkyl amine phosphate salt	Flame retardant chemical filler for polypropylene, other olefins and thermoset applications.	19.6
<b>ANTIBLAZE™ NP</b>	Formulated alkyl amine phosphate salt	Flame retardant chemical filler for polyolefins and EVA co-polymers.	15.7
<b>ANTIBLAZE™ TCP*</b>	Tricresyl phosphate		8.3
<b>ANTIBLAZE® TXP*</b>	Trixylenyl phosphate		7.6
<b>ANTIBLAZE® 519*</b>	Triaryl phosphate ester	Flame retardant fluid/plasticizer used in lubricants, hydraulic fluids, PVC, urea-formaldehyde resins and in elastomers.	8.3
<b>ANTIBLAZE® 521*</b>	Triaryl phosphate ester		8.1
<b>ANTIBLAZE® 524*</b>	Triaryl phosphate ester		7.7
<b>TIMBER</b>			
<b>ANTIBLAZE™ ML</b>	Aqueous solution of ammonium polyphosphate	Integral flame retardant for wood-based panel products.	15.7
<b>ANTIBLAZE™ PI</b>	Ammonium polyphosphate	Powder flame retardant for integral treatment of wood-based panel products.	26.0
<b>COATINGS</b>			
<b>ANTIBLAZE™ MC</b>	Ammonium polyphosphate	For use in intumescent coatings.	30.0

\* Available only in the USA



## Phosphorus Specialties

*The Phosphorus Specialties business works directly with customers on an exclusive basis to develop commercial processes and applications for phosphorus chemicals. Product areas include phosphonate esters (e.g. Horner-Emmons reagents), bisphosphonates, monomeric and polymeric phosphonic acids, phosphorylating agents and derivatives and phosphines and phosphine ligands.*

*We have a fully integrated development program where new processes and products are tested in Rhodia's laboratory, pilot plant and semi-works facilities. We closely manage processes to provide safe operation and timely delivery of products and have a complete hazard evaluation program as an integral part of new product introductions.*

*The business continues to evolve as an increasing number of companies source key intermediates and products from Rhodia. The application areas served by this business include pharmaceutical intermediates and fine chemicals, polymers and plastics, electronics, paints and coatings and other areas related to surface property modification and material science. The product range on the following pages represents a small fraction of more than 50 products in the development pipeline.*

*Our monomer products and their homopolymer and copolymer derivatives continue to attract attention as surface property and performance enhancers.*



PRODUCT	DESCRIPTION	APPLICATION
<b>SURFACE TREATMENT CHEMICALS</b>		
VPA	Vinylphosphonic acid	Surface treatment agent to improve bonding to metals and metal complexing agent.
ALBRITECT® CP30	Copolymeric pretreatment	Surface treatment agent to improve binding to metals.
OPA	Octylphosphonic acid	Metal complexing agent, tin ore flotation aid and surface treatment agent for metals and metal oxides.
ACCOMET® C	Chromium based pretreatment	Dry-in-place metal pretreatment process for coil coating applications.
ALBRITECT® Pre-treatment	Non-chrome pretreatment	Dry-in-place metal pretreatment process for coil coating applications; free from heavy metals.
ALBRITECT® D Series Anti-corrosive Pigments	Non-chrome anticorrosive pigment	Non-toxic anticorrosive pigments effective in general industrial paint systems; lead and chromium free.
ALBRITECT® CC Series	Non-chrome anticorrosive pigment	Anticorrosive pigments. Non-toxic pigments effective in a variety of coil coating primer systems; lead and chromium free.
ALBRITECT® 6835	Ethylene methacrylate phosphate	Adhesion promoter and corrosion inhibitor in coatings and adhesives.
Vicro-Pet® 50	Tan, viscous liquids	Excellent inhibitors for steel, aluminum, mixed alloys, used in wafer-based coatings, antifreeze compounds, cleaners and polishes.

## INTERMEDIATES and REAGENTS

<b>TMP-HP</b>	Trimethyl phosphite (high purity)	Intermediate in manufacturing of phosphonate esters and vinyl phosphates; reagent for dehalogenations, dehydrohalogenations and reductive cyclisations.
<b>TEP-HP</b>	Triethyl phosphite (high purity)	Intermediate in manufacturing of phosphonate esters: reagent for halogenations, dehydrohalogenations and reductive cyclisations.
<b>TIPP-HP</b>	Triisopropyl phosphite (high purity)	Intermediate in manufacturing of phosphonate esters; reagent for dehalogenations, dehydrohalogenations and reductive cyclisation.
<b>TBP-HP</b>	Tributyl phosphite (high purity)	Intermediate in manufacturing of phosphonate esters; reagent for dehalogenations, dehydrohalogenations and reductive cyclisation; scavenging agent for sulphur impurities.
<b>TPP-HP</b>	Triphenyl phosphite (high purity)	Reagent for reductions and peptide coupling. Complexes with halogens and ozone for selective halogenations and oxidations.
<b>DMHP-HP</b>		
<b>DEHP-HP</b>	Diethyl hydrogen phosphite (high purity)	Intermediate in manufacturing of phosphonate esters and chlorophosphates.
<b>DBHP-HP</b>		
<b>DMMP-HP</b>	Dimethyl methylphosphonate (high purity)	Intermediate in manufacturing $\beta$ -Ketophosphonates.
<b>AMPA</b>	Aminomethylphosphonic Acid	Intermediate in manufacturing pharmaceutical intermediates (developmental product).
<b>TMPA</b>	Trimethyl phosphonoacetate	Intermediate in manufacturing of fine chemicals via Horner-Emmons reaction (developmental product).

PRODUCT	DESCRIPTION	APPLICATION
<b>INTERMEDIATES and REAGENTS</b>		
DEMPA	Diethyl methyl phosphonoacetate	Intermediate in manufacturing of fine chemicals via Horner-Emmons reaction (developmental product).
TIPMDP	Tetraisopropyl methylenediphosphonate	Intermediate in manufacturing of bisphosphonate esters, acids and salts; reagent for phosphonate preparation via Horner-Emmons reaction.
TEPA	Triethyl phosphonoacetate	Intermediate in manufacturing of fine chemicals and polyester processing acid.
DECMP	Diethyl cyanomethylphosphonates	Intermediate in manufacturing of substituted nitrile via the Horner-Emmons reaction and their amide and heterocycle derivatives.
TEPF	Triethyl phosphonoformate	Intermediate in manufacturing of phosphonoformic acid and its esters and salts.
PDCP	Phenyl dichlorophosphate	Intermediate in selective manufacturing of phosphoric acid diesters; protective agent for hydroxyl groups.
DPCP	Diphenyl chlorophosphate	Intermediate in selective manufacturing of phosphoric acid monoesters; protective agent for hydroxyl and ketone groups.
<b>PHOSPHINES</b>		
TBPinE	Tributylphosphine	Intermediate for phase transfer catalysts, biocides and Wittig reactions; (phosphine oxide by-product is water soluble).
TPPInE	Triphenylphosphine	Intermediate for phase transfer catalysts and Wittig reactions, ligand for hydroformylation catalysts.
TOTPinE	Tri-o-Tolylphosphine	Phosphine ligand for hydroformylation catalysts, used in Heck and Mitsunobu reactions.
dippe	1,2-Bis (Diphenylphosphino) ethane	Bidentate phosphine ligand used with transition metals to provide catalysts for carbonylations, hydroformylations and organic synthesis.
dppp	1,3-Bis (Diphenylphosphino) propane	
dppb	1,4-Bis (Diphenylphosphino) butane	
dppf	1,1-Bis (Diphenylphosphono) ferrocene	



**[www.rhodia.com](http://www.rhodia.com)**

**[www.rhodia-ppd.com](http://www.rhodia-ppd.com)**

Welcome to Rhodia's Phosphorus and Performance Derivatives Customer Service Page.  
Here you will find contacts designed to help you locate the right resources  
where ever you are in the world.

Rhodia also produces a wide range of solutions for the beauty, clothing,  
foodstuffs and healthcare markets in addition to transport, industry and the environment.  
To learn more about all the products we produce, have a look at the Rhodia website.

#### **Head Office**

Rhodia Phosphorus and Performance Derivatives  
Oak House, Reeds Crescent  
Watford, Hertfordshire WD24 4QP  
United Kingdom  
Tel: + 44 (0)1923 485868  
Fax: + 44 (0)1923 211580

#### **Europe/Middle East/Africa**

Rhodia Phosphorus and Performance Derivatives  
Sylvain Dupuislaan 243  
100 Brussels  
Belgium  
Tel + 32 2 529 45 82  
Fax + 32 2 529 45 84  
  
(PPD) European Customer Service  
Trinity Street  
Oldbury, West Midlands B69 4LN  
United Kingdom  
Tel: + 44 (0)121 552 3333  
Fax: + 44 (0)121 541 3235

#### **North America**

Rhodia Phosphorus and Performance Derivatives  
259 Prospect Plains Road CN 7500  
Cranbury, NJ, 08512-7500 USA  
Tel: 1 609 860 3919  
Fax: 1 609 860 0076

(PPD) North American Customer Service  
Tel: 1 609 860 4000 or 1 888 776 7337 (USA only)  
Fax: 1 609 655 8704

#### **South/Central America**

Rhodia Phosphorus and Performance Derivatives  
Temistocles 10 Piso 9  
Col. Chapultepec Polanco  
11560 México, D.F. México  
Tel: + 52 5283 2800 or + 52 5283 2846  
Fax: + 52 5281 5862

#### **Asia/Pacific**

Rhodia Phosphorus and Performance Derivatives  
300 Beach Road  
199555 Singapore  
Tel: + 65 291 1921  
Fax: + 65 296 7249



# **Shell Chemicals**

# **Solvents for Mining**

**ISEC 2002 South Africa**



## Shell Chemicals

Shell Chemicals has a large number of products in its portfolio which are used in the mining industry (see table attached).

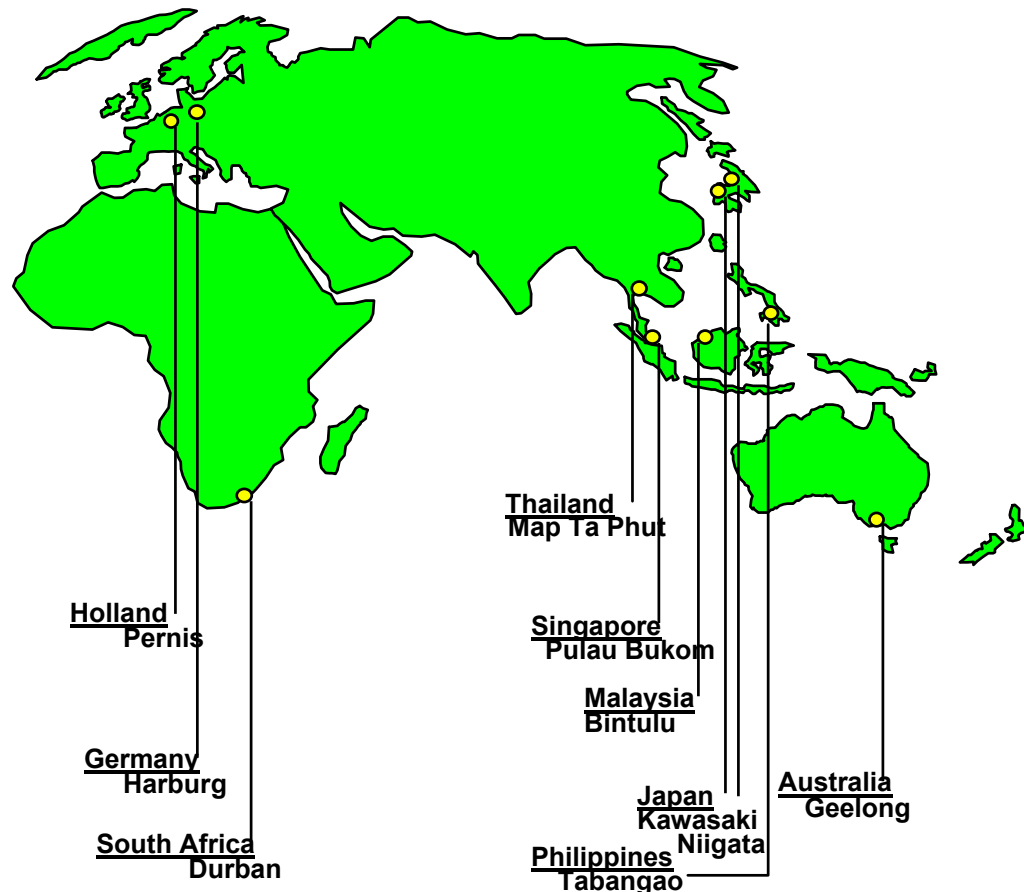
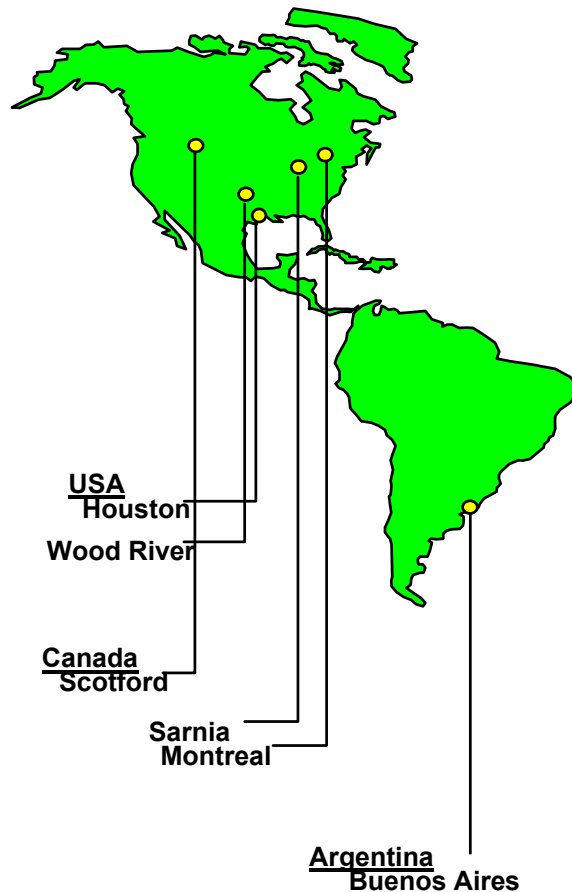
We are able to offer these products worldwide via local Shell Chemicals operations. Currently we supply the in Australasia, Southern Africa, Southern and North America.

For further queries either contact your local Shell Chemicals Company or our mining focal point Mr. Peter Haig  
(tel. number +61 7 5493 2795 e-mail address: [Peter.A.Haig@Shell.com.au](mailto:Peter.A.Haig@Shell.com.au) ) or visit us on our website: [www.shell.com/chemicals](http://www.shell.com/chemicals)



Shell Chemicals

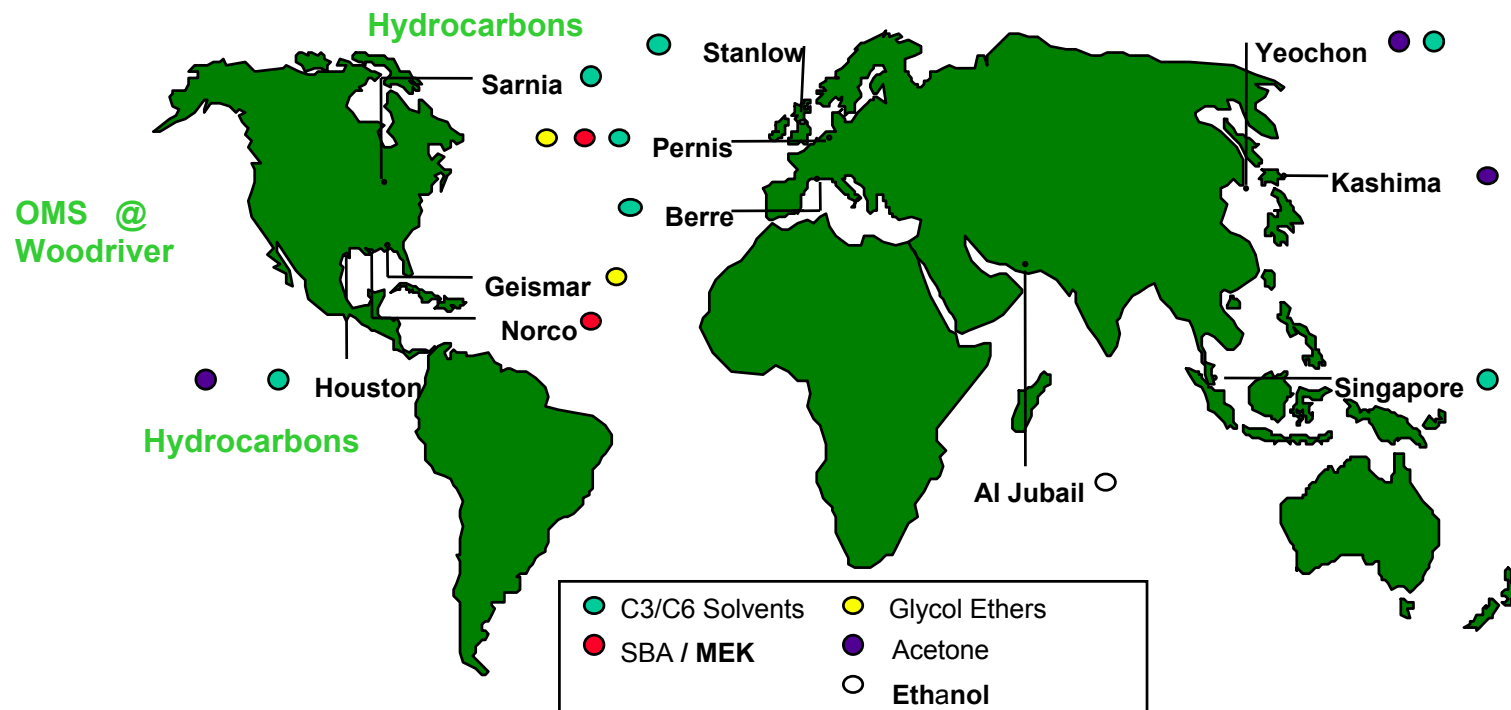
# Shell Hydrocarbon Solvents Plants





Shell Chemicals

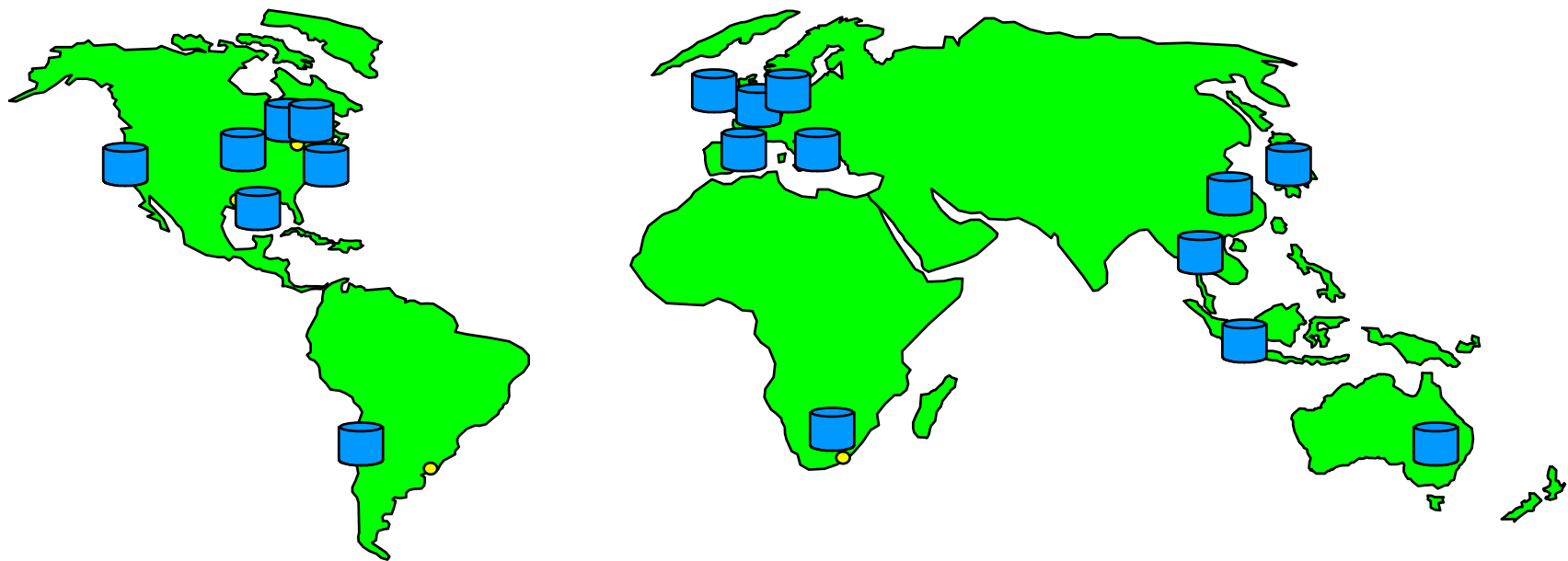
# Shell Solvents Units Worldwide





Shell Chemicals

# Terminals Shell Solvents





Shell Chemicals

# Why buy from Shell Chemicals?

- Multi Site Solvent Manufacture
- Product Quality
- European / Global Specification
- Local Storage
- Security of supply
- Franchised Distributor Network
- R & D facilities : Amsterdam and West Hollow
- On-going Investment
- ISO certification
- Customer Logistics Charter
- Global Website



Shell Chemicals

# Mining Solvents

<u>Application</u>	<u>Shell Solvents</u>
Solvent Extraction	<b>Shellsol 2325</b> <b>Shellsol 2046</b> <b>Shellsol D70</b> <b>Shellsol A150</b> <b>Shellsol D80</b>
Frothing	<b>MIBC</b> <b>HG</b> <b>Shellfroth 10</b> <b>DPM</b> <b>BTTO (bottom from EO glycol ethers)</b> <b>PEG</b> <b>MTTO (bottom PO glycol ether with &gt; MTP)</b>
Coal Flotation	<b>Shellsol 2323</b> <b>Shellsol 2046</b> <b>MTTO (pour point depressant wet coal flow)</b>
Tar Sands Flotation	<b>MIBC</b>